JAE
vol. XLIV s2
2013 September

Official Journal of the Associazione Italiana di Ingegneria Agraria

Member of the International Commission of Agricultural Engineering

Proceedings of the 10th Conference of the Italian Society of Agricultural Engineering

Horizons in agricultural, forestry and biosystems engineering

Viterbo, Italy, September 8-12, 2013

Guest Editors: Danilo Monarca, Massimo Cecchini

Journal of Agricultural Engineering
open access journal - ISSN 1974-7071 - www.agroengineering.org

pagepress

Journal of Agricultural Engineering

pISSN 1974-7071 | eISSN 2239-6268

Publisher

PAGEPress Publications
via Giuseppe Belli 7
27100 Pavia, Italy
Tel. +39.0382.1751762 – Fax. +39.0382.1750481
info@pagepress.org – www.pagepress.org

pagepress

Journal of Agricultural Engineering

The Journal of Agricultural Engineering (JAE) is the official journal of the Italian Society of Agricultural Engineering - AIIA - supported by University of Bologna. The subject matter covers a complete and interdisciplinary range of research in engineering for agriculture and biosystems.

Instructions to Authors

Manuscripts must be written in English. Authors whose native language is not English are strongly recommended to have their manuscript checked by a language editing service, or by an English mother-tongue colleague prior to submission.

Manuscripts should be saved and submitted as a single WORD file containing the full text, references, tables and figures. In case of acceptance, original text and figures must be provided for publication.

Original Articles: should normally be divided into an abstract, introduction, materials and methods, results, conclusions and references. The abstract should contain a maximum of 400 words. *Review Articles:* no particular format is required for these articles. However, they should have an informative, unstructured abstract of about 250 words. *Technical Notes:* are articles with a simple layout and containing limited data (no more than two figures or tables) and a small number of citations (not more than 25). They should be limited to 2,000 words of text (figure captions, table headings and reference lists are additional to this limit).

Manuscripts should be double spaced with numbered lines and wide margins and should be arranged as follows. *Title page:* including the full title, the name(s) of the author(s), their affiliation and the name of the corresponding author to whom proofs and requests for off-prints should be sent. *Abstract:* should not exceed 400 words. *Keywords:* three to six keywords characterizing the content of the article in alphabetical order. *Introduction:* A brief introduction. *Materials and methods:* this section should provide sufficient information and references on the techniques adopted to permit their replication. *Results:* the content of this section should permit full comprehension of the data reported in figures and tables. *Conclusions:* this should underline the significance of the results and place them in the context of previous research. *Acknowledgements:* a brief text. *References* should be prepared strictly according to the instructions given below. *Units:* authors are recommended to use the International System of Units (SI). *Scientific names:* common names of organisms should always be accompanied, when first cited, by their complete scientific name in *italics* (genus, species, attribution and, if appropriate, cultivar). *Formulae:* mathematical formulae must be carefully typed, possibly using the equation editor of Microsoft Word; when a paper contains several equations they should be identified with a number in parentheses (e.g. Eq. 1). Please note that each accepted paper will undergo technical and scientific copyediting before publication. *Tables:* tables are numbered consecutively in Arabic numbers without “no.” before the number. References should be made in the text to each table. The desired style of presentation can be found in published articles. Titles of tables should be descriptive enough to be able to stand alone. Do not present the same data in tabular and graphic form. *Figures*: figures are numbered consecutively in Arabic numbers. References should be made in the text to each figure. Each figure should have a caption. The term "figure" is used also for graphs and photos. *Symbols and abbreviations* used in figures can be defined in the figure caption or note or within the figure itself. Please avoid the use of bold face or greater size for the characters. Symbols and abbreviations used in figures can be defined in the figure caption or note or within the figure itself. The figures must be submitted as .tif or .jpg files, with the following digital resolution: 1. Color (saved as CMYK): minimum 300 dpi; 2. Black and white/grays: minimum 600 dpi; Lettering of figures must be clearly labelled. *Movies*: movies can be submitted and uploaded as "Supplementary Files" during the manuscript submission procedure. Dimension should not exceed 5 MB. *Citations in the text:* the Journal follows the "author, year" style of citation. When a citation has one or two authors, cite the reference throughout using the name(s) and the date. When a citation has more than two authors, cite the reference throughout the text with *et al.* following the last name of the first author. When two or more references are included in a grouping within a sentence, they are arranged and separated by a semicolon. The first criterion is the year (former citations precede recent ones); multiple citations for a given year are further arranged alphabetically and multiple citations for the same initial letter are arranged as follows: first the citation with one author, secondly the citation with two authors, then the other (with *et al.*). When the same author has two references with different dates, cite them in chronological order, separating the dates with a comma; when the same author has two references with the same date, arrange the dates as a and b (also in the reference list) and separated by a comma. Journal titles mentioned in the reference list should be abbreviated according to the following websites (sequenced by relevance): 1. ISI Journal Abbreviations Index (http://library.caltech.edu/reference/abbreviations/); 2. Biological Journals and Abbreviations (http://home.ncifcrf.gov/research/bja/) Example: (Foury, 1967, 1972; Burns *et al*., 1970; Allen *et al*., 1990; Basnizki and Zohary, 1994; White *et al*., 1990a, 1990b). Citation should be made in the text to each reference. Citations are listed in strict alphabetical order by first author' last names. Use capital and lower case letters for authors' names. If all authors are identical for two or more citations, chronological order of publication should dictate the order of citations. When more than one paper in a given year is listed by authors whose names are in the same order in each paper, the papers are arranged in alphabetical order of the paper title. Use the following system to arrange your references:

1. Periodicals: Hennighausen L.G., Sippel A.E. 1982. Characterization and cloning of the mRNAs specific for the lactating mouse mammary gland. Eur. J. Biochem. 125:131-41.

2. Books: National Research Council 2001. Nutrient Requirements of Dairy Cattle. 7th rev. ed. National Academy Press, Washington, DC, USA.

3. Multi-authors books: Brouwer I. 1965. Report of the subcommittee on constants and factors. In: K.L. Blaxter (ed.) Energy metabolism. EAAP Publ. N. 11, Academic Press Ltd., London, UK, pp 441-3.

4. Proceedings: Rossi A., Bianchi B. 1998. How writing the references. Proc. 4th World Congr. Appl. Livest. Prod., Armidale, Australia, 26:44-6. (Or 44, if one page) -

Blanco P., Nigro B. 1970. Not numbered volumes. Page 127 (or pp 12-18) in Proc. 3rd Int. Conf. Cattle Dis., Philadelphia, PA, USA.

5. Thesis: Rossi P. 1999. Stima di parametri genetici nella

pagepress

razza Reggiana. Degree Diss., Università di Milano, Italy.

6. Material from a World Wide Web site: Food and Drug Administration, 2001. Available from: http://www.fda.gov or Food and Drug Administration, 2001. http://www.fda.gov Accessed: May 2012.

7. Regulations:

- Italian Regulation, 1992. Application of the Council Directive (EEC) No. 86/609 regarding the protection of animals used for experimental and other scientific purposes. LD 116/1992. In: Official Journal No. 294, 18/2/1992, pp 5-24.

- European Commission, 1994. Commission Decision of 27 June 1994 concerning certain protection measures with regard to bovine spongiform encephalopathy and the feeding of mammalian derived protein, 94/381/EC. In: Official Journal, L 172, 07/07/1994, pp 23-24.

8. International standards: ISO, 1991. Determination of total fat content - Meat and meat products. Norm ISO R-1443:1991. International Organization for Standardization Publ., Geneva, Switzerland.

9. In press: Manuscripts that have been accepted for publication but are not yet published can be listed in the literature cited with the designation [In press] following the journal title.

10. Other: Citations such as personal communication, unpublished data, etc. should be incorporated in the text and NOT placed into the Reference section.

Copyright

Peer-review policy

All manuscript submitted to our journals are critically assessed by experts in accordance with the principles of Peer Review, which is fundamental to the scientific publication process and the dissemination of sound science. Each paper is assigned to the Chief Editor. The first step of manuscript selection takes place entirely inhouse and has the objective to establish the article's appropriateness for our journals' readership. The articles are then reviewed by two different external referees (second step or classical peer-review) in accordig with the associate editors.

Subscriptions

Italy: € 65.00 per year; one number € 25.00; back issues or double issues: € 25.82; back year: € 72.30

Abroad: annual Subscription € 75.00 - air mail subscription € 90.00.

Autorizzazione Del Tribunale Di Bologna N. 4045 Del 3 Febbraio 1970.

Journal of Agricultural Engineering

Rivista trimestrale registrata al Tribunale di Pavia n. 9/2012/Reg.

Stampa: Press Up s.r.l.
via La Spezia, 118/C 00055 - Ladispoli (RM)
Tel. and Fax: +39.076.15.27.351

Supported by University of Bologna

pagepress

Journal of Agricultural Engineering
volume XLIV, supplement 1, 2013

AIIA13

Proceedings of the 10th Conference of the Italian Society of Agricultural Engineering

Horizons in agricultural, forestry and biosystems engineering

Viterbo, Italy, September 8-12, 2013

Guest Editors
Danilo Monarca, Massimo Cecchini

Table of Contents

pagepress

Scientific Committee

Alessandro Santini (AIIA President)
Danilo Monarca (Vice President)
Antonino Failla (Past President)
Paolo Balsari
Thomas Banhazi
Gualtiero Baraldi
Remigio Berruto
Luigi Bodria
Giovanni Cascone
Raffaele Cavalli
Artemi Cerdà
Giancarlo Dalla Fontana
Mario Falciai
Vito Ferro
Claudio Gandolfi
Emilio Gil
Giuseppe Giordano
Adriano Guarnieri
Joerg Hartung
Dirk Jaeger
Robert Kaufmann
Mario Aristide Lenzi
Sandro Liberatori
Peter Lundqvist
Attila Nemes
Luigi Pari
Antonio Pazzona
Domenico Pessina
Pietro Piccarolo
Felice Pipitone
Elisabeth Quendler
Nunzio Romano
Giacomo Scarascia Mugnozza
Giampaolo Schillaci
Peter Schulze Lammers
Claus Aage Grøn Sørensen
Paolo Spugnoli
Patrizia Tassinari
Alessandro Toccolini
Fedro Zazueta

Organizing Committee

Danilo Monarca
(convener)

Massimo Cecchini,
Stefano Gasbarra (coordinators)

Daniele De Wrachien
(international relationships)

Paolo Biondi,
Maurizio Carlini,
Andrea Colantoni,
Roberto Fanigliulo,
Salvatore Grimaldi,
Antonio Leone,
Angela Lo Monaco,
Alvaro Marucci,
Giuseppina Menghini,
Raffaele Pelorosso,
Andrea Petroselli,
Rodolfo Picchio,
Fabio Recanatesi,
Maria Nicolina Ripa,
Manuela Romagnoli

Scientific Secretariat

Salvatore Grimaldi, Andrea Petroselli (AGR/08)
Massimo Cecchini, Andrea Colantoni (AGR/09)
Alvaro Marucci, Maria Nicolina Ripa (AGR/10)

Organizing Secretariat

DAFNE Department – Tuscia University
Via S. Camillo De Lellis, s.n.c.
01100 Viterbo – Italy

Ce.F.A.S. Special Agency of the Chamber of Commerce
Viale Trieste, 127 01100 Viterbo – Italy
+39.0761.324196

PRINTED WITH THE SUPPORT AND THE PATRONAGE OF THE CARIVIT FOUNDATION OF VITERBO, ITALY

PRESENTATION

The Board of Directors of the Italian Association of Agricultural Engineering, following the well-established tradition to organize every four years a Conference, has chosen Viterbo as venue for the tenth edition which will be held on September 8-12, 2013.

The closer and closer integration of scientific know how, that is demanded in the use of the environmental resources and it is driven by the new developing models, has addressed the agricultural engineering toward the bio-systems engineering, therefore expanding its former expertise-area by incorporating living systems related to both the agriculture and to natural systems. As a consequence, the interests of the Association now spam even over the application of engineering principles to processes governing territorial phenomena with the aim to study, to model, to manage and to set off biology systems toward an optimal agricultural development, crop production, the use of the soil and the environment.

Within such a context the conference, by accomplishing the actual and future needs of the world population, represents an important chance to bring together engineers and researchers to let meeting people working in different, although similar, environments.

In particular, the 2013-conference will focus on: new horizons in agricultural, forestry and bio-systems engineering and, to better homogenize discussions, presentations will be organized according to the listed below sessions:

1 Forest-wood chains
2 Hydrology and dynamics of water and sediments in agricultural and mountain basins: monitoring, modeling and risk analysis
3 Hydraulics and hydro-morphological processes for stream and river restoration and management
4 Information technology, automation and precision farming and forestry
5 Structures and technologies for livestock production: technical, energy and environmental aspects
6 Structures and technologies for protected crop production: technical, energy and environmental aspects
7 Post harvest, food and process structures and technologies
8 Power and machinery in agriculture and forestry
9 Analysis, modeling and planning of rural areas
10 Renewable energy, biomass and biological residues
11 Safety, health and ergonomics - SHWAnet international meeting
12 Sustainable planning and management of soil and water resources

Prof. Alessandro SANTINI
AIIA President

pagepress

Dear colleagues,

it is my pleasure to welcome you to the 10th AIIA Conference: "AIIA13 – Horizons in agricultural, forestry and biosystems engineering", and to welcome you to Viterbo.
For the first time the AIIA conference will be held in English. The purpose of this choice is to involve academics and researchers coming from other nations.
This conference will then be a unique opportunity for scientists, researchers, experts, students and people representing the business world to show, share and discuss the results of their researches. Another goal of this conference is the promotion of the cooperation and networking in the field of Biosystems Engineering, also trying to include the business world in it.
By doing that, we will be able to take on the new challenge of Horizon 2020, the new European Framework Programme. This programme attributes a capital and fundamental role to research and innovation, seen as important means to guarantee an intelligent, sustainable and comprehensive growth to Europe.

Horizon 2020 is articulated on 3 strategic objectives

1) Excellent science, intended to secure Europe's leadership in science worldwide.
2) Industrial Leadership , aimed at supporting research and innovation of European industry, with a strong focus on industrial technologies and investments for SMEs,
3) Societal challenges , aimed at tackling major global challenges in the following areas: health, demographic change and wellbeing, food security, sustainable agriculture, secure, clean and efficient energy, smart, green and integrated transport, climate action, resource efficiency and raw materials, inclusive, innovative and secure societies.

In all these fields Agricultural, Forestry and Biosystems Engineering in the coming years will have a major role.

I conclude by saying that AIIA13 is also an opportunity to know the Tuscia, a still intact territory, in which culture and respect for the land, innovation and tradition come together in a truly original model of sustainable development. I wish all the participants a pleasant stay in Viterbo and Italy.

In closing this brief greeting I want to thank:

- CEFAS, Special Agency of the Chamber of Commerce, for the logistic support to the Conference,
- the Tuscia University, which offered the beautiful and historic seat of the Conference
- the Ministry of Agriculture, the Lazio Region, the Provincial Administration and the Municipality of Viterbo, UNACOMA and CRA-Ing, for their support,
- CIGR and EURAGENG, for their sponsorship,
- FACMA and Enama, sponsors of the Conference.

A special thanks to the Carivit Foundation of Viterbo, whose contribution has enabled the printing of the Conference Proceedings.

Danilo Monarca
AIIA 2013 CONVENER

Chestnut: from coppice to structural timber. The case study of "Uso Fiume" beams sampled in Liguria

Marco Togni, Alberto Cavalli, Davide Mannozzi

GESAAF – Dipartimento di Gestione dei Sistemi Agrari, Alimentari e Forestali, Università di Firenze, Italy

Abstract

Recently Agriculture Department of Liguria Region had supported studies and researches on the timber quality of living trees in local coppice chestnut forests, with the prospect to produce also timber for structural use. Under some *ad-hoc* funds a 30 years old coppice forest in the high Bormida Valley, never thinned after the last utilization, has been chosen for sampling. 18 selected trunks were felled and the assortment called "*Uso Fiume*" (UF) was chosen, getting 49 beams (cross-section from 12×12 to 24×24 cm), by way of saw-mill operations The UF-beam is a structural element, derived from Italian tradition. Such elements are used in Italian buildings over the time, in substitution to structural sawn timber, principally for roofing. The UF-beam is a square edged log with wane; more precisely it is a full log, edged on four sides, maintaining boxed heart and an approximately central pith. Today the features of such a beam is established according to the specific Italian standard UNI 11035-3 for spruce and fir and to the CUAP (Common Understanding of Assessment Procedure) n. 03.24/22 for chestnut and conifers. The beams were visually graded according to the Visual Strength Grading procedure and the physical and mechanical properties (density, modulus of elasticity-MOE and modulus of rupture-MOR) were determined according to the standard requirements (EN 408, EN 384, ISO 3131), disregarding the moisture content: the mechanical tests were performed with wood in green state (moisture content M.C.>30%) because it is the actual condition of use in building, due to the very low permeability of the chestnut heartwood which entails long seasoning time of large cross section beams. The study showed very high yields considering the stems-to-beams volume ratio, close to 70%. Characteristics values of the sample resulted: char. density kg/m³, char. modulus of elasticity $E_{0,mean}$ 10,3 GPa and char. bending strength $f_{m,k}$ 28,5 MPa. These results can be considered very promising because the data match the Strength Class D24 (EN 338), the same Class as full cross-section chestnut beams (at M.C.=12%).

Correspondence: Marco Togni, Alberto Cavalli, Davide Mannozzi, GESAAF – Dipartimento di Gestione dei Sistemi Agrari, Alimentari e Forestali, Università di Firenze, Italy.

Key words: chestnut, structural timber, square edged log with wane, strength, grading.

Contributions: the authors contributed equally.

Conflict of interests: the authors declare no potential conflict of interests.

Funding: the research was supported by a fund of Regione Liguria - Dipartimento Agricoltura, Turismo e Cultura Servizio Politiche della Montagna e della Fauna Selvatica

Journal of Agricultural Engineering 2013; XLIV(s2):e1
doi:10.4081/jae.2013.(s1):e1

Introduction

Liguria is the most forested region in Italy with a forested surface of 62.6% - 71,5% according to different inventory assessments.[1,2] The second inventory,[2] states that chestnut forests cover around 60000 hectares equal to the 16% of the regional forests. Recently some public institutions of Liguria, particularly the Mountain Policies Service (Agriculture Department), had supported studies and researches on the timber quality, beginning from living trees. One of the most important species studied was chestnut (*Castanea sativa* Mill.) whose silvicultural practice is typically coppice.

Since 2010 in Italy it is possible to utilize Chestnut timber with rectangular cross section as visual strength graded structural material. Standard EN 1912:2012,[3] that allocates each visual grade of the structural timber into the Strength Classes listed in EN 338:2009,[4] enumerates also Italian chestnut among the different structural timbers.

Near to this kind of structural element, there is a customary Italian product called Uso Fiume (UF): the UF-beam is a structural element, coming from tradition and used in Italian buildings over the time, in substitution to typical structural sawn timber; today it is described as a strength graded product, used as structural timber, *"square edged logs with wane"* that is *"full logs which are edged on four sides maintaining boxed heart and an approximately central pith"*.[5] This type of products is favoured for rural building, easy to be prepared in self-production and in case of owned forest. But the European standard framework does not *yet al*low the use of not squares edged beams. Due to this reason, for the use in building of such a structural element, since 2010 a new Italian standard[6] (for Norway spruce and fir beams), and a specific CUAP 03.04/22[5] (for conifers and chestnut) have been developed and approved.

In addition it must be remembered that the better mechanical properties of roundwood in comparison to square sawn wood (rectangular cross section) are well known.[7] The UF-beams can be considered an intermediate solution between round wood and sawn timber; hence it is expected for its mechanical characteristics as well for the easiness to use in building (compared to the totally roundwood).

To concretize this idea some Italian private firms in a consortium, co-ordinated by an association that represents primary processing and wooden constructions industries, funded a specific research for the implementation of the use also of UF chestnut by means of an

European Technical Approval (ETA). The document ETA-12/0540[8] gives to the Consortium (not including companies of Liguria region) the possibilities to use the CE marking for chestnut UF-beams, visually strength graded for structural use.

For the chestnut from coppice sampled in Liguria, the aims of the research, strictly regarding the structural use of wood, were:

- the study on relationship between quality of the standing trees and final use,
- the determination of characteristic values used for the structural design,
- the comparison with known values of square edged beams of the species,
- the assessment of the suitability of the combination species/origin/product to the proposed use.

Final objective is the promotion of this timber as structural material and so the enhancement of the utilise.

Materials and methods

A 30 years old coppice forest in the high Bormida Valley, growth in high soil fertility, never thinned after the last utilisation, was chosen for the sampling. Some standing trees were selected following the principles of the cutting diameter (min. 20 cm) and the stem straightness (max. curvature 1 cm/m stem length). No other criterion was chosen for selecting, but all the visible defects were evaluated, to assess the log quality finalized to structural use, following a specific protocol, including also: the ratio between largest branch and stem diameters at the insertion point, the presence/absence of injury on the bark or signs of disease on living tree (e.g. *Cryphonectria parasitica* (Murr.) Barr.) as a warning of the potential presence of ring shake. It is important to remark that at present there is not European standards for the grading chestnut roundwood, unlike that for other species[9], nor for quality grading of standing trees. Mean diameter at 1.3 m of the selected ones was 26.5 cm (minimum 23, maximum 33 cm). 18 trunks were harvested and transported to the local saw-mill and the stems were cutting into drums. The length of each log was determined taking into account the presence of defects or anomalies (e.g. large branches) and to obtain the length/diameter ratio close to 20, between 18 and 22. 50 logs were obtained with a length range between 2.4 and 4.8 m, mean diameter 21.5 cm (minimum 15, maximum 32 cm). A protocol similar to the previous one was applied to the logs, considering also the presence/absence of ring shake and other possible defects, visible on the ends of the logs.

The sawing pattern has been studied to extract squared edge logs but with wide wanes which characterise the UF-beams. As the logs were tapered and the sawn faces are straight and parallel, the changeful dimensions of the wanes were biggest into the top end (minimum diameter) of the log. After the saw-mill operations the beams were transported into the Laboratory for the following tests.

The sample of beams was subjected to a sequence of tests having the aim of: I) visually grading the beams by means of an *ad hoc* strength grading rule, II) measuring the bending Modulus of Elasticity (MOE), III) determining the bending strength (modulus of Rupture – MOR), IV) determining the density, V) measuring the moisture content (M.C.). Finally VI) the physical and mechanical properties II, III and IV, referring to the selected grade (I) were used to derive the characteristic values (modulus of elasticity - $E_{0,mean}$, bending strength - f_k, density - $_k$,) and then to determine the possible Strength Class.[4]

Grading: the strength grading of each timber elements is needful for the structural use; [10] visual or machine grading are acceptable; in the visual grading the strength determining defect is the worst defect of the beam, according to the appropriate visual strength grading rule. In this research a visual strength grading rule was adopted: it was derived by the international document Common Understanding of Assessment Procedure (CUAP) n. 03.24/22[6] (for spruce, fir, larch and chestnut) and by the standard UNI 11035-3:2010[5] (only for spruce and fir). The two rules converge in a unique grade named C, except for the possibility to grade also beams with ring shake defect, accepted for chestnut. The main discriminating defects in this visual strength grading rule, very easy to apply according to the above mentioned standards, were:

- knots dimension (maximum value of the ratio between minimum diameter of the worst knot and the thickness of the beam on which it appears),
- visible ring shake, permitted only on the ends, centred and with a diameter lesser than 1/3 of the minimum side of the cross section,
- the fissures passing through the thickness, permitted only at the ends, with a limited length,
- the slope of grain as general grain direction referring to the longitudinal axis of the beam. Each beam was graded and mechanical properties were determined according to standard EN 408[11] by means of Metro-COM universal testing machine.

Elasticity: the MOE values were determined in a four-points bending test. During the loading tests the neutral axis displacement were measured by means of LVDT transducers and acquired, together with the applied load, with a Measurement Computing 16-bit DAQ connected to a PC. Small steel plates, of length not greater than one-half of the depth of the test piece were inserted between the beam and the loading heads or supports, to minimize local indentation.

Bending strength: after the MOE determination the logs where tested at failure in order to calculate the MOR (according to the EN 408), adopting the same testing geometry. The critical section (the weakest portion of the beam) was positioned inside the inner load points in four-points bending test, where the bending moment is constant, for the correct determination of the MOR value, as set by standard EN 384:2005.[12] Some of the UF-beams after the bending to failure are visible in Figure 1.

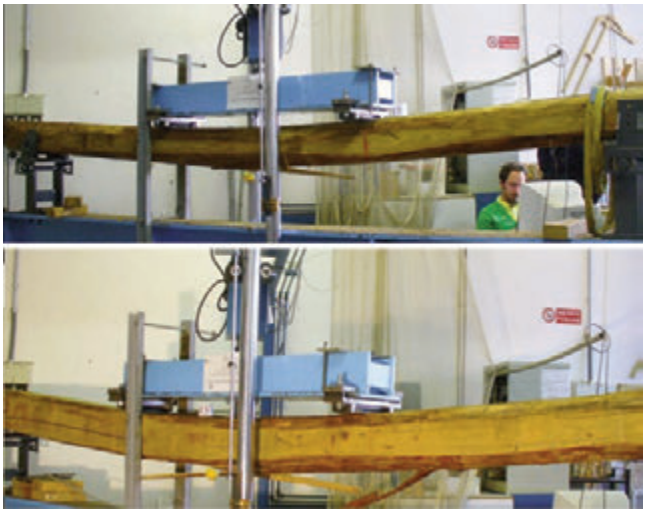

Figure 1. Two tested UF-beams after failure in bending: n. 17a (top of the figure), nominal cross section 220x210 mm, length 4670 mm, MOR 39.3 MPa; n. 15a (bottom of the figure) nominal cross section 240x240 mm, length 4640 mm, MOR 32.4 MPa.

Density and moisture content: after the bending tests, close to the point of rupture, two adjacent specimens (corresponding to the whole cross section of each log) were collected, for the M.C. and density determination. One specimen was used for the M.C. determination adopting the double weighing method.[13] The density have a great importance for timbers, because it affects their mechanical properties and it is related to the M.C., so the second specimen was used to calculate the density at the time of test (as the weight to volume ratio). After that, it has been seasoned and the density was recalculated and corrected to 12% M.C. according to the ISO 3131,[14] for further comparisons.

Derivation of characteristic values: to characterise timber for structure it is necessary to derive the characteristic values, starting from the ones achieved by the physical and mechanical tests. The adjustment and derivation procedures are rigorously indicated in the standard.[12] The density and elasticity values must be adjusted taking into account the M.C.; the bending strength has to be standardised on the actual depth of the beams. Due to the small dimension of the sample (43 beams in 1 only group, the grade C), it was decided to derogate the standard[12] and not to apply the adjusting factor k_s for the number of specimens. The choice is justified by the need to make comparison with existing characteristic values, derived from different samples.

Results and discussion

Through the sawmill operations, 49 UF-beams were achieved. One log was rejected for hard damage during handling. The yield of the sawmill operations was close to 70%, a high value thank to the geometrical characteristics of the assortment. The cross sections of the beams, close to square with approximately central pith, were in the range between 120x120 mm and 240x240 mm; "squared cross section" must be conceived as the circumscribed square. The geometrical features of the sample were distributed as described in Table 1.

According to the visual strength grading rule adopted, the UF-beams graded into the grade C had a very high yield: 43 beams on 49 (=88%); only 6 beams (=12%) were rejected because not grading for structure by the rule. Main reasons of rejection were: ring shake (1 beam), knot dimension (1 beam), anomaly (double pith, 1 beam), passing through fissures (3 beams).

No relationship were founded among the strength quality of the beams (grade C or rejected) and the defects and other characteristics measured on roundwood (trunks and logs), except for 2 events (the anomalies of double pith and ring shake, recorded on roundwood). The grade determining defects "fissures passing through" could not be recorded because their opening is typically delayed due to the seasoning of wood and to the increasing of the internal stress; the values of the ratio between largest branch and stem diameters at the insertion point did not have any relationship with the grade and, successively, with stiffness and strength data.

The main physical and mechanical properties obtained by tests and measures performed, are reported in Table 2.

M.C. resulted very high, as expected from chestnut large cross section beams. The very low permeability of chestnut heartwood is well known:[15] a natural seasoning of such a timber members needs more than 1 warm season to reach a M.C. lower than 20% (reference value in Italian standard[5]). The high M.C. had a reduction effect on MOE so that the average MOE resulted lower than values at normal condition (corresponding to 12%, reference value of the moisture of wood at the standard environment of 20±2°C and 65±5% relative humidity) though the adjusting factor[12] was applied: it can adjust only for a M.C. difference of 6%. The M.C. values had not sensible effects on MOR because on full size timber the defects outweighed any repercussion of the moisture. From the MOE, MOR and density data, were derived the characteristic values concerning the sub-sample of the 43 UF-beams selected in the Grade C. These derivations were done to obtain comparable values for chestnut and it differs from the procedures for the definitive characteristic values for structural timber which require much more specimens. All the data of the whole sub-sample were utilized for the derivations of the MOR characteristic value (f_k), including also logs failed outside the middle third. The final values for the selected 43 beams in Grade C were

- characteristic density: ρ_κ 508 kg/m^3, kg/m^3,
- characteristic modulus of elasticity: $E_{0,mean}$ 10,3 GPa
- characteristic bending strength: $f_{m,k}$ 28,5 MPa.

These results match the Strength Class D24[4], the same Class for Italian chestnut structural timber with rectangular cross section[3], although the characteristic value of modulus of elasticity of Italian chestnut, as stated by the standard[16] (ρ_κ 485 kg/m^3, $E_{0,mean}$ 12,5 GPa, $f_{m,k}$ 28,0 MPa), is ~20% higher than the present one, due to the green condition of the testing sample (M.C.=48%, much higher than wood in normal condition).

Table 1. Main geometrical features of UF-beams* sample.

Depth class [mm]	Number	Average cross sections depth x width [mm]	Average length [mm]
140	4	125x123	3190
160	16	151x151	2888
180	13	179x177	3456
200	10	197x195	3763
220	4	214x211	4278
240	2	235x225	5030
Total sample	**49**	-	-
mean [mm]	-	174x173	3443
minimum [mm]	-	120x120	2430
maximum [mm]	-	240x240	5420
dev. stand. [mm]	-	27÷28	608
C.V. [%]	-	16÷18	17.7

*UF-beams: "Uso Fiume" beams.

Table 2. Main data of the physical and mechanical properties.

	M.C.* [%]	Density$ [kg/m^3]	MOE°$ [kN/mm^2]	MOR# [N/mm^2]
Mean	48	571	10.34	38.5
Minimum	23	485	8.34	22.5
Maximum	74	735	14.20	54.7
Dev. stand.	11.8	49.0	1.27	6.8
C.V.	24.6%	8.6%	12.2%	17.5%

*Moisture content, °Modulus of Elasticity, #Modulus of Rupture. $values adjusted to the reference moisture content 12%.

Conclusions

The research presented showed that from an ordinary coppice forest of chestnut, sampled in Liguria Region, through basic saw mill operation, it is possible to obtain a very performing structural material: the assortment UF-beams. This kind of product summarises by itself very good properties:

- no need of pre-selection, except for straightness and dimensions,
- high sawing yield, close to 70%,
- good grading yield: 88% UF-beams graded for structure (Grade C),
- high structural performances, comparable to the chestnut structural timber with rectangular cross section, and selectable in Strength Class D24,
- immediately usable, without necessity to be seasoned or kiln dried.

In conclusion the large natural wanes did not have any sensible effect on mechanical performances, making UF-beams similar to the ones with rectangular cross section.

References

1. Ministero delle Politiche Agricole Alimentari e Forestali - Corpo Forestale dello Stato Consiglio per la Ricerca e la Sperimentazione in Agricoltura (CRA-MPF), 2005. INFC - L'Inventario Nazionale delle foreste e dei serbatoi forestali di Carbonio. Metodi e risultati Available from http://www.sian.it/inventarioforestale/jsp/01tabelle_superficie.jsp . Accessed: May 2013
2. Camerano P., Grieco C., Mensio F., Varese P. I Tipi forestali della Liguria, Regione Liguria, Erga Edizioni (GE): 336 pp. 2008.
3. EN (European standard). Structural Timber. Strength classes. Assignment of visual grades and species, Norm EN 1912:2012. Brussels, Belgium. European Committee for Standardization, 2012.
4. EN (European standard). Structural timber. Strength classes. Norm EN 338:2009. Brussels, Belgium. European Committee for Standardization, 2009.
5. UNI (Italian standard). Legno strutturale - Classificazione a vista dei legnami secondo la resistenza meccanica - Parte 3: Travi Uso Fiume e Uso Trieste. Norm UNI 11035-3:2010. Milano, Italia. Ente Italiano di Unificazione, 2010.
6. Österreichisches Institut für Bautechnik, 2012. Strength graded structural timber - square edged logs with wane. Common Understanding of Assessment Procedure CUAP 03.04/22. OIB, Vienna, Austria.
7. Ranta-Maunus A. *et al.*, 1999. Round small diameter timber for construction. Final report of project FAIR CT 95-0091. VTT, publication 383 pp:191+19. Espoo, Finland
8. Österreichisches Institut für Bautechnik, 2013. Uso Fiume of chestnut. Strength graded structural timber – Squared edge logs with wane to be used as structural element in buildings and civil engineering works. European Technical Approval ETA-12/0540. EOTA European Organization for Technical Approvals. OIB, Vienna, Austria.
9. EN (European standard). Hardwood round timber. Qualitative classification. Part 1: Oak and beech. Norm EN 1316-1:2013. Brussels, Belgium. European Committee for Standardization; 2013.
10. Italian regulation: 2008. Nuove Norme Tecniche per le Costruzioni. DM 14/01/2008. In G.U. n. 29 4/02/2008 - S.O. n. 30
11. EN (European standard). Timber structures. Structural timber and glued laminated timber. Determination of some physical and mechanical properties. Norm EN 408:2010. Brussels, Belgium. European Committee for Standardization; 2010.
12. EN (European standard). Structural timber. Determination of characteristic values of mechanical properties and density. Norm 384:2005. Brussels, Belgium. European Committee for Standardization; 2005.
13. EN (European standard). Moisture content of a piece of sawn timber. Determination by oven dry method. Norm 13183-1:2002. Brussels, Belgium. European Committee for Standardization; 2002.
14. ISO (International Organization for Standardization). Wood – Determination of density for physical and mechanical tests. Norm ISO 3131:1975. Geneva: International Organization for Standardization Publications; 1975.
15. Giordano G., Tecnologia del legno. Vol. 3**, II edition. Torino, Italy: UTET; 1988.
16. UNI (Italian standard). Legno strutturale - Classificazione a vista dei legnami secondo la resistenza meccanica - Parte 2: Regole per la classificazione a vista secondo la resistenza meccanica e valori caratteristici per tipi di legname strutturale. Norm UNI 11035-2:2010. Milano, Italia. Ente Italiano di Unificazione, 2010.

Harvesting techniques for non-industrial SRF biomass plantations on farmland

Raffaele Spinelli,[1] Janine Schweier,[2] Fabio De Francesco,[1]

[1]CNR IVALSA, Sesto Fiorentino (FI), Italy; [2]Institute of forest utilisation and work science, Alberts-Ludwigs-University, Freiburg i. B., Germany

Abstract

The goal of this study was to compare the technical and economic performance of terrain chipping and roadside chipping, applied to short rotation biomass plantations. The null hypothesis was that no significant difference are in the performance of the two work systems, when applied to short rotation coppices. Those systems especially designed for non-industrial SRF plantations, were used for conventional logging operations. The difference on the above mentioned systems consisted especially in the chipping location: chipping was performed directly to the field (containers reach the chipper in the field) or at the field's edge (roadside chipping). Both systems were tested on two of the most common SRF poplar clones in Italy, namely: AF2 and Monviso. Plots were allocated randomly to the two treatment levels (roadside or field chipping) than blocked for two main clone types (AF2 and Monviso) so that each of the 4 treatments level and clone types has a minimum repetition plot of 6 times (total of 24 replications). The Plot were identified with paint markings at the stump so each plot area could be identified at the ground. Net weight of each charge was obtained by a certified weighbridge, so each plot has its own productivity in terms of weight and time consumption. Results were encouraging: harvesting cost varied from 16.3 to 23.2 € tonne-1, and was lower for terrain chipping and for the most productive clone (Monviso). Despite its higher cost, roadside chipping was preferred for its better terrain capability and for the superior storage quality of uncomminuted biomass. Both systems were suboptimal in their current configurations. They could offer a better performance, subject to minor improvements

Correspondence: Raffaele Spinelli, CNR IVALSA via Madonna del Piano 10 Sesto Fiorentino (FI), Italy.
Tel.+39.055.5225641 - Fax+39.055.5225643.
E-mail: spinelli@ivalsa.cnr.it

Key words: poplar, mechanization, CTL.

Acknowledgements: Support for this study was provided by Pellerei – Ago AG and by COST Action FP0902 within the scope of its 4th STSM programme.

Journal of Agricultural Engineering 2013; XLIV(s2):e2
doi:10.4081/jae.2013.(s1):e2

Introduction

Covering marginal farmland with fast-growing tree species could be a cost-effective way to produce wood biomass for industrial and energy use (Hoogwijk *et al.* 2003). Afforestation, compared to conventional agriculture, offers a better environmental performance due to reduced water (Heller *et al.* 2003), chemical (Sage 1998) and fossil energy (Djomo *et al.* 2011, Hillier *et al.* 2009) inputs. In case of soil and groundwater contamination, planting trees can be a way to filter it (Rockwood *et al.* 2004). After changing land use from farm crops to forest plantations the soil carbon stock increases (Guo and Gifford 2002, Coleman *et al.* 2004) and the farm-scale biodiversity and landscape are also improved (Rowe *et al.* 2011, Weih 2008).

Depending on site conditions and product strategy, modern biomass plantations have a harvesting turnover from 2 to 10 years if established with hardwoods (O'Neill *et al.* 2010). Farmers prefer a very short rotations (2 to 4 years) because they are used to short return times and are generally averse to long waiting times (Londo *et al.* 2004). Due to the small tree size, 2 to 4 years turnover plantations are effectively harvested with modified foragers (Manzone *et al.* 2009). In contrast, bigger investors can afford longer return times and favour slightly longer rotations (5 to 10 years), which generally offer better value recovery (Spinelli *et al.* 2008). These plantations are best harvested with dedicated forest technology, specifically modified for the task (Spinelli and Hartsough 2006, Grosse *et al.* 2008). Many benefits are offered by a rotation between 5 and 10 years because a better capacity to capture growth rate increase as the longer turnover, (Ceulemans and Deraedt 1999; Pallardy *et al.* 2003); a higher resiliency to the effects of the occasional bad season (Badenau and Auclair 1989); the capacity of guaranteeing high biomass yields at lower planting densities (Willebrand *et al.* 1993); a lower bark to fibre ratio (Phelps *et al.* 1985), offering higher pulp (Ai and Tschirner 2010) or energy conversion (Kenney *et al.* 1990) yields, as well as lower ash contents (Tharakan *et al.* 2003). The advantages of extended rotations have finally attracted European farmers (Spinelli *et al.* 2011), who seem increasingly disaffected with traditional short rotation coppice (Helby *et al.* 2006).

However, extended rotations offer relatively large trees, which cannot be harvested with adapted foragers (Spinelli *et al.* 2009a). Unfortunately, most farmers lack the critical mass to acquire highly-productive forestry equipment, just for harvesting their own biomass plantations. Hence, there is a need for adapting conventional forest machinery to use in the new crops. In Europe, that means using cut-to-length (CTL) equipment, especially harvesters and forwarders (Gellerstedt & Dahlin 1999). These machines are designed for felling, delimbing and crosscutting trees directly at the stump site, and then forwarding processed assortments to the nearest landing (Chiorescu and Grönlund 2001). Harvesters and forwarders are not designed for whole-tree harvesting, which has proven the most effective system when handling biomass plantations (Spinelli *et al.* 2009b). However, they can still be used for whole-tree harvesting, although with a some-

what reduced efficiency. The goal of this study was to determine the performance of conventional CTL equipment when used for whole-tree harvesting in biomass plantations. In particular, we determined the unit harvesting cost in financial, energy and emission terms. Suggestions for improvement were also provided.

Materials

The machines used to make this study were a dedicated harvester (Valmet 921), a 10-t forwarder (Valmet 840), an industrial 335 kW chipper (Jenz HEM 561) towed by a 95 kW farm tractor (Valtra 8450) and two tractor-trailer units which have a capacity of 42 m^3. the chips load was moved from the field to the central collection point consisting in a concrete pad, covering a distance of 600 m. The access at the fields is possible only if the soil was not wet. The system was like the type commonly used for the harvesting of conventional poplar plantations (Spinelli *et al.* 2011b).

The system was tested in two different configuration: in the first configuration called "field's edge" trees were felled and bunched by the harvester and then crosscut at mid-length with a chainsaw, than the 10-t forwarder moved the tree sections to the chipper at field's edge, over an average distance of 150 m. Chips were blown into the two tractor-trailer units, and transported to the central collection point.

The second configuration, called "terrain chipping", trees were felled and bunched by the harvester, then reached by the chipper directly in the field, so that neither crosscutting nor separate forwarding were necessary, because the same tractor-trailer units moved the chips from the field to the central collection point. This mode was swifter, because required fewer steps, but could only be applied if the field was accessible to the heavy chipper and the cumbersome tractor-trailer units. It was also least suited to building long-term biomass stores, which should be assembled with tree sections rather than chips, because chips do not store well (Jirijs 2005).

This system was tested on two different poplar clones, among the most common in Italian poplar plantations. These were the hybrid poplar (Populus x euroamericana) clones AF2 and Monviso.

Methods

The experimental design included four treatments, deriving from the combination of clone types (AF2 or Monviso) with harvest modes (terrain chipping or roadside chipping). Each treatment was replicated 6 times. Therefore, the plantations were divided into experimental blocks consisting of 4 rows of 25 trees each. Since the trees had been established at a 3¥2 m spacing the average surface area of the plots was equal to 600 m^2. The blocks were located in two adjacent 5-year-old plantations and were randomly assigned to the harvesting modes in each plantation (Figure 1).

The authors recorded the time spent on each block by each machine, separating productive time from delay time (Björheden *et al.* 1995). Delay time is typically erratic, and it may introduce excessive variability to a study conducted on relatively small blocks. Besides, a short-term study may fail to produce an accurate representation of delay time. For this reason, delay time was averaged for each machine across the whole test (*i.e.* 12 blocks for the chainsaw and the forwarder and 24 blocks for the harvester and the chipper). Hence, the total net time and delay time for each machine were used to calculate an appropriate delay factor, i.e. the ratio of delay time to net work time. Delay factors were then compared to the results obtained from other long term studies, conducted by the same authors on the same machine types under similar work conditions (Spinelli *et al.* 2003, Spinelli and Visser 2008, Spinelli and Visser 2009). Corroboration was obtained for the harvester, the chainsaw and the forwarder, whose measured delay factors were adopted into use. The delay factor calculated for the chipper was not corroborated by existing literature, and was discarded. Instead, we adopted the long-term figures found in the reference material.

Harvested volumes were estimated by taking all chip loads to a certified weighbridge. Loads were separated by block, assembling partial loads when necessary. Moisture content determination was conducted on 6 samples per clone, collected in sealed bags and weighed fresh and after drying for 48 hours at a temperature of 103° C in a ventilated oven.

Machine costs were provided by the contractor and reflected the contracting rates typical of the region. They were: 110 € h^{-1} for the harvester, 15 € h^{-1} for the chainsaw team, 70 € h^{-1} for the forwarder, 240 € h^{-1} for the chipper and 50 € h^{-1} for each tractor-trailer unit. In fact, when chipping was performed at roadside, one driver managed both tractor-trailer units, so that the total cost for the two units dropped from 100 € h^{-1} to 75 € h^{-1}.

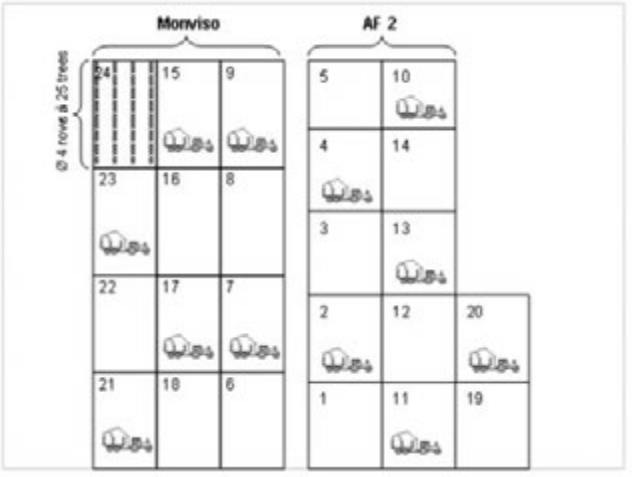

Figure 1. Experiment layout.

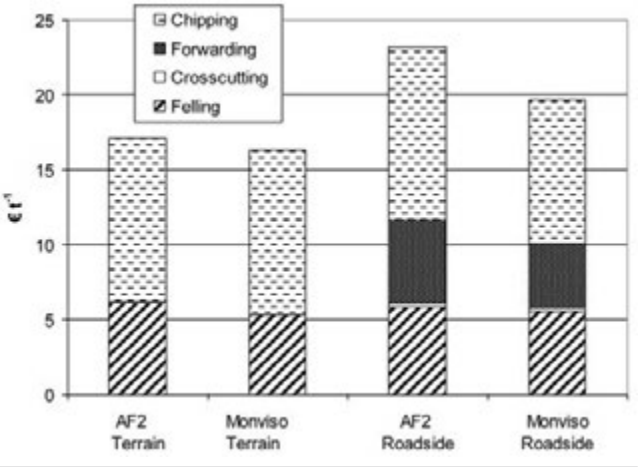

Figure 2. Breakdown of harvest cost by work step.

Results and Discussion

Both clones performed very well, with a high survival rate and a very fast growth: Monviso gave the best results, offering larger tree size and higher stand stocking compared to AF2. All these differences were statistically significant. Monviso trees had a significantly smaller diameter at breast-height compared to AF2 trees. They were also taller, but in this case the difference had no statistical significance. The same accounted for moisture content. Hence, the larger individual weight of Monviso trees must be related to different form, taper or branching. Table 1 shows the basic statistics for the test fields.

Table 1. Stand characteristics and biomass yield by harvesting site.

Clone type	AF2		Monviso		P
	mean	SD	mean	SD	
DBH, cm	16.2	0.7	14.6	0.8	<0.0001
Height, m	18.2	2.3	18.7	1.8	0.7569
Mass, kg tree^{-1}	116.8	12.3	125.5	10	0.0713
Density, trees ha^{-1}	1595.1	33.9	1599.8	20.7	0.6891
Stocking, tonnes ha^{-1}	186.3	19.3	200.9	17.8	0.0669
m.c., %	56.3	1.7	54.7	1.2	0.0839
Stocking, odt ha^{-1}	81.4	8.4	91	8.1	0.0093
Yield, odt ha^{-1} year^{-1}	16.3	1.7	18.2	1.6	0.0093

DBH = tree diameter at breast height; SD = standard deviation; odt = oven-dry tonnes; P= p-value for the clonal difference obtained from the unpaired t-test; Density = tree density at harvest, from a theoretical initial density of 1667 trees ha^{-1}.

Table 2. Machine productivity by clone type and harvest mode.

Harvest mode	Terrain chipping		Roadside chipping	
Clone type	AF2	Monviso	AF2	Monviso
Felling	18.0	21.1	18.9	20.2
Crosscutting	NA	NA	58.3	59.5
Forwarding	NA	NA	12.9	16.4
Chipping	31.2	31.1	28.3	34.3

Productivity figures are in fresh tonnes per scheduled work hour, including delays.

Average yield was 18.2 and 16.3 oven-dry tonnes (odt) per ha, respectively for Monviso and AF2. These figures compared well with the average values measured further north for the best poplar (Karacic *et al.* 2003; Pellis *et al.* 2004; Henderson and Jose 2010) and willow (Nordh and Verwjist 2004, Proe *et al.* 2002) clones. This was a witness to the good quality of the Italian clones and climate. In this respect, it is important to note that the values in this study were net, after harvesting losses, and they were obtained from relatively large plots under operational conditions. As is shown in Table 2 and in Table 3 (ANOVA), the productivity of felling, forwarding and chipping was significantly affected by clone type (Monviso or AF2. The effect of clone type is explained by the different tree size, which has a strong impact, on the other hand, harvest mode (*i.e.* terrain chipping or roadside chipping) doesn't affect machine productivity. That has been demonstrated many times for harvesters (Holtzscher *et al.* 1997), feller-bunchers (Visser and Stampfer 2003), forwarders (Tiernan *et al.* 2004) and chippers (Spinelli and Magagnotti 2010). The lack of any significant effect for harvest mode points at the versatile quality of the machines on test. It may also hint at a suboptimal system, which is not specialised enough for deployment under specific mode and conditions. This point is supported by the superior productivity figures obtained with specialised harvesting systems. Under the very similar conditions of US poplar plantations, the productivities of felling, forwarding and chipping are 35÷45, 30÷45 and 48÷52 t hour^{-1}, respectively (Spinelli and Hartsough 2006). These values are between 1.4 and 2.7 times higher than those obtained from the current experiment. Similar differences are also found for the whole-tree harvesting of eucalypt trees from SRF plantations (Spinelli *et al.* 2009b). The differences are highest for felling and forwarding, which should receive priority when trying to improve the harvesting system under test. Significant improvements could be obtained with limited investment. In particular, the harvester head on the dedicated CTL harvester should be replaced with an accumulating felling-bunching device, capable of multi-tree handling. Specific models are now available for application to conventional CTL harvesters, and can be obtained at a reasonable price (Spinelli *et al.* 2006). On the forwarder, the conventional short-wood bunk should be replaced with an inverted grapple for temporary conversion into a clam-bunk skidder. This machine is best suited to whole-tree extraction, and would offer superior productivity. Both measures would not require large investments and would be reversible. Hence, they could be implemented by small contractors and would maintain the versatile character of existing machinery, which could be reconverted to the old configuration for use in conventional forestry operations.

Table 3. Anova table for machine productivity

	Effect	DF	SS	MS	F-Value	P-Value	Power
Felling	Treatment	1	1.24*10^{-5}	1.24*10-5	3.27*10^{-6}	0.9986	0.05
	Clone	1	29.03	29.03	6.64	0.0180	0.69
	Interaction	1	5.35	5.35	1.23	0.2816	0.18
	Residual	20	87.42	4.37			
Crosscutting	Clone	1	4.61	5.61	0.03	0.8716	0.05
	Residual	10	1677.17	167.72			
Forwarding	Clone	1	35.26	35.26	10.98	0.0078	0.86
	Residual	10	32.12	3.21			
Chipping	Treatment	1	0.14	0.14	0.01	0.9105	0.05
	Clone	1	50.85	50.85	4.57	0.0452	0.52
	Interaction	1	55.84	55.84	5.01	0.0367	0.56
	Residual	20	222.71	11.14			

Table 4. Harvesting cost: financial.

Harvest mode	Terrain chipping		Roadside chipping	
Clone type	AF2	Monviso	AF2	Monviso
Financial (€ t^{-1})	17.1	16.3	23.2	19.7

Table 5.Anova table for the financial, energy and emission cost.

	Effect	DF	SS	MS	F-Value	P-Value	Power
Financial	Treatment	1	133.46	133.46	63.51	<0.0001	1.00
	Clone	1	27.30	27.30	12.99	0.0018	0.94
	Interaction	1	10.83	10.83	5.15	0.0344	0.57
	Residual	20	42.03	2.10			

The monetary cost of harvesting varied between 16.3 and 23.2 € t^{-1}, delivered to the central collection point and excluding further transportation (Table 4). Both clone type and harvest mode had a significant effect on unit cost (Table 5): cost was lower for the Monviso clone, due to its larger tree size; it was higher for roadside chipping, due to the larger number of work steps, each incurring additional expenses (Figure 2). These costs are relatively high, if compared to the costs reported for the industrial harvesting of the US poplar plantations, in the range of 10 US dollars per tonne. The costs recorded in this study were also higher than those reported for harvesting shorter rotations with forage harvesters, which are in the range of 15 – 20 € t^{-1} (Spinelli *et al.* 2009a). However, the costs recorded in this study are still much below the average price offered by most industrial biomass plants in Italy. This is estimated to 48 € t^{-1} delivered to the plant (Spinelli *et al.* 2011c), which leaves between 15 and 22 € t^{-1} to cover plantation costs, after deducting an average transportation cost around 10 € t^{-1}.

Conclusions

Conventional forest machinery can be easily deployed for harvesting biomass plantations established over farmland.

The harvesting system offers a suboptimal performance, but it can be substantially improved, especially when deployed under the roadside chipping mode. This could allow a significant reduction of harvesting cost, for a relatively small additional investment. While terrain chipping incurs the lowest harvesting cost, it may be safest to focus on roadside chipping. This has a higher potential for improvement and offers significant technical advantages. In particular, the forwarders used for biomass extraction have a much better floatation compared to the tractor-trailer units, which allows stand access under wet soil conditions, as well as reduced soil compaction and stool damage. Furthermore, roadside chipping is best suited to building biomass stores, in the form of stacked tree sections at the roadside. As productivity is dependent on tree size, one could expect significant cost reductions if better clones are developed and/or rotations are further extended.

References

Ai J, Tschirner U (2010) Fiber length and pulping characteristics of switchgrass, alfalfa stems, hybrid poplar and willow biomasses. Bioresour Technol 101: 215-221.

Bedeneau M, Auclair D (1989) Effect of coppicing on hybrid poplar fine root dynamics. Ann For Sci 46 (suppl.): 294-296.

Björheden R, Apel K, Shiba M, Thompson M A (1995) IUFRO Forest work study nomenclature. Swedish University of Agricultural Science, Dept. of Operational Efficiency, Garpenberg. 16 p.

Ceulemans R, Deraedt W (1999) Production physiology and growth potential of poplars under short-rotation forestry culture. For Ecol Manag 121: 9-23.

Chiorescu S, Grönlund A (2001) Assessing the role of the harvester within the forestry-wood chain. For Prod J 51: 77-84.

Coleman M D, Isebrands J G, Tolsted D N, Tolbert V R (2004) Comparing Soil Carbon of Short Rotation Poplar Plantations with Agricultural Crops and Woodlots in North Central United States. Environ Manag 33: 299–308.

Djomo S N, Kasmioui O E, Ceulemans R (2011) Energy and greenhouse gas balance of bioenergy production from poplar and willow: a review. GCB Bioenerg 3: 181–197.

European Commission (Ed.). (2010) International Reference Life Cycle Data System Handbook: General guide for Life Cycle Assessment - Detailed guidance. Author: Joint Research Center. 414p.

García S G, Berg S, Feijoo G, Moreira M T (2009) Environmental impacts of forest production and supply of pulpwood: Spanish and Swedish case studies. Int J Life Cycle Assess 14: 340 – 353.

Gellerstedt S, Dahlin B (1999) Cut-to-length: the next decade. J For Eng 10: 17–25.

Guo L B, Gifford R M (2002) Soil carbon stocks and land use change: a meta analysis. Global Change Biol 8: 345–360.

Grosse W, Landgraf D, Scholz V, Brummack J (2008) Ernte und Aufbereitung von Plantagenholz (Harvesting and conditioning of wood from short-rotation plantations). Schweiz Z Forstwes 159: 114–119.

Helby P, Rosenqvist H, Roos A (2006) Retreat from Salix – Swedish experience with energy crops in the 1990s. Biomass Bioen 30: 422-427.

Henderson D, Jose S (2010) Biomass production potential of three short rotation woody crop species under varying nitrogen and water availability. Agrofor Syst 80: 259-273.

Hillier J, Whittaker C, Dailey G, Aylott M, Casella E, Richter G M, Riche A, Murphy R, Taylor G, Smith P (2009) Greenhouse gas emissions from four bioenergy crops in England and Wales: Integrating spatial estimates of yield and soil carbon balance in life cycle analyses. GCB Bioenerg 1: 267–281.

Holtzscher M, Lanford B (1997) Tree diameter effects on cost and productivity of cut-to-length systems. For Prod J 47:25–30.

Hoogwijk M, Faaij A, Van der Broek R, Berndes G, Gielen D, Turkenburg W (2003) Exploration of the ranges of the global potential of biomass for energy. Biomass Bioen 25:119-133.

Jirjis R (2005) Effects of particle size and pile height on storage and

fuel quality of comminuted Salix viminalis. Biomass Bioenerg 28. 193-201.
Karacic J, Verwjist T, Weih M (2003) Above-ground woody biomass production of short rotation populus plantations on agricultural land in Sweden. Scand J For Res 18:427-437.
Kenney W, Sennerby-Forsse L, Layton P (1990) A review of biomass quality research relevant to the use of poplar and willow for energy conversion. Biomass 21: 163-188.
Londo M, Roos M, Dekker J, De Graaf H (2004) Willow short-rotation in multiple land-use systems: evaluation of four combination options in the Dutch context. Biomass Bioen 27: 205-221.
Manzone M, Airoldi G, Balsari P (2009) Energetic and economic evaluation of a poplar cultivation for the biomass production in Italy. Biomass Bioen 33: 1258-1264.
Nordh N E, Verwjist T (2004) Above-ground biomass assessments and first cutting cycle production in willow coppice. Biomass Bioen 27:1-8.
O'Neill M, Shock C, Lombard K, Heyduck R, Feibert E, Smeal D, Arnold R (2010) Hybrid poplar (*Populus* ssp.) selections for arid and semi-arid intermountain regions of the western United States. Agrofor Syst 79: 409-418.
Pallardy S, Gibbins D, Rhoads J (2003) Biomass production by two-year-old poplar clones on floodplain sites in the Lower Midwest, USA. Agrofor Syst 59: 21-26.
Pellis A, Laureysens I, Ceulemans R (2004) Growth and production of a short rotation coppice culture of poplar I. Biomass Bioen 27:9-19.
Phelps J, Isebrands J, Einspahr D, Christ J, Sturos J (1985) Wood and paper properties of vacuum airlift segregated juvenile poplar whole-tree chips. Wood Fiber Sci 17: 529-539.
Proe M, Griffiths J, Craig J (2002) Effects of spacing, species and coppicing on leaf area, light interception and photosynthesis in short rotation forestry. Biomass Bioen 23: 315-326.
Rockwood DL, Naidu C, Carter D, Rahmani M, Spriggs T, Lin C, Alker G, Isebrands JG, Segrest S (2004) Short-rotation woody crops and phytoremediation: Opportunities for agroforestry? Agrofor Syst 61-62: 51-63.
Rowe R L, Hanley M E, Goulson D, Clarke D J, Doncaster C P, Taylor G (2011) Potential benefits of commercial willow Short Rotation Coppice (SRC) for farm-scale plant and invertebrate communities in the agri-environment, Biomass Bioenerg 30: 325-336.
Sage R (19989 Short rotation coppice for energy: towards ecological guidelines. Biomass Bioen 15: 39-47.
Spinelli R, Owende P, Ward S, Tornero M (2003) Comparison of short-wood forwarding systems used in Iberia. Silva Fennica 38: 85–94.
Spinelli R, Hartsough B (2006) Harvesting SRF poplar for pulpwood: Experience in the Pacific Northwest. Biomass Bioenerg 30: 439-445.
Spinelli R, Nati C, Magagnotti N (2006) Biomass harvesting from buffer strips in Italy: three options compared. Agroforest Syst 68: 113-121.
Spinelli R, Hartsough B, Moore P (20089 Recovering sawlogs from pulpwood-size plantation cottonwood. For Prod J 58: 80-84.
Spinelli R, Visser R (2008) Analyzing and Estimating Delays in Harvester Operations. Int J For Eng 19: 35-40.
Spinelli R, Visser R (2009) Analyzing and estimating delays in wood chipping operations. Biomass Bioenerg 33: 429-433.
Spinelli R, Nati C, Magagnotti N (2009a) Using modified foragers to harvest short-rotation poplar plantations. Biomass Bioen 33: 817-821.
Spinelli R, Ward S, Owende P (2009b) A harvest and transport cost model for Eucalyptus spp. fast-growing short rotation plantations. Biomass and Bioenerg 33: 1265-1270.
Spinelli R, Magagnotti N (2010) A tool for productivity and cost forecasting of decentralised wood chipping. For Pol Econ 12: 194-198.
Spinelli R, Magagnotti N, Picchi G, Lombardini C, Nati C (2011a) Upsized harvesting technology for coping with the new trends in short-rotation coppice. Appl Eng Agric 27: 1-7.
Spinelli R, Magagnotti N, Nati C (2011b) Work quality and veneer value recovery of mechanised and manual log-making in Italian poplar plantations. Eur J Forest Res 130:737–744.
Spinelli R, Ivorra L, Magagnotti N, Picchi G (2011c) Performance of a mobile mechanical screen to improve the commercial quality of wood chips for energy. Bioresour Technol 102, 7366-7370.
Tharakan P, Volk T, Abrahamson L, White E (2003) Energy feedstock characteristics of willow and hybrid poplar clones at harvest age. Biomass Bioenerg. 25: 571-580.
Tiernan D, Zeleke G, Owende P, Kanali C, Lyons J, Ward S (2004) Effect of Working Conditions on Forwarder Productivity in cut-to-length Timber Harvesting on Sensitive Forest Sites in Ireland. Biosyst Eng 87: 167–177.
Visser R, Stampfer K (2003) Tree-length system evaluation of second thinning in a loblolly pine plantation. South J Appl For 27: 77-82.
Weih M (2008) Short rotation forestry (SRF) on agricultural land and its possibilities for sustainable energy supply. Nordic Council of Ministers, TemaNord 2008: 543, Copenhagen, 66 p. Online: http://www.norden.org/en/publications/publications/2008-543.
Willebrand E, Ledin S, Verwijst T (1993) Willow coppice systems in short rotation forestry: effects of plant spacing, rotation length and clonal composition on biomass production. Biomass En. 4: 323-331.

Analysis of a double steering forest trailer for long wood log transportation

Francesco Marinello, Stefano Grigolato, Luigi Sartori, Raffaele Cavalli

Department of Land, Environment, Agriculture and Forestry, University of Padova, Legnaro (PD), Italy

Abstract

A cost effective technical solution of a forest double steering trailer was studied and tested, allowing decrease of radius of curvature and increase of the maneuverability, independently from the length of the transported logs. The steering system improves the so called "stinger-type truck" configuration using an articulated frame; through a rearward hinge, the front wheels direction mechanically controls and adapts the direction of rear twin wheels. The study was based on CAD simulations considering the dimensions of the trailer transporting logs with a length up to 12 m. For different log lengths the simulation analyzed the total maneuver area, in terms of minimum curve radius and curve widening. A field test on a prototype operated for transport of long logs along a representative forest road in the Alps was carried out. The results confirm the improvements foreseen by CAD simulations, with allowed curve radius down to 6 m, even with 12 m logs.

Introduction

The transportation of wood both on-road and off-road represents the backbone of harvesting operations over gentle as well as steep terrain (Bont *et al.* 2012).

In mountainous area on-road transport is often operated on steep terrains in which the construction and maintenance of the forest roads determine high costs (Stückelberger, *et al.* 2006). Therefore the forest road networks in mountainous area consist of narrow and single lanes, high road gradients and frequent switchback curves (Cavalli and Grigolato, 2010).

As a consequence road standard characteristics strongly influence the transportation feasibility by truck and trailer system in mountainous area. As a result tractor and forest trailer systems, commonly used for off-road forwarding of logs along the skidding trails network, in the case of extreme conditions represent the only suitable transportation system in such severe conditions (Baldini *et al.* 2010).

A wide range of logging trailers is available. Commonly they are designed in order to minimizing the construction weight and maximizing the payload. The chassis spine (single or double), where the wheels' cross-members and the stake's bolsters are attached, is the fundamental part of the trailer's frame (Jones, 1995).

According to technical reports of forest trailers companies, most popular tractor and trailer systems have payloads ranging from 5 to 10 tons. Lower capacity trailers may have only two wheels but usually most forest models have a four wheel bogie design. Also steerable drawbars are commonly offered on many forestry trailers. This last solution enables the trailer to follow tractor wheel tracks when turning and reduces the need for a wider road in switchback curves.

Even if a tractor with a forest trailer is considered a handy transportation system in forest roads with severe gradients, in the case of long logs transportation such system can be still inadequate when narrow switchback curves have to be run. In the specific scenario of Italian Alps, logs transportation along forest roads most typically makes use of a tractor and trailer system. The performance in terms of maneuverability of such a system is in general acceptable when logs are within 6 m long: on the other hand, when log length exceeds 8-10 m, maneuverability sensibly worsens. As a consequence, forest trailers with improved steering system need to be implemented.

In order to verify the feasibility to transport logs with a length exceeding 8-10 m on narrow and steep forest roads, a prototype of forest double steering trailer was analyzed. The study aimed to evaluate the effectiveness of the technical solution adopted by the transportation system analyzing through a CAD simulation which considered the minimum radius of curvature and curve widening, and the maneuverability, with different length of transported logs. The results of the CAD simulation were then verified by a field test carried out on a forest road in the alpine area of Belluno province.

Materials and methods

Description of the trailer prototype

The prototype is a forest double steering trailer, based on an improved design of the so called "stinger steer truck" configuration. A sketch of the trailer is proposed in Figure 1.

It is a two axle trailer, featuring a front drive axle with differential wheels, coupled with the tractor power take-off shaft, and a twin wheeled idle axle in the rear part. The front part of the trailer is hitched to the rear frame through a central hinge giving an articulated frame. Therefore the trailer is designed to allow the idle axle to rotate relative to the hinge, and to permit also small roll and pitch motions.

The front frame protrudes rearward of the front axle wheels (the so called stinger part in stinger steer trucks), and symmetrically the rear frame protrudes frontward of the rear axle (the so called reach part). Through the hinge, the stinger steers the reach: in such a way the

Correspondence: Raffaele Cavalli, Department of Land, Environment, Agriculture and Forestry - University of Padova, Legnaro (PD), Italy
E-mail: raffaele.cavalli@unipd.it.

Key words: forest double steering trailer, CAD simulations, forest road, wood transport.

Journal of Agricultural Engineering 2013; XLIV(s2):e3
doi:10.4081/jae.2013.(s1):e3

direction of back twin wheels is mechanically controlled and adapted by driving axle rotations.

Two conventional log bunks are pivotally mounted respectively on the front and on the rear frame of the trailer, and complementary support the logs. Logs constrain rear axle distance from the front one, pulling the rear part of the trailer. When the trailer is driven around a curve, orientation and distance between the bunks remain fixed due to the logs constrain, while the reach has to lengthen due to the relative rotation of the two axles. Such extension is compensated by a steel cylindrical telescoping bar implemented between the reach and the hinge on the stinger (the compensator): even when turning on roads with tight turning radii and independently of the load, such element lengthening eventually allows the relative rotation of the rear axle.

Modeling

When the tractor drives the trailer around a curve, particular attention has to be paid to two part of the vehicle: the wheels and the dynamic envelope. Indeed during motion, not only the wheels have to lie always within the roadway, but also vehicle dynamic envelope has not to interfere with elements (*e.g.* plants or walls) alongside the roadway.

Since the vehicle is designed to work at relatively low speeds, a kinematic slip-free condition can be assumed between inner and outer wheels, according to Ackermann condition (Jazar, 2009), getting to the following mathematical model.

With reference to Figure 2, said α_i and α_e the steer angles of respectively the inner and the outer front wheel of the tractor, and l the wheelbase, the mass center of the tractor turns on a circle with radius:

$$R_M = \sqrt{a_2^2 + l^2 \cdot \cot^2 \alpha} \quad (1)$$

where:

$$\alpha = \cot^{-1}\left(\frac{\cot\alpha_i + \cot\alpha_e}{2}\right) \quad (2)$$

and the front part of the trailer follows a circular trajectory with radius R_{Tf}:

$$R_{Tf} = \sqrt{(l \cdot \cot\alpha_i + w/2)^2 + b_1^2} - b_2^2 \quad (3)$$

with a relative angle β with respect to the tractor direction, which is expressed by:

$$\beta = 2 \cdot \tan^{-1}\left(\frac{1}{b_1 + b_2}\left(R_{Tf} - \sqrt{R_{Tf}^2 - b_1^2} + b_2^2\right)\right) \quad (4)$$

Thus the central hinge of the trail turns on a circle with radius:

$$R_T = \sqrt{b_3^2 + R_{Tr}^2} \quad (5)$$

The rear part of the trail, constrained by the logs length between bunks L, has a relative angle with respect to the front part of the trail expressed by:

$$\gamma = \sin^{-1}\left(\frac{L}{R_1}\right) \quad (6)$$

and the rear part of the trailer follows a circular trajectory with radius R_{Tr}:

$$R_{Tr} = R_T \cdot \cos\left(\sin^{-1}\left(\frac{L}{R_1}\right) - \sin^{-1}\left(\frac{b_3}{R_1}\right)\right) \quad (7)$$

Knowing the average track between the wheels of the tractor (w_M) and of the trailer (w_{Tf} and w_{Tr} respectively for the front and the rear axle) and the overall width of the tires (t_M, t_{Tf} and t_{Tr} respectively for the tractor the front wheels and the rear wheels of the trailer), it is possible to calculate the minimum curve radius (measured in the inner side of the road) which can be run from the vehicle:

$$R_{min} = \min\{R_{Mmin}, R_{Trmin}, R_{Tfmin}\} \quad (8)$$

$$R_{Mmin} = \sqrt{R_M^2 - a_2^2} - (w_M + t_M)/2 \quad (9)$$

$$R_{Trmin} = R_{Tr} - (w_{Tr} + t_{Tr})/2 \quad (10)$$

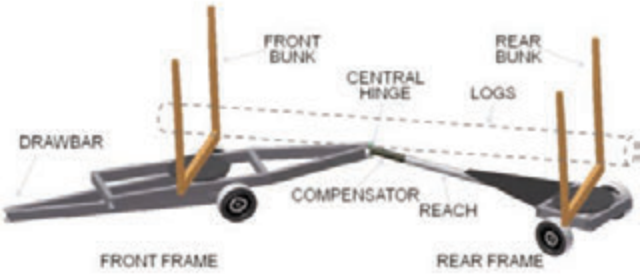

Figure 1. Schematic three-dimensional view of the trailer: a compensator implemented between a reach and a stinger allows rotation of the rear part relatively to the front part, while logs held by front and rear bunks constrain axles distance.

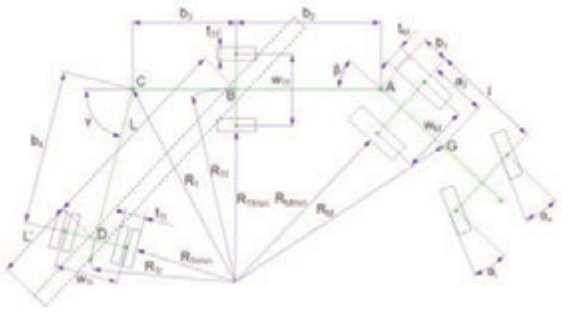

Figure 2. Simplified schematic view of the tractor with trailer and main dimensions.

Figure 3. Schematic view of the tractor with trailer driven into a switchback curve and main dimensions.

$$R_{Trmin} \quad R_{Tr} \quad (w_{Tr} + t_{Tr})/2 \tag{11}$$

The minimum curve radius R_{min} has to be compared with the inner curve radius R_{in} and the following condition has to be verified: $R_{in} \leq R_{min}$.

Similarly the maximum curve radius (measured in the outer side of the road) which can be run from the vehicle in first approximation can be calculated as:

$$R_{max} \quad \max|R_{Mmax}, R_{Trmax}, R_{Trmax}| \tag{12}$$

where:

$$R_{Mmax} \quad \sqrt{R_M^2 \quad a_2^2} + (w_M + t_M)/2 \tag{13}$$

$$R_{Trmax} \quad R_{Tr} + (w_{Tr} + t_{Tr})/2 \tag{14}$$

$$R_{Trmax} \quad R_{Tr} + (w_{Tr} + t_{Tr})/2 \tag{15}$$

The maximum curve radius R_{max} has to be eventually compared with the outer curve radius R_{out}, and the following condition has to be verified: $R_{out} \geq R_{max}$.

Additionally the dynamic envelope of the logs and in particular minimum and maximum radius of curvature traced by the logs R_{Lmin} and R_{Lmax} has also to be taken into account: indeed the projection of the logs has not to exit the roadway, or at least not to interfere with elements (e.g. standing trees or walls) alongside the roadway.

Software simulations

For the present study a mechanical solid modeling design software (Autodesk Inventor®) was implemented. Such software, generally referred as 3D CAD, allows design, visualization and modeling of three-dimensional digital prototypes, simulating different operating conditions in terms of loads and relative movements.

Implementation of simulation software in general brings clear advantages in design and testing of new vehicles: reduces time and costs for development of new products, allows mechanical verification of different design variations both for single elements and for whole structures and eventually allows dynamic simulation to foresee vehicle maneuverability.

For the specific study, 3D design software was implemented in order to recognize vehicle critical parts and verify their mechanical behavior when undergoing high solicitations. Additionally CAD simulations allowed foreseeing trailer dynamics, to better understand motion trajectories and maneuverability (Figure 4).

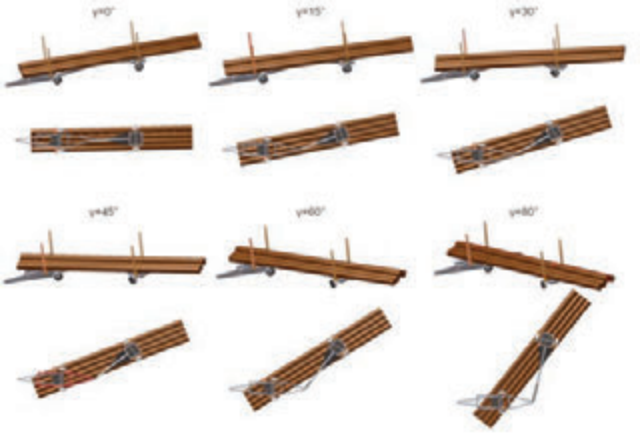

Figure 4. Simulated perspective and bottom view of the trailer at different angles ϒ between the front and the rear part.

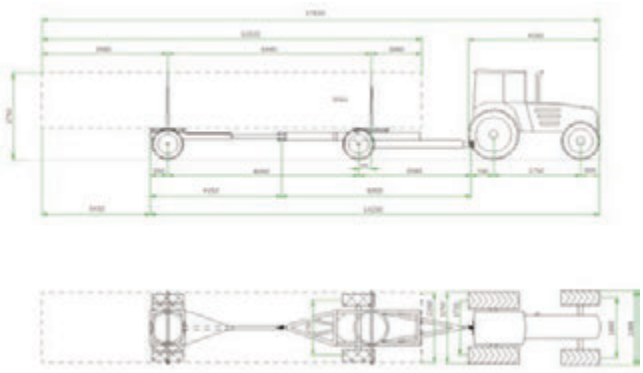

Figure 5. Layout and main dimensions (mm) of the double steering forest trailer prototype.

Field tests

The GPS technology applications for collecting resource measurement and managing forestry operations is well known both for off-roads (Veal *et al.*, 2001; Mc Donald *et al.*, 2005; Pellegrini *et al.*, 2013) and on-roads transportation (Holzleitner *et al.*, 2011; Simwanda *et al.*, 2011). In order to field testing the simulated forest double steering trailer, an existing prototype with a hinge position approximately at the 55% of the wheelbase length was investigated (Figure 5; Figure 6). The trailer motion was monitored through field survey using a GPS device (Trimble@ ProXH coupled with a Trimble@ NOMAD). Additionally a GIS (ArcGIS@ 10.1) view of GPS data was implemented, allowing verifica-

Figure 6. The double steering forest trailer prototype during the test.

tion of the transportation movement along the forest roads, for a better understanding of trailer dynamics and maneuverability. The test considered the use of a D-GPS mounted on the front part of the farm tractor in center position above the front axle. For the analysis, the trailer was driven several times along a 6 km forest road in a forest site on the Eastern Italian Alps. The road showed an average width of 2.7 m and an average road grade of 16%, with a maximum grade of 20%. Switchback curves generally presented a curve radius ranging between 6 m and 7 m. For the test the trailer was loaded with logs longer than 10 m and having an average diameter of 45 cm. The D-GPS measurements were corrected in post-processing with the support of a public antenna available at a distance of 5 km from the test site.

Results

Curve dynamic analysis

The trailer underwent a set of simulations, in order to understand the role of the central hinge into curve dynamics. For this reason a two-axle trailer with a 6 m wheelbase was simulated, and the effect of hinge position was varied from a minimum of zero to 100% of the wheelbase.

The minimum value 0% corresponds to a hinge positioned in correspondence of the center of the front axle: in other words corresponds to a standard two axle trailer with turntable front axle. Conversely, when the hinge is at 100% of the wheelbase, the condition corresponds to a two-axle stinger steer trailer with a stinger part as long as the wheelbase.

Wheels trajectory

Hinge position has no effect on the radius of curvature of the front axle, which is in first approximation insensitive to what stands behind. On the other hand, hinge position has a remarkable effect on trailer rear part.

In terms of radius of curvature, the closer is the hinge to the front axle, the smaller is the radius of curvature traced by the rear wheels (Figure 7). This result brings to a faulty conclusion that the closer is the hinge to the front axle the better is the maneuverability.

This conclusion is not correct: indeed for best maneuverability of the trailer it is desirable to have not just the minimum curvature, but rather the minimum off-tracking between front and rear axles of the trailer. Therefore the maximum difference between the minimum and the maximum radii ΔR_T measured between front and rear outer and inner wheels has to be conveniently taken into account. Such difference has a lower bound which is the track augmented by the width of the tire (i.e. the distance between outer sidewalls of inner and outer wheels):

$$\Delta R_{min} \quad \max\left((w_{Tr} + t_{Tf}),(w_{Tf} + t_{Tr})\right) \qquad (16)$$

The parameter ΔR_T represents the roadway width needed by the trailer to complete a curve. The closer is the difference ΔR_T to the lower bound ΔR_{min}, the smaller is the width needed to maneuver the trailer along the curve.

Simulations showed that the minimum difference is achieved when the hinge is positioned at a distance from the front axle varying between 40% and 80% of the wheelbase, with an optimum close to 60% (Figure 8). For good maneuverability of the vehicle, not only the positioning of the wheels relatively to the road site but also the dynamic envelope has to be considered, with particular attention to the hinge and the logs. The displacement of the hinge should be as small as pos-

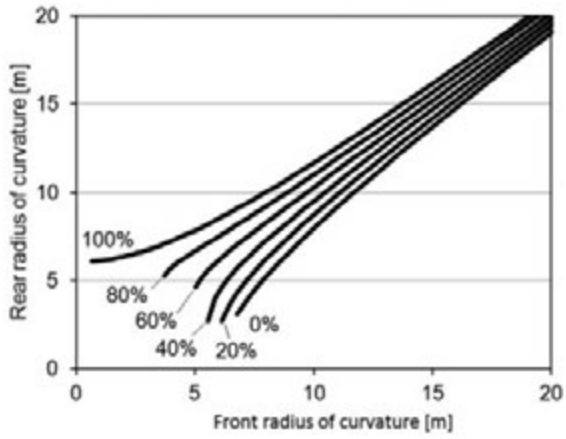

Figure 7. Variation of the rear radius of curvature RTr as a function of the front radius of curvature RTf, at different hinge positions.

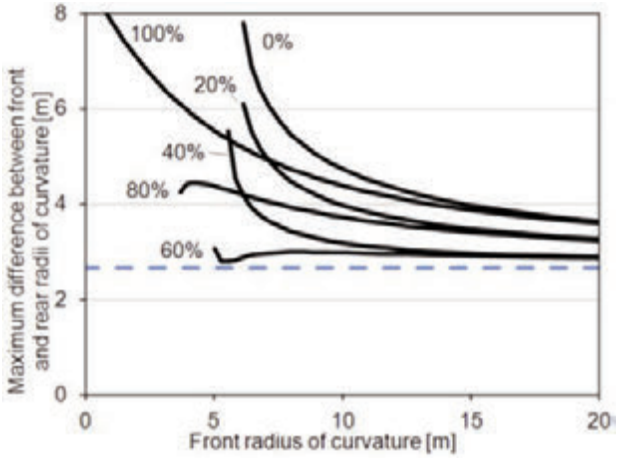

Figure 8. Variation of the difference between front and rear radii of curvature RT as a function of the front radius of curvature RTf; the blue dotted line represent the lower bound, given by the larger axle width.

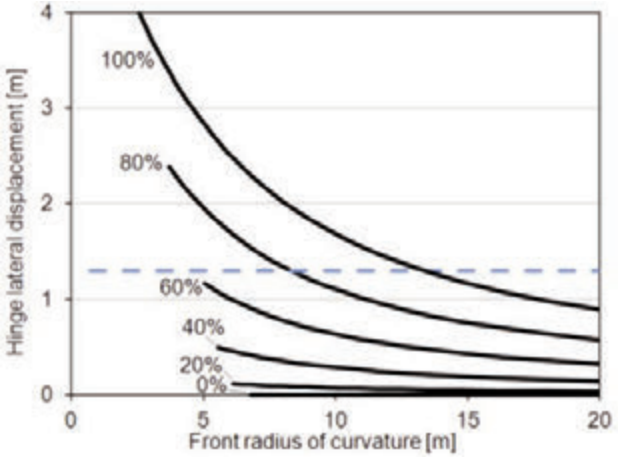

Figure 9. Displacement of the hinge as a function of the front radius of curvature RTf.

sible: indeed even a small interference with external obstacles could bring relevant damages, causing a lock of the two part of the frame, and bringing the trailer out of order. On the other hand the horizontal projection of the logs can exit the road site: nevertheless it has to be as small as possible, in order to minimize the probability of interferences with external obstacles lying alongside the roadway.

Hinge trajectory

Then simulations were carried out, in order to evaluate central hinge displacement and logs dynamic envelope. The same two-axle trailer with 6 m wheelbase was considered, and again the effect of hinge position was varied from a minimum of zero to 100% of the wheelbase. Results are summarized in Figure 7, where the blue dotted line represents half the larger axle width: if the displacement overcomes such values, the hinge is supposed to sticking out from the trailer frame projection. When the hinge is at 0% of the wheelbase, the condition resembles the trivial case of a standard two-axle trailer with turntable front axle: in such state the displacement is constantly equal to zero, independently from front axle radius of curvature. As the hinge moves rearward, the displacement increases. Such displacement comes to critical values as the hinge get closer to the rear axle: in particular high displacements are found with the hinge positioned at a distance larger than 60% of the wheelbase from the front axle.

Logs trajectory

It has been said that the horizontal projection of the logs also plays an important role. Since the tighter trajectory is traced by the rear axle, analysis considered the difference between the minimum radius of curvature traced by the logs projection and the radius of curvature of the external sidewall of the rear wheel standing in the inner part of the curve. The minimum radius of the logs RL_{min} was measured between the bunks in the portion of log most protruding during curve movement (see Figure 3). Results are reported in the graph below (Figure 8). In order to minimize the probability of interferences with external obstacles, the projection of the logs should be always within the wheel tracks. This occurrence is not always possible when using a two axle stinger steer trailer. In particular, as the hinge moves rearward, the probability of interferences with external obstacles increases, since the relative displacement of the logs with respect to the inner wheel R_{Lmin}-R_{Trmin} becomes negative. In other words, as the hinge gets closer to the rear axle, the logs minimum radius of curvature becomes smaller than the inner wheel radius of curvature (i.e. $R_{Lmin}<R_{Trmin}$). To keep the difference always positive (i.e. to avoid interferences of the central part of the logs with external obstacles), the hinge has to be kept at a distance from the front axle smaller than 40% of the wheelbase.

Analyses considered also the maximum radius of curvature produced by the dynamic envelope of the logs. In case of transportation of long logs, the larger trajectory is covered by their extremities, sticking out from the rear part of the trailer. The difference between the maximum radius of curvature traced by the logs projection and the radius of curvature of the external sidewall of the rear wheel standing in the outer part of the curve R_{Lmax}-R_{Trmax} was therefore quantified (Figure 11 and 12). For the simulation 10 m and 12 m long logs were considered, with respectively a 2 m and a 4 m rear sticking out length L' (Figure 2). It is clear how tighter curvatures cause higher widening of the curve, but the effect is somehow reduced as hinge gets closer to the rear axle. The effect is clearly less evident as shorter logs are carried, on the other hand becomes more evident as their length increases.

A best configuration for a two-axle stinger steer trailer cannot be defined a priori. The design necessarily has to take into account the characteristics of the road, of the road sides and of the load type. Comparing the graphs above, in general best tradeoffs can be expected

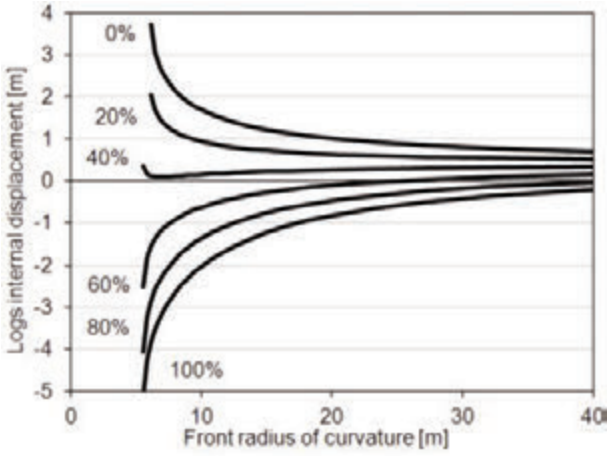

Figure 10. Logs internal displacement (measured as the difference between rear wheels and logs minimum radius of curvature R_{Lmin}-R_{Trmin}) as a function of the front radius of curvature.

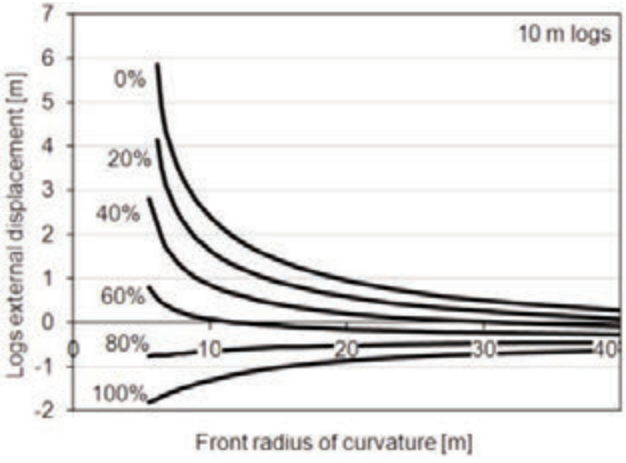

Figure 11. Logs external displacement (measured as the difference between rear wheels and logs maximum radius of curvature R_{Lmax}-R_{Trmax}) as a function of the front radius of curvature in the case of 10 m logs.

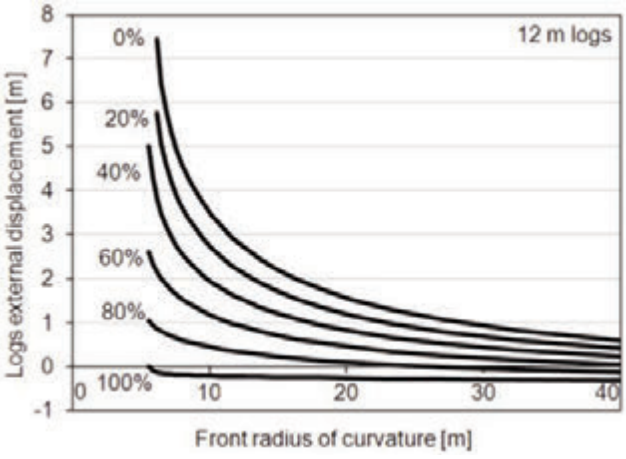

Figure 12. Logs internal displacement (measured as the difference between rear wheels and logs maximum radius of curvature R_{Lmax}-R_{Trmax}) as a function of the front radius of curvature in the case of 12 m logs.

whenever the hinge is positioned at a distance from the front axle ranging between 40% and 60% of the wheelbase, but unfortunately a general statement is not possible.

Field tests

The test carried on the double steering forest trailer prototype highlights a good maneuverability of the transportation system along forest road with high road grade and small switchback curves radius. Both the conditions with loaded and unloaded trailer were tested.

In the case of loaded trailer with logs longer than 10 m (the longest with a length of 12 m, positioned at the center of the trailer), the transportation system was clearly affected by the high transported payload (average speed in loaded condition 4.9 km h^{-1}, average speed in unloaded condition 9.5 km h^{-1}). The minimum switchback curve radius was 6 m with an external widening curve of approximately of 1 m. Such result confirmed simulations, which foresaw an external logs displacement of about 1.5 m (see Figure 9).

The back projection of the logs (approximately 3 m) played an important role during the approach of the switchback curve as the projection of the longest log was very close to the cut-slope of the road prism. For this reason the tractor driver had to continuously modify and correct tractor trajectory acting on the front wheel direction. The result is a trajectory where the center of curvature is not a fixed point coincident with the curve center: conversely the center of curvature of the vehicle is constantly changing during motion. On the other hand, also the curve has not a constant curvature but the radius constantly decreases in the first half, and symmetrically increases during the second half. This behavior is typical of all the roads, and introduces a limitation in reported simulations. Indeed proposed analyses are built on the condition of constant radii of curvature, which is not verified in actual roads. Nevertheless the relevance of the proposed results is not diminished, posing the limits for the maximum performance achievable with the trailer driven in ideal conditions.

Conclusions

In this study a prototype of a double steering forest trailer for long log transportation was analyzed and tested. The simulation of the prototype was supported by dedicated 3D software mainly focusing on the wheels and the dynamic envelope when the transportation system runs switchback curves with challenging curve radii.

The simulation results evidenced how the hinge position influences the radius of curvature of the rear wheels. The simulation allowed identifying an optimum position (between 40 to 60% of the wheelbase respect to the front axle) of the hinge to minimize the off-tracking between front and the rear axle. Such hinge positioning is also suitable to avoid excessive lateral displacement of the hinge, keeping its trajectory always within the track of the trailer.

Simulations evidenced also how logs external displacement is minimized when the hinge is brought closer to the rear axle, however staying within acceptable values when it is positioned at least at 50% of the wheelbase length.

Tests on a prototype (with the hinge location approximately at 55% of the wheelbase) reasonably confirm simulation results in term of transportation system dynamic. Main limitations arise from forest roads poor regularity, which typically replicates the complex morphology of the mountainous terrain. In such conditions software simulations are not sufficient to accurately describe the dynamic of the transportation system, but gives however relevant indications on maximum expectable performance.

References

Baldini S., Cavalli R., Piegai F, Spinelli R., Di Fulvio F., Fabiano F., Grigolato S., Laudati G., Magagnotti N., Nati C., Picchio R. 2009. Prospettive di evoluzione nel settore delle utilizzazioni forestali e dell'approvvigionamento del legname. Atti del Terzo Congresso Nazionale di Selvicoltura per il miglioramento e la conservazione dei boschi italiani. Taormina, 16-19 Ottobre 2008, Firenze: Accademia Italiana di Scienze Forestali, 2:717-728, ISBN/ISSN: 978-88-87553-16-1.

Bont L.G., Heinimann H.R., Church R.L. 2012. Concurrent optimization of harvesting and road network layouts under steep terrain. Ann Oper Res. 1-24.

Cavalli R., Grigolato S. 2010. Influence of characteristics and extension of a forest road network on the supply cost of forest woodchips. J For Res-JPN. 15:202-209.

Holzleitner F., Kanzian C., Stampfer K. 2011. Analyzing time and fuel consumption in road transport of round wood with an onboard fleet manager. Eur J For Res. 130:293-301.

Jazar R.N. 2009. Mathematical theory of autodriver for autonomous vehicles. J Vib Control. 16: 253.

Jones D.H. 1995. Timber trailers for agricultural tractors. Forest Research. Technical Notes. 28. Machynlleth: Forest Commission.

McDonald, T. P., & Fulton, J. P. (2005). Automated time study of skidders using global positioning system data. Comput Electron Agr. 48(1):19-37.

Pellegrini M., Ackerman P., Cavalli R. 2013. On-board computing in forest machinery as a tool to improve skidding operations in South African softwood sawtimber operations. South Forests. 75:89-96.

Sessions J., Wimer J., Boston K. 2009. Increasing Value and Reducing Costs through Hauling Longer Logs: Opportunities and Issues. West J Appl For. 24:157-162.

Simwanda M., Wing M.G., Sessions J. 2011. Evaluating global positioning system accuracy for forest biomass transportation tracking within varying forest canopy. West J Appl For. 26:165-173.

Stückelberger J.A., Heinimann H.R., Burlet E.C. 2006. Modeling spatial variability in the life-cycle costs of low-volume forest roads. Eur J For Res. 125:377-390.

Veal M.W., Taylor S.E., McDonald T.P., McLemore D.K., Dunn M.R. 2001. Accuracy of tracking forest machines with GPS. T ASAE. 44:1903-1911.

Decision analysis for the determination of biomass in the territory Tuscia Romana by geographic information system and forest management plans

A. Colantoni,[1] F. Recanatesi,[1] S.Baldini,[1] M. Felicetti,[2] M. Romagnoli[1]

[1]Department of science and technology of Agriculture Forest Nature and Energy (DAFNE), University of Tuscia, Viterbo, Italy; [2]Bic Lazio – Regione Lazio, Italy

Abstract

The growing interest in the development of chains for the use of agroforestry biomass for energy demand, is due to the awareness they are a crucial element to mitigate the global climatic change effects. The true effort is to have a reliable estimation of biomass availability by some instruments like forest management plans, which allow to locate the forest supply and to know the forest biomass availability in a medium period. In this paper we carried out a decision analysis by geographic information system, in Tuscia Romana area comprising 11 municipalities for a total amount of 813 km^2. An estimation was carried out taking into account the bibliographic data on the analyzed species, reporting the biomass in weight taken out by the forest cut utilization. A comparison was also performed in field on chestnut trees cut in a sampling area near Bracciano and in a close sawmill. The results show long, medium and short-term dynamics, but some critical points were found related to the process of estimation and to the real procurement of biomass in some years. The results suggest to be care in a possible project of a biomass plant.

Introduction

In the energy scenarios developed at international level, the role of renewable energy sources, is become more and more relevant. In this overview the role of biomass is considered crucial for achieving the objectives of climate change mitigation both at International and national level. The role of renewable energy sources (FER) is not limited to the decreasing of pollutants but it goes far beyond, going to affect the great fundamental choices concerning sustainable development, resource conservation, agricultural and rural development, safety of supply, and a hopefulindependence from foreign markets up to the fight against poverty. An increase of FER can also help to overcome the inequalities in access to energy sources that are recorded both at global and national levels, as well as to support the growth of the economy of the developing countries.

In Italy we have moved at an early stage in the exploitation of the great potential that renewable energy sources represents. The barriers to be removed are not only economic, but also social and cultural. The problem of social acceptability is in fact still the second obstacle for the development of FER especially in central-southern Italy. In this area there are many difficulties to apply a regular forest management, because the stumpage value is very often negative and also becausethe woods are often degraded making the priority to recover forest predominant. In such situation biomass supplyfor energetic purposes sometimes fights with the production of wood assortments suitable for other uses (boards, beams etc.) especially in the very few cases where wood quality has some potentiality for the developing economy of the territory.

The exploit the use of biomass for energetic purposes in this area should take into account the existing forest chains and do not depress the possible use of forest in a multipurpose overview, allowing also the productive role where it is a resource for the territory, limiting only to the use of the residuals which cannot find any other possibility of employment.

To address the efforts towards the use of biomass for energetic purposes, being careful of the social and economic equilibrium of some territories, means to operate in a descending approach which can be so organized:

To make a general overview of the biomass availability and the feasibility for energetic purposes.

To verify the estimation by case studies in order to understand the residuals of biomass which could be used after forest harvesting for biomass in energetic purposes. The study is addressed to the knowledge of the biomass which is usually leaved in the forest stand after cutting the trees that means branches and the top of the tress with a diameter below 5 cm.

To enlarge the whole perspective to the forest-wood-chain taking into account the final product that means in central-southern Italy to consider the transformation in the sawmill.

Starting by this assumptions we have carried out this study in the territory of Tuscia Romana in Lazio Region. The aim is to approach a feasibility study based on the information of the potential biomass and verifying the estimated data on one case study during forest harvesting and transformation in the sawmill.

At the moment the case study is related only to chestnut species harvested during winter season at 2012-2013 and worked in the sawmill in order to obtain as final product beams for the buildings.

Correspondence: M. Romagnoli, Department of science and technology of Agriculture Forest Nature and Energy (DAFNE), University of Tuscia, Viterbo, Italy.
E-mail: manuela romagnoli mroma@unitus.it

Key words: G.I.S., biomass, renewable energy, Tuscia.

Journal of Agricultural Engineering 2013; XLIV(s2):e4
doi:10.4081/jae.2013.(s1):e4

Materials and methods.

The estimation of biomass for energetic purposes has been carried out in the territory of Tuscia Romana, which cover 12 municipalities at North of Rome, using the information collected in a prepared form which has been delivered by the professionals foresters of the territory. In our study we were able to collect the information only of 11 municipalities.

The most important required information are: the name of the stand which is going to be harvested in each municipality, the general site characteristics (i.e slope, altitude, viability, civic uses, wildfire accident, accessibility). The collected information was get by means of forest management plans where it is reported the surface and the total biomass in cubic meters which will be cut in each single stand in each year. Such biomass considers the trunk, it does not take into account the branches and the top of the tree which in this area, as custom, is leaved inside the forest .

The transformation of volumetric data to weight has been carried out using the wood density values reported in Hellrigl (2004) for each species, at 33% of hydric content (measured on the fresh weight) i.e. 50% of moisture content (i.e. measured on the dry weight). The water content was chosen because it allows the operation of biomass boilers with enough efficiency, it is well known as too much water makes difficult to burn woody biomass. In order to estimate the total energetic power, it was decided to apply the percentage of 18% at the total weight biomass cut by the forest sands. This value has been considered reasonably usable for energetic purposes considering the species which are widespread in the area (oaks, beech, chestnut) collecting the references on this subject.

The potential basins of biomass (stands to be cut), according to the species and to the year of harvesting, were located on the map by Geographical information System divided in each town of the Tuscia Romana and indifferent colours were used for each year of cut, in order to provide a useful tool for the administrators. For each town it has been calculated the total biomass to be cut on the whole time period considered in the forest management plans and the total energetic power developed. At the end a general graph up to the year 2027 was prepared in order to show the general trend of biomass supply enhancing possible a lack of availability and the prospective in order to build one or more biomass boilers.

Residual Biomass from Harvesting and sawmill operations

In order to verify if the estimation of the biomass carried out by forest management plans, one case study in Vicarello (Bracciano, Central Italy) stand was applied during harvesting operations in winter 2012/2013. In a coppice stands of chestnut a sample area located at about 450 m of altitude, and a slope of 30%-35%, 36 stumps were cut with about seven shoots for each stump. The mean diameter at the bottom of the shoots spans from 15 cm to a maximum of 20 cm.

The harvested trees were weighted considering on one hand separately the tree top, which was cut when the diameter of the stem was below 5 cm, and the branches; on the other hand the whole log was weighted. Moisture contents of fresh wood was measured by means of a gravimetric method. The biomass of the tree top and branches was compared to the weighted whole trunk.

In order to have an idea of a total residual in the entire chestnut chain, 10 logs of chestnut in the sawmill with a diameter at the bottom spanning from 15 to 22 cm and spanning by 8 to 10 cm at the top of the tree, with a total length of about 12 meters, were followed in the sawmill. We could not follow the material coming from Vicarello but some logs coming from the same area that means the municipality of Bracciano. It was measured the starting weight of the logs and their volume in cubic meters. The logs were processed in the sawmill it was possible to obtain poles or boards and small joists using a trimmer and a multi-blade circular saw. The final assortments were weighted again and their sizes were measured. The percentage of the residuals as volume and weight was measured.

Results

The species which are going to be cut in the next years in the area Tuscia Romana are mainly chestnut coppices, and deciduous oaks both in coppice and in conversion from coppice to high forest, sometimes mixed with chestnut; the remaining part is the Mediterranean forest of sclerophyllous and beech forests.

The town in which there is the highest content of biomass to be cut is Tolfa where more of 200.000 $m^3$of wood were estimated as harvested by the foresters freelancers, up to the year 2034 (the forest management plan is actually under revision).

The lowest availability of biomass is in Anguillara where about 5000 m^3 of wood in turkey oak coppice stands were predicted in forest harvesting up to the year 2033.

As regards chestnut the most part of the biomass is in Bracciano site and it is about 80.000 m^3 predicted by a forest management plan which spans up to the year 2019 (Table 1). We report the table and the map of the localization of forest stands which are going to be cut in Bracciano (Figure 1).

Taking into account all the surface which will be interested by forest harvesting in the territory Tuscia Romana, comparing this value with the estimated surafce covered by forests as reported in ISTAT in the year 2000, we could suppose that a further area in all the municipalities could be used as biomass supply for energy. In fact, according to the surface which is classified as forest in ISTAT 2000,we have a gap between what is reported by the prepared forms by forest freelances and that wooden area as reported in each municipaliy by ISTAT. The potential adding biomass supply spans from a remaining potential surface which could be cut by 25% (Manziana) to over 60% in Allumiere. It is not known if such difference is real that means that forest is pres-

Table 1. Biomass supply of Bracciano town.

Municipality	Management	Species	Biomass at fresh state (m3)	Hydric content (%)	Moisture content (%)	Specific density according to the Hydric content kg/m^3	Biomass for energetic purposes (t) 18% of the total amount	Pcs MJ/kg	Pci MJ/kg	Thermal energy production (kWh$_{th}$)
Bracciano	Ceduo	*Quercus cerris*	87.937,49	33	50	900	14.246	18,12	11,74	41.811.638
	Ceduo misto	*Quercus cerris*	16.688,50	33	50	900	2.704	18,12	11,74	7.934.881
	Ceduo	*Castane sativa*	79.341,06	33	50	780	11.139	19,80	12,51	30.193.574

ent and possibly available to be cut, or if the forest is not available because it takes into account the shurbs which are not object of forest management and which are not going to be cut.

The 18% in weight of the total biomass was assumed to be available for energy purposes and the total availability of the areaTuscia Romanais reported year by year in Figure 2. If we assume the total biomass which would be necessary to have a total develop of 2 MW in all the examined period we can see that there are two important minimum in the biomass supply in the year 2021 and 2023

In the analysis of chestnut in Vicarello, during winter forest harvesting we could verify two loads in which 350 and 440 kg of branch and tree top were weighted; the weight of their corresponding tree is respectively 1220 and 2200 kg. Comparing the biomass which could be used for energy we have a percentage of 16.9 and 16.6%. If we transpose this result to the biomass which was reported in the forest management plans it means that we could estimate a percentage of 20% in chestnut in weight which we could use for biomass for energy. Because the wood moisture content we measured in the field is about 50% we can be satisfied because this value approaches the percentage 18% we assumed during the feasibility study.

In the sawmills the percentage of residuals is higher. The percentage of biomass which can be used for energetic purposes increases up to 40% taking into account the log were some block full of defects were eliminated trunks (without tree top and branches) and as final product poles, small joists and boards. In fact the 10 logs were 740 kg in weight and we could obtain 300 kg of small joists and 160 kg of boards, with a residual of 280 kg (Figure 3). To this percentage we would have to add a biomass which was eliminated before

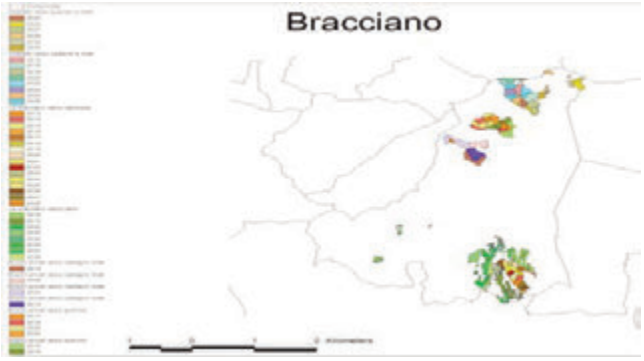

Figure 1. Map of Bracciano with the location of biomass supply.

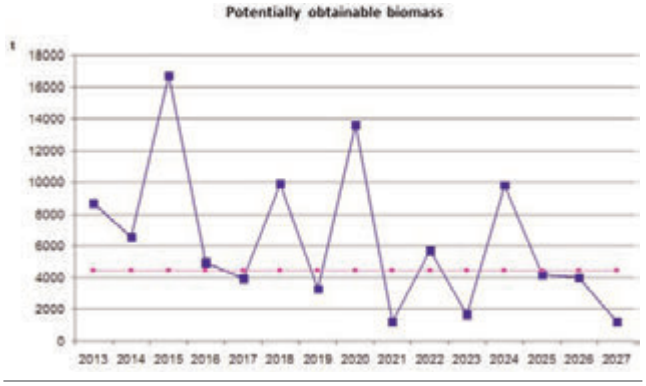

Figure 2.

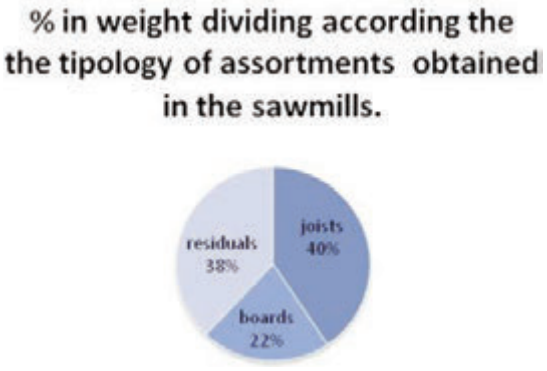

Figure 3. Assortment in the sawmills.

Conclusions

Available residual biomass - obtained from database and our case study can be successfully considered as a real economic opportunity to be used as forest biomass in Tuscia Romana. The large quantities can supply the growing energy demand and can be efficiently used in domestic or district heating. But many information is lacking to have a more reliable biomass estimation which can be used for energy purposes. The first information and may be the most important are the possible roads which can be used for forest harvesting, they can limit the biomass supply really available for energy purposes.

References

AA.VV. Filiere Corte in Liguria. Energia dal bosco per le coltivazioni in serra: l'esperienza del progetto Biomass.

Bagnaresi U., Baldini S., Berti S., Minotta G., 1987. Assessment of the Energy bilance for beech coppices in the Northern Appenines. In: Atti del Convegno "Biomass energy: from harvesting to storage", Marino 19-21 novembre 1986. London, Elsevier Applied Science, p.75-79.

Bagnaresi U., Baldini S., Berti S., Minotta G., 1987. Beech coppice in Italy'sNorthern Appenines: energy balance of logging operations. In: "Fuelwood production strategies", Proceedings of IUFRO Project Group P1.09.00, IUFRO XVIIIth World Congress, Ljubljana, 1986. Uppsala, SwedishUniversity of AgriculturalSciences, p.103-106.

Bagnaresi U., Baldini S., Berti S., Minotta G., 1987. Ricerche sui bilanci energetici e sui costi di utilizzazioni forestali. Annali dell'Accademia Italiana di Scienze Forestali

Helrigl B, 2004. Il potere calorifico del legno. Convegno studio "Le biomasse agricole e forestali nello scenario energetico nazionale". Progetto Fuoco 2004, Verona 18-19 marzo 2004.

Verani S., Nati C., Spinelli R., Nocentini L., 2008. Meccanizzazione avanzata in bosco ceduo. Analisi tecnica dei due cantieri. Sherwood, 144:42-46.

Spinelli R., Nati C., Magagnotti N., Verani S., Raccolta integrata di legna d ardere e cippato dalla gestione dei cedui quercini degradati in Molise. Rapporto tecnico per Regione Molise.

Spinelli R., Magagnotti N., Meccanizzazione spinta nelle fustaie nel diradamento delle fustaie transitorie di faggio. Alberi e territorio: 19-25.

Colour modifications and hyperspectral imaging: non-invasive analysis of photo-degraded wood surfaces

Giorgia Agresti,[1] Giuseppe Bonifazi,[2] Luca Calienno,[3] Giuseppe Capobianco,[2] Angela Lo Monaco,[3] Claudia Pelosi,[1] Rodolfo Picchio,[3] Silvia Serranti[2]

[1]Department of Cultural Heritage Sciences, University of Tuscia , Largo dell'Università, Viterbo, Italy; [2]Department of Chemical Engineering Materials & Environment, Sapienza – Rome University, Rome, Italy; [3]Department of Agriculture, Forests, Nature and Energy (DAFNE), University of Tuscia, Via San Camillo de Lellis, Viterbo, Italy

Abstract

The aim of this investigation is to study the changes occurring on the surface of poplar wood exposed to solar irradiation, in a controlled environment. Poplar is poor of coloured extractive, so that the surface changes are attributed to the main wood constituents' modifications and the contribution of extraneous substances to holocellulose and lignin can be considered negligible. The poplar wood samples were irradiated in a Solar Box chamber, equipped with a 280 nm UV filter, until reaching 504 hours. The colour changes were monitored with the reflectance spectrophotometer of X-Rite CA22 according to the CIELAB system. The surface chemical modifications were evaluated by measuring the infrared spectra with a Fourier Transform Infrared spectrometer (FT-IR) operating in DRIFT modality. Hyperspectral imaging (HSI) was also applied to study the surface wood changes by using a SisuCHEMA XL Workstation operating in the SWIR range (1000-2500 nm). The data obtained from the different techniques applied were put in comparison in order to find possible correlations between them also with the aim to evaluate the applicability of the HSI technique to the investigation of wood modifications, in a totally non-invasive modality. The possibility to find a correlation between colour changes and chemical modifications, investigated both with traditional and innovative methodologies, in wood surfaces can have practical application in cultural heritage and contemporary objects.

Correspondence: Luca Calienno, Department of Agriculture, Forests, Nature and Energy (DAFNE), University of Tuscia, via San Camillo de Lellis, 01100 Viterbo (Italy). E-mail: luca.calienno@unitus.it

Key words: Poplar; Colour measurement, FT-IR spectroscopy, Hyperspectral imaging; wood.

Journal of Agricultural Engineering 2013; XLIV(s2):e5
doi:10.4081/jae.2013.(s1):e5

Introduction

The focus of this work is to study the surface modifications of poplar (*Populus* spp.) wood by reflectance spectrophotometry, Fourier Transform Infrared (FT-IR) spectroscopy and HyperSpectral Imaging (HSI) in order to understand the mechanisms that cause surface changes due to photo-degradation and to suggest possible solutions to avoid the degradation phenomena. The choice of poplar was due to its widespread use in Italy for the creation of statues, ceilings, furniture, doors, painted panels, etc.

In cultural heritage the monitoring of wood surfaces during light exposure should be performed through non-destructive methods to avoid the paradox of damaging a work of art while monitoring its preservation state (Marengo, *et al.* 2003; Marengo, *et al.* 2004). For this reason colour measurements were chosen as possible method to evaluate wood surface changes.

Since colour changes on wood surfaces are due to photo degradation of its chemical constituents, the study of the relationship between CIELAB colour changes and changes in chemical composition due to irradiation is of practical importance both in cultural heritage and in contemporary artefacts and objects (Pandey, 2005)

This work starts from previous studies, developed by the same authors, regarding colour measurements on poplar and chestnut wood (Lo Monaco, *et al.* 2011a; Lo Monaco, *et al.* 2011b; Genco, *et al.* 2011; Pelosi *et al.* 2013). The novelty of this work, in respect of the previous ones, is the attempt to verify the possible correlations existing between colorimetric and chemical data in the perspective to develop simple, fast and reliable techniques to detect wood surface modifications.

The first studies dealing with the application of multi-spectral and HSI based techniques, in the visible region, to wood date back to 1941 (Pillow, 1941) where this approach, based on classical spectra collection, was utilised to identify compression wood in conifers. Compression wood appears more opaque, in comparison with normal wood that appears translucent. Methods based on NIR imaging were thus developed and applied to classify wood (*i.e.* compression and opaque) (Nystrom and Hagman, 1999) and further "refined" to perform regions mapping (*i.e.* bark, compression and normal wood) (Noordam, *et al.* 2005). In the recent years the utilisation of HSI based techniques increased considerably, also in the field of wood studies where they are used especially to perform the chemical surface mapping for obtaining the distribution of lignin, galactose and glucose in different wood species (Thumm, *et al.* 2010).

In this work, the classical colorimetric investigation procedures, the chemical analysis and the proposed HSI based techniques are compared in order to verify the possibility to use colour measurements as a quick and simple method to control the surface modifications, map-

ping (i.e. pixel by pixel) the wood sample surface.

The fulfilment of this goal was achieved by examining the correlations between classical colorimetric and chemical data with wood surface spectral characteristics detected in the i) VIS-NIR (400-1000 nm) and ii) SWIR (1000-2500 nm) wavelength ranges. This approach is of great interest in the perspective to set up efficient, robust, non invasive and not destructive analytical tools addressed to evaluate status and modifications of photo-degraded wood surfaces.

Materials and Methods

Colour monitoring and FT-IR analysis

Wood samples were obtained by a single board of poplar. After cutting, the samples were stored in darkness in a conditioned room at 65% relative humidity and a temperature of 22°C to reach the 12% of moisture content.

The samples dimensions for the colour examination were 235 x 50 x 50 mm.

To perform the FT-IR analysis directly on wood surface, circular slices, diameter 10 mm and 2 mm thick, were obtained from the specimens of poplar. The dimensions of the slices were suitable for the FT-IR diffuse reflectance accessory. The same slices were used to perform the HSI measurements.

The accelerated ageing of the samples was performed in a Model 1500E Solar Box (Erichsen Instruments GmbH & Co), in order to simulate the sunlight exposition. The samples were exposed in the Solar Box chamber from 1 to 504 h at 550 W/m^2, 55°C and the UV filter at 280 nm.

After exposure for a given length of time the samples were removed from the Solar Box chamber and the colour was measured using an X-Rite CA22 reflectance spectrophotometer. The characteristics of the colour measuring instrument are the following: colour scale CIEL*a*b*; illuminant D65; standard observer 10°; geometry of measurement 45°/0°; spectral range 400-700 nm; spectral resolution 10 nm; measurement diameter 4 mm; white reference supplied with the instrument. The CIELAB colour system was used where L* describes the lightness while a* and b* describe the chromatic coordinates on the green-red and blue-yellow axes, respectively. Measurements were taken at the following hour intervals: 0, 1, 2, 3, 4, 5, 6, 7, 8, 9, 10, 11, 12, 24, 48, 72, 96, 120, 144, 168, 216, 312, 408 and 504 h. Ninety colour measuring points were chosen and three measures for each point were performed, according to Normal 14/83, so that two hundred and seventy measurements were realized at each exposure time.

Infrared spectra were obtained using a Nicolet Avatar 360 Fourier transform spectrometer. For each sample 128 scans were recorded in the 4000 to 400 cm^{-1} (2500 - 25000 nm) spectral range in diffuse reflection modality (DRIFT) with a resolution of 4 cm^{-1}. Spectral data were collected with OMNIC 8.0 (Thermo Electron Corporation) software.

To obtain the FT-IR spectra, sample slices were directly inserted in the FT-IR diffuse reflectance accessory unit. As background the spectrum of the KBr powder was used. The spectra were collected in DRIFT modality directly on the wood slices in order to avoid analysing also the unaltered wood. In fact, wood is a good light absorber for infrared, visible and ultraviolet light (Kataoka and Kigushi 2001; George, *et al.* 2005). In particular the UV component of light is totally absorbed in a 75 µm-thick layer (Hon and Shiraishi 2001). Since the change caused by irradiation appears in a thin surface layer, it is not easy to remove the proper thin layer for pellet preparation, as suggested also by other authors (Tolvaj, *et al.* 2011).

FT-IR spectra were recorded at the following time intervals: 0, 6, 12, 24, 48, 72, 96, 120, 144, 168, 216, 312, 408 and 504 hours.

Band assignment was made according to literature references (Moore and Owen 2001; Chang, *et al.* 2002; Colom, *et al.* 2003; Pandey and Pitman 2003).

Peak heights were measured using OMNIC software according to the method described in the literature (Pandey and Pitman 2003).

The colour and FTIR data were analyzed with the StatSoft ® Statistica 2010 advanced statistics software. As a first step, data distribution was plotted and visually checked for normality. Differences between treatments were checked with the standard paired t-test, with ANOVA and M-ANOVA analysis. Post-hoc tests were conducted with Tukey HSD test method. Linear and non-linear regression analysis was used to develop prediction models.

In particular, two-way ANOVA was applied to the infrared peak values to test if significant differences in relation to the samples and to the time could be found.

Hyperspectral analyses

Hyperspectral analyses were carried out in 2 steps: a 1st step addressed to analyse degraded wood surfaces in the wavelength interval 400-1000 nm (VIS-NIR) and a 2nd in which analyses were carried out in the interval 1000-2500 nm (SWIR). Investigations have been developed with 2 different sensing devices, both from SPECIM Ltd, Finland: i) an ImSpector™ V10E acting in the range 400-1000 nm, with a spectral sampling/pixel of 2.8 nm, a dispersion of 97.5 nm/mm and F/2.4 numerical aperture, coupled with a CCD camera (780x580 pixels) and ii) a Specim SISUChema XL™, embedding an ImSpector™ N25E acting in the range 1000-2500 nm, with a spectral sampling/pixel of 6.3 nm, coupled with a MCT camera (320x240 pixels). Pixel resolution was 12 bits for the first device and 14 bits for the second, respectively.

For the 1st set of acquisitions (400-1000 nm) the ImSpector™ V10E was installed on a Leica M205C stereomicroscope. The energysing source was constituted by MI-150 Dolan Jenner fiber optic device equipped with a dicroic lamp. For the 2nd set of acquisitions (1000-2500 nm) the SISUChema XL™ was used, equipped with macro lens allowing the acquisition of wood samples with a resolution of 30 m/pixel. Images were acquired scanning each investigated sample line by line.

The calibration of the procedures was performed recording two black and white reference images. Certified standards were used. Black image (B) was acquired to remove the camera sensor dark current effect. White reference image (W) was acquired using a white ceramic tile, calibrated with a NPL Spectralone® specimen, in the same condition for the raw image acquisition. The image correction was thus performed adopting the following equation:

$$I = \frac{I_0 - B}{W - B} \times 100 \quad (1)$$

where I is the corrected hyper-spectral image in a unit of relative reflectance (%), I_0 is the original hyperspectral image, B is the black reference image (~0% reflectance) and W is the white reference image (~99.9% reflectance). All the corrected images were then used to perform the HSI based analysis, that is to extract spectral information and to select the effective wavelengths for the final classification purposes.

Spectral data analysis was carried out adopting standard chemometric methods (Geladi, *et al.* 2007; Otto 1999), by the PLS_Toolbox (Version 6.5.1, Eigenvector Research, Inc.) running inside Matlab® (Version 7.11.1, The Mathworks, Inc.). Raw spectra were preliminary cut, at the beginning and at the end of the investigated wavelength range, to eliminate unwanted effects due to lighting/background noise. Wavelength reduction, in VIS-NIR, was from 121 to 81 nm so that the investigations was carried out in the spectral range 500-900 nm. As

Table 1. Nonlinear regression analysis applied to the chromatic coordinates at different times of exposure in Solar Box for poplar samples.

Value	Intercept	Significance	Time	Significance	time2	Significance	R2adj.	Significance
L*	83.002	***	-0.045	***	0.00004	***	0.816	***
a*	1.569	***	0.032	***	-0.00003	***	0.954	***
b*	20.108	***	0.00679	***	-0.00008	***	0.857	***

regards SWIR, the reduction was from 256 to 240 nm resulting in a spectral range 1005-2500 nm. Different pre-treatments, e.g.: De-trend 1st polynomial, Mean-center, 1st Derivative, Standard Normal Variation, Generalized Least Square Weighting (GLSW) and Baseline techniques, were applied to classify the different investigated samples.

Principal Component Analysis (PCA) was used to decompose the "processed" spectral data into several Principal Components (PCs) (linear combinations of the original spectral data) embedding the spectral variations of each collected spectral data set. A reduced set of factors is produced. Such a set can be used for discrimination, since it provides an accurate description of the entire dataset.

Partial Least Squares Discriminant Analysis (PLS-DA) was used to find a model able to perform an optimal discrimination among classes of samples and to predict new images. PLS-DA is a supervised classification technique, requiring a prior knowledge of the data (Barker and Rayens 2003). The result of PLS-DA applied to hyper-spectral images is a "prediction map", where the class of each pixel can be identified using color mapping.

Table 2. Non linear regression analysis applied to the time as function of the chromatic coordinates.

Poplar samples	B	Significance
Intercept	1732.326	***
L*	-56.232	***
a*	16.154	***
b*	24.495	***
L^{*2}	0,381	***
a^{*2}	4.376	***
b^{*2}	-0.520	***
R^2adj.=0.947; p<0.001		
T=1732.3-56.2L*+16.2a*+24.5b*+0.4L*2+4.4a*2		

Results and discussion

Colour monitoring and FT-IR analysis

Colour variability of poplar wood was widely discussed elsewhere suggesting the necessity to perform a high number of measurements in order to avoid this variability (Lo Monaco, *et al.* 2011; Ferreira, *et al.* 2012). M-ANOVA and Tukey tests were applied to the chromatic coordinates as function of irradiation times, until 504 hours of exposure. These tests underline that L*, a* and b* undergo statistically significant changes after the exposure times, apart from the first hours of irradiation suggesting the possibility to start the measurements directly after 6 hours of irradiation

In particular L* value decreases from 84.3 to 71.6. The a* and b* coordinates increase from 2.0 to 9.5 and from 16.8 to 33.3 respectively. In general it is possible to state that the greatest change occurs within the first 24 h of exposure and around the 460 nm wavelength (Reflectance% = -28.3) which corresponds in violet/blue shades.

A nonlinear regression analysis was applied to the chromatic coordinates at different time of exposure in Solar Box in order to evaluate the statistical significance of the experimental data. The results reported in Table 1 demonstrate that the various components exhibit a high statistical significance concerning every polynomial function used for the analysis.

A nonlinear regression analysis with three dependent variables was applied to the time in function of colour coordinates. The results shown in Table 2 underline the highly statistical significance of the obtained measures regarding the dependent variable time (T) as function of the colour coordinates (L*, a*, b*).

The irradiating-time dependent diffuse reflectance FT-IR spectra are shown in Figure 1. It can be observed that the intensity of the bands at 1507 cm^{-1}, 1595 cm^{-1} and 1464 cm^{-1}, associated to lignin, decrease dur-

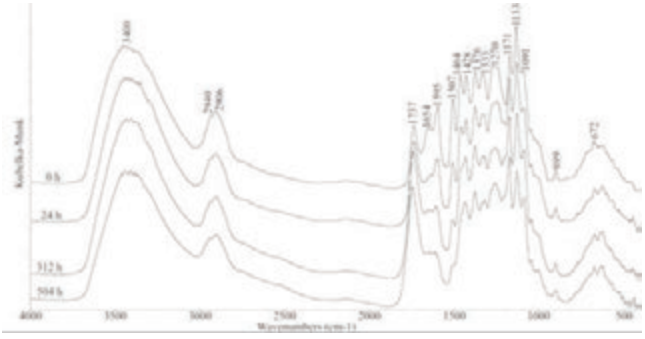

Figure 1. Diffuse reflectance spectra of poplar slices measured at chosen exposure times.

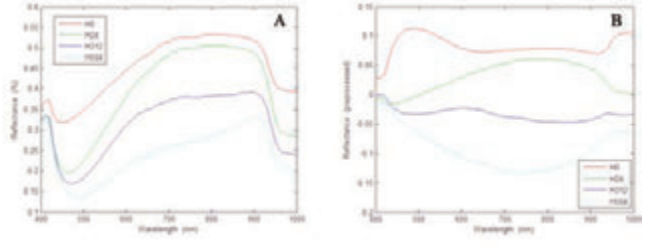

Figure 2. Acquired (2A) and pre-processed (2B) spectra of the different analysed wood slices, in the VIS-NIR field. Spectra pre-processing was carried out adopting a GLSW procedure.

Table 3. Two-way ANOVA test applied to the peak ratios in relation to the poplar samples and to the irradiation time.

Peak ratio	Measures Nr.	Average	Std. Dev.	Samples differences	Time differences
I_{1507}/I_{1376}	42	0.827	0.490	No significance	***
I_{1740}/I_{1376}	42	3.210	1.030	No significance	**
I_{1507}/I_{1737}	42	0.326	0.302	No significance	***

ing photo-degradation. This is accompanied by an increase in the intensity of the band at 1737 cm^{-1}, due to carbonyl absorption. The intensities of the peak associated to carbohydrates at 1376 cm^{-1} is not significantly affected by irradiation, so this band has been used as internal reference to evaluate the lignin decay.

In order to determine the rate of lignin decay and carbonyl formation, the intensities of the lignin band at 1507 cm^{-1}, the carbonyl band at 1737 cm^{-1} and the carbohydrate reference band at 1376 cm^{-1} were calculated (Pandey and Pitman 2003). Then the relative change in ratio of lignin/carbohydrate bands at different exposure times were derived and statistically evaluated.

In particular, two-way ANOVA applied to the infrared peak (Table 3) shows that the differences in the peak ratio with respect to the exposure times are highly significant concerning the I_{1507}/I_{1376} and I_{1507}/I_{1737} ratios. The difference is only significant as regards the I_{1737}/I_{1376} ratio.

Nonlinear regression analysis was also applied to the peak ratio at the different times of exposure in Solar Box. The results are shown in Table 4.

The lignin/carbohydrate intensity ratio decreased with the exposure times and after 48 h of irradiation the experimental value of the I_{1507}/I_{1376} ratio decreased to about 50% of its original value.

The relative increase of the carbonyl groups during photo-irradiation was calculated by considering the ratio of intensity of carbonyl band at 1737 cm^{-1} against reference peak at 1376 cm^{-1}. The intensity of the band of the carbonyl groups increases as function of irradiation time. This can be explained with the liberation of C=O groups of degraded lignin. As the carbonyl groups increase during the photo-ageing whereas the lignin band decreases, the ratio of intensity of the bands at 1507 and 1737 cm^{-1} undergoes a fast and significant decrease after few hours of exposure. In fact, after 12 hours of exposure the experimental value of the I_{1507}/I_{1737} ratio decreased to about 50% of its original value.

The regression analysis clearly demonstrates that for the I_{1507}/I_{1376} and I_{1507}/I_{1737} peak ratios a statistically significant regression has been derived from the experimental data. In the case of the I_{1737}/I_{1376} peak ratio the regression has a low statistical significance.

At last the colour changes of wood during irradiation were correlated with lignin decay and the formation of carbonyl groups produced by the photo-degradation process. In fact, as the colour changes of the surfaces are mainly due to the liberation of C=O groups due to photo-degradation of lignin, there would be a correlation between the colour coordinates and the relative intensity of the infrared peaks associated to lignin. The results showed in Table 5 demonstrate that the lignin decay is related to photo-induced colour changes of wood surfaces.

Hyperspectral imaging on the wood slices

Investigations in the VIS-NIR wavelength range. The acquired and the pre-processed spectra for the different irradiated wood slices, at time 0 (H0), 24 (H24), 312 (H312) and 504 hours (H504) of exposure are shown in Figure 2. The Figure 3 shows the false colour images, as resulting from hypercube data structure. The results of PCA are shown in Figure 4. The spectral data of the four wood samples are clustered into four distinct groups according to their spectral signatures.

A discrimination between the wood samples characterized by differ-

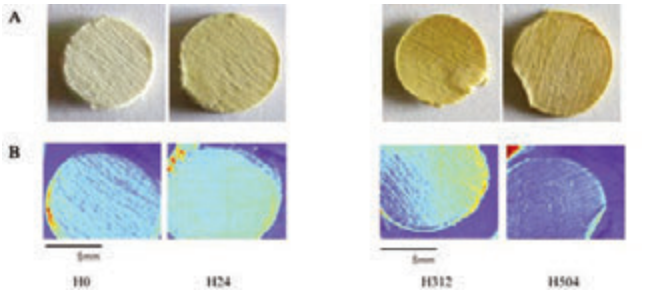

Figure 3. Images of the investigated poplar samples used to build the model. A: acquired images and B: images resulting from hypercube data rendering (i.e. false colours) according to samples spectral response in the VIS-NIR range.

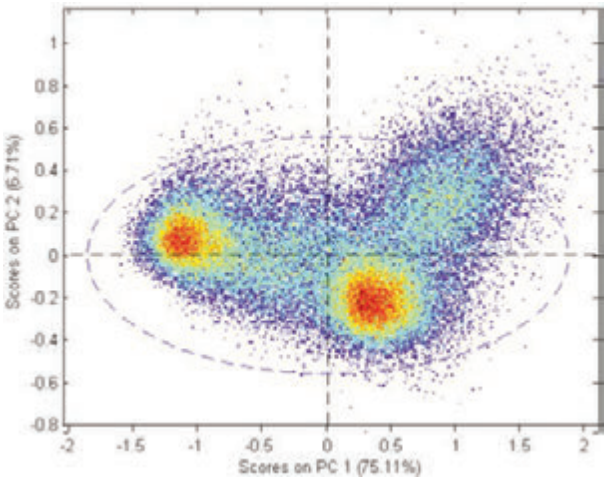

Figure 4. Score plot (PC1 vs PC2), obtained using 81 wavelengths, based on average HSI spectral signatures in the VIS-NIR wavelength region (400–900 nm) for the analysed poplar wood samples.

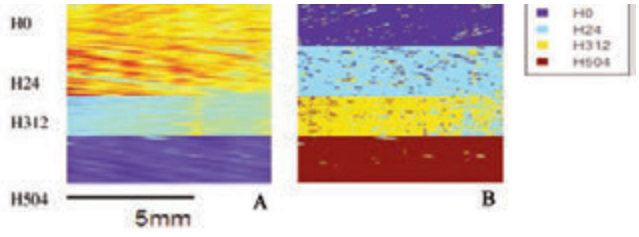

Figure 5. Reconstructed sample image, obtained combining the four different selected ROIs inside the different wood samples, and utilised to perform the hyperspectral based PLS-DA model validation (A). PLS-DA prediction (*most probable class prediction*) (B).

Table 4. Nonlinear regression analysis for the peak ratio at the different times of exposure in Solar Box of poplar samples.

Value	Coefficient	Description	Significance	Time coefficient	Significance	R^2adj.	Significance
I_{1507}/I_{1376}	1.383	e coefficient	***	-0.005	***	0.865	***
Regression				$I_{1507}/I_{1376}=1.383e^{-0.005t}$			
I_{1737}/I_{1376}	2.808	Intercept	***	0.003	*	0.129	*
Regression				$I_{1737}/I_{1376}=2.808+0.003t$			
I_{1507}/I_{1737}	0.995	Intercept	***	0.0031	***	0.924	***
	-0.109	Square root coefficient	***				
			Regression	$I_{1507}/I_{1737}=0.995+0.0031t-0.109t^{0.5}$			

Table 5. Nonlinear regression analysis applied to the peak ratio as function of the chromatic coordinates L*a*b* in poplar wood.

	I_{1507}/I_{1376}			I_{1507}/I_{1737}	
	B	Significance		B	Significance
Intercept	1.4582	***	Intercept	-12.420	***
L^{2}*	0.000092	***	L^{2}*	0.0017	***
a^{2}*	-0.00373	***	a^{2}*	-0.0072	***
b^{2}*	-0.001328	***	b^{2}*	0.0032	***
R^2adj.=0.999	R^2adj.=0.995				
$I_{1507}/I_{1376}=1.4582+0.000092L^{*2}-0.00373a^{*2}-0.001328b^{*2}$I1507/I1737=-12.420+0.0017L^{*2}-0.0072a^{*2}+0.0032b^{*2}					

ent exposure times is obtained, especially concerning H0, H24 and H504, whereas H312 is more dispersed between H24 and H504.

The PLS-DA based classification was calculated using the same pre-treatment technique adopted to perform PCA (GLSW) analyses for reference class definition. Starting from 4 new samples, the same approach previously outlined was thus applied, that is: i) construction of a sample image to verify PLS-DA model, starting from four different ROIs selected inside the wood samples in order to avoid "border effects"; ii) selection of ROIs, inside the reconstructed sample image, to collect spectra representative of the different irradiated wood slices, to validate the model.

The results, as prediction images, indicate that the PLS-DA models allow obtaining a good classification of all the samples (Figure 5). Such results can be evaluated taking into account the values of sensitivity and specificity parameters obtained. These parameters range from 0 to1, being 1 the ideal value for a prediction model. Sensitivity is defined as the proportion of class members correctly classified. Specificity refers to the proportion of non-class members correctly classified.

The sensitivity and specificity of the PLS-DA model are calculated both for *Calibration* and *Cross-Validation*. The values of sensitivity and specificity range between 0.75 (H312) and 0.996 (H0) for *Calibration* and between 0.74 (H312) and 0.996 (H0) for *Cross-Validation*. Good values of sensitivity and specificity are obtained for the classification of the different time exposed wood samples, indicating the robustness of the model. The sample exposed 312 hours was confirmed as the worst classified according to the indications obtained during the explorative analysis based on PCA previously carried out and described.

Hyperspectral imaging on the wood slices

Investigations in the SWIR wavelength range. The acquired and the pre-processed spectra for the different irradiated wood slices, at time 0 (H0), 24 (H24), 312 (H312) and 504 hours (H504) of exposure are shown in Figure 6. In the SWIR range both cellulose and lignin are characterised by absorption bands corresponding to specific wavelengths, that is 1220, 1480, 1930, 2100, 2280, 2340 and 2480 nm for cellulose and 1450, 1680, 1930, 2270, 2330, 2380 and 2500 nm for lignin (Van der Meer and Jong 2002).

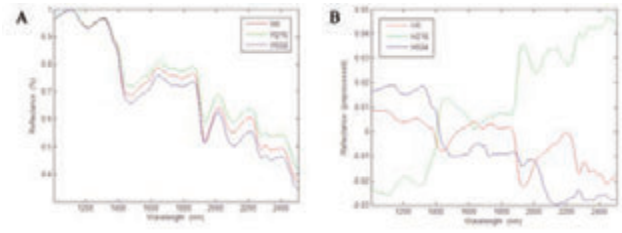

Figure 6. Acquired (A) and pre-processed (B) spectra of the different analysed wood slices, in the SWIR field. Spectra pre-processing was carried out adopting a GLSW procedure.

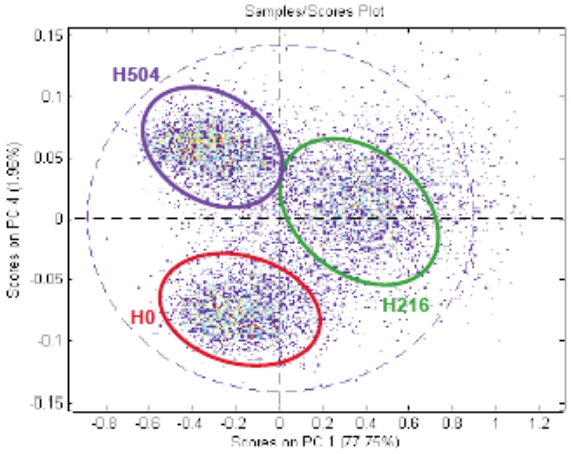

Figure 7. Score plot (PC1 vs PC2), obtained using 240 wavelengths, based on average HSI spectral signatures in the SWIR wavelength region (1005-2500 nm), of the analysed poplar wood samples.

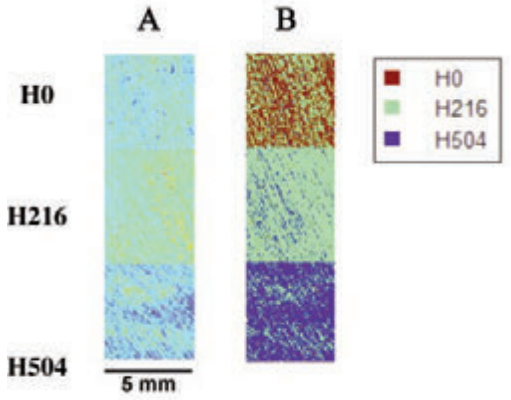

Figure 8. Reconstructed sample image, obtained combining three different ROIs inside the different wood samples, and utilised to perform the hyperspectral based PLS-DA model validation (A). PLS-DA prediction (*most probable class prediction*) (B).

The strong absorptions at around 1460 nm and 1930 nm can be attributed to the combination modalities of OH in water molecules. It should be noted that the water chemical bond vibration around 1460 nm may overlap with those of other OH groups in cellulose molecules or of CH_2 groups in lignin molecules (Van der Meer and Jong 2002), making difficult the accurate band assignment in this region. The weak spectral feature around 1730 nm may be attributed to the presence of OH bond of water molecule in cellulose/lignin and the weak absorption at 1790 nm to O-H stretching in water molecules. The mean absorptions in the 2000-2500 nm wavelength interval can be attributed to the various configurations of the C-H, C=O, C=C, and -COOH functional groups in cellulose and lignin.

Spectra have been acquired performing a preliminary background removal as, differently from the VIS-NIR case; spectral data collection and analysis have been carried out with reference to the entire surface of each wood sample.

The results of PCA, applied to the average spectral signature of the investigated wood samples are shown in Figure 7. The greater part of the variance was captured by the first two PCs. PC1 and PC2 explained 77.75% and 1.96% of the variance, respectively. Spectral data of the 3 wood samples are clustered into 3 distinct groups according to their spectral signatures. A discrimination between the wood samples characterized by different exposure times is thus obtained.

The PLS-DA model was developed, as in the VIS-NIR study, to perform a prediction (i.e. recognition/classification) on unknown wood samples characterised by different exposure times. The PLS-DA based classification was calculated using the same pre-treatment technique adopted to perform PCA (GLSW) analysis for reference class definition. Starting from 3 new samples the following approach was applied: i) construction of a sample image to verify PLS-DA model, performing background elimination, ii) collection of all the spectra related to each sample in order to validate the model. The results indicate that the PLS-DA models allowed to reach, as in the VIS-NIR range, a good recognition/classification, according to their irradiation times for the 3 investigated poplar samples (Figure 8).

The sensitivity and specificity of the PLS-DA model, based on all 240 wavelengths, are calculated both for *Calibration* and *Cross-Validation*. The values of sensitivity and specificity range between 0.896 (H24) and 0.993 (H0) for *Calibration* and between 0.868 (H24) and 0.993 (H0).

Conclusions

The study of colour changes in poplar samples showed the wood surface colour undergoes an important variation due to photo-irradiation. The greatest changes occur within the first 24 hours and they are mainly due to L* decrease and b* increase. M-ANOVA and Tukey tests underline that L*, a* and b* undergo statistically significant changes after the exposure times further demonstrating that surface wood colour remarkably changes due to ligth exposure. The regression analysis, applied both to the chromatic coordinates as function of the time and vice versa, underlines the highly statistical significance of the experimental data.

FT-IR spectroscopy allowed to investigate the rate of photo-degradation of wood surface due to lignin oxidation. The rate of photo-degradation of wood surface was investigated by studying the lignin/carbohydrate intensity ratio as function of time. The results put in evidence that lignin degrades quickly: after 48 hours of irradiation the lignin/carbohydrate ratio (I_{1507}/I_{1376}) decreased to about 50% of its original value. The regression analysis applied to the infrared peak ratios demonstrated that the differences between the values at the various irradiation times are statistically significant, apart from the I_{1737}/I_{1376} ratio. Moreover a correlation between the colour changes and the chemical modifications was investigated in order to assess the applicability of colorimetric measurements in totally non-invasive modality on the works of art.

The most important result was that a correlation of the colour changes may be derived with the photo-degradation of lignin obtained by FTIR analysis. This finding demonstrates that non-invasive colour measurements can be used to evaluate the photo-degradation of wood. In particular the regression analysis showed that the lignin decay is related to the photo-induced colour variations of wood surfaces expressed by the L*a*b* coordinates.

Concerning hyperspectral imaging, the detected spectral features showed in the VIS-NIR range are mainly linked to the spectral shape (i.e. colour variation), whereas in the SWIR range cellulose and lignin affect both shape and reflectance levels.

The PCA applied to hyperspectral images acquired in the wavelength range 400-1000 nm highlighted a significant variation between samples not exposed and exposed after 24 hours. The variations between samples irradiated for 312 and 504 hours are lower, if compared with the previous ones, in any case the results showed that the colour changes is correlated with the lignin photo-degradation. Concernign the SWIR, the PCA demonstrated a correlation between sample spectral profile characteristics and the exposure times.

The application of partial least squares regression (PLS-DA) allowed to perform an good classification and recognition of different irradiated samples in both the investigated wavelength ranges. The proposed approach clearly showed as a correlation can be established between color variation and wood degradation in the VIS-NIR; furthermore in the SWIR range wood surface chemical changes can be assessed.

The results obtained show that colour is a promising tool for non invasive assessment of the chimical variation of wood surface in order to monitor both historycal wood artefacts and contemporary wood objects.

References

Barker M., Rayens W.2003.Partial least squares for discrimination, J. Chemom. 17: 166-173.

Chang H.T., Yeh T.F., Chang S.T. 2002. Comparisons of chemical charac-

teristic variations for photodegraded softwood and hardwood with/without polyurethane clear coatings. Polym. Degrad. Stab. 77: 129-135.

Colom X., Carrillo F., Nogués F., Garriga P. 2003. Structural analysis of photodegraded wood by means of FTIR spectroscopy. Polym. Degrad. Stab. 80: 543-549.

Ferreira R.C., Lo Monaco A., Picchio R., Schirone A., Vessella F., Schirone B. 2012. Wood anatomy and technological properties of an endangered species: Picconia azorica (Oleaceae). IAWA J. 33 (4): 375-390.

Geladi P., Grahn H., Burger J. 2007. Multivariate images, hyperspectral imaging: background and equipment," Techniques and Applications of Hyperspectral Image Analysis, 1-15, Grahn H. and Geladi P. Eds., John Wiley & Sons, West Sussex, England.

Genco G., Lo Monaco A., Pelosi C., Picchio R., Santamaria U. 2011. A study of colour change due to accelerated sunlight exposure in consolidated wood samples. Wood Res-Slovakia 56 (4): 511-524.

George B., Suttie E., Merlin A., Deglise X. 2005. Photodegradation and photostabilisation of wood - the state of the art. Polym. Degrad. Stab. 88: 268-274.

Kataoka Y., Kigushi M. 2001. Depth profiling of photo-induced degradation in wood by FT-IR Microspectroscopy. J. Wood Sci. 47: 325-327.

Hon D. N. S, Shiraishi N. 2001. Color and Discoloration and Weathering and photochemistry of wood. Wood and Cellulose chemistry, Marcel Dekker Inc., New York, 385-442, 513-546.

Lo Monaco A., Marabelli M., Pelosi C., Picchio R. 2011a. Colour measurements of surfaces to evaluate the restoration materials. Proc. SPIE 8084: 1-14.

Lo Monaco A., Pelosi C., Picchio R. 2011b. Colour evolution of wood surfaces in simulated sunlight exposure. Proc. Colour and Colorimetry. Multidisciplinary Contributions, 207-214.

Marengo E., Robotti E., Liparota M. C., Gennaro M. C. 2003. A Method for Monitoring the Surface Conservation of Wooden Objects by Raman Spectroscopy and Multivariate Control Charts. Anal. Chem. 75: 5567-5574.

Marengo E., Robotti E., Liparota M. C., Gennaro. M. C. 2004. Monitoring of pigmented and wooden surfaces in accelerated ageing processes by FT-Raman spectroscopy and multivariate control charts. Talanta 63: 987-1002.

Moore A.K., Owen N.L. 2001. Infrared spectroscopic studies of solid wood. Appl. Spectrosc. 36: 65-86.

Nystrom J., Hagman O. 1999. Methods for detecting compression wood in green and dry conditions. J. *Wood Sci.* 45(1): 30-37.

Noordam J.C, Van der Broek W.H.A.M., Geladi P., Buydens L.M.C. 2005. Detection and classification of latent defects and diseases on raw French fries with multispectral imaging. *Chemom. Intell. Lab. Syst*. 75(2): 115-126.

Otto M. 1999. Chemometrics, statistics and computer application in analytical chemistry. Wiley-VCH, New York.

Pandey K. K., Pitman A. J. 2003. FTIR studies of the changes in wood chemistry following decay by brown-rot and white-rot fungi. Int. Biodeter. Biodegr. 52: 151-160.

Pandey K. K. 2005. Study of the effect of photo-irradiation on the surface chemistry of wood. Polym. Degrad. Stab. 90: 9-20.

Pelosi C., Agresti G., Calienno L., Lo Monaco A., Picchio R., Santamaria U., Vinciguerra V. 2013. Application of spectroscopic techniques for the study of the surface changes in poplar wood and possible implications in conservation of wooden artefacts. In: Proc. SPIE 8790-41: 1-14.

Pillow M. 1941. A new method for detecting compression wood. *J. Forest*. 39: 385-387.

Thumm A., Riddell M., Nanayakkara B., Harrington J., Meder R. 2010. Near infrared hyperspectral imaging applied to ammping cemical composition in wood samples. J. Near Infrared Spectrosc. 18: 507515.

Tolvaj L., Mitsui K., Varga D. 2011. Validity limits of Kubelka-Munk theory for DRIFT spectra of photodegradated solid wood. Wood Sci. Technol. 45: 135-146.

Van der Meer F.D., Jong S.M. (Eds.) 2002. Imaging Spectrometry: Basic Principles and Prospective Applications. Remote Sensing and Digital Image Processing, Vol. 4 Springer, Netherlands, 130-133.

Carbon balance and energy fluxes of a Mediterranean crop

Simona Consoli,[1] Osvaldo Facini,[2] Antonio Motisi,[3] Marianna Nardino,[2] Rita Papa,[1] Federica Rossi,[2] Salvatore Barbagallo[1]

[1]Dipartimento di Gestione dei Sistemi Agro-alimentari e Ambientali (DiGeSA), Università degli Studi di Catania, Italy; [2]Istituto di Biometeorologia, Consiglio Nazionale delle Ricerche, Bologna, Italy; [3]Dipartimento Scienze Agrarie e Forestali (SAF), Università degli Studi di Palermo, Italy

Abstract

This paper is based on the analysis of a long-term mass (carbon dioxide, water vapour) and energy (solar radiation) balance monitoring programme carried out during years 2010 and 2012 in an irrigated orange orchard in Sicily, using the Eddy Covariance (EC) method. Orange (*Citrus sinensis* L.) is one of the main fruit crops worldwide and its evergreen orchard may have a great potential for carbon sequestration, but few data are currently available. In the study, the role of the orchard system in sequestering atmospheric CO_2 was analyzed, thus contributing to assess the carbon balance of the specie in the specific environment.Vertical energy fluxes of net radiation, soil heat, sensible heat and latent heat fluxes were measured at orchard scale by EC. Evapotranspiration (ET) values were compared with upscaled transpiration data determined by the sap flow heat pulse technique, evidencing the degree of correspondence between instantaneous transpirational flux at tree level and the micrometeorological measurement of ET at orchard level.

Introduction

Orange orchards are widely diffused in Mediterranean regions, playing a fundamental role in the economy of the primary sector of these areas (Capra *et al.*, 2011). These species need a large amount of water for sustaining their production, and the determination of their effective water demand is still an important issue of debate in the applied research (Hamdy, 1999; Consoli *et al.*, 2006; Consoli and Papa, 2012; Ballester *et al.*, 2012), similarly to the partition of crop evapotranspiration (ET_c) into transpiration (T) and soil evaporation (E) rates (Cohen *et al.*, 1993; Rana *et al.*, 2005; Consoli and Papa, 2012; Motisi *et al.*, 2012). The role of these species from an ecological point of view in terms of absorbing the atmospheric carbon dioxide (CO_2) is much less discussed and few data are available in the literature. Recent research carried out on the role of Mediterranean orchards (olive and orange) in sequestering atmospheric CO_2 have evidenced them to be high carbon sinks, with respect to other evergreen orchards (Liguori *et al.*, 2009; Nardino *et al.*, 2013). In general, the efficiency of the orchards as carbon sink is favoured by its vigorous growth and high leaf area index, even if human actions (farming management techniques) may influence their physiology and thus carbon sequestration role. Modern concepts of intensive agricultural crop systems and highly efficient irrigation management strategies (i.e. drip irrigation, deficit irrigation, etc…) lead to an intensification of the orange eco-physiological activity and potential carbon sequestration, driving towards advances in crop productivity (Pernice *et al.*, 2009).

The study of the physical relationships between orange orchards and the atmosphere above, allowing the comprehension of the exchange mechanisms of water, carbon dioxide and heat, presents several constraints related to the homogeneous extensions to match the required fetch, the expensive micrometeorological tower to put in operation, and often the complexity of data processing. The Eddy Covariance (EC) technique constitutes the reference method to monitor and measure the above cited flux exchange mechanisms; although its adoption in monitoring networks throughout the world has led to significant advances in defining how ecosystem-level fluxes respond to variability in land cover and climate forcing (Baldocchi, 2003), it is influenced by a series of restrictive assumptions requiring corrections, including: surface homogeneity of the downwind area, sensor misalignment, air density changes, coordinate rotation, etc. Thus, recorded EC data need validation to be representative. Furthermore the inability of EC data to close the energy budget is a well-known issue (Aubinet *et al.*, 2000; Barr *et al.*, 2006; Twine *et al.*, 2000), which has led several authors to emphasize the necessity of finding a way to deal with it (Mahrt, 1998; Wilson *et al.*, 2002; Baldocchi, 2003; Liu *et al.*, 2006, Consoli and Papa, 2012). Despite the sources of errors associated with long-term EC flux measurements, many investigators are producing reasonable estimates of annual carbon exchange. When measurements come from nearly ideal sites the error bound on the net annual exchange of CO_2 is less than ±50 g(C) m^{-2} $year^{-1}$ (Baldocchi, 2003).

This paper aims at analysing the mass (H_2O, CO_2) and heat fluxes

Correspondence: Simona Consoli, Dipartimento di Gestione dei Sistemi Agro-alimentari e Ambientali (DiGeSA), Università degli Studi di Catania, via S. Sofia 100, 95123 Catania, Italy.
Tel. +39.095.7147547 – Fax: +39.095.7147605.
E-mail: simona.consoli@unict.it

Key words: carbon balance, eddy covariance, orange orchard.

Acknowledgements: this work has been carried out in the context of the Project of Relevant National Interest (P.R.I.N.) 2008 "Assessment of mass and energy fluxes for the irrigation management of Mediterranean tree crops" under grant no. 2008CR84NF by Italian Ministry of Research and University (M.I.U.R.). Authors wish to thank the Azienda Tribulato (Lentini, SR) for its hospitality. Authors are also grateful to the Agrometeorological Service (SIAS) of the Sicilian Region for its support.

Journal of Agricultural Engineering 2013; XLIV(s2):e6
doi:10.4081/jae.2013.(s1):e6

exchanged within an orange orchard in Sicily to (i) assess the carbon balance and the role of the orchard system in sequestering atmospheric CO_2; and (ii) determine reliable crop water demand values to be partitioned between crop transpiration and soil evaporation rates.

Materials and Methods

The experimental field, which had an area of approximately 20 ha, is located in Eastern Sicily, where orange orchards are the predominant crop. The plants (15-25 years-old *Citrus sinensis*, cv Tarocco Ippolito) are on a regular grid of 4.0 x 5.5 m^2 (about 455 plants ha^{-1}); the mean canopy height is 3.7 m and the crop ground cover is 70%, with a mean leaf area index (LAI) of 4.3 m^2 m^{-2}, measured by an LAI-2000 Plant Canopy Analyzer (Li-Cor Bioscence, USA). Trees were daily drip irrigated at full rate with four on-line drippers per plant (discharge rate of 4 l h^{-1}). The total volume of water applied during summer was fixed at 5,500 m^3 ha^{-1} and added to precipitation amounts. The site shows good crop homogeneity, no slope, and dominant wind speed and fetch allowing for an ideal application of micrometeorological techniques (Figure 1). During the monitoring period 2010-2012, hourly meteorological data (incoming short-wave solar radiation, air temperature, air humidity, wind speed and rainfall) have been acquired by an automatic weather station located near the orchard (about 7 km far) and managed by SIAS (Servizio Informativo Agrometeorologico Siciliano). The wind data recorded from this station were considered during the tower setting up, with the prevailing wind direction determined to be west (Figure 2).

The Eddy Covariance technique (Swinbank, 1951; Aubinet *et al.*, 2000) was used to directly measure the vertical fluxes of CO_2, H_2O and sensible heat, H, for three consecutive years (from January 2010 to December 2012). A 10 meter mast set up equipped with two 3-dimensional sonic anemometers (Windmaster Pro, Gill Instruments Ltd, at 4m, and a CSAT-3D, Campbell Sci. USA, at 8 m) and an open path gas analyzer (IRGA) (Li7500, LiCor Inc., USA) was positioned in the orchard. The net available energy (R_N, W m^{-2}) at the surface was measured by a four-component net radiometer (CNR1, Kipp&Zonen) deployed at about 8 meters from the ground. Soil heat flux density (G, W m^{-2}) was measured with three soil heat flux plates (HFP01, Campbell Scientific Ltd) placed horizontally 0.05 m below the soil surface. Three different measurements of G were selected: in the trunk row (shaded area), at 1/3 of the distance to the adjacent row, and at 2/3 of the distance to the adjacent row. The soil heat flux was measured as the mean output of three soil heat flux plates. Data from the soil heat flux plates was corrected for heat storage in the soil above the plates.

The raw data was recorded at a frequency of 10 Hz using two synchronized data loggers (CR3000, Campbell Sci.) and data quality was checked during the post processing together with some routines to remove the common errors (Kaimal and Finnigan, 1994).

Unfortunately, during 2011, most data from the gas analyzer were lacking due to necessary maintenance. This loss of CO_2 and H_2O data did not allow to elaborate on carbon and energy balances.

Within the footprint area of the tower, plant transpiration rate was measured by applying the Heat Pulse Velocity (HPV) sap flow technique (Green and Clothier, 1988).

When high frequency micrometeorological fluxes were checked for quality, the percentage of data coverage may have been reduced; thus, procedures of data gap filling were often applied determining the annual and monthly net ecosystem exchange (NEE). In the study, a non linear regression method was applied for filling the gaps (Falge *et al.*, 2001). Missing values of CO_2 flux (F_c, mmol m^{-2} s^{-1}) were calculated using the regression relationship established between F_c and measured air temperature (nighttime) and radiation (daytime) on monthly bases.

For nocturnal respiration fluxes, the Lloyd and Taylor (1994) relation was applied:

$$R_e = b_1 e^{b2\,T_{air}} \quad (1)$$

where, R_e (μmol m^{-2} s^{-1}) is the ecosystem respiration and b_1 and b_2 are the coefficients computed for each month from the experimental data (data not showed). For diurnal fluxes (F_c), the equation of Dagnelie (1991) was adopted:

$$F_c = GPP_{OPT}\left(1 - e^{\frac{aPPFD}{GPP}}\right) - R_{day} \quad (2)$$

where, PPFD is the photosynthetic photon flux density, a is a coefficient, GPP is the gross primary production and R_{day} the diurnal ecosystem respiration.

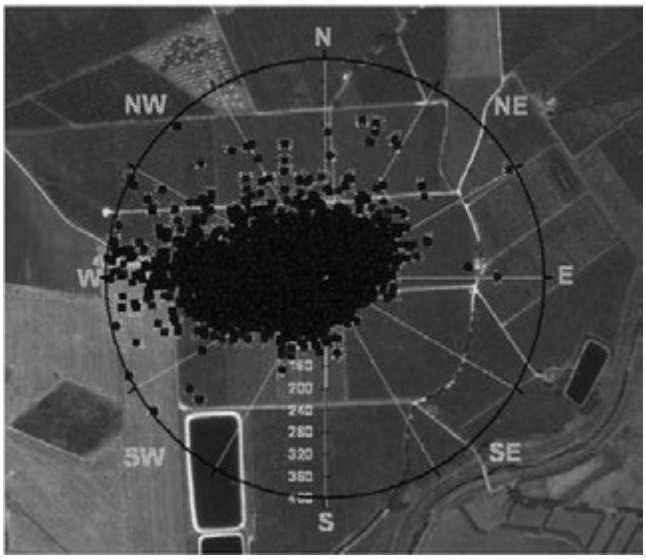

Figure 1. Footprint area (A) where points denote downwind distance where fluxes were mainly captured by the micrometeorological tower; (B) wind rose for a 10° wind sector expressed as a percent of the data over a 5-year period.

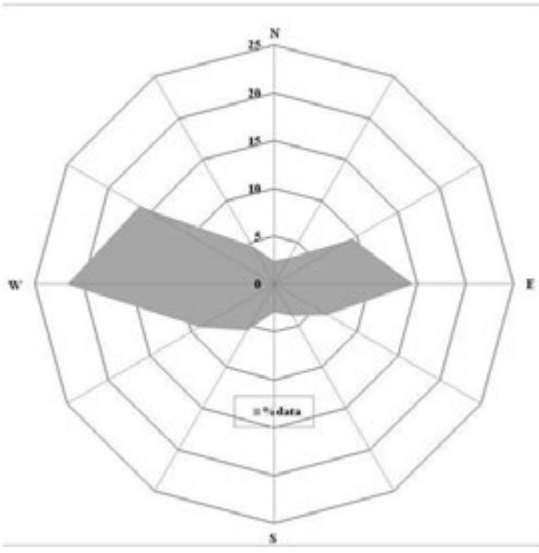

Figure 2. Micrometeorological tower and sap flow sensors location.

Total carbon exchange terms were estimated both at monthly and annual scales. The NEE was computed from the complete series of CO_2 fluxes measured by EC and gap filled using the nonlinear regression method described above. The ecosystem respiration (ER) was estimated according to Falge *et al.* (2001), with the Lloyd and Taylor's equation. In particular, there is negligible photosynthesis at night, so nightime NEE is a measure of ER (Desai *et al.*, 2005).

The gross primary productivity for each 30 min was the difference between NEE and estimated ER.

Additionally, surface energy balance measurements at the experimental site showed that the sum of sensible and latent (LE) heat flux was highly correlated (r^2>0.90) (Figure 3) to the sum of net radiation and soil heat flux. A linear fit between the two quantities showed a certain energy balance un-closure for 2010 and 2012. These percentages of un-closure are in the range reported by most flux sites (Wilson *et al.*, 2002) and provide additional confirmation of the turbulent flux quality (Moncrieff *et al.*, 1996).

Measurements of water consumption at tree level (T_{SF}) were done by using the Heat Pulse Velocity (HPV) technique. For HPV measurements, two 4 cm sap flow probes with 4 embedded thermocouples (Tranzflo NZ Ltd, Palmerston North, NZ) were inserted into the trunks of three trees. The probes were positioned at the North and South sides of the trunk at 50 cm from the ground and wired to a data-logger (CR1000, Campbell Sci.) for heat-pulse control and measurement; the sampling interval was 30 min. Data from the two probes was processed according to Green *et al.* (2003) to integrate sap flow velocity over sapwood area and to calculate transpiration. Therefore, the sapwood fraction of water was determined both on sample trees during the experiment, and directly on the trees with the sap flow probes, at the end of the observation period. Wound-effect correction (Green *et al.*, 2003) was done on a per-tree basis.

Scaling up the sap flow from a single tree to the field scale requires analysing plant size variability, to determine the mean of those monitored. This was obtained by analysing the spatial variability of plant leaf area (Jara *et al.*, 1998). Thus, scaling was done only on the basis of the ratio between orchard leaf area index (LAI) and tree leaf area.

Results and Discussion

Precipitation and temperature regimes were fairly similar during the 3 experimental years, and were typical of a Mediterranean area, with a mean air temperature of about 18.0°C and annual rainfall less than 600 mm. The diurnal flux trend of individual components of the energy balance for the orange orchard showed that the latent heat flux was always in excess of the sensible heat flux during daylight hours and the H was higher than the soil heat flux. At night, the Eddy Covariance results showed H and LE approaching zero (Figure 4).

During typical days of the spring-summer periods (Figures 5 and 6), latent heat (or evapotranspiration) was generally (with the exception of April) the prevalent flux, with a weak midday depression, most likely due to no limit in crop water availability.

The orchard photosynthetic activity (F_c, μmol m^{-2} s^{-1}) showed the typical trend of the evergreen species. Maximum values were observed during May-June and August-September periods; the month of July of the study period was characterized by a reduction in the crop photosynthetic activity, with a shift in the maximum assimilation towards the first daytime hours; this was most likely due to the rise in air temperature, causing stomatal closure.

The net ecosystem exchange was calculated at monthly and annual scales. Figure 7 shows the monthly NEE, ecosystem respiration and gross primary production together with air temperature and cumulative precipitation during 2010 and 2012 periods. The highest NEE values were recorded during the spring-summer period [90-100 g(C) m^{-2} $month^{-1}$]. ER ranged from 40 to 110 g(C) m^{-2} $month^{-1}$, reaching maximum values during the spring and the autumn. The highest values of ecosystem assimilation (GPP) was 180 g(C) m^{-2} $month^{-1}$ in May 2010 and 140 g(C) m^{-2} $month^{-1}$ in the April-June period 2012, the lowest values were in the December-February period of both years.

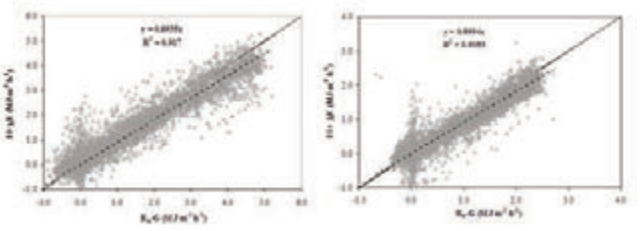

Figure 3. Surface energy balance closure from EC measurements during 2010 and 2012.

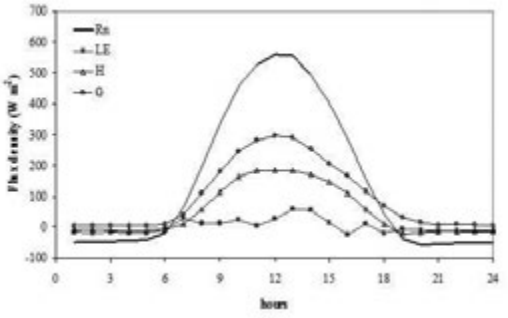

Figure 4. Surface energy balance components during a typical summer day in the experimental period.

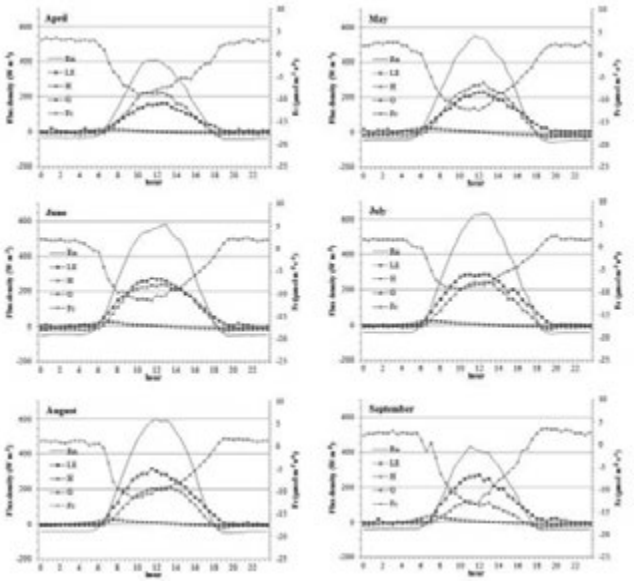

Figure 5. Surface energy balance components and CO_2 fluxes during typical spring-summer days in 2010.

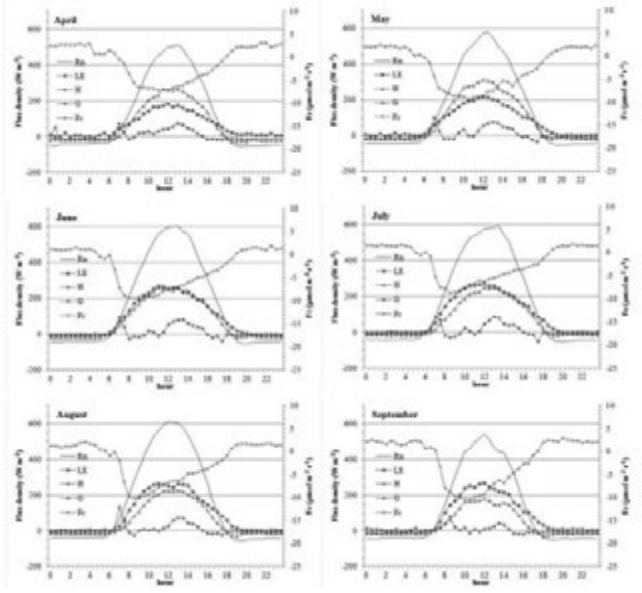

Figure 6. Surface energy balance components and CO_2 fluxes during typical spring-summer days in 2012.

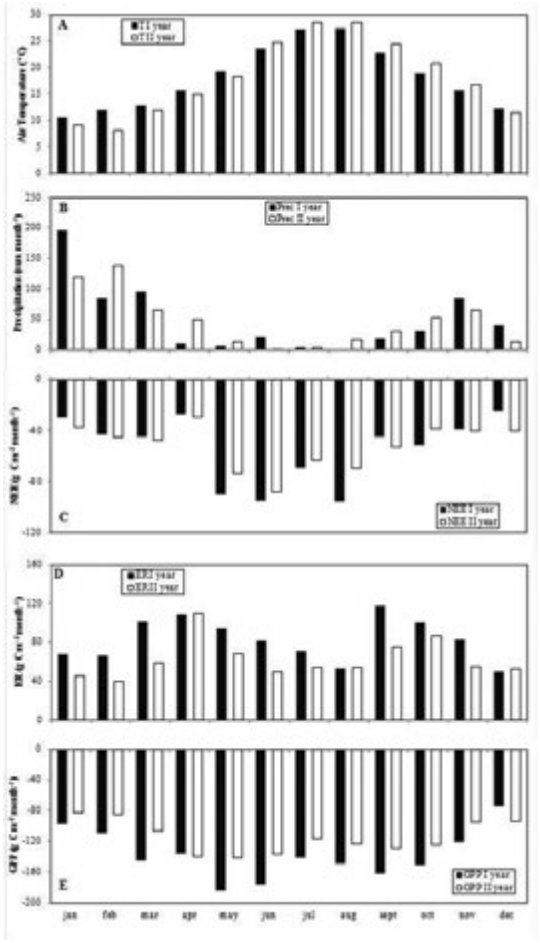

Figure 7. Monthly trends of air temperature (A), cumulative precipitation (B), net ecosystem exchange (C), ecosystem respiration (D) and gross primary production (E) during 2010 and 2012.

The annual carbon uptake of the orange orchard under study was 6.5 t(C) ha^{-1} $year^{-1}$ in 2010 and 6.3 t(C) ha^{-1} $year^{-1}$ in 2012 (Figure 8). Total ER was 9.9 t(C) ha^{-1} $year^{-1}$ in 2010 and 7.5 t(C) ha^{-1} $year^{-1}$ in 2012. Consequently, gross primary production was 16.4 t(C) ha^{-1} $year^{-1}$ in 2010 and 13.7 t(C) ha^{-1} $year^{-1}$ in 2012.

On the whole, the carbon balance during the two years under study was quite similar, indicating similar plant functionality. This corroborates with the same climatic conditions during the examined periods (Figure 7 A and B).

The divergence between sap flow transpiration values and crop evapotranspiration begins at about 09:00 local time. Midday T_{SF} fluxes were almost steady for most of the period while ET_c ones followed the daily trend of atmospheric evapotranspiration demand (Figure 9). Midday differences between T_{SF} and ET_c denote a depletion of plant water content in relation to the imbalance between tree crown water loss by transpiration, as estimated by EC, and water transport from the tree's root mass as estimated by sap flow (SF). This imbalance is recovered in the afternoon and nocturnal hours, with higher T_{SF} than ET_c fluxes. Most of the differences here in water-use dynamics could be interpreted by tree capacitance. The imbalance between canopy transpiration and tree-water uptake is revealed by a large hysteresis (data not shown), with higher afternoon SF values. It is interesting to note that the hysteresis loop appears specularly reflected, with a larger hysteresis in the morning-midday hours (Motisi *et al.*, 2012). During 2012, a decreasing trend was observed on plant T_{SF} values, associated with the inability to recover the daily imbalance between EC estimation of water losses and those estimated by SF. This fact most likely reflects the first symptoms of physiological diseases caused by the CTV virus, that was described to have influenced the crop from the end of 2011 The cumulative values of ET_c and sap flow measurements of transpiration in the May-September periods were about 600 mm and 530 mm, respectively.. The average daily values of ET_c and T_{SF} are 3.9 mm d^{-1} and 3.4 mm d^{-1}, dur-

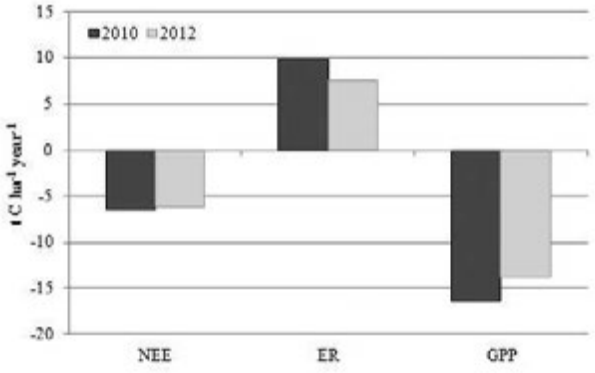

Figure 8. Net ecosystem exchange (NEE), ecosystem respiration (ER) and gross primary production (GPP) in 2010 and 2012.

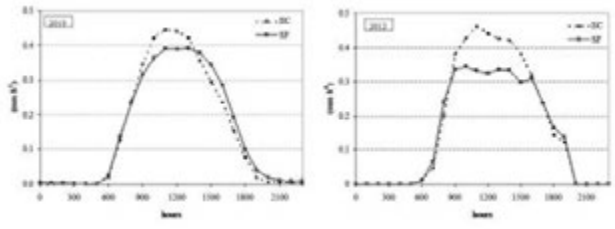

Figure 9. Diurnal changes of up-scaled sap flow (SF) fluxes in orange. Each datapoint represents the average of all the values in the observation period (July-August 2010 and 2012).

ing May-October 2010 and 4.0 mm d^{-1} and 3.5 mm d^{-1} in 2012.

The values of ET_c followed atmospheric demand in both growing seasons, being higher during May-October (from flowering to fruit maturation), with peaks of 6.7 mm d^{-1} and 6.0 mm d^{-1} during 2010 and 2012.

Conclusions

The orange orchard under study has the typical configuration of an intensive system, with about 70% of ground cover by the vegetation. For this system, the net ecosystem exchange and ecosystem respiration were computed from the complete series of the CO_2 fluxes measured by the Eddy Covariance method. The NEE measured for the orchard during the study were 6.5 t(C) ha^{-1} $year^{-1}$ in 2010 and 6.3 t(C) ha^{-1} $year^{-1}$ in 2012, similar to those reported for the same crop by Liguori *et al.* (2009). NEE and ER variations were mainly related to the fluctuation of the meteorological variables at the experimental site. In particular, in the region under study, carbon exchanges were driven by the available radiation and water. However, the scarcity of information on the NEE of fruit tree orchards does not allow a comparative analysis between various species and orchard management practices.

The Eddy Covariance technique allowed to assess water, energy and carbon exchanges from the plant system and it is proved reliable in providing information at the orchard scale and at different temporal scales. Its results are fairly well coupled with transpiration measurements through sap flow.

In conclusion, these preliminary results may allow assessing the sink capacity of an important crop system that is widely present in the Mediterranean agricultural context.

References

Aubinet M; Grelle A; Ibrom A; Rannik Ü; Moncrieff J; Foken T; Kowalski AS; Martin PH; Berbigier P; Bernhofer Ch; Clement R; Elbers J; Granier A; Grünwald T; Morgenstern K; Pilegaard K; Rebmann C; Snijders W; Valentini R; Vesala T. 2000. Estimates of the net annual carbon and water exchange of forests: the EUROFLUX methodology. Adv. Ecol. Res., 30, 113-175.

Baldocchi DD. 2003. Assessing the eddy covariance technique for evaluating carbon dioxide exchange rates of ecosystems: past, present and future. Global Change Biol., 9, 479-492.

Ballester C; Castel J; Intrigliolo DS; Castel JR. 2012. Response of Navel Lane Late citrus trees to regulated deficit irrigation: yield components and fruit composition. Irrigation Science, 31, 333-341.

Barr AG; Morgenstern K; Black TA; McCaughey JH; Nesic Z. 2006. Surface energy balance closure by the eddy-covariance method above three boreal forest stands and implications for the measurement of the CO_2 flux. Agric. Forest Meteorol., 140, 322-337.

Capra A; Consoli S; Scicolone B. 2011. Economic analysis of citrus orchards under deficit irrigation in South Italy. ISHS Acta Horticulturae 922. XXVIII International Horticultural Congress on Horticulture for People (IHC2010).

Cohen M; Girona J; Valancogne C; Ameglio T; Cruizat P; Archer P. 1993. Water consumption and optimisation of the irrigation in orchards. Irrig. Sci., 12(2), 93-98.

Consoli S; O'Connell NV; Snyder RL. 2006. Estimation of evapotranspiration of different orange sized orchard canopies using energy balance. J. Irr. Drain. Eng. ASCE, 32(1), 2-8.

Consoli S; Papa R. 2012. Corrected surface energy balance to measure and model the evapotranspiration of irrigated orange orchards in semi-arid Mediterranean conditions. Irrig. Sci., ISSN 0342-7188, DOI 10.1007/s00271-012-0395-4.

Dagnelie P. 1991. Theorie et methodes statistiques. Presses Agronomiques de Gembloux, Vol.1.

Desai AR; Bolstad PV; Cook BD; Davis KJ; Carey EV. 2005. Comparing net ecosystem exchange of carbon dioxide between an old-growth and mature forest in the upper Midwest, USA. Agri. For. Meteorol. 128, 33-55.

Falge E; Baldocchi DD; Olson RJ; Anthoni P; Aubinet M; Bernhofer C; Burba G; Ceulemans R; Clement R; Dolman H; Granier A; Gross P; Grünwald T; Hollinger D; Jensen NO; Katul G; Keronen P; Kowalski AS; Ta Lai C; Law BE; Meyers T; Moncrieff J; Moors E; Munger JW; Pilegaard K; Rannik Ü; Rebmann C; Suyker A; Tenhunen J; Tu K; Verma S; Vesala T; Wilson K; Wofsy S. 2001. Gap filling strategies for defensible annual sums of net ecosystem exchange. Agric. Forest Meteorol., 107, 43-69.

Green SR; Clothier B. 1988. Water use of kiwifruit vines and apple trees by the heat-pulse technique. J. Exp. Bot., 39, 115-123.

Green SR; Clothier B; Jardine B. 2003. Theory and Practical Application of Heat Pulse to Measure Sap Flow. Agron. J., 95, 1371-1379.

Hamdy A. 1999. Water resources in the Mediterranean region: from ideas to action. In: Background documentation for thematic session. Consultation of experts from MENA region on: World Water Vision-Water for Food and Rural Development. CIHEAM-IAMB, Valenzano, 27-29 May, pp. 1-23.

Jara J; Stockle CO; Kjelgaard J. 1998. Measurement of evapotranspiration and its components in a corn (Zea mays L.) field. Agric. Forest Meteorol., 92, 131-145.

Kaimal JC; Finnigan JJ. 1994. Atmospheric boundary layer flows. Oxford Univ. Press, pp. 289.

Liguori G; Gugliuzza G; Inglese P. 2009. Evaluating carbon fluxes in orange orchards in relation to planting density. J. Agr. Sci., 147, 637-645.

Liu H; Randerson JT; Lindfors J; Massman W; Foken T. 2006. Consequences of incomplete surface energy balance closure for CO2 fluxes from open-path CO2/H2O infrared gas analyzers. Bound.-Layer Meteorol., 120, 65-85.

Lloyd J; Taylor J.A. 1994. On the temperature dependence of soil respiration. Funct. Ecol., 8, 315-323.

Mahrt L. 1998. Flux sampling errors for aircraft and towers. J. Atmos. Oceanic Technol., 15, 416-429.

Moncrieff JB; Malhi Y; Leuning R. The propagation of errors in long-term measurements of land-atmosphere fluxes of carbon and water. 1996. Global Change Biol., 2, 231-240.

Motisi A; Consoli S; Rossi F; Minacapilli M; Cammalleri C; Papa R; Rallo G; D'Urso G. 2012. Eddy covariance and sap flow measurements of energy and mass exchange of woody crops in a Mediterranean environment. In: 8th international workshop on sap flow, Volterra, May 8-12.

Nardino M; Pernice F; Rossi F; Georgiadis T; Facini O; Motisi A; Drago A. 2013. Annual and monthly carbon balance in an intensively managed Mediterranean olive orchard. Photosynthetica, 51(1), 63-74.

Pernice F; Motisi A; Rossi F; Georgiadis T; Nardino M; Fontana G; Dimino G; Drago A. 2009. Micrometeorological and sap flow measurements of water vapour exchanges in olive: scaling up from canopy to orchard. Acta Hort., 846, 159-166.

Rana G; Katerji N; de Lorenzi F. 2005. Measurement and modelling of evapotranspiration of irrigated citrus orchard under Mediterranean conditions. Agric. Forest Meteorol., 128, 199-209.

Swinbank, WC. 1951. The measurement of vertical transfer of heat and water vapour by eddies in the lower atmosphere. J. Meteorol., 8, 135-145.

Twine TE; Kustas WP; Norman JM; Cook DR; Houser PR; Meyers TP; Prueger JH; Starks PJ; Wesely ML. 2000. Correcting eddy-covariance flux underestimates over a grassland. Agric. Forest Meteorol., 103, 279-300.

Wilson K; Goldstein A; Falge E; *et al.* 2002. Energy balance closure at fluxnet sites. Agric. Forest Meteorol., 113, 223-243.

Runoff and sediment yield modeling in a medium-size mediterranean watershed

Ossama. M.M. Abdelwahab, Tiziana Bisantino, Fabio Milillo, Francesco Gentile

Department of Agro – Environmental and Territorial Science (DISAAT), University of Bari, Italy

Abstract

The AnnAGNPS model was used to estimate runoff, peak discharge and sediment yield at the event scale in the Carapelle watershed, a Mediterranean medium-size watershed (506 km^2) located in Apulia, Southern Italy. The model was calibrated and validated using five years of runoff and sediment yield data measured at a monitoring station located at Ordona – Ponte dei Sauri Bridge. A total of 36 events was used to estimate the output of the model during the period 2007-2011, in comparison to the corresponding observations at the watershed outlet. The model performed well in predicting runoff, as was testified by the high values of the coefficients of efficiency and determination during the validation process. The peak flows predictions were satisfactory especially for the high flow events; the prediction capability of sediment yield was good, even if a slight over-estimation was observed. Finally, the model was used to evaluate the effectiveness of different Management practices (MPs) on the watershed (converting wheat to forest, using vegetated streams, crop rotation corn/soybean, no tillage). While the maximum reduction in sediment yield was achieved converting wheat to forest, the best compromises between soil conservation and agriculture resulted to be crop rotations.

Correspondence: Ossama. M.M. Abdelwahab,
Department of Agro – Environmental and Territorial Science (DISAAT),
University of Bari, via Amendola 165/A 70126 Bari (Italy).
Tel. +39.080.5442211 - Fax: +39.80.5443061.
E-mail: el.khwaga_eng@yahoo.com

Key words: watershed modeling, AnnAGNPS, suspended sediment transport, Best Management practices, crop rotation.

Acknowledgements: the present work was financially supported by the Italian Ministry of Education, Universities and Research (MIUR), Project "National network for monitoring, modelling and sustainable management of erosion processes in agricultural land and hilly-mountainous area", in the framework of the PRIN 2010-2011.

Journal of Agricultural Engineering 2013; XLIV(s2):e7
doi:10.4081/jae.2013.(s1):e7

Introduction

Soil erosion can lead to reduction of soil fertility, loss of nutrients, and declines of crop yields in farmlands. In a review of mechanized agricultural systems in which wheat, corn, soybean and barley were planted, Bakker *et al.* (2004, 2005) found that on average, soil erosion reduced crop productivity by about 4% for each 10 cm of soil lost. In recent years, it is widely recognized that more site-specific approaches are needed to assess variations in erosion susceptibility in order to select the most suitable land management method (Pandey *et al.*, 2008). Structural and non structural measures to control negative impacts of runoff and erosion processes can be properly addressed through reliable prediction models. Although there has been considerable effort, additional work is needed to assess and improve the reliability of available prediction models in different environmental contexts. Reliable prediction models can help to select the most practical and effective tools in reducing erosion problems and developing appropriate land use planning (Licciardello *et al.,* 2007).

Continuous distributed simulation models (as AnnAGNPS, WEPP, SWAT) provide great advantages as they allow watersheds response to be studied over a longer time period and can help to select the most practical and effective tools in reducing erosion problems (Zema *et al.*, 2010).

AnnAGNPS has been implemented to assess runoff and water quality as well as sediment yield in small to large watersheds under different environmental conditions. Assessments of model performance, frequently coupled with calibration/validation trials in monitored watersheds ranging from 32 ha to 2500 km^2, have recently been published (Licciardello *et al.*, 2007; Yuan *et al.*, 2008; Parajuli *et al.*, 2009; Zema *et al.*, 2010)

Few studies have been conducted using AnnAGNPS at the watershed scale in semi-arid environments. Here the quantification of sediment transport is quite difficult due to the high variability of rainfalls and water flows. The semi-arid areas receive low annual rainfall, have nutrient-poor soils, short-grass or shrublands vegetation and the actual evapotranspiration is recognised as the main hydrologic loss (50-60 % of the mean annual rainfall). In particular, after long-lasting periods with no rains and high temperatures, the soil can be very dry at the time of the storm. On the contrary in humid and hyper-humid climates, because of the high number of rainy days, the rainfall responsible for the flood peak is likely to occur when the infiltration rate into the soil is close to the gravitational capacity (Fiorentino and Iacobellis, 2001).

With particular reference to the Mediterranean environment, tests of the single-event model AGNPS were carried out in Italy, where hydrological effects of different land uses in an alpine environment (Cazorzi and Dalla Fontana, 1996; Cazorzi, 1996; Lenzi and Di Luzio, 1997) as well as soil erosion in southern small watersheds characterized by ephemeral streams (Morgagni *et al.*, 1993; Licciardello and Zimbone, 2002) were successfully predicted.

In order to estimate erosion and sediment transport processes in semi-arid environments the AnnAGNPS - Annualized Agricultural Non-

point Source model was selected and applied in the Carapelle watershed (Southern Italy). The model structure is suitable as it contains both empirical and quasi-physically based algorithms, it is fully distributed with land surface runoff and sediment processes modelled for the individual grid cell, and the output is routed to the catchment outlet. The data requirements and computational complexity of the AnnAGNPS allow the model to be used as a tool for watershed management planning. (Bisantino *et al*, 2013).

The AnnAGNPS model was developed to analyze and provide estimates of runoff with primary emphasis upon sediment and nutrients transport from agricultural watersheds, and to compare the effects of various conservation alternatives. Simulations under various combinations of different scenarios of land and water management can provide comparative analysis of different options and prove to be very useful as a guide to what Best Management Practices (BMPs) can be adopted to minimize pollution from point and nonpoint sources (Shrestha *et al.*, 2006).Best Management Practices (BMPs) are structural and nonstructural approaches used to reduce pollutant loads in watersheds draining both urban and rural areas. The Soil and Water Conservation Society (SWCS) defines a BMP as "a practice or combination of practices that are determined by a state or designated area-wide planning agency to be the most effective and practicable (including technological, economic, and institutional considerations) means of controlling point and nonpoint source pollutants at levels compatible with environmental quality goals" (Barry *et al.*, 2001).

Vegetation plays a critical role in flow resistance, particularly in relation to relaxation times and thresholds for flood erosion effects. Because of the resistance of vegetation-mantled banks and flood plains, there may be progressive, long-term encroachment of vegetation into the channel, especially on small streams. This vegetation increases roughness so reduces flow conveyance (Wolman and Gerson, 1978). The vegetation could retain from 30 to 70 percent of the deposited sediments. The ability of vegetation to entrap and retain sediment is related to the length and cross-sectional area of the vegetation (Thornton *et al.*, 1997). Early research on the hydrologic impacts of vegetation management practices began in the 1910s, was expanded into the 1930s and 1940s, and continuing in the 1980s to further evaluate the effects of vegetation manipulations on the basin's water resources and other multiple uses (Zou *et al.*, 2010). The impact of vegetation on the system is overwhelming. Vegetation produces an erosion-resistant peat layer, stabilizes channel banks and slows down the water flow. Vegetation also stimulates aggradation of bed load material on the channel bottom, and contributes to avulsion by blocking the channels. The channel network owes its origin to repeated though infrequent avulsion (Gradzinski *et al.*, 2003).

Another important management practice is the no-till farming. No-till farming, due to an associated increase in surface residue and reduction in surface runoff, has been recommended as a best management practice to reduce soil erosion. Surface residues affect erosion by decreasing the soil surface area susceptible to raindrop impact, reducing the velocity of runoff and hence its transport capacity, and by creating mini-ponds that result in deposition behind clumps of residue (Fu *et al.*, 2006).

Another conservation practice is the crop rotation (often called conservation crop rotation), that is defined as the use of different crops in a specified sequence on the same farm field. There are several reasons for using crop rotations; although the primary one is to reduce soil erosion, thereby reducing the quantities of sediment and sediment-bound pollutants such as nitrogen, phosphorus and pesticides. (Barry *et al.*, 2001).

The objective of this paper is to evaluate the AnnAGNPS model prediction capability for runoff and sediment yield using a five years data base in a middle sized Mediterranean watershed located in Southern Italy. A continuous simulation process of runoff and sediment yield has been carried out comparing the simulation outputs to the corresponding observed data measured during the period 2007-2011. A calibration process for the model parameters that have a large impact on the prediction capacity of the model has been performed at the event scale utilizing the events recorded in the period 2007-2008, then a validation process to evaluate the model performance using the events recorded in the period 2009-2011. Finally, after validation, the model has been used to evaluate the effectiveness of alternative MPs on sediment yield at the watershed scale.

Materials and methods

AnnAGNPS Model Description

The Annualized Agricultural Nonpoint Source Pollution model (Theurer and Cronshey, 1998; Bingner and Theurer, 2005; USDA-ARS, 2006) was developed by the USDA Agricultural Research Service (ARS) and Natural Resources Conservation Service (NRCS) to predict sediment and chemical delivery from un-gauged agricultural watersheds up to 300,000 ha (Bosch *et al.*, 2001). AnnAGNPS is a continuous simulation, grid-based, batch-process computer program where runoff, sediment, nutrients and pesticides are routed from their origins in upland grid cells through a channel network to the outlet of the watershed (Binger and Theurer, 2005). The climatic data requirements for simulations include daily maximum and minimum temperature, precipitation, average daily dew point temperature and wind speed, and sky cover (Bingner and Theurer, 2005). The ArcView interface for AnnAGNPS incorporates the Generation of weather Elements for Multiple applications (GEM) climate generation model (USDA-ARS, 2005) which generates daily precipitation, maximum and minimum temperature, and solar radiation. AnnAGNPS users also have the option to input measured climate data by uploading the data into the input editor.

AnnAGNPS hydrology is based on a simple bookkeeping of inputs and outputs of water during the daily time steps (Bingner and Theurer, 2005). The hydrologic processes simulated in the model include interception, evaporation, surface runoff, and evapotranspiration, subsurface lateral flow and subsurface drainage (Yuan *et al.*, 2006). In AnnAGNPS, runoff is predicted using the SCS curve number technique (USDA-SCS, 1986), and sheet and rill erosion are predicted with the Revised Universal Soil Loss Equation (RUSLE, Renard *et al.*, 1997). Soil moisture balance is calculated on a sub-daily time step using a simple constant-time step procedure for both the tillage and below tillage composite soil layers (Bingner and Theurer, 2005). Sediment transport in channels is computed using a modified Einstein equation, and the Bagnold (1966) equation is used to estimate sediment transport capacity of the flow (Bingner and Theurer, 2005). AnnAGNPS utilizes the HUSLE (Hydro-geomorphic Universal Soil Loss Equation) model (Theurer and Clarke, 1991) to determine sediment delivery ratios of total sediment to the stream network.

Study area

The Carapelle watershed is located in Puglia region (Southern Italy). It originates from the flyschoid formations of the Daunia Mountains and crosses the Tavoliere floodplain before flowing into the Adriatic sea (Figure 1; Table 1). Soils predominantly belong to the class of Entisols and have a fine clayey-loamy texture, are low in organic matter content, natural fertility and water-holding capacity. The plain and the low hilly areas (80% of the watershed surface) are mainly used for cereal cultivation and olive orchards, whereas in the higher slopes deciduous oaks

and hardwoods (*Quercus pubescens* and *Quercus cerris*) and pasture conditions are present. The climate is typically Mediterranean, with rainfalls ranging from 450 to 800 mm/year and average temperatures from 10 to 16°C. The flow regime is torrential and flood events are mainly associated with intensive, short-term rainfalls. Suspended sediment, even during floods, is mainly characterized by fine particles.

Monitoring stream flow and suspended sediment

Continuous stream flow and sediment load data derived from the monitoring station located in the Carapelle torrent at Ordona-Castelluccio dei Sauri Bridge (Figure 2). The station is equipped with an ultrasound water stage meter and a water stage recorder, with remote data transmission. Runoff is determined by converting the record of water levels into a record of flows using the experimental water discharge rating curve given by the National Hydrografic Service, that is responsible for the runoff measurements. An infrared optic probe (Hach-Lange SOLITAX Hs-line) is used to monitor suspended sediments. The probe measures suspended sediments by coupling backscattering and nephelometric photodetectors (Gentile *et al.*, 2010). The instrument is contained in a shelter tube through a pulley, a float and a counterweight group that is anchored to a bridge pier to protect the instrument from the impact of coarse material in the flow and to prevent any potential measuring errors caused by incident radiant energy straying into the infrared field. The instrument is controlled through a data acquisition system that is powered by solar panels and is able to measure high solid concentrations with the capability to reduce watery medium and light interferences.

Gentile *et al.* (2010) tested the probe in the laboratory in order to evaluate the functional capacity of the instrument and to assess the effects of the different grain size and solid fractions on measurements. The instrument was field calibrated during the flood events of 2007-2009 to evaluate the efficacy of the housing system, to identify a calibration curve of the instrument for the specific torrent and to assess the type of the relationship between the SSC measured by the instrument and the gravimetric SSC. The SSC of all samples was measured using the gravimetric method and compared with the data observed by the optical sensor.

Thirty-six events observed during 2007-2011 were used for the application of the AnnAGNPS model, this does not include all runoff and sediment yields that occurred in the watershed, some storm events were not sampled due to equipment malfunctions or temporary lack of power to the sensor, caused by the solar panels. In general, the small number of flood events during the rainy season is another characteristic of Mediterranean watersheds.

Considering that AnnAGNPS do not consider base flow, the surface runoff separation from baseflow was performed (Figure 3) using the filtering algorithm developed by Eckhardt (2005). Baseflow separation is required in numerous widely used hydrological and erosive models and must be considered in monthly models (Mouelhi *et al.*, 2006). The filtering algorithm has the following equation:

$$b_k = \frac{(1-BFI_{max})ab_{k-1} + (1-a)BFI_{max}Q_t}{1-aBFI_{max}} \quad (1)$$

where b_k is the base flow at time stamp k; b_{k-1} is the base flow at the previous time step; Q_t is the measured total flow; BFI_{max} is a constant that can be interpreted as the maximum value of long term ratio of base flow to total stream flow; a is the recession constant. The filter parameter "a" and BFI_{max} were calculated using the hydrograph recession curve analysis and the optimization module developed by Kyoung *et al.* (2010).

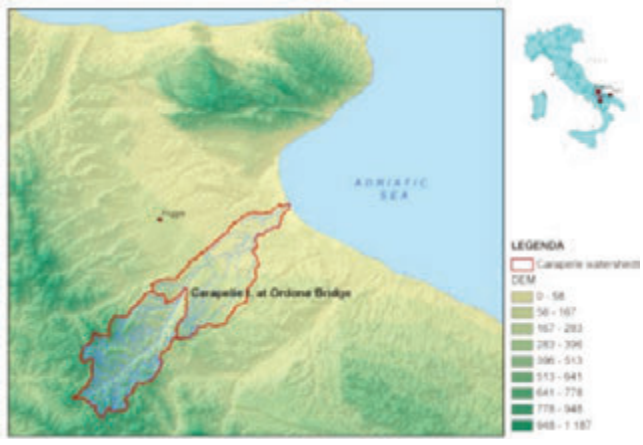

Figure 1. Carapelle watershed in Southern Italy.

Figure 2. Continuous stream flow and sediment load data monitoring station.

Table 1 Main characteristics of the Carapelle watershed, mouth at Ordona bridge.

Watershed area	km2	506.2
Maximum altitude	m a.s.l	1075.0
Average altitude	m a.s.l.	466.0
Minimum altitude	m a.s.l	120.0
Main channel length	km	52.2
Main channel slope	%	1.8
Mean watershed slope	%	8.2
Time of Concentration	hour	10

Input Data Preparation

Topography

The topographic features were defined using the Digital elevation map (90m) of the Carapelle watershed provided by the SRTM (Shuttle Radar Topographic Mission) project carried out by the NASA (National Aeronautics and Space Administration) and the NGA (National Geospatial-Intelligence Agency).

The watershed discretization into homogeneous drainage areas ("cells") and the hydrographic network segmentation into channels ("reaches") was performed using the GIS interface incorporated into AnnAGNPS. The geometry and the density of the drainage network were modeled by setting the critical source area to 50 ha and the minimum source channel length to 250 m, resulting in 1006 cells and 416 reaches, which allowed a suitable representation of the watershed.

Land Use and Field Management

Land use data are based on the 1:100 000 CORINE Land Cover data set (CLC2000). The accuracy of the data set has been validated in other studies by comparing images with ground based photography and field surveys (EEA, 2006). Based on the CLC2000 dataset, land uses were grouped in six main classes: cropland (winter wheat and olive-groves), rangeland, forest, urban, fallow and pasture. Figure 4 reports the surface area covered by each land use. The CORINE data set only distinguishes between arable land and agricultural or non-agricultural land use types, therefore information on crop growth and cropping methods were needed. In particular the crop data and management information required by the model include the units harvested, surface and subsurface decomposition, crop residue, root mass, canopy cover, management scheduling and agricultural operations.

The winter wheat crop parameters were based on RUSLE guidelines and internal databases (Renard *et al.*, 1997) while four management practices were assigned to represent the local conditions of the watershed (Table 2).

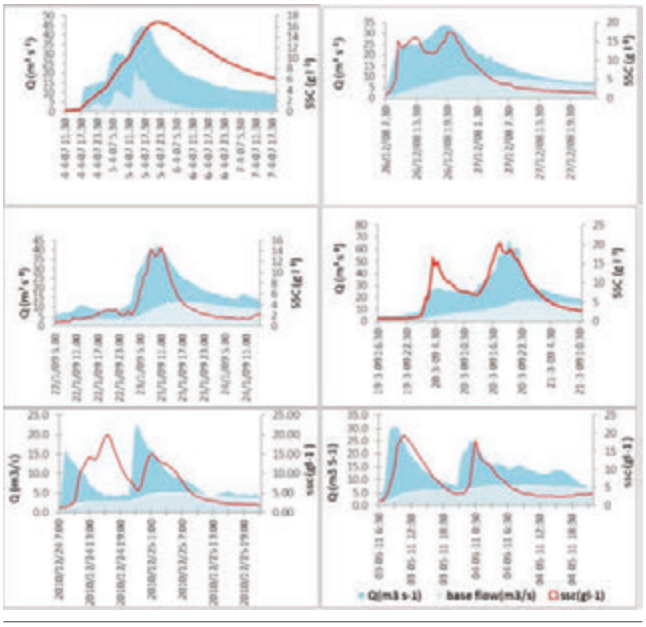

Figure 3. Measured stream flow, suspended sediments and calculated baseflow for some flow events registered during the period 2007-2011

Planting operations occurred in September and harvesting operations occurred in June. After harvest, the land is prepared with other management practices (tillage, semi-deep drill). The tillage effects are linked to the management of crop residues, control of competing vegetation, incorporation of amendments, preparation of the seedbed and, in semi-arid zones, moisture conservation.

A new database was created for the olive grove crops describing: the root density, the estimated aerial coverage of the crop canopy and the average rainfall drop height, which were assumed to remain constant respectively at 30000 kg ha-1, 50 % and 1 m (Galvagni *et al.*, 2006). Tillage operations and organic fertilizers applications were scheduled (Table 2) as they are required to aerate soil, improve water storage,

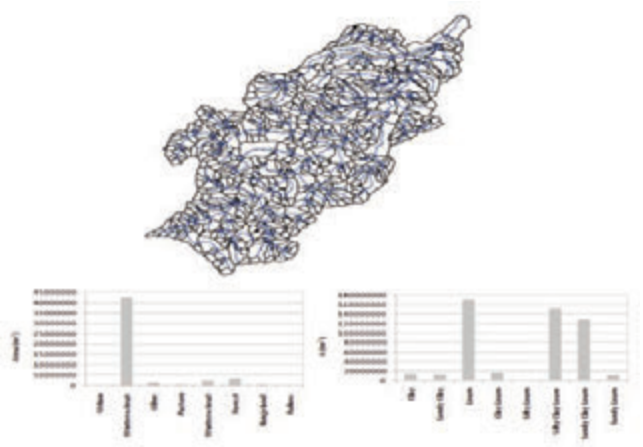

Figure 4. Layout of the discretized watershed with the surface area covered by each land use and soil texture class.

Table 2. Management scheduling for cropland.

Winter wheat		Olive grove	
Event date	Management scheduling	Event date	Management scheduling
06/01	Harvest grain	01/01	Organic fertilizer application
09/01	Tillage	04/01	Tillage operation
09/20	Begin crop growth	06/01	Shallow tillage operation
12/15	Semi-deep drill	08/01	Shallow tillage operation
11/01	Harvest	12/01	Organic fertilizer application

Table 3. Soil properties for each textural class.

Soil structure	K factor (t h MJ^{-1} mm^{-1})	Wp (%)	Fc (%)	ks (mm h^{-1})
Clay	0.035	0.3	0.42	4.5
Sandy clay	0.034	0.26	0.37	14.89
Loam	0.043	0.11	0.24	12.7
Clay Loam	0.03	0.2	0.34	2.02
Silty clay	0.035	0.27	0.42	1.49
Silty-loam	0.044	0.1	0.27	9.88
Silty-clay-loam	0.043	0.18	0.37	4.59
Sandy-clay-loam	0.033	0.17	0.26	4.83
Sandy-loam	0.006	0.2	0.1	32.92

remove weeds and avoid soil compaction.

Single non-cropland databases were assigned to rangeland, forest, urban, fallow and pasture field types. The root system parameters of the forest field type were derived from literature (Galvagni *et al.*, 2006).

The crop management factor C for each period was calculated by the model based on land use, canopy cover, surface cover, surface roughness and soil moisture conditions. The P factor used was set to 1 since no significant management operations were implemented to reduce soil erosion.

Soil properties

Soil parameters such as the textural classes, saturated hydraulic conductivity and soil depths were extracted from the project ACLA2 (scale 1:100 000), a research program funded by the Puglia Region aimed at agro-ecological characterization of the region on the basis of laboratory tests, field observations and photo interpretation of aerial photographs and satellite images (Caliandro *et al.*, 2005). The soil depth is considered as the portion of soil that allows the development of functional and organic roots, where the term "functional" refers to soil moisture dynamics while "organic" considers the interactions involved in the organic matter production (Caliandro *et al.*, 2005). On the basis of the USDA triangle the mean percentages by weight of sand, clay and silt, were assigned to each textural class. The percentage of organic matter was derived from the project Octop of the European Soil Data Centre (ESDAC, 2003).

In the Carapelle watershed soils have weak or no diagnostic subsurface layers and are generally well drained. Hydraulic conductivity decreases as soil pore diameters decreases: in the root zone (h<110 cm) saturated hydraulic conductivity can be assumed to have high values (k_{sat}>3.6 cm/h), but the drainage can be restricted below the root zone (k_{sat}<0.036 cm/h).). For this reason the permeability of the soil layer used to simulate subsurface flows and to account for the groundwater processes was referred to the less permeable layer at 150 cm. The average soil hydraulic properties, water content at wilting point Wp, field capacity Fc and saturated hydraulic conductivity ks, were calculated for each soil type (Table 3) using the Saxton and Rawls (2006) pedotransfer functions.

The RUSLE soil erodibility factor "K", was estimated using the Lal and Elliot (1994) equation. Nine types of soils were identified and the average erodibility factors were calculated (Table 3). Based on each land use (cropland, fallow, rangeland, forest, pasture, urban) and Hydrologic Soil Group (A, B, C, D) the initial Curve Numbers were defined (Table 4).

Climate

Meteorological data such as daily maximum temperature, daily minimum temperature, daily precipitation, daily sky cover, daily wind speed and daily dew point temperature were used as the input climate data for the simulations. The spatial distribution of climatic data were assessed using the Thiessen weighting procedure related to the eight rain gauges located in the watershed or in the surrounding area.

The rainfall erosivity factor R was estimated by (Bisantino *et al.*, 2013) considering the mean monthly precipitation of the period 1979-1999, according to Ferro *et al.* (1999), resulting in 960.70 MJ mm ha^{-1}year^{-1}.

Model calibration and validation

Both the hydrological and erosion components of AnnAGNPS were calibrated/validated in a logical order taking into account a previous sensitivity analysis performed by Bisantino *et al* (2013) for the most meaningful parameters of the model (R, K, C and P factors of USLE equation, CN curve number and MN Manning's roughness coefficient). The parameter calibration order used was first surface runoff, then peak flow and finally sediment load. Input parameters affecting surface runoff and peak flow were first calibrated because of their influence on the other output.

The calibration/validation process of runoff was carried out by modifying the initial values of CN, which represent a key factor in obtaining accurate prediction of runoff and sediment yield (Yuan *et al.*, 2001; Shrestha *et al.*, 2006) and the most important input parameter to which the runoff is sensitive (Yuan *et al.*, 2001; Baginska *et al.*, 2003).

For the calibration of peak flows and sediment yields, both 24 h rainfall distributions (types I and Ia) typical of a Pacific maritime climate with wet winters and dry summers outlined by the Natural Resource Conservation Service (NRCS) and described by SCS (1972) were considered. Based on the analysis of observed rainfall events at different rain gauges performed by Bisantino *et al* (2013) it was found that both storm types well represent the meteorological conditions of Mediterranean zones. The storm type "I" was found to give better predictions of peak discharge so it was set during simulations.

The sediment yields were evaluated at the event scale by adjusting the Manning's roughness coefficient (whichaffects the RUSLE C factor).

The observed flood events have runoff volumes ranging from 0.2 to 8.6 mm (94593 to 4336938 m^3), peak discharges between 1.6 and 73.6

Table 4. Initial curve number values.

Cover type	Initial curve numbers for hydrologic soil groups			
	A	B	C	D
Cropland	72	81	88	91
Fallow	76	85	90	93
Rangeland	35	56	70	77
Forest	43	65	76	82
Pasture	49	69	79	84
Urban	89	92	94	95

Table 5. Coefficients and difference measures for model evaluation and their range of variability.

Coefficient	Equation	Range of variability
Coefficient of efficiency (Nash and Sutcliffe, 1970)		-∞ to 1
Willmott index 1982		0 to 1
Coefficient of determination R^2		0 to 1
Coefficient of residual mass (Loague and Green, 1991)		-∞ to ∞
Root mean square error		0 to ∞

m^3/s and sediment loads between 202 to 103216 t (0.4 to 204 g m^{-2}).The years considered (2007-2011) had precipitation rates ranging from 544.0 mm in 2007 to 873 mm in 2010 .

Model Performance Assessment

The model performance was evaluated at the event scale by qualitative and quantitative approaches. The qualitative approach consisted of visually comparing observed and simulated values. For a quantitative evaluation, a range of both summary and difference measures were used. The summary measures utilized were the mean and standard deviation of both observed and simulated values. For difference measures five evaluation criteria were used to evaluate the model performance: the coefficient of determination (R^2), the Nash-Sutcliffe coefficient of efficiency (NSE), the Willmott index of agreement (W), the coefficient of residual mass (CRM), and the root mean square error (RMSE). The coefficient of determination, R^2, describes the proportion of the total variance in the observed data that can be explained by the model, R^2 is an insufficient and often misleading evaluation criterion as large values of R^2 can be obtained even when the model-simulated values differ considerably in magnitude; the Nash and Sutcliffe (1970) coefficient of efficiency (NSE) was also used to assess the model efficiency (Table 5). In particular, some authors discussed that NSE is more sensitive to extreme values (Legates and McCabe, 1999; Krause *et al.*, 2005). Willmott (1982) sought to overcome the insensitivity of correlation-based measures to differences in the observed and model-simulated means and variances by developing the index of agreement. The Coefficient of Residual Mass (CRM) was used to indicate a prevalent model over- or underestimation of the observed values (Loague and Green, 1991). The values considered optimal for these criteria were one for "R^2", "NSE" and "W" and zero for "CRM". According to common practice, simulation results are considered good for values of NSE greater than or equal to 0.75, satisfactory for values of NSE between 0.75 and 0.36, and unsatisfactory for values below 0.36 (Van Liew and Garbrecht, 2003). Finally, the RMSE describes the difference between the observed and simulated values in the unit of the variable, and it ranges from 0 to ¥, where zero indicates that there is no difference between model simulations and field observations.To quantify the model accuracy in simulating runoff, peak discharge and sediment load, AnnAGNPS was applied to simulate the entire period 2007-2009. The output efficiency was evaluated as relative error (RE).The RE is the ratio of the total difference between simulated and observed values versus the total observed value. It ranges from minus one to ∞ while zero indicates that there is no difference between model simulation and field observation. The smaller the absolute value of a RE, the better performance of the model is:

$$RE = \frac{|P-O|}{O} \quad (2)$$

where P is the predicted value and O is the observed value. The relative error was used to solve the problems of significance and units, as it is the ratio between the absolute error and the absolute value of the correct value.

Management Practices

The management practices have an important role when applied as a plan of soil and water conservation. The aim of the simulation was to understand the entity of the sediment yield reduction at a watershed scale in a Mediterranean environment when applying agricultural or environmental measures of soil erosion control; for this reason these measures were applied at a very large scale in the watershed. The different scenarios that have been considered are representative of situations that it is difficult to find in real cases; nevertheless, they could be

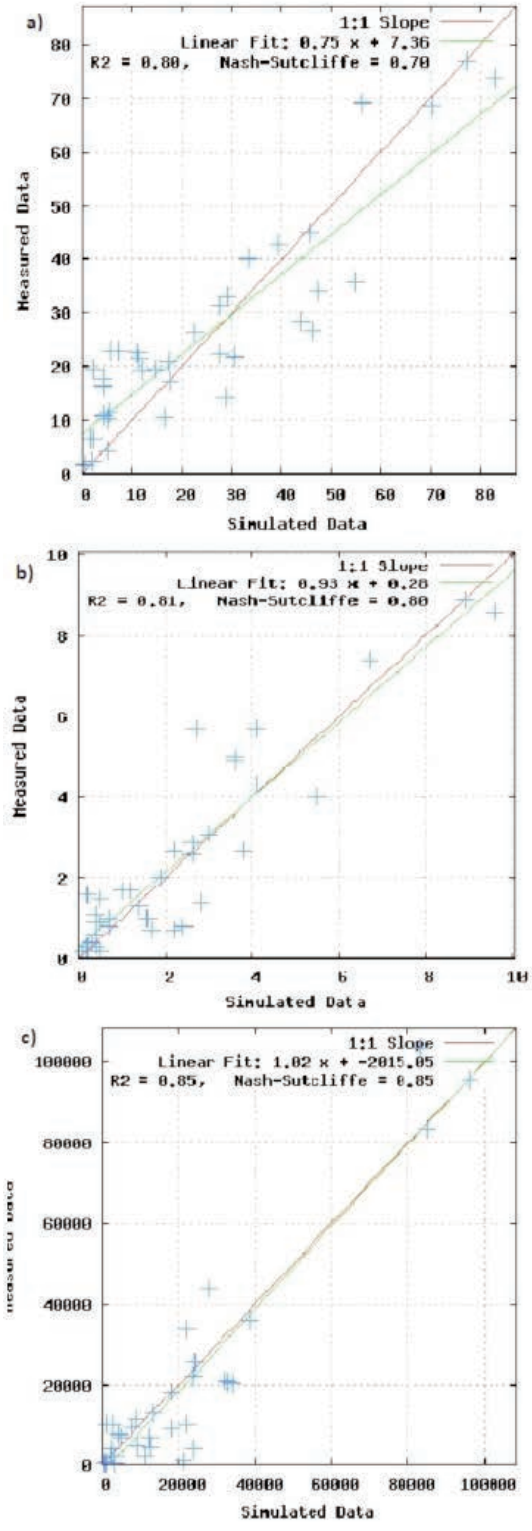

Figure 5. Comparison of 36 observed and simulated events: (a) peak flow, (b) runoff and (c) sediment yield in the Carapelle watershed

a good starting point to design a combination of agricultural and environmental measures that can have a good impact on the reduction of sediment yield in the watershed. Such a process, that should be carefully carried out to take into account the real conditions of the watershed in terms of physical, environmental, agricultural and socio-economic features, could drive to the definition of the so called Best management practices.

To evaluate the effectiveness of Management Practices (MPs) on sediment yield, the following alternative scenarios were simulated using AnnAGNPS at the monitoring site, and the sediment yield at the watershed outlet was compared with the results obtained from the validation simulation file:

1st scenario (S1) the wheat crop was assumed to be converted into forest. During this simulation, the input file was modified to replace the field land use type "Winter wheat" into the "Forest" land use type; CN and MN were set to forest. This scenario can be considered representative of the situation before the establishment of agriculture in the area.

2nd scenario (S2) using the Vegetated Streams. In this simulation, the reach vegetation code was changed to assign a code for a vegetated stream instead of no-vegetated streams.

3rd scenario (S3) A crop rotation of Corn & soybean was assumed to be planted instead of the winter wheat crop. The winter wheat cover crop was not planted and the field was fallow, with residue from soybeans and cotton left on the surface. The data base of corn and soybean were based on the internal data base of the model: the corn was planted in 15th of April of the 1st year of simulation and harvested in the 25th of October of the same year, while the Soybean was assumed to be planted in the 1st of April of the following year and harvested in the 25th of October of the same year. For both crops, no tillage operations were supposed, and the plant residues were left in place.

4th scenario (S4) no tillage in winter wheat. In this simulation, the input file was modified to exclude any crop tillage operation in the Management operation data.

Results and Discussion

Calibration and validation

The model performance was calibrated at the event scale utilizing 11 observed erosive events registered during the period 2007 -2008. In uncalibrated mode, the model tends to over-predict the runoff volumes, so the initial CNs were properly decreased to get runoff results closer to the observed ones. The same results were found in semi-arid conditions by Licciardello *et al.* (2007).

At the end of calibration, runoff depths were in general slightly over predicted (see the negative value of the CRM coefficient in Table 6). The mean value and the standard deviation of the simulated runoff depths were close to the observed corresponding values, with a difference equal approximately to 10 and 2 % respectively. The coefficient of determination and the Nash-Sutcliff efficiency factor achieved after the runoff calibration were good (Table 6). Similar results were found at the event scale by other authors like Yuan *et al.* (2001), Shrestha *et al.* (2006) and Shamshad *et al.* (2008).

After calibration, the mean predicted value of peak flow was 14 % different from the mean observed value, however, the difference between predicted and simulated values raises for the standard deviation to be more than 40 % (Table 6). High efficiency is shown by the coefficient of determination R^2 value (R^2=0.81), while other statistical indexes (NSE and RMSE) show a satisfactory prediction (Table 6). Other authors (Zema *et al.*, 2010; Shrestha *et al.*, 2006; Licciardello *et al.*, 2007) found that the model unsatisfactory predicted peak flows. To calibrate the sediment yield, the MN's roughness coefficient of each cell was modified starting from the initial values taken from TR55

Table 6. Statistics concerning the AnnAGNPS calibration and validation in the Carapelle watershed.

Calibration			Runoff (mm)				
Observed	1.5	1.9	-	-	-	-	-
Default simulation	2.1	2.4	0.38	0.65	-0.42	1.4	0.88
Calibrated model	1.7	1.9	0.76	0.78	-0.1	0.91	0.93
			Peak flow (m^3/s)				
Observed	16	14	-	-	-	-	-
Default simulation	27	31	-1.4	0.86	-0.75	21	0.78
Calibrated model	18	20	0.54	0.81	-0.14	9.2	0.92
			Sediment yield (kg/m2)				
Observed	0.018	0.025	-	-	-	-	-
Default simulation	0.037	0.044	-0.81	0.62	-1.04	0.33	0.77
Calibrated model	0.024	0.028	0.67	0.74	-0.35	0.01	0.92
Validation			Runoff (mm)				
Observed	2.56	2.22	-	-	-	-	-
Simulated	2.28	2.18	0.81	0.82	0.11	0.99	0.95
			Peak flow (m^3/s)				
Observed	29	18	-	-	-	-	-
Simulated	26	22	0.69	0.82	0.11	10.2	0.93
			Sediment yield (kg/m^2)				
Observed	0.036	0.05	-	-	-	-	-
Simulated	0.038	0.04	0.86	0.86	-0.06	0.02	0.96

(SCS, 1986). For forest and rangeland, MN values respectively equal to 0.8 and 0.13 were set , while for urban areas, cropland and pasture the initial value of 0.15 was considered. Increasing the value of MN for the different land uses and especially for the cropland (wheat) and urban areas, the tendency of the model to overestimate the suspended sediment yield that is clear in the un-calibrated mode was reduced (see the CRM values before calibration in default simulation and after calibration in Table 6). Generally, a good correlation between observed and simulated data was obtained, as reported by the Nash Sutcliffe efficiency index and the coefficient of determination R^2; the value of the root mean square error was close to zero, showing a good model efficiency in predicting sediment yield.

The results obtained in the calibration phase were used for model validation, that was carried out using 25 events recorded during the period 2009-2011. As confirmed by the statistical indexes, an excellent performance of the model was observed in simulating runoff volumes (Table 6). The model performance in predicting peak discharges is satisfactory (see RMSE and NSE values) although according to the R^2 values a good correlation between observed and simulated data exist. Sediment yield values were perfectly predicted and an acceptable overestimation is observed.

Figure 5 reports the visual comparison between simulated and observed data for the entire period (thirty-six events). As expected using the calibrated SCS-CNs, the model prediction is good for runoff and sediment yield and satisfactory for peak discharge.

After the validation process, it was observed, comparing the statistical indexes, that the model prediction was better in the validation than in the calibration process. To better understand this finding, the relative error (RE) was calculated for two groups of events and represented on a box plot (Figure 6).The first group (26 events) has peak discharges $Q_p \leq 30$ m^3 s^{-1} and is representative of low flow events, as previously stated by Gentile *et al.* (2010) in the same watershed; the second group (10 events) has peak discharges $30 < Q_p \leq 73.6$ m^3 s^{-1} and is representative of high flow events. A difference in the RE values between the two groups was observed, showing that the model better predicts sediment yield for high intensive events and that a larger scatter between simulated and observed sediment yield values exists for low flow events. The same behaviour was observed for peak flows.

As the number of high flow events included in the validation process (25 events, 3 years) is greater than those included in the calibration (11 events, 2 years), this could be the reason why the model did not perform as well in calibration than in validation.

Sediment yield response to alternative Management Practices

Figure 7 shows the average annual sediment yield (t/ha) at a watershed scale obtained applying four alternative scenarios of Management practices that could be used to reduce soil erosion and sediment loads in the watershed.

In the first scenario (S1), when all the cropland wheat is substituted with forest, the sediment yield is reduced in the watershed, with an average value of 60 % during the whole period of simulation; this land use change would save a total amount of 9.3 t/ha of sediments.

In the second scenario (S2) the use of vegetation along the whole stream network (vegetated streams) reduces the average annual sediment yield by 18.5% (a total amount of 3 t/ha), due to the effect of vegetation in retaining sediments from being eroded and conveyed to the watershed outlet.

In the third Scenario (S3) a crop rotation of corn-soybean is hypothetically applied instead of the overall cropland wheat. The average annual sediment yield is reduced by 34 %, due to the effect of the continuous cover offered by the crop residue that helped in protecting soil from being eroded. As a quantity, a total amount of 5.3 t/ha of sediments could be saved.

The last scenario (S4) is corresponding to the application of no tillage practices in cropland. Herethe sediment yield could be reduced by up to 18.5%, preventing approximately 3 t/ha of sediments from being lost.

The S1 scenario, that means converting all the cropland into forest and gives the better results in terms of soil erosion control, could be considered as representative of the ancient conditions in the Puglia region (eighteen century) when forest was the prevailing land use and agriculture was not yet extensively estabilished.

The S3 and s4 scenarios can be considered as agriculture-targeted, both give good results in terms of sediment yield reduction, even if the efficiency of crop rotations is approximately two times that of the conservation tillage (no-tillage) practices. Finally, the S2 scenario, that could be considered as environmentally-targeted, has the same efficiency of the agricultural S4 scenario.

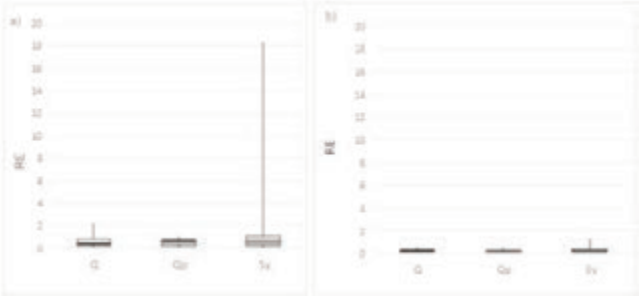

Figure 6. Average relative error (RE) for low flow events (a) and high flow events (b).

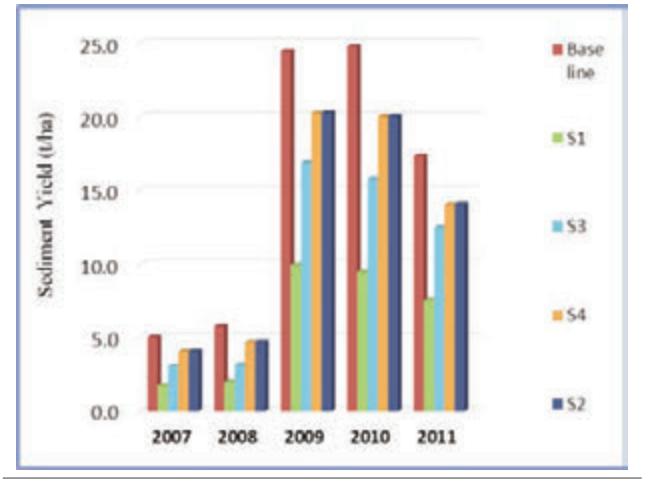

Figure 6. Average relative error (RE) for low flow events (a) and high flow events (b).

Conclusions

The AnnAGNPS Model was implemented in the Carapelle, a medium size Mediterranean watershed in southern Italy, using 36 erosive events recorded during the period 2007-2011. The objective of this work was to evaluate the model capacity of predicting sediment yield, runoff, and peak flow in the watershed through a continuous monitoring of runoff and sediment loads. The evaluation process included 2 phases, the first one was the model calibration and the second one was the model validation. The model calibration was performed following an order in which runoff was calibrated first by adjusting the initial curve number values modifying the retention S factor. The impact of the SCS types Ia and I synthetic rainfall distribution was investigated; the SCS storm type I gave the highest efficiency in predicting peak flows and was used in the simulation. Finally, the sediment yield was calibrated by adjusting the Manning roughness coefficient. Comparing predicted to observed data visually and using different statistical indexes, the results showed a good model performance in predicting runoff and sediment yield on the event basis in calibration and validation, while its performance was satisfactory for peak discharge. Generally, the model showed a tendency to better predict high flow events while a great scatter was found between observed and predicted values in case of low flow events. This result is important in semi-arid conditions where the annual sediment transport rate is mostly concentrated in a small number of high erosive events.

Successively the effectiveness of applying some Management practices on the sediment yield reduction at a watershed scale was determined. Based on the simulation results, it is concluded that substituting cropland wheat with forest achieved the highest reduction in sediment yield. A good compromise between agriculture and soil conservation was represented by the crop rotation of corn and soybean, while the scenarios corresponding to the revegetation of the stream banks ("environmentally targeted") and the conservation tillage (no-tillage) in cropland achieved almost similar results. Further analyses need to be performed to evaluate the management practices that are more suitable with the real agriculture and land conditions in the watershed and consequently to assess possible Best management practices (BMPs) in terms of soil erosion control and sediment yield reduction.

References

Baginska B, Milne-Home W., Cornish P.S. 2003. Modelling nutrient transport in Currency Creek, NSW with AnnAGNPS and PEST. Environ. Modell. Softw. 18: 801-808.

Bagnold, R.A. 1966. An approach to the sediment transport problem from general physics. Prof. Paper 422-J. U.S. Geol. Surv., Reston, VA.

Bakker M.M., Govers G., Rounsevell M.D.A.. 2004. The crop productivity–erosion relationship: an analysis based on experimental work. Catena. 57: 55–76.

Bakker M.M., Govers G., Kosmas C., Vanacker V., Oost K.V., Rounsevell M. 2005. Soil erosion as a driver of land-use change. Agr Ecosyst Environ. 105: 467–481

Evans B.M., Corradini K.J. 2001. BMP Pollution Reduction Guidance Document. Available from: http://www.predict.psu.edu /Downloads/BMPManual.pdf Accessed: January 2013.

Bingner R.L., Theurer F.D. 2005. AnnAGNPS technical processes documentation, version 3.2. Oxford. Miss.: USDA ARS National Sedimentation Laboratory.

Bisantino T., Gentile F., Trisorio Liuzzi G. 2011. Continuous Monitoring of Suspended Sediment Load in Semi-Arid Environments. In: S.S. Ginsberg (ed.) Sediment Transport. ISBN 978-953-307-189-3. InTech, Available from: http://www.intechopen.com/articles/show/title/continuous-monitoring-of-suspended-sediment-load-in-semi-arid-environments Accessed: May 2012

Bisantino T., Bingner R., Chouaib W., Gentile F., Trisorio Liuzzi G. 2013. Estimation Of Runoff, Peak Discharge And Sediment Load At The Event Scale In A Medium-Size Mediterranean Watershed Using The Annagnps Model. Land Degrad. Dev. doi: 10.1002/ldr.2213.

Bosch D., Theurer F., Binger R., Felton G., Chaubey I. 2001. Evaluation of the AnnAGNPS water quality model. In. J.L. Parsons, D.L. Thomas, and R.L. Huffman (eds.): Agricultural Non-point Source Models: Their Use and Application. Southern Cooperative Series Bulletin 398. Available at: http://s1004.okstate.edu/S1004/Regional-Bulletins/Modeling-Bulletin/modeling-bulletin.pdf. Accessed: March 2012.

Caliandro A., Lamaddalena N., Stellati M., Steduto P. 2005. Caratterizzazione agroecologica della Regione Puglia in funzione della potenzialità produttiva: Progetto Acla 2. Bari.

Cazorzi, F. 1996. Watershed oriented digital terrain model. User manual, Win95 version, 80. Internal report. Padua, Italy: University of Padova, Agripolis Campus, IDEA Laboratory.

Cazorzi, F., Dalla Fontana G. 1996. Un modello distribuito per la valutazione degli effetti idrologici dei mutamenti d'uso del suolo. Proc. Problemi dei grandi comprensori irrigui: esercizio, manutenzione e ammodernamento delle reti di irrigazione. Associazione Italiana di Ingegneria Agraria (1st section), Novara, Italy.

Chow V.T., Maidment D.R., Mays L.W. 1988. Applied Hydrology. McGraw-Hill Publishing Company, New York.

Eckhardt K. 2005. How to construct recursive digital filters for baseflow separation. Hydrol Process 19: 507-515.

EEA-European Environmental Agency. 2006. The thematic accuracy of Corine land cover 2000 - Assessment using LUCAS. Technical report.

European Soil Data Centre (ESDAC), 2003. The map of organic carbon in topsoils in Europe. Available from http://eusoils.jrc.ec.europa.eu Accessed December 2011.

Fiorentino M, Iacobellis V. 2001. New insights about the climatic and geologic control on the probability distribution of floods. Water Resour. Res. **37(3)**: 721–730.

Ferro V., Porto P., Yu B. 1999. A comparative study of rainfall erosivity estimation for southern Italy and southeastern Australia. Hydrolog. Sci. J. 44: 3–23.

Fu G., Chen S., McCool D.K. (2006). Modeling the impacts of no-till practice on soil erosion and sediment yield with RUSLE, SEDD, and ArcView GIS. Soil Till. Res. 85(1-2): 38-49.

Galvagni D., Gregori E., Zorn G. 2006. Modelli di valutazione della biomassa radicale di popolamenti forestali. L'Italia forestale e Montana 61 (2): 101-118.

Gentile F., Bisantino T., Corbino R., Milillo F., Romano G., Trisorio Liuzzi G. 2010. Monitoring and analysis of suspended sediment transport dynamics in the Carapelle torrent (southern Italy). Catena 80: 1-8.

Gradzinski R., Baryla J., Doktor M., Gmur D., Gradzinski M., Kedzior A., Paszkowski M., Soja R., Zielinski T., Zurek S. (2003). Vegetation-controlled modern anastomosing system of the upper Narew River (NE Po-land) and its sediments. Sediment Geol, 157(3-4): 253-276. doi: 10.1016/S0037-0738(02)00236-1.

Krause P, Boyle D.P., Base F. 2005. Comparison of different efficiency criteria for hydrological model assessment. Adv. Geosci. 5: 89–97.

Kyoung J.L. , Youn Shik P., Jonggun K., Yong-Chul S., Nam Won K., Seong Joon K., Ji-Hong J., Bernard A.E. 2010. Development of genetic algorithm-based optimization module in WHAT system for hydrograph analysis and model application. Computers &

Geosciences 36(7): 936-944.
Lal R., Elliot W. 1994. Erodibility and erosivity. In: R. Lal (ed.), Soil Erosion Research Methods. Soil and Water Conservation Society and St. Lucie Press.USA., pp 181–208.
Lenzi M.A., Di Luzio M. 1997. Surface runoff, soil erosion, and water quality modelling in the Alpone watershed using AGNPS integrated with a Geographic Information System. European J. Agron. 6(1-2): 1-14.
Legates D.R., McCabe G.J. 1999. Evaluating the use of 'goodness of fit' measures in hydrologic and hydroclimatic model validation. Water Resour. Res. 35: 233–241.
Loague K, Green R.E. 1991. Statistical and graphical methods for evaluating solute transport models: overview and application. J. Contam. Hydrol. 7: 51–73..
Licciardello F., Zimbone S.M. 2002. Runoff and erosion modeling by AGNPS in an experimental Mediterranean watershed. Proc. ASAE Annual Intl. Meeting/CIGR XVth World Congress. St. Joseph, Mich.: ASAE
Licciardello F., Zema D.A., Zimbone S.M., Bingner R. L. 2007. Runoff and soil erosion evaluation by the AnnAGNPS model in a small Mediterranean watershed. Transactions of the American Society of Agricultural and Biological Engineers (ASABE) 50(5): 1585-1593
Loague K., Green R.E. 1991. Statistical and graphical methods for evaluating solute transport models: Overview and application. J. Contam. Hydrol. 7(1 2): 51 73.
Mohammed H., Yohannes F., Zeleke G. 2004. Validation of agricultural non-point source (AGNPS) pollution model in Kori watershed. South Wollo, Ethiopia. Int. J. Appl. Earth Obs. Geoinf. 6: 97-109.
Morgagni A., Marsigli M., Todini E. 1993. Assessment of soil erosion in a number of small ephemeral streams in Calabria and Sicily. Proc. Workshop on Soil Erosion in Semi arid Mediterranean Areas, 137 148. European Society for Soil Conservation, Centro Studi per l'Economia applicata all'Ingegneria.
Mouelhi S., Michel C., Perrin C., Andreassian V. 2006. Stepwise development of a two-parameter monthly water balance model. J Hydrol 318: 200–214.
Nash J.E., Sutcliffe J.V. 1970. River flow forecasting through conceptual models: Part I. A discussion of principles. J Hydrol 10: 282–290.
Pandey A., Chowdary V.M., Mal B.C., Billib M. 2008. Runoff and sediment yield modeling from a small agricultural watershed in India using the WEPP model. J. Hydrol. 348: 305-319.
Parajuli PB, Nelson NO, Frees LD, Mankin KR. 2009. Comparison of AnnAGNPS and SWAT model simulation results in USDA-CEAP agricultural watersheds in south-central Kansas. Hydrological Processes 23(5): 748-763.
Renard K.G., Foster G.R., Weesies G.A., McCool D.K., Yoder D.C. 1997. Predicting Soil Erosion by Water: A Guide to Conservation Planning with the Revised Universal Soil Loss Equation (RUSLE). USDA Handbook No. 703.
Saxton K.E., Rawls W.J. 2006. Soil water characteristic estimates by texture and organic matter for hydrologic solutions. Soil Sci. Soc. Am. J. 70: 1569-1578.
SCS. 1972. National Engineering Handbook, Section 4. Hydrology Soil Conservation Services, U.S., Department of Agriculture, Washington DC.
SCS. 1986. Technical Release 55: Urban Hydrology for small watersheds. Soil Conservation Service, USDA.
Shamshad A., Leow C.S., Ramlah A., Wan Hussin Sanusi W.M.A., Mohd S.A. 2008. Applications of AnnAGNPS model for soil loss estimation and nutrient loading for Malaysian conditions. Int. J. Appl. Earth Obs. Geoinf. 10: 239–252.
Shrestha S., Mukand S.B., Gupta A., Kazama F. 2006. Evaluation of annualized agricultural nonpoint source model for a watershed in the Siwalik Hills of Nepal. Environ. Model. Softw. 21: 961–975.
Suttles J. B., Vellidis G., Bosch D.D., Lowrance R., Sheridan J.M., Usery E.L. 2003. Watershed scale simulation of sediment and nutrient loads in Georgia coastal plain streams using the annualized AGNPS model. Trans. ASAE 46(5): 1325-1335.
Theurer F.D., Clarke C.D. 1991. Wash load component for sediment yield modeling. Proc. of the Fifth Federal Interagency Sedimentation Conf., Las Vegas, NV, March 18-21,1991. pp. 7-1 to 7-8.
Theurer F.D., Cronshey R.G. 1998. AnnAGNPS – Reach routing processes. Proc. First Federal Interagency Hydrologic Modeling Conference. Las Vegas, NV, April 19-23, 1998. pp. 1-25 to1-32.
Thornton C. I., Abt S. R., Clary W. P. 1997. Vegetation influence on small stream siltation1. J. Am. Water Resour. Assoc., 33(6): 1279-1288.
USDA-ARS. 2005. Generation of weather Elements for Multiple applications. Available online: http://www.nwrc.ars.usda.gov /models/gem/index.html (verified May 2007)??.
USDA-ARS. 2006. AnnAGNPS - Annualized Agricultural Non-point Source Pollution Model. Available from: http://www.ars.usda.gov/Research/docs.htm?docid=5199 Accessed November 2011.
USDA-SCS. 1986. Urban hydrology for small watersheds. Technical release 55, 2nd ed., NTIS PB87- 101580. USDA, Springfield, VA.
Van Liew M.W., Garbrecht J. 2003. Hydrologic simulation of the Little Washita River experimental watershed using SWAT. J. Am. Water Resour. Assoc. 39: 413–426.
Van Liew M. W., Garbrecht J. 2003. Hydrologic simulation of the Little Washita River experimental watershed using SWAT. J. Am. Water Resour. Assoc. 39(2): 413 426.
Willmott C.J. 1981. On the validation of models. Phys. Geogr. 2: 184–194.
Willmott C.J. 1982. Some comments on the evaluation of model performance. Bull. Am. Meteorol. Soc. 63: 1309–1313.
Wolman M.G., Gerson R. 1978. Relative scales of time and effectiveness of climate in watershed geomorphology. Earth Surface Processes. 3(2): 189-208.
Yuan Y., Bingner R.L., Rebich R.A. 2001. Evaluation of AnnAGNPS on Mississippi Delta MSEA watershed. Trans. ASAE 44(5): 1183-1190.
Yuan Y., Bingner R.L., Theurer F.D. 2006. Subsurface flow component for AnnAGNPS. Appl. Eng. in Agric. 22(2): 231-241.
Yuan Y, Locke MA, Bingner RL. 2008. Annualized Agricultural Non-Point Source model application for Mississippi Delta Beasley Lake watershed conservation practices assessment. Journal of Soil And Water Conservation 63 (6): 542-551.
Yoon J. 1996. Watershed scale non-point source pollution modelling and decision support system based on a model- GIS-RDBMS linkage. Proc. AWRA Symposium on GIS and Water Resources, Ft Lauderale, FL, 2-16.
Zema D.A., Bingner R.L., Denisi P., Govers G., Licciardello F. Zimbone, S.M. 2010. Evaluation of runoff, peak flow and sediment yield for events simulated by the AnnAGNPS model in a belgian agricultural watershed. Land Degrad. Develop. Land Degrad. Develop. 23: 205–215.
Zou C.B., Ffolliott P.F., Wine M. 2010. Streamflow responses to vegetation manipulations along a gradient of precipitation in the Colorado River Basin. For. Ecol. Manage., 259(7): 1268-1276. doi: DOI: 10.1016/j.foreco.2009.08.005.

Runoff generation processes in a Mediterranean research catchment (Sardinia)

Marcello Niedda, Mirko Castellini, Filippo Giadrossich, Mario Pirastru

Department of Agraria, University of Sassari, Italy

Introduction

In recent decades the hydrological community has increasingly improved its understanding of the runoff generation in river basins. Since Horton (1933), numerous studies have investigated these mechanisms at the plot, hillslope and catchment scale (e.g.: Betson, 1964; Dunne and Black, 1970; Pilgrim *et al.*, 1978; Kirkby, 1978; Mosley, 1979; Beven, 1989; Anderson and Burt, 1991). The primary processes that have been observed and described to explain runoff generation in a catchment area are: (1) Hortonian Overland Flow (HOF), which occurs when rainfall intensity exceeds the infiltration capacity of the soil; (2) Saturation Overland Flow (SOF), which occurs when the storage capacity of the soil is exceeded and defines the concept of contributing saturated areas, which expand as rainfall volume increases; (3) Saturated Subsurface Flow (SSF), which occurs when the water in the soil flows along lateral paths and thus contributes to streamflow as return flow from the groundwater aquifer.

Since the 1960s researchers have appreciated the importance of SSF mechanism in runoff formation, particularly in natural landscapes. Research into catchment hydrology has led to the development of models, such as Topmodel (Beven and Kirkby, 1979) or SMR (Frankenberger *et al.*, 1999), which aim to represent the varying extension of the saturated areas in relationship to the topography. This is one of the main factors governing stream discharge and water-table dynamics, especially in natural mountain catchments. Topography controls the flow-path geometry, the saturated area formation, depending on the water-table depths, and the SSF runoff production. Soil water content and water-table data combined with hydrograph separation techniques were the basis of the first investigations on runoff formation by Dunne and Black (1970). Improved computing and data storage capacity has played an important role in improvement the modelling of runoff formation processes, and has allowed these mechanisms to be simulated by spatially distributed mathematical models (e.g.: Abbott *et al.*, 1986; Grayson *et al.*, 1992; Beven *et al.*, 1995; Refsgaard, 1997). However not all these processes are well understood, such as, to take one example, the mechanism by which SSF enters streams quickly enough to contribute to storm-flow (Sophocleous, 2002). One reason for this is that natural soils are very heterogeneous and respond to rainfall in different ways, as Brooks *et al.* (2007) pointed out in their conclusion. These problems are accentuated in the semi-arid Mediterranean climate, where runoff formation processes are particularly variable over time because of the marked irregularity in rainfall and the seasonal mismatch between evaporation and rainfall. These factors amplify oscillations in soil moisture and the depth of the water-table.

Detailed catchment studies that use distributed data collected continuously over a long period of time are uncommon, and this is particularly true in the semi-arid Mediterranean region. In response to this, a small natural catchment in Sardinia (Italy), an island at the center of the Mediterranean, was chosen as the experimental site for a long term field study. The study focused particularly on the dynamics of the runoff generation processes through field observations of rainfall, soil water content, water-table depths, and stream discharge. A physically-based distributed rainfall-runoff model was used. The model suitability was evaluated, using integrated (outlet discharge) and distributed (water-table depths) catchment response. Water-table depths are very sensitive to the hydrological properties of the catchment, and this makes them excellent distributed indicators of model performance. Despite that, only few studies have used these measurements to evaluate the predictive ability of hydrological models (Lamb *et al.*, 1997; Seibert *et al.*, 1997; Molénat *et al.*, 2005; Brooks *et al.*, 2007; Gascuel-Odoux *et al.*, 2010; Vansteenkiste *et al.*, 2012). The aims of this work are identifying the main characteristics of runoff generation mechanisms from observations carried out in a small catchment of central Mediterranean dominated by SSF; simulating these mechanisms with a distributed hydrological modelling; and verifying if this model is appropriate for predicting simultaneously stream discharge and water-table dynamics.

Correspondence: Marcello Niedda, Department of Agraria, University of Sassari, Italy.
E-mail: niedda@uniss.it

Key words: storm-flow coefficient; runoff generation; physically based model.

Journal of Agricultural Engineering 2013; XLIV(s2):e8
doi:10.4081/jae.2013.(s1):e8

Materials and methods

The study area

The study was conducted in the Baratz basin, located in North-Western Sardinia, Italy (Figure 1). The contributing area, at the outlet height of 40 m a.s.l., is 7.4 km^2, the maximum catchment height is 410 m, the mean height 156 m and the mean slope 15.6%. The climate is semi-arid Mediterranean, with mean annual temperature of 15.8 °C and minimum and maximum mean daily temperature of 3 °C and 29 °C, respectively. Average annual precipitation is 590 mm and average potential evapotranspiration is about 900 mm. In the central-northern part of the basin the geological substratum consists of fractured sericite phyllite on the metamorphic Paleozoic base of Sardinia, while in the Southern part it is Permian sandstone and conglomerates of

alluvial deposits, with Permo-carboniferous and Triassic volcanic insertions. The morphology of the basin is narrow valleys covered in woods. The soils in the North of the basin were either thin or of medium depth, from loam to loamy sand, sub-acid, and partially desaturated. The soils in the South were deep, sandy loam in the surface layers and from sandy clay loam to clay in the deeper layers, and from sub-acid to acid. The most widespread land-use was natural pasture, followed by deciduous forest and maquis. These characteristics are reported in Table 1.

The instrumentation

An automatic station was set up in 2008, located at the catchment outlet, with sensors for rainfall, air temperature and relative humidity, wind velocity, net solar radiation, atmospheric pressure, soil moisture, groundwater level and temperature, and depth and velocity of surface flow, described in detail in Pirastru and Niedda (2013). All automatic measurements were executed every 300 s, and were logged using a CR1000 Campbell Scientific Inc. datalogger, a SonTek Argonaut-SW current meter and three Schlumberger mini-divers. A V-notch was installed on the stable bed of a trapezoidal concrete channel, immediately downstream from the current meter, to stabilize the low flow and facilitate the measurements. Groundwater levels were taken in five boreholes located in the valley bottom, as shown in Figure 1a, by using mini-divers and manual measurements every one-two weeks.

Storm-flow coefficients

From the four year series of data, from 2008 to 2012, the storm-flow coefficients at the event scale were computed. All the events more than 5 mm of rain, and separated by time intervals of more than 24 hours with less than 1 mm of rain, were chosen. Sixty-nine such events were identified during this period, and the following variables were calculated for each of them: rainfall depth, maximum hourly rainfall intensity, storm-flow discharge, storm-flow coefficient, base-flow discharge, the average soil moisture (the first metre) and the water-table depth at the valley bottom at the start of the event. The storm-flow discharge was separated from the base-flow discharge using the classic method of Hewlett and Hibbert (1967). Beginning from the foot of the rising limb of the streamflow hydrograph, base-flow was then increased by a constant value until it intersected the falling limb of the hydrograph, which indicated the end of the storm-flow event. An increment of the base-flow of 10 l/s per day was chosen after analysis of all the hydrographs observed in the basin. Figure 2a shows the seasonal evolution of the rainfall depths for each of the 69 chosen events during the four years of monitoring. Winter was the season with the greatest number of events (40%), and summer the fewest (9%). The other events were equally divided between spring and autumn, although the rainfall depths in autumn were greater, with a maximum value of 108 mm. Figure 2b shows the seasonal evolution of the storm-flow coefficient for each event. The highest values were clearly concentrated in winter. In the other seasons, and particularly from the middle of March to the middle of November, even rainfall which had higher depths than those of the winter did not generate significant storm-flow discharge, with storm-flow coefficients of less than 2%.

The correlations between the storm-flow coefficient and the maximum hourly rainfall intensity and also the base-flow were analyzed. The first correlation was found to be statistically non-significant (r=-0.1), which indicates that rainfall intensity had little influence on hydrological response in forested basins, in agreement with the studies by Hewlett *et al.* (1977) and Lana-Renault *et al.* (2007). The correlation between the storm-flow coefficient and the base-flow was, however, statistically significant (r=0.76), which is in line with the results obtained by Latron and Gallart (2007) and Lana-Renault *et al.* (2007) for other

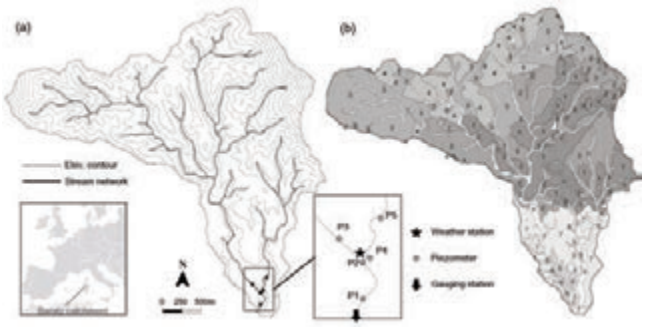

Figure 1. (a) Map of the Baratz catchment in North-Western Sardinia, Italy (elevation contour interval: 25 m from 50 to 400 m asl) and location of the main monitoring instruments; (b) map of soil and land-use type (classes in Table 1).

Table 1. Soil and land-use properties for the Baratz basin.

Type (Figure 1b)	1	2	3	4	5	6	7	8	9	0	S
Geology	Paleozoic metamorphic				Permian sandstone		Pliocene alluvial deposits			Olocene alluvial deposit	
Surface cover	Pasture	Maquis	Forest	Pasture	Forest	Pasture			Maquis	Pasture	Riparian
Soil thickness H (m)	0.25		0.35		0.5		1.0	0.5	0.3	3.0	
Texture	Loam		Loamy sand		Sandy loam					Loam	Sand
Soil porosity f_c (cm³/cm³)	0.463		0.437		0.453					0.463	0.437
Soil moisture at –33 kPa q_{33} (cm³/cm³)	0.270		0.125		0.207					0.270	0.091
Saturated hydraulic conductiv. K_s (mm/h)	12		70		30					12	220
Relative area (%)	19.1	22.3	22.0	14.7	1.1	0.5	8.7	0.9	1.8	0.3	8.5

small Mediterranean basins. Because base-flow is governed by the soil moisture and the water-table depth, this correlation shows the influence of the pre-event values of these variables on the rainfall-runoff processes. Figures 2c,d,e,f show the seasonal dynamics for average moisture in the first metre of soil (four TDR probes) and the depth of the water-table at piezometers P1, P2 and P4. These figures show some regularities in each season, despite the great variability in rainfall and stream discharge from one year to another. The differences in soil moisture and the water-table depth in the four years are more to do with the rapid autumnal increase and the rapid decrease in summer, and less with the maximum and minimum values. Figure 3 shows the relationships between the storm-flow coefficients and soil moisture and the water-table depth at the start of each event, at piezometer P1 near the basin outlet. The correlation is very high, which agrees with those for their seasonal evolutions. The storm-flow coefficients increase as soil moisture increases and the water-table depth in the valley bottom decreases. Storm-flow coefficients were greater than 2% only when soil moisture was more than 30% and the water-table depth less than 1 m, a depth which corresponded with that of the streambed.

Runoff generation mechanisms

The monitoring with TDR probes indicates that soil moisture in winter was higher than 30%, with peak levels of over 40% during the most intense rainfall events (Figure 2c). In this season the water-table was at the same level as the streambed, about 1-1.5 metres deep, with higher peaks during the most intense rainfall events (Figure 2d,e,f). The height of the peaks also increased with the distance of the piezometers from the streambed. This was capable of draining the nearest piezometers P1 and P2, a few metres from the streambed, more rapidly than it did P4, which was 17 metres from the streambed. Only at piezometer P4 did the water-table reach the ground surface and the soil become saturated for brief periods, as shown in Figures 2d,e,f. As can be seen in Figure 2b, the winter period from November to March was the only with high storm-flow coefficients (>2%). In this period of rapid runoff after rainfall, the storm-flow peaks were a result of the SOF mechanism over large saturated areas, which are controlled by the SSF. The high runoff during the recession after the rainfall shows that the SSF enters streams quickly enough to contribute to discharge, in the form of storm-flow.

In spring, the soil moisture of the surface layers begins to decline rapidly, due to the great increase in evapotranspiration, until they reach minimum levels in late spring. The water-table in the valley bottom stays at the same level as the streambed. This serves to feed the streambed, generating the slow response and the long recessions typical of the base-flow. The generation mechanism is the exfiltration of the SSF within the soil matrix. Only in summer does the water-table begin to fall to a greater depth than the streambed of the valley bottom.

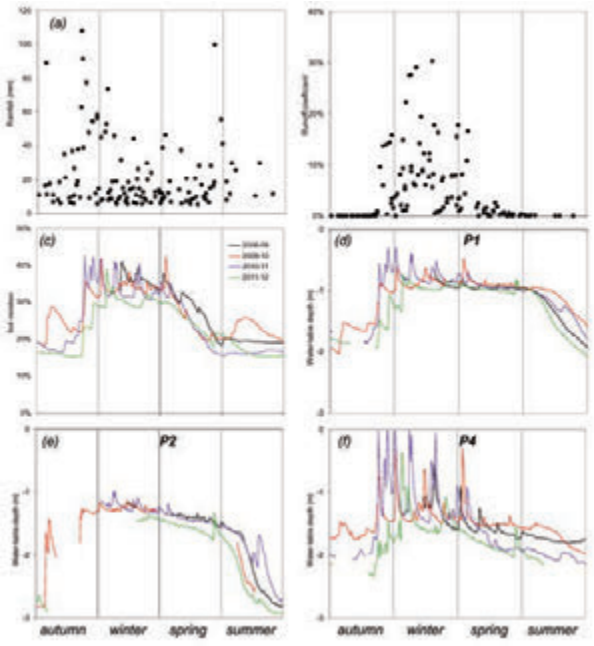

Figure 2. Seasonal patterns throughout the years 2008-2012 of (a) the rainfall depth; (b) the maximum hourly rainfall intensity; and (c) the storm-flow coefficient.

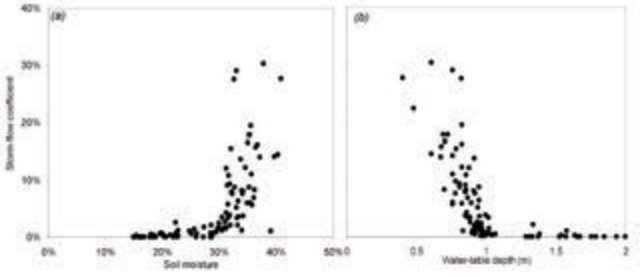

Figure 3. Relationships between the storm-flow coefficients and (a) the average soil moisture, observed near P4; and (b) the water-table depth at the start of each event, observed at piezometer P1.

Table 2. Annual components of the catchment water balance: *P* precipitation, *R* runoff, *R/P* runoff coefficient, *ET* actual evapotranspiration, *E* evaporation from surface interceptions, *I* percolation; and efficiency coefficients *EF* for the four hydrological years of continuous simulation

	Measured			Simulated				
Water year	*P* (mm)	*R* (mm)	*R/P* (%)	*ET*(mm)	*E* (mm)	*I* (mm)	*R* (mm)	*EF*
2008-2009	775	97.7*	12.6	435.4	88.2	92.6	124.6	0.87
2009-2010	700	32.2*	4.6	490.6	108.5	36.0	51.3	-1.30
2010-2011	801	195.4	24.3	437.6	91.1	107.3	176.5	0.82
2011-2012	596	15.1	2.5	473.7	84.9	31.1	31.2	-1.50
av.2008-2012	718	91.3	11.9	459.3	93.2	66.8	95.9	0.83

* Missing observed runoff data filled in with simulated values.

The base-flow stops and the streambed dries up until the autumn recovery. As shown in Figure 2, summer and autumn are characterised by low water-table heights and low soil moisture. This usually lasts until the middle of November when, after the most intense rainfall of the year, both these values increase rapidly and reach their annual maximum values. Before this, in summer and early autumn, there was no measurable discharge, despite various rainfall events, some of which were very intense. This can be seen from the seasonal evolution of the rainfall and storm-flow coefficients in Figures 2a and 2b. This shows that during these seasons the non-saturated soils, which extend towards the valley bottom, are able to absorb large, high-intensity rainfall events. This means that the HOF is a negligible mechanism in this environment.

The SSFR model

The Saturated Subsurface Flow Routing model (SSFR) is a GIS-based distributed model for the continuous simulation of the coupled subsurface-channel flow, which neglects the vertical distribution of soil moisture and the unsaturated flow processes. The SSFR model used in this project is a modified version of a previous model, which was developed for basins with steep and shallow soil in Mediterranean environment (Niedda, 2000; Niedda and Pirastru, 2012; Niedda and Pirastru, 2013). SSFR is based on the modelling principles of Grayson *et al.* (1992), who minimized the number of parameters and processes represented, so that the simplified structure of the model is in balance with the amount of available field data, while the flow components are physically based. Surface interception and soil moisture store dynamics, percolation into the bedrock, evapotranspiration, 1D open channel flow and 2D horizontal saturated subsurface flow are modelled, based on the water balance at each cell of the grid discretization, and for each time step. Conceptual representation of the vertical and lateral water flows for each grid-cell are shown in Figure 4. Since HOF is a negligible mechanism, all excess precipitation P_e from interception storage S infiltrates, unless the soil thickness H is saturated (Frankenberger *et al.*, 1999; Moore and Grayson, 1991; Wigmosta *et al.*, 1994). Soil moisture varies between soil porosity and residual content, set at zero for a forest ecosystem. It is assumed that soil thickness first becomes wet up to the moisture content θ_{33}, held at –33 kPa matric potential. Only when the soil moisture exceeds $_{33}$ do excess volumes constitute an input for the SSF governed by Darcy's law. Following Dupuit's approximation, the mass and momentum conservation equations for unsteady 2D saturated subsurface flow were used, with parameters the soil hydraulic conductivity decreasing with depth, from K_S at the surface and 0 at the bottom. When the height of the water-table h exceeds a threshold value $_i$, the soil percolation I is activated. When the height of the water-table intercepts the ground surface ($h > H$), saturation-excess R is an input in surface runoff Q. In accordance with the Saint-Venant equations and the kinematic approximation, the mass and momentum conservation equations for 1D gradually varied surface flow were used, with parameter the Manning's roughness. The partial differential equations for surface and subsurface flow, described in Niedda and Pirastru (2012), were solved by conventional finite difference schemes. The same numerical discretization was used for the soil and channel flow components, the space cells of grid-DEM and the other landscape parameters.

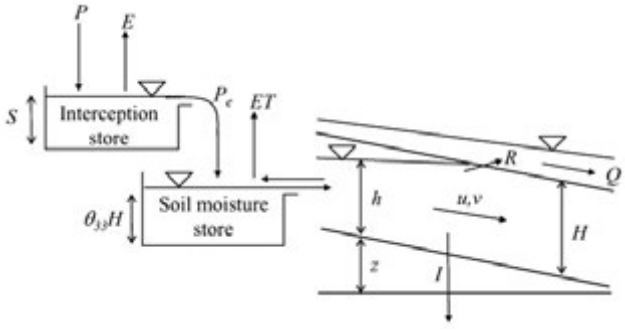

Figure 4. Conceptual representation of the vertical and lateral flows between soil, bedrock, surface and atmosphere domains simulated by the distributed catchment hydrologic model at each cell of the grid discretization.

Model parameterization

The model input are digital elevation data, soil and land-use maps, precipitation, and evapotranspiration. The terrain properties were organized into eleven types, as shown in Figure 1b, identified as areas with the same soil depth, texture, land-use and geology (see Table 1). Manning's roughness coefficient n=0.03 $m^{-1/3}s$ was used. The interception storage capacity S was determined from the Leaf Area Index (LAI): S(mm)=0.2·LAI (Dickinson *et al.*, 1991), with LAI=2 for pasture and 10 for maquis and forest. Soil porosity φ, moisture content θ_{33} and hydraulic conductivity KS were estimated from soil texture (Rawls *et al.*, 1993); but the effective hydraulic conductivity was obtained as α·KS, where α is a fitting amplification factor. This step was applied because the hydrological conservation equations are derived at the point-scale within a differential control volume, and their use at catchment scales may require effective parameters that differ from those estimated in field plots or laboratory studies.

The simple percolation mechanism used for the Baratz basin was optimised by the calibration procedure, as information on the hydraulic properties of the fractured bedrock was unavailable. Unlike other models, in which percolation feeds a deep aquifer generally represented as a linear reservoir which feeds the base-flow (Frankenberger *et al.*, 1999; Gascoin *et al.*, 2009), in this case percolation becomes a net loss subtracted from the soil water content of each cell. This hypothesis is suggested by the fact that in the Baratz basin the upstream aquifer of the fractured metamorphic rock is not connected to the soil of the valley bottom. The fractured bedrock is, indeed, only present in the hillier central-northern part of the basin (about 80% of the area), while in the southern flatter part, where there is the basin outlet, the bedrock consists of Permian sandstone which has very low permeability and percolation is not activated.

The actual evapotranspiration *ET* of the different canopy covers was calculated from reference evapotranspiration *PET* using the ECOWAT model: $ET=k_m \cdot k_v \cdot k_d \cdot k_s \cdot PET$. The details of the ECOWAT model are described in Spano *et al.* (2009), where the model was tested at a wide range of sites, including one which is very close to Baratz catchment (7 km away). As in this study, microclimate factor k_m and vegetation factor k_v are set at 1.2 and 0.92, respectively, k_d is set to 0.8 for pasture and 0.6 for maquis and forest, and $k_s=\sin(\theta/\theta c \cdot \pi/2)$ for $\theta < \theta_c$, where $\theta_c=0.5 \cdot \theta_{33}$.

The continuous simulation was run from 2008 to 2012, using a time-step equal to 300 s and a space-step equal to 5 m. The soil was considered completely dry as an initial condition, as there had been severe droughts in the previous periods. Fit calibration process was applied in an attempt to make model predictions consistent with both the observed stream discharge and the distributed water-table depths. The goodness-of-fit was evaluated using the coefficient of efficiency *EF* (Nash and Sutcliff, 1970) for hourly stream discharge. Three parameters were considered for the model calibration: the soil conductivity amplification factor α; the percolation velocity into the fractured

bedrock I; and the water-table height threshold H_i above which percolation begins.

Results and discussion

Calibration results

The comparisons between the simulated and observed streamflow at the basin outlet are shown in Figure 5, and water-table depths at each piezometer in Figure 6. The water balance between September 2008 and September 2012 (Table 2), shows that total precipitation P was divided up as follows: 64% actual evapotranspiration ET, 13% evaporation from surface interceptions E, 13.4% surface runoff R and 9.3% soil percolation I. In the first water year, there was a high value of P, a runoff coefficient of 12.6 % and a good efficiency of the simulation of the stream discharge, as shown in Table 2. In 2009-10, despite P was above the long-term average, ET was high and the runoff coefficient small. The simulation overestimated the stream discharge, and so was little efficient. In 2010-11 there was the highest P, the highest runoff coefficient and a good efficiency of the simulation. Finally, in 2011-12, when there was low P and the ET was high, the simulation overestimated the small observed stream discharge and was little efficient.

Two amplification factor values were obtained: α=100 for maquis and forest, and α=5 for pasture and riparian areas. These calibrated values are much larger than the soil conductivities found in the literature at the point scale, and similar in magnitude to the values found by Dunne and Black (1970) and Brooks *et al.* (2004) in their hillslope trench studies of forested soil horizons. These values take into account different effects, among which the macropore flow, mainly present for maquis and forest, and the parameter scaling due to the topography resolution adopted in the numerical scheme (Niedda, 2004; Jana and Mohanty, 2012). Percolation velocity was obtained by calibrating the simulated storm-flow peaks with those that were measured. The optimised value I=4 mm/h was found to be compatible with the conductivities of the fractured rock that are estimated in the literature, though these vary widely (Smith and Wheatcraft, 1993; Pirastru and Niedda, 2010). The water-table height threshold H_i=0.15 m, above which percolation begins, was obtained by attempting to close the poly-annual water balance at the basin scale. These parameter values show that deep percolation, physically justified by the presence of highly fractured bedrock in the Baratz basin, is a fundamental part of the model. The percolation was a key component of the catchment water balance, which is of the same order as surface runoff and significantly reduces the storm-flow. Without this component, the simulated storm-flow peaks would have been one order higher than those actually measured. The latter were, indeed, significantly lower than those for similar basins with impermeable bedrock.

Despite great differences in annual rainfall and stream discharge, one can identify common characteristics in the pattern of the water-table, simulated with relatively high efficiency (Figure 6a). During winter and spring the water-table is close to the streambed incised in the valley bottom, and this is well simulated. Most difficulty was experienced in simulating the water-table during the gradual recession in the dry season, due to the effects of ET, and the successive autumnal rise. In general the simulated recession during the dry season was in advance of the observed results, while during the autumnal rise the simulation lagged behind the observed results. The spatial variations in the water-table levels show that there were great differences in the rate and the size of the recession during the dry period. The simulation reproduced the recession found by piezometer P1 very well, while it underestimated the results for P2 and overestimated those for P4 (Figure 6). The simulation estimated most efficiently the results for P1, than P2 and P4, also because the calibration was optimised for the stream discharge measured at the basin outlet, where P1 is situated. It is important to note that the piezometers closest to one another, P2 and P4, showed the greatest differences in the evolution of the water-table, with rapid falls in summer in P2 and much slower in P4, above all in the first year of monitoring. These great differences in the behaviour of the water-table, even over a short distance, are probably due to the complex geometry of the bedrock surface and the alluvial strata with different hydrological characteristics. The fact that the two piezometers are on different branches of the stream network which join just before the basin outlet may also have an influence on these differences. These characteristics are very difficult to survey in detail at the basin scale and therefore to represent in the model.

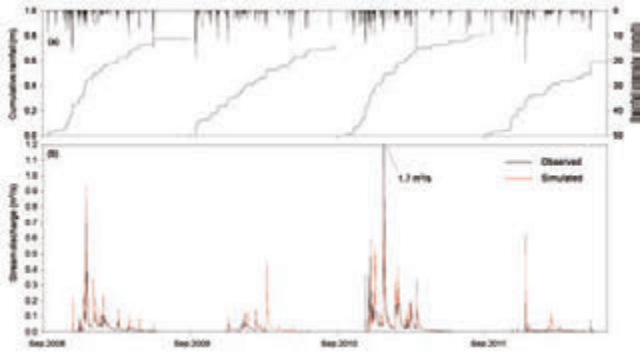

Figure 5. Comparison between (a) cumulative rainfall, rainfall intensity and (b) simulated and observed hourly stream discharge at the basin outlet from September 2008 to June 2012.

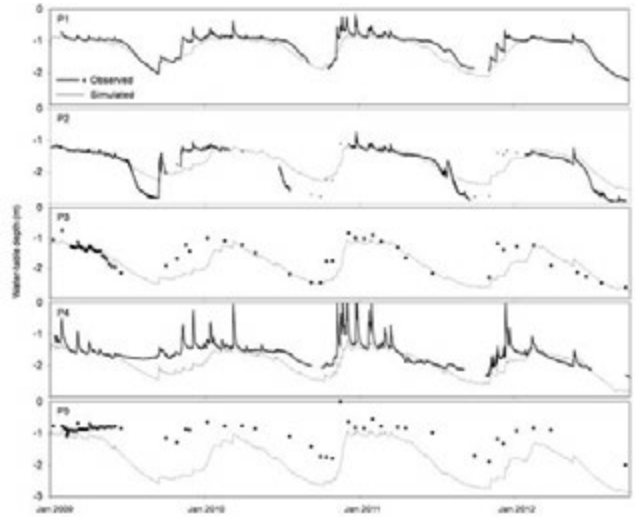

Figure 6. Observed and simulated water-table depth at the five piezometers from January 2009 to September 2012.

Discussion

The SSFR model simulated the hydrological processes of the Baratz basin continuously for a series of four years. It used a limited number of parameters to represent the subsurface and surface flow, generated through the SOF and SSF mechanisms. The main simplifications were with respect to the vertical distribution of soil moisture, the unsaturated flow and the HOF. Ignoring these processes allowed us to reduce the simulation of the 3D subsurface flow to a 2D sub-horizontal scheme, limited only to the saturated part of the soil. This was very advantageous for implementing and resolving the numerical scheme. This simplified scheme, despite the smoothing effect on the observed data of the water-table, was still able to reproduce the runoff generation through exfiltration of SSF and through SOF over the variable saturated areas, so that stream discharge at the basin scale was efficiently simulated. One of the principal objectives of this work was to evaluate the errors which occur when simulating stream discharge and shallow water-table dynamics with these modelling hypotheses. Theseassumptions are generally satisfactory in forested hillslopes where the soil is thinner and there is high hydraulic conductivity, due to the presence of a thick network of macropores. Experimental observations have, indeed, always shown that in such environments SSF is dominant, the infiltration capacity of the soil exceeds rainfall intensity, and that overland flow is extremely rare (Hewlett and Hibbert, 1967; Dunne and Black, 1970). One major critical problem whether these modelling hypotheses can be used for valley bottoms, where the thickness of alluvial soils may be greater, and deforesting and agricultural practices commonly used in the Mediterranean have reduced the drainage capacity of the surface soil. In such cases, the unsaturated soil between the ground surface and the water-table may have a great influence both on the recharge, and thus on the SSF of the valley bottom, and on the HOF mechanism.

In this respect, the water-table depths observed in the valley bottom showed that intense rain in the wet seasons, when the water-table was near the soil surface, resulted in a rapid rise in its level, and SSFR was unable to reproduce this in its entirety. This fast response, observed by many authors (Molénat *et al.,* 2005; Brooks *et al.*, 2007; Lana-Renault *et al.*, 2007), was because of the high water content of the unsaturated soil near the ground surface in winter. This make the effective porosity very small, so that only small amounts of water are necessary to saturate the whole soil profile (Pirastru and Niedda, 2012). The SSFR model does not represent the water content of unsaturated soil greater than $_{33}$, showing pre-event soil moisture as being less than the actual value, and thus underestimates the rise of the water-table, as shown in Figure 6. The piezometers also showed that the amount of rise during storm-flow in wet seasons was proportional to the distance from the streambed. This can be seen from the smaller peaks at P1 and P2, which were only a few metres from the stream, and the larger peaks at P4, 17 m from the stream (Figure 1). This difference is due to the hydraulic gradients of the water-table, which feeds the stream discharge through the lateral SSF. The fact that the rapid water-table rises could not be fully reproduced by the model meant that the simulated gradients of the water-table were lower that those observed. Therefore, in order to generate the observed streamflow, a higher value of K_s was necessary in simulating SSF. This is one of the reasons for increasing the calibrated values of soil conductivity at the basin scale in SSFR.

By contrast in spring, when *ET* is the active process that quickly dries the surface soil while the water-table is still high in the valley bottom, as shown in Figure 2, there are high vertical gradients in the soil water potential. The SSFR model was also unable to simulate this, as it cannot represent soil water content of less than θ_{33} before the water-table level reaches zero. As a result, since the modelled *ET* subtracts water first from the water-table and then from the soil moisture below $_{33}$, the simulated water-table depths tend to anticipate the start of the recession observed in field, as shown in Figure 6. The rapid rise of the water-table in response to intense autumnal rainfall, but when its level is low and the soil was still dry, is perplexing. Here generally the simulation tended to delay the time at which the water-table rises. One reason for this is because the simulated volume of the infiltrated water are retained throughout the whole depth of the soil layers until θ_{33} is reached, and only then does the rise of the water-table begin. The mechanism by means of which the water-table can rise rapidly even when its level is low and the soil is still dry is a matter of debate. It may be due to both the effect of the macropores and the lateral contribution of wet soil under the streambed (Sophocleus, 2002). It may also be influenced by the vertical distribution of the drainable porosity and the hydraulic conductivity, which locally control the water-table variations and water flux. SSFR takes into account decreasing hydraulic conductivity with depth and uniform drainable porosity. Different vertical distribution would have to be verified by a quantity of field data generally too large to be collected at the catchment scale. These are complex processes that still need to be investigated experimentally and simulated by modelling. This lack of information is probably one of the reasons that less simplified models than the one we used, which simulate the 3D unsaturated flows, such as e.g. MIKE SHE (Abbott *et al.*, 1986) or ParFlow (Kollet and Maxwell, 2006), produce equally satisfactory results at the basin scale (Vansteenkiste *et al.*, 2012). Indeed, as stated by Brooks *et al.* (2007), the accuracy of any distributed hydrologic model is limited by our ability to characterize the spatial heterogeneity in soil hydraulic properties.

Conclusions

In this small Mediterranean research catchment, dominated by the SSF mechanism of runoff production, the relationship between rainfall and storm-flow depth at the event scale confirmed the strong non-linearity of these two variables, as has also been shown in other Mediterranean catchments (Ceballos and Schnabel, 1998; Martınez-Mena *et al.*, 1998; Latron and Gallart, 2007, Lana-Renault *et al.*, 2007). The storm-flow coefficient was mainly related to soil moisture and water-table depth, with values higher than 2% only during the wet winter period, suggesting that subsurface flow played a primary role in runoff production at the basin scale. The seasonal dynamics of soil moisture, water-table depth and stream discharge observed at the valley bottom of the Baratz catchment enabled us to recognize three seasonal periods of the water year, characterised by different dominant runoff formation processes: 1) summer and autumn, which have high water-table depths, low soil moisture and no stream discharge even when there is intense rainfall, which infiltrates into the soil and increases the water content and water-table level, without producing HOF; 2) winter, which has low water-table depths, high soil moisture and storm-flow generated by the SOF over saturated areas and by the SSF through pipes, macropores and seepage zones in the soil; 3) spring, which has low water-table depths, low soil moisture and slow base-flow generated by the exfiltration of SSF through the soil matrix. These results indicate that the dominant mechanism in runoff formation is the SSF, which gives rise to base-flow, controls the saturated areas formation and enters streams quickly enough to contribute to the storm-flow together with the SOF, while the HOF mechanism can be ignored.

References

Abbott M.B., Bathurst J.C., Cunge J.A., O'Connel P.E., Rasmussen J. 1986. An introduction to the European hydrological systems–systeme hydrologique Europeen, 'SHE'. 2. Structure of a physically based distributed modelling system. Journal of Hydrology 87:61–77.

Anderson M.G., Burt T.P. 1991. Process studies in hillslope hydrology: an overview, in: Process studies in hillslope hydrology, Wiley & Sons, Chichester: 1–8.

Betson R.P. 1964. What is watershed runoff?. J. Geophys. Res. 69:1541–1552.

Beven K., Lamb R., Quinn P., Romanowicz R., Freer J. 1995. TOPMODEL. In Computer Models of Watershed Hydrology, Singh V.P. (Ed.), Water Resour. Publ., Highlands Ranch, Colo.:627–668.

Beven K.J., Kirkby M.J. 1979. A physically based variable contributing area model of basin hydrology. Hydrological Sciences Bulletin 24:43–69.

Beven K.J. 1989. Interflow, in: Unsaturated Flow in Hydrologic Modelling Theory and Practice, edited by: Morel-Seytoux H.J., Kluwer Academic Publishers:191–219.

Brooks E.S., Boll J., McDaniel P.A. 2004. A hillslope-scale experiment to measure lateral saturated hydraulic conductivity. Water Resources Research 40: W04208. doi:10.1029/2003WR002858.

Brooks E.S., Boll J., McDaniel P. 2007. Distributed and integrated response of a geographic information system-based hydrological model in the eastern Palouse region, Idaho. Hydrological Processes 21:110–122.

Ceballos A., Schnabel S. 1998. Hydrological behaviour of a small catchment in the dehesa landuse system (Extremadura, SW Spain). J. Hydrol. 210:146–160.

Dickinson R.E., Henderson-Sellers A., Rosenzweig C., Sellers P.J. 1991. Evapotranspiration models with canopy resistance for use in climate models, a review. Agricultural and Forest Meteorology 54:373–388.

Dunne T., Black R.D. 1970. An experimental investigation of runoff production in permeable soils. Water Resources Research 6:478–490. doi: 10.1029/WR006i002p00478.

Frankenberger J.R., Brooks E.S., Todd Walter M., Walter M.F., Steenhuis T.S. 1999. A GIS-based variable source area hydrology model. Hydrological Processes 13:805–822. doi: 10.1002/(SICI)1099-1085(19990430)13.

Gascoin S., Ducharne A., Ribstein P., Carli M., Habets F. 2009. Adaptation of a catchment-based land surface model to the hydrogeological setting of the Somme River basin (France). J. Hydrol. 368:105–116.

Gascuel-Odoux C., Weiler M., Molénat J. 2010. Effect of the spatial distribution of physical aquifer properties on modelled water table depth and stream discharge in a headwater catchment. Hydrol. Earth Syst. Sci. 14:1179–1194.

Grayson R.B., Moore I.D., McMahon T.A. 1992. Physically based hydrologic modeling 1. A terrain-based model for investigative purposes. Water Resources Research 28:2639–2658.doi: 10.1029/92WR01258.

Hewlett J.D., Fortson J.C., Cunningham G.B. 1977. Effect of rainfall intensity on storm flow and peak discharge from forest land. Water Resources Research 13(2):259–266.

Hewlett J.D., Hibbert A.R. 1967. Factors affecting the response of small watershed to precipitation in humid areas. In: Sopper W.E., Lull H.W. (Eds.), International Symposium of Forest Hydrology. Pergamon Press: 275–290.

Horton R.E. 1933. The role of infiltration in the hydrologic cycle. Trans. American Geophysical Union 14:446–460.

Jana R.B., Mohanty B.P. 2012. On topographic controls of soil hydraulic parameter scaling at hillslope scales. Water Resources Research 48: W02518, doi:10.1029/2011WR011204.

Kirkby M.J. (Eds.) 1978. Hillslope hydrology, Wiley and Sons, Chichester.

Kollet S.J., Maxwell R.M. 2006. Integrated surface-groundwater flow modeling: A free-surface overland flow boundary condition in a parallel groundwater flow model. Adv. Water Resour. 29(7):945– 958.

Lamb R., Beven K., Myrabø S. 1997. Discharge and water-table predictions using a generalized TOPMODEL formulation. Hydrological Processes 11:1145–1168.

Lana-Renault N., Latron J., Regüés D. 2007. Streamflow response and water-table dynamics in a sub-Mediterranean research catchment (Central Pyrenees). J. Hydrol. 347:497– 507.

Latron J., Gallart F. 2007. Seasonal dynamics of runoff-contributing areas in a small mediterranean research catchment (Vallcebre, Eastern Pyrenees). J. Hydrol. 335 (1–2):194–206.

Martınez-Mena M., Albaladejo J., Castillo V. 1998. Factors influencing surface runoff generation in a Mediterranean semiarid environment: Chicamo watershed, SE Spain. Hydrological Processes 12:741–754.

Molénat M., Gascuel-Odoux C., Davy P., Durand P. 2005. How to model shallow water-table depth variations: the case of the Kervidy-Naizin catchment, France. Hydrological Processes 19(4):901–920.

Moore I.D., Grayson R.B. 1991. Terrain-based catchment partitioning and runoff prediction using vector elevation data. Water Resources Research 27:1177–1191.doi: 10.1029/91WR00090.

Mosley P.M. 1979. Streamflow generation in a forested watershed, New Zealand. Water Resources Research 15:795–806.

Nash J.E., Sutcliffe J.E. 1970. River flow forecasting through conceptual models, part I - a discussion of principles. J. Hydrol. 10:282–290. doi: 10.1016/0022-1694(70)90255-6.

Niedda M. 2000. Simulation of ground-water flow in steep basin with shallow surface soil. J. Hydraul. Eng. 126:670–678.

Niedda M. 2004. Upscaling hydraulic conductivity by means of entropy of terrain curvature representation. Water Resources Research 40: W04206. doi:10.1029/2003WR002721.

Niedda M., Pirastru M. 2012. Hydrological processes of a closed catchment-lake system in a semi-arid Mediterranean environment. Hydrological Processes, doi: 10.1002/hyp.9478.

Niedda M., Pirastru M. 2013. Modelling stream discharge and shallow water-table dynamics in a Mediterranean natural catchment (Sardinia). Hydrological Processes, in press.

Pilgrim D.H., Huff D.D., Steele T.D. 1978. A field evaluation of subsurface and surface runoff. II. Processes. J. Hydrol. 38:319–341.

Pirastru M., Niedda M. 2010. Field monitoring and dual permeability modelling of water flow through unsaturated calcareous rocks. J. Hydrol. 392: 40–53. doi: 10.1016/j.jhydrol.2010.07.045.

Pirastru M., Niedda M. 2013. Evaluation of the soil water balance in an alluvial flood plain with a shallow groundwater table. Hydrological Sciences Journal, 58:898–911, doi 10.1080/02626667.2013.783216.

Rawls W.J., Ahuja L.R., Brakensiek D.L., Shirmohammadi A. 1993. Infiltration and soil water movement. In Handbook of hydrology, Maidment D.R. (ed.), McGraw-Hill, New York, 5.1.

Refsgaard J.C. 1997. Parameterisation, calibration and validation of distributed hydrological models. J. Hydrol. 198:69–97.

Seibert J., Bishop K.H., Nyberg L. 1997. A test of TOPMODEL's ability to predict spatially distributed groundwater levels. Hydrological Processes 11:1131–1144.

Smith L., Wheatcraft S.W. 1993. Groundwater flow. In: Maidment D.R. (Ed.) Handbook of Hydrology, McGraw-Hill, Inc., New York. 6.1-6.58.

Sophocleous M. 2002. Interactions between groundwater and surface water: The state of the science. Hydrogeology Journal 10:52–67.

Spano D., Snyder R.L., Sirca C., Duce P. 2009. ECOWAT—A model for ecosystem evapotranspiration estimation. Agricultural and Forest Meteorology 149:1584–1596. doi:10.1016/j.agrformet.2009.04.011.

Vansteenkiste T., Tavakoli M., Ntegeka V., Willems P., De Smedt F., Batelaan O. 2012. Climate change impact on river flows and catchment hydrology: a comparison of two spatially distributed models. Hydrological Processes, doi: 10.1002/hyp.9480

Wigmosta M.S., Vail L.W., Lettenmaier D.P. 1994. A distributed hydrology-vegetation model for complex terrain. Water Resources Research 30:1665–1679, doi:10.1029/94WR00436.

Application of the new Morphological Quality Index in the Cordevole river (BL, Italy)

E. Rigon, J. Moretto, F. Delai, L. Picco, D. Ravazzolo, R. Rainato, M.A. Lenzi

Department of Land, Environment, Agriculture and Forestry, University of Padova, Italy

Abstract

The evaluation of the morphological quality of rivers is essential to define the level of alteration and for implementing future management strategies that consider also hazards related to fluvial processes and channel dynamics. This type of evaluation is particularly significant for the Italian rivers, that, as in many other European countries, have a very high level of human pressure. Recently, in Italy, the National Institute for Environmental Protection and Research has promoted a methodology named IDRAIM for hydromorphological analysis of streams that pursues an integrated approach aimed at a harmonized implementation of both the EU Water Framework Directive (WFD, 2000/60/EC), and the EU Floods Directive (2007/60/EC). In this paper we present the application of the Morphological Quality Index (MQI) protocol, which is part of IDRAIM, to determine the assessment of the morphological quality of the Cordevole River. The water network (only collectors greater than third-order were considered), has been divided, through GIS software, into 132 river reaches of homogeneous morphological characteristics, according to the first phase of the method. At this stage the semi-automatic calculation of lateral confinement (defined by "degree of confinement" and a "confinement index") was tried, in order to reduce the implementing time. The application of 28 indicators was made for 42 reaches representing the major river types and human pressures in the site investigation. The results showed that 48% of the analyzed reaches have a very good or good quality status, 38% have a moderate morphological quality, while only 14% have the characteristics of poor or very poor quality. The main causes that lead to a strong alteration of the terms of reference are linked to i) poor connectivity between hillslopes and river corridor, that is very important for the natural supply of sediment and large wood; ii) absence of vegetation in the river corridor, that is functional to a range of geomorphic processes; iii) presence of artificial elements, particularly the bed-load interception structures in the catchment, bank protection along the reach, and the removal of sediment, large wood and vegetation.

Correspondence: Emanuel Rigon, Department of Land, Environment, Agriculture and Forestry, University of Padova, Italy.
E-mail: emanuel.rigon@unipd.it

Key words: Hydromorphology, river network segmentation, morphological recovery, Water Framework Directive, Cordevole River (Bl, Italy).

Acknowledgments: this research was founded by both the University of Padua Strategic Research Project PRST08001, "GEORISKS, Geological, morphological and hydrological processes: monitoring, modelling and impact in North-Eastern Italy", Research Unit STPD08RWBY-004 and the Project "SedAlp": sediment management in Alpine basins, integrating sediment continuum, risk mitigation and hydropower", 83-4-3-AT, in the framework of the European Territorial Cooperation Programme "Alpine Space" 2007-2013.

Journal of Agricultural Engineering 2013; XLIV(s2):e9
doi:10.4081/jae.2013.(s1):e9

Introduction

Many European rivers suffered different ranges and types of human pressure that modified their morphology and altered their hydrological processes (Liébault and Piégay, 2001; Gurnell *et al.*, 2009). In the recent years, it was necessary to have a tool to assess the ecological, morphological, hydrological conditions and the alteration level respect the reference conditions of rivers. The main purpose of this tool is to define strategies of morphological recovery and plan river restoration management. The EU Water Framework Directive (WFD; European Commission, 2000) and EU Floods Directive (European Commission, 2007), defines a series of innovative criteria and actions necessary for the ecological classification and management of European rivers. The WFD introduces the term "hydromorphology", which requires the consideration of any modifications of flow regime, sediment transport, river morphology, and lateral channel mobility.

The evaluation of the hydromorphological quality is particularly significant for the Italian rivers, that, as in many other European countries, have a very high level of human pressure (e.g. Surian *et al.,* 2009; Rigon *et al.,* 2012b; Moretto *et al.*, 201). The National Institute for Environmental Protection and Research (ISPRA) has recently promoted a new and innovative methodology for the hydromorphological evaluation, analysis, and monitoring of Italian streams (IDRAIM). In this paper we present the application of the Morphological Quality Index (MQI) protocol, which is part of IDRAIM, (Rinaldi *et al.*, 2013) in the Cordevole River, a main tributary of the Piave River. The first phase of the MQI procedure (general setting and segmentation) was implemented for the whole catchment area and was classified by remote sensing with GIS techniques in 132 segments between the sixth and fourth order. The 28 indicators contained in the evaluation forms were applied in second phase for 42 reaches, about 30% of the total river network. In addition, we propose a methodology for the semi-automatic calculation of lateral confinement (defined by "degree of confinement" and a "confinement index"), in order to reduce the time of river network segmentation.

Study area

The Cordevole river (Figure 1) has a length of about 79 km, entirely within the province of Belluno (Italy north-east). It rises at the

Pordoipass (1919 m a.s.l.), in the municipality of "Livinallongo del Col di Lana" and flows into the Piave river near the town of Mel, (275 m a.s.l.). The major tributaries are the Fiorentina and Pettorina (near Caprile), the Biois (Cencenighe) and Tegnas (Taibon). Downstream of Agordo the stream continues along a narrow valley where sometimes remains dry, due to the hydroelectric derivations. A few kilometers from the mouth receives the Mis stream.

The catchment area (Figure 1), which accounts for 843 Km² (hydro GIS analysis, see below), has a mountainous planform, and gives to the hydrographic network a tormented morphology typical of Alpine basins. Woodlands cover about 40% of the territory, and are mainly spruce, and the local climate is very influenced by altitude and exposure (mean annual temperature is ≈ 7° C and mean annual precipitation is ≈ 1100 mm).

The geology of the area is very complex . The higher parts of the basin are generally composed of dolomite, limestone, and volcanic rocks forming subvertical cliffs, whereas the lower slopes, deeply incised by rivers, are formed by highly erodible sedimentary rocks and quaternary deposits, with diffuse mass wasting processes (Picco *et al.*, 2012)

The flow regime (contributions from rain and snowmelt) has a high runoff during the months of May-June and low flows during the months of January-February (colder months). In the autumn often occur intense and short duration rains, causing flash flood. Part of the territory of the basin lies within the Belluno Dolomites National Park and there are several natural areas and landscapes of Regional interest.

The artificial interventions (check-dams, transversal and crossing structures, bank protections) are very present in the stream and are located near population centers and roads. Many of these interventions were built in the years following the 1966 flood that showed how these areas can be dangerous. There are mainly transversal structures and check-dams very large and close-ups, now filled with sediment, and thus no longer functional. In the recent years there is a tendency to naturalistic intervene, but overall the interventions are few and only built in cases of extreme necessity for the hydrogeological safety. The interventions for hydroelectric power production, already designed in the 1930 for the presence of two natural basins (Marmolada Glacier and Alleghe Lake) are mainly represented by the Masarè spillway (Alleghe), the Ghirlo dam (Cenceninghe) and the Mis dam, that has a height of 91 m.

Materials and methods

The MQI evaluation provides a first phase of initial analysis and subdivision in homogeneous reaches, analyzing existing information and remote sensing data by GIS, and a subsequent application phase of the evaluation procedure (Rinaldi *et al.*, 2013). In this work, during the river network segmentation, various tools and scripts were implemented to reduce the application time , as the semi-automatic calculation of the indices needed to define the degree of confinement. During the second phase we analyzed the information derived from the first phase, and field surveys were made in 42 reaches with the support of the evaluation forms in order to define the geomorphic functionality, artificiality and channel adjustments for each reach.

General setting and segmentation

The initial setting and river network segmentation into relatively homogeneous reaches, considering the valley form, slope, flow and sediment load conditioning (Brierley and Fryirs, 2005) was carried in GIS project (ArcGIS 10, ESRI®) in which it was implemented a database with the following metadata:

- Digital color orthophotos for the years 2000, 2003, and 2006 available in Web Map Service mode on the National Geoportal (http://www.pcn.minambiente.it/GN/)
- Digital Terrain Model (DTM) in "ascii" format, downloaded from the Regional Geoportal (http://idt.regione.veneto.it/app/metacatalog/index?deflevel=165) and subsequently converted to raster with 5mX5m cell.
- Regional Technical Maps (CTR Veneto Region, from Geoportal)
- Regional Physiographic Units Map available from site of Agency for Environmental Protection and Prevention of Veneto, ARPAV (http://www.arpa.veneto.it/temi-ambientali/suolo)
- Regional Geolitological Map (downloaded from Regional Geoportal)
- Artificial Intervention Database (watershed management and torrent control structures) of the Belluno Province, provided by the Regional Hydrological Service.

These last metadata are organized according to types of structures, in different shapefiles that report essential information (eg. year of construction, geometric dimensions, etc.) for both the first as well as the second phase of the MQI evaluation.

The catchment area definition and the identification of the synthetic hydrographic network was made with the Arc Hydro Tools (ESRI®) setting the blue lines threshold value = 16 ha. From the DTM the Slope and Exposure Maps were derived. This geospatial information jointly the 2006 orthophotos were utilized for the photo-interpretation (Figure 2) and editing of active channel and alluvial plain (which is defined as the maximum width of the investigation river region). This editing work has been carried out throughout the river network from the 4th to 6th order (Horton-Strahler classification; Strahler, 1964).

The segmentation methodology was based on the MQI protocol application (Rinaldi *et al.*, 2012), but has been applied to a slightly different steps sequence and have been implemented some semi-automatic GIS processes. Initially it was carried out a first segmentation (editing of lines) considering the physiographic units, hydrological discontinuities (from hydro elaboration and artificial intervention database), relevant changes in channel width and alluvial plan width (obtained from

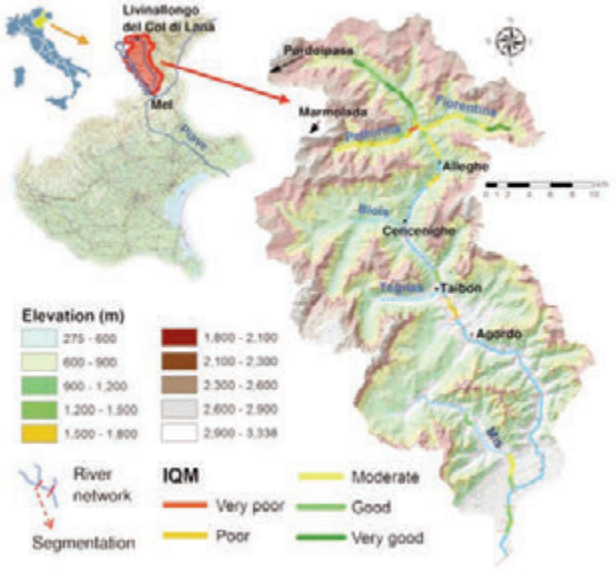

Figure 1. Map of the Cordevole basin, hydrograph segmentation and MQI evaluation results.

photo-interpretation), bed slope (slope map), and variations in geolitology. The active channel and alluvial plain shapes has been subdivided into various polygons with the segmentation lines intersection. The outer area of these polygons (buffer of 20 m) was intersected with the slope map, and has been calculated automatically the percentage of banks directly in contact with the hillslopes, identified as the terrain portions with a slope greater than 20° (Figure 2). In other words, it has been defined for each reaches the "degree of confinement". With other semi-automatic procedures was calculated the polygons area and perimeter and then the ratio between the alluvial plain width and the channel width for each reaches, called the "confinement index". Putting together these two indices could be computed rather quickly the lateral confinement (for more details on the classification see Rinaldi *et al.*, 2012). Eventually, according to this lateral confinement, appropriate adjustments have been carried on the initial division, and then we proceeded in the definition of river morphology taking into account the specific Italian Alpine context (e.g., Lenzi *et al.*, 2000).

Evaluation procedure

After the segmentation phase, for each identified reach were summarized data and information needed to apply the evaluation procedure. The field surveys were made in the period August 2012 – May 2013 with the support of the evaluation forms. 31 reaches of the upper part of the Cordevole (76% of reaches identified in segmentation phase) were analyzed and 11 other reaches representative of the downstream area. The water conditions during the measurements were of low flow and no significant flood events in prior periods. As required by the protocol different indices of geomorphological functionality, artificiality, and only for two reaches (channel width greater than 30 m) the channel adjustments, were analyzed. The evaluation of the 28 indicators was complete with the application MQI evaluation forms, which can be of two types, one for confined channels, and one for semi-confined and unconfined (Rinaldi *et al.*, 2013). The number and type of indicators are not the same in these two evaluation forms.

The main attention was paid to the analysis in the continuity (lateral and longitudinal) of river processes, channel morphological conditions and vegetation. Most of the applied indices were evaluated thanks to the information obtained during the first phase of general settings and segmentation. Three classes are generally defined for each indicator evaluating with a score of 0 in the case of absence or negligible presence of alteration, intermediate alteration score of 2-3, and highest alteration score 5-6. In cases of extremely dense and dominant presence of artificial elements are awarded additional points of alteration.

Results

The segmentation phase has identified 62 reaches of 4th, 33 of 5th, and 37 of 6th order (132 in total). For each of them, through the GIS analysis, segment length, average width of the active channel and alluvial plain, average slope, and drainage area were obtained. Furthermore, the degree of confinement and confinement index (Table 1) were calculated. All these data have been included in the GIS project database. The results show that the average length of river segments obtained is between 951 m (5th order) and 1347 m (6th order). The average width of the active channel is strictly linked to the reach order, and changes from 15 m (4th order), to 31 m (5th order) and 88 m for the

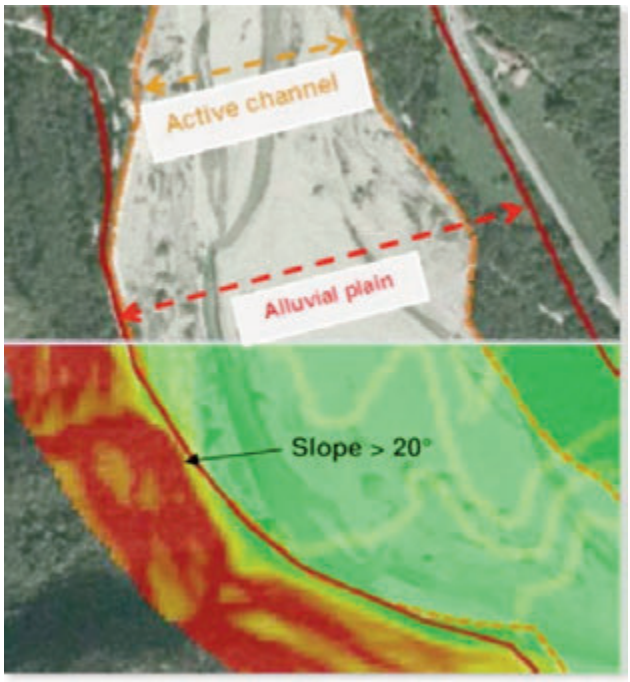

Figure 2. Segmentation phase and calculation of the indices of confinement.

Table 1. Characteristics of the reaches obtained in the segmentation phase of MQI protocol.

Stream order	Reaches identified		Length (m)	Width Alluvial plain (m)	Active channel (m)	Elevation (m.a.s.l.)	Degree of confinament	Confinament Index	Mean Channel Slope (m/m)	Drainage Area (km^2)
6th	37	Mean	1347	218	88	583	0.2	2.4	0.016	522
		Max	2923	920	310	1000	0.7	4.3	0.109	844
		Min	465	40	26	278	0.0	1.1	0.0004	222
5th	33	Mean	951	68	31	758	0.3	2.3	0.035	81
		Max	1940	188	86	1115	0.8	5.0	0.078	163
		Min	404	21	12	325	0.0	1.1	0.007	35
4th	62	Mean	1124	24	15	1091	0.3	1.6	0.091	27
		Max	1907	72	48	1634	0.9	2.5	0.259	70
		Min	345	6	5	425	0.0	1.1	0.011	8

reach of 6th order (Table 1). The degree of confinement, calculated with semi-automatic GIS methods has an average value of 0.2-0.3 with a maximum of 0.9 (90% of channel in contact with the slopes) in the smaller streams (Figure 3). The confinement index (relationship between the width of the alluvial plain and bankfull) is in general directly proportional to the stream order, with average values of between 1.6 and 2.4 (Figure 3), although higher values are observed in the case of 5th order.

The application of MQI evaluation forms has required about 3 hours of field surveys for each reach analyzed, for a total of 15 days of activity. 10 reaches of 6th order (27% of this order reaches identified in segmentation phase), 14 of 5th order (42%) and 18 of 4th order (27%) were analyzed. The results derived from the application of various indices have been organized in the summary sheets (one for each reaches) that contains tables with the general settings (location, confinement and morphology), scores attributed to each indicator and the calculation of MQI and the corresponding class quality. This data are summarized in Table 2 that contains the name of the river, reach order, the class of confinement, Morphological Alteration Index (MAI), MQI and the quality class represented with different. The MQIs obtained were also implemented in the GIS database from which it was obtained a layout summary (Figure 1) where the quality classes (with different colors) for each reach analyzed can be observed. On average, the lower values of MQI are observed in the Pettorina reaches and in 4th order reaches, as can be seen from the box plot in Figure 4. The distribution of MQI seems more linked to the collectors that the river order. These results show

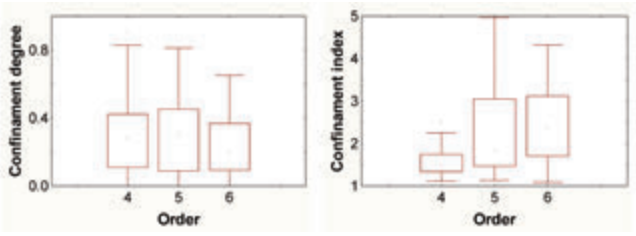

Figure 3. Degree and index of confinement in relation to order for the 137 reaches identified in segmentation phase of MQI protocol. The square within each box indicates the median value, box ends are 25th and 75th percentiles, whiskers are the 10th and 90th percentiles, and dots are outliers.

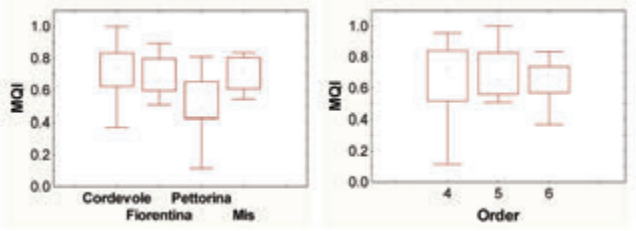

Figure 4. MQI evaluation results of the different streams and in relation to order for the 42 reaches analyzed. The square within each box indicates the median value, box ends are 25th and 75th percentiles, whiskers are the

Table 2. Morphological Quality Index results for the 42 reaches analyzed. Contains the name of the river, reach order, the class of confinement (Conf. class) and Morphological Alteration Index (MAI). The quality class is represented with different colors in MQI index cells: red, very poor; orange, poor; yellow, moderate; light green, good; dark green, very good. Look at the Figure 1 for the distribution into the river network of morphological quality class evaluated.

ID	60102	60103	60119	60120	60124	60133	60134	60135	60136	60137	50138	50139	50140	50141
River	Cord	Cord	Cord	Cord	Cord	Cord	Cord	Cord	Cord	Cord	Cord	Cord	Cord	Cord
Order	6	6	6	6	6	6	6	6	6	6	5	5	5	5
Conf. class	S-NC	S-NC	S-NC	S-NC	S-NC	S-NC	C	S-NC	S-NC	C	S-NC	S-NC	C	C
MAI	0.26	0.17	0.63	0.43	0.17	0.30	0.52	0.38	0.32	0.27	0.38	0.47	0.27	0.17
MQI	0.74	0.83	0.37	0.57	0.83	0.70	0.48	0.62	0.68	0.73	0.62	0.53	0.73	0.83

ID	50142	50143	40144	40145	40146	40147	40148	50201	50202	50203	50204	50501	50502	50503
River	Cord	Cord	Cord	Cord	Cord	Cord	Cord	Mis	Mis	Mis	Mis	Fior	Fior	Fior
Order	5	5	4	4	4	4	4	5	5	5	5	5	5	5
Conf. class	C	C	S-NC	C	C	C	C	S-NC	S-NC	S-NC	S-NC	S-NC	C	C
MAI	0.00	0.12	0.16	0.05	0.25	0.25	0.11	0.22	0.46	0.33	0.17	0.49	0.41	0.44
MQI	1.00	0.88	0.84	0.96	0.76	0.75	0.89	0.78	0.54	0.67	0.83	0.51	0.59	0.56

ID	50504	40501	40502	40503	40504	40505	40601	40602	40603	40604	40605	40606	40607	40608
River	Fior	Fior	Fior	Fior	Fior	Fior	Pett	Pett	Pett	Pett	Pett	Pett	Pett	Pett
Order	5	4	4	4	4	4	4	4	4	4	4	4	4	4
Conf. class	C	C	C	C	C	S-NC	C	C	C	C	S-NC	C	C	C
MAI	0.39	0.33	0.20	0.33	0.12	0.11	0.89	0.54	0.19	0.56	0.49	0.59	0.31	0.38
MQI	0.61	0.67	0.80	0.67	0.88	0.89	0.11	0.46	0.81	0.44	0.51	0.41	0.69	0.62

Cord, Cordevole; Fior, Fiorentina; Pett, Pettorina. C, confined; S-NC, semi-confined/unconfined.

Figure 5. Photos of some reaches evaluated and MQI results.

that 48% of the reaches analyzed have a good or high quality, and these are mainly located in the High Cordevole or in the less hydrographic network (four examples shown in Figure 5a, 5b, 5c, 5d). 38% present a moderate quality, and in particular different reaches of the Fiorentina, Cordevole from Caprile to Alleghe and Pettorina (Figure 5e 5f) . Only 14% is in poor or very poor quality, such as the Pettorina reach immediately upstream of the confluence with the Cordevole (Figure 5e 5f).

Discussion and final remarks

This work shows the successfully use, in a dolomite basin (Torrente Cordevole, Bl), of the new MQI protocol evaluation (Rinaldi *et al.*, 2013). The implementation of some semi-automatic GIS tools has allowed us to greatly speed up the first phase of the general setting and segmentation. It was also possible to determine in the laboratory, some indicators of alteration, in particular those that have a flood plain or basin scale application. Some limitations or problems arising during this first phase can be summarized as follows: i) the need of very good capacity of GIS analysis and editing; ii) limit of spatial analysis linked both the quality of the DTM and images, and the strong disturbance (shadows, vegetation, narrow valleys): in our case study it is seen that the hydrographic network lower of the fourth order are difficult to analyze; iii) need for a complete and updated of Artificial Intervention Database. In the analyzed area there are gaps in this database also of great works, such as the dam of Mis.

The second phase of indicators implementation has highlighted a low availability of some information necessary for the evaluation, such as the management of artificial structures and river clear-cut operation, and information of morphometric changes of the last 50 years of the great reaches. Some indicators are extremely simplified as shown by the MQI authors (Rinaldi *et al.,* 2103) and there is a strong subjectivity in the scoring of the indices in relation to the experience and training of the operators.

The sub-reaches that have the greatest degree of morphological alteration present i) poor connectivity between hillslopes and river corridor, mainly caused by the presence of roads, that is very important for the natural input from the slopes of sediment and large wood; ii) absence of vegetation in the river corridor, almost always as a result of human alteration, that is functional to a range of geomorphic processes; iii) presence of artificial elements, particularly the bedload interception structures in the catchment, bank protection along the reach, and the removal of sediment, large wood and vegetation, already highlighted in Rigon *et al.*, (2012a). A partial restoration of these reaches could be implemented by converting the old interception structures in new constructions designed by the criteria of natural engineering. In addition, it would be desirable to carry out the analysis of priorities, and implementing intervention only where really necessary, possibly with low-impact structures (e.g. wood retention structures with rope nets or rakes).

References

Brierley G.J., Fryirs K.A., 2005. Geomorphology and River Management: Applications of the River Style Framework. Blackwell, Oxford, UK . 398 pp.

European Commission, 2000. Directive 2000/60/EC of the European Parliament and of the Council of 23 October 2000 Establishing a Framework for Community Action in the Field of Water Policy. Official Journal L 327, 22/12/2000, Brussels, Belgium. 73 pp.

European Commission, 2007. Directive 2007/60/EC of the European Parliament and of the Council of 23 October 2007 on the Assessment and Management of Flood Risks. Official Journal L 288/27, 6/11/2007, Brussels, Belgium. 8 pp.

Gurnell A, Surian N, Zanoni L. 2009. Multi-thread river channels: a perspective on changing European alpine river systems. Aquatic Sciences 71: 253-265.

Lenzi M.A., D'Agostino V., Sonda D. (2000) - "Ricostruzione morfologica e recupero ambientale dei torrenti", + CD rom "Le morfologie d'alveo dei corsi d'acqua alpini", 208 pp., Bios, Cosenza, (ISBN 88-7740-302-0).

Liébault F., Piégay H. 2001. Assessment of channel changes due to long-term bedload supply decrease, Roubion River, France. Geomorphology 36: 167–186.

Moretto J., Rigon E., Mao L., Picco L., Delai F., Lenzi M.A. 2012. Medium- and short-term channel and island evolution in a disturbed gravel bed river (Brenta River, Italy). Journal of Agricultural Engineering. Vol. 43, 4; 176-188. DOI: 10.4081/jae.2012.e27.

Picco L., Mao L., Rigon E., Moretto J., Ravazzolo D., Delai F., Lenzi M.A. 2012 An update of the sediment fluxes investigation in the Rio Cordon (Italy) after 25 years of monitoring. Journal of Agricultural Engineering. Vol. 43, 3; 108-113; doi: 10.4081/jae2012e17

Rigon E., Comiti F., Lenzi M.A. 2012a. Large wood storage in streams of the Eastern Italian Alps and the relevance of hillslope processes.

Water Resources Research VOL. 48, W01518, doi:10.1029/2010WR009854

Rigon E., Moretto J., Mao L., Picco L., Delai F., Ravazzolo D., Lenzi M.A. & Kaless G, 2012b. Thirty years of vegetation cover dynamics and planform changes in the Brenta River (Italy): implications for channel recovery; IAHS Publication N. 356, pp. 178-186; ISSN 0144-7815.

Rinaldi M., Surian N., Comiti F., Busettini M., 2013. A method for the assessment and analysis of the hydromorphological condition of Italian streams: The Morphological Quality Index (MQI). Geomorphology 180-181: 96-108.

Rinaldi M., Surian N., Comiti F., Bussettini M., 2012. Guidebook for the Evaluation of Stream Morphological Conditions by the Morphological Quality Index (MQI). Version 1.1. 85 pp Istituto Superiore per la Protezione e la Ricerca Ambientale, Roma. ISBN: 978-88-448-0487-9.

Strahler, A. N. 1964. Quantitative geomorphology of drainage basins and channel networks, Handbook of Applied Hydrology, section 4-IIV. T. Chow, McGraw-Hill, New York.

Surian N., Ziliani L., Comiti F., Lenzi M.A., Mao L. 2009. Channel adjustments and alteration of sediment fluxes in gravel-bed rivers of north-eastern Italy: Potentials and limitations for channel recovery. River Research and Applications 25: 551-567.

Displacement length and velocity of tagged logs in the tagliamento river

Diego Ravazzolo,[1] L. Mao,[2] B. Garniga,[1] L. Picco,[1] M.A. Lenzi[1]

[1]Department of Land, Environment, Agriculture and Forestry, University of Padova, Padova, Italy

[2]Department of Ecosystems and Environment, Pontificia Universidad Catolica de Chile, Santiago, Chile

Abstract

Large wood enhance the dynamics of geomorphic processes in river systems, increases the morphological complexity of the channel bed, and provides habitats for fish and invertebrates. On the other side, if transported during high-magnitude events, large wood pieces can increase flood risks in sensitive places such as bridges and narrow cross sections prone to outbank flows. However, the dynamics and mobility of logs in rivers is poorly understood, especially in wide gravel-bed rivers. Recent studies have employed fixed video cameras to assess logs velocity, but little evidence is still available about travel length during flood events of different magnitude. This study was conducted in a valley reach of the Tagliamento river, located in the North East of Italy. The Tagliamento river is approximately 800 m wide in the study area, and is characterized by relatively high natural conditions and complex fluvial dynamics. Log mobility have been studied from June 2010 to October 2011, a period characterized by a relatively high magnitude flood in November 2010. Log mobility and displacement during floods have been measured by implanting active radio transmitters (RFID) in 113 logs and GPS track devices in 42 logs. The first devices allow to recover the log after flood events by using a portable antenna, and to derive the displacement length over the monitoring period, whereas the second devices allows to calculate instantaneous (1 sec) and average log velocity of moving logs. Recovery rate of logs equipped with RFID and GPS was about 50% and 60%, respectively. A preliminary analysis of the data collected indicates that there is a positive relationship between displacement length and the peak of flood events, as well as a positive relationship between log velocity and the flood magnitude. Also, a critical flow rate over which logs stranded on active bars can be transported has been identified. The ability to predict wood mobility in gravel-bed rivers could allow to define better strategies of river management and restoration, by improving the ability to understand wood transport processes and calibrate budgets of wood in rivers.

Correspondence: Diego Ravazzolo, Department of Land, Environment, Agriculture and Forestry, University of Padova, Padova, Italy.
E-mail: diego.ravazzolo@studenti.unipd.it

Key words: Large wood transport, Tagliamento river, gravel-bed river, wood characteristics, tracking systems.

Aknowledgement: this research was founded by both the Italian National Research Project PRIN20104ALME4-ITSedErosion: "National network for monitoring, modeling and sustainable management of erosion processes in agricultural land and hilly-mountainous area"; and The EU SedAlp Project: "Sediment management in Alpine basis: Integrating sediment continuum, risk mitigation and hydropower",83-4-3-AT, in the framework of the European Territorial Cooperation Programme Alpine Space 2007-2013.

Journal of Agricultural Engineering 2013; XLIV(s2):e10
doi:10.4081/jae.2013.(s1):e10

Introduction

Wood is an important component of river systems, as it could contribute to determine geomorphic (Brookes, 1988), hydraulic, and ecological processes (Gurnell *et al.*, 2002; Sedell *et al.*, 1988). Despite some positive effects in river systems, wood in-channel could represent an issue to some human activities on rivers, as it may disrupt navigation, including commercial marine operations on large rivers (Gurnell *et al.*, 2002; Piégay, 2003) and also might damage infrastructure when it accumulates on or near sensitive structures as bridge piers for example increasing bridge scour (Diehl, 1997; Wallerstein, 1998; Kothyari and Ranga Raju, 2001). Wood budgeting in mountain basin is thus of the highest importance in terms of morphodynamics studies of river systems and hazard mapping of floodplains and critical areas (bridge, in-channel structures, etc). However, a there still a considerable lack of knowledge on the complex set of processes involved in the recruitment, transport, deposition, and decay of wood pieces in fluvial systems, and even more on the quantification of these processes at the rage of spatial and temporal scales at which they occurred. Some previous studies have attempted to assess wood budget in mountain catchments trying to give a conceptual framework on how to approach the budgeting (Benda *et al.*, 2003; Martin & Benda *et al.*, 2001; Marcus *et al.*, 2011; MacVicar and Piégay, 2012) but there is a lack of knowledge on some factors on the formulas. In particular, entrainment threshold for log movement and displacement lengths during floods of different magnitude are still poorly quantified and scarcely measured in the field.

Recently, Marcus *et al.*, 2011 proposed an annual wood budget using a relation between transport rate and flow discharge. Beside, in the French Rhone River, Moulin and Piégay, (2004a) found a positive correlation between flood magnitude and volumes of transported. More recently, MacVicar & Piégay (2012) used a streamside video cameras to observe wood transport during floods, and correlated it with the water discharge in a wandering piedmont river, the Ain River in France. Other studies (Braudrick *et al.*, 1997; Braudrick and Grant, 2001; Haga *et al.*, 2002) investigated the relationship between the distance travelled by a single piece of wood and the local properties of the flow, observing that the travel distance depends on the wood size (i.e. length or diameter) and density, the water depth and velocity, and the channel bed roughness. Physical modelling of wood transport and displacement lengths with steady flow condition were carried out by Bocchiola *et al.* (2006a) and Bocchiola *et al.* (2008), who also explored

the behavior of logs in presence of obstacles.

This paper presents some novel data on log incipient motion and displacement lengths during floods of different magnitude in a large, braided gravel-bed river of the Eastern Italian Alps (Tagliamento).

Studyarea

This research was carried out in Tagliamento River, a braided gravel-bed river located in Friuli region in north-eastern Italy. The Tagliamento River has a basin area of 2871 km^2 and drains for about 172 km from the Italian Alps (1195 m a.s.l.) to the Adriatic Sea (Figure 1). The river has a straight course in the upper part, while most of its course is braided shifting to meandering in the lower part where dykes have constrained the lower 30 km. In the study reach, the river flows in a width of about 800 m and with a slope of about 0.003 mm^{-1}.

A strong gradient exists along the length of the river which has a big influence on precipitation, temperature, humidity and consequently vegetation patterns. In fact in the Tagliamento River there is an annual precipitation ranges from 3100 to 1000 mm per year and mean annual temperature from 5 to 14°C. Peak river flows usually occur in spring and autumn due to snowmelt and intense precipitation respectively.

The Tagliamento River is one of the few European gravel-bed rivers still retaining a highly dynamic nature and ecomorphological complexity because of a relatively low human impact (Tockner *et al.,* 2003), it is considered as the last morphologically intact river in the Alps and is an ecosystem model for large temperate rivers indeed, along most of its course, the river is enclosed by riparian woodland dominated by *Populus nigra* and *Salix alba* (Bertoldi *et al.*, 2013; Francis *et al.*, 2008) especially along the margins and on the many islands within the active, increase the supply of LW in-channel. Whereas the gravel bar surfaces stored 1-6 t ha^{-1} of wood and vegetated patches stored more than 1000 t ha^{-1}. However, it was observed in study area through field survey a wood storage of 6 t ha^{-1} (Gurnell *el al*., 2000).

Materials and methods

Log mobility was studied from June 2010 to October 2011, a period characterized by a relatively high magnitude flood in November 2010 recorded at Villuzza's gauging station (Figure 2). Woody elements of different size and typology were measured to analyses the log mobility and displacement length during flood events. Active radio transmitters (RFID) and LandAirSea's 3100-EXT passive GPS track (below called GPS track) devices were implanted in 113 and 42 logs respectively (Figure 3).

RFID devices, the same tested in Ain River by MacVicar *et al.* (2009), were installed in little holes on the trunk and they were isolated from the water by a cover of silicone. These devices allow to recover the log after flood events by using a portable antenna, and to derive the displacement length over the monitoring period, whereas the GPS track allows calculating instantaneous (1 sec) and average log velocity of moving logs. These devices, never tested in rivers before, have dimensions in cm of 8.64 W x 10.67 L x 4.32 H and powered by 4AA batteries. They are equipped with an external GPS antenna and up to 300 hours of internal GPS flash data storage-tracking capacity. The devices have a cold start GPS acquisition time, warm start and hot start GPS of 90, 50 and <10 seconds respectively. Each GPS track was waterproofed using a plastic box , where a RFID was placed as well in order to allow post-event recovery. Plastic boxes were fixed to woody elements tying them to the trunk with metal chains and cable ties.

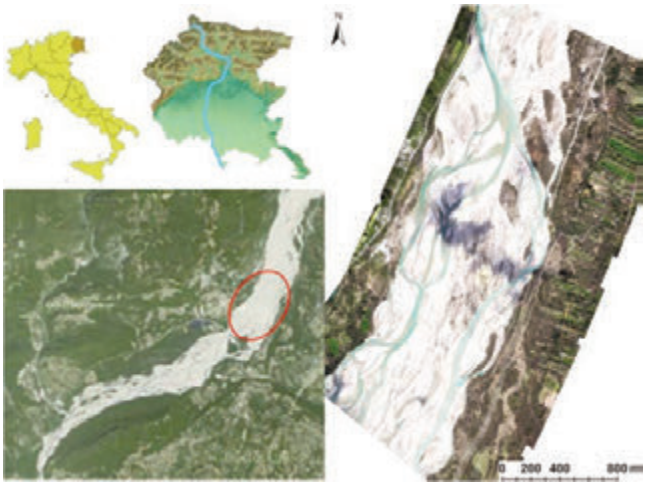

Figure 1. Location of Tagliamento river and the Cornino sub-reach.

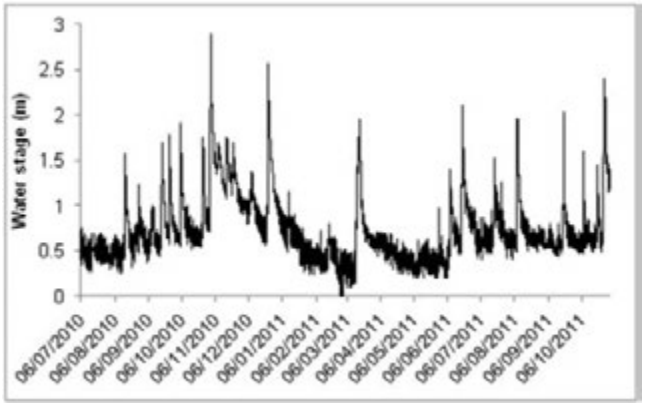

Figure 2. Water stage recorded at Villuzza's gauging station in Tagliamento river.

Figure 3. Example of the different devices installed on the logs in Cornino sub-reach: LandAirSea's 3100-EXT passive GPS track (a) and Active radio transmitters (RFID) (b).

The devices were installed at three different times during the study period. 21 GPS track and 75 RFID were installed in August 2010, further 7 RFID and 6 GPS were installed in December 2010, and lastly, 31 RFID and 15 GPS were installed in March 2011.

All the woody elements were tagged in low bars (Rinaldi, 2000) in order to have similar incipient motion conditions. Each tagged log was measured using a spread sheet and the volume was calculated using its mid-diameter and length taken by a tree caliper and tape, respectively (Mao *et al.*, 2008). Additional data concerning tree species, orientation to flow, state of decay, delivery mechanism and position in the channel were collected for each log analyzed. The positions of all tagged log was recorded before and after the flood events using a DGPS Leica series Viva. DGPS data were surveyed and geo-referencing of the same control network (stable points along the floodplain).

Results

From June 2010 to March 2011, 113 RFID and 42 GPS track were installed in 155 logs. The recovered logs accounted for 56 RFID and 26 GPS track (Table 1). During the flood events of the study period, 31 RFID and 5 GPS track were mobilized. Furthermore, 15 GPS track recorded an activation signal (e.g. the plastic box floated around the log, which was not transported by the flood) but they were not mobilized. On the Figure 4 are indicated the logs with GPS track that have been displaced and the logs which have only been activated but not transported. The highest recorded rates of GPS track activation were recorded on 15/08/2010 and 05/10/2010, with peaks flow high 1.57 and 1.91 m at Villuzza, respectively. On the other hand, the highest recorded rates of GPS track with movement were recorded on 15/08/2010 and 19/06/2011, with peaks flow high of 1.57 and 2.11 m, respectively. GPS_8a was transported for more than 51000 m during the flood event of the 19/06/2011.

Most of the tagged logs, were entrained during the rising limb or at the peak of the hydrographs. Also, most of the immobile GPS tracks have recorded a signal of activation during the rising limb of the lowest floods. It is important to note that during the falling limb of the flood event in November 2010, the GPS_4 recorded two signals of movement, 03/11/2010 and 06/11/2010 respectively.

The median value of the flow which have activated but not moved the logs with GPS track installed is around 38% of the bankfull stage, whereas a 40% of bankfull stage is required to entrain the tagged logs.

To assess the relation between high flow discharge and logs displacement length, the flow duration curves have been calculated, taking into account the whole period in which the RFID remained installed in the field before being recovered, and the period in which GPS Track devices moved. From the flow duration curves, the following percentiles were calculated: h_{25}, h_{50}, h_{75} and h_{100} (i.e. the maximum registered flow stage). Figure 5 shows that there is a certain correlation between the displacement length and the peak of hydrograph that caused the entrainment. Beside, this relationship increased in statistical significance if h_{25} and h_{75} are taken into account as well.

Knowing the log's travel distance and the duration of their movements, it was possible to calculate log's velocity during floods. Because logs could temporarily stop during the events, their velocity is called "virtual velocity", *sensu* Wilcock (1997). It was observed that there is a relatively poor correlation between the peak of transporting floods and virtual velocity. However, using the (h_{75}-h_{25}) ratio, the regression sensibly increases its statistical significance. Because velocities calculated from data collected by the GPS Track devices is a real velocity, as it considers only the interval in which the log actually moved, it is surprising that there appears to be no relation between velocity and the water stage of hydrograph. This is likely due to the reduced number of observation, and to the fact that considerable velocity fluctuations were observed.

Discussion and Conclusions

A proper assessment of wood budgeting at the basin and reach scale of a river system is crucial for engineering, geomorphological, and ecological purposes. However, the current knowledge of physical processes involved in the recruitment, entrainment, transport and deposition of logs in rivers is very poor due to the complexity of these phenomena and the lack of field observation. This study provides one of the few field evidence of log transport during floods in a wide, braided gravel-bed river. Displacement length and virtual velocity data have been col-

Table 1. Summary of recovery rate of GPS Track and RFID devices during the study period.

% Lost		GPS Track 38.1	RFID 50.4
Found	Moves	11.9	27.4
Found	Immobile	50	22.1

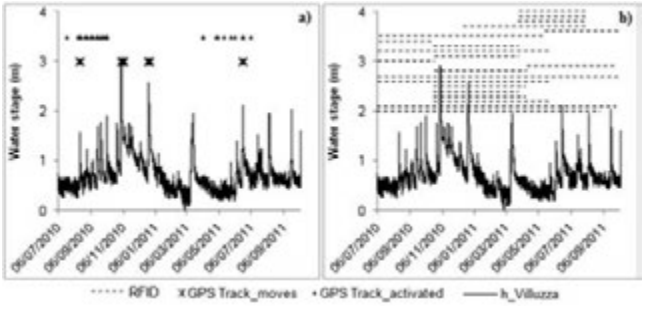

Figure 4. Flood events during the study period with the identification of the activation and displacement of the GPS Track devices (a) and the installation days and recovery of RFID devices (b).

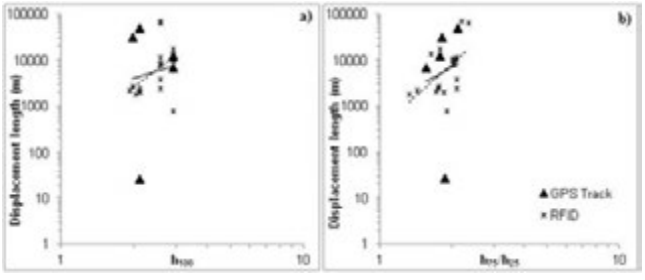

Figure 5. Power trend lines that analyze the relation between logs displacement length in function of the percentile 100 of the GPS Track and RFID flow duration curves (GPS Track R^2=0.0102 RFID R^2=0.2399) (a) and in function of the ratio between the percentiles 75 and 25 (GPS Track R^2=0.0107 RFID R^2=0.3011) (b).

lected using active radiotransmitters (RFID) and GPS antennas with dataloger fixed to logs lying on low, active bars. The devices proved to work reasonably well, as the recovery rate was quite high, and comparable with what reported by MacVicar *et al.* (2009). Large wood transport has been recently analyzed by MacVicar and Piégay, (2012) using a video camera fixed to the bank of a river, and a LSPIV tracking software. Even if this method does not work overnight, it allowed to observe that log transport is higher during the rising limb of hydrographs. This has been verified in the Tagliamento as well, and is likely to be related to the transport of ready-available logs stranded in the low bars. As expected, logs are likely to be deposited in low bars during the falling limb of hydrographs, at a lower discharge than the required for its entrainment. As to the relationship between wood transport and flood peak magnitude, the study suggests that there is a poor direct correlation. This is in agreement with what previously observed by Moulin and Piégay (2004a) and modeled by Marcus *et al.* (2011), who suggested that this relationship is highly non-linear.

This preliminary results reported in this study are to be enriched by further time series analysis and an attempt of numerical modelling, but represent one of the first attempts of measuring log entrainment, travel distance and velocity in a gravel-bed river in Italy. Further studies could increase our current understanding of these processes in rivers, with important practical applications such as risk analysis in floodplains, design of in-channel structures, and river ecology application.

References

Benda LE, Sias JC. A quantitative framework for evaluating the mass balance of in-stream organic debris. In: Forest Ecology and Management, 172; 2003. pp 1–16.

Bertoldi W, Gurnell AM, Welber M. Wood recruitment and retention: The fate of eroded trees on a braided river explored using a combination of field and remotely-sensed data sources. In: Geomorphology, 180-181; 2013. pp 146–155.

Bocchiola D, Rulli MC, Rosso R. Transport of Large Woody Debris in the presence of obstacles. In: Geomorphology, 76; 2006a. pp 166–178.

Bocchiola D, Rulli MC, Rosso R. A flume experiment on the formation of wood jams in rivers. In: Water Resources Research, 44; 2008. pp 17.

Braudrick C.A, Grant G.E, Ishikawa Y, Ikeda H. Dynamics of wood transport in streams: a flume experiment. In: Earth Surface Processes and Landforms, 22; 1997. pp 669-683.

Braudrick CA, Grant GE. Transport and deposition of large woody debris in streams: a flume experiment. In: Geomorphology, 41(4); 2001. pp 263–283.

Brookes A. Channelized Rivers, Perspectives for Environmental Management. In: Wiley, New York; 1988. pp 362.

Diehl TH. 1997. Potential drift accumulations at bridges. US Department of Transportation, Federal Highway Transportation.

Francis RA, Petts GE, Gurnell AM. Wood as a driver of past landscape change along river corridors. In: Earth Surface Processes and Landforms, 33; 2008. pp 1622–1626.

Gurnell AM, Petts GE, Hannah DM, Smith BPG, Edwards PJ, Kollmann J, Ward JV, Tockner K. Wood storage within the active zone of a large European gravel-bed river. In: Geomorphology, 34; 2000. pp 55–72.

Gurnell AM, Piégay H, Swanson FJ, Gregory SV. Large wood and fluvial processes. In: Freshwater Biology, 47; 2002. pp 601–619.

Haga H, Kumagai T, Otsuki K, Ogawa S. Transport and retention of coarse woody debris in mountain streams: An in situ field experiment of log transport and a field survey of coarse woody debris distribution. Water Resources Research, 38; 2002. pp 1126.

Kothyari UC, Ranga Raju KG. Scour around spur dikes and bridge abutments. In: Journal of Hydraulic Research, 39(4); 2001. pp 367–374.

MacVicar BJ, Piégay H. Implementation and validation of video monitoring for wood budgeting in a wandering piedmont river, the Ain River (France). In: Earth Surface Processes And Landforms, 37; 2012. pp 1272–1289.

MacVicar BJ, Piégay H, Henderson A, Comiti F, Oberlin C, Pecorari E. Quantifying the temporal dynamics of wood in large river: field trials of wood surveying, dating, tracking, and monitoring techniques. In: Earth Surface Processes and Landforms, 34; 2009. pp 2031–2046.

Mao L, Burns S, Comiti F, Andreoli A, Urciolo A, Gavino-Novillo M, Iturraspe R, Lenzi MA. Acumulaciones de detritos lenosos en un cauce de Montaña de Tierra del Fuego: Analisis de la movilidad y de los efectos hydromorfologicos. In: Bosque, 29 (3); 2008. pp 197-211.

Marcus WA, Rasmussen J, Fonstad MA. Response of the fluvial wood system to fire and floods in northern Yellowstone. In: Annals of the Association of American Geographers, 101; 2011. pp 22–44.

Martin DJ, Benda LE. Patterns of instream wood recruitment and transport at the watershed scale. In: Transactions of the American Fisheries Society, 130; 2001. pp 940–958.

Moulin B, Piégay H. Characteristics and temporal variability of large woody debris trapped in a reservoir on the River Rhone (Rhone): implications for river basin management. In: River Research and Applications, 20; 2004a. pp 79–97.

Piégay H. Dynamics of wood in large rivers. In: Gregory, S.V., Boyer, K.L., Gurnell, A.M. (Eds.), The Ecology and Management of Wood in World Rivers. American Fisheries Society, Bethesda, MD; 2003. pp 109–134.

Rinaldi M. 2000. "Erosione del suolo, fenomeni franosi e dinamica fluviale". Dispense del corso di Geologia Applicata. Università degli studi di Firenze. Corso di Laurea in Ingegneria per l'Ambiente e il Territorio. pp. 180.

Sedell J.R, Richey J.E, Swanson F.J. The river continuum concept: a basis for the expected ecosystem behavior of very large rivers? In: Canadian Special Publication of Fisheries and Aquatic Sciences, 106; 1989. pp 49–55.

Tockner K, Ward JV, Arscott DB, Edwards PJ, Kollmann J, Gurnell A.M, Petts GE, Maiolini B. The Tagliamento River: a model ecosystem of European importance. In: Aquatic Sciences, 65; 2003. pp 239-253.

Wallerstein NP. Impact of LWD on fluvial processes and channel geomorphology in unstable sand bed rivers. PhD thesis, University of Nottingham, UK; 1998.

Wilcock PR. Entrainment, displacement and transport of tracer gravels. In: Earth Surface Processes and Landforms, 22; 1997. pp. 1125–1138.

The influence of the net rainfall mixed Curve Number – Green Ampt procedure in flood hazard mapping: a case study in Central Italy

Andrea Petroselli,[1] Ettore Arcangeletti,[1] Elena Allegrini,[1] Nunzio Romano,[2] Salvatore Grimaldi[3]

[1]Dipartimento di scienze e tecnologie per l'agricoltura, le foreste, la natura e l'energia (DAFNE), University of Tuscia, Viterbo, Italy; [2]Dipartimento di Agraria, Sezione di Ingegneria Agraria,

Abstract

A net rainfall estimation procedure, referred to as Curve-Number For Green-Ampt (CN4GA), combining the Soil Conservation Service - Curve Number (SCS-CN) method and the Green and Ampt (GA) infiltration equation was recently developed, aiming to distribute at sub-daily time resolution the information provided by the SCS-CN method. The initial abstraction and the total volume of rainfall provided by the SCS-CN method are used to identify the ponding time and to quantify the hydraulic conductivity parameter of the GA equation, whereas the GA infiltration model distributes the total volume of the rainfall excess provided by the SCS-CN method. In this study we evaluate the proposed procedure with reference to a real case comparing the flood mapping obtained applying the event-based approach for two different net rainfall scenarios: the proposed CN4GA and the common SCS-CN. Results underline that the net rainfall estimation step can affect the final flood mapping result.

Introduction

Since floods can alter even seriously the environment and compromise human activities and economic development, flood hazard mapping is considered as the optimal non-structural tool for sustainable urban and land planning. It plays a fundamental role in flood prevention and protection. According to the European Directive 2007/60, the assessment and management of flood risks should lead to reduce negative consequences on people and environment. As a result, effective flood prevention and mitigation are strongly needed to successfully overcome impacts of flood events [European Directive, 2007/60].

A preliminary floodplain characterization at the basin scale can be carried out applying simplified hydrogeomorphological methods, which mainly refer only to terrain analysis and Digital Elevation Models (DEMs) [Dodov and Foufoula-Georgiou, 2006; Nardi *et al.*, 2006]. However, in order to gain inundation maps useful for urban and land planning, advanced hydrologic and hydraulic modeling are required. While the former provides flood peak discharges or flow hydrograph with a given return period, the latter employs a monodimensional (1D) or bidimensional (2D) hydraulic propagation models in order to accurately evaluate the spatial flow distribution. In the past years, the complex 2D models suffered from the limited amount of input data and computational burdens. Nevertheless, these limitations have been recently overcome leading to advanced approaches for accurate spatial and temporal flooding process simulations [Grimaldi *et al.*, 2013a; Horritt *et al.*, 2007]. As a consequence, nowadays, detailed urban development projects should include 2D modeling as a mandatory solution.

In general, the hydrological-hydraulic procedure for flood mapping includes several steps as follows [Petroselli, 2012; Sampson *et al.*, 2012]: (1) terrain analysis for morphometric attributes; (2) design hyetograph estimation (3) net rainfall evaluation (4) rainfall-runoff modeling (5) design hydrograph quantification, and (6) hydraulic propagation model.

The present paper explores the third stage of the above sequence by providing an evaluation of a recently proposed procedure [Grimaldi *et al.*, 2013b, 2013c], known as Curve-Number For Green-Ampt (CN4GA) that combines the Soil Conservation Service - Curve Number (SCS-CN) method and the Green-Ampt (GA) infiltration equation. A real case study in a small watershed –for which rainfall and flood inundated areas are available– is further investigated in the present work. Starting from gross rainfall observations, two net rainfall scenarios – namely CN4GA and SCS-CN respectively– are estimated and routed by the use of 2D modeling in the selected case study. The comparison of the two flooded areas with the observed one allows to evaluate if the CN4GA procedure provides reliable results.

Correspondence: Andrea Petroselli, DAFNE, Università degli Studi della Tuscia, via San Camillo de Lellis snc, 01100, Viterbo.
Tel. +39.0761.357348. E-mail:petro@unitus.it

Key words: CN4GA, flood mapping, rainfall–runoff modelling, SCS-CN method, WFIUH.

Journal of Agricultural Engineering 2013; XLIV(s2):e11
doi:10.4081/jae.2013.(s1):e11

Material and methods

The SCS-CN method [Soil Conservation Service, 1972] is a lumped approach describing the runoff or precipitation excess P_e (mm) as a function of the accumulated gross precipitation depth P (mm) according to:

$$P_e = \frac{(P - I_a)^2}{P - I_a + S} \quad , \quad I_a = 0.2 \cdot S \quad , \quad S = 254 \cdot \left(\frac{100}{CN} - 1 \right) \qquad (1)$$

where I_a is the initial abstraction (mm), S is the maximum potential retention (mm), and CN is the Curve Number, ranging from 0 (null

runoff) to 100 (runoff equals the gross rainfall).

The Green-Ampt (GA) method [Green and Ampt GA, 1911; Mein and Larson, 1973] is an infiltration equation exploiting Darcy's law and is based on the following expression:

$$I(t) = K_s t + \Delta h \cdot \Delta\theta \cdot \ln\left[1 + \frac{I(t)}{\Delta h \cdot \Delta\theta}\right] \quad (2)$$

where $I(t)$ is the cumulative infiltration rate (mm), K_s the saturated hydraulic conductivity (mm/h), t is the time (h), Δh the driving matric pressure-head (mm), and $\Delta\theta$ (-) is the change in soil moisture content between the saturation condition and the initial condition (*i.e.* $\Delta\theta = \theta_{sat} - \theta_{init}$). In Eq. 2 four parameters need to be quantified in order to estimate the cumulative infiltration function: θ_{sat}, θ_{init}, Δh and K_s.

Since it is inappropriate to apply the SCS-CN at sub-daily time resolution, recently, an empirical and iterative procedure [Grimaldi *et al.*, 2013b, 2013c] (CN4GA, Curve Number for Green-Ampt) combining GA and the SCS-CN methods has been introduced. In the mixed procedure the cumulative P_e and I_a values are derived using the SCS-CN method and then used to estimate the ponding time and the GA hydraulic conductivity K_s, since this latter is the most difficult parameter to quantify. The others GA parameters, as shown in Grimaldi *et al.*, 2013c, are insensitive in the CN4GA procedure and then literature values are taken into account, considering simple soil properties and assuming the permanent wilting condition as the initial dry state for θ_{init}. In doing so, two different net rainfall scenarios can be obtained: SCS-CN and CN4GA, both having the same cumulative rainfall excess value and ponding time.

The selected case study is the Fiora watershed located in Central Italy, with basin area equal to 821 km^2 and with elevations ranging from 75 to 1660 m a.s.l.; the average basin slope is 9.8% while the land cover was derived from CORINE project [CORINE Project, 2000], and an average value of 72.45 was assigned to CN according to [USDA-NRCS, 2010]; for the CN4GA application, average values of the hydraulic parameters pertaining to sandy clay loam soil were used.

Four rain gauges (namely Montalto, Pitigliano, Sorano, Vulci) are available with rainfall observations at 1 hour time resolution: the rainfall event of November 11-13, 2011, has been selected and, moreover, the Thiessen polygon and the areal reduction factor methods have been employed in order to determine the average gross rainfall hyetograph. SCS-CN and CN4GA methods have been applied as previously described and the two net rainfall scenarios have been convolved with the basin IUH in order to obtain the resulting hydrographs. As IUH, the parsimonious WFIUH-1par was applied as described in [Grimaldi *et al.*, 2010, 2012]. The concentration time T_c = 18 hours and has been obtained using the NRCS empirical relation [Natural Resources Conservation Service (NRCS), 2008].

The two corresponding hydrographs have been routed implementing the 2D hydraulic model FLO-2D [FLO-2D, 2012]; topography and roughness conditions of the 2D hydraulic modeling project were derived by integrating the available digital data with field campaign. The selected hydraulic modeling domain, shown in Figure 2, is located in the proximity of the basin outlet within a large floodplain which has been flooded during the selected rainfall event: the observed flood area extension was digitized starting from orthophoto maps provided by Regione Toscana and Autorità di Bacino Interregionale del Fiume Fiora. In doing so, it is possible to compare the observed flood area with the two simulated ones.

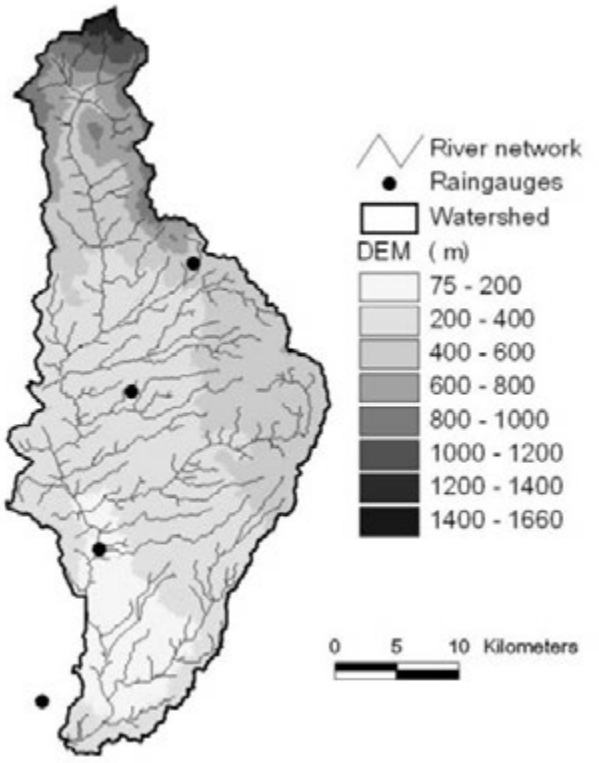

Figure 1. Case study DEM, rain gauges and drainage network.

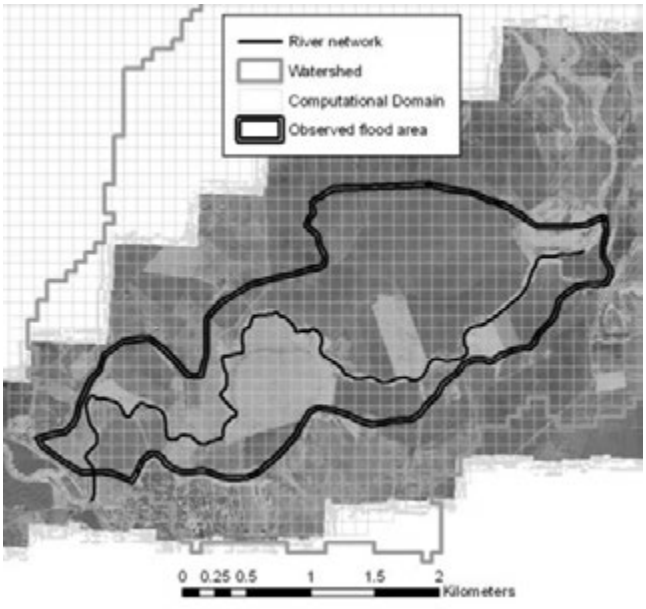

Figure 2. Case study 2D hydraulic modeling domain. Cell size resolution is 100 m.

Results and discussion

In Figure 3 the results of rainfall runoff modeling are reported; in the upper x axis the average gross hyetograph is shown together with the two estimated net hyetographs, while the two hydrographs are reported in the lower x axis. With specific regard to the considered rainfall event, the observed hydrograph is not available. The gross rainfall amount is 213 mm, while the net rainfall amount is 130 mm for both SCS-CN and CN4GA. Confirming previous literature results [Grimaldi *et al.*, 2013b, 2013c], CN4GA is more able, as respect to SCS-CN, to follow the shape of gross hyetograph, providing in this circumstance a peak discharge of 1844 m^3/s, while SCS-CN method provides a peak discharge of 1541 m^3/s. It is noteworthy that the Basin Authority "Autorità di Bacino Interregionale del Fiume Fiora" has estimated a peak discharge of 1911 m^3/s for the considered event, with a return period of 361 years.

In Figure 4 the results of 2D hydraulic modeling are shown. With respect to the observed and digitized flooded area, the CN4GA flood area is similar to the corresponding one obtained with the SCS-CN application. However, considering only the area that has been flooded, the CN4GA application provides, with reference to the SCS-CN application, 19 more cells, each one characterized by an area corresponding to 1 hectare, that appears to be inundated as it happened, while this situation does not happen with the SCS-CN application. This is mainly due to the fact that CN4GA rainfall-runoff modeling provides a higher peak discharge, resulting in a greater flooded volume and area. Anyway, differences among the flooded areas are moderate: SCS-CN flooded area is 4.26 km^2, and CN4GA flooded area is 4.49 km^2, being the differences around 5%. Regarding total flooded volumes, SCS-CN is 13,170,000 m^3, while CN4GA is 14,930,400 m^3, with a difference of 13%.

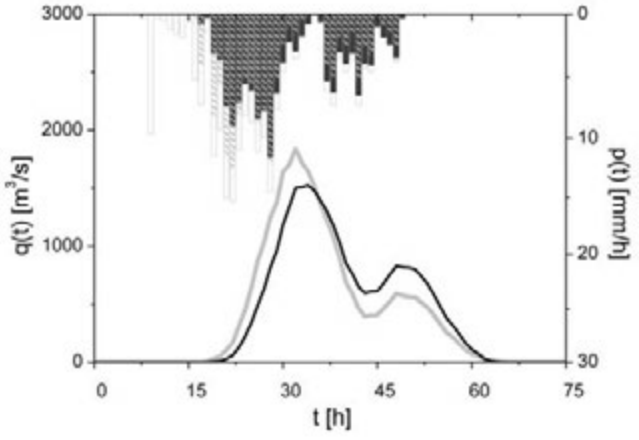

Figure 3. Results of rainfall runoff modeling. Upper x axis: gross rainfall (light gray), SCS-CN net rainfall (thick black), CN4GA net rainfall (thick gray). Lower x axis: SCS-CN net discharge (thick black), CN4GA net discharge (thick gray).

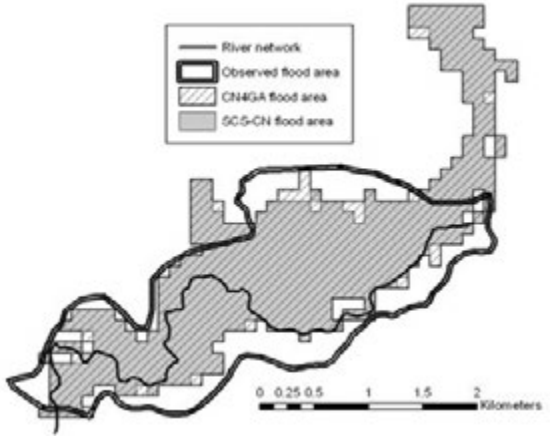

Figure 4. Results of 2D hydraulic modeling. Observed, SCS-CN and CN4GA flooded areas

Conclusions

A recently proposed mixed procedure, named CN4GA, specifically designed to distribute in time - according to the Green-Ampt infiltration equation - the total runoff volume provided by the SCS-CN method, is here applied on a case study in Central Italy in hydrologic-hydraulic event-based approach to derive flood maps. Three flood maps have been compared: one observed and digitized from aerial photos, two simulated with event-based approach adopting CN4GA and SCS-CN methods in the net rainfall step. The results show that the CN4GA modeled flood area is more similar to the observed one, although differences are moderate, being around 5% for flooded areas and 13% for flooded volumes among the two modeling approaches.

References

CORINE (Coordination of Information on Environment) Project, 2000. CORINE Database, a key database for European integrated environmental assessment. Programme of the European Commission, European Environmental Agency (EEA).

Dodov, B., Foufoula-Georgiou, E., 2006. Floodplain morphometry extraction from a high resolution digital elevation model: a simple algorithm for regional analysis studies. IEEE Geosci. Remote Sens. Lett. 3 (3), 410–3.

European Directive 2007/60

FLO-2D. 2012. FLO-2D Reference Manual (https://www.flo-2d.com/)

Green WH, Ampt GA. 1911. Studies on soil physics. J. Agr. Sci. 4(1): 1–24.

Grimaldi S, Petroselli A, Alonso G., Nardi F. 2010. Flow Time estimation with variable hillslope velocity in ungauged basins. Adv. Water Resour. 33:1216-23,

Grimaldi S, Petroselli A, Nardi F. 2012. A parsimonious geomorphological unit hydrograph for rainfall runoff modeling in small ungauged basins. Hydrolog. Sci. J. 57(1): 73–83.

Grimaldi, S., Petroselli, A., Arcangeletti, E., Nardi, F., 2013a. Flood mapping in ungauged basins using fully continuous hydrologic-hydraulic modeling. J. Hydrol. 487:39-47.

Grimaldi, S., Petroselli, A., Romano, N. 2013b. Green-Ampt Curve-Number mixed procedure as an empirical tool for rainfall-runoff modelling in small and ungauged basins. Hydrol. Process. 27(8):1253-64

Grimaldi, S., Petroselli, A., Romano, N. 2013c. Curve-Number/Green-Ampt mixed procedure for streamflow predictions in ungauged basins: Parameter sensitivity analysis. Hydrol. Process. 27(8):1265-75

Horritt, M.S., Di Baldassarre, G., Bates, P.D., Brath, A., 2007. Comparing the performance of a 2-D finite element and a 2-D finite volume

model of floodplain inundation using airborne SAR imagery. Hydrol. Process. 21:2745-59http://dx.doi.org/10.1002/hyp. 6486.

Mein RG, Larson CL. 1973. Modeling infiltration during a steady rain. Water Resour. Res. 9(2): 384–94.

Nardi, F., Vivoni, E.R., Grimaldi, S., 2006. Investigating a floodplain scaling relation using a hydrogeomorphic delineation method. Water Resour. Res. 42, W09409. http://dx.doi.org/10.1029/2005WR004155.

Natural Resources Conservation Service (NRCS). 2008. part 630 Hydrology, National Engineering Handbook. U.S. Department of Agriculture: Washington, DC.

Petroselli, A., 2012. LIDAR Data and Hydrological Applications at the Basin Scale. GIScience & 652 Remote Sensing, 49(1): 139-62.

Sampson, C.C., Fewtrell, T.J., Duncan, A., Shaad, K., Horritt, M.S., Bates, P.D., 2012. Use of terrestrial laser scanning data to drive decimetric resolution urban inundation models Adv. Water Resour. 41:1-17,

Soil Conservation Service (SCS). 1972. National Engineering Handbook, Section 4, Hydrology, (NEH-4), U.S. Department of Agriculture, Washington D.C..

USDA-NRCS. 2010. National Engineering Handbook, Part 630 - Hydrology. (http://www.info.usda.gov/viewerFS.aspx?hid=21422).

Erosion - deposition evaluation through hybrid DTMs derived by LiDAR and colour bathymetry: the case study of the Brenta, Piave and Tagliamento rivers

J. Moretto, F. Delai, E. Rigon, L. Picco, M.A. Lenzi

Department of Land, Environment, Agriculture and Forestry, University of Padova, Italy

Abstract

Risk management and flood protection are frequently assessed through geo-morphometric evaluations resulting by floods events. If we aim at elevation models with high resolutions and covering large areas, airborne LiDAR surveys can represent a good compromise among costs, time and uncertainty. The major limitation of the non-bathymetric LiDAR surveys consists in the detection of wet areas. Indeed, accounting for more than 20 cm of water depth, LiDAR signal increases exponentially its error. In this paper we present a comparison of the results concerning the application of a colour bathymetry methodology for the production of hybrid DTMs (HDTM). These elevation models were derived by merging LiDAR data for the dry areas and colour bathymetry for the wet areas. The methodological approach consists in a statistical regression between water depth and RGB band intensity values from contemporary aerial images. This methodology includes the use of filters in order to reduce possible errors due to the application of the model, to estimate precise "in-channel" points. The study areas are three different human impacted gravel-bed rivers of the North-East of Italy. This methodology has been applied in three sub-reaches of Brenta River, two of Piave River and two of Tagliamento River before and after relevant flood events with recurrence interval ≥ 10 years. Potentials and limitations of the applied bathymetric method, the comparison of its use in different fluvial contexts and its possibility of employment for geo-morphometric evaluations, were then tested.

DGPS control points (1841, 2638, 10473 respectively for Brenta, Piave and Tagliamento River) were finally used to evaluate the accuracy of wet areas. Results showed that, in each model, wet areas vertical errors were comparable to those featured by LiDAR data for the dry areas.

Correspondence: Johnny Moretto, Department of Land, Environment, Agriculture and Forestry, University of Padov, Italy.
E-mail: johnny.moretto@studenti.unipd.it

Key words: LiDAR data, DGPS survey, Colour bathymetry, Floods,Geomorphic changes, Gravel Bed River.

Acknowledgements: this research was founded by the University of Padua Strategic Research Project PRST08001, "GEORISKS, Geological, morphological and hydrological processes: monitoring, modelling and impact in North-Eastern Italy", Research Unit STPD08RWBY-004; the Italian National Research Project PRIN20104ALME4-ITSedErosion: "National network for monitoring, modeling and sustainable management of erosion processes in agricultural land and hilly-mountainous area"; and The EU SedAlp Project: "Sediment management in Alpine basis: Integrating sediment continuum, risk mitigation and hydropower", 83-4-3-AT, in the framework of the European Territorial Cooperation Programme Alpine Space 2007-2013.

Journal of Agricultural Engineering 2013; XLIV(s2):e12
doi:10.4081/jae.2013.(s1):e12

Introduction

The study of river morphology and dynamics is essential to understand the factors (natural and anthropic) determining sediment erosion, transport and deposition processes (Moretto *et al.*, 2013a). To better analyse the magnitude of different fluvial morphological adjustments, quantitative approaches are needed. Different methods proved to be able to provide high-resolution Digital Elevation Models (DEMs) of fluvial systems. Recent studies on morphological channel changes have used passive remote sensing techniques such as digital image processing (Legleiter and Roberts, 2009), digital photogrammetry (Lane *et al.*, 2010), active sensors including Laser Imaging Detection and Ranging (LiDAR) (Hicks *et al.*, 2012), Terrestrial Laser Scanner (Picco *et al.*, 2012) and acoustic methods (Rennie, 2012). The main problem related to the production of precise fluvial DTMs without using bathymetric sensors is due to the absorption of natural (solar) or artificial (LiDAR) electromagnetic radiation in the wetted channel. The survey of wetted areas can be thus approached using techniques based on the calibration of a depth-reflectance relationship of images, which can be in grey-scale (e.g. Winterbottom and Gilvear, 1997), coloured (Carbonneau *et al.*, 2006 and Moretto *et al.*, 2012) or multispectral (Legleiter *et al.*, 2011). All the solutions need a field survey, contemporary to the flight, to allow the availability of calibration depth points.

The present work proposes the analysis, on the Brenta, Piave and Tagliamento Rivers, of the Moretto *et al.*, (2012) methodology. This approach consists of a calibration of a depth-colour model to estimate channel water depths. After a filtering process, the bathymetric points for the wet areas and the LiDAR points for the dry areas will be merged to produce the final Hybrid Digital Terrain Models (HDTMs).

The specific objectives can be summarized as follows: i) analyse the results of a bathymetric approach in three different braided river systems; ii) evaluate limits and potentials of this procedure with attention to the factors significantly influencing the quality of the final results; iii) provide generic rules to minimize the possible source of errors.

Study area

Brenta river

The Brenta River, is located in the southeastern Alps covering a drainage basin of approximately 1567 km^2 and a length of 174 km. The study reaches, located between Bassano Del Grappa and Carturo (Figure 1), have a braided and wandering morphology, active channel width ranges between 300 m and 800 m and the average slope is 0.36%. Human impacts on this river were very intense; dams, gravel mining and torrent control works have caused severe effects. The average annual precipitation, mainly concentrated in spring and autumn seasons, is about 1100 mm. Three sub-reaches 1.5 km long and 5 km apart from each other were selected and named according to the nomenclature of the nearby villages: Nove, Friola and Fontaniva (Figure 1). For more details see Moretto *et al.*, (2013a).

Piave river

The Piave River, drainage area 4500 km^2, lies in the Eastern Italian Alps. The main channel flows in the south direction for 220 km from its headwaters to the outlet in the Adriatic Sea, near to Venice. The climate is temperate-humid with an average annual precipitation of about 1350 mm. Two study reaches have been selected in the middle portion of the river course (drainage area 3180 km^2 at the Busche dam; Figure 1). The first one, Belluno, features a length of about 2.2 km, whereas the second, Praloran, 3.2 km. The river morphology in the study sub-reaches is dominated by braided and wandering channel patterns; the slope is around 0.45%. For more detail see Delai *et al.*, (2013).

Tagliamento river

The Tagliamento River is a gravel-bed river located in the Southern Alps in North-Eastern Italy (Friuli Venezia Giulia Region) and is one of the last European rivers still maintaining a high degree of naturalness. It originates at 1195 m a.s.l. and flows for 178 km to the northern Adriatic Sea, thereby forming a link corridor between the Alps and the Mediterranean zones. Its drainage basin covers 2871 km^2 (Figure 1).

The hydraulic regime of the Tagliamento River is characterized by an irregular discharge and a high sedimentation load; due to the climatic and geological conditions of the upper part (annual precipitation can reach 3000 mm). Two sub-reaches located near to the town of Forgaria nel Friuli were analyzed. The upstream sub-reach "Cornino" shows a predominant braided morphology, with a slope of around 0.35%. Flagogna sub-reach has a predominant wandering morphology with a slope of around 0.30%. For more detail see Moretto *et al.*, (2013b).

Materials and methods

Data acquisition

Two LiDAR surveys were commissioned: the first in 2010 and the second in 2011 after the significant floods registered on November and December 2010 (Figure 2). For each LiDAR survey a point density able to generate digital terrain models with 0.5 m of resolution was required. LiDAR data were taken together with a series of RGB aerial photos with 0.15 m pixel resolution. In-channel DGPS points acquisition was performed, taking different depth. Overall, 399 (2010) and 1421 (2011) points for the Brenta River, 337 (2010) and 2301 (2011) points for the Piave River, 1107 (2010) and 9366 (2011) points for the Tagliamento River were acquired.

Indirect estimates of the water level and dataset preparing

Edges of the "wet area" through shape polygon and reliable LiDAR points able to represent the water surface elevation (*Zwl*) in our inference zone were selected. The correspondent intensity of the colour bands and *Zwl* were added to the points acquired in the wetted areas (DGPS wet-area survey) obtaining a shape file of points containing five fields (in addition to the spatial coordinates X and Y): the intensity of the three colour bands, Red (*R*), Green (*G*), Blue (*B*), the elevation of the channel bed (*Zwet*) and *Zwl*. Finally, the channel depth was calculated as $Dph = Zwl - Zwet$.

Figure 1. Study area of Brenta, Piave and Tagliamento River.

Figure 2. Floods of November 2011, Brenta River - Friola reach.

Hybrid DTM creation and validation

The best bathymetric model was applied to the georeferenced photos (raster calculator - ArcGIS® 10) to determine the RDph. The *RD*ph was then filtered in order to delete incorrect points, mainly due to sunlight reflections, turbulence, and elements (wood or sediment) above the water surface (Moretto *et al.*, 2012).

The corresponding *Zwl* was added to the corrected points (*D*ph model) to obtain, for each point, the estimated elevation of the river bed (*Zwet* = *Dph* + *Zwl).* Hybrid DTMs (HDTM) were built up with the natural neighbor interpolator, integrating Zdry points (by LiDAR) in the dry areas and Zwet points (by colour bathymetry) in the wet areas.

The final step was the validation of the HDTM models which was carried out by comparison with DGPS surveys (1841 points on Brenta River, 2638 points on Piave River, and 10473 points on Tagliamento River). The accuracy of the hybrid DTMs was estimated for wet areas considering colour bathymetry errors at different water stage levels grouped in classes incremented of 20 cm (see Table 1).

Results

Brenta river

The statistical regressions performed have produced the best bathymetric models for each inter-flood period. The maximum water depth estimated with an error lesser than ± 0.20 m has reached 0.80 m (Table 1) for this colour model:

$$Dph = 5.31 + 0.07513\ R - 0.1869\ G - 0.01475\ B - 0.0004582\ RB + 0.001056\ G^2 + 0.0003352\ B^2 - 0.000002142\ G^3 \quad (2)$$

where *Dph* is the estimated water depth and R, G and B are the red, green and blue bands, respectively. A similar model structure was found on the 2011:

$$Dph = -0.607 + 0.03508\ R - 0.06376\ G - 0.1377\ B + 0.002257\ RG - 0.001096\ RB + 0.002303\ GB - 0.0007273\ R^2 - 0.002956\ G^2 + 0.0009993\ B^2 + 0.000002837\ G^3 - 0.00000685\ B^3 \quad (3)$$

In this case the water depth estimated, lesser than ± 0.20 m of error has reached the same results of 0.80 m obtained for the 2010 (Table 1).

Piave River

From the statistical regressions performed in 2010, as in the Brenta River all the three colour bands have proved to be significantly correlated with the water depth:

$$Dph = 6.96 + 0.06222\ R - 0.01419\ G - 0.2581\ B - 0.0001518\ R^2 + 0.002002\ B^2 - 0.000005091\ B^3 \quad (4)$$

Table 1. Error analysis of depth-colour models applied at different water stages for 2010 and 2011 on Brenta, Piave and Tagliamento River.

REACH Depth	Brenta 2010 Dph (R, G, B)			Piave 2010 Dph (R, G, B)			Tagliamento 2010 Dph (R, G, B)		
	Error (m)	dev. St. (m)	Calib. points	Error (m)	dev. St. (m)	Calib. points	Error (m)	dev. St. (m)	Calib. points
0.00 - 0.19	0,26	0,22	107	0,43	0,28	7	0,15	0,11	232
0.20 - 0.39	0,26	0,24	87	0,21	0,16	42	0,10	0,09	327
0.40 - 0.59	0,21	0,20	75	0,08	0,15	81	0,10	0,09	275
0.60 - 0.79	0,22	0,18	59	0,00	0,17	70	0,18	0,13	184
0.80 - 0.99	0,26	0,15	32	0,08	0,18	50	0,32	0,19	64
1.00 - 1.19	0,51	0,21	20	0,20	0,23	38	0,54	0,22	15
1.20 - 1.39	0,69	0,14	13	0,11	0,22	27	0,46	0,21	9
1.40 - 1.59				0,29	0,23	11	-	-	1
1.60 - 1.79				0,13	0,13	8			
1.80 - 1.99				0,25	0,33	3			
> 2.00									
TOTAL			393			337			1107

REACH Depth	Brenta 2010 Dph (R, G, B)			Piave 2010 Dph (R, G, B)			Tagliamento 2010 Dph (R, G, B)		
	Error (m)	dev. St. (m)	Calib. points	Error (m)	dev. St. (m)	Calib. points	Error (m)	dev. St. (m)	Calib. points
0.00 - 0.19	0,27	0,11	61	0,05	0,09	221	0,37	0,11	127
0.20 - 0.39	0,18	0,11	248	0,04	0,11	967	0,21	0,11	599
0.40 - 0.59	0,13	0,11	427	0,19	0,11	628	0,14	0,11	1631
0.60 - 0.79	0,14	0,13	343	0,31	0,13	301	0,12	0,10	2233
0.80 - 0.99	0,24	0,19	187	0,45	0,18	123	0,13	0,10	2089
1.00 - 1.19	0,32	0,19	100	0,51	0,29	36	0,15	0,13	1419
1.20 - 1.39	0,40	0,13	35	0,62	0,30	8	0,18	0,16	755
1.40 - 1.59	0,56	0,10	20	0,69	0,56	4	0,26	0,18	341
1.60 - 1.79				0,59	0,70	7	0,38	0,21	123
1.80 - 1.99				1,08	0,54	6	0,49	0,19	39

This model reaches 1.40 m of water depth, with an error lesser than ± 0.20 m . Similarly, a regression model for 2011 was performed:

$$Dph = 0.83 - 0.004607\,R + 0.009665\,G - 0.04102\,B - 0.000205\,R^2 - 0.0006412\,G^2 + 0.0002062\,B^2 + 0.000002987\,G^3 + 0.0005447\,RG + 0.0005339\,RB - 0.000004473\,RGB \quad (5)$$

In this case, the maximum reached depth with an error lesser than ± 0.20 m is equal to 0.60 m (Table 1).

Tagliamento river

The 2010, statistical regression has demonstrated that, as in the Brenta and Piave River all the colour bands are significantly correlated with the water depth:

$$Dph = -0.207 + 0.09R + 0.1151G + 0.007827B + 0.001573G^2 + 0.0006577B^2 - 0.000005273G^3 - 0.000002425B^3 - 0.0006273RG - 0.0008327RB - 0.0004865GB + 0.00000649RGB \quad (6)$$

This model is able to reach such as for the Brenta River 0.80 m of water depth with an error lesser than ± 0.20 m (Table 1). Similar results were featured for 2011:

$$Dph = -0.69 + 0.0235R - 0.02822G + 0.008599B + 0.000061G^2 + 0.00009621B^2 - 0.00000006799R^3 - 0.0000004239B^3 - 0.00009157RG - 0.00004429RB - 0.00004228GB + 0.0000005079RGB \quad (7)$$

An example regarding the result of the model application is reported in Figure 3. From a general point of view the model seems to be able to produce a good water depth estimation comparing with the aerial photos.

This model, compared with the control points, estimates the wet area with an average error lesser than ± 0.20 m up to 1.40 m (Table 1) of water depth.

Discussion

The different water depth errors estimated from LiDAR and from the proposed colour bathymetric approach have been compared to the 2010 and 2011 Brenta, Piave and Tagliamento DGPS surveys and reported on Table 1.

The statistical analysis showed that all the three bands (R G B) and also some of the other constituent factors (interactions among bands and square and cubic terms) are significant ($P<0.05$) for each river and each year to predict the water depth.

The results confirm that more the depth increases, greater is the light adsorbed, as described by Legleiter (2012), raising the variability of R, G and B colour bands. This greater variability decreases the quality of the results of the colour models. Despite this decrease in quality, an adequate number of calibration points allow to reach an acceptable error in function of the final goal.

To provide some guidelines to project the "colour bathymetry survey", the expected error associated with the depth and the calibration points was implemented in Figure 4. Four "error model" are reported, one for each river (interpolating the 2010 and 2011 error data reported in Table 1) and one that is the average "error trend" obtained by interpolating all "error data" from each river. To provide more solid general rules, suspicious points were deleted. Therefore for the 2010 Piave points above 0.8 m (Table 1) of water depth were not considered. The lower error resulting seems to be erroneous if compared with the other survey. The reason is due to the bad luminosity conditions of the aerial photos. The different calibration point number among the different years and surveys at different water level, seems to suggest that: i) a minimum number of 200 - 250 calibration points for each water range level (with a step of 0.2 m) seems able to guarantee an average error lesser than ± 0.2 m, from 0 to 1.5 m of water depth; ii) between 1.5 m and 2 m of depth (the deepest range surveyed), the error is generally greater than ± 0.2 m and between 0.3 – 0.4 with at least 250 calibration points; iii) the different "error" trend among the analysed rivers suggest that the error is not only in function with the different depth and calibration points, but also with the "photo conditions" such as luminosity, hour of fly, etc.

Other important rules to produce a reliable colour bathymetry are: i) commissioning LiDAR and aerial photo surveys with the lowest water

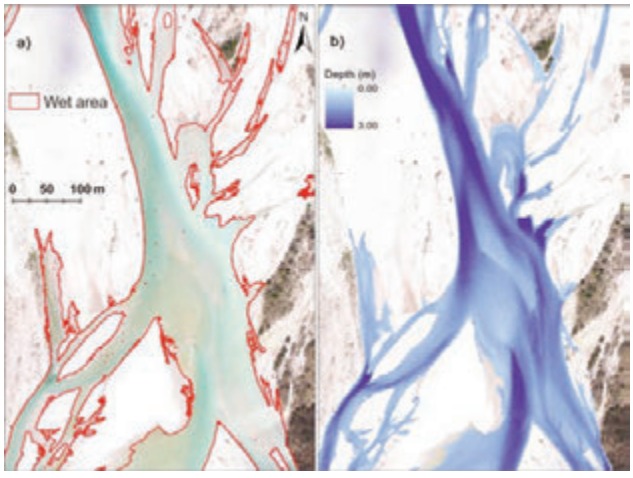

Figure 3. Wet area and colour bathymetry application on a sub-reach of Cornino 2011 (Tagliamento River).

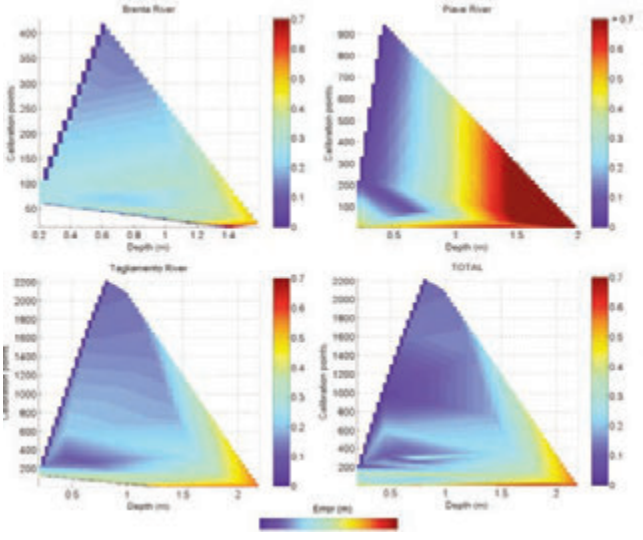

Figure 4. Error expected (with our surveys) at different water depth and number of calibration points.

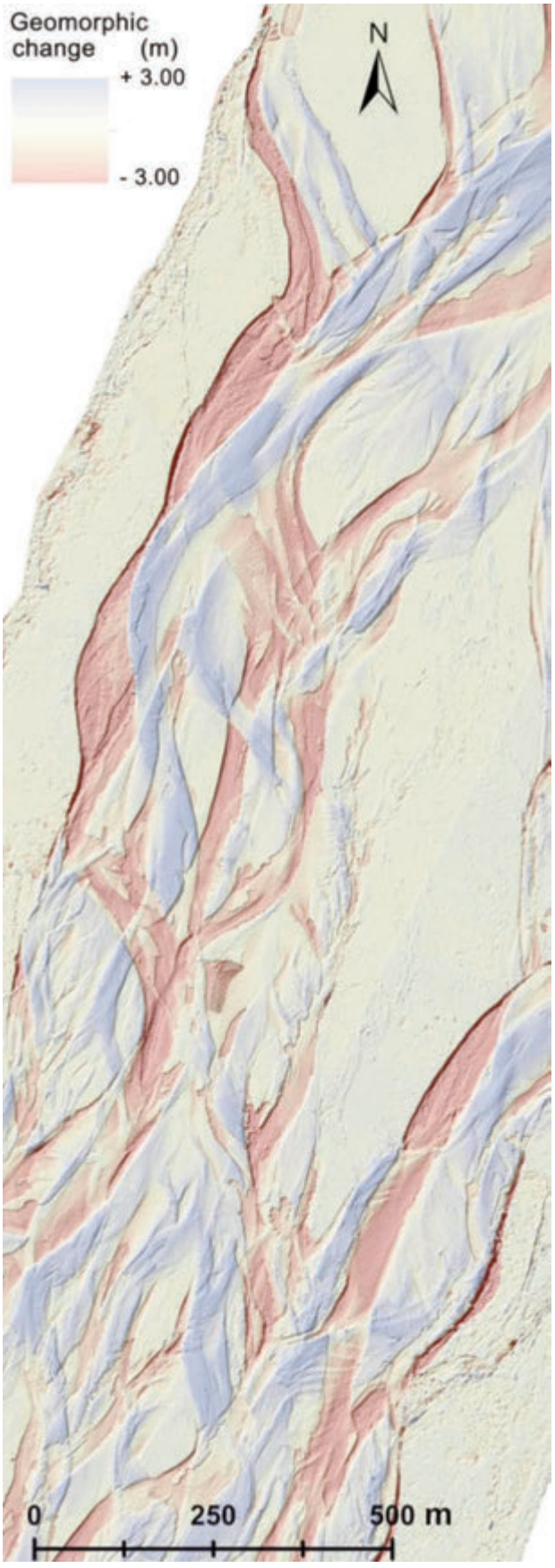

Figure 5. Difference of DEMs (DoD) of Cornino reach.

depth and suspended sediment load; ii) flight time around midday, to avoid shadows which can introduce more errors on the colour models; iii) perfect photo-georeferenziation; iv) good water level estimation in the whole reach. Finally, an "ad-hoc" calibration of a depth-colour model, for each river and for each year, is necessary to have more precise water depth estimation. Indeed among different rivers and temporal surveys, change the luminosity condition, the channel bottom colour, the water turbidity and other factors that can change the colour at the same water depth.

However, thinking about a depth-colour model generalization, this work suggest that is important to use models with three colour bands (if we are using RGB photos) to allow a better colour combination and avoid as much as possible, the noise effects due for example, to the presence of pheriphyton in the bottom (Moretto *et al.*, 2012). The depth-colour model could be calibrated by using all the data from each river and years together, but if we aim at precise volumetric change evaluation, as highlighted above, an ad-hoc calibration (depth models 2 – 7) results more accurate.

The difference of DEM (DoD), is reported (Figure 5) for the Cornino reach, derived from the 2011 and 2010 HDTMs difference. These changes are due to the flood events of November-December 2010 (RI > 10 years). The most part of the variations have occurred in the wet areas; as highlighted in Moretto *et al.*, 2012, Delai *et al.*, 2013 and Moretto *et al.*, 2013b. The results confirm that if we aim at geomorphic changes evaluation in environments with a significant presence of the wet areas, bathymetric techniques are required to not provide far results from the reality.

Conclusions

The proposed methodology allows the production of high-resolution DTMs of wetted areas with an associated uncertainty which is comparable to LiDAR data (Moretto *et al.*, 2012). The statistical analyses have demonstrated that all the three colour bands (R, G, B), in all the three rivers are significantly related to water depth.

The different number of calibration points acquired (Table 1) also at different water level, has shown that the error of the colour bathymetry is significantly related to water depth and water stage.

A minimum number of 250 calibration points for each water range level (with a step of 0.2 m) seems to be the threshold to guarantee an average error lesser than ± 0.2 m from 0 to 1.5 m of water depth.

The raster of difference (DoD) highlights the consequences of the flood events of November–December 2010 (RI > 10 years), indicating that deposition and erosion areas are more concentrated in the wet areas. In the analysis of braided morphologies, the calculation of not corrected estimations of change in those areas can lead to volumetric results far from the real values. The results of this study can be a valuable support to generate precise elevation models, also for the wet areas, that can be useful to evaluate erosion-deposition patterns, to improve sediment budget calculation, numerical modeling and to develop more effective river management strategies.

References

Burnham K.P., Anderson, D.R. 2002. Model Selection and Multimodel Inference: A Practical Information-Theoretic Approach. 2nd New York, ed. Springer, pp. 488.

Carbonneau P.E., Lane S.N., Bergeron N.E. 2006. Feature based image processing methods applied to bathymetric measurements from

airborne remote sensing in fluvial environments. Earth Surface Processes and Landforms 31: 1413–1423.

Delai, F., Moretto, J., Picco, L., Rigon, E., Ravazzolo D., Lenzi, M.A. 2013. Analysis of Morphological Processes in a Disturbed Gravel-bed River (Piave River): Integration of LiDAR Data and Colour Bathymetry. Journal of Civil Engineering and Architecture, USA JCEA-E 20130528-4. (In press)

Hicks, D.M. 2012. Remotely sensed topographic change in gravel riverbeds with flowing channels. In Church M., Biron P.M., and Roy A.G. Gravel-bed Rivers: Processes, Tool, Environments. Wiley-Blackwell, pp. 303-314.

Lane S.N., Widdison P. E., Thomas R.E., Ashworth P.J., Best J.L., Lunt I.A., Sambrook Smith G.H., Simpson C.J. 2010. Quantification of braided river channel change using archival digital image analysis. Earth Surface Processes and Landforms **35**: 971–985. DOI: 10.1002/esp.2015.

Legleiter, C.J. 2012. Mapping river depth from publicy available aerial images. River Research and Applications, doi: 10.1002/rra.2560

Legleiter, C.J., Kinzel, P.J., Overstreet, B.T. 2011. Evaluating the potential for remote bathymetric mapping of a turbid, sand-bed river: 1. Field spectroscopy and radiative transfer modeling. Water Resour. Res., 47, W09531, doi:10.1029/2011WR010591.

Legleiter, C.J., Roberts, D.A. 2009. A forward image model for passive optical remote sensing of river bathymetry. Remote Sensing of Environment 113: 1025–1045.

Moretto, J., Rigon, Mao, L., E., Picco, L., Delai, F., Lenzi, M.A. 2013a. Channel adjustments and island dynamics in the Brenta River (Italy) over the last 30 years. River Research and Applications. (In press)

Moretto, J., Delai, F., Picco, L., Rigon, E., Ravazzolo D., Lenzi, M.A. 2013b. Integration of colour bathymetry, LiDAR and DGPS survey for assessing fluvial changes after floods events in the Tagliamento River (Italy). Agricultural Sciences. ISSN Print: 2156-8553. (In press)

Moretto, J., Rigon, E., Mao, L., Picco, L., Delai, F., Lenzi, M.A. 2012. Assessing morphological changes in gravel bed rivers using LiDAR data and colour bathymetry. IAHS-AISH Publication, Issue 356: 419-427.

Picco, L., Mao, L., Cavalli, E., Buzzi, E., Rigon, E., Moretto J., Delai F., Ravazzolo D., Lenzi M.A. 2012. Using a Terrestrial Laser Scanner to assess the morphological dynamics of a gravel-bed river. IAHS-AISH Publication, Issue 356: 428-437.

Rennie, C.D. 2012. Mapping water and sediment flux distributions in gravel-bed rivers using ADCPs. Gravel-bed Rivers: Processes, Tool, Environments. Wiley-Blackwell, pp. 342-350.

Winterbottom, S.J., Gilvear, D.J. 1997. Quantification of channel bed morphology in gravel-bed rivers using airborne multispectral imagery and aerial photography. Regulated Rivers: Research and Management 13: 489–499.

The contribution of chestnut coppice forests on slope stability in abandoned territory: a case study

Chiara Bassanelli, Gian Battista Bischetti, Enrico Antonio Chiaradia, Lorenzo Rossi Chiara Vergani

DiSAA - Università degli Studi di Milano, Italy

Abstract

Sweet chestnut has been for many centuries fundamental for the Italian mountainous economies, where this kind of forest was traditionally managed in short rotation to rapidly produce wood biomass. Due to the social and economic changes, which made such management scheme unprofitable especially on the steep and remote slopes, such practice has been mainly abandoned and most of chestnut forests became over-aged and very dense, causing an increase of localized slope instability. In this work the effect of over-aged chestnut coppice forests on shallow landslides was analysed by evaluating and comparing mechanical contribution to soil shear strength provided by root systems in differently managed chestnut stands. The study area is located in Valcuvia (Lombardy Prealps) where three different stands, one managed and the others abandoned (over 40 year aged), established on cohesionless slopes (quaternary moraine deposits) were chosen having care to select homogeneous conditions in terms of substrate, aspect and elevation. As slope steepness strongly affects forestry practices and steeper stands are more frequently abandoned, the considered stands have different terrain inclination, 30-35° in abandoned stands and 13° in the managed one. Slope stability of the three sites was evaluated by applying the infinite slope approach accounting for additional root cohesion and tree surcharge. Additional root cohesion was estimated through the Fiber Boundle Model approach by collecting roots in the field and measuring their resistance in laboratory, and by measuring root diameter and density distribution with depth by the wall technique method.

The results, as expected, showed that over-aging does not affect root mechanical properties, whereas it significantly affects root distribution within the soil. In terms of slope stability, when steepness exceeds 35°, instability phenomena can be triggered by high level of soil saturation in the case of over-aged forests, whereas for less extreme cases chestnut forests, although over-aged, are able and fundamental to guarantee safe conditions.

Correspondence: Gian Battista Bischetti, DiSAA via Celoria 2 , 20133 Milano, Italy.
Tel. +39.0250316904 - Fax +39.0250316911. E-mail bischetti@unimi.it

Key words: root cohesion, slope stability, sweet chestnut.

Contributions: the authors contributed equally.

Conflict of interests: the authors declare no potential conflict of interests

Funding: the work was supported by Regione Lombardia – DG Agricoltura under "Programma Regionale di Ricerca in campo agricolo - Piano della ricerca 2004" - "Progetto Cedui e Dissesto Idrogeologico" ProCeDI.

Journal of Agricultural Engineering 2013; XLIV(s2):e13
doi:10.4081/jae.2013.(s1):e13

Introduction

The role of forests in contrasting many natural hazards is well established from ages (e.g. Motta and Haudemand 2000), especially when slope stability is the considered threat (e.g. Sakals *et al.* 2006). In the last decades a great number of studies have been carried out aiming to explain and quantify the effect of vegetation on slope stability (e.g. Bischetti *et al.* 2009; Schwarz *et al.*, 2010) and to model the soil reinforcement by roots (e.g. Wu, 2013).

Considerable less attention has been dedicated to the role of forest management on slope stability (e.g. Sidle, 1991), although a great part of forests around the world are now managed and nearly all the European and Italian forests have been managed from centuries. Among the most anthropised forests in the Alps and in the Apennines, sweet chestnut represents one of the most important and common case. Chestnut, in fact, for a long time has been the basis for many traditional mountain economies, which used it for fire, food, livestock feeding, manufacturing of daily tools, etc. (Del Favero, 2002). As chestnut has a naturally tendency to develop from the same stool several adventitious shoots characterised by a rapid growth, a common practice adopted to maximize the biomass increase is coppicing with a short rotation length (<20 years) and such a practice can be considered as the standard management scheme for chestnut in Italy.

Things have changed from the second half of XX century when the great socio-economic transformation which occurred in mountain society structure led to abandon many forests (Del Favero, 2002; Vogt *et al.*, 2006). Chestnut forests passed this from being over-managed, to be under-managed with a consequent over-aging of shoots and stools (several times the usual rotation length).

In such a situation a central question raises regarding the capability of over-aged coppiced sweet chestnut forests to guarantee the slope stability, especially in the many cases where steepness is high and soils are cohesionless. In many areas of Italian Alps and Prealps, in fact, demographic increase forced people to plant sweet chestnut also on very steep slopes, which were the first to be abandoned when the economic situation improved.

The aim of this paper is to improve our knowledge on the role of over-aged sweet chestnut forest in hillslopes stability by quantifying the contribution of roots in terms of additional cohesion. Three sites

were taken in Valcuvia (Varese, Italy) as a case study of over-aged sweet chestnut forests on cohesionless and steep terrains, that is a typical conditions of many hillslopes of Lombardy.

Material and methods

Slope stability model

In the case of shallow landsliding phenomena triggered by intense rainstorms, the infinite slope approach represents a standard among the different geotechnical models that can be adopted (Sidle and Ochiai, 2006). As all approaches referring to General Limit Equilibrium principle, the infinite slope method expresses the stability of hillslopes in terms of factor of safety, FoS, representing the ratio between stabilizing and destabilizing forces.

Under this approach, FoS for forest hillslopes can be calculated as (Hammond *et al.*, 1992):

$$FoS = \frac{c_r + c_s + \cos^2\alpha\left[q0 + \gamma(D - D_w) + (\gamma_{sat} - \gamma_w)D_w\right]\tan\phi}{\sin\alpha\cos\alpha\left[q0 + \gamma(D - D_w) + \gamma_{sat}D_w\right]} \quad (1)$$

where α is the angle of ground surface (°), D is soil thickness (m), D_w is saturated soil thickness (m), c_r is tree root reinforcement expressed as cohesion (N/m^2), q_0 is tree surcharge (N/m^2), c_s is soil cohesion (N/m^2), φ is the effective friction angle (°), γ is moist soil unit weight (kg/m^3), γ_{sat} is saturated soil unit weight (kg/m^3) and γ_d is water unit weight (kg/m^3). In equation 1 the effect of vegetation is fundamentally accounted for by means of the additional root cohesion and the tree surcharge values (besides hydrological control which reflects on D_w). Estimation of c_r, that is recognized as playing a key role (Wu *et al.*, 1979; Pollen and Simon, 2005), as a consequence, has been the object of a great number of studies in the last years. The most commonly adopted models for c_r estimation refer to the Wu (1976) and Waldron (1977) model, the Fiber Bundle Model (FBM; Pollen and Simon, 2005) and the Root Bundle Model (Schwarz *et al.*, 2010). In the present paper the FBM model has been adopted under the static fiber bundle approach and equal load sharing, as it has been proven to provide safer values (Ji *et al*, 2010).

FBM basically requires as input parameters the number of roots of different size that are present at different depth and their tensile resistance. According to the literature (e.g. Bischetti *et al.*, 2009; Genet *et al.*, 2010), only roots in the range 1-10 mm have been considered.

The infinite slope model is generally solved considering a shear plane parallel to topographic surface, but in the case of shallow landslides in forest hillsopes also the vertical shear surfaces is considered as resistant and c_r is estimated accounting the roots crossing both the vertical and basal planes (see e.g. Roering *et al.*, 2003).

Study area

The sites where studies have been conducted are located within the boundary of Comunità Montana Valli del Verbano (Figure 1), which is representative of a larger area in Lombardy and in the Prealps where a lot of over-aged coppice chestnut forests established on very steep cohesionless slopes. Within the study area, have been identified three different hillslopes covered by the same chestnut forest type, classified as "Castagneto delle cerchie moreniche occidentali" (Del Favero, 2002), but with different characteristics: A) over-aged coppice chestnut on a hollow topography; B) managed coppice chestnut (approximately 25 years old) and C) over-aged chestnut coppice on a nose topography (Figure 2).

The three sites are homogenous in terms of geology, aspect and elevation, but different in terms of steepness. As inclination strongly affect forest practices, in fact, all managed coppice forests are now limited to gentle and easily accessible slopes. According to USCS (Casagrande, 1948) soil in all sites has been classified as SM "silty sand, sand-silt mixture", and according to the literature and previous studies in similar areas (Bischetti *et al.*, 2004), geotechnical properties have been estimated in a safely perspective as c'=0 and ϕ'=27°. The characteristics of the three sites are reported in Table 1.

Table 1. Site characteristic.

Site	Site A	Site B	Site C
Number of trenches	2	2	2
Elevation(m a.s.l.)	600	580	595
Average inclination (°)	35	13	30
Average trees diameter (cm)	24,23	21,46	17,1
Distance between stools (m)	3,85	4,19	5,8
Average trees hight (m)	14,58	11,68	12,51
Basal area (m2/ha)	50,87	47,08	62,41
Live/dead	35/43	54/38	68/124
Management	Over-aged coppice	Managed coppice	Over-aged coppice
Topography	Concave	Convex	Convex
Soil depth (m)	0,8	0,5	0,9

Figure 1. Study area map and location of experimental sites.

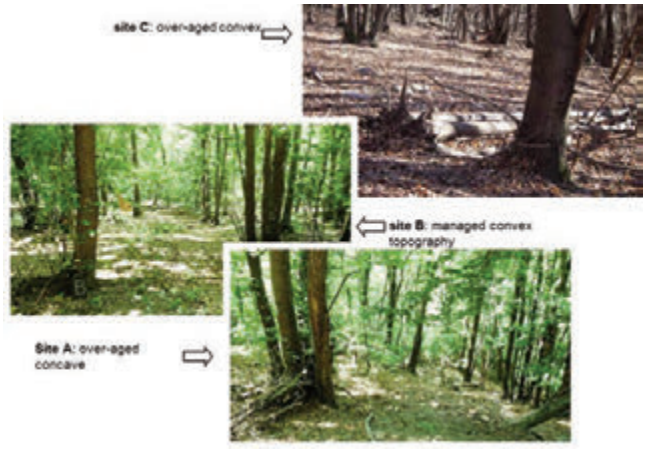

Figure 2. The investigated sites A) over-aged chestnut on hollow, B) managed chestnut and C) over-aged chestnut on nose.

In each site two trenches were dug to the parental material and until roots were no more present, in all cases trenches were located in the middle of a group of stools where the effect of roots is likely to be the lowest.

Root tensile tests

Roots for tensile resistance tests were collected by digging pits in the middle between adjacent stools, having care to do not damage them and sampling the full diameter range between 1 and 10 mm. Samples were preserved to deterioration maintaining roots in a 15% alcohol solution (Meyer and Gottsche, 1970; Bischetti *et al.*, 2003) until tensile tests were carried out.

Tensile test were performed by a device consisting of a strain apparatus (test speed 10 mm/min) controlled by an electrical motor, equipped with a load cell (F.S. 500 N, accuracy 0.1% F.S.) and special clamping devices able to avoid root damage at the clamping points (see Bischetti *et al.*, 2009 for details). Only specimens that broke near the middle of the roots between clamps were considered valid. Root size was estimated as the average of three values taken with an electronic caliper at three points near the section of the potential breaking (Abdi *et al.*, 2010; Vergani *et al.*, 2012).

Root density measures

Root density was measured at each dug trench by the trench wall method combined to image analysis (Bischetti *et al.*, 2009; Hales *et al.*, 2009). The method consists in cleaning the trench wall from all organic materials different from roots, putting a frame 0.3×0.3 m as reference, and taking a series of images to obtain a vertical profile; to increase the contrast between soil and roots the trench wall were wetted and a great care was given to the scene illumination. Images were then rectified to correct geometrical deformations through a specific software (GIMP 2 www.gimp.org) and roots diameter and position were measured through manual digitalization of each root using GIS software (MapWindow 4.6 ww.mapwindow.org).

Result

Root resistance

Roots sampled at the different sites have been tested in terms of tensile resistance, obtaining a number of valid tests between 40 and 56 for each site. Statistics of tensile tests summarized in Table 2 show that the mean tensile resistance values resulted comparable between the three sites (36,98 N for abandoned chestnut coppice in watershed; 34,53 N for managed chestnut coppice and 40,85 N for abandoned chestnut coppice on slope).

As force values (F) depends on root diameter (d) a regression F-d relationship has been obtained and, in agreement with what already found by other studies (e.g. Vergani *et al.*, 2012), this is a power – law type:

$$F = ad^{b} \quad (2)$$

Regression parameters are reported in Table 2 and show that the relationship is strong and highly significant in all the cases.

To verify a possible influence of over-aging and/or topography on root resistance, force-diameter data from the three different sites have been analysed by ANCOVA using diameter as a covariate. Results (Table 3) indicate that no significant difference can be detected between the resistance of roots sampled in the three sites.

As a consequence, it was possible to build a F-d relationship by using all values in a single power – law regression (Figure 3):

$$F = 10{,}80d^{1{,}57} \quad (3)$$

Root density distribution

The general trend in all sites, as expected, is a decrease in root density with depth, although in site C such a trend is less clear compared to sites A and B.

Table 2. Statistics of tensile tests and parameters of regression F-d power – law relationship

Site valid tests (#)	Site A 48	Site B 40	Site C 56
Diameter (mm)			
Aver.	1,87	1,88	2,05
Max	6,8	5,46	4,96
Min	0,6	0,55	0,34
Force at rupture (N)			
Aver.	36,98	34,53	40,85
Max	200,15	230,19	150,64
Min	3,83	4,67	2,49
a[1]	11,4	10,47	10,6
b[1]	1,56	1,52	1,6
R^2	0,87	0,82	0,93
p	< 0,001	< 0,001	< 0,001
F	297,9	176,5	717

[1]regression parameters of Equation 2.

Table 3. Results of ANCOVA between F-d series; Test L is Levene test for homoschedasticity, Test KS is Kolmogorov-Smirnov test for normality, Test Par. is the parallelism test and Test Int. is the intercept test.

Comparison	Test L	Test KS	Test Par.	Test Int.
A-B	$F_{1;84}$ = 0,42 Pr(>F) = 0,52	p-value = 0.89	$F_{1;84}$ = 467 Pr(>F) < 0,001	$F_{1;85}$ =472 Pr(>F) < 0,001
A-C	$F_{1;102}$ = 1,88 Pr(>F) = 0,17	p-value = 0,70	$F_{1;100}$ = 960 Pr(>F) < 0.001	$F_{1;101}$ = 968 Pr(>F) < 0.001
B-C	$F_{1;94}$ = 3,59 Pr(>F) = 0,06	p-value = 0,76	$F_{1;92}$ = 802 Pr(>F) < 0.001	$F_{1;93}$ = 807 Pr(>F) < 0.001

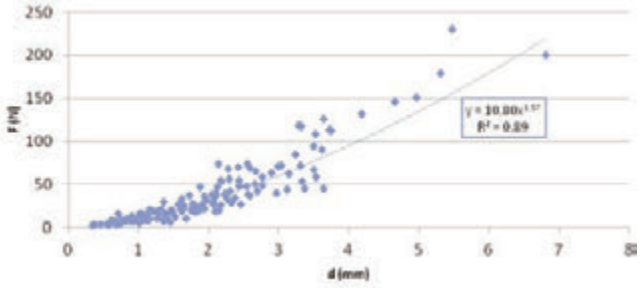

Figure 3. Force – diameter power – law relationship valid for all sites (R^2 = 0,89).

Rooting depth corresponds approximately to the pedologically active layers and then is shallower in the case of site B. Despite this difference, however, the total number of roots per unit width of soil is greater in the case of site B compared to sites A and C (2745, 2533 and 1878 roots/m, respectively). An important difference can also be noted in terms of size distribution (Figure 4); in site A and B, 1-2 mm class dramatically prevails on other size classes at all depths (between 70% and 80%), whereas in site C it represents only a little more than a half (between 40% and 60%).

Additional root cohesion

Additional root cohesion values were calculated at different depths in each site basing on root *F-d* relationship (Equation 2) and root density distributions, as previously introduced.

c_r values range between 5-25 kPa in shallower layers (10-20 cm) to 5-10 kPa in deeper layers (50-90 cm). Looking c_r distribution with depth for the three sites (Figure 5), it can be noted that they agree quite well with root density and size distributions as expected.

Slope stability

Slope stability at the three sites have been estimated by the infinite slope model implemented by Equation 1, fixing the potential shear surface at a depth of 0,9 m. In sites A and C, in fact, it is at such depth that shearing is most likely to occur, being a significant change in soil horizons (from A to B) and roots density.

In general it is worth to note that under the General Limit Equilibrium framework, it is evident that without any contribution from vegetation sites A and C would be intrinsically unstable as in cohesionless soils the FoS in dry conditions simply reduces to the ratio between the friction angle and the slope inclination.

Equation 1 was firstly applied to site A and C with different soil saturation levels to estimate the present level of stability (Figure 6). It can be observed from FoS curves that site A become unstable when saturation level exceeds 70% and at risk of instability also for smaller values. Site C can be considered stable for all level of saturation except for values higher than 60-70% for which it is moderately stable.

Due to uncertainty and space variability of c_r values, equation 1 was solved also combining site A with c_r profile of site C and vice-versa. The results show that in both cases, FoS values are between the actual ones and nearly always greater than 1,0 (except for fully a saturated condition in site A).

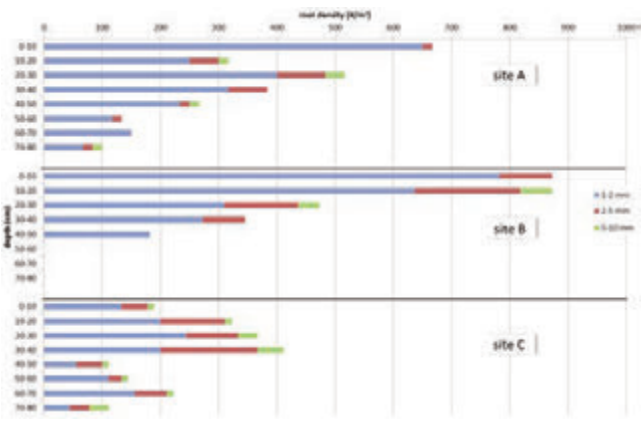

Figure 4. the distribution of root diameters resulted quite different for the three investigated sites in terms of maximum depth, number at different depth and size; in site B roots are shallower and denser with respect to other sites; in site C roots are about half compared to other sites and fine roots don't prevail on thicker classes.).

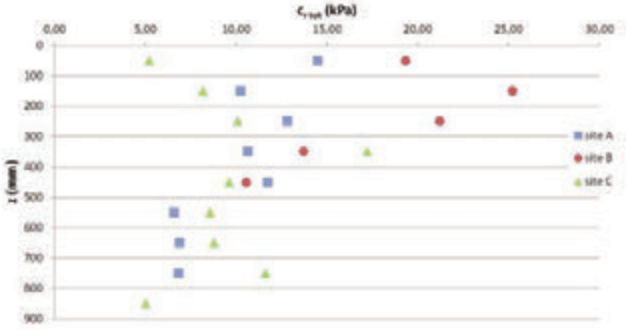

Figure 5. c_r values distributions with depth at the three considered sites show that the contribution of roots can be significant also in depth.

Discussion

The results of tensile tests indicate that root sampled at the three considered sites are not significantly different in terms of tensile resistance. The over-aging of coppice chestnut and/or the topography, as consequence, do not affect root tensile resistance, confirming that the main drivers of such a property are diameter and species, as found by previous researches (e.g. Genet *et al.*, 2005; Vergani *et al.*, 2012).

Root density and size distribution, on the contrary, showed several differences. First in sites A and C (over-aged forests) the rooting depth is higher than site B, where forest is managed (although at the end of its rotation). In principle, this could be explained by the charactersitic of chestnut stools to renew completely their root system at each coppicing operation (Bedeneau e Pagés, 1984) because this could keep roots shallower. Despite steepness, however, in sites A and C present an accumulation of soil, likely to arrive from the upper part of hillslope, and this makes roots deepening easier than in site B. Steepness itself, moreover, requires a deeper rooting to balance overturning moments.

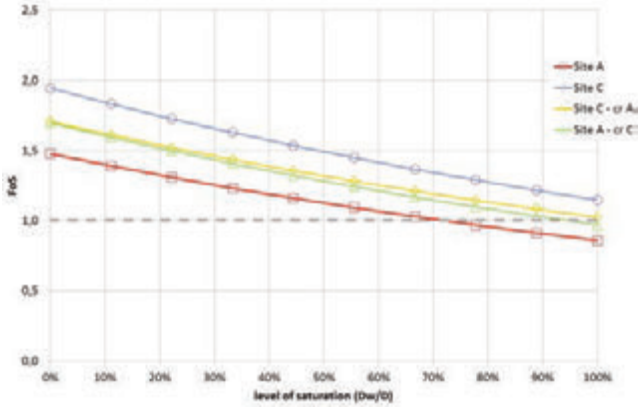

Figure 6. FoS values at sites A and C for increasing levels of saturation showing the level of instability.

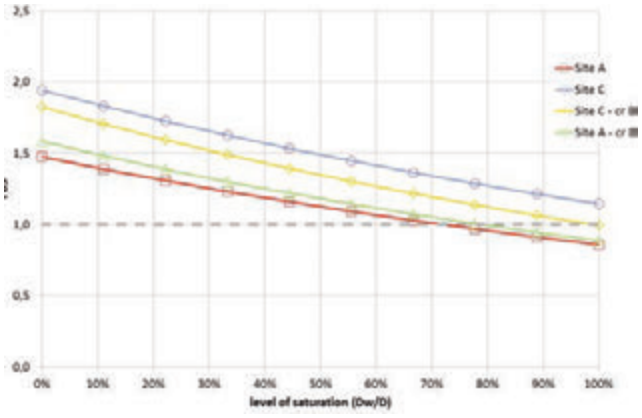

Figure 7. Comparison of FoS at sites A and C by adopting original cr values and values obtained from site B.

Besides rooting depth, a second point concerns the size distribution that is fairly similar in site A and B; the total number of roots is approximately the same, as well as the proportion of fine roots (1-2 mm class). On the contrary, in site C total root number is 75% of those at site A and, more relevant, fine roots are only a half of the total.

Such findings, which can have important implication on root cohesion, can be explained looking at the site characteristics. At site C, in fact, stools are sparser and dead stools are more in comparison to sites A and B (Table 1).

In any case, taking site B as a reference for managed condition, c_r distribution estimated at site B was applied to sites A and C (keeping shear plane depth at 0.9 m) for evaluating possible consequences of a restart in managing over-aged chestnut forests on steep slopes. Basing on the unfortunately scarce literature, in fact, a continuous renewal of root system consequent to coppicing could change root size distribution (Bedeneau e Pages, 1984; Aymard e Fredon, 1986; Bagnara e Salbitano, 1998).

The results (Figure 7) basically show a reduction in slope stability for site C, that for higher level of saturation could be critical, whereas in the case of site A changes are negligible.

Concluding remarks

This paper has shown that over-aged coppiced sweet chestnut forests, as well as managed ones of course, are fundamental in guarantee hillslope stability in those territories where steepness and poor geotechnical properties of soil make hillslopes intrinsically unstable.

The results of this study, in particular, show that root tensile resistance of single roots seems to do not be affected by over-aging, whereas on the contrary, root density and size distribution can be.

By estimating hillslope stability including overload and additional cohesion due to forest, it has be shown that in the case of steep and cohesionless terrains covered by over-aged chestnut forests, instability phenomena can be triggered by high level of soil saturation when steepness exceeds 35°. For less extreme case, instead, chestnut forests, although over-aged, are fundamental in guarantying stability. As over-aged coppiced forests, however, are subject to extensive overturning phenomena which could evolve in more severe phenomena, coppicing operations should be incentivized giving a higher priority to steeper hillsopes.

References

Abdi E:, Majnounian B., Genet M., Rahimi H. (2010) Quantifying the effeects of root reinforcement of Persian Ironwood (Parrotia persica) on slope stability; a case study: Hillslope of Hyrcanian forests, northern Iran. Ecol. Eng. 36:1409-1416

Aymard M., Fredon J-J (1986) Etude de realtion entre une racine et les rejets de la souche chez Castanea sativa Miller. Ann. Sci. For., 43,3,351-364.

Bagnara L., Salbitano F., 1998. Struttura delle ceppaie e dei sistemi radicali in cedui di faggio sui monti Sibillini. Sherwood, 30: 31-34

Bedeneau M., Pagès L. (1984) Etudes des cernes d'accroissement ligneux du système racinaire d'arbres traits en tallis. Ann. Sci. For., 41, 59-68.

Bischetti G.B., Bonfanti F., Greppi M. (2003) Misura della resistenza a trazione delle radici: apparato sperimentale e metodologia di analisi. Quad. Idronomia Mont 241

Bischetti G.B., Simonato T., Chiaradia E.A. (2004) Valutazione del contributo degli apparati radicali nell'analisi di stabilità ei movimenti franosi superficiali, Riv. Ing. Agr., 3, 33-40.

Bischetti, G.B., Chiaradia, E.A., Epis, T., Morlotti, E. (2009) Root Cohesion of forest spe-cies in the Italian Alps, Plant and Soil. DOI 10.1007/s11104-009-9941-0.

Casagrande A. 1948. Classification and Identification of Soils. Transactions ASCE. p. 901.

Del Favero R. (ed.). 2002. I tipi forestali nella regione Lombardia, Regione Lombardia, Cierre edizioni, Verona (Italy), 506 pp.

Genet M., Stokes A., Salin F., Mickovski S.B., Fourcaud T., Dumail J-F, van Beek R. 2005, The influence of cellulose content on tensile strength in tree roots, Plant and Soil, 278:1–9

Genet M., Stokes A., Fourcaud T., Norris J. (2010) The influence of plant diversity on slope stability in a moist evergreen deciduos forest. Ecol. Eng. 36:365-275

Hammond C., Hall D., Miller S., Swetik P. (1992) Level I Stability Analysis (LISA) Documentation for Version 2.0. United States Department of Agriculture, Intermountain Research Station, General Technical Report INT-285.

Hales T.C., Ford C.R., Hwang T., Vose J.M., Band L.E. (2009) Topographic and ecologic controls on root reinforcement. J. Geophys. Res. 114, F03013.

Ji J., Kokutse N., Genet M., Forcaud T., Zhang Z. (2012) Effect of spatial variation of tree root characteristics on slope stability. A case study on Black Locust (Robinia pseudoacacia) and Arborvitae (Platycladus orientalis) stand on the Loess Plateau. China. Catena. 92:139-154

Mao R., Zeng D.-H., Li L.-J. (2012) Engineering ecological protection against landslides in diverse mountain forests: Choosing cohesion models. Ecol. Eng. 45:52-69

Meyer Fh., Gottsche D. (1970) Distribution of root tips and tender roots of beech. In: Ellenberg H. (ed) Ecological studies. Analysis and synthesis. Vol. 2 Springer – Verlag. Berlin. pp. 47-52

Motta R., Haudemand J.C. (2000) Protective forests and sylvicultural stability: an example of planning in the Aosta Valley. Mt Res Dev 20: 180-187

Pollen N., Simon A. (2005) Estimating the mechanical effect of riparian vegetation on streambank stability using fiber bundle model. Water Resour. Res. 41:W07025

Roering J.J, Schmidt K.M., Stock J.D. *et al.* (2003) Shallow landsliding, root reinforcement, and the spatial distribution of trees in the Oregon Coast Range. Can. Geotech. J. 40:237-253

Sakals M.E., Sidle R.C: (2004) A spatial and temporal model of root cohesion in forest soil. Can. J. For. Res. 34:950-958

Schwarz M, Cohen D, Or D. 2010. Root-soil mechanical interactions during pullout and failure of root bundles, J.Geophys. Res.: 2156-2202.

Sidle RC, Ochiai H. 2006. Landslides: Processes, prediction, and land use. Washington, DC: American Geophysical Union.

Vergani C., Chiaradia E.A., Bischetti G.B. (2012) Variability in the tensile resi stance in Alpine forest tree species. Ecol. Eng. http://dx.doi.org/10.1016/j.ecoleng.2012.04.036

Waldron, L.J. (1977) The shear resistance of root-permeated homogeneous and stratified soil, Doil Science Society of America Journal, 41, 843-849.

Wu, T. H. (2013). Root reinforcement of soil: Review of analytical models, test results, and applications to design. Canadian Geotechnical Journal, 50(3), 259-274

Wu, T.H. McKinnel, W.P., Swanston, D.N. (1979) Strength of tree roots and landslides on prince of Wales Island, Alaska, Canadian Geotechnical Journal, 16, 19-33.

A simple field method to measure the hydrodynamic properties of soil surface crust

Vincenzo Alagna, Vincenzo Bagarello, Simone Di Prima, Giuseppe Giordano, Massimo Iovino

Dipartimento di Scienze Agrarie e Forestali, Università degli Studi di Palermo, Italy

Abstract

The hydraulic resistance of the surface crust was determined by a combination of two infiltrometric techniques: first, a surface measurement of steady-state infiltration rate is conducted by a mini-disk tension infiltrometer (MDI); then, the surface crust is removed, its thickness is measured, and a ponded infiltration test is performed at the same site. The Beerkan Estimation of Soil Transfer parameters (BEST) method is applied to estimate the hydraulic properties of the underlying soil provided the particle-size distribution and the bulk density are known. Under the assumption of a unit gradient of hydraulic head below the soil crust, the pressure head at the interface crust-soil is derived. Finally, the hydraulic conductivity of the crust is calculated from the steady-state water flow measured by the MDI and the Darcy law. The method was tested in a sandy loam and a clay soil. In the sandy loam soil, a 2-3 mm thick slaking crust was visually observed, but no increased surface hydraulic resistance was detected in 10 out of 11 cases. In the clay soil, a 5-7 mm thick crust was formed by gradual coalescence of the plastic, wet aggregates by rainfall compaction. In 10 out of 15 tests, the steady-state infiltration rate with the crust was lower than the underlying soil saturated hydraulic conductivity, denoting an increased hydraulic resistance of the surface crust. For the clay soil, the mean value of the hydraulic resistance was practically independent of the crust thickness and varied between 78 and 81 min.

Correspondence: Massimo Iovino, Dipartimento di Scienze Agrarie e Forestali, Università degli Studi di Palermo, viale delle Scienze, ed. 4, ingr. E, 90128 Palermo, Italy.
Tel. +39.091.23897070 - Fax +39.091.484035.
E-mail: massimo.iovino@unipa.it

Key words: soil surface crust, mini disk tension infiltrometer, BEST procedure.

Acknowledgements: the authors would like to thank Giuseppe Nicolosi for his help in the experimental work.

Contributions: theory was developed by V. Bagarello and M. Iovino. All authors analyzed the data and contributed to write the manuscript.

Funding: the study was supported by grants of the Sicilian Region (Progetto Tristezza).

Conference presentation: this paper was presented at 10th AIIA Conference: "AIIA13 – Horizons in agricultural, forestry and biosystems engineering", Viterbo, Italy, September 8-12, 2013.

Journal of Agricultural Engineering 2013; XLIV(s2):e14
doi:10.4081/jae.2013.(s1):e14

Introduction

In many arid and semi-arid regions, the combination of high intensity rainfall and unstable soil aggregation frequently leads to the development of a surface crust characterized by higher bulk density and lower porosity than the underlying soil. It acts as a barrier to water infiltration, hampers germination of seeds and reduces root aeration and water availability. Preventing these problems requires an understanding and prediction of how soil degradation develops in the field (Bresson and Boiffin, 1990). In the formation of surface crusts, aggregate stability plays a key role. Rainfall or irrigation water may destroy soil aggregates by two processes. First, breakdown of aggregates as consequence of slaking when immersed in water. Second, mechanical destruction of aggregates as consequence of water drop impacts (De Jong *et al.*, 2011). In both cases, the loose particles are partially moved by splash erosion and carried into the soil mass by the infiltrating water where they fill the voids between the aggregates. Valentin and Bresson (1992) referred to this as *structural crust*. Fine particles, resulting from aggregates breakdown, can be translocated to a certain distance from their original location. After the rainstorm, a *depositional crust* of variable thickness can be deposited on the soil surface, mainly consisting of clay that was in suspension during rainstorms. A detailed classification of structural and depositional crusts was proposed by Valentin and Bresson (1992).

Investigations on the effects of surface crusting on infiltration rate were conducted since the middle of the 20th century. A review of laboratory and field studies aimed at investigating the factors involved in rainfall-induced seal formation and improving the knowledge about soil crusting effects can be found in Assouline (2004). A simple approach to model the effect of surface sealing on infiltration consists of considering a well established saturated crust with constant thickness and saturated conductivity. Hillel and Gardner (1969) accounted for the crust effect through the hydraulic resistance which is the ratio between the crust thickness and the corresponding conductivity. Under ponded condition, if the crust is less pervious than the lower layer, a negative pressure head can develop in the subsoil (Hillel and Gardner, 1969). A measurement of the pressure head at the crust-soil interface can be obtained by minitensiomenter horizontally inserted beneath the soil crust.

Vandervaere *et al.* (1997) proposed a method which uses tension disk infiltration data at several water supply potential, together with information from pre-installed minitensiometer below the soil crust to estimate hydraulic conductivity, matric flux potential and sorptivity. An alternative approach involves the use of the inverse solution and two transient infiltration experiments conducted in the same site by a disk infiltrometer before and after the removal of the soil crust (Šimůnek *et al*, 1998). However, tensiometers insertion may be problematic in situ whereas the inverse modeling raises problems of non-uniqueness of the solution (Šimůnek and van Genuchten, 1997). Touma *et al.* (2011) proposed a method to determine the surface crust resistance

that combines two types of in situ experiments: i) a rain simulation experiment, and ii) a single ring infiltration test on the same soil after removal of the crust. Steady state infiltration rate through the crust is calculated as the difference between the runoff rate and the applied rainfall intensity. The subsoil hydraulic properties are determined by the combination of pedotransfer functions and a transient model for 3D infiltration in a homogeneous, uniformly unsaturated soil. The method appeared reliable even if it was applied to only one soil type and texture. However, the field use of the rainfall simulator is complicated and the spatial support for the proposed method is questionable. In fact, the two experiments do not sample the same area (1 m^2, or more, for the simulated rainfall against <0.02 m^2 for ring test).

An alternative to the rainfall simulator for measuring the steady state infiltration rate through the soil crust could be the use of the minidisk tension infiltrometer (MDI) that requires a small amount of water and it is easily transportable in the field (Lichner *et al.*, 2007; Madsen and Chandler, 2007; Dohnal *et al.*, 2010). A laboratory application of the MDI to measure the infiltration rates of badlands crust was conducted by Li *et al.* (2005). The MDI samples a limited area (approximately 15 cm^2) with a very limited disturbance of soil surface. This small sampled area implies that local crust characteristics, including thickness, can be precisely determined. The minimization of disturbance is a great advantage for the characterization of the soil surface crust in the field given the nature of the thin sealing layer, that can easily be disrupted under minimal mechanical action.

The purpose of this investigation was to develop and test a simplified method to determine the hydrodinamic properties of the surface crust. Following the approach by Touma *et al.* (2011), the hydraulic resistance of the crust is determined by a combination of two infiltrometric techniques: first, a surface measurement of steady-state infiltration rate is conducted by a MDI; then, the surface crust is removed, its thickness is measured, and a ponded infiltration test is performed at the same site. The Beerkan Estimation of Soil Transfer parameters (BEST) procedure (Lassabatère *et al.*, 2006) is applied to estimate the hydraulic properties of the underlying soil provided the particle-size distribution and the bulk density are known. The method was tested in a sandy loam and a clay soil exhibiting a structural crust that developed due to the autumn-winter rainstorms typically occurring under Mediterranean climate.

Theory

The method is based on the earlier work by Hillel and Gardner (1969). The flux across a surface crust of thickness L_c (L) is given by:

$$q_c = -K_c \frac{h_s - L_c - h_0}{L_c} \quad (1)$$

in which h_0 (L) is the water pressure head at the crust surface, h_s (L) is the pressure head at the soil-crust interface and K_c (L T^{-1}) is the hydraulic conductivity of the soil crust. For zero ponded conditions, h_0 becomes zero; furthermore, the thickness of the crust (of the order of a few mm) can be neglected in the numerator of eq. (1) which becomes:

$$q_c = -K_c \frac{h_s}{L_c} = -\frac{h_s}{R_c} \quad (2)$$

where R_c (T) is the crust resistance. For a transient infiltration process, h_s increases with time up to a constant value when steady state condition is reached. Then, the water flux entering the subsoil, q_s (L T^{-1}), can be calculated by the Darcy law:

$$q_s = -K(h_s)\left(\frac{dh}{dz} - 1\right) \quad (3)$$

where $K(h_s)$ is the unsaturated hydraulic conductivity of the subsoil corresponding to a pressure head h_s and (dh/dz -1) is the hydraulic gradient at soil-crust interface. Due to the continuity of the flux at the soil-crust interface, $q_c = q_s$. Furthermore, when steady state is reached, dh/dz tends to become a negligible quantity and eq. (3) reduces to:

$$q_s = K(h_s) \quad (4)$$

Combining eqs. (2) and (4), the following equation for the crust hydraulic resistance is obtained:

$$R_c = -\frac{h_s}{K(h_s)} \quad (5)$$

When the crust thickness cannot be neglected in the numerator of eq. (1), the crust resistance will be given by:

$$R_c = -\frac{h_s - L_c}{K(h_s)} \quad (6)$$

Therefore, determination of the soil crust resistance needs the knowledge of the soil hydraulic properties of the subsoil, $\theta(h)$ e $K(h)$, and execution of an infiltration test in which water is supplied at the upper surface of the soil crust under zero ponded conditions. Under steady state conditions, the unsaturated hydraulic conductivity of the subsoil $K(h_s)$ is determined by eq. (4) and, then, the pressure head at the crust-subsoil interface is derived by inverting the $K(h)$ relationship. Crust hydraulic resistance is finally obtained by eqs. (5) or (6).

The hydraulic properties of the subsoil can be determined by the BEST method (Lassabatère *et al.*, 2006) that focuses specifically on the van Genuchten (1980) relationship for the water retention curve with the Burdine (1953) condition and the Brooks and Corey (1964) relationship for hydraulic conductivity:

$$\frac{\theta - \theta_r}{\theta_{fs} - \theta_r} = \left[1 + \left(\frac{h}{h_g}\right)^n\right]^{-m} \quad (7a)$$

$$m = 1 - \frac{2}{n} \quad (7b)$$

$$\frac{K(\theta)}{K_{fs}} = \left(\frac{\theta - \theta_r}{\theta_{fs} - \theta_r}\right)^{\eta} \quad (8a)$$

$$\eta = \frac{2}{m \times n} + 3 \quad (8b)$$

where θ (L^3L^{-3}) is the volumetric soil water content, h (L) is the soil water pressure head, K (L T^{-1}) is the soil hydraulic conductivity, n, m and η are shape parameters, and h_g (L), θ_{fs} (L^3L^{-3}, field saturated soil water content), θ_r (L^3L^{-3}, residual soil water content) and K_{fs} (L T^{-1}, field saturated soil hydraulic conductivity) are scale parameters. In the BEST procedure, θ_r is assumed to be zero.

Estimation of the shape parameters is based on the soil particle size distribution (PSD), whereas the scale parameter are estimated by means of an inverse analysis of infiltration data. Cumulative infiltration data, I (L), are fitted to the analytical formulation derived by Haverkamp *et al.* (1994) for a transient zero ponded infiltration from a circular surface:

$$I(t) = S\sqrt{t} + \left(A S^2 + B K_{fs}\right)t \quad (9)$$

where t (T) is the time, S (L T$^{-1/2}$) is soil sorptivity, and A (L^{-1}) and B are constants that depend on the shape parameter η, the scale parameter θ_{fs}, the ring radius, r (L), and the initial water content, θ_0 (L^{3}L^{-3}). The initial and field saturated water contents are measured at the beginning and the end of the infiltration experiment, respectively. BEST first estimates sorptivity by eq.(9) with K_{fs} replaced by its sorptivity function and the experimental steady state infiltration rate, i_s (L T^{-1}):

$$K_{fs} = i_s - A S^2 \quad (10)$$

Once sorptivity is estimated, K_{fs} is driven through eq.(10), assuming that steady state has been reached. As eq.(9) is valid only at transient state, the considered duration of the experiment has to be lower than a maximum time, t_{max} (T):

$$t_{max} = \frac{1}{4(1-B)^2}\left(\frac{S}{K_{fs}}\right)^2 \quad (11)$$

The pressure head scale parameter, h_g, is finally estimated by the following relationship (Lassabatere *et al.*, 2010):

$$h_g = -\frac{S^2}{c_p K_{fs}\left(\theta_{fs} - \theta_0\right)\left[1 - \left(\frac{\theta_0}{\theta_{fs}}\right)^{\eta}\right]} \quad (12)$$

in which c_p is a texture parameter that can be derived from the shape parameters (m, n and η).

Materials and methods

Validation of the proposed method was performed in two differently textured soils. The first experimental site (Site 1) is located near the Agricultural Faculty of the University of Palermo (UTM: 355500E, 4218950N) in a citrus orchard having a canopy that covers almost completely the soil surface. The soil had received no tillage in the last three years and, in late autumn when the experiments were conducted, uncontrolled weeds covered diffusely but not uniformly the soil surface. According to the USDA classification, the soil is sandy loam with percentages of clay, *cl* = 15.6% silt, *si* = 27.4% and sand, *sa* = 50.7%. Hydraulic resistance of the surface crust was measured at 11 randomly selected points in which a surface crust was visually observed. Site 2 is located in a vineyard near Marsala, western Sicily (UTM: 286250E, 4187250N). The soil is classified as clay (*cl* = 54.3%, *si* = 29.2%, *sa* = 16.5%). In late spring, after the winter rainfalls, 15 measurement points were randomly selected approximately in the middle of the crop rows (spaced 2.50 m) where soil was not covered by vegetation.

Measurement of the hydraulic resistance of the crust involved a two step experiment (Figure 1). First, the MDI was applied on the surface of the crust to measure the steady state infiltration rate, q_c. The original MDI device (Decagon Devices, Inc., Pullman, WA) with a disk diameter of 3.2 cm was used. The pressure head at the soil surface can be regulated from -0.5 to -7 cm by a suction control tube at the top of the infiltrometer. A very thin layer of contact material (Spheriglass no.2227, Potter Industries, LaPraire, Canada) was spread on the surface crust to level small irregularities and assure a good hydraulic contact between the porous disk and the soil. Then the MDI was accurately placed on the surface to avoid any disturbance of the crust and the air tube open to start infiltration. The instrument was assured to a rod to keep it in vertical position and to avoid loss of contact with the crust surface during infiltration (Figure 1). The imposed pressure head at the base of the device was not set to zero, as established by theory, but a small suction (approximately 5 mm) was applied to consider the thickness of the contact material layer and also to avoid lateral leakage when water is applied onto an unconfined surface at zero (or positive) pressure head. According to Reynolds (2006), the imposed pressure head on the soil surface is higher than the one established at the base of the device by a quantity depending on the thickness of the contact

Figure 1. Experimental procedure for determining the hydraulic resistance of the surface soil crust: a) surface crust; b) MDI experiment; c) crust removal; d) ring infiltration test.

material (i.e., established h_0 value > 5 mm). In addition, considering the low porosity of the sealed surface soil, the use of a slightly negative pressure head at the soil surface should not influence the measurement of the hydraulic resistance of the crust. Visual readings of the water level in the MDI supply tube were taken at 30 s interval until the complete empting of the reservoir that occurred in approximately 8 min in the sandy loam soil and 15 min in the clay soil. Apparent steady-state infiltration rate was deduced from the slope of the linear portion of the cumulative infiltration vs. time plot.

Three days after the MDI measurement, the surface crust was accurately removed and its thickness measured by a gauge. The average of 5-6 measurements was assumed as thickness of the crust at a given measurement point. A ring with an inner diameter of 80 mm was inserted into the subsoil to a depth of about 10 mm to avoid lateral loss of the ponded water. A known volume of water (50 mL) was poured in the cylinder at the start of the measurement and the elapsed time during the infiltration was measured. When the amount of water had completely infiltrated, an identical amount of water was poured into the cylinder, and the time needed for the water to infiltrate was logged. The procedure was repeated until the difference in infiltration time between three consecutive trials became negligible, signaling a practically steady-state infiltration. To avoid disturbance of the soil surface, the water energy was dissipated against a shield placed 10-20 mm above the soil surface (Figure 1). The number of collected (t, I) data points varied with the run between 10 and 16.

Before conducting the experiment, a disturbed soil sample was collected to estimate the initial gravimetric water content and to determine the PSD, using conventional methods following H_2O_2 pretreatment to eliminate organic matter and clay deflocculation using sodium hexametaphosphate and mechanical agitation (Gee and Bauder, 1986). When the last volume of water had infiltrated, a small sample was collected within the ring to determined the field saturated gravimetric water content. Both initial and field saturated gravimetric water content values were converted into volumetric ones, i.e. θ_0 and θ_{fs}, by the dry soil bulk density, ρ_b (Mg m^{-3}), measured on an undisturbed soil core (0.05 m in height by 0.05 m in diameter) collected in the subsoil in close vicinity of the infiltrometer ring.

Results and discussion

In site 1, the steady state infiltration rate, q_c, through the surface crust ranged from a minimum value of 390 to a maximum value of 755 mm h^{-1} with a mean value of 561 mm h^{-1} (Table 1) In site 2, q_c ranged from 117 to 200 mm h^{-1} (average 147 mm h^{-1}). As expected, a lower q_c values were observed in the clay soil where the relatively weaker structure of the soil aggregates lead to the formation of a more compact surface crust (Figure 1). The coefficient of variation of q_c in the two soils were similar, even if the hydrodinamic characteristics of the surface crust could be considered more homogeneous in the clay soil (CV = 23%) than in the sandy loam soil (CV = 19%) at the time of field tests.

The hydraulic properties, *i.e.* the water retention curve and the hydraulic conductivity function, of the soil underneath the crust showed similarities between the two soils. The relationships $\theta(h)$ were more variable with the considered run in the sandy loam soil than in the clay soil. The opposite result was found for the hydraulic conductivity functions (Figure 2). The shape parameters (n, m and η), that basically depend on the PSD, were characterized by small coefficients of variation (CV < 2.5%) for both soils. For the sandy loam soil, the average values of n, m and η (N = 11), were 2.15, 0.07 and 16.0. For the clay soils (N = 15), n = 2.07, m = 0.03 and = 31.4. These results did not coincide with the mean values listed by Minasny and McBratney (2007) for the USDA textural categories, which is obvious given the differences in terms of both origin and sample size of the datasets. However, the shape parameters of this investigation were relatively close to the ones reported by the cited Authors and also in line with the circumstance that a lower n and a higher value should be expected for a clay soil than a sandy loam soil.

The mean values of θ_{fs} were 0.62 cm^{3}cm^{-3} (CV = 5.0%) in site 1 and 0.56 cm^{3}cm^{-3} (CV = 5.8%) in site 2. Actually, estimations of total porosity conducted from independently measured soil bulk densities by assuming a particle density of 2.65 kg m^{-3}, yielded similar results, i.e. a mean value of 0.59 cm^{3}cm^{-3} for the sandy loam of site 1 and 0.55 cm^{3}cm^{-3} for the clay soil (site 2). The pressure head scale parameter, h_g, and the field saturated hydraulic conductivity, K_{fs}, that mainly depend on the infiltration experiments, were characterized by a greater variability. The mean values of the two scale parameters were h_g = 87 mm (CV = 61%) and K_{fs} = 346 mm h^{-1} (CV = 44%) for site 1, and h_g = 241 mm (CV = 118%) and K_{fs} = 731 mm h^{-1} (CV = 87%) for site 2. The estimated values of h_g are in agreement with the texture of the two soils given that a higher absolute value of the pressure scale parameter is expected in fine soils exhibiting a smaller modal pore size (Haverkamp *et al.*,

Table 1. Statistics of the hydraulic parameters of the van Genuchten-Broooks and Corey model (n, m, η, θ_{fs}, hg and K_{fs}) for the subsoil and steady state infiltration rate through the surface crust (q_c).

	n	m	η	θ_{fs} (m^{3}m^{-3})	h_g (mm)	K_{fs} (mm h^{-1})	q_c (mm h^{-1})
Site 1 sandy loam N = 11							
min	2.149	0.069	15.6	0.576	-180	193	390
max	2.159	0.074	16.4	0.649	-26	623	755
mean	2.154	0.071	16.0	0.615	-87	346	561
CV (%)	0.2	2.5	2.2	5.0	61.0	43.5	23.2
Site 2 clay N = 15							
min	2.067	0.032	30.5	0.514	-886	14	117
max	2.073	0.035	33.0	0.622	-51	1777	200
mean	2.070	0.034	31.4	0.557	-241	731	147
CV (%)	0.1	2.4	2.3	5.8	118.0	86.6	18.7

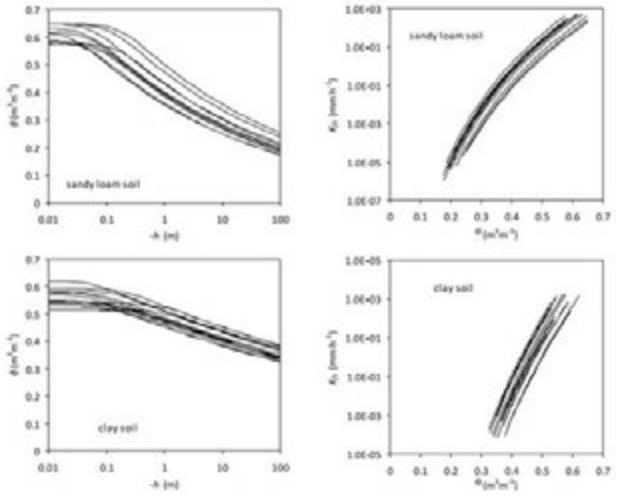

Figure 2. Water retention curves and hydraulic conductivity functions for the subsoil of site 1 (a and b) and site 2 (c and d).

2006). A higher mean K_{fs} value in the clay soil probably occurred because soils rich in clay often show macropores, microcraks and other structural discontinuities that help water transmission (Bagarello *et al.*, 2010). In this case, the variability of the measured K_{fs} also increases depending on whether the macropores are sampled or not (Bagarello *et al*, 2012). In fact, the K_{fs} values measured by the BEST procedure in the clay soil extended over two orders of magnitude from a minimum of 14 mm h^{-1} to a maximum of 1777 mm h^{-1} whereas in the sandy loam soil the field saturated hydraulic conductivity values differed, at the most, by a factor of 3.2.

In site 1, the ratio of the steady state flow rate though the crust to the field saturated hydarulic conductivity of the subsoil, q_c/K_{fs}, was greater than one in 10 out of 11 experiments (mean value, q_c/K_{fs} = 1.56) and also for the only experiment in which $q_c < K_{fs}$, the ratio q_c/K_{fs} was very close to one (q_c/K_{fs} = 0.93). It was concluded that the visually observed surface crust was not hydraulically effective in reducing infiltration in this soil. Surface soil crust in the sandy loam site was thinner (L_c = 2-3 mm) and less developed than in the clay soil. As can be seen in Figure 3, it includes many sand particles that avoided excessive compaction of the surface layer. According to Valentin and Bresson (1992), in cultivated soils of loamy type slaking crusts develop as a result of aggregate breakdown probably induced by entrapped air compression when the soil is dry before rainfall. Such crusts are thin (1-3 mm), rather porous with a no clear textural separation between coarse and fine particles and the infiltration rate is relatively high (De Jong *et al.*, 2011). Another factor that lead to the formation of a slaking crust in the sandy loam soil of site 1, could be the protective effect of the tree canopy that prevented the soil surface from the direct impact of the drops. Therefore, the main mechanism for disaggregation was the wetting of the dry aggregate rather than the kinetic energy of the rainfall.

In the clay soil, the condition $q_c/K_{fs} < 1$ was observed in 10 experiments out of 15 experiments denoting an increased hydraulic resistance of the surface crust. With the exclusion of one experiment that yielded a value of q_c/K_{fs} = 9.1, mainly as a consequence of an extremely low value on the subsoil field saturated hydraulic conductivity (K_{fs} = 14 mm h^{-1}), the q_c/K_{fs} values ranged from 0.09 to 1.59 with a mean value of 0.49 (CV = 108%). Therefore, the formation of a surface crust acted as a barrier to water infiltration in the clay soil. The crust in clay soil was thicker (L_c = 5-7 mm) and probably more compact than in the sandy loam soil (Figure 4). Physical characterization of the soil crust should be carried out in additional testing of the proposed field method. However, visual inspection of the removed crust showed a distinct structural separation between the compacted surface layer and underlying undisturbed subsoil that, according to Valentin and Bresson (1992), typical occurs in the coalescing crust. Such crusts results mainly from gradual compaction due to aggregate coalescence by deformation under plastic conditions. This crusting process is observed in wet soils under heavy rainfall intensity.

For the experiments in which $q_c/K_{fs} < 1$ (N = 10), the pressure head at the soil-crust interface, h_s, varied between 263 and 77 mm with a mean value of 180 mm (CV = 35.5%) (Table 2). Considering that water is supplied at the surface of the crust with a pressure head close to zero ($h_0 \approx$ 5 mm) this result shows what marked reduction of the water pressure head occurs in the first mm of the profile due to the hydraulic resistance of the crust. If the thickness of the crust is neglected, the hydraulic resistance calculated from eq. (5) ranged from 0.39 to 2.24 h with a mean value of 1.31 h (78 min). The corresponding mean value

Table 2. Statistics of the pressure head at the crust-subsoil interface, h_s, crust thickness, L_c, hydraulic resistance, R_c and hydraulic conductivity, K_c, of the surface crust of the clay soil determined for the experiments in which $q_c/K_{fs} < 1$ (N = 10).

Statistic	q_c/K_{fs}	h_s (mm)	L_c (mm)	R_c (h) eq. (5)	K_c (mm h^{-1}) eq. (5)	R_c (h) eq. (6)	K_c (mm h^{-1}) eq. (6)
min	0.09	-263	5	0.385	2.68	0.41	2.62
max	0.84	-77	7	2.241	12.97	2.29	12.18
mean	0.24	-180	6	1.312	5.77	1.35	5.53
CV (%)	97.6	35.5	11.1	47.8	53.5	47.0	51.9

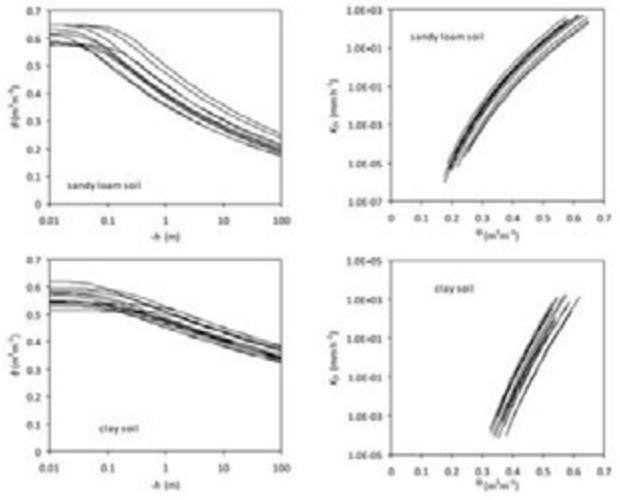

Figure 2. Water retention curves and hydraulic conductivity functions for the subsoil of site 1 (a and b) and site 2 (c and d).

Figure 3. Slaking structural crust on the sandy loam soil of site 1 (a) and coalescing crust on the clay soil of site 2 (b).

of the hydraulic conductivity of the crust was 5.8 mm h^{-1}. Considering the thickness of the crust (6) the mean value of the crust hydraulic resistance was 1.35 h (81 min), with a mean value of the hydraulic conductivity of 5.5 mm h^{-1}. Therefore, calculation of the hydraulic parameters of the crust were not appreciably affected by L_c. A practical implication of this result is that measuring the crust thickness is not strictly necessary to calculate its conductivity and hydraulic resistance.

Conclusions

Soil surface crusting may severely affect agricultural soils as it significantly reduces infiltration, hampers germination of seeds and reduces root aeration and water availability. Knowledge of the hydrodinamic properties of the surface soil crust is important to predict and mitigate its negative effects. A simplified method to determine the hydraulic resistance of the surface crust is presented that is based on the approach by Hillel and Gardner (1969). It requires the knowledge of the steady state infiltration rate in the crusted soil and the hydraulic properties of the soil underlying the crust and combines two in situ infiltrometric experiments. A mini-disk tension infiltrometer is first conducted at the soil surface to measure the steady-state infiltration rate. Then, the surface crust is removed, its thickness is measured, and a ponded infiltration test is performed at the same site to determine the hydraulic properties of the underlying soil by the Beerkan Estimation of Soil Transfer parameters (BEST) procedure.

The method was tested in a sandy loam and a clay soil after a prolonged rainfall period that allowed the formation a surface crust. In the sandy loam soil, a 2-3 mm thick slaking crust was visually observed, but ratio of the steady state flow rate to the field saturated hydarulic conductivity of the subsoil, q_e/K_{fs}, was greater than one in 10 out of 11 experiments thus detecting no increase of the surface hydraulic resistance. In the clay soil, a 5-7 mm thick crust was formed that was attributed to gradual coalescence of the plastic, wet aggregates by rainfall compaction. In this soil, the condition $q_e/K_{fs} < 1$ was observed in 10 out of 15 experiments denoting an increased hydraulic resistance of the surface crust. The hydraulic resistance was not appreciably affected by the crust thickness. The mean value of the crust hydraulic resistance was 1.31-1.35 h (78-81 min), with a mean value of the hydraulic conductivity of 5.5-5.8 mm h^{-1}. The developed method is particularly simple and appears to be suitable to discriminate between different levels of the hydraulic resistance of the surface crust. However, further investigations involving different soil and crust types is necessary in order to confirm its reliability.

References

Assouline S. 2004. Rainfall-induced soil surface sealing: a critical review of observations, conceptual models, and solutions. Vadose Zone Journal, 3:570-591.

Bagarello V., Di Stefano C., Ferro V., Iovino M., Sgroi A., 2010. Physical and hydraulic characterization of a clay soil at the plot scale. Journal of Hydrology, 387: 54-64.

Bagarello V, D'Asaro F, Iovino M. 2012. A field assessment of the Simplified Falling Head technique to measure the saturated soil hydraulic conductivity. Geoderma 187-188: 49-58.

Bresson L.-M., Boiffin J. 1990. Morphological characterization of soil crust development stages on an experimental field. Geoderma, 47:301-325.

Brooks R.H., Corey C.T. 1964. Hydraulic properties of porous media. Hydrol. Paper 3, Colorado State University, Fort Collins.

Burdine N.T. 1953. Relative permeability calculation from pore size distribution data. Petr. Trans. Am. Inst. Min. Metall. Eng., 198:71-77.

De Jong S.M., Addink E.A., van Beek L.P.H., Duijsings D. 2011. Physical characterization, spectral rensponse and remotely sensed mapping of Mediterranean soil surface crusts. Catena, 86:24-35.

Dohnal, M., Dusek, J., Vogel, T., 2010. Improving hydraulic conductivity estimates from minidisk infiltrometer measurements for soils with wide pore-size distributions. Soil Sci. Soc. Am. J. 74(3), 804-811.

Gee G.W., Bauder J.W. 1986. Particle-size analysis. In Methods of soil analysis. Part 1, Klute A (ed), 2nd ed, ASA and SSSA, Madison, WI, USA, 383-411.

Haverkamp R., Debionne S., Vialet P., Angulo-Jaramillo R., de Condappa D. 2006. Soil properties and moisture movement in the unsaturated zone. In J.W. Delleur (ed.), The handbook of groundwater engineering, CRC, Boca Raton, FL.

Haverkamp R. Ross P.J., Smettem K.R.J., Parlange J.Y. 1994. Three-dimensional analysis of infiltration from the disc infiltrometer. 2. Physically based infiltration equation. Water Resources Research, 30:2931-2935.

Hillel D., Gardner W.R. 1969. Steady infiltration into crust-topped profiles. Soil Science, 180(2):137-142.

Lassabatère L., Angulo-Jaramillo R., Goutaland D., Letellier L., Gaudet J.P., Winiarski T., Delolme C. 2010.. Effect of settlement of sediments on water infiltration in two urban infiltration basins. Geoderma, 156:316-325.

Lassabatère, L., Angulo-Jaramillo, R., Soria Ugalde, J.M., Cuenca, R., Braud, I., Haverkamp, R., 2006. Beerkan estimation of soil transfer parameters through infiltration experiments – BEST. Soil Science Society of America Journal 70, 521-532.

Li X.-Y., González A., Solé-Benet A. 2005. Laboratory methods for the estimation of infiltration rate of soil crusts in the Tabernas Desert badlands. Catena, 60:255-266.

Lichner L., Hallett P.D., Feeney D.S., Ďugová O. Šír M., Tesař M. 1997. Field measurement of soil water repellency and its impact on water flow under different vegetation. Biologia, 62(5):537-541.

Madsen M.D., Chandler D.G. 2007. Automation and use of Mini Disk Infiltrometer. Soil Science Society of America Journal, 71:1469-1472.

Minasny B., McBratney A.B. 2007. Estimating the water retention shape parameter from sand and clay content. Soil Science Society of America Journal, 71:1105-1110.

Reynolds W.D. 2006: Tension infiltrometer measurements: implication of pressure head offset due to contact sand. Vadose Zone Journal, 5:1287-1292.

Šimůnek J., Angulo-Jaramillo R., Schaap M.G., Vandervaere J.P., van Genuchten M.T. 1998. Using an inverse method to estimate the hydraulic properties of crusted soils from tension disc infiltrometer data. Geoderma, 86:61-81.

Šimůnek J., van Genuchten M.Th. 1997. Estimating unsaturated soil hydraulic proper-ties from multiple tension disc infiltrometer data. Soil Science, 162(6):383-398.

Touma J., Raclot D., Al-Ali Y., Zante P., Hamrouni H., Dridi B. 2011. In situ determination of the soil surface crust resistance. Journal of Hydrology, 403:253-260.

Valentin C., Bresson L.-M. 1992. Morphology, genesis and classification of surface crusts in loamy and sandy soils. Geoderma, 55:225-245.

van Genuchten M.Th. 1980. A closed form equation for predicting the hydraulic conductivity of unsaturated soils. Soil Science Society of America Journal, 44:892-898.

Vandervaere J.P., Peugeot C., Vauclin M., Angulo-Jaramillo R., Lebel T. 1997. Estimating hydraulic conductivity of crusted soils using disc infiltrometers and minitensiometers. Journal of Hydrology, 188-189:209-223.

Evaluation of short-term geomorphic changes along the Tagliamento river using LiDAR and terrestrial laser scanner surveys

R. Rainato,[1] L. Picco L,[1] M. Cavalli,[2] L. Mao L.,[3] F. Delai,[1] D. Ravazzolo,[1] M.A. Lenzi[1]

[1]Department of Land, Environment, Agriculture and Forestry, University of Padova, Italy; [2]CNR-IRPI, Padova, Italy; [3]Department of Ecosystems and Environment, Pontificia Universidad Catolica de Chile, Santiago, Chile

Abstract

In the recent years a change in the predominant morphology of several river environments has taken place, consisting in a reduction of the braided pattern in favor to wandering or straight configurations. This evolution seems to be due, according to the scientific community, to anthropic causes and, in particular, to the alteration of flow regimes as well as the reduction of sediment transport. Braided rivers are characterized by two or more active channels, separated by bars and fluvial islands and normally feature a high morphological dynamism. This dynamism is the result of the interaction among different elements as sediment supply, flow regime and in-channel and perifluvial vegetation. These factors have a fundamental role in the erosion and deposition processes which are the basis of the morphological changes. The aims of this study are the assessment of the short period geomorphic and volumetric changes occurred along a reach of the Tagliamento River and the comparison between the results obtained from LiDAR (Light Detection and Ranging) and TLS (Terrestrial Laser Scanner) data. The Tagliamento river is a natural gravel-bed river located in the NE of Italy, characterized by a relatively low degree of human disturbances. The analyses were carried out considering two different scales (a reach of about 430 ha and a sub-reach of about 25 ha) and were based on two subsequent datasets in order to investigate the short-term geomorphic changes due to eight significant floods. The surveys were performed using two different datasets derived from LiDAR and TLS technologies and used to analyze the reach and sub-reach respectively. The short-term estimates of geomorphic and volumetric changes were performed using DEMs of Difference (DoD) based on a Fuzzy Inference System. The results have confirmed the high dynamism of the Tagliamento river, estimating a prevalent deposition at reach and a predominant erosion at sub-reach levels. Finally, a comparative qualitative assessment of the output derived from the different data sources was performed, showing little differences between the two survey methods that proved to be both precise and reliable.

Correspondence: Riccardo Rainato, Department of Land, Environment, Agriculture and Forestry, University of Padova, Italy.
E-mail: riccardo.rainato@studenti.unipd.it

Key words: geomorphic changes, gravel bed braided river, LiDAR, Tagliamento River, Terrestrial Laser Scanner.

Acknowledgements: this research was founded by both the Italian National Research Project PRIN20104ALME4-ITSedErosion: "National network for monitoring, modelling and sustainable management of erosion processes in agricultural land and hilly-mountainous area"; and The EU SedAlp Project: "Sediment management in Alpine basis: Integrating sediment continuum, risk mitigation and hydropower",83-4-3-AT, in the framework of the European Territorial Cooperation Programme Alpine Space 2007-2013.

Journal of Agricultural Engineering 2013; XLIV(s2):e15
doi:10.4081/jae.2013.(s1):e15

Introduction

Rivers are exposed to changing environmental conditions over multiple spatial and temporal scales, with the imposed environmental conditions and response potential of the river modulated to varying degrees by human activity and our exploitation of natural resources (Buffington, 2012). The watershed features that control river morphology include topography, sediment supply, discharge (Lisle *et al.*, 2000) and vegetation (Picco *et al.*, 2012). Among the various fluvial morphologies, the braided rivers represent very dynamic systems, in which even ordinary flood events can trigger morphologically active processes. Braided gravel-bed rivers are defined as streams which flow in multiple and migrating channels across an alluvial gravel bed, containing numerous and changing bars, ponds and islands (Gray & Harding, 2007). This fluvial pattern is localized mainly in the piedmont areas, where the proximity of mountains brings large amount of coarse sediment supply, as well as rapid and frequent variations of flow discharge, and thus braided gravel bed rivers present high amounts of energy which makes them respond dynamically to any change (Picco, 2010).

Also in the field of study of fluvial geomorphology a valuable aid is represented by the recent advances in survey equipment and software, that allow the production of high-resolution Digital Elevation Models (DEMs). This new generation of DEMs offers an excellent opportunity to measure and monitor morphological changes across a variety of spatial scales (Heritage & Hetherington, 2007). Coupled with this, the development of topographic survey techniques, *i.e.* airborne and terrestrial LiDAR, GPS, photogrammetry, has led to an increase in the amount of data collected during fieldwork in riverine environments, offering new insights into fluvial dynamics (Brasington *et al.*, 2000). These advances allow the monitoring of geomorphic changes and the estimation of sediment budgets through the application of the morphological method (Church & Ashmore, 1998). This method, in the last decades, has been expanded to include the use of repeat topographic

surveys from which DEMs could be built and differenced to produce DEMs of Difference (DoD) (Wheaton *et al.*, 2010). In fact, as shown by different authors (Brasington *et al.*, 2003; Rumsby *et al.*, 2008), a DoD may provide a high resolution, spatially distributed surface model of topographic and volumetric changes through time.

The aims of the present research are the assessment of the short period geomorphic and volumetric changes occurred along a braided reach of the Tagliamento River, and the comparison between the results obtained from LiDAR and TLS data.

Study area

The Tagliamento river is a gravel-bed river, located in the North-Eastern Italy. It originates at 1195 m a.s.l. and flows for 178 km from the Alps to the northern Adriatic Sea. Its catchment covers 2871 km^2. The river has a straight course in the upper part, while most of its course is braided shifting to meandering in the lower part where dykes have constrained the last 30 km. However, the upper reaches are more or less intact, thus the basic river processes, such as flooding and the erosion and accumulation of sediment, take place under near natural conditions (Picco *et al.*, submitted). A strong climate gradient exists along the length of the river which has a big influence on precipitation, temperature, humidity and consequently vegetation patterns. Another peculiarity of the Tagliamento river is the fact that within its catchment are located very rainy areas, where the annual precipitation can reach 3100 mm per year. The precipitation regime, as well as the temperatures, present a north-south gradient. Following this trend the first ranges from 3100 to 1000 mm per year, while the mean annual temperatures varies from 5 to 14°C. The upper part of the catchment (Carnian and Julian Alps) receives very intensive rain-storms, resulting in severe erosions; torrential rainfalls, steep slopes and extensive sediment sources that, in turn, generate high floods and massive sediment transport rates (Tockner *et al.*, 2003). In this sense, it is important to note as more than 70% of the basin is located in the Alpine area. The study areas, a braided reach of about 430 ha (Figure 1), inside which it was identified a sub-reach of about 25 ha, are localized at the end of the mountain basin, near to the village of Forgaria nel Fiuli (UD).

During the study period significant flood events were recorded (Figure 2). Between August 2010 and September 2011, for 8 times the water stage has exceeded 1.6 m. The events of November 2010 (2.90 m) and December 2010 (2.57 m) were significant with a recurrence interval (R.I.) of around 3 years.

Materials and methods

As said the surveys analyses were carried out considering two different scales. The reach has been detected by two airborne LiDAR flights, carried out in August 2010 and April 2011 (adopting orthometric elevations, estimated vertical error ± 0.20 m) (Picco *et al.*, 2013). The datasets produced by LiDAR surveys (called L2010 and L2011) were filtered using the software Terrascan, developed by Terrasolid. This step was necessary in order to obtain the ground points, necessary for the creation of the DEMs. For this purpose the filtered datasets were imported into ArcGIS 10.1 (ESRI). After the filtering was reached a mean point density of 2/m^2 for L2010 and a value of 2.66/ m^2 for L2011. These density values allowed us the adoption a cell size of 0.50×0.50 m, for the DEMs derived from LiDAR surveys (Figure 3).

The sub-reach was detected via TLS surveys, carried out in August 2010 and in September 2011, using a Leica ScanStation2. During the 2010 survey (T10), the sub-reach presented a low discharge level, while

Figure 1. The Tagliamento river basin (on the left), the reach localization along the main course (in the middle), and the entire reach of about 430 ha (on the right).

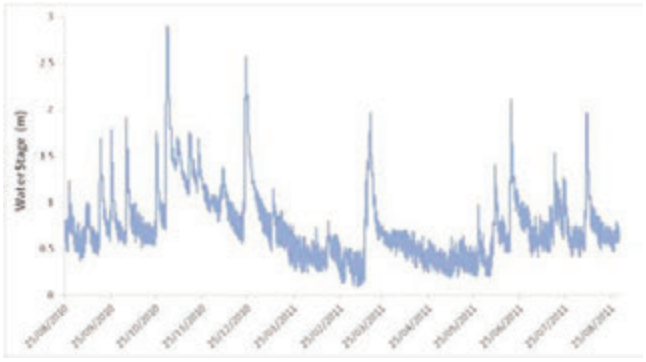

Figure 2.The flood events occurred during the study period along the reach, on the Tagliamento river.

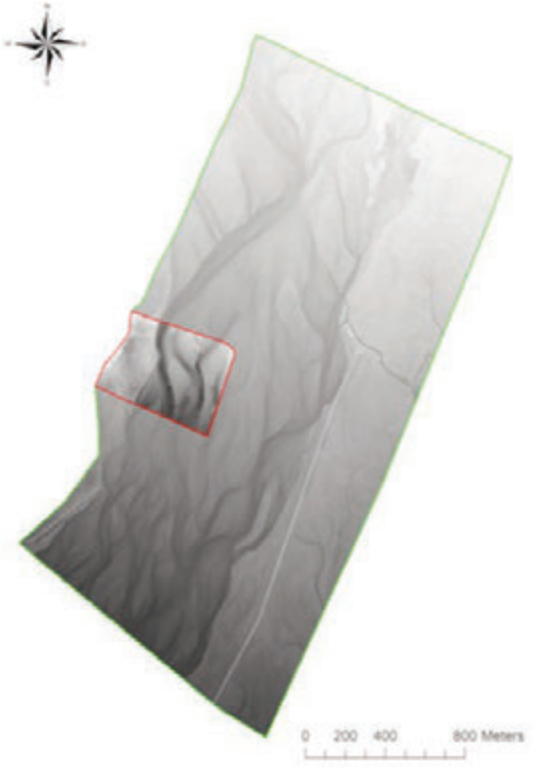

Figure 3. DEM of the study areas in 2010. In red is delimited the sub-reach (25 ha), while in green the reach (430 ha).

during the 2011 investigation (T11) the channels were nearly dry. In the first case, 241 points were measured, within the active channels, using a differential Global Position System (dGPS) in order to collect ground data given that the TLS data is not accurate for the submerged areas (Milan *et al.*, 2007). The individual scans were registered, georeferenced and filtered. These operations were performed using the software Cyclone 7, developed by Cyra Technologies Inc. Also in this case, the filtered point clouds were imported into ArcGIS 10.1, and were integrated with points collected with dGPS along the submerged areas (only for T10). After the integration a mean point density of 68.46/m^2 for T10 and 201.91/m^2 for T11 was reached. In this case, the mean density values allowed us the adoption a cell size of 0.15×0.15 m (Figure 3). Root mean square error (RMSE) analysis was conducted to define the DEM vertical accuracy using a series of dGPS data (vertical quality lower than 0.02 m) as control points. The errors were computed as the difference between the control point elevation and the cell elevation value in the DEM. The RMSE analysis resulted in the following values: 0.052 on DEM T10 and 0.048 on T11 depicting the high accuracy of the surveys. In addition, the average vertical error analysis resulted in the following values: 0.055 m on DEM T10 and 0.026 m on DEM T11.

The availability of subsequent surveys, concerning the same study areas, allows to analyze the geomorphic changes. To perform this type of analysis, we have used the Geomorphic Change Detection 5.1.0 (GCD) software (http://gcd.joewheaton.org). This is a plug-in that can be utilized in ArcGIS environment and allows the monitoring of geomorphic changes through the creation of DoD, in other words through the comparison of repeat and subsequent DEMs. In the case of the present study a not simplistic difference between DEMs but an *ad hoc* Fuzzy Inference System (FIS) was developed to estimate the DEM uncertainty. This FIS (Table 1) was also used in other works (Picco *et al.*, submitted) concerning this study area, and uses as inputs: slope, point density and roughness. For the detailed explanation of GCD software we refer to Wheaton *et al.* (2010). After defining the spatial variability of the uncertainty, the DoDs were recalculated and thresholded at a 95% confidence interval, also using the Bayesian updating method, that re-elaborate the DoDs on the basis of the spatial coherence of erosion and deposition units.

Results

The first result concerns the geomorphic variations occurred within the entire reach. The DoD obtained (Figure 4) from the comparison between the L2011 (April 2011) and the L2010 (August 2010) shows the changes occurred in about 8 months. In the DoD are shown in red the areas prone to erosion, while in blue the surface prone to deposition. We can observe that the most part of the geomorphic changes occur within the active channel areas, without significant variations in the perifluvial zones. The most important erosion phenomenon, from the point of view of extent and incision degree, occurs as bank erosion. This type of scour affects the floodplain areas, as we can observe especially in the middle of the sub-reach, along the main channel, on the right side.

In the upper part of reach other erosions take place, in this case due to the development of some new secondary channels. A significant aggradation occurred along the course of the main channel, on the right side. Here are located the maximum values of deposition. Others considerable depositional phenomena take place downstream, where the channels have deposited in the central part, eroding the lateral floodplain through bank erosions.

Table 2 shows the main results obtained from the comparison between L2011 and L2010. The *Total Net Volume Difference* (+ 145898 m^3) highlights how, in the study reach, there was a prevalent trend of deposition, during the study period. Nearly all values concerning erosion and deposition do not show large differences. For example the *Total Area of Erosion* features the value of 1135232 m^2, a result very similar to the *Total Area of Deposition* that is 1584695 m^2. Also the volumetric results, in particular the percentages, are quite similar with 43% of *Erosion* and 57% of *Deposition*. According to this trend, also the

Table 1. FIS rules used in this work.

ROUGHNESS	SLOPE	DENSITY	UNCERTAINTY
low	low	high	LOW
medium	low	high	LOW
high	low	high	LOW
low	medium	high	LOW
medium	medium	high	LOW
high	medium	high	AVERAGE
low	high	high	LOW
medium	high	high	AVERAGE
high	high	high	AVERAGE
low	low	medium	LOW
medium	low	medium	AVERAGE
high	low	medium	AVERAGE
low	medium	medium	AVERAGE
medium	medium	medium	AVERAGE
high	medium	medium	HIGH
low	high	medium	AVERAGE
medium	high	medium	HIGH
high	high	medium	HIGH
low	low	low	HIGH
medium	low	low	HIGH
high	low	low	EXTREME
low	medium	low	HIGH
medium	medium	low	HIGH
high	medium	low	EXTREME
low	high	low	EXTREME
medium	high	low	EXTREME
high	high	low	EXTREME

Table 2. Results of comparison L2011-L2010.

Maximum positive variation (m)	3.56
Maximum negative variation (m)	-3.06
Average variation (m)	0.05
Standard deviation	0.53
Total Area of Erosion (m^2)	1 135 232
Total Area of Deposition (m^2)	1 584 695
Total Volume of Erosion (m^3)	468 223
Total Volume of Deposition (m^3)	614 121
Total Volume of Difference (m^3)	1 082 343
Total Net Volume Difference (m^3)	145 898
Percent Erosion (by volume)	43%
Percent Deposition (by volume)	57%

Average Variation takes a value of 0.05 m, very close to zero. However, meaningful is the assessment of the *Total Volume of Difference* equal to 1082343 m^3.

The geomorphic changes occurred within the sub-reach were analyzed through two DoDs. The first one was produced by comparing high-resolution DEMs (T11-T10), in other words using the maximum resolution (0.15 m) offered by TLS surveys. The further DoD (T11_05-T10_05) was made by comparing the same data acquisition, but producing DEMs with lower resolution (0.50 m), as in the case of the LiDAR DEMs. These two DODs, characterized by different resolutions, are shown in Figure 5. In both comparisons we can clearly identify the erosion and depositional phenomena, taking place in approximately 12 months between the two data acquisitions. First of all we can observe as the erosion phenomena occur in two main areas: along the main channel an extended and deep bank erosion affects the contiguous floodplain on the right side (maximum values of erosion), and in the middle of the sub-reach, due to the creation of two new secondary channels. The depositional phenomena were concentrated on the left side, where was situated a vegetated bar, and along the course of the main channel, where a wide aggradation has taken place.

Table 3 shows the main results obtained from the comparison between T11-T10, T11_05-T10_05 and, in the last column, the percentage difference between these two results. First of all, we can observe how both the DoDs have estimated a prevalence of erosion within the sub-reach, with values of *Total Net Volume Difference* of -68351 m^3 and -68604 m^3 respectively. In the results of T11-T10 this trend is also confirmed by the considerably higher value of the *Total Volume of Erosion* (96638 m^3) in respect to the *Total Volume of Deposition* (28287 m^3). Also the extension of the areas affected by the phenomena, are in line with these results, with the *Total Area of Erosion* equal to 148186 m^2, while the *Total Area of Deposition* amounting to 75333 m^2, nearly a 2/1 ratio (1.97). Other results according to this trend is the *Average Variation* that accounts for -0.31 m, featuring a negative value. All the results obtained from the comparisons T11_05-T10_05 are in line with the values seen before. It is interesting to note how the percentage difference achieves a maximum value of 12.58%, as in the case of the *Total Area of Deposition*, while in other cases the difference is always maintained below 10%. Very significant is the estimate of the *Total Net Volume Difference* that differs by only 0.37%.

Table 3. Results of comparison T11-T10, T11_05-T10_05 and the percentages differences between them.

Maximum positive variation (m)	1.74	1.68	-3.45
Maximum negative variation (m)	-2.96	-2.94	-0.68
Average variation (m)	-0.31	-0.34	9.68
Standard deviation	0.68	0.70	2.94
Total Area of Erosion (m^2)	148 186	136 036	-8.20
Total Area of Deposition (m^2)	75 333	65 856	-12.58
Total Volume of Erosion (m^3)	96 638	95 806	-0.86
Total Volume of Deposition (m^3)	28 287	27 202	-3.84
Total Volume of Difference (m^3)	124 924	123 008	-1.53
Total Net Volume Difference (m^3)	-68 351	-68 604	0.37
Percent Erosion (by volume)	77%	78%	1.00
Percent Deposition (by volume)	23%	22%	-1.00

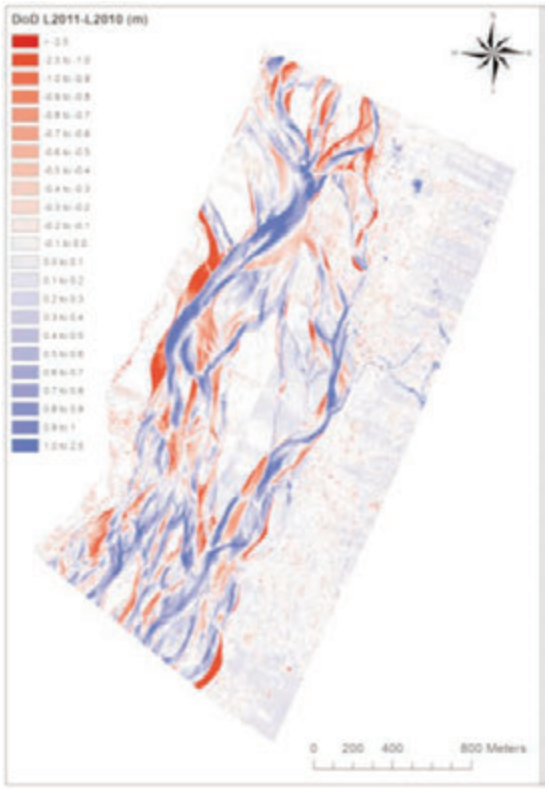

Figure 4. DoD relative to the comparison L2011-L2010.

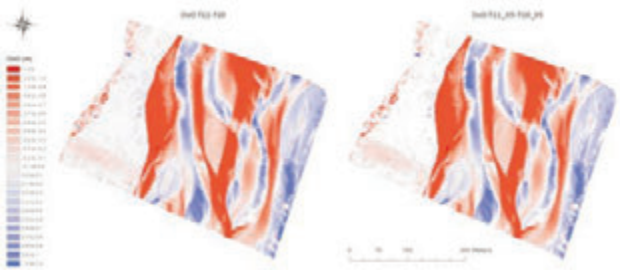

Figure 4. DoD relative to the comparison L2011-L2010.

Discussion

The analysis carried out showed how the floods events occurred during the study period have caused consistent geomorphic variations along the study areas. The DoD obtained from the comparison between L2011 and L2010 has analyzed the changes along the entire study reach, estimating a positive budget (+ 145898 m^3) However, this trend is weak given that there was no prevalent phenomena: a sort of balance between erosion and deposition has taken place. The analysis carried out by comparing the TLS surveys allowed us to study in detail the changes that took place within the sub-reach. In this study area it is observed a clear prevalence of erosion phenomena with a value of *Total Net Volume Difference* of -68351 m^3, in the comparison T11-T10, and -68604 m^3 in T11_05-T10_05. The formation of two new secondary channels, in the middle of the sub-reach, has certainly influenced these results. But a key role can be attributed especially to the extended and deep bank erosion which affected the contiguous floodplain, on the right side. Concerning the third comparison (T11_05-T10_05) that calculates the difference between low-resolution DEMs (0.50 m) the volumetric data were compared with the results obtained by T11-T10 (resolution 0.15 m). This comparative relation (Table 3) allowed to high-

light as the percentages difference never exceed the 12.6%, with the most of the differences that were maintained below 10%. Analyzing individually the results, we can observe how the use of a cell size of 0.50×0.50 m has caused a reduction in the values of *Maximum Negative Variation* (-0.68%) and *Maximum Positive Variation* (-3.45%), in other words a sort of flattening of this punctual values. Differences of more than 8% are related only to the *Average Variation* (9.68%), the *Total Area of Erosion* (-8.20%) and the *Total Area of Deposition* (-12.58%). In this case, the lower resolution caused an underestimation of the areas affected by erosion and depositional phenomena.

Conclusions

The aims of this study was the assessment of the short period geomorphic and volumetric changes occurred along a reach of the Tagliamento River and the comparison between the results obtained from LiDAR and TLS data. Regarding the latter aim a comparative assessment of the output derived from the different data sources was performed, showing little differences between the two survey methods that demonstrated, anyway, to be both precise and reliable. The comparison between different resolution DoDs has shown that even the lower resolutions (0.50 m) allow to obtain significant results, with differences that at most have reached 12.58%, if compared to those obtained by higher resolutions (0.15m). This prove how, in this context, also the use of medium resolutions permits a correct assessment of geomorphic changes, and in particular of volumetric variations. On the other hand the use of high resolutions is confirmed as essential for a correct analysis of specific parameters, as roughness. The GCD method, used in this study, thanks also to the use of an *ad hoc* FIS has proved to be an efficient tool that allows the estimation of volumetric and geomorphic variations, not using a simple difference between DEM, but rather by a accurate multi-parametric analysis, that permits to eliminate the higher uncertainties. Moreover a proper assessment of these variations represents a valuable data that can be used in the flood management programs. In conclusion, the analyzes performed have confirmed the high dynamism of the Tagliamento river, typical feature of gravel bed rivers, especially if characterized by braided morphology, as in this case.

References

Brasington J., Langham J., Rumsby B.T., 2003. Methodological sensitivity of morphometric estimates of coarse fluvial sediment transport. Geomorphology 53, 299–316. DOI: 10.1016/S0169-555X(02)00320-3.

Brasington J., Rumsby B.T., McVey R.A., 2000. Monitoring and modeling morphological change in a braided gravel-bed river using high resolution GPS-based survey. Earth Surf. Processes and Land. 25, 973–990. DOI: 10.1002/1096-9837(200008)25:9<973.

Buffington J.M., 2012. Changes in channel morphology over human time scales. Gravel-bed Rivers: processes, tools, environments. Edited by Michael Church, Pascale Biron, Andrè G. Roy. Wiley-Blackwell, 435-463. DOI: DOI: 10.1002/9781119952497.ch32.

Church M., Ashmore P., 1998. Sediment transport and river morphology: a paradigm for study. In Gravel-Bed Rivers in the Environment, Klingeman PC (ed). Water Resources Center: Highlands Ranch, CO.

Gray D., Harding J.S., 2007. Braided river ecology, a literature review of physical habitats and aquatic invertebrate communities, Science for conservation 279, Science & Technical Publishing, Department of Conservation, Wellington, New Zealand.

Heritage G.L., Hetherington D., 2007. Towards a protocol for laser scanning in fluvial geomorphology. Earth Surf. Processes Land. 32, 66–74.

Lisle T.E., Nelson J.M., Pitlick J., Madej M.A., Barkett B.L., 2000. Variability of bed mobility in natural, gravel-bed channels and adjustments to sediment load at local and reach scales. Water Resources Research, Vol. 36, No. 12, 3743-3755. DOI:10.1029/2000WR900238.

Milan D.J., Heritage G.L., Hetherington D., 2007. Application of a 3D laser scanner in the assessment of erosion and deposition volumes and channel change in a proglacial river. Earth Surf. Processes Land. 32, 1657–1674. DOI: DOI: 10.1002/esp.1592.

Picco L., 2010. Long period morphological dynamics in regulated braided gravel-bed rivers: comparison between Piave River (Italy) and Waitaki River (New Zealand), PhD thesis, University of Padova, 190 p.

Picco L., Mao L., Rigon E., Moretto J., Ravazzolo D., Delai F., Lenzi M.A., 2012. Riparian forest structure, vegetation cover and flood events in the Piave River, WIT Transactions on Engineering Sciences, Vol.73, 137-147, ISSN: 1743-3553, DOI: 10.2495/DEB120121.

Picco L., Tonon A., Ravazzolo D., Rainato R., Rigon E., Moretto J., Delai F., Lenzi M.A., 2013. Monitoring river islands dynamics using aerial photographs and LiDAR data: the Tagliamento river study case. Atti del Convegno "The Role of Geomatics in Hydrogeological Risk". Padua, Italy, 27-28 February 2013.

Picco L., Mao L., Cavalli M., Buzzi E., Rainato R., Lenzi M.A., (submitted). Evaluating short-term morphological changes in a gravel-bed braided river using Terrestrial Laser Scanner. Geomorphology.

Rumsby B.T., Brasington J., Langham J.A., McLelland S.J., Middleton R., Rollinson G., 2008. Monitoring and modeling particle and reach-scale morphological change in gravel-bed rivers: Applications and challenges, Geomorphology 93(1-2), 40-54. DOI: 10.1016/j.geomorph.2006.12.017.

Tockner K., Ward J.V., Arscott D.B., 2003. The Tagliamento River: a model ecosystem of European importance. Aquatic Sciences 65, 239-53. DOI 10.1007/s00027-003-0699-9.

Wheaton J.M., Brasington J., Darby S.E., Sear D.A., 2010. Accounting for uncertainty in DEMs from repeat topographic surveys: improved sediment budgets. Earth Surf. Processes Land. 35, 136–156. DOI: 10.1002/esp.1886.

LiDAR derived high resolution topography: the next challenge for the analysis of terraces stability and vineyard soil erosion

Federico Preti,[1] Paolo Tarolli,[2] Andrea Dani,[1] Simone Calligaro,[2] Massimo Prosdocimi[2]

[1]Dipartimento di GESAAF, Sezione di Ingegneria Agraria, Forestale e dei Biosistemi Agrari, Università di Firenze, Firenze, Italy; [2]Department of Land, Environment, Agriculture and Forestry University of Padova, Agripolis, Legnaro (PD), Italy

Abstract

The soil erosion in the vineyards is a critical issue that could affect their productivity, but also, when the cultivation is organized in terraces, increase the risk due to derived slope failure processes. If terraces are not correctly designed or maintained, a progressively increasing of gully erosion affects the structure of the walls. The results of this process is the increasing of connectivity and runoff. In order to overcome such issues it is really important to recognize in detail all the surface drainage paths, thus providing a basis upon which develop a suitable drainage system or provide structural measures for the soil erosion risk mitigation. In the last few years, the airborne LiDAR technology led to a dramatic increase in terrain information. Airborne LiDAR and Terrestrial Laser Scanner derived high-resolution Digital Terrain Models (DTMs) have opened avenues for hydrologic and geomorphologic studies (Tarolli *et al.*, 2009). In general, all the main surface process signatures are correctly recognized using a DTM with cell sizes of 1 m. However sub-meter grid sizes may be more suitable in those situations where the analysis of micro topography related to micro changes is critical for slope failures risk assessment or for the design of detailed drainage flow paths. The Terrestrial Laser Scanner (TLS) has been proven to be an useful tool for such detailed field survey. In this work, we test the effectiveness of high resolution topography derived by airborne LiDAR and TLS for the recognition of areas subject to soil erosion risk in a typical terraced vineyard landscape of "Chianti Classico" (Tuscany, Italy). The algorithm proposed by Tarolli *et al.* (2013), for the automatic recognition of anthropic feature induced flow direction changes, has been tested. The results underline the effectiveness of LiDAR and TLS data in the analysis of soil erosion signatures in vineyards, and indicate the high resolution topography as a useful tool to improve the land use management of such areas. The stability conditions have been analyzed under the influence of the measured geometry alterations of the wall structure.

Correspondence: Paolo Tarolli, Department of Land, Environment, Agriculture and Forestry, University of Padova, Agripolis, viale dell'Università 16, 35020, Legnaro (PD), Italy.
E-mail: tarolli.paolo@gmail.com

Key words: Soil erosion, terraced slopes, vineyard, LiDAR, TLS, DTM.

Acknowledgements: the Riegl LMS-620 data were elaborated by the Interdepartmental Research Center for Cartography, Photogrammetry, Remote Sensing and GIS at the University of Padova (CIRGEO). Airborne LiDAR data were provided by the Ministry for Environment, Land and Sea (Ministero dell'Ambiente e della Tutela del Territorio e del Mare, MATTM), within the framework of the 'Extraordinary Plan of Environmental Remote Sensing' (Piano Straordinario di Telerilevamento Ambientale, PST-A).

Journal of Agricultural Engineering 2013; XLIV(s2):e16
doi:10.4081/jae.2013.(s1):e16

Introduction

Extended terraced slopes are a distinctive characteristic of landscapes all over the Italian peninsula. The terraces, in fact, allow the farming of many precious products, such as wine, also on very steep slopes. In this terraced landscape, the human interference on the natural morphology is evident, but terraces represent also a typical case of the ancient blending of anthropic communities and lands. Terraced vineyards, as much as olivegrove, are probably the most typical landscape in Tuscany, and the Chianti wine is one of the most prestigious wine produced in Tuscany, exported and appreciated all over the word. Neverthless, these terraced rural areas have gone through a series of social and economical changes that caused, since the Sixties, a gradual abandonement of the traditional agricultural practices and of the maintenance of the rural landscape. A serious consequence following the lack of maintenance of terraced slopes is the increasing erosion due to the loss of efficiency of drainage systems (Crosta *et al.*, 2003). Uncontrolled erosion in agricultural lands causes not negligible soil and nutrient losses (Poesen and Hooke, 1997; Douglas *et al.*, 1998; Corell *et al.*, 1999; Steegen *et al.*, 2001; Verstraeten and Poesen, 2002; Ng Kee *et al.*, 2002; Ramos and Martìnez-Casanovas, 2004) and the long-term productivity loss of degraded soil and plot level (Roose, 1996; Woodward, 1999), with a severe economic impact on farms (Martìnez-Casanovas *et al.*, 2005). The consequences of a strong soil erosion in terraced areas are serious, with possible negative effects over people's safety. In terraced slopes, in fact, concentrated flow incises rills and gullies that can damage retaining walls (Figure 1) and trigger small slides and slumps (Crosta *et al.*, 2003).

Due to the flow concentration during high-intensity or moderate-intensity but prolonged rainstorms, or after snow melting, small slides can evolve in shallow landslides (Moser and Hohensinn, 1983; Crosta, 1998; Crosta e Frattini, 2002) such as soil slips and debris flow that can travel distances up to several hundred meters (Crosta *et al.*, 2003).

According to Crosta *et al.* (2003), terraces produce great changes in slopes hydrologic setting enhancing flow concentration and infiltration at specific sites. This explains the important role of morphology-derived hydrologic factors as triggering process of landslides. It is also clear the importance of having effective instruments to assess in a

detailed way the morphology, to recognize those areas subject to potential erosion and slides. In the last year, many works have demonstrated the effectiveness of high resolution topography derived by Laser Scanner (LiDAR) to generate accurate Digital Terrain Models (DTM) to be considered in many different areas of research. Nowadays, common meter resolution DTMs are useful to recognize all the main surface processes signatures (Tarolli and Dalla Fontana, 2009; Passalacqua *et al.* 2010; Sofia *et al.* 2011; Tarolli *et al* 2012; Sofia *et al.* 2013a,b). In some specific situation, however, where the surveyed processes are related to micro morphologies, as in the case of terraced vineyard, a sub-meter DTM might be more suitable (Tarolli *et al.*, 2012; Lin *et al.*, 2013). Centimetric resolution DTMs are derivable from spatial data acquired through Terrestrial Laser Scanner (TLS), a LiDAR instrument that has been proven to be a useful tool for such detailed field survey at a hillslope scale. In this context, the aim of this paper is to present the TLS survey and the consecutive spatial data processing of a terraced vineyard subject to soil erosion risk in the typical landscape of "Chianti Classico" wine at Lamole (Tuscany, Italy). High-resolution results are compared with traditional resolution digital topography derived by airborne LiDAR.

Materials and methods

TLS survey and derived DTMs

The TLS survey was performed in March 2013. A "time-of-fly" Terrestrial Laser Scanner System Riegl® LMS-Z620 was used. This laser scanner operates in the wavelength of the near infrared and provides a maximum measurement range of 2 km, with an accuracy of 10 mm and a speed of acquisition up to 11000 pts/s. For each measured point, the system records the range, horizontal and vertical alignment angles, and the backscattered signal amplitude. The laser scanner was integrated with a Nikon® D90 digital camera (12.9 Mpixel of resolution) equipped with a 20 mm lens, that provided an RGB value to the acquired point cloud (Figure 2).

The TLS survey at Lamole was carried out from six scan positions, in order to capture precisely the complex morphology of the terraced slopes: one position was used for a panoramic high resolution scan of the main terraced slope, and five were considered to model, with a very high resolution, the recently restored wall, displaying signs of failures (see Figure 8 Chapt 3, and Figure 2). From the "panoramic" scan position 5,352,080 elevation points were collected with a resolution of 0.1 m at 200 m from the scanner. From the other scan positions 1,452,944 points were measured on the retaining wall and on its close proximity with a resolution of 0.02 m at 10 m from the scanner; other 1,737,818 points with a resolution of 0.05 m at 20 m from the scanner plus 2,254,414 points with various resolutions were acquired on the surrounding area (Figure 3).In order to georeference the survey in a global coordinate system, a GNSS network was set up. A couple of Topcon HiPer Pro® dual-frequency and dual-constellation receivers were employed. These differential GPS+GLONASS receivers guarantee a horizontal precision of 3 mm + 0.5ppm (per baseline length) and a vertical precision of 5mm + 0.5ppm (per baseline length) if used in static or rapid static mode.

The raw spatial data (X, Y, Z measurements) acquired were processed in two steps: first to georeferece them and filter all non-ground points, and then to create the DTMs.

The whole processing procedures have been carried out using the Riegl proprietary software RiscanPro®. In particular, with RiscanPro a semi-automatic iterative surface based approach is available to detect non-ground points within a defined range from the real ground surface.

Figure 1. Terraced walls with an implemented drainage system (A), and effects of a failed maintenance (B).

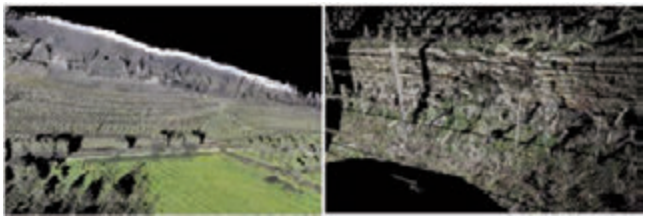

Figure 2. Point cloud derived with TLS with RGB color overlapped to each point.

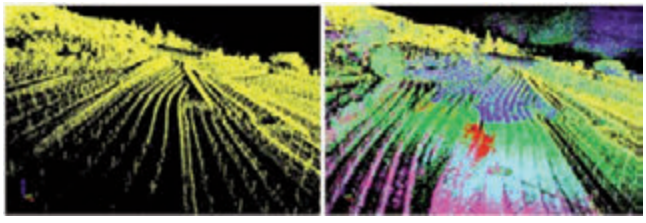

Figure 3. Example of point cloud taken from a single position (left), and overlapping of multiple scans (right).

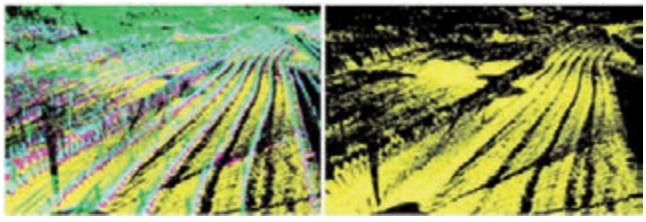

Figure 4. Detail of point cloud of Lamole study area in false colors: yellow points are the groundpoints; fuchsia points are points included from the ground and 50 cm height from the ground; blue points are points with a distance from the ground range from 50 cm to 1m; green points are points above 1m from the ground.

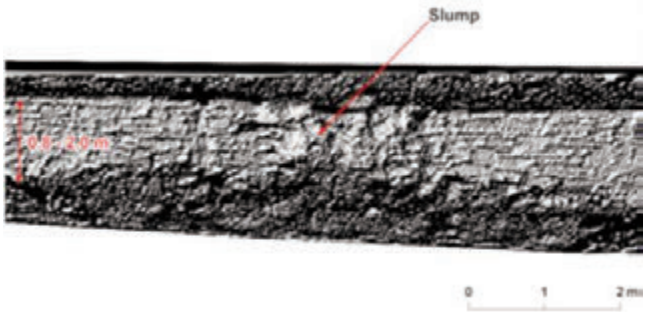

Figure 5. Surveyed retaining wall model hillshade at 0.01 m resolution.

Thanks to the algorithm, more and more fitting meshes are created applying a 2.5D raster filter – this filter generates a 2.5D raster point cloud of source data; in which that each raster cell will be represented by a single point. The points that lie over a threshold defined from the generated mash are eliminated. In the Lamole case, the minimum distance considered from the ground surface was been 0.2m. After this iterative process some corrections were necessary, because of the particular morphology, characterized regular big steps rich in vegetation, not easy to model by 2.5D filter. Figure 4 shows an example of the raw point data (A) and the ground point data (B) derived after the filtering procedure. Spatial coordinates of the remaining ground points were exported and elevation values were interpolated by the natural neighbors method (Sibson, 1981) to generate 0.2 and 0.5 m resolution DTMs of the terraced slope. The ground points density is really irregular on the study area, but at the center of the surveyed terraced slope average ground points density is more than 1000 pts/m^2. The absolute vertical accuracy, evaluated by a ground differential DGPS, was estimated to be less than 0.1 m.

Wall modeling

A centimetric survey of a 120 m long stretch of wall was carried out from four different scans positions. After a hand-made filtering of vegetation, the topographic information was exported flipping the order of x, y, z values: the coordinates of each point were exported as –y; z; x. Therefore, a front viewed 3D digital model of the retaining wall was generated interpolating x value by the natural neighbors method (Sibson, 1981). In the created wall model, with a resolution of 0.01 m, every single stone that compose the wall can be individuate (Figure 5). This level of precision allows to simulate the behavior of the wall in response to back load with a high detail and without many artifacts and much approximations.

Topographic analyses

To quantify the effect of retaining walls on contributing area distributions (and therefore, on flow paths) within catchments, we applied the Relative Path Impact Index (RPII) index proposed by Tarolli *et al.* (2013) to quantify the forest road effects on slope stability. This morphometric index is calculated as follows:

$$RPII = ln\left(-\frac{A_{sm} - A_r}{A_{sm}}\right) \quad (1)$$

where A_r is the contributing area (computed according to the D-Inf method proposed by Tarboton 1997) evaluated in the presence of any roads or paths on hillslopes, while A_{sm} is the contributing area without morphological alterations on hillslopes.

The negative sign and the logarithmic function is applied to emphasize and map only those areas where an increasing of drainage area is observed due to human induced alteration. The higher the RPII index, the stronger the alteration.

To simulate the absence of anthropogenic features (roads, paths, walls), a smoothed DTM is considered, based on an approximation of the original surface solved within a local moving window. To produce this smoothed surface, we decided to use the bivariate quadratic function introduced by Evans (1979), expressed as:

$$Z = ax^2 + by^2 + cxy + dx + ey + f \quad (2)$$

where x, y, and Z are local coordinates, and *a* to *f* are quadratic coefficients. This function was found to perform well in the presence of elevation errors (Albani *et al.* 2004; Florinsky 1998), and it has been successfully applied also in several other analysis on Earth surface morphology and feature extraction (Pirotti and Tarolli, 2010; Sofia *et al.*, 2011; Tarolli *et al.*, 2012, Sofia *et al.* 2013a,b).

Study area

The study area is in the "*Chianti Classico*" wine area, in the center of Tuscany, and it is located in the small village of Lamole (Figure 6) within the municipality of Greve in Chianti (province of Florence).

The study area is a typical hilly environment, along a slope facing North-North West, on soils that have been developed from sedimentary rocks such as sandstones and marls. Vineyards here are growth on terraces made only of dry-stones, that represent a typical landscape element of this region (Figure 7).

The terraces have been restored since 2003 in order to maintain their original role of soil erosion prevention, and to realize the production of a very fine wine. Few months after the restoration, one of the terraces displayed deformations and slumps (Figure 8). This particular wall was therefore considered as an interesting element for the analysis described in the following chapters.

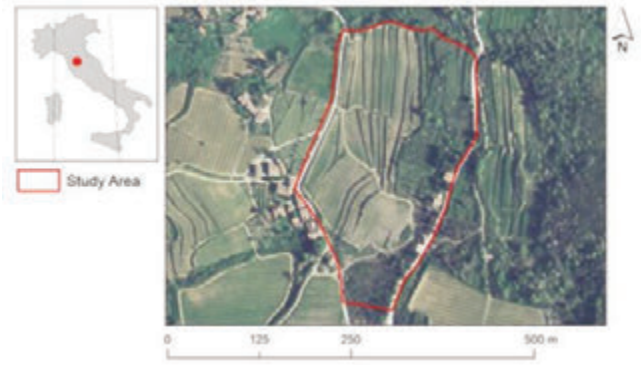

Figure 6. Geographical setting of study area of Lamole.

Figure 7. Panoramic picture of the Lamole area and its terraces.

Figure 8. Surveyed terraced walls with slumps and erosion

Available data

Airborne LiDAR elevation data

For the study area, a DTM with a 1 m resolution derived from Airborne LiDAR survey is available (Figure 9). This model is readily accessible to public authorities in Italy, and it is promoted by the Ministry for Environment, Land and Sea (*Ministero dell'Ambiente e della Tutela del Territorio e del Mare, MATTM*), the Department of Civil Protection and the Mininstry of Defense, in agreement with the regional governments. The DTM has a horizontal accuracy of about ±0.3 m and vertical accuracy of ±0.15 m (RMSE estimated using DGPS ground truth control points).

Results

The lamole study case highlights the effectiveness of TLS surveys for two different analysis at least. The first is that the super resolute and systematic short range scan of a retaining wall allows the generation of a centimetric resolution 3D digital model of the wall with a very high accuracy. A model with this high resolution could be used in strengths and stability simulations. With centimeter wall-model, the behavior under soil pressure of the most of the stones can be correctly simulated and therefore, the final results might be more realistic than the results achievable with a totally artefacted wall-model.

The second result is the RPII index calculation. Figure 10 shows the RPII index evaluated using the ALS-Derived DTM with 1 m resolution (A) and the TLS DTMs with 0.5 m (B) and 0.2 m (C) resolution.

Using a common ALS-derived DTM, the RPII does not detect any flow alteration, and so any soil erosion, due to terraces and any possible damage to the retaining walls (Figure 10 A). With a TLS survey derived topographic base of 0.5 m resolution (Figure 10B) results are better but not yet completely satisfactory: just the most intense flow alterations are shown in the RPII map. In the RPII map of the terraced slope of Lamole a strong flow concentration is shown in corresponding of slump of the surveyed retaining wall. But the high values of the index are reported only below the collapsed stretch of the wall, and this could clearly appear as a not univocal result. In the 0.2 m resolution RPII map (Fig. 10C) there is no doubts that the flow deviation and concentration in corresponding of the slump are processes beginning above the slump, and they are due to the presence of the above terraces. In the 0.2 m resolution RPII map a considerable increase of contributing area due to terraced morphology is reported also in corresponding of a deformed segment of the surveyed retaining wall.

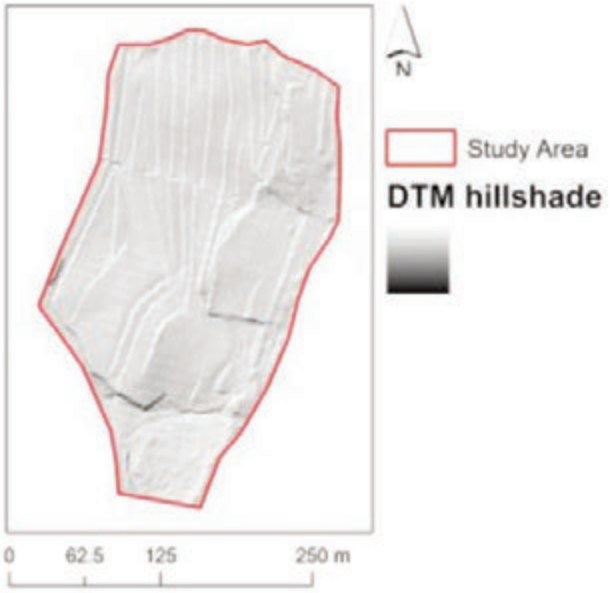

Figure 9. Airborne-LiDAR DTM (1m resolution) available for the study area.

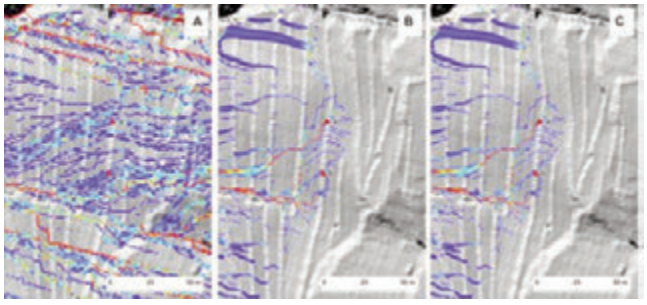

Figure 10. The RPII index evaluated using the ALS-Derived DTM with 1 m resolution (A) and the TLS DTMs with 0.5 m (B) and 0.2 m (C) resolution. a and b represent the wall deformation surveyed on the field.

Conclusions

This paper highlights the effectiveness of a centimetre resolution topography obtained from TLS survey in the analysis of terrace failure processes in vineyards. In the landscape of "*Chianti classico*" wine, the TLS has been proved to be a useful instrument to perform quickly high resolution and high accuracy topographic surveys. Interpolating the acquired points, two high resolution DTMs (0.5 m and 0.2 m resolution) have been obtained, and then a simple morphometric and hydrological analysis is performed. Using a 0.2 m resolution TLS derived DTM, overflow convergences are recognizable exactly where in the field erosion evidence were surveyed. This proves that TLS and the derived high resolution topography can be a useful tool to improve the land use management and planning for the maintenance of terraced areas. However, this method needs to be improved, to clean the alteration that might derive from complex terraced morphology by thick vegetation and DTM artefacts.

References

Albani M., Klinkenberg B., Andison D.W., Kimmins J.P. 2004. The choice of window size in approximating topographic surfaces from digital elevation models. International Journal of Geographical Information Science, 18(6): 577-593.

Corell D.C., Thomas E., Jordan E., Weller D.E. 1999. Precipitation effects on sediment and associated nutrient discharges form Rhode river watersheds. Journal of Environmental Quality 28, 1897-1907.

Crosta G.B. 1998. Regionalization of rainfall threshold: an aid to landslides hazard evaluation. Env. Geol. 35 (2-3): 131-145.

Crosta G.B. and Frattini P. 2002. Rainfall threshold for triggering soil slips and debris flow. Proc. 2nd Plinius Int. Conf. on Mediterranean Storms, Siena, Italy, [in press].

Crosta G.B., Dal Negro P., Frattini P. 2003. Soil slips and debris flows on

terraced slopes. Natural Hazards and Earth System Sciences 3: 31-42.

Douglas C.L., King K.A., Zuzel J.F. 1998. Nitrogen and phosphorous in surface runoff and sediment from a wheat-pea rotation in north-eastern Oregon. Journal of Environmental Quality 27: 1170-1177.

Evans I.S. 1979. An integrated system of terrain analysis and slope mapping. Final report on grant DA-ERO-591-73-G0040, University of Durham, England.

Florinsky I.V. 1998. Accuracy of local topographic variables derived from digital elevation models. International Journal of Geographical Information Science 12(1): 47-61.

Lin C.W., Tseng C.M., Tseng Y-H., Fei L.Y., Hsieh Y.C., Tarolli P. 2013. Recognition of large scale deep-seated landslides in forest area of Taiwan using high resolution topography. Journal of Asian Earth Sciences 62: 389-400.

Martìnez-Casanovas J.A., Concepcion Ramos M., Ribes-Dasi M. 2005. On-site effects of concentration flow erosion in Vineyard fields: some economic implications. Catena 60: 129-146.

Moser M. and Hoensisnn F. 1983. Geotechnical aspect of soil slips in Alpine regions. Eng. Geol. 19: 185-211.

Ng Kee Kwong K.F., Bholah A., Volcy L., Pynee K., 2002. Nitrogen and phosphorous transport by surface runoff from a silty clay loam soil under sugarcane in the humid tropical environmental of Mauritius. Agriculture, Ecosystems and Environment 91: 147-157.

Passalacqua P., Tarolli P., Foufoula-Georgiou E. 2010. Testing space-scale methodologies for automatic geomorphic feature extraction from lidar in a complex mountainous landscape. Water resources research, 46, W11535. doi:10.1029/2009WR008812.

Pirotti F., Tarolli P. 2010. Suitability of LiDAR point density and derived landform curvature maps for channel network extraction. Hydrological Processes 24: 1187-1197. doi: 10.1002/hyp.758.

Poesen J. and Hooke J.M. 1997. Erosion, flooding and channel management in the Mediterranean environments of southern Europe. Progress in Physical Geography 21: 157-199.

Ramos M.C., Martinez-Casanovas J.A. 2004. Nutrient losses from a Vineyard soil in Northeastern Spain caused by an extraordinary rainfall event. Catena 55: 79-90.

Roose E. 1996. Land Husbandry: Components and Strategy. 70 FAO Bulletin. Food and Agriculture Organization of the United Nations, Rome.

Sibson R. 1981. A brief description of natural neighbor interpolation (Chapter 2). In: V. Barnett Interpreting Multivariate Data. John Wiley, Chichester, 21-36.

Sofia G., Tarolli P., Cazorzi F, Dalla Fontana G. 2011. An objective approach for feature extraction: distribution analysis and statistical descriptors for scale choice and channel network identification. Hydrol. Earth Syst. Sci.; 15, 1387–1402,doi:10.5194/hess-15: 1387-2011.

Sofia G., Pirotti F., Tarolli P. (2013a). Variations in multiscale curvature distribution and signatures of LiDAR DTM errors, Earth Surf. Process. Landforms, DOI: 10.1002/esp.3363

Sofia G., Dalla Fontana G.,. Tarolli, P. (2013b). High-resolution topography and anthropogenic feature extraction: testing geomorphometric parameters in floodplains. Hydrol. Process.. doi: 10.1002/hyp.9727.

Steegen A., Govers G., Takken I., Nachtergaele J., Poesen J., Merckx R. 2001. Factors controlling sediment and phosphorous export from two Belgian agricultural catchments. Journal of Environmental Quality 30: 1249-1258.

Tarboton D.G. 1997: A new method for the determination of flow directions and upslope areas in grid digital elevation models. Water Resources Research 33: 309-319.

Tarolli P. and Dalla Fontana G. 2009. Hillslope to valley transition morphology: new opportunities from high resolution DTMs. Geomorphology 113: 47-56.

Tarolli P., Arrowsmith J R., Vivoni E.R. 2009. Understanding earth surface processes from remotely sensed digital terrain models. Geomorphology 113: 1-3.

Tarolli P., Sofia G., Dalla Fontana G. 2012. Geomorphic features extraction from high resolution topography: landslide crowns and bank erosion. Natural Hazards 61: 65-83.

Tarolli P., Calligaro S., Cazorzi F., Dalla Fontana G. 2013. Recognition of surface flow processes influenced by road and trails in mountain areas using high-resolution topography. European Journal of Remote Sensing 46: 176-197.

Verstraeten G. and Poesen J. 2002. Regional scale variability in sediment and nutrient delivery from small agricultural watersheds. Journal of Environmental Quality 31: 870-879.

Woodward D.E. 1999. Method to predict cropland ephemeral gully erosion. Catena 37: 393-399.

Actual evaporation estimation from infrared measurement of soil surface temperature

Davide Pognant, Davide Canone, Stefano Ferraris

Interuniversity Department of Regional and Urban Studies and Planning, Politecnico e Università di Torino, Italy

Abstract

Within the hydrological cycle, actual evaporation represents the second most important process in terms of volumes of water transported, second only to the precipitation phenomena. Several methods for the estimation of the *Ea* were proposed by researchers in scientific literature, but the estimation of the *Ea* from potential evapotranspiration often requires the knowledge of hard-to-find parameters (e.g.: vegetation morphology, vegetation cover, interception of rainfall by the canopy, evaporation from the canopy surface and uptake of water by plant roots) and many existing database are characterized by missing or incomplete information that leads to a rough estimation of the actual evaporation amount. Starting from the above considerations, the aim of this study is to develop and validate a method for the estimation of the *Ea* based on two steps: i) the potential evaporation estimation by using the meteorological data (i.e. Penman-Monteith); ii) application of a correction factor based on the infrared soil surface temperature measurements. The dataset used in this study were collected during two measurement campaigns conducted both in a plain testing site (Grugliasco, Italy), and in a mountain South-East facing slope (Cogne, Italy). During those periods, hourly measurement of air temperature, wind speed, infrared surface temperature, soil heat flux, and soil water content were collected. Results from the dataset collected in the two testing sites show a good agreement between the proposed method and reference methods used for the Ea estimation.

Correspondence: Davide Canone, DIST, Politecnico e Università di Torino, Viale Mattioli 39, Torino 10125, Italy.
Tel. +39.011.0907427
E-mail: davide.canone@unito.it, davide.canone@polito.it

Key words: Hydrology, surface evaporation, heat fluxes, infrared temperatures, eddy covariance.

Journal of Agricultural Engineering 2013; XLIV(s2):e17
doi:10.4081/jae.2013.(s1):e17

Introduction

Changes in the hydrological cycle induced by global warming may affect society deeply, especially with regard to flood and drought risks, water availability and water quality.[1]

This consideration was comprehensible since by Rind *et al.*,[2] who highlighted that climate changes, caused by increasing atmospheric concentrations of greenhouse gases, would have important effects on water circulation and water availability with significant environmental and economic consequences on agriculture, forestry and river flow. Also the scenario analysis on the climate change performed by Arnell predicted that by 2025 five billion people will risk to live in areas subject to water stress, with an increase of potential evaporation in the Eastern Europe even up to 25% and more.[3,4] In consideration with this, since evaporation represents the second most important phenomenon in terms of volumes of water transported in the hydrological cycle, all the connected processes will be surely affected by climate changes. Due to the importance of the evaporation on water balances, both direct and indirect methods were developed and improved to estimate it.

The three most commonly used direct methods to estimate the actual evaporation rate are i) eddy correlation, ii) the Bowen ratio, and iii) the lysimeters, but each of the mentioned method can show different advantages and disadvantages. The applications of eddy covariance and Bowen ratio methods are many nowadays, but limited by the requirement of advanced equipments and a large uniform test area.[5] Lysimeters are also expensive. Finally, the use of micro-lysimeters has the advantage that the spatial variability of evaporation can be directly examined, but measurements are difficult and time consuming.[6] On the other hand, some popular indirect methods are used to assess actual evaporation starting from either the Penman Monteith potential evaporation model, or the Priestley and Taylor potential evaporation model,[7] It is sometime used also the advection-aridity actual evaporation model based on the Bouchet complementary relationship.[8,9] The use of the Penman Monteith equation, as proposed by Allen *et al.*,[10] allows rapid estimates of potential evaporation (loosely defined as the evaporation from surfaces where water is not limiting) in different sites (basically, all the sites with meteorological equipment). The equations for wet surface evaporation can be used to determine actual evaporation by means of the reductions factors as a function of moisture availability.[11] On the other hand, to better estimate the actual evaporation, Brutsaert obtained a theoretical formulation of the scalar roughness length for rough surfaces on the basis of a local Reynolds number.[12,13] Afterwards, Parlange and Katul proposed an advection-aridity complementary model to estimate actual evaporation which requires,[14] as input, the meteorological data used in the classical Penman Monteith equation.

Recently, several attempts have been made to improve these methods in order to provide better estimates of actual evaporation. Surface temperatures, combined with meteorological factors were used to provide estimates of actual evaporation,[15] and remote-sensed surface

temperatures in conjunction with net radiation, air temperature, wind speed and surface roughness were used to map both soil moisture and actual evaporation.[16]

In this context, also the method developed by Ben-Asher *et al.* allows the actual soil evaporation estimation.[17] It starts from the daily surface temperatures of three soil samples in different hydrological conditions: steady state saturation, steady state dry, and a drying soil. In particular, by relating the surface temperature of the drying soil sample to the other ones, a relative evaporation index (*RE*) can be calculated to estimate the soil actual evaporation starting from the potential Penman Monteith estimation. Moreover, Kerridge *et al.* improved the study of Ben-Asher *et al.* by estimating the *RE* index for a drip irrigated vineyard site,[18] starting from infrared temperature measurement collected by a sensors mounted on a quad bike, on several days of the 2009–2010 season. Obviously, the need of two reference soils in steady state conditions (saturation and dry) during in situ monitoring would become a disadvantage extremely hard-to-manage.

Taking into consideration all the mentioned aspects and to create an efficient and less expensive way to estimate the actual soil evaporation both in plain and in mountain conditions, this study aims to modify the Ben-Asher method, in an effort to overcome those in situ monitoring difficulties that can represent an operational limit. An additional goal of this study would be the application of the proposed method also in mountain conditions.

Hence, the goodness of the proposed method is tested not only with the Parlange and Katul method applied to the meteorological data collected in the University Campus of Grugliasco,[14] River Po plain (North-West Italy), but also with the Eddy covariance experimental data collected in the mountain test site of Cogne, Aosta Valley (North-West Italy).

Materials and methods

Theory and formulations

The methodology proposed by Ben-Asher *et al.* and improved by Kerridge *et al.* allows estimation of actual evaporation based on *RE* calculated on the basis of the soil surface temperature.[17, 18]

In particular, Ben-Asher *et al.* expressed the relationship between soil temperature and evaporation as:[17]

$$\int_{t1}^{t2} \lambda E_d \, dt = S_d \Delta T_{d,max} \quad (1)$$

$$\int_{t1}^{t2} \lambda E_s \, dt = S_s \Delta T_{s,max} \quad (2)$$

where λE_d and E_s are the actual evaporation from, respectively, a dry and a saturated soil, (W m^{-2}); $\Delta T_{d,max}$ and $\Delta T_{s,max}$ represent the difference between maximum and minimum temperatures, (°C), daily based; and S_d and S_S are coefficients of proportionality that are mainly function of convective and radiative transfer of energy. From theoretical findings, Ben-Asher *et al.*,[17] discovered that this two coefficients can be considered nearly equal and directly computable from the $\Delta T_{d,max}/\Delta T_{s,max}$ ratio.

On the basis of the above mentioned assumptions, the daily latent heat flux from soil to the atmosphere can be calculated starting from the difference of the maximum and the minimum temperature measured on the soil surface in saturated and dry conditions. This imply that during any field survey, saturated and dry soil samples must be maintained near the investigated site with a labor-intensive approach. In the original method,[17, 18] the reference dry soil was established in a plastic bucket buried in the soil and protected from rain and irrigations, while the reference saturated soil was put in a similar bucket and daily refilled with water.

The RE was expressed as a linear function of the difference between maximum minimum soil surface temperatures:

$$RE = -a\left(T_{d,max} - T_{d,min}\right) + b \quad (3)$$

where

$$a = \frac{1}{\Delta T_{s,max}} \quad (4)$$

$$b = \frac{T_{0,max} - T_{0,min}}{\Delta T_{s,max}} \quad (5)$$

$$\Delta T_{s,max} = T_{s,max} - T_{0,max} \quad (5)$$

T is the soil infrared temperature, (C°), the subscripts *0*, *d* and *s* denote respectively dry, drying and saturated soil, and the subscripts max and min indicate the highest and the lowest daily temperature.

Unfortunately, the Ben-Asher method highlights some technical and practical limits: i) in particular conditions, when the reference dry and saturated soils have similar surface temperatures (max and min) , the RE value become close to 1 and its application in a potential evaporation models lead to an actual evaporation equal to the potential one; ii) as stated also from the author, when there are large temperature changes referred to small evaporation amounts, as well as, when soil evaporation amount decrease down to the zero level, the proposed method becomes unreliable; iii) operational difficulties in maintaining the proper conditions for the reference soils in case of field monitoring are quite complicated.[17] Moreover the Ben-Asher method cannot be applied on common meteorological databases, and on databases of satellite measurements, both of which do not contain soil surface temperature measurements of reference samples.

To overcome such limitations, we propose to estimate the surface temperatures $T_{0,min}$, $T_{0,max}$ and $T_{s,max}$, (°C), starting from measurements collected in specific reference days of the growing season. Namely, when the soil water contents are supposed to be very close, respectively, to the minimum and to the maximum values achievable in the investigated area. The proposed method is based on the assumption that the diurnal temperature variation at the surface of the earth is mainly determined by the global short-wave radiation, according to Lonnqvist,[19] and by the air temperature in the lower layer of the atmosphere. The reference days were identified (within the same growing season) as the days with lowest and highest soil water content respectively and good weather conditions (namely after large spring rainfalls the first and in midsummer the second). Then we employed the values of maximum and minimum soil temperature measured in these two days to estimate $T_{0,min}$, $T_{0,max}$ and $T_{s,max}$ by means of the following relations:

$$T_{0,min} = T_{lo,m} \frac{Rg_{d,M}}{Rg_{lo,M}} \frac{Ta_{hi}}{Ta_{lo}} \quad (7)$$

$$T_{0,max} = T_{lo,max} \frac{Rg_{d,max}}{Rg_{lo,max}} \frac{Ta_{lo}}{Ta_{hi}} \quad (8)$$

$$T_{s,max} = T_{hi,max} \frac{Rg_{d,max}}{Rg_{lo,max}} \frac{Ta_{lo}}{Ta_{hi}} \quad (9)$$

where *Rg* is the global radiation, (W m^{-2}); *Ta* is the air temperature of the lower layer of the atmosphere when the global radiation reach its daily maximum value, (°C); the subscripts *lo* and *hi* refer to the reference days with lowest and highest soil water content respectively; the

subscripts m and M refer to the average value between sunrise and midday, and the average value between sunrise and the maxΔimum daily solar radiation respectively.

The air temperature correction on $T_{0,min}$, $T_{0,max}$, and $T_{s,max}$ by mean of the terms Ta_h/Ta_{lo} on $T_{0,min}$ and Ta_{lo}/Ta_{hi} on $T_{0,max}$ and $T_{s,max}$, reduce the discrepancy between T_0 and T_s due to the difference of air temperature between the reference days.

The parameters a and b were calculated according to Ben-Asher *et al.*,[17] while RE was given by:

$$RE = \left[-a\left(T_{d,max} - T_{d,m}\right) + b\right]\frac{\Delta T_d}{\Delta T_0} \quad (10)$$

where ΔT_d and $\Delta\Delta T_0$, (°C), are given by

$$\Delta T_d = T_{d,max} - T_{d,m} \quad (11)$$

$$\Delta T_0 = T_{0,max} - T_{0,m} \quad (12)$$

and they represent the differences of soil surface temperature, respectively, in a normal drying day, and in the lowest soil water content reference day.

Finally, a validation procedure was performed by testing the output data with, respectively, the advection aridity evaporation model proposed by Parlange and Katul at the Grugliasco test site (plain conditions) and the Latent Heat values measured with the Eddy covariance station in the Cogne test site (mountain conditions).

Validation

River Po plain test site

The actual evaporation values are referred to the meteorological dataset collected during the growing season 2009. The proposed method were compared to the actual evaporation data obtained from the advection aridity model proposed by Parlange and Katul.

In this hourly model, the potential evaporation is computed using a Penman equation,[20] while the reference wet surface evaporation is computed using the Priestley-Taylor approach.

Mountain test site

The validation in the Cogne test site was performed directly on the latent heat flux data obtained from the eddy covariance station.

The turbulent fluxes sensible heat (H) and latent heat (LE) were calculated using the following equations:

$$LE = \lambda \rho w' q' \quad (13)$$

$$H = \rho C_p T' w' \quad (14)$$

where λ is the latent heat of vaporization, (J kg^{-1}), E the water vapor flux, (kg m^{-2} s^{-1}), ρ the density of dry air, (kg m^{-3}), w the vertical wind speed, (m s^{-1}), q the specific humidity, (kg kg^{-1}), Cp the specific heat capacity of dry air (1013 J kg^{-1} K^{-1}), and T the sonic temperature (°C).[21] The quantities $w'q'$ and $T'w'$ represent the covariance between vertical wind speed and vapor density, and between vertical wind speed and temperature, respectively.

On these quantities it was applied the rotation of coordinates proposed by Kaimal and Finnigan.[22] The sonic anemometers' virtual air temperature was corrected, accounting for wind speed normal to the sonic path and humidity effects.[23,24] On both the sensible heat flux and the latent heat flux, the correction for the density effects given by Webb *et al.* was carried out.[25]

Two ground heat flux plates were installed parallel to the slope near the base of the station, at 15 cm depth in the soil. The ground heat flux term G was obtained directly from the average of these two heat flux plates. The net radiometer provides the net radiation flux Rn.

The sensible heat flux H, the latent heat flux LE, and the ground heat flux G are defined as positive away from the surface, while the net incoming radiation Rn is positive toward the surface.

Changes in heat energy stored S in the shallow soil were computed using measurements of soil temperature change in the soil column and soil-moisture content.

The change in soil heat energy was computed as:[26,27]

$$S = \frac{10000\Delta T_s\, C_s d}{\Delta t} \quad (15)$$

where 10,000 is a conversion factor; ΔT_s is the soil temperature change, (°C); C_s is the volumetric heat capacity of the soil, (J g^{-1} °C^{-1}); d is the soil layer thickness (8 cm); and Δt is the time interval (1800 seconds). The soil heat capacity C_s was estimated from the relation:

$$C_s = D_s(C_{sd} + C_w X_w) \quad (16)$$

where D_s is the dry-soil bulk density (1,5 g cm^{-3}); C_{sd} is the specific heat capacity of the dry soil (assumed to be 0.840 J g-1 °C^{-1}); C_w is the specific heat capacity of water (namely 4.190 J g^{-1} °C^{-1}); and X_w is the mass fraction of water in the soil.

Finally, to evaluate the energy fluxes on the slope we considered the correction of net radiation due to the inclined surface and its effects on eddy fluxes following the procedures proposed by Kondratiev *et al.*[28] The zenith and the azimuth angles of the sun requested to estimate the solar radiation on sloping surfaces were calculated with the Solar Position Algorithm developed by Reda and Andrea for the National Renewable Energy Laboratory-U.S Department of Energy.[29]

Sites description

River Po plain test site

The measurement site is located in Grugliasco (Torino), in the northwestern part of the Po river plain - Italy (45° 03' 52" latitude, 7° 35' 34" longitude) at 290 m a.m.s.l., as shown in Figure 1.[30, 31]

The Italian Geological Map identifies this area as an aeolian deposition zone which was formed by the accumulation of wind-blown sediment. The soil is mainly composed of sand and the slope is about 1% (Table 1). Soil analysis shows the presence of two different soil horizons: the first one is a typical surface horizon (A) placed between the surface and 1.0 m depth, and the second one is a mineral horizon (C) placed from 1.0 m down to 3.0 m depth.

An Apogee Instruments IRTS-P infrared sensor was used to perform measurements of soil surface temperature during the experimental period.

Mountain test site

The study was carried out on a slope in the NorthWest Italian Alps near Cogne, Italy at 45°36' 48" latitude, and 7° 21'29" longitude (Figure 1). The experimental site is located at 1730 meters above sea level on a slope facing East- Southeast (120°) with an inclination of about 26°. The vegetation is characterized by herbaceous and shrub components typical of degraded pastures at high altitudes, therefore it is representative of wide mountain areas. This region belongs to a continental climatic zone that is characterized by cold winters and hot summers; rainfall occurs mainly in spring and autumn, with an average of 650 mm y^{-1}. The average annual temperature is about 4°C. The experimental site is characterized by high incident solar radiation due to its aspect resulting in strong turbulent energy fluxes (sensible heat and latent heat) and large temperature differences between day and night. The incident radiation also speeds up the dynamics of snow melting and soil drying.

The eddy covariance station is located in the middle of the slope and consists of a data logger (Campbell Sci., CR3000), a three-dimensional sonic anemometer (Campbell Sci., CSAT3), an open path infrared gas

analyzer (Licor, Li-7500A), and a Krypton hygrometer (Campbell Sci., KH20). These three sensors were placed parallel to the ground at an height of 2.10 meters. The sample frequency was settled at 10 Hz and the measurements were collected as averages over 30 min periods.

The experimental site is also equipped with the following additional sensors: a Vaisala HMP45C probe for detecting the air temperature and humidity; a Kipp&Zonen NR-LITE net radiometer; a Campbell Sci. CS616 probe for the measurement of water content using Time Domain Reflectometry technique; two Campbell Sci. TCAV thermocouple probes for the measurement of the soil temperature; two Hukseflux HFPS01C plates for the measurement of heat fluxes within the soil; and an Apogee Instruments IRTS-P infrared sensor for the measurement of the soil surface temperature. All the above mentioned sensors collect data each 10 min and all the collected values are also averaged on 30 min periods.

Independent soil water content measurements (performed with a Time Domain Reflectometer Campbell TDR100) were carried out since October 2010.

Results

River Po plain test site

In order to estimate the *RE* index, two reference days, necessary for the $T_{0,min}$, $T_{0,max}$ and $T_{s,max}$ calculation, were chosen within the growing season 2009. The selection criteria was based on the hourly soil water content Time Domain Reflectometry (TDR) monitoring. The following dates were selected:

Reference day for T0,min and T0,max: September, the 6th 2009 - when the soil reached its seasonal minimum value of water content (0.035 m^3/m^3). On that day, the minimum surface temperature of the ground was 25.2 °C while the maximum reached 46.8°C.

Reference day for TS,max: April, 29th 2009 - characterized by high soil water content (0.28 m^3/m^3) and absence of clouds. On that day, a minimum temperature of 11.6 °C and a maximum temperature of 19,4°C were recorded.

Starting from the parameters collected during the above mentioned days, the RE index values have been calculated for each day related to four evaporation transients during the growing season 2009 (Table 2). In detail, for the Grugliasco site, the RE values range from a minimum of 0.18 and a maximum of 0.76, with an average value of 0.52.

The application of the estimated *RE* index to the potential evaporation quantities highlights that the values of "corrected" potential evaporation match quite well the actual evaporation values calculated with the Parlange and Katul method (Figure 2a-d). This matching is particularly evident on clear days with high evaporation, namely for all the days with high solar radiation and high potential evaporation (e.g. July 19th and 20th; and August 4th and 5th).

Conversely, on days when there are irregular trend of potential evaporation due to cloudy weather or partially overcast sky (es. July 21st, 22nd and 23rd; and August 3rd, 27th, and 31st) the proposed method shows poor results: those days are all characterized by an RE index extremely low with respect to the average value.

For all those days, except for August the 31st, the low value of *RE* is due to the low difference between maximum and minimum daily surface temperature (<9°C). Since soil surface temperature values are highly sensitive to slight changes in sun exposure, in case of irregular solar radiation the soil temperature can be more influenced by other factors such as either air temperature or soil moisture.

The low value of *RE* for August the 31st depends on the solar radiation of the previous day (i.e. August the 30th), that was rather low dur-

Table 1. Textural properties of the Grugliasco test site .

Horizon A 0 - 1 m	15.5	50.1	16.1	5.3	8.2	4.8	1.4	1.55
Horizon C 1 - 3 m	35.5	54.9	5.5	0.9	1.8	1.4	0.4	1.7

Table 2. Variables for the RE index calculation for the Grugliasco test site.

31/05/2009	11.43	17.76	57.95	28.67	0.03	1.37	0.52
01/06/2009	25.45	24.02	68.09	33.69	0.03	1.28	0.64
02/06/2009	17.88	24.02	68.31	33.79	0.03	1.28	0.63
03/06/2009	16.85	23.22	66.77	33.03	0.03	1.29	0.61
04/06/2009	18.66	21.08	67.65	33.47	0.03	1.36	0.70
19/07/2009	8.86	23.24	69.19	34.23	0.03	1.31	0.43
20/07/2009	14.31	22.62	67.65	33.47	0.03	1.32	0.59
21/07/2009	5.70	13.87	53.32	26.38	0.04	1.46	0.33
22/07/2009	5.55	14.11	51.12	25.29	0.04	1.43	0.31
23/07/2009	5.03	18.75	63.02	31.18	0.03	1.39	0.29
24/07/2009	8.66	20.85	63.68	31.51	0.03	1.33	0.42
03/08/2009	8.24	12.67	48.26	23.87	0.04	1.46	0.43
04/08/2009	15.41	21.40	65.00	32.16	0.03	1.33	0.61
05/08/2009	13.65	20.51	61.70	30.52	0.03	1.32	0.56
06/08/2009	13.39	19.35	61.04	30.20	0.03	1.35	0.57
07/08/2009	12.98	22.07	59.71	29.54	0.03	1.25	0.49
26/08/2009	13.41	15.99	56.63	28.02	0.03	1.42	0.59
27/08/2009	8.92	20.17	57.73	28.56	0.03	1.29	0.40
28/08/2009	21.68	20.85	63.68	31.51	0.03	1.33	0.66
29/08/2009	20.31	20.40	58.83	29.11	0.03	1.29	0.57
30/08/2009	15.75	8.22	40.32	19.95	0.05	1.58	0.58
31/08/2009	31.44	20.13	55.09	27.25	0.04	1.26	0.18
01/09/2009	20.81	13.33	57.07	28.23	0.03	1.52	0.76

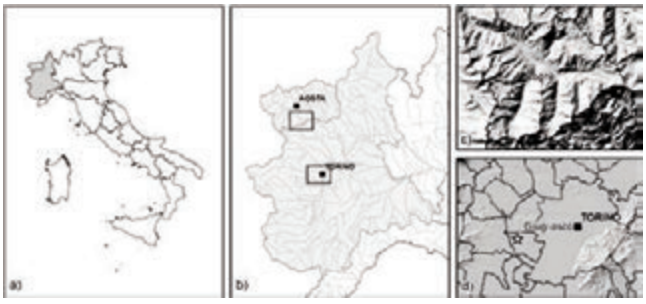

Figure 1. Map of the North-West Italy. The black dots and white stars highlights the experimental test sites of Cogne and Grugliasco.

ing the afternoon. Hence, the *RE* index value is extremely low because of the high value of the term $T_{d,max} - T_{d,min}$ in the equation (3). In Figure 2d it is highlighted that the low solar radiation on August the 30th caused a minimum value in the soil surface temperature during the early hours of August the 31st quite lower than the average value referred to the same considered period. Only the strong incident radiation, which occurred during the following days, leads to a significant soil temperature increase. In Figure 3 it is shown the agreement between the Parlange-Katul actual evaporation values and our calculated soil evaporation. The results have been obtained without considering the above mentioned days characterized by low temperature differences.

The poor results on days with cloudy conditions are mentioned also by Kerridge *et al.*: they suggested that a change in weather conditions during the survey time can affect the results of the correction.[18]

Mountain test site

As in the Grugliasco site, the following dates were chosen to estimate the *RE* for the site of Cogne:

Reference day for $T_{0,min}$ and $T_{0,max}$: August, the 8th 2012 - when the soil reached its seasonal minimum value of water content (0.034 m^3/m^3). On that day, the minimum surface temperature of the ground was 19.5°C while the maximum reached 31.2 °C.

Reference day for $T_{s,max}$: May, the 8th 2012 - characterized by high soil water content (0.190 m^3/m^3) and absence of clouds. On that day, a minimum temperature of 20.6 °C and a maximum temperature of 26.1 °C were recorded.

Starting from the parameters collected during the above mentioned days, the *RE* index values have been calculated for each day. They are related to two transient evaporation during the growing season 2012 (Table 3). In detail, for the Cogne site, the *RE* values range from a minimum of 0.30 and a maximum of 0.69, with an average value of 0.44.

From an analysis of the results highlighted in Figure 4a-d, it is possible to assess that the proposed correction method seems to works bet-

Table 3. Variables for the RE index calculation for the Cogne test site. .

31/05/2009	11.43	17.76	57.95	28.67	0.03	1.37	0.52
01/06/2009	25.45	24.02	68.09	33.69	0.03	1.28	0.64
02/06/2009	17.88	24.02	68.31	33.79	0.03	1.28	0.63
03/06/2009	16.85	23.22	66.77	33.03	0.03	1.29	0.61
04/06/2009	18.66	21.08	67.65	33.47	0.03	1.36	0.70
19/07/2009	8.86	23.24	69.19	34.23	0.03	1.31	0.43
20/07/2009	14.31	22.62	67.65	33.47	0.03	1.32	0.59
21/07/2009	5.70	13.87	53.32	26.38	0.04	1.46	0.33
22/07/2009	5.55	14.11	51.12	25.29	0.04	1.43	0.31
23/07/2009	5.03	18.75	63.02	31.18	0.03	1.39	0.29
24/07/2009	8.66	20.85	63.68	31.51	0.03	1.33	0.42
03/08/2009	8.24	12.67	48.26	23.87	0.04	1.46	0.43
04/08/2009	15.41	21.40	65.00	32.16	0.03	1.33	0.61
05/08/2009	13.65	20.51	61.70	30.52	0.03	1.32	0.56
06/08/2009	13.39	19.35	61.04	30.20	0.03	1.35	0.57
07/08/2009	12.98	22.07	59.71	29.54	0.03	1.25	0.49
26/08/2009	13.41	15.99	56.63	28.02	0.03	1.42	0.59
27/08/2009	8.92	20.17	57.73	28.56	0.03	1.29	0.40
28/08/2009	21.68	20.85	63.68	31.51	0.03	1.33	0.66
29/08/2009	20.31	20.40	58.83	29.11	0.03	1.29	0.57
30/08/2009	15.75	8.22	40.32	19.95	0.05	1.58	0.58
31/08/2009	31.44	20.13	55.09	27.25	0.04	1.26	0.18
01/09/2009	20.81	13.33	57.07	28.23	0.03	1.52	0.76

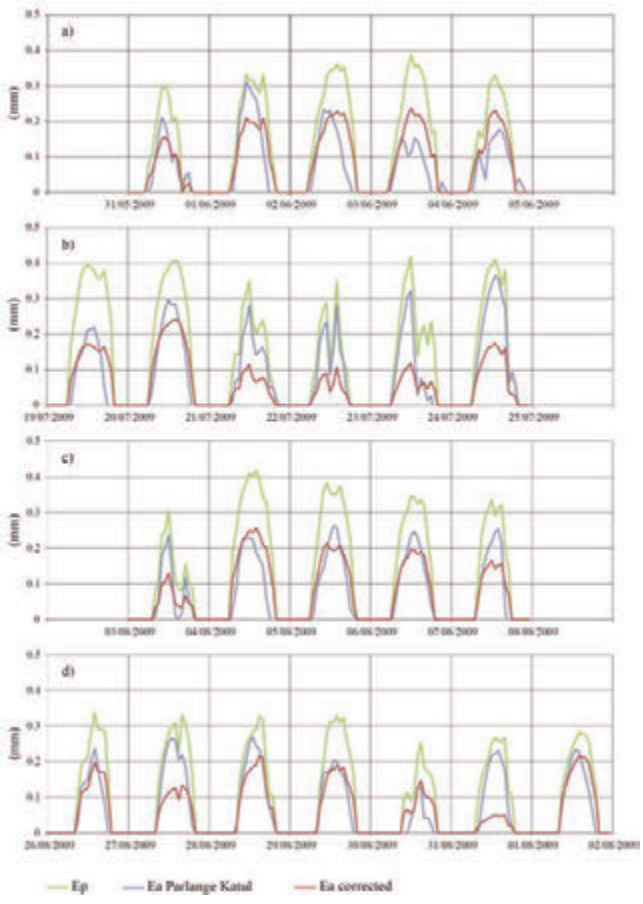

Figure 2. Values of Ep Penman-Monteith, Ea Parlange and Katul and Ea corrected calculated for the field site in Grugliasco in four periods of the year 2009: a) between May the 31st and June the 5th; b) between July the 19th and 25th; c) between August the 3rd and 8th and d) between August the 26th and September the 1st.

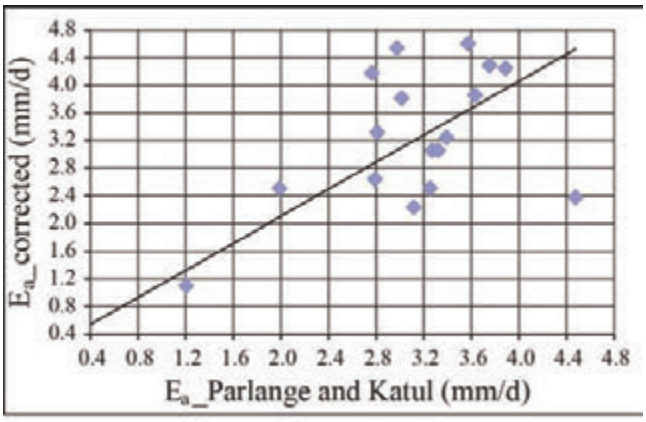

Figure 3. Parlange – Katul actual evaporation compared to the soil evaporation estimated from RE × Ep – Grugliasco site

ter in the experimental site of Cogne than in the Grugliasco test site.

Only on May the 12th (Figure 4b) the results of the correction are difficult to assess, and the extreme variability of the potential evaporation reflects the extremely irregular results measured by the eddy covariance station. For all the other days within the investigated period, the correction of the potential evaporation shows a good agreement with the results obtained by the eddy covariance survey.

In contrast with the Grugliasco results, even the days characterized by partially covered sky (hence with an irregular solar radiation) have returned values of actual evaporation very similar to those measured in situ (e.g. May 6th, 19th; and August 12th).

In the experimental site of Cogne the relationship between the actual evaporation from eddy covariance measurements and the evaporation corrected with the proposed method is much more noticeable with respect to the site of Grugliasco (Figure 5), with a coefficient of determination of 0.788. This can be related to the method used to calculate *Ea* in Grugliasco. The eddy covariance method is one of the best methods for measuring actual evaporation and it provides more accurate results than the estimations computed with the Parlange Katul method.

Also, the vegetation cover of the Cogne test site is more uniform than the Grugliasco one and it probably leads to better measurements of the surface temperature.

Conclusions

In the present work we developed and validated a method for the estimation of the actual evaporation starting from the Ben-Asher approach.[17] In particular we proposed the application of a correction factor on the potential evaporation, calculated on the base of easy-to-find parameters (namely the usual meteorological variables and the infrared soil surface temperatures), starting from two reference days in soil saturated and soil dry conditions. The method was tested both in a plain test site and mountain conditions.

The proposed correction model provided a good estimation of actual evaporation especially in sunny weather conditions, both in the mountain test site, and in the plain experimental area. When there are irregular trends of potential evaporation due to cloudy weather or partially overcast sky the proposed method can lead to poor results. On the other hand, in the mountain test site, the proposed model seems to provide acceptable results also in not completely sunny meteorological conditions. This is certainly a limitation of the methodology, but the days when it is not possible to provide accurate estimates of actual evaporation are typically characterized by little incident radiation, hence, also little evaporation. Given the increasing use of infrared satellite images (e.g. Landsat, Modis) to determine the surface temperature of the soil, the proposed method could be probably applied on a large scale in the future with large advantages for the water-resources management and planning.

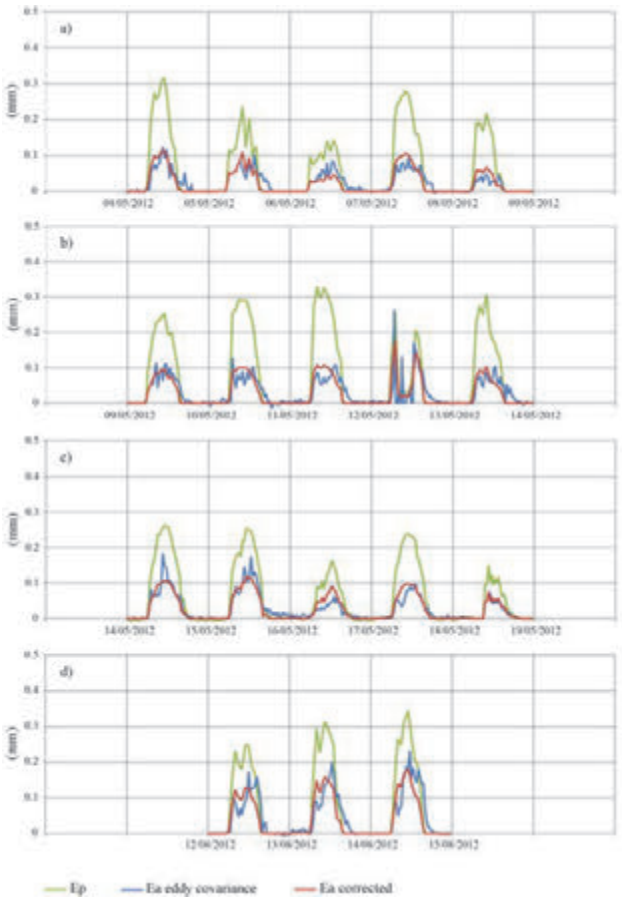

Figure 4. Values of Ep calculated with the Penman-Monteith equation, actual evapotranspiration measured by the eddy covariance station located in Cogne field site and Ea "corrected" in four periods of the year 2012: a) between May the 4th and 9th; b) between May the 9th and 14th; c) between May the 14th and 19th and d) between August the 12th and 15th.

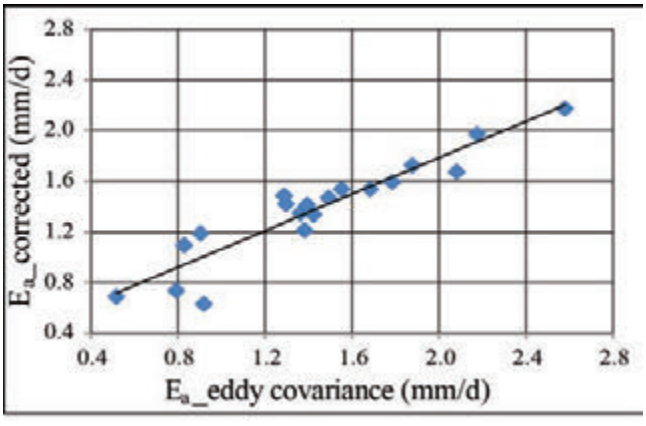

Figure 5. Measured soil evaporation compared to calculated soil evaporation from RE × Ep for the Cogne site.

References

1. Kabat, P. 2006. Climate change impacts on global water cycle and implications for water management in Europe. International Workshop on Climate Change Impacts on the Water Cycle, Resources and Quality.
2. Rind D, Rosenzweig C, Goldberg R. Nature 1992; 358:119–122.
3. Arnell NW. Climate change and global water resources, Glob. Environ. Change 1999; 9(1):S31-S49.
4. Arnell NW. The effect of climate change on hydrological regimes in

Europe: a continental perspective. Glob. Environ. Change 1999; 9(1):5-23.
5. Qiu GY, Yano T, Momii K. An improved methodology to measure evaporation from bare soil based on comparison of surface temperature with a dry soil. J. Hydrol. 1998; 210(1-4):93-105.
6. Evett SR, Warrick AW, Matthias AD. Wall material and capping effects on microlysimeter temperatures and evaporation. Soil Sci. Soc. Am. J. 1995; 59:329–36.
7. Priestley CHB and Taylor RJ. On the assessment of surface heat flux and evaporation using large-scale parameters. Mon. Weath. Rev. 1972; 100:81-92.
8. Brutsaert W and Stricker H. An advection-aridity approach to estimate actual regional evapotranspiration. Water Resour. Res. 1979; 15(2):443–450.
9. Bouchet, R. J., 1963. Evapotranspiration reelle evapotranspiration potentielle, signification climatique, Symp. Publ. 62, Int. Assoc. Sci. Hydrol., Berkeley, Calif., 134–142.
10. Allen RG, Pereira LS, Raes D, Smith M. Crop Evapotranspiration: Guide-lines for Computing Crop Water Requirements, FAO Irrigation and Drainage Paper 56, Rome, FAO; 1998.
11. Crago RD and Brutsaert W. A comparison of several evaporation equations. Water Resour. Res. 1992; 28:951-954.
12. Brutsaert W. A theory for local evaporation (or heat transfer) from rough or smooth surfaces at ground level, Water Resour. Res. 1975; 11(4):543-550.
13. Brutsaert W. Evaporation into the atmosphere. Dordrecht, Holland, D. Reidel Publishing Company; 1982.
14. Parlange MB and Katul GG.. An advection-aridity evaporation model. Water Resour. Res. 1992; 28:127–132.
15. Kalma JD, McVicar TR, McCabe MF. Estimating Land Surface Evaporation: A Review of Methods Using Remotely Sensed Surface Temperature Data. Surv. Geophys. 2008; 29(4-5):421-469.
16. D browska-Zieli ska K, Budzy ska M, Kowalik W, Turlej K. Soil moisture and evapotranspiration of wetlands vegetation habitats retrieved from satellite images, HESS, Special Issue: Earth observation and water cycle science, Copernicus Publications; 2010.
17. Ben-Asher J, Matthias AD, Warrick AW.. Assessment of evaporation from bare soil by infrared thermometry. Soil. Sci. Soc. Am. J. 1983; 47:185–191.
18. Kerridge BL, Hornbuckle JW, Christen EW, Faulkner RD. Using soil surface temperature to assess soil evaporation in a drip irrigated vineyard. Agric. Water Manage. 2013; 116(C):128-141.
19. LőnnqvistO. On Diurnal Variation of Surface Temperature. Tellus 1962; XIV:96 -101.
20. Katul GG and Parlange MB. A Penman-Brutsaert model for wet surface evaporation. Water Resour. Res. 1992; 28:121–126.
21. Massman W, Lee X, Law BE. Handbook of Micrometeorology. A Guide for Surface Flux Measurements and Analysis. Boston, Kluwer Academic Publishers; 2004.
22. Kaimal JC and Finnigan JJ. Atmospheric Boundary Layer Flows. New York, Oxford University Press; 1994.
23. Schotanus P, Nieuwstadt FTM and De Bruin HAR. Temperature Measurement with a Sonic Anemometer and its Application to Heat and Moisture Fluctuations. Boundary-Layer Meteorol. 1983; 26:81–93.
24. Turnipseed AA, Blanken PD, Anderson DE, Monson RK. Surface energy balance above a high-elevation subalpine forest. Agric. For. Meteorol. 2002; 110:177–201.
25. Webb EK, Pearman GI, Leuning R. Correction of flux measurements for density effects due to heat and water vapor transfer. Quart. J. Roy. Meteorol. Soc. 1980; 106:85–100.
26. Campbell Scientific, Inc., 1990, TCAV averaging soil thermo-couple probe instruction manual: Logan, Utah, 2p.
27. German ER. Regional evaluation of evapotranspiration in the Everglades: U.S Geological Survey Water Resources Investigations Report 00-4217; 2000.
28. Kondratiev KJ, Pivovarova, ZI, Fedorova MP. The radiation regime of sloping surfaces. Hydrometeoizdat 1978; 216 p.
29. Reda I, Andrea A. Solar Position Algorithm for Solar Radiations Application. Sol. Energy 2004; 76(5).
30. Baudena M, Bevilacqua I, Canone D, Ferraris S, Previati M, Provenzale A. Soil water dynamics at a midlatitude test site: Field measurements and box modeling approaches. J. Hydrol. 2012; 414-415:329-340.
31. Canone D, Ferraris S, Sander G, Haverkamp R. Interpretation of water retention field measurements in relation to hysteresis phenomena, Water Resour. Res. 2008; 44:W00D12, doi:10.1029/2008 WR007068.

Estimating the contribution of rainfall, irrigation and upward soil water flux to crop water requirements of a maize agroecosystem in the Lombardy plain

Michele Rienzner, Sandra Cesari de Maria, Arianna Facchi, Fatma Wassar, Claudio Gandolfi

Department of Agricultural and Environmental Sciences (DiSAA), Università degli Studi di Milano, Italy

Introduction

The unsaturated zone plays an important role in the hydrological cycle, since it is at the interface between atmosphere and groundwater circulation. Water fluxes in the unsaturated zone affect water status, development and production of crops; by an environmental point of view, these fluxes determine mobilization and transport of solutes and pollutants from the soil surface to the aquifer system.

There are several reasons for modelling hydrological processes in the unsaturated zone, one of them is definitely the existing limit at the possibility of measuring all the variables we need to know about the physical system. The models are used to perform extrapolations or predictions that, reasonably, are expected to be useful in decision-making processes focused on hydrological issues (Beven, 2001).

Water movements in the unsaturated zone can be described with mathematical formulations based on different approaches (e.g. Gandolfi *et al.*, 2006) going from very simplified conceptual schemes to models, as SWAP (Kroes and van Dam, 2003), Hydrus-1D (Šim nek *et al.*, 2008), U3M-1D (Vaze *et al.*, 2004), implementing the numerical solution of the Richards' differential equation. The latter set of models simulate soil, plant and atmosphere as a continuous system in which water movements are driven by potential gradients. In case a thorough analysis of the physical processes is required and all the needed information is available, complex models are usually preferred.

A modelling approach is particularly interesting in sites where there is a strong interaction between the processes occurring at the soil surface and the groundwater, as in areas characterized by shallow groundwater tables. In such situations, a water flow towards the roots zone is triggered by the strong potential gradient that occurs when the soil water content nearby the roots becomes very negative. A model simulation can be very useful in the estimation of this upward flux since a reliable direct measurement is at least a complex task.

Numerous studies, performed by different approaches, attempted to quantify the contribution of the capillary rise to the root zone soil water balance, taking into account several variables including, particularly, the crop type and the groundwater depth. Kahlown *et al.* (2005) reported that with a groundwater depth of 0.5 m irrigation of wheat was no longer required, while in the case of sunflower an irrigation supply equal to the 20% of the evapotranspiration volume showed to be sufficient. Prathapar and Qureshi (1999) showed that with a groundwater depth within 2 m from the topographic surface, crops were able to extract a considerable fraction of the water they needed. Kahlown *et al.* (1998) illustrated how a groundwater depth of 1 m represents the optimum situation for the growth of many crops, while the capillary rise contribution to the root zone water balance becomes negligible when the groundwater depth becomes 2-3 m. Liu and Luo (2011) suggested a groundwater table at 1.5 m from the soil surface as the optimum for the winter wheat, since this depth allows its complete root development. Kahlown *et al.* (2005) suggested the optimal groundwater depth to be between 1 and 2 m for all the crops they investigated. For the maize crop, the same authors reported a required irrigation contribution of 75 mm when the groundwater depth was 1 m, this contribution was shown to increase approximately linearly with the increasing of the water table depth (the linear decrease was highlighted for all the crops examined). A linear relationship between the groundwater depth and the required irrigation amount was also detected by other authors, including Sepaskhah *et al.* (2003). Authors, however, came to different conclusions, since factors such as climate of the experimental areas or soil types therein play a non-negligible role.

Although maize is a crop fairly affected by water ponding (often happening when shallow groundwater combines with heavy rains or abundant irrigation), massive roots uptake and yields are documented also with groundwater depths of few tens of centimetres. With a water table depth of 0.5 m several authors found groundwater contributions around 40% of the crop water requirements and an increase in yield (Follett *et al.*, 1974; Cavazza and Pisa, 1988; Pisa and Ventura, 1991). The same contribution was observed by Kahlown *et al.* (2005) for maize in an arid region of Pakistan. These authors also reported that the contribution decreases to 30% of the crop water requirements with a groundwater depth of 1 m and to 7.5% with a groundwater depth of 1.5 m. Soppe and Ayars (2003) showed that the contribution of shallow

Correspondence: Michele Rienzner, Dipartimento di Scienze Agrarie e Ambientali (DiSAA), Università degli Studi di Milano, Via Celoria 2, 20133, Milano (MI), Italy.
Tel. +39.02.50316901 - Fax: +39.02.50316911.
E-mail: michele.rienzner@unimi.it

Key words: SWAP, calibration, SCEM-UA, maize water requirements, capillary rise

Acknowledgements: the authors would like to thank Regione Lombardia for funding the AC-CA project, as well as those who took part in for their meaningful contribution. The first author thanks the MIUR as well for financing his research grant.

Contributions: the authors contributed equally.

Conflict of interests: the authors declare no potential conflict of interests.

Funding: MIUR, Regione Lombardia

Journal of Agricultural Engineering 2013; XLIV(s2):e18
doi:10.4081/jae.2013.(s1):e18

water tables is not constant in time but increases with the increasing of the rooting depth, reaching its maximum value at the end of the growth phase of the plant, when roots are fully developed. Liu and Luo (2011) concluded their study proposing irrigation systems in which the water table depth could be maintained at a depth of 1.5 m or less, allowing an increase in crop production and a reduction in the use of surface irrigation.

In order to have a reliable model estimation of the water fluxes, especially in case of complex physically based models (i.e. implementing the Richards' equation), a relevant effort has to be spent for the quantification of the model parameters. Some of the needed parameter values are difficult to be quantified, even in presence of in-field or lab measurements. Among them, the effective soil saturated hydraulic conductivity (K_s), which is the value needed by the model (valid under the hypothesis of spatial homogeneity), is actually a virtual value since it does not correspond to any specific conductivity that can be measured in the field where a relevant spatial variability usually exists. The calibration of K_s can be done through inverse modelling (i.e. finding the value of the parameters giving the best fit between field measurements and model outputs) adopting the algorithms available in literature for the global optimum search (e.g. SCE-UA, SCEM-UA, PEST, SWARM).

This research aims at estimating the upward groundwater flux in an experimental case characterized by a shallow groundwater table (as it is typical for large areas of the Po valley plain) in order to assess its contribution to the satisfaction of maize water requirements among the other water inputs (rain and irrigation). For this purpose, the hydrological model SWAP (Soil Water Atmosphere Plant model, Kroes and van Dam, 2003) has been implemented using detailed monitoring data collected in field. For the calibration of the saturated hydraulic conductivity, the model has been coupled with the algorithm SCEM-UA (Vrugt *et al.*, 2003), which is effective and efficient in locating the optimal values in multidimensional parameters spaces in case of highly-non-linear systems. In this paper, preliminary results concerning one site and one year are presented and discussed.

Materials and methods

Monitoring activity

In the agricultural seasons 2010 and 2011, an intensive monitoring activity was carried out for quantifying fluxes and storage of water and carbon in two maize agro-ecosystems of the Lombardy plain, according to the purpose of the AC-CA project (Gandolfi *et al.*, 2012), funded under the Lombardy agricultural research program 2007-2009. The experimental site this paper is concerned is a 10 ha field located in Landriano (Figure 1 – 45°19' N, 9°15' E, 88 m a.s.l), characterized by a shallow groundwater table depth (0.6 to 1.5 m).

In both the years the field was seeded with a long season Zea Mays variety (class 600-700) and a border irrigation was applied just in the first one. The monitoring setup involved an eddy covariance tower measuring water and carbon fluxes and instruments for the continuous monitoring of the soil water status installed in six Intensive Monitoring Plots (IMPs hereafter). Each IMP was provided with: (i) a FDR Sentek soil water content probe (sensors placed at 7, 27, 47, 67 cm depth), (ii) 4 tensiometers (installed at the same depths of the soil water content sensors) and (iii) a 3 m piezometric pipe equipped with a STS pressure transducer. Moreover, about 8 campaigns per agricultural season were carried out in each IMP to measure crop biometric parameters (leaf area index, crop height and rooting depth) and to collect soil samples for assessing soil physico-chemical properties (soil texture, organic matter content, bulk density). At the same dates also saturated hydraulic conductivity measurements with two Guelph permeameters and one tension infiltrometer were carried out at the same sites (Rienzner *et al.*, 2011). Finally, undisturbed soil samples were extracted in September 2010 for the laboratory determination of soil retention curves (by tension plates and the Richards' pressure plate apparatus).

The SWAP hydrological model

Among the numerical models solving the Richards' equation in the one-dimensional vertical form, SWAP (Soil Water Atmosphere Plant model, Kroes and van Dam, 2003) is one of the most widely used and best documented. It adopts the modified differential Richards' equation which includes a sink term representing the macroscopic flow extracted by the vegetation (depending on plant characteristics, local soil water potential and transpiration demand due to climate). SWAP solves the Richards' equation by a finite difference scheme adapted from those described by Haverkamp *et al.* (1977) and Belmans *et al.* (1983); initial and bottom boundary conditions must be provided as input.

The soil profile is modelled as a sequence of layers, each one with its own hydraulic characteristics. The layers are further discretized into smaller compartments adopted in the finite differences solution scheme. Soil retention curves $\theta(h)$ and unsaturated hydraulic conductivity $K(\theta)$ of the layers are described by the analytic equations of Van Genuchten (1980) and Mualem (1976) respectively. Regarding the crop development, SWAP includes a detailed crop growth model (WOFOST 6.0, Spitters *et al.*, 1989; Hijmans *et al.*, 1994) and, alternatively, a simple module needing the time series of leaf area index (LAI) or soil cover fraction (CF), crop height, roots depth and distribution. The interception is modelled by the analytical model proposed by Von Hoyningen-Hune (1983) and Braden (1985). The potential evapotranspiration can be calculated either by the Penman-Montieth equation (Allen *et al.*, 1998) or by applying crop factors to a reference evapotranspiration given in input. Then, the actual transpiration is derived from the potential accounting for soil cover, moisture and salinity conditions in the root zone (weighted by the root density), while the actual evaporation depends on the capacity of the soil to transport water to the soil surface. As regards irrigation, it can be fixed or scheduled by SWAP choosing among different time and depth criteria.

Figure 1. Location of the experimental site (black dot) within the Lombardy region.

Input data and SWAP parameterization

Among the collected data (6 IMPs and two years), IMP-5 year 2010 was chosen as case study for this contribution. The chosen simulation period starts on 08/05/2010 (2 days before crop emergence) and ends at the maize harvesting (11/09/2010). The initial conditions of soil water potential were fixed according to the groundwater level measured in the day the simulation starts (1 cm below the soil surface) and the bottom boundary condition was fixed by the daily series of groundwater depth. Soil profile was divided into four layers having their centre at the sensors depth (Section 2.1), further divided in 1cm-thick compartments; the fourth layer was extended up to the bottom of soil profile (4 m).

The four retention curves were obtained by least squares regression, on the pairs of water content (θ) and water potential (h) values measured at the four different depths, with the Van Genucthen curve. The calibration values were the collected field measurements (along the season) and the laboratory test out comes made with tension and Richards' plates apparatus on undisturbed soil samples taken in September 2010 at the same depths of the sensors. Van Genucthen curve calibration was performed by using a MATLAB algorithm solving nonlinear curve-fitting problems in least-squares sense (lsqcurvefit.m of the MATLAB Optimization Toolbox; Coleman and Li, 1996) for all the parameters except of the saturated water content, which was selected according to field measurements.

Maize growth was computed using the simple crop module since the crop biometric measurements were directly collected in field (linear interpolation was used to obtain the complete time series).

Daily meteorological data recorded by a 200m-far meteorological station were used, i.e. solar radiation (KJ m^{-2}), maximum and minimum temperature (°C), air humidity (KPa), wind speed (m s^{-1}) and rain (mm). As regards irrigation, on day 25/07/2010 a water amount was supplied by border irrigation which produced in IMP-5 an estimated infiltration of 65.9 mm (obtained assessing local water table fluctuations and changes in soil moisture).

SCEM-UA

SCEM-UA (Shuffled Complex Evolution Metropolis - usable algorithm (Vrugt *et al.*, 2003a; Vrugt *et al.*, 2003b) is an algorithm for optimization, inverse modeling and assessment of hydrologic model parameters. It provides an estimate of the most likely parameter set and its underlying posterior probability distribution. The algorithm is a Markov Chain Monte Carlo (MCMC) sampler, which generates multiple sequences of parameter sets that converge to the stationary posterior distribution for a large enough number of simulations. For further details of SCEM-UA's functioning the reader should refer to Vrugt *et al.*, 2003a; Vrugt *et al.*, 2003b.

Among the automatic calibration procedures, SCEM-UA has been chosen as it is consistent, effective and efficient in locating the optimal model parameters in multidimensional parameters spaces which may not be smooth. As a matter of fact, the case study performed required a calibration of a highly-non-linear system with a four-dimensional parameters space (saturated hydraulic conductivity at four depths).

A pre-alpha version of SCEM-UA (MATLAB version) was used and coupled with the stand-alone model (SWAP.exe) through a set of MATLAB functions and scripts written in order to virtually make SWAP running within the MATLAB environment.

The objective function leading the assessment of the "best" parameter set was defined as a weighted mean of the squared error between measured and simulated values (i.e. soil water potential, soil water content and water table depth). The weight of each term was set according to the reliability of the corresponding measured data. Results of the calibration procedure are described in Section 3.

Results

In this section are presented both the optimal K_s sets given by SCEM-UA for the four soil layers the profile was divided in, along with some details of the calibration, and an analysis of the corresponding SWAP outputs.

K_s estimation

A wide range of K_s values, going from 0.01 to 1000 cm d^{-1}, was given to SCEM-UA as prior distribution of the parameters (actually the inverse problem was performed on decimal log-transformed K_s ranging from -2 to 3). After some exploratory SCEM-UA applications (changing e.g. the weights in the objective function), a suitable inverse solution was obtained with a 15,000 simulations run. The main SCEM-UA output is a matrix having in each row the four parameters corresponding to each SWAP run and the resultant value of the objective function. A selection of 100 parameter sets (100-Opt hereafter) was obtained by extracting the rows having the best 100 values of the objective function, the same was done for the 20 best sets (20-Opt hereafter).

Figure 2 shows the four frequency distributions, one for each layer, of 100-Opt (light grey) and 20-Opt (dark grey). The distributions are bell-shaped and their ranges, compared with their mean values, are quite narrow indicating that the optimization, after a thorough investigation of the whole space, converged to a small area corresponding to the optimal solution in the 4D parameter space.

The values of the objective function of 100-Opt, divided by the overall worst value, range from 0.0128 to 0.0132. As different combinations of the four parameters gave nearly equivalent scores of the objective function, the results of the inverse problem consist of multiple solutions for the saturated hydraulic conductivities of the soil profile. The means of the calibrated K_s (100-Opt), going from the first layer (close to the soil surface) to the fourth one, are 10.96, 1.76, 3.74 and 4.79 cm d^{-1} showing some variation along the profile. Notice the conductivity is smaller in the layers containing the plough pan.

A confirm of the SCEM-UA estimation for the shallower layers is

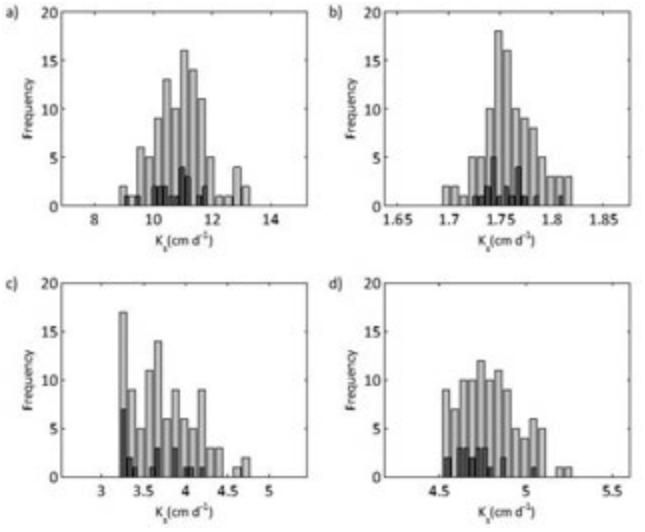

Figure 2. Posterior distribution of the Ks values estimated for the layers: (a) 0-17 cm, (b) 17-37 cm, (c) 37-57 cm, (d) 57-77 cm.

found in the results of the Guelph permeameter campaigns (Rienzner *et al.*, 2011; Gandolfi *et al.*, 2012) conducted in the same period and IMP. In fact, the measured values of K_s, involving the first 30 cm, ranged from 2.8 to 9.1 cm d^{-1}, in agreement with the calibration results for the first two layers.

SWAP outputs

The SWAP model was run with the 100-Opt K_s set in order to quantify the upward flux. Capillary rises were thus computed on each day of simulation as the upward fluxes pouring out from the model compartment immediately below the root depth (which changes in time according to the field measurements). The 100 total upward fluxes were then replicated proportionally to their objective score (100 replicates for the best simulation and 1 to the 100th); the histogram of the upward flux is reported in Figure 3.

As an example of the model fitting, Figure 4 shows the measured and simulated soil water contents along the crop season for the 20-Opt K_s set. In the figure, the 20 lines cannot be distinguished due to an overlying of the results, confirming the modelling error to be equivalent in the set.

Finally, Table 1 reports the different contribution to the maize water requirements due to rain, irrigation and capillary rise (100-Opt set), and the water percolation computed in the same way of the upward flux.

Conclusions

In order to compute a complete water balance of a Lombardy maize field, including percolation and capillary rise, the SWAP model was implemented with a complete set of field measurements accounting for meteorology, soil properties, measurable water fluxes and crop features. Nevertheless, a calibration procedure of the saturated soil hydraulic conductivities along a layered profile was needed for a reliable application of the model, since it is rather unrealistic to measure directly the effective values of K_s within some square meters and at different depths without disturbing the cropped soil. For this purpose, the MATLAB SCEM-UA toolbox was coupled with the SWAP model in order to obtain an optimal estimation of K_s sets able to represent the experimental soil profile.

The preliminary results for IMP-5–year 2010 show that the potential evapotranspiration (464 mm) is not fulfilled since actual transpiration amounts to 403 mm. It is worth to stress that, while irrigation and rain contribute to the satisfaction of both the soil evaporation and the plant transpiration, the upward flux (237 mm) contributes mainly to transpiration. Moreover, most of rain and irrigation (379 mm) percolate (308 mm) but, due to the shallow groundwater table, capillary rise compensates almost 80% of the same percolation losses, greatly increasing the water efficiency of the whole system.

Rain, irrigation and capillary rise account, respectively, for 67%, 14% and 51% of the crop water requirements represented by the potential evapotranspiration. A significant contribution of capillary rise was thus noticed in case of shallow groundwater which ensured about half the potential evapotranspiration flux; this percentage is even greater than the values found by other authors (i.e. up to 40% with a water table 50 cm below the soil surface in Follett *et al.*, 1974; Cavazza e Pisa, 1988; Pisa e Ventura, 1991; Kahlown *et al.*, 2005).

Concluding, the adopted approach involving the inverse calibration of a physically based model is a promising tool to enhance the analysis of the soil-water-plant system with particular reference to the interactions between the groundwater and the root zone which significantly influence the whole system.

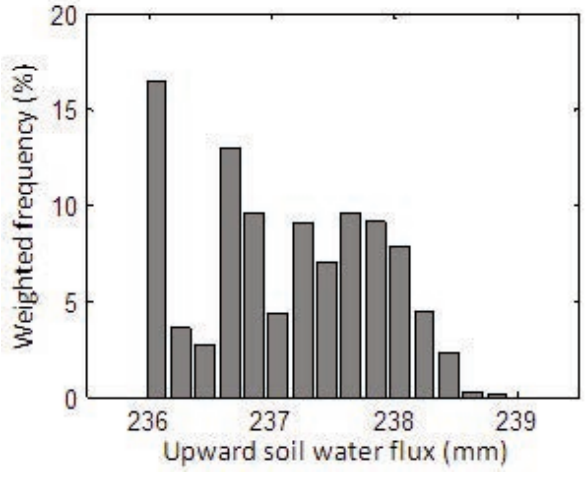

Figure 3. Histogram of the 100-Opt upward flux, weighted in frequency proportionally to the corresponding value of the objective function.

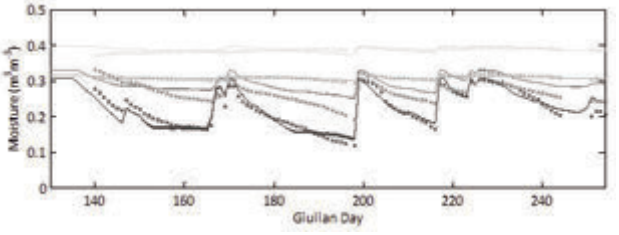

Figure 4. Moisture trends for the four layers: measured data at the sensors depths (squares) and model outputs for the 20-Opt set at the same depths (straight lines); grey getting lighter moving downward the soil profile.

Table 1. Average fluxes as obtained by the 100-Opt SWAP simulations, percentage of satisfaction of the potential evapotranspiration are also provided (E and T are the evaporation and transpiration components)

Potential ET (mm)	Net rain (mm)	Irrigation (mm)	Mean Actual ET (mm)	Mean percolation (mm)	Mean upward flux (mm)	
464 (E 293, T 171) (86%)	313 (-66%)	66 (51%)	403 (E 255, T 148)	-308	237 (67%)	(14%)

References

Allen, R.G., Pereira, L.S., Raes, D., Smith, M. 1998. Crop evapotranspiration: guidelines for computing crop water requirements, Irrigation and Drainage Paper 56. United Nations FAO, Rome, pp 300.

Belmans C., Wesseling J.G., Feddes R. 1983. Simulation of the water balance of a cropped soil: SWATRE. J Hydrol. 63:271-286.

Beven K. 2001. Rainfall-Runoff Modelling. The Primer.Wiley & Sons, Ltd.

Braden H. 1985. Ein Energiehaushalts – und Verdunstungsmodell for Wasser und Stoffhaushaltsuntersuchungen landwirtschaftlich genutzer Einzugsgebiete. Mittelungen Deutsche Bodenkundliche Geselschaft. 42:294-299.

Cavazza L., Pisa P.R. 1988. Effect of watertable depth and waterlogging on crop yield. Agr Water Manage. 14:29-34.

Coleman T.F., Li Y. 1996. An Interior, Trust Region Approach for Nonlinear Minimization Subject to Bounds. SIAM J Optimiz. 6:418-445.

Follett R.F., Doering E.J., Reichman G.A., Benz L.C. 1974. Effect of irrigation and water-table depth on crop yields. Agron J. 66:304– 308.

Gandolfi C., Facchi A., Gharsallah O., Wassar F., Rienzner M., Chiaradia E., *et al.* 2012. Progetto ACCA. Relazione finale: Regione Lombardia. http://www.lavoro.regione.lombardia.it/ shared/ccurl/291/119/ACCA_Relazione%20Finale.pdf

Gandolfi C., Facchi A., Maggi D. 2006. Comparison of 1D models of water flow in unsaturated soils. Environ Modell Softw. 21:1759-1764.

Haverkamp R., Vauclin M., Touma J., Wierenga P.J., Vachaud G. 1977. A comparison of numerical simulation models for one-dimensional infiltration. Soil Sci Soc Am J. 41:285-294.

Hijmans R.J., Guiking-Lens I.M., van Diepen C.A. 1994. User's guide for the WOFOST 6.0 crop growth simulation model. Technical Document 12, Alterra Green World Research, Wageningen, pp 144.

Kahlown M.A., Ashraf M., Zia–ul–Haq. 2005. Effect of shallow groundwater table on crop water requirements and crop yields. Agr Water Manage. 76:24–35.

Kahlown M.A., Iqbal M., Skogerboe G.V., Rehman 1998. S.U. Water logging, salinity and crop yield relationships. Mona Reclamation Experimental Project, WAPDA. Report No. 233.

Kroes J.G., van Dam J.C. 2003. Reference Manual SWAP version 3.0.3. Alterra-report 773. Wageningen, Alterra, Green World Research. ISSN 1566-7197.

Liu T., Luo Y. 2011. Effects of shallow water tables on the water use and yield of winter wheat (Triticum aestivum L.) under rain-fed condition. Aust J Crop Sci. 5(13):1692-1697.

Mualem Y. 1976. A new model for predicting the hydraulic of unsatured porous media. Water Resour Res. 12:513-522.

Pisa P.R., Ventura F. 1991. Groundwater table contribution to crop water budget: a review. Irrigazione e drenaggio. 38(1): 3-14.

Prathapar S.A., Qureshi A.S. 1999. Modelling the effects of deficit irrigation on soil salinity, depth to water table and transpiration in semi-arid zones with monsoonal rains. Int J Water Resour D. 15:141-159.

Rienzner M., Garlaschelli F., Gandolfi C. 2011. Analisi statistica della conducibilità idraulica satura stimata in campo per un suolo superficiale. Convegno di Medio Termine dell'Associazione Italiana di Ingegneria Agraria; Belgirate, 22-24 settembre 2011. http://www.aiia2011.unimi.it/chiave/memorie/2.pdf

Sepaskhah A.R., Kanooni A., Ghasemi M.M. 2003. Estimating water table contributions to corn and sorghum water use. Agr Water Manage. 58:67–79.

Šimůnek J., Šejna M., Saito H., Sakai M., van Genuchten M.Th. 2008. The Hydrus-1D Software Package for Simulating the Movement of Water, Heat, and Multiple Solutes in Variably Saturated Media, Version 4.0. HYDRUS Software Series 3. Department of Environmental Sciences, University of California Riverside, Riverside, California, USA, pp 315.

Soppe R.W.O., Ayars J.E. 2003. Characterizing ground water use by safflower using lysimeters. Agr Water Manage. 60:59–71.

Spitters C.J.T., van Keulen H., van Kraalingen D.W.G. 1989. A simple and universal crop growth simulator: SUCROS87. In: Rabbinge R, Ward SA, van Laar HH (Eds.) Simulation and systems management in crop protection, Simulation Monographs, Pudoc.

Van Genuchten M.Th. 1980. A closed form equation for predicting the hydraulic conductivity of unsatured soils. Soil Sci Soc Am J. 44:892-898.

Vaze J., Tuteja N.K., Teng J. 2004. CLASS Unsaturated Moisture Movement Model U3M-1D. User's Manual. NSW Department of Infrastructure, Planning and Natural Resources, Australia and Cooperative Research Centre for Catchment Hydrology, Australia. ISBN 0 7347 5513 9.

Von Hoyningen-Hüne J. 1983. Die Interception des Niederschlags in landwirtschaftlichen Beständen. Schriftenreihe des DVWK. 57:1-53.

Vrugt J.A., Gupta H.V., Bouten W., Sorooshian S.A. 2003a. A Shuffled Complex Evolution Metropolis algorithm for optimization and uncertainty assessment of hydrologic model parameters. Water Resour Res. 39(8), 1201.

Vrugt, J.A., Gupta H.V., Bastidas L., Bouten W., Sorooshian S. 2003b. Effective and efficient algorithm for multi-objective optimization of hydrologic models. Water Resour Res. 39:1214.

Hydrometeorological monitoring for water balance determination at plot scale

A. Sommella,[1] Mario Palladino,[1] A. Comegna,[2] A. Coppola[3]

[1]Division of Water Resources Management, University of Naples "Federico II", Italy; [2]School of Agricultural Forestry Food and Environmental Sciences (SAFE), University of Basilicata, Potenza, Italy

Abstract

To provide adequate answers to recurring problems in land and water resources management, nowadays the use of physically based models is widespread. The reliability of the responses of this kind of model is closely linked to the precision with which model parameters are determined, such as soil hydraulic characteristics and meteorological variables. In this work, we set up a complete station for the monitoring of both meteorological and soil variables, as well as a soil hydraulic characterization. The experimental site shows vertic characteristics and is in Guardia Perticara, Basilicata region, Italy.

Introduction

The water balance of soil-plant-atmosphere system can be studied at different scales. The study at a smaller scale is useful if the goal is to define the basic laws concerning the physical phenomena occurring in the soil and the physiological processes occurring into plants; the medium scale when interested in the control of hydrological parcels of land cultivated mainly for agricultural purposes; bigger scale is most appropriate for comprehensive evaluations that affect entire river basins.

Medium scale approach is based on the definition of water balance, represented by an expression which summarizes the water cycle accomplished through fluxes of water in the soil and represented by the following relationship:

$$N + I = ET + Pr \pm D$$

where the symbols, for a given period of time, are: N = natural incomes of water; I = irrigation amount; ET represents evapotranspiration fluxes over the period, Pr = loss of water to deep percolation and runoff; D = variations in water content of soil profile.

Correspondence: A. Comegna, School of Agricultural Forestry Food and Environmental Sciences (SAFE), University of Basilicata, Potenza, Italy.
E-mail: alessandro.comegna@unibas.it).

Key words: soil hydraulic characterization, soil water balance, TDR.

Journal of Agricultural Engineering 2013; XLIV(s2):e19
doi:10.4081/jae.2013.(s1):e19

In recent years it became common to physically based models to provide adequate answers to recurrent problems of management of land and water resources (Hillel, 1980; Santini 1992; Simunek *et al.*, 1998). The reliability of these models is closely linked to the degree of accuracy with which the parameters are determined, such as soil hydraulic properties and meteorological variables.

To this end, on two plots of an experimental field site in Guardia Perticara (Potenza, Italy), was set up a complete instrumentation for the detection of these parameters.

The processes of transpiration, evaporation, infiltration and formation of runoff are largely determined by the content and the energy state of water in the unsaturated zone of the soil. Knowledge of the evolution in time and space of these quantities is a prerequisite for the identification of mass exchanges between the different components of the soil-plant-atmosphere through which compute comprehensive and reliable water balances.

Although physically based mathematical models allow very detailed descriptions of water transfer processes, their degree of accuracy in terms of predicting accuracy is however conditioned by the large number of input parameters involved. Because these parameters are used also in the process of validation of the models, it is necessary for them to be observed through accurate evaluation that require a large number of observations, given the inherent spatial-temporal variability of the porous media in the study.

The burden of such determinations in the open field has necessitated the development of measuring devices and automatic acquisition system, which also require sophisticated instrumentation and specifically developed control software.

This study provides details of the experimental installation characterized by a high degree of automation and the detailed space-time acquisitions of the variables in the study. As such, it allows us to come to a complete hydrological balance, whose reliability is verified through a simulation of water exchange processes in the soil-atmosphere, conducted using only input parameters independently determined. In the simulation the crop has been neglected, because during the period under investigation, the soil is without vegetation.

Materials and methods

The experimental area falls within the Agri basin, sub-basin of the Sauro, in Guardia Perticara, Potenza (Italy), at an altitude of 720 m above sea level, with an average annual temperature of 12 °C and an average annual precipitation of about 790 mm.

The area is located on a geological formation defined as polychrome shale claystones and, in the superficial part, affected by landslides. The soil type falls within the "vertic ustorthens", according to the classification USDA. Other important properties are represented by a low permeability and vertic characters from the top of the clay soil, well evi-

dent during the summer because of the cracks. The soil profile shows the presence of an Ap horizon, which extends between 0 cm and 30 cm and a second horizon Cca, which develops from 30 cm up to more than 100 cm. The soil was characterized hydraulically through undisturbed soil sampling at three different depths in ten stations. In the laboratory, retention and hydraulic conductivity curves were determined (Sommella and Gaetani, 1990; Santini *et al.*, 1995). For each depth investigated the average curves characteristics showed no significant differences between the different location (Figure 1). The field was divided into 16 plots, arranged in subplots of rectangular shape with a width of 15 m and a length equal to 40 m, the average slope of each plot according to the longest side is equal to 14% while the transverse slope is virtually zero (Figure 2).

The 8 downstream plots have been hydraulically isolated from the others in order to precisely define the boundary conditions. For the rainfall measures three pluviographs were installed. To measure the parcels outflows were prepared three channels of 5 m length, made of sheet metal, immediately downstream of each parcel parallel to the shorter side. For each plot, the water runoff intercepted by the collecting channels were connected through PVC pipes with a diameter of 140 mm to a channel of supply; outflows were finally collected in a tank with a volume of 1 m^3. For direct estimation of the volumes of groundwater a drainage system has been buried in the first soil horizon. With reference to the investigation in this study, the tests involved two of the eight parcels of the experimental field on which, in addition to the instrumentation described above, have been installed for each plot 6 access tubes for the use of the neutron probe and TDR probes, for water content monitoring, as well as tensiometers, for water potential measurements. For a complete and accurate data acquisition a centralized system was installed, which allowed the contemporary taking of the measures. The system is based on a data logger of Campbell Scientific mod. CR10 complete with two multiplexers for the extension of acquisition channels of analog data and contact closure. The programmability of the datalogger has allowed to establish the frequency with the maximum freedom for the acquisition and storage of data, allowing it to suspend all operations in the case of power failure. This allows the battery to hold a charge up to 4 days and then to preserve the CR10 from the loss of the program and data, and the system to resume working properly to restore the power supply.

CR10 has a circular buffer data memory, so the data stored once saturated the capacity of the data logger, go to fill the memory locations in which they were already stored previous acquisitions. The program prepared, described in a later paragraph, has allowed the data memory of the CR10 maintained data for the last six days of acquisition. To overcome this limit, the CR10 has been linked with two serial micromodem to a computer on which a program, at predetermined time intervals, automatically transferred to the hard disk data recorded by CR10 after last query, making the storage capacity of the system virtually unlimited. The CR10 has two program tables, which can be assigned different execution intervals. The first table was used for the acquisition of outflow data and the second for the acquisition of environmental parameters and inflows.

The execution interval of the first table was 5 seconds, and the signals from the level sensors and rain gauge of the drain, which through the appropriate calibration scales, were converted respectively in heights and volumes of water; every two minutes were the heights stored snapshots and the total volume passed through the drain.

The second table acquires every 10 seconds signals from environmental sensors and the three rain gauges and converted in the respective physical variables; every 10 minutes the height of rain was totalized and stored and every 30 minutes the average of the data read from environmental sensors has been stored.

Sensors description

Acquisition system has been linked to magnetic switches of the three rain gauges. For the acquisition of meteorological data, the system has been connected to sensors for detecting speed and wind direction, temperature, relative air humidity and solar radiation.

For the measurements of the levels in the tank, were used probes that return a current signal, so that the measures were not influenced by the length of the connecting cables to the datalogger. Initially, they were used to position sensors that exploit the principle of magnetostriction created by a permanent magnet placed in a point of a conductor; in a second time levels were measured with pressure transducers (designed to work in adverse conditions) characterized by a single circuit for the power supply and measurement.

For drain outflow measurement a rain gauge was installed with contact closure device connected with the effluent flow from the drains and the measurement was carried out as is set for the measurement of inflows.

Soil sensors

For the acquisition of data relating to soil, in particular water content and potential, in two plots were prepared 6 measurement stations equipped with an access tube for the probe to neutrons, three TDR probes (Topp, 1980) and two tensiometers. The aluminium tube for the neutron probe access has been driven into the soil to a depth of 1.5 m; the measurements were made weekly at six different depths, in the range 20-110 cm. The tensiometers were positioned at a depth of 80 cm and 100 cm. The readings were taken every three to four days. The neutron probe measurements of water content, allow good spatial resolution but, being related to the presence of an operator in the field, have a limited temporal frequency. To overcome this drawback, the stations have been completed with three TDR probes for the automatic measurement at three different depths, more specifically, a probe has been stuck in the surface region in vertical position between 0 cm and 15 cm, the other two positioned horizontally at depth 30 cm and 60 cm.

The instrument used for the TDR measurements is Tektronix 1502C equipped with a serial interface (SP 232) that allows the connection to the computer through the RS 232 serial port.

To be able to simultaneously detect soil moisture in several places, a multiplexer was built, controlled through the computer, which allows the connection to the tester up to 36 TDR probes. The multiplexer consists of seven coaxial relays in six positions, characterized by an insertion loss, for signals with a frequency of 18 GHz, lower than 0.5 dB. The tester is connected to a relay to the outputs of which were connected inputs of the other six relays. In this way they are made 36 ports for the connection of the probes

The probes used were built with two steel conductors of diameter 0.5 cm, length 15 cm, with a distance of 5 cm and the balun drowned in the resin that constitutes the head of the probe to minimize the dispersion of the signal (Zegelin *et al.*, 1989). Since the theoretical calculations for the construction of the balun does not produce accurate results in reality (Spaans and Baker, 1993), because of uncertainty relative to the properties of ferrites and the components of the coils, the best way to identify suitable materials is a trial and error procedure (Grant and Phillips, 1990).

The control of the TDR acquisition system was operated by an already developed software (Damiani, 1996) originally developed for the single measurement acquisition, modified using the libraries provided in Quick Basic to control the multiplexer (Heimovaara and Bouten, 1990).

Results

In the graph of Figure 3 shows the time course of water content, at all three measuring depth, measured by the neutron probe and TDR, as well as the rainfall occurred during the observation period from March 1997 to December 1997. The relative homogeneity found between the measurements carried out in six different locations of the same parcel has permitted the use of average values of the observed quantities. During periods in which it was possible to carry out measurements using both the neutron probes and the TDR, the comparison verifies a substantial agreement in the time evolution of the medium-term water content. As expected on the other hand for the considerations previously developed, the reflectometric method allows to follow this trend with greater detail, highlighting all the short-term variations in the water content in the three horizons also in response to modest rainfall. In contrast, the neutron method, not allowing acquisitions in automatic, is capable of providing only information about the evolutionary trend of the profiles of water content after each rain event.

It is possible to observe how in the initial part of the observation period and following the winter precipitation, the water content in the upper layer reaches values close to saturation and also it is highlight an extremely sensible response to the meteoric inputs. By contrast, the deeper layer shows lower water contents and is less affected and with delay respect the same rain inputs. With the drying of the soil occurring in the summer period a stable water content of 10-15% is reached for the three layers, then returned to their initial values, according to an evolution which is obviously linked to precipitation events.

The evolution of the profiles of water content acquired using the neutron probe and, alternatively, of TDR measurements was compared with the result of a simulation conducted by applying the model POLICORO (Santini, 1992), widely verified for different soils and crops. The use of the simulation model is particularly useful in the interpretation of experimental tests, in addition to allowing for a relatively easy assessment of the influence of soil and meteorological parameters on the distribution of water in the system.

In the simulation as input data were used the daily actual evapotranspiration data in mm/d determined by applying the Pennman-Monteith equation, as well as the rain in mm/d. The hydrological behaviour of the soil has been described by solving the equation of Richards, using the hydraulic properties, retention curves and hydraulic conductivity (Figure 1). With reference to boundary conditions adopted for the simulation, the surface processes of infiltration and evaporation were controlled by external environmental conditions. In this hypothesis, the evaporation is determined by radiation external conditions until reaching a critical potential to the soil surface; achieved that value instead of the evaporation is governed by the profile of water content in the soil. On this basis the model returns in output, among other things, the actual evapotranspiration as permitted by the actual conditions of soil moisture. At the lower boundary is hypothesized a condition of free drainage. In the input data runoff has been neglected, because in the observation period were absent. As an example, in Figure 4 is represented the comparison between the water content measured by the neutron method and simulated, which refers to the three measuring depth.

The reliability of the experimental methodology adopted is confirmed by the good correspondence between field measurements and simulation results, the latter regardless of the characterizations obtained using laboratory on soil undisturbed samples. Of course, with reference to the TDR measurements, not shown here, the periodic fluctuations are followed by the simulation described in more detail.

The importance of monitoring water content profiles with high time frequency is evident when one wants to follow the evolution of the vol-

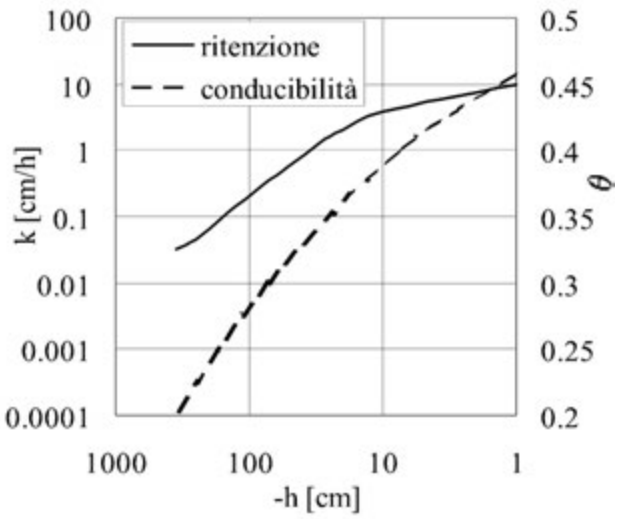

Figure 1. Mean soil hydraulic characteristics.

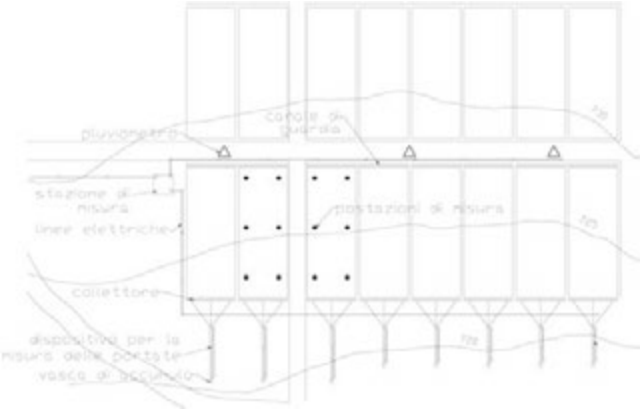

Figure 2. Guardia Perticara experimental plots.

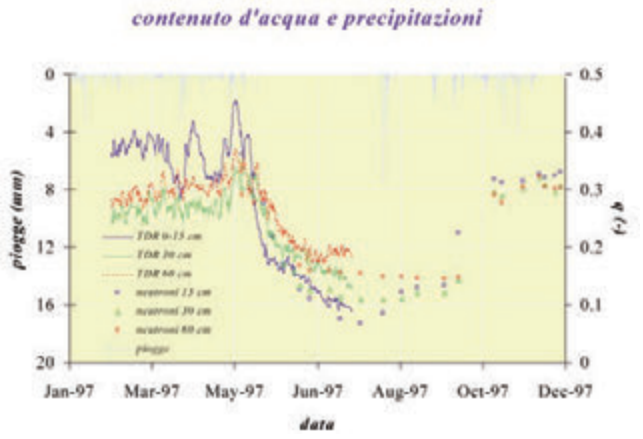

Figure 3. Water content measurements.

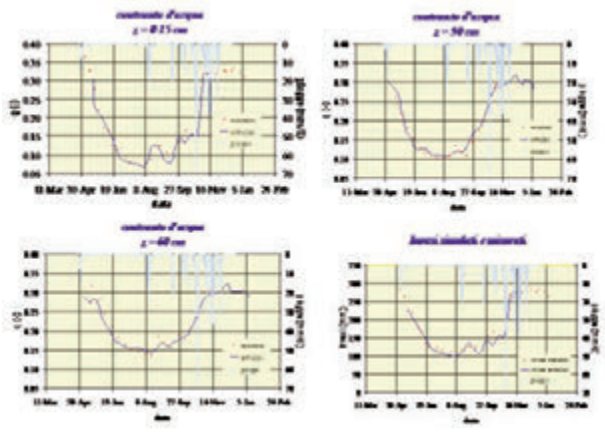

Figure 4. Comparison between experimental and simulated data.

ume of water stored in the soil profile investigated after dry and rainy periods . The fourth graph of Figure 4 shows the trend of the heights of water stored up to a depth of 80 cm, calculated with reference to the profiles of water content measured and simulated respectively. It is a soil that has an average water capacity corresponding to about 170 mm of water with a maximum in the rainy period of about 280 mm and a minimum in the dry months of about 110 mm. These values are consistent with those expected given the retention characteristics of the medium under consideration.

Conclusions

In hydrological sciences is widespread the use of simulation models in the interpretation of real world phenomena. The physical concepts on which the models are often based specifications need to be tested through field experiments that must necessarily involve multi-disciplinary skills. In this sense, the use of sophisticated equipment for the measurement of all variables needed for the quantification of a soil water balance, allowed to describe to a high degree of detail the evolution of the complex exchange processes in the system.

Particular attention was paid to the acquisition and subsequent processing of meteorological and soil data, using instruments that are suitable to be automated, allowing measurements with high spatial and temporal resolution. The reliability of TDR has been verified through the comparison with the neutron method, practically considered a reference for soil water content methods.

The simulation results allow, on the one hand, to verify the usefulness of models in the interpretation of experimental tests, and confirm on the other hand that field experiments conducted through appropriate methodologies are essential for the validation of the models themselves.

References

Damiani, P., 1996 Tecnica di utilizzo del TDR per la misura del contenuto volumetrico d'acqua nel suolo. Dipartimento Tecnico-Economico per la gestione del Teritorio Agricolo-Forestale.

Grant, I.S., Philips, W.R., 1990: Electromagnetism. John Wiley & Sons, Chichester, England.

Heimovaara, T.J., Bouten, W., 1993: A computer-controlled 36 channel time domain reflectometry systemfor monitoring soil water contents. Water Resour. Res. 26, 2311-2316.

Hillel, D., 1980: Applications of soil physics. Academic press.

Santini, A., 1992: Modelling water dynamics in the soil-plant-atmosphere system for irrigation problems. Excerpta 6, 133-166.

Santini, A., Romano, N., Ciollaro, G., Comegna, V., 1995: Evaluation of a laboratory inverse method for determining unsaturated hydraulic properties of a soil under different tillage practices. Soil Sci. 160 (5),340-351.

Simunek, J., Sejna, M., Van Genuchten, M. Th., 1998: The HYDRUS-1D software package for simulating water flow and solute transport in two dimensional variably saturated media. International Grownd Water Modeling Center, Colorado

Sommella, A., Gaetani, G., 1990: Impianto sperimentale per la misura del deflusso superficiale e dell'erosione. Pubblicazione dell'Università degli Studi della Basilicata. Istituto di Genio Rurale e Forestale.

Spaans, E.J.A., Baker, J.M., 1993: Simple baluns in parallel probes for Time Domain Reflectometry. Soil Sci. Soc. Am. J. 57, 668-673.

Topp, G.C., 1980: Electromagnetic determination of soil water content: measurements in coaxial trasmission lines. Water Resour. Res. 16, 574-582.

Zegelin, S.J., White, I., Jenkins, D.R., 1989: Improved fields probes for soil water content and electrical conductivity measurements using time domain reflectomety. Water Resour. Res. 25, 2367-2376.

A 2D hydrodynamic-sedimentological model for gravel bed rivers. Part II, Case study: the Brenta River in Italy

Gabriel Kaless,[1] Johnny Moretto,[1] Fabio Delai,[1] Luca Mao,[2] Mario A. Lenzi[1]

[1]Dipartimento Territorio e Sistemi Agroforestali, Università di Padova, Italy; [2]Departamento de Ecosistemas y Medio Ambiente, Pontificia Universidad Católica de Chile, Santiago, Chile

Abstract

A 2D depth average model has been used to simulate water and sediment flow in the Brenta River so as to interpret channel changes and to assess model predictive capabilities. The Brenta River is a gravel bed river located in Northern Italy. The study reach is 1400 long and has a mean slope of 0.0056. High resolution digital terrain models has been produced combining laser imaging detection and ranging data with colour bathymetry techniques. Extensive field sedimentological surveys have been also carried out for surface and subsurface material. The data were loaded in the model and the passage of a high intense flood (R.I. > 9 years) was simulated. The model was run under the hypothesis of a substantial equilibrium between sediment input and transport capacity. In this way, the model results were considered as a reference condition, and the potential trend of the reach was assessed. Low-frequency floods (R.I. » 1.5 years) are expected to produce negligible changes in the channel while high floods may focalize erosion on banks instead than on channel bed. Furthermore, the model predicts well the location of erosion and siltation areas and the results promote its application to other reaches of the Brenta River in order to assess their stability and medium-term evolution.

Correspondence: Gabriel Kaless, TeSAF, Facoltà di Agraria, Università degli Studi di Padova, via dell'Università 16, 35020 Legnaro (PD), Italy.
Tel. +39.049.8272675 – Fax. +39.049.8272686.
E-mail: gabriel.kaless@unipd.it

Key words: gravel-bed rivers, 2D depth-average model, hydrodynamic-sedimentological simulations, high-resolu-tion digital terrain models, Brenta River.

Acknowledgements: This research has been carried out within the frame of the UNIPD Project "CARIPARO-Linking geomorphological processes and vegetation dynamics in gravel bed rivers" and the UNIPD Strategic Project GEORISKS, Research Unit TeSAF Department. Part of this research was also founded by both, the SedAlp Project: Sediment Management in Alpine Basins: integrating sediment continuum, risk mitigation and hydropower, 83-4-3-AT, in the framework of the European Territorial Cooperation Programme Alpine Space 2007-2013, and the PRIN20104ALME4-ITSedErosion: "National network for monitoring, modelling and sustainable management of erosion processes in agricultural land and hilly-mountainous area".

Journal of Agricultural Engineering 2013; XLIV(s2):e20
doi:10.4081/jae.2013.(s1):e20

Introduction

Many gravel bed rivers in Italy have been disturbed over the last decades by human interventions. The recent changes of Brenta River have been analyzed by means of aerial photographs (Moretto, 2010). In other cases, such as the Piave River, the availability of historical documents has allowed the reconstruction of a chronology of changes in the last 200 years (Comiti *et al.*, 2011). Human interventions have affected directly and indirectly the fluvial systems. Basin works such as reforestation, check-dams along tributaries and the construction of dams for electric energy generation purposes have severely reduced the sediment supply. Moreover, in-channel activities such as gravel mining and bank protections have also increased the sediment deficit (Surian and Rinaldi, 2003). Nowadays, there is the agreement that sediment supply change has been the key factor in determining channel adjustments (Rinaldi *et al.*, 2005; Comiti *et al.*, 2011). Hence, in most cases management strategies have been directed to operate on sediment supply for enhancing channel dynamics.

Sediment transport is not usually directly measured in large gravel bed rivers, and indirect strategies are employed instead. Up to the present, transverse sections have been surveyed and compared along the reaches of Brenta River (Surian and Cisotto, 2007) and Piave River (Comiti *et al.*, 2011), involving standard GPS procedures. Recently, the combined use of laser imaging detection and ranging (LiDAR) data and elevation reconstruction by colour bathymetry techniques has produced high resolution digital terrain models (DTMs) which allow detailed studies at the reach scale (Moretto *et al.*, 2012). Another strategy recently employed for the quantification of sediment transport has involved the use of numerical models. Ziliani and Surian (2012) have applied a cellular model for interpreting past changes in the Tagliamento River and to assess possible evolutionary trajectories according to different flow regime scenarios.

The aim of this paper is to interpret morphological changes at a reduced spatial and temporal scale occurred in a reach of the Brenta River, using a 2D-depth average hydrodynamic and sedimentological model. High resolution data have been elaborated and DTMs are available before and after an intense flood event (R.I. > 9 years).

Brief history of the evolution of Brenta River

As a result of the need of electric energy generation and new irrigation systems, during the first years of the 20th century many dams were built, most of which were completed before the '60s (see Table 1). Dams have a scarce capacity for storing water volumes during flood events and, hence, to reduce the peak discharge. The main effect of dams has affected the regime of sediment delivery, interrupting the natural sediment flow during floods and, hence, affecting the sediment

balance in the fluvial network placed downstream.

The decrease of sediment supply has also been a consequence of other human interventions, namely bank protection occurring mainly during the 19th century and the implementation of torrent control works from the '20s, both promoting channel stability due to the increase of bank strength and fixing the stream bottom bed.

More recently, another human activity has altered the dynamics of these fluvial systems. Between the '60s and '90s, intense gravel mining was carried out. According to the official data, 8.6 million of cubic meters of sediments were supposed to have been mined between 1953 and 1977, but aerial photographs taken in those years indicate that the volume of sediments removed from the channel was much larger (Surian and Cisotto, 2007).

The Brenta River has experienced a dramatic narrowing process in the last decades, being 442 m wide at the beginning of 20th century and reducing to 224 m in 2003. This process has been accompanied by incision up to 2.5 m. The mean channel slope has slightly increased, from 0.0033 m/m to 0.0036 m/m over the same period.

Materials and methods

The study reach of the Brenta River is placed 4.7 km downstream Bassano del Grappa, near to Nove village. The river reach is 1400 m long and the active channel is on average 73 m wide with a slope of 0.0056. The mean depth accounts for 1.4 m with a maximum depth in the pools of 2.8 m. The bed material (substrate) is composed by a gravel-sand mixture with D_{50} = 21 mm and a sand content of 15%. The bed is armoured and the surface layer is coarser than the substrate material (D_{50} = 49 mm).

The Brenta River exhibits a single-thread channel which is mainly incised and has a floodplain confined by levees. Along the left bank protections, control works consisting on rip-rap inhibit channel widening; however, the right bank is free to evolve.

Data acquisition and digital terrain model development

The study reach of Nove was scanned with LiDAR technology at two different times: the 23rd of August 2010 by Blom G.C.R. S.p.A. which used a sensor OPTECH ALTM Gemini; the 24th of April 2011 by O.G.S. which used a sensor RIEGL LMS-Q560. The raw LIDAR data were filtered to obtain ground points with the software "TerraScan". Because no bathymetric LiDAR surveys were available colour bathymetry method was used to create a more accurate and detailed DTM of the wetted areas. This methodology consists on calibrating a regression model between water level depth measurements, assessed by Differential Global Positioning System (DGPS), and Red, Green and Blue bands values of aerial photos taken contemporary to the LiDAR survey. Through the integration of LiDAR points for exposed areas and colour bathymetry points foreign-channel areas, the subsequent DTMs were compared creating a DoD (Digital elevation model of Difference) and identifying deposition and erosion processes. The accuracy of the models was then tested through DGPS control points (Moretto *et al.*, 2012).

Sedimentological surveys

Samples of surface material were taken at 5 cross sections in order to describe the spatial variability (covering a sequence riffle-pool-riffle-pool-riffle).The random walk approach (Wolman, 1954) was applied at each cross section collecting a minimum of 120 pebbles.

Two samples of substrate material were also taken from lateral bars. The surface armour layer was removed and then the material was extracted; coarse pebbles were classified and weighted in the field and a sample of gravel and sand (D < 25mm) was later analyzed in the laboratory.

Boundary conditions and numerical settings

The Lican-Leufu model was employed for assessing the morphological evolution of the reach. The model solves the depth-averaged Reynolds's equations that incorporates the standard k-e model for turbulence closure. The sedimentological modulus solves the Exner's equation for bed elevation change and a two-layers scheme is used for modelling the armour layer (for further details see Kaless *et al.*, 2013).

Sediment supply

A recirculation scheme was adopted so as to simulate a condition of mass balance, i.e., the reach can transport all the sediment supplied. Then, the stability state of the actual River Brenta could be assessed considering the model results as a reference of equilibrium.

Water discharge

The data available for the period 23/8/2010 - 24/4/2011 consisted of mean daily discharges, with a period length of 244 days. Since low discharges did not produce morphological changes, a minimum discharge of 150 m^3/s was selected. This discharge can entrain at least 41% of the bed material (considering a reference dimensionless shear stress of 0.045). Discharges below 150m^3/s were removed from the original record but the sequence was conserved. The resulting record to be modelled had a length of 35 days.

Numerical settings

The domain was divided in 111 cells in the downstream direction and 60 cells across the channel. Cell sizes were not constant and averaged 12.60 m in length and between 2.00 to 4.00 m in width.

Although a short period of 35 days was simulated, the model was operated under the "medium-term" scheme (see Kaless *et al.*, 2013). The discharge-tolerance was 10% and the tolerance for bed elevation change was set at 5%. At the downstream boundary, a minimum bed elevation was imposed (no erosion could have taken place below this level) and the water surface elevation was fixed at the uniform-flow depth. The minimum water depth was set at 0.25 m for the hydrodynamic model and 0.30 m for the sedimentological routine.

On sites where banks are protected with rip-rap to prevent erosion, a high friction angle was set in the model (e.g. 89°).

Results

Comparison of mass balance

Cross sections were analyzed computing the volume difference between final and initial elevations. The difference has been expressed in terms of volumes (Figure 1). The predicted variation of volumes relies above the observed one, indicating that incision has taken place at the present condition of the Brenta River.

When the variation of volumes in the downstream direction is observed, it appears that both curves exhibit similar patterns. In order to evidence this fact, the model output was adjusted with a constant equal to the difference in predicted and observed total volumes. The

dashed line in Figure 1 shows a good concordance for most of the reach. The first 15 cross sections exhibit clear differences: while erosion took place in the model, deposition was observed.

Comparison of spatial patterns

The DoD was calculated with the available DTMs of the Brenta River (Moretto *et al.*, 2012) and the results of the simulation (Figure 2). The flow in the Brenta River was mainly concentrated in the active channel as indicated by the pattern of erosion/deposition, while all over the lateral floodplain a small erosion (10 cm on the mean) took place indicating conditions of lower flow. On the contrary, the lateral channel was activated in the simulation and a high erosion process took place at the upstream end.

Due to the passage of these high floods, bank erosion occurred along the pool sectors, i.e., the upper left bank (cross section 30) and the subsequent in the right bank (cross section 70). There should have been erosion on the next left side near cross section 90 but at this place bank was protected with rip-rap. Erosion was also significant on the right bank between sections 20 and 30 (see also Figure 2). This bank was not eroded in the simulation but at the same place erosion was present within the channel. However, it is evident the coincidence of erosion pattern with alternating sides, between observations and simulation.

Although the net mass balance is negative in the Brenta River, the DoD reveals that siltation also occurred within the channel. There was a large supply of material deposited at the upstream extremity of the reach, with positive mass balance at the beginning of the reach and modest net erosion downstream (see in Figure 1 the first 10 cross sections). Furthermore, downstream deposits were also generated immediately downstream the eroded sectors in the same side of the channel (see cross sections 70 and 90 in Figure 2). Since sediment was recirculated in the simulation, more material was available for bar formation and, hence, deposition sectors result more frequent in the predicted DoD. Those sectors observed in the field featuring siltation or low erosion are instead covered with sediments in the simulation, as shown between cross sections 50 and 100.

Two cross sections were chosen for a local comparison. Figure 3 shows cross section 61 which was highly eroded during the flood events, in fact, the right bank retreated of about 11m. Siltation occurred along the opposite bank aggrading the bed level by nearly 1m. The model also predicted erosion in the same bank although it was not so significant as observed. Siltation was also correctly located on the left side of the channel with the same levels.

On the other hand, the comparison of the upstream cross section 50 results difficult because of the secondary channel activation during the simulation that diverted discharge and reduced the flow in the main channel. This fact, beside the imposition of a high friction angle for bank stability, may represent the reason of the lack of bank erosion sectors in the predicted cross section (Figure 4).

Discussion

The Brenta River has been dramatically disturbed by human activities during the last decades. Dams built in the upper basin have retained sediments in the catchment, protections works along the banks have limited the local sources of sediment and in-channel gravel mining has produced a deficit in sediment balance. The sediment dynamics in the Brenta River has recently been studied by Surian and Cisotto (2007). These researchers compared cross sections and aerial photographs and calculated sediment transport rates within the channel. As a result, they concluded that transport rate may range between 0 – 12.200 m^3/year in the reach analyzed by this study.

There are some issues that should be considered before attempting

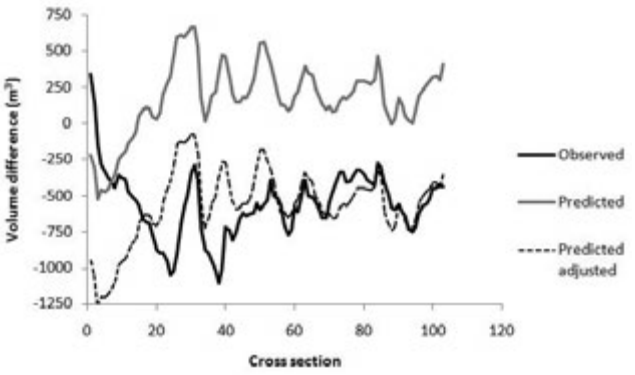

Figure 1. Comparison of mass distribution along the study reach. Volumes have been calculated considering the difference of DTMs at each cross section (see Figure 2 for location of sections).

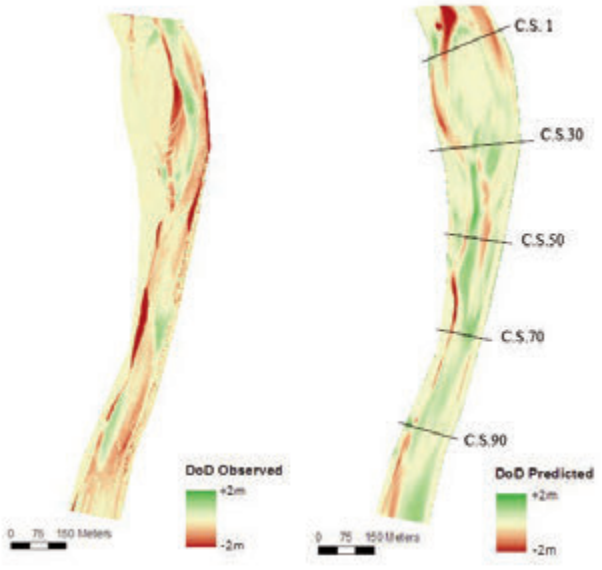

Figure 2. Comparison of measurements and model results. Left: Difference of DTMs measured in the field (Moretto *et al.*, 2012); and right: Difference of DTMs simulated with the model. Cross sections (C.S.) are indicated.

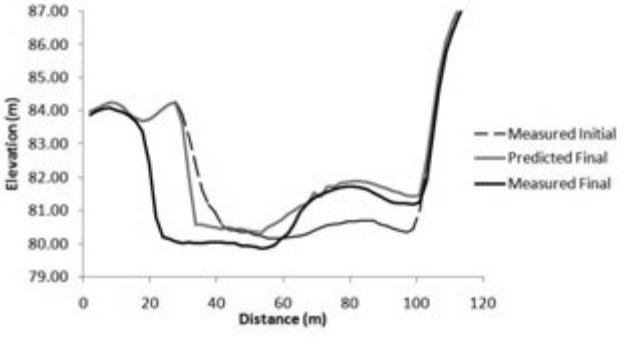

Figure 3. Comparison of a cross section with protection works on the right bank, at cross section 92 (see Figure 2 for location).

a comparison of results. Firstly, there are spatial scales and data resolution differences between this study and the previously mentioned that have to be underlined. Surian and Cisotto evaluated sediment transport analyzing changes in 12 cross sections distributed along a 23 km long reach. In this study, high resolution DTMs were employed covering a shorter reach about 1400 m long. Secondly, these researchers did not consider the sand content because they assumed it was wash material. Subsurface surveys were conducted in this study indicating that sand content is 15.1%. On the contrary, sediment transport and bed changes were computed in the numerical modelling using Wilcock and Crowe's (2003) model, which includes the sand fractions. Finally, the aforementioned input annual bulk of 12.200 m^3 was added by the authors to the budget so as to have positive sediment transport; and they further indicated that at the Barzziza gauging station the total load was estimated in 37.000 m^3/year. Therefore, budgets provided by Surian and Cisotto will be considered as indication of "order of magnitude" and corrected to incorporate the sand content.

Total sediment volumes (V_{TS}) are related with gravel volumes (V_{gravel}) by means of:

$$V_{Ts} = \frac{V_{gravel}}{(1 - SF)}$$

where in SF is the sand content. DoD volumes () are also corrected to take into consideration porosity:

$$V_{Ts} = (1 - \lambda) \cdot V$$

Surian and Cisotto reported a sand content of 20.8% and hence their informed volumes were multiplied by 1.263. The bed porosity was estimated using an empirical formula proposed by Wu and Wang (2006) accounting for 0.241Hence volume differences have to be multiplied by the factor 0.759.

The model was run under conditions of mass balance, i.e., the reach transport capacity was equal to the sediment supply. Figure 5 shows the sediment transport rate for different discharges as predicted by the model. According to the model, transport rate increases lowly up to discharges above bankfull, but surpassing a discharge of 380 m^3/s, transport rate goes up quickly.

The mean annual sediment transport rate was calculated using the duration curve of discharges for the last 50 years, and resulted to be 77.210 m^3. The recirculated total sediment volume for the studied events was 160.000 m^3, i.e., the required volume for mass balance during these events could not be supplied with the ordinary curve of discharges. Furthermore, if the calculated transported discharge is adopted as an estimation of the actual sediment transport, then the sediment supplied can also be assessed. The difference in the DTMs indicates that the reach lost 57.810 m^3 and hence the supply should be in the order of 10^5 m^3, which is one order of magnitude higher than the Surian and Cisotto estimation for the annual transport rate of 15.400 m^3 / 37.000 m^3.

Erosion along the active channel may be conditioned by several factors: channel widening, the development of a static armour, or by fixing the boundary conditions at the bridge located near downstream of the reach. Figure 2 shows that most part of the material deficit was due to erosion along the banks of the channel. Computing the volumes it turned out that bank erosion furnished 21.750 m^3 of material during the floods, which is 38% of the total mass deficit. One possible river restoration scenario could entail the elimination of protection works existing along the right bank at the downstream part of the reach, where it would be possible to relocate three houses and to build a new

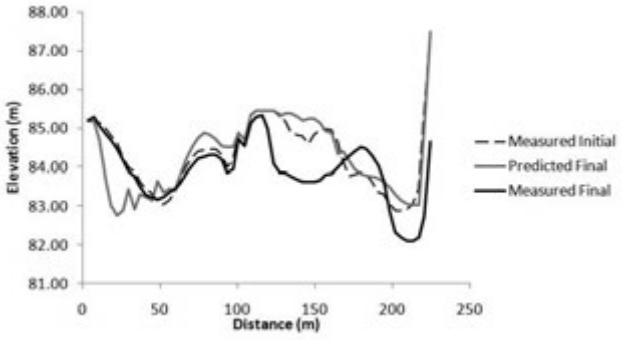

Figure 4. Evolution of the historical cross section after the passage of floods in the period 2010-2011. See cross section 30 in Figure 2 for location.

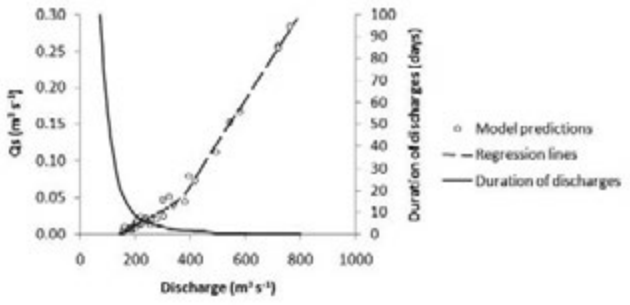

Figure 5. Predicted sediment transport rate in the Brenta River for the simulated period. Frequency of discharges was calculated using records from the last 50 years.

Table 1. Dams constructed in the Brenta River basin. The drainage area upstream the dam is indicated (modified from Surian and Cisotto, 2007).

River	Dam	Drainage area upstream (km^2)	Year of construction
Cismon Torrent	Ponte Serra	497	1909
Costa Brunella Torrent	Costa Brunella	0.7	1941
Cismon Torrent	Corlo	628	1954
Senaiga Torrent	Senaiga	58	1954
Noana Torrent	Val Noana	8	1958
Cismon Torrent	Val Schener	204	1963

levee 100 m to 150 m apart from the current bank position. Under this scenario, channel widening would promote channel stability by providing material and reducing the transport capacity as shear stress would reduce. A recent research carried on by Rigon *et al.* (2012) has pointed out the relation between flood magnitude and channel widening, and stressed the role of riparian vegetation. In general, a higher magnitude of flooding corresponds to a higher active channel widening; and a reduction of the active channel width is due to the expansion of riparian vegetation establishing in floodplains and islands during periods of lack of major disturbance processes.

The development of a static armour is crucial for the channel stability. Laboratory experiments revel that two phases are present during the development of the armour: a first phase of incision and a second phase of coarsening (Church *et al.*, 1998; Wilcock *et al.*, 2001; Mao *et al.*, 2011). Furthermore, static amour layers are highly structured and imbricated with higher thresholds for entrainment. The Brenta River is highly armoured, with a reach-average absolute armouring index of 2.32 (3.58 at riffles and 1.72 at pools). Considering reach-average values, the surface D_{90} is nearly 181 mm and the maximum diameter (D_{99}) is 335 mm. This surface material is much coarser than the competence of high flows (RI > 9 years) which according to the model is D_{90} = 73 mm and D_{99} = 155 mm. This difference may be an indication that the surface has developed a static armour that is resistant to high floods.

Conclusions

The 2D-depth average model described well the location of siltation areas and bank erosion, although it was run under a condition of unlimited sediment supply which was not the actual situation in the Brenta River. The applied model, based on high-resolution DTMs, estimated annual sediment transport in the order of $8 \cdot 10^4$ m^3 which is higher in respect to previous studies results based on cross sections.

The response of the channel in the medium-term has to distinguish ordinary events (above bankfull discharge, with Q = 350 m^3/s and R.I. »1.5 years) and high floods with recurrence interval above 9 to 10 years. With regards to ordinary events, due to the presence of a well armoured bed and low transport rates, not significant or negligible changes are expected to be observed in the channel bed (considering also errors in determination of volume changes that render difficult to discern small changes). On the other hand, high floods are expected to focalize erosion on banks instead on channel bed.

In general, the model provided good results that promote its application to other reaches of the Brenta River in order to assess their stability and medium-term evolution.

References

Church M, Hassan MA, Wolcott JF. Stabilizing self-organized structures in gravel-bed stream channels: field and experimental observations, Water Resour Res 1998; 34, 3169-79.

Comiti F, Da Canal M, Surian N, Mao L, Picco L, Lenzi MN. Channel adjustments and vegetation cover dynamics in a large gravel bed river over the last 200 years, Geomorphology 2011, doi: 10.1016/j.geomorph.2010.09.011.

Kaless G, Lenzi MA, Mao L. A 2D hydrodynamic-sedimentological model for gravel bed rivers. Part I: theory and validation. Proceedings of the Italian Society of Agricultural Engineering Associazione Italiana, 2013; In Press.

Mao L, Cooper J, Frostick L. Grain size and topographical differences between static and mobile armour layers. Earth Surf Processes 2011, DOI: 10.1002/esp.2156.

Moretto J. Caratterizzazione dei fiumi ghiaiosi naturali ed antropizzati e analisi delle modificazioni morfologiche più recent del Fiume Brenta tra Bassano del Grappa e Carturo. Degree Diss. Università degli Studi di Padova, Italy; 2010.

Moretto J, Rigon E, Mao L, Delai F, Picco L, Lenzi MA. Assessing morphological changes in gravel bed rivers using LiDAR data and colour bathymetry. Erosion and Sediments Yields in the Changing Environments, Proceedings of a symposium held at the Institute of Mountain Hazards and Environment 2012. IAHS Publ. 356, 419-427.

Rigon E, Moretto J, Mao L, Picco L, Delai F, Ravazzol D, Lenzi MA, Kaless G. Thirty years of vegetation cover dynamics and planform changes in the Brenta River (Italy): implications for channel recovery. Erosion and Sediments Yields in the Changing Environments, Proceedings of a symposium held at the Institute of Mountain Hazards and Environment 2012. IAHS Publication 356, 178-86.

Rinaldi M, Wyzga B, Surian N. Sediment mining in alluvial channels: physical effects and management perspectives. River Res Appl 2005; 21: 805–28.

Surian N, Rinaldi M. Morphological response to river engineering and management in alluvial channels in Italy. Geomorphology 2003; 50, 307-26.

Surian N, Cisotto A. Channel adjustments, bedload transport and sediment sources in a gravel-bed river, Brenta River, Italy. Earth Surf Processes 2007; 32, 1641-56.

Wilcock PR, Kenworthy ST, Crowe J. Experimental study of the transport of mixed sand and gravel. Water Resour Res 2001; 37, 3349-58.

Wilcock PR, Crowe JC. Surface-based transport model for mixed-size sediment, J Hydrol Eng 2003; 129, 120-8.

Wolman MG. A method of sampling coarse bed material. American Geophysical Union, Transactions 1954; 35, 951-6.

Ziliani L, Surian N. Evolutionary trajectory of channel morphology and controlling factors in a large gravel-bed river. Geomorphology 2012; doi:10.1016/j.geomorph.2012.06.001.

A 2D hydrodynamic-sedimentological model for gravel-bed rivers. Part I: theory and validation

Gabriel Kaless,[1] Mario A. Lenzi,[1] Luca Mao[2]

[1]Dipartimento Territorio e Sistemi Agroforestali, Università di Padova, Italy; [2]Departamento de Ecosistemas y Medio Ambiente, Pontificia Universidad Católica de Chile, Santiago, Chile

Abstract

This paper presents a novel 2D-depth average model especially developed for gravel-bed rivers, named Lican-Leufú (Lican=pebble and Leufu=river, in Mapuche's language, the native inhabitants of Central Patagonia, Argentina). The model consists of three components: a hydrodynamic, a sedimentological, and a morphological model. The flow of water is described by the depth-averaged Reynolds equations for unsteady, free-surface, shallow water flows. It includes the standard k-e model for turbulence closure. Sediment transport can be divided in different size classes (sand-gravel mixture) and the equilibrium approach is used for Exner's equation. The amour layer is also included in the structure of the model and the surface grain size distribution is also allowed to evolve. The model simulates bank slides that enable channel widening. Models predictions were tested against a flume experiment where a static armour layer was developed under conditions of sediment starvations and general good agreements were found: the model predicted adequately the sediment transport, grain size of transported material, final armour grain size distribution and bed elevation.

Correspondence: Gabriel Kaless, TeSAF, Facoltà di Agraria, Università degli Studi di Padova, Via dell'Università 16, 35020 Legnaro (PD), Italy.
Tel. +39.049.8272675 – Fax. +39.049.8272686.
E-mail: gabriel.kaless@unipd.it

Key words: gravel-bed rivers, 2D-depth-average model, hydrodynamic-sedimentological model, bed load, armour layer, bed evolution.

Acknowledgements: this research has been carried out within the frame of the UNIPD Project "CARIPARO-Linking geomorphological processes and vegetation dynamics in gravel bed rivers" and the UNIPD Strategic Project GEORISKS, Research Unit TeSAF Department. Part of this research was also founded by both, the SedAlp Project: Sediment Management in Alpine Basins: integrating sediment continuum, risk mitigation and hydropower, 83-4-3-AT, in the framework of the European Territorial Cooperation Programme Alpine Space 2007-2013, and the PRIN20104ALME4-ITSedErosion: "National network for monitoring, modelling and sustainable management of erosion processes in agricultural land and hilly-mountainous area". We are very grateful to Robert Bernard for providing useful suggestions while developing the hydrodynamic model.

Contributions: the authors contributed equally.

Conflict of interests: the authors declare no potential conflict of interests.

Funding: the laboratory experiments were supported by a Marie Curie Intra European Fellowship (219294, FLOODSETS) within the 7th European Community Framework Program while Luca Mao was based at the Department of Geography of the University of Hull (UK).

Journal of Agricultural Engineering 2013; XLIV(s2):e21
doi:10.4081/jae.2013.(s1):e21

Introduction

The observed shape of a river is the consequence of controlling processes such as the flow of water and sediments, and the forces of boundary conditions such as valley confinement and slope, vegetation, etc. The resulting river morphology is the complex result of the complex interactions between sediment transport, flow of water, and channel morphology. In the last years several models have been developed for explaining and predicting the shape of a river. These models constitute the everyday growing discipline of Computational Fluid Dynamics. Many models have been especially created for reproducing the complex flow in meandering rivers (Wu *et al.*, 2000; Ferguson *et al.*, 2003; Abad *et al.*, 2008). The flow of water in meandering rivers is highly disturbed by channel sinuosity that induces secondary currents (Rozovskii, 1961). Sediment is transported both in suspension and as bed load and comprises fine sizes, *i.e.*, sand. Moreover, bank failure models have to consider material cohesion due to the presence of silt and clay (Darby *et al.*, 2002).

Gravel-bed rivers are usually located within mountain landscapes. They present several features that differentiate them from meandering rivers: both bed and banks are composed of non-cohesive material (mixture of sand, gravel and cobbles, although a "virtual" cohesion can be provided by vegetation roots), the aspect ratio(width/depth) is higher because channels are wider and shallower; bed load sediment transport is responsible of channel form been material in suspension negligible for channel change (Leopold, 1992), and the bed is usually armoured, which regulates the interaction between bed surface and sediment transport. These features impose new and different challenges for modelling. Also, the last years have witnesses the production of numerical models that consider some of the aforementioned features: Nataga *et al.* (2000) developed a depth-average shallow water model including a sediment transport model (with only one grain size) and a bank failure model for gravel-bed rivers. Later, Jang and Shimizu (2005) and Garcia-Martinez *et al.* (2005) developed models for wide channels using the Meyer-Peter and Müller sediment transport formula for uniform material. Finally, Li and Millar (2007) extended the Mike 21C model implementing Parker's (1990) sediment transport model for mixtures.

The main objective of this paper is to present a novel numerical model especially design for assessing morphological changes in grav-

el-bed rivers, called Lican-Leufú 2D model (Lican and Leufu are two words two words of the Mapuche language, the native inhabitants of Central Patagonia, Argentina; the words indicate the two key aspects of the new model: the flow of water, Leufu = river, and the processes related with gravel transport, Lican = pebble). The model considers the presence of an armour layer, the transport of sand-gravel mixtures, and bank erosion processes.

The 2D hydrodynamic and sedimentological model

Hydrodynamic model

The governing equations are composed of the depth-averaged versions of mass balance and momentum balance for shallow water, unsteady flows:

$$\frac{\partial z_{ws}}{\partial t} + \frac{\partial (hU)}{\partial x} + \frac{\partial (hV)}{\partial y} = 0 \qquad 1$$

$$\frac{\partial U}{\partial t} + U\frac{\partial U}{\partial x} + V\frac{\partial U}{\partial y} = -g\frac{\partial z_{ws}}{\partial x} + T_x - Ch^{-1}U|U| \qquad 2$$

$$\frac{\partial V}{\partial t} + U\frac{\partial V}{\partial x} + V\frac{\partial V}{\partial y} = -g\frac{\partial z_{ws}}{\partial y} + T_y - Ch^{-1}V|U| \qquad 3$$

where in z_{ws} is the water surface elevation, h is the flow depth, U and V are the depth-average quantities of local velocities, |U| is the modulus of the depth-averaged velocity vector, T is the force due to viscous effects, and C, a friction factor. This coefficient is related to the bed roughness using Keulegan's (1938) equation and Kamphius's (1974) experimental results supported by field measurements (Kaless, 2013):

$$C^{-2} = 2.5ln\left(11\frac{h}{2D_{90}}\right) \qquad 4$$

Viscous forces are the result of turbulent flow. Viscous force T represents the turbulence effects on the mean flow. Bernard (1993) proposed the following expressions:

$$T_x \approx h^{-1}\nu_t\nabla\cdot(h\nabla U) + 2\frac{\partial \nu_t}{\partial x}\frac{\partial U}{\partial x} + \frac{\partial \nu_t}{\partial y}\left(\frac{\partial U}{\partial y} + \frac{\partial V}{\partial x}\right) \qquad 5$$

$$T_y \approx h^{-1}\nu_t\nabla\cdot(h\nabla V) + 2\frac{\partial \nu_t}{\partial y}\frac{\partial V}{\partial y} - \frac{\partial \nu_t}{\partial x}\left(\frac{\partial U}{\partial y} + \frac{\partial V}{\partial x}\right) \qquad 6$$

where ν_t represents the depth-averaged kinematic eddy viscosity. The standard k-e model is used for the turbulence closure. The kinematic eddy viscosity is evaluated by an empirical formula in terms of the turbulent kinetic energy (k) and the energy dissipation rate (ε). Both variables, k and e, have to be found solving two transport-type partial differential equations (for a thorough exposition see Rodi, 1993, and Bernard, 1993).

Finally, sidewall effects are considered negligible in shallow water flows which are usually observed in gravel-bed rivers.

Sediment transport model

Sediment transport is modelled assuming local equilibrium conditions (Wu, 2007), and using the Exner's equation which relates spatial changes in sediment transport with temporal variation of bed elevation. It is expressed in the following way:

$$(1-\lambda_p)\frac{\partial z_b}{\partial t} = -\sum_k \nabla\cdot q_k \qquad 7$$

where λ_p is the bed material porosity, z_b is the bed elevation and q_k is the sediment transport vector for the k^{th} grain size class, which is evaluated with a sediment transport model. The sum on the right side indicates that the divergence must be evaluated for all the grain size classes. The temporal evolution of the surface grain size distribution is described using the active layer approach (Hirano, 1971; Parker and Southerland, 1990). The mass balance is applied to analyze interactions between sediment transport, active layer and sublayer:

$$\frac{\partial (L_a F_k)}{\partial t} = \frac{\nabla\cdot q_k}{(1-\lambda_p)} + f_{lk}\left(\frac{\partial L_a}{\partial t} - \frac{\partial z_b}{\partial t}\right) \qquad 8$$

where in L_a is the height of the active layer, F_k and f_{lk} are the surface and interface exchange grain fractions (for the k^{th} grain size class), respectively. The active layer has a height of the same order that the largest particles: $L_a = 2\partial$.The interface grain size distribution f_{lk} depends on whether the bed is degrading or aggrading. When the bed degrades f_{lk} is equal to the substrate grain size distribution. On the contrary, when bed aggrades a mixture between the bed load and the active layer material is adopted (Parker *et al.*, 2006). The evaluation of the sediment transport vector q_k requires the definition of its modulus (transport intensity) and its direction, i.e., the components along the x and y axes. The bulk transport of the k^{th} grain size class is calculated using the Wilcock and Crowe's (2003). Bed load direction is evaluated according to the near-bed flow direction and bed topography as well (see Parker, 2006). Sediment transport direction depends on the flow direction but is influence by gravity effects due to bed slope and grain size (for a thorough exposition see Kaless, 2013).

Bank erosion model

Sediment transport near the banks is expected to produce local erosion. This process increases the bank slope, and when this exceeds the response angle it collapses. The heuristic model proposed by Jang and Shimizu (2005) has been adopted for modelling the bank failure. When the slope exceeds the angle of repose (assumed to be ϕ=??, the dynamic Coulomb coefficient) a failure surface inclined at the angle of repose is extended up to the floodplain surface. All the sediment above the failure lines moves downslope to form a deposit with a linear upper surface. Furthermore, the new surface grain size distributions for deposited and eroded areas are evaluated considering a mixture between the previous surface layer and the substrate material (see Kaless, 2013 for further details).

Boundary conditions

The solution of the governing equations requires the specification of the boundary conditions and the initial condition. The boundary conditions consist of the specification of water and sediment fluxes and their distribution along the upstream cross section and water level at the downstream end, for which the normal flow is adopted. Flow through the lateral boundaries is not allowed. Because flow is unsteady, a specific treatment (drying/wetting processes) was considered for inner and lateral boundaries.

Numerical methods

A finite-volume discretization scheme with a curvilinear boundary-fitted grid was adopted. The location of dependent variables is specified according to a staggered grid: fluxes (Q_u and Q_v) are calculated at face-centre, and scalar variables (water elevation, turbulent kinetic energy k, dissipation rate ε, sediment transport, bed elevation and grain size distributions) are calculated at cell-centre. The cell-centred depth-averaged velocities U and V are computed from Q_u and Q_v only when they are needed, for instance, to compute the viscous, friction forces and bottom shear stress.

The governing equations are transformed from Cartesian (x, y) coordinates to curvilinear coordinates ξ = ξ(x,y) and η = η(x,y). Each cell

is composed of four nodes that can be placed arbitrarily, so spacing Dx and Dy are variable. Conversely, in the computational domain the spacing is constant: $\Delta\xi = 1$ and $\Delta\eta = 1$. Using the coordinate transformation $\xi = \xi(x,y)$ and $\eta = \eta(x,y)$, it is possible to obtain the corresponding expression for each differential operator in the governing equations (Bernard, 1993). Advection terms require specific numerical methods in order to avoid instabilities: a) the momentum equation is solved applying the MacCormack's predictor-corrector scheme, adapted from Bernard's (1993) for solving a free surface flow; b) the transport equations of the Standard k-ε model are solved using the Euler (first order) upwind scheme; and c) the Exner equations (for bed elevation and grain size distribution) employ the Euler's scheme with the HLPA interpolation method for the divergence term (Zhu, 1991).

Flow and sediment transport calculations are decoupled because bed changes are very slow. First, the flow equations are solved considering a fixed bed, and then sediment transport is calculated considering water surface and discharge fixed (but water depth and mean velocity are adjusted considering bed elevation changes). For low-term simulations a tolerance is imposed for bed change and when this is exceeded, the hydraulic parameters are updated solving the flow equations. Instead, for a long-term simulation that normally spans several days, hydraulic parameters are hold fixed during the time step (normally assumed to be one day).

Because flow is unsteady a criterion was established to assess when the flow has reached a steady condition. The hydrodynamic calculation stops when the difference between the discharge through all the cross sections and the incoming discharge is below a given tolerance.

Validation against a flume experiment

The model has been tested using the results from a flume experiment carried on to develop a static armour layer under conditions of sediment starvation. Four parameters were used for the comparison: load and grain size distribution of the outgoing sediment transport during the armouring process, and the final bed elevation and surface grain size distribution.

Experimental settings

The physical experiment was conducted at the laboratory of the University of Hull (U.K.), within the facilities of the Total Environmental Simulator. The flume was a 2 m wide and 11 m long with a longitudinal slope of 0.005 m m^{-1}. At its downstream end, eight traps covering the whole flume width were used to collect the transported sediments. Traps were collected and emptied at variable intervals in order to derive bedload transport rates and grain size. The bulk gravel-sand mixture had the following percentiles: D_{16} = 4.1 mm, D_{50} = 6.4 mm and D_{84} = 13.1 mm. At the beginning of the experiment sediments were screeded flat to the specified bed slope. Only one run was performed with a water discharge of 340 l s^{-1} m^{-1}. Pressure transducers were placed beneath the sediments along the channel centre for measuring the water surface elevation.

The experiment run until the outgoing sediment transport was 1% the initial value. At this moment photographs of the bed surface were taken and after, the grid-by-number approach was used to evaluate the average surface grain size distribution. Bed elevations were also measured along the left wall of the flume.

Numerical method settings

Because there was no armour at the initial state the surface grain size distribution was assumed equal to the bulk sand-gravel mixture. The initial water surface elevation was calibrated against measurements so as to assure similar hydrodynamic conditions in the flume and in the model. The porosity of the mixture was not measured. Instead it was calculated using an empirical formula proposed by Wu and Wang (2006), giving the value λ_p=0.27.

The boundary conditions assumed for the simulations are: a) Fixed downstream water surface elevation; b) Constant upstream incoming water discharge; c) Null sediment supply; and d) Fixed bed elevation at the downstream end. The model was run under the "low-term" configuration.

Several parameters were selected for analyzing the model sensibility (Table 1). They belong to three groups: a) the mesh density represented with the downstream spacing (Δx), b) hydrodynamic parameters including the convergence tolerance (Tol_Q) and the downstream water surface elevation (H_{dw}); and c) sedimentological parameters including the tolerance for bed elevation change (Tol_Z) and bed porosity (λ_p).

Results

During the experiment, the bed experienced a degradation in its upstream end and a progressive bed surface coarsening. An erosion scour formed at the upstream end of the flume. Sediment transport rate reached the highest intensity at the beginning of the experiments (53 gr m^{-1} s^{-1}) and decreased quickly been below 1% of the initial rate after 45 hr.

Two indexes were used to summarize the model performance: abosolute difference (AD) employed for comparing predicted and observed bed elevations (z_{pred} and z_{obs} respectively) and the absolute logarithmic ratio (ALR), in the case of discharges (q):

$$AD = \frac{1}{N}\sum_{i=1}^{N}\left|z_{pred,i} - z_{obs,i}\right| \quad (9)$$

$$ALR = \frac{1}{N}\sum_{i=1}^{N}\left|log\left(\frac{q_{pred,i}}{q_{obs,i}}\right)\right| \quad (10)$$

where in N is the number of observations. The entire numerical runs exhibit the exponential-type tendency observed in the experiment (Figure 2). The grid spacing affects little the predicted outgoing sediment flow, due to similar ALR values (Table 2). Also, low changes are observed when Tol_Q is relaxed (see runs 8, 9 and 10). The model is quite

Table 1. Variation in selected parameters for model sensibility analysis: grid spacing in the downstream direction (x) and across the flume (y); downstream water depth (H_{dw}); tolerance for model convergence (Tol_Q); tolerance for bed elevation change (Tol_z) and bed material porosity (λp).

Run	Δx	Δy	H_{dw}	Tol_Q	Tol_z	λp
W1	0.500	0.125	0.195	1%	2%	0.27
W2	0.250	0.125	0.190	1%	2%	0.27
W3	0.125	0.125	0.185	1%	2%	0.27
W4	0.125	0.125	0.185	1%	5%	0.27
W5	0.125	0.125	0.185	1%	10%	0.27
W6	0.250	0.125	0.200	1%	2%	0.27
W7	0.250	0.125	0.210	1%	2%	0.27
W8	0.125	0.125	0.185	1%	2%	0.34
W9	0.250	0.125	0.190	2%	2%	0.27
W10	0.250	0.125	0.190	5%	2%	0.27

sensitive to changes in the downstream water surface elevation (runs 2, 6 and 7): when the depth is increased the initial transport rate decreases significantly as evident from the reduction in the relative peak discharge (Table 2). The best agreement corresponds to calibrated boundary condition (Run 2). Finally, the change in Tol_z (runs 3, 4 and 5) did not affect the exiting sediment transport.

With regards to the grain size distribution (GSD) of outgoing bed load (Figure 3), all the runs predicted the same distribution. The predicted GSD approximated very well the observed GSD for the lower percentiles (D_{16}, D_{50}, Table 3), i.e., the predicted median diameter was very near the observed mean value. There is a clear discrepancy for the coarser fractions: the predicted percentile 84 % is somewhat lower than observations.

In general, bed was incised not uniformly across the flume (Figure 3), with the deepest sector in the channel centre and almost no erosion at the sidewalls. Erosion was higher at the downstream end in contradiction with observations. Changing the grid spacing, porosity or tolerance Tol_z produced only slight changes. On the contrary, the model was more sensible to changes in boundary conditions. The rise in the downstream water surface elevation (H = 0.19; 0.20 and 0.21 m) reduced the amount of erosion and the final bed profile was progressively at higher levels (note that AD decreases in Table 2 for runs 2, 6 and 7). The model was also sensible to changes in the discharge convergence tolerance (Tol_0, see AD change in runs 8, 9 and 10, in Table 2).

Table 3 also includes representative diameter for the final surface material. With regards to measurements, Figure 5 shows the mean distribution from 10 photographs and it also includes enveloping maximum and minimum curves. It is noted that the predicted grain size distribution is very similar to that measured and is within the aforementioned band. The predicted D_{50} was7.5 mm while the predicted was D_{50} = 8.1 mm.

Discussion

Lican-Leufú predictions have been tested against a flume experiment that involves a change in bed elevation, surface grain size distribution, flow hydraulics and sediment transport as well. Because all these factors are tightly related, the experiment constitutes a good opportunity to assess the model capabilities.

The model was very sensitive to boundary conditions. A slight change of the downstream water surface elevation had an evident effect on the transported sediment flux and final bed elevation because the higher water surface reduced flow velocity and bottom shear stress. Then, as there was a no-linear relation between shear stress and sediment transport, a small reduction in τ was amplified into the transport rate. The higher the water surface elevation, the lower the shear stress, sediment transport and hence, the final bed elevation was higher.

Previous researches have shown that armouring development occurs into two phases: a first phase were bed degrades and then a second phase where the surface coarsens due to selective transport of fine sediments at flows below the threshold for entrainment of larger grain sizes, such that the bed surface is winnowed of the most easily moved fine sediment (Church *et al.*, 1998; Wilcock *et al.*, 2001; Mao *et al.*, 2011). When the static armour layer has developed sediment transport vanishes.

The application of the model shows that during the first phase sediment transport decreases as bed slope reduces (i.e., it is entirely governed by hydraulics). The second phase was also present in the experiment: although the final surface grain size distribution was only slightly coarser than the initial one, an incipient static armour developed. The measured absolute degree of armouring was D_{50}/D_{50ss} = 1.26, while the predicted one was 1.17. This indicates that selective transport took place in the flume. In order to verify this affirmation, fractional rates were calculated using sediment transport rates at the beginning and the end of the experiment. For the initial state, the initial bulk grain size distribution was considered, while the final surface grain size distribution was considered for the final fractional rate. Resulting curves (not showed) showed that at the beginning of the experiment, when there was no armour layer, all the grain fractions were transported (full transport). On the contrary, by the end of the experiment partial transport occurred. Coarse material remained in the bed while fine grains were winnowed.

Table 2. Comparison of model predictions against observations. Sediment transport is compared using the absolute logarithmic ratio (ALR), while med bed elevations are compared with the absolute difference index (AD).

Run	Sediment	Relative	Mean bed trans-
W1	0.25	0.62	0.031
W2	0.26	0.73	0.034
W3	0.27	0.73	0.036
W4	0.28	0.81	0.036
W5	0.28	0.76	0.038
W6	0.23	0.52	0.027
W7	0.26	0.35	0.021
W8	0.24	0.71	0.037
W9	0.24	0.78	0.033
W10	0.26	0.59	0.032

Table 3. Comparison between predicted and observed grain size distributions (GDS) of outlet sediment transport and final surface material.

D16 (mm)	3.0	3.6	4.5	4.1
D50 (mm)	5.4	5.6	7.5	8.1
D84 (mm)	8.0	10.3	16.1	17.7

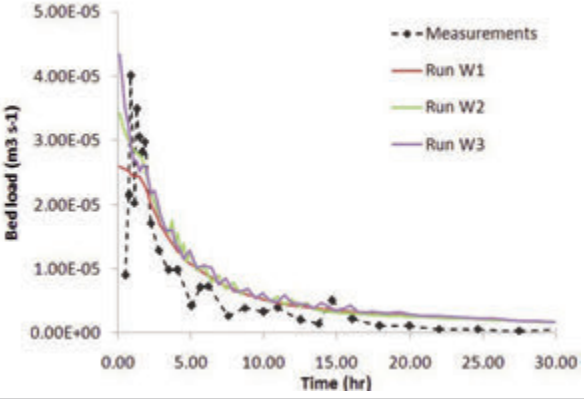

Figure 2. Comparison of predicted and observed outgoing sediment transport. Different curves evidence the sensibility of the mode predictions to changes in grid spacing (runs 1, 2, 3, see Table 1).

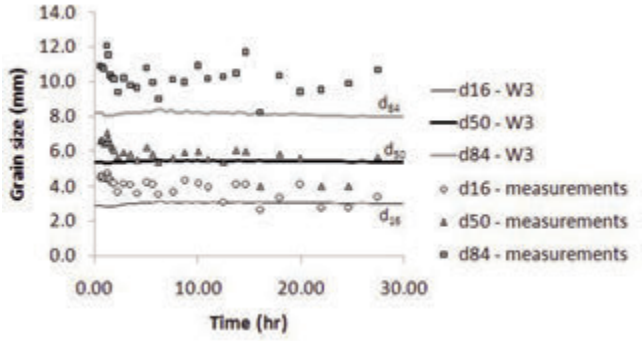

Figure 3. Comparison between predicted and observed bed load grain size. Because all the runs have almost identical values, only results from run 3 are shown.

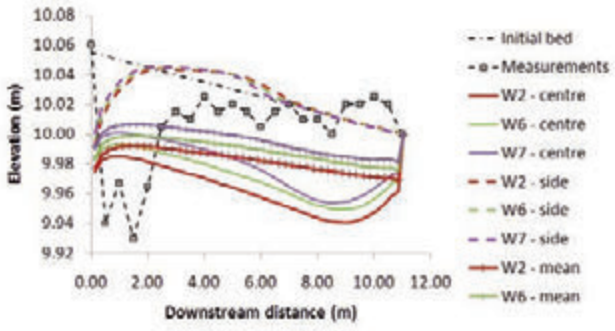

Figure 4. Comparison between observation and prediction for the final bed elevation. Model sensibility has been assessed by changing the downstream water surface elevation (runs 2, 6 and 7, see Table 1).

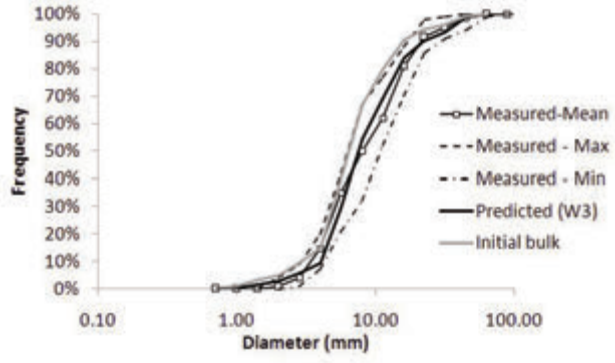

Figure 5. Comparison between predicted and observed final grain size distributions of surface material. Because the observed curve is the result of the analysis of 10 photographs a mean curve is exposed and enveloping curves are also provided.

Conclusions

Overall, Lican-Leufú model proved to perform remarkably well in reproducing the experimental runs because: a) the outgoing sediment flux was correctly predicted in terms of transport rate and calibre; b) final mean bed elevation was very similar to that measured (considering that only near sidewalls elevations were available); and c) the predicted surface grain size distribution was in agreement with observations.

Previous researchers have identified two phases during the development of static armour layers. The application of Lican-Leufú indicates that the interaction between hydraulics and bed degrading was the main factor driving sediment transport and full transport prevailed in the initial phase of the experiment. By the end of the experiment, partial transport occurred due to bed coarsening, coarse material remain in the flume and fine sediments were winnowed.

References

Abad JD, Buscaglia G, Garcia MH. 2D stream hydrodynamic, sediment transport and bed morphology model for engineering applications. Hydrol Process 2008; 22: 1443-59.

Bernard RS. Numerical model for depth-averaged incompressible flow. US Army Corp of Engineers, Waterways Experimental Station, Technical Report REMR-HY-11, 1993.

Church M, Hassan MA, Wolcott JF. Stabilizing self-organized structures in gravel-bed stream channels: Field and experimental observations. Water Resour Res 1998; 34: 3169–79.

Darby SE, Alabyan AD, Van de Wiel MJ. Numerical simulation of bank erosion and channel migration in meandering rivers. Water Resour Res 2002; 38, doi:10.1029/2001WR000602.

Garcia-Martinez R, Espinoza R, Valera E, Gonzalez G. An explicit two-dimensional finite element model to simulate short- and long-term bed evolution in alluvial rivers. J Hydraul Res 2005; 44, 755-66.

Ferguson RI, Parsons DR, Lane SN, Hardy RJ. Flow in meander bends with recirculation at the inner bank. Water Resour Res 2003; 39, 1322, DOI:10.1029/2003WR001965.

Hirano M. River bed degradation with armouring. Proceedings of the Japan Society of Civil Engineering 1971, 55-65.

Jang CL, Shimizu Y. Numerical simulation of relative wide, shallow channels with erodible banks, J Hydraul Eng 2005; 131: 565-75.

Kaless G. Stability analysis of gravel-bed rivers: Comparison between natural rivers and disturbed rivers due to human activities. PhD Diss., Università degli Studi di Padova, Italy, 2013.

Kamphuis JW. Determination of sand roughness for fixed beds. J Hydraul Res 1974; 12: 193–203.

Keulegan GH. Laws of turbulent flow in open channels, National Bureau of Standards Research Paper RP 1151, Washington D.C., 1938.

Leopold LB. Sediment size that determines channel morphology. In Billi P, Hey RD, Thorne CR, Tacconi P, eds. Dynamics of Gravel-bed Rivers. Chichester: John Wiley and Sons; 1992: 297-311.

Li SS, Millar RG. Simulating bed-load transport in a complex gravel-bed river. J Hydraul Eng 2007, 133, Doi:10.1061/(ASCE)0733-9429(2007)133:3(323).

Mao L, Cooper J, Frostick L. Grain size and topographical differences between static and mobile armour layers. Earth Surf Proc Land 2011, DOI:10.1002/esp.2156.

Nagata N, Hosoda T, Muramato Y. Numerical analysis of river channel processes with bank erosion. J Hydraul Eng 2000; 126: 243-52.

Parker G. Surface-based bedload transport relation for gravel rivers, J Hydraul Res 1990, 28: 417–36.

Parker G. Transport of gravel and sediment mixtures. In: Garcia MH, ed. Sedimentation Engineering, Processes, measurements, modelling and practice; ASCE Manuals and Reports on Engineering Practice No. 110, ASCE 2006: 165-251.

Parker G, Sutherland AJ. Fluvial armor. J Hydraul Res 1990; 28: 529-44.

Parker G., Hassan M, Wilcock P. Adjustment of the bed surface size distribution of gravel-bed rivers in response to cycled hydrographs. In: Habersack H, Piegay H, Rinaldi M, eds. Gravel Bed Rivers 6: From process understanding to river restoration, Amsterdam, Elsevier Science 2006: 241-85.

Rodi W. Turbulent models and their applications in hydraulics, A state-of-the-art review, 3rd Edition. IAHR Monograph Series, New York ,Taylor & Francis 1993.

Rozovskii IL. Flow of water in bends of open channels. Translated by Y. Prushansky, Jerusalem Program Sci. Translation, 1961.

Wilcock PR, Kenworthy ST, Crowe J. Experimental study of the transport of mixed sand and gravel. Water Resour Res 2001; 37, 3349-58.

Wilcock PR, Crowe JC. Surface-based transport model for mixed-size sediment, J Hydraul Eng 2003; 129: 120-8.

Wu W, Wang SSY. Formulas for sediment porosity and settling velocity. J Hydraul Eng 2006; 132: 858–62.

Characterization of fluvial islands along three different gravel-bed rivers of North-Eastern Italy

L. Picco,[1] R. Rainato,[1] L. Mao L,[2] F. Delai,[1] A. Tonon,[1] D. Ravazzolo,[1] M.A. Lenzi M[1]
[1]Department of Land, Environment, Agriculture and Forestry, University of Padova, Padova, Italy
[2]Department of Ecosystems and Environment, Pontificia Universidad Catolica de Chile, Santiago, Chile

Abstract

River islands are defined as discrete areas of woodland vegetation located in the riverbed and surrounded by either water-filled channels or exposed gravels, exhibiting some stability and remaining exposed during bank-full flows. Islands are very important from both morphological and ecological points of view, representing the most natural condition of a fluvial system and are strongly influenced by human impacts. This study aims at analyzing the morphological and vegetation characteristics of three different typologies of islands (pioneer, young and stable) in three distinct rivers in the NE of Italy, affected by different intensities of human pressure. The study was conducted on several sub-reaches of the Piave, Brenta and Tagliamento rivers. The first is a gravel-bed river, which suffered intense and multiple human impacts, especially due to dam building and in-channel gravel mining. The same alterations can also be observed in the Brenta river, which also presents bank protections, hydropower schemes and water diversions. On the other hand, the Tagliamento river is a gravel-bed river characterized by a high level of naturality and very low human pressures. The analyses were conducted using aerial photographs and LiDAR data acquired in 2010 in order to define and distinguish the three different island typologies and to obtain a characterization of ground and vegetation features. The results suggest that the fluvial islands lie at different elevations and this fact implies a different resistance capacity during flood events. Pioneer islands and young islands lie at lower elevations than stable islands causing a lower capacity to survive during considerable flood events, in fact in most cases those islands typologies were removed by ordinary floods. Stable islands lie at higher elevations and only intense and infrequent flood events (RI > 10-15 years) are able to determine considerable erosions. Regarding the characteristics of vegetation, we can observe a strong distinction between the three typologies. Stable islands always exhibit the greatest vegetation height and the presence of these plants, sometimes higher than 30 m, contributes to increase the resistance and the stability of these components of fluvial systems.

Correspondence: Lorenzo Picco, Department of Land, Environment, Agriculture and Forestry, University of Padova, Italy.
E-mail: lorenzo.picco@unipd.it

Key words: fluvial island, gravel bed river, piave river, tagliamento river, Brenta river.

Acknowledgements: this research was founded by both the Italian National Research Project 20104 ALME4 -ITSE: "National network for monitoring, modeling and sustainable management of erosion processes in agricultural land and hilly-mountainous area"; and The EU SedAlp Project: "Sediment management in Alpine basis: Integrating sediment continuum, risk mitigation and hydropower", 83-4-3-AT, in the framework of the European Territorial Cooperation Programme Alpine Space 2007-2013.

Journal of Agricultural Engineering 2013; XLIV(s2):e22
doi:10.4081/jae.2013.(s1):e 22

Introduction

River islands are defined as discrete areas of woodland vegetation surrounded by either water -filled channels or exposed gravel (Ward *et al.*, 1999) which exhibit some stability (Osterkamp, 1998) and remain exposed during bankfull flows. Islands have the potential of enhancing the biodiversity within the riparian zone, because their shorelines are characterized by a mosaic of habitat patches of different ages which are uncommon features along heavily managed river banks (Gurnell *et al.*, 2001). Since islands are separated from the floodplain, they may offer a safe refuge for the wildlife from many predators. Arscott *et al.* (2000) found that on the Tagliamento river, the aquatic habitat complexity was greater in the island-braided section if compared to the island-devoid section. In the same river, Van der Nat *et al.* (2003) showed that aquatic habitats were more stable in regions of vegetated islands if compared to bar-braided regions. Stanford *et al.* (1996) showed that islands are most likely to be found in areas of high dynamic fluvial processes that would account for high species diversity within a wide range of riparian habitats. An early classification of straight, braided and meandering channel patterns (Leopold *et al.*, 1964) implicitly incorporates island development through two different processes: a) the evolution of relatively stable medial bars on which vegetation can establish itself within braided channels; b) the isolation of a section of vegetated floodplain through avulsion and cut-off along meandering channels. Kellerhals *et al.* (1976) further discriminated between occasional, frequent, split and braided island patterns. The type of islands present in a riverine system can also help to describe the river processes. Gurnell & Petts (2002) determined that most European rivers were once islands-dominated (pre-1900), but have become devoid of islands due to human interference. Away from areas of agricultural or urban development in Europe, islands remain a common feature of riverine landscapes, such as in the Tagliamento river (Ward *et al.*, 1999). The presence of a certain species of plant on the island can help to determine the flow conditions in the area. Some plant species require specific growth conditions, such as inundation duration, grad ient, and particle size (Picco *et al.*, 2012b).

Nearly all large European rivers are flow-regulated to some degree. This can have implications for fluvial islands development and stability. Dams reduce flood peaks, increase base flow, and store sediments (Kondolf, 1997; Braatne *et al.*, 2003). The sediment transported downstream a dam can be only a fraction of the normal sediment load. The reduced flow peaks downstream eliminate most processes of channel erosion, overbank deposition, and sediment replenishment. This also generally reduces the biologic habitat, diversity, and interactions between biotic and hydrologic processes (Poff *et al.*, 2007). Osterkamp (1998) describes several scenarios in which islands could disappear. Perimeter sediment deposition could eliminate an island by several processes. The first is by preferential in-filling of one of the side channels that effectively raises the bed level in one anabranch but not in the other, and thereby shifts the flow into a single path. The second is by sedimentation around the whole perimeter of the island until it eventually coalesces with other nearby islands or the floodplain, again forcing the flow into a single path. A third method of island elimination occurs when the flow preferentially incises one of the side channels and leaves the other anabranch 'high and dry'. This is common downstream dams after peak flows have been reduced. If a low flow regime persists for long enough, vegetation may accumulate between an island and its floodplain. Floods can eliminate an island by two processes. The first is by simply increasing the flow to levels high enough that the entire island is eroded away. The second is by changing the main direction of the flow during a flood, thereby altering the angle of attack from the water and gradually wearing away the island by abrasion (Wyrick, 2005).

The aim of the present study is to analyze the characteristics of fluvial islands along three gravel-bed rivers affected by different levels of human pressure, as well as to better comprehend the different response to floods and to obtain more information to define more effective flood management programs, precautionary actions and to predict hydraulic hazards.

Study area

The study was conducted along three different sub-reaches of the Brenta, Piave and Tagliamento Rivers (Figure 1).

Brenta river

The Brenta River basin is located in the eastern Italian Alps (Italy) and its course interests Trentino -Alto Adige and Veneto Region (Figure 1). The study reach, called Fontaniva, features a length of around 3 km and it is located downstream in respect to the mountain hydrological basin (1567 km^2) between Bassano del Grappa and Carturo Featuring an average annual precipitation of 1100 mm (spring and autumn are the rainiest seasons), the area presents an intermediate position between the piedmont and the floodplain. The dominant morphology of the reach is braided; the width is around 800 m and the average slope is 0.003, it flows being divided in several channels which contribute to form many fluvial islands (braided pattern). The Brenta river is characterized by the presence, all over its basin, of dams, hydrological derivations and embankments. It is possible define the Brenta river as a strong affected river by human pressures.

Piave river

The Piave River rises at an elevation of 2037 m.a.s.l. and has a length of 222 km. It flows from its source in the Dolomites to the Adriatic Sea. The drainage basin is composed mainly of sedimentary rocks (predominantly limestone and dolomite) and has an area of 4500 km^2. The study reach (Figure 1) is around 3 km long and is located along the middle course of the Piave River, within the mountain district. The average valley gradient is about 0.004 m m^{-1} and the channel width ranges from 100 m to 1000 m. The study reach may be described as transitional between wandering and braided morphology.

Tagliamento river

The Tagliamento River is located in the southern Alps of North-Eastern Italy. It originates at 1195 m a.s.l. and flows for 178 km to the northern Adriatic Sea, thereby forming a link corridor between the Alpine and the Mediterranean zones. Its drainage basin covers 2871 km^2 (Figure 1). The hydraulic regime of the Tagliamento River is characterized by irregular discharges and high sedimentation load, due to the climatic and geological conditions of the upstream portion of the basin. The river is considered as the last morphologically intact river in the Alps, and therefore constitutes an invaluable resource. In fact the extensive vegetated islands and gravel bars are key indicators of its natural conditions, while engineering works for flood control or navigation have eliminated such features in most European water courses.

Materials and Methods

The analyses were conducted on a single dataset relating to 2010 for each river under consideration. Aerial photographs and LiDAR data were used. Aerial photographs were rectified and co-registered to a common mapping base at 1:5.000 by a GIS software (*Esri ArcGIS 9.2*). Approximately 30 ground-control points were used to rectify each single frame and a second order polynomial transformations were then applied. The active channel area and width were defined using the different aerial photographs and correspond to the area of water and unvegetated sediment bars.

Assuming the conceptual model of island dynamics proposed by Edwards *et al.* (1999), vegetated bars and pioneer islands were classified as distinct morphological units, the latter being areas with vegetation higher than 3 m. Pioneer, young and stable islands were distinguished based on the maturity and size of the vegetation (Kollman *et al.*, 1999). In the aerial photos, distinction between arboreal and shrubby vegetation was made by estimating vegetation height based on canopy texture, shape and shadows. Pioneer islands were defined as surfaces on bars with patchy vegetation covered with spots of vegetation 3-5 m high. Young islands were distinguished because of the higher extension and dimensions, whereas stable islands were defined as older (15-20 years) areas with a high dense vegetation cover (Gurnell & Petts, 2002). Canopy height derived from the LiDAR was used to complement the aerial photographs (Zanoni *et al.*, 2008). One airborne LiDAR flight for each river, carried out in August allowed us to analyze the vertical characteristics of the ground and vegetation of the islands. Point density of 2-3/m^2 was reached after filtration. Digital Terrain Model (DTM) and Digital Surface Model (DSM) were created at 0.5 m resolution for each river. Based on the 0.5 m LiDAR resolution, the raster subtraction of the original DTM layer and the DSM layer generated the Canopy Height Model (CHM), which was used to obtain the maximum elevation of island ground and the maximum height of the island vegetation (Picco, 2010). analyzed reaches related to the active channel extension. It is possible to observe as the Brenta reach and the Tagliamento reach show similar differences, with much greater stable island sizes than the other two typologies, while along the Piave reach there is a less clear distinction between the sizes of the three different island typologies. It is rather interesting to see as, looking at the values reported in the graphs, there is a strong difference between the exten-

sion of the islands related to the active channel area along the Brenta sub-reach than the other two rivers, in fact, for example, the median value for the stable islands is around 0.025 along the Brenta river and around 0.001 and 0.005 along the Piave river and Tagliamento river, respectively.

In Figure 3 are reported the characteristics of the ground elevation and the vegetation height of the Brenta river s ub- reach islands. We can observe a clear distinction in both the analyzed characteristics, with a significant distinction in the median values reported.

In Figure 4 are reported the characteristics of the ground elevation and the vegetation height on the Belluno reach islands. A lower difference, in respect to the Brenta river reach, between the ground elevation of the three different fluvial island typologies can be highlighted. In fact, there is only a difference between the median values of about 0.5 m, while in the Fontaniva reach that value rises until around 1.3 m. Looking at the vegetation height, it is possible to observe a clear distinction between the Piave and the Brenta river reaches, with a consistent decrease in the median values all over the three island typologies under consideration.

Finally, looking at the Cornino reach (Figure 5), it is possible to observe as, also in this case, there is a lower difference between the ground values in respect with those registered along the Brenta river. It is also interesting to see as, along the Taglimento river, some vegetated patches that could be classified as islands can rise into some hollows.

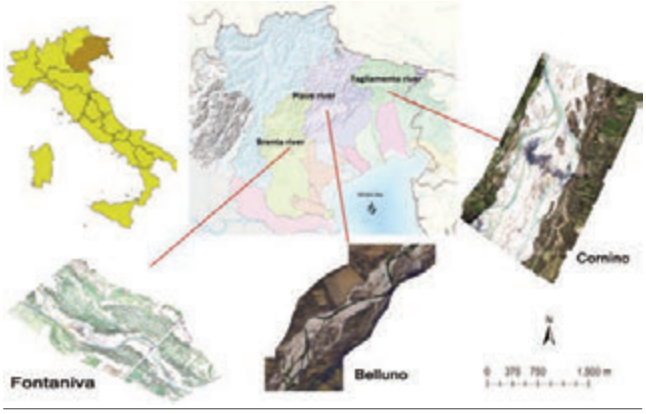

Figure 1. The study areas are located in the North-Eastern Italy, from west to east it is possible to see the Brenta river sub-reach called Fontaniva (on the bottom left), the Piave river sub-reach called Belluno (on the bottom middle) and the Tagliamento river sub-reach called Cornino (on the right). Flow direction is always from top to down.

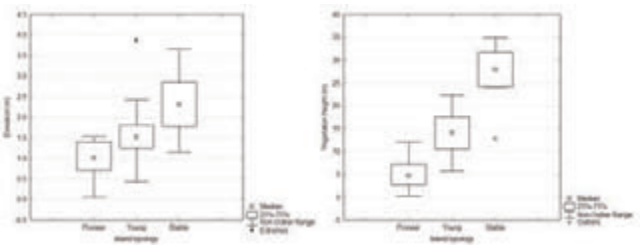

Figure 3. Maximum ground elevation of the Fontaniva sub-reach islands (on the left) and maximum vegetation height (on the right).

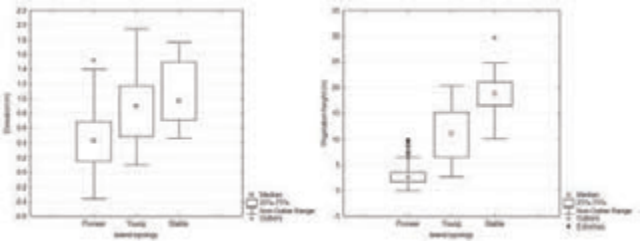

Figure 4. Maximum ground elevation of the Belluno sub-reach islands (on the left) and maximum vegetation height (on the right).

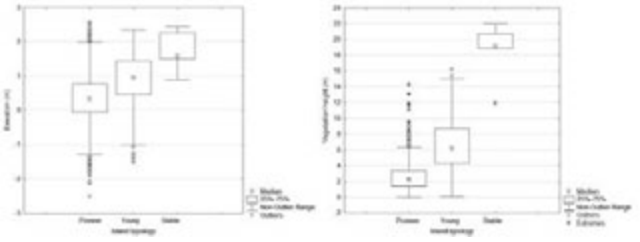

Figure 5. Maximum ground elevation of the Cornino sub-reach islands (on the left) and maximum vegetation height (on the right).

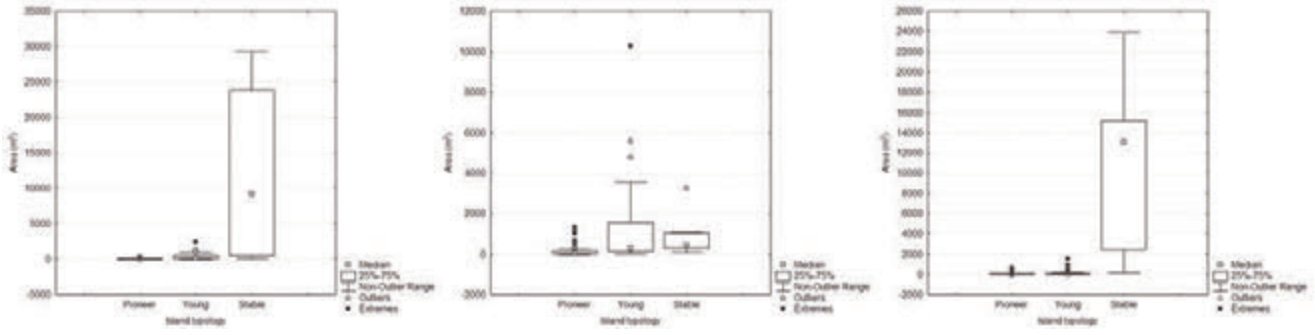

Figure 2. Variation in island size related to the active channel area along the Brenta river (on the left), the Piave river (in the middle) and the Tagliamento river (on the right).

Discussion and Conclusions

The analysis here presented allowed us to better understand how and how much the islands can be affected by the surrounded environment. The results, in fact, show consistent differences between the three analyzed river systems. Taking into account the different human impact intensity all over the basins and along the fluvial corridor it is possible to connect the differences in size and cover, ground elevation and vegetation height of the fluvial islands with the human activities overall. In fact, the systems under consideration are theoretically comparable by the morphological, biogeographical and hydrological point of view, but these systems are affected in very different manners by human activities.

Looking at the higher cover of fluvial islands along the Brenta reach, this phenomenon is probably due to the high level of embankments that do not permit a constant sediment recruitment from the banks with consequent channel narrowing processes that allow an easier vegetation stabilization over the higher bars that are not disturbed periodically by the floods. On the other hand, along the Tagliamento river there is a higher difference between the sizes of the stable islands and the other two typologies, this is probably due to the fact thatonly the more stable islands are able to resist to the very common flood events that could happen different times per year moving huge volumes of sediments (Picco *et al.*, submitted). These observations matched with those made by different authors (Bertoldi *et al.*, 2009; Comiti *et al.*, 2011; Picco *et al.,* 2012a) wherein the island dynamics were found to be strictly associated to the occurrence of major floods (RI > 10-15 years), which are the only ones able to generate substantial island erosions.

Thanks to the LiDAR data was possible to analyze important morphometric characteristics of the different typologies of islands. As expected, stable islands lie at higher elevation. This is due to the fact that older vegetation growing on stable islands allows the deposition of fine sediments which, in turns, enhances the conditions for vegetation growth, providing even better circumstances for the vegetation to establish on stable islands (Picco *et al.*, 2012a). The flood control (by dams) and the sediment recruitment control (by embankments), can be the factors by which dependsalso the lower difference in the ground elevation between the three island typologies along the Cornino reach, than the higher difference that is registered along the strongly affected Brenta river. In fact, a more active environment permits a mixed distribution of channels, bars and islands that, ultimately, maintain similar morphological characteristics all over the active channel do not allowing the narrowing processes seen along the Brenta river. This higher stability of the stable islands along the Fontaniva reach is, also, reflected by the very high vegetation that composes this island typology, in respect of the lower maximum height observed along the two more natural rivers under consideration.

This important analysis can be carried out with the simple detection starting from aerial photographs. This kind of analysis can be helpful also to predict the hydraulic hazard linked to the morphological changes and to formulate more effective flood management programs. Analyzing the island characteristics it is possible to observe how the fluvial system is stable, permitting to predict the potential increase in hydraulic hazards depending on the conditions and expansion of perifluvial vegetation and fluvial islands. Using LiDAR data it is possible to predict the LW characteristics, dimensions and volumes that could be moved downstream during floods in case of island erosion processes, permitting to localize areas of storage or areas that can be affected by the direct impact of LW (eg. bridges, check dams, bank protections); on the other hand it is possible to define the potential volume of sediment that can be released during island erosion. All this important information can be really useful to better define flood management programs and precautionary action such as, for example, the removal of the biggest trees from the islands located close to critical sections.

References

Arscott, D.B., Tockner K. and Ward J.V., 2000. Aquatic habitat diversity along the corridor of an Alpine floodplain river (Fiume Tagliamento, Italy), Archiv für Hydrobiologie, 149, 679-704.

Bertoldi W., Zanoni L., Tubino M., 2009. Planform dynamics of braided streams. Earth Surfaces Processes and Landforms 34, 547-557.

Braatne J.H., Rood S.B., Simons R.K., Gom L.A. and Canali G.E., 2003. Ecology of riparian vegetation of the Hells Canyon corridor of the Snake River: field data, analysis and modeling of plantresponses to inundation and regulated flows. Technical Report Appendix E. 3. 3-3. Idaho Power Company. Boise, Idaho, USA.

Comiti F., Da Canal M., Surian N., Mao L., Picco L., Lenzi M. A., 2011. Channel adjustments and vegetation cover dynamics in a large gravel bed river over the last 200 years. Geomorphology 125, 147-159.

Edwards, P.J., Kollman J., Gurnell A., Petts G.E., Tockner K. and Ward J.V., 1999. A conceptual model of vegetation dynamics on gravel bars of a large alpine river. Wetlands Ecology and Management, 7,141–153.

Gurnell A.M., Petts G.E., Hannah D.M., Smith B.P.G., Edwards P.J., Kollmann J., Ward J.V. and Tockner K., 2001. Riparian vegetation and island formation along the gravel-bed Fiume Tagliamento, Italy. Earth Surf. Processes and Landforms, 26, 31-62.

Gurnell A.M. and Petts G.E., 2002. Island-dominated landscapes of large floodplain rivers, a European perspective. Freshwater Biology, 47, 581-600.

Kellershals R., Asce M., Church M. and Bray D.I., 1976. Classification and Analysis of River Processes. Journal of the Hydraulics Division, July, 1976.

Kondolf G.M., 1997. Hungry water: effects of dams and gravel mining on river channels. Environ. Mgmt, 21 4, 533-551.

Leopold L.B., Wolman M.G. and Miller J.P., 1964. Fluvial processes in Geomorphology. Freeman; San Francisco, USA.

Osterkamp W.R., 1998. Processes of fluvial island formation, with examples from Plum Creek, Colorado and Snake River, Idaho. Wetlands, 18, 530-545.

Picco L., 2010. Long period morphological dynamics in regulated braided gravel-bed rivers: comparision between Piave River (Italy) and Waitaki River (New Zealand), PhD thesis, University of Padova, 190 p.

Picco L., Mao L., Rigon E., Moretto J., Ravazzolo D., Delai F. and Lenzi M.A., 2012a. Medium term fluvial island evolution in relation with flood events in the Piave River. WIT Transactions on Engineering Sciences, Vol.73, 161 -172, ISSN: 1743-3553 (on-line). doi: 10.2495/DEB120141.

Picco L., Mao L., Rigon E., Moretto J., Ravazzolo D., Delai F. and Lenzi M.A., 2012b. Riparian forest structure, vegetation cover and floods events in the Piave River (Northeast of Italy). WIT Transactions on Engineering Sciences, Vol 73, 161-172, ISSN 1743-3533 (on-line). doi:10.2495/DEB120141.

Picco L., Mao L., Cavalli M., Buzzi E., Rainato R., Lenzi M.A., (submitted). Evaluating short-term morphological changes in a gravel-bed braided river using Terrestrial Laser Scanner. Geomorphology.

Poff, N.L., Olden J.D., Merritt D.M. and Pepin D.M., 2007. Homogenization of regional river dynamics by dams and global biodiversity implications. Proceedings of the National Academy of Sciences, 104,5732–5737.

Stanford, J.A., Ward J.V., Liss W.J., Frissell C.A., Williams R.N., Lichatowich J.A. and Coutant C.C., 1996. A general protocol for restoration of regulated rivers, Regulated Rivers: Research & Management, 12, 391-413.

Van der Nat, D., Tockner K., Edwards P.J., Ward J.V. and Gurnell A.M., 2003. Habitat change in braided flood plains (Tagliamento, NE-Italy), Freshwater Biology, 48, 1799- 18 12.

Ward J.V., Tockner K., Edwards P.J., Kollmann J., Bretschko G., Gurnell A.M., Petts G.E. and Rossaro B., 1999. A reference river system for the alps: the Fiume Tagliamento. Regulated rivers: Research & Management, 15, 63-75.

Wyrick J.R., 2005. On the formation of fluvial islands. PhD Thesis, Oregon State University, USA. 302 p.

Zanoni L., Gurnell A., Drake N. and Surian N., 2008. Island dynamics in a braided river from analysis of historical maps and air photographs. River Research and Applications, 24, 1141-1159.

Evaluation of short-term geomorphic changes in differently impacted gravel-bed rivers using improved dems of difference

F. Delai,[1] J. Moretto,[1] L. Mao,[2] L. Picco,[1] M.A. Lenzi[1]

[1]Department of Land, Environment, Agriculture and Forestry, University of Padova, Padova, Italy
[2]Department of Ecosystems and Environment, Pontificia Universidad Catolica de Chile, Santiago, Chile

Abstract

The evaluation of the morphological dynamics of rivers is increasingly focusing, in recent years, on the achievement of quantitative estimates of change in order to identify geomorphic trends and forecast targeted restoration actions. Thanks to the development of more effective and reliable survey technologies, more accurate Digital Elevation Models (DEM) can be produced and, through their consequent differencing (DoD), extremely useful geomorphic analyses can be carried out. In this situation, a major role is played by uncertainty, especially in the final volumetric rates of erosion and deposition processes, that may lead to misinterpretation of spatial and temporal changes. This paper aims at achieving precise geomorphic estimates derived from subsequent hybrid (LiDAR and bathymetric points) surface representations. The study areas consist of gravel-bed reaches of two differently impacted fluvial environments, Piave and Tagliamento rivers, that were affected by two severe flood events (Piave, R.I. of 7 and 10 years and Tagliamento, R.I. of 15 and 12 years) in the inter-surveys period. The basic Hybrid Digital Elevation Models (HDTM) were processed accounting for spatially variable uncertainty and considering, beside slope and point density input variables, a novel component measuring the quality of the bathymetric derived points. In fact, since the major changes occur within river channels, the integration of this variable evaluating the precision of the bathymetric channel elevations in the HDTMs, has allowed, through the creation of targeted FIS (Fuzzy Inference System) rules, to obtain reliable geomorphic estimates of change. Volumes and erosion and deposition patterns were then analyzed and compared to outline the different dynamics among the sub-reaches and the two river systems.

Correspondence: Fabio Delai, Department of Land, Environment, Agriculture and Forestry, University of Padova, Italy.
E-mail: fabio.delai@studenti.unipd.it

Key words: DoD, geomorphic changes, gravel bed braided river, LiDAR, Piave River, Tagliamento River.

Acknowledgements: this research was founded by the University of Padua Strategic Research Project PRST08001, "GEORISKS, Geological, morphological and hydrological processes: monitoring, modelling and impact in North-Eastern Italy", Research Unit STPD08RWBY-004; the Italian National Research Project PRIN20104ALME4-ITSedErosion: "National network for monitoring, modeling and sustainable management of erosion processes in agricultural land and hilly-mountainous area"; and The EU SedAlp Project: "Sediment management in Alpine basis: Integrating sediment continuum, risk mitigation and hydropower", 83-4-3-AT, in the framework of the European Territorial Cooperation Programme Alpine Space 2007-2013.

Journal of Agricultural Engineering 2013; XLIV(s2):e23
doi:10.4081/jae.2013.(s1):e23

Introduction

The estimation of close-to-real rates of geomorphic changes has become a major issue of river geomorphology in the recent years. Beside qualitative evaluations, the achievement of reliable amounts of erosion and deposition processes represents a great help for identifying the current state of a river environment and plan future management actions. The advances in the different survey technology methods, such as total stations (Fuller *et al.*, 2005), dGPS (Brasington *et al.*, 2003), aerial LiDAR (Devereux and Amable, 2009) and TLS (Milan *et al.*, 2007; Heritage and Milan, 2009), have allowed a quicker acquisition of topographic data over larger extents and with very fine resolutions (Marcus and Fondstad, 2008; Notebaert *et al.*, 2008). Thanks to the development of GIS tools capable to process large datasets, the interpolation of Digital Elevation Models (DTMs) has become the most common procedure to represent and analyze topographic surfaces (Milan *et al.*, 2011). A problem in the reproduction of river environments is featured by the representation of wet areas where, normally, the most significant scour and fill processes take place. Without the use of bathymetric sensors (*i.e.* bathymetric LiDAR), technologies still characterized by high costs, scarce data quality and relatively rough resolutions (Hilldale and Raff, 2008), the representation of river channels results limiting, since signals undergo absorption by water. To solve these problems, a cost-effective detection method for wet areas can be the calibration of depth-reflectance relationships, using grey-scale, colour-scale and multispectral imagery, even considering that they need depth points from a contemporary field survey (Moretto *et al.*, 2012). After achieving precise DEMs, their difference can produce reliable Dems of Difference (DoDs) where scour and fill areas and volumes can be analyzed (Lane *et al.*, 2003). In all this process, a decisive role is played by uncertainty that in wet areas often exceeds the real change (Wheaton *et al.*, 2010). A novel reliable approach introduced by Wheaton *et al.* (2010) and packaged in a wizard-driven Matlab software application (Geomorphic Change Detection), presents a robust and spatially variable estimation of DEM uncertainty in order to achieve precise rates of geomorphic changes. The cell-by-cell use of a Fuzzy Inference System (FIS) to obtain a spatially variable elevation uncertainty and the modification of the resulting sediment budget on

the basis of probabilistic spatial coherence of erosion and deposition units are the key innovations of this method (Wheaton *et al.*, 2010).

In the present work we aim at performing and interpreting accurate and reliable estimates of short-term geomorphic changes of study reaches of two differently impacted gravel-bed rivers of North-Eastern Italy: Piave and Tagliamento rivers. Starting from hybrid DTMs (Moretto *et al.*, 2012) derived by integrating LiDAR and colour bathymetry data sources, precise DoDs showing scour and fill estimates will be produced using the Geomorphic Change Detection (GCD) software (Wheaton *et al.*, 2010). The two novel methodological aspects regard: first, the use of hybrid DTMs in a the GCD environment and, second, the creation of an "ad hoc" FIS script where, beside the commonly used slope and point density inputs, a third factor evaluating the accuracy of the bathymetric points (derived using the Moretto *et al.* 2012 method) used to represent in-channel areas (zones normally featuring the greatest changes) will be presented.

Study areas

Piave river

The Piave River basin (drainage area 3900 km^2) lies in the Eastern Italian Alps. The main channel flows in the south direction for 220 km from its headwaters to the outlet in the Adriatic Sea, near to Venice. The analyzed portion of the Piave river is located in its middle course and features an average annual precipitation of about 1350 mm and a very wide gravel bed, characterized by a multithread channel pattern. Two study sub-reaches that have been selected are (drainage area until the Belluno station equal to 1965 km^2; Figure 1): Belluno featuring a length of about 2.2 km and Praloran with a length of 3.2 km. Their morphology is dominated by braided and wandering channel patterns, the slope is around 0.45%, and the D_{50} ranges between 20 and 50 mm (Comiti *et al.*, 2011; Kaless *et al.*, 2013).

The Piave river has suffered intense and multiple human impacts which reached their peak between the 1960s and the 1990s with heavy gravel mining activities (Comiti *et al.*,2011).

Tagliamento river

The Tagliamento river is a natural gravel-bed river, located in the North-Eastern Italy. It originates at 1195 m a.s.l. and flows for 178 km from the Alps to the northern Adriatic Sea, thereby forming a link corridor between the Alpine and the Mediterranean zones. Its catchment covers 2871 km^2. It is considered one of the most natural European river environments and its basin is located in one of the wettest areas of Europe, where the annual precipitation can reach 3100 mm per year. The two study sub-reaches (Figure 2) are located in the piedmont area of the river where the prevalent morphology is braided and the average D50 is equal to 36 mm (Mao *et al.*, in preparation). The first one, Cornino, features a length of 3 km while the second, Flagogna, a length of 3.5 km (Picco *et al.*, submitted).

Materials and methods

The survey analyses consist in three different data sources acquired before and after the severe flood events (Fig. 3) occurred in November-December 2010 (Piave, R.I. of 7 and 10 years and Tagliamento, R.I. of 15 and 12 years): LiDAR, dGPS and aerial photos. LiDAR and aerial photo captures were performed in August 2010 (for both rivers) and in February 2011 (for the Piave river) and April 2011 (for the Tagliamento river) by Blom GCR SpA using an OPTECH ALTM Gemini Sensor (flight height ~ 850 m). The data acquisition was carried out with the best weather and low water level conditions and the LiDAR points were filtered from vegetation using the Terrascan software (Terrasolid). The point density was commissioned in function of the required DTM resolution (0.5 m cell-size) accounting for at least two ground points per m^2 and the average vertical error was estimated through dGPS points comparison in the final surface models. LiDAR acquisition was associated with a series of RGB aerial images featuring 0.15 m of pixel resolution. Finally, dGPS points were taken contemporary, covering different morphological units and water stages. Totally, 537 dGPS points in 2010 and 4006 dGPS points in 2011 for the Piave river and 1107 dGPS points in 2010 and 9366 dGPS points in 2011 for the Tagliamento river were surveyed (dGPS average vertical error ± 0.025 m).

Through the Moretto *et al.* (2012) method that derives water depths by calibrating a regression model between the Z-detrended dGPS coordinate and the photo colour bands (Red, Green and Blue), bathymetric points for the wet areas and LiDAR filtered points for the dry areas were integrated to build accurate hybrid DTMs (for 2010 and 2011).

Figure 1. The Piave river basin and (below) the two study sub-reaches, Belluno and Praloran.

Preparation of Fuzzy Inference System (FIS) variables and rules

In Matlab environment (Fuzzy Logic application) an "ad hoc" FIS file considering as inputs slope, point density and bathymetric points quality and as output elevation uncertainty was edited. Slope and point density categorical limits (*i.e.* low, medium, high) were chosen taking into consideration the literature values (Wheaton *et al.*, 2010) and our fluvial environments (gravel-bed rivers) and related field experience. The third input variable, the bathymetric points quality, represents an innovation inasmuch the colour bathymetry derived points (Moretto *et al.*, 2012) that were used to interpolate the wet areas of the DTMs were also evaluated in their accuracy. The achievement of reliable final geomorphic estimates considering the precision of in-channel depths was here considered as fundamental since the most significant scour and fill processes occur in the wet areas. For this input variable, we needed to consider only in-channel elevations so that, beside the common low, medium and high categories, a fourth "out channel" category including all the points elevation of the dry areas was added. The categorical limits of this bathymetric accuracy input feature small differences among the considered years and rivers (Table 1) depending on the number of dGPS points used to calibrate the model (Moretto *et al.*, 2012). All the categorical limit values of this input variable were increased by 10 in order to avoid problems of having negative and "crossing-zero" values in the Fuzzy Logic application. Finally, 36 FIS rules were edited, setting the output qualities of the elevation uncertainty according to Wheaton *et al.* (2010) as low, average, high and extreme. For details on the FIS logic and procedure we refer to Wheaton *et al.* (2010).

Preparation of the associated input DTMs

In ArcGIS 10.0 (ESRI) environment the three DTMs associated to the input variables (slope, point density and bathymetric points quality) were then created for each sub-reach and year (2010 and 2011) using, as basis source, the hybrid DTMs. The slope and point density DTM were interpolated using the correspondent ArcGIS tools. Concerning the "bathymetric points quality" DTM, a surface interpolating in the wet areas the points (increased by 10) derived by the Moretto *et al.* (2012) procedure and in the dry areas a unique value of 11 m to include all the outer channel surface was finally built.

Final DoD production using the GCD software

At this point, the basic hybrid DTMs, the FIS files ("Piave", "Tagliamento 2010" and "Tagliamento 2011" differing only in the class limits of the input variable "bathymetric points quality") and the associated input DTMs (slope, point density and bathymetric points quality) were ready to be run in the Geomorphic Change Detection 5.0 (GCD) software (Wheaton *et al.*, 2010; http://gcd.joewheaton.org). Through the creation of associated uncertainty surfaces derived by the combination of the input DTMs and FIS rules, the basic hybrid DTMs and the error rasters were differenced producing reliable DoDs. Geomorphic changes were calculated, following literature (Wheaton *et al.*, 2010), by using a spatially variable uncertainty thresholded at 95% C.I. and the Bayesian updating method which accounts for spatial coherent erosion and deposition units (5×5 mobile windows). For details on the GCD software we refer to Wheaton *et al.* (2010).

Results

The main results of the study concern the production of precise DoDs and consequent change estimates accounting for uncertainty by

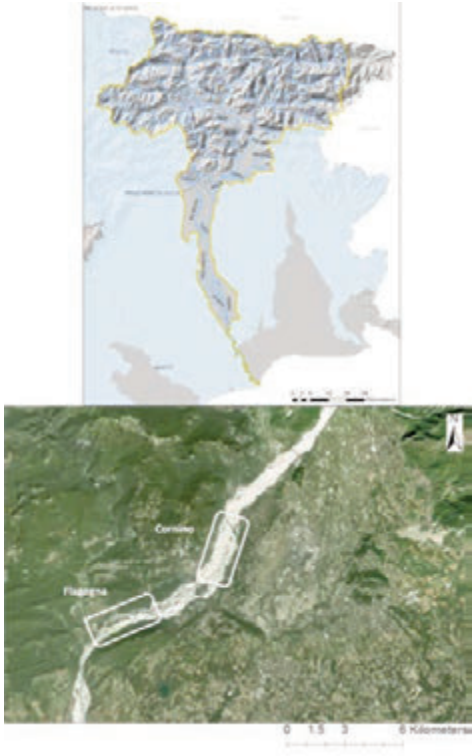

Figure 2. The Tagliamento river basin and (below) the two study sub-reaches, Cornino and Flagogna.

Figure 3. Belluno sub-reach (Piave river) during the flood events of November-December 2010.

Table 1. Original categories and limits used to describe in the FIS file the novel input variable: bathymetric points quality.

	Piave				Tagliamento 2010				Tagliamento 2011			
Low	-3	-3	-1.4	-1.3	-3	-3	-0.8	-0.7	-3	-3	-1.5	-1.4
High	-1.4	-1.3	-0.3	-0.2	-0.8	-0.7	-0.25	-0.15	-1.5	-1.4	-0.3	-0.2
Medium	-0.3	-0.2	0.25	0.3	-0.25	-0.15	0.25	0.3	-0.3	-0.2	0.25	0.3
Out Channel	0.25	0.3	1	1	0.25	0.3	1	1	0.25	0.3	1	1

using an innovative multi-input GCD analysis. In Figure 4 we can observe the DoDs of Belluno and Praloran sub-reaches (Piave river). In both models, a first visual inspection underlines a fluid representation of erosion and deposition dynamics, especially in the wet channels that are the areas featuring the major variations. The use of the novel input variable evaluating the precision of the bathymetric derived elevation points seems to help to better define the underwater zones contributing to more reliable scour and fill estimates. The parts of the DoD maps featuring no colors represent either areas where no change has occurred or areas with a too high uncertainty. Even though an accurate filtering process deleting the vegetation interference were carried out in the first phases of data management (using Terrascan software), possible errors due to the residual presence of misleading elevations should be taken into account. Considering the volumetric estimates, as we can observe in Table 2, a comparison between the raw and the spatially-variable thresholded volumes is presented. The estimates obtained using the GCD analysis, improved with the bathymetric quality evaluation input, result more conservative and provided with an accurate uncertainty quantification. In both sub-reaches net erosion has considerably prevailed as a consequence of the flood events of November-December 2010 with an associated error calculation that in Praloran overtakes the estimate of plausible change.

In the case of the Tagliamento river, the DoDs of Cornino and Flagogna sub-reaches (Figure 5) represent, similarly to those of the Piave river, very precisely the geomorphic changes occurred after the 2010 flood events. The alternation of scour and fill areas results very fluid producing a reliable basis for volumetric change estimates. In Table 3 raw and thresholded volumes of erosion and deposition processes and the consequent sediment storage are reported, confirming the conservative output of the GCD analysis accounting for the novel bathymetric quality evaluation. In the first sub-reach, Cornino, net erosion significantly prevails while in Flagogna sub-reach a final difference indicating a predominant deposition is present. Noteworthy is the comparison of the sediment volumes mobilized by the two rivers: the Tagliamento features a significantly higher order of magnitude in respect to the Piave.

Discussion

The detection and quantification of the geomorphic changes occurred as a consequence of the 2010 flood events by using an improved GCD analysis have shown precise and meaningful results. The use of "basis" hybrid DTMs (LiDAR and colour bathymetry derived) and the creation of an *ad hoc* FIS file including an innovative input that evaluates the accuracy of the wet channel points derived by colour bathymetry (Moretto *et al.*, 2012) have contributed to improve the reliability of the volumetric estimates. In fact, considering the precision of

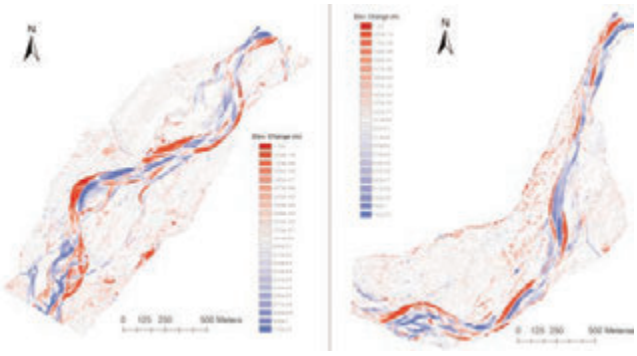

Figure 4. DoDs of Belluno and Praloran sub-reaches (Piave river) obtained using the improved GCD analysis.

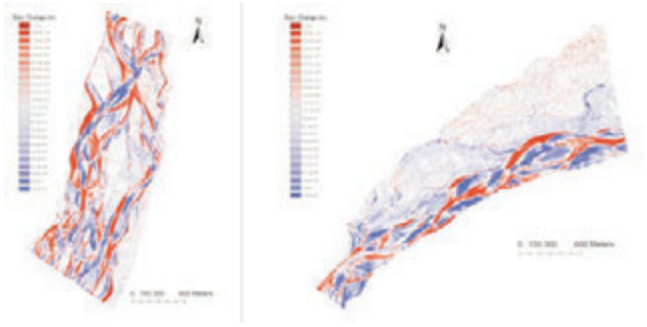

Figure 5. DoDs of Cornino and Flagogna sub-reaches (Tagliamento river) obtained using the improved GCD analysis.

Table 2. Raw and thresholded volumes of geomorphic changes accounting for uncertainty for the Piave river.

	Belluno sub-reach			Praloran sub-reach		
	Raw	Thresholded DoD Estimate ± Error Volume	% Error	Raw	Thresholded DoD Estimate ± Error Volume	% Error
Total Volume of Erosion (m^3)	216.365	198.040±50.527	26%	231.035	206.460±73.205	35%
Total Volume of Deposition (m^3)	127.570	114.112±19.820	17%	158.440	139.511±28.804	21%
Total Net Volume Difference (m^3)	-88.795	-83.927±54.276	-65%	-72.595	-66.949±78.668	-118%

Table 3. Raw and thresholded volumes of geomorphic changes accounting for uncertainty for the Tagliamento river.

	Cornino sub-reach			Flagogna sub-reach		
	Raw	Thresholded DoD Estimate ± Error Volume	% Error	Raw	Thresholded DoD Estimate ± Error Volume	% Error
Total Volume of Erosion (m^3)	767.006	744.173±89.317	12%	440.610	415.077±72.787	18%
Total Volume of Deposition (m^3)	523.068	503.779±61.277	12%	564.462	538.138±85.722	16%
Total Net Volume Difference (m^3)	-243.938	-240.394±108.316	-45%	123.852	123.061±112.456	91%

the representation of the wet channel landforms, a volumetric rate closer to the real change can be achieved. The spatially variable assessment of the uncertainty through the production of error surfaces by combining the associated input DTMs (slope, point density and bathymetric points quality) regulated by the FIS rules has finally allowed to recover some information normally below the chosen uniform $_{min}$LoD (minimum Level of Detection). The use of the probabilistic Bayesian updating for identifying coherent units of erosion and deposition (using the contiguity index) has also helped to recuperate low magnitude volumes of change. Even though the present study represents a very accurate and reliable attempt of geomorphic change estimation, further improvements could be carried out to reduce possible sources of error such as, in this case, small areas of vegetation interference.

Concerning the resulting sediment budget, we can observe a common deficit of sediment in the two sub-reaches of the Piave river, whereas in the Tagliamento river the situation seems to be more equilibrated with erosion dominating the budget in the first sub-reach and deposition in the second. In this sense, future management strategies accounting for the achievement of a sediment continuum should be though, especially for the Piave river, to re-establish a dynamic equilibrium in the fluvial environment.

Conclusions

The recent investigation of river dynamics relies always more on quantitative amounts of change to analyze the present condition of fluvial environments and choose the more effective restoration actions. The detection of the short-term geomorphic variations occurred as a consequence of the 2010 flood events through the proposed improved GCD analysis (evaluating also the bathymetric points quality) has demonstrated to be a reliable method to achieve precise volumetric estimates. These erosion and deposition trends can thus represent a trustworthy basis on which effective restoration measures can be undertaken.

References

Brasington J., Langham J., Rumsby B.T. 2003. Methodological sensitivity of morphometric estimates of coarse fluvial sediment transport. Geomorphology. 53: 299–316.

Comiti F., Da Canal M., Surian N., Mao L., Picco L., Lenzi M.A. 2011. Channel adjustments and vegetation cover dynamics in a large gravel bed river over the last 200 years. Geomorphology. 125: 147 – 159.

Devereux B., Amable G. 2009. Airborne LiDAR: instrumentation, data acquisition and handling. In: G.L. Heritage, A.R.G Large (ed.) Laser Scanning for the Environmental Sciences. Wiley-Blackwell, Chichester, UK.

Fuller I.C., Large A.R.G., Heritage G.L., Milan D.J., Charlton M.E. 2005. 35. Derivation of reach-scale sediment transfers in the River Coquet, Northumberland, UK. In: M. Blum, S. Marriott, S. Leclair (ed.) Fluvial sedimentology VII. : International Association of Sedimentologists Special Publ. N. 35, Wiley-Blackwell, Chichester, UK, pp 61–74.

Heritage G.L., Milan D.J. 2009. Terrestrial laser scanning of grain roughness in a gravel-bed river. Geomorphology. 113: 4 -11.

Hilldale R.C., Raff D. 2008. Assessing the ability of airborne LiDAR to map river bathymetry. Earth Surface Processes and Landforms. 33: 773-783.

Kaless G., Mao L., Lenzi M.A. 2013. Regime theories in gravel-bed rivers: models, controlling variables, and applications in disturbed Italian rivers. Hydrol. Process. (published online). DOI: 10.1002/hyp.9775.

Lane S.N., Westaway R.M., Hicks D.M. 2003. Estimation of erosion and deposition volumes in a large, gravel-bed, braided river using synoptic remote sensing. Earth Surface Processes and Landforms. 28: 249–271.

Mao L., Picco L., Cooper J., Lenzi M.A. (in preparation). How surface grain organization influences the relationship between grain size and roughness in gravel-bed rivers?

Marcus W.A., Fonstad M.A. 2008. Optical remote mapping of rivers at sub-meter resolutions and watershed extents. Earth Surface Processes and Landforms. 33: 4–24.

Milan D.J., Heritage G.L., Hetherington D. 2007. Application of a 3D laser scanner in the assessment of erosion and deposition volumes and channel change in a proglacial river. Earth Surface Processes and Landforms. 32: 1657–1674.

Milan D.J., Heritage G.L., Large A.R.G., Fuller I.C. 2011. Filtering spatial error from DEMs: Implications for morphological change estimation. Geomorphology. 125: 160–171.

Moretto J., Rigon E., Mao L., Picco L., Delai F., Lenzi M.A. 2012. Assessing morphological changes in gravel bed rivers using LiDAR data and colour bathymetry. Erosion and Sediment Yields in the Changing Environment, IAHS Publ. 356: 419-427.

Notabaert B., Verstraeten G., Govers G., Poesen J. 2008. Qualitative and quantitative applications of LiDAR imagery in fluvial geomorphology. Earth Surface Processes and Landforms. 34: 217-231.

Picco L., Mao L., Cavalli M., Buzzi E., Rainato R., Lenzi M.A. (submitted). Evaluating short-term morphological changes in a gravel-bed braided river using Terrestrial Laser Scanner. Geomorphology.

Wheaton J.M., Brasington J., Darby S.E., Sear D.A. 2010. Accounting for uncertainty in DEMs from repeat topographic surveys: improved sediment budgets. Earth Surface Processes and Landforms. 35: 136-156.

Comparison of different methods to predict the mean flow velocity in step-pool channels

T. Michelini, V. D'Agostino

University of Padova, Dept. TeSAF, Legnaro (PD),, Italy

Abstract

Steep mountain streams have irregular bed topography, where the mean flow velocity is heavily affected by the coarsest bed components and by their arrangement to form step pools, cascades, and rapids. According to literature findings the mean flow velocity is often related with water discharge, channel slope, and grain-size related variables through power relationships. Several approaches consider dimensionless hydraulic geometry terms to develop the analysis over a wide range of channel sizes and hydraulic conditions. The aim of this research is to test the performance of some literature formulas to directly compute the mean flow velocity (*V*) in step-pool sequences.

The study area deals with two fish ladders located in the Vanoi torrent (Trento Province, Italy), which were built by mimicking the step-pool morphology. Three reaches were selected to cover different channel slopes (2.6-10%). Data collection entailed three main phases: (1) topographical surveys, (2) granulometric analysis, and (3) flow discharge measurements (salt dilution method). Geometric and hydraulic variables were measured for the following step-pool cross sections: step head, pool center, and intermediate position between pool end next step. Particular attention has been reserved to determine the effective mean flow velocity over the whole path of each step pool sequence. The performance of different literature equations to predict V has been verified. The relations have been shared in three groups: dimensional (*V*), dimensionless with respect to the grain size (*V**) or to a combination of grain size and slope (*V***). In general, the *V* group of equations has produced the highest errors between computed and measured values. The dimensionless *V**, *V*** groups have shown the best performance. In particular the *V** equations, which use unit discharge and channel slope, have provided the better fitting, and the lowest root mean square error. The results highlight the difficult to estimate flow velocity in step-pool sequences, and the attitude of this channel-bed morphology to be highly dissipative. The good performance of some dimensionless equations to predict V could also support the hydraulic designer in case the 'morphological rebuilding' of mountain creeks is opportune. Further analyses are required to better understand the flow behavior in streams where very rough bed forms and hydraulic drops are the primary sources of flow energy dissipation.

Correspondence: Tamara Michelini, University of Padova, Dept. TeSAF
Viale dell'Università, 16 - 35020 Legnaro (PD), Italy.
Tel. +39.049.8272700 - Fax +39.049.8271686
E-mail: tamara.michelini@studenti.unipd.it

Key words: flow velocity, morphology, steep channels; step-pool]

Journal of Agricultural Engineering 2013; XLIV(s2):e24
doi:10.4081/jae.2013.(s1):e24

Introduction

In mountain environments, alluvial channels with gradients greater than 0.02 (Grant *et al.*, 1990) can form step-pool sequences, which are characterized by large-scale roughness. Step-pools are functionally important in river systems because they maximize flow resistance and increase the bed stability (Abrahams *et al.*, 1995; Chin, 2003; Curran and Wohl, 2003; MacFarlane and Wohl, 2003). The step-pool regime alternates supercritical and subcritical flow conditions and results very similar to that of consolidation check-dams. Previous investigations suggest that the step-pool reach gradient (S) and liquid discharge represent dominant controls of the flow kinematic of mountain creeks (David *et al.*, 2010). In field study of rough and narrow streams the flow discharge measurement is usually more accurate than the flow depth measurement. In fact, these streams exhibit irregular bed topography that makes difficult the determination of a representative flow depth (Rickenmann and Recking, 2011). Consequently several authors have calibrated equation for the direct estimation of the mean flow velocity (V) using both field data (Jarrett, 1984; Rickenmann, 1994; Ferguson, 2007; Comiti *et al.*, 2007) and laboratory data on self-formed steps (Comiti *et al.*, 2009; Zimmermann, 2010). These equations have the following form:

$$V \propto g^{0.20}\, S^{0.20} q^{0.60} D_c^{-0.40} \quad [1]$$

where q is the unit discharge, D_c the grain roughness, and g the gravity acceleration. Rickenmann (1991) proposed to use $D_c = D_{90}$ (diameter for which the 90% of the sieve diameter is finer), while Aberle and Smart (2003) and Zimmermann (2010) adopted the standard deviation of bed longitudinal profile (σ_z), resulting more appropriate in streams with substantial bed forms.

Comiti *et al.* (2007) introduced the hydraulic geometry equation in a dimensionless form:

$$V^* = \alpha\, q^{*m} \quad [2]$$

being α and m two empirical parameters and:

$$V^* = \frac{V}{\sqrt{g\, D_c}} \quad [3]$$

$$q^* = \frac{q}{\sqrt{g\, D_c^{\,3}}} \quad [4]$$

Ferguson (2007) has remarked that [Eq. 2] performs better than other equations since q^* is a better predictor than the depth (h) over

grain size ratio (h/D_c) and is probably less affected by measure error.

Rickenmann and Recking (2011) introduced the following new dimensionless terms:

$$V^{**} = \frac{V}{\sqrt{g\,S\,D_c}} \quad [5]$$

$$q^{**} = \frac{q}{\sqrt{g\,S\,D_c^{\,3}}} \quad [6]$$

and then they formulated a hydraulic-geometry type equation:

$$V^{**} = a\,q^{**m} \quad [7]$$

The authors calibrated equation [Eq. 7] through a data set of 2890 field measurements. They divided the result into three different domains as to q^{**} ($q^{**} \geq 100$; $1 \leq q^{**} < 100$; $q^{**} < 1$). To obtain a smoother transition for the velocity predictions between the three domains, the authors used the logarithmic matching technique proposed by Guo (2002). The aim of this research is to test the predictive capacity of available literature formulas, which are more appropriate to compute directly the mean flow velocity in channels with a step-pool morphology. The verification has been carried out by using field data of small-scale step-pool sequence and assessing the performance of the equations listed in Table 1.

Materials and methods

A dataset of hydraulic and geometric variables were collected in three artificial step-pool reaches, which were built with the function of fish ladders by passing check dams in the Vanoi torrent (Trento Province, Italy). Three step-pool reaches (*TA*, *TB*, *TS*; channel widths from 0.62 to 1.65 m) were selected in order to test different channel slopes (6.0%, 10.0%, and 2.6% respectively). Field experiments were performed in three main phases: (1) topographical surveys, to draw longitudinal profiles and cross-sections of the channel; (2) grain-size measures of the bed surface; the sediment sampling was conducted by line (fixed spacing) and using a caliber; (3) measurements at controlled steady conditions of flow depth and water discharge using the salt dilution method. A number of 65 cross-sections were surveyed in the following characteristics positions: step heads (SH), pool centers (PC), and intermediate positions (INT) between the pool end and the following step. The mean flow velocity (V) in each cross-section was back-calculated as the ratio discharge (Q) flow area (A). In the elaboration of field data particular attention was reserved to quantify the effective mean flow velocity over the whole path of each step-pool reach. This velocity, here defined as 'reach-averaged flow velocity', resulted from the ratio between the sequence length and the total travel time, which was calculated accounting for partial mean velocities within the all sub-reaches SH-PC, PC-INT, and INT-SH. The reach-averaged V values were compared with V values that can be computed via the

Table 1. Equations for flow velocity prediction tested in this study; Rh=hydraulic radius; hm = hydraulic depth (m); H/L = step height-length ratio; σ_z = standard deviation of the residuals of a thalweg longitudinal profile regression (m); D_{90} (diameter for which the 90% of the sieve diameter is finer) (see text for the other symbols).

Matakiewickz (1932)	$V = 2.38\,Rh^{0.70}$	[8]
Bray (1979)	$V = 8\,Rh^{0.60}S^{0.29}$	[9]
Jarrett (1984)	$V = 3.17\,Rh^{0.83}\,S^{0.12}$	[10]
Rickenmann (1991)	$V = 1.3\,g^{0.20}S^{0.20}q^{0.60}D_{90}^{-0.40}$	[11]
Rickenmann (1994)	$V = 0.37\,g^{0.33}S^{0.20}Q^{0.34}D_{90}^{-0.35}$	[12]
Aberle and Smart (2003)	$V = 0.96\,g^{0.20}S^{0.20}q^{0.60}\sigma_z{}^{-0.40}$	[13]
D'Agostino (2005)	$V = 1.42\,q^{0.48}$	[14]
D'Agostino et al. (2006)	$V = 1.21\,g^{0.245}S^{0.16}q^{0.51}D_{84}^{0.265}$	[15]
Comiti et al. (2007)	$V^* = 0.29\,q^{*\,0.66}$	[16]
Comiti et al. (2007)	$V^* = 0.74\,q^{*0.59}\left(\frac{H/L}{S}\right)^{0.52}$	[17]
Ferguson (2007)	$V^* = 1.44\,q^{*\,0.60}S^{0.2}$	[18]
Comiti et al. (2009)	$V^* = 1.24\,q^{*\,0.83}$	[19]
Zimmermann (2010)	$V^* = 0.58\,q^{*\,0.39}$	[20]
Yochum et al. (2012)	$V^{**} = q^{**\,0.16}$	[21]
Yochum et al. (2012)	$V^{**} = 0.9\left(\frac{hm}{\sigma_z}\right)^{**\,0.16}$	[22]
Rickenmann and Recking (2011)	$V^{**} = 1.5471\,q^{**0.7062}\left[1+\left(\frac{q^{**}}{10.31}\right)^{0.6317}\right]^{-0.4930}$	[23]

relationships listed in Table 1. Observed values were then plotted against measured values. The predictive performance of each equation was assessed by means of the normalized root mean square error (*RMS*), quantifying the following standard deviation of residuals:

$$RMS = \sqrt{\frac{\sum \left(\frac{V_{predicted} - V_{observed}}{V_{predicted}}\right)^2}{N}} \quad [24]$$

Results

The main results of topographical surveys, granulometric analysis and flow measurements are summarized in Table 2 and Table 3. The reach-averaged V data versus predicted values are shown in Figure 1 along with *RMS*, which was calculated both separately for each reach (TA, TB, TS) and for the whole sample (Tot in Figure 1). All comparisons and performance evaluations were conducted in terms of dimensional flow velocity (V), thus always transforming the equation results

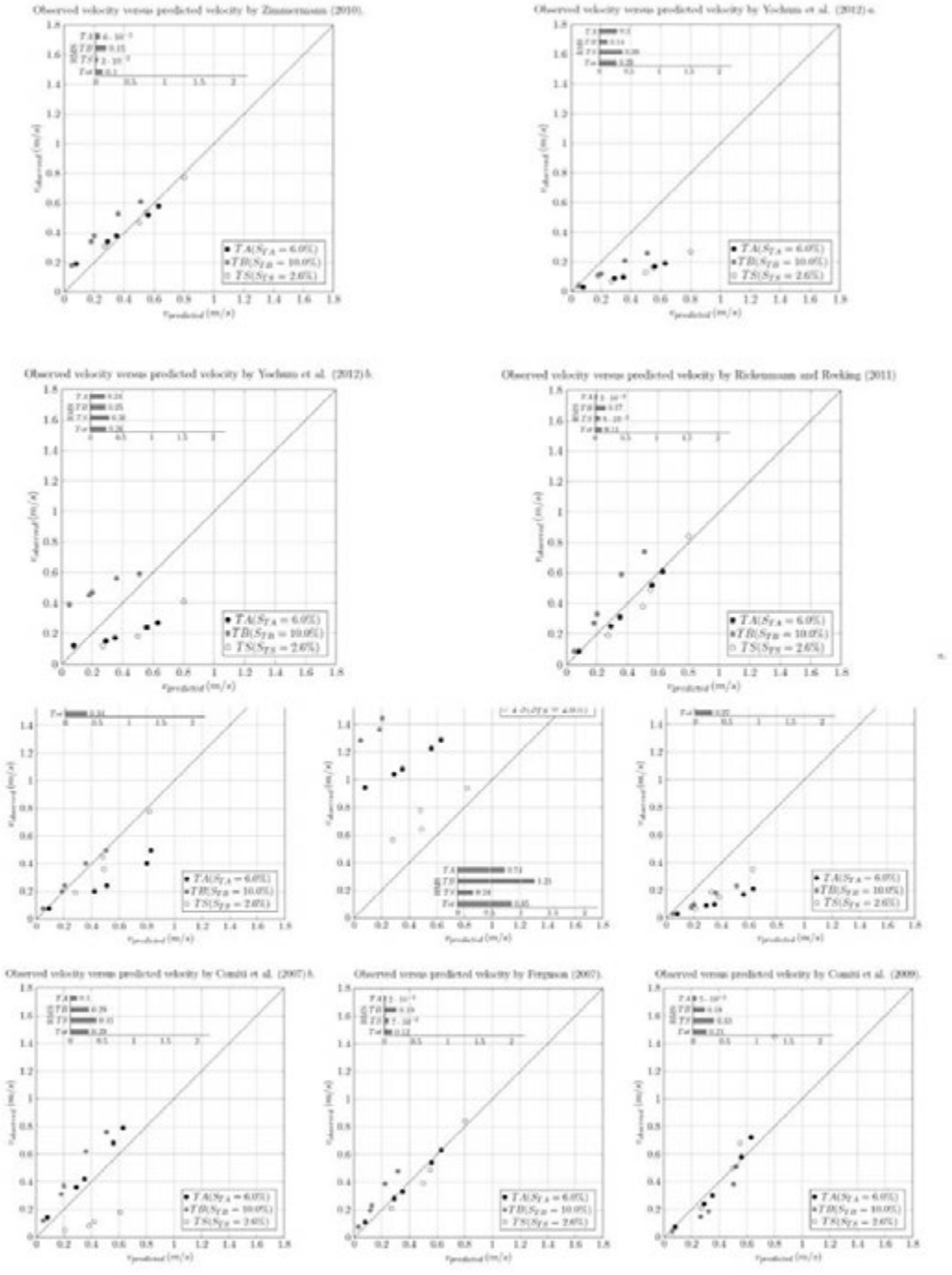

Figure 1. Observed values of mean flow velocity ($V_{observed}$) versus predicted values ($V_{predicted}$) from the application of equations in Table 1.

of those equations (e.g. Eq. [17] or [23], Table 1), which adopt dimensionless variables.

Between the classical power law relationships directly computing the mean velocity (*V*), the D'Agostino (2005) equation provided predictions with the best performance (lowest *RMS* = 0.297). Considering the equations based on the *V** group, that of Zimmermann (2010) produced the lowest *RMS* (0.098) and this value was also the best one on the whole (V, V* and V** group). A quite similar *RMS* value (0.121) resulted from the relations of Ferguson (2007) and Comiti *et al.* (2009), and both equations showed a general tendency to an overestimation. Analysing the dimensionless *V*** group of equations, the lowest *RMS* (0.109) was generated by the equation of Rickenmann and Recking (2011), with a *RSM* value very close to that Zimmermann (2010). Equation 22, proposed by Yochum *et al.* (2012), is the only one containing a relative submergence, and exhibited a tendency of underestimation. Comiti *et al.* (2007) equation, which employs a steepness factor, produced a high dispersion of data around the line of perfect agreement.

Looking at the three reaches (*TA*, *TB*, and *TS*) separately, the Ferguson (2007) equation provided the lowest *RMS* (0.020) and the best fit for the reach TA. Good predictions for the reach *TA* was also obtained with Rickenmann and Recking (2011) and Comiti *et al.* (2009) relations. For the reach *TB*, Yochum *et al.* (2012), equation [21], and Zimmermann (2010) predicted the more correct values. It was also observed that the dimensionless equation introduced by Zimmermann (2010) provided the lowest sum of the three partial *RMS* values.

Table 2. Principal results of topographical and grain-size measurements.

Reach	Cross-sections	Total Length (m)	Slope (m/m)	D_{84} (m)	σ (m)
TA	22	35.39	0.060	0.26	0.244
TB	19	19.99	0.100	0.26	0.279
TS	23	42.98	0.026	0.18	0.078

Table 3. Data set of the experiments in the artificial step-pool reaches.

Reach aged	Experiment	Discharge Q (m^3/s)	Reach-ave flow velocity V (m/s)
TA	TA_1	0.01	0.627
	TA_2	0.03	0.048
	TA_3	0.04	0.185
	TA_4	0.12	0.204
	TA_5	0.18	0.357
TB	TB_1	0.01	0.505
	TB_2	0.03	0.275
	TB_3	0.04	0.492
	TB_4	0.11	0.426
	TB_5	0.19	0.823
TS	TS_1	0.01	0.069
	TS_2	0.04	0.151
	TS_3	0.07	0.224
	TS_4	0.23	0.412

Discussions and conclusions

The capability to predict the mean flow velocity V for a given discharge is essential for hydraulic and hydrological modelling, stream restoration design, geomorphic analysis, and ecological studies (Yochum *et al.*, 2012). An unique approach is not available to predict V in each fluvial-morphological type, and, in particular, in steep channels. As to step-pool sequences the application of traditional laws of flow resistance provides serious problems because the V estimation is highly sensitive to the choice of representative cross-sections and roughness parameters due to great irregularity of thalweg and stream banks. Therefore, when the discharge is known, the direct estimation of V from the unit water discharge is preferable (Rickenmann, 1990; Aberle and Smart, 2003; D'Agostino, 2005; Ferguson, 2007). In this research, a new database of cross section geometry and hydraulic variables was collected for small-scale step pools under well controlled steady flow conditions. The mean flow velocity has been extracted in terms of a reach-averaged velocity resulting from the 'travelling' time along the whole step-pool sequence. The study results indicate the dimensionless unit discharge, [Eq. 4], is a robust predictor of V over a significant range of step-pool slopes (3-10%). The Zimmermann (2010) equation generated the best fit and the lowest errors, hinting that the used roughness parameter (D_e=σ_z) is more suitable for the V assessment in step-pools. Furthermore Yochum *et al.* (2012) equation, [Eq. 22], which also contains σ_z and well predicts V, confirms the previous remark. In few words, the standard deviation σ_z of the residuals of the thalweg profile regression allows capturing the influence of the largest clast on the flow resistance and then avoiding a more problematic grain size sampling. The good performance of Rickenmann and Recking (2011), Comiti *et al.* (2009), and Ferguson (2007) equations has turned out to be in accordance with Comiti *et al.* (2007) and David *et al.* (2010) findings. In fact, our study confirms that variations in flow resistance are mostly explained by unit discharge and slope, whereas the relative submergence hm/D_{84} is not an appropriate explanatory variable of V for step-pool creeks, and a macro-roughness variable, like the step height-length ratio, can be more effective. Finally, the good predictions provided by the Rickenmann and Recking (2011) equation for the three step-pool reaches suggest to better investigate on the transitional behaviour between shallow and deep flows and to dedicate further efforts in assessing the boulder concentration and protrusion (Nitsche *et al.*, 2012), which interact with such a transition.

References

Aberle J., Smart G. M. 2003. The influence of roughness structure on flow resistance on steep slopes. J. Hydraul. Res., 41(3): 259-269.

Abrahams A. D., Li G., Atkinson J. F. 1995. Step-pool streams: adjustment to maximum flow resistance. Water Resour. Res. 31: 2593-2602, doi:10.1029/95WR01957.

Chin A. 2003. The geomorphic significance of step-pools in mountain streams. Geomorphology, 55: 125-137.

Comiti F., Cado D., Wohl E. 2009. Flow regimes, bed morphology, and flow resistance in self-formed step-pool channels. Water Resour. Res. 45: W04424, doi:10.1029/2008WR007259.

Comiti F., Mao L., Wilcox A., Wohl E. E., Lenzi M. A. 2007. Field- derived relationships for flow velocity and resistance in high-gradient streams. J. Hydrol., 340: 48-62, doi:10.1016/j.jhydrol.2007.03.021.

Curran J. H., E. E. Wohl 2003. Large woody debris and flow resistance in step-pool channels, Cascade Range, Washington. Geomorphology, 51: 141-157, doi:10.1016/S0169-555X(02)00333-1.

D'Agostino V. 2005. Velocità media della corrente in torrenti fortemente scabri. In: Proc. of the Italian Congress AIIA2005, Catania, Italy, June: 27-30.

David G. C. L., Wohl E. E., Yochum S. E., Bledsoe B. P. 2010. Controls on spatial variations in flow resistance along steep mountain streams. Water Resour. Res., 46(3): W03513, doi:10.1029/2009WR008134.

Ferguson R. 2007. Flow resistance equations for gravel- and boulder-bed streams. Water Resour. Res., 43(12): W05427, doi:10.1029/2006 WR 005422.

Grant G. E., Swanson F. J., Wolman M. G. 1990. Pattern and origin of stepped-bed morphology in high- gradient streams. Western Cascades, Oregon. Geol. Soc. Am. Bull., 102: 340-352.

Guo J. 2002. Logarithmic matching and its application in computational hydraulics and sediment transport. J. Hydraul. Res., 40(5): 555-566.

Jarrett R. D. 1984. Hydraulics of high-gradient rivers. J. Hydraul. Eng., 110(11): 1519-1539.

MacFarlane W. A., Wohl E. E. 2003. Influence of step composition on step geometry and flow resistance in step-pool streams of the Washington Cascades. Water Resour. Res., 39(2): 1037, doi:10.1029/ 2001WR001238.

Nitsche M., Rickenmann D., Turowski J. M., Badoux A., Kirchner J.W. 2011. Evaluation of bedload transport predictions using flow resistance equations to account for macro-roughness in steep mountain streams. Water Resour. Res., 47(8): W08513, doi:10.1029/2011 WR010645.

Rickenmann D. 1991. Hyperconcentrated flow and sediment transport at steep slopes. J. Hydraul. Eng., 117(11): 1419-1439.

Rickenmann D. 1994. An alternative equation for the mean velocity in gravel-bed rivers and mountain torrents. In: G. V. Cotroneo, R. R. Rumer (eds.), Hydraulic Engineering, vol. 1, Am. Soc. of Civ. Eng., New York, pp. 672-676.

Rickenmann D. 1990. Bedload transport capacity of slurry flows at steep slopes. Mitt. der Versuchsanstalt fur Wasserbau, Hydrologie und Glaziologie, ETH Zurich, 103.

Rickenmann D., Recking A. 2011. Evaluation of flow resistance in gravel-bed rivers through a large field data set. Water Resour. Res., 47(7): W07538, doi:10.1029/2010WR009793.

Yochum S. E., Bledsoe B. P., David G. C. L., Wohl E. E. 2012. Velocity prediction in high-gradient channels. J. Hydrol., 424: 84-98, doi:10.1016/j.jhydrol.2011.12.031.

D'Agostino V., Zasso M., Vianello A., Cesca M. (2005). Nuovi contributi sulla velocità media della corrente nei corsi d'acqua montani. Quaderni di Idronomia Montana, 25, Bios, Cosenza, pp. 117-129 (ISBN – 10: 88-60-93-014-6).

Zimmermann A. 2010. Flow resistance in steep streams: An experimental study, Water Resour. Res., 46: W09536, doi:10.1029/2009WR 007913.

Proposal of a local telemetry network for the monitoring the thermodynamic and environmental performances of farm tractors

Fabrizio Mazzetto, Marco Bietresato

Free University of Bozen-Bolzano, Faculty of Science and Technology – Fa.S.T., Bolzano, Italy

Abstract

The TRAKTnet.one project aims to identify and develop new solutions to remotely monitor the efficiency of farm-tractors engines included in a local voluntary network. The knowledge of tractors' efficiency can give important information concerning machines' consumption, emissions and need for servicing, thus contributing to a more environmentally-sustainable agriculture. Engines will be monitored by measuring rpms, exhaust gas temperature and oxygen content (through lambda sensors) and then analysing and inferring the data through procedures, which algorithms will be an integral part of the project's results.

Trials will be performed on different engines and at different speeds/loads. The choice of the thermocouple type and installation point must be done carefully for not influencing sensitivity and response time. The final outcome of the project is expected to be an automatic system, based on an inference software-engine able to correctly interpreting the sensors outputs. The advantage of this proposal is to exploit a farm monitoring network, previously designed for managing the information related to the automatic compilation of records in the country, by simply equipping data loggers with two additional sensors.

Correspondence: Marco Bietresato, Free University of Bozen-Bolzano, Faculty of Science and Technology – Fa.S.T., piazza Università 5, P.O. Box 276, I-39100 Bolzano (BZ), Italy.
Tel. +39.0471.017181 – Fax: +39.0471.017009.
E-mail: marco.bietresato@unibz.it

Key words: Farm tractors; engine performances; remote monitoring; telemetry.

Acknowledgements: the authors wish to thanks Dr. Aldo Calcante of Università degli Studi di Milano and Dr. Carlo Bisaglia of CRA-ING for their assistance during the experimental surveys at the test bench.

Conflict of interests: the authors declare no potential conflict of interests.

Conference presentation: this paper has been submitted to The Italian Society of Agricultural Engineering for the 10th AIIA Conference "AIIA13 – Horizons in agricultural, forestry and biosystems engineering", which will be held in Viterbo, University of Tuscia, Italy, on September 8-12, 2013.

Journal of Agricultural Engineering 2013; XLIV(s2):e25
doi:10.4081/jae.2013.(s1):e25

Introduction

General considerations and problem description

The necessary condition for developing a sustainable agriculture is to raise the overall efficiency of farm machines by: (1) increasing their annual exploitation, (2) keeping constant their performance over the time. This intensive control on machines must necessarily imply: (a) the implementation of a Farm-Information-System (FIS) based on a client-server approach, to acquire and manage information needed for taking decisions at both farm and territorial scale, through a Farm-Operational-Monitoring, using telemetry and data-loggers on tractors and implements (Mazzetto, Calcante, & Salomoni, 2009; Sahu & Raheman, 2008; Yule, Kohnen, & Nowak, 1999), (b) the proposal of solutions that are economical, simple, robust, reliable and effective in acquiring selected engine parameters (Singh & Singh, 2011).

The TRAKTnet.one project of the Free University of Bolzano aims to identify and develop new solutions to remotely control the efficiency (hence: consumption, emissions and need for servicing) of farm-tractors engines included in a local voluntary network all along their lifespan, thus contributing to a more environmentally-sustainable agriculture. The proposed solutions will be based on remote measurements of exhaust gases' temperature (De Souza & Milanez, 1987; Friso, 1988; Pang, Zoerb, & Wang, 1985) and oxygen; these parameters will be analysed and inferred through procedures, which algorithms will be an integral part of the project's results.

Several experiences reported in literature (Friso, 1988; Goering, Hansen, Lyne, & Meiring, 1986) show that the EG temperature is proportional to the engine torque, thus allowing for an indirect calculation of engine load and related instant power (this is possible only knowing a priori the maximum rated power each engine can provide). The combustion quality, on the other hand, can be related to the oxygen concentration in the EGs, measured through lambda sensors, thus enabling a rough estimate of the engine efficiency.

Engines will be monitored by measuring rpms, EGs' temperature and oxygen content (as indexes indirectly estimating consumption and efficiency) and then analysing and inferring the data through procedures, which algorithms will be an integral part of the project's results (Alvarez & Huet, 2008). This implies: (1) the existence of a service centre controlling all farm machines and managing a FIS network through simple logical connections according to a client-server approach, (2) a database relative to all the monitored engines when they are new, in order to have a comparison term with the data collected by the network. This database will be compiled starting from the data reported on the OECD test reports and from properly tuned numerical models, without any additional test to be performed during the type-testing of a tractor.

Aim of the research

The final outcome of the project is expected to be an automatic system, based on an inference software-engine able to correctly interpreting the sensors' outputs. It could be used by tractors' owners for being

advised about the need for servicing their vehicles but also by local authorities for monitoring tractors' environmental impact in a territory and, maybe, for tailoring the subsidies to the farmers (e.g., on a rewarding-score in accordance to the detected performances).

The advantage of this proposal is to exploit a farm monitoring network, previously designed for managing the information related to the automatic compilation of records in the country, by simply equipping data loggers with additional sensors.

Materials and Methods

System definition and implementation

The system and its components at every level have been defined by using a *top-down approach*, hence, after formulating the general task(s) of the system, its main elements (*i.e.*, the first-level subsystems) have been specified but not detailed. The detailed refinement of each subsystem is the final task and will be afforded afterwards.

The system general architecture has been defined starting from the following needs/technical requirements:

- collecting a series of data on vehicles operating in an environment presenting several potential problems for electronic devices (*e.g.*, humidity, dust, heat sources);
- interpreting the collected data to obtain therefore information concerning the functioning of farm engines;
- putting this information at the disposal of the farmers and/or local authorities.

After defining the architecture, four steps will be followed: (1) preliminary assessment of sensors features (*e.g.*, number, type, position); (2) numeric modelling of a compression-ignition engine to understand the effects of ageing and bad maintenance on its performances; (3) evaluation of possible modifications of commercial sensors (*e.g.*, K- or J-type thermocouples, zirconium-oxide lambda sensor); (4) execution of bench and field tests to validate the system.

The choice of the thermocouple type (band/rod) and installation point (manifold/pipe) must be done carefully for not influencing sensor's sensitivity and response time. The combustion quality can be related to the oxygen concentration in exhaust gases (EG). Trials will be performed on different engines (*e.g.*, naturally-aspired/turbocharged, with/without EGR/SCR or analogous devices) and at different speeds/loads (full load, partial loads, idle).

Preliminary bench tests

Some preliminary bench tests were carried out at the CRA-ING OECD laboratory centre (Treviglio, BG, Italy) with the aim of finding the best position for recording the EG temperature. The tests concerned three farm tractors covering a wide range of powers and engines types (Table 1). The experimental procedure consisted of several bench tests (163 trials in total, 48-60 per tractor) aimed to record engines' performances (instant torque, power and brake specific fuel consumption-BSFC) and the relative EG temperatures in their operating ranges (Jahns *et al.*, 1990); each test started only after the engine warmed up and included:

- a classic OECD bench test with the fuel-pump rack fully-opened;
- other four tests with the fuel-pump rack at intermediate positions between the maximum and the minimum (each spaced approximately of 200 rpm).

During the tests, three thermocouples were used to measure the EG temperature in three different points of the exhaust pipeline:

- one mineral-insulated *K-type* thermocouple, with its tip inserted inside the exhaust manifold (in direct contact with the gas) and fixed to the manifold through a bayonet coupling (→temperature measured with this thermocouple: TcK);
- two *J-type* thermocouples, fixed through hose clamps respectively in contact with the second cylinder's exhaust pipe (→temperature: TcJ-cyl) and outside of the exhaust manifold (→temperature: TcJ).

EGs' temperature was sampled only after 5 minutes the engine was subjected to a set brake force (time interval tuned after the first surveys) to have a stable value of the temperature for each operating condition.

The *Response Surface Modelling-RSM* (Maheshwari *et al.*, 2011) was used to study the test results. Previous works (Friso, 1988; Goering *et al.*, 1986) showed that the relationship existing between torque-*M*, engine speed-*n* and EG temperature-*T* can be numerically approximated by third-degree full-cubic polynomials. If y_k and $x_{i,k}$, are, respectively, the *k-th* predicted value of a generic response and the corresponding values of the x_i (i=1, 2) generic factors, i.e. independent variables, non-coded, a_0 is the interception coefficient, a_i, a_{ii}, a_{iii}, a_{ij} and a_{ijh} ($i \neq j \neq h$) are the coefficients of the linear, quadratic, cubic, 2nd-order and 3rd-order interaction terms, the generic regression model used in RSM is:

$$y_k(x_i; i=1,2) = a_0 + \sum_{i=1}^{2} a_i x_{i,k} + \sum_{1\le i\le j\le 2} a_{ij} x_{i,k} x_{j,k} + \sum_{1\le i\le j\le h\le 2} a_{ijh} x_{i,k} x_{j,k} x_{h,k} \quad (1)$$

Design-Expert 7.0.0 (Stat-Ease, Minneapolis, MN, USA) was used to analyse the collected data and propose for each response a regression model with only the significant terms (*ANOVA/RSM*; the terms have been chosen according to RSM-software suggestions).

Table 1. Tractors' engine main specifications.

Engine technical characteristic	Unit	Farm tractor		
		Same Explorer 70 DT	Same Explorer 80 DT	Same Laser 130 DT
Manufacturer/type	-	Same, 1000.4 A	Same, 1000.4 A1	Same, 1056 P
Cylinders/configuration	nr.	4, straight	4, straight	6, straight
Piston bore/stroke	mm, mm	105.0, 115.5	105.0, 115.5	105.0, 120.0
Compression ratio	-	17.1	17.1	n.a.
Total displacement	cm^3	4 000	4 000	6 234
Max power value/engine speed	kW, rpm	47.07@2350	54.20@2509	92.00@2260
Engine speed range	rpm	675-2509	700-2712	n.a.

n.a.: not available data

First model of the engine

With the aim of calculating the EG temperature of the new engine of each model of tractor connected in the network, a numerical/analytical model should be created with a certain degree of detail from the OECD test report's data. In this case, the analyst has a great freedom in how creating the engine model, in the achievable level of detail and in the choice of the software to be used. In fact, he may:

- implement a series of thermodynamic transformations (more or less ideal) using equations directly written within a program; the software used in this case can even have a purely textual interface (*e.g.*, Microsoft Visual Basic; Mathworks Matlab);
- approach the problem through precompiled or writable function blocks, properly connected to each other to describe exchanges of matter, energy or information, graphically building a layout similar to the real one; the suitable software have a graphical interface and adopt a single-port (*e.g.*, Mathworks Simulink) or a multi-port icons description (*e.g.*, Gamma Technologies GT-Power, LMS Imagine.Lab AMESim);
- opt for a multi-dimensional simulative approach (2D, 2D axially-symmetric, 3D) adopting a discretization of the domain (finite element method, geometric element method, boundary element method) useful in the detail modelling of the heat transfer phenomena.

The software used for the creation of the first models is AMESim 12.0.0 (LMS Imagine, Leuven, Belgium). In AMESim each individual element/component is associated to a subroutine whose inputs can be entered by the user or come from other elements/components. The exchange quantities for each block are written in terms of power (Bond-Graph approach) and therefore are always expressed as a scalar product of two vector quantities. The used elements are zero- or one-dimensional, require limited computational times and give in the meantime the possibility of simulating also very complex systems (e.g. a complete engine). AMESim uses a lumped and distributed parameter approach in which the necessary ordinary (for 0D-elements) or partial (for 1D-elements) differential equations of the system are automatically written by the software.

Results

System components

The monitoring system is composed of three basic elements (Figure 1 *left*):

- *hardware devices*, for collecting and/or storing the data (sensors, data logger with communication capabilities, servers with storage units);
- a set of *automatic computing procedures*, based on several physical models of the engines (one model per each engine) to obtain time-related information about the engine performances from the raw data achieved; the output formats can be both tabular and graphical;
- *interfaces*, to enable the users the access and use of the information.

The system presented here will be fully interfaced with a FIS (Mazzetto *et al.*, 2009) and can be seen as completion of it: some important data collected by the farm monitoring network (e.g., concerning field operations), will be related to the acquisitions of additional sensors on engines, thus extending the FIS monitoring also to all the involved power units. In particular, the field-event data-logger (FDL), already present on board all the vehicles connected in a FIS network, will be completed of the following components, connected to its input and output ports (Figure 1 *right*):

- two/three input units, *i.e.* an engine speed sensor, an EG temperature sensor (thermocouple) and, eventually, also a zirconium-oxide lambda sensor;
- one/two output unit(s), *i.e.* a GPRS antenna and, eventually, a liquid crystals display positioned on the tractor's dashboard.

The FDL, powered by the 12-V-DC electrical system of the tractor, is the kernel of the on-board system and has several functions:

- it is necessary for the power supply of all the connected I/O units, which are typically passive, i.e. not powered independently;
- it collects and stores temporarily the data collected by the sensors, providing to send the raw data (or the interpreted data; see below) to a remote server via GPRS;
- if provided with the correct calibration curves, it is capable to interpret directly the sensors' analogue/digital signals as physical quantities (engine speed, EG temperature, EG oxygen concentration) before sending them to a server.

System conceptual functioning

The system operates conceptually in *three different phases*:

- usage of the OECD test results for tuning a physical model of the

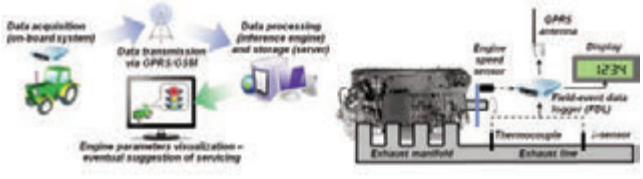

Figure 1. (left) general functioning of the monitoring system for the tractors; (right) on-board components involved in the engine monitoring (dashed/continuous arrows indicate raw/interpreted data flows; power-supply connections are not represented).

Table 2. Main results of bench tests and RSM analyses (M: torque; P: power; S: speed; T: temperature).

Tr.	Operating point	Experimental measurements						R^2 of $T=f(M,S)$ fitting		
		M (Nm)	P (kW)	S (rpm)	TcK (K)	TcJ (K)	TcJ-cyl (K)	TcK	TcJ	TcJ-cyl
SAME 70	Idle	-	-	221	377	336	318	0.9986	0.9968	0.9691
	Max P	423	45	1024	832	449	320			
	Max M	548	34	588	832	492	336			
SAME 80	Idle	-	-	381	413	357	342	0.9960	0.9889	0.9344
	Max P	465	47	956	880	449	346			
	Max M	582	37	613	855	472	356			
SAME 130	Idle	-	-	325	393	407	342	0.9966	0.9738	0.9799
	Max P	804	84	995	981	594	462			
	Max M	913	55	572	923	612	490			

engine; usage of the tuned physical model for correlating the EG temperature and the specific consumption/efficiency with the torque and the speed, thus developing some mathematical models with different degrees of detail/complexity (Figure 2);
- usage of the temperature data, recorded during the normal operating of a tractor, together with the time history of field operations recorded through the FDL for correlating together torque, speed and efficiency of a model of tractor with some hours of operation (Yule *et al.*, 1999; Kolator and Białobrzewski, 2011); integration of this model into the main FDL inference engine to have an estimate of the engine torque or efficiency;
- comparison of the efficiency values predicted by the two models to quantify the performance decrement of the engine (Alvarez and Huet, 2008) and suggestion to the driver of eventual extraordinary maintenance interventions to the vehicle.

RSM will be used in the first phase (Figure 2) and in particular in two different sub-phases:
- to approximate the equations of torque, power, BSFC and efficiency as a function of the engine speed, starting from standard OECD test results (full-load curve, part-loads curves at rated engine speed and at PTO speed);
- to build 2-variable models of the EG temperature and engine efficiency as a function of torque and engine speed from the output data coming from a tuned physical model of the engine.

Positioning of the EG thermocouple

The bench tests and the subsequent RSM confirmed the experiences reported in literature, showing that, for a set engine speed, the EG temperature T is positively correlated with the torque M ($R^2 \geq 0.9344$; Figure 3; Table 2). The K-thermocouple gave the most statistically-significant measurements (best R^2) and had the higher instrumental sensitivity (or "gain", here: $\partial T/\partial M$) in the engine torque range ($\Delta T_{TcK} \geq 450°C$, *i.e.* more than 3 times ΔT_{TcJ} and up to 34 times $\Delta T_{TcJ\text{-}cyl}$ during the same tests), surely due to the absence of an interposed (pipe's) material, having an its own inertia and thermal conductivity.

Engine model

The first developed model reproduces the layout of a hypothetical single-cylinder Diesel engine. It has the same geometric-functional characteristics of a single cylinder of SAME Explorer 70's engine (obtained from the OECD test report and by modelling the piston; Figure 4).

The model layout includes also the intake and the exhaust systems (respectively: from the air filter to the motor, from the motor to the exhaust pipe; Figure 5).

This model uses:
- 67 input parameters (geometrical, thermodynamic, functional) entered by the user, deduced from the OECD test report's data directly or indirectly (with the aid of a spread sheet)
- The Barba combustion model (dual-zone, specific for Diesel engines)
- The Annand model for the gases-combustion chamber's walls heat exchange, with the value of the convection and radiation coefficients taken from the software library
- The values of the properties of fuel and metallic materials of the intake and exhaust pipes, of the convective and radiative coefficients taken from the software library
- The values of direct and inverse flow coefficients through the valves, valves lift function, IVO and EVC angles, injection map, injector flow profile and nozzle sizes taken from the software library

After simulating 10 seconds of engine operation at 2350-rpm rotational speed (i.e., 196 cycles), the torque stabilizes at 56.03 Nm, corre-

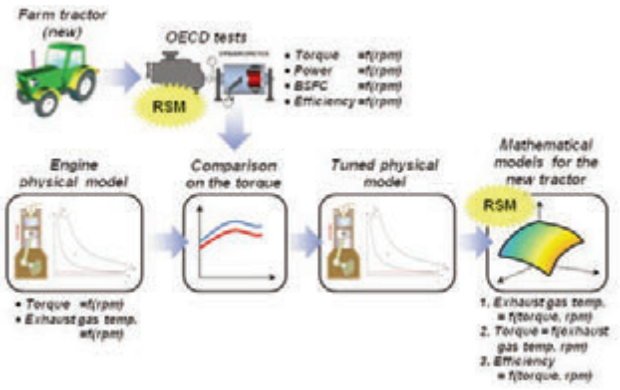

Figure 2. First phase of the conceptual functioning of the system, concerning the modelling of a new engine; in evidence the sub-phases in which Response Surface Modelling (RSM) can be used.

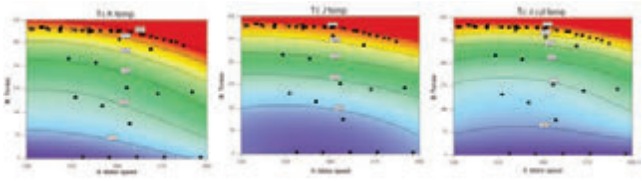

Figure 3. Contour plots of the temperatures regression models for Same

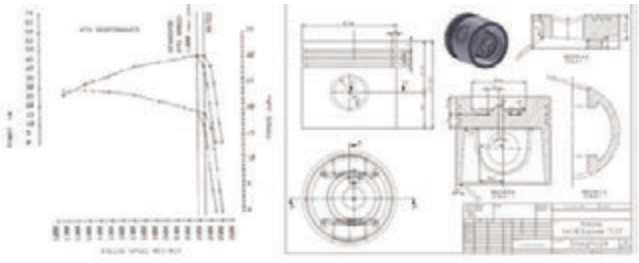

Figure 4. SAME Explorer 70's characteristic curves (left; source: OECD test report) and piston (right).

Figure 5. Layout of the model of a tractor engine, complete of the intake (red) and exhaust (blue) pipelines.

sponding to a power of 13.79 kW, net of any frictional loss. The OECD power value is 47.07 kW, therefore 15% lower than the value (55.16 kW) obtainable by simply multiplying by 4 (number of engine's cylinders) the value obtained above. Although the multiplication of the single-cylinder engine output to have the output of a similar multiple-cylinder engine gives approximate results and the obtained difference is significant, this result is promising. In fact it should be considered that it was obtained with a not-yet tuned model and, especially, without taking into account any mechanical (engine, transmission) and viscous (fan) friction which are normally present in a real motor, and not considering the interactions between input and output gas flows that will surely exist in a multi-cylinder engine. The model gives the analyst the chance to have a graphical-numerical output of many physical quantities in several points of the layout (e.g., see Figure 6) ad in particular to check the EG temperature (Figure 7).

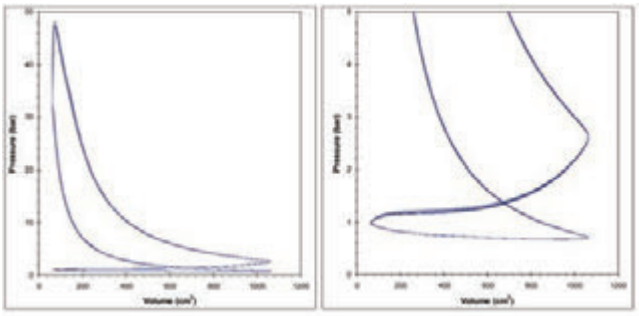

Figure 6. (left) Clapeyron diagram of the combustion chamber; (right) magnification of the passive part of the engine cycle in which inlet and outlet phases are visible.

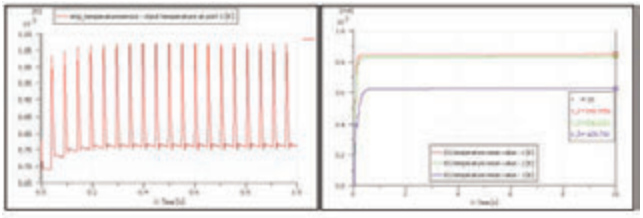

Figure 7. (left) instant EG temperature at the cylinder's outlet (first second); (right) EG mean temperature at three different points of the exhaust (cylinder's outlet; collector's outlet; muffler's outlet).

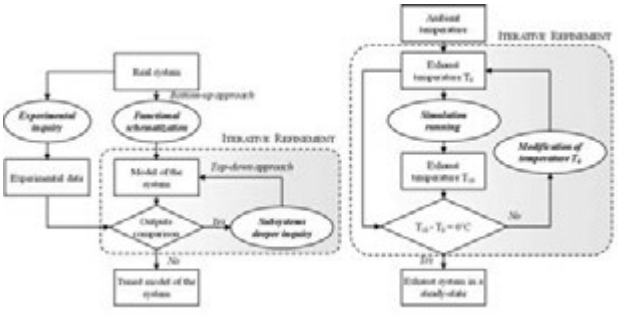

Figure 8. (left) process of system modelling and model calibration; (right) process of finding a steady-state operation for the exhaust system (T0: initial temperature; T10: temperature at 10 s).

Conclusions and future work

Thanks to some preliminary bench tests, the correlation of the EG temperature with the torque and engine speed was fully confirmed and hence will be used in the project. Thinking about the monitoring system, the same tests were useful to realize that a thermocouple placed outside the exhaust manifold/pipe, although very easy to install, could be a feasible solution only if stating that the acquisitions can be taken after the engine keeps its speed constant for a certain period. As this situation could rarely happen during the normal operation of a tractor, and considering also the higher sensitivity shown by the thermocouple with the tip inside the exhaust line, this latter solution revealed to be the best one to be applied in the tractors. A first numerical model of an engine shows the high potential of the used software (LMS Imagine.Lab AMESim): it can simulate real combustion and heat transmission phenomena and lets the user access to many physical quantities in every point of the layout. Notwithstanding the many assumptions done and without tuning the model, the torque output (calculated for four cylinders) differs only of 15% from OECD data. The next two phases will involve the completion of the model with other three cylinders and its subsequent calibration. The tuning will involve all those aspects for which there are no details/data (e.g., intake and exhaust ducts length, localized pressure losses, IVO and EVC values). A diagram of the (iterative) procedure for setting up a numerical model of an engine is visible in Figure 8. The further phase will involve the reaching of a thermal steady-state for the exhaust system. Since it would be impossible to simulate 10 minutes of engine operation (11760 cycles at 2350 rpm; 60 Gb of hard disk occupancy), the initial temperature of the exhaust pipes' metal will be modified in order to have a constant temperature during the simulation time (10 s; Figure 8).

References

Alvarez, I., & Huet, S. (2008). Automatic diagnosis of engine of agricultural tractors: The BED experiment. Biosystems Engineering, 100(3), 362–369. doi:10.1016/j.biosystemseng.2008.04.003

De Souza, E. G., & Milanez, L. F. (1987). Indirect evaluation of the torque of diesel engines. Transactions of the ASAE, 31(5), 1350–1354.

Friso, D. (1988). Modello matematico per l'ottenimento rapido del piano quotato dei consumi di un motore diesel [Mathematical model to obtain quickly the contour map of diesel engine specific fuel consumptions]. Rivista di Ingegneria Agraria, 1, 56–61.

Goering, C. E., Hansen, A. C., Lyne, P. W. L., & Meiring, P. (1986). Model for predicting tractor engine performance. In International Symposium on Agricultural Engineering. Pretoria, South Africa.

Mazzetto, F., Calcante, A., & Salomoni, F. (2009). Development and first tests of a farm monitoring system based on a client server technology. In Precision Agriculture '09. 7th European Conference on Precision Agriculture 2009 (pp. 389–396). Wageningen, The Netherlands.

Pang, S. N., Zoerb, G. C., & Wang, G. (1985). Tractor monitor based on indirect fuel measurement. Transactions of the ASABE, 28(4), 994–998.

Sahu, R. K., & Raheman, H. (2008). A decision support system on matching and field performance prediction of tractor-implement system. Computers and Electronics in Agriculture, 60(1), 76–86. doi:10.1016/j.compag.2007.07.001

Singh, C. D., & Singh, R. C. (2011). Computerized instrumentation system for monitoring the tractor performance in the field. Journal of Terramechanics, 48(5), 333–338. doi:10.1016/j.jterra.2011.06.007

Yule, I. J., Kohnen, G., & Nowak, M. (1999). A tractor performance monitor with DGPS capability. Computers and Electronics in Agriculture, 23(2), 155–174. doi:10.1016/S0168-1699(99)00029-0

Speeding up innovation in agricultural IT

Hannu E. S. Haapala

Agrinnotech, Kalevankatu, Seinajoki, Finland

Abstract

An OECD funded research was conducted where methods and processes for speeding up innovation in agriculture were assessed. A global web-based questionnaire was sent to experts in agricultural engineering, research, marketing, education and users of new technologies. Interviews of selected experts were done to deepen the analysis. The results show that considerable part of the relatively slow innovation comes from the fact that users do not trust in new technologies or that the usability of them is unacceptable. The experts suggest that education of the engineers and designers should include more elements from User-Centered Design (UCD) and also User-Driven Innovation methods should be more used. As a conclusion a new 'Dream Team' of agricultural innovation was developed where user interaction and marketing professionals were given more roles.

Introduction

An innovation, by definition, needs to be widely adopted by its users. The Oslo manual of innovation (OECD 2005) claims that technological innovations consist of implemented products and processes. The original definition of innovation by Schumpeter (1934, ref. Drejer 2004) claims that it is essential for an innovation that it is applied in practice. The definition also tells that users typically spread innovations through imitation. As the innovation is found useful, it finds new users. Consequently, because of this crucial role, the end-users should be involved in the innovation process. In past decades, researchers and designers of agricultural technologies have created new ideas to meet the urgent global challenges in food, feed, fibre, and fuel production. Consequently, quite a few new technologies have been developed.

Precision Farming (PF) is a good example of this development. PF applies accurate control technologies to plant production. Measurement and control technologies enhance the efficiency and, simultaneously, reduce the negative impacts of production. The goal is to produce accurately according to the needs of the soil and plants, thus optimizing the use of inputs. (Haapala 1995). Uptake of PF technologies by the end-users, however, has not been very effective. As the adoption is weak, the technologies do not provide all their potential benefits. Only some individual technologies, such as row guidance and yield mapping, have been adopted in large farms (Diekman & Batte 2010, Winstead *et al.* 2010). The vision of a fully integrated Precision Farming system (e.g. Haapala 1995) has not, however, been realised in such a magnitude that it could be called an innovation. As argued before, weak adoption stops the innovation process. That is true in the case of Precision Farming as well. If the PF technologies are not applied effectively and widely enough, the users get limited benefits and they eventually stop using PF. Generally, one evident reason for weak adoption is that potential users are conservative and do not trust enough in new technologies (Kaasinen 2005, Li *et al.* 2008). In order to be better adopted, the new technologies need to show remarkable benefits as compared to the old ones. Changing from old technologies has to be profitable. To be acceptable, they also need to be easy to learn, easy to use, dependable and ergonomically sound (Nielsen 1993). This is true also in agricultural technologies (Haapala & Nurkka 2006). A successful innovation process can be divided in subsequent phases that all must be efficient (Haapala 2012a, 2012b). The technological level of the product must be at an appropriate level, the technology must be acceptable, and it has to be purchased and applied in a correct way. Furthermore, the volume of application has to be wide enough. In other words, the R&D process must produce suitable technologies for the users and their needs, and the users must use the technologies in a correct way. Since the end-users are in a crucial role, User-Centered Design methods (UCD) can enhance the innovation process. UCD methods help to choose appropriate technological level of the product. Especially UCD enhances acceptability of the product. An acceptable product is more likely to become an innovation since it produces positive user experience that boosts the imitation process. Consequently, UCD enables the purchase and use of a new technology. (Haapala 212a, 212b). As derived above, UCD could help to design better tools for PF so that it could be better adopted and utilized by the end-users of these technologies. The goal of this research was to test this hypothesis. (Haapala 2012a, 2012b). End-users of technologies have a central role in Living Lab methodologies. In agricultural engineering Living Labs have been used for User-Centered RDI but also for education (Haapala & Pasila 2008, 2009, Wolfert *et al.* 2010). Living Labs were included in this research as a potential realization of the UCD in agricultural engineering.

Correspondence: Hannu Haapala, Agrinnotech, Kalevankatu 12b A26, 60100 Seinajoki, Finland.
Tel. +358400814808.
E-mail: hannuhaapala1@gmail.com

Key words: innovation, agriculture, IT, User-Centered Design.

Acknowledgments: the author would like to thank OECD Co-operative Research Programme for the research fellowship, and IVIA, Spain for the possibility to stay as a visiting researcher during the project.

Contributions: the author is solely responsible for the entire work.

Funding: the work was supported by an OECD CRP (Co-operative Research Programme) Fellowship.

Conference presentation: part of this paper was presented at the CIGR-AgEng 2012 Conference in Valencia, Spain, July 8-12, 2012 and AiiA13 Conference in Vitebro, Italy, September 8-12, 2013.

Journal of Agricultural Engineering 2013; XLIV(s2):e26
doi:10.4081/jae.2013.(s1):e26

Materials and Methods

The research was performed as a literature review, an internet-based Webropol® questionnaire for experts (sent to over 500 recipients, 341 opening the questionnaire, answering rate 12%, resulting N=41) and interviews of selected experts (N=10). The recipients were from all continents except Africa.

Acceptability of PF technologies was evaluated in modified categories of Nielsen (1993). Some detailed features of economy, benefits and technical compatibility and reliability were added. The concept of trust was also added.

In the questionnaire, the PF technologies were split into classes related to field operations, planning and control, and quality aspects. The questionnaire had four topics: technological level of PF products, application rate of PF, acceptability of PF, and the applicability of UCD to R&D in agricultural engineering.

The experts used the same topics but additionally they gave their opinions and visions of the most important research and development topics of UCD in Agricultural Engineering. Finally, the experts evaluated pre-set arguments of the potential of User-Centered Design (UCD) in the agricultural innovation process. They also rated the importance and urgency of UCD and PF related actions in research policy.

Results

In every class of PF technologies, the experts would like the current level of technology to be better than it is. In other words, they were disappointed on the past development. However, they were optimistic about the future and believed that R&D will be capable to narrow the technological development gap. Some technologies, such as the measurement of weather parameters or yield quantity, are not expected to develop much until 2020. Most potential development is expected to be in the planning algorithms. (Haapala 2012b)

Also in the case of application rate of PF technologies the experts were not satisfied with the current situation. Nor did the experts believe that the future application rate of PF technologies meets the expectations. Most potential growth in application was expected to be in the measurement of plant parameters and in the development of Farm Management Information Systems (FMIS). (Haapala 2012b)

The experts argued that efficiency of use is the most important component in usability. Economic aspects including awareness of the costs and benefits are also significant. Reliability and trust building were also ranked high. (Haapala 2012b)

The experts agreed that the current innovation process is not perfect. The end-users are not adequately involved in the R&D process and even if they are the designers do not understand them well enough. Experts think that UCD could bring more speed into the innovation process. However, the designers are not familiar with the UCD methods. There is an agreement among experts that UCD and related methods would yield to better products that would help the users to better adopt new technologies. Also trust in new technologies would be built with the use of UCD. (Haapala 2012b, Figure 1)

During the interviews of selected experts it became evident that the subject of the research was ranked as highly important. The interviews revealed a widespread concern on the situation in agricultural innovation processes. The interviewed experts agreed that the new technologies will not be applied enough if the user issues are ignored. The developers shoud know the user benefits in much more detail.

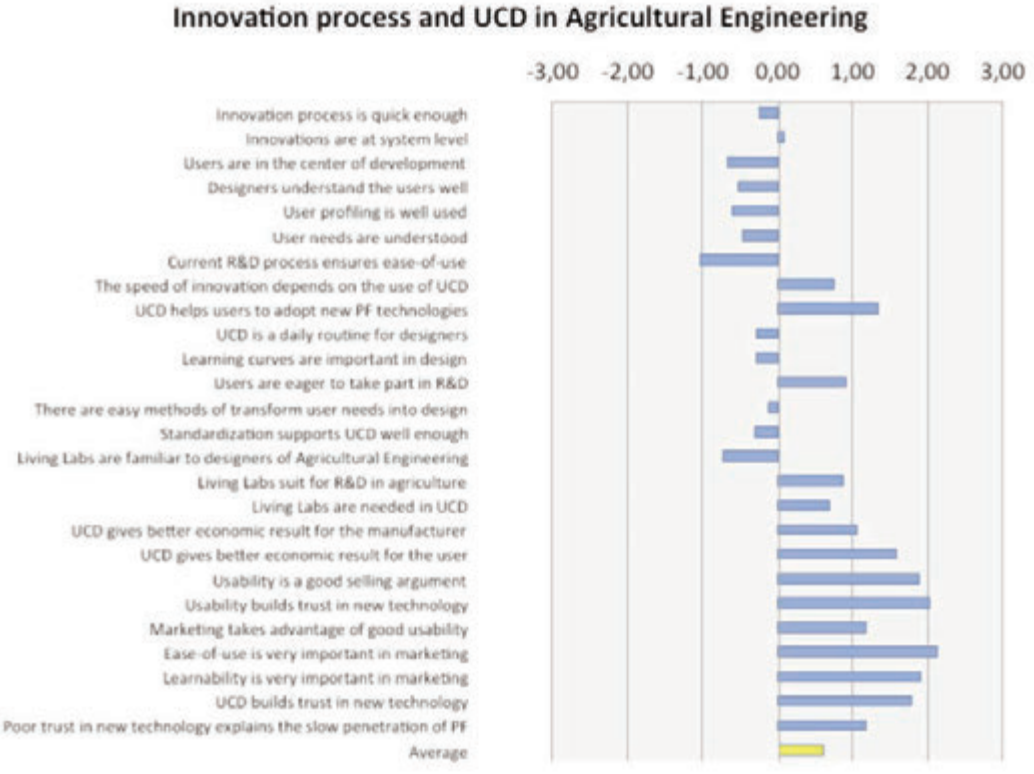

Figure 1. Innovation process and UCD in Agricultural Engineering. Arguments (-3=argee, 0= neutral, 3=agree).

Concervatism of farmers was pointed out to be an important fact limiting risk taking. Marketers of agricultural technologies should be more integrated in the innovation process since they have much contact to the end-users so that they have the potential to enhance innovation. On the other hand, marketers need reliable information about customer benefits.

Discussion

The respondents' competence profile was variable. In general, they were strong in engineering, research and practical use of technologies at the farm level. They evaluated themselves to have weaknessess in skills considering marketing, sales and teaching of design.

According to the feedback received, the questionnaire was heavy (over 40 pages). This limited the number of recipients. On the other hand, the recipients who dedicated their time for the questionnaire felt that the questions were relevant for the research topic.

The literature review revealed that there has not been much research on the subject of acceptability of argicultural engineering. Comparable research has mainly been done in other industries (e.g. Nielsen 1993, Kaasinen 2005, Li *et al.* 2008). Comparison of the results is somewhat difficult since agriculture is a very seasonal profession. The processes that apply technologies are not continuous so that the technologies are used in short periods of time that occur only a couple of times during the year. The users of agricultural technologies are often different from other workers because of their comparably high middle age, low educational level and low motivation to use the latest developments.

Conclusions

The results show that, in order to increase the speed of innovation, the end-users of new sustainable production systems such as Precision Farming (PF) need to trust better in the technologies involved. Acceptable products increase adoption of new technologies in agriculture. A deeper involvement of end-users in the design process yields products that are more acceptable. Using User-Centered Design (UCD) methods shortens the design phase in R&D because less iteration is needed to design an acceptable product. Therefore, UCD speeds up the innovation process. Since innovation is spread through imitation, the lead users need to have good experiences of using new technologies. Consequently, Living Labs where the lead users act as developers could be used to efficiently spread the good image of UCD-designed products. In future, education of the engineers and designers in agricultural R&D should include more elements from User-Centered Design (UCD) and also User-Driven Innovation methods should be more used.

The 'Dream Team' of agricultural innovation experts would consist of the traditional engineer-designer working partners but enhanced with the end-users and marketing specialists. This would add the needed user interaction and marketing expertise to the innovation process (Figure 2).

Figure 2. Innovation Dream Team. In addition to the traditional Enginee-Designer team the End-Users and Marketers of the technology should be integrated into the innovation process.

References

Diekmann, F. & Batte, M. 2010 Ohio Farming Practices Survey: Adoption and Use of Precision Farming Technology in Ohio. Experimentation report AEDE-RP-0129-10. http://tiny.cc/Diekmann _Batte.

Drejer, Ina 2004. Identifying innovation in surveys of services: a Schumpeterian perspective. http://dx.doi.org/10.1016/j.respol.2003.07.004. In: Research Policy. Elsevier. Vol. 33, 3: 551–562.

Haapala, H. & Nurkka, P. 2006. Usability as a Challenge in Precision Agriculture – case study: an ISOBUS VRT. Agricultural Engineering International: the CIGR Ejournal. 9 p.

Haapala, H. & Pasila, A. 2008. Agro Living Lab as a Tool to Teach R&D. 2008 ASABE Annual Meeting June 29 – July 2, 2008.

Haapala, H. & Pasila. A. 2009. Agro Living Lab - an R&D platform- ensuring acceptability of new technology among farmers. 67th International Conference on Agricultural Engineering LAND.TECHNIK AgEng 2009.

Haapala, H. 2012a. Speeding up innovation in agriculture. Questionnaire for Experts. Webropol questionnaire. http://agrinnotech.com.46 p.

Haapala, H. 2012b. The potential of User-Centered Design (UCD) to make radical agricultural innovations. In: International Conference of Agricultural Engineering. CIGR-AgEng 2012. July 8-12. Valencia, Spain.

Kaasinen, E. 2005. User acceptance of mobile services – value, ease of use, trust and ease of adoption. Espoo 2005. VTT Publications 566. 151 p. + app. 64 p.

Li, W., Hess, T. & Valacich, J. 2008. Why do we trust new technology? A study of initial trust formation with organizational information systems. The Journal of Strategic Information Systems. http://dx.doi.org/10.1016/j.jsis.2008.01.001. Elsevier. Vol 17, 1: 39–71

Nielsen, J. 1993. Usability Engineering. Academic Press Inc. 362 p.

OECD 2005. Oslo Manual. The measurement of scientific and technological activities. Proposed guidelines for collecting and interpreting technological innovation data. European Commission. Eurostat. www.oecd.org/sti/oslomanual. ISBN 978-92-64-01308-3. 3rd ed. 163 p.

Winstead, A., Norwood, S., Griffin, T., Runge, M., Adrian, A., Fulton, J. & Kelton, J. 2010. Adoption and Use of Precision Agriculture Technologies by Practitioners. In: Proc.the 10th International Conference on Precision Agriculture, 18-21 July 2010. Denver, Colorado.

Wolfert, J., Verdouw, C., Verloop, C. & Beulens, A. 2010. Organizing information integration in agri-food—A method based on a service-oriented architecture and livinglab approach. Special issue on Information and Communication Technologies in Bio and Earth Sciences. http://dx.doi.org/10.1016/j.compag.2009.07.015. Computers and Electronics in Agriculture. Elsevier. Vol. 70, 2: 389–405.

GNSS-based operational monitoring devices for forest logging operation chains

Raimondo Gallo,[1] Stefano Grigolato,[2] Raffaele Cavalli,[2] Fabrizio Mazzetto[1]

Free University of Bozen-Bolzano, Faculty of Science and Technology, Bolzano, Italy; Forest Operation Management Unit, [2]Dept. Land, Environment, Agriculture and Forestry, University of Padova, Italy

Abstract

The first results of a new approach for implementing operational monitoring tool to control the performance of forest mechanisation chains are proposed and discussed. The solution is based on Global Navigation Satellite System (GNSS) tools that are the core of a data-logging system that, in combination with a specific inference-engine, is able to analyse process times, work distances, forward speeds, vehicle tracking and number of working cycles in forest operations. As a consequence the operational monitoring control methods could provide an evaluation of the efficiency of the investigated forest operations.The study has monitored the performance of a tower yarder with crane and processor-head, during logging operations. The field surveys consisted on the installation of the GNSS device directly on the forest equipment for monitoring its movements. Simultaneously the field survey considered the integration of the GNSS information with a time study of work elements based on the continuous time methods supported by a time study board. Additionally, where possible, the on-board computer of the forest machine was also used in order to obtain additional information to be integrated to the GNSS data and the time study. All the recorded GNSS data integrated with the work elements study were thus post-processed through GIS analysis.

The preliminary overview about the application of this approach on harvesting operations has permitted to assess a good feasibility of the use of GNSS in the relief of operative times in high mechanised forest chains. Results showed an easy and complete identification of the different operative cycles and elementary operations phases, with a maximum difference between the two methodologies of 10.32%. The use of GNSS installed on forest equipment, integrated with the inference-engine and also with an interface for data communication or data storage, will permit an automatic or semi-automatic operational monitoring, improving the quantity of data and reducing the engagement of the surveyor.

Correspondence: Raimondo Gallo, Free University of Bozen-Bolzano Faculty of Science and Technology Piazza Universitá 5, 39100 Bolzano BZ Italy.
Email: raimondo.gallo@natec.unibz.it

Key words: precision forestry, forest operation performance, operational-monitoring, time study.

Journal of Agricultural Engineering 2013; XLIV(s2):e27
doi:10.4081/jae.2013.(s1):e27

Introduction

As in agriculture, also in the forest sector the information technology has been introduced with the aim to improve the efficiency and performance of this sector. Indeed the Precision Forestry is the approach that employs the well known strategies and methodology of Precision Agriculture and Precision Farming to the forest sector in order to obtain a decision support system (DSS) (Lubello *et al.*, 2006). The Precision Forestry, starting from the well-established Precision Agriculture, presents some research topics not yet completely explored. One of these is the study of operational monitoring in automatic ways. Considering the equipment on which the Precision Forestry bases its applications, the Global Navigation Satellite System (GNSS) device is one of the most important.

The aim of this study is to detect the operative times through the use of a GNSS device that, at each fixing point, is able to perform also a time acquisition. The operational time study is considered as "a set of procedures for determining the amount of time required, under certain standard conditions of measurement, for tasks involving some human, machine, or combined activities" (Mundel and Danner, 1994). At this regard, the operational time study became an important parameter for the assessment of the productivity. Indeed, thanks to the time survey, it is possible to evaluate which is the efficiency of the entire work systems (machineries and humans activities), the singular equipment or the team of workers.

The analysis of the operational times or time consumption measurement, in forestry sector is usually done thanks to the use of time study boards or hand held computers or by automated data collectors attached to forest machines' computers and CAN-bus channels (Nuutinen *et al.* 2010). Automatic operational time study based on the installation of GNSS on machineries that operate in forest are also quite common. This methodology is mainly applied for the tracking of the movements of the machineries for felling and skidding operations in forest (Taylor *et al.*, 2006; Cordero R., *et al.*, 2005; McDonald and Fulton 2005, McDonald *et al.*, 2001, Taylor, *et al.*, 2001; Veal, *et al.*, 2001; McDonald 1999) and for tracking the trucks for timber haulage (Simwanda *et al.*, 2011; Devlin and McDonnell, 2009; Devlin *et al.*, 2008; Sikanen *et al.*, 2005). Only a document on the use of GPS for the analysis of tower yarder was found (Nitami *et al.*, 2011).

The aim of this study is to verify the feasibility to develop a methodology for acquisition, elaboration and interpretation of the data autonomously. The methodology must recognizes and reliefs the num-

ber of cycles of work, each elementary phase and also the respective operational time. This will be possible thanks to the development of an inference-engine able to transform satellite raw data into intelligible management information (Mazzetto *et al.*, 2012). The operational time data acquisition system was then validated through the comparison with an operational monitoring relief with stopwatch. This paper presents the preliminary results and discussions.

Materials and Methods

Study area

The study-case was set during the logging operations of conversion of a secondary forest of Norway spruce (*Picea abies* L.) in a mixed forest mainly composed of beech (*Fagus sylvatica* L.). The forest yard, interested by the cultural operation, was organized in pre-alpine region, in the N-E of Italy (Pordenone Province – Friuli Venezia Giulia Region). The machineries that compose the mechanisation chain were chains saw and Mayr-Melnhof®-MM *Syncrofalke*, mobile tower yarder with crane and processor-head. The employed carriage was a MM *Sherpa* with 3 t payload.

The *data-logger* used for the automatic reliefs was a Geographical Position System (GPS) mobile device installed on the cable yarder's carriage. The GPS unit is an ASCTECH® MobileMapper 6, a 12-channel singular frequency device; which runs Windows Mobile 6, and the specific software MobileMapper Field on a 400 MHz cpu. In order to assure a better reception of the satellite's signals, an external antenna was connected. In order to protect the GPS from any accidental shocks, a plastic box with layers of foam was built. Finally the box, which carried the GPS, was fixed to the internal body of the carriage (Figure 1a) with plastic ties. Meanwhile the external antenna was placed on top of the frame by means of a magnet. The antenna connection cable was fixed to the lateral frame of the carriage with scotch tape in order to avoid any entanglement with branches (Figure 1b).

The GNSS device was set with an automatic data acquisition of the carriage's position every 3 seconds.

A time study board with three decimal stopwatches was used for the manual relief of operative times necessary to the validation of the data. The manual time relief was based on the continuous time methods. The methodology requires the presence of two surveyors: one placed in the felling point and the other one placed on the temporary storage area for the relief of possible operative down-time during the downloading operations as well as the relief of timber's volumes exploited. The communication between the surveyors was supported by radio. The operational monitoring was based on the identification of elementary operations for operative times as following:

- Travel empty: when the carriage starts movement from the unhooking site (landing) to when it stops along the line for starting the hooking phase;
- Hooking: from when the carriage stops to when the log movements start;
- Side-lining: from the start of the log movements to the unlock of the carriage;
- Load travel: from the unlock of the carriage to the next lock in proximity of the tower yarder for the unhooking;
- Unhooking: from the lock of the carriage and start of the download operation to the unlock for the start of the next cycle;

Meanwhile, the operative down-times were identified due to: mechanical reasons (in the case of machine break-down), operative reasons (delay because the operator is interested in more than one activity), operator's personal reasons (personal needs) or study reasons.

Elaboration data

Data acquisition that, set with a period of collection of 3 seconds of interval, was post-processed through the use of the software MobileMapper Office 4.0. The elaboration returned correct coordinates, altitude as well as recording time. Using these data following values of instantaneous speeds, movements, advancement direction were obtained. Since the system must work without any reference data , and also reduce the influence of possible low accuracy of the data, a methodology to establish an initial reference point P_r (x_r; y_r) – external to the points cloud in proximity of the starting point – was necessary (Figure 2).

The determination of P_r is done in order to obtain a starting point as reference for the detection of all distances of the entire points of the data-set. The first point collected by GNSS device identifies the start of the relief, then, the recognition of the logging direction establishes the choice of the coordinates for P_r. The attribution is done considering the maximum or minimum coordinates of the points of the cloud in the proximity of the initial point. When the referencing point of the system is detected, the distances from P_r of the entire set of points were calculated in order to have a common variable to analyse the relationship between variables.

Figure 1. Installation of GNSS device on carriage (a: particular view; b: during detecting operations).

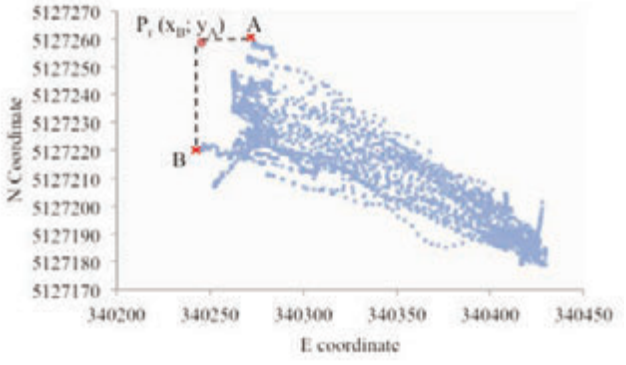

Figure 2. Distribution of GPS detections and identification of the point of reference P_r recognising A and B as the extreme point of the cloud and N-E as logging direction.

Results and Discussions

During this study case a total of 2 days of automatic and manual monitoring were done. Only the data collected during the second day were usable for the elaborations. Due to the low precision and accuracy of the first day's acquisitions it was not possible to perform the post-processing elaboration of the raw data. Therefore only one data-set was post-processed and elaborated; it is represented in Figure 2. The relief consists in an effective survey of 3.6 hours of work with a data-set of 3093 records. In fact the number of records is lower than what corresponds to 3.6 hours. This lack of time information occurred as empty spaces during the data acquisition and also as drift points. In fact the expected result from GPS detection should be a series of points more or less along the same line. Anyhow correlating the times gap with the respective distances of the registered position (Figure 3) and comparing them with the other graphs that describe the carriage's kinematic behaviour, (Figure 4; Figure 5a; Figure 5b), it was possible to detected that this phenomenon occurred mainly when the carriage is blocked for hooking or unhooking operations.

These time gaps happen rarely during the advancement. The drifting of the points could be due to several factors as: the canopy coverage (McDonald and Fulton, 2005), the loss or the acquisition of new satellite's signal (Taylor *et al.*, 2006) – that determine a recalculation of the GNSS device position –, the insufficient satellites coverage or their geometric distribution (Naesset *et al.*, 2000) during the acquisition data. But in this case it is possible to say that the drift is caused by multipath interference due to the closeness with steel equipment (truck and carriage frame), that bounced the satellite's signal, and also by the bad weather with fog and fine rain during the relief, which influenced the speed at which the satellite radio waves travelled (Naesset *et al.*, 2000). For making a first description of carriage's kinematic behaviour data about distances, advancement speeds and advancement directions were necessary (Figure 4; Figure 5a; Figure 5b).

In Figure 4 the advancement direction of the carriage during its movements and during the hooking and unhooking operations is reported. Its relationship with the distances from the point of reference highlights two distinguished families of points. Each in correspondence to the average values of 110° and 290°. These represent the direction of movement of empty and loaded travels respectively. While the carriage stops the advancement and during the hooking and unhooking operations the values of direction do not have linear distributions. This is due to the oscillation caused by the weight of the logs during the load or unloads operations. As far as the analysis of the advancement speeds is concerned, it is possible to say that the carriage travels with an advancement speed higher than 2.5 m/s during its travel operations. It is also possible to note that the advancement speed is split in two different families of points, better visible in figure 5b, with different average values of speed: 2 m/s for the lower and 3 m/s for the higher, respectively for loaded and empty travel. Besides this, in figure 5a it is easy to identify also the points where the carriage blocks its advancement in correspondence to the hooking area as well as the point of automatic arrest in proximity of the tower yarder during the empty travel (red arrows in the Figure 5a).

After that, analyses of the working cycles (Figure 6) were done in order to obtain the gross cycle time and the elementary operational times. Through this elaboration it was possible to analyse the relationship between the progressive time (considered as the sum time difference between two sequent points) and the respective distance from the point of reference.

Results of the gross and elementary study time are summarized in the following tables (Table 1, 2).

To facilitate the procedure of operational times recognition they are not considered at net to down-times. During the study a total of 21 cycles was monitored, the first one, being a trial run, was not considered. McDonald (2005) reported that the automatic time study with the use of GNSS device is able to correctly recognize at least 90%, of the cycles, in the present study the result is better because all cycles were recognized. The very good results obtained are also demonstrated by the high value of correlation between the manual relief and the automatic ones (Figure 7). Anyhow, in total, a difference below 4 minutes was observed between the two methodologies of relief. Probably these

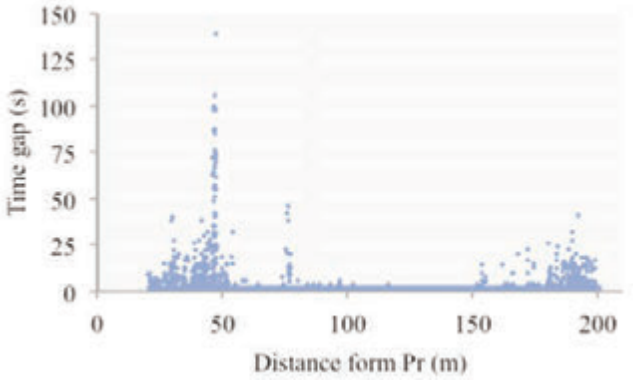

Figure 3. Times gap distribution in relation to the distance from P_r.

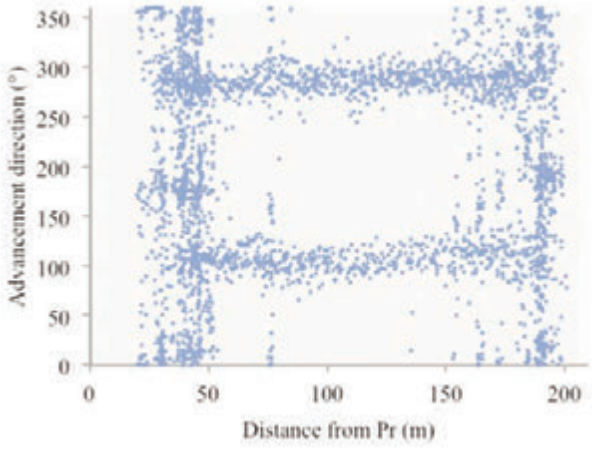

Figure 4. Distribution of the advancement directions in relation to distance from P_r.

Table 1. Number of cycles and gross operative time summary.

	Operative Cycle N	Gross operative time min
Automatic relief GNSS (AR)	20	135.12
Manual relief Clock (MR)	20	131.51
Difference	-	*-2.75 [%]*

are due to recording discontinuities during time detections, and to the presence of communications delays between the two surveyors due to transmission troubles of the walkie-talkie. Meanwhile for what concerns the elementary time study, the side-lining operations were not identifiable, because the detected parameters were not sufficient for that. So, in order to proceed with the analysis, hooking and side-lining operations were considered together. Also in this case all operative phases were recognized. For the elementary phases, substantial time differences between the GNSS and clock detections were found (Figure 7). These are mainly present during travels. Explanation of that could be associated to the difficulties during the determination of the shift values between sequent phases (Table 2).

Table 2. Operative time summary for each elementary phase.

Operative cycle	Empty travel		Hooking		Loaded travel		Unhooking	
	GNSS min	Clock min	GNSS min	Clock min	GNSS	Clock	GNSS	Clock
1	0.80	0.85	0.63	0.52	1.57	1.52	1.68	1.77
2	1.12	0.71	1.60	1.45	1.47	1.37	1.33	1.47
3	0.97	0.81	1.72	1.82	2.55	1.91	3.78	3.33
4	1.08	0.92	1.60	1.64	1.87	1.75	1.00	1.08
5	0.80	0.85	0.77	0.84	1.50	1.44	2.97	3.00
6	0.90	0.65	1.00	1.17	2.73	2.45	1.17	1.52
7	0.97	0.92	1.23	1.44	2.85	2.75	0.48	0.47
8	1.15	1.06	1.95	1.86	3.53	3.61	0.97	0.93
9	1.07	1.09	3.80	3.83	1.67	1.70	3.00	3.00

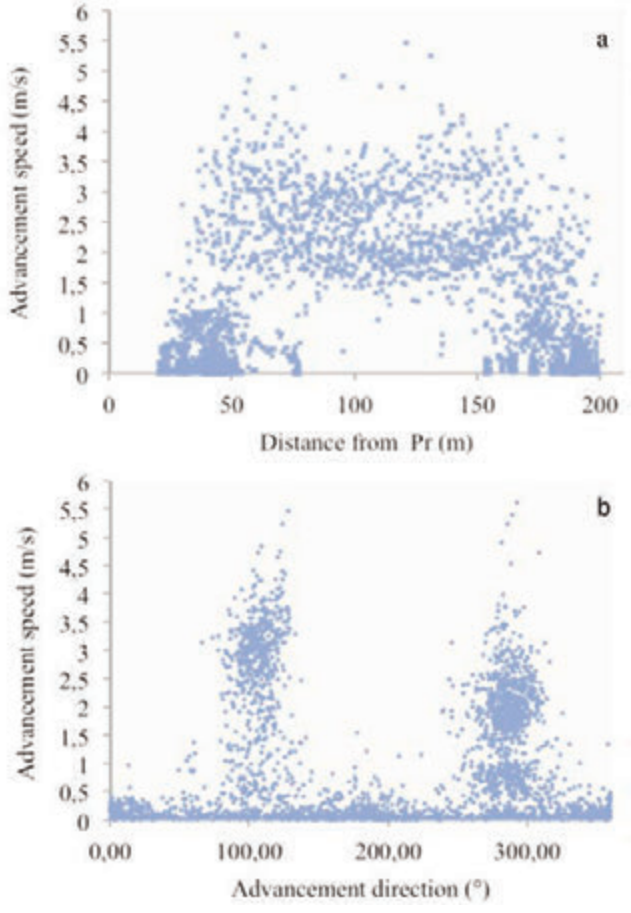

Figure 5. a) distribution of the advancement speeds in relation to distance from P$_r$; b) distribution of the advancement speeds in relation to advancement directions.

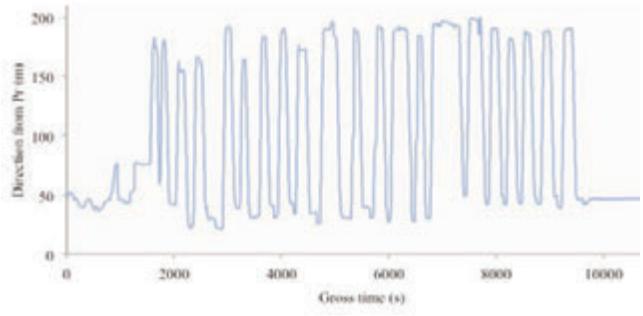

Figure 6. Representation of the entire cycling work.

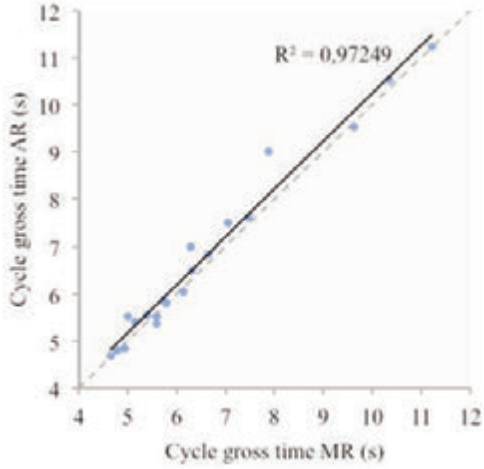

Figure 7. Correlation between manual relief (MR) and automatic relief (AR) with GNSS device.

Conclusions

Despite the short test period, experiences obtained very interesting and important results for further improvement of the assess methodology. This initial part of the research has shown that the use of GNSS devices presents a very interesting feasibility for performing operational time monitoring in forest logging operations. All operative cycles and all elementary operations have been exhaustively recognized. Considering the cycle's gross times the differences are lower than 2.75%, corresponding to 3.61 minutes. Meanwhile the differences between the elementary operations are higher. Indeed the two methodologies present a maximum difference of 9.24%, which means a maximum average error lower than 0.46% (0.18 minutes) for each cycle. This value could be considered acceptable. In order to increase the accuracy of the automatic time relief it could possible employ GNSS devices those reach signal from both satellite constellation: GPS and GLONASS.

From these first results several open points were found, next steps of the research will be the identifications of the reasons of the drifting phenomena during the GNSS detection and also of the discrepancy between the times relieved mainly during travel operations. Besides this, new strategies for the detection of side-lining operations will be analysed. The possibility of including further sensors (such as load cells for measuring the weight of timbers hooked to the crane) will be considered as well, in order to provide more information for a better performance of the inference-engine.

References

Cordero R., Mardones O., and Marticorena M. 2006. Evaluation of forestry machinery performance in harvesting operations using GPS technology. In: Precision Forestry in Plantations, Semi-Natural and Natural Forests, Proceedings of the International Precision Forestry Symposium, Stellenbosch University, South Africa. pp 163-73

Devlin G.J., McDonnell K. 2009. Assessing Real Time GPS Asset Tracking for Timber Haulage. Open Transportation Journal 3: 78-86.

Devlin G. J., McDonnell K., Ward S. 2008. Timber haulage routing in Ireland: an analysis using GIS and GPS. Journal of Transport Geography 16(1): 63-72.

Lubello D., Cavalli R. 2006. Ambiti applicative della Precision Forestry. Sherwood Foreste 125: 11-16.

Mazzetto F., Sacco P., Calcante A. 2012. Algorithms for the interpretation of continuous measurement of the slurry level in storage tanks. Journal of Agricultural Engineering 43(1), e6.

McDonald T. 1999. Time Study of Harvesting Equipment Using GPS-Derived Positional Data. Notes. http://treesearch.fs.fed.us/pubs/1411

McDonald T., Fulton J. 2005. Automated time study of skidders using global positioning system data. Computers and electronics in agriculture 48(1): 19-37.

McDonald T., Rummer B., Taylor S. 2001. "Automating time study of feller-bunchers." In Proceedings of the Canadian Woodlands Forum's 81st Annual Meeting and Council on Forest Engineering's 23rd Annual Meeting- Technologies for New Millennium Forestry, Kelowna, BC.

Mundel M., Danner D. 1994. Motion and time study – improving productivity. 7th ed. Prentice Hall, Upper Saddle River, NJ. 770pp.

Nitami T., Soil S., Kataoka A., Mitsuyama T. 2010. Tower Yarder operation in Japan and the performance analysis by GPS-based system. In: Pushing the boundaries with research and innovation in forest engineering. FORMEC 2011, Proceedings of the 44th International Symposium on Forestry Mechanisation, 9-13 October 2011. Graz, Austria.

Naesset E., Bjerke T., Bvstedal O., Ryan L. H. 2000. Contributions of differential GPS and GLONASS observations to point accuracy under forest canopies. Photogrammetric Engineering & Remote Sensing 66(4). pp 403-07.

Nuutinen Y., Väätäinen K., Asikainen A., Prinz R. & Heinonen J. 2010. Operational efficiency and damage to sawlogs by feed rollers of the harvester head. Silva Fennica, 44. pp 121-39.

Sikanen L., Asikainen A., Lehikoinen M. 2005. Transport control of forest fuels by fleet manager, mobile terminals and GPS. Biomass and Bioenergy 28(2). pp 183-91.

Simwanda M., Wing M. G., Sessions J. 2011. Evaluating Global Positioning System Accuracy for Forest Biomass Transportation Tracking within Varying Forest Canopy. Western Journal of Applied Forestry 26(4). pp 165-73.

Taylor S. E., McDonald T., Veal M. W., Grift T. E. 2001. Using GPS to evaluate productivity and performance of forest machine systems. In Proceedings of the First International Precision Forestry Cooperative Symposium: University of Washington, College of Forest Resource. pp 151-55.

Taylor S., McDonald T., Fulton J., Shaw J., Corley F., Brodbeck C. 2006. Precision forestry in the southeast US. In Proceedings of the 1st International Precision Forestry Symposium. pp. 397-14.

Veal M., Taylor S., McDonald T., McLemore D., Dunn M. 2001. Accuracy of tracking forest machines with GPS. Transactions of the ASAE 44(6). pp 1903-11.

Sustainable management of waste in green nursery: the Tuscan experience

Daniele Sarri, Riccardo Lisci, M. Rimediotti, M. Vieri

Department of Agricultural, Food Production and Forest Management University of Florence Firenze, Italy

Abstract

The green nursery sector in Europe involves 90,000 ha of cultivated land and 120,000 ha for the nurseries (MiPAAF, 2012), reaching 19.8 billions of Euros in 2011. Every year, nurseries produce waste about 4 kg of the residual biomass for each m^2 of the potted plants cultivation.

Nurseries waste make up a substantial quantity of organic materials e.g. wood biomass-substrate, which could be retrieved and valorized. With the expansion of potted plants cultivation and the resulting increase in discarded products a number of companies have begun to setting up solutions for the recovery of materials accumulated.

Analysis led to the development of a separating system based on trunk vibration technology. To this end, two shaker yard were identified, developed and tested for the recovery of residual biomasses. With these solutions, green waste can be easily grasped by a clamp device able to convey strong vibrations to the trunk (or to the aerial part of the plant) to the point that the soil materials are detached from the vegetable portions.

Correspondence: Daniele Sarri, GESAAF Department of Agricultural, Food Production and Forest Management, Scuola di Agraria, University of Florence, Piazzale delle Cascine 15, 50144 Firenze, Italy
Tel. +39 055 3288320 - Fax +39 055 331794
E-mail:daniele.sarri@unifi.it

Key words: biomass recovery, substrate reuse, mechanical shaker separation.

Acknowledgments: Authors wish to acknowledge the Vannucci's nursery that hosted the tests and supplied a lot of the information contained in the present work filling in specific questionnaires. Furthermore, authors wish to thank the company A. Spedo e Figli for the logistic assistance and the cooperation.

Contributions: the authors contributed equally.

Conflict of interests: the authors declare no potential conflict of interests.

Funding: the work was supported by Regione Toscana, project VIS Vivaismo Sostenibile 2013.

Journal of Agricultural Engineering 2013; XLIV(s2):e28
doi:10.4081/jae.2013.(s1):e28

Introduction

The Italian nursery sector involves 13,000 ha of potted flowers and plants and represent the second most important European market with an annual average turnover of 2,5 billions of Euros.

Although the significant economic potential, the sector is characterised either by limited size companies, i.e. less than 10.000 m2 and, either by a limited number of extensive nurseries. Consequently, these conditions, influence the potential level of innovation that the companies choose and that could implement. The small nursery employ standard stage processes and mechanization, vice versa the big companies, in the last years, started to implement innovative solutions in the productive processes. Many studies developed in Oregon (CFNP, 2011) analyse the impacts associated to the nurseries, recommending best practices for energy reductions and wastes recycle or reuse. Furthermore, the worldwide financial crisis and the rising cost of raw materials, has also affected the nursery sector specifically for the supply of raw materials such peat (basic element of the substrates) and mineral fertilizers.

About this the University of Florence research unit worked on the VIS (Sustainable Plant Nurseries Project) on a study to identify solutions for the green nursery wastes recovery. Green waste products in nurseries and the derivatives of dried and unsalable plants, of lifting plants and pruning, make up a substantial quantity of organic materials e.g. wood biomass and substrate, which could be retrieved and valorized. The wastes of farm that works on full field cultivations, are usually made up of dried plants and pruning byproducts while the reverse is the case for those raising crops in containers, whose waste is mainly substrate. Moreover, the latter fraction shows a high concentration of controlled-release-fertilizers, which gives great potential and high economic value to the recycled substrate (Figure 1). Up to few years ago, the common management was carried out through the disposing of all the biomass, i.e. the wood, the roots, the substrate and other waste materials. With the expansion of cultivating crops in containers and the resulting increase in discarded products a number of companies have begun setting up work-sites for the management of the materials accumulated. Currently, for wastes recovery, the most widespread technique is to sent the biomass to a treatment plant where shredding and wind separating are performed, producing powdery substrate, wood with substrate traces, iron and stony materials. The powdery substrate may be mixed with the virgin substrate with a variable share, whilst the wood is used for biofilters production. Another type of management involves the biomass shredding and a storage phase with a variable duration in function of the weather, features of the stock site, raw matter quality, type and number of processing stages. This management ensures a fermentation of the biomass with a potential reduction of the pests level. However, the resulting biomass, has a more concentration of wood parts than the other one.

The components which can be recovered on industrial work-sites following bioshredding take on characteristics which make it difficult to get two fractions of optimum quality (Figure 2). This operations are more effective if the different typologies of the residual biomass (i.e.

the wood and the substrate) are separated, before the shredding phase, in order to guarantee their better reuse and a more significant substitution of the raw materials needed in the nursery. Particularly, depending on the level of separation of the main components and on the quality of the recovered products in terms of purity, size, etc., the shredded wood may be applied as biofilter or as solid biofuels. The recovered substrate may be mixed to the virgin one in quantities as higher as the wood and the other minor compounds (e.g. stones, ferrous materials, plastics, etc.) are much limited.

On these bases, the work has focused to identify solutions for separating substrate and wood biomass components with processes, which do not allow interaction. Analysis led to the development of a separating system based on trunk vibration technology.

Materials and methods

The concept singled out is based on the knowledge that the biomass, to be worked, must be moved in any case in the nursery. On this basis a solution able to simultaneously perform the step of handling and separation was defined. The general principle is: the biomass may be easily grasped by a clamp device able to convey strong vibrations to the trunk to the point that the substrate is detached from the vegetable portions. In so doing the two components can be managed separately, as green discard and earth-peat for reusing in the production process. Then the whole plant is chipped obtaining wood that may be used as solid biofuel in small or medium sized boilers for heating. The recovered substrate may be used instead of the virgin one. To this end, two yards were identified, developed and tested for an efficient use on residual biomass with a mass of up to 800 kg.

Selected as a solution to apply in smaller nurseries with plants of no more than 100 kg was a small yard "Unifi prototype" made of a track-laying walking tractor equipped with a shaker clamp with a motorized frame equipped with power points and a lift (Figure 3). The drive transmission is hydrostatic: a tandem pump is connected to the engine, which in its turn controls two orbital motors with direct power take-off from the cog wheels; the control unit for forward movement and the steering is the only lever, so the vehicle can be driven with one hand. Speed variation is continuous up to a maximum of 6 km/h both forward and in reverse.

The clamp weigh about 100 kg and is coupled with the closure jaws for work on trees of up to 150 mm in diameter. The vibration is made by an eccentric mass driven by an hydraulic motor; this configuration, with a 16 cm^3 hydraulic motor, produces centrifugal force of vibration about 120 N at the frequency of 69 Hz. Hydraulic plant, with a capacity of 45 L min^{-1}, is required for operations. Moreover, the prototype is furnished with a setup for the shaker that includes a steel frame, for regulating and positioning the vibrating jaws. The movement of the vibrating clamp is driven by a horizontal forked boom with manual regulation equipped with a hydraulic piston linking it to the lift column, also with a hydraulic control lever. With this configuration, the clamp can be positioned from 0,3 m to 1 m above the mean ground elevation and a further 0,5 m with the regulation for inclination. Used for handling plants with mass of more than 100 kg is the vibrating clamp made by the company A. Spedo e Figli in Badia Polesine, near Rovigo, capable of dealing with trees with masses of up to 800 kg and diameters of up to 0,4 m. The technical specification of the yard make it possible to cope with all types of plant discards which can be found a nursery. For this purpose, the yard includes a 110 kW tractor equipped with a front loader and the clamp (Figure 4). This configuration is a solution suitable for medium size and big nurseries or contractor services. The vibrating clamp, with opposing jaws, is oil hydraulic driven. By the rota-

Figure 1. Green nursery waste: pile of discarded plants.

Figure 2. Green waste after the bio-shredding phase: the two fractions present a high level of contamination.

Figure 3. The "Unifi prototype" made of a small track-laying walking tractor equipped with a shaker clamp.

tion of an inertial mass driven by a hydraulic motor, it originates a variation of centrifugal strength, which in its turn generates vibration. Micro-vibration can be regulated for amplitude and frequency and is controlled independently of the shaker on the basis of the diameter of the tree gripped to ensure the complete detachment of the soil. The design configuration enables rotation of 60° for facilitating gripping and moving the tree. The jaws are easy for the operator to maneuver with great precision and safety through a joystick in the tractor cab or report control and the electro-hydraulic device enabling movement at proportional speeds. The original closing clamps on the jaws were modified with the addition of structures and raised steel staffs for a steady grip during shaking. The logistics for operations call for the following phases: gripping the tree, recovery of the containers, shaking, heaping up the biomass. (Figure 5) Work on the single tree appears laborious but it must be pointed out that this operation does not entail further steps because with present management each tree is gripped and lifted with a lift for the container recovery.

Figure 4. The implemented yard based on a shaker A. Spedo e Figli company.

To study the effectiveness of the yards, some tests were conducted in the Vannucci Green Nursery Company in the city of Pistoia located in the centre of Italy. The field tests were performed with two types of green waste species: *x Cupressocyparis leylandii* commonly called Leyland Cypres and *Cedrus atlantica "Glauca Pendula"* commonly called Weeping Atlas Cedar. The first specie tested were raised 5 years in containers of 50 L and they had a single trunk height 3,5 m on average. The Weeping Atlas Cedar, were raised in container, with variable volumes from 240 to 300 L of substrate for the same time, they had reached 4,5 m in height and they were structured in single trunk with the upper part curved to the ground. The average trunk diameters, of the two tree kinds, were respectively 0,065 m for the Leyland Cypres and 0.1 m for the Weeping Atlas Cedar.

Trials were carried out on twenty trees by applying the force to the trunk at an approximate height of 0.1 m from the upper level of the substrate. The UNIFI prototype worked only the species Leyland Cypres because it is designed to work with biomasses with maximum mass of 100 kg while the Spedo yard worked both the specie. Each tree was weighed before and after the shaker stage by means of a load cell brand DG model MCWL600 with a sensitivity of 0.05 kg and full scale at 600 kg. Measurements were performed up to the complete separation the substrate from the wood biomass storing the time required.

Figure 5. The operative logistics: grip the tree, containers recovery, shaking, heaping up the biomass.

Results

Both the yards developed have allowed to effectively separating the residual biomass. The Unifi prototype has employed an average of 34 seconds to work each plant (shaking stage) while the Spedo yard, with the Weeping Atlas Cedar, it took 32 seconds and 31 seconds for the Leyland Cypres. About the quantity of recovery materials, preliminary tests conducted have highlighted for the Weeping Atlas Cedar mean values of 40 kg of green waste and 250 kg of substrate. In the case of Leyland Cypres were obtained average values of 18 kg of green waste and 34 kg of substrate. Regarding the quality of the recovery portions, in the case of the powdery substrate these were cleaned by the visual point of view with only some leaf and small parts of the root system. The latter appear completely separated from the substrate so immediately ready to the shredding stage. Also the characteristics of the recycled powdery substrate allow to mix instantaneously with the virgin matters, reducing the demand of non-renewable raw material.

Conclusions

Present work has focused to the possible recovery of the residual biomasses, i.e. the wood and the substrate, of the potted plants that are discarded in the nursery production chain. To recognize the value of green waste, different ways and equipment can be employed, so it is necessary a careful reflection on the design of the more suitable yard in function of the type of nursery. In particular, it is essential to consider the available spaces and the economic feasibility: the yards configurations depend by the structural and organizational conditions of the nursery, but also by its investment capability. Other essential variables are the amount of waste produced annually, their features, in terms of botanical species and size of plants. All these aspects affect the choice of machines. The use of shaker machines to residual biomasses recovery is an alternative technique that, properly developed and industrialized, may be effectively introduced in the nursery chain. The adoption of innovative technologies for green waste recovery described in this study can afford on the one hand the exploitation of by-products, on the other to obtain significant benefits in terms of environmental protection thanks to the recovery of biomass for energy purposes.

References

CFNP, 2011.Climate Friendly Nurseries Project, Best management practices for climate friendly nurseries, Oregon Association of Nurseries, Oregon Environmental Council, Oregon State University, Advantage IQ, Version 2.0, August 2011.

MiPAAF, 2012. Lettera UE 13-05, Situazione attuale del settore florovivaistico Europeo, 19 luglio 2012.

Sarri D, Rimediotti M, Vieri M, Recupero degli scarti verdi Chapter 3 in final report book Gestione sostenibile dei vivai 2013. Available from: http://www.cespevi.it/vis/Manuale_VIS.pdf Accessed: May2013.

Selective spraying of grapevine's diseases by a modular agricultural robot

R. Oberti,[1] M. Marchi,[1,2] P. Tirelli,[1,2] A. Calcante,[1] M. Iriti,[1] M. Hočevar,[3] J. Baur,[4] J. Pfaff,[4] C. Schütz,[4] H. Ulbrich[4]

[1]DiSAA, Dipartimento di Scienze Agrarie e Ambientali, Università degli Studi di Milano, Italy, [2]Applied Intelligent Systems–AIS Lab, Dipartimento di Informatica, Università degli Studi di Milano, Italy; [3]University of Ljubljana, Faculty of Mechanical Engineering, Ljubljana, Slovenia; [4]Institute of Applied Mechanics, Technische Universität München, Garching, Germany

Abstract

In current viticulture protection of grapevine is obtained with uniform distribution of fungicides, typically repeated according a regular calendar. This continuous protection approach can easily result in ten to fifteen treatments per season in vineyards of several wine-producing regions. Primary infections exhibit nevertheless discrete foci, with uneven spatial distribution. Hence it can be argued that detection of symptoms at early disease stages and their targeted treatment would reduce the spread of the infection to wider patches in the vineyard, while enabling reduced use of pesticides. Within the UE-project CROPS, a modular and multifunctional agricultural robot system for specialty crops is being developed and one of the tasks that has to accomplished is selective spraying of diseases. The robotic system set-up integrates a six degrees of freedom manipulator, an optical sensor system and a precision spraying actuator. After a brief description of the requirements of the system, this contribution gives a detailed description of its components and discusses the results obtained in first experiments. As case study we consider here the automatic detection and selective spraying of grapevine canopy areas exhibiting symptoms of powdery mildew (Erysiphe necator), one of the major diseases for this crop. Based on optical sensing feedback, the precision spraying actuator is positioned by the manipulator to selectively and accurately apply pesticides solely to infected areas.

Disease foci identification and localization is based on on-the-go processing of images sensed by a multispectral camera inspecting the vertical structure of the grapevine canopy. At the end of the manipulator arm is located the precision spraying actuator, constituted by an axial fan with a flow straightener and an axially mounted spraying nozzle. The sprayer can deliver an air-carrier flow with an adjustable velocity, producing a circular spraying pattern of a constant diameter of 0.15 m over a wide range of spraying distances.

A first experiment was conducted in an experimental greenhouse, where vineyard canopy conditions were recreated by aligning plants of grapevine grown in pots. Within the recreated canopy, diseased plants with different levels of disease symptoms were used as targets of automated selective spraying performed by the agricultural robot. The results of these experiments are discussed in view of a possible intelligent, close precision crop protection framework.

Correspondence: Roberto Oberti, DiSAA, Dipartimento di Scienze Agrarie e Ambientali, Università degli Studi di Milano, via Celoria 2 - Milano, Italy.
E-mail: roberto.oberti@unimi.it

Key words: Precision spraying , agricultural robot, crop protection, automation, disease sesning.

Acknowledgements: CROPS (GA-246252) is funded by the European Commission under the 7th Framework Programme within the theme "Automation and robotics for sustainable crop and forestry management"

Journal of Agricultural Engineering 2013; XLIV(s2):e29
doi:10.4081/jae.2013.(s1):e29

Introduction

In current farming practice, pesticides are typically applied uniformly to the fields. This, despite several pests and diseases exhibit an uneven spatial distribution, with typical patch structures evolving around discrete foci, especially during early stages of development. Grapevine is not an exception and, in current viticulture practice, fungicides are applied uniformly through the vineyard according a spraying calendar, commonly based on regular and frequent fungicide applications, more rarely triggered by experts decisions or objective data. For powdery mildew (*Erysiphe necator*) and downy mildew (*Plasmopora viticola*), two major grapevine fungal diseases, this continuous protection approach can easily result in ten to fifteen treatments per season, often at application rates of 500-1000 dm^3/ha each, for many vineyards in some of the most advanced wine-producing regions worldwide.

Pesticides are recognised to play a major role in environmental pressure and production costs of agricultural activity, as well as in public concerns about healthiness and wholesomeness products. There is then an increasing interest in developing suitable techniques and equipment able to selectively target the application of pesticides where and when needed by the crop, with the aim of preventing or inhibiting the establishment of the infection and its epidemic spread to the whole field.

Growing labor costs and unavailability of skilled personnel during work-peak periods in most European countries, promote the research on advanced automation for selective agricultural cultivation processes. Since growing of crops requires several operations with a huge variety of combinations in parameters, only a highly modular and reconfigurable robotic system suitable for different specialty crops (grapes, sweet-pepper, apples) as well as for multiple tasks (spraying, selective harvesting), can achieve high utilization grades.

The main task of UE project CROPS (www.crops-robots.eu) is to

develop, optimize and demonstrate a multipurpose, modular and lightweight manipulator able to cope with these specific requirements. The adopted approach it's clearly distinguished from that of other research groups which use non-modular and heavy standard industrial manipulators (see e.g. Baeten *et al.*, 2008; Katupitiya *et al.*, 2008) or which focus on one specific fruit and purpose (see e.g. Guo *et al.*, 2010; Kitamura/Oka, 2005).

One of the challenging applications of the new CROPS manipulator is the selective, intelligent targeting of pesticides distribution on diseased or susceptible areas of the crop plants.

Among possible sensing technics for disease symptoms detection, proximal optical sensing has specific characteristics especially relevant for field applications on grapevine and other specialty tree-crops. In particular, it can inspect the vertical structure of the canopy, allowing for potential on-the-go detection of early symptoms even at centimeter/sub-centimeter scale.

The possibility to optically detect disease symptoms relies on the modifications induced by the pathogen in the plant tissue and, in turn, in the way how light interacts with it. Beside disease-specific pigmentation, main optical effects of plant diseases are associated to spectral absorption bands of chlorophyll, where tissue degradation induced by pathogens is especially emphasized.

As case studies we consider here the fully automatic selective spraying of powdery mildew diseased areas on grapes leaves as they are encountered in vineyard conditions. This paper reports on first results of a session of greenhouse experiments, with the objective of identifying disease foci within healthy canopy based on optical sensing and by sensing feedback to position a precision spraying actuator by the manipulator to selectively and accurately apply pesticides solely onto infected areas.

The robot system

Robotic manipulator

The manipulator was designed for agricultural applications in selective harvesting and precision spraying. The selective harvesting task has the highest requirements on the dexterity and accuracy in positioning of the end-effector tool. Thus, this application was the basis for the kinematic and mechatronic design, resulting in a nine degrees-of-freedom (DoFs) manipulator. For further details on the design refer to Baur *et al.* (2012).

For the precision spraying application, the end-effector must be roughly positioned at a distance of 0.4 – 0.6 m in front of the canopy and dealing with a canopy height of about 0.9 m. Furthermore, the end-effector should be able to spray on a target area from several directions to improve the spray coverage. Since the sprayer is rotationally symmetric, only the rotations about the x – and z – axis (cf. Figure 2) are relevant. Due to the modular design, the nine DoFs manipulator can be reconfigured to a six DoFs manipulator (the kinematic scheme is shown in Figure 1) which is more suitable for this application.

For having the manipulator ready to work under greenhouse conditions, it was necessary to build an extra cover to protect the robot against spray droplets which in addition to the high humidity conditions in the environment could lead to a short circuits on the electronics. As a results, a hard cover encloses the carriage of the linear bearing while a flexible shell protects the subsequent five joints. The casing is built up of several pieces of polyoxymethylen which are glued to two main parts. One part covers the backside, the other part is fixed at the front and serves as intersection to the soft cover. This shell is welded together out of four pieces of ripstop-nylon which is coated with a film of Thermoplastic polyurethane. The resulting tube can be wear on the arm, fixed at the sliding and is finished with an angle bracket, which is fastened to the manipulator. The bracket serves both as mounting point and for the connection of a waterproof plug. Thus power and data signals for the end effector are provided from within the protection.

A microcontroller interface board (Atmel® AT90CAN32) which provides several digital and analog IO's for various end-effectors (precision sprayer, apple gripper, and sweet-pepper fruit removal unit) as well as a CAN interface to the manipulator real-time control unit was designed. Thus, the nozzle as well as the fan speed of the precision sprayer can be controlled by simple ROS (Open Source "Robot Operating System" by Willow Garage, http://www.ros.org) messages.

For the positioning, the goal coordinates of the tool-center-point of the sprayer are send to the real-time control unit via the ROS interface

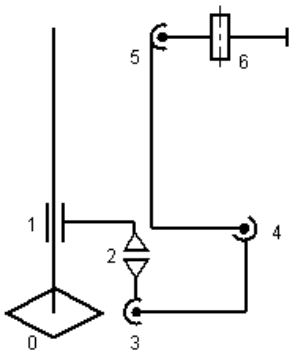

Figure 1. Kinematic scheme of the manipulator in spraying configuration

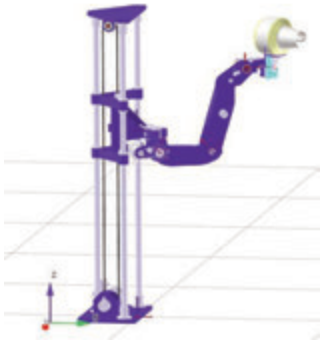

Figure 2. Visualization of the manipulator equipped with the spraying end-effector.

Figure 3. Manipulator System with waterproof cover.

(cf. Figure 4). The inverse kinematics is computed on the real time PC on the velocity level (Siciliano (2009)). To avoid instability of this computation close to kinematic singularities, a configuration dependent damping factor is added. This results in a stable, but less accurate solution of the inverse kinematics close to kinematic singularities. The computed joint trajectory is than sent to the low level motor controllers of the manipulator in each time step.

Disease sensing

Disease sensing was based on multispectral image analysis of canopy under diffuse illumination. All the equipment was installed in a dockable aluminum frame which contained an RGB color camera (acA1300, Basler, Germany), an R-G-NIR multispectral camera (MS4100, DuncanTech, USA), a data acquisition PC, panels for diffuse illumination of the imaged area and power supply. The cameras were mounted on a sliding structure allowing position adjustments in height. During the experiments the cameras position was kept constant at an height of 1,4 m. To provide background regularization and avoid multiple viewing across glass walls in the greenhouse, a black, low-reflective shield was positioned on the back of the imaged plants.

For disease detection only R-G-NIR multispectral camera was used. The multispectral camera acquires 1912x1076 pixels, 8 bit images in three distinct spectral channels: green (540 nm), red (660 nm) and near infrared (800 nm). The area imaged was about 1.0x0.5 m, resulting in a spatial resolution of about 0.5 mm/pixel. At each acquisition, raw pixels intensity in each channel was normalized using reflectance standard panels (Spectralon 20%, 50% and 99%, Labsphere, USA) kept in the field of view of the camera. Disease symptoms identification is based on the combination of two approaches: one based on the value of two spectral indexes calculated at pixel level, and the other based on relative variations (local gradients) of grey level intensity in the red channel.

A fairly clear discrimination between healthy and diseased areas can be obtained by considering for each pixel the pair of values obtained with the two spectral indexes:

$$I1 = Red/(Red+Green+NIR) \quad [1]$$

$$I2 = (Red*Green)/NIR\text{^}2 \quad [2]$$

These indexes are designed to capture the reflectance variations in either red or green channel, or a combination of both, related to chlorophyll absorption band which is especially expected to respond to local tissue degradation linked to a pathogen attack (Oberti *et al.*, 2012).

Nevertheless, disease classification results based only on (I1, I2) combinations appears to be prone to significant false positive detections (i.e. non diseased areas classified as diseased). This was found to be especially related to specular reflections on glossy leaf tissue and to specific structures as leaf veins or young, green branches. To reinforce the classification robustness, a local approach was adopted, based on gradient intensity of pixel levels in the red spectral band, allowing to discriminate between smooth changes in intensity and sharp changes more likely due to reflections effects.

The two approaches are integrated within a classifier and when the two methods agree above a certain probability threshold, a set of binary regions in the image. After morphological filtering aimed to remove isolated pixels and small areas, regions left are then assumed as diseased tissue, while the rest of the foreground is assumed to correspond to healthy tissue.

Sprayer end effector

The sprayer end effector consists of an axial fan as airflow generator, an airflow duct, a pesticide nozzle with anti-dripping device, an electrical connector for power supply and control signals, all enclosed in a plastic chassis. The sprayer end effector was designed with the main goal of performing precision spot spraying of small patches of infected areas. In operation the end-effector has to be connected to a pumping station and a pesticide formulation tank placed at the base of the manipulator. The pesticide delivery flow-rate ranges from 15 ml/min to 50 ml/min, depending on the selected nozzle tip. The one used during the experiments has a flow-rate of 30 mL/min at a pressure of 4 bars, with a full cone pattern of 30° and an average diameter of spray droplets of about 150 µm. The fan features PWM control for rotational speed, allowing to set the air-carrier flow velocity from 5 to 30 m/s. As overall result, the sprayer end effector delivers a circular spraying pattern of a constant diameter of 0.15-0.2 m over a wide range of spraying distances (0.4 - 1.5 m).

Greenhouse experiments

Plant material preparation and canopy setup

Selective spot spraying concept was tested in a session of greenhouse experiments conducted in early 2013 on grapevine canopy with localized symptoms of powdery mildew (*Erysiphe necator*), one of the major diseases for this specialty crop.

To this aim in spring 2012, 180 plants of *Vitis vinifera* L. cv Cabernet Sauvignon were propagated from wood, and nursed in 30 cm diameter pots by maintaining greenhouse environment under controlled conditions at 25/20 °C day/night temperature, with 50-75% relative humidity and a 16-h photoperiod (40 µmol quanta m^{-2} s^{-1}). Grapevine plants were pruned in autumn so that they reached full development stage in February 2013. This schedule enabled off-season use of the CROPS manipulator after field experiments on other agricultural operations in other sites considered within the project.

A subset of grown grape plants was inoculated by brushing *Erysiphe necator* conidia onto the adaxial (upper face) epidermis of healthy leaves in order to induce powdery mildew infection. The infected plants were nursed in a separated greenhouse room where favourable environmental conditions for disease development were maintained.

For purpose of experimenting the selective spraying system, the plant material was arranged in a greenhouse setup in order to simulate vineyard canopy conditions by aligning healthy grapevine plants in pots on tables (Figure 4, right). Within the recreated canopy wall, diseased plants with different levels of symptoms were positioned in order to simulate the presence of localised disease foci within healthy vegetation, representing the actual targets of selective spot spraying to be performed by CROPS robot.

Different replicates of grapevine canopy plot (5 m in length x 1,8 m in height) were obtained by preparing different plants arrangements by substituting healthy and diseased plants with other spare samples and/or changing their position in the line.

Prior to each robotic spraying pass, the canopy plot was accurately monitored by visual inspection by a plant Pathologist. Position, size and intensity of disease foci symptoms were recorded and used for assessing the results obtained with each robotic spraying treatment.

Robotic system setup and experimental procedure

For the spot spraying experiments session, the disease detection system and the manipulator equipped with precision spraying actuator were integrated on a trailer platform, hosting the PC for data acquisition and real-time processing and the controller of the manipulator. The manipulator geometrical coordinates system was then registered

with the coordinates system of the multispectral camera. With this procedure, the position of a point at a known frontal distance X from the camera and having coordinates (yi, zi) in an acquired image, can univocally translated in a vector of coordinates (xm, ym, zm) of the manipulator reference system.

During the experiments, the trailer holding the robotic system was positioned frontally to the recreated canopy and while traveling was kept at a constant distance from the midline of the vegetation. The trailer was moved in front of the canopy wall at steps of 10 cm. At each position a multispectral image of the canopy was acquired and processed in real-time.

The obtained results in terms of presence and position of disease symptoms were written in to a spraying targets queue file. Concurrently, the targets in the queue list identified by previous acquisitions and having a position in the canopy reachable by the manipulator at current trailer standing, were aggregated in single spray spots (i.e. within circles having a diameter of 15 cm). The coordinates of the center of each resulting spray spot were then passed to the manipulator controller through ROS messages. The corresponding targets were assumed treated and consequently removed from the queue list.

In order to maximize the homogeneity of spraying deposit and covering of targets, each single spot (i.e. a circular area of the canopy with a diameter of 15 cm) was sprayed from three different directions. For each spot to be sprayed the manipulator was then commanded to bring the end effector in three positions from where the nozzle was operated to deliver one third of the nominal flow (0.5 s on a total of 1.5 s of spraying time). The sequence of three positions was: i) distance from spot's center d= 0.6 m, latitude angle α=30°, longitude angle γ=0°; ii) distance from spot's center d= 0.6 m, latitude angle α=-30°, longitude angle γ=+30°; iii) distance from spot's center d= 0.6 m, latitude angle α=-30°, longitude angle γ=-30°.

With this spraying sequence timing, each identified target received a corresponding application rate of 375 L/ha$_{foliage}$ which is a representative value of current grapevine protection treatments.

After all the targets in queue falling in the workspace of the manipulator at current trailer standing were sprayed, a message of duty accomplished was generated and trailer was then moved by 10 cm to next step.

In order to assess the performance of the automatic disease detection system the algorithm output for each robotic pass was compared with the visual inspection records (position, size, intensity of symptoms) made by plant Pathologist. The final spray deposit on the canopy, and specifically on individual disease foci, was evaluated by spraying a fluorescent dye mixture.

Results

The operative results obtained with robotic selective spraying of disease symptoms were quantitatively assessed through three parameters:

- the *sensitivity* of the selective treatment, which expresses the capability of real covering the targets (numerically defined as the fraction of canopy area to be sprayed which was actually sprayed by the robot);
- the *specificity* of the selective treatment, which expresses the capability of avoiding excess of unnecessary spraying (numerically defined as the canopy area fraction of the area not to be sprayed which was actually left unsprayed by the robot);
- the *pesticide reduction* of the selective treatment, which expresses the reduction of used pesticide in comparison of a conventional uni-

Figure 4. Hardware and software architecture of the robotic manipulator.

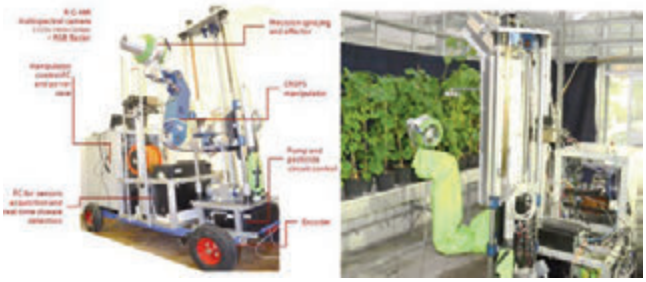

Figure 5. The robotic setup integrated on a trailer during preparation in the lab (left), and during experiments of selective spraying on grapevine

Figure 6. Example of grapevine plants setup to recreate a vineyard canopy wall in greenhouse conditions. Among aligned healthy plants, powdery mildew infected plants with different levels of disease symptoms were positioned to simulate the presence of localised disease foci (in red) within healthy vegetation.

Figure 7. Example of detected diseased areas as automatically identified by the robotic system and corresponding spray spots (blue circles) commanded to the sprayer effector. There is an evident overlap with Pathologist prescription (Fig.5 as ground truth) for two foci at position around 170-200 and around 300-340, while around position 100 the robotic system has erroneously treated two false positive regions

form spray distribution operated at the same application rate (numerically defined as the ratio of canopy area sprayed, including multiple sprayings from overlapping spots, on the area of the canopy plot).

Figure 5 shows an example of the different replicates of grapevine canopy plots prepared for the experiments. Red frames in the image indicate the disease foci positions as obtained by plant Pathologist monitoring, hence representing the actual target of selective spraying. In Figure 6, the corresponding symptoms map as automatically detected by the robotic system is shown. In the same chart, the blue circles represent the spray spots which the manipulator was commanded to apply to the canopy. It can be noticed that there is a remarkable qualitative overlap between results in Figure 6 and the plant Pathologist prescription (red frames in Figure 5) for what concerns two disease foci located around position x=170-200 and around position x=300-340 in the chart. On the other hand, the robotic system erroneously detected and treated two false positive regions around position x=100.

In this specific example the actual disease area represents the 1.6% of the total canopy area. The sensitivity of the robotic selective spraying resulted 85%, while the selectivity was 92% meaning that only 8% of the total healthy area was sprayed unnecessary. The total amount of sprayed pesticide was 16% of the amount used in a conventional uniform treatment, with a remarkable reduction of 84%.

Even if described just as an illustrative example, these results are at our best knowledge the first application of selective, intelligent treatment of plant diseases, representing a possible steps towards new developments in precision pest management and precision protection of crops.

References

Baeten J., Donné K., Boedrij S., Beckers W., Claesen E. 2008. Autonomous fruit picking machine: A robotic apple harvester, Tracts in Advanced Robotics, Vol. 42, pp. 531–539.

Baur J., Pfaff J., Ulbrich H., Villgrattner T. 2012. Design and development of a redundant modular multipurpose agricultural manipulator, Advanced Intelligent Mechatronics (AIM), 2012 IEEE/ASME International Conference on', Kaohsiung, Taiwan, 823-830.

Guo J., Zhao D., Ji W., Xia W. 2010. Design and control of the open apple-picking-robot manipulator, Proc. IEEE Int. Conf. on Computer Science and Information Technology (ICCSIT), Vol. 2, pp. 5–8.

Katupitiya J., Eaton R., Cole A., Meyer C., Rodnay G. 2005. Automation of an Agricultural Tractor for Fruit Picking, in Proc. IEEE Int. Conf. on Robotics and Automation (ICRA), pp. 3201–3206.

Kitamura S., Oka, K. 2005. Recognition and cutting system of sweet pepper for picking robot in greenhouse horticulture, Proc. IEEE Int. Conf. on Mechatronics and Automation (ICMA), Vol. 4, pp. 1807–1812.

Oberti R., Tirelli P., Marchi M., Calcante A., Iriti M., Borghese N.A. 2012. Automatic diseases detection in grapevine under field conditions. Proc. of the first International Conference on Robotics and associated High-technologies and Equipment for agriculture applications. 2012, p. 101-106, Pisa University Press, ISBN: 9788867410217

Siciliano, B.; Sciavicco, L. & Villani, L., 2009. Robotics: modelling, planning and control, Springer Verlag.

Open problems in traceability: from raw materials to finished food products

Lorenzo Comba,[1] Fabrizio Dabbene,[2] Paolo Gay,[1,2] Cristina Tortia[1]

1 DI.S.A.F.A, Università di Torino, Grugliasco (TO), Italy; [2]CNR–IEIIT, Torino, Italy

Abstract

Even though the main EU regulations concerning food traceability have already entered to force since many years, we still remark very wide and impacting product recalls, which often involve simultaneously large territories and many countries. This is a clear sign that current traceability procedures and systems, when implemented with the only aim of respecting mandatory policies, are not effective, and that there are some aspects that are at present underestimated, and therefore should be attentively reconsidered. In particular, the sole adoption of the so-called "*one step back-one step forward traceability*" to comply the EC Regulation 178/2002, where every actor in the chain handles merely the data coming from his supplier and those sent to his client, is in fact not sufficient to control and to limit the impact of a recall action after a risk notification. Recent studies on lots dispersion and routing demonstrate that each stakeholder has to plan his activities (production, transformation or distribution) according to specific criteria that allow pre-emptively estimating and limiting the range action of a possible recall. Moreover, these new and very recently proposed techniques still present some limits; first of all the problem of traceability of bulk products (e.g. liquids, powders, grains, crystals) during production phases that involve mixing operations of several lots of different/same materials. In fact, current traceability practices are in most cases unable to deal efficiently with this kind of products, and, in order to compensate the lack of knowledge about lot composition, typically resort to the adoption of very large lots, based for instance on a considered production period. Aim of this paper is to present recent advances in the design of supply chain traceability systems, discussing problems that are still open and are nowadays subject of research.

Correspondence: Paolo Gay, DI.S.A.F.A – Università di Torino, 44 via Leonardo da Vinci, 10095 Grugliasco (TO) – Italy.
E-mail: paolo.gay@unito.it

Key words: traceability, supply chain, bulk products.

Acknowledgements: this work was partially supported by the grants of the projects Namatech-Converging Technologies (CIPE2007), Regione Piemonte, Italy and PRIN 2009 (prot. 2009FXN7HW_002), MIUR, Italy.

Journal of Agricultural Engineering 2013; XLIV(s2):e30
doi:10.4081/jae.2013.(s1):e30

Introduction

A traceability system (TS) has to the assignment to provide strategic information in the unfortunate case when a lot of product has to be recalled. Product recalls are an increasing concern for food companies and government agencies (e.g. FDA for US and RASFF for EU). Traceability can be voluntary, when disposed by the food manufacturer itself, or forced (Kramer *et al.*, 2005).

The main causes of product recalls are incorrect labelling and packaging, failures in good manufacturing practice, and, of course, the identification of conditions that can compromise the safety of the food and consumer's health (chemical contamination, microbial agents, foreign material, undercooking of product etc.). Another frequent cause is the (undeclared or accidental) contamination of raw and semi-processed materials with allergens (especially eggs, peanuts, dairy and wheat). The occurrence of food and feed recalls is increasing (Potter *et al.*, 2012) and in the EU, in 2011, exceeded 3700 notification cases. This fact can also be imputed to food safety standards and new government regulations, to the development of new detection technologies and the increasing importation from low-cost countries, where food safety standards are frequently less severe.

The management of a recall procedure involves many activities, ranging from the risk assessment, the identification of the interested products, the notification of the measure to the actors of the supply chain (suppliers, distributors, buyers etc.), and, finally, the recall action. Wynn *et al.* (2011) identified common data requirements for traceability and data exchange, and analysed opportunities for the automation of the notification process in the case of a recall.

There are many consequences in a recall action. One of the first, is the potential drop in consumer confidence (Kumar and Budin, 2006; Skees *et al.*, 2001). Indeed, a negative image of the brand can remain in the subconscious of potential consumers for long periods. The company has then to incur costs related to the logistics of the recall and the destruction of all the products that are, in some way, connected with the incriminated batch (Jacobs, 1996).

Since this could be absolutely critical for a company, it is important to prepare action plans to be ready to such undesired event. Some studies have been carried on for modelling and forecasting the effects of recall actions (e.g., see Kumar and Budin, 2006, Randrup *et al.*, 2008 and Fritz and Schiefer, 2009). What resulted is that most companies do not have reliable methods to manage a recall strategy on the basis on estimation the real amount of product that has to be discarded in the case of a recall. The recall of a product typically follows two steps that should be be performed in very short time: the backward identification of potential deficient lots and then the forward identification of potentially affected products that have to be withdrawn (Fritz and Schiefer, 2009). Considering the main task of TS, the performances of a TS can therefore be associated to its ability to react to a crisis, holding down the amount and the costs of the product to be recalled.

Following the entering to force of EC Regulation 178/2002 and subsequent normative, traceability has evolved in different directions, engaging many aspects among which the definition of optimal lot sizes

and mixing routing rules, the tracking of products in distribution networks and the embedding of product quality information for supply chain managements purposes.

This paper presents a brief overview of the state of the art of the research on traceability and the open problems nowadays subject of research. To enter in a deeper detail, authors have chosen two two specific aspects: the definition and the evaluation of the performances of a traceability system (TS) connected to the minimization of the impact of a possible product recall, and the management of traceability information related to bulk products. These research lines have been selected considering their impact on the supply chains, on the market, and on the consumer, and the very recent results published in literature. These arguments are very up-to-date and rich of ongoing applications in different food supply chains. The paper is organized in two main sections dedicated to these topics and a Conclusions section where future trends and perspectives are discussed.

Performances evaluation of traceability systems

The definition and the evaluation of the performance of a traceability system is a fundamental step to compare different approaches and technologies and to judge new possible traceability oriented management policies. Many different criteria have been proposed which are mainly based on these factors:

- the cost of a possible product recall;
- the degree of dispersion of raw materials and intermediates;
- the speed of the TS in supplying information and to act to a crisis.

Most part of the performance definitions presented in literature allows the determination of quantitative indexes that can be used by optimization procedures. In this case, performances can be enhanced acting on logistics, lot definition and sizing, and, more in general, production management rules and plans. In other cases, e.g. the reduction of the response time of the TS, an enhancement of the performances can be obtained upgrading and expanding the information management tools and the level of automation in the supply chain, i.e. investing in the TS.

To formalize some elements in performance measurement criteria, some nomenclature concerning lots, their management, and size has to be introduced. Moe (1998), following the terminology firstly introduced by Kim *et al.* (1995), introduced the *traceable resource unit* (TRU) as *"unique unit, meaning that no other unit can have exactly the same, or comparable, characteristics from the point of view of traceability"*. This concept has been then described in ISO Standard 22005/2007 (ISO, 2007). Here the lot is defined as "*set of units of a product which have been produced and/or processed or packaged under similar circumstances*".

A further elaboration of this concept was proposed by Bollen *et al.* (2007) introducing the *identifiable unit* (IU), which represents the unit of product that have to be uniquely identifiable within each system. From the size of IUs it descends the *granularity* of the traceability system, which can be expressed as the size of the smallest TU managed by the TS (Karlsen *et al.*, 2012). Indeed, granularity level is determined by size and number of batches. A finer granularity allows adding even more detailed information about the product, and acting at a more detailed and range-limited level in the case of a possible recall. The size of batches is important for companies in reducing risk and the wideness of repercussions. The optimal granularity level is very difficult to determine, since it depends on product type and customer. Indeed, it should be remarked that the simple implementation of a finer granularity has no value by itself, unless it provides more precise traceability. Moreover, the way a product is processed has to be taken into account. In particular, whether the product is processed in completely separated sessions (i.e. separated batches), or if some mixing can occur between products of two succeeding batches. In the case of mixing, which is typical for bulk commodities (liquids, powders, crystals, grains etc.), is still an open problem and is discussed in Section 4.

A first approach for performance measurement is to consider a *recall cost* (*RC*) connected to the material that has to be recalled in the case of crisis. Such cost depends on different factors such as i) the size of the batches that have been individually tracked and managed by the traceability system, ii) the way the batches of the different materials have been processed and mixed to obtain the final product, and iii) the level of segregation adopted by the firm to manage and maintain separated different batches of product. Direct costs associated to a recall action include the costs for the notification of the recall, the logistics to retrieve the product and lost sales. Resende-Filho and Buhr (2010) consider all these cost components, as a whole, as directly proportional to the amount of product to be recalled, that is $RC=\alpha P_r Q_R$ where Q_R represents the quantity of product to be recalled, P_r the retail value of the product, and α is a coefficient accounting for notification and logistics. Analogously, Fritz and Schiefer (2009) express the overall recall cost of a TS as the sum of the cost of the system *C(tt)*, the costs induced by the possible reductions in efficiency *C(e)* and in quality *C(q)* caused by the adoption of the tracking and tracing system, i.e. $C(overall)= RC+C(tt)+C(e)+ C(q)$

In other cases the performances were associated to the degree of dispersion of the lot of products. This indirect measure of *RC* was firstly proposed in Dupuy *et al.* (2005) as *downward* and *upward dispersion indices* and, more in general, as *batch dispersion cost* (*BDC*). The downward dispersion of a lot represents the number of batches of finished product that contains part of the lot, while the upward dispersion of a finished lot of product is constituted by the number of raw material lots used to produce the lot. The sum of downward and upward dispersion indices of all raw materials gives the measure of the total batch dispersion of a system. It follows that when the performance of a traceability system is associated to batch dispersion, it is measured by the number of active paths (links) between raw materials and finished products. Rong and Grunow (2010) introduced the *chain dispersion measure*, which can be specifically applied to the distribution phase, defined as

$$D_b = \frac{n(n-1)}{2}$$

where η is the number of retailers served by the lot b. As for the batch dispersion cost, the chain dispersion measure depends on the number of links, but it increases quadratically for n>1. However, it should be remarked that the typical interest of a company is to know the worst-possible amount of product that could be necessary to recall. For this reason, Dabbene and Gay (2011) associated to the performance measure of a TS the *worst-case recall cost* (*WCRC*) index, defined as the largest amount of product that has to be recalled when a batch of raw material results unsafe. Analogously, the *average recall cost* (*ARC*) index was introduced to represents the average mass of product to be recalled when one of the entering material is found inappropriate. The formalism introduced in Dupuy *et al.* (2005) and then in Dabbene and Gay (2011) stems from the consideration that, from a traceability viewpoint, the production process can be modelled as an interconnected graph, where nodes represents the different lots of raw/intermediate materials, and the arrows represent the mixing operations that lead to the final lots of product.

Degradation in the TS performance occurs whenever systematic

information loss takes place, as for instance when information about the composition or process conditions is not properly linked to the product and systematically recorded. This corresponds to a loss in precision and of the granularity level of the TS. Karlsen *et al.* (2010) defined the point where this loss occurs as *critical traceability point* (CTP). Following a similar to HACCP approach, the identification and mapping of CTPs is performed by qualitative methods (direct observation, structured interviews and document analysis), and leads to the definition of a *critical traceability point analysis* plan (Karlsen and Olsen, 2011). Some application of CTP mapping and validation can be found in Donnelly *et al.* (2009); see also Karlsen *et al.* (2011) and references therein. Finally, an important aspect of the TS and its performance evaluation, as also reported in ISO Standard 22005/2007, is the definition of monitoring procedures and schemes to evaluate the effectiveness of the system. For some particular types of foodstuff, specific physicochemical and microbiological analytical techniques have been developed for determining the origin with a good level of precision (Peres *et al.*, 2007). Validation should be performed periodically by verifying the fulfilment of the desired level of the TS performances, for instance by simulating product recalls. A study on simulated recall in the case of Nordic fish products is reported in Randrup *et al.* (2008).

Traceability of bulk products

In many food plants, raw or semiprocessed products are handled as liquids (as e.g. milk, vegetal oils, etc.), powders (e.g. cocoa, powdered milk, flour etc.), crystals (e.g. salt, sugar) or grains. These products, for which is in almost all cases impossible to associate a label, a marker or any other identifier, are usually stored in tanks or huge silos, which are very rarely completely emptied. It follows that many lots are contemporarily kept in the same container. During the production phases, ingredients are mixed to obtain the desired final or semiprocessed product. There are indeed situations in which different lots cannot be mixed. This is the case, for instance, of products subject to religious specifications (e.g. Kosher or Halal certifications), or military supply contracts, or the case of products subject to very particular safety issues and constraints. In these cases, the only possible way to process raw materials and food is to guarantee complete and absolute segregation of lots using separated containers and/or accurately washing (or even sterilizing) the processing plants before their use with these lots. For these cases, the problem of traceability is even simpler, because raw materials and products are managed at whole lot level. However, in the great majority of cases, lots of bulk products are somehow mixed and/or they make use of the same facilities and plants, and are therefore naturally subject to thresholds. As an example, even the differentiation between non-GM from GM grains, which has important economical and ethical implications, is formally established and verified using a threshold where, in detail, EC Regulation No 1829/2003 (European Commission, 2003) for genetic modified (GM) and non-GM grains labelling guarantee that any food containing material that contains more than 0.9% of GM would be labelled as "contains GM". The problem of the traceability of fluid products has been first addressed as *fuzzy traceability* by Skoglund and Dejmek (2007) where dynamic simulation of continuous processing is used to model the changeover of lots of liquid product, in a pipe. In absence of a cleaning operation between the processing of two subsequent lots, portions of product, defined as *virtual batches*, deriving from the partial mixing of two lots are generated. This methodology is especially addressed for continuous processes on fluid products as sterilization and pasteurization where lots of products are supplied in sequence to the plant. In some case the flow of a product can be monitored mixing to the product specific identifiers that can be detected by the TS. This is the case, for example, of particular pill-size food-grade tracers inserted into grains (Liang *et al.*, 2012; Lee *et al.*, 2010) carrying identity information by means of printed bar codes or data matrix. For the cases in which this solution cannot be pursued, Comba *et al.* (2013) recently proposed a methodology based on compartmental models (Godfrey, 1983), which is applicable to any kind of bulk product including powders, grains, and fluids, where the definition of lot given in the ISO Standard 22005/2007 is rigorously formalized introducing a criterion, named *composition-distance*, to formally establish the homogeneity of a lot from the point of view of its composition in terms of raw materials that need to be tracked. The composition distance measures the difference of two products in terms of percentage content of *supply-lots* (raw materials), thus leading to formal definition of homogeneity: two portions of product can be considered as homogenous (and hence part of a single lot) if their composition-distance is less than a given quantization level. This approach is in accordance with the current regulation for the management and traceability of genetically modified (GM) products (European Commission 2003a,b), which states that a product can be labelled as GM-free if its percentage GM content is less than 0.9%. The management of homogenous lots of products (referred to as *cohorts*) and of their flow inside the production line is then governed by means compartmental models. This methodology allows to track the composition, in terms of lots of raw material, of any portion of product processed in the plant, and has been previously successfully used in (Comba *et al.*, 2011) to determine precise thermal conditions of fluid product processed in mixed continuous-discontinuous condition (i.e. plants with valves and pumps that can introduce discontinuities in the product flow). Another interesting approach has been proposed by Bollen *et al.* (2007) and by Riden and Bollen (2007). They considered the transport of discrete items (apples) that, once fluidized considering average flows, can be connected to flow of any bulk material. In their setting, apples, supplied to the packhouse in bulk bins, are moved in a water dump bulk flow up to the grader operators that handle single fruits and directs them into packaging lines of the sorting machine. At the end of these lines the fruits are placed into colour/size homogeneous packs. During their flow in the water dump and then in the packaging lines, a level of mixing among lots of apples occurs. In their first paper, Bollen *et al.* (2007) developed and validated a set of statistical models, using the measured arrival sequence of 100 blue marker balls, that indicates the composition, in a probabilistic setting, of a outgoing lot. The proposed models are indeed able to assign a probability of bin origin to any individual fruit in the final packs.

Conclusions

Traceability is becoming more and more a strategic tool that, in addition to its first task of guaranteeing consumers' safety, can help companies in the management of the production. The definition and the optimization of performance measures of the TSs lead to the a-priori determination and reduction of the risk at which a company is exposed in the case of possible product recall. The availability of this information will help companies in designing plant facilities and planning the production. What we expect in the next future is the development at a commercial level of these new tools as an integral part of ERP and traceability software. This is a living matter and therefore standards have even now to be accepted. The availability of reliable methods to estimate and trace the composition of lots, especially for bulk products, without resorting to the currently often-adopted process of oversizing the lots, allows the proper identification and definition of batches of homogeneous product. In particular, the availability of precise information about the composition, in terms of lots of raw or intermediate

ingredients, introduces the possibility to correlate product data with raw materials and then to optimise the recipes for each final product type. Also in this case we expect the development of new traceability software able to manage this kind of information and the tuning of sensors and identification devices able to guarantee a real-time validation of the simulated results.

References

Bollen, A. F., Riden, C. P., & Cox, N. R. (2007). Agricultural supply system traceability, Part I: Role of packing procedures and effects of fruit mixing. Biosystems Engineering, 98(4), 391–400. doi:10.1016/j.biosystemseng.2007.07.011

Comba, L., Belforte, G., & Gay, P. (2011). Modelling techniques for the control of thermal exchanges in mixed continuous–discontinuous flow food plants. Journal of Food Engineering, 106(3), 177–187. doi:10.1016/j.jfoodeng.2011.04.015

Comba, L., Belforte, G., Dabbene, F., & Gay, P. (2013). Methods for traceability in food production processes involving bulk products, Biosystems Engineering, in press.

Dabbene, F., & Gay, P. (2011). Food traceability systems: Performance evaluation and optimization. Computers and Electronics in Agriculture, 75(1), 139–146. doi:10.1016/j.compag.2010.10.009

Donnelly, K. A.-M., Karlsen, K. M., & Olsen, P. (2009). The importance of transformations for traceability – A case study of lamb and lamb products. Meat Science, 83(1), 68–73. doi:10.1016/j.meatsci.2009.04.006

Dupuy, C., Botta-Genoulaz, V., & Guinet, A. (2005). Batch dispersion model to optimise traceability in food industry. Journal of Food Engineering, 70(3), 333–339. doi:10.1016/j.jfoodeng.2004.05.074

European Commission (2002). Regulation (EC) No 178/2002 of the European Parliament and of the council of 28 January 2002 laying down the general principles and requirements of food law, establish the European Food Safety Authority and laying down procedures in matters of food safety. Official Journal of the European Union, L31, 1-24 (28.01.02).

European Commission. (2003a). Regulation (EC) No 1829/2003 of the European Parliament and of the Council of 22 September 2003 concerning the traceability and labeling of genetically modified organisms and the traceability of food and feed products produced from genetically modified organisms and amending directive 2001/18/EC. Official Journal of the European Union L268, 1–23.

European Commission (2003b). Regulation (EC) No 1830/2003 of the European Parliament and of the Council of 22 September 2003 concerning the traceability and labeling of genetically modified organisms and the traceability of food and feed products produced from genetically modified organisms and amending directive 2001/18/EC. Official Journal of the European Union, L268, 18/10/2003, 24-28

Fritz, M., & Schiefer, G. (2009). Tracking, tracing, and business process interests in food commodities: A multi-level decision complexity. International Journal of Production Economics, 117 (2), 317-329, doi:10.1016/j.ijpe.2008.10.015

Godfrey, K. (1983). Compartmental Models and Their Applications. Academic Press, London and New York.

ISO (2007). ISO Standard 22005/2007. Traceability in the feed and food chain: general principles and basic requirements for system design and implementation.

Jacobs R.M. (1996): Product recall – a vendor/vendee nightmare. Microelectronics reliability, 36 (1), 101-103, doi: 10.1016/0026-2714(95)00001-I

Karlsen, K.M., Donnelly, K.A.-M., & Olsen, P. (2010). Implementing traceability: practical challenges at a mineral water bottling plant. British Food Journal, 112 (2), 187-197

Karlsen, K.M., & Olsen, P. (2011). Validity of method for analysing critical traceability points. Food Control, 22 (8), 1209-1215, doi:10.1016/j.foodcont.2011.01.020

Karlsen, K. M., Donnelly, K. A.-M., & Olsen, P. (2011). Granularity and its importance for traceability in a farmed salmon supply chain. Journal of Food Engineering, 102(1), 1–8. doi:10.1016/j.jfoodeng.2010.06.022

Karlsen, K.M., Dreyer, B., Olsen, P., & Elvevoll, E. (2012). Granularity and its role in implementation of seafood traceability. Journal of Food Engineering, 112 (1-2), 78-85, doi:10.1016/j.jfoodeng.2012.03.025

Kim, H., Fox, M., & Gruninger, M. (1995). An ontology of quality for enterprise modelling. Proceedings of the Fourth Workshop on Enabling Technologies: Infrastructure for Collaborative Enterprises , 105-116.

Kramer, M., Coto, D., & Weidner, J. (2005). The science of recalls. Meat Science, 71 (1), 158-163, doi:10.1016/j.meatsci.2005.04.001

Kumar, S., & Budin, E. (2006). Prevention and management of product recalls in the processed food industry: a case study based on an exporter's perspective. Technovation, 26 (5), 739-750, doi:10.1016/j.technovation.2005.05.006

Lee, K.-M., Armstrong, P. R., Thomasson, J. A., Sui, R., Casada, M., & Herrman, T. J. (2010). Development and Characterization of Food-Grade Tracers for the Global Grain Tracing and Recall System. Journal of Agricultural and Food Chemistry, 58(20), 10945–10957. doi:10.1021/jf101370k

Liang, K., Thomasson, J. A., Lee, K.-M., Shen, M., Ge, Y., & Herrman, T. J. (2012). Printing data matrix code on food-grade tracers for grain traceability. Biosystems Engineering, 113(4), 395–401. doi:10.1016/j.biosystemseng.2012.09.012

Peres, B., Barlet, N., Loiseau, G. and Montet, D. (2007). Review of the current methods of analytical traceability allowing determination of the origin of foodstuffs. Food Control, 18(3), 228-235, doi:10.1016/j.foodcont.2005.09.018

Potter, A., Murray, J., Lawson, B., & Graham, S. (2012). Trends in product recalls within the agri-food industry: Empirical evidence from the USA, UK and the Republic of Ireland. Trends in Food Science & Technology, 28, 77-86, doi: 10.1016/j.tifs.2012.06.017

Moe, T. (1998). Perspectives on traceability in food manufacture. Trends in Food Science & Technology, 9(5), 211–214. doi:10.1016/S0924-2244(98)00037-5

Randrup, M., Storøy, J., Lievonen, S., Margeirsson, S., Árnason, S. V., Ólavsstovu, D. í, … Frederiksen, M. T. (2008). Simulated recalls of fish products in five Nordic countries. Food Control, 19(11), 1064–1069. doi:10.1016/j.foodcont.2007.11.005

Riden, C. P., & Bollen, A. F. (2007). Agricultural supply system traceability, Part II: Implications of packhouse processing transformations. Biosystems Engineering, 98(4), 401–410. doi:10.1016/j.biosystemseng.2007.07.004

Resende-Filho, M. & Buhr, B.L. (2010). Economics of Traceability for Mitigation of Food Recall Costs. Available at: http://ssrn.com/abstract=995335, doi:10.2139/ssrn.995335

Rong, A., & Grunow, M. (2010). A methodology for controlling dispersion in food production and distribution. OR Spectrum, 32(4), 957–978. doi:10.1007/s00291-010-0210-7

Skees, J., Botts, A., & Zeuli, K. (2001). The potential for recall insurance to improve food safety. International Food and Agribusiness Management Review, 4, 99-111, doi: 10.1016/S1096-7508(01)00072-6

Skoglund, T., & Dejmek, P. (2007). Fuzzy Traceability: A Process Simulation Derived Extension of the Traceability Concept in Continuous Food Processing. Food and Bioproducts Processing, 85(4), 354–359. doi:10.1205/fbp07044

Wynn, M., Ouyang, C., ter Hofstede, A., & Fidge, C. (2011). Data and process requirements for product recall coordination. Computers in Industry, 62, 776-786, doi:10.1016/j.compind.2011.05.003

An automatic system for the detection of dairy cows lying behaviour in free-stall barns

Simona M.C. Porto, Claudia Arcidiacono, Umberto Anguzza, Andrea Giummarra, Giovanni Cascone

Department of Agri-food and Environmental Systems Management, Building and Land Engineering, University of Catania, Italy

Abstract

In this paper, a method for the automatic detection of dairy cow lying behaviour in free-stall barns is proposed. A computer vision-based system (CVBS) composed of a video-recording system and a cow lying behaviour detector based on the Viola Jones algorithm was developed. The CVBS performance was tested in a head-to-head free stall barn. Two classifiers were implemented in the software component of the CVBS to obtain the cow lying behaviour detector. The CVBS was validated by comparing its detection results with those generated from visual recognition. This comparison allowed the following accuracy indices to be calculated: the branching factor (BF), the miss factor (MF), the sensitivity, and the quality percentage (QP). The MF value of approximately 0.09 showed that the CVBS missed one cow every 11 well detected cows. Conversely, the BF value of approximately 0.08 indicated that one false positive was detected every 13 well detected cows. The high value of approximately 0.92 obtained for the sensitivity index and that obtained for QP of about 0.85 revealed the ability of the proposed system to detect cows lying in the stalls.

Correspondence: Giovanni Cascone, DiGeSA, Section: Building and Land Engineering, University of Catania, via S. Sofia n.100, 95123 Catania, Italy.
Tel. +39.0957147571 – Fax: +39.0957147600
E-mail: gcascone@unict.it

Key words: Precision livestock farming, image analysis, loose housing system.

Acknowledgements: this research was financed by MIUR within a PRIN 2008 project entitled Innovative techniques for behaviour analysis of dairy cows in barns equipped with automatic milking systems. Local coordinator of the research unit of the University of Catania: prof. Giovanni Cascone.

Contributions: Ph. D. Eng. Simona M.C. Porto carried out the field trial, elaborated the data, and wrote the text; Prof. Claudia Arcidiacono contributed to the writing of the text; Ph. D. Eng. Umberto Anguzza developed the software tools of the system and contributed to data elaboration; Ph. D. Student Andrea Giummarra contributed to the field trial and carried out the validation of the system by carrying out the visual analysis of camera images; Prof. Giovanni Cascone coordinated the research.

Conflict of interests: the authors declaire no potential conflict of interests.

Journal of Agricultural Engineering 2013; XLIV(s2):e31
doi:10.4081/jae.2013.(s1):e31

Introduction

Nowadays, the possible occurrence of pandemics caused by the diffusion of diseases transmitted from animals to humans represents one of the most threatening risk for human health. Therefore, operators and researchers of the livestock and veterinary sectors as well as the public opinion assign a great importance to those specific problems of intensive livestock farming which affect animal welfare, product quality and, as a consequence, consumers' health.

Recently, modern Information and Communication Technology (ICT) applications to animal breeding produced the development of the Precision Livestock Farming (PLF) which regards the study of systems and methods to monitor, store and continuously assess data related to processes regarding the animal and its breeding environment. The modelling of these data makes it possible to obtain information suitable to assess animal health status, comfort and productivity, and adopt smart management protocols of livestock farming in real time (Cangar *et al.*, 2008).

In dairy cow farming, PLF may represent a useful application for the study of animal behaviour. In this context, this study aims at designing and implementing a system, which was based on the automatic analysis of digital images, for behaviour detection of dairy cows housed in free-stall barns.

The automatic analysis of digital images has been utilised in several research work (Shao *et al.*, 1998; Noldus *et al.*, 2001; Shao and Xin, 2008) that had the objective to monitor animal behaviour in different breeding environments. Automatic systems of detection based on this technique require the adoption of image processing algorithms when relevant brightness and background variations reduce detection of the significant content of the image (foreground), i.e., the presence of the animals and the activities they carry out. Furthermore, the methodologies proposed in these studies regarded laboratory trials or tests in small breeding environments which entailed that the designed systems were very simple since the video-recording system included only one camera or video-camera, and the automatic detection system elaborated images acquired from only one source.

The main objective of this research, which was part of a wider project (PRIN 2008 - Innovative techniques for behaviour analysis of dairy cows in barns equipped with automatic milking systems), was the attainment of the automatic detection of some behaviours of dairy cows bred in a free-stall barn by using classifiers based on the Viola Jones algorithm (Viola and Jones, 2001, 2004). This algorithm, which was originally elaborated for human face detection, could be suitable to obtain an accurate recognition also in presence of relevant varia-

tions of brightness and background in the analysed image sequence.

The behaviours considered in this research were the following: feeding at the manger, lying in the stalls, and standing and walking in the feeding alley and the service alleys. For each behaviour, one or more classifiers were modelled.

In this paper the main information related to the modelling of the classifiers that were built to detect the presence of dairy cows lying within the stalls is reported. Furthermore, in order to improve the readability of the paper, a brief description of the Viola Jones algorithm is provided in the section below. Further information can be found in Porto *et al.* (2011, 2013).

Training and execution of a classifier based on the Viola Jones algorithm

The classifier based on the Viola Jones algorithm (Viola and Jones, 2001, 2004) is a *cascade* of stages, each one of them being a strong classifier composed of a combination of weak classifiers.

In the training phase, the classifier requires samples of positive images and samples of negative images that both have sizes of $w \times h$ pixels. To obtain these samples from the frames acquired by the video-cameras, it is required that an operator extracts a set of positive images that has a size of $W \times H$ pixels (with $W > w$ and $H > h$) and a set of negative images that has a size of $W' \times H'$ pixels (with $W' > w$ and $H' > h$). A positive image contains the object to be recognized whereas a negative image contains only parts of the objects that constitute the image background. In the extraction process, all the positive images must maintain the same aspect ratio w/h. The sizes of the negative images, on the other hand, must not be smaller than those of the largest positive image.

The sample of positive images is obtained by automatically reducing all the positive images selected by the operator to $w \times h$ pixels. The sample of negative images, instead, is generated by the algorithm through the automatic execution of multiple scans of the negative images selected by the operator. In detail, a first scan is carried out by using a sliding window of $w \times h$ pixels.

During the training process, the algorithm classifies a negative image as false positive if it has wrongly recognised the target object in the image. Likewise, the algorithm classifies a positive image as true positive if it has correctly recognised the target object in the image. Therefore, along with the maximum number of stages (*ns*) that compose the cascade, the training phase requires the definition of the maximum value for the false positive rate (*MaxFPR*), and the minimum value for the true positive rate (*MinTPR*). The *MaxFPR* and *MinTPR* fixed values must be equal for all stages.

The *MinTPR* parameter is obtained from the equation:

$$MinTPR = \left(TPR_{cas}\right)^{1/ns} \quad (1)$$

by fixing the minimum value of the true positive rate that the cascade must produce (*TPRcas*), and the value of *ns*.

At the end of the training process the minimum false positive rate of the cascade (*FPRcas*) is obtained. If *FPRcas* is of the order of magnitude 10^{-6} (Viola & Jones, 2001, 2004), it demonstrates that the classifier has the ability to distinguish the background from the object to be detected.

In the execution phase, the Viola Jones algorithm utilises an image scanning process by using a sliding window similar to that used in the training phase. Ultimately, each stage of the cascade establishes if the area of the image contained within the sliding window must be classified as *not an object* or as *probably an object*. If one of the stages establishes that the content is classified as *not an object*, that part of the image is definitively discarded and classified as background, whereas if it is classified as *probably an object* the next stage will analyse the content. The higher the number of stages used to evaluate the content of the sliding window the higher the possibility that the sliding window contains the object to be detected.

Materials and methods

The breeding area under study

The research trials were conducted in a cubicle free-stall barn for dairy cows located in the province of Ragusa (Sicily, Italy). A group of 15 cows were monitored. The breeding environment considered in the trials was composed of a resting area subdivided in two rows of head-to-head stalls with sand beds, a feeding alley adjacent to the resting area, a service alley, and two service passages (Figure 1). In this breeding environment, the factors that may complicate the automatic detection of the lying cows within the stalls are the following: variability of colour tone of the sand which constitutes the lying surface of the stalls; the considerable variability of environment brightness in the proximity of the open side of the building; the high quantity of solar radiation that is reflected by the sand beds and the metal surfaces constituting the cross bars; the lack of homogeneity in colour and reflectance of the alleys' surfaces, which is caused by the presence of slurry.

To design and build the video-recording system, video-cameras Vivotek FD7131 were chosen, which have a maximum resolution of 640 × 480 pixels and a maximum image-capture capability of 30 fps, equipped with an hypertext transfer protocol interface (HTTP) and a LED (light emitting diode) for illumination in night vision. With the aim to obtain a planimetric top-view of the breeding environment considered in the trial, ten video-cameras were utilised, six of them were placed above the feeding alley at an height of 4.40 m from the floor, and four were installed above the resting area at an height of 4.05 m (Figure 1). Image acquisition was carried out by utilising a specific software developed in Microsoft® Visual C# Express, which allowed the acquisition of one snapshot for each video-camera with a frequency of one fps. Through the additional use of OPENCV graphical libraries, the software applied operations of synchronization, calibration, rotation, resizing and union to the ten obtained snapshots, in order to produce as output an image which had a size of 1044×1920 pixels and contained the plan view. The outcome of these operations was a sequence of panoramic top-view images with a frequency of 0.5 fps.

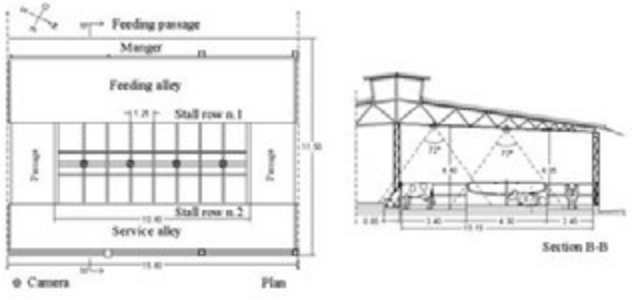

Figure 1. Plan and section of the study area in the barn considered in the trial.

Training of the classifiers

The panoramic images, which were utilized to train the cow lying behaviour detector, were extracted from the video-recordings acquired between the 1st and the 7th of August 2011.

Though the camera model was equipped with a built-in LED illuminator, it did not provide sufficient lighting inside the building during the evening and night. Therefore, the panoramic top-view images used in the training phase referred to the time interval between 6:00 a.m. and 8:00 p.m. However, this time interval did not affect the modelling of the detectors because it included the most significant herd management tasks and variations in the surfaces' illumination. In particular, it included feeding distribution, the two milking operations during which the animals left the resting area, the activation of the evaporative cooling devices and the direct dripping system that produced a significant variation in the colour of the sand beds in the stalls, the cleaning of the feeding alley that determined a variation of the appearance of the floor, and light intensity variations in the different areas of the breeding environment throughout the day.

Since the stalls had a head-to-head layout and a classifier based on Viola Jones algorithm is unable to find the object to be detected if its image is rotated compared to that used during the training, in this phase two classifiers were modelled: classifier 1a to detect the presence of cows lying in the first row of stalls which can be reached from the feeding alley, and classifier 1b to detect the presence of cows when they are lying in the second row of stalls which can be reached from the service alley.

By applying a sampling time of ten minutes, 84 panoramic top-view images of the resting area were considered in each of the seven days analysed. From these panoramic images an operator selected the positive and negative images required to train the classifiers.

Testing of the classifiers

The objective of the classifiers' testing phase was to verify the functioning of each trained classifier without performing time-consuming visual recognition activities required to validate the detection results.

As for the training phase, the panoramic images were extracted from video-recordings acquired between the 1st and the 7th of August 2011 from 6:00 a.m. to 8:00 p.m., with a 10-min scan sampling. However, acquisition was delayed by five minutes in comparison to that employed in the training phase. For each classifier and each instant of acquisition, the panoramic image was selected on the basis of the average pixel brightness level of the image of the stalls. In detail, the panoramic image that had the average of stalls' pixel brightness values closest to the weekly mean, which was obtained by averaging the brightness values of the same instant of acquisition for each of the seven days of the week, was selected.

As for the training phase, an operator extracted a set of positive images and a set of negative ones. The images utilised for the testing phase were built by a specific software that allowed the overlapping of each positive image on each one of the panoramic negative images, i.e., selected among those where the cows were absent from the resting area. The overlapping area was randomly selected among the areas of the negative images that corresponded to the stalls. The obtained test images were then subject to three image alteration techniques: smoothing, erosion, and dilatation. Finally, the software stored the coordinates of the vertices of each positive image by fixing one of the vertices of the panoramic negative image as origin of the coordinate system. Within the same software, two classifiers were implemented to assess the accuracy of the detection of the cows that were present in the test images. During the execution of the classifiers, the software labelled a test image as true positive (TP) if the cow was correctly detected in its position, or else as false negative (FN) if the cow though it was present in the test image, was not detected by the classifier. Furthermore, the software assigned a value equal to the number of false positives (FPs) eventually found, i.e., areas of the background which were wrongly detected as cows, to each test image. Next, the software counted the images labelled as TP and FN, computed the sum of the FPs found in the images, and quantified the following accuracy indices: i) Hit rate (HR): ratio between the total number of TPs and the total number of the images utilised in the testing phase; ii) Miss rate (MR): ratio between the total number of FNs and the total number of the images utilised in the testing phase; iii) False positive rate (FPR): ratio between the total number of FPs and the total number of the images utilised in the testing phase.

Validation of the system

Once verified the functioning of the two classifiers by means of the testing phase, the overall performance of the CVBS was assessed by finding the position of the cows displayed in the sequence of the panoramic images. To this aim, another software that allowed the comparison between the data obtained from the simultaneous execution of the two classifiers and those derived from the visual analysis of the panoramic images carried out by the operator was elaborated. This comparison made it possible to compute the following accuracy indices:

i) Branching factor (BF): ratio between the total number of FPs and the total number of TPs obtained from the panoramic images. Low values of the BF index indicate a good ability of the classifier to discern the cows from the background:

$$BF = \frac{FP}{TP} \tag{2}$$

ii) Miss factor (MF): ratio between the total number of FNs and the total number of TPs obtained from the panoramic images. Low values of the index show the good ability of the classifier to recognize the cows:

$$MF = \frac{FN}{TP} \tag{3}$$

iii) Sensitivity: percentage of cows correctly classified, (i.e., true positives), over the total number of cows which are actually present in the panoramic images:

$$Sensitivity = \frac{TP}{TP + FN} \times 100 \tag{4}$$

iv) Quality Percentage (QP): in comparison to the sensitivity index, this ratio takes into account the presence of FPs in the analysed panoramic image, i.e., areas of the background incorrectly classified as cows:

$$QP = \frac{TP}{TP + FN + FP} \times 100 \tag{5}$$

The validation phase was carried out by using the video recordings acquired between the 8th and the 14th of August, 2011, during the time interval between 6:00 a.m. and 8:00 p.m. An operator performed the visual analysis of the video-recordings by using the software and marked the stalls occupied by the animals by selecting a point inside it. This information was then stored in a database. To reduce the time needed to perform the visual analysis, the panoramic images were selected at a 10-min scan sampling.

The number of positive images used in the training phase, equal to 826 and 319 for classifier 1a and classifier 2a respectively, was obtained by extracting from each panoramic image the image subsets of all the rectangular areas of 224×140 pixels, related to the stalls occupied by

the cows (Figure 2A). Similarly, the number of negative images was equal to 600 and was obtained from stalls areas unoccupied by the cows (Figure 2B). The dimensions of the sliding window were set to 40×25 pixels. In all, 600 positive images samples and about 50×10^7 negative images samples of 40×25 pixels were obtained.

During the testing phase, the use of weekly data of stalls' pixel brightness values (Figure 3) produced a sequence of video-recordings composed of 84 panoramic images from which 346 positive images of 224×140 pixels were extracted. In detail, 274 images obtained by selecting all the cows lying in the stalls of row n.1 were utilised to test the classifier 1a. The other 72 images obtained from images where the cows were lying in the stalls of row n.2, were used to test the classifier 1b. As for the number of negative images, two images were selected at 6:30 a.m. and at 6:30 p.m., i.e., when the cows were in the milking area, other two images were selected slightly before and after the cleaning of the feeding alley, which was carried out at about 8:00 a.m., when the cows were confined in the service alley (Figure 1).

Results and discussion

For both the classifiers the *MaxFPR* value, which was set equal to 0.5, allowed a rapid decrease of the FPR_{cas} value as the number of stages increased, with a maximum number of stages *ns* equal to 30.

Under the hypothesis that the TPR_{cas} value was at least equal to 0.90, the parameter *MinTPR* computed according to Eq. (1), was equal to 0.9965. The training of the classifiers ended at the 27^{th} stage when FPR_{cas} values reached the order of magnitude 10^{-7} for both classifiers.

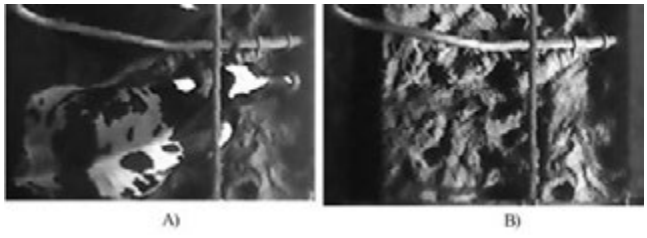

Figure 2. A) Example of positive image. B) Example of negative image

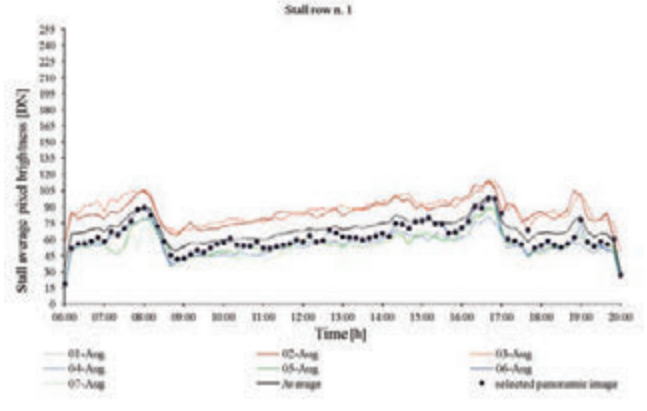

Figure 3. Average of the pixel brightness values composing the areas of the panoramic images of stall row n.1, computed at 10-min intervals and for each acquisition instant of the seven days considered; weekly means of the average of the pixel brightness values related to the stall row n.1; panoramic images selected to produce the sequence of images.

Similarly to the outcomes of a previous study carried out to detect cow presence at the feed barrier (Porto *et al.*, 2011), in this trial a lower number of both positive and negative images than that utilised by Viola and Jones (2001, 2004) for human face detection, made it possible to obtain very low FPR_{cas} values equal to 3.09×10^{-7} and 7.93×10^{-7} for classifier 1a and classifier 1b, respectively, and at the same time assured considerably high TPR_{cas} values equal to approximately 0.90 for both classifiers. This result could be explained by the fact that the classifiers modelled in this study, thanks to the use of Viola Jones algorithm, proved to be robust with regard to the significant background variations which occurred in the breeding environment during the daytime hours.

The operations of overlay and alteration of the images determined the use of 4384 test images for classifier 1a and 1152 for classifier 1b.

On the basis of the high value of HR which resulted about equal to 0.88 for both the classifiers, it can be highlighted that the testing phase proved the high ability of the classifiers to detect the cows even when noise affects the processed images, still yielding a low FPR which resulted equal to about 0.08 for both the classifiers. This result confirmed the outcome of the training phase where a very low value of FPR_{cas} was obtained.

In the validation phase, 589 panoramic top-view images were analysed in which 2281 images of cows lying in the cubicles were present. The overall number of cows correctly detected was 2088 and, therefore, the number of unclassified cows resulted 193. The number of false positives given by the system was 167. The accuracy indices calculated on the basis of these values were: BF = 0.08; MF = 0.09; sensitivity = 0.92; QP = 0.85.

The values obtained for the BF and MF indices showed that for every 11-13 cows correctly detected, the cow lying behaviour detectors made two errors: an omission error, i.e., they did not detect a cow in the resting area, and a commission error, i.e. they produced a false positive. However, the good ability of the classifiers to detect the cows is proved by the high value of the sensitivity obtained. This index which is directly comparable to the HR value obtained in the testing phase, revealed that in the validation phase both the classifiers improved of about 4% their ability to detect the cows in comparison to the testing phase. This improvement in the validation phase was not found in a previous trial carried out with the aim to detect the cows at the feed barrier (Porto *et al.*, 2011). This result is due to the smaller number of postures the animals assume while lying in the stalls compared to that found when they are in the feeding alley, close to the feed barrier. Furthermore, the stalls geometrically identify the area where cow presence is possible and thus it facilitates the selection of positive images which contain the body of just one animal.

By considering that the operations carried out to obtain the plan view of the resting area produced sequences of panoramic top-view images with a frequency of 0.5 fps and that the time needed to classify the content of a panoramic top-view image using an Intel Core (TM) 2 Quad CPU Q670 processor was approximately 320 ms, the automated detection of a cow in the stalls can be considered to be a real-time operation. During the execution of the cow lying behaviour detectors, this characteristic allowed results to be stored within text files, or in a database, therefore avoiding the storage of video-recordings.

Conclusions

This study aimed at building an automatic system for the detection of cows lying in the stalls. To this purpose two classifiers were modelled, which were based on the algorithm proposed by Viola and Jones.

Since the proposed system did not require the use of image quality

enhancement techniques applied to the outcome of the classifiers, both in the training and the execution phases, its application could be more suitable than that of other systems proposed in literature when the images of the breeding environment do not allow an easy extraction of the animal shape from the background.

The results obtained in the training phase highlighted that the use of a small number of both positive and negative images makes it possible to obtain a low false positives rate, while maintaining a good cow detection ability within the stalls. The importance of this result lies in the reduction in the operator's time required to select positive and negative images used for the training of the classifiers.

The results of the testing phase proved that the two classifiers have a good ability to detect cows even when noise affects the processed images, and making a few errors in the background.

Finally, since the classification speed of the information contained in the panoramic images allowed the recognition of the dairy cows in real time, the system was able to store the results of the detection in text files or in databases that allow an easy data management, and thus avoids the onerous storage of video-recordings.

References

Cangar, Ö., Leroy, T., Guarino, M., Vranken, E., Fallon, R., Lenehan, J., Mee, J., Berckmans D. 2008. Automatic real-time monitoring of locomotion and posture behaviour of pregnant cows prior to calving using online image analysis. Computers and electronics in agriculture, 64, 53-60.

Noldus, L. P. J. J., Spink, A. J., Tegelenbosch, R. A. J. 2001. Ethovision: a versatile video tracking system for automation of behavioral experiments. Behavior Research Methods, Instruments, & Computers, 33(3), 398-414.

Porto, S.M.C., Arcidiacono, C., Guarnera, G. C., Cascone, G. 2011. Preliminary study for the implementation of an image analysis algorithm to detect dairy cow presence at the feed barrier. Journal of Agricultural Engineering, 4, 17-23.

Porto, S.M.C., Arcidiacono, C., Anguzza U., Cascone, G. 2013. A computer vision-based system for the automatic detection of lying behaviour of dairy cows in free-stall barns. Biosystems Engineering, 115 (2), 184-194.

Shao, B., Xin, H., Harmon, J.D. 1998. Comparison of image feature extraction for classification of swine thermal comfort behaviour. Computers and Electronics in Agriculture, 19, 223-232.

Shao, B., Xin, H. 2008. A real-time computer vision assessment and control of thermal comfort for group-housed pigs. Computers and electronics in agriculture, 2008, 62, 15- 21.

Viola, P., Jones, M. 2001. Rapid object detection using a boosted cascade of simple features. In: IEEE Computer Society Conference on Computer Vision and Pattern Recognition, Kauai, Hawaii, 1, 511-518.

Viola, P., Jones, M. 2004. Robust real-time face detection. International Journal of Computer Vision, 57(2), 137-154

Economic and environmental benefits of using a spray control system for the distribution of pesticides

F. Calegari,[1] D. Tassi,[2] M. Vincini[1]

[1]Centro Ricerca Analisi Spaziale e Telerilevamento, Università Cattolica del Sacro Cuore, (PC) Italy; [2]Azienda Sperimentale "V. Tadini", Podenzano (PC), Italy

Abstract

Agrochemical distribution accuracy is critical for an effective intervention with a significant impact both on production costs and on the environment. Here we present the results obtained on processing-tomato crops using a sprayer boom with and without nozzle control integrated with an RTK (Real Time Kinematic) automatic guidance system. The trials were carried out on tomato crops cultivated in fields of different shapes in a farm located in the Po' Valley (Piacenza), using a self-propelled sprayer with a capacity of 1000 L and a 14 m opening boom, with a three-channel direct injection distribution system. The self-propelled sprayer was equipped with an automatic guidance system and integrated nozzle control on each boom section. Several parameters were recorded including the speed (km/h) and treated surface (ha). The analysis of the data collected shows an average overlap reduction of 15% compared to conventional guidance, a value that increases with the irregularity of the field. This technology can improve the environmental sustainability of agrochemical distribution due to the reduction in the consumption of pesticides and can improve the overall welfare of the operator as well.

Introduction

In recent years agricultural opportunities for precise management of field operations have increased considerably due to the availability of geospatial information and technology such as GPS (Global Positioning System), GIS (Geographic Information System), sensors, control systems and remote sensing. Development of new automated systems for agricultural machinery helps to improve competitiveness and sustainability in agriculture with a positive impact on the quality of yields. RTK (Real Time Kinematic) GPS provides high-precision positioning of the machine avoiding problems for the operator due to poor vision of reference points in the field, in particular when there are no visual cues available because the crop has not yet emerged or is in the early stages of growth. The GPS system is not based on visual reliefs so its activity is not adversely affected by poor lighting or from other conditions that reduce the view of the operator (Perez-Ruiz *et al.*, 2012; Reyns *et al.*, 2002; Servadio and Blasi, 2003; Zhang *et al.*, 2002). This allows high precision driving and a highly effective input distribution. The main advantage deriving from the assisted driving in a self-propelled sprayer with an RTK-GPS guidance system associated with a control system of sectors of the boom, is overlap elimination (i.e. the interruption of the distribution of a crop protection product over areas already treated in a previous path, and the interruption of the distribution over areas that do not require any treatment (edges of the field, etc.). It must be emphasized that for operations that involve the use of external inputs such as fertilizers, pesticides, etc., the application of this modern technology allows the recording of sprayer paths and product consumption and, as a consequence, provides an economic analysis of the sprayer operation (Batte and Reza Ehsani, 2006; Gualandi, 2011; Luck *et al.*, 2010).

The main advantages of using a system with these features, both in pesticide treatment and in foliar fertilization, are the following:

- Application accuracy (i.e. distribution of the right amount of product);
- Avoiding overlapping zones or areas not treated so as to optimize the dosage per area avoiding waste, voids or overages of the products used;
- Higher speed of the operation (i.e. work area covered in a given time);
- Traceability of interventions, with recording of all the operational data (e.g. speed, location, product consumption);

In order to assess the benefits of the technique, the treatment trial was made using a self-propelled sprayer, combining the automatic guidance and nozzle-control systems on irregular shaped fields of tomato crops.

Methodology

The trial was carried out using a self-propelled sprayer with a capacity of 1000 L and an open boom 14 m wide, divided into five sections, with a distribution system with a three-channel direct injection. The sprayer adopted a GPS RTK (Real Time Kinematik) automatic guidance system with an integrated nozzle-control system of each section of the boom (i.e. with the capability of opening and closing the sections according to needs). The integrated system recorded several parameters including speed (km/h) and the area treated (ha). A speed

Correspondence: Ferdinando Calegari, Centro Ricerca Analisi Spaziale e Telerilevamento, Università Cattolica del Sacro Cuore, (PC) Italy.
E-mail: ferdinando.calegari@unicatt.it

Key words: automatic guidance system, precision agriculture, precision spraying, processing tomato.

Journal of Agricultural Engineering 2013; XLIV(s2):e32
doi:10.4081/jae.2013.(s1):e32

record control was set up to record averaged data every 20 m. The comparison involved the use of a sprayer with and without the boom control system. The trial was carried out on 4 fields of irregular shape, with a surface area ranging from 3.05 to 8.48 ha, in a farm located in Piacenza countryside. Processing tomato was planted in the fields in single rows with row spacing of 1.50 m, a density of 35000 transplant seedlings/ha with a drip irrigation system. The transplant was carried out the first week of May. Throughout the season 10 treatments were performed with pesticides (herbicide, fungicide and insecticide). Data collection was performed during the treatment at the end of June. In the first phase, spreading operations were performed without the automated system (conventional way) using only water, while in the second phase carried out immediately after the first, automatic guidance and boom control systems were used and the spreading of pesticide was performed.

The use of the sprayer, with the control system of the boom activated, followed this procedure:

- A first step in order to treat a 14 meter-band along the field boundary was carried out (total width of the boom) so as to define the boundaries of the field;
- The remaining area was treated advancing in the direction of the rows and following the path pointed out by the guidance system. Once the path was intercepted, the autopilot itself drove the machinery, so that the operator was allowed to check on the boom and the operation of the nozzles.

The system is completely automatized. However, it still requires the presence of an operator and a beeping warning alarm when the machinery is approaching the end of the field. The self-propelled sprayer is also equipped with an on-board computer able to keep the amount of distributed water constant, even if speed of advancement is changed. The controller can report, in real time, any anomaly in the pump flow rate that measures the product and water, for instance, if the speed of work is increased without allowing the pumps to achieve the set dosage or in case of a slight clogging of filters that cause an abnormal water supply to the injection system. The system permits the recording of all previously set parameters (speed, level, time, etc.) which can then be downloaded, as georeferred data, into farm information systems.

Results

In the period in which comparisons were made between the two systems of treatment, the crop was at its highest vegetative growth, in good nutritional status and plant health. The weather conditions were in the normal range of temperatures and with normal humidity.

It can be noted in Figures 1 and 2 that where the treatments are performed with the control system of the boom activated, the sprayer speed in tracks near the edges of the field are higher and more homogeneous rather than where the operations are performed using the conventional approach. This is due to the increased comfort of the operator that must not continuously check obstacles on the boundaries and in previously treated areas need not manage the opening and closing of boom sections.

In Table 1 are reported the surfaces treated with the conventional system and with the automatic system. The area treated for the conventional approach is higher for all 4 fields.

The relative difference in the treated area, between the conventional and automatic approaches, should in general reduce with the increase in the size of the field and should increase with the degree of irregularity of the field.

Table 1 reports the treated surfaces and the percentage of treated

Figure 1. Shows the sprayer tracks during the treatment with the conventional system, distributing only water. The data indicates the path of the machine during the treatment in field n. 3; different colours indicate different speeds during the treatment.

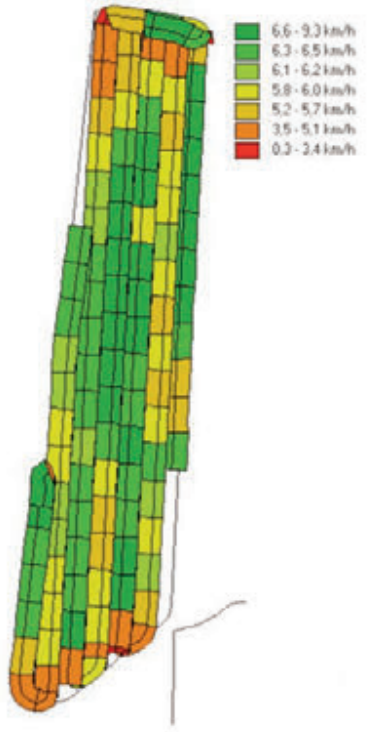

Figure 2. Shows the same parameters measured before, with automatic guidance and boom control activated. The blue colour indicates the first step of the treatment performed around the borders of field n. 3.

Table 1. Treated surfaces and the percentage of saving with the treatment carried out with the automatic control system of the boom compared to the conventional automatic guidance only, for each field.

Field	Surface treated (ha)		%	Saving
	Conventional system		Boom control system	
1	8.48		7.58	10.6
2	7.75		6.65	14.2
3	6.33		5.18	18.2
4	3.05	2.53	17.0	
			Mean	15.0

area saved with the treatment carried out with the automatic control system of the boom compared to the conventional automatic guidance only for each field. We also have indicated the differences for each individual field, ranging from 18.2 to 10.6% with an average of 15%. The difference in the treated surface is inversely proportional to the size of the field.

Conclusions

This technology drastically reduces the overlap, compared to the treatment performed in the conventional way. A significant reduction (15%) of the quantities of agrochemicals distributed was obtained, thus improving the environmental sustainability and avoiding at the same time, areas with overages or areas not treated that could become the source of many plant diseases (fungal disease, etc.). Furthermore, in the overall assessment of this system the positive impact in terms of the well-being of the operator, arising from the reduction of working time and from a better operational comfort should be considered.

References

Batte M.T., Reza Ehsani M. 2006. The economics of precision guidance with auto-boom control for farmer-owned agricultural sprayers. Comput. Electron. Agr. 53: 28–44.

Gualandi E. 2011. Quanto si può risparmiare nelle operazioni colturali. Agricoltura, supp. 46: 30-36.

Luck J.D., Zandonadi R.S., Luck B.D., Shearer S.A. 2010. Reducing pesticide over-application with map-based automatic boom section control on agricultural sprayers. T. ASABE 53(3): 685-690.

Perez-Ruiz M., Slaughter D.C., Gliever C., Upadhyaya S.K. 2012. Tractor-based Real-time Kinematic-Global Positioning System (RTK-GPS) guidance system for geospatial mapping of row crop transplant. Biosyst. Eng. 111: 64 -71.

Reyns P., Missotten B., Ramon H., De Baerdemaeker J. 2002. A Review of Combine Sensors for Precision Farming. Precis. Agric. 3: 169–182.

Servadio P., Blasi E. 2003. I GIS e le loro applicazioni nel settore agricolo. L'Informatore Agrario n. 49, 51-56.

Zhang N., Wang M., Wang N. 2002. Precision agriculture - a worldwide overview. Comput. Electron. Agric. 36: 113-132

Analysis of poultry eating and drinking behavior by software eYeNamic

A. De Montis,[1] A. Pinna,[1] M. Barra,[1] E. Vranken[2,3]

[1]University of Sassari, Dipartimento di Agraria, Sassari, Italy; [2]Fancom B.V., Panningen, The Netherlands; [3]KULeuven, Division M3-BIORES, Heverlee, Belgium

Abstract

Constant presence of at least one operator in livestock buildings for broilers would allow a perfect control of animal behaviour and, especially, deviations in feeding and drinking patterns, in the perspective of a high welfare status. However, as nowadays it is impossible for a farmer to be present in the farm all day long, automatic monitoring systems are required. The purpose of this paper is to introduce a system (eYeNamic) for automatic monitoring and analyzing broilers' behavior in a farm. eYeNamic is a camera system introduced and produced by Fancom BV, a company operating in the field of automation of livestock facilities. It includes three cameras located on the ridge of the broiler house and able to monitor chickens' behaviour twenty-four hours a day. Through eYeNamic it is possible to process the images and to obtain a measure of animals' distribution and activity, which can be conceived as valuable indicators of animal welfare. The study presented in this paper was divided into several phases: data collection, images visualization, observation of the distribution and activity of the chickens, and statistical analysis of the observations. The analysis of correlation between the number of 14 days old broilers near the feeding line (manual counted) and the average occupation density measured with eYenamic indicates that the best conditions have occurred with a 50 cm by 75 cm area around each feeding pan. With reference to the drinking line, the best response was found in an area 50 cm wide and the whole drinking line long. For the activity behavior, there was no significant correlation between activity and number of chickens eating from all the pans: this confirms that broilers while eating reduce their activity. It was concluded from this study that eYeNamic is a good system to observe animal behavior and, especially, to take care of their drinking and eating behaviour. A satisfactory correspondence between eYeNamic remote and human observations depends on a correct definition of animals' eating behaviour. In our case, this correspondence is established for the manual labeling, only if a broiler maintains its whole head inside the pan for a period lasting 20 seconds. In many cases the simple closeness to the pan or drinking line does not guarantee that a broiler is eating or drinking.

Correspondence: Andrea De Montis, University of Sassari, Dipartimento di Agraria, viale Italia, 39, 07100 Sassari, Italy.
E-mail: andreadm@uniss.it

Key words: broilers, remote control, precision farming.

Journal of Agricultural Engineering 2013; XLIV(s2):e33
doi:10.4081/jae.2013.(s1):e33

Introduction

Nowadays, animal welfare is an important public concern and unlimited access to food and water are important parameters in relation to welfare. These conditions result in improved animal performance, stronger growth, less illness, and lower mortality rates.

Hence, continuous observation of animal performance is very important because it is impossible for farmers to be present in the animal houses the whole day. Since today there is lack of systems able to autonomously observe specific animals, such as broilers, Fancom BV, a company operating in the field of automation of livestock facilities, has introduced the system eYeNamic. The experimentation of eYeNamic has to be referred to a panorama of research studies, which recently have focused on the requirements for remote and continuous livestock monitoring systems. The purpose of this paper is to introduce a system for automatic monitoring and analyzing broilers' behavior in a farm located in the Limburg province, The Netherlands and to demonstrate its usefulness in detecting and correcting unusual or inconvenient animals' behaviour. In the next section, a brief literature review on animals' remote monitoring systems is presented. In the third section, the monitoring system selected for the experimentation is introduced and commented. In the fourth section, the results of this work are discussed, while in the fifth section the conclusions are proposed.

Animals' remote monitoring systems: a brief literature review

According to Laurence (2008), applied behavioural scientists will focus not just on animal behaviour per se, but specifically on the resolution of key issues about animal welfare. He observes that today public concern about welfare in livestocks and, generally, quality of animal life is still expanding being comparable to other conteporary issues, such as food supply. A particular interest is devoted to the development of experimental modelling able to offer proper welfare assessment measures. In this respect, research studies have focussed on the integration of a number of livestock monitoring systems through software and hardware able to gather and organize a wealth of information. Technological advances include sensors management and image capture and analysis capable of control key variables, such as animal identity, weight, and behaviour, physiological and environmental factors, and body conformation and composition, and odours and sounds (Frost *et al.*, 1997).

The panorama of studies on livestock monitoring systems and animal behaviour embraces works on a number of species including broiler chickens. We report some examples as follows.

Dawkins et at (2012) study broilers' behaviour by means of camera equipment and statistical analysis of optical flow patterns and found that collective movements of the flock are significantly correlated with

relevant welfare measures, i.e. mortality, hockburn, and abnormal walking. Kristensen and Cornou (2011) focus on deviations from normal activity level of broiler chickens behaviour. They experimented with an overhead video camera system coupled with an outliers filtering software based on linear dynamic modeling. One of the main findings of these authors is the test of a device able to automatically detect abnormal activity levels and emit an alarm to immediately notify producers. Aydin *et al.* (2010) start from the evidence that metabolic and locomotive problems are related to fast growth rate and inactivity. Thus they study the activity level of broiler chickens by means of camera recording and processing software EyeNamic (Leroy *et al.*, 2006) and found high correlation between gait score and activity level.

As this paper refers to the aforementioned software, in the next section we present the features of this monitoring system and the experimentation developed.

Materials and methods

EYeNamic is a camera system used to monitor the behaviour of animals. There are three cameras mounted in the ridge of the chicken house that steadily monitor the floor, so you can analyze the behaviour of broilers and follow it from minute to minute. A scheme explaining the detail of cameras' location is reported in Figure 1. Afterwards, analysis software translates these images into an index for animal distribution and activity in the house, both valuable indicators of animal welfare. EYeNamic software allows to:

-- Measure the distribution and activity level of animals (broiler chickens) in real time.
- Localize the occupation density and activity by measuring it for different pre-defined zones.
- Freely choose the number and placement of the zones using a configuration tool.

The occupation density is the percentage of pixels representing chickens in the pictures in relation to the total amount of pixels in one zone: therefore, it is obtained by calculating the ratio between the number of object pixels over total pixels. A uniformity index was defined in order to know which percentage of occupation density values fall within the (+/- 20 %) range around the average occupation density. A scheme of the processing rationale is reported in Figure 2.

The average activity index is a measure of the animals' dynamics and is calculated by processing the data of the activity density index. The activity density index is calculated by confronting pictures taken by the same camera during a time period equal to 1 second. A scheme of the processing rationale is reported in Figure 3.

As the scheme reported in Figure 4 shows, the system includes a monitoring and a processing module: livestock floor pictures are taken every second by the three cameras, sent continuously in a storing device and analyzed through the software eYeNamic in order to obtain automatically a characterization of animals' activity and distribution. In addition, the number of eating and drinking chickens is manually

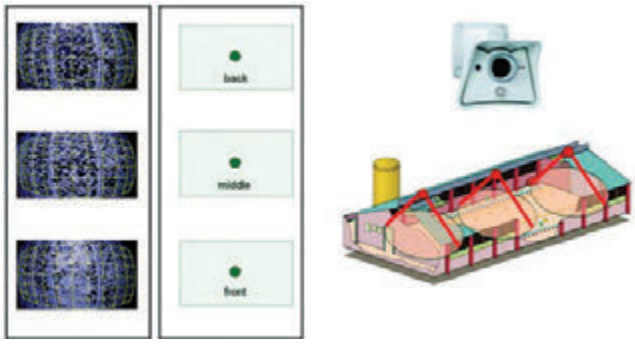

Figure 1. eYeNamic positioning and perspective of the three cameras.

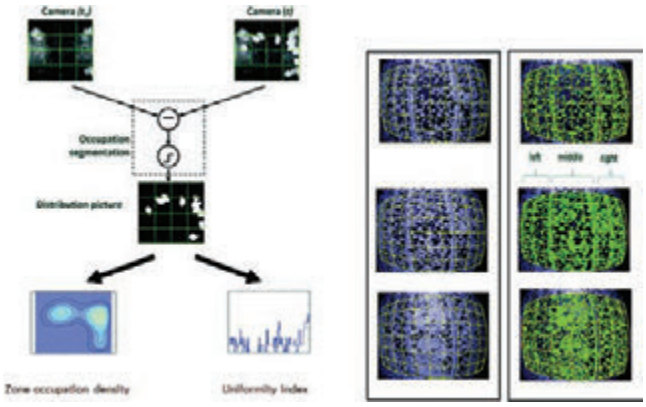

Figure 2. eYeNamic scheme of calculation for chickens' occupation index.

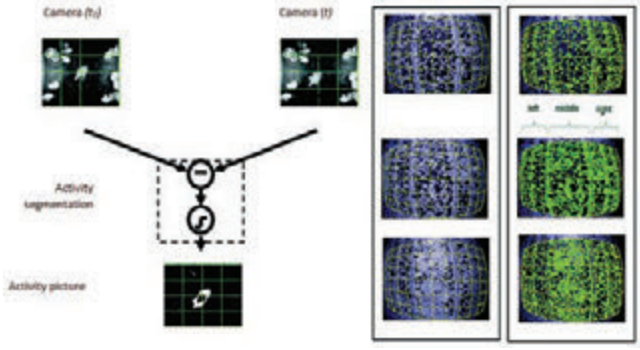

Figure 3. eYeNamic scheme of calculation for chickens' activity index.

Figure 4. Scheme of processing and comparing automatically versus manually retrieved information.

calculated and confronted with the automatically processed figures obtained by means of correlation analysis.

The images have been collected each 7th day of the week, during the period from July 15 to August 19, 2010, and light period from 3:00:00 AM to 7:00:00 AM. The manually count of eating and drinking chickens has been executed on pictures shot every five minutes. Hence, information from eYeNamic processing and manual observation has been synchronized in a compact dataset covering 42 days. For the manual labeling, only the chickens with their whole head inside the pan in the period from 10 seconds before until 10 seconds after the picture were counted at four feeding pans in the camera image. In Figure 5, the localization of the feeding pan is reported. These data were compared with the results of eYeNamic in which we selected the data of the occupation density in the zones around the feeding pans.

Different combinations of zones were used for the automatic analyses (see figures 6; 7; 8; 9; and 10). In total, we have considered five different configurations for the whole chickens growth cycle; afterwards, we defined the optimal area in the pictures occupied by chickens eating at the feeding pan. Then we checked the best configuration of eating zones by comparing data from eYeNamic with the data of the manual observations.

A similar procedure was used also to calculate the average density for drinking lines: drinking pattern with eYeNamic data have been compared with numbers of drinking animals manually observed (see Figure 11). Different configurations of zones were used also for this analysis.

In this way, it is possible to assess the effectiveness of eYeNamic as an animals' behavior automatic detection system. In the next section, the results of the behavior analysis is presented and referred to 14 days old chickens.

Results

We develop a correlation analysis to inspect the interaction between the number of eating chickens and average occupation density of a specific zone around each pan for five configurations. The analysis allows to see the best configuration around each pan. In Table 1, we report the correlation coefficients.

We can infer that for each pan the highest correlation coefficient corresponds to configuration 3 (average value 0.66), even though high correlation coefficients occur for some other pans; (see, for example, pan three, configuration 4, and 5). So, we can confirm that the highest concentration of chickens eating around the pans occurs on average for configuration 3. By contrast, in configuration 1 the average correlation coefficient is the lowest (0.53): this means that there are more chick-

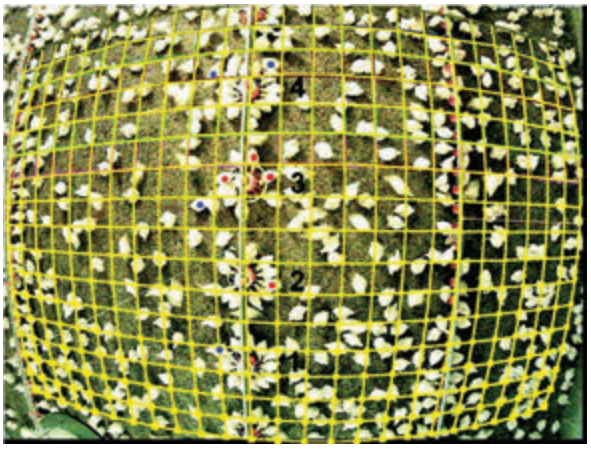

Figure 5. Chickens' feeding behavior around the pans: red points correspond to eating and blue points to not eating animals.

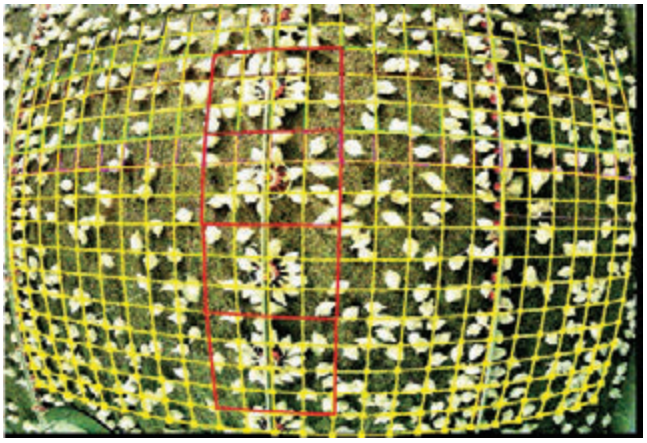

Figure 6. Areas around the pans adopted as reference zones to calculate the average density for configuration 1.

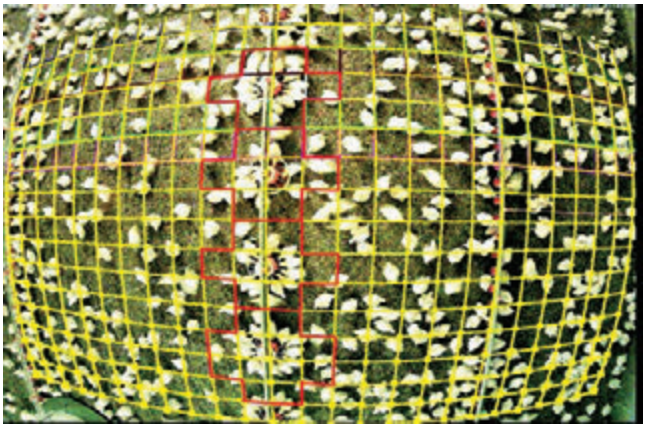

Figure 7. Areas around the pans adopted as reference zones to calculate the average density for configuration 2.

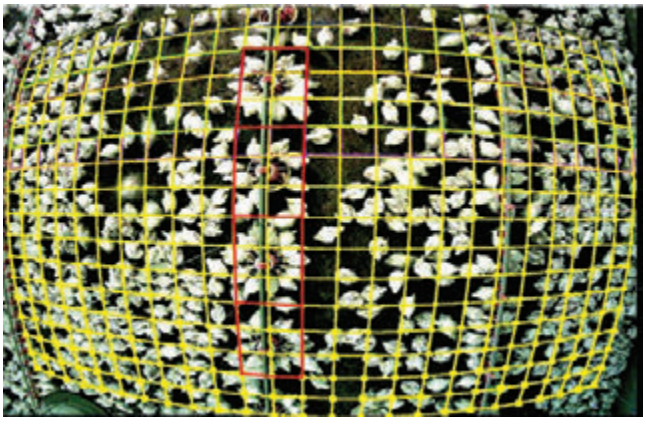

Figure 8. Areas around the pans adopted as reference zones to calculate the average density for configuration 3.

Table 1. Correlation analysis of average occupation density versus eating pattern and average activity density versus eating pattern.

Feeding pan	Configuration	Correlation coefficient (R)	
		Average occupation density vs eating pattern	Average activity vs eating pattern
1	1	0.55	0.48
	2	0.60	0.52
	3	0.73	0.27
	4	0.63	0.24
	5	0.55	0.37
2	1	0.63	0.30
	2	0.59	0.35
	3	0.69	0.18
	4	0.71	0.19
	5	0.51	0.14
3	1	0.54	0.22
	2	0.63	0.14
	3	0.68	0.00
	4	0.72	0.04
	5	0.72	0.04
4	1	0.42	0.23
	2	0.52	0.13
	3	0.53	0.16
	4	0.47	0.13
	5	0.57	0.10

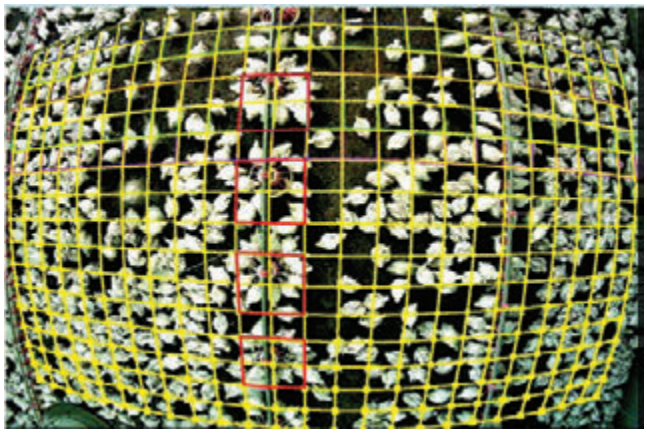

Figure 9. Areas around the pans adopted as reference zones to calculate the average density for configuration 4.

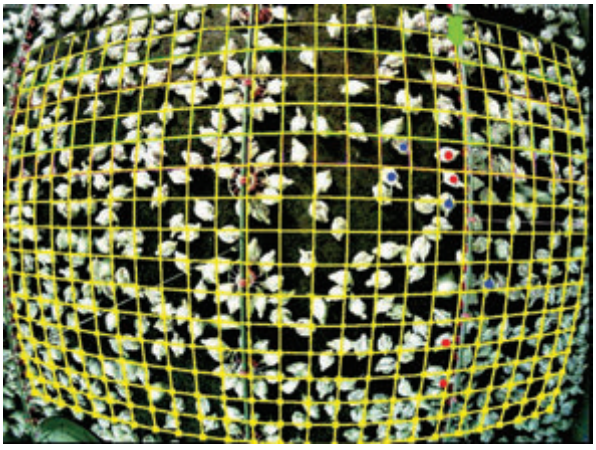

Figure 11. Analysis of drinking behavior: the green arrow indicates the drinking line; red points identify drinking and blue point not drinking chickens.

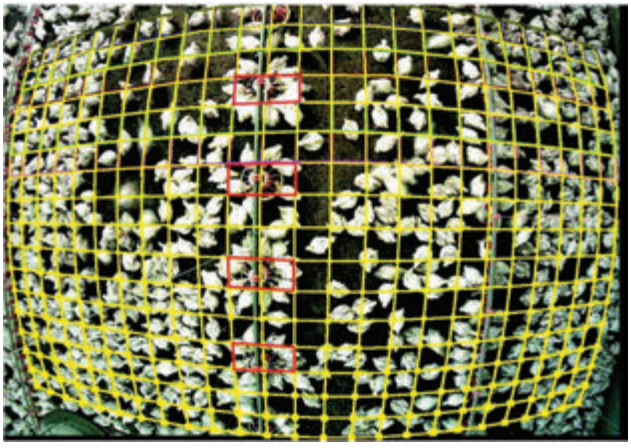

Figure 10. Areas around the pans adopted as reference zones to calculate the average density for configuration 5.

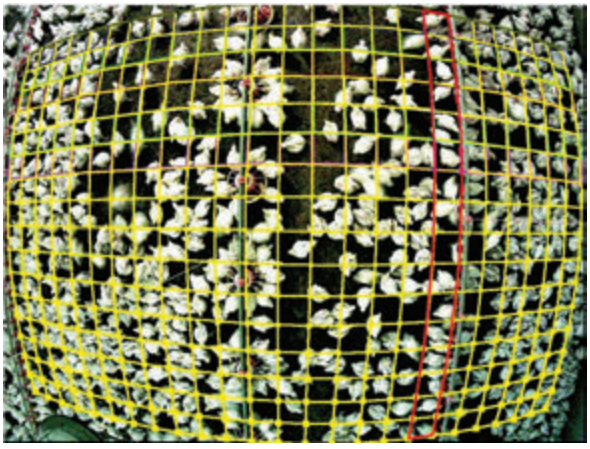

Figure 12. Area around the drinking line adopted as reference zone to calculate the average density for configuration A.

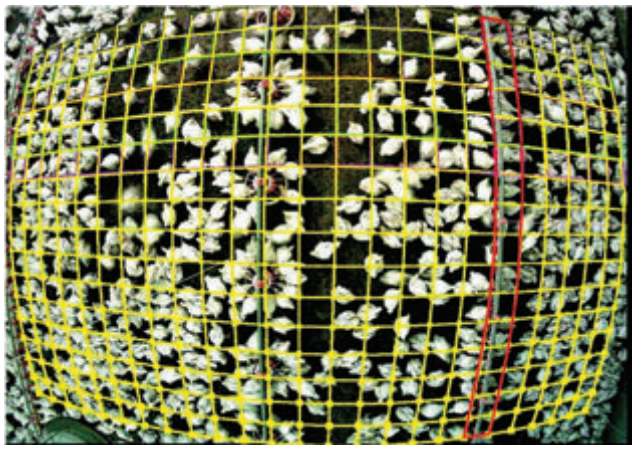

Figure 13. Area around the drinking line adopted as reference zone to calculate the average density for configuration B.

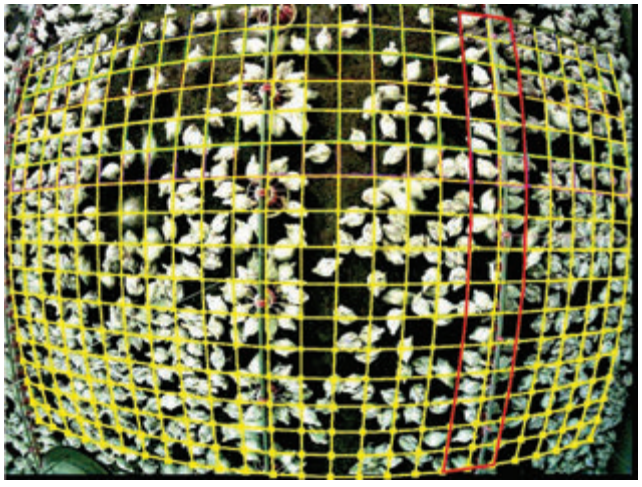

Figure 14. Area around the drinking line adopted as reference zone to calculate the average density for configuration C.

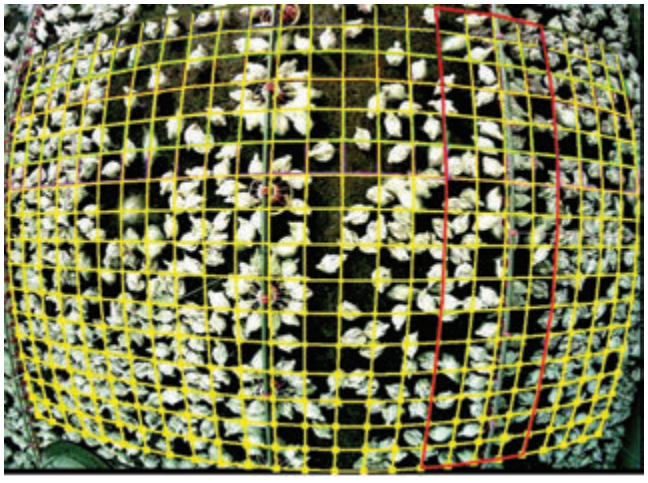

Figure 15. Area around the drinking line adopted as reference zone to calculate the average density for configuration D.

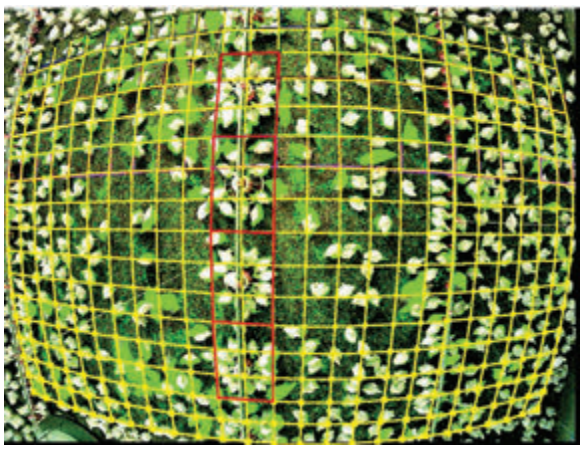

Figure 16. Analysis of chickens' movements: the green arrows describe the activity for configuration 3.

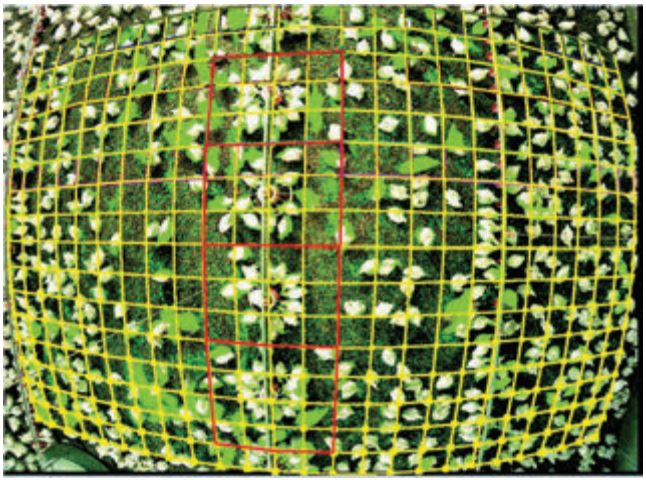

Figure 17. Analysis of chickens' movements: the green arrows describe the activity for configuration 1.

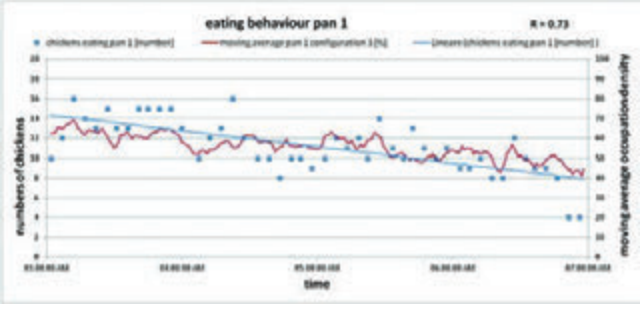

Figure 18 Functional relation between number of chickens eating at pan 1 and average occupation density for configuration 3.

ens that are not eating in the feeding zones in configuration 1 than in configuration 3.

Table 1 also reports correlation coefficients relating number of eating chickens and average activity for each pan and for five configurations. Results show that for configuration 3 a much lower correlation coefficient (average 0.15) is found compared to other configurations. This implies clearly that birds do not move, while eating, i.e. their level of activity is usually low. The high correlation coefficient for configuration 1 means that eating chickens have been moving with a more intense activity.

Figures 16 and 17 report the same image but with two different configurations; it is possible to monitor the activity of the chickens and also select a number of not eating animals.

In Figures 18 and 19, we report graphs about the functional relation between the numbers of eating chickens at pans 1 and 4 and the average occupation density for configuration 3. The horizontal axis indicates a time period from 3:00:00 AM to 7:00:00 AM, while the primary vertical axis indicates the number of eating chickens manually counted every five minutes. The second vertical axis shows the moving average occupation density. It is possible to see a better correlation for pan 1 through the correlation coefficient.

The number of chickens eating, like the moving average occupation density, decreases with time from 3:00:00 AM to 7:00:00. It is possible to see that they are concentrated especially in the first hour of the light period.

A similar work was done for inspecting the drinking behavior. We calculated the correlation coefficient for the whole drinking line for four configurations: in this way it is possible to see the best configuration of the zones around the drinking line. Correlation analysis results are reported in Table 2.

We found the highest correlation coefficient (0.65) for configurations C: this implies that most of the chickens around the drinking line with combination C are drinking. By contrast, for configuration D the correlation coefficient is not significant: hence in this case, there are a lot of chickens not drinking.

Figure 20 reports on the functional relation between the number of (manually counted) drinking chickens, and the average occupation density for combination C. The horizontal axis indicates the time period of the observation, the left hand side vertical axis indicates the number of drinking chickens, and the right hand side vertical axis indicates the moving average occupation density during the 4 hours. The number of drinking chickens decreases very slightly with time. By contrast, the average occupation density is constant over time: there are a lot of chickens that are not drinking in that area.

Figure 21 report a graph concerning chickens' eating behavior during the whole growth cycle. The highest correlation coefficients occur for 2 weeks old chickens for all configurations. Moreover, configuration 3 is the best for 7 to 42 days old chickens. For 5 and 6 weeks old chickens correlation coefficient is lower than for 14 days old animals: this phenomenon occurs since in the last 2 weeks there are less eating chickens in a larger surface, as some animals are not eating, while moving around the pan. It is important to see that with all the configurations for one week old chickens correlation coefficient increases in the period from 15/07/2010 until to 22/07/2010 and over time also the number of eating chickens increases. Afterwards, correlation coefficient is always lower in each configuration.

Conclusions

In this section, we discuss the results of this paper. We have presented a remote monitoring system able to control chickens' behaviour by

Table 2 Correlation analysis of average occupation density versus drinking pattern.

Drinking line configuration	Correlation coefficient (R)
A	0.60
B	0.45
C	0.65
D	0.43

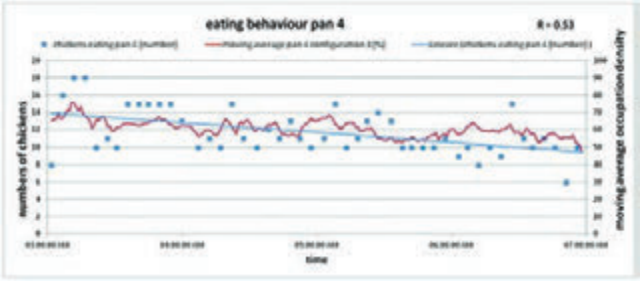

Figure 19 Functional relation between number of chickens eating at pan 4 and average occupation density for configuration 3.

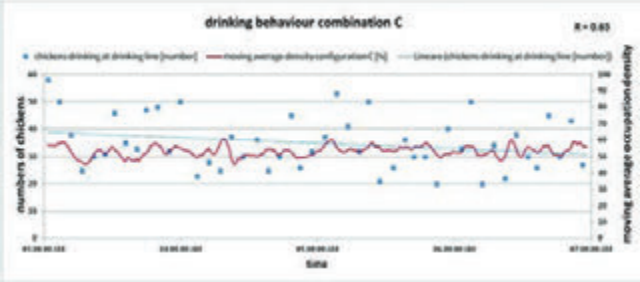

Figure 20 Functional relation between number of drinking chickens and average occupation density for configuration C.

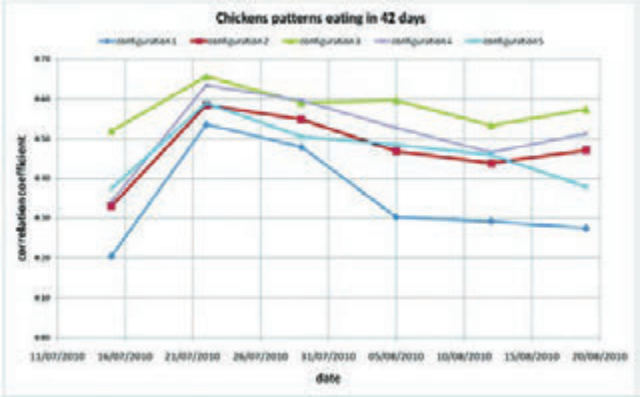

Figure 21 Chickens' eating behavior by configuration during the whole growth cycle.

processing images taken from three fixed cameras. We found that for eating behaviour there is a good correlation between the number of eating chickens and average occupation density for 14 days old chickens. The highest correlation coefficient (average value equal to 0.66) was found at pan 4 for configuration 3 referring to an area extending 50*75 cm around the feeding line. For drinking behavior, there is a good correlation coefficient for configuration C (0.65) corresponding to a zone 50 cm wide around the drinking line. For the activity behaviour there is no significant correlation for all the pans, and especially for configuration 3. In fact, for this configuration there is a low correlation coefficient for the activity (0.15), in contractition to the highest correlation for occupation density.

As a conclusion of these analyses, we can say that eYeNamic is a good system to observe animal behaviour, especially to take care of the animals' welfare. However, it is necessary to find a good definition of eating and drinking chickens to improve the correspondence between data processed through eYeNamic system and the real manually counted values. Moreover, with an overview of that relationship we can say that it is very important to analyze the areas close to the feeding pan and drinking line. That because usually with a bigger raster we observe a number of birds in the specific zones that are not eating or drinking.

References

Aydin A., Cangar O., Eren Ozcan S., Bahr C., Berckmans D. 2010. Application of a fully automatic analysis tool to assess the activity of broiler chickens with different gait scores. Computers and Electronics in Agriculture 73: 194-199.

Dawkins M.S., Cain R., Roberts S.J. 2012. Optical flow, flock behaviour and chicken welfare. Animal Behaviour 84: 219-223.

Frost A.R., Schofield C.P., Beaulah S.A., Mottram T.T., Lines J.A., Wathes C.M. 1997. A review of livestock monitoring and the need for integrated systems. Computers and Electronics in Agriculture 17: 139-159.

Kristensen H.H., Cornou C. 2011. Automatic detection of deviations in activity levels in groups of broiler chickens - A pilot study. Biosystems Engineering 109: 369-376.

Lawrence A.B. 2008. Applied animal behaviour science: Past, present and future prospects. Applied Animal Behaviour Science 115: 1-24.

Leroy T., Vranken E., Van Brecht A., Struelens E., Sonck B., Berckmans D. 2006. A computer vision method for on-line behavioral quantification of individually caged poultry. Transaction of ASABE 49 : 795-802.

Satellite guidance systems in agriculture: experimental comparison between EZ-Steer/RTK and AUTOPILOT/EGNOS

P. D'Antonio, C. D'Antonio, C. Evangelista, V. Doddato

School of Agricultural Sciences, Forest and Environmental, University of Basilicata, Potenza, Italy

Abstract

The research has been conducted using two different satellite-guidance devices and two different correction systems of the GPS signal: the EZ-Steer/RTK and Autopilot/EGNOS. The machines used in the tests were the tractor New Holland T7060, the rotary harrow Alpego DG-400 and the burier Forigo DG-45, in order to determine which of the two systems ensured the best quality of work. On the basis of the results obtained it is clear that the EZ-Steer/RTK system, guarantees a lower stability of the theoretical trajectory compared to the Autopilot/EGNOS system, above 1,77%. From the elaboration of data of the two guidance systems behavior to manage the only width of transposition, it is observed that the EZ-Steer/RTK system is able to guarantee a better hold of the line compared to the Autopilot/EGNOS system, which provides a mistake of 164 cm on the total width of transposition and 2 cm on the mean value. In the matter of the normalized transposition surfaces, the Autopilot/EGNOS system ensures a better work quality.

Introduction

The precision farming is a form of agriculture multidisciplinary and technologically advanced, which recourses to machines equipped with "intelligent systems", able to dose the productive factors (fertilizers, pesticides, etc.) according to the real needs of the homogeneous areas constituent the plot (*Verghagen and Bouma, 1997*). The farming tends to manage every factor of production in varying measure, treating small areas inside the lot as separate surfaces. By doing so, the economic margin of crops can be increased, reducing the input of the technical means. Furthermore, the environmental impact and the quantity of the production factors used, such as pesticides and fertilizers, are significantly reduced. Therefore, the precision farming aims to adapt the contributions in a point manner, taking into account the local variability of the physical, chemical and biological characteristics of the field, and the timing of implant (*Pierce and Sadler, 1997*); at the same time, also the soil preparation work must be performed accurately, in order to avoid overlap, which would cause an increase of the costs. For this aim, a detailed mapping of the physical, chemical and biological properties of the field has been used, so that they can be managed by the control computer of the cultivation operations, placed beside the machines. Therefore, the implementation of the actions demands an automatic positioning system (GPS, Global Positioning System), which allows to the machine to recognize the exact location on the map, differentiating the agricultural operation to carry out. A group of 24 satellites in orbit around the earth forms the GPS. With three satellites, a receiver and through the three-dimensional triangulation, the receiver will indicate its position on the earth. That is done through the analysis of the high frequency signals, that the satellites send to the receiver, which calculates how long it takes to receive the signal and its position is displayed on a screen (Satellites 2006). In addition, it reduces the environmental damage and the risks in agriculture. During the crop production, the uncertainty of the yield may be reduced and the safety of the farmers incomes can be increased if the technological elements are used and combined correctly (*Auernhammer 2001; Gandonou et al 2004; Chavas, 2008*).

Correspondence: C. D'Antonio, School of Agricultural Sciences, Forest and Environmental, University of Basilicata, via dell'Ateneo – 85100 Potenza, Itly. Tel.+39.0971205471, Fax: +39.0971205429,
E-mail: c_dantonio@yahoo.it

Key words: Precision farming, guidance assistance, transposition

Journal of Agricultural Engineering 2013; XLIV(s2):e34
doi:10.4081/jae.2013.(s1):e34

Methods

The experimentation has been carried out on two plots (A1 and A2), with temperatures around 22-25° C and a relative humidity (RH) between 60% and 65%. The climate in this area is arid Mediterranean.

The surveys were conducted on two different satellite guidance devices using two different correction systems of the GPS signal:

- the EZ-Steer, with RTK precision system;
- the Autopilot, with EGNOS precision system.

The EZ-Steer is an assisted guidance system, wherein the management of the tractor direction happens by a motorized roll, placed beside the steering, which is operated by the control unit positioned in the tractor cabin. This system doesn't overcome the value of 90 points (on a scale that ranges from 50 to 150), because of a non-instantaneous reaction of the starter to the course correction pulses issued by the control unit and because of the roll slipping light on the wheel; it was observed that, using a precision RTK and setting a value more than 90 points, the EZ-Steer system get in overcorrection, since the course corrections operated by the control unit, called in this article T2, can't be handled by the roll placed on the wheel and for this the tractor is not perfectly able to follow the direction assigned through GPS, but it accentuates the sine frequency around this. The Autopilot, instead, is an integrated system, which uses the hydrostatic guidance system for the management of the tractor through a hydraulic control unit, which

communicates with the control unit, called in this article, T3, placed in the control room. The control unit T3 communicates, both, with the GPS antenna and with the sensors proximal to the wheels, which indicate how the feed axis divert respect to the orthogonal of the tractor. The Autopilot's hydraulic circuit, differently from the EZ-Steer, allows to work with a value up to 135 points before going in overcorrection, that means it has a remarkable ability to maintain the correct trajectory also on land full of holes and/or soft. The GPS with EGNOS error correction can obtain a positioning accuracy, that is a precision between consecutive passes, of 20 cm and a repeatability year after year of 90cm (it's a free service); the RTK, instead, is a high-precision technology, with an accuracy between consecutive passes of 2.5 cm and a repeatability year after year of 2.5 cm. The RTK is able to provide an elevation accuracy of 5 cm, with an improvement of almost two orders of height compared to the GPS standard (DGPS), since this system is able to extract the additional information, examining the carrier wave of the GPS signal (*Tyler et al., 1997*). The RTK system's disadvantages are: a higher cost, the need to establish a local base station and a significant decrease compared to the GPS standard methods. A light-bar provides information of the visual guide to the operator, who may make some corrections of manual steering (*Trimble Navigation, Ltd., 2005*). An assisted steering system makes automatic these adjustments and the operator directs only the tractor and his intention to turn at the end of the field (*Grisso and Alley, 2002*).

For the tests, the tractor used was the New Holland T7060 and as machines the rotary harrow, Alpego DG-400 and the buriers Forigo DG-45.The operating machines have been used to improve the quality of work, understood as a shorter overlap or a shorter deviation between wipes contiguous. The tractor New Holland T7060 is operated by a NEF motor, which has been designed to minimize the vibrations. It is a 6-cylinder engine capable of developing a stable power at any speed. In addition, this engine has a low speed that reduces the noise and the vibrations. The harrow Alpego DG-400 is a folding rotary harrow, used to break up the clods after the plowing to prepare the seeding or planting bed. It has a width of 4.10 m and a work front of 4.00 m. It is a harrow that can fold on itself turning into a little shape, below 2.50 m in width. With regard to the harrowing depth, the value set up was 10 cm; a sampling was performed and the related data were shown in the table 6. The buriers is a machine used for the preparation of the seedbed on soil with a good supply of skeleton, allowing to obtain a surface layer well refined. Its mechanical action is due to the rotation impressed by the power takeoff tractor to a rotor with vertical teeth (knives) type milling cutter. In front, the Forigo DG45 - 400 is provided with a pair of the conveyor discs, which represent the most protruding part of the operating machine, characterizing the amplitude of the work front. The researches carried out on flat surfaces, so that the rover and the eventual antenna RTK could be used by the largest number of satellites (in fact, leaning both to GLONAS and to GPS, it has been detected on the user interface display, placed in the driver's cab, a medium of 10 satellites); for the same reason we worked on flat areas without the presence of trees, power lines, farms or similar facilities, which would block out the signal in case it interposes between the receiver and the satellite. The surveys have been performed using a tape measure of 20 m, a tape measure of 3 m, steel rods, a carpentry line and a land surveyor squaring. Between two passes perfectly contiguous, it can see the entire line of juncture, which in the absence of transpositions, keeps perfectly linear along the entire route. Combining the line of juncture with the land surveyor squaring thread and working backwards through armor rods, it was possible to align and stake out the extremes of the linear transpositions along the joint. Then, it was detected the distance between the stakes, obtaining the so-called length of transposition and also connecting the two pegs with a line, it was possible to detect the maximum distance, identifying in this way, the width of transposition. The surveys were performed over several days in the countryside on a route of 13.000 m and 80 observations for each plot. The basic parameters that have characterized the two test scenarios are summarized in the Table 1 and in the Table 2 there are the machine operating data.

The surveys have been performed on pairs of contiguous swaths, to identify areas where happen an overlap or some variations, so that even the measure results reasonable.

The principle is as follows: let us suppose that the work front amplitude of the operating machine is fixed, for example of 4.00 m for the Alpego DG-400, it follows that two swaths pull in parallel between them, will show a constant amplitude of 8.00 m, for which any section (orthogonal to the advance direction of the tractor) will not show neither overlaps or derivations, and therefore, the satellite guidance system will have done a good work. In the overlap areas we will have a reduction of this width, which will be of value below 8.00 m, for example, it will be of value 7.50 m. Therefore, the lateral transposition datum reported on the land book will be the result between the width measured in the field, in this case 7.50 m, and the nominal width of the two contiguous swaths, in the case 8.00 m. The transposition length, that is the transposition entity in the direction of tractor advancement, was measured detecting the distance between the point in which the tractor deflected the ideal trajectory and the point where the tractor inserted again on the ideal trajectory. In the areas of deviation, instead, the front is greater than the front that would occur if the swaths were maintained tangential, for which, in this case the lateral transposition datum reported on the land book will be the result of the difference between the width actually measured in the field, for example 8.50 m, and the nominal width of the two adjacent swaths, 8.00 m. For each transposition, then, has been calculated the apparent area, multiplying the transposition length for its width. Obviously, since in the variance analysis for one factor (ANOVA) it is necessary to standardize the number of the detected data, to the non-existent data have been assigned a value of 0 and the average was calculated considering these terms.

Table 1. Basic nominal geometric parameters.

	EZ-Steer/RTK	Autopilot/EGNOS
A swath average length(m)	250	271
Total number of passes made	52	48
Meters travelled (m)	13000	13000
Contiguos passes number	26	24
Single pass width (m)	3,8	4
Two contiguous passes width (m)	7,6	8
Swath total width (m)	197,6	192
Two contiguos passes surface (m2)	1900	2168
Σof work surface (m2)	49400	52032

Table 2. Machine operative data.

	Forigo DG45 + New H. T7060	Alpego+ New H. T7060
Average speed (Km/h) m/min)	3,6; 60	4,0; 66,7
Work front width (m)	3,8	4
Processing depth (m)	0,2	0,1
Fuel consumption (l/h)	15,4	15,8

Results and discussion

From the elaboration of data in relation to the behavior of the two satellite guidance systems, that manage the only direction of tractor advancement, we have obtained the following results (Table 3).

On the basis of these results you gather that the EZ-Steer/RTK system ensures a lower capacity of the theoretical path, in fact, the total of the travelled route shows an error of 229.42 m respect to the Autopilot/EGNOS system, above 1.77%. From the elaboration of data relating to the behavior of the two guidance systems in manage only the transposition width, we have obtained the following results (Table 4). So it can be observed that the EZ-Steer/RTK system ensures a better approximation of the tractor trajectory to the theoretical path respect to the Autopilot/EGNOS system, which provides an error greater than 1.64 m over the total transposition width and 2 cm over the average transposition width. This is because the RTK, proposing a greater precision lead the EZ-Steer system to approach more to the theoretical path, differently from the EGNOS system, which manages an accuracy of 20 cm, therefore, despite the Autopilot control ability on the tractor, at the end you can get more lateral transposition. As regards the latitudinal parameter, unlike the transposition length, has not been considered the percentage of the transposition width respect to the total of the work front, in that, at least in this location, not actually being in possession of an adequate amount of data, the transposition width and the total width of the work front are not connected with each other; it follows that, the total work front is not derived from the quality of latitudinal work and the use of two machines has been exclusively as tracer, because all this, the piloting, being automated, will repeat the lateral transposition error despite you will work on 3.80 m, 4.00 m to 20.00 m. From the elaboration of data relating to the behavior of the two guidance systems in managing the areas of normalized transposition, we obtained these results (Table 5).

About these values is possible to observe that the Autopilot/EGNOS system is capable of ensure a better quality of work than the EZ-Steer/RTK system, in fact, it provides a precision on the transposition total area, equal to 6.396 m^2. The area of transposition, therefore, is the parameter that most of all allows to compare the two combinations of guidance systems, as it is a datum that merges the longitudinal behavior of transposition with the latitudinal one. As for the transposition width also for the surface of transposition is not considered the proportion (%) of the transposed area respect to the total of worked area, in that, with increasing of the work front, and therefore, the surface unitarily worked, the surface transposed being equal, it follows its reduction if we consider it in percentage terms.

As you can see the average depth of work respects the operating nominal depth when the tractor is supported either by the system EZ-Steer/RTK or by the Autopilot/EGNOS system. The variance analysis (ANOVA) affected parameters such as: transposition length, transposition width and normalized areas. For the calculation of the variance of the transposition length we have analyzed the data obtained, which have reported in the graph relative to the transposition lengths provided by the two guidance systems (Figure 1).

The results obtained showed that the values of transposition length surveyed in the field for the EZ-Steer/RTK and the Autopilot/EGNOS systems one deviate significantly from the average. Similarly to the calculation of the variance of the transposition width have been analyzed the data collected which have shown in the graph of the transposition

Table 3. Transposition length results.

	EZ-Steer/RTK	Autopilot/EGNOS	VARIAZIONE
Swath average length (m)	250	271	-21
Route travelled (m)	13000	13000	0
Transposition totallength (m)	998,64	769,22	229,42
Transposition average length (m)	12,483	9,6153	2,8677
Transposition length of total travelled route (%)	7,682	5,917	1,77
Length min. of transp(m)	1,3	2,45	-1,15
Length max oftransp(m)	28,7	17,1	11,6

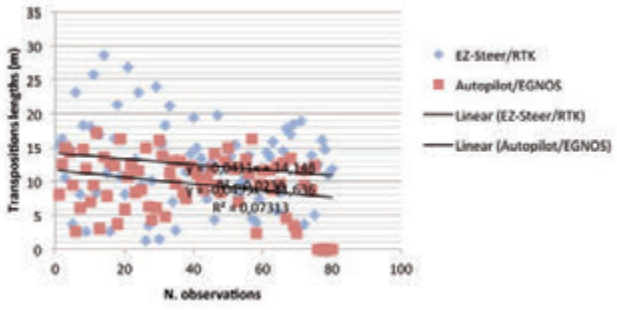

Figure 1. Transposition lengths provided by the two guidance systems.

Tabella 4. Results about transposition width.

	EZ-Steer/RTK	Autopilot/EGNOS	VARIAZIONE
Work front widh (m)	3,8	40,2	
Two passes contiguous width (m)	7,6	80,4	
Swath width(m)	197,6	192-5,6	
Total transposition width(m)	11,6	13,237	1,637
Average transposition width (m)	0,145	0,165	0,02
Length min. of transp(m)	0,05	0,08	0,03
Length max.oftransp(m)	0,355	0,375	0,02

Table 5. Results on the surface of transposition.

	EZ-Steer/RTK	Autopilot/EGNOS	VARIAZIONE
Swath average length (m)	250	271	-21
Route travelled (m)	13000	13000	0
Transposition totallength (m)	998,64	769,22	229,42
Transposition average length (m)	12,483	9,6153	2,8677
Transposition length of total travelled route (%)	7,682	5,917	1,77
Length min. of transp(m)	1,3	2,45	-1,15
Length max oftransp(m)	28,7	17,1	11,6

widths provided by the two guidance systems (Figure 2.).

For the calculation of the variance of the transposition normalized areas, obtained by multiplying for each survey, the transposition length for its width, we have analyzed the collected data which have shown in the graph (Figure 3).

The variance analysis on the normalized areas shows that the values obtained from the systems EZ-Steer/RTK and Autopilot/EGNOS do not deviate significantly from the average.

The survey results are summarized in the following table (Table 7) to deduce the behavior of the two systems and draw conclusions.

In longitudinal terms, a good work quality is given by the null transposition length. It's clear from the comparison with the data that the EZ-Steer/RTK system, provides a lower capacity of the theoretical trajectory. In fact, the total of the carried out route, shows a longitudinal transposition of 229.42 m more than the Autopilot/EGNOS system, equal to 1,77% of the 13,000 m routes. It follows that, between the two systems, the Autopilot/EGNOS is able to correct before and better the deviation from the theoretical route. The device EZ-Steer is an assisted guidance system and the tractor is operated by a motorized roller, whose management is assigned to the control unit T2 placed in the tractor's cab. The starter, which is the limit of the EZ-Steer system, is unable to handle the multiple impulses of course correction issued by the control unit causing a light slipping on the wheel, reducing the system sensitivity. All these elements are summarized from the parameter aggressiveness, which expresses the ability of the system to allow the tractor to point out the theoretical trajectory. Increasing the aggressiveness the systems helps the tractor to follow a rectilinear profile and faithful to the theoretical trajectory. It exists, however, a limit called overcorrection that is proportional to the architecture of the system. The EZ-Steer, in fact, does not allow to go over 90 points of aggressiveness, because exceeding this threshold it is in overcorrection and instead to follow the theoretical trajectory increases the error around it. This implies a greater transposition length, and, therefore, a lower quality of work. The Autopilot system, instead, allows to reach an aggressiveness of 135 points, justifying the different length of transposition, found in the experimental stage, between the two systems. The EZ-Steer system, however, differently from the Autopilot, is implemented by a correction RTK that according the test it should have offset the reduced aggressiveness, and therefore, it would have to reduce the transposition length but it was not like. In fact, the EZ-Steer/RTK system has found a transposition length equal to 998.64 m, while the Autopilot/EGNOS system has found a transposition length of 769.22 m. The control ability of the actual trajectory on the ideal trajectory and the aggressiveness of the two guidance systems, the EZ-Steer and the Autopilot prevail against the accuracy correction of the satellite signal took place by the RTK and EGNOS devices. The results on the transposition widths point out the different ability of the precision correction accomplished by both systems. While, with the Autopilot/EGNOS system has a transposition average width equal to 16.5 cm, the EZ-Steer/RTK system has a transposition average width equal to 14.5 cm. For the combination EZ-Steer/RTK, the 14.5 cm are, however, a result that does not respect the power of the RTK correction (2.5 cm), while the Autopilot/EGNOS combination is fully integrated within the 20 cm guaranteed by EGNOS correction. The system Ez-Steer/RTK's transposition average width (14.5 cm) does not respect the potential of the RTK correction (2.5 cm), while, the system Autopilot's transposition average width is included in the correction EGNOS's 20 cm. The motivation, also in this case, is referable to the different aggressiveness of the two satellite guidance systems, this is because a 90 points' aggressiveness induces the tractor to move away from the ideal trajectory, unlike what happens with a 135 points' aggressiveness obtained by the Autopilot system. Comparing the two systems on the basis of the transposition

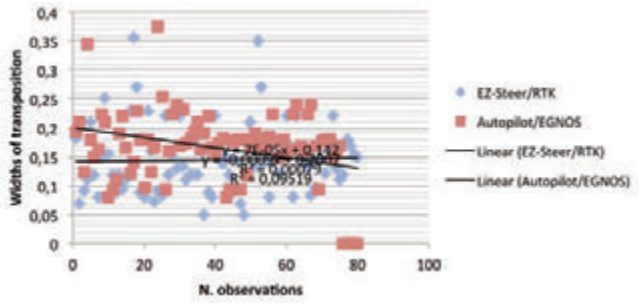

Figure 2. Comparison between the transposition widths provided by the two guidance systems.

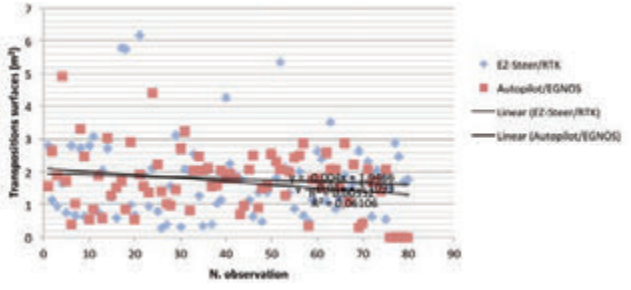

Figure 3. Comparison between the transposition normalized surfaces provided by two guidance systems.

Table 6. Results on the work depth of the machines.

	Forigo DG45	Alpego DG – 400
Work nominal depth (m)	0,2	0,1
Work total depth (m)	16,078	8,002
Work average depth (m)	0,200975	0,100025

Table 7. Results about the performances of two guidance systems.

	EZ-Steer/RTK	Autopilot/EGNOS	VARIAZIONE
Transposition total length (m)	998,64	769,22	229,42
Transposition average length (m)	12,483	9,6153	2,87
Variance–Transposition average length	38,3352	18,3766	19,96
Percentage of the transposition length on the total of travelled route (%)	7,682	5,917	1,77
Transposition total width (m)	11,6	13,237	-1,64
Transposition average width (m)	0,145	0,165	-0,02
Variance – Transposition average width	0,0037	0,0043	0,00
Transposition total surface(m^2)	142,672	136,276	6,40
Transposition average surface(m^2)	1,7834	1,7035	0,08
Variancetransposition average surface	1,5861	0,888	0,70

normal areas show that both are characterized by a good reliability that is even higher in the case of the Autopilot/EGNOS association, able to contain the transposition surface of only 6.396 m^2, thanks mainly to the lower longitudinal transposition. As you can see, the machines using the two systems, the Autopilot/EGNOS and the EZ-Steer/RTK had an homogeneous regularity of work. These results, however, can be attributed to the capability of the tractor New Holland T7060's active suspensions and to the regularity of the surfaces which have not produced a considerable pitch stress to the tractor. The regular work depth doesn't result from the control units of control, because although the T3, compared to T2, also manages the pitch, this capacity has to be understood in terms of the tractor's apparent position respect to the real position and therefore it has to be understood in terms of geo-referencing, not mechanical. There will be different results from the ones found when the control unit T3 have planned with a pitching control that operates on the suspension hydraulic circuit.

Conclusions

The conducted experimentation shown the way the two satellite guidance systems examined don't have a significant differences in the quality of work, although the Autopilot/EGNOS system has a greater reliability on the transposition length. It follows that the two combinations of satellite guidance, in view of the similar amount of latitudinal transposition, are suitable for all those jobs which tolerate some mistakes, such as: plant protection treatments, fertilizing, harrowing, mowing, reaping and so on, while for a high precision work, such as the sowing, weeding, planting, processing among rows, there is the need to use a combination that guarantees a maximum precision, and for this it will be necessary to optimize the system Autopilot supporting by the RTK correction. The maximum precision that comes from, however, can entail the saving on factors of production and this solution would be hoped for the increase of their purchase cost and for the growth of company. An entrepreneur who wants the growth of his company, adopting the two systems must consider several aspects, such as: the current size and the expansion potential of company, the crops ordering current and future, the possibility of entering in the subcontracting's business, the EZ-Steer's versatility compared to the Autopilot, but also the Autopilot's precision potentials against the EZ-Steer and therefore an actual concrete opening towards a thrust precision farming. The disadvantage of the Autopilot and that since it has the integrated system, it can be disassembled by a tractor and the reassemble on another one which may be suitable for the performed work. These systems make independent the tractor feed from the operator's view; this is an advantage for the operator who will have a less workload and more time to focus his attention on what it is important, that is, the processing. These are systems that allow to reduce the overlaps. This condition implies a better quality of work, also motivated by a reduced compaction of land (for minor steps), by an increase in fertility, by a reduction of erosion, by a less disturbance to crops in progress, with a higher productivity of the yards, thanks to the use of the front work, and the decrease of passes number being equal surface and a greater speed of execution. This in turn, entails a decrease in costs, a greater productivity and a better management of company. The satellite guidance systems, in fact, allowing the tractor in the field to geo-reference, which are validly supported by remote sensors, from information derived from remote sensors and therefore by the prescription maps (which quantify the intensity of interventions in various areas of the field), in conjunction with appropriate technologies, which allow you to practice the VRA (variable distribution of inputs with sensors), find step by step the physical-chemical state of the soil, the nutritional state of the crop, the plant health state of the same, and the degree of production maturation etc.. An further advantage of these systems is a less pollution of water and air and a traceability of products, in fact, the geo-referencing, supported by the context of precision agriculture, identifies the exact point of origin of the product and the treatments to which it was subjected. The EZ-Steer's advantage regards the possibility of being applied to over several tractors, in fact, within a couple of hours it can be disassembled by a machine and reassemble on another one. The Autopilot, instead, is an integrated system, placed on the guidance hydraulic circuit, which greatly improves the precision of the assisted driving (in fact, you get to 130 of aggressiveness), at the same time has the disadvantage of not be able to be moved by a tractor to another one, and therefore, to a greater precision of the guidance system there is the cost of a less versatility. The disadvantages are: a precision work not very good, the occasional loss of the satellite signal (attributable to several factors: power lines, trees, houses, water openings for irrigation, etc..), and a substantial purchase for the systems more advanced.

References

Auernhammerr H. Precision farming – the environmental challenge. Computer and Electronics in agriculture 2001; 31:43- 30.

Chavas J. P. A cost approach to economic analysis under state-contingent production uncertainty. American Journal of Agricultural Economics. Blackwell Publishing Co 2008; 435: 446 - 90 (2).

Gandonou, J M, Dillon C, Harman W, Williams J. Precision farming as a tool in reducing environmental damages in developing countries: a case study of cotton production in Benin. American Agricultural Economics Association 2004. Annual Meeting. Available from:http://ageconsearch.umn.edu/bitstream/20086/1/sp04ga02.pd

Grisso R. and M. Alley. (2002). Precision farming tools – light bar navigation. Publication 442-501. Blacksburg: Virginia Cooperative Extension Service

Pierce F.J., Sadler E.J. (1997). The state of site specific management for agriculture, ASA Publ., ASA, CSSA e SSSA, Madison, WI, USA.

Tyler D A,. Roberts D W, Nielsen G A. (1997). Location and guidance for site-specific management. In: The State of Site-Specific Management for Agriculture1997. ASA, CSSA, SSSA, Madison, WI; 1997. pp. 161-181.

Trimble Navigation, Ltd. EZ SteerTM System reference guide. Overland Park, Kan; 2005.

Verhagen J , Bouma J, 1997. "Modeling soil variability". In Pierce F.J., Sadler E.J. (ed).The state of site specific management for agriculture 1997: ASA Publ., ASA, CSSA e SSSA, Madison, WI, USA; 1997.

New solutions for horse shelters to connect to the equestrian paths

Gianluca Bambi, Massimo Monti, Matteo Barbari

Dipartimento di Gestione dei Sistemi Agrari, Alimentari e Forestali, GESAAF, Firenze, Italy

Abstract

A rational and modern network of riding trails involves the building of specific structures for the horses according to the new needs of equestrian tourists. These shelters require appropriate technical models that today cannot be found easily in the Italian or foreign literature. Over the years this gap has led to the development of the practice "do it yourself", following old techniques of construction, not able to meet the new demands of the market of horse tourism. This research has highlighted two different solutions that can meet the needs of tourists riding today, in accordance with the laws about the construction and the health part. These structures have been designed observing the principles of low impact, low cost, easy installation, complete reuse. Two kinds of structures have been planned. Temporary stay horse shelter: building to put in resting places of interest along the path (historic villages, monasteries, etc.), where it is possible to arrange the horses for a few hours and allow to the riders to make a careful visit of places of interest. Overnight stay horse shelter: structure to put in particular points where horses and riders can spend the night. A new type of horse barn with annexed feed storage and saddle room. The structure is dynamic, due to the possibility to change quickly the position of the horses (max 8 places).

Introduction

In Italy a growing number of projects involves the creation or promotion of riding trails. These projects are often developed by public offices, such as regions, provinces and natural park authorities. Therefore the horse tourist sector has become part of the dynamics of territorial development.

The "*equitourism*" is one of best hiking ways to live landscape intimately and naturally, to arouse emotions in the rider that only the horse can transmit. Tuscany is a region that definitely offers an exceptional opportunity for the development of equestrian tourism, thanks to the wealth of its natural and environmental heritage and to the craft traditions, history and culture of its inhabitants. Today the equestrian tourism is not any more a small market, but has become a true form to spend time to discover the landscape. It is like a return to tradition: the horse is no longer used only for sports, but to travel from one point to another, as has been for many centuries, like a true travel companion that can help to relate better with the nature.

In Europe there are already two important cases of successful integrated offering of equestrian tourism. The first system is represented by Ireland (already fully operational), the second is located in Italy and is represented by the Abruzzo Region. In particular, this project looks at the model of Ireland, which has been able to relate public and private initiatives by creating a tourism product that has turned the horse culture of the territory in a special tourist offer "all season" and to generate local economic value.

A rational and modern network of riding trails involves the building of specific structures for the horses according to the new needs of equestrian tourists. The Department of Tourism of Tuscany Region, in collaboration with the Fitetrec Tuscany (Italian Federation Equestrian Tourism), identified two years ago five rings of horse trails. The project "Riding Trails Tuscan" is part of the interregional cooperation actions for the development of Equestrian Tourism, following a strategic segment of a new tourist offer based on criteria of sustainable development.

Correspondence: Matteo Barbari, Dipartimento di Gestione dei Sistemi Agrari, Alimentari e Forestali, GESAAF – via San Bonaventura 13 50145 Firenze-Italy.
E-mail: matteo.barbari@unifi.it

Key words: horse shelter, horse paths, wood building

Journal of Agricultural Engineering 2013; XLIV(s2):e35
doi:10.4081/jae.2013.(s1):e35

Materials and methods

The research was developed thanks the interaction between the Department and the Tuscany Region, for the realization of a guidelines manual for the realization of riding trails. The research has started with an analysis of the accommodation requests made by the riders about the horse shelter. This survey was done in collaboration with the Italian Equestrian Federation. To facilitate the construction by private people and for a quick approval and inclusion in the local laws, the horse shelter have been designed following these principles: low impact, low cost, easy installation, complete reuse. One of the problems that emerged during the research was the opportunity or less of the realization of one building for the manure storage. The research, after a series of meetings with the local health office of the Tuscany Region, has shown some final considerations very helpful for the local authorities. The shelters are completely made in wood and include, when required, the use of reinforced concrete. The cladding is made in wood as well as the internal partitions among horses. The internal cladding, in one of the two types designed, is completely removable thanks to rails, hooks and iron chains.

Results

In this first phase, the research has identified two different propos-

als of horse shelter, with solutions that can satisfy the needs of modern tourist riding and have correspondence with the legislation about constructive sanitation. These buildings, preferably made with materials and according to traditional types, must follow the criteria of correct insertion into the landscape and reducing environmental impact.

Overnight stay horse shelter

This type of horse shelter must be connected to an official accommodation for the riders (according to the regional law LR 42/2000). It is an innovative type of horse shelter, designed to meet the different needs. In fact, the structure can be used like a loose box or a single stall, with easy operations to change disposition requiring few minutes. In this way two possibilities of housing can be offered, taking into account that some horses do not tolerate conditional admission in stall. The building allows to accommodate up to 8 horses in stalls or 4 horses in loose boxes. The number can change in mixed solutions (4+2, 6+1, 2+3).

Close to the area for horse shelter there is a room used to store feed and saddles and also used as emergency shelter for riders. The module is dimensioned so that the horses are placed head-to-head and have a width at minimum of 1.47 m and a length of 3.07 m. The building must be equipped with artificial lighting, fixed or mobile in order to ensure the inspection operations during the night. Inside every stall a drinking trough and a manger are placed in the corners opposite the opening (Figures 1 and 2).

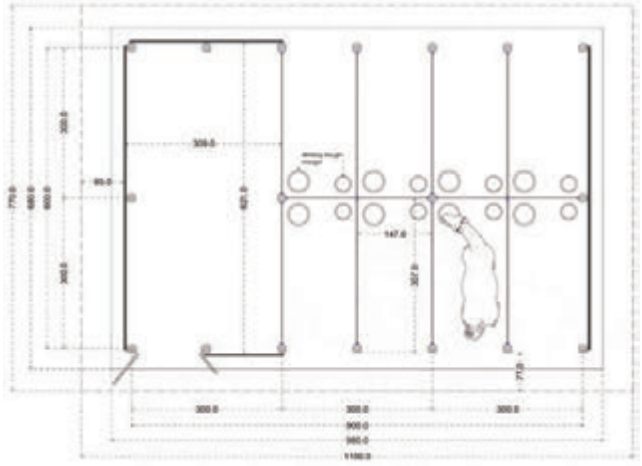

Figure 1. Layout of the overnight stay horse shelter.

Figure 2. Perspective view of the overnight stay horse shelter.

Temporary stay horse shelter

This type of shelter is based on the concept of old horse post station, to put in resting places of interest along the path. The building is modular and does not have the room for storage of saddles and feed. It is advisable nevertheless to provide a fence to support the saddles. An external drinking trough has to be provided (Figures 3 and 4)
In both the structures the following elements must be present:

- iron ring to tie in correct way the horses, preferably with a rope fitted with a counterweight to avoid accidents;
- sink to wash the horse tack and a rubber tube (at minimum 4 m) to clean the horses;
- chain needed in the bottom of the stall (behind the horse), designed to contain and give security to fearful or nervous horses.

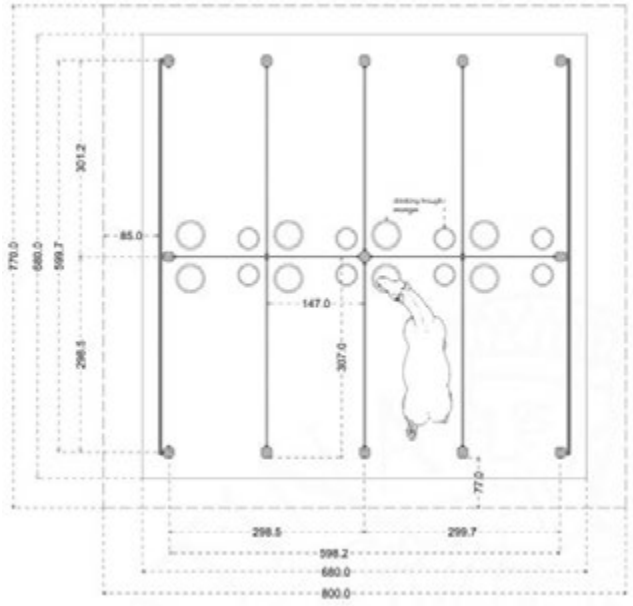

Figure 3. Layout of the temporary stay horse shelter.

Figure 4. Perspective view of the temporary stay horse shelter.

Health and hygiene guidelines for the manure

The health and hygiene standards to build these particular temporary horse shelters is quite complex because the local municipal regulations of hygiene are quite different in the Tuscany Region. Indeed, if it is true that this building constructed for the custody of horses in theory should follow the veterinary police regulations, it is also true that it is a temporary shelter, where the horses remain inside for few hours. This has led to different interpretations by the veterinary offices dislocated in the Region.

The legislation imposes a waterproof flooring for a complete disinfection and cleaning. However, taking into account that the shelter has to be suitable for temporary use, different design solutions could be provided. These include the creation of stalls with interlocking concrete tiles or the preparation of the simple bare ground with several layers of cobblestones. The proposed solutions are based on the use of reinforced concrete foundation, that is the most request.

Another consideration regards the possibility or not to build the place for the manure storage. One solution is represented by the possibility to put the manure in special sealed containers (such as garbage bin), to empty into an official place for the manure. Alternatively a plastic sheet on the ground could be used, with the disadvantage that it must be replaced each time the manure is removed.

The municipal regulations often require the presence of a reinforced concrete flooring, increasing the total cost of construction. Other national regulations to follow are those concerning the distances for positioning and for sizing. The storage period for the horse manure can be smaller than for others animals (up to 90 days). Usually a surface of 3 m^2/horse for a storage period of 180 days is planned, so 1.5 m^2/horse for 90 days. Considering a presence of horses of 2-3 days per week (35 days in the 3 months of storage), and occupation of the shelter mainly overnight (10-12 hours/day), a further reduction of 50% can be considered. Therefore for a shelter with 8 horses a rectangular surface of about 3 m^2 is required. The catch basin for the urines is not required because these are totally absorbed by the litter (straw, wood shavings or other).

Conclusions

The main aim of the research was to propose a series of projects for housing of horses to service riding nets. The structures were designed following the general principles of the Horse Code for the Protection and Management prepared by the Ministry of Labour, Health and Social Policies.

The proposed solutions can meet the needs of the modern tourist riding and have correspondence with the local and regional legislation.

The designed solutions have to be considered type-projects, to be built in the whole national territory, leaving the final structural calculations to specific individual cases.

References

Barbari, M., Conti, L., Monti, M., Pellegrini, P., Rossi, G., Simonini, S., Sorbetti Guerri, F. (2012). Antropizzazioni decostruibili per il non-consumo del territorio rurale - Parte I: dallo sviluppo sostenibile alle antropizzazioni decostruibili. L'Edilizia Rurale tra Sviluppo Tecnologico e Tutela del Territorio. Firenze: AIIA - Associazione Italiana di Ingegneria Agraria.

Barbari, M., Conti, L., Monti, M., Pellegrini, P., Rossi, G., Simonini, S., Sorbetti Guerri, F. (2012). Antropizzazioni decostruibili per il non-consumo del territorio rurale - Parte II: progettazione per la decostruibilità. L'Edilizia Rurale tra Sviluppo Tecnologico e Tutela del Territorio. FIRENZE: AIIA - Associazione Italiana di Ingegneria Agraria.

Barbari, M., Monti, M., Pellegrini, P., Sorbetti Guerri, F. (2003). La costruzione di edifici agricoli in legno massiccio sulla base di progetti tipo. In Costruire in legno - Progetti tipo di fabbricati ed annessi agricoli (2 ed.). Firenze, Italia: ARSIA Regione Toscana.

Giordano, G., Ceccotti, A., Uzielli, L. (1999). Tecnica delle costruzioni in legno (5th ed.). Milano, Italia: Hoepli.

Monti, M., Pellegrini, P. (2005). Impiego strutturale del legno massiccio negli edifici agricoli alla luce dell'evoluzione normativa. L'ingegneria agraria per lo sviluppo sostenibile dell'area mediterranea. Catania.

Schouten, J., Addis, W. (2004). Design for deconstruction. Principles of design to facilitate reuse and recycling. CIRIA.

Environmental assessment of individual and collective manure management systems

Giorgio Provolo, Aldo Calcante, Francesca Perazzolo, Alberto Finzi, Filippo Volontè, Davide Grimaldi, Mauro Pinnetti, Giorgia Cocolo, Ezio Naldi, Giorgio Galassi, Elisabetta Riva

Department of Agricultural and Environmental Science, University of Milan, Italy

Abstract

In intensive livestock area with large nutrient surplus collective management systems can be a suitable solution. However, the collective system should carefully evaluated for environmental sustainability to avoid cross effects. The aim of this study was to evaluate the environmental effects of the introduction of a collective treatment plant for energy production and nitrogen removal. For this purpose an assessment methodology, for individual farms and collective treatments plants, has been defined to estimate the emissions of the main pollutants to the air (CO_2, CH_4, N_2O, NH_3) and to the soil (N). The method devised has been assessed in a case study (a treatment plant collecting manure from 12 farms). The main effect of the introduction of the collective management system from the environmental point of view is a reduction of greenhouse gases emissions of 61% due to methane emission reduction and renewable energy production. Furthermore, it reduces the amount of nitrogen to be applied to land from 430 kg ha^{-1} to about 220 kg ha^{-1}, decreases the emission of ammonia in the air by about 17% due to lower amount of nitrogen that is managed by farms in the storage and spreading operations.

Introduction

The environmental impact related to intensive livestock farming is often determined by manure management systems that do not use best available techniques. Furthermore, in areas with a high density of animals, the load of nutrients exceed crop requirements, causing a relevant environmental problem. As livestock intensification continues, there is a need for development of technology and strategies to control the associated environmental problems (Petersen *et al.*, 2007).

In this framework and considering the regulatory constraints (Community directives 91/676/EEC and 2010/75/EU), the application of different techniques of collective treatment and management of manure, represents a possible solution to the sustainability of livestock farms.

A manure management system needs to address the principal local environmental risks and any excess of nutrient over the requirements of the local crop production, since manure disposal will often be (either directly or indirectly) by land application. Good strategies enable a targeted application of nutrients that meets, but does not exceed local crop needs. Criteria for the design of the future waste management systems and the improvement of existing ones include the maximization of nutrient recycling and of social acceptance, the protection of air, soil and water resources, human health and safety, the control of manure application rates, and the minimization of capital and operating costs and energy requirements (Lagüe *et al.*, 2005). The present concern about global climate change should stimulate practical solutions in areas with nutrient surplus towards a contribution of the manure management to an effective reduction of greenhouse gases (GHGs). The implementation of some technologies and practices can mitigate the impact of agriculture on Climate Change (IPCC, 2006). At the same time such solutions must also bring a reduction in other emissions to air (especially ammonia), as well as further environmental protection for water and soil. In order to control nutrient surpluses and other risks, environmental technologies and management strategies are needed. Unfortunately, the development is impeded by the lack of well-defined market conditions. Economic and market policies and regulations of manure management present boundary conditions which determine if a given technology is attractive to the farmer. Moreover a gap between the development in scientific understanding of the multiple risks of manure management and the take-up of this knowledge by policy makers still exists, it is now understood that cost-effective solutions can only be found in integrated policies (Petersen *et al.*, 2007).

Therefore, integrated assessment tools and decision support systems are now required which have yet to be developed. The regulation aiming to minimise the environmental impact of livestock manure becomes one of the many external constraints that farmers – and these assessment tools – have to consider. When dealing with livestock manures in a whole-farm perspective, the evaluation of cross- and side-effects of regulations based on scientific knowledge still poses significant challenges. For this reason collective systems might be an interesting solution but it should carefully evaluated for environmental sustainability to avoid cross effects and the increase of emissions to air. The main emissions to air from farms are: methane (CH_4) produced by ruminal digestion and stored manure, ammonia (NH_3) and

Correspondence: Giorgio Provolo, Department of Agricultural and Environmental Science, University of Milan, via Celoria 2, 20133 Milano (Italy) Tel.+39.02.5031 6855. E-mail: giorgio.provolo@unimi.it

Key words: nutrient surplus, treatment plant, anaerobic digestion, nitrogen removal.

Acknowledgments: this research was financially supported by the MANEV project No. LIFE09 ENV/ES/000453.

Journal of Agricultural Engineering 2013; XLIV(s2):e36
doi:10.4081/jae.2013.(s1):e36

carbon dioxide (CO_2) as a result of animal respiration and manure stored. Finally, during the spreading phase produces losses of NH_3 volatilization and nitrous oxide (N_2O). NH_3 causes acidification of soil and water. Approximately, 90% of NH_3 emissions are due to agriculture in several European countries, 40% of which coming from animal housing and manure storage (Rigolot *et al.*, 2010). CO_2 emissions in agriculture is negligible because it is derived mainly from burning fossil fuels. The amounts of CH_4 and N_2O emitted to the atmosphere are low compared to CO_2, but their global warming potentials are, respectively, 21 and 310 times higher than that of CO_2. Within the European Union, agriculture has been estimated to contribute 49% of anthropogenic CH_4 emissions and 63% of N_2O emissions (Sommer *et al.*, 2004). The extreme involvement of agriculture and livestock farming on environmental issues, involves using computer models to estimate the pollutants emissions of during farm activities. These models can be used both to highlight the criticality of the farms and to establish sustainable manure management systems (Burton and Turner, 2003).

Therefore, when a new treatment facilities is introduced, the reduction of GHGs and ammonia emissions has to be assessed together with the nutrient load on the land receiving the treated manure.

This study has been developed in the framework of the LIFE+ 2009 "Evaluation of manure management and treatment technology for environmental protection and sustainable livestock farming in Europe (MANEV)" project (http://www.lifemanev.eu/). MANEV is an European project of large-scale demonstration framed within the LIFE + Programme of Environment Policy and Governance, whose main objective is to improve environmental protection and sustainability of livestock promoting the use of treatment technologies in different saturated or surplus areas in the production of livestock manure across Europe. Eight partners will assess 13 treatment technologies and manure management systems, located in eight regions with high pig production belonging to four European countries, following a common monitoring and assessment protocol that has been developed in the project. The results of each assessment could be referred to CO_2 equivalent units in order to assess its contribution to fight against climate change.

A software tool will be developed based on the results and all the information and data obtained from the technology assessments developed in the project, which is intended to provide an objective decision support tool to determine the most appropriate treatment according to the local circumstances, without being these mere technological comparison but taking into account aspects like for example environment, society, economics, local regulation,… of every case study. Europe will be endowed with a common decision support tool to the various technologies beneficial for both farming sector (search for the optimal technology) and the administration (environmental control and promotion of the use of technologies).

The activity carried out in the project include the definition of a common protocol to assess the emissions of the different treatment systems studied within the project.

The aim of this study was to evaluate the environmental effects of the introduction of a collective treatment plant for energy production and nitrogen removal. For this purpose the assessment methodology defined in the MANEV project, for individual farms and collective treatments plants, has been adopted to estimate the emissions of the main pollutants to the air (CO_2, CH_4, N_2O, NH_3) and to the soil (N). The method devised has been assessed in a case study (a treatment plant collecting manure from 12 farms).

Materials and methods

The monitored plant

The studied management system is a collective treatment plant with an anaerobic digestion phase for energy production and a nitrogen removal phase. It is located in northern Italy, Bergamo province, in an intensive livestock area where there is a high surplus of nitrogen and has been designated as vulnerable zone.

The treatment plant involves 12 livestock farms (mainly pigs, but also cows and poultry), located 0.5 to 6 km far away from the plant, for a total daily production of around 220 m^3 of manure (Table 1). The manure is transported by slurry tankers with the exception of the nearby farm, connected by mean of a pipeline. At first, manure is processed in an anaerobic digestion reactor for the production of energy. This step consists of two digesters, with a volume of 2280 m^3, and a post-digester (of 3185 m^3 volume). One of the two digesters is fed with manure and other biomasses (silage) around 10 t per day, while the second one is fed with raw manure. The digestate is then conveyed to the post digester. The digested effluent is then separated, in order to reduce load and to separate most of the phosphorus. The solid-liquid separation treatment is performed by two screw press separators. The solid fraction is sold, while the liquid fraction is treated for biological nitrogen removal. This process is carried out by two Sequencing Batch

Table 1. Main characteristics of the farms of the collective management system examined.

Farm	Type of livestock	Number of heads	Total live weight (t)	Total N (kg)
A1	dairy cows	640	204	26628
A2	dairy cows	560	175	22049
A3	dairy cows	790	246	30833
A4	hens	70000	70	16100
A5	dairy cows	322	100	12636
A6	dairy cows	999	333	43955
A7	beef cattle	80	25	2134
A8	dairy cows	527	164	20639
A9	fattening pigs	1400	102	11154
A10	fattening pigs	3500	271	29684
A11	fattening pigs	1800	142	15583
A12	dairy cows	1190	371	46900

Reactors (SBRs), having a capacity of 660 m^3 each, which operate in parallel. The cycles consist of four steps: feed (15-20 m^3 in 20 minutes), mixing (90 minutes), aeration (230 minutes) and settling (20 minutes).

The effluent is finally stored in three storage tanks. Then, it is transported to the farms by slurry tankers or pipelines.

Methodology used

The assessment protocol developed include the following four different steps:

- Step 1. Farm storage: This step would assess the impact of storage tank period inside the farm and its consequences in its subsequent treatment.
- Step 2. Transport and intermediate storage: This step would assess the impact of the transport of raw manure or to an intermediate storage of the treatment plant.
- Step 3. Treatment: the treatment plant has been monitored in order to provide a complete assessment of the treatment and its main process units. Moreover, raw manure and other materials fed to the process has been be characterized so as to the end-products of the process.
- Step 4. End-products management: End-products has been characterized and its transport and storage has been assessed with methodologies specified for steps 1 and 2. Same methodologies will be used for land spreading.

Environmental impact of the construction step was not considered at the moment. Nevertheless, it will be a further improvement by including information according to average European values for different materials and equipment. All the emissions related to the management of cosubstrates or additional material included in the process, before its treatment, has not been assessed within our system. These emissions are considered to belong to the system of the process that generates them. Emissions related to the treatment period and up to its final destiny are assessed all together with manure evaluation as part of the treatment technology impact.

Environmental assessment

The methodology used for the calculation of the emissions was applied for each pollutant and for each step of the manure management (De Vries and de Boer, 2010).

CO_2 emission are not considered for farm storage. For transport the Tier 2 methodology of IPCC 2006 has been used. Emissions were estimated from the fuel consumed and the distance travelled. In general, the fuel consumed is appropriate for CO_2 and the distance travelled by vehicle type and road type is appropriate for CH_4 and N_2O (IPCC, 2006). The average values of fuel consumption per distance unit travelled by the vehicles has been obtained by direct measurement during the monitoring period. The CO_2 emission value has been obtained using as emission factor the carbon content of the fuel multiplied by 44/12.

Energy balance in the treatment plant (expressed as CO_2) has been obtained by the difference of energy produced and the energy required to run the treatment. Data derives from plant monitoring.

The estimate of CH_4 and N_2O emissions has been obtained by using IPCC 2006 (Tier 2) methodology. For this purpose, the information has been obtained from the characterization of manure (Total nitrogen, volatile solids, etc.). For the other factors of this methodology, the default values has been used.

This method has been used for: Farm storages, intermediate farm storages, off-road transportation. The methane emissions during treatment have been obtained from literature values for similar treatments. In the biogas production emissions has been considered 5% (leackage) and in the SBR treatment 10% of the potential value (Loyon, 2006; Hansen, 2006; Brown, 2008).

For emissions related to land application the farm practice has been obtained from the recordkeeping of the farms.

Ammonia emission takes place in all those activities in which pig manure is in contact with air (storage, land application and tanks without cover in treatment plants) and transport activities.

When calculating emissions of NH3 using a mass flow approach, a system based on Total ammoniacal nitrogen (TAN) is preferred to one based on total N, as is used by IPCC to estimate emissions of N2O (EMEP/EEA, 2009).

EMEP/EEA 2009 Tier 2 methodology has been used to calculate ammonia emissions from the manure management.

To evaluate emissions from farm and intermediate storage, data of the different type of pits available in each farm has been collected. As the storage period (Hydraulic retention time) is limited when the manure is transported to the treatment plant, a duration factor has been introduced to avoid overestimation of the emissions. For this reason a linear trend of emissions has been considered and the default emission factor has been reduced according the ratio between the actual duration and a duration of 180 days.

Ammonia emissions during treatment has been obtained by literature. For the final storage the same EMEP/EEA 2009 Tier 2 methodology has been used but the TAN content was calculated according to the transformation in the treatment plant. To evaluate emissions during distribution the average conditions, derived from farm recordings was used in order to obtain an average emission factors.

To assess the water pollution risk, the crop balance method has been used. A modeling approach to nitrogen leaching and to nutrients in runoff was outside the scope of this work and the information required for this evaluation was not readily available (including soil analyses). The crop requirements were obtained by the farm records, using the average yields and nutrient content of the products according to the local data.

For the treatment plant the removal efficiencies were obtained from the monitoring data. The following values were used:

- Volume=1,01 (consider the addition of biomass and the solid manure produced in separation step)
- Total solids= 0,46 (consider the reduction in the anaerobic digestion, the separation and the biological treatment)
- Volatile solids= 0,35 (consider the reduction in the anaerobic digestion, the separation and the biological treatment)
- Total nitrogen= 0,55 (consider the addition of nitrogen with the biomass, ammonia emissions and the nitrogen removal in the biological treatment)
- Ammoniacal nitrogen=0,46 (consider also the mineralization of the organic nitrogen)

The emissions factors from the treatment plant, according the methodology explained resulted as follows:

- Emission of NH_3=7,59% of total nitrogen
- Emission of N_2O= 2,17% of total nitrogen
- Emission of CH_4=179,1 m^3 (t Volatile Solids input)$^{-1}$
- Emission of CO_2=-458,71kg CO_2 (t Volatile Solids input)$^{-1}$

The methodology reported has been applied to two different scenarios:

- Scenario 1: all the farm act individually and spread the produced manure in their fields
- Scenario 2: all the manure produced in individual farms is transported to the collective treatment plant and, after treatment, is transported back to each farm that provides to store it and to land spreading according to the manure management plan.

Results

The evaluation of the emissions related to each livestock is summarized in Table 2. It should be noticed that for the scenario 2, the results are reported for each livestock also if a collective treatment plant is adopted, in order to better compare the two scenarios.

The average reduction of ammonia emissions resulted of 17%. This value might be considered low compared to the nitrogen removal efficiency of the treatment plant (55%). However it should be considered that the emissions from the buildings are not affected and that the nitrogen remaining in the final product is mineralized thus the emissions during storage and spreading are higher.

The effect of the collective management system on ammonia emissions varies among livestock farms (Figure 1). This variation is explained by the different influence of the emissions before the treatment on the total emissions. In fact, the manure removal system and the amount of solid manure affect the ammonia emissions in this step of the management and have a different share of the total ones.

The emissions of GHGs are greatly influenced by the collective treatment system (Figure 2). Nitrogen oxide emissions are more than two times higher due to the negative effect of the treatment system. On the other hand, the methane emissions lower a lot (51%) due to the recovery of the biogas plant. Of course, the methane emissions in the intermediate storage before the transportation to the treatment plant entails some methane emissions (collection is made weekly in each farm) and the end product has still some methane production potential (the volatile solids are 2-2.4% of the total mass of the slurry applied to the land). However the main methane emissions in the scenario 2 are related to the losses of methane produced, due to leakages. The value used for this purpose (5% of the methane produced) might be overestimate, but there are limited information about losses from the biogas plants and further investigation are needed to have a better assessment.

The additional benefit of the treatment plant refers to the reduction of CO_2 emissions due to the energy production. The overall benefit in term of total CO_2 eq. reduction is 61% that seems a very good achievement. Figure 3 shows the comparison of the two scenarios for each farm. The only situation with a limited reduction of GHGs is the farm A4 (egg production) where the manure management in building and

Table 2. Emissions estimated by the two management systems (scenario 1 and 2) for each farm.

farm	scenario 1 NH_3 (kg year^{-1})	scenario 2 N_2O (kg year^{-1})	CH_4 (kg year^{-1})	CO_2 (kg year^{-1})	NH_3 (kg year^{-1})	N_2O (kg year^{-1})	CH_4 (kg year^{-1})	CO_2 (kg year^{-1})
A1	16,735	627	26,275	16,150	13,558	1,007	16,460	-525,710
A2	14,560	458	22,516	12,365	11,659	824	13,221	-376,130
A3	21,319	515	32,100	15,460	17,047	1,166	15,864	-321,080
A4	32,081	1,400	1,879	2,675	30,670	1,814	3,533	-214,531
A5	8,578	228	13,031	9,309	6,901	483	6,398	-123,865
A6	28,636	529	47,462	24,528	22,466	1,436	23,581	-483,113
A7	1,817	25	2,174	3,549	1,405	84	1,162	-23,095
A8	14,390	222	22,254	13,288	11,165	682	11,187	-236,864
A9	9,335	3	25,699	6,930	7,829	371	10,890	-125,491
A10	23,336	6	68,433	15,828	19,572	925	28,997	-369,624
A11	12,002	3	35,909	9,064	10,065	477	15,216	-179,273
A12	32,296	554	50,499	22,633	25,235	1,578	25,309	-539,228
total	215,085	4,571	348,231	151,780	177,572	10,848	171,817	-3,518,004

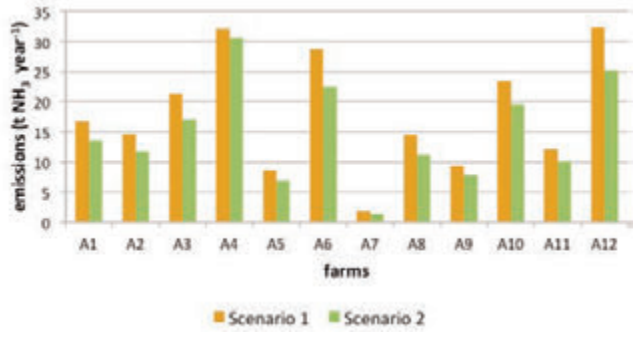

Figure 1. Comparison of the ammonia emission of the farms for the two management systems considered.

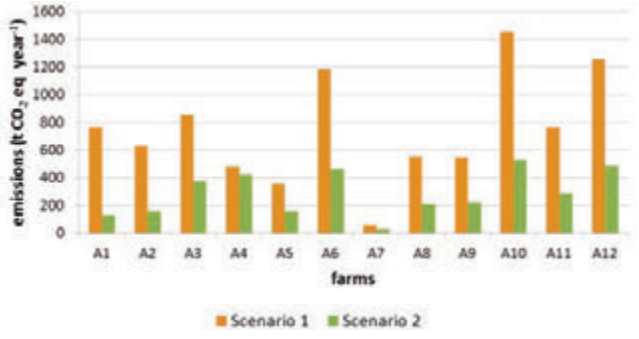

Figure 2. Comparison of the emission of CO_2 equivalents for each farm for the two management systems considered

storage has a limited production of methane.

The reduction of GHGs obtained demonstrate how this collective management systems might be sustainable despite the higher emissions due to transportation. This operation should be carefully considered as it can contribute significantly to the emissions. In the case study considered, the CO_2 emissions in scenario 2 are almost twice than in scenario 1 as most of the slurry is transported with slurry tankers. The balance without considering the CO_2 saved by renewable energy production is however positive, also if at lower level (18% reduction) due to the general decrease of methane emissions.

A further evaluation of the effect of the introduction of the collective management system can be obtained from the two indicators reported in Figure 3. The first expresses the nitrogen losses to air compared to the nitrogen excreted by animal. The value of scenario 1 (55%) is reduced of 18% in scenario 2, confirming the benefit in terms of acidification effect and eutrophication potential.

The second one refers to nitrogen load and indicates the average amount of nitrogen applied to each hectare of land (arable or grassland). The assessment in this case should be carried out considering two aspects: the nutrient balance and regulation. The crop requirement in the area, considering the nitrogen efficiency, has an average of more than 500 kg of nitrogen per hectare due to the intensive cropping system, but the area has been classified as vulnerable and therefore a limit of 170 kg of nitrogen from animal should be considered. The nutrient removal treatment allows a reduction of 50% of the total nitrogen. Although this resulted in a nitrogen load not jet completely under the limits, it can be considered as an effective reduction of the potential release of nitrates in the waters and of the eutrophication effect. In fact considering an average nitrogen efficiency of 50% the introduction of the collective treatment plant can reduce the nitrogen release after incorporation from 215 kg ha^{-1} to 108 kg ha^{-1}.

Conclusions

The methodology defined in the framework of the MANEV project was effective to assess the environmental impact of different manure management systems. The case study used has highlighted how a collective treatment system might be effective in the reduction of emissions to air and potential nitrogen pollution of surface and ground waters. The combination of anaerobic digestion and nitrogen removal treatment has demonstrated to be sustainable also from the environmental point of view also if the benefits of renewable energy production are not considered. The reduction of emissions related to methane can compensate the increase in CO_2 emissions for the transport of manure from the livestock farms to the treatment plant and vice versa. The removal treatment can reduce the nitrogen load to land at acceptable values. Although the economic assessment was outside the aim of this work, it can be considered how the possibility to have an income selling electric energy can compensate the cost of the nutrient removal treatment, making this solution sustainable also from the economic point of view. Further benefits derives from the reduction of odors and the production of a stabilized effluent that can be used as fertilizer more efficiently, with a possible reduction of mineral fertilizers and the consequent further economic and environmental benefits. Although the methodology used proved to be adequate for the assessment, it should be pointed out that there are some aspects, like the emissions from the different treatments, that will benefit of further studies in order to better consider the possible effect of different options on the emissions to air.

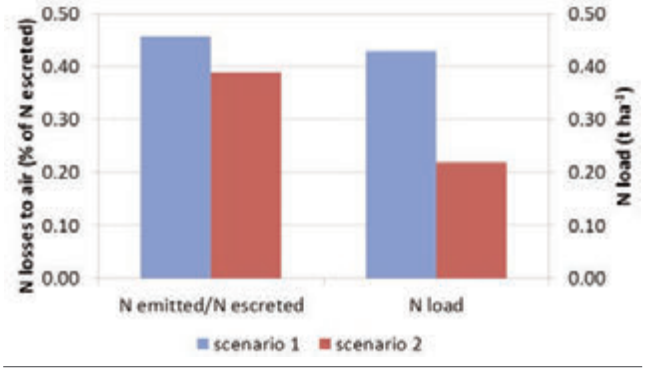

Figure 3. Nitrogen losses to air (ammonia, nitrous oxide) referred to total nitrogen excreted and total nitrogen load to the available land for the two management systems.

References

Brown S., Kruger C., Subler, S. 2008. Greenhouse Gas Balance for Composting Operations. J. Environ. Qual. 37: 1396-1410.

Burton C.H., Turner C. 2003. Manure Management – Treatment Strategies for Sustainable Agriculture (second edition). Silsoe Research Institute.

De Vries, M., de Boer, I.J.M., 2010. Comparing environmental impacts for livestock products: a review of LCA. Livest Sci.128: 1-11.

EMEP/EEA. 2009. 2009 air pollutant emission inventory guidebook. European Environment Agency.

Hansen M.N., Henriksen K., Sommer S.G. 2006. Observations of production and emission of greenhouse gases and ammonia during storage of solids separated from pig slurry: Effects of covering. Atmos. Environ. 40: 4172-4181.

IPCC 2006, 2006 IPCC Guidelines for National Greenhouse Gas Inventories, Prepared by the National Greenhouse Gas Inventories Programme, Eggleston H.S., Buendia L., Miwa K., Ngara T. and Tanabe K. (eds). Published: IGES, Japan.

Lague C., Landry H., Roberge M. 2005. Engineering of land application systems for livestock manure: A review. Can. Biosyst. Eng. 72: 9-16.

Loyon L., Guiziou F., Béline F., Peu P. 2006. Gaseous emissions (NH3, N2O, CH4, CO2) during pig slurry biological aerobic treatment and treatment by-product storages. International Congress Series 1293: 299-302.

Petersen S.O., Sommer S.G., Béline F., Burton C., Dach J., Dourmad J.Y., Leip A., Misselbrook T., Nicholson F., Poulsen H.D., Provolo G., Sørensen P., Vinnerås B., Weiske A., Bernal M.-P., Böhm R., Juhász C., Mihelic R. 2007. Recycling of livestock manure in a whole-farm perspective. Livest. Sci.112: 180-191.

Rigolot C., Espagnol S., Pomar C., Dourmad J. 2010. Modelling of manure production by pigs and NH3, N2O and CH4 emissions. part I: Animal excretion and enteric CH 4, effect of feeding and performance. Animal. 4(8):1401-12.

Sommer S.G., Hansen M.N., Søgaard H.T. 2004. Infiltration of Slurry and Ammonia Volatilisation. Biosystems Eng. 88, 359-367.

A partial life cycle assessment approach to evaluate the energy intensity and related greenhouse gas emission in dairy farms

Lelia Murgia, Giuseppe Todde, Maria Caria, Antonio Pazzona

University of Sassari, Department of Agraria, Sassari, Italy

Abstract

Dairy farming is constantly evolving towards more intensive levels of mechanization and automation which demand more energy consumption and result in higher economic and environmental costs. The usage of fossil energy in agricultural processes contributes to climate change both with on-farm emissions from the combustion of fuels, and by off-farm emissions due to the use of grid power. As a consequence, a more efficient use of fossil resources together with an increased use of renewable energies can play a key role for the development of more sustainable production systems. The aims of this study were to evaluate the energy requirements (fuels and electricity) in dairy farms, define the distribution of the energy demands among the different farm operations, identify the critical point of the process and estimate the amount of CO_2 associated with the energy consumption. The inventory of the energy uses has been outlined by a partial Life Cycle Assessment (LCA) approach, setting the system boundaries at the farm level, from cradle to farm gate. All the flows of materials and energy associated to milk production process, including crops cultivation for fodder production, were investigated in 20 dairy commercial farms over a period of one year. Self-produced energy from renewable sources was also accounted as it influence the overall balance of emissions. Data analysis was focused on the calculation of energy and environmental sustainability indicators (EUI, CO_2-eq) referred to the functional units. The production of 1 kg of Fat and Protein Corrected Milk (FPCM) required on average 0.044 kWh_{el} and 0.251 kWh_{th}, corresponding to a total emission of 0.085 kg CO_2-eq). The farm activities that contribute most to the electricity requirements were milk cooling, milking and slurry management, while feeding management and crop cultivation were the greatest diesel fuel consuming operation and the largest in terms of environmental impact of milk production (73% of energy CO_2-eq emissions). The results of the study can assist in the development of dairy farming models based on a more efficient and profitable use of the energy resources.

Correspondence: Lelia Murgia, University of Sassari, Department of Agraria viale Italia 39, 07100 Sassari, Italy.
E-mail: dit_mecc@uniss.it

Key words: elecricity, fuel, carbon footprint, LCA.

Journal of Agricultural Engineering 2013; XLIV(s2):e37
doi:10.4081/jae.2013.(s1):e37

Introduction

Energy consumption, water utilization and environmental impact are becoming the major issues in the agro-food sector that is called to respond adequately to the climate change problems. Agricultural and livestock activities are important sources of primary greenhouse gases (GHGs). These sectors have been estimate to contribute for about 10-12% to global anthropogenic GHG emissions (Grosson *et al.*, 2011; Smith *et al.*, 2007). Furthermore, agriculture is responsible of indirect emissions in other industrial sectors which supply the resources consumed in the agricultural processes (IPCC 2006). The usage of fossil energy in agricultural processes contributes to climate change both with on-farm emissions from the combustion of fuels, and by off-farm emissions due to production and transport to the farm of agricultural inputs (West *et al.*, 2010). As a consequence, a more efficient use of fossil resources together with an increased use of renewable energies can play a key role for the development of more sustainable production systems.

The methodology that is internationally applied to assess the global impact associated to production activities or products is Life Cycle Assessment (LCA). LCA allows to analyse all the inputs and outputs of a system to estimate the potential environmental impact of a product or service through its life cycle (UNI EN ISO 14040-44 2006). The stages of LCA are: goal and scope definition, inventory analysis, impact assessment an interpretation of results. The system boundaries are used to define the limit of the study and results of LCA are expressed for functional unit of product. All data concerning the use of resources, the energy requirements, the emissions and the products resulting from each process are collected during the inventory analysis. As the impact categories and the level of detail of the analysis can be chosen and specified, the LCA procedure can be tailored to the goals of the study.

The aims of this study were to evaluate the energy requirements in dairy farms, define the distribution of the energy demands among the different farm operations, identify the critical point of the process and estimate the amount of CO_2 associated with the energy consumption. The study, based on a simplified LCA approach, involved 20 dairy conventional farms over a period of one year, half of which have a photovoltaic system for electricity generation.

Materials and methods

This work is a part of a larger research project (*Dairy Carbon Footprint-Filiera AQ*) involving 285 dairy farms located in the centre and south Italy and which aims to assess the potential environmental impact of milk production at farm level. A sample of 20 dairy farms, located in the Arborea area (Sardinia, Italy) are analysed in this study to quantify the fossil energy flows and the carbon dioxide equivalent (CO_2-eq) emissions associated to farming activities.

Data inventoried in each farm, related to year 2011, include general information such as herd size, animal categories, land used, milk quality and production, and a detailed description of cultivated crops, farm structures, equipment and machinery.

Detailed statistics of the monthly energy flows, such as consumption bills of fuels and electricity and the self-produced energy from photovoltaic (PV) generators, were recorded.

The overall data were structured in a data base created on Microsoft Excel. Further calculations were performed to determine sustainability indicators, such as Energy Utilization Indices (EUI) and CO_2-eq emissions referred to functional units (cows, kg of Fat and Protein Corrected Milk -FPCM), that can be compared to literature data.

A detailed energy auditing was performed to allocate the energy consumptions among the different farm activities. All the electrical appliances operating at farm level have been inventoried, reporting the power of each equipment and its usage time (hours per day, days per year) to obtain the annual electricity consumption. Additionally, comparison between the audit data and the electricity bills were performed to evaluate the conformity of the results.

The following farm activities have been detailed:

Lighting: type and power of lamps, as well the illumination time, were collected from barns and farm's facilities

Ventilation and misting: used to lower the air temperature in cowsheds and reduce cow's heat stress during the warm season. These equipment run only when the temperature is above 20-25°C, and the usage time was obtained from the manager interview.

Brushing: 65% of the farm's sample uses mechanized brush to increase cow's comfort. The system is equipped with an electric motor that allows brush rotation as soon as the cow touches it. Operating time of cow brushing was set at 6 minutes/day per milking cow (DeVries, 2007).

Milking: the inputs due to the use of vacuum pump, milk pump and air compressor have been summed together to outline the total consumption of the milking operation. Additionally, the presence of a Variable Drive Speed (VDS) system was taken into account when assessing the electrical consumption of the vacuum pump. The VDS device allows reducing the speed of the vacuum pump based on the vacuum level requirement during milking, thus diminishing of 40-50% the electrical consumption. The 60% of the investigated farms were provided of a VDS system. Electrical consumptions of milk pump and air compressor were set as a 4% of the vacuum pump consumption.

Milk Cooling: electrical consumption for milk refrigeration shows high variations due to the presence or not of the pre-cooling system. The following procedure was used to assess the annual energy consumption (RE_{el})of the milk tank:

$$RE_{el} = \frac{m \times c_p \times (t_1 - t_2)}{COP \times \eta \times 3.6} \quad [\text{kWh} \cdot \text{y}^{-1}]$$

where m (kg · year^{-1}) is the mass of milk, c_p (MJ kg^{-1} °C^{-1}) the milk specific heat value, t_1 and t_2(°C) the initial and final milk temperatures, COP and η are respectively the coefficient of performance and the efficiency of the refrigeration system, 3.6 the conversion factor from MJ to kWh. The electricity required milk cooling is reduced by the use of pre-coolers which lower the temperature of the milk entering the tank. The magnitude of this reduction depends on the temperature of the cooling media; a decrease of 16°C was set in t_1 value when the pre-cooler was available (30% of the farms).

Water heating: both the milking system and the cooling tank need high volumes of water in order to clean and disinfect all the equipment used during the milking operation. Hot wash water (50÷65°C) was used in 19 farms over 20, while only one used warm water (40°C). Different water heating systems were found during the survey: 85% of the investigated farms were equipped with an electrical water heater and 90% with heat recovery systems (HRS) which recuperate the heat given off by the condenser of the refrigeration circuit. The quantities of hot water produced vary based on the quantity of milk refrigerated.

The following equation was used to assess the energy () related with hot water consumptions:

$$RE_{el} = \frac{m \times c_p \times (t_1 - t_2)}{COP \times \eta \times 3.6} \quad [\text{kWh} \cdot \text{y}^{-1}]$$

where m (kg · year^{-1}) is the mass of wash water set at 12 kg per milking unit per milking (SCE, 2004) plus 150-200 L per day for the bulk tank, cp (MJ kg^{-1} °C^{-1}) the water specific heat value, t_1 and t_2 (°C) the initial and final water temperatures, η the efficiency of the electric boiler, 3.6 the conversion factor from MJ to kWh. Different Δt values were applied according to the presence/absence of HRS and the final water temperature required.

Water supply: energy consumptions have been split among water pumping, related only to cowshed and parlour water requirements, and irrigation, associated with the water distribution systems. All farms use an irrigation system of cultivated fields, but only 10% of them use water pumping.

Slurry management: energy consumptions are related to all the equipment used for manure removal, storage, and treatment.

Other: this section includes the operations with lower impact on dairy farm energy demands such as water treatment, feed preparation and high pressure cleaning.

Farm fuel consumptions have been grouped in three main processes:

Field operations, related to forage and animal feed production. The overall tasks carried out for crop cultivation were divided into four sections: slurry distribution; soil tillage; sowing; fertilization and treatment; harvesting and storage of the product.

Slurry management, including operations as sewage management and treatment.

Feeding operations, regarding feed preparation and distribution by means of mixer trailers.

To estimate the tractor diesel consumption due to each operation, the usage time of the machinery, the power of the tractor and the fuel consumption at partial load (Q) have been considered. Q was derived from the following equation (Grisso *et al.*, 2004): $Q = (0.22\,X + 0.096) \cdot P_{pto}$ (L· h^{-1}) which considers the rated power of the machinery(P_{pto}, *kW*) and the estimated ratio (*X, decimal*) of the rated power being used during field operations. A value of 0.30 was set for light operations till to a value of 0.65 for the heaviest ones. A conversion factor of 0.835 kg·L^{-1} was then used to transform the equation results in kg of diesel.

The carbon dioxide emission derived from energy uses was calculated multiplying the total consumptions to the following specific emission factors: 0.4103 kg CO_2-eq kWh^{-1} (ISPRA 2011), based on the energy mix used to produce electricity in Italy, and 3.15 kg CO_2-eq kg^{-1}(ENEA 2010) to assess the emission from diesel combustion.

On farm renewable energy production was monitored in 10 farms which produce photovoltaic electricity. The total production of each PV system (kWh·year^{-1}) was analysed to determine the efficiency (kWh per kW_p^{-1}) and to assess the reduction of carbon dioxide release into the environment. Per each kWh produced, a net emission factor of -0.3813 kg CO_2-eq was considered, derived from the difference between the index of the Italian energy mix (0.4103 kg CO_2-eq·kWh^{-1}, ISPRA 2011) and the CO_2 emitted during the photovoltaic system production (0.029 kg CO_2-eq·kWh^{-1}, Raugei *ethh al.*, 2009).

Results

The characteristics of the studied farms and the annual energy consumptions are summarized in Table 1. The average herd dimension was 320 heads (range 158-500), of which about 44% are milking cows with an average yearly milk production of 10.1 t per cow. The annual energy requirement accounted for 29,519 kg of diesel fuel and 55,843 kWh of electricity, which approximately correspond to an expenditure of 38,500 € per year.

Expressing the farm energy demand in terms of primary energy, which allows to compare the prevalence of the different energy resources, the diesel fuel accounts for about 70% of the total direct energy consumption at farm level, while the electricity represents the 30%.

The farm average emission of carbon dioxide, due to all energy usages, was 120 t CO_2-eq per year that corresponds to 0.085 kg CO_2-eq per kg of FPCM. Preliminary results on GHG production from the dairy farms included in the larger study indicate a prevalence of about 9% of the emissions due to fossil energy among the total GHG emissions.

The energy intensity of dairy farms represents the measure of energy efficiency and it is calculated as index of energy used (EUI) per unit of herd size or milk production. For the electricity, the EUI_s resulted 401 kWh per milking cow and 0.044 kWh/kg per FPCM per year. These results are lower than those found in similar studies carried out on European dairy farms. In a French study conducted by L'Institut de l'Elevage (2009) which involved 60 dairy farms (milk yield 7.2 t cow^{-1}·year^{-1}) the EUI was 420 kWh/lactating cow and 0.059 kWh/kg of milk per year. These values are 4.5% higher than the present study in terms of kWh for lactating cows and 25% higher if referred to the unit of milk. Greater values are reported in an Italian study carried out on 60 dairy farms (milk yield 8 t cow^{-1}·year^{-1}) in the Emilia Romagna region (Rossi, 2012): 510 kWh per cow per year and 0.064 kWh per kg of milk per year. A German study (Jäkel, 2003) carried out on 41 dairy farms shows an average EUI of 0.09 kWh per kg of milk, a value that is more than double of the present result. The EUI per unit of milk mirrors the value of 0.05 kWh obtained in a previous study carried on in the same region (Murgia *et al.*, 2008), while the index per cow was much larger (466 kWh per lactating cow). The differences in farm technological levels and in yield per cow affect the energy efficiency indicators. Large productions of milk allows reducing the consumption of electricity per unit of milk sold.

The carbon dioxide emissions associated with the electricity inputs were 176 kg CO_2-eq/cow per year and 0.019 kg CO_2-eq /kg of FPCM per year.

The annual consumption of diesel was 92 kg per cow, which corresponds to 0.021 kg diesel per kg of FPCM. The annual emissions deriving from these inputs were 289 kg CO_2-eq per cow and 0.066 kg CO_2-eq per kg of FPCM milk per year. When referred to the cultivated land, these indexes were 396 kg of diesel·ha^{-1} and 1248 kg CO_2-eq ·ha^{-1} per year.

As shown in figure 1A, milk refrigeration and milking result the most demanding operations in all the dairy farms examined, requiring respectively 23% and 19% of the annual electricity consumption. Also, other processes that affect significantly the electricity requirements are: slurry management (12%), water pumping (11%), irrigation (10%), fan-misting operations (9%) and water heating (8%).

Analysing the diesel fuel consumption associated to farm and field processes (Figure 1B), the feed preparation and distribution represent together the 51% of the total fuel utilization, the land operations related to crop production account for 42% and the sewage management for 7%.

Crop selection of the investigated farms was based on: corn silage (*Zea Mays L.*, 100% of the farms, average cultivation 26±12 ha/farm); grass forage (*Lolium spp.,* 100% of the farms, 25±13 ha/farm); Alfalfa forage (*Medicago Sativa L.*, 55% of the farms, 10±4 ha/farm).

Figure 2 illustrates the total carbon dioxide emission (diesel plus electricity) attributed to each farm operations. Diesel consumption, being responsible of 79% of the total emission from energy usages, represents the most pollutants process of the farms. Feed management represent the 40% of the total carbon dioxide emissions, followed by land operations (33%) and slurry management (6%). The use of electricity accounts for 21% of the total carbon dioxide emissions.

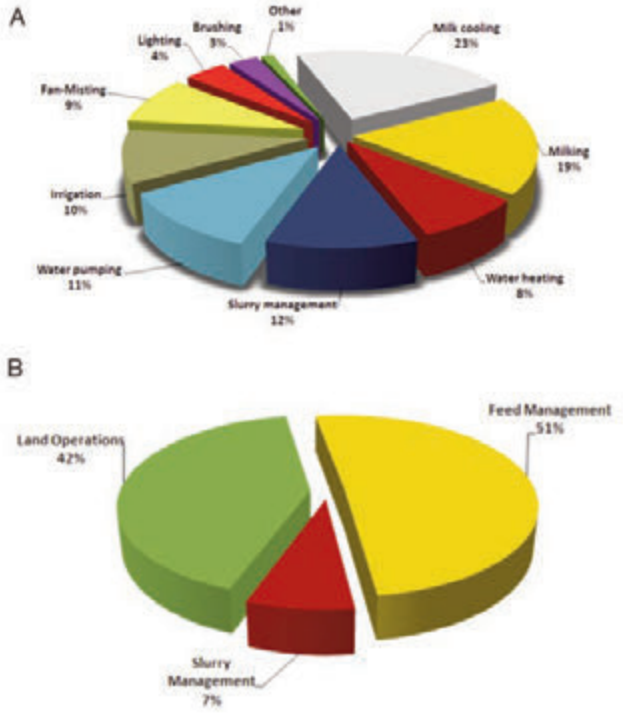

Figure 1. Allocation of fossil energy consumptions (A, electricity; B, diesel) among farm and field operation. Data from 20 dairy farms, referred to an average milk production of 10.1 t.cow^{-1}.year^{-1}.

Table 1. Data summary of the examined farms (N=20)

	Cows (n)	Land (ha)	Milk (t y^{-1})	Diesel (kg y^{-1})	Electricity (kWh y^{-1})
Minimum	158	14	822	12320	31343
Mean	320	47	1412	29597	55843
Maximum	500	95	2678	58394	163893

Photovoltaic energy analysis

The production of energy by PV systems is able to fit the electricity trend demand in dairy farms, as shown in the example of figure 3. The electricity consumption shows peak of request during the summer period due to the higher requests of energy for cooling the cowshed, milk refrigeration and irrigation. Photovoltaic generation follows the natural variability of solar radiation, with higher production during the summer period, peak value in July and minimum during winter months. Therefore PV energy generation can partially supply the demand of electricity during the lower peak of energy generation, but even exceed during the higher peak production. In this case, the surplus of electricity production is injected to the grid and sold.

The study has involved 10 farms which have installed a PV generator integrated on the roof top of the cowsheds. The total PV power installed accounts for 1,122 kWp (corresponding to 0.37 kWp per cow), with an average value of 112 kWp per farm (range 25-250 kWp). The analysis of the PV recorded productions indicates a specific production of about 1,387±14 kWh/kWp per year, which leads to a total electricity generation of 1,559,192 kWh per year.

The PV electricity generation allows to decrease the high peak demand of grid energy during summer period, reducing the emission of carbon dioxide and the cost of the electricity purchased.

Results on yearly base show a positive balance in electricity net production. The surplus of electricity generation was sold, increasing the economic benefits of the farms and reducing the carbon footprint of the milk produced. Final analyses have shown on average a reduction of carbon dioxide emission of 0.023 kg of CO_2-eq per kg of FPCM (from 0.085 to 0.062). The total carbon dioxide reduction was 29,726 kg of CO_2-eq $\cdot y^{-1}$ which represents a 25% decrease of the total amount released by the whole group of farms.

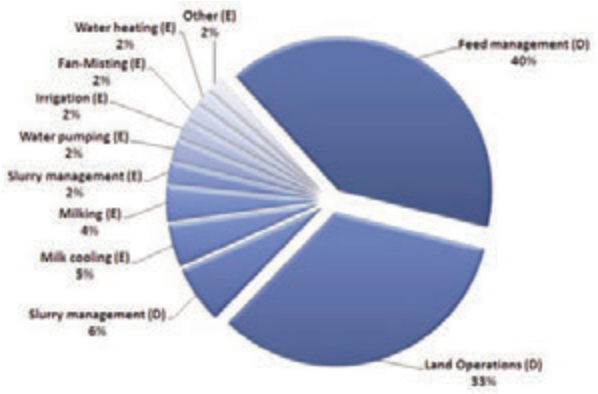

Figure 2. Allocation of GHG emissions from electricity (E) and Diesel (D) to different farm operations.

Figure 3. Monthly electricity consumptions and photovoltaic production

Table 2. Annual electricity and diesel consumptions (average ±st.dev) and associated CO_2-eq emissions.

	Electricity		Diesel		
	Consumption (kWhel y-1)	Emission (kg CO2-eq)	Consumption (kg y-1)	Consumption (kWhth)	Emission (kg CO2-eq)
Cow	176 (±74)	78	92 (±21)	1099	289
Lactating Cow	401 (±180)	176	209 (±47)	2496	658
Land (ha)	768 (±358)	338	396 (±123)	4730	1248
FPCM Milk (kg)	0.044 (±0.03)	0.019	0.021 (±0.005)	0.251	0.066

Table 3. Summary of the electricity comparison between farms with PV and without PV system; the results are expressed per year

	No PV system		PV system		
	Consumption (kWh)	Emission (kg CO_2-eq)	Consumption (kWh)	Production (kWh)	Emission* (kg CO_2-eq)
Cow	156	69	196	514	-121
Lactating Cow	349	154	453	1187	-280
Land (ha)	647	285	889	3476	-986
FPC Milk (kg)	0.035	0.016	0.052	0.12	-0.026

*Negative results indicate the avoided emissions due the surplus of PV energy produced

Conclusions

Electricity and fuel consumption in dairy farms represent an important source of GHG emission into the environment. The present study determined the energy requirements for diesel and electricity at farm level, also underlining the critical point where mitigation strategies are needed. Additionally photovoltaic electricity generation was considered as a mitigation strategy to compensate the GHG impact of milk production. PV electricity can also help reducing the demand in dairy farms, especially decreasing the high peak of consumptions.

Electricity requests in the dairy farms involved in the study were mainly due to the operations regarding the milking parlour (milking, milk refrigeration and water heating), which required 50% of the total electricity consumption.

A large number of the investigated farms already use energy saving technologies, such as heat recovery system from cooling tanks (90% of farms), variable speed drive for the vacuum pump (60%) and milk precoolers (30%). Improving energy savings allow to reduce the electricity demand, especially for those equipments that need high electricity input. The estimated electricity emissions of CO_2-eq were 78 kg per cow that correspond to 0.019 kg CO_2-eq per kg of FPCM.

Diesel consumption was assessed for land operations, feed management and slurry management and corresponds to 92 kg of diesel per cow and 392 kg per ha^{-1}. The operations related to animal feeding, as crop cultivation, feed preparation and distribution, require the largest quota of total fuel consumption (42% and 52% respectively). The emissions associated to diesel combustion were 289 kg CO_2-eq per cow and 0.066 kg CO_2-eq per kg of FPCM.

Final results of carbon dioxide emissions from fuel and electricity usage showed that 79 % of the emissions were due to the use of diesel. These results underline the need to focus the mitigation strategies in fuel usage, especially for feed management and land operations.

Reducing electricity and diesel consumption leads to decrease anthropogenic gas emissions into the environment, to reduce costs for the farms and to improve the efficient use of natural resources.

References

Crosson P., Shalloo L., O'Brien D., Lanigan G.J., Foley P.A., Boland T.M. 2011. A review of whole farm systems models of greenhouse gas emissions from beef and dairy cattle production systems. Animal Feed Science and Techology, 166-167:29-45

DeVries T. J., Vankova M., Veira D.M., Keyserlingk, 2007. Usage of Mechanical Brushesby Lactating Dairy Cows. Journal of Dairy Science 90:2241-2245.

ENEA, 2010. Inventario annuale delle emissioni di gas serra su scala regionale, Le emissioni di anidride carbonica dal sistema energetico. Rapporto 2010.

Grisso R.D., Kocher M. F., Vaughan D.H. 2004. Predicting Tractor Fuel Consumption. Applied Engineering in Agriculture, 20(5):553–561

Institut de l'Elevage 2009. Les consommations d'energie en bâtiment d'elelevage laitier. Reperes de consommations et pistes d'economies. Collection : Synthese, Janvier

IPCC 2006. Guidelines for National Greenhouse Gas Inventories. Volume 4: Agriculture, Forestry and Other Land Use. Chapter 10: emissions from Livestock and Manure Management.

ISPRA 2011. Produzione termoelettrica ed emissioni di CO_2. Fonti rinnovabili e impianti soggettia ETS. Rapporto 135/2011.

Jäkel K. 2003. Analyse der Elektroenergieanwendungund Einsparpotentialeam BeispielsächsischerMilchviehanlagen. Forschungsbericht Agrartechnik, 414, Mertin-Luther-Universitat Halle/Saale

Murgia L., Caria M., Pazzona A. 2008. Energy use and management in dairy farms. International Conference "Innovation technology empower safety, health and welfare in agriculture and agro-food systems", Ragusa, Italy, sept. 15-17, pp.1-7.

Raugei M., Frankl P. 2009. Life cycle impacts and costs of photovoltaic systems: Current state of the art and future outlooks. Energy 34: 392–399

Rossi P., Gastaldo A. 2012. Consumi energetici in allevamenti bovini da latte. Informatore Agrario 3(Suppl):45-47.

Smith, P., D. Martino, Z. Cai, D. Gwary, H. Janzen, P. Kumar, B. McCarl, S. Ogle, F. O'Mara, C. Rice, B. Scholes, O. Sirotenko 2007. Agriculture. In "Climate Change 2007: Mitigation. Contribution of Working Group III to the Fourth Assessment Report of the Intergovernmental Panel on Climate Change" [B. Metz, O.R. Davidson, P.R. Bosch, R. Dave, L.A. Meyer (eds)], Cambridge University Press, Cambridge, United Kingdom and New York, NY, USA.

Southern California Edison 2004. Dairy Farm Energy Management Guide California.

UNI EN ISO 14040, 2006. Environmental management, Life cycle assessment, Principles and frame work.

UNI EN ISO 14044, 2006. Environmental management, Life cycle assessment, Requirements and guideline.

West T. O., Marland G. 2002. A synthesis of carbon sequestration, carbon emissions, and net carbon flux in agriculture: comparing tillage practices in the United States. Agriculture, Ecosystems and Environment, 91: 217–232.

Implementation of a genetic algorithm for energy design optimization of livestock housing using a dynamic thermal simulator

Maria Elena Menconi, Massimo Chiappini, David Grohmann

Department Uomo e Territorio, University of Perugia, Italy

Abstract

A Genetic Algorithm (GA) is an optimization process inspired by natural systems ability of surviving in many different environments through the mechanisms of natural selection and genetics. The pairing of GA-based optimization techniques with dynamic energy models is a common and effective practice to find energy efficient design solutions. In this paper is implemented an optimization tool that use a GA and a dynamic energy model. Efficiency of GAs depends largely on the coding strategy and on the parameters selection. In order to test the code and to find the best combination of parameters, a parametric analysis of GA's performances is carried out. The algorithm, coded in Matlab, works with populations of strings. Each string, that represents a complete design solution, is initially randomly generated by the GA and evaluated in terms of energy performances by the dynamic thermal simulator. A new population is then generated using three different GA stochastic operators: reproduction, crossover and mutation, by selecting, mixing and randomly modifying the fittest solutions of the previous generation. Each generation is energetically evaluated and thus the fitness of the strings, that represent the energy efficiency of the design solutions, improves every cycle till eventually converge to the best solution. This whole methodology is well documented and applied in residential buildings design but can be easily extended to livestock housing. In this paper the algorithm is coded to be applied on a simple sheepfold model in order to optimize only passive design solutions.

Introduction

Objectives of the research

In this work is investigated the interaction between various parameters of an implemented Genetic Algorithm (GA) for the analysis of the energy efficiency of the external envelope of sheepfolds, with the aim to identify the best combinations of these parameters.

The interaction between the parameters depends mainly on the type of function to be optimized (Hart W.E. and Belew R.K., 1991). Many studies have been conducted to find the optimal parameter setting of GAs (De Jong K., 2007), some of them take into consideration the interaction between only two parameters and analyze the variations that the pairing generates in the algorithm performance (Goldberg D.E. *et al.*, 1992). In some cases, empirical studies have been conducted (Wu. A. *et al.*, 1997) or complex stochastic models like the Markov chains (Chakraborty U. *et al.* 1996; Chakraborty U and Janikow C.Z., 2003) have been used.In this paper, which is inspired by a work of Kalyanmoy Deb (1998), we addressed the effects induced by five parameters of the GA: population size, crossover probability, mutation probability, encoding and reproduction strategy.

Genetic Algorithm

The GAs are research and optimization systems which are inspired by the evolution of natural systems and by their ability to adapt to many and varied external conditions in effective and efficient manner.

Their strength, compared to other search systems, is given by three factors: the GA do not operate on individual points but on populations of points, reducing the likelihood of running into local minima; they act directly on the code and not on the functions, making them difficult to deceive; they make use of semi probabilistic operators, enabling a highly exploratory research (Goldberg D.E., 1989).

Before a GA can be developed it is necessary to choose the type of encoding to be used for the representation of the chromosome's parameters. The quality of a GA depends largely on the coding strategy adopted and on its interaction with the operators of crossover and mutation, in respect of the variables and constraints of the problem. Binary type is one of the most used encodings.

As schematically represented in Figure 1, the basic element of a GA, the individual, is constituted by a string, chromosome, containing a set of sequenced parameters, said genes. Each individual represents a possible solution to the given problem, more individuals form a population.

The algorithm is initialized with the random generation of the first population. The iterative loop begins with the evaluation of the quality of an individual (that is how good the solution is to the problem) which is measured by a fitness function.

At each generation, the individuals of the population are stochastically selected in agreement with the value of the fitness function and are paired to generate better individuals.

The evolutionary process is carried out by three basic operators: reproduction, crossover and mutation:

- with the reproduction the strings are selected according to their fitness value and are copied to the mating pool to generate the next population;
- through crossover couples of chromosomes are randomly paired to generate new individuals;

Correspondence: Maria Elena Menconi, University of Perugia, Uomo e Territorio Department
e-mail of corresponding author: mariaelena.menconi@unipg.it

Key words: Genetic algorithm, building energy optimization, dynamic thermal model, parametric analysis.

Journal of Agricultural Engineering 2013; XLIV(s2):e38
doi:10.4081/jae.2013.(s1):e38

- finally, the mutation involves the random variation of values of the genes of the individual and has the important task to prevent the premature convergence and therefore the loss of important genetic material (Haupt R. and Haupt S.E., 2004).

The purpose of the GA is the identification of chromosomes that optimize the fitness function.

Materials and methods

Flowchart of working methodology

The methodology adopted for the performance analysis of the implemented GA is shown in Figure 2.

The work can be divided into three main steps:

- analysis of the energy performance of the building;
- implementation of the GA;
- encoding of the statistical cycle and parametric analysis of the GA performance.

In optimizing the energy efficiency of building envelopes, the coupling between thermal simulation models and optimization algorithms is a widely tested practice(Caldas L.G. and Norford L.K., 2002; Znouda E. *et al.*, 2007). One of the most common methodologies involves the continuous exchange of data between the simulation and the optimization models, where the first carries out the task of calculating the energy performance of the building, and therefore the values assumed by the objective function, while the second identify the best technological and constructive solutions. In this study has been adopted a simplified interaction methodology between the simulation model and the energy optimization algorithm. In our case, in fact, using the simulation energy model, all the different construction types examined have been simulated in advance, analyzing the effects of a single construction element at a time, not taking into account the interaction between the different components of the building envelope. The different energy consumption values thus obtained were subsequently placed inside the optimization algorithm GA through a legend function that associates to each type of construction a corresponding sequence of integers.

Not considering the interactions between the various types of casing and being the simulation model and the optimization algorithm unable to exchange data in real time, make it impossible to conduct a rigorous analysis of the energy performance of the building, but only a qualitative analysis of the energy efficiency of three types of coating (vertical wall, windows and roof). However, for the purpose that has been set in this work, namely the analysis of the performance of the GA varying some significant parameters, the use of this simplified approach is more than justified, not going to affect any of the obtained results.

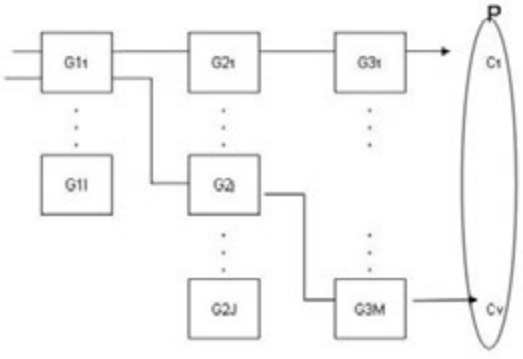

Figure 1. Representation of the constituent elements of the GA, genes, chromosomes and population. Genes: G1i, G2j, G3m, represent the different parameters that we want to optimize (in this case 3 parameters); variables counter i, j and m that vary respectively from 1 to I, J, M (the number of decision alternatives for each gene). Chromosome : Cv (G1i, G2j, G3m), represents a combination of the selected parameters, with v that varies from 1 to V (total number of chromosomes that constituting the population). Population: P (C1,…,CV) represents the set of chromosomes. Each iteration of the GA provides for the generation of new chromosomes, which will form a new population.

Energy simulation software and building model

The chosen software for the energy performance analysis of the building is Energy Plus, that can be downloaded from the following site: http://apps1.eere.energy.gov/buildings/energyplus/energyplus_download.cfm.

This software has been selected as it is free downloadable and is one of the most complete software for dynamic simulation of the energy performance available. In the present work it was decided to act only on existing sheepfolds, choosing between the range of passive solutions available, the most simple and immediate interventions on the exterior of the building. The building model includes the definition of its exact geographical location, its orientation, the geometric characteristics (3D model), a detailed description of the materials (properties and thickness) that compose the opaque and transparent surfaces, the modeling of infiltration, the description of the gain / consumption factors (people, animals, lights, electric equipment, air conditioning sys-

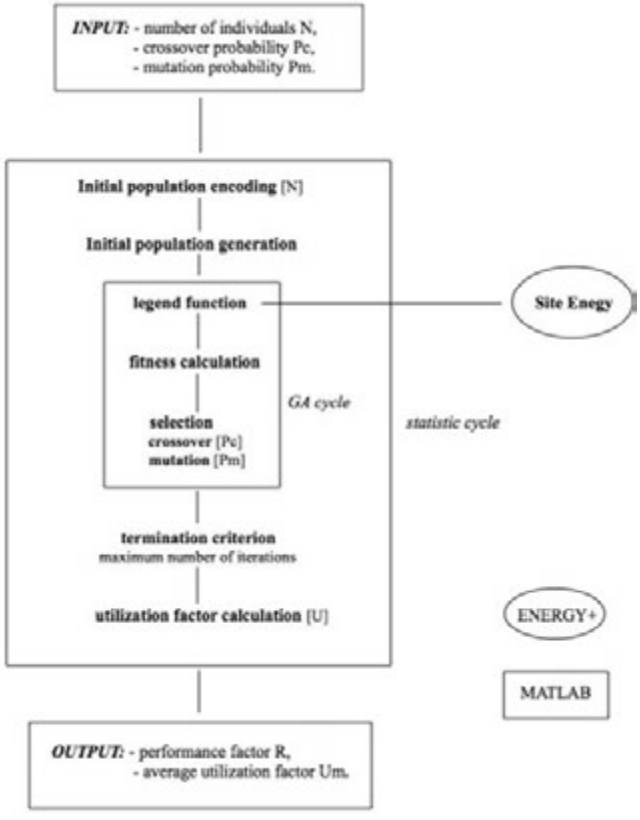

Figure 2. Flowchart of the adopted methodology. Starting from three GA parameters (input), number of individuals (N), mutation probability (Pm) and probability of crossover (Pc), have been obtained and analyzed the algorithm performance, by examining the performance parameter (R) and the average utilization parameter (Um).

tems). Between all the parameters listed above, those chosen to be varied are the genes of the GA developed in this work. The first step concerns the choice of the number of parameters to be varied in energy simulations (number of genes) and, for each parameter, the number of changes (for example the gene "wall's insulation" may differ depending on type, thickness or position of the insulation layer). The existence of an ideal HVAC system has been hypothesized to evaluate the energy savings that can be achieved by the introduction of an intervention on the building enclosure. The different Site Energy values, that are generated by the Energy Plus run varying the individual parameters, are the input values for the genes of the GA, according to which the chromosomes and the population are formed.

GA implementation

The GA developed for this study was coded using Matlab (MATLAB Version 7.1.0.124 (R14)), a programming language that works with matrices, strings and numeric operations. For the main functions of the GA a toolbox for Matlab developed by the University of Sheffield was used (Chipperfield A. *et al.*, 1995).

The first step is to choose the encoding strategy, in our specific case, having to deal with numbers that vary in discrete terms and that are included in well-defined intervals, was chosen a binary type encoding. All evolutionary processes take place through the manipulation of binary strings that represent, through sequences of integers, different configurations of the outer shell (Figure 3).

In this step, in addition to the type of encoding, all the data that characterize the structure of the population, such as the number and the length of the individuals are inserted. Following the coding of the population, the algorithm is initialized with the random generation of the first population. The iterative cycle begins with the assignment, to each gene, of the corresponding value of Site Energy, so that the value of the objective function can be calculated and its fitness assigned. The objective function was defined as the average of the three values of Site Energy associated with the genes of each chromosome, a function that the GA has the aim to minimize. The next step is the selection of individuals for the reproduction via Stochastic Universal Sampling, a selection method consisting of a semi-probabilistic roulette with X equally spaced arms, that, at every cycle, select X individuals arranged in sectors whose size is proportional to the owned fitness (Baker E., 1987). The selected individuals are then mated through single point crossover, a type of crossover through which the strings are broken in a single point and the resulting segments are crossed together. Following the crossover operator there is the mutation one which, randomly varying bits of individuals, introduce new genetic material. Both crossover and mutation do not automatically apply to every individual, but in accordance with determined probabilities.

To facilitate the algorithm convergence has been adopted an elitist reproduction strategy, that consists in keeping the best individuals of each generation and to insert them directly into the next one. This allows to avoid the destruction of valuable genetic material, thus improving the performance of the algorithm (Dumitrescu D. et al, 2000). In the implemented GA a 10% of individuals go directly to the next generation, the selection of these individuals is carried out based on the fitness value, in order to retain only those most efficient. The cycle ends when it reaches a predetermined number of generations.

Parametric analysis

In this paper we addressed the effects induced by five parameters of the GA: population size, crossover probability, mutation probability, encoding and reproduction strategy. Since in actual optimization and research problems, as in the case of energy optimization, the main source of expenditure of computational resources is the evaluation of the values of the objective function (Deb K. and Agrawal S., 1998), the maximum number of evaluations to be performed in the various cycles of the GA needed to reach the optimal solution is fixed in advance (S).

If S is such a number, a GA with a population of N individuals requires a maximum of T = S / N generations, since at each generation are evaluated N functions. The value of S depends essentially on the complexity of the function to be solved and on the length of the string, as evidenced by Heinz Muhlenbein (1992).

Since the global optimal solution is known beforehand (given, for each variable in the GA, by the sum of genes that have the lower value of Site Energy), is possible to set up a statistical analysis of the effectiveness of the implemented GA, by reiterating several times (Cs) the basic cycle of the GA, consisting of T generations, and then evaluate a performance factor, called R, and a Utilization Factor, called U.

R is an indicator of the ability of the algorithm to find the optimum solution within the predetermined number of T generations and is calculated as: R = O / Cs, where O is the number of times that the algorithm is able to identify the optimal solution.

U studies the degree of utilization of the evaluations of the objective function, since not all S evaluations are always used to find the optimal solution, and is given by: U = 1 - F / S, where F is the number of evaluations actually carried out to reach the optimal solution.

R is calculated at the end of the Cs iterations of the statistical loop, while U is calculated at the end of every GA cycle. Once the GA cycle is

Table 1. Energy plus IDF Editor: variable instantiation for option zero - Envelope. Sheepfold building located in central Italy (Umbria; lat 42.87, long 12.96), time zone 1 and elevation 974 m a.s.l. The total building area is 777.35 m^2. The weather file used is Perugia – ITA IGDG WMO#=161810 and the hours simulated are 8760.

Variable name	Range or value	
Orientation (degree from true North)	120	
Window-wall ratio (%)	4.89	
Window type	Simple glazing	
	U-factor (W/m2-K)	6
	Solar heat gain coefficient	0.7
Door type	Wood	
	Thickness (m)	0.009
	Conductivity(W/m-K)	0.14
	Density (Kg/m^3)	530
	Specific heat (J/Kg-K)	900
Floor type	Concrete	
	Thickness (m)	0.1
	Conductivity(W/m-K)	1.6
	Density (Kg/m^3)	2300
	Specific heat (J/Kg-K)	850
Wall type 1	Concrete block	
	Thickness (m)	0.2032
	Conductivity(W/m-K)	1.11
	Density (Kg/m^3)	800
	Specific heat (J/Kg-K)	920
Wall type 2	Metal	
	Thickness (m)	0.0008
	Conductivity(W/m-K)	45.28
	Density (Kg/m^3)	7824
	Specific heat (J/Kg-K)	500
Roof type	Fiber concrete	
	Thickness (m)	0.0065
	Conductivity(W/m-K)	0.35
	Density (Kg/m^3)	1500
	Specific heat (J/Kg-K)	1030

repeated Cs times, it is possible to calculate the average utilization factor Um, which represents the U average for the Cs simulations.

R can vary between 0 and 1 where R = 1 means that the algorithm always found the optimal solution in the Cs carried out simulations and 0 that it has never succeeded.

U can also vary between 0 and 1, with U = 1, the algorithm is able to identify the optimal solution in the first generation, while U = 0 means that S evaluations were not enough to identify the optimal solution.

Results

This section presents the results of the parametric analysis performed. The zero-building is a sheepfold located in central Italy, at an altitude of 974 meters above sea level (Figure 4). The building houses 200 sheep at full capacity and has two births periods per year, the operators are 2. The characteristics of the envelope are described in Table 1.

The GA structure was coded to represent the problem under consideration. The evaluation of the GA was made by varying, for the zero-building, the materials used for windows and for the insulation of the walls and cover, as shown in Table 2, in which are also reported the values of the Site Energy generated from different simulations, using the weather file of Perugia. From the dynamic energy simulation, the solution for the building which presents the best conditions for energy saving has shown that the best materials, respectively for glazed surfaces, insulation of the vertical walls and insulation of the roof are: aerogel, mineralized wood and polyurethane.

The 3 variables represented in table 2 are the 3 input variables in the GA. Each chromosome has then 3 genes of which the first, the windows, with values between 1 and 4, the second, the wall's insulation, and the third, the cover's insulation, with values between 1 and 8. Since with 2 bits is possible to represent 2^2 elements, and with 3 bits 2^3 elements, we have strings of 8 bits. Therefore 8 is the length of the population (L).

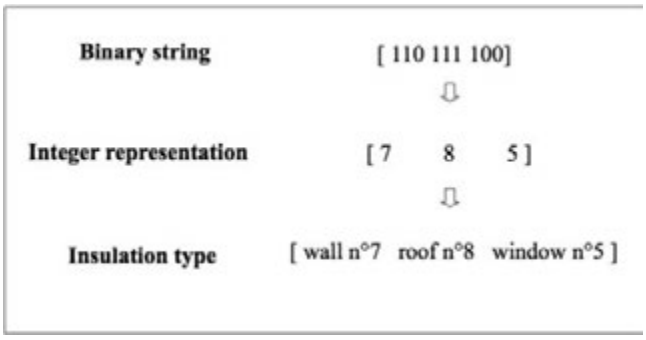

Figure 3. Example of a string structure and decoding methodology: a binary string is converted into integer values that are then associated to insulation types.

Figure 4. Sheepfold model.

Table 2. GA: variable instantiation.

Variable name	Variable type	Value	Site Energy (GJ)
Wintype (xi; i:1-4)	discrete	option zero	114.72
		low emission	113.26
		selective	113.06
		aerogel	112.43
Wall type: insulation (yj; j: 1-8)	discrete	option zero	114.72
outside layer: concrete block		sheep wool	103.57
layer 2: insulation		mineralized wood	102.34
(thickness: 0.05 m)		thatch	103.74
layer 3 : Lime-cement plaster (thickness: 0.01 m)		glass wool	103.94
		rock wool	103.24
		sintered polyester foam	103.48
		polyurethane	103.32
roof type: insulation (zm; m: 1-8)	discrete	option zero	114.72
outside layer: Fiber concrete (thickness: 0.0065 m)		sheep wool	41.97
layer 2: insulation		mineralized wood	45.13
(thickness: 0.05 m)		thatch	48.83
layer 3 : Lime-cement plaster (thickness: 0.01 m)		glass wool	43.78
		rock wool	42.37
		sintered polyester foam	41.69
		polyurethane	40.98

The simulations were conducted varying the number of the population N (4, 8, 12, 16, 20, 30, 60, 100, 150) and for various combinations of mutation probability (Pm) and crossover probability (Pc) respectively: 1/L – 0; 0.5/L – 0 ; 0 - 0.9; 1 / L - 0.9 ; 0.5 / L - 0.9 and 0.1 / L - 0.9. The combinations were selected so as to investigate the effects of the application of only crossover (for example the 0-0.9 combination), mutation alone (for example the 1/L -0 combination), or combinations of the two. S was set at 300, Cs at 600, this means that for each combination of N, Pc, Pm studied were carried out, for the calculation of R and Um, 300x600 = 180,000 evaluations of the objective function. From the analysis of the parameter R performance (Figure 5) it is possible to derive the algorithm's ability to identify the optimal solution: the algorithms with a high Pm behave very well and evenly from small to medium-high populations, 4 - 60 individuals, finding the optimal solution in 90% of cases. With decreasing of Pm, the curve loses its uniformity by presenting lower performance values, especially for medium-low populations. The algorithms based on crossover (high Pc) begin to give good results passed the threshold of 20 individuals, reaching peak performance, more than 90% success rate, at around the 60 individuals. Passed the peak the number of successes returns to decline with the increase of the population. This behavior can be explained considering that the crossover-based GA can rely solely on the genetic variability of the initial population, that clearly increases with a higher number of individuals present at the beginning of the simulation. All the analyzed types have a performance drop for large populations since, remaining unchanged the maximum number of evaluations of the objective function, decreases the number of cycles available to apply evolutionary operators, turning essentially from a semi-probabilistic to a random research method. The analysis of the U (Figure 6) enables to assess the efficiency of the algorithm in terms of speed (number of generations) of finding the optimal solution. For small populations (N = 4) all combinations have poor results (Um > 0.3). The combinations with low Pm tend to improve passed the threshold of 16 individuals, confirming previous observations. On the other hand, the combinations with high Pm tend to worsen with increasing number of individuals going from about 0.7, for 16 individuals, to about 0.57, for over 60 individuals. The best performances (Um > 0.7) were obtained by combining high Pc and Pm, in a population range between 8 and 30 individuals.

Further analysis was conducted on the effectiveness of the elitist strategy adopted (Table 3). Two series of simulations were carried out, one for a medium-low population (12) and another for a medium-high (60) one, in the absence of elitist strategy, that is letting participate to the processes of selection, reproduction and mutation all individuals of a given generation.

The parameters of performance and utilization were then compared with the relative series in the presence of elitist strategy. In both cases, the lack of this arrangement has led to a considerable decrease of the operating parameter, as shown in table 3, especially in combination

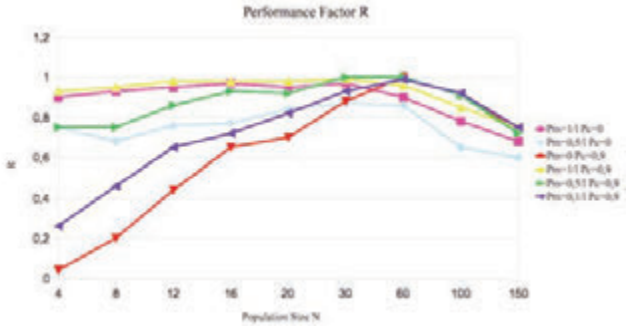

Figure 5. Performance Factor R varying population size for different combinations of crossover and mutation probability, Pc and Pm.

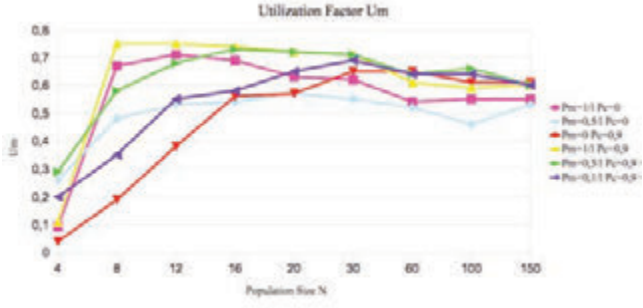

Figure 6. Average Utilization Factor Um varying population size for different combinations of crossover and mutation probability, Pc and Pm.

Table 3. Confrontation between different Um changing the number of chromosome reinsertion in the elitist strategy approach. Et=0,9 means 90% offspring reinsertion into the next generation, Et=1 means 100% offspring reinsertion (absence of elitist strategy).

N	Um		Pm	Pc
	Et 0,9	Et 1		
12	0,71	0,26	1/L	0
12	0,75	0,29	1/L	0,9
60	0,54	0,38	1/L	0
60	0,61	0,45	1/L	0,9
60	0,64	0,51	0,5/L	0,9
60	0,64	0,57	0,1/L	0,9

Table 4. Confrontation between Performance Factor R and Average Utilization Factor Um using Standard binary code and Gray code changing different input parameters.

	Input			Output	
	N	Pc	Pm	R	Um
Standard	8	0	1/L	0,93	0,67
Gray				0,99	0,76
Standard	8	0,9	0,5/L	0,75	0,58
Gray				0,98	0,76
Standard	8	0,9	0,1/L	0,46	0,35
Gray				0,76	0,49
Standard	12	0,9	0,5/L	0,84	0,68
Gray				0,99	0,76
Standard	12	0,9	0,1/L	0,6	0,49
Gray				0,84	0,62
Standard	16	0	1/L	0,97	0,69
Gray				0,99	0,76
Standard	16	0,9	0,5/L	0,93	0,73
Gray				0,99	0,75
Standard	16	0,9	0,1/L	0,72	0,58
Gray				0,9	0,62

with high Pm (1 / L). The effect tends to diminish in the series with the largest population, but it remains significant.

Finally, an analysis was performed on the type of encoding used. In general, the binary coding presents problems related to the so called Humming Cliff (Schaffer J.D. *et al.*, 1989). A coding problem that consists in phenotypic values (the values that assume the bit sequences of binary strings,) close to each other, described by totally different genotypic structures (the bit sequences of binary strings). To overcome the Humming Cliff problems is commonly used the Gray encoding (Caruana R.A. and Schaffer J.D., 1988), in which to variations of adjacent bits correspond minimal deviations of the values which those bits assume. In order to assess the effects of the binary encoding type on the performance of the algorithm, simulations were repeated in Gray code and then the performance and use of the parameters were compared with the relative simulations carried out in standard binary code. Going from a standard binary encoding to a Gray coding (tab.4) there are, for small and medium small populations (N = 4-16), improvements in both the performance and parameters utilization, in almost all the studied combinations. The improvement effect lowers with the increase of the population. With a population of 30 individuals are not observed substantial differences. The best results have been reported for small Pm (Pm = 0.5 / L or 0. 1 / L).

Conclusions

The carried out parametric analysis allowed us to measure the trend of the algorithm performance varying the size of the population (N), the probability of crossover (Pc) and mutation probability (Pc), in order to identify the best combination to be used in the energy optimization of the building enclosure.

We recall that the GA has been realized in standard binary code, with the use of an elitist strategy, the selection based on fitness using a Stochastic Universal Sampling, and the use of single point crossover.

From the obtained results (Figures 5 and 6), it can be deduced that the best overall performance (R and Um) can be attributed to an algorithm consisting of a population of 12 or 16 individuals, with Pc equal to 0.9 and Pm equal to 1 / L = 0.12, to which are associated a R equal to 0.98 and a Um of 0.75. Despite the small size of the space of solutions, 256 in total, however, it has been awarded the combination of parameters with the highest exploratory capacity (high values of both Pc and Pm).

The elitist strategy has certainly played an important role, in this mechanism, enabling not to waste the best solutions despite the high variability of the research process. This statement can be confirmed by observing the drastic reduction of Um, from 0.75 to 0.3, with the elimination of the elitist strategy (Table 3).

The overall picture changes going from a standard binary to a Gray encoding. Using a Gray encoding, the same performance (R = 0.99 and Um = 0.75) can also be obtained with the following combinations of N-Pc-Pm: 8-0-0,12 ; 8-0,9-0,06 ; 12-0,9-0,06 ; 16-0-0,12 ; 16-0,9-0,06 (Table 4). This result confirms that the Gray encoding is preferable in the development of GA similar to that used in this work.

This study is a preliminary work aimed at the realization of an energy optimization model for livestock production buildings. The next step would be to replace the simplified interaction methodology between the optimization algorithm and thermal simulation model used in this paper, with a complete methodology that allows the two systems to communicate simultaneously, taking into account all the interactions between the various components that contribute to the energy behaviour.

References

1. Baker E., 1987. Reducing bias and inefficiency in the selection algorithm. Proceedings of the 2nd International Conference on Genetic Algorithms. Lawrence Erlbaum Associates, Hillsdale, New Jersey, 14–21.
2. Caldas L. G. and Norford L. K, 2002. A design optimization tool based on a genetic algorithm. Automation in Construction. 11, 173–184.
3. Caruana R. A., Schaffer J. D., 1988. Representation and hidden bias: Gray vs. binary coding for genetic algorithms. Proceedings of the Fifth International Workshop on Machine Learning, Eds. San Mateo, CA: Morgan Kaufmann, 153–161.
4. Chakraborty U., Deb K., Chakraborty M., 1996. Analysis of selection algorithms: A Markov chain approach. Evolutionary Computation. 4 (2), 132–167.
5. Chakraborty U., Janikow C.Z., 2003. An analysis of Gray versus binary encoding in genetic search. Information Science. 156, 253–269.
6. Chipperfield A., Fleming P., Pohlheim H., Fonseca C., 1995. Genetic Algorithm TOOLBOX For Use with MATLAB. User's guide, version 1.2. Retrieved from http://www.geatbx.com/ea_matlab.html
7. De Jong K., 2007. Parameter setting in Eas: a 30 year perspective, parameter setting in evolutionary algorithms. Studies in Computational Intelligence.54, 1–18.
8. Deb K., Agrawal S.,1998. Understanding interactions among genetic algorithm parameters, in Foundations of Genetic Algorithms V, Banzhaf W. and Reeves C., Eds. San Mateo, CA: Morgan Kauffman, 265–286.
9 Dumitrescu D., Lazzerini B., Jain L.G., Dumitrescu A., 2000. Evolutionary Computation, CRC Press LLC.
10. Goldberg D. E., 1989. Genetic algorithms in search, optimization, and machine learning. New York: Addison-Wesley.
11. Goldberg D. E., Deb K., Clark. J. H., 1992. Genetic algorithms, noise, and the sizing of populations. Complex Systems. 6, 333–362.
12. Hart W. E., Belew R. K., 1991. Optimizing an arbitrary function is hard for the genetic algorithm. Proceedings of the Fourth International Conference on Genetic Algorithms, 190–195.
13. Haupt R. L., Haupt S.E., 2004. Practical Genetic Algorithms. 2nd edition, John Wiley & Sons, Haboken, New Jersey.
14. Muhlenbein H., 1992. How genetic algorithms really work I: Mutation and hillclimbing. Foundations of Genetic Algorithms II, Eds. R. Ma:nner and B. Manderick, Amsterdam: North-Holland, 15-25.
15. Schaffer J. D., Caruana R. A., Eshelman L. J., Das R., 1989. A study of control parameters affecting online performance of genetic algorithms for function optimization. Proceedings of the Third International Conference on Genetic Algorithms. Eds. San Mateo, CA: Morgan Kaufmann, 51–60.
16. Wu A., Lindsay R. K., Riolo R. L., 1997. Empirical observation on the roles of crossover and mutation. Proceedings of the Seventh International Conference on Genetic Algorithms.362–369.
17. Znouda E., Ghrab-Morcos N., Hadj-Alouane A., 2007. Optimization of Mediterranean building design using genetic algorithms. Energy and Buildings. 39, 148–153.

Influence of feed delivery frequency on behavioural activity of dairy cows in freestall barns

Elisabetta Riva, Gabriele Mattachini, Luciana Bava, Anna Sandrucci, Alberto Tamburini, Giorgio Provolo

Department of Agricultural and Environmental Science, University of Milan, Italy

Abstract

Research on feeding management in more competitive free-stall settings indicates that frequency of delivery of fresh feed stimulates feed bunk attendance and can affect other aspects of cows' time budgets apart from feeding such as time spent standing vs. lying down. The objective of this study was to examine how the frequency of feed delivery affects the behavior in two farms, one with a conventional and one with automatic milking system (AMS). The feeding frequency was varied from two to three times per day in the conventional dairy farm; one to two times per day in the AMS farm. The experiment was carried out in two different seasons. All behaviours of the cows were monitored in continuous by video recording. As expected, behavioral indices have been significantly affected by environmental conditions both in conventional farm and AMS farm. The variation in the frequency of feed delivery seems to affect the cow behavioural activity only in a limited way and modify only slightly the daily averages of the time spent in different activities mainly increasing the time cows spend standing (+4-5%).

Introduction

During the past few years, there has been increased interest in determining the effects that feeding frequency has on the performance of lactating dairy cows. Feeding is normally the predominant behavior in dairy cattle (Grant and Albright, 2001). Dairy cows spend 3 to 5 h/d eating, consuming 9 to 14 meals per day. In addition, they ruminate 7 to 10 h/d, spend approximately 30 min/d drinking, 2 to 3 h/d being milked, and require approximately 10 h/d of lying and (or) resting time (Grant and Albright, 2000). Typically, group-housed dairy cows are provided with fresh feed twice per day (2×), or only once per day (1×) to reduce labor costs. Research on feeding management in more competitive free-stall settings indicates that frequency of delivery of fresh feed stimulates feed bunk attendance (DeVries *et al.*, 2003) and can affect other aspects of cows' time budgets apart from feeding such as time spent standing or ruminating while standing vs. lying down (Phillips and Rind, 2001). DeVries and von Keyserlingk (2005) showed that the time of provision of fresh feed strongly influenced the feeding behavior of dairy cows, these authors also found that the time of feed delivery affected lying behavior. DeVries *et al.* (2005) showed that increasing the frequency of feed delivery allowed the cows to increase their daily feeding time and increase the distribution of feeding time over the course of the day, improving access to fresh feed for all cows and to reduce sorting. Mäntysaari *et al.* (2006) compared cows fed a total mixed ration (TMR) once or 5 times a day and also found total eating time was longer when feed was delivered more often, but, cows fed 5 times a day increased restlessness and decreased lying time than cows fed once times a day. Haley *et al.* (2000) showed that individually housed cows in tie stalls tended to eat the majority of their feed during the day, and peak feeding activity occurred immediately following milking and feed distribution. Similar responses to milking and feeding have also been demonstrated for cows in free-stall housing (Tanida *et al.*, 1984; DeVries *et al.*, 2003; Wagner-Storch and Palmer, 2003). Heat stress, particularly temperature-humidity index (THI), reduce dry matter intake (DMI) and milk yield in lactating cows (West, 2003; West *et al.*, 2003) and were also found to influence the dairy cows' time budget (Cook *et al.*, 2007).

The effect of feeding frequency on the performance of dairy cows has been examined in many studies. Time spent feeding has also been shown to be correlated with milk production (Shabi *et al.*, 2005). Gibson (1984) concluded that increasing the feeding frequency of dairy cows increased the milk fat percentage by an average of 7.3% and increased milk production by 2.7%. In the studies by Shabi *et al.* (1999), Le Liboux and Peyraud (1999), and Kudrna *et al.* (2001), increasing feeding frequency increased the DMI of the TMR, but had no effect on milk production. Contrary to these results, in the study by Phillips and Rind (2001), the DMI and milk yield were higher with feeding once a day compared with 4 times a day and concluded that frequent feeding disturbed the cows and reduced milk production.

Conventional milking systems provide a more structured daily routine, whereas automatic milking systems (AMS) allow for more flexibility in milking times for individual cows (Wagner-Storch and Palmer, 2003). According to Melin *et al.* (2005) the motivation to eat is a better incentive in attracting the cows to the milking unit than the motivation to be milked (Prescott *et al.*, 1998; Halachmi *et al.*, 2000). Oostra

Correspondence: Giorgio Provolo, Department of Agricultural and Environmental Science, University of Milan, via Celoria 2, 20133 Milano Italy. Tel.+39 02 5031 6855.
E-mail: giorgio.provolo@unimi.it

Key words: dairy cows; behaviour; environmental condition, automatic milking system.

Acknowledgements: this research was financially supported by the Ministry of University and Research (Italy) within the PRIN 2007 project on Innovative technical solutions for improving the production efficiency and the animal welfare in dairy cow housing.

Journal of Agricultural Engineering 2013; XLIV(s2):e39
doi:10.4081/jae.2013.(s1):e39

et al. (2005) reported that the daily number of visits to the AMS was not affected by the feeding frequency, however, an increase of frequency had a positive effect on the utilization of the cowshed facilities, such as the occupation of the feeding fence, cubicles, and feed alley. The daily feeding time is also influenced by the cow traffic system (Hermans *et al.*, 2003).

The objective of this study was to examine how the frequency of feed delivery affects the time budget, considering also feed intake and milk production, in lactating dairy cows in conventional and AMS farms.

Materials and Methods

Housing system and animals

The study was carried out between April and November 2009 in two dairy farms located in Lombardy (Italy) where animals were kept in loose housing condition with cubicles.

In the first farm (conventional) animals were milked in a herringbone milking parlour (12+12) twice daily and were divided in two groups (primiparous and pluriparous). Milking occurred twice a day at 05:00 and 17:00 h. The barn is oriented NW-SE, the studied a group of 96 primiparous was housed in the NE side equipped with 100 cubicles (2 rows) with mattress covered with chopped straw. At the beginning of the data collection period, cows were 214 ± 9.37 (mean ± SD) days in milking (DIM) and the average milk yield was 27.1 ± 0.66 kg/d. The manger has 90 feeding space and there are 8 fans for summer ventilation. The layout of the barn is reported in Figure 1. Cows were fed with total mixed ratio (22 kg of dry matter head^{-1}).

In the second farm cows were milked in two AMS (VMS, DeLaval, Tumba, Sweden). A forced traffic was applied so the animals were forced to pass through the AMS before they could reach the feed troughs. Cows were divided in two pens but all animals had access to the both AMS 24 h/d (while a total of 0.5 h/d was dedicated to the cleaning of the system from 5.30 to 6 a.m.). Cows were granted milking permission after 6 h from previous milking, unless a milking failure occurred, in which case cows would be allowed permission to be milked again immediately. Cows with more than 12 h since last milking were fetched and forced to visit AMS.

The barn is oriented E-W, the studied a group of around 50 primiparous and multiparous cows (parity 1.83 ± 0.03, milk yield 30.0 ± 3.05 kg/d, DIM 193 ± 17.8; mean ± SD) was housed in the N side equipped with 61 cubicles (4 rows) with mattress covered with sawdust. The manger has 39 feeding space and there are 2 fans for summer ventilation. The layout of the barn is reported in Figure 1. Cows were fed with total mixed ratio (19.8 kg of dry matter head^{-1}).

Environmental monitoring

Two data loggers, for each farm, were used for the measurement of the air temperature, relative humidity and light intensity (HOBO U12 Temp/RH/Light/External Data Logger, Onset Computer Corporation, Bourne, MA, USA). The data loggers were located in the barn at a height of about 2m above the floor in order to measure the air temperature as close as possible to the animals without being affected by the animals. The microclimatic data interval time recording was set at 15 min. The temperature-humidity index (THI), which is widely utilized in literature, was used to consider the temperature and the humidity jointly. The THI was calculated for each position in the barn and an overall value for the THI was obtained by averaging the data obtained from each data logger. The equation used to calculate THI was: THI = Tdb + 0.36 × Tdp + 41.2, where Tdb is the dry bulb temperature in ºC, and Tdp is the dew point temperature in °C (Yousef, 1985).

Feeding frequency

The treatments were applied to entire pen with primiparous cows in conventional farm and one pen in AMS farm and consisted in two periods with two different feeding frequency distribution replicated in two different season. Each period lasted two week: one week for adaptation and one for trial.

The feeding frequency was two (7.00 h and 17.00 h) or three (8.00 h, 11.00 h and 17.00 h) and season summer and autumn in the conventional dairy farm; in AMS dairy farm the feeding frequency was one (9.00 h) or two (9.00 h and 18.00 h) and season spring and summer. All cows in the AMS farm received a TMR at feed bunk and a different amount of concentrate at the AMS during milking depending on milk yield.

Behavioural recording

All behaviours of the cows were monitored in continuous by video recording system for all duration of the study. The video surveillance system consisted of four IR day/night weather-proof varifocal cameras with 42 infrared led for night vision (420SS-EC5, Vigital Technology Ltd., Sheung Wan, Hong Kong) and a recording personal computer based on Windows XP Professional. The cameras each had a protective aluminium housing (IP66) and a 4.0 to 9.0 mm varifocal lens. The four cameras were placed about 5 m above the pen floor to allow for the complete visualization of the pens. The cameras were connected to a four channel video capture DVR4200 card (Huper Laboratories Co., Ltd., Taipei, Taiwan) that was integrated into the PC and that converted the analogue signal to a digital signal for subsequent storage on a hard disk. Each camera was set to continuously record at 640 × 480 resolution and 1 frames/s.

The analysis of the video recording data consisted of the evaluation of the number of dairy cows engaged in different behavioural activities (i.e., feeding, lying, and standing). Standing was considered to be an upright posture (i.e., motionless or walking), while the lying category included only cows that were observed in total lateral or sternal recum-

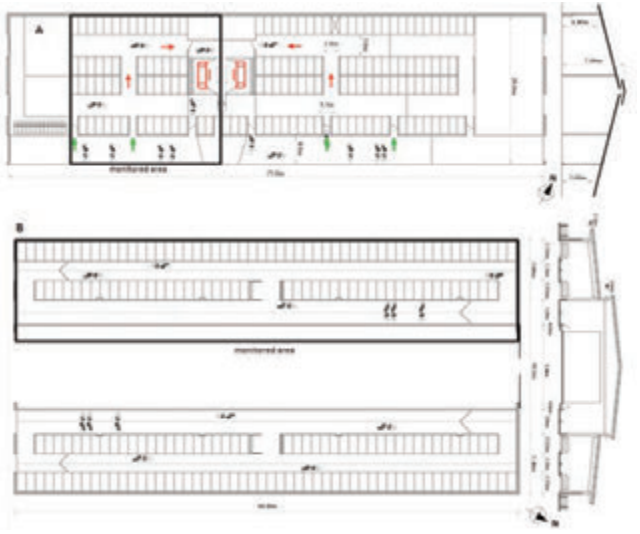

Figure 1. Layout of the monitored barn for the AMS farm (A) and the conventional farm (B).

bency within the confines of a stall (Overton *et al.*, 2002). Eating was defined as actively ingesting feed or water, or standing within 0.6 m of the feed bunk and oriented toward the feed (Overton *et al.*, 2002). Behavioural activities were analysed at scan intervals of 60 min (Mattachini *et al.*, 2011) for each barn to create 2 databases. For each database and for each hour, specific cow behavioural indices were calculated, namely CLI, SUI, CSI, SPI, and CFI. The cow lying index (CLI) describes the number of animal resting in the stall and is defined as total number lying in free stalls divided by the total number of cows in the barn. The free-stall use index proportion of eligible lying (SUI) was defined as total number of cows lying in free stalls divided by the total number of cows in the barn that were not eating during that time period (Overton *et al.*, 2002). The cow standing index (CSI) was calculated as the number of cows observed standing (not lying and eating), divided by the total number of cows in the barn. The stall perching index (SPI) defined the proportion of cows touching a stall that were standing with only the front 2 feet in the stall and the rear feet in the alley (Cook *et al.,* 2005). The cow feeding index (CFI) was obtained counting the cows at the feed bunk (Wagner-Storch and Palmer, 2003). The entire behavioural observation period covered 8 d for each treatment in each period for a total of 32 d for each farm.

Table 1. Climatic and feeding frequency effects on behaviour indices

farm	Factor	CLI	CSI	SUI	SPI	CFI	AMS
AMS farm	Weather	**	**	**	**	*	*
	Feeding frequency	**	n.s.	n.s.	n.s.	*	**
	Hour	**	**	**	**	**	**
	Environmental condition x Feeding Frequency	*	n.s.	*	n.s.	n.s.	*
Conventional farm	Weather	**	**	**	**	n.s.	-
	Feeding frequency	n.s.	*	n.s	n.s.	n.s.	-
	Hour	**	**	**	**	**	-
	Environmental condition x Feeding Frequency	n.s.	**	n.s.	**	n.s.	-

** P≤0.01; * P≤0.05; n.s. not significant

Table 2. Mean values of the indices and THI for the two frequencies of feed delivery (1× vs 2) and for the two periods (hot and cool) for the automatic milking system farm.

	Number of feeding distribution per day							
	1				2			
	Weather				Weather			
	hot		cool		hot		cool	
	Mean	Standard deviation	Mean	Standard deviation	Mean	Standard deviation	Mean	Standard deviation
CLI	0.47	0.13	0.54	0.12	0.46	0.14	0.50	0.14
CSI	0.28	0.10	0.22	0.08	0.26	0.09	0.22	0.08
SUI	0.62	0.14	0.70	0.12	0.63	0.12	0.69	0.12
SPI	0.14	0.06	0.11	0.06	0.14	0.06	0.11	0.05
CFI	0.17	0.09	0.18	0.09	0.18	0.11	0.19	0.09
AMS	0.08	0.08	0.06	0.05	0.09	0.07	0.09	0.07
THI	72.91	3.88	60.32	3.09	71.36	3.63	66.43	3.47

Table 3. Mean values of the indices and THI for the two frequencies of feed delivery (2× vs 3×) and for the two periods (hot and cool) for the conventional farm.

	Number of feeding distribution per day							
	2				3			
	Weather				Weather			
	hot		cool		hot		cool	
	Mean	Standard deviation	Mean	Standard deviation	Mean	Standard deviation	Mean	Standard deviation
CLI	0.54	0.20	0.62	0.21	0.52	0.17	0.61	0.19
CSI	0.21	0.09	0.14	0.07	0.23	0.09	0.14	0.06
SUI	0.71	0.15	0.79	0.15	0.68	0.14	0.79	0.16
SPI	0.08	0.04	0.06	0.04	0.09	0.04	0.05	0.03
CFI	0.25	0.18	0.24	0.20	0.25	0.13	0.25	0.18
THI	71.93	3.50	58.40	2.91	74.31	3.12	56.96	3.13

Statistical analysis

Behavioural indices were not normally distributed as defined by the Kolmogorov–Smirnov test and these indices were then square root-arcsine transformed to achieve normal distribution (Mitlohner *et al.*, 2001). For the analysis of behaviours (CLI, CSI, SUI, SPI, CFI, AMS), both farms were considered as the experimental unit, with measures from multiple days and cows averaged to create one observation per hour of the day, per farm, per treatment (1 vs. 2; 2 vs. 3) and per environmental condition (cool and hot). Effect of the hour of the day was considered in both farms. In conventional farm milking hours were excluded. An ANOVA was carried out considering as factors: feeding frequency, environmental condition, hour and interaction feeding frequency x environmental condition.

DMI, milk yield, and THI were tested by ANOVA using the same factorial model for daily values.

In statistical analysis, significance was declared when $P < 0.05$ (* $P < 0.05$; ** $P < 0.01$; *** $P < 0.001$).

Results

As expected, almost all behavioral indices have been significantly affected by environmental conditions both in conventional and AMS farm (Table 1).

Although the THI values were not particularly high also in the hot period (< 73) the differences in the behavioral activity in comparison to the cool period were marked (table 2): CLI decreased of 10-15% while cows were standing longer (23-50%). Thus also the SUI decreased in hot conditions. The SPI shows an significant increment in both farms (>30%) revealing cows were less comfortable. CFI has been affected in a very limited way in the conventional farm and the differences are not significant while slightly decreased in the AMS farm (-5%).

The increase in the feeding frequency has caused different effect in the two farms.

In AMS farm significantly affected CLI, CFI and AMS (Table1). As expected, CLI was reduced when the number of the feeding distribution per day increased, but the effect is significantly higher (interaction significance P<0.05) in the cool period. In hot period the variation of this index is very limited. The consequence is a higher CFI that resulted 8% higher in both periods. As the traffic is forced through the milking, also a significant increase of the time spent in this area has been recorded. Thus the effect in the AMS farm of the increase of the number of feeding distribution per day has been to reduce the time spent lying and an increase of the time spent trying to reach the manger and in feeding.

The effect in the conventional farm confirms a tendency of reduction of the CLI (not significant) and an increase of time spent standing mainly in the hot period, confirmed by a significant interaction (Table 1). In this farm the increase of the number of distribution per day seems to have induced cows to rise and to stand. Although they did not spend a significant longer time at the manger, the tendency also in this case was to increase the time spend feeding (Table 3).

Figure 2 reports the average hourly behavior of cows in the experimental periods. The indices were of course significantly affected by the time of the day. It can be noticed that the conventional farm cows is to rest just after the morning milking but, when the feed is distributed a great number of cows reach the manger. After the afternoon milking

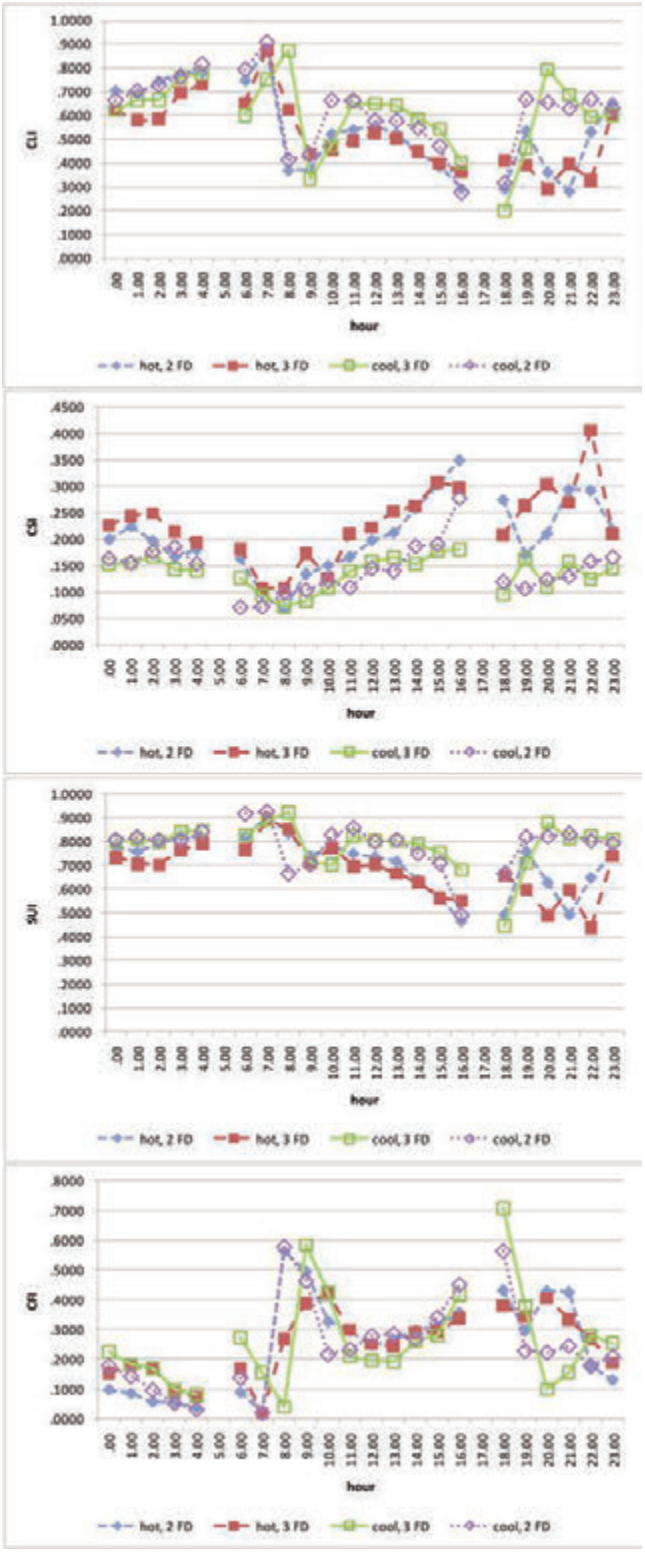

Figure 2. Hourly means of the behavioural indices for the two farms in the four test conditions: two weather (hot and cool) and two feed delivery frequencies (2 and 3 times a day for the conventional farm; 1 to 2 times a day for the AMS farm).

cows go directly to the manger as feed is already available. In AMS farm the feeding activity is reduced from 10 p.m. to 8 a.m. and then remain quite high (more than 20% of cows) during the day. The effect of the number of feeding distribution during the day is not evident in both farms. This is probably due to the operation of pushing feed in the manger that is carried out by both farms periodically during the day.

The effect of the number of distribution of feed per day results clearly also by the comparison of the daily time budget of the two test conditions for the two farms (Figure 3).

The variations are similar in both farms. When the number of distributions rise, the feeding time increase while the lying and standing time decrease. From figure 3 it can also be noticed that in both farms the daily time a cow spend for lying and feeding seems to be constant as well as the time spent standing and milking. In AMS farm cows significantly increase the time spent in the AMS holding area, while in conventional farm they increase the standing time. In any case, the variation of the feeding distribution affected negatively the daily time budget.

Conclusions

The most significant effect on cow behavioural activity is however related to THI also when daily values are in the range where heat stress should not occur.

The variation in the frequency of feed delivery seems to affect the cow behavioural activity but only in a limited way and to modify only slightly the daily averages of the time spent in different activities. The increase of the standing time for the conventional far and time spend in the holding area for the AMS farm is the main effect recorded in this experiment.

Further investigations are required to evaluate other aspects like the number of bouts and the duration of each lying period. Of course, in farms where the feeding operations are not automatized, the farmer should evaluate carefully if the higher cost of an extra feeding delivery is compensated by the increase in milk production.

The adverse effect of a more frequent feed distribution on cow daily time budget should therefore be carefully considered. Although it seems to have limited effect, the longer standing time cannot be ignored especially in farm equipped with AMS where the cow traffic system might worsen the consequences of a more frequent feed delivery.

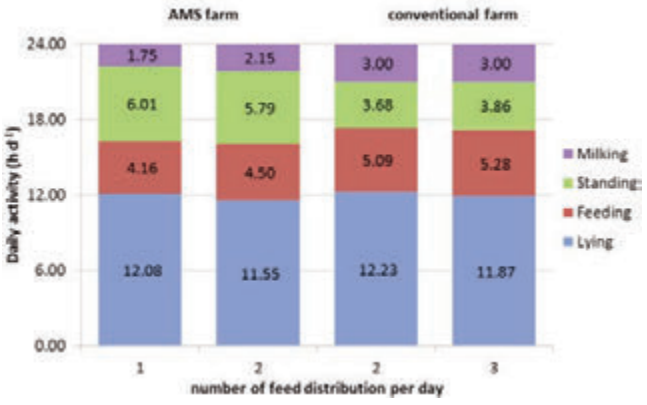

Figure 3. Comparison of the Daily Time Budget for the two farms considered in relation to the number of feed distributions per day.

References

Cook N. B., Mentink R.L., Bennet T.B., Burgi K. 2007. The effect of heat stress and lameness on time budgets of lactating cows. J. Dairy Sci. 90:1674-1682.

DeVries T.J., von Keyserlingk M.A.G., Weary D.M., Beauchemin K.A. 2003. Measuring the feeding behavior of lactating dairy cows in early to peak lactation. J. Dairy Sci. 86:3354-3361.

DeVries T.J., von Keyserlingk M.A.G. 2005. Time of feed delivery affects the feeding and lying patterns of dairy cows. J. Dairy Sci. 88:625-631

DeVries T.J., von Keyserlingk M.A.G., Beauchemin K.A., 2005. Frequency of feed delivery affects the behavior of lactating dairy cows. J. Dairy Sci. 88:3553-3562

Gibson J. P. 1984. The effects of frequency of feeding on milk production of dairy cattle: An analysis of published results. Anim. Prod. 38:181–189.

Grant R. J., Albright J. L. 2001. Effect of animal grouping on feeding behavior and intake of dairy cattle. J. Dairy Sci. 84:E156-163

Grant R. J., Albright J. L. 2000. Feeding behaviour. Page 365-382 in Farm Animal Metabolism and Nutrition. J.P.F. D'Mello, ed. CABI Publishing,Wallingford, Oxon, UK

Kudrna V., Lang P., Mlazovska P., 2001. Frequency of feeding with TMR in dairy cows in summer season. Czech J. Anim. Sci. 46:313–319.

Haley D. B., Rushen J., de Passillé A. M. 2000. Behavioural indicators of cow comfort: activity and resting behaviour of dairy cows in two types of housing. Can. Vet. J. 80.2:257 -263

Halachmi I., Metz J. H. M., Maltz E., Dijkhuizen A. A., Speelman L. 2000. Designing the optimal robotic barn. Part 1: Quantifying facility usage, J. Agric. Eng. Res. 76:37–49.

Hermans G. G. N., Ipema A. H., Stefanowska J., Metz J. H. M. 2003. The effect of two traffic situations on the behavior and performance of cows in an automatic milking system. J. Dairy Sci. 86:1997–2004.

Le Liboux S., Peyraud J.L., 1999. Effect of forage particle size and feeding frequency on fermentation patterns and sites and extent of digestion in dairy cows fed mixed diets. Anim. Feed Sci. Tech. 76:297–319.

Mäntysaari P., Khalili H., Sariola J., 2006. Effect of feeding frequency of a total mixed ration on the performance of high-yielding dairy cows. J. Dairy Sci. 89:4312-4320.

Mattachini G., Riva E., Provolo G. 2011. The lying and standing activity indices of dairy cows in free-stall housing. Appl. Anim. Behav. Sci. 129:18-27.

Melin M., Wiktorsson H., Norell L. 2005. Analysis of feeding and drinking patterns of dairy cows in two cow traffic situations in automatic milking systems. J. Dairy Sci. 88:71-85.

Mitlohner F.M., Morrow-Tesch J.L., Wilson S.C., Dailey J.W., McGlone J.J. 2001. Behavioral sampling techniques for feedlot cattle. J. Dairy Sci. 79:1189-1193.

Overton M.W., Sischo W.M. Temple G.D. Moore D.A. 2002. Using time-lapse video photography to assess dairy cattle lying behavior in a free-stall barn. J. Dairy Sci. 85:2407-2413.

Oostra H.H., Stefanowska J., Sallvik K., 2005. The effects of feeding frequency on waiting time, milking frequency, cubicle and feeding fence utilization for cows in an automatic milking system. Acta Agr. Scand. A-An. 55.4:158 - 165.

Phillips C.J.C., Rind M.I. 2001. The effects of frequency of feeding a

total mixed ration on the production and behavior of dairy cows. J. Dairy Sci. 84:1979–1987.

Prescott N.B. Mottram, T.T., Webster A.J.F. 1998. Relative motivations of dairy cows to be milked or fed in a Y-maze and an automatic milking system. Appl. Anim. Behav. Sci. 57:23-33.

Shabi Z., Bruckental I., Zamwell S., Tagari H., Arieli A. 1999. Effects of extrusion of grain and feeding frequency on rumen fermentation, nutrient digestibility, and milk yield and composition in dairy cows. J. Dairy Sci. 82:1252–1260.

Tanida H., Swanson L.V., Hohenboken W.D. 1984. Effect of artificial photoperiod on eating behavior and other behavioral observations of dairy cows. J. Dairy Sci. 67.3:585–591

Wagner-Storch A.M., Palmer R.W. 2003. Feeding behavior, milking behavior, and milk yields of cows milked in a parlor versus an automatic milking system. J. Dairy Sci. 86:1494-1502

West J. W., 2003. Effects of heat-stress on production in dairy cattle J. Dairy Sci. 86:2131–2144.

Wes, J.W., Mullini, B.G., Bernar, J.K., 2003. Effects of hot, humid weather on milk temperature, dry matter intake, and milk yield of lactating dairy cows. J. Dairy Sci.86: 232-242.

A survey on Italian compost dairy barns

Lorenzo Leso,[1] Maurizio Uberti,[2] Wasseem Morshed,[1] Matteo Barbari[1]

[1]Departement of Agricultural, Food and Forestry Systems, University of Florence, Italy; [2]Freelance veterinarian

Abstract

Compost-bedded pack barns, generally known as compost dairy barns, are alternative housing systems for dairy cows. In these barns, the whole surface of the resting area is covered with a deep-bedded pack that is frequently stirred in order to incorporate fresh manure into the pack and to enhance the evaporation of water. Experiences with compost bedded pack barns for dairy cows are reported in literature from the USA, Israel, the Netherlands and Austria. The main advantages of these housing systems regard animal welfare and manure management. Since 2006, this housing system has been applied consistently in Italy. However, scientific knowledge about Italian compost barns is still lacking. This study aims at describing housing system, assessing producers' satisfaction and measuring performance of dairy cows housed in compost bedded pack barns. Ten commercial dairy farms in northern Italy was involved in the study. All pens in each farm were surveyed to determine the surface of total available area, bedded area and pack depth. In order to investigate management practices, labor requirement, consumption of bedding materials and producers satisfaction, a questionnaire was submitted to each farm manager. The temperature of the bedded pack was measured in each farm during summer and winter. Moreover, data from Italian Breeder Association were collected for each herd over a period of one year (from September 2011 to September 2012). For the ten compost barns involved in the study the average total available area was 10.9 m^2 per cow and the average pack area was 6.7 m^2 per cow. The bedded pack was aerated 1.4 times per day. The most commonly used bedding material in these farms was dry sawdust. The consumption of bedding materials was 8.1 m^3 per cow per year. A clear tendency to inverse correlation was found between the space per cow and the amount of bedding needed per cow (R^2= 0.395; p-value=0.051). Operations related to pack management require 4.1 hours of labor per cow per year. Direct relationship was found between the bedded area space per cow and the annual labor required for pack management per cow (R^2=0.505; p-value=0.048). Performance of cows housed in compost barns included in this study was encouraging and although some concerns about the cost of bedding, overall producers were satisfied with this housing system.

Correspondence: Matteo Barbari, Departement of Agricultural, Food and Forestry Systems. University of Florence, Italy
E-mail: matteo.barbari@unifi.it

Acknowledgements: the authors wish to thank all the dairy producers for their kind collaboration. We also acknowledge the Associazione Italiana Allevatori and the APA of Mantua and Cremona for their important contribution in providing data.

Journal of Agricultural Engineering 2013; XLIV(s2):e40
doi:10.4081/jae.2013.(s1):e40

Introduction

Compost-bedded pack barns, generally known as compost dairy barns, are an alternative loose housing system that appears to offer excellent comfort level for dairy cows. In this type of barn, cows are provided with a large bedded area for resting rather than individual stalls. Compost bedded pack refers to a mixture of feces and urine produced by the cows and organic bedding. Unlike conventional straw-bedded yards, the whole surface of compost packs is cultivated once or twice daily to dry the surface and incorporate manure into the pack (Klaas and Bjerg, 2011). A properly managed bedded pack provides a dry, comfortable and healthy surface on which cows lie, stand and walk. Compost-bedded pack barns for dairy cows are spread in the USA, Israel, Europe and South Korea (Galama, 2011). By analyzing international literature two main types of compost-bedded pack barns could be identified. Although both two types seem to be based on the evaporation of water from the pack, management practices, type of bedding materials and barn's characteristics are significantly different (Galama 2011; Klaas and Bjerg, 2011).

The first type, which was initially developed in the USA and applied with some modifications also in the Netherlands and Austria, is based on the development of heat in the pack. In this type of compost barns the most important issue is to maintain adequate chemical and physical characteristics into the substrate in order to promote aerobic microbial activity (Black *et al*., 2013). The recommended bedded area space per cow for this type of housing system ranges from 7.4 to 12.5 m^2/cow (Janni *et al*. 2007; Galama, 2011; Black *et al*., 2013). The most commonly used bedding materials are sawdust, wood shavings and wood chips. The second type of compost barn takes advantage from the natural drying potential of the air rather than heat production into the pack (Galama, 2011). This type of housing system has been developed in Israel and is receiving an increasing interest in the Netherlands. The recommended bedded area space per cow in this type of compost barns ranges from 15 to 20 m^2/cow in barns provided with scraped feeding alleys and up to 30 m^2/cow in systems without concrete alleys (Klaas *et al*., 2011).

Since 2006, compost-bedded pack barn for dairy cows has spread in Italy. Actually, Italian compost dairy barns are about 50, mostly located in the Po Plain, northern Italy. Although in other countries this housing system has evolved mainly with the aim of increasing the welfare of dairy cows (Barberg *et al*., 2007a; Klaas *et al*., 2010), in Italy it was developed initially to reduce the risk of mastitis in deep straw-bedded yards. Compost bedded pack was quickly appreciated by Italian farmers for its benefits towards udder health (Vighi *et al*., 2009). Few years later, also the positive effects on lameness prevalence and longevity became evident and many more farmers shifted to compost bedded pack.

As a matter of fact, one of the most noticeable benefits of compost bedded pack regards cow comfort and feet and legs health (Ofner-Schröck *et al*. 2013; Barberg *et al*., 2007b; Fulwider *et al*., 2007;). Lobeck *et al*. (2011) found that dairy cattle housed in compost bedded barns had reduced lameness and hock lesions compared with those housed in free stall barns. Observations of lying behavior, social interactions, and natural lying positions indicated that compost dairy barns could be an adequate housing system for dairy cows (Enders and Barberg, 2007). Overall, producers are satisfied with this housing system, especially for improved animal welfare, but some concerns regard pack management and the cost and availability of bedding (Shane *et al*., 2010).

Besides the benefits mentioned above, this alternative housing system could represent an effective tool to reduce the costs for manure management, especially in areas where there is a high density of dairy production, such as Po Plain, Italy. Compared with free stall barns, compost bedded pack barns produce less slurry, and solid manure has higher agronomic value (Galama, 2011). The interest of Italian farmers and researchers towards compost dairy barns is rapidly and consistently increasing (Ventura, 2011). However, scientific knowledge about the application of this housing system in Italy is still lacking. The objective of the current study was to describe housing system and management practices, assess producers satisfaction and measure performance of dairy cows housed in Italian compost-bedded pack barns.

Materials and methods

This observational study was performed on ten dairy farms in the provinces of Mantua (n. 7) and Cremona (n. 3). All farms included met the following criteria: shifted to compost bedded pack at least two years before the start of the study, all lactating cows are housed in compost bedded pack barns, pack is cultivated at least once per day, drive-through TMR feeding and use corn silage in lactating cows' ration. The primary breed in all farms was Holstein. Monthly dairy herd records were obtained from Italian Breeders Association (Associazione Italiana Allevatori, www.aia.it) for each farm included. To assess herds' performance the following data were collected over a period of one year (from September 2011 to September 2012): herd mean daily milk yield, 305 mature equivalent milk production, days in milk (DIM), fat and protein content, herd mean somatic cells count (SCC), age at first calving, mean number of parity, calving interval and mean number of services per pregnancy.

Each farm was visited once between July and September 2012 to collect on-farm data which included: barn dimensions and layout, total available area space per cow, lying area space per cow, bedding type and pack depth. Barns dimensions was measured using a Leica DISTO A5 laser distance meter (Leica Geosystems, Heerburgg, Switzerland). A questionnaire was submitted to the herd manager at the time of the visit. The first part of the questionnaire included 25 questions regarding pack management practices, machines and equipment used, labor required and consumption of bedding. In the second part of the questionnaire producers were asked to express their satisfaction with the alternative housing system in regards to the following features: animal welfare, cow cleanliness, udder health, claw and leg health, fertility, longevity, milk yield, ease of management, costs and manure management. Satisfaction levels was expressed using a 4-point scale where 1=very dissatisfied, 2= dissatisfied, 3=satisfied and 4= very satisfied.

In addition, five farms were visited twice, once in winter (January 2012) and once in summer (August 2012), to measure the temperature of the pack and the air temperature inside the barn. Pack temperatures were taken in ten points across the resting area at 20 cm depth. Air temperature was measured in five positions inside the barn at 1 m above the pack surface. Temperature measurements were performed by the same operator using a DO 9847 portable multifunction data-logger (Delta Ohm, Padua, Italy).

Statistical analysis

Descriptive statistics (mean, SD and range) were used to describe herds' characteristics, spaces per cow, pack depth, pack temperatures, air temperatures, quantitative data regarding management practices and producers' satisfaction scores. Results are presented in text as mean ±SD and range. Linear regression analyses were performed to identify variables affecting consumption of bedding and labor requirement. Residuals were visually checked. Coefficient of determination (R^2) was calculated to assess the goodness of fit of the model and t-test were performed to determine whether there is a significant linear relationship between variables. All analyses were performed using the "base" and "stats" packages of R (R Development Core Team, 2011).

Results

The size for the herds included in this study was 112 ±58.8 lactating cows ranging from 42 to 192. Descriptive statistics for the herds' performance are reported in Table 1. All the compost barns visited had a flat concrete floor under the bedded pack and nine out of ten barns have an indoor (n. 6) or outdoor (n. 3) scraped feed alley. The width of the feed alleys resulted in 4.32 ±1.54 m while the space per cow at the feed fence was 0.58 ±0.20 m/cow. In one barn there was no scraped alley. Total available area space per cow was 11.0 ±4.1 m^2/cow. The resting area (compost-bedded pack) space per cow was 6,8 ±2.2 m^2/cow (range of 3.56 to 10.18 m^2/cow). The depth of the bedded pack at the moment of farm visits was 25.6 ±9.4 cm (range from 15 to 40 cm).

Management

Management practices applied in the farms included in this study was quite heterogeneous. However, the most commonly used technique can be described as follows. To start a compost-bedded pack a layer of 10-20 cm of organic bedding is distributed on the floor of the lying area. During the first 5-10 days the pack is not aerated and no bedding is added. After this starting period the surface of the bedded pack is stirred on a regular basis once or twice daily while cows are being

Table 1. Descriptive statistics for the herds' performance between September 2011 and September 2012.

Parameter	Min	Mean(SD)	Max
Milk yield (kg/cow*day)	24.8	30.8 (3.05)	35.2
DIM	184	209 (29.1)	273
305 mature equivalent milk production (kg)	9205	10541 (667)	11458
Milk fat (%)	3.43	3.67 (0.17)	3.88
Milk protein (%)	3.33	3.48 (0.10)	3.62
SCC (cell*1000/mL)	132	354 (121.1)	548
Age at firs calving (months)	22	29 (4.0)	35
Number of parity	2.01	2.39 (0.26)	2.74
Calving interval (days)	395	450 (35)	494
Number of services per pregnancy	1.84	2.67 (0.47)	3.53

milked in the parlor. A layer of fresh dry bedding is added every 12±17 days (range from 1 to 55 days) mainly to keep the moisture content of the pack under control. Most producers add a consistent amount of fresh dry materials only when the bedding particles start to adhere to the cows but in some dairies a smaller amount was added more frequently, up to once daily. The bedded pack area was completely cleaned out every 30±35 days (range from 10 to 90 days) when the moisture content of the bedded pack exceeds a critical level at which cows start to sink deep into the pack and the aerations become difficult.

In 6 farms the pack was aerated once a day and twice a day in the remaining 4, averaging 1.4 aeration per day. Typically a tractor provided with a tines cultivator was used to stir the bedded pack. The power of tractors used for cultivating the pack was 62±16.1 kW (range from 37 to 88 kW). On average the pack was aerated at a depth of 19±7.6 cm, ranging from 10 to 30 cm. Stirring the pack required 41±47 min/day (range from 5 to 150 min/day) and the productivity of this operation resulted in 2610.9±2425.7 m^2/hour (range from 725 to 8006.5 m^2/hour). All the operations related to compost-bedded pack management (start-up, aeration, bedding addition and barn cleaning) required 356±274 hours/year (range from 136 to 1002 hours/year). By comparing the annual labor requirement for pack management with the number of cows housed in each barn, the annual labor per cow resulted in 4.2±2.1 hours/cow*year (range from 1.2 to 6.7 hours/cow*year). Since the labor for pack cultivation primarily depended on the surface of bedded pack, a significant relationship (R^2=0.505; p-value=0.048) was found between the space per cow and the annual labor requirement for pack management (Figure 1).

Bedding

In compost dairy barns included in this study dry sawdust and wood shavings (mainly from pine wood) are used for bedding. Seven producers used only sawdust while 3 preferred a mixture of sawdust and wood shavings. During winter one farmer tried to add a load of coconut fiber but he reported problems due to rapid rise in moisture content which resulted in a consistent loss of structure. In warm periods some producers successfully reused sun-dried manure coming from compost-bedded pack barns. The amount of fresh bedding materials needed was 875.2 ±469.7 m^3/year (range from 575 to 1600 m^3/year). Annual bedding requirement compared with the bedded area surface and the number of cows housed in each barn resulted respectively in 1.4 ±2.9 m^3/m^2*year (range from 0.3 and 2.6 m^3/m^2*year) and 8.2 ±2.9 m^3/cow*year (range from 3.2 and 13.4 m^3/cow*year).

The amount of bedding as well as the frequency whit which is added and the time between complete pack renovations strongly depended on season and weather conditions. In all farms included the consumption of bedding was concentrated in the winter period when the evaporation of water from the pack was limited due to low air temperature and high relative humidity. Most of the dairies did not add any bedding to the pack in the period between May and late September. Although climate plays a major role, also the bedded area space per cow affected the amount of bedding needed in compost dairy barns. Increasing the bedded area surface resulted in greater amount of bedding used to start-up the pack. On the other hand larger space per cow allowed to reduce consistently the need of bedding in the following phases. A clear tendency to inverse correlation (R^2= 0.395; p-value=0.051) was found between the space per cow and the annual amount of bedding used per cow (Figure 2).

Pack temperature

The temperature of the pack measured during summer was 29.6 ±3.7°C (range from 24.2 to 33.4°C). In the same period the air temperature inside the barn was 29.3±1.6°C (range from 27.3 to 31.4°C). During winter the temperature of the pack was 11.7±6.0°C (range from 6.4 to 21.6°C) while the air temperature was 4.4±1.9°C (range from 2.3 to 7.2°C). Both in summer and winter the temperatures of the pack were not sufficient to identify a composting process. However the difference between pack and air temperatures measured during winter indicated that pack was biologically active. In few barns, especially during summer, the temperature of the pack was lower than air temperature. Probably this was due to the intense evaporation of water from the surface of the pack.

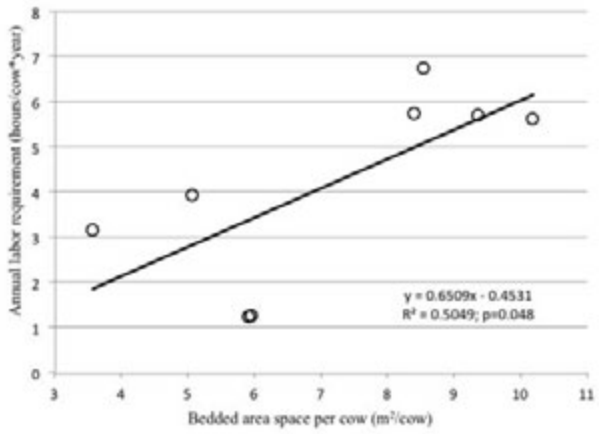

Figure 1. Scatter plot of the relationship between the bedded area space per cow and the annual labor requirement for pack management (data from 2 farms were not available).

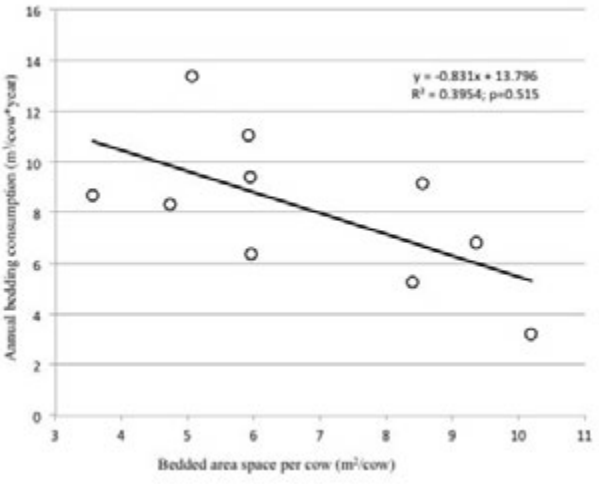

Figure 2. Scatter plot of the relationship between the bedded area space per cow and the annual amount of bedding used.

Producers' satisfaction

Overall producers were satisfied with their compost-bedded pack barns. Almost all producers identified cows' welfare and legs and feet health as the main benefits of this alternative housing system. High satisfaction levels were also found towards udder health, fertility and manure management. Many farmers spontaneously remarked a reduced presence of flies in compost barns, especially during the summer period. Major concerns regard ease of management and costs. Results of the survey on producers satisfaction are summarized in Table 2.

Table 2. Producers' satisfaction levels with compost bedded pack housing system in regards to different features.

Feature	Satisfaction level[a]		
	Min	Mean	Max
Animal welfare	3	3,65	4
Cow cleanliness	2	3,00	4
Udder health	3	3,25	4
Claw and leg health	3	3,50	4
Fertility	2	3,13	4
Longevity	2	3,00	4
Milk yield	2	3,00	4
Ease of management	2	2,88	4
Costs	2	2,63	4
Manure management	2	3,25	4

aSatisfaction reported on a 4-point scale, from 1 (very dissatisfied) to 4 (very satisfied).

Discussion

Many farmers shifted from deep straw-bedded yard to compost-bedded pack to reduce SCC. The satisfaction level towards this aspect leads to think the objective has been achieved. In dairies included in the current study the herd mean SCC was 354,000 ±121,100 cells/mL. Other studies on compost dairy barns reported similar SCC. In a survey carried out in Kentucky the herd mean SCC was 318,000 cells/mL (Black *et al*., 2013). Barberg *et al*. (2007b) reported a mean SCC of 325,000 ±172,000 cells/mL for 12 herds housed in compost barns in Minnesota. In the same study a reduction in mastitis infection rate was found in 6 out of 9 herds after shifting to compost-bedded pack barns. Lobeck *et al*. (2011) compared welfare of dairy cows housed in compost barns and free stall barns finding no significant difference in mastitis infection rate. Although udder health in compost barns seems to be adequate, difficulties in keeping dry the pack could pose challenges towards cow cleanliness, especially during winter period. Many authors emphasized that a high hygiene level at milking and proper management of the pack are essential for achieving high quality milk in this housing system (Barberg *et al*., 2007b; Janni *et al*., 2007; Black *et al*., 2013).

Producers interviewed in the current study were widely satisfied with the increased welfare of cows housed in compost-bedded pack barns. Similarly Minnesota dairy farmers identified animal welfare as the main reason to build a compost barn (Barberg *et al*. 2007a) and increased cow comfort compared to free stalls was the most frequently cited benefit of this alternative housing system among dairy producers in Kentucky (Black *et al*., 2013). Experimental data confirmed that compost-bedded pack barns have positive impact on the welfare of dairy cows (Barberg *et al*., 2007b; Fulwider *et al*. 2007; Lobeck *et al*., 2011). However many authors remarked that cost and availability of bedding could limit the use of compost barns (Barberg *et al*., 2007a; Shane *et al*., 2010). Also Italian producers expressed quite clearly their concern about this issue.

In the compost barns included in the current study the annual amount of bedding used was 8.2 m^3/cow*year. Considering an average cost for dry sawdust of 18 €/m^3, the annual bedding cost resulted in 148 €/cow*year. Janni *et al*. (2007) estimated an annual bedding consumption in Minnesota compost barns of 19.6 m^3/cow*year and a total annual bedding cost of 181 $/cow*year. Although the annual cost for bedding was similar due to the difference in sawdust price, the amount of bedding used in Italian compost barns was sensibly lower than that used in Minnesota. Climate and weather conditions could partially explain the amount of bedding needed but pack management and barns' characteristics have to be considered as well.

The space per cow is considered by many authors as a key factor in compost-bedded pack barn management (Klaas and Bjerg, 2011). Janni *et al*. (2007) recommended a minimum pack area space per cow of 7.4 m^2/cow for a 540 kg cow. More recently researchers from Kentucky suggested that the optimal space per cow ranges from 9.3 to 10.2 m^2/cow (Black *et al*., 2013). Considering the only bedded area, the space allotment in compost barns included in the current study was 6,8 ±2.2 m^2/cow. Since an inverse relationship was found between the space per cow and the amount of bedding used per cow (Figure 2), increasing the space per cow should results in a reduction in bedding consumption. As a matter of fact, considering the only barns which had more than 8 m^2/cow (n. 4) the average annual amount of bedding used and the annual cost for bedding resulted respectively in 3.0 m^3/cow*year and 54 €/cow*year. On the other hand an increase in the space per cow may result in an increase in labor requirement for pack aeration. The productivity of pack stirring operations varied considerably among compost barns included (from 725 to 8006.5 m^2/hour). Producers remarked that shape and dimensions of the barn strongly affected the amount of time needed to stir the pack. Regular shape of the bedded areas minimized the time required for aerating the pack.

The space per cow and the shape of the bedded area can affect significantly the costs for compost-bedded pack barns management. However even the temperature of the pack should be taken into account. The heat produced by the microbial activity into the pack increases the evaporation of water and thus reduces the amount of bedding needed to maintain dry the pack (Janni *et al*., 2007). Smits and Aarnink (2009) calculated that the evaporation of water from a bedding that is composting is higher than from a non-composting pack. Black *et al*. (2013) fount that in Kentucky compost barns the ideal pack temperature is between 43 and 60°C. Nevertheless high pack temperature seems to be necessary only in compost barns with relatively high animal density (7.5-12.5 m^2/cow) and in cold climates, especially during winter. In Israeli climatic conditions by providing each cows with at least 15 m^2 it was possible to maintain dry pack during the whole year, even though the heat generation was limited (Klaas *et al*. 2010). In compost barns included in the current study the temperatures of the pack (winter: 11.7 ±6.0°C; summer: 29.6 ±3.7°C) and the bedded area space per cow (6,8 ±2.2 m^2/cow) seem to be insufficient to allow adequate evaporation from the pack, especially during winter.

Low bacterial activity in the pack could be explained by high animal density which leads to excessive bedding moisture content and thus limits the growth of aerobic bacteria. Black *et al*. (2013) found that maximum pack temperatures tend to be achieved when the bed moisture content is between 40 and 60%. Moreover in order to keep the heat produced into the pack, relatively high pack depth are needed. Experiences from the Netherlands indicated that a layer of at least 50 cm is needed to avoid excessive heat dissipation during pack stirring

(Galama, 2011). In addition higher pack depth allows to store manure into the barn for longer periods reducing the need of external storage and the labor required for pack renovations. In compost barns included in the current study the pack depth ranges from 15 to 40 cm. Most producers reported difficulties in increasing the pack depth because the bed moisture content raised too rapidly and cows sunk deep into it. In Italian compost barns lower animal densities seem to be necessary to maintain adequate pack moisture content and decrease the amount of bedding needed, especially during winter. Further studies are needed to identify the ideal space per cow and develop management recommendations for compost dairy barns in Italian climate.

Conclusions

Italian compost-bedded pack barns may represent an effective solution for housing dairy cows. Producers identified animal welfare as the main benefit of this system and overall they appeared to be very satisfied. Nevertheless concerns about the cost of bedding led to think that pack management and barns' characteristics have not been optimized yet. Results obtained confirmed that animal density is a key factor in compost-bedded pack barns.

References

Barberg A.E., Endres M.I., Janni K.A. 2007a. Compost dairy barns in Minnesota: a descriptive study. Appl. Eng. Agric. 23(2):231-238.

Barberg A.E., Endres M.I., Salfer J., Reneau J. 2007b. Performance and welfare of dairy cows in an alternative housing system in Minnesota. J. Dairy Sci. 90(3):1575-83.

Black R., Bewley J., Taraba J., Day G., Damasceno F.A. 2013. Kentucky compost-bedded pack barn project. Cooperative extension service, University of Kentucky, College of agriculture. Lexington, KY, 40546.

Enders M.I., Barberg A.E. 2007. Behaviour of dairy cows in an alternative bedded-pack housing system. J. Dairy Sci. 90(9):4192–4200.

Fulwider W.K., Grandin T., Garrick D.J., Engle T. E., Lamm W. D., Dalsted N. L., Rolling B. E. 2007. Influence of free-stall base on tarsal joint lesions and hygiene in dairy cows. J. Dairy Sci. 90(7):3559–3566.

Galama P. 2011. Prospects for bedded pack barns for dairy cattle. WUR Livestock Research, Wageningen, NL.

Janni K.A., Endres M.I., Reneau J.K., Schoper W.W. 2007. Compost dairy barn layout and management recommendations. Appl. Eng. Agric. 23(1):97-102.

Klaas I.C., Bjerg B. 2011. Compost barns - an alternative housing system for dairy cows? CAB Reviews: Prospectives in Agriculture, Veterinary Science, Nutrition and Natural Resouces. 45(6):1-9.

Klaas I.C., Bjerg B., Friedmann S., Bar D. 2010. Cultivated barns for dairy cows - an option to promote cattle welfare and environmental protection in Denmark? Dansk Veterinærtidsskrift. 93(9):20-9.

Lobeck K.M., Endres M.I., Shane E.M., Godden S.M., Fetrow J. 2011. Animal welfare in cross-ventilated, compost-bedded pack, and naturally ventilated dairy barns in the upper Midwest. J. Dairy Sci. 94(11):5469–5479.

Ofner-Schröck E., Zähner M., Huber G., Guldimann K., Guggenberger T., Gasteiner J. 2013. Kompoststall - funktionell und tiergerecht? Bautagung Raumberg-Gumpenstein. 2013, 15–22.

R Development Core Team. 2011. R: A language and environment for statistical computing. R Foundation for Statistical Computing, Vienna, Austria. ISBN 3-900051-07-0, URL http://www.R-project.org/.

Shane E.M., Endres M.I., Janni K.A. 2010. Alternative bedding materials for compost bedded pack barns in Minnesota: a descriptive study. Appl. Eng. Agric. 26(3):465-73.

Smits M.C.J., Aarnink A.Y.A. 2009. Verdamping uit ligbodems van vrijloopstallen; oriënterende modelberekeningen. Rapport 230. Animal Sciences Group. Wageningen UR.

Ventura P.G. 2011. Un modello innovativo per le stalle europee. Stalle da latte. 29:30-32.

Vighi P., Uberti M., Calamari L. 2009. Più benessere per le bovine con l'erpicatura della lettiera. Terra e Vita. 24:43-46

Use of a proactive herd management system in a dairy farm of northern italy: technical and economic results

Stefania Leonardi,[1] Gabriele Marchesi,[2] Francesco Maria Tangorra,[1] Massimo Lazzari[1]

[1]Department of Health, Animal Science and Food Safety, Università degli Studi di Milano;
[2]Milkline® S.r.l., Italy

Abstract

Reproductive and economic data were recorded before and one year after the installation of Herd Navigator™ in a dairy farm with AMS (Automatic Milking System) located in a mountain area of Northern Italy. Number of days open reduced from 166 to 103 days, number of days between the first and second insemination decreased from 45 to 28 days, and days for identifying an abortion were 80 % less, from 31 to 6 days. The preliminary results highlight the usefulness of the proactive herd management system installed for the reproduction management. A basic economic model is proposed to evaluate the potential economic benefits coming from the introduction of this technology. The model considers the benefits deriving from the reduction of reproduction problems and, consequently, of days open. Considering the effects related to the above mentioned aspects in a case study involving 60 dairy cows, a return on investment over 5 years has been calculated.

Introduction

One of the major factors influencing the profitability of a dairy herd is reproductive performance. Following mastitis, failure in detection of oestrus is the second largest cause of economic losses to

dairy farmers (Maatje *et al*., 1997). Inefficient detection of oestrus has been found to be the leading cause of extended calving intervals (Rounsaville *et al*., 1979) and the main contributor to the lowering of fertility (Lopez *et al*., 2004). On the contrary, increasing the detection of oestrus reduces days open and increases profitability with a higher impact at lower oestrus detection rates (Pecsok *et al*., 1994).

Farris (1954) first described the increased physical activity of dairy cows during oestrus. Later studies have confirmed that the measurement of the increase in the number of steps is a useful tool for the detection of oestrus, especially if associated with a specific algorithm (Moore and Spahr 1991; Lehrer *et al* 1992; Liu and Spahr 1993; At-Taras and Spahr, 2001; de Mol *et al*., 2001; Firk *et al*., 2002; Roelofs *et al*. 2005).

Many oestrus detection systems are used in attempt to improve conception rates, ranging from the simple visual observation of the animals to more specific systems based on the measurement of the cows' activity through pedometers or collar activity meters (Holman *et al*., 2011). The effectiveness of pedometer-aided detection of oestrus, when compared with visual observation, is quite variable and ranges from 60 to 100%, depending on the study (Lehrer *et al*., 1992). Pennington (1986) reported an efficiency for visual observation of 45% and for pedometers between 78 % and 96%.

Another system for oestrus detection is the analysis of progesterone in milk (Bulman and Lamming, 1978; O'Conner, 1993; Royal *et al*., 2000; Friggens and Chagunda, 2005). In the literature, concentrations less than 3 ng/ml were considered indicative of an oestrus (Lamming and Bulman 1976). In test carried out on Danish dairy herds, an oestrus breakpoint level of 5 ng/ml was determined (Friggens *et al*., 2006).

In 2008 an advanced milk analysis tool (Herd Navigator, DeLaval, Sweden) was developed for heat detection, by measuring progesterone, mastitis detection, by measuring lactate dehydrogenase (LDH), and ketosis detection, by measuring beta-hydroxybutyrate (BHB). This system automatically takes representative milk samples of individual cows from specific milking points during milking and automatically selects, through a specific algorithm called "biomodel", which cows must be monitored and sampled at each milking session, and which parameters should be measured when the animals arrive to the milking parlour (Mazeris, 2010).

Field tests carried out in Denmark between 2008 and 2009 on three farms with more than 150 animals in lactation showed a heat detection rate (HDR) between 95% and 97%, and a conception rate (CR) ranging from 40% to 63%, using Herd Navigator (HN). Moreover, HN reduced the number of days open on an average of 22 days (Blom and Ridder, 2010). Further tests carried out in 2009 on three farms in Denmark and two farms in Holland, with an average of about 180 heads of Holstein Frisian, had showed an HDR between 97% and 100% and an improvement of pregnancy rate (PR) from a minimum of 7.7% to a maximum of 44.4% (Vreeburg, 2010).

The aim of the study was to evaluate the technical and economic benefits on reproductive management deriving from the introduction of HN in a dairy cow farm located in a mountain area of northern Italy and characterized by robotic milking.

Correspondence: Massimo Lazzari, Department of Health, Animal Science and Food Safety, Università degli Studi di Milano, Via Celoria 10, 20133, Milano, Italy.
E-mail: massimo.lazzari@unimi.it

Key words: days open, oestrus detection, proactive herd management.

Journal of Agricultural Engineering 2013; XLIV(s2):e41
doi:10.4081/jae.2013.(s1):e41

Materials and methods

The study was carried out from September 2011 to September 2012 in a dairy cows farm located in a mountain area of Northern Italy (Trentino-Alto Adige). On average, during the experimental period 60 cows (Holstein Frisian and Brown Swiss) were milked with a Voluntary Milking System (VMS, DeLaval, Sweden) and managed through the integrated herd management software DelPro(DeLaval, Sweden). A HN was installed on September 2011.

- HN is basically composed of:
- a milk sampling station, placed within the VMS, to collect milk samples from individual cows;
- an analysis unit, placed into the milking room, to analyse milk samples for progesterone, LHD, and BHB concentrations.

While cows are being milked, representative milk samples are taken and sent, one-by-one, to the analysis unit. A specific algorithm selects which cow to sample during a certain milking session and which parameters to measure. In particular, the prediction of the reproductive status is driven by the progesterone concentrations in milk. HN takes milk samples for progesterone analysis at varying intervals during the heat cycle, especially on the period up to a new event. After a heat the model asks for samples from day 5 to day 14 to asses if the cow is pregnant or has developed a follicular cyst. Further, the model asks for other samples after day 18 in the heat cycle to find the next heat. In cows that are bred the model follows the development in progesterone: if at day 30 after breeding the progesterone concentration is high, the model assumes that the cow is pregnant and follows the cows for the next 25 days to check for pregnancy.

Basic information describing the farm before the installation of HN such as average number of milking cows over the last 12 months, milk yield per lactation, annual culling rate, etc. were collected through the help of the farmer and the veterinarian of the farm.

During the experimental trial the reproductive status of the cows was monitored using HN. A start time of 20 days before the end of the voluntary waiting period (VWP) was set as start for progesterone measurements and when alarms occurred (follicular or luteal cist, pregnancy attention, abortion, etc.) the cows were examined by the veterinarian at the earliest convenience.

A partial budget analysis was carried out to assess the potential savings on reproductive management of dairy cows, as a consequence of the HN installation. The cash flows changes were identified at the HN introduction, and costs and benefits were evaluated over a period of 8 years from HN installation.

Results and discussion

Table 1 summarizes some basic information of the farm involved in the study, before the HN installation. The milk yield level and the difference in milk yield between 3rd and 1st lactation cows are equivalent to the values of the "Po Valley" intensive dairy farms.

The main reproductive data recorded before and after the HN installation are shown in table 2.

The absence of an electronic oestrus identification before the HN installation was the main responsible for the low HDR (45 %) and PR (18 %), and the high number of days open (166 days) recorded in the farm.

After the HN installation a strong improvement of the reproductive performance was observed. In particular the abortion identification reduced from 31 days to 6 days (-80 %), the days from 1st and 2nd insemination decreased of about 38 % (from 45 days to 28 days), while the average days open changed on average by 63 days (from 166 days to 103 days). As a consequence, the HDR has more than doubled (from 45 to 96 %), the CR increased from 40 % to 64 %, and the PR grew strongly from 18 % to about 61 %.

Main benefits and costs related to the reproductive management, resulting from the HN installation, are summarized in Table 3.

Table 1. Farm overview.

Cows in lactation [n]	60
Milk yield level [kg/lactation]	11,000
Difference in milk yield between 3rd and 1st lactation cows [kg]	1,300
Days per year with reduced attention to heats (harvest, holidays etc.) [gg]	90
Annual culling rate [%]	30
Average salary for own work [€/h]	20.00
Milk price [€/kg]	0,40
Average price for heifers - 24 months [€/heifer]	2,000.00
Slaughter price per cow culled due to reproduction problems [€/cow]	500.00
Price per insemination (semen + labour) [€]	23.00
Cost per pregnancy check [€/day]	4.00
Cost per days open [€/day]	€ 2,00
Voluntary waiting period (VWP) [days]	60

Table 2. Main reproductive data before and after the HN installation.

Reproductive data	Before HN installation	After HN installation
No. of pregnancy check per cow per lactation [n]	3.0	1.0
Veterinarian cost [€]	40.00	-
Surveillance of pregnancy check [h/check]	0.04	0.04
Time spent to heat detection [h/days]	1.0	1.0
Avg. of Days In Milk (DIM) at the first insemination [days]	85	65
Days after latest heat for identify luteal cysts (before typically by the time of pregnancy check) [days]	40	20
Cystic cows culled [%]	35.0	5.0
Days after abortion/1st heat [days]	31	6
HDR [%]	45.0	96.0
CR [%]	40.0	64.0
PR [%]	18.0	61.4
Days from 1st to 2nd insemination [days]	45	28
Average days open [days]	166	103

Table 3. Main benefits and costs related to the reproductive management, resulting from HN installation

Benefits	[euro/year]
Increase in average milk yield and less feed due to reduced days open.	7,560.00
Reduced labour	7,300.00
Reduced veterinarian costs	4,800.00
Reduced insemination costs	2,760.00
Reduced cull cows	2,092.50
Total benefits	24,512.50
Costs	
Service and sticks (130 €/year*cow)	7,800.00
Electrical power	547.50
Other	182.50
Total costs	8,530.00

Considering an initial investment of 70,000 € for the HN, a real interest of 1.5 % (net inflation), an estimated shelf life of 8 years, a recovery value of 10% compared to the initial value, and an extraordinary maintenance after 4 years as 10% of the investment value, the following indexes were calculated:

- a five-year Return on Investment (ROI);
- a net annual value of 48,500 €;
- an Internal Rate of Return (IRR) of 15%.

Up to the time in which the test was ended, the other HD function associated to mastitis and ketosis detection do not have shown their utility in improving the herd status probably due to the fact that this last was initially of a good level.

Conclusions

The test has been carried out in a mountain area farm situation in which the herd initial status was characterized by a limited cows number, good milk yield and quite low reproductive indexes. In this specific situation, the HD has shown its capacity to assure a single cow better control that has leaded to an high improvement of the average reproductive indexes. The enhancement of the economic performances related only on this aspect it has been sufficient to guarantee an acceptable ROI value for the economic investment associated to the HD adoption. It can be supposed that these encouraging results would be further improved in the future when the additional management HN management options (LDH analysis for mastitis detection, Urea and RHR for ketosis detection and feeding improvement) will produce their effect on the herd.

References

At-Taras, E.E., Spahr, S.L. (2001). Detection and characterization of heat in dairy cattle with an electronic heatmount detector and an electronic activity tag. J. Dairy Sci. 84, 792–798.

Blom J, Ridder C. (2010). Reproductive Management and Performance Can be Improved by Use of DeLaval Herd Navigator®. The First North American Conference on Precision Dairy Management.

Bulman D.C., Lamming G.E. (1978). Milk progesterone levels in relation to conception, repeat breeding and factors influencing acyclicity in dairy cows. Journal Reproduction Fertility 54, 447–458.

de Mol R.M., Ouweltjes W., Kroeze G.H., Hendriks M.M.W.B. (2001). Detection of estrus and mastitis: field performance of a model. Applied Engineering Agricultural 17, 399–407.

Firk R., Stamer E., Junge W., Krieter J.(2002).Automation of oestrus detection in dairy cows: a review. Livestock Production Science. 75:219–32.

Friggens N.C., Chagunda M.G.G. (2005).Prediction of the reproductive status of cattle on the basis of milk progesterone measures: model description. Theriogenology. 64, 155–190.

Holman A., Thompson J., Routly J. E., Cameron J., Jones D. N., Grove-White D., Smith R. F., Dobson H. (2011). Comparison of oestrus detection methods in dairy cattle. Veterinary Record 2011 169: 47.

Lamming G.E., Bulman D.C. (1976). Use of milk progesterone radioimmunoassay in diagnosis and treatment of subfertility in dairy cows. Br Vet J 132, 507–517.

Lehrer A.R., Lewis G.S., Aizinbud E. (1992). Oestrus detection in cattle: recent developments. Animal Reproduction Science. 28:355–61.

Liu, X., Spahr, S.L., (1993). Automated electronic activity measurement for detection of oestrus in dairy cattle. Journal of Dairy Science 76 (10), 2906–2912.

Lopez H., Satter L.D., Wiltbank M.C. (2004). Relationship between level of milk production and estrous behaviour of lactating dairy cows. Animal Reproduction Science 81:209-223.

Maatje, K., S. H. Loeffler, and B. Engel. 1997. Predicting optimal time of insemination in cows that show visual signs of oestrus by estimating onset of oestrus with pedometers. J. Dairy Sci. 80:1098.

Mazeris F. 2010. DeLaval Herd Navigator® Proactive Herd Management. The First North American Conference on Precision Dairy Management 2010. Toronto, Canada.

Moore A.S., Spahr S.L. (1991). Activity monitoring and an enzyme immunoassay for milk progesterone to aid in the detection of estrus. Journal of Dairy Science 74 (11), 3857–3862.

O'Connor M.L. (1993). Heat detection and timing of insemination for cattle. Penn State University College of Agricultural Sciences. Extension Circular 402, 19

Pecsok, S. R., M. L. McGilliard, and R. L. Nebel. 1994. Conception rates.1. Derivation and estimates for effects of estrus detection on cow profitability. J. Dairy Sci. 77:3008.

Pennington, J. A., J. L. Albright, and C. J. Callahan. 1986. Relationships of sexual activities in oestrous cows to different frequencies of observation and pedometer measurements. J. Dairy Sci. 69:2925.

Roelofs J.B., van Eerdenburg F.J.C.M., Soede N.M., Kemp B. (2005). Pedometer readings for estrous detection and as predictor for time of ovulation in dairy cattle. Theriogenology 64 (8), 1690–1703.

Royal M.D., Darwash A.O., Flint A.P.F., Webb R., Woolliams J.A., Lamming G.E. (2000). Declining fertility in dairy cattle: changes in traditional and endocrine parameters of fertility. Animal Science 70, 487–501.

Rounsaville, T. R., P. A. Oltenacu, R. A. Milligan, and R. H. Foote. 1979. Effects of heat detection, conception rate, and culling policy on reproductive performance in dairy herds. J.Dairy Sci. 62:1435.

Vreeburg N. (2010). Precision Management On Two Dutch Dairy Farms By Use Of Herd Navigator®. The First North American Conference on Precision Dairy Management.

Optimization of sustainable buildings envelopes for extensive sheep farming through the use of dynamic energy simulation

Maria Elena Menconi, David Grohmann

Department Uomo e Territorio, University of Perugia, Italy

Abstract

Extensive sheep farming can be seen as a marginal market, compared to other livestock and agricultural activities, taking into account only the economic absolute values. But for many rural marginal areas within the European Community member states, in particular for those located in the Mediterranean area on hills or mountains with high landscape value, extensive sheep farming is not only the longest practiced animal farming activity, but also the most interesting considering its adaptability to the territorial morphology and the restrictions that have been established over the years in terms of sustainable rural development practices.

At the moment, most of the structures used in this type of farming are built using low cost and sometimes recycled, but often unsuitable, materials. Few specific studies have been carried out on this particular issue assuming, presumably, that the very low profit margins of these activities made impossible any restructuring.

Taken this into account, the new Rural Development Plans that will be issued in 2014 will surely contain some measure dedicated to innovations in farming structures and technology towards facilitating the application of the principles of energy optimization. This is the framework in which the present research has developed.

The software that has been applied to perform the energy optimization analysis is the dynamic energy simulation engine Energy Plus.

A case study farm has been identified in the small village of Ceseggi (PG), situated in Central Italy. For the case study optimum thermo hygrometric conditions have been identified to ensure the welfare of animals and operators and it has been hypothesized the insertion of an ideal HVAC system to achieve them. Afterwards were evaluated the different energy requirements of the building while varying the insulation material used on the vertical surfaces. The greater goal is to verify which could be the best insulation material for vertical surfaces from energy requirement, primary energy and cost points of view and to verify as well if it would be possible to achieve optimum environmental conditions by using only passive solutions.

Correspondence: Maria Elena Menconi, Department Uomo e Territorio, University of Perugia, Italy

Key words: Dynamic energy simulation, sustainable building envelopes, vertical surface insulation, extensive sheep farming.

Journal of Agricultural Engineering 2013; XLIV(s2):e42
doi:10.4081/jae.2013.(s1):e42

Introduction

As a result of sensitization to the issues of energy saving, efficient use of resources and fight against pollution, the trend in European Union regulation is to place more stringent requirements on the energy performance of buildings, (2002/91/EC, 2012/27/EC) acknowledged by the Italian National Energy Strategy (D.lgs 192/2005, D.M. 8/03/2013). Numerous studies have amply demonstrated that the best solutions related to energy conservation should be strongly anchored to the geographical context of reference (Znouda E. et al., 2007; Ihm P. and Krarti M., 2012) and then consider all aspects as the enclosure, the orientation, the shape (Wang K.S.Y. and Yik F.H.W., 2004), the distribution of the functional areas, the materials, the openings, the loads, the energy sources (http://www.activehouse.info/). There are many tools for the verification of the energy performance of buildings that differ in the level of detail required in the input data and then in the ease of obtaining the results and their reliability.

The main distinction is between stationary and dynamics simulations. Stationary simulations use as input data average monthly temperature and radiation, instead simulations carried out under dynamic conditions use as input a weather file that has a hourly scan of the main meteorological variables, allowing much more realistic and complete surveys. Energy Plus is one of the most well-known free software dedicated to the simulation of building energy working under dynamic conditions. This software was elaborated to primarily assess the performance of residential buildings. There are also publications of the same kind for livestock infrastructures, but are mostly dedicated to cattle and swine intensive farming (Jäkel K., 2003; Kraatz S. and Berg W., 2007; Fabrizio E. and Airoldi G., 2012).

Extensive farming, due to its generally lower management costs in comparison with intensive practices, and especially dairy sheep farming, until now has received little attention.

In this paper is used Energy Plus applying it to a dairy sheep farming. Sheep farming can be considered a niche market within the vast framework of agriculture activities, representing just 7% of the European livestock market (European Commission, 2012).

Especially in the last decade, the entire national agriculture production has identified, in quality products, strongly connected with the territorial context in which are produced, their most important resource (ARSIA, 2006). Olive oil and wine have been trailblazer products in this regard and sheep's products (milk, meat and wool) could represent equally important resources for those areas in which they are produced. Extensive sheep farming plays other pivotal roles; one of this

is the territorial protection in marginal rural territories, with a low level governance, otherwise destined to depopulation and abandonment; moreover can be considered one of the livestock activities more sustainable from an environmental point of view (Thompson R., 2009).

The buildings in service of extensive sheep farming are quite heterogeneous in terms of material and geometries (Chiappini U. *et al*., 1994), having been realized in a rather extended period, but it can still be clearly identified a trend toward low cost materials and structures greatly simplified from the design point of view (U.N.A.P.O.C., 1992).

This generally translates into greater difficulties in the control of environmental conditions within the structures and the lack of dedicated HVAC systems also contributes to worsen the problem (Capronese M., 2008).

Most of the contact with the external environment of a building occurs through opaque surfaces such as walls, roof and floor. It is evident the role played by these elements in maintaining comfort in indoor environments. In this regard, for the design of a building so that it can be affected as little as possible by the external conditions and temperature changes or when operating on an existing building, the first option is to intervene on the thermal inertia of the opaque surfaces. The thermal inertia can be increased by using high-density materials, increasing the capacity of accumulation of the heat. It is also possible to intervene with cavities or with insulating coatings, which have a further damping effect of the oscillations of internal temperature. The outer envelope becomes the first element on which is possible to work for improving the energy efficiency of a building.

This paper is focused on existing buildings, exploring the possibilities offered by vertical surfaces in order to identify the best solutions in terms of overall energy savings (reducing building energy consumption and primary energy embodied in the selected materials) and reduction intervention costs.

Material and methods

The developed methodology includes the following steps (Figure 1):

1 Construction of the 3D model of the building. For this purpose is possible to use the free software SketchUp (http://www.sketchup.com/intl/en/download/index.html) that allows you also to define the building orientation with respect to the wind rose.
2 Definition of the thermal zones. Thanks to an interesting plug-in called Open Studio (http://apps1.eere.energy.gov/buildings/energyplus/energyplus/openstudio.cfm) is possible to draw in SketchUp the building directly divided into thermal zones, which are not determined by the internal subdivisions of the building, but by the volumes with constant air temperature (for example, two contiguous rooms maintained at the same temperature are part of the same thermal zone).
3 At this point is possible to import the file into Energy Plus (http://apps1.eere.energy.gov/buildings/energyplus/energyplus_download.cfm), in IDF format, and to characterize the properties of building components (n. layers, materials, layout) 4 - Within the component of Energy Plus called IDF Editor is also possible to define the characteristics of the used materials (thickness, conductivity, specific heat, density).
5 Then internal gain space data must be compiled for every thermal zone (for example for animals housed the internal gain tool requires to divide them into sheep and lambs and to define their level of activity and the timetable of their presence in the stable; similarly for operators; for lighting requires lighting level (W) and switching times; for electric equipment design level and switching timetable; for zone infiltration requires value and method of design of the flow rate)
6 Configuration of an ideal HVAC system that will be used to estimate the margin of improvement of the energy performance of the building. Is important to emphasize that the choice of an ideal system has been made because in real situations, in the sheepfold buildings is not present an HVAC system. The objective is to have a reference value with which to compare the various proposed solutions, with a more ambitious overall goal of verifying the possibility to ensure the optimum environmental conditions (Chiumenti R., 1987) for animals and operators exclusively through design solutions and insulation, without the introduction of an actual HVAC system; The considered optimal and critical temperature ranges are the following:

Sheep	optimal T range 10-17 °C;	critical T range 6-25 °C
Lamb 0-2 weeks	optimal T range 20-22 °C;	critical T range 17-25 °C
Lamb 3-4 weeks	optimal T range 15-18 °C;	critical T range 13-25 °C

7 Acquisition of a weather file for the selected location. The weather data file contains hourly data (8760 data per year) for 27 climate parameters, Numerous weather files are available on the U.S. Department of Energy website (http://apps1.eere.energy.gov/buildings/energyplus/weatherdata_about.cfm?CFID=775268&CFTOKEN=44dffced5c01a022-A76E7BE2-E559-85AF-AD92C8E8EDC0CCBB), once the location is identified (name, latitude, longitude, time zone, elevation) the closest available weather file is selected. The Weather File and the IDF are the two input file of the Energy Plus component EP-launch, this tool allows to run the simulation of the building energy performance for a user-defined period (in this work is one year). Therefore, at this point, it is possible to make a first evaluation of the energy that is required by the building in the current state (defined *reference*) to achieve and maintain during the year the optimum conditions for animals and operators.
8 Construction of alternative IDF models, varying the caulking materials used to insulate the vertical walls, using natural and synthetic materials;
9 Comparison of the various results, in term of total site energy, primary energy and cost, using the Simple Additive Weighting (SAW) multi criteria analysis;
10 Evaluation of the best solutions concerning insulation's options.

Results

Case study

The developed methodology was applied in a dairy sheep livestock farm building. The case study sheepfold is located in Ceseggi, part of the municipality of Sellano (Umbria region- Central Italy) and about 1 km away from the border with the Marche region. The building is situated at south-east of Sellano city and its elevation is 974 m a.s.l..(Figure 2)

The building is organized in three structures: the stable, the milking parlor and the warehouse and occupies a total area of 766 m^2 and a volume of 3648,31 m^3 (Figure 3). The building is exposed to the North-East along the longitudinal axis of the fold, the openings are represented by aluminum doors and by single glass aluminum frame windows. The gross wall area is 732,87 square meters and the windows opening area is 35,84 square meters, with a window-wall ratio of 4,89%. The 3D model of the building is represented in Figure 4.

Construction materials consist of steel for structures such as pillars and trusses, concrete blocks for the infill and concrete slabs for cover.

The sheepfold, at full capacity, can accommodate about 200 sheep. The births take place twice a year, in winter from January to March and during the summer from June to August.

For each of these periods there are approximately 80 births. The sheep are housed the whole day in the stable only in winter; in summer only those with lamb. For the rest of the year all the animals are located in the barn only at night. For the periods from April to June and from September to December, the animals are milked twice a day. For these periods, in the simulations, values of activity level are associated to sheep, lambs and operators (Table 1), in order to identify the internal gain values.

The electric equipment is represented by a pump and a compressor serving the milking parlor and a mill and hay cutting machine in the warehouse.

The selected weather file is the Perugia one.

The choice of the weather file of Perugia represents an approximation and to get more accurate results would be necessary to have a more specific weather file. This choice has been made as, form the available dataset from the U.S. Department of Energy, this Perugia dataset is the best fitting one (http://apps1.eere.energy.gov/buildings/energyplus/cfm/weather_data3.cfm/region=6_europe_wmo_region_6/country=ITA/cname=Italy).

The present work provides the simulation, via Energy Plus, of the thermal behavior of the case study building adding to the vertical opaque surfaces an outer 1 cm layer of plaster and an inner layer of 5 cm of insulation.

The insulating materials to be used as design options have been selected from the Umbria Regional pricing 2012 (http://www.operepubbliche.regione.umbria.it/Mediacenter/FE/CategoriaMedia.aspx?idc=323&explicit=SI) choosing only simple insulating panels for vertical surfaces, which are the most economical solutions available.

The characteristics of the various materials were taken, when pres-

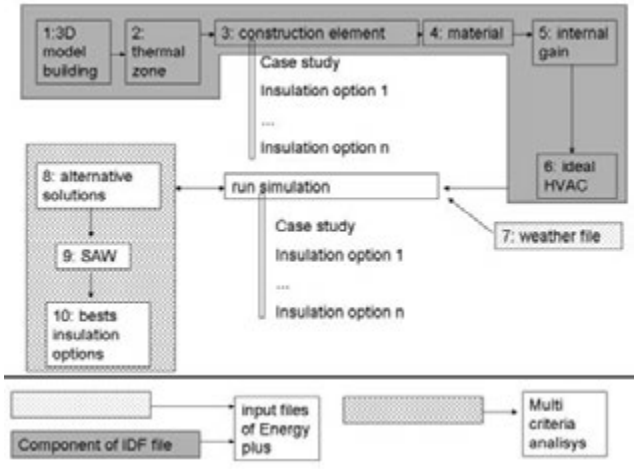

Figure 1. Methodology flowchart.

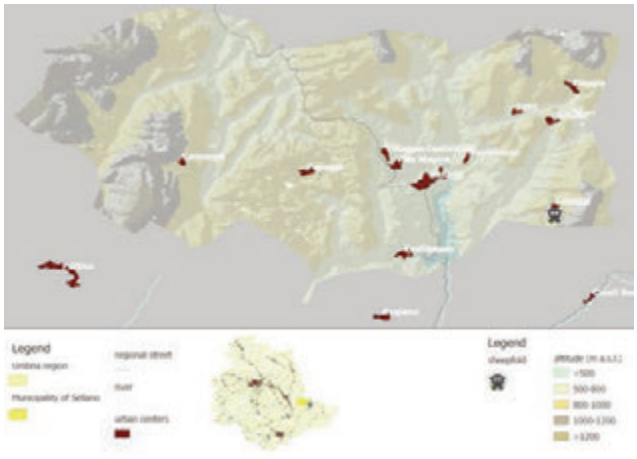

Figure 2. Location of the study case sheepfold.

Table 1. Activity levels

	Activity level w/element
People	216
Sheep	115
Lamb	50

Figure 3. Case study sheepfold.

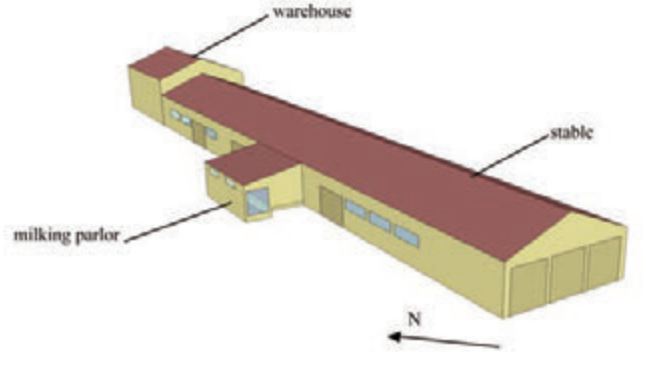

Figure 4. Case study sheepfold 3D model.

ent, always in the same Umbria Regional price list and supplemented by findings from other sources (Rossi M., 2007; Emilia Romagna Regional price list, Chamber of Commerce of Verona price list)

Nine internal insulation materials were evaluated: 5 of natural origin, and 4 of synthetic origin (Table 2).

Discussion of results

The results of the simulation (Figure 5 and 6) show that introducing an insulating layer a substantial energy saving it's achievable, between 10 – 12 %, in term of *Site Energy* (GJ/year), where Site Energy indicates the amount of heat and electricity consumed by the building .

Both synthetic and natural materials, as was to be expected, can achieve excellent results in term of thermal inertia.

Another parameter that should be taken into account is the *Primary Energy Input* (*PEI*) of the various materials, in order to embody in the comparison the sustainability aspects, as well.

PEI is a measure of the non renewable resources consumed for the production of a certain good.

Comparing the Site Energy and the PEI for natural and synthetic materials (fig. 7) it is evident that natural materials have a significant lower embodied energy, which would lead the choice of the most suitable material in their direction. On the other hand, under such difficult economic conditions, every *costs* and supplementary outlay must be carefully considered to avoid overloading the enterprises financial balances. This leads to the difficult task of singling out a price for every material used in the simulations.

The price of construction materials depends by regional price lists that are, generally, updated yearly. In this work the Umbria Regional pricing 2012 is used to define different prices, because the case study building is located in Umbria. One of the simplest multicriteria analysis techniques, the Simple Additive Weighting (Alireza A. *et al*., 2010), can help us identifying the best insulation solution on the basis of these 3 parameters (Site Energy, PEI, cost; Table 3). Its formula is as follows:

$$S_i = \frac{\sum_{j=1}^{n} w_j xi_j}{\sum_{j=1}^{n} w_j} \quad (1)$$

where the counter i is related to the alternatives (the alternative 0 relative to the non-intervention and the other relative to the various insulation materials for the vertical wall) and ranges from 1 to 9, the counter j is related to the considered parameters and varies from 1 to 3, w is the weight assigned to each parameter and x is the value that each alternative i assumes with respect to each parameter j, appropriately normalized. We have chosen to assign to all the parameters the same weight $w_j = 1$, j:1-3, normalizing their values with the minimum and maximum value criterion (equ.2). This linear normalization allows having values evenly distributed inside a closed variation interval [0-1].

$$S_i = \frac{\sum_{j=1}^{n} w_j xi_j}{\sum_{j=1}^{n} w_j} \quad (2)$$

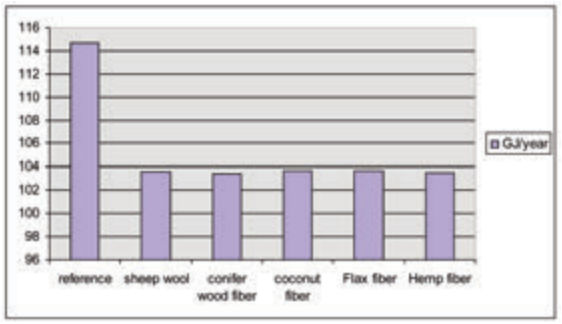

Figure 5. Site Energy results (Energy Plus simulation) for natural materials.

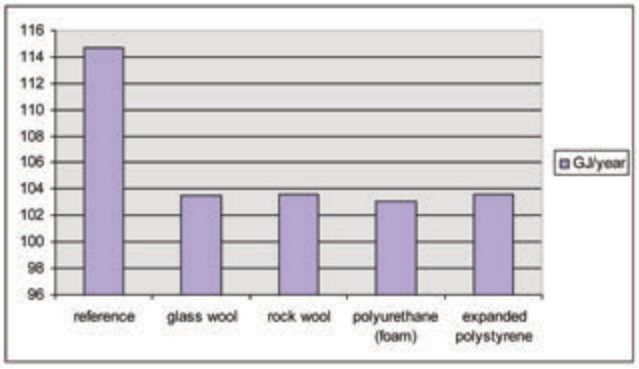

Figure 6. Site Energy results (Energy Plus simulation) for synthetic materials.

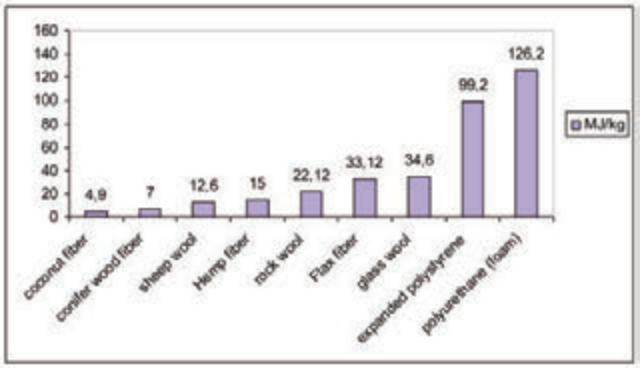

Figure 7. Primary Energy Input.

where y_i are the x_i normalized value, Xmax and Xmin are respectively the maximum and the minimum value of x_i.

From Table 4 it can be seen that, from the multicriteria analysis based on the considered parameters, the rock wool appears to be the best insulating material for the vertical walls of a buildings with the same localization characteristics. This material would be suitable for this type of applications as it's a widely used material with high availability and for its ease of installation.

Conclusions

The results show that by applying a 5 cm insulation internal layer substantial energy savings can be achieved (around 10%), in order to maintain optimal environmental conditions.

The differences between the various materials (around 1 GJ per year) seem to suggest that the most viable solution for this type of building, taking into account the low economic margin of the activity of

Table 2. Material used to change vertical opaque surfaces in the case study.

Material	Thickness (cm)	Origin	Thermal conductivity λ (W/m K)	Density (kg/m3)	Specific heat (J/kg K)
Insulation					
sheep wool	5	natural	0,037	17,9	1720
conifer wood fiber	5	natural	0,04	150	2100
coconut fiber	5	natural	0,043	70	1300
glass wool	5	synthetic	0,032	13,5	850
rock wool	5	synthetic	0,04	80	840
polyurethane (foam)	5	synthetic	0,024	34	1250
expanded polystyrene	5	synthetic	0,036	24	800
Flax fiber	5	natural	0,04	30	1660
Hemp fiber	5	natural	0,039	40	2100
Plaster					
plaster	1		1	1800	910

Table 3. Considered criteria in the SAW analysis. Source of data: Site Energy is an output of Energy plus run simulation, PEI by Colombo (2006) and cost by Umbria Regional pricing 2012.

Insulation alternatives i:1-9	Site Energy (x_1) GJ	PEI (x_2) MJ/Kg	Cost (x_3) euro/m^2
without insulation (reference)	114.72	0	0
sheep wool	103,60	12,6	25
conifer wood fiber	103,44	7	23,25
coconut fiber	103,65	4,9	29,2
glass wool	103,48	34,6	7,2
rock wool	103,62	22,12	8,1
polyurethane (foam)	103,05	126,2	18,88
expanded polystyrene	103,62	99,2	10,26
Flax fiber	103,68	33,12	19,55
Hemp fiber	103,55	15	21,25

Table 4. Simple Additive Weighting Results: S.

Material	Site Energy* GJ/year	PEI* MJ/Kg	Cost* euro/m^2	S
without insulation (reference)	0.00	1.00	1.00	2.00
sheep wool	0.95	0.90	0.14	2.00
conifer wood fiber	0.97	0.94	0.20	2.11
coconut fiber	0.95	0.96	0.00	1.91
glass wool	0.96	0.73	0.75	2.44
rock wool	0.95	0.82	0.72	2.50
polyurethane (foam)	1.00	0.00	0.35	1.35
expanded polystyrene	0.95	0.21	0.65	1.81
Flax fiber	0.95	0.74	0.33	2.01
Hemp fiber	0.96	0.88	0.27	2.11

(* this columns show normalized parameters values)

which are in service, is the most economical, in terms of both materials and labour, and the most sustainable in terms of materials PEI. But we must take into account that the costs, as they have been considered in the work, are related to the initial investment (and therefore refer only to the first year of operation), while the energy savings continue in subsequent years. This consideration is likely to lean toward different materials such as conifer wood fiber that appears to have a better performance of the rock wool, on the basis of the first two evaluation parameters Site Energy and PEI (Table 4). A necessary development of this research should include an analysis of performance variations including interventions on roofs and windows, because acting only on vertical opaque surfaces the objective of lowering to zero the energy requirement of the building, to achieve optimal environmental conditions, is not attainable. It is also clear that could emerge an issue about the feasibility of such interventions, considering the limited profit margins of enterprises with characteristics similar to the study case. These enterprises operate, and have always operated, in the absence of a dedicated HVAC system, and then to simulate its presence may appear to be forced, as we did to obtain the reference value used in the comparison. This choice may seem arbitrary, but it is not in view of the fact that, in the continuous search for improvement of our production facilities, towards greater environmental sustainability, achieving adequate standards, in terms of optimal environmental conditions for operators and animals, should be considered an essential starting point. On the other hand working with the aim of improving the environmental conditions for workers and animals could also led to the improvement of the productivity livestock performances and to the maintenance of high quality standards of products (Sevi A. *et al*., 2001; Sevi A. *et al*., 2003).

In an ideal situation it would be preferable to design the structures from scratch, incorporating in the process, in addition to the aspects listed above relative to the thermal inertia of the enclosure, also structural solutions such as the shape, orientation, and optimal distribution of the functional areas. However, this is often not feasible because of the high costs involved.

Trying to improve the existing structures, also in consideration of the contributions made in this regard by the EU in compliance with the principles of sustainability of the agricultural sector, is an objective actually pursuable.

References

Alireza A., Majid M., Rosnah M.Y., 2010. Simple Additive Weighting approach to Personnel Selection problem. International Journal of Innovation, Management and Technology. 1 (5), 511-515.

Agenzia Regionale per lo Sviluppo e l'Innovazione nel settore Agricolo-forestale (ARSIA) Regione Toscana, 2006. Guida per la valorizzazione dei prodotti agroalimentari tipici (Guide for the valorisation of typical food products). ARSIA.

Capronese M., 2008. Sheep housing and welfare. Small ruminant research. 76, 21-25.

Chiappini U., Fichera R. C., Mennella V., 1994. Metaprogettazione per l'edilizia zootecnica (Meta-design for the livestock building). C.N.R.

Chiumenti R., 1987. Costruzioni rurali (Rural constructions). Edagricole.

Colombo G., 2006. Lo stato dell'arte nella progettazione passiva degli edifici (State of the art in the design of passive buildings). Alinea, Firenze.

European Commission, 2012. Agriculture, fishery and forestry statistics. Main results –2010-11, Eurostat, Retrieved from http://europa.eu;

Fabrizio E., Airoldi G., 2012. Simulazione termoenergetica dinamica di un edificio per l'allevamento suinicolo: strategie edilizie e impiantistiche per l'ottimizzazione del benessere termo igrometrico (Thermo-energetic dynamic simulation of a building for the swine farming: building and plant strategies for optimizing the welfare thermo hygrometric). AIIA 2012, Conference proceedings. Firenze, 20-22 September 2012.

Ihm P., Krarti M., 2012. Design optimization of energy efficient residential buildings in Tunisia. Building and Environment. 58, 81-90.

Jäkel K., 2003. Analyse der Elektroenergieanwendung und Einsparpotentiale am Beispiel sächsischer Milchviehanlagen (Analysis of the electrical energy input and saving potentials at the example of Saxon dairy farms). Forschungsbericht Agrartechnik, 414, Martin-Luther-Universität, Halle/Saale.

Kraatz S., Berg W., 2007. Energy demand for milking dairy cows. Asabe Annual Intl. Meeting, paper n. 074175, Minneapolis.

Rossi M., 2007. Soluzioni tecniche per involucri ad alta efficienza energetica. L'isolamento termico (Technical solutions for high energy efficiency enclosures. The thermal insulation). Costruire. 288, 72 – 76.

Sevi A., Annicchiarico G., Albenzio M., Taibi L, Muscio A., Dell'Aquila S., 2001. Effects of solar radiation and feeding time on behaviour, immune response and production of lactating ewes under high ambient temperature. Journal of Dairy Science. 84, 629-640.

Sevi A., Albenzio M., Muscio A., Casamassima D., Centoducati P., 2003. Effects of litter management on airborne particulates in sheep houses and on the yield and quality of ewe milk. Livestock Production Science. 81, 1-9.

Thompson R., 2009. Sustainability of hill sheep flocks in England, Small Ruminant Research. 86, 71–73.

U.N.A.P.OC. (Unione Nazionale Associazioni Produttori Ovi-Caprini), 1992. Ovinicoltura (Sheep husbandry). UNAPOC.

Wang K.S.Y., Yik F.H.W., 2004. Representative building design and internal load patterns for modelling energy use in residential buildings in Hong Kong. Applied Energy. 77, 69–85.

Znouda E., Ghrab-Morcos N., Hadj-Alouane A., 2007. Optimization of Mediterranean building design using genetic algorithms. Energy and Buildings. 39, 148–153.

Influence of low vacuum levels on milking characteristics of sheep, goat and buffalo

Maria Caria,[1] Carlo Boselli,[2] Lelia Murgia,[1] Remo Rosati,[2] Antonio Pazzona[1]

[1]Dept. of Agraria, University of Sassari, Italy; [2]Istituto Zooprofilattico Sperimentale delle Regioni Lazio e Toscana, Roma, Italy

Abstract

Different settings of the operating parameters (pulsator rate, pulsator ratio and vacuum) are used for milking dairy species in different parts of the world. The level of the operating vacuum in machine milking is one of the principal factors which influence the integrity of the tissues and the milk quality. High vacuum levels (>42 kPa) are often used to facilitate the opening of the teat canal by overcoming the biological closing forces whithin the teat sphincter, but can result in severe machine-induced teat tissue damage. In this study characteristics and performances of mechanical milking at low vacuum levels have been investigated in different dairy species. Milking times and milk productions have been obtained from milk emission curves, recorded by electronic milk-meters (LactoCorder®) during the milking at different vacuum levels of sheep, goats and buffaloes. The results of the comparative experiments clearly indicate that a low vacuum level modifies the kinetics of milk emission, the machine-on time and, thus, the throughput of milking system, in all the dairy species considered. Milk yield was satisfactory at any level tested, showing that low vacuums can be adequate to completely empty the udder. Slight differences were found across species concerning the increase in the milking time per head associated with low levels of milking vacuum Our study represents a contribution to encourage the decrease of the working vacuum during mechanical milking, also for those dairy species generally considered hard to be milked, as buffaloes. Milking should be performed applying the lowest vacuum level, compatible with not excessively prolonging milking time, in line with the animal welfare on dairy husbandry.

Correspondence: Maria Caria, Dept. of Agraria, University of Sassari, viale Italia 39, 07100 Sassari, Italy.
E-mail: mariac@uniss.it

Key words: milking machine, vacuum, sheep, goat, buffalo.

Acknowledgements: t,his study was supported by grants from the MIUR-PRIN 2008 “Valutazione di alcune innovazioni per il miglioramento del benessere, dello stato di salute e della qualità produttiva dei ruminanti da latte”.

Journal of Agricultural Engineering 2013; XLIV(s2):e43
doi:10.4081/jae.2013.(s1):e43

Introduction

There are three operative parameters that regulate mechanical milking: working vacuum, pulsator

rate, and pulsator ratio. In general, the parameters of the pulsations are specific for each species of animal, while the vacuum is regulated on the basis of the type of milking system (high and low level) and the customs of the country and area (Billon *et al*.,1999).

High vacuum levels (>42 kPa) are often used to facilitate the opening of the teat canal by overcoming the biological closing forces whithin the teat sphincter, but can result in severe machine-induced teat tissue damage. These vacuum levels seem to be extremely high when compared with the vacuum needed to open the teat canal in Sarda sheep (26 kPa), Lacaune sheep (25.0 to 35.9 kPa; Marnet *et al*., 1999), the mountain Greek breed Boutsiko (16.59 kPa; Sinapis *et al*., 2007), Saanen goats (34.6 kPa; Le Du and Benmederbel, 1984), and buffaloes (over 30 kPa; Aliev, 1969).

High vacuum levels can cause several undesirable effects in small ruminants, such as an increase in somatic cell count (Sinapis and Vlachos, 1999; Le Du, 1983, 1985; Pazzona and Murgia, 1993) even when combined with a low pulsator rate (Fernandez *et al*., 1999). By contrast, Peris *et al*. (2003) reported that in the short term neither somatic cell count of the milk nor teat thickness changes were affected by differences in vacuum level (36 vs. 42 kPa). It is well known that application of the vacuum slows blood circulation in the teat tissue, thus influencing its temperature. Recent studies (Stelletta *et al*., 2007) have shown that the teat returns to its normal physiological temperature more rapidly if the milking vacuum is reduced. Increase in milking time and increased frequency of the teatcups falling off are the principal negative factors that have up to now discouraged the use of low vacuum (Spencer and Rogers, 1991). In recent years, there has been a tendency to reduce the vacuum level used for milking small ruminants (34 tom 36 kPa). In Sardinia, most systems used for milking sheep and goats operate at vacuum levels between 41 and 44 kPa, with a maximum level of 50 kPa (Pazzona and Murgia, 2003).

A positive relationship between increasing working vacuum and the milk SCC has been found in buffalo (Badran, 1992; Pazzona and Murgia, 1992), which confirms preceding works on cows where raising the vacuum from 33 to over 50 kPa had a negative effect on teat condition (Langlois *et al*., 1980) and increased mastitis incidence (Galton and Mahle, 1980; Langlois *et al*., 1980; Osteras and Lund, 1988). By contrast, increase in milking time and increased frequency of the teat cups falling off are the principal negative factors caused by lowering the milking vacuum level (Spencer and Rogers, 1991). Because little or

no cisternal milk is available in buffalos, the animals are often exposed to a long period of vacuum without any ejection of milk. The use of high-working vacuums combined with the absence of milk can cause irritation in the delicate mammary tissues and, thus, stress the animals (Bruckmaier and Blum, 1996).

Buffalo are considered to be slow and hard milkers (Sastry *et al.,* 1988) because of their slow milk ejection reflex and their sphincter muscle around the streak canal is thicker than in cattle (Stahl Hogberg and Lind, 2003). For these reasons the working vacuum applied to buffalo is generally higher than the level used in cows so as to shorten the milking time. In a recent field survey carried out in 189 installations for buffalo milking in Italy, the working vacuum levels varied from 40 to 53 kPa. The most frequent values (45%) ranged between 44 and 46 kPa, whereas only 4% of the installations were set at ≥50 kPa (Assaociazione Italiana Allevatori in 2009, Rome, Italy, personal communication) .

In line with the current interest in animal welfare, this study investigates characteristics and performances of mechanical milking at low vacuum levels in dairy. sheep, goats and buffaloes.

Materials and methods

Sheep

A prototype milking system specifically designed to optimize vacuum stability and allow low vacuum milking was used in the experiment. The milking parlor prototype was one platform with 24 sequentially gated stalls, with 12 milking units in a low line system. The technical innovation of the prototype is the internal diameter of the milk line, 74 mm instead of 50 mm normally used for sheep (UNI 11008, 2002). The greater diameter of the milk line optimizes the flow conditions even when air suddenly enters, a very common event during sheep milking due to the short milking time for this species (Pazzona and Murgia, 1997). Stabilizing the vacuum in the milking system minimizes the possibility of the clusters falling off (Pazzona and Murgia, 2001). The milking units were assembled from different types of components, chosen taking into consideration both the suitability of the teatcups for the flock and the total mass of the components. This mass was 490 g, the average mass for clusters commonly used in sheep milking, which vary between 390 and 640 g in mass based on our own survey of eight commercial units. The experiment was carried out on 48 pluriparous Sarda breed sheep. The animals were randomly divided into two groups of 24, and one group was assigned the working vacuum of 28 kPa while the other was assigned the 42 kPa. Milking was performed twice daily at 6.00 a.m., and 6.00 p.m.; for the trial the data was recorded one time a day for three months, at the afternoon milking. During the experiment, the operator's work time for each sheep was measured, including access time and downtime. The milking routine was performed by two operators, each of whom managed six milking units. From these data, the throughput of the milk installation, in terms of sheep milked per hour and sheep milked per man hour, was calculated for both low vacuum and standard vacuum (Pazzona *et al*., 2009). The milking routine did not include any form of preparation of the udder or mechanical stripping.

Goats

Comparative tests were carried out to evaluate the effect of the two operative vacuum levels during milking of goats (35 and 44 kPa). Forty Camosciata breed goats were milked in the experiment, using a bucket milking system equipped with two milking units. The data obtained from the test were then used to simulate the milking routine applied in a 12 stalls in a low-line system, equipped with 12 milking units and automatic cluster removal. The throughput of the milking installation and the operator performance, was calculated for both vacuum levels tested, using the mathematical model developed by Caria *et al*. (2011).

Buffalo

A herd of 450 milking Mediterranean breed buffalo, in different parity and stage of lactation, were used in the experiment. The milking system was a 2 × 28 parallel parlor with a low-level milking system equipped with a light-weight (1.80 kg) cluster (Harmony Plus, DeLaval, Tumba, Sweden), automatic cluster removers, and electronic herd management system (Alpro system, DeLaval). The cluster was equipped with conic rubber liners and the pulsator rate was set at 60 cycles/min and 65% ratio. The working vacuum was tested for values of 42 kPa and 36 kPa. Milking took place at intervals of 9 h (daytime) and 15 h (overnight). The milking routine involved the attachment of the milking unit, without any preparation of the udder either by pre-stimulation or pre-dipping, and the manual removal of the teat cups without mechanical or manual stripping. During milking the animals were not given any concentrates. The operator work time for each buffalo was measured, including access time and idle/waiting times. These data allowed us to calculate the throughput of the milking system and the operator performance at vacuums of 36 and 42 kPa (Caria *et al*., 2011).

Equipment used and statistical analysis

For all the experiments carried on, the milking time (the time from attaching to removing the teat cups) and the milk yield were recorded using electronic mobile milk flow meter (Lactocorder®, WMB, Balgach, Switzerland).

Statistical analysis was carried out by comparing the milking time and milk yield between low vacuums and standard vacuums, using a Mann Whitney *U* test from SPSS (ver. 15.0, Chicago, Ill.: SPSS, Inc.).

Results and discussion

Table 1 reports the statistics on milking performances of all the dairy species investigated.

The tests on ewe milking have shown no significative differences on milk production (0.49 kg) when milking at 42 and 28 kPa, while milking time increased ($P<0.01$) passing from 0.94 min to 1.10 min (+17%). This is due to the lower pressure difference across the teat canal exerted by the teatcups on the udder, that lowers the milk flow rate through the teat, prolonging the milking time.

The delay of the milking time for an individual ewe obtained using the vacuum of 28 kPa do not affect so consistently the total session milking time, when the operator managing 6 milking units. The throughput of milking system obtained by specific equations (Pazzona *et al*., 2009) shows a little difference between the two levels of vacuum: 333 sheep/h at 42 kPa *vs* 321 at 28 kPa (Table 2).

In goats, in contrast to what is observed in ewes, both the time and the milk produced per milking were increased when lowering the vacuum from 44 to 35 kPa. As a consequence, also for this specie the throughput of the milking system, equipped with automatic cluster removals, as hypothesized in this study, resulted lower than 12 goats/h (-7%) using the vacuum of 35 kPa (Table 2). The difference between the average milk yield/goat per milking was statistically different at the two vacuum levels: 1.24 kg at 35 kPa and 1.05 kg at 44 kPa). These values could be interpreted as the longer milking time due to low vacuum level allows to remove both the cisternal and alveolar milk.

The response of buffaloes to the decrease in milking vacuum was

Table 1. Mean milk production and milking time per all dairy species studied for 2 vacuum levels tested.

	Sheep		P	Goat		P	Buffalo		P
Vacuum (kPa)	28	42	-	35	44	-	36	42	-
N	108	117	-	335	323	-	192	288	-
Milk yield (kg)	0.49	0.49	N.S.	1.24	1.05	< 0.01	3.6	4.1	N.S.
SE	0.01	0.01	-	0.02	0.02	-	0.15	0.14	-
Milking time (min)	1.10	0.94	< 0.01	2.51	2.13	< 0.01	8.13	7.36	< 0.01
SE	1.61	1.49	-	0.04	0.04	-	0.34	0.24	-

similar to ewes. Comparison of the milk yield was not statistically different at the two vacuum levels (Table 1). The average values obtained during our tests, 3.6 kg/milking at 36 kPa and 4.1 kg/milking at 42 kPa, mirror the data recorded in previous studies (Bava and Zucali, 2007; Borghese *et al*., 2007). The high variability in individual milk production was related to the presence of animals at different stages of lactation.

During the whole milking session, the duration of each phase of the routine was analyzed, to define the operator performance and the milking system throughput as a function of the individual milking time at the working vacuums of 36 kPa and 42 kPa (Table 2). The optimal number of milkers is calculated to ensure the presence of the operator at the end of milking of the first buffalo that has had the clusters attached.

Referring to the 28 + 28 stalls milking system and to the results obtained from the milk curves, the model was applied to a milking routine without pre-stimulation or post-milking treatment, stripping of the udders, and the use of automatic cluster removers set at 0.20 kg/min. Considering 2 milkers, the total herd milking time resulted in 3.25 h at 42 kPa of vacuum and 3.36 h at 36 kPa, corresponding to a throughput of the milking system (*Co*) of 139 and 134 buffalo/h, respectively. Operator performance *(P)* is 69 buffalo/man-hour, at a vacuum of 42 kPa and 67 buffalo/man*hour at a vacuum of 36 kPa, with a difference of 2 buffalo/man*hour.

These results clearly showed that even a vacuum of 36 kPa is more than enough to guarantee that the teat canal opens. By contrast there was a significant increase in milking time (0.77 min) due to a longer latency time and a prolonged time for the complete emptying of the udder. Anyhow, this aspect should be taken into account considering that the duration of milking in cows seems to influence teat tissue reactions less than the high vacuum (Hamann *et al*., 1993). In farms where the latency time could be shortened by inducing milk let down through pre-stimulation of the udders along with feeding concentrate in parlor, the use of a low milking vacuum level might represent an appropriate choice, considering the advantages which it offers in terms of animal health and well-being.

Table 2. Throughput of milking system and operator performance at different vacuum levels as a function of the routine.

	Sheep[1]		Goat[2]		Buffalo[3]	
Vacuum (kPa)	28	42	35	44	36	42
Co (heads/h)	321	333	152	164	134	139
P (heads/man*h)	161	166	152	164	67	69

Co = throughput of the milking system; P = operator performance. [1]Two milkers; [2]One milker; [3]Two milkers.

Conclusions

The results of the study concerning the effects of dairy milking at low vacuum levels on both milk emission parameters and milking parlour throughput showed that:

- Considerations concerning the effect of vacuum setting on the milking time and consequently the throughput of the milking system, are similar for all three dairy species examined.
- The milking time for small ruminants increased on average by 17.0 – 17.8% using the lower levels of vacuum. In buffalo the milking time increased by just 10.5%, probably because of the difference between the vacuum levels tested, that was 6 kPa for this specie instead of 14 and 9 kPa, respectively for sheep and goats.
- As a consequence, the efficiency of milking routine was also influenced by the level of working vacuum. When reduced, it slightly affected the throughput of milking system and the operator performance. The Co was decreased of about 12 heads/h, corresponding to 3.6 and 7.3% for sheep and goats respectively. In buffalo milking, the Co was reduced of about 3.6%, corresponding to about 7 minutes increase in the time spent for the whole milking session. This short time does not compromise the management of the milking and the farm labour organization, considering that the use of automatic cluster removal strongly reduces the milking time.
- The results obtained show that the choice of setting the milking vacuum at a lower level than those commonly used, for all the species investigated, is not compromised by the slight decrease of throughput, especially if the amount of milk yield per milking is the same as found in sheep and buffalo or even higher (+18%, P<0.01, in goats).

References

Aliev, M. G. 1969. Physiology of machine milking of buffaloes. Dairy Science Abstr. 32:329–332.

Badran, A.E.1992. Effect of vacuum and pulsation rate on milking ability in Egyptian buffaloes. Buffalo J. 1:1–7.

Bava L., Zucali M. 2007. Una buona mungitura con una giusta routine. Informatore Zootecnico 18:156–169.

Billon P., Ronningen O., Sangiorgi F., Schuiling E. 1999. Quantitative requirements of milking installations for small ruminants: Survey in different countries. In Proc. 6th Intl.Symposium in Machine Milking of Small Ruminants: Milking and Milk Production of Dairy Sheep and Goats, 209-215.

Borghese A., Mazzi M., Rosati R., Boselli C. 2007. Milk flow pictures in Mediterranean Italian buffaloes, through LactoCorder instrument. pp 60-63 in Proc. Int. Symp. Teagasc/IDF on advances in milking, Cork, Ireland.

Bruckmaier R. M., Blum J. W. 1996. Simultaneous recording of oxytocin release, milk ejection and milk flow during milking of dairy cows with and without prestimulation. J. Dairy Res. 63:201–208.

Caria M., Murgia L., Pazzona A. 2011. Effects of the working vacuum level on mechanical milking of buffalo. J. Dairy Sci. 94: 1755-1761.

Fernandez N., Diaz J. R., Peris C., Rodriguez M., Molina M. P., Torres A. 1999. Machine milking parameters for the Manchega sheep breed. Pages 233–238 in Proc. Sixth International Symposium in Machine Milking of Small Ruminants, Athens, Greece. European Association for Animal Production (EAAP) Publication no. 95. Wageningen Academic Publishers, Wageningen, the Netherlands.

Galton D. M., Mahle D. E. 1980. Effects of vacuum level and pulsation ratio on udder health. Proc. Annu. Mtg. Nat. Mastitis Council Inc. 19:39–43.

Hamann J., Mein G. A., Wetzel S. 1993. Teat tissue reactions to milking: Effects of vacuum level. J. Dairy Sci. 76:1040–1046.

Langlois B. E., Cox J. C., Hemken R. W., Nicolai J. 1980. Effect of milking vacuum on some indicators of bovine mastitis. J. Dairy Sci. 63(Suppl. 1):116–117.

Le Du J. 1983. Comparaison d'un lactoduc en ligne haute et en ligne basse: Incidence sur la traite des brebis de races Lacaune et Manech. Ann. Zootech. 32: 43-52.

Le Du J., Benmederbel B. 1984. Aptitude des chevres de race Saanen a la traite mecanique: Relation avec les caracteristiques physiques du trayon. Ann. Zootech. 33: 375-384.

Le Du J. 1985. Parametres de fonctionnement affectant l'efficacite des machines a traire pour brebis et chevres. Pages 430–431 in 36eme Reunion Annuelle F.E.Z., Ed. Giahoudi Bros Publication, Thessalonique, Grece.

Marnet P. G., Combaud J. F., Dano Y. 1999. Relationships between characteristics of the teat and milkability in Lacaune sheep. In Proc. 6th Intl. Symposium in Machine Milking of Small Ruminants: Milking and Milk Production of Dairy Sheep and Goats, 41-44

Osteras O., Lund A. 1988. Epidemiological analyses of the associations between bovine udder health and milking machine and milking management. Prev. Vet. Med. 6:91–108.

Pazzona A., Murgia L. 1992. Effect of milking vacuum on leucocyte count in buffalo milk. Pages 691–694 in Proc. 24th International Conference on Agricultural Mechanization, Zaragoza, Spain.

Pazzona A., Murgia L. 1993. Effetto del vuoto di mungitura e delle frequenze di pulsazione sulla carica leucocitaria del latte di pecora. L'Informatore Agrario 42:43–46.

Pazzona A., Murgia L. 1997. Dimensionamento e prestazioni del lattodotto nelle mungitrici per ovini. L'informatore Agrario 8: 89 93.

Pazzona A., Murgia L. 2003. Stato attuale degli impianti per la mungitura di ovini e caprini. Informatore Zootecnico, Supp. No.12: 42-50.

Pazzona A., Caria M., Murgia L. 2009. Effects of a low vacuum level on vacuum stability and milking parlor performance for sheep. Trans. ASABE 52:247–252.

Peris C., Diaz J. R., Balasch S., Beltran M. C., Molina M. P., Fernandez N.. 2003. Influence of vacuum level and overmilking on udder health and teat thickness changes in dairy sheep. J. Dairy Sci. 86(12): 3891 3898.

Sastry N. S. R., Bhagat S. S., Bharadwaj A. 1988. Aspects to be considered in milking management of buffaloes. Indian J. Anim. Prod. Manag. 4:378–393.

Sinapis E., Vlachos I. 1999. Influence du niveau de vide de la machine a traire et des facteurs zootechniques sur le comptages de cellules somatiques chez les chevres locale grecque. Pages 513–518 in Proc. Sixth International Symposium in Machine Milking of Small Ruminants, Athens, Greece. European Association for Animal Production (EAAP) Publication no. 95. Wageningen Academic Publishers, Wageningen, the Netherlands.

Sinapis E., Marnet P. G., Skapetas B., Hatziminaoglou I. 2007. Vacuum level for opening the teat sphincter and the change of the teat end wall thickness during the machine milking of mountainous Greek breed (Boutsiko) sheep. Small Rumin. Res. 69(1/3): 136-143.

Spencer S. B., Rogers G. W. 1991. Effect of vacuum and milking machine liners on liner slip. J. Dairy Sci. 74:429–432.

Stahl Hogberg M., Lind O. 2003. Milking the buffalo. Buffalo milk production. Ari. Lic. Animal Husbandry, Department of Nutrition and Management, Sweden.

Stelletta C., Murgia L., Caria M., Gianesella M., Pazzona A., Morgante M. 2007. Thermographic study of the ovine mammary gland during different working vacuum levels. In Proc. ASPA XVII Congress. Italian J. Animal Sci. 6(supp. 1): 600.

UNI 11008. 2002. Impianti per la mungitura meccanica delle specie ovina e caprina. Milan, Italy: Ente Nazionale Italiano di Unificazione.

Biodegradable films and spray coatings as eco-friendly alternative to petro-chemical derived mulching films

G. Vox,[1] G. Santagata,[2] M. Malinconico,[2] B. Immirzi,[2] G. Scarascia Mugnozza,[1] E. Schettini[1]

[1]Department of Agricultural and Environmental Science (DISAAT), University of Bari, Bari, Italy; [2]Institute of Chemistry and Technology of Polymers, CNR, Pozzuoli, Naples, Italy

Abstract

The use of plastic mulching films in horticulture causes the serious drawback of huge amount of wastes to be disposed of at the end of their lifetime. Several pre-competitive research products based on raw materials coming from renewable sources were recently developed to be used as biodegradable materials for soil mulching. Biodegradable materials are designed in order both to retain their mechanical and physical properties during their using time and to degrade at the end of their lifetime. These materials can be integrated directly in the soil in order to biodegrade because the bacterial flora transforms them in carbon dioxide or methane, water and biomass. The innovative materials can be obtained using natural polymers, such as starch, cellulose, chitosan, alginate and glucomannan. Biodegradable extruded mulching films were performed by means of thermo-plasticizing process. Spray mulch coatings were realized directly in field, by spraying water solutions based on natural polysaccharides, thus covering the cultivated soil with a protective thin geo-membrane. In this paper an overview on the formulation development, processing understanding, field performance, mechanical and radiometric properties of these innovative materials for soil mulching is presented. In field the biodegradable mulching films showed suitable mechanical properties if compared to the low density polyethylene films. The radiometric properties and their effect on the temperature condition and on weed control in the mulched soil were evaluated too. At the end of their lifetime the biodegradable materials were shattered and buried into the soil together with plants.

Correspondence: Evelia Schettini, Department of Agricultural and Environmental Science (DISAAT) – University of Bari, via Amendola 165/A - 70126 Bari, Italy, giuliano.vox@uniba.it
E-mail: evelia.schettini@uniba.it

Key words: spray technique, polysaccharides, eco-sustainability, mechanical properties.

Acknowledgements: the research described has been carried out under the project EC RTD QLRT 'Environmentally friendly mulching and low tunnel cultivation - Bioplastics' (Contract n° QLK5-CT-2000-00044) and under the project LIFE Environment "Biodegradable coverages for sustainable agriculture - BIO.CO.AGRI" (LIFE03 ENV/IT/000377), both funded by the European Commission.
The experimental tests, the data processing and the editorial work must be shared, within the competencies of the research groups, equivalently among the Authors.

Journal of Agricultural Engineering 2013; XLIV(s2):e44
doi:10.4081/jae.2013.(s1):e44

Introduction

Synthetic petro-chemical based mulching films are worldwide used in agriculture to suppress weed, to reduce the loss of moisture from the soil, to preserve the plants and the edible products from the soil diseases and from the dirt. The main advantages of the plastic mulches are the decrease of the use of chemicals in weed control, the reduction of water consumption, the faster crop development, the improvement of the plants health and of the yield quality. In intensive cultivation low density polyethylene (LDPE) mulching films are commonly used for their mechanical and thermo-optical properties, chemical and microbial degradation resistance, easy processability and low cost. Opaque mulching films do not allow photosynthetically active radiation (PAR) passing through thus preventing weed growth, while transparent mulches warm the substrate hastening early growth and blooming. At the end of their lifetime the plastic films must be removed with high cost for the growers and with environmental negative consequences connected to their collection, disposal of and recycling process.

In order to develop eco-friendly alternatives to synthetic petro-chemical polymers, novel biodegradable materials have been developed using raw materials from renewable origin. The biodegradable materials have to retain their mechanical and physical properties while in use and must be biodegradable or compostable at the end of their life, degrading via micro-organisms into carbon dioxide or methane, water and biomass. These materials can be obtained by means of thermal film forming processes, casting and spraying techniques.

Biodegradable mulching films can be made by thermo-plasticizing film forming process, using natural or synthetic biodegradable polymers such as starch, poly(lactic acid) (PLA) or polyvinyl alcohol (PVOH) as raw material. Starch based films (Mater-Bi, Novamont Co., Novara, Italy) have been successfully tested (Bastioli, 1998; Briassoulis, 2006a, 2006b, 2007; Martin-Closas *et al*., 2008; Scarascia *et al*., 2004; Scarascia *et al*., 2006; Vox and Schettini, 2007; Malinconico *et al*., 2008), but their cost was higher than the cost of LDPE films.

Biodegradable mulching coatings can be made by spraying water solutions directly in field thus covering the soil with a protective thin geo-membrane. The water solutions are based on natural polysaccharides, such as sodium alginate, galactomannan, chitosan and cellulose (Schettini *et al*., 2007; Schettini *et al*., 2013; Immirzi *et al*., 2009), and on hydrolyzed proteins (Sartore *et al*., 2013).

This paper investigates the formulation development, processing

understanding, field performance and the mechanical properties of starch-based extruded films and spray mulching coatings. These biodegradable mulches, prepared using natural polymers, were tested in field also in order to verify if they accomplish the mulching task of weed control and if they have the required lifetime.

Materials and methods

Biodegradable mulching films and water-born spray coatings were tested at the experimental farm of the University of Bari from 2001 to 2005 (Scarascia *et al*., 2004; Schettini *et al*., 2007; Vox and Schettini, 2007). The biodegradable mulches and commercial LDPE films, used as control, were applied inside greenhouses, under low tunnels and in open-air; they varied in thickness and colour, as shown in Table 1.

The use of biodegradable films and spray coatings did not require any particular change in agronomical practices. The soil preparation, such as ploughing and tilling, do not differ for the application of an extruded film or a spray coating (Malinconico *et al*., 2008). The soil and the growing media should be without residues of previous cultivations and large size stones; the surface should be flat to prevent holes and cracks of the film or coating, which can facilitate weed growth. Drip irrigation, irrigation by hose and by porous tube, which are the irrigation methods used in presence of plastic mulching films, were also suitable for the biodegradable mulches. The agrochemical products, such as fertilizers, insecticides, fungicides, herbicides and so on, were employed both for biodegradable mulches and for LDPE films in the same period and at the same doses.

The starch-based raw material (Mater-Bi, Novamont Co., Novara, Italy) was extruded using the LDPE film extrusion line with minor modifications (Briassoulis, 2006b, 2007). The films tested varied in different kind and quantity of biodegradable master batches and of stabilizers used, with a percentage not revealed since these formulations are proprietary. As done for LDPE films, the installation of biodegradable mulching films in field was performed by machine (Figure 1) or manually.

An innovative approach of mulch forming is the use of the spray methodology (Figure 2; Malinconico *et al*., 2008). Polysaccharides, as agarose, galactomannans (guar gum, locust bean gum) and sodium alginate, are chosen as basic ingredients of the water-born solutions for their biodegradability, biocompatibility and non-toxicity and for their intrinsic properties to form water resistant coatings (Avella *et al*., 2007; Mormile *et al*., 2007). In order to improve the mulching function and the tensile strength of the spray coating, fillers (cellulose fibres, carbon black, fine bran of wheat and powdered seaweeds), plasticizing polymers (hydroxyethylcellulose), and natural plasticizers (glycerol and polyglycerol) were mixed to the polymeric matrices. Three different spray mulching coatings were developed (Malinconico *et al*., 2008) and the polysaccharides concentration used determined coating's thickness and lifespan. The coating coded MY consisted of a water mixture of locust bean gum and guar gum (PSS20 Protective Surface System, PSI Polysaccharide Industries AB, Stockholm, Sweden), with a concentration of about 1.5% of each component with the addition of a non-gelling concentration of agarose. To this blend 1.5% of glycerol and 2% of carbon black were added; the latter was added to the water solution to make the coating opaque to the PAR radiation in order to control the weed growth (Figure 2(a)). The coating coded MC was based on PSS20

Figure 1. Mechanical installation for soil mulching of the biodegradable melt-extruded film for a low-tunnel cultivation at the experimental farm of the University of Bari (Italy).

(a) (b)

Figure 2. Soil mulching made by means of spraying techniques applying biodegradable water-born solutions: MY on soil raised beds inside a greenhouse (a) and MA on the growing media in a cultivation carried out in pots (b).

Table 1. Biodegradable and LDPE extruded mulching films and biodegradable water-born spray coating tested at the University of Bari.

Code	Technique	Raw material	Colour	Thickness (µm)
MB1	Extrusion	Mater-Bi	Black	50
MB2	Extrusion	Mater-Bi	Black	25
MB3	Extrusion	Mater-Bi	Black	15
MP1	Extrusion	LDPE	Black	40
MY	Spray	PSS20, carbon black	Black	18-35
MC	Spray	PSS20, cellulose paper	White	1500-2500
MA	Spray	Sodium Alginate, seaweeds, bran of wheat	Brown	3000-5000

formulation added with cellulose fibres, able to improve the mechanical resistance of the coating in wet environment, by forming a polymeric texture. Under wetting conditions the MC coating could follow the ground shape withstanding the forces of cracking soil due to the plasticizing action of water. The coating coded MA was developed by using sodium alginate for 33%, hydroxyethylcellulose for 17% and polyglycerol for 50%. This blend was sprayed on the soil, which was previously covered with a pulverized mixture of seaweeds flour and fine bran of wheat in order to improve the mechanical response of the coating.

The three water-born solutions were applied by means of an airbrush, using a high pressure spray machine, commonly employed in agriculture. The side slope of raised beds should be limited in order to avoid a possible sliding of the water-born coating at the liquid state during the spraying before the dry process (Figure 2 (a)). In pot cultivation the level of the growing media must be lower than the edge of the pot in order to contain the spray coatings (Figure 2(b)). In presence of plants a protection must be used to maintain plants clean during the spraying (Figure 3). In case of seeds or bulbs sowed before the spraying, buds hole the coatings without any problem (Figure 4) while seedlings transplanting can be performed holing the coating when the drying process of the coating is completed.

After the harvests, the biodegradable films and water-born coatings were shattered together with the plants, by means of tilling machine, in order to accelerate the degradation process by the action of the microorganisms (Figure 5).

Mechanical laboratory tests were carried out at ICTP on samples of the biodegradable and LDPE mulching films taken before their installation, and on laboratory samples of the water-born biodegradable coatings, obtained spraying the water-born solutions on glasses and peeling them once dried. Mechanical properties play a fundamental role for mulches, influencing their durability and functionality. The tensile stress and strain at break for the LDPE, the biodegradable films and the MY water-born coating were measured by a dynamometer (Instron Mod. 4301), in accordance with the ISO 5893 standard (ISO 5893, 2002). For each sampling five specimens, obtained with a regular punch cutter and with the dimension of 0.5 cm x 2.5 cm, were tested at room temperature, at crosshead rate of 10 mm min-1 and at relative humidity equal to 35 %.

The MA and MC water-born coatings were not self-standing materials but they took their support from the soil beneath, thus the mechanical characterization of the MA and MC coating samples was not feasible with the dynamometer and it was carried out by the "puncture test", an empiric test described by Malinconico *et al* (2008). The puncture test consists in penetrating the specimens with a spherical dart that, moving at constant rate, pierces the samples until the laceration of the same; for this kind of empirical test, the maximum load (N) as a func-

Table 2. Mechanical properties of the biodegradable and LDPE extruded mulching films and of the MY biodegradable water-born coating.

	Young Modulus (MPa)	Tensile stress at break (MPa)	Tensile strain at break (%)
MB1	246 (± 20%)	11 (± 20%)	380 (± 30%)
MB2	456 (± 20%)	11 (± 20%)	262 (± 30%)
MB3	265 (± 20%)	18 (± 20%)	255 (± 30%)
MP1	270 (± 13%)	20 (± 20%)	578 (± 30%)
MY	48.8 ± 6.4	2.45 ± 0.21	4.10 ± 1.2

Figure 3. Soil mulching with the MA biodegradable water-born coating realised by means of spraying techniques in a cultivation carried out in pots at the experimental farm of the University of Bari (Italy).

Figure 4. Emergence of bulbs sowed before the spraying, in a cultivation carried out in pots at the experimental farm of the University of Bari (Italy).

tion of the displacement (mm) was recorded. For each time of samples drawing out, seven specimens were tested.

Results and discussion

The average values of the tensile stress and strain at break, and of the Young Modulus relative to the biodegradable and LDPE mulching films and to the MY water-born coating are reported in Table 2. The mechanical tests were carried out in the longitudinal direction (extrusion direction) because in this direction the tensile properties of the biodegradable films vary more regularly than in transversal direction. This was probably due to the anisotropy of biodegradable material respect to the enhanced regular macromolecular organization of LDPE film.

The thickness of the MY water-born coating varied from 18 to 35 µm, due to the presence of carbon black whose distribution was not homogeneous. The biodegradable films and the MY coating showed lower values of tensile stress and strain at break than the value obtained for the MP1 LDPE film (Table 2). The MB2 biodegradable mulching film was characterised by the highest value of the Young Modulus, equal to 456 MPa, while the MY coating by the lowest value of tensile stress at break (2.45 MPa), of tensile strain at break (4.10 %) and of the Young Modulus (48.8 MPa). According to the EN 13655 (EN 13655, 2003), black LDPE mulching films must have a tensile stress at break higher than 16 MPa and a tensile strain at break higher than 180-250%, being the above range a function of the thickness. Even though the values of the tensile stress at break evaluated for the MB1 and MB2 black biodegradable films were lower (Table 2), their mechanical properties were sufficiently in the range necessary to be installed and to be used from planting to harvesting applying the same cultivation techniques currently used for LDPE mulching films (Vox *et al*., 2005; Briassoulis, 2006a; Scarascia Mugnozza *et al*., 2006; Malinconico *et al*, 2008).

The mechanical properties of the MC and MA water-born coatings, i.e. the maximum load and the displacement evaluated by means of the "puncture test", are reported in Table 3. The MC and MA coatings were characterised by inhomogeneous surfaces and irregular thickness: the MA coating had a thickness from 3000 to 5000 µm while the MC coating from 1500 to 2500 µm. The mechanical performance was adequate for their durability and functionality from planting to harvesting.

The biodegradable mulching films and the water-born coatings created a physical barrier to prevent airborne weed seeds.

The MB1 and MB2 films lasted 9 months during a strawberry cultivation (Scarascia Mugnozza *et al*., 2006) and MB3 was used for 5 months during a melon cultivation (Vox *et al*., 2005). The Mater-Bi mulching films recorded a lifetime longer than the one of other biodegradable films reported in literature: from 2 to 5 months when Mater-Bi mulching films are used in an open-air cultivation (Novamont, 2007); 1.5 months for a Mater-Bi mulching film of 18 m (Martin-Closas *et al*., 2002); 3 months for a copolyester biodegradable mulching film (Tocchetto *et al*., 2002), and 3.5 months for a modified starch polymer blended with aliphatic polyesters (Halley *et al*., 2001).

The MA and MC coatings lasted for 6 months and the MY coating for almost 5 months. These water-born coatings can be compared in literature to a sprayable mulch colour synthetic latex film (Mahmoudpour and Stepleton; 1997) and to a biodegradable polymeric mulching spray coatings based on hydrolyzed proteins (Sartore *et al*., 2013). The sprayed mulch described by Mahmoudpour and Stepleton (1997) was used in open air and it was damaged after two weeks after their application due to a hail storm. The mulching coating based on hydrolyzed proteins remained continuous and regular for 9 months keeping its mulching effect with few irregularities on the surface around the plants, where water was delivered by the drip irrigation system (Sartore *et al*., 2013).

Table 3. Mechanical properties of the MA and MC water-born coatings.

	Maximum load (N)	Displacement (mm)
MA	3.4±1.6	1.058±0.015
MC	122.5±2.3	0.408±0.030

Figure 5. Shattering by a milling machine of biodegradable mulching films at the end of the cultivation at the experimental farm of the University of Bari (Italy).

Conclusions

The employment of biodegradable materials based on renewable raw sources represent a valid challenge for the development of eco-friendly materials able to compete with petro-chemical polymers due to their sustainability and inexhaustibility. The biodegradable starch-based extruded films and the biodegradable sprayable water-born polysaccharides based coatings had mechanical properties and field performance comparable to low density polyethylene mulching films. Future research will be particularly addressed at improving the mechanical properties, in order to lengthen their lifetime and also to produce films having a higher roll width.

References

Avella M., Di Pace E., Immirzi B., Impallomeni G., Malinconico M., Santagata G. 2007. Addition of glycerol plasticizer to seaweeds derived alginates: Influence of microstructure on chemical–physical properties. Carbohyd Polym 69 (3): 503-511.

Bastioli C. 1998. Properties and applications of Mater-Bi starch-based materials. Polym Degrad Stabil 59: 263-272.

Briassoulis D. 2006a. Mechanical behaviour of biodegradable agricultural films under real field conditions. Polym Degrad Stabil 91 (6):

1256-1272.
Briassoulis D. 2006b. Mechanical performance and design criteria of biodegradable low-tunnel films. J Polym Environ 14 (3): 289 - 307.
Briassoulis D. 2007. Analysis of the mechanical and degradation performances of optimised agricultural biodegradable films. Polym Degrad Stabil 92 (6): 1115-1132.
EN 13655 2003. Mulching thermoplastic films for use in agriculture and horticulture. CEN - European Committee for Standardization, Bruxelles.
Halley P., Rutgers R., Coombs S., Kettels J., Gralton J., Christie G., Jenkins M., Beh H., Griffin K., Jayasekara R., Lonergan G. 2001. Developing biodegradable mulch films form starch-based polymers. Starch 53: 362-367.
Immirzi B., Santagata G., Vox G., Schettini E. 2009. Preparation, characterisation and field testing of a biodegradable sodium alginate-based spray mulch. Biosyst Eng 102: 461 – 472.
ISO 5893 2002. Rubber and plastics test equipment - Tensile, flexural and compression types (constant rate of traverse) – Specification. International Organization for Standardization.
Mahmoudpour M. A., Stepleton J. J. 1997. Influence of sprayable mulch colour on yield of eggplant (Solanum melongena L. cv. Millionaire) Sci Hortic 70 (4): 331-338.
Malinconico M., Immirzi B., Santagata G., Schettini E., Vox G., Scarascia Mugnozza G. 2008. Chapter 3: An overview on innovative biodegradable materials for agricultural applications in "Progress in Polymer Degradation and Stability Research", H. W. Moeller Editor, Nova Science Publishers, Inc. NY USA, ISBN: 978-1-60021-828-6: 69-114.
Martin-Closas L., Soler J., Pelacho A. M. 2002. Effect of different biodegradable mulch materials in an organic tomato production system. Proc. "Biodegradable materials and natural fibre composite in agriculture and horticulture". Hannover, Germany, 2-4/06/2002. p. 78-85.
Martin-Closas L., Pelacho A.M., Picuno P., Rodríguez D. 2008. Properties of new biodegradable plastics for mulching, and characterization of their degradation in the laboratory and in the field. Acta Horticulturae 801(1): 275-282
Mormile P., Petti L., Rippa M., Immirzi B., Malinconico M., Santagata G. 2007. Monitoring of the degradation dynamics of agricultural films by IR thermography. Polym Degrad Stabil 92: 777-784.
Novamont. 2007. Mater Bi. http://www.materbiagro.com/ing/caratteristiche.html
Scarascia-Mugnozza G., Schettini E., Vox, G. 2004. Effects of the Solar Radiation on the Radiometric Properties of Biodegradable Films for Agricultural Applications. Biosyst Eng 87 (4): 479-487.
Scarascia-Mugnozza G., Schettini E., Vox G., Malinconico M., Immirzi B., Pagliara S. 2006. Mechanical properties decay and morphological behaviour of biodegradable films for agricultural mulching in real scale experiment. Polym Degrad Stabil 91 (11): 2801-2808.
Schettini E., Vox G., De Lucia B. 2007. Effects of the radiometric properties of innovative biodegradable mulching materials on snapdragon cultivation. Sci Hortic. 112 (4): 456-461.
Schettini E., Santagata G., Malinconico M., Immirzi B., Scarascia Mugnozza G., Vox G. 2013. Recycled wastes of tomato and hemp fibres for biodegradable pots: Physico-chemical characterization and field performance. Resour Conserv Recy 70: 9– 19.
Sartore L., Vox G., Schettini E. 2013. Preparation and Performance of Novel Biodegradable Polymeric Materials Based on Hydrolyzed Proteins for Agricultural Application. J. Polym. Environ. doi: 10.1007/s10924-013-0574-2
Tocchetto R. S., Benson R. S., Dever M. 2002. Outdoor weathering evaluation of carbon-black-filled, biodegradable copolyester as substitute for traditionally used, carbon-black-filled, nonbiodegradable, high-density polyethylene mulch films. J Polym Environ 9 (2): 57-62.
Vox G., Schettini E., Scarascia-Mugnozza, G. 2005. Radiometric properties of biodegradable films for horticultural protected cultivation. Acta Hort. 691(2): 575-582.
Vox G., Schettini E. 2007. Evaluation of the radiometric properties of starch-based biodegradable films for crop protection. Polym Test 26 (5): 639-651.

Hydrogen and renewable energy sources integrated system for greenhouse heating

Ileana Blanco, Alexandros Sotirios Anifantis, Simone Pascuzzi, Giacomo Scarascia Mugnozza

Department of Agro – Environmental Science (DISAAT), "Aldo Moro" University of Bari, (Italy)

Abstract

A research is under development at the Department of Agro-Environmental Sciences of the University of Bari "Aldo Moro" in order to investigate the suitable solutions of a power system based on solar energy (photovoltaic) and hydrogen, integrated with a geothermal heat pump for powering a self sustained heated greenhouse. The electrical energy for heat pump operation is provided by a purpose-built array of solar photovoltaic modules, which supplies also a water electrolyser system controlled by embedded pc; the generated dry hydrogen gas is conserved in suitable pressured storage tank. The hydrogen is used to produce electricity in a fuel cell in order to meet the above mentioned heat pump power demand when the photovoltaic system is inactive during winter night-time or the solar radiation level is insufficient to meet the electrical demand. The present work reports some theoretical and observed data about the electrolyzer operation. Indeed the electrolyzer has required particular attention because during the experimental tests it did not show a stable operation and it was registered a performance not properly consistent with the predicted performance by means of the theoretical study.

Introduction

Advanced greenhouses mainly need heating systems, in addition to electrical energy for ventilation, irrigation and fertilization. In detail, in horticultural and floricultural context, winter heating for greenhouses can be the 70% of production costs, being often a limit to an optimal vegetative development of protected crops for unsustainable costs (Scarascia Mugnozza G. et Anifantis A., 2009).

The use of suitable microclimate control systems, energy efficiency strategies and renewable energy sources could provide a significant impetus for greenhouse gases reduction and contribute reaching legislated energetic and environmental targets and improving the environmental performance of the greenhouses (Scarascia Mugnozza *et al*., 2011), ensuring at the same time optimal microclimate conditions for protected crops (Ozgener *et al*., 2005).

Geothermal heat pumps potentiality in the agricultural sector and especially for greenhouse heating demands have been successfully estimated (Dickson *et al*., 2004); in these circumstances heating plants are economically advantageous having a low environmental impact too (Benli, 2013; Chai *et al*., 2012; Scarascia Mugnozza *et al*., 2011; Ozgener, 2010; Kondili et Kaldellis, 2006; Adaro *et al*., 1999).

The urgent need to pass from conventional energetic systems, based on fossil fuel resources, towards energetic systems based on solar and wind energy, has to face the problems related to variable and unpredictable energy availability from renewable sources. Consequently it is necessary to provide this systems with a power back up arrangement as in example batteries, which are commonly used for this purpose but have also some limitations such as limited lifetime and low energy storage capacity. Fuel cells application, fuelled with hydrogen, is better than batteries when used to support solar energy power plants (Ro et Rahman, 1998).

Renewable sources energy can be used to generate high purity hydrogen gas through water electrolysis process; produced hydrogen, as energy vector, can serve to store energy produced in excess when compared to demand, and at a later stage it can be used as a fuel to reproduce electricity through fuel cell systems.

At present a lot of researches have been carried out and are still being developed on modelling, analysing and optimization of solar (photovoltaic and wind)-electrolyzer-fuel cell hybrid power systems with backup consisting in hydrogen storage systems (Khan et Iqbal, 2005; Jallouli et Krichen, 2012) with the hydrogen stored as liquid, as gas under pressure or through metal hydrides (Miland et Ulleberg, 2012); such researches sustain feasibility and reliability of solar hydrogen power systems.

However few studies have been done regarding the integration of solar hydrogen power systems with greenhouses, supporting that these systems provide a viable option for powering stand-alone greenhouse in a self-sustained manner (Ganguly *et al*., 2010).

Therefore a research is under development at the Department of Agro-Environmental Sciences of the University of Bari "Aldo Moro" in order to investigate the suitable solutions of a power system based on solar energy (photovoltaic) and hydrogen, integrated with a geothermal heat pump for powering a self sustained heated greenhouse. The present work reports some theoretical and observed data about the electrolyzer operation.

Correspondence: Ileana Blanco, Department of Agro – Environmental Science (DISAAT), "Aldo Moro" University of Bari, via Amendola 165/A, 70126, Bari, Italy.
Tel. /fax: +39. 080 544 29 77.
E-mail: ileana.blanco@uniba.it

Key words: greenhouse heating, energy savings, electrolyser, hydrogen, fuel cell, ground source heat pump.

Journal of Agricultural Engineering 2013; XLIV(s2):e45
doi:10.4081/jae.2013.(s1):e45

Materials and methods

The experimental greenhouse

The experimental study was carried out at the experimental farm University of Bari sited in Valenzano (Bari, Southern Italy), latitude 41° N. A greenhouse-integrated system composed of photovoltaic panels, electrolyser bank, Polymer Electrolyte Membrane fuel cell stacks and a geothermal heat pump was set up.

A system of equipments have been designed and installed in order to produce electricity from solar photovoltaic source (PV) and hydrogen gas from water by means of an electrolyser powered by PV. The produced hydrogen is stored in a pressure tank and than it is used as fuel by a fuel cell system producing electricity for greenhouse energy demands when photovoltaic is inactive (during night time or overcast sky).

The electrical energy produced was used for powering the heating system set in order to satisfy the thermal energy demand of 48 m^2 double plastic skin greenhouse; therefore the use of renewable energy was combined with passive techniques of energy saving using an inflated double film for increasing thermal transmittance.

The main structure of the greenhouse, arched roof one, is made of tubular galvanized steel. The coverage is made of a double ethylene vinyl acetate film (multiEVA 33 AD AF), each one having a thickness of 200 m, with an interposed 2 cm air space, which is kept under constant pressure by an air pump. The base and the warheads (east and west-facing greenhouse surface) are corrugated sheets made of polyester reinforced with glass fibers (PRFV). Each greenhouse is provided with a sliding door, a vertical fan/air extractor and an air inlet louver, all of which are placed on a single warhead.

Another greenhouse unheated, with the same geometric and constructive characteristics, has been realized for comparison (Figure 1).

The two greenhouses are east-west oriented, being 8 m in length and 6 m in width, 3.5 m in height. Therefore the surface coverage is about 120 m^2 and the volume is about 150 m^3.

The distance between the two greenhouses is 12 m; therefore there is no mutual shading.

The necessary heating power Q_H was evaluated using the heat balance with the main power losses between the air inside the greenhouse and the external ambient. Thus Q_H was calculated by means of the following equation (1):

$$Q_H = Q_c + Q_v + Q_i \quad [W] \quad (1)$$

where:

Q_c is the conduction and convection power loss through the greenhouse covering system [W];

Q_v is the inside air leakage power loss between the internal and external ambient [W];

Q_i is the power loss by radiation from covering film to blue sky [W].

The greenhouse heating system was realized through black plastic hose supplied by a 7.2 kW low-enthalpy geothermal heat pump equipped with 120 m vertical double U-bend ground heat exchangers.

The hybrid system

The power plant has been designed with the purpose of using the photovoltaic production also directly, avoiding the double energy conversion involving energy losses (electricity hydrogen electricity) when there is simultaneity between photovoltaic energy production and greenhouse energy demands. The designed passive loads are seasonally dependent.

The system (Figure 2) can be powered through the national electric grid in order to guarantee always the energy supply in case of default of the power system.

The whole energy system, except for PV modules and storage tanks, is enclosed in a steel cabinet (Figure 3) subdivided into two separate chambers, one encloses the process unit, the second one encloses the power supply unit. The process unit contains all equipment, piping and field instruments necessary for carrying out the water electrolysis process, and also the fuel cells.

The array of photovoltaic panels consists of 24 modules of 240 W peak power, maximum operating voltage 29.64 V. Modules were grouped in two series, grouped in parallel, in order to achieve a nominal voltage of the array of 360 V. The PV modules have a total area around 39 m^2, south-oriented with an elevation angle of 30° in order to maximize annual energy production (Figure 4). The PV modules have been set up on a tubular galvanized steel structure.

Figure 1. Experimental greenhouses.

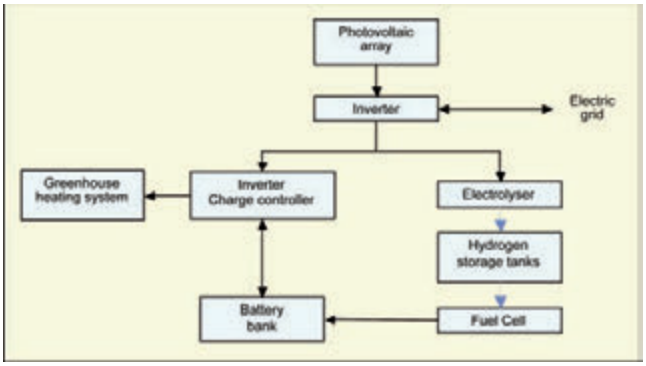

Figure 2. Functional diagram of the power plant.

Figure 3. Plant external layout.

The renewable energy produced by the aforesaid PV modules was converted to AC power by an inverter in order to feed the water electrolyser sited in the cabinet. Furthermore the AC power could also feed the grid. The inverter has an input voltage of 300-600 VDC and an output AC voltage of 230 VAC.

The electrolyser unit has an input voltage of 230 VAC and its consumption is of 3.55 kW. The hydrogen nominal production rate (dry gas) is 0.4 Nm^3/h with output pressure of 3 MPa. Moreover the hydrogen production rate is directly proportional to the AC flow set to be conducted along the cell stack. It has been chosen to add Potassium Hydroxide (KOH 28%) to the contained water for forming the electrolyte, in order to make it highly conductive.

The produced hydrogen is stored under pressure at 3 MPa in two steel tanks of 0.6 m^3 placed outside the cabinet (Figure 3). The fuel cell system is based on the proton exchange membrane (PEM) technology and is set in the process unit of the cabinet; it is designed with modular cartridge technology, having a peak power of 2 kW.

The fuel cell requires industrial grade hydrogen (99.95%) and oxygen (air) and has as by-products pure water/vapor and heat; the output voltage is of 48 VDC and the consumption is of 30 standard liter per minute (slpm) at 2 kW (operation temperatures 0°C÷ 46 °C).

The energy produced by the fuel cells is used to charge a battery bank consisting of six 12V cells connected in series and in parallel providing a global energy of 900 Ah.

Finally an inverter is connected to the battery terminals in order to be used as a stand-alone sinusoidal AC voltage provider.

The system monitoring and control, placed in the control unit, is based on a programmable logic controller (PLC) and is integrated with a power supply unit. The PLC manages all the processes and safety.

This system has been set up and it has been finished in April 2013. During the month of May 2013 operation tests have been carried out paying attention on the functionality of the electrolyzer; the amount of hydrogen produced was evaluated during daytime hours of different days.

Theoretical considerations concerning the electrolyzer

According to Faraday's law, the production rate of hydrogen M_{elec} in a water electrolyzer, consisting of a certain number of electrolyzer cells connected in series, can be calculated by (Li *et al*., 2009):

$$M_{elec} = \eta_F \, x \, N_{elec} \, x \, I_{elec} / (n \, x \, F) \qquad [\text{mol s}^{-1}] \qquad (2)$$

where:
η_F is the Faraday efficiency;
N_{elec} is the number of electrolyzer cells in series;
I_{elec} is the current through the electrolyzer [A];
n is the number of moles of electrons per mole of water, n = 2;
F is the Faraday constant (96487 C mol^{-1}).

The Faraday efficiency, that is often called the "current efficiency", is defined as the ratio between the actual and the theoretical maximum amount of hydrogen produced in the electrolyzer (Ulleberg, 2003).

According to the manufacturer of the electrolyzer the value of $_F$ is equal to 91%.

To produce hydrogen the working voltage U (V) between the two electrodes must be higher than the minimum decomposition voltage U_{tn}:

$$U_{tn} = \Delta H / nF \qquad [\text{V}] \qquad (3)$$

where:
ΔH is the standard enthalpy for splitting water of hydrogen [286 kJ mol^{-1}];
n = 2.

At standard conditions $U_{tn} = 1.482$ *V* (Ulleberg, 1998).

The voltage efficiency η_V is defined by:

$$_V = U_{tn} / U \qquad [\%] \qquad (4)$$

According to the manufacturer of the electrolyzer the value of $_V$ is equal to 80%.

Considering the registered values of the working voltage of the experimental electrolyzer, the η_V can be calculated by means of eq. 4; thus the actual voltage efficiency η_V will be 75%.

The power consumption of an electrolyzer can be expressed as (Li *et al*., 2009):

$$P_{elec} = I_{elec} \, x \, U \, x \, N_{elec} \qquad [\text{W}] \qquad (5)$$

Thus the hydrogen production by the electrolyzer, taking into account equation 2, can be calculated as:

$$M_{elec} = \eta_F \, x \, P_{elec} / (U \, x \, n \, x \, F) \qquad [\text{mol s}^{-1}] \qquad (6)$$

Considering the registered values of the hydrogen production, the power consumption and the working voltage of the experimental electrolyzer, the Faraday efficiency η_F can be calculated by means of eq. 6; thus the actual voltage efficiency η_F will be 87%.

The electrolyzer unit has a built-in gas compressor in order to store the produced hydrogen in tanks. The power necessary to compress the gas can be calculated by (Li *et al*., 2009):

$$W_c = m_c \, x \, C_p \, x \, T_1 \, x \, (1/\eta_c) \, x \, [(P_2/P_1)^{(r-1)/r} - 1] \qquad [\text{W}] \qquad (7)$$

where:
m_c is the flow rate of hydrogen through the compressor [kg s^{-1}];
C_p is the specific heat oh hydrogen at constant pressure (14304 kJ (kg K)$^{-1}$);
T_1 is the inlet gas temperature of the hydrogen compressor (313.15 K);
η_c is the isentropic efficiency of the compressor [%];
P_2 is the output gas pressure of the hydrogen compressor (3 MPa);
P_1 is the inlet gas pressure of the hydrogen compressor (0.6 MPa);
r is the isentropic exponent of hydrogen (1.4).

The mole mass of hydrogen is 2.016 (g mol^{-1}); therefore $m_c = M_{elec} \, x \, 2.016 / 1000$ (kg s^{-1}). The value of η_c in this work is assumed equal to 68% according to manufacture data.

Figure 4. The photovoltaic array.

Results and discussion

Figure 5 shows the photovoltaic electrical production (kW) as a function of the hour during a day of May 2013; this day was characterized by a highly variable weather similarly to the other days of the month and then the evaluated day can be considered representative for May 2013. The electrolyzer started to produce hydrogen when the photovoltaic production was greater than 1.6 kW, that is in the periods 8-10 and 11-14. Figure 6 shows through a dashed line the amount of produced hydrogen as a function of the stack power consumption. These experimental data are compared, in the same Figure, with data (through a continuous line) calculated by means of equation 6.

According to the experimental data aηnd by means of theoretical considerations (Figure 6), we have assessed the actual voltage efficiency (η_V = 75%) and the actual Faraday efficiency (η_F = 87%) which are clearly lower than the manufacturer efficiency values. The actual production of hydrogen is slightly different from the calculated one obtained by means of theoretical conditions (Figure 6).

These disagreements between expected and registered values are probably due to the mathematical model. Effectively this model contemplates electrolyser working at atmospheric pressure and at constant temperature. Furthermore the compression of the hydrogen (equation 7) takes place after its production in suitable compressor.

The realized electrolyzer besides works under pressure of 0.3 MPa with a changeable operative temperature (20 °C-80 °C) and the produced hydrogen is already pressed (0.3 MPa), ready to be stored in the tanks. Consequently the power necessary to compress the hydrogen is secondary if compared to the one related to the theoretical model (equation 7).

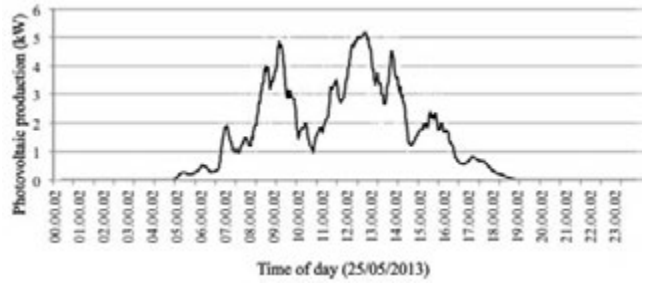

Figure 5. The daily photovoltaic production

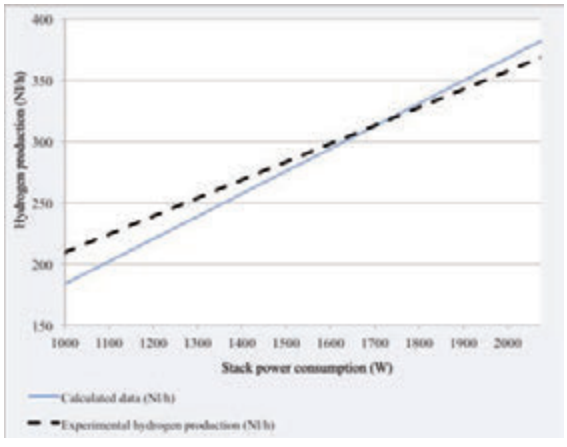

Figure 6. The hydrogen production.

Conclusions

The realized system has required the analysis of different technical characteristics related to the heating demands of the experimental greenhouse, the ground source heat pump, the hydrogen production, the storing system, the photovoltaic system. Further studies have been carried out to evaluate the connection and the affects among the members in order to obtain a hybrid system for the production and storing of green hydrogen. Above all the electrolyzer has required particular attention because during the experimental tests it did not show a stable operation and it was registered a performance not consistent with the predicted performance by means of the theoretical study. Some technical operations are being carried out for enhancing the system functionality, making it suitable to the designed task of supplying electrically the greenhouse heating system during cold periods.

References

Adaro J. A., Galimberti P. D., Lema A. I., Fasulo A., Barral J. R. 1999. Geothermal contribution to greenhouse heating. Appl. Energ. 64: 241-249.

Benli H. 2013. A performance comparison between a horizontal source and a vertical source heat pump systems for a greenhouse heating in the mild climate Elazig, Turkey", Appl. Therm. Eng. 50 (1): 197-206.

Chai L., Ma C., Ni J.Q. 2012. Performance evaluation of ground source heat pump system for greenhouse heating in norther China. Biosyst. Eng. III: 107-117.

Dickson M., Fanelli M. 2004. What is geothermal energy? Istituto di Geoscienze e Georisorse, CNR, Pisa, Italy. Available from: http://www.unionegeotermica.it/What_is_geothermal_en.html Accessed: May 2013.

Ganguly A., Misra D., Ghosh S. 2010. Modeling and analysis of solar photovoltaic-electrolyzer-fuel cell hybrid power system integrated with a floriculture greenhouse, Energ. Buildings. 42: 2036 – 2043.

Jallouli R., Krichen L. 2012. Sizing, techno-economic and generation management analysis of a stand alone photovoltaic power unit including storage devices. Energy. 40 (1): 196–209.

Khan M. J., Iqbal M. T. 2005. Pre-feasibility study of stand-alone hybrid energy systems for applications in Newfoundland. Renew. Energ. 30 (6): 835-854.

Kondili E., Kaldellis J.K. 2006. Optimal design of geothermal-solar greenhouses for the minimisation of fossil fuel consumption. Appl. Therm. Eng. 26 (8-9): 905-915.

Li C.-H., Zhu X.-J., Cao G.-Y., Sui S., Hu M.-R. 2009. Dynamic modeling and sizing optimization of stand-alone photovoltaic power systems using hybrid energy storage technology. Renew. Energ. 34 (3): 815-826.

Miland H., Ulleberg Ø. 2012. Testing of a small-scale stand-alone power system based on solar energy and hydrogen. Sol. Energy. 86 (1): 666–680.

Ozgener O., Hepbasli A. 2005 Performance analysis of a solar assisted ground – source heat pump system for greenhouse heating: an experimental study. Build. Environ. 40: 1040-1050.

Ozgener O. 2010. Use of solar assisted geothermal heat pump and small wind turbine systems for heating agricultural and residential buildings. Energy 35: 262–268.

Ro K., Rahman S. 1998. Battery or fuel cell support for an autonomous photovoltaic power system. Renew. Energ. 13 (2): 203-213.

Scarascia Mugnozza G., Anifantis A. 2009. Dal fotovoltaico al termico.

Colture Protette 6: 40-43

Scarascia Mugnozza G., Pascuzzi S., Anifantis A. 2011. Impianto sperimentale geotermico a bassa entalpia per riscaldamento serricolo. Prime valutazioni. Proc. Congr. Medio termine dell'Associazione italiana di Ingegneria Agraria AIIA, Belgirate, Italia. Available from: http://www.aiia.it/images/Atti/ Belgirate_2011/142.pdf Accessed: May 2013.

Ulleberg Ø. 1998. Stand-Alone Power Systems for the Future: Optimal Design, Operation & Control of Solar-Hydrogen Energy Systems. PhD thesis, Norwegian University of Science and Technology, Trondheim.

Ulleberg Ø. 2003. Modeling of advanced alkaline electrolyzers: A system simulation approach. Int. J. Hydrogen Energ. 28 (1): 21-33.

Variation of physical properties of LDPE greenhouse films due to agrochemicals used during cultivation

Evelia Schettini*, Giuliano Vox

Department of Agricultural and Environmental Science, University of Bari, Italy

Abstract

During protected cultivation, the use of agrochemicals influence the degradation of the greenhouse plastic films. A research was carried out to evaluate how agrochemicals contamination and solar radiation influence the physical properties of low density polyethylene (LDPE) films. The LDPE films were manufactured on purpose adding different anti-UV stabilizer systems and were exposed to natural outdoor weathering at the experimental farm of the University of Bari (Italy; 41° 05' N). Each film was tested as covering of two low tunnels: one was sprayed from inside with commercial agrochemicals containing iron, chlorine and sulphur while the other one was not sprayed and used as control. Radiometric tests were carried out on the new films and on film samples taken at the end of the trial. Analyses on absorption of the selected contaminants were carried out in laboratory on the samples taken at the end of the exposure in the field in order to compare the relative effectiveness of the stabilizing systems under evaluation. The experimental tests showed that the natural weathering together with the agrochemicals did not modify significantly the radiometric properties of the films in the solar and PAR wavelength range. Significant variations were recorded for the stabilised films in the LWIR wavelength range.

Correspondence: Evelia Schettini, Department of Agricultural and Environmental Science, University of Bari, via Amendola 165/A – 70126 Bari, Italy.
Tel. +39 080 5443060- Fax+39 080 5442977.
E-mail: evelia.schettini@uniba.it

Key words: chlorine, HALS, iron, radiometric properties, solar radiation, sulphur.

Acknowledgements: the present work has been carried out under the projects funded by P.A.T.I. S.p.A. (San Zenone degli Ezzelini, TV, Italy) during the period 2006-2009.
The authors thank C. Anifantis and F. Ferrulli of the University of Bari for their cooperation in the field test.
The experimental tests, the data processing and the editorial work must be shared equivalently among the Authors.

Journal of Agricultural Engineering 2013; XLIV(s2):e46
doi:10.4081/jae.2013.(s1):e46

Introduction

The radiometric properties of films used for crop protection influence the microclimate of the protected volume, i.e. the air temperature and relative humidity, the soil temperature, the quantity and quality of the solar radiation, modifying the growing condition of the crop in comparison with the external climatic conditions. The time stability of the radiometric properties of the film during the crop cycle cultivation is important when assessing the potential benefits of different materials on microclimate and on crop growth. The average service life for plastic films used to cover greenhouses ranges from some months up to three or four years in the Mediterranean region. Film lifetime is influenced by parameters related both to the film itself and to the environment in which the film is used (Desriac, 1991; Dilara and Briassoulis, 2000; Briassoulis, 2005; Ruiz *et al*., 2006; Stefani *et al*., 2008).

The ultra violet (UV) radiation in the solar spectrum, especially the UV-B and UV-A radiation that occur in the wavelength range from 280 nm to 400 nm, is one of the factors that mainly influences the ageing degradation process by leading to bond cleavage and depolymerisation (Nijskens *et al*., 1990; Dilara and Briassoulis, 1998). The use of UV-stabilizers, such as UV absorbers, hindered amine light stabilizers (HALS) and nickel quenchers, mitigates the degradation through the prevention of solar radiation absorption as well as minimizing any subsequent radical oxidation reactions. UV stabilisers absorb UV radiation and dissipate it into heat; HALS additives decompose radicals while nickel quencher deactivate radicals, hampering the degradation process (Sanchez-Lopez *et al*., 1991).

Agrochemical substances influence greenhouse film degradation due to their active principles, method of application and frequency, greenhouse ventilation and structure (Dilara and Briassoulis, 2000). Agrochemicals based on sulphur and chlorine generate sub-products of the used pesticides that lead to a deterioration of the covering films together with a reducing of their mechanical and physical properties (Kham and Halim, 1995; Rull and Marin, 2006; Espi *et al*, 2007; Vox *et al*., 2008; Stefani *et al*., 2011; Schettini and Vox; 2012).

Aim of the research is to study the effects of agrochemicals containing iron, chlorine and sulphur, which are sprayed during cultivation, on greenhouse plastic films degradation. Three low density polyethylene (LDPE) greenhouse films were tested changing the UV-stabilizers added to the base polymer. Natural outdoor weathering, radiometric tests, and analyses on the absorption of selected contaminants were carried out to evaluate the detrimental effect of ageing and of agrochemical application on different covering films actually used in the Mediterranean region.

Materials and methods

Low density polyethylene (LDPE) films were manufactured on purpose by P.A.T.I. S.p.A. company (San Zenone degli Ezzelini, TV, Italy)

with a nominal thickness of 100 m, using the single layer blow-extrusion technology. The UV stabilizers, such as triazine UV absorbers, benzophenone UV absorbers, polymeric HALS, and N-alkoxy (NOR) HALS, were added to the basic polymers with a percentage not revealed, since these formulations are proprietary. Each film was identified by a code as shown in Table 1.

The films were exposed to natural outdoor weathering at the experimental farm of the University of Bari (Valenzano, Bari, Italy; 41° 05' N, 16° 53' E, 85 m asl). The test started in Spring 2009, allowing the highest solar irradiation of the films during the warmest period of the year, and ended when the first film was broken. Each film was used to cover two low tunnels (Figure 1): one of the tunnels was sprayed (code S) with the agrochemicals while the other one was not sprayed and used as control (code C). Each low tunnel had a length of 20.0 m, a width of 1.0 m and a height of 0.8 m, with N-S orientation.

The agrochemicals were sprayed onto the films by a system consisting of a pump connected with pipes and nozzles located inside the low tunnels. A water solution with a foliar fertilizer containing iron (Sequestrene® Life, Syngenta Crop Protection S.p.A., Milan, Italy), a fungicide containing sulphur (Tiovit® Jet, Syngenta Crop Protection) and a fungicide containing chlorine (Topas®, Syngenta Crop Protection) was sprayed weekly during the period test. The doses of the active principles of the agrochemicals were: 0.500 g/m^2 for sulphur; 0.028 g/m^2 for chlorine; 0.034 g/m^2 for iron.

Solar radiation was measured by a pyranometer (model 8-48, Eppley Laboratory, Newport, RI, USA) in the wavelength range 0.3-3 mm; data were recorded by a data logger (CR10X, Campbell, Logan, USA) every 60 s and stored as 15 min average values. The cumulative solar radiation for the exposure period was calculated.

Radiometric tests on the new films and on samples taken at the end of the trial were carried out at the University of Bari. Spectral transmissivity $\tau(\lambda)$ of a material is the fraction of the incident energy radiant flux that is transmitted at a specific wavelength λ. Spectral direct transmissivity in the wavelength range between 300 and 2500 nm were measured by means of a spectrophotometer (UV-VIS-NIR Lambda 950, Perkin-Elmer Instruments, Norwalk, CT, USA) in steps of 10 nm using radiation with a direct perpendicular incidence. Spectral total transmissivity was measured by means of an integrating sphere (diameter 60 mm) used as receiver of the Lambda 950 spectrophotometer. Spectral diffuse transmissivity was calculated by subtracting the direct transmissivity from the total transmissivity. The transmissivity coefficients were calculated as weighted average values of the transmissivity over the wavelength interval between 300 and 2500 nm for the solar range, and between 400 and 700 nm for the photosynthetically active radiation (PAR) range using the spectral distribution of the terrestrial solar radiation as weighting function (Vox and Schettini, 2007). The transmissivity in the long wave infra-red radiation (LWIR) range between 2500 and 25000 nm was measured by a spectrophotometer (FT-IR 1760X, Perkin-Elmer Instruments, Norwalk, CT, USA) in steps of 4 cm^{-1}. Spectral transmissivity was measured using radiation with a direct perpendicular incidence. The transmissivity coefficient in the LWIR range was calculated as average value of the spectral transmissivity in the wavelength range from 7500 to 12500 nm, where the bodies at ambient temperature have the maximum energy emission as expressed by Planck's spectral distribution of emissive power (Vox and Schettini, 2007).

The absorption of chlorine, iron and sulphur was estimated at the Venezia Tecnologie laboratories (Venice, Italy), using fluorescence X-ray elementary semiquantitative analysis.

Table 1. LDPE greenhouse covering films.

Film code	Stabilizers
A4	No stabilizers
D4	NOR-HALS + triazine UV filter
H4	HALS + benzophenone UV filter

Figure 1. The experimental field at the University of Bari (Italy).

Results and discussion

Table 2 show the radiometric parameters of the films tested, i.e. the total transmissivity coefficients calculated in the solar (300-2500 nm),

Table 2. Radiometric coefficients of the LDPE films; 0: new film; C: control film; S: sprayed film; trans.: transmissivity.

Film	Exposure time, days	Cumulative solar radiation, MJ/m^2	Total solar trans., %	Total PAR trans., %	Total UVA trans., %	LWIR trans., %
A4_0	0	0	89.2	88.6	80.5	78.8
A4_C	108	2428	90.7	90.9	79.6	67.9
A4_S	108	2428	89.8	89.0	72.4	55.5
D4_0	0	0	89.4	90.2	49.3	74.2
D4_C	108	2428	90.0	90.3	50.5	71.9
D4_S	108	2428	89.2	88.6	55.3	60.8
H4_0	0	0	88.1	88.4	30.2	72.1
H4_C	108	2428	88.2	87.3	28.1	70.4
H4_S	108	2428	87.7	86.6	31.6	60.4

in the PAR (400-700 nm), in the UVA (320-380 nm) and in the LWIR (7500-12500 nm) wavelength range. These coefficients were evaluated at the beginning of each trial for the new films (coded 0) and at the end of the trials both for the control films (coded C), subjected only to the natural weathering, and for the sprayed films (coded S), subjected to the natural weathering and to the spray of the agrochemicals. The cumulative solar radiation was calculated from the day of the film installation. In the solar and in the PAR wavelength range the radiometric properties of all the films varied less than 5% between the values measured at the beginning of the trial and the end of the trial.

In the LWIR range the stabilised films showed variations less than 20% between the values measured at the beginning of the trial and the end of the trial; the A4 film, a not stabilised film, showed a higher decrease (about 30% from its initial value). Figures 2 shows the spectral transmissivity of the H4 films in the LWIR wavelength range, between 2500 and 25000 nm; the curves concern the new film (H4_0), the control film (H4_C) and the sprayed film (H4_S) after the exposure in the field. The H4 film showed changes of its radiometric properties at the end of the exposure in the field. The variation of the transmissivity in the LWIR range suggests changes in the chemical structure of the films. Greenhouse covering films must satisfy the EN 13206 (2001) standard; it establishes that the films, with a thickness of 100 m, must have a PAR total transmissivity coefficient higher than 85%. The films were always characterised by higher values for the PAR total transmissivity coefficient, ranging from 86.6% (H4_S) to 90.9 % (A4_C).

Table 3 shows the absorption of the chemical contaminants, such as chlorine, iron, and sulphur, of the films tested at the end of their exposure in the field. The H film was characterised by the highest sulphur and chlorine absorption in comparison with the other films sprayed in the same way and at the same time intervals.

Table 3. Contaminants in the LDPE films at the end of film exposure in the field.

Film	S (ppm)	Cl (ppm)	Fe (ppm)
A4_S	1600	250	150
D4_S	2100	170	150
H4_S	3600	300	150

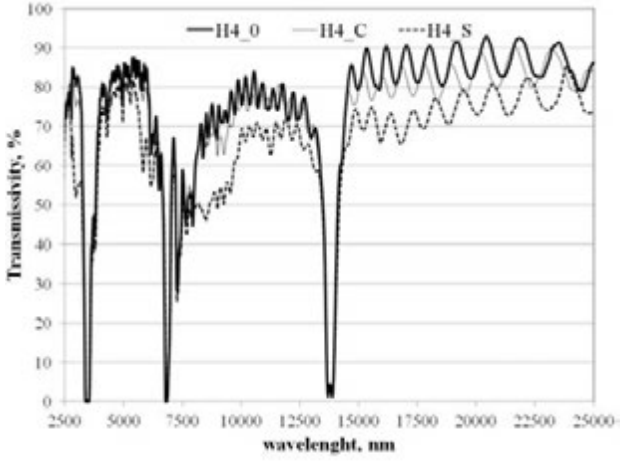

Figure 2. Long wave infrared (LWIR) spectral transmissivity of the H4 film in the wavelength range 2500-25000 nm; H4_0, new film; H4_C: control film exposed only to natural weathering; H4_S: film exposed to natural weathering and to agrochemicals.

Conclusion

The research showed that the radiometric properties of the films in the solar and in the PAR wavelength range were not significantly modified during their exposure to climatic agents and to the agrochemicals; the variation of the transmissivity coefficients was less than 5%. Variations less of 20% of the initial value were recorded between the values measured at the beginning and the end of the test for the radiometric coefficients of the stabilised films in the LWIR wavelength range.

References

Briassoulis D. 2005. The effects of tensile stress and the agrochemical Vapam on the ageing of low density polyethylene (LDPE) agricultural films. Part I. Mechanical behaviour. Polym. Degrad. Stabil. 88: 489-503.

Desriac Ph. 1991. The effect of pesticides on the life of greenhouse films. Plasticulture 89: 9-16.

Dilara P. A., Briassoulis D. 1998. Standard testing methods for mechanical properties and degradation of low density polytehylene (LDPE) films used as greenhouse covering materials: a critical evaluation. Polym. Test. 17: 549-585.

Dilara P. A., Briassoulis D. 2000. Degradation and stabilization of Low-density Polyethylene films used as greenhouse covering materials. J. Agric. Eng. Res. 76: 309-321.

EN 13206. 2001. Covering thermoplastic films for use in agriculture and horticulture. Comité Européen de Normalisation (C.E.N.), Brussels.

Espí E., Salmerón A., Fontecha A., García Y., Real, A. I. 2007. The effect of different variables on the accelerated and natural weathering of agricultural films. Polym. Degrad. Stabil. 92 (12): 2150-2154.

Khan J. H., Hamid S. H. 1995. Durability of HALS-stabilized polyethylene film in a greenhouse environment. Polym. Degrad. Stabil. 48: 137-142.

Nijskens J., Deltour J., Albrecht E., Grataud J., Feuilloley, P. 1990. Comparative studies on the ageing of polyethylene film in the laboratory and in practical use. Plasticulture 87: 11-20.

Ruiz P., Pagani F., Vulic I., Lobo F. 2006. Is the service life of greenhouse covers determined by exposure to the sun or by contact with agrochemical substances? Plasticulture 125: 37-49.

Rull F., Marin A. 2006. The influence of metham-sodium on the degradation of films used as covers in greenhouse. Plasticulture 126: 7-19.

Sanchez-Lopez S., Prado H. L., Ramirez E., Mendoza N. 1991. Recycling of waste agricultural polyethylene film. Plasticulture 92: 49-53.

Schettini E., Vox G. 2012. Effects of Agrochemicals on the Radiometric Properties of Different anti-UV Stabilized EVA Plastic Films. Acta Horticulturae 956: 515-522.

Stefani L., Schettini E., Vox G. 2011. Correlation between agrochemicals, solar radiation and mechanical properties of greenhouse plastic films. Acta Horticulturae 893: 281-288.

Stefani L., Zanon M., Modesti M., Ugel E., Vox G., Schettini E. 2008. Reduction of the Environmental Impact of Plastic Films for Greenhouse Covering by Using Fluoropolymeric Materials Acta Horticulturae 801: 131-138.

Vox G., Schettini E. 2007. Evaluation of the radiometric properties of starch-based biodegradable films for crop protection. Polym. Test. 26 (5): 639-651

Vox G., Schettini E., Stefani L., Modesti M., Ugel E. 2008. Effects of Agrochemicals on the Mechanical Properties of Plastic Films for Greenhouse Covering. Acta Horticulturae 801: 155-162.

Comparison of different estimation procedures for the hydraulic properties of horticultural substrates by One-Step technique

Carlo Bibbiani,[1] Carlo A. Campiotti,[2] Luca Incrocci,[3] Alberto Pardossi[3]

[1]Department of Veterinary Science, University of Pisa, Italy; [2]Department UTEE-AGR, ENEA, Italy; [3]Department of Agriculture, Food and Environment Science, University of Pisa, Italy

Abstract

The improved iterative method for the simultaneous determination of the hydraulic properties of growing media from One-Step experiment by Bibbiani, is performed and compared with simplified equations by Valiantzas and Londra. Brooks and Corey equation for water retention, and Kozeny power equation for hydraulic conductivity characterized the hydraulic properties of the porous media. The iterative procedure is applied on pure peat, pumice, and their mixes. The One-Step method has been previously optimized: processing the mean cumulative outflow curves recorded versus time, an estimation of diffusivity, and therefore of the hydraulic functions, is derived. Estimated water retention curve is compared with nine experimental data, and with the estimation of the Van Genuchten model, via the RETC code. Bibbiani's and Van Genuchten's models overlap except for the "very wet" range near saturation, whereas the Valiantzas and Londra's procedure didn't get satisfactory results. In regard to diffusivity, a good similarity between Bibbiani's and Van Genuchten-Mualem's curves can be assessed, while Valiantzas and Londra's procedure generally results in higher values. Due to the lack of estimation of the water retention curve, Valiantzas and Londra's procedure fails to estimate the hydraulic conductivity function, whereas Bibbiani's and Van Genuchten-Mualem's curves match together in most cases.

Correspondence: Carlo Bibbiani, Department of Veterinary Sciences, University of Pisa, Viale delle Piagge 2, 56124 Pisa, Italy.
Tel.: +39.050.2216813 - Fax: +39.050.2216706.
E-mail: carlo.bibbiani@vet.unipi.it

Key words: hydraulic characteristics of substrates, parameter estimation, one-step experiment.

Contributions: the authors contributed equally.

Journal of Agricultural Engineering 2013; XLIV(s2):e47
doi:10.4081/jae.2013.(s1):e47

Introduction

Water flow and solute transport modelling must rely on the knowledge of water retention and hydraulic conductivity curves, namely (h) and K(θ) or K(h). Computed water balances are very sensitive to soil hydraulic parameters and therefore their accurate determination is essential (Jhorar *et al*., 2004; Schneider *et al*., 2009). Experimental methods have been set for this task, with varying complexity and accuracy of measurements. The substrate moisture retention curve is rather easily achieved. On the contrary, the determination of the hydraulic conductivity function requires the establishment of steady-state moisture profiles under unsaturated conditions, which is a tough assignment. This difficulty led scientists to conceptual models which could predict K(θ) from the moisture retention curve coupled by Ks measured independently (conductivity at saturation, where simple permeameters have been manufactured either constant head or falling head). Gardner (1962) introduced another method which relies on the determination of diffusivity D(θ) relationship with one-step outflow data, being diffusivity the ratio of conductivity to the specific water capacity C(h)=d /dh. Henceforth, many authors developed more accurate equations.

In this paper the cumulative outflow data obtained by one-step outflow experiment are used for the prediction of D(θ) employing equations from Valiatzas (1989), Bibbiani (2002), Valiantzas *et al*. (2007), Valiantzas and Londra (2012), and Van Genuchten-Mualem model (Mualem, 1976; Van Genuchten, 1980). Bibbiani's method, assuming a particular power form with a small number of parameters for the θ(h) and K(h) curves, leads to the estimation of the hydraulic characteristics. The estimated hydraulic functions are compared with experimental data, and with the Van Genuchten-Mualem model curves.

Materials and methods

Five replications of peat, pumice, and a peat/pumice (1Pe:1Pu) [1:1 (v/v)] mix were packed in 347.5 ml cylindrical aluminum tubes (7.6 cm in diameter, 7.6 cm in height). The pumice is a 'tout-venant' material sieved at 8 mm maximum particle size. At the end of the procedure, the substrate samples were seated on a grid for a 30 minutes 'free drainage'. Samples were then weighed to determine the water content θ_{fd}. At this time, samples were subjected to the One-Step procedure. Firstly, they were seated on the porous plates of Buchner filter funnels with an air-entry pressure > 16 kPa and a plate conductivity equal to 2.28 cm/hr. An airtight lid was placed on the top of each funnel and a positive air pressure was applied. An initial pressure equal to -1 kPa referred to the core centre was applied; once equilibrium was reached,

the core was weighed and replaced in the funnel, and a sudden application of a positive gas pressure increment marked the initiation of the outflow process recorded with time until equilibrium at the new pressure. The couple of pressure [-1;-10] kPa was chosen as it was the most accurate (Bibbiani, 2002). A duration of 48 hours proved to be sufficient to allow for the necessary equilibrium and calculations. To make a comparison with experimental moisture retention data, the above samples were resaturated: a drying retention curve was determined applying -1.0; -2.0; -3.0; -5.0; -10.0; -15.0; -23.0 kPa matric potential referred to the core centre. After -23.0 kPa measurement, the samples were removed and put in a ventilated oven at 105 °C for 24 hours and weighed. Then, the cylinder was clamped in a constant volume air pycnometer device to determine the total porosity θ_{TP}. To measure saturated hydraulic conductivity, the modified constant head method described by Da Silva (1991) was followed in its main steps using Plexiglas™ cylinder (20.0 cm in height and 5.1 cm in diameter). The process was replicated three times. The mean value was taken as the saturated hydraulic conductivity Ks.

In order to calculate D(θ) function, Valiantzas (1989) derived an accurate equation, starting from Gardner (1962) and Passioura (1976) approximate equations, as:

$$D(\theta) = -\frac{2 \cdot L^2}{\pi^2}\left(\frac{dq}{d\theta} + \frac{q}{\theta - \theta_f}\right) \quad (1)$$

where q = dθ/dt is the outflow rate, θ_f is the final volumetric water content in One-Step experiment, and L is the height of the sample. Valiantzas *et al*. (1988), and Valiantzas and Kerkides (1990) proposed a simple method for the simultaneous determination of hydraulic properties starting from an estimation of diffusivity function D(θ). Bibbiani (2002), in order to remove the limitation due to the absence of the θr parameter, re-introduced the latter in the relative water content equation. Thus, the proposed Θ equations are written as:

Brooks and Corey's (B&C, as referred herein after), for water retention

$$\Theta = \left[\frac{He}{h}\right]^{\lambda} \qquad h > He \quad (2)$$

$$\Theta = \frac{\theta - \theta r}{\theta s - \theta r} = 1 \qquad 0 \le h \le He \quad (3)$$

Kozeny's (KO, as referred herein after), for conductivity

$$Kr(\Theta) = \frac{K(\Theta)}{K_s} = (\Theta)^p \quad (4)$$

where θs is the saturated water content, θr is the residual water content, He is the air-entry value, p and λ are fitting parameters.

Eqs. 2, 3, and 4 can be substituted for D(Θ) equation obtaining:

$$D(\Theta) = B\,(\Theta)^A \quad (5)$$

$$B = \frac{Ks\,He}{\lambda(\theta s - \theta r)} \quad (6)$$

$$A = p\text{-}1\text{-}\frac{1}{\lambda} \quad (7)$$

The problem appears as an identification problem of parameters A, B, λ, and θr, while θs is taken as a known parameter, and calculated in this paper as:

$$\theta_S = \frac{3\theta_{TP} + \theta_{fd}}{4} \quad (8)$$

The outflow rate q(θ(t)) is related to diffusivity D(θ) by approximate analytical expressions, λ(μ) and $\theta_L(\mu)$, μ depending on (θ; θr; A), as proposed by Valiantzas and Kerkides (1990) and modified by Bibbiani (2002):

$$q(\theta) = \frac{B\lambda^*(\mu)}{(A+1)\,L^2\,(\theta s - \theta r)^A}\cdot[(\theta_L(\mu) - \theta r)^{A+1} - (\theta f - \theta r)^{A+1}] \quad (9)$$

Each θr value leads to estimate parameters A and B minimizing the difference between simulated and measured outflow rates q(t). Consequently the D(θ) function is calculated. Then, the unknown parameter λ is estimated minimizing the S(θr,λ) objective function, which is the difference between the natural logarithm of measured and simulated relative water content data, calculated as:

$$S(\theta r,\lambda) = \sum_{y=1}^{M} \{\ln[\frac{\theta y - \theta r}{\theta s - \theta r}] - \lambda \cdot \ln[\frac{\lambda(\theta s - \theta r)}{Ks} B_{(\theta)C}] + \lambda \cdot \ln[h_y]\}^2 \quad (10)$$

where M means number of experimental θ(h) data, θ_y is the water content in correspondence with h_y value of matric potential.

Thus, the minimum value function S(θr,λ) can be plotted, and its minimum singles out the best fitting vector [θ_r, λ_r]. Eq. 6 and 7 give parameters He and p, and so functions θ(h) and K(h) are plotted. In order to neglect the porous plate impedance effect on the results, which might be significant at the early stages of the outflow process, Valiantzas *et al*. (1988) forced the procedure for estimating D(θ) analyzing only the part of the curve where the cumulative outflow V ceases to be linear with respect to the square root of time √t. Later on, Valiantzas *et al*. (2007) and Valiantzas and Londra (2012) derived some simplified equation for the determination of the hydraulic properties of horticultural substrates, applying respectively Eq. 1 in the former, and B&C equation and Burdine model (Burdine, 1953) in the latter; they introduced in Eq. 1 a new dimensionless variable obtained from the outflow data as well, the fraction of the remaining outflow water volume S_{out}, as:

$$S_{out} = \frac{\theta - \theta_f}{\theta_i - \theta_f} = F(\sqrt{t})^G \quad (11)$$

which is related to cumulative outflow V vs. the square root of time √t with a power form similar to that of Eq. 5, where θ_i and θ_f are respectively the initial and final volumetric water content in One-Step experiment, F and G are fitting parameters. In this context, they derived the following:

$$D(\theta) = -\frac{2\cdot(G-1)\cdot L^2 \cdot F^{2/G}}{\pi^2}\left(\frac{\theta - \theta f}{\theta i - \theta f}\right)^{-2/G} \quad (12)$$

In order to evaluate the hydraulic functions, they proposed to measure experimentally the water retention, or alternatively, in their latter paper, to run the One-Step procedure fixing θ_f as close as possible to the 'real' θ_r value.

In the present paper, in order to compare all the previous estimated water retention and hydraulic conductivity curves, the Van Genuchten–Mualem (VG-M, as referred herein after) combined model (Mualem, 1976; Van Genuchten, 1980) was applied to experimental retention

data, having fixed their parameters respectively as m=1-1/n, l=0.5, and θs from Eq. 8. The fitting program RETC (Van Genuchten *et al*., 1991) estimated θr, α, and n unknown parameters, computing both experimental retention data coming only from One-Step experiment and diffusivity data calculated by Eq. 5.

$$\Theta(h) = \frac{\theta - \theta r}{\theta s - \theta r} = \left[1 + (\alpha \cdot |h|)^n\right]^{-m} \quad (13)$$

$$C(\Theta) = \alpha n m(\theta_s - \theta_r)\Theta^{1/m}\left(1 - \Theta^{1/m}\right)^m \quad (14)$$

$$K(\Theta) = Ks \cdot \Theta^{1/2}\left[1 - \left(1 - \Theta^{1/m}\right)^m\right]^2 \quad (15)$$

$$D(\theta) = \frac{K(\theta)}{C(\theta)} \quad (16)$$

Finally, RETC code estimated D(θ) taking as input only 9 experimental moisture retention data, thus resulting in the VG-M (Retention only) curve.

Table 1. Water retention data-sets, and One-Step pressure heads set-up.

Pure Peat		1Peat:1Pumice		Pure Pumice	
Pressure Head h	Water Content θ	Pressure Head h	Water Content θ	Pressure Head h	Water Content θ
3.8 = 'θfd'	0.879	3.8 = 'θfd'	0.729	3.8 = 'θfd'	0.465
3.8 = 'θfd'	0.879	3.8 = 'θfd'	0.729	3.8 = 'θfd'	0.465
20	0.501	20	0.525	20	0.380
30	0.435	34	0.471	30	0.370
50	0.379	50	0.447	50	0.364
104 = 'θf'	0.329	104 = 'θf'	0.395	100 = 'θf'	0.347
140	0.318	147	0.376	140	0.340
230	0.309	233	0.361	230	0.335

Table 2. Measures parameters at saturation, and parameter estimation obtained for Eqs. 2-7. B&C-KO model.

Substrate	ρ kg m^{-3}	θ_{TP} m^{3}m^{-3}	θs m3m^{-3}	Ks cm min^{-1}	$\overline{\theta}_r$ m^{3}m^{-3}	A($\overline{\theta}_r$, λ) -	A($\overline{\theta}_r$, λ) -	λ -
Peat	115	0.94	0.92	3.360	0.298	2.7498	33.8752	1.1285
1Pe:1Pu	307	0.86	0.83	1.44	0.206	6.1897	19.715	0.3315
Pumice	830	0.68	0.62	180.0	0.248	6.827	100.75	0.1665

Table 3. Parameter estimation obtained for Eq. 12. Nonlinear least-squares analysis by RETC program (l = 0.5). Fit of 9 experimental retention data only for Eq. 13. VG-M (Retention only) model. Simultaneous fit of Retention and Diffusivity data from One-Step experiment for Eq. 13. VG-M model.

	Pure Peat		1Peat:1Pumice		Pure Pumice	
Variable	Value	St.dev.	Value	St.dev.	Value	St.dev.
Parameter for Eq. 12						
F	6.793		10.13		324.2	
G	-1.767		-1.433		-2.439	
Fit of 9 experimental retention data only for Eq. 13						
θr	0.3030	0.0058	0.2907	0.0102	0.3283	0.0091
α	0.1042	0.0030	0.2348	0.0113	0.8385	0.2135
n	2.3396	0.0700	1.5093	0.0298	1.6297	0.1234
m	0.5725		0.3374		0.3864	
R2	0.9993		0.9995		0.9964	
Simultaneous fit of retention and diffusivity data from One-Step experiment for Eq. 13						
θ_r	0.3072	0.0007	0.3069	0.0074	0.2788	0.0040
α	0.0984	0.0015	0.7149	0.0782	2.7400	0.1434
n	2.3681	0.0244	1.3873	0.0221	1.2906	0.0093
m	0.5777		0.2792		0.2252	
R^2	0.9993		0.9541		0.9923	

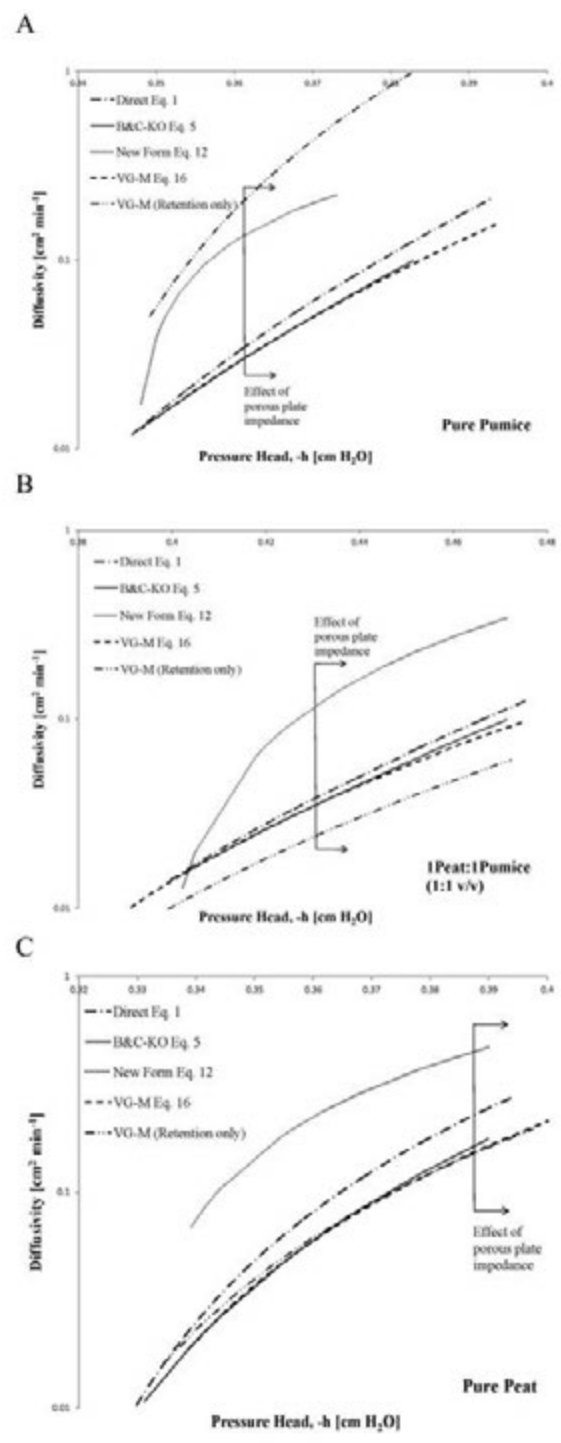

Figure 1. Substrate water diffusivity as a function of volumetric water content, D(θ), estimated by various equations. (A). Pure Pumice (B). 1Peat:1Pumice (1:1 v/v) (C). Pure Peat. The short vertical line labeled "Effect of the porous plate impedance" defines the region where the plate impedance is not negligible.

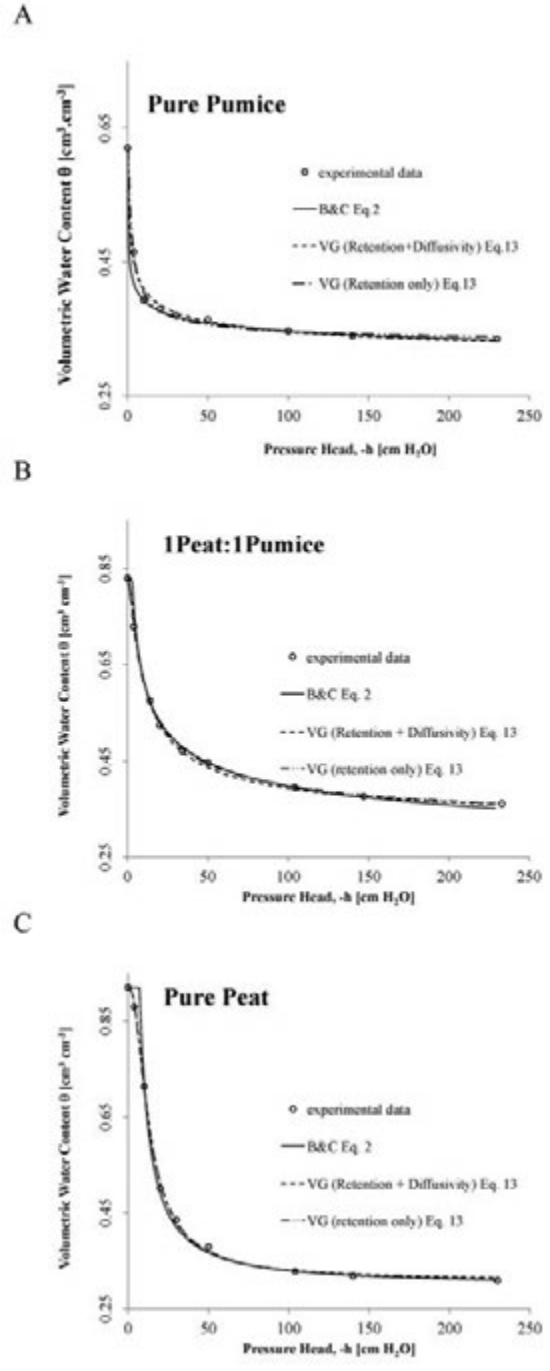

Figure 2. Substrate water retention θ(h) as a function of pressure head -h, measured and estimated by B&C and VG equations. (A). Pure Pumice (B). 1Peat:1Pumice (1:1 v/v) (C). Pure Peat.

Results and discussion

Table 1 reports all the measured moisture retention points for the three substrates, and the initial and final pressure heads set-up for One-Step experiment. Table 2 shows the estimated parameters for Eqs. 2 and 5, as related to the B&C-KO model improved by Bibbiani (2002).

Table 3 refers to Eq. 12, giving parameters of the new dimensionless variable S_{out}, obtained by Valiantzas *et al*. (2007). Moreover, it reports the estimation by RETC code for the VG-M model related to Eq. 13, with the analysis of 9 retention data only (derived from independent measurements), and both retention and diffusivity data derived from One-Step experiment. A comparison of diffusivity functions, $D(\theta)$, estimated by the above discussed equations, is well-drawn in Figure 1. Irrespective to the substrate nature, there is a good agreement between the direct calculation of $D(\theta)$ by Eq. 1, and both the B&C-KO model by Eq. 5 and the VG-M model by Eq. 16 (retention and diffusivity data). The VG-M (Retention only) curve shows a variable and unpredictable behavior, suggesting a non-reliable estimation based only on retention data. The prediction of $D(\theta)$ by Eq. 12 doesn't match any other ones in this experiment. Since Valiantzas *et al*. (2007) reported a substantial identity between their estimation and Eq. 1, the huge discrepancy in the present work might depend on the different final pressure at the end of the outflow procedure $h(\theta_f)$ that they fixed in the range -14÷-18 kPa. Doing this way, they assumed that θ_f is very close to the θ_r value, thus letting the estimation of θ_r^0; on the contrary, in this paper, $h(\theta_f)$ was chosen by analogy to the well-known tension range for the calculation of the hydraulic properties of horticultural substrates, such as the 'easy available water' value. On the basis of these results, the comparison of the water retention function gives us a deeper understanding of the whole estimation capability. Figure 2 shows the experimental data, the B&C and VG plot of the function, as well. As one can see, the main difference between B&C Eq. 2 and VG Eq. 13 estimated curve lies in the very wet range (i.e. $h(\theta)<-1$ kPa), being all the rest almost overlapped. Both the predictions by Valiantzas *et al*. (2007) and Valiantzas and Londra (2012) don't match the experimental water retention results (data not shown), most likely because of the same reason above explained. Moreover, the B&C Eq. 2 model, related only to One-Step procedure, seems to have the same power of estimation of the VG Eq. 13 model, both of them being in optimal agreement with the experimental water retention data.

Figure 3 provides us information about the sensitivity of Eq. 16 calculating $K(\theta)$ as unknown variable. In fact, despite the large difference between the estimation of $D(\theta)$ with VG-M (retention and diffusivity data) and VG-M (retention only) curve by Eq. 15, the influence of the specific water capacity $C(h)$, being the first derivative of the $\theta(h)$ curve, results in a much narrow gap between the respective $K(\theta)$ curves. In fact, except for the VG-M (retention only) model applied to Pure Pumice, which leads to a remarkable discrepancy in the wet range, the estimated functions are close to each other, relatively to each substrate. In this respect, the RETC code computation of experimental data coming only from One-Step procedure provides a sound basis comparison with the improved iterative method by Bibbiani (2002).

Conclusions

This study aims to compare different methods for the simultaneous determination of the hydraulic properties of growing media from One-Step experiment, exploiting the capability of the latter procedure to estimate the diffusivity function. Valiantzas *et al*. (1988, 1990, 2007) and Valiantzas and Londra (2012) set up attractive equations for this task. From their approach stems the Bibbiani (2002) improvement of the estimation method, based on Brooks and Corey equation for water retention, and Kozeny power equation for hydraulic conductivity. An independent set of 9 water retention experimental data allows the comparison of estimated curves. Moreover, the RETC software with the Van Genuchten model is performed, resulting in other two estimations of the hydraulic function: the first one coming only from water retention experimental data, the second one computing retention and diffusivity

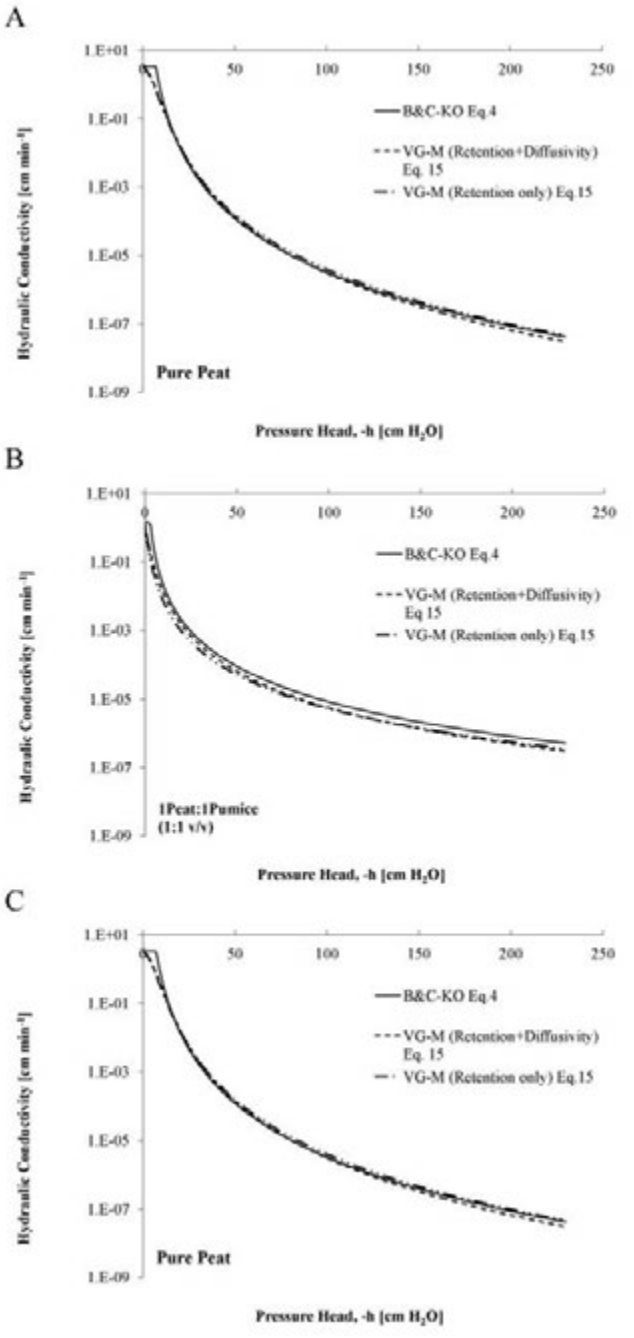

Figure 3. Substrate water conductivity K(h) as a function of pressure head -h, estimated by various equations. (A). Pure Pumice (B). 1Peat:1Pumice (1:1 v/v) (C). Pure Peat.

data from One-Step experiment.

Due to different requirements related to the final pressure head applied in One-Step experiment, Bibbiani's method leads to a good estimation of hydraulic functions for the three horticultural substrates in agreement with the Van Genuchten model, while the Valiantzas and Londra (2012) set of equations show poor applicability to this particular choice of the final pressure head.

References

Bibbiani C. 2002. An iterative procedure to estimate hydraulic characteristic of plant substrates from One-Step outflow data. Agricoltura Mediterranea 132:232-245.

Burdine, N.T. 1953. Relative permeability calculation from pore size distribution data. Trans. Am. Inst. Min. Eng., 198, 71-78.

Da Silva F.F. 1991. Static and dynamic characterization of container media for irrigation management. Thesis for MSc, Faculty of Agriculture; Hebrew University of Jerusalem.

Gardner W.R. 1962. Note on the separation and solution of diffusion type equation. Soil Sci. Soc. Am. Proc. 26, 404.

Johrar R. K., van Dam J. C., Bastiaansan W. G. M., Feddes R. A. 2004. Calibration of effective soil hydraulic parameters of heterogeneous soil profiles, J. Hydrol., 285, 233–247.

Mualem Y. 1976. A new model for predicting the hydraulic conductivity of unsaturated porous media. Water Resour. Res. 12:513-522.

Passioura J.B. 1976. Determining soil water diffusivity from one-step outflow experiments. Aust. J. of Soil Res. 15, 1-8.

Schneider C.L., Attinger S., Delfs J.O., Hildebrandt A. 2009. Implementing small scale processes at the soil– plant interface—the role of root architectures for calculating root water uptake profiles. Hydrol. Earth Syst. Sci. Discuss., 6, 4233-4264. http://www.hydrol-earth-syst-sci-discuss.net/6/4233/2009/

Valiantzas J.D., Kerkides P., Poulovassilis A. 1988. An improvement to the One-Step method for the determination of soil water diffusivities. Water Resour. Res. 24:1911-1920.

Valiantzas J.D. 1989. A simple approximate equation to calculate diffusivities from One-Step experiments. Soil Sci. Soc. Am. J. 53, 342-349.

Valiantzas J.D., Kerkides P. 1990. A simple iterative method for the simultaneous determination of soil hydraulic properties from One-Step outflow data. Water Resour. Res. 26:143-152.

Valiantzas J.D., Londra P.A., Sassalou A. 2007. Explicit formulae for soil water diffusivity using the Ona-Step outflow technique. Soil Sci. Soc. Am. J. 71:1685-1693.

Valiantzas J.D., Londra, P.A. 2012. Simplified equations for the determination of the hydraulic properties of horticultural substrates by One-Step outflow experiments. J. Plant Nutr. Soil Sci. 175:49-52.

Van Genuchten M.Th. 1980. A closed-form equation for predicting the hydraulic conductivity of unsaturated soils. Sci. Soc. Am. J. 44:892-898.

Van Genuchten M.Th., Leij F.J. and Yates, S.R. 1991. The RETC code for quantifying the hydraulic functions of unsaturated soils. Robert S. Kerr Environmental Research Laboratory Office of Research and Development, U.S. Environmental Protection Agency, ADA, Oklahoma 74820.

Production and reuse of waste in rural area with high density of greenhouse

Giovanni Russo, Giuseppe Verdiani

Department of Agro, Environmental Science (DISAAT), "Aldo Moro" University of Bari, Italy

Abstract

Agricultural activities cause the production of considerable amounts of waste sometimes dangerous that must be properly handled to avoid negative impacts on rural areas and on agroecosystems. The estimation of qualitative and quantitative characteristics of agricultural waste products and the capacity of rural land of transposing organic matter deriving from the processes of composting, is a key point for the planning and management of the waste integrated cycle. The aims of this study are the evaluation of the quantities of various types of agricultural waste on territorial scale, the amount of compost that can be used in rural areas affected by different cultures and the effectiveness of community composter in the treatment of vegetable agricultural waste for the production of green composted soil. These assessments were carried out in an area of study characterized by a high spatial density of greenhouses. The methodological procedure used is based on the use of agricultural waste production coefficients and maximum application rates of compost for cultivation. The results show the role and potential of the agricultural areas in the waste cycle from production to the potential reuse of recovered material.

Introduction

The rural areas plays a key role in the mitigation of environmental risks related to the management of urban and agricultural wastes. Besides the production of waste produced by farms, may be present in a rural area municipal or industrial wastes treatment plants that increase the environmental risk. In addition, rural areas are the final delivery for many organic wastes.

The industrial waste treatment facilities in the rural areas can cause negative impacts on the ecological balance, landscape, degree of naturalness (Pivato *et al*., 2012). The construction and operation of these plants is, however, necessary in order to reduce the environmental impact of the production of urban and special waste. These plants allow the recovery/recycling, volume reduction, mitigation of hazards, disposal in sanitary safety. The need to build and operate landfills, recycling and composting plants, waste to energy and waste collection centers must therefore be combined with the simultaneous target to protect the environment, the landscape, human health and quality of agricultural and livestock production. In this context is necessary mitigate the health and environmental risks determined by waste treatment plants. For the prevention and reduction of pollution caused by waste management activities, the European Directive 2008/1/EC identifies the measures to be adopted to reduce emissions to air, water and soil. According to this Directive, waste treatment plants must be built and operated by applying the "Best Available Techniques" in order to reduce the overall impact on the environment.

It 'also necessary to act on the management of waste from the stage of production, collection and transport through proper planning and organization (Calabrò, 2009).

The management of agricultural waste in rural areas is a complex problem that must, therefore, be addressed in the context of proper coordination between land use, planning and integrated cycle of wastes (Dal Sasso *et al*., 2009). Waste management plans are identified by Legislative Decree no. 152/06 as important tools to make sustainable waste cycle, in terms of environmental and economic possibilities. These plans should indicate the method of the collection and treatment of wastes at regional and provincial level on the basis of qualitative and quantitative characteristics.

In Italy, the evaluation of agricultural waste is uncertain because they are left in the environment, burned in an uncontrolled manner (Picuno and Scarascia Mugnozza, 1994) and transferred illegally in road bins for the collection of municipal waste. The above reasons prevent a proper evaluation of the amount of agricultural waste produced especially in rural areas characterized by the presence of small farms, this makes difficult the drafting of management plans for agricultural waste.

The agricultural waste management plans of the Abruzzo Region and the Florence Province have made a significant and concrete impulse to the proper management of national agricultural waste.

It is expected in them the selective collection of recyclable fraction of the waste (cardboard, plastic and wood, used oil, batteries and accumulators) by means of the operators of waste management services and the creation of centers of collection of separated waste in accordance with Ministerial Decree 08/04/2008 and Ministerial Decree of 13/05/2009. These collection centers may be used for the transfer of many different types of agricultural waste for recovery/recycling. In this way are increased the "indices of recovery/recycling" of agricultural waste and emissions are reduced due to transport with the ability to

Correspondence: Giuseppe Verdiani, Department of Agro, Environmental Science (DISAAT), "Aldo Moro" University of Bari, via Amendola 165/A 70126 Bari (Italy). Tel./Fax: +39.080.544 2960.
E-mail: giuseppeverdiani@hotmail.it.

Key words: agricultural waste, compost, environmental sustainability

Contributions: the paper is to be attributed to the authors in equal measure.
Acknowledgments: this research has been funded by the Italian Ministry of Agriculture, Food and Forestry MIPAAF, programme OIGA III, 17/10/2010 - ID 145– "SEABIA - Ecological and low impact substrates".

Journal of Agricultural Engineering 2013; XLIV(s2):e48
doi:10.4081/jae.2013.(s1):e48

organize and plan the itineraries of collection vehicles in the area.

The environmental impacts associated with the management of agricultural organic waste can be further reduced through their treatment and recovery on site. Are in fact available small plants (community composters, biomass heating plants, bio-gas plants) that can be installed in the farm. These plants are used to treat organic waste and to obtain compost and/or energy for use in agro-industrial processes and in particular in greenhouse sector. In fact, the compost can be used as a component of growing media of ornamental potted plants to reduce the amount of peat (De Lucia et al., 2009) and the renewable thermal energy can be used for greenhouse heating to reduce the consumption of fossil fuels (Scarascia Mugnozza *et al*., 2012).

The assignment of agricultural waste collection service to the municipal waste management services and the installation of on-site organic waste treatment plants, can improve the financial statements of farms, the rural landscape and the environment. These aspects have significant importance because the agricultural sector in 2008 was responsible for the production of about 440,000 t year^{-1} of waste on a national scale (ISPRA, 2011) and 9,000 t year^{-1} in the Puglia Region (ARPA Puglia, 2010). In Italy, in recent years, have been reduced environmental burdens connected to the waste cycle and has been improved the human/environment interaction thanks to the increase of the recovery of agricultural waste and a simultaneous reduction in the use of landfills (Atrigna *et al*. 2011).

A large quantity of agricultural waste consists of plastics (Scarascia Mugnozza *et al*., 1999) due to the increasing use of plastic films in agriculture for greenhouses covering, mulching and crop protection (Scarascia Mugnozza *et al*., 2007). During their use, the plastic films are subject to the reduction of mechanical strength (modulus of elasticity and elongation % at break) and radiometric characteristics (reduction of transmissivity in PAR) due to the action of external climatic factors and therefore are periodically replaced (Picuno *et al*., 2009). In fact, we can estimate the production of agricultural waste plastic films consist of about 110,000 t year^{-1} in Italy (Dal Sasso *et al*., 2009) equal to 25% of total agricultural waste. These plastic wastes are often used in cement industries, however, their qualitative characteristics and the percentage of contaminants depend on the previous use (greenhouses, tunnels, mulching, etc.). (Briassoulis *et al*., 2012). The other agricultural waste, are made by: agrochemicals containers, tires and batteries of agricultural vehicles, paper/cardboard packaging, wood, iron.

At the same time, in agricultural activities can be used plastic film, produced through recycling of plastic waste (Picuno *et al*., 2009) and substrates products through composting of pruning and organic waste (De Lucia *et al*., 2009).

The composting process reproduces, under controlled conditions, the natural decomposition and humification of organic substances (Zorzi *et al*., 2010) by the combined action of microorganisms and chemical-physical reactions. The correct evolution of biological and biochemical reactions that characterize the composting process is related to chemical - physical parameters such as: moisture, pH, carbon/nitrogen ratio in the treated waste (Atrigna *et al*., 2011). The composting determines the mineralization of the organic substance, the production of humic acids and the production of a stable end-product defined by Italian legislation "composted soil". The composting process can be realized in industrial plants with high potential of treatment, in domestic composters and in the modern electromechanical composter plants for community with treatment capacity of about 25 waste tons year^{-1} (Figure 1). Community composting is a intermediate level between home composting and industrial composting and may be able to provide a treatment of organic waste physically near the production site (Accotto, 2011). The large distance of the rural areas by industrial composting facilities makes this solution economically and ecologically interesting (Silingardi, 2011) although the energy consumption is about 15 kWh t^{-1} treated.

Depending on the type of organic waste that are subjected to composting, soil improvers are classified by Legislative Decree n. 75/2010 as "Mixed composted soil improvers" (MCSI) and "Green composted soil improvers." (GCSI). The GCSI is produced exclusively from vegetable organic wastes (crop residues, agricultural residues, pruning of urban green) while the MCSI is produced from the treatment of municipal organic waste, sludge from the treatment of urban waste water and agro-industrial wastes, cuttings and prunings.

The composting of organic waste and the use of MCSI or GCSI in different agricultural sectors can help to solve two problems at the planetary level: the disposal of organic waste and the reduction of the environmental burden of agricultural process.

The use of quality compost in agriculture can make a significant improvement for agricultural food production more environmentally friendly, and allows to increase the fertility of agricultural soil, reduce erosion and irrigation requirements of the crop (Favoino and Hogg, 2002). Furthermore, the application of compost improves the biological conditions of agricultural soil by increasing the level of organic matter and humus and ensuring an adequate supply of nutrients to maintain the crops in an appropriate vegetative state with repercussions on productivity (Baldi *et al*., 2008).

In 2009, 3.715.302 tons of organic waste were transferred to national composting plants and 976,424 tons of soil improvements, which complies with the quality standards imposed by Legislative Decree no. 75/2010, were produced (ISPRA, 2011). The soil improvements have been used in agriculture, in open field cultivation (70%) and in gardening and landscaping sector (30%) (Centeremo, 2011). Landfill disposal of 3,715,302 tons of organic waste would have resulted in the consumption of useful volumes for other waste, leachate, emission of approximately 7,200,000 tonnes of biogenic CO_2. The qualitative and quantitative characteristics of the leachate and biogas produced in landfills are in fact strongly influenced by the mineralization of available organic matter and biokinetic (APAT, 2005). In landfills, the high moisture content of the organic wastes produces percolate with a high content of organic substances that together with the production of biogas results in sagging of the final cover.

The objective of this study was to determine a methodology for the evaluation of the quantity and typologies of agricultural waste and, at the same time, to quantify the amount of compost used in the agricultural sector in a particular rural area. In order to assess the role of the agricultural land in the integrated waste cycle, this methodology was applied to a rural sample area. The qualitative characteristics of an GCSI obtained from a community composter were determined using data from a greenhouse farm present in the area sample as standard. The proposed methodology allows to steer management of the collection, transport and treatment of agricultural waste to environmental sustainability.

Materials and methods

Within of the present study were evaluated potential production of agricultural waste in a rural area sample of the Puglia Region, the amount of soil improver that can be used in agriculture and the effectiveness of a community composting plant fueled by pruning .

In order to estimate the flows of waste and soil improvers used in a territory, a methodology based on the analysis of cartographic data and information relating to the production of waste was used (geographical information system - GIS). For each crop present in the analyzed area were acquired application rates of soil improver from reference data

(Agricultural Integrated Management Regulation of the Tuscany Region, 2004).

Sample area

The sample area analyzed is the Optimal Collection Area no. 1 (ARO 1) which includes the municipalities of Bitonto, Corato, Molfetta, Terlizzi, Ruvo di Puglia (Figure 2). This geographical area has been identified according to the Puglia Regional Law no. 24/2012 for improving the waste management in compliance with the principles of differentiation, adequacy and efficiency. The area object of study is characterized by a total surface of 69,470 ha, from a suburban area with a strong agricultural vocation, by the high presence of greenhouse and the absence of widespread abandonment cultivation

Community composter

The community composter has been installed in the Municipality of Molfetta within the greenhouse farm "Primavita Srl". In order to compost organic waste coming from: the farm's pruning, horticultural residues and olive pruning produced in the study area, an automatic composter "BEETLE 50" (Comar Ecology) (Figure 3) was used. The plant consists of a cylindrical tank in insulated stainless steel, inside which there is a composting chamber characterized by a volume of 1.32 m^3. The composting process is automatically controlled because turning over and the progress of the organic material is carried out by an electromechanical system with shovels. The heating of the composter is provided by n. 2 electric heaters and is thermostatically controlled. The aeration in the composted mass is realized by a geared motor that moves the waste at time intervals ensuring optimal oxygenation and reduction of the size of the particles produced by the process. The composter is equipped with an automatic ventilation system that draws air from the outside and feeds it into the composting chamber with recirculation. The waste water resulting from the composting process is collected in a tank of 10 lt. for subsequent treatment (reuse in community composter) or for disposal. The composter has been combined with a Honda GX340 shredder to ensure adequate and uniform size of the vegetable organic material to be composted.

Applied methodology

Analysis of the rural territory

Territorial analysis of the ARO 1 was conducted using geographical information systems (GIS) with the support of the ESRI ArcMap software. The data provided by the software and analyzed were: land use, spatial distribution of crops, greenhouses, tunnels and tendone systems. Specifically, have been used the land use thematic map of the Puglia Region at 1:5000 scale according to standard European CORINE

Figure 1. Community composter.

Figure 2. Municipal Limits of ARO 1.

Table 1.Coefficients of agricultural waste production.

Type of waste products	Description of owaste	Type of ocultivation	Coefficient of production	Unit of measure	Bibliographic source
Plastic waste from primary production	Plastic films for greenhouse covering	Horticultural greenhouse Vineyards covered	1.25	t ha^{-1} $year^{-1}$	ANPA, 2000
	Plastic films for mulching	Horticultural	0.3	t ha^{-1} $year^{-1}$	Cadir - Lab, 1994
	Irrigation pipes	Irrigation crops	0.06	t ha^{-1} $year^{-1}$	ANPA, 2000
	Nets storm and shade	Vineyards	0.04	t ha^{-1} $year^{-1}$	ANPA, 2000
Plastic packaging	Packaging of fertilizers and soil improvers	Arable crops	0.0027	t ha^{-1} $year^{-1}$	Cadir - Lab, 1994
		Fruit trees	0.0018	t ha^{-1} $year^{-1}$	Cadir - Lab, 1994
		Horticultural	0.003	t ha^{-1} $year^{-1}$	Cadir - Lab, 1994
Agrochemical waste	Empty agrochemicals containers	Arable crops	0.0005	t ha^{-1} $year^{-1}$	Cadir - Lab, 1994
		Vineyards and olive trees	0.0012	t ha^{-1} $year^{-1}$	Cadir - Lab, 1994
		Fruit trees	0.0028	t ha^{-1} $year^{-1}$	Cadir - Lab, 1994
		Horticultural	0.0009	t ha^{-1} $anno^{-1}$	Cadir - Lab, 1994
Vegetable waste from primary production	Cuttings and prunings	Vineyards	2.4	t ha^{-1} $anno^{-1}$	ANPA, 2000
		Fruit trees	2.75	t ha^{-1} $anno^{-1}$	ANPA, 2000
		Olive trees	1.7	t ha^{-1} $anno^{-1}$	Cotana e Cavalaglio, 2008

Land Cover and regional digital color orthophoto with a ground pixel resolution of 50 cm. In order to extract information on the area: occupied by the different agricultural crops (olive groves, vineyards, orchards, crops, vegetables), covered by greenhouses and screenhouse, mulched with plastic film areas, were realized photo-interpretation and geo-processing on the cartographic bases employed.

Calculation of agricultural waste production on a regional scale

The quantitative and qualitative evaluation of the typologies of agricultural waste in the study area was carried out by applying the factors of production that combine the spatial extent of the different cultivated areas to the quantities of waste produced. The coefficients of production of agricultural waste typologies that characterize the different cultivations (Table 1) were thus extrapolated from literature sources.

Evaluation of the amount of MCSI that can be used in the agricultural areas

The evaluation of the amount of MCSI that can be used in the area was made on the basis of maximum doses of nutrients (N, P, K) that can be applied to the soil. These quantities are given in the Agricultural Integrated Management Regulation of the Tuscany Region (2004) for each crop and take into account the expected normal fertilization. The maximum amount by weight of MCSI that can be applied annually to different crops is shown in Table 2.

These collected data have allowed to calculate the mass of organic wastes from urban and agricultural areas required for the production of MCSI that can be applied within the study area. This calculation was performed assuming the hypothesis that 1 kg of organic waste produces 0.3 kg of MCSI. It was also verified whether the amount of municipal organic waste in the ARO 1 may be entirely destined for composting and reused in the provenance rural areas.

Assessment of the community composter effectiveness

For the assessing the effectiveness of the composter are ongoing experimental composting tests by different agricultural organic matrices. Were carried out chemical - physical analysis of composted organic matrices and produced GCSI. In the composter were conferred: pruning olive trees, and horticultural and floricultural organic waste. In order to enter in the chamber of composting a mixture with particle size between 1-10 cm, low percentage of impurity, moisture content of between 50-70% and a C/N ratio between 20 and 30, the organic material was triturated in Honda GX340 shredder. The analysis carried out (Table 5) On organic matrices showed a reduced nitrogen content. For this reason, in the composting chamber was introduced Urea for ensuring an adequate ratio C/N needed to start the process. This additive is permitted by the legislation on the environment and fertilizers.

Figure 3. Beetle community composter.

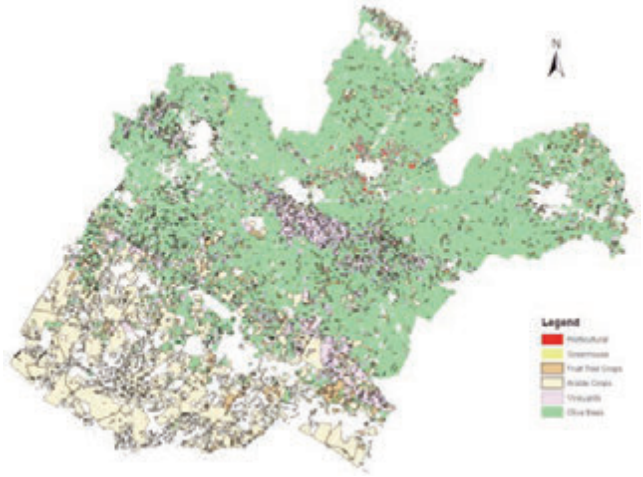

Figure 4. Land use in rural areas of ARO.

Results and discussion

Characteristics of the rural territory of ARO 1

The utilized agricultural area (UAA) in the ARO 1 is about 54,990 ha and is being used for the cultivation of: horticultural crops (330 ha) and flower (700 ha) in the open field and greenhouse, cereal (13730 ha), grapes (3760 ha), olive trees (34850 ha) and fruit trees (1620) (Table 3 - Figure 4). The cultivated area is partially characterized by the presence of greenhouse and tunnels (about 338 ha), plastic film (about 81.0 ha) and plastic nets (about 564.0 ha) for "tendone systens" used for grapefruit cultivation.

Table 2. Maximum application rate of compost.

Type of cultivation	Maximum application rate of compost	Unit of measure
Arable crops	7.3	t ha^{-1} $anno^{-1}$
Horticultural	14.3	t ha^{-1} $anno^{-1}$
Fruit trees and vineyards	7.1	t ha^{-1} $anno^{-1}$

Table 3. Agricultural use of land.

Type of cultivation	Surface [ha]	%
Horticultural crops	330	0.6
Flower	700	1.3
Arable crops	13,730	24.9
Olive trees	34,850	63.5
Vineyards	3,760	6.8
Fruit trees	1,620	2.9
Total	54,990	10

Table 4. Production of agricultural waste in ARO 1.

Type of waste	Description of waste	Amount of waste produced	Unità di misura
Plastic waste from primary production	Plastic films for greenhouse covering	523.75	t year^{-1}
	Film plastici per la pacciamatura	99.0	t year^{-1}
	Plastic films for mulching	384.6	t year^{-1}
	Irrigation pipes	22.56	t year^{-1}
Plastic packaging	Packaging of fertilizers and soil improvers	110.47	t year^{-1}
Agrochemical waste	Agrochemicals empty containers	58.03	t year^{-1}
Vegetable waste from primary production	Cuttings and prunings	72724.0	t year^{-1}

Table 5. Chemical properties of the organic matrices.

Chemical element	Value for olive pruning	Value for horticultural vegetable waste	Unit of measure
Nitrogen	0.45	0.49	g/100g of dry matter
Organic carbon	42.4	40.5	g/100g of dry matter
Rate Organic carbon/Nitrogen	94	83	
Phosphorus	0.04	<0.01	g/100g of dry matter
Potassium	0.51	0.51	g/100g of dry matter
Sodium	0.188	0.063	g/100g of dry matter
Calcium	1.58	1.16	g/100g of dry matter
Magnesium	0.27	0.09	g/100g of dry matter
Iron	258	227	g/100g of dry matter
Copper	266	5	g/100g of dry matter
Zinc	47	17	g/100g of dry matter

Production and management of agricultural waste

In the rural area of the ARO no. 1 are produced about 1,030 t year^{-1} of plastic waste annually, 73,000 t year^{-1} of cuttings and prunings and 58 t year-1 of pesticides used containers. In Table 4 are specified the quantities of each type of waste products estimated through the production coefficients extrapolated from the literature and shown in Table 1.

Plastic wastes, mainly composed of film for covering greenhouses and plastic nets for tendone system, represent the fraction of agricultural waste that creates more environmental and landscape issues. The organization of the collection of this waste for delivery to collection centers may represent a useful solution economically and environmentally.

The collection of plastic waste can have an economic benefit to be distributed among the municipal authority and the service provider for the collection and, to confer this waste to recycling facilities thus avoiding mismanagement of plastic waste by farmers (eg. uncontrolled burning, abandonment, illegal dumping).

A particularly dangerous agricultural waste are used containers of agrochemicals that may have a significant environmental and health risks both. These containers must be disposed of as special waste (Legislative Decree 152/2006) for the serious damage to the environment and persons that substances contained are likely to cause. The collection of these containers from the waste management urban services could allow a correct treatment thus avoiding illegal disposal. Are widespread in northern Europe washing plants for empty containers of agrochemicals which allows to reduce the hazardous properties and to promote recycling as plastic. The washing procedure allows the removal of agrochemicals inside the containers and purification of wastewater deriving from the washing. The wastewater is then treated in bio-filters that are made from organic material called "bio-beds".

Table 6. Amount of MCSI usable in the ARO 1.

Type of cultivation	Maximum application of compost	Unit of measure
Cereal crops	100229	t year^{-1}
Horticultural crops	4719	t year^{-1}
Fruit trees and vineyard	38198	t year^{-1}

The organic matter present in the bio-bed absorb pollutants and facilitate their biodegradation due to metabolic activity of the microbial component.

The cuttings and prunings are in some cases re-used in farms (green manure, fuel, etc.) and it is therefore necessary to provide for collection in composting plants, only for farms that want this service. An interesting solution for the recycling of organic waste produced in rural areas far from composting plants is represented by the composter community. At community composting plant installed in the greenhouse company "Primavita Srl" were introduced the pruning of olive tree and horticultural and floricultural residues. The organic matrices treated were analyzed for their chemical and physical characterization (Table 5) as well as the product compost. The compost was used to replace in whole or in part the peat used in the substrates. This practice reduces the environmental load because the peat comes from Northern Europe and is being depleted.

Compost usable in ARO 1

The application of MCSI on agricultural soil of the ARO 1 must not exceed 143,146 t year-1. This amount is allocated to the agricultural areas used for cultivation of different crop types as specified in Table 6. The application of these quantities can improve the chemical - physical

and microbiological soil property thus avoiding nitrate leaching and, therefore, without compromising the groundwater quality.

The amount of organic waste required for the production of MCSI is about 429,438 tonnes. In the ARO 1 in the year 2012 were produced 102,263.2 tons of municipal solid waste (MSW) which are composed by 35% of organic material (www.rifiutiebonifica.puglia.it). The municipal organic waste produced by domestic users and non-domestic (schools, offices, commercial activities) in the in the ARO 1 are approximately about 108,516 tons and can therefore be entirely destined for composting and be used in local agriculture. To achieve high levels of use in agriculture of GCSI and MCSI are needed adequate awareness and incentives for farmers. The use of MCSI and GCSI is, in fact, a complementary activity to the recycling of organic waste that needs adequate support through Measure 214 "Payment Agro - Environmental" of the Rural Development regarding the adoption of sustainable methods of agricultural production and land management.

Conclusions

The carried out work provides an appropriate methodology for evaluating the amount of agricultural waste generated and the calculation of the maximum amount MCSI applicable on agricultural soil on a territorial scale.

The evaluation of the maximum utilization rate of MCSI on a territorial scale, and the drafting of appropriate fertilization plans can improve the characteristics of the soil and of agricultural production without damaging the quality of the environmental matrices.

The ability to obtain information on the production of agricultural waste, divided by type, allowing both rapid quantitative estimate, and the correct programming of the collection, transport and disposal/reuse. In this context, the activation of the collection service of plastics waste (plastic films for greenhouses and tendone system, mulching films, agrochemicals empty containers) can increase separate plastic waste collection and their recycling. This collection service may be entrusted to the manager of waste management services or to farmers. The use of GIS can provide valuable support to the organization of the routes and frequencies of collection of agricultural waste as it allows to identify the spatial distribution of production.

The organic vegetable waste, can be transferred and processed in community composters placed in rural areas for the production of GMSI, to be used then for the crops, thus reducing transport for disposal. In order to reduce emissions due to uncontrolled burning or transport, this use permits reuse for agricultural purposes with clear environmental benefits.

The present study thus shows that the rural areas can play an important role in the waste cycle from production to recycling.

References

ANPA, Agenzia Nazionale per la Protezione dell'Ambiente. 2000. I rifiuti del comparto agricolo.

APAT, Agenzia per la Protezione dell'Ambiente e per i Servizi Tecnici. 2005. Criteri metodologici per l'applicazione dell'analisi assoluta di rischio alle discariche.

ARPA Puglia, Agenzia Regionale per la Protezione Ambientale. 2010. Relazione sullo stato dell'ambiente.

Atrigna M., Canditelli M., Faustini N., Pescheta G. 2011. La gestione della frazione umida/biodegradabile dei rifiuti urbani. Rifiuti Solidi. 2:101-109.

Baldi E., Toselli M., Marangoni B., Innocenti A., Scudellari D. 2008. Pesco, l'uso del compost migliora la fertilità del suolo. Agricoltura. 1:101-102.

Briassoulis D., Hiskakis M., Babou E., Antiohos S.K., Papadi C. 2012. Experimental investigation of the quality characteristics of agricultural plastic wastes regarding their recycling and energy recovery potential. Waste Management. 32(6):1075–1090.

CADIR-LAB. 1994. Ipotesi di progetto pilota per la raccolta e lo smaltimento di rifiuti agricoli e contenitori esausti di fitofarmaci nell'alessandrino.

Calabrò P.S. 2009. Greenhouse gases emission from municipal waste management: The role of separate collection. Waste Management. 29:2178-2187.

Centeremo M. 2011. Stato dell'arte del compostaggio e digestione anaerobica da rifiuto organici in Italia. Atti della Conferenza nazionale sul compostaggio e la digestione anaerobica, Ecomondo November 2011, Rimini, Italy.

Cotana F., Cavalaglio G. 2008. La valorizzazione energetica delle potature di ulivo. Quaderni Ercole Olivario. 5.

Dal Sasso P., Scarascia Mugnozza G., Marinelli G. 2009. La raccolta di rifiuti plastici in agricoltura: proposta di organizzazione territoriale nelle zone agricole dell'area metropolitana di Bari. Atti del IX Convegno Nazionale dell'Associazione Italiana di Ingegneria Agraria "Ricerca e innovazione nell'ingegneria dei biosistemi agro-territoriali", September 14-16, Ischia, Italy

De Lucia Zeller B., Ingravalle S., Russo G., Scarascia Mugnozza G., Vecchietti L. (2009). Analisi ambientale e agronomica di substrati per piante in vaso da rifiuti organici e agroindustriali. Atti del IX Convegno Nazionale dell'Associazione Italiana di Ingegneria Agraria "Ricerca e innovazione nell'ingegneria dei biosistemi agro-territoriali", September 14-16, Ischia, Italy

Legislative Decree n. 36/2003. Attuazione della direttiva 1999/31/CE relativa alle discariche di rifiuti.

Legislative Decree n. 152/2006. Norme in materia ambientale.

Legislative Decree n. 75/2010. Riordino e revisione della disciplina in materia di fertilizzanti.

Ministerial Decree of 08/04/2008. Disciplina dei centri di raccolta dei rifiuti urbani raccolti in modo differenziato.

Ministerial Decree of 13/05/2009. Modifiche al Decreto Ministeriale del 08/04/2008 sulla disciplina dei centri di raccolta dei rifiuti urbani raccolti in modo differenziato.

European Directive 2008/1/CE. Prevenzione e riduzione integrate dell'inquinamento.

Favoino E., Hogg D. 2002. Biowaste and climate change: a strategic assessment of composting. Gestion des d'echets et changement climatique.

ISPRA, Istituto superiore per la Protezione e la Ricerca Ambientale. 2011. Rapporto sui rifiuti speciali

Picuno P., Scarascia Mugnozza G. 1994. The management of agricultural plastic film wastes in Italy. Proceedings of the International Agricultural Engineering Conference, 6-9 December, Bangkok, Thailandia.

Picuno P., Scarascia Mugnozza G., Sica C. (2009). Proprietà meccaniche e radiometriche di film plastici rigenerati da granulo riciclato di origine agricola. Atti del IX Convegno Nazionale dell'Associazione Italiana di Ingegneria Agraria "Ricerca e innovazione nell'ingegneria dei biosistemi agro-territoriali", September 14-16, Ischia, Italy.

Pivato A., Vanin S., Palmeri L., Barausse A., Mangione G., Rasera M., Monego G. (2012). La Biopotenzialità come indicatore di compensazione ambientale per un impianto di compostaggio. Rifiuti

Solidi. 1:23-31.
Regione Toscana. 2004. Disciplinare di produzione integrata.
Scarascia Mugnozza G., Vox G., Picuno P. 1999. Metodologie di analisi territoriale in relazione all'uso di plastiche per le coltivazioni protette. Atti del Seminario dell'Associazione Italiana di Ingegneria Agraria "Le colture protette: aspetti agronomici, territoriali e tecnico-costruttivi", June 24-26 , Ragusa, Italy.
Scarascia Mugnozza G., Dal Sasso P. 2007. Film biodegradabili: aumenta il loro impiego nelle colture protette. Colture Protette. 36(8):85-94.
Scarascia Mugnozza G., Pascuzzi S., Anifantis A., Verdiani G. 2012. Use of low-enthalpy geothermal resources for greenhouse heating: an experimental study. Acta Scientiarum Polonorum. 11:13-19.
www.rifiutiebonifica.puglia.it
Zorzi G., Silvestri S., Cristoforetti A. 2010. Il compostaggio e il suo ruolo strategico in un sistema integrato di gestione dei rifiuti. Rifiuti Solidi. 2:105-117.

Solar radiation inside greenhouses covered with semitransparent photovoltaic film: first experimental results

Alvaro Marucci,[1] Adolfo Gusman,[2] Barbara Pagniello,[1] Andrea Cappuccini[1]

[1]Department of Agriculture, Forests, Nature and Energy (D.A.F.N.E.); University of Tuscia, Viterbo, Italy; [2]External collaborator

Abstract

The southern Italian regions are characterized by climatic conditions with high values of solar radiation and air temperature. This has allowed the spread of protected structures both as a defense against critical winter conditions both for growing off-season. The major energy source for these greenhouses is given by solar energy and artificial energy is used rarely. So the problem in the use of greenhouses in these areas, if anything, is opposite to that of the northern areas. In these places you must try to mitigate often the solar radiation inside the greenhouses with suitable measures or abandon for a few months the cultivation inside these structures. The solar radiation intercepted by passive means can be used for other purposes through the uptake and transformation by the photovoltaic panels whose use however is problematic due to complete opacity of the cells. New photosensitive materials partially transparent to solar radiation onto flexible media, allow to glimpse the possibility of using them to greenhouses cover, getting the dual effect of partially screen the greenhouse and use the surplus to generate electricity. The research was carried out to evaluate the possibility of using a flexible photovoltaic film realized by the University of Rome Tor Vergata (research group of ECOFLECS project coordinated by prof. Andrea Reale) for covering greenhouses. Two greenhouses in small scale were built: one covered with photovoltaic film and one covered with EVA film for test. In both greenhouses during the first research period it was grown a variety of dwarf tomato.

The research was carried out comparing the solar radiation that enters into greenhouse in the summer (August 2012) and in winter conditions (December 2012) in both greenhouses.

The result show that the average ratio between the daily global solar radiation under the photovoltaic film and outside radiation is about 37%, while between the radiation under EVA film and outside radiation is equal to approximately 63%.

These result allow us to assert that during the hot season the use of photovoltaic film might be useful to mitigate the excesses of solar radiation into the greenhouse. During the cold season the use of this film not allows to achieve the minimum indoor climate conditions for the cultivation, however, it is possible to think to remove it in the periods of low solar radiation because it is a very flexible film.

Correspondence: Alvaro Marucci, DAFNE, Department of Agriculture, Forests, Nature and Energy, University of Tuscia, 01100 Viterbo – Italy.
Tel. +39.0761.357365 - Fax: +39.0761. 357453
E-mail: marucci@unitus.it

Key words: Mediterranean greenhouse, photovoltaic film, solar energy

Acknowledgements: The work was carried out in the research project "ECOFLECS" – leader: Aero Sekur SpA.

Journal of Agricultural Engineering 2013; XLIV(s2):e49
doi:10.4081/jae.2013.(s1):e49

Introduction

The Italian agricultural landscape is often characterized by the presence of greenhouses for horticulture that ensure the continuity of production during all year independently of seasonal climate change. These structures, using the greenhouse effect produced by solar radiation that passes through the transparent surfaces, allow to reach and maintain the values of the different climate parameters, such as the indoor air temperature and relative humidity to suitable levels for the needs of plants.

The greenhouses are widespread in central and northern Europe, where it is difficult to cultivate horticultural crop in the field for long periods of the year due to the unfavorable climate. In the southern Europe, however, they are mainly used for the cultivation of vegetables and flowers out of season. In these "Mediterranean greenhouses", the main supply of energy for creating the microclimatic conditions is given by solar energy and the artificial energy only in the short cold periods (mostly at night). The agronomic research, the last building technology of greenhouses and the choice of transparent cover materials are today increasingly oriented to reduce the use of artificial energy to contain the cost of production and the environmental impact (Vox *et al.,* 2010; Marucci *et al.,* 2011a; Campiglia *et al*., 2007).

These greenhouses are especially prevalent in the central and southern Italy and in all countries bordering the Mediterranean such as Spain, Greece, Israel, etc. In these locations the intensity of solar radiation reaching the Earth's surface during some periods of the year is often excessive in relation to the needs and it causes the raising of the indoor air temperature to levels that are not tolerated by crops and by workers. Not long ago, during the summer months, the productive activity in greenhouses was suspended or if the cost of roofing materials was low, the transparent covering was removed transforming the protected crop in an open field cultivation. This practice has been recently resumed using the open roof greenhouse that completely cancels the greenhouse effect during periods of intense solar radiation. As an alternative to these solutions, we can use shade cloth that is placed on the greenhouse roof, cooling systems or, more simply, we can increase the natural ventilation through large openings or use mechanical ventilation. These solutions involve a significant increase in the costs of construction and operation.

Therefore, the main problem in these geographical areas is to try to

reduce the solar radiation into the greenhouse during summer months. Passive systems, such as the shade cloth or painting the cover (no longer in use), are able to reject only a portion of solar radiation through a significant reduction of the optical transmittance of the covering. This reduction can also reach very high values (greater than 80%) but it depends by the needs of the plants that require well identified quantitative and qualitative levels of light for their biological activity (Hurd, 1983; Kittas and Bailie, 1998 ; Kittas *et al.,* 1999).

The solar radiation rejected by passive means of protection (shade cloth and nets, etc..) could be more conveniently used for other purposes with appropriate means of uptake and transformation. Among these are of particular interest the photovoltaic panels that turn the solar energy into electrical energy.

The complete opacity of the material used for the cells (silicon), however, hinders the use of photovoltaic on greenhouses because the cells can be not crossed, at least in part, by solar radiation. The research of other materials to the photovoltaic energy production in substitution of silicon (Hua *et al*., 2009; Shin *et al*., 2010) that are partly transparent to solar radiation and the possibility of using flexible substrates for cells, give us a hope to apply such materials on greenhouse covering. The effect of the application of such materials is to reduce the radiation inside the greenhouse during periods of excess and use the surplus to produce electricity (Marucci *et al.*, 2012; Marucci *et al.*, 2013a).

A recent study on the applicability of photovoltaic systems on the Mediterranean greenhouses showed that the crop planning allows us to make better use of solar energy (Marucci *et al.*, 2013b*;* Marucci *et al.*, 2011b; Rouphael *et al*., 2010). For example, the tomato cultivation from October to April as well as having some energy surplus in the clear days of growing period, gives the full availability of solar energy in the summer months when the crop in the greenhouse is suspended.

At the University of Tuscia there is an ongoing research to evaluate the possible use of semi-transparent photovoltaic film as a greenhouse covering material. The work shows the results obtained by this research.

Materials and methods

The research was carried out on a recent model of organic photovoltaic film developed by the University of Rome Tor Vergata.

This film was made by inserting semitransparent photovoltaic modules between two layers of poly-vinyl-butyral. Spectrophotometric laboratory analysis has showed that the photovoltaic film has a transmittance of 48% and 69% respectively in the field of visible and near infrared radiation (Figure 1) (Marucci *et al.,* 2013a).

The refractive index of this material was calculated to determine the solar radiation reflected by a transparent surface, using the following equation:

$$\tau = \frac{4n_1 n_2}{(n_1+n_2)^2} \quad (1)$$

where τ t is the transmittance, n_1 is the refractive index of air and n_2 is the refractive index of the film. The values of this index were 4.341326 and 4.206651 respectively between 380 nm and 760 nm (visible) and 380 nm 1100 nm (visible and near infrared).

This photovoltaic film was used for covering the roof of a model of greenhouse specifically developed. A second model was covered with Eva film (Figures 2,3 and 4).

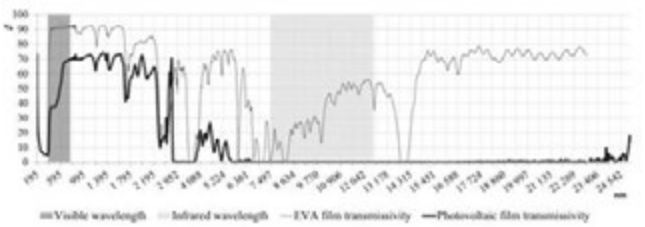

Figure 1. Transmissivity of photovoltaic and EVA films to solar radiation.

Figure 2. The two models covered with photovoltaic and EVA films.

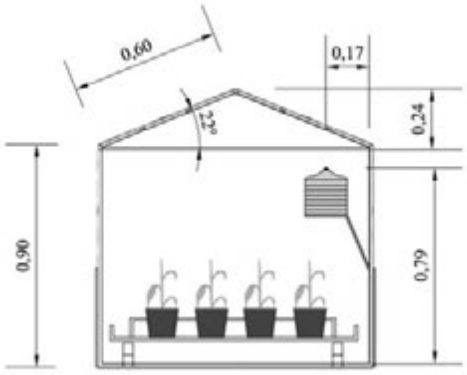

Figure 3. Section of the experimental model.

Figure 4. Models during the test.

In particular each model has, in plan, a length of 1.60 m, a width of 1.13 m, a height to the eaves of 0.90 m and to the ridge of 1.14 m. The roof pitch angle is 22°.

This angle value was chosen to make most similar models to full-scale greenhouses although it is known that an angle between 33° and 40° it seems, at latitude of Italy, more convenient to pick up the greatest amount of solar energy by south oriented surfaces. These last values of the roof pitch for a greenhouse do not allow to capture the greatest amount of solar energy (Candura and Gusman, 1977) and create different problems in form and static structure.

The two transversal walls of each model were coated with a four layers polycarbonate sheet. In one a fan of 1000 m^3h^{-1} was installed while in the other an aluminum manually adjustable shutter. The longitudinal walls were closed with opaque panels to a height of 0.40 m while the remaining 0.50 m were closed with an EVA film of 0.18 mm completely rolled up to the eaves. This closure has been used since the end of September while in the months of August and September has been kept rolled to promote a more effective ventilation.

Sensors to measure temperature, relative humidity of the air and solar radiation were installed, in each model, and precisely:

- N° 1 Thermo-hygrometer CS215 with weather shelter
- N° 1 Pyranometer CS300

The same instruments were installed in the greenhouse models and outside.

The data collected from these sensors were gathered into a CR1000 Datalogger with 16 channels and 8 IO ports. On a solid memory the instantaneous values of minimum, maximum and mean of temperature and air humidity, at 15-minute intervals, were recorded. Regarding the measurement of radiation, always with the same scan time, the instantaneous value in kWm^{-2} and the cumulative value in MJm^{-2} were recorded.

Identification of clear days

In order to evaluate the possibility of adopting the photovoltaic film for covering greenhouses, have been taken into account the solar radiation data on clear days of August and December. In the place where the greenhouses have been installed these months are usually characterized by extreme weather conditions.

For identifying the clear days, the values of the solar radiation measured by the outside radiometer with those obtained by the calculation with the mathematical model proposed by Hottel (Duffie *et al*., 1991) were compared. The model uses the extraterrestrial solar radiation, the Julian day, the zenith angle of the sun and the transmittance of the atmosphere:

Rg = global radiation at ground= Rb + Rd $[Wm^{-2}]$ (2)

Rb = direct radiation at ground = $Re_b \cos q_z$ $[Wm^{-2}]$ (3)

Rd = diffuse radiation at ground = $Re_d \cos q_z$ $[Wm^{-2}]$ (4)

where:

Re = outer radiation= 1367 (1 + 0.033 cos (360/365*n)) $[Wm^{-2}]$

n = Julian day

τ_b = transmissivity of the atmosphere to the direct radiation =

$$A_0 + A_1 \times e^{\frac{-K}{\cos\theta_z}}$$

τ_d = transmissivity of the atmosphere to the diffuse radiation= 0.271 - 0.294 τ_b

$$A_0 = [0.4237 - 0.00821(6 - A)^2]\left[1 + 0.03 \sin\left(\pi\left((91 + n)/182\right)\right)\right]$$

$$A_1 = [0.5055 - 0.00595(6.5 - A)^2]\left[1 + 1.01 \sin\left(\pi\left((91 + n)/182\right)\right)\right]$$

$$K = [0.2711\ 0.01858(2.5 - A)^2]\left[1.01 - 0.01 \sin\left(\pi\left((91 + n)/182\right)\right)\right]$$

A= altitude [km];

$$\cos\theta_z = \sin\phi \sin\delta + \cos\varphi \cos\delta \cos\omega$$

ϕ = local latitude;
δ =Inclination of the sun
ω = hour angle.

Twelve clear days in August and twelve clear days in December have been identified (Figure 5, 6 and 7).

Calculation of the solar radiation in the greenhouse models

For each of these clear days was quantified global solar radiation (direct and diffuse) recorded inside the two prototypes and outside of them. Comparing these values, it was possible to calculate the global average transmittance of the two types of coverage.

For each clear day and for each transparent surface, the solar radiation inside of the prototypes has been evaluated by a mathematical model that uses the data of theoretical and measured solar radiation outside the prototypes, the values of the transmittance of the materials and the calculated refractive indices. In this model the reflection phe-

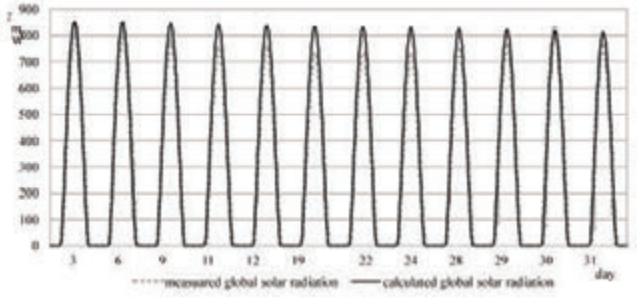

Figure 5. Global solar radiation measured and calculated in August.

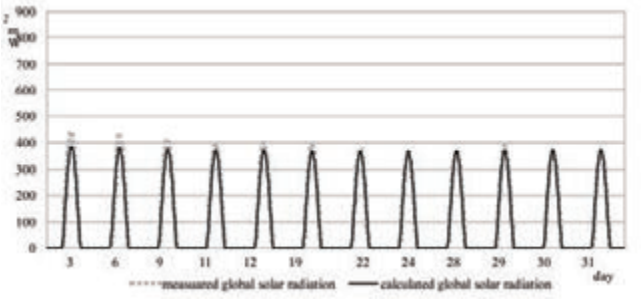

Figure 6. Global solar radiation measured and calculated in December.

nomenon that has been considered ,essentially depends on the refractive index and the angle of incidence of the solar rays that is particularly important for the material of the photovoltaic film.

Daily values of global solar radiation that passes through the individual transparent surfaces were calculated on the level of the radiometers located in each model. This evaluation was made using the solar radiation values calculated by Hottel equation and those recorded by the outside radiometer.

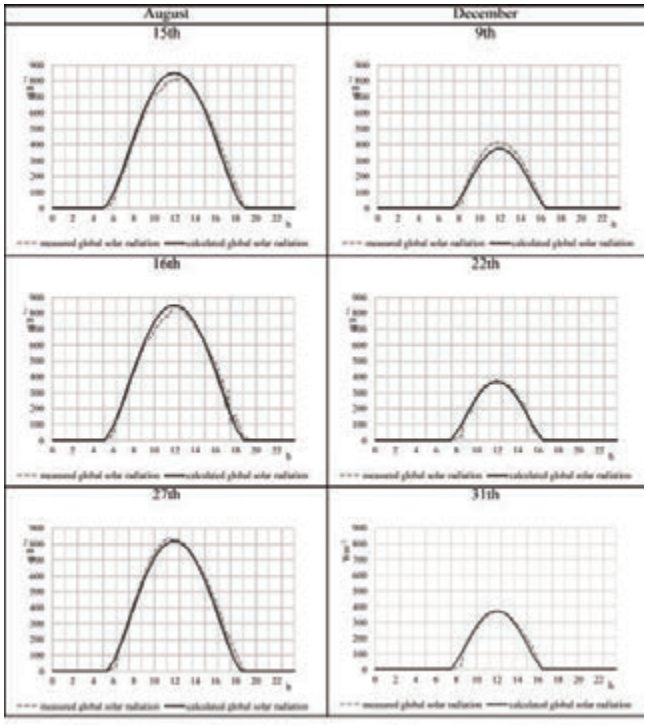

Figure 7. Global solar radiation measured and calculated in some representative days.

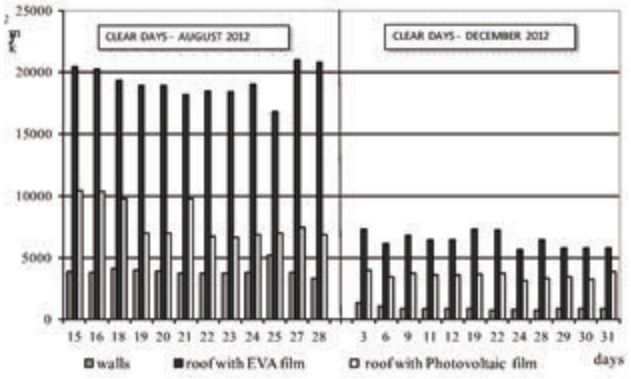

Figure 8. Comparison of solar radiation measured for transparent walls and roof.

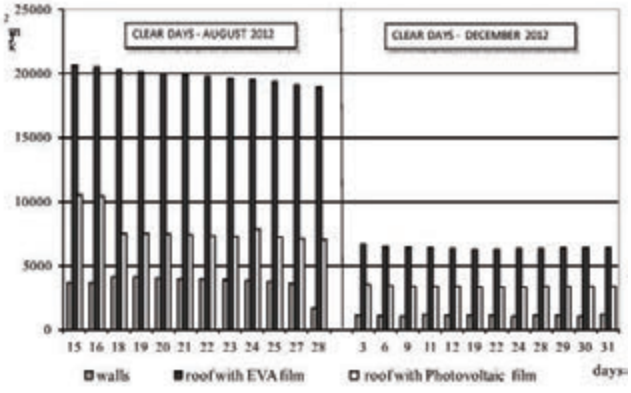

Figure 9. Comparison of solar radiation calculated for transparent walls and roof.

Table 1. measured and calculated global solar radiation.

Clear days	August 2012 Measured global solar radiation [kJm^{-2}]	Calculated global solar radiation [kJm^{-2}]	Clear days solar radiation	December 2012 Measured global solar radiation [kJm^{-2}]	Calculated global solar radiation [kJm^{-2}]
15	24110	24402	3	8729	7869
16	23644	24261	6	7647	6872
18	22434	23972	9	8198	7335
19	21919	23825	11	7864	7064
20	21647	23678	12	7861	7085
21	21055	23529	19	7492	6759
22	21018	23377	22	7086	6431
23	21198	23224	24	6890	6222
24	21818	23068	28	7313	6568
25	20138	22909	29	7568	6804
27	22663	22749	30	7100	6381
28	21128	24402	31	7184	6461

Table 2. Measured global radiation inside and outside of models and transmittance of EVA and photovoltaic films.

Clear days	August 2012 Global solar radiation [kJm^{-2}]	Radiation in Greenhouse with photovoltaic film [kJm^{-2}]	Radiation in Greenhouse with EVA film [kJm^{-2}]	Mean global transmittance of photovoltaic film [%]	Mean global transmittance of EVA film [%]
15	23892	9920	15638	42	65
16	23153	9085	14667	39	63
18	22441	8899	14388	40	64
19	21938	8711	13878	40	63
20	21673	8702	13566	40	63
21	20993	8431	13059	40	62
22	21003	8467	13004	40	62
23	21187	8359	12891	39	61
24	21875	8239	12764	38	58
25	19327	7268	10964	38	57
27	22561	8098	13111	36	58
28	21086	7712	12776	37	61
Mean	21761	8491	13392	39	61

Results

The analysis of the global radiation measured outside (Table 1) shows that in the clear days of August, the mean global radiation outside is about 21897 kJm^{-2} while in the clear days of December, this value drops to about 7577 kJm^{-2}.

Comparing the measured values to those calculated using the model proposed by Hottel, it appears that there is an overestimation of the mean global radiation about 7.8% in days of August, while in December there is an underestimation of around 9.9%. These differences, in our opinion, are essentially due to the haze in August caused by air humidity. In winter, however, the clear days almost always coincide with the days when the wind blows from the northern quadrant and removes the haze. For these reasons, we have decided that it was possible to use the calculated values of solar radiation to evaluate the solar energy inside the greenhouse models.

Table 2 shows that in the clear days of August into greenhouse covered with photovoltaic film, the radiation is 37% less than the radiation recorded in the greenhouse covered with the EVA film. This difference increases to 45% in December.

In absolute terms, the maximum daily global radiation measured in August into the greenhouse covered with photovoltaic film was 9920 kJm^{-2} against 15638 kJm^{-2} into the greenhouse covered with EVA film. During the month of December, these values decrease respectively to 2926 kJm^{-2} and 5319 kJm^{-2}.

Considering that in the experimental area the clear days were about 30% of the days of the month, it is to be inferred that this type of the greenhouse would be unusable especially for most of the month of December. During this month, the average daily radiation in the greenhouse covered with photovoltaic film amounted to 2077 kJm^{-2} against 3648 kJm^{-2} measured in the greenhouse covered with EVA film.

These results are an obvious consequence of the lower transmittance of the photovoltaic film -38% than EVA film) that, if during August this characteristic can mitigate the excesses of radiation, during December doesn't allows to achieve a functional use of greenhouse without artificial energy subsidies (heating and lighting).

Another test was performed using mathematical models for determining the single rates of solar energy that penetrated into the green-

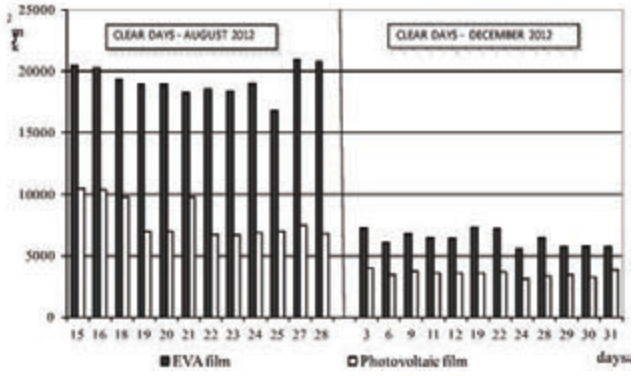

Figure 10. Comparison of the measured solar radiation transmitted by EVA and Photovoltaic films.

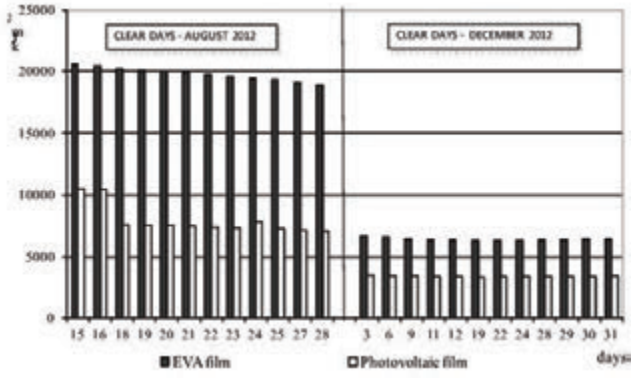

Figure 11. Comparison of the calculated solar radiation transmitted by EVA and Photovoltaic films.

house models through the transparent surfaces using both the solar radiation calculated values and those measured with the radiometer placed outside. The results of this analysis are shown inFigures 8, 9, 10 and 11.

The comparison between the global solar energy into greenhouse model and the energy that passes through the roof reveals that through this surface penetrates inside the 85% of energy in the case of EVA film and the 73% in the case of photovoltaic film.

It should be remembered, moreover, that the incidence of the transparent surface of the vertical walls on the roof surface of the models used is greater than that which occurs generally in the greenhouses in real scale. We tried to reduce this difference by making opaque the lower parts of these structures.

These results confirm that in a greenhouse the greater contribution of solar energy occurs through the roof and considering that the effect of transversal and longitudinal walls is greater when the greenhouse is covered with photovoltaic film, it is advisable to use highest greenhouses with large transparent longitudinal and transversal walls to try to improve the level of inside radiation.

Analyzing the figures 10 and 11 we clearly see the marked difference between the solar energy that pass through the roof in EVA film and the one in photovoltaic film. This difference is about 70% in August and 50% in December and this is due to the effect of the reflection of sunlight on the covering. In winter, because of the lower altitude of the sun on the horizon, the rays of the sun hit in oblique the covering increasing its reflectivity.

Conclusions

The experimental results and those obtained by comparison with the mathematical models used allow us to make some final considerations.

The photovoltaic film would be useful in the summer to mitigate the excesses of solar radiation that occur especially in central and southern areas of Italy. In these areas, in fact, during the summer season the cultivations inside greenhouses are always difficult and often these structures are left unused if there are not efficient cooling systems. Also, the reduction of brightness into the greenhouse, due to low transmissivity of photovoltaic film, can be considered as a positive element for the species that do not tolerate high light levels.

The biggest problems you have, of course, during the winter season when in greenhouses covered with traditional plastic films occurring micro indoor climate conditions were not always favorable for culture due to a not sufficient greenhouse effect. If you reduce the contribution of solar energy with a less transparent coverage as the photovoltaic film, it is difficult to think about the use of this material for covering greenhouse. The values measured inside the photovoltaic greenhouse, in our opinion, are quite low to ensure an adequate greenhouse effect also for cultivation of plants which are thermally less demanding. You might think about removing the photovoltaic film during wintertime (e.g. rolling up the film) and as soon as the solar radiation exceeds certain levels, this covering could be extended to capture solar energy and reduce internal levels of energy.

The difficulties in applying similar solutions are technical and economical. A cost benefit analysis only, which involves the entire greenhouse system can give a more certain answer to the possibility of produce photovoltaic energy using these systems.

References

Campiglia E., Colla G., Mancinelli R., Rouphael Y., and Marucci A. 2007. Energy balance of intensive vegetable cropping systems in central Italy. Acta Horticulturae, vol. 747, 185–191.

Candura A., Gusman A. 1977. Studio per una migliore utilizzazione dell'energia solare nelle serre in vetro. Colture protette, no. 10, 23-40.

Duffie J. A. and Beckman W. A. 1991. Solar Engineering of Thermal Processes. John Wiley & Sons, New York, NY, USA.

Hailin Hua, Sheng-ChinKung, Li-MeiYang, Nicho, M.E., M.Penner, R. 2009. Photovoltaic devices based on electrochemical–chemical deposited CdS and poly3-octylthiophene thin films Solar EnergyMaterials & Solar Cells, 93, 51-54.

Hurd, R.G. 1983. Energy saving techniques in greenhouses and their effects on the tomato crops, Scientia Horticulturae, 33, 94-101.

Kittas C. and Bailie A. 1998. Determination of the spectral properties of several greenhouse cover materials and evaluation of specific parameters related to plant response. Journal of Agricultural Engineering Research, vol. 71, no. 2, 193–202.

Kittas C., Baille A., and Giaglaras P. 1999. Influence of covering material and shading on the spectral distribution of light in greenhouses. Journal of Agricultural Engineering Research, vol. 73, no. 4, 341–351.

Marucci A., Campiglia E., Colla G., and Pagniello B. 2011a. Environmental impact of fertilization and pesticide application in vegetable cropping systems under greenhouse and open field conditions. Journal of Food, Agriculture and Environment, vol. 9, no. 3-4, 840–846.

Marucci A. and Pagniello B. 2011b. Simulation of the growth and the production of the tomato in typical greenhouses of the Mediterranean environment," Journal of Food, Agriculture and Environment, vol. 9, no. 3-4, 407–411.

Marucci A., Monarca D., Cecchini M., Colantoni A., Manzo A., Cappuccini A. 2012. The semitransparent photovoltaic films for Mediterranean greenhouse: A new sustainable technology. Mathematical Problems in Engineering, vol. 2012, Article ID 451934, 14 pages.

Marucci A., Monarca D., M. Cecchini, M., Colantoni, A., Allegrini E., and Cappuccini A., 2013a. Use of Semi-transparent Photovoltaic Films as Shadowing Systems in Mediterranean Greenhouses. ICCSA 2013, Part II, LNCS 7972, 231–241.

Marucci A., Gusman A., Pagniello B., Cappuccini A., 2013b. Limits and prospects of photovoltaic covers in mediterranean greenhouse. Journal of Agricultural Engineering, vol. 44, no. 1, 1-8.

Rouphael Y., Cardarelli M. T., Ajouz N., Marucci A., and Colla G. 2010. Estimation of eggplant leaf number using thermal time model. Journal of Food, Agriculture and Environment, vol. 8, no. 2, 847–850.

Shin G.H., Allen C.G., Potter B.G. Jr. 2010. RF-sputtered Ge–ITO nanocomposite thin films for photovoltaic applications. Solar EnergyMaterials & Solar Cells, vol. 94, 797-802.

Vox G., Teitel M., Pardossi A., Minuto A., Tinivella F., Schettini E. 2010. Chapter 1: Sustainable Greenhouse Systems in "Sustainable Agriculture: Technology, Planning and Management", Augusto Salazar e Ismael Rios Editors, Nova Science Publishers, Inc. NY USA, ISBN: 978-1-60876-269-9: 1-79.

Building green covering for a sustainable use of energy

C.A. Campiotti,[1] E. Schettini,[2] G. Alonzo,[3] C. Viola,[1] C. Bibbiani,[4] G. Scarascia Mugnozza,[2] I. Blanco,[2] G. Vox[2]

[1]ENEA - Italian National Agency for New Technologies, Energy and Sustainable Economic Development - Technical Unit Energy Efficiency - Agriculture Unit, Rome, Italy; [2]Department of Agricultural and Environmental Science, University of Bari, Italy; [3]Dipartimento di Scienze Agrarie e Forestali, University of Palermo, Italy; [4]Department of Veterinary Science – University of Pisa, Italy

Abstract

Nowadays the growth of the cities increased built and paved areas, energy use and heat generation. The phenomenon of urban warming, called urban heat island, influences negatively outdoor comfort conditions, pollutants concentration, energy demand for air conditioning, as well as increases environmental impact due to the demand of energy generation. A sustainable technology for improving the energy efficiency of buildings is the use of green roofs and walls in order to reduce the energy consumption for conditioning in summer and improve the thermal insulation in winter. The use of green roofs and walls can contribute to mitigate the phenomenon of heat island, the emissions of greenhouse gases, and the storm water runoff affecting human thermal comfort, air quality and energy use of the buildings. Recently, a number of municipalities started to adopt regulations and constructive benefits for renovated and new buildings which incorporate green roofs and walls. The aim of this paper is to describe the green roofs and walls plant technology.

Correspondence: Evelia Schettini, Department of Agricultural and Environmental Science, University of Bari, via Amendola 165/A - 70126 Bari, Italy. Tel. +39.080.5443060 - Fax+39.080.5442977.
E-mail: evelia.schettini@uniba.it

Key words: air-conditioning, energy savings, urban ecology, green roofs, green walls.

Acknowledgements: the present work has been carried out under the "Piano triennale 2012-2014 per la Ricerca di Sistema Elettrico Nazionale, progetto C.2 'Sviluppo di modelli per la realizzazione di interventi di efficienza energetica sul patrimonio immobiliare pubblico', Piano Annuale di Realizzazione (PAR) 2012", funded by the Italian Ministry of Economic Development.
The data processing and the editorial work must be shared, within the competencies of the research groups, equivalently among the Authors.

Journal of Agricultural Engineering 2013; XLIV(s2):e50
doi:10.4081/jae.2013.(s1):e50

Introduction

The phenomenon of urban warming, known as urban heat island, influences negatively outdoor comfort conditions, pollutants concentration, as well as increases the environmental impact due to the energy demand for air conditioning (Karlessi *et al*., 2009; Karlessi *et al*., 2011; Santamouris, 2012). A sustainable technology for improving the energy efficiency of buildings is the use of green roofs and green walls in order to reduce the energy consumption for conditioning in summer and to increase the thermal insulation in winter (Cheng *et al*., 2010; Jim and Tsang, 2011; Köhler and Poll, 2010; Perini *et al*., 2011).

The technique of establishing vegetation on rooftops and facades of buildings, known as Green Roofs and Facades (GRF), has seen a growing interest in many cities. It can be considered a solution for providing insulation to buildings and thus contributing to save energy consumption by reducing energy demand for space conditioning (Pérez *et al*., 2011). Besides GRF can increase the life span of a typical roof by protecting the roof components from solar radiation and extreme temperatures. The elevation of the temperature in the cities (the so called urban heat island effect), due to the high concentration of heat absorbed and re-irradiated by rooftops and pavements, can be reduced by the extensive use of the GRF technique. The plants that improve the air quality in the urban areas by emitting oxygen can also remove airborne pollutants and provide a more aesthetically pleasing environment to live and work. Due to contribution which GRF give to the general topic of decrease the CO_2 in the air, a widespread use of "green roofs," "living roofs,", "green facade" and "eco roofs" can become a part of the solution and an action response to the Kyoto Protocol. It is reported a worldwide surface of 234 ha of GRF, while in Italy there are about 1000 m^2 of Green Roofs. Because the building sector in Europe consumes 40% of the total end-energy, there is an increasing interest in using such "green option" to improve the energy efficiency of civil buildings in Europe, and the green roofing and facades technology is to become common in the building of new construction industry. However, there is still a lack of quantifiable data to definitely account either the materials and techniques or the benefits that green roofs and facades can really provide to the efficiency and energy saving of buildings, its occupants, and the nearby community. Although data are available for some areas, mainly Germany and North America, most of them are not transferable to specific climatic conditions of other countries. Recently, ENEA has started a project using some experimental facilities available at the Centre ENEA, located at 30 km in the north of Rome (latitude: 42°02'36", longitude: 12°18'28"). The priority established by the project team was to start developing a feasibility study in order to define materials, energetic parameters, adapted plant species and options for the green roofs and facades systems, and to collect existing performance data and scientific information on construction,

maintenance, costs and plant systems. This paper is also part of a research activity in progress at ENEA to explore the potential of GRF systems as sustainable and innovative tools for improving energy efficiency by the use of "green insulation" of buildings, and their contribute to aesthetic and eco-urban life in the cities.

Energy fluxes in Green Roofs and Walls

Aim of the green wall or roof is to reduce solar energy absorbed by the wall/roof by screening the exposed surface and to increase thermal insulation; this allows the reduction of the energy demand for air conditioning used to reduce high temperatures in the warm periods.

Figure 1 shows the energy fluxes occurring in the green roof/wall system, and the symbols used in this figure are shown in Table 1. Heat is exchanged by means of conduction (C), convection (A) and radiation (E in the solar range and R in the long wave infrared range); solar radiation (E_s) increases energy of the whole system, thus a reduction of the solar transmissivity of the plant wall results in a decrease of the temperature inside the building. Solar transmissivity of the plant wall mainly depends on the percentage of building surface covered with the plants. When the plants wall strongly reduces solar transmissivity, heat transfer from the plant wall to the building surface mainly occurs by convection and by long wave infrared radiation. Heat transfer by convection depends on the air velocity in the gap. Radiation heat transfer in the long wave infrared range depends on the emissivity of the surfaces; a suitable choice of the building surface emissivity can increase the thermal insulation of the building. Natural ventilation occurring through the green wall/roof, if it is permeable to the air, influences the air gap temperature and consequently the building air temperature.

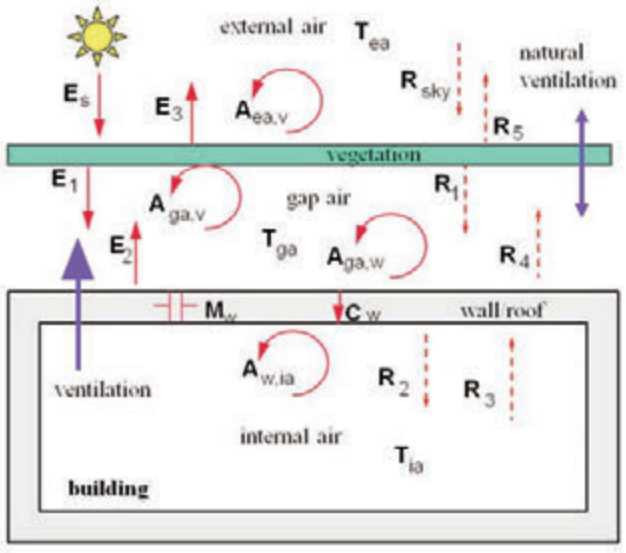

Figure 1. Energy fluxes in a green roof/wall system; symbols are described in Table 1.

Table 1. List of Symbols

A = heat transfer by convection [W]
C = heat transfer by conduction [W]
R = heat transfer by irradiation [W]
H = heat transfer by ventilation [W]
E = incident solar radiation heat flux [W]
M = heat storage [W]
T = temperature [K]
Subscripts
ea=external air
ga=gap air
ia=external air
s=solar
v= vegetation
w= wall/roof

The design of the GRF systems

The growing of plants either on the rooftop or on the outside walls of buildings implies that plants should be selected according to a number

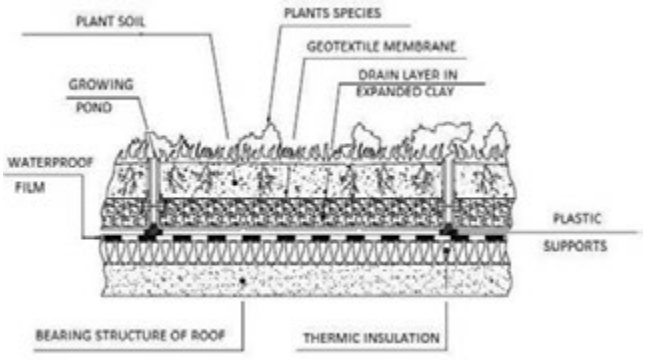

Figure 2. Detail of hydroponic substrate.

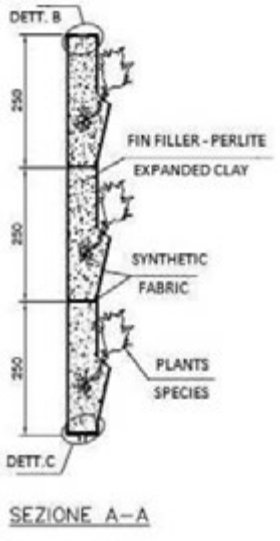

Figure 3. Section modular system.

of technical considerations and parameters, e.g. plants should not modify the structural parts of buildings, plant species should be chosen to establish green coverage in a short time, plants should have high drought tolerance and finally plants should not create conflicts with local or native species and should be most suited to each aspect of the built environment. Appropriate evaluation should be done to choose what plant species are most suitable either for rooftop or for facades. Criteria for selecting plant material include design intent, aesthetic appeal, local environmental conditions, plant characteristics such as rate of establishment, longevity, disease and pest resistance, the substrate composition and depth available for planting, the eco-system service potential. Tables 2-3 report a selection of plants species that can be used for GRF and their biological characteristics (Niachou *et al*., 2001; Dunnet *et al*., 2008; Kristin *et al*., 2008; Trepanier *et al*., 2009; Blanusa *et al*., 2013).

Although some plants are able to grow directly on walls by taking root

Table 2. Plants species used for Green Roofs.

Species	Family	Type or features
Sedum sp	Crassulaceae	Evergreen (5-7 cm in height). Flowering in summer. Mild climate, sun exposure, drought tolerance
Dianthus sp	Caryophyllaceae	Herbaceous plant. Red and white flowers. Tropical and temperate climate.
Allium	Alliaceae	Annual / perennial bulbous plants. White, rose, violet inflorescence. Temperate climate
Achillea	Ateraceae	Perennial herbaceous. White and rose flower. Sun exposition
Arabis	Cruciferae	Perennial herbaceous plant. White flower. Temperate and cold climate.
Aster	Asteraceae	Perennial herbaceous plant. Inflorescence of different colors. Temperate and cold climate.

Table 3. Plants species used for Green Walls.

Species	Family	Type or features
Hedera sp	Araliaceae	Evergreen climbing shrub (to 20 m h). Cold and mild climate.
Parthenocissus sp.	Vitaceae	Deciduous climbing shrub (to 20 m h). Temperate climate.
Bignonia capreolata	Bignoniaceae	Evergreen climbing (to 12 m h). Mild climate.
Clematis montana	Ranunculaceae	Deciduous vigorous climbing (to 10 m h). Cold climate.
Wisteria sinensis	Fabaceae	Deciduous climbing shrub (to 20 m h). Rapid growth. Temperate climate and mild.
Jasminus officinalis	Oleaceae	Deciduous resistant climbing (to 6-7m h). Temperate climate and sun exposure (no wind).
Actinidia colomikta	Actinidiaceae	Deciduous resistant shrub climbing (to 4 m h). Cold and mild climate
Ampelopsis	Vitaceae	Deciduous shrub climbing (to 8 m h). Temperate climate (full to partial sunlight).
Rhyncospermum jasminoides	Apocynaceae	Evergreen resistant climbing (to 20 m h). Temperate climate (more suitable above 10°C).
Adiantum sp	Pteridaceae	Perennial herb. Tropical - temperate climate (shady - wetlands)
Rododendron obtusum	Ericaceae	Perennial sub shrubs. Temperature above 5° C.
Vriesea splendens	Bromeliaceae	Succulent plant. Tropical climate.
Dieffenbachia picta	Araceae	Perennial evergreen ornamental plant. Tropical climate
Dracena godseffiana	Liliaceae	Evergreen ornamental plant (to 2 m h). Tropical climate

in the substance of the wall itself, it is advisable not to create conditions which could promote little deterioration in the building surface. Therefore, to grow plants on walls and buildings some kind of support structure is usually essential. Facade could incorporate structures where plants are planted or allowed to take root by structures made of cables, rope or netting, wide-meshed grid structure to which plants can be attached and trained into place, special containers planted at different levels on the facade.

Whenever possible it is advisable to leave a small gap between the facade of the building and the supporting structure in order to maximize the effects of summer cooling and winter insulation.

The design of the GRF systems must take into account the load-bearing capacity of the structure, the design of waterproofing and irrigation systems (hydroponics system) and the methods of getting soil and other necessary materials onto the roof.

Many possibilities exist for constructing of green roofs, depending on the characteristics of both buildings and local climate. Plants can be established directly upon the green roof media via seed, plugs, and cuttings or plants can be pre-grown at ground level on a blanket, mat, or tray and then placed on the roof. Both the green facades and the green roofs use a hydroponics system to grow plants. The hydroponics systems used are closed-loop systems provided with a biofiltration and nutrient recycling system, which will allow to capture, reuse and treat nutrient solutions and water (Bibbiani *et al*., 2011; Massa *et al*, 2010).

The plant grow system is fed by appropriate nutrient solution which is re-circulated from a manifold, located at the top or at the bottom of the wall, and then collected in a gutter were is filtered and recirculated to the plants. However, new building construction can include GRF systems which can use the grey water from inside the building, with significant water saving of the building's potable water use. Figure 2 and Figure 3 show the modular system under experimentation at ENEA.

Conclusions

Green roofs and facades (GRF) systems represent a class of plant technology still absent from conventional roof and walls of civil buildings but with a high potential to be used as innovative solutions for improving energy efficiency and saving in the sector of construction industry. GRF, like other constructing component and technology, can be used as a biological insulation system either for reducing energy for conditioning in summer or to increase the thermal properties of buildings in winter. In addition, these natural insulating systems can also improve the quality of air and the aesthetical impact of buildings in high constructed areas in cities, and have the potential to recreate natural ecosystem with trees, bushes and crops and thus contributing also to combat the global climatic changes by decreasing both the heat's island and the CO_2 emissions in the city's centers.

References

Bibbiani C., Incrocci L., Campiotti C. A. 2011. A fast procedure to estimate hydraulic characteristics of greenhouse substrates from one-step outflow data. Acta Horticulturae 893: 979-986.

Blanusa T., Vaz Monteiro M.M., Fantozzi F., Vysini E., Li Y., Cameron R.W.F. 2013. Alternatives to Sedum on green roofs: Can broad leaf perennial plants offer better 'cooling service'? Build. Environ. 59: 99-106.

Cheng C.Y., Cheung K. K.S., Chu L.M. 2010. Thermal performance of a vegetated cladding system on facade walls. Build. Environ. 45 (8): 1779-1787

Dunnett N., Nagase A., Booth R., Grime P. 2008. Influence of vegetation composition on runoff in two simulated green roof experiments, Urban. Ecosyst. 11: 385–398

Jim C.Y., Tsang S.W. 2011. Biophysical properties and thermal performance of an intensive green roof. Build. Environ. 46 (6): 1263-1274.

Karlessi T., Santamouris M., Apostolakis K., Synnefa A., Livada I. 2009. Development and testing of thermochromic coatings for buildings and urban structures. Sol. Energy 83: 538-551

Karlessi T., Santamouris M., Synnefa A., Assimakopoulos D., Didaskalopoulos P., Apostolakis K. 2011. Development and testing of PCM doped cool colored coatings to mitigate urban heat Island and cool buildings. Build. Environ. 46: 570-576.

Köhler M., Poll P. H. 2010. Long-term performance of selected old Berlin greenroofs in comparison to younger extensive greenroofs in Berlin. Ecol. Eng. 36 (5): 722-729.

Getter K. L., Rowe D. B. 2008. Media depth influences Sedum green roof establishment, Urban. Ecosyst. 11: 361–372.

Massa D., Incrocci L., Maggini R., Carmassi G., Campiotti C.A., Pardossi A. 2010. Strategies to decrease water drainage and nitrate emission from soilless cultures of greenhouse tomato. Agric. Water Manage. 97 (7): 971-980.

Niachou A., Papakonstantinou K., Santamouris M., Tsangrassouls A., Mihalakakou G. 2001. Analysis of the green roof thermal properties and investigation of its energy performance, Energy Build. 33: 719-729.

Pérez G., Rincón L., Vila A., González J. M., Cabeza L. F. 2011. Green vertical systems for buildings as passive systems for energy savings. Appl. Energy 88 (12): 4854-4859

Perini K., Ottelé M., Fraaij A.L.A., Haas E.M., Raiteri R. 2011. Vertical greening systems and the effect on air flow and temperature on the building envelope. Build. Environ. 46 (11): 2287-2294

Santamouris M. 2012. Cooling the cities – A review of reflective and green roof mitigation technologies to fight heat island and improve comfort in urban environments. Sol. Energy, http://dx.doi.org/10.1016/j.solener.2012.07.003

Trepanier M., Boivin M.A., Lamy M.P., Dansereau B. 2009. Green Roof and living walls, Chronica Horticulture 49 (2): 5-7.

Temperature conditioning in ornamental plant production with a prototype device: root zone cooling in protected environments

Gianluca Burchi,[1] Sonia Cacini,[1] Marco Fedrizzi,[2] Mauro Pagano,[2] Mirko Guerrieri,[2]

[1]CRA-VIV Research Unit for Nursery Plant Production and Management of Landscape and Ornamental Plants, Pescia (PT), Italy; [2]CRA-ING Research Unit for Agricultural Engineering, Monterotondo (Rome), Italy

Abstract

One of the greatest growing costs in greenhouse floriculture is for energy. To reduce energy costs for thermal conditioning was projected an innovative root zone cooling system characterized by two coaxial pipes with hydraulic countercurrent flows. This new system was compared with a traditional system with hydraulic flows cocurrent. The plants were equipped with coolers for obtaining flowering in the summer period by a culture of Alstroemeria spp and were measured energy consumption in each root zone cooling system. The tests also focused on a particular change, made during the tests of previous years, which allows the coaxial system in turning his operation from countercurrent flows to cocurrent flows. The results obtained show that the root zone coaxial cooling system allows to obtain, in comparison to the traditional type, a better temperature uniformity of the root zone ground, both when it is used with countercurrent flows both when it is used with cocurrent flow. The system also allows a slight overall reduction in energy consumption.

Correspondence: Marco Fedrizzi, CRA-ING Research Unit for Agricultural Engineering, via della Pascolare 16, 00016 Monterotondo (Rome), Italy.
Tel. +39.0690675253 - Fax: +39.0690625591.
E-mail: mauro.pagano@entecra.it

Key words: cut flowers, greenhouse, energy consumption, root zone cooling.

Acknowledgments: this study is part of the National Research Project "Florovivaismo: LOgistica e Risparmio ENERgetico F.LO.R.ENER.", financed by the Italian Ministry of Agriculture, in order to study the optimisation of energy use along the flower and ornamental plant production and distribution chain.

Contributions: the authors contributed equally.

Conflict of interests: the authors declare no potential conflict of interests

Journal of Agricultural Engineering 2013; XLIV(s1):e51
doi:10.4081/jae.2013.(s1):e51

Introduction

Cultivation of horticultural crops in protected environments is an industry of considerable economic importance in Italy. Greenhouses can greatly increase the productivity of agricultural soil by accelerating and thus shortening the life cycles of many species, both of vegetables and flowers, promoting crop planning and diversification and also the optimization of inputs.

A technique commonly used in greenhouse management is the root zone heating of seeds, cuttings, transplanted seedlings and plants (Roberts and Mears, 1989; Takakura et al., 1994; Diver, 2002). This method allows the cultivation of ornamental species even when temperature is not optimal for plant growth and development. The most widely used technique for root zone heating involves the use of pipes, laid at the bottom of the benches, in which warm water circulates, heated by a heating boiler.

One of the major problems with this technique is the significant reduction of water temperature along the pipeline, especially in the terminal portion where it arrives after yielding heat to the ground. As a consequence, the tube fails in conditioning the cultivation substrate homogeneously and thus development differs between plants placed at the initial or at the final portion of the heating line.

With the aim of reducing the problems described above, research was carried out by the Research Unit for Agricultural Engineering, Monterotondo, Rome (CRA-ING), at the experimental farm of the Research Unit for Nursery Plant Production and Management of Landscape and Ornamental Plants in Pescia (PT), Italy (CRA-VIV).

Materials and methods

The aim of this work was to test the ability of an innovative root zone cooling system, characterized by the presence of coaxial pipes, to heat homogeneously potted plants placed on benches, in comparison with the traditional method. The tests were conducted in the experimental farm of CRA-VIV, in a greenhouse consisting of a galvanized iron structure with a polycarbonate roof and a fully automated and motorized opening system.

Eight rectangular concrete benches (0.70 m width x 7.25 length m x 0.30 m height) were placed on concrete blocks raising them 0.35 m above the soil level. The interior walls and bottom were coated with polystyrene panels to a thickness of 5 cm.

Two hydraulic systems, a traditional and a coaxial pipes type, were installed in a greenhouse and were originally used, starting in 2008, for carrying out root zone heating tests (Figure 1) in flower cultivation (Fedrizzi et al., 2006). The innovative root zone temperature conditioning system was placed at the bottom of 4 benches. The innovative feature of this system consist in the presence of a pair of coaxial poly-

ethylene radiant pipes: in the inner pipe flows the cold water coming from a cooling water plant and in the interstice between the two pipes (return line) flows the water returning to it.

The use of coaxial pipes is widespread for general purpose (Carnavos, 1985; Horton et al., 1975), in heat exchange systems or equipment such as air conditioning and refrigeration circuits (Edwards, 1981), in carrying toxic or hazardous gases (Spiegelman, 1992), in pneumatic servo and control systems (Wolf and Reichert, 1995), in dangerous conditions such possibility of air contamination (Wolf, 1996), in thermally insulating systems (Ziemek and Schatz, 1972).

However, nowadays, it's not the same in agriculture because of the lack of specific facilities: in fact to realize the system, it was used an italian patent (Rosati, B., 2004) that allows the connection between the internal and external coaxial pipes through a specific junction element. The baseline consisted of a smaller pipe (diameter 16 mm), with the hot water flow inside, and a larger pipe (diameter 32 mm), coaxial to the first, through which the water returned to the cooling plant, connected by means of junction elements. The inner tube was inserted manually for the whole length in the outer one that was closed at the end by a cap. The water passed from the inner pipe to the outer one due to the presence of this closure. The contact between the coaxial pipes results in a continuous transfer of thermal energy between the fluid in the inner pipe and the fluid in the outer pipe. Since the flow rate of water is the same, the difference between the area of the section of the inner tube and the area of the interstice between the pipes in which the water flows back to the cooler, induces a different speed of the fluid in the two hydraulic lines. The characteristics of the innovative pipelines are shown in Table 1.

The hydraulic network, having a total length of 112 m, consisted of a series of 4 benches in which four hydraulic lines, 28 m long, were arranged in parallel. The connection pipes between the benches were insulated with neoprene to prevent heat absorption.

The cooling system was completed by:

a) an air cooled water chiller;
b) a thermocouple sensor for cooling plant management, placed inside the greenhouse above the aerial part of the crop;
c) a thermocouple sensor for cooling plant management, placed into the substrate at the centre of the hydraulic line (Figure 2, position 2);
d) an electric power meter (kWh).

In order to compare the innovative system with the traditional one, a second cooling system was set up within the same greenhouse. It was completely independent from the innovative system and a cooling plant of the same model was used (Figure 1 and 2). This traditional system was realized by a unique Polyethylene (PE) pipeline (diameter 32 mm)

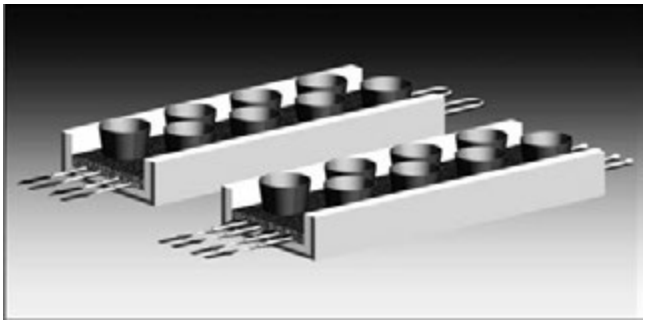

Figure 1. Water flow in winter using condition (heating mode) in the traditional (left) and in the innovative (right) system placed below the pot cultivation.

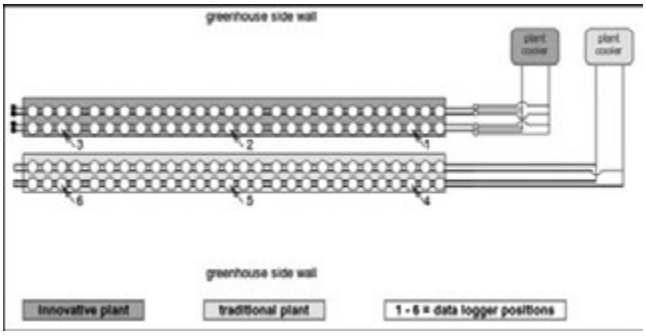

Figure 2. Scheme of the cooling systems with the position of data loggers

Table 1. Main characteristics of coaxial pipes

Characteristics	Return line (outer tube)	Delivery line (inner tube)
External diameter (mm)	16.0	32.0
Inner diameter (mm)	12.5	23.2
Tube section area (mm2)	122.7	422.7
Area of the interstice between the pipes (mm^2)	122.7	221.7

Table 2. CV and energy consumption.

innovative plant operation mode	Counter current	Counter current	Counter current	Counter current	Counter current	Counter current
Starting test date	03/08/2011	19/08/2011	30/08/2011	11/08/2011	24/08/2011	26/09/2011
End test date	11/08/2011	24/08/2011	26/09/2011	19/08/2011	30/08/2011	04/10/2011
Average CV of 3 measured points in innovative plant	0,04	0,03	0,03	0,04	0,03	0,08
Average CV of 3 measured points in traditional plant	0,10	0,09	0,10	0,11	0,09	0,06
Traditional system-total energy consumption (kWh/ 24 h)	22,36	28,75	17,57	25,34	25,33	22,13
Innovative system-total energy consumption (kWh/ 24 h)	17,38	27,96	16,94	24,60	20,36	21,06
Total energy consumption: difference (kWh/ 24 h)	-4,98	-0,79	-0,63	-0,74	-4,96	-1,07
Total energy consumption: difference (%)	-21,85	-2,72	-7,93	-2,93	-20,41	-4,77

that was connected to the cooler at both extremities. Thus, both the outlet and the return branch of the same pipe were located under pots.

Each of the two coolers had cooling capacity of 10.8 kW, 3 kW power draw and were equipped with: hermetic compressor with thermal protection, plate evaporators, condensers battery materials come from copper pipes and storage tanks of water having a function of buffer tanks for the reduction of ignitions of the compressors and to standardize the delivery water temperature. The hydraulic circuits were equipped with water circulation pump, expansion vessel, safety valve, Y-strainer to retain impurities contained in the water circuit.

The fan groups were constituted by helical fans in thermoplastic material, directly driven by single-phase asynchronous electric motors. The cooling circuits were made of copper pipe with welded joints silver alloy comprising capillary or thermostatic expansion valve with external equalizer that modulates the flow of gas as a function of the cooling load.

There were pressure fixed setting, mechanical filters driers able to retain moisture and impurities present in the circuit, differential pressure between the inlet and outlet of the evaporator with the function of flow switches.

There were present also the switchboards, for the protection and control in accordance with International Standard IEC60335-2-40, which included a microprocessor which, among other things, served to control the water temperature and the setting of the set of operation.

The coolers were able to cool output water up to a temperature of 7°C. Each of the 8 benches (4 heated by the innovative system, 4 by the traditional one) contained 2 rows of 12 plastic pots (diameter 30 cm, volume 18.5 l) (Figure 2) placed directly above the radiant pipes. The empty spaces between pots inside the benches were filled with a 15 cm layer of medium-thickness expanded clay.

The temperature, in different positions along the cooling lines, was measured through the use of specific data logger with 2-channel, model Testo 175-T2 (Testo AG, Germany), with internal and external sensors. The instruments were placed in three positions along the pipelines: at the start (Figure 2, position 1 and 4), in the middle (Figure 2, position 2 and 5) and at the end (Figure 2, position 3 and 6) of the coaxial and the traditional system respectively. The data logger were synchronized to the solar time and were programmed to acquire data every 15 minutes.

In the 2011 summer season, the two cooling systems were set up and observation tests were carried out on the efficiency of the different plants. With the aim to test the cooling systems in real operating conditions, two bulbs of Zantedeschia aethiopica were previously transplanted into each pot, filled with peat and pumice, in October 2010. This species was chosen because, in order to obtain the flowering in the summer season, the temperature of the culture substrate must be constantly maintained at about 14 ° C.

Temperature data were acquired by a PC and were organized in the form of a database together with the consumption of liquefied petroleum gas (LPG) and electricity for both systems.

For the analysis of the uniformity of root zone cooling, contemporaneous records of temperatures in three different positions of each line were used.

The measures obtained by data logger placed near the thermocouple sensors into the pots in the central positions 2 and 5 (Figure 2) were taken as reference to evaluate differences with the measures recorded by data loggers placed at the beginning and at the end of both systems.

In the course of 24 hours the soil temperature varied under the influence of many external factors (solar radiation, heating the greenhouse, irrigation, etc..), and so the sum of substrate temperature differences between individual measures recorded in three different points into the bench in both systems was calculated. The electrical energy consumption was recorded for each cooling plant.

In the course of the comparative tests carried out in the winter of 2007-2008, coaxial plant heating, due to operational differences between the two systems in terms of inertia in the achievement of the thermal regime, during periods in which they alternated days characterized by temperatures daily myths and nights with cold temperatures (between late autumn and early winter or late winter and early spring), presented in consumption higher than those in the traditional plant.

To resolve this problem, it has been designed and built a prototype device with hydraulic valve that can change the direction of fluid flow in coaxial pipes, allowing you to transform the mode of operation according to the Italian Patent No. 1351132 (hydraulic flows countercurrent) or according to the traditional type (hydraulic flows cocurrent) and vice versa, with regard to these critical periods characterized by intermittent operation.

Upstream of each pair of patented devices of coaxial coupling have been inserted two three-way valves which allow the orientation in the same direction of the flow of fluids in the two coaxial tubes, thus allowing to transform the operation of two pairs of coaxial pipes from the traditional to the innovative type, and vice versa.

After actuation of the valves, the water flow within the coaxial pipes occurs in the same direction (cocurrent) in the inner pipe and the external one. Obviously, to enable the return of water to the boiler, the coaxial pipes, which originally had an end cap on the external pipe, were hydraulically connected in pairs with a pipeline with a diameter equal to that of the external tube, equipped with a valve that must be kept open for operation in the traditional mode and closed for the coaxial.

During year 2011, since August 4 to October 10, the two hydraulic systems (traditional and innovative) were tested in root zone cooling function. Moreover, in consequence of the changes described above, the new coaxial system has been tested also in the cocurrent mode, which corresponds to the operation mode of the traditional plant.

To evaluate the total energy consumption of the systems compared, the data related to electricity consumption (kWh) detected during the tests were converted to units of energy (J) at a rate of 3.6 MJ / kWh, in reference a time duration of periods of tests and evidence and expressed in MJ consumed within 24 hours (MJ / d).

Results

In table 2, the data referred to the average CV of the 3 measured points of the plants indicate that from day 04/08/2011 to 4/10/2011 the innovative plant, in any mode would be used, has always obtained good conditions of cooling uniformity in the terrain of culture, compared to traditional plant. In fact, in the period from day 11/8/2011 to 19/8/2011 the average CV value of the 3 temperatures in innovative plant (coax mode, cocurrent) is 0,04 while in the traditional system is 0,11.

In the period from day 24/8/2011 to 30/8/2011 the same values were equal to 0,03 and 0,09 respectively. In the period from day 26/9/2011 to 4/10/2011 values were 0,08 and 0,06.

This shows that, for each test of the cooling plants, the traditional system showed much higher values than the innovative one. Since a higher value corresponds to a less uniformity in temperature recorded along the pipeline, it appears that the innovative system allows a greater uniformity in cooling the cultural substrate along the bench than the traditional one.

The results show that the innovative system, in relation to his functional characteristics, always consumed lower amounts of energy compared to the traditional one, ranging from 2,72% to 21,85%.

Conclusions

An innovative root zone cooling system was described and tested in this work. The main objective of this research, consisting in obtaining as homogeneous as possible temperature conditions in protected crop cultivation in relation to the different distances from the cooler, was achieved. The results of the trials carried out during year 2011 showed that the new root zone cooling system resulted in a much higher temperature uniformity than in the traditional one. The goal achieved is even more interesting considering that the innovative system also showed a lower energy consumption compared to the traditional one.

References

Carnavos, T.C., 1985. Coaxial finned tube heat exchanger, Noranda Metal Industries, Inc. (Newton, CT) United States Patent n° 4554969

Diver S., 2002. Root zone heating for greenhouse crops. Appropriate Technology Transfer fo Rural Areas (ATTRA). http://www.attra.org/attra-pub/ghrootzone.html

Edwards, R.C., 1981. Coaxial tube in tube heat exchanger with inner tube support, Edwards Engineering Corporation (Pompton Plains, NJ) United States Patent n° 4286653

Fedrizzi, M., and Bozzoli, M., 2006. Un sistema innovativo di riscaldamento basale per colture sotto serra. Colture protette 3: 63-69

Horton, L.R., Jackson, C.A., Holcomb, W.P., and Horton, C., 1975. Coaxial Tube Coupler Assembly, United States Patent n° 3860269

Roberts W. J., Mears, D. R., 1989. Floor heating of greenhouses. Acta Hort. (ISHS) 257: 189-200

Spiegelman, J.J., 1992. Coupling for interconnection of coaxial tubing, Tylan General, Inc. (San Diego, CA) United States Patent n° 5088774

Takakura T., Manning T. O., Giacomelli G. A. , Roberts W. S., 1994. Feedforward control for a floor heat greenhouse. Transactions of the ASABE. 37(3): 939-945.

Wolf, F.J., and Reichert, U., 1995. Fluid containing coaxial tube for control systems, WOCO Franz-Josef Wolf & Co. (Bad Soden-Salmunster, DE) United States Patent n° 5433252

Wolf, L.W., 1996. Vented bending sleeves for coaxial tubing systems, United States Patent n° 5497809

Ziemek, G., and Schatz, F., 1972. Spacing in coaxial pipes system, Kabel-und Metallwerke Gutehoffnungshutte Aktiengesellschaft (Hannover, DT) United States Patent n° 3670772

Rosati, B., 2004. Nuovo tubo e valvola di flusso per una migliore gestione dell'acqua calda Italy patent n° 0001351132

International Standard IEC60335-2-40:2003/A13:2012 Household and similar electrical appliances - Safety - Part 2-40: Particular requirements for electrical heat pumps, air-conditioners and dehumidifiers

A new method for Espresso Coffee brewing: Caffè Firenze

Alessandro Parenti, Lorenzo Guerrini, Piernicola Masella, Riccardo Dainelli, Paolo Spugnoli

Dipartimento di Gestione dei Sistemi Agrari, Alimentari e Forestali, Università di Firenze, Italy

Abstract

Espresso coffee is the most popular choice for Italian coffee consumers. It has been estimated that every day, in the world, over of 50 million of Espresso cups are taken. As a consequence of this success, a large number of devices to make Espresso have been developed. In this scenario, a new device has been recently developed and patented (Eu. Patent 06 023 798.9; US 2010/0034942 A1). This brew method, named "Caffè Firenze", uses a sealed extraction chamber, where water and gas provides pressure higher than the other extraction methods. Three main parts compose the apparatus: the gas source, the extraction chamber and the heat exchanger. The gas source provides the pressured gas required to raise the pressure of the system. The extraction chamber is made with chrome-brass and accessorized with two heating glow plugs. Many are the factors affecting Espresso quality: it is known that, coffee type, roasting conditions and degree, grinding and storage strongly affect the obtained brew. Also, several studies have been carried out on the effect of the setting parameters on quality, for example water pressure, water temperature, and brew time. Among the characteristics that determine Espresso quality, the main attribute for the visual analysis is, without doubts, the foam, also called "crema". Indeed, height, aspect, and persistency of foam are features much appreciates by consumers. Two distinguish Espresso foam parameters are the persistency and foam index. Equipping a commercial bar machine with the new designed extraction chamber makes feasible the comparison between the traditional way to brew Espresso and the new device. The comparison was made holding the previous mentioned conditions, and differences were evaluated in terms of physical parameters and aromatic profiles.

Caffè Firenze shows pronounced differences compared with traditional Espresso in term of foam-related parameters. Also, the new extraction device produces coffees with higher values of body-related parameters, such density and viscosity. The two kinds of Espressos are perceived different at visual analysis and taste by a panel test.

Correspondence: Lorenzo Guerrini, Dipartimento di Gestione dei Sistemi Agrari, Alimentari e Forestali, Università degli Studi di Firenze, Piazzale delle Cascine 15, 50144, Firenze (Italy).
Tel.+39.0553288352 - Fax: +39 0553288316.
E-mail lorenzo.guerrini@unifi.it

Key words: coffee extraction method, coffee foam, coffee device

Contributions: the authors contributed equally.

Conflict of interests: the authors declare no potential conflict of interests.

Funding: the work was supported by La Marzocco s.r.l. and Francesco Illy.

Journal of Agricultural Engineering 2013; XLIV(s1):e52
doi:10.4081/jae.2013.(s1):e52

Introduction

Espresso coffee (EC) is a popular choice of coffee consumers. Illy *et al*. (2005) estimate that, every day in the world, over of 50 million of EC cups are taken, and in the same work, give EC definition as "a brew obtained by percolation of hot water under pressure through tamped/compacted roasted ground coffee, where the energy of the water is spent within the cake". For this reason, a large number of devices and methods to produce EC are known. The conventional way to brew EC is the bar machine. This device consists of three main parts: a rotative pump, a heat exchanger, and an extraction chamber (Illy *et al*., 2005). It is known that, coffee type, roasting conditions and degree (Sanz *et al*., 2002), grinding and storage (Anese *et al*., 2006) strongly affect EC quality. Also, several studies have been carried out on the effect of the setting parameter on brew quality, for example water pressure (Andueza *et al*., 2002), water temperature (Andueza *et al*., 2003) and brew time (Ludwig *et al*., 2012). Hence, the brew could be considered as influenced by several factors and the overall quality of the EC is hardly predictable.

Among the characteristics that determine EC quality, the main attribute for the visual analysis is without doubts the foam, also called "crema" (Illy *et al*., 2005). In fact an expert consumer can immediately detect from foam colour, texture and persistency dissimilarity possible errors in grinding, percolation, temperature or extraction level (Illy and Navarini, 2011). Physically the crema is a biphasic system compounded by a gas phase surrounded by a liquid phase, named lamellae. The gas phase is compounded by the carbon dioxide originated during roasting and the water vapour made during the percolation process. During the percolation, the hot water flows through the grounded coffee panel, solubilizing and emulsifying proteins and low-molecular weight surfactant, which are responsible for the physical properties of the crema. Particularly some of the oils are emulsified by the pressure provided by the espresso machine and give the creamy sensation of the foam (Piazza *et al*., 2008). Two distinguish EC foam features are the persistency and foam index. The latter is defined as the ratio between the foam and liquid volumes; this index should be, for a quality EC, at least 10%. Persistency is defined as the time before foam breaking up and the underlying brown liquid phase became visible. This shouldn't happen before two minutes since the EC was brewed (Illy *et al*., 2005). Since height, aspect and persistency of foam are much appreciate by consumers, a new device able to improve these characteristic have been recently developed and patented (Eu. Patent 06 023 798.9; US 2010/0034942 A1). This brew method, named "Caffè Firenze" (CF), uses a sealed extraction chamber where water and air provides pressure higher than the other extraction methods. For better understand-

ing the physical and the chemical difference of EC brewed with this technique, CF was compared with a Bar Machine (BM), the traditional way to produce EC.

Materials and Methods

Caffè Firenze method description

The method for preparing CF could be summarized in four subsequent main steps. First, 7g of grinded coffee are added to the extraction chamber, which is sealed. Than, pressurized air is introduced to the system. In this process the pressure rises until 15 bar. Afterward, hot water is introduced in the chamber. The water further comprises the gas, and pressure reach 20 bar. After a pre-infusion phase of 10 s, the coffee flows out.

Device description

To perform the tests a commercial bar machine (Strada, La Marzocco, Italy) was modified, replacing one of the brewing chambers with a Caffè Firenze chamber. The new bar machine arrangement is shown in Figure 1.

The CF group is made in AISI 316 steel, with an internal chamber volume of about 200 cm^3.

The cylinder has internal diameter of 49 mm, and support the air and the water entries. The external cylinder is provided with three thermo resistances thermometer managed with a PID. A compressor provides the required air pressure.

Coffee

The tests were performed (nine replicates per treatment) using a commercial blend (Amici Red, 100% arabica). For every coffee a single serving pod was used. This to minimize the impact of the milling, storage, and dosing related parameters.

All brewed coffees were immediately sampled at the outflow from the machines in a glass weighing bottle (named sampling vessel, 75 ml volume, 53 mm of internal diameter and 34 mm of height). With the purpose of homogeneity, the ECs were sampled by targeting at the same weight of percolated liquid into the sampling vessel, regardless the coffee flow rate or percolation time. Thus, a digital balance (max capacity 300.0 g; precision 0.1 g, D-mail srl, Italy,) was placed under the vessel and the coffee collected until the preselected weight of 25 g. The resulting final brew weight was of 25.7±0.6 g averaged over all the samples.

All the sampled ECs were analyzed and evaluated for the following parameters.

Foam Index and persistency: Foam index is defined as the ratio between foam and liquid volume (vol vol-1 %) measured 30 s after the extraction (geometry of the sampling vessel as above reported). Persistency is defined as the time (in minutes) before foam breaking, leaving a first uncovered black spot on the surface of the beverage (Petracco, 2001).

Density and viscosity: Before performing these measurements samples were cooled to 20 °C. Density was measured with a pycnometer (g ml-1) with 25 ml of capacity. Viscosity was measured with a capillary viscometer (Ostwald) fitted with an automatic optical reader (model Viscoclock, SCHOTT Instruments GmbH, Germany) and expressed as mN s m-2.

Panel test: the sensorial characteristics were evaluated with a descriptive and quantitative analysis. Nine people made up the panel. On the evaluation sheet, each panellist had to report the following features on a straight line of 20 cm of length:

- visual: foam amount, colour;
- olfactory: fresh fragrances, toasted fragrances;
- gustatory: body, bitter, sweet, sour, salty, umami, astringency, persistency, burned;
- a global evaluation.

Results and Discussion

The Caffè Firenze brewing method produces a well-characterized EC, as shown in Figure 2.

The first noticeable distinctive trait is the foam amount and its persistency. The traditional bar method return a foam index value, in the experimental conditions, of 32.4±7.3, three times higher to the literature reference minimum value for EC quality of 10%. The foam index obtained with CF brewing method is 117.6±21.7. Hence, at a visual analysis the difference between the traditional EC and CF results immediately clear, because of the different foam/liquid ratio. Even the

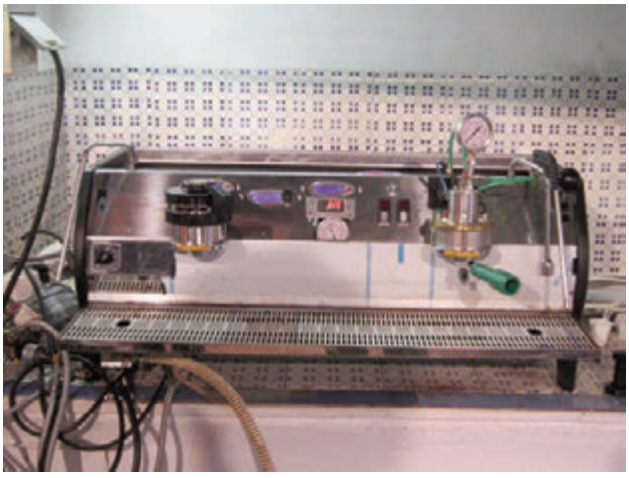

Figure 1. Modified "Strada" Bar Machine. The left brewing chamber is the standard equipment; the right one is the Caffè Firenze device.

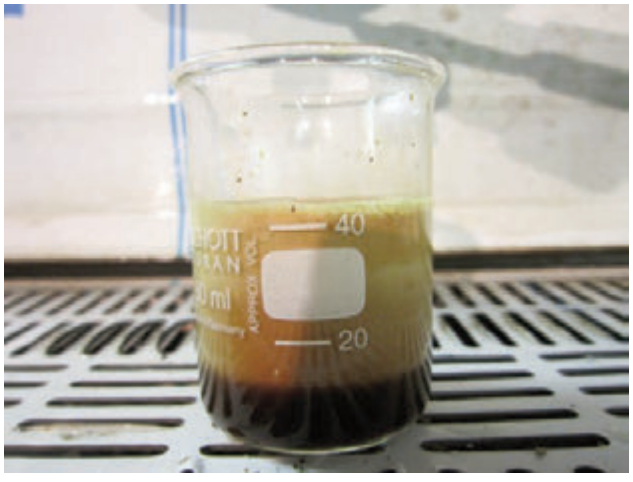

Figure 2. Caffè Firenze.

Figure 3. Sensorial profile of the two kinds of Espresso.

Table 1. Measured density and viscosity of produced espresso coffee. Different letters indicate significant difference at t-test (p=0.05).

	Bar method	Caffè Firenze
Density (g ml-1)	1.026 b	1.057 a
Viscosity (mNm-2s)	1.38 b	1.59 a

persistency of the foam is higher in CF than EC. In the EC the first black spot of liquid uncovered with foam appear after 3.88±0.93 minutes, greater than the literature value of two minutes too. Instead, CF shows a foam persistency larger than 8 hours. Even these data indicates a good EC quality in term of foam related parameters; CF is immediately recognisable at visual analysis for the greater amount of foam and its persistency. The difference produced with the two different brewing methods could be also noticed in term of two body-related physical parameters, such as density, and viscosity, as seen in table 1.

Even in this case the traditional EC shows significant lower value (t-test, p=0.05) than the CF. However, the less value of BM in the body related parameters was not perceived by panel test. In fact, for both ECs, the body score were 10/20. The results of the descriptive sensorial analysis are reported in Figure 3. At visual analysis, panellists notice the already mentioned difference in foam index and some differenced in colour. In fact, CF is characterized by light brown foam and a dark brown, while BM shows the typical hazelnut foam with the tiger skin effect. CF taste results less intense in term of physical sensations such as bitter, acid, and umami than BM. Also, CF reveals less pronounced burned-roasty flavour. Otherwise, panellist perceived more fresh fragrances such as flower and hazelnut scents. As global evaluation panellists prefer CF respect to BM.

Conclusion

The new device for Espresso Coffee brew is able to produce a well-defined kind of coffee, named Caffè Firenze. This coffee is recognisable at a visual analysis because of the large amount of light brown foam on top of the beverage. Furthermore, the performed panel tests and the analysis of density and viscosity highlight additional difference between the two kinds of Espressos. Eventual, on the basis of the global evaluation on panel tests a hypothetical consumer acceptance of this product should be imagined.

References

Andueza, S., Maeztu, L., Dean, B., De Peña, M. P., Bello, J., & Cid, C. (2002). Influence of water pressure on the final quality of arabica espresso coffee. Application of multivariate analysis. Journal of agricultural and food chemistry, 50(25), 7426–31.

Andueza, S., Maeztu, L., Pascual, L., Ibanez, C., De Peña, M. P., Cid, C., & N. (2003). Influence of extraction temperature on the final quality of espresso coffee. Journal of the Science of Food and Agriculture, 83(3), 240–248.

Anese, M., Manzocco, L., & Nicoli, M. C. (2006). Modeling the secondary shelf life of ground roasted coffee. Journal of agricultural and food chemistry, 54(15), 5571–6.

Illy, E., & Navarini, L. (2011). Neglected Food Bubbles: The Espresso Coffee Foam. Food biophysics, 6(3), 335–348.

Illy A., Viani R., & Suggi Liverani F., (2005). Espresso coffee: the science of quality. Elsevier Academic Press.

Ludwig, I. A., Sanchez, L., Caemmerer, B., Kroh, L. W., De Peña, M. P., & Cid, C. (2012). Extraction of coffee antioxidants: Impact of brewing time and method. Food Research International, 48(1), 57–64.

Piazza, L., Gigli, J., & Bulbarello, A. (2008). Interfacial rheology study of espresso coffee foam structure and properties. Journal of Food Engineering, 84(3), 420–429.

Petracco M., (2001). Technology IV: Beverage preparation: brewing trends for the new millennium, in Coffee recent development Ed by Clarke R. J. and Vitzthum O. G., Blackwell Science, Oxford, pp 140–164.

Sanz, C., Maeztu, L., Zapelena, M. J., Bello, J., & Cid, C. (2002). Profiles of volatile compounds and sensory analysis of three blends of coffee: influence of different proportions of Arabica and Robusta and influence of roasting coffee with sugar. Journal of the Science of Food and Agriculture, 82(8), 840–847.

Screening of grated cheese authenticity by nir spectroscopy

Chiara Cevoli, Angelo Fabbri, Alessandro Gori, Maria Fiorenza Caboni, Adriano Guarnieri

Department of Agricultural and Food Science, University of Bologna, Italy

Abstract

Parmigiano–Reggiano (PR) cheese is one of the oldest traditional cheeses produced in Europe, and it is still one of the most valuable Protected Designation of Origin (PDO) cheeses of Italy. The denomination of origin is extended to the grated cheese when manufactured exclusively from whole Parmigiano-Reggiano cheese wheels that respond to the production standard. The grated cheese must be matured for a period of at least 12 months and characterized by a rind content not over 18%. In this investigation the potential of near infrared spectroscopy (NIR), coupled to different statistical methods, were used to estimate the authenticity of grated Parmigiano Reggiano cheese PDO. Cheese samples were classified as: compliance PR, competitors, non-compliance PR (defected PR), and PR with rind content greater then 18%. NIR spectra were obtained using a spectrophotometer Vector 22/N (Bruker Optics, Milan, Italy) in the diffuse reflectance mode. Instrument was equipped with a rotating integrating sphere. Principal Component Analysis (PCA) was conducted for an explorative spectra analysis, while the Artificial Neural Networks (ANN) were used to classify spectra, according to different cheese categories. Subsequently the rind percentage and month of ripening were estimated by a Partial Least Squares regression (PLS). Score plots of the PCA show a clear separation between compliance PR samples and the rest of the sample was observed. Competitors samples and the defected PR samples were grouped together. The classification performance for all sample classes, obtained by ANN analysis, was higher of 90%, in test set validation. Rind content and month of ripening were predicted by PLS a with a determination coefficient greater then 0.95 (test set).

These results showed that the method can be suitable for a fast screening of grated cheese authenticity.

Correspondence: Chiara Cevoli, Department of Agricultural and Food Science, University of Bologna, P.zza Goidanich n.60 - 47521, Cesena (FC). E-mail:chiara.cevoli3@unibo.it

Key words: Parmigiano Reggiano cheese, NIR spectroscopy, artificial neural network, multivariate statistics.

Journal of Agricultural Engineering 2013; XLIV(s1):e53
doi:10.4081/jae.2013.(s1):e53

Introduction

Parmigiano–Reggiano (P-R) cheese is one of the oldest traditional cheeses produced in Europe, (Zannoni, 2010). It carries the prestigious appellation of Protected Denomination of Origin (PDO), and the production is regulated by the Parmigiano-Reggiano Cheese Consortium (CFPR)

The denomination of origin is extended to grated P-R cheese made exclusively with whole cheese. The grating operation must occur in the defined geographical area of cheese production, and packaging must take place immediately, without any processing or addition of substances to modify the conservation and the original organoleptic characteristics. The grated cheese must be characterized by the absence of additives, moisture no less than 25% and no more than 35%, matured for a period of at least 12 months, rind not over 18%, typical amino-acid composition of the cheese, not crumbly in aspect and with homogeneous particles with a diameter inferior to 0.5 mm and not exceeding 25% (D.P.C.M. 4/11/1991), in addiction to the specific rules and compliance to the standard that local processors must attain to during production.

Therefore, to guarantee the quality and authenticity of grated P-R, it is important to monitor the preparation of the grated product in the diary factories. Food frauds and deceptive practices, carried out by unscrupulous producers solely oriented to the misrepresentation, have always been a serious problem because of the economic advantages deriving from partial replacement of high-priced ingredients with low cost ones. In particular, for foodstuffs produced, processed and prepared in a specific geographical area using recognized methods, objective and exhaustive food authenticity information is the major concern for food producers, retailers and consumers, against fraudulent practices. The main concern during the cheese grating operations, is the loss of the stamp embossed on the rind as a symbol of authenticity and guarantee to costumers, that will be printed afterwards on the package. In this way, the grated P-R can be easily mixed with low quality cheeses, extra rind and non-compliant P-R samples

The traditional analysis to discriminate P-R cheese from others brands of hard cheese, are based on the determination by wet chemistry of some technological parameters (Panari *et al*., 2009).

More efficient but expensive spectroscopic techniques to determine the authenticity of Parmigiano Reggiano cheese are stable isotope analysis and nuclear magnetic resonance (Consonni and Cagliani, 2008; Camin *et al*., 2012).

To determine the rind percentage and the months of ripening of the grated P-R by referring only to moisture value of the product is difficult because the packs are filled with grated cheese from different areas of the wheel. The cheese making technology and the dimension of the wheel (22–24 cm high, 40–45 cm diameter) of this long-ripened cheese (minimum 12 months of ripening) lead to differential evolution of the chemical /physical parameters between the inner and the outer zones during the ripening (Malacarne *et al.,* 2009; Tosi *et al*., 2008; De Dea Lindner *et al.,* 2008; Panari *et al.,* 2003; Careri *et al.,* 1996; Pecorari *et al.,* 1995).

The possibility of detecting the addition of extra rind to grated cheese (Grana Padano) and the ripening time of the P-R cheese has been studied by means of destructive chemical methods (Cattaneo *et al.,* 2008; Consonni *et al.,* 2008; Shintu and Caldarelli, 2005).

It therefore becomes important to find a method to determine authenticity, rind percentage, and months of ripening of the grated P-R cheese based on a non destructive, fast and high-throughput techniques. In this way the infrared spectroscopy (IR) combined with the chemiometric technique, can be represent a good alternative (Reid *et al.,* 2006; Luykx and van Ruth, 2008). With regards to near infrared spectroscopy (NIR), investigations combined with chemometric methods were carried out for cheese authentication (Pillonel *et al.,* 2003; Ottaviana *et al.,* 2012), prediction of sensory attributes (González-Martín *et al*. 2011), and determination of physicochemical properties of cheese (Karoui *et al*., 2003; Karoui *et al.,* 2006; Sánchez-Macías *et al.,* 2010).

The present research intends to investigate the potential of the use of NIR coupled to different chemiometric techniques to discriminate grated P-R cheese from non-compliance P-R (defected P-R; P-R with rind >18%) and competitors and to predict the rind percentage and months of ripening of the grated P-R.

Materials and methods

Samples

For the experimentation 400 grated cheese samples classified as compliance P-R, competitors, non-compliance P-R (defected P-R) and P-R with rind content >18% were used.

Compliance P-R samples (140) derived from certified whole cheese wheels, grated and packaged in the area of origin as quoted in the product specification (D.P.C.M. 4/11/1991).

Non-compliance P-R, were grated samples derived from certified whole cheese wheels, but characterized by the presence of extra rind content varying from 25% to 50% (106). A further class of non-compliance P-R was represented by the grated cheese samples derived from defected uncertified whole P-R cheese wheels (38). The compliance and non-compliance grated P-R cheese samples were of known month of ripening (from 12 to 32 circa), and provided by the CFPR which guaranteed the origin.

The competitor group (116) was composed by commercial brands of Italian, European and extra-European grated cheeses of unknown age, collected at local markets.

Particle size of the samples ranged between 0.5 and 1.5 mm.

NIR spectroscopy

NIR spectra were obtained using a spectrophotometer Vector 22/N (Bruker Optics, Ettlingen, Germany) in diffuse reflectance mode. The instrument was equipped with a rotating integrating sphere that allows a wide illumination of the sample and a better reduction of scattering due to the irregularity of the surfaces. Before every analysis, each box containing grated cheese was stirred. NIR spectrum was obtained by average of 32 scans of each sample and three replicates were collected for each individual sample (50 g of grated cheese) by using standard cups with quartz base. Background was defined by acquiring the spectrum of the quartz support without the sample, in the same instrumental conditions (25°C). The speed of acquisitions was 10 kHz in a range from 12500 cm^{-1} 4000 cm^{-1} to and 8 cm^{-1} of spectral resolution

Data processing

To remove the effects of light scatter, NIR spectra were pre-treated with multiplicative scattering correction (MSC). Data were also treated by applying the first derivative (Savitsky-Golay) to the absorbance data. Mean-centred spectral data were subjected to PCA, ANN and PLS analysis.

Principal component analysis (PCA) was applied as an exploratory analysis in order to define a possible discrimination between samples of compliance P-R and non-compliance P-R or competitors and based on rind percentage and months of ripening (The Unscrambler ver. 9.7, CAMO, Oslo, Norway).

To discriminate among specific classes, artificial neural network models (ANN) were performed by using STATISTICA Neural Networks 4.0 (StatSoft Inc., Tulsa, OK, USA). A Multi-Layer Perceptron (MLP) neural network was built to predict the specific classes to which the samples belong. To perform classification tasks, four nominal output variables (I, II, III and IV) were used: I for compliance P-R samples, II for competitors samples, III for defected P-R samples (not-compliance) and IV for P-R samples with a rind percentage higher than 18% (non-compliance). For input and hidden layers, linear and logistic activation function were used, respectively, while for output layer the *softmax* function was used. From a statistical point of view, with the *softmax* activation function and the cross-entropy error, neural network model can be seen as a multilogistic regression model, and the outputs are then interpretable as posterior probabilities for categorical target variables (Bishop, 1995).

Looking for the best classification ability, different node numbers in the hidden layer and combinations of momentum and learning rate were tested. The convergence of ANNs was ruled by a back propagation algorithm. The original datasets were randomly divided into training set (70%), verification set (15%) and test set (15%). It was checked that samples from all classes were contained in the test set.

Subsequently two Partial Least Squares regression (PLS) models were built to predict the rind percentage and the month of ripening from the NIR spectra of the samples. Particularly for the prediction of months of ripening, only the spectra of compliance P-R samples were used. The models were calibrated using 80% of the data set, selected as representative of the population variance, and validated by means of leave-one-out full cross validation and test set validation (performed using the remaining 20% of the data set).

Results

The score plot of the PCA performed to discriminate between compliance P-R, competitors and defected P-R samples is reported in Figure 1. A clear separation between compliance P-R samples and the others samples was observed. Defected P-R and competitors samples were grouped together. It can be see that both the PC1 (89%) and the PC2 (3%) contributed to the discrimination. that might be attributed to spectral regions that previous investigations associated with moisture and lipid contribution (Karoui et al., 2005 and 2006). Furthermore, during the ripening, complex chemical–physical modification might occur: particularly proteolysis and lipolysis are the most important biochemical processes, which cause a variation in the state of the nitrogen fraction as well as a modification of the lipid composition (Pellegrino *et al.,* 1997; McSweeney, 2004; Tosi *et al.,* 2008).

The score plot concerning the discrimination between samples characterized by different rind percentage, is reported in Figure 2. The technique was unable to achieve a clear separation between samples with different rind percentage. Only the samples characterized by a rind

content 18% were grouped. An insufficient separation may be due to the fact that in addition to the rind percentage, also the months of ripening varied (from 12 to 32 months).

Considering only the compliance samples (rind content <18%), it is possible to observe for both spectroscopic techniques (Figure 3) that the samples distribution take place according to the months of ripening. Particularly, the samples with less than 17 months of ripening and the sample with more than 27 months of ripening are grouped separately.

Concerning the ANN results, an early stopping technique was used to select the number of training cycles to avoid overfitting, using the verification set to monitor the prediction error. The learning rate and momentum parameters were used to control the size of weight adjustment along the descending direction and for dampening oscillations of the iterations.

The power of the classification model was evaluated by using three parameters: (I) classification ability: percentage of correctly classified samples in both training, verification and test sets; (II) recognition ability: percentage in the training and verification set; (III) predictive ability: percentage of correctly classified samples in the test set during the training step (Cajka *et al.,* 2009).

In Table 1 are reported the results of the neural networks tested to discriminate the compliance P-R, the competitors, the defected P-R and P-R with rind content>18%.

The best prediction results were obtained with a three layer network, having 5 nodes in the hidden layer. A large number of nodes did not increase the network performance. All the ANNs were obtained with a learning rate of 0.01 and a momentum of 0.8.

The classification, recognition and predictive ability were 98.5, 97, 100 and 97 %, 100, 97.8, 100 and 100% and 95.5 95.5, 100, and 91%,

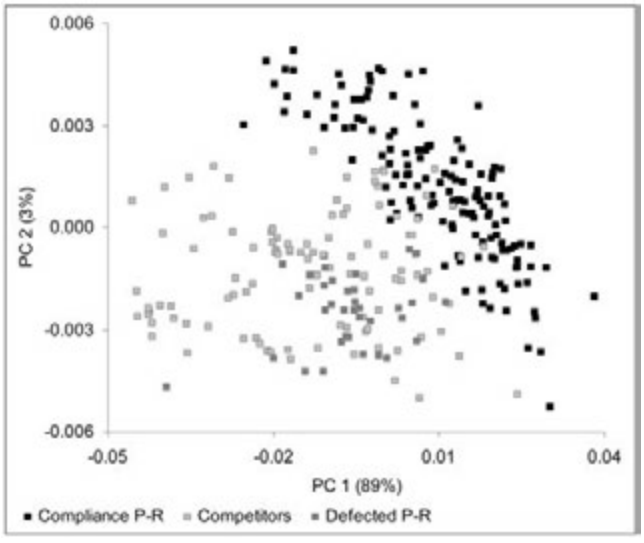

Figure 1. Score plot obtained by PCA analysis to discriminate the compliance P-R from non compliance (competitors and defected P.

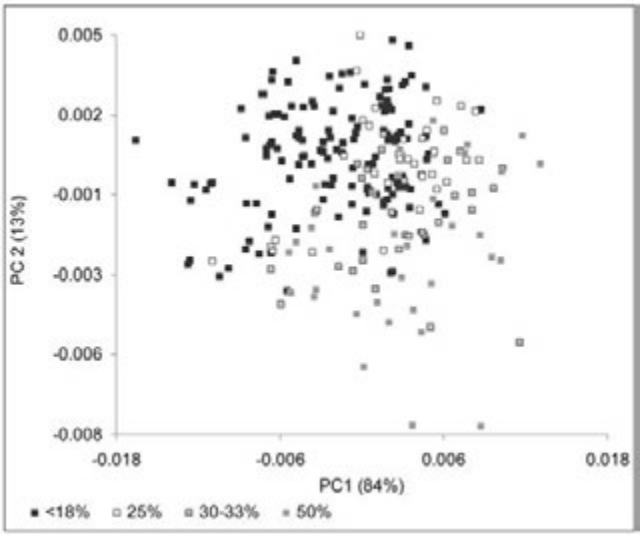

Figure 2. Score plot obtained by PCA analysis (compliance P-R and P-R with rind >18%) to discriminate the rind percentage.

Table 1. Classification results obtained by artificial neural network (ANN).

Classes	Corrected classified cases (%)		
	Training set	Validation set	Test set
Compliance P-R	100	100	95.5
Competitors	100	95.5	95.5
Defected P-R	100	100	100
Rind >18%	100	100	91

Table 2. Prediction results obtained by Partial Least Squares regression models (PLS).

		PCs	R^2	RMSE
Rind (%)	Calibration	15	0.982	1.473
	Cross validation	15	0.953	2.227
	Test set	13	0.95	2.319
Months of ripening	Calibration	14	0.986	0.805
	Cross validation	14	0.95	1.491
	Test set	12	0.942	1.562

Note: PCs, number of Principal Component; R^2, determination coefficient; RMSE, Root Mean Square Error.

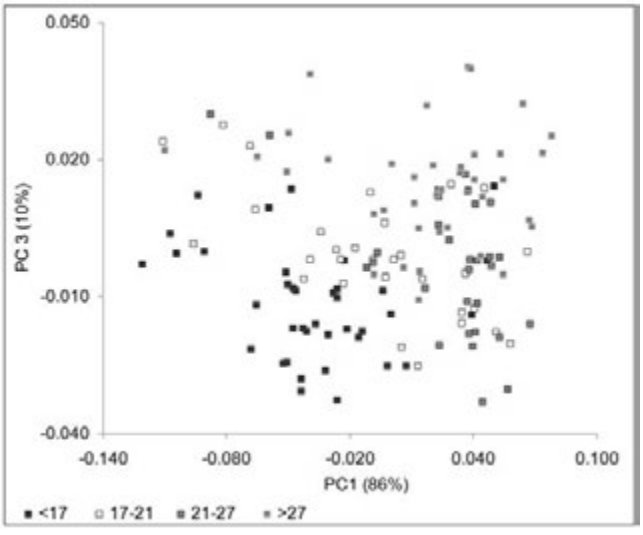

Figure 3 .Score plot obtained by PCA analysis of the compliance P-R spectra to discriminate the months of ripening.

respectively for compliance P-R, competitors, defected P-R and P-R with rind content >18%.

The results of the PLS analysis, in terms of determination coefficient (R^2) and root mean square error (RMSE) in calibration, cross validation e test set validation were reported in Table 2.

For all data sets, it can be seen that the rind percentage is predicted by a R^2 greater than 0.95 and a maximum RMSE of about 2.4% (test set validation), while months of ripening, by a R^2 0.942 and a maximum RMSE of 1.562 months (test set validation). The exact rind percentage of the compliance P-R samples was not known, in fact these samples were characterized by a rind percentage between 12% and 18%. Consequently a not accurate reference data can be negatively influence the results.

Conclusions

Near infrared spectroscopy coupled with advanced statistical techniques (PCA and ANN), were able to discriminate in a fast and reliable way the grated samples of the PDO P-R cheese from major commercial brands of competitors and from non-compliance P-R (samples with extra rind content or defect). ANN resulted to be able to classify correctly in the test set the 95.5 % of compliance.

Rind content and month of ripening were predicted by PLS analysis with a determination coefficients in test set validation of 0.95 (RMSE= 2.4%) and 0.942 (RMSE=1.562 months), respectively.

The results obtained confirms the use of spectroscopic as method suitable for a fast screening of grated cheese authenticity.

References

Bishop C.M., 1995. Neural Networks for Pattern Recognition. Oxford University Press, Oxford, UK.

Cajka T., Hajslova J., Pudil F., Riddellova K. 2009. Traceability of honey origin based on volatiles pattern processing by artificial neural networks. J. Chromatogr. A. 1216:1458-1462.

Camin F., Wehrens R., Bertoldi D., Bontempo L., Ziller L., Perini M., Nicolini G., Nocetti M., Larcher R. 2012. H, C, N and S stable isotopes and mineral profiles to objectively guarantee the authenticity of grated hard cheeses. Anal. Chim. Acta. 711:54-59.

Careri M., Spagnoli S., Panari G., Zannoni M., Barbieri, G. 1996. Chemical Parameters of the Non-volatile Fraction of Ripened Parmigiano-Reggiano Cheese. Int. Dairy J., 6:147-155.

Cattaneo S., Hogenboom J.A., Masotti F., Rosi V., Pellegrino L., Resmini P. 2008. Grated Grana Padano cheese: new hints on how to control quality and recognize imitations. Dairy Sci. Technol. 88:595–605.

Consonni R., Cagliani L.R. 2008. Ripening and geographical characterization of Parmigiano Reggiano cheese by 1H NMR spectroscopy. Talanta, 76:200-205.

Council Regulation (EC) n° 510/2006, On the protection of geographical indications and designations of origin for agricultural products and foodstuffs. Official Journal of the European Union, 93:12-25.

D.P.C.M. 4/11/1991. Estensione della denominazione di origine del formaggio «Parmigiano Reggiano» alla tipologia «grattugiato». Gazzetta Ufficiale, n. 83, 8 /4/1992.

De Dea Lindner J., Bernini V., De Lorentiis A., Pecorari A., Neviani E. Gatti M. 2008. Parmigiano Reggianocheese: evolution of cultivable and total lactic microflora and peptidase activities during manufacture and ripening. Dairy Sci. Technol. 88:511–523.

González-Martín M.I., Severiano-Pérez P., Revilla I., Vivar-Quintana A.M., Hernández-Hierro J.M., González-Pérez C., Lobos-Ortega I.A. 2011. Prediction of sensory attributes of cheese by near-infrared spectroscopy. Food Chem. 127: 256-263.

Karoui R., Mouazen A. M., Dufour E., Pillonel L., Schaller E., de Baerdemaeker J., Bosset J. O. 2006. Chemical characterisation of European emmental cheeses by near infrared spectroscopy using chemometric tools. Int Dairy J. 16:1211-217.

Karoui R., Dufour E., Pillonel L., Schaller E., Picque D., Cattenoz T. 2005. The potential of combined infrared and fluorescence spectroscopies as a method of determination of the geographic origin of Emmental cheeses. Int Dairy J. 15:287-298.

Karoui R., Mazerolles G., Dufour E. 2003. Spectroscopic techniques coupled with chemometric tools for structure and texture determinations in dairy products: a review. Int Dairy. 13:607–62.

Luykx D.M.A.M., & van Ruth S.M. 2008. An overview of analytical methods for determining the geographical origin of food products. Food Chem. 107:897-911.

McSweeney P.L.H. 2004. Biochemistry of cheese ripening. Int. Dairy J. 57:127–144.

Malacarne M., Summer A., Franceschi P., Formaggioni P., Pecorari M., Panari G., Marian P. 2009. Free fatty acid profile of Parmigiano–Reggiano cheese throughout ripening: comparison between the inner and outer regions of the wheel. Int Dairy J. 19:637-641.

Panari G., Filippi S., Caroli A., Pecorari A., Nocetti M. 2009. Analytical methods to distinguish Parmigiano-Reggiano cheese from similar varieties of cheese. Scienza e Tecnica Lattiero-Casearia, 60:25-29.

Panari G., Mariani P., Summer A., Guidetti R., Pecorari M. 2003. Variazione della composizione e andamento della proteolisi del Parmigiano–Reggiano nel corso della maturazione in riferimento al profilo (centro e periferia) della forma. Scienza e Tecnica Lattiero Casearia, 54:199–212.

Pecorari A., Gambini G., Panar, G., Nocetti M. 2007. The characterisation of 12 months old Parmigiano–Reggiano cheese. Scienza e Tecnica Lattiero Casearia, 58:205–217.

Pellegrino L., Battelli G., Resmini P., Ferranti P., Barone F., Addeo F. 1997. Effects of heat load gradient occurring in moulding on characterization and ripening of Grana Padano. Lait, 77:217–228.

Pillonel L., Luginbühl W., Picque D., Schaller E., Tabacchi R., Bosset J O. 2003. Analytical methods for the determination of the geographic origin of Emmental cheese: mid- and near-infrared spectroscopy. Eur Food Res Technol, 216:174–178.

Reid L.M., O'Donnell C.P., Downey G. 2006. Recent technological advances for the determination of food authenticity. Trends Food Sci Tech, 17:344-353.

Sánchez-Macías D., Fresno M., Moreno-Indias I., Castro N., Morales-delaNuez A., Álvarez S., Argüello A. 2010. Physicochemical analysis of full-fat, reduced-fat, and low-fat artisan-style goat cheese. J Dairy Res, 9:3950-3956.

Savitzky A., Golay M.J.E. 1964. Smoothing and differentiation of data by simplified least-squares procedures. Anal Chem, 36:1627-1639.

Shintu L., Caldarelli S. 2005. High-Resolution MAS NMR and Chemometrics: Characterization of the Ripening of Parmigiano Reggiano Cheese. J. Agric. Food Chem. 53:4026–4031.

Tosi F., Sandri S., Tedeschi G., Malacarne M., Fossa E. 2008. Variazione di composizione e proprietà fisico-chimiche del Parmigiano Reggiano durante la maturazione e in differenti zone della forma. Scienza e Tecnica Lattiero Casearia, 59:507-528.

Zannoni M. 2010. Evolution of the sensory characteristics of Parmigiano-Reggiano cheese to the present day. Food Qual Pref. 21:901-905.

Application of Computer Vision for quality control in frozen mixed berries production: colour calibration issues

D. Ricauda Aimonino, P. Gay, L. Comba

DI.S.A.F.A, Università di Torino, Grugliasco (TO), Italy

Abstract

Computer vision is becoming increasingly important in quality control of many food processes. The appearance properties of food products (colour, texture, shape and size) are, in fact, correlated with organoleptic characteristics and/or the presence of defects. Quality control based on image processing eliminates the subjectivity of human visual inspection, allowing rapid and non-destructive analysis. However, most food matrices show a wide variability in appearance features, therefore robust and customized image elaboration algorithms have to be implemented for each specific product. For this reason, quality control by visual inspection is still rather diffused in several food processes. The case study inspiring this paper concerns the production of frozen mixed berries. Once frozen, different kinds of berries are mixed together, in different amounts, according to a recipe. The correct quantity of each kind of fruit, within a certain tolerance, has to be ensured by producers. Quality control relies on bringing few samples for each production lot (samples of the same weight) and, manually, counting the amount of each species. This operation is tedious, subject to errors, and time consuming, while a computer vision system (CVS) could determine the amount of each kind of berries in a few seconds. This paper discusses the problem of colour calibration of the CVS used for frozen berries mixture evaluation. Images are acquired by a digital camera coupled with a dome lighting system, which gives a homogeneous illumination on the entire visible surface of the berries, and a flat bed scanner. RBG device dependent data are then mapped onto CIELab colorimetric colour space using different transformation operators. The obtained results show that the proposed calibration procedure leads to colour discrepancies comparable or even below the human eyes sensibility.

Correspondence: Davide Ricauda Aimonino, Dipartimento di Scienze Agrarie, Forestali e Alimentari (DI.S.A.F.A.) Università degli Studi di Torino, via Leonardo da Vinci, 44, 10095 Grugliasco (TO), Italy.
Tel. +39.011.6708890, Fax +39.011.6708591
E-mail: davide.ricauda@unito.it

Key words: computer vision, colour calibration, food quality, frozen berries.

Acknowledgements: this work was partially supported by the grants of the project FoodVision (POR-FESR – Regione Piemonte).

Journal of Agricultural Engineering 2013; XLIV(s1):e54
doi:10.4081/jae.2013.(s1):e54

Introduction

Over the last two decades, image processing has been rapidly diffused in food industry as instrument for automatic food quality evaluation and control (Du and Sun, 2004; Jackman *et al*., 2012). Computer Vision Systems (CVSs) can effectively replace visual (human) inspection in different contexts of food industry. Furthermore, they provide more objective and standard evaluation of some food quality parameters over a great number of samples (Du and Sun, 2004; K. León *et al*., 2006).

Most food products have a heterogeneous matrix; therefore their appearance properties (colour, texture, shape and size) can be strongly variable, even for the same product category. For this reason specific image processing tools have to be developed for every specific product as well as *ad hoc* image acquisition systems have to be implemented in same particular cases. These aspects are the main limitation to a large-scale deployment of CVS in food industry, in particular in small and medium enterprises, where quality control is mainly entrusted to trained inspectors.

Among food quality evaluations based on products appearance, one of the most repetitive and tedious is the quality control of frozen mixed fruits or vegetables. An example is the production of frozen mixed berries. Usually, berries are severally frozen and then mixed together, in different amounts, according to a recipe. Since producers have to ensure the correct quantity (within a certain tolerance) of each kind of fruit in the mixture, quality control consists in manually counting the amount of each of them in samples (with the same weight) collected by different production lots.

This task could be efficiently carried out by a CVS, analysing a whole product sample in few seconds.

The identification of different objects within a digital image of a food product is typically based on shape and colour appearance attributes, even if texture and size are also used in many cases (Du and Sun, 2004; C. Zheng *et al*., 2006; Jackman and Sun, 2013). Different classification methods can be adopted to classify the objects in a number of classes with similar appearance properties. Statistical, fuzzy logic and neural network are the most used ones (Du and Sun, 2004). While shape analysis can be usually performed adopting morphological operations available in image processing tools, colour measurement is a nontrivial task. Digital colour images are acquired in RGB colour space, which is not a colorimetric space (Hong *et al*., 2001; Green, 2003). RGB signals provided by an image acquisition system (camera, scanner) are device-dependent, i.e. different devices (even of the same type) can give different responses. Therefore, a colour space transform that maps RGB values of a digital image onto a device-independent colorimetric colour space, such as CIELab, has to be defined for accurate colour measurements (Hong *et al*., 2001; Westland and Ripamonti, 2004; K. León *et al*., 2006; Wu and Sun, 2013). This procedure is usually called device colour characterization.

A preliminary study about the development of a laboratory CVS for

frozen mixed berries quality inspection is presented in this paper. In particular, the article is focused on the colour characterization of the imaging system. A target-based approach has been adopted, in which a set of colour samples, with known XYZ and/or Lab values, is considered as reference. Different polynomial transforms (from RGB to CIELab colour space) for colour characterization were compared and applied to two image acquisition systems: a flat bed scanner and a CVS based on a digital camera. Performances of the calibration models were evaluated in terms of colour measurement accuracy and calculation times.

Image acquisition systems

A simple way to classify and count fruits in a sample of frozen mixed berries is to spread them randomly on a flat surface painted with al light colour, in order to have a good contrast between berries and background in the digital image. This layout suggested to carried out tests collecting images both by a flat bed scanner and a CVS equipped with a digital camera.

In the first case an A4 Microtek ScanMaker i900 flat bed scanner was adopted. Scan surface was covered with a wooden cover (210 mm × 290 mm × 50 mm) to shield ambient light, whose internal walls were painted with a light grey paint, similar to the standard grey for cameras white balance (X-rite ColorChecker white balance card).

The CVS consisted of a Nikon D5100® colour digital camera coupled with a dome lighting system, which ensured a uniform illumination of berries without shadows. A white plastic hemisphere (350 mm diameter) reflects the light provided by two LEDs arrays, obtaining a colour temperature of about 5500 K. The camera was mounted on a stand together the hemisphere as shown in Figure 1. Lifting up them, berries samples can be arranged within the circular surface defined by the LEDs support. Images acquisition and camera set up were remotely controlled by NKRemote® software (Breeze System - UK) installed on Laptop PC connected to the camera with the USB port. The camera and the illumination system were placed into a (500 mm × 600 mm × 900 mm) wooden box internally painted black to avoid external light and reflections (Valous *et al*., 2009). A manual camera white balance was carried out, using an X-rite ColorChecker white balance card, before device characterization. A set of card images was collected changing the camera colour temperature parameter, until the three histograms of the RGB channels were exactly overlapped. The obtained value was adopted in all subsequent image acquisitions, maintaining the automatic white balance disabled as suggested by (Cheung *et al*., 2004).

Devices colour characterization

Device characterization mainly consists in to find one or more transforms between the device RGB values and an absolute device-independent, metric, colour space, usually CIELab. The result of this process is an image represented in L*a*b* colour coordinates on which colorimetric measurements can be performed. In target-based approach, an image of a reference colour card with a number of colour samples is acquired by the CVS to obtain their mean RGB values, while the correspondent XYZ values are measured by a spectrophotometer. Different methods can be applied to derive the RGB-XYZ transform: look up tables with interpolation, polynomial regressions and neural network among all (Hong *et al*., 2001; Wu and Sun, 2013). CIELab colour coordinates are then calculated applying the following standard transformation:

$$L^* = \begin{cases} 116\left(\frac{Y}{Y_n}\right)^{1/3} - 16 & if \left(\frac{Y}{Y_n}\right) > 0.008856 \\ 903.3\left(\frac{Y}{Y_n}\right) & if \left(\frac{Y}{Y_n}\right) \le 0.008856 \end{cases}$$
$$a^* = 500\left[\left(\frac{X}{X_n}\right)^{1/3} - \left(\frac{Y}{Y_n}\right)^{1/3}\right] \quad (1)$$
$$b^* = 200\left[\left(\frac{Y}{Y_n}\right)^{1/3} - \left(\frac{Z}{Z_n}\right)^{1/3}\right]$$

where X_n, Y_n and Z_n are the tristimulus values of a reference white for a certain CIE standard illuminant (Green, 2003).

A X-right ColorChecker passport (a poked-size version of traditional ColorChecker) was used as colour reference in present work. This card is a collection of 24 (20 mm × 20 mm) coloured patches, which XYZ val-

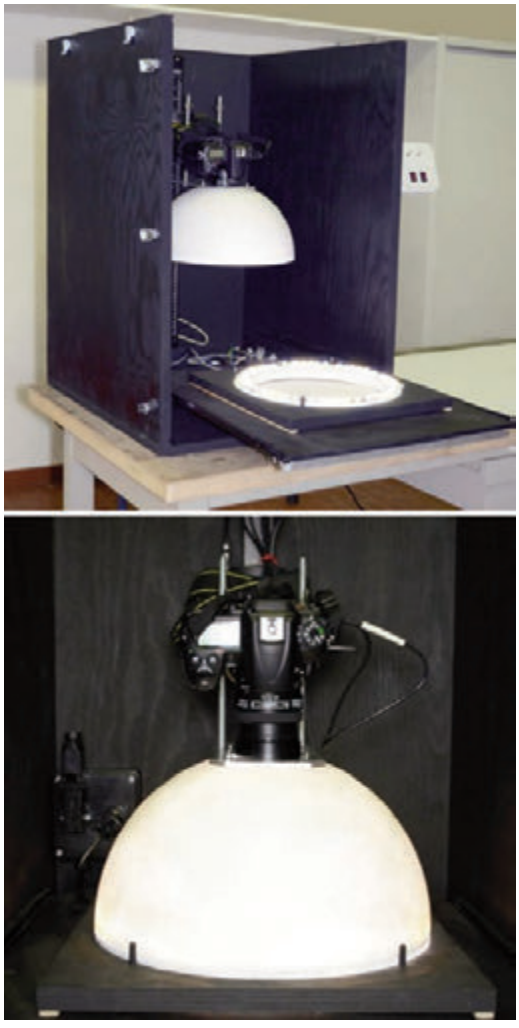

Figure 1. The Computer Vision System (without front and top walls) in which camera and the white hemisphere are lifted up to allow samples arrangement (on left); the same system during image acquisition (on right).

ues of each patch are collected as a result of five subsequent measurements carried out with a X-rite spectrophotometer (D50 illuminant, 2° observer). Digital images of the ColorChecker were acquired by the scanner and the CVS to obtain the input devices RGB values of the 24 coloured patches. These values were calculated as the average of the RGB values of all pixels corresponding to each colour patch, excluding boundary pixels. CEI tristimulus values (XYZ) of ColorChecker card and the corresponding device RBG ones were used to carry out colour characterization considering different polynomial regression models with least-squares fitting. The transform from RGB device values to XYZ can be performed applying the following relationship to each pixel of an image:

$$\begin{bmatrix} X \\ Y \\ Z \end{bmatrix} = C\,p \qquad (2)$$

where C is the $(3\times n)$ calibration matrix calculated with the last squares fitting polynomial regression (see e.g. (Hong *et al*., 2001) for a detailed decryption of the method), and p is a vector whose $n \times 1$ elements are the terms of the correspondent polynomial calculated with the r, g, and b normalized values of the pixel. The following polynomials were compared in this paper:

	Calibration Model	*n*
p_1	$r\ g\ b$	3
p_2	$r\ g\ b\ 1$	4
p_3	$r\ g\ b\ rgb$	4
p_4	$r\ g\ b\ rgb\ 1$	5
p_5	$r\ g\ b\ rg\ rb\ gb$	6
p_6	$r\ g\ b\ r^2\ g^2\ b^2$	6
p_7	$r\ g\ b\ rg\ rb\ gb\ 1$	7
p_8	$r\ g\ b\ rg\ rb\ gb\ rgb$	7
p_9	$r\ g\ b\ r^2\ g^2\ b^2\ 1$	7
p_{10}	$r\ g\ b\ r^2\ g^2\ b^2\ rgb$	7
p_{11}	$r\ g\ b\ rg\ rb\ gb\ rgb\ 1$	8
p_{12}	$r\ g\ b\ r^2\ g^2\ b^2\ rgb\ 1$	8
p_{13}	$r\ g\ b\ r^2\ g^2\ b^2\ rg\ rb\ gb$	9
p_{14}	$r\ g\ b\ r^2\ g^2\ b^2\ rg\ rb\ gb\ 1$	10
p_{15}	$r\ g\ b\ r^2\ g^2\ b^2\ rg\ rb\ gb\ rgb$	10
p_{16}	$r\ g\ b\ r^2\ g^2\ b^2\ rg\ rb\ gb\ rgb\ 1$	11
p_{17}	$r\ g\ b\ r^3\ g^3\ b^3\ r^2\ g^2\ b^2\ rg\ rb\ gb\ rgb\ 1$	14
p_{18}	$r\ g\ b\ r^4\ g^4\ b^4\ r^3\ g^3\ b^3\ r^2\ g^2\ b^2\ rg\ rb\ gb\ rgb\ 1$	17
p_{19}	$r\ g\ b\ r^5\ g^5\ b^5\ r^4\ g^4\ b^4\ r^3\ g^3\ b^3\ r^2\ g^2\ b^2\ rg\ rb\ gb\ rgb\ 1$	20
p_{20}	$r\ g\ b\ rg\ rb\ gb\ r^2\ g^2\ b^2\ rgb\ r^2g\ g^2b\ b^2r\ r^2b\ g^2r\ b^2g\ r^3\ g^3\ b^3\ 1$	20
p_{21}	$r\ g\ b\ r^6\ g^6\ b^6\ r^5\ g^5\ b^5\ r^4\ g^4\ b^4\ r^3\ g^3\ b^3\ r^2\ g^2\ b^2\ rg\ rb\ gb\ rgb\ 1$	23

However, usually, colour characterization cannot be directly applied to normalized RGB values of an image, because most image acquisition devices show nonlinearities between the input light intensity and the response of the colour channels. Although CCD sensors are characterized by a linear response to light intensity, a nonlinearity was added by manufacturers according to sRGB standard (gamma correction). Therefore a linearization process is recommended before applying colour characterizations transformations, even in the case of polynomial (nonlinear) models (Cheung *et al*., 2004). The linearization consists in to find the inverse function of added nonlinearity. Luminance (Y coordinate of XYZ colour space) and reflectance of grey colour samples are almost constant within the visible light spectrum; therefore RGB channels response is described by the trend of these parameters depending on RGB values obtained for the same grey samples (Westland and Ripamonti, 2004). Figures 2 and 3 show the nonlinear relationships between RGB responses and mean reflectance of the six ColorChecker grey samples for CVS and scanner respectively. The same behaviour is shown for luminance (not reported). These relationships represent the linearization functions for R, G and B channel, which can be calculated by least-square polynomial regression. Four polynomial (3-rd, 4-th, 5-th and 6-th degree) fitting are tested evaluating their effect on scanner and CVS colour characterization. The measure of the colour difference between the values estimated by colour characterization (, , and) and those measured with spectrophotometer (, , and) was calculated, for the 24 ColorChecker patches.

$$\Delta E = \sqrt{(L_e^* - L_m^*)^2 + (a_e^* - a_m^*)^2 + (b_e^* - b_m^*)^2} \qquad (2)$$

Calculation times for linearization and colour characterization procedures are also calculated as performance index, adopting 1280 × 848 pixels images as reference.

All algorithms for channel response linearization, colour characterization and results comparison were implemented with Matlab® (MathWorks, USA).

Results

CVS camera and scanner channels responses (Figures 2 and 3) show a power law trend, typical of gamma corrections. Increasing the order of the polynomial fitting for channel response linearization, R^2 regression coefficient increases as well as calculation times (Table 1), denot-

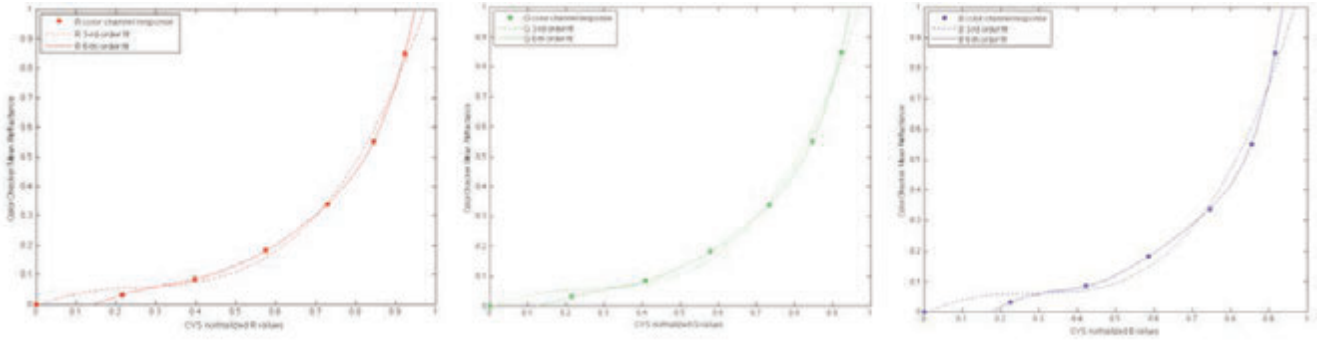

Figure 2. CVS camera RGB channels response (relationships between normalized RGB values of ColorChecker grey patches and Mean Reflectance), and corresponding 3-rd and 6-th order linearization polynomial fits.

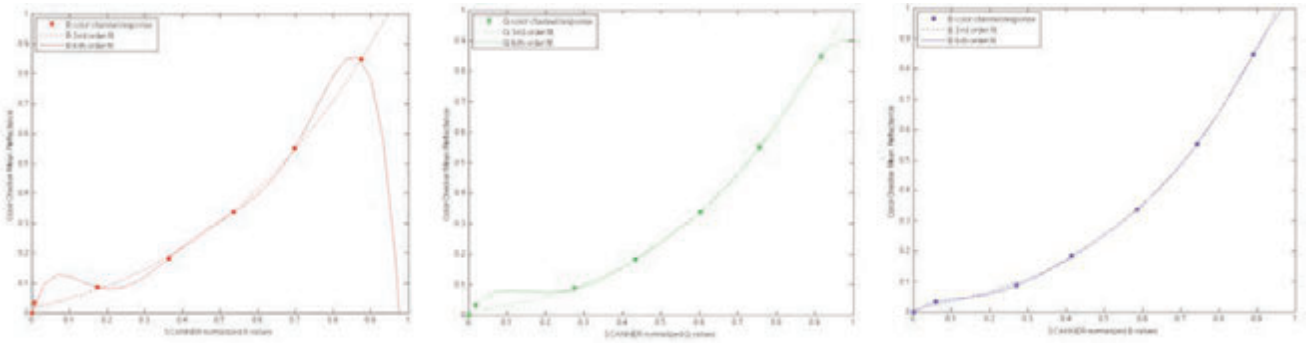

Figure 3. Scanner RGB channels response (relationships between normalized RGB values of ColorChecker grey patches and Mean Reflectance), and corresponding 3-rd and 6-th order linearization polynomial fits.

Table 1. Regression coefficients (R^2) and calculation times for R, G and B channels linearization (for 3-rd, 4-th, 5-th and 6-th degree polynomials models) adopting mean reflectance and luminance.

Image acquisition system	Polynomial degree	Calculation time [ms]	Mean Reflectance			Luminance		
			R^2_R	R^2_G	R^2_B	R^2_R	R^2_G	R^2_B
CVS	3	138	0.9936	0.9930	0.9863	0.9828	0.9822	0.9755
	4	146	0.9987	0.9985	0.9958	0.9879	0.9876	0.9850
	5	154	0.9998	0.9998	0.9993	0.9889	0.9890	0.9885
	6	165	1.0000	1.0000	1.0000	0.9891	0.9891	0.9891
Scanner	3	138	0.9995	0.9998	0.9997	0.9886	0.9889	0.9888
	4	146	0.9998	0.9999	0.9997	0.9889	0.9890	0.9888
	5	154	0.9999	0.9999	0.9999	0.9890	0.9890	0.9890
	6	165	1.0000	1.0000	1.0000	0.9891	0.9891	0.9891

Table 2. Performances of CVS colour characterization polynomial models with different mean reflectance linearization functions (3-rd, 4-th, 5-th and 6-th degree polynomials fitting).

		Linearization polynomials degrees (mean reflectance)											
		3			4			5			6		
Model	# terms	ΔE_{min}	ΔE_{max}	ΔE_{avg}	ΔE_{min}	ΔE_{max}	ΔE_{avg}	ΔE_{min}	ΔE_{max}	ΔE_{avg}	ΔE_{min}	ΔE_{max}	ΔE_{avg}
p_1	3	3.658	28.245	11.749	2.764	28,407	10,426	3,049	30,250	10,336	2,981	28,437	10,064
p_2	4	3,222	28,774	12,115	1,196	28,846	10,868	3,186	30,465	10,707	3,695	28,846	10,134
p_3	4	1,624	20,975	10,634	0,729	22,401	9,667	1,461	25,164	9,990	1,734	22,863	9,442
p_4	5	0,928	18,552	10,479	1,775	18,455	9,801	1,842	20,649	9,647	1,976	19,119	9,646
p_5	6	1,403	21,738	9,104	1,023	21,263	7,857	1,285	18,919	7,316	1,444	19,306	7,648
p_6	6	3,324	27,178	8,862	1,780	40,124	8,221	1,168	63,498	9,064	1,263	40,920	7,083
p_7	7	1,656	19,370	9,071	1,363	21,076	7,917	1,673	18,006	7,476	1,726	19,180	7,756
p_8	7	0,482	23,913	8,853	0,450	20,084	7,284	0,318	15,428	6,843	0,324	16,978	6,679
p_9	7	2,439	26,356	9,136	1,090	45,150	9,128	1,437	67,519	10,227	1,292	45,663	8,288
p_{10}	7	0,859	16,281	6,497	0,475	10,066	4,799	0,560	15,415	5,648	0,594	9,523	4,423
p_{11}	8	0,573	19,057	8,185	0,502	20,602	7,119	0,402	19,003	6,425	0,358	18,712	6,475
p_{12}	8	0,590	15,036	6,225	0,267	27,641	5,342	0,292	19,387	6,370	0,243	24,343	4,964
p_{13}	9	0,597	13,410	5,495	0,340	8,023	3,197	0,146	9,639	3,475	0,381	6,945	2,796
p_{14}	10	0,688	13,768	5,515	0,424	9,515	3,277	0,230	10,218	3,618	0,096	9,703	2,977
p_{15}	10	0,236	15,816	5,561	0,278	8,036	3,095	0,201	9,164	3,431	0,116	7,015	2,752
p_{16}	11	0,534	13,964	5,597	0,276	18,204	3,464	0,220	8,708	3,535	0,116	7,033	2,793
p_{17}	14	0,403	10,489	3,707	0,225	17,422	3,021	0,140	7,577	2,713	0,108	6,467	2,609
p_{18}	17	0,047	7,812	2,450	0,041	6,199	2,272	0,022	9,260	2,236	0,027	6,351	2,255
p_{19}	20	0,027	5,911	1,638	0,010	5,903	1,534	0,013	5,674	1,707	0,019	6,909	1,934
p_{20}	20	0,011	7,553	1,799	0,024	5,523	0,936	0,035	2,939	0,920	0,014	2,442	0,742
p_{21}	23	0,012	2,252	0,644	0,015	1,003	0,201	0,005	1,053	0,316	0,013	2,558	0,419

Table 3. Performances of p19 , p20 and p21 colour characterization models with different linearization functions (3-rd, 4-th, 5-th and 6-th degree polynomials fitting).

		Linearization polynomials degrees (mean reflectance)											
	Model	3			4			5			6		
	# terms	ΔE_{min}	ΔE_{max}	ΔE_{avg}	ΔE_{min}	ΔE_{max}	ΔE_{avg}	ΔE_{min}	ΔE_{max}	ΔE_{avg}	ΔE_{min}	ΔE_{max}	ΔE_{avg}
CVS													
Mean	p_{19} (20)	0,027	5,911	1,638	0,001	5,903	1,534	0,013	5,674	1,707	0,019	6,909	1,934
Refl.	p_{20} (20)	0,011	7,553	1,799	0,024	5,523	0,936	0,035	2,939	0,92	0,014	2,442	0,742
	p_{21} (23)	0,012	2,252	0,644	0,015	1,003	0,201	0,005	1,053	0,316	0,013	2,558	0,419
Lum.	p19 (20)	0,020	7,004	1,963	0,009	7,011	1,634	0,012	8,800	2,074	0,016	7,302	2,156
	p20 (20)	0,009	7,721	1,847	0,021	5,487	0,927	0,033	3,356	1,280	0,011	3,097	0,789
	p21 (23)	0,009	2,333	0,626	0,023	1,773	0,406	0,007	1,540	0,291	0,015	3,347	0,589
Scanner													
Mean	p_{19} (20)	0,029	6,065	1,848	0,017	5,939	1,857	0,020	5,857	1,530	0,028	10,028	2,837
Refl.	p_{20} (20)	0,021	3,395	0,860	0,022	3,701	0,844	0,021	3,810	0,886	0,036	11,739	2,696
	p_{21} (23)	0,012	4,062	0,774	0,013	3,436	0,672	0,015	3,757	0,906	0,008	8,882	1,378
Lum.	p_{19} (20)	0,026	6,081	1,864	0,015	5,987	1,879	0,019	5,973	1,517	0,028	10,087	2,775
	p_{20} (20)	0,020	3,304	0,850	0,022	3,526	0,801	0,023	3,892	0,888	0,028	10,413	2,432
	p_{21} (23)	0,012	4,190	0,784	0,012	3,672	0,711	0,014	3,796	0,939	0,008	8,209	1,282

ing a better fitting. Linearization with luminance gives slightly lower R^2 values than the case with mean reflectance for both acquisition systems, even if the polynomial fitting seems to perform better for the flat bed scanner.

Regarding to colour characterization (Table 2) colour differences between values estimated by the different models and measured values generally decreases increasing the number of polynomial terms, even if this is not always the case. According to Hong *et al*. (2001), models performances depend on the terms used. Considering colour differences obtained with 7 terms polynomial models, better performances of p_{10} respect to the other models (p_7, p_8, p_9) can be observed regardless the adopted linearization fitting. In particular the term *rgb* determines lower ΔE values respect to the term 1, as can also be noted for p_2 and p_3 models.

However, in order to obtain accurate colour measurements, average ΔE should be less than 2.2, since this is considered the minimum value of colour difference distinguishable by human eyes (Valous *et al*., 2009). For this reason only the last three models (p_{19}, p_{20}, p_{21}) were compared for CVS camera and scanner considering the different linearization polynomial fittings. A progressive reduction of ΔE values was observed increasing the degree of the linearization polynomial fitting for CVS, using both mean reflectance and luminance (Table 2 and 3). Colour characterization performances for the scanner show a different behaviour, with an initial reduction of ΔE, adopting 3-rd and 4-th degree polynomials, and a subsequent colour difference increase with higher order polynomials. This behaviour can be explained comparing the shape of approximating polynomials graphs in Figures 2 and 3. Note that, both polynomial fits are increasing functions in the case of CVS (Figure 2), moreover 6-th order polynomial fit provides a better fitting than the 3-th one. On the contrary, 3-th and 6-th order approximating polynomials have different behaviours for scanner linearization. The first one is an increasing function, which mind a typical gamma correction, whereas the 6-th order polynomial fit shows a relative and an absolute maximum for R and G channels. This means that in this case polynomial fit does not approximate a gamma correction curve correctly, in spite of R^2 of the 6-th order R and G channels polynomial fits are greater than the 3-th order ones. Therefore, high R^2 values in linearization process do not necessarily correspond to better colour characterization performances.

It also important to note that CVS provides better performances than the scanner (Table 3). This difference can be attribute to the white balance performed for CVS camera that probably improves its accuracy.

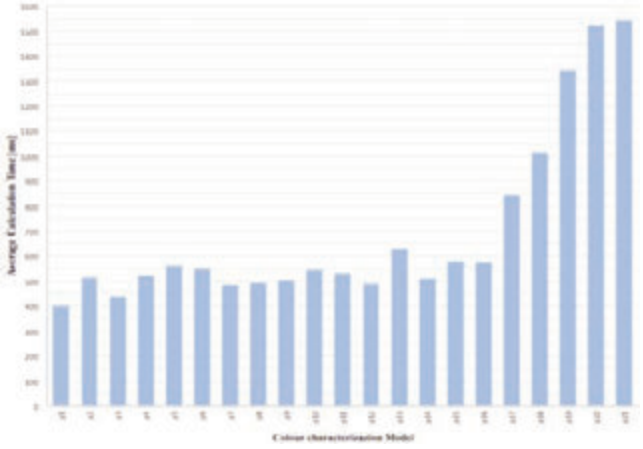

Figure 4. Average calculation times of colour characterization process for the adopted models.

Average calculation times were evaluated for all colour characterization models, applying the characterization algorithm to ten different images (1280 × 848). Data reported in Figure 4 show that processing times are absolutely compatible with laboratory analyses even adopting high performances models (about 1.5 seconds).

Conclusions

Colour characterization of an imaging system is an essential step for colour measurements on food products. Food quality controls, based on products appearance properties, require accurate colour measurements to adequately detect defects and/or products classification. Polynomial characterization models, preceded by a RGB channel response linearization, can achieve high accuracy with reasonable cal-

culation times. Therefore this technique can be profitably employed in laboratory applications. Approximating polynomials can be adopted even in channel response linearization process. However, increasing the order of the polynomial fits do not generally correspond to a performance improvement of the whole colour characterization. Therefore this issue has to be taken in account if an automatic calibration tool is developed.

Further investigations about colour characterization will be carried out evaluating models performances in berries classification in order to look for the best trade of between classification accuracy and calculation times.

References

Cheung, V., Westland, S., Thomson, M. 2004. Accurate estimation of the nonlinearity of input/output response for color cameras. Color Res. Appl. 29: 406–412.

Du, C.-J., Sun, D.-W. 2004. Recent developments in the applications of image processing techniques for food quality evaluation. Trends Food Sci. Technol. 15: 230–249.

Green, P. 2003. Colorimetry and colour difference, in: Colour Engineering Achieving Device Independent Colour, Display Technology. John Wiley & sons, 49–77.

Hong, G., Luo, M.R., Rhodes, P.A. 2001. A study of digital camera colorimetric characterization based on polynomial modeling. Color Res. Appl. 26: 76–84.

Jackman, P., Sun, D.-W. 2013. Recent advances in image processing using image texture features for food quality assessment. Trends Food Sci. Technol. 29: 35–43.

Jackman, P., Sun, D.-W., ElMasry, G. 2012. Robust colour calibration of an imaging system using a colour space transform and advanced regression modelling. Meat Sci. 91: 402–407.

León, K., Mery, D., Pedreschi, F., León, J. 2006. Color measurement in L a b units from RGB digital images. Food Res. Int. 39: 1084–1091.

Valous, N.A., Mendoza, F., Sun, D.-W., Allen, P. 2009. Colour calibration of a laboratory computer vision system for quality evaluation of pre-sliced hams. Meat Sci. 81: 132–141.

Westland, S., Ripamonti, C. 2004. Characterization of Cameras, in: Computational Color Science Using Matlab. Wiley, 127–140.

Wu, D., Sun, D.-W. 2013. Colour measurements by computer vision for food quality control – A review. Trends Food Sci. Technol. 29: 5–20.

Zheng, C., Sun, D.-W., Zheng, L. 2006. Recent developments and applications of image features for food quality evaluation and inspection – a review. Trends Food Sci. Technol. 17: 642–655.

Near-infrared spectroscopy is feasible to discriminate hazelnut cultivars

Elisabetta Stella,[1] Roberto Moscetti,[1] Letizia Carletti,[1] Giuseppina Menghini,[1] Francesco Fabrizi,[1] Valerio Cristofori,[1] Danilo Monarca,[1] Massimo Cecchini,[1] Riccardo Massantini[1]

[1]Department of Agriculture, Forest, Nature and Energy, University of Tuscia, Italy; [2]Department for Innovation in Biological, Agro-food and Forest system, University of Tuscia, Italy

Abstract

The study demonstrated the feasibility of the near infrared (NIR) spectroscopy use for hazelnut-cultivar sorting. Hazelnut spectra were acquired from 600 fruit for each cultivar sample, two diffuse reflectance spectra were acquired from opposite sides of the same hazelnut. Spectral data were transformed into absorbance before the computations. A different variety of spectral pretreatments were applied to extract characteristics for the classification. An iterative Linear Discriminant Analysis (LDA) algorithm was used to select a relatively small set of variables to correctly classify samples. The optimal group of features selected for each test was analyzed using Partial Least Squares Discriminant Analysis (PLS-DA). The spectral region most frequently chosen was the 1980-2060 nm range, which corresponds to best differentiation performance for a total minimum error rate lower than 1.00%. This wavelength range is generally associated with stretching and bending of the N-H functional group of amino acids and proteins. The feasibility of using NIR Spectroscopy to distinguish different hazelnut cultivars was demonstrated.

Correspondence: Riccardo Massantini, DIBAF, Tuscia University, Via S. Camillo de Lellis snc, 01100, Viterbo, Italy.
Tel. +39.0761.357496 - Fax: +39.0761.357498. E-mail: massanti@unitus.it

Key words: *Corylus avellana L.*, Near Infrared spectroscopy, hazelnut sorting

Contributions: the authors contributed equally.

Conflict of interests: the authors declare no potential conflict of interests.

Funding: this work was supported by the Ministry of Agricultural and Forestry Policy (MIPAAF MI.F.COL. 2012 – D.D. 17304).

Conference presentation: part of this paper was presented at the 10th Italian Conference AIIA (Associazione Italiana di Ingegneria Agraria), 2013 September 8-12, Viterbo, Italy.

Journal of Agricultural Engineering 2013; XLIV(s1):e55
doi:10.4081/jae.2013.(s1):e55

Introduction

Hazelnuts are one of the most important raw material for the confectionary and chocolate industries and they are generally marketed shelled. They are also used to add fiber, flavor and texture to various foods (Kibar and Ortzuk, 2009). Moreover, hazelnuts are a source of bioactive compounds that might be incorporated into new health-related products or serve as substitutes for synthetic ingredients (Contini *et al.*, 2008). Different uses of hazelnuts are being explored including the use of unripe fruit (Moscetti *et al*., 2012).

According to qualitative standards of the confectionary industry, the main commodity-related characteristics of the fruits, in relation with the process and use, are: fruit morphology, moisture content, shape uniformity, percent kernel, flaw incidences and the peelability as a consequence of the roasting process.

Moreover, the confectionary industries and the markets require whole hazelnuts from specific cultivar to enhance the characteristic of the traditional product with the aim of releasing a high quality product (Massantini *et al*., 2009).

The most suitable techniques for sorting and grading commodities are based on electrical properties, near-infrared (NIR) Spectroscopy, sound/noise/vibration, ultrasound nuclear magnetic resonance, X ray, volatile emission and other (Sun, 2010; Singh *et al*., 2010; Wang *et al*., 2011). NIR spectroscopy has a number of desirable qualities including minimal need for sample preparation, good sample penetration, and a wide range of applications. It is fast, easy to use, environmentally benign, and is highly suited to rapid on-line inspection (Pasquini, 2003; Wang *et al*., 2010).

NIR spectroscopy was used to compare moisture and acidity of several varieties of hazelnuts (Bellincontro *et al*., 2005). More recently Bellincontro *et al*. (2009) evaluated the quality of hazelnuts during the storage by NIR spectroscopy and finally Moscetti *et al*. (2013) identified hazelnuts flaw by Vis/NIR spectroscopy.

The aim of this paper was to demonstrate the feasibility of the NIR spectroscopy use for hazelnut-cultivar sorting of 'Tonda Gentile Romana'(TGR), 'Nocchione' (NOC) and 'Tonda di Giffoni' (GIF) that represent the main-grown varieties in Central Italy. The reason is to comply with the confectionary-industries' expectation that require special characteristics in relation with the specific use of the raw material itself and comply with the requirements of the regulation (G.U. n.186, 12-08-2009) that sets in 90% the maximum percentage of 'Tonda Gentile Romana' plus 'Nocchione' and 'Tonda di Giffoni'.

Materials and methods

Whole hazelnut kernels (round shape cvs. 'Tonda Gentile Romana', 'Nocchione' and 'Tonda di Giffoni') were obtained from the Assofrutti

facility (Caprarola, Viterbo, Central Italy) in October 2012. The moisture content was, for all the samples, 4.00±0.11%. Hazelnut spectra were acquired from 600 fruit per each cultivar sample, using a Luminar 5030 Acousto-Optic Tunable Filter-Near Infrared (AOTF-NIR) Miniature "Hand-held" Analyzer (Brimrose Corp., Baltimore, USA). The instrument was equipped with a reflectance post-dispersive optical configuration and an indium gallium arsenide (InGaAs) array (range 1100-2300 nm, 2-nm resolution) with a scanning time of 60 ms. Each acquired spectrum was the average of 10 scans. The reference spectrum was automatically measured by the instrument as described by Cayuela and Weiland (2010). Two spectra were acquired from opposite sides of the same hazelnut. Diffuse reflectance spectra were acquired and converted to transmittance measurements using SNAP! 2.04 software (Brimrose Corp.). Transmittance spectral data were transformed into absorbance ($A = \log T^{-1}$) using R 2.15.2 statistics software.

Features for use in classification were extracted from the spectra as raw absorbance values at each wavelength. Further, these features were extracted following a variety of spectral pretreatments including row-Mean Centering (rMC), Standard Normal Variate (SNV), Multiplicative Scatter Correction (MSC), and Savitzky-Golay first and second derivatives (d*f*, d2*f*) with second order polynomial (from 9 nm to 57 nm smoothing points with a step of 6 nm) (Savitzky and Golay, 1964; Boysworth and Booksh, 2008). High frequency noise was filtered from rMC, SNV, MSN and non-pretreated spectra by applying a Savitzky-Golay filter with 5-nm smoothing points. For each pre-treated and not-pre-treated dataset, Mean Centering (MC) was also tested, and a simulated annealing algorithm (SAA) was used to seek k-feature subsets (where k ranged from 2 to 6) which are optimal, as surrogates for the whole dataset (Cerdeira *et al.*, 2012). A maximum of 6-feature selection was computed to minimize the overfitting. An iterative Linear Discriminant Analysis (LDA) algorithm was used to choose a relatively small set of variables for the ability to correctly classify the samples. For each iteration of the algorithm, 50% of the samples were used as a training set, 25% were used for validation and 25% were used as test set. No outlier selection was computed.

The optimal group of features selected for each trial was analyzed using Partial Least Squares Discriminant Analysis (PLS-DA). For each combination of features a Receiver Operating Characteristics (ROC) graph was plotted for 20 instances (from 0.0 to 1.0 sound prior probability and from 1.0 to 0.0 unsound prior probability with a step of 0.05). The ROC curve is a two-dimensional depiction of classifier (combination of features) performance. It contains plots of the 'false positive rate' and the 'true positive rate' (also respectively called '1 – specificity' and 'sensitivity') as a function of the threshold value (Fawcett, 2006):

$$\text{False positive rate} = 1 - \frac{\text{True negatives}}{\text{False positives} + \text{True negatives}} \quad (1)$$

$$\text{True positive rate} = \frac{\text{True negatives}}{\text{Total positives}} \quad (2)$$

The total error rate represents the percentage of hazelnuts in the validation set incorrectly classified. False positive (fp) errors occur when a good product is classified as bad, while false negative (fn) errors occur when a defective product is misclassified as good.

For each ROC plot the relative Area Under the ROC Curve (AUC) was additionally used to evaluate the performance of each computed linear discrimination function (Fawcett, 2006), because it is statistically consistent and more discriminating than the total error rate, as demonstrated by Ling *et al*. (2003). Consequently, this makes it possible to obtain different AUCs for linear discrimination functions providing the same error rate for a given threshold value. The AUC takes on values between 0.5 and 1.0. An AUC value close to 0.5 indicates that the two groups are not distinctly different and therefore the classifiers have a weak discriminative ability. An AUC value close to 1.0 indicates that the features have strong discriminative power and a low tendency for overlap in the distributions of the group scores (Luo *et al*., 2012). The AUC value corresponds to the percentage of time a random selection from the positive group will produce a score greater than a random selection from the negative group (Fielding and Bell, 1997). For this research, an AUC of 0.9 was used as a threshold for acceptable discriminative performance. Thus, classifiers with an AUC equal to or less than 0.9 were discarded.

Statistical pretreatments and analysis, and data normalizations were performed using R 2.15.1 statistics software in combination with TISEAN 3.0.1 package (Hegger *et al*., 2012), and MASS 7.3-21, hyperspec 0.98, mda 0.4-2, PLS 2.3-0 and RTISEAN 3.0.14 R-packages (CRAN, 2012).

Results and discussions

There are no scientific studies on NIR spectroscopy to recognize different hazelnut varieties and it is impossible to find data for wavelength selection related with hazelnuts discrimination. Spectra included in the range 1100-2300 nm were acquired because this range was positively used in other studies on vegetable oil characterization (Yildiz *et al*., 2001), representing the main constituent of hazelnuts with a content above 60% on dry weight (Cristofori *et al*., 2008; USDA, 2009). Consequently the knowledge of chemical composition of the hazelnut and relative bibliography informs of the relation between molecules and wavelength that are more frequently selected from statistical models during the experimental phase. To recognize the three varieties (GIF, NOC, TGR) a predictive model LDA was tested. However, the

Test #	Dataset				Features (nm)						Error rates (%)			AUC (%)
	Scatt. C.	Norm.	SG*	Deriv.	1	2	3	4	5	6	fp	fn	total	
01	MSC	-	45	df	1136	1822	1848	2026	-	-	0.00	0.02	0.01	99.98
02	-	-	45	-	2000	2060	-	-	-	-	0.00	0.02	0.01	99.94
03	-	-	53	-	1360	1888	2000	2058	2182	-	0.00	0.02	0.01	99.89
04	MSC	-	57	df	1142	1552	1726	1872	2034	-	0.00	0.02	0.01	99.87
05	-	-	13	-	1518	2016	2050	2174	-	-	0.00	0.02	0.01	99.81
06	-	MC	21	-	1990	2058	2136	-	-	-	0.00	0.02	0.01	99.68

obtained discriminating performances are not suitable because they showed a high classification error for 'Nocchione' and 'Tonda Gentile Romana' cultivars. Therefore, the initial purpose for developing a 3-classes discriminant function was discarded. Consequently, the spectral data from the NOC and the TGR samples were merged into a new class sample, corresponding to 'Nocciola Romana DOP' (NRM) and a new 2-classes discriminant model (GIF and NRM) was developed.

The spectral region most frequently selected by the 2-classes-iterative LDA was the 1980-2060 nm range, which corresponds to best discrimination performance for a total minimum error rate lower than 1.00%. This wavelength range is generally associated with stretching and bending of the N-H functional group of amino acids and proteins. Features from the aforementioned range were frequently coupled with the wavelengths included in the 2120-2180 nm range, which typically represent the vibrations of C-H/C=O groups of lipids and N-H/C=O groups of proteins and amino acids (Workman and Weyer, 2008).

Discriminant functions with excellent performances were also obtained using features selected from the 1150-1650 nm spectral region, which represents the first overtone of stretching vibrations of O-H group (water, free fatty acids and monoglycerides) and overtone and stretching of combination and deformation of the –CH group (CH_3–, –CH_2– and *cis* R_1-CH=CHR_2CH_3–) (Yildiz *et al*., 2001; Christry *et al*., 2004). In addition, other wavelengths close to 1800 nm, which are descriptive of the fatty acid composition (Bewig *et al*., 1994), were also chosen by the iterative LDA function as features having good classification performances.

The most accurate classification of 0.00% fp, 2.00% fn and 1.00% total error was achieved using first derivative preprocessing combined with a Savitzky-Golay filter with 45 smoothing points and a Multiplicative Scatter Correction algorithm (Test #1) (Table 1). Features selected were *Abs*[1136 nm], *Abs*[1822 nm], *Abs*[1848 nm] and *Abs*[2026 nm]. For these features, the AUC value was 0.9999, corresponding to an excellent discrimination performance of the selected classifier. However, the amount of wavelengths required in an online sorting device would be conditional on the spectral pretreatment used. Obtaining scatter-corrected spectrum requiring to datasets of full spectra. Consequently, Test #1 and other Tests performed with scatter correction techniques are not suitable for fast- and inexpensive-online-detection devices. With this in mind, the best classification resulted from a Savitzky-Golay filter with 45 smoothing point (Test #02), resulting in excellent discrimination between classes (0.9995 AUC): *Abs*[2000 nm] and *Abs*[2060 nm], which correspond to overtones related with amino acids and proteins composition of hazelnut (Figure 1). The PLS-DA of test #10 indicates that the 96.91% of the variance was explained by LV1 and the 3.09% of residual variance from LV2 was essential was a complete description of the samples (Figure 2).

These results need to be supported by chemical assessments to confirm the potential compositional differences observed by NIR spectroscopy and this would be a great reason to continue the experimentation.

Conclusions

In the present study, the feasibility of using NIR Spectroscopy (from 1100 nm to 2300 nm) to discriminate different hazelnut cultivars (cvs. 'Tonda Gentile Romana', 'Nocchione' and 'Tonda di Giffoni') was demonstrated. Features for discriminant analysis that showed the best classification results were generally in the 1150-1650 nm, 1800 nm, 1980-2060 nm and 2120-2180 nm spectral bands. The 2 classes discriminant models showed a very high performance of the NIR Spectroscopy for a suitable classification of 'Nocciola di Giffoni IGP' and 'Nocciola Romana DOP'. The best classification performance (0% fp, 2% fn, 1% total error and 0.9995 AUC) were obtained using a Savitzky-Golay filter with 45-smooting points, and *Abs* [2000 nm] and *Abs* [2060 nm] wavelengths.

Finally, the method used here allows reliable classification of hazelnuts cultivars based on a maximum of 6 wavelengths selected from within the spectral range from 1100-2300 nm, thus providing the means for a rated, on line detection system.

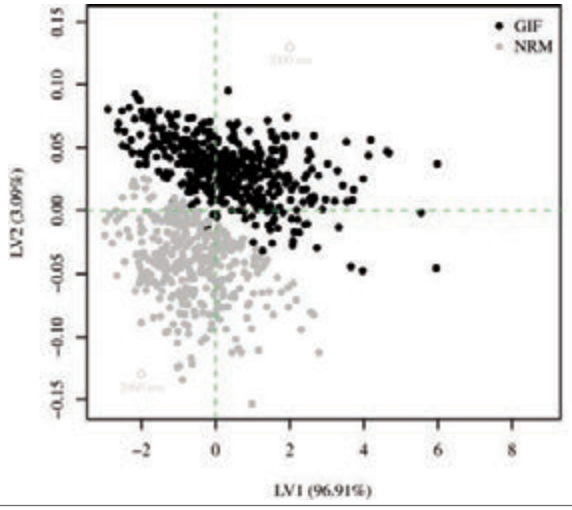

Figure 1. Classes spatial distribution along the LD1 dimension and relative overlayed density plot obtained from the three features selected from the spectra acquired from the flat side (fs) of the fruit. Spectra pretreated with the Savitzky-Golay filter (45-smoothing points).

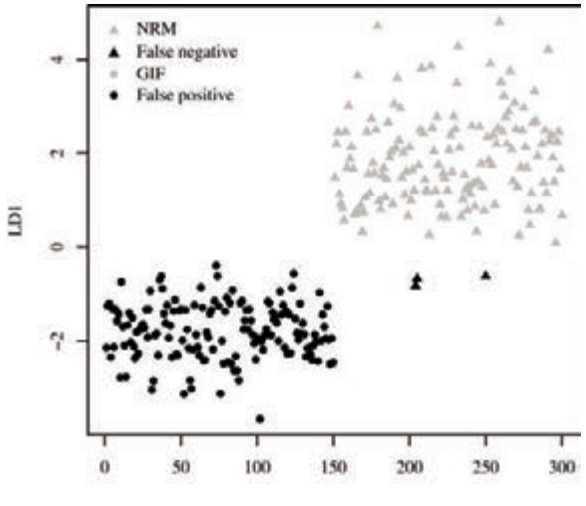

Figure 2. PLS-DA score plot of the two features selected during the Test #10 (Table 1). Dataset pretreated with the Savitzky–Golay filter (45-nm smoothing points). Percents of the explained variance are reported in

References

Bellincontro, A., Fracas, A., Anelli, G., Mencarelli, F., Di Natale, C., Esposito, G. Use of NIR Technique to measure the acidity and water content of hazelnuts. Proc. VI Intern. Congress on Hazelnut published Tous, J., Rovira, M. and Romero, A. Acta Horticult. 2005;686:499-503.

Bellincontro, A., Mencarelli, F., Forniti, R., Valentini, M. Use of NIR-AOTF Spectroscopy and MRI for quality detection of whole hazelnuts. Proc.VII Intern. Congress on Hazelnut published Varvaro, L. and Franco, S. Acta Horticult. 2009;845:593-7.

Bewig, K.M., Clarke, A.D., Roberts, C., Unklesbay, N. Discriminant analysis of vegetable oils by near-infrared reflectance spectroscopy. J. Am. Oil Chem. 1994;2:195-200.

Boysworth, M.K., Booksh, K.S. Aspects of multivariate calibration applied to near-infrared spectroscopy. In Burn, D. A., & Ciurczak, W. E. (Eds.), Handbook of Near-Infrared Analysis (3rd ed.) 2008;207-29. CRC Press.

Cayuela, J.A., Weiland, C. Intact orange quality prediction with two portable NIR spectrometers. Postharvest Biol. Tec. 2010;58:113–20.

Cerdeira, J.O., Silva, P.D., Cadima, J., Minhoto, M. Package 'subselect' 0.12-2 for use with R. Selecting variable subsets. 2012.

Christry, A.A., Kasemsumran, S., Du, Y., Ozaki, Y. The detection and quantification of adulteration in olive oil by near-infrared spectroscopy and chemometrics. Anal Sci 2004;20:935-40.

Contini, M., Baccelloni, S., Massantini, R., Anelli, G. Extraction of natural antioxidants from hazelnut (*Corylus avellana* L.) Shell and skin wastes by long maceration at room temperature. Food Chem 2008;110:659-69.

Cristofori, V., Ferramondo, S., Bertazza, G., Bignami, C. Nut and kernel traits and chemical composition of hazelnut (*Corylus avellana* L.) cultivars. J. Sci. Food Agr. 2008;88:1091-8.

Fawcett, T. An introduction to ROC analysis. Pattern Recognition Letters 2006;27:861–74.

Fielding, A.H., Bell, J.F. A review of methods for the assessment of prediction errors in conservation presence/absence models. Environ. Conserv. 1997;24:38–49.

Italian Regulation. Disciplinare di produzione della denominazione di origine protetta 'Nocciola Romana' DOP. In: Official Journal No. 186, 12/8/2009.

Hegger, R., Kantz, H., Schreiber, T. Nonlinear Time Series Analysis (TISEAN). 2012.

Kibar, H., Öztürk T., The effect of moisture content on the physico-mechanical properties of some hazelnut varieties. J Stored Prod Res 2009;45:14-8.

Ling, C.X., Huang, J., Zhang, H. AUC: a better measure than accuracy in comparing learning algorithms. Lect. Notes Artif. Int. 2003;2671:329-41.

Luo, X., Takahashi, T., Kyo, K., Zhang, S. Wavelength selection in VIS/NIR spectra for detection of bruises on apples by ROC analysis. J Food Eng. 2012;109:457–66.

Massantini, R., Moscetti, R., Monarca, D., Cecchini, M., Contini, M., Mordacchini Alfani, M.L. Influence of cover crop and double harvest on storage of fresh hazelnuts (Corylus avellana L.). Adv. Hortic. Sci 2009;23:231-7.

Moscetti, R., Frangipane, M.T., Monarca, D., Cecchini, M., Massantini, R. Maintaining the quality of unripe, fresh hazelnuts through storage under modified atmospheres. Postharvest Biol. Tec. 2012:65:33-8.

Moscetti, R., Haff, R.P., Aernouts, B., Saeys, W., Monarca, D., Cecchini, M., Massantini, R. Feasibility of Vis/NIR spectroscopy for detection of flaws in hazelnut kernels. J Food Eng 2013;118:1-7.

Pasquini, C. Near infrared spectroscopy: fundamentals, practical aspects and analytical applications. J. Braz. Chem. Soc. 2003;14:198-219.

Savitzky, A., Golay, M.J.E. Smoothing and differentiation of data by simplified least squares procedures. Anal. Chem. 1964;36:1627–39.

Singh, C.B., Jayas, D.S., Paliwal, J., White, N.D.G. Identification of insect-damaged wheat kernels using short-wave near-infrared hyperspectral and digital colour imaging. Comput. Electron. Agr. 2010;73:118-25.

Sun, D. Hyperspectral imaging for food quality analysis and control. Academic Press, 2010. London.

United States Department of Agriculture (USDA). National nutrient database for standard reference - Release 22, 2009. URL http://ndb.nal.usda.gov/

Wang, J., Nakano, K., Ohashi, S., Takizawa, K., He, J.G. Comparison of different modes of visible and near-infrared spectroscopy for detecting internal insect infestation in jujubes. J. Food Eng. 2010;101:78-84.

Wang, J., Nakano, K., Ohashi, S. Nondestructive detection of internal insect infestation in jujubes using visible and near-infrared spectroscopy. Postharvest Biol. Tech. 2011;59:272-9.

Workman, J. Jr., Weyer, L. Practical Guide to Interpretive Near-Infrared Spectroscopy. CRC Press, 2008;51-69.

Yildiz, G., Wehling, R.L., Cuppett, S.L. method for determining oxidation of vegetable oils by near-infrared spectroscopy. J. Am. Oil Chem. Soc. 2001;5:495-502.

Assessment of the energy and separation efficiency of the decanter centrifuge with regulation capability of oil water ring in the industrial process line using a continuous method

Biagio Bianchi, Antonia Tamborrino, Francesco Santoro

Department of Agricultural and Environmental Science, University of Bari, Italy

Abstract

The third era in olive oil extraction sees a new generation of decanter that give the operator the possibility to chose time by time the type of working: two or three phase shifting from one solution to the other without stopping the machine and even intermediate solutions between two or three phase, making the most suitable adjustments, following olive variety, just as the machine works. A decanter centrifuge was employed during the experimental tests with variable differential speed between bowl and screw conveyor (n) and with regulation capability of oil-pulp ring levels. Thus permit to shift from three to two phase, reducing water added and discharging the following by-products: dehydrated husk similar to that of three-phase and recovers a wet pulp that is the between the liquid phase and the solid phase.

This paper aims to report the preliminary results of the energy and functional efficiency of the decanter when it works in the industrial scale plant and using a continuous method. The tests were carried out at two different flow rate values; for each flow rate the different variable differential speed between bowl and screw conveyor was varied at 15,50, 17,50 and 19,50. Quality olive, operating speed of the crusher machine and relative feed flow rate of the machine, the malaxing time and the degree of dilution of the paste, as well as the oil-pulp ring level were the same for all the trials. Irrespective of the flow rate and n used, the machine tends to stabilize energy consumption in a very short time and values were quite similar to each other. The reductions in flow rate do not involve reductions of energy consumption indeed lead to the increase of absorption per unit mass of product worked. For all thesis studied, no significant changes of the oil recovery efficiency were found, indeed changing the flow rate and the n a different distribution of the not extracted oil was found in the pulp and in the husk. To complete the knowledge, a set of tests changing also the oil-pulp ring levels, has been provided for the next olive oil season.

Correspondence: Antonia Tamborrino, DISAAT, University of Bari, via Amendola 165/A – 70126 Bari, Italy.
Tel.: +39.080.5443122 - Fax: +39 080 5443122.
E-mail: antonia.tamborrino@uniba.it

Key words: olive oil extraction; decanter centrifuge; energy and separation efficiency.

Contributions: the authors contributed equally.

Conflict of interests: the authors declare no potential conflict of interest.

Journal of Agricultural Engineering 2013; XLIV(s1):e56
doi:10.4081/jae.2013.(s1):e56

Introduction

Industrial production of olive oil is supported by centrifugal extraction since the 1970s. Until well into the 1970s, after crushing, stirring and heating it was standard practice to squeeze the olive using hydraulic presses and to separate the liquid obtained into oil and water phases in small disk separators or static sedimentation tanks – a very complex procedure with relatively low outputs. Initially 3-phase decanters were introduced. This 3-phase technology involved diluting the olive pulp with water, enabling the oil to be separated from the solid matter and water – an economical method, but one which, because of its requirement for huge volumes of fresh water, placed a significant burden on the environment. The quantities of wastewater also proved to be an ecological problem (Roig *et al.,* 2006).The 3-phase decanters are able to separate oil from the husk (solide residues of olive) and waste water; due to the large amount of water added to the process a considerable reduction of natural antioxidant in the resulting olive oil is observed. The crucial advance came in the form of the 2-phase system. This was a method developed in the early 1990, which uses no added water for dilution and produces correspondingly less wastewater. What both processes have in common is that the olives are initially reduced to a pulp. With 3-phase technology, this olive pulp must be diluted with warm water so a layer forms between the oil and solids in the decanter. This is the only way to achieve the subsequent separation into oil phase, husk and wastewater. Depending on the type of olive, the required volume of water is 15 to 30 percent, in rare cases as much as 50 percent. The amount of loaded wastewater produced by this process is correspondingly high. In the 2-phase system, the preliminary treatment of the olives is essentially the same as in a 3-phase system. However, the fruits are milled smaller and malaxed for longer. The 2-phase decanters are able to separate the oil from the olive paste producing a pomace only, and for this reason are called '2-phase decanters'. They produce a very wet husk, with water content between 65 and 70% by weight. In addition to the ecological issues, the 2-phase system is also impressive from an economic perspective. It ensures the best possible oil quality by retaining the highest possible polyphenol content. The taste is intense, because many flavours and ingredients are washed out to a much lesser extent due to the addition of less water. At the same time, these oils have an exceptionally long shelf life (Alburquerque *et al.,* 2004). In 1997 an innovative type of decanter (VDP-decanter) was introduced with a more advanced system to regulate the processing conditions. This allows to obtain better results

according to the variation of the ratio between liquid and solid phases, thus optimizing operational performances in relation to the rheological features of olive oil pastes. The decanter centrifuge were design with an innovative geometry, made by a longer cylindrical part of the bowl and shorter beach sections, and a special bowl with a variable dynamic pressure (VDP) cone system. This makes it possible to electronically adjust the speed of the screw according to the torque on the conveyor screw. Moreover, with the VDP the automatic control of differential speed depends on the twisting moment, thus obtaining drier discharged solids, with lower oil residue contents (Catalano *et al.,* 2003). This decanters are able to work using a small amount of added water (0 to 20 percent of the weight of the olives) reducing the waste water discharged and producing a pomace with a water content between 55 and 60%.

The latest development in this field is the new generation of decanter that give the operator the possibility to chose time by time the type of working: 2 or 3-phase shifting from one solution to the other without stopping the machine and even intermediate solutions between 2 or 3-phase, making the most suitable adjustments, following olive variety, just as the machine works. Thus permit to shift from 3 to 2-phase, reducing water added and discharging the following by-products: dehydrated husk similar to that of three-phase and recovers a wet pulp that is the between the liquid phase and the solid phase (Altieri 2010). Regarding the energy consumption in the olive oil extraction plants few studied have been done. In 1994 Morello studying continuous plants of the low work capacity (about 1500kg/h) highlighter that the utilization of the installed electrical power varies between 20 and 40%, with values minimum (20-25%) for the extraction equipment: feed pumps, decanter, vibrating screens; the same equipment commits about 25% of the electricity used, with a power consumption of primary specific energy about 70-100 MJ/t of olives, equal to about 20% of the total energy. The optimization of the energy consumption of the decanter thus assumes considerable importance in the total energy balance and in production costs of the extra virgin olive oil.

This paper aims to report the preliminary results of the energetic and functional efficiency of the decanter when it works in the industrial scale plant and using a continuous method. The purpose has been to evaluate the performance of the decanter with appropriate adjustments of the functional parameters: different conveyor/bowl differential speed (Dn) and different mass flow rate of olive paste (Qp).

Materials and methods

Industrial tests

The experimental tests were carried out in an industrial olive oil mill located in Trani (BA), Italy. The extraction plant was equipped with a hammer crusher followed of a set of malaxer machine connected in series. The number of malaxer used was four; in this condition the paste fell, helped also to the movement of the reel, in the next malaxer and later in the next one until to feed the decanter. The paste was discharged by means at a "mono" type pump that feeds a centrifuge machine for oil recovery. The decanter centrifuge used was designed and built by the Barracane company (Modugno - BARI, ITALY) - MEGA-LA 650; the continuous extraction olive oil plant work up to 6500 kg/h as a maximum work of throughput. This type of decanter is an two-phase decanter that produce, as a by-products, a dehydrated husk similar to the one coming from a three-phase decanter and a wet pulp called "pâté" made up the only pulp of olives without any traces of kernel.

Design features of the decanter centrifuge

The decanter centrifuge with variable differential speed between bowl and screw conveyor (Δn) and with regulation capability of oil-water ring level was used. The power-transmission technology between the conveyor and bowl developed in this decanter could be defined "electro-mechanical recovery":

- Maximum work of throughput: 6500 kg/h;
- Main electric power: 75 kW;
- Supply voltage: 380 V three-phase;
- Rated power asynchronous bowl electric motor: 45 kW;
- Rated current bowl electric motor: 80 A;
- cos ϕ bowl electric motor: 0.87;
- Rotational speed of the bowl electric motor: 1475 rev/min;
- Rated power asynchronous screw conveyor electric motor: 30 kW;
- Rated current screw conveyor electric motor: 54.4 A;
- cos screw conveyor electric motor: 0.87;
- Rotational speed of the screw conveyor electric motor: 1470 r/min.

In Figure 1 is sketched the electro-mechanical transmission that characterizes the external bowl and the coaxial inner screw conveyor motion. At the end of the cylindrical section of the bowl there are the exits of the olive oil and of the semifluid fraction made of pitted pulp and water. At about 1/3 of the screw conveyor hollow shaft total length there is the input section of the braked olive paste. The external bowl electric motor is powered by an inverter that is itself controlled by a knob in order to modify the rotation speed of the olive pasta; in the same way the supply of the screw conveyor electric motor is made whose rotation speed is controlled also by a planetary gearbox which fixes a 1:3 constant transmission ratio.

The bowl electric motor inverter is connected in series to the one of the screw conveyor electric motor which is itself connected to the public power supply network.

The olive paste, once has been introduced into the decanter, is obliged to rotate at the same angular speed of the bowl forcing the internal screw conveyor to rotate at the same angular speed which is however set to be lower; so the screw conveyor electric motor behaves as a generator so that the produced energy is used by the bowl electric motor with a fewer public supply network energy consumption.

The machine is also equipped with a system of pick-up diameters setting of both olive oil and olive paste. On the external bowl conical part surface, near its end, there are the husk exit holes.

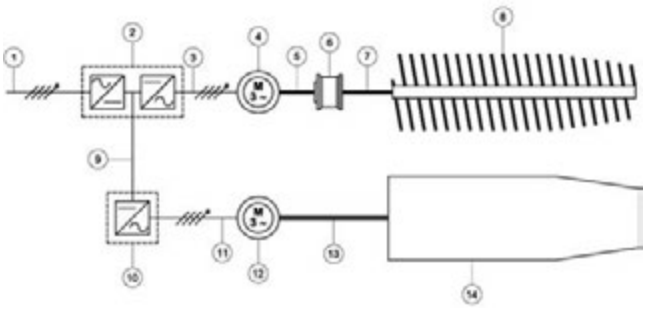

Figure 1. Decanter electro-mechanical transmission: 1 power supply, 2 screw conveyor energy recovery inverter, 3 screw conveyor electric motor power supply, 4 screw conveyor electric motor, 5 electric motor shaft, 6 planetary gearbox, 7 screw conveyor belt transmission, 8 screw conveyor, 9 inverter series connection, 10 bowl inverter, 11 bowl electric motor power supply, 12 bowl electric motor, 13 bowl belt transmission, 14 bowl.

Experimental procedure

Olive fruits of constant quality (cv. Peranzana) were used for the trials. After the leaf-removal the olives were crushed and malaxed in continuous. The trials were divided in six tests and to ensure an average working time of about 60 minutes were used 10 minutes to stabilize the functioning of the decanter centrifuge and 50 minutes available for sampling. For each test paste was malaxed for 60 minutes at 28°C.

During the continuous process of extraction were tested 2 different nominal values of paste mass flow rate, 4800 kg/h and 4000 kg/h. For each value of paste mass flow rate the differential speed between the screw conveyor and bowl (Δn) was varied at 15.50, 17.50, 19.50. For all the tests no variation of the ring level was done as well as the water flow rate added to the process that was equal to 380 kg/h. This corresponds to about 8 % of the first value of paste mass flow rate and about 10 % of the second value.

Industrial tests: power consumption

In order to carry out the power consumption related industrial tests a measurement instrumentation chain has been arranged:

1 Digital built in frequency, current and voltage RS232 output of the KEB COMBIVERT F6-K - inverter;
2 RS232 to USB converter;
3 Personal computer;

To achieve the desired differential speed Dn above specified for each test, the frequency of the input voltage of the two electrical motors of both screw conveyor and bowl, has been controlled; these values has been continuously verified during the tests.

The instrumentation chain was arranged to a data acquisition rate of 106 data per second (dps). The parameters monitored during the tests were:

- Bowl electric motor current consumption;
- Bowl electric motor power consumption;
- Screw conveyor electric motor current consumption/production;
- Screw conveyor electric motor power consumption/production.

The acquired data were processed using software specifically designed for this aim and the data have been treated with a statistical software.

Industrials tests: mass balance

The parameters used for the mass balance of the decanter centrifuge are: Q_p: actual olive paste flow mass, (kg/h); Q_o: Olive oil flow mass (kg/h); Q_w: Process water flow mass (kg/h); Q_{wp}: Wet pulp flow mass (kg/h); Q_h: Husk discharge flow mass (kg/h). In the mass balance the following Q are known: Q_p, Q_o, Q_w and Q_{wp} whereas the Q_h was obtained by application of the following equation: $Q_h = Q_p - Q_o - Q_{wp}$.

For each test a sample was taken of olive, of olive paste and two samples (one every 20 minutes) of wet pulp and husk. Moisture content of olive paste, husk and wet pulp were done. The analysis was based on weigh difference after sample drying, according to the official method. Fat content was assessed using a solvent extractor based on the Randall 148 extraction technique (VELP SCIENTIFICA). All analyses were carried out in triplicate. The separation efficiency was calculated from values obtained, as a percent ratio between oil extracted during process and oil contained in olives, as well as oil lost in wet pulp and husk.

Statistical analysis

Statistical analysis and plotted results were carried out using Statistica software (STATISTICA; Statsoft version 9.1).

Results and discussions

Energy efficiency

Based on experimental tests results, it's possible to note that irrespective of the flow rate and Δn used, the machine tends to stabilize energy consumption in a very short time (less than 10,0 s) and values are quite similar to each other. The reductions in flow rate do not involve reductions of energy consumption indeed lead to the increase of absorption per unit mass of product worked. The machinery energy consumption (Table 1) can be considered fairly constant with Δn variation. Irrespective of the studied working condition, even if the energy consumption are almost equal each other with current consumptions that varies from 50 to 60 A, it's possible to detect a trend in electric power consumption rising when lowering Δn and vice versa: the higher Δn values carried out tests show lower electric power consumption for both the studied supply flows.

This result can be explained if it is considered that rising the bowl-screw conveyor differential speed involves a fewer time during which the olive paste stays in the machine which in turn involves a more fluid olive paste with a lower resistant torque on the screw conveyor.

This last eventuality also shows that the energy lost due the resistant torque on the screw conveyor is much more greater than the one lost in the planetary gearbox even if it should increase with higher Δn. However the machinery energy recovery system allows the bowl electrical motor to really use fewer electric energy from the public electric energy network then theoretically needed; in fact during regime phase, the screw conveyor is dragged along by the bowl, so its electrical motor acts as a generator and the produced energy is used by the bowl electrical motor.

This behavior is shown by negative current measurement at the screw conveyor electrical motor during regime phase (Table 1). With an independent transmission system, the bowl electrical motor used energy would have been greater.

Collected energy data analysis shows a not significant variation related to a paste flow supply reduction thus it should be better to let

Table 1. Experimental test measured energetic parameters mean values.

Test	BC_S (A)	ε	SCC_S (A)	ε	BC_R (A)	ε	SCC_R (A)	ε	TC_R (A)	ε
A	77	3,04	25	0,95	68	3,24	- 16	3,12	52	3,49
A+	76	1,98	24	1,31	67	1,74	- 17	2,34	50	1,83
A-	78	2,87	27	0,92	67	3,76	- 12	2,97	55	1,85
B	74	3,65	26	1,65	68	2,48	- 10	3,12	58	1,74
B+	76	3,88	24	1,42	66	3,01	- 10	3,47	56	2,23
B-	77	2,62	26	0,57	69	2,12	- 9	3,21	60	2,43

BC_S: Bowl current consumption at start-up phase; SCC_S: Screw conveyor current consumption at start-up phase; BC_R: Bowl current consumption at regime phase; SCC_R: Screw conveyor current consumption at regime phase; TC_R: Total current consumption at regime phase.

Table 2. Oil balance for all the trials as a function of the processing conditions.

Test	Qp (kg/h)	Processing water (%)	Δn	Extraction efficiency (%)		Residual oil content (kg/100 kg)			
						Husk		Wet pulp	
				m	DS	m	DS	m	DS
A	4809,6	8	17,50	90,2	±0.11	3,68	±0.01	6,08	±0.02
A -	4809,6	8	15,50	88,7	±0.12	8,94	±0.02	2,35	±0.03
A +	4809,6	8	19,50	89,3	±0.19	7,62	±0.02	3,11	±0.01
B	4075,2	10	17,50	89,3	±0.20	7,88	±0.03	2,79	±0.03
B -	4075,2	10	15,50	90,4	±0.12	7,27	±0.01	2,31	±0.02
B +	4075,2	10	19,50	90,3	±0.19	6,99	±0.01	2,71	±0.02

the machine work at its maximum working capacity because the power consumption per mass unit should be the lowest. This result could be useful in the olive mill management; as a matter of fact the paste flow supply rate is the main operating parameter modified in order to solve abnormal working conditions. Conversely, on this specific machinery, since a lot of working parameters can be modified without outages, the energy consumption could be optimized modifying other working parameters such as Δn or the pick-up diameters instead of paste flow supply.

Separation efficiency

The extraction efficiency varies from 80 to 90% of the oil content of the olives, because the oil in the olive paste is only partially free to escape and part of it remain in unbroken olive cells or is trapped in the tissues of cytoplasm or is emulsified in the aqueous phase. The residual oil in the olive by-products is a critical point in the olive oil extraction process. Furthermore, the olive husk is sold to other factories, where the olive oil residual is extract by solvent extraction to obtain the "olive pomace oil". But, before this, the by-products could be sent to another decanter associated to the firsts extractions equipment line, in the same facilities, where usually is added water and started a process to recovery the amount of oil residual, obtaining the oil so called "oil from ripasso".

The results of trials, are reported in Table 2, as a function of the processing conditions, i.e. feeding, and differential velocity of the conveyor to the bowl. For all conditions studied, there have been no significant changes in the performance of the machine in terms of oil extracted. In particular, the total amount of oil that has been not extracted, thus present in the husk and in the wet pulp, is never greater than 2.8% on the total mass of the obtained residues (13% on the oil present in olives). Besides, in all samples of wet pulp, no fragment of stones has been detected; this open an interesting scenario in the reuse of this by-product for composting or animal feeding.

A complete analysis of the effects of the various process parameters on the extraction efficiency of this type of decanter was performed: the oil content in the wet pulp and in the husk has been determined and in the Table 2 the main differences between the different operating conditions are shown. The composition of the by-products, in terms of oil residual, is influenced by the operating conditions used: flow mass rate and Dn. Different flow mass rate and different Dn determines a different amount of the residual oil in the two by-products discharged: wet pulp and husk. The condition of the Test A determines an amount of residual oil in the wet pulp greater than that present in the husk. This condition makes much convenient to extract the residual oil only from the wet pulp using a intended decanter ensuring, besides, the highest amount of residual oil in the lower quantity of by-product treaty allows to reduce both investment costs, relative to the machines and the overall dimensions allocated to this operation, both the costs of management. Reducing the nominal work throughput at 4000kg/h and setting 19,50 as Dn (test B), the greater amount of residual oil was founded in the husk with the same extraction efficiency for both the tests (test A and test B). The evaluation of mass balances and the comparison of results in different operating conditions can suggest optimal operating conditions of the extraction process.

Table 3. Flow mass balance for all tested conditions.

Test	Qp (kg/h)	Qw (kg/h)	Qo (kg/h)	Qwp (kg/h)	Qh (kg/h)
A	4809,6	379,5	1005	1551	2633,1
A -	4809,6	379,5	888	1332	2969,1
A +	4809,6	379,5	966	1212	3011,1
B	4075,2	379,5	768	990	2696,7
B -	4075,2	379,5	828	999	2627,7
B +	4075,2	379,5	788	987	2679,7

Conclusions

The peculiarity of the present study is the use of an industrial olive mill. So on the one hand has been difficult to identify the right process-ruling parameters, and sometimes even understand them, but on the other hand the obtained results are immediately usable by the olive mills managers because these results are obtained on a real-scale model towards an experimental-scientific approach.

The obtained experimental tests results shows high performances and significant flexibility potential of the studied machine both by an energy consumption point of view and by a functional one if referring to oil extraction efficiency and wastes management.

Some of the obtained results are the basis of the present study hereinafter that should be held in the next olive production season. During the following research step, the decanter will be optimised in order to achieve the higher yield, the lowest energy consumption and an easy management of residual oil both in the wet pulp and in the husk, with the final result to produce easy to use iso-yielding charts.

References

Alburquerque, J.A., Gonza lvez, J., Garcı a, D., Cegarra, J. Agrochemical characterisation of ''alperujo'', a solid by-product of the two phase centrifugation method for olive oil extraction. Bioresource Technology. 2004; 92(2): 195–200.

Altieri, G., Comparative trials and an empirical model to asses throughput indices in olive oil extraction by decanter centrifuge. Journal of food engineering. 2010; 97:46-56.

Catalano, P., Pipitone, F., Calafatello, A., Leone, A. Productive Efficiency of Decanters with Short and Variable Dynamic Pressure Cones. Biosystems Engineering. 2003; 86(4):459–464.

Morello G., Peri G., Planeta A. Aspetti energetici dell'estrazione dell'olio di oliva in impianti a ciclo continuo. Proceedings book "Aspetti Energetici del Sistema Agro-Industriale e Loro Influenza sul Territorio". 1994; 1:199-215.

Roig, A., Cayuela, M.L., Sa nchez-Monedero, M.A. An overview on olive mill wastes and their valorisation methods. Waste Management. 2006; 26:960–969.

An integrated mechanical-enzymatic reverse osmosis treatment of dairy industry wastewater and milk protein recovery as a fat replacer: a closed loop approach

F. Sarghini,[1] A. Sorrentino,[1] P. Di Pierro[2]

[1]Department of Agriculture, University of Naples Federico II , Portici (NA), Italy; Department of Chemical Sciences, University of Naples Federico II , Portici (NA), Italy

Abstract

The dairy industry can be classified among the most polluting of the food industries in volume in regard to its large water consumption, generating from 0.2 to 10 L of effluent per liter of processed milk. Dairy industry effluents usually include highly dissolved organic matter with varying characteristics, and a correct waste management project is required to handle. In a framework of natural water resource availability and cost increase, wastewater treatment for water reuse can lower the overall water consumption and the global effluent volume of industrial plants. Moreover, correct dismissal of dairy industry wastewater is sometimes neglected by the operators , increasing the environmental impact due to the chemical and biological characteristics of such effluents. On the other hand, in the case of whey effluents, several by-products are still present inside, such as lactose and milk proteins. Membrane technology has some advantages including a high degree of reliability in removing dissolved, colloidal and particulate matter, like the selectivity in size of pollutants to be removed and the possibility of very compact treatment plants. For example, Reverse Osmosis (RO) technology has been successfully applied for the treatment of dairy wastes (1), and as a technology for concentration and fractionation of whey. In this work a membrane treatment approach using reverse osmosis technology is investigated and implemented: the permeate obtained can be reused as clean warm water for cleaning and sanitation of production plants, while concentrated milk proteins are modified by using transglutaminase enzyme obtaining a high temperature resistant fat replacer to be used in different low-fat products like for example mozzarella cheese.

Correspondence: Fabrizio Sarghini, DIAAT, Via Università, 100 - 80055 Portici (NA), Italy.
E-mail: sarghini@unina.it

Key words: dairy industry waste recovery, enzymatic treatment, low fat mozzarella cheese, whey.

Acknowledgements: Regione Campania, PSR 2007-2014 under 1.2.4 program is gratefully acknowledged for financial support.

Journal of Agricultural Engineering 2013; XLIV(s1):e57
doi:10.4081/jae.2013.(s1):e57

Introduction

The dairy industry produces an high amount of wastewaters characterized by a severe chemical oxygen demand (COD) and biological oxygen demand (BOD) representing their high organic content (Orhon *et al*, 1993). Furthermore, the dairy industry is one of the largest sources of industrial effluents in Europe: a typical European dairy industry generates a large amount of effluent ranging from 0.2 to 10 L per liter of processed milk.

Dairy waste effluents are usually concentrated, and the main contributors of organic load to these effluents are carbohydrates, proteins and fats originating from the milk (Kasapgil *et al*.,1994 and Perle *et al*.,1995).

While the cheeses have always been a production priority, the main by-product, i.e whey, representing a very high percentage of processed milk, has been greatly neglected in the past, both in terms of characterization and possible use. In fact, whey main use consists in swine feeding if not disposal, with the relative costs of the process, sometimes even outside of compliance with environmental regulations.

As a matter of fact, such wastewaters cannot be simply dismissed, and they require a chemical or mechanical processing, with a significant economic cost.

Among several possible approaches, membrane technologies, and more specifically Reverse Osmosis (RO) technology has been successfully applied for the treatment of dairy wastes (Vourch *et al*., 2005), and as a technology for concentration and fractionation of whey.

Generally speaking two different strategies can be adopted: the first simply aimed to dismiss the dairy waste minimizing the economic and environmental impact (clean water production + concentrated products) , the second considering such wastes as a resource and focused on recovery by-products from the wastewaters in order to increase the economic value of the overall chees production process.

Specifically, whey protein represents one of the most interesting by-products, although some technical difficulties can arise when the final transformation is not performed in the dairy industry itself, due to the fact that refrigeration is required to preserve their properties.

In this work a membrane treatment approach using reverse osmosis technology is investigated and implemented: the permeate obtained can be reused as clean warm water for cleaning and sanitation of production plants, while concentrated milk proteins are modified by using transglutaminase enzyme obtaining a high temperature resistant fat replacer to be used in different low-fat products like for example mozzarella cheese.

Materials and methods

Reverse Osmosis Plant description

The first part of the work consisted in selecting an appropriate membrane treatment plant to be introduced in a cheese factory (Caseificio Campolongo Srl), with the aim of producing high quality whey protein and clear water from separation process.

Reverse Osmosis (RO) is a system of concentration of liquid alternative to thermal evaporation systems, with operating costs lower than in conventional evaporators, and an appropriate RO concentration plant was built on skids for easy handling and a more rational layout, equipped with 24 elements polymeric spiral membranes.

The plant was fed from a reservoir operated by a level control automatic system for the whey filling. A centrifugal pump with an installed power of 0.75 kW was used to collect the serum from the food reservoir of food and to send, after safety filtration using a polypropylene bag filter with a filtration network of 50 microns, into a heat exchanger for inlet temperature control.

The system can work in two temperature conditions: cold (10°C - 15°C) or warm (50°C) operative mode, as working at intermediate temperatures promotes bacterial growth, causing the fouling of the membranes. The serum, after being set to the appropriate temperature in the heat exchanger, was pressurized using a multi-impeller centrifugal pump with an installed capacity of 7.5 kW, controlled by an inverter, and then sent to double multi-impeller centrifugal recirculating pumps with an installed capacity of 4 kW for each loop on the membranes.

The two pumps ensure the serum to make the loop into the 24 polymeric spiral membranes with a pressure up to 40 bar. The concentrate is then transferred to another tank after a second heat treatment. An automatic control system governs the operation of all devices installed on the system and automatically controls the exercise cycles, as well as membrane rinsing and washing.

Operating conditions are listed in Table 1.

Serum feeding should be pre-filtered on a dry filter, degreased ((to 0,05% fat final content) at 10°C -15°C or 50°C. In case the system works at low temperature, the plant efficiency is expected to decline in the order of 20-25%.

Protein concentration

The whey is what remains of the milk as a result of the process of curdling, necessary for the production of dairy products of all kinds. In addition to serum, other liquid waste are generated by the production process of the cheese, like ricotta cheese and butter.

In the considered dairy industry, production data are reported in Table 2.

The quantities of the latter are usually of the order of 20% of the total liquid waste products, depending on seasonal production of the cheese. The final concentrations of retentate is approximately around 18% and the permeate presents low values of conductivity (low salt content).

Low-Fat Mozzarella cheese production

While traditional products like mozzarella are widely present on any market shelf, reducing economic income for the producer due to their saturated market, some low fat cheeses can be sold in niche markets with high added value.

A major problem in low-fat mozzarella cheese production is related to the choice of fat replacer: as a matter of fact, most of industrial fat replacers are not able to preserve their structure at spinning temperature, e moreover they tend to change texture and flavor of the final product. Being mozzarella a well characterized cheese, this would involve a low acceptance from the final consumer. In our approach, whey proteins obtained from RO concentration and previously treated with an enzymatic process using Transglutaminase (TGase), were used as fat replacer.

Several tests were performed, adding proteins at concentrations gradually higher, starting at 1% and reaching 10%.

In this work, the low fat mozzarella cheese, with characteristics in line with the traditional mozzarella, is obtained using a skimmed milk with a fat content of 2% (approximately 50% less than the initial content). To this milk, suitably heated, is added the curd and whey protein concentrate suitably modified. After pH stabilization, the coagulation is carried out at a temperature of about 35 °C; when pH reaches the optimal value for the processing and the spinning is performed.

Subsequent industrial tests have indicated as an optimal percentage the addition of 10% of the modified proteins, performing mechanical spinning with acceptable results from a point of view of workability of the product.

Chemical Analysis of Low-Fat mozzarella cheese

Cheese moisture was determined by microwave oven by drying the samples to a constant weight (i.e., <0.1 mg change over 10 s) at 50% power. Protein and fat contents were determined respectively by Kjeldhal method and according to García-Ayusousing L. E. *et al*., 1999. Each assay was performed in triplicate.

Instrumental texture analysis of mozzarella cheese.

Mozzarella cheese's texture Mozzarella was evaluated using an Instron universal testing instrument model no. 5543A (Instron Engineering Corp., Norwood, MA, USA) equipped with a 2 kN load cell in compression mode with a cylindrical probe (55 mm diameter). The instrumental Texture Profile Analysis (TPA) test described by Bourne,1978 was used. The test was configured for analyzing the four TPA parameters, hardness, springiness, chewiness, and cohesiveness. Pre- and post-test speeds were 2.0 mm/sec, while test speed was 1.0 mm/sec. Mozzarella was removed from the refrigerator and allowed to heat up at room temperature (1-2 h) and then, three cylinder of 30 mm diameter were cut from each samples. Samples, prepared as described above, were centered and compressed to 20% of deformation. All the analyses were performed with at least eight samples per batch.

Table 1. Operating conditions for the RO plant.

Final water quantity	max 2.000 l/h
Working cycle	max 10 hours
Concentration ratio	3
Filtered serum per cycle	max 30.000 l
Operative pressure	25-35 bar
Temperature	max 50 °C

Table 2. Production data.

Transformed milk	18000 kg/day
Working days	300 /year
Serum quantity	16000 kg/day
Serum /Milk(%)	90%
Low fat serum(%)	60%
Scotta (%)	20%

Results

Power consumption

It was possible to estimate that the specific consumption of electrical energy (absorbed by the processing equipment: equipment, pumps and refrigeration unit) to concentrate whey is equal to 7 kWh/m^3 , while the specific fuel consumption (used in the boiler to heat the water necessary for the process) is equal to 2 kg fuel/m^3 of treated serum.

Since on average there are approximately 240 m^3 of serum per month, it is estimated an electricity consumption equal to 1680 kWh/month and a fuel consumption of 480 kg of fuel per month. The hot operative working condition, as explained in the previous section, it is recommended with respect to the cold working. The proposed approach allowed an annual save of 30k € respect to the previous system in which an external company was paid for concentrated protein transportation.

Low-fat mozzarella cheese characteristics

The reduction of fat in Mozzarella cheese often leads to various defects such as rubbery texture, as well as poor meltability and stretchability, principally due to its low moisture. Water is thought to act as a lubricant or plasticizer between the proteins, and in fact it is well known that increasing the ratio of water to cheese proteins makes the cheese softer.

Ismail *et al*.,2011 suggest the use of denatured whey protein to improve low fat Mozzarella cheese properties by increasing water holding. Di Pierro *et al*., 2010 used enzyme Transglutaminase (TGase) to produce a novel, so-called "crosslinked cheese" with increased water content and cheese yield. In this work we have used TGase to crosslink the two times concentrated whey proteins in order to produce covalent micro-particulates. Afterwards the TGase-modified proteins were added to defatted milk at a concentration of 10 % (MS-10) and 12 % (MS-12) (v/v) before the manufacture of Mozzarella cheese.

We compared such new product with conventional Mozzarella (control). It is possible to note from Table 3 that the water holding in Mozzarella cheese is directly correlated to the amount of TGase-treated whey added.

However, only in Mozzarella cheese obtained with 10% of TGase-treated whey showed a significant increase of protein content. These results can be explained by hypothesizing the increase of serum bound to the gel network reinforced by additional covalent bonds, and the incorporation of casein fines or whey proteins into the gel network, due to the activity of the enzyme added together with the treated whey (Di Pierro *et al*., 2010;Sayadi *et al*.,2013).

It is well known that textural properties (hardness, cohesiveness, springiness, and chewiness) are important functional properties of Mozzarella and any attempt to reduce the fat content of Mozzarella have to take into account these aspects. We have compared the textural properties of Mozzarella cheese using a Texture Profile Analyses (TPA). Results reported in Table 4 showed no significant differences in respect to springiness, chewiness and cohesiveness were observed between MS-10 and control Mozzarella cheeses, while hardness significantly increased, probably due to the TGase crosslinks which increase water retention. On the contrary, MS-12 Mozzarella cheeses showed a significant reduction of both hardness and chewiness, suggesting that a higher number of crosslinks is responsible for a greater amount of serum retained in this type of Mozzarella cheese which increased the structure volume providing a softer texture. In fact, it is well known that increasing the ratio of water to cheese proteins makes the cheese softer. Water is thought to act as a lubricant or plasticizer between the protein molecules, making the cheese more pliable (Glicksman, 1991; Tunick, 1991). Our results suggest that 10% is the highest amount of TGase-treated whey that do not affect the rheological properties of Mozzarella cheese. Moreover, pre-treatment of whey with the enzyme TGase is an effective strategy to produce defatted Mozzarella cheese with textural properties comparable to the normal one.

Table 3. Effect of the addition of TGase-treated whey on chemical composition of Mozzarella cheese.

Mozzarella cheese	Water content (%)	Protein content (% DM)	Fat (% DM)
Control	63.18±1.2	16.03±0.35	16.71±1.2
MS-10	66.26±1.9	18.23±0.68	9.40±0.9
MS-12	69.28±1.3	17.97±0.92	9.72±2.2

Values are mean ± standard deviation (SD). DM, Dry Matter.

Table 4. Effect of the addition of TGase-treated whey on rheological properties of Mozzarella cheese.

	Hardness (N)	Springiness (mm)	Chewiness (N mm)	Cohesiveness
Control	70.35±13.52^a	20.2 ±1.5^a	913.4±155.4^a	0.63±0.04^a
MS-10	80.13±7.07^b	19.9 ±4.5^a	847.3±232.7^a	0.53±0.06^a
MS-12	47.12 ±8.35^c	20.7 ±2.2^a	565.6±163.7^b	0.57±0.04^a

Values are mean ± standard deviation (SD). Mean followed by the same letters are not significant (Tukey-Kramer test $p<0.05$)

Conclusions

The proposed approach couple a standard reverse osmosis membrane technology with an advanced enzymatic treatment of whey protein to obtain a high value secondary product which can be used as a fat replacer. This product can be locally used to produce high value salutistic cheeses, like a low fat mozzarella cheese. The low-fat mozzarella cheese was subjected to sensory analysis and did not show significant differences from the traditional mozzarella. It seems to preserve the same taste and texture of the classic mozzarella produced by Campolongo Srl but with 50% less fat, and the product is going to be soon commercialized.

A significant economic saving was obtained locally using concentrated whey proteins, without considering the added value of low-fat mozzarella cheese. Moreover, tests are currently performed to introduce whey modified proteins in other cheese typologies.

References

Bourne, M.-C. 1978. Texture profile analysis. Food Technology, 32 (7), 62–66,72.

Di Pierro, P., Mariniello, L., Sorrentino, A., Gosafatto, C. V. L., Chianese, L., & Porta, R., 2010. Transglutaminase induced chemical and rheological properties of cheese. Food Biotechnology, 24, 107-120.

García-Ayuso L. E., Velasco J., Dobarganes M. C. and Luque de Castro M. D.,1999. Accelerated Extraction of the Fat Content in Cheese Using a Focused Microwave-Assisted Soxhlet Device. J. Agric. Food Chem., 47 6: 2308.

Glicksman, M., 1991. Hydrocolloids and the search for the "Oily Grail". J. Food Technol. 10:94.

Ismail M., Ammar E.T., and El-Metwally R., 2011. Improvement of low fat mozzarella cheese properties using denatured whey protein. International Journal of Dairy Technology, 64 (2): 207.

Kasapgil B, Anderson G.K., Ince O.,1994. An investigation into the pretreatment of dairy wastewater prior to aerobic biological treatment. Water Sci Technol;29:205–12.

Orhon D, Gorgun E, Germirli F, Artan N.,1993. Biological treatability of dairy wastewaters. Water Res. ;27:625–33.

Perle M, Kimchie S, Shelef G.,1995, Some biochemical aspects of the anaerobic degradation of dairy wastewater. Water Res.,29:1549–54.

Sayadi A., Madadlou A., Khosrowshahi A.,2013. Enzymatic cross-linking of whey proteins in low fat Iranian white cheese. International Dairy Journal, 29, 88-92

Tunick, M. H., Mackey K. L., Smith P. W., and Holsinger V. H.,1991. Effects of composition and storage on the texture of Mozzarella cheese. Neth. Milk Dairy J. 45:117.

Vourch, M., Balannec, B., Chaufer, B., Dorange, G., 2005. Nanofiltration and reverse osmosis of model process waters from the dairy industry to produce water for reuse, Desalination, 172, 3:245-256.

Safety performance assessment of food industry facilities using a fuzzy approach

F. Barreca, G. Cardinali, C.R. Fichera, L. Lamberto, G. Modica

Dipartimento di Agraria, Università degli studi Mediterranea di Reggio Calabria, Reggio Calabria, Italy

Abstract

The latest EU policies focus on the issue of food safety with a view to assuring adequate and standard quality levels for the food produced and/or consumed within the EC. To that purpose, the environment where agricultural products are manufactured and processed plays a crucial role in achieving food hygiene. As a consequence, it is of the utmost importance to adopt proper building solutions which meet health and hygiene requirements and to use suitable tools to measure the levels achieved. Similarly, it is necessary to verify and evaluate the level of safety and welfare of the workers in their working environment. The safety of the workers has not only an ethical and social value but also an economic implication, since possible accidents or environmental stressors are the major causes of the lower efficiency and productivity of workers. However, the technical solutions adopted in the manufacturing facilities in order to achieve adequate levels of safety and welfare of the workers are not always consistent with the solutions aimed at achieving adequate levels of food hygiene, even if both of them comply with sectoral rules which are often unconnected with each other. Therefore, it is fundamental to design suitable models of analysis that allow assessing buildings as a whole, taking into account both health and hygiene safety as well as the safety and welfare of workers. Hence, this paper proposes an evaluation model that, based on an established study protocol and on the application of a fuzzy logic procedure, allows evaluating the global safety level of a building. The proposed model allows to obtain a synthetic and global value of the building performance in terms of food hygiene and safety and welfare of the workers as well as to highlight possible weaknesses. Though the model may be applied in either the design or the operational phase of a building, this paper focuses on its application to certain buildings already operational in a specific productive context.

Correspondence: Francesco Barreca, Dipartimento di Agraria, Università degli studi Mediterranea di Reggio Calabria. Località Feo di Vito, 89122 Reggio Calabria, Italy.

Key words: Safety Performance Assessment, Agri-food industry facilities, Post Occupancy Evaluation (POE), Global Safety Buildings Index (GSBI), Fuzzy sets.

Acknowledgements: this research was partly funded by the QUASIORA (Quality Safety Origin of the food), which was granted within the Framework Program "APQ Ricerca Scientifica e Innovazione Tecnologica nella Regione Calabria" (Scientific Research and Technological Innovation in the Calabria Region) involving the European Union, the Calabria Region and the Italian Ministry for Education, University and Research.

Journal of Agricultural Engineering 2013; XLIV(s1):e58
doi:10.4081/jae.2013.(s1):e58

Introduction

Recent statistical surveys show that, in Europe (European Commission, 2007), food manufacturing companies are about 310.000 and workers in the sector are over 4.688.000, for an annual turnover of over 850 billion Euros. These figures give an idea of the importance of this productive sector and, above all, of its significance for the whole European economy. On the other hand, consumers demand more and more guarantees of safety and sustainability of the entire chain of production.

In order to ensure suitable health and hygiene standards, it is fundamental to consider the whole manufacturing cycle in all types of agri-food companies: from the supply of raw material to the sale of the product. In fact, during all the phases of its manufacture, the product risks of being contaminated by pathogenic microorganisms for reasons related not only to the productive process but also to the indoor environmental conditions of hygiene of the manufacturing facility, which are strictly connected with the adopted technical and management solutions (Lelieveld H.L.M., *et al*., 2005).

However, agri-food facilities must assure not only the consumers' hygiene safety, by adopting all the precautions and building solutions which may ensure adequate safety levels for product contamination, but also an adequate safety level for workers (Sinisammal J. *et al*.; 2012). Recently, EU-27 has implemented the European strategy on health and safety at work for the period 2007-2012 ("Improving quality and productivity at work: Community strategy 2007-2012 on health and safety at work") establishing six intermediate objectives in order to achieve a 25% reduction in the total incidence rate of accidents at work. As recently reported, the Strategy has met this ambitious goal. Currently, the Health and Safety Strategy for the period 2013-2020 is under implementation.

Therefore, productive facilities must ensure adequate performances in terms of health and hygiene standards and of workers' safety (Jacinto C.*et al*., 2009). These performances must be carefully taken into account during the building design process and regularly verified during its use. To that purpose, Post Occupancy Evaluation (POE) (Joon-Hoa *et al*. 2012) is particularly important. Another significant aspect to consider is that the building performances may also depend on how the manufacturing process is managed and conducted (Leppälä 2012). For instance, hygiene conditions are influenced by sanitation procedures as well as the noise level is strictly connected with the machines, plants and operation modes used (Parejo-Moscoso

et al. 2013). One of the main goals of this paper is to obtain a synthetic value of global safety that can be referred exclusively to the building (Fabiano *et al*. 2004) and to its components and plants. Specifically, this paper proposes a model for the evaluation of the Global Safety Building Index (GSBI), which is based only on the evaluation of the performances of the technical elements and of the plants of the building and does not take into account the contingent conditions of the manufacturing process and, therefore, the company operation modes (Stave and Törner 2007). This approach allows applying the model also in the design phase and evaluating the global safety level of the building even before it starts operating. Thus, the model highlights the most important weaknesses in global safety and verifies the effects of possible interventions and corrections.

Materials and Methods

The model for the evaluation of the Global Safety Buildings Index

The building system evaluation, encapsulated through the Global Safety Buildings Index (GSBI), is carried out by means of specific performance indicators. Such indicators can be measured either objectively, through an instrumental survey, or subjectively, through a qualitative judgment expressed by an expert surveyor.

GSBI set of indicators was organized into a four-level tree structure (Figure 1). In particular, the first level was divided into the two established safety categories: workers' safety and hygiene safety. This hier-

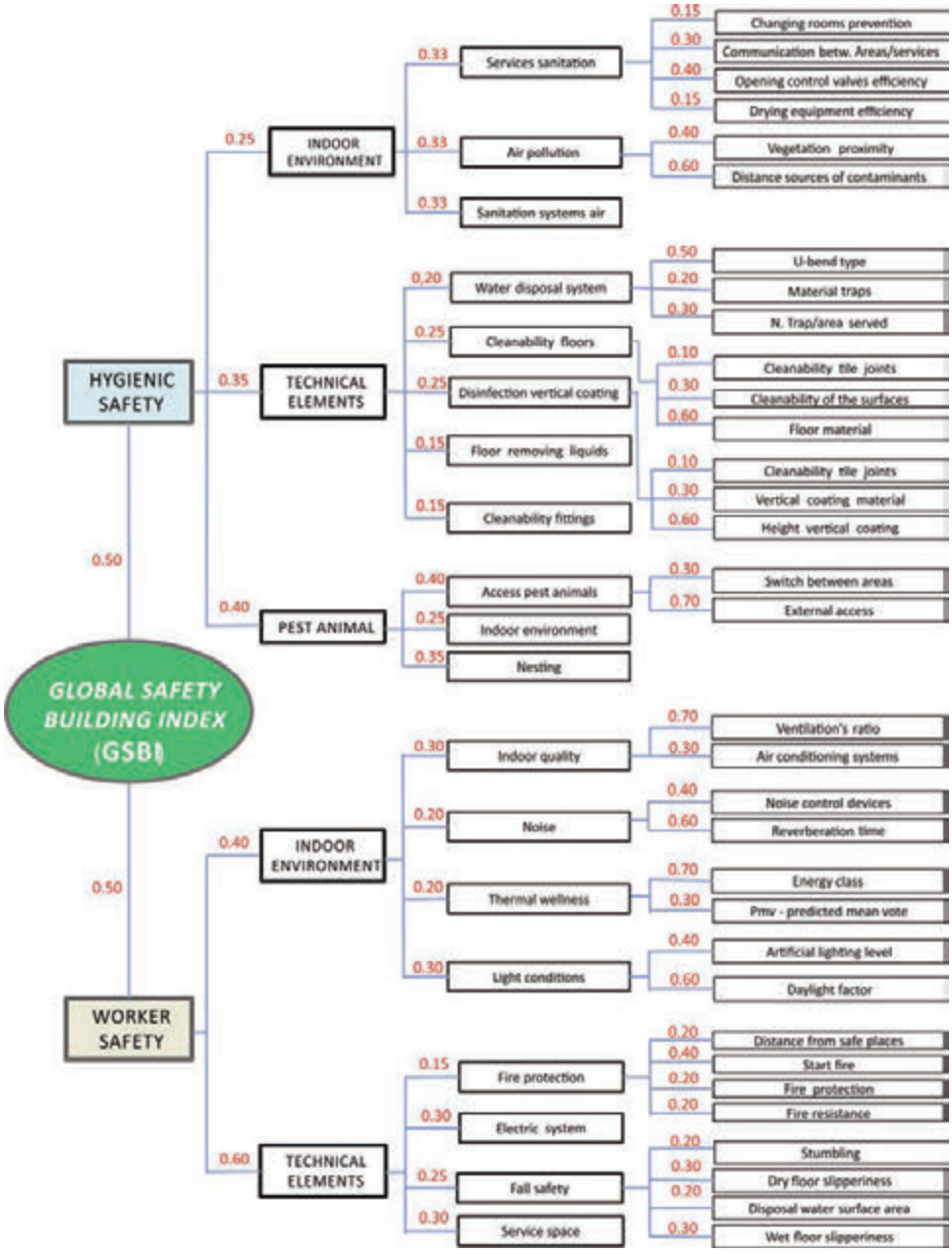

Figure 1. Chart showing the hierarchical structure of the model for the evaluation of the Global Safety Buildings Index (GSBI). For each indicator, the relative weight [0, 1] corresponding to each hierarchical level, is reported.

archization allows evaluating each category separately, thus showing in which category the building may reveal greater weaknesses. For each category on the second hierarchical level, evaluation was carried out on the adequacy of the technical system (building components which are directly related to safety) and on the environment safety (referred to the performances of the class of the technical elements that indirectly contribute to creating internal environmental and functional conditions that enhance safety).

Set of quantitative and qualitative indicators

On the basis of their different typology, selected indicators were distinguished in quantitative and qualitative indicators. Quantitative indicators are characteristics of the building that can be instrumentally measured or evaluated through calculation procedures; while qualitative indicators are based on the judgment of a surveyor/assessor. For instance, in the category of workers' safety, the slip, trip and fall safety of the building was evaluated. The risks of slipping and tripping are among the main risk factors for workers in the agri-food sector. The loss of grip between foot and floor may be induced either by an inadequate value of floor roughness or by the presence of liquids that alter the surface of the material, or by both conditions. A useful element to quantify the workers' risk of slipping is the measurement of the coefficient of sliding friction between sole and floor (Malkin and Harrison 1980). The proposed model evaluates fall safety by referring to the following specific indicators: slipping on wet and dry floor; tripping due to loss of balance; quick liquid removal from the floor. In this case, indicators are evaluated by referring to instrumental measurements. For instance, slip safety is evaluated by measuring slipperiness with the Tortus method, which was developed by Malkin and Harrison at British Ceramic Research Association (1980) and is based on the measurement of the sliding friction value of a slipping element (in rubber for wet floors and in leather for dry floors). Slipperiness is measured by means of a Tortus digital tribometer FSC 2011 (Figure 2).

Data analysis and aggregation

The numerical analysis and the aggregation of the values of the qualitative and quantitative indicators were carried out by means of fuzzy logic (Beriha *et al*. 2012).

The main property of fuzzy logic (Zadeh 1965) is that it translates the linguistic judgments, expressed by man in a vague and inaccurate manner, into numerical and mathematical terms. Therefore, the use of this logic allows overcoming the uncertainty of the qualitative evaluation of the single building technical element, conducted by a surveyor, as well as considering the difficulty in estimating how the performance of each component contributes to the value of the global safety of the building (Pinto *et al*. 2012). Furthermore, the standardization of values in hierarchical levels allows expressing GSBI in a variable interval between 0 and 1, where 0 corresponds to the worst value while 1 corresponds to the best one. In the implemented model, the values of indicators were transformed into fuzzy membership values by using a specific transformation function of triangular type that takes into account three levels of judgment. For instance, in the case of slip safety, safety is very low if the coefficient of sliding friction is below 0.4; it is acceptable if the coefficient is between 0.4 and 0.74; and, finally, it is good if the coefficient is above 0.74. The aggregation of the four levels composing the hierarchical model was carried out on the elements belonging to the same hierarchical level by means of a normalized fuzzy weighted average procedure. The weights of each level of evaluation, whose sum was equal to 1 (Figure 1), were defined with a group of field experts. In particular, the relative weight of each element was defined in relation to its contribution to global safety, to the level of measurement accuracy, to the adopted measurement method (instrumental or subjective), to literature data, to the acquired scientific knowledge and to the values of National and international regulations.

Results

The validation of the model required the development of a specific procedure (Figure 3). Such a procedure includes consecutive steps

Figure 2. Survey of coefficient of friction on the floor by the Tortus digital tribometer FSC 2011.

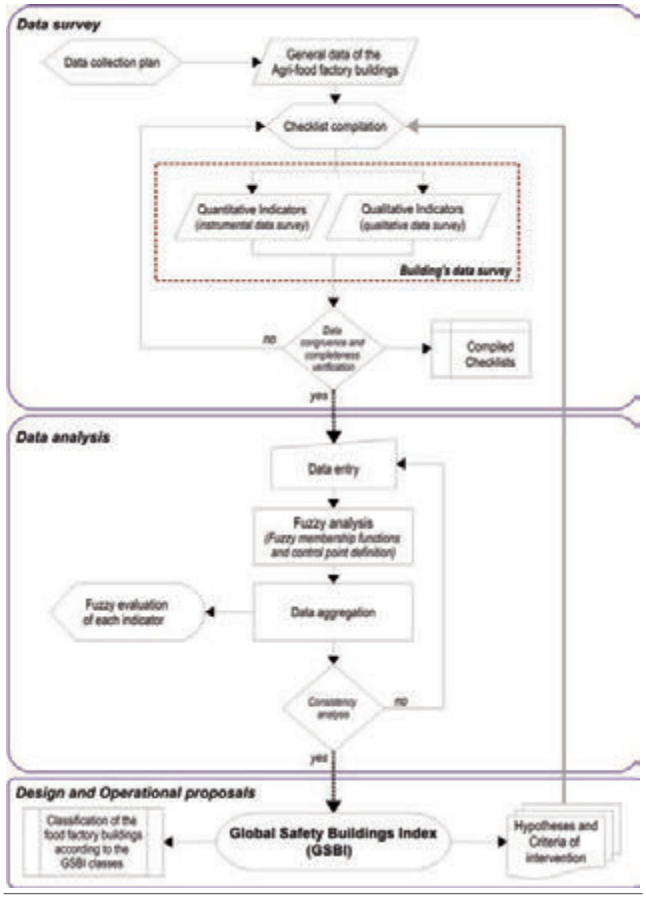

Figure 3. Flow-chart of the procedure for the evaluation of the Global Safety Buildings Index (GSBI).

that, in each phase, allow checking proper progress and making corrections.

In particular, such steps can be summarized as follows:

- Planning of the survey campaign and preliminary investigation of the manufacturing facility, preliminary building survey.
- Collection of data on the company that uses the building and on its organization.
- Recording and acquisition of detailed data and performance evaluation of the building and of its components through instrumental measurements and evaluation judgments expressed by the surveyor and organized according to a specially prepared checklist.
- Data analysis and verification of the congruency of recorded data and measures with the performance specifications of the elements.
- Compilation of the checklist and filling in of a survey form.
- Input of the acquired data in the analysis model and transformation of data into fuzzy values.
- Implementation of the model of analysis and aggregation of the different hierarchical levels through established weight functions.
- Verification of the consistency of the results obtained from the model and possible adjustment and improvement of data.
- Comparison and analysis of the results obtained from the model, observations on the results obtained in the different hierarchical levels of the model.
- Calculation of the Global Safety Building Index (GSBI) and of the relative values for each environmental unit and category.
- Analysis and identification of possible weaknesses in health and hygiene safety and in workers' safety.
- Development of possible proposals and corrections on the building in order to improve performances in the hygiene safety of products and in the workers' safety. (Figure3)

At this point, the application of the model may end or, starting a loop procedure from the initial phases of surveying, it may allow verifying the effectiveness of the corrections put in place or only envisaged.

This organization of the model allows evaluating the global safety level of the building or calculating it already during the phase of design. Moreover, it enables to verify the effectiveness of possible corrections or modifications in the technical elements of the buildings.

In addition, the possibility to compare the value of the building global safety and established benchmark values is particularly important.

The application of the whole procedure to a manufacturing area of a dairy farm located in the plain of Gioia Tauro, Reggio Calabria, is described below.

The manufacturing facility covers two storeys, each of about 250 m^2; the manufacturing area in on the ground floor and covers around 130 m^2 (Figure 4).

After a first inspection, the building was surveyed and then, following the checklist, metrical data and judgments on the performance of the main building components, in terms of hygiene safety of the products and workers' safety, were acquired.

The values of the fuzzy functions obtained from the application of the proposed model (Figure 5) allowed carrying out a first series of analyses and evaluations on the safety level of the manufacturing area of the analyzed building. In particular, the geometric centre of the fuzzy function, which describes global safety calculated through the illustrated procedure, has a value (0.439) that is slightly lower than the average value (0.50). This means that the global safety of the building is certainly acceptable, even if it shows further room for improvement. The disaggregate values of the centres of the functions related to the workers' safety and health and hygiene safety (0.439 and 0.644 respectively) are also close to the average value. The comparison between the two membership functions allows further considerations. In fact, the membership function of the workers' safety has a value of maximum membership equal to 0.565, while the value of the membership function of the health and hygiene safety of the building is 0.725, though it shows greater dispersion of values. This result shows that, though the global health and hygiene safety of the building (considering the geometric centre of the function) is lower than the workers' safety, it would be sufficient to act on a few negative causes of dispersion, and therefore on those technical elements showing the lowest efficiency judgment, to considerably improve the global value and, as a result, to increase the GSBI final value.

Discussion and Conclusions

The application of the proposed procedure allowed verifying not only if the developed model was correct but also if it was easy to apply. To that purpose, in the phase of the model definition, particular importance was given to the determination of the sets of indicators concern-

Figure 4. Lay-out of the surveyed dairy farm.

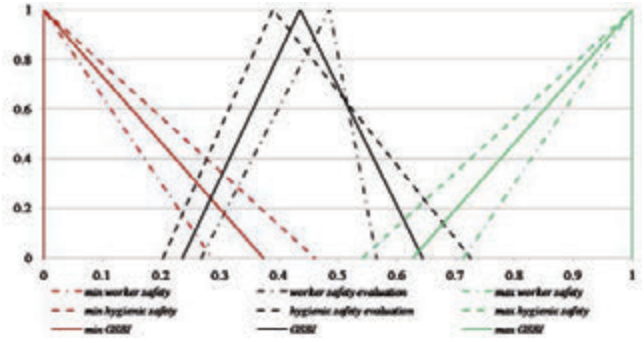

Figure 5. Graph showing the fuzzy membership function of the Worker Safety Evaluation (WSE), the Hygienic Safety Evaluation (HSE) and the Global Safety Buildings Index (GSBI). For each of these indexes, the minimum and the maximum values are reported.

ing the hygiene safety of products and the workers' safety. Specifically, though indicators were limited in number to facilitate the phase of data acquisition and the application of the model, they were chosen according to the following characteristics:

- Being easy to assess by means of not particularly complex instruments;
- Being exclusively referred to technical building components;
- Being independent from contingent factors or from the boundary conditions of the manufacturing process;
- Being independent per environmental unit and field of evaluation.

In fact, the number of evaluation indexes must be adequate to describe the building performances correctly and quite accurately in relation to health and hygiene safety and workers' safety and must take into account current regulations and the most dangerous risks inside buildings. Finally, it is worth mentioning that the structure of the model allows necessary adjustments and improvements during all the phases of the process and it is so general that it may be applied to all types of agri-food production. Therefore, this paper will be further developed to allow its application to other functional fields of the manufacturing facility and to various types of production.

References

Abouelnaga A., Metwally A.,Aly N., Naguib A.; Nagy M., Agamy S. 2010. Assessment of nuclear energy sustainability index using fuzzy logic. Nuclear Engineering and Design, 240 (2010), pp.2820-2830.

Beriha G.S., Patnaik B., Mahapatra S., Padhee S. 2012. Assessment of safety performance in Indian industries using fuzzy approach. Expert Systems with Applications, 39(3), pp.3311–3323.

Joon-Hoa C., Vivianb L., Azizanb A. 2012. Post-occupancy evaluation of 20 office buildings as basis for future IEQ standards and guidelines. Energy and buildings, 46 pp. 167-175.

European Commission, 2007. Community strategy on health and safety at work (2007-2012). Brussels. Available at: http://europa.eu/legislation_summaries/employment_and_social_policy/health_hygiene_safety_at_work/l10114_en.htm#

Lelieveld H.L.M., Mostert M.A., Holah J. 2005. Handbook of hygiene control in the food industry. 1th rev. ed Woodhead Publishing Limited, Cambridge,UK.

Fabiano B., Currò F., Pastorino R. 2004. A study of the relationship between occupational injuries and firm size and type in the Italian industry. Safety Science, 42(7), pp.587–600.

Jacinto C., Canoa M., Guedes Soares C. 2009. Workplace and organisational factors in accident analysis within the Food Industry. Safety Science, 47(5), pp.626–635.

Leppälä J.M.. 2012. Integrated production and safety risk management on. Proc. International Conference of Agricultural Engineering, Valencia, Spain, July 8-12.

Malkin F., Harrison R. 1980. A small mobile apparatus for measuring the coefficient of friction of floors. Journal of Physics D: Applied Physics, 13, pp.77–79.

Parejo-Moscoso J.M., Rubio-Romero J.C.,Pérez-Canto S., Soriano-Serrano M. 2013. Health and safety management in olive oil mills in Spain. Safety Science, 51(1), pp.101–108.

Pinto, A., Ribeiro R., Nunes L. 2012. Fuzzy approach for reducing subjectivity in estimating occupational accident severity. Accident; analysis and prevention, 45, pp.281–90.

Sinisammal J., Belt P., Härkönen J., Möttönen M.,Väyrynen S. 2012. Managing Well-Being at Work during 2010 – Expert Viewpoints. Open Journal of Safety Science and Technology, 2, pp.25-31.

Stave C., Törner M. 2007. Exploring the organisational preconditions for occupational accidents in food industry: A qualitative approach. Safety Science, 45(3), pp.355–371.

Zadeh L.A. 1965. Fuzzy sets. Information and Control, 8, pp. 338

UHF-RFID solutions for logistics units management in the food supply chain

Paolo Barge, Paolo Gay, Valentina Merlino, Cristina Tortia

DI.S.A.F.A – Università degli Studi di Torino, Grugliasco (TO), Italy

Abstract

The availability of systems for automatic and simultaneous identification of several items belonging to a logistics unit during production, warehousing and delivering can improve supply chain management and speed traceability controls. Radio frequency identification (RFID) is a powerful technique that potentially permits to reach this goal, but some aspects as, for instance, food product composition (e.g. moisture content, salt or sugar content) and some peculiarities of the production environment (high moisture, high/low temperatures, metallic structures) have prevented, so far, its application in food sector. In the food industry, composition and shape of items are much less regular than in other commodities sectors. In addition, a wide variety of packaging, composed by different materials, is employed. As material, size and shape of items to which the tag should be attached strongly influence the minimum power requested for tag functioning, performance improvements can be achieved only selecting suitable RF identifier for the specific combination of food product and packaging. When dealing with logistics units, the dynamic reading of a vast number of tags originates simultaneous broadcasting of signals (tag-to-tag collisions) that could affect reading rates and the overall reliability of the identification procedure. This paper reports the results of an extensive analysis of the reading performance of UHF RFID systems for multiple dynamic electronic identification of food packed products in controlled conditions. Products were considered singularly or arranged on a logistics pallet. The effects on reading rate and reading zone of different factors, among which the type of product, the number and position of antennas, the field polarization, the reader RF power output, the interrogation protocol configuration as well as the transit speed, the number of tags and their interactions were analysed and compared.

Correspondence: Cristina Tortia, DI.S.A.F.A, Università degli Studi di Torino, 44 Via Leonardo da Vinci, 10095 Grugliasco (TO), Italy
Tel. +39.011.6708845- Fax: +39. 011.2368845
E-mail: cristina.tortia@unito.it

Key words: UHF, logistics, food supply chain.

Acknowledgements: this work was partially supported by the grants of the projects Namatech-Converging Technologies (CIPE2007), Regione Piemonte, Italy and PRIN 2009 (prot. 2009FXN7HW_002), MIUR, Italy.

Journal of Agricultural Engineering 2013; XLIV(s1):e59
doi:10.4081/jae.2013.(s1):e59

Introduction

Traceability systems represent an important tool for companies to ensure the quality and safety of products, to increase the efficiency of managing of products and information flows and logistics, thus promoting their competitiveness within the supply chain and the market.

To cope with increasing complexity and globalization of supply chains, investments on ICT are constantly growing to improve information management and product identification systems efficiency. In particular, radio frequency identification (RFID) offers several advantages, as contactless and automatic identification of single or multiple products, which bestow an added value on this technology in comparison, for example, with barcodes. However, data transmission between the transponder and the reader takes place through electromagnetic waves and therefore without the need of free paths. Indeed, RFID tags are part of a technology that, when combined with databases or shared in communication networks, become an effective tool for the stakeholders involved in the supply chain, for new services and applications even in hostile environments. To reduce costs, for instance in logistics, transponders are usually inserted into labels to distinguish each unit of product of a specific production lot and to trace its position and path along the supply chain.

In the retail sector, RFID are commonly used for pallets, packing cases and/or single items identification to increase supply chain transparency, to reduce labour and optimize warehousing. Several important companies, e.g. Wal-Mart, Best Buy, Target and Albertson's, have already taken this opportunity. At receiving, RFID reduces labour, enabling the quick scanning of pallets and eliminating the need to open packing cases to get inventory down to item level. Benefits include reducing out-of-stocks through item-level visibility of storeroom and shelf inventories, reducing the mis-shipments by promoting more accurate shipping, and preventing product counterfeiting, diversions and theft through mass, reliable, item-level identification (Penttilä *et al.,* 2006).

RFID systems operating at UHF band can be used to improve single items, automatic, simultaneous and contactless data capture. RFID can be applied at different level as wholesale distributors for automatic inventory management, at partner/supplier depots, on the loading dock for automatic identification of pallet. In food supply chains some issues remain to be addressed for the application of this technology. These include reading reliability, which in some cases and with certain products is still to be improved, the lack of homogeneity of the standards governing their use in different countries at the global level, the investment costs and the need to involve stakeholders and upstream and downstream. For these reasons, although this represents a potential solution for goods traceability and for supply chain logistics control, the introduction of RFID UHF technology in different food sectors is currently being researched. There are some noticeable technical difficulties to obtain exhaustive and reliable identification of food items in critical production environments (Clarke *et al.,* 2006; Mühlmann and Witschnig, 2007). The main responsible of the negative effects on tag performances, both in static and dynamic condi-

tions, is the variation of the electric field in the proximity of a food object due to its dielectric properties which influence reflections, transmission and absorption rates. It is therefore important to assess food behaviour in processes where electromagnetic fields are involved, in order to avoid scarce reliability of the system that could definitively lead to the loss of confidence by the end user.

Collisions among tags in a dense population conditions is another critical aspect.

The EPCglobal Gen2 protocol regulates the interaction between RFID reader and tags operating in the 860 MHz – 960 MHz frequency range defining the physical and logical requirements for a passive-backscatter, interrogator-talks-first system. This standard is widely used for supply chain management where medium-range and high-speed identification is required (Wen-Tzu and Wen-Bin, 2011). In EPC Gen2 protocol, which is nowadays the widespread adopted UHF standard, interrogation phase is controlled adjusting some key-parameters that influence the duration and the accuracy of a complete tag inventory. The tuning of these parameters is crucial in dynamic applications, as the collisions must be quickly solved, while the objects to be identified are still in the reading area.

To read multiple tags simultaneously in a dense population, an anti-collision algorithm (Q), based on dynamic framed slotted ALOHA method, was developed. As soon as the tag enters the RF field domain, is enabled to accept the interrogator request. A selection of a group of tags can be made by a query command which communicate to the tag one among four sessions: S0, S1, S2 and S3. Each session is provided with a two-state inventoried flag (A or B). When the tag is energized, the persistence time of the inventoried flag value is indefinite for S0, S2 and S3, while is in the range 0.5-5 s for S1 session. The algorithm implements a number of slotted frames equal to 2^Q-1. Each of the selected tags randomly choose one among the available time slot (in the range 0, 2^Q-1) and will backscatter a 16-bit random number (RN16) when the interrogator calls for the specified time slot. Upon receiving a tag RN16, the interrogator acknowledges the tag with the same RN16. If the RN16 is correct, the tag will finally backscatter its 96-bits ID. At this point, the tag commutates to the acknowledged state and also inverts the Inventoried flag specified by the 'Query' command.

In this paper, technological solutions for packed food products automatic and simultaneous identification based on RFID-UHF system were reported and discussed. The system is intended to improve the internal logistics (identification, localization, automatic count, inventory management) and through the supply chain, as well as to allow the automatic collection of production process information. A very diffused RFID solution at industrial level is the portal (or gate) layout, which is generally implemented across conveyor belts or in loading dock area for the automatic loading/unloading of pallet in warehouses. At this purpose a RFID gate, constituted of a metallic structure and equipped with 4 UHF antennas, was constructed to perform simultaneous reading of a large number of tags attached on packed food arranged on a pallet. Different kinds of food materials were used for trials: dry food, beverage and their respective empty packaging were selected to compose the pallet for electronic identification. Different technological solutions were evaluated in terms of reading accuracy of tags applied on secondary packaging, considering static and dynamic reading conditions and different antenna layout.

Materials and Methods

To evaluate the performances of UHF identification of food packed products, an experimentation on items housed in secondary packaging was carried out at first in static conditions.

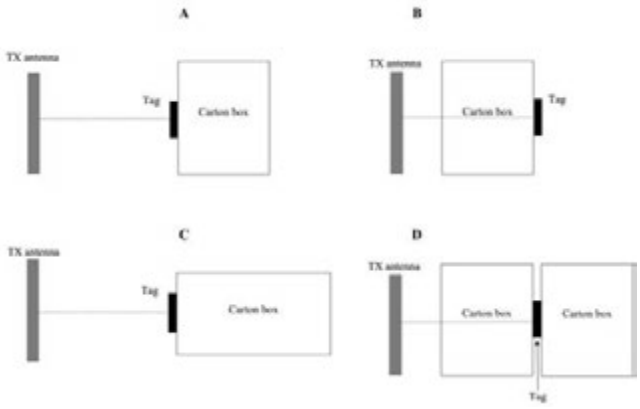

Figure 1. Position of food items, transmitting and receiving antennas in the four configurations A, B, C, and D.

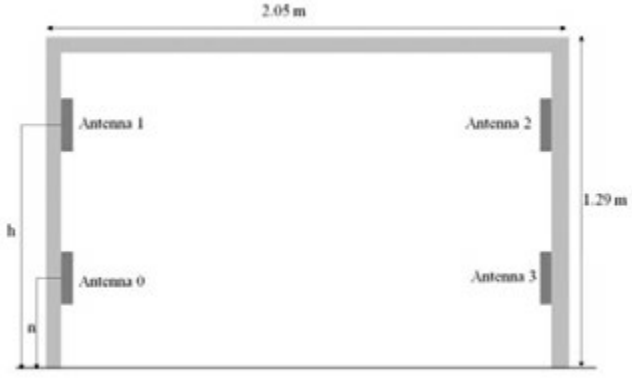

Figure 2. Gate framework: dimensions and antennas position.

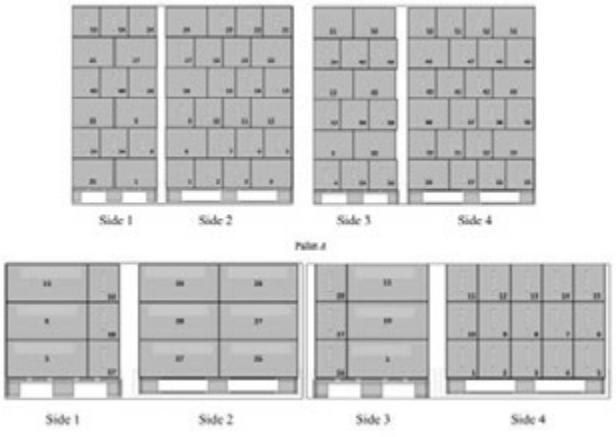

Figure 3. Snacks and empty boxes (Y) and sweetened tea (Z) pallet setup.

At this purpose, tag interrogation was carried out using a Caen RFID R4300P standalone reader connected to a linear (Caen RFID, model Wantenna X007, 8 dBi gain) or to a circular polarized antenna (Caen RFID, model Wantenna X005, 7 dBi gain). The system is ISO 18000-6C compliant. The effect of the packed food on minimum transmitter power output (TPO) to activate the tag and correctly receive the EPC ID was evaluated measuring the parameter P_{min} (dB), as described by Rao *et al.* (2005) and Nikitin *et al.* (2007). P_{min} was determined in semi anechoic chamber, at a fixed distance, modulating TPO by a power sweep in the range 0 ÷ 2000 mW till tag detection (Tortia *et al.,* 2012).

Five tags, LabID UH100 (*a*), LabID UH3D40 (*b*), LabID UH331 (*c*), Alien 9634 (*d*), and Alien 9662 (*e*), were tested in free space or directly attached on the secondary packaging of the food products. Firstly, to compare transponders performances, the minimum power to activate each of the considered tag models was measured with the transponder attached to a very thin plastic tape suspended in free space by means of a light wood frame. The tag-to-reader antenna distance was maintained constant at 0.5 m. Both circular and linear polarized antennas were used for tests. UHF attenuators (-10 dBm for circular polarized antenna and -20 dBm for linear polarized antenna) were used to maintain the reader in the nominal output power range.

In a second trial, tags were attached directly on a carton box filled with sweet snacks or sweetened tea in four configurations to simulate possible item positioning scenarios (Figure 1). Sweet snacks were singularly packed by a carton/polypropylene film primary packaging; 120 single items were then inserted in a secondary carton box (0.3 x 0.4 x 0.25 m). Sweetened tea was contained in plastic cups welded at the top in group of six items and secondarily packed stacking 72 single items in a carton box (0.28 x 0.56 x 0.22 m). A single electronically identified carton box in absence (configurations A, B, and C) or presence (D) of another identical item in proximity was adopted in this trial. In configuration B and D the product is interposed between reader (TX) and tag (RX) antennas, while only free space separates RX and TX antenna in A and C configurations. Tag-to-reader antenna distance was maintained constant at 1 m.

This approach allows assessing the power levels to be employed by the reader antenna to identify food materials with different dielectric properties. Then, dynamic reading efficiency (DRE % - tag correctly identified/tag present) was evaluated simulating identification in dynamic condition, i.e. with the product moving through a portal, using a UHF gate with several of the previous product items arranged on a moving pallet.

The evaluation of the performances of the UHF systems in dynamic conditions was carried out employing a portal where four UHF antennas were mounted. In Figure 2 the portal framework with the layout of the four antennas (named 0, 1, 2, and 3) is reported.

No metals were present in the working environment as the gate was in a large empty room. The major contribution to reflection, apart of the gate metal framework, is due to the floor (Sydänheimo *et al.,* 2006). Caen A941 standalone reader controlled by the RFID Caen Easy Controller software was used. To compare performances in dynamic conditions, the variable tag was excluded, using only tag *c*. Each carton box was arranged on a pallet following the scheme in Figure 3 and then electronically identified. Tags were always attached on the external minor side of the carton box. Pallet *Y* (1.80 x 1.15 x 1.20 m) was composed of 54 carton boxes arranged in six horizontal rows of nine carton boxes for each level. Carton boxes in this pallet were empty or filled with sweet snacks for a total of 648 primary packed items. Pallet *Z* (0.84 x 1.10 x 0.78 m) was composed by three horizontal rows and seven carton boxes filled with sweetened tea per each level for a total of 21 carton boxes.

Identification of empty boxes pallet was used to verify the reading coverage of the gate at different combinations of linear and circular antennas. Firstly, two linear (n=0.73 m - antennas 0 and 3) and two circular (h=1.34 m - antennas 1 and 2) polarized antennas were mounted on the gate. TPO was set to 1000 mW. In dynamic identification trials pallet was manually moved through the gate using a forklift at different speeds ranging from 0.5 to 1.5 ms^{-1}. Pallet was always forked from the narrow side: in this way, the pallet larger side was parallel to the antennas plane. On the contrary, for the static tests, pallet was positioned under the RFID portal until the end of the reading cycle (10 seconds).

In the following, four linear polarized antennas were used both for dynamic and static readings using both *Y* configuration with carton boxes empty or filled with sweet snacks and *Z* configuration for tea.

Table 1. Configurations of the four linear polarized antennas in the gate. n is the height of antennas 0 and 3, while h is the height of antennas 1 and 2. Horizontal shift is the distance from the antenna centre to the gate vertical central axis. Elevation angle is the angle between the antenna and the horizontal plane.

Configurations	Height (m)		Antennas Horizontal shift (m)	Elevation angle
1	n	0.73	0	90°
	h	1.48		
2	n	0.25	+ 0.16	90°
	h	1.48	0	110°
3	n	0.44	+ 0.16	90°
	h	1.35	0	90°
4	n	0.44	0.16/-0.16	100°
	h	1.35	-0.16/0.16	75°
5	n	0.44	-0.16/0.16	100°
	h	1.15	0.16/-0.16	90°
6	n	0.65	0*0	90°
	h	1.46		

Table 2. Mean P_{min} of each tag model attached on a thin plastic tape suspended in free space by means of a light wood frame. Tag to reader antennas distance was equal to 0.5 m.

Tag	Model	P_{min}	
		Circular polarization antenna	Linear polarization antenna
a	UH100	10.7	2.0
b	UH3D40	12.3	9.5
c	UH331	9.8	2.1
d	ALIEN9634	10.1	1.3
e	ALIEN9662	11.0	2.4

Table 3. Pmin (dBm) to activate tag c by CAEN linear polarized antenna. Tag was attached on carton box filled with sweet snacks or plastic cups of sweetened tea in different reading configurations. Tag to antenna distance was equal to 1 m.

Configurations	Pmin	
	Sweet dry Snack	Sweetened tea
A	17.2	22.8
B	17.4	Out of range
C	20.7	24.1
D	22.4	Out of range

Table 4. Dynamic reading efficiency (DRE% = n° tags correctly identified/n° tags present) of electronic identification of pallets Y and Z, also with empty carton boxes, by means of four linear polarized antennas, adjusted in different configurations, in static and dynamic conditions in functions of Q and S values and, in the case of dynamic conditions, of pallet speed through the gate.

Carton box	Q	S	Static or dynamic (S/D)	Speed (m/s)	Antennas configuration	DRE%
Empty	1	2	S	0	1	96
	1	2	D	0.80		94
	2	2	S	0	1	100
	2	2	D	0.55÷0.80		100
	2	2	D	0.99÷1.21		90
	3	2	S	0	1	100
	3	2	D	0.53		100
	3	2	D	0.57÷0.60		98
	3	1	S	0	1	100
	3	1	D	0.40 ÷0.70		94
Dry Snack	2	2	S	0	3	100
	2	2	D	0.50÷0.70		100
	3	2	S	0	1	96
	3	2	S	0	2	100
	3	2	D	0.50÷0.60		100
	3	2	D	1.24		88
Sweetened tea	2	2	S	0	4	80
	2	2	S	0	5	100
	2	2	D	0.30÷0.50		100

Several configurations with variable antennas heights, positions and orientations were tested (see Table 1 for details) to verify the coverage zone and reading efficiency of the gate.

Four linear polarized antennas were fixed on the portal in configuration 6 (Table 1). The adopted power level ranged from 200 mW to 800 mW, while the forklift speed through the gate was ranging from 0.5 to 2 ms^{-1}. Electronic identification of pallets *Y* was performed also rotating the external carton boxes in order to position the tag on the internal side of the pallet.

Both in static and dynamic trials, Session (S0, S1, S2, and S3) and Q values were changed in the different repetitions to evaluate the influence of these parameters of the ALOHA anti-collision algorithm on reading efficiency.

Results

Minimum power levels to be delivered from the reader to obtain tag activation at 0.5 m distance are reported, for each tag model and receiving antenna combination, in Table 2. As we refer to the power at the cable before the antenna panel, Equivalent Isotropic Radiated Power (*EIRP*) in the tag direction is different for antennas with higher/lower gain. Since to detect the tag the electromagnetic signal has to cover both forward and backward paths, the transmitter and tag antenna gains influence twice the required power levels.

As for passive tag the power received at the reader goes as the inverse fourth power of the distance between reader and tag antennas, and it is also proportional to the square of antenna gain, this latter plays a large role in achievable read range. For this reason, P_{min} mean values (TPO at the cable, dBm) are different, even for the same tag model, when using circular or linear antennas.

The comparison among tags was done ranking results obtained with the same antenna. As can be seen, the activation of tag *b* is critical and higher power levels are needed in both linear and circular polarization cases (Table 2), even if in the case of circularly polarized field the difference with other tags is less evident. This could be explained considering that tag *b* is a double dipole cross-shaped which can receive power at different field polarization orientations.

Table 5. Dynamic reading efficiency (DRE%) at different power levels and pallet speeds. Portal was in configuration 6 and both snacks (Y) and tea pallets (Z) were used.

Pallet	Repetitions (n)	TPO (mW)	Speed range (m/s)	Medium speed (m/s)	DRE%
Y	15	200	1.30- 2.10	1.45	100
Z	4	100	0.50-0.90	0.73	84.75
Z	11	200	0.50-1.50	1.08	97.8
Z	2	400	0.11- 0.9	0.51	100
Z	3	800	0.9-1.4	1.10	100

The power requested to activate tag *d* resulted low, but from our previous experiences (Barge *et al.,* 2013), performances of this transponder type are strongly reduced when attached to food products. On the basis of these results, tag *c* was chosen for static performances evaluation on food items contained in their secondary packaging both in static and dynamic conditions.

Table 3 reports minimum power levels to activate transponder *c* attached to the carton box filled with snacks or tea in different configurations. The correct identification of the tag was always possible at 1m distance for carton filled with snacks, even when the packed product was interposed between reader and tag antennas (B and D). It can be noticed that, for snacks, the positioning of the tag on the minor side, leaving a thicker mass behind the tag in length (C), has a stronger effect on the required power than the interposition of the object in front of the tag (A). For sweetened tea, tag reading was possible only if tea was not interposed among tag and reader (B and D).

In dynamic trials, when the gate was composed by a combination of two linear and two circular polarized antennas and empty carton boxes were stacked on the pallet following scheme *Y*, mean *DRE%* was not acceptable (93%), even at low speed (<0.3 ms^{-1}) and with session set to S0. It has to be reminded that, at constant Q value, the probability to have collisions increases if in the field are present a larger number of

tags matching the chosen flag value. In case of session S0, when the tag has already transmitted its EPC code the inventoried flag changes value (e.g. from A to B) till tag is energized, but if tag is not powered, even if for a very short period, it returns to the default value (e.g. A) thus participating again to the group of tags not yet inventoried.

In dynamic conditions, the probability that tag loses its power, is very high and thus, if session is S0, as the group of tags to be selected is always large, collisions are increased.

In static conditions, when tags are continuously energized, all the transponders were correctly detected.

As the low gain of circular polarization antenna resulted in a more difficult detection of the tags, only linear polarized antennas were considered in the following trials. Circular polarization antennas, however, must be considered in case of misalignment between field orientation and tag.

Different session and Q values combinations were then used, as reported in Table 4.

When Q value was set to 1 only two slotted frame are available for tags to send their RN16 code. As the tag number is 54, collisions are very frequent and the reading is difficult even in static condition. In fact, if Q was set to 2 and 3 in static conditions the complete reading of tag present in the field for empty boxes was always obtained. The Q value must be well adapted to the number of expected tag as the bigger the number of slot, the longer is the reading cycle to acknowledge all tag IDs. As in case of Q set to 3 was not observed a great improvement of DRE, for sake of reading speed, Q value 2 should be preferred. If session was set to S1 even on empty boxes and at low speed the complete reading of tag was not achieved. This is probably due to the inventoried flag persistence time which is in the range 0.5 – 5 s, even if the tag is in energized state. In fact, when working with session 0 and 1, each tag code was acquired more than two times per inventory round. As configuration 1 was not optimal when in cartons food products were present, antenna position was changed (configurations 2-5). In particular antenna height was changed as floor acted as reflector, and horizontal position was shifted to increase reading volume.

In configuration 2 and 3 the DRE was 100% at speed up to 0.6 $ms^{-1}$for sweetened snacks.

Reading results for tea were better than expected as dynamic reading of all the 21 tags was possible, even if the speed should be maintained up to 0.5 ms^{-1}.

In Table 5 is highlighted the effect of increasing TPO on the reading efficiency for tea, at different speed, in configuration 6, which resulted to be optimal for each kind of tested product.

In this configuration, for snacks, some of the boxes of pallet *Y* were turned and the tag remained internal to other boxes. Also in this critical tag position a 100% *DRE* was obtained.

Conclusions

The influence of tag positioning on food products was assessed comparing two food types, characterized by different dielectric properties as well as their empty packaging.

Dynamic efficiency of RFID UHF portal were compared in various antennas geometries, TPO levels and EPC Gen2 protocol parameters tuning using three pallet setup assembling both empty, dry snacks and sweetened tea carton boxes.

In the case studied, where tag were all optimally oriented for linear polarized antennas, the circular polarization antenna resulted less efficient in dynamic conditions.

The dynamic reading efficiency as well as the time to complete the inventory are strongly dependent on anti-collision algorithm parameters. The parameter Q must be optimized in function of the number of the expected tag and the speed of object moving through the portal. The persistence of the inventoried flag of the tag, which is typical for different sessions, is relevant to limit collision during inventory, increasing accuracy.

As often, at shipping, different products are picked and a heterogeneous pallet composition is obtained, if RFID is used as tracking device, the scheme used for positioning of the packed products must be optimized in function of the discussed results.

References

Barge, P., Gay, P., Merlino, V., Tortia, C., 2013. Effect of packaging on Radio Frequency Identification of food products. From effective to intelligent agriculture and forestry, XXXV CIOSTA & CIGR V Conference 2013, 3 – 5 July, Billund, Denmark. In press.

Clarke, R.H., Twede, D., Tazelaar, J.R., Boyer, K.K., 2006. Radio frequency identification (RFID) performance: the effect of tag orientation and package contents. Packaging Technology and Science 19, 45–54.

EPCGlobal Inc™ , 2005. EPC™ Radio-Frequency Identity Protocols Class-1 Generation – 2 UHF RFID – Protocol for communications at 860 MHz – 960 MHz. Version 1.0.9.

Mühlmann, U., Witschnig, H., 2007. Hard to read tags: an application-specific experimental study in passive UHF RFID systems. Elektrotechnik und Informationstechnik, 124(11), 391-396.

Nikitin, P.V., Rao, K.V.S., Lazar, S., 2007. An Overview of Near Field UHF RFID, in: IEEE International Conference on RFID, 2007. Presented at the IEEE International Conference on RFID, 2007, 167 –174.

Penttilä, K., Keskilammi, M., Sydänheimo, L., Kivikoski, M., 2006. Radio frequency technology for automated manufacturing and logistics control. Part 2: RFID antenna utilisation in industrial applications. The International Journal of Advanced Manufacturing Technology 31, 116–124.

Rao, K.V.S., Nikitin, P.V., Lam, S.F., 2005. Antenna design for UHF RFID tags: a review and a practical application. IEEE Transactions on Antennas and Propagation 53, 3870 – 3876.

Sydänheimo, L., Ukkonen, L., Kivikoski, M., 2006. Effects of size and shape of metallic objects on performance of passive radio frequency identification. The International Journal of Advanced Manufacturing Technology 30, 897–905.

Tortia, C., Barge, P., Gay, P., Merlino, V., Serale, S. and C. Gandini, 2012. Key technological factors for successful RFID systems application in food supply chain management. CIGR-AGENG 2012, International Conference of Agricultural Engineering "Agriculture and Engineering for Healthier Life", July 8-12, Valencia, Spain.

Wen-Tzu, C., Wen-Bin, K., 2011. A Novel Q-algorithm for EPCglobal Class-1 Generation-2 Anti-collision Protocol. World Academy of Science, Engineering and Technology 54, 801-804.

An overview of emerging techniques in virgin olive oil extraction process: strategies in the development of innovative plants

Maria Lisa Clodoveo

Department of Agro-Environmental and Territorial Sciences, University of Bari, Bari, Italy

Abstract

Currently the systems for mechanically extracting virgin oils from olives are basically of two types: discontinuous-type systems (obsolete and dying out) and continuous-type systems. Systems defined as "continuous-type" are generally comprised of a mechanical crusher, a malaxer and a horizontal-axis centrifugal separator (decanter). The "continuous" appellation refers to the fact that two (mechanical crusher and decanter) out of the three machines making up the system operate continuously; the malaxer, which actually is a machine working in batches, is located between these two continuous apparatuses. Consequently the malaxation represents the bottleneck of the continuous extraction process. The entire virgin olive oil (VOO) process has changed very little over the last 20 years. One of the essential challenges of VOO industrial plant manufacturing sector is to design and build advanced machines in order to transform the discontinuous malaxing step in a continuous phase and improve the working capacity of the industrial plants. In recent years, rapid progress in the application of emerging technologies in food processing has been made, also in VOO extraction process. Ultrasounds (US), microwaves (MW), and pulsed electric fields (PEF) are emerging technologies that have already found application in the VOO extraction process on pilot scale plants. This paper aims to describe the basic principles of these technologies as well as the results concerning their impact on VOO yields and quality. Current and potential applications will be discussed, taking into account the relationship between the processing, the olive paste behavior and the characteristics of the resultant VOO, as well as recent advances in the process development.

Correspondence: Maria Lisa Clodoveo, Department of Agro-Environmental and Territorial Sciences, University of Bari, Via Amendola 165/A, 70126 Bari, Italy.
Tel. +39 080 5442514 - Fax: +39 080 5442504; mobile phone: +39.334.6053 605.
E-mail: marialisa.clodoveo@ uniba.it

Key words: virgin olive oil extraction process; emerging technology; ultrasound; microwave; sustainable plant engineering solutions.

Maria Lisa Clodoveo is assistant professor with tenure at the Department of Agro-Environmental and Territorial Sciences, University of Bari, Italy. She teaches classes on Food science and technology and Food quality control. She also teaches a specialized course in olive-oil processing plants. Her research interests include innovation in optimization of agro-food industry plants and process settings, influence of industrial processes on food quality, real time control of processes, recycling of agro-food by-products, and waste management.

Journal of Agricultural Engineering 2013; XLIV(s1):e60
doi:10.4081/jae.2013.(s1):e60

Introduction

All operations required in the oil extraction process take aim at to obtaining the highest quality of oil from fruits. Crushing and malaxation are the most important critical points of the oil mechanical extraction process (Amirante *et al*., 2010a; Clodoveo, 2012; Amirante *et al*., 2010b; Parenti *et al*., 2006; Masella *et al*., 2011; Parenti *et al*., 2008). Malaxation can largely affect the oil yields and also the healthy proprieties of virgin olive oil (VOO) (Clodoveo, 2012). In the olive fruit, only the 80% of oil can be easily extracted because it is located in the vacuoles of olive pulp cells, the rest can be found dispersed in the cytoplasm as microgels and thus, is difficult to extract (Aguilera *et al*., 2010). The effect of traditional malaxing is to disrupt the interfacial films in the olive paste modifying the dispersion degree of oil droplets and promoting the coalescence phenomena, but it requires a long mixing time. Actually, considering the yield as the main economical parameter, oil millers tend to increase malaxing time or temperature with detrimental effect on VOO quality (Clodoveo, 2012). So, it is important to find an innovative technology able to enhance the extraction yields, reducing the process time and preserving the VOO quality.

The VOO plant manufacturers are interested to the searching for new alternative extraction processes able to increase the yield reducing the producing cost of the resulting product (Di Renzo & Colelli, 1997). They have to respond to the changed market needs by offering highly efficient plants for supporting and increasing income of olive millers restricting the plant investment (with a minor number of malaxer) and reducing the working time optimizing the plant working capacity. In order to reach these goals, emerging technologies, such as PEF, US and MW can be employed. This review aims to describe the basic principles of these technologies as well as the state of the art concerning their applications in VOO extraction process. Future trends and potential applications will be discussed, focusing on the relationship between the raw and in-process materials, the processing techniques and the final product quality, as well as recent advances in the process development.

Traditional voo extraction systems

As is well known, currently the systems for mechanically extracting virgin oils from olives are basically of two types: discontinuous-type systems and continuous-type systems. Discontinuous-type systems, generally comprised of a millstone combined with hydraulic presses, generally have a low working capacity and unavoidably require a high amount of labour (Amirante *et al*., 2010 a). For these reasons they are deemed obso-

lete and are dying out, superseded by continuous-type systems. The systems defined of continuous type generally are constituted by a mechanical crusher, a malaxer and a horizontal-axis centrifugal separator (decanter). The designation "continuous" relates to the fact that two of the three machines composing the system operate continuously (crusher and decanter), the malaxer, which actually is a machine operating in batches, is placed between these two continuous apparatuses (Clodoveo, 2012). Traditionally, the malaxation phase consists in slow mixing (12-18 revolutions per minute) the olive paste at 27-32°C for a period of time comprised between 30 and 60 minutes depending upon the features of the raw material. The malaxation purpose is to promote the coalescence of the tiny oil drops in drops with greater sizes which can be separated more easily in a centrifugal field on one hand, to reduce the olive paste viscosity value so as to optimize the phase separation inside the decanter (oil /vegetable water / pomace) on the other hand. The malaxation phase actually represents the "bottleneck" of the continuous extraction process. Currently the system used to guarantee continuity to the process, without interrupting the activity of the machines upstream and downstream of the malaxer, consists in placing several malaxing machines in parallel (Figure 1), with the burden of a heavy investment in plant engineering (Amirante *et al*., 2011). The oil mills which are not equipped with several malaxers actually operate in a discontinuous way and they do not fully exploit the work capacity of crusher and decanter. One of the critical factors determining so long malaxation time is constituted by the period necessary so that the just crushed olive paste reaches the process temperature (27-32°C) (Clodoveo, 2013a). Such period on the average lasts at least one third of the total malaxation time. The malaxer usually is a semicylindrical tank equipped with a rotating arms shaft and stainless steel blades. The walls of the malaxing tank are hollowed so that warm water flows through the jacket heating the olive paste (Clodoveo, 2012). The malaxer is a heat exchanger characterized by a low overall heat transfer coefficient because the ratio (r) of surface area (S) to volume (V) is disadvantageous (r = S/V), so it is important to find an innovative technology able to improve heat-exchange (Amirante *et al*., 2006). In this sense, pulsed electric field (PEF), power ultrasound (US) and microwave (MV) are considered to be emerging and promising technologies for VOO industry.

Principles and mechanism of PEF

PEF treatment involves the application of short pulses of high voltage in order to disrupt biological cells in the food material. The concept was established and reported for the first time more than 50 years ago (Toepfl *et al*., 2006). However, besides some sporadic industrial applications conducted in the following decades it was just recently, that the technology was introduced at an increasing number as large scale commercial application. Depending on the treatment intensity (electric field strength, number and duration of the electric pulses) and cell properties (size, shape, orientation, conductivity) the pore formation may be permanent or temporary (Zimmermann *et al*., 1974; Zimmermann *et al*., 1976; Angersbach *et al*., 2000). The treatment consists of the application of very short electric pulses (1 – 100 s) at electric field intensities in the range of 0.1 – 1 kV/cm (reversible permeabilization for stress induction in plant cells), 0.5 – 3 kV/cm (irreversible permeabilization of plant and animal tissue) and 15 – 40 kV/cm for the irreversible permeabilization of microbial cells. The aforementioned field intensities lead to the formation of a critical transmembrane potential, which is regarded to be the precondition for cell membrane breakdown and electroporation (Tsong, 1990) (Figure 2). The irreversible electroporation results in a loss of turgor, the leakage of cytoplasmic content and lysis (Rubinsky, 2010). Reversible permeabilization leads to the formation of conductive channels across the cell membrane but electrically insulating properties will recover within seconds (Angersbach *et al*., 2000).

PEF mechanical effect

Cell membrane acts as a physical barrier in removing the intracellular substances (water, oil, and antioxidants) from plant tissues in solid-liquid extraction (Puértolas *et al*., 2012).

The disintegration or permeabilization of the cell membrane in a plant food tissue can allow the release of intracellular water, oil and solutes (secondary metabolites) to migrate in an external medium (Ade-Omowaye *et al*., 2001). Application of PEF of high intensity, due to it mechanical effect, can cause temporary or permanent rupture of cell membranes (Barbosa-Cánovas *et al*., 1999). An irreversible perforation of the cell membrane reduces its barrier effect and, applied to fruit and vegetable cells, mass transfer processes like pressing or extraction are more effective (Jaeger *et al*., 2009). Its ability to permeabilize cellular tissue in a short time can be utilized to replace energy- and time-consuming conventional thermal or mechanical techniques (Toepfl *et al*., 2001).

PEF thermal effect

Although the PEF treatment is defined as a non-thermal food processing technology, there is a significant temperature increase during high intensity PEF treatment due to Joule heating (Sastry & Barach, 2000). Many authors have described the temperature distribution in a PEF treatment chamber and reported the occurrence of high local temperatures due to inhomogeneous field distribution of the electrical

Figure 1. VOO extraction plant equipped with plural malaxing machines in parallel (Photography courtesy Alfa Laval Olive Oil S.p.A.).

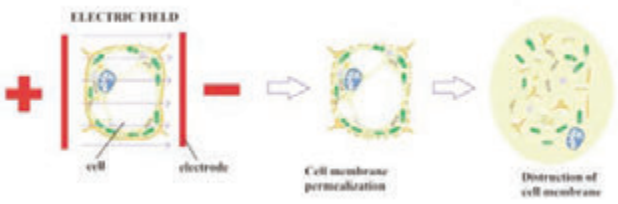

Figure 2. When external applied electric field reaches to the threshold values of the cell membrane, then cell membrane can permeabilize to deliver cytoplasmic content. Applying an intense electric field, which exceeds certain critical value, irreversible electroporation can occur resulting cell membrane rupture.

field, limited flow velocity and recirculation of the liquid (Fiala *et al*., 2001; Lindgren *et al*., 2002; van den Bosch *et al*., 2002; Gerlach *et al*., 2008; Jaeger *et al*., 2009). The increase in product temperature dependent on the energy input (Toepfl, *et al*., 2003) in comparison to conventional thermal processing is quite low (from 30 to 80°C) and in general do not affect the functional and nutritional value (e.g. vitamin content) of the food in contrast to traditional heating methods (Olsen *et al*., 2010). Traditional heating methods always include a temperature gradient, which causes areas of high temperature at the surface resulting in an overtreatment, Using PEF, the applied energy causes a temperature increase, which is a volumetric heating. The PEF process can be used for liquids, also containing particles. Field strength of about 20 kV/cm, depending on the product, and 3.000 to 6.000, very short pulses (microseconds), results in a slight increase of temperature and a decrease of processing time.

Applications of PEF technology in VOO extraction process

PEF has been already used in food processing for sterilization and preservation and has been shown to increase yields in the extraction of fruit juices, such as from oranges (Rivas *et al*., 2006). Recent research reveals its potential for making olive oil (Figure 3).

Abenoza *et al*. in 2012 studied the effect of the application of PEF treatments of different intensities (0–2 kV/cm) on Arbequina olive paste in reference to olive oil extraction at different malaxation times (0, 15, and 30 min) and temperatures (15 and 26 °C). They observed that when the olive paste was treated with PEF (2 kV/cm) without malaxation the extraction yield improved by 54 %. At 15 °C, a PEF treatment of 2 kV/cm improved the extraction yield by 14.1 %, which corresponded with an enhancement of 1.7 kg of oil per 100 kg of olive fruits. So, they suggested the application of a PEF treatment could permit reduction of the malaxation temperature from 26 to 15°C without impairing the extraction yield. These data confirm that Therefore, the treatment of the olive paste with PEF has the potential to induce cell disintegration and to facilitate the release of the small oil droplets. The facilitated release of oil from the cell provides the potential to perform the malaxation at lower temperature with beneficial effects on the oil quality (Kalua *et al*., 2007): regard to the parameters legally established (acidity, peroxide value, K232, and K270), VOO were not affected by the PEF treatments like the sensory analysis. Moreover, PEF also has potential to increase VOO phytonutrient content and to improve consumer health benefits and olive oil shelf life. PEF treatment also provides energy and time savings – compared to thermal or enzyme treatment – and improving oil quality. These preliminary results stimulated the scaling up of this technology and a commercial product was developed (Figure 4).

PEF equipment

The PEF process is based on pulsed electrical currents delivered to a product placed between a set of electrodes. The electric field may be applied in the form of exponentially decaying, square wave, bipolar, or oscillatory pulses and at ambient, sub-ambient, or slightly above-ambient temperature. The high intensity PEF processing system is a simple electrical system (Figure 4). Generation of pulsed electric fields requires a fast discharge of electrical energy within a short period of time. This is accomplished by the pulse-forming network, an electrical circuit consisting of one or more power supplies with the ability to charge voltages (up to 60 kV), switches (ignitron, thyratron , tetrode, spark gap, semiconductors), capacitors (0.1-10 F), inductors (30 H), resistors (2 Ω – 10 MΩ), and treatment chambers (Gongora-Nieto *et al*., 2002). A PEF treatment chamber can consist of at least two electrodes and insulation zone, where the foods receive pulses. The electrodes are made of inert materials, such as titanium (Figure 5).

Figure 3. Setup for a pilot plant to study the PEF assisted VOO extraction process. A) pulse generator; B) Crusher feed hopper and screw; C) Crusher; D) PEF treatment chamber; E) malaxer; F) decanter.

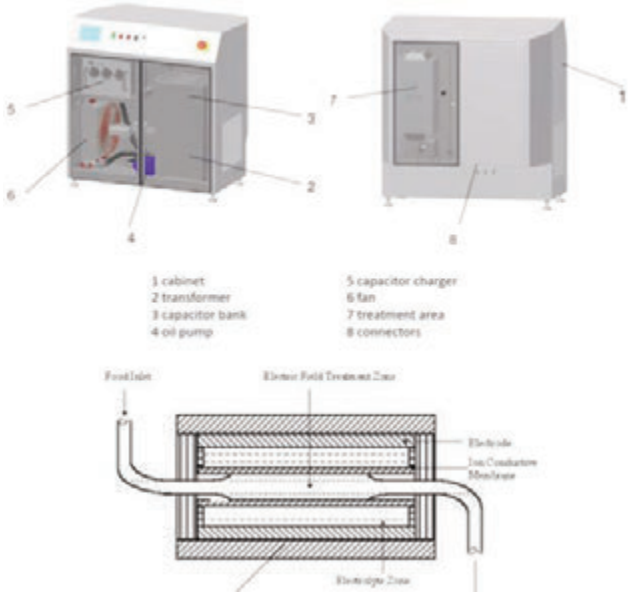

Figure 4 PEF industrial device available for VOO extraction process (Image courtesy Diversified Technologies, Inc.)

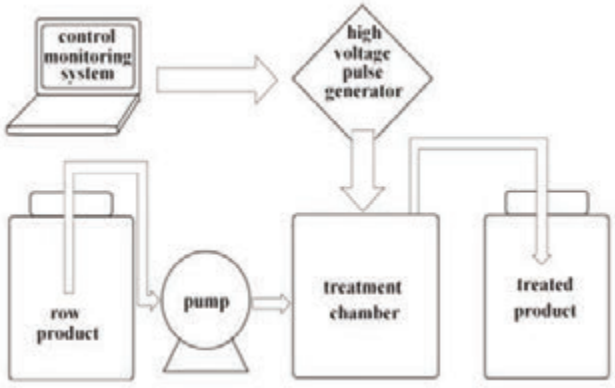

Figure 5. Flow chart of a PEF food processing system with basic components.

Economic aspects of PEF technology

PEF equipment uses ordinary electricity. The facility meets electrical safety standards and no harmful environmental by-products are produced (Ramaswamy *et al*., 2005). PEF is an energy efficient process compared to thermal processes (Vega-Mercado *et al*., 1997). A commercial-scale PEF system can process between 1,000 and 5,000 liters of liquid foods per hour and this technology is easy scalable (Sampedro & Zhang, 2012). Generation of high voltage pulses having sufficient peak power (typically megawatts) is the limitation in processing large quantities of fluid economically (Gaudreau *et al*., 1998). The emergence of solid-state pulsed power systems, which can be arbitrarily sized by combining switch modules in series and parallel, removes this limitation (Gaudreau *et al*., 2001).

Principles and mechanism of us

US are a form of energy generated by sound waves of frequencies above 16 kHz (Jayasooriya *et al*., 2004). Two main mechanisms of US could be useful to optimize the VOO extraction process: the mechanical and the thermal effects (Clodoveo, 2012). Mechanical action is due to the cavitation phenomena (Luque Garcìa & Luque de Castro, 2003) which disrupt the biological cell walls (Cravotto, *et al*., 2008). Heating occurs as the ultrasonic energy is absorbed in a medium (Jayasooriya *et al*., 2004; Zheng & Sun, 2006).

US mechanical effect

During the sonication process, longitudinal waves are created when a sonic wave meets a liquid medium, thereby creating regions of alternating compression and expansion (Piyasena *et al*., 2003) (Figure 6).

These regions of pressure change cause the phenomena of cavitation (Bove *et al*., 1969). Cavitation can be defined as the formation, growth and subsequent collapse of vapor and/or gas-vapor filled bubbles in the liquid (Zhou *et al*., 2009). The energy which the cavity gains during its growth over terms of microseconds is released during its subsequent implosive collapse in a time-duration of few microseconds. The implosion of cavitation bubbles generates macro-turbulence, high-velocity inter-particle collisions and perturbation in micro-porous particles of the biomass which accelerates the diffusion of cellular content (Vilkhu *et al*., 2011). Moreover, the cavitation near the liquid–solid interface sends a fast moving stream of liquid through the cavity at the surface. Cavitation on the product surface causes impingement by micro-jets that result in surface peeling, erosion and particle breakdown. This effect provides exposure of new surfaces further increasing mass transfer (Vilkhu *et al*., 2008).

US thermal effect

The thermal effect occurs as kinetic energy from the ultrasound waves is absorbed by a medium (Wu & Nyborg, 2008). Ultrasound kinetic energy when absorbed by tissues can also be converted into heat (Nussbaum, 1997). This phenomena is called attenuation. Whenever ultrasonic energy is propagated into an attenuating material, such as a vegetal tissue, the amplitude of the wave decreases with distance (Ma *et al*., 2008). This attenuation is due to either absorption or scattering. Absorption is a mechanism that represents that portion of ultrasonic wave that is converted into heat, and scattering can be thought of as that portion of the wave, which changes direction (O'Brien Jr, 2007). Because the medium can absorb energy to produce heat, a temperature rise may occur as long as the rate of heat production is greater than the rate of heat removal. Attenuation increases if frequency increases (Gammell *et al*., 1979).

Applications of US technology in VOO extraction process

One of the latest challenges for the VOO industrial plant manufacturing sector is the conversion of the traditional malaxing batch process into a continuous operation (Clodoveo, 2012). The first step towards the continuous process consists in reducing the duration of malaxation. In order to reduce the malaxing time enhancing the quality of the product, Clodoveo *et al*. (2013a & b) tested an ultrasound assisted VOO extraction processes against the traditional method (Figure 7).

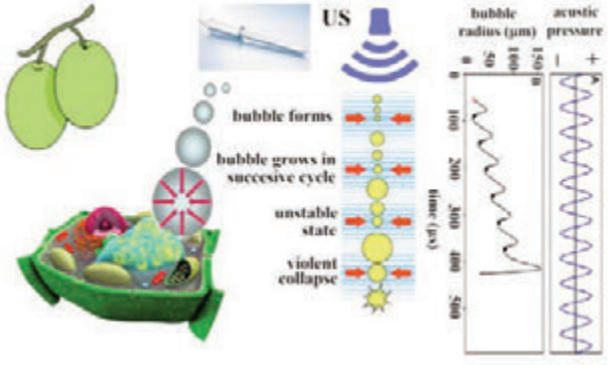

Figure 6. Cavitation phenomena.

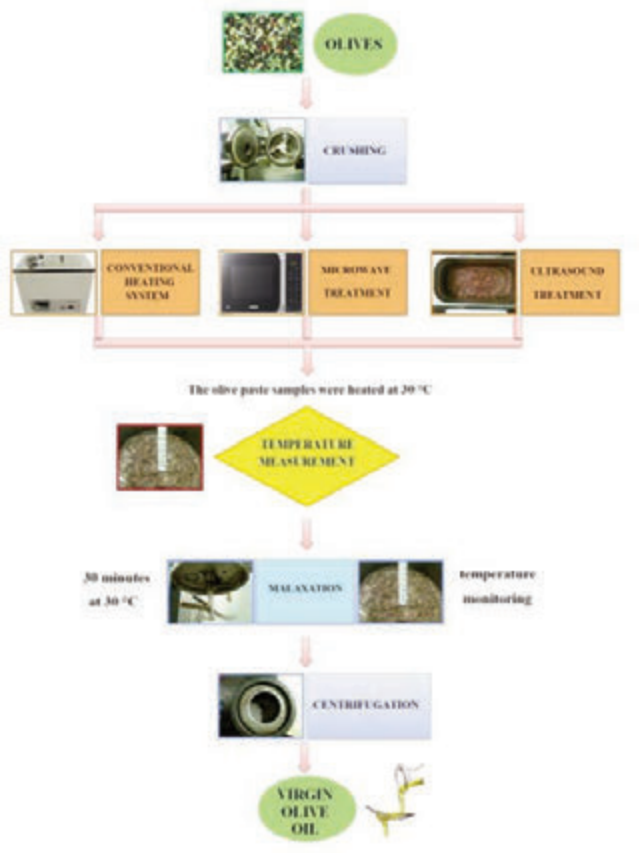

Figure 7. The flow chart of the method used to evaluate the thermal effect of US and MW on olive paste and its influence on the length of malaxation in a pilot scale plant.

The sonication treatment was applied on olive paste after the crushing. As mentioned, the malaxing phase can theoretically be divided into two different stages. The first stage is definable as "pre-heating", i.e. the time required to the olive paste to achieve the process temperature (30 °C). The second stage is definable as the "effective malaxation". The duration of the pre-heating stage is about 50% of the total process time and is also influenced by the room temperature (the oil mill temperature depends on whether condition and is about 10–20°C during the olive harvesting season, from September to January). In this experimental plan (Figure 7), malaxation time was established as a function of two factors: a) the time required to reach 30°C (pre-heating) b) the fixed time of 30 min needed to complete the oil coalescence. When the US treatment to the olive paste (cv. Coratina) was applied instead the conventional heating system (Clodoveo *et al*., 2013 b & c), a quick heating of the product occurs. Applying the conventional heating method of the olive paste, the length of the pre-heating stage was about 45% of the total process time (Figure 8A), taking 25 minutes to carry the olive paste up 30°C before the "effective malaxation" stage. Applying the US treatment (35 kHz – 150 W) on the olive paste (2.5 kg) the pre-heating length was about 10 minutes (Figure 8B), corresponding to a 60% reduction in respect to the conventional system.

Parameters legally established (acidity, peroxide value, K_{232}, and K_{270}) to measure the level of quality of the virgin olive oil were not affected by the US treatments.

A sensory analysis revealed that the application of a US treatment did not generate any bad flavor or taste in the oil. The ultrasound technique improved antioxidant content in VVOs, and in Coratina VOO improved its taste by reducing the bitter and pungent notes, which are not always accepted by consumers. Ultrasound treatment of olive paste before malaxation increases the process efficiency by reducing the malaxation step, so it represents a useful strategy to reduce the number of malaxers thus reducing the plant costs. Moreover, US treatment significantly improves the extractability of "Coratina" VOO (Clodoveo 2013 a). These results are in agreement with a previous study made by Jiménez *et al*. (2007). In the considered experimental conditions, at pilot plant scale, the average increase of extracted VOO after sonication treatment was about 8 g/kg of olives. In an industrial full scale plant with a 2000 kg of olives/h working capacity, if the plant works 8 h/day, with an average extraction yield of 16%, it produces about 2500 kg of VOO per day. Employing the ultrasound technology for 10 min (ultrasonic frequency – 35 kHz; effective ultrasonic power – 150 W), assuming at least an increase of about 5 g of extracted VOO per kilogram of olives, the quantity of extracted VOO per day could increase of about of 80 kg with an increment of 3% of the total VOO production. Moreover, this calculation does not take into account that the ultrasound treatment determines a 70% reduction of the duration of the pre-heating ; this could also contribute to increase the quantity of extracted VOO per day because of the higher working capacity of the innovative plant in comparison with the traditional system. Other results obtained excluding the malaxation are even more interesting: at laboratory scale, Clodoveo *et al*. (2013 c) observed that when the VOOs were extracted without malaxing, the extraction yield of untreated sample was 1.0 % (± 0.1), while US treatment of olive paste produced a significant increase in extraction yields equal to 5.4 % (± 0.3). The results, obtained without malaxation in the laboratory procedure, open up new prospects for developing innovative continuous extraction system to overcome the actual obsolete malaxing batch technology. Moreover, reducing the length of the pre-heating malaxation stage could present energy savings for the olive oil extraction industry.

US equipment

In order to develop an industrial ultrasonic plant feasible for VOO extraction plant (Clodoveo 2013 a) (Figure 9) it is possible retrofitting the existing devices collocating a rod-style piezoelectric transducer into the malaxer with the aim to sonicate the olive paste. Moreover, as an alternative, a new device, an ultrasonic reactor, placeable between the crusher and the malaxer can be developed. An ultrasonic reactor consists of a holding tank and an ultrasonic sonotrode.

After the crushing, olive paste can fall into the closed ultrasonic reactor, and at the end of sonication treatment, a pump can be used to move the sonicated and preheated olive paste into the malaxer.

In order to reduce the duration of sonication treatment it is also possible to combine a heat exchanger with the ultrasonic reactor (Amirante *et al*., 2006).

Economic aspects of US technology

Ultrasonic processing is a technology with good payback on capital investment (Ashokkumar *et al*., 2009). Significant improvements process enhancement and cost reduction are achievable on a commercial scale (Patist & Bates, 2011). The efficiency of ultrasonic generators and transducers has been improved: current systems have an energy efficiency around 85% which simply means that most of the power send to the transducer is transferred into the medium. The transducers are easily installed into an existing facility. The amount of energy required per liter material treated (often defined as kWh/L) is comparable to any other unit operation in the industry and the maintenance cost are low. The payback (defined here as investment cost over the benefit) is in general less than 1 year (Patist & Bates, 2008).

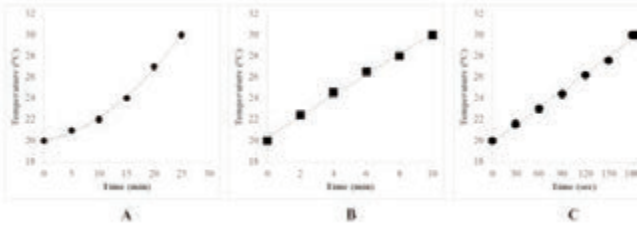

Figure 8. Influence of the olive paste heating system on the duration of the pre-heating stage: conventional heating method (A), US treatment(B) MW treatment(C).

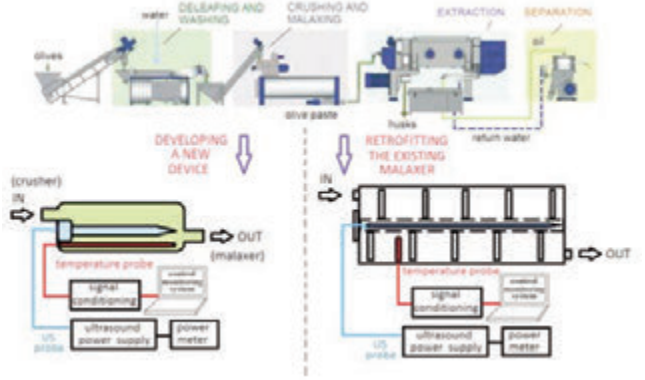

Figure 9. Scaling up of ultrasounds application in VOO industry.

Principles and mechanism of mw

MW are non-ionizing electromagnetic waves of frequency between 300 MHz to 300 GHz (Banik, 2003). MW is a technology applied in many food processes enables to reduce processing times (Mullin, 1995). MW operations have extensive applications in food technologies such as solvent lipid extraction from seed, pasteurization, sterilization, baking, blanching, cooking, drying, and thawing of different food products (Ramaswamy, & Marcotte, 2005). But, before the olive harvesting seasons 2011-2012 and 2012-2013, the MW treatment of olive paste has never been applied (Clodoveo 2013 c). The MW treatment of olive paste presented many advantages due to its mechanical and thermal effects.

MW thermal effect

Microwave heating is a process in which the materials couple with microwaves, absorb the electromagnetic energy volumetrically, and transform into heat (Zhao *et al*., 2000). This is different from conventional methods where heat is transferred by the mechanisms of conduction, radiation and convection (Oghbaei & Mirzaee, 2010). In conventional heating, the material's surface is first heated followed by the heat moving inward. This means that there is a temperature gradient from the surface to the inside. However, microwave heating generates heat within the material first and then heats the entire volume (Yadoji *et al*., 2003). This heating mechanism is advantageous due to the following facts: enhanced diffusion processes, reduced energy consumption, very rapid heating rates and considerably reduced processing times, improved physical and mechanical properties, simplicity and lower environmental hazards. These are features that have not been observed in conventional processes (Yadoji *et al*., 2003; Leonelli, *et al*., 2008).

MW mechanical effect

MW technology presents also a mechanical effect due to the heating which determines an increasing of the vegetal tissue volume and, in this way, cells explode releasing their content into the liquid phase. Moreover, when the liquid phase absorbs the MW, the kinetic energy of its molecules increases, and consequently, the diffusion rate increases too (Kratchanova *et al*., 2004; Mandal *et al*., 2007).

Applications of MW technology in VOO extraction process

Considering the thermal and mechanical effects of this emerging technology, it is reasonable to hypothesize that the MW can reduce the length of malaxation improving the oil releasing. Experimental trials were carried out in a pilot scale plant applying MW treatments on olive paste (Figure 7). Applying the MW treatment (800W) on the olive paste (2.5 kg) the pre-heating length was about 3 minutes (Figure 8C), corresponding to an 88% reduction in respect to the conventional system.). Table 1 summarizes data relative to the qualitative parameters of extracted VOOs using the conventional and MW heating employing a pilot scale plant. All the examined VOOs, regard the considered parameters, belong to the extra VOO commercial class. In fact, all the samples showed very low percentages of free fatty acids and peroxide value (index of primary oxidation), and all the samples were always below the legal limit. No differences attributable to this innovative technologies were highlighted confirming that MW, in these experimental conditions (temperature treatment: 30°C), did not affect oil acidity and peroxide value. Also the values of K_{232} (another index of primary oxidation) and K_{270} (an index of hydroperoxides degradation) were not influenced by the MW treatment. All the oils were free of defects. The oils obtained by applying the MW treatment on olive paste were more pigmented than the conventional ones. This result was due to the MWs which cause the increase of vegetal tissue volume disrupting the cells and releasing the pigments. This visual observation was confirmed by the analytical data. Considering the total chlorophylls and carotenoids content, the lower values were obtained from olive paste untreated with 164 ± 17 and 33 ± 6 (mg/kg), respectively. The highest values were obtained when the MW treatment was applied with 219 ± 23 for the total chlorophyll and 81 ± 6 (mg/kg) for the total carotenoid contents. Aware that these compounds act as prooxidants in the light, these olive oils should be stored in the dark and in adequate bottles (Malheiro *et al*., 2013) to more preserve the VOO quality and shelf-life. Considering the effect of MW treatment on extraction yields, employing the pilot scale plant, the extraction yield was 16.7 % (± 0.2), and 17.1 % (± 0.1) for the conventional and MW treatment respectively. When the VOOs were extracted without malaxing, the extraction yield of untreated sample was 1.0 % (± 0.1) while the MW treatment produced a significant increase in extraction yields equal to 5.4 % (± 0.3). These results demonstrate that this innovative treatment has a mechanical effect on olive paste causing the rupture of cell walls and recovering the oil trapped in the uncrushed olive tissue (Li *et al*., 2004; Cravotto *et al*., 2008). This data open up new prospects for developing innovative continuous extraction system to overcome the actual obsolete malaxing batch technology. In fact, a secondary effect should be considered: the crushing step may create an emulsion that impedes the complete separation between the oil and water; the emerging MW can facilitate the emulsion phases' separation determining the coalescence phenomena in a shorter time compatible with the development of a continuous system (Nour *et al*., 2010)

MW equipment

There are many options to develop a continuous MW system placeable between the crusher and the malaxer. The easier apparatus could be constituted by a MW tunnel: A modular microwave tunnel oven can be easily developed projecting equipment with multiple microwave sources and the possibility to control the atmosphere for the continuous processing of olive paste. A conveyor belt can run for carrying olive past from the crusher outlet through the oven cavity, to the malaxer. Microwave energy can be launched into the cavity above and below the conveyor belt. A more complex system could be represented by a continuous a rotating tube system: this system can be consisted of a screen and reverberant cavity inside which there is a slightly inclined pipe in which the olive paste is irradiated. The rotating tube, in addition can transferring the olive paste from loading to unloading, favors its constant mixing and reduces the risk that an uneven heating occurs. It could be easily monitored the temperature, the microwave power, and the speed, with a management system based on electronic logic PLC.

Economic aspects of US technology

Conventional industrial heating method using steam or electric heaters may be more efficient compared to microwave heating in terms of converting the energy into a useful heat. It is difficult to estimate the total economic value for microwave technology when considering the complete extraction process, because, even if this technology has the lower energetic efficiency (42%) (defined as the ratio, expressed as a percent, between the transferred heating power necessary to warm up the olive paste and the input electric power) if compared to the conventional (49,5%) and the US heating treatment, the higher speed in reach the process temperature can allow a high increase in plant working capacity and a high reduction of investment costs. Moreover, other new values are added by using versatile novel technology that offers advantages over traditional processing such as: more rapid heating, preservation of sensory and nutritional quality, high throughput of processed

foods, and possibility of incorporation of microwave processing equipment in the existing processing lines.

Conclusion

The application of new emerging technologies, such as PEF, US and MW, in the VOO extraction process offers a number of advantages due to their mechanical and thermal effects. In contrast with the existing technology, the considered emerging ones are able to cause the rupture of cell walls and recovering the oil and minor compounds trapped in the uncrushed olive tissue, increasing the work capacity of the extraction plant and reducing the process time. PEF, US and MW can be retrofitted to existing VOO extraction plants or be engineering into new systems. The industrial application of these technologies could represent the first step toward a continuous malaxing phase. A continuous process presents potential advantages such as minor operating costs, minor capacity limitations, faster return on investments, lower cost of production, reduced energy demands, reduced work-in-progress, faster and easier cleaning, real-time quality control and significantly reduced footprint facility (Clodoveo *et al*., 2013 a). In recent years many efforts were spent to increase the overall heat transfer coefficient of the malaxer improving the ratio between the surface area of the malaxing tank and the volume of olive paste. Moreover, sophisticated system for the real time monitoring of the malaxing condition (temperature, atmosphere composition, viscosity, etc.) were tested in order to design the most innovative malaxer without resolving the question of the batch process (Amirante *et al*., 2008 a & b) (Figure 10).

The relative increment of the plant costs discourages the VOO plant manufacturers to continue towards this direction, also considering the negative trends of virgin olive oil prices in the worldwide market, which is a real impediment for the olive millers to invest money in new expensive machines. The actual trend is developing new apparatus to reduce plant investments increasing the extraction yields. If it is possible to apply a thermal and mechanical action on the olive paste before the inlet in to the malaxer, a high constructive simplification of this machine can be realize reducing its cost: in fact, the malaxer can be transformed in a thermally isolated tank equipped with a rotating arms shaft and stainless steel blades, excluding the jacket for heating the olive paste. Future researches should be developed to evaluate the significance of these technologies assessing their potential using the following criteria: energy savings, first costs, and other benefits, all being compared to existing technologies.

Figure 10 Malaxer equipped with sensors in order to control the oxygen concentration in the head space of the tank and in the olive paste. Besides, a system to inject oxygen was introduced on this machine.

ABBREVIATIONS
VOO: Virgin Olive Oil
PEF: Pulsed Electric field
US: Ultrasound
MW: Microwave
r: ratio of surface area to volume
S: surface area of the malaxer
V: volume of the malaxer

References

Aguilera, M. P., Beltran, G., Sanchez-Villasclaras, S., Uceda, M., & Jimenez, A. (2010). Kneading olive paste from unripe 'Picual'fruits: I. Effect on oil process yield. Journal of Food Engineering, 97(4), 533-538.

Abenoza, M., Benito, M., Saldaña, G., Álvarez, I., Raso, J., & Sánchez-Gimeno, A. C. (2012). Effects of pulsed electric field on yield extraction and quality of olive oil. Food and Bioprocess Technology, 1-7.

Ade-Omowaye, B. I. O., Angersbach, A., Taiwo, K. A., & Knorr, D. (2001). Use of pulsed electric field pre-treatment to improve dehydration characteristics of plant based foods. Trends in Food Science & Technology, 12(8), 285-295.

Amirante, P., Clodoveo, M. L., Dugo, G., Leone, A., & Tamborrino, A. (2006). Advance technology in virgin olive oil production from traditional and de-stoned pastes: Influence of the introduction of a heat exchanger on oil quality. Food chemistry, 98(4), 797-805.

Amirante, P., Clodoveo, M. L., Leone, A., & Tamborrino, A. (2011). Innovation in olive oil processing plants to produce an excellent olive oil and to reduce environmental impact. Italian Journal of Agronomy, 4(1s), 147-162.

Amirante, P., Clodoveo, M. L., Tamborrino, A., & Leone, A. (2008b). A new designer malaxer to improve thermal exchange enhancing virgin olive oil quality. Acta Horticulturae 949 (pp. 455-462).

Amirante, P., Clodoveo, M. L., Tamborrino, A., Leone, A., & Dugo, G. (2008a). Oxygen Concentration Control during Olive Oil Extraction Process: a New System to Emphasize the Organoleptic and Healthy Properties of Virgin Olive Oil. Acta Horticulturae 949 (pp. 473-480).

Amirante, P., Clodoveo, M.L., Tamborrino, A., Leone, A. & Paice, A. (2010a). Influence of the Crushing System: Phenol Content in Virgin Olive Oil Produced from Whole and De-stoned Pastes. In: Victor R. Preedy and Ronald Ross Watson - Olives and Olive Oil in Health and Disease Prevention., p. 69-76, ACADEMIC PRESS LTD ELSEVIER SCIENCE LTD, 24-28 OVAL RD, LONDON, ENGLAND

Amirante, P., Clodoveo, M.L., Tamborrino, A., Leone, A. & Patel, V. (2010b). Influence of Different Centrifugal Extraction Systems on Antioxidant Content and Stability of Virgin Olive Oil. In: Victor R. Preedy and Ronald Ross Watson - Olives and Olive Oil in Health and Disease Prevention. vol. UNICO, p. 85-93, ACADEMIC PRESS LTD ELSEVIER SCIENCE LTD, 24-28 OVAL RD, LONDON, ENGLAND

Angersbach, A., Heinz, V., & Knorr, D. (2000). Effects of pulsed electric fields on cell membranes in real food systems. Innovative Food Science and Emerging Technologies, 1, 135–149.

Ashokkumar, M., Bhaskaracharya, R., Kentish, S., Lee, J., Palmer, M., &

Zisu, B. (2009). The ultrasonic processing of dairy products–An overview. Dairy Science & Technology, 90(2-3), 147-168.

Banik, S., Bandyopadhyay, S., & Ganguly, S. (2003). Bioeffects of microwave—a brief review. Bioresource Technology, 87(2), 155-159.

Barbosa-Cánovas, G. V., Pothakamury, U. R., Gongora-Nieto, M. M., & Swanson, B. G. (1999). Preservation of foods with pulsed electric fields. Academic Press.

Bove, A. A., Ziskin, M. C., & Mulchin, W. L. (1969). Ultrasonic detection of in-vivo cavitation and pressure effects of high-speed injections through catheters.Investigative Radiology, 4(4), 236-240.

Clodoveo, M. L. (2012). Malaxation: Influence on virgin olive oil quality. Past, present and future–An overview. Trends in Food Science & Technology, 25(1), 13-23.

Clodoveo, M. L., & Hachicha R. (2013c).Beyond the traditional virgin olive oil extraction systems: earching innovative and sustainable plant engineering solutions. Food Research International. In press.

Clodoveo, M. L., Durante, V., & La Notte, D. (2013a). Working towards the development of innovative ultrasound equipment for the extraction of virgin olive oil. Ultrasonics Sonochemistry. 20 (5) , pp. 1261-1270.

Clodoveo, M. L., Durante, V., La Notte, D., Punzi, R. & Gambacorta, G. (2013b). Ultrasound-assisted extraction of virgin olive oil to improve the process efficiency. European Journal of Lipid Science and Technology. In press. DOI:10.1002/ejlt.201200426

Cravotto, G., Boffa, L., Mantegna, S., Perego, P., Avogadro, M. & Cintas, P. (2008). Improved extraction of vegetable oils under high-intensity ultrasound and/or microwaves. Ultrasonic Sonochemistry, 15(5), 898-902.

Di Renzo, G. C., & Colelli, G. (1997). Flow behavior of olive paste. Applied engineering in agriculture, 13.

Fiala, A., Wouters, P. C., van den Bosch, E. and Creyghton, Y. L. M. (2001). Coupled electrical-fluid model of pulsed electric field treatment in a model food system. Innovative Food Science and Energing Technologies 2: 229-238.

Gammell, P. M., Le Croissette, D. H., & Heyser, R. C. (1979). Temperature and frequency dependence of ultrasonic attenuation in selected tissues. Ultrasound in medicine & biology, 5(3), 269-277.

Gaudreau, M. P. J., Hawkey, T., Petry, J., & Kempkes, M. (1998). Pulsed Power systems for Food and Wastewater processing. In Twenty Third International Power Modulator Symposium, Rancho Mirage.

Gaudreau, M. P., Hawkey, T., Petry, J., & Kempkes, M. A. (2001). A solid state pulsed power system for food processing. In Pulsed Power Plasma Science, 2001. PPPS-2001. Digest of Technical Papers (Vol. 2, pp. 1174-1177). IEEE.

Gerlach, D., Alleborn, N., Baars, A., Delgado, A., Moritz, J., & Knorr, D. (2008). Numerical simulations of pulsed electricfields for food preservation: A review. Innovative Food Science & Emerging Technologies, 9, 408–417.

Góngora-Nieto, M. M., Sepúlveda, D. R., Pedrow, P., Barbosa-Cánovas, G. V., & Swanson, B. G. (2002). Food processing by pulsed electric fields: treatment delivery, inactivation level, and regulatory aspects. LWT-Food Science and Technology, 35(5), 375-388.

Heinz, V., Toepfl, S., & Knorr, D. (2003). Impact of temperature on lethality and energy efficiency of apple juice pasteurization by pulsed electric fields treatment. Innovative Food Science & Emerging Technologies, 4(2), 167-175.

Jaeger, H., Balasa, A., & Knorr, D. (2009). Food industry applications for pulsed electric fields. In Electrotechnologies for Extraction from Food Plants and Biomaterials (pp. 181-216). Springer New York.

Jayasooriya, S.D., Bhandari, B.R., Torley, P. & D'Arcy B.R. (2004). Effect of high power ultrasound waves on properties of meat: a review. International Journal of Food Properties,7(2), 301-319

Jiménez, A., Beltràn, G. & Uceda, M. (2007). High-power ultrasound in olive paste pretreatment. Effect on process yield and virgin olive oil characteristics. Ultrasonic Sonochemistry, 14, 725–731.

Kalua, C. M., Allen, M. S., Bedgood Jr, D. R., Bishop, A. G., Prenzler, P. D., & Robards, K. (2007). Olive oil volatile compounds, flavour development and quality: A critical review. Food Chemistry, 100(1), 273-286.

Kratchanova, M., Pavlova, E., & Panchev, I. (2004). The effect of microwave heating of fresh orange peels on the fruit tissue and quality of extracted pectin.Carbohydrate Polymers, 56(2), 181-185.

Leonelli, C., Veronesi, P., Denti, L., Gatto, A., & Iuliano, L. (2008). Microwave assisted sintering of green metal parts. Journal of materials processing technology, 205(1), 489-496.

Li, H., Pordesimo, L.O. & Weiss, J. (2004). Wilhelm High intensity ultrasound-assisted extraction of oil from soybeans. Food Research International 37,731–738

Lindgren, M., Aronsson, K., Galt, S. and Ohlsson, T. (2002). Simulation of the temperature increase in pulsed electric field (PEF) continuous flow treatment chambers. Innovative Food Science and Emerging Technologies 3: 233-245.

Luque Garcìa, J.L. & Luque de Castro, M.D. (2003). Ultrasound: a powerful tool for leaching TRAC. Trends in Analytical Chemistry, 22 (1), 41–47.

Ma, Y., Ye, X., Hao, Y., Xu, G., Xu, G., & Liu, D. (2008). Ultrasound-assisted extraction of hesperidin from Penggan (Citrus reticulate) peel. Ultrasonics Sonochemistry, 15(3), 227-232.

Malheiro, R., Casal, S., Teixeira, H., Bento, A. & Pereira, J.A. (2013). Effect of olive leaves addition during the extraction process of over mature fruits on olive oil quality. Food Bioprocess Technology, 6,509–521

Mandal, V., Mohan, Y., & Hemalatha, S. (2007). Microwave assisted extraction—an innovative and promising extraction tool for medicinal plant research.Pharmacognosy Reviews, 1(1), 7-18.

Masella, P., Parenti, A., Spugnoli, P., & Calamai, L. (2011). Malaxation of olive paste under sealed conditions. Journal of the American Oil Chemists' Society, 88(6), 871-875

Mullin, J. (1995). Microwave processing. In New methods of food preservation(pp. 112-134). Springer US.

Nour, A. H., Yunus, R. M., & Anwaruddin, H. (2007). Water-in-crude oil emulsions: its stabilization and demulsiflcation. Journal of Applied Sciences, 7(22), 3512-3517

Nussbaum, E. (1997). Ultrasound: to heat or not to heat—that is the question. Physical Therapy Reviews, 2(2), 59-72.

O'Brien Jr, W. D. (2007). Ultrasound—biophysics mechanisms. Progress in biophysics and molecular biology, 93(1-3), 212.

Oghbaei, M., & Mirzaee, O. (2010). Microwave versus conventional sintering: A review of fundamentals, advantages and applications. Journal of Alloys and Compounds, 494(1), 175-189.

Olsen, N. V., Grunert, K. G., & Sonne, A. M. (2010). Consumer acceptance of high-pressure processing and pulsed-electric field: a review. Trends in Food Science & Technology, 21(9), 464-472

Parenti, A., Spugnoli, P., Masella, P., Calamai, L., & Pantani, O. L. (2006). Improving olive oil quality using CO2 evolved from olive pastes during processing. European Journal of Lipid Science and Technology, 108(11), 904-912.

Parenti, A., Spugnoli, P., Masella, P., & Calamai, L. (2008). The effect of malaxation temperature on the virgin olive oil phenolic profile under laboratory scale conditions. European Journal of Lipid Science and Technology, 110(8), 735-741.

Patist, A., & Bates, D. (2008). Ultrasonic innovations in the food industry: From the laboratory to commercial production. Innovative food science & emerging technologies, 9(2), 147-154.

Patist, A., & Bates, D. (2011). Industrial applications of high power ultrasonics. In Ultrasound Technologies for Food and Bioprocessing (pp. 599-616). Springer New York.

Piyasena, P., Mohareb, E., & McKellar, R. C. (2003). Inactivation of microbes using ultrasound: a review. International journal of food microbiology, 87(3), 207-216.

Puértolas, E., Luengo, E., Álvarez, I., & Raso, J. (2012). Improving mass transfer to soften tissues by pulsed electric fields: Fundamentals and applications. Annual review of food science and technology, 3, 263-282

Ramaswamy, H. S., & Marcotte, M. (2005). Food processing: principles and applications. CRC Press.

Ramaswamy, R., Jin, T., Balasubramaniam, V. B., & Zhang, H. (2005). Pulsed Electric Field Processing. Fact sheet for food processors, Extension Fact Sheet, 2-05.

Rivas, A., Rodrigo, D., Martínez, A., Barbosa-Cánovas, G. V., & Rodrigo, M. (2006). Effect of PEF and heat pasteurization on the physical–chemical characteristics of blended orange and carrot juice. LWT-Food Science and Technology, 39(10), 1163-1170.

Rubinsky, B. (eds) (2010) Irreversible Electroporation. Springer, Heidelberg.

Sampedro, F., & Zhang, H. Q. (2012). 13 Recent Developments in Non-thermal Processess. Food and Industrial Bioproducts and Bioprocessing, 313.

Sastry, S. K., & Barach, J. T. (2000). Ohmic and inductive heating. Journal of food science, 65(8), 42-46.

Toepfl, S., Heinz, V., & Knorr, D. (2001). Overview of Pulsed 4 Electric Field Processing for Food. Introduction to Food Engineering, 69.

Toepfl, S., Mathys, A., Heinz, V., & Knorr, D. (2006). Review: potential of high hydrostatic pressure and pulsed electric fields for energy efficient and environmentally friendly food processing. Food Reviews International, 22(4), 405-423.

Tsong, T.Y., 1990. Review: on electroporation of cell membranes and some related phenomena. Bioelectrochemistry Bioenergetics 24, 271—295.

van den Bosch, H. F. M., Morshuis, P. H. F., & Smit, J. J. (2002). Temperature distribution in fluids treated by pulsed electric fields. Proceedings of the International Conference on Dielectric Liquids, Graz (Austria)

Vega-Mercado, H., Martin-Belloso, O., Qin, B. L., Chang, F. J., Marcela Góngora-Nieto, M., Barbosa-Canovas, G. V., & Swanson, B. G. (1997). Non-thermal food preservation: pulsed electric fields. Trends in Food Science & Technology, 8(5), 151-157.

Vilkhu, K., Manasseh, R., Mawson, R., & Ashokkumar, M. (2011). Ultrasonic recovery and modification of food ingredients. In Ultrasound Technologies for Food and Bioprocessing (pp. 345-368). Springer New York.

Vilkhu, K., Mawson, R., Simons, L., & Bates, D. (2008). Applications and opportunities for ultrasound assisted extraction in the food industry—A review.Innovative Food Science & Emerging Technologies, 9(2), 161-169.

Wu, J., & Nyborg, W. L. (2008). Ultrasound, cavitation bubbles and their interaction with cells. Advanced drug delivery reviews, 60(10), 1103-1116.

Yadoji, P., Peelamedu, R., Agrawal, D., & Roy, R. (2003). Microwave sintering of Ni–Zn ferrites: comparison with conventional sintering. Materials Science and Engineering: B, 98(3), 269-278.

Zhao, C., Vleugels, J., Groffils, C., Luypaert, P. J., & Van der Biest, O. (2000). Hybrid sintering with a tubular susceptor in a cylindrical single-mode microwave furnace. Acta materialia, 48(14), 3795-3801.

Zheng, L. & Sun D.-W. (2006). Innovative applications of power ultrasound during food freezing processes – a review. Trends in Food Science & Technology, 17, 16-23.

Zhou, Z. A., Xu, Z., Finch, J. A., Masliyah, J. H., & Chow, R. S. (2009). On the role of cavitation in particle collection in flotation–A critical review. II. Minerals Engineering, 22(5), 419-433.

Zimmermann, U., Pilwat, G. & Riemann, F. (1974). Dielectric breakdown in cell membranes. Biophysical Journal. 14: 881-899.

Zimmermann, U., Pilwat, G., Beckers, F. & Riemann, F. (1976). Effects of external electrical fields on cell membranes. Bioelectrochemistry Bioenergetics 3: 58-83.

Mild separation system for olive oil: quality evaluation and pilot plant design

Francesco Genovese, Giovanni Carlo Di Renzo, Giuseppe Altieri, Antonella Tauriello

University of Basilicata, School of Agricultural, Forestry, Food & Environmental Science (SAFE), Potenza, Italy

Abstract

The entire process of olive oil extraction involves the breakage of olive fruits to obtain a paste, the kneading of the paste, a centrifugation, and a further cleaning, performed by a disc stack centrifuge, to separate the residual water. In this research, in order to evaluate the effect of final centrifugal separation on olive oil quality and to both define and design the settings of a innovative separation system, olive oil was separated off from water using an accelerated separation process, tested in comparison with a disc centrifuge. The laboratory plant used for the trials was constituted by a twin cylindrical separator equipped with 4 variable frequency inverters, in order to regulate the fluid flow rates in the plant. Oil samples were collected during the trials to evaluate the influence of the proposed innovative process on oil quality; measuring some parameters as free acidity, peroxides (PV), specific extinction coefficients K_{232} and K_{270}, chlorophylls , carotenoids, total polyphenols (POL) and turbidity. Results showed statistically significant differences (p-values<0.05) in some parameters as POL, PV, and ultraviolet absorption K232 and K270.

Introduction

The final quality of olive oil, a vegetable oil obtained directly from olive fruits (Olea europea) and essential in the Mediterranean diet, is strictly related to some processing parameters (i.e. type of crusher, decanter geometry, added process water, malaxation time and temperature). The process generally consists of four phases: (a) breakage of olive fruits (carried out by several type of crushers) producing a paste composed by a mixture of two distinct liquid phases (raw oil and water); (b) kneading of the paste, in order to facilitate cohesion of smaller oil droplets into larger ones; (c) centrifugation, to separate the different phases, which occurs in a horizontal screw conveyor centrifuge with continuous discharge of solid phase (decanter); (d) oil cleaning.

After extraction using decanter, the oil yet contains a small amount of residual water and impurities, requiring a further cleaning, that is performed by washing the oil in a vertical centrifuge with lukewarm tap water added (Di Giovacchino *et al*., 2002), which could produce negative effects on the quality (loss of aroma) and loss of stability of the final product (oxidative reactions), mainly due to oil heating and amount of dissolved oxygen (Masella *et al*., 2009).

Considering the latest developments (Amirante P. and Catalano, 1993; Amirante R. and Catalano, 2000; Catalano *et al*., 2003; Daou *et al*., 2007; Boncinelli *et al*., 2009; Altieri, 2010) in decanter centrifuge design, modeling and construction that allow the production of a cleaner oil both in terms of suspended solid and water content, the use of vertical disc stack centrifuge separator could result excessive; moreover in recent years there is an increasing interest in cloudy (veiled) extra-virgin olive oil since it is considered less processed by some consumers (Del Giovine *et al*., 2005; Koidis *et al*., 2008).

In this paper authors, evaluating some chemical and physical attributes of olive oil, propose a mild separation system for its cleaning; collected data allow to define the design parameters of a prototype system based on natural sedimentation in comparison with traditional centrifugal separation used to clean the raw oil (after the decanter extraction).

Correspondence: Francesco Genovese, University of Basilicata, School of Agricultural, Forestry, Food & Environmental Science (SAFE), Viale dell'Ateneo Lucano, 10, 85100 Potenza, Italy.
Tel. +39.0971.205256 - Fax: +39.0971.204322.
E-mail: francesco.genovese@unibas.it

Key words: vertical centrifugation, virgin olive oil quality, separation.

The authors contributed equally.

The authors declare no potential conflict of interests.

Journal of Agricultural Engineering 2013; XLIV(s1):e61
doi:10.4081/jae.2013.(s1):e61

Materials and methods

The experimental trials were carried out using a laboratory plant, based on a gravity separating system, constituted by a twin cylindrical oil-water separator (two cylindrical columns connected in series). Each cylindrical column (made of transparent material suitable for contact with olive oil) was 2 m high (0.27 m internal diameter, 0.29 m external diameter), and has a total volume of about 114 dm^3.

In order to balance the inlet flow rate to the outlet flow rate of both clean oil and oily deposits 4 volumetric pumps (2 for each column) with flexible impeller were used, controlled by a variable frequency inverter drive (VFD).

Raw oil, extracted from olive variety "Coratina" by decanter separation, was fed into the first column with a constant rate of about 1 dm^3/min. After about 90 min, considering the columns internal volume, the raw oil leaves a sediment on the bottom of the column that is composed by high density suspended solids and residual water, while cleaned oil and low density suspended solids float to the surface of the

cylinder. Cleaned oil extracted by the second pump, very close to the surface level (4 cm under the free surface level), was transferred into the second column, at a constant rate equal to the inlet. Maintaining constant the oil inlet and the outlets in the two columns, after the settling time of about 180 min, clean oil resulted about 90%, while the residual dirty oil mixed with the water and settled materials was treated in a centrifugal separator.

In order to define the design criteria of the innovative plant prototype, oil samples were collected after the following processing operations: 1) extraction by centrifuge, the sample were collected on decanter exit (Control); 2) improved natural settling (sedimentation) performed in a laboratory plant (Sedoil); 3) centrifuge separation performed in a vertical disc stack centrifuge that represents the traditional oil cleaning operation (Cenoil).

Nine samples of olive oils were analyzed (within 48 hours after the treatment) for each treatment and for each sample composition, Sedoil and Cenoil samples were evaluated with reference to Control.

The non parametric Kruskal-Wallis test with Scheffe procedure was performed on the relative differences setting the multiple comparison post-hoc tests at 10% familywise error rate level.

Analytical methods

Free acidity (FA), peroxide value (PV), UV specific extinction coefficients (K232, K270) were determined according to the analytical method of the European Official Method of Analysis (EU Regulations 2568/91).

FA was determined by titration of a mixture of oil in ethanol/ether 1:2 (v/v) with potassium hydroxide 0.1 N. PV was determined as follows: a mixture of oil and chloroform/acetic acid 2:3 (v/v) was left to react in darkness with a saturated potassium iodine solution; the released free iodine was titrated with a sodium thiosulphate solution (0.01 N).

K232 and K270 extinction coefficients were calculated from absorption at 232 (K232) and 270 nm (K270), respectively, with a spectrophotometer (UV/Vis Spectrophotometer, Ultraspec 2100 pro) using isooctane as a blank.

Chlorophylls (CHLO) and carotenoids (CAR) concentrations were spectrophotometrically determined fixing the wave length at 670 nm and 470 nm respectively, in hexane. The maximum absorption at 670 nm is related to the chlorophyll fraction, while the maximum absorption at 470 nm is related to the carotenoid fraction. The values of the applied coefficients of specific extinction were E0 = 613 for pheophytin, a major component in the chlorophyll fraction, and E0 = 2000 for lutein, a major component in the carotenoid fraction.

Total polyphenols (POL) contents were evaluated by a spectrophotometric method. Phenolic compounds were isolated by a double extraction of oil (10 g) with a methanol-water mixture (80:20 v/v). The Folin-Ciocalteau reagent was added to a suitable aliquot of the extracts, and the absorption of the solution at 765 nm was measured. Gallic acid standard solutions were used to calibrate the method (linear concentration interval 15-500 mg/dm^3). Turbidity measurements (TUR) were carried out by the nephelometric method with a Turbidimeter Model (Delta Ohm HD25.2) The turbidimeter used in the study was carefully calibrated with formazin standards (0.05-800 NTU).

Results and discussion

In Table 1 are shown the results obtained performing the chemical and spectrometric analysis associated with the collected data.

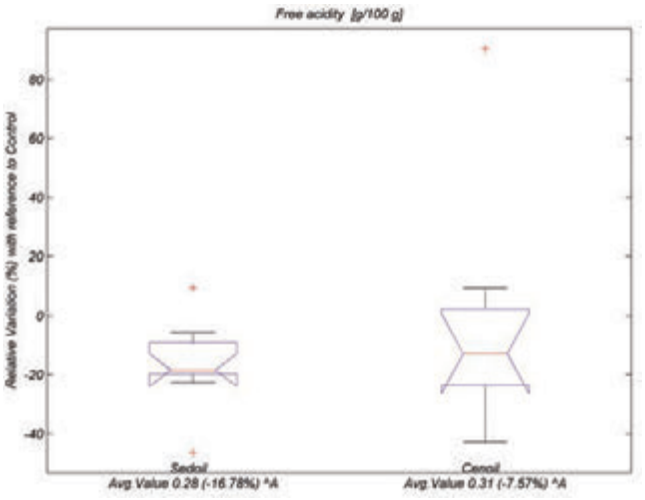

Figure 1. Free acidity values box plot of relative difference with reference to Control.

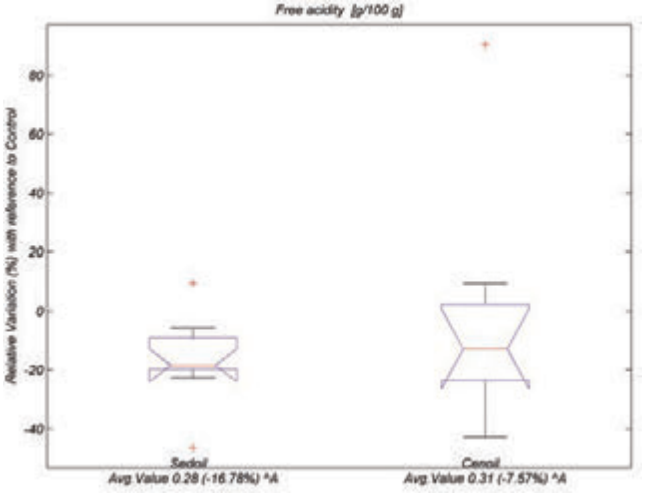

Figure 2. Peroxide values box plot of relative difference with reference to Control.

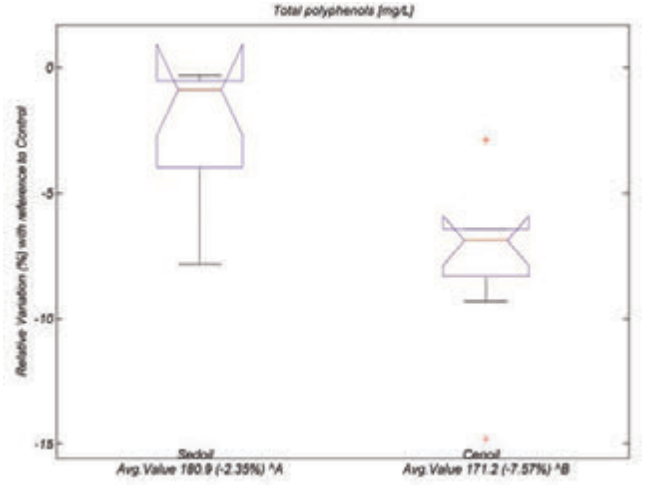

Figure 3. Total polyphenols values box plot of relative difference with reference to Control.

Measured average water content was 0.9% and 0.7% in Sedoil and Cenoil respectively. The values did not result significantly different when referred to Control, thus proving that using the enhanced sedimentation process allows achieving an efficient water separation with a reduction of water content of 69.56%.

Further, the measured oil temperature results significantly different between Sedoil and Cenoil; Sedoil treatment causes a temperature reduction from 33.3°C to 29.8°C with a reduction of 10.42%. Cenoil treatment causes a temperature average value of 34.0 °C that represents an increase of the olive oil temperature (+2.10%) after the extraction by decanter centrifuge.

In most cases the analysis of data shows that the value of each parameter evaluated in the Sedoil is not significantly different from the corresponding value in the raw olive oil obtained from decanter (Control), while the value of the same parameter in the Cenoil resulted significantly different: this demonstrates that the final centrifugal separation of raw olive oil from water and suspended solids by disc stack centrifuge produces modifications of the olive oil quality parameters respect to natural settling.

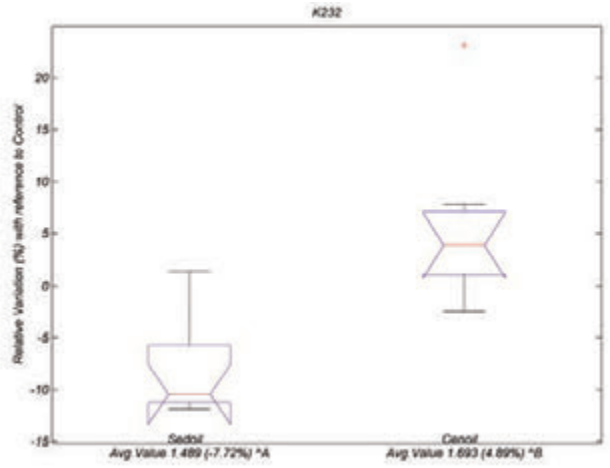

Figure 6. K232 values box plot of relative difference with reference to Control.

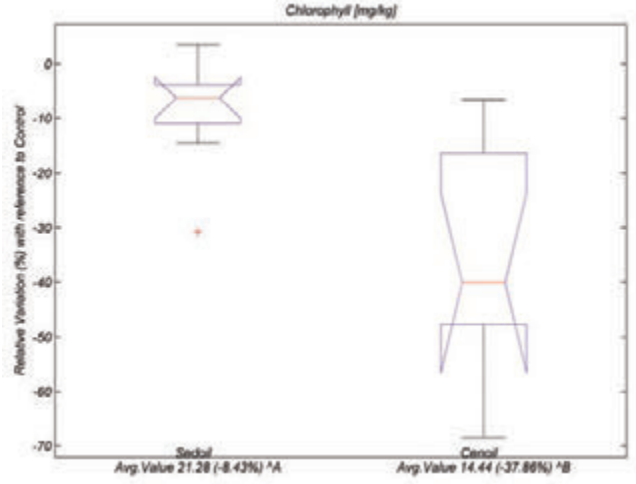

Figure 4. Chlorophyll values box plot of relative difference with reference to Control.

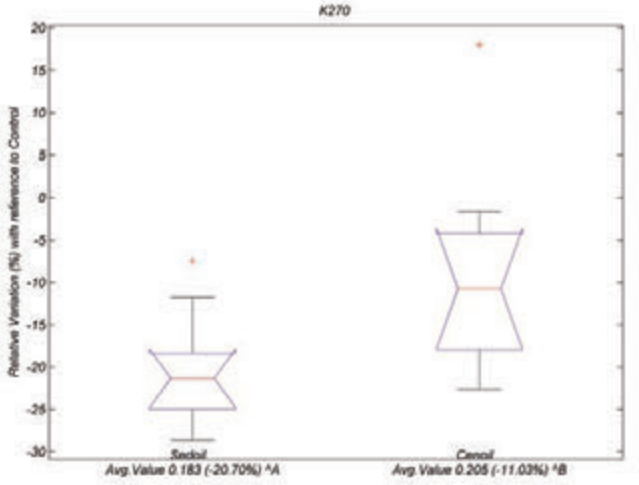

Figure 7. K270 values box plot of relative difference with reference to Control.

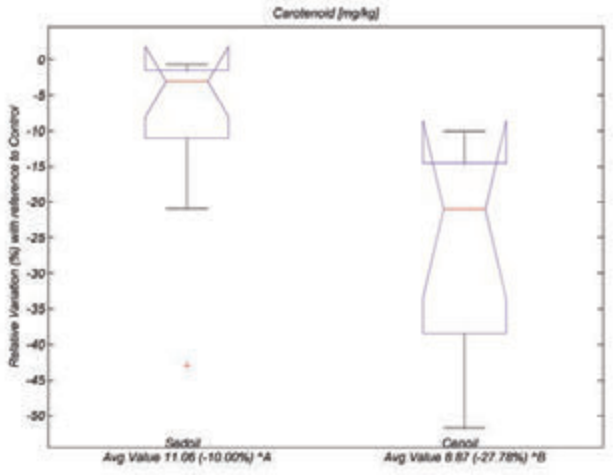

Figure 5. Carotenoid values box plot of relative difference with reference to Control.

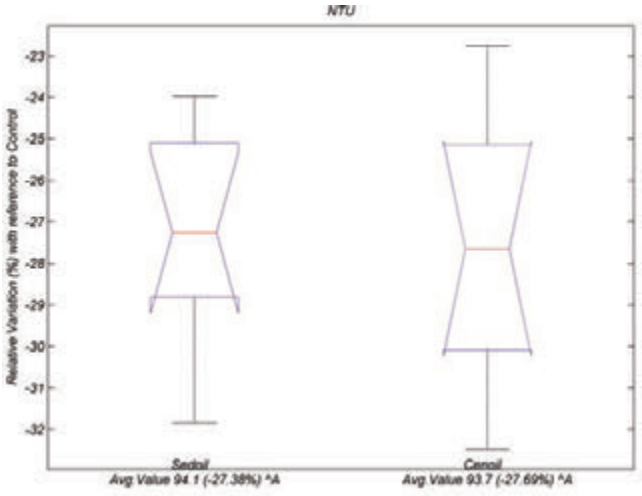

Figure 8. Turbidity values box plot of relative difference with reference to Control.

Table 1. Kruskal-Wallis test on the relative differences respect to the reference treatment Control. Multiple comparison tests at 10% significance level. In the bracket the relative percentage variation. Same letter in each row means no significantly difference at stated significance level.

Parameter	Control	Sedoil	Cenoil	p-value
Free acidity [g/100 g]	0.34	0.28 (-16.78%)[a]	0.31 (-7.57%)[a]	0.724
Peroxide value [meq/kg]	3.4	2.9 (-16.15%)[a]	3.9 (14.63%)[b]	0.001
Total polyphenols [mg/dm^3]	185.2	180.9 (-2.35%)[a]	171.2 (-7.57%)[b]	0.009
Chlorophyll [mg/kg]	23.24	21.28 (-8.43%)[a]	14.44 (-37.86%)[b]	0.003
Carotenoid [mg/kg]	12.29	11.06 (-10.00%)[a]	8.87 (-27.78%)[b]	0.009
K232 [AU]	1.614	1.489 (-7.72%)[a]	1.693 (4.89%)[b]	0.001
K270 [AU]	0.231	0.183 (-20.70%)[a]	0.205 (-11.03%)[b]	0.024
Turbidity [NTU]	129.6	94.1 (-27.38%)[a]	93.7 (-27.69%)[a]	0.825
Water content %	3.0	0.9 (-69.56%)[a]	0.7 (-76.51%)[a]	0.566
Temperature [°C]	33.3	29.8 (-10.42%)[a]	34.0 (2.10%)[b]	0.000

Nevertheless this behaviour is not general.

Figure from 1 to 8 show the box plot of relative variation (%) of evaluated parameters in both Sedoil and Cenoil with reference to Control. Boxes represent the first quartile (q1), median and third quartile (q3) of the evaluated parameters, and lower (L) and upper (U) limits are defined as:

$$L = q1 - 1.5 \times IQR \text{ and } U = q3 + 1.5 \times IQR, \text{ where } IQR = q3 - q1.$$

The average FA value of Sedoil and Cenoil did not differ significantly from Control, despite average FA value of Sedoil results lower than the other. The FA parameter is related to the hydrolytic enzymes activities in presence of water and with optimal temperature level in the range 30 to 40 °C.

PV measures the formation of hydroperoxides in presence of oxygen pointing out the effect on the quality of the processing operation, in terms of oxygen contact with olive oil during the cleaning operation (Boskou, 2006).

In the olive oil samples of Cenoil the average PV results equal to 3.9 meq/kg significantly different from the average value of 2.9 meq/kg measured in Sedoil samples. Furthermore the Cenoil treatment increases the PV with respect to Control by 14.63%, whereas Sedoil treatment lowers the PV value by -16.15% showing a significantly increase in the oil quality.

This result confirms that the deep contact between oil and oxygen caused by the use of the disc stack centrifuge represents an important oxidative effect and the residual water in the oil is an additional source of oxidation.

POL average value observed in Sedoil was equal to 180,9 mg/dm^3 and the difference resulted not significant from that observed for the Control (185.2 mg/dm^3), but the average value measured in Cenoil (171.2 mg/dm^3) resulted lower and the difference significant. Probably, considering the high water solubility of POL, the highest PV value found in Control samples could be related to an higher residual water content after the extraction performed by the decanter, that was found to be 3.0% respect to the water content of Sedoil and Cenoil equal to 0.9% and 0.7%. CHLO, CAR, K232 and K270 in Sedoil were found to be significantly different respect to the Cenoil samples.

The TUR average value resulted 93.7 in Cenoil, lower than the average value of 94.1 measured in Sedoil, but the difference was not significant.

Conclusions

In this paper the authors describe the results on olive oil quality obtained in trials carried out to define the design parameters of a prototype system based on natural sedimentation to separate olive oil with highest quality in comparison with traditional centrifugal separation and raw oil (before cleaning operation). The experimental trials were carried out using a laboratory plant, based on a separating system constituted by a twin cylindrical oil-water separator, in order to define the design criteria of the innovative plant prototype, oil samples were collected and analyzed after the processing operations.

The separation system proposed by the authors allows achieving an efficient water separation and doesn't affect the olive oil temperature. The separation system had a significant effect on the chemical attributes of the olive oil: from the obtained results Sedoil was characterized by significant differences in POL, PV, CHLO, CAR, K232 and K270. No significant differences were found in FA e TUR.

Oil obtained by the innovative plant showed an higher POL content (180.9 mg/l vs. 171.2 mg/l) and a lower PV (2.90 vs. 3.90). Considering the general increasing of olive oil quality induced by non-centrifugal final separation an innovative plant was designed using the collected data. Further investigation will be made to evaluate the shelf life of Sedoil after 3, 6 and 12 months, at last the industrial innovative plant will be designed.

References

Altieri G. 2010. Comparative trials and an empirical model to assess throughput indices in olive oil extraction by decanter centrifuge. Journal of Food Engineering. 97(1):46-56.

Amirante P., Catalano P. 1993. Analisi teorica e sperimentale dell'estrazione dell'olio d'oliva per centrifugazione. La rivista italiana delle sostanze grasse. LXX:329-335.

Amirante R., Catalano P. 2000. Fluid dynamic analysis of the solid–liquid separation process by centrifugation. Journal of Agricultural Engineering Research. 77 (2):193-201.

Boskou, D. Olive Oil: Chemistry and Technology. 2th. AOCS Publishing. 2006.

Boncinelli P., Daou M., Cini E., Catalano P. 2009. A Simplified Model for Designing and Regulating Centrifugal Decanters for Olive Oil Production. Transactions of the ASABE, American Society of Agricultural and Biological Engineers. 52(6):1961-1968.

Catalano P., Pipitone F., Calafatello A., Leone, A. 2003. Productive efficiency of decanters with short and variable dynamic pressure cones. Biosystems Engineering 86 (4): 459-464.

Daou M., Furferi R., Recchia L., Cini E. 2007. A modelling approach to extra virgin olive oil extraction. Journal of Agricultural Engineering. 38(4):11-20.

Del Giovine L., Fabietti F. 2005. Copper chlorophyll in olive oils:identification and determination by LIF capillary electrophoresis. Food Control. 16:267-272.

Di Giovacchino L., Sestili S., Di Vincenzo D. 2002. Influence of olive processing on virgin olive oil quality. Eur J Lipid SciTechnol. 104:587-601.

Koidis A., Triantafillou E., Boskou D. 2008. Endogenous micro-flora in turbid virgin olive oils and the physicochemical characteristics of these oils. Eur J Lipid Sci Tech. 110:164-171.

Masella P., Parenti A., Spugnoli P., Calamai L. 2009. Influence of vertical centrifugation on extra virgin olive oil quality. J. Am. Oil Chem. Soc. 86:1137-1140.

Numerical models of mass transfer during ripening and storage of salami

Angelo Fabbri, Chiara Cevoli, Giulia Tabanelli, Fausto Gardini, Adriano Guarnieri

Department of Agricultural and Food Science, University of Bologna, Italy

Abstract

Ripening, in the dry sausages manufacturing process, has an influence over the main physical, chemical and microbiological transformations that take place inside these products and that define the final organoleptic properties of dry sausages. A number of study about the influence of ripening conditions on the main chemical and microbiological characteristics of dry sausages is available today. All these studies indicate that the final quality and safety standards achieved by the sausage manufacturing process can be considered to be strictly dependent from the specific ripening conditions. The water diffusion inside a seasoned sausage is surely an aspect of primary importance with regard to the quality of final product. As a consequence the aim of this research was to develop two parametric numerical models, concerning the moisture diffusion physics, describing salami ripening and storage. Mass transfer equations inside the sausage volume were numerically solved using a finite element technique. A first model describes diffusion phenomena occurring inside the salami and the exchange phenomena involving the surface of the product and the environment. After the ripening, the salami are stored in waterproof packaging, consequently an additional model able to describe also the evaporation and condensation phenomena occurring between the salami surface and the air in the package, was developed. The moisture equilibrium between salami surface and conservation atmosphere is mainly ruled by the temperature changes during storage. Both models allow to analyze the history of the moisture content inside the salami and are parametrised on product size and maturation/storage conditions. The models were experimentally validated, comparing the numerical outputs of the simulations with experimental data, showing a good agreement.

Introduction

Dry sausages are the result of a fermentation process and a ripening period during which the products reach the desired characteristics. From several centuries, different kind of dry fermented sausages have been produced in the Mediterranean area (Toldrá *et al*., 2007; Zeuthen, 1995). The wide variety of dry fermented sausages is a consequence of variations in formulation, raw material, and manufacturing processes which come from the traditional habits of different countries and regions (Zanardi *et al*., 2010). Often sausages get different names according to geographic origin (Toldrá, 2006). Salami are typical European dry sausage manufactured with pork, beef, or veal, added with salt, spices, and sometimes herbs and/or other ingredients.

The primary European countries producing salami with a traditional seasoning process are Germany, Italy, Spain, France, and Hungary, with an amount of production of several hundred-millions kg per year, and consequently it is clear that ripening and storage treatment plays an important role (Bertolini *et al*., 2006). In the dry sausages industry, ripening is nowadays considered to be one of the most important stages of the integrated supply chain needed to ensure that the end products have the final requirements in terms of quality and safety standards (Grassi *et al*., 2005). Particularly the ripening stage influences over the main physical, chemical and microbiological transformations that take place inside of salami.

A large number of study regarding the influence of ripening conditions on the microbiological, physical and chemical properties of dry sausages is available (Baldini *et al*., 2000; Campbell-Platt, and Cook, 1995; Zanardi *et al*., 2010). All these researches show that the final quality and safety standards achieved by the sausage manufacturing process can be considered to be strictly dependent from the way the ripening stage is designed and carried out (Rizzi, 2002).

Two simultaneous mass transport phenomena occur inside the matrix during the drying process: water and solutes transfer. Many theoretically and experimentally study about transfer of water and solutes through meat and meat products matrices are reported in literature (Costa-Corredor *et al*., 2009; Graiver *et al*., 2006; Hansen *et al*., 2008; Sabadini *et al*., 1998; Unal *et al*., 2004).

As reported in many specific reviews, the recent progress in computing efficiency coupled with reduced costs of codes has set out the numerical simulation as a powerful tool to study many food processes with the aim of providing effective and efficient plant design or operating solutions (Scott and Richardson, 1997; Xia and Sun, 2002; Wang and Sun, 2003; Norton and Sun, 2006; Smale *et al*., 2006; Verboven *et al*., 2006; Mirade, 2008). In this regard, the numerical simulation was used to study the mass transfer in various food during drying, baking, freezing and ripening (Mirade, 2008; Sakin *et al*., 2007; Lemus-Mondaca *et al*., 2013; Floury *et al*., 2008).

The aim of this research was to develop two parametric numerical models, concerning the moisture diffusion physics, describing salami ripening and storage. Mass transfer equations inside the sausage volume were numerically solved using a finite element technique. A first model describes diffusion phenomena occurring inside the salami and the exchange phenomena involving the surface of the product and the environment, while a second one describes also the evaporation and condensation phenomena occurring between the salami surface and the air in the package. The models were experimentally validated, comparing the numerical outputs of the simulations with experimental data.

Correspondence: Chiara Cevoli, P.zza Goidanich n.60 - 47521, Cesena (FC).
E-mail: chiara.cevoli3@unibo.it

Key words: numerical simulation, water diffusion, salami, ripening, storage.

Journal of Agricultural Engineering 2013; XLIV(s1):e62
doi:10.4081/jae.2013.(s1):e62

Materials and methods

Ripening model

The equations regarding mass transfer inside the salami during ripening were solved using Comsol Multiphysics 4.3 (COMSOL Inc., Burlington, MA, USA), a commercial partial differential equations solver, based on finite element technique.

The model considers both diffusion phenomena inside the salami and exchange phenomena between product and air of the ripening environmental.

In order to limit the computation time, an one-dimensional model was built and then, with a simple geometric operation, a 2D model can be visualized. In fact, salami geometry is axisymmetric and a simple radius, comprised between the longitudinal axis and the external cylindrical surface, was considered. The geometry dimensions reflect the real ones of the salami considered (radius, *r*: 20 mm, length: 200 mm).

The moisture transfer is governed by Fick's law:

$$\frac{\partial C}{\partial t} = D_{H2O}\left(\frac{\partial^2 C}{\partial x^2}\right) \quad (1)$$

where C is calculated moisture concentration (mol m^{-3}) at time t and coordinate x.

The mass diffusivity (D_{H2O}) through the involved material was estimated by an inverse method (2.74E-12 m^2s^{-1}).

The initial and boundary conditions are:

- initial moisture concentration (C_{inR}) was considered constant in space and defined as following:

$$C_{inR} = \left(\frac{M_{H2O}}{PM_{H2O} \cdot V_s}\right) \rightarrow C_{inR} = \left(\frac{X_{inR} \cdot \rho_s}{PM_{H2O}}\right) \quad (2)$$

where X_{inR} is the initial moisture content on dry basis (experimental determination: 1.14 $kgkg^{-1}$), ρ_s is the salami density (experimental determination: 600 kgm^{-3}), while PM_{H2O} is the molecular weight of the water (0.018 kg mol^{-1});

- on the interface between the surface of the salami and the air, a flux condition was imposed:

$$N_R = k_{ex}\left(C_{bound} - C\right) \quad (3)$$

being N_R (mol m^{-2} s^{-1}) the flux, k_{ex} (ms^{-1}) the mass exchange coefficient and C_{bound} the moisture concentration of salami at equilibrium.

Concerning the mass exchange coefficient (k_{ex}: 1E-6 ms-1), it can vary within very broad limits, without problems of physical model fidelity: for high values could be compromised convergence, while for small values could introduce an artificial resistance to the moisture passage. The value must therefore be determined empirically by choosing a level slightly lower than that which causes convergence problems.

Moisture concentration of salami at equilibrium was defined by following equation:

$$C_{bound} = \left(\frac{X_{bound} \cdot \rho_s}{PM_{H2O}}\right) \quad (4)$$

where X_{bound} is the dry basis moisture content at equilibrium. This value was determined by using the Oswin law:

$$X_{bound} = A\left[\frac{a_w}{(1-a_w)}\right]^B \quad (5)$$

being a_w the room relative humidity (0.7), while A e B are two parameters extrapolated by fitting absorption isotherms with Oswin law. In this research, the absorption isotherms, at different temperatures, of a similar product to salami, were used (Palatoglu *et al*., 2011):

$$A = 129028\exp^{-0.033T} \quad (6)$$

$$B = 0.1199\exp^{0.0053T} \quad (7)$$

where T is the temperature (K).

Model was validated by comparing dry basis moisture content, numerically and experimentally determined on salami after 12 an 24 days of ripening at 75% of relative humidity.

Storage model

For the model of salami storage in waterproof packaging, the same software geometry and physical parameters of the salami (D_{H2O}) used for the ripening model were considered.

The model considers both diffusion phenomena inside the salami and exchange phenomena (evaporation and condensation) between product and headspace. The total water mass of the salami/air system was imposed constant.

Even in this case, the phenomenon of mass transfer is governed by Fick's law.

The initial and boundary conditions are:

- initial moisture concentration (C_{in}) was considered constant in space and defined as follows:

$$C_{inS} = \left(\frac{M_{H2O}}{PM_{H2O} \cdot V_s}\right) \rightarrow C_{inS} = \left(\frac{X_{inS} \cdot \rho_s}{PM_{H2O}}\right) \quad (8)$$

where X_{inS} is the initial dry basis moisture content (experimental determination: 0.97 $kgkg^{-1}$);

- on the interface between the surface of the salami and headspace, a flux condition (N_S [$molm^{-2}s^{-1}$]), as function of the partial pressure, was imposed:

$$N_S = k_{ex}\left(C_{\varphi_{air}} - C_{aw_{air}}\right) \quad (9)$$

where:

$$C_{\varphi_{air}} = \left(\frac{X_{\varphi_{air}} \cdot \rho_{air}}{PM_{H2O}}\right): \quad (10)$$

moisture concentration of the air/water vapour mixture;

$$X_{\varphi_{air}} = \left(\frac{PM_{H2O}}{PM_{air}}\right) \cdot \left(\frac{\varphi_{air} \cdot P_{airSat}}{P_{atm} - \varphi_{air} \cdot P_{airSat}}\right): \quad (11)$$

moisture content in the air/water vapour mixture (Mujumdar and Menon, 1995);

$$C_{aw_{air}} = \left(\frac{X_{aw_{air}} \cdot \rho_{air}}{PM_{H2O}} \right);$$

moisture concentration of the air near to salami; (12)

$$X_{aw_{air}} = \left(\frac{PM_{H2O}}{PM_{air}} \right) \cdot \left(\frac{aw_{air} \cdot P_{airSat}}{P_{atm} - aw_{air} \cdot P_{airSat}} \right);$$

moisture content in the air near to salami (Mujumdar and Menon, 1995); (13)

$$\rho_{air} = \left(\frac{P_{atm} \cdot PM_{air}}{RT} \right);$$ air density [kgm^{-3}]; (14)

P_{atm}: atmospheric pressure [1E+5 Pa];
PM_{air}: air molecular weight [28.84 gmol^{-1}];
R: gas constant [8.314 JK^{-1}mo^{-1}];
T: temperature [K];

$$P_{airSat} = \left(10^{\left(8.07131 - \frac{1730.63}{233.426+T}\right)} \cdot \frac{P_{atm}}{760} \right);$$

saturation pressure of water vapour in air as function of temperature (August-Antoine, 1888) [Pa]; (15)

$$\varphi_{air} = \frac{P_{air}}{P_{airSat}};$$ relative humidity of air/water vapour mixture; (16)

$$P_{air} = \frac{M_{air} \cdot RT}{PM_{H20} \cdot V_{air}};$$ partial pressure of water vapour [Pa]; (17)

V_{air}: headspace volume [m^3];

$$M_{air} = (M_{Tot} - M_S - M_{Lq});$$

water mass in the headspace [kg] calculated considering mass conservation equation; (18)

$$M_{Tot} = M_{Sd} \cdot X_{in};$$ total water mass in the system [kg]; (19)

$$M_{Sd} = V_s \cdot \rho_s;$$ dry salami mass [kg]; (20)

$$V_s = \left(r^2 \pi L \right);$$

salami volume (r: salami radius, L:salami lengh) [m^3]; (21)

$$M_S = (\bar{\rho}_{H2OS} \cdot V_s);$$ water mass in salami [kg]; (22)

$$\bar{\rho}_{H2OS} = \bar{C} \cdot PM_{H2O};$$

mean water density as function of mean water concentration [kgm^{-3}]; (23)

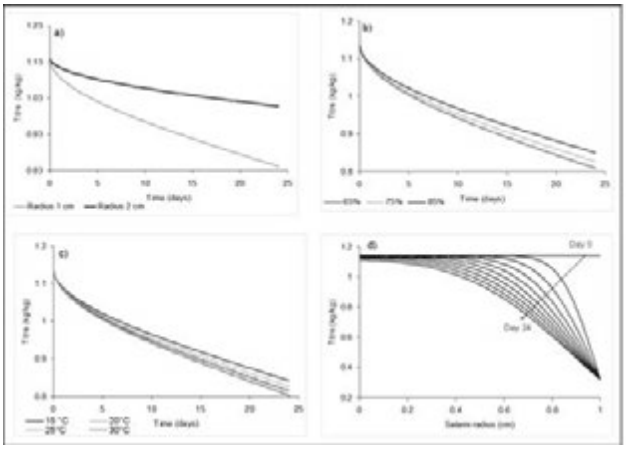

Figure 1. Mean dry basis titres of water, determined numerically, as function of salami radius (a), humidity (b), temperature (c) and position inside of salami (c).

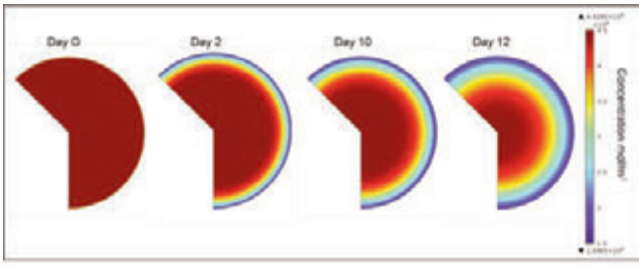

Figure 2. Simulated moisture concentration inside of a salami characterized by a radius of 1 cm, for 12 day of ripening.

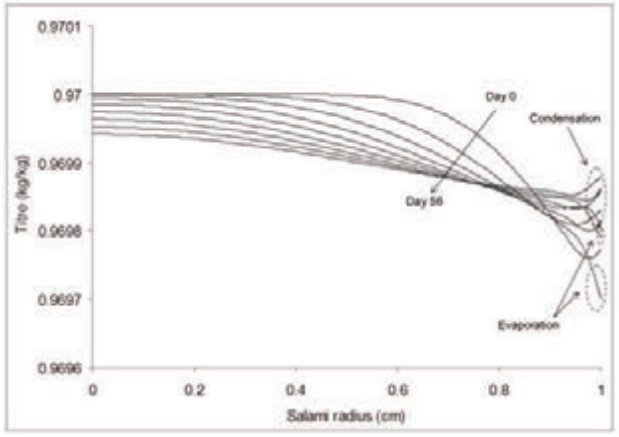

Figure 3. Dry basis titre of water as function of storage time and position inside of salami.

$$\frac{dM_{Lq}}{dt} = Fc - Fe$$

water mass conservation equation as function of evaporation and condensation phenomenon [kg]; (24)

$$Fc = Kc \cdot (\varphi_{air} - 1) \cdot \left(\frac{M_{air}}{M_{Tot}}\right) \cdot \overline{A}$$

mass flow of condensing water (when air/water vapour humidity is greater or equal to 1) [kgs^{-1}]; (25)

$$Fe = Ke \cdot (1 - \varphi_{air}) \cdot \left(\frac{M_{Lq}}{M_{Tot}}\right) \cdot \overline{A}$$

mass flow of evaporating water (when air/water vapour humidity is less than 1) [kgs^{-1}]; (26)

$$\overline{A} = L\pi \cdot (r + r_c)$$

mean exchange area (r_c: packaging salami); (27)
Kc: condensation parameter [1E-3 kgs^{-1}m^{-2}];
Ke: evaporation parameter [1E-3 kgs^{-1}m^{-2}];

$$aw_{air} = \left(\frac{\left(\frac{X_{H2OS}}{A}\right)^{\left(\frac{1}{B}\right)}}{1 - \left(\frac{X_{H2OS}}{A}\right)^{\left(\frac{1}{B}\right)}} \right)$$

relative humidity of air near to salami by using Oswin law; (28)

$$X_{H2OS} = \left(\frac{\overline{C}_c \cdot PM_{H2O}}{\rho_s}\right)$$

dry basis moisture content of salami surface as function of mean water concentration determined on the exchange surface ($\overline{C}_c$). (29)

Model was validated by comparing the dry basis moisture content, numerically and experimentally determined on salami after 56 days of storage in waterproof packaging.

Results

To validate the ripening model, experimental and calculated values of dry basis moisture content determined after 12 and 24 days of ripening at 75% of humidity, were compared. Experimentally values of 0.978±0.072 and 0.841±0.049 were found, respectively for 12 and 24 days of ripening, while values of 0.962 and 0.835 were determined by model. The simulated and experimental data appear to be in good agreement. This result shows that the numerical model is able to reproduce the mass transfer phenomenon inside of salami.

To evaluate the effect of salami size on the mass transfer, the mean moisture con content on dry basis, determined numerically, for a salami of radius varying from 1 to 2 cm, are reported in Figure 1a. It can be see that the salami size affects significantly the mass transfer, in fact, doubling the salami radius, the final value of dry basis moisture content decreases of about 0.2. This aspect highlights that the assessment of size is an important aspect for the ripening stage.

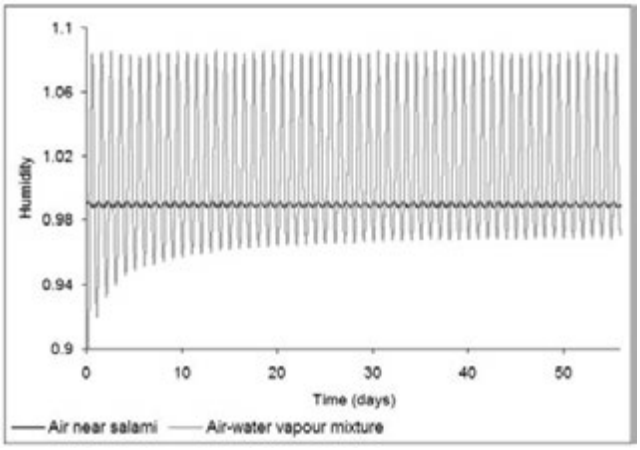

Figure 4. Trend of air humidity near to salami and of air-water vapour mixture humidity, during 56 days of storage.

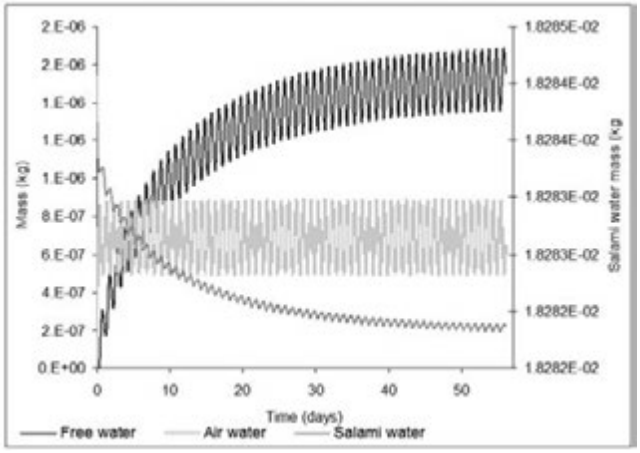

Figure 5. Mass of water free (available for evaporation and condensation), water in packaging air and in salami.

The mean moisture contents on dry basis, for a relative humidity of 65, 75 and 85% are reported in Figure 1b. The humidity not affects significantly the mass transfer, in fact it is possible observe a moisture content decrease of about 0.05, passing from a humidity of 0.65 to 0.85 %. To evaluate the effect of ripening temperature on the mass transfer, the mean dry basis moisture content, determined numerically, for a ripening temperature of 15, 20, 25 and 30°C, are reported in Figure 1c. Passing from 15 to 30 °C, only a moisture content decrease of 0.05 was observed, therefore it possible to assert, also in this case, that temperature not affect significantly the mass transfer inside of salami.

Dry basis moisture content as function of ripening time and position inside of salami is reported in Figure 1d. In the salami centre (r=0), moisture content is unchanged, while on the surface, is in equilibrium with the environment. A moisture content decrease along the salami radius was observed.

In figure 2 the simulated moisture concentration inside of a salami characterized by a radius of 1cm, during 12 days of ripening is reported. It can be seen that after 12 days of ripening, the moisture inside the salami is not uniformly placed, there is a considerable difference

between centre (about 15000 mol m^{-3}) and surface (about 45000 mol m^{-3}). To validate the storage model, experimental and calculated values of moisture content on dry basis determined after 56 days of storage in waterproof packaging at temperature variable from 20 to 30°C 75% of humidity, were compared.

Experimentally, a slightly lower moisture content (0.95) than the initial one (0.97) was obtained. By using the model, after 56 days of storage, the moisture content value decreases of only about 0.01 (final value of about 0.96). This result shows that the numerical model is able to reproduce the mass transfer, evaporation and condensation phenomena during the storage of packaged salami.

Room temperature variation produces condensation and evaporation phenomena on the salami surface causing small oscillations. In fact the water can not diffuse out of salami because the waterproof packaging makes closed the system.

Dry basis moisture content as function of storage time and position inside of salami is reported in Figure 3. It can be seen that the moisture content variation is vary small and that in the salami centre (r=0), is unchanged, while on the surface (r=1), evaporation and condensation phenomena causing more variation. Particularly, when temperature increases, water evaporates and moisture content decreases, while when temperature decrease, water condenses and moisture content increases.

Trend of air humidity near to salami and of air-water vapour mixture humidity, during 56 days of storage, are reported in figure 4. Air humidity is characterized by more small variation (from 0.991 to 0.988), compared to air-water vapour mixture humidity (from 0.94 to 1.08). These trends, due to temperature oscillation, control evaporation and condensation phenomena, in fact when air-water vapour mixture humidity is greater than 1, water free condenses, on the contrary, when it is less or equal to 1, water free evaporates.

Mass changes of liquid water (available for evaporation and condensation), in packaging air and inside of salami, during storage, are shown in figure 5. According to figure 3, it can be seen that salami water mass, decreases very little during the storage. This reduction causes a free water increase during about the first twenty days of storage. In fact the water moves from salami to packaging air until the air is saturated.

Conclusions

The numerical models allowed to study the mass transfer of the water inside of salami, during the ripening and storage phases, with a detail unreachable by any experimental technique.

The results of the models, in integral form, are in good agreement with those experimentally observed.

The model clarify the mass diffusion mechanism that move moisture from the inner part of salami to its surface: whatever are the environmental conditions, the moisture in the headspace reach an equilibrium with the moisture inside the meat. During the conservation the moisture concentration tends, by mass diffusion, to became uniform in space, flowing from the centre to the periphery. As the temperature decrease, the head-space air became over-saturated releasing some water. This liquid state water drops on the salami surface, significantly compromising the conservation conditions. During the conservation time, every temperature oscillation activates this water movement mechanism.

Ultimately the numerical model represents a powerful and versatile industrial instrument and being parametric, wide spanning data input regarding time, ripening and storage temperatures, size and type of sausage etc., can be tested.

References

Baldini P., Cantoni E., Colla F., Diaferia C., Gabba L., Spotti E., Marchelli R., Dossena A., Virgili E., Sforza S., Tenca P., Mangia A., Jordano R., Lopez M.C., Medina L., Coudurier S., Oddou S., Solignat G. 2000. Dry sausages ripening: influence of thermohygrometric conditions on microbiological, chemical and physico-chemical characteristics. Food Res Int, 33:161-170.

Bertolini M., Ferretti G., Grassi A., Montanari R. 2006. Seasoning process design optimization for an ascending flow ripening chamber. J. Food Eng, 77:529-538.

Campbell-Platt G., Cook P.E. 1995. Fermented meats. Glasgow: Blackie Academic and Professional.

Costa-Corredor A., Pakowski Z., Lenczewski T., Gou P. 2010. Simulation of simultaneous water and salt diffusion in dry fermented sausages by the Stefan–Maxwell equation. J. Food Eng, 97:311-318.

Floury J., Le Bail A., Pham Q.T. 2008. A three-dimensional numerical simulation of the osmotic dehydration of mango and effect of freezing on the mass transfer rates. J. Food Eng, 85:1-11.

Graiver N., Pinotti A., Califano A., Zaritzky N. 2006. Diffusion of sodium chloride in pork tissue. J. Food Eng, 77:910-918.

Grassi A., Montanari R. 2005. Simulation of the thermodynamic patterns in an ascending flow ripening chamber. J. Food Eng, 68:13-123.

Hansen C.L., van der Berg F., Ringgaard S., Stodkilde-Jorgensen H., Karlsson A.H. 2008. Diffusion of NaCl in meat studied by 1H and 23Na magnetic resonance imaging. Meat Sci, 80:851–856.

Lemus-Mondaca R.A., Zambra C.E., Vega-Gálvez A., Moraga N.O. 2013. Coupled 3D heat and mass transfer model for numerical analysis of drying process in papaya slices. J. Food Eng, 116:109-117.

Mirade P-S. 2008. Computational fluid dynamics (CFD) modelling applied to the ripening of fermented food products: Basics and advances. Trends Food Sci Tech, 19:472-481.

Mujumdar. A.S., Menon. A.S., 1995. Drying of Solids, pp. 1-46, in A.S. Mujumdar (Ed.) Handbook of Industrial Drying, 2nd Edition, Marcel Dekker, New York.

Norton T., Sun D.W. 2006. Computational fluid dynamics (CFD) e an effective and efficient design and analysis tool for the food industry: a review. Trends Food Sci Tech, 17:600-620.

Polatoğlu B., Vildan Beşe A., Kaya M. & Aktaş N. 2011. Moisture adsorption isotherms and thermodynamics properties of sucuk (Turkish dry-fermented sausage). Food Bioprod Process, 89:449-456.

Rizzi A. 2003. Development of a numerical model for the fluid dynamic simulation of an ascending flow ripening chamber. J. Food Eng, 58:151–171.

Sabadini E., Carvalho B.C., do A. Sobral P.J., Hubinger M.D. 1998. Mass transfer and diffusion coefficient determination in the wet and dry salting of meat. Drying Tech, 16:2095–2115.

Sakin M., Kaymak-Ertekin F., Ilicali C. 2007. Simultaneous heat and mass transfer simulation applied to convective oven cup cake baking. J. Food Eng, 83:463–474.

Scott G., Richardson P. 1997. The application of computational fluid dynamics in the food industry. Trends Food Sci Tech, 8:119-124.

Smale N. J., Moureh J., Cortella G. 2006. A review of numerical models of airflow in refrigerated food applications. Int J. Refr, 29:911-930.

Toldrá F. 2006. Meat fermentation In Y. H. Hui, E. Castell-Perez, L. M. Cunha, I. Guerrero-Lagarreta, H. H. Liang, Y. M. Lo, D. L. Marshall, W. K. Nip, F. Shahidi, F. Sherkat, R. J. Winger, & K. L. Yam (Eds.), Handbook of food science, technology and engineering, Florida, USA: CRC Press.

Toldrá F., Nip W. K., Hui Y. H. 2007. Dry-fermented sausages: An overview. In F. Toldrá (Ed.), Handbook of fermented meat and poultry. Iowa, USA: Blackwell Publishing.

Unal B.S., Erdog˘du F., Ekiz H.I., Ozdemir Y. 2004. Experimental theory, fundamentals and mathematical evaluation of phosphate diffusion in meats. J. Food Eng, 65:263–272.

Verboven P., Flick D., Nicolaı B.M. Alvarez G. 2006. Modelling transport phenomena in refrigerated food bulks, packages and stacks: basics and advances Int J. Refr, 29:985-997.

Wang L., Sun D.W. 2003. Recent developments in numerical modelling of heating and cooling processes in the food industry e a review. Trends Food Sci Tech,14:408-423.

Xia B., Sun D.W. 2002. Applications of computational fluid dynamics (CFD) in the food industry: a review. Comput Electron Agric, 34:5-24.

Zanardi E., Ghidini S., Conter M., Ianieri A. 2010. Mineral composition of Italian salami and effect of NaCl partial replacement on compositional, physico-chemical and sensory parameters. Meat Sci, 86:742–747.

Zeuthen P. 1995. Historical aspects of meat fermentations. In G. Campbell-Platt, & P. E. Cook (Eds.), Fermented meats. Glasgow, UK: Blackie Academic & Professional.

Mechanical grading in *PGI Tropea red onion* post harvest operations

Bruno Bernardi, Giuseppe Zimbalatti, Andrea Rosario Proto, Souraya Benalia, Antonio Fazari, Paola Callea

University Mediterranea of Reggio Calabria, Department of AGRARIA, Reggio Calabria, Italy

Abstract

The growing interest expressed by consumers toward food products quality as well as toward their linkage to the territory, has led producers to fit to the continuous rising demand for "typical products", and to look for new and more efficient production and marketing strategies. An emblematic case is represented by Tropea red onion that, as a typical product, plays an important role in economical and rural development of the territory to which it is linked. The organoleptic features offered by "Tropea Red Onion", PGI certified (Calabria), have to be associated as well to the quality of services that accompanies its processing. Technology application in post-harvest operations, has certainly contributed to make faster and less tiring all processing tasks. The main problem related to the mechanization of Tropea red onion post-harvest operations lies in the removal of the various layers of the external tunic, making it impossible for optical or electronic grader to achieve this task in a satisfactory way since the sensors are not able yet to separate the "bulb" from its involucre. In this context, the current study aims to assess the productivity of three different machines used for round Tropea red onion grading, and determine their work efficiency. The carried out analysis highlighted the ability of the studied machines to ensure a high work capacity, while maintaining a high level of precision during calibration process. Such precision allows to decrease laborer employment and increase processing chain speed, rising as well the annual use of the machines, allowing consequently processing cost savings. For a more profitable employment of such graders, it is, however, necessary from one hand, to properly form the technicians responsible of processing plants management, and from the other hand, to be able to take advantage of a technical assistance network, able to serve users in a short time.

Correspondence: Bruno Bernardi, University Mediterranea of Reggio Calabria, Department of AGRARIA, Località Feo di Vito, 89122 Reggio Calabria, Italy.
E-mail: bruno.bernardi@unirc.it

Key words: Mechanical grading, PGI Tropea red onion, productivity, working capacity.

Authors have contributed equally to present work.

Journal of Agricultural Engineering 2013; XLIV(s1):e63
doi:10.4081/jae.2013.(s1):e63

Introduction

Nowadays, the modern agri-food chain requires an increasingly advanced planning that aims to improve and increment productions qualitative level (Cavalli *et al.*, 2011). The added value associated to the "territory" of some products, such as the Red Onion of Tropea (Calabria- Southern Italy), can therefore assume a great importance and contribute considerably to rural development and agricultural diversification (Gulisano *et al.*, 2000). In addition, organoleptic features provided by this product that has PGI label (EC, 2008), should be connected as well to the quality of services that accompanies its processing and marketing (Fafani *et al*., 1997). Such scenario should lead the agri-food industries to strengthen their productive systems and modify the current production, distribution and marketing settings (Fabbris, 1989), that are still not suitable to supply markets of typical products. Consumers' expectations and consequently global markets require standardized and homogeneous products with quality and size tolerances tending to zero. Moreover, productions should be characterized by a continuity of supply that have a strict compliance with delivery time, as well as bargaining forms for consistent provisions programmable for the medium and long terms. Regardless intrinsic qualitative features that provides the red onion of Tropea (nutritional, organoleptic and sanitary ones), the optimization of some post-harvest operations such as those related to its grading can certainly contribute to make faster and less burdensome this processing phase. Diverse types of machines and plants are available to carry out this operation (Amirante *et al.*, 1988; Baraldi *et al.*, 1998; Peri, 1986; Oberti *et al.*, 2001; Mignani, 2001). But, the main problem concerns the removal of the external layers of the "protection coat", which make difficult to employ optical or electronic graders in a satisfactory way. In this context, the present experimental study has been achieved in order to analyze one of the most important post-harvest processing phases, which is grading, and assess work efficiency of Tropea red onion mechanical graders, considering productive outputs and highlighting critic points and optimization possibilities of the employed machines.

Materials and methods

Experimental trials have been carried out in two firms, indicated in this paper as A and B, among the most advanced technologically within Tropea red onion production area. Processing chain in these firms is almost standardized. Grading, that is products sorting according to their size (Menesatti, 2000; Ortiz-Cañavate *et al.*, 2002), begins with manual sorting of the bulbs and the subsequent "tailing" that consists in the removal of the dried leaves, also known as tail, at about one centimeter from the bulb. The process then, continues by placing the onions in the graders, to which follow weighing and packing operations. Grading in firm A is achieved by mean of two different machines: the first one (Figure 1) presents three processing lines,

composed of opposite and divergent pairs of counter-rotating endless belts. The bulbs move on between the rollers, whose difference creates a growing gap through which the onions fall according to their size, inside of hoppers, from where they are then sent in apposite bins.

The second machine, however, is a continuous cycle rollers type composed of a sequence of forced rotation bobbins pairs that create a gap equal to onions size between two consecutive pairs, thanks to the inclination they undergo (Figure 2).

Bobbins system ensure the continuous and independent adjustment of grading size in each separate section, enclosing so, the largest dimensional range, while the forced rotation of the bobbins ensure the ideal positioning that enable grading of each single product.

Firm B, however, employs a grade screen sizer (Figure 3): a conveyer belt carries the products to the sorting zone, where metallic cylinders with holes of diverse dimensions are set up. While vibrating, they grade the onions according to their size, and then, unload the processed products in the appropriate bins.

The conducted trials, aimed to determine grading operations accuracy of the considered processing lines. A series of bulbs with different size have been selected to verify the influence of the product size on the precision. The bulbs have been numerated, then, the maximum diameter of the transversal section of each one has been measured manually with a Vernier caliper. Such diameter is commonly known as maximum "equatorial diameter", although the largest transversal section of the bulb is rarely encountered in the median zone. Subsequently, onions underwent a normal grading cycle in order to assess machines working efficiency. Moreover, working time as well as graders performances have been analyzed, according to C.I.O.S.T.A. ranking requirements (Bolli *et al*., 1987), considering machines starting as the beginning of trials, the final point, however, corresponded to the end of products unload.

Results and discussion

Firm A

As reported previously, in this firm, there are two onions graders, the first one with inclined belts, and the second one with rollers, having the same four dimensional classes or grading issues (30-50; 51-70; 71-90; > 90). Graphic 1 sums up percentages of onions that fell in the different dimensional classes, in both graders of firm A. It provides a first indication about the size of processed onions in this firm, which is over 70 mm for almost all samples.

Figure 1. Onion grader with inclined belts.

Figure 2. Onion grader with rollers.

Graphic 2 reports, however, the average size of graded onions samples, as well as the respective standard errors. It can be observed that onions appertaining to lower dimensional classes are hardly identified by both graders, while, onions that belong to the most frequent commercial classes, that is, equal or more than 70 mm are graded with more accuracy independently from grader type.

According to Graphic 3, the highest graders efficiency is reached when values obtained from the ratio between not correctly graded onions and total graded one for each dimensional class, are closed to zero. Explaining so, the capability of the grader to recognize the highest number of onions appertaining to a specific dimensional class. In general, a high accuracy is recorded for both graders, even if the most reliable one was the grader with inclined belts. It has to be noted that for extreme calibres, there was some difficulties to recognize the correct issue, however, the highest accuracy was obtained for the dimensional class of 71-90 mm.

Working time measurements achieved during trials for both graders of firm A are shown in Table 1. Reference timing unit corresponded to the amount of minutes required to grade one hundred kilograms of the product. Operative time could be calculated as well.

These data, show that the lowest operative working time (TO), equal to 3.20 min/100 kg, was recorded for onion grader with inclined belts,

Figure 3. Onions grade screen sizer (firm B).

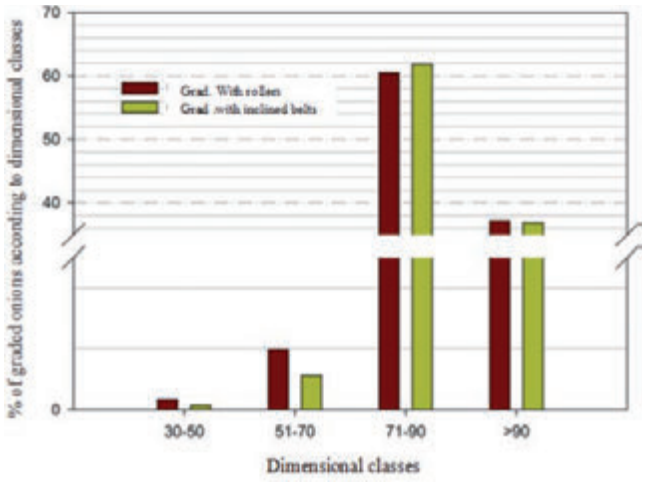

Graphic 1. Percentage of graded onions according to the different dimensional classes in firm A.

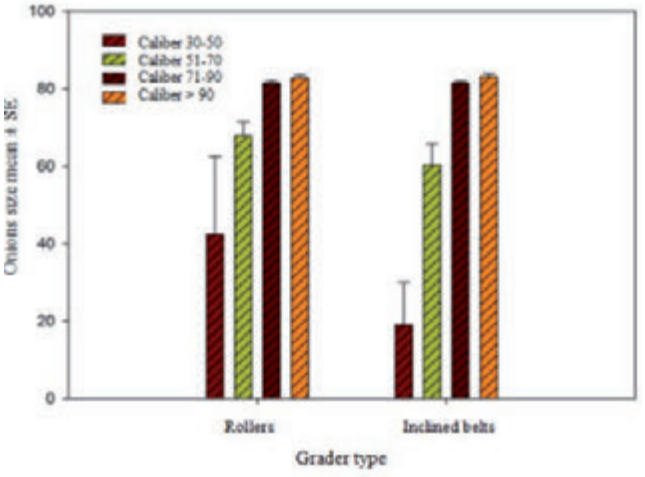

Graphic 2. Onions size mean ± standard error for each dimensional class according to grader type.

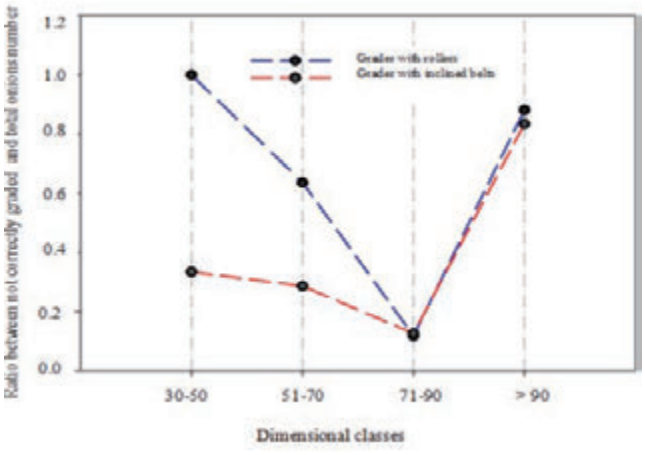

Graphic 3. Graders working efficiency in firm A.

however, the grader with rollers presented almost the double value (5.43 min/100 kg). Idle time has not been registered, showing so the good functioning of both graders and the ability of laborers charged of processing. From working time values, it was possible to obtain working capacity and productivity for the analyzed graders, whose values are reported in Table 2, taking into account the employment of three processing units for each machine. Operative working capacity of the grader with inclined belts according to TO had a value of 1,800 kg/h while operative working productivity (PO) had a value of 600 kilograms per hour per operator (kg/hop). For the grader with rollers, these parameters assumed respectively the values of 1,040 kg/h for working capacity and 349 kg/hop for operative working. Therefore, it clearly emerges that the grader with inclined belts is better than the other one in terms of both working capacity and productivity.

Firm B

In this firm, there are six dimensional classes for onions grading, divided as follows: 25/40, 40/50, 50/60, 60/70, 70/80, 80/100. Graphics 4 and 5 indicate that the greatest number of graded onions appertained to dimensional classes having the caliber between 60 and 80 mm. Furthermore, product size differences between the two firms can be observed, processed onions in firm B being smaller.

Graphic 6 reports however the onions grade screen sizer efficiency. A high accuracy is observed even in this case. But differently from firm A, here, there are some difficulties for the recognition of the correct caliber of big size onions, however, the highest grading precision is obtained for the smallest dimensional class 25-50 mm.

Table 3 show the recorded effective and operative working times during onions grading by mean of the screen sizer.

These data, reveal that operative working time (TO) of the last grader, equal to 6.25 min/100 kg, is the highest one. Indeed, although still technologically valid, it represents a less recent model than the previous two graders. However, There were not idle times, highlighting once more the good functioning of the machine and the ability of laborers that accompany graders. From time values, it was therefore possible to obtain work capacity and productivity of the grade screen sizer, whose values are reported in Table 4, considering the employment of three working units. Operative working capacity (according to TO) had a value of 935 kg/h while, operative working productivity (PO) was equal to 311 kg/hop.

Conclusions

The conducted analysis on onions post-harvest operations, highlighted that the employed graders are able to ensure a high working capacity, maintaining a notable accuracy during grading and weighing operations. Such precision allows to reduce man power employment and make faster processing chain, engendering machines annual utilization increase and processing costs saving. It is to be noticed that the employment of two processing lines in firm A is excessive, given that the grader with inclined belts is enough for achieving rapidly and accurately this operation. Obtained data support therefore the managerial decision to substitute the grader with rollers by more graders with inclined belts. First models of optical grading machines start to be employed, however, these one do not represent an easy solution for onion grading, because external protective coats could highly interfere

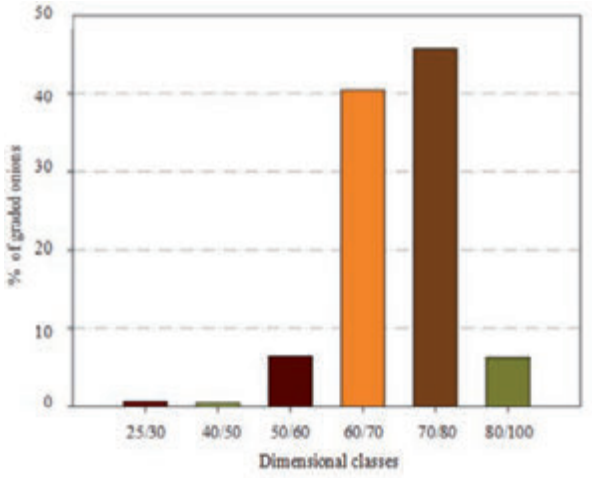

Graphic 4. Percentage of graded onions according to the different dimensional classes in firm B.

Table 1. Graders average working time in firm A.

Grader type	TE [min/100 kg]	TA [min/100 kg]			TO [min/100 kg]	TM [min/100 kg]	
		TAS	TAC	TOTAL		TME	TMI
Inclined belts	3.00	0.20	-	0.20	3.20	-	-
Rollers	5.13	0.30	-	0.30	5.43	-	-

TE: Effective working time; TA: Accessory time; TAS: Accessory time for unloading; TAC: Accessory time for handling; TO: Operative working time; TME: Evitable idle time; TMI: Inevitable idle time.

Table 2. Working capacity and productivity of the employed graders in firm A.

Grader	Working capacity				Working productivity
	Referred to TE		Referred to TO		Referred to TO
	[min/100 kg]	[100 kg /h]	[min/100 kg]	[100 kg /h]	[100 kg /hop]
Inclined belt	3	20	3.20	18	6
Rollers	5.13	11.50	5.43	10.4	3.49

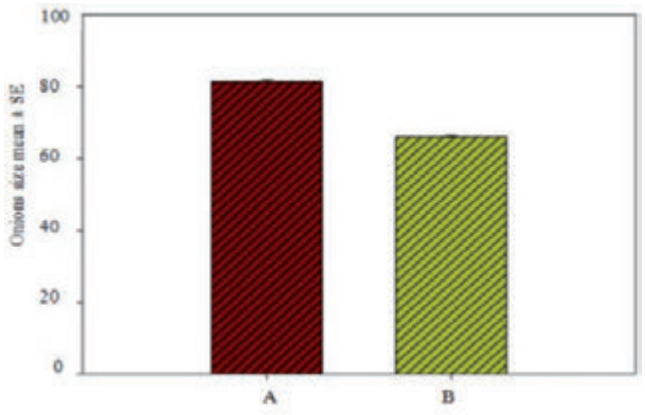

Graphic 5. Dimensional differences of the processed onions between firms *A* and *B*.

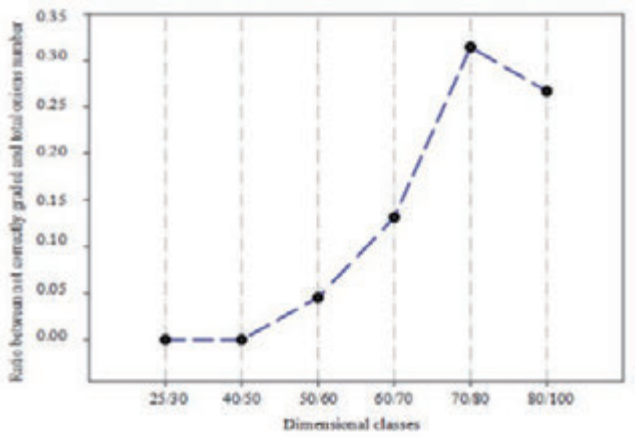

Graphic 6. Working efficiency of the onions grade screen sizer used in form B.

Table 3. Average working times of the onions grade screen sizer used in firm B.

Grader	TE [min/100 kg]	TA [min/100 kg]			TO [min/100 kg]	TM [min/100 kg]	
		TAS	TAC	TOTAL		TME	TMI
Screen sizer	5.35	0.25	0.25	0.50	6.25	-	-

Table 4. Working capacity and productivity of the onions grade screen sizer used in firm B.

Grader	Working capacity				Working productivity
	Referred to TE		Referred to TO		Referred to TO
	[min/100 kg]	[100 kg /h]	[min/100 kg]	[100 kg /h]	[100 kg /hop]
Screen sizer	5.35	10.74	6.25	9.35	3.11

reception and transmission sensors. For these reasons, optical systems do not respect perfectly accuracy threshold declared by their constructors, although they are among the most advanced and accurate systems. Competition capability recovery passes through the valorization of typical products, accompanied by the rigorous and complete application of high quality standards, excellent presentations and various assortments. The introduction of graders such as those analyzed in this study, can certainly contribute for the accomplishment of the above cited objectives, since they present suitable features for post-harvest processes optimization.

Acknowledgement

This work is part of the ongoing project Dolce Rossa supported by the APQ "Scientific Research and Technological Innovation" (Az. 2 and Az. 3) financed by Calabria Region-Department of Research, European Community, Italian Ministry of Economic Development (MISE) and Italian Ministry of Research Science and Technology (MIUR).

References

Amirante P., Cappiello M., Di Renzo G.C. 1988. Meccanizzazione delle operazioni post-raccolta come cerniera tra produzione e commercializzazione. IV Convegno Nazionale di Genio Rurale, Porto Conte - Alghero, Maggio.

Baraldi E., Ragni L. 1998. La moderna tecnologia per la meccanizzazione dei processi post-raccolta. L'Informatore Agrario. 28: 25-48.

Bolli P., Scotton M. 1987. Lineamenti di tecnica della meccanizzazione agricola. 1a Edizione. Edagricole, Bologna, Italia. 221 pp.

Cavalli R., Monarca D. 2011. Lo stato e le prospettive della ricerca nel settore AGR/09. Convegno di Medio Termine dell'Associazione Italiana di Ingegneria Agraria. Belgirate, 22-24 settembre 2011.

EC, 2008. Regolamento (CE) N. 284/2008 della commissione del 27 marzo 2008 recante iscrizione di alcune denominazioni nel registro delle denominazioni d'origine protette e delle indicazioni geografiche protette.

Fabbris L. 1989. Consumatore e mercato. Sperling & Kupfler Editori.

Fafani R., Sullace S. 1997. I consumi alimentari in Italia ed in Europa,

cambiamenti strutturali, convergenza e differenziazione. La questione agraria. n. 67.

Gulisano G., Privitera D. 2000. Strategies of marketing of a traditional vegetable product: the red onion in Tropea. Proc. XIVth Intrnational Symposium on Horticultural Economics, 12-15 September, Acta Horticulturae, ISHS.

Menesatti P. 2000. Misura strumentale della qualità in ortofrutticoltura. Italus Hortus. 2: 12-19.

Mignani I. 2001. Gli aspetti fisiologici delle tecnologie non distruttive. Atti del convegno: La qualità dei prodotti ortofrutticoli: stato dell'arte sull'uso delle tecnologie non distruttive, MACFRUT, Cesena, maggio.

Oberti R., Guidetti R., Naldi E. 2001. Progettazione di un sistema di calibrazione ottico a basso costo per prodotti ortofrutticoli. Congresso A.I.I.A., Vieste (FG), settembre.

Ortiz-Cañavate J., Moreda G., Homer I., Morabito S., Ruiz-Altisent M. 2002. Fruit size determination by a new optical sensor. International Conference on Agricultural Engineering (AgEng), Budapest, Hungary.

Peri C. 1986. Nuove frontiere della tecnologia alimentare: le mild tecnologies", progetto finalizzato IPRA del CNR. Atti del convegno "Nuove frontiere della tecnologia alimentare: le mild tecnologies", Roma, novembre.

Technical and economic evaluation of maceration of red grapes for production everyday wine

F. Pezzi,[1] C. Caprara,[2] D. Friso,[3] B. Ranieri[4]

[1]Department of Agricultural and Food Sciences, University of Bologna, Italy; [2]Department of Agricultural Sciences, University of Bologna, Italy; [3]Department of Land, Environment, Agriculture and Forestry - TeS.A.F., University of Padova, Italy; [4]Winery of Forlì and Predappio, Italy

Abstract

For red wines, the phase of maceration is fundamental as it affects important features such as colour, aroma and flavour. For wines for everyday consumption these features must provide an easily drinkable product with a good quality basis that is consistent over time. In recent years two methods of maceration seem to guarantee these objectives better than others, while also allowing good work organization and automation: hot maceration and pneumo-carbonic pumping over. These techniques have been evaluated in a large winery, defining their production potential, labour requirements, energy consumptions and economic costs. Chemical and sensory evaluations were carried out on wines produced from grapes with the same characteristics.

Introduction

Although consumer attention is increasingly directed towards top of the range wines, most of the wine drunk in this country and in other parts of the world is table wine for everyday use in the home.

These everyday wines, while falling into a limited price range, must be easily drinkable and with a good basic quality that remains constant over time.

The most important quality aspects for red wines regard the colour, flavour and aromas. A vinification phase that can have a significant influence on these characteristics is the maceration (Arfelli *et al.* 2001; Lambri and Silva 2004).

Correspondence: Fabio Pezzi, Department of Agricultural and Food Sciences, University of Bologna, Via G. Fanin 50, 40127 Bologna, Italy.
Tel. +39.051.2096187.
E-mail: fabio.pezzi@unibo.it

Key words: grape maceration, energy consumptions, economic costs

Contributions: the authors contributed equally.

Conflict of interests: the authors declare no potential conflict of interests.

Journal of Agricultural Engineering 2013; XLIV(s1):e64
doi:10.4081/jae.2013.(s1):e64

In the last years two methods of maceration appear to guarantee the quality aspects of wines better than the others, while also allowing a good organization and automation of the work: hot maceration and pneumo-carbonic pumping over (Amati, 1985; Celotti and Rebecca 1998; Celotti and Franceschi 2004)

The objective of this research was to evaluate these two techniques in a large winery, analysing the production potential, labour requirements, energy consumption and economic costs.

Chemical and sensorial evaluations were also conducted of the wines obtained, which were produced from grapes with the same characteristics.

Materials and methods

The vinification trials were conducted at the Forlì-Predappio Winery (FC) during the 2012 grape harvest.

The plant productivity and energy consumptions were evaluated during the entire wine-making process of 2012, while the product quality was evaluated on volumes of around 1000 hl of wine obtained from Sangiovese grapes with homogeneous sanitary and chemical characteristics.

The plants were:

- Hot macerator constituted by the BioThermo/Cooler System of Della Toffola S.p.A (BioThermo/Cooler System Guide).
- Pneumo-carbonic fermentation tanks based on the Ganimede Method of Ganimede S.r.l. (Metodo Ganimede Guide).

Della Toffola hot macerator

The hot maceration plant used in the winery forms a continuous process as shown in Figure 1.

After the crushing/stemming, the crushed grapes are treated with sulphur dioxide and then accumulated in a stopover tank (A) for an estimated time of approximately 60 min. In this tank the crushed grapes undergo enzymatic activity and continuous agitation for the homogenization of the mass.

The crushed grapes are then continuously withdrawn by a Monho pump to pass through the tube heat exchanger (B), which is fed with hot water at 93°C produced by the boiler (E), through which the product passes 18 times within 2 minutes.

The crushed grapes enter the exchanger at a temperature of about 25-27°C and exit at 80.5°C. The sharp rise in temperature is obtained not only with the contribution of the hot water but also by the reuse of a part of the hot must drained by the drum separator (C). This fraction of must is further heated inside the exchanger and is united to the crushed grapes on entry to increase the temperature and make the mass more fluid.

From the separator, the must not reused for the pre-heating of the crushed grapes is reunited with the pomace in a tank (D) equipped

with an agitator and placed under vacuum (-0.928 bar) by a liquid ring vacuum pump.

In this phase the product is flash cooled by the joint action of the vacuum and a heat exchanger (L) that acts as a steam condenser for the reintegration of the condensate.

The product exits the vat at a temperature of 45°C and is sent to a continuous drip-press (I) for the definitive separation of the pomace.

The extracted must is filtered by a rotating filter (H), cooled in the exchanger (G) and collected in the tank (F) where it is inoculated with selected yeasts, cooled for 4-5 days and maintained at a temperature of 20°C by indirect cooling with glycol.

The end product then undergoes a tangential filtration.

Ganimede fermentation tanks

Wine-making with the Ganimede plant is a discontinuous process that in the Forlì-Predappio winery is done with 7 tanks, four of which are of 74 m^3 and three of 184 m^3. As the tanks are used approximately 80% full, the useful capacity results as being 678 m^3 of crushed grapes that, considering a density of $_{\text{crushed grapes}}$=1090 kg m^{-3}, corresponds to a mass of 739 t.

The Ganimede process (Figure 2), after filling the vat with the crushed grapes, is based on the exploitation of the CO_2 freed by the fermentation. This is collected below the funnel-shaped diaphragm and as it leaks, gradually remixes the cap of pomace that has formed in the upper part of the mass (stage 1). At regular intervals, the opening of the by-pass rapidly releases the CO_2 upwards and causes the fall and complete immersion of the cap of pomace in the liquid mass (stage 2). The closing of the by-pass restarts the cycle with the stratification of the pomace in the upper part and the accumulation of CO_2 below the headspace (stage 4). During this sequence, the mass may be drained (délestage) with the complete extraction of the must, followed a few hours later by its reintroduction on the cap of pomace to accentuate the action of leaching and extraction (stage 3). In the controlled plant the délestage was realized twice per cycle.

At the end of maceration the product is extracted with a belt conveyor and sent by a series of screw conveyors to a dripper that partially separates the must then consigns the pomace to a membrane crusher-stemmer for a complete extraction.

This maceration process is also completed by a tangential filtration.

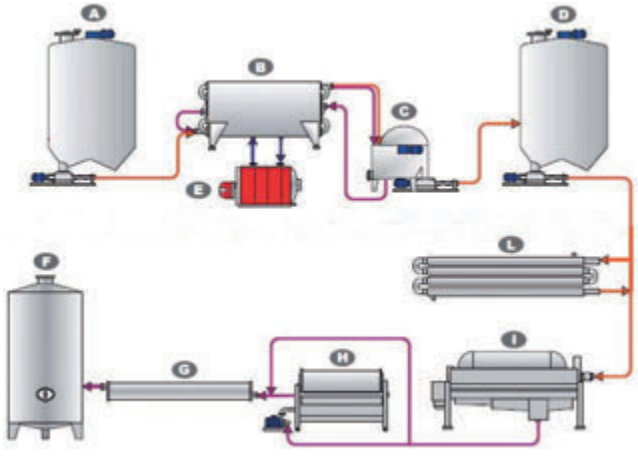

Figure 1. Flow chart of the thermal maceration plant. A: stopover tank; B: tube heat exchanger; C: drum separator; D: storage tank; E: boiler; F: fermentation tank; G: thermal exchanger; H: rotating filter; I: continuous drip-press; L: vacuum and heat exchanger.

Evaluation of the processes

The electricity and thermal consumption have been evaluated for both processes, considering the individual elements and their use for the execution of the operating cycles. The comparison of the two maceration techniques was only made between the characteristic elements of each plant, excluding the phases in common: crushing and stemming, plant loading, final tangential filtration and storage in tank.

An economic evaluation was done on the basis of the measured energy consumption and the parameters reported in Table 1 to obtain a unit cost of the process based on the productivity observed in the winery (ASAE Standards 2011).

The same elements were also used to extend the evaluation by hypothesizing different production levels.

A chemical analysis and sensorial analysis by means of the recognition test (triangle test, preference test and descriptors test) were conducted on the wines obtained.

Results

During the 2012 grape harvest, the Della Toffola hot maceration plant in the Forlì-Predappio winery was utilized for 22 days with a daily use of 20 h, and an hourly productivity of around 15 t h^{-1}.

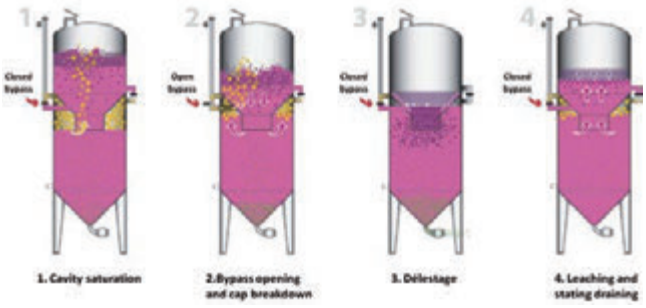

Figure 2. Stages of the maceration process in the Ganimede fermentation tank.

Table 1. Elements used for the economic evaluation.

Economic parameters	Hot maceration	Ganimede system
Market price – MP (€)	320000	825000
Residual value (%MP)	5	10
Max. economic life (years)	15	20
Plant use life (h)	5000	8000
Daily use (h day^{-1})	20	24
Interest rate (%)	5	5
Labor hours/hours of plant use	1.50	0.57
Annual maintenance:		
- labor (h)	70	50
- spare parts (€)	5000	2500
Wage (€ h^{-1}) 16 16		
Energy cost:		
- electricity (€ kWh^{-1})	0.08	0.08
- methane (€ m–3)	0.40	-

The Ganimede plant was instead used for 4 production cycles, each one lasting 6 days for a total of 24 days. Considering the overall capacity of the plant, the daily productivity is around 141 t.

Energy consumption

Figure 3 reports the electricity consumption on an hourly basis for the different phases of the Della Toffola hot maceration process, obtained from the sum of the individual elements utilized in the plant. The total electricity consumption amounts to 169.8 kWh, with a higher incidence in the phases of vacuum cooling (D-L), pressing (I) and filtering (H) that follow the central phase of hot maceration.

For the thermal consumptions linked to the hot maceration, with a flow of crushed grapes of 15 t/h, the parameters characterizing the process are:

$m_{crushed}$=15 t

$c_{crushed}$=0.86 kcal/kg°C

$T_{in\_crushed}$=27°C

$T_{out\_crushed}$=80.5°C

The amount of heat necessary to warm the crushed grapes in stationary conditions is:

$$\Delta Q_{crushed} = m_{crushed} \cdot c_{crushed} \cdot \left(T_{out\_crushed} - T_{in\_crushed}\right) \cong 690150 kcal \quad (1)$$

Corresponding to 46010 kcal t^{-1} that, with a calorific power of methane of 8200 kcal m^{-3}, is equivalent to a theoretical methane consumption of 5.61 m^3.

When the crushed grape is heated reusing a part of the hot must, as happens in the process, part of the heat is supplied by the must. However, this in turn cools down, so the thermal energy provided by the water from the boiler must finish the heating of the crushed grape (up to 80.5°C) and return the cooled must to the same temperature.

From the point of view of energy requirements, the situation does not change substantially from that with only water heating. The benefits of reintroducing part of the hot must are mainly linked to a better homogenization of the system, improved product flow and a reduction in thermal shock.

Figure 4 reports the electricity consumption for the different phases of the Ganimede process for the entire 6-day maceration cycle. Total electricity consumption amounts to 1759.6 kWh, with the highest incidence (43%) for the transport phase that, in this case, is penalized by a considerable distance of the tanks from the draining-pressing area.

Given that every maceration cycle lasts 144 h, an average hourly energy consumption of 12.22 kWh can be estimated.

Economic evaluations

For the Della Toffola plant the calculation of the operating cost, based on the 2012 figures and the economic parameters in Table 1, provides an annual quota of fixed costs of 42634 €, which is equal to 96.9 € h^{-1}. The hourly incidence of the variable costs corresponds to 71.2 € h^{-1}, of which 24 € h^{-1} is for labour, 13.6 € h^{-1} for electricity and 33.7 € h^{-1} for thermal energy. The total hourly cost is therefore 168.1 € h^{-1}, which corresponds to a unit cost of 11.2 € t^{-1} of processed product.

For the Ganimede plant the fixed costs are affected by the high purchasing cost of the plant and correspond to 82854 € $year^{-1}$, with an average hourly incidence of 143.8 € h^{-1}, while the share of variable costs is 10.1 € h^{-1}, of which 9.1 € is for labour and 1 € for electricity. The total hourly cost is 153.9 € h^{-1}, corresponding to a unit cost of 30 € t^{-1}, about three times that of the Della Toffola plant.

In theory the trend of the costs of the two plants can be simulated taking into account a variability in annual production. The result (Figure 5) shows a fairly flat curve for the hot maceration plant, affected by the high incidence of variable costs. On the contrary the Ganimede plant, because of the greater weight of the fixed costs, shows a clearly decreasing trend. Despite this, considering also a particular situation of underutilization of the Della Toffola plant and greater utilization of the Ganimede plant, the difference between the unit costs reduces but still remains evident.

Chemical and sensorial analyses

Despite coming from grapes with homogeneous characteristics, the chemical analyses have demonstrated different values for the two wines. More specifically, the values in the wine obtained with hot maceration are lower: total acidity 4.91 vs. 6.05 g l^{-1}; volatile acidity 0.17 vs. 0.23 g l^{-1}; total SO_2 56 vs. 72 m gl^{-1}; total polyphenols 1572 vs. 2043; colour intensity 7.19 vs. 8.73. The low levels of the first 3 parameters are positive for the characteristics of the wine, while the last two may be signs of weakness.

The sensorial analysis, conducted with a panel of 27 expert wine-tasters, displayed a significant difference (p=0.001) between the two

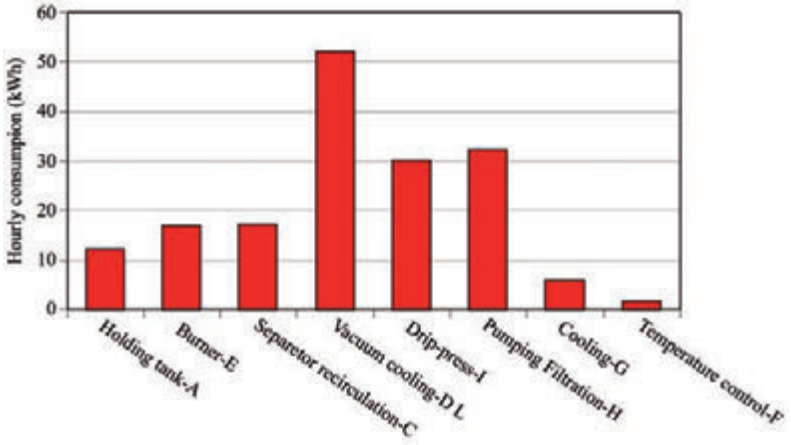

Figure 4. Electricity consumption for an operating cycle of the Ganimede plant.

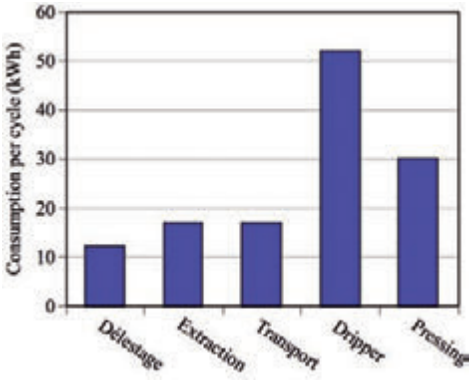

Figure 5. Unit costs according to annual productivity.

wines. The preference of 15 out of the 27, even if not significant, was for the hot macerated product. The descriptive evaluation (Figure 6) identified two wines with completely different sensorial characteristics. The wine obtained from the hot maceration was distinguished by greater aroma and freshness, resulting as suitable to be drunk young. The wine obtained with the Ganimede system instead showed a more complex and evolved structure, destined to improve over time.

The chemical and organoleptic differences of the two wines obtained determine a different market destination: the hot macerated product is mainly suitable for integration with other wines to enhance the levels of freshness and aromas; the wine produced with the Ganimede system is instead destined to the production of more traditional wines that maintain the characteristics of the grape variety.

The commercial value of the two wines, destined mainly for everyday consumption, is quite similar, even if the increased demand for hot macerated wine in recent years has allowed selling prices to rise by around 10%.

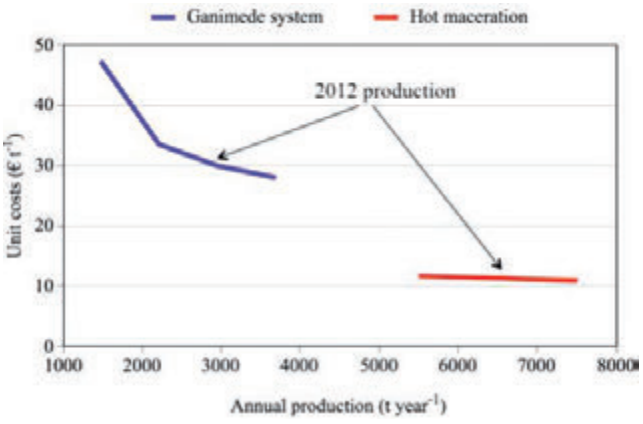

Figure 6. Descriptive evaluation of the two wines obtained.

Conclusions

The analysis of the maceration processes has demonstrated clear differences in the productivity, energy consumption and unit costs of production of the two plants.

The hot maceration uses more energy, but, thanks to the speed of the process that guarantees high productivity, the unit cost is lower. Furthermore, due to the high incidence of the variable costs, it appears less important that the production potential of this plant is fully exploited.

On the contrary the Ganimede plant has a higher unit cost that, due to the high purchase price, requires maximum exploitation of its annual production potential.

The chemical and sensorial evaluations describe two extremely diverse wines that, although being in the same commercial price range, can have two different and complementary destinations: the aroma and freshness of the hot macerated product makes it more suitable for integrating and improving other wines, while the other appears to be destined to the production of more traditional wines.

This quality difference fully justifies the choice of the Forlì-Predappio winery, which, although involving different production costs, has recently introduced both maceration systems to widen its range of red wines and respond more efficiently to the varied demands of the market.

References

Amati, A. 1985. Le possibili utilizzazioni della termomacerazione in enologia. Atti dell'Accadademia Italiana della Vite e del Vino. 37:143-155.

ASAE Standards 2011. EP497.7. Agricultural Machinery Management. St. Joseph, Mich., USA.

Arfelli, G., Sartini, E. and Gennari, L. 2001. La vinificazione in rosso. Il divulgatore. 24 (4/5): 34-37.

BioThermo/Cooler System Guide. 2013. Available from: http://www.dellatoffola.it Accessed: May 2013.

Celotti, E. and Rebecca S. 1998. Expériences récentes de thermomacération des raisins rouges. Revue des Œnologues. 89:14-18.

Celotti, E. and Franceschi, D. 2004. Gestion de certaines variables dans la macération des raisins rouges. Revue des Œnologues. 110:24-27.

Lambri, M. and Silva, A. 2004. Tecniche di macerazione e caratteri qualitativi dei vini rossi. L'informatore Agrario. 13:77-81

Metodo Ganimede Guide. 2013. Available from: http://www.ganimede.com Accessed: May 2013.

Control of mixing step in the bread production with weak wheat flour and sourdough

Alessandro Parenti,[1] Lorenzo Guerrini,[1] Lisa Granchi,[1] Manuel Venturi,[1] Stefano Benedettelli,[2] Fabrizio Nistri[3]

[1]Dipartimento di Gestione dei Sistemi Agrari, Alimentari e Forestali, Università di Firenze, Italy; [2]Dipartimento di Scienze delle Produzioni Agroalimentari e dell'Ambiente, Università di Firenze, Italy; [3]Tecnologie per l'arte bianca di Fabrizio Nistri & C. Sas, Prato, Italy

Abstract

Recently, several old Italian grain varieties have been reinstated, and the market seems to reward the breads made with these flours. Among such varieties, cultivar Verna appears to be interesting because the regular consumption of bread obtained by this variety and sourdough provides beneficial effects on human health such as the improving of the lipid, inflammatory, and hemorheological profiles. However, flours derived from Verna shows low technological performances. For example, the W value of these flours, obtained with alveoghraphic tests and considered as the commercial standard for the flour "strength" evaluation, is largely inferior than the W values of the commercial flour blends currently used in the bread making process. Moreover, the W values broadly change among the batches of Verna flours, whereas, usually, commercial blends are provided to bakeries with standard technological properties. Hence, these properties of Verna flour could lead to developed or overworked doughs and therefore to breads of worse quality. In addition, the previous mentioned large variability of flours from Verna can affect also the sourdough microbiota. For these reasons the composition and activity of the sourdough microorganisms should be controlled while the mixing process should be able to adapt to the different flour properties. Some works, in literature, report that monitoring the electrical consumption could provide useful information about the dough rheology, and this could be used to monitor the mixing step. In the present work the effect of different mixing times are evaluated on breads made with Verna flour type 2 leavened with sourdough. Tests were carried out at industrial scale in two different days. During the tests the electric consumption was monitored to highlight some features suitable for the mixing phase control. The breads were evaluated in terms of loaf volume measurement, crumb image analysis and losses of moisture content during storage. The results show that the composition of the sourdough microbiota and the mixing time affects the produced bread, especially when it is baked with low technological performance flours. Bread baked with an appropriate mixing time shows higher loaf volumes and lower water losses during storage.

Correspondence: Lorenzo Guerrini, Dipartimento di Gestione dei Sistemi Agrari, Alimentari e Forestali, Università degli Studi di Firenze, Piazzale delle Cascine 15, 50144, Firenze, Italy.
Tel. +39.055.3288352 - Fax: +39.055.3288316.
E-mail: lorenzo.guerrini@unifi.it

Key words: baking, sourdough, mixing, old wheat varieties, Verna

Contributions: the authors contributed equally.

Conflict of interests: the authors declare no potential conflict of interests.

Funding: the work was supported by Panificio Menchetti Pietro di Santi e Figli snc, Marciano della Chiana-AR, Italy

Journal of Agricultural Engineering 2013; XLIV(s1):e65
doi:10.4081/jae.2013.(s1):e65

Introduction

During the last 50 years, wheat breeding strategies were direct to the yield production improvement, to the kernel protein content increase, and to select plant with high response to chemical fertilization input (Sofi *et al.*, 2010). Gradually, in this scenario, old varieties are less and less suitable in agricultural production, and they were confined to germoplasm collections and seed servers. Nowadays, however, this trend seems to be reversed. In fact, in Tuscany, breads made with type 2 flours from these varieties and sourdough as leavening agent restart to spread, and the market seems to reward these breads. This could be due to the increased consumer attention to healthy and functional foods. Particularly, a study on regular consumption of bread made with Verna flour and sourdough shows beneficial in several aspects associated to the consumer health. Indeed, the lipid, inflammatory, and hemorheological profiles results improved by Verna bread regular consumption (Sofi *et al.*, 2010). In terms of bread productive process, the spread of old varieties, and the use of sourdough, raise up some issues. Currently, bread makers work blend of flours, with standard technological characteristics, and perhaps adopt a standard recipe, with well-defined working conditions, *i.e.* temperature, water content, absence/presence of salt and surfactant, amount of mixing work input and baker's yeast as leavening agent. These conditions are widely considered important to the success of the productive process (Campos et al, 1997; Anderssen *et al.*, 1997). In bakery, the commercial standard for the flour strength evaluation, is the alveographic test; with the reference value of the parameter "W", which summarizes technological flours performance. In normal bread-making process, blends shows constant W values, so a standard work-input could be provided in the mixing phase, guaranteeing the final bread acceptability. On the other hand, with old varieties flours, the W is largely variable among the batches and a standard recipe could not be adopted

anymore. Also, the W value of these flours is lower than those of the commonly used flour. For Verna, to provide an example of the working difficulties in bakery of these flours, W value of about 100 could be found in literature (Parenti *et al.*, 2012), while Quaglia (1984) identified wheat with W lower than 110 as "not for bread-making use". The various flour characteristics and process parameters affect also the performances of the sourdough that is used in the leaving step during the bread making in order to improve rheological, organoleptic and nutritional properties of the final products (Arendt *et al.*, 2007). Indeed, the sourdough microbiota, including lactic acid bacteria mostly of the genus *Lactobacillus* and yeast species belonging to genera *Candida* and *Saccharomyces*, are known to be dependent on some process parameters such as dough yield (water activity), addition of salt, number of propagation steps, and fermentation time (De Vuys and Neysens, 2005). On the contrary, surveys on the possible effect of the dough mixing time on the microbial ecology of the sourdough fermentation are lacking.

These issues point out the importance to investigate the effect of mixing work input amount from both technological and microbiological points of view.

The mixing work input provides to flour and water the energy allowing the development of a protein matrix, including starch granules, and giving dough the peculiar viscoelastic behaviour (gluten network). During the mixing step, after the complete flour hydration, the adjunctive energy is used for stretching and orienting the protein electronegative groups, to allow the formation of covalent bounds among cysteine residues, and other kinds of bounds, such as dipolar, ionic, hydrogen and Van der Walls forces. A well-hydrated dough, with insufficient mechanic deformation is named undeveloped dough and present worse rheological and baking properties than a correct developed one (Campos *et al.*, 1997). Even overworked dough shows mediocre technological properties, with decreased resistance and extensibility before the breaking (Gras, 2000). Hence, to obtain quality breads (in rheological terms) is important to provide a well-defined mixing work input. In the present work, a monitoring of the effects at industrial scale of different work input on breads has been carried out.

Materials and methods

Trials were carried out at Panificio Menchetti Pietro di Santi e Figli snc (Marciano della Chiana-AR, Italy), during two tests days. The used mixer was a twin arm type with 80 kg of maximum capacity, filled with 60 kg of dough, working at 30 rpm of mixing rate. The adopted proportion among ingredient was: 30 kg Verna type 2 flour (Table 1), 15 kg of sourdough, 15 kg of water.

In the two tests the effect of mixing were evaluated after 12, 17, and 22 minutes in the first one (PM1), and after 17, 22, and 27 in the last one (PM2). At the chosen moments three samples of dough per each time were collected and put in mould. Afterwards, the samples were put in leavening cell at 30°C and 75% of relative humidity. The proofing trend was monitored with pH measures performed every 30 minutes, and putting another sample in a graduate cylinder. Microbiological analysis of different samples were performed at the beginning and at the end of the fermentation. The proofing ended at 3.5 of pH value; this happened before 3 and 2.5 hours respectively, in the first, and in the second test. Then, samples were baked. The steam oven annular tubes (Spighi, Italy), was set up to 240°C and, after the bread introduction the heating system was turned off. The chosen baking time was 55 minutes.

Table 1. Flour technological characterization.

Rheological characteristics		Chemical characteristics (%)	
W	100-120* 10^{-4} J	Humidity	11
P/L	1.09	Total Protein	11
Falling Number	310-330	Insoluble Protein	10
Stability	>6'	Ashes	1.50
Water absorption	>45 %	Cellulose	>1.6
Volume	>550 ml/100 g	Lipids	0.50

pH measurement: pH was measured with a Crison pHmeter (mod GLP 21), after dissolving a small dough sample of about 10 g in distilled water.

Microbiological analysis: Dough samplings and platings were carried out at the manufacture soon after the mixing step and at the end of fermentation. Lactic acid bacteria, plated on maltose-MRS agar integrated with pimaricin (50 mg/L) at pH 5.6, were counted after incubation for 48-72 h at 30°C under anaerobic conditions. Yeasts, plated on WL agar (Oxoid Ltd, Basingstoke, Hampshire, UK) containing sodium propionate (2 g/L) and streptomycin (30 mg/L), were counted after incubation for 48 h at 30°C under aerobic conditions. Identification of microbial isolates was attained by molecular methods: PCR-RFLP of ITS region for yeasts and PCR-ARDRA for lactic acid bacteria according to Venturi *et al.* (2012).

Volume increase monitoring: 500 g of dough were putted into the leavening cell into a graduated cylinder. Dough height was recorded every 30 minutes.

The results of the different mixing time were evaluated in term of final loaf height, crumb image analysis, and losses of moisture during storage.

Final loaf height: three samples of 1000 g of dough were collected for each time and put in a mould. The mould was parallelepiped with internal dimension of mm 105x250x60 with the upper side open to allow the dough proofing. These moulds, hence, permit to compare different thesis during proofing.

Crumb image analysis: three slices of each loaf were analysed according to the method already described in Fois *et al.* (2012).

Moisture losses: changes in crumb moisture content were evaluated with a loss on drying method. About 5 g of crumb were exactly weighted and put in oven overnight at 103°C. Afterwards, the sample was weighted again, and the water content determined from the difference. The measures were performed after 1, 3, and 7 days since baking.

Results and discussion

The three different working times return breads with different appearance. During the leavening phase, the different mixing time produces different leavening behaviour (Figure 1A and 1B).

The sample with the lower mixing input (12 minutes), and those with the higher one (27 minutes) showed less volume increase in the proofing phase, than the sample picked at 17 minutes that showed the highest value in both tests.

Such differences couldn't be attributed to microbial populations occurring in dough after the different mixing time and at the end of fermentation. Indeed, in both trials, independently of the mixing and fermentation time, the yeast population, consisting of the species *Candida milleri*, achieved comparable cell densities (Table 2). In addition, although, soon after the mixing step, bacterial populations decreased progressively with the increase of working time, at the end

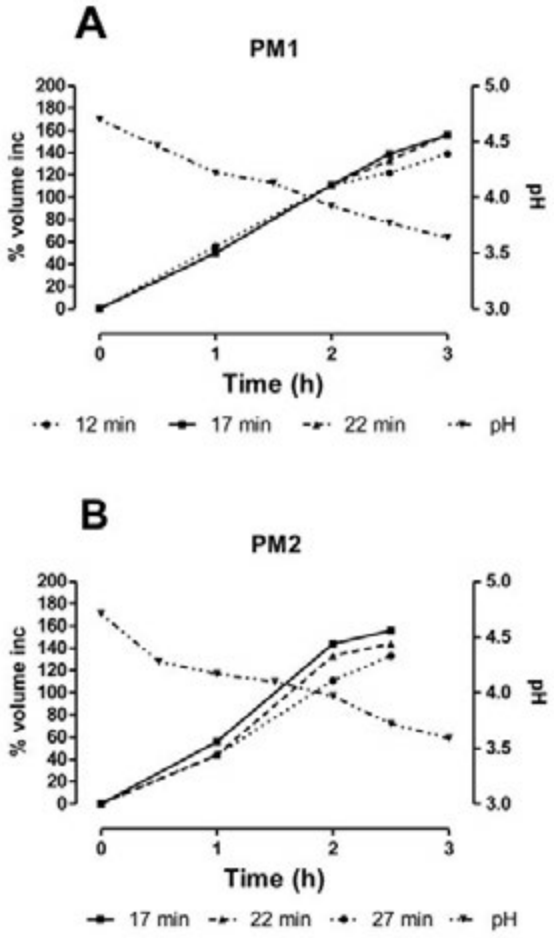

Figure 1. Volume increase (%) and pH courses during the fermentation in the two trials; A: PM1; B: PM2.

Table 2. Microbiological counts (CFU/g) and standard deviations (sd) of *Lactobacillus sanfranciscensis* (Ls) and *Candida milleri* (Cm) at the beginning (T0) and at the end of the fermentation after 3 (T3) or 2.5 (T2.5) h in the trials PM1 and PM2, respectively. Numbers at pedice after F indicate the minutes of dough mixing time.

PM1	Ls CFU/g	Cm sd		
			CFU/g	sd
F_{12} T0	2.62×10^{8}	3.32×10^{7}	6.10×10^{6}	5.66×10^{5}
F_{17} T0	1.28×10^{8}	1.48×10^{7}	4.75×10^{6}	3.54×10^{5}
F_{22} T0	9.85×10^{7}	9.19×10^{6}	4.60×10^{6}	7.07×10^{5}
F_{12} T3	4.70×10^{8}	2.26×10^{7}	1.89×10^{7}	3.59×10^{5}
F_{17} T3	4.05×10^{8}	2.47×10^{7}	1.24×10^{7}	1.64×10^{5}
F_{22} T3	9.70×10^{8}	1.13×10^{7}	1.63×10^{7}	3.01×10^{5}
PM2	**Ls CFU/g**	**Cm sd**		
			CFU/g	sd
F_{17} T0	2.09×10^{8}	1.13×10^{7}	4.50×10^{6}	5.66×10^{5}
F_{22} T0	1.53×10^{8}	1.56×10^{7}	3.00×10^{6}	1.41×10^{5}
F_{27} T0	9.85×10^{7}	1.34×10^{7}	4.35×10^{6}	7.78×10^{5}
F_{17} T2,5	6.05×10^{8}	1.20×10^{7}	8.70×10^{6}	5.46×10^{5}
F_{22} T2,5	8.90×10^{8}	5.66×10^{6}	1.28×10^{7}	1.62×10^{5}
F_{27} T2,5	1.03×10^{9}	7.78×10^{6}	2.66×10^{7}	6.49×10^{5}

of fermentation, they didn't show significant differences. This means that the longer was the mixing time the higher was, during the fermentation, the number of generations of *Lactobacillus sanfranciscensis*, the only bacterial species found. Nevertheless, no relationships between the extent of growth and fermentation performances were established. Anyway, it is pointed out that, as expected, lactic acid bacteria was the predominant population in dough,

The volume increase was only partially reflected in the height of the breads showed in Figures 2A and 2B.

In the first test, the heights among the mixing times are well pronounced, in fact the Tukey post-hoc test shows significant difference (P=0.05) among the three treatments. On the other hand, in the second test the baking process partially overcome the proofing difference and difference could be found only between 22 and 27 minutes. In the crumb image analysis the holes were divided in three class: I ≤ 0.05 mm^3, 0.05 mm^3 ≤ II ≤ 3 mm^3, III > 3 mm^3. Also, the ratio between total and alveolated surface was determined and express in percentage (Table 3).

Data didn't show pronounced differences among the mixing time, except for the under mixed dough. In fact, the slice image analysis revealed, in comparison *i.e.* with the 22 minutes of mixing of the same test, the same percentage of alveolated surface, but larger and irregular holes on the slice. The crumb water content during storage is shown in Figures 3A and 3B.

In this case, differences in bread water retention could be noticed for

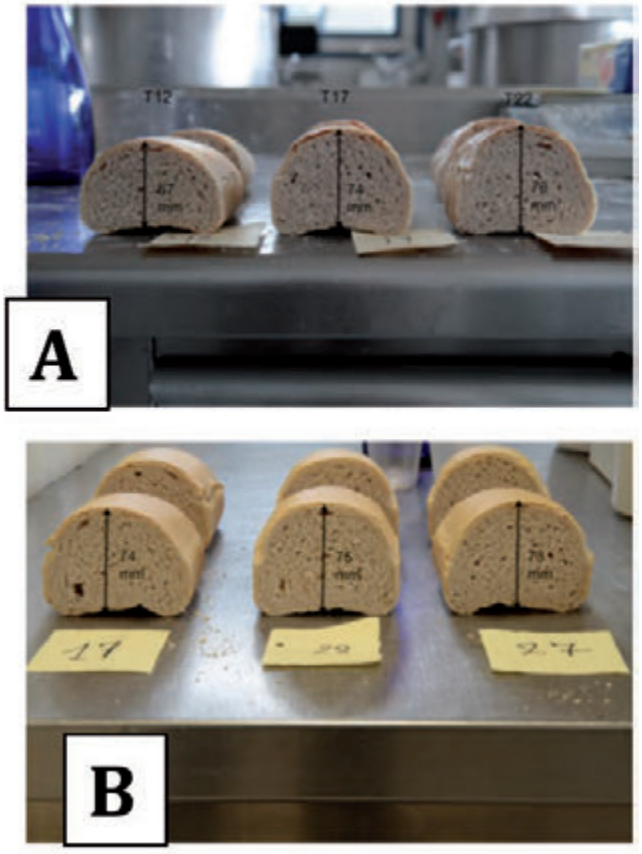

Figure 2. Height of the breads with different mixing times. A: PM1; B: PM2.

Table 3. Results of crumb image analysis of the loafs in the two trials.

PM1	Class distribution (%)			Average hole surface (mm³) per class			Alveolated surface (%)
	I	II	III	I	II	III	
T12	67.45	21.25	11.30	0.169	1.249	8.283	29.10
T17	72.55	17.90	9.55	0.174	1.298	7.859	25.05
T22	71.55	21.20	7.25	0.176	1.091	10.654	29.10
PM2	**Class distribution (%)**			**Average hole surface (mm³) per class**			**Alveolated surface (%)**
	I	II	III	I	II	III	
T17	71.33	22.30	6.38	0.166	1.234	7.383	31.20
T22	73.83	19.18	6.98	0.161	1.190	7.900	27.00
T27	72.50	21.03	6.48	0.161	1.181	10.809	31.70

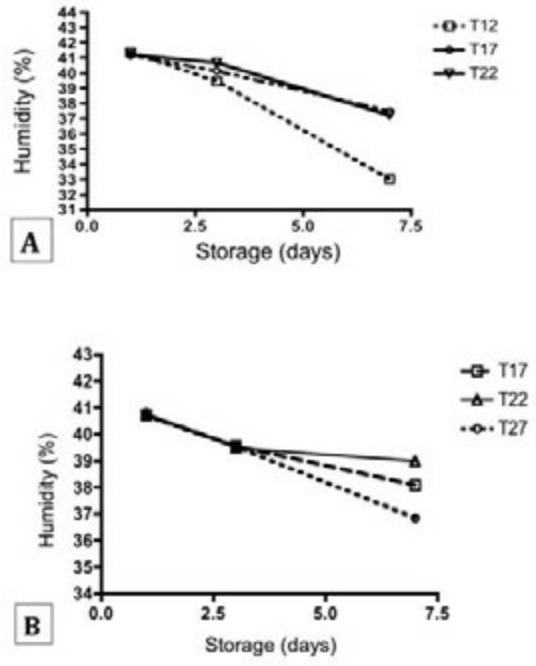

Figure 3. Humidity trend during storage of the different breads . A: PM1; B: PM2.

breads mixed for a different time. Particularly, in the first test, there is a significant difference between the 12 minutes treatment, and the others. On the other hand, in the second test, there are differences among the three times. These changes in moisture are less pronounced during the first days of storage, and became significant after a week.

Conclusions

In the present work some effect of the mixing time on the produced Verna breads could be noticed. Particularly, those effects appear more pronounced during the proofing phase, and could be revealed in terms of dough growth and bread final volume. Furthermore, the mixing time affect the humidity retention capacity of the breads during storage. In literature (Zheng *et al.*, 2000; Shehzad *et al.*, 2012), some works pointed out that electrical consumption could be suitable to monitor the dough behaviour during the mixing step. Considering the importance of this step on bread production and the already seen effects of mixing time, further development should be oriented to the use of this parameter to attempt establishing the optimal mixing end.

References

Anderssen, R. S., Gras, P. W., & Macritchie, F. 1998. The rate-independence of the mixing of wheat flour dough to peak dough development. J Cereal Sci. 27, 167–177.

Arendt, E. K., Ryan, L. A. M., & Dal Bello, F. Impact of sourdough on the texture of bread. 2007. Food Microbiol., 24, 165-174.

Campos, D. T., Steffe, J. F., & Ng, P. K. W. 1997. Rheological behavior of undeveloped and developed wheat dough. Cereal Chem., 489–494.

De Vuyst, L., & Neysens, P. The sourdough microflora: biodiversity and metabolic interactions. 2005. Trends Food Sci. Tech., 16, 43 - 56.

Fois, S., Fadda, C., Tonelli, R., et al. 2012. Effects of the fermentation process on gas-cell size two-dimensional distribution and rheological characteristics of durum-wheat-based doughs. Food Res. Int., *49*(1), 193–200.

Gras, P. 2000. Modelling the developmental rheology of wheat-flour dough using extension tests. J Cereal Sci., *31*(1), 1–13.

Parenti, A., Guerrini, L., & Spugnoli, P. Dough buoyancy to monitor bread production process. In: AgEng2012: proceedings of the international conference of agricultural engineering. 2012, July 8-12.

Shehzad, A., Chiron, H., Della Valle, et al. 2012. Energetical and rheological approaches of wheat flour dough mixing with a spiral mixer. J. Food Eng., *110*(1), 60–70.

Sofi, F., Ghiselli, L., Cesari, F., et al. 2010. Effects of short-term consumption of bread obtained by an old italian grain variety on lipid, inflammatory, and hemorheological variables: an intervention study. J. Med Food, *13*(3), 1–7.

Quaglia G. 1984. *Scienza e tecnologia della panificazione*. Chirotti editori. Pinerolo - Italy

Venturi M., Guerrini S., & Vincenzini M. 2012. Stable and non-competitive association of *Saccharomyces cerevisiae*, *Candida milleri* and *Lactobacillus sanfranciscensis* during manufacture of two traditional sourdough baked goods. Food Microbiol. 31, 107e115.

Zheng, H., Morgenstern, M. P., Campanella, O. H., & G, L. N. 2000. Rheological properties of dough during mechanical dough development. J Cereal Sci. *32*(3), 293–306.

Kinetic and thermodynamic properties of soybean grains during the drying process

Daniel Emanuel Cabral de Oliveira,[1] Osvaldo Resende,[2] Jaqueline Ferreira Vieira Bessa,[2] Adrieli Nagila Kester[2]

[1]UFMT. Av. Alexandre Ferronato, Setor Industrial Sul Sinop; [2]IF Goiano. Rodovia Sul Goiana, Rio Verde, GO

Abstract

The aims of this work were to adjust different mathematical models to experimental data describing the drying of the Valiosa cultivar soybean grain, to determine and to evaluate the effective diffusion coefficient and to obtain the activation energy and the thermodynamic properties of the drying process under different air conditions. The experiments were conducted at the Federal Institute of Education, Science and Technology of Goiás (Instituto Federal de Educação, Ciência e Tecnologia Goiano – Câmpus Rio Verde). The Valiosa cultivar soybean grains, with an initial moisture content on a dry basis of 0.56 (d.b., decimal), were dried in an oven with forced air ventilation at five different temperatures (40, 55, 70, 85 and 100°C) until reaching a moisture content of 0.133±0.019 (d.b.). Of the models analyzed, Page's model was selected to best represent the drying phenomenon. The effective diffusion coefficient of soybeans increased with the air temperature and was described by the Arrhenius equation; an activation energy of 22.77 kJ mol^{-1} was reported for liquid diffusion in the drying of the soybeans. The enthalpy and entropy decreased with increasing temperature, while the Gibbs free energy increased with increasing drying temperature.

Introduction

The soybean (*Glycine max*) is the most commonly grown oilseed in the world because of its high protein content, which is important for the diets of humans and animals raised for human consumption (Carvalho, 2012). The soybean culture is one of the most important cultures in Brazil, as it corresponds to 40% of the total grain produced in the country and 27% of the grain produced worldwide. Brazil is the second largest producer and the largest exporter of soybeans, and soybeans account for 20% of exports in Brazilian agribusiness (Vernetti and Vernetti Junior, 2009).

The purpose of drying agricultural products is to ensure their quality during storage, as the reduction in the moisture content reduces the biological activity and the chemical and the physical changes that occur during storage.

The study of drying provides information on the heat and mass transfer that occur between the biological material and the drying element (usually heated or non-heated atmospheric air), which is crucial for the design, operation and simulation of drying systems and dryers (Correa *et al.,* 2003). The use of mathematical models to simulate the drying process in dryers that operate at high temperatures is an important tool for engineers who work in the field of drying and storage of grains (Queiroz *et al.,* 1999).

The liquid diffusion theory has been widely used to study the drying of vegetable products. According to Corrêa *et al.* (2006), the liquid diffusion mechanism is complex because of the diversity in chemical compositions and physical structures of the product. Water diffusion in agricultural products involves different mechanisms, including molecular diffusion, capillary diffusion, surface diffusion, hydrodynamic flow, vapor diffusion and thermal diffusion (Goneli *et al.,* 2009).

Knowledge of the thermodynamic properties involved in the drying of agricultural products allows engineers to design better drying equipment, to calculate energy requirements necessary for the process, to study the properties of adsorbed water, to evaluate the microstructure of food and to study the physical phenomena that occur at the material surface (Corrêa *et al.,* 2010).

The aim of this study was to obtain the drying curves and evaluate the liquid diffusion and the thermodynamic properties of Valiosa cultivar soybean grains dried under different air- drying conditions.

Materials and methods

The experiments were conducted in the Laboratory for the Postharvest of Vegetables Products (Laboratório de Pós-colheita de Produtos Vegetais) at the Federal Institute of Education, Science and Technology of Goiás (Instituto Federal de Educação, Ciência e Tecnologia Goiano – Câmpus Rio Verde) with Valiosa cultivar soybean grains from the municipality of Santa Helena de Goiás (GO). The initial moisture content of the grains on a dry basis was 0.56 (d.b., decimal); these grains were dried in an oven with forced air ventilation at five different temperatures (40, 55, 70, 85 and 100°C), leading to relative humidities of 25.3, 12.5, 5.7, 3.5 and 2.2%, respectively. The drying con-

Correspondence: Osvaldo Resende, Instituto Federal Goiano, Rodovia Sul Goiana, Km 01. Zona Rural. C. Postal 66. Rio Verde, GO
E-mail: osvresende@yahoo.com.br

Key words: *Glycine max*, liquid diffusivity, enthalpy, entropy, Gibbs free energy.

Acknowledgements: the authors extend thanks to CNPq, CAPES and IF for their financial support for this work.

Journal of Agricultural Engineering 2013; XLIV(s1):e66
doi:10.4081/jae.2013.(s1):e66

tinued in an oven at 105 ± 1°C for 24 h in three replications until the grains reached a moisture content of 0.133±0.019 (d.b.) (Brazil, 2009).

The reduction in the moisture content during drying was monitored with the gravimetric method (mass loss) using a scale with a resolution of 0.01 g; knowing the initial moisture content of the product, the drying continued until the desired moisture content was achieved.

The temperature and relative humidity of the external ambient environment of the drying chamber were monitored with a psychrometer, and the internal temperature was monitored with a thermometer installed inside the oven. The relative humidity of the drying air was obtained by means of the basic principles of psychrometry, using the software GRAPSI.

The moisture content ratios of the soybeans during drying were determined with the following expression:

$$R X \quad \frac{X - X_e}{X_i - X_e} \tag{1}$$

where:
RX: ratio of the moisture content of the product, dimensionless; X: moisture content of the product (kg of water kg^{-1} dry weight);
X_i: initial moisture content of the (kg of water kg^{-1} dry weight); and
X_e: equilibrium moisture content of the product (kg of water kg^{-1} dry weight).

The equilibrium moisture content of the soybeans at each temperature was obtained

with the modified version of Henderson's equation, as reported by Asae (1988).

The experimental data describing the drying process of the soybeans were adjusted with mathematical models commonly used to represent the drying of agricultural products; these models are presented in Table 1.

The mathematical models were fitted using nonlinear regression with the Gauss- Newton method using statistical software. The models were selected according to the determination coefficient (R^2), the chi-square test (χ^2), the relative average error (P) and the standard deviation of the estimate (SE). A relative average error of less than 10% was considered a criterion for model selection, as recommended by Mohapatra and Rao (2005).

$$P = \frac{100}{N}\sum \frac{\left|Y - \hat{Y}\right|}{Y} \tag{13}$$

$$SE = \sqrt{\frac{\sum\left(Y - \hat{Y}\right)^2}{GLR}} \tag{14}$$

$$\chi^2 = \frac{\sum\left(Y - \hat{Y}\right)^2}{GLR} \tag{15}$$

where:
Y: experimental value;
$\hat{Y}$: value calculated by the model;
N: number of experimental observations;
GLR: degrees of freedom of the model (number of experimental observations minus the number of model coefficients).

The liquid diffusion model for the spherical geometric form with the approximation of eight terms (Equation 2) was fitted to the experimental data describing soybean drying according to the expression:

$$RX = \frac{X - X_e}{X_i - X_e} = \frac{6}{\pi^2}\sum_{n=1}^{\infty}\frac{1}{n^2}\exp\left[-\frac{n^2\cdot\pi^2\cdot D\cdot t}{R_e^2}\cdot\right] \tag{16}$$

where:
RX: ratio of the moisture content of the product, dimensionless;
t: time, s;
n: number of terms;
D: liquid diffusion coefficient, m2.s^{-1}; and
R_e: equivalent radius, m (2.95 x 10^{-3} m)

The volume of each grain (V_g) was obtained by measuring the three orthogonal axes (length, width and thickness) of fifteen grains at the end of drying with a digital caliper with a resolution of 0.01 mm, according to the expression proposed by Mohsenin (1986):

$$V_g = \frac{\pi\cdot A\cdot B\cdot C}{6} \tag{17}$$

were:
V_g: grains volume, mm-3; A: length, mm;
B: width, mm; and
C: thickness, mm.

The relationship between the effective diffusion coefficient and the increase in drying air temperature was described with the Arrhenius equation.

Table 1. Mathematical models used to predict the drying of agricultural products.

Model equation	Model	
RX = 1+a t+b t 2	Wang and Sing	(2)
RX = exp(-k · t^n)	Page	(3)
RX = exp(-k · t)	Newton	(4)
RX = a · exp(-k · t)+c	Logarithmic	(5)
RX = a · exp(-k · t)	Henderson and Pabis	(6)
RX = a · exp(-k · t^n)+b · t	Midilli	(7)
RX = a · exp(-k · t)+(1 - a)exp(-k · a · t)	Two exponential terms	(8)
RX = a · exp(-k$_o$ · t)+(b · exp(-k$_1$ · t)	Two terms	(9)
RX = a · exp(-k · t)+(1 - a) · exp(-k · b · t)	Diffusion approximation	(10)
RX = a · exp(-k · t)+(1 - a)exp(-k$_1$ · t)	Verma	(11)
RX = exp ((-a (-a^2+4 · b · t)^{0,5}/2 · b	Thompson	(12)

where: t: drying time, h; k, k$_o$, k$_i$: drying constants h^{-1}; and a, b, c, n: models coefficients.

$$D = D_O \cdot \exp\left(\frac{-E_a}{R \cdot T_{ab}}\right) \quad (18)$$

where:
D_o: pre-exponential factor;
E_a: activation energy, kJ.mol^{-1};
R: universal gas constant, 8.134 kJ.kmo^{-1}1.K^{-1}; and
T_{ab}: absolute temperature, K.

The thermodynamic properties of the drying of soybean grains were obtained with the method reported by Jideani and Mpotokwana (2009):

$$\Delta H = E_a - R \cdot T \quad (19)$$

$$\Delta S = R \cdot \left(\ln k - \ln \frac{k_B}{h_p}\right) - \ln T_{abs} \quad (20)$$

$$\Delta G = \Delta H - T_{abs} \cdot \Delta S \quad (21)$$

where:
ΔH: enthalpy, J mol^{-1};
ΔS: entropy, J mol^{-1};
ΔG: Gibbs free energy, J mol^{-1};
k_B: Boltzmann constant, 1.38×10^{-23} J K^{-1}; and
h_p: Planck constant, 6.626×10^{-34} J s^{-1}.

Results and discussion

The average values of the moisture content ratio of the soybean grains dried under different air conditions are shown in Table 2. The times required for the grains to reach the moisture content of 0.133±0.019 (kg water kg^{-1} dry weight) were 18.6, 11.6, 7.7, 5.9 and 4.7 h for the drying temperatures 40, 55, 70, 85 and 100°C, respectively.

The increase in air temperature was found to cause a reduction in the grain drying time. The reduction in drying time is related to the greater difference between the partial pressure of water vapor in the drying air and in the product caused by the increase in temperature. This greater difference promotes an easier and more rapid water removal; similar observations were made by other authors for numerous products (Resende *et al.,* 2008; Almeida *et al.,* 2009; Sousa *et al.,* 2011; Costa *et al.,* 2011; Oliveira *et al.,* 2012).

The values of the determination coefficient (R^2) and the relative average error (P) of the eleven models adjusted during the drying of the soybeans at different temperatures are shown in Table 3. The determination coefficient (R^2) was above 99% for all models and all drying temperatures, indicating, according to Madamba *et al.* (1996), a satisfactory representation of the phenomenon under study.

Table 2. Moisture content ratio (RX, decimal) of Valiosa cultivar soybean grains during drying time (h) under five temperature conditions (°C).

40°C		55°C		70°C		85°C		100°C	
Time	RX	Time	RX	Time	RX	Time	RX	Time	RX
0.00	1.00	0.00	1.00	0.00	1.00	0.00	1.00	0.00	1.00
0.67	0.97	0.42	0.96	0.25	0.97	0.22	0.97	0.18	0.97
1.30	0.92	0.78	0.92	0.60	0.92	0.48	0.92	0.40	0.90
2.00	0.86	1.13	0.88	0.93	0.87	0.65	0.88	0.60	0.85
2.40	0.84	1.52	0.84	1.20	0.83	0.85	0.84	0.77	0.81
3.02	0.79	1.83	0.81	1.45	0.79	1.08	0.80	0.93	0.77
3.58	0.76	2.22	0.77	1.68	0.76	1.37	0.75	1.10	0.72
4.37	0.71	2.60	0.74	1.92	0.73	1.60	0.72	1.25	0.69
4.85	0.68	2.98	0.70	2.17	0.70	1.80	0.68	1.42	0.66
5.45	0.65	3.37	0.67	2.48	0.66	2.02	0.65	1.63	0.62
6.43	0.61	3.83	0.64	2.78	0.63	2.25	0.61	1.85	0.58
7.05	0.58	4.32	0.60	3.17	0.59	2.48	0.58	2.05	0.55
7.72	0.55	4.78	0.57	3.52	0.55	2.70	0.55	2.23	0.51
8.55	0.52	5.25	0.54	3.87	0.52	2.97	0.51	2.43	0.47
9.58	0.48	5.82	0.50	4.25	0.48	3.20	0.48	2.65	0.44
10.50	0.45	6.27	0.48	4.63	0.45	3.55	0.44	2.90	0.41
11.53	0.42	6.80	0.45	4.97	0.42	3.85	0.41	3.13	0.38
12.62	0.38	7.50	0.42	5.33	0.39	4.08	0.39	3.35	0.35
13.55	0.35	8.05	0.39	5.65	0.36	4.32	0.36	3.55	0.32
14.60	0.32	8.70	0.36	6.10	0.33	4.60	0.33	3.77	0.30
15.68	0.29	9.45	0.33	6.62	0.30	4.88	0.30	3.97	0.27
16.55	0.26	10.00	0.31	6.95	0.28	5.25	0.28	4.17	0.25
17.38	0.24	10.85	0.28	7.30	0.26	5.58	0.25	4.38	0.23
18.58	0.21	11.57	0.25	7.67	0.24	5.87	0.23	4.75	0.21

The models presented relative average error values (P) less than 10% for the five conditions analyzed, indicating, according to Mohapatra and Rao (2005), that they provide suitable representations of the drying phenomenon. However, the Wang and Sing (2), Newton (4), Exponential of Two Terms (8) and Thompson (12) models had the highest values of P.

The chi-square (χ^2) values and the estimated average error (SE) obtained for the different models adjusted to the different conditions used to dry the soybean grains are described in Table 4.

The eleven models analyzed showed low values of estimated average errors (SE), which suggests good adjustments of the models to the experimental data. All models showed significant chi-squared values. Günhan *et al.* (2005) reported that the lower the value of chi- square, the better the fit of the model. The Page (3), Logarithmic (5) and Midilli (7) models had the lowest chi-square values.

The analyzed models satisfactorily represented the process of soybean grain drying; however, the Page (3), Logarithmic (5) and Midilli (7) models had the best overall fits. Thus, due to its simplicity, the Page model was selected to represent the phenomenon of soybean grain drying.

Figure 1 shows the drying curves for soybean at the different studied temperatures generated from the experimental data and the values

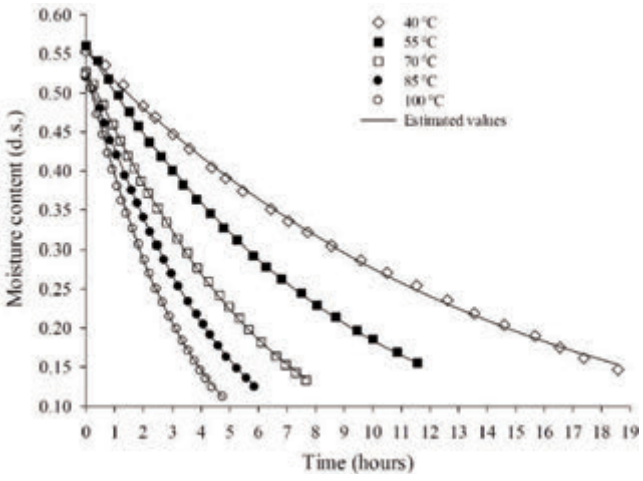

Figure 1. Drying curves, experimental data and values estimated by Page model for the soybean grains at temperatures of 40, 55, 70, 85 and 100°C.

Table 3. Determination coefficient (R^2, %) and relative average error (P, %) for the models analyzed during the drying of soybean grains under various temperature conditions (°C).

Models	Temperature (°C) 40		55		70		85		100	
	R^2	P	R^2	P	R^2	P	R^2	P	R^2	P
2	99.75	2.41	99.92	1.18	99.97	0.55	99.97	0.46	99.96	0.68
3	99.88	1.69	99.98	0.43	99.98	0.68	99.99	0.48	99.96	0.83
4	99.84	1.78	99.96	0.49	99.62	0.68	99.39	3.47	99.58	3.27
5	99.91	1.48	99.98	0.39	99.98	0.38	99.97	0.61	99.97	0.74
6	99.88	1.70	99.98	0.39	99.82	1.89	99.72	2.21	99.78	2.11
7	99.93	1.19	99.98	0.41	99.99	0.39	99.99	0.31	99.97	0.68
8	99.84	1.78	99.96	0.49	99.62	2.80	99.98	0.39	99.58	3.27
9	99.89	1.64	99.98	0.39	99.82	1.89	99.72	2.21	99.97	0.71
10	99.89	1.63	99.96	0.49	99.97	0.46	99.94	0.90	99.96	0.71
11	99.89	1.67	99.97	0.41	99.97	0.46	99.94	0.90	99.95	0.80
12	99.84	1.78	99.96	0.49	99.62	2.80	99.39	3.47	99.58	3.27

Table 4. Values of the chi-square test (2, decimal x10-3) and estimated average error (decimal, SE) obtained for ten models used for the representation of kinetics of drying of Valiosa cultivar soybean grains.

Models	Temperature (°C) 40		55		70		85		100	
	2	SE	2	SE	2	SE	2	SE	2	SE
2	0.152	0.012	0.046	0.007	0.015	0.004	0.020	0.005	0.027	0.005
3	0.071	0.008	0.013	0.004	0.014	0.004	0.009	0.003	0.026	0.005
4	0.095	0.010	0.020	0.004	0.013	0.004	0.352	0.019	0.254	0.016
5	0.060	0.008	0.010	0.003	0.010	0.003	0.020	0.004	0.023	0.005
6	0.077	0.009	0.009	0.003	0.108	0.010	0.170	0.013	0.129	0.011
7	0.049	0.007	0.010	0.003	0.007	0.003	0.006	0.003	0.020	0.004
8	0.099	0.010	0.021	0.005	0.227	0.015	0.010	0.003	0.266	0.016
9	0.073	0.009	0.010	0.003	0.119	0.011	0.187	0.014	0.023	0.005
10	0.072	0.008	0.022	0.005	0.018	0.004	0.040	0.006	0.026	0.005
11	0.074	0.009	0.017	0.004	0.018	0.004	0.040	0.006	0.035	0.006
12	0.099	0.010	0.021	0.005	0.227	0.015	0.368	0.019	0.266	0.016

estimated by the Page model. A satisfactory adjustment of the model to the experimental values was.

The drying time of the product was inversely proportional to the temperature; in other words, the higher the temperature, the shorter the drying time. The drying times for 40°C and 100°C were 18.6 hours and 4.7 hours, respectively. Corrêa *et al.* (2010) reported that the reduction in the moisture content of agricultural products, especially of grains and seeds, occurs with decreasing order with increasing temperature due to the difference in the surface moisture and the size of the whole grain. Sousa *et al.* (2011) and Oliveira *et al.* (2012) reported similar results for the drying of forage turnip seeds and corn, respectively.

Table 5 shows the values of the coefficients "k" and "n" of the Page model fitted to experimental data describing the kinetics of soybean grain drying at different temperatures.

The magnitude of the drying constant k for the Page model represents the phenomenon whereby temperature increases in the drying air result in increasingly favorable external drying conditions. However, the coefficient n of the Page model was not affected by drying temperature. Thus, for the range of temperatures studied, the drying of soybean grains can be estimated using the following expression:

$$RX \quad exp \quad 0.0702 \quad 0.0033T \quad t^{1.0764} \qquad (22)$$

where:
T: drying temperature (°C)
t: drying time (h)

Figure 2 shows the experimental and the estimated data for the moisture content ratio (RX) obtained using the Page model, the values obtained using equation 22 and the values presented in Table 2. This model provided a good adjustment to the data while adequately describing the process of soybean grain drying. The reduction in the moisture content ratio leads to a greater discrepancy between the estimated and experimental values.

The values of the effective diffusion coefficient of soybeans as a function of the conditions of the drying air are shown in Figure 3.

The effective diffusion coefficient increased linearly with increasing temperature of the drying air, with values of 0.847×10^{-11} to 3.46×10^{-11} $m^2\ s^{-1}$ for temperatures ranging from 40 to 100° C, indicating a greater intensity of water transport from the inside to the periphery of the grain and corroborating results obtained by Mohapatra and Rao (2005), Resende *et al.* (2008), Almeida *et al.* (2009), Costa *et al.* (2011), Corrêa *et al.* (2011) and Siqueira *et al.* (2012). Madamba *et al.* (1996) reported that the effective diffusion coefficients were on the order of 10^{-11} to 10^{-9} $m^2\ s^{-1}$.

Sousa *et al.* (2011) studied the drying of fodder radish seeds and obtained values similar to those found in the present work on the order of 3.23×10^{-11} to 10.42×10^{-11} $m^2.s^{-1}$ at temperatures of 30 and 70°C, respectively. Gely and Santalla (2007) and Oliveira *et al.* (2009) encountered values on the order of 1.18×10^{-12} to 6.76×10^{-12} $m^2.s^{-1}$ and 1.54×10^{-13} to 4.85×10^{-13} $m^2.s^{-1}$ $m^2.s^{-1}$ for the diffusion coefficients of quinoa seeds and corn grains, respectively. Thus, water is removed more rapidly from soybeans than from quinoa seeds and corn grains.

The dependence of the effective diffusion coefficient of the soybean grains on the drying air temperature was represented by the Arrhenius expression, as illustrated in Figure 4.

The activation energy is defined as the ease with which water molecules overcome the energy barrier for migration from the interior of the

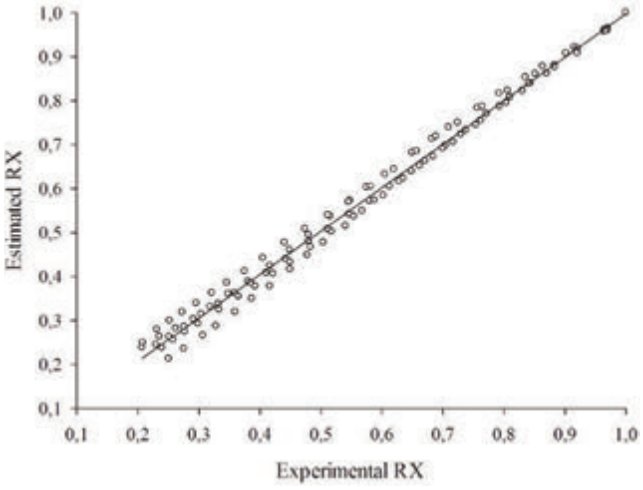

Figure 2. Experimental and estimated values of the moisture content ratio obtained using the Page model as a function of soybean drying temperature.

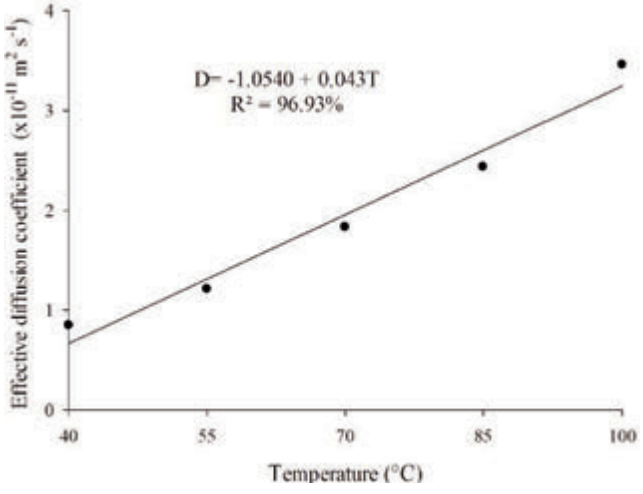

Figure 3. Average values of the effective diffusion coefficient ($m^2.s^{-1}$) obtained for soybean grains drying at temperatures of 40; 55; 70; 85 and 100°C.

Table 5. Coefficients of the Page model adjusted for different drying conditions of Valiosa cultivar soybean grains.

Coefficient	Temperature (°C) 40	55	70	85	100	Average values
K	0.0727*	0.1138*	0.1505*	0.1962*	0.2813*	k= -0.0702+0.0033T
N	1.0327*	1.0178*	1.0981*	1.1311*	1.1022*	1.0764

*Significant at 1% by test t.

Table 6. Values of enthalpy (H, J mol^{-1}), entropy (S, J mol-1 K^{-1}) and Gibbs free energy (G, J mol^{-1}) for different conditions of drying air used for Valiosa cultivar soybean grains.

Thermodynamic properties	Temperature (°C) 40	55	70	85	100	Equation	R² (%)
H	20164.4	20039.7	19914.9	19790.2	19665.5	H=20496.9-8.3T	
S	-267.1	-263.8	-261.8	-259.9	-257.3	S=-272.9-0.16T	
G	103810.6	106596.0	109758.2	112899.5	115683.5	G=95726.6+200.3T	

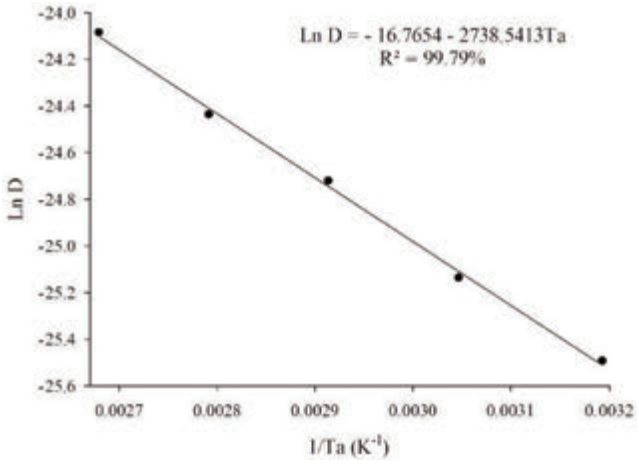

Figure 4. Arrhenius representation for the effective diffusion coefficient for soybean drying at temperatures of 40; 55; 70; 85 and 100°C.

product to its exterior (Resende *et al.,* 2005). In the present work, the activation energy for the liquid diffusion of soybeans was 22.77 kJ.mol-1 in the studied temperature range. According to Zogzas *et al.* (1996), the activation energy for agricultural products ranges from 12.7 to 110 kJ.mol-1; thus, the value obtained in the present study is within this range.

Kitic and Viollaz (1984) obtained a value close to that found in the present work. These authors reported an activation energy for the soybean of 28.80 kJ.mol^{-1}. Gely and Santalla (2007) and Costa *et al.* (2011) evaluated the drying of quinoa and crambe and reported activation energies of 37.97 and 37.07 kJ.mol^{-1}, respectively. The activation energy of soybean encountered in the present study was lower than that found in other studies; this may be due to the more unstable bond between water and the product evaluated, as reported by Siqueira *et al.* (2012).

Table 6 shows the values of enthalpy, entropy and Gibbs free energy for the different drying conditions. The enthalpy and entropy decreased while the Gibbs free energy increased linearly with increasing drying temperature.

The enthalpy is related to the energy required to remove water from the product during the drying process; thus, the enthalpy decreases with increasing drying temperature (Oliveira *et al.*, 2010). This behavior was observed for soybean grains during the reduction of the moisture content, indicating that lower temperatures require more energy.

According to Goneli *et al.* (2010), the entropy is a thermodynamic property that can be related to the degree of disorder between the water and the product. The entropy decreases with increasing drying air temperature. Corrêa *et al.* (2010) reported that this behavior is expected because the decrease in drying temperature decreases the excitation of water molecules of the products and increases the order of the water-product system.

The Gibbs free energy is related to the work required to produce available sorption sites (Nkolo Meze'e *et al.,* 2008). The Gibbs free energy can be positive for endogenous reactions where it is necessary to add energy from the environment. The Gibbs free energy can be negative when the phenomenon occurs spontaneously without the addition of energy. The Gibbs free energy of soybean grains was found to be positive and increased with increasing drying temperature. This behavior was also observed by Corrêa et al. (2011) when studying the thermodynamic properties of corn cobs drying at temperatures of 45, 55 and 65°C.

Equations used to determine the enthalpy, the entropy and the Gibbs free energy for the temperature range studied can be found in Table 6. These thermodynamic properties behaved in a linear manner and were characterized by high coefficients of determination.

Conclusions

All of the analyzed models satisfactorily represented the drying of grains; however, the Page model, due to its simplicity, was chosen to best represent the phenomenon.

The effective diffusion coefficient of soybeans increased with increasing drying air temperature; this phenomenon was described by the Arrhenius equation and characterized by an activation energy of 22.77 kJ.mol^{-1}.

The enthalpy and entropy decreased with increasing drying temperature and the entropy was negative at all temperatures studied. The Gibbs free energy was positive for the analyzed conditions and increased with increasing drying temperature.

References

Almeida, D.P.; Resende, O.; Costa, L.M.; Mendes, U.C.; Sales, J.F. 2009. Cinética de secagem do feijão adzuki (*Vigna angularis*) [Drying kinetics of adzuki beans (*Vigna angularis*)]. Gl. Sci Technol. 2:72-83.

American Society of Agricutural Engineers (ASAE). 1988. Agricultural Engineers Handbook.

ASAE, 35th, St. Joseph.

Brasil, Ministério da Agricultura e Reforma Agrária. Secretaria Nacional de defesa Agropecuária. 2009. Regras para Análise de Sementes [Regulations for Testing Seeds]. Brasília, 395p.

Carvalho, P.T. 2012. Balanço de emissões de gases de efeito estufa de biodiesel produzido a partir de soja e dendê no Brasil [Balance of emissions of greenhouse gases from biodiesel produced from soybean oil and palm oil in Brazil]. 2012. 166f. Dissertação (Mestrado)

apresentada ao Programa de Pós-graduação em Planejamento Energético, COPPE, da Universidade Federal do Rio de Janeiro.

Corrêa, P.C.; Araújo, E.F.; Afonso Júnior, P.C. 2003. Determinação dos parâmetros de secagem em camada delgada de sementes de milho doce (*Zea mays* L.) [Determination of the parameters related to thin-layer drying of sweet corn seeds (*Zea mays* L.)]. Rev. Bras. Milho e Sorgo. 2:110-9.

Corrêa, P.C.; Resende, O.; Goneli, A.L.D.; Botelho, F.M.; Nogueira, B.L. 2006.

Determinação do coeficiente de difusão liquida dos grãos de feijão [Determination of the liquid diffusion coefficient of bean grains]. Rev. Bras. Prod. Agro. 8:117-126.

Corrêa, P.C.; Oliveira, G.H.H.; Botelho, F.M.; Goneli, A.L.D.; Carvalho, F.M. 2010.

Modelagem matemática e determinação das propriedades termodinâmicas do café (*Coffea arábica* L.) durante o processo de secagem [Mathematical modeling and determination of the thermodynamic properties of coffee (*Coffea arabica* L.) during the drying process]. Rev. Ceres. 57:595-601.

Corrêa, P.C.; Botelho, F.M.; Oliveira, G.H.H.; Goneli, A.L.D.; Resende, O.; Campos, S.C.

2011. Mathematical modeling of the drying process of corn ears. Acta Scientiarum. Agronomy. 33:575-581.

Costa, L.M.; Resende, O.; Sousa, K.A.; Gonçalves, D.N. 2011. Coeficiente de difusão efetivo e modelagem matemática da secagem de sementes de crambe [Effective diffusion coefficient and mathematical modeling of the drying of crambe seeds]. Rev. Bras. Eng. Agr. Amb. 15:1089-1096.

Gely, M.C.; Santalla, E.M. 2007. Moisture diffusivity in quinoa (*Chenopodium quinoa*

Willd.) seeds: Effect of air temperature and initial moisture content of seeds. J. Food Eng.

78:1029-1033.

Goneli, A.L.D.; Corrêa, P.C.; Afonso Júnior, P.C.; Oliveira, G.H.H. 2009. Cinética de secagem dos grãos de café descascados em camada delgada [Kinetics of thin-layer drying of peeled coffee beans]. Rev. Bras. Arm. 11:64-73.

Goneli, A.L.D.; Corrêa, P.C.; Oliveira, G.H.H.; Botelho, F.M. 2010. Water desorption and thermodynamic properties of okra seeds. Transactions of the ASAE. 53:191-197.

Günhan, T.; Demir, V.; Hancioglu, E.; Hepbasli, A. 2005. Mathematical modelling of drying of bay leaves. E. Conv. Manag. 46:1667-1679.

Jideani, V.A.; Mpotokwana, S.M. 2009. Modeling of water absorption of botswana bambara varieties using Peleg's equation. J. Food Eng. 92:182–188.

Kitic, D.; Viollaz, P.E. 1984. Comparison of drying kinetic of soybean in thin layer and fluidized beds. Int. J. Food Sc. Tech. 19:399–408.

Madamba, P.S.; Driscoll, R.H.; Buckle, K.A. 1996. Thin-layer drying characteristics of garlic slices. J. Food Eng. 29:75-97.

Mohapatra, D.; Rao, P. S. 2005. A Thin layer drying model of parboiled wheat. J. Food Eng.

66: 513-518.

Mohsenin, N.N. 1986. Physical properties of plant and animal materials. New York: Gordon and Breach Publishers.

Nkolo Meze'e, Y.N.; Noah Ngamveng, J.; Bardet, S. 2008. Effect of enthalpy–entropy compensation during sorption of water vapour in tropical woods: the case of bubinga (*Guibourtia Tessmanii* J. L Eonard; G. *Pellegriniana* J.L.). Therm. Acta. 468:1–5.

Oliveira, D.E.C.; Resende, O.; Smaniotto, T.A.S.; Campos, R.C.; Chaves, T.H. 2012. Cinética dos grãos de milho [Kinetics of corn grains]. Rev. Bras. Milho Sorgo. 11:189-201.

Oliveira, G.H.H; Corrêa P.C.; Araújo E.F.; Valente, D.S.M.; Botelho F.M. 2010. Desorption isotherms and thermodynamic properties of sweet corn cultivars (*Zea mays* L.). Int. J. Food Sc. Tech. 45:546-554.

Queiroz, D.M.; Corrêa, P.C.; Souza, C.M.A. 1999. Simsec – Um programa para simulação de secagem [SIMSEC – A software for drying simulation]. In: Conferência Brasileira de Pós-Colheita, 1, Porto Alegre, 1999. Anais. Passo Fundo: Abrapós; Cesa; Embrapa Trigo, p.248.

Resende, O.; Corrêa, P.C.; Goneli, A.L. D.; Botelho, F.M.; Rodrigues, S. 2008. Modelagem matemática do processo de secagem de duas variedades de feijão (*Phaseolus vulgaris* L.) [Mathematical modeling of the drying process of two varieties of common bean (*Phaseolus vulgaris L.*)]. Rev. Bras. Prod. Agro. 10:17-26.

Resende, O.; Corrêa, P.C.; Goneli, A.L.D.; Martinazzo, A.P.; Ribeiro, R.M. 2005. Contração volumétrica na difusão líquida durante o processo de secagem do arroz em casca [Volumetric contraction in liquid diffusion during the drying of paddy rice]. Rev. Bras. Arm. 30:163-171.

Siqueira, V. C.; Resende, O.; Chaves, T. H. 2012. Difusividade efetiva de grãos e frutos de pinhão-manso [Effective diffusivity of grains and fruits of *Jatropha curcas*]. Sem. Ci. Agr. 33:2919-2930.

Souza, K.A.; Resende, O.; Chaves, T.H.; Moreira, L.C.; 2011. Cinética de secagem do nabo forrageiro (*Raphanus sativus* L.) [Drying kinetics of forage turnips (*Raphanus sativus L.*)]. Rev. Ci. Agro. 42:883-892.

Vernetti, F.J.; Vernetti Junior, F.J.; 2009. Genética da Soja: Caracteres Qualitativos e Diversidade Genética [Soybean Genetics: Genetic Diversity and Qualitative Characteristics]. Embrapa Informação Tecnológica, Brasília- DF, 221p.

Zogzas, N.P.; Maroulis, Z.B.; Marinos-Kouris, D. 1996. Moisture diffusivity data compilation in foodstuffs. Drying Technology. 14:2225-2253.

Traction performance simulation for mechanical front wheel drive tractors: towards a practical computer tool

A. Battiato,[1,2] E. Diserens,[1] L. Sartori[2]

[1]Agroscope Reckenholz-Tänikon Research Station ART, Ettenhausen, Switzerland;
[2]Land, Environment, Agriculture and Forestry Department, University of Padua, Italy

Abstract

An analytical model to simulate the traction performance of mechanical front wheel drive MFWD tractors was developed at the Agroscope Reckenholz-Tänikon ART. The model was validated via several field tests in which the relationship between drawbar pull and slip was measured for four MFWD tractors of power ranging between 40 and 123 kW on four arable soils of different texture (clay, clay loam, silty loam, and loamy sand). The pulling tests were carried out in steady-state controlling the pulling force along numerous corridors. Different configurations of tractors were considered by changing the wheel load and the tyre pressure. Simulations of traction performance matched experimental results with good agreement (mean error of 8% with maximum and minimum values of 17% and 1% respectively). The model was used as framework for developing a new module for the excel application TASCV3.0.xlsm, a practical computer tool which compares different tractor configurations, soil textures and conditions, in order to determine variants which make for better traction performance, this resulting in saving fuel and time, *i.e.* reducing the costs of tillage management.

Correspondence: Andrea Battiato, Agroscope Reckenholz-Tänikon Research Station ART, Tänikon 1, 8356 - Ettenhausen, Switzerland.
Tel. +41.(0)52.368.3332 - Fax: +41.(0)52.365.1190.
E-mail:andrea.battiato@agroscope.admin.ch
andrea.battiato@studenti.unipd.it

Key words: Drawbar pull, MFWD tractor, Traction performance, Wheel slip.

Contributions: the authors contributed equally.

Conflict of interests: the authors declare no potential conflict of interests.

Acknowledgements: we wish to acknowledge the Swiss Federal Office for the Environment FOEN and the tyre manufacturer Michelin for providing the financial support for this study.

Journal of Agricultural Engineering 2013; XLIV(s1):e67
doi:10.4081/jae.2013.(s1):e67

Introduction

Since the traction performance of a tractor has a major impact on both fuel consumption and the time required for soil tillage, optimising this performance is clearly of crucial importance in tillage management.

The traction performance of a tractor depends on many factors such as soil mechanical behaviour, wheel load, tyre inflation pressure, wheel dimensions and number, tractor geometry (wheelbase and drawbar height), engine power, and inclination of the pulling force. While most of these factors are more or less constrained, some of them, such as wheel load, tyre pressure, or number of drive wheels, can be easily managed in order to improve the traction performance of the tractor.

Effects of tractor configuration on fuel consumption, specific fuel consumption, and work-rate were reported by Lyne *et al.* (1984) and Serrano *et al.* (2009). Jenane *et al.* (1996) observed that operating at optimum tractive efficiency allows the minimum specific fuel consumption.

This study was aimed to develop a practical computer application for simulating traction performance of MFWD tractors under several configurations and on different soils. This application will be presented as a new module of the software TASC developed at the Agroscope Reckenholz-Tänikon Research Station ART (Diserens *et al.*, 2003).

The application is based on an analysis of the stress-strain interaction at soil-tyre contact surface with the model presented by Shmulevich and Osetinsky (2003) and Osetinsky and Shmulevich (2004). Models of soil-pneumatic wheel interaction based on Bekker's theory (Bekker, 1956) were previously presented by Bekker (1960), Fujimoto (1977) and Schmid (1995). Bekker (1960) assumed the contact surface between soil and tyre to be a combination of a flattened portion and the unloaded contour, Fujimoto (1977) proposed to replace the elastic tyre with a bigger rigid wheel within the area of contact with soil, whilst Schmid (1995) introduced a parabolic configuration of the tyre-soil contact surface with the apex at the front point of contact. The approach of a parabolic shaped contact surface was used later, in a modified form, by Shmulevich and Osetinsky (2003).

Materials and methods

Soil-tyre interaction modelling for a MFWD tractor

The main forces acting on the driven pneumatic wheel are shown in Figure 1, with a detail of the elementary forces acting at soil-tyre contact, according to Shmulevich and Osetinsky (2003).

The model assumes the soil to behave as a plastic non-linear medium, the wheel to roll in steady-state motion at a low velocity, and the tyre to deform in linear elasticity. The soil-tyre contact surface in the longitudinal direction has a parabolic form with the apex at the rear

point of contact *A* (Figure 1), and the wheel-soil interaction is two dimensional (plane-strain problem). This latter assumption implies that the rut depth is the same across the width, and the width is the same along the contact surface, moreover all values are referred to the unit width of the wheel.

The soil-tyre interaction model was adapted for a MFWD tractor by introducing the load transfer effect and the multipass effect.

The dynamic wheel load due to load transfer effect was considered on the basis of the equilibrium condition of the tractor body (Figure 2), as follows:

$$W_f = W_{0,f} - \Delta W \tag{1}$$

for the front wheel and

$$W_r = W_{0,r} + \Delta W \tag{2}$$

for the rear wheel.

The terms $W_{0,f}$ and $W_{0,r}$ are the stationary wheel loads on the front wheel and rear wheel, respectively, whereas W_f and W_r are the wheel loads in dynamic conditions on the front wheel and rear wheel, respectively. The term DW is the load transferred, calculated as:

$$\Delta W = \frac{T_f + T_r + (NT_f + NT_r)(h - R_{r,r}) + NT_f(R_{r,r} - R_{r,f})}{L} \tag{3}$$

in which T_f, NT_f, $R_{r,f}$ and T_r, NT_r, $R_{r,r}$ are in order the total driving torque, the net traction and the rolling radius of the front wheel and the rear wheel, respectively, h is the height of the drawbar measured on the field in the operating configuration and L is the wheelbase of the tractor (Figure 2).

Equation 3 is derived assuming the rolling radius to be a good approximation of the height of the wheel hub and to be constant, and the rut depth small enough to be neglected in the calculation. Moreover this equation is valid when the pulling force is applied horizontally, which means that the total tractor weight remains constant and only its distribution between the front and rear axles changes.

The multipass effect accounts for the different mechanical behaviour of soil interacting with the front wheel and the rear wheel, this was considered by means of a differentiated soil mechanical characterization with bevameter tests before tractor passage as well as on the rut left from the passage of the front wheel, according to Bekker (1960).

For a tractor with rigid coupling between the front and the rear axles, the ratio of the theoretical speed of the front wheel to that of the rear wheel K_s is fixed, and therefore there is a precise relationship between the slip of the front wheel i_{front} and that of the rear wheel i_{rear} in straight line motion:

$$i_{front} = 1 - \frac{(1 - i_{rear})}{K_s} \tag{4}$$

Preliminary tests with the four MFWD tractors, in all configurations considered, have indicated values of K_s very close to 1 (between 0.993 and 1.016), this allowed a simplified analysis in which the slip of the front wheel and that of the rear wheel were assumed to be the same.

Design of field tests

Several traction tests were carried out with a Hürlimann H488 DT (65 kW, 40.8 kN) chosen as reference tractor for this study. Additional traction tests were carried out with a FIAT 50-66 DTS (40.4 kW, 25.3 kN), a John Deere 6920 (110 kW, 66.7 kN), and a John Deere 6930 (123 kW, 68 kN).

The pulling force was obtained by means of a second tractor used as braking machine. In this case were used different tractors having weight always higher than the pulling tractor.

The pulling and the braking tractors were connected by a steel cable and moved aligned as sketched in Figure 3. The traction force was measured by a load cell in section with the steel cable. The actual forward velocity was measured by a radar velocity sensor, whilst the wheel rolling velocity was registered by means of a wireless wheel speed sensor of two pulses per wheel revolution set on a rear wheel of the pulling tractor. All these parameters were recorded and displayed by an auto-

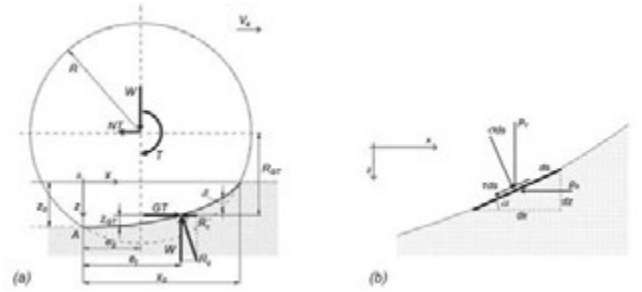

Figure 1. Interaction between soil and a driven pneumatic wheel (a) with the detail of the elementary forces at soil-tyre contact (b) according to Shmulevich and Osetinsky (2003).

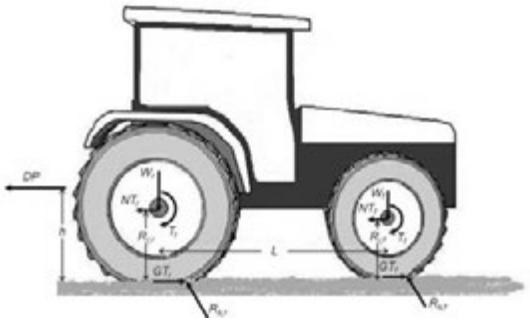

Figure 2. Forces on a MFWD tractor.

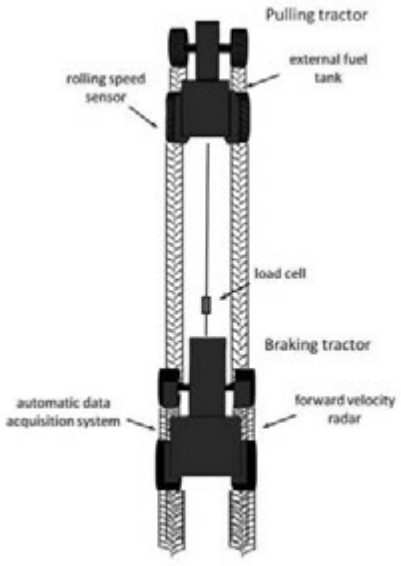

Figure 3. Layout of the tractor pulling test.

matic acquisition system in the braking tractor. The stationary wheel load was measured with flat bed scales.

Different tractor configurations were considered by changing tyre inflation pressure and wheel load (Table 1).

The traction tests were carried out on four sites having different soil textures. Physical and mechanical parameters of topsoil (0-10 cm depth) of the four sites are reported in Table 2. The volumetric water content was measured by means of a time domain reflectometry (TDR) device with two-rod single diode probes at a depth of 10 cm. The water potential at 10 cm of depth was measured with field tensiometers.

The mechanical parameters of soil required for the simulation were obtained on the basis of vertical plate penetration tests and horizontal plate shear deformation tests (Bekker, 1960) with a tractor-mounted bevameter (Figure 4) (Diserens and Steinmann, 2003). The bevameter has a massive frame with a central jack powered by the hydraulic system of the tractor. A laptop is used as datalogger. The vertical force and the axle torque are measured by a load cell and a torque cell, respectively. The soil sinkage is measured by means of an ultrasound sensor which stands on a tripod frame and reflects the signal on a specific surface on top of the compression plate (Figure 4B). The rotation of the lugged plate (Figure 4C) is measured by a tachometer.

The penetration tests were repeated with two circular plates of 20 and 30 cm in diameter in order to account for the influence of the tyre width on the pressure-sinkage relationship of soil (Bekker, 1960). Both the penetration tests and the shear deformation tests were executed according to indications reported by Bekker (1956) and Bekker (1960), and parameters K_c, K, n, c, and k (Table 2) were determined according to the procedure described by Wong (1980).

In order to consider the multipass effect, the mechanical tests were executed before tractor passage as well as on the rut left from the passage of the front wheel. Parameters K_c, K and n calculated before and after the passage of the front wheel changed significantly in the clay soil but not in the other locations which were widely trafficked, conse-

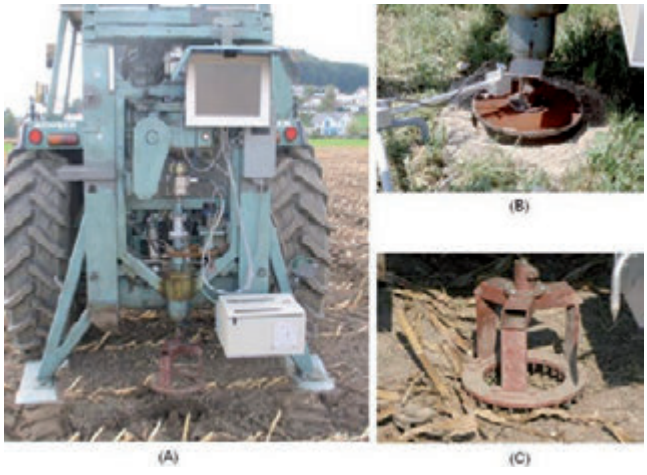

Figure 4. The tractor-mounted bevameter (A), the circular plate (30 cm wide) for compression tests (B), and the lugged plate for shear tests (C).

Table 1. Configurations of tractors.

Tractor	Configuration	Tyre F / R*	Wheel load [kN] C / CL / SL / LS**	Tyre Pressure [kPa] C / CL / SL / LS
Hürlimann H488 DT	1	F	9.1 / 9.1 / 9.1 / 9.1	60 / 60 / 60 / 60
65 kW		R	10.9 / 10.9 / 10.9 / 10.9	60 / 60 / 60 / 60
F = (380/85R24)	2	F	9.1 / 9.1 / 9.1 / 9.1	160 / 160 / 160 / 160
R = (420/85R34)		R	10.9 / 10.9 / 10.9 / 10.9	160 / 160 / 160 / 160
	3	F	10.3 / 10.3 / 10.3 / -	60 / 60 / 60 / -
		R	14.3 / 14.3 / 14.3 / -	60 / 60 / 60 / -
	4	F	10.3 / 10.3 / 10.3 / -	14.3 / 14.3 / 14.3 / -
		R	160 / 160 / 160 / -	160 / 160 / 160 / -
FIAT 50-66 DTS	1	F	- / 5.8 / - / -	- / 60 / - / -
40.4 kW		R	- / 6.3 / - / -	- / 90 / - / -
F = (8.3R24)	2	F	- / 5.8 / - / -	- / 160 / - / -
R = (230/95R36)		R	- / 6.3 / - / -	- / 180 / - / -
	3	F	- / 7.0 / - / -	- / 60 / - / -
		R	- / 10.7 / - / -	- / 90 / - / -
	4	F	- / 7.0 / - / -	- / 160 / - / -
		R	- / 10.7 / - / -	- / 180 / - / -
John Deere 6920	1	F	- / 14.1 / - / -	- / 50 / - / -
110 kW		R	- / 19.1 / - / -	- / 50 / - / -
F = (540/65R28)	2	F	- / 14.1 / - / -	- / 140 / - / -
R = (650/65R38)		R	- / 19.1 / - / -	- / 140 / - / -
John Deere 6930	1	F	- / - / - / 14.7	- / - / - / 60
123 kW		R	- / - / - / 19.3	- / - / - / 60
F = (540/65R28)	2	F	- / - / - / 14.7	- / - / - / 140
R = (650/65R38)		R	- / - / - / 19.3	- / - / - / 180
	3	F	- / - / - / 14.3	- / - / - / 60
		R	- / - / - / 31.0	- / - / - / 60
	4	F	- / - / - / 14.3	- / - / - / 140
		R	- / - / - / 31.0	- / - / - / 180

*F, Front tyre; R, Rear tyre. **C, clay; CL, clay loam; SL, silty loam; LS, loamy sand.

quently they were differentiated for soil interacting with the front wheel ($K_{c,f}$, $K_{,f}$, n_f) and soil interacting with the rear wheel ($K_{c,r}$, $K_{,r}$, n_r), as reported in Table 2. The shear parameters c, and k did not change significantly before and after the passage of the front wheel in all locations and for these a unique characterization was adopted.

The tyre rolling radius R_r was determined according to the ASAE Standard S296.2 as the distance travelled per revolution of the wheel divided by 2π when operating at the specified zero condition. This latter was assumed as the vehicle operating in self-propelled condition on a hard surface, such as a smooth road, according to Wismer and Luth (1973).

The stiffness of the tyre was calculated on the basis of tyre dimensions, according to Lines and Murphy (1991).

Results and discussion

Results of field tests

Influence of tractor size and power on traction performance is pointed out in Figure 5A, where measured and simulated drawbar pull for

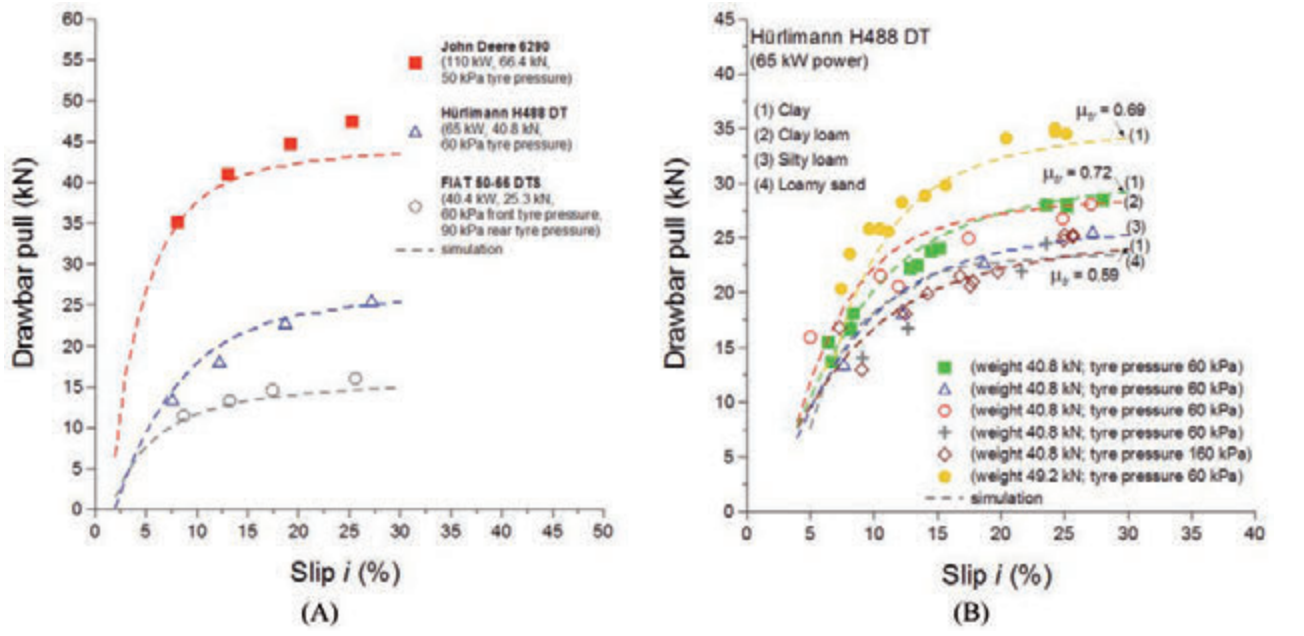

Figure 5. Measured and simulated traction performance: (A) influence of tractor power on the clay loam; (B) influence of wheel load, tyre pressure, and soil texture.

Table 2. Physical and mechanical parameters of topsoil in the four locations considered.

Soil property 0-0.10 m depth	C*	CL*	SL*	LS*
Sand [%]	20	31	20	84.2
Silt [%]	32	34	53	10.1
Clay [%]	48	35	27	5.7
Texture (USDA)	clay	clay loam	silty loam	loamy sand
Volumetric water content θ [%]	27.0	28.4	40.2	15.2
Water potential s [kPa]	6.11	9.45	1.27	57.40
Cohesive modulus of deformation (front) $K_{c,f}$ [kN/m$^{(n+1)}$]	2354.1	4554.8	298.2	1208.2
Frictional modulus of deformation (front) $K_{\varphi,f}$ [kN/m$^{(n+2)}$]	-4130.0	-3036.5	479.0	-805.5
Exponent of deformation (front) n_f	1.01	0.90	0.77	0.81
Cohesive modulus of deformation (rear) $K_{c,r}$ [kN/m$^{(n+1)}$]	2168.9	4554.8	298.2	1208.2
Frictional modulus of deformation (rear) $K_{\varphi,r}$ [kN/m$^{(n+2)}$]	-3498.3	-3036.5	479.0	-805.5
Exponent of deformation (rear) n_r	0.79	0.90	0.77	0.81
Cohesion c [kPa]	15.5	5.0	15.9	29.2
Angle of shear resistance φ [°]	26.5	30.0	25.6	6.4
Shear deformation modulus k [m]	0.014	0.010	0.010	0.012

*C, clay; CL, clay loam; SL, silty loam; LS, loamy sand

the FIAT 50-66 DTS, the Hürlimann H488 DT and the John Deere 6920 are compared on the clay loam. As expected, tractors of bigger size and more powerful have higher traction performance.

Influence of variations in wheel load and tyre inflation pressure on traction performance are simulated consistently, as reported in Figure 5B. Here measured and simulated drawbar pull of the Hürlimann H488 DT are compared with and without ballast and at two tyre inflation pressures (60 kPa and 160 kPa) on the clay soil. The effect of variations in wheel load and tyre inflation pressure is also compared in terms of traction coefficient whose value is reported for a slip of 30%, this coefficient is defined as the ratio between the drawbar pull and the tractor load:

$$\mu_{tr} = \frac{DP}{W_{Tractor}} \quad (5)$$

The traction performance depends on the extension of the soil-tyre contact surface as well as on the stress state along this latter. Both the extension and the stress state are controlled by the stiffness of the tyre, the wheel load, and the mechanical behaviour of soil.

According to results reported by Turner (1993) and Zoz and Grisso (2003), an increase in tractor weight (wheel load) makes for higher drawbar pull, however, it doesn't seem to produce a significant variation in terms of traction coefficient.

Increasing wheel load causes, on the one hand, an increase in soil deformation and compaction resistance, on the other hand, the soil-tyre contact surface to become more extended. This produced an increase in drawbar pull but did not improve traction performance in terms of the traction coefficient, which decreased slightly (Figure 5B).

With regard to the variation in tyre inflation pressure, many authors have shown the benefits on traction performance of tractors of reduced inflation pressure (Burt and Bailey, 1982; Wood and Mangione, 1992; Upadhyaya and Wulfsohn, 1993; Turner, 1993; Zoz and Grisso, 2003).

A decrease in tyre inflation pressure produces an increase in the traction force as well as in the traction coefficient (Figure 5B), this effect is due to a bigger contact surface between soil and tyre which allows a better use of topsoil strength, especially in cohesive soils which usually present low frictional component of resistance and high cohesive component.

At low tyre inflation pressure the tractor develops, for the same slip, higher drawbar pull than with high tyre inflation pressure or, analogously, it develops the same traction force with less slip. This fact has evident consequences on the energy efficiency of the traction development.

In Figure 5B the measured and the simulated drawbar pull of the Hürlimann H488 DT are also compared in the four terrains considered. Physical and mechanical parameters of the topsoil in the four locations were widely different (Table 2), as a consequence, the same tractor configuration produced different traction performance. This confirming that tractor traction performance depends on the tractor-terrain system, being not exclusive peculiarity of tractor configuration.

For a fixed contact surface, the maximum traction is controlled by soil strength, whereas the way the traction is developed with slip is

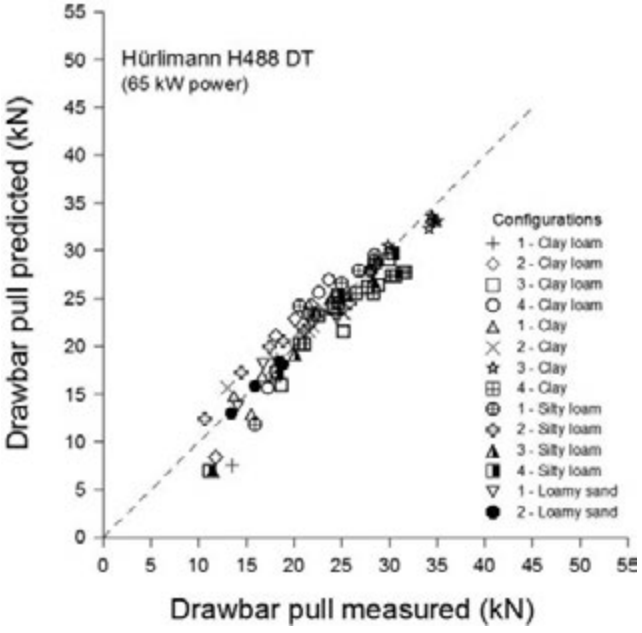

Figure 6. Comparison between measured and simulated drawbar pull of the Hürlimann H488 DT on the four sites for the different configurations considered.

Table 3. Accuracy of traction performance simulations.

Tractor	Configuration C / CL / SL / LS*	Mean residual [kN] C / CL / SL / LS*	Mean error
Hürlimann H488 DT	1	1.00 / 1.86 /1.61 / 0.98	0.05 / 0.13 / 0.08 / 0.05
65 kW	2	0.94 / 2.88 / 1.69 / 0.31	0.05 / 0.17 / 0.10 / 0.02
	3	1.04 / 2.37 / 1.92 / -	0.03 / 0.10 / 0.13 / -
	4	1.66 / 2.26 /1.60 / -	0.06 / 0.10 / 0.12 / -
FIAT 50-66 DTS	1	- / 0.73 / - / -	- / 0.05 / - / -
40.4 kW	2	- / 0.86 / - / -	- / 0.09 / - / -
	3	- / 0.16 / - / -	- / 0.01 / - / -
	4	- / 0.35 / - / -	- / 0.02 / - / -
John Deere 6920	1	- / 2.07 / - / -	- / 0.05 / - / -
110 kW	2	- / 2.71 / - / -	- / 0.10 / - / -
John Deere 6930	1	- / - / - / 4.35	- / - / - / 0.14
123 kW	2	- / - / - / 1.22	- / - / - / 0.04
	3	- / - / - / 1.93	- / - / - / 0.06
	4	- / - / - / 2.22	- / - / - / 0.06

*C, clay; CL, clay loam; SL, silty loam; LS, loamy sand.

controlled by the stiffness of soil under shear stress, as measured in the bevameter tests.

From the point of view of the tractor configuration, the drawbar pull rises when the area of interaction between soil and tyre increases. This could be obtained by means of a decrease in tyre inflation pressure, an increase of wheel load or by using dual tyres.

In Figure 6 the measured and predicted drawbar pull of the Hürlimann H488 DT are compared for the different configurations considered (Table 1) in the four sites (Table 2).

In Table 3 the accuracy of the simulation of the drawbar pull is reported in terms of mean residual and mean error for all the configurations considered in our tests.

Model simulations matched experimental measurements with general good agreement within the slip range considered (mean error of 8% with maximum and minimum values respectively of 17% and 1%).

Development of a new module for TASCV3.0.xlsm

The validated approach to model tractor traction performance was used as framework for developing a new excel module for the third version of TASC (http://www.agroscope.admin.ch/praxis/00220/06773/06777/index.html?lang=en). This module also simulates the topsoil damage from cutting effect due to tyre slip on the basis of an analysis of the stress state at soil-tyre contact surface (Battiato and Diserens, 2011).

For the farmers, three practical tests were set up to allow a fast, simple and reliable mechanical characterization of the topsoil behaviour.

Different tractor configurations, soil textures and conditions can be confronted. TASCV3.0.xlsm offers a valuable support to find out tractor configurations and soil conditions which optimise traction, this resulting in saving fuel and time, *i.e.* reducing the costs of tillage management.

Conclusions

This study aimed to develop an analytical model to simulate the traction performance of MFWD tractors on the basis of an analysis of the stress-strain interaction at soil-tyre contact surface.

The model presented matched experimental results with good agreement (mean error of 8% with maximum and minimum values respectively of 17% and 1%). Moreover, it provided consistent simulations of the effect of variations in tyre pressure and wheel load, and besides, of the influence of soil texture.

A new module for the third version of the excel application TASC is developed on the basis of this model.

This practical computer tool offers a valuable support to find out tractor configurations and soil conditions which optimise traction performance, *i.e.* which reduce the costs of tillage management.

References

American Society of Agricultural Engineers 1983. Agricultural engineers yearbook of standards. ASAE Standard S296.2 - Uniform terminology for traction of Agricultural Tractors, Self-Propelled Implements, and other Traction and Transport Devices. ASAE, St. Joseph, MI, USA.

Battiato A., Diserens E. 2011. Predicting topsoil damage from slip of tractor tires. Bodenkundliche Gesellschaft der Schweiz. Bulletin 32:21-6.

Bekker M.G. 1956. Theory of Land Locomotion. University of Michigan Press, Ann Arbor, MI, USA.

Bekker M.G. 1960. Off-the-Road Locomotion. University of Michigan Press, Ann Arbor, MI, USA.

Burt E.C., Bailey A.C. 1982. Load and inflation pressure effects on tires. Trans. ASAE. 25:881-4.

Diserens E., Spiess E., Steinmann G. 2003. TASC: a new practical computer tool to prevent soil compaction damage in arable farming. Proc. Int. Conf. Geo-Environmental Engineering, Singapore, pp. 85-92.

Diserens E., Steinmann G. 2003. In-situ determination of the fracture point of an agricultural soil using the plate penetration test, comparison with the oedometer method and validation. Proc. Int. Conf. Geo-Environmental Engineering, Singapore, pp. 93-106.

Fujimoto Y. 1977. Performance of elastic wheels on yielding cohesive soils. J. Terramech. 14:191-210.

Jenane C., Bashford L.L., Monroe G. 1996. Reduction of fuel consumption through improved tractive performance. J. Agric. Eng. Res. 64:131-8.

Lines J.A., Murphy K. 1991. The stiffness of agricultural tractor tyres. J. Terramech. 28:49-64.

Lyne P.W.L., Burt E.C., Meiring P. 1984. Effect of tire and engine parameters on efficiency. Trans. ASAE 27:5-7.

Osetinsky A., Shmulevich I. 2004. Traction performance simulation of a pushed/pulled driven wheel. Trans. ASAE 47:981-94.

Schmid I.C. 1995. Interaction of vehicle and terrain results from 10 years research at IKK. J. Terramech. 32:3-26.

Serrano J.M., Peça J.O., Silva J.R., Márquez L. 2009. The effect of liquid ballast and tyre inflation pressure on tractor performance. Biosystems Eng. 102:51-62.

Shmulevich I., Osetinsky A. 2003. Traction performance of a pushed/pulled drive wheel. J. Terramech. 40:35-50.

Turner R.J. 1993. A simple system for determining tractive performance in the field. ASAE/CSAE meeting presentation, ASAE paper No. 93-1574. ASAE, St. Joseph, MI, USA.

Upadhyaya S.K., Wulfsohn D. 1993. Traction prediction using soil parameters obtained with an instrumented analog device. J. Terramech. 30:85-100.

Wismer R.D., Luth H.J. 1973. Off-road traction prediction for wheeled vehicles. J. Terramech. 10:49-61.

Wong J.Y. 1980. Data processing methodology in the characterization of the mechanical properties of terrain. J. Terramech. 17:13-41.

Wood R.K., Mangione D.A. 1992. Tractive benefits of properly adjusted inflation pressure: Farmer experiences. ASAE paper No. 92-1583. ASAE, St. Joseph, MI, USA.

Zoz F.M., Grisso R.D. 2003. Traction and tractor performance. ASAE distinguished lecture series (Tractor design No. 27), ASAE publication No. 913C0403. ASAE, St. Joseph, MI, USA.

Soil management effect on soil penetration resistance in the vineyard

Pietro Catania,[1] Mariangela Vallone,[1] Felice Pipitone,[1] Gioacchino Francesco Argento,[1] Giuseppe Spartà,[2] Vito Armando Laudicina[1]

[1]University of Palermo, Dipartimento di Scienze Agrarie e Forestali, Palermo, Italy; [2]Assessorato Regionale Risorse Agricole e Alimentari, Palermo, Italy

Abstract

In environments characterized by steep slopes or arranged in terraces, among the shallow tillage systems, rototilling is extensively used. However, the effect of the repeated use of rototilling has a considerable influence on soil characteristics; it appears finely powdered, soft and without structure. In order to limit these inconveniences, an innovative self-propelled machine equipped with working tools as a spade, to be used in steep slopes or arranged in terraces areas, was designed by the Mechanics Section of the SAF (Scienze Agrarie e Forestali) Department of the University of Palermo in cooperation with Agrotec company, Padua, Italy. The aim of this study is to compare the effects of three machines for shallow tillage: a chisel plough (CP), a rototilling (RT) and a spading machine (SM) on penetration resistance in semi-arid environments of the Mediterranean basin. No tillage was also included. Penetration resistance (PR) was surveyed for all the treatments to a depth of 300 mm with an electronic dynamometer. The treatments consisted in the execution of a shallow tillage to a depth of 150 mm. SP treatment allowed us to obtain PR lower values throughout the tillage profile than RT, CP and NT. It follows that the type of machine used influences soil PR, and then the soil water storage capacity, key factor for the agricultural productions in semi-arid environments as in Sicily.

Correspondence: Pietro Catania, University of Palermo. Dipartimento di Scienze Agrarie e Forestali, Viale Delle Scienze Edificio 4, 90128 Palermo, Italy.
Tel. +39.91.23865608.
E-mail: pietro.catania@unipa.it

Key words: penetration resistance, spading machine, tillage

Contributions: the authors contributed equally.

Conflict of interests: the authors declare no potential conflict of interests.

Conference presentation: part of this paper was presented at the 10th Italian Conference AIIA (Associazione Italiana di Ingegneria Agraria), 2013 September 8-12, Viterbo, Italy.

Journal of Agricultural Engineering 2013; XLIV(s1):e68
doi:10.4081/jae.2013.(s1):e68

Introduction

In environments characterized by steep slopes or arranged in terraces, among the shallow tillage systems, rototilling is extensively used. This is because this machine allows in one step to clean the soil from weeds, to obtain it well crumbled and in excellent condition for the subsequent operations. It can also be adjusted to enhance the tractor coupling and optimize the balance between energy cost and quality of work (Pezzi, 2005, Hendrick, 1980).

However, the effect of the repeated use of rototilling has a considerable influence on soil characteristics; it appears finely powdered, soft and without structure.

This phenomenon is even more favored in environments with volcanic soils (island of Pantelleria, mount Etna, island of Salina, etc.) with predominantly pyroclastic deposits, characterized by compositional and textural heterogeneity, high porosity and poor mechanical strength properties. Therefore, these soils have an high degree of vulnerability and are closely prone to surface instability and erosion (Vallone *et al.*, 2007). Soil pulverization causes a lack in soil structure and this immediately causes the loss of its storage capacity of water reservoir and, consequently, of its fertility.

In order to limit these inconveniences, an innovative self-propelled machine equipped with working tools as a spade, to be used in steep slopes or arranged in terraces areas, was designed by the Mechanics Section of the SAF (Scienze Agrarie e Forestali) Department of the University of Palermo in cooperation with Agrotec company, Padua, Italy.

The aim of this study is to compare the effects of three machines for shallow tillage: a chisel plough (CP), a rototilling (RT) and a spading machine (SM) on penetration resistance in semi-arid environments of the Mediterranean basin. No tillage was also included.

Materials and methods

The innovative spading machine (SM) is self-propelled and is equipped with five working tools of the spade-type with two blows each moved by the hydraulic circuit of the machine. The rototilling (RT) has got eight elements, inserted into the central rotor, driven by the PTO of the tractor. The chisel plough (CP) has got five chisels. The machines used in the tests are shown in Fig.1. Four treatments were realized, including no tillage.

The tests were performed in the spring of 2012 (April-May) on a sandy clay loam soil. The experimental plot was inside the Faculty of Agriculture of the University of Palermo, it was covered in vineyard and located at 38 ° 06' N and 13 ° 20' E, 48 m above sea level. The area's climate is mild with rainfall largely concentrated in the winter.

Penetration resistance (PR) was surveyed for all the treatments to a depth of 300 mm with an electronic dynamometer (IMADA, DPS 5R – USA) detecting forces up to 500 N, connected to a mechanical stand

(IMADA MX2-500N - L). The measured values, recorded by the software IMADA ZP Recorder, were downloaded to a spreadsheet for further processing. The penetrometer used for the tests was equipped with a cone having 10 mm diameter base; it was mounted to the dynamometer through a 6 mm diameter steel bar (Fig. 2).

The treatments consisted in the execution of a shallow tillage to a depth of 150 mm using the three different machines; three blocks were located inside the experimental plot and divided into four subplots where the treatments were randomly performed. Penetration tests were performed soon after tillage at the time called T1 on the four treatments (SP, RT, CP and NT) till 300 mm depth. Penetration resistance was also evaluated 30 days after tillage at the time called T2. Statistical analysis was performed using Statgraphics Centurion by Statpoint inc., USA.

Results

Figure 3 shows penetration resistance soon after tillage (T1) for the four treatments till 300 mm depth.

The lowest PR values were obtained in SM treatment, then RT and CP and lastly NT. Note that, till 200 mm depth, PR values at 75, 100, 150 and 200 mm depth in SM treatment show statistically significant differences respect to the other treatments at the same depths. In particular, note that these differences were obtained for a layer corresponding to 50% of that entirely tilled. At the depth of 75 mm, the average values obtained by SM are lower by about 62% than those of RT, 74% of CP and 80% of NT. At the depth of 100 mm the average values obtained by SM are lower by about 74% than those of RT, 77% of CP and 83% of NT. At the depth of 150 mm, the average PR values for SM are lower by about 52 % of RT, 70% of CP and 58% of NT.

Penetration resistance data 30 days after tillage (T2) for the four treatments till 300 mm depth are shown in Figure 4. It comes out that thirty days after tillage there is an increase in the value of PR in all the treatments. SM treatment gave PR average values lower than the others with statistically significant differences in the soil layer between 50 and 110 mm, equal to 40% of the tilled soil.

In particular, note that at the depth of 75 mm, the average values obtained by SM are lower by about 77% than those of RT, 64% of CP and 80% of NT. At the depth of 100 mm the average values obtained by SM

Figure 1. Machines used during the tests. a) Spading machine (SP), b) Rototilling (RT), c) Chisel plough (CP).

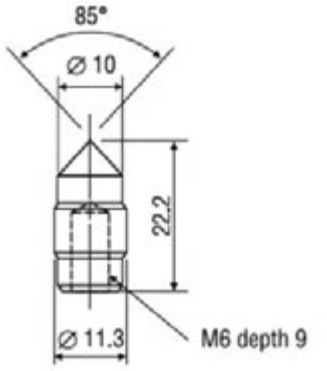

Figure 2. Cone penetrometer section used to measure penetration resistance.

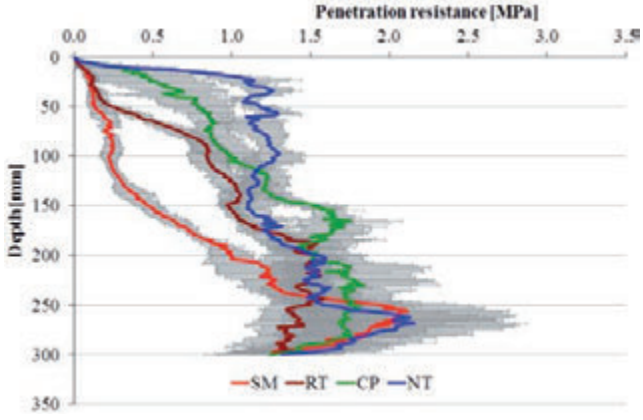

Figure 3. Penetration resistance for Spading Machine (SM), Rototilling (RT), Chisel Plough (CP) and No Tillage (NT) treatments soon after tillage (data are reported as means ± standard deviations of the three replicates).

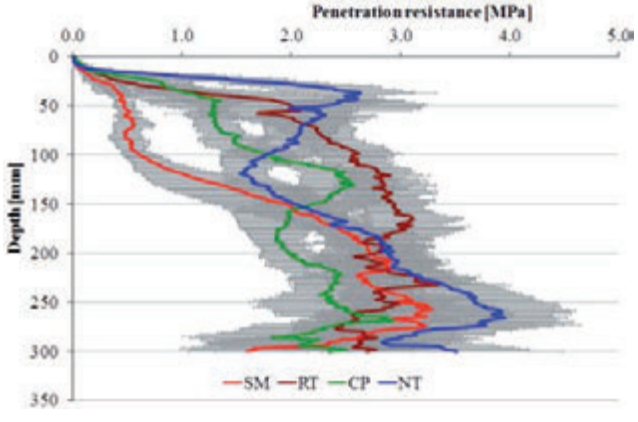

Figure 4. Penetration resistance for Spading Machine (SM), Rototilling (RT), Chisel Plough (CP) and No Tillage (NT) treatments 30 days after tillage (data are reported as means ± standard deviations of the three replicates).

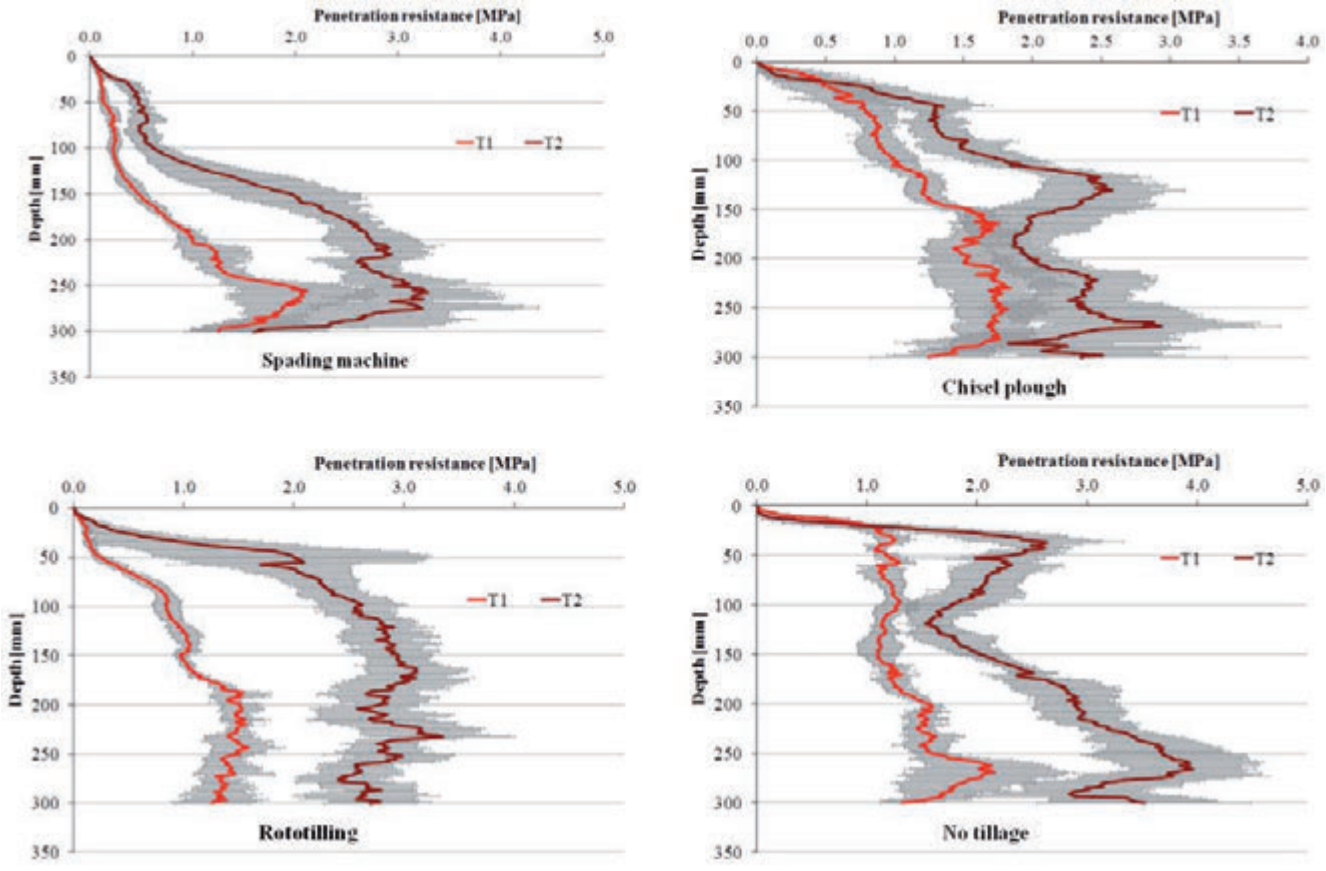

Figure 5. Penetration resistance for Spading Machine (SM), Rototilling (RT), Chisel Plough (CP) and No Tillage (NT) treatments soon after (T1) and 30 days after tillage (T2)(data are reported as means ± standard deviations of the three replicates).

are lower by about 76% than those of RT, 66% of CP and 65% of NT.

Finally, comparing PR values in the four treatments, there are not statistically significant differences.

In Figure 5 we report the penetration resistance data collected individually in the four treatments in the two periods, immediately after tillage (T1) and thirty days after (T2).

Comparing the PR mean values obtained immediately after tillage (T1) and thirty days after it (T2) it comes out that RT is the treatment that undergoes a significant increase. The PR average values, in fact increase, with statistically significant differences between T1 and T2, of about 1.75 MPa at 50 mm depth, of about 1.71 MPa at 100 mm depth and of about 1.97 MPa at 150 mm depth. MS treatment thirty days after tillage, shows PR average values higher by about 0.34 MPa at 50 mm depth, by about 0.39 MPa at a depth of 100 mm and about 1.49 MPa at 150 mm depth with statistically significant differences between T1 and T2. CP and NT treatments show PR increases less considerable than the other.

Conclusions

The study was aimed at comparing the effects of three machines for shallow tillage: a chisel plough (CP), a rototilling (RT) and a spading machine (SM) on penetration resistance in a semi-arid environment of the Mediterranean basin. No tillage was also included.

SP treatment allowed us to obtain PR lower values throughout the tillage profile than RT, CP and NT. As regards the PR values obtained along the soil profile between 0 and 150 mm, it appears that:

- in SP treatment PR does not exceed 2 MPa immediately after and 30 days after tillage in the whole layer interested in tillage;
- in RT treatment PR reaches 3 MPa at about 150 mm depth 30 days after tillage;
- in CP treatment PR reaches 2.5 MPa at about 150 mm depth 30 days after tillage;
- in NT treatment PR reaches 2.5 MPa in the first 50 mm of depth 30 days after tillage.

It follows that the type of machine used influences soil PR, and then the soil water storage capacity, key factor for the agricultural productions in semi-arid environments as in Sicily.

References

Bachmann J., Contreras K., Hartge K.H., MacDonald R. 2006. Comparison of soil strength data obtained in situ with penetrometer and with vane shear test. Soil & Tillage Research, 87, 112-118.

Hendrick J.G., 1980. A powered rotary chisel. Transactions of the ASAE, 1349-1352.

Lopez M.V., Arrue J.L., Sanchez-Giron V. 1996. A comparison between seasonal changes in soil water storage and penetration resi stance under conventional and conservation tillage systems in Aragon.

Soil & Tillage Research, 37, 251-271.
Pezzi F., 2005. Traditional and new deep soil tillage techniques in Italy. Transactions of the ASAE, 48(1), 13-17.
Sandri R., Anken T., Hilfiker T., Sartori L., Bollhalder H. 1998. Comparison of methods for determining cloddiness in seedbed preparation. Soil & Tillage Research, 45, 75-90.
Singh B., Malhi S.S. 2006. Response of soil physical properties to tillage and residue management on two soils in a cool temperate environment. Soil & Tillage Research, 85, 143-153.
Vallone M., Catania P., Pipitone F. Carrara M., 2007. Analisi delle modalità di gestione dei suoli di Pantelleria al fine di preservarne la fertilità - Atti del Convegno Nazionale AIIA 2007: Tecnologie innovative nelle filiere: orticola, vitivinicola e olivicolo-olearia, 5-7 Sept, Pisa e Volterra, Italy, II, 44-47.

Study of a test methodology to assess potential drift generated by air-assisted sprayers

Paolo Balsari, Paolo Marucco, Claudio Bozzer, Mario Tamagnone

Dipartimento di Scienze Agrarie Forestali e Alimentari, DiSAFA, Università di Torino, Italy

Abstract

During pesticide application spray drift may cause diffuse pollution phenomena in the environment. In the last years the European Union, through the Directive on the sustainable use of pesticides (128/2009 EC), has recommended the adoption of measures enabling to prevent spray drift. Among these measures, the adoption of buffer zones beside the sprayed fields requires to consider different widths for these no spray zones according to the amount of spray drift generated by the spraying equipment used for application. It is therefore necessary to classify the different sprayer models according to drift risk. For what concerns the sprayers used on arboreal crops, in order to make this classification in a simple and quick way as it was already proposed for the field crop sprayers (ISO FDIS 22369-3), a study was started aimed at defining a methodology to assess potential drift produced by the different sprayer models in absence of wind, using ad hoc test benches. On the basis of the positive first experimental data obtained, a first proposal for a new ISO standard methodology was prepared.

Introduction

The European Directive 128/2009 EC on sustainable use of pesticides prescribes to use the most efficient spraying equipment in order to prevent environmental contamination risks, especially those related to aquatic organisms. Prevention of spray drift is therefore a key aspect, as the dispersion of part of the droplets sprayed on crops outside the target field may cause not negligible contamination risks for the surrounding environment and even for bystanders. On the other hand, the recent amendment of the Machinery Directive (127/2009 EC) requires that all new sprayers comply with a set of technical features which are relevant to guarantee the environmental safeguard in spray application.

In recent years several European countries have already adopted some measures to prevent risks of environmental contamination with pesticides, establishing buffer zones along water courses and sensitive areas. Generally, the width of the buffer zone is defined according to the type of plant protection product applied (toxicity, dose), to the characteristics of the area adjacent to the sprayed field (*e.g.* water courses, urban areas, other sensitive crops) and to the features of the spraying equipment used.

Classification of sprayers according to drift risk is therefore necessary in order to modulate the width of buffer zones in function of the sprayer type used. Actually ISO standard 22369 defines the classes of drift reduction with respect to a reference sprayer and refers to ISO standard 22866 for the assessment of spray drift in the field. This methodology, however, is rather complex, reproducibility of results is poor and results are strictly related to the agro-environmental context in which tests are carried out.

As there is a huge number of types and configurations of air-assisted sprayers for arboreal crops, their classification applying ISO 22866 test methodology would be long and expensive. Moreover, it should be repeated in each country/region taking into account the most common characteristics of the vineyards/orchards (layout, training system, plant size, etc.). Aim of the present study was therefore to develop a simpler methodology for assessing the potential drift generated by air-assisted sprayers for arboreal crops in absence of wind.

Materials and methods

Tests were made using two different air-assisted sprayers: one for orchards (Nobili Oktopus 1000, equipped with 7+7 nozzles, radial fan and multiple hoses to convey the air to the air spouts positioned in correspondence of the nozzles) and one for vineyards (Dragone k2 500, equipped with 4+4 nozzles, axial fan and tower shaped air conveyor). Each sprayer was tested using either conventional hollow cone nozzles or air induction flat fan nozzles (Table 1). In all trials a forward speed of 6 km/h was adopted and 5 replicates were made.

Volume application rate for the orchard sprayer was 1000 l/ha, assuming to operate with a distance between rows of 4 m, while for the vineyard sprayer it was 340 l/ha, assuming to operate with a distance between rows of 2.5 m.

Tests were carried out in absence of wind (maximum wind velocity < 0.5 m/s), operating the sprayer along a track made of concrete 50 m long and 3 m wide, in order to minimise the effects of eventual jerks on spray distribution. On the right side of the track, perpendicular to the sprayer forward direction, four arrays of Petri dishes were placed. In each array the first sampler was positioned at 2 m distance from the centre of the sprayer, the following samplers were positioned every one meter until 20 m distance from the centre of the sprayer (Figure 1A). The first array of Petri dishes was left always uncovered while the

Correspondence: Paolo Marucco, Dipartimento di Scienze Agrarie Forestali e Alimentari, DiSAFA, Università di Torino, via L. da Vinci 44, 10095 Grugliasco (TO), Italy
Tel. +39.011.6708599 - Fax: +39.011.2368599.
E-mail: paolo.marucco@unito.it

Key words: sprayer, drift, classification, test bench.

Journal of Agricultural Engineering 2013; XLIV(s1):e69
doi:10.4081/jae.2013.(s1):e69

other three arrays were placed in ad hoc test benches designed at DiSAFA – University of Torino (Balsari *et al.*, 2007). These test benches are provided with a sliding cover that is automatically activated by the tractor pass through a pneumatic system. In practice, a tractor mounted appendix hits a vertical pole that is linked to the mechanism of the sliding covers. Position of the vertical pole was established in such a way that test benches were uncovered after the sprayer pass when the spraying nozzles were, respectively, at distances of 2, 4 and 6 m with respect to the benches (Figure 1B).

The system of samplers therefore enabled to assess to projection of the spray jet on the permanently uncovered Petri dishes and to evaluate, on the Petri dishes revealed only after the sprayer pass, the fraction of droplets that remain suspended in the air after the sprayer pass and then fall down to the ground. The latter represents the part of droplets more prone to drift as they can be blown out of the treated area by environmental wind.

Tests were carried out spraying a water solution of yellow tracer Tartrazine E 102 (10% v/v). Amount of spray deposits collected on plastic Petri dishes (15 cm diameter) were measured in laboratory by means of spectrophotometric analysis.

Results

Test results pointed out that the orchard sprayer is featured by a longer spray jet range (about 20 m distance from the centre of the sprayer) with respect to the vineyard sprayer, whose spray jet range is limited to about 14 metres from the sprayer centre (Figure 2). Profiles of spray jet range registered in the five replications of each test presented a good reproducibility in terms of sum of spray deposits registered at the difference sampling distances (Table 2).

Use of air induction nozzles on the orchard sprayer did not have a significant impact on the profile of the spray jet range (Figure 3A) while it reduced consistently the length of the spray jet range for the vineyard sprayer; in this latter case spray deposits were concentrated at 4-5 m from the centre of the sprayer (Figure 3B).

The spray deposits detected on the samplers positioned along the test benches resulted lower with respect to those measured on the permanently uncovered samplers. Deposits decreased according to the distance of the test bench from the point of activation of the sliding covers. This fact resulted more evident when air induction nozzles were used, either on orchard or on vineyard sprayers (Figures 4 and 5).

Discussion

On the basis of the results obtained a method for calculating a drift potential index (DPI) for each thesis examined was studied. As a first step, it was considered necessary to estimate the amount of spray recovered on the permanently uncovered samplers with respect to the

Table 1. Sprayers and operative parameters examined in the trials.

Test	Sprayer model	Nozzles	Pressure (MPa)	Sprayer flow rate (l/min)	Fan air flow rate (m3/h)
1	Nobili Oktopus	Teejet TXB 8004	1.0	40.3	14000
2	Nobili Oktopus	Teejet AI 11004	1.0	40.3	14000
3	Dragone k2 500	Albuz ATR yellow	1.0	8.4	20000
4	Dragone k2 500	Lechler ID 12002	0.5	8.4	20000

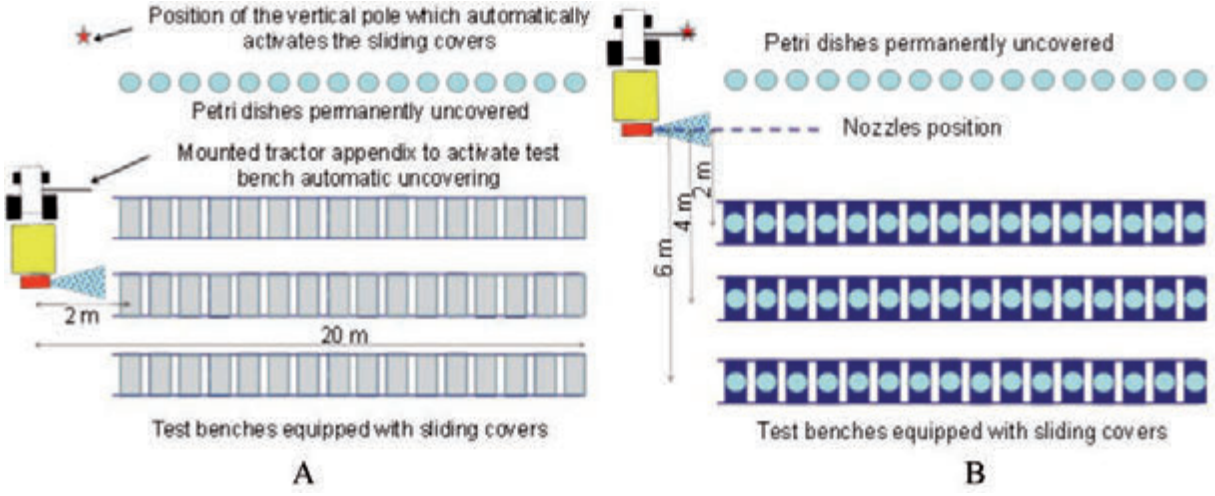

Figure 1. Scheme of samplers disposal to assess the range of the spray jet generated by the sprayer (permanently exposed collectors) and of the test benches disposal to detect the spray deposits which fall on the ground after the sprayer pass. A) Situation while the sprayer is passing besides the test covered benches; B) Just after the sprayer pass the test benches are uncovered and the samplers are revealed.

Table 2. Values of the sum of spray deposits (µl/cm2) obtained on the Petri dishes permanently exposed, measured in each of the five replicates made for each test (see Table 1) and coefficient of variation (CV) between the replicates.

Test	Rep 1	Rep 2	Rep 3	Rep 4	Rep 5	Mean	CV
1	8.4	10.0	8.0	8.0	8.2	8.5	10%
2	9.9	9.2	10.6	9.1	8.5	9.5	9%
3	1.7	1.9	1.9	1.5	2.0	1.8	11%
4	2.9	3.2	1.7	2.8	3.5	2.8	24%

amount sprayed by the machine. Therefore, taking into account the operative parameters adopted, for each thesis the amount of liquid sprayed per cm of advancing was calculated according to the following equation [1]:

$$E = Q/v \quad [1]$$

where:
E is the amount of liquid sprayed per cm of advancing (expressed in µl/cm);
Q is the total sprayer flow rate on one side of the machine (expressed in µl/s);
v is the sprayer forward speed (expressed in cm/s).

The percentage of liquid recovered on the Petri dishes permanently exposed with respect to the amount sprayed was then calculated through the following equation [2]:

$$RR = [\ \sum D_i \times 100 / E\ ] \times 100 \quad [2]$$

where:
RR is the percentage of liquid recovered on the samplers;
D_i is the spray deposit (µl/cm2) registered at every sampling distance i;
100 is the distance (expressed in cm) between two adjacent samplers.

In order to simplify the test method, concerning the spray deposits collected on the test benches, it was chosen to consider just the ones measured on the test bench positioned at 4 m distance from the nozzles when the bench was uncovered.

On the basis of the data registered on the test benches potential drift (DP) was calculated through the following equation [3]:

$$DP = \sum Si \times d_i \times 100 \quad [3]$$

where:
DP is the potential drift;
S_i is the spray deposit (µl/cm2) measured at each sampling distance i along the test bench;
d_i is the sampling distance (expressed in cm) of each sampler i from the sprayer centre.
Finally, thanks to the parameters calculated in the equations [2] and

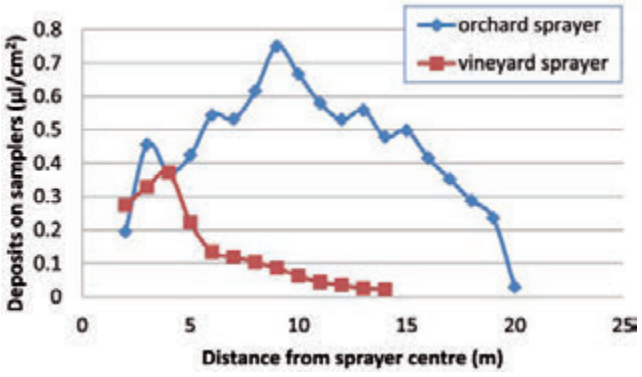

Figure 2. Profiles of spray jet ranges registered for the orchard and for the vineyard sprayers, both equipped with conventional hollow cone nozzles.

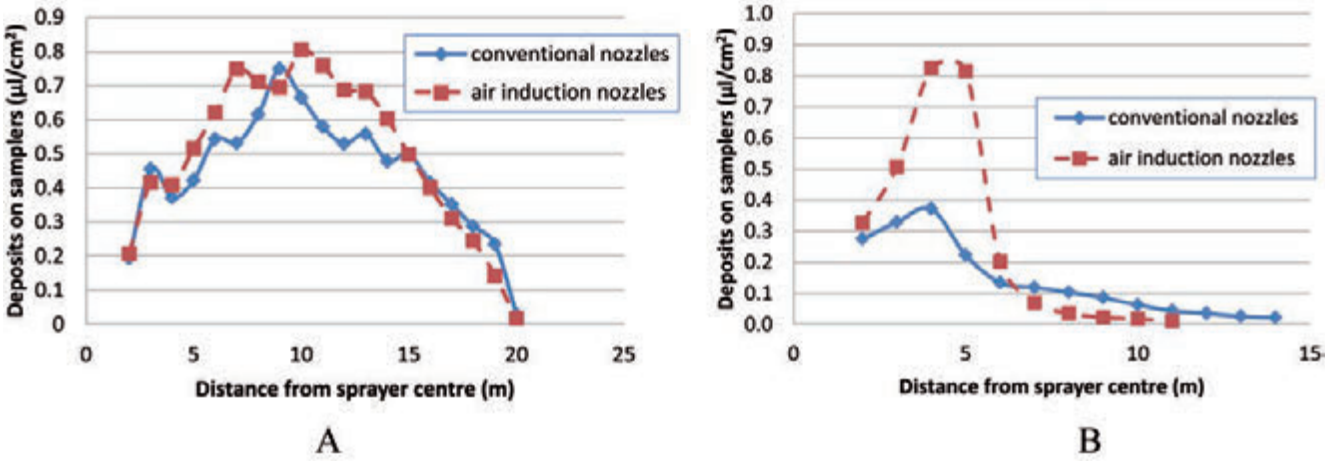

Figure 3. Profiles of spray jet range obtained with the orchard sprayer (A) and with the vineyard sprayer (B) in function of the nozzle type employed.

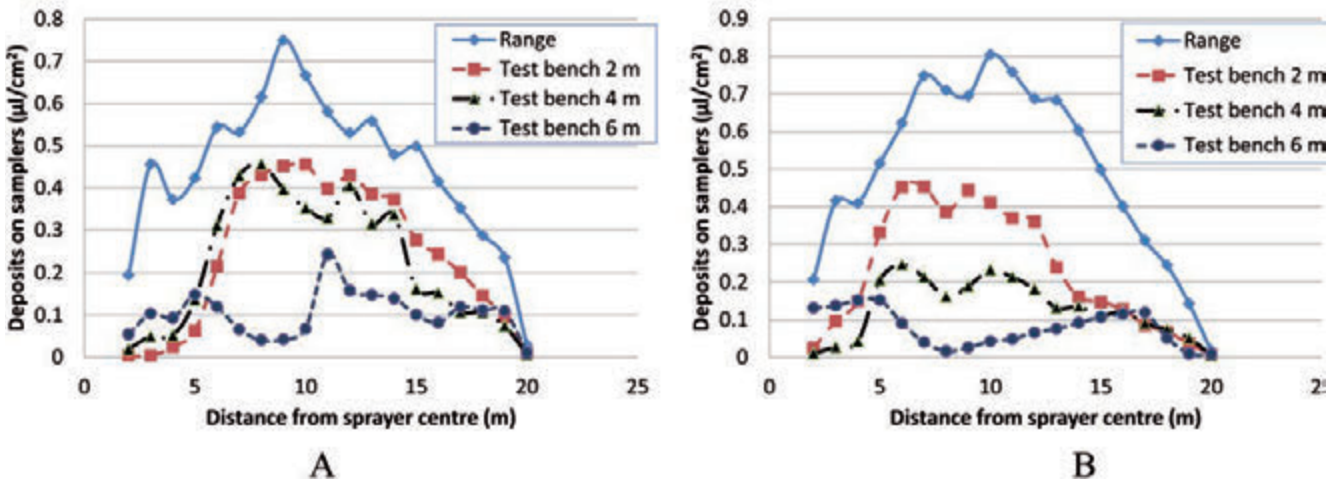

Figure 4. Orchard sprayer: profile of the spray jet range and trend of spray deposits detected on samplers positioned along the test benches using conventional hollow cone nozzles (A) and air induction flat fan nozzles (B).

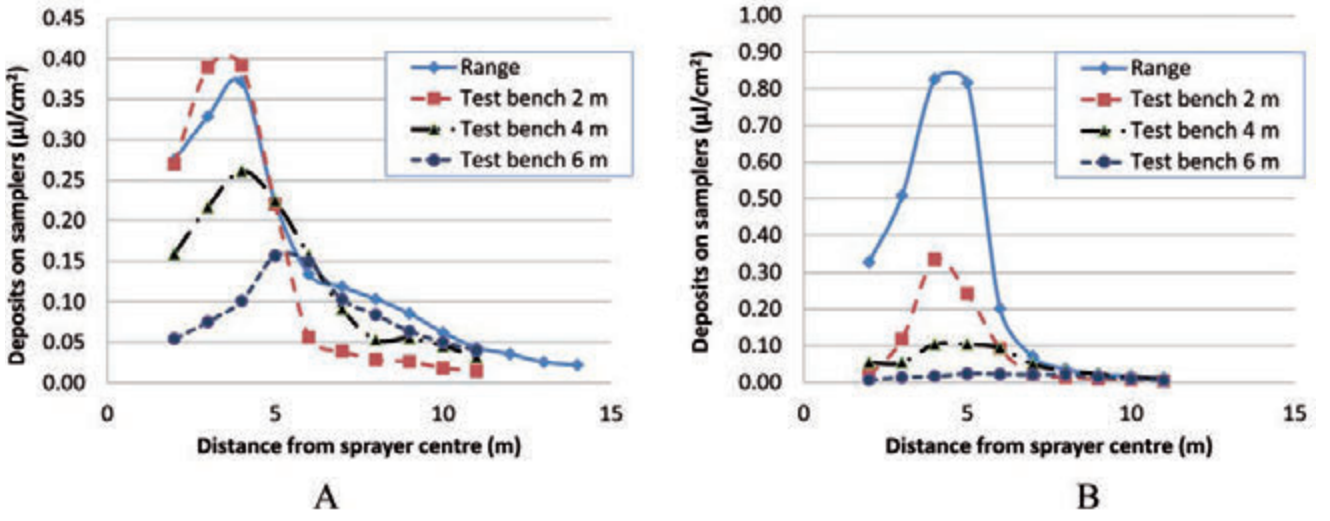

Figure 5. Vineyard sprayer: profile of the spray jet range and trend of spray deposits detected on samplers positioned along the test benches using conventional hollow cone nozzles (A) and air induction flat fan nozzles (B).

[3], the index of potential drift DPI was calculated applying the following equation [4]:

$$DPI = DP \times (100\text{-}RR) / 1000 \quad [4]$$

Applying the above mentioned equations to the data collected in the four experimental thesis examined the values of drift potential index (DPI) reported in Table 3 were obtained.

Table 3. Values of drift potential index calculated for the 4 thesis examined in the experiments.

Test	Sprayer and nozzle type	Drift potential index (DPI)
1	Orchard, conventional hollow cone	254
2	Orchard, air induction flat fan	134
3	Vineyard, conventional hollow cone	36
4	Vineyard, air induction flat fan	9

Conclusions

Comparing the drift potential indexes obtained using the air induction nozzles with respect to those obtained with conventional nozzles it was found a reduction of 48% for the orchard sprayer and a reduction of 75% for the vineyard one. However, it was noticed that the absolute value of DPI considerably varied in function of the sprayer type (vine-

yard or orchard) and, therefore, in order to make a consistent classification of sprayers according to drift risk it will be necessary to define a reference sprayer (type and configuration) either for vineyard or for orchard sprayers. Classification in terms of drift reduction (see ISO 22369-1) could be done comparing the DPI of a candidate sprayer with respect to that of the reference sprayer. With the aim to implement the proposed test method in an ISO standard, further tests are on their way aiming at acquiring further data related to different models and configurations of vineyard and orchard air-assisted sprayers.

References

Balsari, P., Marucco, P., Tamagnone, M., 2007. A test bench for the classification of boom sprayers according to drift risk. Crop protection, 26, 1482-1489.

ISO 22866, 2005. Equipment for crop protection - Methods for field measurement of spray drift.

ISO 22369-1, 2006. Crop protection equipment - Drift classification of spraying equipment - Part 1: Classes.

Repair and maintenance costs of 4WD tractors and self propelled combine harvesters in Italy

Aldo Calcante,[1] Luca Fontanini,[2] Fabrizio Mazzetto[3]

[1]Department of Agricultural and Environmental Sciences, Università degli Studi di Milano, Italy; [2]Effelle Solution, Italy; [3]Faculty of Science and Technology, Free University of Bolzano, Italy

Abstract

Purchasing and maintaining tractors and operating machines are two of the most considerable costs of the agricultural sector, which includes farm equipment manufacturers, farm contractors and farms. In this context, repair and maintenance costs (R&M costs) generally constitute 10-15% of the total costs related to agricultural equipment and tend to increase with the age of the equipment; hence, an important consideration in farm management is the optimal time for equipment replacement. Classical, R&M cost estimation models, calculated as a function of accumulated working hours, are usually developed by ASAE/ASABE for the United States operating conditions. However, R&M costs are strongly influenced by farming practices, operative conditions, crop and soil type, climatic conditions, etc. which can be specific for individual countries. In this study, R&M cost model parameters were recalculated for the current Italian situation. For this purpose, data related to the R&M costs of 100 4WD tractors with engine power ranging from 59 to 198 kW, and of 20 SP combine harvesters (10 straw walkers combines and 10 axial flow combines) with engine power ranging from 159 to 368 kW working in Italy were collected. According to the model, which was obtained by interpolating the data through a two-parameter power function (proposed by ASAE/ASABE), the R&M cost incidence on the list price of Italian tractors at 12,000 working hours (estimated life of the machines) was 48.6%, as compared with 43.2% calculated through the most recent U.S. model while, for self propelled combine harvesters, the R&M cost incidence at 3,000 working hours was 23.1 % as compared with 40.2% calculated through the same U.S. model.

Correspondence: Aldo Calcante, Department of Agricultural and Environmental Sciences, Università degli Studi di Milano, via Celoria 2, 20133 Milano, Italy.
Tel. +39.02.50316854.
E-mail: aldo.calcante@unimi.it

Key words: repair and maintenance costs, 4WD tractors, self propelled combine harvesters, cost estimation models.

Contributions: the authors contributed equally.

Conflict of interests: the authors declare no potential conflict of interests.

Journal of Agricultural Engineering 2013; XLIV(s1):e70
doi:10.4081/jae.2013.(s1):e70

Introduction

Purchasing and maintaining tractors and operating machines are two of the most considerable costs of the agricultural sector (Buckmaster, 2003; Mazzetto and Calcante, 2010), which includes farm equipment manufacturers, farm contractors and farms. In particular, for farms, mechanization costs can constitute 15-50% on the total costs of crop production (mean data related to field crops, E. U. FADN, 2007).

The operating costs of an agricultural machine are calculated using methodologies that are similar to those employed for calculating a balance sheet. Briefly, a balance sheet consists in the registration of a series of economic events linked to the flows of materials (or services) in input or output categories. At the end of a financial period, all the budgeted entries are included in the so-called final balance, *i.e.*, the result of the economic activity of a company. In our case, it was necessary to apply analytic accounting rules by dividing investment over a predefined number of years (amortization) and adding all the items that, in a specific year, represented the real cost of agricultural machines (taxes and insurances, hours of ordinary maintenance, spare parts, etc.) and the overall costs due to consumables, which are directly proportional to the effective working hours of a machine (for example, lubricants, fuels, etc.)

It is even possible to calculate a capital budget, which is a kind of forecast of the economic events that are expected to occur during a productive period. This strategy allows predicting potential costs of materials (supply of production factors) and financial terms, such as allotted capital or funds for the acquisition of new resources. Compared with a final balance, the budget is obviously more simplified because it is not based on real items. Moreover, the economic scenario of a tentative budget is based on a rational hypothesis that depends on former experiences. In addition, the estimated cost of agricultural machines is usually calculated when planning a new purchase or when assessing the performances of possible alternative scenarios that involve the use of different machines. Because real data are not available, the calculation methodology is based on simplifications and conventions that estimate single item costs, usually split in annual ownership costs and annual operating costs. In this context, repair and maintenance costs (R&M costs), which are included in annual operating costs, represent about 10-15% of the total mechanization costs (Rotz and Bowers, 1991). R&M costs tend to increase depending on the age of a machine and, hence, become an important criterion in determining the optimal time to replace machine itself.

Farm equipment manufacturers design agricultural machines to perform for a maximum number of hours, which is called "estimated life" (Df, hours). Considering the physical wear of tractors and self propelled (SP) combine harvesters, and the current construction tech-

nology, the life of a tractor ranges between 10,000 and 14,000 hours (up to 16,000 hours for high power tractors, Lazzari and Mazzetto, 2009) whilst the life of a SP combine harvester is estimated to 3,000 hours. Yet, the estimated life is highly variable for each type of machine because it depends on its use. Specifically, the estimated life depends on several factors, such as intensity of use per year, propensity to buy new machines to maintain a high technological level, quantity and quality of ordinary maintenance, and compliance with programmed extraordinary maintenance intervals (for example, rebuilding the clutch and brakes). Theoretically, R&M costs could be a function of the intensity of use of a particular machine, at least, for some wear parts. However, other factors are involved in R&M costs, such as operative conditions, crop and soil type, climatic conditions, mean engine load required by different operations, and machine maintenance level. Because of the aforementioned difficulties, the most convenient method to correctly estimate R&M costs is based on a modeling approach. Therefore, the R&M cost estimation requires a calculation model that is 1) appropriate for the temporal dynamic of predictable expenses of different machines types and 2) able to extrapolate average behaviors from a sufficiently wide sample.

At the methodological level, different models are available for calculating R&M costs. One the most well-known and used model is the one proposed by Bowers and Hunt (1970), which is a three-parameter model that starts with R&M costs associated with a large sample of machines. Fairbanks *et al.* (1971) developed two models with data collected through interviews related to a sample of 114 farmers from Kansas: one model referred to tractors (2WD and 4WD) and the other model referred to self-propelled harvesting machines. The model proposed by Fairbanks *et al.* (1971) is based on a two-parameter equation (power function) suggested by the ASAE D 230.1 (1966). This model estimates the repair and maintenance costs according to equation (1)

$$Crm = RF1 \cdot \left(\frac{h}{1000}\right)^{RF2} \quad (1)$$

where:
Crm = total cumulative repair and maintenance costs (expressed as the percentage of the list price of a machine);
h = working hours accumulated by each machine.
RF1 and RF2 = dimensionless coefficients that affect the shape of the interpolating curve.

In particular, RF1 describes the amount of R&M costs while RF2 represents the distribution of R&M costs during the estimated life of a machine (Sartori and Galletto, 1992).

Nowadays, the standard applied at international level is the ASAE D497.7 (2011), whose RF1 and RF2 parameters are calculated for the U.S. operating context. Obviously, since the R&M R&M costs are strongly influenced by farming practices, operative conditions, crop and soil type, climatic conditions, etc. which can be specific for individual countries, it would be necessary to adapt the RF1 and RF2 parameters to specific local situations in order to refine the results of cost calculation methodology (Ward *et al.*, 1985; Rotz, 1987; Morris, 1988; Gliem *et al.*, 1989; Wahbi and Al-Suhaibani, 2001; Frank, 2003; Knoub Bacht *et al.*, 2008).

Table 1 shows the RF1 and RF2 parameters proposed by ASAE D497.7 (2011) for 4WD tractors and SP combine harvesters, respectively, the values of Df (in hours, estimated life of machines) and total life of R&M cost: this latter parameter represents the amount of R&M costs, expressed as a percentage of the list price, used for maintenance and repairs on average during all the Df period of machine.

Total life of R&M costs are expressed as a percentage of the list price. For 4WD tractors, at 16,000 accumulated working hours ASAE D497.7 (2011) standard estimates R&M costs equal to 76.8% of the price list whilst, for SP combines, at 3,000 accumulated working hours the same standard proposes an incidence of R&M costs equal to 40.2% on the price list of the machine. The objective of the present work was to collect and analyze real data on the R&M costs of tractors and SP combine harvesters working in Italy in order to recalibrate RF1 and RF2 parameters to have a predictive model suitable for the local situation. The obtained models would provide planners, manufacturers of agricultural machinery and farmers with an opportunity to evaluate the economic performances of tractors and SP combines in Italian contexts. The possibility of using local models allows to carry out accurate economic analysis of agro-mechanical investments and enables to help farmers and contractors to take the better decisions related to farm mechanization planning (for example it is possible to carry out comparison between different extended warranty plans, Calcante *et al.* 2013); indeed, all these aspects are based on the estimated costs of agricultural machine use.

Materials and methods

The present study compiled data on the R&M costs (ordinary and extraordinary) of tractors and SP combine harvesters belonging to farmers and contractors working in Italy. The research considered 100 models of 4WD tractors of several brands (Italian and foreign) with engine power ranging from 59 to 198 kW, and 20 SP combine harvesters (10 straw walkers combines and 10 axial flow combines) with engine power ranging from 159 to 368 kW. Considered SP combines were used especially for grain and ear corn harvesting. Three of them were used also for rice harvesting. The characteristics of the considered population of machines are summarized in Table 2.

The mean ages of the sampled machines was 8 years (minimum, 1 year; maximum, 22 years) for tractors and 9 years for SP combines (minimum, 2 year; maximum, 19 years). Noted that mean annual use of tractors was clearly higher than the Italian average (less than 500 h/year for tractors, Pawlak *et al.*, 2001), but it was lower than the U.S.

Table 1. RF1 and RF2 parameters proposed by ASAE D497.7 (2011) for 4WD tractors and SP combine harvesters.

Machines	RF1	RF2	Df (h)	Total life R&M cost (%)
4WD Tractors	0. 300	2.000	16,000	76.8
SP combine harvesters	4.000	2.100	3,000	40.2

Table 2. Characteristics of the considered population of agricultural machines.

Machines		Sample size	Power (kW)	Working hours (h/year)	Age (years)
4WD tractors	100	Min.	58	213	1
		Max.	198	2,217	22
		Ave.	113	798	8
SP combine harvesters	40	Min.	151	197	2
		Max.	368	833	19
		Ave.	236	367	9

average (970 h/year, Pawlak *et al.*, 2001). For SP combines, no data are available in literature. A survey conducted by us in collaboration with some of the most important farm equipment manufacturers (CNH and John Deere), indicated about 500-600 h/years as mean annual use of SP combines in U.S. operating conditions.

To achieve a satisfactory level of completeness of the dataset, data related to maintenance and repair costs were collected using the following sources:

1) Direct contact with tractors' and SP combines' owners (filling forms). In this way, it was possible to collect data related to the maintenance activities performed in farms' workshops.
2) Queries to dealers' and authorized workshops' databases, in which ordinary, programmed and extraordinary maintenance interventions are registered. These databases represented the most complete source of repair and maintenance activities (especially extraordinary and programmed activities, with relative R&M costs) that are rarely performed in farms.

The costs of ordinary maintenance were obtained from information provided by tractors' and SP combines' owners and, in the absence of such information, from the reported information on the use and maintenance manuals of each single machine. The cost of labor for ordinary maintenance was estimated to be 35 €/hour (this value was corrected for inflation as a function of the moment of the intervention). Lubricant costs were not considered because such costs are conventionally included in the cost calculation of consumable materials (fuels and lubricants). Therefore, we considered only the labor cost necessary for replacing lubricants. Thus, an accurate and complete survey was obtained as a result of the completeness of the dataset. Unlike other papers, where R&M costs were grouped on an annual basis, here, they were linked to working hours measured at the moment of ordinary or extraordinary maintenance interventions. From the operative point of view, recorded data were managed and assembled through a normal spreadsheet (Microsoft Excel 2010). Once data from all the considered machines were grouped, the R&M costs – expressed as a percentage of the list price as a function of the accumulated working hours – were plotted on two two-dimensional plots, one for tractors and one for SP combines. Interpolation of values performed through a two-parameter power function allowed us to calculate RF1 and RF2 parameters for tractors and SP combine harvesters working in Italy.

Results and discussion

Table 3 shows the average, standard deviation, minimum and maximum values and the coefficient of variation of all the considered machines.

According to Bowers and Hunt (1970) and Rotz (1987), the high variability of data present in this type of analysis is evident. Indeed, for tractors, the coefficient of variation of labor is 70%, that of spare parts is 84%, and that of accumulated R&M costs is 77%. For SP combines, the coefficient of variation of labor is 53%, that of spare parts is 42%, and that of accumulated R&M costs is 40%. Therefore, such costs are not dependent only on the age of the machine and its yearly working hours. The high observed variability likely depends on the following factors: a) the fulfillment of programmed maintenance plans; b) the engine power and list price of a machine (*i.e.* more powerful tractors are involved in heavy operations and, therefore, are subject to higher wear); c) the intensity and modality of use of a single machine (tractor and SP combine); and d) the ability of driver.

Therefore, obtaining a general model that is useful for each farm and each specific machine is difficult because of the need to consider several different variables (Ward *et al.*, 1985). Because we were able to compile information for each single machine, it was possible to assign several extraordinary maintenance interventions to the involved electromechanic parts. Figure 1 highlights the part that required more extraordinary maintenance interventions for 4WD tractors and SP combines. For tractors, the part most subject to issues was the engine (25 % of total interventions), followed by the electronic system (18%) and the transmission (15%). Because tractors are normally involved in heavy operations, the engine and transmission are the most vulnerable parts to wear and breakage. In contrast, the electronic system is surprisingly the next most vulnerable part. Certainly, the electronic system is open to significant improvements, especially concerning its reliability. For SP combines, the component that required more extraordinary maintenance events was the header unit (49.3%) followed by the threshing system (12.5%), the hydraulics (8.2%) and the classic wear and tear parts (feeder conveyor, 7.6%, grain tank unloading auger, 6.9%).

To estimate the RF1 and RF2 parameters for tractors and SP combines, the interpolation of R&M cost values, referred to list price and expressed as a function of accumulated working hours, was performed using equation (1). The obtained model (2) for 4 WD tractors presents $R^2 = 0.82$, RF1 = 1.945 and RF2 = 1.295

$$Crm = 1.945 \cdot \left(\frac{h}{1000}\right)^{1.295} \quad (2)$$

while the model for SP combine harvesters (3) presents $R^2 = 0.80$, RF1 = 4.095 and RF2 = 1.591

$$Crm = 4.095 \cdot \left(\frac{h}{1000}\right)^{1.591} \quad (3)$$

Table 3. Variability of labor, spare parts accumulated working hours and R&M costs of the considered machines.

		Labor (€)	Spare parts (€)	Accumulated working hours	Accumulated R&M costs (€)
4WD tractors	Average	5,098	11,671	5,626	15,702
	Standard Dev.	3,595	9,780	2,955	12,085
	Minimum	77	79	400	319
	Maximum	18,935	50,001	15,450	60,621
	CV	70%	84%	55%	77%
SP combine harvesters	Average	5,554.65	25,374.52	2,996	30,739.70
	Standard Dev.	1,664.83	10,731.10	1,211	13,425.34
	Minimum	1,496.00	9,824.89	1,200	12,448.39
	Maximum	10,565.05	47,862.80	4,970	58,269.30
	CV	53%	42%	40%	44%

Clearly, both models are the result of R&M cost analyses – based on real data - on a non-homogeneous sample of machines. In this population, in fact, it is possible to find: a) new and old machines with few working hours that have undergone only the ordinary maintenance, b) tractors and SP combines with high number of working hours and high number of ruptures, c) new machines with high number of working hours and high number of repairing. It is reasonable to expect that the age of the machines (in terms of years since their first registration, or construction, *i.e.* its calendar-age) can somehow influence on the cost of R&M, due to phenomena related to natural aging of individual components. However, these phenomena act in combination with the direct wear due the actual operation of the machine and the models proposed so far tend to see the effects due to these causes prevailing as compared to the calendar-age of the machines. To this aim, it should be mentioned that also the engine load may influence the course of R&M costs along timeline: regular use of machines in heavy work enhances wear phenomena, especially for tractors. These considerations would lead to the definition of estimation models with a greater number of variables, with the need to redefine the methods of investigation and render useless comparisons with conventional models used so far. Therefore, in this study we considered useful to apply again the approach already proposed by Bowers and Hunt (1970) that evaluates the accumulated R&M costs of each machine with its accumulated work hours.

The resulting pattern for 4WD tractors compared with the ASAE D497.7 (2011) model is highlighted in Figure 2 (we assumed Df of 12,000 hours for tractors, which corresponds to total life of R&M cost = 48.6%). From a strictly theoretical point of view, for tractors, it would be possible to extend the Df value (Df = 16,000 hours, total life of R&M cost of 70.5%, a smaller value than that estimated by the U.S. model, table 1). However, considering that the analyzed population of tractors has average annual working hours of 798 hours, the estimated life of each tractor would be 15 years. This value does not coincide with the amortization period, which is usually estimated in 12 years for these categories of tractors (Lazzari and Mazzetto, 2009). Further, this value not only has economic meaning but also represents the time point when it is advisable to substitute a machine for technical limits, better safety and comfort as well as to reduce the environmental impact of the equipment. In other words, increasing the years of estimated life might mean owning technically obsolete machines for farmers and contractors.

For 4WD tractors, the R&M costs in Italy are higher than those in the U.S. (48.6% vs. 43.2%). In particular, the maximum distance between the two curves corresponds to 7,600 working hours (Crm = 27% and Crm = 17% of price list, respectively). Moreover, the two curves tend to converge in the proximity of the end of the estimated life. Indeed, with a hypothetical Df of 16,000 hours, the two curves practically show sim-

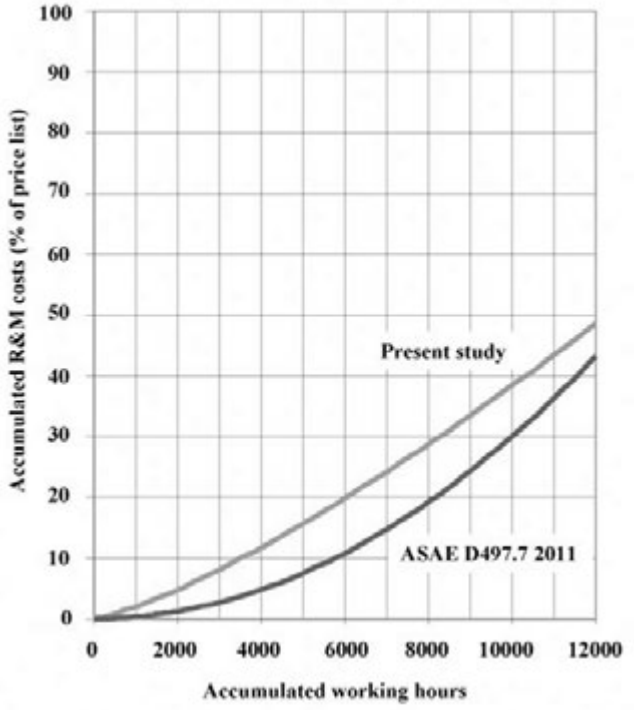

Figure 2. Comparison between our model for 4WD tractors (Present study) and that proposed by ASAE D497.7 (2011).

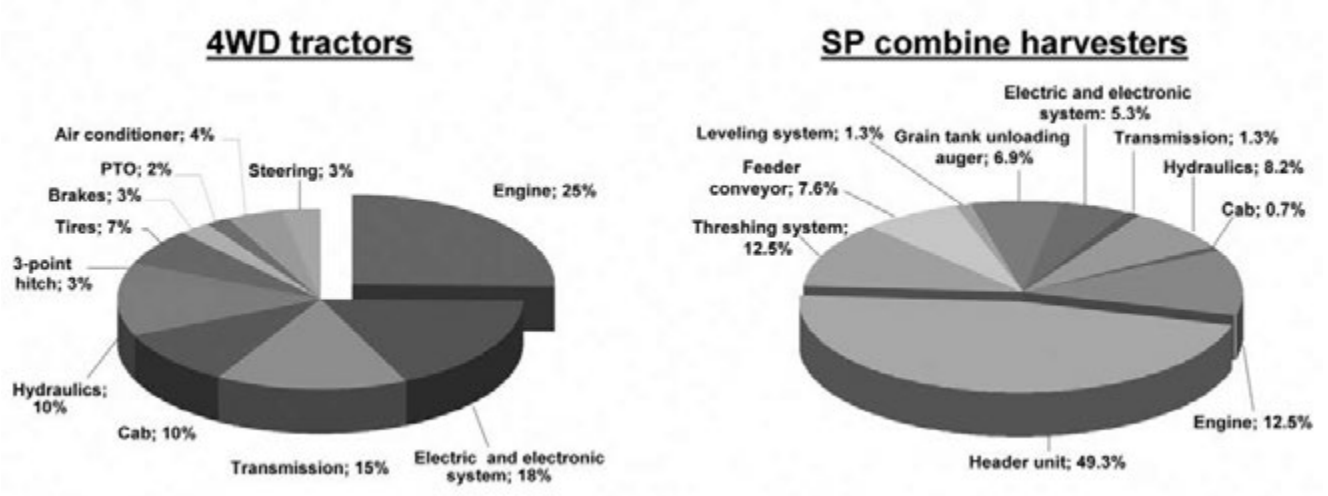

Figure 1. Distribution of extraordinary maintenance events as a function of the considered agricultural machine parts.

ilar values at approximately 14,000 hours. This means that, in Italy, we have a greater incidence of Crm than estimated by ASAE D497.7 (2011) especially for the younger machines with high number of working hours. So, this is an important criterion in order to choose the right time for the tractor substitution, both for contractors (who tend to substitute, anyhow, their tractors more frequently than farmers) and farmers that often keep obsolete and uneconomic machines in their fleet of tractors.

For SP combine harvester, we obtained opposite results (Figure 3): in U.S the R&M costs are much higher than those obtained in Italy. In fact, considering Df = 3,000 hours, the model proposed by ASAE D497.7 (2011) for U.S. context, estimates a R&M costs incidence = 40.2% whilst our model only 23.1%. This means that, in U.S, there's a greater incidence of Crm than in Italy probably due to the different intensity of use (over 500 vs. 367 h/year) and to the different operating conditions in the two countries. Further, it is important to note that RF1 and RF2 parameters proposed by ASAE/ASABE are related to generic "self propelled combines" whilst our research has considered particularly SP combine harvesters for wheat and ear corn (the most diffused crop productions in Italy). On the other hand, is the crop that requires the adoption of a specific header unit and, as a consequence, determines the machine working parameters in terms of energy requirements, working speed, rpm of engine and threshing systems etc.. This, certainly, has a great influence on breakage and wear and tear of specific mechanical parts (Srivastava *et al.*, 1990; Mao *et al.*, 2007).

In conclusion, the differences between the ASAE D 497.7 models and models calculated for the considered agricultural machines operating in the Italian context are evident. This confirms the need to recalibrate RF1 and RF2 parameters for local conditions.

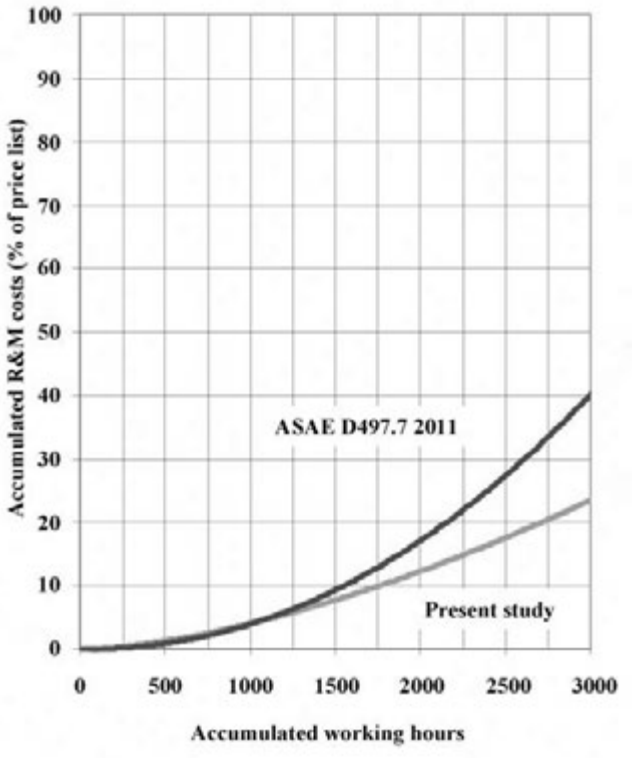

Figure 3. Comparison between our model (Present study) for SP combine harvesters and that proposed by ASAE D497.7 (2011).

Conclusions

The aim of the present work was to calculate - for the Italian situation - the RF1 and RF2 parameters of the model based on a power function normally used to estimate R&M costs of 4WD tractors and SP combine harvesters. Data on ordinary and extraordinary maintenance interventions of the considered machines were collected through direct contact with tractors' and SP combines' owners and through queries to dealers and authorized workshops' databases. The obtained results were compared with results reported in the last release proposed by ASAE/ASABE (ASAE D497.7, 2011) that are currently the standard for this type of analysis. Our model for 4WD tractors shows that, for a total life of 12,000 hours, the R&M costs (expressed as a percentage of the list price) are 48.6%, whilst model related to SP combine harvesters shows that, for a total life of 3,000 hours, R&M costs are 23.1%. The comparison between our models and the most recent ASAE models showed higher incidence of R&M costs in the Italy than in the U.S for tractors and an opposite behavior for SP combines. Therefore our results confirm the need to have models based on local conditions in order to improve the R&M costs estimation for each agricultural context. For future, it would be useful to increase the sample size and to create an operational tool at a national level that is able to collect data linked to the maintenance and repair interventions of agricultural machines. However, such information system cannot be successful without the adoption of telemetry devices and/or operating monitoring systems installed on-board of tractors. Thus, the collection process of work parameters related to agricultural machines would be completely automated. Some tractors and SP combines are already provided with built-in devices to continuously monitor their performances. In other situations, it is possible to adopt data-loggers, normally employed for the monitoring of farm activities, for managerial purposes (Mazzetto *et al.*, 2009). In any case, a complete and objective analysis can be performed on a large scale only with the participation of farm equipment manufacturers, dealers, agro-mechanical companies and farmers' associations.

References

ASAE STANDARDS, 58th D497.7: Agricultural machinery management data. St. Joseph, Mich.: ASABE; 2011

ASAE STANDARDS, 13th D230.1: Agricultural machinery management data. St. Joseph, Mich.: ASAE: 1966

Bowers W, Hunt DR, Application of mathematical formulas to repair cost data. Trans. ASAE 1970;13:806-9.

Buckmaster DR, Benchmarking tractor costs. Applied Eng in Agric 2003;19:151-4.

Calcante A, Fontanini L, Mazzetto F, Repair and maintenance costs of 4WD tractors in Northern Italy. Trans ASAE 2013;56:355-62.

E.U. FADN; 2007. Available from: http://ec.europa.eu/agriculture/rica/index.cfm.

Fairbanks GE, Larson GH, Chung DS, Cost of using farm machinery. Trans ASAE 1971;14: 98-101.

Frank L, Coefficients of repair and maintenance costs for axial and transverse combine harvester in Argentina. Span J Agric Res 2003;1:81-97.

Gliem JA, Persinger KM, Carpenter TG, Holmes RG, A comparison of ASAE estimated tractor and combine repair and maintenance costs to actual repair and maintenance costs of selected farms. 1989; ASAE Paper No. 89-1024. St. Joseph, Mich.: ASAE.

Knoub Bacht GM, Ahmadi H, Akram A, Karimi M, Repair and maintenance cost model for MF285 tractor: A case study in central region

of Iran. American- American-Eurasian J of Agric and Environ Sci. 2008;4:76-80.

Lazzari M, Mazzetto F, Chapter 3: Analisi economica delle macchine agricole (Economical analisys of agricultural machines). In Prontuario di meccanica agraria e meccanizzazione (Agricultural mechanic and mechanization handbook). Reda ed. Torino; 2009.

Mao Z, Wei Q, Zhang Q, Power efficiency analysis of combine harvester in field operation. Paper No 071027, ASAE Annual Meeting. St. Joseph, Mich.: ASAE; 2007.

Mazzetto F Calcante A, Come valutare i costi della manutenzione (How to evaluate maintenance costs). Il Contoterzista 2010;3:1-6.

Mazzetto F, Calcante A, Salomoni F, Development and first tests of a farm monitoring system based on a client-server technology. Proc. Precision Agriculture '09. Wageningen, the Netherlands, July 6-8; 2009. pp: 389-96.

Morris J, Estimation of tractor repair and maintenance costs. J of Agric Eng Res 1988;41: 191-200.

Pawlak J, Pellizzi G, Fiala M, Development of agricultural mechanisation to censure a long-term world food supply. General background information and requirements. Proc. of XII Meeting Club of Bologna. Bologna, Italy, November 18-19; 2001. pp. 24-47.

Rotz CA, A standard model for repair costs of agricultural machinery. Applied Eng in Agric 1987;3: 3-9.

Rotz CA, Bowers W, Repair and maintenance cost data for agricultural equipment. 1991; ASAE Paper No 91-1531. St. Joseph, Mich.: ASAE.

Sartori L, Galletto L, Costi di riparazione e manutenzione dei trattori nella Provincia di Padova (Repair and maintenance costs of tractors in the Padua district). Rivista di Ingegneria Agraria 1992;23:81-9.

Srivastava AK, Mahoney WT, West NL, The effect of crop properties on combine performance. Trans ASAE 1990;33:63-72.

Ward SM, McNulty PB, Cunney MB, Repair costs of 2 and 4 WD tractors. Trans ASAE 1985;28:1074-6.

The RHEA-project robot for tree crops pesticide application

Marco Vieri, Riccardo Lisci, Marco Rimediotti, Daniele Sarri

Department of Agricultural, Food Production and Forest Management University of Florence Firenze, Italy

Abstract

The sustainable use of pesticide and the need of a renewed integrated system of agricultural knowledge and management, focus the designing of the EU FP7 RHEA Project. The objectives are the design, development, and testing of a new automatic generation of robotic systems to perform field operations for the sustainable crop management. The project affects three case study: chemical, physical, mechanical and thermal effective weed management in maize and wheat cultivations and chemical pesticide management in woody crops. To achieve the goals, a fleet of small and heterogeneous robots, ground and aerial, equipped with advanced sensors, innovative end actuators and decision control algorithms were realized. Present work is related to the third case study considered *i.e.* the spraying in woody crops specifically in olive trees. The final decision on woody perennial crops treatment device system, was oriented toward a complete double side air blast sprayer with eight separate spraying modules on four vertical bands of the canopy. Rhea air blast sprayer introduces some important innovations in the studies concerning the pesticide variable rate treatment, *i.e.* the management possibility of air flow in site specific way and in real time in function of the target.

Correspondence: Marco Vieri, GESAAF Department of Agricultural, Food Production and Forest Management, Scuola di Agraria, University of Florence, Piazzale delle Cascine 15, 50144 Firenze, Italy.
Tel. +39.055.3288320 - Fax +39.055.331794.
E-mail:marco.vieri@unifi.it

Acknowledgments: authors wish to acknowledge the Nobili.

Key words: precision farming, sustainability, variable rate treatment, air-blast sprayer, robot.

Contributions: the authors contributed equally.

Conflict of interests: the authors declare no potential conflict of interests.
Funding:

Dedication: none

Journal of Agricultural Engineering 2013; XLIV(s1):e71
doi:10.4081/jae.2013.(s1):e71

Introduction

Our society is evermore demanding lower impacts on environment and higher standards in food safety. The new Community rules on the risks reduction to the environment and food safety require a breakthrough innovation in all sectors especially in agriculture at which there is a strong pressure due to the remarkable use of chemicals. The sustainable use of PPP (Plant Protection Products) (Vieri & Spugnoli, 1996), the need of a renewed integrated system of agricultural knowledge and management, focus the designing of the EU FP7 RHEA Project (Robot fleets Highly for Effective Agriculture and forestry management).

The objectives of the RHEA project are the design, development, and testing of a new automatic generation of robotic systems to perform field operations for the sustainable crop management. To achieve this goal, a fleet of small and heterogeneous robots – ground and aerial – equipped with advanced sensors, innovative end actuators and decision control algorithms was realized. RHEA can be considered a cooperative robotic system, falling within an emerging area of research and technology.

Six integrated modules make up the RHEA system: Mission Manager (MM), Perception System (PS), Communication and location System (CS), Actuation System (AC) divided into High Level and Low Level Decision, Mobile Units (MUs) and the Base Station and Graphic User Interfaces (GUI) (Gonzales *et al.*, 2011). The project affects three case study: chemical, physical, mechanical and thermal effective weed management in maize and wheat cultivations and chemical pesticide management in woody crops. Present work is related to the third case study considered *i.e.* the mobile unit development for spraying in woody crops specifically in olive trees. The design involved the analysis of the following variables:

- Equipment configuration; single side or double side and the number of modules;
- Device system (DS) and the control system or Low Level Actuation System (LLAS);
- Main parameters controlled: spray cloud features, liquid flow rate, air flow rate and the air jet variable direction.

Materials and methods

The initial project proposal about the RHEA ground mobile units (GMUs) configuration, took into account very small vehicles with mass of 200-400 kg and less than 15 kW power, operating at a forward speed of 1.5 m s^{-1} with only one operating arm. This setting, is really feasible only for spot spraying technique *e.g.* in the insects control, but it is not appropriate for other diseases like fungi etc. .In these cases, at least, two problems arise: the first one is the dosage that, even in a modern intensive tree plant with an average of 5000 m^2 of canopy surface per hectare, requires not less than 100-200 l ha^{-1}. The second is the necessity of an air assisted device to optimize the distribution inside the

canopy. Furthermore, the use of one single spray diffuser, at the prescribed forward speed, produces an unacceptable unequal sinusoidal application. Because of these issues, the RHEA Consortium approved a more suitable ground mobile unit with other new specifications: 4x4 wheel drive, CVT transmission, 37.3 kW gross power, with a 10% of which available as electric power, maximum mass of 1600 kg, three hitch points lift and standard 52 rad s^{-1} p.t.o. . These new features, make it possible to adopt a common ready to use and innovative air assisted sprayer.

Another important choice, was the scenario for the final demonstration trials: the RHEA Consortium approved an intensive olive plantation. This decision was taken because the olive growing is, at the same time, quite similar to modern orchard crops and woody tree crops. The plantation pattern (Figure 1) was 4.0 m inter-row and 1.5 m distance on the row to reach a foliar wall as flat and regular as possible.

With these variables, different solutions about pesticide spraying and air vector devices management were investigated (Figure 2). The final judgment was oriented toward a complete double side air blast sprayer (based on Nobili Oktopus air blast sprayer) with eight separate spraying modules on four vertical bands of the canopy. For the machine automation, three types of kinematic coupling driven by stepper motors were built. These are managed by the motion controller, which allows an accurate motor control both in speed and position. Moreover, they are fully programmable and they can be interfaced with a standard P.L.C. (Programmable Logic Controller). A detection system consisting of eight ultrasonic sensors permits to reach data about the canopy width of each vertical band. Finally, actuation rules (Figure 3) for every one device to better fit optimum spray features (air and liquid flow rate) on each vertical bands of the canopy were defined.

Results

The design has led to the development of an air blast sprayer (Figure 5); with the following features:

- maximum height of the vertical boom 2.5 m;
- canopy band to be treated 2.7 m (3.0 - 3.5 m maximum crop height);
- total equipment mass (empty tank) 400 kg;
- tank 300 L;
- hydraulic pump with maximum flow rate of 100 L min^{-1} at 25 bar and maximum 5 kW of power requirement to the p.t.o. ;
- fan maximum 15 kW to the p.t.o.;
- the equipment is semi-loaded and coupled at the three hitch point lift but when it is working, floating and resting on its wheels.

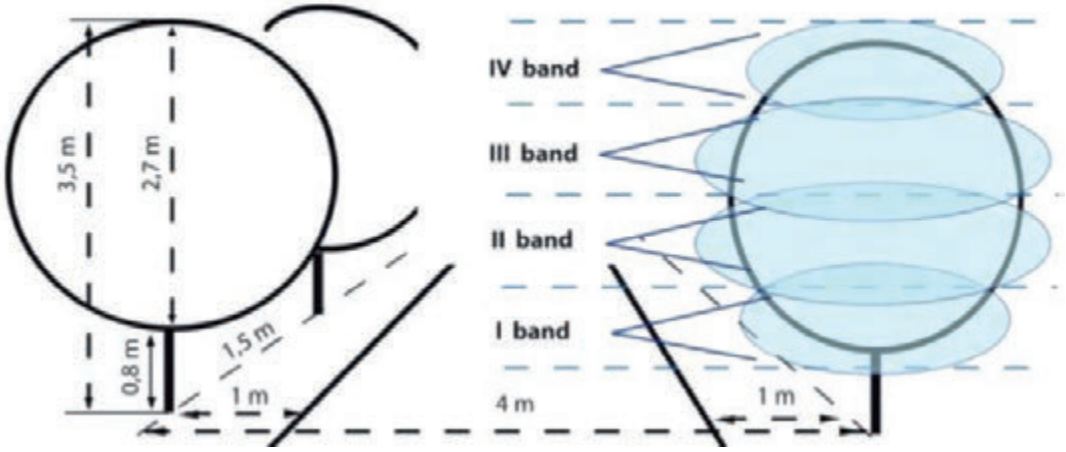

Figure 1. Demonstration woody perennial plant and definition of the four horizontal canopy bands.

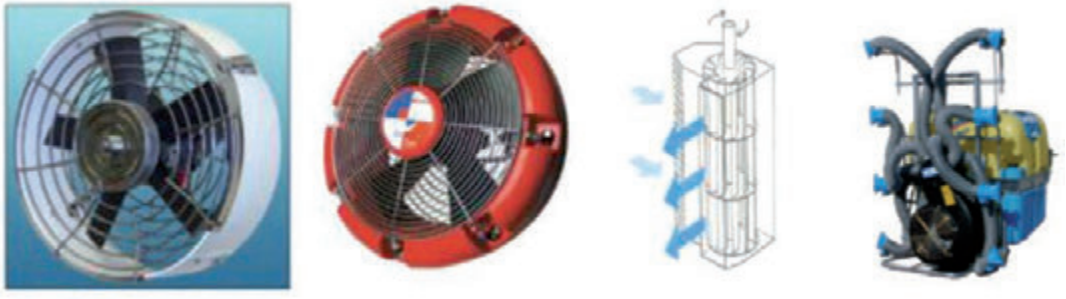

Figure 2. Spraying and air vector devices solutions evaluated for the air blast sprayer configuration: left to right; the Proptec rotary atomizers which use mechanical centrifugal force to atomize fluids; The Sardi fan Multiple air-assisted sprayers, with a series of spray heads with a direct blast axial flow fan and a series of hollow cone nozzles; The tangential cross-flow fan; The Nobili Oktopus sprayer with eight spraying modules manually adjustable.

In view of the objectives, and starting from the basic configuration of the Nobili Oktopus air blast sprayer, the following changes were designed:

- detection system composed of eight ultrasonic sensors to reach data on canopy width of each vertical band;
- variable control of the liquid flow rate in each module to adapt dosage at the canopy thickness on each band with the following rules: 100% canopy thickness 100% dose; 50% canopy thickness 70% dose; < 50% canopy thickness 30% dose, absence of canopy 0 dose;
- to control flow rate two solutions were developed and tested: an intermittent spray nozzle driven by frequency and duty cycle electronically managed and double nozzles on each module with 70% and 30% of needed flow rate on each band simultaneously open with full canopy (Figure. 5);
- for the air flow adjustment in the main entrance a fan inlet manifold throttle valve controlled by a stepper motor was built (Figure 4);
- the variable inclination (step motor controlled) of the four terminal modules (top and bottom) to improve the deposition in these sensitive areas of the canopy (Figure 4);
- to control the airblast flow rate on each module, eights butterfly valves (step motor controlled) located on each pipe of the eight fan calotte collector were designed (Figure 4);

The entire equipment, with the whole system of devices (DS), was monitored by the LLAS that consist in the PLC (Figure 5) and related algorithms. All this is controlled, in its turn, by the HLDMS and upstream from the MM of the RHEA system.

Conclusions

The Rhea air blast sprayer introduces an important innovation in the studies concerning the pesticide variable rate treatment, *i.e.* the management possibility of air flow in site specific way and in real time in function of the target. The innovative devices developed and the wide versatility of the actuators designed, makes it possible to adapt the air flow in function of the canopy thickness. The spraying configuration designed provides eight different vertical bands of independent treatment with the possibility to manage, in a site specific way, the pesticide dose applied and the air flow direction and its rate. The spray robot module has both remote and proximal controls; remote for tractor control and proximal for spraying. This choice has a double aim *i.e.* to have an innovative sprayer usable and testable as independent autonomous equipment or else, coupleable with standard tractors. The expected pesticide dosage saving is about 50% of the conventional application rate maintaining, at the same time, the quality of the foliage deposition.

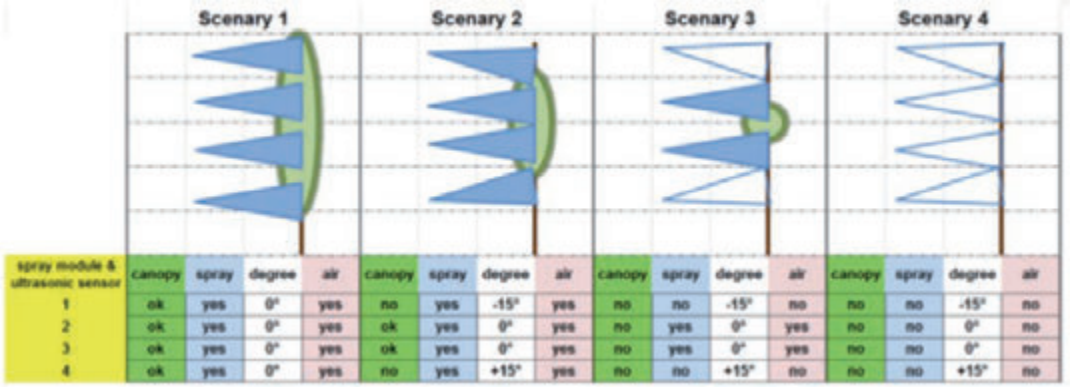

spray module & ultrasonic sensor	Scenary 1				Scenary 2				Scenary 3				Scenary 4			
	canopy	spray	degree	air	canopy	spray	degree	air	canopy	spray	degree	air	canopy	spray	degree	air
1	ok	yes	0°	yes	no	yes	-15°	yes	no	no	-15°	no	no	no	-15°	no
2	ok	yes	0°	yes	ok	yes	0°	yes	no	yes	0°	yes	no	no	0°	no
3	ok	yes	0°	yes	ok	yes	0°	yes	no	yes	0°	yes	no	no	0°	no
4	ok	yes	0°	yes	no	yes	+15°	yes	no	no	+15°	no	no	no	+15°	no

Figure 3. Rules on spray modules to adapt dosage at the canopy thickness on each band: scenario 1 corresponding to the presence of 100% of canopy 100% dose, scenario 2 presence of 50% 70% dose, scenario 3 presence < 50% canopy thickness 30% dose and absence of canopy 0 dose.

Figure 4. Devices developed for the air flow control left to right: fan inlet manifold throttle valve in the main entrance; actuation system for the upper and lower spray modules based on kinematic coupling driven by the stepper motor. This solution allows to obtain 30 ° of rotation, thus the orientation of air flow; butterfly valves located on the exit of fan calotte to selective opening of the spray modules.

Figure 5. On the left solutions developed for the liquid flow rate control: dual nozzles on each module electronically controlled by two solenoid valves with 70% and 30% of needed flow rate on each band simultaneously open with full canopy. Centre: electronic plant, center of the low level actuation system. On the right general view of the RHEA air blast sprayer prototype coupled with the ground mobile unit.

References

Sarri D, Lisci R, Rimediotti M, Vieri M. The RHEA-project: a new generation of air-blast sprayer for tree crops pesticide application. In proceedings of the 9th European Conference on precision Agricolture, 2013 Jul 7-11, Lleida, Spain. In press in Precision Agricolture ed. Springer.

Gonzalez-de-Santos P, Vieri M, Ribeiro A, Raffaelli M, Emmi L, Fontanelli M, Rimediotti M, Frasconi C, Sarri D. & Peruzzi A. 2011. The RHEA project: a fleet of autonomous robots for precision chemical and no chemical weed management in arable crops and on-canopy spraying in tree crops. In Proceedings of the Convegno di Medio Termine dell'Associazione Italiana di Ingegneria Agraria, Belgirate, 22-24 settembre 2011.

Vieri M, & Spugnoli P. 1997. An high pressure injection system for precision application of pesticide. BIOS Scientific Publishers Limited, Oxford 1997.

Vieri M, Lisci R, Rimediotti M, Sarri D. (2012). The innovative RHEA airblast sprayer for tree crop treatment. In proceedings of the first International Conference on Robotics and associated High-technologies and Equipment for agriculture. Application of automated systems and robotics for crop protection in sustainable precision agriculture. (RHEA 2012) Pisa, Italy, September 19-21, 2012. Pg. 93-98.

Vieri M, Sarri D, Rimediotti M, Lisci R, Peruzzi A, Raffaelli M, Fontanelli M, Frasconi C, Martelloni L. (2012). RHEA project achievement: an innovative spray concept for pesticide application to tree crops equipping a fleet of autonomous robots. Proceedings of the International Conference of Agricultural Engineering. CIGR-AgEng2012 – Valencia Conference Center, 8-12 July 2012, Valencia, Spain. Report 1356. ISBN 978-84-615-9928-4.

Experimental tests on a new harvesting system for Burley tobacco

Salvatore Faugno,[1] Collins Okello,[1,2] Roberta Infascelli,[1] Francesca Audino,[1] Luca Ardito,[1] Stefania Pindozzi[1]

[1]Dipartimento di Agraria, Università di Napoli Federico II, Italy; [2]Department of Biosystems Engineering, Gulu University, Uganda

Abstract

The globalization of the tobacco production has led to a drop in competitiveness of the Italian tobacco on the world market. Burley is the main variety of tobacco cropped in Campania region of Southern Italy. Its leaves have to be sewn, in the curing phase. Aim of this work is to show the results of the implementation of a new harvest machine prototype. Basically, the machine used for Bright tobacco, totally mechanical harvested, which doesn't need to be sewn because it requires an indirect-fire treatment into the curing furnaces. The machine was modified in order to mechanize harvesting of Burley tobacco, and tested on four cultivars of Burley tobacco under three different planting layouts. The Burley tobacco leaves can be harvested mechanically by pulling individual leaves off the stalk; leaves are then sorted and tied in bundles prior to sewing. A mechanical burley tobacco harvesting system was evaluated. This machine consists in realizing a leaves orientation system based on the different weight between the leaf blade and the stalk enhanced by an air flow. The measurements taken were harvest timing, work capacity, and quality standards of the work carried out. The results, in terms of user time, range from 6.67 h/ha to 7.80 h/ha while in terms of operational efficiency are between 88% and 89%. The average user capacity recorded for the four cultivars is equal to 0.14 ha/h, a value far from the one recorded for the same harvesting machine used for Bright tobacco (0.25 ha/h). The harvest timing capacity, range from 0.51 t/h to 0.99 t/h. The work productivity goes from 0.17 t to 0.33 t per hour of human unit respectively. The average number of detached leaves, depending on the cultivar, has been between 523 and 744. Concerning the leaf orientation, a general percentage of 73% was achieved.

Correspondence: Stefania Pindozzi, DIA, Università degli Studi di Napoli Federico II, via Università 100, 80055 Portici (NA), Italy.
Tel. +39.081.2539128.
E-mail: stefania.pindozzi@unina.it

Key words: Burley tobacco, mechanical harvesting, harvest timing.

Contributions: the authors contributed equally.

Conflict of interests: the authors declare no potential conflict of interests.

Funding: the work was supported by Campania Region with Tab.It Project.

Acknowledgments: The research activities were made under the project "Technical innovations and organizational restructuring of the tobacco sector in Campania region, in compliance with quality productions (Tab.IT)", funded by the Rural Development Policy 2007-2013, Measure 124 of Campania Region aimed at identifying techniques of cultivation of burley tobacco with low energy input pursuing the complete mechanization of the crop cycle. The authors would like to thank Spapperi s.r.l. and prof. I. Sifola for their support.

Journal of Agricultural Engineering 2013; XLIV(s1):e72
doi:10.4081/jae.2013.(s1):e72

Introduction

Tobacco cultivation in Europe is not immune to the effects of markets globalization which has created a sudden loss of competitiveness of Italian products compared to those available on the world market. The Italian agricultural system is burdened with a high cost of labor, because the crops are not fully mechanized.

The imbalance between production costs and the tobacco price was attenuated until 2006 due to the direct subsidy under the Common Agricultural Policy (CAP) and the Tobacco Common Market Organization (CMO). Since 2003, after an important reform in the CAP, subsidies were "decoupled" from particular crops. This led to a tremendous reduction of lands under tobacco cultivation. In Italy, the total area of land under tobacco cultivation reduced by approximately 28%. In the North of Italy, there was an increase in the average size of specialized tobacco farms, while the average size of the farms remained unchanged in Campania region (ISTAT, 2010). The decrease in production in Campania region was more than 43%. This difference in production between Campania region and other Italian areas is attributable to discrepancy in the production cycle. The bright-leaf tobacco is the variety mainly grown in the North of Italy, for which it is possible to implement the mechanical harvesting. However, harvesting of the burley tobacco cultivar, which is cultivated in the South Italy, remains highly labor intensive.

Despite these difficulties the Italian tobacco industry occupies a prominent position in the international scene, with a production of 89 kt y^{-1}, represents 26% of the total European production (NOMISMA, 2011). The cultivation of tobacco contributes less than 1% on the gross marketable production of Italian agriculture, and is mainly concentrated in four Italian regions of Campania, Tuscany, Umbria and Veneto. The tobacco industry employs approximately 204,000 persons throughout the supply chain (Di Carlo, 2012).

The mechanical systems for burley tobacco harvesting has not been investigated adequately despite numerous efforts to develop mechanize the operation over the last 30 years (Casada *et al.* 1972; Yoder & Henson, 1974; Duncan *et al.* 1996, 1999; Wells *et al.* 2011). One of the major limitations in the mechanical harvesting of burley tobacco is

related to the disposition of the leaves, which are not orderly arranged during harvesting and must be reorganized and put in bundles before being stuck for air-curing.

The aim of this study is to evaluate a new harvester prototypes realized within the project "Technical Innovations and Organizational Restructuring of the Tobacco sector in Campania region, Respecting Quality Production" (Tab.IT). The project aimed at identifying techniques of cultivation of Burley tobacco with low energy input and implementing the complete mechanization of the crop cycle. The prototype consists of a leaves orientation system based on the difference in weight between the leaf blade and the petiole and enhanced by an air flow. The prototype was the result of collaboration between the Department of Agriculture of University of Naples Federico II and an agro-machinery manufacturing company, Spapperi Srl of San Secondo (PG). The prototype was a modification of the bright-leaf tobacco harvesting machine. The system was improved and results of field tests were reported in order to evaluate the functionality of the system, the quantity and quality of work. The tests were carried out on four cultivars of Burley tobacco and with three different planting densities, with variation only in the distance between plants in the row. The row spacing was kept constant to allow the passage of the harvesting machine.

Materials and methods

Collection technique

The prototype was designed based on the Bright-leaf tobacco harvesting system. The Bright-leaf tobacco is intended for kiln-drying; therefore, the leaves collected are discharged directly in the loading system of the drying oven. However, burley tobacco is air-cured and the leaves have to be bundled and sewed after harvesting. The bundles are then hanged on special supports in cold greenhouse and allowed to dry. In order to perform the sewing, the leaves have to be mostly intact and all arranged with the stalk from the same side. This diverse need of care is the main challenge mechanical harvesting burley tobacco. Currently this type of tobacco is collected by workers, who advance between the rows, manually detaching the leaves and forming bunches, already oriented to be allocated to the next phase of sewing. As reported by CRAA in 2006, the manual labor requirement, for conventional harvesting is approximately 74 w-h/ha, including the time required for retrieving filled sticks from fields and hanging in barns for curing.

Experimental site

The experimental tests were carried out on a plot of 1 ha, located in Vitulazio in the South of Italy. Harvesting operations were observed and documented during the 2012 burley season at the Società Agricola Alessia Srl. The harvesting trials were carried out with four cultivars of Burley tobacco *i.e.*, CD, DD, BD and PM34, which is typically grown in the Caserta province, as the control. The first three cultivars reached a height of around 2.20 m. All the cultivars were planted at spacing between plant in rows of 0.25 m, 0.30 m and 0.33 m, while row length was kept constant at 0.90 m.

Description of machinery and harvesting mode

The Spapperi prototype, a modification of the Bright tobacco harvesting machine, is able to obtain pre-orientation of leaves, forming bunches ready for sewing, which takes place in the field. The system for the orientation of leaves is based on the weight difference between the leaf lamina and petiole, and on the increased aerodynamic drag of leaves. To this end a tapered section downwards metallic channel, has been mounted on the machine.

A blower (Figure 1a), was positioned at the base of the hopper to create an ascending air current that ensure orientation of leaves. The leaves from the elevation system are conveyed up in a pneumatic hopper from where they fall on a conveyor belt (Figure 1b). During the descending phase they are positioned with down stem. At the exit of the hopper the leaves are intercepted by a conveyor belt which transfers them in a container (Figure 1c).

Data collection

The experimental tests were carried out to evaluate system productivity. The measurements taken were harvesting time, working time, and quality of work. Analysis of working times was conducted according to the CIOSTA (Commission Internationale de l'Organisation Scientifique du Travail in Agriculture) official methodology and to recommendations of Italian Association of Rural Engineering (AIGR) 3A R1. Working times were split into time elements of the functional process analyzed, and consisted of the gross working time, which included the accessories times and unproductive times (Magagnotti *et al.* 2013, Fedrizzi *et al.* 2012). All time elements and the related time-motion data were recorded with a chronograph. Measurements were made timing the various phases at the cycle level, where the harvesting of a full unit was considered as a complete cycle (Magagnotti *et al.* 2013).

The tests were carried out over the length of the 400 m rows of four

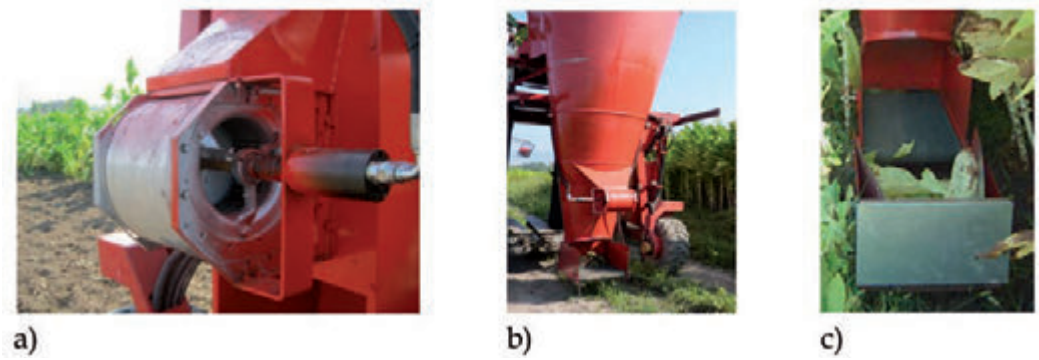

Figure 1. a) The blower; b) pneumatic hopper; c) Conveyor belt and container.

cultivars with three planting densities. The times recorded were, effective time (T_E), (h/ha); accessories time (T_A) required for turning, driving in and out for refueling, transferring the load and calibration on field (h/ha). The sum of T_E and T_A is equal to the operating time (t_o) and is defined as the actual time for harvesting (Bolli *et al.* 1987). User working time (t_u) that includes the preparation time on the field and operator rest was expressed as worker hour per hectare (w-h/ha). Row spacing and row length were also measured and used for calculating harvested area and associated to mass output in order to estimate average net yield.

Quality of work

Evaluation of the quality of work involved assessment of the integrity of the harvested leaves and their orientation. The harvested leaves were divided into three categories (Figure 2) *i.e.*, i) intact leaves, that are those with whole leaf blade; ii) partially intact leaves, but totally appropriate, with less damages in the foil or damaged petioles; and iii) damaged leaves not suitable for further processing.

Data were collected on the first 50 m of each row. During the test, detached leaves were controlled by an operator and divided into damaged and undamaged. At the same time another operator examined every single plant and recorded the number of leaves removed per plant. To determine exactly the number of detached leaves from the plants fresh scars on the drums were counted. The orientation of leaves were also evaluated.

Field capacity and productivity were calculated from the times recorded in the field. Field capacity is defined as the rate at which a farm machine performs its primary function (Mark Hanna, 2001) and is expressed in ha/h. Productivity is the ratio of the unit yield to workers hours (w-h) required for the farm machine and is expressed as the kg/w-h.

Results and discussion

Table 1 presents the results of time analysis of operations on the four cultivars.

User working time (t_u), that is of greatest interest to farmers, ranged from 6.67 for the PM34 cultivar at a planting density 0.33 m to 7.80 h/ha for the PM34 cultivar at a planting density 0.25 m. Data reported in Table 1 shows that increase in plant density results in higher number of hours required to harvest an hectare. This is because of the reduced working speed observed when the plant density was increased.

Field capacity, productivity and gross-effective productivity associated with the operation of the prototype harvesting machine are shown in Table 2. The user field capacity showed no substantial differences with an average value of about 0.140 ha/h, standard deviation (σ) equal to 0.006 and Coefficient of variation (CV) equal to 4% for the effective and

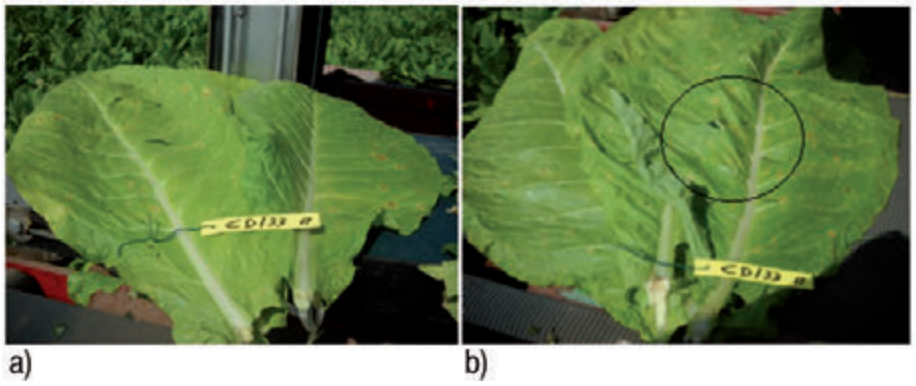

Figure 2. Quality of work parameters a) Intact leaves; b)Partially intact leaves.

Table 1. Times results associated with the operation of Spapperi prototype burley harvesting machine.

Cultivar/ planting density (cm)	Time elements			
	T_E (h/ha)	T_A (h/ha)	t_o (h/ha)	t_u (w-h/ha)
PM 34/25	6.7	0.84	7.54	7.8
PM 34/30	6.17	0.8	6.97	7.2
PM 34/33	5.65	0.77	6.42	6.67
CD/25	6.25	0.81	7.06	7.31
CD/30	6.13	0.82	6.94	7.16
CD/33	5.79	0.77	6.56	6.8
DD/25	6.27	0.83	7.1	7.36
DD/30	6.2	0.79	6.98	7.21
DD/33	5.98	0.76	6.74	6.99
BD/25	6.23	0.84	7.08	7.32
BD/30	6.21	0.8	7.01	7.25
BD/33	6.02	0.77	6.79	7.01

Table 2. Field capacity, productivity and gross-effective productivity associated with the operation of Spapperi prototype burley harvesting machine.

Cultivar/ planting density (cm)	Field capacity (ha/h)			Productivity (kg/wh*)			Gross-effective productivity (kg/ha)	Average value (%) of intact leaves
	Effective	Operative	User	Effective	Operative	User		
PM 34/25	0.149	0.133	0.128	206	183	177	5199	63.95
PM 34/30	0.162	0.144	0.139	231	205	198	3877	79.8
PM 34/33	0.177	0.156	0.015	33	29	279	5147	74.3
CD/25	0.16	0.142	0.137	207	183	177	5199	60.35
CD/30	0.163	0.144	0.014	387	342	331	5510	58.55
CD/33	0.173	0.152	0.147	319	282	272	7119	62.2
DD/25	0.159	0.141	0.136	273	242	233	4545	55.4
DD/30	0.161	0.143	0.139	245	217	21	3669	66.95
DD/33	0.167	0.148	0.143	293	26	251	4974	62.75
BD/25	0.016	0.141	0.137	278	245	237	5741	62.15
BD/30	0.161	0.143	0.138	197	174	169	5256	69
BD/33	0.166	0.147	0.143	273	242	235	4929	61.2

operative capacity. However, the field capacity is very far from that reported for bright-leaf tobacco harvesting machine that is about 0.25 ha/h.

Quality of work

Results of the quality of work are reported in the Table 2. The number of tobacco plants uprooted or broken during the harvesting test was about two to three plants per row, caused by a misalignment of the plants, or from an oblique growth. The mean value of intact leaves for the four cultivars was 64.7%, and the four cultivars showed very little variation in quality with a CV value of 10%. This corresponds to a loss of 0.17 t/ha of fresh tobacco, which is less significant for the case of the PM34 cultivar.

The last work quality parameters evaluated was the leaves orientation efficiency. These tests were carried out both with stationary machine and with moving machine. In the first case, the leaves were fed in manually. The best results were obtained in tests with stationary machine, with about 75% of the leaves well oriented. Tests carried out in the field showed a reduction in the percentage well oriented of leaves to 70%. This difference depends on the number of leaves that reach the hopper. It was observed that lower value of well oriented always corresponded to overloading of the hopper.

Future work

The Tab.IT project, is a three-year project beginning from 2010 to 2013, and will continue for another burley tobacco season. The first year was used to study and design the prototype. During the first burley tobacco season involved organizing the first version of the prototype, in which the sewing phase was on the top of the harvesting machine. This prototype required three workers to operate it and was considered unsuitable for both the excessive human labor and for safety reasons. The second prototype, presented in this paper, did not show encouraging results. This because an harvesting machine must guarantee a certain amount of work and at the same time must guarantee the commercial quality of the harvested product. Future work will aim at improving these attributes.

Conclusions

In this study, we developed and evaluated a prototype barley tobacco harvester. The best operating time performance obtained was 6.67 h/ha, far less from than performance of Bright-leaf tobacco harvester, which is reported to be 4 h/ha. Also, the harvested product quality highlighted unacceptable losses of approximately 30%. However, results showed very good levels of leaves orientation made directly on the machine of about 73%. Even in this case an improvement of the prototype will still be advantageous.

The poor performance in terms of field capacity of the machine, which advance with an average speed of 0.5 m/s, is probably caused by excessive plant density, which results in very tall tobacco plants. The very tall plants results in forward bending and consequently damage to leaves. Also this aspect has to be considered, in fact even if the burley tobacco has generally a lower height of tobacco Bright, it is not possible to perform topping operation. This because topping operation would entail an excessive accumulation of nicotine in the leaves, aspect considered negative.

References

Bolli P. Scotton M. Lineamenti di tecnica della meccanizzazione agricola. - Bologna :edagricole, 1987. - p. 47-56,107-120.

Casada JH, EM. Smith, CF. Abrams. 1972. A mechanical harvester for stalk-cut tobacco. Tobacco Science 16:147–149.

C.R.A.A. 2006. Miglioramento dell'efficienza della fase primaria nella filiera del Burley available on line: http://www.agricoltura.regione.campania.it/erbacee/pdf/report-burley.pdf

Di Carlo M. 2012. L'incerto futuro del tabacco italiano - L'Informatore Agrario. 15: 16.

Duncan GA, SA. Shearer, B. Tapp, CL. King. 1999. A new floating spear

mechanism for impaling burley tobacco plants onto a wooden stick. Applied Engineering in Agriculture 15(5):383–387.

Duncan GA, LR. Walton, JH. Casada, LD. Swetnam, B. Tapp. 1996. Development and evaluation of a cable-hoist system for housing burley tobacco. Applied Engineering in Agriculture 12(4):411–416.

Hanna M. 2001. Estimating Field Capacity of Farm Machines - Machinery Management – available on line at http://www.extension.iastate.edu/publications/pm696.pdf

ISTAT Istituto Nazionale di Statistica [Italian National Institute of Statistic], 2010. 6th General Census of Agriculture, Italy.

NOMISMA, 2011. La filiera del tabacco in Italia - Impatto socioeconomico ed aspetti di politica fiscale XV Rapporto (available on line at http://www.nomisma.it/fileadmin/User/XV_rapp_tabacco_2011.pd)

Wells L.G., Smith T.D., Day V G.B., Harpring M. 2011. On-farm performance of a mechanical burley tobacco harvesting system. Tobacco Science. 48:1–6

Yoder EE, WH. Henson, Jr. 1974. Handling burley tobacco on portable curing frames. Agricultural Information Bulletin No. 366. GPO, Washington, DC.

Numerical and experimental analysis of vertical spray control patternators

F. Sarghini,[1] G. Pergher[2]

[1]University of Naples Federico II, Dept. Of Agriculture, Portici (NA), Italy; [2]University of Udine, DISA, Udine, Italy

Abstract

The experimental vertical spray control walls have the purpose of picking up the liquid delivered by trained sprayer for providing the liquid distribution profile in height. Theoretically this should correspond to the ideal profile, which consists in a uniform distribution on the vegetation. If the profile is different from the ideal, a parameter setup is required on the sprayer. Nonetheless, some problems are hidden in the aforementioned statements: i) no wall measures exactly the distribution profile (*i.e.* the flow through the sections in the vertical plane, parallel to the direction of advancement of the sprayer). Compared to real profile, sensitive errors are introduced: the evaporation of the drops, the deviation of the air flows caused by the sensors panel themselves; by the possibility that the drops bounce on the wall panels, also due to the current of air that can push the liquid veil laterally or upwards, Moreover, everything varies depending on the geometry of the sensors, air velocity, air humidity; ii) no one knows what exactly is the optimal distribution profile. It is often considered as optimal a profile that reflects the amount of leaf area subtended by each section absorber: however, it is evident that the path of the droplets changes according to the sprayer typology (eg. radial-flow or horizontal flows). In this work a combined numerical-experimental approach is adopted, in order to assess some of the aforementioned issues: numerical data obtained by using computational fluid dynamics models are compared and validated with experimental data, in order to assess the reliability of numerical simulations in configurations which are difficult to analyze using an experimental setup.

Introduction

The distribution of pesticides through traditional trailed sprayers , the most common configuration for this this type of agricultural operation, represents an unresolved problem because of complicated interactions between operating parameters like the air flow rate and the pesticide nozzle orientation and constructive related parameters such as the fan geometry or the nozzle topology used for the atomization. In addition, pesticide distribution in the open field further complicates the framework, through the effects due to the advancement speed or the presence of wind.

This often involves a considerable deposition off-target, with consequences not only on treatment efficiency itself but also involving a serious environmental impact and safety for the operator.

Sprayer calibration is generally considered as an essential factor in determining the effectiveness of spray application in agriculture. Proper calibration should provide a constant deposit of the pesticide per unit of target area. In spray applications to orchards or vineyards, the spatial distribution of leaves fruits or other parts of the plant may vary considerably depending on the crop, growing system, growth stage, purpose of the application, or other factors (Pergher, 2004). Therefore, calibration should include a proper adjustment of the directions of spray and air flows in order to provide a good deposition uniform.

One possibility consists in calibrating the sprayers in a control station, where pesticide distribution is analyzed using experimental vertical spray control walls or patternators; based on the liquid distribution of the pesticide some adjustment can be done, working on nozzle orientation for example. Nonetheless such approaches rely on a certain degree of heuristic intuition, due to the complexity of the flow field dynamics.

Because of the complexity of the experimental approach, in these cases the numerical modeling is an investigative tool almost indispensable. In this work an experimental validation of the numerical approach is presented and some details of the flow field are analyzed.

Materials and methods

Numerical liquid droplet tracking in trained atomizer flow field is a very complex task. As a matter of fact, the dispersion of small inertial particles in inhomogeneous turbulent flow has been long recognized as crucial in a number of industrial applications and environmental phenomena: mixing, combustion, spray dynamics, pollutant dispersion, or cloud dynamics are all example of such phenomena involving droplet transport.

In all these problems accurate predictions are important, but they not trivial to obtain because of the complex phenomenology controlling turbulent particle dynamics.

Direct numerical simulations (DNS) of turbulence coupled with Lagrangian particle tracking (LPT) (Wang and Maxey,1993; Uijttewaal and Oliemans, 1996; Rouson and Eaton, 2001) have demonstrated their capability to capture the physics of particle dynamics in relation with turbulence dynamics and have highlighted the key role played by inertial clustering and preferential concentration in determining the rates of particle interaction, settling, deposition, and entrainment.

Correspondence: F. Sarghini, DIAAT, Via Università, 100, 80055 Portici (NA), Italy.
E-mail: sarghini@unina.it

Key words: deposition, patternator, numerical simulation, sprayer, Vineyard.

Journal of Agricultural Engineering 2013; XLIV(s1):e73
doi:10.4081/jae.2013.(s1):e73

Due to the computational requirements of DNS, however, analysis of applied problems characterized by complex geometries and high Reynolds numbers demands alternative approaches.

Turbulent flows are characterized by eddies with a wide range of length and time scales. The largest eddies are typically comparable in size to the characteristic length of the mean flow (for example, shear layer thickness). The smallest scales are responsible for the dissipation of turbulence kinetic energy.

It is possible, in theory, to resolve directly resolve the whole spectrum of turbulent scales using an approach known as direct numerical simulation (DNS), where no turbulence modeling is required . However, DNS is not feasible for practical engineering problems involving high Reynolds number flows. The cost required for DNS to resolve the entire range of scales is proportional to Re^3, where Re is the turbulent Reynolds number, but for high Reynolds numbers the cost becomes prohibitive.

In Large Eddy Simulation (LES) large eddies are resolved directly, while small eddies are modeled. The rationale behind LES can be summarized saying that momentum, mass, energy, and other passive scalars are transported mostly by large eddies, although some problems arise when particles or droplet interacts with the filtered flow field (Bianco et al, 2012). Large eddies are related to the geometries and boundary conditions of the modeled flow, while small eddies tend to be more isotropic, and are consequently more universal. As a consequence the possibility of finding an universal turbulence model is much higher for small eddies. In this work a scale similar model was adopted inside the framework of LES approach, (see Sarghini et al.,1999, for a summary of LES equations and scale similar models, and Sarghini et al, 2003 for the current implementation)

Droplet modeling

After the spray is generated from the nozzle, secondary droplet breakup (Fritsching, 2004; Markus and Fritsching, 2006) can appear. This break-up is mainly caused by the aerodynamical forces acting on the droplets and is classified by the Weber number. A droplet exposed to a relative velocity difference will eventually break up if the Weber number is large enough. The time it takes to deform and disrupt a droplet is described by the characteristic break-up time which is a result of Rayleigh-Taylor or Kelvin-Helmholtz (Levich, 1962; Bradley, 1973) instabilities. The spheroidization time for a droplet (Nichiporenko and Naida, 1968; Markus and Fritsching, 2006) after break-up is comparably small and hence the new droplets can be assumed to be spherical immediately after break-up. Depending on the initial Weber number, the droplets will deform and eventually break up in different sized fragments. Obviously, a high Weber number leads to a very disruptive break-up, while the break-up for small Weber numbers is slower and less disruptive. The different break-up regimes are to be distinguished by different sub-models.

In the numerical simulation several particle interaction models were introduced for particle secondary breakup, collision and coalescence.

Secondary breakup: Taylor analogy model

The Taylor analogy breakup (TAB) model (Taylor, 1981) is a classic method for calculating droplet breakup, which is applicable to many engineering sprays. This method is based upon Taylor's analogy between an oscillating and distorting droplet and a spring mass system.

The external force is given by aerodynamic droplet drag force, the damping force is due to the viscous forces, and the restoring force of the spring is given by surface tension forces

Droplet collision and coalescence: O'Rourke algorithm

Collision calculation is a time consuming task, considering that for N droplets, each one has N-1 possible collision partners, setting the number of possible collision pairs to 0.5 N^2 approximately. The algorithm of O'Rourke (O'Rourke, 1993), a stochastic estimate of collisions, reduces the computational cost of the spray calculation assuming that two parcels may collide only if they are located in the same continuous-phase cell. This method can be reasonably adopted only when the continuous-phase cell size is small compared to the size of the spray, being in this case the method second-order accurate at estimating the chance of collisions.

Droplet size

A Rosin-Rammler distribution was adopted, with an average D_{50} size equal to 250 mm and limit diameters D_{10}=100mm and D_{90}=500mm (Nuyttens et al, 2009) .

The numerical solver adopted in this work is OpenFoam (OpenFoam v2.2.0), a free, open source CFD software package. Several mesh configurations were tested, ranging from 300x10^3 up to 3×10^6 control volumes, and grid independence was tested on simplified test cases.

Results

Numerical results were compared with experimental data obtained from ENAMA certification report 05-109b - Poly 800/8 for an Agricolmeccanica SrL Poly 1000/8 trained atomizer. In particular, data related to liquid distribution were compared with numerical results obtained by collecting data on 2 virtual vertical spray control wall (P1 and P2, see Figure 1) , positioned at 1.25 m from the symmetry plane on the sprayer and considering all the particle passing through a 4.15m high x 2 m window during 20 s of computational time interval after the transient startup of the fan.

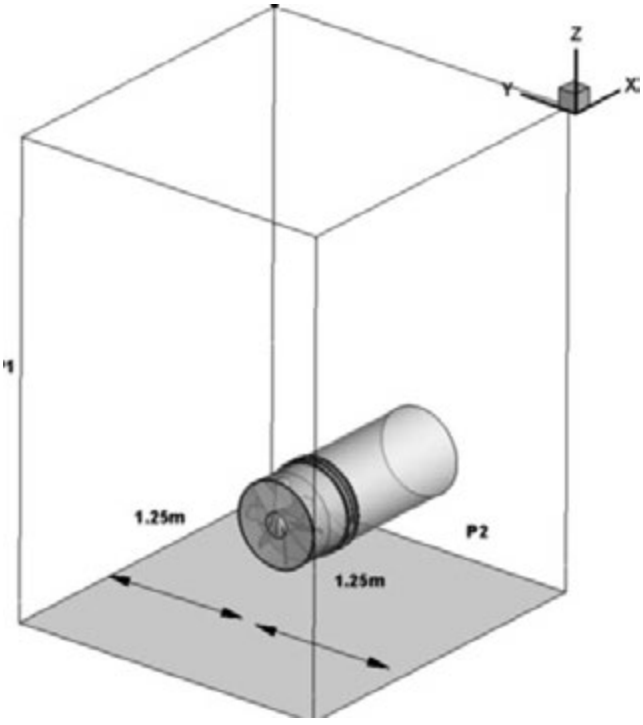

Figure 1. Numerical virtual vertical captation wall P1 and P2.

Such data were normalized using a captation index, computed at the end of the numerical measurement, showing the collected volume (vi, in ml) as a function of the measuring range for each virtual collecting panel as a percentage of the maximum value detected.

$$d_i = 100\frac{v_i}{v_{i(\max)}}$$

where v_i, in ml, is the volume captured by each captation panel i and $v_{i(max)}$, in ml, is the volume collected by the captation panel providing the maximum volume.

Operative parameters considered in the simulation are: axial fan rotational speed 1836 giri/min, nozzle mass flow rate /water) 1.06 liter/min at 10 bar, total volumetric fan flow rate 33800 m3/h.

In Figure 2 a comparison between experimental and numerical captation index is presented, showing a good agreement with an asymmetric distribution between the two sides, although a small quantitative divergence is present. Moreover, numerical results tends to distribute the droplets in the higher panels of the captation wall, probably due to the presence of a secondary break-up phenomena.

In Figures 3 and 4 frontal and lateral views of droplets distribution for a tracking time equal to 1 s are presented. Notice that the geometrical axial fan configuration, without any device to straighten the internal flux and to reduce the swirl due to blades rotational movement, generates a strong asymmetry which is responsible of the difference in results between right and left side showed in Figure 2. Moreover, axial momentum generates also the dispersion of the droplets also on an inclined radial cone, as showed in Figure 4.

In Figure 5 and 6 velocity contours are shown on both frontal and lateral planes, showing that although at a certain distance from the nozzle

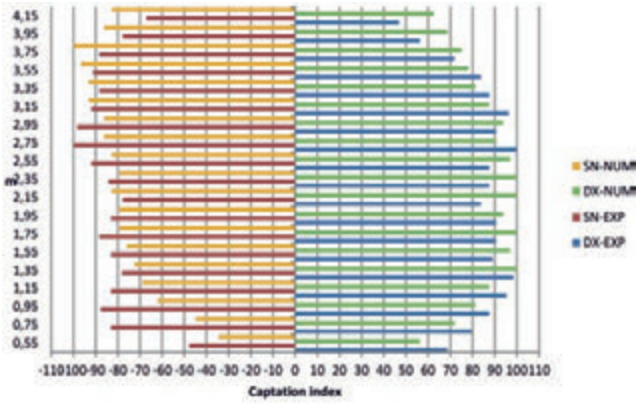

Figure 2. Experimental and numerical captation index diagram.

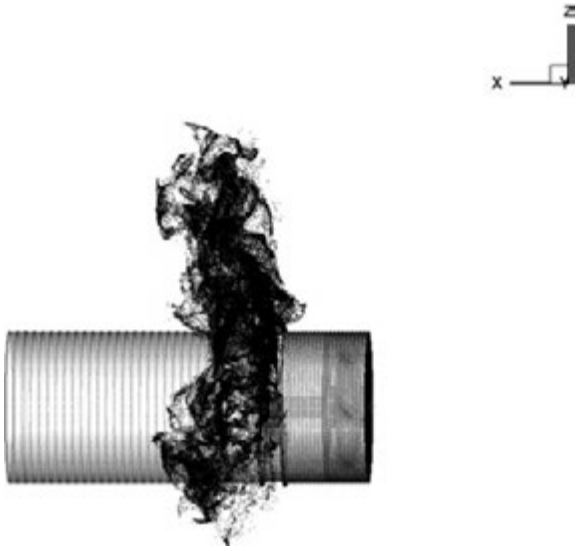

Figure 4. Droplets distribution (lateral view) - axial fan without swirl control (rotor only).

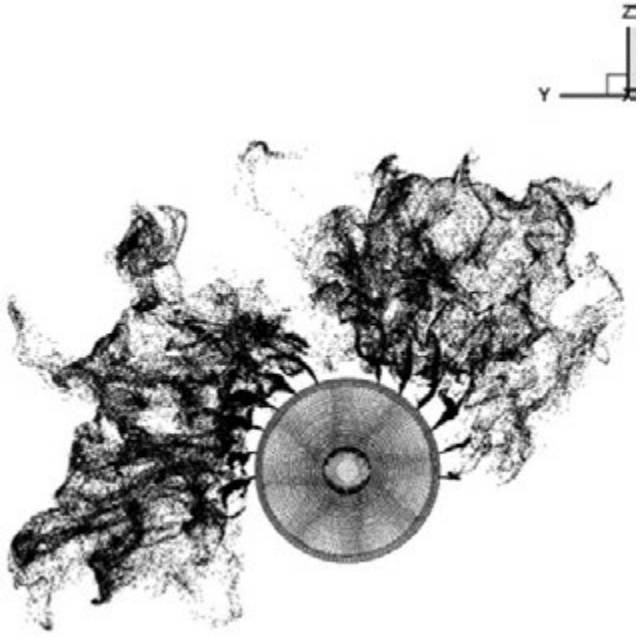

Figure 3. Droplets distribution (frontal view) - axial fan without swirl control (rotor only).

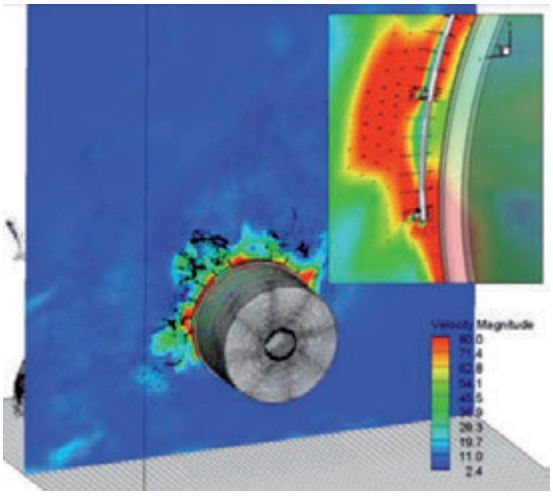

Figure 5. Velocity contour distribution (frontal view) - axial fan without swirl control (rotor only).

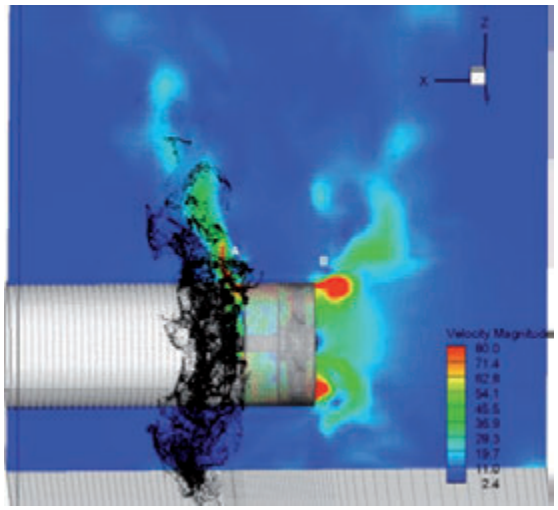

Figure 6. Velocity contour distribution (lateral view) - axial fan without swirl control (rotor only).

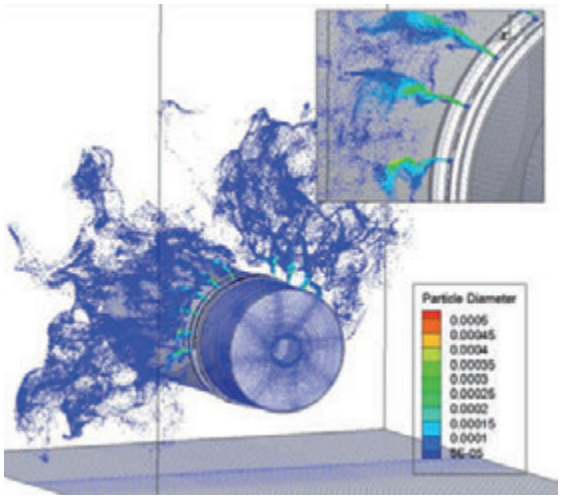

Figure 7. Droplets size distribution (frontal view) - axial fan without swirl control (rotor only).

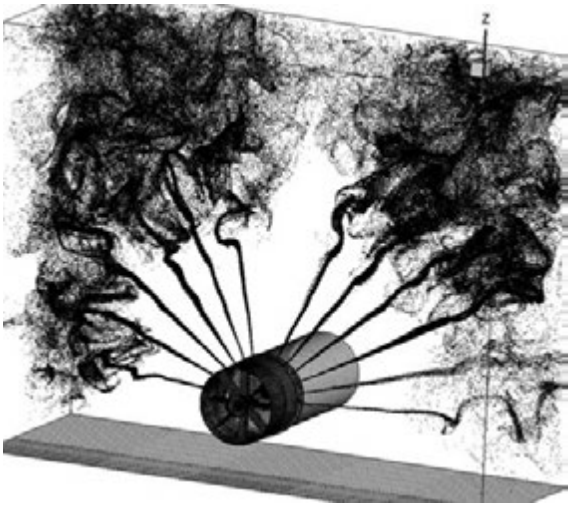

Figure 8. Droplets distribution - axial fan without moving part (uniform inflow) and direction control (stator only).

ring, air speed is order of 10 m/s, near the nozzle air speed peaks are higher than 80 m/s, generating 2 main effects: an unsteady vortex shedding (Figure 6) and a secondary droplets break-up, generating a different droplets diameter distribution as showed in Figure 7.

In Figure 8 droplets distribution is showed for a simulation on a slight different configuration: rotating blades are replaced by a uniform inflow velocity distribution followed by a static blades geometry (stator), where swirl effects can be neglected: in this case vortex shedding and related particles entrainment is strongly reduced, and radial asymmetry disappears.

Conclusions

Results obtained using computational fluid dynamics technique showed a good agreement with experimental data, although a slight difference is still present. This difference can be attributed to geometrical details and secondary break-up modeling. In any case, ad-hoc experiments should be carried out in order to match all geometrical and operative parameter details.

Nonetheless, numerical experiments showed that a main role is played by the internal flow field of the axial fan, which is responsible for the unsteady flow and related vortex shedding in proximity of the nozzle's ring, inducing a backward radial bending of the nozzle jet. Another detail to be assessed is the influence of the fan inflow flow field with the flow field near the nozzle in case of short fan configuration, which is related to axial fan blade geometry.

The presence of unsteady vortices generates a strong vortex entrainment where a high number of droplets collision coalescence happens because of vortex entrainment.

Results showed that numerical simulation can be used to design more efficient patternators, allowing to gain an important insight in droplet - flow field interactions, almost impossible to obtain in an experimental setup.

References

Bianco F., Chibbaro S., Marchioli C., Salvetti M. V., and Soldati A., 2012. Intrinsic filtering errors of Lagrangian particle tracking in LES flow fields, Phys. Fluids, 24, 1.370- 1378.

Bradley D., 1973. On the atomization of liquids by high-velocity gases, Part 1. J. Phys. D: Appl. Phys. 6:1724–1736, and Part 2., J. Phys. D: Appl. Phys. 6:2267–2272.

Fritsching U., 2004. Spray Simulation: Modelling and Numerical Simulation of Sprayforming Metals. Cambridge University Press, Cambridge, UK.

Fritsching U., Zhang H., Bauckhage K.,1994. Numerical simulation of temperature distribution and solidification behaviour during spray forming, Steel Res., 65,273–278.

Markus S., Fritsching U., Bauckhage K., 2002. Jet break up of liquid metals in twin fluid atomization, Materials Science and Eng., A 326:122–133.

Nichiporenko S, Naida YI.1968. Heat exchange between metal particles and gas in the atomization process. Soviet Powder Metall. Metal Ceramics, 7(7):509–512.

Nuyttens, D., Schampheleire, M. de, Verboven, P., Brusselman, E., Dekeyser, D., 2009. Droplet size and velocity characteristics of agricultural sprays ,Transactions of the ASABE, Vol. 52 No. 5 pp. 1471-1480.

O'Rourke P. J. ,1981. Collective Drop Effects on Vaporizing Liquid Sprays". PhD thesis. Princeton University, Princeton, New Jersey.

OpenFoam, The free CFD Toolbox, www.openfoam.org. , accessed 20.04.2013.

Pergher G., 2004, Field evaluation of a calibration method for air-assisted sprayers involving the use of a vertical patternator, Crop Protection, 23, 5 , Pages 437-446.

Rouson D. W. and Eaton J. K., 2001. On the preferential concentration of solid particles in turbulent channel flow, J. Fluid Mech. 428, 149.

Sarghini, F., U. Piomelli,, Balaras E.,1999. Scale-Similar Models for Large-Eddy Simulations, Physics of Fluids, 11, 6:1596.

Sarghini, F., De Felice, G., Santini, S., 2003, Neural networks based subgrid scale modeling in large-eddy simulations, Computers and Fluids, 32,1:97-108.

Taylor G. I. , 1963. The Shape and Acceleration of a Drop in a High Speed Air Stream, Technical Report. In the Scientific Papers of G. I. Taylor. ed., G. K. Batchelor.

Levich VG, 1962. Physicochemical Hydrodynamics. Prentice Hall, Upper Saddle River, NJ, 501–667.

Uijttewaal W. S. J. and Oliemans R. W. A.,1996. Particle dispersion and deposition in direct numerical and large eddy simulations of vertical pipe flows, Phys. Fluids 8, 2590.

Wang L. P. and Maxey M. R., 1993. Settling velocity and concentration distribution of heavy particles in homogeneous isotropic turbulence, J. Fluid Mech., 256, 27.

Preliminary evaluation of a short rotation forestry poplar biomass supply chain in Emilia Romagna Region

L. Pari,[1] Massimo Brambilla,[2] V. Civitarese,[1] C. Bisaglia[2]

[1]Consiglio per la Ricerca e la Sperimentazione in Agricoltura, Unità di Ricerca per l'Ingegneria Agraria, Monterotondo (Roma), Italy; [2]Consiglio per la Ricerca e la Sperimentazione in Agricoltura, Unità di Ricerca per l'Ingegneria Agraria, Laboratorio di Treviglio (BG), Italy

Abstract

Woody Biomasses (from agriculture and forestry activities) are among the most promising renewable energy sources. Current literature describes woody biomass feedstock supply chains supporting biofuels and utilities industries: the potentially productive land area overheads required for biomass production may results in a complex logistic within the whole chain. Its effective enhancement requires significant changes in the logistics environment of energy plants for sustainable energy production and the sequence-dependent procurement chains for biomasses furthermore complicate these changes. According to this, optimizing harvesting and supplying operations turns out to be strategic within the framework of the current energy policy. In this work we present a case study carried out monitoring 57 short rotation forestry (SRF) production sites placed in Emilia Romagna Region, Northern Italy, all supplying the harvested biomass to the same biomass power plant placed in the province of Ravenna (Italy). The overall average yield of these sites was 55 t/ha, the site surfaces ranged from 0.3 to 20 hectares and the distance from the power plant ranged between 8.2 to 102 km with one production site only within 10 km from the power plant. Harvest and transport costs were calculated according to two different harvesting scenarios: *i)* single phase harvesting (one cutting/chopping machine + tractors and trailers); *ii)* double phase harvesting (cutting/mowing machine followed after 80 days by chopping machine + tractors and trailers). Results show that, according to the first scenario, at increasing distances overall harvesting and transport costs ranged from 8.9 to 21.0 ± 1.3 €/t (average ± standard deviation), while, with reference to the second scenario, they increased from 10.3 to 23.8 ± 1.5 €/t with the transportation costs accounting from 16 to almost 70% of the total costs.

Correspondence: Massimo Brambilla, Consiglio per la Ricerca e la Sperimentazione in Agricoltura, Unità di Ricerca per l'Ingegneria Agraria, Laboratorio di Treviglio, via Milano 43, 24047 Treviglio (BG), Italy.
Tel./Fax.: +39.0363.49603
E-mail: massimo.brambilla@entecra.it

Keywords: SRF biomass harvesting optimization, transport costs.

Contributions: the authors contributed equally.

Conflict of interests: the authors declare no potential conflict of interests.

Conference presentation: this paper was presented at the 10th AIIA Conference: "AIIA13 – Horizons in agricultural, forestry and biosystems engineering", Viterbo, University of Tuscia, Italy, on September 8-12, 2013.

Funding: the work was supported by the SUSCACE project (Scientific Support to Agricultural Conversion towards Energy Crops).

Acknowledgments: the Authors acknowledge the role of the "SUSCACE" Project (Scientific Support to Agricultural Conversion towards Energy Crops) for funding the study.

Journal of Agricultural Engineering 2013; XLIV(s1):e74
doi:10.4081/jae.2013.(s1):e74

Introduction

The rises of fossil fuel derived energy prices, and the increasing environmental concern, encourage the use of alternative and renewable energy sources as woody biomasses (Goldstein, 2006): low carbon power sources whose energy exploitation has the advantage that the emitted greenhouse gases (GHG) amounts are the same of those absorbed during the growth phase (Dubuisson and Sintzoff, 1998; Walle *et al.*, 2007; Djomo *et al.*, 2011).

Short rotation forestry (SRF) programs, made these woody fuel sources widely available allowing increases in production quality maintaining the competitiveness of the production costs: as far as woody fuel quality is concerned studies pointed out the importance of proper storage and handling of these biomasses (Lehtikangas, 2000; Jirjis, 2001; Lehtikangas, 2001; Pettersson and Nordfjell, 2007; Noll *et al.*, 2010) and production management criteria were addressed as way to maintain and increase the sustainability of this production (Cherubini and Strømman, 2011; Stolarski *et al.*, 2011; González-García *et al.*, 2012). With particular reference to harvesting operations, one recent study of Fiala and Bacenetti (2012) pointed out, with reference to poplar trees, how plantation characteristics strongly influence machine productivity together with biomass transport system efficiency introducing a big tricky point of this energetic sector: biomass production and transportation account for a significant part of the whole bioenergy costs (Zhang *et al.*, 2005) affecting plants' profitability, which is known to be highly geographically dependent (Noon and Daly, 1996). Transporting loose comminuted biomass is, at the moment, the most effective method for biomass supplying provided that close coordination of the transportation fleet is arranged (Spinelli and Hartsough, 2006).

Transportation costs from the sources to the energy plants take a significant proportion of the overall production costs of woody biomasses: hauling distance, load bulk density and delivered material

moisture content can accounting up to 50 per cent of delivered costs (Angus-Hankin *et al.*, 1995; Zhan *et al.*, 2005; Pan *et al.*, 2008). Increasing the transportation efficiency of woody biomass should significantly reduce overall production costs as well as environmental impacts (Palmgren *et al.*, 2004). To achieve this, many models and decision systems relying on GIS approach have been developed to define planning and management strategies for the optimal logistics for energy production from woody biomass, such as forest biomass, agricultural scraps and industrial and urban untreated wood residues (Andersson *et al.*, 1995; Frombo *et al.*, 2008; Sang-Kyun *et al.*, 2012). These decision support systems have been set up to select least-cost bioenergy locations when more than one bioenergy plant is present in the region and there is significant variability in biomass farm-gate price or in supply costs (Ranta, 2005; Panichelli and Gnansounou, 2008) or to facilitate the definition of sound policies and strategies based on a comprehensive perspective of the whole energy system (Mitchell, 2000; Masera *et al.*, 2006).

Within this framework, with the final aim to assess the effective account of delivery costs on woody biomass price, we present a case study carried out monitoring short rotation forestry (SRF) production sites placed in Emilia Romagna Region, Northern Italy, all supplying the harvested biomass to the same biomass power plant placed in the province of Ravenna (Italy).

Material and methods

Fifty seven short rotation forestry biomass production sites (Figure 1) growing poplar tree (*Populus spp.*) or locust tree (*Robinia pseudoacacia*) were monitored with reference to biomass production and transport to the power plant site. According to the distance from the centralized power plant, biomass production units were divided in the following groups: *i*) within 10 km; *ii*) from 10 to 30 km; *iii*) from 30 to 40 km; *iv*) from 40 to 60 km; *v*) from 60 to 70 km; *vi*) more than 70 km.

For this production site characterization, two different scenarios (namely, "single phase harvesting" and "double phase harvesting" procedures) have been taken into account.

According to single phase harvesting scenario, biomass was harvested and chopped with a CLAAS forager (Jaguar series, CLAAS KGaA mbH, Germany) powered by an engine rated at 372 kW. The unit, fitted with one "GBE-1" header for SRF crop harvesting (Figure 2) cuts the stems and moves them toward the horizontal in feed rollers built into the forager unit. This harvesting-chipping machine enters the field followed by tractors with trailers or by lorries providing for chopped biomass transport to the plant site.

The double phase harvesting scenario considers two separate passes. In the first pass, a semi-trailed cut-windrower (applied to a 60 kW tractor at least), cuts the stems and lays them in the inter-row parallel with the advancing direction of the tractor while, in the second pass, a forage harvester equipped with a pick up head collects and chip the windrowed stems. The pick-up gathers the plants from the ground and the concomitant action of the forward moving of the tractor and of the conveyor device allows for the loading of the trees towards the feeding rolls of the chipping device and the offloading of the chips into the trailers. While the first pass is conducted in winter and during the dormant season, the second pass occurs in late spring, after the stems have been partially dehydrated. Information about production rates and costs of each of these scenario are reported in Tables 1 and 2. For each production unit, the distance from the centralized power plant was determined and according to this, harvesting and transporting costs were calculated as follows:

$$Harvesting\ Costs\ (€/t) = \frac{Produced\ Biomass\ (t)}{Machine\ operative\ capacity\ (ha/h)}\ x\ hourly\ Costs\ (€/h)$$

$$Transport\ Costs\ (€/t) = \frac{Time\ required\ (h)}{Lorry\ hourly\ cost\ (€/h)}\ x\ Number\ of\ required\ trips\ x$$

$$Overall\ Costs\ (€/t) = Harvesting\ costs\ (€/t) + Transport\ Costs\ (€/t)$$

The obtained data underwent statistical analysis by means of *Minitab® 16 Statistical Software* (2010) to perform descriptive statistics and analysis of variance ($P<0.05$).

Results

Biomass production units of the considered scenario turn out to be quite unevenly distributed among the considered distance ranges (Figure 3), nevertheless the average surface used for biomass production turned out not to be significantly different (Figure 4) at $P < 0.05$: as a matter of fact only one production site (whose production accounts for

Figure 1. Geographical distribution of the biomass production sites (green markers) and of the power plant (red marker). Image from Google Earth®.

Figure 2. Particular of the GBE-1 header for SRF harvesting.

1.3% of the total produced biomass) is located within 10 km from the power plant and 4 plants only (7.0% of the total) are placed from 10 to 30 km of distance while great part of them are placed more than 40 km far (Figure 3).

The comparison carried out on overall costs and on the per cent weight of transport costs (Table 3) shows that overall costs range from 8.92 – 10.26 € t^{-1} to 20.97 – 23.79 € t^{-1} increasing, as expected, at increasing distances from the power plant with similar percentage incidences of the transport costs.

If, on one hand, generally speaking, the costs related to the double phase harvesting procedure are always higher than those related to the one phase harvesting, on the other the one way ANOVA shows that in three cases only this difference turns out to be significant.

The same analysis carried out on the incidence of transport costs, shows that for production sites placed from 40 to 60 km and from 60 to

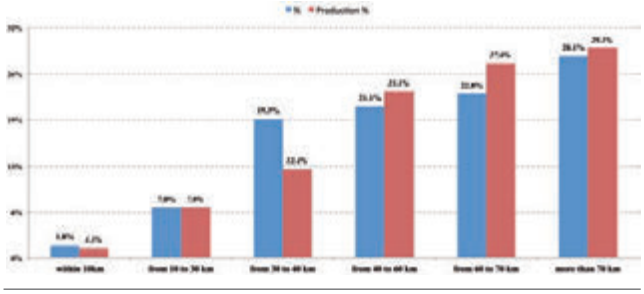

Figure 3. Distribution of the biomass production units in the distance range as percentage of their number (blue columns) and of the whole produced biomass (red columns).

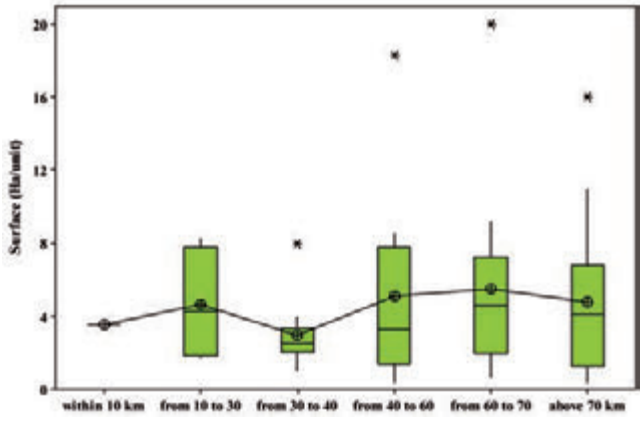

Figure 4. Boxplot chart of the average unit surface (Ha/unit) for the considered distance ranges.

Table 1. Main economic and technical features of the *single phase harvesting procedure*.

Cutting/Chopping machine hourly cost (€/h)	411.00
Productivity (Ha/h)	1.0
Woody Biomass Yield (Mg/ha)	55.0
Tractor + trailer hourly cost (€/h)	42.00
Trailer maximum capacity (t)	0.37
Tractor average speed (km/h)	35.0
Lorry hourly cost (€/h)	65.00
Maximum capacity of the lorry (t)	21.00
Average speed of the lorry (km/h)	50.0

Table 2. Main economic and technical features of the *double phase harvesting procedure*.

1st phase: cutting and mowing		2nd phase: chipping and transporting	
Cutting hourly cost (€/h)	67.00	Pick-up Hourly Cost (€/h)	308.50
Operative Capacity (Ha/h)	1.40	Operative capacity (Ha/h)	0.85
Biomass Yield (Mg/ha)	55.0	Biomass Yield (Mg/ha)	46.7
Tractor + trailer hourly cost (€/h)	42.00	Tractor + trailer hourly cost (€/h)	42.00
		Maximum trailer capacity (Mg)	0.70
		Lorry for biomass transport (€/ha)	73.00

Table 3. Average harvesting and transporting overall costs as well as average per cent accounting of transport costs on the total costs. Uppercase letters indicate significant differences among mean values along the same column (p<0.05), lowercase letters indicate significant differences (p<0.05) between values belonging to different harvesting procedures.

Distance ranges from the power plant	N. of units	Single phase harvesting		Double phase harvesting	
		Overall costs (€/t)	Transport costs (%)	Overall costs (€/t)	Transport costs (%)
Within 10 km	1	8.92 A	16.3 A	10.26 A	15.8 A
From 10 to 30 km	4	10.91±0.90 (B, a)	31.2±5.62 (B, a)	12.49±1.01 (B, a)	30.6±5.60 (B, a)
From 30 to 40 km	11	13.56±0.46 (C, a)	44.8±1.84 (C, a)	15.47±0.52 (C, b)	44.1±1.80 (C, a)
From 40 to 60 km	12	17.66±0.28 (D, a)	57.7±0.69 (D, b)	20.08±0.31 (D, a)	56.9±0.69 (D, a)
From 60 to 70 km	13	18.37±0.23 (E, a)	59.3±0.50 (E, b)	20.87±0.26 (E, b)	58.6±0.54 (E, a)
More than 70 km	16	20.97±1.34 (F, a)	64.2±2.00 (F, a)	23.79±1.51 (F, b)	63.5±2.02 (F, a)

70 km from the power plant, the incidence of these is significantly, despite slightly, lower when harvesting is carried out according to the double phase system.

With reference to transport costs incidence on overall costs, these results fully comply with the finding of Spinelli *et al.* (2006), who assessed that transportation accounts for 30-50% of the total costs on the short haul, and 60-70% of the costs on the long one when SRF poplar for pulpwood is concerned. Nevertheless, when transport cost values are concerned, according with Sultana and Kumar (2011), both fixed costs and distance related variable should be considered with the latter depending on the type of biomass being transported, on the form of biomass, on the equipment used for loading–unloading and any existing contractual agreement (Searcy *et al.*, 2007). Mahmudi and Flynn (2006) assessed the fixed costs of woody chips transport at 4.07 € t^{-1} and the variable component at 0.06 € t^{-1}. Transport costs recalculation with these values (converted into euros) give rise to an great overestimation of transport costs for the production unit closer to the power plant, while for the other groups of biomass production sites the predicted values are 24% higher than ours in case of units ranging from, 10 to 30 km from the plant, while for all the others the estimated values are from 29 to 60 % lower. This trend is confirmed also by comparing overall costs with those of 49.46 € t^{-1} for 16 km distance and 36.33 € t^{-1} for 27 km distance presented by Perrin (2012) who worked on corn-stover biomass supply of ethanol production facility. The reason of this can be ascribed, on one hand, to the costs of the fuel for transport which, has high impact on transport costs in the European context, while on the other to the high variability of duty trucks which can differ substantially around the world and even in the same country (Widerberg *et al.*, 2006). Moreover, with reference to data provided by Perrin *et al.* (2012) their value is unavoidably affected by the higher value of fixed and variable components that, according to Kumar and Sokhansanj (2007),are quite higher than those provided by Mahmudi and Flynn (2006).

Conclusions

A case study on the effective costs related to biomass supply chain in the Emilia Romagna region was carried out considering a number of SRF production sites within 70 km of distance from the power plant. At increasing of the distance, overall cost can almost double passing, at varying of the hypothesized scenario, from 8.92 – 10.26 € t^{-1} to 20.97 – 23.79 € t^{-1} where transport costs incidence varies from 31 to 64%.

References

Andersson G., Flisberg P., Lidén, B, Rönnqvist, M. 2008. RuttOpt – a decision support system for routing of logging trucks. Can J Forest Res 38 (7): 1784-1796.

Angus-Hankin C., Stokes B., Twaddle A. 1995. The transportation of fuel wood from forest to facility. Biomass Bioenerg 9 (1-5): 191-203.

Cherubini F., Strømman A.H. 2011. Life cycle assessment of bioenergy systems: State of the art and future challenges. Bioresource Technol 102 (2): 437–451.

Djomo S.N., Kasmioui O.E., Ceulemans R. 2011. Energy and greenhouse gas balance of bioenergy production from poplar and willow: a review. GCB Bioenerg 3: 181–197.

Dubuisson X., Sintzoff I. 1998. Energy and CO_2 balances in different power generation routes using wood fuel from short rotation coppice. Biomass Bioenerg 15: 379-390.

Fiala M., Bacenetti J. 2012. Economic, energetic and environmental impact in short rotation coppice harvesting operations. Biomass Bioenerg 42: 107-113.

Frombo F., Minciardi R. , Robba M., Rosso F., Sacile R. 2009. Planning woody biomass logistics for energy production: A strategic decision model. Biomass Bioenerg 33 (3): 372–383.

Goldstein N. 2006. Woody biomass as a renewable energy source. Biocycle 47(11): 29-31.

González-García S., Bacenetti J., Murphy R.J., Fiala M. 2012. Present and future environmental impact of poplar cultivation in the Po Valley (Italy) under different crop management systems. J Clean Prod 26: 56-66

Jirjis R. 2001. Forest residue-effect of handling and storage on fuel quality and working environment. Forest Research Bulletin 223: 136-145.

Kumar A., Sokhansanj S. 2007. Switchgrass (*Panicum virgatum L.*) delivery to a biorefinery using integrated biomass supply analysis and logistics (IBSAL) model. Bioresource Technol 98: 1033-1044.

Lehtikangas, P. (2000). Storage effects on pelletised sawdust, logging residues, and bark. Biomass Bioenerg 19: 286-293.

Lehtikangas, P. (2001). Quality properties of pelletised sawdust, logging residues, and bark. Biomass Bioenerg 20: 351-360.

Mahmudi H., Flynn P.C. 2006. Rail vs Truck transport of biomass. Appl Biochem Biotech 129 (1-3): 88-103.

Masera O., Ghilardi A., Drigo R., Trossero M.A. 2006. WISDOM: A GIS-based supply demand mapping tool for woodfuel management. Biomass Bioenerg 30: 618-637.

Minitab® 16 Statistical Software (2010). [Computer software]. State College, PA: Minitab, Inc. (www.minitab.com)

Mitchell C.P. 2000. Development of decision support systems for bioenergy Applications. Biomass Bioenerg 18: 265-278.

Noll M., Naumann A., Ferrero F., Malow M. (2010). Exothermic processes in industrial-scale piles of chipped pine-wood are linked to shifts in gamma-, alphaproteobacterial and fungal ascomycete communities. International Biodeter Biodegr 64, 29-637.

Noon C.E., Daly J.M. 1996. GIS-based biomass resource assessment with BRAVO. Biomass Bioenerg 10: 101-109.

Panichelli L., Gnansounou E. 2008. GIS-based approach for defining bioenergy facilities location: A case study in Northern Spain based on marginal delivery costs and resources competition between facilities. Biomass Bioenerg 32: 289-300.

Palmgren M., Rönnqvist M., Varbrand P. 2004. A near-exact method to solve the log truck scheduling problem. International Transactions in Operational Research, 11: 447–464

Pan F, Han H-S, Johnson L, Elliot W. 2008. Production and cost of harvesting and transporting small-diameter trees for energy. Forest Prod J 58 (5): 47-53.

Pettersson M., Nordfjell T. 2007. Fuel quality changes during seasonal storage of compacted logging residues and young trees. Biomass Bioenerg 31: 782-792.

Ranta, T. 2005. Logging residues from regeneration fellings for biofuel production–a GIS-based availability analysis in Finland. Biomass Bioenerg 28: 171-182.

Spinelli R., Nati C., Magagnotti N. 2006. Recovering logging residue: experiences from the Italian Eastern Alps. Croat J For Eng 28: 1-9.

Spinelli R., Hartsough, B.R. 2006. Harvesting SRF poplar for pulpwood: Experience in the Pacific Northwest. Biomass Bioenerg 30: 439-445.

Stolarski, M.J., Szczukowski S., Tworkowski J., Klasa A. 2011. Willow biomass production under conditions of low-input agriculture on marginal soils. Forest Ecol Manag 262 (8): 1558-1566.

Sultana, A., Kumar, A. 2011. Optimal configuration of multiple lignocellulosic biomass feedstocks delivery to a biorefinery. Bioresource Technol 102: 9947-9956.

Walle I.V., Camp N.V., Van de Casteele L, Verheyen K, Lemeur R. 2007. Short-rotation forestry of birch, maple, poplar and willow in Flanders (Belgium) II. Energy production and CO2 emission reduction potential. Biomass Bioenerg 31:276-283.

Widerberg J., Dahlber E., Svensson M. 2006. Study of stability measures and legislation of heavy articulated vehicles in different OECD countries. Conference proceedings/ISHVWD-9.

Zhan F.B., Chen X., Noon C.E., Wu. G. 2005. A GIS-enabled comparison of fixed and discriminatory pricing strategies for potential switchgrass-to-ethanol conversion facilities in Alabama. Biomass Bioenerg 28: 295–306.

Chipping machines: disc and drum energy requirements

Alessio Facello,[1], Eugenio Cavallo,[1] Raffaele Spinelli[2]

[1]CNR IMAMOTER, Torino, Italy; [2]CNR IVALSA, Sesto Fiorentino (FI), Italy

Abstract

Air pollution and fossil fuel reserves exhaustion are increasing the importance of the biomass-derived products, in particular wood, as source of clean and renewable energy for the production of electricity or steam. In order to improve the global efficiency and the entire production chain, we have to evaluate the energetic aspects linked to the process of transformation, handling and transport of these materials. This paper reports results on a comparison between two chippers of similar size using different cutting technology: disc and drum tool respectively. During trials, fuel consumption, PTO torque and speed, processing time and weight of processed material were recorded. Power demand, fuel consumption, specific energy and productivity were computed. The machine was fed with four different feedstock types (chestnut logs, poplar logs, poplar branches, poplar sawmill residues). 15 repetitions for each combination of feedstock-tool were carried out. The results of this study show that the disc tool requires, depending on the processed material, from 12 to 18% less fuel per unit of material processed than the drum tool, and consequently, from 12 to 16% less specific energy. In particular, the highest difference between tools was found in branches processing whereas the smallest was in poplar logs. Furthermore the results of the investigation indicate, that, in testing conditions, the productivity of drum tool is higher (8%) than disc tool.

Introduction

The use of fossil energy sources like petrol and carbon has a strong consequence on greenhouse effect, climate change and acidification of water and soil (de Wit and Faaij, 2010). Biomass-derived products are an important source of renewable energy and can reduce the global pollution. Traditional agricultural crops, dedicated energy crops and residues from agriculture and forestry have high potential for the production of heat, steam, electricity and transportation fuels (Chum and Overend, 2001).

Various type of processing machines are used to facilitate handling and transport of wood (Hillring, 2006), that is one of the most important source of biomass. The energetic aspects linked to the process of transformation, handling and transport of these materials have to be considered in order to optimize and improve the entire process.

This paper refers result on a comparison between two chippers of similar size using different cutting technology: disc and drum tool respectively. Trials has been performed to investigate the differences in terms of energy requirements, hourly production and type of raw material processed by the two machines.

Correspondence: Alessio Facello, Strada delle Cacce 73, Torino, Italy.
Tel. +39.011.3977721.
E-mail: a.facello@ima.to.cnr.it

Key words: chipping, energy, fuel consumption, power, tractor.

Journal of Agricultural Engineering 2013; XLIV(s1):e75
doi:10.4081/jae.2013.(s1):e75

Materials and methods

Chippers used during tests are small-scale machines designed for operate with medium power agricultural tractor. They have the same log diameter capacity (250 mm max) and they use different cutting technologies: disc tool and drum tool respectively. In both cases chippers mount two blades with a offset of 13 and 15 mm respectively, in order to obtain the same final cut length. The disc machine has a piece breaker and the drum chipper mounted a 50x50 mm mesh sieve to reduce the oversize particles output.

A 100 kW agricultural tractor powered the machines, setting the Power-Take-Off to the speed recommended by the chippers manufacturer: 540 rpm for the disc chipper and 750 rpm for the drum chipper respectively.

The tractor was equipped with transducers measuring:
- Torque and rotating speed of the power-take-off;
- Fuel consumption;
- Fuel temperature.

A strain-gauge based torque meter, giving a rated voltage output of 2 $mV \cdot V^{-1}$ @ 2250 Nm, was used to measure continuously the torque adsorbed by the machines. Power-take-off rotating speed was detected with a 60 tooth gear coupled with a magnetic pick-up that give a pulse output directly proportional to the speed (1 $Hz \cdot rpm^{-1}$, max 5000 rpm).

Fuel consumption measurement was carried out with a volumetric fuel meter directly connected with the engine feed line (send and return pipe). This device returns a pulse signal proportional to the volume of fuel that flow through the meter. Rated output is 2000 pulse per dm^3, that is equivalent at 1.8 Hz per $dm^3 \cdot h^{-1}$ in terms of hourly consumption. The fuel meter was equipped with two PT100 thermocouples connected respectively to the send and return lines in order to know the fluid temperature and deduce the fuel density.

Trials were performed processing different feedstock types (poplar logs, chestnut logs, poplar sawmill residues and poplar branches). The moisture content was in the range 44-52% and was determined with the gravimetric method according to the European standard CEN/TS 14774-2 collecting one sample at the end of each repetition. For each combination feedstock-machine were performed 15 repetitions obtaining a total of 120 repetitions manually feeding the machines with loads

of around 100 kg. In order to reduce the effect of the progressive blade wear, a random machine feeding sequence was used (Nati *et al.*, 2010).

Productivity was determined measuring the exact time required to process the material excluding the machine-feed operation. The exact working time was calculated in the post-processing operation looking at the power adsorption graph.

In order to evaluate the weight of processed material a load cell between the metal bin used to collect the chips produced by the machine and its support was installed. In this way, for each repetition, was possible to know the exact weight of processed material and, in post-processing operation, to calculate the productivity.

All sensors were connected to a pc-based multichannel acquisition system that filter, elaborate, display and record the incoming signals. The instrument can acquire up to 8 analog channels and up to 24 digital channels with a maximum sample rate of 10 ks·s^{-1}. For this study the recording sampling rate was fixed to 200 Hz and were used 3 analog channel (torque meter and thermocouples) and 2 digital channels (speed sensor and fuel meter).

The acquisition software can be configured to make real-time computation on the basis of the acquired data. With these feature is possible directly evaluate other derived parameters as the instantaneous power delivered to the chipper and total fuel consumption. The acquisition system also permit graphical visualization of the acquired data for better monitoring and interpretation.

Figure 1 show a typical screen used during the tests. On the right a graphical representation of the instantaneous power (up) and fuel consumption (down), on the left, in numerical form, PTO torque and rpm, engine power and rotational speed, fuel consumption. On the bottom the average values obtained during the test.

In the post-processing operation specific power and specific fuel consumption were computed using the equations reported below:
specific power (SP) equation:

$$SP = \frac{Pw}{p} \left[kWh \cdot t^{-1}\right]$$

where "*p*" is the productivity in tons per hour and "*Pw*" is the average power required in kW.

Specific fuel consumption (SFC) equation:

$$Sfc = \frac{c}{p} \left[dm^3 \cdot t^{-1}\right]$$

where "c" is the fuel consumption in dm^3·h^{-1}and "p" is again the productivity in tons per hour.

All the recorded data were analyzed to extract the net values of power requirements and fuel consumption. To obtain the net value of these parameters were conducted some data acquisitions in idle conditions setting the tractor engine at the rated working conditions obtaining the results showed in Table 1.

Furthermore the exact processing time was determined on the basis of the power absorption level introducing a power threshold value that is equal to the average power needed when the chipper runs in idle conditions. Above this value we can assert that the machine is processing material and it is running status (Figure 2).

Threshold values are necessary to calculate the net values of power, fuel consumption, specific power an specific power consumption subtracting the threshold values to the gross data. Net values are useful to better compare results obtained with different machines that work in different conditions. With this approach is possible to evaluate the amount of power (or other quantity studied) that is due to the material processing operation, removing the "mask effect" introduced by the idle values.

Results

Table 2 reports the average values of net power adsorption of the two machines.

Table 1. Average values obtained in idle conditions.

Device	Power [kW]	Fuel [dm^3 · h^{-1}]	Speed [rpm]
Drum	4.9	8.4	776.7
Disc	4.6	6.3	521.3

Table 2. Average net power for disc and drum machines.

Average net power [kW]	Disc	Drum
Chestnut logs	30.8	41.4
Poplar branches	17.0	23.9
Poplar logs	33.3	41.1
Poplar mill	23.2	29.6
TOTAL	26.1	34.0

Figure 1. Typical acquisition system screen.

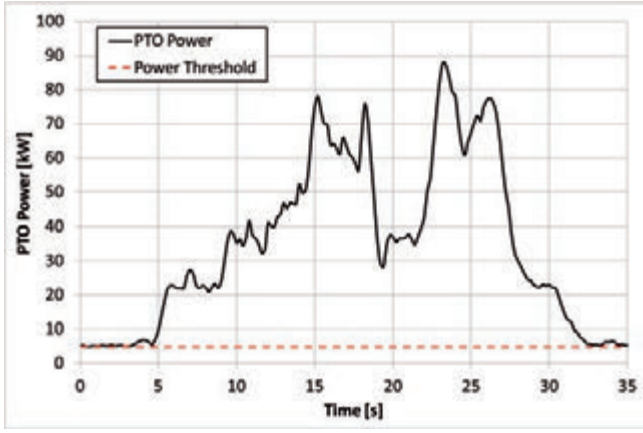

Figure 2. PTO power graph obtained processing a single 89 kg poplar logg.

The drum tool machine requires the highest average net power (34.0 kW vs 26.1 kW obtained with disc tool) and the highest difference is in poplar branches processing were drum machine require up to 41% more power than disc machine. This suggest more difficulty to comminute this kind of material for drum machine.

Looking at the productivity (Table 3) poplar logs obtained higher values, but considering dry values, chestnut has the best values. This difference is due to the different levels of moisture content of the two materials.

Dry productivity was calculated considering the moisture content of each sample that were 44.7% for chestnut, 50% for poplar branches, 53% for poplar logs and 49% for poplar mill. Using dry productivity values is useful to compare the results with other machines removing the influence of the water content.

Table 4 shows the average values of specific fuel consumption obtained with the four different type of feedstock. The "fresh" column has been calculated considering the total weight of the material and the total fuel consumption. On the other hand, net dry values have been computed using the dry weight and net fuel consumption values (subtracting the idle value). Poplar mill gives the higher "fresh" value for both machines and this may indicate a lower efficiency of the machines comminuiting this kind of feedstock. Looking at the "net dry" values drum machine has higher values (+15%).

Another important efficiency indicator is the specific energy required to process the material. Table 5 reports average values of specific energy. Again, poplar mill requires the higher amount of specific energy, whereas poplar branches needs the lowest quantity of energy per unit of material processed.

Disc machine gives lower values of specific energy (average -15%) with all kinds of feedstock-indicating a better efficiency in compared with the drum machine.

We have to focus that the values thus described are uniquely referred to the comminution work without delays and time needed by other operations like machine feeding. Delays may take up to 50% of the total working time (Spinelli and Visser, 2009) affecting heavily productivity and fuel consumption. This variation is a consequence of the operator effect that introduce a high variability in the measurement of this parameters as described by Harstela (1988).

In this study, to eliminate this effect, all the data were computed only during the comminution time interval not considering all the other accessory operation.

Table 3. Productivity values for disc and drum chippers.

Productivity [t·h^{-1}]	Disc		Drum	
	Fresh	Dry	Fresh	Dry
Chestnut logs	11.0	6.1	12.3	6.7
Poplar branches	7.5	3.7	8.3	4.1
Poplar logs	11.7	5.5	12.4	5.9
Poplar mill	7.8	3.9	8.0	4.2
TOTAL	9.5	4.8	10.3	5.2

Table 4. Average specific fuel consumption values.

Specific fuel consumption [dm^3·t^{-1}]	Disc		Drum	
	Fresh	Net dry	Fresh	Net dry
Chestnut logs	1.3	1,3	1.5	1,5
Poplar branches	1.5	1,1	1.7	1,3
Poplar logs	1.3	1,5	1.5	1,8
Poplar mill	1.6	1,5	1.9	1,6
TOTAL	1.4	1,3	1.7	1,5

Table 5. Average specific energy.

Specific energy [kWh·t^{-1}]	Disc		Drum	
	Fresh	Net dry	Fresh	Net dry
Chestnut logs	3.3	5,1	3.8	6,1
Poplar branches	3.0	4,6	3.5	5,8
Poplar logs	3.3	6,1	3.7	7,0
Poplar mill	3.7	6,1	4.4	7,2
TOTAL	3.3	5,5	3.8	6,5

Conclusions

The average productivity obtained during the tests was 10.3 t·h^{-1} for the drum machine and 9.5 t·h^{-1} for the disc machine. Specific fuel consumption was 1.7 dm^3·t^{-1} and 1.4 dm^3·t^{-1} for drum and disc tool respectively. These values can be compared with other chippers of similar size (Spinelli *et al.*, 2012). Also the specific power adsorption values (average 3.3 and 3.8 kWh·t^{-1}) are aligned with those obtained with machines that adopt similar cutting system. These values, if compared with those obtained by Facello *et al.*, (2012) testing a converted grinder, in general are lower and this suggest a different efficiency of the cutting technology used by the machine.

Using disc or drum machines give significant differences in terms of specific energy adsorption and productivity.

References

Chum, H.L., and Overend, R.P. (2001). Biomass and renewable fuels. Fuel Process. Technol. *71*, 187–195.

Facello, A., Cavallo, E., and Spinelli, R. (2012). Chipping vs grinding, net energy requirements. In FORMEC 2012, (Cavtat), 8-12 september 2012.

Harstela, P. (1988). Principle of comparative time studies in mechanized forest work. Scand. J. For. Res. *3*, 253–257.

Hillring, B. (2006). World trade in forest products and wood fuel. Biomass Bioene. *30*, 815–825.

Nati, C., Spinelli, R., and Fabbri, P. (2010). Wood chips size distribution in relation to blade wear and screen use. Biomass Bioen. *34*, 583–587.

Spinelli, R., and Visser, R.J.M. (2009). Analyzing and estimating delays in wood chipping operations. Biomass Bioen. *33*, 429–433.

Spinelli, R., Cavallo, E., and Facello, A. (2012). A new comminution device for high-quality chip production. Fuel Process. Technol. *99*, 69–74.

De Wit, M., and Faaij, A. (2010). European biomass resource potential and costs. Biomass Bioen. *34*, 188–202.

Tractor accelerated test on test rig

M. Mattetti,[1] Giovanni Molari,[1] A. Vertua,[2] A. Guarnieri[1]

Dipartimento di Scienze e Tecnologie Agro-alimentari, Università di Bologna, Bologna, Italy

Abstract

The experimental tests performed to validate a tractor prototype before its production, need a substantial financial and time commitment. The tests could be reduced using accelerated tests able to reproduce on the structural part of the tractor, the same damage produced on the tractor during real life in a reduced time. These tests were usually performed reproducing a particular harsh condition a defined number of times, as for example using a bumpy road on track to carry out the test in any weather condition. Using these procedures the loads applied on the tractor structure are different with respect to those obtained during the real use, with the risk to apply loads hard to find in reality. Recently it has been demonstrated how, using the methodologies designed for cars, it is possible to also expedite the structural tests for tractors. In particular, automotive proving grounds were recently successfully used with tractors to perform accelerated structural tests able to reproduce the real use of the machine with an acceleration factor higher than that obtained with the traditional methods. However, the acceleration factor obtained with a tractor on proving grounds is in any case reduced due to the reduced speed of the tractors with respect to cars. In this context, the goal of the paper is to show the development of a methodology to perform an accelerated structural test on a medium power tractor using a 4 post test rig. In particular, several proving ground testing conditions have been performed to measure the loads on the tractor. The loads obtained were then edited to remove the not damaging portion of signals, and finally the loads obtained were reproduced in a 4 post test rig. The methodology proposed could be a valid alternative to the use of a proving ground to reproduce accelerated structural tests on tractors.

Correspondence: Giovanni Molari, Dipartimento di Scienze e Tecnologie Agro-alimentari, Università di Bologna, viale Fanin 50, Bologna Italy.
Tel. +39.051.2096191 - Fax: +39.051.2096178.
E-mail: giovanni.molari@unibo.it

Key words: durability, accelerated test, tractor, 4-post rig.

Journal of Agricultural Engineering 2013; XLIV(s1):e76
doi:10.4081/jae.2013.(s1):e76

Introduction

Recently the competitiveness between different tractor manufacturers has increased in particular with reference to the increasing of the reliability (Strutt and Hall, 2003) and to the reduction of the time-to-market similarly to the automotive trend (Hughes *et al.*, 2005). One of the development steps more involved in this tendency is the durability approval due to the high time-consumption (Oelmann, 2002). This development phase consists of an application of a load sequence, representative of the real use of the machine, to the whole vehicle or to a specific component (Garcia *et al.*, 2010). The load sequence reproduces in the structure a damage equivalent to that obtained by the farmer's use in the whole life of the tractor. A detailed measure of the real loads on a similar machine during the customer usage, a removal of the not damaging cycles (Lee *et al.*, 2005), and the reproduction of the load cycle obtained on a tractor prototype are therefore necessary.

The reproduction of the load cycle on a real field is difficult, not only due to the dependency on weather conditions, but also for the reduced occurrence of the applied loads and, as a consequence, a long time necessary to reproduce the entire cycle. To overcome these problems, particular tracks with defined bumps were designed, but despite a reduction of the test time they have not permitted an accurate reproduction of the load cycles (Mattetti *et al.*, 2012). In the recent years different studies have been performed to improve the feasibility of these tests (Thomas *et al.*, 1999; Renius, 1977; Kim et al, 2006; Kim *et al.*, 2006). One of these methods involved the use of proving grounds, special tracks with different types of pavements that are possible to meet during the real car driving (Ensor and Cook, 2007). The use of proving grounds permits a

reduction of the testing time due to a high occurrence of the stress and due to the high occurrence of higher damaging events with respect to the field. The use of the proving grounds have permitted to reproduce a load cycle of a medium power tractor with an acceleration factor of about three (Mattetti *et al.*, 2012). This acceleration factor is around three times, lower with respect to the usual one obtained for cars (Braccesi *et al.*, 2005), due to the lower speed of the tractor and the difficulties in the reproduction of the horizontal loads. Other problems related to the use of the proving grounds are the weather conditions and the necessity to change the drive after some hours. To further increase the acceleration factor of the tests a 4 post test rig could be used. This rig is provided by hydraulic cylinders, transducers and control systems used to replay the load cycle on the vehicle. The reproduction of the load cycle on the 4 post test rig could reduce the time of the proving ground tests due to the possibility to perform these tests in the lab without a driver on the tractor (Ledesma *et al.*, 2005). The goal of the paper is the definition of a methodology to reproduce the load cycles necessary for the durability approval also in a 4 post test rig with an acceleration factor higher with respect to that obtained with only proving grounds.

Table 1. Measured channels list

Channel	Measured channel	Hand
1	Lift arm load	Left
2	Lift arm load	Right
3	Top link load	-
4	Lower arm axial load	Left
5	Lower arm axial load	Right
6	Vertical front axle load	Left
7	Vertical front axle load	Right
8	Vertical front axle acceleration	Left
9	Vertical front axle acceleration	Right
10	Vertical rear axle acceleration	Left
11	Vertical rear axle acceleration	Right

Materials and methods

The methodology was applied to a 80 kW power tractor. In the tractor the transducers indicated on Table 1 were fitted to measure the load on the lift arm, on the top link, on the lower arm, on the vertical front axle; and the accelerations on the vertical front and rear axle.

The test schedule has been defined in Mattetti *et al.*, (2012) to reproduce the loading cycle derived from the signals obtained during tests on field. In particular the test schedule was composed of a combination of different proving grounds (PG) travelled a defined number of times and two field operations (FO), also repeated a defined number of times. The signals correspondent to the channels 1-7 reported on Table 1 were edited to reproduce a part of the test schedule on the 4 post test rig. The editing was obtained using the software nCode GlyphworksTM (). In particular the editing was realised splitting the signals into temporal windows in which the pseudo-damage was calculated according to:

$$PD = \sum_i n_i S_i^4$$

where:
S_i: load amplitude derived from rainflow matrix;
n_i: cycle number counted in a generic time history;
with S_i and n_i calculated using the rainflow algorithm (Downing and Socie, 1982; Rychlik, 1987).

The signals were edited removing the less damaging portions, and maintaining a damage higher than 95% of the total damage. The removal of some portions of the signal introduces unwanted spikes that modify the frequency content of the signal and could damage the rig. For this reason the not continuous windows were connected with half-sine joining functions. Once defined the windows of the force signals, the correspondent windows of the acceleration signals were composed to be reproduced in the 4 post test rig. From the acceleration the drives of the hydraulic cylinders of the 4 post test rig were obtained to reproduce the load cycle on the different channels (Kelly *et al.*, 2002).

Results

The signals of one test condition with the deleted parts highlighted are reported in Figure 1. The deleted parts of the signals are in preponderance in the starting and final parts of the signals.

The edited signals have a similar trend with respect to the measured ones with the only difference being the duration of the signal. In Figure 3 the power spectrum densities are compared, in particular the two trends are very similar due to the fact that the editing does not introduce anomalous peaks.

The tractor could be tested on the 4 post test rig for a reduced duration with respect to the different tests on proving grounds (PG) and on

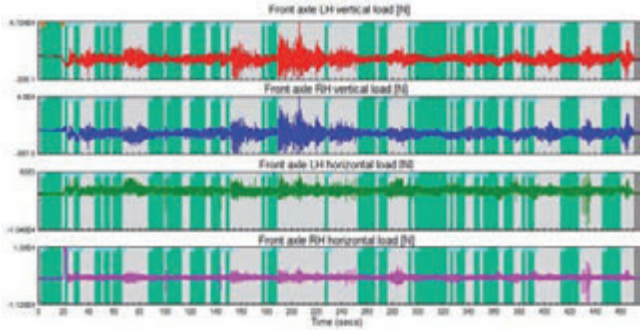

Figure 1. Editing of the signals: the green parts are the not damaging part of the signals.

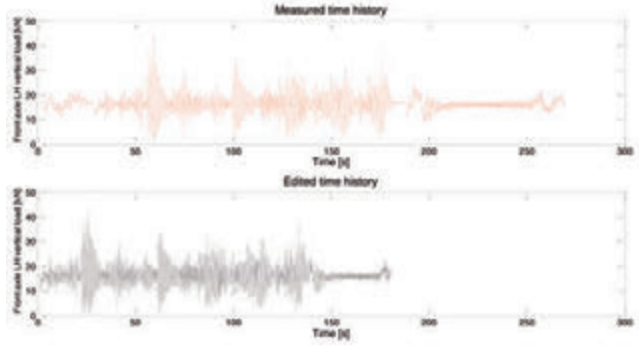

Figure 1. Editing of the signals: the green parts are the not damaging part of the signals.

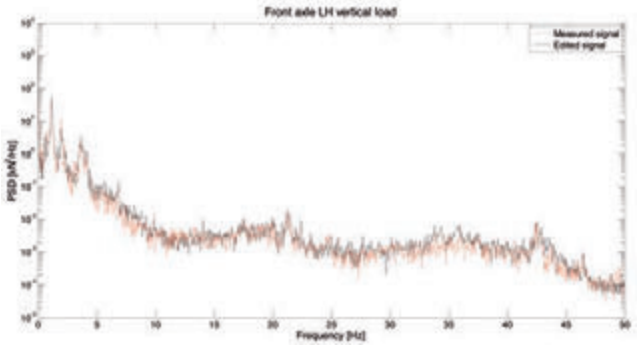

Figure 3. Comparison between the Power Spectrum Density of the measured signal and the edited one.

Table 2. Reduction factor for each test condition.

Testing condition	Duration of the tests without/with the combination with the test on 4 post test rig [s]	Reduction factor [%]
PG test condition 1	181	33
PG test condition 2	270	41
PG test condition 3	373	11
PG test condition 4	373	9
PG test condition 5	368	8
PG test condition 6	**370**	**15**
FO test condition 1	42	69
FO test condition 2	49	78

field (FO). The reduction factor for each test condition with respect to the time necessary on PG and on FO are reported on Table 2.

Testing condition Duration of the tests without/with the combination with the test on 4 post test rig [s] Reduction factor [%] PG test condition 1 181 33 PG test condition 2 270 41 PG test condition 3 373 11 PG test condition 4 373 9 PG test condition 5 368 8 PG test condition 6 370 15 FO test condition 1 42 69 FO test condition 2 49 78

The two field operations are the activities with the highest reduction coefficients due the higher portion of not damaging signals. But the two field operations are the activities with the higher influence on the total time of the test. The using of the 4 post test rig permits a reduction of the total time of the test into only 500 hours instead of the 1100 hours obtained by Mattetti *et al.* (2012) with the use of PG and FO only.

Furthermore the test on the 4 post test rig can be performed without interruption due to the change of the driver or unfavourable weather conditions as for the proving ground and field work tests.

Conclusions

In the paper a methodology to perform accelerated structural tests on a tractor has been presented. In particular, starting from a test schedule composed of a combination of proving grounds and field works, tests on a 4 post test rig have been performed to reduce the total time of the test. The use of the 4 post test rig permits a reduction of the total time of the test in only 500 hours instead of the 1100 hours obtained with the use only of proving grounds and field works. The total acceleration factor with the 4 post test rig was about 6.

References

Braccesi C, Cianetti F, Pioli D. Optimisation of the process of experimental sign off of a vehicle. Int J Heavy Veh Syst 2005;12:193-206.

Downing SD, Socie D. Simple rainflow counting algorithms. Int J Fatigue 1982; 4:31-40.

Ensor D, Cook C. Derivation of Durability Targets and Procedures Based on Real World Usage. SAE Technical Paper 2007; 2007-26-074.

Garcia C, Araan J, Ruiz S. Design of reliable accelerated test programs based on real market use 2010; 2010-36-0029.

Hughes S, Jones RP, Burrows AJ. Application of System Modeling to Road Load Data Synthesis for Automobile Product Development. In Proceedings of the ASME Computers and Information in Engineering Division ASME Conference Proceedings, 2005 Nov 5-11, Orlando, Florida. Michingan:ASME; 2005. pp31-40.

Kelly J, Kowalczyk H, Oral HA. Track Simulation and Vehicle Characterization with 7 Post Testing. SAE Technical Paper 2002; 2002-01-3307.

Kim, HE, Kim DS, Lee YP, Yoo YC. Accelerated Life Testing Method of Transmission. Key Eng Mat 2006; 326-8:1865-8.

Ledesma R, Jenaway L, Wang Y, Shih S. Development of Accelerated Durability Tests for Commercial Vehicle Suspension Components. SAE Technical Paper 2005; 2005-01-3565.

Lee YL, Pan J, Hathaway RB, Berkley ME. Fatigue testing and analysis: theory and practice. Burlington, MA: Butterworth-Heinemann. Burlington;2005.

Mattetti M, Molari G, Sedoni E. Methodology for the realisation of accelerated structural tests on tractors. Biosyst Eng 2012; 113:266-71

Oelmann B. Determination of load spectra for durability approval of car drive lines. Fatigue Fract Eng M 2002; 25:1121-5.

Renius KT. (1977). Application of cumulative damage theory to agricultural tractor design elements. Konstruktion 1997; 29:85-93.

Rychlik I. A new definition of the rainflow cycle counting method. Int J Fatigue 1987; 9:119-21.

Strutt JE, Hall PL. Global vehicle reliability: prediction and optimization techniques. Suffok: Professional Engineering Pub; 2003.

Thomas JJ, Perroud G, Bignonnet A, Monnet D. Fatigue design and reliability in the automotive industry. Esis Publ 1999; 23:1-11

Monitoring of the tractor working parameters from the CAN-Bus

Giovannni Molari,[1] Michele Mattetti,[1] Daniela Perozzi,[1] Eugenio Sereni[2]

[1]Dipartimento di Scienze e Tecnologie Agroalimentari, Università di Bologna, Bologna, Italy; [2]CNH Italia, Modena, Italy

Abstract

The analysis of the tractor mission profile is one of the main objectives for tractor manufacturers. The mission profile has usually been estimated through the use of questionnaires submitted to consumers. This procedure is time-consuming and not totally reliable due to the trustworthiness in the questionnaire compilation. In all the high power tractors numerous transducers are fitted to monitor some parameters to optimise the operation of the machines. All of these transducers are connected to an electronic central unit or with the tractor CAN-Bus. In this context, a system able to monitor the working parameters of the machines capitalising the existing transducers could represent the optimal solution for monitoring tractors distributed in different regions. The high number of signals are in any case difficult to memorise without a high quantity of memory. The goal of the paper is to define a methodology to memorise the operation parameters useful to define the mission profile of a tractor using a small memory. A tractor of a nominal power of 230 kW was selected and a system able to measure the signals acquired by the transducers fitted on the tractor was connected to the CAN Bus of the tractor. After a detailed analysis of the parameters measured on the tractor, the useful parameters were defined and acquired in different working conditions. The analysis of the parameters stored in the memory has allowed a detailed analysis of the operational parameters of the tractor in different applications. These parameters could be used by engineers to design tractors with a higher quality and reliability and also to define predictive maintenance criteria and reduce unexpected tractor failures.

Introduction

Reliable tractors can be built only if designed to sustain loads really recorded during the use of the machine on field from different farmers (Strutt and Hall, 2003). These loads are determined through a recording of the signals obtained from defined transducers fitted on a specific tractor (Ledesma *et al.*, 2005). In this way, however, the measurements are time-consuming, expensive, and often not reliable due to the impossibility to measure the loads obtained with a high number of tractors and a low measuring time with respect to the whole useful life of the machine (Socie, 2001). The load variability is in any case high due to different effects. The most relevant effects are the driver (Socie and Pompetzki, 2004), the application of the machine (Mattetti, 2012), and the market. A poor evaluation of the loads has, as a consequence, the use of higher safety coefficients with an increase of production costs, the design of tests not able to reproduce real working conditions, and an underrate of the loads with consequent problems like errors in engine mapping. These problems have been addressed using questionnaires to define the main use frequency of the tractor from the drivers (Dressler *et al.*, 2009). The questionnaires allow to define a mission profile of the vehicle, to produce a sample of accurate measurements able to better reproduce the real life of the tractor and, therefore, to supply a useful instrument to the designers. However, the information obtained with the questionnaires is

subjected to imprecise evaluations (Hayes, 2008). These problems could be overcome through the use of a data-logging system integrated on the machine able to monitor the functional parameters of the vehicle. In different vehicles, transducers necessary for vehicle operation are mounted. These transducers are usually connected to the CAN-Bus introduced by Robert Bosch, in 1986, to reduce the number of connections from the different electrical devices, increasing the strength of the connections and reducing the costs (Emadi, 2005). The transducers connected to the CAN-Bus have been used to measure the functional parameters of different vehicles (Mueller *et al.*, 2012) and have also been used to acquire the load spectrum in automotive transmissions (Willmerding and Häckh, 2007). With reference to tractors, on the contrary, data-logging systems have been used to measure only field work performances (Al-Suhaibani and Al-Janobi, 1996; Culpepper, 1979) without the evaluation of the mission profile of the machine. With reference to the mission profile of the tractor, previous studies have highlighted the necessity to exactly evaluate the idle time without a request of power from the engine (Mattetti *et al.*, 2012). The work cycle of the tractor could be acquired using transducers connected to the CAN-Bus, however, a high dimension memory would be required, but it would be difficult to fit it on a commercial tractor. The goal of the paper is to define a methodology to acquire, rework and memorise the operation parameters useful to define the mission profile of a tractor or a subsystem using a small memory.

Materials and methods

The measurements were performed on a CNH T8.360 tractor with a PTO nominal power of about 229 kW. The main characteristics of the tractor are reported on Table 1. The model was selected in this range

Correspondence: Giovanni Molari, Dipartimento di Scienze e Tecnologie Agroalimentari, Università di Bologna, viale Fanin 50, Bologna Italy.
Tel.. +39.051.2096191 - Fax: +39.051.2096178.
E-mail: giovanni.molari@unibo.it

Key words: CAN-Bus, tractor, customer correlation, tractor usage, mission profile.

Journal of Agricultural Engineering 2013; XLIV(s1):e77
doi:10.4081/jae.2013.(s1):e77

Table 1. Tested tractor specification.

Engine type	6/vertical in-line, 6728 cm^3, super charged, Tier III
Max power [kW]	229, 263 with powerboost
Width [mm]	2235
Wheelbase [mm]	3450
Front wheel type	420/90R 30
Rear wheel type	710/70R 42
Total mass [kg]	12100
Load on the front axle [%]	36
Transmission type	Powershift with 19 forward and 4 reverse speeds

of power due to the high number of transducers connected to the CAN-Bus.

The tractor was used by a farmer located in the Emilia Romagna Region in different working conditions : trailer transportation, cultivation and ploughing. Each work was executed for one hour. The signals were read from the CAN-Bus using the data logger Vector CANcaseXL log (https://vector.com) and memorised on a SD card. The signals were then sampled at the CAN sample rate, converted through the software Vector CANalyzer (https://vector.com) and analysed through the software Matlab (http://www.mathworks.com). To memorise the operational parameters using a reduced memory, the data were clustered in matrices as performed with strain gage signals (Downing & Socie, 1982). In function of the signal type, the data were transformed in a univariate histogram through the "hist" command of Matlab, or converted on a bivariate histogram matching different signals.

Between the different signals monitored, the channels correspondent to the gear selected and the engine torque percentage, were analysed. In particular, the combination of the signals to evaluate the durability

target of some tractor components, were evaluated. Previous studies have highlighted the necessity to evaluate with more precision the time without power request (Mattetti *et al.*, 2012). For this reason, the time of use of each gear was evaluated.

Results

In this paper the results of one working condition is reported, and in particular the distribution of the different gears used during the use of a disc cultivator is reported in Figure 1.

The distribution of the used gears show how the gear F9 is the one most used during the work with the cultivator. The percentages of use in the other gears are reduced. Also the percentage of use in the neutral position is very low. All the other gears and the neutral position were used during the end field manoeuvres.

In Figure 2 the engine torque distribution in the different gears is reported. The tractor was mainly used with an engine torque between 70 and 80 % of the maximum torque. The value of the torque in the neutral position is very low with a correspondent absence of power request in the neutral position.

In Figure 3 the time distributions of the transmission in neutral position are reported. Only two intervals with the transmission in neutral position are highlighted, both with a duration lower than 30 s, probably due to the start and stop procedures.

Conclusions

In this paper a methodology to record a large quantity of information on tractor use has been presented using a device than could be fitted on any produced tractor with an easy and quick procedure. The infor-

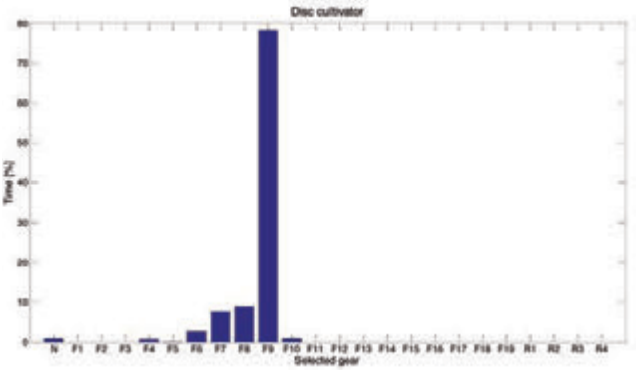

Figure 1. Gear usage histogram.

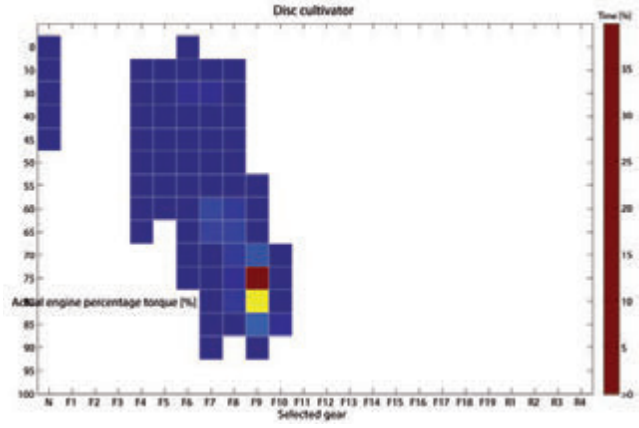

Figure 2. Engine torque used in the different gears.

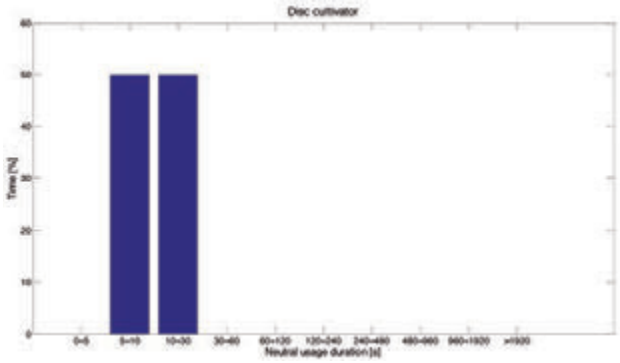

Figure 3. Neutral usage duration of the transmission in neutral position.

mation acquired has been reworked with adequate statistical methods to identify some uses of the machine.

This information could be used from the designers to define suitable targets for each component. The data obtained from the analysis could be employed to obtain a better prediction of the simulation subsystems of the vehicle and to optimise their performances.

Finally, this information could be used to correctly calibrate the functionality of the after-treatment device. The possibility of the farmers to identify the use of the tractor to optimise the performance and the costs is not negligible.

The activity will be extended to other signals not considered in the present work, as those connected with the three point hitch use. Other combinations useful to identify the degree of use of these machines to increase reliability will also be defined.

References

Al-Suhaibani SA, Al-Janobi A. An instrumentation system for measuring field performance of agricultural tractors. Misr Journal of Agricultural Engineering - M.J.A.E 1996; 13: 516–28.

Culpepper WJ. Description of a Data Logger/Analysis Field Test System. SAE Technical Paper 1979; 790522.

Downing SD, Socie D. Simple rainflow counting algorithms. Int J Fatigue 1982; 4:31–40.

Dressler K, Speckert M, Müller R, Weber C. 2008. Customer loads correlation in truck engineering. In Proceedings of FISITA 2008: world automotive congress, 2008 Sept 14-19, Munich, Germany.

Emadi A. Handbook of Automotive Power Electronics and Motor Drives. New York (NY): CRC Press; 2005.

Hayes BE. Measuring customer satisfaction and loyalty: survey design, use, and statistical analysis methods. Milwaukee, WI: ASQ Quality Press; 2008.

Ledesma R, Jenaway L, Wang Y, Shih S. Development of Accelerated Durability Tests for Commercial Vehicle Suspension Components. SAE Technical Paper 2005; 2005-01-3565.

Mattetti M. Accelerated structural tests on agricultural tractors PhD Diss., University of Bologna, Bologna, Italy; 2012

Mattetti M, Molari G, Sedoni E. Methodology for the realisation of accelerated structural tests on tractors. Biosyst Eng 2012; 113:266–71

Mueller C, Daily J, Papa M. Assessing the Accuracy of Vehicle Event Data Based on CAN Messages. SAE Technical Paper 2012; 2012-01-1000.

Socie D. Modelling expected service usage from short-term loading measurements. Int J Mater Prod Tec 2001; 16:295–303.

Socie D, Pompetzki M. Modeling Variability in Service Loading Spectra. Journal of ASTM International 2004; 1:46–57.

Strutt JE, Hall PL. Global vehicle reliability: prediction and optimization techniques. Suffok: Professional Engineering Pub; 2003.

Willmerding G, Häckh J. Load spectrum prediction for transmission under realistic use combining test and computer simulations. In Proceedings of FISITA 2007: world automotive congress, 2007 Jul 15-18, Budapest, Hungary.

Harvest of table olives by mechanical harvesting equipment

Filippo Gambella

Università degli Studi di Sassari, Dipartimento Agraria, Sassari, Italy

Abstract

In this work, we have evaluated the performance, of an electric comb equipped with five undulated fingers used for mechanized the harvesting of table olives. The first aim of the work was to test three different types of coating materials used for covering the fingers: Silicon (S), Vulcanized rubber (VR) and Natural rubber (NR). The diameter of the coating materials tested were 7mm (D1), 14 mm (D2), 19 mm (D3) in order to evaluate the damage of different working conditions on the intact olives. During harvesting, silicon at 7mm and 14mm resulted in the largest percentage of undamaged the fruit (67% and 65%), natural rubber 63% and vulcanized rubber at the 54%. The second aim was to evaluate the combination, in terms of the best performance, of the machines used for mechanized harvesting of table olives. Several factors have been examined: undulating fingers variation thickness, different rotational speeds and different coating materials used to reduce the impact damage on olives. From the tests on olive tree we have determined that while plastic materials (S) and (NR) appear to have a positive role in harvest quality, the vibration transmitted to the operator's hand is great from 6.48 m/s2 for S to 6.31 m/ s2 for NR and 2.92 m/s2 for VR, respect to the materials used.

Introduction

Hand harvesting of table olives is expensive because it involves a large number of workers and thus high labor costs, but it does ensure a high quality of the final product. To reduce production costs, many olive operation are now using mechanical harvesting equipment (Ferguson, 2006). The use of hand-held machines in olive harvesting have always been marked by a lack of information from an ergonomic point of view. The hand-held harvesting can expose the workers to noise, vibrations transmitted to the hand-arm system (Cerruto *et al.*, 2009; Deboli *et al.,* 2008; Gambella *et al.* 2012; Pretti *et al.* 2013) and arm muscle fatigue due to the machine weight. Essentially, tables olive harvesters can use three different systems to detach the fruit: 1) shaking the trunk, applied in traditional or intensive groves; 2) directly shaking specific areas of canopy using hand portable vibrating combs with rotating heads, suitable even for large trees and expanded canopies; 3) laterally shaking the canopy of the entire plant using a straddle engine with bilateral sets of shaking rods, borrowed from viticulture, on hedge trained plants. Trunk shakers, electrical comb, rake stripper and others typologies of harvesters are widely used in the mechanical harvesting of oil olive groves (Gil-Ribes *et al.,* 2009, Paschino *et al*. 2010). However, the table olives had a number of various factors that make the use of the shakers difficult and among that limits its use are: high fruit retention force, high fruit bruise susceptibility, lack of tree pruning adaption to mechanical harvesting and the hand-arm vibration transmitted to operators. All of these limitations imply in some cases a low harvesting efficiency and high percentage of damaged fruit (Kouraba *et al.,* 2004; Ferguson *et al*., 2010;) A preliminary study on the fruit damage was carried out by Paschino *et al.* (2010) on the use of electric hand-held harvesters, equipped with titanium undulating fingers coated with silicon, and on the damage produced by the different working conditions during harvesting of table olives. Experiments in the field have highlighted that during table olive harvesting contact between undulating teeth with reduced coating thickness and the fruit increased the damage by nearly 60% (Paschino *et al.* 2010). Another study investigated the level of vibration generated by three different types of plastic coating materials used on titanium fingers in order to minimize the damage to the olives. The mechanical damage during harvesting consists of local tissue degradation combined with an output of intracellular water and the oxidation of phenolic compounds after impact (Segovia-Bravo *et al.*, 2009). The oxidation process produces a darkening of the green color on the olive surface. After some time, depending on the intensity and characteristics of the impact, the area effected begins to darken, first superficially, then spreading deeper into the flesh until it reaches the endocarp (Ben-Shalom *et al.,* 1978) of the olive.

Correspondence: Filippo Gambella. Sezione di Ingegneria del Territorio. Dipartimento di Agraria, Università degli Studi di Sassari, Viale Italia 39, 07100 Sassari, Italy.
Tel. +39079229281- Fax +3909229285.
E-mail: gambella@uniss

Key words: electric comb; tables olives; harvesting tools.

Journal of Agricultural Engineering 2013; XLIV(s1):e78
doi:10.4081/jae.2013.(s1):e78

Aim of the work

The purpose of this study was to evaluate the performance of an hand-held olive harvester consisting of an electric comb equipped with fingers coated with various materials and to assess olive the damage during harvesting. Additionally we measured the level of vibration transmitted to the operator's hand by the harvesting equipment.

Materials and methods

The harvesting trials were carried out on a farm which specialized in table olives production, located in the plain of Ozieri, northern

Sardinia, Italy. The "Manna" (*Olea Europea L.*) cultivar was used in this experiment. the harvesting test was conducted in the first 10 days of January 2012 during the green maturation stage. The olives were harvested from 54 plants and graded by size with divergent wires. The electric comb used was mounted on a telescopic pole and powered by an electrical DC power pack (ISO-Tech). In order to reduce the probability of impact damage, three different coatings for undulating fingers were prepared with overall diameter of 7.1 mm (D1), 13.9 mm (D2) and 19.2 mm (D3). Three different types of elastic material, Silicon (S), Vulcanized rubber (VR) and Natural rubber (NR), with three different hardness value in Sh.A scale were also used for each diameter: Silicon (Sh.A 50); Natural Rubber Sh.A (45-55) Vulcanized Rubber Sh.A (80-90) (Fig. 1). An acquisition system (Larson Davis, model HVM1009) for measuring vibrations was used to measure and recording hand-arm vibration exposure. A triaxial accelerometer, which measures the vibrations along the three axes (x, y and z) simultaneously, was used. The accelerometer model was SEN020 PCB (ICP Company) positioned on the top of the hand grip, to assess the tool vibration.

Damage evaluation of fruit

The harvested olives were classified according to the different kinds of damage that was found on the skin and based on previous experiments carried out with the same harvester. For each classified group of olives, all were exposed to air for 24 hours to allow for oxidation. This allowed on damage caused by harvesting equipment to become visually evident. The impact damage caused by undulating fingers contact was visually assessed using the system proposed by Mohsenin, (1996) and Treeamnuk *et al*. (2010) as shown in Figure 2. The biological damage was classified using the system proposed by Riquelme *et al.* (2007). Three types of damage were identified for all the harvested olives and these were divided up as follows:

- 1st class-damaged olives during the harvesting phase (Fig. 2a and 2b).
- 2rd class-biologically damaged olives.
- 3th class-intact or undamaged olives after harvesting.

The following formulae were used to classify the harvested olives, based on the detected damage:

Damage % per class of olives 1st, 2nd and 3th = (n° of damaged olives/n° of olives harvested from the plant) 100*

In each individual case, the percentage of intact olives was obtained from the difference between the overall total, the percentage of damaged olives and the percentage of olives with biological damage.

Statistical analysis results

The General Linear Model (GLM) procedure of Minitab 16 Ltd software was used to statistically analyze the data on the percentage of intact fruit and the damaged percentage of olives harvested with three different thicknesses of undulating fingers, the three different speeds and with three different types of plastic materials. The following formula was used, y=D+V+M+D*V+D*M+M*V, where y, each time, is the percentage of intact olives and the percentage of olives damaged by impact; D, each time, is the overall diameter of the coating of undulating fingers (3 levels: D1, D2 and D3); V each time, is the rotational speed of undulating fingers (3 levels: V1; V2 and V3); M is the type of plastic material used for coating the undulating fingers (3 levels: M1, M2 and M3). D*V, D*M and M*V are the interactions between the above listed factors. The multiple comparisons were computed using Tukey's test (confidence = 95%). The data of the level of vibration transmitted to the operator's hand were statistically analyzed by simple analysis of variance (ANOVA). The means were separated with the Kruskal-Wallis test. The level of statistical significant was stabled at $p \leq 0.005$

Results

Table 1 outlines the percentages of intact olives. The variance analysis for damage showed significant results only for materials. The thickness of the coating also had a significant impact on the percentage of damage. Specifically, 35% of olives harvested with a thickness of D1 showed significant more damage than those harvested with thicknesses of D2 and D3. Average damage (5.34%) was markedly less when vulcanized rubber was used than when silicon (19.48%) or natural rubber (19.89%) was used (Table 1). In terms of the efficiency of the material used, if one adds the percentage of impact damage to those of intact

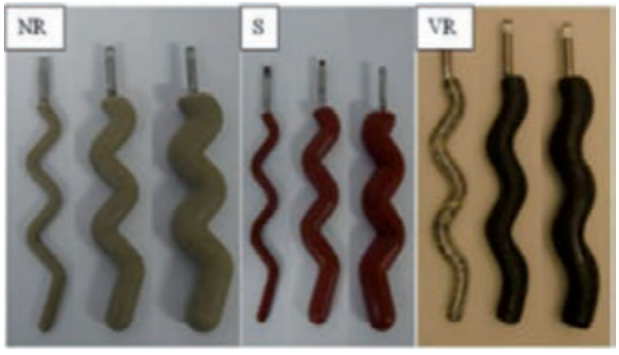

Figure 1. The different types of plastic material applied to the rotating fingers: (NR) natural rubber, (S) silicon and (VR) vulcanized rubber.

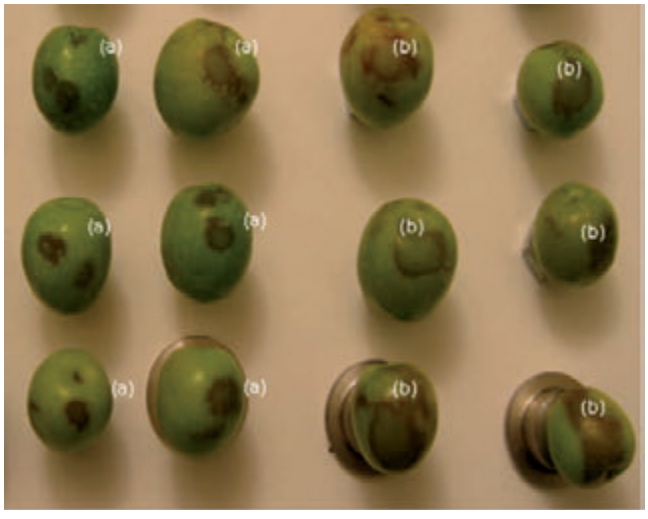

Figure 2. Classification of damages detected during mechanized harvesting and 24 hours ofter the exposure of drupes to air: (a) example of superficial impact damage caused by undulating teeth consequently the combing operation; (b) deep damage caused by the insertion of the drupe between the undulating teeth and the rotation block of the mechanical harvesting tools.

olives, then the percentages of potentially transformable fruit are 85.9%, 95.1% and 97.7% for VR, NR and S, respectively. Direct observation of the olives also showed that olives harvested with undulating fingers coated with silicon were more intact than those harvested with undulating fingers coated with vulcanized rubber (Table 1). There were significant differences in the percentages of intact olives, depending on the thickness of the coatings. The results were 36.75% intact with D1, 56.00% intact with D2 and 61.89% intact with D3. These results highlight that the best results are obtained with coatings D2 and D3 (Table 1). The rotational speed also had a significant effect on the results. As the rotation of the fingers increased the percentage of intact olives decreased (62.31% with V1, 56.07% with V2 and 36.16% with V3), irrespective of the thickness of the coating (Table 1). The material used did not significantly affect on the percentage of intact olives. This type varied from 47% for natural rubber to 56% for silicon (S).

There were significant differences in results depending on the coating material used when the smallest thickness was used (D1), but this was not true for D2 and D3. Table 2 illustrates the percentages of intact olives. There were a significant percentage of olives harvested suitable for transformation in brine, when the silicone or natural rubber was used for coatings the finger, while for the fingers coated with vulcanized rubber the percentage of intact olives were 54.1% and 54.4%.

When the D1 and D2 thickness in natural rubber or in silicon was used, the percentage of intact olives decrease from 63.8% to 60.8% to the first and from 67.5% to 65.0% to the second. Vulcanized rubber with D1 and D2 thickness, had the same percentage of intact olives 54.1% and 54.4%. The percentage of intact fruit rose from 17.6% to the natural rubber, to the 42.2% of the vulcanized rubber respectively (Table 2). In terms of operative parameters, the best combination appear when was used the natural rubber or the silicon at the D1 or D2 thickness. All the plastic materials utilized show a low quality of the olives harvested when were used with the thickness D3 (Table 2).

Table 3 shows the values of acceleration weighted with the machines used on olive trees at the rotation speed of 4000 rev/min, set by the producer, but considering all the sizes of finger coated (D1, D2 and D3) and types of material used (natural rubber, silicon, and vulcanized rubber). Data were also analyzed to assess rotational speed of the combing fingers. The fingers coated with silicon and vulcanized rubber produced dynamic acceleration levels increasing in function of the thickness. Different outcome had the rake type NR. In fact, it, with a thickness D2, the acceleration value was 5.73 m/s^2, lower than the thickness D1 and D3 (6.31 m/s^2 and 9.59 m/s^2 respectively.

The value of maximum acceleration equal to 11.38 m/s^2 was produced by silicon comb with a thickness D3, while the vulcanized rubber comb had values of 7.19 m/s^2. Also during the dynamic combing, the fingers mounted in the harvesting head produced an abnormal kinematic behavior, due to the excessive thickness of the material used for the fingers coating. For the D2 thickness the vulcanized rubber had a value of acceleration equal to 3.92 m/s^2 (almost three times less than the fingers coated with silicon, 11.37 m/s^2), while the natural rubber reported 5.73 m/s^2. For the thickness D1 and D3, the lower acceleration values are 2.92 m/s^2 and 7.19 m/s^2 for fingers coated with the material vulcanized rubber. For the thickness D1, the highest acceleration value is 6.48 m/s^2, produced by the silicon type. For the natural rubber type, the maximum acceleration was 9.59 m/s^2 for the thickness D3, while for the thickness D1 was 6.31 m/s^2 at the same rotation speed. The statistical analysis with rotation speeds of 4000 rev/min shows a significant difference in working conditions considered. The significant statistical differences assigned to all the three materials three different behaviors, even if the minimum values of acceleration were recorded for all

Table 1. Variance analysis of foliage and branches damage, impact damage and intact fruits.

Thickness	Foliage and branches	Impact	Intact fruits
7 mm (D1)	14.62 (± 3,36)	34.49^a (± 3,10)	36.75^a (± 5,41)
14 mm (D2)	16.58 (± 3,36)	24.94^b (± 3,10)	56.00^b (± 5,41)
19 mm (D3)	13.51 (± 3,36)	20.13^b (± 3,10)	61.80^b (± 5,41)
Speed (rpm)			
V1	11.68 (± 3,36)	23.36 (± 3,10)	62.31^b (± 5,41)
V2	14.08 (± 3,36)	21.64 (± 3,10)	56.07^b (± 5,41)
V3	18.96 (± 3,36)	34.56 (± 3,10)	36.16^a (± 5,41)
Materials (Type)			
Natural rubber (NR)	19.89a (± 3,36)	27.83 (± 3,10)	47.38 (± 5,41)
Vulcanized rubber (VR)	5.34b (± 3,36)	30.39 (± 3,10)	50.26 (± 5,41)
Silicon (S)	19.48a (± 3,36)	21.39 (± 3,10)	56.91 (± 5,41)

Means that do not share "a" letter are significantly different (p≤0.005). Grouping information using tukey method and 95,0% confidence.

Table 2 The percentage values of intact fruits harvested with undulating teeth coated with different plastic materials: natural rubber (NR), Silicon (S) and Vulcanized rubber (VR).

Thickness	Percentage of intact olives (Natural rubber)	Percentage of intact olives (Silicon)	Percentage of intact olives (Vulcanized rubber)
7 mm (D1)	63.8^a	67.5^a	54.1^{ab}
14 mm (D2)	60.8^{ab}	65.0^a	54.4^{ab}
19 mm (D3)	17.6^b	38.2^{ab}	42.2^{ab}

Means that do not share "a" letter are significantly different (p≤0.005).

Table 3. RMS acceleration measured on the olive tree tests with the three different types of plastic materials: silicone, vulcanized rubber and natural rubber.

Teeth Material S = Silicone NR = Natural rubber VR = Vulcanized rubber	Thickness mm	Operative condition Revolution per minutes rpm	Olive tree working condition	Global acceleration (RMS) (m/s^2)
S	7 (D1)	4000 (V3)	combing	6,48[a]
NR	7 (D1)	4000 (V3)	combing	6,31[a]
VR	7 (D1)	4000 (V3)	combing	2,92[b]
S	14 (D2)	4000 (V3)	combing	11,37[a]
NR	14 (D2)	4000 (V3)	combing	5,73[b]
VR	14 (D2)	4000 (V3)	combing	3,92[c]
S	19 (D3)	4000 (V3)	combing	11,38[a]
NR	19 (D3)	4000 (V3)	combing	9,59[b]
VR	19 (D3)	4000 (V3)	combing	7,19[c]

Averages where do not appear the letter a are statistically different for p≤0,05

the tests conducted with the protective material with greater rigidity as that of vulcanized rubber type (Table 3). From tree tests, it can be deduced that in tests on olive tree materials silicon and natural rubber appear to have a positive role in increasing vibration (from 6.48 m/s^2 for silicon to 6.31 m/s^2 for natural rubber and 2.92 m/s^2 for vulcanized rubber), with respect to the material used.

Conclusions

This research demonstrated that the type and thickness of materials used on the harvesting fingers are important consideration when harvesting table olives.

The tests using natural rubber or silicon with D1 and D2 thicknesses resulted in between 65% and 67% of intact fruit. These results are significantly higher than those for fruit harvested with undulating fingers coated with vulcanized rubber for all three types of undulating fingers considered. The working conditions used allowed for variations in the rotational speeds. When the percentage of intact drupes is added to those potentially transformable (foliar and branches damage and contact damage), the percentage of transformable fruit ranges from 85.6% with D1 to 97.5% with D2 and 95.4% with D3. In terms of the material used the trend is similar, with the percentage of transformable drupes rising from 85.9% when vulcanized rubber is used to 95.1% with natural rubber and 97.7% with silicon.

The hand-arm vibration from the different comb models tested depended mainly from kinematics of the comb used, varying in the different trials from a minimum of 2.92 m/s^2 to a maximum of 11.38.4 m/s^2. Probably this aspect is the main element to be taken into account by the ergonomic point of view. With the same diameters (D2 and D3), silicon, natural rubber and vulcanized rubber, in all tests, produced higher levels of acceleration (*i.e.*11.38 m/s^2 11.37 m/s^2) in silicon D2 and D3. Finally, even for the thickness of 7 mm was found the same results with the silicon and natural rubber with acceleration levels higher than the vulcanized rubber (6.48 m/s^2 silicon, 6.31 m/s^2 natural rubber and 2.92 m/s^2 vulcanized rubber).

The statistical analysis showed similar behavior for the two materials of the elastic type, different from the more rigid material (vulcanized rubber). The action of the foliage certainly affects the level of acceleration transmitted to the hands of workers, because of olive trees have been recorded different global acceleration values. Finally, taking into account the measurements made during collection, can derive specific guidelines on the use of personal protective equipment.

This results in the later formation of more or less extensive superficial browning, and injuries of different depths. The value of the product is reduced and there is a loss of product consistency. The information obtained on table olive damage during fruit detachment with an electric comb can be used by the producers to determine how to reduce and prevent bruising during harvesting operations.

References

Ferguson L. Trends in olive fruit handling previous to its industrial transformation. Grasas y Aceites 2006, 57 1:9–15.

Cerruto E., Manetto G., Schillaci G. 2009. Electric Shakers to Facilitate Drupes Harvesting: Measurement of the Vibrations Transmitted to the Hand-Arm System. XXXIII CIOSTA-CIGR V Conference on "Technology and management to ensure sustainable agriculture, agro-systems, forestry and safety", Reggio Calabria, June 17-19, 2009.

Deboli R., Calvo A., Preti C. The Use of a Capacitive Sensor Matrix to Determine the Grip Forces Applied to the Olive Hand Held Harvesters, Proceedings of the International Conference on "Innovation Technology to Empower Safety, Health and Welfare in Agriculture and Agro-food Systems", Ragusa, September 15–17, 2008.

Gambella F., Deboli R., Preti C., Calvo A. Vibration transmitted to operator's hands by a new type of rotary pick-up for the harvest of table olives. International Conference RAGUSA SHWA 2012, September 3-6, 2012, Ragusa - Italy "Safety Health and Welfare in Agriculture and in Agro-food Systems", 381-387.

Preti C., Gambella F., Deboli R., Calvo A., Inserillo M., Dau R. and Casu E. C. Vibration level generated by a rotary pick-up for the harvest of table olives. AIA – DAGA 2013 Conference on Acoustics March 18-21 2013. Merano.

Gil-Ribes JA, Blanco-Roldán GL, Castro-García S, 2009. Mecanización del cultivo y de la recolección en el olivar. Junta de Andalucía, Sevilla, Spain. 195 pp.

Paschino F, Caria M, Gambella F. The Harvest of Table Olives from the Plant by Means of an Hand Harvester" International Conference Ragusa SHWA-September 16-18, 2010 Ragusa Ibla Campus- Italy "Work Safety and Risk Prevention in Agro-food and Forest Systems" 2010, 656-663.

Kouraba K, Gil-Ribes JA, Blanco-Roldán GL, De Jaime- Revuelta MA, Barranco D,. Suitability of olive varieties for mechanical harvester shaking; Olivae; 2004 101: 39-43.

Ferguson L., Rosa UA, Castro-Garcia S., Lee SM, Guinard JX, Burns J, Krueger WH, O'Connell NV, Glozer K. Mechanical harvesting of California table and oil olives. Adv. Hort. Sci., 2010 24 (1): 53-63

Segovia-Bravo KA, Jaren-Galan M, García-García P, Garrido-Fernández A, 2009. Browning reactions in olives: mechanism and polyphenols involved. Food Chem 114: 1380-1385.

Ben-Shalom N, Harel E, Mayer AM, 1978. Enzymic browning in green olives and its prevention. J Sci Food Agric 29: 398-402.

Mohsenin N.N. Physical properties of plant and animal materials. New York: Gordon and Breach Science Publishers; 1996. Chapter 8 page 383-493.

Treeamnuk K, Pathaveerat S, Terdwongworakul A, Bupata C. Design of machine to size java apple fruit with minimal damage. Biosystem Engineering 2010 7:140-148.

Riquelme MT, Barreiro P, Ruiz-Altisent M, Valero C. Olive classification according to external damage using image analysis. Journal of Food Engineering 2008, 87 371–379.

Experimental tests on winter cereal: Sod seeding compared to minimum tillage and traditional plowing

Antoniotto Guidobono Cavalchini,[1] Gian Luca Rognoni,[2] Francesco M. Tangorra,[1] Annamaria Costa[1]

[1]Department of Health, Animal Science and Food Safety, Università degli Studi di Milano, Milano, Italy; [2]Agronomist

Abstract

Compared to traditional plowing and minimum tillage, the sod seeding technique has been tested in order to evaluate the differences in energy consumption, labor and machinery requirement and CO_2 emission reduction. The experiments were conducted on winter cereal seeding in a Po valley farm in October 2011. The tests were carried out as follows: wheat variety seeding, over corn and alfalfa crops, in large plots with three repetitions for each thesis. They included: *sod seeding* anticipated by round up weeding in the case of the plots over alfalfa; *traditional plowing* at 35 cm followed by rotary tillage and combined seeding (seeder plus rotary tiller); *minimum tillage* based on ripping at the same depth (35 cm) and combined seeder (seeder plus rotary tiller). The following farm operations - fertilizer, and other agrochemical distributions- have been the same in all the considered theses. The results, statistically significant ($P<0.001$) in terms of yields, highlighted slight differences: the best data in the case of the traditional plowing both in the case of wheat crop over corn and alfalfa (84.43 and 6.75 t/ha); slightly lower yields for the sod seeding (6.23 and 79.9 t/ha for corn and alfalfa respectively); lower in the case of minimum tillage (5.87; 79.77 t/ha in the two situations). Huge differences in energy and oil consumption have been recorded: in the case of succession to corn 61.47; 35.31; 4.27 kg oil/ha respectively for, traditional plowing, minimum tillage and sod seeding; in the case of alfalfa 61.2; 50.96; 5.14 kg oil/ha respectively for traditional plowing, minimum tillage and sod seeding. The innovative technique, highlighted huge energy saving with an oil consumption equal to 92% and 89% ($P<0.001$) of what happens in traditional plowing and minimum tillage. Large differences concern labor and machine productivity. These parameters together with oil consumption and machine size [power (kW) and weight (t)] lead to even greater differences in terms of energy consumption, efficiency and CO_2 emission savings. Considerations related to the different mechanizations chains, investments required and to some new practices to be introduced, such as low pressure tires or crawlers, ideal lanes, GPS and automatic guide systems to follow the ideal lanes, conclude the study.

Correspondence: Antoniotto Guidobono Cavalchini, Department of Health, Animal Science and Food Safety, Università degli Studi di Milano, Via Celoria 10, 20133, Milano, Italy.
E-mail: antoniotto.cavalchini@unimi.it

Key words: cropping system, sod seeding, energetic balance, CO_2 emissions.

Journal of Agricultural Engineering 2013; XLIV(s1):e79
doi:10.4081/jae.2013.(s1):e79

Introduction

The first proposals and tests on sod seeding cropping systems date back to the 1940s in England, but only the arrival on the market of Gramoxone (Syngenta,Switzerland), a non-selective herbicide, allowed the follow up and development of trials to study the tillage system. The development of this technique, dates back to the end of the 70s in South America (Argentina and Brazil), and North America (USA). Currently sod seeding is practiced on about 110 million hectares, mainly in South America. No wonder sod seeding tillage machine manufacturers are mostly Argentine and Brazilian. However, in the last decades many models have been produced by Italian and European manufacturers.

In Italy, sod seeding is a cropping system in development, especially practiced in central Italy, but it is also moderately used in certain flat areas as the Pianura Padana. Thanks to the interest shown by researchers and associations whose aim is the development of the tillage system. In fact, some Italian regions provide funding to anyone who uses this technique for at least 5 years.

The standard cropping method in Italy (conventional tillage, CT), with slight modifications depending on crop and type of soil, includes mouldboard ploughing to a depth of 30-40 cm, field cultivation, one or more harrowing passages and sowing. Reduced tillage methods allows energy savings of between 32 and 57% in corn (Cantele and Zanin, 1983), and greater savings can be achieved by no-tillage (Sartori and Peruzzi, 1994; Tebriigge *et al.*, 1994).

It is worthwhile to study alternative soil tillage methods. In Italy, on average, they account for around a third of the energy input (Bonari *et al.*, 1992). They also influence other production factors (Toderi and Bonari, 1986), which in turn contribute to total energy costs in different ways.

The purpose of this study, therefore, wishes to compare three cropping systems (sod seeding *vs.* minimum tillage and conventional plowing) in a flat area of Northern Italy characterized by clay soils, focusing on aspects of energy such as fuel consumption per unit area, energy efficiency, reduction of emissions and implications on agricultural mechanization. The aim of this research is also the definition and design of machines specifically made for hilly farming. Machinery produced in South or North America, is not suitable for marginal hill – mountain areas. While in the flat areas, the benefits are basically energetic and economic; in hilly farming sod seeding also ensures a substantial reduction in soil erosion and instability, usually induced by conventional techniques.

Materials and methods

The tests were carried out in the 2011-2012 period in the Oltrepò Pavese plains, an area characterized by silt-clay soils (Table 1), while other preliminary tests took place in the Appennino Ligure Piemontese, 750 m above sea level (Borgo Adorno, Cantalupo Ligure, AL).

While in the latter, the purpose of the tests was to check the operability of the machines, in the former a strict protocol was followed in order to obtain reliable results.

Thus, two sets of large lots (around 0.5-1 ha) were considered. The first over corn, the second over alfalfa (at end of cycle, V year).

In both cases, the same variety of wheat was sowed (Asuncion by APSOV).

The sod seeding system was compared to other two techniques:

- conventional plowing at 35 cm depth, followed by secondary preparation of the soil by rotary harrow (10 cm deep) and seeding with combined machinery (drill coupled to rotary harrow);
- reduced tillage by ripper (35 cm depth), followed by seeding with drill coupled to rotary harrow.

For each thesis three repetitions were carried out. The rectangular, contiguous parcels were chosen in order to avoid discontinuities and interference due to the headland and drainage channels.

Plowing and subsoiling depth was intentionally limited to 35 cm, while the local practice is 40-45 cm: this was done so as not to penalize conventional techniques and because depths greater than 35 cm in tillage are not justified.

A 75 kW tractor (Fendt 311, AGCO Corporation, Germany) was used on sod seeding parcels, while 150 kW tractor power (John Deere 7530, John Deere, USA) was used on the other two parcels.

Machine features are shown in Table 1.

The investment in seeds was 400 seeds/m^2, about 170 kg/ha in all the compared theses. Only the sod seeding over alfalfa required additional weed control with glyphosate (0.9 kg/ha) ten days before drilling. All other operations as fertilizing, post emergency weeding and phytosanitary treatments were carried out in the same manner in all theses.

The following data were recorded:

- speed and work efficiency of the single operations;
- fuel consumption, using a completely full and subsequent refilling of the tank after working in each parcel;
- slips via speed measurement;
- yields, by weighing the harvested product.

Figure 1 shows the climatic data of the period (October 2011-July 2012); it also shows the dates of the cultural practices.

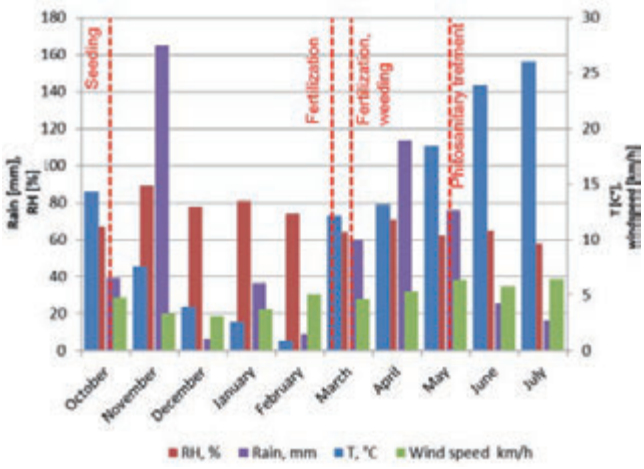

Figure 1. Climatic data, wind speed and rain intensity during the trial.

Table 1. Description of the trials.

	Item	Machines	Machine mass (t)	Speed (km/h)	Work capacity (ha/h)	Man work (man h/ha)	Consumption (kg/ha)	Yield (t/ha)	Slipping (%)
Over corn	Sod seeding	Fendt (75 kW) + Semeato	4.1 4.4	7.35	0.99	1.01	4.3	6.23	4
	Conventional plowing	JD 7530 (150kW, 1700 rpm) plow Vittone 3 plowshares + Alpego rotiller + + Amazone D9 special combined	10.1 1.6 1.6 1.5	1.25 5.3 rotiller 8.5 combined seeding	0.65 plowing 1.71 rotiller 1.65 seeding	 2.7	34.2 14.5 12.7	6.78	23
	Minimum tillage	JD 7530 (150 kW) + ripper Alpego + Amazone combined	10.1 1.2 1.5	 5.9 rip 6.0 combined seeding	 1.29 rip 1.23 seeding	 1.6	 20.03 16.6	5.87	 17
Over alfalfa	Sod seeding	Fendt (75 kW) + Semeato	4.1 4.4	7.40	1.04		5.1	8.13	4
	Early weeding	Landini 7000+ barrel Berthoud		7.5	6.7	1.1	1.6		
	Conventional plowing	JD 7530 (150kW, 1700rpm) plow Vittone 3 plowshares + Alpego rotiller + + Amazone D9 special combined	10.1 1.6 1.5	 5.2 rotiller 8.0	0.59 1.76 rotiller 1.6 combined seeding	 2.9	34.3 12.1 14.0	8.44	27
	Minimum tillage	JD 7530 (150 kW) + ripper Alpego + Amazone combined	10.1 1.2 1.5	 .4.21 ripper 6.10 seeding	 0.91 1.15 combined seeding	 1.9	 29.7 21.2	79.7	 28

On the basis of recorded data, machine mass and agrochemicals used (Tables 1, 2 and 3), energy and CO_2 emissions analyses were subsequently carried out according to established methodologies.

Results

Production

As summarized in Table 4, in both trials (over corn and over alfalfa), the production obtained from the sod seeding cropping system was lower than that obtained with the traditional tillage, but higher than with the minimum tillage technique.

The results are very satisfactory although the conclusions can be drawn only after a number of years. Moreover, the sod seeding technique maximizes the benefits after at least 5 years, during which the crop residues (straw, stalks, etc.) are left on the ground in order to increase surface organic substance resulting in significant advantages.

Capacity and productivity

Sod seeding

- Weeding is only necessary in cases of seeding on lawn, in our case over alfalfa. With a working width of 15 m and a speed of 7.3 km/h the actual working capacity was 6.7 ha/h;
- Seeding: the speed recorded in the two trials (over corn and over alfalfa) was the same, while the work efficiency was slightly higher for the trial over alfalfa: 1,04 ha/h compared to 0.99 ha/h (over corn). This was due probably to the sporadic blockage of the machine with crop residues (Figure 2). In both situations, however, the ability to work effectively deviates significantly from the theoretical one. This is due to drill size used on sod seeding, of drawn

Figure 2. Seeding on alfalfa residues.

Table 2. Agrochemicals used in the trials.

Intervention	Time	Fertilizer/ substance used	Amount distributed (kg /ha)	Energetic costs (MJ/ha, kep/ha)
Preventive weed (only sod seeding over alfalfa)	October, 2, .2011	Glyphosate	0.92	2.3 kep/ha
Fertilization	March, 10, 2012	Ammonium nitrate 33.5%	Theses over alfalfa 54 kgN/ha Theses over corn 50 kgN/ha	99.36 kep/ha 92 kep/ha
Weed	March 29, 2012	Ioxinil-otanoato +bromoxinil+sorbitan monooleato etossilato	0.86	2.15 kep/ha
Fertilization	March, 10, 2012	Ammonium nitrate 33.5%	Theses over alfalfa 47 kgN/ha Theses over corn 110 kgN/ha	86.5 kep/ha 184 kep/ha
Phytosanitary treatment	May 13 2012	Tebuconazole+ deltamethrin	0.23	0.575 kep/ha

Energy equivalents used are shown in Table 3.

Table 3. Energetic equivalents adopted.

Machines, agrochemicals		Equivalent	
Trucks, 7500 h of life		11.5(MJ/t.h)	0.27*10-3tep/t.h
Plow, reaper, 5000 h of life		8.6 (MJ/t.h)	0.20*10-3tep/t.h
Seeders, sprayers, manure spreaders, 5000 h of life		17.3(MJ/t.h)	0.41*10-3tep/t.h
Fertilizers	(N) (K_2O) (P_2O_5)	77 (GJ/t) 14.6 (GJ/t) 9.7 (GJ/t)	1.84 (tep/t) 0.35 (tep/t) 0.23 (tep/t)
Phytosanitary products		105 (GJ/t)	2.50 (tep/t)
Fuel		46 (GJ/t)	1.1 (tep/t)
Oil		84 (GJ/t)	2.0 (tep/t)
Seeds (cereals)		21 (GJ/t)	0.5 (tep/t)
Man work		2 MJ/h uomo	0.05 (kgep/h man)

kind and to the distance between the drawbar and the axis of the machine used that requires a large space or headlands of 20 m.

For sod seeding tillage less than 1h man/ha is required over corn and a little more than 1 hour man/ha (1.1 hours man/ha) over alfalfa, which requires a weeding quote.

Traditional plowing

- Plowing: the working speed showed no significant differences between the operations conducted over corn and alfalfa, with an average value of 5.0 km/h which corresponds to a theoretical working capacity of 0.8 ha /h. Work efficiency, higher in the case of parcels cultivated over corn with 0.65/ha *vs.* 0.59 ha/h over alfalfa, may depend on the different sizes of parcels.
- Preparation of the soil with rotary harrow: the working speed detected was 5.3 km/h, in this case with limited speed differences, while the actual working capacity was 1.7 ha/h;
- Sowing: when performed in combination with rotary harrow at a speed of 8.0 km/h showed a work capacity of 1.6 ha/h. For traditional methods, 2.89 hours man/ha were required.

Minimum tillage

- Subsoiling: in this operation, significantly different values were found between over corn and over alfalfa: 5.9 km/h and 1.5 ha/h, 4.2 km/h and 0.99 ha/h over alfalfa respectively. Differences may be due to different soil conditions with particular reference to the precession: 5-year lawn, corn. The value is confirmed by the significantly higher slip and consumption.
- Sowing in combination: the considerations relative to subsoiling can also be applied to cases of sowing carried out with combined machines (rotary harrow and drill). The advancement rate, and the effective work capacity, were substantially the same - 6.0 km/h and 1.23 ha/h for over corn, and 6.10 km/h and 1.15ha/h for over alfalfa, consumptions were significantly higher in the case of over alfalfa.

1.6 and 1.9 man hours/ha were needed respectively in the case over corn and over alfalfa for minimum tillage.

Fuel consumption

The results (Table 5) are striking and are confirmed in both situations: succession over corn and alfalfa. For the sod seeding, in the first case, the recorded fuel consumption was 4.27 kg oil/ha; higher consumption was measured in the trial over alfalfa (6.74 kg/oil) either for its higher tensile forces or for the additional weeding.

On the contrary, conventional methods required the same fuel consumption in both cases: 61.5 kg/ha in the former; 61.2 kg/ha in the latter, the results are multiples ranging from 8 to 14 times.

Even in the case of minimum tillage, the differences are small: 35.31 and 50.96 kg/ha respectively for the succession over corn and alfalfa. Compared to plowing, the savings are considerable, but higher 8 (succession over corn) and 7 times (succession over alfalfa) than for sod seeding.

Consumption and energy waste are further confirmed by the high values of slipping reported in Table 2, 25% for plowing with peaks of 28% for the subsoiling on alfalfa. In the latter, in fact, consumption was significantly higher than in succession over corn. The slipping recorded in sod seeding tillage was, however, limited to 5%.

Energy balance and emissions

Evaluations on energy efficiency ($\eta = \frac{output}{input}$) and emissions of CO2 were carried out on the entire crop cycle, and on the soil tillage operations in order to highlight phase differences, since the other interventions, including agrochemical applications, were the same for all three treatments compared. In fact, energy use in agriculture can be divided into two components: (1) indirect consumption, necessary for production and delivery of farm inputs (fertilizers, pesticides, non-farm feedstuffs, etc.), machinery and equipment, etc.; (2) direct consumption of fuels and electrical energy in the various cropping operations (Cavalchini, 1977, Borin *et al.*, 1997).

As expected, due to lower fuel consumption and machinery requirements, significantly better results were obtained with sod seeding even for the thesis over alfalfa with pre-emergence weed control.

On the other hand, there were no differences in η values obtained with conventional methods (plowing) and minimum tillage (ripping).

Traditional plowing was more efficient with regard to thesis over corn, minimum tillage was better in the case of over alfalfa, but it is worth pointing out that this is due to yields that are affected not only by tillage and seeding, but by many other factors. In the case of the entire crop cycle, the differences obviously are less evident, but η for sod seeding was always higher (Table 6).

Economic evaluations

Table 7 shows a summary of costs and incomes of the 3 cropping systems: reported costs are repeatable, those related to incomes are only indicative, since they refer to the specific situation and seasonal trends in which the trial was conducted. The economic benefits coming from the sod seeding when compared to the other two techniques was +230 and +129 €/ha (compared to tillage and minimum tillage) over alfalfa; +79 and +219 € / ha compared to tillage and minimum tillage over corn.

Conclusions

The tests confirmed sod seeding theories which have been substantiated in agricultural systems worldwide, but still little used in Italy. Energy savings, erosion reduction, conservation of organic substances in relation to production obtained using traditional methods.

On the other hand, the acquired data showed that reduced work techniques resulted in lower production compared to those obtained using either traditional methods or sod seeding, confirming past experience. In spite of this, in the last decades the minimum tillage technique has become quite common, this is due to: increased productivity of machines and operators, intervening swiftly , access of machines and workers to larger areas, lower machine costs.

These factors are the result of sod seeding which are its main

Table 4. Yields obtained in the trial.

Yield kg /ha	Minimum tillage	Sod seeding	Traditional plowing
Over corn	5.87	6.23	6.75
Over alfa alfa	79.77A	79.90	84.43B

Table 5. Fuel consumption in the trial.

Oil consumption kg /ha	Minimum tillage	Sod seeding	Traditional plowing
Corn	35.43^{A}	4.27^{B}	61.47^{C}
Alfalfa	50.96^{A}	6.74^{B}	61.20^{C}

Table 6. Energy efficiency and CO_2 production.

Item	η=out/inp		kg CO_2/ha kg		CO_2/kg product	
	At the end of seeding	Whole crop cycle	At the end of seeding	Whole crop cycle	At the end of seeding	Whole crop cycle
Sod seeding over alfalfa	21.85	8.53	349.4	895.3	0.043	0.110
Sod seeding over corn	17.41	5.00	335.9	1169.8	0.054	0.187
Plowing over alfalfa	14.75	7.37	530.1	1075.7	0.063	0.127
Plowing over corn	12.22	4.70	521.1	1354.1	0.077	0.200
Minimum tillage over alfalfa	15.34	7.20	487.6	1039.5	0.061	0.130
Minimum tillage over corn	12.01	4.31	458.8	1280.0	0.078	0.218

Table 7. Economic evaluation of the trial (prices are referred to OltrePo pavese farms).

Item	Operation		Income	
	Type	Cost*(€/ha)	Yield (t/ha)	PLV (€/ha) (275 €/t)
Traditional	Plowing	180		
	Soil preparation (rotary tillage)	105	6.78 (over corn)	1864
	Combined seeding	120		
	Total cost of mechanical interventions	405	8.44 (over alfalfa)	2321
Minimum tillage	Ripping	140		
	Combined seeding	120	5.87 over corn	1614
	Total cost of mechanical interventions	260	7.97 over alfa alfa	2192
Sod seeding over corn	Sod seeding	120	6.23	1713
Sod seeding over alfalafa	Preventive weed	40		
	Product	15		
	Sod seeding	120	8.13	2236
	Total	175		

appeal; and because of this will most likely spread quickly. According to the authors, however, besides the environmental advantages shown in the Tables, the most interesting feature is the mechanization required. In sod seeding a low-medium horsepower tractor (75kW) is employed which can also be used for other operations such as the spreading of agrochemicals. For a cereal farm this means an investment on mechanization of less than 40% compared to conventional systems.

Anotheer factor of great importance is that this technique can be used in hilly areas where plowing creates soil movement and instability. In addition, conventional cultural practices are extremely expensive if compared to the production attained. The tests carried out during this experiment demonstrated the advantages of sod seeding for autumn **vernini** cereals in terms of: speed, minimal use of manpower, reduced investment and operation costs, limited erosion and instability. Factors which can relaunch the agro-animal husbandry sectors in the alpine and appenine areas; consequently keeping and protecting the territory and its environment.

References

Bonari, E., Mazzoncini, M., Peruzzi, A. and Silvestri, N., 1992. Valutazioni energetiche di sistemi produttivi a divers.0 livello di intensificazione coltmale. Inform. Agrar. Suppl., 1: l-25.

Borin M., Menini C., Sartori L. 1997. Effects of tillage systems on energy and carbon balance in north-eastern Italy. Soil & Tillage Research 40 (1997) 209-226.

Cantele, A. and Zanin, G., 1983. Diserbanti ed energia: considerazioni sul loro impiego in agricoltura. Riv. Agron., 17: 65-17.

Cavalchini A.G. 1977. Valutazione delle diverse tecniche di raccolta e conservazione dei foraggi prativi in funzione del rendimento energetico. Rivista di Ingegneria Agraria. N° 5-4.

Derpsch R, Friedrich T., Kassam A., Houghven L. 2010. Current status of adoption of no-till farming in the world and some of its major benefits. Int. J. Agric. & Biol. Eng. 3,1: 1-26.

Manby T. 1975. Energy use in Agriculture. The agricultural Engineer. N° 3.

Ribera L. A., Honsb F. M., Richardsona J.M, James W. 2004. An Economic Comparison between Conventional and No-Tillage Farming Systems in Burleson County, Texas Agronomy Journal 96,2 :415-424.

Sartori, L. and Peruzzi, A., 1994. The evolution of no-tillage in Italy: a review of the scientific literature. Proc. 1st EC Workshop on Experience with the Applicability of No-tillage Crop Production in the West.

Terbrigge, F., Grol3, U., Bohmsen, A. and During, R.A., 1994. Advantages and Disadvantages of Conservation- and No-Tillage Compared to Plough Tillage. Proc. hit. Agric. Eng. Conf., Bangkok, 6-9 December 1994.

Toderi, G. and Bonari, E., 1986. Lavorazioni de1 terreno: aspetti agronomici. I. Interazioni tra lavorazioni e terreno, clima, altre tecniche agronomiche. Riv. Agron., 2@2-3): 85-105.

Water sensitive papers simulation to assess deposits on targets

Emanuele Cerruto, Claudia Aglieco

Department DiGeSA, Section of Mechanics and Mechanisation, University of Catania, Catania, Italy

Abstract

Aim of the study is to assess the possibility to use water sensitive papers to estimate, beside the superficial coverage, also the amount of deposit on the target at varying the spray features. To point out the main quantities influencing the deposit, the behaviour of the water sensitive papers was simulated by assuming some simplifying hypotheses: log-normal distribution of the diameter population of the drops and circular spots. Several images (630) of water sensitive papers, sprayed with drops of different mean diameter (from 100 up to 500 µm), constant coefficient of variation (0.50), and theoretical percentage of covered surface ranging from 10 up to 100%, were produced by means of simulation. These images were considered as effective water sensitive paper images and then analysed by means of an image processing software. The correlations between measured and effective values were studied and they allowed for an estimate of deposit and spray features from the image data. This implies that the analysis of the water sensitive paper images allows the determination of more complex parameters such as the unitary deposit and the impact density, all data strictly related to the efficacy of a phytosanitary treatment.

Introduction

Several studies have pointed out that, even if the evaluation of a phytosanitary treatment should be related to the biological results, a proper calibration of the sprayer is necessary in order to avoid off-target losses, to apply the pesticide uniformly on the canopy or where it is required, and to minimise the impact on the environment (Vanella *et al*., 2010). The European Directive 2009/127/CE recognises the use of pesticides "as posing threats both to human health and the environment" and that "the design, construction and maintenance of machinery for pesticide application play a significant role in reducing the adverse effects of pesticides on human health and the environment". The European Directive 2009/128/CE enforces these aspects and states that a "common legal framework for achieving a sustainable use of pesticides should be established, taking account of precautionary and preventive approaches".

The assessment of the distribution of the active substance on the canopy (leaves, fruits) is currently performed by measuring via proper techniques (Cerruto, 2007) the amount of mixture or microelements, sprayed together with the mixture, that reach the target, or by analysing the impacts of the drops on suitable artificial targets (Salyani and Fox, 1999; Cerruto and Failla, 2003; Pergher *et al*., 2008).

The most common artificial targets are water sensitive papers and PVC targets covered with silicon oil. Water sensitive papers allow for a quick assessing of the superficial coverage, while PVC targets allow for a better study of the spots, as they also can be used with high volume rates. The spot size distributions in the two targets are strictly correlated (Cerruto *et al*., 2009).

In the present study the behaviour of water sensitive papers was simulated, so to estimate, in addition to the superficial coverage, the spray features and the amount of deposit on the target. In a previous study (Aglieco and Cerruto, 2012), producing by means of simulation some images of water sensitive papers sprayed with droplets of different pulverisation degree and different coefficients of variation of the droplet diameter, it was found a significant correlation between spray volume collected by the water sensitive papers and data achieved from the images. In this paper the Authors intend to investigate this aspect thoroughly, by extending the study to sprays characterised by wider ranges of mean diameters and to water sensitive papers with greater superficial coverage.

Correspondence: Cerruto Emanuele, Dipartimento DiGeSA, Via S. Sofia 100, 95123 Catania, Italy.
Tel. +39.095.7147514 - Fax: +39.095.7147600.
E-mail: ecerruto@unict.it

Key words: pesticides, image analysis, drop pulverisation.

Contributions: the authors contributed equally.

Conflict of interests: the authors declare no potential conflict of interests.

Journal of Agricultural Engineering 2013; XLIV(s1):e80
doi:10.4081/jae.2013.(s1):e80

Materials and methods

The experimental activity

Sprays with different mean drop diameter were simulated, ranging from 100 up to 500 µm with step of 20 µm. Drop diameters were log-normal distributed, with constant (50%) coefficient of variation (CV). Images of water sensitive papers 2 cm × 7 cm in size were produced, with theoretical values of superficial coverage (not considering overlapping), ranging from 10 up to 100% with step of 10%. For each value of mean diameter and theoretical superficial coverage, three replicates were carried out, so producing a total of 630 images.

Simulation was developed according to the following procedure:

1. Given mean diameter (D_m) and CV, produce the drop diameter population (D_d). The number of drops was preliminarily computed on the basis of the desired theoretical value of superficial coverage.

2. Given the drop diameters D_d (µm), produce the corresponding spot diameters D_s (µm). Spot diameters were estimated by analysing the spread factor (ratio between spot diameter and drop diameter, Figure 1, Novartis) and using the equation:

$$D_s = 0.938 \cdot D_d^{1.1438} \quad (1)$$

3. Produce the water sensitive paper images by randomly allocating the spots, circular shaped, up to the desired theoretical superficial coverage. Images were produced with a resolution of 1200 dpi, enough to detect spots of 24 µm in diameter.
4. Store all the main data used to produce each image (drop diameter population, number, total volume (µL), and volume mean diameter (VMD) of the drops).

All the procedures were implemented by using the open source software *R* (R Development Core Team, 2012).

Data analysis

The images produced via simulation were analysed by means of the *ImageJ* (Abramoff *et al*., 2004) software as effective water sensitive paper images. The software detects the particles, without distinguishing among overlapped particles, and provides some data for each image, among which percentage of covered surface, number of spots and area of each spot were selected.

Subsequently, studying the area of each spot detected by *ImageJ*, other quantities were computed, among which:

- the equivalent diameter D_s' of each spot (that of the circle with the same area);
- the diameter of the drop D_d' capable of producing a spot with diameter D_s' (the calculation was carried out by inverting Equation 1);
- the CV and the mean diameter D_m' of these drops;
- the volume transported by these drops.

All these data were correlated with the theoretical ones used to produce the images so to analyse their trend at varying spray and image features. All the statistical analyses and graphical representations were carried out by using the same software *R*.

Results and discussion

Superficial coverage

Figure 2 show two examples of the simulated water sensitive papers.

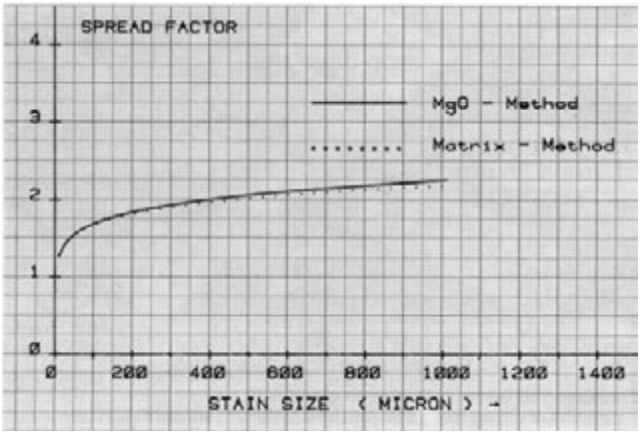

Figure 1. Spread factor *vs.* spot diameter (Novartis).

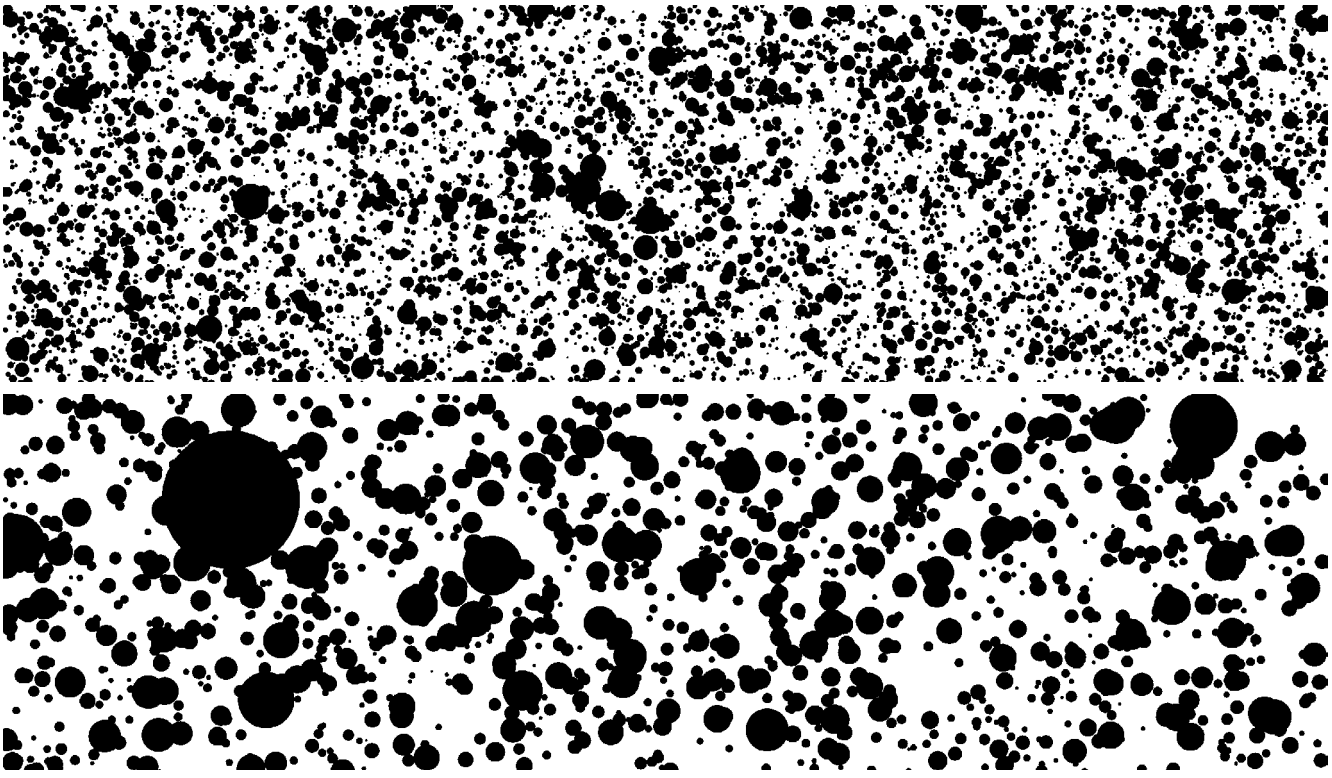

Figure 2. Examples of water sensitive papers produced by the simulations.

The first refers to a spray with mean drop diameter equal to 160 µm, theoretical value of percentage of covered surface equal to 50%, and theoretical deposit equal to 1.97 µL/cm^2. The corresponding values for the second image are 320 µm, 50% and 3.65 µL/cm^2, respectively.

The theoretical (S_T, %) percentage of covered surface is related to the measured one (S_M, %) by the equation:

$$S_T = 101.7827 \cdot \ln \frac{100}{100 - S_M} \quad (2)$$

reported in Figure 3. The coefficient of determination R^2 is equal to 0.9988, highly significant. When the measured value of percentage of covered surface increases towards 100%, the theoretical one tends to infinity asymptotically. Moreover, the result is independent from the mean drop diameter. According to the equation (2), when the theoretical percentage of covered surface ranges from 10 up to 100%, the measured one ranges from 9.4 up to 62.5% and then the overlap ranges from 0.6 up to 37.5%.

Unitary deposit

Figure 4 reports the trends of the theoretical deposit *vs.* the measured percentage of covered surface, at varying the mean drop diameter. The trends are well explained by quadratic relations, whose coefficients are functions of the mean drop diameter. The coefficients of determination range from 0.9887 up to 0.9995, highly significant. So, when the drop diameter CV is equal to 0.5, the unitary deposit can be estimated by knowing mean drop diameter and percentage of covered surface only.

However, in the previous study (Aglieco and Cerruto, 2012), where CVs equal to 0.4, 0.5 and 0.6 were considered, it was found that the relations between unitary deposit and percentage of covered surface are affected by the CV values, and then an appropriate estimate of this parameter should be extracted from the images. This aspect will be investigated in further studies.

As an alternative way, the unitary deposit was computed by analysing the spots, namely by computing the equivalent diameters D_s' of the spots and then the corresponding drop diameters D_d' . In the previous study (Aglieco and Cerruto, 2012), the relation between theoretical deposit and deposit computed by analysing the spots, was found to be independent from the drop diameter CV, even if this aspect should be more investigated by considering wider ranges of CV*s*.

According to this approach, the relation between deposit computed by analysing the spots V_C (µL/cm^2) and theoretical deposit V_T (µL/cm^2) was that showed in Figure 5. The interpolating functions are of the form:

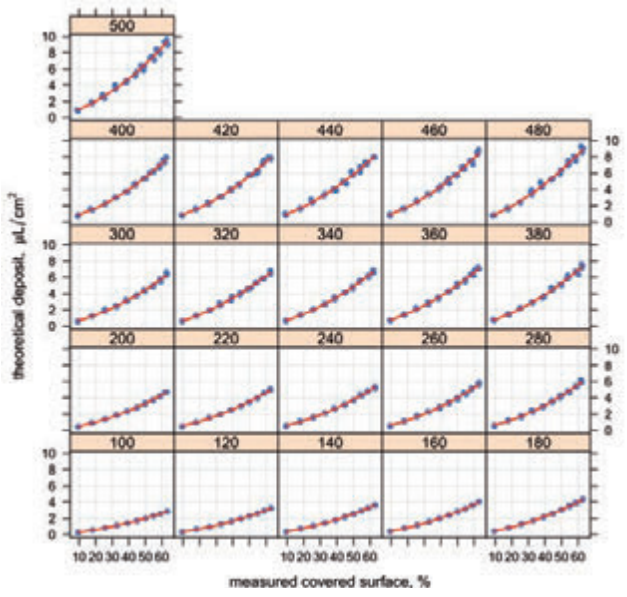

Figure 4. Correlation between measured percentage of covered surface and theoretical deposit at varying mean drop diameter (µm).

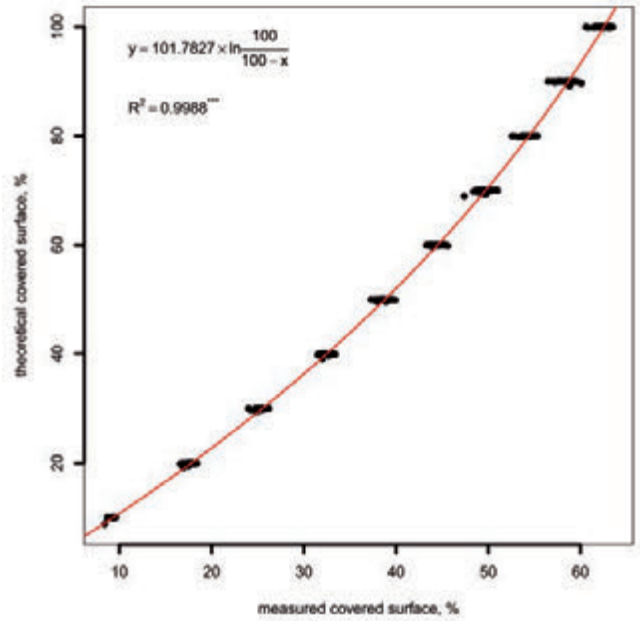

Figure 3. Correlation between theoretical and measured percentage of covered surface.

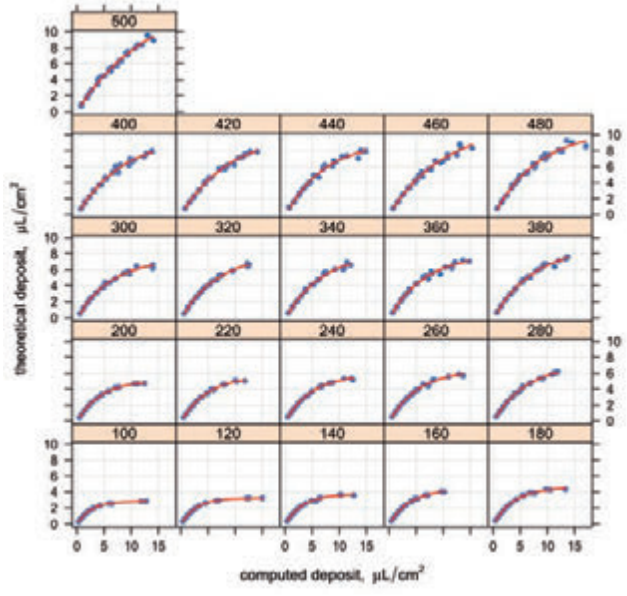

Figure 5. Correlation between computed and theoretical deposit at varying mean drop diameter (µm).

$$V_T = a_0 + a_1 \cdot e^{-a_2 \cdot V_C}, \quad (3)$$

being a_0, a_1 and a_2 coefficients depending on the mean drop diameter. If the independence from the drop diameter CV is confirmed, only an estimate of the mean drop diameter is necessary to compute the deposit starting from the spot analysis on water sensitive paper images.

This estimate can be achieved by computing the linear regression D'_m of on S_M considering the images with S_M<40%only, and predicting the response at S_M=5%. The error was always between 4.2% and 3.6%.

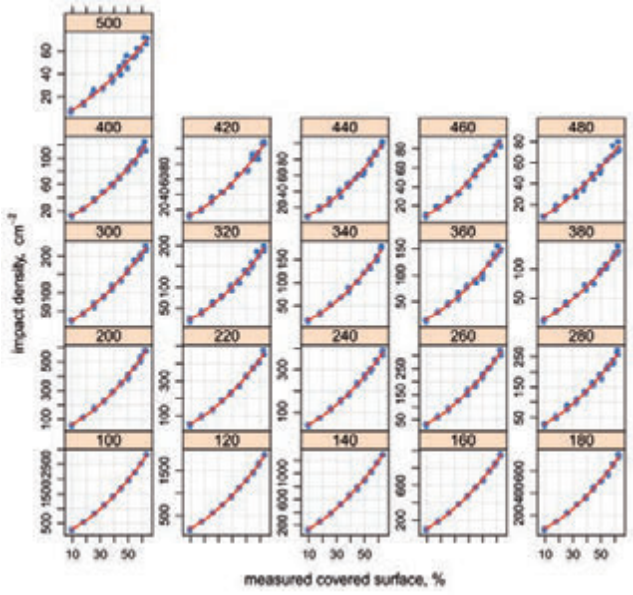

Figure 6. Correlation between impact density and measured percentage of covered surface at varying mean drop diameter (μm).

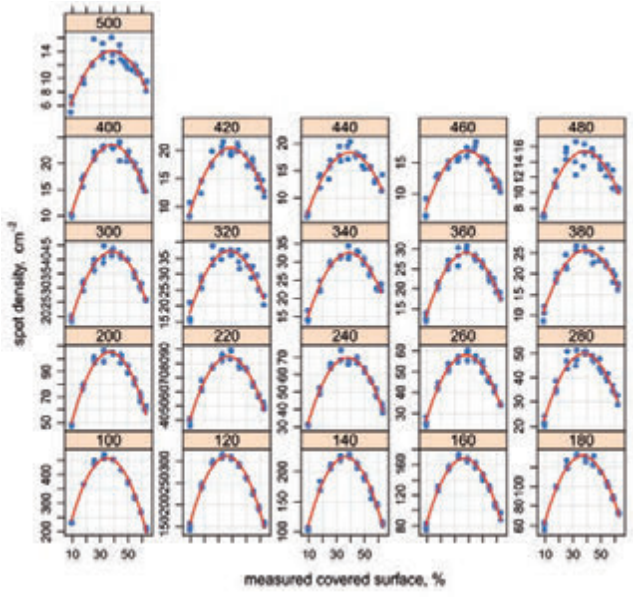

Figure 7. Correlation between spot density and measured percentage of covered surface at varying mean drop diameter (μm).

Impact and spot density

The impact density (number of drops per square centimetre) increases when the percentage of covered surface increases (Figure 6). The regression equations, depending on the mean drop diameters, are of quadratic type, with coefficients of determination ranging from 0.9816 up to 0.9993. As an influence of the drop diameter CV should be expected, even this aspect will be investigated thoroughly in the prosecution of the research.

The spot density (number of spots per square centimetre), at the contrary, due to the overlapping, increases up to a maximum, and then decreases (Figure 7). The maximum is reached when the percentage of covered surface is between 35 and 39%, confirming the results of the previous study, and decreases when the mean drop diameter increases.

Conclusions

The results of this study confirm and enforce those obtained in the previous one (Aglieco and Cerruto, 2012). In particular:

Theoretical and measured percentage of covered surface are related by a simple relation (Equation 2), independently from the spray features. This allows for a quick estimate of the overlap, potentially cause of run-off.

The theoretical deposit is related to the measured percentage of covered surface by a quadratic relation, but influenced by the mean drop diameter. As the previous study revealed an influence of the drop diameter CV, a more accurate estimate of the deposit requires an analysis of the spots.

The analysis of the spots allows for an estimate of the deposit higher than theoretical one, but computed and theoretical deposit are strictly correlated. In the previous study, the regression equations were independent from the drop diameter CV, but dependent only from the mean drop diameter. A dedicated study on this aspect, by considering wider ranges of CV, will be developed in the prosecution of the research.

The effective mean drop diameter can be achieved from the images by using the regression equation of the computed mean drop diameter on the measured percentage of covered surface.

All considered, the analysis of the water sensitive paper images allows for a complete description of the treatment in terms of unitary deposits, drop diameter, spot and impact density. Further studies are necessary to cover other situations (different CV, different diameter distributions, lower mean diameters) and to experimentally verify the models.

References

Abramoff M.D., Magelhaes P.J., Ram S.J. Image Processing with ImageJ. Biophotonics International, 2004, vol. 11, issue 7, 36-42.

Aglieco C., Cerruto E. Theoretical analysis of sprays by simulation on water sensitive papers (Italian). Proceedings of Giornate Fitopatologiche 2012, Milano Marittima (RA), Italy, March 13-16, vol. 2, 79-88.

Cerruto E., Failla S. Spray trials in vineyard using air carrier sprayer. 2nd part: artificial targets analysis (Italian). Riv. di Ing. Agr., 2003, 3, 13-22.

Cerruto E. Influence of Airflow Rate and Forward Speed on the Spray Deposit in Vineyard, J. of Ag. Eng.-Riv. di Ing. Agr., 2007, 1, 7-14.

Cerruto E., Balloni S., Conti A., Caruso L. Caratteristiche di bersagli artificiali per lo studio delle gocce in prove di irrorazione.

Proceedings on CD-ROM of the IX National Congress AIIA 2009 "Ricerca e innovazione nell'ingegneria dei biosistemi agro-territoriali", Ischia (NA), September 12-16, 2009.

Directive 2009/127/EC of the European Parliament and of the Council of 21 October 2009 amending Directive 2006/42/EC with regard to machinery for pesticide application.

Directive 2009/128/EC of the European Parliament and of the Council of 21 October 2009 establishing a framework for Community action to achieve the sustainable use of pesticides.

Novartis. Water-sensitive paper for monitoring spray distribution. 5th edition.

Pergher G., Petris R., Biocca M., Menesatti P. Prime verifiche di campo di un'irroratrice schermata ad aeroconvezione di nuova concezione. Proceedings of Giornate Fitopatologiche 2008, Cervia (RA), March 12-14, vol. 2, 51-58.

R Development Core Team. 2012. R: A Language and Environment for Statistical Computing. R Foundation for Statistical Computing, Vienna, Austria. ISBN 3-900051-07-0, URL http://www.R-project.org.

Salyani M., Fox R.D. Evaluation of spray quality by oil- and water sensitive papers. Transactions of the ASAE, 1999, vol. 42(1), 37-43.

Vanella G., Marucco P., Balsari P. È possibile ottenere il numero di impatti (gocce) per unità di superficie desiderato? Proceedings of Giornate Fitopatologiche 2010, Cervia (RA), March 9-12, vol. 2, 27-34.

Procedure and layout for the development of a fatigue test on an agricultural implement by a four poster test bench

M. Cutini, C. Bisaglia

Consiglio per la Ricerca e la Sperimentazione in Agricoltura, Unità di Ricerca per l'Ingegneria Agraria, Laboratorio di Treviglio (BG), Italy

Abstract

The increasing demand in agricultural vehicles' power requirements, payloads and driving speeds increases issues related to tractors and farm implements exposure to solicitations. One of the main factors to be taken into account for fatigue test developing on agricultural machines is the heterogeneity of the environment and activity in which the tractor operates. In particular, for contractors the use in transport conditions both on terrain and road becomes important. As far as transport is concerned. factors mainly affecting solicitations on carried implement are soil profile roughness, tractor settings and forward speed. In this paper, CRA-ING laboratory of Treviglio, Italy, together with Frandent Group s.r.l. (Osasco, Italy), analyse the possibility of creating a solicitation profile by means of one four poster test bench for fatigue test on a carried implement simulating transport conditions. Accelerations at the hubs of the tractor were acquired during transport on terrain and reproduced with one electro-hydraulic four posters test bench on one dummy of a tractor developed for carrying the implement. Artificial bumps were mathematically created and introduced in the time history to simulate squares solicitations. Twelve hours of test were carried out. This experience confirmed the possibility of carrying out laboratory fatigue test on agricultural implements by reproducing specific field conditions solicitations with four poster test bench.

Correspondence: Maurizio Cutini, Consiglio per la Ricerca e la Sperimentazione in Agricoltura, Unità di Ricerca per l'Ingegneria Agraria, Laboratorio di Treviglio, via Milano 43, 24047 Treviglio (BG), Italy.
Tel./Fax.: +39.0363.49603.
E-mail: maurizio.cutini@entecra.it

Key words: vibration, solicitation, tractor.

Contributions: the authors contributed equally.

Conflict of interests: the authors declare no potential conflict of interests.

Conference presentation: this paper was presented at the 10th AIIA Conference: "AIIA13 – Horizons in agricultural, forestry and biosystems engineering", Viterbo, University of Tuscia, Italy, on September 8-12, 2013.

Journal of Agricultural Engineering 2013; XLIV(s1):e81
doi:10.4081/jae.2013.(s1):e81

Introduction

When normal conditions of use are concerned, irregularity of working terrains and forward speed are the most important causes of vibrations transmitted to agricultural tractors (Scarlett *et al.*, 2007) with subsequent tool oscillation and work quality impairment (Cutini *et al.*, 2011).

For several years tires have been the main element for mechanical vibrations attenuation on agricultural tractors : their effectiveness depends on factors such as eccentricity, load, resonance frequency, and elasticity characteristics (Nguyen *et al.*, 2011; Sherwin *et al.*, 2004; Park *et al.*, 2004; Taylor *et al.*, 2000).

This phenomenon originates from the fact that the tire can be modeled as a series of radial and contiguous spring elements subjected to compressing and recovering forces when entering and exiting the road contact area (Witzel *et al.* 2011; Pacejka, 2010). Variations in the spring constants cause variations in the compressive and restorative forces as the tire rotates.

These forces variations run from tire centre toward the tread, and from the roadway through the tire centre toward the vehicle affecting handling and comfort.

So most of the studies have been directed to the tires' properties, dumping systems and/or their interaction.

However, as aforementioned, in agricultural machines an important factor characterizing the amplitude and frequency of vibrations is represented by the environment, in particular by the soil unevenness.

Soil unevenness has a stochastic character; its deformation has a non-linear, visco-elastic-plastic behaviour and its condition depends on a wide range of parameters (cultivation, cropping/tillage history, texture, organic residue, drainage conditions, etc.) so that it is almost impossible to standardize testing conditions in fields.

To analyze the effect of the surface on the vehicle is necessary to obtain the displacement or the accelerations acting under the tires.

Actually it's possible to measure forces at the hubs but it considers the contribute of the tires. Using measured soil profiles (obtained for example with optical technology) as system inputs is not sufficiently precise and repeatable because of soil deformations.

The most common existing approach (Anthonis, *et al.* 2007; Bisaglia *et al.*, 2006) consists in an iterative methodology. During the field test, accelerations are measured at specific locations of the machine (usually at the hubs), then the machine is put on a test bench and the actuators of the bench are driven in order to create, by deconvolution method, input signals so that sensor signals match with the measurements obtained in the field.

The project foresees to:

1) acquire, during transport on field, time histories representatives of severe conditions,
2) reproduce these situations in laboratory at a four poster test bench,
3) create a "standard" time history,
4) replicate it for a required number of hours.

Theoretical considerations

An iterative deconvolution method is a computerized control technique that enables to duplicate vehicle or component responses measured during field testing in laboratory conditions. The calculation of the control signals for the actuator of the test bench, called "drive signals", is a multivariable tracking problem, currently solved with the so-called iterative deconvolution (ID) procedure (Soderling *et al.*, 1999), which is an off-line iterative feed forward procedure where drive signals are updated based on the measured frequency response function matrix (FRF) of the test arrangement and on the tracking errors obtained in the previous iteration.. During laboratory tests the Remote Parameter Control (RPC®) software from MTS Systems Corporation has been used. The drive signals obtained with this procedure can be considered an approximation of the real field surfaces subject to deformations.

The following steps represent a brief overview of the process:

1. Acquisition of road or service data: to record the road data, transducers are placed on the component and/or vehicle at sites remote from the input forces. These transducers measure accelerations, strains, or displacements. Field or service history data are recorded in either analog FM tape format or digital format. Typically, the number of transducers used for data acquisition exceeds the number of control channels on the simulator.
2. Transfer of (digitized) data to the personal computer.. After the data are recorded and digitized, they are transferred to a Windows based computer for analysis and editing to shorten the test time.
3. Measurement of the system frequency response function: a random noise drive signal is generated to drive the test system and measure its response. The response information is then used to calculate the system model.
4. Estimation (calculation) of the initial drive signal: during this step, the system model measured in Step 3 and the desired response time history from Step 2 are used to create an estimation of the initial drive signal.

$$Desired\ signal \times FRF\text{-}1 \times gain = initial\ drive\ estimate$$
$$0 < gain < 1$$

5. Performing iterations. Because the test system (which includes the mechanical fixturing, hydraulics, and test specimen) is nonlinear and may have some inherent cross coupling, the difference between actual and desired time history responses is repeatedly measured to correct the subsequent drive files. This results is one drive signal inducing the desired response when used to command the test system.
6. Testing (i. e. durability). Once suitable drive signals are derived they are used as controller input commands to perform durability tests.

Materials and methods

Four terrain test bench differing for roughness and hardness, one agricultural tractor and one carried combined implement were used for these tests.

The worst case scenario was selected and reproduced in laboratory. The displacement of the plates defined the simulation of the vertical input of the fields' surfaces.

Evaluations were made with the manufacturer for choosing the level of amplitude of the time history respect to the nominal 100% of the field.

Tractor and implement

The test was carried out on one combined implement, harrow and seeder (Table 1).

The implement was carried by a four wheel drive tractor of 116 kW during test on field to acquire acceleration data from the four hubs.

Terrain test bench

The solicitation acting on the implement has been evaluated testing the machine on four different terrain surfaces chosen as test bench.

The adopted operations and the surfaces were:

- farming road (forward speed till 25 km/h max);
- farming road on maize terrain cultivation (forward speed till 15 km/h max);
- on the transverse way of the sorghum cultivation (forward speed till 25 km/h max);
- on the transverse way of the maize cultivation (looking for the speed inducing tires' resonance).

The last condition was chosen as worst case scenario, in particular the conditions of the lanes were of 0.7 m distance and 0.14-0.17 m depth and the forward speed causing tires' resonance was 6 km/h (Figure 1).

Table 1. Characteristics of the tested vehicle.

Machine	Characteristics		
Tractor	Type		4WD
	Power (kW)		116
	Mass	Front	2450
	with implement	Rear	7950
	(kg)	Total	10400
Harrow:	Width (m)		3
	Mass (kg)		1400
Seeder	Width (m)		3
	Mass (kg)	Machine	900
		Ballast	1000

Figure 1. The tractor with the implement on the transverse way of the maize lanes.

The dummy tractor

A dummy of tractor was developed. It consists of a front axle of a 100 kW tractor joined to a rear axle of a 200 kW tractor by two iron beam HEB 240x240x17 and two plates of 40 mm width. Its rear was equipped with a three point linkage system, category 3.

Tires were 340/85 R28 on the front and 650/65/38 on the rear, the wheelbase was 2965 mm, the masses of the unloaded dummy were 1250 kg on the front, 2280 kg on the rear for a total weight of 3530 kg.

During the test 3400 kg of ballast were fitted on the front axle (Figure 2).

Four poster test bench

The CRA-ING four-poster test bench is specifically designed to test large and heavy vehicles up to 15 t in off-road low-medium range forward speed conditions.

The stand is composed of a seismic mass of the weight of 408 t, isolated from the ground by means of pneumatic springs; four servo-hydraulic actuators articulated for wheel-base/track adjustment on the seismic mass and supporting four vibrating plates upon which the tires of the vehicle are placed; a power hydraulic and a control unit, including a computer-based controller and a data acquisition unit.

Each actuator is controlled in position (up to a frequency of 100 Hz and a peak-to-peak amplitude of 250 mm) and excites one tire of the vehicle in vertical direction.

The displacements of the actuators are measured through linear variable differential transformer (LVDT) transducers, whose output signals are acquired and recorded.

Measure instrumentation

The vehicle has been instrumented with a set of four piezo-electric monoaxial accelerometers (range ±50 g, sensitivity 100 mV/g) to measure the wheel hubs vertical acceleration and a triaxial seat accelerometer (range ±50 g, sensitivity 100 mV/g) placed in correspondence of the seat surface to evaluate operator comfort.

Figure 2. The test layout with the dummy tractor.

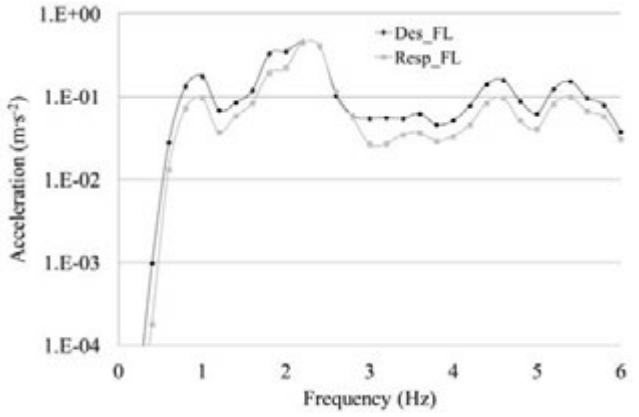

Figure 3. Example of the reproduction of the time history as frequency on the front left hub.

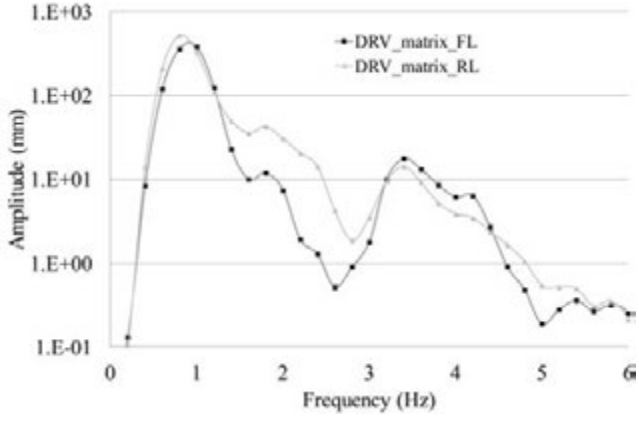

Figure 4. The spectrum of the displacement of the plates of the reproduced TH.

Results

The roughness of the surface combined with the forward speed causes the excitation of the frequencies of the elastic parts and characteristic of the vehicle: tires, cab support, pitch, roll, etc…

The most severe solicitation acquired on the implement is characterized by the pitch of the tractor. This is further enhanced by the weight of the implement itself overhanging on the rear.

The spectrum of the acceleration at the front left hub, and characterizing the pitch, is reported in figure 3 (Des_FL).

It's possible to see the acceleration at about 2 Hz both on the front and on the rear axle.

The reproduction of the time history (TH) at the test bench has been addressed to obtain the main content in frequency acting on the whole vehicle. The time history of interest was reproduced with a mean RMS error of 38 (dimensionless) on the four channels (hubs). An example of the accuracy of the induced acceleration to field data is reported in Figure 3 with reference to the left channel. The final output of the signal reproduction process is the TH of the vertical displacement of the plates. Figure 4 shows that the spectrum of the obtained TH, with one high energy peak at 1 Hz can contribute up to 4 Hz.

The first evaluation of the effect on the vehicle underlines the linearity of the solicitation or, on the contrary, the absence of shock on the implements that could happen as consequence of one not linear response of the vehicle to an obstacle.

For this reason artificial solicitations simulating the effect of bumps have been developed exciting the pitch of the tractor on the front tires by a 4 Hz sine, and combining it with a rear sine of 2 Hz not in phase. The result is shown in Figure 5.

Combining the reproduced TH with the bumps artificially obtained, it was possible to produce the desired solicitation that resulted in a cycle length of 55 s. (Figure 6)

While performing simulation tests, the amplitude of the reproduced solicitation has been tested at 80%; 90%; 100%; 105%; 112% of the acquired one. The implement has been tested both empty and full with sand simulating the presence of seeds in the hopper. According to observations, working at 105% of the amplitude was chosen to carry out the fatigue test with bumps set at 16 mm.

The test with the setting of the implement without ballast resulted more severe.

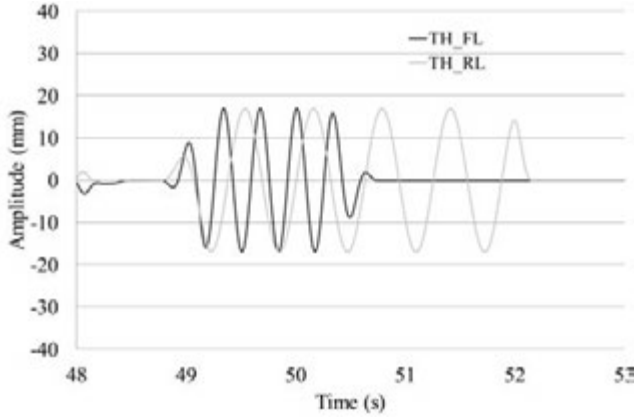

Figure 5. The developed bump for simulating vertical shock.

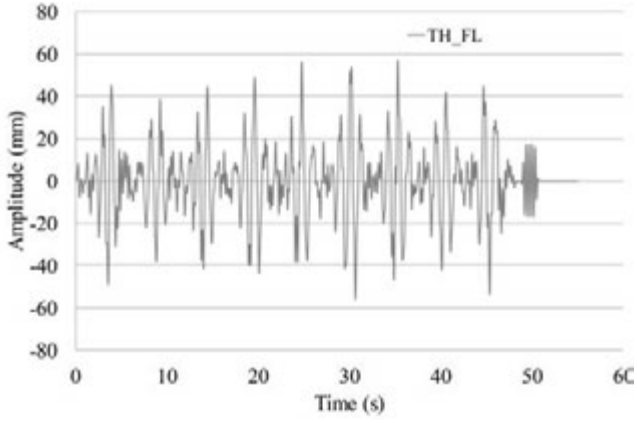

Figure 6. Graphic representation of the developed TH.

Conclusions

A combined implement, carried on a tractor, has been conducted in different fields and conditions for determining the solicitations considered severe for mechanical durability of the implement itself.

Among the time histories acquired during these real conditions of transport on terrains the most representative in terms of mechanical solicitations was selected. This last has been reproduced at an electro-hydraulic four poster on a dummy of tractor especially developed for the implement couplement. Moreover, artificial bumps 16 mm height were introduced in the time history for simulating not linear solicitations as shocks.

The possibility of carrying out a fatigue test on a carried implement simulating the transport condition by a four poster test bench has been verified. Key aspects of the trial are resulted the choice of the conditions to reproduce both in terms of spectrum and amplitude.

References

Anthonis J., et al. 2007. Feedback Approach for Reproduction of Field Measurements on a Hydraulic Four Poster. Biosystems Engineering. 2007. 96(4), pp. 435-445.

Bisaglia C., Cutini M., Gruppo G., Assessment of vibration reproducibility on agricultural tractors by a "four poster test stand", proceedings of the XVI CIGR. EurAgEng 2006. 64th VDI-MEG and FAO joint "World Congress - Agricultural Engineering for a Better World", Bonn, Germany, September 3-7. 2006. pp.1-6.

Cutini M., Bisaglia C., Romano E., Measuring the radial eccentricity of agricultural tires for ride vibration assessment. Proceedings of the 39. International symposium on agricultural engineering "Actual tasks on agricultural engineering", p. 63-72 (ISSN 1333-2651), 22-25 February 2011, Opatija, Croatia.

Nguyen V. N., Inaba S., Effects of tire inflation pressure and tractor velocity on dynamic wheel load and rear axle vibrations, Journal of Terramechanics, 2011, vol.48, pp.3–16

Pacejka H. B. (2010) Tyre and vehicle dynamics. Oxford, Butterworth Heinemann

Park S., Popov A. A., Cole D. J., Influence of soil deformation on off-road heavy vehicle suspension vibration, Journal of Terramechanics, 2004, vol.41, pp.41-68

Scarlett A. J., Price J. S., Stayner R. M., Whole body vibration: Evaluation of emissions and exposure levels arising from agricultural tractors, Journal of Terramechanics, 2007, vol.44, pp.65-73

Sherwin L. M., Owende P. M. O., Kanali C. L., Lyons J., Ward S. M.. Influence of tyre inflation pressure on whole-body vibrations transmitted to the operator in a cut-to-length timber, Applied Ergonomics, 2004, vol.35 (3), pp.235-261

Soderling, S., Sharp, M. and Leser, C. 1999. Servo Controller Compensation Methods Selection of the Correct Technique for Test Applications. VII International MobilityTechnology Conference & Exhibit. Sao Paulo, Brazil : s.n., 1999. pp. 30-35.

Taylor R. K., Bashford L. L., Schrock M. D., Methods for measuring vertical tire stiffness, Transactions of the ASAE, 2000, vol.43 (6), pp.1415-1419

Witzel P., Bottinger S. (2011), Upgrading of the Hohenheim Tyre Model to a radial approach, Landtechnik, 2.2011, 144-146

Application of software for the optimization of the surface shape of nets for chestnut harvesting

Andrea Formato, Giampiero Scaglione, Domenico Ianniello

Department of Agricultural Science. University of Naples "Fed. II", Portici (NA), Italy

Abstract

In this research conveyance nets for the chestnuts harvest have been considered and the optimization of the surface shape of the chestnuts harvest nets has been performed. Indeed, a steep zone with chestnut trees has been considered, with maximum length of 90 m and maximum width of 60 m and the geometric model of the considered zone has been obtained, by mean GIS system and "Archicad 14" program code, obtaining also the soil local slope distribution. The chestnuts fallen have been simulated by mean a "rain device" available in "Sitetopo" program code. This program has allowed to evaluate the rain draining in function of the considered surface slope. Further, the zone with lower quote, for the considered surface, is the zone in that the chestnuts have to be convoyed, "basin zone". Indeed, by mean "Sitetopo" program code, it has been possible to evaluate the rain draining contour-plot, and the conveyance effect, that is, where the rain flow is convoyed. This has been obtained by changing of the net surface slope on that, the rain (simulating the chestnuts) fallen. Indeed the nets have been located following the determined optimal surface. In such way all the fallen chestnuts have been convoyed and picked in a determined zone, "basin zone", and subsequently they have been loaded on the truck for the following workmanships. The evaluated losses have been of around 6-8 % due to chestnuts entangle or little branches obstacle.

Introduction

The chestnut crops, represents an important resource for the national collectivity, considering also the function that the chestnut crop develops inside the wooded sector (Bassi *et al*.,2001; Biondi *et al*.,2001, Formato *et al*.,2008;). Since the chestnut production involves different operational phases, they have to be performed in effective way, keeping in mind all the requirements for the chestnut tree plant. (Bergantz R. 1987 New, 1988, Formato *et al*.,2011). Numerous farms perform chestnut crop activity using different levels of mechanization (Rutter 1987; Monarca *et al*.,2004). To make not expensive and efficient this activity, it is necessary to use the best available technologies to rationalize the harvest production (Monarca *et al*.,2004; Formato *et al*.,2012). Insofar, it results extremely essential, the analysis and the planning of a system in which the machineries and machines are essential components, for the chestnuts harvest and transport. The promotion of the technological innovations to perform this type of work by mean the use of machineries is aimed to facilitate the work of the operators obtaining a lower risk for them and for the environment. Besides the planning, the organization of the works and the improvement of the roads, inside the chestnut tree plant, allow to develop the activities in the considered plant in way more effective and efficient. The mechanization, therefore, is the most important methods that can be considered to perform in the best way the chestnuts crops. Insofar the purpose of this report is that to put in evidence the systems of chestnuts harvest by nets in the chestnut tree plant, keeping in mind the today's mechanical and technological innovations. In fact, by year in year it becomes more and more pressing the demand to improve the chestnuts harvest in mountainous and forestry zones on which the soil morphological conditions make it absolutely unproductive in terms of cost-proceeds. The most part of the zones for the chestnut cultivation, is characterized by excessive soil slope and by difficulty of access. The chestnut harvest machines available on the market still have notable operational limits as it regards the steep zone of the soil considered, sensibly reducing their performances with soil slope higher than 20%. In such case, only the harvest by mean harvest nets it is possible.

Correspondence: Andrea Formato, Department of Agricultural Science. University of Naples "Fed. II", Via Università 100, 80055 Portici (NA), Italy.
E-mail: formato@unina.it

Key words: nets for chestnut harvesting, surface optimizing, net design.

Journal of Agricultural Engineering 2013; XLIV(s1):e82
doi:10.4081/jae.2013.(s1):e82

Materials and Methods

For soil zones with slopes over 25%, it is not possible to use any type of harvesting machine, for which it is possible to perform only the aided harvesting by mean the use of harvest nets and aiding machineries. A method of chestnuts harvest in the steep zones has been studied, testing in the considered chestnut tree plant special types of nets, and using aiding machines: tendering – rewinding machines. Indeed, a steep zone with chestnut trees has been considered, with 90 m of maximum length and 60 m of maximum width. Methods for the conveyance and to pick up of the fallen chestnuts have been tested, by mean study aimed to determine the best geometric shape to realize during the layout of nets. Insofar it has been necessary to realize a digital elevation model (DEM) of the zone of the considered soil, starting from the site map with level quotes of the considered zone. (Figure 1 and Figure 2).

A Digital Terrain Model (DTM) is a topographic model of the bare hearth - terrain relief - that can be manipulated by computer programs. The data files contain the spatial elevation data of the terrain in a digital format which usually presented as a rectangular grid. Vegetation,

buildings and other artificial features are removed digitally, leaving just the underlying terrain, namely the Digital Surface Model (DSM). Satellite provides orthorectified images and aerial photography which can be processed for visualization of terrain conditions in three dimensions (3D), leading to a Digital Elevation Model (DEM). DEMs are used often in Geographic Information Systems (GIS), such as ArcGIS and GRASS GIS system , and are the most common basis for digitally-produced relief maps. While a DSM may be useful for landscape modelling, city modelling and visualization applications, a DTM is often required for flood or drainage modelling, land-use studies, geological applications, and other applications. Common uses of DEM include: extracting terrain parameters, modelling water flow or mass movement (for example, landslides), creation of relief maps, rendering of 3D visualizations, creation of physical models (including raised-relief maps), rectification of aerial photography or satellite imagery, reduction (terrain correction) of gravity measurements (gravimetry, physical geodesy), terrain analyses in geomorphology and physical geography. Several factors are important for quality of DEM-derived products: terrain roughness, sampling density (elevation data collection method), grid resolution or pixel size, interpolation algorithm, vertical resolution, terrain analysis algorithm. The intervals between each of the grid points will always be referenced to some geographical coordinate system. This is usually either latitude-longitude or UTM (Universal Transverse Mercator) coordinate systems. The closer together the grid points are located, the more detailed information will be in the file. The details of the peaks and valleys in the terrain has been better modelled with small grid spacing than when the grid intervals are very large. Elevations other than at the specific grid point locations are not contained in the file. As a result peak points and valley points not coincident with the grid has not been recorded in the file. A DEM can be represented as a raster (a grid of squares, also known as a height-map when representing elevation) or as a vector-based triangular irregular network, generally constructed using the Delauny. The TIN DEM dataset is also referred to as a primary (measured) DEM, whereas the Raster DEM is referred to as a secondary (computed) DEM. TIN's are sets of adjacent, non-overlapping triangles computed from irregularly spaced points (mass point) with (x,y,z) coordinates. TIN models are used to provide better control over terrain slope, aspect, surface areas, volumetric and cut-fill analysis and generating contours. Mass points can occur at any location, the more carefully selected, the more accurate model of the surface. Well-placed mass points occur where there is a major change in the shape of the surface, for example, at the peak of a mountain, the floor of a valley, or at the edge (top and bottom) of cliffs. The TIN model is attractive because of its simplicity and economy and is a significant alternative to the regular raster of the GRID model. The TIN's vector data structure is based on irregularly-spaced point, line and polygon data interpreted as mass points and break-lines and stores the topological relationship between triangles and their adjacent neighbours. Break-lines define and control surface behavior in terms of smoothness and continuity. As their name implies, break-lines are linear features. They have a significant effect in terms of describing surface behavior when incorporated in a surface model such as a TIN. Break-lines can describe and enforce a change in the behavior of the surface. Two types of break-lines are included in this layer: hard and soft. Hard break-lines define interruptions in surface smoothness and are typically used to define streams, ridges, shorelines, building footprints, dams, and other locations of abrupt surface change. Soft break-lines are used to ensure that known "Z" (elevation) values along a linear feature (such as a roadway) are maintained in a TIN. Soft break-lines can also be used to ensure that linear features and polygon edges are maintained in the TIN surface model by enforcing the break-line as TIN edges. Soft break-lines, however, do not define interruptions in surface smoothness. The Delauny triangulation is a proximal method used to generate the TIN. The vertices of the contour lines are used as mass points for triangulation. In many cases this will cause the presence of flat triangles in the surface (Figure 3). Subsequently on the considered model the study of the local slopes and of the director cosines has been performed, and it has been possible to determine the accumulation zones, where to install the harvest tank. The manipulation of the considered model (Figure 4) it has been performed by mean "Archicad 14" program code (Figure 5). Further, the chestnuts fallen has been simulated by mean a "rain device" like "Sitetopo" code. In this way, it has been possible to evaluate the draining of the rain simulating the fruits fallen. By mean iterations, it has been possible to obtain the optimal net geometric shape that convoyed the rain (chestnuts fallen) in the desired "basin zone" (Figure 6). Indeed the nets have been located following the determined surface. In such way all the chestnuts have been picked in an only determined zone, "basin zone". Then, the nets have been pretensioned following the surface determined with the design method described above. In such way the chestnuts have been rolled down and converged to a single point inside the catchment area, known as "sink" and then loaded on the truck for the following workmanships. Indeed, having such TIN DEM of the area considered, it is possible to shape the net, so that all the fruits can roll down in the harvest tanks. The problem of obtaining a suitable shape of the net regards the design process of pretensioned structures such as cable nets and membrane structures. Available design methods have in common that no material laws are

Figure 1. Site map considered.

Figure 2. Site map with level quotes.

necessary to find an equilibrium of the three dimensional shape for given stress distributions, boundary conditions and supports. These shapes of equilibrium should ensure in the built structure an homogeneous distribution of the tension stresses. In reality the material behaviour, process of cutting patterns, manufacturing and pretensioning on site influencing the stress distribution, wrinkles and regions of over stress are obvious, can be seen and measured. (Figure 7)

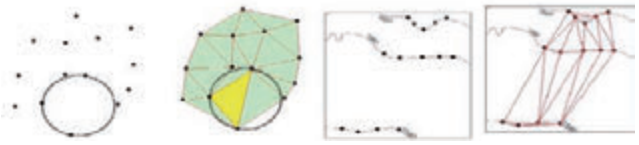

Figure 3. Delaunay triangulation.

Nets for chestnuts conveyance and harvest

Particular types of nets has been considered and precisely: ELAION CANDIA: Strong and heavy net, is defined "anti -thorn" since the textile scheme reduces the possibility of rubbing or hookup, determined by brambles and asperity of the soil. Net with high no-break-up characteristic, weights g. 95/m^2, green color. The considered net has the characteristic followings: low weights, resistance to the tear, low wrinkledness to facilitate the slip/rolling of the fruits, not expensive, large versatility of assemblage; possible versatility to use it, in the harvest yards of other fruits in hull (core) in the steep zones.

Figure 4. 3-D model of the considered soil zone.

Tension structures design

The design process of tension structures such as double curved cable nets or membrane structures such as tents can be divided into form finding, static analysis and cutting pattern. The result of the form finding is a shape of equilibrium for a certain stress distribution and boundary conditions. The shape of equilibrium ensures the geometry of the double curved surface which has only tension and avoids compression in the surface. From this geometry the structural behaviour is exanimated and the cutting pattern is made. An enhanced design concept is based on five design steps defining the shape of equilibrium, generating the cutting pattern, reassembling and pre-tensioning the cutting pattern, the structural analysis of the reassembled structure and the evaluation of the structural behaviour. The material behaviour is considered in the last three steps: flattening the shape of equilibrium, reassembling and load bearing behaviour. The length and the width of the strips has an influence to the shear deformation of the coated fabric. The orthotropic behaviour of coated fabric influences the process of pretension and the stress distribution in the reassembled structure. The numerical process allows after evaluation modifications to reach better results in the reassembled structures considering stress distribution and deformations. (Figure 8). The development of Computer Aided Design marked the start of changes in geometry endorsing new and free forms. This generation of double curved 3-dimensional surfaces is restricted by few limitations. Theoretically there are an unlimited number of forms to be numerical generated and represented. However, the manufacture and realization of such double curved surfaces are subject to numerous boundary conditions and restrictions. Using cables and membranes for the load transfer only tension forces can be carried, the cables and membranes can not withstand bending moments and compression forces in a global point of view. The structures have to be pre-tensioned in order to activate the geometric stiffness or to be able carrying compression forces by reducing the pretension. The shape of equilibrium defines a pre-tensioned geometry of a doubled curved surface for a cable net or a membrane structure. The relation between the tension stress, geometry and equilibrium allows three possibilities to introduce the tension into the membranes and influences the shape of equilibrium (Figure 9). Membrane - textile structures can be designed in three general ways.

Figure 5. 3-D TIN DEM model of the considered soil zone.

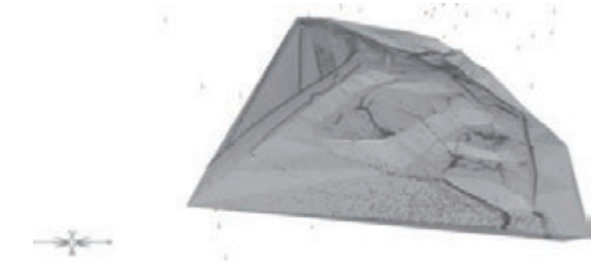

Figure 6. 3 D TIN DEM model with the zone where the harvesting tanks have been located.

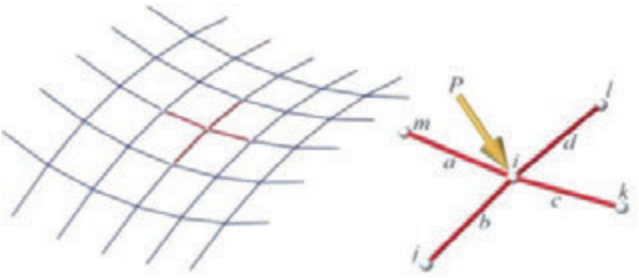

Figure 7. Part of a cable network.

Non-computational: physical models are used to form-find the prestress surface geometry and create the cutting patterns. Simplified "hand calculations" are used to predict structural response.

Non-specialised software: non-equilibrium computational modelling software, such as 3DS Max, is used to generate the pre-stress surface geometry and cutting pattern generation. Standard finite element (FE) software, such as Ansys 14.5 code, is used to perform non linear structural analysis.

Specialised software: lightweight structure task-specific equilibrium based computational modelling software is used to perform form-finding, load analysis and cutting pattern generation. The non-computational method has the advantages that it is intuitive, the form can be realised, it can be implemented with low initial investment, and modification of conceptual forms is quick and simple. It suffers from its lack of computational non-linear structural analysis, low precision and lack of computational mesh for rendering. Its slowness, particularly with respect to making modifications to the production form and cutting patterns, makes it operationally expensive. Using the non-specialised software method leverages existing CAD and analysis software skills and provides many sophisticated geometric tools. With few exceptions, the forms generated are, however, not force equilibrant. Consequently they can not necessarily be realised with a tensile surface. Lack of integration between the mesh generation and analysis leads to slow design modification cycles. Conventional FE software is often inappropriate for use with textile models. In particular, convergence problems are usually experienced by standard FE systems when dealing with textile slackening on-off non-linearity. Specialist textile structure software systems quickly provides high confidence, high precision, integrated solutions. Initial investment is higher but when design volume is adequate, per-design costs are low.

Experimental tests

In the case in study, a farm has been considered constituted by around 10 hectares of chestnut tree. In a meaningful part of the considered area, because of the high slope, the harvest and the workmanships of cleaning pre-harvest, they are effected completely by hand. The tests have been performed in a chestnut tree plant of about 25 years of age, constituted by a steep soil, with different slope values. The nets were located following the optimal shape determined by using machines aiding the operation of net rewind.(Figure 10 and Figure 11). Insofar , experimental tests have been effected both on the materials of the considered nets and on the realized equipments, and models have been used for verifying the obtained results. For the forces' determination, the structural parts have been sensitized, opportunely through movements and strengths transducers connected to a system of data acquisition with frequency of sampling of 1 hz. The equipment is composed by tubular structure, transportable by mean the pitchforks of the anterior lifter of the tractor. It is possible to move the tool with a lifter connected to the three back points. The structure contains a galvanized plate tank for the chestnuts and two sidely arms sustaining the net. The tank for the chestnuts has an opening with counter for the transfer of the chestnuts in the large case for the transport. The arms sustaining the net are composed by 2 segments that refold on it.

Data results analysis

The nets have been located following the determined optimal surface (Figure 12 and Figure 13). In such way all the chestnuts have been

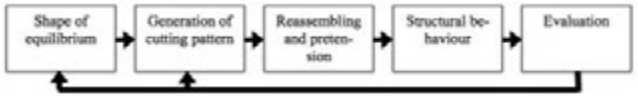

Figure 8. Enhanced design process of membrane curvature.

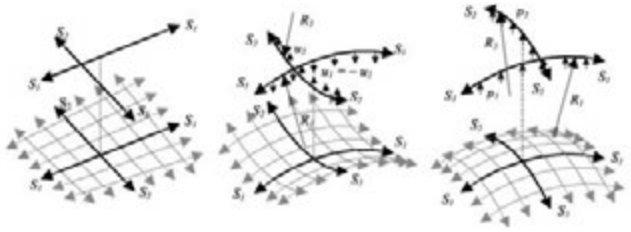

Figure 9. Relation between tension forces and curvature.

Figure 10. Aiding machine to rewind the nets.

Figure 11. Aiding machine to rewind the nets.

Figure 12. Harvest nets.

Figure13. Harvest nets.

picked in an only determined zone, "basin zone", and subsequently they have been loaded on the truck for the following workmanships. The evaluated losses have been of around 6-8 % due to chestnuts entangle or little branches obstacle. The picked production during the tests has been determined by the presence of a notable quantity of product on the soil (0,264 kg/m^2).The analysis of the picked product has been effected, to the purpose to underline the working quality performed by the harvest system considered. It is been noticed as in the picked product there were impurities equal to 2,2%. Such level of cleaning can also be defined good in consideration of the washing operation in water of the chestnuts that is performed as a rule subsequently in the farm center.

Conclusions

An application of software for the optimization of the surface shape of nets for chestnut harvesting has been set-up, for steep soil (slope >25%), not being possible some type of mechanization, then nets opportunely designed have been used. Such nets have been installed according to a geometry determined through computational codes, in way that the chestnuts, when they fall, because the geometry of the nets used, they are convoyed in the harvest tank. Besides with such research it has been validated the use of machine to stretch and to rewind the nets. Such machine has resulted, not heavy, manageable and effective.

This research is at the basis of possible further development of the study aimed to reduce the "mountain marginal areas", that is to obtain a productive activity in this type of areas, avoiding the abandonment of them.

References

Bassi D., Casiraghi M.C., Magnani I., Vercesi A., Delaidelli G. 2001 - Effetto dei trattamenti post raccolta e dei metodi di conservazione sulla qualità delle castagne. In: Atti del convegno nazionale sul castagno 2001, Marradi 25- 27 ottobre 2001, 244-249.

Bergantz R. 1987. Experiences with the California chestnut industry. In Proceedings of the Second Pacìfic Northwest Chestnut Congress, Oregon State University.33-5 l.

Biondi P., Monarca D., Panaro V. 2001. Influenza della raccolta meccanica delle castagne sulla qualità dei frutti raccolti. Convegno Nazionale Castagno 2001.

Formato A., Scaglione G.P, Carillo M., Federico R. 2008. *Performance Evaluation of Pneumatic Machines for Hazelnut Harvesting* Conv. AgEng2008. Hersonissos. Crete. Greece. 23-25 June 2008.

Formato A., Scaglione G., Pucillo G., Abagnale A., Milano G. 2011. Chestnuts facilitated harvest systems in steep zones XXXIV CIOSTA CIGR V Conference 2011: Efficient and safe production processes in sustainable agriculture and forestry 29 June - 01 July 2011 - Vienna, Austria. ISBN:978-3-200-02204-1

Formato A., Guida D., Lenza A., Palcone C., Scaglione S. 2012. A machine prototype for the chestnut mechanical harvest in steep zone. CIGR-AgEng2012 International Conference of Agricultural Engineering. Valencia, Spain - July 8 - 12, 2012.PAPERS BOOK. ISBN 10 84-615-9928-4 and ISBN13 978-84-615-9928-8

Formato A., Guida D., Lenza A., Palcone C., Scaglione G. 2012. A machine to improve the safety during the chestnut mechanical harvest in steep zone. International Conference RAGUSA SHWA "Safety Health and Welfare in Agro-food Agricultural and Forest Systems". September 3-5, 2012 Ragusa – Italy. ISBN 978-88-905473-4-8

Monarca D., Cecchini M., Massantini R., Antonelli D., Salcini M.C., Mordacchini M.L. 2004. Mechanical harvesting and quality of ''marroni'' chestnut. Acta Horticolturae.

New E. 1988. The chestnut industry in New Zealand. Proc. 2nd PNW Chestnut Congress. Chestnut Growers Exchange P.O. Box 12632, Portland, OR 97212. OR Dept. Ag. Chestnut blight quarantine 1987. OAR 603-52-075. Oregon Dept. Agric., 635 Capitol Street NE, Salem, OR 97310.

Rutter P. 1987 . Chestnut ecology and the developing orcharding industry. In Proceedings of the Second Pacific Northwest Chestnut Congress, Oregon State University.

Aerodynamic properties of six organo-mineral fertiliser particles

Marcello Biocca, Pietro Gallo, Paolo Menesatti

CRA-ING, Consiglio per la Ricerca e la sperimentazione in Agricoltura, Agricultural Engineering Research Unit, Roma, Italy

Abstract

Agricultural fertilisers are generally applied by means of centrifugal disk spreaders. The machinery, the working conditions and the physical characteristics of fertilizers (including the aerodynamic characteristics of particles) may affect the behaviour of particles after the discarding from the spreader. We investigated the aerodynamic properties of organo-mineral fertilisers (a class of slow release fertilisers that are less investigated since they are relatively new in the market) using a vertical wind tunnel similar to an elutriator. In the same time, the morphological characteristics of individual fertilizer particles were measured by means of an image analysis procedure. In the study we compare six different fertilisers and we discuss the suitability of the employed methods. The results provide the terminal velocity – Vt – (the velocity value that overcome the gravity force of the particles) of the particles, ranging from 8.60 to 9.55 m s^{-1}, and the relationships between Vt and some physical properties (mass, shape, dimensions) of the fertilizers. Moreover, the results of field distribution trials show the behaviour of the tested fertilizers during practical use. Such data can contribute to enhance the quality of application of these products in field.

Introduction

Granular fertilisers are the most common type of agricultural fertilisers since they are easily produced, transported and applied. Many studies give emphasis on the proper application methods of agricultural fertilisers in order to increase crop yield, reduce costs, and minimise environmental pollution. In fact, to be efficiently applied in field, granular fertilisers must be properly handled and distributed.

The most common granular fertiliser application devices is the centrifugal disk spreader. The main advantages of this spreader are the large spread width, the simple and robust construction and the low cost. In this machinery, the distribution pattern of fertilizer is affected by many variables, depending on machinery model, on working conditions and on physical characteristics of fertilizer, including the aerodynamic characteristics of granular fertilizers, that affect the behaviour of particles after the discarding from the spreader (Allaire and Parent, 2004; Macmillan, 2007). This study intends to determine some physical characteristics of organo-mineral fertilisers, an interesting type of slow release fertilisers that are less investigated since they are relatively new in the market.

A common attribute used in aerodynamic investigations on particles is terminal (or floating) velocity (Vt). Particles with higher Vt would travel farther than particles with a lower Vt. (Lee and Yates, 1977). Terminal velocity is determined by morphology and mass, and can be measured by two methods (Jongejans and Schippers, 1999): (1) a dropping method, using a fall tower in which particles are dropped from a certain height in motionless air (Grift *et al.*, 1997) and (2) a floating method, using a vertical wind tunnel in which particles can float while the necessary upward air flow is determined (Bilanski and Lal 1965, Law and Collier 1973, Hofstee 1992). The advantage of the floating method is that the terminal velocity can be obtained directly and that the apparatus can be relatively small. A disadvantage consists in the difficulty to obtain a smooth air flow with little turbulence.

To study the aerodynamic properties of some organo-mineral fertilisers we designed and realized a vertical wind tunnel (elutriator) and we measured the Vt of six commercial organo-mineral fertilizers; then we determined their morphology by means of an image analysis technique. Moreover, in field tests we studied the behaviour of fertilizers during practical application.

Correspondence: Marcello Biocca, CRA-ING, via della Pascolare 16, 00015 Monterotondo, Roma, Italy.
Tel. +39.06.90675215 - Fax: +39.06.90625591.
E-mail: marcello.biocca@entecra.it

Key words: organo-mineral fertilisers, spreading, image analysis, aerodynamic.

Contributions: the authors contributed equally.

Conflict of interests: the authors declare no potential conflict of interests.

Journal of Agricultural Engineering 2013; XLIV(s1):e83
doi:10.4081/jae.2013.(s1):e83

Materials and methods

Fertilizers

The study was carried out on six commercial organo-mineral fertilisers, named "A", "F", "N", "O", "S" and "M" (see Table 1 for characteristics). Each product was sieved at the following diameters: 1.4; 2.0; 3.35; 4.75 mm and samples consisting of ten particles for each product and each diameter class were collected and weighed.

Elutriation test

To investigate the aerodynamic properties of the fertilizers a vertical wind tunnel similar to an elutriator was designed and constructed (Law and Collier, 1973). In the apparatus (Figure 1) air is blown through a duct equipped with an anemometer to measure air velocity.

A fan driven by a 85 W a.c. motor (Vortice CA 150-V0 D) is placed in the wind tunnel of 10 cm of diameter. The velocity of the airflow in the wind tunnel is regulated by a voltage regulator and it ranges from 5.2 to 12.3 m s-1 (at the exit). In the duct a honeycomb section is mounted to straighten the flow and reduce the turbulence. A probe anemometer (Schiltknecht MiniAir 6) was used to measure air velocity in the test section. To measure floating particle velocity, at first the sample was loaded on a net placed at 19.5 cm to the tube exit, then the fan was turned on and the velocity was adjusted until the first five particles out of ten were discarded from the device. The air velocity at that point was acquired as terminal average velocity (Vt).

Distribution trials

The fertilizer "N" was distributed in field and the product was collected with 42 trays (500X500x100 mm), placed long a line transverse to the direction of forward motion of the tractor (Figure 1). We used a double disk spreader "Amazon" trailed by a "Landini Globus 80" tractor. The forward speed was 8.1 km h-1 and the test was replicated three times. The fertilizer of each tray was collected and weighed with a technical balance (Gibertini). The content of the tray placed at a distance of 0, 2.75, 4.75, 6.75, 7.75, 8.75, 10.25 and 10.75 m from the centre of the sampling line (on both sides), undergone to the image analysis to assess the dimensions of the individual particles contained in each tray.

Image analysis

The morphological characteristics of individual fertilizer particles were measured by means of an image analysis procedure. Images of the particles were acquired by means of an high resolution scanner and analysed by k-means unsupervised clustering method acting on multiple features autoscaled values (RGB channels; sum of RGB channels, grey value and whole RGB channels ratio) (Menesatti *et al.*, 2008).

In the elutriation tests, three images with ten particles for each fertilizer and for each diameter class were acquired, up to a total of 72 acquired images. The individual particles were described by image analysis in terms of several morphological parameters and in this study we utilized: the area (the image area of the particle), the maximum and minimum lengths. As derived variables, we considered: 1) a shape factor (S = length max/length min - *i.e.* a spherical particle has a S value of one); 2) an index ma (the mass divided by the frontal area of the particle in pixel); 3) an index Sw (the shape factor divided by the mass).

In the distribution tests, images of 26,531 single objects in total were acquired. The image analysis output for these particles was the same of the elutriation test.

Results

The average values of terminal velocities, mass and shape of fertilisers particles are summarised in Figure 2, where the data are referred to samples formed by ten particles for each size class. Each measurement was replicated three times.

The analysis of variance (ANOVA) performed on the data (Table 2) showed that the fertilisers have statistically significantly different Vt. Moreover, the fertilisers significantly differ in term of shape factor (S) (Table 3). The product named "A" shows in the meantime the highest value of S and the lowest Vt.. The fertilizers are more uniform in terms of particle weight.

To analyse the effect of the physical characteristics of particles on Vt, a multiple regression analysis was performed on Vt (dependent variable) and the following both measured and calculated variables (predictors): the area A (the image area of the particle), the maximum and minimum lengths, the mean weight particles, the shape factor S, the estimated particle diameter (in pixel), the index ma, the index Sw (the shape factor divided by the mass). The simple correlations between Vt (y) and these variables (x) are showed in Figure 3.

To choice the best variables for the terminal velocity, a stepwise (backward) multiple regression automatic procedure was applied (R Core Team, 2012). The Table 4 shows the result.

Regarding the application tests with the centrifugal spreader, the Figure 4 shows the distribution pattern of particles in terms of some morphological characteristics of individual particles (*i.e.* weight, area, major axis and shape – all values are standardized). The curves show that the mass of particles of the fertilizer "N" appear as the most important factor in determining the different distribution of particles. In other terms, the heaviest particles travel longer.

Conclusions

This study investigated the aerodynamic features of fertilizer parti-

Table 1. Characteristics of the tested products.

Name	Manufacturer	NPK content [%]	Bulk density [kg m^{-3}]
A	1	18.5-0-0	823.9
F	1	9-14-13	947.8
M	2	7-7-7	960.3
N	1	8-15-0	935.7
O	1	15-5-5	856.9
S	1	9-12-21	831.2

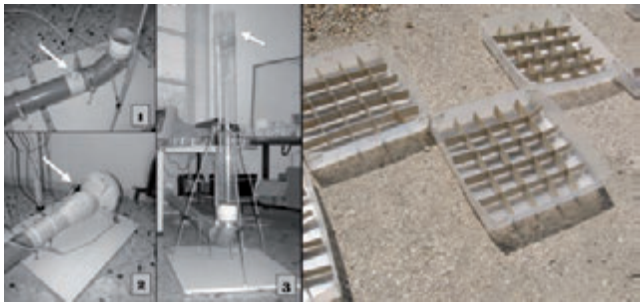

Figure 1. The apparatus used in the test (left): 1) the anemometer position; 2) the engine; 3) the terminal tube and the measurement zone; (right) the trays for the distribution tests.

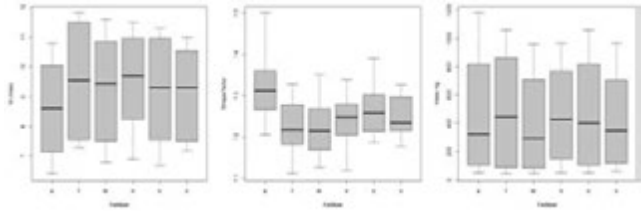

Figure 2. Some morphological characteristics of fertilizer particles of the six tested products (n=120); from left to right: terminal velocity (m s-1), shape (dimensionless) and mass (mg).

Table 2. ANOVA results for the Vt values for the tested fertilisers and different particle diameters.

EFFECT	SS	DF	MS	F	Prob F	Sign.
Diam.	189.6283	3	63.209	654.831	6.3735×10^{-39}	**
Fertil.	7.405	5	1.481	15.342	5.33563×10^{-9}	**
Diam. x Fertil.	5.8083	15	0.3872	4.011	0.000118607	**
Residual	4.633	48	0.0965			
Total	207.475	71				

Table 3. ANOVA results for the S (shape factor) values for the tested fertilisers and different particle diameters.

EFFECT	SS	DF	MS	F	Prob F	Sign.
Diam.	0.050921	3	0.01697	4.82859	0.00512	**
Fertil.	0.074345	5	0.01487	4.22990	0.00289	**
Diam. x Fertil.	0.076050	15	0.00507	1.44230	0.16666	
Residual	0.168730	48	0.00352			
Total	0.370045	71				

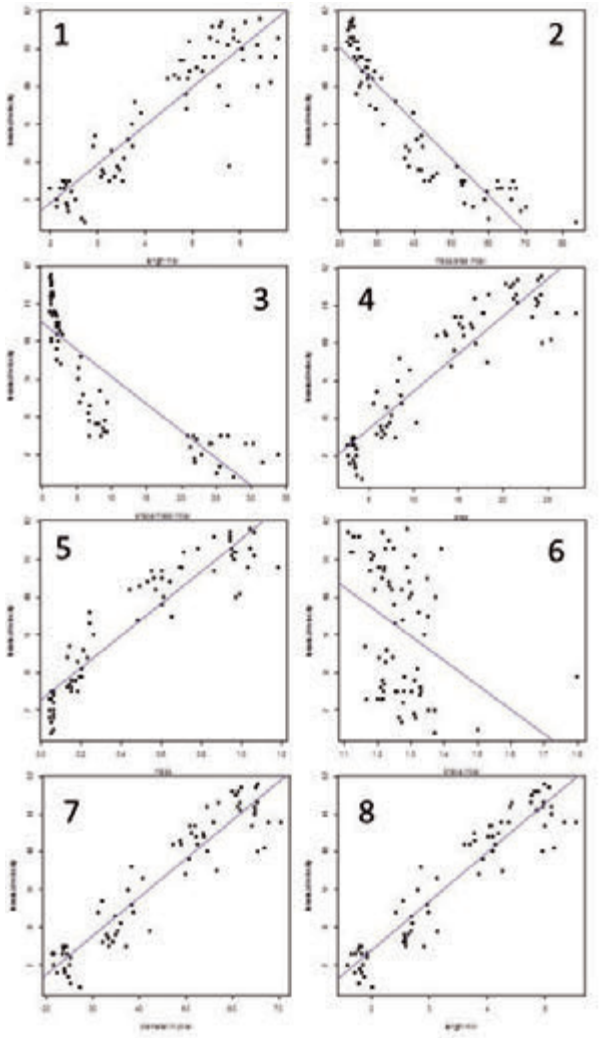

Figure 3. The simple correlations between terminal velocity (y) and the measured (or estimated) morphological and physical properties of particles. 1: ×= length maximun; 2: ×= Ma index; 3: ×= Sw index; 4: ×= area; 5: ×= mass; 6: ×= shape index; 7: ×= diameter in pixel; 8: ×= length minimum.

Table 4. Multiple regression results after stepwise backward procedure for terminal velocity.

	Estimate	Std. Error	t value	Pr(>|t|)	
(Intercept)	6.84356	2.10699	3.248	0.001852	**
Mass	4.04972	1.32340	3.060	0.003231	**
Area	-0.64592	0.10898	-5.927	1.35e-07	***
Length max	0.90897	0.54046	1.682	0.097477	.
Shape index	-3.93612	1.43684	-2.739	0.007964	**
Diameter	0.24683	0.06798	3.631	0.000562	***
S_w index	0.11129	0.02738	4.064	0.000134	***
M_a index	-0.05744	0.01431	-4.013	0.000160	***

Signif. codes: 0 '***' 0.001 '**' 0.01 '*' 0.05 '.' 0.1. Residual standard error: 0.3736 on 64 degrees of freedom. Adjusted R-squared: 0.9522. F-statistic: 203.2 on 7 and 64 DF, p-value: < 2.2e-16.

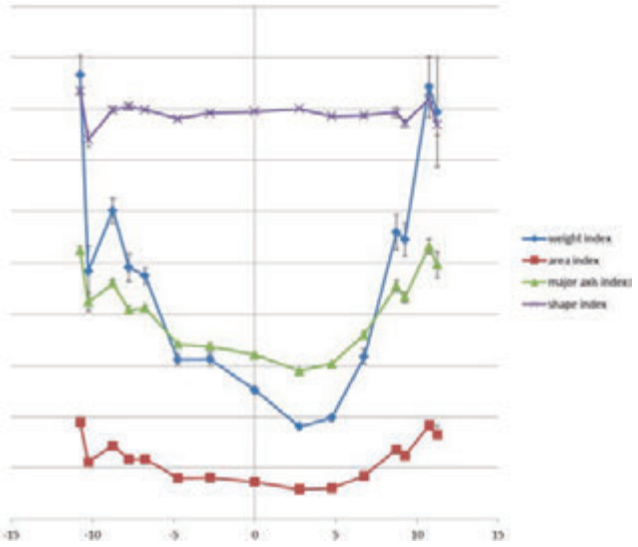

Figure 4. The distribution pattern of particles of fertilizer "N", in terms of weight, area, major axis and shape. All values are standardized.

cles, to contribute to enhance the quality of application of these products in field.

We found that the terminal velocity of fertiliser particles is related to measurable physical properties of the product. The developed elutriator could be used successfully for determining the terminal air velocity of the particles. Moreover the performed image analyses has been useful for determining the particle morphology characteristics considered in the paper.

When a fertilizer having heterogeneous distribution of particles is distributed by a spreader, physical features of the individual particles determine the distribution pattern. In conclusion, the terminal velocity is an aerodynamic characteristic that is easily measured to characterise such materials. But because the terminal velocity allows the drag coefficient to be determined for one condition only, its use is not applied in predictive models. A knowledge of the terminal velocity (or floating velocity) is however useful both in designing a system for separating one fraction of a mixture from another in a vertical column (elutriator) and to describe different products in terms of mechanical characteristics.

Further works are needed to put in relation the terminal velocity with the results obtained in field distribution.

References

Allaire, S. E. and L. E. Parent, 2004. Physical Properties of Granular Organic-based Fertilisers, Part 1: Static Properties. Biosystems Engineering, [87] 1, 79-87.

Bilanski, W. K. and R. Lal, 1965. Behavior of threshed materials in a vertical wind tunnel. Transactions of the ASAE, 8, 411-413.

Grift, T. E., J. T. Walker and J. W, Hofstee, 1997. Aerodynamic properties of individual fertilizer particles. Transactions of the ASAE, 40, 13-20.

Hofstee, J. W., 1992. Handling and spreading of fertilizers: part 2, physical properties of fertilizer, measuring methods and data. J. Agric. Eng. Res. 53: 141-162.

Jongejans, E. and P. Schippers, 1999. Modeling seed dispersal by wind in herbaceous species. Oikos 87: 362-372.

Law, S. E. and J. A. Collier, 1973. Aerodynamic resistance coefficients of agricultural particulate determined by elutriation. Transactions of the ASAE, 5. 918-922.

Lee, K.C. and W.E. Yates, 1977. A rotary cylinder spreader for aircraft granular applications. Transactions of the ASAE [20] 5, 801-805.

Macmillan, R.H., 2007. The Mechanics of Fluid – Particle Systems, with special reference to agriculture. Available at http://eprints.unimelb.edu.au/archive/00001514/ (accessed on May, 2013).

Menesatti, P., M. Biocca, S. D'Andrea and M. Pincu, 2008. Thermography to analyze distribution of agricultural sprayers. QIRT Journal (Quantitative Infrared Thermography Journal) [5] 1, 81-96

R Core Team, 2012. R: A language and environment for statistical computing. R Foundation for Statistical Computing, Vienna, Austria. ISBN 3-900051-07-0, URL http://www.R-project.org/.

Dynamic-energetic balance of agricultural tractors: active systems for the measurement of the power requirements in static tests and under field conditions

Daniele Pochi, Roberto Fanigliulo, Mauro Pagano, Renato Grilli, Marco Fedrizzi, Laura Fornaciari

Consiglio per la ricerca e la sperimentazione in agricoltura, CRA-ING, Unità di ricerca per l'ingegneria agraria, Agricultural Engineering Research Unit, Monterotondo (Roma), Italy

Abstract

Modern tractors are characterized by the introduction of devices designed to increase the operative performances of the machines, such as systems for monitoring and controlling various functions (through a massive use of electronics and hydraulics), or deputed to improve the comfort of the driver (paying more attention to ergonomics, air-conditioning, noise and vibration). Such devices need energy to be operated, affecting the energetic balance of the tractor. In this context, the availability of suitable methodologies and instrumental systems could be useful to provide objective, accurate and reliable measurements of the performances of the tractors under different conditions, also considering the power requirements from ancillary services and/or simulating the coupling with operating machines. The tests on the performances of tractors are now made using different methods, including the trial codes issued by the OECD Codes. Beyond their undoubted validity, they fix standard test conditions that often do not adequately represent the operative reality, so that, much remains to investigate on the actual performances provided by the tractors. From this point of view and with reference to fixed point tests, a test bench was developed for the measurement of the power required by various devices, such as transmission and air conditioning. It was used in experimental tests on a tracked tractor and on a wheeled tractor, aimed at validating the test device, measuring the power absorption related to the rotational speed of the organs of propulsion and to the characteristics curves, in order to quantify the power drawn by the transmission and by the air conditioning and assess the residual power for other tractor functions. As to field conditions, a study is being conducted at CRA-ING, within the project PTO (Mi.P.A.A.F.), to develop a mobile test bench aimed at evaluating the power required by different operations, such as self displacement, traction, use of power take off, their combination. The system simulates such operations by applying to the tractor, by means of a system of sensors and actuators operated by feedback signals, work cycles combining force of traction, p.t.o. torque, hydraulic power, derived from data recorded during real field test with agricultural machines.

Correspondence: Daniele Pochi, Unità di ricerca per l'ingegneria agraria, Via della Pascolare, 16, 00015 Monterotondo (Rome), Italy.
Tel. +39.06.90675232 - Fax: +39.06.90625591.
E-mail: daniele.pochi@entecra.it

Key words: agricultural machines, transducers, data acquisition system, operative performance, tractor test bench.

Contributions: the authors contributed equally.

Conflict of interests: the authors declare no potential conflict of interests.

Journal of Agricultural Engineering 2013; XLIV(s1):e84
doi:10.4081/jae.2013.(s1):e84

Introduction

Modern tractors are characterized by the introduction of devices designed to increase the operative performances of the machines, such as systems for monitoring and controlling various functions (through a massive use of electronics and hydraulics), or deputed to improve the comfort of the driver (paying more attention to ergonomics, air-conditioning, noise and vibration). Such devices need energy to be operated, affecting the energetic balance of the tractor (Pochi *et al*., 1996; Bodria *et al.*, 2006; Al-Suhaibani *et al*., 2010).

In this context, the availability of suitable methodologies and instrumental systems could be useful to provide objective, accurate and reliable measurements of the performances of the tractors under different conditions, also considering the power requirements from ancillary services and/or simulating the coupling with operating machines (Casini Ropa, 1975; Gasparetto *et al*., 1985; Fanigliulo *et al*., 2004).

The tests on the performances of tractors are now made using different methods, including the trial codes issued by the OECD (2005). Beyond their undoubted validity, they fix standard test conditions that often do not adequately represent the operative reality, so that, much remains to investigate on the actual performances provided in field by tractors (Marsili and Servadio, 2001).

The main items for further studies are: at fixed point, the distribution of engine power to move the various internal components of the tractor (gearbox, transmission, air conditioning, hydraulic system, etc.); under actual field conditions, the work of hydraulic lift in terms of actual control of the mounted implement and the work for self-displacement on different surfaces.

This work is framed in the context of activities the goal of which is to establish a test protocol for measuring the dynamic and energetic balance of the tractor in real operating conditions, on completion and integration of the tests according the OECD standards and in support of ENAMA protocols for the tests of operating machines.

In the first step it has been faced the aspect of the relief, in tests at a fixed point, of the power required for the operation of various organs of the tractor. To do this, a dynamometric brake, commonly used in power-take-off tractor tests, has been combined with a special device (which is presented below for a description) suitably designed for accurate measurements of the power required by different tractor services. The detailed information provided allows better evaluation of actual power requirements of the machines for primary and secondary soil tillage. Finally, the second part of the paper reports the results of tests aimed at measuring the power absorbed by the motion transmission systems from the flywheel to the organs of propulsion of two tractors and by the air conditioning system of a tractor.

Furthermore, the study of the performances of tractors under field conditions became the main subject of the research project "Methodologies and instrumentations for the measurement of the Performances of Tractors under Operative conditions – Integration of the tests indicated in the OECD Codes No. 2 and 5" (acronym: PTO – Mi.P.A.A.F., DM 2148 - 20/03/2009). The projects aims at developing a mobile test bench that, coupled to the tractor, is capable to simulate the action of operating machines, both passive (pulled machines as ploughs) and driven by the tractor PTO.

The system is based on hydraulic actuators generating the desired load condition on the tractor (force of traction and/or torque at the PTO, hydraulic power) controlled by electronic elements. A feedback system allows the application of work cycles based on the combination of data recorded during the test of real operating machines. Basing on such an approach it should be possible to develop a test methodology based on standard simulated work cycles that allow to test tractors under real conditions (in field or road, in plain or in hilly surfaces etc) and to reliably compare their performances. The project is in progress and in the following a description of the equipment already made will be provided.

Materials

Static tests

Equipment used for static test

The bench for the testing of tractors, made at the headquarters of CRA-ING (Monterotondo, Italy), is arranged in two separate rooms: the actual test room and the cockpit.

Inside the test room, there is an electro-magnetic dynamometric brake for testing, at the PTO, of tractors with maximum power of 300 kW.

Backward, the brake is connected by means of a driveshaft, to a three-phase asynchronous electric motor (Figure 1) with nominal power of 30 kW (at 1000 min^{-1}), controlled by an inverter, which allows adjustment of frequency and voltage in order to control the speed and torque, both positive and negative (the torque is measured by a load cell specially installed to lock the stator of the electric motor).

A system of 8W resistances (installed in series) has the function of dissipating as heat, the electric energy generated by the conversion of the kinetic energy of the rotor while it works in addition to the dynamometric brake. The electric motor was used in tests aimed to study of the absorption of power by the transmission and subsidiary systems.

On one side of the test bench, a box houses a weight fuel consumption measurer, suitably connected to the tractor feed (Figure 2). Changes in weight, referring to the time they have been detected, to measure the time consumption and therefore the introduction of fuel.

The cockpit houses the console for the control of the brake and the electric motor, and for monitoring test parameters and plant working parameters. All data (brake torque, torque electric motor and turns of both) are collected by a computer equipped with a PCI card for immediate processing.

Tractors used in static tests

The tests were conducted on a tractor with steel tracks (A) and on a wheeled tractor (B). Their main characteristics are summarized in Table 1.

Test of tractors under operative conditions

The realization of the mobile test bench mentioned in the point 2 is still in progress. It will be based on a vehicle (pulled by the tractor) modified according to Figure 3 that schematically shows the main interventions to be made on an old truck.

The test bench in his final version will be capable to apply to the tractors load conditions as force of traction, torque at the PTO and hydraulic power requests (and the combination of them), while travelling on any type of surface.

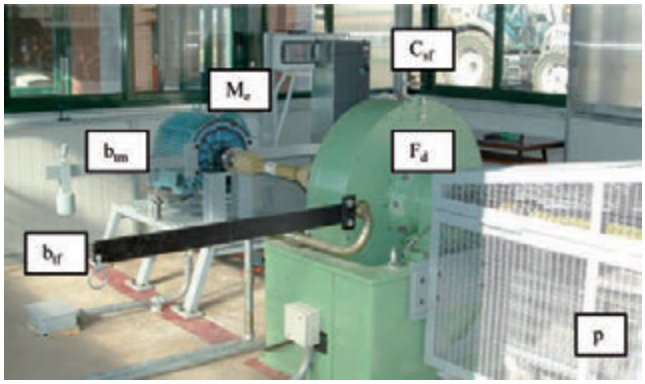

Figure 1. Test bench: F_d, dynamometric brake; M_e, three-phase electric motor connected to F_d by means of a cardan joint; C_{sf}, frequency static converter; B_{tf}, steel bars used for calibrating the load cell of the dynamometric brake; b_{tm}, steel bars used for calibrating the load cell of the electric motor; p, protection frame of the cardan joint between dynamometric brake and tractor power take off.

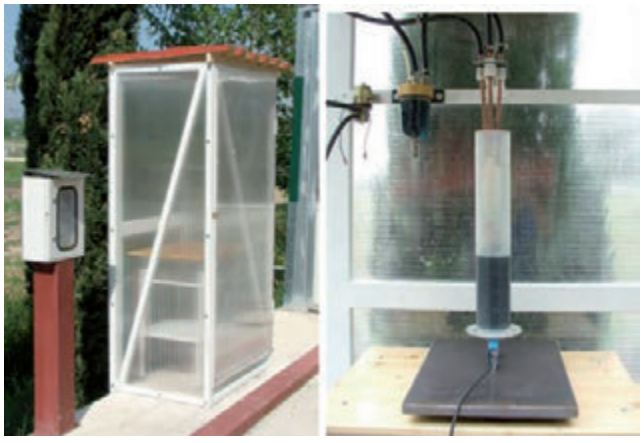

Figure 2. Left: box with the fuel consumption measurer. Right: weight fuel consumption measurer.

Methods

Static tests

The tractors were positioned at the dynamometric brake with wheels/tracks lifted from the ground. The power take off was connected to the brake by means of a drive shaft, as second drive shaft linked the brake and the electric motor, as described above. Before the tests, the actual transmission ratios between engine drive shaft, PTO, final transmission and peripheral speed of tires and tracks were recorded on both tractors (Table 2).

The tests were divided into three phases: 1) determination of the characteristic curves, at the PTO, of each tractor according to the OECD standard (using only the dynamometric brake, with and without transmission and air conditioning system working). 2) relief of the power requirements by the connection of pre-selected transmission gear ratios, by means of the combined action of the electric motor and the Brake, starting from the maximum power characteristic curve. 3) determination of the power absorbed by the air conditioning in the cab of the tractor B, by means of both brake and electric motor, always starting from the curve of maximum power.

Characteristic curves of the engines

All the test providing the engine characteristic curves were performed in accordance with the requirements of the OECD Code No. 2 for the tests at the PTO of tractors. The environmental parameters that can affect the results of the trials have been monitored, such as, for fuel consumption, the temperature of fuel, lubricating oil and air and the atmospheric pressure. This made it possible to standardize the data using correction functions officially recognized [1], which take into account the above parameters.

Table 1. Main characteristics of the tested tractors.

	Main characteristics	Tractor A	Tractor B
Engine	Cylinders (n) / displacement (cm^3)	4 / 4000	4 / 4000
	Nominal power (kW) / engine speed (min^{-1})	75/2500	84/2300
	Max power engine speed. (min^{-1})	2500	2300
	Maximum torque. Nm / engine speed (min^{-1})	355 /1400-1600	395 / 1400 / 1600
Transmission	Gear box	4 synchronized gears, 2 gear ranges with speed reducer	5 synchronized gears, 3 gear ranges with Power Shift speed reducer
	Rapports (n.)	16FW+ 16 Rev	20 AV+20 Rev
	Reversing idler	mechanic. synchronized	mechanic. synchronized
	Nominal speed - minimum / maximum ($m\,s^{-1}$)	0.17 / 3.05	0.14 / 11.11
	PTO clutch	multiple discs in oil bath	multiple discs in oil bath
	PTO speed gear adopted in the tests (min^{-1})	750 min^{-1} (at nominal speed)	540 Eco (743 min^{-1} at nominal speed)
	Max engine speed with PTO insertion (min^{-1})	2980	2512
	Max engine speed without PTO insertion (min^{-1})	2985	2518
	Transmission ratio engine drive shaft PTO	3.123	3.003

Table 2. Characteristics of the gear boxes of the two tractors with reference to the ratios adopted in the tests.

Tractor A					Tractor B				
reducer	gear range	gear	τ	vp * $m\,s^{-1}$	gear range	gear	Power-Shaft	τ	vp * $m\,s^{-1}$
Low speed (R)	Turtle	1	183.53	0.45	Low speed (R)	1	rated	360.51	0.55
		2	164.31	0.51			base	301.80	0.66
		3	127.15	0.66		3	rated	244.04	0.81
		4	92.36	0.90			base	170.19	1.17
	Hare	1	177.47	0.47		5	rated	129.09	1.54
		2	136.26	0.61			base	88.35	2.25
		3	106.60	0.78	Medium speed (M)	1	rated	203.67	0.98
		4	76.81	1.08			base	140.86	1.41
High speed (V)	Turtle	1	71.44	1.17		3	rated	114.16	1.74
		2	54.86	1.52			base	78.51	2.53
		3	42.49	1.96		5	rated	59.91	3.32
		4	31.01	2.69			base	40.67	4.89
	Hare	1	59.35	1.40	High speed (V)	1	rated	60.12	3.34
		2	45.82	1.82			base	47.12	4.22
		3	35.35	2.36		3	rated	39.03	5.09
		4	25.74	3.24			base	26.44	7.51
						5	rated	19.93	9.97
							base	13.64	14.57

* vp, peripheral velocity of wheels and steel tracks referred to the engine nominal speed of the two tested tractors.

Power absorbed by the transmission

Characteristic curves with clutched gear

Starting from the characteristic curves under conditions of maximum fuel delivery, the clutching of a specific gear box ratio determines a resistive torque that the engine must overcome to allow the rotation of transmission system and wheels or tracks. As a consequence, the power requirement increases depending on the rotational speed of wheels (or tracks) and a new balance working point will be reached on the engine speed-power diagram (and on engine speed-torque diagram as well). As previously mentioned, the tractors at the dynamometric brake were lifted from the ground in order to detect the characteristic curves of the motor without and with gear. Comparing them, the power absorbed by the transmission can be evaluated for each gearbox ratio, throughout the range of engine operation. This procedure was applied, on both tractors, for some gearbox ratios. The results were reported in diagrams.

Tests with the electric motor connected to the dynamometric brake

The coupling of the dynamometric brake with the electric motor allows rapid reproduction of single points of the characteristic curves corresponding to engine working conditions observed during field operations. For each point the system provides accurate measurement of the total power and of the power absorbed by the transmission. The test procedure is based on the following points:

1. adjustment, by means of the dynamometric brake, of engine speed, torque and power on values corresponding to desired operative conditions and acquisition of the data;
2. clutching of a gearbox ratio: this determines, on the engine speed-torque and speed-power diagrams, new points of equilibrium of the system, consisting on reduction of the speed and variation of torque and power measured by the data acquisition system connected to the brake;

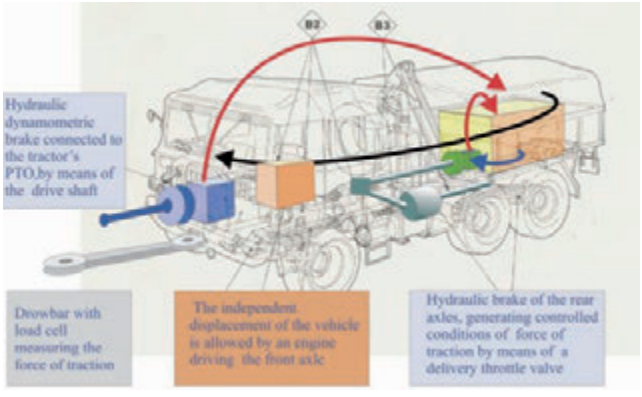

Figure 3. Vehicle to be modified in order to lodge equipments, instruments and control systems generating the simulate operative conditions derived from field tests with real operating machines.

3. restoration of initial conditions of point 1, by means of a positive torque provided by the electric motor, bringing the engine speed, torque and power to the initial values detected by acquisition system. The electric motor then provides a couple (measured by the load cell) and a power equal to that absorbed by the insertion of the specific gear box ratio;
4. disconnection of the gear-box and elimination of the positive torque of the electric motor, returning to the conditions set out in point 1 (without the help of the electric motor).

According to such a procedure, it is possible to move along the curve of power (it can be the curve of maximum power or can be obtained under condition of partial fuel introduction) and to observe further points of working in order to measure the power required by the insertion of different gear-box ratios and by auxiliary devices.

The power requirements by transmission were measured starting from the full admission curves of power of each tractor. After having identified a point of working near the maximum power, the power required at the insertion of different gear box rations were measured adopting the above described procedure.

Tests of tractors under operative conditions

The mobile test bench should allow to simulate the action of any operating machine coupled to the tractor. This is possible through adjustments and combination of the different types of solicitations applicable to the tractor during its travel. As to the origin of said solicitations, the workgroup involved in the project (CRA-ING - Agricultural Machinery Testing Center, certified by ACCREDIA as Lab. No. 1141 according the standard EN ISO/IEC 17025:2005), during more than 15 years, has been making tests on agricultural equipments, recording field test data on force of traction, p.t.o. torque, velocity, slip and other significant parameters, especially with regard to soil tillage machines and sowing machines. Such data series can be indefinitely reproduced by the feedback control system of the mobile test bench. Combining the data series of different operations, for time intervals representative of their real execution in farm, will allow to "build" artificial work cycles, applicable to the tractor under test, in a pre-defined test track with different conditions of surface, slope. The work cycles will be representative of the typical use of the tractors during the year, and will be calibrated on the type of machines and on their dimensions and power class. Similar tractors will undergo the same work cycle. The method will provide information on the real performances of the tractors and reliable comparative data among machines of the same category.

Results

Static tests

The diagrams of Figure 4 show, for each tractor, a series of curves, obtained at the dynamometric brake, which describe the behaviour of torque and power provided by the engine and the fuel consumption under three conditions of working.

It can be noticed the almost perfect overlap of the curves of consumption, which indicates that in all the tests, the engine globally provided the same power. As to power and the torque, each of them presents three different curves monitored by the system and depending on the different conditions of working: the higher curve refers to the performances of the sole engine, as the other two are related to new points of balance determined by the insertion of two gearbox ratios (the lower refers to the ratio corresponding to higher speed) that made the wheels turn. Each curve describes the torque and the power still available (at the p.t.o.) and measured by means of the dynamometric brake, after the insertion of a gearbox ratio. When the engine works in given operating conditions (of power, torque and fuel consumption) the insertion of gearbox ratio represents an additional resistant load. As a conse-

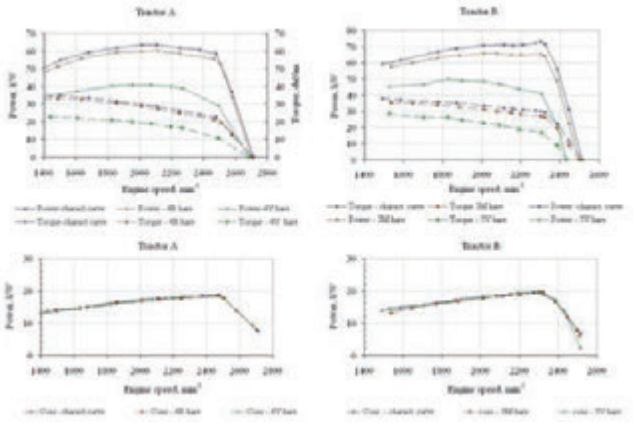

Figure 4. Engine characteristic curves under maximum fuel supply conditions. Each diagram shows the curves referred to only-engine working conditions and to the clutching of two different gears.

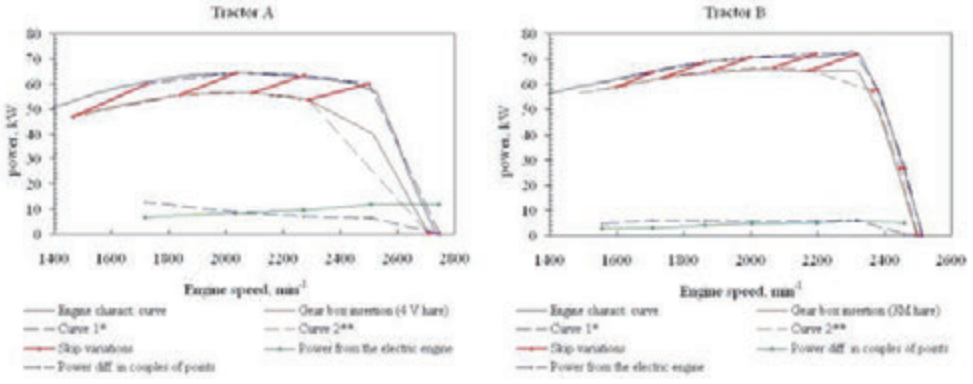

Figure 5. Tests with the electric motor.

quence, the engine-brake system looks for a new point of balance, skipping from a curve of couple (and power) to another, with an engine speed change, at the same time, with reference to the starting value.

In the engine-brake system, such an additional resistant load (and the relative power), needed for operating any service at a certain engine speed, can be measured by means of the system based on the electric motor (2.1) used as an active system for restoring the operating conditions prior to the insertion of the gear, without disconnecting it. By applying the procedure described in 3.1.2.2, it was possible to make direct measurements of the torque applied by the electric motor and of its rotation speed, allowing to calculate the power required by the transmission, for the gear box ratio adopted. The test started from the characteristic curves at maximum fuel introduction, according to the OECD Code n. 2. The results of these tests are reported in the diagrams of Figure 5 referred to the two tested tractors.

Each diagram shows two characteristic curves described by continuous lines: the blue line is the characteristic of the sole engine; the dark red line is the curve obtained after the insertion of a gear box ratio. Moreover, several couples of points are visible, each couple joined by a red straight line segment. The segments describe the variation of the engine working conditions (speed and power) as a consequence of the insertion of a gear box ratio (the above mentioned skipping from a curve to another). As expected, for each couple of points, one point lays on a curve (blue dashed line) overlapping the characteristic curve without gear box insertion (continuous blue line), as the other point lays on a lower curve (dark red dashed line) that coincides with the characteristic curve obtained with gear box insertion (continuous blue line).

For each couple of points, the electric motor was used to restore the initial engine speed, torque and power conditions (upper curve, as detected by the brake measuring system), The torque required by the operation was measured and multiplied by the rotation speed, directly provided the power absorbed by the gear box. Its behaviour is described by the bottom green continuous line that connects the detected points and decreases for engine speed decreases.

Finally, the bottom blue dashed line shows the behaviour of the power differences calculated in each couple of points. In describes what occurs when a gear box ratio is inserted and allows to assess the power actually available for the work. In this case it increases at engine speed decreasing.

The diagrams of Figure 6 show the results of the measurements of the gear box power requirements as a function of the peripheral velocity of tracks/wheels. For tractor A, the power increases rather constantly with the speed and a single regression curve is capable to accurately describe the behaviour. For tractor B, the behaviour I more complex because of the overlaying of the speed values of different gear ranges. For this reason, the regression curves referred to the different gear ranges are reported nearby the regression curve of all points, summarizing the average variation of power *vs.* peripheral velocity.

Further information can be achieved from the data of the power required by the transmission. Considering them as function of the engine speed at which they were observed and reporting them in the diagrams of the characteristic curves of power, provided the diagrams of Figure 7, where green coloured areas are visible, representing the power available from the engine after the insertion of the gear box ratios: of course, it decreases with engine speed, as a consequence of the greater absorption due to higher velocities. For each value of the engine speed into the interval of the green area, the available power can be calculated as the difference between the regression functions reported in the diagrams with reference to the section of the curves interested.

Finally, the Figure 8 shows the comparison between the characteristic curves of power and torque drawn, for the tractor B, with and without operating the air conditioning system in the cab. A difference of about 2 kW is clearly visible along the whole engine working range.

Tests under operative conditions

At present time, the stage of development of the mobile test bench includes the realization of the active system for the control of the p.t.o. power requirements, shown in Figure 9 and provisionally installed on a trailer. It is complete with sensors, data acquisition system and feedback control system.

First tests were made using the data series recorded during the work

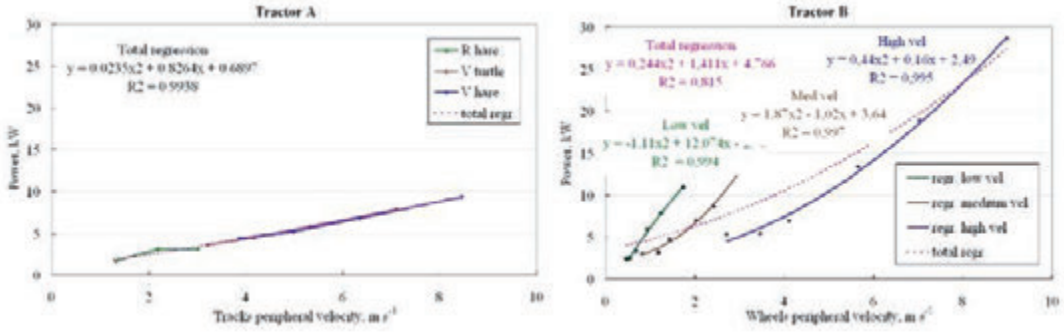

Figure 6. Power absorbed by the transmission as a

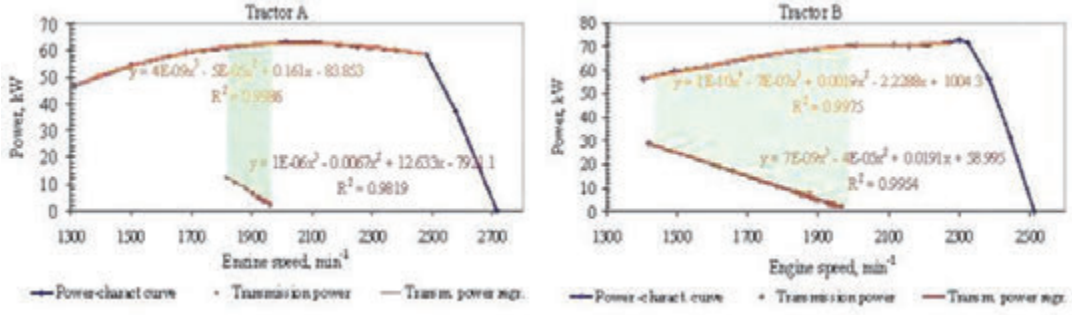

Figure 7. Power absorbed by the transmission and characteristic curves of power. The coloured areas represent the power availability cleared of the transmission requirements.

executed by a medium dimension rotary harrow. The mobile test bench was coupled to the power take off of a 59 kW tractor and its control system appeared capable of correctly adjusting the values of torque, following the behaviour and the variation recorded in the field test. The development activity is going on and, at the moment, concerns the control system of the force of traction. At the same time the study is proceeding aimed at defining work cycles representative of the operational reality.

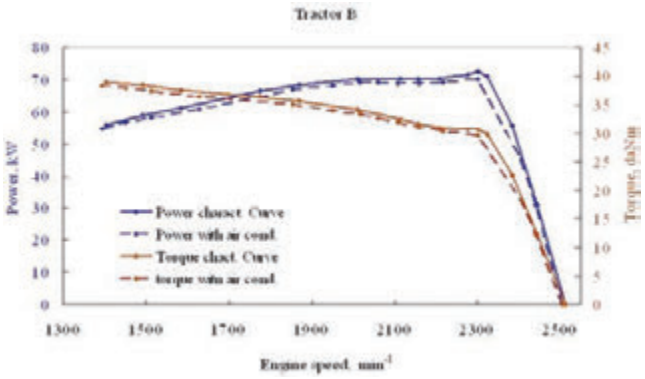

Figure 8. Power absorbed by the air conditioning system in the cab of the tractor B.

Figure 9. Mobile test bench for testing tractor power take off performances in field. It is the first step in the realization of the equipment subject of the p.t.o. project. It consists of a hydraulic dynamometric brake in which a throttle valve is electronically controlled (in feedback) with the purpose of applying the desired condition of torque (and power) measured by means of a torque meter.

Conclusions

The capability to ascertain the actual performances of a farm tractor can be increased by deepening the analysis of the functions the tractor is required to provide. Such analyses need the development of suitable methods and of the equipments for their application.

The integration between the new information and the more established methods, such as those indicated by the OECD codes, can provide a comprehensive picture of the characteristics of the tested machines, creating an instrument for guidance in the choice of operators.

The proposed insights concern both tractor tests at a fixed point and under operative condition aimed at investigating the power required by the different services such as transmission, hydraulic system, air conditioning system.

The described equipment for static tests based on the integration of a dynamometric brake and an electric motor has proven to be capable to quickly provide detailed information on the power required by mechanic transmission, as a function of the travel speed, allowing to assess the actual power available for further operations different from the displacement, depending on the initial conditions of engine operation. Further studies will determine whether the proposed system can be used with transmissions of more recent introduction (eg, those with continuous variable speed) and to define a methodology that codifies the procedures and test.

As to the tractor tests under operative conditions, the proposed test bench, still under development, will represent an additional tool capable of providing new elements for the evaluation of tractors, completing the picture resulting from the tests required by the OECD code.

References

Al-Suhaibani S.A., Al-Janobi A. A., Al-Majhadi Y. N. 2010. Development and evaluation of tractors and tillage implements instrumentation system. Am. J. of Eng. and Appl. Sci. 3 (2): 363-371.

Bodria L., Pellizzi G., Piccarolo P. 2006. Meccanica agraria Volume I – Il trattore e le macchine operatrici. Edagricole, Bologna, Italia, pp 32-56.

Casini Ropa G. 1975. A testing vehicle for checking the performance of the tractor drawbar. J. Agr. Eng. 2: 87-96.

O.E.C.D., 2012. OECD standard code for the official testing of agricultural and forestry tractor performance, Code 2, Paris Cedex, France.

Fanigliulo R., Pochi D., Volpi C., Santoro G. 2004. A mobile system to evaluate the performances of agricultural machinery under field conditions. J. Agr. Eng. 4: 89-95.

Gasparetto E., Trolli C., Viola L. 1985. Sono utili per le trattrici agricole le prove di trazione su pista?. L'Informatore Agrario 2: 43-49.

Marsili A., Servadio P. 2001. Prova in campo – Fendt 716 Vario. Macchine e Motori Agricoli 3: 34-37.

Pochi D., Ragni L., Santoro G. 1996. A mobile laboratory for the analysis of the tractor-implement-soil interactions. Third part: comparison between methodologies to evaluate the power adsorbed by implements. J. Agr. Eng. 27 (4): 193-197.

Effect of different winter pruning systems on grapes produced

Claudio Caprara,[1] Fabio Pezzi[2]

[1]Department of Agricultural Sciences, University of Bologna, Italy; [2]Department of Agrifood Sciences and Technologies, University of Bologna, Italy

Abstract

The purpose of these trials was to evaluate possible effects on properties of grapes, particularly the physical and mechanical features, depending on the winter pruning system. The following pruning techniques were carried out: manual pruning (m); mechanical pruning (M); mechanical pre-pruning and subsequent manual finishing (Mm); mechanical pre-pruning and contemporary fast manual finishing, using a wagon facility with two operators equipped with pneumatic scissors (Mw). The trials were carried out on Sangiovese trained to spurred cordon. During the trials were measured: time and cost of pruning, quality of pruning and the vegetative-productive response of vines. During grape harvesting a consolidated analytical method of texture analysis was applied to evaluate the physical parameters of grapevine cultivar: pedicel detachment, skin perforation, skin thickness, grape features as hardness, cohesiveness, springiness. Analysis of working time showed that the manual pruning (m) determined a greater commitment of time, while the mechanized pruning (M) presented a time reduction of 95%. The two mechanized pruning associated with manual finishing reduced the time of 21% (Mm) and 69% (Mw). The lowering cost is less evident but important anyway. Regarding the quality of pruning, the increase in the level of mechanization has produced an increase of spurs and buds density. It was also detected a higher percentage of damaged spurs and in wrong position. The increasing of mechanization levels of pruning also has produced smaller and sparser bunches with smaller berries. The study of mechanical properties of berries showed significant differences in the mechanical behaviours of the different pruning tests. The mechanized pruning presented higher values for the pedicel detachment, skin perforation and cohesiveness, while it gave lower values for thickness of skin and springiness. The results showed that mechanical pruning can modify properties of the berries which influence mechanical harvesting on vineyard.

Correspondence: Claudio Caprara, Department of Agricultural Sciences, University of Bologna, Via G. Fanin 48, 40127 Bologna, Italy.
Tel. +39.051.2096192.
E-mail: claudio.caprara@unibo.it

Keywords: mechanical pruning, vineyard, grape mechanical properties.

Contributions: the authors contributed equally.

Conflict of interests: the authors declare no potential conflict of interests.

Journal of Agricultural Engineering 2013; XLIV(s1):e85
doi:10.4081/jae.2013.(s1):e85

Introduction

Winter pruning of the vineyard is one of the most important cultural practices for its physiological and productive influence on plants. In Italy the manual pruning is still prevalent and appreciated for quality of work, when performed by experienced operators.

In recent years, the difficulty to have skilled labor and the overall growth of production costs have increased the interest towards the mechanical pruning. After about forty years of experimentation in Italy (Baldini and Intrieri, 1984; Gubiani *et al.*, 1994; Intrieri and Poni, 1995; Brancadoro *et al.*, 1997; Intrieri *et al.*, 1999; Poni *et al.*, 2004), the approach is still partial and mechanical pruning is done mostly as an operation that includes a final manual trimming. Against clear economic advantages (Pergher and Gubiani, 1995; Brancadoro and Marmugi, 1997; Pezzi and Bordini 2006), the main concerns that limit the mechanical pruning are the vegetative and productive behavior of plants, especially their capacity of spurs renewing and control of buds number. Other problems may involve the plant health area for the greater probability of wood disease attributable to drying up of shoots aged or damaged by the machines.

To provide further information to winegrowers, an experimentation was begun a decade ago that aims to evaluate the agronomical, economical and operational aspects of pruning mechanization (Pezzi and Bordini, 2006). In the last year the study also wanted to test the possible influences that the mechanical pruning can have on physical and mechanical characteristics of the grapes (Pezzi *et al.*, 2012), because these factors could affect the mechanization of other operations, in particular the harvesting.

The aim of this research was to evaluate the effects of mechanical pruning on Sangiovese, one of the most diffused vines in Italy where mechanization is increasing.

Materials and Methods

The trial of mechanical pruning is in progress at the experimental farm "Terre Naldi" in Faenza (Italy) which collaborates with the University of Bologna. In this farm some grape varieties, grown with different forms of training systems, are pruned with different levels of mechanization to evaluate the performance and cost of pruning techniques, the quality of work and plant behavior.

The trials were carried out on Sangiovese vines grown on medium

fertility flat land. The vineyard was trained to spurred cordon, with a plant distance of 1.1 m by 2.5 m.

The considered tests for winter pruning were:

(m) - manual pruning, done by operators who proceeded walking and used manual scissors. The work plan provided 7 spurs plant^{-1} with 2 buds.

(Mm) - mechanical pruning and subsequent manual finishing. The work plan included a cut of the spurs by the mechanical pruner to 2 buds and a subsequent manual thinning of the spurs done by operators who proceeded walking and used manual scissors.

(Mw) - mechanical pruning and contemporary manual finishing, performed with pneumatic shears by two operators placed on a wagon trailed by the tractor carrying the mechanical pruner. The work plan included a cut of the spurs by the mechanical pruner to 1-2 buds and a quick manual thinning of the spurs, less accurate than tests m and Mm.

(M) - mechanical pruning done only with the machine. The work plan included a cut of the spurs by the mechanical pruner to 1-2 buds.

The mechanical pruner was the "Trimmer" model by Tanesini Technology Company with a swinging cutter bar and a tool for vine-branch detachment. In the test the mechanical pruner has been set up raw straddling with three blades, to cut the cordon above and laterally in one step. The blade for horizontal cutting was mobile with spring return to overcome the poles. The machine has been carried anteriorly by a 59 kW four-wheel drive tractor. The wagon used had perimetral railings, systems for adjusting the height and the lateral displacement and a compressor for the supply of compressed air.

In each test we measured the work time, the result of pruning, and yield response. From the work time and the parameters listed in Table 1 it has been possible to make a hypothesis of cost (ASAE, 2011).

At harvest, the grapes were subjected to laboratory measurements with Texture Analyser (TA-HDi model by Stable Micro Systems, UK) to measure detachment of pedicel, break and thickness of skin (Figure 1) (ASAE, 1997; Stable Micro Systems, 2005). The Texture Profile Analysis (TPA) was also carried out obtaining several parameters including hardness, cohesiveness and springiness (Bourne, 2002; Rolle *et al.*, 2011; Pezzi *et al.*, 2012). Each test was carried out on 50 samples.

Results

The desired accuracy with manual pruning (m) and the need to manually remove the vine-branches from the wires has limited the forward speed of operators (Table 2) who worked with a frequency of 30 cut min^{-1}.

In the mechanical pruning (M) the machine was used with a forward speed of only 1080 m h^{-1} to maintain high precision of height cutting.

In Mm test the machine forward speed was the same of M test. After the machine passage, the operators manually cut only spurs in excess advancing with speed almost double compared to that of m test, keeping a cut frequency of 39 cut min^{-1}.

In Mw test the forward speed was reduced to 580 m h^{-1} to allow an acceptable manual finishing. The cut frequency in this test was 50 and 35 cut min^{-1} respectively for the first and the second operator.

Consequently the unit effective working times were very different (Figure 2). Compared to m test the mechanical pruning (M) reduced of 95% required time. Mechanical pruning and subsequent manual finishing (Mm) allowed a reduction of 47% of working time, while mechani-

Table 1. Elements used for the economic evaluation.

Economic parameters	Values
Market price (€) - MP	
- mechanical pruner	9.500
- wagon	3.500
Residual value - RV	10% MP
Machine life - N	2.000 h
Vineyard area	10 ha
Max years of use - n	10
Fixed costs (€ year^{-1}):	
- amortisation	(MP-RV)/n
- interests	5% (MP+RV)/2
- other costs	3% MP
Variable costs (€ h^{-1})	
- repairs	60% MP/N
- maintenance	10% working time
- tractor with operator	35
- labor	12

Table 2. Results at harvest.

Tests	Forward speed		Number of operator (n)	Operator's cut frequency (cut min^{-1})
	Machine (m h^{-1})	Labour (m h^{-1})		
m	-	48.6	1	30
Mm	1080	100.8	1	39
Mw	576	576.0	2	50 - 37
M	1080	-	-	-

Table 3. Results of pruning tests.

Tests	Buds	Spurs						
	(n plant^{-1})	total (n plant-1)	1 bud (%)	2 buds (%)	3 buds (%)	>3 buds (%)	damaged (%)	well positioned (%)
m	15.29 a[1]	7.33 a	22.85 ab	49.37 ab	26.85 a	0.93 a	0 a	89.32 c
Mm	20.33 ab	10.17 b	19.70 a	59.47 b	19.23 a	1.60 a	2.95 b	79.14 b
Mw	24.42 b	14.17 c	46.36 c	38.69 a	12.78 a	2.17 a	1.74 ab	65.64 a
M	35.46 c	17.58 d	34.08 bc	44.84 a	15.55 a	6.53 b	4.11 b	64.63 a

[1]values followed by different letters within the same column differ statistically for P≤0.05.

cal pruning and contemporary manual finishing (Mw) allowed a reduction of 75%.

Compared to m test, the unit costs calculated on 10 ha vineyard showed a clear advantage for M test, with a saving of 71% equivalent to 703 € ha^{-1} (Figure 2). The cost reduction for tests Mm and Mw was less important, respectively of 23% and 35%.

The vineyard minimum sizes for economical purchase of the machine are of 3.9 ha for Mm method, 4.0 ha for Mw and 1.7 ha for M.

With regard to the result of pruning the four tests have been characterized by a different density of spurs and buds with values increasing with the mechanization level. The statistical analysis showed significant differences among the tests (Table 3). With regard to the distribution of buds on each spur, it was observed that m and Mm tests have a wider presence of spurs with 2 buds, while M and Mw tests have a prevalence of spurs with 1 or 2 buds.

Using a low forward speed of machine, the presence of damaged spurs was low, with higher value for M test (4%). The manual finishing after mechanical pruning (Mm and Mw tests) reduced the damaged spurs. With manual pruning (m) the spurs were well positioned on the upper side of the permanent cordon (89%), while using only mechanical pruning (M) the well positioned spurs were lower (65%). The result was intermediate in Mm and Mw tests, where operators have improved the selection.

The greater presence of buds left by mechanical pruning did not affect the yield and its quality characteristics (Table 4). The production was instead different in bunch and berry sizes, with a weight reduction in more mechanized interventions (M and Mw).

Mechanical pruning has also affected the physical and mechanical features of grapes (Table 5). The two prunings more mechanized (M and Mw) have increased the energy required for the pedicel detachment from berry. They also have influenced resistance and thickness of skin.

The results obtained using the Texture Profile Analyzer were quite interesting: the mechanical pruning test (M) was marked by lower values of cohesiveness and higher values of springiness and hardness (Table 6).

Figure 1. Texture analyzer used.

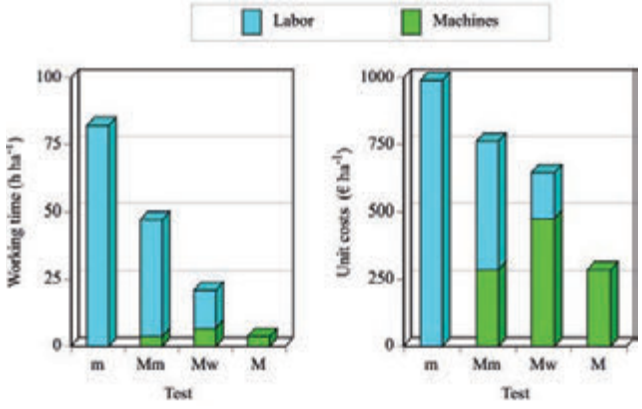

Figure 2. Working time and unit costs of the four pruning tests.

Table 4. Results at harvest.

Tests	Yield (t ha^{-1})	Weight of bunches (g)	Weight of berries (g)	°brix	Acidity (g L^{-1})	pH
m	25.21 a[1]	231 b	2.50 bc	19.0 a	7.53 a	3.19 a
Mm	24.85 a	244 b	2.63 c	18.5 a	7.93 a	3.16 a
Mw	23.15 a	229 ab	2.40 ab	18.4 a	7.93 a	3.17 a
M	25.33 a	215 a	2.31 a	18.6 a	7.33 a	3.18 a

[1]values followed by different letters within the same column differ statistically for P≤0.05.

Table 5. Mechanical parameters measured on berries.

Tests	Detachment of pedicel		Break of skin	Thickness of skin	
	Force (N)	Energy (mJ)	Force (N)	Energy (mJ)	(mm)
m	5.41 a[1]	18.81 a	4.62 a	13.26 ab	0.237 b
Mm	5.43 a	19.70 a	4.53 a	13.06 a	0.219 ab
Mw	5.53 a	21.78 ab	5.00 b	14.71 c	0.210 a
M	5.78 a	24.83 b	4.92 b	14.26 bc	0.210 a

[1]values followed by different letters within the same column differ statistically for P≤0.05.

Table 6. Texture Profile analyzer parameters.

Tests	Hardness	Cohesiveness	Springiness
	(N)		
m	4.73 b[1]	0.451 b	0.185 a
Mm	4.63 ab	0.446 ab	0.184 a
Mw	4.51 a	0.450 b	0.187 a
M	4.92 c	0.443 a	0.197 b

[1]values followed by different letters within the same column differ statistically for P≤0.05.

Conclusions

The evaluation of different levels of mechanization in the winter pruning of the Sangiovese grapes has provided some useful information to winegrowers for the choice of technique to use.

The operational and economical aspects repeated generally those already in evidence from other experiences and they gave very favorable indications to the total or partial application of mechanical pruning.

Mechanical pruning performed carefully by the tractor driver has allowed an acceptable quality of intervention by size, positioning and integrity of the spurs. The possibility of completing mechanical pruning with a more or less careful manual finishing can improve the result by removing part of the less suitable spurs and reducing the number of buds.

The adaptability of plants to the higher number of buds left by mechanical pruning appears positive with a reduction in the size of bunches and berries. The modification of the berries has also affected their mechanical properties which may be important, especially in view of a mechanical harvesting.

Some modifications of these properties, such as increased resistance to detachment of the pedicel, appear to hinder the work of grape harvesters, while others such as springiness and resistance to breakage of the skin, can be beneficial to better protect the integrity of the berries and thus better preserve the quality of the grapes harvested by machine.

References

ASAE, 1997. ASAE Standard S368.2: Compression test of food materials of convex shape. ASAE, St. Joseph, MI.

ASAE Standards 2011. EP497.7. Agricultural Machinery Management. St. Joseph, Mich., USA.

Baldini, E. and Intrieri, C. 1984. Meccanizzazione della vendemmia e della potatura. Ed. CLUEB, Bologna, Italy.

Bourne, M. C. 2002. Food texture and viscosity: concept and measurement. 2nd Ed., Academic Press, New York, USA.

Brancadoro, L., Maccarone, G. and Scienza, A. 1997. Potatura invernale della vite: risultati vegeto-produttivi. L'Informatore Agrario. 48:59-62.

Brancadoro, L. and Marmugi, M. 1997. Rapporto tra i sistemi di potatura invernale e tempi di lavoro nella vite. L'Informatore Agrario. 23:71-74.

Gubiani, R., Pergher, G. and Gasparinetti, P. 1994. La potatura meccanica della vite nell'ambito della meccanizzazione integrale. L'Informatore Agrario. 44:27-34.

Intrieri, C. and Poni, S. 1995. Integrated evolution of trellis training systems and machines to improve grape quality and vintage quality of mechanized italian vineyards. Am. J. Enol. Vitic. 46(1):116-126.

Intrieri, C., Silvestroni, O., Filippetti, I., Lia, G., Borghesi, L. and Colucci, E. 1999. Comportamento operativo e funzionale di "Trinova II" e di "Trinova II-Prunner" in prove di vendemmia e di potatura su "cordone libero mobilizzato. Frutticoltura. 9:89-97.

Pergher, G. and Gubiani, R. 1995. Analisi dei tempi di lavoro nella potatura del vigneto. m&ma. 7/8:49-53.

Pezzi, F. and Bordini, F. 2006. La potatura meccanica nel vigneto: aspetti tecnici, qualitativi ed economici di differenti livelli di meccanizzazione. Rivista di Ingegneria Agraria. 1:57-65.

Pezzi, F., Balducci, G., Barca, F. and Caprara, C. 2013. Effects of Winter Pruning on Physical and Mechanical Properties of Grapes. Proc. 1st IW on Vineyard and Mechanization & Grape & Wine Quality, Ed.: S. Poni, Acta Hort. 978, ISHS 2013: 347-352.

Poni, S., Bernizzoni, F., Presutto, P. and Rebucci, B. 2004. Performance of Croatina under Short-Cane Mechanical Hedging: A Successful Case of Adaptation. Am. J. Enol. Vitic. 55(4):379-388.

Rolle, L., Giacosa, S., Gerbi, V. and Novello V. 2011. Comparative Study of Texture Properties, Color Characteristics, and Chemical Composition of Ten White Table-Grape Varieties. Am. J. Enol. Vitic. March 62:49-56.

Stable Micro Systems, Texture Analyzer User Guide, UK , 2005.

The cross-border project between France and Italy MARS+. Sub-project - *Innovative technologies for the mechanization of the areas hard to reach*

G. Tirrò, R. Lisci, M. Rimediotti, D. Sarri, M. Vieri

Department of Agricultural, Food Production and Forest Management University of Florence, Firenze, Italy

Abstract

The care and protection of the mountain areas and their traditional crops were some of the reasons that led regional governments of Liguria and Tuscany to participate in the strategic project "Sea, Countryside and Land: potentiate the strategic unitarily" (MARS +). This project has also involved the participation of the four cross-border regions: Tuscany (leader), Sardinia, Liguria and Corsica. The aim was to promote the development of the innovations and entrepreneurship in the rural areas in order to increase competitiveness. In particular, the subproject SC has provided the transfer of innovations to facilitate the processes of mechanization in vineyards and olive orchards in contexts defined as "heroic", areas of high landscape and environmental value in which the typical cultures has been always carried out, generally, on terraces or slopes. These conditions require a great effort by the farmers and result in high production costs. The transfer of the innovations has provided the organization of demonstration days in which the technological solutions for the management of the farming operations in vineyards and olive orchards were proposed and tested. During these events, the participative process was fundamentally reconfirmed, not only as a means to expand the knowledge of innovative products, but also as an opportunity for farmers, retailers, manufacturers, researchers, and local administrators to interact and facilitate the development of other technologies. The parameters that led to the innovative solutions included: the small size, user-friendliness, agility, and the ability of operating on systems not easily accessible. These products must also ensure the ergonomics and safety of workers performing all the growing operations. A thorough research of the available technologies and prototypes, still under development, affirms the presence of many innovations. These innovations not only allow the execution of all the field operations in the vineyard and olive orchards and significant time and cost reduction but also ensure the performance in complete safety. This research has shown the constant development of these products and how the use of electronics and mechatronics is becoming more prevalent.

Correspondence: Gaetano Tirrò, GESAAF Department of Agricultural, Food Production and Forest Management, Scuola di Agraria, University of Florence, Piazzale delle Cascine 15, 50144 Firenze, Italy
Tel. +39.055.3288260 - Fax +39.055.331794.
E-mail: gaetano.tirro@unifi.it

Key words: conservative agriculture, steep slopes, innovations, Mars+.

Contributions: the authors contributed equally.

Conflict of interests: the authors declare no potential conflict of interests.

Funding: the work was supported by the Europen Comunity.

Conference presentation: work never presented.

Dedication: none.

Journal of Agricultural Engineering 2013; XLIV(s1):e86
doi:10.4081/jae.2013.(s1):e86

Introduction

In the month of May 2013 is ended the Cross-Border Project MARS PLUS, where the Division of Agricultural Mechanics, University of Florence was directly responsible for the specific subproject the introduction and testing of innovative technologies for growing grapes and olives grown into steep slopes. This Unit has studied, until the 50s, the problem of mechanization in hilly areas and in the 90s made the first Italian project (Project Candia) on the mechanization of "heroic" viticulture, with the preparation of an experimental plans connected , where it is possible to have a mechanization through the use of innovative mini track drive characterized by size, agility and safety typical of minidumpers.

The Region of Tuscany, under the Programme for cross-border cooperation between Italy and France "Maritime" 2007-2013, has been the leader of the strategic project "Mars + - Sea, Countryside and Land: Increasing unified strategy", which has been also attended by Regions Liguria, Sardinia and Corsica.

The strategic project has intervened on the management of the land and its agricultural food production, and on the development of these productions and multi-functionality of the agricultural and fisheries.

Overall, the project was divided into 6 sub-projects and a system action. The sub-SC was divided into a set of actions aimed at the introduction of innovations and achievements of pilot projects in the field of "difficult" contexts agricultural and rural border area.

In particular, the ACTION 3.1 of the subproject SC has provided for the transfer of innovation for the facilitation of the processes of mechanization and management of herbaceous cover soil on the areas under grape and olive-growing in difficult positions (areal heroic) and terraced, Tuscany (Lunigiana, Island of Elba and Giglio Island) and Liguria (Cinque Terre, Levanto, Sestri Levante, Genoa hinterland,

Arroscia and Intemelia) with the involvement of local institutions and associations.

The specific objectives of the subproject were:

- Helping to avoid the abandonment of the area, promote the recovery of cultivated areas, even in a sustainable way, to ensure the conservation and the protection of the landscape and the environment as a whole and promoting the preservation of local natural and genetic resources;
- Implement the promotion and diffusion measures of technological innovation, scientific and service in the productive chains that characterize our rural areas - Contribute to the achievement of sustainable production models both from an environmental and economic / social.

The demonstration days

Within the project MARS + Liguria and Tuscany, the Operational Unit in Agricultural Mechanics, University of Florence, have realized sixteen demonstration days addressed to professionals, technical and agricultural operators for the presentation and demonstration of technological innovations for the facilitation of the processes of mechanization of farming operations in vineyards and olive-growing, situated in difficult and terraced areas as the provinces of Genoa, Savona, Imperia, La Spezia, Massa Carrara, Livorno and Grosseto.

The demo day is an occasion in which farmers have the opportunity to take vision of the innovations on the market, to see how they work and to try them in person. The sharing of proposals, criticisms and relative valuations has led manufacturers to improve further their machines, farmers to adapt cultivation techniques and practices of use, researchers and administrators to calibrate their intervention actions. In fact, during the demonstration days, manufacturers often presenting new products based on the development of existing ones.

All areas involved in the project are in the nature of heroic viticulture and olive growing, steep slopes, the presence of narrow terraces, small owners, very high risk of dropping out.

The demonstration days involved all the operations carried out in the vineyards and in the olive orchards as: pruning, canopy and soil management, pest management, harvest and waste management.

Before the execution of each demonstration day was made a careful study of the characteristics of the site in order to contact only the appropriate companies.

The careful search has given the opportunity to contact and involve a large number of companies, both Italians and foreign, which produce innovative technologies that are well suited to work in the typical conditions of heroic agriculture. Among the factors that were considered for the choice of products, safety, ergonomics and comfort are those taken into greater consideration. The development of new technologies has allowed, in fact, to ensure that it is possible to perform the collection and the harvest and the pruning of olive trees without the use of the stairs. Furthermore has been researched all the innovations that permit to control and reduce the use of chemical substances, in accord to the European Directive on the sustainable use of pesticides requires new management strategies of pest management, which provide an optimization of the treatments on the vegetation and the reduction of environmental release.

Results

The research of the companies producing innovative technologies showed a constantly evolving sector, ready to receive any suggestions likely to improve what is already in production.

Currently available on the market there are different types of products that allow you to perform mechanically and safely all farming operations, both in the olive groves and in the vineyards, situated in areas where accessibility is limited.

Over the years the introduction of innovative products has affected all aspects of viticulture and olive cultivation: handling, soil management, canopy management, the plant protection, harvesting.

The sector that has seen major innovations is the one of minidumper. The first minidumper presented in the '90s (Avidor, Collar, Chappot) (Vieri *et al*., 1997) have been constantly evolved and all construction companies have been trying to meet the needs of farmers each time proposing ever more performing products .

There are different types of products on the market, but they all have in common the small sizes (also 65 cm wide), easy of driving, extreme stability even at steep slopes.

It is possible to make a first distinction according to the driving position: on the ground, or on the vehicle (Figures 1 and 2).

Usually all these vehicles are equipped with rubber tracks in order to avoid excessive soil compaction, increased grip, allow the lower center of gravity, reducing the turning radius and make possible maneuvering in tight spaces, typical of mountain and terraced environments, allowing the movement in land not practicable by wheeled vehicles.

Another common feature of most of this vehicles is the presence of a dumper. Its tipping could be either manual or hydraulic (Figure 1), on the front and in certain cases also lateral. There are also dumpers with extensible side according to the specific requirements (Figure 3).

The versatility makes these machines necessary in a farm. All vehicles are equipped with a hydraulic pump which allows, for example, the connection to the atomizer (Figure 4).

The presence of the power takeoff (PTO), in front or rear position, makes possible the management of soil and pruning residues through the connections with small shredder or cultivators. (Figures 5 and 6).

Canopy management (grapevine)

The grapevine canopy management consists of many operations that take a long time if they are carried out manually. The main innovations consist of all those machines which, when applied to minidumpers, enable the carrying out of the binding, pre-pruning and leaf removal. The operation of such equipment takes place through the connection to the hydraulic circuit. (Figures 7-10)

Pruning (grapevine/olive)

In this sector the innovations include the introduction of scissors (Figure 11) and saws (Figures 12 and 13) applied to the telescopic rods that allow cutting up to 5 meters in height. These products allow, therefore, the performance of this operation without the use of ladders, reducing the operating time and, especially, ensuring the total safety of the farmer. Another innovation is the development of special blades, that don't lose the sharpness and ensure a clean cut in few shots. These innovations permit not only to spend less time, but reduce the operator fatigue.

The introduction of technologies that facilitate this operation allows a considerable reduction of operating times, of the efforts needed to make the cut, avoiding the use of ladders. These goals have been achieved thanks to the scissors, electronic and pneumatic loppers, with

Figure 1. Grillo – mini crawler dumper- 406. The compact size (161×71×110 mm) permit to work in narrow space. The driving position is on the ground, it is provided with the automatic parking brake. Manual tipping.

Figure 2. Hinowa – Mini crawler tractor D.O.C. Track 37.100. Equipped with brushwood shredder, pneumatic tipping dumper, prepared to use the atomizer.

Figure 3. Sabre Italia – Mini crawler dumper – Bp 30. Dump with expandable sides- Dimension: Length 75 cm (90) - Width 53 cm (83) - Height 21 cm.

Figure 4. Ro.Da.G – Mini crawler tractor – HT 200 – The tank contains 25l, max flow rate 24l/m.

Figure 5. Fratelli Camisa - TP 480H Crawler tractor with guidance from the ground and power takeoff.

Figure 6. Hinowa – HS 1200 Compact track tractor with guidance on the footboard. The most important characteristics are the roadway with variable pitch from 76 to 106cm and the electric and hydraulic arrangement for mounting various agricultural kit.

Figure 7. Clemens - Pre-pruner vario. The pre-pruner is designed to adapt to the working conditions of each vineyard. Each cutting head is driven through its own hydraulic circuit.

Figure 8. Clemens - EL 30 - Leaf remover - Due to the weight and reduced dimensions, it is possible to use even in tight rows, and can also be worn by a mini-track tractor. The vine leaves are drawn in between a rubber roller and a perforated drum by a suction fan, removed from the vine and ejected from the machine. Thanks to a parallelogram joint, the leaf remover glides gently over the grape area.

Figure 9. Clemens – Leaf cutter - Thanks to special manufacturing techniques, the aluminium blade holder of the leaf cutter is itself very strong and yet very light. This increases its stability and makes it possible to work on steep slopes and gradients. The sickle-shaped cutting tools made from tempered knife steel produce a clean cut. The large upper blade is surrounded by a guard that prevents the driver from being exposed to the cuttings. Thanks to special drive belts, the device is very low maintenance. The blade holder has vibration-free bearings, and the impact protection works at both front and back.

Figure 10. Clemens – Shoot binder tandem - The shoots are tied in synchronization with the driving speed. With good soil conditions, working speeds up to 7 km/h are possible. With three-dimensional adjustments, the shoot binder can be adapted to suit various types of vines and conditions in the vineyard.

Figure 11. Pellenc – Trelion - Electronic scissors.

Figure 12. Pellenc – Selion – Electric chainsaw applied on a telescopic pole. Allows cutting branches thick over 30cm, up 5 m in height. It is also possible tilt the head up to 90°. All the Pellenc gears are powered by lithium-ion battery, which is characterized by the high autonomy offered and the possibility of being applied equally on each of them.

endothermic engine placed on telescopic rods that allow the cutting of thick branches.

These products play an important role with regard to the prevention of accidents at work because they avoid the operator having to climb on the trees and stand on the stairs to carry out the pruning.

Also the use of electronic scissors affects the healthy aspect because the operator, requiring less effort to make the cut, reduces the occurrence of musculoskeletal diseases.

Management of by-products of pruning (grapevine/olive)

The management and recovery for energy production pruning residues has previously been a problem that now finds the optimal solution with the use of shredders and chippers (Figures 14 and 15). These machines are characterized by their small size and limited weight and are equipped with wheels or tracks. These characteristics mean that they can carry easily in every part of the vineyard or olive growing, thus avoiding unnecessary loss of time for the collection and transportation of waste outside the orchards. It is also possible to reuse the waste for energy purposes.

Pest management (grapevine/olive)

In the agricultural realities difficult to reach, one of the main problems for the mechanization of operations, certainly regards the execution of phytosanitary treatments, which led some manufacturers to the preparation of spraying modules on mini-track tractors. They consist of a diffuser cannon which has the ability to rotate 270° on the horizontal plane and 120° in the vertical plane, allowing to treat up to 20 m, with a feed speed of 3 km / h and an estimated labor capacity in 500 plants per hour. This system allows you to cover areas not accessible to conventional means (Figure 16).

Another valid solution is offered by Tifone, which introduces an innovative crawler atomizer, consisting of a cannon orientable instantaneously by remote control. It is characterized by the production of a range that can reach 40 m, m against 15-20 of a normal hand lance.

Soil management

The machineries for soil management are many and of different types, concerning different types of processing.

There are portable equipment, such as brush cutters, brushwood shredder machines, even with remote control (Figure 17), lawnmowers tracked, and spaders to steep slopes. These allow the processing of the soil to a depth of 15 cm and, being only 90cm wide and equipped with tracks, make possible to access at the terraces, in the steep slopes vineyards.

The cultivators with the block of the rotating parts, as required by European Standard EN 709/2010, play a very important role. This device makes immediate the block of the rotating parts and stopping the machine as soon as the clutch is released.

Weeding

An innovation in the field of weed control is represented by the

Figure 13. Pellenc – Selion – Electric chainsaw.

Figure 14. Eliet – Super Proof 2000 – Shredder. Allows to chip the waste from eight hours of pruning in one hour and it is easily maneuvered past all garden entrances and gates thanks to the tracks.

Figure 15. Bear Cat – Chipper 4.5".

Figure 16. Martignani - Phantom B 748 "Minor-Trekker" - Nebulizer cannon.

Figure 17. Energreen - Robogreen - , Brushwood shredder machines. Allows to work on slopes up to 50°, and the remote control ensures the complete security of the workers.

Figure 18. Simeoni - Fertil Dispenser – Knapsack. Allows an operator to fertilize uniformly from 600 to 1500 plants per hour.

devices for localized weed control that allow the reduction of waste in the environment. In addition, the delivery of the active substance in micro doses allows a considerable reduction of the product used. These products manuals are very light, easily transportable and their use is possible even in the most difficult to reach.

Fertilization

Even in this sector the innovations directly affect both the environmental aspect that the ergonomics. The first because the use of knapsack allows the timely delivery and controlled granular fertilizer allowing a reduction of the product used. Also, allow the operator to maintain the upright position for the execution of this operation, for the benefit of both the speed of dispensing that of working conditions. (Figure 18)

Collection (olive)

The manual picking of olives is a very expensive operation, which takes a long time and that, moreover, forces workers to use the stairs, the main cause of accidents and injuries that involves the growers.

The introduction of innovative products has not only concerned the olive harvest but also the recovery and the cleaning of the olives collected.

There are several kind of innovations that permit to speed up and make it safer, thanks to the use of equipment capable of reaching every part of the canopy without the use of ladders. It is possible make a distinction between the facilitators of collection and the shaking machines. Facilitators are tools already present on the market from many years and allows to collect efficiently up to 5m, without damaging the trees and the olives themselves.

The various models differ for the type of vibrating head and for the operation, pneumatic or electric. The introduction of new light and resistant materials, electronics, electric motors more and more reliable has allowed the production of tools that are widely distributed in the territory with a progressive decrease in the cost of purchasing and management. The most important innovation was the introduction of really light batteries, that are easily transported by the operator in a backpack. These batteries also have the advantage of being able to be used on many other electronic devices: scissors, binders, blowers, etc..

In addition, the olive harvest can be done through the use of heads shakers that apply to tractors or excavators, allow the separation of all the fruits.

This technology is evolving and spreading very fast, the technical improvements of the machine have been remarkable. The positioning times of the shaker has been reduced by increasing the speed of movement obtained by electro-hydraulic actuators controllable also by a radio control. It was also improved the "grip on the plant" with pliers that do not produce barking. Has been modified the configuration of "jaws" and adopted multiple layers of friction that allow you to maintain a constant pressure of closing.

The possibility of coupling tools collection to mini-excavators are particularly common even in small farms, has allowed optimize the operations of detachment and recovery even in marginal areas. In this sense, the experiences of the Agricultural Mechanics Unit of the University of Florence, led in 2000 to the creation the first integrated yard for the olive harvest. In place of the bucket was present head shaker and a reverse umbrella, with hydraulic opening, applied to the front blade and a rear apparatus, equipped with a vacuum cleaner and a cyclone for the cleaning of olives and storage in bins. (Figure 19)

The tests conducted have shown that in yard with two operators, in a rational installations, it has an average productivity of collection of 180 plants per day.

The application of the shakers headshot or combing the arm of mini excavators can operate in a small space and with extreme efficiency.

Further the possibility to apply the head shaker, in the 90s the U.O. has projected and realized a head with vibrating combs.

The vibrating combs are particularly indicated in the case of trees of high size, spread in the southern part of Tuscany and Liguria, because allow to harvest over 7 meters high. The prototype developed by the University of Florence in 1998, was resumed and completed by the company Viviani agricultural machinery, which has developed a head comber applicable to the excavators, characterized by patented teeth, whose shape greatly improves the separation of the fruit, decreasing the risks of damage to the plant (Figure 20).

The use of these technologies has found wide diffusion and application by many manufacturers that offer different types of products able to carry out the collection in any type of soil.

The recovery of the olives is a crucial aspect, very often overlooked. The machines for intercepting are essentially aimed to the rationalization of the yard collection and the reduction of costs through an increase in labor productivity. In fact, the recovery represents a considerable part in the times and costs of collection, in particular in such areas. There are interesting solutions, the automatic umbrellas able to facilitate and optimize the recovery operations. There are manual versions, even for very small economic reality olive-growing (Figure 21), and motorized, for the reduction of efforts while traveling in the field; also placed on the mini-track tractor for more professional business. All

Figure 19. The integrated yard. The head shaker and the reverse umbrella on the front and the cleaner system on the back.

Figure 20. Viviani – Combers.

Figure 21. Bosco.-.Olivspeed. The manual umbrella is a revolutionary solution for the recovery of the olives and it is is available with a diameter of 4, 5 and 6 meters.

types of innovations allow you to eliminate the nets and can be coupled to various collection systems, facilitators, tested shakers or combers, allowing for greatly reducing the operation time and optimize the logistics of recovery operations.

Another operation it is possible perform on the field, immediately after the harvest and before the transfer to the mill, refers to the cleaning of the olives. In fact, there are defoliators, electric or internal combustion engine, easily transportable in the field, that allow to eliminate the leaves and twigs present among the olives and can also increase the volume by 30% and 15% the weight of each box.

Conclusions

The Strategic Project MARS + provided an opportunity to study in detail the areas in which it is practiced the "heroic" viticulture and olive growing, to know directly the small local manufacturers and understand their relevance to social, economic and environmental.

The organization of demonstration days, and the strong participation of exhibiting companies, has allowed to see and test directly many innovative technologies. From this it is found that the technologies available on the market allows farmers to speed up and make safer all the cultivation operations, reduce fatigue and reduce the production costs.

In order to present the information activities carried out under the project MARS + has been specially created website www.martepiumeccanizzazione.it

The main purpose of the website is to collect all the references and information about the realities encountered during the project, on the innovations presented, on companies and retailers who kindly brought the machines to the demo days. The section "Repertorio delle Tecnologie" is particularly important because it contains a detailed list of all the innovative products in the industry, not just those of the companies that took part in the demonstration days.

In this collection, the products are listed and divided according to their use, there is a small technical details, with images showing the characteristics of the product and shows the web contacts and e-mail of all the manufacturers.

The use of all these technologies must be accompanied by the rationalization of farms and spaces within them that have to allow the access and the movement of the equipment, through the use of appropriate naturalistic engineering works. (Vieri, *et al.*, 1998, Ferretti, 1997, Ramos *et al.*, 2007).

It is observed that all the manufacturers are particularly interested in these areas and on the problems present in them, the products are constantly being improved and will always try to follow the advice of farmers.

References

Ramos M.C., Cots-Folch R., Martínez-Casasnovas J.M. *Sustainability of modern land terracing for vineyard plantation in a Mediterranean mountain environment – The case of the Priorat region (NE Spain).* Geomorphology 86 (2007) 1-11

Vieri M., Chiostri C., *Meccanizzazione dei vigneti a forte declività: esperienze in Toscana.* Viticoltura di montagna. 9, (1998), 9-18

Vieri M., Giovannetti M., Lorieri P. P., Tarducci S., Zoli M., Beltrami. *Progetto di meccanizzazione di vigneti su pendici a forte declività.* 1997 Quaderno ARSIA 2/97

Any additional information on innovative products and manufacturing companies are available on the website www.martepiumeccanizzazione.it

Static consolidation of a renaissance palace by resins, pins and connecting rods

Antoniotto Guidobono Cavalchini,[1] Martino Guidobono Cavalchini,[2] Elena Poverello[3]

[1]Department of Health, Animal Science and Food Safety, Università degli Studi di Milano, Milano, Italy; [2]Architect; [3]Engineer, Bossong S.p.A.

Abstract

The paper reports the results of a research on the static consolidation of an important XV century tower by Bramante belonging to an important monumental complex located in the Po Valley which was showing worrying structural conditions . The tower, 19 m high, very thin, lacking connections in the highest part, showed overturnings of the four façades not in plumb by over 150mm; Due to the presence of architectural terracotta elements, it was not possible to intervene on the external facades. This is why the authors decided to create a sort of hoop from inside using a U (120 mm) steel profile fastened to the walls by means of steel pins anchored with epoxy resins. The pins (12 mm, 350 mm length) have been positioned at a distance of 50 cm inclined by 30° alternatively downwards and upwards in order to get at minimum of 2+2 courses of bricks. Then, by a series of steel tie rods it was possible to tie the opposite walls. Finally, triangular frames have been positioned on the 4 corners in order to avoid teething collapse in case of great stress. Before starting with the strengthening work, as described above, experimental tests, supported by the Bossong company, were conducted to verify tensile stress resistance of each pin. The tests studied different solutions in terms of diameter and anchoring material. The tensile tests , carried out by using a specific hydraulic puller equipped with a dynamometer and a displacement transducer, showed very high allowable loads , between 20 and 60 kN/pin depending on the pin and fastening type. According to data obtained, the most suitable solution was chosen; it was also used in other parts of the castle. The behavior of the reinforced structure , which withstood the February 2012 earthquake without any problem demonstrated the validity of the proposed technique which is an interesting, non invasive solution for historical buildings.

Correspondence: Antoniotto Guidobono Cavalchini, Department of Health, Animal Science and Food Safety, Università degli Studi di Milano, Via Celoria 10, 20133, Milano, Italy.
E-mail: antoniotto.cavalchini@unimi.it

Key words: historical building restoration; anchoring means; static consolidation.

Journal of Agricultural Engineering 2013; XLIV(s1):e87
doi:10.4081/jae.2013.(s1):e87

Introduction

The work was carried out in the castle-palace, built around 1490, by a leading Milanese courtier, Bergonzo Botta, in Branduzzo (PV) on the right bank of the Po. Although there are no sure documents, Bramante is given credit for the palace, and in any case to his circle, which at the time worked in Milan and to whom, besides Amadeo, Botta had already tapped to build his own palace in Milan [1, 2, 3].

The Branduzzo complex is completely built with terracotta bricks produced locally. It is made up of two rectangular courts having a common quarter, of which one smaller so called noble, and one larger used for agricultural purposes. The former is closed on three sides by two-storey buildings,; the fourth side overlooks the Bramante palace. Four towers in the court corners complete the court. Of these the two shortest ones joint the three short bodies and are extremely simple, they date back to the middle of the 400s, while the two that joint the body of the palace are decidedly taller and stylistically homogenous with the same palace (Figures 1 and 2).

As for the one facing north (Figure 1), poor upkeep, structural modifications in the XVIII c., and time itself have caused severe settling. The object of this paper is in fact static consolidation.

The north tower, state (Figure 3): the 19-metre tower at its eaves leans on two sides, one to the side of the palace and the other to the bottom of the building, giving it significant strength. In section (Figure 3) we notice that from a continuous 0.60m thickness to 12m, up to the first floor vault, the masonry decreases to just 0.40. From 12m up to the top the masonry is free without floors or other connecting elements. It's what gives it its slenderness. This could lead to bucking because at the top the walls are stressed by horizontal forces of the roof hip rafters. The main frame of the roof, is in fact made up of a roof truss from which four hip rafters set out resting on the arris creating a horizontal thrust. Furthermore, the roof truss, originally facing south-north, was subsequently (XIX c.) moved to the east-west axis facing west (towards the garden); here the masonry was weakened further due to a flue. In the XVIII c. new openings were made and balconies built in the north facade, modifying the original structure and its static balance.

For the above reasons as well as for time and lack of maintanance, the structure is in a precarious state resulting in toothing loss on the arris and out of plumb on all 4 facades. Thanks to the building that leans on the west facade up to 15m, the west façade shows modest settling signs the flue mentioned above notwithstanding. Out of plumb is mainly towards the outside, the greatest are along the boundary fascia at cornice level which is mostly decorative. In said fascia we noticed out of plumb 150, 180, 110 mm respectively in the South, East, and North facades.

Consolidation interventions: in such situation, in order to strengthen the structure and avoid further deterioration it was decided to carry out a reversible intervention resorting to:

- a hoop around the tower in order to contain settling towards the outside;

- a network of tie-beams between opposite facades so as to create an intermediary joint capable of reducing the slenderness of the walls;
- joint tie-beams between hip-rafters on opposite ends so as to eliminate horizontal thrust.

As it was not possible to use a hoop from the outside, so as not to alterate the facade, we opted to intervene from the inside employing section irons anchored to the masonry using steel pins and mortar and/or epoxy.

Materials and methods

In order to test the anchors to be used in the project, extraction trials were carried out on different types of sample anchors.

Given the difficulties to carry out extraction trials on the structure itself and at the same time avoid weakening the masonry around the area to be consolidated, it was decided to run the tests at the base of the twin tower, easily done with the equipment used. The two towers are contemporary, with same-size bricks (26×13×6,5) made in a special furnace specifically built locally so the structure of the two towers is anologous. Today, a patch on the outskirts of the complex still keeps its old name "*campo furnasa",* here while working the land one can still find objects made of terracotta. A mensiochronological trial analysis revealed no important differences between the bricks with which the various 14th c. structures (the object of this study) were built. On the contrary, behavioural differences have to be presumed and can be assessed with data made available from literature books in the masonrysection on the ground floor, were extraction trials were carried out, and the portion + 16m where the consolidation intervention was made due to the different influence of the vertical load which burden the two areas. Nevertheless, the test results are of extreme importance for this intervention and for similar situations. The different tests are summarized in table 1, the test site is shown in Figure 4. For the research the behaviour of two different types of injected anchorage were tested: controlled injection anchorages with sock and mortar and anchorages with epoxy, even though project needs specifically the high number of joints to connect the profile in the hoop of the Bramante tower with perimetrical masonry, favoured, during application, the second type, above all for the smaller of the hole.

Once the perforations were made using a core boring machine, the steel bars were have been anchored with binders using the procedure indicated in table 1. Time was allowed for the mortar and resin to dry; subsequently extraction trials were carried out using a manually activated pierced piston oleodynamic cylinder extractor able to exert a maximum force of of 576 kN, measured by means of a pressure transducer applied to the hydraulic circuit. In relation to the applied load, movements were measured using a straight transducer potentiometer with a ball-like sounder having a resolution of 0.01 mm positioned on top of the steel bar. To read and record test data, an acquisition digital system, made up of a personal computer linked to an acquisition/conversion A/D (anologic/digital) electronic control unit, was used. Recording of instrument indications (load or pressure and movement) was carried out every 0.5 seconds. Figure 5 shows an outline of the trial equipment used.

Results

Figures 7 and 8 show the behavioral graphs of the different anchorage systems tested, while the main values are outlined in table 2. As regards controlled injection anchorage with sock, the results are of great importance in the case of mortar type Hs cement-based mixture, where we reach linear field values higher than 100kN in both repetitions. Instead in the Ls theses, lime-based mixture, the values as always in linear field are decidedly lower around 35÷40 kN, with an ini-

Figure 1. General view of Branduzzo palace.

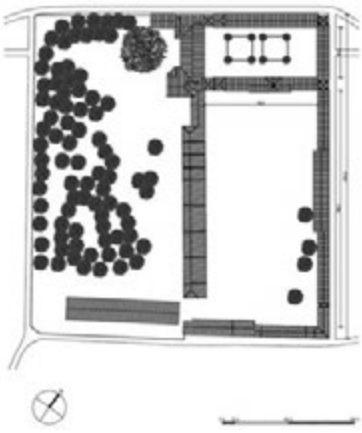

Figure 2. General plan of Branduzzo complex.

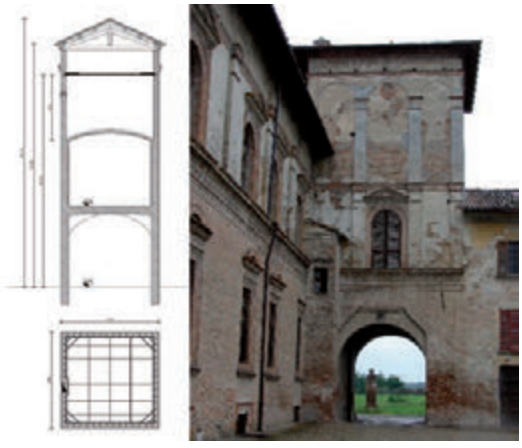

Figure 3. Above: vertical section of the tower; below: cross section and the structural interventions; right: the north tower.

tial breaking of the substratum and subsequent unthreading of the anchorage bulb.

In the two these with resin anchorage, the E20 solution with a 20 mm diameter pin and anchorage length of 400 mm (surface adherence to the sustratum being 30144 mm^2) reveal good results in both repitions : maximum peak load, is around 60÷70 kN.Peak values around 70kN are also reached with E12 with 12mm diameter pins and 350 mm anchorage length (surface anchorage at substratum being 13188 mm^2). This is true only in one of the two repitions since in the second one the maximum load is around 47 kN. With the same maximum load E12 theses movements were much more significant compared to the E20 theses (Table 2). Table 2 also shows rigidity K values and tension in keeping with what Algeri Poverello *et al.* found in similar trials carried out on anchorages with sock and mortar cement-based mixture (HS) and lime (LS) both in the laboratory and on site [5,7].Carefully analyzing the graphs (Figures 7 and 8) and taking into account the age of the bricks, only the linear loads were considered, or characterized by displacements 1 (mm): Using this approach the feasible loads are lower: HS.162,43=HS.255,16=90kN; LS.138,09=35kN; LS.246,69=45kN; E20.147,78=42kN; E20.2=66,4060kN; E12.132,27=32kN; E12.226,58=27kN.

Consolidation intervention: thanks to the results, we proceeded to define and realize the above mentioned consolidation work. For the hoop a UPN 120 profile was chosen easy to place, perforate and capable of following the curvilinear profile of the brickwork, while guaranteeing good resistance to flexion in terms of y (Wy=11,1cm3). The section was fastened to the walls with 14 pins 12 mm (wall holes 14 – ideal anchorage length 350.mm) using epoxy. Wheel-base between the pins is variable to avoid the perforations from falling in the joints between the single bricks, is circa 50 cm. Then, by a series of steel tie rods it was possible to tie the opposite walls . Finally, triangular frames have been positioned on the 4 corners in order to avoid teething collapse in case of great stress (Figure 9). Cautiously taking into consideration a load of 10kN/pin determined by using a safety coefficient=4, the system should be able to resist lateral thrusts of 140kN

Conclusions

The solution proposed was supported by on site tests which allowed us to reach a detailed definition of the best type of anchorage most suitable to the application: resistance and size of the anchorage, type of brickwork and geometry of the structural elements, these are the parameters on which the choice was based. By simply modifying one of

Table 1. Characteristics of the different anchoring systems tested

Thesis	Diameter of the hole (mm)	Diameter of the pin (mm)	Anchorage system	Lenght of the anchorage (mm)
Hs	62	20	Controlled injecion anchorage with sock and mortar Bossong BCM Hs with a cement basea	550
Ls	62	20	Controlled injecion anchorage with sock and mortar Bossong BCM Ls with a lime base	550
E20	24	20	Epoxy anchorage Bossong	400
E12	14	12	Epoxy anchorage Bossong	350

Figure 4. The test site and the tower to be consolidated.

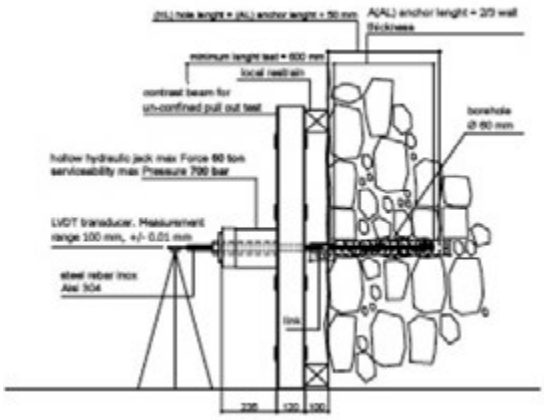

Figure 5. Trial equipment used.

Figure 6.The equipment during the extraction trials.

Table 2. Main data recorded in the tests.

Test	$F_{50\%}$ linear value [kN]	F_1 load at a displacement of 1mm [kN]	F_{max} max load [kN]	F_{post} final value after the peak [kN]	$S_{50\%}$ displacement at 50% [mm]	S_{max} displacement at the peak [mm]	$K_{50\%}$ fastening stiffness at 50% [kN/mm]	$\tau_{hole\ 50\%}$ [N/mm^2]	$\tau_{bar\ 50\%}$ [N/mm^2]	$\tau_{hole\ max}$ [N/mm^2]	$\tau_{bar\ max}$ [N/mm^2]	Failure mode
HS.1	70,93	62,43	141,85	114,44	1,33	4,98	53,33	0,73	2,26	1,46	4,52	masonry failure and pull out of the bar (loss of adherence between bar and grout)
HS.2	64,17	55,16	128,34	111,43	1,19	4,60	53,93	0,66	2,04	1,32	4,09	masonry failure and pull out of the bar (loss of adherence between bar and grout)
LS.1	44,69	38,09	89,38	------	1,48	22,70	30,20	0,46	1,42	0,92	2,85	masonry failure and pull out of the anchor (loss of adherence between grout and masonry
LS.2	40,28	46,69	80,56	------	0,68	17,89	59,23	0,41	1,28	0,83	2,57	pull out of the bar
E20.1	21,26	47,78	62,52	30,09	0,27	2,29	115,78	0,71	0,85	2,07	2,49	masonry failure
E20.2	36,64	66,40	73,28	62,41	0,10	5,07	366,4	1,22	1,46	2,43	2,92	masonry failure
E12.1	42,28	32,27	84,56	------	1,49	13,31	28,37	2,75	3,21	5,50	6,41	masonry failure
E12.2	23,28	26,58	47,61	19,32	0,90	4,25	26,45	0,18	0,21	3,09	3,61	masonry faiure

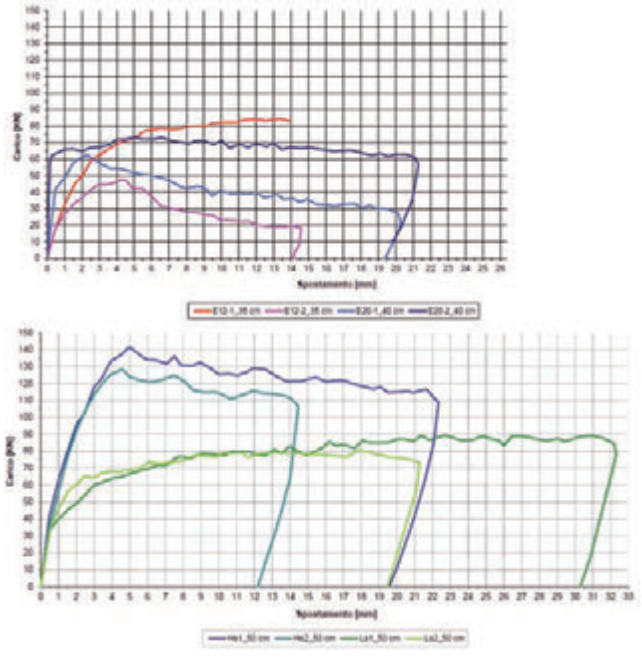

Figures 7 and 8. Load=f(displacement) in the tested achoring solutions.

Figure 9. The loop created from inside: the U profile fastened to the masonry by the anchored pins, the triangular frame at the corner and the steel tie rods are shown.

the parameters, for example the type of masonry, stone rather than brick, can change the surrounding conditions, thus the choice could be made for a different type of anchorage compared to the one chosen for the Bramante tower.

Globally speaking regardless of the type of anchorage used for the connection of the profile, the method used makes it possible to build an efficient containment of the tower walls, in order to create the box-shaped structure and efficacy of the walls to support horizontal thrusts that may occur during earthquakes. The metal elements bond the walls stressed orthogonally on its floor, impeding overturning.

References

1) P.Merzagora a.a. 1992-93 "L'influsso del Bramante a Milano nell'architettura privata:il palazzo di Bergonzo Botta "degree diss. Politecnico di Milano, Faculty of Architecture.
2) E.Rossetti a.a. 2005-06" Residenze aristocratiche , spazi urbani e interventi principeschi nella Milano di Lodovico il Moro" Università degli Studi di Milano, Faculty of Phylosofy
3) L.Giordano 1978 Branduzzo in A.Peroni et al "Pavia architetture dell'età sforzesca"- Ist.bancario S.Paolo di Torino- Torino pp 231-284
4) A.Falcone, V.Pracchi, E.Romoli "Indagini e consolidamento strutturale Palazzo Botta-Adorno Castelletto di Branduzzo", Scuola di Specializzazione in Restauro dei Monumenti a.a. 1993/'94 Politecnico di Milano
5) Felicetti R., Gattesco L., penetration test to study the mechanical responce of mortar in ancient masonry buildings in Materials and Methods RILEM vol 31, june 1998 pp350-356
6) C. Algeri, E.Poverello,E. Giuriani, G.Plizzari 2010 "Experimental study on the injected anchors behaviour" in Structural Analysis of Historical Constructions Xianglin Gu and Xiaobin Song. Shanghai pp 423-428
7) C.Algeri, E.Poverello, 2010 "La ricerca sul comportamento degli ancoraggi iniettati nelle murature storiche in situ" Atti Convegno Ricerca e Innovazione nel consolidamento delle strutture in muratura in zona sismica. Ferrara- Salone internazionale del Restauro.
8) Algeri, E.Poverello,E. Giuriani, G.Plizzari 2010 "Prove sperimentali di estrazione di ancoraggi iniettati in murature storiche" Atti Convegno "Evoluzione nella sperimentazione per le costruzioni" Madrid 2010
9) L.Jurina 2007 *Sperimentazione e didattica per la comprensione delle strutture storiche*, "XXX Curset - Jornadas Internacionales sobre la intervencion en el patrimonio arquitectonico", Barcellona, 13 – 16 dicembre 2007.

The study of rural landscape at the farm scale: changes in traditional signs and structures

Z. Ludwiczak, S. Benni, P. Tassinari

University of Bologna, Department of Agricultural Sciences, Bologna, Italy

Abstract

The importance of cultural, historical and identity values of traditional rural landscapes is widely acknowledged in the relevant scientific fields and in legislation. Furthermore, the knowledge of their evolution represents a fundamental basis in order to manage landscape transformations appropriately. The work is part of a broader research aimed at developing and testing a method for the systematic high time and spatial resolution assessment of changes in traditional rural landscape signs. We describe here the main phases of this original quantitative method and a summary of the first results over an Italian case study. A set of parameters allows to provide complementary information about the evolution of the main characters of rural settlements and their components. This proves to be essential to achieve a deep understanding of the traditional physiognomy of places, and to support landscape management and restoration, and the definition of transformation projects.

Introduction and aims

The importance of cultural, historical and identity values of traditional rural landscapes is widely established both in legislation and at the scientific level. The knowledge of their evolution also represents a fundamental basis for the proper management of future changes of rural landscapes. In fact several studies have dealt with the issue of increasing importance on the recognition and preservation of all types of traditional landscape values (Antrop, 1997; 2000; Pedroli, 2000; Nohl, 2001; Van Eetvelde and Antrop, 2005). However, at present appropriate methods and techniques aimed at creating specific cognitive frameworks in support of policies, plans and projects concerning the extra-urban areas are generally lacking (Antrop 1997, Scazzosi 2002, Castelnovi 2004, Van Eetvelde e Antrop 2005, Agnoletti 2013, Cullotta e Barbera, 2011).

The authors have carried out several studies about the analysis of landscape changes of rural landscapes and the rural built heritage (Tassinari *et al.*, 2008; 2010a, 2011). Meta-design criteria to improve the quality of the rural settlement system have been defined, and methodologies addressed to integrate analyses and interpretative tools have been proposed (Tassinari *et al.*, 2010b; 2013). Moreover the authors have adopted an original approach considering jointly the rural built environment and the farmyards based on postulates of typological consistency with historic farmsteads (Benni *et al.*, 2012). In fact this study is part of a broader research aimed at defining and testing a high time and spatial resolution systematic method for the assessment of changes in traditional rural landscape signs. This work presents the main phases of the quantitative method developed by the authors and its application to a pilot study case. The goal of the study is the definition of a set of parameters suitable to provide a framework of the evolution of the main characters of the rural built environment and its components. The specific goals consist in the characterization of the traditional landscape arrangements, identification of the trends of landscape evolution (direction and intensity), and recognition of the level of preservation of their signs and structures.

Materials and methods

The research was developed by referring to a sample of study areas located in the area of the Imola plain (Emilia-Romagna region, Italy). In particular we considered a set of 11 farms with total area of about 200 ha, which had belonged to the institution *Hospital Santa Maria della Scaletta*, founded in the 15th century (Figure 1). The landscape context of the study area has been characterized since ancient times by a strong farming system - whose traditional signs can be ascribed to the Roman centuriation (Sereni, 1961) – having a prevailing scattered settlement system with open farmyard (Gambi, 1977; Gaiani and Zagnoni, 1997; Ortolani, 1953).

The analysis of the changes of the rural landscape signs at the scale of the farm, together with the broad study of the scientific literature, was conducted based on different sources. In particular we analyzed, besides the various statistical and archival materials, the historical cadastral maps (Nelli Cadastre of 1633-36, Guerrini Cadastre of 1739-41, Gregorian Cadastre of 1817-35), cabreos and historic maps (*Visite Fondi Rustici Appartenenti all'Ospedale S. M. della Scaletta,* 1820; *Inventario della proprietà terriera appartenente all'ente ospedaliero di Imola,* 1932-33; *Inventari di consegna dell'ente ospedaliero "Ospedale S. M. della Scaletta di Imola"*, 1969-71), Italian Military Geographic Institute (IGMI) maps (1892, 1911, 1956), Regional Technical Maps (1975, 1985, 1994), satellite and aerial orthoimages (IGMI fly of 1954-55, Emilia-Romagna fly of 1969-71 and 1976-78, Italy 2000 fly of 1999 QuickBird satellite images of 2003, AGEA fly of 2005). The cartographic

Correspondence: Patrizia Tassinari, University of Bologna, Department of Agricultural Sciences, viale G. Fanin 48, 40127 Bologna, Italy.
E-mail: patrizia.tassinari@unibo.it

Key words: traditional rural landscapes, change detection, rural settlements.

Journal of Agricultural Engineering 2013; XLIV(s1):e88
doi:10.4081/jae.2013.(s1):e88

materials, considered as privileged sources for the ad hoc creation of geo-referenced databases, were acquired in high resolution raster format and processed in GIS environment, using standard procedures (ESRI ArcGIS 9.2).

The general architecture of the method is based on the widely shared and reliable principles of landscape structural analysis, which consist in the decomposition of landscape into its elementary components and the subsequent identification of the structure and their relationships. The main steps of the method named *Traditional Rural Landscape Analysis* (TRuLAn), based on inputs deriving from both the critical analysis of the state of art and tests over study cases, involve parallel investigation with high time and spatial resolution at the scale of the whole farm and the farmstead.

Phase I. Landscape identification and characterization

The preliminary phase of characterization of the landscape context involves the identification (through the analysis of literature and available cartographic and descriptive sources) of those elements that make up the formal structure *i.e.* the physiognomy of landscape. At the farmstead scale, in order to fully grasp the meaning and value of the peculiarities of the settlement system under investigation, it is necessary to identify and characterize its shape and predominant typology within the context, paying particular attention to the settlement structure and the main relationships established between the house and the other components of the agricultural-settlement arrangement. This phase also focuses on the farmstead components attributable to the constructed space, to the open space, with their specialized categories (portions of the farmyard with a functional specialization related to agricultural production or processing of agricultural products, distinct among them also for their physiognomic structure), and the boundary elements.

Phase II. Inventory and parameterization

This phase is divided into two stages conducted in parallel with continuous interactions: the synchronic and diachronic inventory of countryside signs (stage IIA) and the definition and application of analytical and interpretative tools (stage IIB). In the first step, through a systematic inventory in GIS environment, we identified the basic areal units for the parameterization of the land-use categories recognized at the highest spatial resolution allowed by the cartographic sources (also considering the historical ones that are not coded in the most recent institutional land-use databases) and linear natural or anthropic boundary elements, whose presence within a given land-use areal units generates different land parcels. In stage IIB, we defined and applied the parameters for the characterization of presence/absence and number/variety of elements as well as for the quantification of the distinctive geometric characteristics (size, shape, spatial structure, etc.) and the relationships between the different categories.

Phase III. Analysis and interpretation of changes in rural landscape signs

This phase is aimed at the integrated interpretation of the results obtained from the computation of two sets of parameters determined at the scale of the farm and the farmstead, using all the available cartographic sources, including those that were not directly used for definition and calculation of the parameters, allowing to more accurately detailing the evolutionary processes, complementing and enriching the data obtained from the quantitative analysis and providing the information for the periods not covered by the parametric analysis.

Results

The main results about the application of the proposed method to the scale of the farmstead, describing the evolution of the main characteristics of rural settlement and its components, are described below.

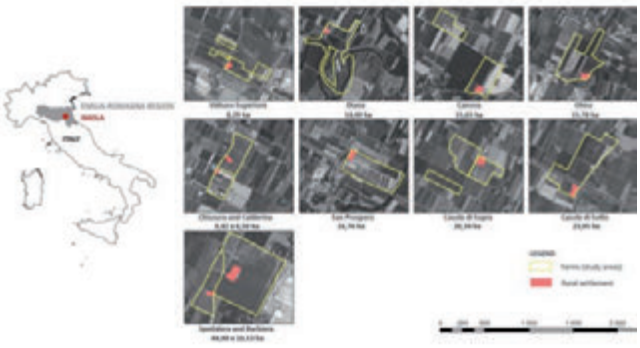

Figure 1. Study areas: geographic location, farm boundaries and farmstead areas (AGEA orthophotos, flight 2005).

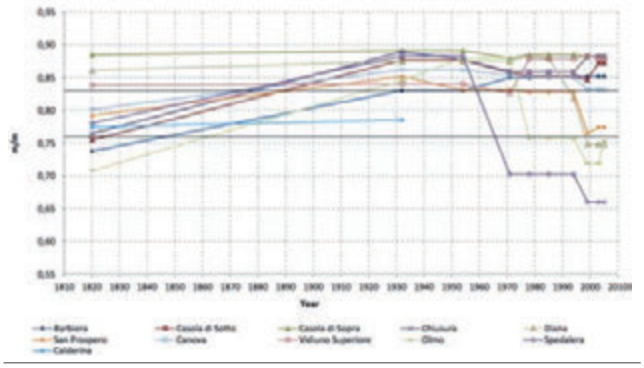

Figure 2. Time changes in CRS (compactness of the rural settlement form) in the analysed farms.

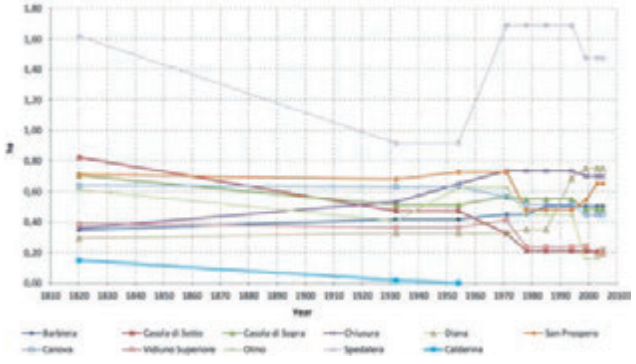

Figure 3. Time changes in ARS (area of the rural settlement) in the analysed farms.

Table 1. Parameters for the diachronic analysis of the main characters of rural settlements and their elements.

PARAMETER	DESCRIPTION
The rural settlement	
Area of the rural settlement [ARS] (ha)	It is the area covered by the farm center, separated from the surrounding cultivated land by the system of boundary elements.
Compactness of the rural settlement form [CRS] (m/m)	$\frac{2\sqrt{\pi A}}{P}$ where A: farm center's area - P: farm center's perimeter This index (Turner and Garden 1991) reaches its maximum value (1) for a circle, while all the other forms show lower values. The index is equal to 0,88 for a square, and to 0,83 and 0,76 for a rectangle whose sides are in the ratio 1:2 and 1:3 respectively.
The built system	
Built-up area [BA] (m²)	All the farm buildings and other build elements are considered. The diachronic analysis of this parameter agrees to quantify the development of the built system within the farm.
Number of buildings and built elements [NB]	This value, to be interpreted jointly with the changes in BA, provides information about the characteristics of changes in the built system, highlighting also the enlargement of existing building units resulting from the increase of their size or rather from the juxtaposition of minor building volumes.
Number of buildings and built elements located on the historical position of buildings - Share of built-up area covering the historic position of buildings [NBH-SBH] (%)	These parameters quantify the number of buildings and the share of the total built-up area located on the historical position as shown in the 1820 maps, respectively. The diachronic reading of this parameter allows a better interpretation of the degree of preservation of the traditional characters related to the arrangement of buildings and other built elements within the farm center.
Ratio of the built-up area to the total area of the rural settlement [RBA] (%)	Besides quantifying the share of the farm center area covered by buildings, this parameter provides information about the open spaces (its complement, varying in inverse proportion).
The system of open spaces	
Ratio of the area covered by specialized open spaces to the overall farmyard area [RSO] (%)	The sum of the areas of all the categories of specialized open spaces is related to the total area of the farmyard, defined as the difference between the area of the rural settlement and the area of the farmstead.
Number of specialized open spaces [NSO]	The number of specialized areas of the farmyard belonging to the various functional categories.
Variety of specialized open spaces [VSO]	The number of different categories of open spaces which can be found in the farmyard.
The system of boundary elements	
Share of the perimeter of the rural settlement covered by physical boundary elements [SPB] (%)	It is calculated for each type of vegetation or built boundary element which defines the boundaries of the farm center.
Share of the perimeter of the rural settlement covered by vertical boundary elements [SPVB] (%)	It is calculated focusing on the overall length of the vegetation and built elements with a significant vertical development.

Table 2. Synthetic characterization of the boundary systems of the analysed farms.

	SPB [%]		Detailed description of the categories of (vegetational and built) vertical boundary elements	
	1820	2011	1820	2011
Barbiera	57,3	79,8	row of trees, hedgerow with trees	hedgerow, row of trees
Caldevino	74,3	-	row of trees, hedgerow -	-
Canova	94,8	100	mixed hedgerow with trees	mixed hedgerow with fence
Casale di Sopra	97,6	17,5	row of trees with nushes, hedgerow	row of trees
Casale di Sotto	98,6	80,3	row of trees, hedgerow	linear vegetation
Chiesura	98,5	44,0	row of trees, hedgerow, hedgerow with fruit trees and vineyards	hedgerow, single trees, linear vegetation
Diana	61,8	48,3	hedgerow with trees	hedgerow
Ginna	72,5	25,9	hedgerow with trees, mixed hedgerow	fence
San Prospero	94,9	34,0	row of trees, hedgerow	linear vegetation, walls with linear vegetation
Spedalera	86,6	13,9	row of trees, hedgerow	linear vegetation
Vidiana Superiore	47,2	0	mixed hedgerow	-

Phase I. Physiognomic analysis

The analysis of literature and historical documents performed on the sample of the study areas led to the determination of the fundamental components and main characteristics of form and composition of the settlement system investigated, focusing especially on the traditional arrangements. The essential elements of the organization of the rural settlement with open farmyard are attributable to:

- its localization (the farmyards may arise along carriage roads or in the midst of cultivated land);
- the built environment consisting of all the farm buildings and other built elements variables within the farmstead;
- the open spaces of the farmyard, which may include the traditional categories: "macero" (an artificial pond for steeping hemp); "vivajo" or "spinaja" (a plant nursery usually surrounded by hedges); "brolo" or "orto" (orchard or vegetable garden usually surrounded by hedges); "vitaja" (an area for the cultivation of grape); "aia" (threshing floor in clay or bricks);
- the system that defines the farmyard boundaries consisting in vegetation elements (such as hedges, rows of trees with or without grapevine) and manufactured (such as public and rural roads, ditches, walls and other fences).

Phase II. Inventory and parameterization

In Table 1 the main spatial parameters (phase IIB) are presented, first those referring to the whole rural settlement, and subsequently those relative to its components (built space, open space, boundary elements).

Phase III. Analysis and interpretation of changes in rural landscape signs

To enable an integrated interpretation of the multidimensional nature of the space-time diversification of physiognomic characters (parameters), the results have been analyzed together with the support of complementary interpretations of different forms of representation. Each parameter has been interpreted by tracing its changes for all the rural settlements, allowing a synthetic study of the trend of each traditional character in a spatial perspective. The temporal variations of all the parameters for each rural settlement have been interpreted together, providing an overview of the respective physiognomic evolution. We carried out the analysis of temporal changes in the coefficient of variation of each parameter, allowing a diachronic reading of the degree of homogeneity/diversity of different physiognomic characters of the rural settlements investigated. The approaches described above call for further integration through a multi-perspective interpretation able to consider the temporal evolution of all the parameters for all rural settlements. To this end, the joint analysis of the groups of parameters, of which the main results are reported in below, proved very useful.

The rural settlement and the built system

In 1820 rural settlements were characterized by high diversification with regard to their size, shape and built area. From 1820-1932 a trend was detected toward uniformity in the character of shape and size (Figures 2 and 3): the size of smaller farmsteads increased and that of larger ones decreased, the traditional long and narrow shape became more compact and the parameters BA and NB did not vary significantly.

However, putting the relationship these results with RBA and the SBH, we found that the buildings have undergone (partly) demolitions and reconstructions.

In the period 1932-1954 almost all settlements kept their size and shape, whereas in all cases BA began to increase, despite the fact that the total NB usually did not change. The decrease in NBH showed that this increase cannot be attributed only to the widening of existing buildings. Subsequently, in the period 1954-1971, BA kept on growing, while the total ARS remained almost constant, except in some cases where significant increases or vice versa reductions were detected due to external forces (*e.g.* the transfer of part of the farm for the construction of road infrastructure). In 1971-1978 ARS did not vary, however, the growth of BA was detected. From 1978 to 1994, the values were in line with the previous period. On the contrary, in 1994-1999 several changes were observed that do not allow to identify common trends. Until 2005 (the final time step) no substantial change was detected (Figure 3).

Traditional arrangements of the specialized open spaces

The evolution of farmyard size since 1820, when a clear diversification was detected (with values between 0.15 and 0.70 ha), showed an homogeneous trend until 1932, with an increase of minimal areas until 1971, and then a decrease until 1994. In 1971-1978 there was a more significant reduction of size with an overall decrease of ARS and an increase in BA. Until 1994 there were no significant changes and higher variations (both increase and decrease) can be identified in 1994-2005.

As for the study of changes of specialized open spaces, there was a lack of detailed information in the technical topographical maps and aerial and satellite images, which made unfeasible a diachronic and systematic study of variations in such areas. The integrated analyses of the Gregorian cadastre and cabreos, however, allowed us to return a detailed picture of their traditional arrangement. At present, as shown by surveys, in certain farmyard we observed the presence of specialized open spaces, but they show drastically reduced and the traditional ones are in almost all cases disappeared. At the same time, in relation to the new functions of rural settlements, new categories of such spaces were detected such as ornamental gardens and parking areas.

System of elements which defines the boundaries of the farmyard

For the diachronic analysis of the elements which defines the boundaries of the farmyard, we applied the same considerations about the use and usefulness of the cartographic sources considered for the specialized open spaces. In particular, the structure of the traditional boundaries of the farmyard was reconstructed by means of a thorough reading of the documents of 1820 and compared with the current one (Table 2), through on-site surveys which allowed us to assess their degree of conservation. The surveys carried out showed that traditional vertical boundary elements (mainly vegetation), except in a few cases, occupied between 72 and 100% of the perimeter of the farmyard. To date, in most cases, vegetation boundary elements have been reduced (they have been preserved mainly along public and rural roads or along farmyards sides adjacent to buildings) or completely disappeared. In the cases in which the vegetation typologies have been preserved, it was noted that over time they have changed their appearance (*e.g.* following the regular pruning and use of non-native species), often deeply changing the relationships between the perception of the farmstead and its surroundings. Moreover new categories of these elements, *e.g.* fences, have appeared, partly replacing those missing.

Conclusions

The TRuLAN method was conceived as a tool of general validity and has been applied and validated on a specific area (Imola plain area). On the one hand, this method is applicable in landscape contexts characterized by agricultural systems and rural and natural conditions which are widely present in the European reality as it is recognized by the scientific literature (Antrop, 2005; Claval, 2005; Skaloš *et al.*, 2011). On the other hand, the structure of the proposed method is applicable in contexts where different types and shapes of rural settlements prevail or the natural and semi-natural elements have greater relevance. However the application of the specific phases requires a calibration of the method, using appropriate checks, integrations and adaptations both of the elements and signs synchronically and diachronically inventoried, and the parameters for their quantitative analysis, whose definition is an essential part of the method.

The high spatial and temporal resolution of the analyses allows to identify and quantify objectively the most minute modalities and trends of changes in rural settlements. The analytical and interpretative tools, aimed at assessing the importance of the diversification of characters in contexts with various sizes and their stay in the short, medium or long term, allow to identify areas with similar characteristics, according to the morphological traits or the physiognomic aspects of certain portions of the territory. This specific landscape characterization is applicable to the field of landscape planning and land-use planning, and in particular in the determination of objective cognitive frameworks as the basis for guidelines and policies at national and regional level, as well as for more specific actions on a local scale, aimed at the preservation, conservation, redevelopment and revitalization of rural areas.

References

Antrop M. 1997. The concept of traditional landscapes as a base for landscape evolution planning. The example of Flanders Region. *Landscape Urban Plan.* 38:105-117.

Antrop M. 2000. Background concepts for integrated landscape analysis. *Agric., Ecosystems Environ.* 77:17-78.

Antrop M. 2005. Why landscapes of the past are important for the future? *Landscape Urban Plan.*70:21-34.

Agnoletti M. (ed.) 2013. *Italian Historical Rural Landscapes. Cultural Values for the Environment end Rural Development*. Springer.

Benni S., Torreggiani D., Carfagna E., Pollicino G., Dall'Ara E., Tassinari P. 2012. A methodology for the analysis of dimensional features of traditional rural buildings to implement the FarmBuiLD model. *Trans. ASABE*, 55(1):241-248.

Castelnovi P. 2004. *Il senso del paesaggio e la convenzione europea.* In Sargolini M. (ed.) *Paesaggio, territorio del dialogo*, 59-70. Rome: Kappa.

Claval P. 2005. Reading the rural landscape. *Landscape and Urban Planning*, 70, 9-19.

Cullotta S. & Barbera G. 2011. Mapping traditional cultural landscapes in the Mediterranean area using a combined multidisciplinary approach: Method and application to Mount Etna (Sicily; Italy). In *Atti di 13° Conferenza Nazionale ASITA*, Bari 1-4 December, 859-864.

Gaiani M. & Zagnoni S. 1997. *Iconografia dell'insediamento rurale tra XVI e XIX secolo.* In Zaffagni M. (ed.) *La casa della Grande Pianura*, 169-233. Florence: Alinea.

Gambi L. 1977. *Cultura popolare nell'Emilia-Romagna. La casa dei contadini.* Milan: Amilicare Pizzi.

Nohl W. 2001. Sustainable landscape use and aesthetic perception – preliminary reflections on the future landscape aesthetics. *Landscape Urban Plan.:* 54:223-237.

Ortolani M.1953. *La casa rurale nella pianura emiliana*. Firenze –

Empoli: Poligrafo toscano.
Pedroli B. 2000. *Landscape – our Home. Lebensraum Landschaft, Essays on the Cultural of the European Landscape as a Task*. Stuttgart: Indiago.
Skaloš J., Weber M., Lipský Z., Trapàkovà I., Šantr kovà M., Uhli ovà L. & Kukla P. 2011. Using old military survey maps and ortophotograph maps to analyse long-term land cover changes – case study (Czech Republic). *Applied Geogr.* 31:426-438.
Scazzosi L. 2002. Valutare I paesaggi. In Clementi A. (ed.) *Revisioni di paesaggio: studi metodologici per l'applicazione della Convenzione europea del paesaggio*. Roma: Meltemi, 217-241.
Sereni E. 1961. *Storia del paesaggio agrario italiano*. Bari: Laterizia.
Tassinari P., Carfagna E., Benni S., Torreggiani D. 2008. Wide-area spatial analysis: A first methodological contribution for the study of changes in the rural built environment. *Biosystems Eng.* 100(3):435-447.
Tassinari P., Carfagna E., Torreggiani D., Benni S., Zagoraiou M. 2010a. The study of changes in the rural built environment: Focus on calibration and improvement of an areal sampling approach. *Biosystems Eng.* 105(4):486-494.
Tassinari P., Torreggiani D., Benni S., Dall'Ara E. 2010b. Research model for farm building design: General structure and physiognomic characterization phase. *Agric Eng Int: CIGR J.* 12(1):47-54.
Tassinari P., Torreggiani D., Benni S., Dall'Ara E., Pollicino G. 2011. The FarmBuiLD model (farm building landscape design): First definition of parametric tools. *J. Cultural Heritage* 12(4):485-493.
Tassinari P., Torreggiani D., Benni S. 2013. Dealing with agriculture, environment and landscape in spatial planning: A discussion about the Italian case study. *Land Use Policy*, 30(1):739-747.
Turner M. G. & Gardner H. 1991. *Quantitative methods in landscape ecology: the analysis and interpretation of landscape heterogeneity*. New York: Springer-Verlag.
Van Eetvelde V. & Antrop M. 2005. The significance of landscape relic zones in relation to soil conditions, settlement pattern and territories in Flanders. *Landscape Urban Plan.* 70:127-141.

Historical road system and farmhouses in Apulia

L.P. Caliandro,[1] R.V. Loisi,[2] P. Dal Sasso[2]

[1]Department of Agricultural Sciences, food and environment, University of Foggia, Italy, [2]Department of Agro-Environmental and Territorial Science (Di.S.A.A.T.), Agriculture Faculty, University of Bari, Italy

Abstract

Human settlements often originate from the presence of such natural sustaining water bodies as springs, rivers, or rather from the proximity of relevant infrastructure (roads, harbours, etc.). Rural residential buildings, however, are generally closely linked to the cultivated fields of a farm. A significant example of rural buildings, that particularly identifies some national or regional areas, is that of the Apulian farmhouses known as "*masserie*", which are considered as an important cultural heritage in the rural territories of that region. These buildings, featuring relevant architectural and landscape characteristics, encompass several functions within them and often host more than one family living there permanently. Territorial distribution of rural buildings and farmhouses in Apulia is diversified and, in general and as already stated, it can depend on the close relationship between the building and its adjacent agricultural lot. Moreover, in the case of the Apulian farmhouses, owing to their specific role in overseeing the territory and asserting land tenure rights, this distribution may have "genetic" origins influenced by other elements, too. The efforts of the present work regarding this issue are to investigate the existing relationships between the Apulian farmhouses system and the "historical" roads already existing when they were built (XII-XIX centuries). Particularly, the study proved if there are any correlations among the Roman roads, the sheep's paths (*tratturi*) crossing the Apulia region and the farmhouses, both from the point of view of the distance from the roads and the importance of the individual farmhouses. Using GIS software and overlay mapping procedures it was possible to quantify the amount of farmhouses and their concentration within the catchment areas of the aforementioned historical roads, while through historical and territorial in-depth analysis those elements characterizing the most interesting farmhouses from the historical and architectural point of view were identified. The research provided interesting information on the existing relations between historical roads and farmhouses, leading to further considerations on the possibility to enhance some of these monuments, located in rural areas, through the promotion of the "integrated" asset represented by the historical road system, with particular reference to the sheep's paths (tratturi).

Correspondence: Lucia Patrizia Caliandro, Department of Agricultural Sciences, food and environment, University of Foggia, Via Napoli, n. 25, 71100 Foggia, Italy.
Mobile: +39.320.4394648 - Fax: +39.080.5442962.
E-mail: lucia.caliandro@unifg.it; l.caliandro@unifg.it

Key words: Historical road system, Farmhouses, Integrated recovery, GIS.

The work is due in equal parts to the authors.

Journal of Agricultural Engineering 2013; XLIV(s1):e89
doi:10.4081/jae.2013.(s1):e89

Introduction and objectives

The growing demand for rural and cultural tourism contributed to the revaluation of both the representative role of cities and the "open" territories emphasizing the integrated promotion of the excellences.

In this context, a number of studies were carried out aimed at recognizing elements of historical and cultural importance and identifying structural invariants to be interpreted as strength and starting points in the enhancement of the territory.

The knowledge of the endogenous resources of a territory provides information for its preservation and leads to the individualization of promoting actions consistent with other socio-economic aspects belonging to the territory, in the perspective of its environmentally sustainable development.

A similar virtuous project of wide areas enhancement is connected to the possibility of restoring existing linear elements, such as the historical road system, which possess interesting features increasing their specific cultural value.

Among the characterizing assets of the historical and cultural heritage in the Apulian rural territory there are the "*masserie*" (as the farmhouses are known in Italian), the most significant architectural emergencies in the rural constructions. They are considered as symbols of the land-owner middle class and emblem of a strong relationship between shape and function, cultivation and agricultural firm.

Indeed, the historical road network is the conceptual and physical medium by which the landscape, environmental and cultural resources are linked, contributing to add value to the whole territory.

Stated the importance of the two systems, the farmhouses and the historical road system (the sheep's paths - "*tratturi*" - of the sheep pasture - "*mena delle pecore*" - and the consular roads), it is necessary to find integrated recovery forms concerning their functional and physical connections, too. The very existence of a historical road can favour the restoration of farmhouses and, similarly, the farmhouses restoration can ensure the enhancement of the historical routes. In this way, saving one of the two assets categories will have positive effects on the other.

In the light of such considerations, the aim of the present study is to identify the connections and the interrelations between the farmhouse buildings and the historical road system, *i.e.* the territorial links existing between the most relevant architectural emergencies of the

peasant culture and the most important historical infrastructure of the territory, in order to distinguish in quality and quantity those manufacts to be more easily restored and reused due both for their closeness to the above mentioned roads and for their intrinsic value. The study has been carried out on the whole territory of the province of Taranto, after a preliminary analysis of the regional context.

Materials and methods

Materials

Apulia region is characterized by a relevant presence of farmhouses, scattered in the whole territory. These farmhouses embody the architectural symbol of the peasant culture and the greatest expression of the rural building, typical of the medieval age till the end of the XIX century (Figure 1).

Surrounded as they were by huge cultivated lands, farmhouses represented the centre of production and organization of the rural work (Calderazzi, 1989). They often offered valuable architectural features, integrated in rural landscape of great suggestion and identification (Figure 2).

Since each farmhouse has its own features due to the social, economic and agricultural reality of the territory to which it belongs, there are no recurrent building techniques but only improvements or differences between one another which stress their identity. This aspect represents the real value of the farmhouses as being tout court cultural assets, not only limited to the peasant world (Dal Sasso *et al.*, 2009)

According to a study carried out by the Department of Agro-Environmental and Territorial Science of the University of Bari, about 8 000 farmhouses were surveyed in the Apulia region, as reported in the 1:25 000 scale official cartography of the Military Geographic Institute (IGM), produced in 1950 (Table 1 - Dal Sasso *et al.*, 2009).

Some of these present relevant historical-architectural features identified in the Cultural Heritage Chart recently produced by the Apulian Regional Administration for the creation of the new Regional Landscape Plan (Piano Paesaggistico Territoriale Regionale or PPTR - Figure 3 -).

The historical routes crossing the regional territory that have been taken into consideration in this study are the Roman consular roads and the "*tratturi*" (as the sheep's paths are known in Italian).

Until the IV century before Christ, in Southern Italy all the cultural and commercial relationships developed through the pre- or proto-historic road network. It was with the advent of the Romans, between the end of the IV and the beginning of the III century before Christ, that an organized road plan was conceived by the central government.

Despite the almost complete disappearance of the consular roads, they still represent a notable functional and structural example.

Roman roads were born for military reasons. Indeed, the Appia road was built in stages, as the Roman conquest of new territories expanded. Moreover, from the IV to the II centuries before Christ, the "*Appula"* (Apulian) road system represented the main path for the commercial exchanges with Greece and the East Mediterranean.

Among the 29 Roman roads spreading from Rome to the rest of Italy, the Appia road and the Trajan road are those crossing the Apulian territory (Figure 4).

The first road, built in 330 before Christ by the Consul Appio Claudio, stretched from Rome to Benevento and Taranto, and, later, under the Emperor Traiano, it reached Brindisi.

The Trajan road, also known as "*Appia-Traiana* or *Minuccio Traiana*", linked Benevento to Brindisi, passing from Troia, Ordona and Canosa, while on the way between Bitonto and Egnazia, it was made of two stretches, the coastal Trajan road, the "*Traiana Costiera*" and the Internal Trajan road, the "*Traiana Interna*". In the Apulian Territory, the Trajan road extends for about 505 kilometres, while the Appia Road is about 194 kilometres long.

Today little is remained of this road system because its long use destroyed many of its archeological traces and also because those paths, which were included in the major routes of the Imperial Age and often used till nowadays, have been rearranged or restored in the course of the centuries (Cippone, 1993).

In this study the historical cartography has been adopted (Otranto, 2007) which reproduces the original map of Giovanni Antonio Rizzi

Table 1. Named farmhouses surveyed by IGM cartography (scale 1:25 000) and by the Apulian Cultural Heritage Chart.

Province	Foggia	Bat	Bari	Brindisi	Taranto	Lecce	Total
Farmhouses surveyed by IGM cartography	2 587	507	1 820	980	1 157	1 419	8 470
Farmhouses surveyed by	1 144	211	321	539	606	127	2 947

Figure 1. Apulian farmhouse.

Figure 2. Farmhouses integrated in rural landscapes.

Figure 3. Farmhouses surveyed by IGM cartography (scale 1:25 000) and by the Apulian Cultural Heritage Chart.

Zannoni drawn for the reign of Naples and dating back to the last twenty years of the XVIII century.

The sheep's paths (Figure 5), deserted or substituted by the ordinary road system in some stretches, nowadays still constitute essential elements of the territorial organization and undoubtedly a symbol of the agro-pastoral civilization (AA.VV., 1999)

In the protohistoric period, the sheep's paths already represented long "grassy roads" where herds and sheep grazed, allowing the transfer out of the coastal lands to the internal ones. Transhumance required a long journey and so it should ensure food (green roads) and resting places (stations, *jazzi*, hunting lodges, etc.) for the cattle.

For a long time the sheep's paths have been linking roads between the Abruzzo and Molise Appennine pasture and the Apulian plains, representing the core of a fundamental commercial activity for all the different populations developed in Southern Italy, from the Sanniti to the Kingdom of the two Sicilies.

At the beginning of summertime the herd was shepherded towards the mountains. In autumn it was brought back to the plains where it spent winter, through grassy roads called "*calles publicae*" which could be passed under payment of a duty to the State.

Later on, as deduced by Emperors Teodosio and Giustiniano Codes it's known that these roads were called "*tractoria"*, from which derived the term "*tratturi"* that is still in use.

The origin of transhumance is very ancient and widespread in a lot of regions, both Italian and foreigner, where, under different names, it is possible to distinguish these pasture communicating roads.

The sheep's paths usually took their name from the arrival lands or a nearer centre.

Their economic role is already present in the Roman times. Their use was subdued to the payment of a tax, the "*publicum vectigal*", which varied according to the number and the weight of the animals.

In the Middle Ages Alfonso I d'Aragona established the "*Regia dogana per la mena delle pecore in Puglia*", the institution which administered the sheep's paths system and was in charge of collecting the Royal tax by the herds owners who used the State property lands for the cattle-rearing.

The *Regia Dogana* had its first venue in Lucera and later in Foggia, where it was present from 1447 to 1806.

The golden age of the sheep's paths lasted till 1806, when Giuseppe Bonaparte abolished the *Regia Dogana*. Since then the transhumance roads decayed and any law effort of protection and restoration failed (Colapietra, 1985)

The main sheep's paths were linked by a series of branches and little sheep's paths; the width of the first was fixed in 60 steps or Neapolitan steps, corresponding to 111,11 metres; the second has a 30 steps (55,55 metres) width and the third, which linked the sheep's paths and gave access to the mountain pastures and locations, has a width that varied from 20,15 steps (37,31 metres) to 10 steps (18,52 metres).

According to a list compiled in 1912, the entire extension of the sheep's paths system amounted to 2 978.29 kilometres for a total of 21 000 hectares and included five regions: Abruzzo, Molise, Apulia, Campania and Basilicata.

As far as the Apulian territory is concerned, the sheep's paths system extends for about 1 990 kilometres (Figure 6) and crosses the territories of the province of Foggia, where the sheep's paths network is very dense, and the province of Bari, mainly in the pre-Murgia and Murgia area, to become thicken again in the province of Taranto.

In this study the sheep's paths map was adopted, as reported by the Apulian Territorial Urban Planning/Landscape Map (*Piano Urbanistico Territoriale Tematico/Paesaggio* or PUTT/P). Apulian Regional Administration is working on the identification of restored, not yet restored and/or deserted stretches, through a photographic interpretation of the regional ortho-photography (Figure 7).

As this study area the province of Taranto was chosen, due to the fact that it is largely affected by the presence of farmhouses recognized as cultural heritage and, more specifically, for the massive concentration of valuable farmhouses (reported in the Cultural Heritage Chart) in the central area of the province, including the municipalities of Martina Franca, Grottaglie and Taranto, crossed by a thick net of sheep's paths and by the historical Appia road.

Moreover, new forms of rural tourism have been developing in this area. Those are recently aimed at the quality of products and services, and tend to promote the cultural, landscape and environmental peculiarities which give an effective contribution to the identification and enhancement of the heritage linked to the historical road system.

Methodology

The research work is composed by four phases. In the first, data concerning farmhouses located in the territory of Taranto have been analyzed, with a particular reference to those buildings having a significant historical and architectural value. To this aim, the data gathered by the project of the Apulian farmhouses classification, already started by the Department of Agro-Environmental and Territorial Science of the University of Bari, have been used.

The final result of cited work has been the synthesis of the specific features of the analyzed farmhouses (location, territorial layout, surface, volume, typological, structural, functional and architectural characteristics, historical information, present destination, maintenance status, firm peculiarities).

Moreover, using a GIS tool (Arcview 9.3.2 software package), it was created the identification map of the valuable farmhouses, as detected from the ones reported in the 1:25 000 scale cartography of the Military Geographic Institute (IGM). Those map was then overlapped to the

Figure 4. Roman consular roads.

Figure 5. Part of a neglected sheep's path.

Figure 6. Sheep's paths system in Apulia.

Apulian Cultural Heritage Chart, which in turn reports further valuable farmhouses.

The second phase consisted in the analysis of the main historical paths of the Apulian territory, the georeferencing of the historical cartography concerning the consular roads and the sheep's paths system (Otranto, 2007), and the identification of those stretches which mark the territory of Taranto.

In the third phase the correlation between the farmhouses system and the historical path network in the province of Taranto has been evaluated, according to the following principle.

With the help of a GIS tool, the catchment area (a buffer having a distance of 1 km) of the historical paths crossing the analyzed territory (the Appia Roman road and the sheep's paths) has "built". Subsequently those farmhouses falling within the aforementioned areas, and related to each path, have been detected (Figures 8 and 9).

This last phase led to the quantitative evaluation of the farmhouses set in the catchment area of the historical road system.

Results and discussion

This study allowed the evaluation of the existing correlation between the farmhouses and the main historical paths in the province of Taranto.

It was noticed that a section of the Appia road, about the 48% of its total length, was used as sheep's paths.

The analysis of the catchment area (buffer), derived as previously described, both for the Appia road and the sheep's paths, highlighted the fact that the farmhouses located inside those areas are the 31% of the total amount of farmhouses located within the boundaries of the province of Taranto. On the other side, a considerable number of farmhouses, about the 69% of the total, is scattered outside the catchment area of the various historical paths examined.

Besides, the importance of the farmhouses inside those areas is great, if we particularly consider the fact that they were real landmarks for the internal territories and, for this reason, they were generally built far from the main communication roads and the urban centres.

Being a principal historical road, the Appia road path joins the main functional and structural poles of the territory, as the urban centres, and has a highly value also for its correlation to the farmhouses. This correlation in similar to the one existing between the farmhouses and the sheep's paths, as shown in Table 2, where 1.04 farms/km for the Appia road and 1.02 farms/km for the sheep's paths have been detected.

This is clearly justifiable because, in different periods of time, this road was used as a sheep's paths in the stretch between the Tratturo Melfi – Castellaneta (sheep's paths Melfi-Castellaneta) and the Tratturello Tarantino (Taranto little sheep's paths), for a total length of about 53 kilometres. Considering this common portion (Figure 10), indeed, it can be noticed that, due to the presence of 69 farmhouses in the catchment area, their impact value grows to 1.30 in relation to the length of the path.

The percentage distribution (Table 2) of the farmhouses placed within the catchment area of the sheep's paths (27% out of 1 157 provincial farmhouses) still represents a considerable amount, particularly considering the great extension of the sheep's paths system of the province.

This allow to highlight the functional connection between the sheep's paths and the farmhouses, *i.e.* between the transhumance sheep-breeding and the resident breeding. Moreover, the considerable linear length of the different paths here analyzed, represents a structural and functional axis of the extra urban territory which seems to be

Table 2. Farmhouses placed within the catchment area of the historical paths.

Historical road system	Farmhouses (N)	Road length (km)	Farmhouses/km (N/km)	Farmhouses detected/ Provincial farmhouses (equal to 1 157) (%)
Appia Roman road	114	109	1.04	10
Sheep's paths (tratturi)	314	306	1.02	27
Sheep's paths (tratturi) overlapped with Appia Roman road	69	53	1.30	6
Total	359 (428-69)	362 (415-53)	0,99 (359/362)	31

Figure 7. Ortho-photographic identification of a sheep's path stretch.

Figure 8. Relationships between the Appia Roman consular road and the farmhouses system.

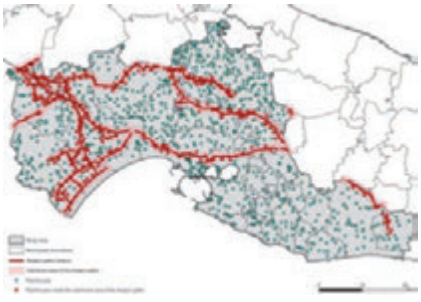

Figure 9. Relationships between the sheep's paths and the farmhouses system.

particularly interesting from the point of view of an integrated restoration of the rural building heritage.

Given that a stretch of the Appia road (the 48% of its length, with the 60% of farmhouses placed in the path buffer) coincides with the Tratturo Melfi – Castellaneta and the Tratturello Tarantino, to be discussed later, the portion which completes the historical path crosses the city of Taranto and presents an interesting concentration of farmhouses exactly in the outskirts of the city.

Among the valuable farmhouses in that area, there is Mucchio farmhouse (Figure 11), articulated around a yard and composed by different structures that started from the original core built to serve the different agricultural, residential and defensive functions. The chapel represents a unique element, since it is completely isolated from the working area of the farm (Mongiello, 1984). Nowadays Mucchio farmhouse lay abandoned in the industrial area of the Italsider of Taranto.

The sheep's paths counting a massive presence of farmhouses in their catchment area are the Tratturo Melfi-Castellaneta, the Tratturello Orsanese and the Tratturello Gorgo-Parco (Table 3). The farmhouses placed in the catchment areas related to the sheep's paths located in the north-west side of Taranto present characteristics that differ to those of the farmhouses placed within the Murgia dei Trulli, where the Tratturello Gorgo-Parco is located.

The first are characterized by largely built areas "due to the extension of the cultivated lands and the distance from the centres of labour recruiting. They looked like small villages, with the peasant houses grouped around the manor house and the church" (Colamonico, 1970).

Among the most valuable farmhouses of this area there is the Tafuri farmhouses, near the municipality of Castellaneta (Figure 12).

The farmhouses placed in the catchment area of the Tratturello Gorgo-Parco are generally characterized by a two-floor building, the manor house, and by rural buildings with the typical shape of "*trullo*" grouped together, in pair or in line creating an open yard with the manor house (Figure13).

Among the most significant examples of this farmhouses typology

Table 3. Farmhouses placed within the catchment area of the individual sheep's paths.

Sheep's paths	Farmhouses (N)	Road length (km)	Farmhouses/km (N/km)
Melfi - Castellaneta	30	14.8	2.02
Santeramo in Colle - Laterza	24	16.2	1.48
Martinese	100	92.5	1.08
Murge	11	6.8	1.61
Tarantino	52	57.8	0.90
Orsanese	30	16.9	1.77
Quero	14	9.8	1.42
Palagiano - Bradano	27	28.6	0.94
Pineto	13	17.6	0.74
Bernalda - Ginosa - Laterza	13	13.5	0.97
Pini	11	8,3	1,34
Ferre	5	4,3	1,16
Gorgo - Parco	33	18,9	1,74
Total	363	306	

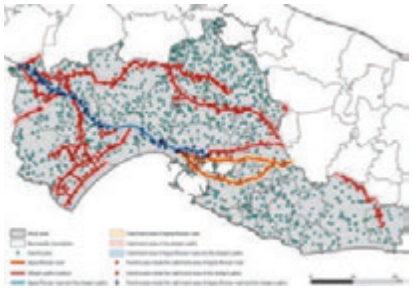

Figure 10. Relationships among the Appia Roman consular road, the sheep's paths and the farmhouses system.

Figure 11. Mucchio farmhouse in Taranto.

Figure 12. Tafuri farmhouse in Castellaneta countryside.

Figure 13. Architectonic survey of a farmhouse with trulli in Martina Franca countryside.

Figure 14. Valuable farmhouses in the catchment area of Tratturello Gorgo-Parco.

within the catchment area of the Tratturello (Figure 14), there are the farmhouses named Motolese Murge (Figure 15a), Paglierone (Figure 15b), Croce Grande (Figure 16a), Cavaliere (Figure 16b), Gorgo (Figure 17a) and Carrucola (Figure 17b).

Along the Tratturello Martinese, the longest in the province of Taranto, presenting a great number of buildings in its catchment area (100 farmhouses), there are stretches presenting a relevant concentration of farmhouses, particularly near Crispiano-Grottaglie and Castellaneta-Laterza, which include on the same path the two typologies of farmhouses above mentioned.

Conclusions

Even if limited to the province of Taranto, this research drew a connection between the two systems, the road and the farmhouses ones, as points of reference for similar studies in those areas affected by the same existing structures.

The study results also suggest a method to identify sheep's paths stretches still to be restored by means of a dedicated photo-interpretation. This study allows to create a link between the farmhouses system and the one relating to the main regional paths having historical and cultural origin.

The results clearly showed a complex relationship between the two systems, so that it can be easily made hypothesis about an integrated use of the territory, that comprehends both the agricultural and livestock realities (the farmhouses), and the cultural touristic value (the routes).

This will mean to support the rural territory development with the enhancement of its cultural resources, that can be pursued both through restoration and re-use of the farmhouses, keeping in mind their touristic, didactic, leisure and research use destination, and increasing the value of the sheep's paths, the role of which could be emphasized through information points, signals, etc.

Figure 15a. Motolese Murge farmhouse (on the left) and Figure 15b. Paglierona farmhouse (on the right), both located in Martina Franca countryside.

Figure 16a. Croce Grande farmhouse (on the left) and Figure 16b. Cavaliere farmhouse (on the right), both located in Martina Franca countryside.

Figure 17a. Gorgo farmhouse (on the left) and Figure 17b. Carrucola farmhouse (on the right), both located in Martina Franca countryside.

All these hypothesis are particularly advisable since most of the farmhouses in the studied area are only partially abandoned. In fact, they are generally used for agriculture or, in some cases, for touristic accommodation.

This research results can also integrate the previous classification work of the farmhouses, adding to them a further significance as to a territorial parameter of evaluation.

In the perspective of a sustainable development, the investigation of integrated endogenous resources is a key action for a correct use of the territory and for a future development respectful of the environment and the landscape.

In conclusion, this work may provide information for the definition of territorial plans which, far from being only an ideal guide, should also constitute practical guidelines for any possible form of intervention.

References

AA.VV. 1999. I territori della transumanza: una rete per i parchi. Dierre edizioni, Chieti.

Calderazzi A. 1989. L'architettura rurale in Puglia: le masserie. Schena, Fasano.

Cippone N. 1993. La Via Appia e la terra jonica. Nuova Editrice Apulia, Martina Franca.

Colamonico C. 1970. La casa rurale nella Puglia. Olschki, Firenze.

Colapietra R. 1985. I grandi tratturi nella tematica attuale dei beni ambientali. Proc. 4th Congr. Prehistory – Proto-history - History of Daunia. Civica Amministrazione-Biblioteca Comunale "A. Minuziano"-Archeoclub d'Italia, San Severo.

Dal Sasso P., Ottolino A., Loisi R.V. 2009. Masserie di Puglia: Censimento e Analisi delle tipologie. Estimo e Territorio vol. II: 42-54.

Mongiello L. 1984 Le masserie di Puglia. Organismi architettonici ed ambiente territoriale. Adda, Bari.

Otranto G., 2007 Cento itinerari più uno in Puglia. Gelsorosso, Bari.

Land use change in the Veneto floodplain and consequences on minor network drainage system

Massimo Prosdocimi, Giulia Sofia, Giancarlo Dalla Fontana, Paolo Tarolli

Department of Land, Environment, Agriculture and Forestry, University of Padova, Agripolis, Legnaro, (PD) Italy

Abstract

Anthropic pressure has been proven to be one of the most evident forces able to alter landscapes. Its impact on the surroundings can be easily detectable especially in a high-density populated country such as Italy. Among the most evident anthropic alterations, the most important are the urbanization processes but also changes in cultural techniques that have been occurring in rural areas. These modifications influence the hydrologic regimes in two ways: by modifying the direct runoff production and by having a strong impact on the drainage system itself. The main objectives of this work are to evaluate the impact of land cover changes in the Veneto region (north-east Italy) on the minor drainage network system, and to analyze changes in the direct runoff in the last 50 years. The study area is a typical agrarian landscape and it has been chosen considering its involvement in the major flood of 2010 and considering also the availability of data, including historical aerial photographs, historical information, and a high resolution LiDAR DTM. The results underline how land cover variations over the last 50 years have strongly increased the propension of the soil to produce direct runoff (increase of the Curve Number value) and they have also reduced the extent of the minor network system to the detriment of urbanized areas and changes of plots of land boundaries. As a consequence, the capacity of the minor network to attenuate and eventually laminate a flood event is decreased as well. These analysis can be considered useful tools for a suitable land use planning in flood prone areas.

Correspondence: Paolo Tarolli, Dipartimento Territorio e Sistemi Agro-Forestali, Università degli Studi di Padova, Viale dell'Università 16, 35020 Legnaro (PD), Italy. E-mail: tarolli.paolo@gmail.com

Key words: land cover change, direct runoff, DTM, minor network system.

Acknowledgements: LiDAR data were provided by the Ministry for Environment, Land and Sea (Ministero dell'Ambiente e della Tutela del Territorio e del Mare, MATTM), within the framework of the 'Extraordinary Plan of Environmental Remote Sensing' (Piano Straordinario di Telerilevamento Ambientale, PST-A).

Journal of Agricultural Engineering 2013; XLIV(s1):e90
doi:10.4081/jae.2013.(s1):e90

Introduction

Significant changes in land use happened over the last few centuries in all European countries and whether the floods experienced in these recent years are triggered or exacerbated by human activities, has been subject of much debate (Bronstert, 1996; Kundzewicz and Takeuchi, 1999; Kundzewicz and Kaczmarek, 2000; Longfield and Macklin, 1999). Alterations in agricultural techniques and the simultaneous increase of urbanization and industrialization processes have increased the extent of impervious areas, causing the so-called soil sealing. Leopold in 1968 demonstrated that passing from a permeable soil type (*i.e.* grassland) to a less permeable one (*i.e.* urbanized area), a faster and higher response of the watershed in generating runoff is expected and thus, a clear modification in the hydrograph shape. As outlined by Bronstert *et al.* (2001), both runoff generation and discharge conditions can be altered by human activities and, in general, field drainage, wetland loss and urbanization result in increased 'flashiness' of runoff, more rapid downstream transmission of flood waves, and less floodplain storage. Recently, Veneto Region has undergone both significant territorial and socio-economic changes. Actual conformation arises due to the expansion of a metropolitan polycentric system, characterized by a dispersion of low-density residential functions and a homogeneous distribution of medium-small size productive activities (Fregolent, 2005). These dispersion processes have been deeply studied since the 80s and a particular attention has been given to the phenomenon called "urban sprawl" (Indovina 1990, 2009; Indovina, Fregolent, Savino 2004; Tosi, Munarin 2004; Fregolent 2005, 2012). This process caused the expansion of new residential neighborhoods and productive/commercial areas to the detriment of agricultural plots. Therefore, in the floodplain context, the natural river system has been deeply modified over time through the artificial management of water levels and discharges. This resulted in an artificial drainage system, in which the flow occurs along a network of regular channels (larger channels and small ditches), often through water pumping. There is no doubt that this type of area is naturally exposed to the danger of floods, whose causes are multiple and often interacting with each other. The principal causes can be generally distinguished between problems related to large rivers unable to manage the incoming flows, and issues directly related to the inability of draining meteoric water through the smaller hydraulic network (ditches). While problems related to the large rivers are mainly connected to choices and actions applied in historical times, the problems of the smaller hydraulic network are due to small and relatively recent territorial changes: fast human settlement in floodplain, and the intense urbanization, have reduced the extent of the network while increasing at the same time impermeable surfaces, with the result that the remaining network drainage capabilities are no longer sufficient (Cazorzi *et al.*, 2013). As a consequence, situations of hydraulic crisis happen with increasing frequency and they affect the most urbanized districts.

This work aims to analyze the effects of land use cover changes,

occurred in the Veneto region over the past 50 years, on the minor drainage network system and direct surface runoff. The study area has been selected because of its involvement in the major flood of 2010 and because of the availability of data, including historical aerial photographs, historical information, and a high resolution LiDAR Digital Terrain Model (DTM). In particular, many recent studies have proved the reliability of these models in many disciplines concerned with Earth-surface representation and modeling, including applications in hillslope (Tarolli and Tarboton, 2006; Lashermes *et al.*, 2007; Booth *et al.*, 2009; Kasai *et al.*, 2009; Tarolli and Dalla Fontana, 2009; Orlandini *et al.*, 2011) and fluvial environments (Charlton *et al.*, 2003; Heritage and Hetherington, 2007; Hilldale and Raff, 2008; Jones *et al.*, 2007; Cavalli *et al.*, 2008; Vianello *et al.*, 2009; Notebaert *et al.*, 2009; Cavalli and Tarolli, 2011; Legleiter, 2012; Cazorzi *et al.* 2013). There is also a growing interest in the application of such information by agencies responsible for land management for the development of automated methods aimed at solving geomorphological and hydrological problems. Automatic feature extraction from LiDAR DTMs can in fact greatly improve databases and it is a useful tool for natural hazard mapping and environmental planning.

Materials and methods

The study is based on the availability of historical aerial images that date back to 1954, 1981 and 2006 and a high resolution LiDAR DTM having 1 m cell size. At first, a semi-automatic approach, developed by Cazorzi *et al.*, 2013, has been applied in order to identify the minor drainage network system and estimate some its parameters such as drainage density and storage capacity, through the DTM which dates back to 2006 and a morphological parameter named Relative Elevation Attribute (REA) derived from it. A thresholding approach based on the standard deviation of REA has been used in order to automatically extract the small-scale topography features (minor drainage network system) (Figure 1).

The procedure divides the area in analysis in square sub-areas whose each one is 100 m x 100 m wide. For each sub-area, are computed the average width of ditches, drainage density and storage capacity values.

Based on the relative available historical images, land use cover maps and drainage network systems have been both drawn. Due to the mediocre resolution and due to black and white colors of the images of 1954 and 1981, it has been possible to identify only two macro-categories of land use cover: agricultural lands and artificial surfaces. For uniformity, such classification has been applied to 2006 as well, although more detailed information were available thanks to the CORINE land cover data. In order to avoid as much as possible misleading identifications, local authorities, such as the Adige-Euganeo Land Reclamation Consortium, and local farmers were interviewed and shown, as validation, the likely land use cover and minor drainage network maps (Figure 2).

By knowing the likely length of the minor drainage network, it has been possible to estimate the variation of drainage densities over time.

By applying the Soil Conservation Service Method (USDA, 1972), such land use cover maps have been combined with data concerning the hydrological soil groups made available by Veneto Region, in order to obtain Curve Number maps for 1954, 1981 and 2006. Since precise CN values did not exist for the land cover categories identified in the study area, such values have been obtained by averaging plausible values concerning artificial surfaces and agricultural lands found in literature. Still according to the SCS-CN method, direct surface runoff has been computed for each year by considering a uniformly distributed rainfall over the study area. Maximum rainfall values for different return times (2, 5, 10, 30, 50, 100 and 200 years) and durations (1 and 3 hours) registered at the meteorological station of Este, have been used for the aforementioned purpose.

The effects of drainage network storage capacity on direct runoff from 1954 to 2006 have been analyzed through the application of the so-called "*Residual runoff*" index (m^3/ha) (Eq.1):

$$\textit{Residual runoff} = \text{Direct runoff} - \text{Storage capacity} \quad (1)$$

The aforementioned index has been computed for each 100 m x 100 m square sub-area.

Since the semi-automatic approach, which has been applied for the 2006, gives, as output for each cell, also the average width and the consequent average cross section area of ditches, it has been possible to estimate the likely storage capacity for 1954 and 1981 as well, by simply multiplying the ditches length by the cross section areas for that cell. For this analysis, the upstream contributions are not accounted for because this assessment aims to identify the presence of areas that may be already in critical condition for the runoff directly produced by the input local rainfall.

Study area

The study site is a small area covering about 266 ha and it is located within a flooded area identified according to warnings made by people

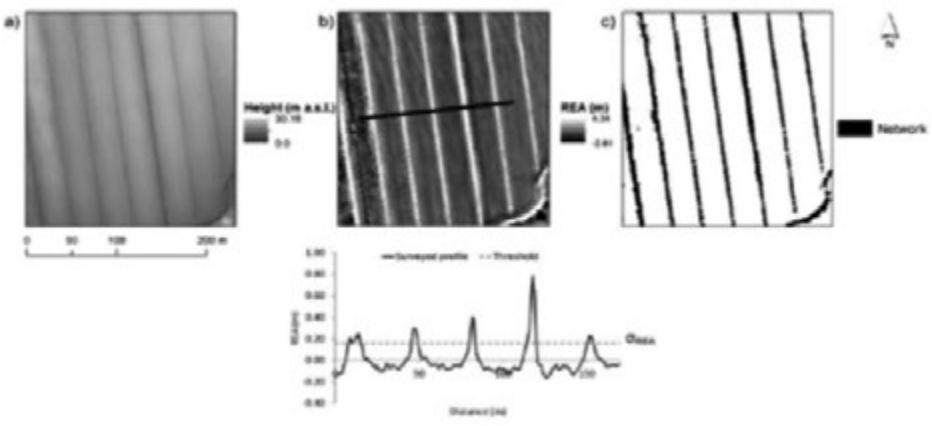

Figure 1. a) Input DTM, b) derived REA map and the threshold identified (standard deviation of REA) to detect the network, c) boolean map obtained from the methodology applied where features can take only binary values: 1 or 0 for network and landscape pixels respectively (modified from Sofia, 2012).

during the major Veneto flood event of 2010. It is placed between the municipalities of Montagnana and Megliadino San Fidenzio (province of Padua), and it is about 12 km far from the meteorological station of Este (Figure 3).

The area belongs to the Brenta-Bacchiglione River Basin Authority and it is located within the boundaries of the Adige-Euganeo Land Reclamation Consortium. Other than for its involvement in the major flood event, the study area has been selected also for the availability of LiDAR DTM and historical images (1954, 1981 and 2006) and because it is a representative of a typical Veneto agrarian landscape.

Results

Land use cover has undergone significant changes from 1954 to 2006. Artificial surfaces increased in extension passing from 16.02 ha in 1954 to 87.57 ha in 2006 to the detriment of agricultural lands. As a consequence, reductions of drainage network length, drainage density and storage capacity values have been registered as well (Table 1 and Figure 4 and 5).

Concerning the effects of drainage network storage capacity on direct runoff, by return times greater than 10 years direct runoff values get much larger than storage capacity ones; therefore, *residual runoff* index starts to lose his meaning. Hence, it is possible to declare that ditches become critical because they already get saturated by considering as input a local rainfall with return times greater than 10 years and 1 hour duration. Given the definition of *residual runoff*, as it gets higher it corresponds to a worsening of the situation (increase in impermeable surfaces) and thus, we move from 1954 to 2006 and vice versa (Figure 6).

Conclusions

This study highlighted the influence of land use changes on drainage network systems and direct runoff. Since drainage networks in agrarian landscapes within floodplains are expected to affect hydrological response during floods (Cazorzi *et al.*, 2013), this assessment becomes a crucial tool for flood management. In fact, low values of

Table 1. Table reporting values concerning the variation of land use change, drainage network system, drainage density and storage capacity from 1954 to 2006.

		1954	1981	2006
Land use cover (ha)	Artificial surfaces	16.02	40.95	87.57
	Agricultural lands	249.98	225.05	178.43
Drainage network system (km)		58.70	47.13	30.08
Drainage Density (km/km^2)		22.07	17.72	11.31
Storage capacity (m^3/ha)		28 600	23 900	18 290

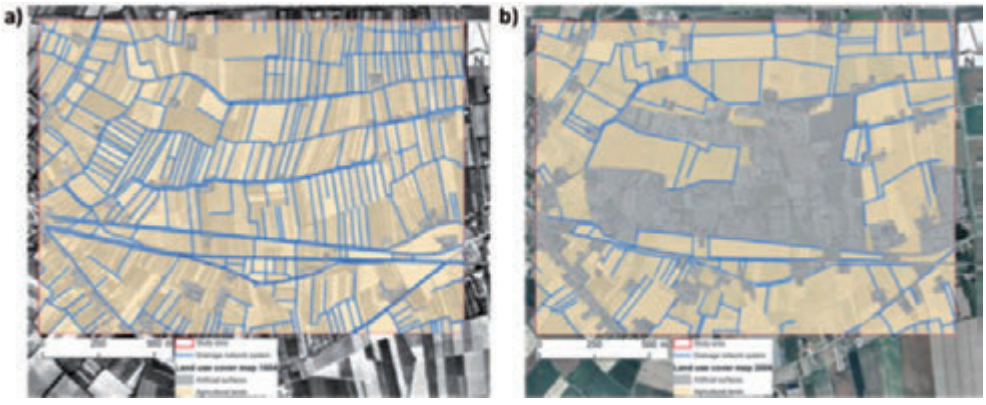

Figure 2. Land use cover maps and likely drainage network system in 1954 (a) and in 2006 (b). In yellowish are represented the agricultural lands while in grayish the artificial surfaces. Blue lines represent ditches and channels.

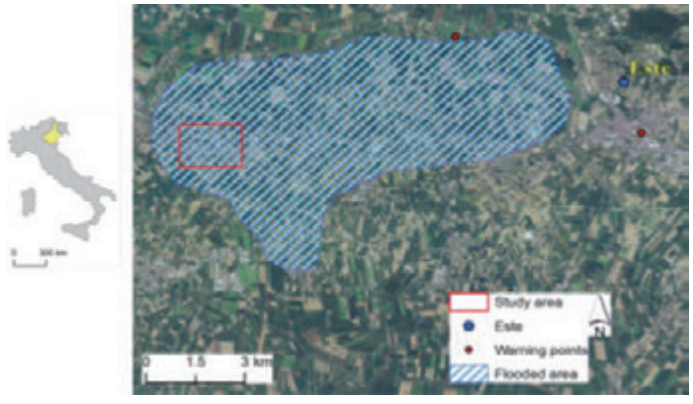

Figure 3. Localization of the study area. It has been selected because of its involvement in the major flood event of 2010.

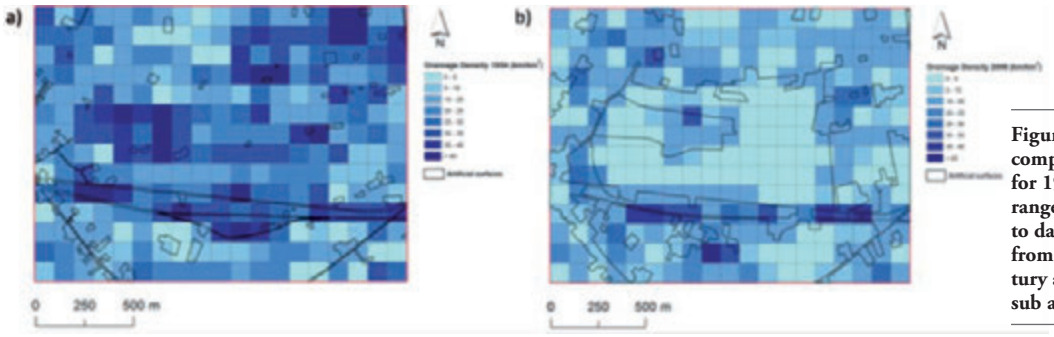

Figure 4. Drainage density maps computed for each sub area (1 ha) for 1954 (a) and 2006 (b). The color ranges from light blue (lower values) to dark blue (higher values). Moving from the 50's to the twenty first century an increase in number of lighter sub areas can be easily detected.

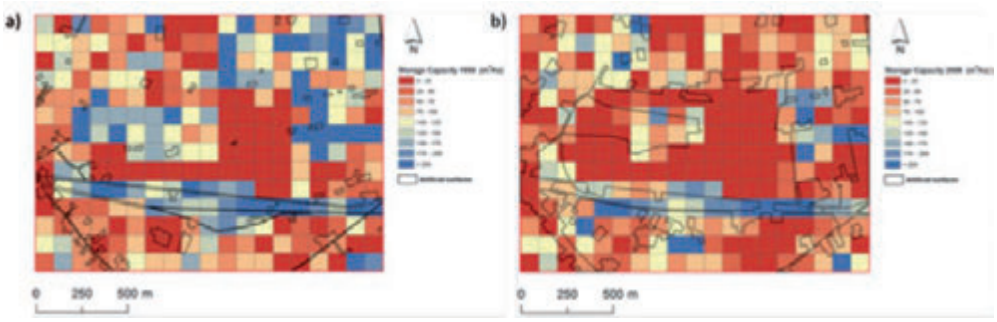

Figure 5. Storage capacity maps computed for each sub area (1 ha) for 1954 (a) and 2006 (b). The color ranges from red (lower values) to blue (higher values). Moving from the 50's to the twenty first century an increase in number of reddish sub areas can be easily detected. Hence, this corresponds to a decrease of the total likely amount of channel storage capacity.

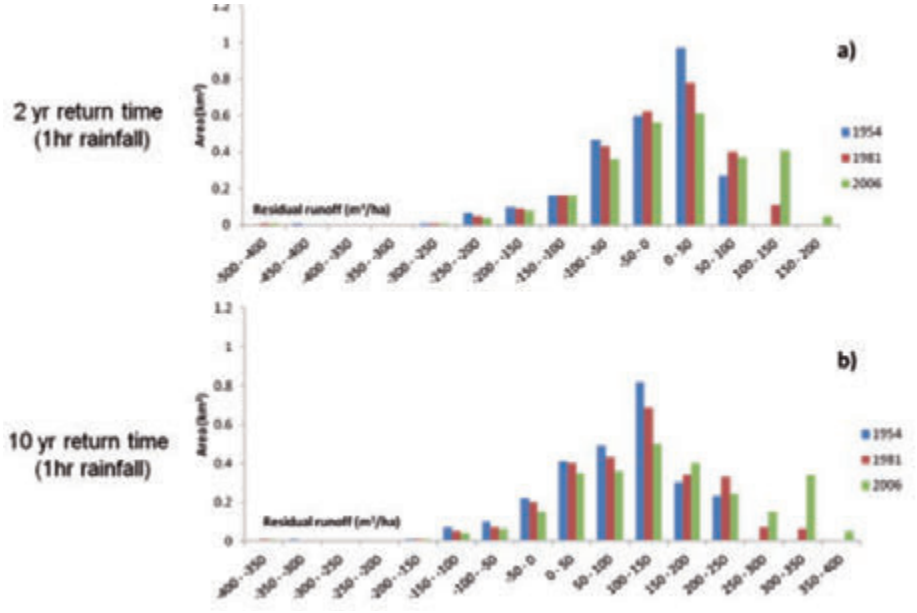

Figure 6. Comparison between the three mean residual runoffs computed for each sub area, by considering a rainfall with return times of 2 and 10 years and 1 hour duration. The lower are the values and the better is the situation from a hydrological point of view. By moving from a 2 years return time to a 10 years return time rainfall, higher residual runoff classes become more representative.

channel storage capacity can i) outline areas whose hydrological behavior is potentially critical during floods, where land use might increase the level of risk, and ii) they allow to identify storage volumes already available on the surface that can contribute to laminate flood peaks. Therefore this work provides an additional proof of suitability of the estimated network parameters (drainage density and storage capacity) in supporting flood management. In addition, by analyzing the effects of drainage network capacity on the direct surface runoff, it has been possible to evaluate the presence of areas that may be already risky simply for the runoff directly produced by the input local rainfall; in this perspective, a simple index (*residual runoff*) has been computed. As main outcomes, this work highlighted that: 1) there might be some issues in the network in the case of rainfall events with return times greater than 10 years and 1 hour duration, and 2) changes in land use should be accounted in planning and managing procedures. The increase of runoff due to land use change should always be accounted for, and it should be operationally compensated by a corresponding increase of the storage capacity. If this is not accomplished,

an increase of the residual runoff should be expected, with problems related to its control, especially when dealing with floods.

References

Booth A.M., Roering J.J., Perron J.T. 2009. Automated landslide mapping using spectral analysis and high-resolution topographic data: Puget Sound lowlands, Washington, and Portland Hills, Oregon. Geomorphology 109: 132-147. doi:10.1016/j.geomorph.2009.02.027.

Bronstert A. 1996. River flooding in Germany: influenced by climatic change? Physics and Chemistry of the Earth 20(5-6): 445-450.

Bronstert A., Niehoff D., Burger G. 2001. Effects of climate and land-use change on storm runoff generation: present knowledge and modeling capabilities. Hydrological Processes 16: 509-529.

Cavalli M., Tarolli P., Marchi L., Dalla Fontana G. 2008. The effectiveness of airborne LiDAR data in the recognition of channel bed morphology. Catena 73: 249-260. doi:10.1016/j.catena.2007.11.001.

Cavalli M., Tarolli P. 2011. Application of LiDAR technology for rivers analysis. Italian Journal of Engineering Geology and Environment. Special Issue 1: 33-44. doi:10.4408/IJEGE.2011-01.S-03.

Cazorzi F., Dalla Fontana G., De Luca A., Sofia G., Tarolli P. 2013. Drainage network detection and assessment of network storage capacity in agrarian landscape. Hydrological Processes. 27(4): 541-553. doi: 10.1002/hyp.9224.

Charlton M.E., Large A.R.G., Fuller I.C. 2003. Application Of Airborne LiDAR In River Environments: The River Coquet, Northumberland, Uk. Earth Surf. Process. Landforms 28: 299–306.

Fregolent L. 2005. Governare la dispersione. FrancoAngeli, Milano.

Fregolent L. 2012. La città a bassa densità: problemi e gestione. TeMA Journal of Land Use, Mobility and Environment, 5(1): 7-19.

Heritage G., Hetherington D. 2007. Towards a protocol for laser scanning in fluvial geomorphology. Earth Surf. Process. Landforms 32: 66–74.

Hilldale R.C., Raff D. 2008. Assessing the ability of airborne LiDAR to map river bathymetry. Earth Surface Processes and Landforms 33: 773-783.

Indovina F. 1990. La città diffusa. Daest-IUAV, Venezia.

Indovina F., Fregolent L., Savino M. 2004. L'esplosione della città. Editrice Compositori, Bologna.

Indovina F. 2009. Dalla città diffusa all'arcipelago metropolitano. FrancoAngeli, Milano.

Jones A.F., Brewer P.A., Johnstone E., Macklin M.G. 2007. High resolution interpretative geomorphological mapping of river valley environments using airborne LiDAR data. Earth Surface Processes and Landforms 21: 1574-1592.

Kasai M., Ikeda M., Asahina T., Fujisawa K., 2009. LiDAR-derived DEM evaluation of deep-seated landslides in a steep and rocky region of Japan. Geomorphology 113: 57-69.

Kundzewicz Z.W., Kaczmarek Z. 2000. Coping with hydrological extremes. Water International 25(1): 66-75.

Kundzewicz Z.W., Takeuchi K. 1999. Flood protection and management: quo vadimus? Hydrological Sciences Journal 44(3): 417-432.

Lashermes B., Foufoula-Georgiou E., Dietrich W.E. 2007. Channel network extraction from high resolution topography using wavelets. Geophysical Research Letters 34, L23S04, doi:10.1029/2007GL031140.

Legleiter C.J. 2012. Remote measurement of river morphology via fusion of LiDAR topography and spectrally based bathymetry. Earth Surface Processes and Landforms 37(5): 499-518.

Leopold B.L. 1968. Hydrology for Urban Land Planning – A Guidebook on the Hydrologic Effects of Urban Land Use. Geological Survey Circular 554. Washington.

Longfield S.A., Macklin M.G. 1999. The influence of recent environmental change on flooding and sediment fluxes in the Yorkshire Ouse basin. Hydrological Processes 13(7): 1051-1066.

Notebaert B., Verstraeten G., Govers G., Poesen J. 2009. Qualitative and quantitative applications of LiDAR imagery in fluvial geomorphology. Earth Surface Processes and Landforms 34, 217-231.

Orlandini S., Tarolli P., Moretti G., Dalla Fontana G. 2011. On the prediction of channel heads in a complex alpine terrain using gridded elevation data. Water Resources Research 47, W02538. doi:10.1029/2010WR009648.

Sofia G. 2012. Digital terrain analysis for hydrogeomorphic feature recognition. PhD Degree Diss., Università di Padova, Italy.

Tarolli P., Tarboton D.G. 2006. A New Method for Determination of Most Likely Landslide Initiation Points and the Evaluation of Digital Terrain Model Scale in Terrain Stability Mapping. Hydrology and Earth System Science 10: 663-677. doi:10: 663-677.

Tarolli P., Dalla Fontana G. 2009. Hillslope to valley transition morphology: new opportunities from high resolution DTMs. Geomorphology 113: 47-56.doi:10.1016/j.geomorph.2009.02.006.

Tosi M.C., Munarin S. 2004. Tracce di città. Esplorazioni di un territorio abitato: l'area veneta. FrancoAngeli, Milano.

Vianello A., Cavalli M., Tarolli P. 2009. LiDAR-derived slopes for headwater channel network analysis. Catena 76, 97-106. doi:10.1016/j.catena.2008.09.012.

Urban-rural gradient detection using multivariate spatial analysis and landscape metrics

Marco Vizzari,[1] Maurizia Sigura[2]

[1]Corresponding Author, Department of Man and Territory. University of Perugia, Perugia, Italy; [2]Department of Agricultural and Environmental Sciences, University of Udine, Udine, Italy

Abstract

The gradient approach allows for an innovative representation of landscape composition and configuration not presupposing spatial discontinuities typical of the conventional methods of analysis. Also the urban-rural dichotomy can be better understood through a continuous landscape gradient whose characterization changes accordingly to natural and anthropic variables taken into account and to the spatio-temporal scale adopted for the study. The research was aimed at the analysis of an urban-rural gradient within a study area located in central Italy, using spatial indicators associated with urbanization, agriculture and natural elements. A multivariate spatial analysis (MSA) of such indicators enabled the identification of urban, agricultural and natural dominated areas, as well as specific landscape transitions where the most relevant relationships between agriculture and other landscape components were detected. Landscapes derived from MSA were studied by a set of key landscape pattern metrics within a framework oriented to the structural characterization of the whole urban-rural gradient. The results showed two distinct sub-gradients: one urban-agricultural and one agricultural-natural, both characterized by different fringe areas. This application highlighted how the proposed methodology can represent a reliable approach supporting modern landscape planning and management.

Introduction

Correspondence: Marco Vizzari, Department of Man and Territory. University of Perugia, Borgo XX Giugno 74, 06131 Perugia, Italy.

Key words: agriculture, kernel density estimation, landscape metrics, multivariate spatial analysis, transitional landscapes, urban-rural gradient.

Acknowledgements: this study was developed within a wider project named "Agricultural peri-urban landscapes of Umbria: identification, planning, and management", funded in 2009 by the Bank of Perugia Foundation.

Journal of Agricultural Engineering 2013; XLIV(s1):e91
doi:10.4081/jae.2013.(s1):e91

European landscapes are intensively changing because human impacts on ecosystems are increasing at unprecedented and accelerated rates (Pearson and McAlpine, 2010). Human activities are the major forces in shaping landscape, creating a mosaic of natural and human-managed patches that vary in type, size, shape, and arrangement. Landscape structure and ecosystem configuration are critical to understanding ecological processes and functions since they directly affect the distribution of energy, materials, and species. Human influences on landscape structure are so numerous and different as to necessitate an analysis of their combined effects through a gradient of landscape modifications (Godron and Forman, 1983). The gradient analysis is a well established approach to study the ecology and the distribution of plants and animals in response to physical, chemical, ecological and climatic conditions of the environment. Simple gradients, as well as complex gradients can be found in landscapes. The former refer to environmental series due to a single measured environmental factor, while the latter are generated by several factors (man-made or natural) some of which may interact (McDonnell *et al.*, 1993). Anthropogenic gradients were defined by Forman and Godron (1986) as the succession in the space of natural–managed–cultivated–suburban–urban landscapes. Along this gradient, a progressive change in the landscape structure can be observed and different characteristics of structural elements can be pointed out. Moving from the most natural to the most humanized landscape, man-made patches tend to increase, while natural resources patches tend to decrease. Patch density, and in general fragmentation, tends to increase as well as the regularity of patch shape, whereas the mean values of patch size and landscape connectivity tend to decrease.

In the gradient view, the urban-rural dichotomy can be thought of as a landscape gradient, if considered as a sliding level of human influence from rural to urban landscape, including ecological processes, flows and movements of goods, energy, people, capital, and information (Modica *et al*., 2012). The urban-rural gradient approach is commonly used to investigate how urbanisation phenomena are changing the ecological patterns and related processes across the landscape (McDonnell and Pickett, 1990; Luck and Wu, 2002; Hahs and McDonnell, 2006; Yang *et al.*, 2010). Urbanization itself can be considered as a particular environmental gradient that produces relevant modifications on the structures and functions of ecological systems (McDonnell and Hahs, 2008). Moreover the urban-rural gradient analysis turns out to be fundamental in the identification and characterization of specific land use/land cover transition areas, characterized by peculiar and crucial ecological processes such as the peri-urban and the agro-forestry fringes. In the light of such complexity, the analysis of spatio-temporal and morpho-functional dynamics of landscape gradients should be supported by efficient and objective quantitative approaches based on methods aimed at the modelling of spatial data. Gradient analysis and landscape pattern analysis seem appropriate for such studies (Luck and Wu, 2002; Zhang et al, 2004). One effective method for representing and analysing landscape gradients is using Kernel Density Estimation (KDE) techniques applied on inten-

sity indicators associated with geographic features (Torrens and Alberti, 2000; Vizzari, 2011a; Vizzari, 2011b; Modica *et al.*, 2012).

The quantification of spatial heterogeneity of landscape is necessary to explore relationships between ecological processes and spatial patterns (Forman & Godron, 1986; Palmer, 2008; Turner, 1990). A great variety of metrics aimed at the study of landscape composition and configuration were developed and applied to the analysis of urbanized systems (Wu, 2000; Botequilha Leitão and Ahern 2002; Li *et al.*, 2005; Uuemaa *et al.*, 2009).

In order to capture the spatial structure generated by land uses, this study integrates gradient analysis with pattern metrics to quantitatively characterize the landscape. The central assumption is that urban-rural gradient structure is mainly determined by three key components which generate, in turn, detectable landscape gradients: urbanization, agriculture and natural elements. Detection and analysis of the spatial organization of these main gradients are key steps for understanding the complexity of anthropized landscapes. Within this framework we aimed to address three core goals: (1) representation and analysis of landscape gradients produced by urbanization, agriculture, and natural elements; (2) urban-rural gradient classification and subdivision through multivariate analysis of said gradients; (3) characterization of the gradient and landscapes obtained from the previous analysis, with a particular focus on peri-urban and agro-forestry fringes.

Figure 1. Geographic location of the area under investigation.

Materials and methods

The 493 Km^2 wide study area comprises the Italian municipalities of Assisi, Bastia, Bettona, and Cannara (Figure 1). The area is characterized by a very typical landscape of central Italy composed of 54% of agricultural land, 34% forests and semi-natural areas, 9% of built-up areas and 3% of wetlands and water bodies (Corine Land Cover 2006, personal elaboration). Morphologically the area is characterized by a central wide plain in which intensive agricultural farms, urban and productive settlements are located. At the edge of this plain (on the NE and SW) there are two low hillsides dominated by very typical olive-growing agricultural area. The innermost higher hills are occupied mainly by agro-forestry areas, woodlands and grasslands of varying extent. In the middle of the area is Mount Subasio (1290 m), which, together with the city of Assisi, is the most prominent element of cultural identity for the entire landscape under investigation. The area, because of its characteristics and ongoing transformations, was considered very appropriate for the application and validation of the proposed methodology. The general purpose was the exploration of the spatio-functional relationships between the key landscape components in order to identify sensible and representative areas on which to define sound guidelines supporting spatial planning. The methodology was developed through three main steps: (a) spatial modelling of gradients generated by key landscape components; (b) multivariate spatial analysis and landscape classification; (c) analysis of landscape structure.

Spatial modelling of gradients generated by key landscape components

Urbanization, agriculture, and natural elements were assumed to be key components of the urban-rural gradient of the area and represented and analysed independently. In view of the specific nature of their landscape gradients, a continuous analytical approach for the representation of these variables was adopted. GIS gridding techniques were applied to interpolate a defined pool of values for variables, referring to known parts of the territory, in order to reconstruct the most likely distribution of the phenomenon in the entire study area (Bailey and Gatrell, 1995; Longley *et al.*, 2005; Smith *et al.*, 2007). Between the various gridding techniques, density analysis makes it possible to transform values measured at specific locations as continuous surfaces representing the general trend of the spatial distribution for the considered variable. Kernel Density Estimation (KDE) is a particular density analysis that produces smoother surfaces, according to a kernel function, that appears more representative of landscape gradients (Vizzari, 2011b). In KDE, a moving window is superimposed over a grid of locations and the density of events is estimated at each location using a distance-weighted function, with the degree of smoothing controlled by the kernel bandwidth (Gatrell *et al.*, 1996). The application of KDE requires the choice of the kernel function (*e.g.*: Gaussian, triangular, quartic) and the definition of three key parameters: bandwidth, cell size and intensity (Silverman, 1986). However the choice among the various kernel functions does not significantly affect the outcomes of the process (Epanechnikov, 1969). Differently, bandwidth definition represents the most problematic step, but also the most useful for exploratory purposes, since a wider radius shows a more general trend over the study area, smoothing the spatial variation of the phenomenon, while a narrower radius highlights more localized effects such as 'peaks and troughs' in the distribution (Jones *et al.*, 1996; Borruso, 2008). Despite the many approaches available in the literature, visual examination of the resulting surfaces for different values of bandwidth remains a common method supporting the definition of this parameter (Bailey and Gatrell, 1995; Lloyd, 2007; Vizzari, 2011b). A bandwidth of 500 m was considered effective for a reliable generalization of landscape gradient at the scale adopted for the analysis. Cell dimension was set to 50 m, a lower value than the coarsest legible resolution according to Hengl (2006).

Multivariate spatial analysis and landscape classification

The spatial relationships between the gradient's components were subsequently analyzed using a multivariate technique based on the ISODATA (Iterative Self-Organizing Data Analysis Technique A) algorithm (Ball and Hall, 1965, Richards, 1999). This technique makes it possible to organize the basic data into a number of groups (or clusters) such that units belonging to the same group are more similar, in accordance to a given similarity measure, than those units belonging to different groups. The number of clusters and their characteristics are to be determined a priori, even if the number of final groups may differ from the initial one as a result of the optimization procedures for this method. Prior to the application of the ISODATA technique, it is appropriate to proceed with suitable variable standardization in order to avoid that the different ranges of variation may alter the final classification. In this application standardization has been performed through a linear normalization between 0 and 1.

Analysis of landscapes structure

A set of landscape metrics was used for this study including patch density (PD), mean patch size (MPS), edge density (ED), largest patch index (LPI), landscape shape index (LSI), Simpson's evenness index (SIEI), and percentage of landscape (PLAND) (Table 1). Certain metrics were used to examine landscape-level properties, *i.e.* to describe the spatial patterns of all land-use types as a whole. Other metrics were used to examine class-level properties, *i.e.* to describe the spatial patterns of different land-use types in the urban-rural and agricultural-forestry fringe areas.

At the landscape level, dynamics of patch size, patch density, shape and landscape diversity were detected and some of the hypotheses on landscape structural responses along a human transformation gradient, as postulated by Forman and Godron (1986), were tested.

Considering the non-normal distribution of the data and the different composition of samples, the influence of urban-rural gradient on the landscape configuration was examined on each metric using a rank-based (Kruskal-Wallis) modified robust Brown-Forsythe Levene-type test based on the absolute deviations from the median (Hines and Hines, 2000). Peri-urban and agro-forestry fringes were analysed on the basis of landscape composition using the PLAND metrics to better understand the roles of the different land uses in influencing the fringe areas (Table 1). In this phase eight classes of land use were considered: woodlands, orchards, olive groves, vineyards, built-up areas, grasslands, arable land with trees, arable land.

Table 1. Landscape metrics (based on McGarigal and Marks, 1995) used to quantify the spatial patterns of landscape types along the urban-rural gradient.

Landscape metric	Abbreviation	Description
Patch Density (n./100 ha)	PD	Number of patche per 100 ha
Edge Density	ED	Amount of edge relative to the landscape area
Mean patch size (ha)	MPS	Average area of landscape patches
Largest patch index (%)	LPI	Ratio between the area of the largest patch and the total landscape area
Landscape shape index	LSI	Total length of patches edges divided by the total area adjusted by a constant for a square standard (raster format)
Simpson's Evenness Index	SIEI	Measure of the distribution of area among patch types
Percentage of Landscape	PLAND	Measure of percentage of patch types

Results

Urban-rural gradient detection and characterization

Landscape gradient generated by urbanization

The landscape gradient determined by urbanization was studied analysing the population density by means of official census data available for the year 2000 (ISTAT, 2001). However, using census zones as a geographic reference of the population data may generate spatial inconsistencies especially in wider, less populated zones. Thus, the positional accuracy of census data was improved using the polygons of built-up classes contained in the 2000 Land Use and Land Cover (RERU, 2002) through a spatial matching process of the two datasets. This approach made it possible to associate every point of the total population of a census zone averaged with the total number of points falling in the same zone. On this last dataset a KDE analysis, using the parameters specified previously, was performed generating a spatial index known as UDI (Urban Density Index). The index, which expresses the number of inhabitants per square kilometre, allowed an effective representation of the urbanization gradient of the area under investigation.

Landscape gradient generated by agriculture

The landscape gradients generated by agricultural land uses were studied separating two different components that appear dominant within the landscape under investigation: arable crops and olive groves. Since these two kinds of cultivations produce very different agro-ecosystems, the relative spatial gradients have been represented and analyzed separately. The spatial distribution of arable crops was obtained through the Common Agricultural Policy (CAP) data for the year 2000 linked with the georeferenced centroids of the cadastral parcels. The use of the parcel centroids, instead of the polygons, helped to solve the problems related to multiple correspondence between CAP and cadastral data, related to the presence of multiple agricultural uses within the same parcel. Landscape gradient generated by olive groves was analyzed using national olive trees inventories available for year 2000. A double KDE procedure based on the parameters defined above produced an Arable crops Density Index (ADI) and an Olive groves Density Index (ODI). The former represents the percentage of total landscape area occupied by arable crops, while the latter expresses the number of olive trees per hectare of surface. The combined interpretation of the two indices supported the analysis of the spatial configuration and composition of the agricultural gradients within the study area.

Landscape gradient generated by natural elements

In order to proceed with the analysis of this gradient, forests and grassland polygons were extracted from the LULC 2000 dataset with the aim of isolating the elements with natural characteristics useful for representing the natural gradient. Again on this dataset we applied the KDE using the same parameters defined above. Analysis of the natural elements density has produced a continuous index, known as NDI (Natural elements Density Index), which expresses locally the ratio between the area occupied by the natural elements and the total land-

scape area. This index made it possible to effectively represent the landscape gradient generated by the natural elements within the landscape under investigation.

Landscape subdivision and classification

Starting from ten classes set initially, the ISODATA multivariate analysis produced eight final clusters which were denominated according to their specific characteristics (Figure 2). The clusters, considering their particular composition, can be ordered according to a typical sequence of an urban-rural gradient of central Italy, plotting on a graph the outcomes of the four gradient indicators (Figure 3). For the purpose of an overall analysis of the agricultural intensity, the two indicators ADI and ODI can be summed into a single indicator for better understand the general trend of the agricultural density along the same gradient (Figure 3).

Landscape pattern analysis

The multivariate analysis allowed the classification of different landscape patterns along the urban-rural gradient. For five of the seven landscape metrics Levene's test highlighted different variances among the eight sample classes (Table 2). Only ED showed homogeneity of variances between the landscape clusters. Patch size coefficient of variation were most distinct in agricultural landscapes (AMI, AHI, AOG, AFN) and natural landscapes (ANT, NL) than in urbanized areas (U, UAT).

In order to study the evolution of the metrics along the gradient, the latter were plotted using box-plot graphs ordered according to the sequence defined previously (Figure 4). Patch Density increases from urbanized areas to agricultural landscape, with the exception of intensive agricultural landscape (AHI) where the value decreases dramatically. The same metric decreases progressively moving from traditional agricultural areas (AOG) to the most natural ones. In general, landscapes dominated by traditional agriculture (AOG, AFM) and natural land covers (ANT, NL), as well as, in the intensive agricultural landscapes (AHI) are characterized by lower variability in PD. Regarding dominance of the landscape by few land uses, LPI shows high variability for all the landscapes defined by the gradient. The highest median values were found for urbanized areas (U), intensive agricultural landscape (AHI) and natural landscapes (NL), as an effect of an extent matrix represented by settlements, croplands and forest habitat respectively.

Information regarding landscape fragmentation also came from the ED index (not represented since highly correlated to PD), as we assumed low values associated with a lower number of interfaces between different types of patches and consequently less variation in patch shape. ED highlights the relative simplification of intensive agricultural landscapes, while transitional ones, both from urban to agricultural (U to AMI) and from agricultural to natural (AOG to NL) are characterized, respectively, by an increasing and decreasing trend of diversity in their structure. These results were confirmed by LSI, showing a parabolic shape trend moving from most urbanized (U) to agricultural intensive landscapes (AHI). The higher shape complexity is associated with traditional agricultural landscapes (AOG), dominated by olive groves, while, moving towards the most natural landscapes (NL), LSI assumes low values on average, but with a high variability, within landscapes oriented to agro-forestry activities (AFM) and in the semi-natural ones (ANT). Landscape simplification for intensive cultivated landscapes are also confirmed by the SIEI, while an even distribution among patch types results especially in transition landscapes from urban to agricultural areas (UAT and AMI) and in less intensive agricultural landscapes (AOG, AFM, and ANT).

The analysis of landscape composition (PLAND), developed specifically for peri-urban and agro-forestry transitional landscapes (UAT, AMI, AFM, ANT), shows a diffuse presence of settlements, but their

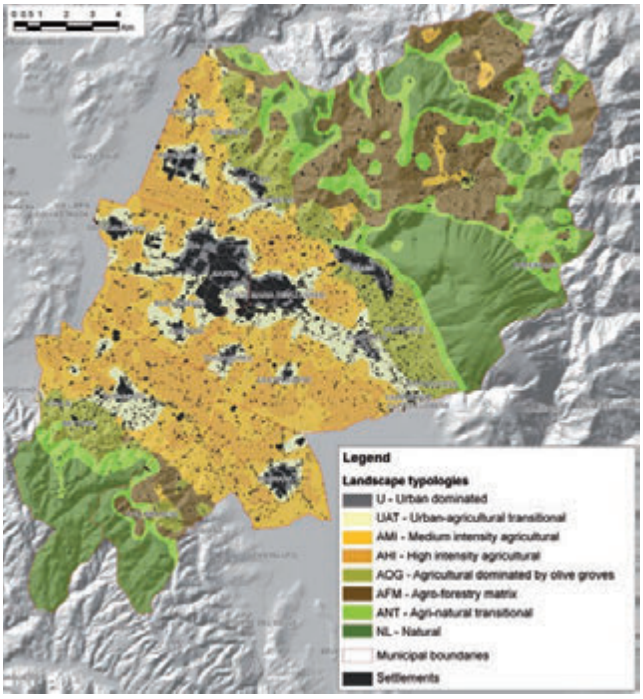

Figure 2. Landscape subdivision generated by cluster analysis.

Table 2. Sample size and mean value of metrics calculated for the landscape types. Modified robust Brown Forsythe Levene type tests were significant showing different variances between the datasets.

Landscapes	U	UAT	AMI	AHI	AOG	AFM	ANT	NL
Sample size	11	16	10	28	9	15	14	14
MPS (ha)	2,44*	1,72*	1,27*	3,28*	1,31*	2,01*	2,37*	8,03*
PD (n./100 ha)	56*	73*	86*	36*	85*	58*	47*	25*
ED (m/ha)	232	297	327	168	305	264	252	169
LPI (%)	67*	40*	52*	82*	37*	39*	46*	62*
LSI	4,44*	6,43*	7,53*	3,36*	9,37*	7,29*	7,00*	4,19*
SIEI	0,54*	0,63*	0,57*	0,22*	0,75*	0,71*	0,69*	0,51*

*= p<0,05.

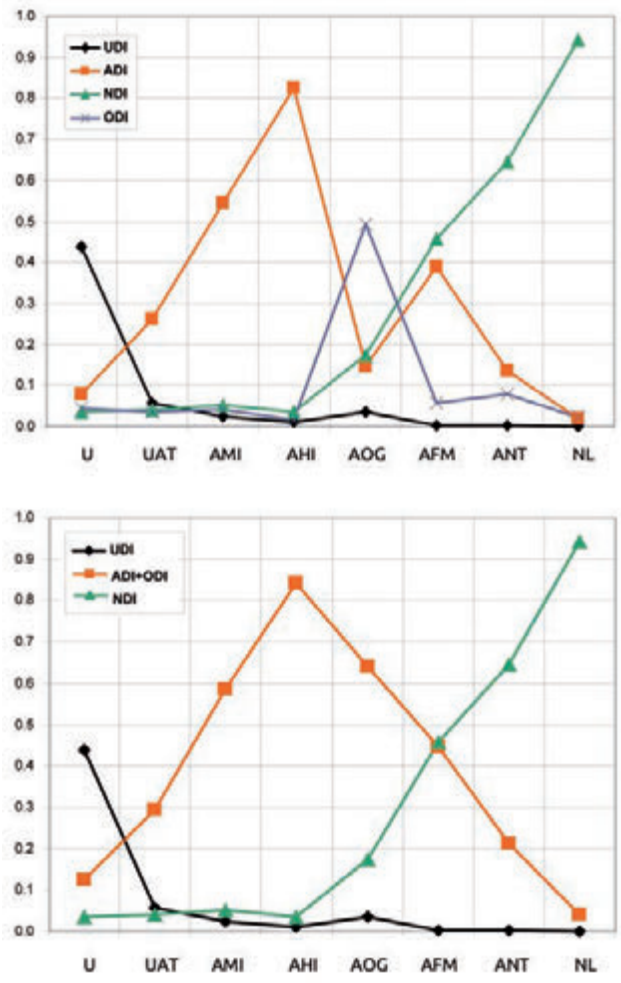

Figure 3. Average values of the four spatial indicators within the landscapes typologies located along the urban-rural gradient.

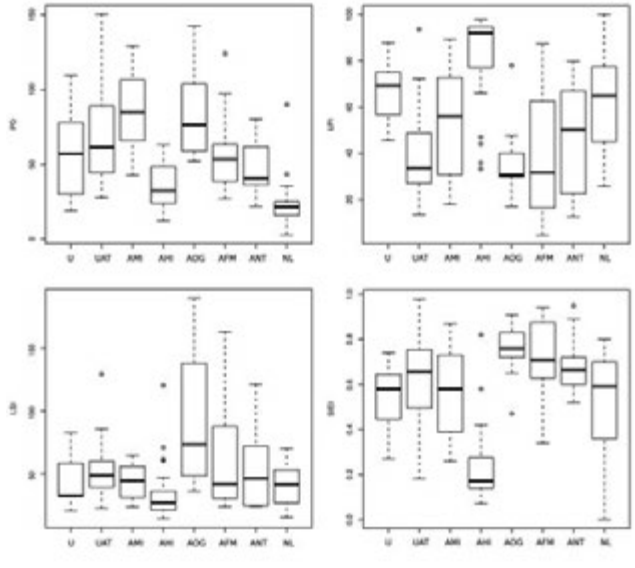

Figure 4. Values of Patch Density index (PD), Largest patch index (LPI), Landscape shape index (LSI), Simpson's Evenness Index (SIEI) for the landscape typologies located along the gradient. Median (line within the white box), upper and lower quartiles (box), maximum-minimum range (whiskers) and outliers are shown.

incidence indicates an evident characterizing function only in transitional urban-agricultural landscapes (UAT) (Table 3). The occurrence of arable land within the four landscape typologies is generally higher, also influencing the most natural landscapes. Semi-natural habitats play an important role only in the rural-forestry fringes, while in the urban rural fringe, a lower percentage of area is occupied by woodlands. Otherwise, the tree crops (olive groves, orchards, and vineyards) are less important for the characterization of the four landscapes.

Discussion

The gradient modelling and the subsequent multivariate analysis conducted to an effective classification in eight landscape typologies, reflects the spatial variability of the area under investigation. Each landscape typology represents a specific portion of the urban-rural gradient and is differentiated by a peculiar composition and configuration.

An overall analysis of the results suggests the subdivision of the general urban-rural gradient of the area into two sub-gradients: an urban-agricultural one (UAsg, from landscapes U to AHI) and an agricultural-natural one (ANsg, from landscapes AHI to N). The former is characterized by a decreasing incidence of urbanization and an increasing level of agriculture, while the latter is distinguished by an increasing level of natural and semi-natural land covers and a decreasing incidence of agricultural uses. Between the extremes of each sub-gradient can be identified interesting transitional landscapes with very peculiar characteristics and transformations related to their diversity and to the relevant spatio-functional interactions between their variegated land uses and covers. The transitional landscape of the UAsg (UAT and AMI) shows a medium diversity and is characterized by a consistent interaction between urban and agricultural areas. The most relevant transformations within these landscapes are related to typical urban dynamics (soil sealing, build-up sprawl and spreading, roads development) to the detriment of agricultural diversity. Differently, the transitional landscapes of AHsg (AOG, AFM, and ANT) are characterized by the higher diversity of the area and enclose a very relevant agro-forestry mosaic. The AFM and ANT landscapes contain the most important high natural value farmland of the area under investigation. Within these contexts the low input and extensive agriculture supports, or is associated with, either a high species and habitat diversity or the presence of species of conservation concern (Andersen *et al.*, 2003; Paracchini *et al.*, 2008).

These results partially confirm the generally predictable characteristics for landscapes in similar human gradients postulated by Forman and Godron (1986). Moreover our results broadly agree with

Table 3. Percentage of landscape (PLAND) of different LULC classes within transitional landscapes.

LULC classes	UAT	AMI	AFM	ANT
Woodlands	3	4	31	58
Orchards	0	0	0	0
Olive groves	1	2	5	6
Vineyards	3	3	0	0
Built-up areas	26	9	4	2
Grasslands	0	0	8	13
Arable lands with trees	4	2	3	1
Arable lands	63	80	49	20

those obtained from analyses of urban to rural gradients in metropolitan areas. Zhang *et al.* (2004) from a GIS-based gradient analysis of urban landscape pattern of the Shanghai metropolitan area, point out an increasing patch density (PD), edge density (ED), and landscape shape complexity (LSI), and sharp decreases in the largest and mean patch size (LPI and MPS). However, in the USA urban land use is associated with the least values for mean patch size and largest patch index and with the largest patch density (Luck and Wu, 2002). A positive relationship between fragmentation and the degree of urbanization has been demonstrated by increases in patch density and decreases in mean patch size from the urban centre to the surrounding fringe areas, while rural landscapes are single land-use dominant and homogeneous (Weng, 2007). In our study this evidence is generally verified except for the traditional rural landscapes which are characterized by a great heterogeneity due to the traditional mosaic of croplands. From the rural-forestry fringes to the natural landscapes, fragmentation of patterns decreased again, but in favour of woodland dominated and well connected natural habitats. Regarding landscape diversity the SIEI shows a quite fluctuating trend. It increased from urbanized areas to urban-agricultural transitional landscapes and then decreased dramatically in intensive agricultural landscape as a consequence of landscape simplification mainly due to agriculture intensification (Kleijn *et al.*, 2011; Bonfanti *et al.*, 1997).

Conclusions

The study adopted a combined method of gradient analysis and landscape metrics to analyze the landscape gradients due to urbanization, agriculture and natural land covers in a typical landscape of central Italy. The urban–rural gradient is one of the techniques commonly used to investigate how urbanisation is changing the ecological patterns and processes across the landscape. The strong interactions between the typical heterogeneous land use of the intermixed fringe areas make it necessary to consider agriculture as a key component of the system. The gradient approach and the multivariate analysis allowed the identification of eight landscape typologies, reflecting the spatial interaction of the landscape gradients considered in the analysis. Calculation of landscape metrics allowed a deeper comprehension of the landscape organization occurring along the urban to rural gradient. As a result, two different sub-gradients were identified: an urban-agricultural one (from urban to agricultural areas) and an agricultural-natural one (from agricultural to natural areas). The overall results pointed out distinct spatial signatures for urban rural fringes and rural-forestry fringes respectively from those of urban and cultivated landscapes. This evidence was found both for land use composition (Table 3) and for landscape configuration, demonstrated by different values of diversity, patch density and patch shape complexity (Figure 4). The specific characteristics of landscape structures reflect different and peculiar processes within the fringes areas. Land-use conflicts, species and habitat conservation, preservation of cultural heritage, changes of lifestyles, products and services from multifunctional agriculture are some of the main issues within peri-urban landscapes. Loss of productive agricultural land, increase in landslide risk, loss of biodiversity associated with agricultural management, degradation of cultural heritage represented by traditional man-made structures are key phenomena associated with agro-forestry landscapes. Identifying the landscape's gradients and patterns and the related ecological and socioeconomic issues is an important preliminary step for an effective spatial planning process.

References

Andersen E., Baldock D., Bennett H., Beaufoy G., Bignal E., Brouwer F., Elbersen B., Eiden G., Godeschalk F., Jones G., McCracken D.I., Nieuwenhuizen W., Van Eupen M., Hennekens S., Zervas G., 2003. Developing a high nature value indicator. Report for the European Environment Agency. Copenaghen.

Bailey T.C., Gatrell A.C., 1995. Interactive spatial data analysis, New York Wiley Geographical Analysis in Baller R.L., Anselin S., Messner G., Hawkins D. (Editors) Longman Higher Education, Harlow.

Ball G.H., Hall D.J. 1965. ISODATA, A novel method of data analysis and pattern classification. Stanford Research Institute, Menlo Park, California.

Bonfanti P., Fregonese A., Sigura M. 1997. Landscape analysis in areas affected by land consolidation. Landscape and Urban Planning, 37(1–2): 91–98.

Borruso G., 2008. Network Density Estimation: A GIS Approach for Analysing Point Patterns in a Network Space. Transactions in GIS 12: 377–402.

Botequilha Leitão A., Ahern J. 2002. Applying landscape ecological concepts and metrics in sustainable landscape planning. Landscape Urban Planning 59 (2): 65–93.

Epanechnikov V.A. 1969. Nonparametric estimation of a multidimensional probability density. Teor. Veroyatnost. i Primenen. 14: 156–161.

Forman R.T.T., Godron. M. 1986. Landscape ecology. John Wiley & Sons, New York.

Gatrell A.C., Bailey T.C., Diggle P.J., Rowlingson B.S. 1996. Spatial point pattern analysis and its application in geographical epidemiology. Transactions of the Institute of British Geographers 21:256–274.

Godron M., Forman. R.T.T. 1983. Landscape modification and changing ecological characteristics. Pages 1-28 in Mooney H. A. and Godron M. (Eds). Disturbance and ecosystems. Springer-Verlag, New York, USA.

Hahs A.K., McDonnell M.J. 2006. Selecting independent measures to quantify Melbourne's urban–rural gradient. Land Urban Plan 78: 435–448.

Hengl T. 2006. Finding the right pixel size. Computers & Geosciences 32: 1283–1298.

Hines W.G.S., Hines R.J.O. 2000. Increased power with modified forms of the Levene (med) test for heterogeneity of variance. Biometrics 56: 451-454.

ISTAT 2001, Italian National Institute of Statistics, "Basi territoriali e variabili censuarie", available from: http://www.istat.it/it/archivio/44523 (accessed on 06/14/2013).

Jones M.C., Marron J.S., Sheather S.J. 1996. A Brief Survey of Bandwidth Selection for Density Estimation. Journal of the American Statistical Association 91: 401–407.

Kleijn D., Rundlöf M., Scheper J., Smith H.G., Tscharntke T. 2011. Does conservation on farmland contribute to halting the biodiversity decline? Trends in Ecology & Evolution 26: 474–481.

Li X., He H.S., Bu R., Wen Q., Chang Y., Hu Y., Li Y. 2005. The adequacy of different landscape metrics for various landscape patterns. Pattern Recognition 38: 2626–2638.

Lloyd: C.D., 2007. Local models for spatial analysis, Population English Edition. CRC Press.

Longley P.A., Goodchild M.F., Maguire D.J., Rhind D.W. 2005. Geographic Information Systems and Science, Information Systems Journal. Wiley.

Luck M., Wu J. 2002. A gradient analysis of urban landscape pattern: a case study from the Phoenix metropolitan region, Arizona, USA. Landscape Ecology 17:327–339.

McDonnell M.J., Pickett S.T.A. 1990. Ecosystem structure and function along urban–rural gradients: an un exploited opportunity for ecology. Ecology 71:1232–1237.

McDonnell M.J., Pickett S.T.A., Pouyat R.V. 1993. The application of the ecological gradient paradigm to the study of urban effects. In: McDonnell, M.J., Pickett, S.T.A. (Eds.), Humans as Components of Ecosystems. Springer-Verlag, New York, NY, 175–189.

McDonnell, M.J., Hahs, A.K. 2008. The use of gradient analysis studies in advancing our understanding of the ecology of urbanizing landscapes: current status and future directions. Landscape Ecology, 23(10): 1143–1155.

McGarigal K., Marks B.J. 1995. FRAGSTATS: Spatial Pattern Analysis Program for Quantifying Landscape Structure, FRAGSTATS Manual. USDA Forest Service.

Modica G., Vizzari M., Pollino M., Fichera C.R., Zoccali P., Di Fazio S., 2012. Spatio-temporal analysis of the urban–rural gradient structure: an application in a Mediterranean mountainous landscape (Serra San Bruno, Italy). Earth System Dynamics 3: 263–279.

Palmer G.C., 2008. Principles and Methods in Landscape Ecology: Towards a Science of Landscape. Austral Ecology 33: 361–362.

Paracchini M.L., Petersen J.E., Hoogeveen Y., Bamps C., Burfield I., Van Swaay C. 2008. High Nature Value Farmland in Europe. An Estimate of the Distribution Patterns on the Basis of Land Cover and Biodiversity Data. Luxembourg.

Pearson D.M., McAlpine C. A. 2010. Landscape ecology: an integrated science for sustainability in a changing world. Landscape Ecology 25:1151-1154.

Richards J.A. 1999. Remote Sensing Digital Image Analysis: An Introduction. Springer-Verlag, Berlin.

Romano B., Ragni B., Orsomando E., Vizzari M., Pungetti G., 2009. Rete Ecologica regionale della Regione Umbria, Petruzzi editore, Perugia.

Silverman B.W., 1986. Density Estimation for Statistics and Data Analysis (Monographs on Statistics and Applied Probability). Chapman and Hall/CRC.

Smith M., Goodchild M., Longley P. 2007. Geospatial Analysis: A Comprehensive Guide to Principles, Techniques and Software Tools (2nd Edn). Matador.

Torrens P.A., Alberti M. 2000. Measuring sprawl. Smart Growth America Washington, DC, London.

Turner M.G., 1990. Spatial and temporal analysis of landscape patterns. Landscape Ecology 4: 21–30.

Uuemaa E., Antrop M., Roosaare J., Marja R., Mander U. 2009. Landscape Metrics and Indices: An Overview of Their Use in Landscape Research. Living Reviews in Landscape Research.

Vizzari M. 2011a. Spatial modelling of potential landscape quality. Applied Geography 31: 108–118.

Vizzari M. 2011b. Spatio-temporal analysis using urban-rural gradient modelling and landscape metrics. Lecture Notes in Computer Science 6782: 103–118.

Weng Y.C. 2007. Spatiotemporal changes of landscape pattern in response to urbanization. Landscape and Urban Planning 81: 341–353.

Wu J. 2000. Landscape Ecology: Pattern, Process, Scale and Hierarchy. Higher Education Press, Beijing, China

Yang Y., Zhou Q., Gong J., Wang Y. 2010. Gradient analysis of landscape pattern spatial-temporal changes in Beijing metropolitan area, China. Science in China. Series E, Technological sciences 53: 91–98.

Zhang L., Wu J., Zhen Y., Shu J. A. 2004. GIS-based gradient analysis of urban landscape pattern of Shanghai metropolitan area, China. Landscape and Urban Planning 69: 1–16.

Determinants of SEA effectiveness: an empirical investigation over municipal spatial planning in Sardinia

Andrea De Montis,[1] Antonio Ledda,[1] Amedeo Ganciu,[1] Mario Barra,[1] Simone Caschili[2]

[1]University of Sassari, Dipartimento di Agraria, Sassari, Italy; [2]UCL QASER Lab & Centre for Advanced Spatial Analysis, University College London Gower Street ,London, UK

Abstract

The late formal tradition of strategic environmental assessment (SEA) European Directive into the Italian planning system has so far induced a variety of behaviour of administrative bodies and planning agencies involved. In Italy and Sardinia, a new approach to landscape planning is characterizing spatial planning practice from the regional to the municipal level. Currently municipalities are adjusting their master plan to the prescriptions of the regional landscape planning instrument (in Italian, Piano Paesaggistico Regionale, PPR), according to processes that have to be integrated with a proper SEA development. With respect to this background, the aim of this paper is to assess the level of SEA implementation on the master plans of Sardinia six years after the approval of the PPR. The first results show that many municipalities are not provided with a master plan (in Italian, Piano Urbanistico Comunale, PUC) and they have in force just an old planning tool. Moreover, just some municipalities have adapted the PUC to the PPR carrying out a SEA process.

Introduction

Italy has acknowledged the European Directive 2001/42/CE (Directive) about the introduction of strategic environmental assessment (SEA) through a series of legislative decrees published from 2006 to 2010. These laws state that SEA must be applied to plans and programs likely to affect the environment and, in particular, interesting given sectors including spatial planning. The Autonomous Region of Sardinia (Region) has acknowledged the Directive by means of two acts approved in 2008 and 2012.

In 2006, the Region has approved a Regional Landscape Plan (in Italian, Piano Paesaggistico Regionale, PPR) constructed according to the Legislative Decree (LD) 42/2004 concerning the code over cultural goods and landscape (Italian Regulation, 2004). The PPR is the main regional landscape planning instrument and it is directed to the protection, valorisation, and promotion of sustainable transformations. The PPR is a spatial coordinator plan, as it indicates guidelines, which need to be implemented by municipal master plan (in Italian, Piano Urbanistico Comunale, PUC). The process of adjustment of the PUC to PPR implies that a SEA procedure is developed in integration with the construction, discussion, and approval of that planning tool.

With respect to this background, the aim of this paper is to assess the level of SEA implementation on the master plans of Sardinia six years after the approval of the PPR.

The paper includes the following arguments. In the next section, the SEA practice context is described, while in the third section some key SEA critical issues are selected and illustrated. In the fourth section, the on-line survey is introduced and referred to the critical issues. In the fifth section, the preliminary results of the survey are shown. In the last section, conclusion is presented.

Correspondence: Andrea De Montis, University of Sassari, Dipartimento di Agraria, Viale Italia 39, 07100 Sassari, Italy.
Tel. +39.079229242 - Fax: +39 079229340.
E-mail: andreadm@uniss.it

Key words: municipal master plans, regional landscape plan, strategic environmental assessment.

Acknowledgement: The authors acknowledge contribution from the research project "Efficacia ed efficienza della governance paesaggistica e territoriale in Sardegna: il ruolo della VAS e delle IDT [Efficacy and Efficiency of landscape governance in Sardinia: the role of SEA and ICT]" founded by the Autonomous Region of Sardinia.

Journal of Agricultural Engineering 2013; XLIV(s1):e92
doi:10.4081/jae.2013.(s1):e92

Materials and methods

SEA implementation on master plans in Sardinia, Italy

Contemporary planning practice in Sardinia is characterized by the design of tools belonging to the last generation of landscape planning instruments. The philosophy of these tools obeys the European Landscape Convention acknowledged in Italy through the LD 42/2004 concerning regulations over cultural goods and landscape (De Montis and Caschili, 2012). In 2006, the Region has approved the PPR and opened a process characterized by the revision of PUCs according to prescriptions and guidelines of the PPR. The adjustment to the PPR is signed by the review of general and special constraints, which represent limitation of property rights and stay in force until master plan design is completed (Aleo, 2012). The first constraints derive from spatial limitations and are imposed by law. The second ones affect goods declared of exceptional importance by means of specific regional administrative acts.

Some authors have pointed out weaknesses and pitfalls. Zoppi (2008) observes how the Region rules over the remaining public bodies according to an inverted subsidiary approach, where local agencies are shadowed by top down hierarchical control processes. In the case of the adjustment of the PUC to the PPR, the municipality plays a marginal role, with respect to planning assumptions and final choices. Deplano and De Montis (2008)

point out a contradiction: on one side, the PPR was approved without SEA, on the other, provincial and municipal landscape planning instruments must be coherent to PPR and subject to SEA.

There is not an organic regulation about SEA implementation of PUCs. The Region has approved so far two directives (Italian acronym DGR, Deliberazione Giunta Regionale) concerning environmental impact assessment and SEA implementation of plans and programs (RAS, 2008, 2012). The acts constitute the acknowledgement of the decrees approved by Italy about the receipt of the Directive (Italian Regulation, 2006, 2008, 2010).

Municipal spatial planning in Sardinia is regulated by Regional Law (RL) 45/1989 concerning land use and protection (RAS, 1989). According to RL 45/1989, the PUC establishes spatial development of a town and its surrounding environment mostly through zoning.

In 2004, RL 45/1989 has been integrated with the publication of RL 8/2004, concerning the institution and management of the PPR (RAS, 2004). According to RL 8/2004, municipalities should have adjusted their PUC to the PPR within one year from the approval of it. Besides, a SEA procedure should have been developed within the municipal master planning process, and the Region has indicated a path for SEA implementation of PUCs through Guidelines (RAS, 2009).

Only a few municipalities have developed SEA processes in a fairly homogeneous pattern. By contrast, the remaining municipalities have delayed their adhesion to the adjustment process. In front of this complex scenario, an analysis of the status of the SEA implementation is useful, as it enucleates concepts recognized as key issues in the international literature. In the next section, these issues are introduced and referred to a specific state of the art summary.

Key issues for a survey on SEA implementation

Scientific literature on SEA effectiveness is very rich. A general concept is that it is useful to measure SEA effectiveness and efficiency by means of indicators able to assess the performance of SEA processes in quali-quantitative terms. Fischer and Gazzola (2006) propose for Italian SEA practice a list of criteria belonging to two groups: the first attains the institutional and participative scenario; the second one reliability and control of focussed, iterative, flexible and informed processes. Jiricka and Pröbstl (2008) study SEA implementation on municipal master planning in alpine states. They focus on these SEA stages: screening, scoping, Environmental Report, consultation, and follow-up. Noble (2009) examines the Canadian SEA system adopting 15 criteria grouped into three areas under these concepts: SEA system, process, and outcomes. De Montis (2013) studies SEA implementation within provincial strategic spatial planning in Italy by developing two questionnaires about general and special aspects.

The focus is now directed to some key issues that are recognized as crucial for SEA implementation on Sardinian municipal master planning (see Table 1): i) general context, ii) participation, transparency and consensus, iii) quality, and iv) monitoring.

With reference to the general context, Hilding-Rydevik and Bjarnadóttir (2007) analyse the relation between context and SEA, and detect a special link connecting context awareness and sensibility to successful SEA implementation in northern European countries. Wirutskulshai *et al.* (2011) examine the recent SEA introduction in Thailand, where traditional top-down approach to spatial planning, the limitation to public participation, and the institutional and cultural context have so far minimized the efficacy of environmental assessment and its influence on development planning.

As far as participation, transparency, and consensus are concerned, Rauschmayer and Risse (2005) develop on a criteria list introduced by Wittmer *et al.* (2006) and propose a framework for the evaluation of conflict resolution strategies in SEA processes. This framework includes criteria referred to the following issues: information, legitimacy, social dynamics, and public participation costs. D'Auria and Ó Cinnéide (2009) analyse SEA integration in development plan construction in the case of Kilrush, Ireland. These authors stress that a clear responsibility attribution to stakeholders enhances their awareness of environmental concerns at hand and encourages decision making grounded on consensus building. Van Buuren and Nooteboom (2010) develop two case studies in The Netherlands and investigate SEA success factors, which help producing collaborative governance processes. These conditions attain the following issues: agreement on the ambitions, consensus about the interpretation, acceptance of facts, flexibility, synergy between acceptance of facts and formation of wishes, development of new roles, and formulation of new requirements. Gauthier *et al.* (2011) refer to the link between spatial planning and public participation in Québec. In Canada, SEA practice is flexible and loosely regulated, and requires an agreement about the decisional process and public participation schedule and methods. Participation is relevant in two major SEA stages: scoping and Environmental Report drafting; but it is crucial also during final decision making and follow-up.

With respect to SEA quality, Bonde and Cherp (2000) measure the quality of the Environmental Report of six spatial plans in UK and Sweden by means of an assessment package including 70 relevant themes grouped into four domains: description of the spatial plan, environment, and starting conditions; identification and valuation of main impacts; alternatives, mitigation strategies, and monitoring; results' communication. Thérivel and Minas (2002) develop on the measurement of SEA efficiency and the identification of the following four main factors: responsible authorities, stages and schedule, resources, and documentation. Authors find that crucial SEA implementation determinants are: team's competences in sustainability issues, and SEA timing. Retief (2007) studies SEA implementation quality in South Africa adopting performance indicators grouped into five areas: context, sustainability, participation, pro-action, and efficiency. Fischer (2010) evaluates the Environmental Report of 117 spatial plans in UK, by means of an evaluation package including 43 indicators clustered into six sections: description of the environment and the spatial plan, SEA integration, illustration of key issues, determination of impacts' intensity, consultation, recommendation on the alternatives, and monitoring. Jie Zhang *et al.* (2013) detect critical factors and stages, which influence SEA implementation and performance. According to these

Table 1. Key issues and scientific literature on SEA.

	Key issues	Reference
1	General context	Hilding-Rydevik and Bjarnadóttir (2007), Wirutskulshai *et al.* (2011)
2	Participation, transparency and consensus	Rauschmayer and Risse (2005), Wittmer *et al.* (2006), d'Auria and Ó Cinnéide (2009), Van Buuren and Nooteboom (2010), Gauthier *et al.* (2011)
3	Quality	Bonde and Cherp (2000), Thérivel and Minas (2002), Fischer (2010), Retief (2007), van Doren *et al.* (2013), Zhang *et al.* (2013)
4	Monitoring	Hanusch and Glasson (2008)

authors, SEA schedule includes always steps belonging to the following five arenas: Pre-SEA, Preparing the ground, Assess and protect, Wrap it up, and Post SEA. Van Doren *et al.* (2013) measure SEA efficiency, with reference to two key concepts: conformance and performance.

As far as monitoring is concerned, Hanusch and Glasson (2008) explore the patterns of follow-up activities in the context of spatial planning in UK and Germany. The study consists of an exam of Environmental Reports about regional spatial strategies and experts' interviews. The authors focus on the following issues concerning follow-up: reasons of activation, processes to be monitored, responsible bodies, management, timing, and expected results.

Managing the survey: a questionnaire

In this section, the focus is on the design of a user friendly on-line tool that includes sections concerning SEA critical issues drawn from the scientific literature. De Montis (2013) has already experimented on-line services able to support an efficient harvest of information. Google Docs™ (Google Inc., Mountain View, CA, USA) was used as platform for the implementation of the questionnaire.

After three years of experience with on-line questionnaires, in this study we have selected the second generation architecture of Google Docs™ documents, *i.e.* Google Drive. In this way, the database obtained describes scenarios, which can be confronted with international SEA practice. The questionnaire includes four parts corresponding to the themes recognized by international literature as key issues (see Table 2). Questions are directed to obtain closed answers with possible integration in a free text box.

Results

Questionnaire outcomes

In this section, we present the results of the questionnaire. The questionnaire has been submitted to officials belonging to municipalities involved in the adjustment of the PUC to PPR. As the PPR is active on the first homogeneous coastal domain, only a subset of 196 municipalities is interested (see Figure 1). This section includes two subsections: the first reports on a preliminary screening of the municipalities involved, while the second on the details of the answers provided by a restricted number of municipalities.

Figure 1. The municipalities aggregated into six groups.

Table 2. Key issues and questions included in the questionnaire on SEA of Sardinian master plans.

	Key issues	Questions
1	General context	1. According to which national regulations is the SEA process being (or has been) developed?
		2. According to which regional regulations is the SEA process being (or has been) developed?
		3. Were (are) the resources adequate to support a SEA process?
2	Participation, transparency and consensus	4. Which competent bodies have been involved?
		5. Which are the measures or tools adopted to encourage and stimulate public participation?
		6. Which communication instruments have been (is being) used to convey public observations?
		7. Which are the main concerns covered during consultation?
		8. Which communication instruments have been adopted to disseminate the results?
		9. What is your judgement on the time span allowed by law for consultation?
3	Quality	10. Does the plan clearly take into account environmental sustainability concerns?
		11. In which stage of the planning process has SEA been developed?
		12. Have realistic and well defined master plan's alternatives been considered?
		13. Which impacts have been identified, described, and evaluated?
		14. Is the controlling authority independent from the proceeding authority (i.e. belonging to another administration)?
4	Monitoring	15. Has the opportunity to monitor the effects of the master plan been considered since the SEA early stages?
		16. Is a monitoring plan already active?
		17. Have specific guidelines been followed in drafting the monitoring plan?
		18. Is the budget sufficient to cover the monitoring plan?
		19. Have subjects and bodies responsible for monitoring been identified?
		20. Are already available instruments, such as the observatory of spatial transformation, being adopted during the monitoring stage?

Preliminary screening

With respect to 196 municipalities contacted, 158 have replied. Phone interviews have revealed that some municipalities showed similar characteristics with regard to issues related to local land use planning. Hence, we have conceived the idea to group those municipalities who had a similar situation. Thus, municipalities can be clustered into six groups, according to master plan type in force, adjustment to PPR process progress, SEA progress, and interview completion (see Table 3).

Group 1 includes municipalities, which are in the early stages of the PUC design in adjustment to the PPR, and are in the early stages of SEA process. Group 2 embraces municipalities where a PUC is in force, but neither PPR adjustment nor SEA process has started. Group 3 includes municipalities where a PUC is in force, and SEA has progressed to the scoping phase. Group 4 clusters municipalities still have a Programma di Fabbricazione, PdF, *i.e.* Building program (a master plan older and with much simpler contents than the PUC) and/or where an old Piano Regolatore Generale, PRG, *i.e.* General Regulatory Plan, the Italian general release of the PUC, is in force. In these cases, PUC design process has been delayed or impeded by many reasons, such as external shocks (natural disasters), and illegal and unauthorized building. In some cases, PUC design process is in the early stages or municipalities have adopted a PUC, but a PdF or PRG is still in force. Group 5 includes municipalities where the PUC adjustment to PPR and its SEA (usually with Environmental Report completed) processes are being finalized and normal procedural stages are on course: adjustment to comments elaborated by RAS, coherence assessment to be performed by RAS, observation period, and SEA assessment by the competent authority. Group 5 also embraces municipalities which have adopted or approved a PUC and developed completely (or nearly so) its SEA. So, the questionnaire has been administered to the municipalities within group 5. We have put municipalities having filled in the questionnaire within group 6: in such cases, officials have totally or partially completed the questionnaire.

Municipalities belonging to groups 1, 2, 3, and 4 (78% of the total), not being at a sufficiently advanced SEA progress, have not been asked to complete the on-line questionnaire.

The details of the answers

In this section, we provide the reader with the details of the answers of municipalities. Thirty-five municipalities have been invited to fill in the questionnaire and just eight have collaborated. This low level of participation is due to a number of factors like unavailability of municipal officers, due to other urgent commitments, and lack of incentive (questionnaire compilation occurs on voluntary basis, without any remuneration).

In the following sections, we develop on the answers following the key issues of the questionnaire.

Context

In three cases, municipalities have referred SEA implementation to LD 152/2006 updated to LD 4/2008: it has more precisely defined the rules, making the LD 152/2006 more responsive to the Directive. The remaining municipalities have referred to the changes introduced by LD 128/2010 (see Figure 2).

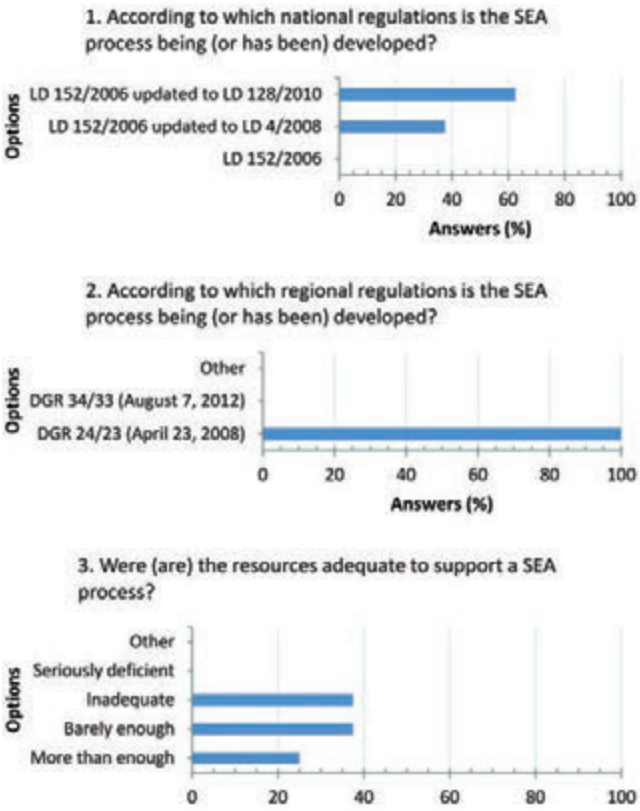

Figure 2. Replies to questions about context: 1. National regulations followed by the municipalities; 2. All municipalities have referred to DGR 24/23 for SEA implementation; 3. Adequateness of financial resources for supporting SEA process.

Table 3. First screening of the municipalities involved.

Group	Number of municipalities	Percentage of contacted municipalities	Master plan instrument in force	Adjustment process of PUC to PPR	SEA progress	On-line survey: interview completed
1	22	14	PUC	Early stages	Not started or very early stages	–
2	44	28	PUC	Not started	Not started	–
3	19	12	PUC	Early stages	Scoping phase	–
4	38	24	PdF, PRG	Not started	Not started	–
5	27	17	PUC	Adopted/completed or nearly so	Environmental report or completed	No
6	8	5	PUC	Adopted/completed or nearly so	Environmental report or completed	Yes

Sardinia does not have a regional law that regulates SEA. With respect to the regional indications, all municipalities have referred to DGR 24/23 issued in 2008.

Finally, municipalities have assessed in different ways the financial resources to carry out the SEA. Three out of eight municipalities believe that the financial resources were insufficient, three barely enough, and two more than enough.

Participation, transparency and consensus

In general, the municipalities have involved almost all the relevant bodies responsible for environmental matters indicated by regional guidelines. Municipalities have always involved the Regional service of environmental sustainability, impact assessment and environmental information systems (Italian acronym SAVI), the corresponding Province and the regional offices for landscape protection (ROLP). Seven municipalities out of eight have involved the Regional agency for environmental protection (Italian acronym ARPAS). Four municipalities have involved management bodies of protected areas (MBPA). In three cases, other actors have been involved, such as the mayors of neighboring municipalities (see Figure 3).

With regard to the instruments used to include the public in the process, the eight municipalities have selected a total of 12 options but none prevails over the others. Public observations have been mainly expressed during meetings.

With reference to nine options selected by the municipalities, the main concern over the public consultation phase refers to time. Problems related to logistics have been considered to be less relevant.

With respect to communication instruments used to disseminate the results, the eight municipalities have selected a total of 11 options. Seven responses have indicated "Documentation on web pages" as the principal tool to inform the public about the results.

Finally, half of the municipalities believes that the time spent in consultations is barely enough.

Quality

Seven out of eight plans have clearly taken into account the goals of environmental sustainability (see Figure 4). In six cases, SEA has been integrated in the early stages of plan preparation. In two cases, it has been integrated in an advanced stage.

Just half of the municipalities have set realistic alternatives with respect to the stated objectives.

All eight municipalities declare to have identified, described and evaluated the direct effects resulting from the adoption of the plan. Indirect effects have been regarded by six municipalities. Half of the municipalities claim to have also described cumulative effects, while just one municipality claims to have also taken into account synergic effects. The controlling authority is always independent from the proceeding authority.

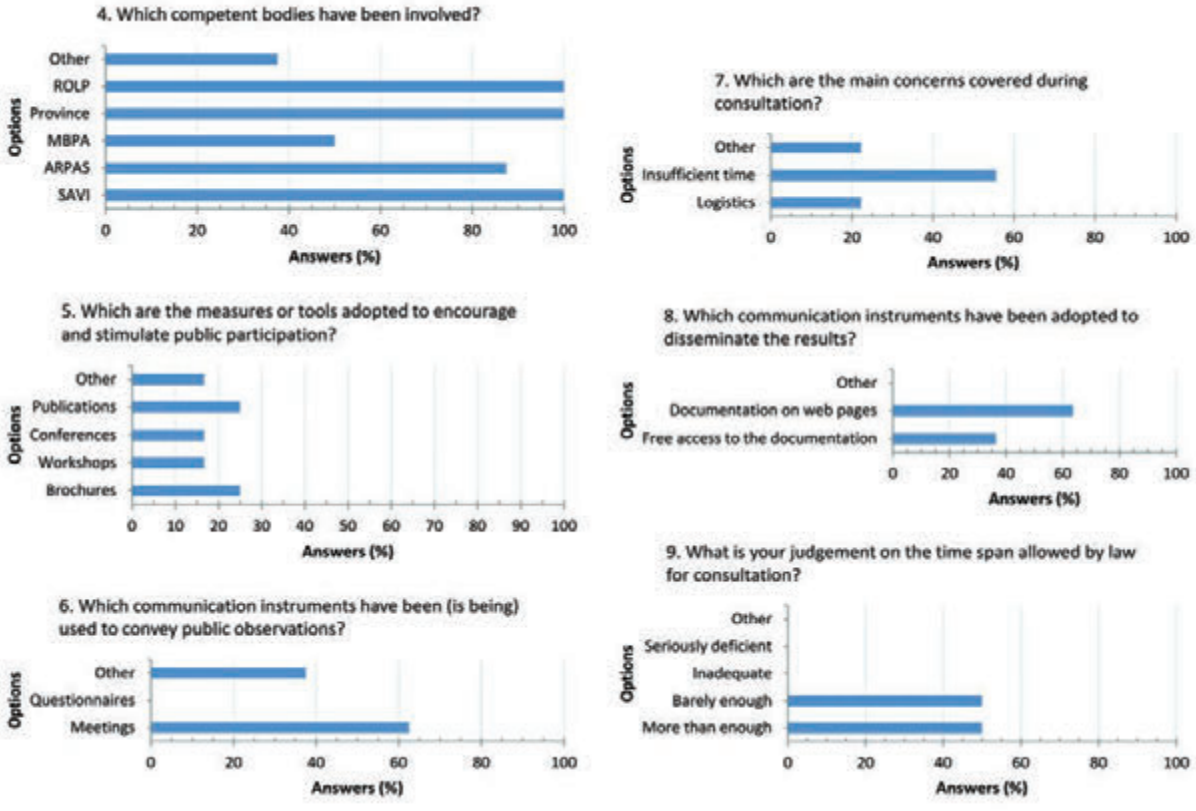

Figure 3. Replies to questions about participation, transparency, and consensus: 4. Competent bodies involved into SEA process; 5. Instruments used to involve the public (question which could be given more answers); 6. Instruments used by the municipalities to convey public observations; 7. The main concerns dealt with during consultation (question which could be given more answers); 8. Communication instruments used by the municipalities to disseminate results (question which could be given more answers); 9. Judgment on the time span allowed by law for consultation.

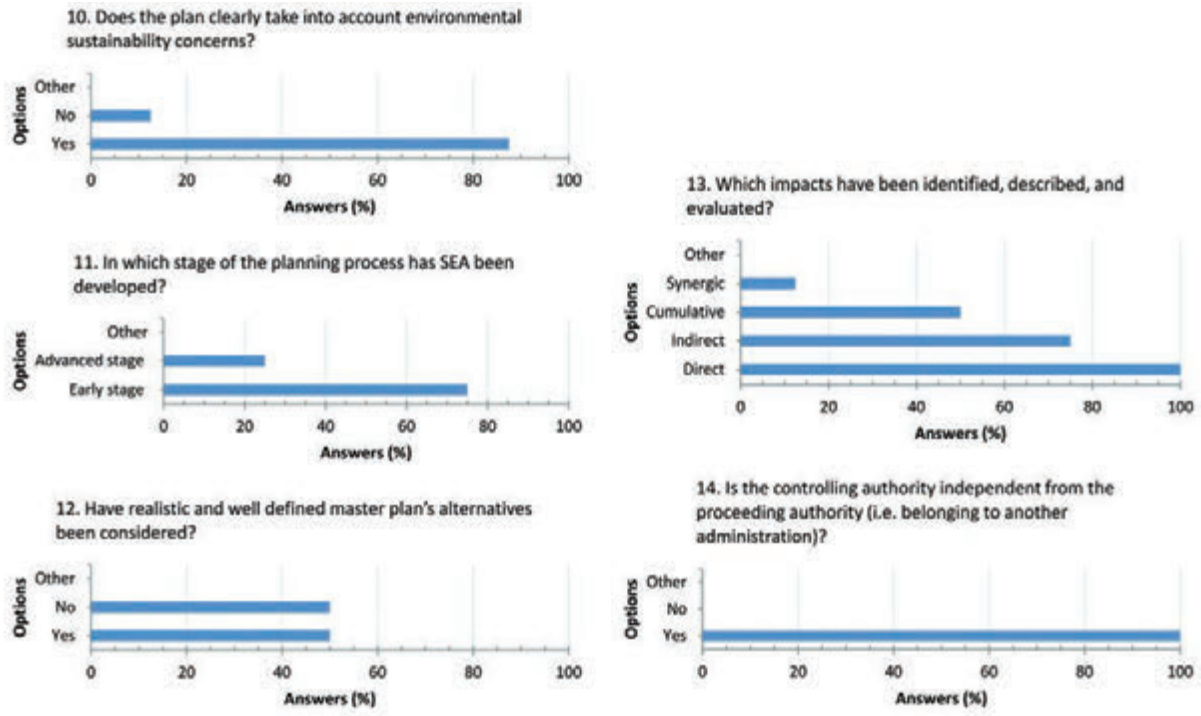

Figure 4. Replies to questions about quality: 10. Environmental sustainability concerns taken into account within plan; 11. Stage in which SEA has been integrated; 12. Master plan's alternatives; 13. Impacts considered; 14. The controlling authority is always independent from the proceeding authority.

Monitoring

With respect to monitoring, most of the municipalities have considered in the scoping phase the ability to track the plan's effects (see Figure 5). In seven out of eight municipalities a monitoring plan is not active yet. Just in three cases, municipalities have followed specific guidelines to elaborate the monitoring plan.

No municipality believes its financial resources are sufficient to carry out the monitoring operations. In five out of eight cases, municipalities have not identified the subjects who would have taken care of the monitoring; in three cases, existing tools will be used for monitoring.

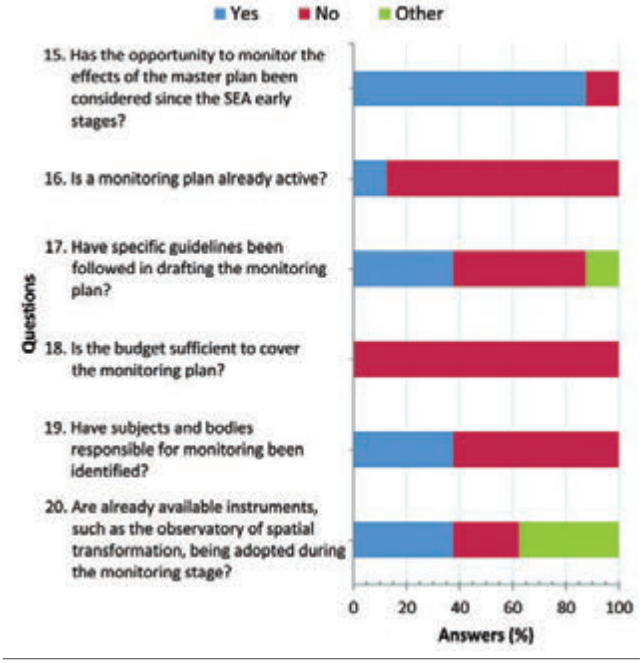

Figure 5. Replies to questions about monitoring within SEA process.

Conclusions

In this paper, the authors discuss a survey about SEA implementation within local master planning, in Sardinia. The main master planning tool, *i.e.* the PUC, is currently subject to renovation in order to adhere to the PPR, Regional Landscape Plan, in force since 2006.

The results of the survey can be analyzed according to two perspectives: the first one relates to the state of local planning, the second relates to SEA implementation at the level of municipal PUCs in coherence with the PPR.

With respect to the first point, results indicate that municipal land use planning still lags behind. Many municipalities involved have an old PdF (or PRG) in force: some of these tools have been approved in the 1980s. Again, many municipalities have approved the PUC, but there is no intention to adapt it to PPR. This is due, in large part, to the absence of political willingness.

With respect to the second point, preliminary results show an overall low level of SEA implementation. Questionnaire responses highlight some critical aspects that are discussed below.

First, contextual aspects regarding SEA procedure have been clarified by national legislation. At the regional level, a law dedicated to SEA still lacks; so far only directives have been issued. Processes of PUC adjustment to the PPR have been delayed because of lack of political interest, and insufficient financial resources.

Second, municipalities have ensured public access to information in a fairly satisfactory way. This is quite a relevant result, since public involvement is a key element in consensus building towards final acceptable decisions.

Third, as far as assessment quality is concerned, almost every municipality has clearly considered in the planning process the environmental sustainability goals. Most municipalities have introduced SEA at the early stages of the planning process. This is crucial, as a lack of adequate consideration of environmental aspects often characterizes SEA processes undertaken at the end of the process. In these case, SEA is meant as a sort of justification for approving a certain plan, and hardly takes into account environmental matters and stakeholders' opinion. Just half of municipalities claim to have developed other solutions with respect to the plan adopted: it would be interesting to investigate how they have studied other options. This is a very critical aspect of SEA implementation worldwide. With respect to the identification, description and assessment of significant effects resulting from the adoption of the plan, all municipalities claim to have taken into account the direct effects. Sometimes indirect effects have been considered. In some other cases, municipalities have also taken into account the cumulative and synergistic effects. It would be necessary to investigate further to understand how municipalities have been able to consider in the planning process these kind of impacts, as they should be particularly difficult to identify, describe and evaluate. According to the literature, we find that the degree of independence of the competent authority against the proceeding authority helps us to define the quality of a SEA. In our survey, the authorities are always independent: self-evaluation is being avoided.

Finally, although in most cases the municipalities have set a monitoring plan, this tool has not been activated by almost no one. In addition, no municipality has clearly indicated a financial support for this phase and just a few municipalities have identified responsible subjects or bodies. So, monitoring is still one of the critical aspects of the SEA process, even though it incontestably improves understanding of significant effects and early identification of relevant environmental concerns. This may be useful to redirect planning choices, in a continuous adaptive process.

References

Aleo M. 2012. Valutazioni ambientali. Le procedure di VAS, VIA, AIA e VI nel governo del territorio, Grafill editore, Palermo, Italy.

Bonde J., Cherp A. 2000. Quality review package for strategic environmental asessments of land-use plans. Impact Assessment and Project Appraisal 18(2):99-110.

D'Auria L., Ó Cinnéide M. 2009. Integrating strategic environmental assessment into the review process of a development plan in Ireland. Impact Assessment and Project Appraisal 27(4):309-19.

De Montis A. 2013. Implementing Strategic Environmental Assessment of spatial planning tools. A study on the Italian Provinces. Environ. Impact Asses. 41:53-63.

De Montis A., Caschili S. 2012. Nuraghes and Landscape Planning: Coupling Viewshed with Complex Network Analysis. Landscape urban plan. 105(3):315-24.

Deplano G., De Montis A. 2008. Pianificazione del paesaggio e valutazione strategica in Sardegna. In: C. Zoppi (ed.) Governance, pianificazione e valutazione strategica – Sviluppo sostenibile e governance nella pianificazione urbanistica, Gangemi, Roma, Italy, pp 266-76.

Fischer T.B. 2010. Reviewing the quality of strategic environmental assessment reports for English spatial plan core strategies. Environ. Impact Asses. 30(1):62-9.

Fischer T.B., Gazzola P. 2006. SEA effectiveness criteria – equally valid in all countries? The case of Italy. Environ. Impact Asses. 26(4):396-409.

Gauthier M., Simard L., Waau J.P. 2011. Public participation in strategic environmental assessment (SEA): Critical review and the Quebec (Canada) approach. Environ. Impact Asses. 31(1):48-60.

Hanusch M., Glasson J. 2008. Much ado about SEA/SA monitoring: The performance of English Regional Spatial Strategies, and some German comparisons. Environ. Impact Asses. 28(8):601-17.

Hilding-Rydevik T., Bjarnadóttir H. 2007. Context awareness and sensitivity in SEA implementation. Environ. Impact Asses. 27(7):666-84.

Italian Regulation, 2004. Code over cultural goods and landscape. LD 42/2004. In: Official Journal No. 45, 24/2/2004.

Italian Regulation, 2006. Environmental Code. LD 152/2006. In: Official Journal No. 88, 14/4/2006.

Italian Regulation, 2008. Additional corrective and supplementary provisions to Environmental Code. LD 4/2008. In: Official Journal No. 24, 29/1/2008.

Italian Regulation, 2010. Amendments and additions to Environmental Code. LD 128/2010. In: Official Journal No. 186, 11/8/2010.

Jiricka A., Pröbstl U. 2008. SEA in local land use planning – first experience in the Alpine States. Environ. Impact Asses. 28(4-5):328-37.

Noble B.F. 2009. Promise and dismay: The state of strategic environmental assessment systems and practices in Canada. Environ. Impact Asses. 29(1):66-75.

RAS 1989. Legge regionale 22 dicembre 1989, n. 45, Norme per l'uso e la tutela del territorio regionale. Testo coordinato, aggiornato alla legge regionale 25 novembre 2004, n. 8, Norme urgenti di provvisoria salvaguardia per la pianificazione paesaggistica e la tutela del territorio regionale, Regione Autonoma della Sardegna.

RAS 2004. Legge regionale 25 novembre 2004, n. 8, Norme urgenti di provvisoria salvaguardia per la pianificazione paesaggistica e la tutela del territorio regionale, Regione Autonoma della Sardegna.

RAS 2008. Deliberazione della Giunta Regionale n. 24/23 del 23 aprile 2008, Direttive per lo svolgimento delle procedure di Valutazione di impatto ambientale e di Valutazione ambientale strategica, Regione Autonoma della Sardegna.

RAS 2009. Linee Guida per la Valutazione Ambientale Strategica dei Piani Urbanistici Comunali, Regione Autonoma della Sardegna.

RAS 2012. Deliberazione della Giunta Regionale n. 34/33 del 7 agosto 2012, Direttive per lo svolgimento delle procedure di valutazione ambientale. Sostituzione della deliberazione n. 24/23 del 23 aprile 2008, Regione Autonoma della Sardegna.

Rauschmayer F., Risse N. 2005. A framework for the selection of participatory approaches for SEA. Environ. Impact Asses. 25(6):650-66.

Retief F. 2007. A performance evaluation of strategic environmental assessment (SEA) processes within the South African context. Environ. Impact Asses. 27(1):84-100.

Thérivel R., Minas P. 2002. Measuring SEA effectiveness. Ensuring effective sustainability appraisal, Impact Assessment and Project Appraisal 20(2):81–91.

Van Buuren A., Nooteboom S. 2010. The success of SEA in the Dutch planning practice. How formal assessments can contribute to collaborative governance. Environ. Impact Asses. 30(2):127-35.

Van Doren D., Driessen P.P.J., Schijf B., Runhaar H.A.C. 2013. Evaluating the substantive effectiveness of SEA: Towards a better understanding. Environ. Impact Asses. 38:120-30.

Wirutskulshai U., Sajor E., Coowanitwong N. 2011. Importance of context in adoption and progress in application of strategic environmental assessment: Experience of Thailand. Environ. Impact Asses. 31(3):352-9.

Wittmer H., Rauschmayer F., Klauer B. 2006. How to select instruments for the resolution of environmental conflicts? Land Use Policy 23(1):1-9.

Zhang J., Christensen P., Kørnøv L. 2013. Review of critical factors for SEA implementation. Environ. Impact Asses. 38:88-98.

Zoppi C. 2008. Politiche territoriali e problematiche partecipative: dialettica e conflitto nella pubblica amministrazione e tra questa e le comunità locali nei processi di pianificazione regionale in Sardegna. In: C. Zoppi (ed.) Governance, pianificazione e valutazione strategica – Sviluppo sostenibile e governance nella pianificazione urbanistica, Gangemi, Roma, Italy, pp 277-97.

Consequence of land use changes into energy crops in Campania region

Stefania Pindozzi, Salvatore Faugno, Elena Cervelli, Alessandra Capolupo, Maura Sannino, Lorenzo Boccia

Dipartimento di Agraria, Università di Napoli Federico II, Italy.

Abstract

Campania region is undergoing a new and important land use change (LUC). Large areas under tobacco are experiencing a severe economic crisis and cereal areas, especially in the hill, are cultivated with increasing difficulty, with poor economic results (yield value of 2.5 t/ha/year) and under the risk of erosion. No-food crops suitable in these contexts are the perennial and in this case, the land use change would certainly lead to a positive impact on reducing erosion, but also on the reduction of nutrient requirement, on fuel consumption and perhaps it would also lead to an increase in profitability. The aim of this work is to identify the areas in which the land use change could be realistic and ecologically compatible and to evaluate the main consequence of the LUC. The study area includes the entire Campania region. It has been assumed that the areas that will undergo the LUC will be the hilly, not-irrigated cereal crop, with altitudes between 400 and 750 m a.s.l., not included in natural parks, in the Site of Community Importance and in the Special Protection Areas. Through the climate model, inferred from the Ground Water Protection Plan, the area to be examined was classified as 'cold Lauretum', which is a good area for the *Arundo donax* crops up to 750 m a.l.s., with recoverable biomass yield of about 12.6 t/year. The erosion has been estimated with RUSLE applied to the whole region. Using the ESRI ArcGis 10.0 software, seven large areas, partially convertible, were identified. The area that is realistic to convert amounted to approximately 500 km2. The value of the biomass production has been evaluated in the order of 25 million euro a year; actual wheat production would be 33 million euro a year but the production costs are far greater.

With LUC there is a reduction in soil erosion in the order of 300000 t/year. This would lead a saving, on global scale, in the order of 10 million tonnes of CO_2 per year.

Correspondence: Lorenzo Boccia, DIA, Università degli Studi di Napoli Federico II, via Università 100, 80055 Portici (NA), Italy.
Tel. +39.081.2539151.
E-mail: lorenzo.boccia@unina.it

Key words: land use change, energy crops, *Arundo donax*.

Contributions: the authors contributed equally.

Conflict of interests: the authors declare no potential conflict of interests.

Funding: the work was supported by Italian Ministry of Education, University and Research. with the PON Project.

Acknowledgments: this research was realized under PON Project 01_01966 "Integrated agro-industrial chains with high energy efficiency for the development of eco-compatible processes of energy and bio-chemicals production from renewable sources and for the land valorization (ENERBIOCHEM)" funded by Italian Ministry of Education, University and Research.

Journal of Agricultural Engineering 2013; XLIV(s1):e93
doi:10.4081/jae.2013.(s1):e93

Introduction

We are certain that Campania region, one of the most important agricultural territory in Italy, is undergoing a new and major Land Use Change (LUC). The analyses of LUC are crucial to understanding several environmental phenomena (Lambin *et al.* 2001; Pelorosso *et al.* 2009) but also to develop the prediction of the new change. The driving forces of the change that we expect, are fundamentally related to economic and social change. Large areas under tobacco and cereals are experiencing a severe economic crisis, especially in the hilly places, which are cultivated with increasing difficulty, with poor economic results and under the risk of erosion (Diodato *et al.*. 2009).

The new LUC will be the consequence of a complex and impetuous LUC that was well studied and analyzed in the past (Di Gennaro and Innamorato, 2005). The further changes that we expect, will take place in an area that has experienced a period of deep transformation in the last forty years, under the pressure of opposite forces, such as the unregulated urban expansion, the intensification and the specialization of agricultural production activities (Fabiani and Favia, 1990; I sistemi di terre della Campania, 2002; Di Gennaro and Innamorato, 2005). The areas that will undergo the land use change, are those that are no longer cost effective for food crops, such as the erosion prone areas under cereal production, in which the no-food crops would also have an environmental value (Fagnano *et al.*,2012 a).

The main driving forces of this process are related to economic factor and to the reduction in the number of farmers in some context, especially in the interior part of the region, far from the main cities. But in some context, there are other driving forces of the LUC. The first is that some areas are polluted due to illegal contamination or fall-out of particulates and pollutants as a consequence of illegal burning of waste. The second is that some irrigated areas have problems of salinity, as a result of excessive withdrawal of groundwater. Considering the incentives for no-food energy crops, it is most likely that in short time some of these areas will be subjected to LUC.

No-food crops suitable in these contexts are the perennials, and the land use change would certainly lead to a positive impact of reducing erosion, but also on the reduction of nutrient requirement, fuel consumption and perhaps it would also lead to increased profitability.

Several studies have demonstrated that in the interior areas of Campania region, the rain erosivity is higher during the months of

September-October (Diodato *et al.*, 2009), which correspond to the period of maximum erodibility of soils also due to the traditional wheat cultivation technique, which provides for the absence of vegetation during these months. As a matter of fact, 80% of the annual erosion occurs during this period. In addition, the wheat yield in these areas is very low (yield value of about 2.5 t/ha/year). Consequently these crops do not seem to be sustainable, in the long term, from an economical and environmental point of view (Fagnano *et al.*, 2012b). No-food crops suitable in these contexts are the perennials and then the land use change would certainly lead to a positive impact of reducing erosion, but also on the reduction of nutrient requirement, on fuel consumption and perhaps an increase in profitability, if under a proper incentive mechanism.

With this background, the aim of this work is to identify the areas in which the land use change could be realistic and ecologically compatible and to evaluate the main consequences of the new land cover mainly in terms of erosion risk reduction.

Materials and methods

Area of study

The study area included the whole Campania region, because the Common Agricultural Policy boundary is the same as the administrative boundary and also because the habitat and topography, change largely due to changes in the surrounding regions. The total area of the territory is about 13,600 km^2, and is made up of mountains, 34.6%, hills, 51%, and plains, 15%. It was assumed that the areas that will undergo the land use change are the hilly cereal growing areas with altitudes between 400 and 750 meters above sea level.

One of the GIS layers used for the land use change study, was derived from the CORINE Land Cover (CLC). The land use map was filtered in ArcGis in order to select the non-irrigated cereal land (Figure 1). Moreover the hilly areas, from the height of 400 to 750 meters above sea level, were obtained by filtering the Digital Elevation Model (DEM) of the Campania region at 20 m resolution (Figure 2).

The eligible areas for land use change was identified by filtering the non-irrigated crop, with altitudes between 400 and 750 m a.s.l., excluding the National Parks, Site of Community Importance (SCI) and Special Protection Areas (SPA).

Climate conditions and suitable crops

The climate model was inferred from the Ground Water Protection Plan (PTA) of the Campania region. The climate in the study areas, can be approximated by the following linear functions:

Mean Annual Temperature = 16.5 - 0.006 height (m.a.s.l.)

Mean Annual Rainfall = 750 mm + height K_2

with K_2 = Coefficient that ranges from 0.40 to 0.70.

Therefore, according to the De Philippis's classification (1937), this area can be classified as 'cold Lauretum', which is a good for the *Arundo donax* crops up to 750 m a.l.s., with recoverable biomass yield in the order of 12.6 t/year after the third year. For hilly wheat areas, a yield value of 2.5 t/ha/year was considered.

Restrictions

The following shapefiles of Campania region were used for the selection of the areas to be converted: natural parks, protected areas (Figure 3), Site of Community Importance (SCI) (Figure 4) and Special Protection Area (SPA) (Figure 4). These layers were imported into ArcGIS in order to exclude them, since they are assumed non-con-

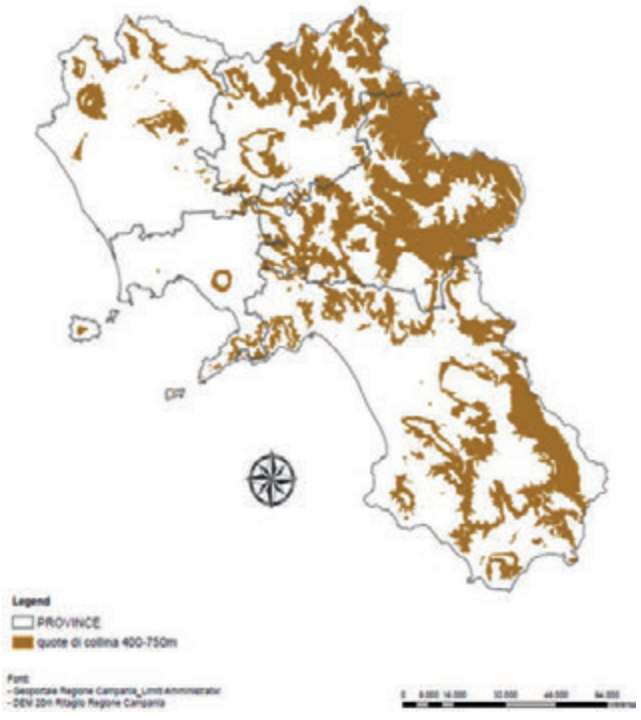

Figure 1. Hill areas, with altitudes between 400 and 750 meters above sea level (DEM of Campania).

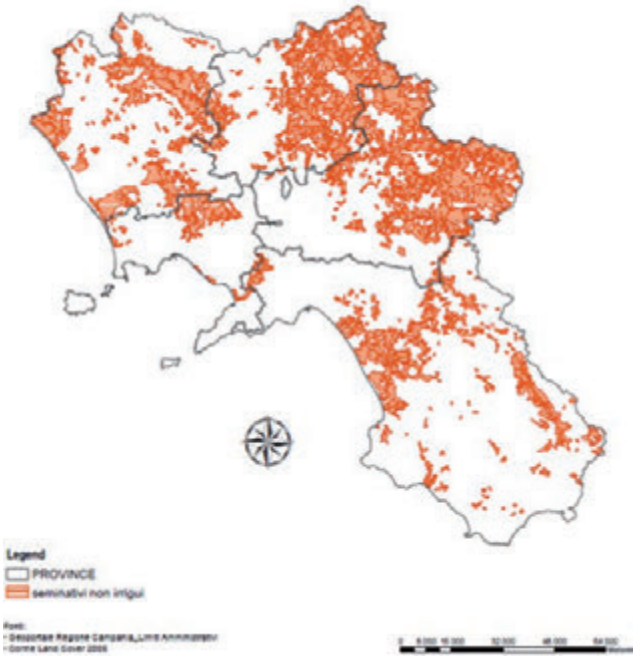

Figure 2. Areas cropped with cereals (CORINE Land Cover).

vertible to energy crops. It's important to note that future management of SCI and SPA could allow the land use change into biomass, but it is not certain, and at date it is correct to exclude these areas.

Soil erosion risk prediction

The soil erosion prediction map was evaluated using RUSLE equation, (Wischmeier, 1959; Wischmeier *et al.*, 1969,1971,1978; Summer *et al.*, 1998) which is not a physically based model, is:

$$A = 2.24\ R\ K\ L\ S\ C\ P,$$

where, A is the average annual soil loss (t/ha/year), R estimates the rainfall erosivity, K estimates the soil erodibility, L is the hill slope, S estimates the hill slope gradient, C is the ground cover factor and estimates the soil susceptibility to the erosive agents and P represents the effect given by any conservative practices of canalization or cultivation. For each parameter, an algorithm was suggested for application to the whole region.

In these areas, erosion has been estimated with the current land use (cereals) compared to the erosion that would occur if the land use were converted to permanent crop.

Methods for estimating the energy potential

The energy potential was predicted for both energy crop and straw, assuming that is possible to collect the straw for energy use

The energy potential of *Arundo donax*, is about 185,000 toe/year (toe is ton of oil equivalent), that was calculated assuming collection 42% of production with moisture content of 30%, with a lower heat value (LHV) for dry biomass of 17.6 MJ/kg. In the case of straw, the value is 70,000 toe/year assuming 90% of the production can be collected and moisture content of 15%.

Results and discussion

Filtering the maps of the studied territory, some areas were identified. For industrial use, only the areas in which it is possible to organize a chain are suitable for LUC. With this approach, using the ArcGIS software, seven large areas were identified. In these seven zones, the land use change with no food crops is possible (Figure 5), without affecting important agricultural land context. The areas identified are only partially convertible.

The total amount of recoverable biomass and its energy value was estimated as reported in Table 1 and Table 2. The total amount of cereals actually produced, the energy cost for mechanization activity and the fertilization requirement were also estimated.

The predicted land use change does not affect all the suitable land, that is 150,000 ha, but only a fraction of these are eligible.

A possible scenario is the one in which, approximately, one-third of eligible zone change land use in the medium term, obtaining a scenario like the one presented in Table 3.

According to this scenario, about 50.000 ha would be converted to energy crops, which is a remarkable surface (4% of whole regional surface of 13,600 km^2) but is quite small compared to Campania region's energy needs. In fact, the biomass production assessed has an energy value of about 160,000 toe/year, equivalent to about 1.5% of the regional energy needs, or only about 3.5% of the regional electricity demand.

Most results of interest are for the potential reduction of soil erosion risk and the reduction of fertilization and machining requirements.

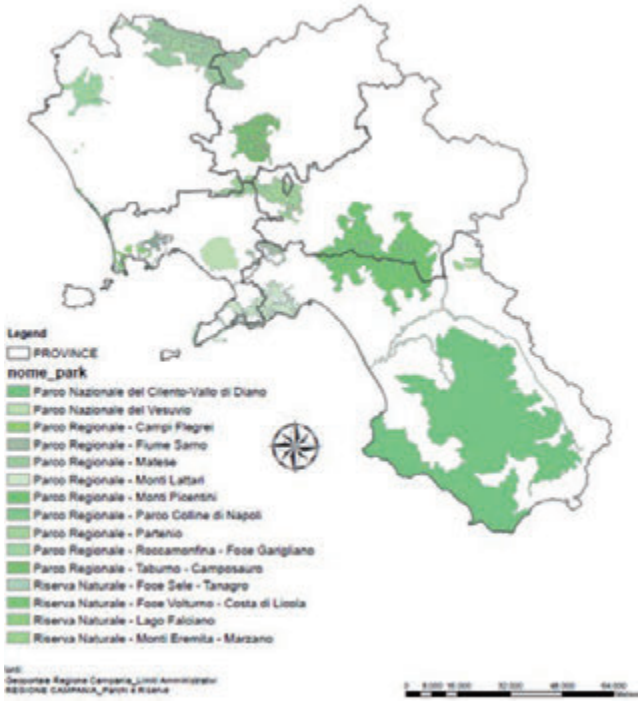

Figure 3. Natural parks and reserves.

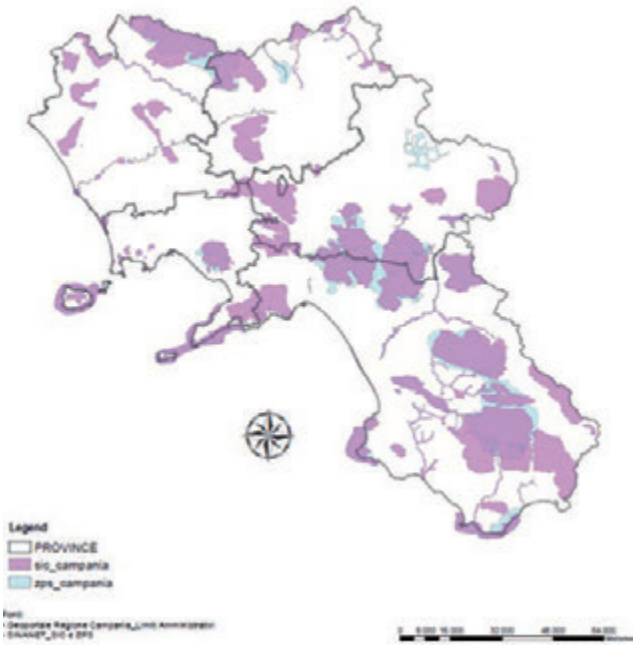

Figure 4. SCI and SPA.

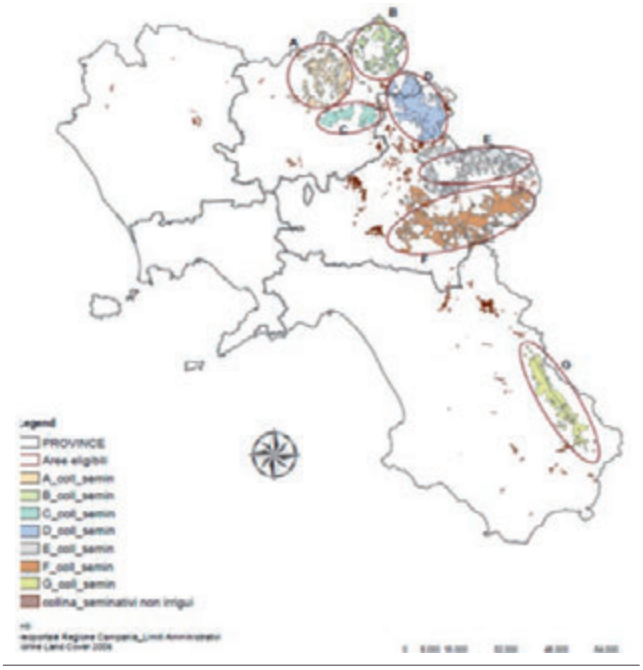

Figure 5. Macroareas resulting from the study.

Conclusions

It is possible to expect a large land use change into energy crops in Campania region. If the goal will be avoid overlap of biomass to arable lands, irrigated crops, parks and reserves, and other protected areas the eligible area remains only 1500 km². Of these 1500 km² it is reasonable to suppose a LUC of only 50,000 ha.

Measures aimed to increased land use change over this value, will lead to conflict with agriculture and environmental constraints.

In this scenario, even with this important LUC, the produced biomass, as an order of dimension, may only compensate the average increase in energy demand of one year in Campania Region.

Value of the biomass production, according to the hypothesis of this study, has been evaluated in the order of 25 million euro a year (assuming a unit price of biomasses of 30 €/t at the plant). This value has to be compared to the value of the actual wheat production, in the same areas. It would be 33 million euro a year (assuming a unit price of 270 €/t of wheat) and would appear more profitable but the production costs are far greater.

Considering the Land Use Change with *Arundo donax* there is a reduction in soil erosion in the order of 300,000 t/year that is one of the main goal of the LUC. This would lead to a saving, on a global scale, in terms of working and fertilization activities, in the order of 10 million tonnes of CO_2 per year.

Table 1. Comparison between biomass produced with actual land use (wheat) and the supposed new land use (*Arundo donax*).

	Zone A	Zone B	Zone C	Zone D	Zone E	Zone F	Zone G	Total
Surface of the eligible area (ha)	10'446	73'713	5'209	15'483	18'046	19'987	9'497	152'381
Straw availability (t/year)	13'985	98'683	6'974	20'728	24'159	26'758	12'714	204'000
Arundo donax availability (t/year)	122'845	866'865	61'258	182'080	212'221	235'047	111'685	1'792'001
Available energy of straw (toe/year)	4'867	34'342	2'427	7'213	8'407	9'312	4'425	70'992
Available energy from *Arundo donax* (toe/year)	33'905	239'255	16'907	50'254	58'573	64'873	30'825	494'592

Table 2. Surface eligible for LUC, surface supposed interested to LUC and production, reduction of predicted erosion.

	Zone A	Zone B	Zone C	Zone D	Zone E	Zone F	Zone G	Total
Surface of the eligible area (ha)	10'446	73'713	5'209	15'483	18'046	19'987	9'497	152'381
Average of soil loss with wheat crop (t/ha)	3.51	8.938	3.83	4.89	2.968	6.796	1.555	
Average of soil loss with *Arundo donax* (t/ha)	0.47	1.19	0.51	0.65	0.40	0.91	0.21	
Predicted annual soil loss with wheat (t/year)	36'697	658'847	19'950	75'712	53'561	135'832	14'768	95'366
Predicted annual soil loss with *Arundo donax* (t/year)	4'893	87'846	2'660	10'095	7'141	18'111	1'969	32'715
Predicted soil loss reduction (t/year)	-31'804	-571'001	-17'290	-65'617	-46'419	-117'721	-12'799	-862'650

Table 3. Evaluation of the consequence of the land use change only a part of eligibile areas.

	Zone A	Zone B	Zone C	Zone D	Zone E	Zone F	Zone G	Total
Surface of the eligible area (ha)	10'446	73'713	5'209	15'483	18'046	19'987	9'497	152'381
Surface with LUC (1/3 of the eligible) (ha)	3'482	24'571	1'736	5'161	6'015	6'662	3'166	50'794
Estimated production of *Arundo donax* (t/year)	40'948	288'955	20'419	60'693	70'740	78'349	37'228	597'334
Total energy value of *Arundo donax*; change supposed in 1/3 of the eligible surface (toe/year)	11'302	79'752	5'636	16'751	19'524	21'624	10'275	164'864
Potential reduction of soil losses (t/year)	-10'601	-190'334	-5'763	-21'872	-15'473	-39'240	-4'266	-287'550

References

De Philippis A. 1937. Classificazione ed indici del clima in rapporto alla vegetazione forestale italiana. N. G. B. I. ns, 44(1); 1-169.

I sistemi di terre della Campania. Carta 1:250.000 e Legenda. Available from: http://www.risorsa.info/files/SK_Carta.htm; Accessed: March 2013.

Di Gennaro A., Innamorato F. P., 2005. Verso l'identificazione dei paesaggi della Campania. Cartografia 1:250.000. Regione Campania, Assessorato al Governo del Territorio. Selca, Firenze

Diodato N., Fagnano M., Alberico I., 2009. CliFERM Climate Forcing and Erosion Response Modelling at Long-Term Sele River Research Basin (Southern Italy). Nat Hazard Earth Sys, 9: 1693-1702.

Fabiani G., Favia F. 1990. Vitalismo produttivo e precarietà strutturale nell'agricoltura campana contemporanea. Studi sull'agricoltura italiana. 25: 586

Fagnano M., Boccia L., Pindozzi S., Infascelli R., Faugno S. 2012.a. Aree Potenzialmente Convertibili a Colture Energetiche: Caso Studio della Regione Campania. Proc. XLI convegno nazionale della società italiana di agronomia. Bari (Italy). Not numbered volumes. Pp 464-466, Ecumenica Editrice scrl, Bari

Fagnano M., Diodato N., Alberico I., Fiorentino N. 2012.b An overview of soil erosion modeling compatible with RUSLE approach. Rend. Fis. Acc. Lincei, 23:69–80.

Lambin E.F., Turner B.L., Geist H.J., Agbola S.B., Angelsen A., Bruce J.W., Coomes O.T., Dirzo R., Fischer G., Folke C., George P.S., Homewood K., Imbernon J., Leemans R., Li X., Moran E.F., Mortimore M., Ramakrishnan P.S., Richards J.F., Skanes H., Steffen W., Stone G.D., Svedin U., Veldkamp T.A., Vogel C., Xu J., 2001. The causes of land-use and land-cover change: moving beyond the myths. Glob. Environ. Change., 11: 261-269.

Pelorosso R., Leone A., Boccia L., 2009. Land cover and land use change in the Italian central Apennines: A comparison of assessment methods. Appl. Geogr., 29: 35-48.

Summer W., Klaghofer E., Zhang W., 1998. Modelling Soil Erosion, Sediment Transport and Closely Related Hydrological Process. Proc. of an International Symposium Held at Vienna. IAHS-AISH Publication N.249, pp.453.

Wischmeier W. H. 1959. A rainfall erosion index for a universal soil loss equation. Soil Science Society of American Journal Procedures. 23:246-249.

Wischmeier W.H., Mannering J.V. 1969. Relation of soil properties to its erodibility. Soil Science Society of America Proceedings. 23:131-137.

Wischmeier W. H., Johnson C. B., Cross B. V., 1971. A soil erodibility nomograph for farmland and construction sites. Journal of Soil and Water Conservation 26:189- 193.

Wischmeier W. H., Smith D. D., 1978. Predicting rainfall erosion losses: A guide to conservation planning. U.S. Department of Agriculture, Washington, DC, USA. Agriculture Handbook 537.

Detection of Landscape patterns in airborne LIDAR data in the Nature Reserve of Castelporziano (Rome)

F. Recanatesi,[1] M. Tolli,[2] M.N. Ripa,[1] R. Pelorosso,[1] F. Gobattoni,[1] A. Leone

[1]University of Tuscia, Dept. DAFNE, Viterbo, Italy; [2]Landscape Architect

Abstract

During the last decades the protection of nature has become a very important aspect due to the anthropogenic interference and structural alteration of the environment, especially in the peri-urban areas. Therefore, for a sustainable forest planning it is fundamental to get information about the actual state and the variation in landscape patterns concerning the forest layers. To this aim, an airborne laser scanning (LIDAR), a type of sensor which explicitly measures canopy height, was used to detect landscape patterns of broadleaf oak forest and for detecting the monumental trees in a peri-urban Natural Reserve: the Presidential Estate of Castelporziano (Rome).

Introduction

The Italian landscape has dramatically changed over the last sixty years, a period in which the major transformations that have deconstructed the traditional representations of our country occurred (Lanzani 2003). In this transformation process, coastal environments and especially the coastal peri-urban areas, have shown particular sensitivity (Falcucci and Maiorano 2008; Paolanti *et al.*, 2013), affected by the typical processes of residential expansion and of deep coastal urbanization.

This impoverishment process of natural coastal environments affects the whole Italian territory and in general all of the Mediterranean coastal areas where, for this reason, biodiversity is profoundly threatened.

Correspondence: F. Recanatesi, University of Tuscia, Dept. DAFNE, Via S.Camillo De Lellis, 01100 Viterbo, Italy.
Tel. +39.0761357357. Fax: +39.0761357453.
E-mail: fabio.rec@unitus.it ; michela.tolli@gmail.com

Key words: LIDAR, landscape patterns, nature reserve.

Acknowledgements: This study was made possible thanks to the environmental monitoring program for the Estate of castelporziano carried out by the National Academy of Sciences" detta dei XL"(Rome).

Journal of Agricultural Engineering 2013; XLIV(s1):e94
doi:10.4081/jae.2013.(s1):e94

In these areas, in fact, lowland forest and ancient dune ecosystems are today represented by sporadic and generally very small size fragments (IUCN Europe, European centre for the Cooperation in the Mediterranean areas).

The context of Nature Reserve of Castelporziano effectively represents the process of coastal urbanization that has concerned the entire Italian Mediterranean area (Tolli & Recanatesi, 2013), in fact, the area near the district Castelporziano-Capocotta-Castelfusano has been affected by the city development model called spontaneous, that is governed only by the laws of the land market and already widely evident in the second half of the '50s. This was later accentuated by the '62 Plan of Rome which has directed most of the urban growth along the sea road director (Marcelloni, 2003). The new urban forecasts do not differ from this trend, providing links to the highway Rome-Latina with a section near the border of the Estate and new residential areas in the Infernetto district and along the Pontine coast.

The process of urbanization has inevitably led to a landscape depleted in its environmental and landscape quality. From a recent study about the ecological relationships between the Nature Reserve of Castelporziano and its territorial context, it is apparent that the Reserve of Castelporziano is the only large area characterized by a prevalence of high and very high environmental quality areas, while everything that is in the immediate context, outside of its administrative boundaries, is mainly defined by low and very low values (Paolanti *et al.* 2013).

It is evident that the Nature Reserve of Castelporziano, with its 6.000 hectares, mainly covered by oak forests with a high density of monumental trees, with a presence of historical and cultural evidences ranging from Roman times to the Renaissance, with significant elements from XIX Century (Giordano *et al.*, 2006), located near the coast and only 20 km South of the urban area of Rome, represents a unique place, both for the environmental role, but also for the scenic charm that these historical and natural stratifications can arouse.

All landscapes are a reflection of an organization of space, a way of every object to organize and order themselves in the territory (Turri 1998). Identify patterns in a particular landscape is equivalent to understand the law that regulates its organization (Morris, 1954, Arnheim 1974). Also according to the Landscape Ecology, every type of landscape can be referred to a template, or a pattern, that varies with the structural aspect of the elementary units, or patches, which compose it. Only by recognizing these patterns and then analyzing scientifically, you may be able to give an unsterile planning policies, in the interests of the protection and enhancement (Forman 1986; Farina, 2002).

In the environment of the Nature Reserve of Castelporziano the detection of landscape pattern is really difficult, mainly for the typical conformation of Mediterranean ecosystems where the multi-specificity and layering structure is difficult to understand if not with field surveys. The mixed oak forests are the most frequent and abundant ecosystems in the Reserve (over 4.000 ha), characterized by extremely variable structure due to the different soil conditions, water availability, upheavals of the urban context (first of all rehabilitation work of the 30s), and the different management over time. There are areas

where the presence of centuries-old individuals, with heights and impressive size of the canopy and brainstem, are evidence of adaptation to an environment that has remained unchanged over time, while in other areas, the control of the Tiber and the impressive reclamation works have led to a slow replacement of deciduous oaks that once dominated the landscape, with those evergreens, more frugal in terms of edaphic and water needs, (Giordano *et al.* 2006). As well as a differentiation of the botanical forests species, also the structural aspect is very variable, in fact there is an alternation of areas with a high density of individual trees of different ages, with areas where the tree cover thins considerably to give more space to open areas of bush and grassland. Another important variant is the alternation of areas where the undergrowth is almost absent with areas where it becomes more dense and rich, represented by a dominated layer not too different from the dominant layer in height and size of the crown. Therefore the Reserve landscape is very varied and complex, consisting of layers that require targeted and careful management. Achieve a so difficult goal is not possible without a detailed knowledge of the structural and compositional aspects of the place. Often is very difficult to obtain a detailed knowledge if not through the direct reliefs on site, especially in Mediterranean areas in which the millennial man action is added to a complexity of natural ecosystems.

Currently the ability to make direct measurements on areas of relevant dimensions as those of the Castelporziano Reserve, is increasingly remote due to the costs and the time required, for these reasons we rely more and more often to the Remote Sensing technology (Fuller *et al.* 1998, Roberts *et al.* 1998, Cho 2009b). The most common method of detection in Remote Sensing is based on the interpretation of aerial images that have been recorded in this area since the 30s. However, a limiting factor in this type of analysis consists in the lack of visibility of the dominated forest structure, this involves difficulties in the relief of different landscapes pattern. This limitation is particularly relevant for natural Mediterranean environment, but today can be overcome through the use of active sensors such as the latest technology LIDAR (Light Detection and Ranging) that today represents the only way to return dendrometric data relating to the distribution and the vertical structure of the forest (Lefsky *et al.* 2005; Levick *et al.*, 2009; Rahman & Gorte 2009; Wessels *et al.*, 2011; Cho *et al.*, 2012; Levick & Asner 2013).

Therefore, the aim of this paper is to identify the different landscape patterns for the oaks forest, furthermore an additional information concerning the census of monumental trees was obtained by processing data aquired from LiDAR and applying an algorithm to extrapolate them. This process is a key requirement for characterizing landscape pattern (Andersen et sl., 2005, Koch, 2006).

Materials and Methods

The study site

The study area is of great historic interest. From the 5th century onwards it was a possession of the Vatican State, until the 19th century, when it was established as a hunting reserve for the Italian Royal Family. Finally, at the end of the Second World War, Castelporziano was chosen as the presidential estate of the Italian Republic, thanks to its rich environmental and cultural heritage

The Presidential estate of Castelporziano, within the territory of Castelporziano and Capocotta, was established as a State nature reserve in the 1999. It covers over about 6000 ha, extending South-South West of Rome (20 km from the city) towards the Tyrrhenian sea (Figure 1). Inside the nature reserve there are two Site of Community Importance (SCI): the coastal area (IT6030027) and the lowland oak

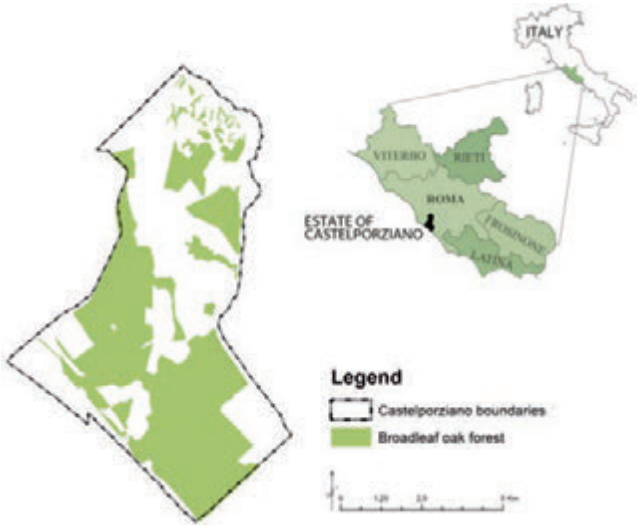

Figure 1. Location of the study area.

woodland (IT6030028). This area, including neighbouring territory of Castelfusano, is what remains of the forest system which once covered the delta of the River Tiber and its neighbouring zones.

The area of the Castelporziano Estate is between 0 and 85 m (a.m.s.l.) and it is mainly flat with a mean slope of 5% to the sea. The climate is meso-Mediterranean with a hot and dry period between May and August and precipitations peaks in spring and autumn, the annual average rainfall is approximately 750 mm. Geo-morphologically, the Estate is divided into two parts: the oldest one (Late Pleistocene) is the Ancient Dune (4/5 of the territory) in northern sector and the newest one (Holocene: 10.000 years ago) is the New Dune near the coast in the southern part.

The type of vegetation was once very common but has now almost disappeared not only in the territory of Rome, but also on many Mediterranean coasts. The territory remained substantially unchanged over the last centuries, allowing an undisturbed growth of the vegetation, which was able to develop and mature considerably. Castelporziano can be considered a unique environment in the Mediterranean due to the concentration of very old plants (*Quercus cerris* L., *Quercus pubescens* Willd., *Quercus robur* L.) which, in consideration of their age and size (many are more then 400 years), can be defined as "monumental trees" (Pignatti *et al.*, 2001; Giordano *et al.*, 2006).

Characteristics of Lidar data set

In this study we used LiDAR data, an active sensor that emits laser pulses and measures the return time for each beam to travel between the sensor and a target using ultra-accurate clocks. The location of every laser return within a coordinate system is achieved by precise kinematic positioning using differential GPS and orientation parameters obtained by an inertial measurement unit (IMU). The IMU captures orientation parameters of the scanner such as roll, pitch and heading angles. Thus, the GPS provides the coordinates of the laser source and the IMU the direction of the pulse. With the ranging data accurately measured and time-tagged by the clock, the position in the horizontal and vertical planes of the return pulses can be calculated. Data are captured as the aircraft moves forward, a scanning mirror directs laser pulses back and forth across the flight line. As a result, the data are spatially distributed as a sawtooth arrangement of points. The majority of the commercial sys-

tems can collect between 20.000 and 75.000 records per second and the LiDAR data sets are normally distributed as large point files in an ASCII XYZ format. Data point density depends on the number of pulses transmitted per unit time, the scan angle of the instrument, the elevation of the aircraft above ground level, and the forward speed of the aircraft. The system is capable of achieving high vertical and horizontal accuracies. This may vary between 15 and 20 cm RMS vertically, while horizontal accuracies are about 20–30 cm. For this study we used data detected in June 2010 with a resolution of 1 m.

Landscape pattern

The location of forest stands characterized by deciduous oak forest has been detected through the woodcut paper on the occasion of Forest Management Plan (FMP) (Giordano *et al.*, 2006).

The determination of the landscape pattern was performed by referring to the definition of Forman & Godron (1986) in which "*... the landscapes are systems of environmental systems that exist at the scale of kilometers and include recognizable elements, related to types of ecosystems and human settlements and / or other manmade elements ...* ". In the natural environments present in Castelporziano, characterized by oak forests (2.890 ha), the detection of the different landscape patterns has been performed by a classification of the territory finalized to the identification of two basic components:

1. The analysis of the spatial structure of forest stands with a predominance of broadleaf oaks;
2. The census of all trees with dendrometric characteristics of monumentality.

With regard to the structure of forest stands, in the present study, this refers to the spatial distribution of plants and their membership in the different layers of the forest (dominant layer and dominated layer) and the type of management (coppice and high forest).

Given the high historical environmental component of these stands was also conducted an investigation to determine the number and spatial distribution of the plants that, by extension of the crown and to the size dendrometric reached, can be considered as monumental trees as provided by current legislation LR n. 39 28/10 2002.

The census of all plants monumental and their spatial distribution have allowed an implementation of the state of knowledge concerning the landscape features of the area in question.

The detection of landscape patterns for broadleaf forest oak was obtained using LIDAR data. These data were employed to analyze the forest layers by means of horizontal sections, detected at different heights from the ground. To this aim we have been consulted data collected in the field related to the heights for different forest layers. (Means *et al.*, 1999; Andersen *et al.*, 2005; Angelo *et al.*, 2010; Giordano *et al.*, 2010; Eysn *et al.*, 2012).

The census of monumental trees

We used ArcMap software in processing LIDAR data. A raindrop algorithm is used to estimate both tree tops and corresponding "light crown boundaries" in the DSM (Suarez *et al.*, 2005; Koch *et al.*, 2006). The algorithm assumes the input data describing a "mountain range". Firstly the local maxima are calculated, pixel that present larger values than their 4 connective neighbors are marked as maxima. Secondly, starting from these maxima an expansion is done until the valley bottoms are reached, like raindrops running downhill in all possible direction. This part of the algorithm continues as long as the examined points found are smaller or equal.

Once got the perimeter, and then the surfaces of the crowns of all the trees, was performed Reclass to isolate all the plants with a surface of the crown equal to or greater than 110 m2. This value has been identified by the consultation of the data collected in sample plots.

Data field

Information regarding the heights of the different layers that characterize the different types of forest were obtained from geo-referenced data, collected in 53 sample plots (30 m radius), carried out during the updating of the Forest Management Plan, 2010 (Giordano *et al.*, 2013). In the sample plots were recorded classical dendrometric parameters: forest structure, species composition; heights of forest layers; management system and plant density. In the sample plots the census of monumental trees present are also reported. These data concerning the surface of the crown coverage and their location in the territory have been used in the validation of the results obtained from the raindrop algorithm analysis of LIDAR data.

Results

The analysis of LIDAR data allowed the determination of four landscape patterns, of which follows a brief description about their structure and considerations regarding the perceptual analysis. Figure 2 shows the inherent thematic mapping of their distribution in the Estate of Castelporziano:

1. Natural coastal landscape (NCL);
2. Anthropogenic trasformation landscape (ATL);
3. Changing coastal plain landscape (CCPL);
4. Stable lowland ancient oak landscape (SLAOL).

Natural coastal landscape

Landscape composed of dune ridges semi stabilized or stabilized by intercropping endemic flora characterized by juniper (Juniperus oxycedrus) with a prevalence of low mediterranean macchia characterized by heather and phillyrea. The innermost part of the territory, for this class of landscape, is characterized by stabilized dune ridges, with maquis and holm oak, and depressions interdunal. From a perceptual point of view this landscape has a twofold component, the first is a low bush, where the trees never grow to over one meter and a half, an

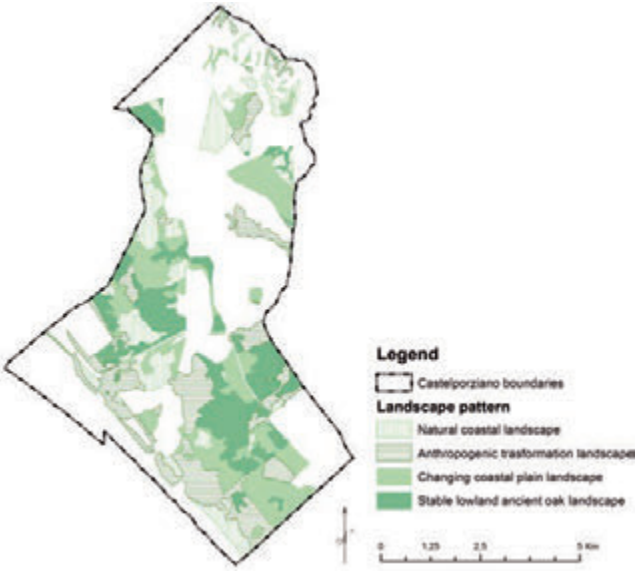

Figure 2. Landscape Pattern detected and localization of sample areas (black dots).

aspect that allows an overview with extensive visual framing the pattern in its context, and the second one is a spot more than two meters high and impenetrable that arises then as a barrier perception.

Anthropogenic transformation landscape

Landscape pertaining to the flood plain behind the dunes in which are obvious effects of land management aimed at the exploitation of forest resources it has, over the centuries, changed the original natural structure of the forest. The effects of such a harvesting have resulted in the depletion in the number of plant species of trees and a simplification of the vertical structure of the same. The selective cuts, perpetrated until the 80s, at regular intervals (for these kind of coppice the rotation was established in 18 years) have shaped the forest structure whose effects, in terms of ecosystem, are due to the simplification of the landscape reduced to a single layer with a predominance of an unique arboreal species. In some areas it was found a plan dominated by shrub consists of a high spot in the prevalence of heather and phillyrea. Because of the abundance of suckers, given the rigid cycles of use followed in the past, this landscape is perceived as an element that is free of visual cones that allow the perception of the internal structure and a contextualization with the surrounding landscape

Changing coastal plain landscape

Landscape represented by all those forest that were excluded from harvesting programs and that, for this reason, today appear in an intermediate evolutionary stage between a management characterized by coppice and the stable formation represented from lowland oak. In this class of landscape stand still signs of coppicing, interrupted over 60 years ago, that has led to an increasing age of the stumps with the consequent self selection of the suckers. Forest ecosystems begin to present the characteristics of vertical diversification with the intrusion of accompanying species such as hornbeam, and occasionally the maple tree which presents heights dendrometric between the high spot and the deciduous oak forest. This structure makes it very varied the visual perception, in fact, it passes from areas in which the forest layer is very fraught, and it behave as a visual screen, with the other in which the visual perception dilates in open areas as visual cones that, in this way, allows the perception the complex stratification that characterizes it.

Stable lowland ancient oak landscape

Stable landscape, characterized by the presence of oaks with senescent characteristics and dendrometric monumentality. These environments have more characters of stability as they have reached a climax status. From a perceptual point of view this is a landscape pattern extremely interesting for its characterization, in fact there are alternation of full and empty that determine open visual spaces and a depth field always variables.

Figure 3 shows a schematic diagram of the landscape patterns detected, where, from the calculations of the LIDAR data, the vertical structures emerge for each type of landscape detected. On the patterns SLAOLA and CCPL, by way of example, have been superimposed information pertaining to the census of monumental trees detected by the raindrop algorithm used. These information has also allowed a spatial representation of the forest area in the three dimensions allowing a classification of the entire territory in landscape structures.

It was also quantified, Figure 4, at the scale of landscape pattern, the functionality in terms of: stability, naturalness, complexity and vulnerability. This representation was carried out with purely subjective criteria, and has the simple purpose of comparing the patterns detected.

The geo-referenced data regarding the number, size and shape of the patches for individual landscape patterns have been developed for the determination of the main indices of the metric own of the landscape metrics.

In Table 1, we report the values distributed according to the four patterns identified. The most significant data indicate a high degree of fragmentation observed on all patterns, this data determine, as a result, an average size of the patch somewhat reduced. Significant also appear the results obtained for the edge metrics, where the values inherent in the edge density expressed per hectare, show an irregular spatial distribution of patches of different patterns. The shape metrics, finally,

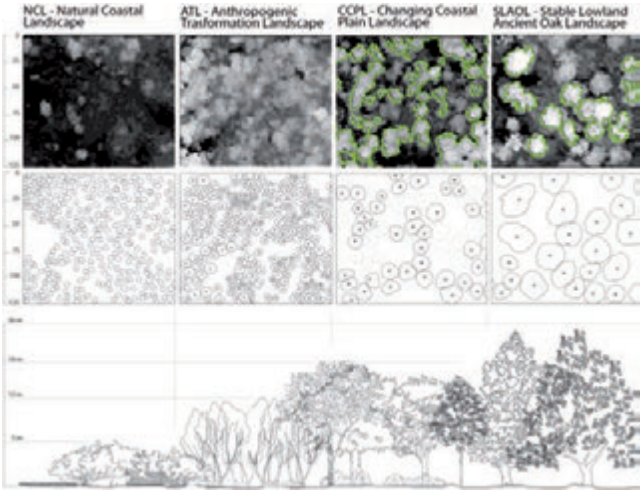

Figure 3. Conceptual framework on the census of landscape pattern in the Estate of Castelporzianothe. The green lines show the detection of monumental trees obtained by LIDAR data for CCPL and SLAOL landscapes.

Table 1. Landscape indices for landscape patterns.

Landscape Pattern	Patch Density & Size Metrics				Edge metrics		Shape metrics		
	Surface (ha)	Number of Patches	Mean Patch Size	Median Patch Size	Total Edge (m)	Edge Density (m)	MSI	AWMSI	Mean Perimeter-Area ratio
Natural Coastal Landscape	574,1	42,0	13,7	5,4	72258,4	25,0	1,6	1,9	7294,1
Anthropogenic Transformation Landscape	741,1	22,0	33,7	10,2	90309,1	31,2	2,1	3,0	247,6
Changing Coastal Plain Landscape	871,5	34,0	25,6	10,7	90472,1	31,3	1,7	2,0	1915,9
Stable Lowland Ancient Oak Landscape	705,1	23,0	30,7	11,8	69596,2	24,1	1,9	2,3	1266,5

shows the above in terms of spatial distribution and irregular shapes.

With regard to the census of monumental trees, in the study area were surveyed a total of 412 trees with a surface of the crown that can be considered monumental (> 110 m^2). Compared to field data concerning the crown coverage of monumental trees the method presented delivers a K of 0.8 for the study area, Figure 5.

Conclusions

The determination of landscape pattern plays a key role in the identification and management of multifunctionality and externalities that a protected area such as peri-urban Nature Reserve Castelporziano is able to express.

To this aim, the use of LIDAR data proved to be a versatile and effective tool above all considering the geographical location of the study area falling in the Mediterranean environment. The ability to analyze the forest area in terms of its vertical structure allows you to compensate for the limitations of the usual remote sensing instruments (photo interpretation and/or images obtained from satellite platforms) that do not allow investigations below the plane of the dominant topsoil thus making it necessary inspections in the field with inevitable repercussions on the execution times and costs.

With regard to the census of woody plants monumental, the high-resolution LIDAR data, together with the use of the raindrop algorithm, present in the suite of ArcMap have provided a comprehensive census of the plants monumental in size and number.

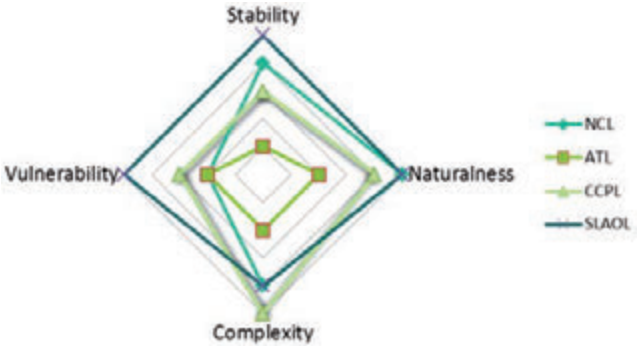

Figure 4. Functionality of the landscape patterns detected.

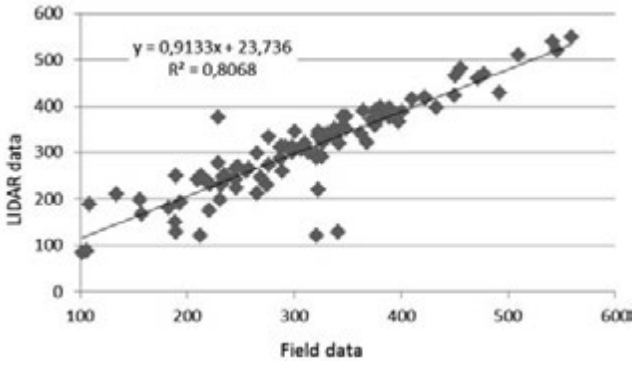

Figure 5. comparison between LIDAR and field sample data in crown coverage detection for monumental trees.

References

Andersen H, McGaughey R, reutebuch S. 2005. Estimatig forest canopy fuel parameters using LIDAR data. Remote Sensing of Environment. Vol. 94, pp. 441 – 449

Arnheim R, 1974. Il pensiero visivo. La percezione come attività conoscitiva. Einaudi (TO)

Angelo J, Duncan B, Weishampel J. 2010. Using LIDAR derived vegetation profiles to predict time since fire in an oak scrub landscape in East central Florida. Remote sensing. Vol. 2, pp. 514 – 525

Eysn L, Hollaus M, Schadauer K, Pfeifer N. 2012. Forest Delineation Based on airborne LIDAR data. Remote Sensing. Vol. 4, pp. 762 – 783

Falcucci A, Maiorano L, 2008. Uso ed abuso del suolo: la trasformazione del paesaggio in Italia dal 1950 ad oggi. In: Riconquistare il paesaggio. La Convenzione Europea del Paesaggio e la Conservazione della Biodiversità in Italia. MIUR.

Gazzetta Ufficiale della Repubblica Italiana. Legge Regionale n. 39 del 28 ottobre 2002.

Giordano E, Maffei L, , Recanatesi F, Tinelli A. 2013. Aggiornamento del Piano di Gestione Forestale per i boschi della Tenuta Presidenziale di Castelporziano. In: Il Sistema Ambientale della tenuta Presidenziale di Castelporziano (Roma). Accademia Nazionale delle Scienze *detta dei XL*. Scritti e documenti.

Giordano E, Capitoni B, Eberle A, Maffei L, Musicanti A, Recanatesi F, Torri V. 2006. Proposta per il piano di gestione forestale della tenuta presidenziale di Castelporziano. In: Il Sistema Ambientale della Tenuta Presidenziale di Castelporziano – ricerche sulla complessità di un ecosistema forestale costiero mediterraneo. Accademia Nazionale delle Scienze *detta di XL*.

Falcucci A, Maiorano L, 2008. Uso ed abuso del suolo: la trasformazione del paesaggio in Italia dal 1950 ad oggi. In: Riconquistare il paesaggio. La Convenzione Europea del Paesaggio e la Conservazione della Biodiversità in Italia. MIUR.

Farina A, 2002. Ecologia del paesaggio. Principi metodi e applicazioni. UTET Università.

Forman R T, Gordon M. 1986. Landscape Ecology. Springer-Verlag, (NY).

Fuller et al. 1998. The integration of field survey and remote sensing for biodiversity assessment: A case study in the tropical forests and wetlands of Sango bay, Uganda. Biological Conservation, 86(3), pp. 379-391.

Koch B, Heyder U, Weinacker H. 2006. Detection of individual tree crowns in airborne LIDAR data. Photogrammetric Engineering & Remote sensing. Vol. 72, n. 4, pp. 357 – 363

Lanzani A., 2003. I paesaggi italiani. Maltemi editore (Rm)

Levick S, Asner G. 2013. The rate and spatial pattern of tree fall in a savanna landscape. Biological Conservation. Vol. 157, pp. 121 – 127

Marcelloni M., 2003. Pensare la città contemporanea. Il nuovo piano regolatore di Roma. Editori LaTerza (Roma-Bari)

Means J, Acker S, Harding D, Blair J, Lefsky M, Cohen W, Harmon M, McKee A. 1999. Use of large-Footprint scanning airborne LIDAR to estimate forest stand characteristics in the western cascades of Oregon. Remote Sensing Envoronment. Vol. 67, pp. 298 – 308

Morris Ch, 1954. Lineamenti di una teoria dei segni. Paravia (TO)

Paolanti M, Blasi C, 2013. Valutazione delle relazioni ecologiche e degli impatti tra la Tenuta di Castelporziano e il suo contesto territoriale. In: Il sistema ambientale della Tenuta Presidenziale di Castelporziano (Rm). Accademia Nazionale delle Scienze *detta dei XL.* Scritti e documenti.

Rahman M, Gorte B. In: Laser scanning. Vosselman G (Eds). IAPRS, Vol. XXXVIII. Paris, 2009

Suarez J, Ontiveros C, Smith S, Snape S. 2005. Use of airborne LIDAR

and aerial photography in the estimation of individual tree heights in forestry. Computer & Geoscience. Vol. 31, pp. 253 – 262

Turri E., 1998. Il paesaggio come teatro. Dal territorio vissuto al territorio rappresentato. Marsilio Editore (VE)

Tolli M, Recanatesi F. 2013. Variation in landscape patterns and vegetation cover between 1930 and 2010 in a coastal Mediterranean natural reserve. Conference Uniscape: Landscape & Imagination, Paris 2-4 may.

The assessment of the visual perception in viewshed analysis for the landscape settings

Enrico Fabrizio,[1] Gabriele Garnero[2]

[1]University of Torino, DISAFA (Dept. of Agricultural, Forest and Food Sciences), Torino, Italy; [2]University and Polytechnic of Torino, DIST (Dept. of Regional and Urban Studies and Planning), Torino, Italy

Abstract

Visibility studies for rural and forest landscape are well established and conducted by means of standard GIS tools that compute the viewshed (a binary representation of the visibility of a location from a certain viewpoint) and cumulative viewsheds (integer representations of the visibility of a location from more viewpoints obtained with raster algebra). However, in order to go beyond the sole geometric information if a cell is visible or not, some authors have introduced various concepts that are based on the visual magnitude or visual exposure. These concepts also take into account the target magnitude, the atmospheric extinction, the colour difference to the background and the visual acuity. These calculations may be complex, extremely time consuming and not affordable with standard GIS tools, because they require specific programming tools. Besides, depending on the application, the factor that affects the visibility may be the distance, the atmospheric extinction, the contrast, etc. In this work, we concentrate on the problem of the calculation of the landscape sensitivity, which defines the degree to which a given landscape is potentially affected by possible changes by means of viewsheds analyses. An example in rural settings is presented in order to demonstrate the problems that arise in real applications and the possible solutions.

Correspondence: Gabriele Garnero, DIST, Università e Politecnico di Torino
Via Leonardo da Vinci, 44, 10095 Grugliasco (TO), Italy.
Tel. +39.011.670.5518 - Fax + 39.011.670.5516.
E-mail: gabriele.garnero@unito.it

Key words: viewshed analysis; landscape; visual perception.

Contributions: the authors contributed equally.

Conflict of interest: the authors declare no potential conflict of interests.

Funding: no source of funding.

Journal of Agricultural Engineering 2013; XLIV(s1):e95
doi:10.4081/jae.2013.(s1):e95

Introduction

It is well known that a new development can modify the viewing conditions of a landscape. This is indicated as a visual impact, however it is seldom an easy task to determine the effect of the view obstructions and the re-shaping of the skyline, both in urban (Moser *et al.*, 2010) and rural areas. It is necessary to take into account, besides the topography, the building elevations and the urban atmospheric visibility. New cartographic products can give new instruments to regional planners. The DTM and orthoimages databases can produce cartography useful in doing the regional planning such as the landscape sensitivity maps. The landscape sensitivity can be defined as the degree to which a given landscape could potentially be affected by possible changes, such as development (Bell, 2012). The metrics of a landscape sensitivity map should be able to identify:

- how much territory can be seen from a certain viewpoint (quantitative concept indicating if the viewpoint can be seen from large areas or only from some specific points);
- how a portion of territory is seen (qualitative concept indicating from which distance it is seen and if this vision is impacting on the observer).

In order to perform maps of the landscape sensitivity it is necessary to use GIS procedures that consider together both terrain and built environment representations and model the interaction between humans and the space. However, visibility studies, especially those referring to rural and forest landscape analysis, are usually based on only terrain representations (triangulated irregular network – TIN or regular square grid of elevations – DEM) and must recur to some simplifications in order to take into account vegetation and other obstacles that affects the visibility (*e.g.* create a vegetation elevation model that is summed to the DEM).

Another characteristic of this work is to go beyond the standard binary approach that is used in visibility analysis (an integer result to identify if the cell of a raster is visible or not), taking into account more realistic factors that depend on the human vision and on the outdoor environment.

Materials and methods

Visibility studies were conducted in the past by means of isovists (Benedikt, 1979). An isovist may be defined as the visual field (set of points) that is wholly visible from a certain single point that is the feature of interest and that is called vantage point. If the isovist is computed on a plan, in a 2D representation the isovist is the set of points that are visible from the vantage point, disregarding the effect of the terrain morphology and the different heights of the surrounding buildings. In this case, an isovist is mapped as the continuous area of a two

dimension polygon. With the creation of isovist generating computer applications (Dalton& Dalton, 2001), there has been the possibility of moving the vantage point along a path generating a field of isovists and studying how the isovist properties vary along the path. However the drawback of an isovists is that in 2 D an isovist does not take into account the possibility to look beyond an obstacle (Llobera, 2003).

A viewshed is a binary representation of the visibility of a location from a certain viewpoint and is usually computed by means of standard functions of GIS software tools from the DTM (Digital Terrain Model). The result is a Boolean variable that identifies if each cell is visible (value 1) or not (value 0) from a certain viewpoint. When the results of various viewsheds from different viewpoints are added up using raster algebra of GIS tool, the result is called cumulative viewshed and is characterized by an integer result: in this way how many viewpoints are seen at cell can be identified.

In order to go beyond the sole information if a cell is visible or not which is typical of the viewsheds, some authors have introduced the visual magnitude, which takes into account also the amount of a specific feature that is visible on the observer view. The first consideration on which this concept is based is that the visible size of an object diminishes as the view distance increases. The visual magnitude result is a floating point whose values are from 0 (no visibility) to 1 (complete visibility) and is computed taking into account the fact that the visible area decreases with the square of the distance. Different formulations for the calculation of the visual magnitude can be found on the literature (Grêt-Regamey *et al.*, 2007; Chamberlain & Meitner, 2013). As can be easily understood, in reality visual magnitude assumes very low values, because they have the physical meaning of the amount of area occupied on an observer view. Again, also in the case of the visual magnitude only geometrical aspects are considered, while other authors have introduced the concept of visual exposure (Domingo-Santos *et al.*, 2011) in order to take into account also the atmospheric extinction, the colour difference to the background and the visual acuity.

Visual magnitude and visual exposure concepts have been widely used in the rural and forest landscape analysis (Kearney *et al.*, 2008; Domingo-Santos *et al.*, 2011; Jakab & Petluš, 2012; Chamberlain & Meitner, 2013).

Viewsheds and cumulative viewsheds can be easily calculated by means of standard GIS tools, however they suffer from the limitation due to the lack of the visual attenuation with distance, so that when the distance increases the results of a viwesheds analysis are merely theoretical.

The effect of the visual attenuation with distance is due, from a physical point of view, to:

- the visual acuity of the human eye;
- the atmospheric visibility;
- the contrast between the target and the surrounding (*e.g.* the sky).

The visual acuity is defined as the inverse of the minimum apparent diameter a, measured in minutes of arc. The arc a can be obtained from the distance of observation d and the object size D as

$$a = \frac{180 \cdot 60}{\pi} \arctan\left(\frac{D}{d}\right) \quad (1)$$

The visual acuity depends on the age of the subject, on the illuminance level and on the contrast, and ranges from 2 (that is 0.5') for young people with the greatest contrast, to 0,2 (that is 5') for elderly people with the lowest contrast (Fortuin, 1951). Usually a value of about 1, that is an angle of 1' (minute), is considered to be a threshold value of visibility in many applications. The limit visibility distance due to visual acuity will be indicate hereinafter as $d_{l,v}$ and is equal, from Eq. 1, to

$$d_{l,v} = \frac{D}{\tan\left(a \frac{\pi}{60 \cdot 180}\right)} \approx D \frac{60 \cdot 180}{a \pi} \quad (2)$$

Considering an object that has a size of 20 m, the maximum distance at which it can be seen is 69 km with a visual acuity of 1.

Even though visual acuity sets a physical limit to the mutual view distance between two points in a GIS model, only in some particular weather conditions (*e.g.* clear winter days) the visual acuity limitation may be the predominant one. In fact, in practice in many cases the atmospheric visibility may limit the maximum visibility distance rather than the visual acuity, however, this aspect is of little interest in the field of landscape sensitivity studies because the landscape perception is supposed to be evaluated during good weather conditions.

The third aspect that affects the visibility of an object in the landscape is the colour contrast between the target and the immediate surroundings. In many procedures for the visual impact assessment (*e.g.* Torres-Sibille, 2009; Chiabrando *et al.*, 2011) this aspect is taken into account computing the colour difference – sometimes erroneously called contrast – expressed as the Euclidean distance between the two points in the CIELAB colour space. In visibility studies other authors calculates the contrast as the difference between the average lightness of the object and the background object (*e.g.* Shang & Bishop, 2000), thus considering only a difference in lightness on a gray scale.

Implementation on a case study

The visibility analysis was conducted on the case study of a path of 14 stages (called "stations") that connects the house of Don Bosco to that of S. Domenico Savio in the province of Asti. The 14 "stations" are dedicated to 14 young people in the history of salvation in the Scriptures. This path is intended to be traveled on foot and is 1200 m long. A representation of this path is reported in Figure 1. This path is currently under construction and is called "Strada del Papa" (Path of the Pope) since it is the normal road for access to the Salesians sites, built in 1988 on the occasion of visit of Pope John Paul II for the centenary of the death of Don Bosco. A firt part of this route, from the house of Don Bosco (the saint of youth) to Saint Dominic Savio (the first young Santo), will be equipped. It is an itinerary in the green of the hill

Figure 1. The path from the house of Don Bosco to the house of S. Domenico Savio.

of Asti already used by groups, families and individuals to take walks or meditate in a favorable, full of silence, beautiful and peaceful natural environment (Figure 2).

Along this path the "Way of biblical youth" will be built. It is a journey dotted with 14 modern kiosks, as many are the Stations of the Cross, but focusing on young people of the Old Testament (*The Sacrifice of Isaac; Joseph, savior of its people; the calling of Samuel, David, the boy anointed king by Samuel; Esther, the girl who saves his people; the vocation of the prophet Jeremiah; Hananiah, Mishael and Azariah, the three youth loyal to God against the idolatrous king of Babylon*) and the New Testament (*Mary of Nazareth, the girl of the Magnificat; the Holy Innocents; twelve year old Jesus among the Doctors in the Temple of Jerusalem; the resurrection of the son of the widow of Nain; the vocation of Andrew and John; the boy the multiplication of the loaves and fishes; the blessing of children*).

The kiosks, made of metal and designed by Aldo Gervasio, will host the paintings by the two Polish Salesians painters, the brothers Robert and Leszek Kruczek.

Digital terrain model - DTM

The new DTM of Piedmont Region has a cell size of 5 m x 5m. Data for the present work have been provided by Regione Piemonte survey aimed to the production of a digital orthoimage at 1:5000 scale and a digital terrain model at Level 4 in accordance with Intesa specifications (CISIS, 2011) as reported in Table 1 (Godone and Garnero, 2013).

A LIDAR survey was carried out by the employment of ALS 50 II sensor (Leica Geosystems) with MPIA (Multiple Pulse In Air) technology, with the following features:

- Maximum Pulse Rate: 150.000 Hz (150.000 points/second);
- Maximum scanning frequency: 90 Hz (90 lines/second);
- 4 echoes (1°, 2°, 3°and last);
- Flying height: 200 - 6000 m above ground;
- Field Of View (FOV): 10° – 75 °;
- Side overlap: 200 - 600 m;
- Intensity measured each echo.

The LiDAR survey of the complete territory of Regione Piemonte was characterized by the following parameters:

- FOV (Field Of View): 58°;
- LPR (Laser Pulse Rate): 66.400 Hz;
- Scan Rate: 21.4 Hz;
- Average Point Density:0.22 pts/m²;
- Average Point Spacing: 2.12 m;

The study area refers to the 156160, 157130, 174040 and 175010 Sections of the regional DTM (Digital Terrain Model), which has a cell size of 5x5 m. The representation of this DTM is reported in Figure 3 where it can be noted that the "Path of Pope" is on a hill and that can be seen from both the valleys on east and west.

Base cartography

The base map produced by the *Unione Collinare Alto Astigiano in 2009* was used for this work. Specifically, it is part of a series of productions partially financed by the Fondazione CRT (Cassa di Risparmio di Torino) executed on the basis of common specifications promoted by the Piedmont Region in the implementation of the national rules that go under the *IntesaGIS* programme. The standardization includes specific standardized contents both in the various productions and at different scales, so that it is possible for the higher-level Public Administration, to retrieve information in order to update their territorial databases.

Table 1. Specifications of the DTM level 4 - CISIS document "Ortoimmagini e modelli altimetrici a grande scala - Linee Guida (Large scale orthoimagery and elevation models – Guidelines)" shows Level values (meters)

Type	DEM or DSM
Accuracy: bare ground PH(a)	0.30
Height accuracy: with tree cover > 70% PH(b) (DEM)	0.60
Height accuracy: buildings (DSM) PH(c)	0.40
Height tolerance: bare ground TH(a)	0.60
Height tolerance: with tree cover > 70% TH(b) (DEM)	1.20
Height tolerance: buildings (DSM) TH(c)	0.80
Planimetric accuracy: PEN	0.30
Planimetric tolerance: TEN	0.60
Cellsize:	5

Figure 2. A view from the "Path of Pope".

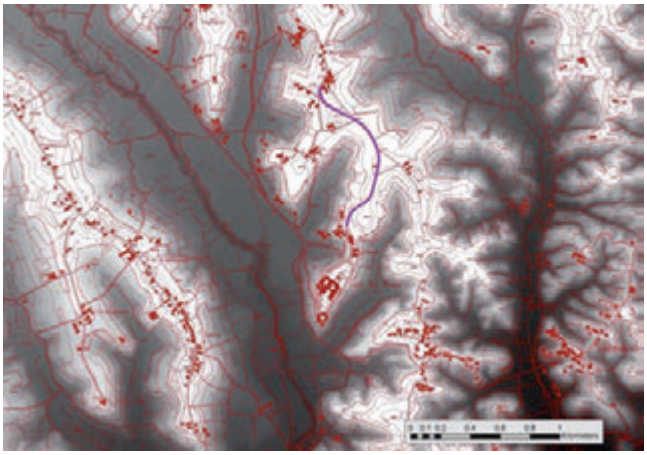

Figure 3. DTM of case study area with the indication of the "Path of Pope" under consideration.

GIS processing

The ArcGIS 10.1 tool was used in all the processing. It is believed that, in a journey on foot, portions of land that are at different distances from the viewers should be classified with a different landscape sensitivity: it is evident from everyday experience that near objects can cause a perception of greater evidence than distant objects, even though those last are, from the point of view of the visibility, are within the visible space and have a size above the threshold level of visual acuity (see Eq. 2).

For the implementation of this work the following classification as a function of visual depth was adopted, in accordance with the indications found in the literature (de la Fuente de Val *et al.*, 2006; Brabyn and Mark, 2011). The levels of visual depth identified were the followings:

- foreground, with 0-500 m visual depth. In the foreground individual components of the scene are distinguishable and multi-sensory factors intervene (sounds, smells);
- intermediate ground 1, with 500-1000 m visual depth. In the intermediate ground individual elements are noticeable compared to the background;
- intermediate ground 2, 1.000- 2.000 m visual depth;
- background, 2.000 m visual depth. The background is of interest only in case of relevant size of the objects or distinguished elements.

The previous values of distance are suitable for the specific contest; different distances may be defined for other topographic and landscape contexts (*e.g.* the visibility of a prominent mountain into an alpine landscape or the visibility of a skyscraper into a urban landscape).

The horizontal aperture angle was set to 360° (full horizontal visibility).

The analyses were then performed by adopting the Multiple Ring Buffer analysis tool available in the ArcGIS Geoprocessing tools.

No limit visibility distance for the atmospheric extinction was assumed since the landscape sensitivity should be studied in the best visibility conditions.

Figure 4. Visibility map of the "Path of Pope" under consideration with the three levels of visual depth (green: visible, red: invisible).

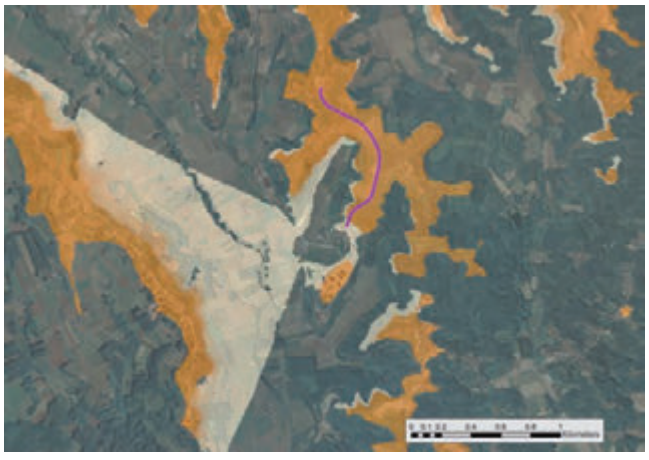

Figure 5. Landscape sensitivity of the "Path of Pope" under consideration.

Results

In the following Figures 4 and 5 the visibility maps are reported. The first map is the visibility of the "Path of the Pope" computed with a discretization of the path with the indication of the various visual depths for foreground (inner curve), intermediate grounds and background. A green land unit means that this land unit sees or can be seen from at least one point of the "Path of the Pope". As can be seen from the figure, large extent of the study area can be seen from the path, especially in the foreground level.

In order to give a quantitative evaluation of the landscape sensitivity, using raster algebra, in Figure 5 each visible land unit is classified as a function of the occurrence of the visibility for the various points in which the "Path of the Pope" was discretized. It can be seen that the for most of the green area of Figure 4, the landscape sensitivity is maximal, because the land unit can see or can be seen from all points in the path. This mapping was obtained by discretizing the path in all the characteristic points, inserting also other 100 points: overall, a total of 443 points were considered and each land unit is classified depending on the incidence of the number of points that see / are seen from the territory.

Conclusions

The modern cartographic supports that are already entered in the normal production process, may be used, in addition to the technical applications for which they are ordinarily prepared, also as interesting databases that allow rethinking the traditional cartography currently used by city and landscape planners.

The examples presented in this paper can in fact provide those involved in the design of planning instruments and operators that check the landscape compatibility of new developments with objective instruments for assessing the actual degree of visual impact of the works under project and, equally objectively, the various proposals (transformation or not, mitigations, green screens, etc....). It is in fact possible to predict the points of visibility and the landscape sensitivity in order to guide and generate an urban development that does not interfere with the landscape settings. In the particular study case, the locations that should be prevented from a large urban development can for example be seen on Figure 4.

Visibility analyses can also be a valuable means for the tourist development of a territory, also by means of new technologies (Garnero *et al.*, 2013; Minucciani *et al.*, 2013).

References

Bell S. 2012. Sustainable Landscape. In: R.A. Meyers (ed.) Encyclopedia of Sustainability Science and Technology. Springer Science, New York, pp 10360-90.

Bendikt M.L. 1979. To take hold of space: isovists and isovist fields. Environment and Planning B. 6:47-65.

Brabyn L., Mark D.M. 2011. Using viewsheds, GIS, and a landscape classification to tag landscape photographs. Applied Geography. 31:1115-1122.

Chamberlain B.C., Meitner M.J. 2013. A route-based visibility analysis for landscape management. Landscape Urban Plann. 111:13-24.

Chiabrando R., Fabrizio E., Garnero G. 2011. On the applicability of the visual impact assessment OAI_{SPP} tool to photovoltaic plants, Renew Sust Energy Rev. 15:845-850.

Dalton R.C., Dalton N. 2001. OmniVista. An Application for Isovist Field and Path Analysis. In Proceedings . 3rd International Space Syntax Symposium Atlanta 2001, pp. 25.1-25.10.

de la Fuente de Val G., Atauri J.A., de Lucio J.V. 2006. Relationship between landscape visual attributes and spatial pattern indices: A test study in Mediterranean-climate landscapes .Landscape Urban Plann. 77:393-407.

Domingo-Santos J.M., de Villaran R.F., Rapp-Arraras I., de Provence E.C.P. 2011. The visual exposure in forest and rural landscapes: An algorithm and a GIS tool. Landscape Urban Plann. 101:52-58.

Fortuin G.J. 1951. Visual power and visibility. PhD Dissertation, University of Groningen (NL).

Garnero G., Corrias A., Manigas L., Zedda S.V. 2013. VGI, Augmented Reality and Smart Web Application: Projects of Development in the Territory of the Sardinia Region, in B. Murgante et al. (Eds.): ICCSA 2013, Part IV, LNCS 7974, pp. 77—92. Springer, Heidelberg.

Godone, D., Garnero G. 2013. The role of morphometric parameters in Digital Terrain Models interpolation accuracy: a case study. European Journal of Remote Sensing, 46(1), 198-214.

Grêt-Regamey A., Bishop I.D., Bebi P. 2007. Predicting the scenic beauty value of mapped landscape changes in a mountainous region through the use of GIS. Environment and Planning B. 34:50-67.

Jakab I., Petluš P. 2012. Development of a program tool for the determination of the landscape visual exposure potential. Developments in Environmental Modelling. 25:375-390.

Kearney A.R. Bradley G.A., Petrich C.H., Kaplan R., Kaplan S., Simpson-Colebank D. 2008. Public perception as support for scenic quality regulation in a nationally treasured landscape. Landscape and urban planning. 87:117-128.

Llobera, M. 2003. Extending GIS-based visibility analyses: the concept of visualscapes. Int. J. Geogr. Inf. Sci., 17 (1), 25-48.

Minucciani V., Garnero G. 2013. Available and Implementable Technologies for Virtual Tourism: A Prototypal Station Project, in B. Murgante et al. (Eds.): ICCSA 2013, Part IV, LNCS 7974, pp. 193—204. Springer, Heidelberg.

Moser J., Albrecht F., Kosar B. 2010. Beyond visualisation – 3D GIS analyses for virtual city models. International Archives of the Photogrammetry, Remote Sensing and Spatial Information Sciences. vol. XXXVIII-4/W15:143-146.

Shang H., Bishop I.D. 2000. Visual thresholds for detection, recognition and visual impact in landscape settings. Journal of environmental psychology. 20:125-140.

Torres Sibille A., Cloquell-Ballester V., Cloquell-Ballester V., Ramirez M. 2009. Aesthetic impact assessment of solar power plants: an objective and subjective approach. Renew Sustain Energy Rev. 13:986–999.

Evolution of some Mediterranean landscapes of Central Italy from historical aerial photographs

Maria Nicolina Ripa, Francesco Ciapanna, Goffredo Filibeck, Federica Gobattoni, Antonio Leone, Raffaele Pelorosso, Matteo Piccinno, Carlo Maria Rossi, Fabio Recanatesi

Dipartimento di scienze e tecnologie per l'agricoltura, le foreste, la natura e l'energia (DAFNE), University of Tuscia, Viterbo, Italy

Abstract

Aerial photos represent the main existent database providing evidence of landscape changes with high detail. The analysis of land cover changes plays a key role in understanding a great variety of phenomena in several research fields. Landscapes are made by society and reflect the changing society and attitude towards the environment. The reorientation of farming system, the practical results of planning processes, the rate and magnitude of the changes in the landscape are some of the most important factors relating to the evolution of our landscapes and are very helpful for the understanding of evolution processes and consequently for the design of landscape-orientated policies. Pressures upon the landscape and values of our landscapes can be defined according to their traditional characteristics; traditional landscapes can be defined as those landscapes having a distinct and recognizable structure, which reflect relations between the composing elements and have a significance for natural, cultural or aesthetical values. In most cases, such landscapes evolved slowly and took centuries to form their values. Sometimes land changes happen fast and spread in vast areas so that some agricultural or natural landscapes, widely perceived as traditional, have very recent origin. In this paper, some preliminary observation and case-studies performed on a set of historical photos are dealt with. In 1935, the Italian Land Register Department commissioned SARA company to survey Viterbo province between 1935-1938 through aerial photographs. During the survey, 5,000 photographs on glass plates were taken at a very low altitude, featuring a very high resolution. Thus, they represents a valuable source of information for documenting past and present land-use practices, local cultural heritage and changes in the landscape. Processing this set of historical photos has started, aimed to quantitatively and qualitatively analyse the 1935-1938 landscape patterns and their role in the development of nowadays landscapes.

Correspondence: Maria Nicolina Ripa, DAFNE, Università degli Studi della Tuscia, Via San Camillo de Lellis snc, 01100,Viterbo.
Tel. +39.0761.357362.
E-mail: nripa@unitus.it

Key words: Aerial photos, traditional landscape, landscape transformation, land use/land cover change.

Journal of Agricultural Engineering 2013; XLIV(s1):e96
doi:10.4081/jae.2013.(s1):e96

Introduction

Changes in land use and land cover are some of the most evident effects of human activities giving rise to modern landscapes. Mainly the agricultural (cultural) landscapes showed (and are probably going to show in the future) the far reaching changes which occurred as a result of technological, socio-economic and political developments as well as global environmental change. The intensification of agricultural production, the retreat of agriculture from unfavourable sites, the processes of urbanization but also afforestation and the natural processes of secondary succession of fallow fields, have produced deeply different modern landscapes in terms of structure, functions and patterns from those pre-existing in many areas of our country and in many other European areas (Bender, 2005; Bouma, 1998, Calvo-Iglesias, 2009, Antrop, 2004; Van Eetvelde, 2004). Under these pushes, in many cases, changes occurred very quickly, particularly during the 20th century, often with no connection with past landscapes, but as a result of consecutive land reorganization in order to better adapt its use and spatial structure to the changing societal demands.

If landscapes changes are the natural expression of the interaction between natural and cultural forces, nevertheless changes today are often seen as a threaten for landscape integrity and for the cultural identity of population.

These concerns are expressed in the European Landscape Convention (ELC) which highlights two fundamental issues, among the others: i) the importance of landscape as an expression of cultural and natural heritage of a population ("… recognize landscapes in law as an essential component of people's surroundings, an expression of the diversity of their shared cultural and natural heritage, and a foundation of their identity" Art. 5, a), and ii) the need of implementing landscape policies "…aimed at protection, management and planning through the adoption of specific measures"(Art 5, b).

A historical perspective is desirable for the comprehension of landscape origin and transformation and for the identification of traditional landscapes. Some authors define traditional landscapes as those one which evolved during centuries (Antrop, 1997), but, according to the ELC, the cultural significance of some landscapes and the link with population must be considered too. Some landscapes can have a recent origin but they can represent the history of a population. It is also desirable to identify and implement those landscape policies invoked by ELC for landscape protection in a perspective of sustainability, but tradition and sustainability (considering its comprehensive meaning), not always overlap (Bouma, 1998; Carmona, 2010; Antrop, 2005; Angelstam, 2013, Puddu et al, 2009; Vos, 1999; Recanatesi, 2010; Antrop, 2006).

Actually the ELC is aimed "… to promote landscape protection, management and planning, and to organize European co-operation on landscape issues", but does not suggest methods or criteria to be adopted.

The detection of land use/land cover change and the consequent analysis of landscape dynamics has become more and more important and it is fundamental to comprehend the genesis of nowadays landscapes.

The production of thematic maps, representing both actual and past conditions, is a main issue in understanding landscape dynamics as well as natural and anthropogenic processes (Pelorosso, 2009).

Aerial photographs represent an important source of information about landscapes of the past, being the main existent database providing high detailed evidence of landscape changes .. In 1935, the Italian Land Register Department commissioned the survey of the whole Viterbo province (352,000 hectares) through aerial photographs. This material, forgotten for a long period, was recently re-discovered and moved to the Viterbo State Archive.

This is by far the oldest Italian example (and one of the oldest in the world) of a large aerial-photograph survey systematically covering a wide, continuous region. Furthermore, the photos were taken at a very low altitude, thus featuring a very high resolution. Thus, they are an invaluable resource to study the historical development of cultural and natural landscapes in C-Italy. A project aiming at digitalizing, orthorectifying and geo-referencing this huge set of historical photos has recently started, in order to quantitatively and qualitatively analyse the landscape patterns of 1935-1938 and their role in the development of present-day landscapes.

This paper presents a still in progress work, whose purpose is the establishment of a province scale diachronic information system focused on the landscape dynamic and evolution allowing cultural and environmental evaluation. It will collect information on the territory coming from aerial photographs, historical maps (Catasto Gregoriano) and archive documents related to the Riforma Fondiaria of 1951. A Web-Catalogue of one century of landscape evolution in the Province of Viterbo is going to be implemented. It can represent an important source of memory for scientists, land planners, and local administrations.

This web catalogue will allow to analyse landscape in terms of biodiversity variation through the last century, or in terms of effectiveness of agricultural policies on agricultural development, or in terms of effectiveness of land planning on nowadays landscape.

Material and methods

In the period between 1935 and 1938, on behalf of the Ministry of Finance (Direzione generale del Catasto e dei Servizi Tecnici), S.A.R.A. (Società per Azioni Rilevamenti Aerofotogrammetrici), established in 1921 by Umberto and Amedeo Nistri, started an aerial survey aimed to produce new cadastral maps with the photogrammetric method that could update the Pontifical cadaster still in use after the unification of Italy 1860 (Figure 1). (Scardozzi).

For this purpose Airplanes of the "Ala Littoria S.A.", established by the fascist regime annexing in 1934 several private company, were used. The aircrafts were equipped with a machine Nistri AFL7 (AFL92) with a Goerz-Geodar F/7.7 lens having a 199, 8 mm focal length. Stereoscopic sequences (consisting in pairs of images of the same area taken from different angles), taken with an angle of 6 degrees have been realized.

In order to obtain final maps at a scale 1:2000, the flight altitude was fixed at 1600-1800 m for images taken on rural areas, and 800-1000 m for urban areas.

8 seconds and 4 seconds were the shooting intervals for rural and urban areas, with a flight speed of 150 Km/h.

The so-called "Fondo Nistri" is constituted by approximately 7.000 aerial photographs on glass plate 13 x 18 cm at a scale of about 1:10.000/1:11.000 (Figure 2). No date is reported on the plate, but, from the examined documents, it emerges that the survey started in the southern part of the province of Viterbo in May 1935 and ended in 1938. Most of the photos were taken in winter because the absence of foliage made it easier the identification of boundaries between the fields. Photograms in the same stripe present an overlay rate ranging from 25 to 45%, parallel adjacent stripes shows an overlay of about 55-70% often resulting redundant (Figure 3). This great quantity of images has been very profitable in the phase of image processing, since during the time, some photographic plates have been damaged or corrupted and the presence of different shooting of the same area anyway allowed, in most cases, a complete reconstruction of land cover.

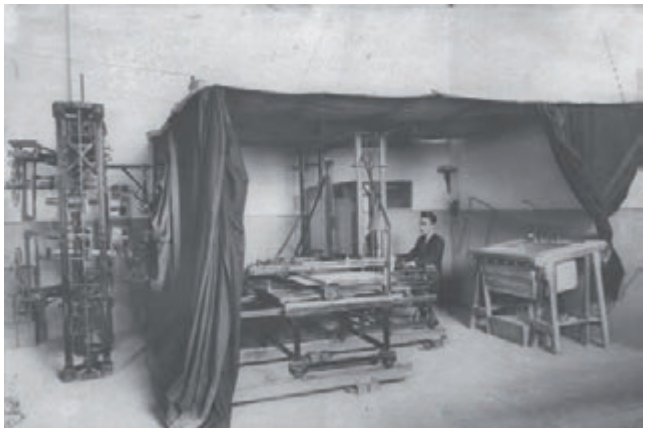

Figure 1. Laboratory of SARA Nistri.

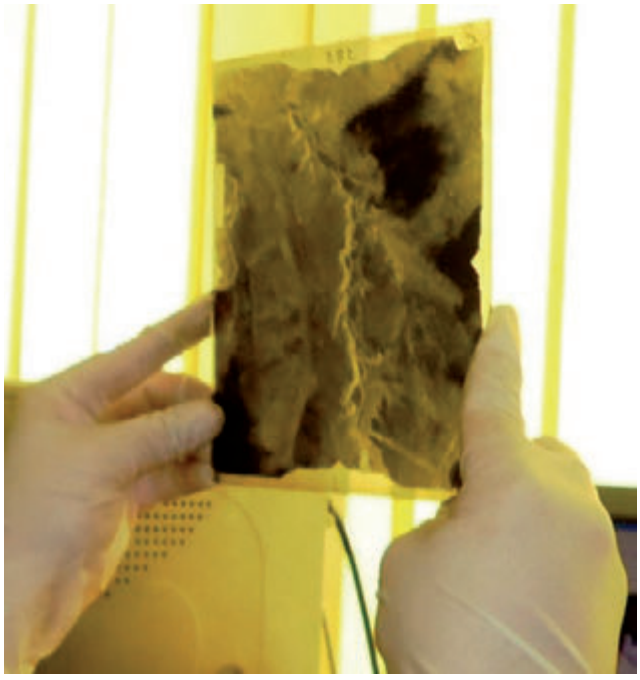

Figure 2. A glass plate of "Fondo Nistri".

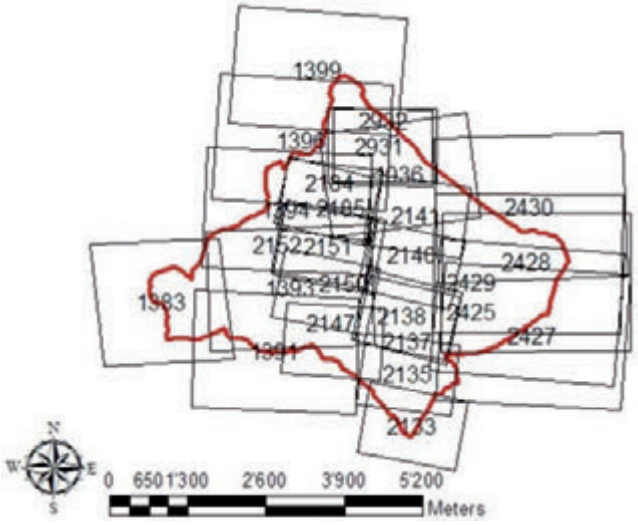

Figure 3. An example of the scheme of photographic shooting.

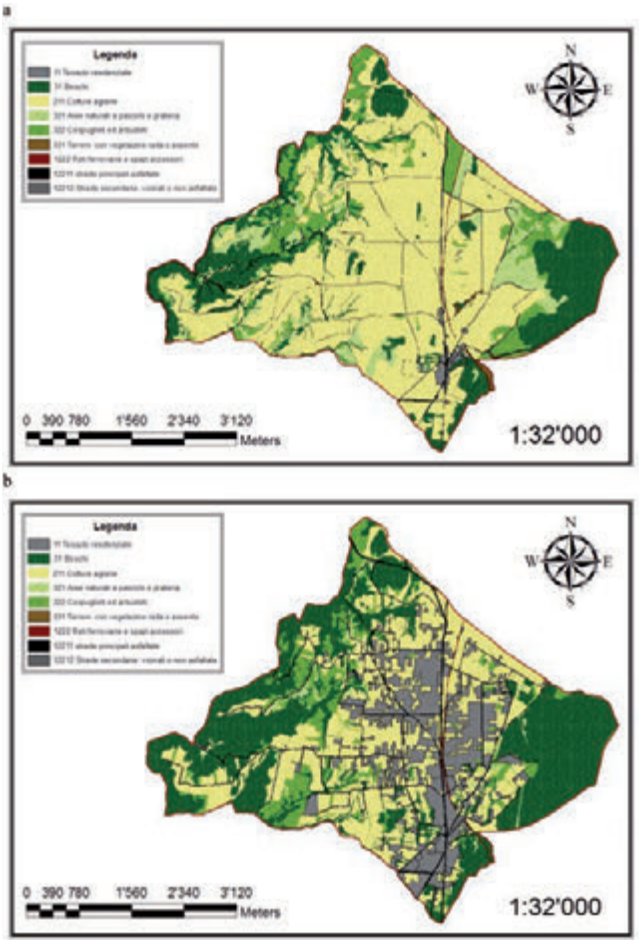

Figure 4. Land use in the municipality of Oriolo Romano a) 1936, b) 2010.

The experimental survey covered the whole territory of the province of Viterbo and it represents a unique document. It allows the reconstruction of land use/land cover in 1935-40 capturing an image of our country preceding the deep important changes occurred during the twentieth century. This huge material has never been inventoried, probably for the outbreak of the Second World War, and its inventory and cataloguing represents one of the goals of the project.

Each glass plate needs to be scanned with an appropriate scanner for transparent glass with low positional error adopting a resolution of 1600 dpi which preserves the resolution of the photos. Great care must be put in handling the glass plate to protect the emulsion covering the impressed side of the glass plate. The scanned images are processed and orthorectified in order to correct the deformations due to the characteristics of the camera and to the relief. The procedure proposed for the landscape dynamics analysis consists of six sequential steps: (1) Aerial photos orthorectification; (2) Orthophotosradiometric correction; (3) Orthophotos mosaicking,; (4) Photo interpretation and land cover map building, and (5) land cover change analysis (Gennaretti *et al.*, 2011).

The accuracy of the orthorectification process has been verified by the RMSE (Root Mean Square Error) index applied on the GCP position.

In most cases, while all land cover classes were easier to distinguish in the 2010 ortho-photos, in the historical ones some cover classes were hard to detect due to their monochrome greyscale, the winter shooting and the condition of the glass plate. Macro classes have been found out with a thematic resolution which, at this phase of the work, can change according to the characteristics of the different areas.

Photo interpretation has been firstly performed for the recent images (2010); subsequently, this base layer has been updated with the photos taken in 2010 and in 1935. This procedure allows to minimize the errors of change detection (sliver polygons and spurious changes, Genaretti *et al.*, 2011). The obtained land use maps have been compared with present land use to point out the landscape dynamics, which can be the starting point for further analysis and considerations.

Image processing and analysis have been performed using the software ArcGis (ESRI) and Orthoengine (PCI Geomatica).

Results and discussion

Although the work is going to be carried out on the whole territory of the province of Viterbo, in this paper preliminary results concerning some selected areas are presented.

The selected areas are Oriolo Romano, Vitorchiano, Canino and Barbarano Romano. Ortho-rectification accuracy gave satisfactory results in all the processed images; in most cases the ground X and Y RMSE were found to be lower than 3 m.

Oriolo Romano

In this area the aerial photos were taken during the winter of 1936; the photo interpretation allowed the identification of 9 types of land use that have been used also for the map of 2010 (Figure 4; Table 1). The comparison between the land use maps of 1938 and 2010 shows: a loss of agricultural areas that evolve either into shrublands due to abandonment, or into urban areas. The relevant growth of urban areas occurred mainly with detriment of agricultural areas and, to a very lesser extent, of natural and semi-natural areas; the expansion of the town follows the path of the main road network (Table 2; Figure 5).

Table 1. Oriolo Romano - Land use in 1936 and 2010.

Land use	1936 (Ha)	2010 (Ha)	Change (Ha)	Change (%)
Agricultural	1065,84	656,93	-408,90	-38,36
Wood	422,40	695,96	273,57	64,76
Urban areas	14,60	306,82	292,23	2002,22
Natural grassland	164,12	33,47	-130,65	-79,61
Bushes and shrubs	190,04	178,39	-11,65	-6,13
Areas with rare vegetation cover	8,02	0,00	-8,02	-100,00
Main roads	13,43	16,69	3,26	24,25
Secondary roads	36,85	26,86	-9,99	-27,11
Railway networks and ancillary areas	5,01	5,16	0,15	2,95

Table 2. Oriolo Romano - Transition matrix 1936 - 2010.

1936	Areas with rare vegetation over	Railway networks	Main roads	Secondary roads	Natural grassland	Bushes and shrubs	Urban areas	Agricultural	Wood	2010
Areas with rare vegetation cover	0	161	0	0	190	4.847	12.730	26.126	36.117	80.171
Railway networks	0	50.137	0	0	0	0	0	0	0	50.137
Main roads	0	0	131.076	100	0	0	3.137	0	0	134.313
Secondary roads	0	176	7.663	214.323	4.730	11.331	6.020	22.530	101.746	368.519
Natural grassland	0	0	135	5.572	36.226	219.413	39.815	471.956	868.097	1.641.215
Bushes and shrubs	0	0	5.221	6.411	94.575	374.159	66.532	306.127	1.047.342	1.900.366
Urban areas	0	0	250	3	0	422	133.391	10.138	1.748	145.952
Agricultural	0	1.143	17.461	34.977	182.015	1.043.325	2.738.931	5.527.536	1.093.509	10.638.897
Wood	0	0	5.072	7.233	16.986	128.937	67.664	186.895	3.811.203	4.223.990
Tot. 2010	0	51.617	166.879	268.618	334.721	1.782.433	3.068.221	6.551.309	6.959.762	Tot. 1936

Vitorchiano

In this area the aerial photos were taken probably during the winter of 1938; the photo interpretation allowed the identification of 3 macro-classes of land use that have been used also for the map of 2010 (Figure 6; Table 1 e 2). The comparison between the land use maps of 1938 and 2010 shows, also for this municipality, a relevant growth of urban areas and a reduction of agricultural areas while natural areas are substantially unchanged (Table 3; Figure 6).

Although in both cases a quite usual and widespread phenomenon can be observed, the spatial pattern of the growth of urban areas in these territories is quite different. In the territory of Vitorchiano the sprawl urbanization predominates over a compact growth of the town; this behaviour can be ascribed to the building of an important highway which crosses the territory of Vitorchiano and connects the city of Viterbo with an important railway and highway junction. Nearby the highway, the development of some residential areas quickly approachable from the town has been promoted. Nevertheless it must be noticed a spread presence of buildings also in the photos of 1938 suggesting a different settlement pattern whose origin could be sought in the history of the territory.

Although the analysis regarding the areas of Canino and Barbarano Romano are still in progress, the results coming out are very interesting. From a preliminary evaluation a trend of landscape transformation similar to the previous described and quite common in many areas of our country, can be observed. It can be summarized in an increase of urban areas, a slight increase of wood and natural areas with shrubs and bushes and a decrease of agricultural areas. Nevertheless a peculiar phenomenon emerges in both areas thanks to the information derived from the analysis of the aerial photos. In fact they provide an

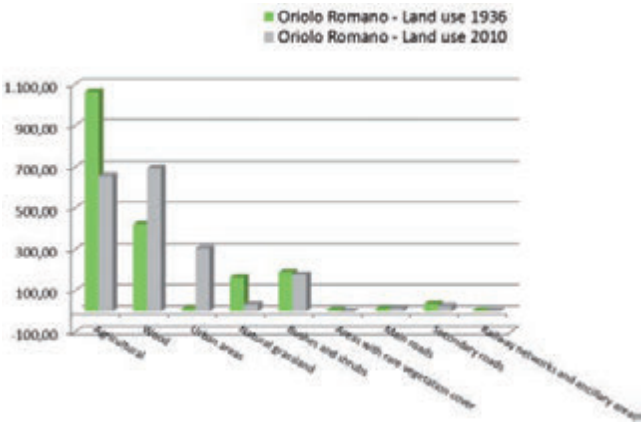

Figure 5. Oriolo Romano – comparison between land use in 1936 and 2010.

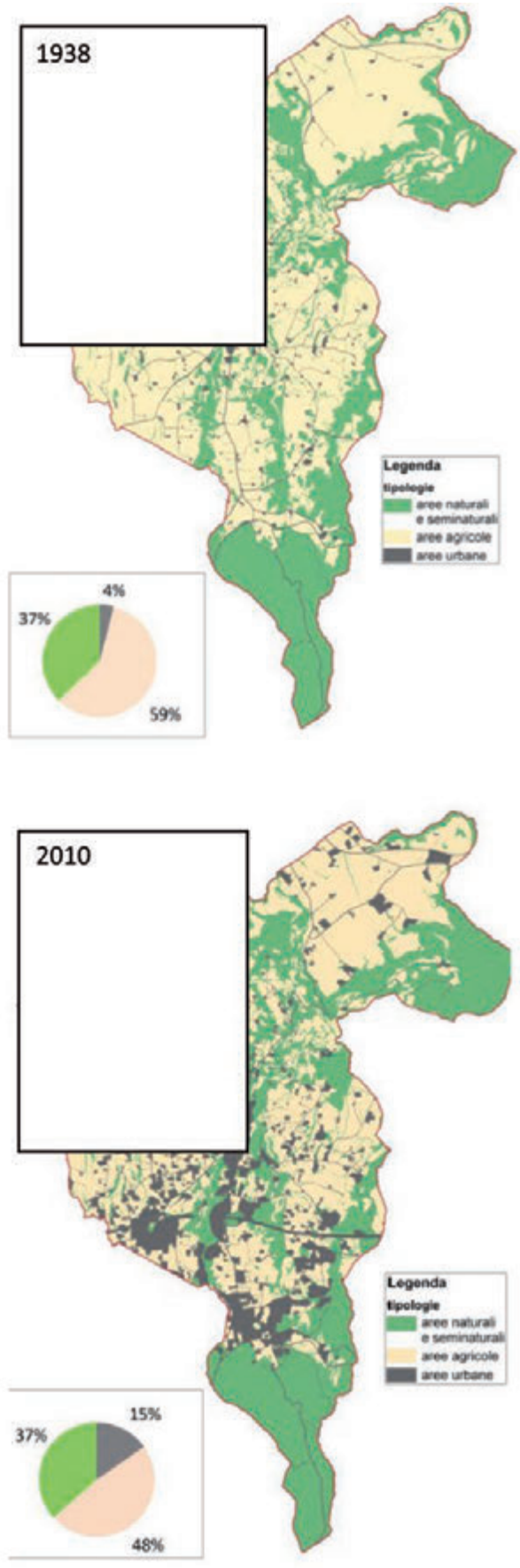

Figure 6. Land use in the municipality of Vitorchiano a) 1938, b) 2010.

imagine of the territory preceding many important events, primarily the socio-economic changes of the 1950's - incl. the "Riforma Fondiaria" (land reclamation), which started in 1951.

In the territory of Canino olive groves presently cover 2.400 Ha, producing a good quality and typical oil. Olive groves landscape as well is considered as typical and traditional, dating back to Etruscan age. Archival sources (*e.g.* "Inchiesta Jacini", 1883) easily show that a hundred years ago Canino had only 300 ha of olive groves. The 1936 aerial photographs show a presence of olive groves only in the area adjacent the town and a landscape dominated by herbaceous crops and grazing land. During the 1951-1954, following the "Riforma Fondiaria" of 1950, the "Ente Maremma" planted 350.000 olive trees in the Viterbo and Grosseto provinces shaping a landscape which, from then on, would be considered "traditional" for that territory. (*"...è, infatti, intendimento dell'Ente dare grande diffusione all'olivo; colline spoglie di ogni vegetazione verranno rivestite di olivi (...). Si è dovuto far ricorso in alcuni casi, oltre che alla potente attrezzatura meccanica dell'Ente, anche all'uso di esplosivi. Su terreni ove vegetava stentatamente il cespugliato, ad una anno appena di distanza dall'esproprio sono stati impiantati gli oliveti" (*Ente Maremma, 1953).

For the territory of Barbarano, comparing the land cover obtained by the aerial photographs of 1936 with the present one, it can be noticed

Table 3. Vitorchiano - Land use in 1938 and 2010.

Land use	1938 (Ha)	2010 (Ha)	Change (Ha)	Change (%)
Agricultural	1755,35	1465,37	-289,98	-16,52
Urban areas	117,89	454,91	337,02	285,88
Natural	1112,06	1065,02	-47,04	-4,23

Table 4. Vitorchiano - Transition matrix 1938 - 201

2010 1938	Agricultural	Urban areas	Natural	Total 1938
Agricultural	1356,61	283,81	114,93	1755,35
Urban areas	4,91	110,63	2,35	117,89
Natural	103,85	60,47	947,74	1112,06
Total 2010	1465,37	454,91	1065,02	

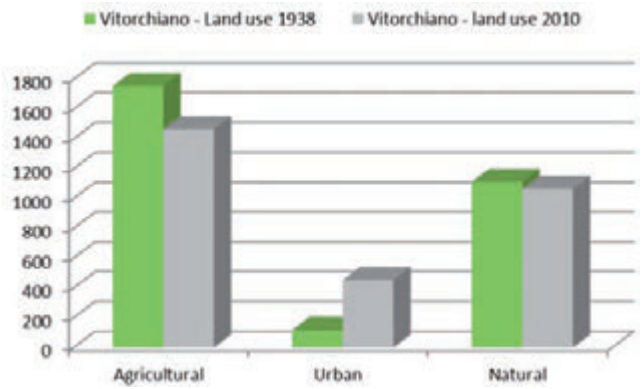

Figure 7. Vitorchiano – comparison between land use in 1938 and 2010.

an expansion of natural areas represented by shrubland and grasslands mainly in the neighboring of Tolfa Mountain with detriment of arable land. This kind of landscape is today perceived as "typical" (and actually has a very high diversity of flora and fauna showing a strong ecological significance); but it is derived from the abandonment of "Quarteria" (four-year rotation of arable and pasture).

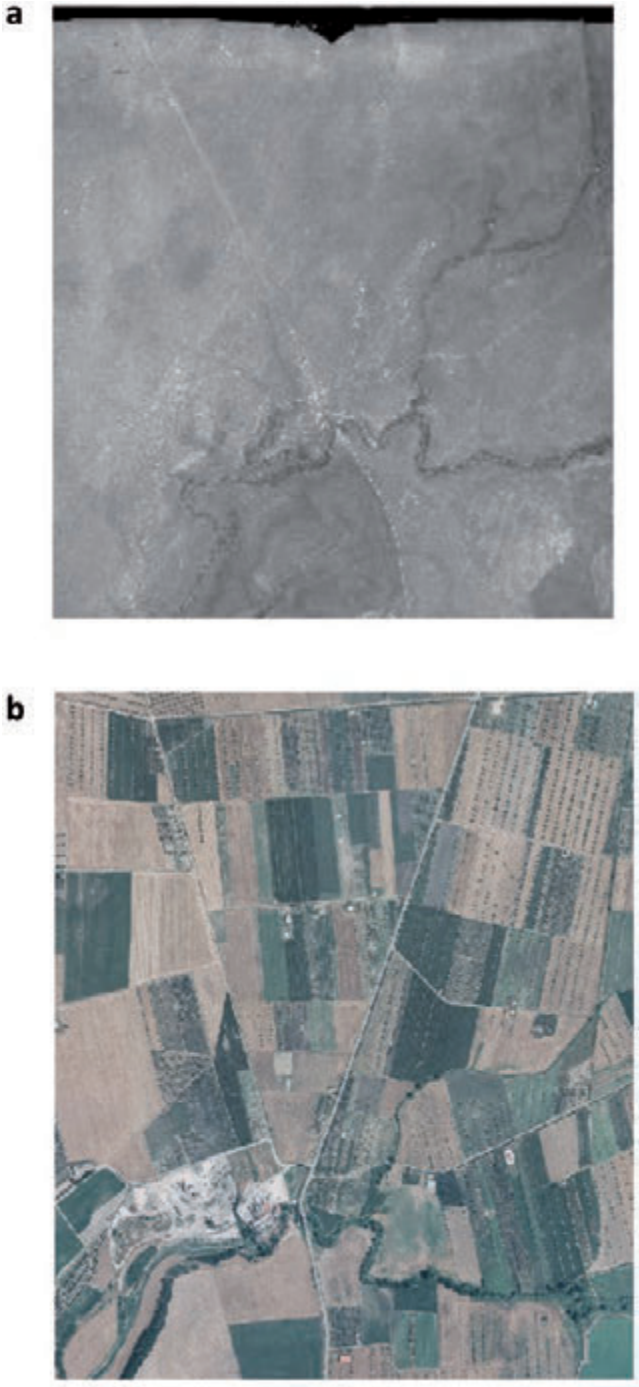

Figure 8. Aerial Photos of the municipality of Canino a) 1938, b) 2010.

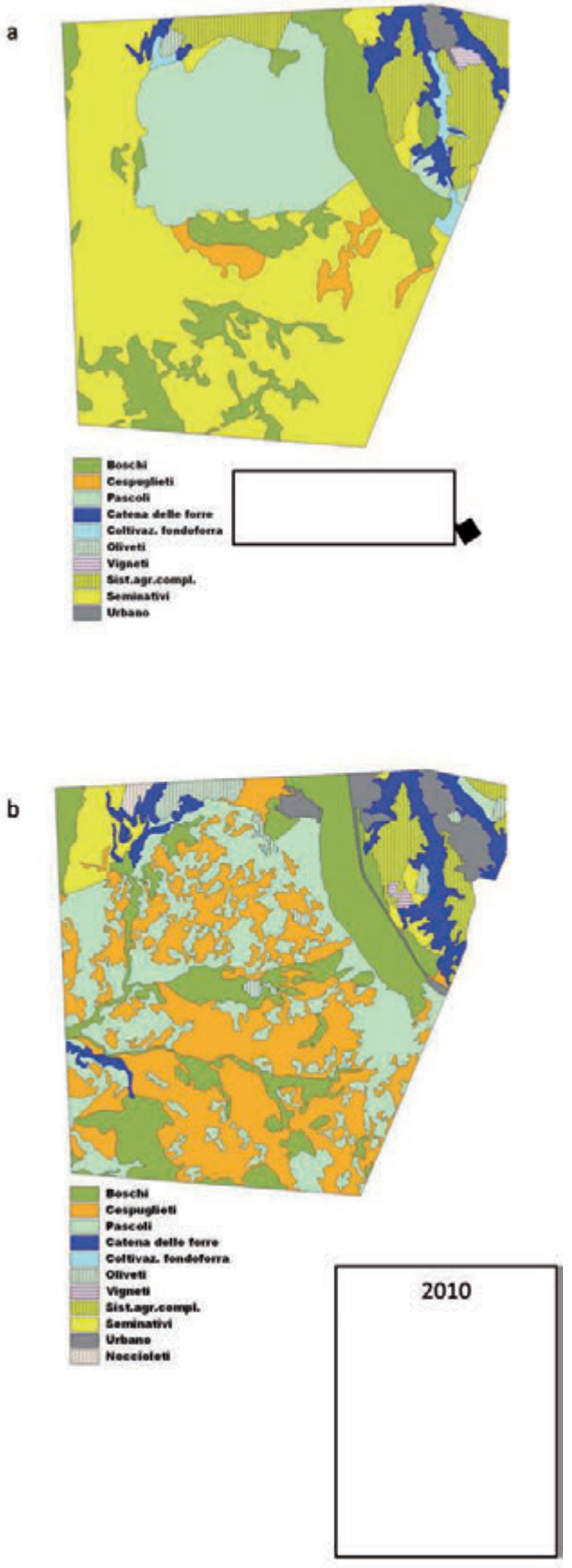

Figure 9. Land use in the municipality of Barbarano Romano a) 1936, b) 2010.

Conclusions

The first goal of setting up a methodology for processing and analysing these old aerial photographs has been very satisfactorily achieved. It represents a first step towards the implementation of the Web Landscape Catalogue for the territory of the Viterbo Province. The preliminary results reported in the present paper, underline how the research applications of such an old (and at the same time high-resolution) collection of digitalized aerial photographs are endless. If compared with the 1954 "Volo GAI", they have a much higher resolution and quality, and they were taken before the socio-economic changes of the 1950's - incl. the "Riforma Fondiaria" (land reclamation), which started in 1951 so that they can provide a snapshot of the whole territory before many changes in agricultural pattern and management occurred.

Compared with the 1943-44 RAF photos, they have a better resolution and a complete coverage of a broader region. The only disadvantage of the Fondo Nistri is represented by the fact that pictures were taken during the winter, making the photo interpretation and the singling out of many types of land use/land cover difficult. The adopted method (proposed in Gennaretti et al, 2011) allows to overcome this inconvenience.

Important information can be derived from these images for land planners and managers regarding the purposes of landscape management and planning. In many cases the restoration of traditional landscape is invoked considering "traditional" equal to natural. The preliminary results obtained for the territory of Canino and Barbarano provide and tickle insights concerning the origin and development of some types of landscapes that are commonly viewed as "traditional" – although historical and archival sources suggest they had a recent origin.

References

Angelstam P., Andersson K., Isacson M., Gavrilov D.V., Axelsson R., Bäckström M., Degerman E., Elbakidze M., Kazakova-Apkarimova E., Sartz L., Sädbom S., Törnblom J., (2013), Learning About the History of Landscape Use for the Future: Consequences for Ecological and Social Systems in Swedish Bergslagen, Ambio, 146-159.

Antrop M., (1997), The concept of traditional landscapes as a base for landscape evaluation and planning. The example of Flanders Region, Landscape and Urban Planning 38: 105-117

Antrop M., (2004), Landscape change and the urbanization process in Europe, Landscape and Urban Planning 67: 9-26

Antrop M., (2005), Why landscape of the past are importante for the future, Landscape and Urban Planning 70: 21-34

Antrop M., (2006), Sustainable landscapes: contradiction, fiction or utopia?, Landscape and Urban Planning 75: 187-197

Baudry J., Burel F., Thenail C., Le Coeur D., (2000), A holistic landscape ecological study of the interactions between farming activities and ecological patterns in Brittany, France, Landscape and Urban Planning 50: 119-128

Bouma J., Varallyay G., Batjes N.H., (1998), Principal land use changes anticipated in Europe, Agriculture, Ecosystems and Environment 67: 103-119

Bender O., Boehmer H.J., Jens D., Schumacher K.P. (2005), Using GIS to analyse long-term cultural landscape change in Southern Germany, Landscape and Urban Planning 70: 111-125

Calvo-Iglesias M.S., Fra-Paleo U., Diaz-Varela R.A., (2009), Changes in farming system and population as drivers of land cover and landscape dynamics: The case of enclosed and semi-openfield systems in Northern Galicia (Spain), Landscape and Urban Planning 90: 168-177

Carmona A., Nahuelhuala L., Echeverríab C., Báezc A., (2010), Linking farming systems to landscape change: An empirical and spatially explicit study in southern Chile, Agriculture, Ecosystems and Environment 139: 40-50

Cassinis G.- Aerofotogrammetria e Catasto - Comunicazione presentata al 2° Congresso Nazionale degli Ingegneri Italiani- Roma, 1931.

Gennaretti F., Ripa M. N., Gobattoni F., Boccia L., Pelorosso R. (2011). A methodology proposal for land cover change analysis using historical aerial photos. Journal of Geography and Regional Planning, 4(9): 542-556

Pelorosso R, Leone A, Boccia L (2009). Land cover and land use change in the Italian central Apennines: A comparison of assessment methods. Appl. Geogr., 29: 35-48.

Puddu G., Pelorosso R., Gobattoni F., Ripa M.N. (2010). Landscape transformations seen through the historical cartography: Sardinia as case study. Proceedings of "Forest Landscapes and Global Change-New Frontiers in Management, Conservation and Restoration" IUFRO Landscape Ecology Working Group International Conference, September 21-27, 2010, Bragança, Portugal. J.C. Azevedo, M. Feliciano, J. Castro & M.A. Pinto (Eds.) Instituto Politécnico de Bragança, Bragança, Portugal.

Recanatesi F., M.N. Ripa, A. Leone (2011), Landscape Change (1930-2010) in a Mediterranean Natural Reserve, Journal of Geography and Regional Planning, Vol. 4(5): 261-272, ISSN 2070-1845.

Scardozzi G. - Studi di Aerotopografia Archeologica, Archeologia Aerea 3'8

Van Eetvelde V., Antrop M., (2004), Analyzing structural and functional changes of traditional landscapes—two examples from Southern France, Landscape and Urban Planning 67: 79-95

Vos W., Meekes H., (1999), Trends in European cultural landscape development: perspectives for a sustainable future, Landscape and Urban Planning 46: 3-14

Esperimenti di fotogrammetria aerea per la formazione delle mappe del catasto italiano- Comunicazione presentata dalla direzione generale del catasto e dei servizi tecnici alla I Riunione dell'Associazione Ottica Italiana. Firenze, 21-24 maggio 1934-XII.

Geomatica Orthoengine, User guide (2003).

PCI- Use'r Guide, Version 8.2 (2001).

Identification of rural landscape classes through a GIS clustering method

Irene Diti, Daniele Torreggiani, Patrizia Tassinari

University of Bologna, Department of Agricultural Sciences, Bologna, Italy

Abstract

The paper presents a methodology aimed at supporting the rural planning process. The analysis of the state of the art of local and regional policies focused on rural and suburban areas, and the study of the scientific literature in the field of spatial analysis methodologies, have allowed the definition of the basic concept of the research. The proposed method, developed in a GIS, is based on spatial metrics selected and defined to cover various agricultural, environmental, and socio-economic components. The specific goal of the proposed methodology is to identify homogeneous extra-urban areas through their objective characterization at different scales. Once areas with intermediate urban-rural characters have been identified, the analysis is then focused on the more detailed definition of periurban agricultural areas. The synthesis of the results of the analysis of the various landscape components is achieved through an original interpretative key which aims to quantify the potential impacts of rural areas on the urban system. This paper presents the general framework of the methodology and some of the main results of its first implementation through an Italian case study.

Introduction and aims

The actual configuration of the territorial and landscape mosaic is characterized from mixed urban and rural macro-systems that create hybrid spaces with intermediate characteristic. This calls for new methods suitable for classifying rural areas based on their vocations, critical issues and potentials, in order to define consistent evolution scenarios. The relationships between natural and manmade landscape components are widely described in the scientific literature through the *urban footprint* (Socco *et al.*, 2004) and *ecological footprint* (Rees and Wackernagel, 1996). Comprehensive evaluation of the characteristics of rural areas and agricultural activities can lend useful support to urban and landscape planning and rural development policies. Therefore, the goal of the research is to develop an innovative quantitative and multicriteria method aimed at classifying rural areas based on their agricultural, environmental, socioeconomic and landscape profile, referring to an original *"Agri-Environmental Footprint"* (AEF) postulate. In particular, this research focuses on a methodology for the geographical definition of periurban contexts aimed to support the calibration of policies for the preservation of the agricultural characters of these areas. This is fundamental in order to safeguard the countryside (Tassinari *et al.*, 2007a), as underlined by the European Landscape Convention.

Correspondence: Irene Diti, Daniele Torreggiani, Patrizia Tassinari, University of Bologna, Department of Agricultural Sciences, Viale G. Fanin 48, 40127 Bologna, Italy.
E-mail: irene.diti@unibo.it, daniele.torreggiani@unibo.it, patrizia.tassinari@unibo.it

Key words: countryside classification, GIS model, periurban agricultural areas, rural planning.

Journal of Agricultural Engineering 2013; XLIV(s1):e97
doi:10.4081/jae.2013.(s1):e97

Materials and methods

The proposed methodology is currently being tested, in order to validate it, on the New District of Imola (Figure 1), a study-area in northern Italy, where several information were already available thanks to previous studies (Tassinari *et al.* 2007a, 2007b).

Data used in our study consisted in spatial information widely used in planning processes: land use maps, cadastral data, statistical georeferred information. Such databases have been elaborated through ArcMap GIS by ESRI. The indexes have been defined based on a critical analysis of the scientific and technical literature.

Results

Figure 2 shows the main result of our work, that is the architecture of the multilevel methodological approach for the classification of the countryside.

A first set of indicators is used in the first-level analysis (*Overall AEF land Classification*) to achieve a preliminary identification of homogeneous extra-urban areas based on the agro-environmental, socio-demographic and infrastructural land's profile. The resulting *Rural Land Classes (RLCs)* are described and grouped according to their specific characteristics. Intermediate urban-rural areas represent the spatial domain for the second-level analysis (*Periurban AEF Land Classification*), aimed to identify different typologies of *Periurban Land Classes (PLCs),* mainly based on their agricultural peculiarities and farm structure.

Some of the indices used in the first level of analysis derive from the fields of Landscape Ecology (as *Shannon Entropy Index*, *Fragmentation Index* or *Corrected Perimeter-Area Index*) and Agronomy (such the *Land Suitability*), while others were conceived for this methodology, in order to describe the recreational and ecological value of the analized countryside (as the *Ecological/Recreational Value* that describe the density of natural and protected areas in the case study area) or in

Figure.1. The study area (New District of Imola, Bologna, Italy).

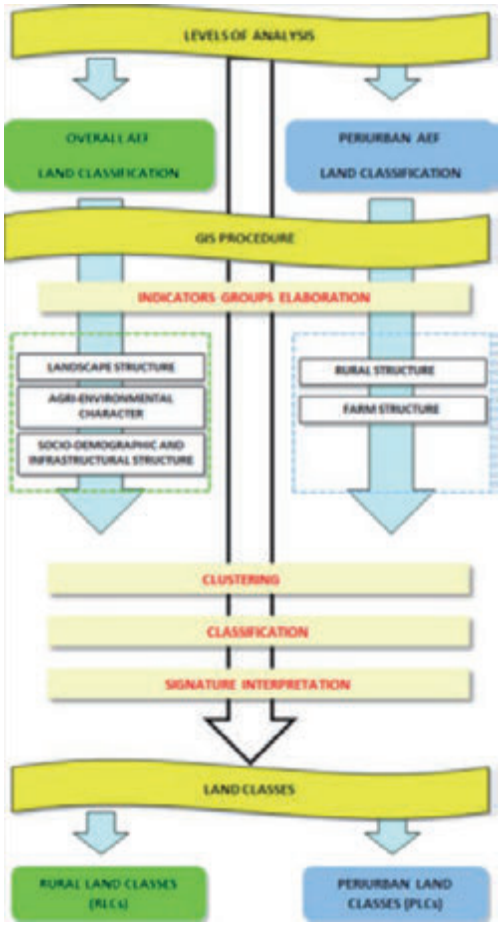

Figure 2. The structure of the model.

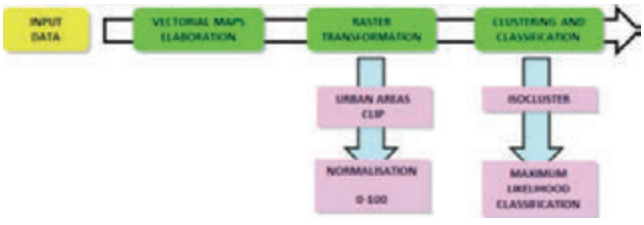

Figure 3. GIS analysis model.

order to quantify the presence/absence of agri-environmental CAP measures, or the impact of multifunctional agricultural activities such as holiday or educational farms. Some indexes were designed with the intent of describing the population characteristics (as the *Population Density* or the *Old-Age Index*) and the impact of the infrastructure on the open spaces outside the cities (*Road density*).

At each level of the analysis vector maps (made for each indicator analized) were converted to raster maps and elaborated to obtain multilevel raster maps that were analysed through suitable cluster analysis algorithms to identify the main landscape patterns (Figure 3).

This GIS procedure and interpretation of the signature of each cluster resulting from the analyses carried out on the study area allowed us to define three landscape classes:

High nature value areas with mainly extensive farming system

Areas with a significant agricultural matrix

Areas with a significant agricultural matrix and remarkable urban-rural interference

The last one represents the spatial domain for the second-level analysis (Periurban AEF Land Classification), allowing to identify "periurban agricultural areas" where agricultural characters and high farming potentiality prove more relevant.

Conclusions

The main strength of the proposed methodology is that of consisting in a systematic and objective procedure that allows to analyze intact multi-thematic data and to aggregate them without any a priori assumption or reclassification filter typical of overlay zoning procedures. This method can be implemented in the land analysis process to support local authorities in spatial planning decisions.

Furthermore, starting from the same general land classification of the first AEF level, the iterative analysis process at the second level of analysis can be used also to identify other specific homogeneous areas using different sets of variables.

Future in-depth studies and applications will mainly focus on the calibration and selection of most important and influential indicators through the comparison of the results obtained from the application of the methodology to different geographical contexts.

References

Rees, W., Wackernagel, M. 1996. Urban ecological footprints. Why cities cannot be sustainable and why they are a key to sustainability. Environment Impact Assess Rev, 16, 223-248.

Socco C. (ed.),2007. Il manuale urbanistico invisibile. La sintassi della città disgregata, Working Paper 06/07.

Tassinari, P., Torreggiani, D., Benni, S. 2007a. Agriculture and Development Processes: Critical Aspect, Potential and Multilevel Analysis of Periurban Landscapes. Part I, *E-Journal – CIGR*, 9,1-14.

Tassinari, P., Torreggiani, D., Benni, S. 2007b. Agriculture and Development Processes: Critical Aspect, Potential and Multilevel Analysis of Periurban Landscapes. Part II, *E-Journal – CIGR*, 9,1-21-

Application, validation and comparison in different geographical contexts of an integrated model for the design of ecological networks

C.R. Fichera,[1] R. Gianoglio,[2] L. Laudari,[1] G. Modica[1]

[1]Dipartimento di Agraria, Università degli studi Mediterranea di Reggio Calabria. Località Feo di Vito, Reggio Calabria, Italy; [2]Seacoop arl, Torino, Italy

Abstract

The issue of the fragmentation of natural habitats is increasingly at the core of the scientific debate, yet it is not taken into account in planning tools, with particular reference to the dynamism and complexity of landscapes. As it has been recognised at a European level, in order to enable different species to remain in good functional status, a network of green infrastructures is required. The concept of "ecological island" is no longer sufficient to adequately protect the fauna and the ecosystem it lives in. As a consequence, ecological islands must turn into ecological networks. The Ecological connectivity refers to the way habitats are physically connected to each other and how easy it is for species to move in. Good ecological connectivity is fundamental to the effective conservation of biodiversity considering that most species and ecological functions provided by ecosystems (ecosystem services) require a much wider space than that available within the boundaries of a single protected area. The main objective of this paper is to critically compare the application of a model for the design of ecological networks to two very different environmental contexts. This model was first tested in a Mediterranean area (the Province of Reggio Calabria) in 2008; the goal was to integrate the traditional (physiographic and functional) approaches into the design of ecological networks by taking into account biological and orographic elements as well as the anthropic structure of the territory. In 2011, within the ECONNECT European project, the model was applied to the pilot region of South-Western Alps (including the French region of Provence-Alpes - Côte d'Azur and the Italian regions Piedmont and Liguria), which is one of the richest transnational districts in Europe in terms of biodiversity. In such a region, the issue of multidisciplinary ecological connectivity was tackled in order to provide a series of proposals aiming at the development of the ecological potential of the area. The two applications allowed to further investigate the strengths and weaknesses of the implemented model by integrating its validation with information on faunal presence, which obviated one of the major limitations occurred in the first application.

Correspondence: Luigi Laudari, Dipartimento di Agraria, Università degli studi Mediterranea di Reggio Calabria, Località Feo di Vito, 89122 Reggio Calabria, Italy.
E-mail: luigi.audari@unirc.it

Key words: ecological networks design, ecological connectivity, geographical information systems, sustainable planning.

Journal of Agricultural Engineering 2013; XLIV(s1):e98
doi:10.4081/jae.2013.(s1):e98

Introduction

Over the last decade, the concept of ecological network has increasingly established itself in the European technical and scientific scenario (Rientjes & Roumelioti, 2003). Nevertheless, the term "ecological network" is not defined univocally and it is subject to different interpretations (Boitani, Falcucci, Maiorano, & Rondinini, 2007).

A first widely recognised approach is the *structural* (physiographic) one, which is based on the patch-matrix-corridor paradigm (Godron & Forman, 1983) where an ecological network is simplified in landscape morphological elements, such as core areas, corridors and buffer zones (R. Jongman & Pungetti, 2004). This interpretation derives from the assumption that the ecological management of the environmental mosaic should be investigated in an integrated manner and considering various space and time scales. Later on, this led to the concept of Multiple-Use Modules (MUM) (Noss & Harris, 1986) and to the use of the structural approach to define networks of habitats (Hobbs, 2002) (*e.g.* the Natura 2000 network, the centerpiece of EU nature and biodiversity policy).

A second widespread approach is the *functional* one, where the elements of the ecological network are interpreted as a whole of ecosystems (core areas) connected through channels of functional relationships between the organisms of the ecosystem (Opdam, Steingröver, & Rooij, 2006). These differences in interpretations are one of the major problems concerning the technical and operational proposals aimed at the definition of ecological networks (Rientjes & Roumelioti, 2003). Actually, this was the theoretical and operational starting point of this research work, which aims at identifying a method that may integrate the above-mentioned approaches obviating the need of detailed spatialized bio-ecological observations that are not often available or based on reliable time and space data. Yet, at the same time, such a method should not lead to the mere identification of physical constituent elements but to a procedure with clear impacts on sustainable spatial planning at a medium and small scale.

In particular, a model for the definition of an ecological network as a guideline in the planning process (Fichera, Laudari, & Modica, 2009a, 2009b) was implemented within a wider research activity carried out by the authors to define models of sustainable landscape planning which take into account ecological connectivity (Fichera, Laudari, & Modica, 2007). From a methodological point of view, the developed model is composed of a system of algorithms operating on a specially structured and implemented geodatabase in a dedicated GIS that, through repeated processing of habitat quality and definitions of core areas, is able to determine the organization of the ecology connectivity

matrix. The model combines the two classical approaches for the definition of ecological networks and sets out an integrated ecological network that corresponds to the real territorial structure and actual ecological needs. The model was applied to the territory of the province of Reggio Calabria (Italy) emphasizing its potentials and limitations as a guiding tool for a sustainable land-use planning (Fichera, Laudari, & Modica, 2010).

The resulting network design allows obtaining spatial continuity functional to faunal dispersion without any excessive impact on the study area. Data inputs were implemented on a *FunConn* (*Functional Connectivity*) model (Theobald, Norman, & Sherburne, 2006). Such a model, which provides graph-theory based analysis methods for landscape connectivity, was modified and adapted for its application to the specific areas.

Materials and methods

Study area

Within the "Alpine Space Programme" (ETC - European Territorial Cooperation, 2007), the European Union has launched the project ECONNECT with the purpose of implementing an ecological continuum across the alpine region over the three years 2008/2011. The main goal of the project is to increase the ecological connectivity of the Alps through a holistic and multidisciplinary approach based on a model that is centred on the qualitative and quantitative selection of the areas of significant ecological value and on the analysis of their levels of interconnection.

In order to achieve that goal, the workgroup, which was entrusted with the implementation of the project in the Alps South-West pilot region (one of the seven ECONNECT regions which are evenly distributed throughout the Alps), adopted the model for the design of ecological networks that (Fichera, Laudari, & Modica, 2009c) had elaborated by adapting and modifying the FunConn model.

This opportunity allowed comparing the design of two ecological networks obtained with the same model applied to territorial contexts (Figure 1) that are deeply different from the administrative, bioecological and geographical point of view:

- The Province of Reggio Calabria, which belongs to the Mediterranean biogeographical region;
- The side of the Maritime Alps that is part of the Province of Cuneo and belongs to the alpine biogeographical region.

Comparison of the model in the two different geographical contexts

The research work was organized in distinct and consequential steps that were carried out at the same time in the two study areas:

Definition of the integrated ecological networks on the two areas;
Selection of common indicators for the context analysis;
Comparison of the two ecological networks.

Ecological networks were elaborated in the two following steps (Figure 2):

- In the first step, a specific ecological network was elaborated for each focal species found in the study areas (Battisti & Luiselli, 2011; Boitani, 2000; Watts *et al.*, 2010). This allowed identifying specific core areas and their related corridors (Bennet & Wit, 2001; Bennett & Mulongoy, 2006).
- In the second step, after identifying the portions of core areas of greatest ecological importance through overlay mapping, the specific ecological networks were aggregated to the "institutional" core areas found in the study areas (Kunzl *et al.*, 2011). The resulting configuration corresponded to the main design of the core areas of the integrated ecological network. Starting from such core areas, the model was used again to calculate the corridors, which, in this network, are plurispecific transit areas.

In this first phase, a difference in the application of the model to the two study areas should be highlighted. In fact, while the identification of the core areas in the Province of Reggio Calabria took into account Park's Integral Reserves, SCIs (92/43/CEE) and SPAs (79/409/CEE) of

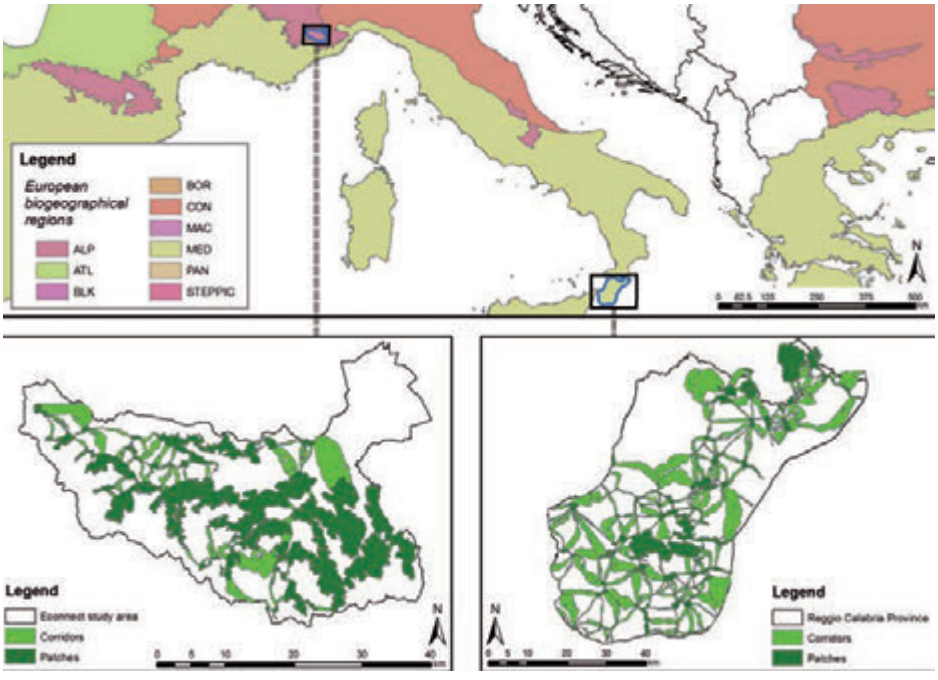

Figure 1. Location of the study areas in their European Biogeographical Regions and organization of the two ecological networks.

the Natura 2000 network (Boitani *et al.*, 2007), in the case of the Maritime Alps, Integral Natural Reserves and Special Natural Reserves (areas of great natural value defined by the Regione Piemonte) were considered. However, this choice was suggested by objective reflections: actually, in the Piedmontese study area, the Natura 2000 system is particularly extended and not completely differentiated according to specific ecological needs. Therefore, it appears as a continuum of protected areas which would make any resulting ecological network, made up of short corridors, completely useless.

The indicators for the network analysis were selected by referring to four indexes which had already been adopted in previous studies (Fichera *et al.*, 2009b) to validate the networks obtained through various methodological approaches (Bennett & Mulongoy, 2006; Boitani *et al.*, 2007; Franco, 2003; R. H. G. Jongman, 1995; Mortelliti, Amori, & Boitani, 2010):

- Biopermeability: the ease with which an animal organism can cross a territory with certain environmental characteristics (APAT, 2003; Fiduccia, 1998; Romano, 2000).
- Anthropic disturbance: the impact generated by population density and vehicular load per road class section (Forman 2000).
- Landscape Fragmentation: level of territorial destructuring caused by the interference of anthropic activity (Jaeger, 2000; Romano, 2003, 2005).
- Environmental sustainability Index (ESI): an indicator of ecological stability determined by the balance of pressure effects and by the regeneration potential typical of each territorial typological unit (Magoni, M. Steiner, 2001).

The values of the indicators were grouped into classes according to their similar impact and the results obtained were shown separately for each of them in the following graphs and figures.

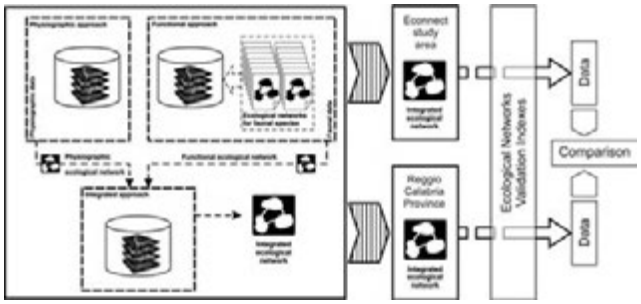

Figure 2. Diagram of the general model and flow chart of the analysis and comparison operations.

Discussion of results

Landscape biopermeability index (LBI)

The landscape biopermeability index (Bona, Badino, & Isaia, 2006) was obtained by reclassifying the codes of the Corine Land Cover Map (EEA (European Environment Agency), 2000) and assigning a permeability value to each class. Such values were obtained by averaging those found in the literature (Drielsma, Ferrier, & Manion, 2007; Fiduccia, 1998; Metzger & Dècamps, 1997; Romano, 2000), which are strictly linked to the habitat preferences in terms of land-use categories of the focal species and ability of focal species in crossing a certain land-use category (Pelorosso *et al.*, 2008).

The spatial representation of this index can be defined as a map illustrating the ability of focal species to pass through or to adapt to a given vegetational or land-use category (Bona *et al.*, 2006). A biopermeability map was created for each study area and the portions of the two ecological networks were extracted from each map (Figure 3). The surface values of biopermeability were grouped into four classes and were made comparable through the calculation of their incidence rates (Figure 4).

As the graph shows, the landscape biopermeability index has a similar trend in the study areas and in the corresponding ecological networks, which expresses a clear improvement in the conditions of biopermeability within the territories of the ecological networks in comparison with the overall surfaces of the study areas.

Anthropic disturbance index (ADI)

The Anthropic disturbance index was obtained by integrating the urban area map and the road network map. Both maps were classified in relation to population density and potential vehicular load per road section (Forman & Alexander, 1998) within the land cover map. The resulting values allowed measuring the variation in the disturbance effect as the distance from the source increased (Forman, 2003).

The cartography highlighted the spread of anthropic disturbance phenomena on the examined territories. An anthropic disturbance map was created for each study area and the portions of the two ecological networks were extracted from each map (Figure 5). The surface values of anthropic disturbance were grouped into four classes and made comparable through the calculation of the relative incidence rates (Figure 6).

In this case, the graph shows a trend that does not perfectly coincide with the index spatial distribution on the study areas as well as a certain difference, between the ECONNECT study area and its ecological network, in the land cover rates of the third disturbance class. This discrepancy is due to the composition of the territorial mosaic (Forman, 2008) of this area, which has neither infrastructures with high disturbance level nor areas with urbanization density that compares with the Province of Reggio Calabria.

Landscape fragmentation Index (LFI)

Sprawl phenomena show that anthropic expansion (Forman, 2008; Harris, 1984; Saunders, Hobbs, & Margules, 1991) has led to a remarkable qualitative and quantitative reduction in rural areas (Modica et al., 2012) with consequent ecosystemic changes caused by the progressive isolation of the residual natural areas and the interruption of the ecological connections existing between spatially separate landscape elements (Haber, 1993).

The index adopted to measure this phenomenon integrates three territorial parameters:

- The level of organization of biopermeable areas, which is useful to identify situations characterized by high spatial variability in land use and, therefore, by a well-organized environmental mosaic (Forman, 2008):

$$Tbiop = \sum Abiop / Au$$

  Where: *Abiop* indicates biopermeable areas and *Au* is the area of the reference territorial unit.
- The urbanization density index (Romano, 2003, 2005), which was adopted to measure the built area per reference unit:

$$DUu = \sum Aurb / Au$$

Where: *Aurb* indicates the urbanized areas and *Au* is the area of the reference territorial unit.

- Infrastructure-related fragmentation index (Romano, 2003, 2005), which measures the density of the road network that is diversified according to the level of congestion:

$$IFI = \sum l_i * o_i / Au$$

Where: l_i is the length of the single road sections, o_i is the congestion coefficient of each type of road (in percent values) and Au is the area of the reference territorial unit.

Once such parameters were mapped and displayed using simple overlay map types, nine landscape fragmentation classes were derived from them (Table 1).

A landscape fragmentation index map was created for each study area and its ecological networks (Figure 7). The corresponding surface values were grouped into four classes and made comparable through the calculation of their incidence rates (Figure 8).

The graph shows a similar trend of the values of the indicator for the two study areas and for the two ecological networks. The variation observed in the III (F and G) and IV (H and I) classes is due to the weak urban dominance of the ECONNECT study area.

Table 1. Landscape Fragmentation Index (LFI) types

Classes	Description of the characteristics
A	Very high fragmentation with agricultural hyper-dominance
B	High fragmentation with urban hyper-dominance
C	High fragmentation with urban dominance
D	High fragmentation with agricultural dominance and strong infrastructural sub-dominance
E	High fragmentation with agricultural dominance and weak infrastructural sub-dominance
F	Average fragmentation with urban dominance
G	Average fragmentation with agricultural dominance
H	Low fragmentation with high urban dominance
I	Very low fragmentation with weak urban dominance

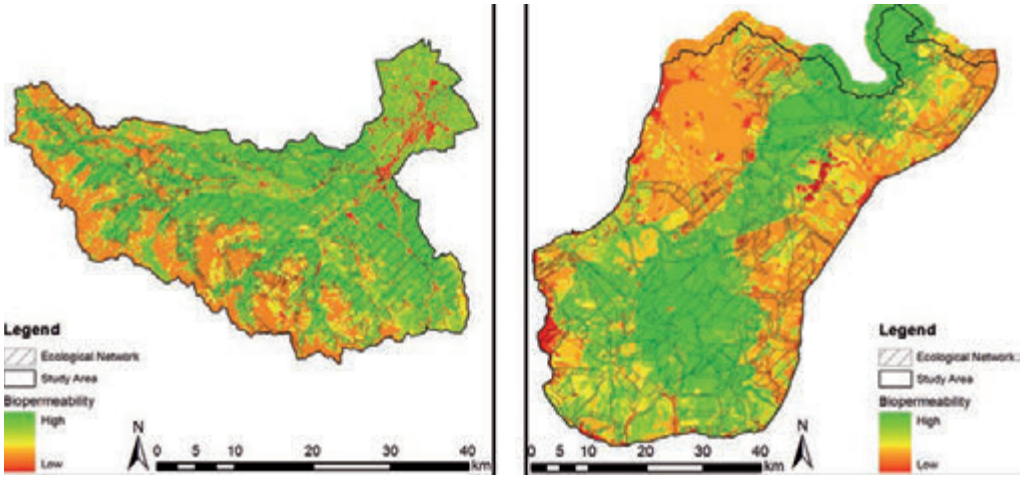

Figure 3. Landscape biopermeability index distribution map.

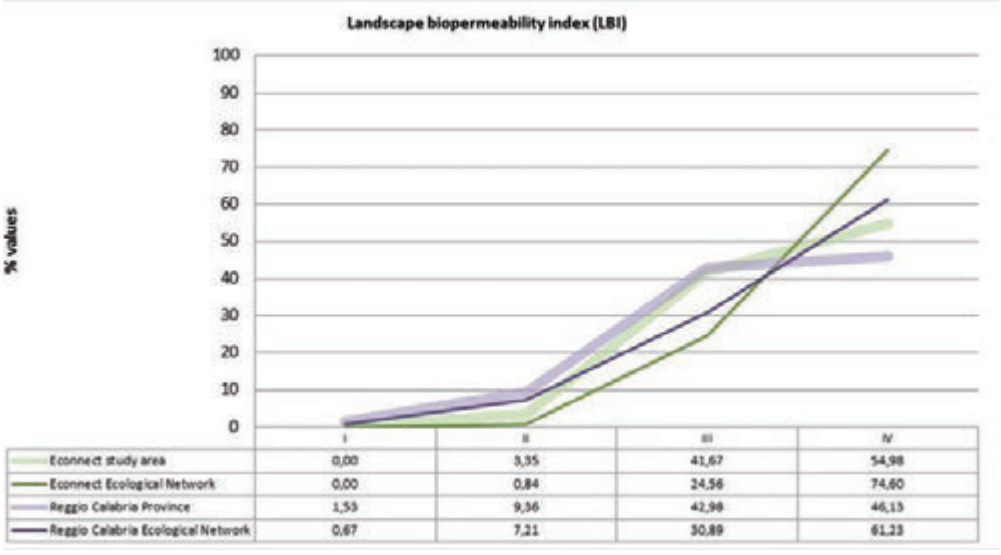

Figure 4. Graph of the distribution of biopermeability classes on the study areas and on the related ecological networks.

Environmental Sustainability Index (ESI)

The Environmental Sustainability index (ESI) (Magoni, M. Steiner, 2001; Treu, Magoni, Steiner, & Palazzo, 2005) is an indicator of the level of ecological stability of the landscape based on models of compartmental land management (Odum, 1983) that give the different land uses the capacity to perform different (or even conflicting) functions. As a result, a condition of sustainable development may be achieved through a balanced dimensional ratio and an effective interaction between the various land covers, which depends on the different pressure and regeneration processes they can carry out (Fichera et al., 2010).

Once the eigenvectors of pressure (AP, Anthropic Pressure) and regeneration (ER, Environmental Regeneration) matrices were calculated, ESI was calculated through the following passages:

- areas covered by the land uses were multiplied by the respective values of AP and ER;
- ESI was calculated as the ratio between the total equivalent area of regeneration ($VA_{regeneration}$) and the overall equivalent area ($VA_{regeneration} + VA_{pressure}$), which were defined for each land use class (equivalent area is meant as the estimate of the equivalent area of ER necessary to rebalance a unit of equivalent area of AP):

$$ESI = {}^{VA_{regeneration}}\Big/_{(VA_{regeneration} + VA_{pressure} * \alpha)}$$

Where is the coefficient of ecological stability used to set the indicator (Table 2).

ESI values were associated to each land cover class for each study area and for the corresponding ecological networks (Figure 9). Surface values were grouped into three classes and made comparable through the calculation of their incidence rates (Figure 10).

Also in this case, the graph shows a marked difference in the index spatial distribution in the two study areas (second and third class) but a certain consistency in the trend of the values on the networks. This discrepancy is due to the higher incidence of agricultural areas (ESI average values) on the territory of the Province of Reggio Calabria and, as a consequence, to the higher proportional weight of forestry areas (high ESI values) on the ECONNECT study area.

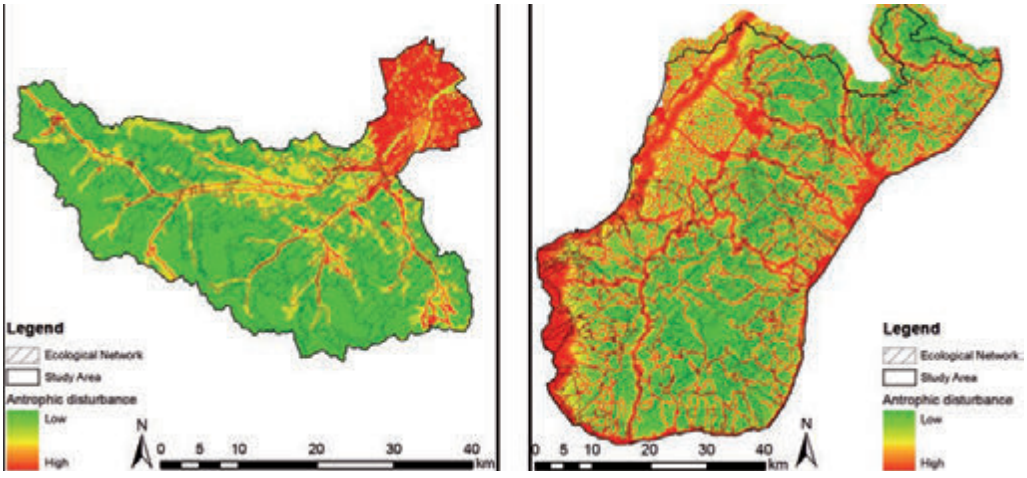

Figure 5. Anthropic disturbance index distribution map.

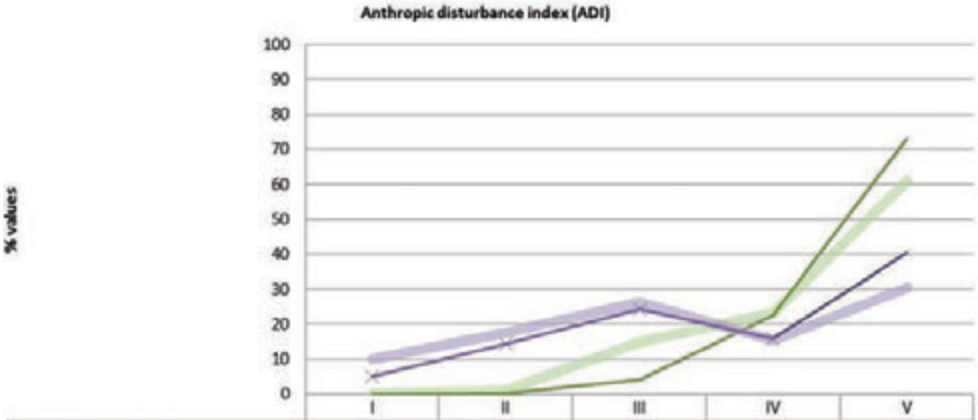

	I	II	III	IV	V
Econnect study area	0	0,90	14,84	23,30	60,96
Econnect ecological network	0	0,32	4,02	22,62	73,04
Reggio Calabria Province	10,0453788	17,69	26,30	15,38	30,58
Reggio Calabria Ecological Network	4,986916993	14,32	24,40	15,85	40,44

Figure 6. Graph of the distribution of anthropic disturbance classes on the study areas and on the corresponding ecological networks

Table 2. Environmental Sustainability Index (ESI) values for each of the defined land cover classes

Land cover classes	Values of each land cover class		ESI
	VA Regeneration	VA Pressure	with ? = 1.4
Forestry areas	99738.81	6642.6046	0.9147
Bush-lands	20241.23	2412.16	0.85
Grasslands	4164.68	541.46	0.84
Agro-forestry areas	1126.29	262.27	0.75
Extensive arable lands and pastures	3756.52	2186.11	0.55
Complex cultivation patterns	42675.04	38243.29	0.44
Intensive arable lands	6598.74	12154.92	0.27
Discontinuous urban fabric	164.83	1168.54	0.09
Continuous urban fabric	659.40	7208.65	0.06
Yards	113.02	1808.41	0.04

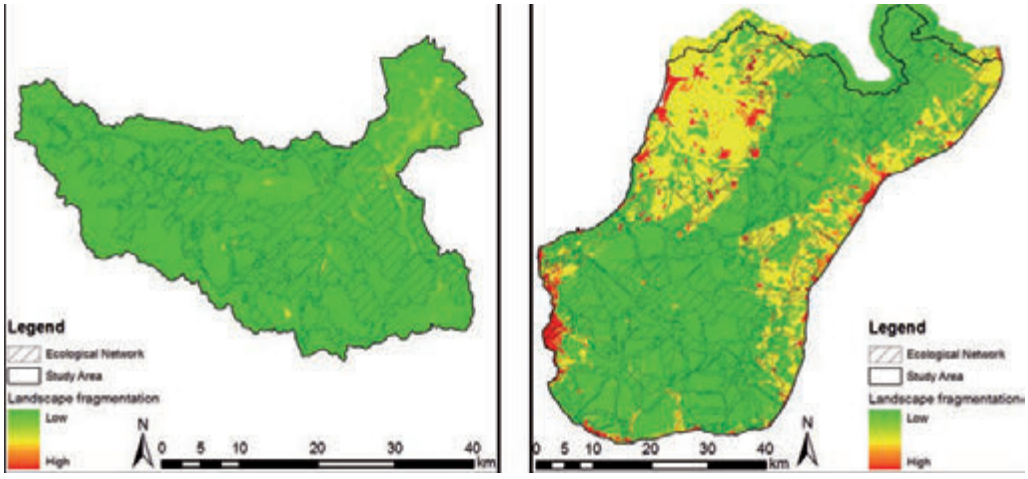

Figure 7. Landscape fragmentation index distribution map.

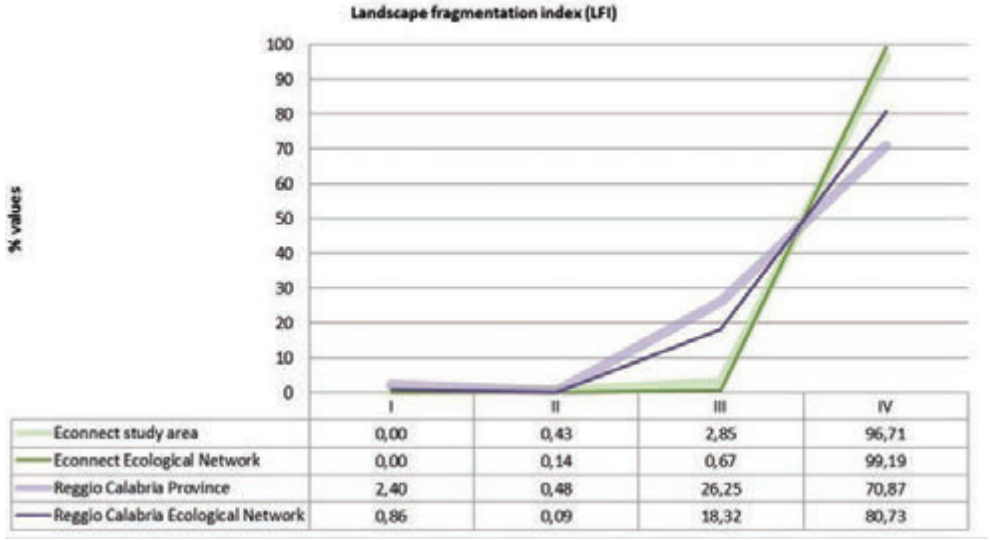

Figure 8. Graph of distribution of the landscape fragmentation classes on the study areas and on their ecological networks

Conclusions

To curb the phenomena of territorial fragmentation is one of the objectives of a correct policy of environmental conservation. As a matter of fact, any treatment of the theme of natural conservation, which is linked to spatial planning based on the mere delimitation of areas and on forms of elementary protection, is anachronistic. The focus must shift from the site or the species to the ecosystem or the habitat so as not to be constrained by the concept of geographical or administrative border. In this new planning scenario, the terms "delimitation" and "zoning" are meant as "structuring of a permeable territorial fabric" able to interconnect the different natural areas as elements of a large system and to guarantee the regular internal dynamics of biological systems.

The model allowed obtaining the design of an ecological network that complies with the theoretical physiographic and functional aspects and with the fundamental characteristics of ecological networks (Bennet & Wit, 2001; A. F. Bennett, 1999; G. Bennett & Mulongoy, 2006). This resulted in an integrated approach to planning that may ensure ecological consistency and territorial multifunctionality (G. Bennett & Mulongoy, 2006). In other words, it would be a wide-ranging green infrastructure aimed at integrating the maintenance of ecological functionality and the real needs and potential expressions of the landscape (Lafortezza, Davies, Sanesi, & Konijnendijk, 2013).

The comparison showed that, in order to effectively model core areas and corridors, the best research scale should be that of a large area (medium spatial scale). This parameter influences not only the applicative importance of results but also the design of networks. In fact, a large-scale application imposes the presence of cutting lines that directly depend on the imposed limits. The application of the model, with the same parameters but on different borders, generates different networks that are not significant at a local scale, though they still allow getting information on the quantity and on the location of high quality habitats for each species.

Particularly referring to the design of networks, in case of high ecological fragmentation, the model tends to generate small patches scattered on the territory. In this situation, corridors are oversized and play a dominant role within the network, thus making their precise analysis unavoidable for an interim validation of the network. When fragmentation is lower and characterized by large and evenly distributed patches, the model generates shorter corridors, since it can at most delimit the

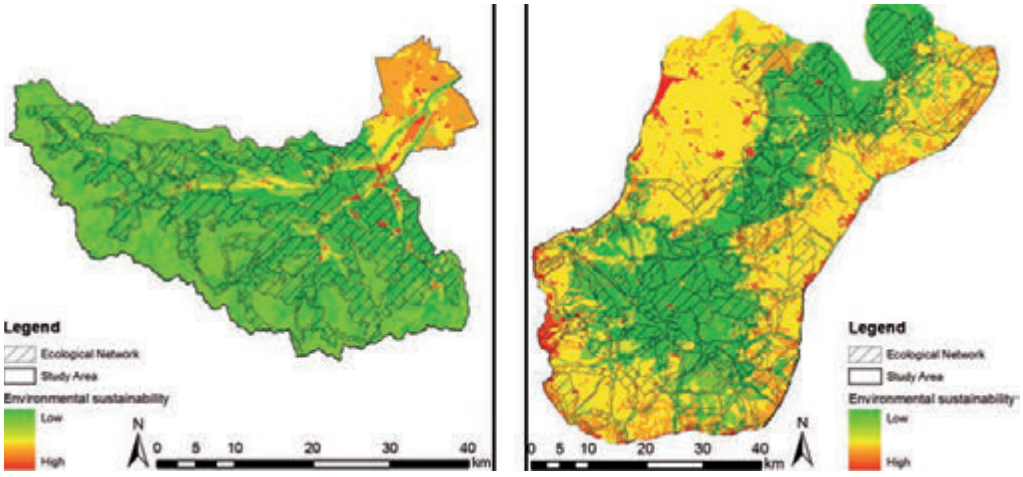

Figure 9. ESI index distribution map.

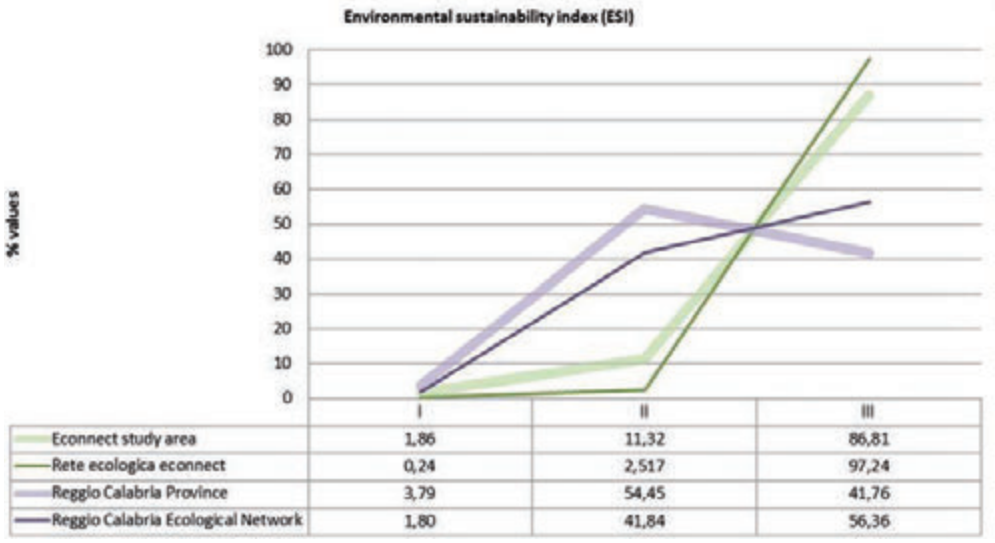

Figure 10. Graph of distribution of the environmental sustainability classes in the study areas and in the corresponding ecological networks.

width of the lower-friction directrices, depending on the biological and ecological characteristics of the faunal species.

An important result is certainly the replicability of the model, which can be used again to integrate further species. Therefore, it proves to be a tool that may be normally used in a system of collection and organization of faunal data and information. Then, the creation of the integrated network must be seen as a result that allows making planning and programming choices able to meet requirements of synthesis and analysis.

Furthermore, the available faunal information for the ECONNECT project territory showed that the presence and location of the species investigated corresponded to the most fitting areas identified by the model. It also provided consistent data related to the clash between fauna and infrastructures.

The analysis carried out demonstrated that, thanks to its characteristics of synthesis, replicability and integrability, the model allows obtaining consistent and similar responses on territories that are orographically, structurally and biologically different.

References

APAT (2003). *Management of the areas for ecological-functional connection. Guidelines and operating procedures for the adjustment of the instruments of spatial planning in relation to the construction of ecological networks at the local level*. APAT manuals and guidelines.

Battisti, C., & Luiselli, L. (2011). Selecting focal species in ecological network planning following an expert-based approach: Italian reptiles as a case study. *Journal for Nature Conservation*, *19*(2), 126–130. doi:10.1016/j.jnc.2010.10.001

Bennet, G., & Wit, P. (2001). *The Development and Application of Ecological Networks. A Review of Proposals, Plans and Programmes* (p. 131). Amsterdam: AIDenvironment.

Bennett, G., & Mulongoy, K. (2006). *Review of experience with ecological networks, corridors and buffer zones* (p. 100). Montreal: Secretariat of the Convention on Biological Diversity, Technical Series No. 23.

Boitani, L. (2000). National Ecological Network and biodiversity conservation. *Parchi*, *29*, 66–74.

Boitani, L., Falcucci, A., Maiorano, L., & Rondinini, C. (2007). Ecological networks as conceptual frameworks or operational tools in conservation. *Conservation biology : the journal of the Society for Conservation Biology*, *21*(6), 1414–22. doi:10.1111/j.1523-1739.2007.00828.x

Bona, F., Badino, G., & Isaia, M. (2006). Designing a "tailor-made" ecological network using geographical information systems. *Ecological Research*, *21*(4), 605–610. doi:10.1007/s11284-006-0157-y

Drielsma, M., Ferrier, S., & Manion, G. (2007). A raster-based technique for analysing habitat configuration: The cost–benefit approach. *Ecological Modelling*, *202*(3-4), 324–332. doi:10.1016/j.ecolmodel.2006.10.016

EEA (European Environment Agency). (2000). *CORINE land cover technical guide – Addendum 2000*. (EEA (European Environment Agency), Ed.) (p. 105). Copenhagen.

ETC - European Territorial Cooperation. (2007). Alpine Space Programme. Retrieved from http://www.alpine-space.eu/

Fichera, C. R., Laudari, L., & Modica, G. (2007). The implementation of an environmental connection matrix for the exploitation of marginal rural areas. The case study of the Tyrrhenian coast of Reggio Calabria. *Multifunctionality and sustainable development of rural areas. Technological innovation and enhancement of typical marginal areas* (p. 236). Reggio Calabria: Iiriti.

Fichera, C. R., Laudari, L., & Modica, G. (2009a). A model for the structuring of ecological networks to support the landscape planning. The case of the province of Reggio Calabria. *IX National Congress of the Italian Association of Agricultural Engineering "Research and innovation in engineering of agro-territorial biosystems"*. Ischia Porto: AIIA.

Fichera, C. R., Laudari, L., & Modica, G. (2009b). Ecological networks as a key in sustainable landscape planning to solve landscape fragmentation. *XXXIII CIOSTA CIGR V Conference on "Technology and management to ensure sustainable agriculture, agro-systems, forestry and safety"* (Vol. 3, pp. 1707–1711). Reggio Calabria.

Fichera, C. R., Laudari, L., & Modica, G. (2009c). A GIS for the definition of the ecological network in the Province of Reggio Calabria (Un GIS per la definizione della rete ecologica della Provincia di Reggio Calabria). *XII ESRI Conference*. Rome, Italy.

Fichera, C. R., Laudari, L., & Modica, G. (2010). From the construction of an ecological network to the definition of an environmentally sustainable planning model for periurban space. *XVII World Congress International Commission Of Agricultural And Biosystems Engineering (cigr)*. Quebec, Canada.

Fiduccia, A. (1998). GIS techniques for environmental planning. *MondoGIS*, *11*.

Forman, R. T. T. (2000). Estimate of the Area Affected Ecologically by the Road System in the United States. *Conservation Biology*, *14*(1), 31–35. doi:10.1046/j.1523-1739.2000.99299.x

Forman, R. T. T. (2003). *Road Ecology: Science and Solutions* (p. 481). Island Press.

Forman, R. T. T. (2008). *Land Mosaics: The Ecology of Landscapes and Regions* (p. 656). Cambridge, UK: Cambridge University Press.

Forman, R. T. T., & Alexander, L. E. (1998). Roads and their major ecological effects. *Annual Review of Ecology and Systematics*, *29*(1), 207–231. doi:10.1146/annurev.ecolsys.29.1.207

Franco, D. (2003). Sustainable landscapes and biodiversity: motives, objectives and opportunities for implementation of ecological networks (Paesaggi sostenibili e biodiversità: motivi, obiettivi ed opportunità di realizzazione delle reti ecologiche). *Genio Rurale*, *10*, 52–64.

Godron, M., & Forman, R. T. T. (1983). Landscape modification and changing ecological characteristics. In H. A. Mooney & M. Godron (Eds.), *Disturbance and ecosystems* (pp. 12–28). Berlin: Springer Berlin Heidelberg. doi:10.1007/978-3-642-69137-9_2

Haber, W. (1993). *Ökologische grundlagen des umweltschutzes*. Bonn: Umweltschutz : Grundlagen und Praxis.

Harris, L. D. (1984). *The fragmented forest; island biogeography theory and the preservation of biotic diversity* (p. 211). Chicago, IL (USA): Univ. of Chicago Press.

Hobbs, R. J. (2002). Habitat Networks and Biological Conservation. In K. J. Gutzwiller (Ed.), *Applying Landscape Ecology in Biological Conservation* (pp. 150–170). New York, NY, USA: Springer. doi:10.1007/978-1-4613-0059-5_9

Jaeger, J. A. G. (2000). Landscape division , splitting index , and effective mesh size : new measures of landscape fragmentation, 115–130.

Jongman, R. H. G. (1995). Nature conservation planning in Europe: developing ecological networks. *Landscape and urban planning*, *32*(3), 169–183. Retrieved from http://www.sciencedirect.com/science/article/pii/016920469500197O

Jongman, R., & Pungetti, G. (2004). *Ecological networks and greenways: concept, design, implementation* (p. 368). Cambridge, UK: Cambridge University Press.

Kunzl, M., Badura, M., Heinrichs, A.-K., Plassmann, G., Haller, R., &

Walzer, C. (2011). *econnect Implementation & Recommendations*. *Nursing Outlook* (Vol. 58, p. 24). Innsbruck, Austria: STUDIA Universitätsbuchhandlung und –verlag.

Magoni, M. Steiner, F. (2001). The Environment in the Provincial Plan of Cremona, Italy. *Environmental Management*, *27*(5), 639–654.

Metzger, J., & Dècamps, H. (1997). The structural connectivity threshold: an hypothesis in conservation biology at the landscap scale, *18*(1), 1–12.

Modica, G., Vizzari, M., Pollino, M., Fichera, C. R., Zoccali, P., & Di Fazio, S. (2012). Spatio-temporal analysis of the urban–rural gradient structure: an application in a Mediterranean mountainous landscape (Serra San Bruno, Italy). *Earth System Dynamics*, *3*(2), 263–279. doi:10.5194/esd-3-263-2012

Mortelliti, A., Amori, G., & Boitani, L. (2010). The role of habitat quality in fragmented landscapes: a conceptual overview and prospectus for future research. *Oecologia*, *163*(2), 535–47. doi:10.1007/s00442-010-1623-3

Noss, R. F., & Harris, L. D. (1986). Nodes, networks, and MUMs: Preserving diversity at all scales. *Environmental Management*, *10*(3), 299–309. doi:10.1007/BF01867252

Odum, E. P. (1983). *Basic ecology*. (Saunders College Pub., Ed.) (p. 613). University of Michigan.

Opdam, P., Steingröver, E., & Rooij, S. van. (2006). Ecological networks: A spatial concept for multi-actor planning of sustainable landscapes. *Landscape and Urban Planning*, *75*(3-4), 322–332. doi:10.1016/j.landurbplan.2005.02.015

Pelorosso, R., Boccia, L., Amici, A., Tuscia, U., Federico, N., Lorenzo, P., & Dipartimento, B. (2008). Simulating Brown hare (Lepus europaeus Pallas) dispersion : a tool for wildlife management of wide areas, 335–350.

Rientjes, S., & Roumelioti, K. (2003). *Support for ecological networks in European nature conservation: an indicative social map*. (D. Groels, Ed.) (European C., p. 55). Tilburg, Netherlands: European Centre for Nature Conservation.

Romano, B. (2000). Continuity and environmental reticularity, new protagonists of the territorial plan. *International Conference "Ecological Networks - Local actions of territorial management for the conservation of the environment"*. Gargnano: Study center Valerio Giacomini.

Romano, B. (2003). Evaluation of urban fragmentation in the ecosystems. *International conference on mountain environment and development (ICMED)*. Chengdu, Sichuan, Chima.

Romano, B. (2005). The indicators of ecological fragmentation in land use planning. *Proceedings of the national conference "ecoregions and ecological networks: planning meets conservation*. Roma: WWF - UPI.

Saunders, D. A., Hobbs, R. J., & Margules, C. R. (1991). Biological Consequences of Ecosystem Fragmentation: A Review. *Conservation Biology*, *5*(1), 18–32. doi:10.1111/j.1523-1739.1991.tb00384.x

Theobald, D. M. ., Norman, J. B. ., & Sherburne, M. R. (2006). *FunConn v1 User's Manual: ArcGIS tools for Functional Connectivity Modeling.* (p. 51). Fort Collins, CO.: Natural Resource Ecology Lab, Colorado State University.

Treu, M. C., Magoni, M., Steiner, F., & Palazzo, D. (2005). Sustainable landscape planning for Cremona , Italy, *47*(2000).

Watts, K., Eycott, A. E., Handley, P., Ray, D., Humphrey, J. W., & Quine, C. P. (2010). Targeting and evaluating biodiversity conservation action within fragmented landscapes: an approach based on generic focal species and least-cost networks. *Landscape Ecology*, *25*(9), 1305–1318. doi:10.1007/s10980-010-9507-9.

Livestock system as a mitigation measure of a wind farm in a mountain area

Antoniotto Guidobono Cavalchini, Gabriele Daglio, Massimo Lazzari, Stefania Leonardi

Department of Health, Animal Science and Food Safety, Università degli Studi di Milano

Abstract

The study concerns a mountain territory, bordering Liguria, Piemonte, Lombardia and Emilia, where a high power 151 MW wind farm, with 42 tower of 3.6 MW power, has been proposed. As a measure of environmental mitigation, the realization of a livestock system of a herd of sucker cows pasturing in the wind farm areas is proposed. This has implications for environmental maintenance, employment in a territory gradually losing its population, and for tourism. The study, having focused on those aspects that reduce landscape impact and carrying out an analysis of the individual areas to evaluate forage resources and the different pastoral indexes, identifies the maximum sustainable load of animals (335 UBA/ha) in the current conditions of neglect. So, some measures to improve and increase sustainable herds have been proposed and examined. The operations include: stone removal; light harrowing; overseeding; creation of fodder reserves for periods of shortage; and grazing will be managed by taking turns. Based on the results of two other studies, both previous tests carried out on site, encourage us to think that we will be able to increase the maximum sustainable seasonal load for the current situation by more than 50%. This means a herd of 500 UBA equal to a gross PLV, for the grazing period of 180 days, of €400,000 and so guarantee an adequate income to 3-4 UL (labor unit), and of €650,000/year in case the chain is completed during the winter months in structures located in the valley. In this case, the PLV obtained could assure income to 6-7 employees, which would be extremely important for the socio-economic conditions of the valley; in consideration of the induced activities- meat processing, marketing and tourism facilities- which could be made available. Experimental tests of the technical improvements described will be carried out in the next season.

Correspondence: Antoniotto Guidobono Cavalchini, Department of Health, Animal Science and Food Safety, Università degli Studi di Milano, Via Celoria 10, 20133, Milano, Italy.
E-mail: antoniotto.cavalchini@unimi.it

Key words: wind farm; livestock system, mitigation measure, mountain area,

Journal of Agricultural Engineering 2013; XLIV(s1):e99
doi:10.4081/jae.2013.(s1):e99

Introduction

The area studied includes the Giarolo, Roncassi and Ebro mountain crests bordering on Liguria, Piemonte, Lombardia and Emilia, also called of *"the Quattro Regioni"*. The territories are going through a period of severe depopulation causing an almost deanthropic state. Consequently also the agro-zootecnical activities have dropped in the past years (Figure 1). Among the major causes are: the lack of productive job alternatives to replace the agricultural ones after the war during which in Italy industry replaced agriculture; shortage of efficient infrastructures to link the urban/industrial centers, and, above all an impervious territory with few resources.

Yet, one of the resources is the wind. Until recently it was considered a nuisance, but today it has regained its importance also in economic terms. Anemologic studies carried out on crests revealed that median annual speed is higher than 5 m/s with peaks above 6 m/s in the winter months, with an annual production of 2800 kWh/kW installed power (Figure 2). This is why in these last few years many wind farm proposals have been put forward; our studies concern the installation of 42 wind generators, 3.6 MW nominal power, totaling 151,2 MW (Figure 3).

Obviously such an intervention is harmful, having a permanent environmental impact, especially on the landscape, which should not to be taken lightly. The repercussions for the expected economic gains (7-9% of revenues from energy produced) are significant for the area. The study proposes the environmental mitigation measures to be taken; improvement and realization of pasture-land resources and a cow calf animal husbandry system. It's an interesting paradox, the solution to the negative technological impact could well be found in traditional measures.

Pastures: the crests studied were once a precious resource, but they have been progressively neglected. Up to the 50s the pastures, besides being used for grazeland, they were cut to create a fodder reserve and were mostly commonly managed. Instead today, while the local population has almost completely given up the use of the pastures, due to the lack of livestock; the grazeland is utilized by lowland livestock breeders for **summer grazing** thanks to regional incentives. It is obviously a non-solution with little attention paid to the needs of the territory.

Materials and methods

The fodder resource studied was assessed by locating plant species via satellite image photo-interpretation using a GSI. The areas located were thus divided into virtual polygons of which the area was calculated. Through video observation each polygon was assigned a "Su" parameter which expresses the percentage of grazeland surface and its *Valore Pastorale* (VP) (Pasture Value). The polygons were given a conversion coefficient K for VP and a fragility coefficient CF, according to a proven method (Cavallero *et al.*, 2002; 2007).

Thus applying to each polygon the formula CMMU = VP * K * S_u * CF for each one we can determine *Carico Massimo Mantenibile Unitario (CMMU) (Unitary Maintainable Maximum Load), expressed in* [UBA * ha^{-1} * $anno^{-1}$ (UBA= Adult Bovine Unit)]. By multiplying the *Unitary Maintainable Maximum Load* by the area of the polygon and the period of summer pasture (180 days), subsequently we referred to the Carico Massimo Mantenibile Stagionale (*Maintainable Maximum Seasonal Load)* referred to the pastureland expressed in [UBA/area,season]. So the Reduction "Kr" coefficient was introduced, which, according to species and breed, (Cavallero *et al.*, 2007), allows the calculation of the Suggested Maintainable Load for the whole area expressed in [UBA/area,season].

Finally, by applying the formula: VP = $\Sigma(CS_i * I_{Si})$ * 0,2, (Daget & Poissonet, 1969; 1971), by determining plant composition we were able to calculate Pasture Value. The Pasture Values used were taken from a previous study in the same area (Giordano and Terzolo 2001), after verifying, by chance, some values.

Results

From the studies carried out using the methods described above, the results are as follows:

The sum of the areas of the individual polygons digitized gives a comprehensive value of 626 Ha. However, for various reasons, (*e.g.* excessive steepness, low pasture value, roads, high number of not edible species, etc.), use of the pastures is limited. Only 444 ha. can be used for pasture. Pasture values VP and *Carico Massimo Mantenibile Unitario (CMMU) (Unitary Maintainable Maximum Load),* calculated with the method above, are broken down for the single areas in Figure 4.

In conclusion the following values were obtained:

- *Unitary Maintainable Maximum Load:* 0,309 [UBA /ha, year]; average value referred to the whole area;
- *Maintainable Maximum Seasonal Load: 447* [UBA /area ,summer pasture period]; total value referred to the whole area studied;
- Suggested Maintainable Load: 335 [UBA /area ,summer pasture period]; total value referred to the whole area studied.

Following the analysis of the fodder resources agro-zootecnical interventions are proposed to improve productivity and efficiency in the area. The interventions include stone removal in some pasture areas and light harrowing the area to remove agricultural residues of the previous season. In addition, in low value areas (VP<25), were the use of machines is possible, overseeding has been taken into consideration. To manage the area by turns , some infrastructural investments for electric fences, water troughs and feed supplements are required. For the latter, hay is used as part of the turn-taking plan, using rotobalers or STack Hand. In both cases rain resistant hay

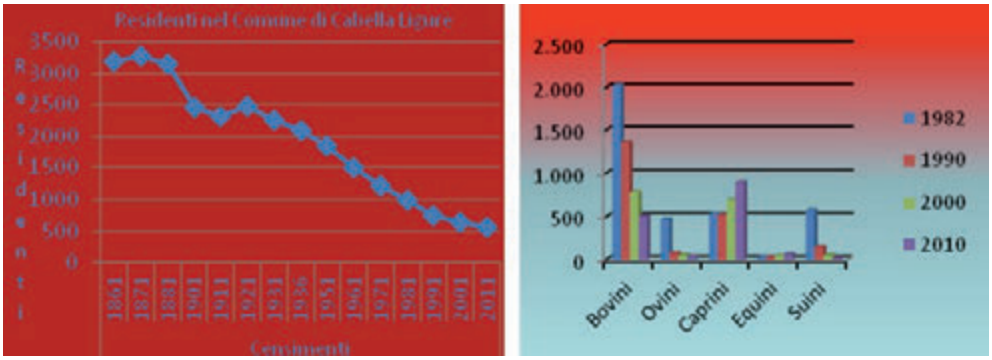

Figure 1. State of the population (Cabella Ligure) and the zootecnical patrimony.

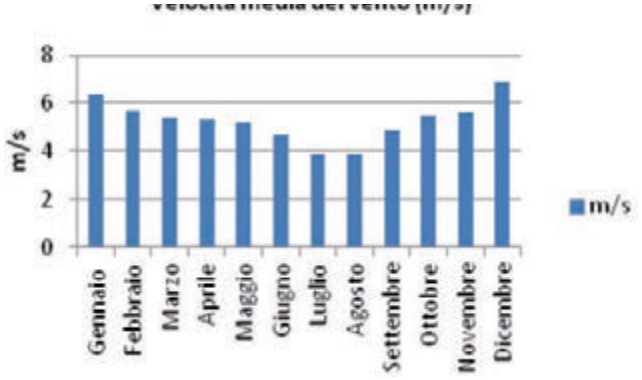

Figure 2. Wind average monthly speed.

Figure 3. Wind generators position.

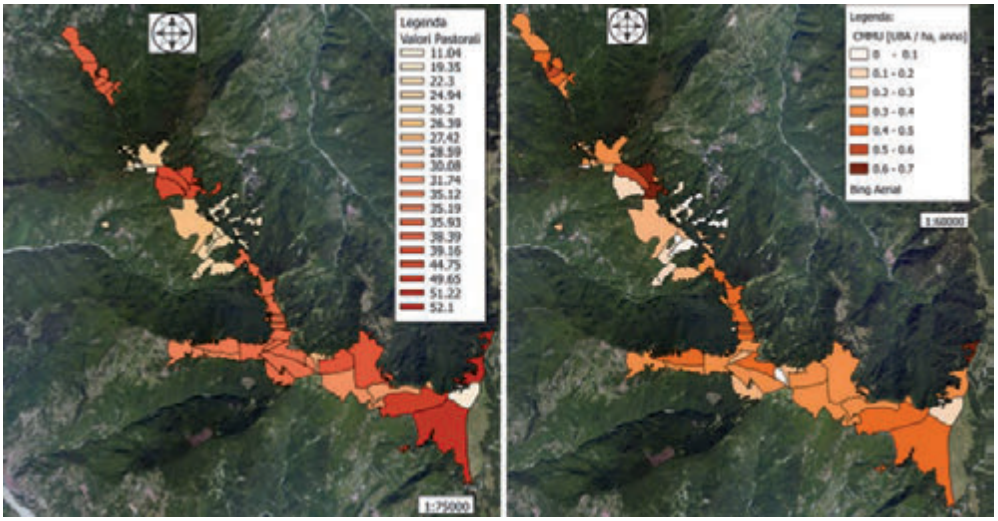

Figure 4. Pasture Values (left) and Unitary Maintainable Maximum Load (right) of the area.

stacks easily accessible to the animals would be made available.

From satellite video analysis stone removal would include a 50 ha area, mostly involving the towns of Cantalupo and Montacuto. Slopes above a 60% inclination would be excluded; light harrowing would be used in a 310 ha area. After a preliminary analysis it was decide that overseeding take place in an area of 30-40 ha/year, in order to assess the benefits and pick out the most productive and suitable species. The areas to be used as fodder reserves, singled out for its productivity, soil morphology and turn-taking plan with reference to the pasture, is 40 ha.

Based on various experiments carried out in the didactic-experimental farm of Borgo Adorno of the University of Milan bordering the areas studied, it was estimated that the proposed improvement interventions, coupled with the turn-taking plan, a Suggested Maintainable Load value near 500 [UBA/area is obtained, in the period of summer pasture period.

Conclusions

The studies clearly show that territorial deterioration and of abandonment will continue unless radical changes take place. A wind farm would be an opportunity for forecasted economic returns if they are shrewdly reinvested on the territory. However, the impact on the landscape and modest employment opportunities are not to be overlooked. The proposed measures concentrating on the primary system by the improvement of a natural resource, the pasture, environmentally valuable, could mitigate the negative impact of a large wind farm. In this way, two different types of businesses could coexist and integrate: the first, of an industrial nature, for the production of renewable energy; the second for the production of quality foods, characterized by a common denominator: the use of natural resources.

As far as employment is concerned, the prime objective of each action on the territory such as the one examined, the zootecnical system proposed, 500 nursing cows, justifies 2-3 Work Units and as such insignificant, but it starts up a PLV of €400,000 not negligible since it is obtained with modest technical means, negligible in terms of economics. To keep in mind also the start of induced consumption with businesses (tourism, meat production, distribution, direct consumption in the local restaurants, etc.) interesting for a valley-based socio-economy in sharp recession.

References

Cavallero et altri. *I tipi pastorali delle Alpi Piemontesi*., Albero Perdisa editore., Bologna., 2007.

Cavallero A., Rivoira G., Talamucci P., *Pascoli.* In Baldoni R. & Giardini L. *Coltivazione erbacee*. Patron editore., Bologna 2002.

Daget P. & Possonet J.: *Analyse Phytologique des pairies.* Document 48, Centre National de la Re Recherche B.P. Montpellier 1969.

Daget P. & Possonet J.,: *Une métode d' analyse phytologique des praires.* Annales Agronomiques 1971.

Geomatics and virtual tourism

Valeria Minucciani,[1] Gabriele Garnero[2]

[1]DAD, Dipartimento di Architettura e Design, Politecnico di Torino, Torino, Italy;
[2]DIST, Dipartimento Interateneo di Scienze, Progetto e Politiche del Territorio, Università e Politecnico di Torino, Torino, Italy

Abstract

The most recent technological revolution, concerning web and "ICT", not only changed individual and collective behaviors, but also allowed experiences no possible before: a real time communication, regardless of the distances; an extended access to disjointed data and sources; the shift in different realities – missing or entirely imaginary. Nowadays, we can think about a new concept of museum, much more inclusive than "objects container": now the museum involves entire countries, entire ecosystems, entire regions. We can speak of "museum outside of the museum", to extend museum "storytelling" to a regional scale, beyond the walls of the traditional museum. On a regional scale experiments entirely convincing have not yet been carried out, but from this point of view cultural lands can be visited as great open air museums, to find objects, artworks or signs: the whole land is a "collection" to be preserved, to be presented and to be interpreted. Thus the visit allows to elicit outstanding objects, to read into landscapes with different filters. Both the physical and virtual visit seem to be a "tour" (Minucciani and Garnero, 2013). To create a virtual tourism prototypal station, we need several and unconventional geometrical data (shared geographic databases, DTMs, digital orthoimages and angle shots, modeling with spherical cameras, ...), thematic data (related to cultural content) and no conventional input units to move and to observe how and where the observer prefers. Authors report here their experience to carry out a prototypal station, able to relate geomatics references to cultural content and to offer a whole experience, involving users also from the sensory point of view.

That's nowadays a specific purpose of new technologies applied to cultural heritage.

Correspondence: Gabriele Garnero, DIST, Università e Politecnico di Torino
Via Leonardo da Vinci, 44, 10095 Grugliasco (TO), Italy.
Tel. +39.011.670.5518 - Fax: +39.011.670.5516.
E-mail: gabriele.garnero@unito.it

Contributions: the authors contributed equally.

Conflict of interest: the authors declare no potential conflict of interests.

Funding: no source of funding

Key words: museography, virtual tourism, geomatics and shared databases, human computer interaction, social inclusion.

Journal of Agricultural Engineering 2013; XLIV(s1):e100
doi:10.4081/jae.2013.(s1):e100

ICT and virtual tours

The concept of virtual museum is by now established, multi-faceted and so widespread that it is now inflated: but a shared definition isn't given yet, and it indicates the possibility of access to the historical, artistic and cultural heritage through the network, sometimes replacing sometimes integrating the real experience of visit.

Then we have "virtual museums" that simply are "catalogs" on line, but we have also cases in which, with more or less interaction, we can perform via video real visits (selecting paths, objects, information). The static nature of these experiences is often the weakest point, despite considerable progress (Caraceni 2012; Minucciani, 2009a; Minucciani 2009b; Antinucci, 2007). In general, they interpret "virtual" as "simulation" (on the screen) of a real experience.

This "replacement" (which anyway provides immediate availability and accessibility everywhere - sometimes more than in the real situation) nevertheless pays a price, that's - above all - disorientation and barrier effect of the screen.

Even very recent projects (*e.g.* Google Maps service "Google Business Photos": after Spain, Denmark and Sweden it's now running available also for Italy - see the "Museo dell'Automobile" case, in Turin), providing an access to interiors thank several 360°pictures, don't completely overcome this hurdle. Fundamentally, they hat replicate indoor the Street View solution.

Likewise if we mean "virtual tourism" reductively as "access to information" related to a place, it seems to be aseptic and far, via video. We cannot define it as "tourism", but rather as "cultural or touristic information".

The loss of the viewer's corporeality creates alienation and separation, thus we need a kind of "*alter ego*" to fill this gap. So, if we attribute to the term "virtual" its scientific meaning, *i.e.* simulation of reality (and consequently simulation of experience), new scenarios open (Vince, 2004): not only the computer version of a real place, but also a place that does not exist - or that no longer exists…

Some experiments have enhanced museums by "virtual guides", *i.e.* synthetic characters that can interact with visitors in a more or less advanced way (Minucciani, 2009a). In other cases, they attempted to give back a "physical", bodily dimension to the virtual tour: in Italy one of the pilot cases goes back to 1994, and it concerned the virtual reconstruction of Nefertari tomb (Antinucci, 2007) ("Nefertari: Luce d'Egitto", temporary exhibition in Rome, Palazzo Rispoli, 1994).

But in this field there have been many other experiments, (in particular, see V-MusT.net NoE experiments during 2012-2013 period (www.v-must.net), more or less immersive, someone scientifically rigorous, someone similar to videogame *tout court*, someone very poor

from the cultural point of view (Minucciani, 2009a; Minucciani, 2009b). They're studying solutions - using geo-caching, geolocation in interior (still a bit problematic) – that offer really educative "games" involving the entire web community: in this regard it should be noted that the Web 2.0 advent has given further impetus to virtual experiences, enriching the cultural impact with socialization and sharing (See Tate Gallery case (www.tate.org.uk/britain/exhibitions/howweare/) or Brooklyn Museum of NY (*Click! A crowed-curated exhibition*: www.brooklynmuseum.org/exhibitions/click/)), (Proctor, 2010).

Furthermore, the new concept of museum (Poulot, 2005), much more inclusive than simple "objects container", enclosed by walls and clearly divided between "inside" and "outside. Now the museum could involve entire countries, entire ecosystems, entire regions. We can speak of "museum outside of the museum" (Minucciani, 2005), that extends museum "storytelling" to a regional scale, beyond the walls of the traditional institution. On a regional scale experiments entirely convincing have not yet been carried out, but from this point of view the cultural lands can be visited as great open air museums, with transversal or theme paths, to find objects, artworks or signs: the whole land is a "collection" to be preserved, to be presented and to be interpreted. Thus the visit allows to elicit outstanding objects, to read into landscapes with different filters. Both the physical and virtual visit seem to be a "tour".

In fact, the new concept of "virtual tourism" is very similar to "virtual museum", but it's more inclusive (Wang, 2011a; Gerosa, 2011; Gärtner at al., 2010; Gretzel *et al.*, 2010; Minucciani, 2009a; Minucciani, 2009b; Hyun *et al.*, 2009; Cheong, 1995; Williams e Hobson, 1995).

Its own meaning is still not universally shared, anyway it originates from the advent of new technologies in the tourism industry: not only regarding new channels of information and purchase, but also the "virtual tours", exploring synthetic worlds (sometimes encroaching on videogame) or the real world. Nowadays the attention is focusing on the second one. Often the "virtual tourism" is defined as "stationary tourism", but they're trying to overcome this feature also because territory perception and his understanding are more complex than a remote visit to museum.

Actually, we could define "virtual tourism" two different cases: a virtual trip in a virtual site (that's a model, mirroring the real world or not) and a real trip (that's powered by another reality – the augmented one). Of course, there is a lot of intermediate options, and we have to take account of specific purposes and different goals (commercial, cultural, entertaining…). But we would like to focus on solutions that don't resort to models and virtual worlds, but instead aim to face to real environment.

About database construction, in addition to traditional, cartographic bases are now achievable different information sources (orthoimagery, digital models produced by photogrammetric correlation to LiDAR takes ...).

Current technology is mature to support specifically these applications with products as UAV shootings (made with extremely manageable and low cost aircrafts, operating with a high degree of automation to realize updated shooting at sustainable costs); reliefs by single "session" (with equipped aircrafts and high-performance vehicles, to acquire information components – photographic - and metric components - LiDAR); use of spherical cameras, able to acquire "views" to be freely visited by user (Figure 1).

Real sites, virtual tourism

Focusing on tourism in real sites, they're attempting to expand the perception and knowledge modes, also thank to open databases more and more extensive.

We can acquire information in increasingly articulated ways, in order to rejoin virtual world and real experience.

For a long time the Authors are interested in this field (Minucciani, 2012; Vaudetti *et al.*, 2012; Minucciani, 2009a; Minucciani, 2005). They believe that communication of cultural heritage has yet to fully benefit from the new technologies chances, not only in Italy (where the matter is particularly urgent and strategic, although their country isn't an emerging model about ICT exploitation for Cultural Heritage). In addition, they trust in a cultural and social mission of virtual tourism: it shouldn't not only enhance already known and possible functions (increasing the commerce and information occasions), but it should also broaden avails to situations and categories of people who have so far been excluded, in different ways.

They are convinced that the time savings should not sacrifice the awareness of real parameters (distances, differences) and that the so-called edutainment shouldn't be a simple compromise between different needs, but rather a richer opportunity. Thus their interest is addressed to technologies able to tie virtual visit and *real site*. Furthermore, they want to pay more attention to "visitor's body", *i.e.* his physical involvement, in virtual experiences.

Many projects facing this issue are already been carried out: from simple "virtual books or tables" to particular experiments as *PointAt*, (These solutions are interactive installations, the first one to consult documents, while *PointAt* allows to learn more about a digital version of an artwork, just pointing the finger on details - that's a very instinctive gesture (Museo del Palazzo Medici Riccardi, Firenze, 2003)), *Museum Wearable*, (This small, lightweight computer, in a carrying backpack, was connected to a body motion sensor and to augmented reality glasses and headphones, in order to support and enhance the museum visit (temporary exhibition "Robots and Beyond", MIT Museum, Boston 2000)), *Cave*, (An enterely virtual, immersive environment you can visit thank stereoscopic glasses and special "mouses" (*e.g.* Kivotos system, Foundation of Hellenic World, Athens 1999)), haptic interfaces, holograms and so on. In these cases, anyway, virtual real-

Figure 1. Multiple access to information.

ity integrates real environment – through 3D models and simulations.

The Authors have just developed a project aiming to explore the opposite situation, integrating the virtual environment by *real elements*.

About this issue, an interesting project has already been carried out: the virtual "Trans Siberian Railway". Thanks to a simple video camera system, it offers the real sights from the train window along the 9000 km travel. The website also features images of small cities crossed, as well as tourist information, related to Google Maps (http://www.google.ru/intl/ru/landing/transsib/en.html. The project was originated from a collaboration between Google Maps and Russian Railways). However, they miss an element that Authors consider crucial: the real interaction with physical movement of the user. Although friendly and shared, a map is an abstraction and cuts immersive effect. All information access should be strictly related with a real sight, and originated from it: interaction interface is crucial.

Thus, as the objective is to merge physical and virtual reality, involving the body motion, the challenge is interesting because they want to present the real views, without 3D models. Another issue becomes crucial: the increase of data sharing, *e.g.* data related to systems as primarily Google Earth, Google Maps and Street View - now in common use. They already can provide, completely free, real images of the sites on global scale. Their content are by now integrated tools, namely repository of territorial data that we can integrate and share.

Recently, another opportunity has been jointed: integration of local and remote databases of images, and implementation in GIS systems (Ferrante and Garnero, 2013, Pirotti *et al.,* 2011).

Virtual Earth and Google Earth use a cartographic representation system not yet implemented – in Italy – in other applications (http://www.google.ru/intl/ru/landing/transsib/en.html. The project was originated from a collaboration between Google Maps and Russian Railways). Particularly interesting for our purpose are the geo-referenced images of Google Street View, implemented within Google Maps and Google Earth that provides panoramic views of 360° horizontally and 290° vertically along the streets (at a minimum distance of 10-20 meters apart). It was introduced in May 2007, and it runs in Italy since October 2008: Street View allows users to view portions of cities around the world at ground level, by placing on the map a little orange man.

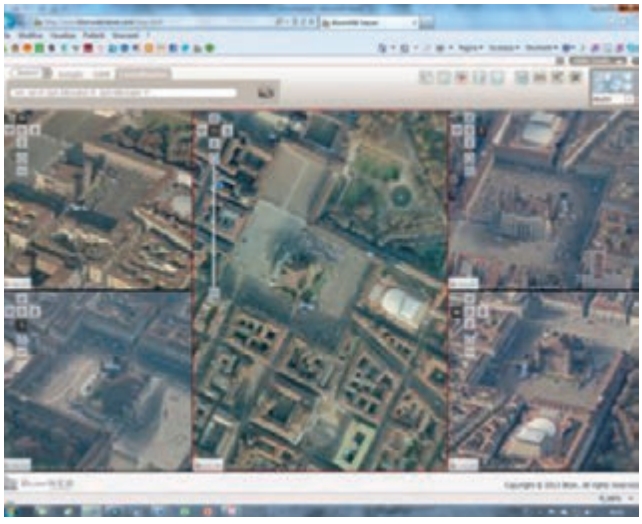

Figure 2. Nadir sight and 4 angle shots of Turin – area of "piazza Castello".

Google Street View uses special cameras (the Dodeca 2360, with 11 goals and produced by the Canadian company Immersive Media) located on the roof of cars or equipped bikes. The service is now extended to main roads and urban streets of large and small centers, across all Italian regions (The updated coverage is available online at http://www.google.com/help/maps/streetview/learn/where-is-street-view.html).

The images quality is satisfying, although they may perceive the "junctions" among consecutive shots.

Furthermore, there are other databases of images that can integrate "real" views (*i.e.* at eye level), to offer to users a complete description of sites. First, the digital orthoimages (high definition) and angle shots (able to acquire buildings facades). The industrial solutions (*Pictometry* ®, *Midas* ® of *Track'air*, *iOne* ® *Visual Intelligence*,...) use systems of cameras, connected to each other and assembled on a single support (Pictometry and Midas systems have 5 cameras: 4 are installed with an inclination of 40-45 ° from the vertical and according to the four directions of view perpendicular to each other (forward, backward, left and right); the fifth camera takes from the zenith. Thus different frames share the same take instant).

In fact, in order to know and document the buildings appearance without performing measurements, less expensive systems are available: *e.g.* drones (UAV, Unmanned Aerial Vehicle) with photographic equipment. The APR (Aircraft Pilot in Remote) will be able to perform low altitude shots everywhere.

Finally, is now possible to create *3D City Models*, namely consultation environments where the buildings are geometrically modeled and then "dressed" with their facades. 3D City Models are one of geomatic products available for a long time, but only the recent improvements in the autocorrelation techniques may allow automatic generation processes, therefore openings to more generalized use.

All of these activities are nowadays made possible by the generalized availability of digital terrain models (DTM). They're got thank to photogrammetric autocorrelation techniques, cartographic data and - as it often happens by now - specific LiDAR shootings (Pelagatti *et al.*, year not specified; INSPIRE, 2007).

Digital Terrain Models (DTM) are a resource in environment and land related applications. They can be employed in several way in order to deepen the comprehension of an area investigated by extracting morphometric parameters or to perform complex analyzes on the DTM alone or by combining it with other data sources with modeling purposes (Godone and Garnero, 2013; Pirotti *et al.*, 2012; Chiabrando *et al.,*. 2011) (Figure 2).

A further contribution comes from the increasing standardization of cartographic production, advocated by the INSPIRE Directive and recently inserted in the current Italian regulations (Garnero *et al.,* 2013; Ferrante and Garnero, 2013, INSPIRE, 2007).

State-of-the-art: the case study of Turin

Other, different databases can be related: information about history, architecture, cultural heritage. An interesting case study is *MuseoTorino*.

Launched during the celebrations for the 150th Anniversary of Italian Unification, it's the new on line museum of Turin and it aims to collect, preserve and communicate information about cultural, historical and artistic heritage of the city, and more. The website (www.museotorino.it) is conceived and structured as a museum, where you can find information on places, people, events, itineraries (thank a browsable map of the contemporary city). Each item has a brief label and a file containing notes and information. The most inter-

esting feature is the use of the latest platforms and technologies based on the Web 3.0 (semantic web) and Linked Open Data philosophy. Museum staff has been working on the website creation and data collection since 2009, and they have produced so far more than 15.300 files on places, events, themes and characters. Each file has been stored in a new generation database, a GraphDB providing excellent performances in data management.

This database is "museum catalogue", which can be consulted online, open to free searches. You can also move across the contemporary city, through a Google Maps application, and travel through time by visiting the permanent historical exhibition on the history of the city. MuseoTorino aims to involve the largest possible number of people, by sharing their knowledge and memories, suggesting ideas and projects. Icom Italia has awarded to MuseoTorino the prize Information Communication Technology (in occasion of *Premio Icom Italia - Musei dell'anno 2011*).

Thus, if the physical environment can be re-composed, instead of modeled, and if data and information can be collected and related, the visitor will be able to perform a "tour" without traveling. But his experience will be really "immersive" only if his motion and his perception of physical environment can be preserved.

So he will have several tools to move, literally, and to observe how and where he prefer (as if he were walking, for instance, but also turning his eyes or his head), namely natural ways with which he normally explores the world.

Suitable I/O peripherals will ensure the correspondence between the physical motion of visitors and views (and a crucial requirement will be the level of immersion of output).

Furthermore, transposition of user' real motion along a trajectory, identified on Google Maps, will be put in relation in real-time with street view images. Several markers on these will allow to access (even through queries in natural language) not only to tourist information but also to cultural ones, detailed and specific, that will catch from different databases. Travel will be featured by shots specially made, in order to access also to particular interiors.

A prototypal station

Starting from aforesaid notes, the Authors believe users can really appreciate und understand the land features, with distances, relations, proportions and morphologies (*i.e.* the territories as "systems"). Among the requirements of a "real" tour, there is the free motion in places and the "guides'" support. The new functions and services of augmented reality, in addition to unstoppable spread of smartphones (which nevertheless don't break the barrier effect of display), still require a cultural, strategic reflection.

The project therefore intends to explore a tour simulation with three basic features:

it offers to the "tourist" a *real* and *immersive vision* of what he would see across the places he's visiting, without turning to city models or synthetic worlds;

it brings together the virtual displacement on sites with a *physical motion really made* by the "tourist";

it uses *shared databases*.

The final prototype (replicable for different contexts - in urban environment and in extra-urban context - and for different situations of use) will allow to visit remote sites, without turning to traditional station in front of a monitor, but recovering movement and free choice of timing and sequences.

The virtual tourist would thus have the opportunity to visit any place, stopping when and how he wants.

The experience will provide most of the functions available for real tourism, improving them: among these, virtual tourists will be able can make stops, get into some interiors and benefit of observation points that are not possible in physical reality, but easily achievable in virtual way (elevations of points of view, spherical shooting etc..).

At last, there are different uses of databases: cloud systems availability and adequate, technological infrastructure allow creation of data bases adaptable to different needs, for scholars, conservation institutions, or simple curious and tourists.

Just the "virtual tourism" is the most attractive form to consult and use such information, because the observer-visitor, according to our project, can access specialized information in intuitive way, thank to navigation tools as described, maybe with virtual assistants and so on.

Of course, such information bases could be available also to users physically visiting real places, thank to positioning instruments (GNSS, gyroscope, compass, ...) already provided on smartphones and tablets . Real tourists will able to access to same information body than virtual one, and to navigate by using the information architectures as geometric and thematic index, data retriving, metadating repertoire ….

Furthermore, at even larger scale, they will enter into the building / museum: dedicated systems will recreate a reference system (radio apparatus as GNSS systems emulators, objects identifications through QRcode, and so on) to enable real user to automatically synchronize, from its location, to available data bases.

Interaction should be as natural as possible, using also natural language and virtual assistants.

The project encompasses several disciplinary cores: museography (that's exhibition strategy and communication of cultural heritage, complemented by historical and technical disciplines); geomatics and image processing (connection between the visitor's motion, the geo and cartographic reference and related databases); virtuality (and web 2.0.), ontologies (and web 3.0); tourism sociology and marketing (implementation of investigation/verification techniques, and their transposition to the virtual tourism) (Figure 3).

Conclusions

The matter the Authors wish point out, in conclusion, relates to the use of technologies and databases now widely available.

Figure 3. Immersive and interactive virtual reality, at LAQ (High Quality Laboratory) "Auditorium", Politecnico di Torino.

In fact, in addition to the scientific and experimental contents in itself, from their use can arise important effects for people.

Indeed it concerns not only economic and commercial business (even if the creation of new jobs and new employment sectors is undoubtedly important). Let's rather consider the social importance of a tourism solution that does not exclude whole, weak segments of population, due to income, age or disability.

In addition to effects of social inclusion (which is a main goal of European Strategy for 2020) should also be underlined the opportunity for a greater access to culture, that's a primary factor of human development and progress.

The territorial information systems leave "technical" fields and gain application contexts related to large public. For this reason, transversal use is crucial: we don't need "new knowledge bases", but to integrate them and provide *interpretations* (ontologies; network systems; systems person-based; systems on geographic key; various access systems, mutually integrated …).

Also "closeness" is, in the most recent project, a crucial key to access information. In this field, due to great amount of interrelated information, and to worldwide spread, the Wikipedia project "Nearby" has really an excellent chance (http://blog.wikimedia.org/2013/05/29/wikipedia-nearby-beta/) (Figure 4).

The information of the largest free encyclopedia in the world will be connected with their geographical reference, so tourists or professional operators will able to browse starting from their real location and then accessing related information. "Nearby" application is already active.

But a true, "intelligent access" has to provide to you information you need, or tailored for you: nowadays, thank to information available *e.g.* on social networks, particular interests of any visitor can be saved and considered. Not only "where you are" is important, but also "who and how you are", because in the information sea you should find what you are really interested to know. Of course, this goal requires a great work on ontologies that have to cross with "social" data, very heterogeneous: each user has the right to receive "his ownr" information output.

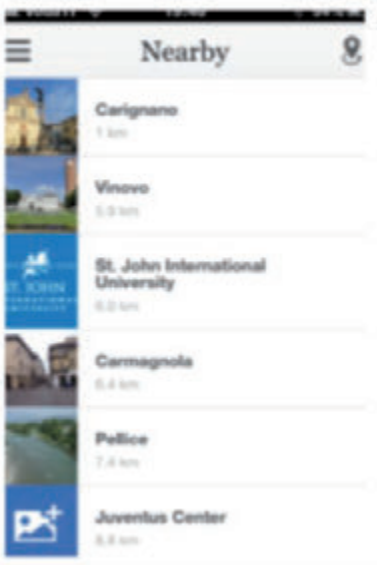

Figure 4. The Nearby feature on iPhone device.

References

Agarwal, J., Sharma, N., Kumar, P., Parshav, V., Srivastava, A., Goudar, R.H.: *Intelligent search in E-Tourism services using Recommendation System: Perfect guide for tourist* (2013) 7th International Conference on Intelligent Systems and Control, ISCO 2013, art. no. 6481190, pp. 410-415.

Antinucci, F.: *Musei virtuali: come non fare innovazione tecnologica* (2007), Roma-Bari Laterza

Barabé, A.: *Evaluation of virtual learning environments : Analysis of an experimental activity related to training in sustainable tourism* [Évaluation des environnements d'apprentissage virtuels : Analyse d'une expérimentation reliée à la formation en tourisme durable] (2003) Loisir et Societe, 26 (1), pp. 211-233+9.

Caraceni, S.: *Musei virtuali-Augmented heritage. Evoluzioni e classificazione delle tipologie di virtualità in alcuni case histories,* (2012), Rimini Guaraldi

Chase-Levenson, A.: *Annihilating time and space: Eclecticism and virtual tourism at the Sydenham Crystal Palace* (2012) Nineteenth-Century Contexts, 34 (5), pp. 461-475.

Cheong, R.: *The virtual threat to travel and tourism* (1995) Tourism Management, 16 (6), pp. 417-422.

Chiabrando, R.; Fabrizio, E.; Garnero, G.: *On the applicability of the visual impact assessment OAISPP tool to photovoltaic plants*, Renewable and Sustainable Energy Reviews (ISSN:1364-0321) , pp. 845- 850, Vol. 15 (2011)

Cozzi, P.: *Turismo e Web. Marketing e comunicazione tra mondo reale e virtuale,* Milano, Franco Angeli (2010)

Davenport, E.: *Localisation, globalisation and SMEs in European tourism: The 'virtual enterprise' model of intervention* (2000) Proceedings of the ASIS Annual Meeting, 37, pp. 309-318.

Dong, H.: *Review on the websites and virtual tourism of World Heritage sites in China* (2010) 2nd International Conference on Information Science and Engineering, ICISE2010 - Proceedings, art. no. 5691830, pp. 6112-6114.

Ferrante, F.; Garnero, G.: *Tecnologie e dati spaziali per una moderna governance del territorio. Strumenti a supporto della riforma del Catasto* (Technologies and spatial data for modern land governance. Tools to support the cadastral reform.), Territorio Italia - Governo del Territorio, Catasto, Mercato immobiliare, n. 01/2013, p. 9-26 (Italian and English version)

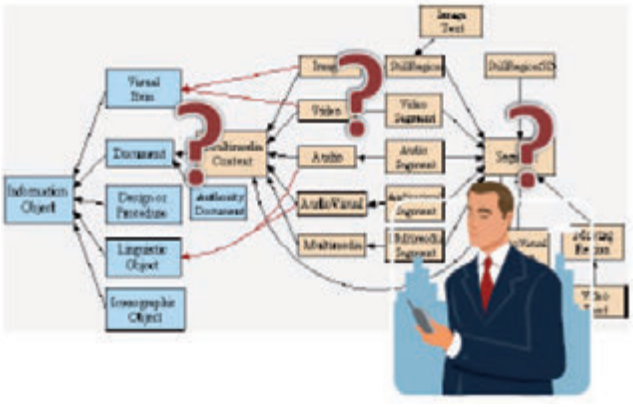

Figure 5. Ontologic interrogation of geographic and thematic DB.

Gale, T.: *Urban beaches, virtual worlds and 'the end of tourism'* (2009) Mobilities, 4 (1), pp. 119-138.

Garnero, G.; Corrias, A.; Manigas, L.; Zedda, S.V.: VGI, *Augmented Reality and Smart Web Application: Projects of Development in the Territory of the Sardinia Region*, in B. Murgante et al. (Eds.): ICCSA 2013, Part IV, LNCS 7974, pp. 77—92. Springer, Heidelberg (2013)

Gärtner, M., Seidel, I., Froschauer, J., Berger, H.: *The formation of virtual organizations by means of electronic institutions in a 3D e-Tourism environment* (2010) Information Sciences, 180 (17), pp. 3157-3169.

Germann Molz J.; Gibson S.: *Mobilizing Hospitality,* Farnham, Ashgate (2007)

Gerosa, M.; Milano, R.: *Viaggi in rete. Dal nuovo marketing turistico ai viaggi nei mondi virtuali* (2011), Milano FrancoAngeli

Godone, D.; Garnero G.: *The role of morphometric parameters in Digital Terrain Models interpolation accuracy: a case study*, European Journal of Remote Sensing, (ISSN:2279-7254) 46: 198-214 [doi: 10.5721/EuJRS20134611] (2013)

Granieri G.; Perri G.: *Linguaggi digitali per il turismo,* Milano, Apogeo (2009)

Gretzel U.; Law R.; Fuchs M.: *Information and Communication Technologies in Tourism 2010,* Wien-New York, Springer (2010)

Hashim, K.H.B.: Jusof, M.J.B., *Spherical high dynamic range virtual reality for virtual tourism: Kellie's Castle, Malaysia* (2010) 2010 16th International Conference on Virtual Systems and Multimedia, VSMM 2010, art. no. 5665945, pp. 297-300.

Hernández, L.A., Taibo, J., Seoane, A.J.: *Immersive video for virtual tourism* (2001) Proceedings of SPIE - The International Society for Optical Engineering, 4520, pp. 63-73.

Hopeniene, R., Railiene, G., Kazlauskiene, E.: *Potential of virtual organizing of tourism business system actors* [Turizmo verslo sistemos dalyviu{ogonek} virtualaus organizavimosi potencialas] (2009) Engineering Economics, 3 (63), pp. 75-85.

Hsu, C.: *The feasibility of Augmented Reality on virtual tourism website* (2011) Proceedings - 4th International Conference on Ubi-Media Computing, U-Media 2011, art. no. 5992081, pp. 253-256.

Hu, Z., Cao, Z., Shi, J.: *Research of interactive product design for virtual tourism* (2012) Lecture Notes in Electrical Engineering, 140 LNEE, pp. 411-416

Hyun, M.Y., Lee, S., Hu, C.: *Mobile-mediated virtual experience in tourism: Concept, typology and applications* (2009) Journal of Vacation Marketing, 15 (2), pp. 149-164

INSPIRE Directive Of the European Parliament and of the Council of 14 March 2007 establishing an Infrastructure for Spatial Information in the European Community - Directive 2007/2/EC (2007)

Kapp K. M.: *The Gamification of Learning and Instruction: Game-based Methods and Strategies for Training and Education.* John Wiley & Sons (2012)

Kim, L.C., Lam, T.K., Talib, A.Z.: *Acoustical heritage for virtual tourism on mobile platform* (2011) Proceeding of the International Conference on e-Education Entertainment and e-Management, ICEEE 2011, art. no. 6137804, pp. 273-276.

Kuntarto, G.P., Gunawan, D.: *Dwipa search engine: When E-tourism meets the semantic web* (2012) 2012 International Conference on Advanced Computer Science and Information Systems, ICACSIS 2012 - Proceedings, art. no. 6468741, pp. 155-160.

Maymand, M.M., Farsijani, H., Tahery Moosavi, S.S.: *Investigation of the key success factors in virtual tourism,* (2012) Indian Journal of Science and Technology, 5 (7), pp. 3073-3080.

Minucciani, V.; Garnero, G.: *Available and Implementable Technologies for Virtual Tourism: A Prototypal Station Project*, in B. Murgante et al. (Eds.): ICCSA 2013, Part IV, LNCS 7974, pp. 193-204. Springer, Heidelberg (2013)

Minucciani, V.: *Pensare il museo. Dai fondamenti teorici agli strumenti tecnici.* p. 1-199, Rivoli (TO):CET - Casa Editrice Torinese, ISBN: 9788896470060 (2012)

Minucciani, V.: *Musei e tecnologie virtuali*, Tafter Journal, ISSN: 1974-563X (2009a)

Minucciani, V.: *Artifici tecnologici al servizio della narrazione archeologica*. In: Celada, G.; Gentilini, C.; Martinelli, C.: *Palestrina. La città e il tempio*. p. 199-211, Maggioli, ISBN: 9788838743382 (2009b)

Minucciani, V.: *Il museo fuori dal museo*, ISBN 9788882230739, Milano, Lybra Immagine (2005)

Pelagatti et al.: *SpatialDBgroup Weblink* to a page about IDT http://spatialdbgroup.polimi.it/visione/ (year not specified)

Pirotti, F., Grigolato, S., Lingua, E., Sitzia, T., Tarolli, P.: *Laser scanner applications in forest and environmental sciences*, Italian Journal of Remote Sensing / Rivista Italiana di Telerilevamento, 44 (1), pp. 109-123 (2012)

Pirotti, F., Guarnieri, A., Vettore, A.: Collaborative Web-GIS Design: A Case Study for Road Risk Analysis and Monitoring, (2011) Transactions in GIS, 15 (2), pp. 213-226.

Poulot, D.: *Musée et muséologie* (2005), Paris La Découverte

Proctor, N.: *Digital Museums as Platform, Curator as Champion, in the Age of Social Media*, Curator (2010)

Roberta, K.V., Wisudawati, L.M., Razi, M., Agushinta R., D.:*Web based virtual agent for tourism guide in Indonesia* (2011) Communications in Computer and Information Science, 191 CCIS (PART 2), pp. 146-153.

Vaudetti, M.; Minucciani, V.; Canepa, S. (a cura di): *The Archaeological Musealization Multidisciplinary Intervention in Archaeological Sites for the Conservation*, Communication and Culture, p. 9-280, Torino, Allemandi & C., ISBN: 9788842221203 (2012)

Vince, J.A.: *Introduction to Virtual Reality* (2004), London Berlin Heidelberg, Springer-Verlag

Wang, F.-X.: *Design and implementation of Hainan tourism spots virtual reality system* (2011a) Key Engineering Materials, 474-476, pp. 2217-2220

Wang, C.: *Application of virtual reality technology in digital tourism* (2011b) Proceedings - 3rd International Conference on Multimedia Information Networking and Security, MINES 2011, art. no. 6103831, pp. 537-541.

Williams, P., Hobson, J.P.: *Virtual reality and tourism: fact or fantasy?* (1995) Tourism Management, 16 (6), pp. 423-427.

Zhang, Y., Zhang, X.: *An integrated application of tourism planning based on virtual reality technology and indicator assessment* (2012) Lecture Notes in Electrical Engineering, 107 LNEE, pp. 1435-1442.

Production of renewable energy in agriculture: current situation and future developments

Carlo Pirazzoli, Alessandro Ragazzoni

Department of Agricultural Sciences, University of Bologna, Bologna, Italy

Introduction

In recent years there has been growing interest in the development of renewable energy due to the need to solve problems related to the increase in energy consumption and the instability of prices for raw materials of fossil origin, and because of concerns about pollution and the effects on climate change. In order to solve these problems there have been extensive studies to research systems and processes capable of limiting the increase in "greenhouse" and so-called "climate changing" gases and, at the same time, to make countries increasingly independent from the energy point of view.

In Italy, similar considerations have taken on a special significance, precisely because of the increasing dependence on foreign energy (equal to over 83% in 2009) (For further details see "Rapporto energia e ambiente: analisi e scenari 2009 (Energy and Environment Report: Analysis and Scenarios 2009)" ENEA 2010), the cost of energy and emissions harmful to the climate, all running counter to the objectives laid down at international level on the subject of global warming.

To try to tackle these issues, there has been an increase in the need to promote efficient long-term energy planning and to provide adequate public incentives for technological innovation and research in the context of saving and improving energy efficiency and technical alternatives to the consumption of fossil fuels.

In particular, the ongoing climate change will require a greater commitment to take all possible measures to reach conditions of equilibrium and overall efficiency in the production and use of energy according to models of sustainability.

Faced with this scenario, the agricultural sector can also play an important role in contributing to increased production of energy from renewable sources. Climate-related problems are directing agriculture towards new challenges and new opportunities, specifically in relation to local presence that characterizes the strategic activities of the sector.

In addition, agriculture can contribute, also directly, to reducing net emissions of carbon dioxide (CO_2) and other greenhouse gases, both through the exploitation of various types of biomass for energy purposes, to be used as a substitute for fossil fuels, and through the adoption of agricultural practices that favour the accumulation of carbon in cultivated plants and the soil.

Indeed, the ability of plants to trap solar energy, converting and storing it permanently in the form of chemical energy is well known, as well as their ability to capture carbon dioxide from the atmosphere, retaining the carbon and emitting oxygen. Remember that in 1.0 g of dry matter there is about 0.5 g C which is obtained from 1.83 g of fixed atmospheric CO2 (D. Coiante, 2010).

Therefore, the role of agriculture in the field of energy is part of a wider framework of services that can it can provide to the community, integrating the concept of multifunctionality that has been attributed to it. Without forgetting that agricultural activity represents an excellent opportunity to protect and enhance the territory, the production of agro-energy could become an opportunity for farmers, who would find new outlets, not only for their crops, but also for by-products and agro-livestock waste/slurry.

In this regard it is noted that, in order to meet obligations under the Kyoto Protocol, as well as the latest EU energy plan, decisive action must be taken to expand the contribution of alternative sources to current overall energy needs with promotional actions aimed at taking advantage of all the opportunities that they offer. In fact, people are aware that there cannot be a single rapid replacement of existing energy resources with other more sustainable ones, and that the possible complementarity of new renewable energy sources (RES) must be studied in relation to the vocation of the territory in which its development is to be planned.

Agro-energy production chains

From the foregoing it can be said that energy production represents an important opportunity for farmers to diversify their business, broadening the prospects and scenarios for the agricultural and livestock farms.

The energy potential of a rural area through the use of biomass produced in by agricultural activity will now investigated in depth: we will therefore describe the agro-energy production chains using biomass specifically, while ignoring other technologies (primarily photovoltaic and solar thermal) that can be developed, even with a profit, by the farmer, but which are not directly related to the traditional activity of a farm.

Raw materials of agricultural origin can be destined mainly for the production of electricity, heat or biofuels depending on the intrinsic characteristics, following a variety of transformation processes. As shown in Figure 1 the main energy production chains that can be activated in a farm are as follows:

- Chain for production of solid biofuels (thermo-chemical conversion process);
- Chain for production of biofuels (physical-chemical conversion process);
- Chain for production of Biogas (biological conversion process).

Correspondence: Carlo Pirazzoli, Department of Agricultural Sciences - University of Bologna, Italy. E-mail: carlo.pirazzoli@unibo.it

Journal of Agricultural Engineering 2013; XLIV(s1):e101
doi:10.4081/jae.2013.(s1):e101

Solid biofuel production chain

The activation of this chain is linked to certain physical and chemical characteristics of biomass. In particular, this raw material must have a relationship between carbon and nitrogen content (C/N ratio) with values greater than 30 (lignocellulosic biomass) and a low moisture content (less than 30% on a wet basis). The following raw materials are suitable for these specifications:

- crops dedicated to the production of solid biofuels, such as pluriennial tree species a with short rotation (Short Rotation Forestry - SRF), including trees such as poplar, eucalyptus, acacia and willow;
- perennial herbaceous crops, such as the common reed, miscanthus and thistle;
- annual herbaceous crops, including fibre sorghum, kenaf and hemp;
- wood processing waste in the industrial sector;
- felling and pruning in the urban sector;
- copse, high forest, waste products from the use of high forests and intermediate cutting in the forestry sector;
- woody component of Municipal Solid Waste (MSW).

In the case of using dedicated crops, we remind you that, for the economic sustainability of the supply chain, the production of this biomass must be low-input (fertilizers, chemical defence products, mechanical energy, etc.) and using simplified cultivation models; the rapid development and the hardiness of these plant species usually do not justify intensive cultivation methods. The most important stage is harvesting, which must be carried out so as to obtain a low humidity product (less than 30% on a wet basis) and must be logistically well organized, in order to contain costs. Plant biomass for combustion has low energy density. Harvesting of wood chips, shredded sorghum, cane etc. provides a product with very low specific weight, with values of 0.35 - 0.5 t/m^3. A unit of volume of the harvested product is composed, therefore, of more than 50% air. The remaining organic portion is composed of at least 50% of water, for which the cost of transportation per unit of dry matter becomes very high. Furthermore, the low specific weight of the product does not allow maximum capacity of lorries to be reached, increasing the amount of transport necessary per unit of area.

Lignocellulosic biomass intended for direct combustion for the production of heat, before being placed on the market, generally undergoes a more or less complex process of transformation to impart the necessary physical and energy characteristics. The main commercial forms for this category of biomass are:

- firewood (blocks or logs),
- wood chips,
- pellets and briquettes.

Direct combustion exclusively for generation of thermal energy is performed in thermal boilers available on the market with multiple technical solutions (reverse flame boilers, boilers with fixed or mobile grid, boilers with automated loading).

The heat produced may also be used for heating the water circulating in a circuit of pipes. In this way it is possible to heat various environments (up to entire buildings, depending on the size of the plant) using a single boiler. Waste heat recovery significantly improves the energy balance of the system.

It is also possible to produce electricity by expanding steam in a turbine. In this way it is possible to convert thermal energy into electrical energy with an efficiency of 15-38%. Also for this type of energy production there are different technologies that can recover heat from the entire volume of steam produced (backpressure systems) or only from a fraction of the steam (condensing and bleeding systems).

Direct combustion results in technology that is a quite widespread despite its low energy yields, production of potentially hazardous fumes due to the presence of carbon monoxide (CO), oxides of sulphur and nitrogen (SO_x and NO_x), as well as problems regarding management of the ashes. Gasification and pyrolysis have an efficiency that is 30-35% greater than combustion, but the complex technology and difficult purification of the gas produced have greatly limited the spread of these types of systems.

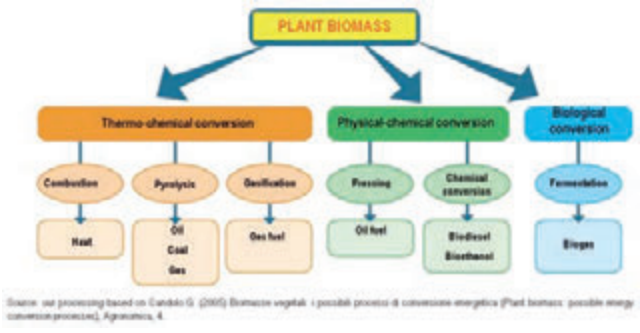

Figure 1. Energy production chains using agro-livestock biomass.

A Ministerial Decree was recently was recently released on thermal energy and energy efficiency (Ministerial Decree 28 December 2012) favouring families and public administrations. In particular, this incentive covers at least 40% of the investment and will be provided over two years *(*five for more costly operationsi).

This measure is an essential step in order to achieve and exceed the European environmental targets for 2020, especially with regard to the quota of thermal energy, for which Italy is still very deficient.

The decree, in fact, sets itself the dual purpose of boosting the production of thermal energy from renewable sources (biomass heating, heat pumps, thermal solar) and accelerating projects for upgrading the energy efficiency of public buildings.

On renewable thermal sources, the new incentive system will promote small scale interventions, typically for domestic and small business use, including greenhouses, which until now have not been encouraged by supporting policies. In this study, it was decided not to investigate this sector any further because:

- the legislation is very recent and still poorly implemented;
- the business reference framework adopted refers to medium-large scale operations and the amount of biomass produced is significant, and would therefore require the possibility of installing greater power.

Biofuel production chain

The physical-chemical conversion of biomass into biofuels requires the prevalent use of dedicated crops (and to a lesser extent of agro-industrial waste) for the production of fuels intended to replace, at least in part, petrol and diesel derived from oil. Despite the many benefits resulting from the use of these biofuels (use of renewable raw material, less dependence on fossil fuels etc.), this energy sector has had limited development in Italy because of very high production unit costs, which prevent biodiesel and bioethanol from competing with fossil fuel. Also, to make matters worse, large expanses of arable land would need to be found in order to meet the current demand for fuel, resulting in radical changes in the traditional destination of food crops. For these reasons, much of public opinion has strongly criticized the development of this technology, which now seems limited exclusively to the presence of a specific financial incentive and a production quota exempt from public excise duty.

The chain in question is classified according to the end product of the physical-chemical conversion of the biomass, namely:

- pure vegetable oils;
- biodiesel;
- bioethanol.

The term pure vegetable oils refers to crude or refined oils produced from oilseeds by pressing or extraction, but not modified from a chemical point of view. Their properties as liquid biofuels, intended for direct combustion in place of diesel fuel, depend on the dedicated crop used. The main oil producing species grown in Italy are sunflower, canola and soybeans, while globally the majority of oil production comes from the palm.

Biodiesel is a liquid fuel, consisting of a mixture of methyl esters, obtained through the trans-esterification (Transesterification is a chemical reaction in which the alcohol group of an ester is replaced by that of another alcohol) of vegetable oils or other raw materials rich in lipids. This biofuel is suitable for replacing fuel in the Diesel cycle engines widely used in the transport sector. In conventional diesel engines, however, it must be mixed with diesel fuel up to a maximum of 30% in volume. Use it in pure form, on the other hand, requires specific technology.

The crops used in the supply chain of biodiesel are the same as those for pure vegetable oils, but animal fats of agro-industrial origin can be used as an alternative, as can cultivations of single-cell eukaryotic algae and/or prokaryotic cyanobacteria, which have a high lipid content, approximately 80% dry matter. The use of the latter type of raw material is still quite experimental, but presents numerous advantages dictated by the speed of growth of the algae and the yield per surface area much higher than traditional crops.

Finally, bioethanol is a liquid biofuel, obtained from the alcoholic fermentation of biomass (plant-based where dedicated crops are used and agri-forestry or animal residues in the case of animal manure) and/or the degradable part of waste (FORSU - agro-industrial residues) and is suitable for replacing petrol in the transport sector.

The main Italian alcohol producing crops that can be used for the production of bioethanol are sugar beet and sorghum due to the high content of simple sugars in the roots and stalks, and maize and wheat for the abundant presence of starch in the grains. In the international arena, however, the production of bioethanol derives primarily from sugar cane.

In conclusion, it can be argued that it is difficult to achieve an organized chain in Italy that would allow biofuels to be produced from domestic raw material: the goal of reaching at least 10% of transport consumption is almost impossible and the multinational oil companies currently find it more economically viable to import finished or semi-finished products from other countries where the availability of dedicated crops is greater and industrial processing has been established for some time (primarily, South America and Eastern European countries).

Biogas production chain

The term biogas refers to a mixture of gases, consisting primarily of methane (50-80%), obtained from the anaerobic fermentation of biomass of plant and animal origin.

This process occurs is performed by microorganisms capable of metabolizing the organic substance with consequent production of gas. Compared to the previously described production chains, that of biogas involves the development of active microorganisms, for which reason it is essential to achieve living conditions optimal for them, and to maintain over time.

The raw materials involved in the biological conversion process are as follows:

- Energy crops: such crops, referred to as "*dedicated*" to energy conversion, are essentially maize, sorghum, triticum, wheat, rye, etc. These are materials with high dry matter content and a high yield in biogas.
- Manure: this biomass has particular importance in the biogas production process because it waste that can be exploited, and it also involves a large amount of micro-organisms which act as inoculum in the transformation of the substrate into biogas. Effluents do not normally have high yields, also due to the small proportion of organic matter (<10% of total).
- Crop residues: these refer to residues from agricultural production such as maize stalks, straw, fruit waste, etc.. It is a material with a good biogas yield, but with variable characteristics that require specific analysis.
- Agro-industrial by-products: this is organic waste matter that is commonly produced in the processing of food products. In particular, it includes slaughter waste, residues from the production of juices, molasses, whey, and so on. These substrates have a high potential, but may be subject to seasonal availability or specific authorizations (such as slaughterhouse waste) (The use of slaughterhouse waste for energy purposes is regulated by specific permits issued by the Veterinary Service on the basis of EC Regulation 1774/2002).
- Organic fraction of municipal solid waste: this category includes numerous materials, difficult to classify and usable only on the basis of the directives on "waste".

Regarding the technology used, the main distinctions concern the total solid content in the biomass used and the temperature of the process (Navarotto, 2010). Digestion, therefore, can be defined as "wet", if the substrate has a total solid content less than 10% and "dry" if the percentage is greater than 20%. In the first case, the material used can be mixable and pumpable, while in the second case, the substrate is not mixable and special techniques are required for loading the plant (For further detials see: Ragazzoni A. (2011), *BIOGAS – Normative e biomasse: le condizioni per fare reddito*, Edizioni L'Informatore Agrario, Verona). As regards the process temperatures, fermentation can be mesophilic, when the temperatures are kept between 38 and 40°C, thermophilic (between 55 and 57°C) or in psychrophilic (below 35°C, but this is uncommon). For each temperature different families of microorganisms develop and suitable for carrying out the digestion process.

Typically a wet digestion biogas plant with mesophilic operation, consists of one or more fermentation tanks made of steel or reinforced concrete equipped with an internal heating system, a biomass mixing system and a gasometric covering capable of accumulating the biogas produced. A system of pipes delivers the gas to a purification complex, normally a chiller (or refrigerator) with a heat exchanger, for the elimination of the water vapour, and subsequently to an internal combustion engine for the production of electricity. The motors used are able to recover the thermal energy deriving from the cooling system in order to heat the fermentation tanks and possibly other production premises or dwellings; in this case, the process is referred to as cogeneration.

The end product of the anaerobic digestion process is the digestate, which takes the form of stabilized organic matter (generally odourless) with organic and chemical characteristics derived from the substrate used as input to the system.

The production of biogas is currently of great interest to the agricultural sector. The ability to use different organic substrates, the characteristics of the digestate (suitable as a soil conditioner and fertilizer) and the current incentive system, make this type of chain one of the most widespread agro-energy technologies in the country.

Faced with a proven technology, the main problems with this energy chain are to be found in the procurement of the biomass, costs for transport and management of the biomass and digestate and in the regulatory framework which is often difficult to interpret at the local level.

As mentioned, the current incentive rate of 0.28 euro/kWh of electricity fed into the grid (valid for plants built and in operation by 31/12/2012) has enabled the activation of large-scale power plants, also in those cases where it was difficult to procure supplies of the biomass necessary for the process, where most of it was purchased on the market and not produced directly on the farm. In these cases, the economic vulnerability of the plants increases, since their sustainability depends economic parameters, which are unlikely to remain stable over time (rental cost of land, cost of the substrates on the market, costs for disposal of the digestate etc.), which must be considered to be at least 15 years, based on the limits for issuing incentive grants. On the basis of these considerations, and with the current reduction in the comprehensive rate, increasing attention has been focussed on the exploitation of waste raw materials to feed the digesters, and to size these according to the actual availability of substrates.

The biogas chain will be examined in more detail below, which has in recent years acquired an important role in rural areas, especially in relation to the significant growth in the number of plants constructed (Figure 2).

Reference standards

The production of energy from biogas is subject to a complex legislative framework that is not always easy to interpret. This chapter summarizes the main aspects that regulate this energy chain, with reference to the legislation that authorizes and incentivises plants at national level (Figure 3); in particular, the examination looks at::

- authorization procedure;
- tax issues relating to the activity of energy production;
- agrifood by-products;
- incentives for the production of renewable electricity (with particular reference to the Ministerial Decree of 6 July 2012).

Plant authorization procedure

The guidelines for authorization to construct and operate plants producing electricity from renewable sources were published in the Official Journal of 18 September, 2010 and inserted definitively in Legislative Decree no. 28 (Legislative Decree no. 28 of 3 March, 2011 Implementation of Directive 2009/28/EC on the promotion of energy from renewable sources, amending and subsequently repealing Directives 2001/77/EC and 2003/30/EC) of 3 March, 2011, which implements the basic Directive 2009/28/EC (Directive 2009/28/EC of the European Parliament and of the Council of 23 April 2009 on the promotion of energy from renewable sources and amending and subsequently repealing Directives 2001/77/EC and 2003/30/EC (Official Journal of the European Union 05/06/2009)) on the promotion of renewable energy. The authorization process, followed by all the Italian Regions, provides the following reference framework:

a. systems considered as freely constructed and subject to simple communication: in the case of installed electrical power <50 kW in a cogeneration scenario, or <200 kW if the property structure of the buildings is not changed;
b. plants that can be constructed through a simplified enabling procedure when the installed electrical power is <250 kW, or <1 MW in the case of cogeneration with heat recovery;
c. installations subject to a single authorization in all other cases.

Plants are, therefore, classified according to the installed power and cogeneration capacity, but the innovation in the Legislative Decree concerns the simplification of procedures introduced in an attempt to speed up the authorization process.

Taxation of energy production

An important element for the economic evaluation the activity in question is the incidence of the tax burden. Art. 1 para. 369 of the 2007 Finance Act (Law no. 296/06) states that «*(…) the production and sale of electric and heating power from renewable agroforestry sources (...) constitute related activities pursuant to Article 2135, third paragraph, of the Italian Civil Code and are considered as producing agricultural income*». In this case, they involve taxation on a cadastral basis of limited importance for the balance sheet of the agro-energy business. The concept of related activity is linked to the principle of prevalence (The principle can be satisfied according to the quantitative requirements (products used in performing related activities obtained from agricultural activity on the farm are prevalent compared to those purchased from third parties) or value (the value of the products obtained from agricultural activity is higher than the cost incurred to purchase third-party products). If neither of the two parameters can be adopted, as in the case of animal slurry, prevalence can be detected by a comparison

Figure 2. Dynamics of the construction of biogas plants in Italy.

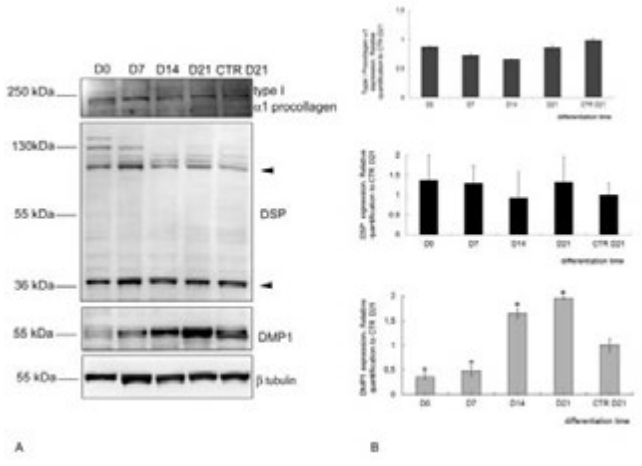

Figure 3.- Key regulatory elements for designing a biogas plant.

between the energy deriving from its own products and that derived from products purchased from third parties), according to which products must derive *primarily* from the main activities or from the use of equipment and/or resources normally used in the business. This taxation on plants has also been maintained in the latest regulatory references for projects that will require authorisation after 31/12/2012.

By-products of organic and agro-livestock origin

Regarding the raw material that can be used for the production of biogas, some recent regulatory specifications have attempted to provide greater clarity. In particular, these include Ministerial Decree no. 205 of 3 December, 2010 and Legislative Decree No. 28 of 3 March 2011 that have better defined the applicability of Legislative Decree no. 4 of 16 January, 2008 on the "definition of by-product".

In essence, the new interpretation amends Part IV of Legislative Decree no. 152/2006 (Environmental Regulations), in Article 183, paragraph 1, letter qq) and defines a by-product, and not waste (pursuant to Article 183, paragraph 1, letter a) as any substance or object that satisfies the conditions and criteria specified by Article 184-bis, paragraphs 1 and 2:

a) the substance or the object originated from a production process, of which it forms an integral part, and the primary purpose of which is not the production of such a substance or object;
b) it is certain that the substance or object will be used, during the same or a subsequent production or use process, by the manufacturer or by a third party;
c) the substance or object can be used directly without any further processing other than normal industrial practice;
d) further use is lawful, in other words, the substance or object fulfils, for the specific use, all the relevant requirements regarding the products and the protection of health and the environment and will not lead to overall adverse impacts on the environment or human health.

The new draft, therefore, of the aforementioned Article 183 states that: «*…by-products include (…): faecal and plant material from cuttings and pruning as part of the maintenance of public and private green areas, or from agricultural activities, which are used in agricultural activities, even outside the place of production, or sold to third parties or used for company inter-corporate plants for the production of energy or heat, or biogas…*».

The digestate obtained from third party manure will retain the possibility for agronomic use integrally, because it derives from by-products and not from waste, naturally always in compliance with the obligations under the Nitrates Directive (Council Directive 91/676/EEC of 12 December 1991 concerning the protection of waters against pollution caused by nitrates from agricultural sources, implemented by the DM 7 April 2006).

Table 1. Basic incentive rates for 2013 and premiums established by the Decree.

BASE INCENTIVE			ADDITIONAL PREMIUMS			
Type of diet used	Power	Base incentive rate 2013 for 20 years	Cogenerator high performance (Art.8 para.3)	High performance cogenerator with nitrogen recovery > 80% to produce fertilizers (Art.26 para.1 and 2)(*)	High performance cogenerator with 20% nitrogen recovery to produce fertilizers (Art.26 para.3a) (*)	Removal of 40% nitrogen, also out in cogeneration (Art.26 para.3b) (*)
	kW	euro/kWh	euro/kWh	euro/kWh	euro/kWh	euro/kWh
Products of biological origin	1<P≤300	0.180	0.040	0.030	0.020	0.015
	301<P≤600	0.160	0.040	0.030	0.020	0.015
	600<P≤1,000	0.140	0.040	0.030	—	—
	1,000<P≤5,000	0.104	0.040	0.030	—	—
	P>5,000	0.091	0.040	0.030	—	—
By-products of biological origin (**)	1<P≤300	0.236	0.010	0.030	0.020	0.015
	301<P≤600	0.206	0.010	0.030	0.020	0.015
	600<P≤1,000	0.172	0.010	0.030	—	—
	1,000<P≤5,000	0.125	0.010	0.030	—	—
	P>5,000	0.101	0.010	0.030	—	—

(*) Premiums cannot be combined with each other (**) The by-products of biological origin are shown in detail in Table 1 attached to the Ministerial Decree of 6 July 2012

Source: our calculations based on Mis Decree

Incentives and tariffs for energy production activity

Crucial elements among the decisive factors for the activation of a plant are the value and duration of financial incentives for the production of energy produced and sold to the network operator. This paragraph describes the procedures that apply the provisions of Ministerial Decree 6 July 2012: *"Implementation of Art. 24 of the Legislative Decree no. 28 of 3 March, 2011 establishing incentives for the production of electricity by plants using renewable sources other than photovoltaic".*

The new incentive system for the production of electricity from renewable sources, as well as providing a mechanism for gradual reduction of the incentive level (Art. 7 comma 1 (*…) for plants that come into operation in the years after 2013, the value of base incentive tariffs is reduced by 2% per year, with commercial rounding to three decimal places (…))*, is also characterized by the introduction of a maximum annual funding quota (5.8 billion euro per year) and the available power of incentivised energy (The definition of these quotas has the function of protecting consumers and users by limiting increases in costs on electricity bills, the proceeds of which finance the promotion of renewable energy) (Table 1). The Decree provides for two types of incentives:

- a comprehensive incentive tariff (To) for plants with power <1 MW;
- an incentive (I) for plants with power > 1 MW and for those with power not exceeding 1 MW that do not opt for the all-inclusive rate, calculated as the difference between a fixed value (total revenue) and the time zone price of the energy (referring to the zone where the electricity produced by the plant it is fed into the grid).

As regards the biomass used, the classes of incentives indicate a desire to reward projects that use, above all, agri-livestock and agro-industrial by-products as substrates, as well as the organic fraction of the waste (in a non-agricultural context), compared to plants designed for the use of "products" (as defined by the regulations) and, therefore, of crops dedicated to energy conversion (specifically, for example, grain silage). In this way, process waste matrices will be better exploited, while it is conceivable that projects related to the exclusive or priority use of dedicated crops will decrease.

As mentioned previously, the other distinguishing feature introduced with the new Decree, is the "size" of the system, understood as the installed electrical power. Five classes have been identified to which different tariffs are applied for the electricity produced and provided. The most important classes for the agricultural refer to power plants included in the category: 1 ≤ 300 kW, those in the range 300 ≤ 600 kW and thirdly, 600 ≤ 1,000 kW.

The most important classes for the agricultural refer to power plants included in the category: 1 ≤ 300 kW, those in the range 300 ≤ 600 kW and thirdly, 600 ≤ 1,000 kW. The introduction of so-called "bonuses" for cogeneration, for the removal of nitrogen and for the containment of emissions, as well as achieving desirable targets for energy and environmental efficiency, also contribute to a further selection criterion for plants, based on the profitability that can potentially be obtained by integrating the various processes. This mechanism seems respond more to business figures who make investments within a complementary framework with local resources and with the need to protect the territory, in reality limiting the spread of initiatives that may, however, be considered as unsustainable (such as high power biogas plants pow-

ered exclusively by maize and concentrated in small areas).

The duration of the new incentives, as defined in Annex 1 of the Decree, is extended to 20 years (compared with the 15-year period up to 2012), in order to provide greater guarantees of stability of profits for the entrepreneur and a longer life time for the plant, so that it will not require final decommissioning after the end of the incentives, but will be allowed to continue operating.

Lastly, the Decree, finally, defines three different modes of access to the incentive mechanisms, depending on the power, which for biogas plants (new, fully rebuilt, re-activated, undergoing renovation or upgrading) are:

- direct access in the case of plants with power <100 kW
- entry in Registers in the case of plants between 100 kW and <5,000 kW;
- competitive downward auction procedures, if the power is > 5,000 kW.

Assessments on the economic sustainability of biogas production plants.

The analysis of the cost-effectiveness of an anaerobic digestion plant for the production of biogas for energy purposes includes certain important decisions that the entrepreneur must face in the design phase: which organic matrices to use for the operation of the digester? What economic advantage can be gained in choosing one "diet" over another? What is the optimum power of the plant?

The uncertainty surrounding the answers and the risk involved in the management decisions of the entrepreneur are not easily solved since there is no single analytical model that can be transferred to all rural contexts and to all businesses. However, we must start from certain basic assumptions: first, that the agro-energy chain must be sustainable from the environmental, territorial and economic point of view. For this purpose, the regulations that are periodically updated and approved at Community, national and local levels must be carefully observed.

The main objective is to chart an analytical path for assessing the economic viability of producing energy from biogas by identifying the elements that the agricultural entrepreneur needs to consider in the decision-making process, especially in light of the new incentive rates promoted by the Ministerial Decree of 6 July, 2012.

To this end, we have identified and explored some useful elements for business choices, which we believe to represent fundamental "nodes" for the approach of the entrepreneur designing a plant for the production of biogas and electricity.

Elements for the evaluation of a plant for the production of biogas

The analysis of the cost-effectiveness of an anaerobic digestion plant for the production of biogas and thermal and electrical energy is detailed and complex. The importance must be stressed of all the stages that characterize the supply chain: from the production of biomass, to transportation, construction and operation of the plant, the production and sale of electricity and thermal energy, and up to the management and transport of the final digestate.

In addition, new regulatory proposals relating to the value of the incentives as regards the all-inclusive tariff outline the analytical path that will be followed. In particular, the distinction of the rates on the basis of "power" and "diet" requires the valuation model to be set up distinguishing projects by the two categories of biomass that are of most relevance to agricultural enterprises (products or by-products of biological origin) and for two power ranges (from 1 kW to 300 kW, and from 301 kW to 999 kW). Therefore, attention will be focused on the four categories of plant resulting from crossing these two variables.

The goal is to verify how costs are distributed by enterprise and, consequently, to outline an economic-profitability framework applicable to different businesses in the biogas sector, according to new specifications for incentive rates. To grasp more clearly the significance of the results obtained from the calculations, it is necessary to specify the basic assumptions used, remembering that the indicators will be expressed in euro/kWh of electricity produced and sold:

1) the dynamics of growth of installed power is included in the range between 100 kW and 999 kW;
2) the crop cost of the biomass from dedicated crops is estimated at around 1,750 euro/ha (based on direct surveys in areas of the Po Valley). To calculate the impact of the spending per unit of electricity produced we adopted the following parameters:
   - average energy yield of biomass: 333 kWh/ton;
   - average yield of maize silage: 55 ton/hectare.

   Therefore, the cost is equal to:

   1,750 (euro/ha) / (55 ton/ha • 333 kWh/ton) = 0.096 euro/kWh
3) the cost of cultivation of biomass was increased in the case where conditions of business self-sufficiency do not exits; it is therefore assume that external land will be obtained with rental agreements to achieve some positive effects on the operation of the plant: the first is to limit external purchasing of biomass, which is certainly subject to the volatility of grain prices; the second is at the same time to meet the minimum requirement necessary so that energy production will be classed as a related activity and, therefore, subject to reduced agricultural taxation (self-production of raw material by the business must be at least> 50%);
4) external supply has been set with incremental quotas of 5% for each additional 90 kW, starting from 100 kW. In terms of value, the land rental cost could, for example, be at a cost of 750 euro/ha equal to:

   (750.00 euro/ha /55 t/ha) /333 (kWh/t) = 0.040 (euro/kWh)

   This additional portion of expenditure must be factored into the cost of cultivation, and therefore for biomass produced on leased land, the total cost becomes:

   0.096 (euro/kWh) + 0.040 (euro/kWh) = 0.136 (euro/kWh)
5) the transport of biomass entering and digestate leaving the plant is based on assumptions of a maximum distance of 15 kilometres for a maximum quantity of the organic matrix of about 64 t/kW (composed partly of silage and solid phase separated from the digestate). In the case of a unit cost of 3 euro/t, the expense per unit of electricity produced is equal to:

   Transport: (3.00 euro/t • 64 ton/kW) / (333 kWh/t biomass • 24 t/kW silage) = 0.024 euro/kWh
6) the construction costs of a plant are normally expressed in euro per kW of installed power. The market is currently oriented to values between 3,500 and 4,500 euro/kW for plants with a capacity up to 1 MW powered primarily by dedicated crops, and 7/8,000 euro/kW for small plants (~100 kW) powered by mostly by manure.
7) the annual cost of operating a plant is mainly composed of: ordinary operating and maintenance costs, annual loan repayments and annual depreciation of capital. As a result, the highest value relates to a 100 kW plant, for which it an estimated a unit expense of more than 7,000 euro/kW is assumed and external financing for 80% of the capital invested. For the 999 kW plant, on the other hand, a cost of approximately 4,000 euro/kW is expected.

Plant management and operating cost

As is well known, the management of an anaerobic digestion plant requires special attention, above all, to ensure continuous operation in

order to achieve high annual production of electricity: an outline time objective of 8,000 hours per year could be assumed. Undoubtedly, attaining this result is only viable if the biological, chemical, technical and mechanical aspects that govern the plant are carefully controlled.

It is, difficult to indicate a value for average expenditure, even if it can be assumed that the unit cost will increase as the installed power decreases, due to the presence of fixed costs that are difficult to eliminate. Therefore, for management expense items we used the same scalar approach as followed for implementation costs: the basic reference figure relates to the management of a plant with a capacity of 999 kW: it is estimated that this would require annual expenditure of approximately 0.030 euro/kWh of electricity produced, which is equivalent to a total amount of about 243 euro/kW per unit of power and approximately 243,000 euro in total.

Finance costs

The financial costs relate to external financing: the amount is proportional to the capital required, the duration and the rate of interest. For the purposes of calculation, it was assumed that the entrepreneur would rely on an outside agency to obtain financing equal to 80% of the total investment, with difference provided by the entrepreneur. For the share of external capital, the time assumed for return of capital to the funding entity is 20 years at a rate of 5.0%, while the owner's capital is allocated in a linear fashion during years in which the incentive rate is provided.

Common management costs of the agricultural business

It was considered appropriate, for the purposes of evaluation, to allocate part of the administration and management costs of the traditional farm enterprise to the management of the biogas plant. In fact, we assumed the project for the digester to be complementary to the agricultural activity, and a portion of more directly agricultural personnel and operating costs would be addressed to this new productive activity. Specifically, we assumed the need at least for an administrative check of about an hour a day and an amount equal to 1% of the value of the plant for management thereof by the employees of the farm.

At this point we have the necessary values to set up the dynamics of the total management cost of a plant. Based on the assumptions, the total annual management cost for a plant can be estimated to be in a range from a minimum of 0.07-0.08 euro/kWh (for systems of high power capacity) up to 0.15-0.16 euro/kWh for small installations (Figure 4).

The decrease in annual running costs is mainly due to the high initial outlay for the construction of the low power plants, which is reflected in an increase in the financial costs related to the issuing of the loan. Therefore, the management of small installed power capacities (for example, <100 kW) must be suitably balanced with a supply of biomass at very low cost, such as the use of biological raw material (for example, manure or waste of agricultural origin), and only a very small proportion of silage.

Risk analysis: comparison between incentive rates before and after 2012

The incentive rate for the production of renewable electricity must be properly compared with the costs described above; the main objective here is to compare the two situations prevailing before and after 2012, when this radical change in the single incentive rate of 0.28 euro/kWh ended 31 December 2012 (Figure 5); In particular, for following assumptions and constants are assumed for the evaluation:

a) plants included in the model have increasing power capacity from 100 to 999 kW;
b) the power diet considered consists of the following:
   - biological products: dedicated crops produced on land belonging to the business and external land;
   - biological products: manure from the farm plus a possible maximum proportion of 30% by weight of silage.
c) Cost values for the various scenarios were considered as common: only the value of the incentive rate and the composition of the diet for powering plant are modified.

The results we wish to obtain from the simulations have a dual purpose: in the first case, concerning the single rate equal to 0.28 euro/kWh, to confirm the behaviour of the entrepreneurs held in choosing to install mainly high power plants (± 999 kW) powered with dedicated crops, and for the new incentive scheme, to identify some strategies that must be followed to achieve a satisfactory level of profitability for the enterprise. Some more detailed clarifications on the results obtained are outlined below.

(A) Plants with increasing power (100 to 999 kW) powered by biological products before 2013

Until 2013, the design of a plant for the production of biogas powered by dedicated crops offered interesting opportunities for entrepreneurs,

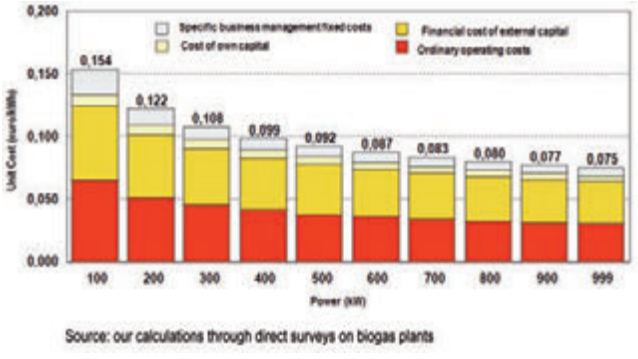

Figure 4. Dynamics of the management cost a biogas production plant with increasing power capacity.

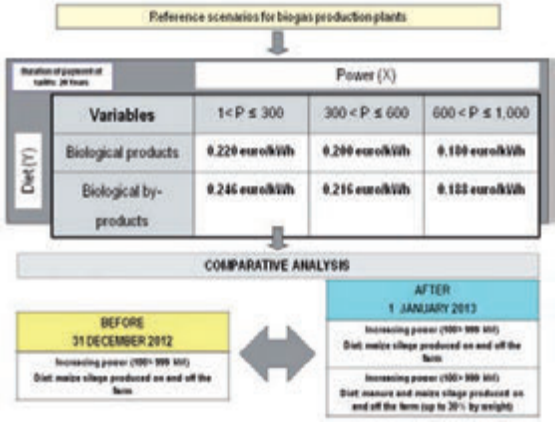

Figure 5. Reference scenarios for the analysis.

especially in the case where they had the entire surface area available necessary to provide silage for the installed power (Figure 6).

As you can see, the absolute growth in profitability was due to two main factors:

- the presence of significant economies of scale that are recorded in the costs for construction and operation of the plant with increasing installed power; starting from 250 kW installed power, the profit started to become very significant;
- the increase in the cost for supply of biomass, in a manner less than proportional to the decrease in the operating costs of the plant; note that in the model a maximum amount of biomass produced externally on rented land of 49% was assumed.

The results obtained under the "old" incentive scheme led to the construction of a large number of installations with powers around the maximum allowed and, only secondly, to consider procurement of biomass as an equally crucial factor for success; as mentioned several times, this strategy was risky and, in fact, we have recently begun to see tensions in grain markets and, above all, in land rental, which can cause problems for the total management cost of the plant.

(B) Plants with increasing power (100 to 999 kW) powered by biological products after 1 January, 2013

The second scenario again considers plants powered by maize silage always with the same cost characteristics as indicated in the previous case, but with revenues enhanced by the incentive rate that began on 1 January, 2013.

The scenario changes dramatically and loses all income opportunities for all installed powers. Indeed, in this specific case, precisely because of the incentive rate that decreases as the power increases, large plants are the most penalized in the overall economic analysis (Figure 7). The opportunity for profit margins does not exist for any installed power. Note, however, that the basic assumptions referred to a portion of leased land: therefore, there cost savings can be achieved if the biomass s completely self-produced, but still with a high degree of risk for the enterprise.

(C) Plants with increasing power (100 to 999 kW) powered by biological by-products after 1 January, 2013

The third scenario takes into consideration plants powered by by-products with a maximum use of dedicated crops <30% by weight. It is assumed that the business has available the manure to be used in the process of feeding the digester. In addition, in the case of power of 100 kW, the diet is composed exclusively of livestock matrix livestock, while as the same power increases, an additional proportion of silage up to a maximum of 30% by weight was considered, as permitted by the regulations.

In this case, the proposed theoretical operation shows the better operating margins. In fact, the net profit for each installed power is always greater than 0.03 euro/kWh, exceeding 0,05 euro/kWh for plants <300 kW (Figure 8).

In absolute terms, it is believed that the most interesting net profit is obtained at two specific points in the growth of the installed power: in fact, around 300 kW the effect of the higher incentive rate becomes relevant for the first stage. At 600 kW, the high power installed and the corresponding electricity produced, can enhance the profit per unit at 0.04 euro/kWh, although this is lower than the plants with power up to 300 kW.

For the purpose of the evaluation, it was not deemed appropriate to further increase the size of the plants, because it would be necessary to have farms with herds not commonly found in the Italian plains.

Brief concluding remarks

In conclusion, it can be argued - albeit with the caution we must exercise in processing data of theoretical approaches - that in the future, the entrepreneur will have interesting opportunities for plants with different power capacity in the context of scenarios that use biological products. In addition, the operating margin that can be obtained

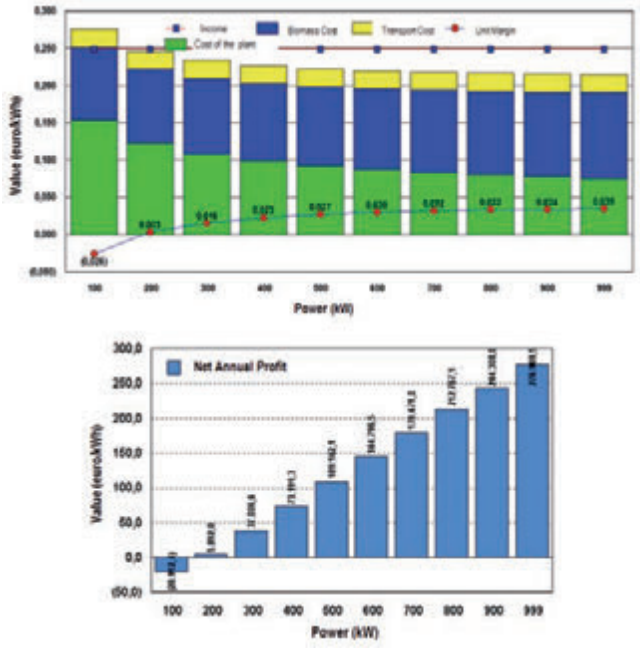

Figure 6. Economic analysis of biogas plants with the incentive rate in force until 31 December 2012.

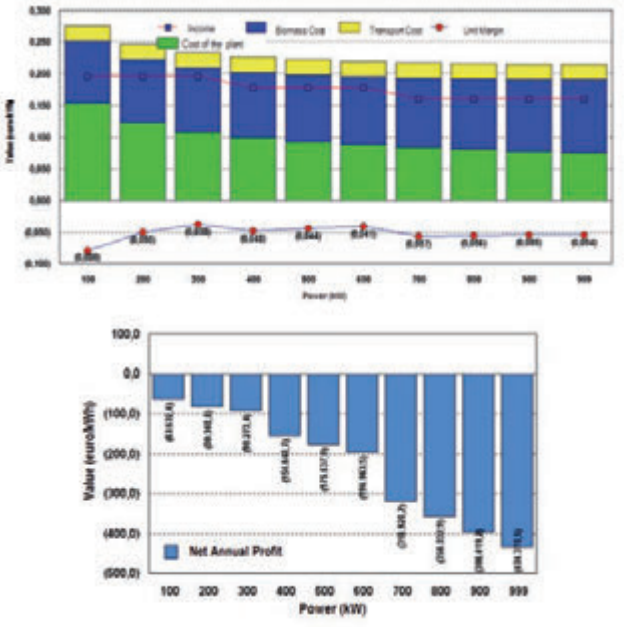

Figure 7. Economic analysis of biogas plants with the incentive rate in force from 1 January, 2013: powered by maize silage.

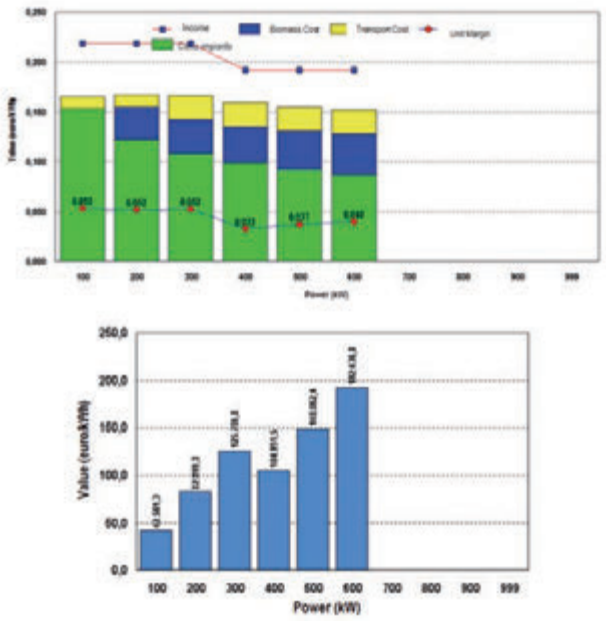

Figure 8. Economic analysis of biogas plants with the incentive rate in force from 1 January, 2013: powered by biological by-products (for example, slurry).

also allows us to consider the possible expensive supply of biomass, in the case where the installed power is to be increased. Conversely, the risks run will be serious if the system is to be powered exclusively with dedicated biomass, especially with cereal silage.

Bibliography

Balsari, P. (2010), Strategie per la delocalizzazione e l'abbattimento delle emissioni dai reflui zootecnici (Strategies for the relocation and reduction of emissions from manure), Università degli Studi di Torino - TECHNICAL DAY "Gestione dei reflui zootecnici: buone pratiche e revisione normativa (Managing manure: good practices and regulatory review)", Carmagnola (TO), 22 June 2010.

Bartonelli V. (2003), Disponibilità di biomassa sul territorio italiano e aspettative reali di sfruttamento (Availability of biomass on the Italian territory and real expectations of exploitation). Il ruolo delle biomasse nell'economia energetica italiana (The role of biomass in the Italian energy economy). in the RECORDS of the APER conference, February, Milano.

Bonari E., Jodice R., Masini S. (2009), L'impresa Agroenergetica: Ruolo e prospettive nello scenario "2 volte 20 per il 2020" (The Agro-energy Company: Role and prospects in the scenario "2 times 20 for 2020"), Edizioni Tellus, Rome.

Bonazzi G. Piccinini S. (2005), Nuove strade per smaltire gli effluenti zootecnici (New ways to dispose of manure), Informatore Agrario, no. 7.

Candolo G. (2005). Biomasse vegetali: i possibili processi di conversione energetica (Plant biomass: possible energy conversion processes), Agronomica, no. 4.

Candolo G. (2006). Energia dalle biomasse vegetali: le opportunità per le aziende agricole (Energy from plant biomass: opportunities for farms), Agronomica, no. 4.

A. Castellini, A. Ragazzoni (2009). Giudizio di convenienza per il trattamento dei liquami zootecnici (Findings on the convenience of slurry treatment). Estimo e Territorio, no. 4.

Coiante D. (2010), "Elettricità da biomasse legnose: effetti economici ed ambientali (Electricity from wood biomass: economic and environmental effects)", in www.aspoitalia.it.

Colonna N., Alfano V., Gaeta M. (2009), La stima del potenziale di biogas da biomasse di scarto del settore zootecnico in Italia (Estimate of the potential of biogas from waste biomass of the Italian livestock sector), ENEA, Report RSE 2009/201.

Fabbri C., Piccinini S. (2008). L'analisi di fattibilità per gli impianti di biogas (Feasibility analysis for biogas plants). Agricoltura, no. 36.

Navarotto P. (2010), L'impianto di biogas: tecnologie costruttive e biomasse (The biogas plant: construction technologies and biomass), in Ragazzoni A. (ed.), BIOGAS, come ottenere nuovo reddito per l'agricoltura (BIOGAS, how to obtain new revenue for agriculture), Edizioni Informatore Agrario, Verona.

Piccinini S. (2000), "Interesting prospects for biogas from slurry", Informatore Agrario, no. 13.

Piccinini S., Rossi L. (2007), Sottoprodotti agro-industriali, un potenziale da sfruttare (Agro-industrial by-products, a potential to be exploited), Informatore Agrario, no. 34.

Ragazzoni A. (2010). Biogas: come ottenere nuovo reddito per l'agricoltura (Biogas: how to obtain new revenue for agriculture). Ed. Informatore Agrario, Verona.

Tiezzi E. (1988), Tempi storici e tempi biologici (Historical times and biological times), in Ceruti M., Laslo E. (ed), "Phisis: Inhabiting the Earth", Feltrinelli, Milano.

Zezza A. (ed.), (2008), Bioenergie: quali opportunità per l'agricoltura italiana (Bioenergy: Opportunities for Italian agriculture), Inea, Edizioni Scientifiche Italiane.

Determining wood chip size: image analysis and clustering methods

Paolo Febbi, Corrado Costa, Paolo Menesatti, Luigi Pari

Consiglio per la Ricerca e la sperimentazione in Agricoltura, Unità di ricerca per l'ingegneria agraria, Monterotondo (Roma), Italy

Abstract

One of the standard methods for the determination of the size distribution of wood chips is the oscillating screen method (EN 15149-1:2010). Recent literature demonstrated how image analysis could return highly accurate measure of the dimensions defined for each individual particle, and could promote a new method depending on the geometrical shape to determine the chip size in a more accurate way. A sample of wood chips (8 litres) was sieved through horizontally oscillating sieves, using five different screen hole diameters (3.15, 8, 16, 45, 63 mm); the wood chips were sorted in decreasing size classes and the mass of all fractions was used to determine the size distribution of the particles. Since the chip shape and size influence the sieving results, Wang's theory, which concerns the geometric forms, was considered. A cluster analysis on the shape descriptors (Fourier descriptors) and size descriptors (area, perimeter, Feret diameters, eccentricity) was applied to observe the chips distribution. The UPGMA algorithm was applied on Euclidean distance. The obtained dendrogram shows a group separation according with the original three sieving fractions. A comparison has been made between the traditional sieve and clustering results. This preliminary result shows how the image analysis-based method has a high potential for the characterization of wood chip size distribution and could be further investigated. Moreover, this method could be implemented in an online detection machine for chips size characterization. An improvement of the results is expected by using supervised multivariate methods that utilize known class memberships. The main objective of the future activities will be to shift the analysis from a 2-dimensional method to a 3-dimensional acquisition process.

Introduction

Correspondence: Paolo Febbi, UniTus-DAFNE, Italy.
E-mail: paolo.febbi@entecra.it

Key words: image analysis, wood chip, size distribution, clustering, sieve result.

Licensee PAGEPress, Italy
Journal of Agricultural Engineering 2013; XLIV(s1):e102
doi:10.4081/jae.2013.(s1):e102

The size distribution of wood chips is recognized as one of the most important parameters for efficient combustion since it affects the storage, the efficiency of energy conversion and environmental emissions (Nati *et al.*, 2010). The dimensions of wood chips are specified by the international standard EN 14961-1:2010 (CSN, 2010) (Table 1).

For fuel chips, mechanically or manually operated screening devices are commonly applied and there is a large variety of applicable systems. The reference methods for size classification of samples are EN 15149-1:2010 (CSN, 2010; oscillating screen method) and CEN/TS 15149-3:2006 (CNS, 2006; rotary screen method). The average relative repeatability limits for horizontal (< 2 w-%) and rotary screenings are exceedingly low. Generally, the relative reproducibility limits based on the median values for horizontal (< 10 w-%) and rotary screening results seem acceptable. On average, reproducibility is better for horizontal screenings than for rotary screening. However, if different measuring principles are applied, particle size analysis of biofuels is associated with high measuring uncertainties (Hartmann *et al*., 2006).

Since the chip form (shape and size) influences the sieve results, the image analysis could provide a method which is sensitive to the geometrical shape for determining a more accurate measure of size integrated with shape (Fernlund, 1998).

Consiglio per la Ricerca e la sperimentazione in Agricoltura, Unità di ricerca per l'ingegneria agraria (CRA-ING) is conducting a research activity for developing a new method, based on the image analysis, for the classification of wood particles, depending on both size and shape.

Materials and Methods

A sample of wood chips (8 liters) was sieved through horizontally oscillating sieves, using five different screen hole diameters (3.15, 8, 16, 45, 63 mm). The wood chips were sorted in decreasing size classes and the size distribution of wood chips was determined. The result is expressed as a percentage of the total mass of all fractions.

The test sample was divided and a wood chip subsample of 1 litre (706 chips) was processed in sequential sieving operations for the determination of its size distribution. Three fractions have been considered: 8÷16 mm, 16÷45 mm, 45÷63 mm. Digital images of all chips in the subsample have been acquired using a high resolution digital scanner A3 (600 dpi; Figure 1). 2-D numerical data have been processed in Matlab (rel. 7.1) environment, specifically developed by CRA-ING. After image segmentation, the following parameters from each object have been extracted: size descriptors (area, perimeter, Feret diameters, eccentricity, etc.) and shape descriptors (99 Fourier descriptors). The Feret diameter is defined as the distance between two parallel tangential lines restricting the object perpendicular to that direction; it measures a particle size along a specified direction. To determine the length and width of a particle area, the algorithm measures Feret diameters in 32 azimuth directions and takes the longest distance as D_{Max} (*length*) and the shortest distance as D_{min} (*width*). The Fourier coefficients can summarize the shape of an object in the frequency domain. Complex shapes can be represented with a small number of invariant coefficients, which can be

viewed as features extracted from the original shapes. Generally, a subset of the components is often enough to capture the overall features of the shape and discriminate different shapes (Zhang and Lu, 2002).

Wang (Wang, 1994) presented a theory suggesting that geometric forms, rectangles, triangles and diamonds, should fall into different areas of a plot of the shape factor, *Sh* (the ratio between the particles perimeter and area, P/A), against the ratio between D_{Max} /D_{min}.

In the present work, some ideal geometric shapes have been considered: rectangles, diamonds, squares and triangles. In order to obtain scale invariant contours from forms, each of them has been normalized by the length of D_{min}=1; so, the shape classification is size independent. This is represented in Figure 2, where diamonds, rectangles and two different kinds of triangles are reported at ratio D_{Max}/D_{min} varying in the range $\sqrt{2}$÷10.

Fernlund (Fernlund, 1998) reported a plot of the shape factor (*Sh*) against the ratio between length and width made for rectangular, triangular and diamond shaped particles. Mathematically the different shapes fall into different areas in this diagram. However, the geometric forms are not easily differentiated using the 32 azimuth directions to compute the Feret diameters. The computed values do not agree with the theoretical ones and so there is a great deal of overlap. The reason for this is assumed to be that the particles are more irregular than they are similar to the typical geometric forms and their perimeters and areas do not agree with the theoretical perimeters and areas (Jansson and Muhr, 1995). It has been demonstrated that in a two dimensional plot it's quite difficult to distinguish enough the different shapes. Wang (Wang, 1994) considered four descriptors (perimeter, area, D_{Max}, D_{min}) to represent forms in a 2-dimensional space; the relative positions of objects in that space cannot be always distinguished. This method reduces the reference space, consequently reducing the distances between objects. Distances between shapes in a 2-dimensional space are smaller than in a *n*-dimensional space.

To discriminate the real forms of chips, it could be helpful to represent the objects in a multidimensional way, with many axes. This is equivalent to dilating the reference space, but augmenting the complexity of the analyses. The shape of chips can be transformed in similarity coefficients in order to quantify the resemblance between objects. Similarities are higher when the two objects are identical and lower when the two objects are completely different. A similarity index (*S*) can be transformed into a distance (*D*) by computing its one-complement. For a similarity measure varying between 0 and 1, the corresponding distance may be computed as (Legendre, 1998).

In an Euclidean space, the objects (chips) may be represented along axes using shape and size descriptors (Costa *et al.*, 2011). The relative position of an object with respect to another one may be used to obtain clusters. Clustering objects is a multivariate operation which partitions the objects into two or more subsets (clusters), using pre-established rules of agglomeration or division, such that each object belongs to one and only one subset of that partition. The subsets form a series of mutually exclusive classes, among which the objects are included.

The adopted clustering method is based on the Euclidean distances among objects, computed using shape and size descriptors (109 variables). The hierarchical clustering routine produces a dendrogram showing how objects can be clustered. A dendrogram is made of branches that meet at nodes which are drawn at the similarity value where fusion of branches takes place.

The dendrogram based on Euclidean distance was performed with the Unweighted Pair-Group Average (UPGMA) algorithm. The highest similarity, or smallest distance, identifies the next cluster to be formed. Following this event, the method computes the arithmetic average of the similarities or distances between a candidate object and each of the cluster members or, in the case of previously formed cluster, between all members of the two clusters. All objects receive equal weights in the computation. Clusters are joined based on the average distance between all members in the two groups. Clustering proceeds by agglomeration as the similarity criterion is relaxed. Each cluster collects objects (chips) that are sufficiently similar, given the variables considered.

Table 1. Specification of the dimensions for wood chips.

Dimensions (mm) for wood chips (UNI EN 14961-1:2010)			
Particle size distribution	Main fraction (min. 75 w-%)	Cross sectional area	Coarse fraction, max length of
P16	3,15÷16 mm	< 1 cm^2	< 31,5/120 mm
P45	8÷45 mm	< 5 cm^2	< 120/350 mm
P63	8÷63 mm	< 10 cm^2	< 350 mm
P100	16÷100 mm	< 18 cm^2	< 350 mm

Results

The result of cluster analysis (UPGMA based on Euclidean distance) on both shape descriptors (Fourier descriptors) and size descriptors (area, perimeter, Feret diameters, eccentricity, etc.) has been reported in Figure 3 to observe the chips distribution according to their descriptors derived from image analysis. For graphical convenience, vertical lines are used to connect branches at the similarity levels of the nodes.

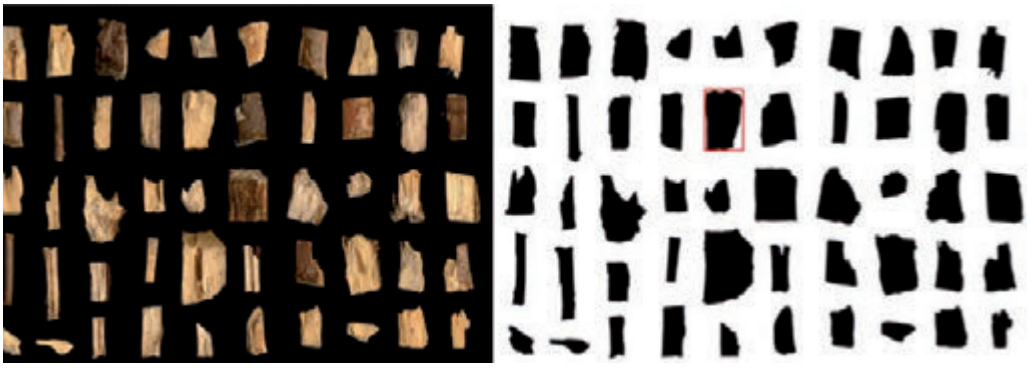

Figure 1. Scanned image of chips (left) and segmented image (right).

Figure 3 represents a summarized version of the whole dendrogram, being it composed by 706 observations. The separation of the main groups is in accordance with the original three sieving fractions. The percentage of chips classified according to the sieving procedure grouping is reported.

Comparing the original assignment of chips made by the sieve method to the assignment made by the clustering method (Table 2), it is possible to determine the number of chips classified in accordance. The method quality is expressed through the percentage of correctly classified units.

Conclusions

The examined data sets consist of chips that belong to three different fractions or groups. A comparison has been made between the traditional sieving and clustering results. The preliminary result shows that the image analysis-based method has a high potentiality for the characterization of wood chip size distribution and could be further investigated. The ability to observe particle groups in accordance with the fractions determined by the screen methods allows the development of a new method for the determination of chip size distribution compatible with the standards EN 15149-1/3. Moreover, this new method could be implemented in an online detection machine for chips size characterization.

Cluster analysis is an unsupervised method that attempts to identify classes (or groups) without using pre-established class memberships. Other works within different scientific fields demonstrated how the integration of complex shape descriptors (such as Fourier descriptors; Menesatti *et al*., 2009) with basic morphometric descriptors (Feret diameters, area, perimeter, etc.) could return better and more accurate descriptions of a phenomena.

In light of this, an improvement of the results is expected by using supervised multivariate methods that utilize known class memberships. Cumulative curves of the size distribution based on image analysis could be constructed. The main objective of the future activities will be to shift the analysis from a 2-dimensional method to a 3-dimensional acquisition process.

Table 2. Chips counts in the three fractions using sieving and clustering methods.

Sieving	Fraction 8÷16	Fraction 16÷45	Fraction 45÷63	Total
Fraction 8÷16	483	-	-	483
Fraction 16÷45	-	220	-	220
Fraction 45÷63	-		3	3

Clustering	Fraction 8÷16	Fraction 16÷45	Fraction 45÷63	Total
Fraction 8÷16	478	36	-	514
Fraction 16÷45	5	184	-	189
Fraction 45÷63	-	-	3	3

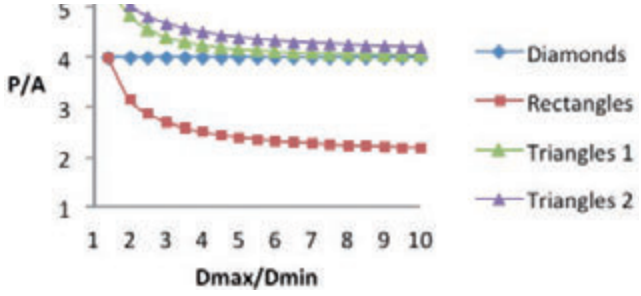

Figure 2. Different areas occupied by the geometric shapes.

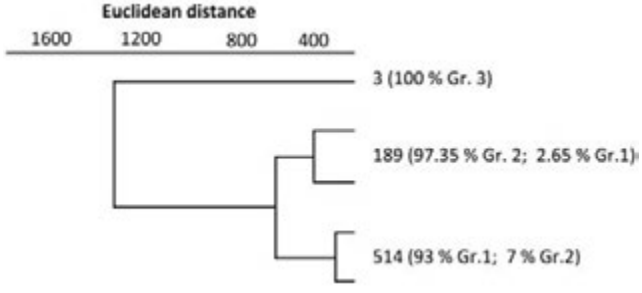

Figure 3: Summarized dendrogram for the cluster analysis on the chips descriptors (size and shape). The groups numbers refers to the sieving procedure grouping

References

Costa, C., Antonucci, F., Pallottino, F., Aguzzi, J., Sun, D.-W., Menesatti, P., 2011. Shape analysis of agricultural products: A review of recent research advances and potential application to computer vision. Food and Bioprocess Technology, 4, 673-692.

CSN P CEN/TS 15149-3:2006. Solid biofuels - Methods for the determination of particle size distribution - Part 3: Rotary screen method.

CSN EN 14961-1:2010. Solid biofuels - Fuel specifications and classes - Part 1: General requirements.

CSN EN 15149-1:2010. Solid biofuels - Determination of particle size distribution - Part 1: oscillating screen method using sieve apertures of 1 mm and above.

Fernlund, J.M.R., 1998. The effect of particle form on sieve analysis: a test by image analysis, Engineering Geology, 50: 111-124.

Hartmann H., Thorsten B., Jensen P.D., Temmerman M., Rabier F., Golser M., 2006. Methods for size classification of wood chips. Biomass and Bioenergy 30: 944-953.

Jansson, M., Muhr, T., 1995. Geometrisk form hos ballast, inverkan på siktresultat och kvalitet. Examensarbete. Avdelningen för Teknisk geologi, Institutionen för Anläggning och miljö, Kungl Tekniska Högskolan.

Legendre P., Legendre L., 1998. Numerical Ecology. 2nd English, ed. Elsevier.

Menesatti P., Aguzzi J., Costa C., García J.A., Sardà F., 2009. A new morphometric implemented video-image analysis protocol for the study of social modulation in activity rhythms of marine organisms. Journal of Neuroscience Methods, ELSEVIER SCIENCE, 184(1): 161-168, ISSN 1872-678X.

Nati C., Spinelli R., Fabbri P., 2010. Wood chips size distribution in relation to blade wear and screen use, Biomass Bioenerg, 34(5): 583-87.

Wang, W.X., 1994. Form analysis of aggregate, for KTH-BASLLAST-standards. June, 1994.

Zhang D. and Lu G., 2002. "A Comparative Study of Fourier Descriptors for Shape Representation and Retrieval," Proc. Fifth Asian Conf. Computer Vision (ACCV '02), pp. 646-651, Jan. 2002.

Sicilian potential biogas production

Antonio Comparetti,[1] Pierluigi Febo,[1] Carlo Greco,[1] Santo Orlando,[1] Kestutis Navickas,[2] Kestutis Venslauskas[2]

[1]Dipartimento di Scienze Agrarie e Forestali, Università degli Studi di Palermo, Italy; [2]Institute of Energy and Biotechnology Engineering, Aleksandras Stulginskis University, Akademija, Kauno r., Lithuania

Abstract

This study is aimed at predicting the Sicilian potential biogas production, using the Organic Fraction of Municipal Solid Waste (OFMSW), animal manure and food industry by-products, in a region where only one biogas plant using MSW and one co-digestion plant are nowadays available.

The statistical data about OFMSW, the number of animals bred in medium and large farms and the amounts of by-products of food processing industries were evaluated, in order to compute the Sicilian potential biogas and energy production. The OFMSW produced in Sicily, that is 0.8 million tons ca. per year (37% of MSW), could be used in a bio-reactor, together with other raw materials, for Anaerobic Digestion (AD) process, producing biogas and "digestate". Moreover, 3.03 million tons ca. of manure, collected in medium and large animal husbandry farms (where cows, pigs and poultry are bred), and 350 thousand tons ca. of by-products, collected in food processing industries (pomace from olive oil mills and grape marc from wineries), might be used for AD process.

The Sicilian potential biogas production from the AD of the above raw materials is 170.2 millions of m^3, that is equal to 1023.4 GWh of energy per year, of which 484 GWh from animal manure, 303 GWh from OFMSW and 236.4 GWh from food industry by-products. The highest biogas production is in the province of Palermo (35.6 millions of m^3), Ragusa (30.8 millions of m^3) and Catania (22.8 millions of m^3), having a potential energy production of 213.8, 185 and 137 GWh, respectively.

Correspondence: Antonio Comparetti, Dipartimento di Scienze Agrarie e Forestali, Università degli Studi di Palermo, Viale delle Scienze, Building 4, 90128 Palermo, Italy.
Tel. +39.091.23897057 - Fax: +39.091.484035.
E-mail: antonio.comparetti@unipa.it

Key words: animal manure, co-digestion, energy, food industry by-products, Organic Fraction of Municipal Solid Waste.

Contributions: the authors contributed equally.

Conflict of interests: the authors declare no potential conflict of interests.

Acknowledgements

The authors acknowledge Dr. Silvia Coscienza, Head of the Waste Department of Sicilian Region, and Francesco Ribaudo, Mayor of Marineo town (Palermo), for their collaboration in data collection.

Journal of Agricultural Engineering 2013; XLIV(s1):e103
doi:10.4081/jae.2013.(s1):e103

Introduction

The biogas produced in a reactor at the end of Anaerobic Digestion (AD) process can be used for the extraction of methane, that can be transferred to the natural gas distribution pipeline or used as vehicle fuel. Another option is to transform the biogas produced into electric and/or thermal energy, in order to contribute to replace fossil-oil based energy sources with renewable ones.

Instead, the other product of AD process, that is the digested substrate or "digestate", is generally separated into a solid and a liquid fraction. The solid fraction can be used as an organic substrate for greenhouse cultivation, while, according to the EU Nitrate Directive (91/676/EEC), the liquid fraction having a chemical composition suitable for plant nutrition can be spread on soils as an organic fertiliser (EU, 1991), in order to minimise the applied rates of nitrogen mineral fertilisers (Weiland, 2010).

The AD process is able to significantly reduce bad smells (up to 80%) and positively change the composition of odours (Weiland, 2010), inactivate weed seeds, bacteria (*e.g. Salmonella* spp., *Escherichia coli*, *Listeria* spp.), viruses, fungi and other parasites in the feedstock (Strauch and Philipp, 2000; Sahlström, 2003).

If a mixture of the Organic Fraction of Municipal Solid Waste (OFMSW), animal manure and food industry by-products, eventually together with herbaceous energy plants and other raw materials, are used for AD, the biogas yield can be increased (Piccinini *et al.*, 2008). Investigations and practical experience show that mixtures of industrial organic wastes with agricultural production ones or plant biomass determine the following benefits: to improve the AD process, so that the digestate can be enriched with various compounds having properties more suitable for plant fertilisation; to increase the biogas yield and, therefore, the biogas plant profitability (Navickas *et al.*, 2004, 2005). Furthermore, after the anaerobic co-digestion, it is possible to minimise the problems related to the collection of some wastes (*e.g.* OFMSW, animal manure, sewage sludge, wastes of slaughter houses), *i.e.* bad smell (due to the concentration of proteins and sulphuric compounds) and high nitrogen concentration (Comparetti *et al.*, 2012).

In Sicily (Italy) about 5 millions of inhabitants (ISTAT, 2012) produce about 2 million tons of Municipal Solid Waste (MSW) per year, of which the 37% can represent the Organic Fraction (OFMSW), and the OFMSW treated is only about the 3% of MSW (Sicilian Region, 2011). The OFMSW could be used in a bio-reactor, together with other raw

materials, in order to produce biogas and "digestate", in a region where only one biogas plant using MSW is operating at the landfill of Palermo (Sicilian Region, 2012) and one co-digestion plant is available at Marianopoli (Caltanissetta). Moreover, in Sicily, the manure produced in medium and large animal husbandry farms (breeding cows, pigs, poultry, etc.) and the by-products of food processing industries (*e.g.* pomace from olive oil mills and grape marc from wineries) would constitute the mixture usable for biogas production (Piccinini *et al.*, 2008).

In this perspective the aim of this study is to predict the Sicilian potential biogas production, using the above unmarketable raw materials, *i.e.* OFMSW, animal manure and food industry by-products.

Materials and Methods

The statistical data about OFMSW, the number of animals bred in medium and large farms and the amounts of by-products of food processing industries were evaluated, in order to compute the Sicilian potential biogas and energy production.

The potential biogas production per year from OFMSW (B_{OFMSW}) was determined according to the following equation, based on the biogas yield (b_w) (Bolzonella *et al.*, 2006) and the mass of this fraction produced per year :

$$B_{OFMSW} = b_w \cdot m_w \quad \text{(Eq. 1)}$$

where : b_w is the biogas yield of OFMSW ($m^3 \cdot t^{-1}$);
m_w is OFMSW mass (t).

The potential energy production per year from OFMSW (E_{OFMSW}) was determined according to the following equation :

$$E_{OFMSW} = B_{OFMSW} \quad e_b \quad \text{(Eq. 2)}$$

where : B_{OFMSW} is the potential biogas production from OFMSW (m^3);
e_b is the energetic value of biogas, depending on the methane concentration in biogas ($kWh \cdot m^{-3}$).

In order to determine the potential biogas production from OFMSW, only the 40% of this fraction produced and collected in Sicily was considered to be used for anaerobic co-digestion process.

The mass of manure produced by each animal species was computed by multiplying the mass of manure produced by each animal (Navickas *et al.*, 2009) per the number of cows, pigs and poultry, drawn from the 6th General Census of Agriculture (ISTAT, 2011).

The potential biogas production per year from animal manure (B_m) was determined according to the following equation, based on the biogas yield (b_m) (Navickas *et al.*, 2009) and the mass of manure (m_m) of each animal species :

$$B_m = b_m \cdot m_m \quad \text{(Eq. 3)}$$

In order to compute the potential biogas production from manure, only the manure produced and collected in medium and large farms (having a minimum number of 50 cows or 100 pigs or 1000 poultry units) was considered to be used for anaerobic co-digestion process.

The potential energy production per year from animal manure (E_m) was determined according to the following equation :

$$E_m = B_m \quad e_b \quad \text{(Eq. 4)}$$

where : B_m is the potential biogas production from manure (m^3).

The potential biogas production per year from food industry by-products (pomace from olive oil mills and grape marc from wine making plants) (B_b) was computed using the following equation, based on the biogas yield (b_m) (Piccinini *et al.*, 2008) and the mass (m_b) of each by-product type (ISTAT, 2011) :

$$B_b = b_b \cdot m_b \quad \text{(Eq. 5)}$$

The potential energy production per year from food industry by-products (B_b) was determined according to the following equation :

$$E_b = B_b \quad e_b \quad \text{(Eq. 6)}$$

Results and discussion

In Sicily 5.05 millions ca. of inhabitants (ISTAT, 2012) produce 2.15 million tons ca. of Municipal Solid Waste (MSW) per year, of which 37% (0.8 million tons ca.) can represent the Organic Fraction (OFMSW). At present only 0.07 million tons ca. of OFMSW (3.17% of MSW) are treated (Sicilian Region, 2011), while 315.3 thousand tons per year of this fraction might be used for biogas production.

Moreover, 3.03 million tons ca. of manure, collected in medium and large animal husbandry farms (where cows, pigs and poultry are bred), and 350 thousand tons ca. of by-products, collected in food processing industries (pomace from olive oil mills and grape marc from wineries), might be used for AD process.

The Sicilian potential biogas production is 170.2 millions of m^3, that

Table 1. Mass, potential biogas and energy production from OFMSW, animal manure and food industry by-products, both in the nine provinces of Sicily and in the whole region.

Provinces	OFMSW			Animal manure			Food industry by-products		
	Mass 10^3 t y^{-1}	Biogas 10^6 m^3	Energy GWh	Mass 10^3 t y^{-1}	Biogas 10^6 m^3	Energy GWh	Mass 103 t y^{-1}	Biogas 106 m^3	Energy GWh
Agrigento	26.6	4.3	25.8	52.6	1.3	8.0	47.4	5.0	30.0
Caltanissetta	15.4	2.5	15.0	85.5	2.1	13.0	22.1	2.6	15.6
Catania	75.0	12.0	72.0	302.0	7.8	47.0	31.6	3.0	18.0
Enna	8.6	1.4	8.4	409.3	10.2	61.0	12.7	1.2	7.2
Messina	40.6	6.5	39.0	311.3	7.8	47.0	15.5	1.5	9.0
Palermo	82.1	13.1	78.6	574.2	14.8	89.0	67.6	7.7	46.2
Ragusa	16.4	2.6	15.6	924.8	26.8	161.0	13.2	1.4	8.4
Siracusa	25.1	4.0	24.0	344.6	8.8	53.0	16.4	1.6	9.6
Trapani	25.5	4.1	24.6	28.7	0.7	5.0	124.0	15.4	92.4
SICILY	315.3	50.5	303.0	3033.0	80.3	484.0	350.2	39.4	236.4

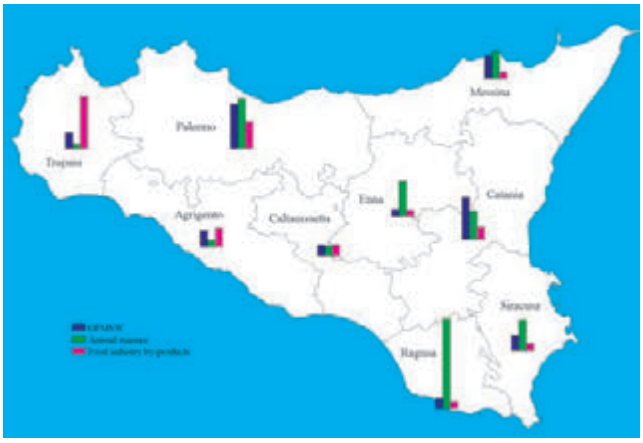

Figure 1. Potential energy production from biogas in the nine provinces of Sicily (GWh).

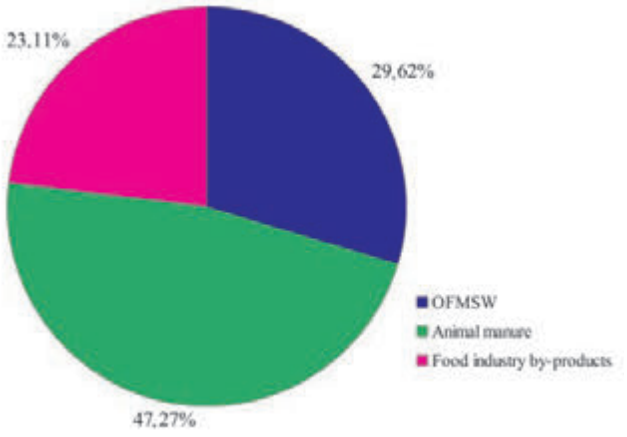

Figure 2. Distribution of Sicilian potential energy production from biogas among the raw materials surveyed.

is equal to 1023.4 GWh of energy per year, of which 484 GWh from animal manure, 303 GWh from OFMSW and 236.4 GWh from food industry by-products.

The highest potential biogas production from the above mixture is in the provinces of Palermo (35.6 millions of m^3, equal to 213.8 GWh per year), Ragusa (30.8 millions of m^3, equal to 185 GWh per year) and Catania (22.8 millions of m^3, equal to 137 GWh per year).

The mass of OFMSW, the manure produced in medium and large animal husbandry farms and food industry by-products, as well as the potential biogas and energy production from these raw materials in Sicily are shown in Table 1.

The potential energy production from OFMSW, animal manure and food industry by-products in the nine provinces of Sicily and in the whole region are presented in Figures 1 and 2, respectively.

The highest potential energy production from OFMSW is in the province of Palermo, due to the highest number of inhabitants and an efficient separate waste collection.

Moreover, the highest potential energy production from manure is in the province of Ragusa, because of the most intensive animal husbandry.

Furthermore, the highest potential energy production from food industry by-products is in the province of Trapani, due to the highest number of food processing industries.

The AD of the mixture surveyed in this study, mainly constituted by animal manure (47%) but also by OFMSW (30%) and food industry by-products (23%), would produce 170.2 million m^3 of biogas, that are equal to 1023.4 GWh per year.

Conclusions

The calculated mass of OFMSW, animal manure and food industry by-products in Sicily is 315.3, 3033 and 350.2 thousand tonnes per year, respectively.

The Sicilian potential biogas production from OFMSW, animal manure and food industry by-products is 50.5, 80.3 and 39.4 million of m^3 of biogas per year, respectively.

The Sicilian total potential biogas production is 170.2 million of m^3 of biogas, that is equal to 1023.4 GWh per year.

The best possibilities for biogas production are in the provinces of Palermo, Ragusa and Catania, having a potential energy production of 213.8, 185 and 137 GWh, respectively.

Waste management is nowadays a problem to be solved in Sicily, as well as in the rest of Italy. In fact, the landfill sites have been or will be filled in with MSW very soon in Italy, where people don't accept the use of new sites in their municipal land. Moreover, the measures aimed at promoting segregated waste collection have been only scarcely implemented in Sicily, as well as in the whole Italy, where the environmentalist movements always fight against the building of incinerators. Therefore, the inefficient waste management has often caused public health problems in whole cities, like recently in Palermo.

In this perspective politicians should promote the valorisation of organic wastes (*e.g.* OFMSW, animal manure and food industry by-products) through AD process. In fact, whether organic wastes were anaerobically digested, it would highly reduce the amounts of these wastes that are nowadays aerobically composted or spread on land as bio-fertilisers after purification or, even worse, landfilled. Therefore, politicians should promote the building of co-digestion plants also in Sicily, in order to contribute to reduce CO_2 emission and, as a consequence, global warming.

References

Bolzonella D., Pavan P., Mace S., Cecchi F. 2006. Dry anaerobic digestion of differently sorted organic municipal solid waste: a full-scale experience. Water Sci Technol 53(8):23-32.

Comparetti A., Greco C., Navickas K., Venslauskas K. 2012. Evaluation of potential biogas production in Sicily. Proceedings of the 11th Int. Scient. Conf. "Engineering for Rural Development", Jelgava, Latvia, 24-25 May, pp. 555-559.

European Union, 1991. Council Directive 91/676/EEC concerning the protection of water against pollution caused by nitrates from agricultural sources. In: Official Journal of the European Communities, 12, pp 1-8.

ISTAT - National Institute of Statistics. 2011. 6th General Census of Agriculture. Sicilian Region.

ISTAT - National Institute of Statistics. 2012. We Italy, 100 statistics to understand the country in which we live. pp. 1-13.

Navickas K., Župerka V., Venslauskas K. 2004. Bioduju gamyba iš organiniu atlieku ir kulturiniu augalu. Šilumos energetika ir technologijos, KTU, pp. 277-282.

Navickas K., Venslauskas K., Župerka V. 2005. Pieno produktu gamybos atlieku anaerobinis perdirbimas. Žmogaus ir gamtos sauga. LŽUU, pp. 46-48.

Navickas K., Venslauskas K., Zuperka V. 2009. Potential and possibilities of biogas production from agricultural raw materials in Lithuania. Rural Development 2009. Lithuanian

University of Agriculture, pp. 365-369.

Piccinini S., Bonazzi G., Fabbri C., Sassi D., Schiff M., Soldano M., Verzellesi F., Berton M. 2008. Energy from biogas produced from livestock manure, dedicated biomass and wastes. Funded by the Autonomous Region Friuli Venezia Giulia, Rural Development Programme 2007-2013, pp. 1-21.

Sicilian Region, Department of Water and Wastes. 2011. Waste Report 2011.

Sicilian Region, Department of Energy. 2012. Energy Report 2011. Energy data in Sicily, pp. 1-122.

Sahlström L. 2003. A review of survival of pathogenic bacteria in organic waste used in biogas plants. Bioresource Technol 87:161-6.

Strauch D., Philipp W. 2000. Hygieneaspekte der biologischen Abfallbehandlung undverwertung. In: Bidlingmaier W. (Ed.) Biologische Abfallbehandlung, Eugen Ulmer, Stuttgart, Germany, pp. 155-208.

Weiland P. 2010. Biogas production: current state and perspectives. Appl Microbiol Biot 85:849-60.

Anaerobic digestion and co-digestion of slaughterhouse wastes

Sonia Castellucci,[1] Silvia Cocchi,[2] Elena Allegrini,[2] Luigi Vecchione[2]

[1]CIRDER, Università degli Studi della Tuscia, Italy; [2]DAFNE, Università degli Studi della Tuscia, Italy

Abstract

The use of renewable energy is becoming increasingly necessary in order to address the global warming problem and, as a consequence, has become an high priority for many countries. Biomass is a clean and renewable energy source with growing potential to replace conventional fossil fuels. Among biomass, residual and waste ones represent a great resource for energy generation since they permit both to eliminate a possible waste and to produce energy. In the present work, the case of slaughterhouse wastes (SHWs) has been investigated. Anaerobic digestion is nowadays considered as one of the most important and sustainable conversion technology exploiting organic matter and biodegradable wastes. Biogas results from this bio-chemical process and mainly consists of methane and carbon dioxide, leading to produce thermal energy and/or electricity. In this paper, the European Regulations on animal by-products (ABPs) are described, and some previous study on anaerobic digestion and co-digestion of ABPs - more precisely SHWs - are considered and compared in order to fix a starting point for future tests on their co-digestion in a micro-scale pilot digester. This is to define optimal feed ratio values which ensure an increasing content of methane in the outgoing biogas.

Introduction

Renewable Energy Sources are increasingly used in order to reduce fossil fuels consumption and consequently those problems linked to global warming (N.L. Panwar *et al.*, 2011). Nowadays, biomass are one of the most widespread sources which can be efficiently used to produce energy in different ways (P. McKendry, 2002). Among them, Anaerobic Digestion (AD) is one of the most interesting energy conversion methods. It involves bacterial fermentation and permits the organic matter decomposition in an oxygen free environment (A. J. Ward *et al.*, 2008). Biogas -primarily consisting of methane (40 - 70%) and carbon dioxide with traces of other gases- derives from AD process (T. Abbasi *et al.,* 2012).

AD leads to several applications and involve different categories of feedstock, *e.g.* industrial and municipal waste-waters, agricultural, municipal, food industry wastes and plant residues. An attractive subject is the possible use on Animal By-Products (ABPs) too (A.J. Ward *et al.*, 2008).

In the present paper, the European Regulations No 1069/2009 and No 142/2011 on ABPs are carefully described in order to identify which animal by-products can be used for biogas production. Furthermore several studies on SHWs anaerobic digestion and co-digestion have been considered and compared in order to fix a starting point for future laboratory tests. This plays a fundamental role if the slaughterhouse wastes produced in the Province of Viterbo have to be reused in a sustainable way by producing energy.

Correspondence: Silvia Cocchi, DAFNE, Università degli Studi della Tuscia, via San Camillo de Lellis snc, 01100 Viterbo (VT), Italy.
Tel. +39.0761.401343.
E-mail: silvia.cocchi@unitus.it

Key words: anaerobic digestion, biogas, slaughterhouse wastes, animal by-products.

Journal of Agricultural Engineering 2013; XLIV(s1):e104
doi:10.4081/jae.2013.(s1):e104

Current regulations on animal by-products

ABPs result from the slaughter of animals for human consumption, the production of dairy products, the disposal of dead animals and during disease control measures. Regardless of their origin, ABPs not intended for human consumption can determine a potential risk to public and animal health and to the environment. The disposal of all ABPs could lead to unbearable costs and risks for the environment which consequently need to be reduced. This problem might be successfully overcome by producing energy with ABPs in a sustainable way. (Regulation EC No 1069, 2009).

The Regulation (EC) No 1069/2009 of the European Parliament and of the Council lays down health rules with specific regard to ABPs and derived products not intended for human consumption. According to the law, ABPs are distinguished in three categories, depending upon the risk they pose towards human, animals and environment, and establishes their potential application (Table 1). Furthermore the corresponding treatments and uses for the treated ABPs categories are defined (Bayr *et al.,* 2012a).

According to the above-mentioned regulation, the use in AD plants is allowed for Category 2 after or without pressure sterilisation – depending on the type of ABPs - and Category 3. For "pressure sterilisation" it is meant the processing of ABPs, after reduction in particle size smaller than 50 mm, to a minimum temperature of 133°C for at least 20 minutes and at an absolute pressure of at least 3 bar (Regulation EC No 1069/2009).

Actually in the Commission Regulation (EU) No 142/2011, implementing Regulation (EC) No 1069/2009, some uses for biogas production are considered for those products derived from processing materials belonging to Category 1. In more detail, the latter products could be transformed into biogas; nevertheless, the digestion residues must be disposed by incineration or co-incineration, as Category 1 materials. If Category 1 materials are subjected to Alkaline hydrolysis pre-treatment, they could be transformed in a biogas plant and subsequently combusted

rapidly at a minimum of 900°C, followed by rapid chilling (quenching), but the transformation shall take place on the same site as the processing and in a closed system. Additionally in the case of high pressure hydrolysis pre-treatment, the product derived from Category 1 material could be used for biogas production, but the whole process must take place on the same site and in a closed system; the biogas produced must be combusted rapidly in the same plant as above explained for the alkaline hydrolysis case. Whereas the products derived from Category 2 and 3 processing can be used for biogas production without restrictions (Commission Regulation (EU) no 142, 2011).

According to Commission Regulation (EU) no 142/2011, a biogas plant must be equipped with a pasteurisation/hygienisation unit, which cannot be by-passed for ABPs or derived products introduced with a maximum particle size of 12 mm before coming into the unit. Nevertheless this unit is not mandatory if the ABPs are processed with the pre-treatments indicated in the Regulation for the specific categories and for some particular ABPs belonging to Category 2 and 3. In Table 2 some pre-treatments are reported.

Anaerobic digestion of SHWs

As indicated in EC 1069/2009, AD represents a treating possibility for ABPs, in order to decrease the environmental impact and to produce energy from biogas for local uses. In this sense, AD is considered an interesting alternative for waste management (Banks and Wang, 1999). Furthermore, digestion effluents can be used as fertilizers in agriculture (Mata-Alvarez *et al.*, 2000; Salminen *et al.*, 2001; Zhang and Banks, 2012).

SHWs represent potentially an excellent substrate for anaerobic digestion because of their high content of lipids and proteins (Hejnfelt and Angelidaki, 2009). However, different studies have proved that the AD of these wastes is practicable only for low organic loading rate (OLR) and hydraulic retention time (HRT) (Salminen and Rintala, 2002) and is particularly prone to failure because of the production of inhibitory compounds: ammonia, volatile fatty acids (VFAs) and long chain fatty acids (LCFAs) (Salminen and Rintala, 2002a; Bayr *et al.*, 2012b; Heinfelt and Angelidaki, 2009; Edstrom *et al.*, 2003; Masse *et al.,* 2002; Broughton *et al.*, 1998; Lokshina *et al.*, 2003).

Co-digestion of SHWs with other biomass, containing low content of nitrogen and/or lipids, permits to improve the process stability and methane production (Bayr *et al.,* 2012a; Salminen *et al.*, 2003; Rosenwinkel and Meyer, 1999).

A two-phase digestion system might represent an alternative solution leading to increase process efficiency, solid reduction, chemical oxygen demand (COD) removal and conversion in biogas (Wang and Banks, 2003; Banks and Wang, 1999).

Several tests were carried out in order to obtain a profitable AD process for biogas production. Thus, evaluations on different parameters variation were investigated as follows: pressure and temperature increases in AD processes or in pre-treatments, but without good results (Cuestos *et al.,* 2010); an increase of lipids or a change of the bacterial community structure, with discrete results (Palatsi *et al.*, 2011). Other studies evaluated the saponification of lipids in SHWs during pre-treatments and the use of ethanol biodegradation: a biogas improvement and, in some cases, the kinetic reactions were shown. However, the results are not enough clear to ensure the success of the process (Battimelli *et al.,* 2009; Battimelli *et al.*, 2010). Other studies concern the effects of influent flow rate variation on biogas production improvement both in BATCH anaerobic digesters (Resch *et al.*, 2006) and in continuously stirred tank reactors (CSTRs) (Marcos *et al.*, 2012).

Table 1. ABPs classification and allowed uses for biogas production according to Regulation (EC) No 1069/2009 of the European Parliament

Category	Animal by-products	Biogas production
1	All body parts of the following animals: suspected of being infected by a TSE; pet, zoo and circus animals; animals used for experiments; wild animals if suspected of being infected with diseases communicable to humans or animals; contained specified risk material. ABPs derived from animals submitted to illegal treatments or containing residues of other substances and environmental contaminants. ABPs collected during waste-water treatments of plants processing Category 1 material or risk material. Catering wastes from means of transport operating internationally. Mixture of Category 1 with Category 2 or 3 material	Not allowed. Allowed after specific pre-treatments, but provided the digestion residues are disposed of by incineration and co-incineration
2	Manure and digestive tract content; ABPs collected during waste-water treatments of plants processing Category 2 material or from slaughterhouses. ABPs containing residues of authorised substances. ABPs declared unfit for human consumption due to the present of foreign bodies. ABPs imported from a third country and fail to comply with Community veterinary legislation. Animals or parts (different than Category 1 and 3) that slaughtered or killed other than for human consumption, foetuses, oocytes, embryos and semen not for breeding purposes; dead-in-shell poultry. Mixture of Category 2 with 3 material. ABPs other than Category 1 or 3	Allowed after pressure sterilisation or in biogas plant with pasteurisation and hygienisation unit. Allowed without pre-treatments only for specific ABPs of this Category
3	Carcases and parts of animals slaughtered or, in the case of game, fit for human consumption but not intended for this use for commercial reasons. Carcases and the following parts of animal slaughtered or game killed for human consumption: parts unfit for human consumption according to Community legislation, heads of poultry, hides, skins, horns, feet, pig bristles, feathers. ABPs from poultry or lagomorphs slaughtered on the farm. Bloods of animals slaughtered in a slaughterhouse and considered fit for human consumption. ABPs arising from the production of products intended for human consumption. Products of animal origin, foodstuffs, pet food or feeding stuffs ,no longer intended for human or animal consumption for commercial reasons. Blood, placenta, wool, feathers, hair, horns, hoof cuts and raw milk, aquatic animals, ABPs from aquatic animals. Eggs, egg by products, including egg shells. Adipose tissue from animals slaughtered in a slaughterhouse. Catering wastes	Allowed after pre-treatments 1 to 6 or 7 or in a plant with pasteurisation and hygienisation unit. Allowed without pre-treatments for specific ABPs if authorised by the competent authority

Mono and co-digestion of pig, poultry and cattle SHWs

Several studies reports experiments on AD of pig SHWs. Tests in BATCH reactor - at 35°C - measured the following methane productions: 428 $dm^3CH_4/kgVS$ (Bayr *et al.*, 2012a) and 580 $dm^3CH_4/kgVS$ (Rodriguez-Abalde *et al.*, 2011). Methane potentials of 225-619 $dm^3CH_4/kgVS$ were evidenced on different pig wastes - meat, bone flour, fat, blood, hair, meat, ribs, raw wastes - at 37 and 55°C in BATCH reactor (Hejnfelt and Angelidaki, 2009).

Experiment results on anaerobic mono-digestion in Continuously Stirred Tank Reactor (CSTR) are not attended, but tests on co-digestion shows the following results: five fractions of rendering wastes with poultry, cattle, pig slaughterhouse wastes with a methane production of 717 $dm^3CH_4/kgVS$ at 35°C (Bayr *et al.*, 2012a); pig mixed SHWs with solid pig manure have a methane yield of 489 $dm^3CH_4/kgVS$ at 37°C (Hejnfelt and Angelidaki, 2009).

Experiments on mono-digestion of poultry SHWs in BATCH reactor shows a methane yield of 262-266 $dm^3CH_4/kgVS$ at 35°C (Bayr *et al.*, 2012a). Whereas tests in CSTRs evidences a methane production of 520-550 $dm^3CH_4/kgVS$ at 35°C (Salminen and Rintala, 2002) and 600-700 $dm^3CH_4/kgVS$ at 34°C (Cuestos *et al.*, 2008). The firsts values are obtained under mesophilic conditions in 2 dm^3 CSTR operating with 0.8 $kgVS/m^3d$ with an HRT of 50 days.

A study on co-digestion of poultry SHWs with Organic Fraction of Municipal Solid Wastes (OFMSWs) - at 34°C, in CSTR - reveals a methane potential of 400-500 dm^3CH_4/kg VS.

A methane yield of 460 $dm^3CH_4/kgVS$ is reported for poultry waste at 35°C (Rodriguez-Abalde *et al.*, 2011) and higher potential is obtained for offal: 210-910 $dm^3CH_4/kgVS$ at 35 and 55°C (Salminen *et al.*, 2003).

Experiments on mono-digestion of bovine SHWs in BATCH reactor shows a methane yield of 572 $dm^3CH_4/kgVS$ at 35°C (Bayr *et al.*, 2012a).

Methane yield of 270-350 $dm^3CH_4/kgVS$ have been measured during co-digestion of solid cattle and swine SHWs with fruit/vegetable wastes and solid cattle/swine manure; the test were carried out in mesophilic conditions (35°C) in a CRST and showed that digestion with mixed substrates is better than with single substrates (Alvarez and Liden, 2008).

Methane yield of 400-500 $dm^3CH_4/kgVS$ has been measured during co-digestion of Poultry SHWs with organic fraction of municipal solid waste (OFMSW); the test were carried out in mesophilic conditions (34°C) in a CRST (Cuestos *et al.*,2008; 2009; 2010). At the beginning of study carried out in 2008, initial problems with accumulation of digestion intermediates occurred, but after an acclimation at low organic loading the mixture could be treated. A dilution of slaughterhouse material with fresh water was used in order to reduce the ammonia concentration.

Methane yield of 400-430 $dm^3CH_4/kgVS$ have been measured during co-digestion of ABPs from meat processing industry with sewage sludge; the test were carried out in mesophilic conditions (35°C) in a CRST (Luste and Luostarinen, 2010).

Co-digestion of manure and rumen (Rosenwinkel and Mayer, 1999) and blood and rumen from cattle and pigs were studied in laboratory in a pilot-scale plant at 37°C and with heating pre-treatments (Edstrom *et al.*, 2003).

A study using fruit and vegetable wastes to improve the nutrient balance in sequencing batch anaerobic digestion was carried out by Bouallagui *et al.* (Bouallagui *et al.*,2009).

Pitk *et al.* studied methane potential of category 2 and 3 SHWs rendering products: melt, decanter sludge, meat and bone meal, technical fat and flotation sludge from wastewater treatments; values in the range 390-978 $dm^3CH_4/kgVS$ were measured (Pitk *et al.*, 2012).

Pre-treatments effects on AD

Several studies evaluated the difference between the biogas production starting from treated and un-treated SHWs.

Some studies were carried out in batch reactor, at 55°C, and on different pig SHWs - meat, bone flour, fat, blood, hair, meat, ribs, raw

Table 2. Some of pre-treatments for ABPs before using in anaerobic digestion plants (Commission Regulation (EU) No 142, 2011)

Category	Uses in biogas plants	Treatments
1-2-3	Standard treatment 1: pressure sterilisation	Particles size ≤ 50 mm; T ≥ 133°C and pressure (absolute) ≥ 3 bar for at least 20 minutes
1-2-3	Standard treatment 2	Particles size ≤ 150 mm; T ≥ 100°C for at least 125 minutes, T ≥110°C for at least 120 minutes, T ≥120°C for at least 50 minutes
1-2-3	Standard treatment 3	Particles size ≤ 30 mm; T ≥ 100°C for at least 95 minutes, T ≥110°C for at least 55 minutes, T ≥120°C for at least 13 minutes
1-2-3	Standard treatment 4	Particles size ≤ 30 mm must be placed in a vessel with added fat: T ≥ 100°C for at least 16 minutes, T ≥110°C for at least 13 minutes, T ≥120°C for at least 3 minutes
1-2-3	Standard treatment 5	Particles size ≤ 20 mm must be heated until they coagulate and then pressed so that fat and water are removed from the proteinaceous material. The latter must then be heated: T ≥ 80°C for at least 120 minutes, T ≥100°C for at least 60 minutes
3	Standard treatment 6	Specific treatment for Category 3 animal by-products originating from aquatic animal or aquatic invertebrates only
3	Standard treatment 7	Other processing method authorised by the competent authority
1-2-3	Alternative treatments Alkaline hydrolysis process	Materials resulting from processing may be transformed in a biogas plant and subsequently combusted rapidly at a minimum of 900°C, followed by rapid chilling ('quenching'); for Category 1, the transformation into biogas shall take place on the same site as the processing and in a closed system;
1-2-3	Alternative treatment: High pressure hydrolysis biogas process After standard method 1.	In the case of starting material of Category 1, the entire process must take place on the same site and in a closed system and the biogas produced during the process must be combusted rapidly in the same plant at a minimum of 900 °C followed by rapid chilling (quenching)

wastes - subjected to the following treatments according to the European Regulation: pasteurization at 70°C for 1 hours, sodium alkali hydrolysis (50 or 100 g NaOH/kgVS), sterilization at 133°C and 300 kPa for 20 minutes; the results show that pre-treatments had no effect on methane yields (Hejnfelt and Angelidaki, 2009).

A methane potential of 351-381 $dm^3CH_4/kgVS$ was determined at 35°C, for AD of meat and bone meat (Wu *et al.*, 2009).

Conversely other studies show some effects of pre-treatments on AD. A potential biogas yield of 1.14 l biogas/gVS is measured for pasteurised SHWs (1 hour at 70°C) is shown, whereas for un-pasteurised ones it is 0.31 l biogas/g VS (the production is about fourfold in the pasteurised case) (Edstrom *et al.*, 2003). A growth in methane potential of about 14-18% is shown for the same pre-treatment with particle sizes lesser than 12 mm and applied to mixture of daily manure and biowastes and in mesophilic conditions (Paavola *et al.*, 2006).

Several pre-treatments were investigated in order to reduce the particle sizes and to promote the lipids solubilisation. An increase of hydrolysis rate was achieved through the following pre-treatments:

- saponification at different temperatures - 60, 120 and 150°C - for 30 minutes and AD tests in mesophilic and thermophilic conditions in batch reactor and on fatty SHWs; the best performances were observed for the treatment at 120 °C (Battimelli *et al.*, 2009;2010);
- enzymatic hydrolysis (Masse *et al.*, 2003)
- enzymatic bio-augmentation (Cirne *et al.*, 2006).

In order to prevent the LCFA inhibition some treatments were studied, such as the use of acclimated biomass (Cavailero *et al.*, 2008), the supplement of adsorbent (biofibers or bentonite) (Palatsi *et al.*, 2009), the use of feeding strategies with sequential LCFA accumulation-degradation steps (Cavaleiro *et al.*, 2009).

Affes *et al.* evaluated different configurations for anaerobic mono-digestion for fat from cattle carcasses in mesophilic conditions (35°C). The system combines saponification wastes pre-treatments, AD in CSTR and solid recirculation. The studies are carried out with/without waste saponification pre-treatments (at 70°C for 60 minutes) and with/without digestate solid fraction recirculation. An enhancement on methane yield and COD degradation efficiency was achieved; the best performance was obtained in the reactor equipped with pre-treatments and recirculation. Indeed saponification enhances the emulsionification and bioavailability of solid fatty residues, whereas recirculation minimizes the substrate wash out and induces the microbial community adaption to the treatment of the lipid/LCFA based substrates (Affes *et al.*, 2013).

Conclusions

The European Regulations describe carefully which SHWs could be used in AD plants and establishes potential applications without any restriction for category 3 only. As for category 2, some restrictions must be applied, whereas with regard to category 1 the use for biogas production is exceptional, complicated and permitted after specific pre-treatments only.

The analysis of different studies on AD of SHWs have shown that a good conclusion of the process can be achieved in mesophilic conditions, whereas it is considerably complicated in thermophilic conditions.

Furthermore co-digestion with other substrates determines better results than mono-digestion of SHWs.

As for pre-treatments effects on AD process, the results are debatable, since pre-treatments influence the biogas production yield according to some authors, whereas other authors demonstrate no effects on the process.

In order to exploit local SHWs by generating energy, future studies will concern co-digestion laboratory tests with different co-substrates. Nowadays, with specific regard to the Province of Viterbo, the following data on SHWs production are available: 2624,1 ton for cattle, 285,7 ton for pigs and 2167,5 ton for ovine and caprine (ISTAT, IZS).

The expected results will help to correctly size digesters in the Province of Viterbo.

References

Abbasi T, Tauseef SM, Abbasi SA. Anaerobic digestion for global warming control and energy generation-An overview. Renew Sust Energ Rev 2012;16:3228-42.

Affes R., Palatsi J, Flotats X., Carrère H, Steyer JP; Battimelli A. Saponification pre-treatment and solid recirculation as a new anaerobic process for the treatment of slaughterhouse waste. Bioresource Technol 2013;131:460-7.

Alvarez R, Liden G. Semi-continuous co-digestion of solide slaughterhouse waste, manure and fruit and vegetable wastes. Ren Energ 2008;33:726-34.

Banks CJ, Wang Z. Development of a two phase anaerobic digester for the treatment of mixed abattoir wastes. Water Sci Technol 1999; 40:69-76.

Battimelli A, Carrere H, Delgenes JP. Saponification of fatty slaughterhouse wastes for enhancing anaerobic biodegradability. Bioresource Technol 2009;100:3695-700.

Battimelli A, Torrijos M, Moletta R, Delgenes JP. Slaughterhouse fatty waste saponification to increase biogas yield. Bioresource Technol 2010;101:3388-93.

Bayr S, Rantanen M, Kaparaju P, Rintala J. Mesophilic and thermophilic anaerobic co-digestion of rendering plant and slaughterhouse wastes. Bioresource Technol 2012; 104:28-36.

Bayr S, Pakarines O, Korppoo A, Liuksia S, Vaisanen A, Kaparaju P. Effect on additives on process stability of mesophilic anaerobic monodigestion of pig slaughterhouse waste. Bioresource Technol 2012;120:106-113.

Bouallagui H, Rachdi B, Gannoun H, Hamdi M. Meshopilic and thermophilic anaerobic co-digestion of abattoir wastewater and fruit and vegetable waste in anaerobic sequencing batch reactors. Biodegradation 2009;20:401-9.

Broughton MJ, Thiele JH, Birch EJ, Cohen A. Anaerobic batch digestion of sheep tallow. Water Res 1998;32:1423-28.

Cavaleiro AJ, Pereira MA, Alves M. Enhancement of methane production from long chain fatty acids based effluents. Bioresource Technol 2008;99:4086-95.

Cavaleiro AJ, Salvador AF, Alves JI, Alves M. Continuous high rate anaerobic tretament of oleic based wastewater is possible after a step feeding start-up. Environ Sci Technol 2009;43:2931-6.

Cirne DG, Bjornsson L, Alves MM, Mattiasson B. Effect of bioaugmentation by an anaerobic lipolytic bacterium on anaerobic digestion of lipid rich waste . J. Chem Technol Biotechnol 2006;81:1745-52.

Commission Regulation (EU) No 142/2011 of 25 February 2011 implementing Regulation (EC) No 1069/2009 of the European Parliament and of the Council laying down health rules as regards animal by-products and derived products not intended for human consumption and implementing Council Directive 97/78/EC as regards certain samples and items exempt from veterinary checks at the border under that Directive. In: Official Journal of the European Union No.54, 25/02/2011, pp 1-254.

Cuestos MJ, Gomez X, Otero M, Moran A. Anaerobic digestion of solid slaughterhouse wastes (SHW) at laboratory scale: influence of co-

digestion with the organic fraction of municipal solide waste (OFMSW). Biochem Eng J 2008;40:99-106.

Cuestos MJ, Moran A, Gomez X, Otero M. Anaerobic co-digestion of poultry blood with OFMSW: FTIR and TG-DTG study of process stabilization. Environ Technol 2009;30:571-582.

Cuestos MJ, Gomez X, Otero M, Moran A. Anaerobic digestion and co-digestion of slaughterhouse wastes (SHW): influence of heat and pressure pre-treatments in biogas yield. Waste Manage 2010;30:1780-89.

Edstrom M, Nordberg A, Thyselius L. Anaerobic treatment of animal by-products from slaughterhouses at laboratory and pilot scale. Applied Biochem and Biotech 2003;109:127-38.

European Regulation (EC) No 1069/2009 of the European Parliament and of the Council of 21 October 2009 laying down health rules as regards animal by-products and derived products not intended for human consumption and repealing Regulation (EC) No 1774/2002 (Animal by-products Regulation). In: Official Journal of the European Union No.300, 21/10/2009, pp 1-33.

Hejnfelt A, Angelidaki I. Anaerobic digestion of slaughterhouse by products. Biomass and Bioenerg 2009;33:1046-54.

Lokshina LY, Vavilin VA, Salminen E, Rintala J. Modeling of anaerobic degradation of dolid slaughterhouse waste: inhibition effects of long-chain fatty acids or ammonia. Appl Biochem Biotechnol 2003;109:15-32.

Luste S, Luostarinen S. Anaerobic co-digestion of meat-processing by-products and sewage sludge-effect of hygenization and organic loading rate. Bioresource Technol 2010;101:2657-64.

Marcos A, Al-Kassir A, Lopez F, Cuadros F, Brito P. Environmental treatment of slaughterhouse wastes in a continuously stirred anaerobic reactor: effect of flow rate variation on biogas production. Fuel processing Technol 2012;103:178-82.

Masse L, Massè DI, Kennedy KJ, Chou SP. Neutral fat Hydrolysis and long-chain fatty acids oxidation during anaerobic digestion of slaughterhouse wastewater. Biotechnol Bioeng 2002;79:43-52.

Masse L, Massè DI, Kennedy KJ. Effect of hydrolysis pretreatment on fat degradation during anaerobic digestion of slaughterhouse wastewater . Process biochem 2003;38:1365-72.

Mata-Alvarez J, Mace S., Llabres P. Anaerobic digestion of solide wastes. An overview of research achievements and perspectives. Bioresource Technol 2000; 74:3-16.

McKendry P. Energy production from biomass (part 2): conversion technologies. Bioresource Technol 2002;83:47-54.

Paavola T, Syvasalo E, Rintala J. Co-digestion of manure and bioeaste according to the EC animal by-products regulation and Finnish national regulations. Water Sci Technol 2006;53:223-31.

Palatsi J, Laureni M, Andres MV, Flotats X, Nielsen HB, Angelidaki I. Strategies for recovering inhibition caused by long chain fatty acids on anaerobic thermophilic biogas reactors. Bioresource Technol 2009;100:4588-96.

Palatsi J, Vinas M, Guivernau M, Fernandez B, Flotats X. Anaerobic digestion of slaughterhouse waste: main process limitations and microbial community interactions. Bioresource Technol 2011;102:2219-27.

Panwar NL, Kaushik SC, Kothari Surendra. Role of renewable energy sources in environmental protection: A review. Renew Sust Energ Rev 2011;15:1513-24.

Pitk P, Kaparaju P, Vilu R. Methane potential of sterilized solid slaughterhouse wastes. Bioresource Technol 2012;116:42-6.

Resch C, Grasmug M, Smeets W, Braun R, Kirchmayr R. Optimised anaerobic treatment of house-sorted biodegradable waste and slaughterhouse waste in a high loaded half technical scale digester. Water Sci Technol 2006;53:213-21.

Rodriguez-Abalde A, Fernandez B, Silvestre G, Flotats X. Effect of thermal pre-treatments on solid slaughterhouse waste methane potential. Waste Manage 2011; 31:1488-93.

Rosenwinkel KL, Meyer H. Anaerobic treatment of slaughterhouse residues in municipal digesters. Water Sci Technol 1999;40:101-111.

Salminen E, Rintala J, Härkönen J, Kuitunen M, Högmander H, Oikari A. Anaerobically digested poultry slaughterhouse wastes as fertiliser in agriculture. Bioresource Technol 2001;78:81-8.

Salminen EA, Rintala JA. Semi-continuous anaerobic digestion of solid poultry slaughterhouse waste: effect on hydraulic retention time and loading. Water Res 2002;36:3175-82.

Salminen E, Einola J, Rintala J. The methane production of poultry slaughtering residues and effects of pretreatments on the methane production of poultry feather. Environ Technol 2003;24:1079-86.

Wang Z, Banks CJ. Evaluation of a two stage anaerobic digester for the treatments of mixed abattoir wastes. Process Biochem 2003;38:1267-73.

Ward AJ, Hobbs PJ, Holliman PJ, Jones DL. Optimisation of the anaerobic digestion of agricultural resources. Bioresource Technol 2008;99:7928-40.

Wu G, Healy MG, Zhan X. Effect of the solid content on anaerobic digestion of meat and bone meal. Bioresource Technol 2009;100:4326-31.

Zhang Y, Banks CJ. Co-digestion of the mechanically recovered organic fraction of municipal solid waste with slaughterhouse wastes. Biochem Eng J 2012;68:129-37.

Energy and pressure requirements for compression of swine solid fraction compost

Niccolò Pampuro, Alessio Facello, Eugenio Cavallo

Istituto per le Macchine Agricole e Movimento Terra (IMAMOTER), Consiglio Nazionale delle Ricerche (CNR), Torino (TO), Italy

Abstract

The excessive amount of pig slurry spread on soil has contributed to nitrate water pollution both in surface and in ground waters, especially in areas classified as vulnerable zones to nitrate in accordance with European Regulation (91/676/CEE). Several techniques have been developed to manage livestock slurries as cheaply and conveniently as possible and to reduce potential risks of environmental pollution. Among these techniques, solid-liquid separation of slurry is a common practice in Italy. The liquid fraction can be used for irrigation and the solid fraction, after aerobic stabilization, produces an organic compost rich in humic substances. However, compost derived from swine solid fraction is a low density material (bulk density less than 500 kg m^{-3}). This makes it costly to transport composted swine solid fraction from production sites to areas where it could be effectively utilized for value-added applications such as in soil fertilization. Densification is one possible way to enhance the storage and transportation of the compost. This study therefore investigates the effect of pressure (20-110 MPa) and pressure application time (5-120 s) on the compaction characteristics of compost derived from swine solid fraction. Two different types of material have been used: composted swine solid fraction derived from mechanical separation and compost obtained by mixing the first material with wood chips. Results obtained showed that both the pressure applied and the pressure application time significantly affect the density of the compacted samples; while the specific compression energy is significantly affected only by the pressure. Best predictor equations were developed to predict compact density and the specific compression energy required by the densification process. The specific compression energy values based on the results from this study (6-32 kJ kg^{-1}) were significantly lower than the specific energy required to manufacture pellets from biomass feedstock (typically 19-90 kJ kg^{-1}).

Correspondence: Niccolò Pampuro, Istituto per le Macchine Agricole e Movimento Terra (IMAMOTER), Consiglio Nazionale delle Ricerche (CNR), Strada delle Cacce, 73, 10135 Torino (TO), Italy.
Tel. +39.011.3977723 - Fax: +39.011.3489218.
E-mail: n.pampuro@ima.to.cnr.it

Key words: density, specific energy, densification, swine manure.

Acknowledgements: This work was carried out within the framework of the "FITRAREF" project, funded by the Italian Ministry of Agriculture and Forestry (Call OIGA, 2009), under the scientific direction of Dr. Eugenio Cavallo (CNR-IMAMOTER). The authors also wish to thank Mr. Giuseppe Paletto and Mr. Guarino Benvegnù (CNR-IMAMOTER) for the technical support.

Journal of Agricultural Engineering 2013; XLIV(s1):e105
doi:10.4081/jae.2013.(s1):e105

Introduction

The excessive amount of pig slurry spread on soil has contributed to nitrate water pollution both in surface and in ground waters, especially in areas classified as vulnerable zones to nitrate in accordance with European Regulation (91/676/CEE).

In order to avoid environmental pollution several technologies have been recently developed. Among these techniques, solid-liquid separation of slurry is a common practice in Italy. It leads to a solid fraction rich in phosphorous and organic matter, and to a liquid fraction which is rich in soluble nitrogen (Fangueiro *et al*., 2012). The liquid fraction can be used in land application or reused on the farm as flushing water (Garcia *et al*., 2009) and the solid fraction can be composted directly and/or co-composted with vegetable residues.

However, compost derived from swine solid fraction is a low density material (bulk density less than 500 kg m^{-3} – Pampuro *et al*., 2012). This makes it costly to transport composted swine solid fraction from production sites to areas where it could be effectively utilized for value-added applications such as in soil fertilization. Densification is one possible way to enhance the storage and transportation of the composted swine solid fraction.

Traditionally, agricultural materials are densified into pellets, cubes and bales. Pellets are the densest of these agglomerates. Therefore, they require the highest amount of input energy (19-90 kJ·kg^{-1}) during manufacturing (Tabil and Sokhansanj, 1996). The manufacture of cubes uses lower pressure than pelletizing. Production of cubes is largely limited to forage crops such as alfalfa (Bernhart *et al*., 2010). Baling is a process that combines compression and packing operations. It is typically used for grassy or fibrous-like materials that are stringy in nature (Bernhart *et al*., 2010). Compost derived from swine solid fraction is not stringy and therefore not suitable for baling.

The overall goal of this study was to investigate the densification process of compost derived from swine solid fraction for efficient transportation and off-site utilization. The first specific objective of this research was to determine the specific energy requirement for compression of compost derived from swine solid fraction at different pressure and at different pressure application time. A second specific objective was to study the equations able to predict compact density and the specific compaction energy required to manufacture compacts from two composts derived from swine solid fraction.

Materials and methods

Sample preparation

The tests were carried out using two different types of compost: swine solid fraction compost (SSFC) and wood chips compost (WCC). SSFC was obtained composting 6,000 kg of swine solid fraction, while WCC resulted by mixing 8,000 kg of swine solid fraction with 2,400 kg of wood chips obtained processing residues from park maintenance.

The initial bulk density of SSFC and WCC were 240 and 480 kg·m^{-3}, respectively.

The initial moisture content of SSFC and WCC were 51.1 and 49.6% (wb), respectively. The moisture content of the samples (mass of 10 kg for each compost type) was reduced to 10% by drying in an oven set to 50°C (Bernhart and Fasina, 2009). Only one moisture level of 10% (wb) was used and this was based upon literature review that at this moisture level, high density and quality pellets/briquettes were produced from various straw and biomass (Li and Liu, 2000; Obernberger and Thek, 2004; Mani *et al*., 2006; Adapa *et al*., 2009).

Compression equipment

The press used to obtain the compressed material has two opposite hydraulic cylinders. The unit, fitted with an oil-hydraulic unit, can deliver up to 297 kN in a time variable from 0 to 210 seconds. The press can be equipped with different compressing chambers as needed. In order to obtain the tests samples, a chamber with a diameter of 45 mm and a volume of 440 cm^3 was used.

Upper and lower cylinders are fitted with load cells (max rated load 200 kN) that give signals proportional to the compressing force. The top of the plunger is connected with a potentiometric displacement sensor (350 mm full stroke) giving the exact position and volume of the compressing chamber. The oil feed line has a pressure transducer. These signals are processed by a pc-based acquisition system capable of acquiring up to 10 ks/s. For this application the sampling rate was fixed to 1 ks/s. All the collected data were recorded with a dedicated software for post-processing operations.

Compression tests and energy calculations

The mass of samples used for making compacts was 55.00 g. Four preset pressures of 20, 50, 80 and 110 MPa corresponding to loads of 31.5, 62.3, 126.1 and 173.4 kN, were used to compress samples in the chamber. Five applications times (5, 10, 40, 90 and 120 s) for each pressure level were applied during densification process. For each material every combination of pressure and time was carried out with five replications (Figure 1).

A digital caliper was used to measure the length and the diameter, while a digital balance accurate to 0.01 g was used to measure the mass of densified material. The densities of the samples were calculated from the ratio of mass to volume.

During the compression of individual compacts, force-displacement data were recorded. Specific compression energy (SCE) was calculated following the methodology of Adapa *et al*. (2006) and Mani *et al*. (2006). The area under the force-displacement curve was integrated using the trapezoid rule (Santamarta *et al*., 2012); when combined with the briquette mass, it yielded the specific energy values in kJ·kg^{-1}.

Data analysis

Regression analysis was performed using the proc reg function in SPSS statistical software package (Version 17.0) and plotted with the experimental data using Microsoft Excel (Microsoft Office 2007). Significance testing was carried out using one way analysis of variance (ANOVA) in the SPSS statistical package.

Results

Compact density

The pressure application time in the compression process has a highly significant effect on the density as well as the maximum applied pressure ($p<0.05$). The interaction between the two parameters is not significant ($p>0.05$).

For WCC the increase in density was significant ($p<0.05$) for an increase of pressure application time from 10 to 40 s and from 90 to 120 s. For SSFC the increase in density was significant ($p<0.05$) for an increase of pressure application time from 5 to 10 s, 10 to 40 s and from 40 to 90 s.

Results from the experiments showed that average density values ranged from 1,001 to 1,435 kg·m^{-3} and from 843 to 1,259 kg·m^{-3} for WCC and SSFC respectively, upon application of pressure in the range of 20-110 MPa (Table 1).

For each pressure level applied, WCC showed density values significantly ($p<0.05$) higher than SSFC.

Eq. (1 and 2) were fitted to the experimental density values as a function of pressure application time and pressure for WCC and SSFC, respectively.

$\rho_{compact} = 179 + 0.5 * t + 260.1 * \ln(p)$ $R^2 = 0.996$ Eq (1)
$5 s \le t \le 120 s$; $20 MPa \le p \le 110 MPa$

$\rho_{compact} = 52 + 0.93 * t + 247 * \ln(p)$ $R^2 = 0.995$ Eq (2)
$5 s \le t \le 120 s$; $20 MPa \le p \le 110 MPa$

Figure 1. Samples obtained applying 50 MPa for 40 s (SSFC on the left and WCC on the right).

Specific compression energy requirement

The ANOVA showed no significant ($p>0.05$) effect of pressure application time on specific compression energy consumption.

For applied pressures of 20, 50, 80 and 110 MPa the average specific compression energy required to form the briquettes was equal to 5.6, 12.7, 19.2 and 24.9 kJ·kg^{-1} for WCC and 9.0, 17.9, 25.4 and 32.2 kJ·kg^{-1} for SSFC.

For each pressure level applied, WCC showed specific compression energy values significantly ($p<0.05$) lower than SSFC. This could be due to the effect of the composting process that leads to a weakening of the wood fires, compared to the swine manure, causing different energy adsorption.

For both materials there is a linear relationship between pressure and specific compression energy following the equation 3 (WCC) and 4 (SSFC).

$SCE_{WCC} = 0.2124 * p + 1.666$ $R^2 = 0.980$ Eq (3)

$20 \text{ MPa} \le p \le 120 \text{ MPa}$

$SCE_{SSFC} = 0.254 * p + 4.694$ $R^2 = 0.962$ Eq (4)

$20 \text{ MPa} \le p \le 120 \text{ Mpa}$

Figure 2 shows the relationship between specific compression energy and density of the densified samples.

For each density value obtained, SSFC showed specific compression energy values significantly ($p<0.05$) higher than WCC (Table 2).

For WCC and SSFC there is a non linear relationship between $\rho_{compact}$ and SCE that can be explained with a exponential equation reported as follow.

$SCE_{WCC} = 0.186\ e^{0.0034 \cdot \rho compact}$ $R^2 = 0.987$ Eq (5)

$950 \text{ kg·m}^{-3} \le \rho_{compact} \le 1450 \text{ kg·m}^{-3}$

$SCE_{SSFC} = 0.735\ e^{0.0030 \cdot \rho compact}$ $R^2 = 0.956$ Eq (6)

$800 \text{ kg·m}^{-3} \le \rho_{compact} \le 1300 \text{ kg·m}^{-3}$

Conclusions

Previous studies conducted by Demirbas (1999) have shown a logarithmic relationship between applied pressure and resulting density of briquettes manufactured from waste paper and wheat straw mixtures and applied pressure. Even though considerably higher pressures were used in that study (300-800 MPa), the briquette densities obtained (50-850 kg·m^{-3}) were lower than the densities obtained in this study. We suspect this is due to the different properties of the materials under test.

Adapa *et al.* (2009) during pellettization of different types of straw, found a polynomial relationship between applied pressure and resulting density. The mean densities of barley, canola, oat and wheat straw compacts increased from 907 to 988 kg·m^{-3}, 823 to 1003 kg·m^{-3}, 849 to 1011 kg·m^{-3} and 813 to 924 kg·m^{-3}, respectively, upon application of pressure in the range of 31.6-138.9 MPa. Although, the moisture level of 10% (wb) used by Adapa *et al.* (2009) was equal to the moisture content used in this study, we have obtained higher density values applying pressure levels of 20-110 MPa. This could be due to the different characteristics of the densification process investigated.

The specific compaction energy values found in this study were considerably higher than those found by Bernhart *et al*. (2010) during the compaction tests of poultry litter. The two main reasons for this difference were that the densities reached by Bernhart *et al*. (2010) were much lower than the densities found for this work and the moisture content of poultry litter was substantially higher.

The specific compression energies calculated for the densification of compost derived from swine solid fraction were lower than the values found by Santamarta *et al*. (2012). Using a moisture content of 10.76%

Table 1. Average density values (kg.m–3) of WCC and SSFC materials obtained using different pressure levels (20, 50, 80 and 110 MPa)

Applied pressure (MPa)	Materials	
	WCC	SSFC
20	1,001±35	843±37
50	1,218±30	1,078±41
80	1,344±32	1,170±32
110	1,435±25	1,259±35

Table 2. Average density and specific compression energy values of WCC and SSFC materials obtained using different pressure levels (20, 50, 80 and 110 MPa)

WCC		SSFC	
$\rho_{compact}$ (kg·m^{-3})	SCE (kJ.kg^{-1})	$\rho_{compact}$ (kg·m^{-3})	SCE (kJ.kg^{-1})
1,001±34	5.6±0.4	843±37	9.0±0.7
1,218±30	12.7±0.6	1,078±41	17.9±0.7
1,344±32	19.2±1.1	1,170±32	25.4±1.1
1,435±25	24.9±1.7	1,259±35	32.2±0.9

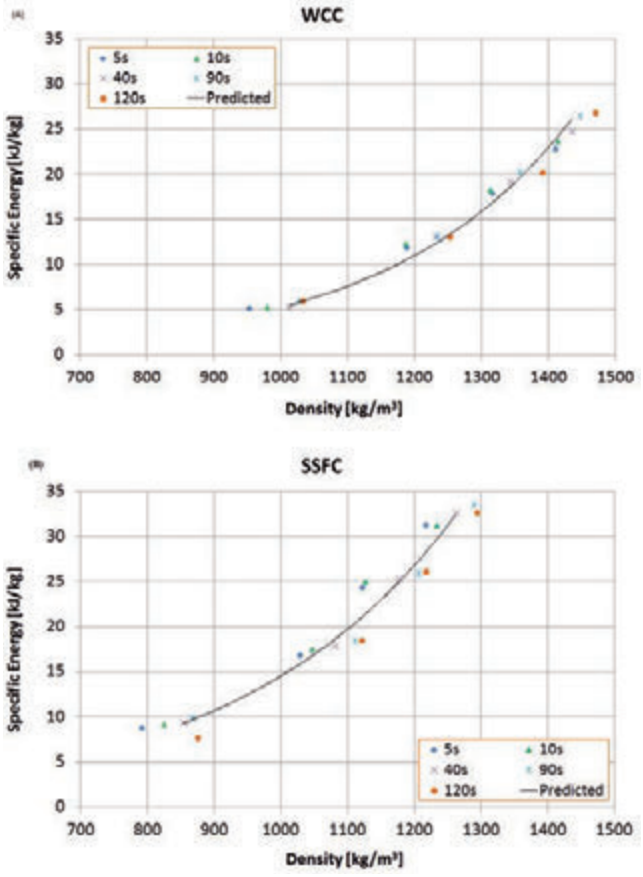

Figure 2. Relationship between specific compression energy and density to form the WCC (A) and SSFC (B) briquettes.

and an applied pressure of 47.7 MPa, the specific energy required to form the OSR straw briquettes was 24.95 kJ·kg^{-1}, compared to 12.7 and 17.9 kJ·kg^{-1} used to produce WCC and SSFC briquettes, respectively, when the applied pressure was 50.0 MPa and the moisture content was 10%.

Moreover the average specific compression energy values found with this trial were lower than the specific energy required to manufacture pellets from biomass feedstock (typically 19-90 kJ·kg^{-1}; Colley *et al*., 2006).

As stated by Mani *et al*. (2004), the energy requirements depend mainly upon the applied pressure and moisture content, but also on the physical properties of the material and the method of compaction.

It can be concluded that the pressure agglomeration process is more efficient than the pellettization process - the specific energy values obtained were significantly lower and the final density values were higher when applying the same compaction pressure level.

The results from this study could be used in the design of economical and simple on-farm pressure agglomeration equipment.

References

Adapa PK, Schoenau GJ, Tabil LG, Sokhansanj S, Singh A, 2006. Compression of fractionated sun-cured and dehydrated alfalfa chops into cubes – specific energy models. Bioresource Technol 98: 38-45.

Adapa P, Tabil L, Schoenau G, 2009. Compaction characteristics of barley, canola, oat and wheat straw. Biosyst Eng 204: 335-344.

Bernhart M, Fasina OO, 2009. Moisture effect on the storage, handling and flow properties of poultry litter. Waste Manage 29: 1392-1398.

Bernhart M, Fasina OO, Fulton F, Wood CW, 2010. Compaction of poultry litter. Bioresource Technol 101: 234-238.

Colley Z, Fasina OO, Bransby D, Lee YY, 2006. Moisture effect on the physical characteristics of switch grass pellets. T ASABE 49: 1845-1851.

Demirbass A, 1999. Physical properties of briquettes from waste paper and straw mixture. Energy Convers Manage 40: 437-445.

Fangueiro D, Lopes C, Surgy S, Vasconcelos E, 2012. Effect of the pig slurry separation techniques on the characteristics and potential availability of N to plants in the resulting liquid and solid fractions. Biosyst Eng 113: 187-194.

Garcia MC, Szogi AA, Vanotti MB, Chastain JP, Millner PD, 2009. Enhanced solid-liquid separation of dairy manure with natural flocculants. Bioresource Technol 100: 5417-5423.

Li Y, Liu H, 2000. High-pressure densification of wood residues to form an upgraded fuel. Biomass Bioenerg 19: 177-186.

Mani S, Tabil LG, Sokhansanj S, 2004. Evaluation of compaction equations applied to four biomass species. Canadian Biosystems Eng 46: 351-361.

Mani S, Tabil LG, Sokhansanj S, 2006. Specific energy requirement for compacting corn stover. Bioresource Technol 30: 648-654.

Obernberger I, Thek G, 2004. Physical characterization and chemical composition of densified biomass fuels with regard to their combustion behavior. Biomass Bioenerg 27: 653-669.

Pampuro N, Facello A, Cavallo E, 2012. Density-pressure relationship in densification of swine solid fraction. Proc International Conference of Agricultural Engineering, Valencia (Spain), July 8-12.

Santamarta LC, Ramirez AD, Godwin RJ, White DR, Chaney K, Humphries AC, 2012. Energy use and Carbon Dioxide emissions associated with the compression of oilseed rape straw. Proc International Conference of Agricultural Engineering, Valencia (Spain), July 8-12.

Tabil LG, Sokhansanj S, 1996. Process conditions affecting the physical quality of alfalfa pellets. Appl Eng Agric 12: 345-350.

Biogas yield from Sicilian kitchen waste and cheese whey

Antonio Comparetti,[1] Pierluigi Febo,[1] Carlo Greco,[1] Santo Orlando,[1] Kestutis Navickas,[2] Arvydas Nekrosius,[2] Kestutis Venslauskas[2]

[1]Dipartimento di Scienze Agrarie e Forestali, Università degli Studi di Palermo, Italy; [2]Institute of Energy and Biotechnology Engineering, Aleksandras Stulginskis University, Akademija, Kauno r., Lithuania

Abstract

The aim of this study is to determine the chemical composition of kitchen waste and cheese whey, as well as the biogas yield obtained from the Anaerobic Digestion (AD) tests of these two raw materials.

Since the separated waste collection is performed in the town of Marineo (Palermo), a sample of kitchen waste, different from food industry one and included in the Organic Fraction of Municipal Solid Waste (OFMSW), was collected from the mass stored at the households of this town. Moreover, a sample of cheese whey was collected in a Sicilian mini dairy plant, where sheep milk is processed. This investigation was carried out inside laboratory digesters of Aleksandras Stulginskis University (Lithuania). Total Solids (TS) resulted 15.6% in kitchen waste and 6% in cheese whey, while both the raw materials showed a high content of organic matter, 91.1% and 79.1%, respectively. The biogas yield resulted 104.6 l kg^{-1} from kitchen waste and 30.6 l kg^{-1} from cheese whey. The biogas yield from TS resulted 672.6 l kg^{-1} using kitchen waste and 384.7 l kg^{-1} using cheese whey. The biogas yield from Volatile Solids (VS) resulted 738.9 l kg^{-1} using kitchen waste and 410.3 l kg^{-1} using cheese whey.

Introduction

The Organic Fraction of Municipal Solid Waste (OFMSW) and/or food industry by-products (*e.g.* cheese whey) and/or animal manure can be processed through Anaerobic Digestion (AD), in order to produce biogas and "digestate". The biogas, mostly containing methane, can be transferred to the natural gas distribution pipeline or Combined Heat and Power (CHP) plants or used as vehicle fuel, while the digestate can be used as bio-fertiliser.

The chemical composition of OFMSW and, therefore, the yield of AD process, is influenced by several factors, including climate, collection frequency and method, season, cultural practices, as well as changes in its solid components (Tchobanoglous *et al.*, 1997; Mace *et al.*, 2000; Pavan *et al.*, 2000; Saint-Joly *et al.*, 2000; Bolzonella *et al.*, 2003a, 2003b, 2005). Several papers focused on the AD of organic wastes according to their origin, *e.g.* OFMSW (Bolzonella *et al.*, 2005), household (Krzystek *et al.*, 2001) and kitchen waste (Rao and Singh, 2004). Many examples exist on the use of AD to treat the mechanically separated biodegradable fraction of municipal waste (Mata-Alvarez, 2003). There are also examples of the processing of mixed source segregated biodegradable wastes, *e.g.* kitchen and garden wastes (Archer *et al.*, 2005), but there are only a few reports on AD plants entirely processing household food waste separated at source (Banks *et al.*, 2011). The interest in this process is growing in Europe, due to the rising energy costs of wet waste processing, the requirement to meet the targets of the EU Landfill Directive (99/31/EC) (EU, 1999) and the need to comply with regulations for the disposal of animal by-products (EU, 2002). According to the regulations of many European countries, whether the waste is not separated at source but the organic fraction is recovered through a Mechanical-Biological Treatment (MBT) plant, the digestate produced is not allowed to be applied on land (Stretton-Maycock and Merrington, 2009). As a consequence, governments and industry are strongly interested in the AD methods of household food waste separated at source (Banks *et al.*, 2011).

Furthermore, kitchen waste was also surveyed as co-substrate for AD (Angelidaki and Ahring, 1997; Brinkman, 1999; Comparetti *et al.*, 2013). Anaerobic co-digestion of mixtures including food industry by-products and animal manure was previously investigated and, among these mixtures, particular interest was paid to the co-digestion of animal manure and cheese whey (Ghaly, 1996; Gelegenis *et al.*, 2007). Several authors focused on the AD of cheese whey for biogas production (Lo and Liao, 1986; Yan *et al.*, 1989; Ghaly and Pyke, 1991). Some studies showed that the co-digestion of cheese whey and other substrata (*i.e.* maize silage, beet pulp, carrot residues and glycerine fraction) can be advantageous inside lab-scale bio-reactors (Kacprzak *et al.*, 2010).

In this perspective the aim of this study is to determine the chemical composition of kitchen waste and cheese whey, as well as the biogas yield obtained from the AD tests of these two raw materials.

Materials and methods

Since the separated waste collection is performed in the town of

Correspondence: Carlo Greco, Dipartimento di Scienze Agrarie e Forestali, Università degli Studi di Palermo, Viale delle Scienze, Building 4, 90128 Palermo, Italy.
Tel. +39.091.23897057 - Fax: +39.091.484035.
E-mail: carlo.greco@unipa.it

Keywords: anaerobic digestion, biogas yield, cheese whey, kitchen waste.

Contributions: the authors contributed equally.

Conflict of interests: the authors declare no potential conflict of interests.

Journal of Agricultural Engineering 2013; XLIV(s1):e106
doi:10.4081/jae.2013.(s1):e106

Marineo (Palermo), a sample of kitchen waste, different from food industry one and included in the Organic Fraction of Municipal Solid Waste (OFMSW), was collected from the mass stored at the households of this town in a day of March 2012.

Moreover, a sample of cheese whey was collected in a Sicilian mini dairy plant, located in Ventimiglia di Sicilia (Palermo) and processing sheep milk, in the same day.

The two samples were transported to the Institute of Energy and Biotechnology Engineering of Aleksandras Stulginskis University (Lithuania).

In the laboratory of this institute, the Total Solids concentration (TS) was determined in each of the two samples, by drying it in an oven at 105 ± 2 °C temperature for 24 hours, as well as Volatile Solids concentration (VS), by burning it at 500 °C temperature. Total organic Carbon concentration (C_T) was determined in each sample, by using an analyser TOC II, as well as Total Nitrogen concentration (N_T), by using a Kjeldahl apparatus.

The AD tests were carried out in two laboratory scale anaerobic digesters under controlled temperature (38 ± 0.5 °C). The sample of kitchen waste (having a mass of 336 g) was added to a laboratory digester, consisting of stainless steel vessels (having a volume of 20 l) equipped with a substrate mixer (having a mixing intensity of 60 min^{-1}). Instead, the sample of cheese whey (having a mass of 26 g) was added to a digester having a volume of 0.5 l. The biogas produced was collected at the top of each digester and conveyed, through a drum type flow meter, to a gasholder (Tedlar® bag, having a volume of 25 l). Later the biogas collected was analysed by using a Schmack SSM 6000 biogas analyser.

The AD tests of kitchen waste were performed in three replications and those of cheese whey in nine replications.

The AD results of kitchen waste and cheese whey were evaluated by means of the following indicators: biogas production intensity b, biogas yield from biomass B_M, biogas yield from biomass Total Solids B_{TS}, biogas yield from biomass Volatile Solids B_{VS}, energy obtained from biomass e_M, from biomass Total Solids e_{TS} and from biomass Volatile Solids e_{VS}. Biogas production intensity b indicates the volume of biogas produced during the time of biomass biological degradation. Biogas yield from biomass B_M, from biomass Total Solids B_{TS} and from biomass Volatile Solids B_{VS} was calculated by means of the following equations (Navickas *et al.*, 2003) :

$$B_M = \frac{b_{dt}}{m}; \quad B_{TS} = \frac{b_{dt}}{m_{TS}}; \quad B_{VS} = \frac{b_{dt}}{m_{VS}} \qquad \text{(Eq. 1, Eq. 2, Eq. 3)}$$

where :
b_{dt} is the volume (l) of the biogas produced (in laboratory) during the time interval dt (duration of biomass biological degradation);
m is the mass (kg) of the biomass sample analysed;
m_{TS} is the mass (kg) of Total Solids in the biomass sample;
m_{VS} is the mass (kg) of Volatile Solids in the biomass sample.

The energy obtained during AD from biomass e_M, e_{TS}, e_{VS} was determined by means of the following equations :

$$e_M = B_M \cdot e_b; \quad e_{TS} = B_{TS} \cdot e_b; \quad e_{VS} = B_{VS} \cdot e_b \qquad \text{(Eq. 4, Eq. 5, Eq. 6)}$$

where :
e_b is the energetic value of biogas (MJ·m^{-3}), depending on methane concentration in biogas (%).

The energetic value of biogas was determined by means of the following equation :

$$e_b = 0.0353 \cdot \frac{C_M}{100} \qquad \text{(Eq. 7)}$$

where :
C_M is the methane concentration in biogas (%).

Results and discussion

The chemical composition of kitchen waste and cheese whey samples are shown in Table 1. Total Solids (TS) resulted 15.6% in kitchen waste and 6% in cheese whey, while both the raw materials showed a high content of organic matter, 91.1% and 79.1%, respectively.

Optimum C/N ratios are generally in the 20-30 range in anaerobic digesters (Themelis and Verma, 2004; Ward *et al.*, 2008). The C/N ratio of kitchen waste resulted 17.4, while that of cheese whey resulted 23.1. Therefore, both values can be assumed to be optimal for AD process. However, Ward *et al.* (2008) reported in a review article that, after an acclimation period, anaerobic bacteria also accept lower C/N ratios (approximately 9).

The results of AD tests, whose duration was five days using kitchen waste and four days using cheese whey, are shown in Table 2.

The biogas yield resulted 104.6 l kg^{-1} from kitchen waste and 30.6 l kg^{-1} from cheese whey. The biogas yield from TS resulted 672.6 l kg^{-1} using kitchen waste (Figure 1) and 384.7 l kg^{-1} using cheese whey (Figure 2).

Table 1. Chemical composition of kitchen waste and cheese whey samples.

Parameter	Measurement unit	Kitchen waste	Cheese whey
Total Solids (TS)	%	15.6	6.0
Organic matter (in TS)	%	91.1	79.1
Organic Carbon	%	5.69	2.29
Total Nitrogen	%	0.328	0.099
C/N ratio	-	17.4	23.1

Table 2. Results of AD tests.

Indicator	Rate	Kitchen waste	Cheese whey
Biogas yield from biomass, B_M	l·kg^{-1}	104.6	30.6
Biogas yield from Total Solids, B_{TS}	l·kg^{-1}	672.6	384.7
Biogas yield from Volatile Solids, B_{VS}	l·kg^{-1}	738.9	410.3

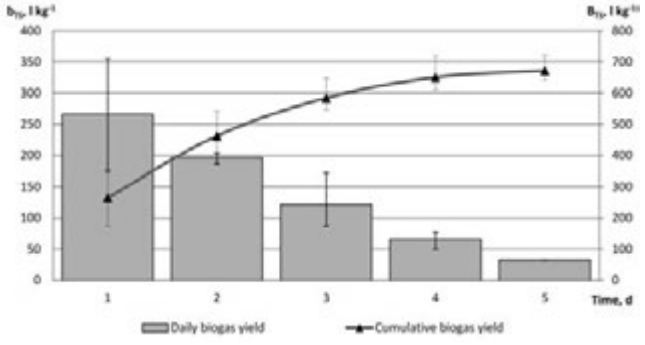

Figure 1. Biogas yield from Total Solids (TS) obtained using kitchen waste during AD tests: the histograms are the daily yield b_{TS}, while the curve is the total cumulative yield B_{TS}.

The biogas yield from Volatile Solids (VS) resulted 738.9 l kg^{-1} using kitchen waste (Figure 3) and 410.3 l kg^{-1} using cheese whey (Figure 4).

Furthermore, other indicators were determined for the kitchen waste sample: methane concentration in biogas of 61.9%, energy obtained from biomass (e_M) of 2.28 MJ·kg^{-1}, energy obtained from dry matter (e_{TS}) of 14.67 MJ·kg^{-1} and energy obtained from organic matter (e_{VS}) of 16.13 MJ·kg^{-1}.

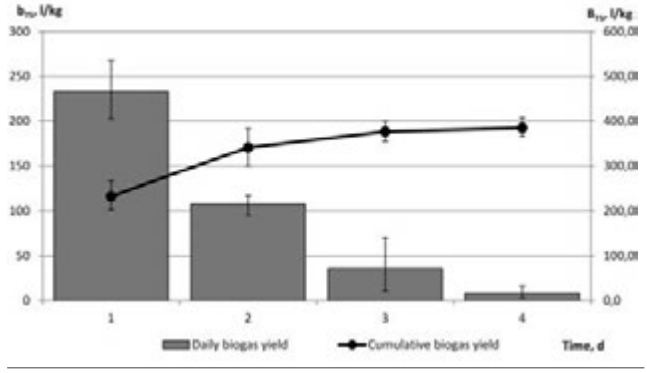

Figure 2. Biogas yield from Total Solids (TS) obtained using cheese whey during AD tests: the histograms are the daily yield b_{TS}, while the curve is the total cumulative yield B_{TS}.

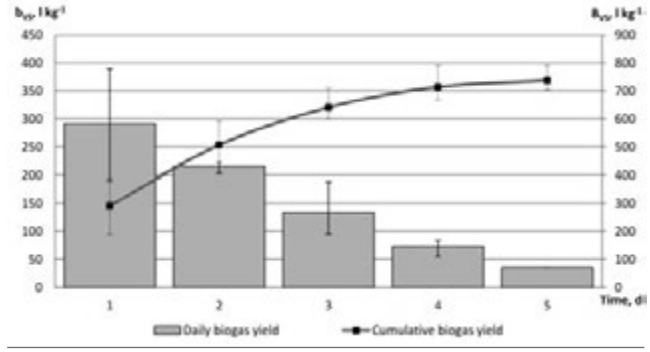

Figure 3. Biogas yield from Volatile Solids (VS) obtained using kitchen waste during AD tests: the histograms are the daily yield b_{VS}, while the curve is the total cumulative yield B_{VS}.

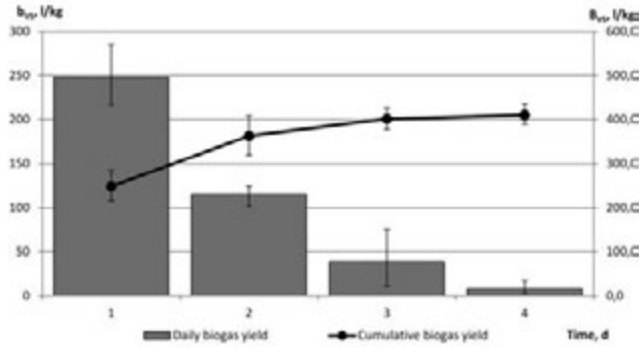

Figure 4. Biogas yield from Volatile Solids (VS) obtained using cheese whey during AD tests: the histograms are the daily yield b_{VS}, while the curve is the total cumulative yield B_{VS}.

Therefore, the biogas yield from VS using both the processed raw materials was comparable with the results of Banks *et al.* (2011) (642 l·kg^{-1} with a methane concentration of 62%) and Bolzonella *et al.* (2006) (700 l·kg^{-1} and 180 l·kg^{-1} from sorted OFMSW with a methane concentration of 56%). However, the biogas yield from organic matter could be temporally variable, due to changing life style and consumed food composition.

Conclusions

Both kitchen waste and cheese whey are reasonable raw materials for biogas production, in terms of Total Solids (TS) and organic matter content, while the C/N ratio obtained (17-23) can be assumed to be optimal for AD process.

The time of biomass biological degradation was five days using kitchen waste and four days using cheese whey.

The biogas yield obtained using kitchen waste was 104.6 l kg^{-1} from biomass, 672.6 l kg^{-1} from TS and 738.9 l kg^{-1} from Volatile Solids (VS). The biogas yield obtained using cheese whey was 30.6 l kg^{-1} from biomass, 384.7 l kg^{-1} from TS and 410.3 l kg^{-1} from VS.

Waste management is a problem to be solved not only in Sicily but in the whole Italy, where the landfill sites have been or will be filled in with MSW very soon, as well as people don't accept the use of new sites in their municipal land. Moreover, the measures aimed at promoting segregated waste collection have been only scarcely implemented in Italy, where the environmentalist movements always fight against the building of incinerators, as well as the inefficient waste management has often caused public health problems in whole cities (*e.g.* Naples and Palermo).

In this perspective politicians should promote the valorisation of organic wastes (*e.g.* kitchen waste and cheese whey) through AD process. In fact, whether kitchen waste was anaerobically digested, it would highly reduce the OFMSW amount that is nowadays aerobically composted or, even worse, landfilled. Moreover, even if the biogas yield from cheese whey resulted about three times lower than that from kitchen waste, the AD of the liquid waste of dairies and mini dairy plants is an interesting option that would solve the problem of its disposal, better than others, *i.e.* purification, aerobic composting and feeding of pigs. These policy measures would contribute to reduce CO_2 emission and, therefore, global warming.

References

Angelidaki I., Ahring B.K. 1997. Codigestion of olive oil mill wastewaters with manure, household waste or sewage sludge. Biodegradation 8(4):221-6.

Archer E., Baddeley A., Klein A., Schwager J., Whiting K. 2005. MBT: A Guide for Decision Makers - Processes, Policies and Markets. Juniper Consulting Ltd., Uley, Gloucestershire, UK.

Banks C.J., Chesshire M., Heaven S., Arnold R. 2011. Anaerobic digestion of source-segregated domestic food waste: Performance assessment by mass and energy balance. Bioresource Technol 102:612-20.

Bolzonella D., Battistoni P., Mata-Alvarez J., Cecchi F. 2003a. Anaerobic digestion of organic solid wastes: process behaviour in transient conditions. Water Sci Technol 48(4):1-8.

Bolzonella D., Innocenti L., Pavan P., Traverso P., Cecchi F. 2003b. Semi-dry thermophilic anaerobic digestion of the organic fraction of municipal solid waste: focusing on the start-up phase. Bioresource Technol 86(2):123-9.

Bolzonella D., Pavan P., Fatone F., Cecchi F. 2005. Anaerobic fermentation of organic municipal solid wastes for the production of soluble organic compounds. Ind Eng Chem Res 44(10):3412-8.

Bolzonella D., Pavan P., Mace S., Cecchi F. 2006. Dry anaerobic digestion of differently sorted organic municipal solid waste: a full-scale experience. Water Sci Technol 53(8):23-32.

Brinkman J. 1999. Anaerobic digestion of mixed slurries from kitchens, slaughterhouses and meat processing industries. In: J. Mata Alvarez., A. Tilche and F. Cecchi (Editors), Proceedings of the 2nd Int. Symp. on Anaerobic Digestion of Solid Waste, Barcelona, Spain, 15-18 June, pp. 190-195.

Comparetti A., Febo P., Greco C., Orlando S. 2013. Current state and future of biogas and digestate production, Bulg J Agric Sci 19(1):1-14.

European Union, 1999. Council Directive 99/31/EC of 26 April 1999 on the landfill of waste. In: Official Journal of the European Communities, 182, 16/07/1999, pp 1-19.

European Union, 2002. Regulation (EC) 1774/2002 of the European Parliament and of the Council, 03/10/2002, laying down health rules concerning animal by-products not intended for human consumption.

Gelegenis J., Georgakakis D., Angelidaki I., Mavris V. 2007. Optimization of biogas production by co-digesting whey with diluted poultry manure. Renew Energ 32:2147-60.

Ghaly A.E., Pyke J.B. 1991. Amelioration of methane yield in cheese whey fermentation by controlling the pH of the methanogenic stage. Appl Biochem Biotech 27:217-37.

Ghaly A.E. 1996. A comparative study of anaerobic digestion of acid cheese whey and dairy manure in a two-stage reactor. Bioresource Technol 58:61-72.

Kacprzak A., Krzystek L., Ledakowicz, S. 2010. Co-digestion of agricultural and industrial wastes. Chem Pap 64(2):127-31.

Krzystek L., Ledakowicz S., Kahle H.J., Kaczorek K. 2001. Degradation of household biowaste in reactors. J Biotechnol 92:103-12.

Lo K.V., Liao P.H. 1986. Digestion of cheese whey with anaerobic rotating biological contact reactor. Biomass 10:243-52.

Mace S., Bolzonella D., Cecchi F., Mata-Alvarez J. 2003. Comparison of the biodegradability of the grey fraction of municipal solid waste of Barcelona in mesophilic and thermophilic conditions. Water Sci Technol 48(4):21-28.

Mata-Alvarez J. (Ed.). 2003. Biomethanization of the Organic Fraction of Municipal Solid Wastes. IWA Publishing, London, UK.

Navickas K., Zuperka V., Janusauskas R. 2003. Energy input for cultivation and preparation of biomass for biogas production / LZUI instituto ir LZU universiteto mokslo darbai / LZUU 35(4):109-16.

Pavan P., Battistoni P., Mata-Alvarez J., Cecchi F. 2000. Performance of thermophilic semi-dry anaerobic digestion process changing the feed biodegradability. Water Sci Technol 41(3):75-82.

Rao M.S., Singh S.P. 2004. Bio energy conversion studies of organic fraction of MSW: kinetic studies and gas yield-organic loading relationships for process optimization. Bioresource Technol 95:173-185.

Saint-Joly C., Desbois S., Lotti J.P. 2000. Determinant impact of waste collection and composition on anaerobic digestion performance: industrial results. Water Sci Technol 41(3):291-7.

Stretton-Maycock D., Merrington G. 2009. The use and application to land of MBT compost-like output - review of current European practice in relation to environmental protection. Science Report - SC030144/SR3. Environment Agency, Bristol, UK.

Tchobanoglous G., Hilary T., Vigil S.A. 1997. Integrated solids waste management: engineering principles & management issues. Mc Graw-Hill Inc.

Themelis N.J., Verma S. 2004. Anaerobic Digestion of Organic Waste in MSW. Waste Management World 20-24.

Ward A.J., Hobbs P.J., Holliman P.J., Jones D.L. 2008. Optimisation of the anaerobic digestion of agricultural resources (review article). Bioresource Technol 99(17):7928-40.

Yan J.Q., Lo K.V., Liao P.H. 1989. Anaerobic digestion of cheese whey using up-flow anaerobic sludge blanket reactor. Biol Waste 27:289-305.

Assessment of energy return on energy investment (EROEI) of oil bearing crops for renewable fuel production

A. Restuccia, S. Failla, D. Longo, L. Caruso, I. Mallia, G. Schillaci

DiGeSA, Mechanics and Mechanization Section, University of Catania, Italy

Abstract

As reported in literature the production of biodiesel should lead to a lower energy consumption than those obtainable with its use. So, to justify its consumption, a sustainable and "low input" production should be carried out. In order to assess the sustainability of *Linum usitatissimum, Camelina sativa* and *Brassica carinata* cultivation for biodiesel production in terms of energy used compared to that obtained, the index EROEI (Energy Return On Energy Invested) has been used. At this aim, an experimental field was realised in the south-eastern Sicilian land. During the autumn-winter crop cycle, no irrigation was carried out and some suitable agricultural practices have been carried out taking into account the peculiarity of each type of used seeds. The total energy consumed for the cultivation of oil bearing crops from sowing to the production of biodiesel represents the *Input* of the process. In particular, this concerned the energy embodied in machinery and tools utilized, in seed, chemical fertilizer and herbicide but also the energy embodied in diesel fuels and lubricant oils. In addition, the energy consumption relating to machines and reagents required for the processes of extraction and transesterification of the vegetable oil into biodiesel have been calculated for each crops. The energy obtainable from biodiesel production, taking into account the energy used for seed pressing and for vegetable oil transesterification into biodiesel, represents the *Output* of the process. The ratio *Output/Input* gets the EROEI index which in the case of *Camelina sativa* and *Linum usatissimum* is greater than one. These results show that the cultivation of these crops for biofuels production is convenient in terms of energy return on energy investment. The EROEI index for Brassica carinata is lower than one. This could means that some factors, concerning mechanisation and climatic conditions, were not suitable to ensure higher crop yields.

Correspondence: Giampaolo Schillaci DiGeSA, Mechanics and Mechanization Section, University of Catania, Via S. Sofia,100, 95123 Catania, Italy
E-mail: giampaolo.schillaci@unict.it

Keywords: Biodiesel, EROEI, net energy balance, oil bearing crops, renewable energy.

Contributions: Restuccia A., data collected, data analyzing, manuscript writing and references search; Failla S., data analyzing, manuscript writing and references search; Longo D., Caruso L. data collected and references search; Mallia I., data collected, data analyzing and reference search; Schillaci G., reviewing.

Conflict of interests: the authors declare no potential conflict of interests.

Funding: the work was supported by the project AGROSO (Evaluation of high erucic acid oilseed species in the Mediterranean environment for use in the energy sector as an alternative to mineral oil with a high environmental impact) funded by MiPAAF (Ministry of Agriculture, Food and Forestry).

Journal of Agricultural Engineering 2013; XLIV(s1):e107
doi:10.4081/jae.2013.(s1):e107

Introduction

In Europe, agriculture plays an important role in providing renewable energy resources. The quote of renewable energy deriving from this sector grew, in recent years, from 3.6% in 2005 to 10.5% in 2010. According to the GSE, in 2012, renewable resources production from agriculture brought in nearly 12,250 GWh (GSE, 2012; Ortenzi, 2013).

To achieve the main objectives set under the NES (National Energy Strategy), which was launched on 8 March 2013, it will need to take into consideration some strategic parameters including that relating to the energetic valorisation of biomass for the production of biofuels. It is also to highlight that the bio-energy production must create jobs as well as important opportunities for safeguarding the land and the national landscapes, especially in marginal lands (Monni, 2013).

In this context, to support the development of agro-energy in , it could be of great importance to focus on crops adapted to marginal land and non-irrigated or historically used for other crops and now being abandoned.

The cultivars of linseed (*Linum usitatissimum L.*) have been widely used in in the past years, recording a yield per hectare almost double the national average (Crescini, 1969: Rivoira, 2001).

The cultivars of *Brassica carinata* has attracted considerable interest also in , thanks to greater vigor, productive potential and increased resistance to biotic and abiotic stress shown by this species in some environments in respect of other varieties (eg. Brassica juncea and Brassica napus) (Mazzoncini *et al.*, 1993; Progetto Fi.Sic.A., 2008; Lazzeri *et al.*, 2009).

In addition, *Camelina sativa* together with other oilseed crops, have garnered interest as potential sources of biodiesel. *C. sativa* has attracted interest as an oil crop because of its ability to grow in various climatic conditions, low nutrient requirements and resistance to disease and pests (Zubr, 1996; Gugel and Falk, 2006; Francis and Warwick, 2009).

In summary, the choice of these high value species erucic, cultivated for energy purposes, derived from their ability to adapt to soil and climatic unfavourable conditions, enhancing thus the marginal areas or abandoned areas of agricultural land.

To be considered sustainable, the production of biodiesel (cultiva-

tion, extraction and trans- esterification) should involve lower energy consumption than those obtainable with its use. From energy audits conducted on rapeseed and sunflower it shows that to the phases of agricultural production and transesterification are attributed, in almost equal parts, about 76% of the total energy used and approximately 15 MJ/kg of biodiesel produced. Considering a calorific value of biodiesel equal to 37.3 MJ/kg, approximately 2.5 units of energy (biodiesel) per unit of energy consumed were obtained (Riva *et al.* 2008).

To assess, from point of view of energetic use, the economic advantages deriving from the cultivation of these crops in order to produce biodiesel, the index EROEI (Energy Return On Energy Invested) has been used. This energetic balance allows to correlate the amount of energy obtained from the crop (Output) with the amount of energy used for its cultivation (Input) as reported in literature (Cosentino *et al.*, 2008; Verani *et al.*, 2008; Lazzeri *et al.*, 2009; D'Avino *et al.*, 2010; Murphy *et al.*, 2010; Unakitan *et al.*, 2010; Pracha and Volk, 2011).

To obtain Input and Output data, energetic equivalents were be used, by choosing those reported in literature and most used (Baldini *et al.*, 1982; Volpi, 1992; Unakitan *et al.* 2010; Fore *et al.*, 2011).

Most recent energetic equivalents are reported in the literature and are worthy of note, but the values are often aggregated or missing and therefore it was not appropriate to consider them in this work (Singh *et al.* 2006; Ozkan *et al.* 2007; Da Silva *et al.* 2010; Zelina *et al.* 2011).

At last, this work is preliminary to a subsequent assessment of emissions of greenhouse gases (GHG), calculated taking into account the data input and output of the cultivation/production. This is to meet the sustainability criteria laid down for the supply chain of biofuels established with the RED (Directive 2009/28/EC).

Materials and methods

The experimental field

The experimental field was carried out in the province of Siracusa in south-eastern Sicily (36 ° 49'02 .61 "N 15 ° 05'33 .81" E); it covers an area of about with a maximum width of about and length of about . For this experiment, three non-irrigated plots were realised, one for each species concerned; each plot covers an area of and has a size ofof 80 m × 62 m. To avoid contamination between different species sown and to facilitate the mechanization of cultural practices, a buffer zones of between the plots and the edge of the area, and between the parcels have been left. The field is flat, rectangular in shape, oriented NW-SE and has an altitude of above sea level. The soil is compact, with lightweight skeleton presence and weaving of medium consistency.

The cultural practices and the machines

Due to the small size of oilseed crops, the tillage were carried out by performing a through preparation of the seed bed. At the beginning of December, a preliminary shredding of existing weed was carried out. The tillage was performed with a shredder having knives on a horizontal rotor, driven by the power take-off, of a width of 2.70 m and mass of 1,130 kg.

Subsequently, to break the compact layer of the surface soil and aerate it a harrowing was carried out. The farm machine used is a cultivator having 9 chisel plow shovels arranged in two rows, of a width of 2.25 m and mass of 500 kg. For the refinement of clods created in the previous tillage a hoeing was conducted. This tillage was carried out with a rotary tiller of a width of 2.05 m and mass of 450 kg.

Sowing and fertilization took place simultaneously in the third decade of December, by distributing 320 kg/ha of complex mineral fertilizer (NP 25-15) and 39 kg/ha of linseed, 4.2 kg/ha of seed *C. sativa* and 5.3 kg/ha of seed *B. carinata*.

For shredding, harrowing, hoeing, the farm machines were connected to a 4 WD tractor of 74 kW and mass of 3,500 kg.

The seeder used for linseed is universal type with mechanical distribution, 19 distributors and mass of 740 kg, double hopper for seed and fertilizer. The width is 2.50 m with adjustable spacing between the distributors (the minimum is 13 cm). In order to obtain a distance between the rows equal to 26 cm the distributors were used alternatively, by closing 9 of them. Because of the small size of the seed, the seed depth was maintained between 0.5 and 1 cm. The seeder was connected to a 4WD tractor of 74.5 kW and mass of 3,500 kg.

The seeder used for seeds of *C. sativa* and *B. carinata* is precision type with pneumatic distribution. It has three binate rows of distributors with a distance of 7 cm between rows and 40 cm between the binate rows, so as to obtain a working width of the machine equal to 1.60 m. In particular, the distance between rows was equal to 2.6 cm and the depth of sowing 1.5 cm for *B. carinata*, while the distance between rows was equal to 1.4 cm and the depth of sowing 0.5 cm for *C. sativa* because of the very small size of the seed. The distance between the binate rows was equal to 40 cm in both cases. The seeder was connected to a 2WD tractor of 44 kW.

After sowing, the rolling to make homogeneous the surface of the soil and a pre-emergence herbicide treatment were carried out. Doses of 1 L/ha of product with active ingredient "Linurom" in concentrations of 45 g/L, for linseed, and doses of 1 L/ha of product with active ingredient "Metazachlor" pure in concentrations of 43.5 g/L for the remaining crops were used. The volumes distributed were respectively 350 L/ha for linseed and 175 L/ha for other crops; these volumes correspond to the minimum recommended doses.

The rolling was performed with smooth roller having a width of 2.4 m and mass of 1000 kg, connected to a 4WD of 78 kW and mass of 2,540 kg.

The pre-emergence weed control was carried out by a bar sprayer 10 m wide and flat spray tips. The pressure during the treatment was 20 bar. The sprayer was connected to a 4WD tractor of 52 kW and mass of 3,200 kg.

During the growing season of the crop, periodic inspections of the experimental field were carried out which did not reveal the need to conduct additional cultural practices.

The harvesting of the experimental field was carried out in the first ten days of June, upon the completion of the seeds maturation, which was tested by sampling in the experimental field.

A combine harvester was used for the harvesting, commonly used for herbaceous crops, of 167 kW, mass of 10,400 kg and cutter bar of 5 m, by properly adjusting the speed of the awner and the opening of the threshing drum. In detail, given the small size of the seeds and not excessive resistance to detachment from the capsule by the same, the speed of rotation of the awner was set relatively low, amounting to about 850 rpm for *L. usitatissimum* and 650 rpm for *C. sativa* and *B. carinata.* The opening of the threshing drum was set of 6 mm anteriorly and 2 mm posteriorly for *L. usitatissimum* and 12 mm anteriorly and 3 mm posteriorly for *C. sativa* and *B. carinata*.

Subsequently, through appropriate laboratory tests were evaluated: the moisture content of the seeds, the thousand seeds weight mass of 1000 seeds and the number of seeds per capsule.

The methodology

In order to assess the sustainability of *Brassica carinata*, *Camelina sativa, Linum usitatissimum* cultivation for biodiesel production in terms of energy used (Input) compared to that obtained (Output), the index EROEI (Energy Return On Energy Invested) has been used.

The Output represents the energy which is possible to obtain by the products used for the cultivation, the Input refers to the factors of production used for the cultivation, whether direct or indirect (machinery

and equipments, diesel fuel and lubricant oil, products for plant protection, fertilizers, etc.).

This methodology involves the use of the so-called energetic equivalents (or indexes), which represent, in the case of Input, the cost of energy incurred for the use of machinery during the various cultural practices and for the consumption of materials necessary for cultivation (seeds, fertilizers, herbicides, etc.), while, in the case of Output, the energy which can be obtained from the crop (vegetable oil, biodiesel, etc..).

For each farm machine used during the experimentation it was possible to find in the literature the energetic equivalent amount (expressed in MJ/h), which indicates the energy used per each hour of machine use; while the consumption of diesel fuel and lubricant oil are calculated separately (Baldini *et al.*, 1982; Unakitan *et al.* 2010). Energetic indexes were found in the literature also for seeds, fertilizers, herbicides, diesel fuel and lubricant oil, oil extraction and transesterification; these are expressed in MJ per unit of product (Baldini *et al.*, 1982; Volpi, 1992; Fore *et al.*, 2011).

To this end, in order to calculate the effective working capacities [ha/h] and then the time units of utilization [h/ha], the effective width of the work [m] and the forward speed [m/s] on the field for each cultural practice were recorded by adopting a standardized methodology.

The diesel fuel consumption was calculated through a direct measurement by using the "top-up" method on the field; furthermore they were verified through the sizing of power, necessary and sufficient, of the tractors used in the different cultural practices.

The consumption of lubricant oil was calculated by taking into account a specific consumption equal to 0,009 kg/kWh (Bodria *et al.*, 2006) and an engine load resulting from the ratio between the ideal power calculated through the sizing and the effective available power of the tractors used in the field.

In the case under consideration, the Output is represented by the energy content of biodiesel produced by the transesterification of vegetable oil mechanically extracted from seeds. The energetic equivalent for the biodiesel is considered equal to the calorific power that is 37.25 MJ/L (Avella *et al.*, 2009).

It is assumed that both for the extraction of oil from seed and for the transesterification of the same are required 5.31 MJ/L of biodiesel (Fore *et al.*, 2011), defined as energy consumed during the processes for machines (screw-press and transesterification machine), electricity, methanol and sodium hydroxide (reagents and catalysts). At the end, these Input data related to the process shall be in addition to those relating to the cultivation in order to obtain the total Input.

Results

Mechanization and agronomic viewpoint

The experimental trials has shown different results for the three species cultivated both for mechanization aspect and for agronomic aspects.

The cultural practices were carried out choosing carefully the machines both for their adaptability to the soil structure and to obtain a good final soil tillage in order to facilitate the crops in the first stages of growth. Moreover, accurate adjustments were carried out on the farm machines both in the farm workshop and in the open field, with particular attention to the seeder and to the harvester in order to optimize their efficiency and to reduce losses.

The three crops were grown in the same experimental field respectively in three similar plots for their physical-chemical features. The pre-sowing and post-sowing cultural practices were carried out at the same time for the three crops, so they gave back the same work capacity [ha/h] and unitary time [h/ha]. At the opposite, the sowing has recorded different values more or less remarkable both for the different wide of the seeders and for the different speed with the same seeder (Table 1). In fact, the mechanical seeder have a width double than the precision seeder. In addition, in order to ensure accurate seeding, the forward speeds were kept lower than those normally used in open fields which are greater to 2m/s with these seeders. For this reason also the working capacity were lower (about 1 ha/h) and unitary times higher of the average values found in field for the sowing. So, the percentage on the total of the cultural practices is quite high and equal to about 20% for *C. sativa* and *B. carinata* while 10% for *L. usitatissimum*.

As a result, the shredding is the practice that recorded the higher incidence on the total in respect to the other practices. It was around 40% for all the crops. The others tillage (harrowing and hoeing) showed similar percentage among 12 and 18% and together account for about 30%. Rolling, weeding and harvesting affect less than 8%, especially the weeding thank to the highest work capacity (about 3.3 ha/h).

The total unitary time is rather high for all three crops considered in respect to other crops, quite similar for the *C. sativa* and *B. carinata*

Table 1. Working capacity in the experimental field.

Cultural practices	Ve m/s	Le m	Ce ha/h	Unitary time h/ha	Incidence *L. usitatissimum*	*C. sativa*	*B. carinata*
Shredding	0.35	2.50	0.32	3.17	42%	38%	38%
Harrowing	1.40	2.05	1.03	0.97	13%	12%	12%
Hoeing	1.10	1.90	0.75	1.33	18%	16%	16%
Sowing and Fertiliz.							
- *L. usitatissimum*	1.55	2.35	1.31	0.76	10%		
- *C. sativa*	1.56	1.15	0.65	1.55		19%	
- *B. carinata*	1.29	1.30	0.60	1.66			20%
Rolling	2.20	2.20	1.74	0.57	8%	7%	7%
Weeding	0.95	9.70	3.32	0.30	4%	4%	4%
Harvesting	1.40	5.00	2.52	0.40	5%	5%	5%
		TOTAL	*L. usitatissimum*	7.51	100%		
			C. sativa	8.29		100%	
			B. carinata	8.40			100%

(8.3-8.4 h/ha) and a little lower for the *L. usitatissimum* (7.5 h/ha) due to a greater work capacity of the sowing.

For each crop, in addition to the yield, the thousand seed weight, the relative humidity and the number of seed for capsule have been evaluated (Table 2).

As a result, the agronomic parameters obtained are comparable with those found in literature, except for the *B. carinata* yield. In this last case, the delayed sowing period for this crop has probably led to a reduction in yield which can still oscillate between 0.1 and 1.2 t/ha (Monti and Venturi, 2007).

The yield of *L. usitatissimum* was very similar (1.45 t/ha) to that reported in literature that is of about 1.52 t/ha (Rivoira, 2001). Even the weight of a thousand seeds is one of the values listed in the bibliography: the thousand seeds weight could be in a range between 3 and 15 g (Crescini, 1969) and for most of commonly variety cultivated between 5 and 10 g (Rivoira, 2001).

In the case of *C. sativa*, the yield was about 1.1 t/ha and the thousand seeds weight was about 1.15 g as reported in other studies where yield was between 1.1 and 3.3 t/ha and thousand seeds weight of about 1.2 g (Crescini, 1969; Zubr, 1996; Gugel *et al.*, 2006).

Regarding *B. carinata*, a recent study performed in Sicily reports a yield of about 1.5 t/ha, that is more than that harvested with the experimental trials and thousand seeds weight of about 3.3 g that is little less than value reported in Table 1 for this crop (Progetto Fi.Sic.A., 2008).

Energetic viewpoint

In order to evaluate the sustainability of the energetic crops the EROEI index was calculated. To do this, the energy gained with the biodiesel producible and that consumed for machines and products used were compared.

In Table 3 is reported the energy consumption for the use of the machine due to the energy embodied in each of them.

The cultural practice that recorded the maximum Energy required was the shredding with an incidence between 34.5 and 38.1% on the total. This result is strictly related to the high unitary time required by the tillage.

Likewise, the sowing was again the practice that recorded the maximum difference among the three crops due to the different seeders used. In fact, for *L. usitatissimum* cultivation a value of about the half than the others two crops was registered. Moreover, only one point percentage of difference between *C. sativa* and *B. carinata* was recorded.

On the other hand, the chemical weeding showed the lower energy consumption a little bit more than 1%, also because of the lowest values of energetic equivalents considered in this cultural practice for the tractor and the operating machine.

The total for each crop shows negligible differences between the species and amounts to a few tens of MJ/ha, due only to the different unitary times of the sowing.

The detailed consumptions of fuel and lubricant are reported in Table 4, where also the percentage of every single practice for each culture is showed.

As already seen for the use of the machines in Table 3, even in this case the differences among the fuel and lubricant consumptions are strictly related to the unitary time needed to carry out each cultural

Table 2. Agronomic parameters.

Crop	Yield	Thousand seeds weight	Relative humidity	Seeds per capsule
	t/ha	g/1000 seeds	%	n
L. usitatissimum	1,45	4,93	8,33%	9
C. sativa	1,10	1,15	6,26%	11
B. carinata	0,85	3,12	11,74%	15

Table 3. Energy consumption due to use of machines.

Cultural practices	Unitary time	Energetic index		Energy required		Total	Incidence		
		tractor	operating machine	tractor	operating machine		*L. usitatissimum*	*C. sativa*	*B. carinata*
	h/ha	MJ/h	MJ/h	MJ/ha	MJ/ha	MJ/ha		%	
Shredding	3.17	27.13[1]	2.26[1]	86.13	7.17	93.30	38.1%	34.9%	34.5%
Harrowing	0.97	27.13[1]	6.07[1]	26.26	5.87	32.13	13.1%	12.0%	11.9%
Hoeing	1.33	27.13[1]	2.51[1]	36.06	3.34	39.39	16.1%	14.7%	14.6%
Sowing and fertilizing									
- *L. usitatissimum*	0.76	27.13[1]	1.76[1]	20.69	1.34	22.03	9.0%	-	-
- *C. sativa*	1.55	27.13[1]	1.76[1]	42.01	2.73	44.73	-	16.7%	-
- *B. carinata*	1.66	27.13[1]	1.76[1]	44.94	2.92	47.85	-	-	17.7%
Rolling	0.57	27.13[1]	6.07[1]	15.57	3.48	19.05	7.8%	7.1%	7.0%
Weeding	0.30	13.08[1]	0.61[1]	3.94	0.18	4.13	1.7%	1.5%	1.5%
Harvesting	0.40	87.63[2]	-	34.77	-	34.77	14.2%	13.0%	12.8%
					L. usitatissimum	244.81			
				TOTAL	*C. sativa*	267.52	100%	100%	100%
					B. carinata	270.64			

[1] Baldini *et al.*, 1982; [2] Unakitan *et al.*, 2010.

practice. In fact, in all cases, the tillage and harvesting recorded in total more than 80% of the consumption, while the rolling and the chemical weeding were always equal or less than 2%. Also the sowing confirmed a big difference when different seeder was used (about 10%) and again a small difference when the same seeder was used in two different species (about 1%).

This result primarily affects the total amount of diesel fuel consumed in three crops. In particular, the cultivation of *L. usitatissimum* involves a saving of about 7-8 kg/ha compared to the other two crops considered.

To assess the total energy consumption for all the products used, fertilizer, herbicide and seeds were considered together to diesel fuel and oil lubricant (Table 5).

Looking at the Table, it appears that the fertilizer represents the product which involves the higher Energy required with value around 7 thousand MJ/ha (about 60% on the total). Also the values of Energy required for the diesel fuel consumption are quite high and around to 3.400 to 3.800 MJ/ha. This two products represent together about 90% of the total of Energy required for the use of the products during the cultivations.

In the case of *L. usitatissimum* the use of seeds is energetically relevant because of the high quantity used for sowing (39 kg/ha). The seed represents about 8% of the total Energy required, while for the other two species it remains around to 1%.

An analysis of the energy consumption relating to machinery, diesel fuel, lubricant oil, fertilizer, herbicide and seed showed that the sowing together to the fertilizing becomes the cultural practice which requires more than 65% of total energy used for the cultivation (Figure 1). The alignment of values concerning the sowing and fertilizing in the three crops is due principally to the amount of energy required to the fertilizer used.

Despite the use of herbicide, the chemical weeding remains, after rolling, the practice that requires the smallest amount of energy. This

Table 4. Diesel fuel and lubricant oil consumption.

Cultural practices	Diesel fuel [kg/ha]	Incidence *L. usitatissimum*	Incidence *C. sativa*	Incidence *B. carinata*	Oil lubricant [kg/ha]	Incidence *L. usitatissimum*	Incidence *C. sativa*	Incidence *B. carinata*
Shredding	17.10	26.6%	23.8%	23.6%	0.55	25.0%	22.7%	22.5%
Harrowing	12.53	19.5%	17.5%	17.3%	0.45	20.6%	18.6%	18.4%
Hoeing	17.21	26.8%	24.0%	23.8%	0.62	28.2%	25.6%	25.3%
Sowing and fertilizing								
- *L. usitatissimum*	2.12	3.3%			0.08	3.5%		
- *C. sativa*	9.54		13.3%		0.31		12.6%	
- *B. carinata*	10.20			14.1%	0.33			13.4%
Rolling	1.10	1.7%	1.5%	1.5%	0.04	1.8%	1.6%	1.6%
Chemical weeding	1.27	2.0%	1.8%	1.7%	0.04	1.9%	1.7%	1.7%
Harvesting	12.99	20.2%	18.1%	17.9%	0.42	19.0%	17.2%	17.1%
TOTAL *L. usitatissimum*	64.32				2.19			
C. sativa	71.75	100%	100%	100%	2.43	100%	100%	100%
B. carinata	72.41				2.45			

Table 5. Energy consumption for all the products used during the cultivation

Product	Quantity kg/ha	Energetic index MJ/kg	Energy required MJ/ha	*L. usitatissimum* %	*C. sativa* %	*B. carinata* %
Diesel fuel						
- *L. usitatissimum*	64,3	52,34[1]	3,366	28.35%		
- *C. sativa*	71,8	52,34[1]	3,756		32.99%	
- *B. carinata*	72,4	52,34[1]	3,789			33.10%
Oil lubricant						
- *L. usitatissimum*	2,20	45,51[1]	100	0.84%		
- *C. sativa*	2,43	45,51[1]	111		0.97%	
- *B. carinata*	2,45	45,51[1]	111			0.97%
Fertilizer	320	22.09[1]	7,069	59.53%	62.09%	61.75%
Herbicide	1.0	343.32[1]	343	2.89%	3.02%	3.00%
Seeds						
- *L. usitatissimum*	39	25.54[2]	996	8.39%		
- *C. sativa*	4.2	25.54[2]	107		0.94%	
- *B. carinata*	5.3	25.54[2]	135			1.18%
TOTAL		*L. usitatissimum*	11,875	100%	100%	100%
		C. sativa	11,386			
		B. carinata	11,448			

[1] Baldini *et al.*, 1982; [2] Volpi, 1992.

is due to the small dose required for after sowing treatment for oilseed crops.

Finally, in order to calculate the total energetic Input for the cultivation of one hectare of the three different oilseed crops, the amount of biodiesel producible from each crop is estimated. By considering the yields reported in Table 2 and an oil yield of 35% for *L. usitatissimum* (Rivoira, 2001), of 38% for *C. sativa* (Gugel and Falk, 2006) and of 36% for *B. carinata*, it is possible to obtain respectively 507, 418 and 306 kilograms of vegetable oil. Moreover, a recent research shows that yields between 88 and 96 kg of biodiesel from transesterification of 100 kg of vegetable oil under alkaline catalysis condition are obtainable (Kumar *et al.*, 2013). The authors also report that the yield differences observed are related to the amount of reagent, catalyst and process temperature employed. Taking into account a mean yield of 92% from the quantities reported above is possible to obtain the biodiesel amounts showed in Table 6.

The total energetic Input data of the process are closely related to the yields and therefore higher values are those of *L. usitatissimum*, follow to the *C. sativa* and *B. carinata*. Similarly also the total amount of energy consumed follows the same order. However, the values obtained are lower than those reported in literature for other crops (Cosentino *et al.*, 2008).

In *L. usitatissimum* and *C. sativa* cases, the EROEI index is bigger than one. It means that these two cultivation are energetically convenient. At the opposite the EROEI index of *B. carinata* is less than one. In this case we spent more energy than we gained from the seeds harvested. However, if we consider the average yield of 1.5 t/ha found by other authors, a biodiesel production of about 596 kg/ha could be obtainable. In this way the biodiesel production could be around to 621 L/ha which determines an EROEI index of 1.7.

Conclusions

The study aimed to verify the technical and economic feasibility of oil bearing crops such as *Linum usitatissimum, Camelina sativa* and *Brassica carinata*, grown for energy purposes for the production of fuel oils and biodiesel. Besides these crops could also get in rotation with durum wheat also in order to improve its productivity.

The experiment performed in Sicily suggests that is possible to use non-irrigated soils for these energetic crops, but the correct cultural practices and sowing period are crucial to obtain good yields. However these were comparable with those reported in literature.

It's important to note, however, that the values of Input are lower than those reported in literature for other crops.

Moreover, in order to decrease the energy input could be reduced the amount of fertilizer to be used. In fact, it represent more than 50% of the totally energy invested.

A correct soil management could be useful to reduce weeds existent and so to eliminate the shredding that is one of the most expensive cultural practices in term of energy consumption.

In order to reduce energetic costs and work time, due to two-three tillage and rolling, the direct sowing with simultaneous tillage and sowing could be checked.

Also a correct use and choosing of the seeder can affect the energy consumptions as in the case object of study. In this regard, the cultivation of *L. usitatissimum* involves a saving of about 7-8 kg/ha compared to the other two crops considered: on larger farms, these differences can have a considerable economic impact.

The EROI index, even with the limitations inherent in the experimental test in object, is bigger than one for *Linum usitatissimum* and *Camelina sativa*, while it is less than one for *B. carinata* because of the delayed of sowing of the crop.

Although the results obtained, using the index EROEI, are partial with respect to an overall assessment which provides also for the calculation of greenhouse gas (GHG) emissions, the study in question is a first step to promote the cultivation of oil bearing crops in agricultural areas marginal or abandoned.

Moreover, it was estimated that biodiesel may be more convenient than diesel when the oil prices reach 75 €/barrel and even greater economic competitiveness may result from the recognition of the environmental benefits coming from the full chain of biofuels (Monti and Venturi, 2007).

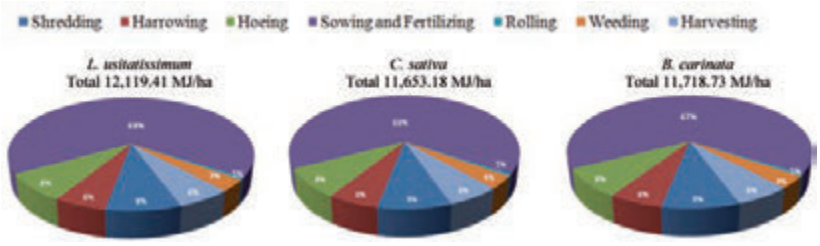

Figure 1. Energy use of machinery, diesel fuel, oil lubricant, seeds, herbicide and fertilizer for each cultural practice in the three crops.

Table 6. Input, output and EROEI index.

Crop	Biodiesel L/ha	Input energetic index MJ/L	Process input MJ/ha	Cultivation input MJ/ha	Total input MJ/ha	Output energetic index MJ/L	Total output MJ/ha	EROEI
L. usitatissimum	583,62	5.31[1]	3099,05	12,118.34	15217,39	37.25[2]	21740,03	1,43
C. sativa	480,70	5.31[1]	2552,52	11,651.06	14203,58	37.25[2]	17906,08	1,26
B. carinata	351,90	5.31[1]	1868,59	11,719.19	13587,78	37.25[2]	13108,28	0,96

[1]Fore *et al.*, 2011; [2]Avella *et al.*, 2009.

References

Avella F., Faedo D., Macor A. Impiego di una miscela gasolio/biodiesel al 30% (B30) nei motori diesel: effetto sulle emissioni inquinanti. La rivista dei combustibili e dell'industria chimica; 2009 vol. 63 n.2, 2-15.

Baldini E., Alberghina O., Bargioni G., Cobianchi D., Iannini B., Tribulato E., Zocca A. Analisi energetiche di alcune colture arboree da frutto. Numero Speciale Rivista di Ingegneria Agraria; 1982 n.2 (giugno).

Bodria L., Pellizzi G., Piccarolo P. Meccanica Agraria Vol I. Edagricole, Bologna, 2006.

Crescini F. Piante Erbacee Coltivate. I Grandi Settori dell'Agricoltura 4. Ramo Editoriale degli Agricoltori, 1969; 221-234.

Cosentino L. S., Copani V., Patanè C., Mantineo M., D'Agosta G. M. Le colture da biomassa per energia per gli ambienti italiani. Attualità e prospettive. Produzione di energia da fonti biologiche rinnovabili. 2 - Le risorse primarie. I Georgofili. Firenze 2008; 163-183.

D'Avino L., Lazzeri L., Dainelli R., Spugnoli P. Un software per la valutazione di sostenibilità delle filiere agro-energetiche. Atti del Convegno "Attualità della ricerca nel settore delle energie rinnovabili da biomassa". Ancona, Facoltà di Agraria, 16-17 dicembre. 2010; 391-400.

Fore S. R., Porter P., Lazarus W. Net Energy balance of small-scale on farm biodiesel production from canola and soybean. Biomass and Bioenergy 35, Elsevier, 2011; 2234-2244.

Francis A., Warwick S.I. The Biology of Canadian Weeds. 142. Camelina alyssum (Mill.) Thell.; C. microcarpa Andrz. ex DC.; C. sativa (L.) Crantz. Canadian Journal of Plant Science 89(4), 2009; 791-810.

GSE 2012. Rapporto Statistico 2011, Impianti a Fonti Rinnovabili.

Gugel R.K., Falk K.C. Agronomic and seed quality evaluation of Camelina sativa in western Canada. Canadian Journal of Plant Science 2006; 1047-1058.

Lazzeri L., D'Avino L., Mazzoncini M., Antichi D., Mosca G., Zanetti F., Del Gatto A., Pieri S., De Mastro G., Grassano N., Cosentino S., Copani V., Ledda L., Farci R., Bezzi G., Lazzari A., Dainelli R., Spugnoli P. On farm agronomic and first environmental evaluation of oil crops for sustainable bioenergy chains.Italian Journal of Agronomy, 2009, Vol. 4 (4), p. 171-180.

Mazzoncini M., Vannozzi G.P., Megale P., Secchiari P., Pistoia A., Lazzeri L. Ethiopian Mustard (Brassica Carinata A.Braun) Crop in Central Italy. Note 1: Characterization and agronomic evaluation. Agricoltura mediterranea 1993; 123, 330-338.

Monni M. La strategia nazionale per lo sviluppo energetico. Mondo Macchina, anno XXII, 2013; n. 3-4. 44-45.

Monti A., Venturi G. Il contributo delle colture da energia alla sostenibilità ambientale. Accademia Nazionale di Agricoltura. Annali Edizione straordinaria CXXVII (Anno 2007). Bologna.

Murphy D. J., Hall C. A. S. Year in review EROI on energy return on (energy) invested. Annals of the New York Academy of Sciences 2010; 1185, 102-118, New York.

Ortenzi M. Europa ed agro energie, un quadro articolato. Mondo Macchina, anno XXII, 2013; n. 3-4; 42-43.

Pracha A. S., Volk T.A. An Edible Energy Return on Investment (EEROI) Analysis of Wheat and Rice in Pakistan. Sustainability 3, Elsevier 2011; 2358-2391.

Progetto Fi.Sic.A. (Filiera Siciliana per l'Agroenergia). Studio di fattibilità per l'introduzione di filiere agro-energetiche in Sicilia. A cura di B. Messina, V. D'Anna, R. Paci, F. Viola. 2008.

Riva G., Foppa Pedretti E., Toscano G. Biocombustili e biocarburanti: aspetti generali e tecnici della loro produzione e utilizzo. Produzione di energia da fonti biologiche rinnovabili. 1 - Le tecnologie. I Georgofili. Firenze 2008; 163-183.

Rivoira G. Lino (Linum usitatissimum L.) - Coltivazioni Erbacee, piante oleifere, da zucchero, da fibra, orticole e aromatiche. vol. 2, 213-218, Pàtron Editore 2001.

Unakitan G., Hurma H., Yilmaz F. An analysis of energy use efficiency of canola production in Turkey. Energy 2010; n.35; 3623-2627.

Verani S., Sperandio G., Picchio R., Savelli S. Nozioni di base per la costituzione di micro filiere energetiche di autoconsumo. Progetto sportello COFEA. Tipografia Bonanni, Roma 2008.

Volpi R. Bilanci energetici in agricoltura. Laruffa Editore, Reggio Calabria 1992.

Zubr J. Oil-seed crop: Camelina sativa. Industrial Crops and Products 6, Elsevier 1996; 113-119.

Harvesting of southern Piedmont's orchards pruning residues: evaluations of biomass production and harvesting losses

M. Grella, M. Manzone, F. Gioelli, P. Balsari

Department of Agricultural, Forest and Food Sciences, DISAFA, University of Torino, Italy

Abstract

In recent years, there has been an increasing interest in respect to all farming residues, including orchard pruning residues. The masses and dimensional characteristics of branches pruned, depend on several factors such as fruit variety, active strength plant, training systems, intensity and periodicity pruning. Many studies were done to fix this type of biomass availability, however they're not up-to-date, and usually they are lacking of accurate surveys. A detailed knowledge of current pruning biomass availability, both qualitative and quantitative, is also necessary for the evaluation of the economic sustainability of their energetic exploitation. In this context, in order to provide an assessment of the real chain potential of energy renewable production, from Cuneo territory pruning residues, a research was conducted on two different orchards species *Actinidia* (Kiwi tree) and *Malus* (Apple tree) pruned in two different ways: "traditional system" and "taille longue system". For each species, pruning residues amount were quantified together with their diameter. The surveys were performed at least on four half trees placed on the same row spacing with three randomized replications in the crop. The amount of pruning residues were determined by a dynamometer (precision 0.02N) whereas the diameter of individual cut-off branches has been detected at the base of the same using a twentieths calliper. Subsequently were performed pruning residues windrowing by rotating rake and the harvest of the same by fixed chamber round baler suitably modified. At the end of these operations have been determined harvesting losses with the same methodology used for the initial quantification of residues. The first result shows that with the "traditional pruning system" the biomass average availability is of 2.5t DM ha^{-1} and 3.0t DM ha^{-1}, respectively for kiwi tree and apple tree. For the latter, the average values are significantly lower 0.5t DM ha^{-1} with "taille longue" pruning system. The harvesting losses have been nearly 19% in kiwi tree and 16% for apple tree (from 95% to 11% according to the variety). In both crops the variation of harvester losses are due mainly to the size and conformation (straight) of pruned branches.

Correspondence: Grella Marco, DISAFA, University of Torino, via Leonardo da Vinci 44, 10095 Grugliasco (TO), Italy.
Tel. +39.011.6708610 - Fax: +39.011.6708591-
E-mail: marco.grella@unito.it

Keywords: biomass, harvest, losses, orchard, pruning.

Contribution: M. Grella, M. Manzone, data collecting and analyzing; M. Grella, manuscript writing and references search; F. Gioelli, P. Balsari, manuscript reviewing; P. Balsari research planning.

Conflict of interest: the authors declare no potential conflict of interest.

Journal of Agricultural Engineering 2013; XLIV(s1):e108
doi:10.4081/jae.2013.(s1):e108

Introduction

Within the national energy scenario, the production of energy from alternative sources is an issue of basic importance and interest, especially in view of two opposing factors: the need to comply the aims of greenhouse gas emissions under the Directive 2009/29 EC so-called "climate-energy package 20-20-20" (reduction of greenhouse gas emissions by 20%, increasing to 20% the share of energy produced from renewable sources and achieve a 20% energy savings, all by 2020), and the growing energy needs that require an organic saving policy. In this regard, the commitments Italy have to respect impose a serious and urgent assessment for using renewable sources for energy. In this context is located the use of biomass energy, as defined by Article 2 of Legislative Decree 29 December 2003, number 387 (text updated according to the changes introduced by Law number 99/2009) as *"the biodegradable fraction of products , waste and residues from agriculture (including vegetal and animal substances), forestry and related industries, as well as the biodegradable fraction of industrial and municipal waste".*

Agriculture is one of the main sectors for supplying renewable fuels. In Italy this sector has particular importance considering that, there are no significant high productive crops (Short Rotation Forestry) specifically dedicated to this purpose (Biomasse Italia S.p.A., 2008; Manzone M., 2006). The main problem of the biomass energy enhancement is in fact related to supply's difficulties: the agricultural sector is able to provide different types of biomass, rising from the herbaceous energy crops to woody, from dedicated to residual productions. In agriculture the potential of residual woody biomass is mostly represented by the pruning of orchards, olive tree and vines (ENAMA, 2011). These biomasses are cut and generally laid down on the soil between the rows or harvested and burned on the sideline. They represent a serious problem for the development of parasites and uncontrolled fires (Vita in Campagna, 2012). Furthermore their management represents a huge additional cost for farmers (Cotana *et al*., 2008). Nevertheless, the use of such wastes for energy production could solve the problem of their disposal, reduce the management costs for the farmer and, at the same time, increase the economic revenue of the farm. Several studies (CNR, 2012; ENAMA, 2011; ENEA, 2010; ISTAT, 2010; ITABIA, 2005) were conducted on the technical characteristics and the availability of biomass and biofuels. Nevertheless the amount of agricultural residues is generally determined by multiplying the cultivated surface with coefficients describing the residues

productivity (CESTAAT, 1990). The information given are consequently often too general and do not allow to be transfer to a specific site.

These studies providing a comprehensive overview, but the heterogeneity of orchards make necessary focused surveys for a new knowledge of framework. Only on the basis of these new knowledge, we will be able to real assess the area vocation for that specific bioenergy supply chain.

The project "Energy from the orchard: an example of supply chain for the production of renewable energy from orchards pruning" (FRUITGAS), funded by the European Union within the Measure 124 of the Rural Development Programme (F.E.A.S.R. 2007/2013 - CHALLENGES "HEALTH CHECK") is carried out nearby two representative orchard farms of Piedmont region, located in the Cuneo (CN) Province.

The project is divided into different activities that can be summarized in the collection, storage and energy use of pruning residues of different fruit tree species.

The project is in its first year of development and to date has been performed pruning, windrowing the harvest and transport to the farm of biomass while are currently an ongoing storage and drying phases.

The work focuses on the quantitative and dimensional characterization of the orchards pruning in order to: understand this influence on the harvesting losses in relation to the machine used. To optimize the harvesting machine collection system of the pruning in function of dimension of the same.

Materials and methods

Two species of fruit tree in terms of woody biomass suitable for energy use have been considered: *Actinidia* spp. (Kiwi tree) and *Malus* spp. (apple tree). These two species are at present the most representative ones of the Cuneo area, covering a surface of 4454.61ha and 3482.53ha respectively (ISTAT, 2010).

For the apple tree two different pruning techniques were compared (Table 1), "traditional" and "taille longue" (pruning method which provides for the free growth of the branches, which are not shortened, and the reduction of bending interventions)(Musacchi *et al.*, 2011; Diemoz *et al.*, 2003), and four different variety: *Gala*, *Scarlett*, *Ambrosia* and *Golden* all spindle trained. The first three varieties have the same rootstock (M9), and the fourth have M26 rootstock. Furthermore, in order to verify a possible effect of the plant age in the production of biomass, orchards of different age (Table 1) were compared. For the Kiwi tree only the crops age (Table 1) was considered due to the fact that *Hayward* is currently the only cultivated variety always managed with the same pruning system called "traditional".

For each species, variety and planting year the mass of the pruning residues through direct surveys within the crops was determined. The size classification of each branch was determined as well.

The surveys were performed on portions of the row spacing at least 4 meters long, at a distance greater than 10 meters from the sideline and on rows not placed on the edge of plot. Adopting these parameters, the number of plants insisting on each survey area was different according to the trees spacing: 4 half kiwi tree and 10 to 20 half apple tree. All measurements were performed with three replicates randomly distributed inside the experimental plot.

The quantification of the cut material was made by the weighing of the branches divided into diameter classes of regular width of 5 millimeters. The determination of the weight was achieved by using a digital dynamometer (Sicutool SCU 4488B) with a precision of 0.02 Newton (N), while for the measurement of the diameters was used a mechanical twentieths Vernier callipers (Valex_1800308).

The biomass production was estimated by analytical calculation between the material weighed in the individual areas of survey and the total crop area. The latter parameter was expressed in dry matter for unit area (t DM ha^{-1}).

The dry matter content of the pruning residues was measured as the difference in weight of fresh material and after drying in a forced ventilation oven (Controls D1396-10) for about 24 hours at a temperature of 103 ° C.

In order to quantify the biomass actually harvestable, the material has been appropriately ordered in swaths through a rake (GIRORAMI new 8BC) and subsequently harvested by a fixed-chamber roundbaler for forages (LERDA 135). The roundbaler was previously modified so that it was able to realize conglomerates of biomass of considerable weight (about 0,5 tons of raw materials with 150 bar (1bar = 10^5 Pa) of pressure in the compression chamber) and to reduce the cost of transportation in a perspective of a future large-scale use of this biofuel.

The harvest losses are detected with the same methodology described above for the quantification of total biomass production (survey area was different according to the trees spacing, with three replicates randomly distributed inside the experimental plot).

Results and discussion

Analysis of diameter classes

The collected data (Figure 1) showed that the kiwi tree has branches of larger diameter than those of the apple tree. A different distribution inside diameter classes is obtained also considering the different apple tree pruning system , in the taille longue over 90% of the diameters fall in the first and second classes, while with the traditional pruning system the majority of the branches (95%) is divided into the first three classes.

In fact, the traditional pruning system reflected in a greater vigor of

Table 1: Technical characteristics of the experimental orchards under investigation.

Species	Variety	Plant year	Rootstock	Coltivation technique	Pruning technique
Kiwi	Hayward	2004	/	Arbor	traditional
Kiwi	Hayward	1988	/	Arbor	traditional
Melo	Scarlett	1999	M9 PAJAN2	Spindle	taille longue
Melo	Gala	1999	M9	Spindle	taille longue
Melo	Ambrosia	2007	M9	Spindle	taille longue
Melo	Gala	2003	M9	Spindle	traditional
Melo	Golden	1990	M26	Spindle	traditional

the plant, promoting the production of branches of greater diameter, while the taille longue system produce a lower woody biomass due to a lower number of cut-off branches for smaller diameter.

Analysis of the amount of biomass produced.

Similarly to what has been observed in the diametric analysis of the cut branches, the amount of produced biomass (Figure 2) reflects the adopted pruning system. Regardless to the considered apple tree varieties, the taille longue pruning system produces an average of 0.46 t DM ha^{-1} while the traditional pruning system 3.04 t DM ha^{-1}.

Within the apple tree pruned by the taille longue techniques the types that contributed to a lesser extent to the production of biomass (0.10 t DM ha^{-1}) was the var. ambrosia (-87.5% compared to var. gala), whereas the greater production was achieved with the var. gala (0.83 t DM ha^{-1}). Intermediate values were obtained with the var. scarlett 0.44 t DM ha^{-1} (-46.6% compared to var. gala). With the traditional pruning system, apple tree produced an average of about 3 t DM ha^{-1} which is approximately 4.5 times higher than the taille longue pruning system. The greatest amount of biomass is obtained with the apple tree var. golden with 3.87 t DM ha^{-1} while the smaller one with the var. gala with 2.21 t DM ha^{-1} (-43.0% compared to var. golden).

For the kiwi tree, the production of biomass on average amounted to 2.51 t DM ha^{-1}, a value very close to that found for the apple tree pruned with the traditional system. The kiwi plants of 2004 produced 3.10 t DM ha^{-1} of biomass corresponding to +37.9% yield when compared to that of the plants from 1988 (1.93 t DM ha^{-1}).

Analysis of losses at harvest

As shown in Figure 3 with the taille longue pruning system on average the 47% of the pruning residues were lost at harvest. Losses recorded with the traditional pruning system were considerably lower (on average of 11% of the residues). However in var. ambrosia the losses are equal to 95%, significantly higher than the losses average of taille longue pruning system. This trend is due to the different conformation of the pruned branches that in the taille longue pruning system are characterized by a small diameter (no more than 15mm), high straightness and limited length (in the ambrosia type the length of the branches never exceeds 300 mm). The traditional pruning system showed losses very similar regardless of the considered varieties of apple tree.

In kiwi tree, regardless to the trees age the values of the harvest losses are around 19% of the available biomass. In this case, the harvest losses are mainly due to the straightness of the branches that barely adapt to harvest mechanical system of the round balers on the market.

Analyzing data of lost biomass expressed as the amount of dry matter (t DM ha^{-1}) the trend is reversed than the losses percentage. The lesser quantity losses ranging from 0.10 to 0.34 t DM ha^{-1} for the apple tree pruned with taille longue system and intermediate values from 0.29 to 0.38 t DM ha^{-1} for the apple tree pruned with the traditional system. The kiwi tree recorded the greatest quantity losses ranging from 0, 38 to 0.58 t DM ha^{-1}.

Conclusions

The processed data show both the kiwi tree, although when affected by bacterial canker (*Pseudomonas syringae* pv *actinidiae*) which limits their vigor (Balestra *et al.*, 2009; Renzi *et al.*, 2012), and the apple tree can guarantee a good production of biomass (2.5 – 3.0 t DM ha^{-1}). Nevertheless the harvest of such potential biofuel is extremely difficult and determines heavy biomass losses (from 11 to 47% of the pruning residues depending on the species, variety and pruning technique).

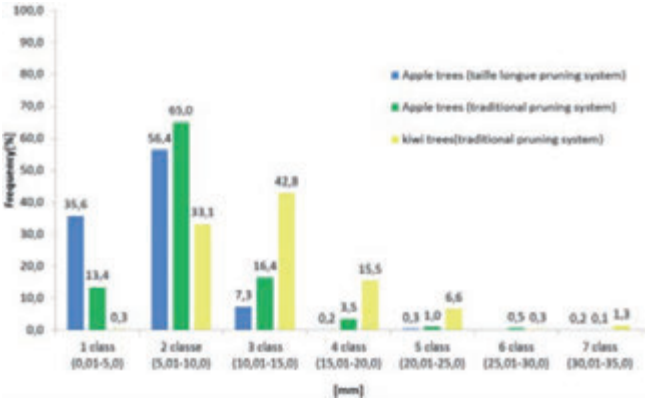

Figure 1. Frequency of pruning branches for diameter class as a function of different pruning systems.

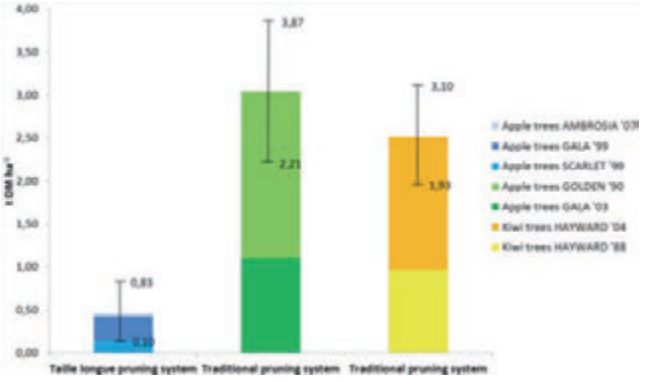

Figure 2. Average pruning residues yield as a function of different pruning system; different colors show how in percentage each variety contributes to the average production.

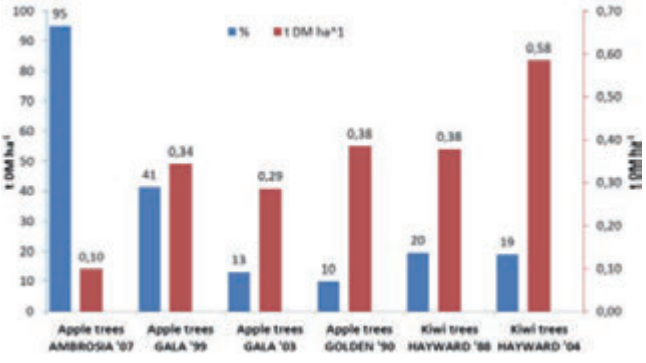

Figure 3. Harvest losses expressed as dry matter [t/ha] and as percentage rates of total biomass production; the data are reported for each species and type.

However, the experiment highlighted how the pruning system adopted for the apple tree (traditional or taille longue) can have a substantial effect on the biomass production,on the physical characteristics (size pruning branches) and on the harvest losses of the produced woody biomass.

Although at present most of the plants are still grown with the traditional pruning system, the projections into the future show a clear transition to the new pruning system taille longue, because it ensures better quality fruits (Diemoz *et al.*, 2003) with a lower production of prunings residues (-80%) that for farms is cost management.

Moreover, it must be pointed out, the new orchards unlike the older ones, having a productive life significantly reduced (max 15 years) inevitably produce a lower amount pruning residues (Bayer Crop Science S.r.l., 2008).

Therefore in the analysis of a possible supply chain aimed at the use of pruning residues as biofuel, we must consider the farming technical evolution (adoption of the new pruning system taille loungue against the traditional pruning system) that underlines a consistent reduction of orchard pruning biomass available. Instead of kiwi tree we must consider the possible removal that potentially could affect all the plants affected by bacterial cancker (no kiwi trees immune to bacterial canker).

In this regard it should be noted that the optimization of the harvesting machine must necessarily be targeted to the harvest of branches characterized by small diameters (max 15 mm) and a high straightness that can't be harvested by the traditional pick-ups fitted to the usual fodder roundbalers.

References

Balestra G. M., Mazzaglia A., Quattrucci A., Renzi M., Rossetti A. 2009. Current status of bacterial canker spread on kiwifruit in italy. *Australasian Plant Disease Notes*. 4(1):34-36

Bayer Crop Science S.r.l. 2008. Il melo. Script marchio editoriale di ART S.p.A., Bologna, Italy.

Biomasse Italia S.p.A., 2008. La filiera da arboricoltura da legno a ciclo breve (S.R.F.)per Biomasse Italia S.p.A. Available from: http://www.biomasseitalia.it/Download/SRF_Presentazione.pdf. Accessed: May 2013

Centro Studi sull'Agricoltura, l'Ambiente e il Territorio (CESTAAT), 1990. Impieghi dei sottoprodotti agricoli e agroindustriali. 1.

Centro Nazionale delle ricerche (CNR), 2012. Progetto "Filiera dell'energia da biomassa". Available from: http://www.agroenergia.net/images/stories/FEB/1_report.pdf Accessed: May 2013.

Cotana F., Cavalaglio G. 2008. La valorizzazione energetica delle potature di olivo. Quaderni Ercole Olivario n.5.

Diemoz M., Vittone G., Pantezzi T. 2003. Potatura del melo: possibili evoluzioni. Terra trentina. Gennaio 2003(1):21-23

ENAMA, 2011. Studio progetto biomasse ENAMA. Available from: http://www.enama.it/it/biomasse_studio.php Accessed: May 2013

ENEA, 2010. Atlante delle Biomasse. Available from: http://www.atlantebiomasse.enea.it. Accessed: May 2013

Isitituto Nazionale di Statistica (ISTAT), 2010. Available from: http://dati-censimentoagricoltura.istat.it/ Accessed: May 2013.

Italian Biomass Association (ITABIA), 2005. Disponibilità, caratteristiche e mercato delle biomasse in Italia. Available from: http://www.itabia.it/conoscenza.php. Accessed: May 2013.

Manzone M., 2006. Meccanizzazione degli impianti di biomassa legnosa a rapido accrescimento (SRF) per la produzione di energia. Vol. 1. PhD Diss., Università di Torino, Italy.

Musacchi S., Colombo R., Mariani M. 2011. Impiantistica e vivaismo. Available from: http://www.crpv.it/doc/44806/DLFE-1402.pdf Accessed: May 2013

Renzi M., Copini P.,Taddei A. R., Rossetti A., Gallipoli L., Mazzaglia A., Balestra G. M. 2012. Bacterial canker on Kiwifruit in Italy: Anatomical changes in the wood and in the primary infection sites. *Phytopathology*. 102(9):827-840

Vita in Campagna, 2012. I lavori di gennaio-febbraio. Supplemento n.1 al n.1 di Vita in Campagna, gennaio 2012, anno 30.

First tests of using an electronic nose to control biogas plant efficiency

Federica Borgonovo, Annamaria Costa, Massimo Lazzari

Department of Health, Animal Science and Food Safety (VESPA), Faculty of Veterinary Medicine, Università degli Studi di Milano, Milan, Italy

Abstract

The demand for online monitoring and control of biogas process is increasing, since better monitoring and control system can improve process plants stability and economy. A number of parameters,such as gas production, pH, alkalinity, Volatile Fatty Acids (VFA) and H_2, in both the liquid and the gas phase have been suggested as process indicators. For different reasons these indicators do not offer enough information to build a consistent feedback control able to promptly forecast and solve plants working problems. The study proposes the use of unconventional complex sensors as a possible solution to engineer a reliable control system. Tests to analyze the biogas coming from a plant were performed using an electronic nose (Airsense PEN 2, AIRSENSE Analytics GmbH). In particular, a 108 olfactometric fingerprinting reference database obtained by different combination of VFA (acetic, propionic e butyric acids, pure or in solution with water) was initially determined. As a second step, the e-nose was tested to verify a potential difference in the analysis of gases emitted by digested manure. Statistic multivariate analysis confirm that the e-nose can distinguish the manure and digester mixed liquor aromatic emission proving the possibility of using this technology as possible base for a biogas control system.

Introduction

The increasing awareness in renewable energy and *green energy* improved the development of biogas technology, especially farm biogas plants (Holm *et al.*, 2009).

Anaerobic digestion (methane fermentation) is a biotechnological process utilizing biomasses, mainly waste, to produce valuablebiogas.

Correspondence: Massimo Lazzari, Department of Health, Animal Science and Food Safety (VESPA), Faculty of Veterinary Medicine, Università degli Studi di Milano, via Celoria 10, 20133 Milan, Italy.
Tel. +39.02.50318047 - Fax: +39.02.50317909.
E-mail: massimo.lazzari@unimi.it

Key words: biogas plant, anaerobic digestion, process overloading, e-nose.

Contributions: the authors contributed equally.

Journal of Agricultural Engineering 2013; XLIV(s1):e109
doi:10.4081/jae.2013.(s1):e109

Biogas can be produced by mesophilic and termophilic plants. During the methanogenesis process, manure, that can be added with biomasses to adjust the anaerobic digestion, is converted to mono and oligomers (aminoacids, long chain fatty acids, saccharides). The substrate fermentation leads mainly to volatile fatty acids (VFA) and acetic acid followed by gases (H_2, CO_2) which,in the last step, are transformed to methane and CO_2. In the meanwhile, the concentration of simple ions and pH varies.

According to environmental fluctuations and for changes in plant feeding, the anaerobic digestion can be altered by many factors(Ward *et al.*, 2008). For this reason a continuous digestion and plant monitoring is needed to avoid the system instability. A wide number of indicators - as volatile fatty acids evaluation (VFAs), pH, redox potential, biogas production rate, and composition - to monitor the correct anaerobic digestion are used. Among these indicators, VFA and biogas production are widely considered as the two most crucial and direct indicators of the system status (Holm *et al.*, 2008), since the increase in VFA concentration is linked tothe methanogenesis inhibition or organic overloading, and implies a risk of process upset (Hansson *et al.*, 2003).

VFAs detection can be performed through fluorescence spectroscopy (Madsen *et al.*, 2011; Pearce *et al.*, 2003), near-infrared (NIR) spectroscopy (Nicolas *et al.*, 2001), titration (Cimander *et al.*, 2002) and gas chromatography(Liden *et al.*, 1998).

Other techniques, extremely useful to detect the quality of the fermentation process status,are the biogas composition and the production rate (Holm et a, 2007; Holm *et al.*, 2008).

Because of the high complexity of biogas plants and fermentation status the interrelations of the many involved parameters remain unclear. In this frame, a wide adopted technique is to set a threshold values for some individual indicators like pH and VFA. These last ones are considered as the most relevant state variables for process monitoring, and are used to judge thereactor status on the basis of the detected values. However, once the threshold values are reached can only reveal the current reactor status, but it is actually, in most cases, too late for an effective process control.

A promising alternative approach is to use the electronic nose.

The electronic nose is a biologically inspired system composed of an array of non-specific gas sensors (Pearce *et al.*, 2003). When sensor responses are put together, they form a pattern, which is typical of the gas mixture. In this way, the sensors responses produce characteristic patterns for each chemical mixture exposed to the sensor array. By presenting many different chemicals to the sensor array, a patterns database is built up and used to train the pattern recognition system that finally allows recognizing a gas mixture. More extensive information about e-nose technology can be found in Pearce *et al.*, 2003.

The first e-nose technology use was applied to the monitoring of the anaerobic digestion process by Nordberg *et al.* 2000. More recently, the electronic nose was proposed as an innovative online monitoring to autoalert and control the system (Adam *et al.*, 2013).

The main aim of this work was to determine the correct technique to use an e-nose as a *discriminator* in anaerobic digestion status.

Indirectly, this study is leaded to investigate the e-nose technology as a new robust, simple, sensitive tool for biogas production monitor-

ing in order to optimize the process and increase gas yield in small scale agricultural plants.

Materials and methods

In the present study, a preliminary test on the e-nose ("Airsense PEN 2", AIRSENSE Analytics GmbH) abilityto detect the biogas plant overloading was performed, analyzing both gases and manure samples collected in vials.To this purpose:

1. As a first step, the olfactometric fingerprints of VFAs (acetic, propionic and butirric acids) in purity or diluted with deionized water (around 108 combinations) were determined, in order to represent the VFAs produced during the anaerobic digestion process. The "training set" obtained in laboratory conditions represented the olfactometric fingerprints reference database of the biogas contained in the headspace of the minireactors.
2. As a second step, the e-nose was tested to verify a potential difference in theanalysis of gases emitted by digested manure (collected in nalophan bags) and by manure itself, in order to set up the proper experimental conditions.

Odor analysis

Manure samples odor were analyzed by means of a PEN 2 electronic nose (WMA Airsense, Schwerin, Germany). It consists of: a sampling unit; a sensor array made up of ten metal oxide semiconductor (MOS, see Table 1) chemical sensors; a software for data storage and multivariate statistical processing (pattern recognition system). During sampling, two hypodermic needles were inserted through the vial rubber cap into the headspace. The first needle was connected to the sampling unit, while the second was connected to a charcoal filter by means of a polytetrafluoroethylene (PTFE, Teflon) hose. Odor analysis was performed in a two step way: measurement and standby. Electro-valves, controlled by a computer program, guided the air through different circuits depending on the stage of the analysis. Irrespective of the phase, airflow in the measurement chamber was kept constant (Table 2). During the measurement phase, the sampling unit "inhaled" the volatile gases present in the vial headspace and sent them - at a constant rate (6.67 mL s^{-1}) - to the measurement chamber causing changes in sensor's conductance: this phase lasted 80 s, which was enough time for the sensor signals to reach a stable value. When a measurement was completed, a standby phase of 160 s was activated.

Table 1. Sensors of the PEN 2 electronic nose (WMA Airsense, Schwerin, Germany).

Number in array	Sensor-name	General description	Reference
1	W1C	Aromatic compounds	Toluene, 10 ppm
2	W5S	Very sensitive, broad range sensitivity, react on nitrogen oxides, very sensitive with negative signal	NO_2, 1 ppm
3	W3C	Ammonia, used as sensor for aromatic compounds	Benzene, 10 ppm
4	W6S	Mainly hydrogen, selectively (breath gases)	H_2, 100 ppb
5	W5C	Alkanes, aromatic compounds, less polar compounds	Propane, 1 ppm
6	W1S	Sensitive to methane (environment) ca. 10 ppm. Broad range, similar to No. 8	CH_3, 100 ppm
7	W1W	Reacts on sulphur compounds, H_2S 0.1 ppm. Otherwise sensitive to many terpenes and sulphur organic compounds, which are important for smell, limonene, pyrazine	H_2S, 1 ppm
8	W2S	Detects alcohols, partially aromatic compounds, broad range	CO, 100 ppm
9	W2W	Aromatics compounds, sulphur organic compounds	H_2S, 1 ppm
10	W3S	Reacts on high concentrations >100 ppm, sometime very selective (methane)	CH_3, 10 CH_3, 100 ppm

Table 2. Summary of the operating conditions of the e-nose during headspace analysis of manureodor).

Operating condition	
Transport gas	Ambient air (cleaned by charcoal filter)
Sampling rate	10 mL s^{-1}
Amount of sample/vial	6.67 mL s^{-1}
Vial volume	20 mL
Data acquisition	
Headspace generation time	1800s
Sampling time	80 s
Flushing time	160s
Total measurement time	240s

Its purpose was to clean the circuit, and the measurement chamber in particular, in order to return the sensor signals to their baselines. During this phase, clean air entered the circuit, crossing the measurement chamber first and pushing the remaining volatiles out of the circuit itself.

The ten MOS chemical sensors comprising the sensor array operated by transduction of the chemical compounds in the manure aroma into electric signals (Yuwono and Lammers, 2004). At the end of the measurement, these signals were recorded and stored, to be analyzed either by the software of the pattern recognition system or by statistical analysis software. One pattern comprises the signals from all ten sensors taken during the measurement of a sample.

The software records the variations occurring in the ratio (G/G0) between the conductance of each sensor, G (Ω-1), at each second of measurement and the reference, G0 (Ω-1), which is the conductance that the sensor shows when clean charcoal-filtered air enters the measurement chamber.

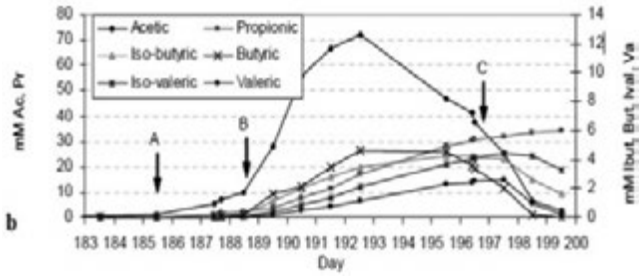

Figure 1. VFA concentration during an organic overloading (in normal conditions before "A", from "A" on adding fiber and rapeseed oil, from point "B" start adding glucose, from point "C" back to normal feed again (from Boe, 2006, *On line monitoring and control of the biogas process*).

PCA and discriminant analysis

To increase the knowledge attained from the considered variables and, according to them, try to discriminate as much as differences as possible during the manure monitoring, data were submitted to principal component analysis (PCA) followed by discriminant analysis. PCA is a linear, unsupervised pattern-recognition technique very useful for analyzing, classifying, and reducing the numerical datasets dimensionality in multivariate problems (Todeschini, 1998).

Linear Discriminant Analysis (LDA) (Meloun *et al.*, 1992) is one of the mostly used classification procedure which maximizes the variance between categories and minimizes the variance within categories. The dataset was preparedusing the signals recorded during the measurement last 5 s when sensor signals were stable meaning that an equilibrium between their sensitivity and the sample manurevolatile compounds was achieved. Statistical analysiswascarried out using Scan for Windows.

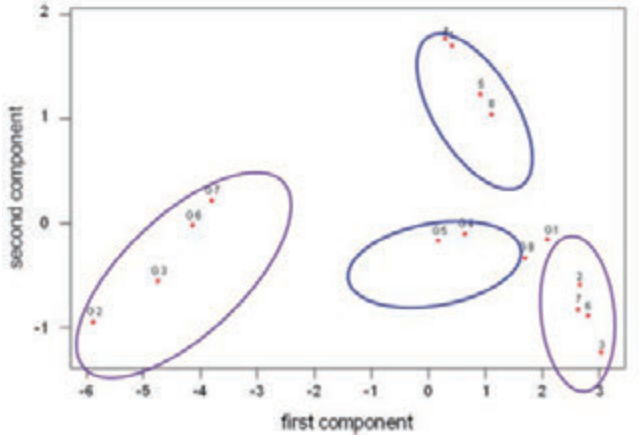

Figure 2. Score plot provided by PCA analysis. Items called with numbers are referred to manure samples (G1…G8) and indicates the air sampled in the minireactors headspace.

Results

Building of an olfactometric "training set" based on odor emitted by mixed compounds of acetic, propionic and butirric acid. The choice to analyse VFA was linked to their capacity to be used as good indicators of digestion process: in particular,as shown in the Figure 1, during overloading or stress episodes corresponding to the rise of the partial hydrogen pressure, propionic acid is more instable than acetate and buthirrate (Boe, 2006).

Results of PCA analysis related to the analysis of gases emitted by digested manure (collected in nalophan bags) and by manure itself are reported in the following Figure 2. Items called with numbers are referred to manure samples (G1…G8) and indicates the air sampled in the minireactors headspace.This preliminary trial was conducted to test the e-nose potential performances differences to detect samples as gases emitted by manure during digestion or as manure itself.

The score plot reported in Figure 2 showed that both procedures gave good results, since either gases samples or manure samples resulted suitable in the two identification groups by the e-nose (G1, G4, G5 and G8 were symmetrically in the graphic opposed to 1, 4, 5 and 8 with respect to the second component; G2, G3, G6 andG7 were opposed to 2, 3, 6 and 7 with respect to the first component.

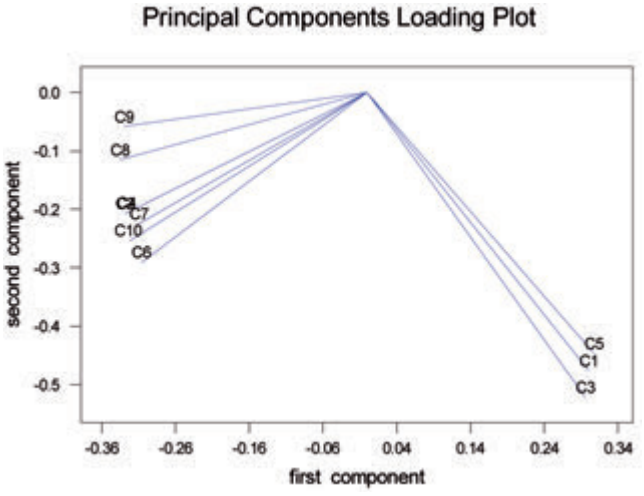

Figure 3. Loading plot provided by PCA analysis.

Conclusions

Electronic nose demonstrated its potential to detect gases emitted by manure during digestion or as manure itself. This procedure can represent a correct technique to monitor, in further studies, the biomethanation process and to discriminate overload situations of anaerobic plants.

References

Boe K, Batstone DJ, Angelidaki I (2007) An innovative online VFA monitoring system for the anaerobic process, based on headspace gas chromatography. BiotechnolBioeng 96(4):712– 721. doi:10.1002/bit.21131

Boe K, Batstone DJ, Steyer J-P, Angelidaki I (2010) State indicators for monitoring the anaerobic digestion process. Water Res 44(20):5973–5980. doi:10.1016/j.watres.2010.07.043

Cimander C, Bachinger T, Mandenius C-F (2002) Assessment of the performance of a fed-batch cultivation from the preculture quality using an electronic nose. BiotechnolProg 18(2):380–386. doi: 10.1021/bp010166j

Cimander C, Carlsson M, Mandenius C-F (2002) Sensor fusion for on-line monitoring of yoghurt fermentation. J Biotechnol 99(3):237–248. doi:10.1016/s0168-1656(02)00213-4

Gilles Adam, SebastienLemaigre, Anne-Claude Romain, Jacques Nicolas, Philippe Delfosse. 2013. Evaluation of an electronic nose for the early detection of organic overload of anaerobic digesters. BioprocessBiosystEng 36:23–33. DOI 10.1007/s00449-012-0757-6

Hansson M, Nordberg A ° , Mathisen B (2003) On-line NIR monitoring during anaerobic treatment of municipal solid waste. Water Sci Technol 48(4):9–13

Holm-Nielsen JB (2008) Process analytical technologies for anaerobic digestion systems. PhDThesis, Aalborg University, Esbjerg. ISBN 978-87-7606-030-5

Holm-Nielsen JB, Al Seadi T, Oleskowicz-Popiel P (2009) The future of anaerobic digestion and biogas utilization. Bioresour Technol100(22):5478–5484. doi:10.1016/j.biortech.2008.12.046

Holm-Nielsen JB, Andre e H, Lindorfer H, Esbensen KH (2007) Transflexive embedded near infrared monitoring for key process intermediates in anaerobic digestion/biogas production. J NearInfraredSpectrosc 15(2):123–135. doi:10.1255/jnirs.719

Holm-Nielsen JB, Lomborg CJ, Oleskowicz-Popiel P, Esbensen KH (2008) On-line near infrared monitoring of glycerol-boosted anaerobic digestion processes: evaluation of process analytical technologies. BiotechnolBioeng 99(2):302–313. doi:10.1002/bit.21571

Lide n H, Mandenius C-F, Gorton L, Meinander NQ, Lundstro¨m I, Winquist F (1998) On-line monitoring of a cultivation using an electronic nose. AnalChim Acta 361(3):223–231. doi:10.1016/

Madsen M, Holm-Nielsen JB, Esbensen KH (2011) Monitoring of anaerobic digestion processes: a review perspective. RenewSustain Energy Rev 15(6):3141–3155. doi:10.1016/j.rser.2011.04.026

Nicolas J, Romain A-C, Andre P (2001) Chemometrics methods for the identification and the monitoring of an odour in the environment with an electronic nose. In: Sensors and chemometrics. Research Signpost, India, pp 75–90

Nordberg A , Hansson M, Sundh I, Nordkvist E, Carlsson H, Mathisen B (2000) Monitoring of a biogas process using electronic gas sensors and near-infrared spectroscopy (NIR). Water Sci Technol 41(3):1–8

Pearce TC, Schiffman SS, Nagle HT, Gardner JW (2003) Handbook of machine olfaction: electronic nose technology. ISBN: 978-3-527-60563-7

Pearce TC, Schiffman SS, Nagle HT, Gardner JW (2003) Handbook of machine olfaction: electronic nose technology. ISBN: 978-3-527-60563-7

s0003-2670(98)00035-x

Ward AJ, Hobbs PJ, Holliman PJ, Jones DL (2008) Optimisation of the anaerobic digestion of agricultural resources. Bioresource Technology 99(17):7928–7940.

Yuwono, A. S., and P. S. Lammers. 2004. Odor polluting in the environment and the detection instrumentation. Agric. Eng. Intl., vol. VI: Invited overview paper.

Evaluation of herbaceous crops irrigated with treated wastewater for ethanol production

Salvatore Barbagallo,[1,4] Antonio Barbera,[2,3] Giuseppe L. Cirelli Giuseppe,[1,4] Mirco Milani,[1,4] Attilio Toscano,[1,4] Roberto Albergo Roberto[3]

[1]Department of Agri-food and Environmental Systems Management, University of Catania, Catania, Italy; [2]Department of Food and Agricultural Production Sciences, University of Catania, Catania, Italy, [3]ENEA, Trisaia Research Centre, Rotondella (MT), Italy; [4]CSEI Catania, Italy

Abstract

The competition for freshwater between agricultural, industrial, and civil uses has greatly increased in Mediterranean basin characterized by prolonged dry seasons. The aim of this study was to evaluate biomass production and the potential ethanol production of promising "no-food" herbaceous crops irrigated with low quality water at different ETc restitutions (0%, 50 and 100%). The research was carried out, in 2011 and 2012, in an open field near the full-scale constructed wetland (CW) municipal treatment plant located in the Eastern Sicily (Italy). The CW effluent has been applied in a experimental irrigation field of *Vetiveria zizanoides* (L.) Nash, *Miscanthus x giganteus* Greef et Deu. and *Arundo donax* (L.). Physical, chemical and microbiological analyses were carried out on wastewater samples collected at inlet and outlet of CW and pollutant removal efficiencies were calculated for each parameter. Bio-agronomical analysis on herbaceous species were made with the goal to evaluate the main parameters such as the plant dimension, the growth response and the biomass production. Biomass dry samples were processed with a three-step chemical pretreatment, hydrolysed with a mix of commercial enzymes and next fermented to obtain the yield of ethanol production. Average TSS, COD and TN removal for CW were about 74%, 67% and 68%, respectively. Although the satisfactory Escherichia coli removal, about 3.5 log unit for both beds on average, CW didn't achieve the restrictive Italian law limits for wastewater reuse. As expected, irrigation was beneficial and the full ET replenishment increase the biomass productivity as compared to the other two treatment. The mean productivity of *Vetiveria zizanoides* and *Myscanthus x giganteus* were about 9, 26 and 38 t ha^{-1} and 3, 7 and 12 t ha^{-1} respectively in 0%, 50% and 100% ETc restitutions. *Arundo donax* gave higher values of dry biomass (78 t ha^{-1} in 100% ETc restitution in 2011 season), and potential ethanol production (about 3,744 kg ha^{-1}). These results suggest the interest in the use of constructed wetland effluents for the irrigation of energy crops to obtain second generation ethanol, particularly in semiarid regions such as the Mediterranean area.

Correspondence: Mirco Milani.
Tel. +39.095.7147 543 - Fax: +39.095.7147.600.
E-mail: mirco.milani@unict.it

Key words: constructed wetland, wastewater reuse, herbaceous crops, evapotranspiration replenishment, ethanol.

Acknowledgements: the research activity was supported by the MIUR (Italian Ministry of Education, University and Research) through the project FITOPROBIO "Production of macrophyte wetland biomasses irrigated with wastewater to obtain second-generation ethanol".

Journal of Agricultural Engineering 2013; XLIV(s1):e110
doi:10.4081/jae.2013.(s1):e110

Introduction

The gradual depletion of petroleum-derived transportation fuels has focused attention on both renewable and environmentally friendly resources (Ge *et al.*, 2011), with ethanol from plants being a possible alternative (Sivakumar *et al.*, 2010). Ethanol produced from lignocellulosic biomass is one of the most suitable alternatives for partial replacements of fossil fuels because it provides energy that is renewable and less carbon intensive than gasoline. Bioethanol reduces air pollution and also contributes to mitigate climate change by reducing greenhouse gas emissions (Gnansounou, 2010).

The success of energy crops is closely linked to the production costs. For this reason it is preferable to grow perennial plants, because they need a limited soil management, and to adopt extensive cultivation systems. However, application of fertiliser and irrigation is generally necessary to achieve high crop productivity, especially in the Mediterranean zones, characterized by a chronic water shortage (Barbera *et al.*, 2009). In this context, the irrigation wastewater reuse is desirable because conserve water resources, reduce disposal of polluted effluents into surface water bodies enhances the economic benefits for farmers due to reduced need for fertilizer (Paranychianakis *et al.*, 2006) improve productivity of crops (Bedbabis *et al.*, 2010).

A viable solution for wastewater treatment could be represented by constructed wetland (CW) which are characterised by low O&M costs and by unskilled manpower requirements and represent environmentally sound alternatives to conventional wastewater treatment plants (Cirelli *et al.*, 2007)

This research activity evaluated: 1) the performances of a constructed wetland (CW) system located in Southern Italy, and its suitability for reusing the effluent; 2) the biomass production of herbaceous species when irrigated with CW effluent; 3) the ethanol yield of three herbaceous species.

Materials and methods

Experimental plans

The study was carried out in a full-scale constructed wetland treatment plant and in an open field of herbaceous species located in San Michele di Ganzaria (Eastern Sicily - Latitude 37° 16' North, Longitude 14° 25' East, altitude 350 m), a rural community of about 5,000 inhabitants. Constructed wetland consists of two Horizontal SubSurface Flow beds (H-SSF1 and H-SSF2) that receive part of secondary effluent (4 L/s) of the conventional wastewater treatment plant of village (Barbagallo *et al.*, 2011). H-SSF1 and H-SSF2 working in parallel and have an almost equal surface area (about 2,000 m^2) but with different operation life: 12 and 6 years of functioning. The terminal section (190 m^2) of H-SSF2 reed bed functions as a free water surface. Both reed beds was vegetated with *Phragmites australis*.

Wastewater treated by constructed wetlands has been used for irrigation of herbaceous crops. To this purpose, an experimental irrigation field of *Vetiveria zizanoides* (L.) Nash, *Miscanthus x giganteus* Greef et Deu. and *Arundo donax* (L.) was established. *V.zizanoides* and *M.giganteus* were transplanted in six plot of 9 m^2 (three repetitions for each species), in July 2008 and May 2009, respectively. *A.donax* was planted, in July 2008, on an area of about 1,000 m^2 divided in three blocks of about 330 m^2. All species were transplanted with a density of about 4 plants/m^2. The wastewaters were supplied by in-line labyrinth drippers system. A meteorological station was installed close to experimental plants, measuring rainfall, temperature, air moisture content, wind velocity, solar radiation and the evaporation. A CR510 automatic weather station (Campbell Scientific, Logan, UT) was installed close to the experimental site for the continuative measure of: rainfall, temperature, air moisture content, wind velocity, solar radiation and the evaporation.

Wastewater irrigation

The water volumes distributed were equal to 0% (S1 and S4), 50% (S2 and S5) and 100% (S3 and S6) of evapotranspiration losses (ETc) (Figure 1).

Wastewater irrigation scheduling was based on water balance equation (Eq. (1)):

$$I = ETc - P + Dp + Rf \quad (1)$$

Where I is irrigation water applied (mm), ETc, crop evapotranspiration (mm) rate calculated as product of Penman-Monteith based reference evapotranspiration (ET0) (ASCE-EWRI, 2004) and the FAO-56 crop coefficient (Kc). ET0 reference data were determined by daily climatic factors using an on-site weather station. Kc ranging from 0.75 to 1.10 for *V.zizanoides* and *M.giganteus* while for *A.donax* varied from 1.00 to 1.30. The terms Dp and Rf represent deep percolation (mm) and runoff (mm), respectively. Since irrigation water was controlled, deep percolation and runoff were assumed negligible. The irrigations were realized from June to October 2011 and 2012.

Analysis

Wastewater analysis

Wastewater quality samples were collected at the inlet and outlet of H-SSF1 and H-SSF2. The following physicochemical parameters were evaluated according to APHA (1998) methods: electrical conductivity (EC), pH, total suspended solids (TSS) at 105°C, COD, total nitrogen (TN) NH_4-N, Total Nitrogen (TN) and PO_4-P. In order to evaluate the microbiological pollution Escherichia coli and Salmonella were also analyzed. *E. coli* was evaluated according to the standard methods (APHA, 1998) and *Salmonella* was examined according to the methodology reported in Barbagallo *et al.* (2003). For each CW were computed the percentage removal efficiencies, for physicochemical parameters, and the log reduction for microbiological parameters.

Bio-agronomical analysis

In the giant reed parcel were identified nine square sampling areas, of one meter side each, where the bio-agronomical survey and sampling activity were carried out during the experimental period. While in the *V.zizanoides* and *M.giganteus* were defined sampling areas of about 4 m^2 in the centre of each plot. In the sampling area, bio-agronomical analysis on tested species were made with the goal to evaluate the main parameters such as the plant dimension, the growth response and the biomass production. Plant samples for the evaluation of productivity were taken in December 2011 and 2012. Biomass dry weight was determined by drying plant tissue samples in a thermo-ventilated oven at 65 °C until constant weight was reached.

At time of harvest, dry biomass samples of each species have been sent to the Biotechnical Laboratory ENEA in Trisaia in order to characterize each species in terms of fiber (hemicellulose, cellulose and lignin). Afterwards all of them were processed with a three-step chem-

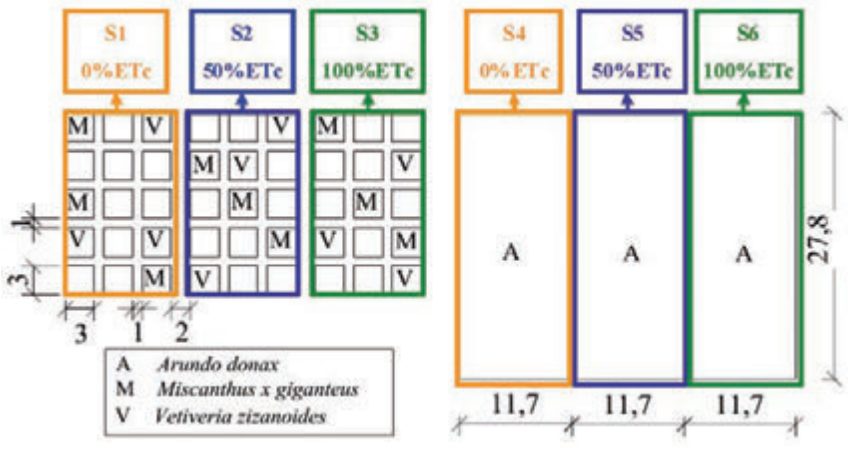

Figure 1. Layout of experimental plant for herbaceous crops.

ical pretreatment to recover most of cellulose and make the biomass more accessible (Borin *et al.*, 2011). This pretreated material was then hydrolysed with a mix of commercial enzymes and next fermented to obtain for each studied plant the yield of ethanol production.

Results and discussion

Constructed wetland performance

During the whole observation period the values of pH and EC of CWs influent and effluent were similar and varied in the range 6.9–7.8 and 1.1–1.7 mS/cm, respectively.

Table 1 shows the average concentrations of the chemico-physical and microbiological parameters in and out of the CWs during the investigation period. The respective mean removal efficiencies are shown in Figure 2.

About 100% and 47% of TSS analysed samples in CWs influent resulted out, respectively, of legislation limits for wastewater reuse (D.M. 185/2003) and for wastewater discharge in water bodies (D.lgs. 152/2006). In the H-SSF1 and H-SSF2 effluent, average TSS concentrations ranged from 6 to 9 mg/L and from 8 to12 mg/L, respectively. The TSS Italian limit for wastewater irrigation reuse was only exceeded by 17% (H-SSF1) and 18% (H-SSF2) of the samples.

In both effluents, COD and TN concentrations were always below the limits imposed by the D.lgs. 152/2006 and D.M. 185/2003, highlighting average removal efficiencies, respectively, of about 55 and 67% in H-SSF1 and 61 and 74% in H-SSF2. Also the average NH_4-N and PO_4-P removal in H-SSF1 (63% and 26%) was lower than in H-SSF2 (71% and 48%). This results could by explained by ability of algae and microphytes to remove the nutrient elements directly on the open water surface at the end of H-SSF2.

The performance was good for *Salmonella* removal, which was never detected in the effluent of CWs. During the 2012 observation period the *E.coli* concentration in the HSSF2 effluent showed an average decrease of 3.5 log units and 3.0 log units in the H-SSF1 effluent. Only 40% of total samples matched the limit of *E.coli* fixed by D.M. 185/2003. However, the *E.coli* concentration in the H-SSF1 and H-SSF2 effluent (always equal or less 10^3 UFC/100 mL) ensure that health-based targets proposed by the WHO (2006) are matched particularly if drip irrigation is used.

Herbaceous crops: biomass and ethanol productivity

Environmental conditions and irrigation volumes

During the two growing seasons, the daily minimum air temperatures ranged from -4.3 to 22.2°C and the maximum from 7.1 to 43.3°C with average seasonal values of 18.8 °C (2011) and 19.9°C (2012). Total rainfall from March to October was 406 mm in 2011 while in 2012 it was only 163 mm (Figure 3), with 179 and 197 days without rain, respectively.

The higher temperature associated with lower precipitation in 2012 irrigation period compared to the same period in 2011 generated the significantly different ETc values. In particular, irrigation water volumes applied in *V.zizanoides* and *M.giganteus* crops were 250 mm and 480 mm (2011 season) and 380 mm and 780 mm (2012 season) at plots

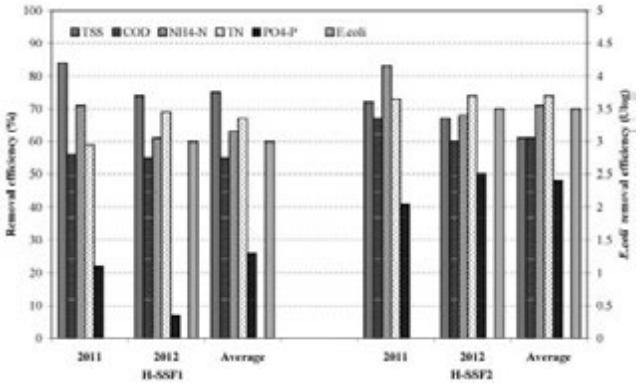

Figure 2. CWs removal efficiency of TSS, COD, NH_4-N, TN, PO4-P and *E. coli* during the observation period

Table 1. Comparison between average pollutant wastewater concentration in the influent (In) and effluent (Out) of H-SSF1 and H-SSF2 with the Italian wastewater discharge limits into surface waters (D.Lgs. 152/2006) and for agriculture reuse (D.M. 185/2003).

Parameters	2011				2012				Average				Law Limits	
	H-SSF1		H-SSF2		H-SSF1		H-SSF2		H-SSF1		H-SSF2		D.Lgs. 152/06	D.M. 185/03
	In	Out	In	Out	In	Out	In	Out	In	Out	In	Out		
TSS (mg/L)	63	9	63	12	42	6	43	8	46	6	47	9	35	10
COD	97	33	97	19	56	19	59	17	63	21	66	18	125	100
(mg/L)														
NH_4-N (mg/L)	24	5	24	3	12	3	13	3	14	4	15	3	-	2
TN (mg/L)	30	11	30	7	28	7	29	6	29	7	29	6	15	35
PO_4-P (mg/L)	4.4	3.5	4.4	2.6	3.3	2.7	3.1	1.3	3.6	2.8	3.3	1. 5	-	-
E.coli (Ulog/100 mL)	-	-	-	-	5.4	2.4	5.4	1.9	5.4	2.4	5.4	1. 9	3.7	1.7*

*Maximum value to be detected in 80% samples for natural treatment systems.

with, respectively, 50% and 100% restitution of ETc. While in *A. donax* plots the irrigation water applied, during spring/summer 2011 and 2012, were 300 mm (50% ETc) and 600 mm (100% ETc) and 480 mm (50% ETc) and 960 mm (50% ETc), respectively.

Crop growth and biomass yield

The increase of ETc restitution, from 0% to 100%, positively influenced the plant higher and, consequently, the aboveground biomass production for all tested species (Table 2) while no significant difference were highlighted for different irrigation thesis. Biomass water content at harvest was lowest in *M.giganteus*, varying from 33 to 38%, compared to *A.donax* (50-56%) and *V.zizanoides* (62-65%). This could be explained with the life cycle of plants: *V.zizanoides* and *A.donax* are active during most of the wintertime in the Mediterranean environment whereas the *M.giganteus* stems dry up completely during winter.

A.donax showed the highest values of dry biomass, with a mean value of about 50 t ha^{-1}, followed by *M. giganteus* (-42%) and *V.zizanoides* (-85%). From first to the second year *Arundo donax* biomass dry yield decreased about 39% due to the reduction (about -50%) of the stalks density. The biomass yield of these species in the tested environment, has been higher (on average +20-30%) than recorded by other authors in two long-term experimental field carried out in Central (Angelini *et al*., 2009) and Southern Italy (Mantineo *et al*., 2009). These differences in yield performance can be linked to density planting (twice more than the other investigations).

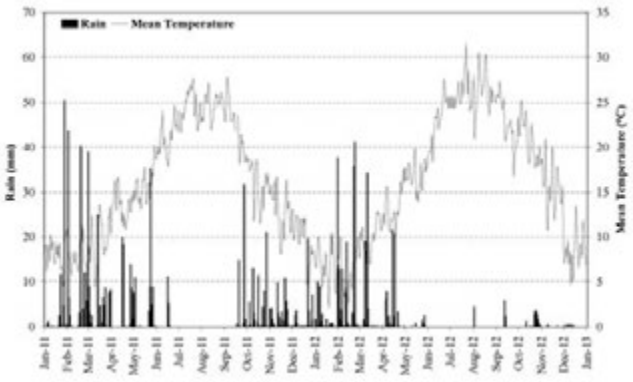

Figure 3. Precipitation and average air temperature series from January 2011 to December 2012.

The yield of *V.zizanoides* determined in this experiment showed values ranging between 2.6 to 16.6 t ha^{-1}, that were comparable to those obtained in other similar field experiments carried out in North Italy ranging between 10 to 12 t ha^{-1} (Monti *et al*., 2005).

With regard to the 2012 yield of *M.giganteus*, it was observed that the high summer temperatures associated with an extended period without significant rainfall events, induced an early senescence state in *M.giganteus* plants without irrigation supply with subsequent dry biomass production failures. These environmental conditions have also influenced the yields of irrigated thesis decreased by 33% (50% ETc) and 31% (10% ETc) than 2011 season. However, the average total biomass produced in the different irrigation treatments was comparable than recorded by other authors in experimental sites with similar climatic and crop management characteristics (Angelini *et al.*, 2009; Mantineo *et al.*, 2009; Zub and Brancourt-Hulmel, 2010).

Ethanol yield

The preliminary study on the chemical composition of biomasses investigated highlighted higher cellulose and hemicellulose concentrations in *A.donax* and *M.giganteus* while the *V.zizanoides* showed lower lignin content (Table 3). These fiber compositions of dry biomass samples were according with the data reported in the Phyllis database (http://www.ecn.nl/phyllis/single.html) and the BioBIB database (http://www.vt.tuwien.ac.at/biobib/). We can suppose that the *A.donax* and *M.giganteus* are the most suitable candidates for the production of fermentable sugars and ethanol by means of the appropriate pretreatment, hydrolysis and fermentation. Infact, the cellulosic and hemicellulosic fractions, are the most important biomass components that hydrolysates produce glucose subsequently fermented into ethanol (Currelli *et al.*, 2002).

Despite the lower concentrations of cellulose and hemicellulose *V.zizanoides* showed higher fermentation yield (glucose percentage fer-

Table 3. Chemical composition of the herbaceous crops.

Species	Extractives (%)	Hemicellulose (%)	Cellulose (%)	Lignin (%)	Ashes (%)
Arundo Donax	14,13±0,13	33,57±0,57	43,69±0,30	8,68±0,25	0,56±0,04
Miscanthus x giganteus	12,35±0,38	34,21±1,24	46,14±0,58	6,14±0,62	1,15±0,02
Vetiveria zizanoides	18,98±0,33	39,77±0,45	34,88±0,46	5,39±0,04	0,80±0,11

Table 2. Mean values of density, height, moisture content and dry biomass evaluated of the herbaceous crops in December 2011 and 2012.

Species	Irrigation thesis	Plant density (n. plant/m^2)		Height (cm)		Moisture content (%)		Dry biomass (t/ha)	
		Dec -11	Dec-12	Dec -11	Dec-12	Dec -11	Dec-12	Dec -11	Dec-12
Arundo donax	0% ETc	22	12	419	392	56	51	48.3	25.6
	50% ETc	22	14	475	437	56	50	59.5	40.9
	100% ETc	24	15	498	453	50	49	78.5	48.5
Mischantus giganteus	0% ETc	83	-	119	-	38	-	19.6	-
	50% ETc	85	73	179	168	37	51	30.6	20.6
	100% ETc	91	80	276	229	33	52	44.6	30.6
Vetiveria zizanoides	0% ETc	4	4	96	91	65	69	2.6	3.7
	50% ETc	4	4	128	136	62	66	3.9	10.8
	100% ETc	4	4	169	168	63	66	7.0	16.6

mented into ethanol) and ethanol production than those obtained for *A.donax* and *M.giganteus* (Table 4). These results could be mainly ascribes to the higher lignin content in *A.donax* and *M.giganteus* biomasses that has reduced the accessibility of cellulose to enzymes decreasing the hydrolysis rate (Currelli *et al.*, 1997).

However, since the aboveground biomass yield per hectare is much higher for *A.donax*, the average ethanol yield per unit of cultivated area (2,400 Kg ha^{-1}) was about 1.1 times the mean ethanol yield calculated for *M.giganteus* (2,190 Kg ha^{-1}) and 3.4 times the average values of *V.zizanoides* (710 Kg ha^{-1}).

Table 4. Glucose and ethanol concentration obtained, respectively, by the hydrolysis and fermentation processes and fermentation and ethanol yields.

Species	Glucose (g/L)	EtOH yield (g/L)	Fermentation production (%)	Ethanol g(EtOH) /100g(S.S.)
Arundo donax	13,7±0,4	4,1±0,4	58,9±3,8	4,8±0,4
Mischantus giganteus	21,1±1,6	6,2±0,9	57,6±3,8	7,5±0,4
Vetiveria zizanoides	21,4±3,5	9,1±0,5	84,0±9,2	9,6±2,6

Conclusions

The results of the experimental activities show that constructed wetlands are able in removing the main chemical and physical pollutants from the secondary effluent of urban wastewaters treatment plant. However, *Escherichia coli* (mean removal efficiency of about 3.3 log unit) in CWs effluents didn't respect the Italian standard for wastewater reuse but complied with the WHO guidelines. In this case stabilisation reservoirs would be used coupling the CWs and would therefore be a reliable and economic solution to further reduce the microbiological load in treated wastewater (Barbagallo *et al.*, 2003b).

The results highlight attractive biomass yield and an interesting crop energy capability by using treated wastewater for irrigation. The aboveground dry matter production, as expected, was positively affected by the full ET replenishment. The higher performance observed under 100% ETc restitution regime indicates that any effort to maximize and stabilize herbaceous biomass production might be subordinated to an adequate water supply. However, the *A.donax* showed significant biomass production even in the absence of irrigation with an average value of about 37 t ha^{-1}.

The biomass and ethanol yield analysis showed highest values for *A.donax* and *M.giganteus*. This suggest the technical feasibility of extensive cultivation of these species on marginal land in the semiarid regions such as the Mediterranean area in order to maximise agricultural profits.

References

Angelini L.G., Ceccarini L., Nassi o Di Nasso N., Bonari E. 2009. Comparison of *Arundo donax* L. and *Miscanthus x giganteus* in a long-term field experiment in Central Italy: analysis of productive characteristics and energy balance. Biomass Bioenerg. 33:635-643.

APHA. Standard methods for the examination of water & wastewater, 21st edn. Baltimore: American Public Health Association (APHA), AmericanWaterWorks Association (AWWA), and American Environment Federation (AEF); 2005.

ASCE-EWRI. The ASCE Standardized Reference Evapotranspiration Equation. Technical Committee report to the Environmental and Water Resources Institute of the American Society of Civil Engineers from the Task Committee on Standardization of Referente Evapotranspiration; 2004.

Barbagallo S., Cirelli G.L., Consoli S. and Somma F. (2003b). Wastewater quality improvement through storage: a case study in Sicily. Water Sci. Technol. 47:169-176.

Barbagallo S., Cirelli G.L., Marzo A., Milani M., Toscano A. 2011. Hydraulics behaviour and removal efficiencies in two H-SSF constructed wetlands for wastewater reuse with different operational life. Water Sci. Technol. 64:1032-1039.

Barbagallo, S., Cirelli, G. L., Consoli, S., Toscano, A., Zimbone, S. M.. Performances and Hydraulics of a H-SSF constructed wetland for municipal wastewater reuse. In: Proceedings of 4th IWA International Symposium on Wastewater Reclamation and Reuse, 2003 November12-14, Mexico City, Mexico.

Barbera, A.C., Milani, M., Bellomia, L., Castiglione, V., Toscano, A., Cavallaro, V.. Effects of wastewater and different fertilization on Sorghum (*Sorghum bicolor* (L.) Moench) biomass production in mediterranean environment. In: Proceedings of 17th European Biomass Conference & Exhibition from Research to Industry and Markets, 2009 June 28 – July 3, CCH-Congress Center, Hamburg, Germany.

Bedbabis S., Ferrara G., Ben Rouina B., Boukhris M. 2010. Effects of irrigation with treated wastewater on olive tree growth, yield and leaf mineral elements at short term. Sci. Hortic-Amsterdam, 126: 345-350.

Borin M., Florio G., Barbera A.C., Cirelli G.L., Albergo R., Palazzo S.. Preliminary evaluation of macrophyte wetland biomasses to obtain second generation ethanol. In: Proceedings of 19th European Biomass Conference and Exhibition, 2011 June 6-10 2011. Berlin, Germany.

Cirelli G.L., Consoli S., Di Grande V., Milani M., Toscano A. 2007. Subsurface constructed wetlands for wastewater treatment and reuse in agriculture: five years of experiences in Sicily, Italy. Water Sci. Technol. 56:183-191.

Curreli N., Agelli M., Rescigno A., Sanjust E., Rinaldi A. 2002. Complete and efficient enzymic hydrolysis of pretreated wheat straw. Process Biochem. 37:937-941.

Curreli N., Fadda M.B., Rescigno A., Rinaldi A.C., Soddu G., Sollai F., Vaccargiu S., Sanjust E., Rinaldi A. 1997. Mild alkaline/oxidative pretreatment of wheat straw. Process Biochem. 32:665-670.

Ge X., Burner D.M., Xu J., Phillips G.C., Sivakumar G. 2011. Bioethanol production from dedicated energy crops and residues in Arkansas, USA. Biotechnol. J. 6: 6-73.

Gnansounou E. 2010. Production and use of lignocellulosic bioethanol in Europe: Current situation and perspectives. Bioresource Technol. 101:4842–485.

Italian regulation, 2003. Italian Technical Guidelines for Wastewater Reuse. D.M. 185/2003. In: Official Journal No. 169, 23/07/2003.

Italian regulation, 2006.

Mantineo M., D'Agosta G.M., Copani V., Patanè C., Cosentino S.L. 2009. Biomass yield and energy balance of three perennial crops for energy use in the semi-arid Mediterranean environment. Field Crop. Res. 114:204-213.

Monti A., Venturi G., Amaducci M.T.. Biomass potential and ash content of switchgrass, giant reed and cardoon in North Italy. In: Proceedings of 14th European Biomass Conference, 2005 october 17-21, Paris, France.

Paranychianakis N.V., Nikolantonakis M., Spanakis Y., Angelakis A.N.

2006. The effect of recycled water on the nutrient status of Soultanina grapevines grafted on different rootstocks. Agr. Water Man. 81: 185-198.

Sivakumar G., Vail D.R., Xu J.F., Burner D.M., Lay J.O., Ge X., Weathers P.J. 2010. Bioethanol and biodiesel: Alternative liquid fuels for future generations. Eng. Life Sci., 10:8-18.

World Health Organization 2006. Guidelines for the safe use of wastewater, excreta and greywater, Volume 2: Wastewater Use in Agriculture. Geneva, Sweezerland.

Zub H.W., Brancourt-Hulmel M. 2010. Agronomic and physiological performances of different species of Miscanthus, a major energy crop. A review. Agron. Sustain. Dev. 30:201–214.

Modelling and optimization of a local smart grid for an agro-industrial site

Enrico Fabrizio,[1] Valeria Branciforti,[2] Marco Filippi,[2] Silvia Barbero,[3] Giuseppe Tecco[3]

[1]University of Torino, Department of Agricultural, Forest and Food Sciences; [2]Politecnico di Torino, Department of Energy; [3]Agrindustria s.n.c., Cuneo, Italy

Introduction

A smart grid is defined where different elements are interconnected between them and with the public utility grid. The development of smart grids is considered a strategic goal at both national and international levels and has been funded by many research programs. Within the BEE (Building Energy Ecosystems) project, funded by the Piedmont Region under the European POR FESR 2007-13 scheme, the creation of an electricity smart grid at a local level in a small agro-industry was done. This industry is one of the so-called *prosumer*, that is both a producer and a consumer of energy. The energy production is done by means of solar photovoltaic and biomass. In this local smart grid, the elements were subdivided in two main groups: loads (process machineries in the case study) and generators (PV and biomass in the case study). The loads may be further subdivided into permanent loads, mandatory loads and shiftable loads. The objective of the smart grid is the minimization of the exchanges between the local grid and the public utility grid. Even though no financial savings occur, this is important for the community grid. The problem is therefore to find the conditions that let the net exported energy going to zero at each time step, so arriving close to a self-sufficient system by modifying the shiftable loads. In a first phase of the study, the consumers were studied and, according to some characteristics of the machineries employed and the production requirements, grouped into production lines that can or not be switched off for intervals of time in order to compensate the smart grid fluctuations. The smart grid balancing may be done on an instantaneous basis, or in a predictive way considering the future weather forecasts and the future production requirements. The demo site was equipped with measurement instrumentation, data acquisition tools and a user interface that may be used to visualize all the quantities that are measured but also to perform the actions suggested by the optimization strategy (start/stop machineries, organization of production, etc).

Correspondence: Enrico Fabrizio, DISAFA, University of Torino, Via Leonardo da Vinci, 44, 10095 Grugliasco (TO), Italy.
Tel. +39.011.670.5525 - Fax: + 39.011.670.5516.
E-mail: enrico.fabrizio@unito.it

Keywords: sustainable factory, energy management, smart grid, production process optimization, energy saving

Contributions: the authors contributed equally.

Conflict of interest: the authors declare no potential conflict of interests.
Funding: POR/FESR 2007-2014, Progetto BEE "Building Energy Ecosystems" del Polo di Innovazione Energie Rinnovabili della Regione Piemonte.

Journal of Agricultural Engineering 2013; XLIV(s1):e111
doi:10.4081/jae.2013.(s1):e111

Introduction

The industrial sector is today responsible of about 20-50% (respectively countries with a long/new productive tradition) of final energy consumptions (Abdelaziz E.A., 2011; ENEA-UTEE, 2010). If considering the world industrial energy consumption over the next 25 years, it is projected to grow continuously, with an average increase of 1,4%. per year from 2006 to 2030. Large margins of improvement still exist and also other positive effects would arrive about various related issues (environmental, social, economical) (Allwood J., 2011).

In industrial settlements it is more and more common to have some on-site generation or co-generation systems (Lazzarin R., 2010; Abdelaziz E.A., 2011). Furthermore industries can be part of energy initiatives at district level (with other industries or with urban centres) (Danestig M., 2011), thus leading to the emerging topic of "smart grids", that has been pointed out as a strategic goal in the future at both national and international levels. The approach that is followed is one of the most promising: the energy generation will be spread on the territory and the number of the so called prosumers, both producers and consumers of energy, will increase (Fabrizio E., 2012).

During the elaboration of innovative tools, aimed to obtain a better energy management, it is important to have a continuous interaction with the subjects who will benefit of these tools, collecting information about daily routine, priorities and possible sudden problems (Asian Productivity Organization , 2008). In this case the chance that the new management strategy will be put in practice is higher. Otherwise, if the provided management system is too difficult or not in accordance with company needs, the proposed innovations, though promising they are, will not be used and no advantages will arrive (Branciforti V., 2013). Concerning energy management, this means that every proposal, aimed to final energy or financial savings, should be flexible enough and should consider some free interventions by workers. In this way energy related goals will be easily achieved without compromising too much company activities. This will encourage people in using the new tools available for them, that would be otherwise immediately abandoned.

In case of on-site energy generation, the aim is to find the best matching between energy demand and supply under some constraints, in order to optimize the system management and exploit its internal potential. Because of self-production and direct consumption of energy, the total amount of energy derived by the external grid decreases and the balance between energy demand and production can arrive

close to zero, if considering one month or all the year. For a more interesting result it is instead necessary to match energy demand and supply in shorter time periods, so going towards a self-sufficient settlement in almost each moment and thus minimizing the interaction with the external grid in both directions, feed-in and delivered energy.

In that sense the optimization helps in exploiting the system potential, by finding the best possible matching between energy demand and supply. The problem is quite difficult because it needs the definition of a complex system in which consumers and producers are different, are present in big number and each with particular needs.

An algorithm is defined in order to find the best management strategy of a system composed by consumers and producers of energy. The general mathematical formulation is useful to extend the approach to systems of different size and composed by various kind and number of subjects (a city with residential, office and industrial buildings that have energy demands and can also have local energy production, or a single firm with internal demands to be supplied and possible energy generators). An application of the latter case is presented in the case study. It is a small enterprise of the agro-food sector that hosts the demonstrative site of the project and that represents in itself an interesting example of internal exploitation of renewable energy sources and biomass.

An applied-research study was carried on by a partnership of academic and industrial subjects in 2011-2012, in order to investigate some new management strategies about electricity use at small district level. The optimization of energy use and the integration with production planning activities, were realized in an industrial demonstrative site located in North Italy. The project was co-financed by Piemonte Regional funds reserved to "research for companies". It was characterized by the involvement of academic, industrial and commercial partners, each interested in getting a more deep experience and knowledge about the smart-grids, a topic that has been pointed out as a strategic goal in the future at national and international level.

According to "20-20-20 scenarios" and to international regulations encouraging renewable energy use - and particularly the exploitation of biomass – the layout of actual energy network will change in future years. It will be probably characterized by many energy producers more and more spread on the territory, with an increasing number of *prosumers*. In recent years many projects are focusing on similar communities. The possible new situation would bear new challenges for the actual infrastructures capability, as the small storage capacity, the high transportation losses and the irregular demand and production profiles of different subjects belonging to the network. The grids should be improved in order to transmit energy in two directions and increasing the storage possibilities. One alternative solution to face all the present limits is the limitation of the storage units and an increased use of energy on site (Fabrizio E., 2012).

The demo site

The buildings

The demonstrative site is the small enterprise named *Agrindustria*, located in Piedmont region, North-west of Italy. The factory processes natural and vegetal materials that, by various working phases (cutting, drying, cooling, etc.), arrive to many final products, directly sent to the market (pellet) or sold to other companies of different sectors (make-up, monument conservation, animal feeds, automotive industry).

The industrial area is composed by 4 main buildings dedicated to different process phases, detached and divided by open areas, plus a civil building hosting the offices and a new structure built to cover the gasifier. The buildings features, their use and size are listed in Table 1. The buildings devoted to productive activities are composed of about 6.000 m^2 of floor area and a corresponding total volume of 67.000 m^3.

The energy system

Agrindustria can be considered a so called *prosumer*, that is a subject being both consumer and producer of energy. Thus the layout of the energy system characterizing the demo-site, both from the energy demand side and from the energy production side, contains many interesting elements that need to be properly considered in their mutual relationships.

The energy demand depends on the activities carried out that can be divided in "civil users" for the office building (ICT, printers and kitchen appliances), "industrial users" (productive machineries) and "building services", aimed at maintaining environmental conditions suitable for the different activities (lighting, environmental heating and cooling, safety systems, automatic gates and transportation systems). Among them, the industrial users represent of course the higher energy demand and are the focus of the present work.

A list of the energy demands and supplies is shown in Table 2. The following energy sources are here exploited:

- Electricity from the public grid;
- Natural gas from the public utility;
- Thermal energy, derived as waste of the syngas combustion process;

Table 1. Description of the buildings composing the industrial area used as demonstrative site.

Building number	Use	Covered area* [m^2]	Volume** [m^3]
Offices	Offices and kitchen		
Building 1	Raw material processing	600	4500
Building 2	Storage of raw material and packaged product	1500	10000
Building 3	Pellet production	840	11350
Building 4	Mais derived production and mais storage	3200	41500
Gasifier roof	Protection of co-generation plant	234	0
	Total	6374	67350

*(closed or not by vertical walls on all sides); **(only completely enclosed spaces).

Table 2. List of the energy demands of the case study and of the different ways they are supplied.

Energy demand	Energy supply and on site production
Electricity	Electricity from the public grid (external supplier)
	Electricity from PV panels (solar radiation on site)
	Electricity from syngas engine (biomas in the gasifier on site)
	Electricity from mini-wind generators (wind generators in chimneys)
Thermal energy	Thermal energy from natural gas (external supplier)
	Thermal energy from syngas combustion (gasifier on site)
Thermal Energy for cooling purposes	Electricity from the public grid (external supplier)

- Self-produced electricity from PV panels present on the buildings roofs;
- Self-produced electricity, deriving by a co-generation plant with internal combustion engine supplied by syngas.

Part of the energy is obtained by renewable energy sources, as:

- Solar radiation, to produce electricity through PV panels;
- Biomass, to produce syngas and consequently thermal energy and electricity;
- Wind-energy, through a small wind generator placed on steam chimneys

A schematic representation of the internal electricity distribution network is displayed in Figure 2, where the all elements listed above, are displayed together with their connections and locations. Different "traditional" energy source and renewable ones (biomass, solar energy, etc.) have been taken into account, because of already existing power plants. On the left side the 3 energy sources used within the factory are listed (electricity from the public grid, solar energy and biomass). On the right side, all final users are described with the name used by the internal staff and they are grouped in 5 clusters, depending on the building they are placed in (grey areas in Figure 2). In the central part of the scheme some converters are represented, as the PV panels and the gasifier. The lines connecting these elements and the arrows, show the way the electricity is distributed from the delivering point to all buildings, and from the arrival point of each building to machineries. All users are identified by their own name and a numeric code, useful to recognize them in all following elaborations. In Figure 3 some energy generators and some productive machineries of the demo site are shown.

The energy demand characterization

In order to characterize the energy demand (requested power and its profile during time), an inventory of the energy users was organized, using data deriving from the owner experience and needs, such as:

1. the list of all engines composing a productive machinery and of their power by target data; each productive line is considered as a single element with total power request equal to the sum of all parts composing it.
2. the average daily working hours of each machinery and the activation days per each week, according to the owner experience during last years.
3. the time that is necessary to conclude a complete working cycle and after which it is possible to stop the machinery.
4. the possibility to stop the activity of each machinery for a certain time – in order to modulate the total load – according to clients request and orders to be dispatched.
5. the location of each machinery in the building, in order to prepare possible monitoring activities for which machineries are connected to each electricity sub-station.

The following information was collected and organized in a table, related to each machinery:

- Numerical code (the same of the previous graphical scheme)
- Name commonly used within the company
- Performed process
- Building location
- Possibility to stop it and time needed to complete a working cycle
- Working hours per day and days of use per week
- Nominal power

Consumption data of the last 4 years were analyzed in order to know the whole system performance before the proposed management strategy. The average electricity consumption of the period 2008-2011 is about 3 GWh each year.

Figure 1. General view of the industrial area hosting the demo-site.

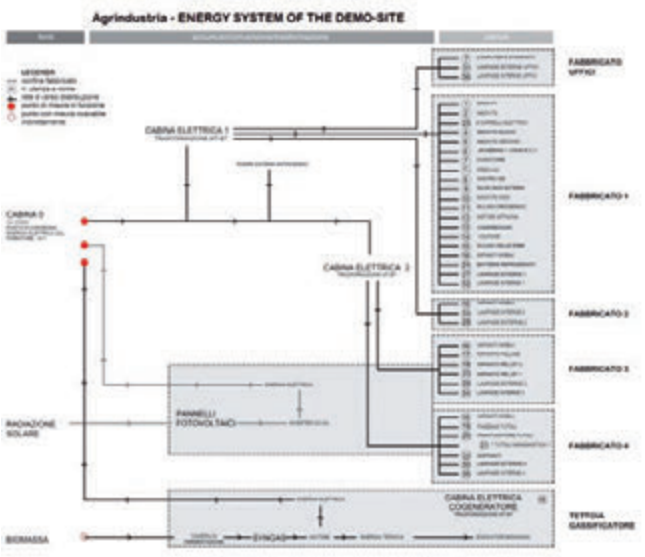

Figure 2. Schematics of the energy system demo-site.

Figure 3. Some energy generators (left picture: gasifier) and loads (right pictures: process machineries) of the demo site.

The modelling framework

Smart grid modelling

The model of a smart grid is reported in Figure 5. The elements can be divided in two main groups: the ones that use energy (loads) and are identified in red with *L*, and the ones that produce energy (generators) and are identified in green with *G*. The model is generalized as a system composed by *n* loads and *m* generators (L_n and G_m). The definition of the system boundaries is of great importance: the elements belonging to the local grid can be seen as an *unicum*: their relationship with the external grid is limited at just one connection point where a measure instrument is usually placed (identified as meter in the figure).

In that way it is possible to quantify:

- the total amount of energy produced by the generators and sent to the external grid (*F*, feed-in energy);
- the total amount of energy demanded by the loads, and provided by the external grid (*D*, delivered energy);
- the net exported energy, *E*, defined as the net energy exported from the system to the external environment (Eq. 1):

$$E(\Delta t) = F(\Delta t) - D(\Delta t) \quad \forall \Delta t \in T \tag{1}$$

The aim of the smart grid management is to find the conditions that limit the import from the external grid and maximize the use of on-site generation. The net exported energy (*E*) should tend to zero at each time step (thus arriving close to a self-sufficient system) or assume positive values (thus resulting in a positive energy system that produces more energy than the energy that is consumed, within a certain time period).

Each load is characterized by a profile of requested energy during time, called $l_n(t)$; similarly for each generator a profile or generated energy during time can be defined and it is called $g_m(t)$.

The energy requested by a generic user *L* during the period Δt is the integral of the function l_n extended to the whole period Δt:

$$L_n = L_n(\Delta t) = \int_t^{t+\Delta t} l_n(t)dt \quad [kWh] \tag{2}$$

In the same way, the energy produced by a generator *G* in the period Δt, can be expressed as:

$$G_m = G_m(\Delta t) = \int_t^{t+\Delta t} g_m(t)dt \quad [kWh] \tag{3}$$

The total energy requested by all users of the local grid in the time period Δt, is called $L(\Delta t)$ and it is defined as the sum of all the requested energy quantities L_n by all loads *L*:

$$L(\Delta t) = \sum_n L_n(\Delta t) \tag{4}$$

Similarly,

$$G(\Delta t) = \sum_m G_m(\Delta t) \tag{5}$$

If the produced energy is not used locally and if no energy storages are present, the net exported energy, according to Eq. 1 can also be expressed as the difference between the total energy produced on site and the total demands,

$$E(\Delta t) = G(\Delta t) - L(\Delta t) \tag{6}$$

Load clustering

In order to define the optimization algorithm, it is necessary to establish some other features of the loads and the generators. An inventory of all energy end-users and generators was produced, characterizing each of them by specific parameters (power, activity period, energy consumed or product). Loads are clustered, with different priority and importance for the company, with a classification that was also used in the domestic sector (Vasquez F. I., 2011). They were subdivided into the following 3 categories (Figure 6):

- *Permanent Loads* (L_{perm}): those use or devices that work continuously over the time period Δt;
- *Mandatory Loads* (L_{mand}): those use that are not always in activity but that, for their function, must be activated immediately when requested;
- *Shiftable Loads* (L_{shift}): those use that are not continuously activated and that, because their function is not essential, can be switched off and satisfied later.

Shiftable loads can be considered as the only free variables of the system, the only elements that can be modified for optimization purposes, because they can be postponed if this is necessary to balance the smart-grid during a certain period Δt.

According to this loads classification, the previous total energy demand, $L(\Delta t)$, can be split into 3 terms, as expressed in Eq. 7. The total number of permanent loads is *a*, of mandatory loads is *b* and of shiftable loads is *c*, being $n=a+b+c$.

$$L(\Delta t) = \sum_n L_n(\Delta t) = \sum_a L_{perm,a}(\Delta t) +$$

CODICE	NOME	LAVORAZIONE SVOLTA	COLLOCAZIONE	LINEA SPEGNIBILE	TEMPO COMPLETAMENTO DI UN CICLO DI LAVORAZIONE	ORE ATTIVITA' GIORNALIERE	GIORNI ATTIVITA' SETTIMANALI	ORE/ANNO DI ATTIVITA' STIMATE	POTENZA INSTALLATA
			n° fabbricato		[min]	[h/g]	[g/settimana]	[h/anno]	[kW]
1	MACH F1	Micronizzazione argilla	1	SI'	10	8	5	2000	25
						TOT ORE/ANNO CALCOLATE			
2	MACH F2	Insaccatrice argilla	1	SI'	3	6	5	1500	6
						TOT ORE/ANNO CALCOLATE			
3	VORTICE smantellato	Mulino a martelli [illegible] per modello 1	1	-	-	0	0	0	0
						TOT ORE/ANNO CALCOLATE			
4	MACH F2 NUOVO	Micronizzazione farine vegetali	1	NO	5	24	4	4800	42
						TOT ORE/ANNO CALCOLATE			

Figure 4. Extract of the energy users inventory.

$$\sum_b L_{mand,b}(\Delta t) + \sum_c L_{shift,c}(\Delta t) \quad (7)$$

Instant optimization

The objective function of the optimization problem is expressed as:

$$f(E(\Delta t)) = 0 \quad \forall (\Delta t) \in T \quad (8)$$

and searches those values able to determine a net exported energy $E(\Delta t)$ close to zero, for each time period Δt.

According to the definition of $E(\Delta t)$ given in Eq. 6 and substituting the value of L with the loads classification provided in Eq. 7, the net exported energy going from the system to the external grid, can be expressed by the Eq. 9:

$$E(\Delta t) = G(\Delta t) - L(\Delta t) = \sum_m G_m(\Delta t) - \sum_a L_{perm,a}(\Delta t) - \sum_b L_{mand,b}(\Delta t) - \sum_c L_{shift,c}(\Delta t) \quad (9)$$

The decision variables of the optimization problem are the shiftable loads. The Boolean parameter π is introduced in the model, associated to each load to indicate its activation in a given period of time (0 indicates the off mode and 1 indicates the on mode).

$$\pi = [0,1] \quad (10)$$

Associating a parameter π to each load, the objective function can be written as:

$$E(\Delta t) = \sum_m G_m(\Delta t) - \sum_a \pi_{Lp,h} L_{perm,h}(\Delta t) - \sum_b \pi_{Lm,j} L_{mand,j}(\Delta t) - \sum_c \pi_{Ls,k} L_{shift,k}(\Delta t) \quad (11)$$

The solution of the optimization problem (expressed by Eq. 12) is a group of n parameters π, one for each load: this combination of various switching on and off modes of the loads satisfies the balance aim, as expressed in Eq. 6 and according to the constraints expressed in Eqs. 13 and 14.

$$\{\pi,\ldots,\ldots,\pi\} : (E(\Delta t)) \to 0 \quad \forall \Delta t \in T \quad (12)$$

$$\pi_{p,i} = 1 \quad \forall i \quad (13)$$

$$\pi_{m,j} = 1 \quad \forall j \quad (14)$$

Each load with π equal to zero should be switched off during the considered time period, while each load with π equal to 1 can be activated during the same time period. This approach is similar to the optimization performed for multi-energy systems in the works (Fabrizio *et al.*, 2009; Fabrizio *et al.* 2010; Fabrizio, 2011).

Predictive optimization

If the instant optimization is repeated for many successive time steps, it is possible to schedule an all day, week or month, thus planning activities in the best way to match both energy optimization goals and production needs. The considered time period is defined in Eq. 15 as T and it includes all time steps Δt_i.

$$T = \sum_{i=0}^{j} \Delta t_i \quad (15)$$

The mathematical expression of the objective function is Eq. 16. It is similar to the instant optimization but with some differences. It is extended to many time periods and the optimization is done on the absolute value of the net exported energy, in order to avoid compensations between positive and negative values of $E(\Delta t)$ in different Δt intervals.

$$f\left(\sum_{i=1}^{q} |E(\Delta t_i)|\right) \to 0 \quad \forall \Delta t \in T \quad (16)$$

The loads classification and the meaning of the parameter π are the same of the instant optimization.

The problem solution is the set of parameters π, referred to the shiftable loads, as expressed in Eq. 17. Those values compose a matrix with q rows, corresponding to the included time periods, and k columns, corresponding to all considered shiftable loads, as shown in Figure 7.

$$\{\pi_{Ls,\Delta t1},\ldots,\ldots,\pi_{Ls,\Delta tq}\} : \left(\sum_{i=1}^{q} |E(\Delta t)|\right) \to 0 \quad \forall \Delta t \in T \quad (17)$$

$$\sum_{k=0}^{c} \pi_{Ls,k} = x \quad \forall L_{s,k} \quad (18)$$

In order to meet the daily company needs, that are independent from the energy issues, a further possibility is provided within the proposed optimization logic. The person or the staff , who are in charge for the production management, can express the total number of activation that each shiftable load must complete in the time period T: these

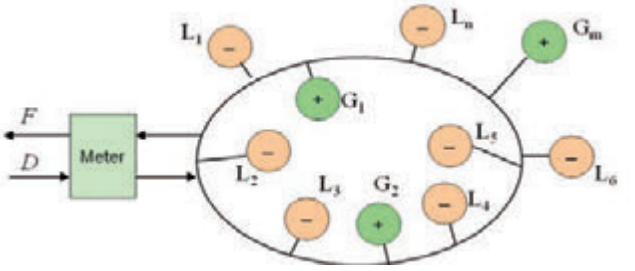

Figure 5. Scheme representing the virtual grid.

Agrindustria - LOADS CLUSTERING IN 3 PRIORITY CATHEGORIES

TIPO DI CARICO	UTENZE	POTENZA TOT. INSTALLATA [kW]	TEMPO COMPLETAMENTO DI UN CICLO PRODUTTIVO [min]
PERMANENTE	17. IMPIANTO PALLINE	340	10
	18. IMPIANTO PELLET 2 (appena ultimato)	200	20
	23. IMPIANTO PELLET 1 GRANDE	395	60
	25. GASSIFICATORE - impianti ausiliari	18	Funzionamento continuo
	TOTALE kW	953	
OBBLIGATORIO	MACCHINE 4. 5. 6. 9. 10. 12. 13. 14. 16. 19. 22. 24	963	Da 5 a 20 min
	16. VARIE: IMPIANTI MOBILI	37	1 min
	27- 36. IMPIANTO ILLUMINAZIONE ARTIFICIALE INTERNA ED ESTERNA	33	Alcune ore
	1. elettrodomestici e ICT uffici	6	Alcune ore
	TOTALE kW	1040	
RIMANDABILE	L_{sm1} 1. MACH F1	25	10
	L_{sm2} 2. MACH F2	6	3
	L_{sm3} 7. COCCITORE	17	15
	L_{sm4} 7 bis. PRESWAC	19	15
	L_{sm5} 8. SASTRI SIL	39	30
	L_{sm6} 11. MULINO CRIOGENICO	34	10
	L_{sm7} 15. MULINO DELLE ERBE	127	10
	L_{sm8} 20. FRANTUMATORE TUTOLI	144	15
	L_{sm9} 21. TUTOLI MAGNOMISTICA	16	15
	L_{sm10} 26. CARRELLI ELETTRICI - N. 6	18	60
	TOTALE kW	439	
	Macchine legate a fasi successive di un unico processo produttivo		

Figure 6. The Loads grouped in the 3 priority categories.

loads, because identified as shiftable, will be considered by the algorithm calculations as machineries whose activation can be planned in the most suitable moment (according to energy matching goals) but with a minimum required number of working cycles that must be completed over the considered period (according to the company orders and needs).

The number of total desired cycles for each shiftable load, is easily provided by the staff and it originates a new constraint for the algorithm during the calculation towards the best solution, represented by Eq. 18. The result is a plan of activities for the period *T*, shown by a user interface, where a combination of various switching on and off of shiftable loads takes the whole system closer to the balance, satisfying both the energy matching goals and the needs of the company about the use of machineries.

The on-off functioning can also be automated but this option needs to be carefully evaluated. Preferably only the information on the best layout of activities is given to the users, that can decide weather or not following the indications.

An intelligent control unit was programmed according to these instructions. In this device some data also converge: they are real time data from measurement tools on the field, weather forecast, estimation based on previous days and constraints decided by the user for that period (urgent orders, priority of some activities, etc.). The intelligent central unit shows information through an interface. Furthermore with very easy calculations it is possible to obtain consumption and production profiles and some indicators of load-matching or grid-interaction, to easily communicate how the system is performing about the desired results.

Smart grid indicators

Some indicators were calculated to analyze the performance of the overall system and the results obtained thanks to the proposed management strategy. They are one load matching indicator and two grid interaction indicators, thus providing some useful information about the reaching of the project goals, the effectiveness of the proposed strategy and the relationship between the system and the external grid.

- *Load cover factor over period T ($\gamma(\Delta t)$)*: it is the ratio between the smallest between the total generated power and the total requested power, over the total requested power. It expresses in percentage which is the part of the total load that was supplied by on site generated energy. In the most successful case, it will be equal to 100%, thus meaning that the all demand was supplied by on site generation.

$$\gamma(\Delta t) = \frac{\min\left[G(\Delta t), L(\Delta t)\right]}{L(\Delta t)}\left[\%\right] \quad (19)$$

- *Relative grid interaction amplitude (A_{gr})*: it is the difference between the maximum and the minimum values of net exported energy registered over period *T*, both normalized by the total design load of the system.

$$A_{gr} = \frac{\max\left[E(\Delta t)\right]}{L(\Delta t)_{des}} - \frac{\min\left[E(\Delta t)\right]}{L(\Delta t)_{des}}\left[-\right] \quad (20)$$

- *No grid interaction probability ($P_{E=0}$)*: it represents the probability that the system is working in autonomy of the grid, by using on site generation to cover the entire load. It is the number of time steps characterized by a value of net exported energy almost equal to zero, over the period *T*, this ration being expressed in percentage.

$$P_{E=0} = \frac{time_{|E(\Delta t)|<0,001}}{T}\left[\%\right] \quad (21)$$

Application

The described logic was applied to the demo-site in an example of predictive optimization. The local grid was defined, to be programmed along a period *T* composed by 8 time intervals Δt, and having the following features:

- 3 generators producing the following design power: G_1=523 kW (PV panels on building 3 and 4); G_2=196 kW (PV panels on building 1 and 2); G_3=200 kW (gasifier); the total produced power is 919 kW, with a time variable production schedule as shown in Figure 8.
- Permanent and mandatory loads, with following features: ΣL_{perm}= 953 kW, ΣL_{mand}= 1040 kW or less, depending on the considered interval (for example because of daily hours of offices activity or evening and night time with light activation). The time schedule of the power requested by these loads is represented in Figure 9.
- Shiftable loads, with the following features: $L_{shift\ 1+2}$ = 31 kW, $_{Lshift}$

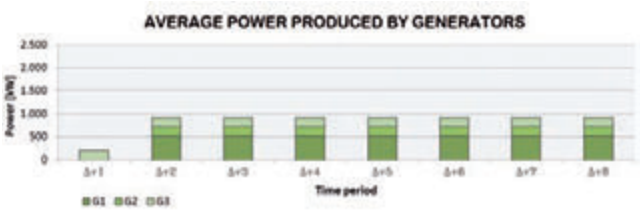

Figure 8. Time schedule of the power requested by permanent and mandatory loads over.

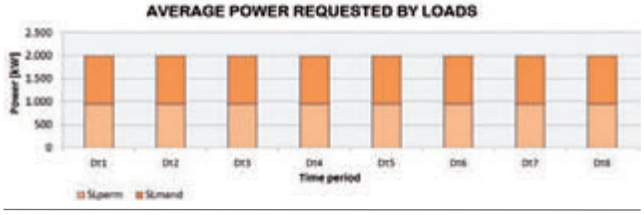

Figure 9. Time schedule of the power produced by generators in the 8 time intervals of the period T.

Figure 7. Matrix resulting from the *predictive optimization* algorithm.

$_{3+4+5}$ = 75 kW, $L_{shift\ 6}$ = 34 kW, $L_{shift\ 7}$ =127 kW, $L_{shift\ 8}$ = 144 kW, $L_{shift\ 9}$ = 10 kW, $L_{shift\ 10}$ = 18 kW.

- For each shiftable load a number of necessary activation periods during was defined. The information is provided as total amount of activations for the 7 identified shiftable loads: $\Sigma\pi L_{shift\ 1+2}$ = 2, $\Sigma\pi L_{\text{shift } 3+4+5}$ = 1, $\Sigma\pi_{Lshift\ 6}$ = 3, $\Sigma\pi_{Lshift\ 7}$ = 1, $\Sigma\pi L_{shift\ 8}$ = 1 $\Sigma\pi_{Lshift\ 9}$ = 2 and $\Sigma\pi L_{shift\ 10}$ = 1, that respectively means that the first group of machineries must be activated twice during the period T, the second only once, the third 3 times and so on.

The constraints are expressed as follows:

πL_n = [0,1] πL_{perm}= 1 πL_{mand}= 1 or 0

$\Sigma\pi L_{shift1+2}$ = 2; $\Sigma\pi L_{shift\ 3+4+5}$ = 1; $\Sigma\pi L_{shift\ 6}$ = 3; $\Sigma\pi L_{shift\ 7}$ = 1; $\Sigma\pi L_{shift\ 8}$ = 1 $\Sigma\pi L_{shift\ 9}$ = 2; $\Sigma\pi L_{shift\ 10}$ = 1

The group of values that, for the given constraints, satisfy Eq. (17) are represented in a matrix in Figure 10. Each column represents one of the 7 shiftable loads and each row represents one of the 8 time intervals Δt. The energy produced by generators is not enough to supply permanent and mandatory loads. The situation changes after the time period Δt_1, when two more generators start to work. This change is shown in the first chart of Figure 11. It is in that phase, since the 2nd time interval, that the problem solution indicates to place the shiftable loads, distributing them in order to arrive closer to the system balance and to satisfy the requested number of working process, expressed as constraint.

The second chart of Figure 11 shows the time intervals in which the energy demand is higher than the energy supply, and the opposite situation. The third chart of Figure 11 represents the value of net exported energy $E(t)$. The negative values highlight a scarcity of self-produced energy in comparison to the energy demand of the same moment, thus imposing to use energy coming from the external grid. This chart is also useful to quantify the distance of the value assumed by $E(\Delta t)$ from the ideal situation of perfect supply-demand matching.

For the present example, the values of the 3 indicators previously described, are shown in Figure 12. Less than a half of the total request was supplied by the generators, with the *Load cover factor over period* T $\gamma(\Delta t)$ corresponding to 40%. The interaction with the external grid was continuous, because at no time step the energy generated on-site was sufficient to totally supply the demands: for this reason the *No grid interaction probability* ($P_{E=0}$) is equal to zero. Nevertheless this interaction was characterized by a quite flat profile, and the quantity requested to the external grid was quite constant during the all period, except for the first time step, as shown in the last chart of Figure 11: the *Relative grid interaction amplitude* (A_{gr}) was in this case 0,3.

Figure 10. The matrix resulting from *predictive optimization*.

Figure 11. Supply and demand and Net Exported Energy over period T.

Conclusions

The optimization algorithm was developed for this case study but the mathematical formulation allows extending it in time and space and to almost any other case study, in terms of different size and also including different final users, dwellings, etc. Moreover it is possible to pursue the optimization of small single smart-grids and then setting a bigger system in order to establish exchanges of energy between them, with a similar optimized logic. In other case studies the results could be more evident according to the energy produces by generators and the number and features of the shiftable loads (that in the presented case study correspond to 1/5 of the total loads in terms of power).

The intelligent central unit shows information through an interface. Furthermore with very easy calculations it is possible to obtain consumption and production profiles and some indicators of load-matching or grid-interaction, to easily communicate how the system is performing about the desired results.

Figure 12. Performance indicators of he smart grid.

It is important to arrive to the matching between demand and supply not only for the obtainable financial advantages (place some loads in the hours of energy surplus, thus profiting of hourly fees) but also because, through a reduced interaction with the external grid, the quantity that is transmitted, and the related distribution losses, decrease.

A deep knowledge of the consumption of factories is among the interests of many actors of the energy supply chain. Because industries are the final clients of this chain, public utilities usually offer specific fees and discounts for those clients who implement some tools to have a more predictable energy profile (monitoring plans for example): in that way the energy trader limits the risk deriving from wrong prediction about the quantity of booked and bought energy quantity, and the consequent penalties for not correct predictions. Moreover the database obtainable with a monitoring activity, with past years data, can be a starting point for a continuous monitoring plan, in order to activate a virtuous process of improvement and control.

Concerning energy management, every proposal, aimed to final energy or financial savings, should be flexible enough and should consider some free interventions by workers. In this way energy related goals will be easily achieved without compromising too much company activities. This will encourage people in using the new tools available for them, that would be otherwise immediately abandoned.

Nomenclature

a	number of permanent loads
b	number of permanen loads
c	number of permanen loads
i	generic time step t
h	number of permanent loads
j	number of mandatory loads
k	number of shiftable loads
n	number of loads
m	number of generators
π, *perm*	permanent
m, mand	mandatory
shift	shiftable
q	number of time step t within period T
D	delivered energy
F	feed-in energy
E	net exported energy
L	load
G	generator
$\varnothing t$	time step
T	total time period
γ	Load cover factor over period T
A_{gr}	Relative grid interaction amplitude
$P_{E=0}$	No grid interaction probability

References

Abdelaziz E.A., Mekhilef S. 2011. A review on energy saving strategies in industrial sector. Renewable and Sustainable Energy Reviews , 15 (1), 150–168.

Abdelaziz E.A., Mekhilef S., Saidur R. 2011. A review on solar energy use in industries. Renewable and Sustainable Energy Reviews , 15, 1777-1790.

Allwood J., Cullen J. 2011. Sustainable Materials - with Both Eyes Open: Future Buildings, Vehicles, Products and Equipment - Made Efficiently and Made with Less New Material. Cambridge, UK, UIT Cambridge.

Asian Productivity Organization . 2008. Working manual on energy auditing in industries - Results of the workshop "Energy efficiency and green productivity". New Delhi, India,: APO and National Productivity Council (NPC).

Branciforti V. 2013. Rational use of energy and materials in industrial areas. Torino: Politecnico di Torino.

Cimren E., Fiksel J., Posner M.E., Sikdar K. 2011. Material Flow Optimization in By-Product Synergy Networks. Journal of Industrial Ecology, 15 (2), 315-33.

Danestig M., Trygg L. Difs K. 2011. Increased use of district heating in industrial processes – Impacts on heat load duration. Energy Procedia IACEED2010, 1584–1588.

ENEA- UTEE Unità Tecnica Efficienza Energetica. 2010. "Rapporto Enea Energia e Ambiente". Roma.

Fabrizio E. 2011. Feasibility of polygeneration in energy supply systems for health-care facilities under the Italian climate and boundary conditions. Energy for Sustainable Development, 15(1), 92-103.

Fabrizio E., Corrado V., Filippi M. 2010. A model to design and optimize multi-energy systems in buildings at the design concept stage. Renewable Energy, 35(3), 644-655.

Fabrizio E., Filippi M., Branciforti V. 2012. Deliverable Progetto Regionale, "BEE Building Energy Ecosystem" . Torino: Politecnico di Torino, Dipartimento Energia, Torino.

Fabrizio E., Filippi M., Virgone J. 2009. An hourly modelling framework for the assessment of energy sources exploitation and energy converters selection and sizing in buildings. Energy and Buildings, 41(10), 1037-1050.

Lazzarin R., 2010. Recupero energetico nei processi industriali, Convegno AICARR "Riduzione dei fabbisogni, recupero di efficienza e fonti rinnovabili per il risparmio energetico nel settore industriale Padova."

Vasquez F. I., K. W. 2011. Electricity load management in smart home control. Sydney: 12th Conference of Building Performance Simulation Association.

Development perspectives for biogas production from agricultural waste in Friuli Venezia Giulia (Nord-East of Italy)

D. dell'Antonia,[1] S.R.S. Cividino,[1] A. Carlino,[2] R. Gubiani,[1] G. Pergher[1]

[1]University of Udine, Department of Agriculture and Environmental Sciences Udine, Italy; [2]Regione Friuli Venezia Giulia, Italy

Abstract

The latest directives of the Energy and Environment Policy of the European Union (EU) established a new framework for renewable sources (Directive EC 28/2009; European Commission, 2009). The Italian Energy Action Plan of 2010 set a target of at least 17% of total energy generated from renewable sources by 2020. In this context biogas from waste and biomass is a potential energy source that can be used for the production of heat, electricity and fuel. The objective of this work was to determine the potential energy production from anaerobic digestion of animal wastes and agricultural residues in Friuli Venezia Giulia (Nord-East Italy).

For an assessment of biogas as an energy source, based on direct conversion by agricultural farms, it is important to establish the amount of the waste. In this study, biogas amount which can be obtained was calculated for all municipalities in the Friuli Venezia Giulia Region (North-East of Italy) by using the number of livestock animals, the cereal area for agricultural residues and also considering various criteria such as the rate of dry matter and availability.

The calculated regional biogas potential is about 187 (N)Gm3 when using animal waste, straw and corn stalk. The potential of biogas energy equivalent of Friuli Venezia Giulia is about 3 600 TJ (LHV) may be able to replace 2.6% of final energy consumption in Friuli Venezia Giulia (3 339 ktoe) and about 10% of the final electricity consumption (864 ktoe) considering an electrical efficiency of 30% with the biogas engine.

Introduction

The latest directives of the Energy and Environment Policy of the European Union (EU) established a new framework for renewable sources (Directive EC 28/2009; European Commission, 2009). The Italian Energy Action Plan of 2010 set a target of at least 17% of total energy generated from renewable sources by 2020. In this context biogas from waste and biomass is a potential energy source that can be used for the production of heat, electricity and fuel. Regarding this, Italy took its first steps at the beginning of the 1980s when realisation of biogas production plants from animal waste was essentially aimed at reducing environmental impact in the agricultural sector rather than providing a clean energy source. At present the situation has changed: while the importance of environmental aspects is still fully recognised, there is now the additional need to increase the use of renewable energy sources in rural areas (Tricase et al., 2009).

The number of anaerobic digestion plants in Italy hasincreased, in recent years, thanks to the old Italian energy law from 244/2007, which provided an all-inclusive feed-in tariff(280 €/MWh for biomass) for electricity production from agricultural biomass, regardless of the feedstock type and the power of the plants.In 2010, some 600 plants in Italy were producing biogas, with a total installed electric power of 350 MW(e) approx. (Piccinini, 2010). Of these plants, 58% of which were working in co-digestion of manure with energy crops and agro-industrial residues.

In July 2012, Italy adopted a new regulation for the production of electricity from biomass, making the public support higher if the production of biogas is derived entirely from animal waste and agricultural by-products (Ministry of Economic Development, 2012).

In relation to the biogas potential from agricultural by-products is important to identify the best farm for the technical and economic convenience of small biogas plants. The objective of this work was to determine the potential energy production from anaerobic digestion of agricultural by-products (animal wastes and agricultural residues) in Friuli Venezia Giulia (Nord-East Italy).

Materials and methods

The agricultural land area in Friuli Venezia Giulia is 218 443 ha (26.5% of total land area; Istat, 2010) with 22 316 agricultural farms (average: 9.8 ha per farm). Only 3 343 farms (15.0%) are raising livestock, including cattle (61.7% of farms), pigs (17.5%), poultry (11.7%), small ruminants (sheep and goats, 8.0%), and rabbits (4.5%). Small ruminants, equines and rabbits were not included in the present analysis.Cattle has the largest share with 89 162 head, 88% of all ruminants. In poultry, 83% aremeat chickens (broilers), 8% are laying hens, 6% are turkeys for a total of 6 951 512 pieces. Finally, pigs are present with 216 430 animal (Table 1).

The total number of cattle, pig and poultry with the relative categorieswas determined using available data for 218 municipalities in Friuli Venezia Giulia (Istat, 2010). These numbers were then used to estimate the potential production of biogas and its energy content for each of the municipalities. There are severalfactors whichaffect the amount of waste and biogas obtainable during livestock operations.

Correspondence: Daniele dell'Antonia, University of Udine, Department of Agriculture and Environmental Sciences, Via delle Scienze, 208 - 33100 Udine, Italy
E-mail: daniele.dellantonia@uniud.it

Key words: biogas, animal waste, straw, corn stalk, feedstock

Journal of Agricultural Engineering 2013; XLIV(s1):e112
doi:10.4081/jae.2013.(s1):e112

These factors include the type and age of animal, body weight, type of breeding, total solids ratio, volatile solids ratio and the availability of waste and biogas yields. The average body weight for the different animal categories was determined using the standards reportedin Italian Law 109/2007 (Table 2).

In the calculation of the amount of waste, the number of animals in each category (cattle, pigs and poultry) and their sub-categories (age of the animal) were multiplied by the body weight to determine the tons of live weight. The live weight for each category(LW, in ton), was calculated as:

$$LW=n°\cdot lw \quad (1)$$

Table 1. The number of livestock farms and total animal numbers for cattle, pig and poultry in Friuli Venezia Giulia.

Animaltype	Live stock farms	Number of animals	Animals per live stock farm
Cattle	2 050	89 162	43
Pig	586	216 430	369
Equine	582	2 815	5
Poultry	392	6 951 512	17 733
Rabbit	152	670 383	4 410
Goats	141	3 285	23
Sheep	126	10 890	86
Italian buffalo	15	1 449	97
Ostrich	2	251	126

Where:

n°, is the number of animal in each category;

lw, in tons, is the live weight per head in each animal category.

According to the standards set by Italian Law 109/2007, concerning the agronomic use of livestock effluents, were defined the wet waste per body weight of each type and age of the animals (annual amounts of wet waste were determined in relation to the type of breeding for each category). The livestock operations slurry (liquid material) and manure (shovelable materials) were considered for the waste yield (Table 3).The amount of annual slurry(S, in m3) was calsutaled as:

$$S=\sum(LW\cdot Sb\cdot B \quad (2)$$

Where:

LW, in tons, is the live weight for each category;

Sb, in m3 t^{-1}, is the slurry per unit live weight for the type of breeding in each category;

Br, in %, is the percentage of the type of breeding.

The amount of annual manure (M, in m^3) wascalsutaled as:

$$M=\sum(LW\cdot Sb\cdot Br) \quad (3)$$

Where:

LW, in tons, is the live weight for each category;

Mb, in m3 t^{-1}, is the manure per live weight for the type of breeding in each category;

Br, in %, is the percentage of the type of breeding.

The biogas yields from cattle, pig and poultry were calculated according to annual amounts of the organic matter in the slurry and manure waste (Table 2). A map of biogas potential production has been produced using GIS-based software. The annual amount of potential biogas (B, in m^3) has been derived from:

$$B=(S\cdot Es)+(M\cdot Em) \quad (4)$$

Where:

S, in m^3, is the amount of annual slurry;

M, in m^3, is the amount of annual manure;

Es, in m^3 ($m^{-3}m^{-3}$), is the efficiency of biogas production fromslurry;

Em, in m3 ($m^{-3}m^{-3}$), is the efficiency of biogas production frommanure.

The data of the biogas obtainable during livestock operations were correlated with the agricultural residues. Operational scenarios provided the utilisation of straw and corn stalk. This allowed to identify the technical potential for the biogas production from the agricultural waste in Friuli Venezia Giulia and afterwards evaluate the economic feasibility of biogas plants in relation to different situations of the area (higher public support for the production of electricity when using by-products).

Results

The biogas potential annual production according to categories and number of animals in designated municipalities in Friuli Venezia Giulia in is presented in Figure 1.

The calculated regional biogas potential is about 38.4 (N)Mm^3 when using only animal waste where 51% of total energy potential is of cattle origin, 32% from pig and 17% of poultry origin. The potential of biogas energy equivalent of Friuli Venezia Giulia is about 777 TJ (LHV) (Table 4).

Table 2. Waste properties and biogas yields of slurry and manure by type of animal.

Feedstock	DM content (% a.r.)	Organic DM content (% a.r.)	Specific weight (t/m^3)	Biogas (Nm^3 t^{-1}Organic DM)	Methane(%) (%)	LHV (MJ/m^3)
Cattleslurry	8.5	6.75	1	230	55	19.6
Cattlemanure	18	14.25	0.3	250		
Pigslurry	6.1	4.9	1	355	55-60	20.5
Pigmanure	22.5	18.75	0.3	450		
Poultryslurry	19.5	14.9	1	300	60	21.4
Poultrymanure	32.25	24.2	0.3	400		
Cornstalks	86	62	0.4	500	54	19.3
Straw	87.5	76	0.04	390	54	19.3

Table 3. The live weight weightand waste yield of the animalsin each category.

Animal type	Categories	Live weight (kg)	Housing system	Waste yield (m^3 $t.l.w.^{-1}$)	
				Slurry	Manure
Cattle	<1 year	150	Freestall with litter	4	22
			Freestallwithoutlitter	22	-
	1-2 years	450	Freestall with litter	10	26.5
			Freestallwithoutlitter	26	-
	>2 years	550	Freestall with litter	10	26.5
			Freestallwithoutlitter	26	-
	Cows	600	Tiestall with litter	9	35
			Tiestallwithoutlitter	33	-
			Freestall with litter	14,5	32
			Freestallwithoutlitter	33	
Pig	20-50 kg	35	Partially-slatted	44	-
			Fully-slatted	37	-
			Straw-bedded	3	28
			Concrete floor	64	-
	50-80 kg	65	Partially-slatted	44	-
			Fully-slatted	37	-
			Straw-bedded	3	28
			Concrete floor	64	-
	80-110 kg	95	Partially-slatted	44	-
			Fully-slatted	37	-
			Straw-bedded	3	28
			Concrete floor	64	-
	>110 kg	110	Partially-slatted	44	-
			Fully-slatted	37	-
			Straw-bedded	3	28
			Concrete floor	64	-
	Boar	250	Fully-slatted	37	-
			Straw-bedded	-	31
	Sow	180	Partially-slatted	44	-
			Fully-slatted	37	-
			Straw-bedded	-	31
			Concrete floor	73	-
	Gilt	100	Partially-slatted	44	-
			Fully-slatted	37	-
			Straw-bedded	-	31
			Concrete floor	64	-
	Layinghens	1.9	Deeplitter with Slatted	0.15	18
			Cage Battery with belt system	0.05	19
			Cage Battery with slurry deep pit	22	-
			Cage Battery with manure deep pit	0.1	17
Poultry	Pullets	1	Deeplitter	1.2	19
	Broilers	1	Deeplitter	1.2	19
	Pharaoh	1	Deeplitter	1.7	13
	Goose	6.5	Deeplitter	0.9	15
	Turkeys	6.7	Deeplitter	0.9	15

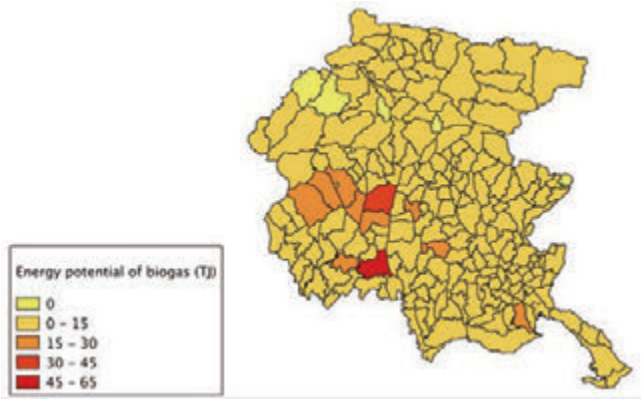

Figure 1. Distributions of the energy potential of biogas production in Friuli Venezia Giulia

In the map the areas with high potential for biogas production are concentrated in Central-Eastern part of the Region. In particular. an area includingsevenmunicipalities (San Vito al Tagliamento, Spilimbergo, Maniago, Montereale Valcellina, San Giorgio alla Richinvelda, Aviano and Vivaro) presents a high potential due to the presence of intensive farming. The area has the potential of about 10.6 (N)Mm^3 (28% of the regional potential). In particular. San Vito al Tagliamento for pig and poultry.whileSpilimbergo for cattle and poultry.

The biogas potential from agricultural by-products is about 187 (N)Mm^3. where 21% from animal waste and 79% from agricultural residues. The energy potential of biogas produced from agricultural by-products may be able to replace the 2.6% of final energy consumption in Friuli Venezia Giulia (3 339 ktoe) and about 3% of the final electricity consumption (864 ktoe) considering a electrical conversion efficiency of 30%.

Conclusions

This work has been a first step in a more complete evaluation of the biogas potential in Friuli Venezia Giulia, which will analyse biogas yields depending on different feedstocks (triticale, straws, agro-industrial waste), plant sizes and logistic solutions, in order to assessthe full technical and economic convenience of small biogas plants in the regional area (100-250 kWe).In this context it is important that the public contribution continue to support biogas plants in order to diversify energy production from the agricultural sector. In fact,the establishment of biogas plants can be a solution to support the agri-food sector (milk, eggs, cheese, meat,etc) in Friuli Venezia Giulia.

Table 4. The total biogas production and relative energy potential from animal waste in Friuli Venezia Giulia

Animaltype	Biogas production (m3)	(%)	Energy potential (GJ)	(%)
Cattle	19 425 929	51	380 748	49
Pig	12 455 854	32	255 345	33
Poultry	6 588 133	17	140 986	18
Total	38 469 916	100	777 079	100

Table 5. The total biogas production and relative energy potential from animal waste in Friuli Venezia Giulia

Agricultural	Cornstalk	Straw	Animalwaste	Total
Area (ha)	73 846	15 974	-	-
By-products (t/year)	406 153	74 949	2 416 102	2 897 204
Biogas ((N) Mm3/year)	126	22	38	187
Energy potential (TJ/year)	2 430	429	777	3 636
Share of energypotential (%)	67	12	21	100

References

European Commission. 2009. Directive EC 28/2009 of the european parliament and of the council on the promotion of the use of energy from renewable sources and amending and subsequently repealing Directives 2001/77/EC and 2003/30/EC. In: Official Journal. L 140. 05/06/2009. pp. 16-62.

Italian Regulation. 2010. Italian Energy Action Plan of 2010 required by Directive EC 28/2009. Ministry of Economic Development.

Tricase C.. Lombardi M. 2009. State of the art and prospects of Italian biogas production from animal sewage: Technical-economic considerations. Renewable Energy 34: 477–485.

Piccinini. 2010. Available from:http://www.progettobiomasse.it Accessed: May 2012.

Italian Regulation. 2012. Decreto Ministeriale of 6 July 2012. Modalità di incentivazione della produzione di energia elettrica da impianti alimentati da fonti rinnovabili.diverse da quella solare fotovoltaica.con potenza non inferiore a 1 kW. Ministry of Economic Development.

Istat Data Warehouse. 2010. Available from: http://dati-censimentoagricoltura.istat.itAccessed: May 2012.

Italianregulation. 2006. Degree 7 April 2006. Criteri e norme tecniche generali per la disciplina regionale dell'utilizzazione agronomica degli effluenti di allevamento.di cui all'articolo 38 del decreto legislativo 11 maggio 1999.n. 152. Gazzetta ufficiale n. 109 del 12/05/2006.

Fantozzi F.. Buratti C. 2009. Biogas production from different substrates in an experimental Continuously Stirred Tank Reactor anaerobic digester.Bioresource Technology 100: 5783–5789.

Onurbas Avcioglu A.. Türker U. 2012. Status and potential of biogas energy from animal wastes in Turkey. Renewable and Sustainable Energy Reviews 16: 1557–1561.

The use of co-digested solid fraction as feedstock for biogas plants

E. Dinuccio, F. Gioelli, D. Cuk, L. Rollè, P. Balsari

Department of Agriculture, Forestry and food science (DISAFA), Università degli Studi di Torino, Grugliasco (TO), Italy

Abstract

A comparative study was set up in order to assess the technical feasibility of the long-term reuse of the mechanically separated co-digested solid fraction as a feedstock for anaerobic digestion plants (ADP). The biogas yields of two feedstock mixtures (A and B) were assessed in mesophilic conditions (40 °C ± 2 °C) using 8 lab-scale continuous stirred-tank reactors (CSRT). Feedstock mixture A (control) consisted of pig slurry (70%), farmyard manure (4%), sorghum silage (12%) and maize silage (14%). Feedstock mixture B was the same as the control plus the solid fraction derived from the mechanical separation of the output raw co-digestate collected on daily basis from the reactors. All reactors were fed simultaneously, three times a week, over a period of nine month. According to the study results, the reuse of the co-digested solid fraction as feedstock for ADP could increase the methane yield by approximately 4%. However, ADP efficiency evaluation (e.g., daily yield of methane per m3 of digester) suggest to limit this practice to a maximum time period of 120 days.

Introduction

Anaerobic digestion of organic substrates for the production and transformation of biogas into electric and thermal energy is experiencing a period of strong growth in Italy. According to a recent survey (Fabbri et al., 2013), approximately 1000 agricultural anaerobic digestion plants (ADP) are currently running on the national territory with an installed electrical capacity of 756 MW. These ADP are generally installed at livestock farms and are mostly fed with animal manure, energy crops and agricultural by-products. Co-digestate is one of the final products of ADP. It contains mostly water, undigested organic matter and readily available inorganic compounds (e.g., nitrogen, phosphorus, potash) to crops. Due to the construction of the ADP often inside intensive livestock production units with insufficient arable land for nutrient recycling, export of nutrients to outside farm areas may be necessary to avoid excess load of nutrients, with special regards to nitrogen (N). For such a reason, in many Italian anaerobic digestion plants, co-digestate is mechanically separated in order to obtain a liquid and a solid fraction (Dinuccio et al., 2010). In the liquid phase the greater amount of potassium and inorganic nitrogen is concentrated, whereas the solid fraction mainly contains organic compounds and phosphorus (Dinuccio et al., 2010). The liquid fraction is generally land applied near the ADP while the solid fraction is exported to outside farm areas or sold to other farmers. Nevertheless, the co-digested solid fraction can still contain a high biogas and methane (CH4) potential (Balsari et al., 2010), due to the presence of residual and undigested volatile solids (VS). Thus, it can be reused as ADP feedstock. Balsari et al. (2010), in a work carried out at a national level through batch trials, found specific CH4 yields of co-digested solid fraction ranging between 71.4 and 156.9 NL/kgVS. According to these figures they estimated that the reuse of the mechanically separated co-digested solid fraction into the digester has the potential to improve the total CH4 production of the ADP by between 4% and 8%, depending on ADP operating parameters (e.g., feedstock type and quality, organic loading rate - OLR, hydraulic retention time - HRT) and the type of separator (e.g., screw press, one stage rotating separator) used to separate the raw co-digested slurry. Moreover, utilizing the co-digested solid fraction in this manner could reduce greenhouse gases (GHG) and ammonia (NH3) normally released (Dinuccio et al., 2013) during its storage. However, specific studies assessing the applicability of such an option in a continuous fed anaerobic digestion system are lacking. This paper presents the results of a laboratory scale experiment carried out with the objective to assess the technical feasibility of the long-term reuse of the mechanically separated co-digested solid fraction as a feedstock for ADP.

Correspondence: E. Dinuccio, Tel. +39 0116708718; Fax: +39 0116708591.
E-mail: elio.dinuccio@unito.it

Keywords: anaerobic digestion, biogas, mechanical separation, solid fraction

Journal of Agricultural Engineering 2013; XLIV(s1):e113
doi:10.4081/jae.2013.(s1):e113

Material and methods

Biomasses collection and characterization

Fresh samples of pig slurry, farmyard manure, sorghum silage and maize silage were collected at a selected full scale ADP (Table 1) operating in the Piemonte region (north western Italy), on the first working day of each month for the duration of the experimental period (270 days). Collected fresh biomass samples were then stored at 5°C for a period of 30 days and used to the anaerobic digestion tests. All biomasses were analysed for pH, total solids (TS), VS, total nitrogen (TN), total ammoniacal nitrogen (TAN), hemicelluloses (HC), celluloses (CE) and lignin (ADL). The pH was measured by a portable pH meter (Hanna Instruments HI 9026) using a glass electrode combined with a thermal automatic compensation system. TS were determined after 24 h at 105 °C. VS were determined according to AOAC (2000), after incineration in a muffle furnace at 550 °C for 4 hours. TN was analysed by the Kjeldahl standard method, after acidification with H2SO4 and mineralisation of the sample; TAN was analysed in accordance with AOAC (2000). HC, CE and ADL were determined by the Van Soest methods (Van Soest et al., 1991).

Figure 1. The lab-scale continuous fed stirred-tank reactors (CSTR) used for the trial

Experimental setup

The biogas yields of two different feedstock mixtures were compared:

- mixture A (control – the same of the selected full scale ADP, Table 1): pig slurry (70%) farmyard manure (4%), sorghum silage (12%), maize silage (14%) - mixture B: the same mixture as the control plus all (100%) the solid fraction obtained after mechanical separation of the output co-digestate collected on daily basis from the digester.

The experiment was carried out under mesophilic conditions (40 °C ± 2 °C), within a temperature-controlled chamber, by using 8 identical lab-scale continuous fed stirred-tank reactors (CSTR). Each reactor (Figure 1), cylindrical in shape, is made up of plexiglass, with a total volume of 6.5L. The biomass within the reactor is continuously mixed at a constant rate of about 4 rpm by a vertical mixer connected to a geared motor installed on the top of reactor. The reactors are equipped with inlet and outlet ports for feeding and effluent discharge. A pipe situated at the top of the reactors is connected to Tedlar® gas bags by means of Tygon® tubing to collect the produced biogas. The experi-

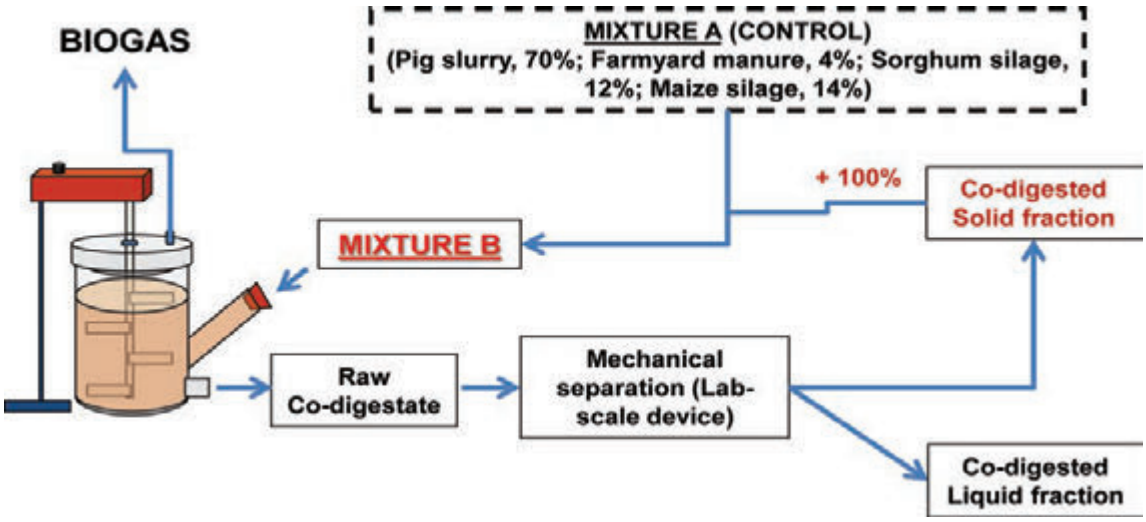

Figure 2. Feeding scheme of the reactors R4-R6.

Table 1: Main operating parameters of the selected anaerobic digestion plant

Feedstock composition	Installed electric power (kWhel)	Temperature (°C)	OLR (kgVS m^{-3} digester day^{-1})	HRT (days)
Pig slurry (70%) Farmyard manure (4%) Sorghum silage (12%) Maize silage (14%)	500	~ 40	~ 2.20	~ 40

Table 2. Main chemical and physical characteristics of the fresh biomasses (standard deviation in parentheses, n=3) used in the trial

	Maize silage	Sorghum silage	Farmyard manure	Pig slurry
PpH	3.75 (0.22)	3.96 (0.19)	8.49 (0.17)	7.26 (0.25)
TS (%)	30.5 (2.96)	27.6 (2.46)	22.3 (2.37	1.13 (0.52)
VS (%TS)	95.5 (0.96)	91.2 (1.05)	78.7 (4.01)	67.6 (4.38)
TN (%)	0.34 (0.10)	0.37 (0.09)	0.48 (0.09)	0.15 (0.07)
TAN (%)	0.03 (0.02)	0.03 (0.01)	0.38 (0.06)	0.11 (0.04)
HC (%)	7.82 (0.74)	6.24 (0.12)	4.20 (0.94)	n.d.
CE (%)	8.16 (0.63)	9.15 (0.72)	7.01 (0.41)	n.d.
ADL (%)	0.99	1.41	2.67	n.d.

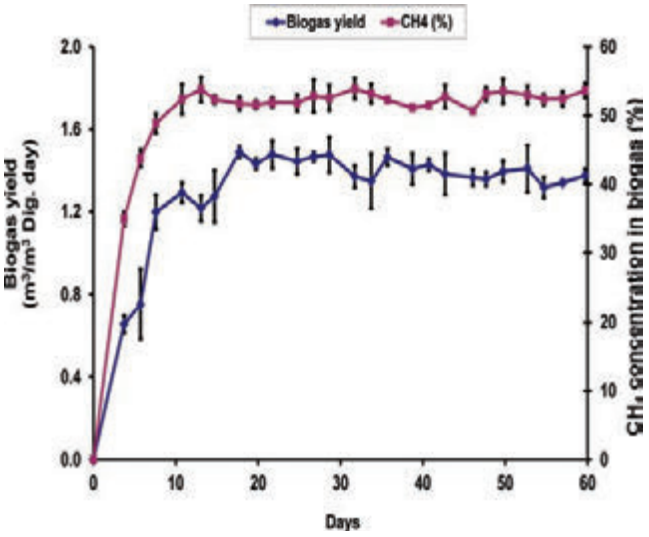

Figure 3. Specific biogas yield and methane concentration recorded from reactors R1-R8 320 during the startup phase (days 0 – 60). Error bars indicate standard deviation (N = 8).

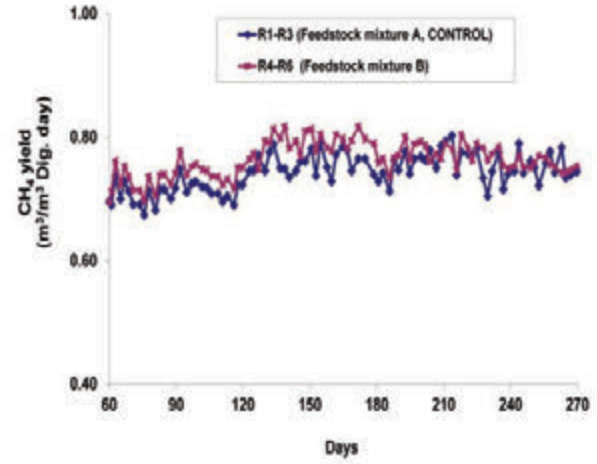

Figure 4. Average volumetric methane yields recorded from day 60 (end of the startup 322 phase) to day 270 (end of the trial) from reactors R1-R3 (feedstock mixture A, control) and 323 from reactors R4-R6 (feedstock mixture B). N = 3; standard deviation removed for clarity. 324

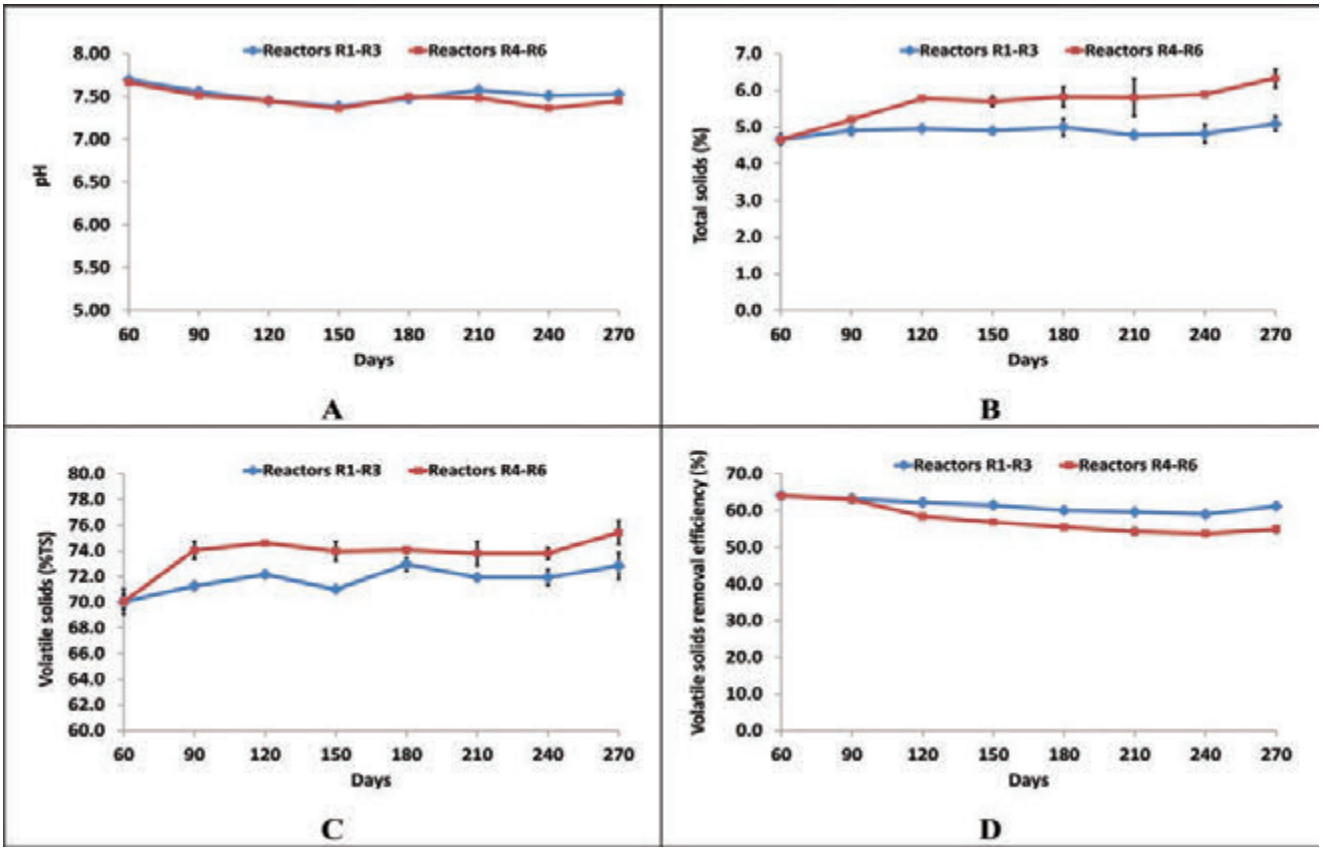

Figure 5. Evolution of pH (A), total solids (B) and volatile solids (C) content in raw co-325 digestate and volatile solids removal efficiencies (D) measured from reactors R1-R3 and 326 reactors R4-R6.

Table 3. Main chemical and physical characteristics of the co-digested solid fraction obtained by mechanical separation of raw co-digestate from reactors R4-R6

Days from the beginning of the experiment	pH	TS (%)	VS (%TS)	TN (%)	TAN (%)	HC (%)	CE (%)	ADL (%)
60 (end of start up phase)	8.26	17.2	85.7	0.43	0.14	5.86	8.51	1.43
90	8.30	18.1	86.6	–	–	–	–	–
120	8.18	17.6	88.8	–	–	–	–	–
150	8.30	16.5	86.9	–	–	–	–	–
180	8.21	16.6	87.6	–	–	–	–	–
210	8.14	16.4	86.9	–	–	–	–	–
240	8.23	17.2	87.5	–	–	–	–	–
270 (end of the experiment)	8.18	17.9	86.5	0.53	0.15	3.75	5.65	5.03

ment lasted 270 days. At the beginning of the experiment (day 0), the reactors were inoculated with 5.5 L of co-digested slurry coming from the selected full scale ADP. Thereafter all reactors (named R1-R8) were fed simultaneously, three times a week, with a determined amount of tested biomasses, throughout the experimental period (270 days). Prior to feeding, an equivalent volume of digester content (raw co-digestate) was discharged. The study was divided into two parts. In the first part of the experiment (startup phase) all reactors were run with feedstock mixture A for 60 days in order to establish a stable digestion process and to ensure steady state conditions. During this period the reactors were operated with an OLR of 2.2 kgVS/ m3 dig. day and a HRT of 40 days, in order to reproduce the same conditions of the selected full scale ADP (Table 1). At the end of the start-up (day 60), two reactors (named R7-R8) were stopped and raw co-

digestate was collected for chemical analysis. The results obtained from these analysis have been used as a baseline to assess the effect of co-digested solid fraction reuse in the digester. In the second part of the experiment (days 61 - 270), a set of three reactors (named R1-R3) continued to be fed with feedstock mixture A (control) and operated as during the startup period (i.e., OLR= 2.2 kgVS/m3 dig. day; HRT= 40 days) while the others three reactors (named R4-R6) were fed using feedstock mixture B (i.e., the same mixture as the control plus all the solid fraction obtained by mechanical separation of the output raw co-digestate collected on daily basis from reactors R4-R6; Figure 2).

Table 4. Average methane yield recorded during the experiment from reactors R1-R3 (feedstock mixture A, control) and from reactors R4-R6 (feedstock mixture B). Standard deviation in parentheses (n=3).

Experimental period (days)	Reactors	Average CH4 yield		Variation compared to control (%)	
		Nm^3 /kgVS	Nm^3/m^3 Dig. day	Nm^3 /kgVS	Nm^3/m^3 Dig. day
61-90	R1-R3	0.320 (0.008)	0.704 (0.018)	-12.2	+3.35
	R4-R6	0.281 (0.007)	0.728 (0.019)		
91-120	R1-R3	0.325 (0.007)	0.715 (0.015)	-11.7	+3.92
	R4-R6	0.287 (0.006)	0.743 (0.016)		
121-150	R1-R3	0.344 (0.008)	0.756 (0.017)	-11.6	+4.42
	R4-R6	0.304 (0.008)	0.789 (0.021)		
151-180	R1-R3	0.345 (0.010)	0.758 (0.022)	-12.0	+4.36
	R4-R6	0.303 (0.006)	0.791 (0.016)		
181-210	R1-R3	0.343 (0.009)	0.755 (0.020)	-13.9	+2.17
	R4-R6	0.295 (0.007)	0.771 (0.018)		
211-240	R1-R3	0.344 (0.014)	0.757 (0.030)	-14.8	+2.19
	R4-R6	0.293 (0.007)	0.774 (0.018)		
241-270	R1-R3	0.342 (0.009)	0.752 (0.020)	-17.1	+0.28
	R4-R6	0.284 (0.003)	0.754 (0.009)		

Table 5. Main chemical and physical characteristics of the raw co-digestate recorded at day 60 (end of the startup phase) and at day 270 (end of the trial) from reactors R1-R3 (feedstock mixture A, control) and from reactors R4-R6 (feedstock mixture B). Standard deviation in parentheses (n=3).

Days from the star of the experiment	Reactors	pH	TS (%)	VS	TN (%TS)	TAN (%)	HC (%)	CE (%) (%)	ADL (%)
60 (end of start up phase)	R1-R6	7.68 (0.07)	4.66 (0.10)	70.0 (0.76)	0.23	0.14	0.47	0.26	0.21
270 (end of experiment)	R1-R3	7.53 (0.07)	5.09 (0.19)	72.8 (1.03)	0.24 (0.03)	0.15 (0.01)	0.84 (0.14)	0.73 (0.12)	1.13 (0.34)
	R4-R6	7.45	6.33	75.4	0.24	0.20	1.90	0.93	2.23

Mechanical separation of the raw co-digestate was performed by using a lab scale mechanical separator as described by Dinuccio et al. (2008). The total amount of separated raw co-digestate, as well as the amount of solid fraction recovered, were weighed and recorded. Biogas and CH4 yields were monitored daily throughout the experimental period. Biogas volume was determined connecting the Tedlar® bags to a Ritter drum-type gas meter type TG05/5 instrument, while CH4 concentration in the biogas was determined using a Draeger XAM 7000 analyzer with infrared sensors. The recorded data were normalized at standard temperature and pressure (0 °C and 1013 hPa) according to German Standard Procedure (VDI 4630, 2006). The specific yields of biogas and CH4 were subsequently expressed as normal m3 per m3 digester and day (Nm/m3 dig. day) or as normal m3 per kg of volatile solids daily fed into the digester (Nm3/kgVS day). During the experimental period the pH, TS and VS of raw co-digestate and co-digested solid fraction were monitored monthly, while TN, TAN and fibres (HC, CE, ADL) were analysed two times: at the end of startup phase (day 60), and at the end of the trial (day 270). All parameters were analysed in triplicate using the same procedures as described in section 2.1. Data were analysed by analysis of variance procedure (ANOVA) followed by Tukey's means grouping tests.

Results and discussion

Characterisation of fresh biomasses and co-digested solid fraction

The main characteristics of fresh biomasses used for the trial are summarized in Table 2. The TS content ranged from 1.13% in pig slurry to about 30% in maize silage, whereas the VS/TS ratio ranged from 0.68 to 0.96. The TAN/TN ratio ranged from 7.43% (sorghum silage) to 78.8% (Farmyard manure). Maize silage had the lowest ADL content, whereas that of farmyard manure was the highest. In Table 3 are shown the main chemical and physical characteristics of the co-digested solid fraction obtained by mechanical separation of raw co-digestate from reactors R4-R6, and used as feedstock for the reactors during the test. Total solids content of co-digested solid fraction ranged from 16.4 to 18.1; VS and TS ratio resulted to be always higher than 0.85 suggesting a residual availability of undigested organic matter. However, the concentrations of HC and CE in co-digested solid fraction tended to decrease over time (Table 3), while, in contrast, the concentration of ADL increased, resulting 1.43% at day 60 (end of startup phase) and 5.03% at day 270 (end of the experiment). The separation efficiency in terms of mass (i.e., the relative amount of co-digested solid fraction obtained by mechanical separation of the raw co-digestate) of the used lab-scale mechanical separator resulted, on average, 9.70% (range 8.70-10.6%).

Continuous anaerobic digestion experiment

Startup phase

During the startup phase (60 days) the average percentage of CH4 in biogas (Figure 3) gradually increased up to the greatest value (53.8%) at day 13; then it stabilized around an average value of 52.4% (range 50.6 - 53.9%). The average biogas yield followed a similar trend; this trend showed a peak (1.49 Nm3/m3 dig. day) at day 18 followed by a steady state period (days 19-60) during which the biogas yield averaged 1.40 (range 1.32 -1.48) Nm3/m3 dig. day. During the 41 days steady state period, the average daily CH4 produced by reactors R1-R8 ranged between 0.313 and 0.353 Nm3/kgVS, comparable to values measured by Gioelli et al. (2012) during a 12 months period of monitoring of the selected full scale ADP; the degree of VS degraded during the anaerobic digestion process resulted 64%. Investigations of 41 biogas plants in Austria by Hopfner-Sixt and Amon (2007) found CH4 yields from co-fermentation of animal manure and energy crops up to 0.39 Nm3/kgVS, with VS degradation rates of 78–84%. The lower degree of degradation found in this study can be explained by the shorter HRT (40 days) of the reactors, which is similar to that of the selected full scale ADP (Table 1) but lesser than the minimum HRT of 45 – 60 days recommended in the literature (e.g., Öchsner and Helffrich, 2005) for an optimal degradation of VS content in energy crops.

Effect of reuse of the co-digested solid fraction as a feedstock on the performances of anaerobic digesters

Figure 4 depicts the average daily CH4 yield for each feedstock mixture (A and B) recorded during the second part (days 61-270) of the experiment. During this 210 days period, the average volumetric CH4 produced by mixture A (control, reactors R1-R3) ranged between 0.674 and 0.802 Nm3/m3 dig. day, reflecting the variability of the characteristics of fresh biomasses (Table 2) collected at the selected ADP during the experiment. The specific CH4 yields, expressed as Nm3/kgVS (Table 4), obtained over the experimental period by feedstock mixture B (reactors R4-R6) were, on average, 17% lower than those recorded from the control (feedstock mixture A reactors R1-R3). However, the average daily volumetric CH4 yields by mixture B (reactors R4-R6) (Figure 4) were generally higher than those obtained by mixture A for most of the experimental period, although such differences were not statistically significant ($p>0.05$). The reuse of the co-digested solid fraction in reactors R4-R6 gradually increased the average volumetric CH4 production rate from 0.728 (days 61-90) to 0.791 (days 151-180) Nm3/m3 dig. day (Table 4). The latter value corresponds to an increase of 4.36% when compared to the average volumetric CH4 production rate (0.758 Nm3/m3 Dig. Day) recorded from reactors R1-R3 (control). After this period such differences did, however, start to decrease, dropping to a value of +0.28% during the last 30 days of trial (Table 4).

The pH values of the raw co-digestate recorded over time (Figure 5A) suggests a regular course of the anaerobic digestion process within all the reactors. The average pH values of co-digestate from reactors R4-R6 ranged between 7.4 and 7.7, within the optimum range (6.5–7.8) for the

adequate growth of anaerobic microorganisms (Liu et al., 2008). This observation indicates that the process adapted well to the introduction of the co-digested solid fraction as co-substrate, as pH fluctuation is a widely used indicator of process stress in anaerobic reactors (Ward et al., 2008). However, the concentration of TAN (Table 5) in raw co-digestate from reactors R4-R6 has shown the tendency to increase, resulting 0.14% at day 60 (end of start up phase) and 0.20% at day 270 (end of the experiment), indicating the possibility of inhibition on the activity of microorganisms. Free ammonia has been suggested to be the main cause of inhibition in anaerobic digesters due to its high membrane permeability (Kroeker et al., 1979; de Baere et al., 1984). Ammonia inhibition was reported to occur above pH 7.4 in the range of 1500–3000 mgTAN/L, whereas at concentrations in excess of 3000 mgTAN/L, ammonia was claimed to be toxic irrespective of pH (Van Velsen, 1979; Koster and Lettinga, 1984). A remarkable increase over time of hemicelluloses, celluloses and lignin content of raw co-digestate from reactors R4-R6 was also observed (Table 5). Lignin is not degradable under anaerobic conditions and may prevent microbial access to hemicelluloses and celluloses (Mussatto et al., 2008). On average, the concentration of TS (Figure 5B) and VS (Figure 5C) in raw co-digestate from reactors R4-R6 resulted, respectively, 15.5% and 18.9% higher than the concentration in raw co-digestate from reactors (R1-R3). An average VS removal efficiency (Figure 5D) of 66.0% and 63.6%, respectively, for reactors R1-R3 and reactors R4-R6 was calculated.

Conclusions

The results obtained in this laboratory-scale study confirm that the co-digested solid fraction can still contain a high biogas and methane potential. The reuse of the co-digested solid fraction as feedstock for ADP seems to be an interesting option. Under the specific laboratory conditions adopted in this study, the long-term reuse of the co-digested solid fraction into the digester improved the total CH4 production by approximately 4%. However, after 120 days of continuous recirculation of the co-digested solid fraction the volumetric CH4 yield of the reactors started to decline, mainly due to the accumulation of recalcitrant organic fibres (e.g., lignin) which are compounds minimally digestible by anaerobic microorganisms. Therefore it is suggested to restrict this practice for limited periods of time, monitoring regularly the productivity of the ADP (e.g., daily yield of biogas and methane per m3 of digester) and the key process parameters (e.g., pH and TAN concentration in raw co-digestate) in order to maintain such variables steady and within the optimal ranges for the adequate growth of anaerobic microorganisms. Nevertheless, full scale ADP conditions may differ from the laboratory. Thus, to confirm the results obtained in this study, experiments should be made in full scale ADP.

References

AOAC 2000. Official Methods of Analysis, fifteenth ed., Association of Official Analytical Chemists, Arlington, VA, USA.

Balsari P., Gioelli F., Menardo S., Paschetta E. 2010. The (re)use of mechanical separated solid fraction of digested or not digested slurry in anaerobic digestion plants. Proceedings paper published in: C.S.C. Cordovil and L. Ferreira (eds.): Proceedings of the 14th Ramiran International Conference, Lisboa, Portugal, 12-15 Sept.

Dinuccio E., Paschetta E., Gioelli F., Balsari P. 2010. Efficiency of mechanical separation of digested and not digested slurry. Proceedings paper published in: C.S.C. Cordovil and L. Ferreira (eds.): Proceedings of the 14th Ramiran International Conference, Lisboa, Portugal, 12-15 Sept.

Dinuccio E., Cuk D., Rollè L., Gioelli F., Balsari P. 2013. GHG emissions from the storage of the liquid and solid fractions of co-digested pig slurry. Proceedings of the International Conference on Greenhouse Gases and Animal Agriculture (GGAA), Dublin, Ireland, 23-23 June.

de Baere L.A., Devocht M., van Assche P., Verstraete W. 1984. Influence of high NaCl and NH4Cl salt levels on methanogenic associations. Water Res. 18:543–548. Dinuccio E., Balsari P., Berg, W. 2008. Gaseous emissions from the storage of untreated slurries and the fractions obtained after mechanical separation. Atmos. Environ. 42:2448-2459.

Fabbri C., Labartino N., Manfredi S., Piccinini S. 2013. Biogas, il settore è strutturato e continua a crescere. L'Informatore Agrario 11:11-16.

Gioelli F., Balsari P., Dinuccio E. 2012. Anaerobic digestion in northern Italy: the situation in Piemonte Region. Proceedings of the CIGR-AgEng conference, 8-12 July, Valencia, Spain.

Hopfner-Sixt K., Amon T. 2007. Monitoring of agricultural biogas plants - mixing technology and specific values of essential process parameters. 15th European Biomass Conference & Exhibition, Berlin, Germany, 7–11 May. Koster I.W., Lettinga G. 1984. The influence of ammonium–nitrogen on the specific activity of palletized methanogenic sludge. Agric. Wastes 9:205–16.

Kroeker E.J., Schulte D.D., Sparling A.B., Lapp H.M. 1979. Anaerobic treatment process stability. J. Water Pollut. Control Fed. 51:718–727.

Liu C., Yuan X., Zeng G., Li W., Li J. 2008. Prediction of methane yield at optimum pH for anaerobic digestion of organic fraction of municipal solid waste. Bioresour. Technol. 99:882–888.

Mussatto S.I., Fernandes M., Milagres A.M.F., Roberto I.C. 2008. "Effect of hemicellulose and lignin on enzymatic hydrolysis of cellulose from brewer's spent grain," Enzyme Microb. Technol. 43:124–129.

Öchsner H., Helffrich D., 2005. Technische Anforderungen an landwirschaftliche Biogsanlagen bei der Vergärung Nachwachsender Rohstoffe, VDI-Richtlinnien 2005, VDI-Berichte 1872. Van Soest P.J., Robertson J.B., Lewis B.A. 1991. Methods for dietary fiber, neutral-detergent fiber and non-starch polysaccharides in relation to animal nutrition. J. Dairy Sci. 74:3583–3597.

Van Velsen A.F.M. 1979. Adaptation of methanogenic sludge to high ammonia–nitrogen concentrations. Water Res. 13:995–999.

VDI 4630 2006. Fermentation of organic materials, Characterisation of Substrate, Sampling, Collection of Material Data, Fermentation Tests, VDI Gesellschaft Energietechnik.

Ward A.J., Hobbs P.J., Holliman P.J., Jones D.L. 2008. Optimisation of the anaerobic digestion of agricultural resources. Bioresour. Technol. 99:7928-7940.

Life Cycle Assessment of maize cultivation for biogas production

J. Bacenetti, A. Fusi, R. Guidetti, M. Fiala

Department of Agricultural and Environmental Sciences. Production, Landscape, Agroenergy, Università degli Studi di Milano, Milano, Italy

Introduction

The renewable sources for energy production is considered to be a potential solution for reducing the environmental problems derived from the fossil fuels use (Gonzalez-Garcia et al. 2012a). Besides the reduction of their consumption, during the past few decades more and more interest has been focused on the production of renewable energy.

In Europe, the interest for Renewable Energy Sources (RES) has strongly increased due to the need to reduce also the greenhouse gas (GHG) emissions, as RED (European Parliament, 2009) indicates.

Energy crops and the derived bioenergy production are expected to bring environmental, social and economic benefits. Several studies have reported benefits in terms of the reduction of GHG, air pollution, acidification or eutrophication (Buratti and Fantozzi 2010; Bacenetti and Fiala 2011; Bacenetti et al. 2012a; González-García et al. 2012b).

However, the environmental impacts concerning bioenergy strongly depend on crops cultivation (Fazio and Monti 2011; Uchida and Hayashi 2012). Among the several possible solutions, the Anaerobic Digestion (AD)represents one of the most promising ways to use RES (Angelidaki and Ellegaard 2003; Jury et al. 2010; Patterson et al. 2011; Capponi et al. 2012).

The agricultural byproducts, such as animal slurry and manure, are commonly used for biogas production; nevertheless, the main biomass for digesters feeding are often represented by cereal silages (maize, wheat and triticale, in particular).

In Italy, about 1000 agricultural biogas plants are currently in function (380 located in Lombardy), for a global electrical power of 156 MW. Although no detailed information concerning the amount of silages used to feed the AD plants is available, the areas in which biogas production is more widespread along with an increase in biomass prices and the value of lands has taken place (Povellato, 2011).

The environmental effects due to energy crop cultivation come not only from field operations but also from the inputs (fuels, fertilizers and pesticides) extraction, production and transportation. Therefore, in order to perform a complete evaluation of the system, all of these aspects must be taken into account.

The aim of this study is to analyze the environmental performances of maize silage for biogas production

Correspondence: M. Fiala, Department of Agricultural and Environmental Sciences. Production, Landscape, Agroenergy, UniversitydegliStudi di Milano, via G. Celoria 2, 20133, Milano, Italy
E-mail: marco.fiala@unimi.it

Key words: biogas production, bioenergy, maize cultivation.

Acknowledgments: the present work is funded by RegioneLombardia - Fondo per la Promozione di AccordiIstituzionali, project BIOGESTECA 15083/RCC". The Authors thank also the RegioneLombardia which financed a Postdoctoral Research Fellowship ("Progetto Dote Ricerca" financed by FSE - RegioneLombardia).

Journal of Agricultural Engineering 2013;XLIV(s1):e114
doi:10.4081/jae.2013.(s1):e114

Introduction

Goal and scope definition

The environmental performances of maize FAO class 700 (maize 700) cultivation were assessed in terms of methane potential production. Maize is commonly used as animal feed, but nowadays -in Northern Italy- it plays an important role for biogas production, too.

This analysis was performed using the Life Cycle Assessment (LCA) methodology able to analyze products, processes or services from an environmental perspective (Guinée et al. 2002; ISO 2006).

Description of the crop cultivation

The cultivation under assessment is carried out in the Po Valley area, district of Milan, Lombardy Region (Italy). The local climate is characterized by an average annual temperature of 12.7°C and the rainfall is mainly concentred in Autumn and Spring (average annual precipitation is equal to 745 mm).

Field and ensilage operations are reported in Table 1 and shown in Figure 1. Field operations can be divided into: (1) soil tillage, (2) crop management (cover fertilization, weed and pest control), (3) biomass harvesting and transport and (4) biomass ensilage.

The crop cultivation starts on May with organic fertilization and ends on September when maize is harvested and immediately ensiled. The biomass yield is 75 twb·ha-1(dry matter content of 34.9%).

Functional unit and system boundaries

Considering that the analysis was performed on the crops that were specifically cultivated for energy generation by means of AD plants, the selected functional unit was 1 tonne of fresh silage (1tWB).

The system boundaries (Figure 1) included crop cultivation and harvesting, biomass transport and ensilage to the close biogas plant.

Life cycle inventory

Data (year 2011) concerning the field operations, ensilage and transport were directly obtained by means of questionnaires (administered to farmers) as well surveys and tests on the field.

Information regarding seeds, fertilizers, pesticides and water use were provided by the farmer as well as the diesel fuel consumption. Emissions due to the fertilizers includenitrogen emissions (nitrate,

ammonia, and nitrous oxide) computed in according to Brentrup et al. (2000). Phosphate emissions were calculated following Smil (2000). Climatic data for year 2011, which were necessary for calculating the fertilizer emissions, were obtained from the meteorological station closest to the farm. Pesticide emissions were also estimated using PestLCI (Birkved and Hauschild 2006).

The emissions due to diesel fuel use were estimated using the Swiss Federal Office for the Environment Database (Federal Department of the Environment, Transport, Energy and Communications, or DETEC); secondary data for seed production, diesel fuel, fertilizers and pesticides were obtained from the Ecoinvent database and the LCA Food DK database (Nielsen et al. 2003).

Considering that the soil was previously dedicated to maize cultivation,zero change in the overall soil carbon content has been assumed.

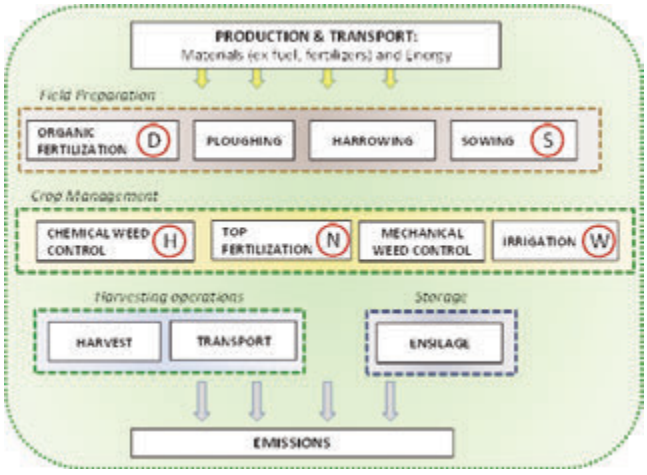

Figure 1. System boundaries

Note: D = digestate, S = seeds, H = herbicide, N = nitrogen fertilizer, W = water

Methods

A life cycle impact assessment (LCIA) was performed using SimaPro software (PRé Consultants - http://www.pre-sustainability.com/simapro-lca-software) and CML 2000 (Guinée et al. 2002) was chosen as a method with which to assess the environmental impact.

Table 2. Scores for all impact categories for the FU

IMPACT CATEGORIES	UNITS	TOTAL
Abioticdepletion	kg Sb eq	0,104624
Acidification	kg SO_2eq	1,378419
Eutrophication	kg PO4eq	0,412833
Global warming (GWP100)	kg CO_2eq	29,75866
Ozonelayerdepletion (ODP)	kg CFC-11 eq	2,11E-06
Human toxicity	kg 1,4-DB eq	3,445905
Fresh water aquaticecotoxicity	kg 1,4-DB eq	0,830076
Marine aquaticecotoxicity	kg 1,4-DB eq	2305,503
Terrestrialecotoxicity	kg 1,4-DB eq	0,023476
Photochemicaloxidation	kg C_2H_4eq	0,003256

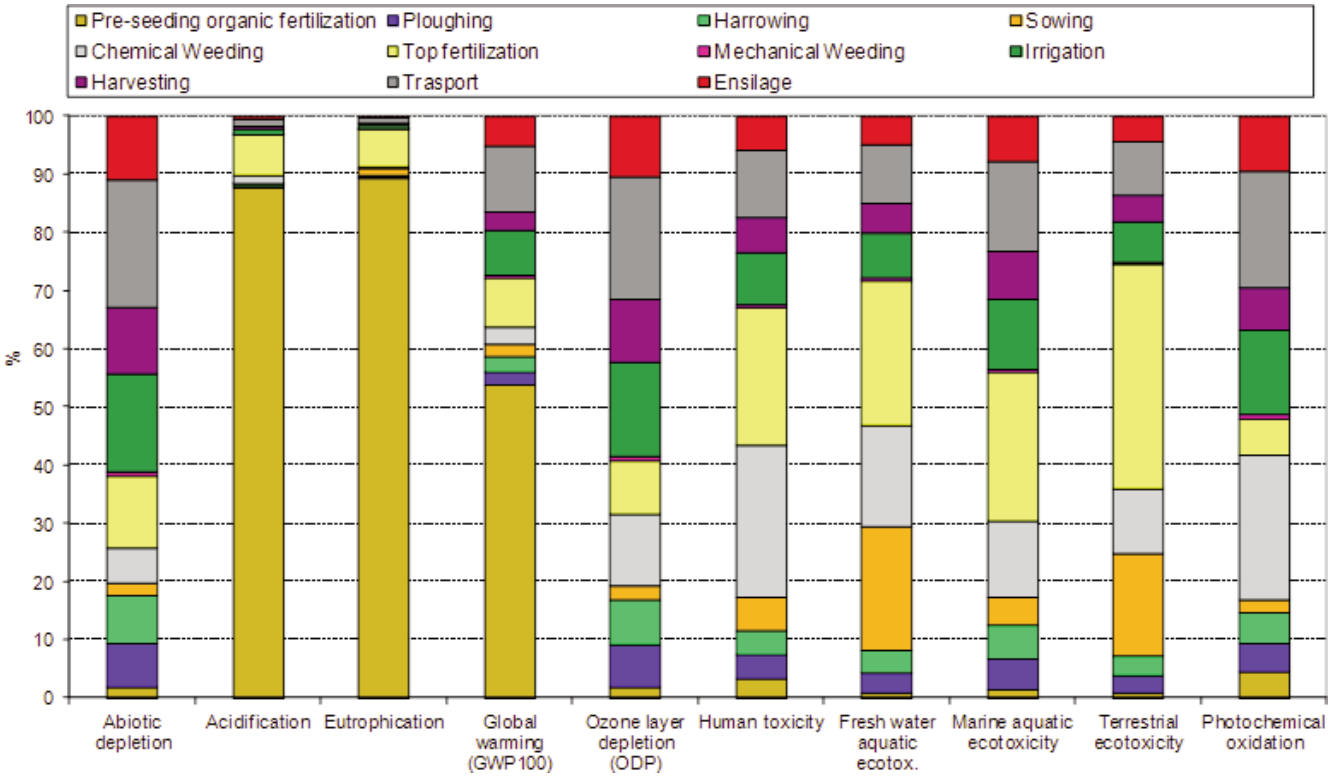

Figure 2. Impact of operations on the different impact categories

Results and discussion

The environmental impact is widely influenced, as expected, by the field operations; on the contrary, less than 5% of the overall environmental impact is due to the ensilage activity. Consequently, the operations carried out on the field are the main responsible (more than 95%) of the environmental burdens for all the 10 impact categories.

Among the different inputs and outputs, the key aspects are: (i) fertilizer emissions (mainly for acidification and eutrophication impact categories), (ii) diesel fuel emissions (mainly for global warming potential impact category), (iii) diesel fuel production (mainly for abiotic depletion and ozone layer depletionimpact categories) and(iv) pesticides production (important for human toxicityimpact category).

Regarding the different field operations, the influence over the 10 impact categories is quite variable (Figure 2);for example, the fertilization is responsible for about 95% of acidification and eutrophication but less than 35% for the others impact categories.

Conclusions

The study assesses the environmental performances of maize FAO class 700; this cereal is the most widespread in Italy and it islargely utilized for biogas production.

The study points out that the environmental burdens of maize 700 cultivation are mainly due to: (i) crop fertilization (in particular nitrogen application, primarily via organic fertilizers) and (ii) mechanization of field operations.

The analysis highlighted that the nitrogen cycle and the linked emissions are relevant for the environmental burden of crop cultivation, especially foracidification and eutrophication. Organic fertilization, carried out with a high-rate of digestate, involves high emissions in atmosphere of ammonia and nitrogen dioxide, especially when the spreading is performed distributing the digestate directly on the soil surface and without a fast burial.The digestateinjection into the soil largely reducesthe ammonia emissions.

Mechanization requiresa high diesel fuel consumption and, consequently, a significant impact on GWP and abiotic depletion as well. Reduction of the diesel fuel consumption, thatcould significantly improve the environmental performances, can be achievedthrough:

1. the introduction of proper technical solutions connected with lower mechanical power requirements (i.e. minimum tillage, sod seeding, slattedmouldboards).

The obtained results represent the environmental evaluation onlyof the first step of the whole biogas process. Future analysis will take into consideration the biogas production (microbiological digestion) and its final conversion into energy by a cogenerated i.c. engine (CHP).

References

1. Angelidaki I., Ellegaard L.,Codigestion of manure and organic wastes in centralized biogas plants: status and future trends. Applied Biochemistry Biotechnology 2003; 109: 95-105.
2. Audsley E.,Harmonisation of environmental life cycle assessment for agriculture. Final Report, Concerted Action AIR3-CT94-2028. European Commission, DG VI Agriculture, 1997, 139 pp.
3. Bacenetti J., Mena A., Negri M., Cantarella P., Bocchi S., Fiala M., Energetic and Environmental Balance of a Biogas Plant in Northern Italy. Proceedings CIGR-AgEng 2012 International Conference on Agricultural Engineering Valencia: CIGR-AgEng, 2012.
4. Bachmaier J., Effenberger M., Gronauer A. Greenhouse gas balance and resource demand of biogas plants in agriculture, Engineering in Life Sciences, 2010; 10: 560-569.
5. Birkved M.,Hauschild M. PestLCI—A model for estimating field emissions of pesticides in agricultural LCA. Ecological Modelling 2006; 198: 433-451.
6. Brentrup F., Küsters J, Lammel J, Kuhlmann H., Methods to estimate on-field nitrogen emissions from crop production as an Input to LCA studies in the Agricultural Sector. Int J Life Cycle Ass 2000;5:349-57.
7. Buratti C., Fantozzi F., Life cycle assessment of biomass production: Development of a methodology to improve the environmental indicators and testing with fiber sorghum energy crop. 2010; 34: 1513-1522.
8. Capponi S., Fazio S., Barbanti L., CO2 savings affect the break-even distance of feedstock supply and digestate placement in biogas pro-

Table 1. Field and ensilage operations for single crop (maize 700)

OPERATION	NN.	MONTH	TRACTOR		OPERATIVE MACHINE			NOTE
			Mass (kg)	Power (kW)	Type Size	Mass (kg)	Time (h/ha)	
Organic fertilization	1	May	5050	(90)	Manure spreader 20 m^3	2000	3.33	85 t·ha^{-1}
								Digestate[a]
Ploughing	1	May	10500	(190)	Plough	2000	1.11	-
Harrowing	1	May	7300	(130)	Rotary Harrow 4,0 m	1800	1.20	-
Sowing	1	May	5050	(90)	Pneumatic seeder 4 rows	900	1.00	20 kg·ha^{-1}
Chemical Weeding	3	May Jun Jun	4450	(80)	Sprayer 15 m	600	0.33	4 kg·ha-1lumax
								1 kg·ha^{-1}dual
								1 kg·ha^{-1} dual
Irrigation	5	Jun Jul Aug	4450	(80)	Pump 950 m^3/h	550	1.20	4400 m3·ha^{-1}
Mechanical Weeding	1	Jun	5050	(90)	Weeder 2,8 m	550	0.33	-
Top fertilization	1	Jun	6850	(120)	Fertilizer spreader 2500 dm^3	500	0.13	60 kg·ha^{-1}Urea
Harvesting	1	Sep	-		Forage harvester	335 kW	13000	1.00

duction. Renewable Energy 2012, 37: 45-52.
9. Casati D., 2011. Le superfici possono ricominciare a salire. Terra e Vita, 35, 40-46.
10. DETEC (Federal Department of the Environment, Transport, Energy and Communications), http://www.bafu.admin.ch/index.html?lang=it last visit 05/02/2013
11. Dressler D., Loewen A., Nelles M., Life cycle assessment of the supply and use of bioenergy: impact of regional factors on biogas production. The International Journal of Life Cycle Assessment 2012; 17 (9):1104-1115.
12. European parliament and council. Directive 2009/28/EC on the promotion of the use of energy from renewable sources. In: Official Journal of the EuropeanCommunities, Vol. L 283/33; 2009.
13. Fazio S., Monti A., Life cycle assessment of different bioenergy production systems including perennial and annual crops, Biomass Bioenerg. 2011, 35, pp. 4868 – 4878.
14. Fiala M., Bacenetti J., Model for the economic, energetic and environmental evaluation in biomass productions. Journal of Agricultural Engineering 2012; 42: 26-35.
15. Goedkoop M, de Schryver A and Oele M., Introduction to LCA with SimaPro 7. PRé Consultants, the Netherlands; 2008.
16. González-García S., Bacenetti J., Murphy R.J., Fiala M., Present and future environmental impact of poplar cultivation in Po Valley (Italy) under different crop management systems. Journal of Cleaner Production. 2012; 26:56-66.
17. González-García S., Bacenetti J., Negri M., Fiala M., Arroja L. Comparative environmental performance of three different annual energy crops for biogas production in Northen Italy. Journal of Cleaner Production 2012; doi:10.1016/j.jclepro.2012.12.017.
18. Guinée J.B. (Ed.), Handbook on Life Cycle Assessment, Operational Guide to the ISO Standards, 2002, 1-708.
19. IPCC, Agriculture, Forestry and Other Land Use. In: Eggleston et al., IPCC Guidelines for National Greenhouse Gas Inventories, Prepared by the National Greenhouse Gas Inventories Programme, 2006.
20. ISO, Environmental management-Life cycle assessment-Principles and framework (ISO 14040), 2006 Brussels: European Committee for Standardization.
21. ISTAT - Istituto Nazionale di Statistica, Tavola C02 - Superficie (ettari) e produzione (quintali): riso, mais, sorgo, altri cereali. Dettaglio per regione - Anno 2011, (http://agri.istat.it/jsp/dwExcel.jsp?q=plC020000010000012000&an=2011&ig=1&ct=244&id=18A|15A|25A last access 21/12/12)
22. Jury C., Benetto E., Koster D., Schmitt B., Welfring J., Life Cycle Assessment of biogas production by monofermentation of energy crops and injection into the natural gas grid. Biomass Bioenerg 2010; 34: 54–66.
23. Lansche J., Müller J., Life cycle assessment of energy generation of biogas fed combined heat and power plants: Environmental impact of different agricultural substrates. Engineering in Life Sciences 2012; 12: 313-320.
24. Nielsen PH, Nielsen AM, Weidema BP, Dalgaard R and Halberg N (2003). LCA food data base. www.lcafood.dk
25. Patterson T., Esteves S., Dinsdale R., Guwy A., Life cycle assessment of biogas infrastructure options on a regional scale. Bioresource Technology 2011; 15: 7313-7323.
26. Povellato A., Aumenta la superficie in affitto delle aziende professionali. L'Informatore Agrario 2011; 40: 32-39.
27. Smil V., Phosphorus in the environment: Natural Flows and Human Interferences 2000 Annu. Rev. Energy Environ. 2000. 25:53–88)
28. Uchida S., Hayashi K., Comparative life cycle assessment of improved and conventional cultivation practices for energy crops in Japan. Biomass Bioenerg 2012;36:302-15.

A farm-scale pilot plant for biohydrogen and biomethane production by two-stage fermentation

R. Oberti, A. Tenca , F. Perazzolo, E. Riva, A. Finzi, E. Naldi, G. Provolo, L. Bodria

DiSAA, Dipartimento di Scienze Agrarie e Ambientali, Università degli Studi di Milano, Milano, Italy

Abstract

Hydrogen is considered one of the possible main energy carriers for the future, thanks to its unique environmental properties. Indeed, its energy content (120 MJ/kg) can be exploited virtually without emitting any exhaust in the atmosphere except for water. Renewable production of hydrogen can be obtained through common biological processes on which relies anaerobic digestion, a well-established technology in use at farm-scale for treating different biomass and residues.

Despite two-stage hydrogen and methane producing fermentation is a simple variant of the traditional anaerobic digestion, it is a relatively new approach mainly studied at laboratory scale. It is based on biomass fermentation in two separate, seuqential stages, each maintaining conditions optimized to promote specific bacterial consortia: in the first acidophilic reactorhydrogen is produced production, while volatile fatty acids-rich effluent is sent to the second reactor where traditional methane rich biogas production is accomplished.

A two-stage pilot-scale plant was designed, manufactured and installed at the experimental farm of the University of Milano and operated using a biomass mixture of livestock effluents mixed with sugar/starch-rich residues (rotten fruits and potatoes and expired fruit juices), afeedstock mixture based on waste biomasses directly available in the rural area where plant is installed.

The hydrogenic and the methanogenic reactors, both CSTR type, had a total volume of 0.7m3 and 3.8 m3 respectively, and were operated in thermophilic conditions (55□ 2 °C) without any external pH control, and were fully automated.

After a brief description of the requirements of the system, this contribution gives a detailed description of its components and of engineering solutions to the problems encountered during the plant realization and start-up.

The paper also discusses the results obtained in a first experimental run which lead to production in the range of previous laboratory results, with a typical hydrogen and methane specific productivity of 2.2 and 0.5 $Nm3/m3_{reactor}$ per day, in the first and second stage of the plant respectively.

At our best knowledge, this plant is one of the very first prototypes producing biohydrogen at farm scale, and it represents a distributed, small scale demonstration to obtain hydrogen from renewable waste-sources.

Correspondence: Roberto Oberti, DiSAA Dipartimento di Scienze Agrarie e Ambientali, Università degli Studi di Milano, via Celoria 2, Milano (Italy).
E-mail: roberto.oberti@unimi.it

Key words: biohydrogen, two-stage anaerobic digestion, farm-scale pilot plant.

Acknowledgments: the authors gratefully acknowledge the support of Regione Lombardia - DG Agricoltura to this research, through the projects AGRIDEN/1181 and BIOGESTECA 15083/RCC.

Journal of Agricultural Engineering 2013; XLIV(s1):e115
doi:10.4081/jae.2013.(s1):e115

Introduction

Hydrogen is considered one of the main possible energy carriers in future, thanks to its energetic and environmental unique properties: indeed, its energy content (120 MJ/kg) is three times higher than liquid fuels -but with a much lower volumetric density- and it can be converted to energy virtually without any exhaust emissions in the atmosphere except for water. In substitution of current fossil-fuel based technologies, renewable production of hydrogen from dark fermentation of biomasses could provide all the potential benefits of hydrogen energy production, especially if obtained by wastewaters or residues digestion.

Biohydrogen production has been demonstrated for a number of organic substrates especially rich in carbohydrates (starch, sugar beets, potatoes processing wastewaters, cheese whey, brewery waste, etc.) with yields typically ranging between 50 and 150 $Ndm^3_{H2}\ g^{-1}_{VS}$, depending on the biodegradability and complexity of the substrate. However, the maximal yield of the process is low (4 $mol_{H2}/mol_{glucose}$) with residual organic matter left unexploited in the process effluent, highly rich in volatile fatty acids (VFAs).

Therefore, recently some studies proposed the coupling of fermentative hydrogen production with traditional anaerobic digestion (AD) process, able to fully exploit the VFAs by converting them to methane and thus increasing the total energy efficiency (Liu et al., 2006; Ueno et al., 2007). Indeed, AD technology is already a well-established bioprocess technology, extensively applied at real-scale, especially in the agricultural sector. In 2010 the 20% of Italian biogas production from biomasses relied on agricultural and livestock residues digestion, which means an opportunity to integrate farmers' income and a contribution to reduce the dependency on fossil energy sources and to progress toward mitigation of emissions in atmosphere especially in areas with high concentration of livestock production such as in specialized districts of Northern Italy.

The transformation of the traditional single-stage AD process in two distinct stages, respectively producing biohydrogen and methane-rich biogases, may therefore represent a feasible and advantageous evolu-

tion of this well established technology, quite promising from a perspectiveof energy and environmental efficiency. Indeed, every single stage may be operated in specifically optimal conditions, likely leading to a larger overall reaction rate and biogas yield and to higher organic matter removal efficiencies, thus improving the reduction of the waste density levels at farm scale.

Furthermore, hydrogen can be processed and upgraded to be suitably employed in end-use zero- emissions technologies like fuel cells, or mixed with the methane produced by the second stage and used in high-effiency low-emission combustion engines (Akansu et al., 2004, Ma et al., 2010) as the new homogeneous charge compression ignition (HCCI) engines (Gomes Antunes et al., 2008).

At laboratory scale, studies on two-stage process mainly addressed possible designs and reactor configurations, operative parameters optimization (pH, temperature, stirring rate), biogas/biohydrogen production maximization, and microorganisms interactions/association within the reactors.

Concerning the scaling up of such a system, just a couple pilot-scale studies were reported at our best knowledge (Cavinato et al., 2011; Lee & Chung, 2010; Ueno et al.,2007; Wang & Zhao, 2009). These plants were operated with heterogeneously concentrated (50-200 g_{VS}/kg) wet biomasses, mainly carbohydrate-rich (food wastes, pulverized garbage and shredded paper wastes, separately collected organic fraction of municipal waste), with average hydrogen yields of 60 Ndm^3_{H2}/kg_{VS}, corresponding to specific volumetric production in the range of 2 - 5 $Nm^3_{H2}/ m^3_{reactor}$•d, at short HRT typically of 1-3 days. The average methane yield from the second CSTR stage ranged between 500 and 650 Ndm^3_{CH4}/kg_{VS}, with HRT variation from 12 to 40 days (Cavinato et al. 2011; Wang & Zhao, 2009).

This paper describes the two-stage pilot-scale plant which was designed, manufactured and installed at "Cascina Marianna" (Landriano, Italy), the experimental farm of the University of Milano. The plant represent the first example of facility for simultaneous biohydrogen and biomethane production. It is based on simple, low-cost and readily applicable technologies, with a general design conceived for farm scale applications. Within this same framework, the reactors were inoculated exploiting mixed culture from natural sources, and fed with a mixture of waste biomasses (fruit and vegetable wastes and livestock residues) directly available in the specific rural area where the plant is installed. Engineering solutions to the problems encountered during the plant realization and start-up are hereby discussed, together with preliminary experimental plant performances.

Materials and methods

Process scheme and pilot-scale plant design

The pilot plant system design combines three cylindrical, heated, continuously stirred tank reactors (CSTRs) made by PVC, one of the most adopted biogas-plant technology for wet biomasses digestion.

With reference to figure 1, the plant operation can be summarized as follows: the feeding substrate mixture is pumped to a first hydrogenic reactor (Fig 1; 3) where the organic matter is hydrolyzed and biologically acidified, producing gaseous hydrogen and carbon dioxide and a effluent digestate rich in VFAs. The digestate is then sent to the second stage of the process, occurring in two identical reactors (Fig 1; 4a and 1; 4b), which together act as a single methanogenic stage, producing a methane-rich biogas and effluent digestate. The end digestate is then stored to be used for fertilizer spreading by the farm.

The two biogases produced by each stage are separately collected in gas bags storage (Fig 1; 6a and 1; 6b) above the reactors.

After preparation by shredding in a biotriturator (Fig 1; 1), the substrate biomass is blended with an appropriate amount of manure. The resulting feedstock is then stored in a 1.2 m^3 pre-feeding refrigerated tank (Fig 1; 2) with a double-walled stainless-steel shell and agitator blades keeping the feedstock at 4 °C and continuously gently mixed. This allows to have an operational autonomy of 3-5 days during experiments, while avoiding major pre-acidification of the substrate.

The hydrogenic reactor (Fig 1; 3) has a capacity of 0.7 m^3 (1.2 m in height x 0.9 m in diameter), while the methanogenic stage occurs in a pair of identical larger reactors (Fig 1; 4a and 4b), with a total capacity of 3.8 m^3, (two reactors 1.95 m in height x 1.1 m in diameter). The operative volumes of each reactor may be individually varied, and in this study they were set to 0.4 m3 for the first stage and to 3.2 m^3 (1.6 m^3 for each reactor) for the methanogenic stage, respectively, resulting in hydraulic retention times ratio of 1 / 8 between the two stages of the process.

Each reactor is provided with a internal folding coil in order to maintain the temperature of the fermentative broth constantly at 55 °C through hot-water circulation, and with mechanical stirring system operated at 60 rpm to keep the substrate homogenously in contact with microorganisms, the temperature uniformly distributed though the broth and to minimize the formation of scum at the surface or solids deposition on the bottom likely leading to blockages in the system.

In each reactor are installed different sensors (Fig 1; 8) for continuous monitoring of the process as well as for automatic control (Fig 1; 9) of the operation of the plant purposes. Pt-100 temperature sensors, pH electrodes and broth levels sensors are installed on the front side of the tank, together with ports designed for physical sampling of fermentative broth.

The biomass is handled to and from different points of the plant by the use of two impeller pumps (Fig. 1; 5a and 5b): loading and unloading of the hydrogenic reactor and methanogenic reactors, as well as transfer from first stage to the second, or recirculation of material if needed. All these configurations of the circuit can be obtained through adequate actuation of eight pneumatically activated valves directly controlled by the digital control system.

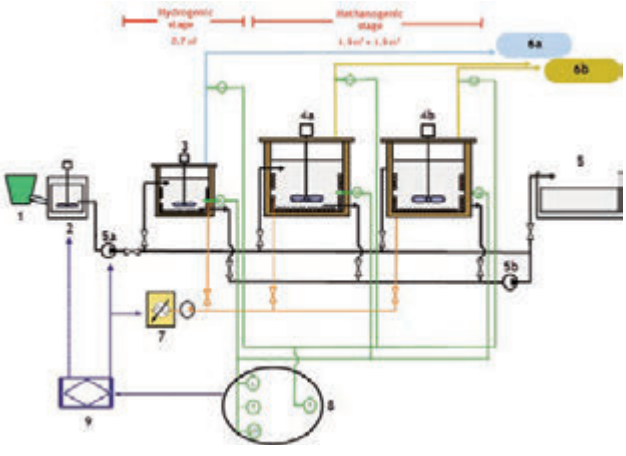

Figure 1. Schematic diagram of the two-stage pilot plant: 1) biotriturator for solid biomass shredding; 2) 1.2 m^3 refrigerated pre-feeding storage; 3) 0.7 m^3hydrogenic reactor; 4a-b) pairs of 1.9 m3methanogenic reactors; 5a-b) impeller pumps for biomass handling; 6a-b) gas bags storage; 7) boiler for heating system; 8) temperature, pH and gas flow-rate sensors; 9) PC based digital control system.

Process monitoring and control

Process parameters monitoring and automatic control of process operations rely on PC-based digital control system (DCS). The custom-made DCS monitors, records and displays on a user-interface the process data transmitted by the sensors. Volumetric biogas production from each reactor is continuously measured by three gas flow meters (LPN/S80 AL G 2.5 SACOFGAS, , Italy). The gas composition was measured once a day by manually taking a sample from the outlet biogas pipe and measuring it with a gas analyzer (ETG-3200L, ETG Risorse e Tecnologia, Italy). Beside data recording, the DCS activates or modulates the biomass flow in to the plant, the reactors' stirring and the hot water circulation for temperature control according to operator's setting.

During all the experiment the temperature was maintained at 55 ± 2.5°C and mixing cycle was set to 2 minutes followed by a 30 seconds of settling stop in the first stage, while in the methanogenic stage the cycle was 1 minute of mixing followed by 1 minute of settling.Loading and unloading of organic substrate was managed on the basis of the two HRTs chosen, set to 2.5 and 20 days for the hydrogenic and methanogenic stage respectively.

The fermentative broths of each reactor were manually sampled four times along the steady state period of the experimental run described in section 3.2, in order to chemically characterize the stages and their removal efficiencies through the measure of total and volatile solids (TS and VS) and of chemical oxygen demand (COD), according to Standard Methods (APHA, 1998).

Feedstocks and inocula

The feeding substrate was a mixture of livestock manure (LM: 65% w/w) and fruit and vegetable waste (FVW: 65% w/w), according to the ratio indicated by previous lab-scale preliminary tests (Tenca et al., 2011). FVW consisted of a mixture of raw and rotten fruits and vegetables residues (mainly potatoes, zucchini and apples). The solid wastes were freshly shredded and mixed together with the fruit juices and the LM. The manure is an ideal co-substrate for FVW fermentation, being an abundant source of alkali and nutrients for cell growth and process pH buffering. LM was not filtered nor treated before feeding. No chemical reagents, buffers or other nutrients were added to the blend, whose TS, VS and pH were 58 ± 4 g/kg, 52 ± 3 g/kg and 7.35 ± 0.1, respectively.

The seed microflora used for the hydrogenic reactor inoculation was a mixture of a livestock manure and a digestate produced in a laboratory-scale thermophilic reactor, fed with glucose and fruit wastes. Methanogenic reactors were inoculated directly with livestock manure, provided directly by the farm where plant is installed.

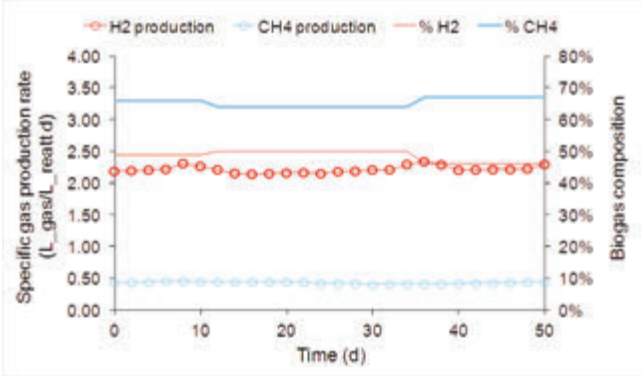

Figure 2. Specific volumetric gas production and composition in the two-stage reactors

Results and discussion

System start-up

Before the start up, the inocula were briefly deaerated with N_2 gas at a flowrate of 100 mL/min to establish the anaerobic conditions favorable to the microflora development and activity. Then the inocula within the reactors were acclimatized for 15 days to thermophilic temperature (55 °C), subjected to a gently stirring. During this time, the first stage was directly fed with the feeding mixture described in section 2.3, and its effluent was simultaneously but partially added to the methanogenic reactors. Indeed, the methanogenic bacteria have slower growth rates and are easier to be subjected to inhibitions, such as by organic shock load, thus the organic load to the second stage was progressively increased during the start-up, until a biogas with methane percentage of 50± 5% was achieved. After 15-20 days, when stable biohydrogen production (H2 content in biogas 40 ± 5%) from the first stage was reached, the hydrogenicdigestate was fully fed to the second reactors, achieving a fully integrated operation of the two-phase AD process.

Two-stage plant performances

The process was continuously operated for more than one month with stable production both in the first and the second stage (Fig. 2). The specific volumetric production rate of hydrogen resulted in 2.1 ± 0.2 $Nm^3_{H2}/m^3_{reactor}$•d with a corresponding yield of 99 ± 10 Ndm^3_{H2}/kg_{VS} (Tab. 1), which is well in the range of other studies on highly degradable feedstock. The biogas produced by the first stage was in average composed by 48% hydrogen without any methane detected, showing that favorable conditions were created by the short HRT and the relative acidity of the fermentation broth. Indeed, the average pH of the hydrogenicstage (5.78 ± 0.10) resulted closely stable around the optimum for hydrogen production without chemicals addiction for pH adjustments, which is quite relevant for practical implementation of the process.

Methane production from the second stage was approximately 0.5 $Nm^3CH4/m^3_{reactor}$•d, with a methane concentration in the biogas of 68% v/v, quite higher than typically reported for similar digestion processes.

Important reductions of the TS, VS and COD contents of the feeding mixtures were noted, with COD reduction after the first stage and after the overall process amounting to 25% and 69%, respectively. At the same time, the system produced a total energy yield of 10-11 MJ/kg_{VS}, with the hydrogen production weighting for nearly the 15% of the total energy produced by the system (Tab. 1).

Conclusions

A two-stage pilot-plant digester at farm scale was successfully run for 1 month, efficiently exploiting typical agricultural and livestock residues, available to the farm (65 % of the organic matter was removed every cycle). Noticeable hydrogen and methane yield were achieved, in particular if related to the overall short cycle time required by the process (20 days). This study also showed higher CH4 content in the biogas from the second stage (≈70%) than the traditional AD, that is advantageous for lowering the biogas upgrading cost.

Table 1. Results overview of the experimental two-stage plant operations

	Hydrogenic stage	Methanogenic stage
Volumetric production rate		
$Nm^3_{H2/CH4}$ / $m^3_{reactor}$•d	2.2 ± 0.2	0.5 ± 0.1
Average content of H_2/CH_4 (%)	48 ± 2	67 ± 1
Biogas yield dm^3_{H2CH4} /kg_{VS}	105 ± 10	290 ± 30
Energy yield MJ /kg_{VS}	1.2 ± 0.1	9.3 ± 1.1
Overall energy yield MJ /kg_{VS}	9.5 - 11.5	

References

Gomes Antunes, J. M., Mikalsen, R., &Roskilly, A. P. 2008. An investigation of hydrogen-fuelled HCCI engine performance and operation. Int. J. Hydr. En., 33, 5823-5828.

Akansu, S. O., Dulger, Z., Kahranman, N., &Veziroglu, N. T. 2004. Internal combustion nginesfueled by natural gas-hydrogen mixtures. Int. J. Hydr. En., 29, 1527-1539.

Ma, F., Ding, S., Wang, Y., Wang, M., Jiang, L., Naeve, N., & Zhao, S. 2009. Performance and Emission Characteristics of a SI Hydrogen-Enriched Compressed Natural Gas Engine Under Various Operating Conditions Including Idle Conditions. Energy &Fuels, 23, 2113-3118.

Cavinato, C., Bolzonella, D., Fatone, F., Cecchi, F., & Pavan, P. 2011. Optimization of two-phase thermophilic anaerobic digestion of biowaste for hydrogen and methane production through reject water recirculation. Bioresource Technology, 102, 8605-8611.

Lee, Y. W., & Chung, J. 2010. Bioproduction of hydrogen from food waste by pilot-scale combined hydrogen/methane fermentation. Int. J. Hydr. En., 35, 11746-11755.

Ueno, Y., Fukui, H., &Goto, M. 2007. Operation of a Two-Stage Fermentation Process Producing Hydrogen and Methane from Organic Waste. Env. Sc. Techn., 41, 1413-1419.

Wang, X., & Zhao, Y. C. 2009. A bench scale study of fermentative hydrogen and methane production from food waste in integrated two-stage process. Int. J. Hydr. En., 34, 245-254.

Liu, D., Zeng, R. J., &Angelidaki, I. 2006. Hydrogen and methane production from household solid waste in the two-stage fermentation process. Water Research, 40, 2230-2236.

Parametric experimental tests of steam gasification of pine wood in a fluidized bed reactor

L. Vecchione,[1] M. Moneti,[1] S. Cocchi,[1] M. Villarini,[1] M. Sisinni,[2] A. Micangeli[2]

[1]DAFNE, Tuscia University, Viterbo, Italy; [2]Dipartimento di Ingegneria Meccanica e Aerospaziale, Sapienza University, Roma, Italy

Abstract

Among Renewable Energy Sources (RES), biomass represent one of the most common and suitable solution in order to contribute to the global energy supply and to reduce greenhouse gases (GHG) emissions. The disposal of some residual biomass, as pruning from pine trees, represent a problem for agricultural and agro-industrial sectors. But if the residual biomass are used for energy production can become a resource. The most suitable energy conversion technology for the above-mentioned biomass is gasification process because the high C/N ratio and the low moisture content, obtained from the analysis. In this work a small-pilot bubbling-bed gasification plant has been designed, constructed and used in order to obtain, from the pine trees pruning, a syngas with low tar and char contents and high hydrogen content. The activities showed here are part of the activities carried out in the European 7FP UNIfHY project. In particular the aim of this work is to develop experimental test on a bench scale steam blown fluidized bed biomass gasifier. These tests will be utilized in future works for the simulations of a pilot scale steam fluidized bed gasifier (100 kWth) fed with different biomass feedstock. The results of the tests include produced gas and tar composition as well gas, tar and char yield. Tests on a bench scale reactor (8 cm I.D.) were carried out varying steam to biomass ratio from 0.5, 0.7 and 1 to 830°C.

Introduction

Nowadays biomass represents an important renewable energy resource because they are present in various form sand species in all parts of the world. Their use allows to not increase the carbon bioxide concentration [1], infact the carbon bioxide emissions quantity during their use is the same of the quantity that the biomass has absorbed from the atmosphere during the cycle life [1].In this way biomass represents one of the most common and suitable solution in order to contribute to the global energy supply and to reduce greenhouse gases (GHG) emissions. Another important feature is represented by a major economic independence from fossil fuels increasing in this way the economy and the development of the agriculture sector of the territory. The disposal of some residual biomass, as pruning from pine trees, represent a problem for agricultural and agro-industrial sectors. But if the residual biomass are used for energy production can become a resource.One of the promising technologies which utilizes the biomass wastes is biomass gasification. The gasification of lignocellulosic biomass is one of the most thermo-chemical conversions technologies developed because it offers high conversion efficiency [2]. It is one of the strategies for exploitation of renewable fuels and power generation. Biomass gasification converts the biomass wastes into clean fuel gases and biofuels. There are two main categories of gasifier, fixed bed and fluidized bed The most suitable energy conversion technology for the above-mentioned biomass is gasification process [3] [4] because the high C/N ratio and the low moisture content, obtained from the analysis. The gasification plants are able to have a primary role in the world system because the electric production is constant and is not necessary any energy storage system, the emissions quantity is controlled, and the energy production is not subjected at aleatory events (as cloud cover or strong winds).

After the gasification process the biomass is transformed in syngas, composed by hydrogen, carbon monoxide, carbon dioxide and methane, with tar, and a solid residue as char and ash.

Furthermore, steam gasification, as the method chosen to gasify biomass in the present work, has other advantages because (i) it produces a gas with higher heating value, (ii) it reduces the diluting effect of N2 from air and (iii) eliminates the need for an expensive oxygen plant when both air and oxygen are used as gasification mediums [5].

The product distribution varies with the biomass used and the gasification temperature. These differences for the H2, CO and CO2 contents in the gas product decrease when the temperature increases to 830°C at which point a gas composition similar for all types of biomass tested is obtained by the achievement of equilibrium in the water-gas shift reaction [6]. The proposed gasification was based on the following reactions:

$C+H2O \rightarrow CO+H2$	R1
$C+CO2 \rightarrow 2CO$	R2
$C+2H2 \rightarrow CH4$	R3
$CH4+H2O \leftrightarrow CO+3H2$	R4
$CO+H2O \leftrightarrow CO2+H2$	R5

But one of the major problems encountered in gasification processes is the tar formation, which reduces the efficiency of gas production and interferes with the equipment operation. Various methods have been investigated to eliminate or reduce the tar formation [5, 6]. Tar are defined as all organic contaminants with a molecular weight larger than benzene Tar removal technologies can broadly be divided into two approaches; hot gas cleaning after the gasifier and

Correspondence: Luigi Vecchione, DAFNE, Tuscia University, Via San Camillo de Lellis, 01100 Viterbo, Italy
E-mail: l.vecchione@unitus.it

Key words: steam gasification, pine wood, Renewable Energy Sources

Journal of Agricultural Engineering 2013;XLIV(s1):e116
doi:10.4081/jae.2013.(s1):e116

treatments inside the gasifier [2]. The different approaches of the second one are a proper selection of operating parameters, use of bed additive/catalyst, and gasifier modifications. The operating parameters such as temperature, gasifying agent, steam to biomass ratio, etc. play an important role in formation and decomposition of tar; using some active bed additives such as dolomite, olivine, char, etc. inside the gasifier can be facilitated the tar reforming. If the gasifier bed is well designed and operated, it can produce a very clean gas with respect to the end user application, eliminating the use of downstream secondary steps. In this work a small-pilot bubbling-bed gasification plant has been designed, constructed and used in order to obtain, from the pine trees pruning, a syngas with low tar and char contents and high hydrogen content. The activities showed here are part of the activities carried out in the European 7FP UNIfHY project. The UNIfHY project includes an innovative fluidized bed gasifier with catalytic filter in the freeboard of the reactor allowing steam reforming process of tar with high temperature keeping high thermic efficiency; it allows to resolve the problem of the high pollutants emissions producing a syngas with high purity and rich of hydrogen. In particular the aim of this work is to develop experimental test on a bench scale steam blown fluidized bed biomass gasifier. These tests will be utilized in future works for the simulations of a pilot scale steam fluidized bed gasifier (100 kWth) fed with different biomass feedstock..

Experimental facility

The installation of the bench scale facility used in this work is shown in Figure 1.

Its major components are: a solid fuel feeding system, a fluidized bed gasifier, a gas cooling system, and metering and analyzing systems for the off-gases. The fluidized bed gasifier consists of an austenitic stainless steel cylindrical vessel of internal diameter 80 mm fitted with stainless steel porous distributor plate, designed to allow a good gas distribution at all temperatures. In particular a sintered stainless steel plate is used. The pressure drops through this plate are higher than 40 % of those through the fluidized bed yet at ambient temperature, in order to guarantee a uniform gas distribution at every temperature. The entire reactor is located in a cylindrical electric furnace provided with temperature and heating rate control systems. Temperature within the reactor is measured by means of two thermocouples, one immersed in the bed and the other located under the distributor. The bed inventory is olivine sand. Fluidized gas is a mix of steam and nitrogen: the flowrate of steam is set to obtain the desired steam to biomass ratio while nitrogen is added to guarantee a superficial velocity equal to two times of the minimum fluidization velocity. Water for the generation of steam is fed to an electrically heated boiler by means of a peristaltic pump at a constant flow rate. The biomass feeding system is designed to properly deliver the biomass inside the bubbling bed. During the start-up, the entire raw gas generated by biomass gasification feeds a torch to be completely burned. When gasification process reaches the steady state condition a heated ceramic filter assures that no fine particles .For each run the permanent gas yield was measured by means of a volumetric gasmeter, after separation of the condensate (water and organic phases) in a cold bath of isopropanol (-10°C). The flow rate of the slipstream was controlled by a needle valve. The TAR was measured after each test by means of Agilent GC-MS. Gas products were analysed by Varian micro-GC.

Process cescription and results

Tests on a bench scale reactor (8 cm I.D.) were carried out varying

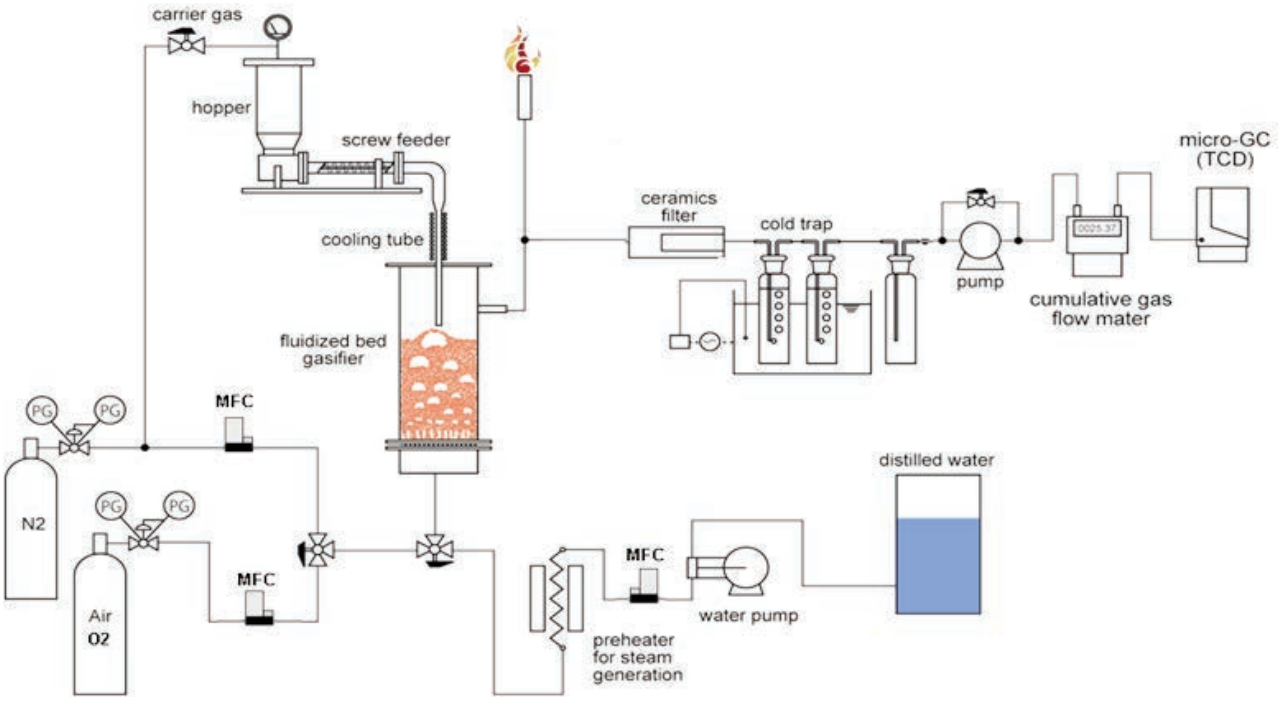

Figure 1. Experimental Facility

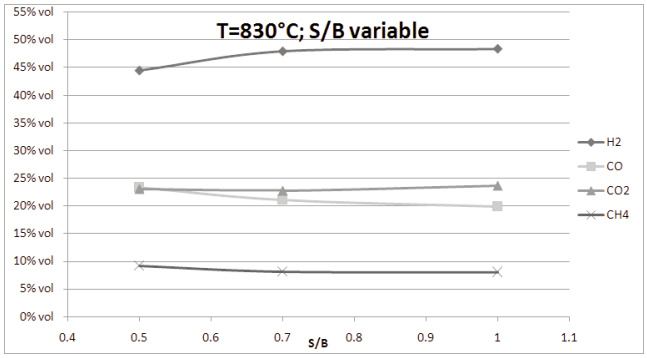

Figure 2. The effect of the steam/biomass ratio on the product distribution

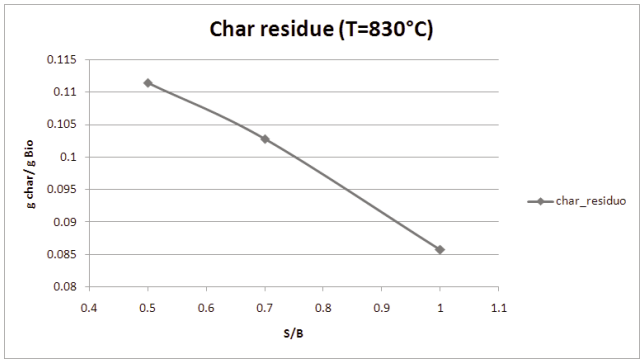

Figure 3. The effect of the steam/biomass ratio on the char residue

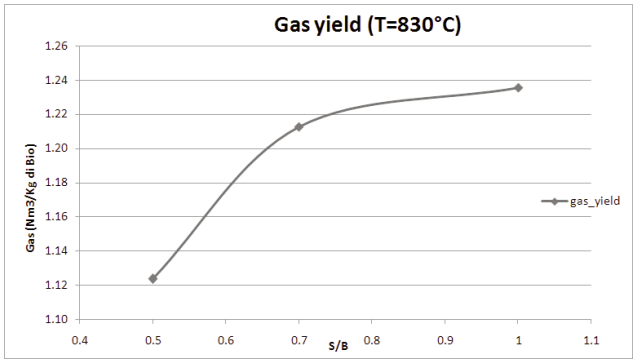

Figure 4. The effect of the steam/biomass ratio on the gas yield

Table 1. Biomass Analysis

Type	Black Pine wood
Status	Raw
Moisture (wt %)	11
Ash (wt %)	0.5
Carbon (wt %)	49,1
Hydrogen (wt %)	6.36
Oxygen (wt %)	44.3
Particle size (mm)	1-2
Particle Density (kg/m3)	510

Table 2. Operating test

Biomass Flow Rate (g/h)	134
Operative Temperature (°C)	**830**
Wind Box Temperature (°C)	450
Vaporize Temperature (°C)	200
S/B	**0.5; 0.7; 1**

Table 3. Results of the tests at different S/B ratios.

T = 830 °C						
S/B	Char (g/gbio)	Gas (Nm3/kg bio)	H2 (%)	CO (%)	CO2 (%)	CH4 (%)
0,5	0,111439162	1,12	0,444323	0,233874	0,230027	0,091777
0,7	0,102801161	1,21	0,479298	0,21113	0,228083	0,081488
1	0,085758049	1,24	0,48372	0,199323	0,236447	0,080509

steam to biomass ratio from 0.5, 0.7 to 1 fixing the temperature at 830 °C. The results of the tests include produced gas and tar composition as well gas, tar and char yield, the wood-gas LHV and process efficiency. Below a preliminary biomass analysis is reported in Table 1, together with average particle size and density.

The main operation parameters are shown in Table 2. The variables studied have been the gasification temperature, and steam/biomass ratio. During tests the temperature was set at 830°C, to assess the effects of the steam to biomass ratio variation and to evaluate the best operative conditions in order to produce high quantity of hydrogen and low tar and char content.

The conversion of char increases with the S/B ratio, as can be seen from Figure 3 . Residual char was varied between 0.11 and 0.08 g/gbio, therefore increases the rate of gas flow product (this is due to an increase in steam). By the formula R1 it is observed that this also increases the production of hydrogen. Instead for the R5 consumption CO which then decreases, as seen from table 3. The CH4 decreases for the reforming R4. The CO2, on the other hand, remains constant because of balance of R5 and R2.

In the table below the effect of steam/biomass ratio on the analysed TARs (Benzene, Xylene, Styrene, Toluene, Naphtalene) is shown.

At this temperature varying the steam to biomass ratio, the total amount of TARs (for Nm3 of syngas) remains practically unchanged.

Bibliography

1. Orecchini, F., Bocci, E.: Biomass to hydrogen for the realization of closed cycles of energy resources. Energy. 32, 1006–1011 (2007).
2. Devi, L., Ptasinski, K.J., Janssen, F.J.: A review of the primary measures for tar elimination in biomass gasification processes. Biomass and Bioenergy. 24, 125–140 (2003).
3. Wang, L., Weller, C.L., Jones, D.D., Hanna, M.A.: Contemporary issues in thermal gasification of biomass and its application to electricity and fuel production. Biomass and Bioenergy. 32, 573–581 (2008).

4. Alauddin, Z.A.B.Z., Lahijani, P., Mohammadi, M., Mohamed, A.R.: Gasification of lignocellulosic biomass in fluidized beds for renewable energy development: A review. Renewable and Sustainable Energy Reviews. 14, 2852–2862 (2010).
5. Franco, C., Pinto, F., Gulyurtlu, I., Cabrita, I.: The study of reactions influencing the biomass steam gasification process☆. Fuel. 82, 835–842 (2003).
6. Herguido, J., Corella, J., Gonzalez-Saiz, J.: Steam gasification of lignocellulosic residues in a fluidized bed at a small pilot scale. Effect of the type of feedstock. Industrial & engineering chemistry research. 31, 1274–1282 (1992).
7. Turn, S., Kinoshita, C., Zhang, Z., Ishimura, D., Zhou, J.: An experimental investigation of hydrogen production from biomass gasification. International Journal of Hydrogen Energy. 23, 641–648 (1998).

Assessment of the energetic potential by hazelnuts pruning in Viterbo's area

D. Monarca, M. Cecchini, A. Colantoni, S. Di Giacinto, A. Marucci, L. Longo

Department of Agriculture, Forest, Nature and Energy (DAFNE), University of Tuscia, Italy

Abstract

In this work the amount of biomass available by the hazelnuts pruning in the province of Viterbo was investigated. At present, the pruning's residues are destroyed by farmers directly in the field, at the end of the pruning; in this way a large quantity of biomass, represented by hazelnut's prunings, is lost; the residues obtained from the hazelnut's pruning, are an important source of biomass that could be used for thermal energy production.

The aim of this work is to realize a map with the estimated energy potential from hazelnut pruning biomass, in the province of Viterbo.

In the first phase the amount of biomass obtained from a hectare of hazelnut's cultivationwas estimated:sampling were carried out in some municipalities of Viterbo while hazelnut pruning was taking place, from January to March.In the field, biomass was weighed and some pieces of wood were collected for laboratory analysis; in particular humidity of biomass, low calorific value, ashand the content of carbon (C), hydrogen (H) and nitrogen (N) were determined. In the calculation of the biomass were considered the age of the plants and the number of plants per hectare.

The results show that the amount of biomass obtained from pruning of hazelnuts varies with the age of plants, but even more so by the number of plants per hectare. The average value of biomass obtained from pruning of a hectare of land is just under 0,9 t. Knowing the net calorific value of the hazelnut wood and the number of hectares cultivated for each municipality, a map of thermal potential energy has been realized..

Correspondence: Massimo Cecchini, Department of Agriculture, Forest, Nature and Energy (DAFNE), University of Tuscia, Via S. Camillo de Lellis snc, 01100 Viterbo, Italy.
Tel.: +39.0761.357.357 - Fax: +39.0761.357.453.
E-mail: ergolab@unitus.it

Key words: biomass, hazelnut's pruning, energy potential from pruning, calorific value.

Contributions: the authors contributed equally.

Conflict of interests: the authors declare no potential conflict of interests.

Conference presentation: part of this paper was presented at the 10th Italian Conference AIIA (Associazione Italiana di Ingegneria Agraria), 2013 September 8-12, Viterbo, Italy.

Journal of Agricultural Engineering 2013;XLIV(s1):e117
doi:10.4081/jae.2013.(s1):e117

Introduction

Among the main treatments on crop management, there are thinning, pruning and fertilizing. These handlings are often applied simultaneously and they interact with each other. As a consequence, they influence the growth and crown of the crop, the branch sizes and the longevity (Forrester et al., 2012a). The three above-mentioned stages affect important aspects of the life crop such as transpiration, photosynthesis and water-use efficiency. From the study of these treatments and their interaction, it is possible to define an efficient and optimal crop management (Forrester et al., 2012b).

Biomass results from pruning crops operation represents an interesting and attractive resource to be exploited in different ways, e.g. fuel for energy production, or transformed into compost and later used as an organic fertilizer. In order to define the most appropriate use of residual biomass from pruning, the attention has to be focused on the amount of pruned material and its physical-chemical characteristics. The former depends on several parameters, namely the type of cultivation, the cultivation site and the planting distance. In case of intensive farming of walnut, hazelnut, olive, grapevine, the pruned biomass reaches 538 kg/ha, 1,848 kg/ha, 2,524 kg/ha and 4,255 kg/ha respectively. Higher quantities of pruned biomass are achieved by apple and pear cultivation, leading to 5,557 kg/ha and 5,818 kg/ha respectively (Bilandzija et al., 2012).

With specific regard to hazelnut crop, in addition to pedo-climatic environment and plant age, the pruning cut method - i.e. manual or mechanical operations - strongly affects the amount of residual biomass and the health conditions of the plant itself.

In more detail, manual pruning leads to produce a higher quantity of biomass if compared to the mechanical method; nevertheless, a decrease in yield was noted for pruned trees. In case of mechanical pruning, an acceptable yield is already expected immediately after the pruning period and leading to a better quality of hazelnut (Sonnati et al., 2009). The intensity of pruning operations in hazelnut cultivations affects the amount of woody biomass and the development of the crop itself. Furthermore, the penetration of light is deeper in the case of a high pruning intensity; in the short term, the yield is greater when low pruning intensity occurs, but higher productivity and growth of the crop result from high-pruning intensity in the long period (Cristofori et al., 2009). The pruning period is strongly linked to the cultivation yield: a limited influence is expected in April, May, June or July, while a significant increase is shown two or three years later after pruning (Ughini et al., 2009).

The biomass resulting from hazelnut plants pruning can be seen as a suitable solution to produce energy by means of thermo-chemical processes, namely combustion, gasification and pyrolysis.

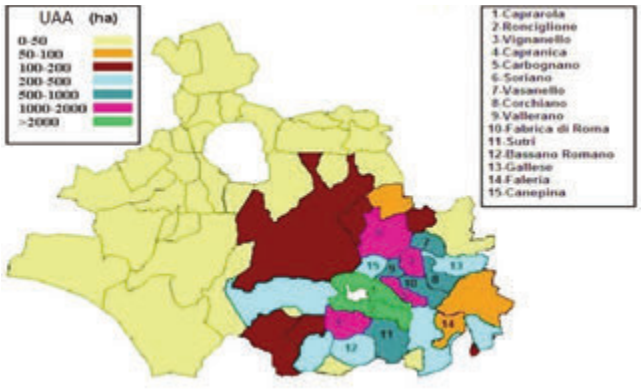

Figure 1. Main hazelnut productive areas in the province of Viterbo. The upper left shows the utilized agricultural area (UAA), with hazelnut cultivation (ha).

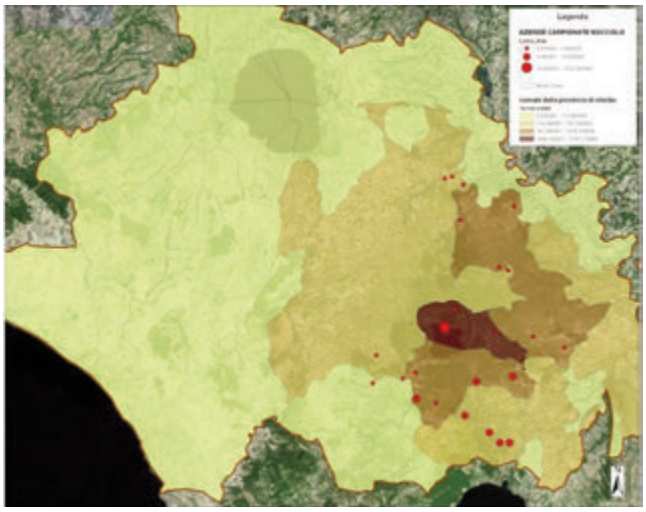

Figure 2. Farm localization and average of biomass.

Figure 3. From left to right: bundles of pruned branches; weighting process with a dynamometer.

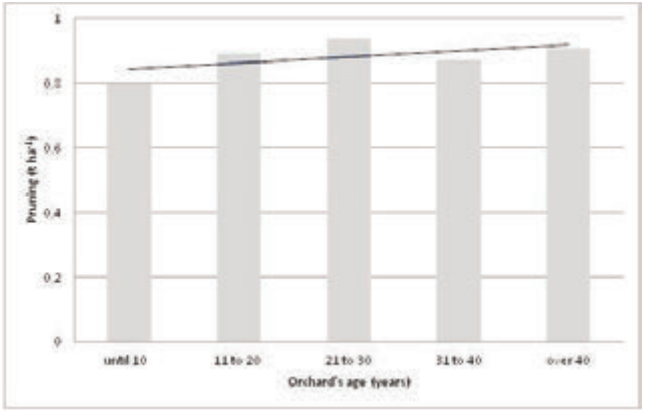

Figure 4. Pruning residues available related to the orchard's age.

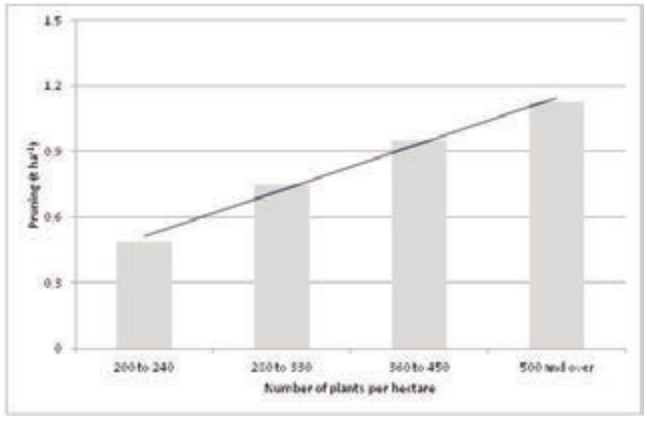

Figure 5. Pruning residues available related to the number of plants per hectare.

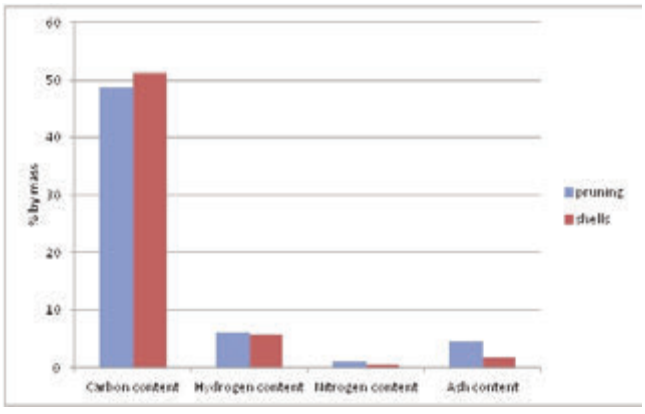

Figure 6. Comparison of biomass characterization between hazelnut pruning and shells.

Table 1. Hazelnut diffusion in the province of Viterbo.

Number of municipality	Number of municipality with hazelnut cultivation	Utilized agricultural area (UAA) (ha)	Utilized agricultural area (UAA), with hazelnut cultivation (ha)	Number of farm	Number of farm with hazelnut cultivation
60	29	21.439	17.735	22.478	9.116

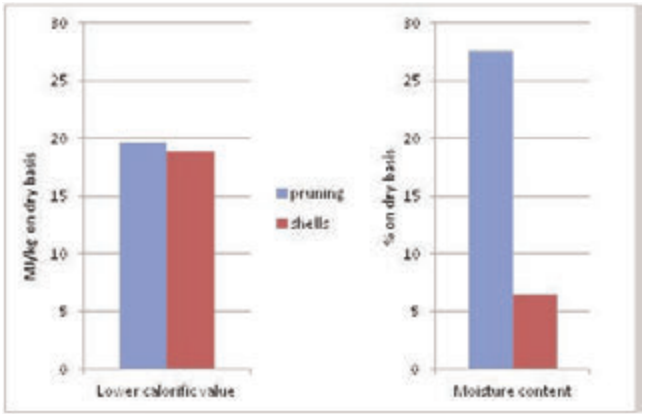

Figure 7. From left to right, lower calorific value and moisture content for hazelnut pruning and shells.

Table 2. Sampled hazelnut groves: main characteristics.

Planting distance (m)	Number of trees ha^{-1}	Number of ha
4.0 x 4.5	556	1
4.5 x 4.5	500	1
5.0 x 4.0	500	22
5.0 x 4.5	450	8
5.0 x 5.0	400	126
5.0 x 5.5	370	1
5.5 x 5.5	331	16
6.0 x 5.0	333	8,5
6.5 x 5.0	308	6
6.0 x 7.0	238	10
6.5 x 8.0	192	2

The present work is aimed at preliminarily evaluating the possible creation of small energy districts in the area of Viterbo (also called Tuscia, in central Italy) (Monarca et al., 2009). This opportunity depends on the amount of available biomass and its conversion technology, since gasification process can be hardly implemented in large scale applications (Monarca et al., 2011). With specific regard to its use as organic fertilizer, the content of nutrient elements and the decomposition level of hazelnut husk - in terms of variations in C/N ratio, organic matter content, organic carbon and nutrients – need to be further investigated and appropriately estimated (Özenç and Özenç, 2009).

This paper shows a study about the amount and use of pruning biomass, particularly about the pruning of hazelnut plants of 25 farm sited in the south-east area of the province of Viterbo.

Two main aspects will be underlined: pruning energy characterization - in terms of calorific value, moisture and CHN content - and availability and distribution in the Province of Viterbo. The former leads to identify the most suitable conversion technology to produce energy from biomass; the latter is addressed to define the potential area where biomass is generated and is strongly related to the location of the plant.

Materials and methods

The crops selected for the present survey are located in some of the most productive areas in the Province of Viterbo; they weren't representatives of the most-spread crop system, because of the large heterogeneity of such a cultivation. The study was carried out on a sample of more than 200 hectares area and involved 25 company (Figure 2).

The pruning residues we considered, belong to the species Corylus avellana L., the cultivar was the Tonda Gentile Romana. For each selected hazelnut crop, surface measure, planting distance and number of trees per hectare were recorded (Table 2). Moreover, every lot was divided into sub-lots, according to the sampling standards (UNI EN 14778:2011), each one delimited by four plants.

Once pruning operations ended, the residual biomass in the sub-lot was bundled and weighted by means of a dynamometer (Figure 3). Weight measurements were carried out in field conditions. Woody samples were put into small closed plastic containers in order to determine chemical and physical characteristics in laboratory conditions.

Later, the average value of the pruning weight per hectare was obtained.

Results

The present study investigates two different aspects: available residual biomass derived from pruning in Corylus avellana L. trees and biomass energy characterization.

The sampled fields examined were divided into age classes - in the case of hazelnut trees - and number of trees per hectare. If we consider the age of the hazelnut tree, as shown in Figure 4, the highest quantities of hazelnut pruning are obtained from 21 to 30 years old-plants. With specific regard to over 40-plants, it seems that the amount of biomass does not show an increasing trend with age. This can be due to the following phenomenon: the over 40-tree volume stops growing. However, a significant difference does not occur if age classes are considered.

Focusing on the number of plant per hectare, a greater difference is noted: as the former increases, the amount of pruned biomass becomes higher, as it can be seen in Figure 5.

In laboratory conditions, biomass characterization was effected. Moisture and ash content were determined on weight fraction on dry basis (wt. % on dry basis). Carbon (C), hydrogen (H), oxygen (O) and nitrogen (N) contents were determined using fraction on mass (% on mass). Also the lower calorific value was determined as a MJ/kg on dry basis (Table 3).

Table 3. Characterization of hazelnut pruning.

Parameter	Value	Unit of measurement
Moisture content	27.59	% on dry basis
Lower calorific value	19.68	MJ/kg on dry basis
Carbon content	48.69	% by mass
Hydrogen content	6.17	% by mass
Nitrogen content	1.09	% by mass
Ash content	4.54	% by mass
C/N	45.69	% by mass

The contents of C, H, N show that these biomass fuels have a higher share of carbon content compared to hydrogen and nitrogen, which increases their energy value.

If we compare the results coming from the energy characterization in laboratory, it can be stated that, with reference to the hazelnut shells, hazelnut trees pruning have similar values in terms of ash content, C, N, H, C/N and lower calorific value: Moisture content is higher in hazelnut residues (Figure 6 and 7).

Conclusions

Available residual biomass, obtained from hazelnut trees pruning, can be successfully considered as a real economical opportunity and as an attractive chance in the Province of Viterbo. The large quantities can supply the growing energy demand and can be efficiently used in domestic or district heating. The energy characterization in laboratory is an important step in choosing the most suitable conversion technology: since this type of woody biomass is similar to hazelnut shells, combustion or gasification seems to be the most appropriate solution (Monarca et al., 2012).

References

Forrester, D.I., Collopy, J.J., Beadle, C.L., Baker, T.G.; Interactive effects of simultaneously applied thinning, pruning and fertiliser application treatments on growth, biomass production and crown architecture in a young Eucalyptus nitens plantation; Forest Ecology and Management. 2012a). 267: 104-16.

Forrester, D.I., Collopy, J.J., Beadle, C.L., Baker, T.G.; Effect of thinning, pruning and nitrogen fertiliser application on transpiration, photosynthesis and water-use efficiency in a young Eucalyptus nitens plantation; Forest Ecology and Management. 2012b). 266: 286-300.

Bilandzija, N., Voca, N., Kricka, T., Matin, A., Jurisic, V. Energy potential of fruit tree pruned biomass in Croatia. Spanish Journal of Agricultural Research. 2012. 10: 292-8.

Sonnati, C., Faciotto, G., Ughini, V. Prune and recycle: mechanical hazelnut pruning and energetic recovery of its biomass. Acta Horticulturae. 2009. 845: 413-18.

Cristofori, V., Cammilli, C., Valentini, F.B., Bignami, C.; Effect of different pruning methods on growth, yield and quality of the hazelnut cultivar 'Tonda Gentile Romana'; Acta Horticulturae 845 , pp. 315-322; 2009.

Ughini, V., Roversi, A., Malvicini, G.L., Sonnati, C. Effects of hazelnut summer pruning performed in different months. Acta Horticulturae. 2009. 845: 363-6.

Monarca, D., Cecchini, M., Guerrieri, M., Colantoni, A. Conventional and alternative use of biomasses derived by hazelnut cultivation and processing. Acta Horticulturae. 2009. 845: 627-34.

Monarca, D., Cecchini, M., Colantoni, A., Marucci, A. Feasibility of the electric energy production through gasification processes of biomass: technical and economic aspects. Lecture Notes in Computer Science (including subseries Lecture Notes in Artificial Intelligence and Lecture Notes in Bioinformatics). 2011. 6785: 307-15.

Özenç, D.B., Özenç, N. Determination of hazelnut husk decomposition level and of the content of some plant nutrient elements under natural conditions. Acta Horticulturae. 2009. 845: 323-30.

Sustainability of grape-ethanol energy chain

G. Riva,[1] E. Foppa Pedretti,[1] G. Toscano,[1] D. Duca,[1] A. Pizzi,[1] M. Saltari,[1] C. Mengarelli,[1] M. Gardiman,[2] R. Flamini[2]

[1]Dipartimento di Scienze Agrarie, Alimentari e Ambientali, Università Politecnica delle Marche, Ancona AN, Italy; [2]Consiglio per la Ricerca e la Sperimentazione in Agricoltura, Centro di Ricerca per la Viticoltura (CRA-VIT), Conegliano TV, Italy

Abstract

The aim of this work is to evaluate the sustainability, in terms of greenhouse gases emission saving, of a new potential bio-ethanol production chain in comparison with the most common ones. The innovation consists of producing bio-ethanol from different types of no-food grapes, while usually bio-ethanol is obtained from matrices taken away from crop for food destination: sugar cane, corn, wheat, sugar beet. In the past, breeding programs were conducted with the aim of improving grapevine characteristics, a large number of hybrid vine varieties were produced and are nowadays present in the CRA-VIT (Viticulture Research Centre) Germplasm Collection. Some of them are potentially interesting for bio-energy production because of their high production of sugar, good resistance to diseases, and ability to grow in marginal lands. LCA (Life Cycle Assessment) of grape ethanol energy chain was performed following two different methods: (i) using the spreadsheet "BioGrace, developed within the "Intelligent Energy Europe" program to support and to ease the RED (Directive 2009/28/EC) implementation; (ii) using a dedicated LCA software. Emissions were expressed in CO2 equivalent (CO2eq). The results showed that the sustainability limits provided by the normative are respected to this day. On the contrary, from 2017 this production will be sustainable only if the transformation processes will be performed using renewable sources of energy. The comparison with other bio-energy chains points out that the production of ethanol using grapes represents an intermediate situation in terms of general emissions among the different production chains..

Correspondence: Daniele Duca, D3A, Università Politecnica delle Marche, via Brecce Bianche - 60131 Ancona (AN), Italy.
Tel.+039 0438 456749, fax +39 0438 64779
E-mail: d.duca@univpm.it

Key words: LCA, biofuel, no-food grapes, sustainability, CO2 emission

Journal of Agricultural Engineering 2013; XLIV(s1):e118
doi:10.4081/jae.2013.(s1):e118

Introduction

Bioethanol is currently produced from raw material obtained from dedicated crops diversified in nature and origin such as, for example, sugarcane, corn, wheat, sugarbeet, grape. Since this production strategy is in direct competition with food production, with a consequent increase in basic foods prices, the trend is to use residual materials (Sarkar et al., 2012) or matrices to be used in bio-refineries (Cherubini, 2010).

In the specific case of bioethanol produced from grape, biofuel fits generally in a larger project for the production of complex molecules such as polyphenols (Kavargiris et al., 2009; Scram et al., 1993). In addition, the cultivation in marginal areas of no-food vine, native throughout Italy (Arroyo and Revilla, 2013), would solve, in this case, most of the issues related to land use competition with the food sector.

Among grapevine beside the V. vinifera varieties used for grapes production for the food industry (as wine, table grapes, raisins or juice), there are many hybrid varieties produced from the innumerable experiments conducted in the past by CRA-VIT. Breeding programs were carried on with the aim of improving grapevine characteristics in particular against diseases, and a large number of hybrid vine varieties was produced. Most of these varieties belong to the "French-American hybrids" (crosses between Vitis vinifera varieties and North American Vitis species) created in Europe to overcome grape phylloxera, powdery mildew and other diseases attack. Some of them potentially are interesting for bio-energy production because have high sugars production, good resistance to diseases, and ability to grow in marginal lands (Esmenjaud and Bouquet, 2009). Moreover, also the production of grape seed oil and biomasses from branches and vine shoots can be significant for bioenergy uses.

In the CRA-VIT grapevine germplasm repository are maintained over 150 different genotypes of hybrid varieties including accessions of complex genealogy obtained crossing several species from the Vitis genus. Data in the literature indicate that there is a large genetic variability among the genotypes about their pest resistance, soil adaptability, length of the cycle, and productivity (from 1-2 to 15-20 kg grape per plant with average sugar content of 13-22 Brix).

Due to technological and legal reasons, the grapes from hybrid vine varieties cannot be used in Italy for winemaking, and nowadays are not significantly used as table grapes. Therefore, these grapes can be included among "no food" products, and their use for energy production overcomes the ethical discussions on the use of food crops for biofuel production.

Given these assumptions, the present work investigates about the chain of bioethanol production from grapes and evaluates the environmental sustainability with respect of greenhouse gas emissions savings, in accordance with the European law which establishes the sustainability criteria for biofuels (Directive 2009/28/EC). A simplified LCA analysis of the chain has been performed to calculate the impact of bioethanol production from grapes on global warming, in order to obtain an indication of its sustainability.

Material and methods

LCA of grape ethanol energy chain was performed following two different methods: (i) using the spreadsheet "BioGrace", developed within the "Intelligent Energy Europe" program to support and to ease the RED implementation (BioGrace, 2010); (ii) using a dedicated LCA software. The analysis entailed the development of different LCA phases, i.e. the choice of the functional unit, the definition of system boundaries, the inventory of inputs and outputs.

To make a comparison of data obtained with those derived from other bioethanol production chains the functional unit chosen for the study was "1 MJ of bioethanol." In a second step, the overall emissions of the supply chain were correlated also to the cultivated hectare.

The inventory phase has been extended both to operations of raw material production (field operations for grape production) and processing for biofuel production (fermentation, distillation) and to its use. The data constituting the inventory were obtained through direct surveys at CRA-VIT or taken from literature. The input and output flows of materials and energy considered as part of the production chain are represented in Figure 1 in order to assess its impact in terms of greenhouse gases (system boundaries).

In compliance with the RED directive, the greenhouse gas emissions of fuels, biofuels and bioliquids were calculated by the following equation:

$$E_B = e_{ec} + e_l + e_p + e_{td} + e_u + e_{sca} + e_{ccs} + e_{ccr} + e_{ee} \quad \text{(Eq.1)}$$

where:

E_B = total emissions from the use of fuel ;

e_{ec} = emissions from the extraction and cultivation of raw materials;

e^l = annualized emissions from carbon stocks changes caused by land use change;

e_p = emissions from processing;

e_{td} = emissions from transportation and distribution;

e_u = emissions from the fuel in use;

e_{sca} = emission saving from soil carbon accumulation via improved agricultural management;

e_{ccs} = emission saving from carbon capture and geological storage;

e_{ccr} = emission saving from carbon capture and replacement;

e_{ee} = emission saving from excess electricity from cogeneration.

When analyzing the grape-to-ethanol chain, the following assumptions were assumed:

- Changes in land use were not considered (e_l);
- Improvements in agricultural practices were not considered (e_{sca});

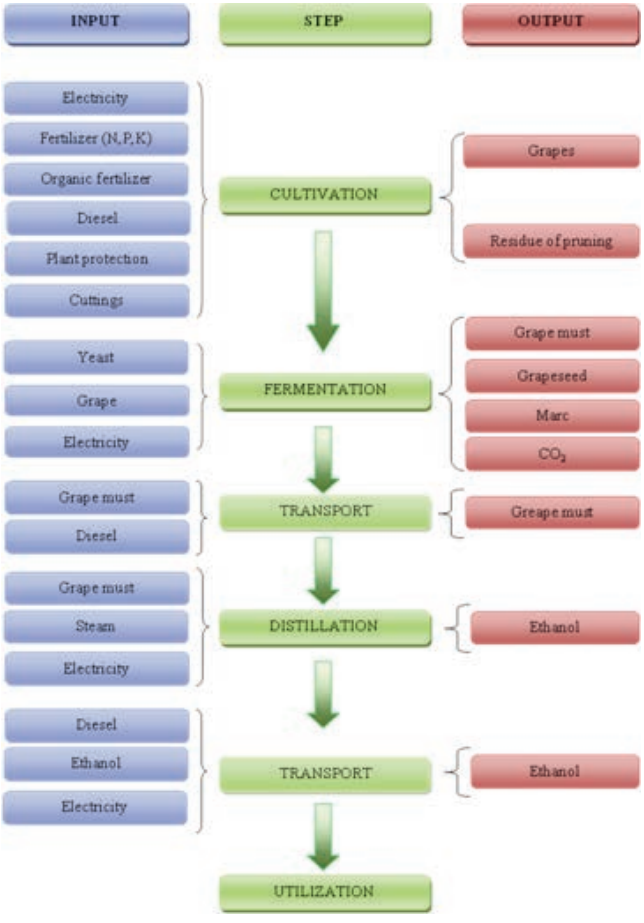

Figure 1. Representation of system boundaries of the analysis

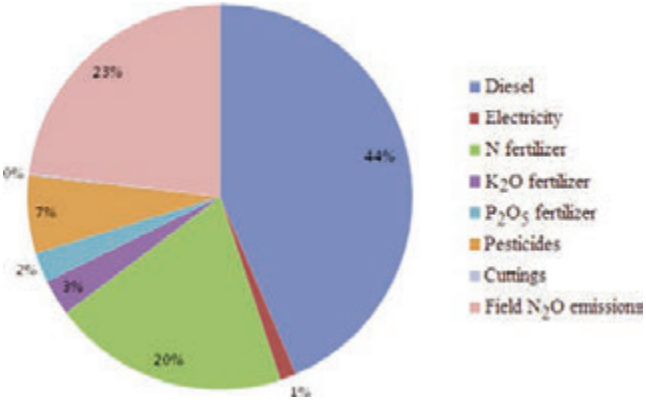

Figure 2. Effect of different inputs used during cultivation stage.

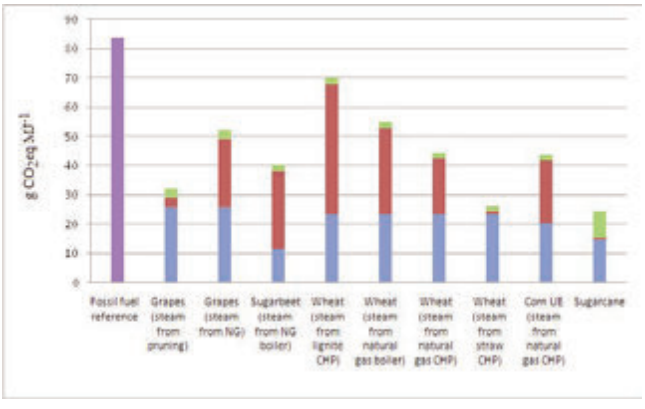

Figure 3. Comparison among overall emissions (g CO2eq MJ-1) of different ethanol production chains and the reference fossil fuel chain.

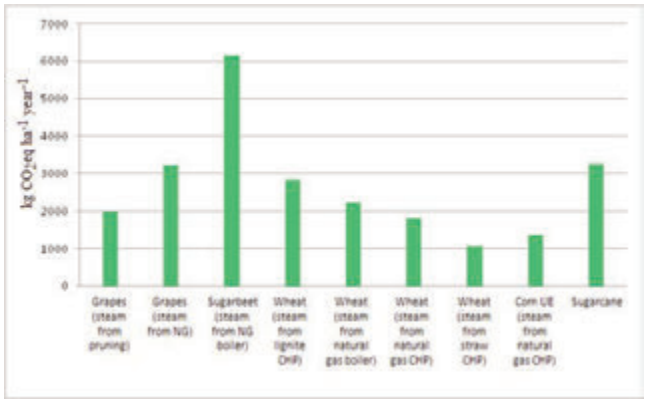

Figure 4. Comparison among overall emissions (kg CO_2eq ha^{-1} $year^{-1}$) of different ethanol production chains.

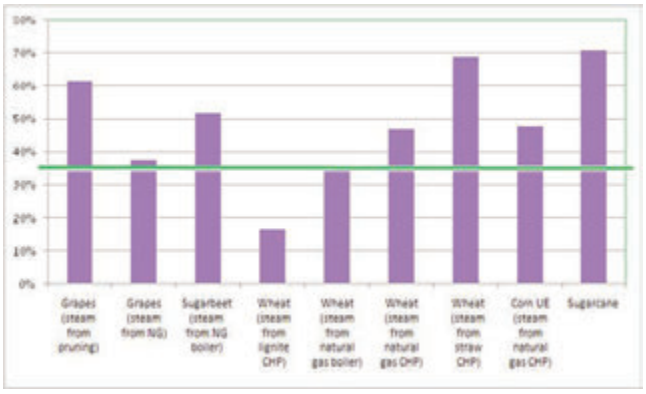

Figure 5. Percentage emission saving compared to the reference fuel. The minimum saving value identified by European Community as threshold is shown in green.

Table 1. Basic assumptions, referring to one hectare, for the calculation of the ethanol-to-energy chain sustainability divided by the steps of production

STEP	Cultivation*	Processing		Transport	
		Fermentation**	Distillation***	Fermented**	Ethanol***
Input	Fuel: 380 l y^{-1} Electricity: 80 kWhy^{-1} Inorganic fertilizer: • 92 kg N y^{-1} • 68 kg P_2O5 y^{-1} • 144 kg K_2O y^{-1} Organic fertilizer (manure): 40.000 kg Plant protection products: 16,2 kg yl of active ingredients (of which approximately 2 kg of copper hydroxide and about 6 kg of Fosetyl-Al) Cuttings: 3500	Electricity 56 kWh y^{-1} Yeasts: 5 kg y^{-1}	Electricity 330 kWh y^{-1} Steam#: 15.120 MJ y^{-1}	Fuel: 33,3 ly^{-1}	Fuel : value from Biograce
Output	Grapes: 40.000 kg y-1 Pruning residues: 70.000 kg y^{-1} with 50% moisture content	Fermented: 5.906 kg y^{-1} Grape seeds: 1.040 kg y^{-1} Marc: 10.960 kg y^{-1} CO2: 2094 kg y^{-1}	Ethanol: 58700 MJ y^{-1}		

Table 2. Allocation percentage (%) of emissions at different steps of the production chain

STEP	Cultivation*	Fermentation**	Distillation***	Transport	
Product				Grape must	Ethanol
Ethanol	55	55	100	100	100
Marc	34	34			
Grapeseed	11	11			

- Operations of carbon capture and geological storage were not considered (e_{ccs});
- Operations of capture and carbon substitution were not considered (e_{ccr});
- Since the cogeneration is not present in the studied chain, the emissions saved as a result of the production of excess electricity were not considered (e_{ee} is however present in some control chain).

The equation used in the specific case can therefore be simplified as follows:

$$E_B = e_{ec} + e_p + e_{td} + e_u (+ e_{ee}) \quad \text{(Eq.2)}$$

The application of Equation 2 made it necessary to start with some assumptions, which focused on inputs and outputs of the different production steps (Table 1).

In the calculation of emissions using the BioGrace method, inputs have been processed using the JEC E3-database, obtaining the three main greenhouse gases (carbon dioxide, methane and nitrous oxide) emitted from the chain, expressed in terms of g CO_2 equivalents (g CO2eq) according to the 2006 and 2007 IPCC guidelines. Emissions relating to the construction of machineries, equipments and structures used were not considered, in accordance with the RED requirements (Annex V, point C).

Using the dedicated LCA software, inputs have been processed using the Ecoinvent database that allows to obtain the emissions evaluation of over fifty greenhouse gases expressed, as in the previous case, in CO_{2eq}.

The emission factors from the Ecoinvent database take into account also emissions related to the construction of machineries, equipments and structures used in their supply chain. In order to evaluate the impacts of biofuels also co-products were considered, using the energy allocation, in agreement with the method used in the BioGrace project and as specifically required by the RED, energy allocation among co-products was adopted in the present work. In particular, the emissions associated with each step in the chain were then distributed in function of the masses and their energy content (Table 2).

Concerning the utilisation step, in accordance with the RED, it was assumed that the combustion of biofuels and biomass generally produces the same amount of CO_2 employed by the plant to grow. Therefore, this contribution should not be recorded in the emission balance.

The percentage in greenhouse gas emission savings were calculated through the ratio shown in Equation 3.

$$ES = (E_F - E_B) / E_F \quad \text{(Eq.3)}$$

where:

ES (Emission Savings) is the percentage of emissions avoided;

E_B is the total emission from the biofuel (bioethanol, in this case);

E_F is the total emission from the reference fossil fuel.

Results and considerations

Through the two softwares (the values coupled in brackets in the text refer to results obtained with BioGrace system and with LCA software respectively. If values are not coupled and no other clarification is given, then it must be considered that the reported value is representative for both the methods) an evaluation of emission level of the studied production chain compared to that of a reference fuel, in accordance to Eupean normatives, was obtained. Results show that the emission level (83,8 g CO_{2eq} MJ^{-1} and 90,8 g CO_{2eq} MJ-1 with BioGrace method and with LCA software respectively) is about 40% lower than the reference value. Thus the studied chain results to be sustainable for the RED parameters. These results became even better if the fossil fuel (methane) used during the distillation step for the production of steam is substituted with a renewable fuel (prunings from cultivation): in this case the emission saving is more than 60%.

Taking into account different production steps (cultivation, transformation, transport), both the methods show that cultivation produces the higher emissions (49-51%), followed by processing (45-44%) and transport (6-5%). The use of prunings as fuel instead of methane for steam production entails significant modifications about emission impacts: 4/5 of total emissions are, in fact, attributed to cultivation while the remaining 1/5 is equally distributed between processing and transport

The analysis of cultivation (Figure 2), carried out with BioGrace method, underlines the important environmental impact of mechanization, followed by inorganic fertilizers and by nitrous oxide emissions, that are however related to fertilization. On the contrary, the environmental impact of cuttings is less than 1%.

Inputs that produce emissions during processing are methane and electricity used mostly for steam production. In particular, methane produces 4/5 of emissions in that step. The substitution of the fossil fuel with wood biomass (prunings) only reduces the electricity input.

During the transport (both the transport of grape must to the distillation step and the transport of ethanol to the pump) the higher contribution in terms of emissions is given by the diesel used for road transports (80%). Electricity used for materials handling contributes for the remaining 20%.

The sustainability of the production chain can be evaluated not only referring to the reference fuel fixed by the normative, but also referring to other well established biofuel production chains. The results reported (Figure 3) refer to elaborations carried out with BioGrace software. The dedicated LCA software produced values in accordance with the previous ones.

The overall emissions impact of ethanol production from grapes is placed in an intermediate position compared to the other production chains considered. The sugarcane-to-ethanol production chain has the lower emission value (24,3 g CO_{2eq} MJ^{-1} of ethanol) while the wheat-to-ethanol production chain that considers the co-generation of lignite appears to be the worst (69,9 g CO_{2eq} MJ^{-1}). If considering the production steps, the grape-to-ethanol production chain has slightly higher emissions during cultivation compared to the other production chains (mean value 20 g CO_{2eq} MJ^{-1}) and in particular compared to those production chains with higher yield for hectare of crops. (beetroot and sugarcane). With the exception of sugar cane-to-ethanol chain (9 g CO_{2eq} MJ^{-1}), where the shipment of ethanol from Brasil has great influence on emissions, the other production chains – including the grape-to-ethanol chain – show low emission deriving from transport (mean value 3 g CO_{2eq} MJ^{-1}). The processing step shows more oscillating emission values. This is evident particularly in the wheat-to-ethanol chain, with values ranging between 0,8 g CO_{2eq} MJ^{-1} and 44,5 g CO_{2eq} MJ^{-1} that refer to wheat-to-ethanol chain through co-generation of straw and lignite respectively.

Figure 4 shows a comparison between the studied production chain with the principal ethanol production chains present in BioGrace (steam production methods are indicated in brackets) in terms of emissions of kg CO_{2eq} ha^{-1} $year^{-1}$.

As it can be seen the overall emission per hectare per year (e.g. in the case of beetroot) does not have the same trend of the overall emission per energy unit, because it takes into account just the territorial unit yield, not the production yield. It is however a useful parameter to identify the magnitude of impacts at local level. In the case of greenhouse gas emission, affecting at global level, this parameter seems to be not significant. For these reasons the RED requires the calculation

of emissions per energy unit, not per territorial unit. Finally (Figure 5), it is shown the emission savings after production and use of 1 MJ ethanol with respect to the reference value (the minimum threshold of 35% indicated in normative is shown in green).

The studied grape-to-bioethanol chains allow to exceed the threshold of 35% greenhouse gas emission saving in all scenarios considered. Using methane as fuel the emission saving is just above the threshold while in the case of using prunings the saving exceeds the 60% (in line with the best bioethanol production chains). This would permit also to stay within the future, and more restricted, sustainability threshold.

Conclusions

Results about the grape-to-ethanol production chain study, with the binding hypothesis of using marginal lands, permit to give a clear indication of its sustainability in terms of greenhouse gas savings compared to the reference fossil chain. The information that emerges with both methods used is that the sustainability is currently respected, considering the threshold limit indicated in the normative. On the other hand, another consideration must be formulated for the future: with a raising of the minimum threshold of emission saving, the grape-to-ethanol chain could be sustainable only if prunings will be used for steam production instead of methane

It must be stressed that all factors used during the cultivation step contribute, directly or indirectly, to increase the production but, at the same time, are also responsible of a certain quantity of emissions. Among them, relevant factors are nitrogen fertilization, diesel (attributable to cultivation) and the type of fuel (prunings or methane) used during the distillation step.

References

1. Sarkar N, Ghosh SK, Bannerjee S, Aikat K. Bioethanol production from agricultural wastes. An overview, Renew Energ 2012;37:19-27.
2. Cherubini F. The biorefinery concept: using biomass instead of oil for producing energy and chemicals. Energy Convers Manage 2010;51:1412-21.
3. Kavagiris SE. Mamolos AP, Tsatsarelis CA, Nikolaidou AE, Kalburtji KL. Energy resources' utilization in organic and conventional vineyards: Energy flow, greenhouse gas emissions and biofuel production, Biomass Bioenerg 2009;33:1239-50.
4. Scram JI, Hall DO, Stuckey DC. Bioethanol from grapes in the European community, Biomass Bioenerg 1993;5(5):347–58.
5. Arroyo Garcia RA, Revilla E. The current status of wild grapevine population (Vitis vinifera spp sylvestris) in the Mediterranean basin. In: Poljuha D and Sladonja B eds. The Mediterranean Genetic Code - Grapevine and Olive. InTech; 2013:Chapter 3, pp.51-72.
6. Esmenjaud D, Bouquet A. Selection and application of resistant germoplasm for grapevine nematodes management. In: Ciancio A, Mukerji KG eds. Integrated management of fruit crops and forest nematodes. Springer; 2009:Chapter 2,pp.195-214.
7. BioGrace (2010), Harmonised calculations of biofuel greenhouse gas emissions in Europe, BioGrace_GHG_calculations_-_version_4b_-_Public.xls. BioGrace, Utrecht, The Netherlands et al.
8. European Union (2009), Directive 2009/28/EC of the European Parliament and of the Council of 23 April 2009 on the promotion of the use of energy from renewable sources and amending and subsequently repealing Directives 2001/77/EC and 2003/30/EC. Official Journal of the European Union L140, pp. 16-61.

Torrefaction of residues and by-products from sunflower chain

G. Riva,[1] E. Foppa Pedretti,[1] G. Toscano,[1] D. Duca,[1] G. Rossini,[1] C. Mengarelli[1]

[1]Dipartimento di Scienze Agrarie, Alimentari e Ambientali, Università Politecnica delle Marche, Ancona, Italy

Abstract

The high heterogeneity of some residual biomasses makes rather difficult their energy use and standardisation is a key aspect for these fuel products. Torrefaction is an interesting process used to improve the quality of ligno-cellulosic biomasses and to achieve standardisation. In the present study torrefaction has been employed on residues and by-products deriving from sunflower production chain, in particular sunflower stalks and oil press cake. The thermal behaviour of materials has been studied at first by thermo-gravimetric analysis in order to identify torrefaction temperatures range. Different residence time and torrefaction temperatures have been employed in a bench top torrefaction reactor afterwards. Analyses of raw and torrefied materials have been carried out to assess the influence of the process. As a consequence of torrefaction, the carbon and ash contents increase while the volatilisation range is reduced making the material more stable and standardised. Mass yield, energy yield and energy densification reach values of about 60 %, 80 % and 1.33 for sunflower stalks and 64 %, 85 % and 1.33 for sunflower oil press cake respectively. As highlighted by results, torrefaction is more interesting for sunflower stalks than oil cake and husks because of the different starting characteristics. Untreated oil cake and husks already show a good high heating value and the eventual torrefaction should be mild. On the contrary for sunflower stalks the process is more useful and could be more severe.

Introduction

Solid biomasses have usually different physical and chemical properties making them difficult to use in combustion systems (Virmond et al., 2012; Wu et al., 2011, Jenkins et al.,1998). The main aspects are the presence of moisture, the heterogeneity of the inorganic fraction and the variability of the organic components, so that many different treatments were studied and developed in order to obtain more homogeneous and standardizable biofuel products. In particular there is a great interest in the torrefaction process, for the energy efficiency of the process and the advantages at a qualitative level (Van der Stelt et al., 2011; Uslu et al., 2008). Torrefaction is a thermo-chemical process similar to pyrolysis and carbonization. The process is performed under an inert atmosphere such as nitrogen. During torrefaction the biomass is treated at high temperature to break the chemical bonds of the organic molecules mainly cellulose, hemi-cellulose and lignin. As a consequence, changes of the biomass structure are caused, with the production of volatile and liquid compounds in addiction to a solid torrefied product. This process causes in wood, and generally in ligno-cellulosic materials, interesting changes for combustion purposes: the increase in energy density, the decrease in hygroscopicity and the ease of grinding (Arias et al., 2008). There are also benefits in terms of biological stabilization and cost reduction during transport and storage, with the possibility to mix the torrefied product with coal for the supply of power plants (Li et al., 2012). In general terms, the behaviour of the torrefied product is similar to that of a traditional solid fossil fuel (Chen and Kuo, 2010).

Torrefaction is a thermal pre-treatment of a solid biomass run without oxygen, at atmospheric pressure and at temperatures between 200 and 300 °C. The first effect on the material is the removal of moisture content and the increase of calorific value. The process determines a loss of solid matter by volatilization up to 30 % by weight, leading inevitably to a loss of energy up to 15 %. The lower energy loss is explained by the decrease of oxygen atoms and partly of hydrogen atoms during the process. Energy and mass balances are therefore key factors for the evaluation of the torrefaction process (Chen et al., 2011). The loss of hydroxyl groups, particularly in wood, but in general in all ligno-cellulosic matrices, is also responsible for the lower hygroscopy of torrefied materials if compared with untreated materials.

The present work was carried out within the "Extravalore" project, funded by MIPAAF (the Italian Ministry of Agricultural, Food and Forestry Policies), about the valorisation of by-products deriving from the biodiesel production process. The present paper aims in particular to find a possible valorisation of sunflower chain residues. The torrefaction of sunflower stalks and oil press cake has therefore been studied in order to evaluate the characteristics and behaviour of the torrefied biomass and to assess the advantages that could be obtained with these different starting materials.

Correspondence: Daniele Duca, D3A, Università Politecnica delle Marche, Via Brecce Bianche, 60131 Ancona (AN), Italy.
Tel. +39 071220429, fax +39 0712204167.
E-mail: d.duca@univpm.it

Key words: stalks, oil press cake, husks, torrefaction.

Journal of Agricultural Engineering 2013; XLIV(s1):e119
doi:10.4081/jae.2013.(s1):e119

Material and methods

Introduction

Materials were obtained within the Extravalore project from seeds and residues of sunflowers cultivated in Osimo (Marche region) and then processed in the Biomass Lab of D3A department of Università Politecnica delle Marche.

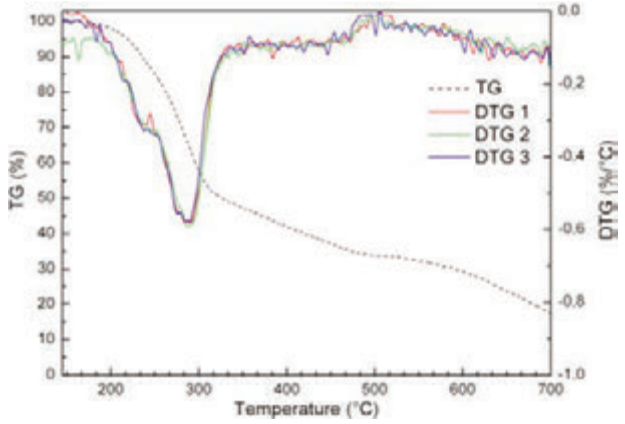

Figure 1. Curves produced from the thermo-gravimetric analysis of sunflower stalks. Overlapping of three repetitions..

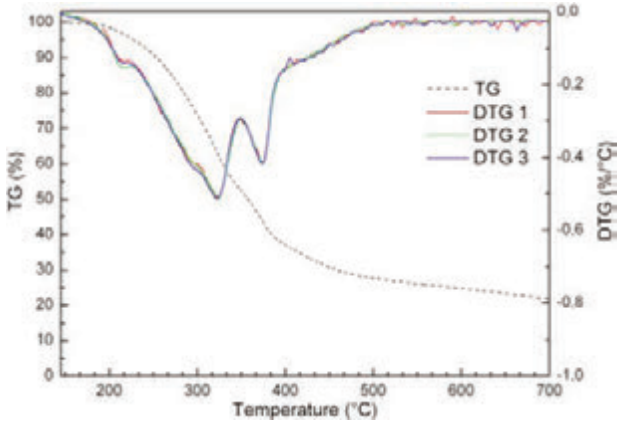

Figure 2. Curves produced from the thermo-gravimetric analysis of sunflower cake. Overlapping of results of three repetitions

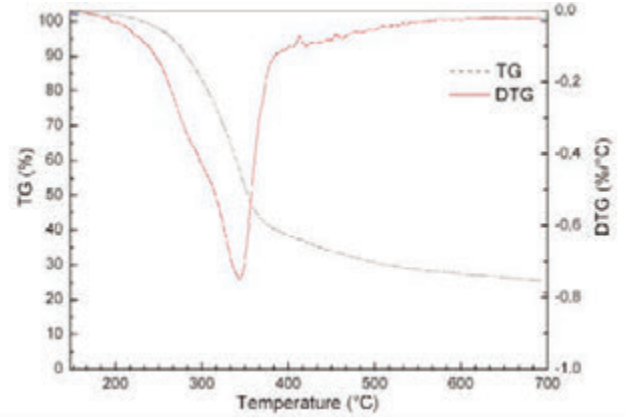

Figure 3. Curves produced from the thermo-gravimetric analysis of sunflower husks

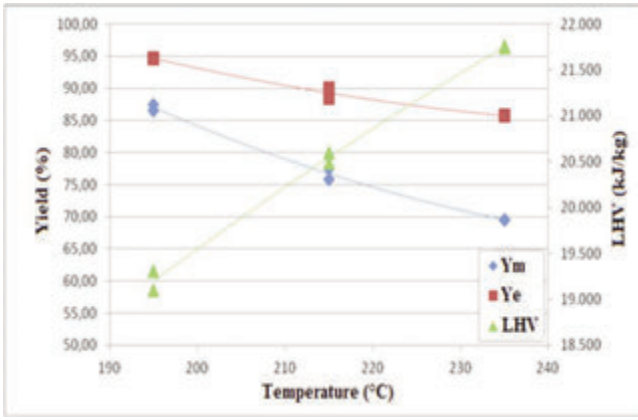

Figure 4. Performance of process yields as a function of temperature (mass yields, "Ym", and energy yields, "Ye") and lower heating value (LHV) in samples of torrefied sunflower stalks at 30 minutes.

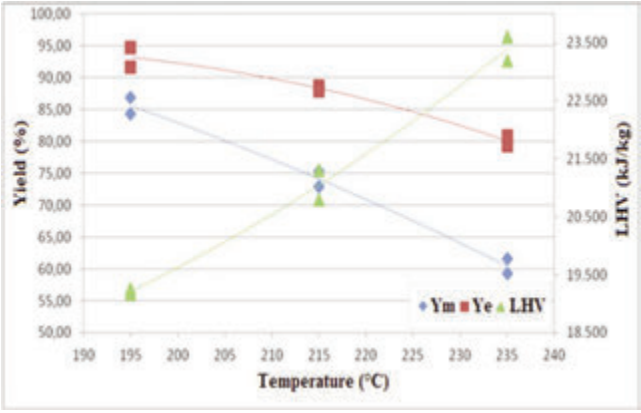

Figure 5. Performance of process yields as a function of temperature (mass yields, "Ym", and energy yields, "Ye") and lower heating value (LHV) in samples of torrefied sunflower stalks at 60 minutes

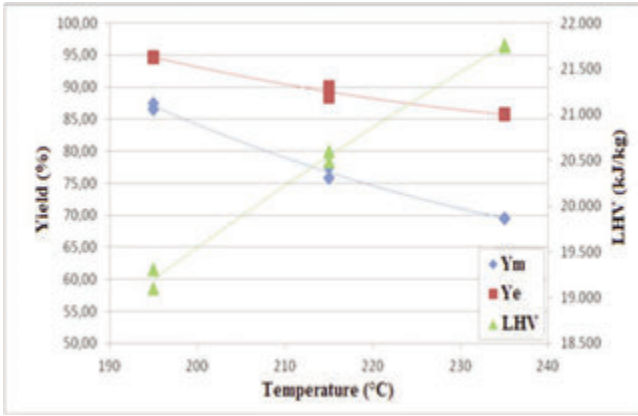

Figure 6. Performance of process yields as a function of temperature (mass yields, "Ym", and energy yields, "Ye") and lower heating value (LHV) in samples of torrefied sunflower cake at 30 minutes

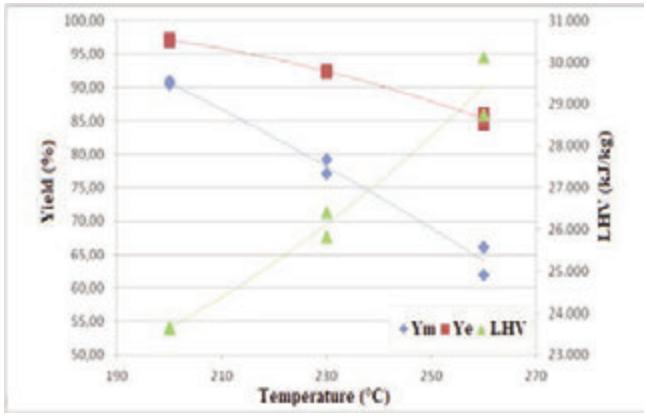

Figure 7. Performance of process yields as a function of temperature (mass yields, "Ym", and energy yields, "Ye") and lower heating value (LHV) in samples of torrefied sunflower cake at 60 minutes

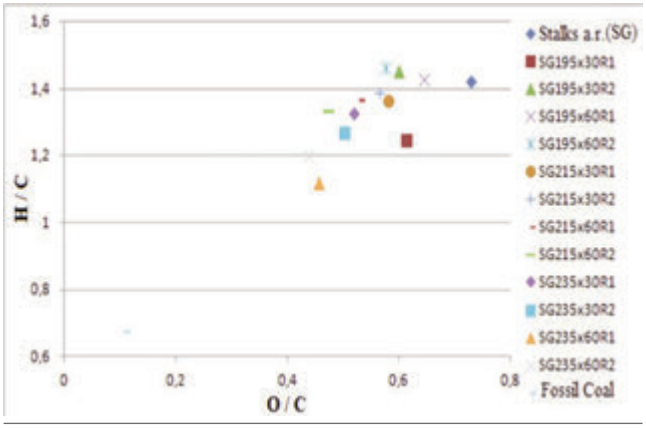

Figure 8. Van Krevelen diagram obtained from the elemental characterisation of row and torrefied sunflower stalks at different conditions. Coal is reported for comparison. (Source for the coal data: Phyllis/ECN, 1998)

The experimental work has been performed as follows:

- sample preparation;
- thermo-gravimetric analysis to define the torrefaction temperatures (Tts) for the later tests in the reactor;
- torrefaction tests;
- characterisation of raw and torrefied materials by thermo-gravimetric, proximate and ultimate analyses;

Table 1. Operative setting parameters used for the tested materials.

sunflower stalks		sunflower cake	
Temp. (°C)	Time (min)	Temp. (°C)	Time (min)
195	30	200	30
	60		60
215	30	230	30
	60		60
235	30	260	91
	60		60

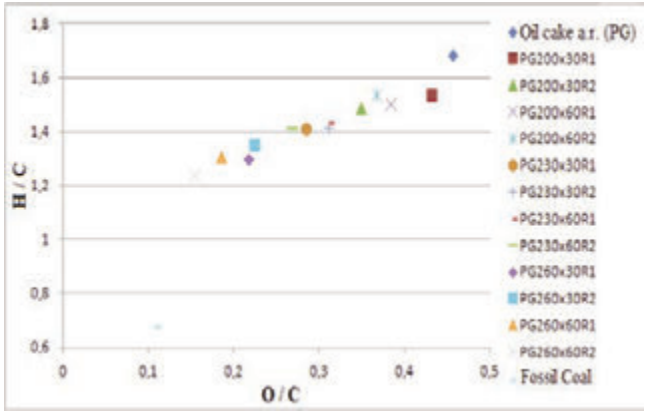

Figure 9. Van Krevelen diagram obtained from the elemental characterisation of row and torrefied sunflower cake at different conditions. Coal is reported for comparison. (Source for the coal data: Phyllis/ECN, 1998)

The steps are described in details.

Sample preparation

The materials employed in the present study and the related moisture contents at sampling are the following:

- sunflower stalks: 18,0%
- sunflower press cake: 9,7%
- sunflower husks: 6,7%

These materials were dried at 105 °C overnight in a forced ventilation oven (MPM INSTRUMENTS), then grinded in a cutting mill (RETSCH). All materials, the raw and processed ones, were stored in air-tight plastic containers at room temperature until analyses were carried out.

Thermogravimetric analysis

The thermal behaviour of raw and torrefied biomass was studied by means of thermo-gravimetric analysis, carried out with a thermo-gravimetric analyser (LINSEIS). The function of weight loss recorded for the whole test, with increasing temperature and time, is called thermo-gravimetric curve (TG). The TG was then processed to obtain the first derivative thermo-gravimetric curve (DTG). For all experimental runs, 20 mg of material were heated from ambient temperature up to 700 °C. The first analysis was made at 5 °C min^{-1} heating rate to define the temperatures for the consecutive torrefaction tests to be performed in the reactor. This rate has been used to allow a more homogeneous sample heating, as reported by some authors (Grønli et al., 2002), and to simulate the heating rate of the reactor. By means of DTG results the Tts for the tests in the torrefaction reactor have been defined. At a later stage, TGs of torrefied and raw materials were carried out to observe the influence of torrefaction conditions on material structure. A faster heating rate (20 °C min^{-1}) was employed in order to reduce analytical time. Nitrogen was used during the analysis at a flow rate of 100 cm3 min^{-1} to maintain an inert environment. To evaluate the experimental reproducibility each sample has been analysed for three times and the DTGs obtained were almost superimposable.

Torrefaction tests

Torrefaction was carried out in a heated bench-top reactor (PARR). The sample (10 g) was inserted in a sample holder and placed in the

Table 2: European standards and instruments employed for heating value, proximate and ultimate analyses

Operation/Analysis	Method	Instrument
Sample preparation	UNI EN 14780	Grinder mill
Moisture content	UNI EN 14774	Stove at T = 105°C – Thermo-gravimetric scale
Ash content	UNI EN 14775	Muffle at T = 550°C – Thermo-gravimetric scale
C,H,N,O	UNI EN 15104	Elemental analyser
High heating value	UNI EN 14918	Calorimeter
Lower heating value	UNI EN 14918	Calorimeter- Elemental analyser
Thermo-gravimetric profile	Internal method	Thermo-gravimetric analyser

Table 3: Sunflower stalks – Analysis of torrefied products (each result is an average of two repetitions)

T	t	Ym	Ye	Ice	HHV	LHV	C	H	N	O	H/C	O/C	Ash
°C	min	% daf			MJ × kg-1 daf	MJ × kg-1 daf	% daf						% s.s.
-	-	100	100	1,00	18,8	17,7	47,31	5,64	1,09	45,96	1,42	0,73	11,57
195	30	87,01	94,65	1,09	20,4	19,2	51,44	5,83	1,19	41,56	1,35	0,61	13,90
195	60	85,58	93,16	1,09	20,5	19,2	51,09	6,20	1,21	41,51	1,45	0,62	13,50
215	30	76,69	89,26	1,16	21,8	20,5	52,52	6,07	1,33	40,09	1,38	0,58	14,80
215	60	74,10	88,32	1,19	22,3	21,0	55,49	6,28	1,26	36,98	1,35	0,50	16,45
235	30	69,55	85,72	1,23	23,0	21,8	55,17	6,00	1,30	37,54	1,30	0,51	16,70
235	60	60,44	80,10	1,33	24,6	23,4	58,25	5,67	1,37	34,72	1,16	0,45	17,80

Table 4: Sunflower cake – Analysis of torrefied products (each result is an average of two repetitions)

T	t	Ym	Ye	Ice	HHV	LHV	C	H	N	O	H/C	O/C	Ash
°C	min	% daf			MJ × kg-1 daf	MJ × kg-1 daf	% daf						% s.s.
-	-	100	100	1,00	23,7	22,1	55,17	7,80	3,47	33,56	1,68	0,46	4,71
200	30	91,70	98,87	1,08	25,3	23,8	58,19	7,39	4,29	30,15	1,52	0,39	5,15
200	60	90,69	97,08	1,07	25,2	23,7	59,16	7,55	3,70	29,59	1,52	0,38	5,20
230	30	81,09	92,20	1,14	26,7	25,1	63,92	7,58	4,55	23,96	1,41	0,28	5,90
230	60	78,18	92,41	1,18	27,7	26,1	63,74	7,62	4,08	24,57	1,42	0,29	5,80
260	30	71,97	89,88	1,25	29,1	27,6	67,69	7,53	4,89	19,90	1,33	0,22	6,40
260	60	64,08	85,27	1,33	31,0	29,4	71,48	7,64	4,75	16,14	1,28	0,17	7,30

Table 5: Energy characterisation of sunflower husks

HHV	LHV	C	H	N	O	H/C	O/C	Ash
MJ × kg -1 daf	MJ × kg -1 daf	% daf						% s.s.
23,2	21,6	56,60	7,55	1,65	34,19	1,59	0,45	3,90

centre of the reactor in order to avoid the direct contact between the biomass and the hot reactor walls. Each test was performed with flowing nitrogen gas to maintain an inert environment inside the reactor. Temperature was controlled during the test using a PID controller. The temperature program consists of a slow heating rate (5 °C min^{-1}) from ambient temperature up to Tt, followed by an isothermal step defined as residence time (Rt). The sample was then cooled to room temperature by a water cooling system under continuous flow of nitrogen through the reactor. The solid sample was then weighted and collected for further analyses. Different Tts and Rts have been evaluated for torrefaction tests. Each test was performed in triplicate. Tts for the torrefaction tests were chosen from DTG at 5 °C min^{-1} within the reactivity range of hemicelluloses, defined as the range between the initial degradation temperature (T_{onset}) and the maximum degradation rate temperature ($T_{shoulder}$). This range has been equally divided into three parts, and the selected Tts are reported in table 1. Sunflower husks were not tested for torrefaction because their energy characterisation gave interesting results and the pre-treatment would not be so useful.

Heating value, proximate and ultimate analyses of materials

To evaluate the influence of the torrefaction conditions on biomass quality, raw and torrefied biomass have been analysed. Heating value, proximate and ultimate analyses were performed for all materials in accordance with the European standards, as summarized in table 2.

Process parameters were calculated to evaluate how temperature and time of the torrefaction treatment influence biomass quality and composition according to the following equations:

$$M_Y\ (\%) = (m_{tor}/m_{bio}) \bullet 100 \qquad \text{(eq.1)}$$

$$I_{ed} = LHV_{tor}/LHV_{bio} \qquad \text{(eq.2)}$$

$$E_Y\ (\%) = M_Y \bullet I_{ed} \qquad \text{(eq.3)}$$

where M_Y and E_Y are mass and energy yields and represent the amount of matter and energy remained after the process; I_{ed} is the energy densification index which represents the increasing of the energy contained in the material; m is the mass of the material, and LHV is the lower heating value. Subscripts *tor* and *bio* are referring to torrefied and raw biomass respectively. All quantities are expressed on dry ash-free base (daf).

Taking into account the results of elemental analysis, H/C and O/C atomic ratios have been calculated and plotted in a Van Krevelen diagram.

Results and discussion

Thermogravimetric analysis

The results of thermo-gravimetric analyses carried out on the starting materials are reported below.

The sunflower stalks produce DTG curves showing a clear overlap of the peak of hemicelluloses with that of cellulose (Figure 1). Unlike classical ligno-cellulosic biomasses the kinetics of thermal degradation is rather low, especially regarding celluloses.

It can be noted also a certain diversity of response among the 3 repetitions and this is related, most likely, to the heterogeneity of the material. The stalk, in fact, consists of two main components, a cortex and a marrow, with different specific weights that are difficult to mix after grinding, and consequently make difficult also the test sample homogenization.

The T_{onset} of this material is about 180-190°C and the $T_{shoulder}$ about 240-250°C. For sunflower stalks were selected a Tmin and Tmax close, respectively, to the point of "onset" and "shoulder" (Tmin = 195 °C, Tmax = 235 °C), and a Tint in the center (215 ° C).

The sunflower cake cannot be considered a classic ligno-cellulosic biomass as surely also consists of fat. Residual oil deriving from the mechanical pressing of seeds in fact still remains inevitably trapped within the matrix of the cake in a variable percentage.

Looking at the thermal profile obtained from the TGA analysis (Figure 2) at least one peak more is observed. The peak corresponding to the volatilization of the oil produces its maximum at a temperature of 375°C.

On the whole, the kinetics of degradation does not reach high values. The first peak that is encountered, probably associated with the decomposition of the hemi-cellulose fraction, appears to be lower and moved to the left.

For this product were chosen 3 temperatures included in the range of holo-celluloses degradation: 200°C, 230°C and 260°C.

The thermal profile obtained from the TGA analysis of sunflower husks (Figure 3) shows a clear overlap of the peak of hemi-celluloses with that of cellulose. The highest cellulose degradation rate is reached at about 340°C, a rather high temperature with respect to the other materials tested. However the degradation kinetics are higher. This behaviour is typical of woody material.

Results of torrefaction tests and characterisation of raw and torrefied materials

The results of chemical and energetic analyses for raw and torrefied samples are listed as follows.

Results of the characterisation of torrefied sunflower stalks are reported in Table 3 together with the process yields.

While the calorific value and the energy concentration index show an increase, the mass yield and energy yield confirm the usual downward trend, reaching values of respectively 60% and 80% with the most critical conditions.

The main results obtained by the treatment of sunflower stalks to different operating conditions are shown in graphic form (Figures 4 and 5).

Table 4 shows the results obtained from the analysis of torrefied sunflower cake: similarly to what observed for the other biomasses, also in this case a torrefaction more extreme in terms of temperature and/or time leads to an increase in carbon content and heating value and, in parallel, a reduction in mass yield and energy yield.

Figures 6 and 7 show in graphic form the values of mass yield, energy yield and lower heating value in function of torrefaction temperature and applying an isotherm of 30 and 60 minutes respectively.

The results of chemical and energetic analyses carried out on sunflower husks are reported in Table 5.

Untreated sunflower husk is an interesting material for energy application due to its high energy content, limited nitrogen and ash content. The most important limit is the poor bulk density but this cannot be solved by torrefaction.

Van Krevelen diagram about sunflower stalks and cake

The torrefaction treatment determines changes in the organic structure of all biomasses. In all cases an increase in the concentration of carbon (C) associated with a decrease of the oxygen content (O) has been observed. On the other hand the concentration of hydrogen (H) oscillates without showing a definable trend.

Generally, the structure of torrefied products tends to assume a composition that more and more resembles to that of conventional solid fuels (e.g. hydrocarbon structure of the coal) when increasing the severity of the process itself.

Plotting the indices O/C (on x-axis) and H/C (on y-axis) of each torrefied product, expressed as atomic ratio, we obtain the so-called "Van Krevelen diagrams." These diagrams highlight the structural changes and allow us to better interpret the effect of torrefaction treatment on the quality of biomasses to be used in combustion.

Figures 8 and 9 show the Van Krevelen diagrams of each material.

In general, it can be seen that the experimental points are arranged along an imaginary line that originates from the characteristic values of the starting biomasses (upper right in the respective graphs) and extends to gradually lower values of H/C and O/C (toward the origin of the axes). The more extreme is the torrefaction (> temperatures and/or> time), the more enriched in carbon than oxygen and hydrogen are the torrefied products. As a consequence their organic structure moves away from that of the original biomass and tends progressively to take on characteristics similar to that of coal, traditional solid fuel, acquiring at the same time also hydrophobic properties typical of non-polar hydrocarbons.

Conclusions

The thermo-gravimetric analyses put in evidence the heterogeneity of the organic fraction which is basically ligno-cellulosic for sunflower stalks while it is much more complex in the cake for the presence of different matrices (oil). Even the inorganic component is present in varying amounts in the different residual biomasses, with values ranging from 3.9% for sunflower husks to 11.6% for stalks. These values are significantly higher than what is found in woody biomasses. The energy concentration, however, proves to be quite interesting, in particular for the sunflower cake and husks.

The torrefaction treatment provides interesting qualitative improvements of all the biomass treated. However, the "price" that is paid in this process is the inevitable loss of mass, and therefore of energy, of the treated material. This depends on the dismissal of organic compounds that are formed by the thermal degradation of macromolecules (hemicelluloses, cellulose and lignin) and that volatilise with different kinetics characteristics of each biomass (as evident in their thermo-gravimetric profiles).

The torrefaction treatment reaches a balance when the quality standard of products finds a compromise with the maximum performance of the treatment in terms of mass and energy. This should be functional to the energy use that it is intended, and therefore to the needs of the energy conversion system powered. The empirical study of the tor-

refaction process is a critical step that should be properly programmed according to the energy performances desired from the torrefied products and in order to identify the best conditions of the treatment. This approach become mandatory due to the structural and chemical variability of biomasses, even within the same product category. Materials with high moisture content and a molecular structure particularly rich in oxygen (and then with higher O/C), such as sunflower stalks, when subjected to heat treatment, undergo more changes in mass but, at the same time, acquire significant benefits in terms of energy concentration.

In this perspective, from a technical point of view, it is better to employ torrefaction with materials such as sunflower stalks, while for sunflower cake and husks a better alternative or a direct energy application should be found. However, from a practical point of view, the torrefaction process is more feasible with residues produced in processing steps than in cultivation, due to logistic aspects.

References

1. Virmond E, De Sena RF, Albrecht W et al. Characterisation of agroindustrial solid residues as biofuels and potential application in thermochemical processes. Waste Manage 2012;32(10):1952-61.
2. Wu MR, Schott DL, Lodewijks G. Physical properties of solid biomass. Biomass Bioenerg 2011;35(5):2093-105.
3. Jenkins BM, Baxter LL, Miles Jr TR et al. Combustion properties of biomass. Fuel Process Technol 1998;54(1–3):17-46.
4. Van der Stelt MJC, Gerhauser H, Kiel JHA et al. Biomass upgrading by torrefaction for the production of biofuels: A review. Biomass Bioenerg 2011;35(9):3748-62.
5. Uslu A., Faaij APC, Bergman PCA. Pre-treatment technologies, and their effect on international bioenergy supply chain logistics. Techno-economic evaluation of torrefaction, fast pyrolysis and pelletisation. Energy 2008;33(8):1206-23.
6. Arias B, Pevida C, Fermoso J et al. Influence of torrefaction on the grindability and reactivity of woody biomass. Fuel Process Technol 2008;89(2):169-75.
7. Li J, Brzdekiewicz A, Yang W et al. Co-firing based on biomass torrefaction in a pulverized coal boiler with aim of 100% fuel switching. Appl Energ 2012;99(0):344-54.
8. Chen WH, Kuo PC. A study on torrefaction of various biomass materials and its impact on lignocellulosic structure simulated by a thermogravimetry. Energy 2010;35(6):2580-86.
9. Chen WH, Cheng WY, Lu KM et al. An evaluation on improvement of pulverized biomass property for solid fuel through torrefaction. Appl Energ 2011;88(11):3636-44.
10. Grønli MG, Várhegyi G, Di Blasi C. Thermogravimetric Analysis and Devolatilization Kinetics of Wood. Ind Eng Chem Res 2002;41(17):4201-08.

Giant reed (*Arundo donax* L.) harvesting system, an economic and technical evaluation

M. Bentini,[1] R. Martelli[1]

[1]Department of Agricultural and FoodSciences, University of Bologna, Bologna, Italy

Abstract

The giant reed is a herbaceous energy crop that demonstrates a good adaptability for areas of central-northern Italy. However, its size and stem resistance to cutting pose problems for harvesting in relation both to the availability of suitable machinery and costs of the operation. A technical and economic evaluation has been conducted of a harvesting system based on an experimental machine, the biotriturator, developed by University of Bologna in collaboration with the Nobili Company (Bologna, Italy) and adapted to field operating conditions.

The harvesting system consists of cutting-shredding and baling in a single pass. The system was evaluated by performing a winter harvest when the crop was in quiescence and had a low moisture content.

The total harvesting costs were evaluated as 11.6 € Mg^{-1} dry biomass. Given that the estimated area that can be covered by the harvesting system was 123 hectares per year the system represents an effective solution for not very large areas and is therefore suitable for the Italian environment where average farm sizes are slightly over seven hectares (ISTAT, 2011).

Introduction

Dedicated energy crops can play a key role in providing substantial amounts of lignocellulosic feedstocks required for the second-generation biofuel production chain as well as heat and electricity production (JRC EC, 2011). The main barrier to the diffusion of crops for bioenergy is cost competitiveness with fossil fuels. To create a reliable supply chain it is necessary to achieve efficient and sustainable cultivation.

The perennial grass giant reed (Arundo donax L.) is considered as particularly promising for Mediterranean regions, because of high yields in lignocellulosic biomass, a good adaptability to these environments and its very low soil tillage, pesticide and fertilizer requirements (Lewandowski et al., 2003; Angelini et al., 2005, 2009)

The harvesting can be a critical phase of giant reed cultivation mainly due to the lack of harvesting machines (Venturi and Bentini, 2005). As well as being very tall and having a high cutting resistance, Arundo is a rhizomatous grass that is not laid out in regular rows and is also sometimes partially lodged (Yitao et al., 2007). It is therefore necessary to design a specific machine or adapt machines developed for other crops.

The harvesting process requires mow-conditioning, raking and baling or loading of loose chopped biomass for delivery to the energy plant. Depending on the moisture content of the biomass a partial drying in the field may be necessary prior to baling or delivery (Trebbi, 1993). The giant reed can also be harvested in winter, with partial drying of the plants in the field improving the characteristics of the biomass in terms of specific energy and reducing the storage and handling costs.

In this paper, a prototype for the cutting and chopping of giant reed has been evaluated. A technical economic analysis has been conducted of a cutting-shredding-baling system that can harvest the crop in a single operation.

Material and methods

Harvesting trials were done on a 7-year-old giant reed crop with a 1 x 1 m planting layout obtained from rhizomes of an ecotype selected at the University of Catania. The crop was harvested at the end of February when plants were in winter quiescence and had a low moisture content. A prototype biotriturator RM 280 BIO was used, which combines cutting, shredding and crop windrowing. The equipment was developed by the Agricultural and Food Sciences Department of the University of Bologna, in collaboration with Nobili S.r.l. (Bologna, Italy). The machine was composed of a cutting shredding chamber surmounted by a dividing conveyor, constituted by a frame to channel the plants into the shredding chamber. The shredding system consisted of a horizontal rotor with 64 half Y-shaped flail blades, the eight rows of flails were staggered. A double auger conveyor situated in the rear of the shredding chamber allowed the biomass to be raked. The biotriturator was front-mounted with a three point hitch on a 4-wheel-drive tractor CNH T6090 (147 kW) (CNH Corporation), with a Kuhn VB2160 round baler (Kuhn S.r.l., Italy) rear-mounted on the same tractor. The baler was a variable chamber that wrapped the bales in nets (Figure 1, 2).

Correspondence: Roberta Martelli, Dipartimento di Scienze e Tecnologie Agro-Alimentari, Università di Bologna, via G. Fanin 50, 40127 Bologna, Italy.
Tel. +39.051.2096175 - Fax: +39.051.2096178
E-mail: roberta.martelli@unibo.it

Key words: cost analysis, giant reed (Arundo donax), harvesting system, herbaceous energy crops.

Journal of Agricultural Engineering 2013;XLIV(s1):e120
doi:10.4081/jae.2013.(s1):e120

Table 1. Implement and tractor cost data

		Tractor	Biotriturator	Baler
Purchase price	€	84000	7500	24000
Estimated life	h	8000	1000	1000
Annual use	h	800	200	200
Remaining value	C1	0.976	0.756	0.852
coefficient	C2	0.119	0.067	0.101
	C3	0.0019		
Insurance and housing	%	1	1	1
RF1		0.019	0.44	0.43
RF2		1.3	2.0	1.8

Table 2. Crop characteristics

Plant age	years	7
Average density	shoots m^{-2}	15
Stem length m	3.7	
Moisture at harvest (wet)	%	41
Average yield (dry)	Mg ha^{-1}	20.1

Table 3. Operative characteristics of harvesting systems

Field speed	km h^{-1}	4.0
Machine working width	m	2.80
Field efficiency		0.55
Effective field capacity*	Mg h^{-1}	12.5
Area covered per year	ha	123

*Referred to dry biomass

Bales were measured and then weighed directly in the field suspended by belts on an electronic dynamometer (Figure 3). The bulk density and moisture content on a wet basis were determined.

The effective field capacity of the machine was evaluated considering the working times measured during the field trials on the basis of Standard ASAE EP496.3.

The total machinery costs are calculated including charges for ownership and operation and are based on buying a new machine and using a tractor for 10 years and implements for 5 years.

The ownership includes depreciation, interest on the investment, insurance and housing of the machine (Standard ASAE S495.1). The purchase price is based on the manufacturer's list price minus a percentage discount indicated by the dealers interviewed (20% for a tractor and 15% for implements). Other variables used in calculating costs are shown in Table 1.

Annual use was assumed as 200 h for implements and 800 h for tractors. The remaining value was calculated on the basis of Standard ASAE D497.7. The other ownership costs, insurance and housing were calculated as a percentage of the purchase price. For the interest charged on borrowing the money a rate of 5% on the average investment was applied.

Labour costs are based on 14.50 euros per hour labour charge, including taxes and social security contributions. Fuel costs are based on diesel fuel priced at 0.93 euros per litre. The total repair and maintenance charges take into account the amount of use and were calculated on the basis of Standard ASAE EP496.3. For the tractor, the repair and maintenance indices relative to the specific Italian situation were used (Calcante et al., 2011).

Figure 1. Baler during ejection phase

Figure 2. Harvesting system

Figure 3. Bale weighing

Results

Table 2 reports average values of the crop characteristics measured at harvesting. The average stem height was 3.7 m with values in the range 2.4-4.4 m, at a density of 15 shoots m-2. The yield represents the amount of biomass collected from the field, not the total amount of above-ground biomass.

For the evaluation of costs and machine performance reference was made to the data obtained in the field trial, which were comparable with average values obtained in other studies done in areas of central-northern Italy (Angelini et al., 2005, 2009).

The field speed was 4.0 km h^{-1}, with a field efficiency of 0.55 limited by the wrapping and ejecting times of the round baler. The effective field capacity was 0.62 ha h^{-1} that, on the basis of the hypothesized annual use, allows an area of 123 hectares per year to be covered (Table 3).

The average volume of the bales was 2.4 m3 (1.6 m diameter by 1.2 m wide) with a mass of 407 kg, moisture content on a wet basis of 41% and density 170 kg m-3.

The cost of the harvesting system amounted to 233.3 € ha^{-1}, due to 78.9 € ha^{-1} for the tractor (including fuel and oil costs), 130.9 € ha^{-1} equipment overheads and 23.5 € ha^{-1} labour cost for the tractor driver. The total harvesting cost per unit of dry biomass was 11.6 € Mg^{-1}.

The cost of net for the round baler was 0.81 euros for bale and was included in the total, while costs to transport the biomass from field to plant and for storage were not included.

The majority of implement costs were for interest and depreciation, corresponding to around 62% of the total cost for the baler and biotriturator and 74% for the tractor excluding the labour cost.

Discussion

The average speed of the harvesting system is 4.0 km h^{-1} and is always lower than 4.5 km h^{-1}, due both to the high cutting resistance of the culms of giant reed and the irregular crop distribution in the field, which over the years tends to invade the inter-rows.

The working capacity of the system is also limited by the baling phase, which has low field efficiency because of the need to stop the machine during the wrapping and ejecting.

Comparison of the biomass harvesting costs with other studies is difficult because of differences in assumption and methods. In addition, while analyses have been done on the harvesting costs of biomass crops such as sorghum and switchgrass (Cundiff and Marsh, 1996; Thorsell et al., 2004; Sokhansanj et al., 2009; Lychnaras and Schneider, 2011), to our knowledge no studies are available on the costs of the mechanised harvesting of Arundo.

Conclusions

The prototype is able to perform properly the harvesting of giant reed even if the crop is not laid out in regular rows but the high shear strength of the culms limits the machine speed. The machine can also used on other energy crops such as sorghum and switchgrass.

This system anyway showed reasonable harvesting costs for not very large areas (around 200 ha) and is therefore suitable for situations like that in Italy, where average farm sizes are slightly over 7 hectares.

In the future, with the expected diffusion of dedicated energy crops with winter harvest, the development of a combine is advisable that both shreds and bales without the feedstock coming into contact with the ground to reduce contamination by inorganic material, and consequently lower the ash content.

References

Angelini L., Ceccarini L., Bonari E. Biomass yield and energy balance of giant reed (Arundo donax L.) cropped in Central Italy as related to different management practices. European Journal of Agronomy 2005;22:375–89.

Angelini L.G., Ceccarini L., Nassi o Di Nasso N., Bonari E. Comparison of Arundo donax L. and Miscanthus x giganteus in a long-term field experiment in Central Italy: Analysis of productive characteristics and energy balance. Biomass Bioenergy 2009;33:635-43.

ASAE. Uniform Terminology for Agricultural Machinery Management. St. Joseph (MI): American Society of Agricultural and Biological Engineers. 2005 Nov. Standard ASAE S495.1.

ASAE. Agricultural Machinery Management. St. Joseph (MI): American Society of Agricultural and Biological Engineers. 2007 Feb. Standard ASAE EP496.3.

ASAE. Agricultural Machinery Management Data. St. Joseph (MI): American Society of Agricultural and Biological Engineers. 2011 March. Standard ASAE D497.7.

Calcante A., Mazzetto F., Fontanini L. Verifica dei parametri del modello per il calcolo dei costi di manutenzione e riparazione di trattori 4rm in pianura padana: primi risultati. Proceedings of the Conference: Gestione e Controllo dei Sistemi Agrari e Forestali, 2011 Sept 22-24, Belgirate, Verbania, Italy.

Cundiff J.S., Marsh L.S. Harvest and storage costs for bales of switchgrass in the southeastern United States. Bioresour. Technol. 1996;56:95-101.

JRC - European Commission 2011. Technology Map of the European Strategic Energy Technology Plan (SET-Plan) Technology Descriptions. Joint Research Centre – European Commission, Luxembourg, EU.

Lewandowski I., Scurlock J.M.O., Lindvall E., Christou M. The development and current status of perennial rhizomatous grasses as energy crops in the US and Europe. Biomass Bioenergy 2003;25:335-61.

Lychnaras V., Schneider U.A. Multi-farm economic analysis of perennial energy crops in Central Greece, taking into account the CAP reform. Biomass Bioenergy 2011;35:700-15.

Sokhansanj S., Mani S., Turhollow A., et al. Large-scale production, harvest and logistics of switchgrass (Panicum virgatum L.)–current technology and envisioning a mature technology. Biofuels, Bioprod. Bioref. 2009;3:124-41.

National Institute of Statistics (ISTAT); 2011. VI Censimento generale dell'agricoltura. Available from: http://censimentoagricoltura.istat.it/fileadmin/template/main/res/comunicato-censimento-agricoltura.pdf Accessed: May 2013.

Thorsell S,. Epplin F.M., Huhnke R.L., Taliaferro C.M. Economics of a coordinated biorefinery feedstock harvest system: lignocellulosic biomass harvest cost. Biomass Bioenergy 2004;27:327-37.

Trebbi G. Power-production options from biomass: The vision of a southern European utility. Bioresour. Technol. 1993;46:23-9.

Venturi P., Bentini M. La logistica delle biomasse: tecnologie di raccolta e stoccaggio. Agroindustria 2005;1:55-60.

Yitao L., Qingxi L., Boping T., et al. Experimental research on the mechanical physical parameters of bottom stalk of the Arundo donax L. in harvesting period. Transactions of the Chinese Society of Agricultural Engineering 2007;23:124-9.

Two prototypes for medium rotation forestry harvesting

L. Pari, V. Civitarese, A. Del Giudice, A. Scarfone

Consiglio per la Ricerca e la Sperimentazione in Agricoltura, Unità di Ricerca per l'Ingegneria Agraria, Monterotondo (Roma), Italy

Abstract

Five years old poplar (Populus spp.) plantation represents an interesting model of productivity. The most attractive characteristics of this energy crop are the handling flexibility, the high yield of biomass per area unit and the good quality of the chips obtainable.

The mechanical harvesting of five-years old poplar plantations requires the use of specialized forest machineries such as harvester, feller, forwarder and chipper. Usually, after felling, the working phases consist of extraction, stacking and chipping. Generally, the last one is carried out in a "static phase", where the product is taken from staked logs by using a hydraulic arm having a gripper that feed the chipping machine.

In order to introduce technological innovations for the medium rotation forestry harvesting, the Consiglio per la Ricerca e la sperimentazione in Agricoltura, Unità di ricerca per l'Ingegneria agraria (CRA-ING) of Monterotondo (Rome, Italy) has developed a five years poplar cut-windrower and a self-propelled chipper equipped with a pick up system.

The prototype of cut-windrower is a semi-trailed machine powered by a 95 kW tractor (at least). It mounts a cutting system and a double pincer with variable positioning. During the cutting phase the plant is grasped by the double pincer which conveys and unloads the stem along the inter-row. The trees are placed parallel to the progress of the tractor, but oriented in the opposite direction.

The biomass windrowed is then chipped in a dynamic phase directly from the inter row using the self-propelled chipper equipped with the pick-up head.

In the first tests, the cut-windrower has reached an operative working capacity of 0.22 ha h^{-1}, with an operative production of 44 t h^{-1}. On the other hand, the self-propelled chipper has showed an operative working capacity equal to 0.18 ha h^{-1}, and an operative production of 35 t h^{-1} about.

Both machines have shown good quality of the work performed and the results obtained indicates that the work phases could be simplified in order to reduce both the time of use and the harvesting costs.

Correspondence: Vincenzo Civitarese, CRA – ING, via della Pascolare 16, 00016 Monterotondo (RM), Italy.
Tel. +39.06.90675235 - Fax: +39.06.90625591
E-mail: vincenzo.civitarese@entecra.it

Key words: poplar, MRF, cut-windrower, wood chip

Acknowledgments: the authors would like to thank the role of the *"SUSCACE" Project (Scientific Support to Agricultural Conversion towards Energy Crops)* for funding the study.

Journal of Agricultural Engineering 2013; XLIV(s1):e121
doi:10.4081/jae.2013.(s1):e121

Introduction

Short-rotation coppice crops (SRCs) are an important resource that can be used as renewable energy (Hansen, 1991; Zamora et al., 2013), and a possible alternative to fossil fuels in Europe (Bergante et al., 2010).

The Italian climatic conditions can be considered optimal for growing poplar tree (Paris et al., 2011) which is one of the most important species for the biomass production. New poplar hybrids and cultivars specifically selected by Italian researcher have showed in experimental trials a very high production capacity (Dillen et al., 2007).

Among the different cropping system, the five years old poplar (Populus spp.) plantation represents a productive model very interesting for its handling flexibility, big yield and good chips quality. The planting distance (3x2 m) and the dimension reached by plant at end of the productive cycle (average basal diameter of 180-200 mm, average height of 15 m) can justify the presence of a forestry yard (Spinelli et al., 2008) organized in compliance with the plants size, the field extension and the productive purpose (Spinelli et al., 2006).

In traditional yard, the trees after felling are generally stacked in designated areas (eg. field sideline) and then chipped by specific machines (trailed or self-propelled chippers) fed by a log grape.

The Engineering unit of the Agricultural Research Council (CRA-ING) of Monterotondo (Rome, Italy) has developed a new harvesting chain for the harvest of five years old poplar plantation.

In this chain the plants are felled , windrowed, and then chipped in a dynamic phase using a prototype of cut windrower (powered by a tractor of 95 kW at least) and a self-propelled chipper equipped with a pick-up head.

The yard proposed and the machines developed for the harvest of five-year old poplar plantations may represent an important innovation for the mechanization of the energy crops. Beside the simplification and the reduction of the harvesting time, this new chain allows to reduce harvesting time and cost, increasing also the number of working hours of tractors. The innovative system was studied by analysing the performance and the quality of the work performed by the new machines during the collection of five years old poplar plantation.

Prototype description

The cut-windrower (Table 1) is a semi-trailed machine having a mass of 2046 kg. The main components of the machine are the cutting system and the double pincer. The double pincer performs different functions such as gripping, transport and unload. The machine is able to cut and leave the plants along the inter-row par-

allel to the progress of the tractor. Once released on the ground, the trees appears with the crowns oriented in the opposite direction respect the advancement of the machine (Fig. 1). The cutting system consists of a sawblade (1000 mm in diameter) that cuts at 2200 rpm. It is installed on a mobile support connected to a spring capable to absorb part of the stress occurred during cutting. The cut-windrower has two wheels that held the machine during work and allow to adjust the cutting height by the action of two jacks (the minimum cut height is 50 mm). The double pincer is composed by two series of mechanic arms (gripping elements) which can be partially overlapped and capable to spin around a master rotary column. When the pincer comes into contact with the tree, it begins to perform a series of operations following a defined time model. These operations consist in griping, lifting, transport toward the inter-row, inclination, release of the plant, and return to the original position.

The time scheduled for opening and tilt of the pincer can be modified with a specific command.

Table 1. technical characteristics of the five years old cut-windrower machine.

Cut windrower machine	
Width and length in working phase (m)	3.21 x 3.60
Width and length in transporting phase (m)	2.35 x 3.60
Maximum height (m)	2.8
Total mass (Kg)	2046
Cutting system	
Diameter of the circular blade (mm)	1000
Circular blade and tooth thickness (mm)	12
Tooth (N°)	36
Rotation speed (rpm/min)	2200
Minimum cut height (mm)	50
Adjustable double pincer	
Mechanic arms (N°)	2
Gripping extent on the trunk (mm)	795
Working phases (N°)	5

The cutting tool and the pincer are able to move laterally from the primary body of the machine, going from the transport configuration to the working configuration.

The self-propelled machine is driven by a 6 cylinders endothermic diesel engine of Iveco FPT (Fiat Powertrain Technologies), with a maximum power of 260 kW. The machine is equipped with four isodiametric wheels (500/18 R22 tires) and the transmission is designed with different driving systems that depending on the needs can be varied using an electric command placed in the cab. The driving configurations are the following: front steering and fixed rear wheels, four-wheel steering, side tractor shift, crab movement.

The machine has a maximum length, width and height of 6390 mm, 2510 mm and 3910 mm respectively, a total weight of 9250 kg, with a tank containing about 300 liters of fuel.

The prototype has a reversible drive, with a tipper for loading having the capacity of 15.7 m3. In order to unload the product directly on the trailers of trucks, the tipper is hinged onto the outer frame of the machine to a height of 3910 mm. Finally, the machine presents frontally the PTO and two arms to connect respectively to the chipping device and to the pick up head.

The chipping system is designed to comminute trees up to a maximum diameter of 380 mm. It consists of a disc with diameter and thickness of 1600 mm and 60 mm respectively working at a speed of 1000 rpm. The disk is directly connected to the PTO by a shaft and two radial blades operate the cut with a fix counter-knife.

The pick-up device consists of a rotary cylinder having diameter and length of 155 mm e 1750 mm respectively. The rotary cylinder has 105 steel reliefs, each one 70 mm long. This tool has both gripping and lifts functions; its rotational axis is 820 mm distant from the power supply system of the machine, presenting a space of 370 mm for unloading impurities.

The conveyor system is implemented by two groups of three counter-rotating toothed drums, which help to direct the material toward the chipping apparatus. Each drum has a diameter of 250 mm and a height of 700 mm.

Moreover, the chipping supply system has two vertical counter-rotating drums, one fixed, the other mobile, whose motion depends on the size of the product. A hydraulic system is installed on the two sides of the pick up head; this allows the contact between the collecting organ and the ground.

During the progress along rows, the self-propelled prototype combined with the pick-up head has been capable to harvest and chipping

Figure 1. Cut windrower machine during the placement of trees on windrow.

Figure 2. Self propelled chipper during the harvest.

trees from the ground, as well as to unload the product on the rear tipper of the machine (Fig. 2) or on trailers.

Materials and methods

Machines performance and work quality were analyzed on three rows (160 m length each) of five years poplar plantation (planting distance 3 x 2 m, plant density 1666 plants ha^{-1}) at the first coppice cycle (root and stem five-years old: R5S5). The harvesting trial was carried out during January 2012 in Savigliano (CN – Italy).

The average height and the diameter of the plants have been evaluated on 30 samples randomly distributed throughout the test area. The diameters have been measured at 100 mm from the ground.

The percentage of dead stools was evaluated along the three harvested rows.

The yield of the plantation was assessed weighting the whole biomass chipped after felling.

Standard harvesting times were registered according to the methodology of the Commission Internationale de l'Organisation Scientifique du Travail en Agriculture (C.I.O.S.T.A.).

The parameters considered to evaluate the work quality of the cut windrower were the cutting height, the stump damage, the regularity of windrows, the percentage of plant not correctly placed along the inter-row. On the other hand, the parameters considered for the work quality of the self-propelled chipper were the product losses and the bulk density, the moisture content, and the particle size distribution of the chips obtained.

The cutting height, the stump damage, the percentage of plants not correctly placed along the inter-row, and the product losses were evaluated on three random plots of 30 m2 from each row.

In particular, the product losses were quantified collecting and weighing all the biomass on the ground after the passage of the self-propelled chipper. The losses have been classified in two categories:

- plants not collected from the pick up head,
- plants not correctly conveyed in the power supply system.

The bulk density was evaluated measuring the weight of five volumetric cylinder after that the product was unloaded on the ground. Five chip samples of 3 kg each were collected into sealed bags, catalogued and transported in laboratory for determining the moisture content and the particle size distribution. The entire procedure was done following the standard methodology of the European Standard EN (UNI EN 15103-2009, UNI EN 14774-2009) and the Technical Specifications (CEN/TS 15149-2006).

Results

The crop was in a good condition of plant health, weeds were almost absent. The average height and diameter of the plants were 18.60 m (std. dev. ± 1.74) and 189 mm (std. dev. ± 30.03) respectively. The percentage of leaks was 1.408% on average, so the real density was 1642 plants ha^{-1}. The harvestable biomass was 198 t ha^{-1}, corresponding to 16.77 odt ha^{-1} $year^{-1}$ (the moisture content of the plants was 57.65%) (Table 2).

The felling-windrowing machine (installed on a tractor Fendt 716 Vario TMS N with a power of 130 kW), working at a speed of 0.24 m s^{-1} (0.87 km h^{-1}) has achieved an operative working capacity of 0.22 ha h^{-1} and an operative hourly production of 44 t h^{-1}.

On the other hand, the self-propelled chipper worked at a speed of 0.18 m s^{-1} (0.65 km h^{-1}) achieving an operative working capacity of 0.18 ha h^{-1} and an operative hourly production of 35 t h^{-1}. Rest and dead time were not recorded while accessory time was represented by time for turns (4.36% for the cut windrowing machine and 6.19% for the self-propelled chipper) and maintenance time (9.40% for the cut windrowing machine and 3.49% for the self-propelled chipper). Table 3 displays times recorded during the harvesting trials.

The cutting height resulted 119.30 mm on average (std. dev. ± 17.13). The percentage of plants not correctly placed along the inter-row was equal to the 3% of the total trees felled.

Table 2. dendrometric parameters registered in the experimental plantation.

Inter-row distance (m)	3
Distance within the plants (m)	2
Dead stools (%)	1.40
Effective density (p ha^{-1})	1642
Shoots/coppice (n.°)	1
Plants diameter (mm)	189□30.03
Plants height (m)	18.60 □1.74
Fresh biomass (t ha^{-1})	198
Moisture content (%)	57.65
Yield (odt ha-1 $year^{-1}$)	16.77

Table 3. performance of the machines.

	Cut windrower	Self propelled chipper
Effective speed (m s^{-1})	0.24	0.18
Operative working capacity (ha h^{-1})	0.22	0.18
Hourly operative production (t h^{-1})	44	35
Accessory time (%)	13.76	9.68
- Time for turns	4.36	6.19
- Maintenance time	9.40	3.49

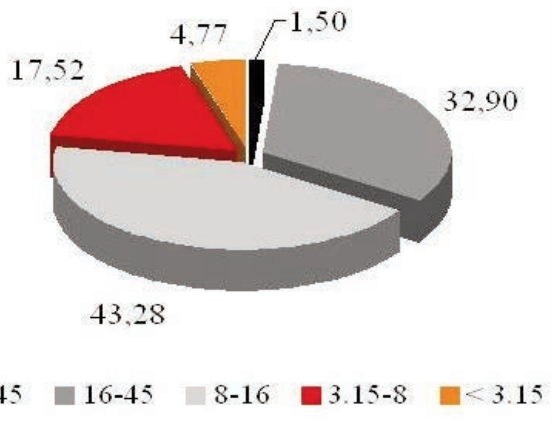

Figure 3. particle size distribution of chips.

The self-propelled machine was able to pick up and chip the 99.15% of the windrowed leaf biomass on the ground (1.68 t representing the 0.85% of the total).

The chips produced had a bulk density of 293.60 kg mc^{-1} (std. dev. ±12.48) and a moisture content equal to 57.65%.

The particle size analysis has shown that the largest part of the product was concentrated in classes of 8-16 mm and 16-45 mm, representing respectively the 43.28% e 32.90% of the total sampling. Impurities or over measured particles were absent (Fig. 3).

Discussion and conclusions

The tests carried out have shown the relevant performance and the good work quality of the machines. CRA ING cut windrower prototype has shown a high working speed, processing about 360 trees per hour. The self-propelled chipper has been able to collect the plants from the ground previously felled and left along inter-rows; it has allowed to operate in a dynamic phase. Similarly to the collection of biennial poplar plantations, the chips produced can be unloaded directly on tractor trailers, reducing the number of the working phases.

Finally, these results show the possibility to optimize the logistic of the whole yard, reducing the harvesting time and the general costs.

References

Bergante S, Facciotto G, Minotta G. Identification of the main site factors and management intensity affecting the establishment of Short-Rotation-Coppices (SRC) in Northern Italy through Stepwise regression analysis. Central European Journal of Biology 2010; 5(4):522-30.

CEN/TS 15149-1:2006. Solid biofuels. Methods for the determination of particle size distribution - Part 1: Oscillating screen method using sieve apertures of 3,15 mm and above.

Dillen SY, Marron N, Bastien C, Ricciotti L, Salani F, Sabatti M, Pinel MPC, Rae AM, Taylor G, Ceulemans R. Effects of environment and progeny on biomass estimations of five hybrid poplar families grown at three contrasting sites across Europe. Forest Ecology and Management 2007;252(1-3):12–23.

Hansen EA. Poplar woody biomass yields: a look to the future. Biomass and Bioenergy 1991; 1:1-7.

Paris P, Mareschi L, Sabatti M, Pisanelli A, Ecosse A, Nardin F, Scarascia-Mugnozza G. Comparing hybrid Populus clones for SRF across northern Italy after two biennial rotations: Survival, growth and yield. Biomass and Bioenergy 2011;35:1524-32.

Spinelli R., Nati C., Magagnotti N. SRF di pioppo – macchine e sistemi per la raccolta. Sherwood - Foreste ed alberi oggi 2006;128:56-9.

Spinelli R., Nati C., Magagnotti N., Picchi G. Harvesting poplar medium rotation coppice with light equipment. Proceedings of 23th International Poplar Commission (IPC, FAO), Pechino, China; 2008 p.168.

UNI EN 14774-2:2009. Solid biofuels. Determination of moisture content. Oven dry method (Part 2): Total moisture - Simplified method.

UNI EN 15103:2009. Solid biofuels Determination of bulk density.

Zamora DS, Wyatt GJ, Apostol KG, Tschirner U. Biomass yield, energy values, and chemical composition of hybrid poplars in short rotation woody crop production and native perennial grasses in Minnesota, USA. Biomass and Bioenergy 2013;49:222-30.

Palms (Phoenix canariensis) infested by red PALM weevil (Rhynchophorus ferrugineus Olivier): insecticidal efficacy tests of chipping treatment

G. Sperandio,[1] M. Fedrizzi,[1] M. Guerrieri,[1] R. Fanigliulo,[1] D. Pochi,[1] M. Pagano,[1] S. Arnone,[2] M. Cristofaro,[2] R. Sasso,[2] S.Musmeci,[2] S.Catarci[3]

[1]CRA-ING, Consiglio per la Ricerca e la sperimentazione in Agricoltura, Monterotondo (Rome); [2]ENEA-UTAGRIECO, Italian National Agency for New Technologies, Energy and Sustainable end Economic development, Sustainable Management of Agro-ecosystems Laboratory, Rome; [3]BBCA-onlus Biotechnology and Biological Control Agency, Rome, Italy

Abstract

The provision n° A6505/29-11-2010 of the Lazio Region Agricultural Department states that the plant material resulting from the felling of palms infested by RPW (Rhynchophorus ferrugineus Olivier) must be disinfested by heat treatment or fine mechanical chipping, ensuring that the resulting materials obtained are of a size smaller than 2 cm. This paper describes changes made on one machine chipper FARMI mod. FOREST CH260 for use in the cutting of trees and palm leaves in accordance with the above mentioned provision. The analyzes carried out on the plant material shredded, according to methodology UNI CEN/TS 15149-1 - 2006, show that 94,78% of the fragments is smaller than 16 mm and a water content of 52.5%. In all fragments of the material shredded at least one of the three dimensions was less than 2 cm. A mix of chipped stipes and leaves of palm tree was tested at ENEA facilities to evaluate the ability of RPW larvae to feed and survive on this substrate. Ten plastic containers (130 liters) were filled up with 26 kg each of chipped matter and infested with larvae grouped by weight into 3 classes ranged from < 0.15 g, 0.15 -;- 0.35 g and > 0.35 g till 2 cm (3 containers for each class and 1 as control; 30 larvae for each container). Containers, covered with a metallic net, were kept in an isolated chamber, controlling temperature in order to maintain the substrate around 30°C. The substrate was inspected at 45 dd after infestation. No survival was recorded on the larvae, indicating that chipping technique could be a suitable method to destroy infested palm avoiding potential risks of re-infestation from the disposal sites.

Correspondence: Mauro Pagano, Consiglio per la Ricerca e la Sperimentazione in Agricoltura, Unità di ricerca per l'ingegneria agraria (CRA-ING), Via della Pascolare, 15- 00016 - Monterotondo (Roma), Italy.
Tel.: +39.06 90675253 - Fax: +39.06 90625591
E-mail: mauro.pagano@entecra.it

Key words: palm, biological residues, Rhynchophorus ferrugineus.

Acknowledgments: authors want to thank *Mrs Celeste Carbone* of S. Marinella (sea-site close to Rome - Italy) that kindly made available her garden for RPW adult trapping and offered infected palms for the experiment.

Contributions: the authors contributed equally.

Conflict of interests: the authors declare no potential conflict of interests.

Journal of Agricultural Engineering 2013; XLIV(s1):e122
doi:10.4081/jae.2013.(s1):e122

Introduction

The introduction of Rynchophorus ferrugineus in Italy in a few years has caused great damage to the wealth of palms that characterizes many Italian areas, causing problems for the landscape changes and the implications for economic issues related to the abatement of the plants affected by the infestation of the pest and the proper and effective disposal of waste material that is difficult to manage in relation to the anatomical and physiological characteristics of the Arecaceae. The implications of the recent epidemic spread of the weevil, now configured as a real biological invasion, have been exacerbated by the difficulties of early diagnosis of insect infestation and the difficulties of operating in an environment often strongly anthropic (Roversi, 2013). It is increasingly necessary to implement preventive measures, such as chopping of trees felled by suitable means to eliminate the pest and then be able to limit the spread, linking the use of biocides synthetic or naturally derived. This aspect is an important element for the protection of the palm trees in the immediate term.

Materials and methods

The tests were conducted in November 2012, at the Research Unit for Agricultural Engineering (CRA-ING) in Monterotondo (RM) and the ENEA Research Center of Rome. At the laboratories of the CRA-ING tests have been carried out mechanical chopping of trees felled because of the infestation of red weevil.

On samples of the chopped material were carried out laboratory tests to determine the density, moisture content and particle size with the European standard method established by CEN (European Committee for Standardization).

For chopping machine was used a wood chipper Farmi CH260 FOREST.

A quota of the chopped material was sent to Entomology laboratories of the ENEA, where a bioassay was set up in order to evaluate the ability of RPW larvae to survive and feed on this substrate. Ten plastic containers, 130 lt of capacity, were filled up with 26 kg of chopped matter

Figure 1. The wood chipper FARMI model - CH260 FOREST Block diagram of workstations.

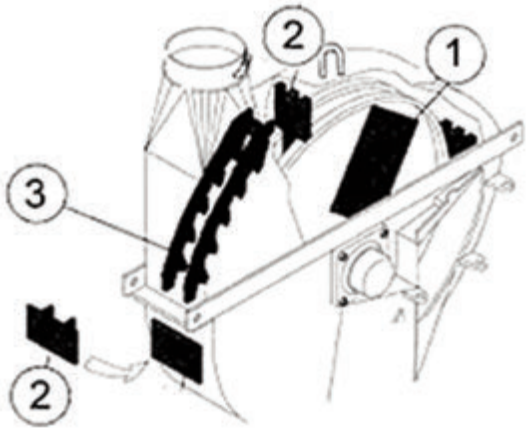

Figure 2. Chipping in 3 stages (for wood chips basis): 1. Double knife on the rotor disk 2. Fixed knives 3. Final knives. (source: http://www.deangeli.bz.it)

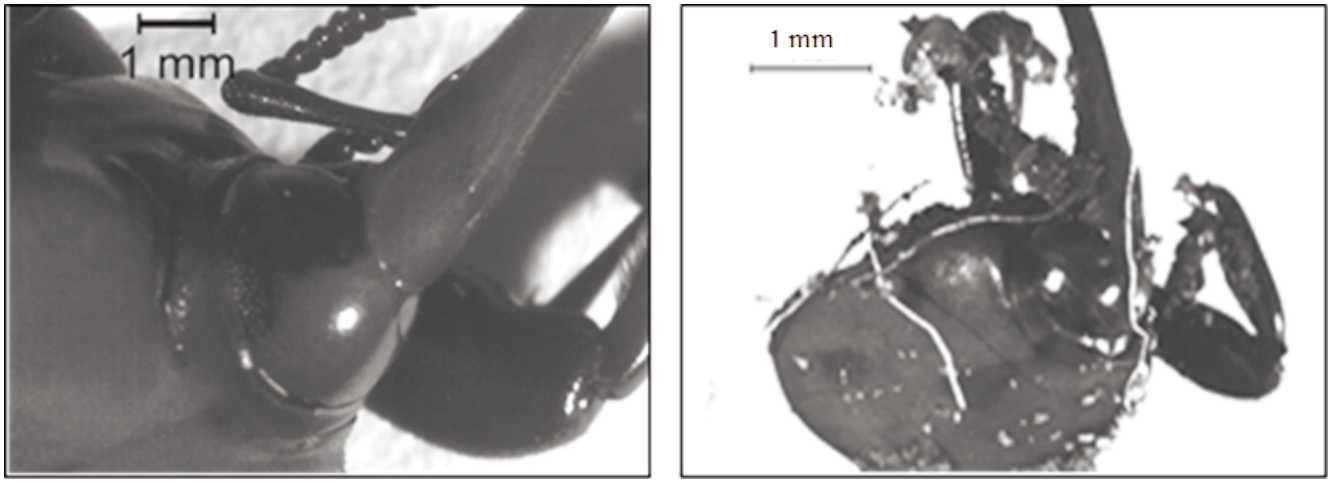

Figure 3. Adult found after 45 days (right) in comparison to normal sized individual.

and infested with larvae. Larvae were obtained in laboratory from eggs laid on pieces of apple by RPW females, reared on apple and grouped into 3 classes as following: less than 0,15 g; from 0,15 g to 0,35 g; from 0,35 to 2 cm of length that is the lowest limit of the size of the chopped material. Each container was infested with 30 larvae, each class of larvae was replicated three times and one container with no larvae was used as control. After infestation, containers were covered with an anti-insect plastic transparent net and kept in climatic chamber in dark conditions. Temperature inside the containers was checked (and temperature control in climatic chamber eventually activated) in order to assure that suitable conditions for larval survival or development were maintained (28°- 32°C). Humidity in the chamber was always close to 100 %.

Since total larval duration in laboratory conditions can range from 70 to 90 dd at 30° C on apple (Cristofaro et al., 2011), or 103 dd and 69 dd at 21°C, respectively on apple and on palm crown (Salama et al., 2009), in order to verify larval survival in our experiment, all the containers were carefully inspected after 45 days. The presence of survived larvae and/or of the eventually developed stages of them (mature larvae, cocoons or adults) was observed.

Machine and work yard description

The wood chipper Farmi CH260 FOREST is constituted by a rotor knife characterized by the ability to adjust the size of the wood chips and the specific allocation of various accessories (Fig. 2) which ensure the correct size and homogeneity of the product. the rotor has the maximum rotational speed of 1000 rpm, has a diameter of 1050 mm and a mass of 240 kg. To avoid the clogging of the machine caused by the compaction of the fragments of palm that adhere to the inner walls of the machine and cause the obstruction, by the chipper has been eliminated a grid which performs the function of retaining the larger pieces of chopped material. The chipper is operated by a tractor 100 kW connected with a drive shaft. The chipper power system is hydraulic and consists of two toothed rollers: the upper roller with greater diameter is installed on a mobile frame with a spring that keeps the roller in contact with the incoming material, ensuring efficient power and high productivity.

The chipping occurs with adjustable knives attached to the rotor by means of screws. Knives are installed into the chipper in a fixed position and participate in the cutting of the material. The maximum size of plant material that can be introduced into the machine is 260 mm,

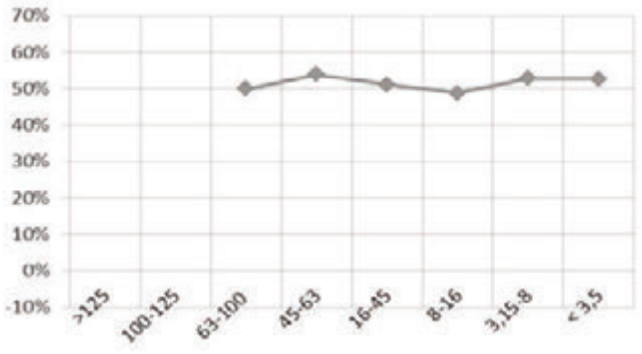

Graph 1. Water content: frequency distribution in classes of wood chips size (at 22 days after felling)

so the stems of palm trees have been previously cut with chainsaw into pieces of appropriate size. Using the machine described chipper is possible to obtain chips with average size between 7 and 25 mm. The resulting material was ejected from the launcher tube and stored in a trailer on the side of the machine.

Results

To allow the machine to perform the work, it was necessary to cut the stems of palm with additional charges for labor.

The distribution in frequency classes of the size of the wood chips shows that over 90% of the sample is in the range between 3.5 and 16 mm. (Fig. 4).

With a mass of about 0.7 t obtained from palm trees, were produced 970 kg of wood chips with a water content of 50% (at 22 days after felling) (Graph 1). The 81.86% of the sample had dimensions of less than 3.5 mm, the 5.22% is in the range between 16 mm and 100 mm, and 0.31% is between 45mm and 100 mm.

A natural increase of the temperature was observed in few days inside all the containers, without any appreciable differences with the control, probably due to the fermentation process of the chopped material. In a week temperature reached a value ranging from 36.9 to 37,1°C. Afterwards a progressive decrease during the experiment was recorded.

When temperature ranged from 22.7 °C to 27.7 °C, it was artificially maintained at about 30 °C.

Results regarding the insect bioassays show that this kind of chopping could be useful for the treatment of stipe and leaves of infested palms destined to disposal sites, avoiding potential risks of re-infestation.

As regard the minuscule adult found, it is known that in unfavorable environments (e.g. unsuitable feeding substrates), the ecdysteroids and JH hormone balance is altered and the chances of untimely metamorphosis processes increases under severe stress conditions (Peri-Mataruga et al., 2006). However, the risk of adult survival and spreading in this form seems very unlikely. Nevertheless, further trials will be set up in order to confirm these results.

Conclusions

The test results show that the chipped material meets the requirements of national and regional legislation. it is possible to enhance the product for direct use in composting or for use as a fuel in a mixture with other waste material (pruning) in the production of thermal energy in small-medium heating systems.

With regard to the quality of work performed, it is observed that the additional operations of cutting of the palm stems represents a further cost increases of chipping.

On a total of 270 individuals, any survived larvae or pupae were found after 45 days from infestation for all the three sized larvae used. However, few hints of very small and empty cocoons were individuated inside the containers infested with the biggest larvae (from 0.35 g to 2 cm of length).

Furthermore, in one of these containers, only a dead minuscule adult was found (Fig. 3). It sized about one third in length (about 1 cm) in comparison to the average of the adults grown on the whole palm.

References

Cristofaro M., Sasso R., Musmeci S., Arnone S., Di Ilio V., De Biase A., Belvedere S., 2011. Primi risultati relativi ad uno studio di fattibilità della tecnica dell'insetto sterile per il controllo di *Rhynchophorus ferrugineus* . XXIII Congresso Nazionale Italiano di Entomologia, Genova 13-16 giugno. http://www.deangeli.bz.it

Perić-Mataruga V., Nenadović V., Ivanović J., 2006. Neurohormones in insect stress: A review. Archives of Biological Sciences, vol. 58, iss. 1, pp. 1-12.

Roversi, 2013, http://sito.entecra.it/portale/cra_progetti.

Salama, H. S. , Zaki, F. N. and Abdel-Razek, A. S., 2009. Ecological and biological studies on the red palm weevil Rhynchophorus ferrugineus (Olivier). Archives Of Phytopathology And Plant Protection, 42: 4, 392 — 399 P. F.

Industrial hemp for biomass production

R. Sausserde, A. Adamovics

Latvia University of Agriculture, Institute of Agrobiotechnology, Republic of Latvia

Abstract

Interest for possibilities of the industrial hemp (Cannabis sativa L.) growing in Latvia is increasing year by year and they are considered as one of the most promising renewable biomass sources to replace non-renewable natural resources for manufacturing of wide range industrial products. The aim of this research was to evaluate of biomass potential of some industrial hemp varieties to be recommended to grow in Latvia and clarify carbon content. The biometric parameters of ten industrial hemp cultivars – 'Bialobrzeskie', 'Futura 75', 'Fedora 17', 'Santhica 27', 'Beniko', 'Ferimon', 'Epsilon 68', 'Tygra', 'Wojko' and 'Uso 31' have been investigated at the Research and Study farm "Peterlauki" of the Latvia University of Agriculture in 2011-2012. The carbon content was determined. The results of investigation show that industrial hemp is promising plant for biomass production in Latvia. Depending on the variety the green over-ground biomass varies from 36 - 54 t ha^{-1} in 2011 and from 48 - 75 t ha^{-1} in 2012. The highest green over-ground biomass was obtained cultivar 'Futura 75' up to 75 t ha^{-1}. The carbon content in hemp stems was found from 41.62 – 45.38 % and it depend on cultivars. Results of investigation of biomass potential of all ten industrial hemp cultivars are presented.

Introduction

The industrial hemp (Cannabis sativa L.) is one of the earliest domesticated and widespread crop all over the world. For many centuries hemp has been cultivated as a source of strong stem fibre and seed oil in Latvia (Ehrensing, 1998). In the 19th century the cultivation of industrial hemp in Europe declined but recently interest has been renewed, for example in Germany, France, the Netherland, the United Kingdom, Spain and Italy, but also elsewhere in the world (Struik et al., 2000). And nowadays industrial hemp has become very important as a crop for biomass production. Environmental concern and recent shortages of wood fibre have renewed interesting hemp as a raw material for a wide range of industrial products including textiles, paper, and composite wood products (Ehrensing, 1998).

It is fast-growing and suitable for Latvia's agro-climate conditions. Latvian hemp sowing areas are registered only in year 2008 and in year 2009 was grown 250 ha. In recent years, the amount of industrial hemp growers and cultivated areas has increased in Latvia and, according to data provided by Association of Industrial Hemp of Latvia, plantations area of hemps is approximately 600 ha in Latvia in 2012. And it means that, interest for possibilities of the hemp growing in Latvia is increasing year by year. And they are considered as one of the most promising renewable biomass sources because it contains the energy which comes from the sun (Adamovi☐s et al., 2012). Through the process of photosynthesis, chlorophyll present in plants absorbs the energy from the sun by converting the carbon-dioxide present in air and water from the ground in carbohydrates.

In Latvia industrial hemp is legally allowed to be grown but the main requirement is that hemp plants should have a low THC (Tetrahydrocannabiol) content (less than 0.2%). The EU common catalogue of varieties of agricultural plant species contains the list with more than 47 industrial hemp varieties (Cannabis sativa..., 2009). And it is difficult to decide which variety from this list could be possible to grow in Latvia with good results and with high biomass yield. The aim of this research was to evaluate of biomass potential of some industrial hemp varieties to be recommended to grow in Latvia and clarify carbon content.

Material and methods

The field trial was carried out in 2011 – 2012 in Research and Study farm "Peterlauki" (56°53'N, 23°71'E) of the Latvia University of Agriculture, in the sod calcareous soils pHKCl 6.7, containing available for plants P 52 mg kg ☐1, K 128 mg kg ☐1, organic matter content 21 to 25 g kg ☐1 in the soil.

There were ten industrial hemp cultivars tested – 'Bialobrzeskie', 'Futura 75', 'Fedora 17', 'Santhica 27', 'Beniko', 'Ferimon', 'Epsilon 68', 'Tygra', 'Wojko' and 'Uso 31'.

Hemp sowing was made by Wintersteiger plot sowing machine in the middle of May. The trial was randomly spaced, triplicate. The plot size 7 m2. Fertilizer application rate – N120P80K112 kg ha^{-1}. Seed rate 50 kg ha^{-1} or average 250 germinate able seeds per 1 m2. In the field rotation, industrial hemp followed previous crop – spring barley. Hemp was harvested by a small mower MF-70 (leaving the stubble of 5 – 8 cm) when the first matured seed appeared.

During both growing seasons the industrial hemp stalk was estimated. Total height of hemp stalk was measured from the soil surface to the tip of plant. No pesticides like insecticides, herbicides, desiccants were used.

The yield of green and dry biomass was evaluated at hemp harvesting time. The main task of research presented here was to evaluate

Correspondence: Rudite Sausserde, Latvia University of Agriculture, Institute of Agrobiotechnology, Republic of Latvia.
E-mail: ruditei@inbox.lv

Key words: hemp, cannabis sativa, ash, carbon

Acknowledgments: the research was supported by the European Regional Development Fund, Agreement No. 2010/0320/2DP/2.1.1.1.0/10/APIA/VIAA/107.

Journal of Agricultural Engineering 2013; XLIV(s1):e123
doi:10.4081/jae.2013.(s1):e123

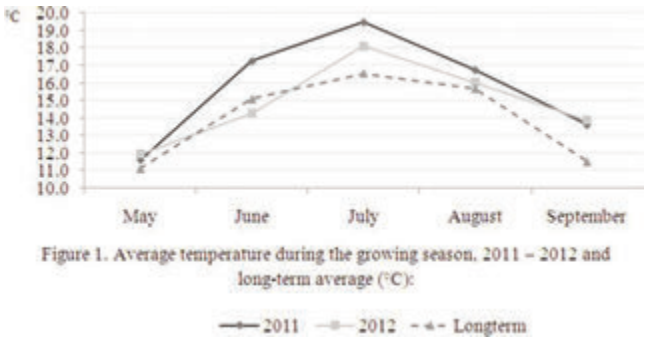

Figure 1. Average temperature during the growing season, 2011 – 2012 and long-term average (°C):

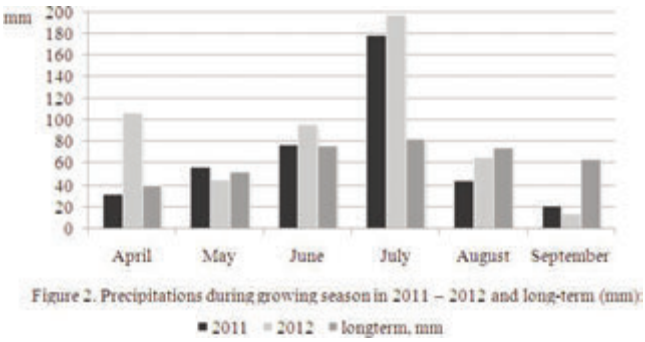

Figure 2. Precipitations during growing season in 2011 – 2012 and long-term (mm):

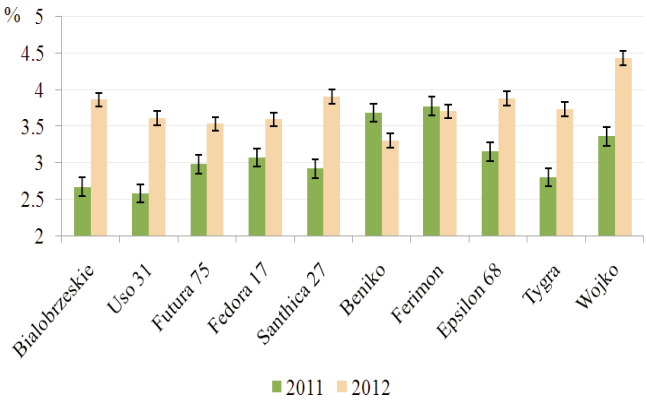

Figure 3. Ash content in hemp of different varieties, %

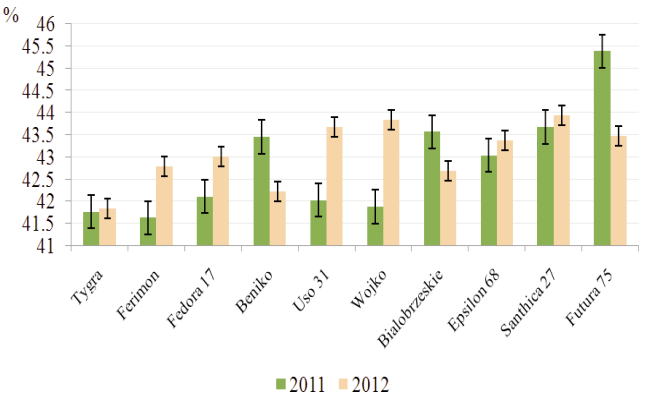

Figure 4. Carbon content in hemp of different varieties, %

biomass potential of ten industrial hemp cultivars under Latvian climatic conditions. The yield of absolutely dry hemp biomass was calculated according to the data of green biomass and its moisture content at harvesting in study years. The carbon content in hemp stem was determined by carbon analyzer Eltra CS-500, which operates on the principles of chromatography. The ash content in hemp stem was determined by a standard method for the rapid ash production method ISO 5984:2002.

Meteorological data as temperature was obtained from Dobele Hydro-meteorological Station (HMS). Precipitations were taken during growing season near to the trials fields in farm Peterlauki. Meteorological conditions during both growing season can be described as good with temperature (Fig. 1) and wet with periodic substantial rainfall (Fig. 2) what was good for hemp growth and development.

A statistical evaluation of the data has been made by ANOVA, variance analysis, the LSD test. Correlation and regression analysis methods were used for data processing.

Results and discussion

Industrial hemp cultivars growth and development is dependent of meteorological conditions during growing period (Struik et al., 2000). Hemp grows best when mean daily temperatures are between 14 °C and 27 °C and it requires abundant moisture throughout the growing season, particularly while young plants are becoming established during the first six weeks of growth (Ehrensing, 1998). According to the data presented in Figure 1 and Figure 2, we can see that meteorological conditions during both trial years were diverse, but both growing seasons were abundant in rainfall which differed only at hemp growing stages and there was good temperature for hemp growth.

According to results, in the years of investigation, the highest stalk length was observed of cultivar 'Bialobrzeskie' (2.63 m) in 2011 and cultivar 'Tygra' (3.06 m) in 2012 (Tab.1). There were significant difference between different cultivars and growing season. The lowest stalk length was observed of cultivar 'Wojko' (1.95 m) in 2011 and cultivar 'Bialobrzeskie' (2.26 m) in 2012.

Statistical evaluation showed that the meteorological conditions during growing season as a factor had an influence on the results of total hemp stalk length.

In 2011, industrial hemp cultivars produced sufficiently high amount of green biomass (Tab.2). Cultivars 'Epsilon 68' and 'Beniko' produced significantly ($p<0.05$) higher amount of green biomass (up to 50 t ha^{-1}) than the other cultivars tested. But in 2012, the green biomass was obtained higher. In this growing season the significantly higher amount of green biomass was obtained cultivar 'Futura 75' (75 t ha^{-1}). The lowest green biomass yield was obtained cultivar 'Uso 31' in 2011.

According to the data of industrial hemp green biomass and amount of plant moisture content at harvesting (it was about 19-45 % in both trial years), the hemp dry biomass yield was calculated. There was significant difference of dry biomass yield between different cultivars in both years. The significantly highest amount of dry biomass yield up to 20 t ha^{-1} was observed from cultivars 'Futura 75' (21.22 t ha^{-1}),

'Beniko' (20.51 t ha^{-1}), 'Wojko' (20.33 t ha^{-1}) and 'Epsilon 68' (20.26 t ha^{-1}) but the lowest – cultivar 'Uso 31' (12.65 t ha^{-1}). In 2012, the significantly highest amount of dry biomass yield was observed from cultivars 'Futura 75' (21.33 t ha^{-1}) and 'Tygra' (20.87 t ha^{-1}) but the lowest from cultivar 'Bialobrzeskie' (11.95 t ha^{-1}). Statistical evaluation showed that the meteorological conditions during growing season as a factor had an influence on the results of total green and dry biomass yield.

The ash content is one of the major qualitative characteristics of biomass. The ash content of all plant sheave must be up to 3%. The ash content should not surpass 5-7% under the conditions of correct stockpile. Nevertheless, the experience shows that the ash content can reach even 20% (Komlajeva et al., 2012). The ash content of hemp cultivars was different and ranged from 2.58 to 3.77 % (Fig.3).

Table 1. Stalk length of industrial hemp varieties

Varieties	Plant stalk length, m		
	2011	2012	Average
Bialobrzeskie	2.63	2.26	2.44
Futura 75	2.54	2.48	2.51
Fedora 17	2.47	2.59	2.53
Santhica 27	2.52	2.66	2.59
Beniko	2.52	2.84	2.68
Ferimon	2.41	2.84	2.63
Epsilon 68	2.50	2.88	2.69
Tygra	2.49	3.06	2.78
Wojko	1.95	2.83	2.39
Uso 31	2.32	2.58	2.45
Average	2.44	2.70	2.57

$LDS_{0.05\ variety} = 0.21$; $LDS_{0.05\ year} = 0.09$; $LDS_{0.05 interaction\ between\ variety\ and\ year} = 0.29$

Carbon is one of the most important products of photosynthesis for biomass production and it is the primary fuel burning element. It has a high caloric value and this accounts for most of the burnt mass (Cars, 2008). According to the research results, there were seen that the carbon content in hemp stems varies from 41.62 – 45.38% in 2011 and from 41.332 – 43.94% in 2012 and it depend on cultivars.

Conclusions

The trial carried out in 2011 – 2012 enables that industrial hemp cultivars tested 'Bialobrzeskie', 'Futura 75', 'Fedora 17', 'Santhica 27', 'Beniko', 'Ferimon', 'Epsilon 68', 'Tygra', 'Wojko' and 'Uso 31' could be successfully grown in Latvia for biomass production. But the highest biomass yield, during both trial years, was obtained from cultivar 'Futura 75'. According to the data we can conclude that the growing season and the selected industrial hemp variety had a significant ($p<0.05$) effect on hemp yield.

According to the results, the ash content was significantly ($p<0.05$) affected by different meteorological conditions during the growing season, but not affected ($p>0.05$) by the selected cultivar.

According to the research results, there were seen that the carbon content in hemp stems varies from 41.62 – 45.38% in 2011 and from 41.332 – 43.94% in 2012 and it depend on cultivars.

References

1. Adamovičs A., Balodis O., Bartušēvičs J., Gaile Z., Komlajeva Ļ., Poiša L., Slepitis J., Straume I., Strikauska S., Višinskis Z. 2012. Enerģētisko augu audzēšanas un izmantošanas tehnoloģijas (Technologies of production and use of production and use of energy crops). In: Atjaunojamā enerģija un tās efektīva izmantošana

Table 2. Biomass yield of industrial hemp varieties, 2011 – 2012

Varieties	Green biomass, t ha^{-1}			Dry biomass, t ha^{-1}		
	2011	2012	Average	2011	2012	Average
Bialobrzeskie	45.80	51.25	48.53	17.15	11.95	14.55
Futura 75	54.56	75.00	64.78	21.22	21.33	21.27
Fedora 17	45.69	57.54	51.61	16.60	18.23	17.42
Santhica 27	47.16	66.43	56.79	19.84	17.39	18.61
Beniko	50.21	48.97	49.59	20.51	19.27	19.89
Ferimon	46.69	52.40	49.55	16.90	18.59	17.75
Epsilon 68	54.13	68.45	61.29	20.26	12.89	16.57
Tygra	44.80	58.83	51.82	18.61	20.87	19.74
Wojko	47.15	59.48	53.32	20.33	19.91	20.12
Uso 31	36.57	51.49	44.03	12.65	17.38	15.01
Average	47.28	58.98	53.13	18.41	17.78	18.09
$LDS_{0.05\ variety}$		10.24			3.45	
$LDS_{0.05\ year}$		4.58			1.54	
$LDS_{0.05 interaction\ between\ variety\ and\ year}$		14.49			4.88	
$\eta 2\%_{variety}$ (impact rate)		26.7 ($p<0.05$)			36.3 ($p<0.05$)	
$\eta 2\%_{year}$ (impact rate)		26.2 ($p<0.05$)			5.9 ($p<0.05$)	
$\eta 2\%_{interaction\ between\ year\ and\ variety}$ (impact rate)		7.6 ($p>0.05$)			16.8 ($p>0.05$)	

Latvijā (Renewable energy and its effective use in Latvia), Jelgava, pp 88 – 91. (in Latvian).
2. Cannabis sativa L. Hemp. 2009. p 199 – 200. Available at: http://eur-lex.europa.eu, 21 April, 2013.
3. Cars, A. 2008. Energoresursi (Energy resources). SIA Baltic Communication Partners, p 102 (in Latvian).
4. Ehrensing D.T. 1998. Feasibility of Industrial Hemp Production in the United States Pacific Northwest. Oregon State Universit. Available at: www.extension.oregonstate.edu/catalog/html/sb/sb681/, 2 April, 2013.
5. Komlajeva L., Adamovics A., Poisa L. 2012. Comparison of different energy crops for solid fuel production in Latvia. Renewable Energy and Energy efficiency, Growing and processing technologies of energy crops. pp 45 – 50.
6. Struik P.C., Amaducci S., Bullard M.J., Stutterheim N.C., Venturi G., Cromack H.T.H. 2000. Agronomy of fibre hemp (Cannabis sativa L.) in Europe. An International Journal Industrial Crops and Products, 11, pp107 – 118.

Mechanized recovery of olive pruning residues: ash contamination and harvesting losses

A. Assirelli,[1] A. Acampora,[1] S. Croce,[1] R. Spinelli,[2] E. Santangelo,[1] L. Pari[1]

[1]Consiglio per la ricerca e la sperimentazione in agricoltura, Unità di Ricerca per l'Ingegneria Agraria, Monterotondo (Roma), Italy; [2]CNR IVALSA, Sesto Fiorentino, Firenze, Italy

Abstract

Agricultural residues represent an important source of biomass for energy. Among the available biomass suitable for energy and available in Italy, pruning represents about the 20% of the total. About 1.184 million of hectares are planted with olive trees; the pruning residues coming from these plantations represent a wide source of biomass at National level. The authors tested six commercial pruning harvesters to determine harvesting losses and product contamination when recovering pruning residues. All harvesters used a mechanical pick-up to collect the residues and a shredder to reduce them into chips. Three different pick-up settings were tested and namely: 1 cm above ground level, manufacturer's specification and 3 cm above ground level. Ash content in the shredded material was taken as a measure of contamination: the uncontaminated branch material collected directly from the trees had a value of 3.5%, whereas in shredded residues varied between 4.5% and over 5.5%, for the shortest and the longest distance between the pick-up and the soil surface, respectively. Harvesting losses were slightly, but significantly, related to pick-up setting, and mainly depended on machine type. Both machines have shown a good quality of the work performed and the results obtained indicates that the work phases could be simplified in order to reduce both the time of use and the harvesting costs.

Introduction

Biomass represents the fourth largest source of energy (after coal, oil and natural gas) and already satisfies about 14% of the energy needs of human society (Parikka, 2004). Large amounts of wood biomass can be obtained from pruning of fruit orchards in the Mediterranean region (FAO, 1997). In Italy, olive groves cover about 1.1 million of hectares, of which about one-third are located in southeastern Italy (Istat, 2001). In Puglia region, these orchards could yield over 800,000 tonnes of dry biomass per year. Nevertheless, the current practice is to dispose of pruning residues through burning or mulching, with no direct economic benefit (Askew and Holmes, 2001). However, research has intensified in recent years, drawing more attention on pruning residue as a possible source of energy (Dalla Marta et al., 2010; Masera et al., 2006). More specifically, several studies have confirmed that agricultural residues may be a suitable source of biomass for the production of thermal and electrical energy (Caputo et al., 2003; Kuiper et al., 1998; Malaspina et al., 1996; Mussatto et al., 2006).

The market offers today various types of machines dedicated to the recovery of pruning residues and their conversion into a biomass product (Magagnotti et al., 2013; Recchia et al., 2009). These implements have received considerable interest and their performances have been documented in several studies, especially concerning the productivity and cost. Much less is known about harvesting losses and product contamination, above all when working on olive orchards (Spinelli et al., 2012; Spinelli et al., 2010). Losses and contamination are probably related, and may in part depend on the machine settings. Losses can be reduced by lowering the pickup device, in order to catch the residues closer to the ground. Moreover, working too close to the ground product may increase soil contamination with soil particles.

The purpose of this study was to determine harvesting losses and product contamination achieved with six commercial machines, under three different settings: standard pick-up height as conventionally set by the manufacturer; pick-up working 1 cm above ground level; pick-up working 3 cm above ground level.

Material and methods

The work took place in Castrigliano de' Greci, southeastern Italy (40°10'32" North, 18°19'11" East). The testing area was a 0.45 ha olive tree plantation, 40 years old and established at a 7.5 x 7 m spacing. Trees had not been pruned for several years, leading to a very large residue yield. Six commercial shredding units were compared and for each (Table 1) three different pick-up settings were considered: standard height set by the manufacturer (setting B); working height 1 cm above ground level (setting A); working height 3 cm above ground level (setting C). Each treatment was replicated three times for each machine, for a total of 54 replications.

In order to evaluate the yield of pruning residues, 12 test windrow were analyzed:

all the residues present in 48 sample areas (1 x 1.5 m) randomly selected has been collected and weighed. Residue was character-

Correspondence: A. Assirelli, CRA – ING, via della Pascolare 16, 00016 Monterotondo (RM), Italy.
Tel. +39.06.90675211 - Fax: +39.06.90625591
E-mail: alberto.assirelli@entecra.it

Key words: biomass, energy, wood, particle size, ash, shredding.

Acknowledgments: the authors would like to thank the role of the "FAESI" Project (Filiere Agro Energetiche nel Sud Italia) for funding the study.

Journal of Agricultural Engineering 2013; XLIV(s1):e123
doi:10.4081/jae.2013.(s1):e123

ized by measuring the diameter and length of individual branches in the sample plots. Harvesting losses were estimated by repeating the same procedure after sampling, this time on 4 sample plots per machine and setting (72 samples). The moisture content was determined on three 250 g samples per plot, according to European standards UNI-EN 14774-1: 2009. Ash content was taken as a measure of contamination and determined on 1.5 kg samples, according to European standard CEN/TS 14775: 2010. Three samples were collected directly from the branches before harvesting, in order to determine a reference ash content before the eventual contamination caused by recovery. Three samples for each treatment (54 samples) were collected from the shredded material accumulated on the sideline.

The study has included the particle size distribution and bulk density. These parameters were determined for one settings only, hypothesizing that product size and density depend by machine characteristics and not by pick-up settings. Bulk density was determined according to European standard UNI-EN 15103: 2009. Particle size distribution was determined on four 4-L samples per machine. Each sample was weighed and the material was divided in three dimensional classes (<5cm, among 5 cm and 10 cm, >10cm). These dimensional classes were weighed again for defining the percent incidence of each class on total sample weight.

The distribution of the data collected was plotted and checked for normality. If complying with normality, the differences between the treatments were tested using analysis of variance. When the data distribution did not accord to normality, the arcsine transformation was used for their normalization. The data were analyzed statistically using Statview for Windows.

Results

All test machines adopted the same working principles. Differences were mainly in some structural details, such as the number of teeth on the pick-up device, or of hammers on the shredder.

The overall amount of pruning residues detected was equal to 14 green tons per hectare. Moisture content at harvest was 22%, defining a good quality fuel. The six tested machines have given a different shredded product, in terms of particle size distribution (Figure 1) and bulk density (Table 2). The Berti and Omat harvesters produced a larger amount of oversize material compared to all other machines, while the Sgarbi, Tierre and the Facma harvesters made much smaller particles, with a low proportion of oversize elements and a high incidence of fines. The length of the shredded material is important for the feeding system of the boilers because, if employing screw systems, a product with particles greater than 10 cm can determine problems of flooding or blockages in the system.

As shown in the table 2, the bulk density of the shredded product was significantly higher for the Sgarbi and the Nobili shredder. The higher value of bulk density relative to the product of the Nobili machine could be justified because the TPR-CV 145 is the only tested model equipped with a system that discharge the chips, at high pressure, in a specific trailer that follows the machine along the working line during the field operations. Respect to the systems used by the other machines, which present their own collection bin, the high pres-

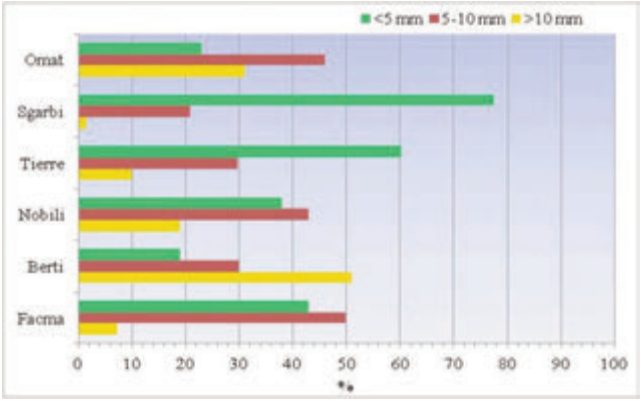

Figure 1. particle size distribution (%) of the shredded olive pruning residues.

Table 1: characteristics of the tested machines.

Make	Tierre	Omat	Nobili	Sgarbi	Facma	Berti
Model	Futura 160	TSB 1900	TRP-CV 145	TR-RAC	Comby TR 200	Piker-Kargo 200
Work width	1.566	1.900	1.450	1.996	1.995	2.000
Diameter pick-up cylinder	127	140	153	Na	95	127
Teeth on pick-up	38	42	32	Na	72	33
Teeth lengh	159	170	156	Na	160	150
Distance between teeth	72	170	170	Na	100	60
Diameter of shredder (mm)	193	480	465	168	229	410
Hammers on shredder (n)	28	22	20	20	27	36

Table 2: bulk density of the shredded olive pruning residues.

	Tierre	Omat	Nobili	Sgarbi	Facma	Berti
Bulk density (Kg m-3)	128	119	174	158	134	124

sure system of the TPR-CV 145 could determine a higher compaction of the shredded product in the trailer. That would explain the higher quantity of product per m3.

The Sgarbi machine produced relatively dense loads, which was likely due to the virtual absence of oversize particles (>10 cm long). In contrast, long fragments tended to structure, increasing the bulk volume of loads (Jensen et al., 2004).

Percent harvesting losses were very low but comparable to those reported in previous studies (Magagnotti et al., 2013). Mean harvesting losses varied from 0.4 to 6% (Table 3), and were significantly related to both machine type and pick-up settings (Table 4). Losses were lowest for the Berti, Omat and Facma harvesters, and highest for the Nobili, Sgarbi and Tierre machines. Machine type had a much stronger effect on losses than pick-up setting. Pick-up teeth number and length were both tested as additional factors in determining harvesting losses, but they did not result to have any significant effect. Attention was then directed to work width, since two of the machines incurring the highest losses also had a reduced work width. It is conceivable that a main cause for high losses could be the mismatch between windrow width and machine work width. In fact, narrower harvesters may have missed the residues placed at the windrow edges. When pruning yield is elevated is difficult to build the narrow swaths, in these conditions the machines should offer the largest possible work width.

Pruning residue was contaminated during recovery, as indicated by the higher ash content of shredded material compared to branch material collected directly from the trees. Mean ash content for the uncontaminated branch material was 3.5%, and was significantly lower compared to all other treatments. Ash content ranged from an minimum of 4% to a maximum of 6%. Mean values varied between 4.6% and 5.7% (Table 5). Ash content was significantly associated to both machine type and pick-up settings, this one having the strongest effect (Table 4). Raising pick-up height to 3 cm above ground level allowed reducing ash content by up to 1% point, compared to working with the pick-up at 1 cm above ground level.

Contamination was effectively reduced by increasing the distance between the pick-up device and the soil surface. Increasing pick-up height also resulted in an increase of harvesting losses, but the effect of pick-up setting on product recovery was much lower than the effect of machine design. In contrast, machine design only had a secondary effect on contamination.

Conclusions

Numerous studies have demonstrated that it is possible to recover and utilize pruning for the production of energy, ensuring economic and environmental sustainability of the supply chain. Regular pruning of olive groves generates large amounts of wood biomass, which can be recovered and processed with commercial pruning harvesters.

Effective recovery implies minimizing product losses and product contamination. The former is mainly related to machine type, the latter to pick-up setting. Product losses might be reduced by selecting

Table 3: harvesting losses (%) as a function of machine type and a pick-up setting (arcsine).

	Height setting		
	A	B	C
Tierre	2.09	3.05	4.01
Omat	0.8	1.1	1.6
Nobili	3.2	3.9	4.2
Sgarbi	4,6	5.4	6
Facma	1	1.3	1.9
Berti	0.4	0.6	0.9

Table 5: percent ash content as a function of machine type and pick-up height setting.

	Height setting		
	A	B	C
Tierre	5.2	4.8	4.7
Omat	Na	4.4	Na
Nobili	5.7	5.3	4.6
Sgarbi	5.2	4.8	4.9
Facma	5.1	5	4.9
Berti	5.6	5.6	4.5

Table 4: result of the analysis of variance for harvesting loss and ash content.

Effect	DF	SS	%	F-value	P-value	Power
Harvesting loss						
Setting	2	0.014	5.9	188.18	<0.0001	1.00
Machine	5	0.22	93.1	1225.12	<0.0001	1.00
Interaction	10	2.79*10-4	0.1	0.78	0.6496	0.36
Residual	54	0.002	0.8			
Ash content						
Setting	2	3.292	43.4	26.27	<0.0001	1.00
Machine	4	0.677	8.9	2.7	0.0493	0.68
Interaction	8	1.739	22.9	3.47	0.006	94.00
Residual	30	1.88	24.8			

for the harvesting loss, the analysis was conducted on arcsine-transformed data; % = incidence of the sum of squares for the individual effect over the total Sum of Squares.

appropriate equipment, offering a good match between work width and expected windrow width. The lowering of contamination level can be achieved by increasing the distance between the soil surface and the machine pick-up, to avoid raking into the soil.

References

Askew M.F., Holmes C. The potential for biomass and energy crops in agriculture in Europe, in land use, policy and rural economy terms. Aspects Appl Biol 2001; 65: 365-374.

Caputo A., Scacchia F., Pelagagge P. Disposal of by-products on olive oil industry: waste-to-energy solutions. Appl Therm Eng 2003; 23: 197-214.

Dalla Marta A., Mancini M., Ferrise R., Bindi M., Orlandini S. Energy crops for biofuel production: analysis of the potential in Tuscany. Biomass Bioenerg 2010; 34: 1041-1052.

FAO. The role of wood energy in Europe and OECD, WETT e wood energy today for tomorrow. Rome: FOPW, Forestry Department; 1997.

ISTAT. V. Censimento Generale dell'Agricoltura. Roma; 2001.

Jensen P., Mattsson J.E., Kofman P.D., Klausner A. Tendency of wood fuels from whole trees, logging residues and roundwood to bridge over openings. Biomass Bioenerg 2004; 26: 107-113.

Kuiper L., Sikkema R., Stolp J. Establishment needs for short rotation forestry in the EU to meet the goals of the commission's white paper on renewable energy. Biomass Bioenerg 1998; 15: 451-456.

Magagnotti N., Pari L., Picchi G., Spinelli R. Technology alternatives for tapping the pruning residue resource. Bioresour Technol 2013; 128: 697-702.

Malaspina F., Cellamare C., Sante L., Tilche A. Anaerobic treatment of cheese whey with a downflow- upflow hybrid reactor. Bioresour Technol 1996; 55: 131-139.

Masera O., Ghilardi A., Drigo R., Trossero M. WISDOM: a GIS-based supply demand mapping tool for wood fuel management. Biomass Bioenerg 2006; 30: 618-637.

Mussatto S., Dragone G., Roberto I. Brewers' spent grain: generation, characteristics and potential applications. J Cereal Sci 2006; 43: 1-14.

Parikka M. Global biomass fuel resources. Biomass Bioenerg 2004; 27: 613-620.

Recchia L., Daou M., Rimediotti M., Cini E., Vieri M. New shredding machine for re cycling pruning residuals. Biomass Bioenerg 2009; 33: 149-154.

Spinelli R., Picchi G. Industrial harvesting of olive tree pruning residue for energy biomass. Bioresour Technol 2010; 101: 730-735.

Spinelli R., Nati C., Pari L., Mescalchin E., Magagnotti N. Production and quality of biomass fuels from mechanized collection and processing of vineyard pruning residues. Appl Energ 2012; 89: 374-379.

A GIS approach for the quantification of forest and agricultural biomass in the Basilicata region

D. Statuto, A. Tortora, P. Picuno

University of Basilicata - SAFE School of Agriculture, Forestry, Food and Environmental Sciences, Potenza, Italy

Abstract

In this paper the attention has been focused on the energy from biomass by-product, including forest biomass and agricultural production, waste and other sources of renewable energy, available in the Basilicata Region. In order to determine the quantity of extractable biomass from the forests of the region data from plans for forest management were used. These data were imported in a Geographic Information System, in order to determine in which part of the Region there is the possibility to find greater quantity of biomass. As for the determination of the quantities of agricultural biomass, the energy crops and the agricultural waste (such as crop residues, grass cuttings, pruning, manure, waste coming from agro-food industries, etc.) were considered too. The reuse and exploitation of these wastes, while contributing to the solution of problems related to their disposal, promote their recovery as a primary source of energy. Once estimated the annual amount of biomass, the percentage of the annual energy contribution which this kind of by-product is able to ensure was determined; this renewable energy source may therefore significantly contribute to the development of the agro-forestry sector.

Introduction

Under the framework of a general analysis that has focused the attention on the energetic vocationality in the Basilicata Region (Statuto et al., 2012), in this paper the analysis especially for what concerns agricultural and forest biomass has been deepened. According with the results that were obtained so far, it was possible to notice that the energy generated from wind and solar source is able, in the regional context, to provide an extremely high potential compared with the biomass analyzed (Hoesen et al., 2010), but both these two renewable sources could not be felt as an important tool for the revitalization and the development of the agricultural and forestry sector (Statuto et al., 2012). So, while retaining as a study area the whole region, the attention was here focused on biomass only as an alternative energy source, including agricultural waste of various origin and biomass arising from the use and maintenance of forests (Yoshioka et al., 2011). This biomass, despite expressing an energy potential much lower than wind and solar power, if properly used could anyway reveal as an important energetic source being able, at the same time, to solve the environmental problems associated with their disposal.

The different biomass here considered are:

- Energy from agricultural biomass: energy derived by crops as Switchgrass pruning residues, agro-food industries residues (marc and exhausted pomace), animal manure;
- Energy from forest biomass, according with data of the forest management plans in the Basilicata Region.

Correspondence: Dina Statuto, University of Basilicata - SAFE School of Agriculture, Forestry, Food and Environmental Sciences, Potenza, Italy

Key words: Renewable Energy, GIS, Forestry Biomass, Agricultural Biomass.

Contributions: the authors contributed equally.

Conflict of interests: the authors declare no potential conflict of interest.

Journal of Agricultural Engineering 2013; XLIV(s1):e125
doi:10.4081/jae.2013.(s1):e125

Material and methods

Study area

The study area consists of the entire regional land. This area, thanks to the morphological and land cover characteristics, can be considered as a good source of renewable energy. As for the energy resulting from agricultural biomass, it was necessary to consider all areas that could potentially be used in the different energy sources. Then, for the entire region, the data of agricultural crops, arable crops, woody crops, breeding and industries processing agricultural products were considered. Particularly, the forest heritage of the Basilicata Region is consistent and in good vegetative conditions, its mapping is entrusted to the Regional Forest Map, while the proper management is entrusted to the forest management plans.

Spatial data

The analysis was performed on a territorial level for all the different types of renewable energy analyzed. The determination of the land suitability to cultivation of energy crops was carried out by evaluating the intrinsic characteristics of the area such as: slope, aspect, land use, in relation to physiological demanding of the considered crop. The input data originates from the Digital Terrain Model and analysis of the vegetation cover. From a territorial basis, only the agricultural areas that complying with specific characteristics (Yoshioka et al., 2011) were considered. Data on woody crops, such as grapevines, olive trees and other tree crops, from which it is possible to obtain pruning residuals, were obtained by statistic information at municipality level (ISTAT, 2011/a, ISTAT, 2011/b).

The same input map was used both for breeding and for the agro-food industries residuals.

Table 1: Classification of diagnostic criteria for territory of Switchgrass

SWITCHGRASS									
Drainage		Weaving (class)		CaCO3		pH		Rainfall (mm) (Apr-Oct)	
weight	0,15	weight	0,05	weight	0,05	weight	0,2	weight	0,4
	Index		Index		Index		Index		Index
No	0	Clay - sandy clay - silty clay	80	Low	100	3 - 4,4	40	100-200	50
Slow	0	Clay loam - silt loam	100	Middle	40	4,5 - 5,5	80	200-300	70
Medium	70	Sandy loam	100	High	10	5,6 - 6,5	100	>300	80
Balanced	100	Sandy clay loam - silty clay loam	90	Very High	0	6,6 - 7,6	80		
Quick	90	Sand - loamy sand	95			7,7 - 8,5	40		
Very rapid	70					8,6 - 9,0	0		

In the forest biomass context, as a territorial unit, the are covered by some previous aggregation of Municipalities – so-called, "Comunità Montane" – were assumed, since the forest management plans are still currently referred to their territories.

Elaborations

Different GIS elaborations were performed with the aim to evaluate the energy suitability in the different territorial levels about the thermal and electric potential of the different energy types, such as the agricultural biomass, resulting from energy crops, pruning residues, agro-food industries residues (marc and exhausted pomace), manures from breeding, and forest biomass, obtained from the maintenance and proper management of the woods in the Region.

Energy from biomass obtained by energy crops

In order to assess the adaptability of the area for cultivation of a plant species suitable for the production of biomass, both the characteristics of the territory and the suitable factors for the production of the species were analyzed. As the reference culture the switchgrass (Panicum virgatum L.) was taken in consideration. The Panicum virgatum is a herbaceous rhizomatous perennial plant, is drought-resistant, tolerant to salinity and acidity; it has demonstrated a good capacity to control the erosion processes too. It adapts to different types of soil, with good drainage and pH between 4.5 and 7.6. (Tenerelli P., 2008). Unlike most other perennial species, it's renewed by sowing. In order to evaluate the suitability of this crop to the territory of the Basilicata Region, the areas defined according with the statistical information as "non-irrigated arable land" with a slope less than 20% were considered.

Furthermore, a series of soil, climatic and environmental parameters were analyzed; their values have been standardized by attributing an index that expresses the limitation factor (from the worst = 0 - to the best = 100). For each diagnostic feature a weight has been assigned, ranging from 0 to 1, basing on the significance of the parameter as a limiting factor for the species. The different parameters classified according with the requirements of the species are shown in table 1.

Once the indices and weights assigned to the various diagnostic criteria, a weighted combination of the different parameters through appropriate functions of Raster Calculator was performed.

From the combination of parameters it has been possible therefore to identify the areas potentially suitable for cultivation of switchgrass; the total area in the region that was calculated amounts to about 259.000 ha. The production of switchgrass that was calculated is about 10-20 tons per hectare, while the yields of dry matter per hectare reach 11 tons per hectare.

Energy from biomass obtained by pruning residues

The crop residues have intrinsic characteristics that make them different from the main products, both for composition of the dry matter, for Lower Calorific Power (LCP) and for the water content at the time of collection. On the basis of an analysis carried out at national level, considering the whole Italian territory, it may be reasonable to consider that the effective availability of fruit trees pruning destined to energy use, varies between 45 to 50% of the total amount of residues produced (ENAMA, 2011). The amount of pruning residues per hectare was therefore estimated by considering a coefficient able to quantify the unit residues per hectare of pruning (Table 2). According with the data resulting from the national context, for the determination of the amount of extractable biomass from residues, only 50% of the total of the pruning scraps has been considered.

The analysis was conducted on a municipal level, considering the data of land use resulting from the 5th General Census of Agriculture (ISTAT, 2010).

Table 2: Pruning residues

Crop	Area (ha) (%)	Unit residues of pruning[t/ha*y]	Total residues of Pruning [t/y]
Grapevine	5626	4,4	24754
Olive Tree	45744	3	137232
Wood Arboriculture	2884	4	11536

Table 3: estimation of scraps from olives processing

Olive varieties	Olive Production (t/ha)	Area (ha)	Olive Production (t)	Virgin Pomace (t)	Exhausted Pomace (t)
Vulture	8	6.815	54.520	16.356	8.178
Maiatica	10	38.928	389.280	116.784	58.392

Table 4: Estimation of energetic potential for various energetic sources treated

Energetic Crops: Switchgrass					
Total Production (t/ha)	D.M. Production (t/ha)	L.C.P (GJ/t)	Energetic Density (MWh/ha)	Potentially Suited Territory (ha)	Electrical Potential (MWh/y)
15	11	15,2	46,31	258.922	11.991.917

Pruning residues: olive tree, grapevine, wood arboriculture					
Crop	Total pruning residues [t/y]	Availability residues (50% of the total (t/y))	L.C.P (kWh/kg)	Thermal Potential (MWh/y)	Electrical Potential (MWh/y)
Grapevine	24754	12.377	4	49.508	18.318
Olive Tree	137232	68.616	4	274.464	101.551
Wood	11536	5.768	4	23.072	8.537
					128.406

Residues by agro-industrial byproducts					
Residue	Total residues [t/y]	Usable residues (50% of the totale (t/y))	L.C.P (kWh/kg)	Thermal Potential (MWh/y)	Electrical Potential (MWh/y)
Exhausted pomace	133.140	66.570	4	266.280	98.524
Exhausted marc	10.352	5.176	3,5	18.116	6.703
					105.227

Manures				
Breeding farms	Effluent Coeff.	Livestock Units	Thermal Potential (MWh/y)	Electrical Potential (MWh/y)
Pigs	0.035	84.387	2.953	1.092
Oxes	1,441	90.602	130.557	48.306
				49.398

Forest Biomass					
Amount of wood to taken (m^3)	Volume (t/m3)	Total of available biomass (t/y)	L.C.P (kWh/kg)	Thermal Potential (MWh/y)	Electrical Potential (MWh/y)
669.231	0,7	468.461	4,4	2.944.616	1.089.508
		Total			13.364.456

Energy from biomass obtained by agro-industrial byproducts

Concerning the agro-food industry, it is possible to identify as significant residues for energy purposes those deriving from the olive oil industry, the exhausted pomace, and those arising by the alcoholic grapevine/wine industry, exhausted marcs.

The main by-products of the oil industry are made from pomace and vegetation water. In the absence of homogenous data about the regional production capacities of the olive oil mills and the real amount of pressed olives, an estimation of process residues was carried out in an indirect manner, starting from the production of olives for industrial use. Starting from the data concerning the average production of olive oil, broken down by geographical area according with the product specification, and considering the spatial data deriving from the Agriculture Census (ISTAT, 2011), the average annual quantity of virgin pomace was calculated as about 30% of the total olive production), and then an estimation of the exhausted pomace was obtained as equal to approximately 50% of virgin pomace (Table 3).

Similarly, the amount of exhausted marcs usable for energy purposes was determined (ENAMA, 2011). Assuming an annual production of about 20 t/ha of grapes and calculating the part of the territory dedicated to the cultivation of vineyards, the amount of extractable exhausted marcs is equal to 4.6% of the production of wine grapes that means, for the entire regional territory, a production of about 5176 t/y.

Energy from biomass obtained by manures

For the evaluation of primary energy obtainable from livestock, in this potential evaluation only the manure produced by the intensive breeding of oxes and pigs have been considered, as other types of farming all over the regional land do not use permanent shelters for the animals (Provolo G., 2005). The total amount of manure per year was so obtained by multiplying the average amount of sewage or manure produced by each animal for the total number of animals present (ISTAT, 2011/b) in the municipality of reference.

The total production of biogas, by type of dejection and animal species, can be calculated with the following formula (Provincia di Latina, 2008)

$$BP=DA \bullet DM \bullet OM \bullet BMP \quad [I]$$

where:
- BP [m^3/y] = Biogas Production
- DA [t] = Dejection amount
- DM [%] = Dry matter
- OM [% di DM]= Organic matter
- BMP [m^3/t] = Biogas Maximum Production = Biogas Yield

The equivalent thermal energy deriving from all this scraps has been calculated without taking into account the different efficiencies of combustion, but only basing on the lower calorific power of the biogas.

Energy by forest biomass

The determination of forest biomass usable for energy purposes was estimated considering the forest management plans of the Basilicata Region with territorial reference to the "Comunità Montane", a previous form of aggregation among different Municipalities that were governing the forest utilizations with a significant environmental importance. Considering the amount of wood obtainable from forests of each "Comunità Montana" and the average

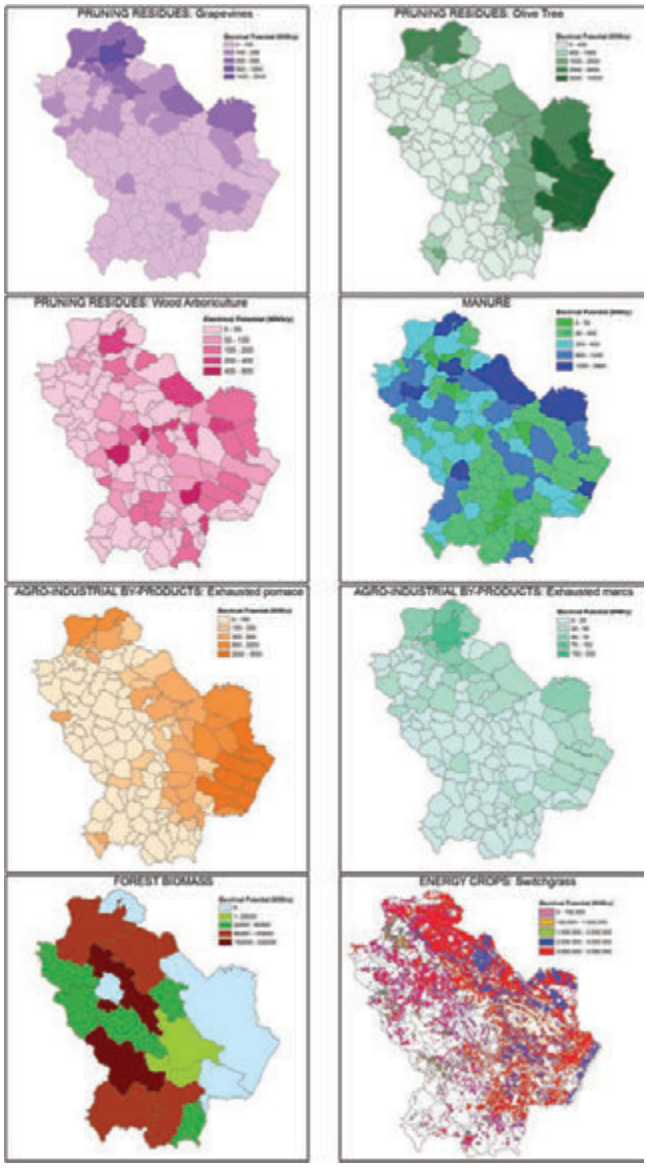

Figure 1. Estimation of Electrical Potential

volume of the different species (0.7 t/m3), the amount of available biomass was estimated as:

TAB=TW*V [II]

- TAB [ton of available dry matter] = Total Available Biomass
- TW [m^3] = Total of Wood that could be obtained from the forest
- V [m^3/t]= Volume relating to each species and derived from tables of volume.

Results

From spatial analysis that the conducted it is clear that the regional land, thanks to its morphological characteristics and to the way of management of the agricultural and forestry activities, can ensure a considerable amount of renewable energy, that is a view to safeguarding the environment and the natural resources (Kinoshita et al.,2009). The estimation of the potential energy resulting from the switchgrass cultivation was determined by considering a LCP average of 15.2 GJ/t and a conversion factor of 1 GJ equal to 0,277 MWh

DMP* LCP*0,277=ED [III]

ED *PST=EP [IV]

where:

- DMP [t/y] = Dry Matter Production
- LCP [GJ/t] = Lower Calorific Power of Switchgrass: expressed in
- ED [MWh/y] = Energetic Density: expressed in
- PST [ha]= potentially suited Territory:
-EP [MWh/y] = Electrical Potential

Assuming a value for the lower calorific power of biomass equal to 4 KWh/kg, the thermal energy equivalent resulting from the enhancement of pruning residues for energy purposes was calculated. The estimation of the potential resulting from the enhancement, for energy purposes, of the agri-food industries scraps was made taking into account a LCP equal to 4 kWh/kg for exhausted pomace and equal to 3,5 kWh/kg for the exhausted marcs (Provincia di Latina, 2008). In estimating the potential arising from the breeding, it has been considered an LCP of biogas equal to 5,3 kWh/Nm^3 (Provincia di Latina, 2008), while for the forest biomass an overall average LCP equal to 4.4 kWh/kg has been used. For the different energetic sources, the energetic electrical equivalent has been estimated considering an efficiency of electricity generation of the electrical Italian mix equal to 37% (Provincia di Latina, 2008).

The results of the estimated productivity are shown in table 4.

Discussion

The values summarized in Table 4 show a significant imbalance between the different energy sources treated. In particular, the main significant aspect seems to be the remarkable electrical potential obtainable from energy crops, in particular the switchgrass (reference culture treated), estimated to be about 12,000 GWh/y. Another important energetic source could be represented by the forest biomass obtainable according with the forest management plans, the estimated potential exceed values of 1,000 GWh/y. In terms of electric potential, the enhancement, for energy pourpose, of agricultural crops, agri-food industries and farms scraps appears to be less effective. Their recovery for energy purposes, however, could be very important since it allows also to the contribution in solving the crucial environmental problem connected with their disposal. The estimated total electric potential for the entire region was therefore approximately calculated into 13,364 GWh/year, a quantity much higher than the total regional energy needs, that was estimated by the Energy- Environmental Plan (Year 2020) into about 3,800 GWh/y.

Conclusions

The objective of this work was to estimate the potential of Basilicata region with reference to the energy capacity obtainable from the enhancement of agricultural and forest biomass (Figure 1). This theme will fit into the objectives that the European Union has set for the year 2020, in particular: a reduction of 20% in emissions of greenhouse gases, an increase up to 20% in the energy saving and consumption of renewable energy sources. From the performed analysis it is possible to note that the energy potential of forest biomass and that

resulting from energy crops is well above the estimation of the expected regional energy needs for the year 2020. Furthermore, the enhancement of agro-industrial residues, although being products with a limited energy potential, will fit into the goals of the general energy efficient conservation and sustainable protection of the natural resources. Taking into account that, given the potential pollutants, these residues pose serious problems for their disposal, and are concentrated in well-defined areas (many of them dictated by the production disciplinary), it is easy to imagine that the potentially obtainable energy could give a strong impetus to the entire agro-forestry district, strongly highlighting the eco-sustainability of this sector also in the production of energy.

References

Consiglio Regionale di Basilicata, Dipartimento Attività Produttive, Politiche dell'Impresa, Innovazione Tecnologica - Ufficio Energia, (2010). PIANO DI INDIRIZZO ENERGETICO AMBIENTALE REGIONALE. [In Italian].

CRA, Consiglio per la Ricerca e la Sperimentazione in Agricoltura, (2006). Energie da biomasse agricole e forestali: miglioramento ed integrazione delle filiere dei biocarburanti e della fibra per la produzione di energia elettrica e termica - Bioenergie. [In Italian].

Disciplinary Production of "Olio extravergine di oliva "MAJATICA" a denominazione di origine protetta (DOP). [In Italian].

Disciplinary Production of OLIO EXTRAVERGINE DI OLIVA "VULTURE" A DENOMINAZIONE DI ORIGINE PROTETTA. [In Italian].

ENAMA, Ente nazionale per la Meccanizzazione Agricola (2011). Biomasse ed Energia. [In Italian].

ENEA (Italian National Agency for New Technologies, Energy and Sustainable Economic Development) Ente per le Nuove tecnologie, l'Energia e l'Ambiente, (2009). Analisi e stima quantitativa della potenzialità di produzione energetica da biomassa digeribile a livello regionale. Studio e sviluppo di un modello per unità energetiche. [In Italian].

INEA Istituto Nazionale di Economia Agraria, - Sede Regionale per la Basilicata, (2006). Carta Forestale della Basilicata. [In Italian].

ISTAT (Italian National Institute for Statistic). (2011). 6° Censimento Generale dell'Agricoltura, - Utilizzazione del terreno dell'Unità Agricola - livello comunale, ISTAT, Roma, Italy [In Italian]

ISTAT (Italian National Institute for Statistic). 2011. 6° Censimento Generale dell'Agricoltura, - Consistenza degli allevamenti, numero di capi - livello comunale, ISTAT, Roma, Italy [In Italian]

Kinoshita T., Inoue K., Iwao K., Kagemoto H., Yamagata Y. 2009. A spatial evaluation of forest biomas usage using GIS. Applied Energy. 86:1-8.

Provolo G. 2005. Manure management practices in Lombardy (Italy), Bioresource Technology. 96:145-152.

Regione Basilicata, Dipartimento Ambiente Territorio Politiche Della Sostenibilità, Ufficio Foreste e Tutela del Territorio, Piani di assestamento forestale. [In Italian].

Regione Marche, Assessorato Agricoltura 2013. Aspetti normativi ed incentivi nel settore delle agroenergie. [In Italian].

Statuto D., Tortora A., Picuno P. 2012. Classificazione di vocazionalità all'impiego di energie rinnovabili mediante grid multi-layer. Congress of AIGR (Italian Association of Agricultural Engineering). "L'Edilizia Rurale tra Sviluppo Tecnologico e Tutela del territorio", Firenze, 20 - 22 Settembre 2012 [In Italian]

Studio per la pianificazione energetico-ambientale della Provincia di Latina, (2008). Provincia di Latina, Volume 1 Tomo II Parte IV. [In Italian] http://www.provincia.latina.it/flex/cm/pages/ServeBLOB.php/L/IT/IDPagina/3094

Tenerelli P. 2008. Analisi Territoriale delle Risorse Agro-Energetiche, Tesi di Dottorato in Ingegneria del territorio e dell'ambiente agro-forestale, Università degli studi di Bari. [In Italian].

Van Hoesen J., Letendre S. 2010. Evaluating potential renewable energy resources in Poultney, Vermont: A GIS-based approach to supporting rural community energy planning, Renewable Energy. 35:2114-2122.

Yoshioka T., Sakurai R., Arugac K., Sakai H., Kobayashi H., Inoue K. 2011. A GIS-based analysis on the relationship between the annual available amount and the procurement cost of forest biomass in a mountainous region in Japan, Biomass and Energy. 35:4530-4537.

Seed losses during the harvesting of oilseed rape (*Brassica napus* L.) at on-farm scale

L. Pari, A. Assirelli, A. Suardi, V. Civitarese, A. Del Giudice, E. Santangelo

Consiglio per la ricerca e la sperimentazione in agricoltura, Unità di ricerca per l'ingegneria agraria (CRA-ING), Monterotondo (Roma), Italy

Abstract

In the Italian environments, the rapeseed (*Brassica napus* L.) is subjected, at ripening, to a seed shattering causing significant losses that reduce the yield and increase the oilseed rape seedbank in the soil. Meteorological events and mechanical harvesting are the main factors affecting the extent of seed dispersal. Lacking the availability of works investigating the actual losses during the harvest at large scale, the Consiglio per la sperimentazione e la ricerca in agricoltura, Unità di ricerca per l'ingegneria agraria (CRA-ING) has conducted a study in order to determine the effective seed losses at on-farm scale.

The amount of losses of two combine headers, traditional for wheat and specific for oilseed rape harvest, was compared. The rapeseed header had a hydraulic sliding cut-bar and two vertical electric blade on both sides in order to reduce the pulling and tearing action between the cut-off plants and those still standing. The seed losses were evaluated before and during the harvesting by using plastic trays placed on the ground within the crop rows. The trays were arranged in a layout allowing the estimation of the seed losses of three different sectors of the combine headers.

The results have demonstrated that, at farm level, the use of a specific oilseed rape header adapted and optimized for the crop requirements allows to obtain a level of seed losses (0,97% of total production), below the values reported in literature. For rapeseed, the higher losses are localized at the final parts of the head, where the plants are strictly intertwined.

Correspondence: Alberto Assirelli, Consiglio per la ricerca e la sperimentazione in agricoltura, (CRA – ING), Via della Pascolare 16, 00016 Monterotondo (RM), Italy.
Tel. +39.06.90675211 - Fax: +39.06.90625591
E-mail: alberto.assirelli@entecra.it

Key words: rapeseed, seed losses, energy crops, combine header

Acknowledgments: this work was supported by the Italian Ministry of Agriculture under the BIOENERGIE Project (Energie da biomasse agricole e forestali:miglioramento ed integrazione delle filiere dei biocarburanti e della fibra per la produzione di energia elettrica e termica).

Journal of Agricultural Engineering 2013; XLIV(s1):e126
doi:10.4081/jae.2013.(s1):e126

Introduction

The prospect of using rapeseed (*Brassica napus* L.) oil for biodiesel production has expanded, in recent years, the cultivation area in Italy, with new sources of income for the farmer. Since previously the oil was destined for food use, the cultivation of rapeseed is well-known and the crop has been introduced in most cropping systems (Venturi and Venturi, 2003; Cosentino et al., 2008). A peculiar trait of rapeseed physiology is the acropetal pattern of fruit (silique) ripening, leading to the simultaneous presence at harvest of both mature and unripe siliques. Upon a short period of rapid dehydration, the siliques may loss until 60% of their water content becoming prone to shattering (Squires *et al.,* 2003) and leading to a significant seed losses.

The loss of seed raises the level of weed infestation for several years, also causing a decrease of yield for the following crop. Gulden *et al.* (2003) observed that, due to the yield losses, the average canola seedbank was approximately 20 times the normal seeding rate. As a consequence the specie can persist as volunteer for many years, because the seeds stored into the soil maintained remarkable ability to germinate up to ten years and beyond (Lutman *et al.* 2003).

Unlike others agricultural contexts, in Italy the oilseed rape is harvested performing just one stage, using the combine harvester with different types of heads and accessories. The timing of harvest is of utmost importance and requires a careful control of both the limitation of losses caused by natural dehiscence and the reduction of the percentage of immature green seeds (Szpryngiel *et al.,* 2003) more sensitive to be damaged (Szwed and Lucaszuk, 2007) and with a lower quality when used for biofuel production (Kachel-Jakubowska and Szpryngiel, 2008). The optimization of machine setting heavily affects all the possible causes of seed dispersal and, hence, the overall performance of the crop.

Aim of this study was the evaluation of the yield reductions of the oilseed rape caused by harvest operations and the identification of the amount of losses registered by different sectors of the combine in the Italian cultivation area on open field conditions and at on-farm scale.

Material and methods

Crop culture

This study was carried out during the summer 2007 in Castelnuovo Scrivia, 44° 58' 53" N latitude, 8° 52' 56" E longitude and 85 m altitude (Piemonte region, Italy). The experimental field was placed within an area of 16 ha cultivated with oilseed rape. Ten plots (5 plots per header), 8 m wide x 50 m long, were considered and arranged in a randomized block design with two blocks to offset the effect of local variation in yield and density of the culture.

Seedbed was prepared at the end of summer, performing first a ploughing (45 cm deep) and then a passage with a rotary harrow. Subsequently the common local agricultural practices for oilseed rape

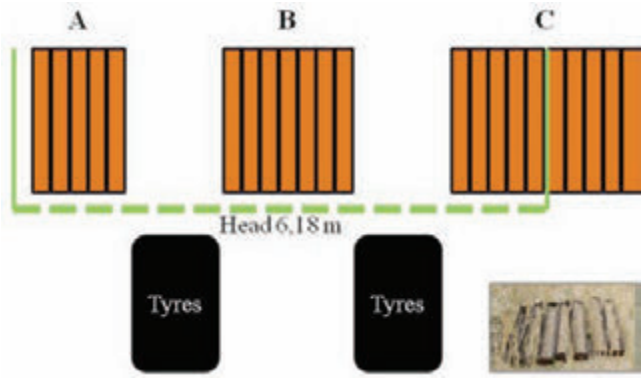

Figure 1. layout of the trays used for the assessment of the seed losses on the ground. The arrangement of the plastic trays inside the canopy is show in the insert.

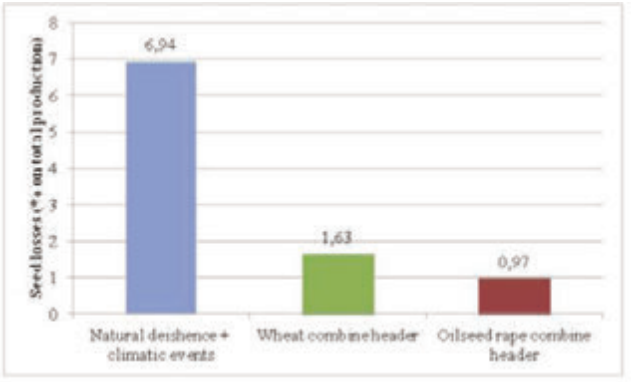

Figure 3. incidence (%) of losses on total production registered for events independent from harvest and for the two headers regardless the sectors of head.

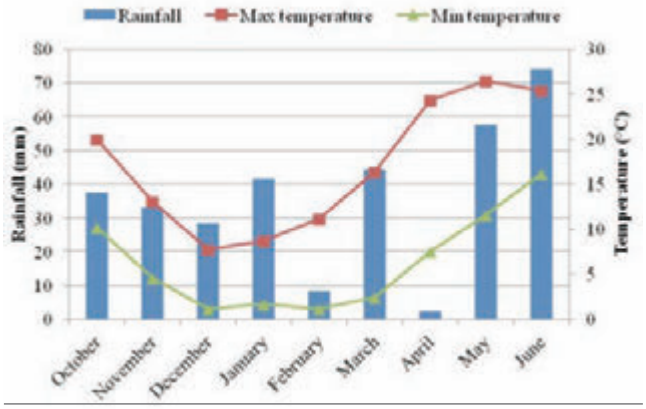

Figure 2. rainfall and temperatures registered for the whole growing season of oilseed rape (October 2006-June 2007) in the experimental field.

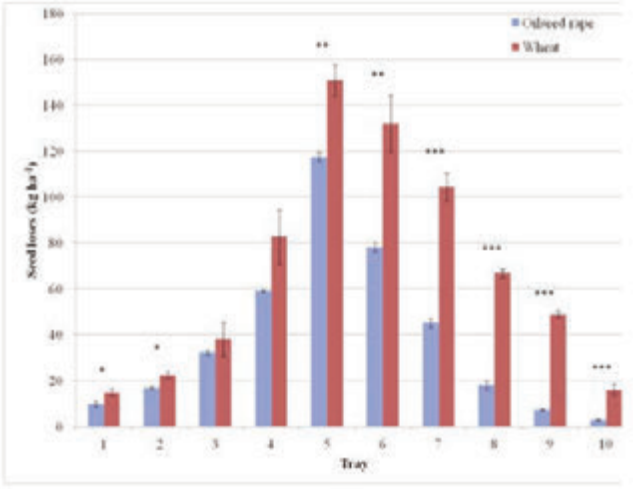

Figure 4. average (±S.E.) seed losses (kg ha^{-1}) recorded for each trays placed below the sector C during the harvest with wheat and oilseed rape headers. Significant differences between headers within tray were determined by Student's t-test. Where reported, *P<0.05, **P<0.01 and ***P<0.001 probability levels.

cultivation were applied. One month after flowering, the turning of seeds color was checked in the whole field (16 ha) in order to determine the proper harvest timing (30-40% of seeds with the color turning from green to brown).

Out of the experimental plots, the whole area (16 ha) were harvested using a combine harvester for wheat and the yield (2.945 t ha-1), net of losses, were used as reference value for the calculation of the percentage of losses on the experimental production.

Evaluation of seed losses

Two different combine headers were compared: a traditional wheat head and a head specifically equipped for rapeseed. This latter mounted a hydraulic sliding cut-bar and two vertical electric blade on both sides in order to reduce the pulling and tearing action between the cut-off plants and those still standing. For both the heads, three defined sectors (named A, B, C) of the combine were considered (Fig. 1): the horizontal cutter bar and the reel (sector A); the horizontal cutter bar, the reel and the threshing and cleaning system (sector B); the horizontal and vertical cutter bar and the reel, for the rapeseed head, or losses due to the horizontal cutter bar and to the effect of tear for the wheat head (sector C). Thus, four sources of losses (A, B, C and B minus A) were assessed for each type of head.

To identify the appropriate work speed, the combine was set in the areas surrounding the plots, maintaining then the same setting for both the wheat and oilseed rape header (Table 1).

Before the harvest, a border strip 12.36 m wide (two passages of the combine) was removed all around the experimental field. Following

Table 1: combine harvester used and setting chosen for the study.

Brand	New Holland
Model	CX8090
Engine power (kW)	337
Rotor diameter (mm)	750
Rotor length (mm)	1,560
Straw walker (n°)	6
Wheat/Oilseed rape header width (m)	6.18
Rotor speed (rad s^{-1})	440
Fan speed (rad s^{-1})	430
Concave clearance (mm)	37
Upper sieve clearance (mm)	4
Lower sieve clearance (mm)	3

Table 3: mean (±S.E.) of the total yield losses and difference (kg ha^{-1}) between headers (Δ_{w-o}) registered for events independent from harvest and for the two headers.

Source of losses	n. of samples	Seed losses (kg ha^{-1}) [a] Total		Δ(W-O)
Natural deishence + climatic events	30	204.34±15.32		
Wheat combine harvester	110	47.96±4.16		
Oilseed rape combine harvester	110	28.64±2.61	***	19.32

[a] Significance of differences between head type for wheat or oilseed rape were determined by Student's t-test. ***P<0.001 probability level.

Table 2: Number and distribution of the trays used for the assessment of the seed losses.

Source of losses	Replicates (n.)	Samples (n.) Combine sector A	B	C	Total
Natural deishence and climatic events	3				30
Header					
Wheat	5	5	7	10	110
Rapeseed	5	5	7	10	110

Table 4: mean (±S.E.) of total yield losses and difference (kg ha^{-1}) between headers (Δ_{w-o}) registered for the different combine sectors analyzed.

Source of losses	Head type	n. samples	Seed losses (kg ha^{-1})[a] Total	$\Delta_{(W-O)}$
Middle (A sector)	Wheat	25	9.97±0.56 E	
	Oilseed rape	25	8.05±0.69 E	1.92
Intersection (C sector)	Wheat	50	67.69±6.87 A	
	Oilseed rape	50	38.63±5.02 C	29.06
Under combine (B sector)	Wheat	35	49.92±5.51 B	
	Oilseed rape	35	29.09±1.84 D	20.83
Threshing and cleaning (B-A sector)	Wheat	25	51.95±5.04 B	
	Oilseed rape	25	26,43±1.25 D	25.52

[a] Different capital letters represent statistically significant differences according to the ANOVA at 0.01 probability level (Duncan's test).

Price et al. (1996) and Klinner *et al.* (1986), small plastic trays (1000 mm long and 160 mm wide) were used for the measurement of seed losses and positioned in each plot (Fig. 1).

In order to evaluate the losses not attributable to mechanical harvesting (natural dehiscence and climatic events), on early June, before the appearing of the first ripen siliques, the plastic trays were randomly placed on three assay areas (1 m wide x 1.8 m long) outside the experimental field (same variety and maturity stage) and removed just before the harvesting.

For evaluating the seed losses during the harvest, the same layout of trays on the ground was adopted for both the heads. The containers were placed 5 m before the plot end in order to allow the combine to pass over them in full workload (threshing, separating and cleaning at work). In total 250 samples of seeds (one sample from each tray) were collected (Table 2).

The meteorological station of Tortona (Alessandria, Italy), belonging to the regional network of environmental monitoring (ARPA), and placed 2.6 km far from test area, recorded the meteorological data of the experimental field.

When performed, the statistical analysis of data were made using MSTAT-C statistical package.

Results

At harvest the crop showed a regular development without lodged areas and with a moisture content of the seeds (9,44%) suitable for the harvest operations. The weather was typical of the region, with minimum and maximum temperatures that progressively decreased from October to February and reached the higher values during the harvest phase (Fig. 2). Just before the harvest, the average temperature progressively increased, peaking (30-31°C) the week preceding the harvest. Concomitantly the solar radiation gradually rose to values above 250 W m-2, thus promoting the uniform ripening of siliques. It should be underline that after the trays for the monitoring of the natural dehiscence have been placed, at least three significative rainfall events occurred. This brought about a seeds dispersal due to the action of natural dehiscence and climatic events (Table 3, Fig. 3), surely consistent (6.94% of total production), but expected for the environmental conditions of the area. The two headers showed a different level (statistically significant) of seed losses. The head for oilseed rape allow a containment of seed dispersal equal to 19.32 kg ha-1, with a decrease of losses from 1,63% (wheat head) to a level of the 0.97% of total production (Table 3, Fig. 3).

Also when considering the different sectors monitored, the rapeseed head achieved values of seed losses lower than the ones for wheat, with a difference statistically significant (Table 4). The amount of seed saved was remarkable for the sector C, where the difference between the two head touched nearly 30 kg ha^{-1}. It should also be noted the difference recorded for the threshing and cleaning apparatus (losses of sector B minus the ones of sector A). The combine header for wheat lost 51.95 kg ha^{-1} (corresponding to 1.76% of the yield) whereas the one for rapeseed 26.43 kg ha^{-1} (0,89% of the yield) with an improvement corresponding to an average potential increase in yield of 25.52 kg ha^{-1}. Such result could be explained assuming a better uniformity of feeding assured by the rapeseed head.

The detailed analysis of losses in the C sector allows to gain additional worthy information (Fig. 4). The reciprocal position of the reel and the cutting mechanism is a key factor: unlike the wheat, for the rapeseed header the losses caused by the reel are intercepted by the head and saved. The difference among the two headers gradually increased until the tray number 5, positioned under the vertical blade.

In this case it is possible to appreciate the differences between a header that cuts (rapeseed) or a head that pulls and tears (wheat) the plants. It should be highlighted that the seeds collected in the first four trays may be attributed to those lost in the sector A.

The effect that the branching of the rapeseed and the resulting intertwining of the plants may have on the seed losses are emphasized by the asymmetry of losses (Fig. 4). For both the heads, the amount of seeds collected by the trays 6 and 7 was higher than the amount registered for the corresponding and symmetric (respect to the tray n. 5, placed under the vertical blade) trays 4 and 3. Considering the rapeseed head, this difference among symmetric trays disappeared by moving towards the trays 8 and 9, falling to zero in the last one. On the contrary, the asymmetry of the curve is more pronounced for the wheat header and the gap between the symmetric trays remain always high. This demonstrates as the action of the vertical blade helps to reduce the losses due to the branching of the rapeseed plants.

Conclusions

To our knowledge, this is the first comparison of seed losses caused by wheat or rapeseed combine headers in open field conditions and at on-farm scale with a more precise quantification of the real yield losses occurring during the industrial cultivation with respect to other similar works (Gulden *et al.,* 2003; Price *et al.,* 1996).

The results underline as the losses are localized, more than ever, in correspondence of the final part of the combine header, where the intertwining of plants increases the seed dispersal. The study has shown how the use of a head with advanced blades allowed the substantial reduction of these losses. The application of lateral electric blades achieves the utmost results when the rubbing action (main cause of ground losses) between the cut-off plants and those that are still standing is knocked down.

Two other technical aspects should be taken into account. Firstly, the increase of the working width plays an important role for the reduction of seed losses. The positive effect is due to the reduction of the number of passages and the separation lines among a passage and the following, but also to a minor rubbing between the crop and the header. Secondly, the increase of the work width requires the use of lower work speed. The plants are picked up less vigorously, thus assuring a more uniform feeding to the combine and a reduction of the collision with the harvester, a significant factor of seed shattering.

The application of a rapeseed head that may be adapted and optimized for the crop requirements allowed a reduction of seed losses (0.97% on total production) at a level below the values reported in literature. The experimental evidences acquired will be of great utility in order to define the aspects of the cultivation technique (such the harvesting) of other crops belonging to the *Brassica* genus (e.g. B. *carinata*) botanically and agronomically related and with a potential interest for their use for bioenergy production.

References

Cosentino S., Copani V., Patanè C., Mantineo M., D'Agosta G.M. 2008. Agronomic, energetic and environmental aspects of biomass energy crops suitable for Italian environments. Italian Journal of Agronomy 3(2):81-95.

Gulden R.H., Shirtliffe S.J., Thomas A.G. 2003. Harvest losses of canola (*Brassica napus*) cause large seedbank inputs. Weed Sci 51(1): 83-6.

Kachel-Jakubowska M., Szpryngiel M. 2008. Influence of drying conditions on quality properties of rapeseed. Int. Agrophys. 22(4): 327-31.

Klinner WE, Neale MA, Arnold RE, Geikie AA, Hobson RN. 1986. Development and first evaluations of an experimental grain stripping header for combine harvesters. Bedford, UK: National Institute of Agricultural Engineering. 43p. Report NIAE-IER-DN—1316.

Lutman PJW, Freeman SE, Pekrun C. 2003. The long-term persistence of seeds of oilseed rape (*Brassica napus*) in arable fields. J Agric Sci 141(2): 231-240.

Price J.S., Hobson R.N., Neale M.A., Bruce D.M. 1996. Seed losses in commercial harvesting of oilseed rape. J Agric Eng Res 65(3): 183-91.

Squires T.M., Gruwel M.L.H., Zhou R., Sokhansanj S., Abrams S.R., Cutler A.J. 2003. Dehydratation and dehiscence in siliques of *Brassica napus* and *Brassica rapa*. Can J Bot 81(3): 248-54.

Szpryngiel M., Wesolowsky M., Szot B. 2003. Economical Technology of Rape seed harvest. Teka Komisji Motoryzacji i Energetyki Rolnictwa Oddział PAN w Lublinie 4: 185-95.

Szwed G., Lukaszuk J. 2007. Effect of rapeseed and wheat kernel moisture on impact damage. Int Agrophys 21(3): 299-304.

Venturi P., Venturi G. 2003. Analysis of energy comparison for crops in European agricultural systems. Biomass Bioenerg 25(3): 235-55.

Enhancement of Palm residues (*Phoenix canariensis*) for a potential use in ruminant feed

G. Sperandio,[1] M. Fedrizzi,[1] M. Iacurto,[2] F. Vincenti,[2] M. Guerrieri,[1] D. Pochi,[1] R. Fanigliulo,[1] M. Pagano,[1]

[1]CRA-ING, Consiglio per la Ricerca e la Sperimentazione in Agricoltura, Unità di ricerca per l'ingegneriaagraria, Monterotondo (Roma), Italy; [2]CRA-PCM, Consiglio per la Ricerca e la Sperimentazione in Agricoltura, Centro di ricerca per la produzione delle carni e il miglioramento genetico, Monterotondo scalo (Roma), Italy

Abstract

The increase of biological residues from numerous fellings of palms (Phoenix canariensis) infested by red palm weevil (Rhynchophorus ferrugineus Olivier) in central Italy and around the Mediterranean basin, has created an important disposal problem. This issue could provide a further use by introducing it as a food in diet of ruminants, beyond that represented by the use as fuel in biomass power plants for heating or electrical energy. The shredded material of palm can be employed to animal nutrition, resulting in interest for the feed industry and livestock sector. Analysis, carried out on samples of shredded palm, made using a chipper machine modified to obtain a product of small size (according to the phytosanitary measures of Lazio Region: n. 390, June 5, 2007), showed an high water content (79%) and therefore a not easy conservation. A conservation technique could be dehydration, in order to make product as flour, pellets, to introduce in unifeed together with the other compounds of the diet (forage, concentrates, etc.). Given the high water content, the dehydration process causes a very high production cost.

About nutritional value, analysis showed 0.65 UF/ kg on dry matter basis, higher than the straw and hay of stable grass in an advanced stage of maturation (0.20 to 0.30 UF/kg). These values are similar to a good hay obtained from mixed grass. As consequence it is possible to use shredded palm as part of energy of the ruminants diet. Is still not clear which component allows the achievement of this value, probably derives in small part by the lipid component and largely by the fibrous component. Moreover data showed that the presence of fatty acid precursors of CLA (Conjugated Linoleic Acid) such as oleic acid and linoleic acid, is much higher than the values of Italian pastures. Utilization of these fatty acids in animal diets improves quality of the final products (milk, cheese, meat). The possibility of introducing shredded palm in ruminants diet, may be topic of interested to feed animal in arid areas of the Mediterranean basin, where it is difficult to find good forages.

Correspondence: Mauro Pagano, Consiglio per la Ricerca e la Sperimentazione in Agricoltura, Unità di ricerca per l'ingegneria agraria (CRA-ING), Via della Pascolare, 15- 00016 - Monterotondo (Roma), Italy.
Tel.: +39.06 90675253 - Fax: +39.06 90625591
E-mail: mauro.pagano@entecra.it

Key words: feed, palm, biological residues, Rhynchophorus ferrugineus.

Contributions: the authors contributed equally.

Conflict of interests: the authors declare no potential conflict of interests.

Journal of Agricultural Engineering 2013; XLIV(s1):e127
doi:10.4081/jae.2013.(s1):e127

Introduction

The epidemic diffusion of the Red Palm Weevil (Rhynchophorus ferrugineus Olivier, 1790), now configured as a real biological invasion, has been exacerbated by the difficulties of disposing of many palm trees torn down and the difficulty of being able to retrieve the necessary material for alternative purposes, considering the high cost of logistics management of such biomass. Is therefore increasingly necessary to implement actions recovery and enhancement of material in compliance with current legislation in the phytosanitary field, implementing specific actions to prevent the diffusion of RWP also in later stages of disposal. In this context, you can insert the action of palm wood shredded reduction, through the use of machines properly prepared to exterminate the phytophagous insect and then be able to avoid the insect reproduction. We describe the actions taken and the means employed for the palms shredded reduction, suggesting a possible re-use of the obtained product as a food supplement in the ruminants diet. The main problem of shredded palm is the water content that is about 79%. A normal corn silage presents a water content between 65% to 70%, depending on harvest time. Different values are reported for cornstalks (values close to 20%); hay (values from 15% to 20%) and wheat straw (values close to 10%). As a consequence of the high water content is very difficult to conserve shredded palm, the best method to conserve could be the ensilage process, but the very low carbohydrate content (9.30 g/100g) causes a low availability of fermentable sugar, needed for a proper acidification of the silage. To solve this problem, it could be hypothesized the addition of sugars during ensiling, in order to guarantee a correct preservation process. Another technique of preservation, may be the dehydration that allows use as flour, pellets, in Total Mixed Ration (TMR) preparation, together with the other compounds (fodder, concentrated, etc.). The process of dehydration could have a very high cost considering the high water content of the product.

Materials and methods

IIn November 2012 at Engineering Research Unit of the Agricultural Research Council (CRA-ING) in Monterotondo (Rome), were conducted the first tests of the palm wood shredded reduction with mechanical shredding action. Have been used a portions of stems and leaves of palm trees (Phoenix canariensis) torn down because it was found that in our country are these to be most affected by the phytophagous insect RPW (Griffo, 2010). In order to conduct the test we used a shredding machine made by FARMI, model FOREST CH 260. From the obtained material (shredded) were taken samples of the product for which were to determine some basic parameters: density, moisture content and size fractions (particle size analysis of the sample of palm wood chips) to European standard established by CEN (European Committee for Standardization). Parallel with other samples of material (placed in polyethylene bags packed in vacuum average weight 2.5 kg) were sent to the laboratories of the Research Centre for meat production and genetic improvement of the Agricultural Research Council (CRA-CPM) Monterotondo (Rome), to carry the appropriate chemical analysis, with the purpose of being able to know the nutritional aspects in the animals diets.

The machine made by FARMI, model FOREST CH-260, is a forestry chipper machine constituted by a rotor disc cutter, with the possibility to adjust the average size of the wood chips to ensure the right size and homogeneity of the product (Fig. 1). The rotor carries out 1.000 rpm max., with a 1050 mm of diameter and 240 kg of weigh. For the chipper has been eliminated the screening grid to prevent clogging of the machine caused by the fibrous palm wood that adheres at inner walls of the machine (Fig. 1).

The chipper machine has been driven by a tractor with 100 kW of power, is connected to it by means of a cardan shaft. The power supply system is hydraulic and composed of two spiked rollers: the upper roller, of greater diameter mounted on a mobile frame compressed by a spring to maintain adherence with the input material to be chipped, ensuring an efficient power and the high productivity result.

The chipping is done primarily through knives mounted on recordable media, attached to the rotor by means of screws. More branches cutting blades mounted inside the housing of the chipper in conjunction with the specific comb rotor perform a secondary processing of wood chips. The maximum diameter of the stems that can be introduced into the machine is about 260 mm, so the stems of palm trees have been previously divided into pieces of smaller sizes through the use of the chainsaw. Using the described chipper machine is possible to obtain chips with average size between 7.00 and 25.00 mm. The material obtained was ejected through a launch tube into a trailer (Fig. 3).

Chipper machine and yard work description

The machine made by FARMI, model FOREST CH-260, is a forestry chipper machine constituted by a rotor disc cutter, with the possibility to adjust the average size of the wood chips to ensure the right size and homogeneity of the product (Fig. 1). The rotor carries out 1.000 rpm max., with a 1050 mm of diameter and 240 kg of weigh. For the chipper has been eliminated the screening grid to prevent clogging of the machine caused by the fibrous palm wood that adheres at inner walls of the machine (Fig. 1).

The chipper machine has been driven by a tractor with 100 kW of power, is connected to it by means of a cardan shaft. The power supply system is hydraulic and composed of two spiked rollers: the upper roller, of greater diameter mounted on a mobile frame compressed by a spring to maintain adherence with the input material to be chipped, ensuring an efficient power and the high productivity result.

The chipping is done primarily through knives mounted on recordable media, attached to the rotor by means of screws. More branches cutting blades mounted inside the housing of the chipper in conjunction with the specific comb rotor perform a secondary processing of wood chips. The maximum diameter of the stems that can be introduced into the machine is about 260 mm, so the stems of palm trees have been previously divided into pieces of smaller sizes through the use of the chainsaw. Using the described chipper machine is possible to obtain chips with average size between 7.00 and 25.00 mm. The material obtained was ejected through a launch tube into a trailer (Fig. 3).

Nutritional aspects: energy content

The energy value, reported as 0.65 UF/kg, was higher than the value of straw and hay of permanent grass harvest in an advanced stage of maturity (0.20-0.30 UF/kg), and it was similar to hay. As consequence of these values it is possible to use this product as part of energy in ruminants diet. Probably the energy value is represented in small part

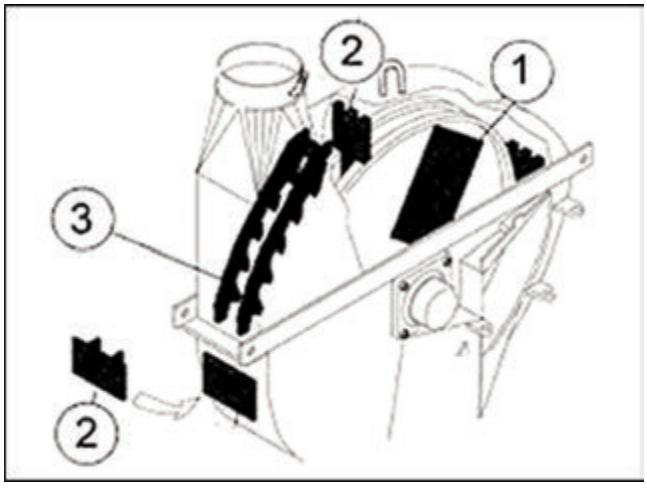

Figure 1. Chipping in 3 stages (for wood chips basis): 1. Double knife on the rotor disk 2. Fixed knives 3. Final knives. (source: http://www.deangeli.bz.it)

Figure 2. Characteristics fibrous palm wood

Figure 3. The wood chipper FARMI model - CH260 FOREST at work

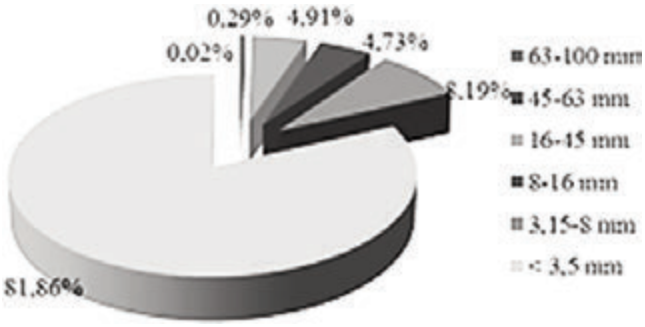

Graph 1. Frequency distribution in weight classes of wood chips size

Table 1. Daily requirements of minerals and vtamine in bovine growth. (source: www.iis-calvi.com)

Live weight (kg)	Growth (g/d)	Ca (g)	P (g)	Mg (g)	K (g)	Na (g)	Cl (g)	A -Vitamins (U. I.)	D - Vitamins (U. I.)
150	1000	27	15	1.9					
	1400	37	19	2.2	11	4.0	5.0	10.000	1.000
250	1000	34	21	3.3					
	1400	44	24	3.9	17	6.0	7.0	15.000	1.500
350	1000	42	35	5.2					
	1400	53	33	5.4	23	7.0	10.0	22.000	2.300
450	1000	52	38	6.8					
	1400	64	35	7.6	29	8.5	12.5	28.000	2.900
550	1000	57	39	7.9					
	1200	68	37	8.8	35	10.5	16.0	35.000	3.500
650	1000	62	37	8.9					
	1200	72	40	9.9	41	11.5	19.5	41.000	4.100

from the lipid component, and largely by the fibrous component of the product. Nevertheless the quality of the fiber present appears to be anomalous. Values of NDF (14.68) are different from the values recorded in the wheat straw (70-75), cornstalks (65-70), hay (60-65) and corn silage (43-45). The same situation was recorded with regard to ADF content, the value of 10.81 was different from the corn silage (30-35), hay and cornstalks (40-45)and wheat straw (50). Therefore, this product seems to have a very digestible fiber, but not so good in terms of functionality and anatomical development of rumen, these aspects may generate an excessive speed of diet transit, resulting in a poor assimilation diet components.

Protein content

Certainly cannot be considered a protein food, in fact proteins content were 0.840 g/100g (0.8% kg / ss) very different from wheat straw (usually not used as protein food (PG = 3.7% / kg DM)) or not good ryegrass hay where we reach values close to 2.5% kg/S.S.

Fatty acid composition

Regarding the fatty acid composition, there was a very high level of palmitic acid. The levels of fatty acid precursors of CLA were high, in particular levels of oleic acid (18.16%) and linoleic acid (15.89%). Linolenic acid content was not good (1.55%). The values of Oleic and Linoleic were higher than the values recorded by Italian pastures where these values are 2.05% about oleic acid and 10.57% about linoleic acid.

Minerals

Regarding the minerals, in particular about those that might cause problems for animal health, was recorded low Zinc content (9 mg/kg), according to European Union Reg. 1334/03 where for ruminants are reported tolerance limits 20-65 mg/kg. Lead content (0.15 mg/kg) was much lower than those reported by European Union Reg. 744/2012, where are reported tolerance limits from 5 mg/kg to 30 mg / kg, depending on the raw material used.

The only trace elements with a good levels were Calcium (54.3 mg/100 g), Phosphorus (53 mg/100 g), Sodium (238 mg/100 g) and Potassium (227 mg/100 g). The levels of these elements might suggest to use as a mineral supplement in the diets of dairy and beef cattle.

Results

The first tests results, show that the material produced meets the requirements of the current legislation at national and regional level. It would therefore be conceivable to enhance the product, assigning it to a direct use in livestock farms. The work carried out by the chipper machine, resulted in the need to further cut of palm trees leading to other costs.

The various size classes differentiation shows that over 90% of the sample falls within a range between 3.5 and 16 mm. (Graph 1). In total have been produced about 910 kg of material crushed to 75,87% of water content representing approximately 1.5 palm trees. As shown in Graph 1, 81.86% showed dimensions of less than 3.5 mm and only 5.22% of the sample falls within a range between 16 mm and 100 mm, while the 0.31% is between 45mm and 100 mm.

Conclusion

In conclusion it is possible to say that the wood chips of palm tree is difficult to use in ruminants diet. First of all, it appears a problem of preservation, due to the high water content. In addition, the chemical analysis showed a very poor nutritional values, in particular respect to protein content. As already mentioned previously, may be used as mineral integration or as energy part of the diet. Regard to the work quality, referring to mechanical shredding operations of palm wood, it highlights the need to intervene with further cuts for the size reducing of the palm stems. This operation increases the whole cost of the shredding.

References

1. P.F. Roversi, 2013, http://sito.entecra.it/portale/cra_progetti. http://www.iis-calvi.com ; http://www.deangeli.bz.it

Determination of the working time requirement for suckling sows in the pen of Wels

E. Quendler[1], P. Pötz[1], W. Hagmüller[2], R. Kogler[1], J. Boxberger[1]

[1]Universität für Bodenkultur, Wien; [2]LFZ Raumberg-Gumpenstein, Wels Thalheim, Austria

Abstract

These days, especially in organic piglet production, it is necessary to reduce the production costs to be competitive on the market. A large proportion of the production costs are caused by labor and construction costs to ensure a high level of animal welfare. The farrowing pen of Wels, currently existing in prototype form, was designed to fulfill organic farming requirements, improve animal welfare, and minimize the costs for construction and labor. The housing system is characterized by four separate functional areas: the lying area, the excretion and moving area, the feeding area for the sow, and a piglet nest. To identify the working time requirements of routine and special tasks, a time study, based on the work element method and an electronic time recording system (ortim b3) (a Pocket PC with time recording software), was conducted. The influencing variables and the time measurements were collected by directly observing work processes in the farrowing unit, which had 5 farrowing pens, over a period of 21 days at the "LFZ Raumberg Gumpenstein." The data were descriptive and statistically analyzed to obtain planning data on the element basis. The time requirement was modeled according to the related task and in total over the suckling period. The routine tasks consisted in transporting the feed to the pen, feeding the sows, monitoring the sows and piglets, mucking out the dung corridor with a tractor and sprinkling straw in it, as well as filling up the hay rack. The labor input was 3.99 AKmin per sow and day in total. The special tasks included inoculating the piglets, marking with ear tags, castrating the male piglets, cleaning the whole pen and the dung corridor, and preparing the farrowing pen for the next sows. Special work required 25.9 MPmin per sow over the keeping period of 21 days. The total working time requirements over the period of 21 days were 1.82 MPh per sow. Overall, the farrowing pen of Wels has low time requirements and can be seen as a good alternative to the existing organic pens.

Correspondence: Elisabeth Quender, UniversitätfürBodenkultur, Peter Jordan Straße 82, 1190 Wien, Austria
E-mail: elisabeth.quendler@boku.ac.at

Key words: Farrowing pen of Wels, organic piglet production, working time requirements

Journal of Agricultural Engineering 2013; XLIV(s1):e128
doi:10.4081/jae.2013.(s1):e128

Introduction

The organic piglet production is currently facing major challenges. Consumers are demanding that sows and piglets are kept in animal-friendly systems, maintaining a high degree of animal welfare and avoiding keeping suckling sows in farrowing crate systems, which do not allow natural movement of the sow and do not meet her natural basic needs, such as her nesting behavior. The different design of farrowing systems leads to differences in labor requirements and hence to significant differences in the cost of production (Weber et al., 1996). Animal-friendly systems are more costly in construction and management than conventional farrowing crate systems. Due to enhanced space with straw bedding, there exist higher resource utilization and sometimes higher piglet losses by crushing (Quendler et al., 2010). These additional investment costs are exacerbated by rising energy and commodity prices, tighter funding conditions, difficult marketing channels for organic piglets and stagnant meat prices. Consequences for farm managers are closing down, especially of small farms, or the change to profitable niche products and the reduction of production costs by growth in order to remain in production. For example, since 1995 the number of pig farmers in Austria has fallen by 74.2%; on a daily basis about 15 farms have given up pig production (Statistik Austria, 2012).The production cost reduction can be achieved through efficient use of resources, high level of performance and growth (Quendler et al., 2010). For organic piglet production, the FAT2 pen, which involves higher total production costs per piglet (by 18.3%) than conventional farrowing crate systems, is predominantly chosen (Quendler et al., 2010). The positioning of the feed trough near the lying area results in an accumulation of food residues in the resting area. The sow uses the outlet as an additional excretion area. This results in additional cleaning activities which contribute to a higher labor requirement. To eliminate these weaknesses, the pen of Wels, which is currently in a prototype stage, has been developed for organic piglet production (Hagmüller et al., 2010). The design of the pen of Wels aims to lower construction costs and fulfill ethological needs of sows. To which extent an optimization has been achieved can only be confirmed by comparison of processing key data. The difficulty of the comparison lies in the missing availability of data for the pen of Wels. To fulfill these objectives processing key data must be collected. For this reason, the determination of the working time requirements for the pen of Wels, based on the work element method, was the aim of this study.

Materials and methods

Experimental farm and pen of wels

The study was carried out in the research center Raumberg Gumpenstein, which is located in Wels (Austria). During the survey, 34 sows were kept and production was done according to the "in-out" method. The farrowing pen of Wels was developed and optimized

according to the requirements of the current EC Organic Regulation 834/2007 (Hagmüller et al., 2010). It consists of a concrete slab; the interior walls are made of three-layer plates (58 mm) while the outlet walls are made of galvanized steel and PVC panels. The lying area is separate from the run-out, manure and feeding area and can be completely closed with an insulating cover. In winter, the lid serves to maintain an optimal temperature of the lying area. The door to the outlet has a suspension system that automatically closes after leaving the pen, so that the temperature in the resting area cannot drop sharply. The piglets can leave the bay via the piglet slip and reach the exit. The piglet net has an area of 1.1 m², is locked with a grafter above the control corridor, mulched with straw and heated with a hotplate from above. The sow and piglets have constant access to the corridor or outlet, which is partly covered and covered by straw in the entire lying area. The only available watering place and the hay rack are installed in the outlet. The feeding area can only be reached through the outlet. The feeding trough is placed in the control corridor.(Figure 1).

Working time measurements

A methodical approach by Auernhammer (1976) was used for the analysis of the pen-related work. With this approach, the total work and the different activities of the piglet production were broken down into tasks and work elements, and their influencing parameters were determined. The smallest unit was represented by the work item. For determining the smallest possible work elements (Centiminutes) of routine, special and monitoring work, a Pocket PC with the time measurement software ORTIMb3 was used. Through the timekeeper, influencing factors such as distance, litter size, and feed and straw amounts used were recorded by on-site measurements (Riegel et al., 2006). The results were tested for randomness, normal distribution and outliers, and the epsilon and variance coefficient values were used for the evaluation of the accuracy of the estimates of the mean values of the population. The standard times and influencing parameters were used to determine the labor time required for each working tasks per passage and year by modeling them in the spreadsheet program.

Results and discussion

Standard times were collected for elements of the tasks and subtasks of routine and special work for the suckling period, which lasted 21 days for each period..

Routine work

The work process of feeding included the subtasks of fetching and rationing the feed. For feed fetching, the labor input was 0.17 MPmin (Man power minutes) per pen and day. This matches the data reported in existing literature on other farrowing crate systems and could be reduced further by shortening the transport routes (Weichselbaumer, 1996; Riegel et al., 2006). The labor time requirement for the distribution was 0.46 MPmin per pen and day. In other systems similar time input exists (Riegel et al., 2006) only WEICHSELBAUER (1996) reports slightly lower input values. For feeding, the labor input was 0.63 MPmin per pen and day. WEICHSELBAUER (1996) reports for other crate systems a value of 0.4 MPmin per crate and day. This could be explained by shorter transport routes and the absence of the protective grid at the feeding trough, which requires a slower allocation of feed in order to avoid loss and pollution in the feed trough environment. The task of the daily health check was carried out after feeding and included examining the sow in the pen and the piglets in the piglet nest. The labor time required for the health check of sow and piglets was 0.37 MPmin per pen and day, although the actual check lasted 4 MPcmin (Man power centiminutes) (2.4 MPsec (Man power seconds)) for the sow pen as well as the piglet nest. This is a labor requirement which is influenced by the construc-

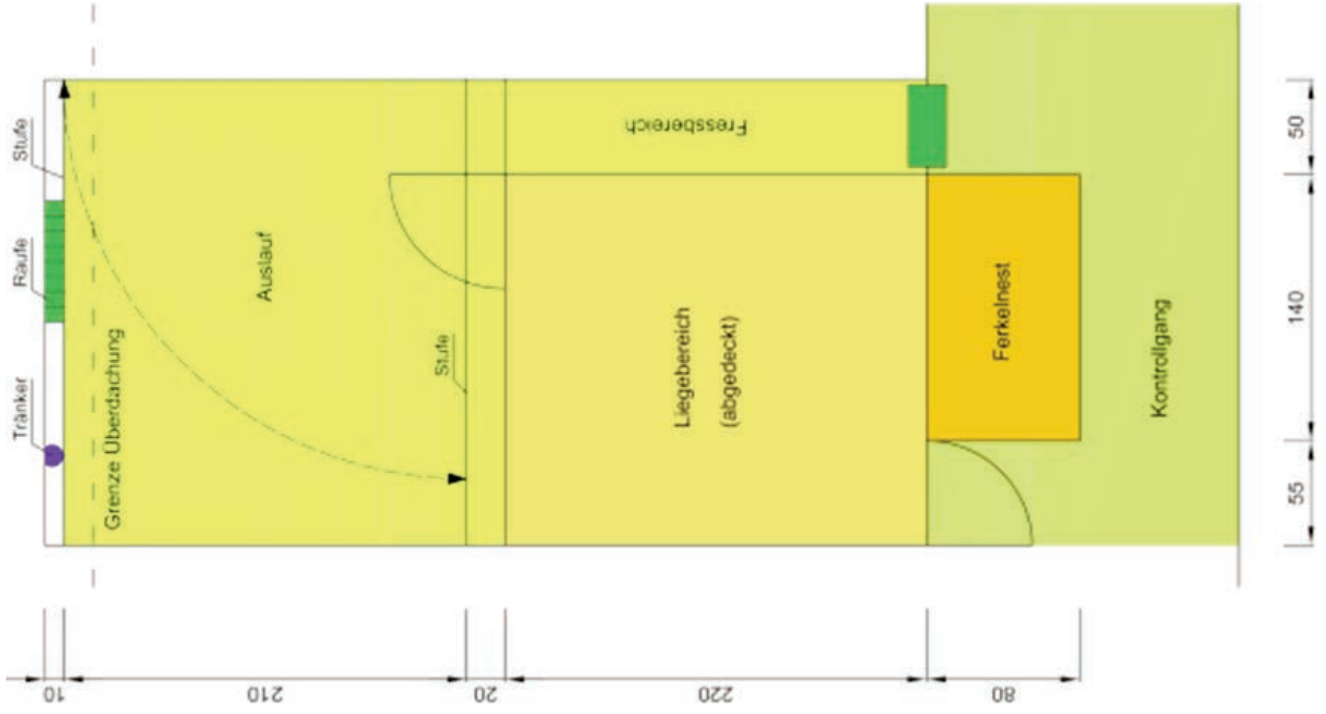

Figure 1. Schematic representation of the farrowing pen of Wels, including dimensions

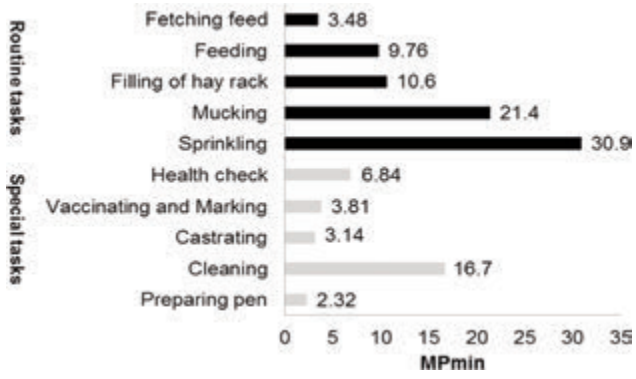

Figure 2. Working times of tasks of a suckling cycle in MPmin

tion design. For example, in the FAT2 or other crate systems it is only partially necessary. The lower time input for the health check of sows in crate systems (2.81 MPcmin, MPsec 1.69) is caused by the better overview of the crate which is not limited by high walls and a lid, but it cannot be avoided when sows are kept without fixation under outdoor climate conditions (Quendler et al., 2010).

The mucking out of the manure of the outlet was done immediately after feeding, while the sow was kept in the feeding area. Since it was carried out with a Hoftrac, it was necessary to open the screen doors. The labor requirement for daily mucking amounted to 1.02 MPmin per sow and day, which is similar to the requirement for FAT2 pens (Riegel et al., 2006). The lying area of sow and piglets had never been mucked during one suckling period, because the outlet area was recognized as manure place.

The sprinkling with straw of the outlet was done immediately after mucking. It consisted of the subtasks of fetching the straw, sprinkling, and closing the screen doors. The labor time required for the task sprinkling was 1.47 MPmin per pen. It is higher than the requirements of other crate systems which have a smaller sprinkling surface, smaller sprinkling amount, and a shorter distance to the straw storage (Weichselbaumer, 1996, 1999). Sows were supplied with hay not only for feeding purposes, but also for the promotion of their species-specific activities. The filling of the hay rack consisted of the subtasks of fetching and allocating the hay into the rack. The time requirement for transportation was 36 MPcmin (21.6 MPsec) and for allocating the hay 14.6 MPcmin (8.75 MPsec). A reduction of the time required would be possible if the distance between rack and hay storage was smaller and if a hay bale was transported while fetching the last straw delivery. The labor time required for routine work was 3.99 MPmin per day and pen, and 83 MPmin per passage (21 days). According to Quendler et al. (2010), the labor requirement for the routine work of FAT2 pen was 1.47 MPmin per sow and day. This lower requirement was achieved with a stock of 100 lactating sows, having no outlet, with semi-automated feeding, and sprinkling and mucking only twice a week. Riegel et al. (2006) determined a labor input of 3.3 to 4.9 MPmin per pen and day of high to low mechanization for group sizes of 40 sows. According to this comparative study, the daily working time requirement for the farrowing pen of Wels can be considered to be low.

Special work

The special work included the tasks of vaccinating, marking with ear tags, castrating piglets, and cleaning and preparing the pen for the next sow or passage. Vaccinating and marking with ear tags were done two days after birth, after feeding, as the sow was at the feeding trough and the piglets in the nest. The labor time needed for piglet handling was 120 MPcmin, for treatment 179 MPcmin, and for marking 82 MPcmin per pen. The treatment and marking of 12 piglets required 3.81 MPmin, which is similar to values of other studies (Riegel et al., 2006). The optimization options are limited to opening and locking the nest lid. Castration was performed in the first week. It included the subtasks of piglet handling (120 MPcmin), administering painkillers (33 MPcmin), and castration (161 MPcmin). The labor time requirement of this task was 0.52 MPmin per piglet, or 3.14 MPmin per pen. Cleaning of the pen after one passage (suckling cycle) included the subtasks of mucking and cleaning. The labor time inputs for sweeping the pen and the piglet nest were 46.4 MPmin (27.8 MPsec) per m^2, or 2.32 MPmin per pen. Washing pen, nest, and feeding place, which had an area of 5.4 m^2, required a working time of 130 MPcmin (78 MPsec) per m^2, or 7.02 MPmin per pen. Cleaning the manure area included the subtasks of opening the screen doors and washing the outside area. The labor time required for cleaning the pen (mucking and washing) was 16.7 MPmin per pen and was the largest labor activity-related time requirement. The time required for sweeping out the pen area was higher than in other studies and was caused by the small nest opening, which is a hindrance during this work process. The reduced labor input for washing one square meter of the pen area corresponded with the lower degree of contamination compared with other systems (Riegel et al., 2006; Quendler et al., 2007). The task of preparing the crate for the next sow included the subtasks of fetching straw and sprinkling. Fetching the straw took 1.67 MPmin and sprinkling 0.66 MPmin. The labor time required for the preparation of the crate was 2.32 MPmin. A reduction of the labor time requirements would be possible if the straw storage was closer.

Working requirements of the farrowing pen of wels

The labor input of the farrowing pen of Wels was 109 MPmin per passage, which corresponded to three weeks. It consisted of 76.1% of routine work and 23.9% of special work. (Figure 2)

For 2.1 litter per year, the labor time requirement per sow and year is 3.81 MPh (Man power hours). Riegel et al. (2006) showed a value of 4.9 MPh for sow and piglets per year in the FAT2 pen at a herd size of 30 animals during a 4-week production cycle with low manual labor input. It increased to 5.9 MPh per sow and year for herd sizes of 20 animals. This would represent a working time requirement of 4.79 MPh per sow and year of a 4-week production cycle for the pen of Wels. According to Quendler et al. (2010), the working time requirement for the pen of Wels is slightly higher (+9.1%) than for the FAT2 pen used for a large herd size of breeding sows (606 sows). The lower labor input for a FAT2 pen can be explained by this pen being managed with a semi-automated feeding system and not having the outlet mandatory for organic piglet production. Overall, the low working time requirement of the pen of Wels is achieved because mucking and sprinkling of the sow pen and piglet nest are unnecessary and mucking and sprinkling of the outlet are performed with machinery.

References

Auernhammer H. 1976. Eine integrierte Methode zur Arbeitszeitanalyse. KTBL-Schrift. 203:95.

Hagmüller W., Preinerstorfer A. 2010. Freies Abferkeln im Außenklimastall – ist das möglich? Der fortschrittliche Landwirt. 24:20-22.

Quendler E., Martetschläger R., Baumgartner J., Boxberger J., Schick

M. 2007. Arbeitszeitbedarfsunterschiede von verschiedenen Abferkelbuchten. 8. Tagung Bau, Technik und Umwelt, Bonn, Deutschland, pp 318-323.

Quendler E., Podiwinsky C., Martetschläger R., Helfensdörfer V., Baumgartner J., Winckler C., Boxbrger J. 2010. Arbeitswirtschaftliche und ökonomische Analyse verschiedener Abferkelsysteme, Die Bodenkultur. 61(1):29-36.

Riegel M., Schick M. 2006. Arbeitszeitbedarf und Arbeitsbelastung in der Schweinehaltung – Ein Vergleich praxisüblicher Systeme in Zucht und Mast. FAT Bericht. 650:5-8.

Statistik Austria 2011. Available from:http://www.statistik.at/web_de/statistiken/land_und_forst-wirtschaft/ viehbestand_tierische_erzeugung/tierbestand/index.html#index2, Accessed: April 2013.

Weichselbaumer L. 1996. Ermittlung des Einstreu- und Arbeitszeitbedarfes von Einzel- und Gruppenhaltungssystemen für ferkelführende Sauen. Diplomarbeit, Universität für Bodenkultur, Österreich.

Weber R., Keil N., Fehr M., Horat R. 2006. Ferkelverluste in Abferkelbuchten – Ein Vergleich zwischen Abferkelbuchten mit und ohne Kastenstand. FAT Bericht. 656:6.

Health and safety challenges associated with immigrant dairy workers

J. Rosecrance, T. Tellechea, L. Menger, D. Gilkey, N. Roman-Muniz

College of Veterinary Medicine and Biomedical Sciences, Colorado State University, USA

Abstract

Faced with increasing industrialization, high demands on production, and decreasing domestic participation in the labor force, dairy producers are employing an immigrant workforce to help meet operational demands. There is little data regarding the number of immigrant workers in the dairy industry, but the trend of hiring immigrant workers in some of the world's highest producing countries is increasing. There are many challenges associated with managing immigrant workers includinghow to effectively train this workforce about safe and efficient work methods.

Methods: Ethnographic methods from the anthropology field served as the primary tool to identify barriers and facilitators of safe work practices in large-herd dairy operations in the United States. Following the weeklong emersion by the research anthropologist at a selected dairy, focus groups were organized at three large-herd dairies. All focus group conversations were tape recorded, transcribed and translated into English. The focus group transcripts were coded for specific themes related to issues that participants felt were barriers or facilitators of worker health and safety.

Results: Twenty-two Latino workers 18 to 58 years of age participated in the three focus groups conducted at one Colorado and two South Dakota dairies. Six major themes relating to barriers and facilitators of worker health and safety were identified and included: communication, integration owner and worker cultures, work organization, leadership, support for animal health, and attention to safety culture within the organization.

Conclusions: Although not often considered by agricultural engineers, an anthropological perspective to challenges involving an immigrant workforce may assist with improved work methods and safe work practices. Through this approach, agricultural engineers may better understand the cultural challenges and complexities facing the dairy industry. Successful integration of immigrant workers relies not only on cultural awareness but also the ability to integrate cultural knowledge, beliefs, values, and traditions into management and work practices.

Correspondence: John Rosecrance, 1681 Campus Delivery, Colorado State University. Fort Collins, Colorado, USA 80523. Tel. +001 970.491.1405. E-mail: john.rosecrance@colostate.edu

Key words: immigrant, safety, anthropologic, ergonomics, dairy, workers

Acknowledgments: the present study was supported by the Center for Disease Control (CDC) / National Institute for Occupational Safety and Health (NIOSH) Mountain and Plains Education and Research Center (grant number: 5T42OH009229-06) and the High Plains Intermountain Center for Agricultural Health and Safety (grant number: 5U54OH008085-09). Its contents are solely the responsibility of the authors and do not necessarily represent the official views of the CDC or NIOSH.

Journal of Agricultural Engineering 2013; XLIV(s1):e129
doi:10.4081/jae.2013.(s1):e129

Introduction

Milk production during the last twenty years in the many parts of the world has increased significantly due to nutritional factors and production methods. During this 20-year period farms with small herds have all but disappeared being replaced by large (>500 head) and mega-herd (>2000 head) dairies. In many countries, profits in the dairy industry are driven by economies of scale, which have resulted in the transition towards large,and mega-herd milking (Reinemann 2001). Production driven by economies of scale result in a cost advantage with the cost per unit of output (milk) decreasing with increasing scale as fixed costs (e.g., equipment) are spread out over more units of output. In the United States for example, there were 650,000 dairy farms in 1970 as compared to 65,000 in 2009 (down 90%). During the same period, milk production and herd size increased significantly (NASS, 2010). Similar trends have been documented in other countries. In Australia, the number of dairy farms fell by 67% over the last three decades from 22,000 in 1980 to just below 7,000 in 2011 (Dairy Australia, 2012). During that same time period average herd size increased 270% and national milk output more than doubled.

The relatively recent shift towards industrialized production systems in the dairy industry has led to health and safety challenges including greater work demands, task specialization, and higher rates of injuries and illnesses among dairy workers (Douphrate, 2009). Studies now indicate that dairy parlor workers involved with large-herd milking tasks are exposed to extreme shoulder postures, high muscle forces, highly repetitive tasks, and insufficient periods of rest (Douphrate, 2011; Douphrate, 2012). Additionally, acute injuries from animal handling (cow kicks, pinned by, and stepped on) have been identified as a significant risk for all dairy workers (Douphrate, 2006). Increased working time, more cows milked per hour, more milking units per parlor, high physical workloads and highly repetitive working routines were potential risk factors associated with musculoskeletal symptoms and disorders in dairy studies (Pinzke, 2003; Patil, 2012). The injuries and illnesses experienced by dairy workers may also be related to a mismatch between equipment design (e.g., milking parlor equipment) and worker anthropometrics.

A growing number of large-herd dairy producers are relying on an immigrant workforce to help meet the demands associated with the increased scope and industrialization of the industry (ILO, 2010; Tipples, 2010; Valentine, 2005). The majority of dairy workers in the United States are considered a vulnerable working population with a high proportion (50% to 84.7%) from Mexico and Central America

(Valentine, 2005; Roman-Muniz, 2006). In Italy, a majority of the dairy workers in the highly productive Lombardy region are immigrants from the Punjab region of India (Lum, 2012). The Indian immigrants are essential to Italy's large production of the well-knownParmigianoReggiano and Grana Padanocheeses (Povoledo, 2011). Although the use of immigrant labor provides economic advantages, it may lead to health and safety challenges among works that are often related to cultural differences (Schenker, 2010). There is evidence suggesting that immigrant workers may be at greater risk of occupational injury and illness than domestic workers. The purpose of this study was toidentify the facilitators and barriers of health and safety practices among immigrant workers at large-herd dairies in the United States.

Methods

Ethnographic methods commonly used in the field of anthropology served as the primary tool to identify barriers and facilitators of safe work practices in large-herd dairy operations. Ethnographic research, as a qualitative research method, assumes there is great variability in how people understand and make their worlds meaningful. Researchers may observe and measure worker behavior in a dairy setting, but such behavior does not exist in a social or cultural vacuum. LeCompte(2010) highlighted a primary distinction between ethnography and other investigative methods carried out in the social and behavioral sciences: "*…ethnography assumes that researchers must first discover what people actually do and the reasons they give for doing it before trying to interpret their actions. That is why the tools of ethnography are designed for 'discovery' prior to 'testing."*

As the growing immigrant labor force brings greater diversity into the dairy industry, it is imperative to take the cultural components of these demographic shifts into account. An ethnographic approach as a mode of discovery aims to tap into the dynamics of the entire dairy worker context, including the workplace, family, and community. This context, which differs across cultures, creates the conditions for the basis of work behaviors. Only by understanding what behavior means from the perspective of the workers will it be possible to design the most effective safety training programs that account for the cultural perceptions. Conversely, traditional safety programs designed by indigenous safety experts and imposed from managers outside of the workers culture often result in little if any transfer of training skills on the job. In the context of the present study, the research team became co-participants in the natural setting of the worker. Through this process, the researcher engages participants in face-to-face interaction; striving for fidelity in the reflection of participant behaviors and perspectives; capturing the local cultural knowledge through 'inductive, interactive and recursive data collection' from multiple sources to understand the human experience within the broader context; and interpreting results through the concept of 'culture as a lens' (Spradley, 1990; DeWalt, 2011).

Consistent with the anthropological approach (LeCompte, 2010), the research team used participant observation, participation, and focus groups in their ethnographic methodology. These methods required the research team to have direct immersion into the context of the dairy workers for an extended period of time. Although several members of the team participated in the participant observation phase at several dairies, the anthropologist was embedded and worked side-by-side with the dairy workers for one-week. This period also included the anthropologist living among the workers at their migrant housing facility. This activity allowed the anthropologist to gain knowledge of the local language and sharing in a wide range of daily routines as full participants in the context of the works lives. This close participation and observation often involves "hanging out" having everyday conversation, which builds trust and reduces the perceived risk of the researcher's presence. An integral part of this process is to normalize the systematic recording of observations in field notes while participating in the worker context (DeWalt, 2011).

Following the weeklong emersion of the anthropologist at the dairy and migrant housing facility, focus groups were organized at the dairy and at two additional dairies in other states. The anthropologist and an additional Spanish-speaking researcher conducted the focus groups. All focus group conversations were tape recorded, transcribed and translated into English at a later date. Data were qualitatively analyzed and grouped into themes for each dairy. The themes for each dairy were then combined to generally represent the three dairies.

Results and discussion

One focus group was conducted at each of three dairies among a total of 22 workers in the states of Colorado and South Dakota in the United States. The focus group participants ranged in age from 18 to 58 years. All participants were Latino / Latina with two females participating. Focus groups were conducted in Spanish language, the native language of the workers.

Although the general topic of the focus groups was related to safety and health, some diversion about issues indirectly related to safety were allowed. The focus group transcripts were coded for specific themes related to issues that participants felt were pertinent to health and safety. The major themes related to both barriers to and facilitators of worker dairy health and safety are illustrated in Figure 1. Six major themes were identified including communication, the integration cultures represented by the owner and workers, work organization issues, leadership, support for animal health and attention to safety culture within the organization.

The theme of *communication* was highlighted by issues related to language, specifically the Spanish spoken by the workforce and English by the dairy owner. Often, the head herdsman, which is supervisory position, spoke a combination of English and Spanish and served as the communication link between the owner and workers. Language difficulties were often mentioned as reasons for miscommunications between workers and owners. Good communication was seen as vital for conducting efficient work and safe work methods within and between areas of the dairy. There also considerable discussion related to how best to communicate safety on the dairy that is discussed in more detail below under the safety culture theme.

The *integration of cultures* theme was focused on various ways to promote understanding and acceptance of differences between the specific cultural facets of workers and managers/owners. Some workers expressed feelings of bias and alienation because they did not speak English or had an undocumented work status. Culturally appropriate health and safety training was also mentioned as a necessity for worker acceptance.

Work organization developed as a major theme contributing to dairy health and safety and was focused around equipment and work schedules. Workers identified the importance of maintaining and fixing equipment in timely manner as well as having adequate tools for conducting their work as essential parts of working in an efficient and safe manner. Good equipment design in terms of reducing reaching away from the body and bending down were also identified as a possible improvement that would lead to a safer workplace. Workers often discussed the difficulties of working long hours (up to 12 hours

Figure 1. Major themes identified that can be facilitators as well as barriers for worker health and safety.

per day) and working six to seven days per week. Often workers did not get the weekend off when their family was at home. Work breaks (for bathroom and meals) were not often built into the production schedule. There was a general feeling that the lack of adequate tools / equipment as well as stressful work schedules contributed to not only poor safety practices but sacrifices in milk production and quality of work.

The theme of *leadership* was discussed in regards to leaders that workers could approach with questions regarding work methods as well as safety concerns. Workers expressed a need for leadership presence during all (3) shifts not just during the dayshift. There were also suggestions regarding an "apprenticeship style" training program as a way of developing leaders from the existing workforce. Incorporating health and safety into leadership training was seen as an important aspect of safety.

There was a consensus among all focus group participants regarding the importance of *animal health* as it related to their daily work tasks as well as their own safety. Animal safety and health was paramount in their work to the degree that it was at times given priority over worker safety. One worker during the focus group explained that *"when the owner heard that the cow kicked someone the cow got the most attention."* The need for training in animal handling and animal behavior issues was noted, as many workers did not have animal handling experience before coming into the dairy industry.

The concept of *safety culture* was discussed indirectly by each focus group and was perceived as being good to low depending on the dairy organization. There were clear differences in perceptions regarding the level of safety culture by dairy. Some workers indicated that consideration of worker safety was non-existent while others described it as adequate. Nonetheless, most workers felt production was more important to management than worker safety and thought that the safety culture could be improved. Workers indicated that they were given video-based safety training but that it was often not pertinent to dairy work or was not relevant to their specific job tasks. Workers also identified production issues that were barriers to implementing some of the safety ideas described in videos.

Although training was not included as a major theme in the model illustrated above, it was discussed with regards to every theme identified. There was a general consensus that culturally appropriate training that was more relevant to the work and workers could have the greatest impact not only on worker health and safety but also work methods. Many workers expressed frustration with a common organizational culture of learning by trial and error with little or no attention to health and safety. One dairy worker expressed the following statement concerning this general frustration: *"In the three jobs I have had in this country nobody has ever explained to me what are the risks of my job and how to prevent them."*

Conclusions

It is clear that the challenges related to improving health, safety, and efficiency on large-herd dairy farms are numerous and significant when immigrant workers are involved. Most of the major themes related to barriers and facilitators to worker health and safety identified are common issues faced by engineers involved in improving health, safety and production efficiency. However, when the majority of the work population involves immigrants, there is a need for focused attention to factors that pertain to the cultural differences between management/owners and workers. The anthropologic methodology incorporated into this study was used to specifically identify (rather than assume) the needs and concerns of a traditionally underserved and vulnerable working population. This study was focused on Latino workers employed in large-herd US dairies. However, countries that experience growth in large-herd milking operations and subsequent growth in immigrant dairy workers likely face similar challenges.

References

Dairy Australia, 2012. http://dairyaustralia.com.au/ (accessed 25 Jul 2012).

DeWalt KM, DeWalt BR, 2011. Participant observation. Lanham, MA: Altamira Press; 2011.

Douphrate D, Rosecrance JC, Wahl H, 2006. Workers' compensation experience of Colorado agricultural workers, 2000-2004. *Am J Ind Med.* 49:900-910.

Douphrate D, Nonnenman M, Rosecrance J, 2009. Ergonomics in industrialized dairy operations. *J Agromed.*14(4):406-412.

Douphrate D. 2011. Musculoskeletal symptoms and physical exposures among U.S. large-herd milking parlour workers.*Proceedings of the Irish Meeting on Agricultural Occupational Health and Safety*; Aug 22nd-24th; Dublin, Ireland.

Douphrate D, Fethke N, Nonnenmann M, Rosecrance J, Reynolds S, 2012. Full shift arm inclinometry among dairy parlor workers: A feasibility study in a challenging work environment. *Appl Ergo.* 43(3):604–613.

International Labour Organization(ILO), 2010. MESHA/2010/10. *Code of practice on safety and health in agriculture.* Geneva, Switzerland: ILO.

LeCompte MD, Schensul JJ, 2010. Design and conducting ethnographic research: An introduction. Lanhan, MD: AltaMira Press.

Lum K, 2012. *The quiet Indian revolution in Italy's dairy industry.*

CARIM India. Report number: 2012/08.
National Agricultural Statistics Service (NASS).2010, *U.S. and all states data:* Dairy.U.S. Department of Agriculture.
Patil A, Rosecrance J, Douphrate D, Gilkey D, 2012.Prevalence of carpal tunnel syndrome among dairy workers. *Am J Ind Med*. 55(2):127–135.
Pinzke S,2003. Changes in working conditions and health among dairy farmers in southern Sweden: A 14-year follow up. *Ann Agric Environ Med.* 10:185-95.
Povoledo E, 2011. In Italian Heartland, Indians Keep the Cheese Coming. http://www.nytimes.com/2011/09/08/world/europe/08iht-italy08.html?pagewanted=all&_r=0(accessed 5 June 2013).
Roman-Muniz IN, Van Metre DC, Garry FB, Reynolds SJ, Wailes WR, Keefe TJ, 2006. Training methods and association with worker injury on Colorado dairies: A survey. *J Agromed*.11(2):19-26.
Schenker MB, 2010. A global perspective of migration and occupational health. *Am J Ind Med*. 2010;53:329-37.
Spradley JP,1980. *Participant observation*. New York, NY: Holt, Rinehart and Winston.
Tipples R,Trafford S, Callister P, 2010. The factors which have resulted in migrant workers being 'essential' workers on New Zealand dairy farms. *Proceedings from Labour, Employment and Work Conference*; Nov 30th-Dec 1st; Wellington, New Zealand.
Valentine BE, 2005. United two cultures: Latino immigrants in the Wisconsin dairy industry. Working Paper 121.

The risk of musculoskeletal disorders due to repetitive movements of upper limbs for workers employed in hazelnut sorting

Andrea Colantoni, Massimo Cecchini, Danilo Monarca, Roberto Bedini, Simone Riccioni

Department of Agriculture, Forest, Nature and Energy (DAFNE), University of Tuscia, Italy

Abstract

In the agro-industrial sector there are many activities whose urgent rhythms can cause a considerable exposure to bio-mechanical risk factors. In the hazelnut sorting, the workers are subject to several biomechanical risks, with repetitive movements, and operations that require a remarkable degree of strength. A thorough study of the workers' exposure to repetitive manual movements has been carried out, with the aim of setting up the necessary measures to reduce the risk factors. The aim of the research is to assess the risk of work-related musculo-skeletal disorders (WMSDs) due to repetitive work, for workers employed to hazelnut shells sorting. The research was carried out in an agricultural cooperative in the Viterbo's area. For risk assessment authors used a method (Occupational Repetitive Actions "OCRA" index according to ISO 11228-3:2009, Ergonomics - Manual handling - Part 3: Handling of low loads at high frequency) which keeps into consideration several risk factors (such as repetitiveness, prehension force, posture). The risk was assessed for 16 female workers (in eight workplaces and in two different shifts) through this classification: workers with experience less than 1 year, from 1 to 10 years and more than 10 years. This classification is very important for knowing if the professional experience could be considered a "prevention measure" for the risk reduction. The results show a high risk level for the right and left limb. The factors which more have contributed to reach such risk level are the great number of movements and the lack of recovering time.

Correspondence: Massimo Cecchini, Department of Agriculture, Forest, Nature and Energy (DAFNE), University of Tuscia, Via S. Camillo de Lellis snc, 01100 Viterbo, Italy.
Tel. +39.0761.357.357 - Fax: +39.0761.357.453.
E-mail: ergolab@unitus.it

Key words: repetitive movements, hazelnut, ergonomics, manual sorting.

Contributions: the authors contributed equally.

Conflict of interests: the authors declare no potential conflict of interests.

Conference presentation: part of this paper was presented at the 10th Italian Conference AIIA (Associazione Italiana di Ingegneria Agraria), 2013 September 8-12, Viterbo, Italy.

Journal of Agricultural Engineering 2013; XLIV(s1):e130
doi:10.4081/jae.2013.(s1):e130

Introduction

The upper limbs have an extremely mobility adapted to human necessities. These common movements are not particularly harmful in the ordinary activities of daily life.

Muscle contraction without sufficient recovery time causes pain as a consequence of lactic acid accumulation, irritating substance. Work-related musculoskeletal disorders (WMSDs) include muscle, tendon and nerve injuries in the shoulder, elbow, forearm, wrist and hand that are not caused by acute trauma (ACGIH, 2001).

Repetitive movements of upper limb and lack of recovery time identified in manual hazelnut sorting could be a risk for WMSDs (Colantoni *et al.*, 2012). A review by the National Institute for Occupational Safety and Health (NIOSH) of epidemiological studies related to WMSDs in the workplace has pointed out their association with the following workplace factors: 1) heavy physical work, 2) lifting and forceful movements, 3) bending and twisting (awkward postures), and 4) exposure to whole-body vibration. Recent innovations at a structural and organizational level, introduced by the European laws, have effectively led to an overall drop, over the last ten years, of the number of injuries and professional diseases. However, although there has been a decrease for "traditional" pathologies, such as hypoacusis, there has been a remarkable increase of musculoskeletal disorders, caused mainly by the lifting and transport of heavy weights, wrong working positions (extreme postures and/or sudden movements) and repetitive movements (INAIL, 2012).

Disorders by repetitive movements represent the main cause of musculoskeletal injuries of workers, which exceeds the number of injuries caused by machinery. WMSDs include carpal tunnel syndrome, tendonitis of the shoulder and wrist, lateral epicondylitis, and others, generally of an etiologic origin. The ISO 11228-3:2009 standard establishes ergonomic recommendations for repetitive work tasks involving the manual handling of low loads at high frequency. It provides guidance on the identification and assessment of risk factors commonly associated with handling low loads at high frequency, thereby allowing evaluation of the related health risks to the working population.

In the agro-industrial sector there are many activities whose urgent rhythms can cause a considerable exposure to bio-mechanical risk factors. In the hazelnut postharvest sector the workers are subject to several biomechanical risks, with repetitive movements, and operations that require a remarkable degree of strength. A thorough study of the workers' exposure to repetitive manual movements has been carried out, with the aim of setting up the necessary measures to reduce the risk factors.

The aim of this research is to assess the risk of musculoskeletal disorders due to repetitive work, for workers employed in manual sorting of hazelnut.

Materials and methods

This study was carried out with the collaboration of Cooperative of

Nut Producers "Colli Cimini and Sabatini" (Capranica, Italy). The establishment is set in an area of 30,000 square meters, and is equipped with modern machinery for all processes.

In the hazelnuts processing cycle, sorting is undoubtedly a fundamental operation. This operation consists in a selection of in-shell hazelnuts and allows to obtain:

full hazelnuts and empty shells (reject);

well formed hazelnuts, with no apparent deformation;

healthy hazelnuts, free of parasites and of defects that can affect the shelf life of the fruit;

clean hazelnuts, free of any visible foreign matter;

dry hazelnuts, free of abnormal external moisture.

Sorting is carried out manually on a conveyor belt (Figure 1) and the operators are standing. Figure 2 shows the block diagram of workstations.

At the aim of the research we assessed the risk for 4 workers (all of them women) of several ages. In Table 1 we can see the number of worker and the ratio age/number of years of work in the company.

The survey was conducted for workers representative of low, medium and high experience: respectively workers n. 1 (low experience), 9 (mid-low experience), 10 (mid-high experience) and 8 (high experience).

There are many ergonomics analysis tools that claim to accurately measure variables associated with WMSDs. They are essentially based on biomechanical, epidemiological and physiological approaches and identify work activities that might cause WMSDs. These tools include: Occupational Safety and Health Administration (OSHA) checklist (Schneider, 1995), Strain Index (Moore and Garg, 1995), American Conference of Governmental Industrial Hygienists (ACGIH) Hand Activity Level (HAL) (ACGIH, 2001), Outil de Repérage et d'Evaluation des Gestes (OREGE) (INRS, 2000), Rapid Upper Limb Assessment (RULA) (McAtamney and Nigel Corlett, 1993) and Occupational Repetitive Actions (OCRA) Index (Occhipinti and Colombini, 1996). For risk assessment authors used the OCRA index method, according to ISO 11228-3:2009, Ergonomics - Manual handling - Part 3: Handling of low loads at high frequency. This method keeps into consideration several risk factors (repetitiveness, prehension force, posture).

Figure 1. Manual sorting: the product passes on a conveyor belt.

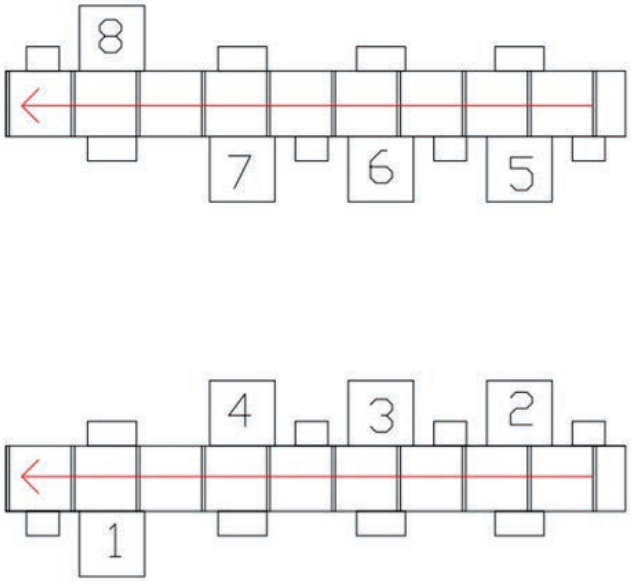

Figure 2. Block diagram of workstations.

Table 1. Workers employed in manual sorting of hazelnuts.

Worker n.	Age/n. years of work
1	19/0
2	45/1
3	51/23
4	58/27
5	52/30
6	57/24
7	55/30
8	58/28
9	49/16
10	51/20
11	50/2
12	48/2
13	51/2
14	43/10
15	50/20
16	28/1

The model is based on three requirements: 1) to thoroughly evaluate the contribution of different multiple risk factors; 2) to develop an index to evaluate the type of risk for various jobs, so that it is possible to compare different indexes and measure the changes should the work shift be re-planned; 3) to determine the repetitive movements of the upper limbs and the maximum frequency of actions per minute recommended in good conditions.

The "exposure index" (*OCRA index*) is defined by the ratio:

$$OCRA\,index = \frac{ATA}{RTA} \quad (1)$$

where *ATA* is the overall number of actual technical actions needed in the workers' shift, and *RTA* is the overall number of reference technical actions (*i.e.*, the total number of actions recommended so as not to expose the workers to risks) in the shift. According to EN 1005-5:2007, an index value of 3.5 means that 95% of *PA* (persons affected) values in the exposed worker population are expected to be higher than twice the 50th percentile (*PA* = 3.7 x 2 = 7.4%) of the reference (not exposed) population. The *RTA* is obtained from the following equation:

$$RTA = CF \times FoM \times PoM \times AdM \times \mathrm{Re}M \times (D \times RcM \times DuM) \quad (2)$$

where *CF* is the "constant of frequency" of technical actions per minute recommended in good conditions; *FoM*, *PoM*, *AdM*, and *ReM* are multiplicative coefficients, relative to each of the *M* jobs carried out by the worker, with values ranging between 0 and 1, chosen according to the behaviour of the risk factors force (*FoM*), posture (*PoM*), additional factors (*AdM*), and repetitiveness (*ReM*); *D* is the net duration of the repetitive task in minutes; *RcM* is the multiplier for the "lack of recovery period" risk factor, ranging between 0 and 1; and *DuM* is the multiplier for the overall duration of repetitive tasks during a shift.

The number of actions recommended for the calculations of the *OCRA index* (*CF* in Eq. 2) is at present 30 actions per minute, although this could vary when more precise experimentation data are available. However, a particularly high frequency of technical actions, for example 40 per minute, is only tolerable for short-term occasional jobs.

Determination of the technical actions

This risk assessment was carried out in a plant for the processing of hazelnuts. Here some workers are engaged in the sorting of hazelnuts.

In order to determine the number of actions carried out, the work shift was studied by analyzing the operations carried out, including the work breaks and their durations (Tables 2 and 3).

The tasks were then analysed by focusing on the different movements performed by the upper limbs. A video camera was used to record the workers at work, and videos then analyzed in slow motion in the laboratory. Camera position was changed several times during the work (videotaping simultaneously both from sagittal and frontal view) in order to have an overall view of the worker's movements. The workers were videotaped for at least one hour while performing a typical work routine. The number of actions carried out was established from a period of observation representative of the whole shift (one hour per site). The calculation of the actions needed to carry out a cycle was determined by slow-motion observation and the number of actions performed by the worker per minute (*FF*) was calculated with the following equation:

$$FF = \frac{NTC \times 60}{FCT} \text{ (actions/min)} \quad (3)$$

where *NTC* is the number of technical actions (for the upper limb) needed to carry out the task during one cycle, *FCT* is the foreseeable duration of the cycle time in seconds, and 60 is a conversion factor (seconds to minutes). The *FF* calculation was repeated for both upper limbs. The overall number of actual technical actions (*ATA*) needed in a shift was calculated with the following equation:

$$ATA = FF \times D \text{ (actions/shift)} \quad (4)$$

where *D* is the shift duration (in min).

Force, posture, additional, and repetitiveness factors

One of the complementary variables to be defined concerns the amount of force needed to perform an action. The greater the force required, the less frequent the number of actions that can be carried out to maintain the same level of risk (CEN, 2007). In order to characterize this variable, the OCRA standard uses Borg scale which measures perceived exertion. The worker assigns for each action a score according to the scale in Table 4; on the basis of Borg score, the multiplicative factor *FoM* is then assigned (Table 5).

Concerning the posture factor, in the literature the presence of repetitive movements for at least 2/3 of the work cycle is considered an element of risk in itself, as is the presence of movements that exceed the articular range by over 50% (Figure 3) for 1/3 of the work cycle.

In OCRA model, as the movements of the shoulders, elbows, wrists, and hands were observed, we also evaluated the simultaneous presence of complementary elements of risk, such as jerky movements, shocks, and vibrations. When a job is analyzed, every gesture is included, and a risk score is assigned to each movement. At the end of the analysis of awkward postures, in order to calculate the equation, the lowest *PoM* multiplier (Table 6) is selected in accordance with the postures and movements of the elbow, wrist, and hand (type of grip).

Next, a score is assigned for the complementary elements that is equal to 1 when they are irrelevant and decreases to as low as 0.80 when they are detected through the whole cycle. If additional factors as listed above are absent throughout most of the task, then the additional factor multiplier (*AdM*) equals 1. Otherwise, *AdM* equals (CEN, 2007):

- 1 if additional factors are present for less than 25% of the cycle;
- 0.95 if additional factors are present for 1/3 (25% to 50%) of the cycle;
- 0.90 if additional factors are present for 2/3 (51% to 80%) of the cycle;

Table 2. Study of work shift (workers n. 1, 9 and 10).

Job	Description	Duration (min)	Type of job (repetitive/not repetitive)
Sorting line	Hazelnut sorting on conveyor belt	210	Repetitive
			Recovery time or not
First break	Lunch break established by worker	40	Recovery time
Second break	Breaks due to cleaning, supply, etc.	110	Recovery time
Total minutes of actual work and breaks		360	

Table 3. Study of work shift (worker n. 8).

Job	Description	Duration (min)	Type of job (repetitive/not repetitive)
Sorting line	Hazelnut sorting on conveyor belt	320	Repetitive
			Recovery time or not
First break	Lunch break established by worker	40	Recovery time
Total minutes of actual work and breaks		360	

- 0.80 if additional factors are present for 3/3 (>80%) of the cycle.

With regard to the repetitiveness multiplier (*ReM*), when the task requires the performance of the same technical actions of the upper limbs for at least 50% of the cycle time or when the cycle time is shorter than 15 seconds, the corresponding multiplier factor (*ReM*) is 0.7. Otherwise, *ReM* is equal to 1 (CEN, 2007).

Recovery period factor

In recovery periods there is a substantial inactivity of the muscular groups used in repetitive movements. Rest breaks, such as the lunch break, are considered recovery periods, as well as periods when the worker performs other jobs without using the muscle group analyzed. Periods when these muscle groups are at rest, provided that they are at rest for at least 10 to 20 seconds, as suggested by the OCRA authors, are considered recovery periods. According to the number of working hours that do not have adequate recovery periods, the value of the multiplicative factor (*RcM*) to be used in Eq. 2 is assigned as shown in Tables 7 and 8. The multiplier for the overall duration of repetitive tasks (*DuM*) during a shift is determined in relation to the overall daily duration (in minutes) of manual repetitive tasks (Table 9).

Results

Table 10 shows, for each worker: the multiplicative coefficients for risk factors (*FoM*, *PoM*, *AdM*, and *ReM*), the multiplier for the "lack of recovery period" risk factor (*RcM*), the multiplier for the overall duration of repetitive tasks during a shift (*DuM)*, the net duration of the repetitive task in minutes (*D*), the number of actions performed per minute (*FF*), the overall number of actual technical actions needed in the workers' shift (*ATA*) and the overall number of reference technical actions (*RTA*). The values for right and left limbs are showed.

Table 11 shows the results of the risk assessment, with the *OCRA index* calculated for each worker.

The *OCRA index* values up to 2.2 are acceptable; values between 2.3 and 3.5 represent a possibility of risk, and values higher than 3.5 are considered unacceptable (more than 4.5 the risk is high, more than 9 the risk is very high), and therefore the way in which the job is carried out should be modified.

Conclusions

The research results indicate that the manual sorting of hazelnuts constitutes a situation of high risk due to repetitive movements of the upper limbs.

Looking at the values in Table 11, it is clear that the risk tends to increase with work experience in the specific task: the latter, in fact,

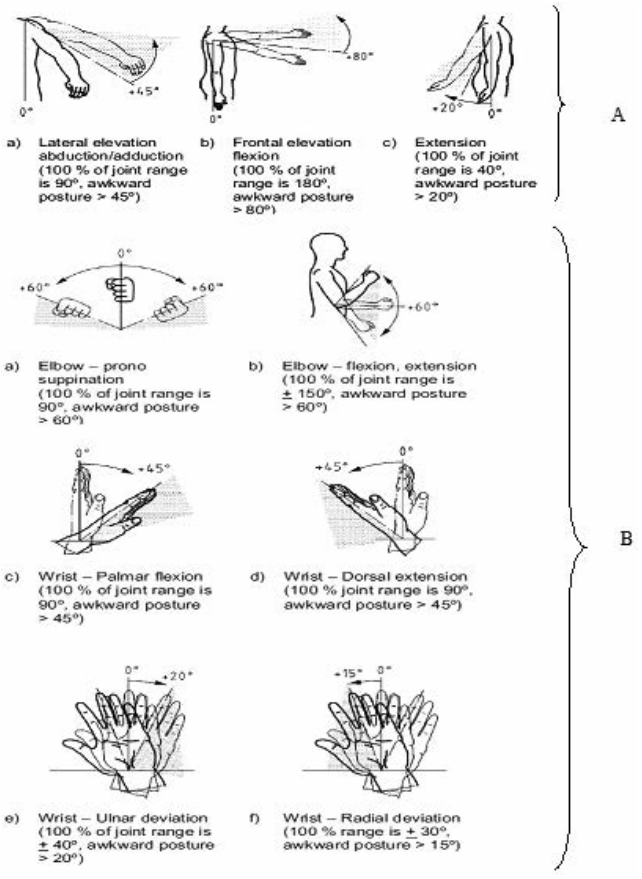

Figure 3. Shoulder postures and movements (A) and elbow and wrist postures and movements (B) (CEN, 2007).

Table 4. Borg scale for the evaluation of muscular force.

Score	Description	Score	Description
0	Completely absent	5	Strong
0.5	Extremely light	6	Strong (+)
1	Very light	7	Very strong
2	Light	8	Very strong (+)
3	Moderate (modest)	9	Very strong (++)
4	Modest (+)	10	Maximum

Table 5. Correspondence between Borg scale score and the multiplicative factor *FoM*.

	Average perceived exertion									
	≤0.5	1	1.5	2	2.5	3	3.5	4	4.5	≥5
Force factor (*FoM*)	1 0.85	0.75	0.65	0.55	0.45	0.35	0.2	0.1	0.01	

Table 6. Multipliers (*PoM*) for awkward postures

Awkward posture (Figure 3)	Portion of the cycle time			
	1% to 24% (<1/3)	25% to 50% (1/3)	51% to 80% (2/3)	>80% (3/3)
Elbow supination (>60°) Wrist extension (>45°) or flexion (>45°) Hand pinch or hook grip or palmar grip (wide span)	1	0.7	0.6	0.5
Elbow pronation (> 60°) or flexion/extension (>60°) Wrist radio-ulnar deviation (>20°) Hand power grip with narrow span (<2 cm)	1	1	0.7	0.6

Table 7. Risk index relative to the relationship between work and rest periods.

Work/Recovery ratio	Recovery	Risk
From 5/1 to 6/1	Adequate	0
From 7/1 to 11/1	Not satisfactory	0.5
>11/1	Not sufficient	1

Table 8. Recovery factor related to the presence or absence of adequate recovery periods.

Number of hours without adequate recovery periods	0	1	2	3	4	5	6	7	8
Multiplicative factor (*RcM*)	1	0.90	0.80	0.70	0.60	0.45	0.25	0.10	0

Table 9. Elements for the determination of the duration multiplier (*DuM*).

	Total time devoted to repetitive tasks during shift (min)			
	≥180	181 to 240	240 to 480	>480
Duration multiplier (*DuM*)	2	1.5	1	0.5

Table 10. Elements for calculating the *OCRA index*.

Worker n.	Limb*	*ReM*	*PoM*	*FoM*	*AdM*	D (min)	*FF* (act/min)	*RcM*	*DuM*	*ATA*	*RTA*
1	R	1	0.6	1	0.9	210	116	0.9	1.5	24360	4593
	L	1	0.6	1	0.9	210	62	0.9	1.5	13020	4593
9	R	0.7	0.7	1	0.9	210	131	0.8	1.5	27510	3149
	L	0.7	0.7	1	0.9	210	85	0.8	1.5	17850	3149
10	R	0.7	0.6	1	0.9	210	120	0.9	1.5	25200	3215
	L	0.7	0.6	1	0.9	210	112	0.9	1.5	23520	3215
8	R	0.7	0.6	1	0.9	320	120	0.7	1.5	38400	3810
	L	0.7	0.6	1	0.9	320	112	0.7	1.5	35840	3810

* R = right; L = left.

Table 11. Risk assessment with *OCRA index*.

Worker n.	Limb*	*OCRA index*	Risk
1	R	5.3	High
	L	2.8	Light
9	R	8.7	High
	L	5.7	High
10	R	7.8	High
	L	7.3	High
8	R	10.1	Very high
	L	9.4	Very high

* R = right; L = left.

leads to a natural increase in the frequency of movements (actions per minute) with a consequent increase of *OCRA index*.

Given the existence of a risk situation related to repetitive activities, the company should plan and implement new prevention strategies. These should consider the fact that the factors that have the greatest impact on the risk associated with repetitive movements, are the incorrect posture and the deficiency of recovery time. On this basis we can identify some measures:

creating a more comfortable workplace, able to meet all the ergonomic standards (*e.g.* workstations adjustable in height depending on the height of workers);

ensuring a higher frequency of rests (recovery time) spread during the workday;

reducing the duration of repetitive work;

improve the structural design of the working environment, for example by providing a second conveyor belt to carry away the rejects, or wider wastebaskets for rejects, in order to facilitate their release by workers.

Finally, the training of workers on the correct methods of work and the health surveillance of workers themselves are very important for the prevention of WMSDs.

References

ACGIH. Threshold limit value for chemical substances and physical agents and biological exposure indices. Cincinnati, Ohio: American Conference of Governmental Industrial Hygienists. 2001.

Apostoli, P., Bazzini, G., Sala, E., Imbriani, M. La versione italiana "OREGE" (Outil de Repérage et d'Evaluation des Gestes) dell'INRS (Institut National de Recherche et de Sécurité) per la valutazione dei disturbi muscolo-scheletrici dell'arto superiore. G. Ital. Med. Lav. Erg. 2002;24: 3-25.

Baar, A.E., Barbe, M.F., Clark, B.D. Work-related musculoskeletal disorders of the hand and wrist: epidemiology, pathophysiology, and sensorimotor changes. The Journal of Orthopaedic and Sports Physical Therapy. 2004;34:610-27.

Barr, A.E., Barbe, M.F. Pathophysiological tissue changes associated with repetitive movement: a review of the evidence. Journal of the American Physical Therapy Association. 2002;82: 173-87.

Borg, G. A. V. Psychophysical bases of perceived exertion. Med. Sci. Sports Exercise 1982;14: 377-81.

Cecchini, M., Bedini, R., Colantoni, A., Menghini, G., Monarca, D. Repetitive movements of upper limbs and risk of musculoskeletal disorders for workers during the cheese production in an Italian agro-food factory. In Proc. Irish Meeting on Agriculture Occupational Safety and Health. Dublin (Ireland), 22 - 24 August 2011.

Cecchini, M., Colantoni, A., Massantini, R., Monarca, D. The risk of musculoskeletal disorders for workers due to repetitive movements during tomato harvesting. J Agric Saf Health. 2010;16: 87-98.

CEN. EN 1005-5 Safety of machinery - Human physical performance - Part 5: Risk assessment for repetitive handling at high frequency. 2007. Brussels, Belgium: European Committee for Standardization.

Colantoni, A., Marucci, A., Monarca, D., Pagniello, B., Cecchini, M., Bedini, R. The risk of musculoskeletal disorders due to repetitive movements of upper limbs for workers employed to vegetable grafting. Journal of Food Agriculture and Environment. 2012;10: 14-8.

Colombini, D., Occhipinti, E. Application of concise exposure index (OCRA) to tasks involving repetitive movements of the upper limbs in various industrial settings: Preliminary experience and validation. Occup. Health and Ind. Med. 1997;37: 76-9.

Colombini, D., Occhipinti, E. Preventing upper limb work-related musculoskeletal disorders (UL-WMSDS): New approaches in job (re)design and current trends in standardization. Appl. Ergon. 2006;37: 441-50.

Davis, T.R.C. Do repetitive tasks give rise to musculoskeletal disorders? Occupational Medicine (Lond) 1999;49: 257-8.

Grieco, A. Application of the concise exposure index (OCRA) to tasks involving repetitive movements of the upper limbs in a variety of manufacturing industries: Preliminary validations. Ergonomics. 1998;41: 1347-56.

INAIL. Rapporto annuale 2012.

INRS. Method de prevention des troubles musculosquelettiques du membre superiore et outils simplex. Doc. Med. Trav. 2000;83: 187-223.

ISO. ISO 11228-3 Ergonomics - Manual handling - Part 3: Handling of low loads at high frequency. International Organization for Standardization. 2009.

Leclerc, A., Landre, M.F., Chastang, J.F., Niedhammer, I., Roquelaure, Y. Upper-limb disorders in repetitive work. Scandinavian Journal of Work Environment & Health. 2001;27:268-78.

Mc Atamney, L., Corlett, E. N. RULA: A survey method for the investigation of work-related upper limb disorders. Appl. Ergon. 1993;24: 91-9.

Merseburger, A. Movimenti ripetitivi degli arti superiori: risultati della valutazione dell'esposizione e dell'indagine clinica nella selezione e confezionamento delle mele. La Medicina del Lavoro. 1996;87: 603-12.

Monarca, D., Cecchini, M., Colantoni, A. 2011. Working posture, repetitive movements of upper limbs and risk of musculoskeletal disorders for workers during the cheese production in an Italian agro-food factory. Vienna (Austria), 29 June- 1 July 2011.

Monarca, D., Cecchini, M., Panaro, V. Analisi dei rischi di affezioni muscolo scheletriche da lavoro ripetitivo per gli addetti ad alcune operazioni agricole e agroindustriali. In Proc. AIIA 2001 Ingegneria Agraria per lo Sviluppo dei Paesi del Mediterraneo.

Moore, J. S., Garg, A. The strain index: A proposed method to analyze jobs for risk of distal upper extremity disorders. American Ind. Hyg. Assoc. J. 1995;56: 443-58.

Occhipinti, E. OCRA, a concise index for the assessment of exposure to repetitive movements of the upper limbs. Ergonomics. 1998;41: 1290-311.

Occhipinti, E., Colombini D. Proposta di un indice sintetico per la valutazione dell'esposizione a movimenti ripetitivi degli arti superiori (OCRA index). La Medicina del Lavoro. 1996;87: 526-48.

Occhipinti, E., Colombini, D. Alterazioni muscolo scheletriche degli arti superiori da sovraccarico biomeccanico: Metodi e criteri per l'inquadramento dell'esposizione lavorativa. La Medicina del Lavoro. 1996;87: 491-525.

Occhipinti, E., Colombini, D. Proposed concise index for the assessment of exposure to repetitive movements of the upper limbs. Occup. Health and Ind. Med. 1997;37: 73-7.

Schneider, S. OSHA's draft standard for prevention of work-related musculoskeletal disorders. Applied Occup. Environ. Hygiene 1995;10: 665-76.

The occupational safety on the construction sites of the farm production buildings in Finland

M. Hellstedt,[1] K.O. Kaustell,[2] T. Kivinen[3]

[1]MTT Agrifood Research Finland, Animal Production Research, Seinäjoki; [2]MTT Agrifood Research Finland, Economic Research, Helsinki; [3]MTT Agrifood Research Finland, Animal Production Research, Helsinki, Finland

Abstract

The size of farms has increased considerably during Finland's EU membership. The growth has meant big investments in the new production buildings. The buildings have been switched to big industrial-hall-like constructions from small-scale ones which have contained own timber and own work contribution. The objective of the project financed by Farmers' Social Insurance Institution was to improve occupational safety on farm building construction and renovation sites by disseminating current safety practices and by developing ways of action which are better than the prevailing ones. The project consisted of a literature review, statistical analysis, as well as a farmer and designer interviews.

In the statistical analysis the MATA occupational injuries insurance claims database on farmers' claims during construction and renovation work for the years 2005 - 2008 was compared with the register of Federation of Accident Insurance Institutions on the construction workers' injuries. In comparing the reasons of the accidents a clear difference was found; poor scaffoldings and ladders are still the main culprits on farm accidents.

Farmer interviews were used to assess occupational safety measures on the construction site, occurred injuries and their types, near-miss situations and the underlying factors which have led to the injuries. Also construction safety deficiencies as well as the direct and indirect costs caused for instance because of the delay in completion of construction project were discussed. Designer interviews aimed to find out how occupational safety and health considerations are taken into account in farm building planning and counseling, and how this experience of the designers should be utilized in order to improve safety at the construction sites on farms.

Farmers knew their obligations on occupational safety poorly. The situation was further worsened by the fact that on the site the supervisor tasks were only nominally executed. The designers knew the occupational health and safety legislation better but this did not help the situation on the sites because designers are not generally involved in the actual implementation of the construction project.

Correspondence: Maarit Hellstedt, MTT Agrifood Research Finland, Animal Production Research, Kampusranta 9 C, 60320 Seinäjoki, Finland
E-mail: maarit.hellstedt@mtt.fi

Key words: construction; safety; production building; agriculture.

Acknowledgments: authors want to thank the Farmers' Social Insurance Institution (MELA) and MTT Agrifood research Finland for their financial support which made this project possible.

Journal of Agricultural Engineering 2013; XLIV(s1):e131
doi:10.4081/jae.2013.(s1):e131

Introduction

The number of farms has decreased but their size has increased considerably during Finlands EU membership. The growth has meant big investments in new production buildings. The buildings have been switched to big industrial-hall-like constructions from small-scale ones that have contained own timber and own work contribution.

The value of Agricultural production buildings is about 350 MEUR which is about 5% of the yearly value of whole construction sector in Finland (MMM 2013). Agricultural buildings form yearly 10% of the whole constructed cubic meters in Finland and about 40 % of the industrial-hall-like construction cubic meters. (Tilastokeskus 2013).

About 1500 different kind of construction projects are accomplished yearly. According to Latvala and Pyykkönen (2009) the average size of loose houses for milking cows during the last years has been 1400 m^2 and 7850 m^3 and the average costs have been about 800 000 €. The construction work is performed by building contractors, competent carpenter groups or by the farmers themselves.

In the beginning of the year 2003 a new law on occupational safety came in to force (Työturvallisuuslaki 2003). Based on the law a new act on occupational safety on construction sites was introduced in 2009 (VnA 2009). The aim of the new law is to enhance proactive occupational safety and hands-on safety control on working places. The act aims to clear the responsibilities each party on the construction site has.

The objective of this project was to improve occupational safety on farm building construction and renovation sites by disseminating current safety practices and by developing ways of action which are better than the prevailing ones.

Materials and methods

The project consisted of a literature review, statistical analysis, as well as a farmer and designer interviews.

Literature review, statistical analysis

Both results of research projects on occupational safety on agricul-

tural production building sites and other examples of good practices in Finland and in other countries were investigated and their usability in Finnish conditions was estimated. Also results of the latest domestic researches on occupational safety on construction sites were examined in order to find practices suitable for agricultural construction sites.

In the statistical analysis the MaTa occupational injuries insurance claims database on farmers' claims during construction and renovation work for the years 2005 - 2008 was used to determine the most common accidents occurred on farm construction sites and their reasons. The Mata database was also compared with the register of Federation of Accident Insurance Institutions from the same years (2005 – 2008) on the construction workers' injuries to find out the possible differences between the most common accidents between these two groups.

Farmer and designer interviews

Farmer interviews were carried out by visiting farms (N=8). The occupational safety measures on the construction site, the possible accidents which had happened and their types and underlying factors which had led to the accident were clarified with the farmer interviews. Also the near accident situations and the safety lacks of the construction work were discussed. Farmers were also asked about their knowledge on the occupational safety legislation and responsibilities on construction sites and their attitude towards safety issues.

Designer interviews (N=10) were made using a web poll. Through the designer interviews it was clarified how the occupational safety issues are taken into consideration in the design of farm production buildings and how attention should be paid to the matter according to the designers' experience so that the occupational safety situation would become better.

Results

During the years 2005 - 2008 a total of 1205 accidents at farm construction work were registered in the Farmers´ insurance database (MATA). The construction work accidents accounted for 5-6 % of all the accidents occurred to farmers at their farm work yearly. The construction work accidents resulted in about 46 500 days of disability, the average period of disability being 38.6 days. During the year 2008 the Farmers' Social Insurance Institution (Mela) paid out to farmers about 1.62 MEUR.

Most of these accidents at construction sites occurred at repairing and maintenance tasks (39.5 %), reconstruction and enlargement sites (18.6 %) and construction of new production facilities (26.5 %). The most common reason for accidents at the construction sites was falling and hitting against something (about 26 % of the accidents). Other common reasons were contact to a cutting object like a knife or some other stabbing edge (11,5 %), and physical stress on muscular and skeletal bodies (10,8 %).

When comparing the reasons of the accidents between the MATA database and the register of Federation of Accident Insurance Institutions (TVL) a clear difference was found; ´poor scaffoldings and ladders´ are still the main reasons of farm accidents (18.2 %) while at other construction sites they were ´ Raw materials, goods, supplies, equipment etc.´ (34.7%) and ´ The terrain (ice) roughness, slipperiness, deceptiveness, soil, obstructions ´(18%) (Table 1).

Farmers found the most hazardous cases at their construction sites to be roof works where tools could drop down or men could drop as well. Helmets were not popular due to hot summer days and thus too much sweating. Scaffoldings were often poor without safety railings. Too often ladders were used as scaffolds which led to accidents when ladders unexpectedly slid down. Lucky enough most workmen used safety boots. Lifting heavy loads caused muscle and bone injuries. Machinery installations caused minor injuries due to sharp metal edges.

According to the interviews the farmers knew their obligations of occupational safety rather poorly. The situation was further aggravated by the fact that on the site the site supervisor tasks including occupational safety issues were usually taken care by nominal and minimal effort and in most cases by the farmer himself. Special plans for occupational safety, which the legislation requires, were very rare. Although construction site meetings were held regularly on most farm construction sites (70%), occupational safety issues were discussed seldom and normally only to remind the constructor of his responsibilities.

The designers knew the occupational health and safety legislation quite well. All the designers knew the law on Occupational safety (Työturvallisuuslaki 2003) although only 40 % of them told that they knew it very well. 30 % of the designers told that they know the Act on occupational safety at construction sites (VnA 2009) well and they take it into account with in their construction plans. However this did not help the situation on the sites because designers are not generally involved in the actual implementation of the construction project

Discussion

Accident risk is high at farm construction sites just like it is at all other construction sites. The culprits differ which is mainly caused by the fact that the farm construction sites are not arranged as professionally as they should from the point of view of their size. The legislation on occupational safety at construction sites, however, is the same for all types of construction sites without any exceptions. In the legislation, there are certain responsibilities and tasks for every worker and party.

Mäkelä (2006) has developed a conceptual system on the safety issues that have to be planned on every construction site. This kind

Table 1. Distribution of the culpits at the construction site for farmers (MATA) and for construction workers (TVL).

Culpits	MATA %	TVL %
The terrain (ice) roughness, slipperiness, deceptiveness, soil, obstructions	16.6	18.0
Raw materials, goods, supplies, equipment, the external environment, fences, loads, tractor accessories and structures	13.2	34.7
Saws, circular saws, field saws, machine tools, cutting machine, slicers, choppers, hand-operated drills and grinding machinery, chain saws	10.0	3.7
Hand tools	9.2	8.6
The external environment (conditions), the work movements and work positions	9.1	0.9
Other culpits	7.6	5.5
Stairs	5.2	2.6
Other buildings, structures and constructions	5.1	0.3

of procedure is not used at farm construction sites because farmers do not recognize the need for this kind of planning. This is partly due to the fact that they do not know well enough their responsibilities on occupational safety issues and partly due to the fact that they are used to do the construction work by themselves and they are not familiar with the procedures on construction sites with workers and constructors. Farmers also lack the information of possible risks at their construction site. It is very difficult to recognize the risks comprehensively. According to Carter and Smith (2006) this is based on lack of common information, knowledge of possible risks and coordinated management. It is possible to enhance risk analysis by using different kinds of checking lists which are available. But the problem still is that the farmers don't even know these checklists.

Conclusions

The direct costs paid out by the insurance company are only part of the total costs caused by the accidents at construction sites. The value of the possible delay of the whole project and the value of other indirect costs is very difficult to estimate. Oinonen & Aaltonen (2007) have estimated that these indirect costs are normally much bigger than the direct costs. Therefore all efforts made to minimize the number of accidents at farm construction sites have a significant influence on the economy of the farm.

A possible solution for enhancing the occupational safety on farm construction sites is that the designers should be given a more visible role in the whole construction process. They have the needed knowledge which should be used for the best of all parties.

In order to get this development in practice, farmers should be given more accurate information on their responsibilities on occupation safety issues and also the economic benefits of the reduction of accidents on their farm construction sites

References

Carter G. & Smith S. 2006. Safety Hazard Identification on Construction Projects. In Journal of construction engineering and management. February 2006. ASCE. p. 197-205.

Latvala, T. & Pyykkönen, P. 2009. Teknotila-hankkeen tuloksia. 20.08.2009. Henkilökohtainen tiedonanto.

MMM 2013. Maa- ja metsätalousministeriö. Maaseudun kehittäminen / Maaseudun rakentaminen / Maatilarakentaminen.
http://www.mmm.fi/fi/index/etusivu/maaseudun_kehittaminen/maaseuturakentaminen/maatilarakentaminen.html

Mäkelä, T. 2006. Pientalojen aluerakentamisen työturvallisuus. VTT tutkimusraportti VTT-R-07902-06.

Oinonen, K. & Aaltonen, M. 2007. Työterveys ja työturvallisuus tuottavuustekijänä. Työtapa-turmien aiheuttamat kustannukset. Työturvallisuuden merkitys työpaikkojen tuottavuuteen –projektin tutkimusosio 2:n loppuraportti Työsuojelurahastolle.

Tilastokeskus 2013. Tilastokeskus. Verkkopalvelut /Suomi lukuina / rakentaminen.
http://www.stat.fi/tup/suoluk/suoluk_rakentaminen.html

Työturvallisuuslaki 2003. Työturvallisuuslaki 738/2002. http://www.finlex.fi/fi/laki/smur/2002

VnA 2009. Valtioneuvoston asetus rakennustyön turvallisuudesta. http://www.finlex.fi/fi/laki/smur/2009/

Methodological approach to assess tractor stability in normal operation in field using a commercial warning device

V. Rondelli,[1] R. Martelli,[1] C. Casazza,[1] A. Guarnieri[1]

[1]Department of Agricultural and Food Sciences, University of Bologna, IT; Dipartimento di Scienze e Tecnologie Agro-Alimentari, Università di Bologna, Italy

Abstract

Since Roll-Over Protective Structures (ROPS) are mandatory on tractors, the number of fatalities caused in the event of an upset is definitely reduced. Nevertheless, fatal accidents caused by machine loss of stability are still of great concern. In fact, despite ROPS have reduced injury to agricultural operators, tractor stability is still a complex issue due to its high versatility in use, especially considering normal operations in field, when interactions with the environment such as soil morphology and climatic conditions are involved, as well as interactions with operator skills and experience.

With the aim of collecting data on different variables influencing the dynamics of tractors in field, a commercial device that allows the continuous monitoring of working conditions and the active configuration of the machines was fitted on standard tractors in normal operation at the experimental farm of the Bologna University.

The device consists of accelerometers, gyroscope, GSM/GPRS, GPS for geo-referencing and a transceiver for the automatic recognition of tractor-connected equipment. A microprocessor processes data and provides information, through a dedicated algorithm requiring data on the geometry of the tested tractor, on the level of risk for the operator in terms of probable loss of stability and suggests corrective measures to reduce the potential instability of the tractor.

Introduction

Tractors are the most widely used machines in agriculture and are responsible for the high number of fatalities related to the use of farm machinery (McCurdy and Carroll, 2000; Nichol et al., 2005). In Italy, data reported by ISPESL (National Institute for Occupational Safety and Prevention) indicate a high number of fatal accidents associated with the use of tractors, 114 in 2008 and 149 in 2009 (Fargnoli et al., 2010). Despite the mandatory application of ROPS to provide a survival volume for the operator, accidents due to tractor rollover are the leading cause of death in farm operations (Pessina and Facchinetti, 2011).

The analysis of tractor upsets is complex because the rollover is influenced by several factors such as interaction among operator, tractor and environment. Major critical variables reducing tractor stability are slopes and rough terrain; these factors interact in a complex manner in determining the risk of rollover, influenced by the position of the tractor's centre of gravity, forward speed and turning angle.

In addition, safe tractor operation also depends on operator skill and experience, reaction time, etc. Interacting factors affect the operator's perception of hazard, using his skill and intuition to evaluate the effects of different environmental factors (Murphy et al., 1985). While most experienced tractor operators have developed an intuitive feel in perceiving hazardous situations, there are many inexperienced young or casual workers who have no specific training in driving the tractor safely (Nichol et al., 2005). Furthermore, the ability to operate safely is further reduced by adverse stressors as vibrations, noise, cold and heat and this is particularly significant when stressor conditions drag on as occurs frequently during farming (Murphy et al., 1985). Other aspects affecting upsets are the characteristics of implements coupled to the tractor

Devices have been developed to inform the operator about tractor stability and warn him in case of overturn risk (Mitchell et al., 1972; Spencer and Owen, 1981) or to alert medical assistance in case of accident (Sarghini and D'Urso, 2010). Frequently, devices evaluating tractor stability conditions take into account mathematical models based on the forces acting on the tractor that can cause the upset. Both the constructive aspects of the tractor, such as weight or the position of the centre of gravity, and those related to its movement such as speed, turning radius and slope are taken into account. Murphy et al. (1985) developed a mathematical model to measure the relative stability of a tractor considering weight and centrifugal force vectors and the effects of ground roughness.

Active systems have been evaluated to stop the tractor in case of rollover risk by cutting fuel supply or ignition system (Murphy et al., 1985). Nichol et al., (2005) developed a low cost device based on sensors and a display to inform the tractor operator of possible instability and to assist him in avoiding dangerous situations. Etzler et al. (2008) proposed a methodology for establishing a risk threshold to inform the tractor operator and assist him in performing corrective manoeuvres for mitigating risks according to risk level. However, only very few commercial warning systems have been developed nowadays and additional research needs to be carried out to assess their performance on tractors operating in farms.

A low-cost commercial warning device (COBO International, USA) is currently under evaluation. The device is fitted with sensors to detect tractor dynamic properties and, through a predictive mathe-

Correspondence: Valda Rondelli, Dipartimento di Scienze e Tecnologie Agro-Alimentari, Università di Bologna, via G. Fanin 50, 40127 Bologna, Italy.
Tel. +39.051.766632 - Fax: +39.051.765318.
E-mail: valda.rondelli@unibo.it

Key words: accident prevention, operator safety, rollover tractor, warning device.

Journal of Agricultural Engineering 2013; XLIV(s1):e132
doi:10.4081/jae.2013.(s1):e132

matical model, process a risk index to inform the operator of potential tractor instability and suggest corrective measures to avoid dangerous operations.

Research objectives are to: i) assess the performance of the commercial device on tractors as they operate in field; ii) collect data on different variables influencing the dynamics of the tractors; iii) verify if the device can be used to improve the operator's risk perception.

Preliminary and methodological aspects of the research are described, providing information on the architecture of the device, tractor field testing and data collection.

Multisensor device

The commercial warning device (COBO International, USA) for tractor stability prediction consists of the following units:

- dual-axis accelerometer as tilt sensor and tri-axial accelerometer to validate the signals from the bi-axial accelerometer and confirm tractor overturn;
- microprocessor to acquire signals and process information;
- gyroscope to measure tractor steering angle rate;
- GPS for tractor geographical localization;

Figure 1. Tractor fitted with multisensor device, main controller (1), visual warning display (2), implement transceiver (3).

Table 1. Parameters recorded by sensors.

Parameter	Units	Notes
Speed	km h^{-1}	
Elevation	m	above sea level
Roll angle	degree	>0 upward
		<0 downward
Pitch angle	degree	>0 clockwise with respect to the advancing direction
		<0 anticlockwise with respect to the advancing direction
Steering	rad s^{-1}	>0 clockwise with respect to the advancing direction

Table 2. Tractors, engine power and working areas.

Tractor code	Power (kW)	Area	Field operations
1	107	hill	harrowing, mowing
2	74	hill	baling, liquid manure spreading
3	200	plain + hill	plowing
4	103	plain	subsoiling, harrowing, baling
5	63	plain	mowing, hay making

Figure 2. Website overview, mapped areas and tractors monitored during operations.

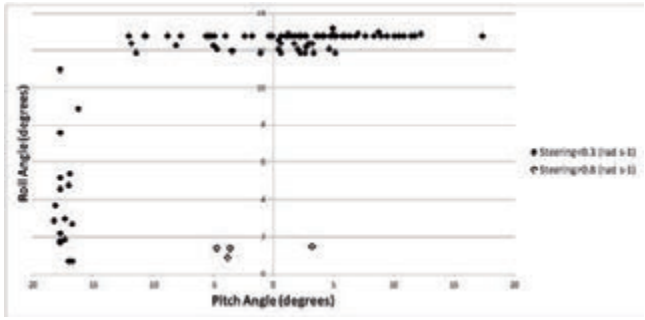

Figure 3. Values of the parameters for warning cases.

Figure 4. Multisensor display device during the static test.

Table 3. Automatically recognized operating machinery.

Transceiver code	Implement	Working area
86	mower	hill
87	tedder	hill
88	liquid manure spreader	hill
89	round baler	hill
90	rotary cultivator (3 m width)	plain + hill
91	rotary cultivator (4 m width)	plain
92	harrow	plain
93	subsoiler	plain
94	mower conditioner	plain
95	plough	plain + hill
96	cultivator	hill
97	round baler	plain

- GSM/GPRS quad-band module for data transmission.

In addition, the multisensor unit recognizes the implements coupled to the tractor by means of a 2.4 GHz transceiver installed on the implements.

The device is completed by a visual warning system based on a mathematical model to alert the operator on rollover risk level (Figure 1).

The risk index, based on a simplified quasi-static model, considers both the geometric parameters of the tractor, or the complex tractor-implement (its overall weight and distribution, centre of gravity, track and wheelbase), and the dynamic operating conditions detected by the sensors (speed, roll and pitch angles, steering rate).

The warning device must be installed by the manufacturer technical staff in order to set up the device, acquiring tractor mass, wheelbase, track and ballasts. The weight of both tractor axles and the overall weight are achieved on the horizontal plane and on a slope in the 8-15 degree range. Weighing is repeated with all implements coupled to the tractor.

The multisensor unit is normally fixed on the tractor roof to be perfectly horizontal, while the visual warning display is fitted on the tractor cab to be monitored from the driver's seat. The device is complemented by a dedicated website, which allows to geo-reference the farm parcels and record tractor types, operators and implements.

Signals detected by sensors (Table 1) are transferred automatically to a database accessible online. Data could be filtered by queries to limit the analysis to interesting information; these could be downloaded as spreadsheets for later evaluation.

Laboratory tests were performed for the device evaluation before field testing. The multisensor was placed on a standard wheeled tractor and this was statically tested on a slope fitted with a commercial digital level. The roll angle was changed and the two different readings were compared. The output of the device was deemed correct.

Field tests

Five warning devices have been installed on standard tractors in use at the experimental farm of the University of Bologna. The monitored machinery includes modern four-wheel drive tractors fitted with a ROPS cab and engine power in the 60 to 100-kW range to carry out normal farm operations (Table 2).

Twelve implements coupled to the tested tractors have been fitted with transceivers for automatic detection (Table 3).

The experimental farm is mainly cultivated with cereal and fodder crops. Fields are located partly in Cadriano, a flat area with altitude in a range of 19 to 40 m above sea level, and partly in Ozzano, in a hilly area with altitude up to 370 m above sea level.

Ten parcels (five on level ground and five on hill) corresponding to the farm's main production units were mapped and recorded on the website to check online the location of the tractors involved in the test (Figure 2). Ten other areas could be mapped as highly hazardous and the device could be set up to alert the operator when the tractor approaches these zones, reaching maximum signal intensity on crossing these boundaries. This function was not checked in the field test.

The five tested tractors were driven by operators employed in the experimental farm and experienced in tractor driving. Tests were arranged to keep the operators in their usual working area, with the exception of the operator driving tractor 3 (Table 2) who usually operated on level ground, but during tests also worked on hills to compare his risk perception in an unusual working area (Table 2).

In addition to the signal detected by the sensor, a data collection form was given to the operators involved in the test, to be filled in after completing the activity to report the operation performed, the working time and the number of events considered potentially dangerous on the basis of a pre-defined scale of estimated risk level. The compiled forms will allow comparing the operators' responses with information provided by the multisensor.

Preliminary results and considerations

The availability of a commercial low cost device, such as the tested warning device, offers the advantage of retrofitting it on tractors. In European Countries since 1974, according to EC Directive 74/150 (EEC, 1974), tractors are fitted with ROPS as a passive means to minimize the risk of injury for drivers in the event of tractor upset. The approach to fit a ROPS was the consequence of verifying that there was only a little chance of preventing tractors from rolling over (Moberg, 1973). Nonetheless, a warning device capable of informing the tractor operator on the stability of his machine during operation could greatly contribute to prevent fatal accidents because he can promptly react and consequently decrease dangerous situations.

The potential of the tested device has positive effects on the operator, with respect to the improvement of the risk perception associated with the stability of the machine, but also offers the employer the chance to evaluate the safety level in the farm through automatic monitoring of fleet equipment, mechanical operations, working areas and dynamic operational conditions.

An experimental methodology was presented at this preliminary stage of research, based on an integrated information system to allow safety evaluation in farm operations. Tests were planned on fields with wide-ranging orographic variability but all tested machinery is modern and operators are experienced. The aim is to monitor tractors in routine operating conditions but with different levels of risk in relation to different land slopes and different working conditions.

The multisensor system, combined with the dedicated web site, allow the recording of events potentially at a risk level above a specific threshold. These records provide the time history of risk events encountered during operations and it is then possible to evaluate the temporal and spatial distribution of the events, analyzing possible causes and comparing the level of safety of the same operation performed by different drivers in different orographic conditions.

Figure 3 shows data of preliminary field tests. Values of pitch and roll angles are displayed when the warning device alerted the operator of tractor 1 during harrowing operation. This activity has been selected because of the high frequency of alarm signals. Absolute values of roll angle are shown due to the symmetrical position of the machinery centre of gravity. Two sets of data are presented, one corresponding to data of steering less than 0.3 rad s-1 and the other higher than 0.8 rad s-1, to point out the prevalent cause, pitch angle, roll angle or steering, that led to the warning.

Clearly the performance of the device in field must first of all be assessed in order to verify the correctness of the sensors' output. The warning device was checked statically in the lab and the results confirmed the acceptable performance of the tilt sensors. However, in field the addition of different forward speeds, different slopes and different steering speeds can interfere with data detected by the sensors. In fact, since many operations are performed with the tractor in field, the device should be able to correctly measure roll and pitch angles at different forward speeds and steering speeds, which means assessing the tractor during normal operation.

It must be underlined that the warning system was designed to help the operator in case of a potential rollover situation suggesting him to act on the parameters under his control, such as speed and turning radius.

Figure 4 shows the display device during the static test. Many indications are provided: speed, pitch and roll angles, warning signal represented by the yellow concentric circles and the condition of prevailing risk, with the suggestion of a corrective action, in the red box. The larger box shows the recording of a device integrated camera.

The operator needs to recognize the dangerous situation on time to correct it and avoid the fatal event. If the device detects the risk level correctly, it can improve operator perception in potentially unstable situations. In this regard it is very important to check whether the display warns too often about potential rollover situations because this can lead the operator to ignore the warning. The levels at which the display shows a near rollover condition need to be optimized to keep the operator's attention.

References

Etzler L., Marzani S., Montanari R., Tesauri F. 2008. Mitigating accident risk in farm tractors.
Ergon. Des. 16:6-13.

European Commission. Commission decision of 4 March 1974 on the approximation of the laws of the Member States relating to the type-approval of wheeled agricultural and forestry tractors, 74/150/EEC. Available on: www/eur-lex.europa.eu.

Fargnoli M., Laurendi V., Tronci M. A risk assessment procedure for the users of narrow track tractors. Proceedings of the 2nd Ragusa SHWA Int. Conf., 2010 Sept. 16-18, Ragusa, Italy.

McCurdy S.A., Carroll D.J. 2000. Agricultural injury. Am. J. Ind. Med. 38:463-80.

Mitchell B.W., Zachariah G.L., Liljedhal J.B. 1972. Prediction and control of tractor stability to prevent rearward overturning. Trans. ASAE 15:838-44.

Moberg, H.A. 1973. Dynamic testing of tractor protection cabs: Development of method, practical experiences. SAE Paper No. 73076. Warrendale, Pa.: SAE

Murphy D.J., Beppler D.C., Sommer H.J. 1985. Tractor Stability Indicator. Appl. Ergon. 16:187-91.

Nichol C.I., Sommer III H.J., Murphy D.J. 2005. Simplified overturn stability monitoring of agricultural tractors. J. Agric. Saf. Health. 11:99-108.

Pessina D., Facchinetti D. Il ruolo del web nel monitoraggio degli incidenti mortali dovuti al ribaltamento dei trattori agricoli. Proceedings of the Conference: Gestione e Controllo dei Sistemi Agrari e Forestali, 2011 Sept. 22-24, Belgirate, Verbania, Italy.

Sarghini F., D'Urso G. An early warning device for identification of tractor accidents, rapid alert and assistance. Proceedings of the 2nd Ragusa SHWA Int. Conf., 2010 Sept. 16-18, Ragusa, Italy.

Spencer H.B., Owen G.M. 1981. A Device for Assessing the Safe Descent Slope of Agricultural Vehicles. J. Agr. Eng. Res. 26:277-86.

Simulated stability tests of a small articulated tractor designed for extreme-sloped vineyards

F. Mazzetto,[1] M. Bietresato,[1] A. Gasparetto,[2] R. Vidoni[1]

[1]Free University of Bozen-Bolzano, Faculty of Science and Technology, Fa.S.T., Bolzano, Italy; [2]Università degli Studi di Udine, Dipartimento di Ingegneria Elettrica, Gestionale e Meccanica, DIEGM, Udine, Italy

Abstract

A new reversible wheeled articulated tractor, designed to work in terraced vineyards trained with "pergola" system, common in mountain areas, is here described in its latest version and analysed through numerical simulations.

This tractor has small dimensions, necessary to operate in that environment, and its central articulation has two rotational degrees-of-freedom. The described features are surely strong design points but could be critical for vehicle's stability, as affecting the supporting base's dimensions and shape. Therefore, the tractor was equipped with a new automatic safety system: a self-locking articulation activated by contact sensors on the wheels. This device makes the vehicle partially-rigid in case of lateral unbalancing, so that rollover can happen only by overcoming the whole vehicle mass.

A mathematical description of vehicle-ground interactions was implemented to deeply inquiry the tractor behaviour in different configurations (straight, angled) at increasing values of ground slope; roll and pitch stability indexes were then computed and used for comparisons with conventional tractors.

Thanks to the low centre-of-gravity, the resulting rollover angle with the vehicle in straight configuration is promising (43.8°→96%): it is greater than the maximum lateral (20°→36%) and frontal (38°→78%) slope angle ever recorded on terraced vineyards. The same rollover angle is lower when the tractor turns.

Correspondence: Marco Bietresato, Free University of Bozen-Bolzano, Faculty of Science and Technology, Fa.S.T., piazza Università 5, P.O. Box 276, I-39100 Bolzano (BZ), Italy.
Tel. +39 0471 017181 - Fax: +39 0471 017009.
E-mail: marco.bietresato@unibz.it

Keywords: articulated tractor; tractor stability; safety index; self-locking articulation, Matlab® simulation.

Acknowledgments: the authors wish to thanks eng. Pietro Afier for his help in the implementation of the simulator.

Conflict of interests: the authors declare no potential conflict of interests.

Conference presentation: this paper has been submitted to The Italian Society of Agricultural Engineering for the 10th AIIA Conference *"AIIA13 – Horizons in agricultural, forestry and biosystems engineering"*, which will be held in Viterbo, University of Tuscia, Italy, on September 8-12, 2013.

Journal of Agricultural Engineering 2013; XLIV(s1):e133
doi:10.4081/jae.2013.(s1):e133

Introduction

General considerations and problem description

Most of the vineyards assigned to the production of high-quality grapes and wines are very problematic by the point of view of the mechanisation. In fact, these vineyards are often placed in steep hillsides and use traditional training systems (such as "pergola"), considered by farmers essential for obtaining a better maturation of grapes and a full development of the aromas which will characterize the wines obtained from those grapes. The only possible mechanization in these difficult environments makes use of small tracked or wheeled tractors capable of operating in: i) very narrow inter-rows, often lower than 1.00 m and with the risk of roll-over, ii) reduced spans under the arbours (commonly ≤1.80 m, often ≤1.60 m); iii) steep and very tight curves in row heads, with great difficulties of manoeuvre.

In particular, the tractor resulting from these design requirements and proposed in this work has small dimensions, necessary to operate in this environment, and presents 4-wheel drive together with a central articulation having two rotational degrees-of-freedom (dof). This joint allows a great manoeuvrability on the horizontal plane and the overcoming of the soil harshness. The described features are surely strong design points but could be potentially critical for the stability of the vehicle since affecting the baseline dimensions and shape. Therefore, a mathematical description of vehicle-ground interactions has been implemented.

The study of the dynamic behaviour of agricultural tractors and of off-road vehicles in general, is a very actual research topic, since it allows having a greater awareness of how design choices influence the stability, the handling and the operational limits of a vehicle, and hence the safety level of the occupants (Guarnieri & Fabbri, 2002).

One of the most interesting topics in studying the stability rollover of agricultural tractors operating on steep hillsides is the capability for the analyst to *predict, prevent or limit the damage caused by a possible overturning*. These situations can be described through analytical equations relating the vehicle attitude to the incipient overturning condition. This problem can be addressed in two different ways: (i) *energetic* or (ii) *Newtonian*.

In (Guzzomi, Rondelli, Guarnieri, Molari, & Molari, 2009), for example, the energetic approach allowed to analyse the different initial rollover conditions of tractors and to evaluate the energy available at rollover start. Thanks to this study it has been possible to realize that the available energy may not be a linear function of tractor mass, as assumed by the international testing procedure, and to define the application range of the energy formula used in Code 6 (OECD, 1990).

State of the art

Most of the works, however, use a Newtonian approach and some of them can consider also a three-dimensional tire–terrain interaction model (Pazooki, Rakheja, & Cao, 2012) or the effects of the rear track width and of an additional weight placed on the wheels on the stability of a tractor when driving on side slopes (Gravalos et al., 2011). Eventual trailers or agricultural implements attached to the tractor change substantially the behaviour of the whole vehicle and could easily lead it to critical conditions, thus they deserve deeper investigations. For example, in (Ji-hua, Jin-liang, & Yan, 2011) a linear dynamics model of tractor/full trailer with six dofs is presented and used to evidence critical situations occurring when avoiding an obstacle (rearward amplification phenomenon).

The model of the lateral dynamics of a tractor with a single-axle grain cart was studied in (Karkee & Steward, 2010); a sensitivity analysis allowed to identify the effect of uncertainty/variation of some parameters on system responses. In (Popescu & Sutru, 2009) the longitudinal stability of the tractor-front-end loader system and of tractor-forklift system was studied in the most difficult work situations: braking and moving the load on the forks while descending on a slope. The same analytical approach is used also in (Guzzomi, 2012) where a geometrical model for predicting the rollover initiation angle of traditional farm tractors fitted with front-axle pivot under quasi-static conditions is presented. The model uses a kineto-static approach based on two rigid bodies: the front axle and wheels (anterior body), and the remaining machine and the rear wheels (posterior body). Conventional tractors have been studied also in (Ahmadi, 2011) through a dynamic model capable of investigating the effects of forward speed, ground slope and wheel–ground friction coefficient on lateral stability at the presence of position disturbances.

The present work uses an approach similar to (Coombes, 1968; Guzzomi, 2012; Scarlett et al., 2006) but deals with *articulated farm tractors*, i.e. wheeled tractors having a central joint used for steering (Mazzetto, Gallo, Vidoni, Bisaglia, & Calcante, 2012; Mazzetto, Gallo, Vidoni, & Bisaglia, 2012). The rollover angle is calculated in a quasi-static condition and the attitude of the tractor in every slope condition is quantified by a *stability index*, in a way similar to (Yisa, Terao, Noguchi, & Kubota, 1998) and (Liu & Ayers, 1999). This index synthetizes possible overturn conditions (e.g., roll and pitch angles) in a single number and it could be very useful if used as input signal for many real-time active safety devices acting on several systems, e.g.: braking systems, limited-slip differentials (Huang, Zhan, & Wu, 2012), variable-geometry roll-over structures (Silleli et al., 2007), self-levelling cab system (Mashadi & Nasrolahi, 2009).

Aim of the research

The aim of this work was to investigate numerically the stability of narrow-track wheeled articulated farm tractors and to evaluate the possibility of introducing a real-time safety device acting on the central joint. The article presents a properly-developed mathematical model, used to simulate the operation of this type of tractors.

Materials and Methods

Central joint design and analysis

A central joint with two dofs was initially selected to be installed on the articulated tractor. This joint allows the steering of the vehicle (*first dof*) and, similarly to conventional tractors with front axle pivot, a simultaneous inclination in the transverse plane when, for instance, a wheel encounters ground harshness (*second dof*). If a static, no slipping wheels condition is considered, the kinematics of lateral overturning of an articulated tractor with a 2-dof joint is similar to the case of conventional tractors (Coombes, 1968; Scarlett et al., 2006), with the only difference that the rollover starts from a single half of the vehicle (the upstream part; Figure 1) and not involves the whole vehicle as for conventional tractors (Figure 2). In particular, the axis of rotation of the overturning part of the articulated tractor would pass by the joint and by the contact point of the lowest wheel of the unstable part (Figure 1). If the downstream half is stable while the upstream part not, the joint position can be thought as fixed.

With the vehicle longitudinal axis perpendicular to the maximum slope direction (advancement along a contour line) the angle of incipient overturning (*stability critical angle*) for this triangular configuration of the supports is (Coombes, 1968; Guzzomi, 2012; Scarlett et al., 2006):

$$\vartheta_{cr} = arctg\left[\frac{w_b(s-s_1)}{2(h_b s - h_1 s_1)}\right] \quad (1)$$

where w_b, s, s_1, h_b and h_1 are defined as in Figure 1 and 2. Since this articulated tractor is thought to be primarily used on slopes, the stability characteristics were enhanced by blocking the second dof of the joint central in conditions of possible rollover. By doing so, the polygon of stability changes from the triangle described above to a quadrilateral which joins all the wheel-ground contact points (Figure 3). That dof will instead remain in the normal operation of the tractor: this increases the comfort of the operator and makes all the wheels touch the ground.

Kinematic models

In order to evaluate the stability and the behaviour of an articulated farm tractor in different working and slope conditions, a simplified model has been developed. The vehicle-system has been evaluated in its main geometrical and mechanical parameters, Figure 4A and Table 1, and the steering articulation has been considered as a revolute kinematic pair. For the reasons previously explained, in this work no pivot on the front axis or independent suspensions have been considered, thus allowing to consider the tractor footprint given by the four wheels in contact with the surface. The revolute joint, that is in charge to simulate the steering system, is the active joint of the tractor and it is limited by the maximum steering angle, max_θ. Moreover, a conventional configuration, i.e. with four wheels and rigid chassis system (without any front axle pivot), Figure 4B, has also been considered to allow a suitable stability comparison and evaluation.

As regards the steering, the overall model has been developed by means of the classical steering kinematics (Genta, 2000), thus neglecting the contributes of sliding and aerodynamic frictions. In such this way, it is possible to evaluate the position of the wheels in a steering condition, i.e. along a circle with different radius, fundamental elements for the stability evaluation.

Quantification of the stability of a tractor

The *conventional agricultural tractor* has been considered as a rigid central body with mass m and four possible contact points with the ground surface. The stability of a tractor can be classified at least into longitudinal (*pitch*) and lateral (*roll*) turning stability, both related to the tractor stability baseline, i.e. the polygonal line that connects all the wheels of the tractor as the wheels set on level ground. Generally speaking, the system is stable if the projection of the centre of gravity (COG) of the system on the travelled plane surface is inside the stabil-

ity baseline. Thanks to this assumption, both the longitudinal and lateral stability can be defined.

In the case of the *articulated tractor*, the stability baseline can be defined in the same way as for the conventional one; the system COG has instead to be computed at each step/configuration since it is directly related to the steering angle. If the COG of the forward and backward parts are considered (COG_b, COG_f), the system COG can be computed.

As the tractor moves at reasonably low speed during its normal operations (lower than 1.5 m s^{-1}), the dynamic stability can be treated with a quasi-static approach, i.e. the inertial terms can be considered negligible, without the risk of invalidating the results. This means that the only force to be considered is the weight (*Fp*), that is distributed on the four wheels (Figure 5A) in correspondence to the four ground-tractor points of contact.

The weight force is applied on the system COG, it is *Fp* = *-mgz*, directed along the absolute vertical axis. Hence, with the aim of evaluating the stability of the system, it has been chosen to simulate the tractor while travelling along a circumference with radius *r* and in different slope conditions, i.e. turning on a plane with different values of the slope (referred to as α).

Following the approach in (Liu & Ayers, 1999), roll and pitch stability indexes have been defined and implemented. The generic (percentage) *stability index* (*SI*) is:

$$SI = \left(1 - \frac{X}{X_{cri}}\right) \cdot 100 \tag{2}$$

where *X* is the state variable for evaluating the stability and X_{cri} its critical value.

In order to compute the *SI*, the following procedure has been followed.

First of all the following data have been computed:

- current position of the four wheels;
- projection of the COG on the inclined plane (*P* in Figure 5B);
- position of the geometric centre of gravity (*GCOG*) with respect to the absolute reference system;
- spatial definition of the tangential (u_2) and orthogonal (u_1) unit vectors with respect to the system path.

With this data available, the indexes are calculated by evaluating the distance of the projection of the tractor COG on the running plane to the symmetry line (*X*), with respect to the zero stability condition (X_{cri}), i.e. when the COG projection falls on the baseline border. In Figure 5B these distances are shown.

For the roll stability index, first of all the COG projection point *P* is evaluated in its u_1 coordinate to select the nearer stability baseline side, e.g. BC in the figure. After that, the line orthogonal to BC and to the point *S*, intersection between this line and the line defined by the unit vector u_2, are computed. Thus, given $P(x_p,y_p)$ and ax+by+c=0, i.e. the equation for BC, the parameters a´, b´ and c´ of the orthogonal line become:

$$\begin{cases} a' = b \\ b' = -a \\ c' = -b\,x_p + a\,y_p \end{cases} \tag{3}$$

while the coordinates of *S* result:

$$\begin{cases} x_s = 0 \\ y_s = -\dfrac{c'}{b'} \end{cases} \tag{4}$$

By computing the coefficients and the coordinates of *S*, it is possible to evaluate the SP and SQ distances, i.e. the *X* and X_{cri} for the roll stability index:

$$SI_{roll} = \left(1 - \frac{SP}{SQ}\right) \cdot 100 \tag{5}$$

The SI_{pitch} is defined and computed in a similar way.

Simulations

The kinematics of the tractors together with the computation of the COG and of the stability indexes have been implemented in a simulator developed in Matlab® (The Mathworks, Natick, Massachusetts, USA), to evaluate and compare the two different tractor architectures and to lay the basis for future safety applications.

In Table 2 the main parameters for the two architectures are reported. As can be appreciated, the total weight of the two tractors is the same, as well the maximum distance between the two wheelbases.

Figure 6 represents a visual output of the Matlab® simulator and shows the different positions of the stability baseline of the conventional tractor along a circular trajectory lying on a sloped plane. The φ angle is the angular coordinate representing the current position of the vehicle along the circumference. The tractor travels anticlockwise along the circumference, starting from the point with maximum x coordinate.

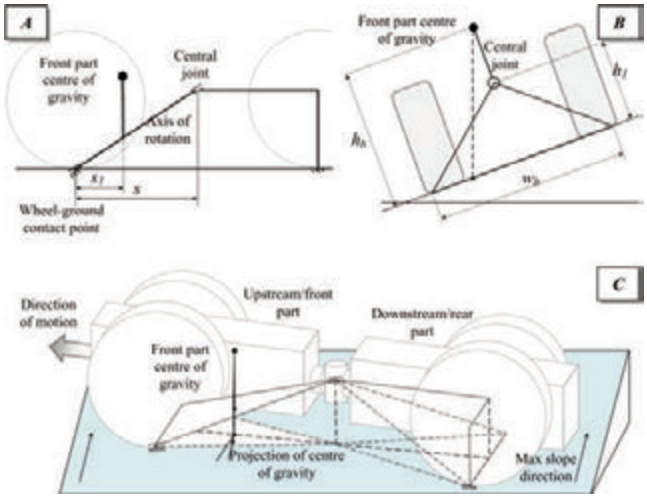

Figure 1. Side (A), front (B) and axonometric (C) views of the equivalent mechanism for an articulated tractor with a 2-dof central joint.

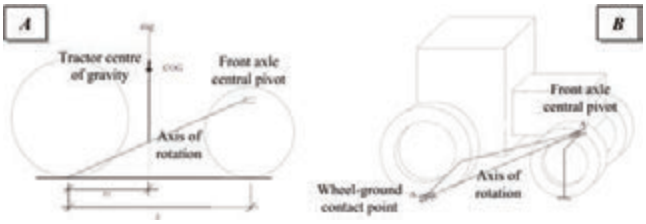

Figure 2. Side (A) and axonometric (B) views of the equivalent mechanism for a conventional tractor with a front axle central pivot (Coombes, 1968; Guzzomi, 2012; Scarlett et al., 2006).

Table 1. Nomenclature.

wb_f	Forward wheelbase width
wb_b	Backward wheelbase width
wb_b_d	Distance joint-backward wheelbase
wb_f_d	Distance joint-forward wheelbase
p_b	Backward tread width
p_f	Forward tread width
COG_b	Backward Centre Of Gravity position
COG_f	Forward Centre Of Gravity position
COG	Centre Of Gravity

Table 2. Stalk length of industrial hemp varieties

Conventional Tractor		Articulated Tractor	
COG coordinates	[0,0.80,0.60]m	COG coordinates (f and b)	[0,0,0.35]m
L	1.20m	L (distance wbvs. joint)	0.60m
wb_f	0.60m	wb_f	0.70m
wb_b	0.80m	wb_b	0.70m
p_b	0.20m	p_b	0.20m
p_f	0.26m	p_f	0.20m
Mass	950 kg	mass (fw, bw)	570,380 kg

Table 3. Values of the S^{lroll} in the two most critical angular positions along the circumference (radius r= 5m)

	φ=90°			φ=270°		
α	Conventional tr.	Articulated tr.	Absolute diff.	Conventional tr.	Articulated tr.	Absolute diff.
10°	83%	89%	+6	79%	83%	+4
20°	62%	74%	+12	59%	67%	+8
30°	39%	57%	+18	34%	51%	+17
40°	11%	36%	+25	6%	30%	+24

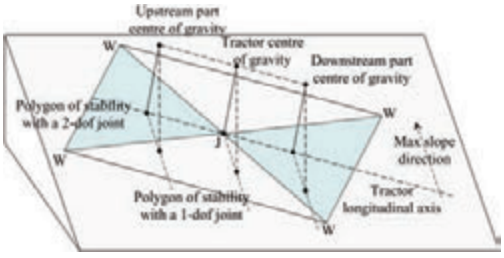

Figure 3. Generic situation of an articulated tractor moving uphill (W: wheel-ground contact point; J: central joint; light-blue triangles: stability polygons with a 2-dof joint); in the represented case, the upstream part would undergo to a lateral rollover (note the projection of the upstream centre of gravity) if the central joint had both the initial 2 dof; with a 1-dof joint the tractor is stable.

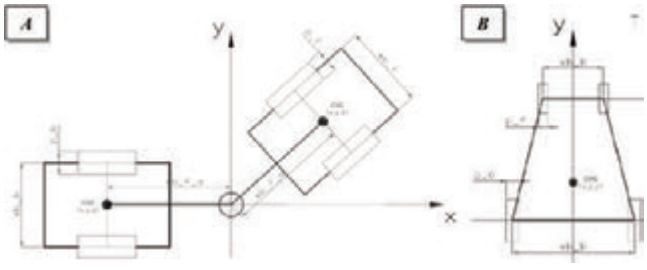

Figure 4. Tractor geometrical parameters (A: Articulated Tractor; B: Conventional Tractor).

Experimental tests

The experimental tests regarded the lateral rollover of the articulated tractor in two different configurations: (a) side overturning of vehicle with the two halves aligned, equivalent to a straight-ahead motion of the tractor along a contour line of a hillside, (b) side overturning of vehicle with the two halves angled, equivalent to a steering manoeuvre of the tractor going upstream from a contour line of a hillside.

When the vehicle was tested in an angled configuration, the longitudinal symmetry axis of the downstream portion of the vehicle passed through the centre of the footprint of a wheel of the other part (according to OECD prescriptions; Figure 7). This configuration corresponds to a steering angle of 30° and a curvature radius of the trajectory of 2.4 m.

Results

Validation of the numerical model

With a *straight configuration*, the experimental test recorded a limit of lateral stability of 43.8° and the numerical model gave a critical angle of 45.7°. The difference between the limit angle measured experimentally and calculated by the simulator (+4%) can be reasonably ascribed to the deformation of the tyres, not accounted in the numerical model presented here. If the deflection of the tyres were taken into account, the lateral inclination of the vehicle would be greater than the slope of the ground and, therefore, the inclination limit would be lower. The angular misalignment found (∅α=1.9°), in fact, corresponds to 2.3 cm if reported on the baseline width of the tractor using the following formula: . This length can be interpreted as the value of deflection undergone by the two tyres of the downstream side and it is compatible with the reduced pressure they had in the tests (1.6 bar, i.e. the value prescribed by OECD protocols). In the same (OECD) *angled configuration*, the experimental test recorded a limit of stability of 41.1° and the numerical model gave a critical angle

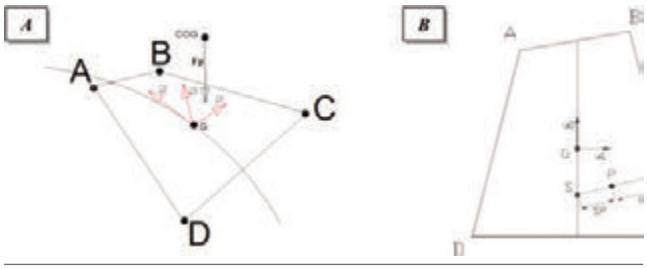

Figure 5. Tractor: A) baseline (ABCD) and weight force; B) stability index computation.

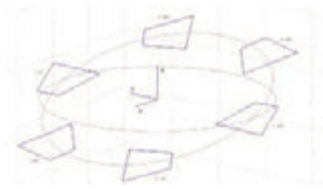

Figure 6. Simulator visual output.

Figure 7. Experimental test of lateral stability with the tractor in an angled configuration.

of 41.5°, hence only +1% than the experimental result. In this case the predictive capabilities of the model are even better than the previous case. Indeed, this configuration is more critical from the stability point of view and the rollover is reached more easily, preventing an excessive load on the tyres sides and hence without an excessive deflection.

Stability evaluations through the numerical model

The simulations have been carried out for different circle radii and slopes. For example, Figure 8 and Figure 9 show the SI_{roll} for the two tractors when describing a circle radius of 5 m, i.e. the angle that spans the entire circumference, and for slope values ranging from 0° to 40°. Looking at the results (Table 3), it can be easily appreciated how, in a quasi-static configuration, the roll stability index for an articulated tractor has better values than a conventional tractor.

Moreover, the adopted approach allows a fast assessment of the system stability and, if proper inertial measurement devices are installed on a tractor, it can be directly exploited for (i) a real-time computation of the system stability degree and (ii) the control and actuation of some active safety devices.

Conclusions and future work

In this work, the stability and human safety of narrow-track wheeled articulated tractors have been evaluated both numerically and experimentally.

First of all, considerations about the central joint and its role in a possible lateral rollover led to identify the opportunity of using a real-time safety device acting on it. This device would act only in case of incipient rollover by blocking the possibility of a part to rotate with

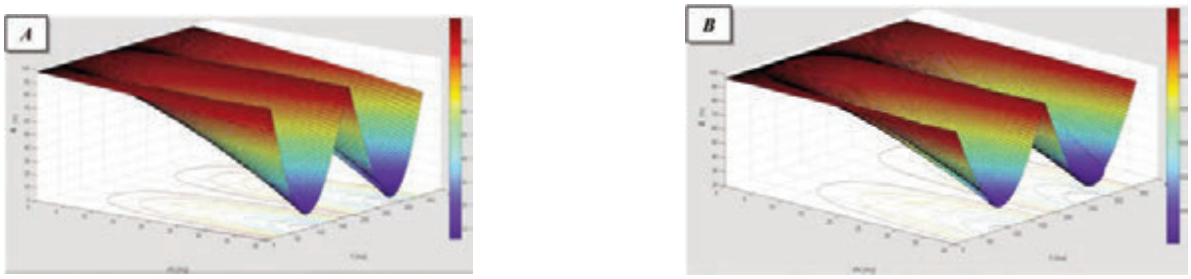

Figure 8. Roll stability index as a function of the slope and the tractor's position on the circumference. A) Conventional Tractor; B) Articulated Tractor.

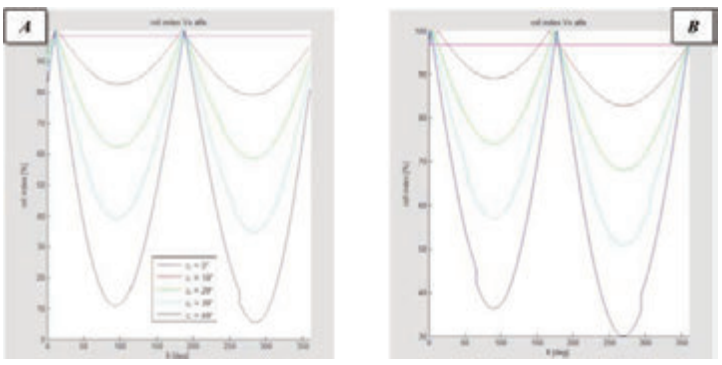

Figure 9. Roll stability index for different slope values. A) Conventional Tractor; B) Articulated Tractor.

respect to the other on a transversal plane. During normal operations this dof is present and allows the tractor overcoming possible ground harshness, hence granting the full adherence of the tyres and the comfort of the operator.

After that, a kinematic model of the articulated tractor was developed using a quasi-static approach and then it was validated with the experimental results of some OECD overturning tests. The numerical results showed a good agreement with the experiments (differences of static results due only to having neglected the tyres' deflection, however within 4%). Subsequently, the simulator was used to study and compare the dynamics of both articulated and conventional tractors. Then, a stability index both for the roll and pitch axis has been defined and the overall algorithm implemented in a Matlab® simulator.

The results show the goodness of the articulated architecture for tractors operating on hillsides (S^{lroll} greater than up to 25 percentage points) and encourage the exploitation, in a future work, of this simplified model for its implementation in real-time safety control systems related to the vehicle stability.

Future activities will cover the completion of the stability index to take also into account the dynamic phenomena, e.g. occurring when travelling on sharp harshness or when transporting fluids in a tank connected to the tractor (i.e., the equipment used for pesticide treatments). Moreover, the model will serve as a base for studying an innovative test platform for real vehicles. The dimension of this platform will allow a tractor to travel on it along a circular trajectory, as simulated in this work. Different road surfaces and obstacles will be used on the platform, to simulate real field conditions. A series of parameters related to the stability of the vehicle and to the operator's comfort will be detected during the movement of the tractor.

References

Ahmadi, I. (2011). Dynamics of tractor lateral overturn on slopes under the influence of position disturbances (model development). *Journal of Terramechanics, 48(5), 339–346. doi:10.1016/*j.jterra.2011.07.001

Coombes, G. B. (1968). Slope stability of Tractors. In Farm Machine Design Engineering (pp. 18–33). Design Engineering Publications.

Genta, G. (2000). Meccanica dell'autoveicolo - Collana di Progettazione e Costruzione di Macchine (p. 568). Torino, Italy: Levrotto & Bella.

Gravalos, I., Gialamas, T., Loutridis, S., Moshou, D., Kateris, D., Xyradakis, P., & Tsiropoulos, Z. (2011). An experimental study on the impact of the rear track width on the stability of agricultural tractors using a test bench. Journal of Terramechanics, 48(4), 319–323. doi:10.1016/j.jterra.2011.04.003

Guarnieri, A., & Fabbri, A. (2002). Le ricerche sul comfort e sulla stabilità delle trattrici agricole [The research on the comfort and stability of agricultural tractors]. In Convegno Nazionale AIIA - La sicurezza delle macchine agricole e degli impianti agro-industriali (pp. 1–21). Alghero - Sassari, Italy: AIIA - Associazione Italiana di Ingegneria Agraria. Retrieved from http://www.aiia.info/Convegni ECongressi/2002/AIIA_2002-Alghero/RelazioniGenerali/relgen-Guarnieri.pdf

Guzzomi, A. L. (2012). A revised kineto-static model for Phase I tractor rollover. Biosystems Engineering, 113(1), 65–75. doi:10.1016/j.biosystemseng.2012.06.007

Guzzomi, A. L., Rondelli, V., Guarnieri, A., Molari, G., & Molari, P. G. (2009). Available energy during the rollover of narrow-track wheeled agricultural tractors. Biosystems Engineering, 104(3), 318–323. doi:10.1016/j.biosystemseng.2009.07.005

Huang, R., Zhan, J., & Wu, J. (2012). Effect of Differential Modeling on Handling and Stability. In SAE-China and FISITA (Ed.), Proceedings of the FISITA 2012 World Automotive Congress (Vol. 198, pp. 441–448). Beijing, China. doi:10.1007/978-3-642-33795-6

Ji-hua, B., Jin-liang, L., & Yan, Y. (2011). Lateral stability analysis of the tractor/full trailer combination vehicle. In 2011 International Conference on Electric Information and Control Engineering (pp. 2294–2298). IEEE. doi:10.1109/ICEICE.2011.5777033

Karkee, M., & Steward, B. L. (2010). Local and global sensitivity analysis of a tractor and single axle grain cart dynamic system model. Biosystems Engineering, 106(4), 352–366. doi:10.1016/j.biosystemseng.2010.04.006

Liu, J., & Ayers, P. D. (1999). Control Strategies and System for Tractor Protective Structure Deployment. In 1999 Summer Conference of the NATIONAL INSTITUTE FOR FARM SAFETY (p. Paper No. 99–11). Ocean City, Maryland, USA. Retrieved from http://lamar.colostate.edu/~jhliu/project/NIFS_99.pdf

Mashadi, B., & Nasrolahi, H. (2009). Automatic control of a modified tractor to work on steep side slopes. Journal of Terramechanics, 46(6), 299–311. doi:10.1016/j.jterra.2009.08.006

Mazzetto, F., Gallo, R., Vidoni, R., & Bisaglia, C. (2012). Development and characterization tests of a small hydraulic-powered tractor prototype for use in extreme sloped vineyards. In International Conference of Agricultural Engineering CIGR-Ageng. Valencia, Spain. Retrieved from http://www.ageng2012.org- www.ageng 2012.org/images/fotosg/tabla_137_C2129.pdf

Mazzetto, F., Gallo, R., Vidoni, R., Bisaglia, C., & Calcante, A. (2012). Designing and testing a new small tractor prototype for the mechanisation of terraced-vineyard farming systems in South-Tyrol. In A. Conti, S. Failla, & D. Camillieri (Eds.), International Conference RAGUSA SHWA 2012 - "Safety Health and Welfare in Agriculture and in Agro-food Systems" (pp. 243–250). Ragusa, Italy: Elle Due. Retrieved from http://www.ragusashwa.it/CD_2012/lavori/TOPIC5/orale/topic 5_243_250.pdf

OECD. (1990). Code 6 - OECD Standard Code for the Official Testing of Front Mounted Rollover Protective Structures on Narrow Track Wheeled Agricultural and Forestry Tractors. Paris, France: Organisation for the Economic Co-operation and Development.

Pazooki, A., Rakheja, S., & Cao, D. (2012). Modeling and validation of off-road vehicle ride dynamics. Mechanical Systems and Signal Processing, 28, 679–695. doi:10.1016/j.ymssp.2011.11.006

Popescu, S., & Sutru, N. (2009). Contributions to the study of the dynamics of agricultural tractors equipped with front-end loader and rear forklift loader. In Engineering for Rural Development - International Scientific Con (pp. 165–170). Jelgava, Latvia. Retrieved from http://www.cabdirect.org/abstracts/20093261569.html

Scarlett, A. J., Reed, J. N., Semple, D. A., Seward, P. C., Stockton, A. D., & Price, J. S. (2006). Operator roll-over protection on small vehicles - Research Report 432 (p. 84).

Silsoe, United Kingdom. Retrieved from http://scholar.google.com/scholar?hl=en&btnG=Search&q=intitle:Operator+roll-over+protection+on+small+vehicles#0

Silleli, H., Dayıoğlu, M. a., Gültekin, A., Ekmekçi, K., Yıldız, M. a., Akay, E., & Saranlı, G. (2007). Anchor mechanism to increase the operator clearance zone on narrow-track wheeled agricultural tractors: Prototype and first tests. Biosystems Engineering, 97(2), 153–161. doi:10.1016/j.biosystemseng.2007.02.016

Yisa, M. G., Terao, H., Noguchi, N., & Kubota, M. (1998). Stability criteria for tractor-implement operation on slopes. Journal of Terramechanics, 35(1), 1–19. doi:10.1016/S0022-4898(98)00008-1

Engineering solutions applied to pneumatic drills to reduce losses of dust from dressed seeds

D. Pochi,[1] M. Biocca,[1] G. Brannetti,[1] R. Fanigliulo,[1] P. Gallo,[1] R. Grilli,[1] S. Montanari,[1] P. Pulcini[2]

[1]CRA-ING, Consiglio per la Ricerca e la sperimentazione in Agricoltura, Agricultural Engineering Research Unit, Roma, Italy; [2]CRA-PAV, Consiglio per la Ricerca e la sperimentazione in Agricoltura, Plant Pathology Research Center, Roma, Italy

Abstract

Neonicotinoid insecticides (imidacloprid, clothianidin, thiamethoxam) and fipronil for maize (*Zea mays* L.) seed dressing have been claimed to play a role in honey bee (*Apis mellifera* L.) decline, since pneumatic precision drills used for sowing contribute to the dispersion of the abrasion dust produced by dressed seeds. The active ingredients (a.i.) can contaminate the environment and can lead to the exposure of operators and bystanders during sowing operations. To achieve a significant reduction of dust drift and to enhance the safety for the operators, CRA-ING studied and developed novel engineering solutions applicable to drills, based on an air-recycling/filtering system. In the first system, the air's excess is forced outward through suitable filters placed on the modified lid of the seed hopper. It can be easily applied to commercial drills in use. The second system was specifically designed for new drills. It consists of a collector duct that receives the air expelled from the vacuum fan opening, creating constant pressure conditions. Part of the air is recycled into the seed hoppers, as the air in excess is directed outward through a single main filter. A third system, based on the second one, entails the use of an electrostatic filter to improve its efficiency. Moreover, to avoid the operator's exposure to the dust during the seed loading, we show an integrated solution based on the use of a modified pre-charged plastic container that replace the drill's hoppers. Preliminary tests ascertained the regular seed distribution with the drills equipped with the prototypes. Then, trials were carried out at fixed point and in field, for detecting the amounts of the drifted a.i., using commercial maize seed dressed with thiamethoxam, imidacloprid, clothianidin and fipronil. The test results show powder and a.i. drift reductions up to a maximum of 94.5% measured at ground level (with fipronil as a.i.) as a consequence of the use of the prototypes.

Correspondence: Marcello Biocca, CRA-ING, via della Pascolare 16, 00015 – Monterotondo, Roma, Italy.
Tel.: +39 0690675215 - Fax: +39 0690625591.
E-mail: marcello.biocca@entecra.it

Key words: dust drift, precision seeder, neonicotinoids, dressed maize.

Contributions: the authors contributed equally.

Conflict of interests: the authors declare no potential conflict of interests.

Journal of Agricultural Engineering 2013; XLIV(s1):e134
doi:10.4081/jae.2013.(s1):e134

Introduction

The pneumatic precision drills implement a seed distribution system based on vacuum effect created by a centrifugal fan. The sucked air in the circuit of the seeder is finally expelled through the fan opening, dragging with it powder and seed particles that can contain dressing substances. Such as machinery are employed in maize sowing (*Zea mays* L.) and insecticides employed in maize seed dressing (namely neonicotinoids and fipronil) have been claimed to play a role in honey bee (*Apis mellifera* L.) mortality and decline (Maini et al., 2010; Apenet, 2011; Tapparo et al., 2012). The situation is particularly serious in Italy, since maize is a major cereal crop, grown on almost one million hectares (Istat, 2011).

In recent years the alarms concerning risks to honey bees have stimulated studies about technical solutions to reduce dust drift and losses from the drills. Some manufacturers proposed devices, called air deflectors, able to redirect the output flow from the fan exit towards the soil, to reduce the diffusion of dust in the atmosphere. In previous works, tests (carried out on four of the above mentioned insecticides) showed that the adoption of the air deflectors determined a reduction of dust drift at least around 50% of the active ingredients (a.i.) amounts observed without deflectors at ground level. In the same trials, it was observed a lesser reduction of active ingredient concentrations in the air (Biocca et al., 2011; Pochi et al. 2011a). However it was ascertained that sub-lethal effects to honey bees are still possible with these levels of dust dispersion (Apenet, 2011; Pochi et al. 2012a), and the Italian Government decided the precautionary suspension of use of all the four a.i. registered for seed dressing (i.e. imidacloprid, thiamethoxam, clothianidin and fipronil).

With the aim of obtaining a further drift reduction, a dedicated study initially started in the framework of a national research project funded by the Italian Ministry of Agriculture called Apenet, and innovative devices were developed at CRA-ING. They are based on the partial recirculation of the air operating the seed distribution in traditional pneumatic drills. The air excess is forced outward through suitable filters and expelled.

Moreover, an additional aspect in the risk assessment involves the operators, since they are potentially exposed to abrasion dust during sowing operations. The exposure can occur differently, such as during the manipulation of dressed seed (opening seed sacks and filling the drill) or in field, during the sowing, at the tractor seat. In order to achieve a higher risk reduction for the operator, we propose an inte-

grated solution based on the use of a modified pre-charged plastic container that replace the drill's hoppers.

The paper refers about the results of tests carried out in order to assess the performances of the innovative prototypes (with particular reference to the prototype 2, named P2), and shows the employ of the innovative seed container.

Materials and methods

Seed. The trials were carried out using commercial maize seed (Pioneer Hybreed PR32G44) dressed with four insecticides (Gaucho™, a.i.: imidacloprid; Poncho™, a.i.: clothianidin; Cruiser™, a.i.: thiametoxam, Regent™, a.i.: fipronil) and a fungicide (Celest™, a.i.: fludioxonil and metalaxyl). According to the manufacturers, the quantities of a.i. were respectively equal to 1.000 mg/seed for imidacloprid, 1.250 mg/seed for clothianidin, 0.600 mg/seed for thiametoxam and 0.500 mg/seed for fipronil. The seed was packed in sacks (25,000 seeds/sack).

Description of prototypes. The first prototype (P1) is based on a partial recirculation of the air operating the seed distribution in traditional pneumatic drills (Figure 1). The air excess is forced outward through suitable filters placed on the modified lid of the seed hopper. The system is suitable to be easily mounted in commercial drill in use. A first version of this prototype was mounted on a Matermacc drill and tested in 2010 (Pochi et al., 2011b; Pochi et al. 2012b). Then, a similar model of the prototype was mounted on a Gaspardo Magica drill. This prototype was equipped with activated charcoal filters for automotive use.

The second prototype (P2) is a modification of the previous one and is designed for ad-hoc developed drills (Figure 2). It consist of a collector duct that receives the air expelled from the vacuum fan opening, creating constant pressure conditions. Part of the air is recycled into the seed hoppers, as the air in excess is directed outward through a single main activated charcoal filter. The prototype was mounted on a Gaspardo Magica, six-rows drill.

Sowing quality assessment. In preliminary tests it was ascertained the regular seed distribution in the drills equipped with the prototypes by means of tests carried out at fixed point (P1) or directly during field sowing (P2); in field the quality of sowing was evaluated according to standard Enama (2003).

Test system (fixed point). The tests were carried out in the workshop's porch of CRA-ING, according to the settings described in Biocca et al. (2011). The drill, suitably placed in the test area, operated the seed distribution *"sur place"*. In the test site artificial wind conditions were produced by means of an axial fan (0.735 m diameter), to obtain a sort of wind gallery with a 22.5 m long sampling area, leeward with respect to the drill position. Along the sampling area a grid of 15 sampling points with Petri dishes (filled with an acetonitrile-water solution) was arranged. The five sampling distances from the drill side were multiples of its working width: 4.5, 9.0, 13.5, 18 and 22.5 m. In the sampling area, five air samplers (TCR Tecora model "Bravo") were set for sucking 100 L of air with a constant flow of 5 $L \bullet min^{-1}$, in order to complete the air sampling 5 min after the end of the seed distribution. Each trial was replicated three times. Each replication consisted of the distribution of 2 sacks of seed, corresponding to a 0.67 ha surface. The drill operated the seed distribution by means of a system allowing to adjust the peripheral speed of the drill's driving wheel. Such a system consisted of an electric engine connected to the driving wheel through a gear-reducer (transmission ratio: 40/1). An inverter (OMRON Varispeed V7) was installed to set the speed of the driving wheel, on the desired value of 1.67 m s^{-1}. The drill was regulated as follows: row distance of 0.75 m; seed distance on the row of 0.18 m; sowing density of 75,000 seeds ha^{-1}; vacuum pressure of 45 mbar.

Field test. The trials were carried out in the experimental farm of CRA-ING (around 42°5'51.26" N; 12°37'3.52" E; 24 m a.s.l.) in 2011 and in the experimental farm of CRA-PCM in 2012 (around 12°47'46" E; 42°26'50" N; 370 m a.s.l.), sowing plots of about 3 ha with all the four a.i.

To detect the a.i. air concentrations, a personal sampler, operating at a constant flow of 4.0 L min^{-1} was placed on the tractor cab.

Moreover, during the tests four air samplers (TCR Tecora, mod. Bravo) were used to collect samples of the powder present in the ambient air. The air sampling heights were 2.0 m and 5.0 m. A couple of samplers were placed at the edge of the field. Considering the prevailing wind direction at the beginning of the trial they were placed leeward. The second couple of samplers were placed in the centre of the sowed field. The pumps of all ambient samplers were calibrated with a constant flow of 15 L min^{-1}. All the portable samplers were equipped with 0.45 m PTFE Millipore diskette filters, without any sampling head. During the tests, the micrometeorological conditions were monitored.

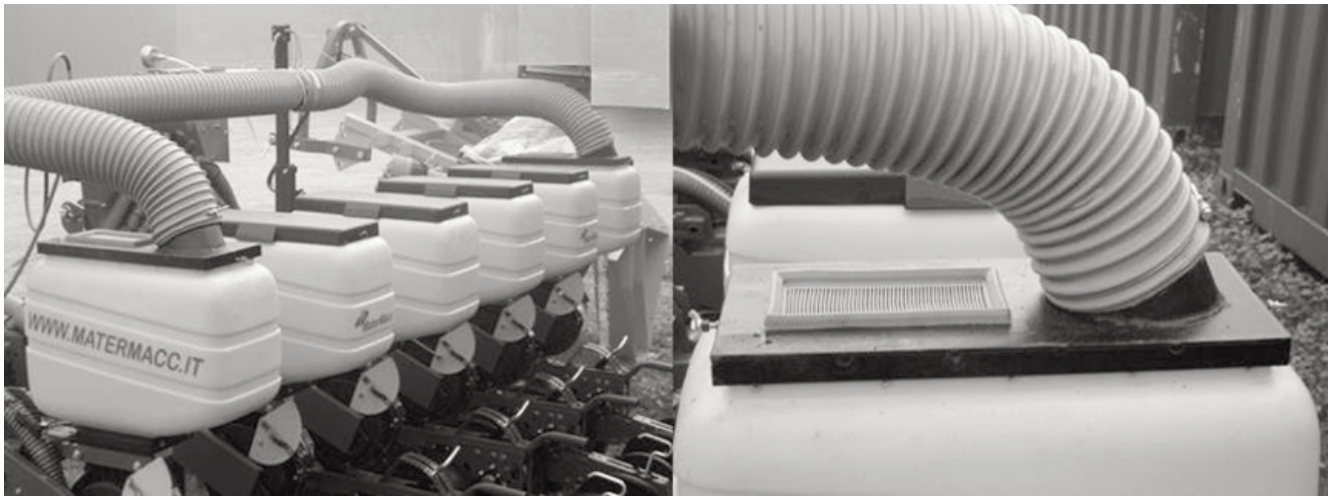

Figure 1. The prototype 1 applied to a Matermacc drill.

Figure 2. The Gaspardo drill equipped with the prototype 2.

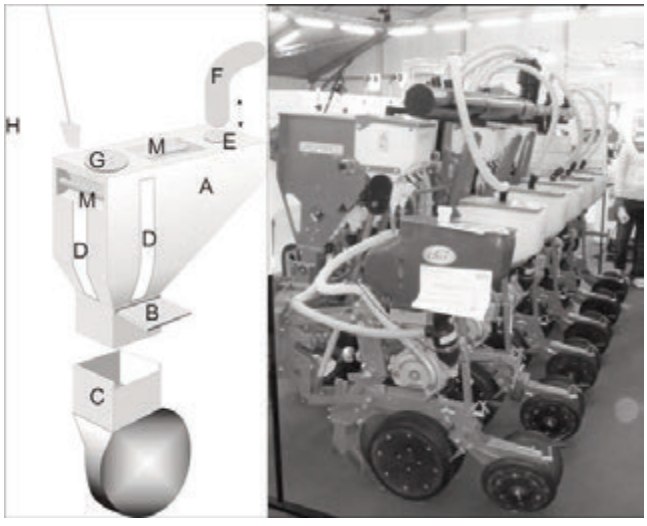

Figure 3. The innovative hopper. Left: layout. Right: mounted on the drill.

Active ingredients determination. The active ingredient determination in the filters was made at CRA-PAV. Active substances were extracted from the samples with acetonitrile. Solutions were sonicated in an ultrasonic bath for 10 min, then filtered with HPLC 0.45 m filters. The analytical determinations were carried out by means of HPLC - ESI - MS – MS and the relative methods were validated in compliance with GLP procedures (Biocca et al. 2011).

Innovative seed container. An innovative hopper was designed and a prototype was built in fibreglass. It consists of containers that can be indefinitely refilled and reused, replacing the conventional hoppers. The introduction of such refill-hoppers involves a modification of the process from the packaging to the sowing. They are filled and sealed in the seed production plant, where all the operations that causing the production and dispersion of dust (with a.i,) can be made under controlled conditions. Each refill-hopper represent a dose of seed. The farmer purchases the number of doses he needs and after the sowing returns the empty hoppers to the plant where they will be prepared for the next season. As to their use, the farmer only must place them on the seed distributor and pull out the closure latch, allowing the seed to fall in the distributor. Then the container was mounted on the Gaspardo drill and checked for its functionality (Figure 3).

Results

The quality of seed distributions of the drill equipped with the prototypes resulted always acceptable, showing the same homogeneity of the sowing carried out with the drill without modifications (Pochi et al. 2012 b).

The Figure 3 shows the residues of a.i. collected in Petri dishes in the tests at fixed point. The amounts (expressed as μg m^{-2}) appear very large as they represent the total dust potentially emitted during the sowing of an area of 0.67 ha. As expected, the quantities of a.i. residues at ground level decrease with respect to the distance from the emission source.

On the other hand, the air concentrations of a.i. in the sampling area appears less linked to the distance (Figure 4). The phenomenon can be

Table 1. Air concentrations of active ingredients recorded during sowing with the prototype (P2) and the conventional drill.

Sampler position	Sampling (n)	a.i	P2 ppb	Conventional ppb
	4	clothianidin	0.012	0.223
field	4	fipronil	0.008	0.057
	4	imidacloprid	0.011	0.025
	4	thiamethoxam	0.009	0.036
	1	clothianidin	0.563	0.236
tractor	1	fipronil	0.087	1.427
	1	imidacloprid	0.129	0.976
	1	thiamethoxam	0.112	8.647

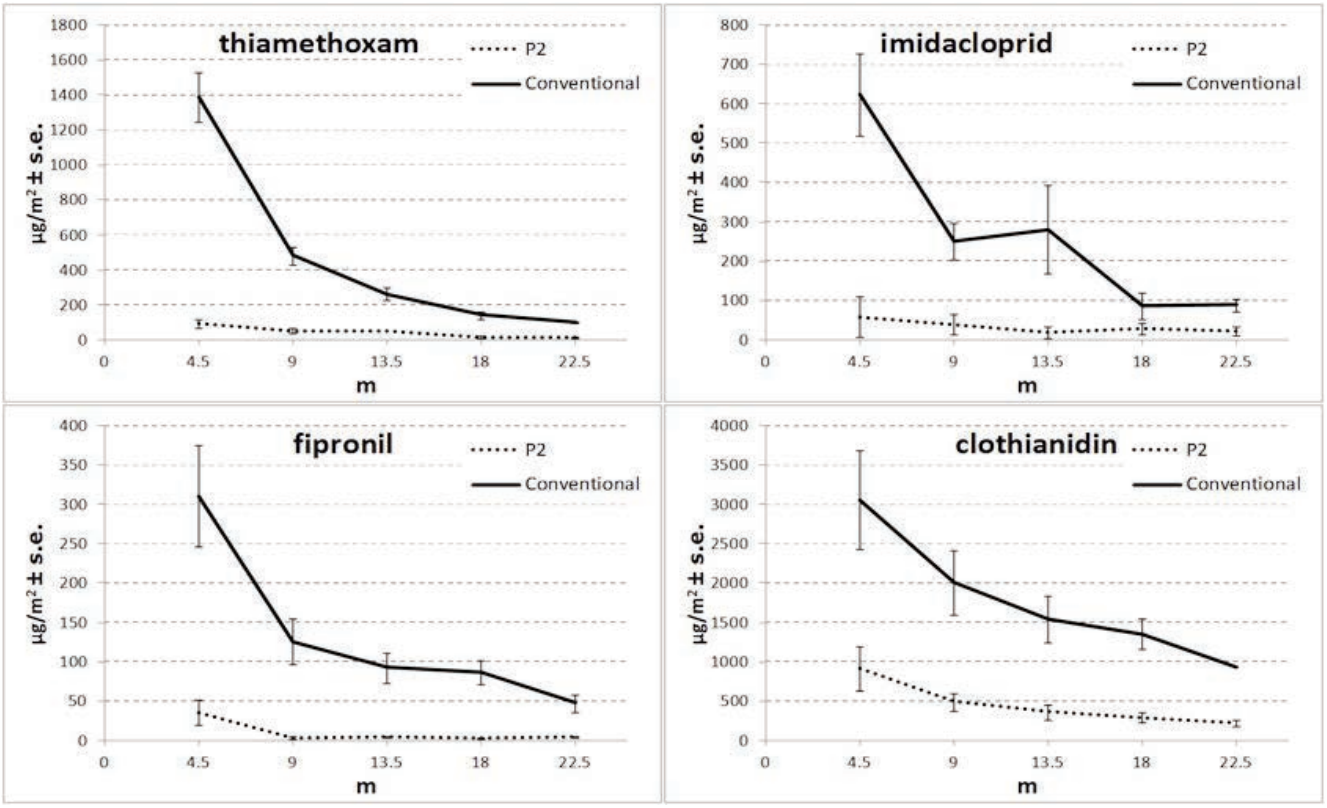

Figure 4. Ground depositions [µg m^{-2} ± s.e.] obtained comparing prototype 2 and conventional drill in fixed point tests.

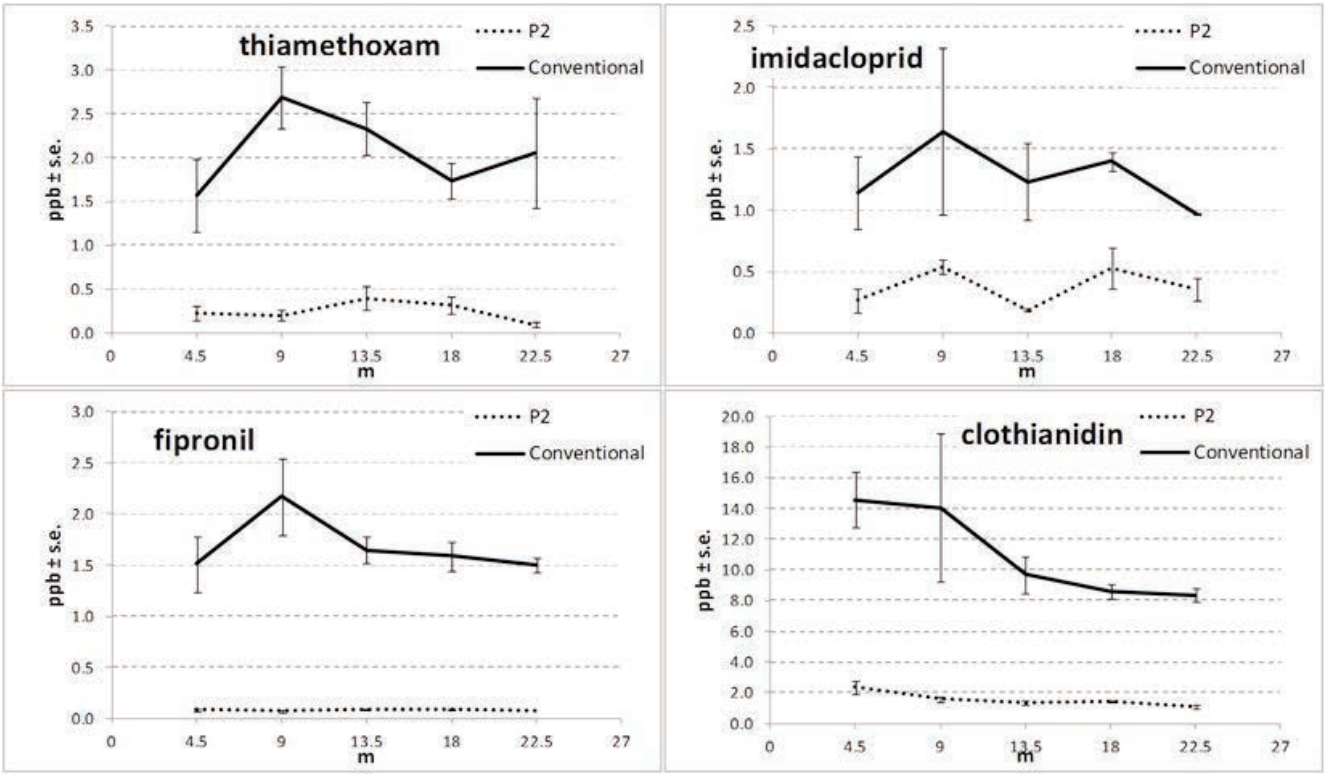

Figure 5. Air concentrations [ppb ± s.e.] obtained comparing prototype 2 and conventional drill in fixed point tests..

related to the presence of very fine particles that can float in the air for long time.

As to the field tests, we sampled the air concentrations of a.i. during the entire sowing of plots of about three hectares. The Table 1 shows the results, as average values of concentrations detected by the four samplers placed in the field (two samplers at the field edge and two samplers in the center of the sowed plot) and the amounts detected by the samplers mounted on the tractor during the sowing. Minor concentrations were always observed with the employ of the prototype, except for the sampling of clothianidin with the sampler placed on the tractor.

In general, in the experiments at fixed point, the drift reduction incited by the prototype is very clear, both at ground level and in the air, ranging from a minimum of about 71% (case of imidacloprid as air concentration) to a maximum of about 95% (case of fipronil as air concentration) (Table 2). Very similar results were also achieved in field measuring the air concentrations into and near the sowed plot. In the case of the sampling on the tractor, it appears that in one case (clothianidin) an increment in the dust drift with the prototype was observed. Such an exception, considering the general significant reduction determined by the use of the prototype, could have been caused by some abnormal event such as contamination of the samples.

Regarding the study of an innovative method to load the drill avoiding the dispersion of dust during the hopper filling, we developed a system based on airtight hoppers used both for the packaging and seed filling. A fiber-glass prototype of such hoppers was realized at CRA-ING and is shown in fig. 3. The introduction of the refill hoppers and of the process related to their utilization completely eliminates the workers exposition to the dust during the seed loading and, in general, reduces the overall risks for the environment. Moreover, because of their indefinite reutilization, the conventional packages are no more requested, saving the cost for their purchasing and avoiding the problem of their disposal as hazardous wastes. The refill hopper can be easily applied to seed drills in use with simple adaptations of the upper opening of the seed distributors in order to lodge them. Further advantages and increased efficiency of the process could be achieved through agreements among the potential stake-holders (seed producers, drills manufacturers, etc.) about the adoption of standard shapes and dimensions of the technical elements, facilitating their diffusion. Similar process could be advantageously adopted in other fields of application in which the manipulation of granular or powder products represent a potential risks for the operators.

Conclusions

This paper shows concentrations of the a.i. emitted by drills equipped with innovative systems developed at CRA-ING. The data are expressed in terms of residue concentrations both in the air and at ground level. Starting from these results, the relative reduction of emission incited by the prototype, was expressed as percentage with reference to a conventional drill. In other terms the comparison of the drill performance were based on real data of a.i. contents.

The results show a remarkable reduction of drift and the efficacy of the innovative systems. The systems were applied to commercial drills without interferences with the quality of seed deposition. The effect of reduction of dust emission incited by the innovative systems was always higher than the one caused by other drift reducing devices (air deflectors) previously tested (Biocca et al., 2011; Pochi et al., 2011a). Nevertheless even with the strongest reductions of dust drift, some undesirable effects for honey bees may occur during their flight in and around contaminated areas due to the high sensitivity of these insects to neonicotinoids and fipronil (Pochi et al., 2012). Consequently, further studies are needed, aimed at providing engineering solutions on the machineries to obtain a better control of dust drift.

Table 2. Relative reductions of a.i. emissions incited by prototype 2, with reference to the conventional drill.

Active ingredient	Fixed point		Field
	Ground [%]	Air [%]	Air [%]
fipronil	92.1	95.0	93.6%
thiamethoxam	90.6	88.2	98.6%
clothiadinin	74.4	86.0	-25.3%
imidacloprid	87.4	70.7	86.0%

References

Apenet, 2011. Effects of coated maize seed on bees. Report based on results obtained from the first year of activity of the APENET project. Pag 131. Available at: http://www.reterurale.it/flex/cm/pages/ServeBLOB.php/L/IT/IDPagina/1289. Accessed: April 10th, 2012.

Biocca, M., Conte, E., Pulcini, P., Marinelli, E. and Pochi, D., 2011. Sowing simulation tests of a pneumatic drill equipped with systems aimed at reducing the emission of abrasion dust from maize dressed seed. Journal of Environmental Science and Health, Part B. 46, 6, 438-448.

ENAMA, 2003. "Protocollo Enama Cat. 04 – Macchine per la semina" (Rev. 2.1 settembre 2003).

ISTAT, 2011. Tavole di dati. On line: http://agri.istat.it. Accessed February 2013.

Maini, S., Medrzycki, P. and Porrini, C., 2010. The puzzle of bee losses: a brief review. Bull Insectology 63, 1, 153-160.

Pochi, D., Biocca, M., Fanigliulo, R., Conte, E. and Pulcini, P., 2011a. Evaluation of insecticides losses from dressed seed from conventional and modified pneumatic drills for maize. Journal of Agricultural Machinery Science, 7, 1, 61-65.

Pochi, D., Biocca, M., Fanigliulo, R., Gallo, P., Pulcini, P. and Conte, E., 2011b. An innovative system to reduce dust drift during sowing of dressed seeds with pneumatic drills. Proceedings of XIV Symposium in Pesticide Chemistry, Piacenza (Italy) 30th August – 1st September 2011.

Pochi D., Biocca M., Fanigliulo R., Pulcini P. and Conte E., 2012a. Potential exposure of bees, *Apis mellifera* L., to particulate matter and pesticides derived from seed dressing during maize sowing. Bulletin of Environmental Contamination and Toxicology. DOI: 10.1007/s00128-012-0664-1.

Pochi D., Biocca M., Fanigliulo R., Gallo P. and Pulcini P., 2012b. Development and testing of innovative devices to reduce the drift of abrasion powder during the sowing of dressed seeds with pneumatic drills. In: International Conference of Agricultural Engineering, CIGR-AgEng 2012, Valencia 8-12 July. ISBN -10: 84-615-9928-4. On-line at: http://cigr.ageng2012.org.

Tapparo, A., Marton, D., Giorio, C., Zanella, A., Soldà, L., Marzaro, M., Vivan, L. and Girolami, V., 2012. Assessment of the environmental exposure of honeybees to particulate matter containing neonicotinoid insecticides coming from corn coated seeds. Environmental Science and Technology, 46,5, 2592–2599.

Exposure to vibrations in wine growing

Domenico Pessina, Davide Facchinetti

Dip. di Scienze Agrarie e Ambientali, Università degli Studi, Milano, Italy

Abstract

Apart the winter period, the activity in specialized agricultural cultivations (i.e. wine- and fruit-growing) is distributed for a long period of the year. Some tasks, such as pesticide distribution, are repeated several times during the growing season. On the other hand, mechanization is one of the pillars on which is based the modern agriculture management.

As a consequence, in wine growing the tractor driver has to be considered a worker potentially subjected to high level of vibrations, due to the poor machinery conditions often encountered, and sometimes to the rough soil surface of the vineyard combined with the high travelling speed adopted in carrying out many operations.

About vibrations, the Italian Decree 81/08 basically refers to the European Directive 2002/44/CE, that provides some very strict limits of exposure, both for whole body and hand-arm districts.

In Oltrepo pavese, a large hilly area located the south part of the Pavia province (Lombardy - Italy) wine growing is the main agricultural activity; for this reason, a detailed survey on the vibration levels recorded at the tractor driver's seat was carried out, in order to ascertain the real risk to which the operators are exposed.

The activity in wine growing has been classified into 6 groups of similar tasks, as follows:

1. canopy management: pruning, trimming, binding, stripping, etc.;
2. soil management: harrowing, hoeing, subsoiling etc.;
3. inter-row management: chopping of pruning , pinching, grass mowing, etc.;
4. crop protection: pesticides and fungicides distribution, sulfidation, foliar fertilization, etc.;
5. grape harvesting: manual or mechanical;
6. transport: from the vineyard to the cellar.

For each group of tasks, the vibration levels on 3 the traditional axes (x, y and z) were recorded, and then an exposure time was calculated for each of them, in order to ascertain the risk level in comparison to what provided by the dedicated standard.

Finally, a detailed study was conducted on the most dangerous working conditions, with the goal to offer solutions able to reduce the overall exposure, as improving the comfort level, as to shorten the working time when possible and/or to provide suitable periods of rest.

Correspondence: Domenico Pessina, Dip. di Scienze Agrarie e Ambientali, Università degli Studi, v. Celoria, 2 - I 20133 Milano, Italy.
domenico.pessina@unimi.it

Key words: vibration risk, exposure, tractor, implement, wine growing

Journal of Agricultural Engineering 2013; XLIV(s1):e135
doi:10.4081/jae.2013.(s1):e135

Introduction

In Europe, the evaluation of the vibrations risk is based on 2002/44/EC Directive, implemented by time in Italy and confirmed in the Decree 81/08, dealing with the safety and comfort of the workers. Also the Machine Directive provides that manufacturers must minimize the vibrations hazard adopting for their production a suitable design and usage conditions. Moreover, in the operation and maintenance manual of a given machine the values of the weighted acceleration of vibration must be reported.

In particular, the Decree 81/08 provides that employers are compelled to ascertain the level of whole-body and hand-arm vibrations in the tasks carried out by the employees under his/her responsibility. For whole-body vibrations, the exposure limits referred to a 8-hours working period are 0,5 m/s2 for the action value and 1,0 m/s2 for the limit value. As an alternative, to the figures indicated by manufacturers in the operation and maintenance manual, information about the vibrations levels can be found in dedicated databases. Unfortunately, the vibration values included in the databases often do not report with a sufficient level of detail the operating condition of the tasks, such as the soil or road surface characteristics, the travelling speed, the tyre inflation pressure, the type and the wear of the seat fitted on the machine and its suspension system, etc. They all are factors influencing remarkably the vibrations level and therefore the operator's exposure. In practice, if reliable data are not available, a direct measurement should be carried out, in accordance with the most known dedicated standards, issued by ISO and CEN, or referring to national guidelines. Moreover, all parameters affecting the operator's level of risk have to be taken into account: axis of perception, frequency, exposure time and obviously vibrations level.

The daily exposure value A(8) normalized to 8 hours must be calculated in accordance with ISO 2631-1, based on the higher of the Root Mean Square (RMS) values of the frequency-weighted accelerations determined on 3 orthogonal axes (awx, awy, awz) for a worker sitting or standing.

For agricultural tasks, the vibrations risk cannot be easily ascertained, because of several sources of disturbance and a very wide variability of operation modes. Therefore, the risk assessment is still often poorly reliable.

In tractors, in addition to the engine, the main vibration sources appear to be the gearbox and the vehicle travelling, due to the rolling/sliding of the tyres/track on the ground, especially if hard and bumpy.

The lack of literature data for a standardized approach to the problem and the need to integrate the existing databases with suitable information, led to the execution of a survey on the exposure to vibrations of agricultural employees in Oltrepo Pavese, a large area particularly suited to wine growing. The measurements were carried out in

collaboration with other local institutions (ASL, UOOML, Maugeri Foundation).

Materials and methods

In order to find the technical meaning of the levels magnitude variation (the range between min and max), 6 groups of common tasks carried out in wine growing have been defined. Also taking into account the machinery characteristics and the operating conditions, the groups were divided as follows:

1. canopy management: pruning, trimming, binding, stripping, etc.;
2. soil management: subsoiling, harrowing, hoeing, etc.;
3. inter-row management: trimming, pruning, suckering, grass mowing, etc.;
4. crop protection: sulfidation, distribution of pesticides and fungicides, foliar fertilization, etc.;
5. grape harvesting: manual or mechanized;
6. transport: mainly from the vineyard to the cellar.

The measurements were performed in 11 wine farms located in Oltrepo pavese. The vibration levels were recorded thanks to a vibration meter make Larson Davis model HVM100, complying the ISO 8041:1990 requirements and a tri-axial accelerometer make PCB model ICB 356B41 (mass 11 g, sensitivity 10,2 mV/ ms-2) placed on the tested tractor seats.

The measurements time was different considering the task features; in any case, the duration, from a minimum of 3 min was defined in order to assure the maximum significance to the data acquired. A dedicated software was then developed to calculate the single axis and the overall levels.

The complementary data, relevant to the task carried out and the machines used have been collected in some paper forms, filled directly in the field. In particular, information about the tractor and the implement technical features, the soil and the working conditions were included (tab. 1).

The table is based on 6 sections, as follows:

- the single task taken into account;
- the test location;
- the main technical features of the tractor and the implement(s);
- the soil conditions and the travelling speed;
- the vibrations levels obtained and the corresponding time of measurements:
- the single axis and the overall levels of vibration.

A general database was finally built, to obtain a overall overview on the survey carried out (tab. 2)

Results and discussion

The standards actually in force provide that the highest of the weighted vibration level recorded on the 3 axes (max (1.4 awx, 1.4 awy, awz) has to be considered as a reference. On the other hand, the dedicated literature highlights an alternative solution, i.e. the RMS value of the levels obtained on each of the 3 axes ($\sqrt{}$ (1.4 awx)^2 + (1.4 awy)^2 + awz^2).

The difference between the two methods is more remarkable as the individual values differ from each other; on the contrary, the two results are fairly similar if the single values are nearly close.

In any case, at present there is no still agreement on which method is able to represent better the effective disturbance. For this reason,

Table 1. An example of the paper form filled in the field for one group of the tasks surveyed.

Chain:	WINE GROWING			
Task:	PRUNING ☐	TRIMMING ☐	STRIPPING ☐	
Wine farm ref.:				
Date:	Operator(s):			
Tractor:	make:	model:	max power: ____ kW ___ CV	wheeldrive: 2WD ☐ 4WD ☐
Driver's seat:	suspension type :	mechanical ☐	hydraulic ☐	pneumatic ☐
Implement:	towed ☐	3-point hitched ☐	3-point hitched with one or more support(s) to the ground ☐	
Working conditions				
1 – Tool type:	vertical blade ☐	horizontal blade ☐	other (specify): _____ ☐	
2 – Soil condition:	FAVOURABLE (wet or dry sandy soil; no gravel or stone content; no or light compaction) ☐	INTERMEDIATE (clay-sandy-loam soil; low gravel and stone content, surface compaction) ☐	POOR (clay and dry soil; high gravel and stone content; high surface and deep compaction) ☐	
3 – Terrain surface:	smooth (i.e. lawn)	fairly rough (i.e.wheat stubble)	rough (i.e. corn stalks)	
4 – travelling speed:	low (< 5 km/h)	medium (5-8 km/h)	high (>8 km/h)	
Measured vibration level:	X axis (lat): _____ m/s^2	Y axis (long.): _____ m/s^2	Z axis (vert.): _____m/s^2	
Measuring time:	X axis (lat.): _____ min	Y axis (long.): _____ min	Z axis (vert.): _____ min	
Value1	max (1,4*X; 1,4 *Y; Z)= _____ m/s^2			
Value 2	$\sqrt{(1,4*X)^2 + (1,4*Y)^2 + (Z)^2}$ = _____ m/s^2			
Note:				

Table 2. Example of database sheets created for the data management and processing.

Azienda	Lavorazione	specifica	Tipologia trattore	Marca e modello	Potenza max	Ruote motrici	Sospensione sedile	Assale trattore	Operatrice (portata semiportata trainata)
Mazzolino	taglio erba		Cingolato	SAME Rock 60	60 CV	2WD	meccanica	tradizionale	trinciaerba gramegna portata
Montello	taglio erba	trinciatura erba	Cingolato	Landini 6830	68 CV	2WD	meccanica		trinciasarmenti calderoni semiportata
Montello	taglio erba	trinciatura erba	Cingolato	New Holland 60-85	60 CV	2WD	meccanica		spollonatrice decespugliatrice Clemens semiportata
Adamo	suolo	fresatura	Cingolato	New Holland TK 85	85 kW	2WD	pneumatica	sospeso e attivato	fresa Nardi 2000 (2002) portata
Adamo	taglio erba		gommato	New Holland TNF90	95 kW	4WD	pneumatica	sospeso e attivato	taglia erba Fischer portata
Costanza	trattamenti		Cingolato	Landini Trekker 85F	58 CV	2WD	meccanica		atomizzatore drageno portata
Montello	trattamenti		gommato	New Holland TK95	95 CV	4WD	pneumatica	sospeso e attivato	atomizzatore trainato vitali SVS GPS 500
Il Bosco	trattamenti		gommato	New Holland 8286	80 CV	4WD	meccanica	tradizionale	atomizzatore Vitifiti 400 S semiportato
Il Bosco	taglio erba		gommato	New Holland TN90F	90 CV	4WD	meccanica	tradizionale	taglia erba semiportata CABE TPR 140-250
Il Bosco	taglio erba		gommato	New Holland TN90F	90 CV	4WD	meccanica	tradizionale	trinciaerba semiportata Nobili VKM 240

A(8) (m/s²)		T max ore		Valori in m/s²						Valori in min		
dopo il 2002	prima del 2002	Livello di azione 0,5	Valore limite 1,15	awx	awy	awz	sup. terreno	terreno	velocità	tempo di rilevazione awx	tempo di rilevazione awy	tempo di rilevazione awz
0,43	0,64	>8 h	>8 h	0,23	0,31	0,36	omogenea	favorevole	bassa	11'45	10'	27'28
0,70	0,91	4	>8 h	0,23	0,36	0,7	irregolare	sfavorevole	bassa	17'43	13'28	27'47
1,07	1,18	2	>8 h	0,27	0,23	1,07	irregolare	sfavorevole	bassa	7'	6'28	14'03
0,35	0,50	>8 h	>8 h	0,13	0,25	0,35		sfavorevole	bassa			2'
0,44	0,63	>8 h	>8 h	0,28	0,25	0,44	omogenea	favorevole	media			2'
1,74	2,19	1	3	0,6	0,73	1,74	omogenea	favorevole	media	17'09	17'09	17'09
0,73	1,03	4	>8 h	0,35	0,52	0,54	omogenea	favorevole	media	27'29	27'29	27'29
0,98	1,26	2	>8 h	0,7	0,43	0,93	omogenea	sfavorevole	media	4'	4'	4'
0,87	1,13	3	>8 h	0,62	0,38	0,49	omogenea	sfavorevole	bassa	11'47	11'47	11'47

the vibration levels obtained with the two methods were compared. In fig. 1 the differences in percentage were shown: for all the 6 groups of similar tasks for the "old" RMS method higher values were calculated, ranging the increases from 26 to 35%. The transport was the more significant task, because when travelling at high speed the levels in all the axis are similar, and therefore the "old" RMS level is much higher than that of the highest among the single axes. In fact, other than the vertical axis (z), also the vibrations in the horizontal axes (x and y) are similarly high, due to the disturbance caused by the trailer (in the longitudinal axis) and the roughness of the road (in the lateral axis).

Analysis for groups of similar tasks

The tasks performed in the canopy management (fig. 2) show the highest values in the vertical axis, being the more involving a hazard for the spinal column. In particular, the 4 cases surveyed were referred to trimmers coupled with tractors ranging from 60 to 100 CV. The lowest values (case 2) was referred to a wheeled tractor, while in the others 3 crawler tractors were considered. The z (vertical) axis showed values very close to or exceeding 1 m/s², the limit value. In the horizontal axes the levels were less hazardous. The vibrations were generated by the travelling of the tractor on the rough soil, while the movement of the trimming blades do not caused significant disturbance.

The vibrations about the soil management tasks (fig. 3) are quite low in two cases, but remarkably high in the other two. The tasks concerned the harrowing and hoeing, but it must be taken into account that all the implements were coupled the crawler tractors having a power ranging between 62 and 115 CV. In particular, the harrowing (cases 3 and 4) showed higher levels in respect to the hoeing (cases 1 and 2); this is because the tine harrow produces more vibration than the hoe and also because the harrowing is normally executed at a higher travelling speed in respect to the hoeing. In fact, in cases 3 and 4 (harrowing) the highest value were recorded in the vertical axis. This is the typical situation of the vehicle travelling at high speed on a rough surface.

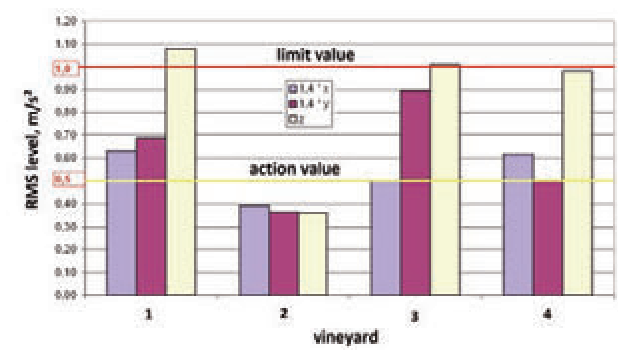

Figure 2. Vibration levels recorded in axes x, y, z during the trimming, carried out with a wheeled tractor (case 2) and 3 crawler tractors (cases 1, 3 and 4).

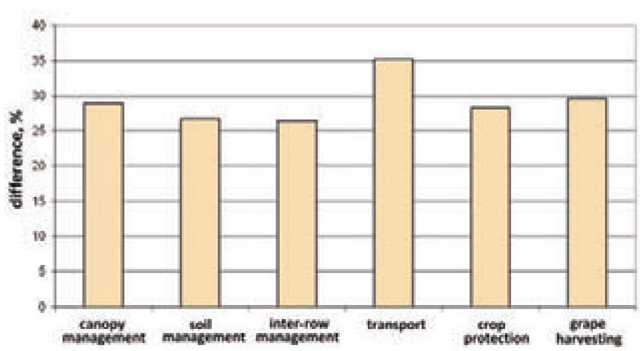

Figure 1. Difference between the "new" (highest single axis value) and the "old" (RMS value of the 3 axes) methods of vibration evaluation, referred to the 6 groups of similar tasks carried out in wine growing.

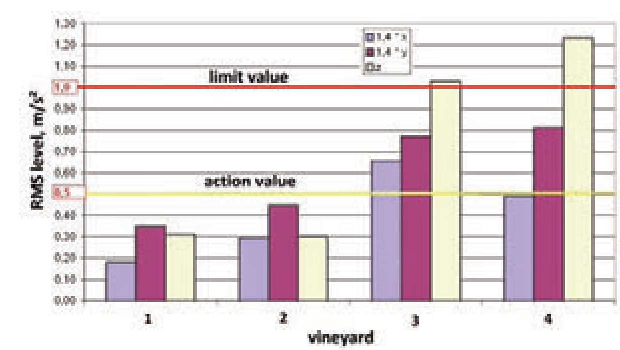

Figure 3. Vibration levels recorded in axes x, y, z during the harrowing (cases 3 and 4) and hoeing (cases 1 and 2) all carried out with crawler tractors.

On the contrary when hoeing the highest levels were recorded in y (lateral) axis, so stressing the work on uneven surface.

In the inter-row management, the chopping pruning, the suckering and the grass mowing were investigated in 13 wine farms. Especially grass mowing was performed in all the surveyed farms, because this is a task very frequently carried out more times during the year. Apart two or 3 situations, in fig. 4 the values are fairly similar. In 3 cases vibrations on z axis were above the limit value, but in many other they were very close to the lower limit of 0,5 m/s^2.

The levels in x axis (long) are often higher than those in y axis (lat): this is due to the technical characteristics of the pruning chopper, based on a rotor placed in a transversal direction in respect to the travelling, on which are running some tools in the longitudinal plane.

Due to the good number of measurements, it was possible to study the obtained data by dividing them between implements coupled only to the 3-point hitch and those having also some wheels (or other meanings) supporting the machine on the ground. In fact, in the first case the implement is entirely loading the tractor, while in the second the vibrations input could be transmitted in a different way to the driver's seat (fig. 5).

As expected, the situation is worsening if the pruning chopper has some meanings touching the ground: in the surveyed cases, at least one of the 3 axes exceeds the action value if 0,5 m/s2, and in just an other in the z axis the remarkable level of 1.9 m/s^2 was reached.

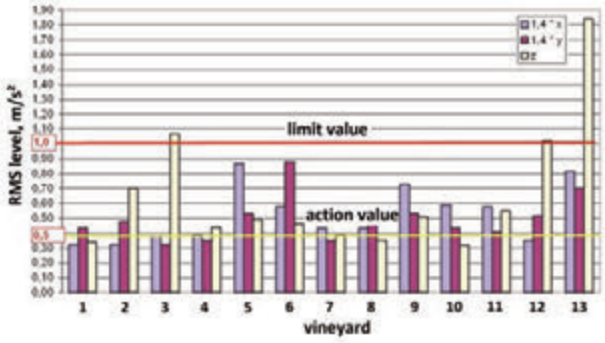

Figure 4. Vibration levels recorded in axes x, y, z during the chopping pruning combined with the grass mowing.

The measurements recorded in the inter-row management tasks were further examined regarding the tractor type used (in any case all of them had a power ranging from 60 and 130 CV). As expected, the fig. 6 shows a clear trend: with the wheeled tractors the vibration levels never exceed the limit value, but in most of them the action limit is reached in at least one of the axes. With the crawler tractors, the Z (vertical) axis levels are quite high.

For the crop protection (pesticide distribution, fig. 7) just in case 1 a crawler tractor was used, showing vibration levels higher than all the other tests. In fact, on the sprayer used in vineyard the pump and the fan do not usually produce hazardous vibration levels, and therefore only the tractor is causing the disturbance.

In any case, the levels generally exceed the action value, but those recorded in the vertical axis are not the highest. The sprayers coupling was equally distributed between towed and hitched to the 3-point linkage.

Apart the case 8, the grape harvesting was executed manually (fig. 8); the measurements refer to the handling of the grape, in particular to the vibration on the seat of the tractor used for the transportation of the bins into the vineyard. On the grape harvester, the levels recorded were lower than the other 7 tractors surveyed, probably because they were all crawler tractors. In respect to the harvest carried out manually, the harvester assures a dramatic increase of the working capacity, but also better comfort conditions, included a lower vibration level.

The grape is normally transported from the wineyard to the cellar with single axle trailers (generally not exceeding 6 t gross weight) towed with tractors. 4 wheeled tractors were investigated, ranging from 60 and 115 CV (fig. 9). In two cases, the levels recorded on the vertical axis are within the action value, but only in one case all the 3 axes values were lower than this limit. In transportation, the travelling speed and the surface conditions are the most important factors influencing the vibrations. The levels in the transversal axis were higher than those in the longitudinal axis, proving that the soil unevenness produced in the surveyed cases more disturbance than the towed trailer input on the tractor.

Operaor's exposure analysis

With reference to the levels obtained from the similar group of tasks, an operator's exposure analysis was carried out, considering the usual reference of 8-hours working time (according to what specified in Italian Decree 81/08), although it is well known that the working day in agriculture is often much longer than this period. In particular, the values were compared with the action and limit values and the relevant limits of

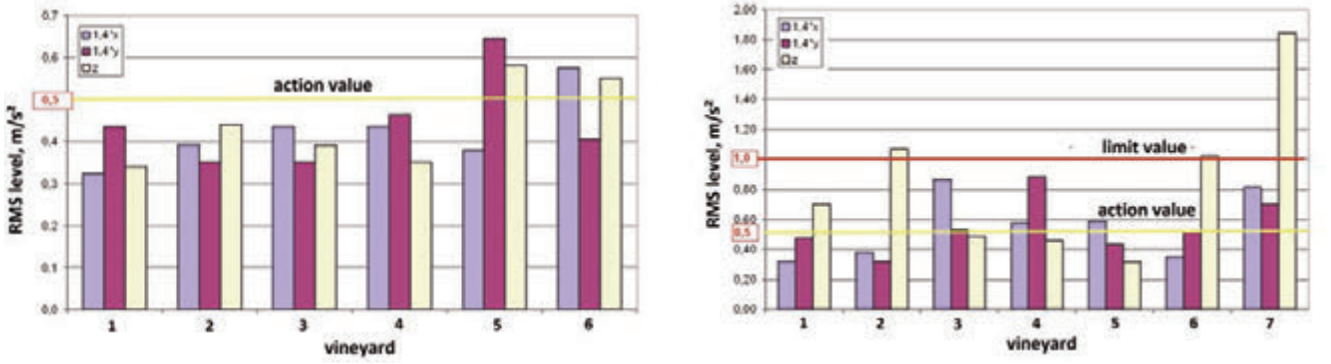

Figure 5. Vibration levels recorded in axes x, y, z during the chopping pruning combined with the grass mowing, divided for implements coupled only to the 3-point hitch (left) and those having also some wheels or other meanings supporting the machine on the ground (right).

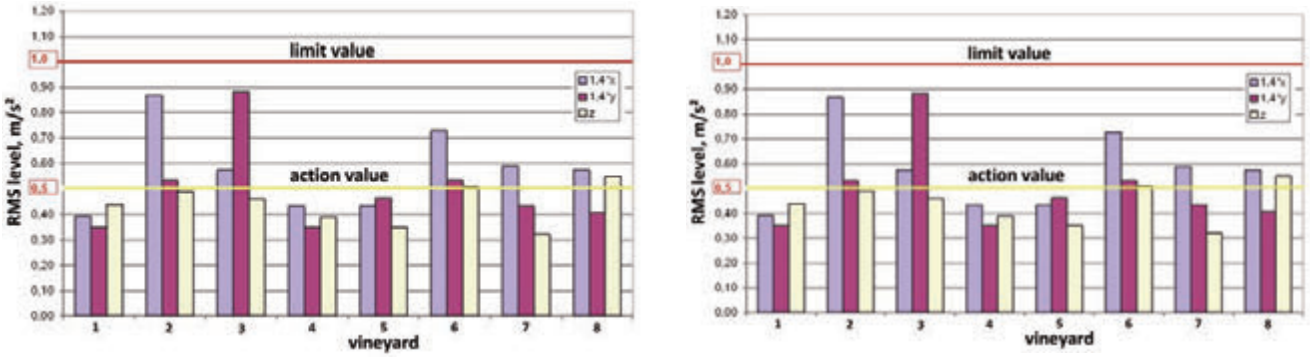

Figure 6. Vibration levels recorded in axes x, y, z during the chopping pruning combined with the grass mowing, divided for wheeled (left) and crawler (right) tractors.

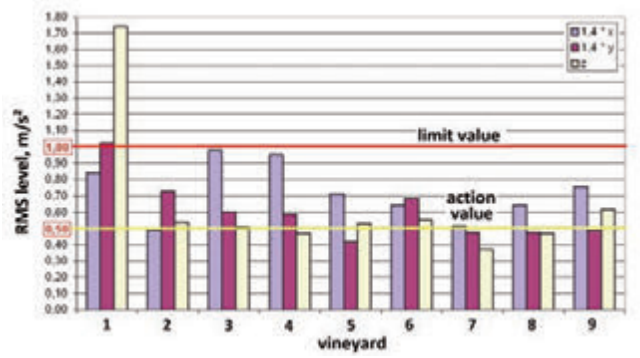

Figure 7. Vibration levels recorded in axes x, y, z during the pesticide distribution.

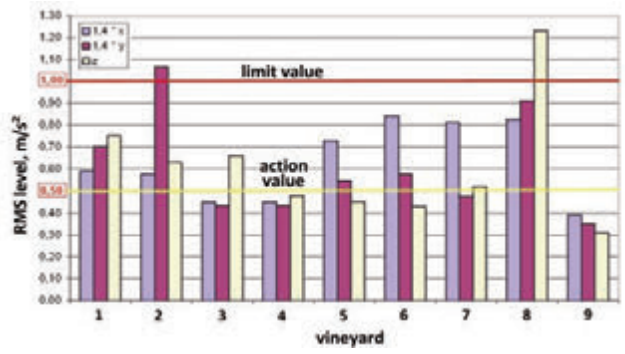

Figure 8. Vibration levels recorded in axes x, y, z during the grape harvesting. Cases 1 to 8 refer to a manual harvesting; case 9 is relevant to the use of a grape harvester.

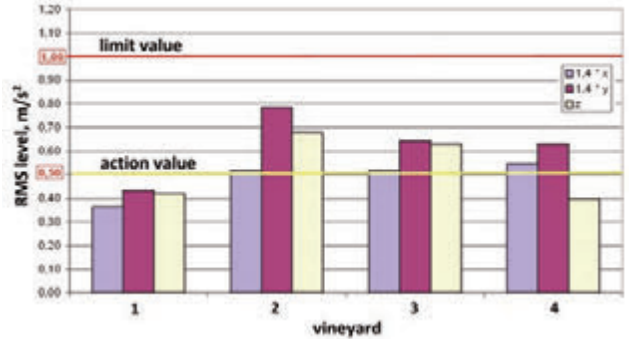

Figure 9. Vibration levels recorded in axes x, y, z during the grape transportation with trailers on the road, from the vineyard to the cellar. In all the 4 cases surveyed, wheeled tractors were used.

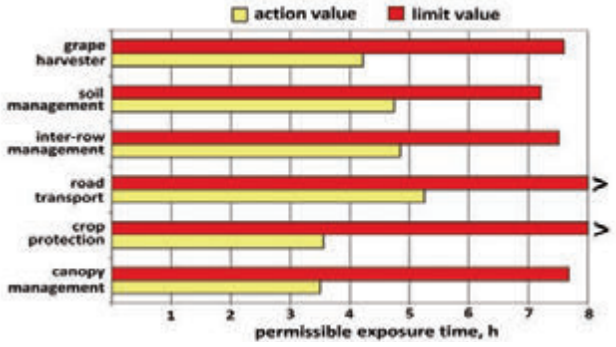

Figure 10. Permissible working time to reach the action (yellow) and limit (red) values of vibration, for 6 groups of similar tasks on wine growing.

working time were calculated, considering the average of the single figures obtained in the cases surveyed in each group of similar tasks.

The results (fig. 10) highlight the permissible working time to reach both the action (0.5 m/s2) and the limit (1.0 m/s2) values.

The transportation and the pesticide distribution tasks seem to be not critical: the limit value is not reached in 8-hours working time. On the contrary, for the soil management, the grape harvesting and the inter-row management the operators should be stop their activity before the end of the working day.

On the other hand, the general situation appears more severe if the action value is considered: for all the tasks, this limit is reached rapidly, ranging from about 3.5 to 5 hours, so creating a lowering of the safety level, due to the increase of physical and mental fatigue of the operator.

Conclusions

In general, the vibrations exposure of operators in wine growing does not appear dramatic for their physical health; however, the work concentration in some periods of the year definitely can lead to some dangerous situations, mainly due to the increase of physical and mental fatigue. In fact, referring to the most severe limit established by the 2002/44 EC Directive, the results show the opportunity to adopt some measures to reduce the vibration disturbance, especially in the vertical direction. The crawler tractors showed high vibrations, while the self-propelled machines (e.g. the grape harvester) highlighted a better level of comfort.

So, some actions could be profitably carried out to improve the situation:

- progressive replacement of crawler tractors with wheeled tractors;
- careful maintenance and adjusting of the driver's seat and its suspension system;
- frequent check of the correct tyre inflation pressure of the wheeled tractors and good maintenance of the track elements for the crawler tractors;
- check of the silent-blocks of the tractor cab or floor;
- careful maintenance of the implements to be attached to the tractor;
- task execution at a suitable travelling speed, not exceeding what provided by the manufacturer;
- assure a correct driving behaviour in transportation at high speed;
- suitable turn over of the tractor drivers, assuring them sufficient periods of rest, in order to recover the best physical and mental efficiency.

Study on the possibility of application of a compact roll over protective structure for agricultural wheeled narrow track tractors

Danilo Monarca, Massimo Cecchini, Andrea Colantoni, Simone Di Giacinto, Giuseppina Menghini, Leonardo Longo

Department of Agriculture, Forest, Nature and Energy (DAFNE), University of Tuscia, Italy

Abstract

Since occupational accidents often occur in farm tractor drivers, it is extremely important to focus the attention on specific devices in order to avoid risks from tractor overturning. This phenomenon is actually considered as the leading cause of deaths or injuries related to agricultural work. The system adopted to reduce the above-mentioned risk consists of passive protection devices aimed at preventing the hazardous event which may affect workers' health. More precisely, the tractor chassis (*i.e.* ROPS) and the proper seat belt define a "safety volume" around the worker. The aim of the present research is to carry out tests on narrow-track wheeled tractors with fixed roll over protective structures in those areas – such as hazel and olive groves and vineyards - where problems related to under–tree activities occur. This is to implement planting layout and/or cultivation techniques which can be considered suitable for tractors with roll over protective structures. According to that, their project parameters – *i.e.* safety volume, seat position and typology, test methods - can be successfully modified and improved. The results show that nowadays only a few agricultural vehicles are provided with specific fixed devices able to work under tree without damaging orchards.

Correspondence: Massimo Cecchini, Department of Agriculture, Forest, Nature and Energy (DAFNE), University of Tuscia, Via S. Camillo de Lellis snc, 01100 Viterbo, Italy.
Tel. +39.0761.357.357 - Fax: +39.0761.357.453.
E-mail: ergolab@unitus.it

Key words: tractor, overturning, roll over protective structure, safety.

Contributions: the authors contributed equally.

Conflict of interests: the authors declare no potential conflict of interests.

Conference presentation: part of this paper was presented at the 10th Italian Conference AIIA (Associazione Italiana di Ingegneria Agraria), 2013 September 8-12, Viterbo, Italy.

Journal of Agricultural Engineering 2013; XLIV(s1):e136
doi:10.4081/jae.2013.(s1):e136

Introduction

In Italy the fatal accidents at work in industry and services have marked, according to the INAIL, a significant drop in the past 10 years (Laurendi and Vita, 2011). Unlike other sectors, where the trend of fatalities follows a trail decreasing for several years, the agricultural sector has also recorded increases (INAIL, 2012). The highest number of fatal accidents, resulting in the death or permanent disability envolving the operators of agricultural tractors, demonstrates the inefficiency of the current safety devices mounted on tractors. The system to reduce the consequences of the overturning of agricultural vehicles is made up of passive protection devices, *i.e.* devices designed to prevent or reduce the severity of the damage caused by the overturning of the machine (Arana *et al*., 2010). The frame structure ROPS (Roll Over Protective Structure), with a restraint system (seat belt) creates and guarantees, around the operator, "a volume of security" or "free zone" (Kim *et al*., 2011). Indeed in the case of overturning, the risk for the operator to remain sandwiched between the constituent parts of the tractor and the ground, is reduced if the operator remains within the volume formed by the protective structure. In smaller tractors, operator, during overturning, must bend his upper body forward until it rests against the steering of the tractor in order to stay in the safety volume. In many tractors protection devices are collapsible in order to facilitate the storage and some working phases. The possibility of lowering the ROPS promotes improper use while working under the canopy of trees, because of their contact with the branches of the trees or the support structures for the breeding of specific crops ("tendone" system). Reduction is obtained by simply sliding a locking pivot without the use of a special tool, contrary to a general principle of security that requires that all protective devices can only be removed using special tools; numerous fatal accidents are determined by the tractor overturning, resulting in crushing the operator due to the failure repositioning in security position of that structure. In Italy the adjustment of tractors in use, through the installation of the protective device, is made compulsory for both employers and the self-employed, by Legislative Decree 81/2008. Point 2.4 of Part II of Annex V to the Legislative Decree 81/2008 refers to the need to limit the risks arising from work equipment rollover (overturning), through the integration of appropriate safety devices (cab or frame protection) .

The Framework Directive 2003/37/EC of 26 May 2003 concerning the type-approval of wheeled agricultural or forestry tractors, their trailers and interchangeable towed machinery, was enacted with the purpose of define processes, whether of a technical nature, to eliminate barriers in the exchange of goods within the European Community. Directive 2003/37/EC repealed Directive 74/150/EEC and all directives for agricultural or forestry tractor. The inefficiency of the safety device of agricultural vehicles can be attributed to a number of factors: the size of the current systems of protection do not allow to work under the canopy of trees; however one of the major causes of accidents can be attributed to incorrect behaviors of users of agricultural machinery,

and also to their poor training in the use of appropriate safety devices for machines and equipment. Today, thanks to compulsory training for tractor drivers, they are more conscious of the risks associated with the use of dangerous machinery. The only front on which you can still work to improve the safety of the machines, concerns the safety devices; it is necessary to study the most efficient systems, able to protect the operator at all times (Myers, 2010). The purpose of this work is precisely to: identify the difficulties of the use of safety devices in the event of rollover in working under canopy when it is in full vigor, and to find effective solutions.

Materials and methods

In this work some farms with the following crops have been selected: hazel, olive, kiwi and vine (the last two grown in tendone system). The choice of these crops is linked to the difficulty of working with tractors under canopy. In the selection of the sample farms the areas with the highest incidence production for individual crops, at the regional level, have been identified.

In Italy the diffusion of crops and methods of cultivation of orchards, are often associated with local traditions of each region. In Latium and Piedmont were analyzed hazel and kiwi plantations, while in Apulia were analyzed vineyards ("tedone" type), and olive groves.

Latium is the region in which are present all the crops under study. The cultivation of hazelnut is concentrated mainly in the province of Viterbo where the growing areas are affected by specific soil and climatic conditions that make the area particularly dedicated to hazelnuts. The planting patterns are the most common ones (5 x 5) m, the territory is mostly hilly. The kiwi cultivation is concentrated almost exclusively in the province of Latina, where the territory is mostly flat.

In Piedmont, the cultivation of the hazelnuts plays a predominant role in the regional economy; the production area par excellence concentrates in Langhe where the topography of the area as strong diversity, alternating plains and hillsides in very steep areas where mechanization is made more difficult. The kiwifruit in this area is not of great importance; however it affects the economy of several local producers. In Piedmont, the actinidia cultivation is usually performed espalier.

The Apulia region is characterized by the presence of olive groves, and in recent years also by younger ones that are best suited to mechanization of the crop as well as its more rational management. Even in these areas is difficult to identify types of farming or planting characteristic patterns considering the great diversity of the farms. In Apulia, the cultivation of the vine is typically "tendone" type and is intended mainly for the production of table grapes of excellent quality. A part of this production is exported. The land is flat and well-suited to mechanization.

For each crop under study was carried out a data acquisition board in which have been reported general indications of the farm and specific indication of the orchard. In addition, for tests carried out in the field with tractors equipped with new rollover protective structures, were prepared technical cards for each machine.

At the stage of identification of the sample farms have followed the acquisition of images in the field and their processing in the laboratory. Sampling was carried out mostly in the period of greatest expansion of the tree crowns, that is, when the situation is worse for the transit of agricultural vehicles in the field. After identifying the firms for which the surveys are carried on the fields were chosen at random, 12 couples of plants in 2 rows (6 couples for each row). The lines were chosen in a central position, so as to be representative of the entire plot (Figure 1).

For each couple 3 photos were taken. In the olive groves and hazel groves were chosen couples of plants in a row. For the vine and for kiwifruit, grown with a tendone or pergola system, the six couples of plants were chosen alternately, so as to have a larger surface area and therefore more representative of the entire plot.

The images collected in the field were taken with camera Canon EOS 1000 D with EF-S 15-55 mm. The camera was positioned on a tripod at a distance from the couples equal to planting pattern and a ground height of 1.30 m (from the center of the lens). To correct the photos by geometric aberration errors and their correct processing it was considered necessary to fix 3 points on each image. The image correction through points spaced according to fixed distance, enables the application of software Autodesk® AutoCAD® Map 3D to obtain images perfectly in line with the plan and overlapping. The 3 points were fixed by the use of a "square" specially designed. The square consists of two aluminum bars 2 m long, hinged so as to form an angle of 90 degrees; on the tree vertices of the square have been applied targets to highlight the known points. On each couple of plants the square has been positioned on the axis joining the two plants. We took advantage of the use of a spirit level to place the bar of the square in a perfectly horizontal position. In order to detect an image that would highlight the edges of the individual couple of plants has been arranged, behind them, a white piece of cloth. The fabric with a width of 5 m and a height of 3 m, was set up with two buckles on the side to be hoisted on two telescopic rods (Figure 2).

The photos taken on the site have been elaborated on the computer through the use of software Autodesk® AutoCAD® Map 3D. The pur-

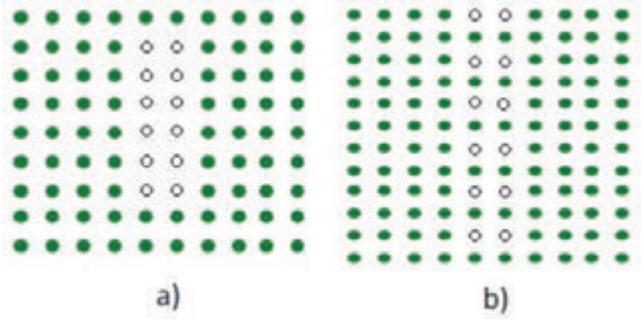

Figure 1. Sampling method: a) olive and hazel groves; b) vineyard and actinidia groves.

Figure 2. Square and cloth.

pose is to define, through polyline, the area for the passage of agricultural machines, with particular reference to cultivation of olives, hazels, vines and actinidia.

The computer elaboration is characterized by three phases: in the first the polyline has been drawn on the image of every couple of plants; in the second the characteristic polyline has been obtained; the third phase consists in the overlapping of the edges of tractors (at present more used in orchards) with the characteristic curve of each cultivation.

The following describes the procedure used for the definition of the characteristic curve of a hazelnut cultivation; the procedure is the same for crops of grapes, olives and actinidia, of which the results will be directly proposed. This survey allows us to simulate the passage of agricultural vehicles between the rows of crops. In the first stage of image processing, a polyline for each couple of plants has been realized; in particular this first phase is constituted by the realization of the anchor square on the photo. The anchor square has been realized by means of a polyline whose sides have real dimensions 2 x 2 m, or the size of the "metal square" in the field. The image put on the work plan has been anchored to the corresponding square with the command: "elastic deformation", which has allowed us to work in scale of proportion, so to keep the size and the actual relations between objects during any stage of computer processing. The anchorage was made by joining the angles of the square, with the three corresponding vertices of the reference square (Figure 3).

Once corrected the photo, a polyline has been realized corresponding to the edge of the couple of plants (Figure 4, 5 and 6).

In the second stage the processing of the polyline feature was carried out by the superimposition of polylines made for each couple of plants. For each polyline has been identified the central point of the base that has been made to coincide with the origin of the Cartesian axes (Figure 7) . Of each polyline have been obtained the coordinates of the vertices (command "list") and processed on an Microsoft® Excel® spreadsheet, obtaining a dispersion diagram. The trend line chosen for the approximation of the characteristic curve is a polynomial of degree ≥ 5.

In the last phase the trend lines, of every culture studied, have been linked with the lines of the silhouettes of tractors. The contour of the machine is obtained with the same methodology as described in phase 1 for the delimitation of areas beneath the canopy of the trees. The machines used in the simulation of passage in the field and which were obtained by the silhouettes are the following: tractor Same Delfino; tractor Goldoni Star 75; tractor Facma Trifrut; self-propelled harvester Facma C 160 S; self-propelled harvester Facma C 180 S; self-propelled harvester Facma C 200 S; self-propelled harvester Facma C 300 S; self-propelled harvester Facma C 380 S; self-propelled harvester Facma Semek 1000.

The tests were performed on, vine, actinidia, hazel and olive groves, where has been tested: the possibility of transit of agricultural tractors equipped with new protective structures (six pillars not lowering); the possibility of approaching the tractor to the trunk of the plant; the possibility of transit under the canopy of plants. The new structures, called CROPS (Compact Roll Over Protective Structure), are lower and compact than those of conventional type, adapting better to orchards with wide crown and "tendone" type plants.

For field tests the following tractors equipped with CROPS have been used: New Holland mod. 4040 T, equipped with open CROPS designed and built by INAIL; SAME mod. 35 Frutteto, equipped with open CROPS, designed and built in collaboration with INAIL; Facma mod. Trifrut 85 HP, equipped with CROPS with roof, designed and built by Facma S.r.l. (Vitorchiano, Italy) specifically for the Trifrut.

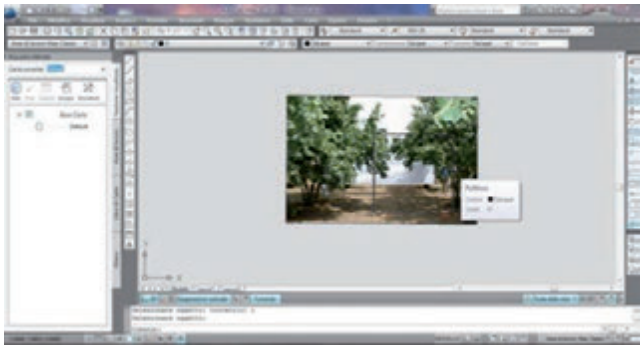

Figure 3. Computer elaboration (step 1).

Figure 5. Computer elaboration (step 3).

Figure 4. Computer elaboration (step 2).

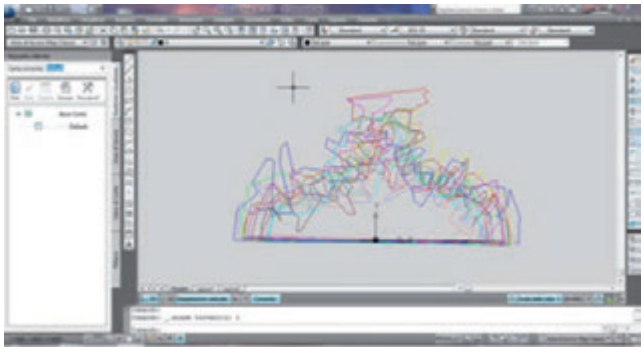

Figure 6. Computer elaboration (step 4).

The CROPS designed by INAIL comply with the standard ANSI/ASAE S478:1995. The clearance zone defined by this standard, with respect to OECD code 7, is characterized that the height in correspondence of SIP is 50 mm lower (Gattamelata *et al.*, 2012).

Results

The characteristic curve of hazelnut has been superimposed on the outlines of some of the most common agricultural vehicles, including the self-propelled harvesters.

In the case of tractors with ROPS raised, the limit is exceeded in height of about 0.5 m, while in the case of the tractor Trifrut, equipped with fixed structure with 6 uprights not folding, exceeding this limit is reduced and is equal to approximately 0.2 m.

Even for the self-propelled harvesting machines the contour exceeds in height the characteristic curve, the height of the machines increases proportionally with the size of the same. Unlike tractors equipped with ROPS, in the self-propelled harvesters, the protection structure has a shape such as to facilitate the sliding of the crown at the time of the passage.

Even the olive tree presents a difficult situation for the passage of tractors with ROPS raised; in particular, the situation more problematic is the Same Delfino (Figure 8), while the Trifrut takes advantage of both the small size and the particular shape of the protective structure which favors the sliding of the branches.

For the kiwifruit canopy grown on a pergola, the difficulty in the passage of agricultural vehicles is accentuated by the presence of fixed structures. On the graphs, the maximum height of the fixed structures from the ground is represented by the brown line. In this case the passage of tractors with ROPS raised is absolutely impossible (Figure 9). Only the tractor Trifrut has the conditions to ensure the safe passage of the machine.

As in the case actinidia, also the tendone vine presents a constraint for the transit of agricultural vehicles represented by fixed structures. Even in this case the maximum limit in height, represented by this constraint, is indicated on the graphs by the brown line (Figure 10).

From the simulations it was possible to observe the difficulty of the most common tractors to transit in orchards; to remedy this problem the new structures of protection in the event of rollover have been developed. In this work we investigated the functionality of tractors equipped with CROPS (Compact Roll Over Protection Structure), testing them in field. These structures were mounted on three tractors: New Holland T 4040 F, SAME 35 Delfino Frutteto, Facma Trifrut. The efficiency of the new compact rollover protective structures, with regard to the transitability in orchards, was observed during the work simulation under canopy.

All field tests have produced encouraging results so that one could say that the new protection structures have helped to make it easier and safer to work under canopy. Some tests are visible at the following link: http://youtu.be/gmddrJg3Btg.

Conclusions

Here is a brief description of the advantages and / or disadvantages

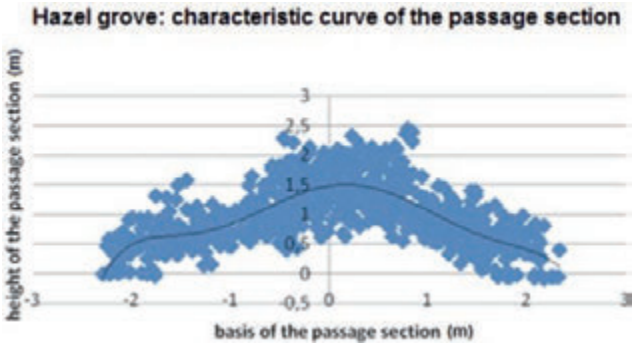

Figure 7. Computer elaboration (step 5).

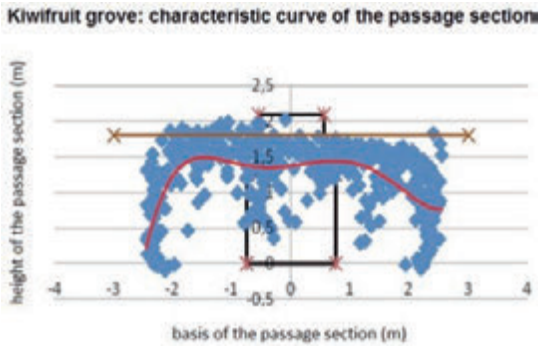

Figure 9. Simulation of transit in kiwifruit grove.

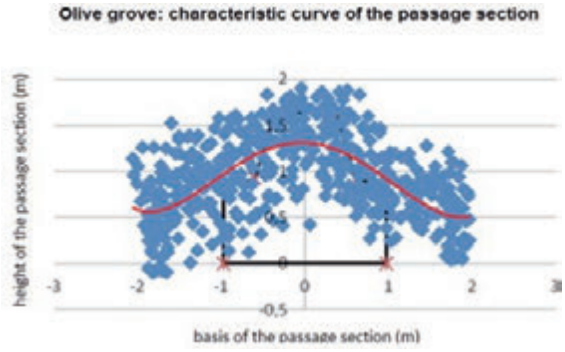

Figure 8. Simulation of transit in olive grove.

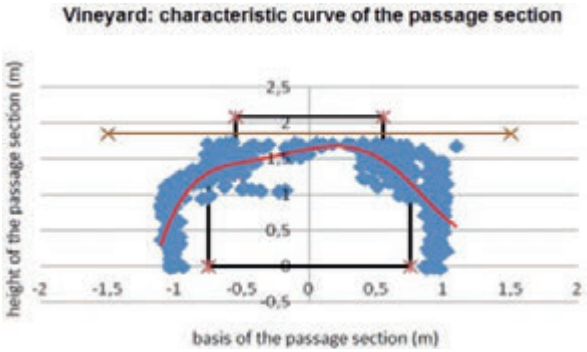

Figure 10. Simulation of transit in vine grove.

related to each of the three frames installed as rollover protective structures: 1) better transitability in the orchard with the presence of dense foliage; the particular conformation of CROPS, especially in the case of the New Holland and Facma, allows a sliding of lower foliage without determining a damage; 2) greater chance of approaching the tractor to the trunk of the plant, the difficulty of working in the vicinity of the foliage often occur in the olive groves; 3) CROPS tractors allow transit below plant canopy for both vineyards and kiwifruit canopy.

It is hoped that these new compact rollover protective structures can have a wide spread. At present there are few agricultural vehicles, equipped with ROPS or other protection systems in the event of rollover, which can perform normal agricultural operations within the orchards, without causing damage to plants.

Two of the tractors tested during the computer simulations, the Same Delfino and Goldoni Star 75, proved to be unfit for transit within an orchard with fixed support structure. From the simulation on computer and from field tests, we observed that the Trifrut works under the canopy of trees and under fixed support structures of some cultivation.

We can say that the field tests can give a measure of the resistance that most branches can oppose to structures of these machines. At the end of the testing phase in the field it will be possible, with the information gathered, to develop new characteristic curves for each cultivation considered, taking into account the actual resistance opposed to the machines by the bigger branches.

References

Arana, I., Mangado, J., Arnal, P., Arazuri, S., Alfaro, J.R., Jarén, C. Evaluation of risk factors in fatal accidents in agricolture. Spanish Journal of Agricultural Research. 2010. 8: 59.

Gattamelata, D., Laurendi, V., Pirozzi M., Vita, L., Puri, D., Fargnoli, M. 2012. Development of a compact roll over protective structure for agricultural wheeled narrow track tractors. in Proc. SHWA, 3-6 September, Ragusa, Italy. pp 131-136.

INAIL (Istituto Nazionale per l'Assicurazione contro gli Infortuni sul Lavoro) - Dipartimento Tecnologie di Sicurezza. 2011. Linee guida adeguamento trattori agricoli o forestali con piano di carico (motoagricole).

INAIL (Istituto Nazionale per l'Assicurazione contro gli Infortuni sul Lavoro). 2012. Rapporto annuale 2012.

Jarén, C., Alfaro, J.R., Arazuri, S., De León, J.L.P., Arana, J.I. Assessing rollover safety provided by ROPS tests following SAE standard J1194 versus OECD code 4. Transactions of the ASABE. 2009. 52: 1453-9.

Kim, H.J., Choi, S., Kim, K.W., Kim, J.S., Kim, J.O., Kim, Y.Y., Kim, H.K., Kwon, S.H. A study on improving the tractor ROPS and seatbelt use of Korean farmers. American Society of Agricultural and Biological Engineers Annual International Meeting. 2011.

Laurendi, V., Vita, L. Documento tecnico redatto dal Gruppo di Lavoro Nazionale istituito presso INAIL. Adeguamento dei trattori agricoli o forestali. INAIL. 2011.

Mangado, J., Arana, J.I., Jarén, C., Arazuri, S., Arnal, P. Design calculations on roll-over protective structures for agricultural tractors. Biosystems Engineering. 2007. 96: 181-91.

Murphy, D.J., Myers, J., McKenzie Jr., E.A., Cavaletto, R., May, J., Sorensen, J. Tractors and rollover protection in the United States. Journal of Agromedicine. 2010. 5: 249-63.

Myers, J.R. Prevalence of roll-over protective structure (ROPS)-equipped tractors on hispanic-operated farms in the United States. Journal of Agromedicine. 2010. 15: 137-47.

OECD Codes. OECD Standard Codes for the official testing of agricultural and forestry tractors. Available at, OECD Headquarters, Paris, France. 2009. http://www.oecd.org

Rondelli, V., Guzzomi, A.L., Selecting ROPS safety margins for wheeled agricultural tractors based on tractor mass. Biosystems Engineering. 2010. 105: 402-41.

Si, J., Wang, G., Yan, Z., Wang, J., Hao, W. Design and performance simulation of ROPS and energy-absorbing device. Nongye Jixie Xuebao/Transactions of the Chinese Society of Agricultural Machinery. 2010. 41: 20-4.

Accident investigation related to the use of chainsaw

Sirio Rossano Secondo Cividino, Rino Gubiani, Gianfranco Pergher, Daniele Dell'Antonia, Emiliano Maroncelli

DiSA, Department of Agriculture and Environmental Sciences, University of Udine, Udine, Italy

Abstract

Operating in woods might be highly dangerous as it takes place in hard environments because of slopes, uneven ground and the presence of the underwood that may prevent machines and operators from moving. The chainsaw is a widely-used tool in agriculture, in forestry as well as for professional and hobby-related purposes. This article has the aim to highlight the state of injuries both for professional and domestic uses. The research focused on web-based report of news published between 2007 and 2012 about mortal and non-mortal accidents occurred in Italy and involving people who were using a chainsaw. On the whole, 336 cases were collected over a 5-year period. The results of the work are represented by a series of thematic maps related to the causative agent, the age of the injured and the seat of the injury. Furthermore, it is confirmed that the operator's head is the most exposed area of the body and is often correlated with the death of the operator (death is often due to collision against the chainsaw blade, facial traumas as well sudden contact with parts of the plant). The study shows the dangers of chainsaw. Even workers experts are involved in serious injury and death. The study highlights the needing of looking for technical solutions and specific procedures for training unskilled worker.

Introduction

Operating in woods might be highly dangerous as it takes place in hard environments because of slopes, uneven ground and the presence of the underwood that may prevent machines and operators from moving. This requires the use of highly dangerous machines and equipment, including sharp tools. The frequency of injuries is, therefore, 1.5 times higher (and their gravity is four times higher) than the average value in domestic industry and tertiary sectors, with an average value of four injuries causing permanent disability or death for every million of hours worked (I.N.A.I.L. source, 1996). Medical costs for chainsaw injuries based amount to about 350 million dollars per year only in U.S. After a web-based research, this study considers all pieces of news concerning the use of a chainsaw. These include mortal and non-mortal deaths involving both skilled woodcutters and unskilled hobbyists. Moreover, this research has included both direct injuries (*i.e.* cuts) and indirect injuries that may be due to a fall from a ladder while trimming a hedge using a chainsaw. The chainsaw as well as all cutting tools may be a highly dangerous source of risk, both for foresters, farm operators as well as hobbyists because of possible contacts with moving parts (Cavazza, 2009). According to FOEN, the Swiss Confederation's Federal Office for the Environment, several accidents occur each year while using a chainsaw and timber harvesting. Several of them are mortal. The main cause is often to be found in lack of knowledge, carelessness and lack of exercise. Most injuries involve persons without any background in forestry-related matters, who were working in woods during their free-time, or farmers who were carrying out complementary activities. In privately owned forests, the frequency of accidents is four times higher than the frequency in firms and logging companies; Very serious injuries have involved persons using a chainsaw for professional purposes or in their free-time, in particular during construction works, gardening, horticulture, maintenance and demolition. Aim of the research is divided into two parts:

- creating a database about accidents with chainsaws;
- propose of management tools for safety. (software PPE safe)

Correspondence: : Cividino Sirio Rossano Secondo Disa,via delle scienze 217, 33100 Udine (UD), Italy
Tel. +39.0432558566.
E-mail: agricolturasicura@gmail.com

Keywords: chainsaw, forestry, safety.

Journal of Agricultural Engineering 2013; XLIV(s1):e137
doi:10.4081/jae.2013.(s1):e137

Materials and methods

The methodology used for the study wanted to define a database, in literature and in official databases (INAIL), there are no aggregated data on accidents with chainsaw. There are only cumulative data associated with professional workers.

The research focused on web-based pieces of news published between 2007 and 2012 about fatal and non-fatal accidents occurred in Italy and involving people who were using a chainsaw. On the whole, 336 cases were collected over a 5 year period. The data source is the web, they are used:

- unofficial database;
- statistics of agricultural unions;
- on-line journals;
- newspaper online;
- blog.

The following parameters were identified for each single accident and later analyzed in an Excel file:

- number of accident per year;
- year in which the accident took place;
- date;
- Region, Province and cause of the accident;
- age, profession and nationality of the injured person;
- seat of the injury;

- link with the news.

The analysis of some parameters required us to assign numeric codes reported as follows in order to allow your faster reading and data analysis (Table 1) (Pessina 2011). Data analyzed were compared with other scientific work. Were excluded from this analysis suicides and homicides with the use of chainsaw.

The second part of the paper analyzes and develops software for the management of risk in forestry work.

The software is divided into three parts:

- type of worker (farmer, gardener, woodcutter, non-professional worker);
- type of activity (use of chainsaw, use tractor, limbing, logging);
- type of workplace (wood, field) .

The program automatically producing devices for the worker and their costs.

Results

The main results are shown in Table 2. The analysis of the data shows that about half of the accidents are fatal. The people involved in accidents are mainly Italian (88,6%) and non-professionals (59.9%).

Areas of the body most vulnerable to injury were: head (34,8 %); trunk (25,0%); and leg (16,8%). This last element is confirmed by the type of event. They are in fact fatal injuries caused by contact / collision with tree or parts of tree, events primarily involving the head, trunk and legs. Contact with moving elements of chainsaw is the second leading cause of injury (39,3%), the other events are more rare.

If you get a closer look at the Regions where the accidents took place, the highest distribution is registered in Lombardia (77 accidents), followed by Toscana, Trentino Alto- Adige and Liguria. In Southern-Italy, fewer accidents are registered. The only Region where no accident took place over the five-year period is Valle D'Aosta.

The distribution of serious or mortal accidents shows a peak between January and April (Figure 1).

This is mostly due to trimming and cleaning and maintenance of green areas as well as loggers' professional activities, which is about to start. The number of accidents is expected to reduce in summer, whereas it strongly increases in autumn and decreases again in winter (December).

Analyzing Table 4 you can see that they are mainly involved in this type of accident the age group 60 - 70

As far as the days of the week are concerned, Friday and Thursday show the highest peaks; the lowest values are registered on Monday.

Figure 3 notes that areas most exposed to a high risk are the hands and legs. It is also noted that there is a difference between the series of the data presented, this element is determined by the fact that the

Table 1. Numeric codes.

deathly	
no	1
yes	2
Nationality	
Italian	1
Rumenian	2
Macedonian	3
Albanian	4
Moroccan	5
Other	6
Injury location	
Hand	1
Arm	2
Leg	3
Foot	4
Head	5
Trunk	6
Event	
Contact with moving elements of chainsaw	1
Contact / collision with tree or parts of tree	2
Infaction	3
Fall from a height	4
Electric shock	5
Burn	6
Position	
non-professional	1
professional	2

Table 2. Results.

deathly	%
no	50,5
yes	49,5
Nationality	**%**
Italian	88,6
Rumenian	5,1
Macedonian	1,8
Albanian	0,6
Moroccan	0,6
Other	3,3
Injury location	**%**
Hand	13,7
Arm	6,1
Leg	16,8
Foot	3,7
Head	34,8
Trunk	25,0
Event	**%**
Contact with moving elements of chainsaw	39,3
Contact / collision with tree or parts of tree	47,7
Infaction	2,7
Fall from a height	7,5
Electric shock	2,4
Burn	0,6
Position	**%**
non-professional	59,9
professional	40,1

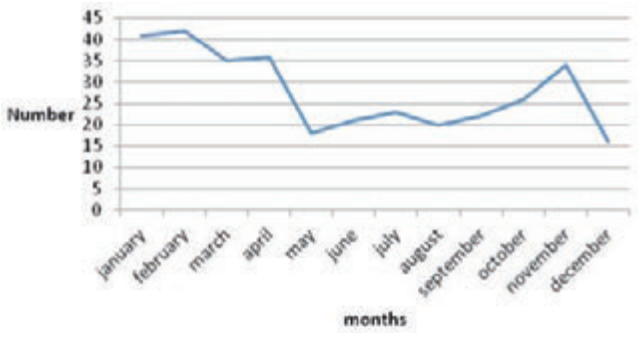

Figure 1. Accident distribution by month.

Table 3. Accident distribution by Region.

Region	Number	%
Abruzzo	15	4,5
Basilicata	1	0,3
Calabria	11	3,3
Campania	12	3,6
Emilia Romagna	24	7,2
Friuli Venezia Giulia	14	4,2
Lazio	11	3,3
Liguria	27	8,1
Lombardia	77	23,1
Marche	9	2,7
Molise	5	1,5
Piemonte	14	4,2
Puglia	4	1,2
Sardegna	5	1,5
Sicilia	8	2,4
Toscana	47	14,1
Trentino Alto Adige	32	9,6
Umbria	3	0,9
Veneto	15	4,5
Valle D'Aosta	0	0,0

Table 4. Victims by age group.

Age	% Wounded	% Dead	Index dead
10 - 20	3,0	2,4	44,4
20 - 30	8,4	9,0	51,7
30 - 40	15,6	14,4	48,0
40 - 50	21,0	17,4	45,3
50 - 60	19,2	15,0	43,9
60 - 70	24,6	25,1	50,6
70 - 80	6,6	13,8	67,6
80 - 90	1,8	1,2	40,0

models presented in the literature do not consider hobbyists. The latter element must be the starting point for new studies that evaluate the overall incidence of accidents related to chainsaw.

Conclusions

Firstly, we deeply analysed and searched for accidents taking place in Italy between 2007 and 2013. By doing this, we were able to perceive how dangerous the chainsaw might be while being used. We later collected a series of key points pertaining education and training within foresters, with an eye to the use of the chainsaw. We started by analysing handbooks by bodies (including Regions, Provinces, Municipalities, several chainsaw manufacturers, Institute of Higher Education for Prevention, Health and Safety at the Workplace, etc.). We later used the information we gathered to develop a model which enables us to verify and to certify correct choice about safety, using PPE Forestry safe 1.1

After the welcoming screen, you have access to the software and can choose among the following options:

- software instructions;
- information key;
- technical aspects;
- personal protective equipment (PPE);
- average cost.

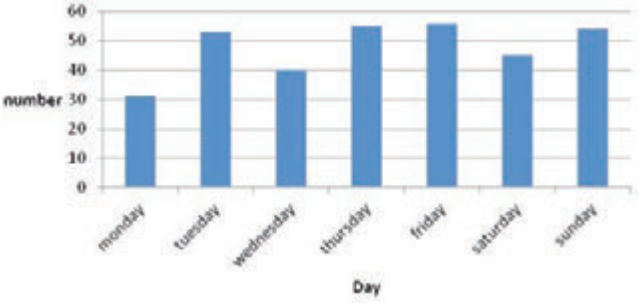

Figure 2. Accident and deaths distribution by day of week.

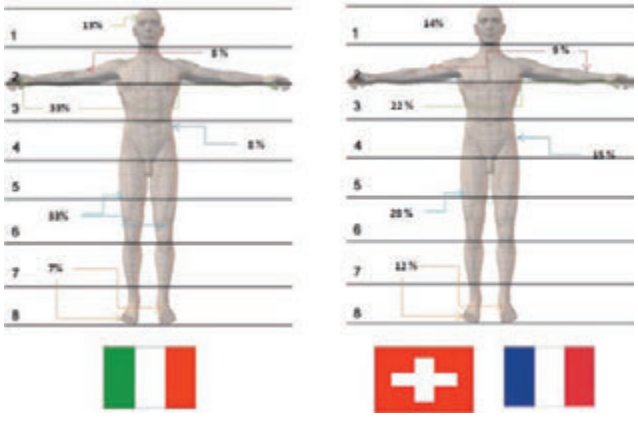

Figure 3. Comparison between the Italian and international data (Suva 2005).

Figure 8. Overwiev PPE safe 1.0.

The program works according to the legislation on safety at workplace 81/2008, the software allows the employer on the basis of precoded parameters (type of chainsaw, chain speed) to choose the correct PPE In conclusion should be underline that employers are required by law to acquaint their workers with any hazards associated with the handling of tools or equipment, such as chainsaws, that they use during their jobs.

References

Astier P. 1982, Les accidents lies a l'emploi de la tronconneuse chez les salaries agricoles de l'Isere de 1976 a 1979, Pages 80-85

Cavazza, N., Serpe, A., 2009. Effects of safety climate on safety norms violations:exploring the mediating role of attitudinal ambivalence towards personal protective equipment. J. Saf. Res., doi:10.1016/j.jsr.2009.06.002.

Cividino Srs,Marroncelli E, 2012,Accident analysis during the chainsaw use: prevention and protection measures to reduce injuries.International Conference RAGUSA SHWA 2012, September 3-6, 2012, Ragusa – Italy "Safety Health and Welfare in Agriculture and in Agro-food Systems" Pages 158-164

D. Pessina, D. Facchinetti , 2011, il ruolo del web nel monitoraggio degli incidenti mortali dovuti al ribaltamento dei trattori agricoli Convegno di Medio Termine dell'Associazione Italiana di Ingegneria Agraria Belgirate, 22-24 settembre 2011

ENAMA, GAS Forum (Global Agricultural Safety Forum), forum mondiale per la sicurezza in agricoltura, Roma, 2008 (http://www.gasforum.eu).

Foen Federal Department of the Environment, Transport, Energy and Communications Workplace safety is first priority

Y.G. Doyle Prevention d Volume 21, Issue 6, December 1989, Pages 529–534 Accident Analysis & Prevention

Wettmann O, Suva 2005, Accidents du travail dans les entreprises forestières en 2003, Pages 19–34, Secteur forêt, arts et métiers.

A Wii-controlled safety device for electric chainsaws

R. Gubiani,[1] G. Pergher,[1] S.R.S. Cividino,[1] R. Lombardo,[2] F. Blanchini[2]

[1]University of Udine, Dept. DISA, Udine, Italy; [2]Innovactors,Udine, Italy

Abstract

Forestry continues to represent one of the most hazardous economic sectors of human activity, and historically, the operation of chainsaws has mainly been restricted to professional lumberjacks. In recent years, because of low cost, chainsaws have become popular among unprofessionals, *e.g.* for cutting firewood and trimming trees. Serious or lethal lesions due to the use of chainsaws or electric chainsaws are often observed by traumatologists or forensic pathologists. Such serious accidents often occur during occupational activities and are essentially due to kickback or uncorrected use of the tool, or when the operator falls down losing the control of the implement. A new device in order to stop a cutting chain was developed and adapted to an electric chainsaw. The device is based on a Wiimote controller (Nintendo™), including two accelerometers and two gyroscopes for detecting rotation and inclination. A Bluetooth wireless technology is used to transfer data to a portable computer. The data collected about linear and angular acceleration are filtered by an algorithm, based on the Euclid norm, capable to distinguishing between normal movements and dangerous chainsaw movements. The result show a good answer to device and when happen a dangerous situation an alarm signal is sent back to the implement in order to stop the cutting chain. The device show a correct behavior in tested dangerous situations and is envisaged to extend to combustion engine chainsaws, as well as to other portable equipment used in agriculture and forestry operations and for this objectives were patented.

Introduction

Forestry continues to represent one of the most hazardous sectors of human activity; however, in the last years the scenario has changed. Historically, the use of chainsaws has mainly been restricted to professional lumberjacks, but in recent years, low-cost models have become popular among unprofessionals, *e.g.* for cutting firewood and trimming trees. Today, over 300 000 chainsaws are sold annually in Italy, while many millions of older models are still in use. The U. S. Bureau of Labour Statistics reported that logging was causing 26% more frequent injures than general industries (Lefort *et al.*, 1999). Accident rates in Sweden among chainsaw operators have been reported to be four times higher than among logging-machine operators (Axelsson, 1998). A German study (1994-1995) found that about 15% of all injures to forestry workers were the direct result of chainsaws (Hartfield , 1997). In the Southeastern United States a study showed that manual chainsaw delimbing, *i.e.* the cutting of branches from stems in felled trees, was the most hazardous activity in partial mechanized logging operations (Shaffer and Milburn, 1999). In Lousiana a study showed that tools and equipment (including chainsaw) were responsible for 19% of the injuries to the body in logging sector (Lefort *et al.*, 1999).

In Italy, Spinelli *et al*. (2010) reported that operators often do not employ a safe technique for starting chainsaws, and do not correctly use PPE (personal protection equipment). Accidents research showed the chainsaw accidents is very high frequency than other operations as a skidding, tending or workplace conditions (Potocnik *et al*., 2009).

Modern chainsaws incorporate numerous safety features to protect the operator from kickback (*i.e.*, the swift reaction upward movement of the chainsaw bar, especially when used with its tip, or "nose") and other hazardous events (particularly when the operator falls down losing the control of the implement). However, such features may be ineffective when correct working procedures are disregarded or even ignored (which often is the case of unprofessional operators). Even the newest models possess, however, some inherent dangers associated with their operation that could result in serious and sometime fatal injuries. Serious or lethal lesions due to the use of chainsaws or electric chainsaws are often observed by traumatologists or forensic pathologists. Such serious accidents often occur during occupational activities, or more rarely during suicidal events. For this kind of accidents, safety protection is possible only if the cutting chain is stopped because often the helmet not is sufficient to safety of kind of accident. The cutting chain is stopped only by activation to chain brake.

Many researchers have tried to set up a system designed to stop the chainsaw when the operator is moving the chainsaw in dangerous mode. One system proposes a capacitive sensor to detect human proximity near the guide bar and chain of a chainsaw. The capacitance sensors are measured using a carrier frequency method and the developed system provides information about human proximity at least for every 0.2 s and hence enables the control unit to react in real time. The system successfully distinguishes between proximity of the human body and wood. The developed system senses human proximity up to 15 cm from the chainsaw (Zangl and Bretterklieber, 2008).

Others researches have set up a brake on electric chainsaw where in that the electric motor is an electronically commutated electric motor having at least three coil windings, and at least one of the run-down and kickback brake and control means adapted to disconnect a driving voltage from each of said motor coil windings except at least one of them and apply a controlled resistive connection across each of said motor coil windings (Jordan *et al*., 2012).

Correspondence: Rino Gubiani, University of Udine, Dept. DISA, Via delle scienze 208, 33100 Udine, Italy.
Tel. -39.0432.558656
E-mail corresponding: Agricolturasicura@gmail.com, rino.gubiani@uniud.it.

Key words: safety, chainsaw, fatal injuries, electronic device.

Journal of Agricultural Engineering 2013; XLIV(s1):e138
doi:10.4081/jae.2013.(s1):e138

Until now, none of these systems reached commercial development, probably due to false response patterns that may decrease the work capacity of the operator. Only Husqvarna has adopted a system called TrioBrake™; it is a safety system where the chain brake can be activated in a third way – with the right hand besides the two customary ways. TrioBrake™ can provide extra protection under situations where a regular chain brake would fail to provide adequate protection. This system forces the worker to assume a more ergonomic position with the body.

The objective of this study has been the development and realization of a new integrated safety system for chainsaws.

Methodology

A new device devised to stop a cutting chain was developed and adapted to an electric chainsaw. The goals to develop this device were:

a) the device must block the cutting chain when a mistake is identified in chainsaw behavior;
b) the device can be adopted in other handheld power equipment (drills, hedge trimmers), including chainsaws powered by 2-stroke engines;
c) device must have a low cost.

The device is based on a Wiimote controller (Nintendo™), including two accelerometers and two gyroscopes for detecting rotation and inclination and thus solve b) and c) goals.

The main problem in a) goal is to identify the mistake in chainsaw behavior and to solve this we had follow path showed in Figure 2.

A Bluetooth wireless technology is used to transfer data to a portable computer. The data collected about linear and angular acceleration are filtered by an algorithm, based on the Euclid norm, capable to distinguishing between normal movements and dangerous chainsaw movements.

In all chainsaws the chain brake is activated if pressure is applied against the guard or when, in the event of kickback, the operator's hand strikes the lever. In chainsaws equipped with electric motor chain movement will be stopped by cutting off the power supply; in chainsaws driven by a 2-stroke motor, a band brake is applied on the clutch drum.

In the realized prototype in case of electric motor the alarm system operates by acting on a potentiometer, in case of a 2-stroke motor the blockage will be integrated on existing chain brake with insertion of a mechanic piston activated by the alarm system.

A cordless electric chainsaw, Black & Decker GKC1817, 18-V 8-in was used in the tests.

Data were collected by a Wiimote controller (Nintendo™) but before to start with tests was necessary to define calibration parameters in order to calculate accelerations from the Wiimote output for (Wiimote reported values 0 to 999). We found this values:

- the value 490 is equal to linear acceleration zero (acclin=0);
- the value 590 is equal to linear acceleration g (acclin=9.8 m/s).

The test for control the level of acceleration was carried out cutting different kind of wood as reported in Table 2.

To optimize the alarm signals was necessary to setting the parameters in order to have the correct sensitivity about these parameters:

1. cut frequency of linear accelerations: cfSlin;
2. cut frequency of angular accelerations: cfSang;
3. linear threshold: thlin;
4. angular threshold: thang;
5. fall threshold: thfall.

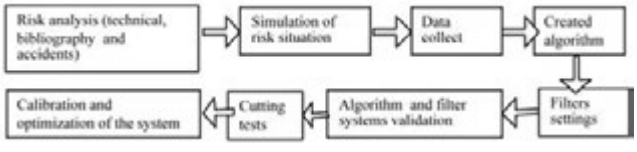

Figure 1. Flow chart of experimental procedure.

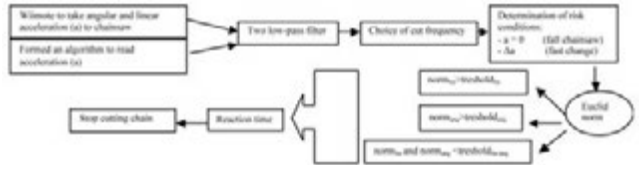

Figure 2. Scheme of algorithm steps.

Table 1. Technical data GKC1817 chainsaw.

Voltage	Vdc	18
Battery capacity	Ah	1.7-1.5 NiCd
Battery mass	kg	0.8
Charging time	h	8
No load chain speed	m/s	3.1
Guide bar length	cm	20
Mass	kg	2.8

Table 2. Test to cut simulation.

Wood	Ø wood (cm)	Replicates (n.)	Mode of cutting
Soft (poplar)	4.0	29	Up-down (lower cutting chain)
Medium soft (fir)	3.3	16	Up-down (lower cutting chain)
Hard (oak)	5.8	10	Up-down (lower cutting chain)
Hard (oak)	5.8	10	Down-up (upper cutting chain)
Hard (oak)	5.8	10	Up-down (lower cutting chain, near to top of guide bar)
Hard (oak)	5.8	10	Down-up (upper cutting chain, near to top of guide bar)

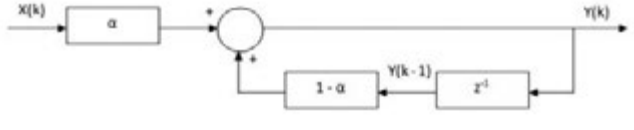

Figure 3. Scheme of low-pass filter (α=parameter with range 0-1; X=Laplace transformed in input; Y= Laplace transformed in output; k=sample; z=coordinate(or x and y)).

Results

The formed algorithm is capable to distinguish this risk situations:

- slipping operator;
- falling operator;
- falling chainsaw;
- kick back chainsaw;
- any another fast movements of chainsaw or operator.

The algorithm calculates the vectorial norm to linear acceleration and angular acceleration (Eq. 1 and 2).

$$norm_{lin} = \sqrt{a^*_{lx}(t)a^*_{lx}(t-1))^2 + (a^*_{ly}(t) - a^*_{ly}(t-1))^2 + (a^*_{lz}(t) - a^*_{lz}(t-1))^2} \quad (1)$$

$$norm_{ang} = \sqrt{a^*_{ax}(t)a^*_{ax}(t-1))^2 + (a^*_{ay}(t) - a^*_{ay}(t-1))^2 + (a^*_{az}(t) - a^*_{az}(t-1))^2} \quad (2)$$

The Euclid norm sphere delimits a space where the chainsaw can be moved. If, in this delimited space, the chainsaw goes through under condition showed in Figure 2, the Wiimote stops the potentiometer to electric chainsaw.

The test carried out for verify the correct correlation to accelerations and alarm signal show:

- that the normal cutting with soft wood has a sufficient uniform linear and angular acceleration (Figure 4).
- the normal cutting with hard wood has a good uniformity as to linear and angular accelerations, but also has more amplitude then in the previous case (Figure 5).
- the cutting in down-up mode with upper cutting chain part do not show more amplitude in accelerations than normal cutting (Figure 6).
- the cutting in up-down or down-up mode near to top of guide bar the acceleration held a large amplitude but not so great to activate the alarm signal (Figure 7) .

In conclusion when the chainsaw works in different mode but always inside a normal condition the alarm signal is not activated.

The test carried out for setting parameters must result in optimized the alarm signals, not to sensitivity because the chainsaw should not be stopped so easily and not too strong.

The data collected were reported in 9 combinations both linear acceleration and angular accelerations with a number of errors reported (from 0 to >50). When cutting wood the alarm doesn't need to be activated and must be considered only those combinations where the value is equal to zero (Tabb. 4 and 5).

At the same mode were setting the parameters also in others different kind of cutting (up-down cutting chain, near to top of guide bar and down-up).

About chainsaw falling down the we know when a body fall the linear acceleration is equal to zero. The threshold value for observer this con-

Table 3. Setting of parameters sampled at 100 Hz by Wiimote.

Wood (n.)	Ø wood (cm)	Reply	Kind of cutting
Hard (oak)	5.8	10	Up-down (lower cutting chain)
Hard (oak)	5.8	10	Down-up (upper cutting chain)
Hard (oak)	5.8	10	Up-down (lower cutting chain, near to top of guide bar)
Hard (oak)	5.8	10	Down-up (upper cutting chain, near to top of guide bar)
Nothing	-	10	Falling chainsaw

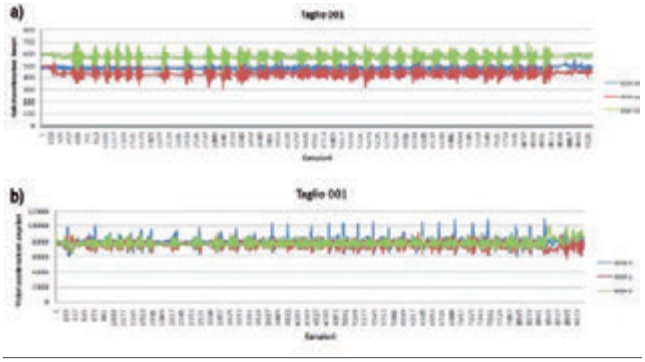

Figure 4. Linear A) and angular B) acceleration with normal cutting to soft wood (up-down with lover cutting chain).

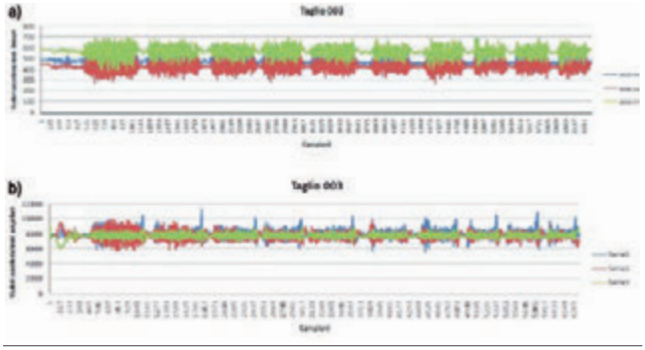

Figure 5. Linear A) and angular B) acceleration with normal cutting to hard wood (up-down with lover cutting chain).

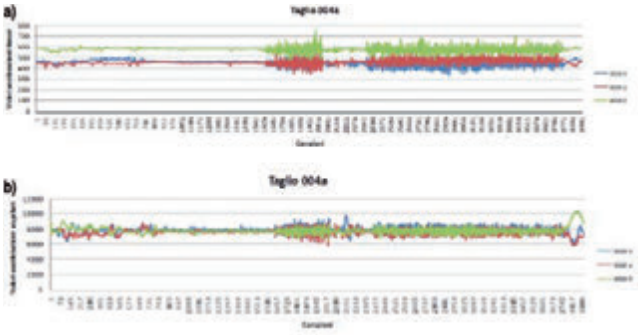

Figure 6. Linear a) and angular b) acceleration with down-up cutting to hard wood.

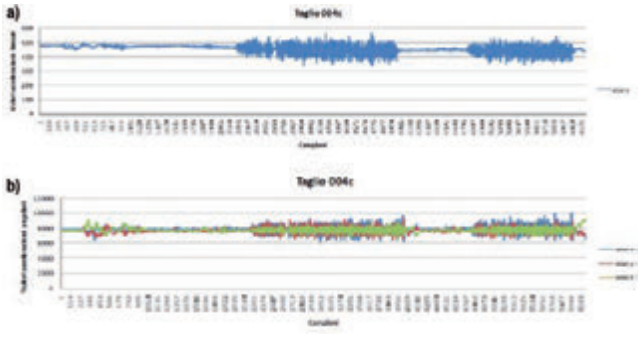

Figure 7. Linear a) and angular b) acceleration with down-up near to top of guide bar cutting to hard wood.

Table 4. Linear cut frequency (cfSlin) and linear threshold (thlin) to cut hard wood.

		Linear cut frequency		
		0.10	0.39	0.60
Linear	3	0	>50	>50
Threshold	5	0	0	>50
	6	0	0	39

Table 5. Angular cut frequency (cfAng) and angular threshold (thang) to cut hard wood.

		Angular cut frequency		
		0.05	0.45	0.60
Angular	50	1	>50	>50
Threshold	250	0	0	1
	450	0	0	1

Table 6. Parameters setup on Wiimote.

Linear cut frequency (cflin)	0.40
Angular cut frequency (cfang)	0.45
Linear threshold (Thlin)	5
Angular threshold (thang)	250
Falling threshold (thfall)	40

dition must be very little and we setup the Wiimote to 40 value.

The parameters setup after test were reported in Table 6.

Conclusion and perspectives

The device show a correct behavior in dangerous situations and it is envisable that it can be extent to combustion engine chainsaws, as well as to other portable equipment used in agriculture and forestry operations. The Wiimote is a easy and cheap device to install to the chainsaw for collect acceleration and position data. The algorithm allows the good control of processing data and send right signal to blocking cutting chain. The idea based on Wiimote device and algorithm based on Euclid norm is patented in 2011 (Blanchini *et al*., 2001) for have a chance to further development as a real application on chainsaw.

References

Axelsson S., 1998. The mechanization of logging operations in Sweden and its effects on occupational safety and health. J. For. Eng. 9(2): 25-31.

Blanchini F., Lombardo R., Battiston G., Cividino S.R.S., Pighin J., Gubiani R., Pergher G. (2011). Patent rif. Glp's ref. A3-8816. State, Italy, filling No. UD2011A000039. Filling date: 15/03/11. International classification B27G.

Bracchetti Montorselli N.; Lombardini C.; Magagnotti N.; Marchi E.; Neri F.; Picchi G.; Spinelli R., 2010. Relating safety, productivity and company type for motor-manual logging operations in the italian Alps. Accidents analysis and Prevention 42, 2013-2017.

Lefort A. J. Jr; de Hoop C.F.; Pine J. C.; Marx B.D., 1999. Characteristics of injuries in the Logging Industry of Louisiana, USA: 1986 to 1998. International Journal of Forestry Engineering, pp 75-89.

Hartfield J., (1997). First Standardized Federal accident statistic – Analysis of accident data of the State Forest Services in Germany. Preceedings of the seminar on safety and health in forestry are feasible herld in Konolfingen, Switerland, October 6-11, 1996, pp 105-126.

Husqvarna, TrioBrake™ AB. SE-104 25 Stockholm S:t Göransgatan 143 +46-3614 65 00 +46-88739 64 50 556000-5331 www.husqvarna.com. Sweden.

Jordan C. Friese A., Heywood P., Barber A. Patent. Application Number: EP20100195647 Publication Date: 06/20/2012 Filing Date: 12/17/2010. International classification B27B 17/08.

Poto nik I, Pentek T., Poje A. (2009). Severity analysis of accidents in forest operations. Cro. J. for. Eng. 30, 2, 171-184.

Shaffer R. M., Milburn J. S., 1999. Injuries on feller-buncher/grapple skidder logging operations in the Southeastern United States. For. Prod. J. 49 (7/8):24-26.

Zangl ,B.G, Bretterklieber T., (2008). A warning system for chainsaw personal safety based on capacitive sensing. IEEE conference "Sensors", Lecce 26-29 October, pages 419-422.

Ergonomic issues in ewe cheese production: reliability of the Strain Index and OCRA Checklist risk assessments

John Rosecrance,[1] Robert Paulsen,[1] David Gilkey,[1] Lelia Murgia,[2] Thomas Gall[2]

[1]College of Veterinary Medicine and Biomedical Sciences, Colorado State University, USA; [2]Department of Agraria, University of Sassari, Italy

Abstract

Occupational ergonomists often use a variety of methods to identify jobs that are considered at high risk for the development of work-related musculoskeletal illnesses. The Strain Index (SI) and the Occupational Repetitive Actions (OCRA) Checklist are two popular upper limb risk assessment tools used in many industries, including the agro-food industry. Both methods are based on similar biomechanical, physiological and epidemiologic principles, but their approach to quantification and estimation of risk factor magnitude is quite different. The purpose of this study was to assess the inter-method reliability of SI and OCRA Checklist. Methods: Twenty-one jobs were video recorded in a Sardinian cheese manufacturing facility. Eight raters were recruited to assess job exposures to physical risk factors using the SI and OCRA Checklist. Inter-method reliability was characterized using proportion of overall agreement, Cohen's kappa, and Spearman and Pearson correlations. Results: Strain Index and the OCRA Checklist assessments produced generally reliable results, classifying the risk of 35 of 42 (83%) job exposures similarly. Conclusions: The OCRA Checklist and SI risk assessments are reliable upper limb measures of physical work exposures. Both measures appear useful for assessing risk of upper limb disorders of work tasks in the agro-food industry. However, the SI is specific to disorders of the distal upper limb and perhaps most useful for assessing risk in work primarily involving the wrist and fingers. Whereas the OCRA Checklist, which includes an assessment of the shoulder, may be more appropriate for evaluating jobs that also require extended periods of reaching and shoulder activity.

Correspondence: Robert Paulsen, 1681 Campus Delivery, Colorado State University. Fort Collins, Colorado, USA 80523.
Tel. +001.970.491.1405.
E-mail: paulsen.rj@gmail.com

Key words: strain index, OCRA checklist, inter-method reliability, musculoskeletal disorders, risk assessment methods

Acknowledgments: the present study was supported by the Center for Disease Control (CDC) / National Institute for Occupational Safety and Health (NIOSH) Mountain and Plains Education and Research Center (grant number: 5T42OH009229-06). Its contents are solely the responsibility of the authors and do not necessarily represent the official views of the CDC or NIOSH.

Journal of Agricultural Engineering 2013; XLIV(s1):e139
doi:10.4081/jae.2013.(s1):e139

Introduction

The Strain Index (SI) (Moore and Garg 1995) and the Occupational Repetitive Actions (OCRA) Checklist (Colombini *et al.,* 2000; Colombini *et al.,* 2011) are two of the most comprehensive and widely used tools used to quantify exposure to physical risk factors for upper extremity musculoskeletal disorders (MSDs). The SI and OCRA Checklist are semi-quantitative observational assessment tools employed by occupational health practitioners and physicians to systematically evaluate ergonomic job hazards in the agro-food industry. Both methods produce a composite risk index that summarizes the magnitude of physical risk factor exposure. The results of an SI or OCRA Checklist assessment are usually interpreted according to tiered risk classification criteria, which usually categorize risk indexes as no risk, moderate risk, or high risk. These categorical risk classifications can be used to map the ergonomic hazards within a facility or a department, to identify the impact of interventions, and to compare an observational risk assessment with other risk assessment methods.

The purpose of this study was to investigate whether the SI and OCRA Checklist would reliably assess risk when they are used to evaluate the same job exposures (inter-method reliability). The SI and OCRA Checklist were used to evaluate physical job exposures to the left and right upper limbs of workers performing 21 different cheese manufacturing jobs.

Methods

The SI is an observational assessment tool used to quantify exposures related to the development of general distal upper extremity MSDs (Moore and Garg 1995). The SI risk index is the product of six task-variable scores determined by an SI rater: (i) *intensity of exertion*, (ii) *duration of exertion*, (iii) *efforts per minute*, (iv) *hand/wrist posture*, (v) *speed of work*, and (vi) *task duration per day* (Moore and Garg 1995).

Similar to the SI, the OCRA Checklist is an observational assessment tool, but it quantifies exposure to physical risk factors affecting the entire upper extremity, including the shoulder. The OCRA Checklist also summarizes exposure in terms of six task-variable scores (i) *frequency of technical actions*, (ii) *force*, (iii) *awkward postures and movements*, (iv) *additional factors*, (v) *lack of sufficient recovery*, and (vi) *task duration* (Colombini *et al.,* 2002; Colombini *et al.,* 2011).

Exposures to physical risk factors for upper extremity MSDs were assessed for 21 cheese manufacturing jobs performed at a facility in

Sardinia Italy. These 21 jobs included all of the major stages of *Pecorino Romano* production, from draining curd to product packaging. Operators performing these jobs were required to exert a variety of repetitive upper extremity movements and forceful exertions. Handheld digital video camcorders were used to record at least five work-cycles of upper limb activity in the frontal and sagittal planes. Job and break/recovery duration information was obtained by direct observation and onsite interviews.

Eight individuals rated the left and right limb exposures for operators performing 21 cheese manufacturing jobs. Regardless of prior experience, raters received structured SI and OCRA Checklist training before evaluating any jobs for the present study.

Raters analyzed videos of each cheese manufacturing job using the SI and OCRA Checklist according to the instructions of the developers of each method (Moore and Garg 1995; Colombini *et al.,* 2011). Raters waited at least three weeks after rating all of the jobs with one method before reevaluating them with the other method.

Data analysis and statistical methods

Strain Index and OCRA Checklist risk indexes, which are continuous variables, can only be compared by categorizing them using common exposure classification criteria (also referred to as hazard thresholds or cut-points). These criteria provide a simple summary of the physical risk factor exposure magnitude experienced by the worker. The exposure classifications chosen for inter-method reliability analyses are shown in Table 1, and they were similar to those used in previous SI and OCRA Checklist or OCRA Index studies (Apostoli *et al.,* 2004; Stevens *et al.,* 2004; Stephens *et al.,* 2006; Spielholz *et al.,* 2008; Jones and Kumar 2010; Colombini *et al.,* 2011; Chiasson *et al.,* 2012).

Inter-method reliability analyses of SI and OCRA Checklist exposure classifications were performed using mean risk indexes based on the eight replicate assessments made of each job (one assessment per rater using both the SI and the OCRA Checklist). The proportion of overall agreement (p_o) for these mean risk indexes was calculated, and Cohen's weighted kappa coefficient using Fleiss-Cohen weights (κ_w) characterized the chance-corrected agreement between both measures. To assist with the interpretation of results, Landis and Koch's (1977) verbal criteria of kappa coefficient magnitude were employed: $\kappa_w < 0.20$, poor or slight agreement; $0.21 \leq \kappa_w \leq 0.40$, fair agreement; $0.41 \leq \kappa_w \leq 0.60$, moderate agreement; $0.61 \leq \kappa_w \leq 0.80$, substantial agreement; and $\kappa_w > 0.80$, almost perfect agreement. Spearman's rank-order correlation coefficient (r_s) was also calculated to represent the strength of association between risk classifications. Additionally, the linear relationship between SI and OCRA checklist continuous risk indexes was characterized by Perason's product-moment correlation coefficient (r). All statistical analyses were completed using SAS/STAT® Software (SAS Institute, Cary, NC) version 9.3 (2012) on a Windows PC. Confidence intervals were calculated with 95% certainty.

Results and discussion

Jobs were predominantly machine-paced and had a mean cycle time of 41.5 seconds (±31.2). The mean risk index for all job exposures was 22.2 for the SI assessments and 19.2 for the OCRA Checklist assessments.

Table 2 displays the distribution of SI and OCRA Checklist risk classifications for the 42 cheese manufacturing exposures (21 jobs x 2 limbs exposed per job). The two methods attributed the same level of risk to 35 of the 42 job exposures (p_o=83.3%). Table 2 also shows that the risk classification for nearly all of the exposures was ranked as "moderate risk" or "high risk" (97.6% for the SI and 92.9% for the OCRA Checklist). The SI ranked more jobs as high risk (61.9%) than did the OCRA Checklist (50.0%). Further, all 7 of the risk classification disagreements were biased toward higher SI risk assessments.

The relatively high level of overall agreement was also substantially greater than would be predicted by chance alone. Cohen's weighted kappa coefficient was 0.76 (95% CI: 0.61-0.92). The lower limit of the κ_w 95% confidence interval was equal to the lower criterion boundary of what Landis and Koch termed "substantial agreement" in ratings beyond chance. The Spearman rank-order correlation coefficient (r_s) for the 42 pairs of risk classifications was 0.80 (95% CI: 0.66-0.89). This strong correlation provides further support for the good inter-method reliability of the SI and OCRA Checklist.

The linear relationship between the SI and OCRA Checklist risk indexes was very strong. For the pairs of 42 continuous risk indexes, the Pearson product-moment correlation coefficient (r) was 0.94 (95% CI: 0.89-0.97). Figure 1 displays this relationship between risk indexes.

The present study appears to suggest a greater inter-method reliability between SI and OCRA Checklist assessments than previous studies have reported. However, directly comparing the present results to these previous studies is somewhat difficult due to methodological differences. Additionally, comparisons between the SI and the OCRA Checklist are rare, and SI comparisons have predominantly been made using the more complex OCRA Index.

Table 1. Strain Index and OCRA Checklist exposure classification criteria used for inter-method reliability analyses.

Risk index classification criteria		
SI		OCRA
<3	No risk	<7.6
3-6.9	Moderate risk*	7.6-14
≥7	High Risk	≥14.1

*Moderate risk indicates a magnitude of exposure that may elevate a worker's risk of developing an upper extremity disorder, and employer action is recommended to reduce the exposure.

Table 2. Distribution of SI and OCRA Checklist risk classifications for 42 upper extremity cheese manufacturing job exposures to physical MSD risk factors.

SI	OCRA			
No. Exposures	Risk index classification criteria			No. exposures
1	<3	No risk	<7.6	3
15	3-6.9	Moderate risk	7.6-14	18
26	≥7	High Risk	≥14.1	21

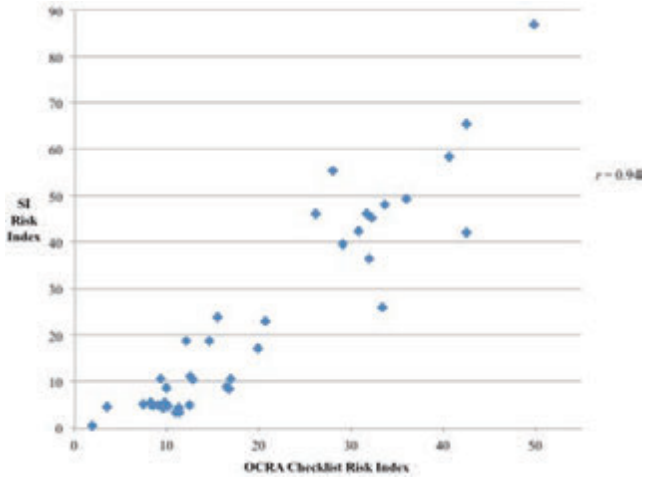

Figure 1. Distribution of SI and OCRA Checklist risk indexes. The Pearson product-moment correlation coefficient (*r*) was 0.94.

Apostoli *et al.*, (2004) used the SI and OCRA Checklist to assess 12 repetitive job exposures using a similar risk classification criterion to that of the present study. The authors observed a relatively low proportion of overall agreement (p_o=41.7%). Of the seven jobs that were classified differently by the two methods, the SI classified them all at a higher level or risk than did the OCRA Checklist. The present study found overall agreement to be double that of Apostoli's *et al.*, results, but the same trend in systematic bias toward higher SI ratings was observed.

Chiasson *et al.*, (2012) reported 60.1% proportion of overall agreement between the OCRA Index and SI risk classifications, and they reported a weak to fair correlation between continuous risk indexes (r=0.32). The authors evaluated 167 different job exposures in a variety of industries. The cheese manufacturing jobs evaluated in the present study exhibited much shorter cycle times on average (mean=41.5 seconds) than those in Chaisson's *et al.*, study. Inter-method reliability may be strong for SI and OCRA Checklist assessments performed in one industry and weak for those performed in a very different industry.

Conclusions

The agreement and strength of association between SI and OCRA Checklist risk classifications was strong for the 42 upper limb cheese manufacturing exposures. Further, the correlation between continuous risk indexes was very high (r = 0.94). Therefore, inter-method reliability was described as good for mean SI and OCRA Checklist assessments of repetitive cheese manufacturing jobs. Both the SI and the OCRA Checklist appear to be reliable measures of exposure to MSD risk factors in cheese manufacturing. For evaluating physical risk in the agro-food industry, either assessment may be appropriate depending on the needs of the evaluation, the type of work performed, and the experience of the raters. However, the SI is specific to disorders of the distal upper limb and perhaps most useful for assessing risk in work primarily involving the wrist and fingers. The OCRA Checklist may be more appropriate when assessing tasks that require extended periods of reaching and shoulder activity, such as picking fruit or harvesting olives. For jobs that expose agro-food industry workers to repetitive upper extremity movements and forces, either the SI or the OCRA Checklist can be used to reliably quantify physical exposure to MSD risk factors.

References

Apostoli, P., Sala, E., Gullino, A. & Romano, C., 2004. [comparative analysis of the use of 4 methods in the evaluation of the biomechanical risk to the upper limb]. *Giornale italiano di medicina del lavoro ed ergonomia,* 26 (3), 223-241.

Chiasson, M.E., Imbeau, D., Aubry, K. & Delisle, A., 2012. Comparing the results of eight methods used to evaluate risk factors associated with musculoskeletal disorders. *International Journal of Industrial Ergonomics,* 42 (5), 478-488.

Colombini, D., Occhipinti, E., Cairoli, S. & Baracco, A., 2000. [proposal and preliminary validation of a check-list for the assessment of occupational exposure to repetitive movements of the upper limbs]. *Medicina Del Lavoro,* 91 (5), 470-485.

Colombini, D., Occhipinti, E., Cerbai, M., Battevi, N. & Placci, M., 2011. [updating of application procedures and criteria for ocra checklist]. *Medicina Del Lavoro,* 102 (1), 1-39.

Colombini, D., Occhipinti, E. & Grieco, A., 2002. *Risk assessment and management of repetitive movements and exertions of upper limbs job analysis, ocra risk indices, prevention strategies and design principles* Oxford: Elsevier.

Jones, T. & Kumar, S., 2010. Comparison of ergonomic risk assessment output in four sawmill jobs. *International Journal of Occupational Safety and Ergonomics,* 16 (1), 105-111.

Landis, J.R. & Koch, G.G., 1977. Measurement of observer agreement for categorical data. *Biometrics,* 33 (1), 159-174.

Moore, J.S. & Garg, A., 1995. The strain index - a proposed method to analyze jobs for risk of distal upper extremity disorders. *American Industrial Hygiene Association Journal,* 56 (5), 443-458.

Spielholz, P., Bao, S., Howard, N., Silverstein, B., Fan, J., Smith, C. & Salazar, C., 2008. Reliability and validity assessment of the hand activity level threshold limit value and strain index using expert ratings of mono-task jobs. *Journal of Occupational & Environmental Hygiene,* 5 (4), 250-257.

Stephens, J.P., Vos, G.A., Stevens, E.M. & Moore, J.S., 2006. Test-retest repeatability of the strain index. *Applied Ergonomics,* 37 (3), 275-281.

Stevens, E.M., Vos, G.A., Stephens, J.P. & Moore, J.S., 2004. Inter-rater reliability of the strain index. *Journal of Occupational & Environmental Hygiene,* 1 (11), 745-751.

Noise risk assessment in a bottling line of a modern Sicilian winery

Mariangela Vallone, Felice Pipitone , Salvatore Amoroso, Pietro Catania

University of Palermo. Dipartimento di Scienze Agrarie e Forestali, Palermo, Italy

Abstract

In wine industry, bottling is a phase of the production cycle characterized by high levels of noise mostly due to repeated collisions between the bottles. In Italy the Law Decree 81/2008 defined the requirements for assessing and managing noise risk, identifying a number of procedures to be adopted at different noise levels to limit workers exposure. This study aims at evaluating the equivalent and peak noise level inside the bottling plant area of a modern Sicilian winery. In particular, the influence of the working capacity (number of bottles produced per hour) on noise levels was evaluated. We considered three test conditions: T1 with working capacity of 4,000 bottles per hour, T2 with working capacity of 5,000 bottles per hour and T3 with working capacity of 6,000 bottles per hour. Fifteen measurement points were identified inside the bottling area. The instrument used for the measurements is a precision integrating portable sound level meter, class 1, model HD2110L by Delta OHM, Italy. The tests were performed in compliance with ISO 9612 and ISO 9432 regulations. The results show that as bottling plant working capacity increases, noise level increases. The measured sound levels exceed the limits allowed by the regulations in all the test conditions; values exceeding the threshold limit of 80 dB(A) were recorded coming up to a maximum value of 95 dB(A) in test T3. In this case, the operator working along the bottling line is obliged to wear the appropriate Personal Protective Equipment.

Correspondence: Mariangela Vallone, University of Palermo. Dipartimento di Scienze Agrarie e Forestali Viale Delle Scienze Edificio 4, 90128 Palermo, Italy.
Tel. +39.91.23865609.
E-mail: mariangela.vallone@unipa.it

Key words: bottling line, noise risk, winery

Contributions: the authors contributed equally.

Conflict of interests: the authors declare no potential conflict of interests.

Conference presentation: part of this paper was presented at the 10th Italian Conference AIIA (Associazione Italiana di Ingegneria Agraria), 2013 September 8-12, Viterbo, Italy.

Journal of Agricultural Engineering 2013; XLIV(s1):e140
doi:10.4081/jae.2013.(s1):e140

Introduction

In wine industry, bottling is a phase of the production cycle characterized by high levels of noise (Lowe and Elkin, 1986; Ologe *et al.*, 2008; Oyedepo and Saadu A., 2010) mostly due to repeated collisions between the bottles. Bottle transport has been identified as one of the main noise-sources in bottling plants (Sivak, 1982); the noise is emitted from the clashing bottles.

Directive 2003/10/EC of the European Parliament was enacted on the minimum health and safety requirements regarding the exposure of workers to the risks arising from physical agents (noise).

It stipulates an upper average limit of noise exposure of a worker during an eight hours shift of work at 85 dB(A). This level is supposed to inhibit hearing impairments of workers (Moselhi *et al.*, 1979). Even the ILO (International Labour Organization) indication agree with this.

In Italy, Law Decree 81/2008 has defined the obligations of noise assessment and risk management, identifying a series of procedures to be adopted at the different noise levels in order to limit the exposure of workers. Excessive noise, in fact, is a global occupational health hazard with considerable social and physiological impacts, including noise-induced hearing loss (NIHL) (Deborah *et al.*, 2005).

Some authors carried out researches aiming at evaluating innovative systems to implement the control of multi-lane conveyors in bottling plants for a noise level reduction. In particular, Sorgatz *et al.* (2012) developed a continuous control algorithm to further reduce the noise emission of multi-lane bottle conveyors. They obtained that the continuous control is less noisy compared with the jam switch control evaluating noise in five measuring points because with the innovative system the velocity of the belts decreased and the impact velocity of the bottles reduced.

In literature, there are few studies concerning the noise level assessment in a bottling plant of a winery. Therefore, this study aims at evaluating the equivalent and peak noise level inside the bottling plant area of a modern Sicilian winery. In particular, the influence of the working capacity (number of bottles produced per hour) on noise levels was evaluated.

Materials and methods

Bottling plant

The bottling plant examined in this study is automated, schematically consisting of the following machines:

- depalletizer (loading empty bottles);
- washing - filling – capping machine;
- washing and drying machine (cleaning the outside of the bottle);
- capper;
- labeling machine;
- vertical cartoner;
- forming machine;
- hive inserting machine;
- closing machine;

- pallettizer;
- wrapping machine.

Five operators control the different phases of the process.

Instruments used during the tests

The instrument used in the tests is a precision integrating portable sound level meter by Delta OHM, Italy, model HD2110L (Figure 1).

Experimental tests

The winery bottling area has an almost rectangular plant with an area of approximately 800 m^2. The 15 measurement points were located through a square mesh whose sides are orthogonal with respect to the sides of the room (Figure 2).

The sound level meter was positioned at a height of 1.50 m from the ground with the aid of a tripod; each measurement had a duration of 2 minutes (the case of stationary noise source) and the parameters were analyzed at intervals of 0.5 seconds.

We measured A-weighted time-averaged sound pressure level (L_{Aeq}) and C-weighted peak sound pressure level (L_{Cpk}). In addition, a C-weighted ex post measurement in the point of greatest noise was realized.

As required by article 189 of Law Decree 81/2008, the worker does not have to be exposed to $L_{Eex,8h}$ values (occupational noise) reported to 8 working hours higher than 80 dB(A) and to L_{Cpk} exceeding 135 dB(C).

$L_{Eex,8h}$ values is given by the following equation:

$$L_{EX,8h} = L_{Aeq,Te} + 10 \log (T_e / T_0)$$

where Te is the effective duration, in hours, of the working day and T_0 is the reference duration equal to 8 hours. In this case Te was assumed to be 7.5 hours.

Before each series of measurements the instrument calibration was performed applying a sound calibrator. The collected data were downloaded to the PC for further processing.

Three test conditions, corresponding to different bottling plant working capacity (as number of bottles per hour) were realized, named T1, T2 and T3:

- T1: working capacity 4,000 bottles per hour;
- T2: working capacity 5,000 bottles per hour;
- T3: working capacity 6,000 bottles per hour.

Tests were carried out in triplicates. Analysis of variance and Tukey's test were performed using Statgraphics Centurion by Statpoint inc., USA.

Figure 1. HD2110L integrating portable sound level meter by Delta OHM, Italy.

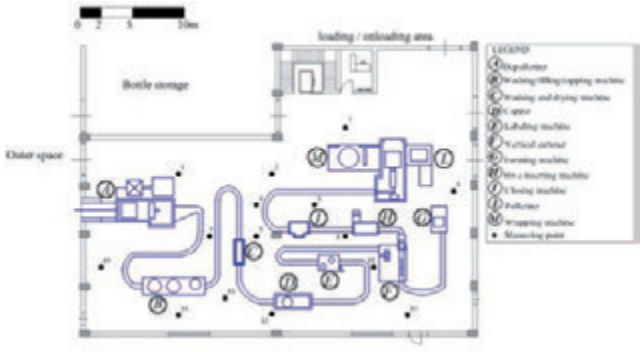

Figure 2. Plan lay out of the bottling area and measurements points.

Results and discussion

A-weighted time-averaged sound pressure levels (L_{Aeq}) for test T1 are shown in Figure 3 for the 15 measuring points.

Noise pressure values obtained in T1 show a minimum of 82.4 dB(A) in the measurement point number 7, near to the palletizer, and a maximum of 89.6 dB(A) in the measurement point number 13, which is located immediately before the capping machine. Figure 3 shows that the exposure limit value established by the article 189 of Law Decree 81/2008 (equal to 87 dB(A)) is reached only in measurement points number 4 and 13 which are located in the vicinity of the conveyor bends. The upper action value of 85 dB(A) is instead achieved in all the measuring stations with the exception of 2, 7, 8, 10 and 14 while the lower action value (equal to 80 dB(A)) is exceeded in all the measuring points. Statistical analysis ($p < 0.05$) shows significant differences between all the measuring points with the exception of 1-12, 1-3, 8-10, 3-12, 6-12, 5-15.

Figure 4 shows the A-weighted time-averaged sound pressure levels (L_{Aeq}) for test T2.

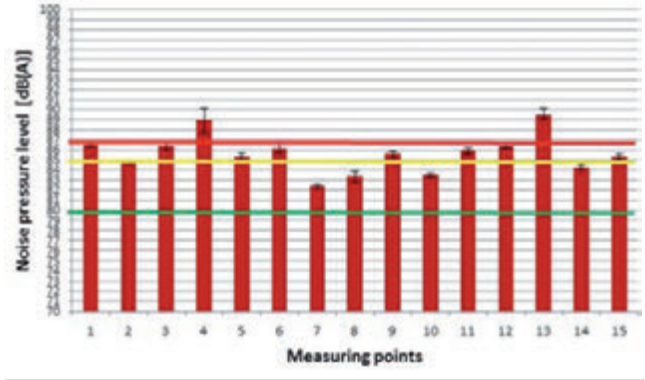

Figure 3. Noise pressure levels (L_{Aeq}) for test T1 in the 15 measuring points (data are reported as means ± standard deviations of the three replicates).

Noise pressure values obtained in T2 show a minimum of 83.8 dB(A) in the measurement point number 7, near to the palletizer, and a maximum of 93.4 dB(A) in the measurement point number 4, which is located immediately after the closing machine. The exposure limit value is reached in measurement points number 3, 4, 5, 9, 11, 12, 13 and 15. The upper action value is achieved in all the measuring stations with the exception of number 7 while the lower action value is exceeded in all the measuring points. Statistical analysis ($p < 0.05$) shows significant differences between all the measuring points with the exception of 2-6, 2-14, 5-15.

Figure 5 shows the A-weighted time-averaged sound pressure levels (L_{Aeq}) for test T3.

Noise pressure values obtained in T3 show a minimum of 84.5 dB(A) in the measurement point number 7, near to the palletizer, and a maximum of 95.6 dB(A) in the measurement point number 4, which is located immediately after the closing machine. The exposure limit value is reached in all the measurement points with the exception of 7, 8 and 10. As obtained in T2, the upper action value is achieved in all the measuring stations with the exception of number 7 while the lower action value is exceeded in all the measuring points. Statistical analysis ($p < 0.05$) shows significant differences between all the measuring points with the exception of 1-2, 1-9, 1-14, 2-9, 2-14, 9-14, 9-15, 14-15.

Data related to the three tests are reported together in Figure 6 in order to highlight the differences, if any, between the noise levels achieved in the various measurement points. Always note statistically significant differences for $p = 0.05$ between the tests T1-T2 (with the exception of the measuring point 6) and T1-T3. The comparison between T2 and T3, however, shows that not all the measurement stations are statistically significant different. Differences were found, for example, at station 4, but not in 13.

The spectral analysis regarding the measurement stations 4 and 13 is reported in Figure 7 for the three test conditions.

C-weighted peak sound pressure levels (L_{Cpk}).obtained in the different tests are shown in Figure 8.

Neither the exposure limit value equal to 140 dB(C) according to the cited art. 189 of Law Decree 81/2008, or the upper and lower action values (equal to 137 dB(C) and 135 dB(C)) are reached or exceeded in any of the measurement points. No statistically significant differences were found between the three tests.

The data obtained by the measurements allowed us to have the equal loudness curves for the tests carried out, thereby evaluating the zones with equivalent average sound levels. Figure 9 shows the map related to T1.

With reference to T2 (Figure 10), you may notice an increase in the noise level compared to T1.

The results of T3 (Figure 11), show overall noise levels higher than the two test conditions discussed above.

Conclusions

The results of the experiments carried out allow us to affirm that increasing the bottling plant working capacity the noise level increases. The highest noise pressure values were obtained in the measurement point number 4 and 13, respectively located immediately after the closing machine and before the capping machine; this occurs in the three test conditions. The results also show that noise pressure values measured during the three tests are always higher than the lower action value identified by law, equal to 80 dB(A) In particular, the upper action value equal to 85 dB(A) is reached in all the measurement points except 2, 7, 8, 10 and 14 in T1. In T2 and T3 this value is reached in every station except number 7. The exposure limit value of 87 dB(A) is reached in T1 only in the stations 4 and 13, in T2 in 3, 4, 5, 9, 11, 12, 13 measurement points and in T3 in all the stations except 7, 8 and 10. As a consequence, the use of appropriate PPE is required when limits imposed by the regulations are exceeded.

With reference to the peak values, neither the exposure limit value equal to 140 dB(C), or the upper and lower action values (equal to 137 dB (C) and 135 dB (C)) are reached or exceeded in any of the measurement points.

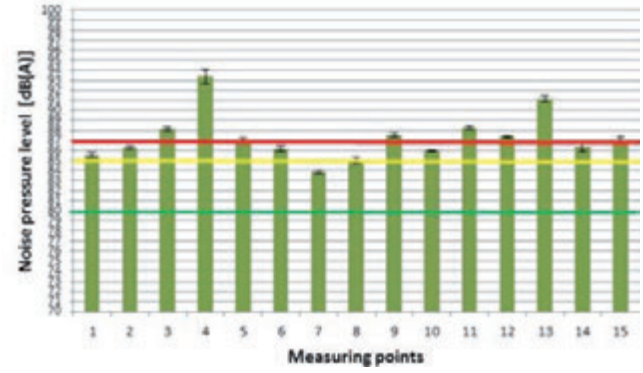

Figure 4. Noise pressure levels (L_{Aeq}) for test T2 in the 15 measuring points (data are reported as means ± standard deviations of the three repli-

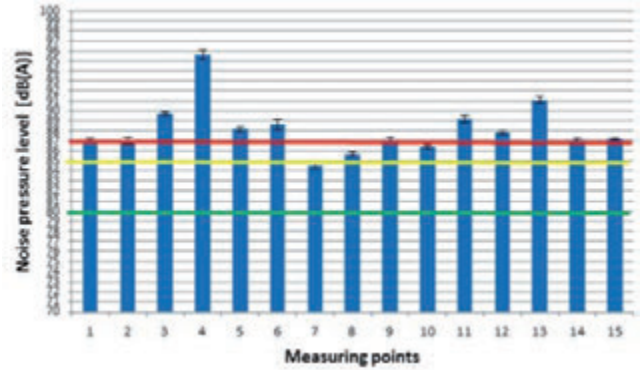

Figure 5. Noise pressure levels (L_{Aeq}) for test T3 in the 15 measuring points (data are reported as means ± standard deviations of the three replicates).

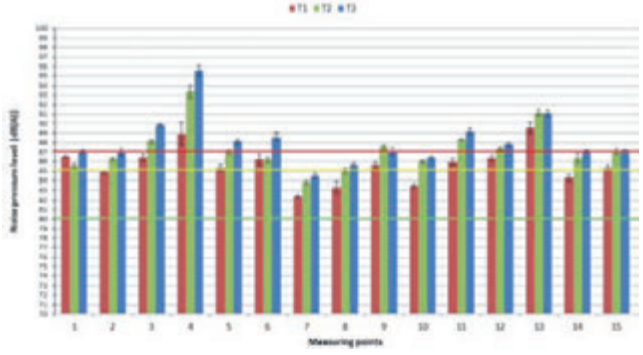

Figure 6. Noise pressure levels (L_{Aeq}) for tests T1, T2 and T3 in the 15 measuring points (data are reported as means ± standard deviations of the three replicates).

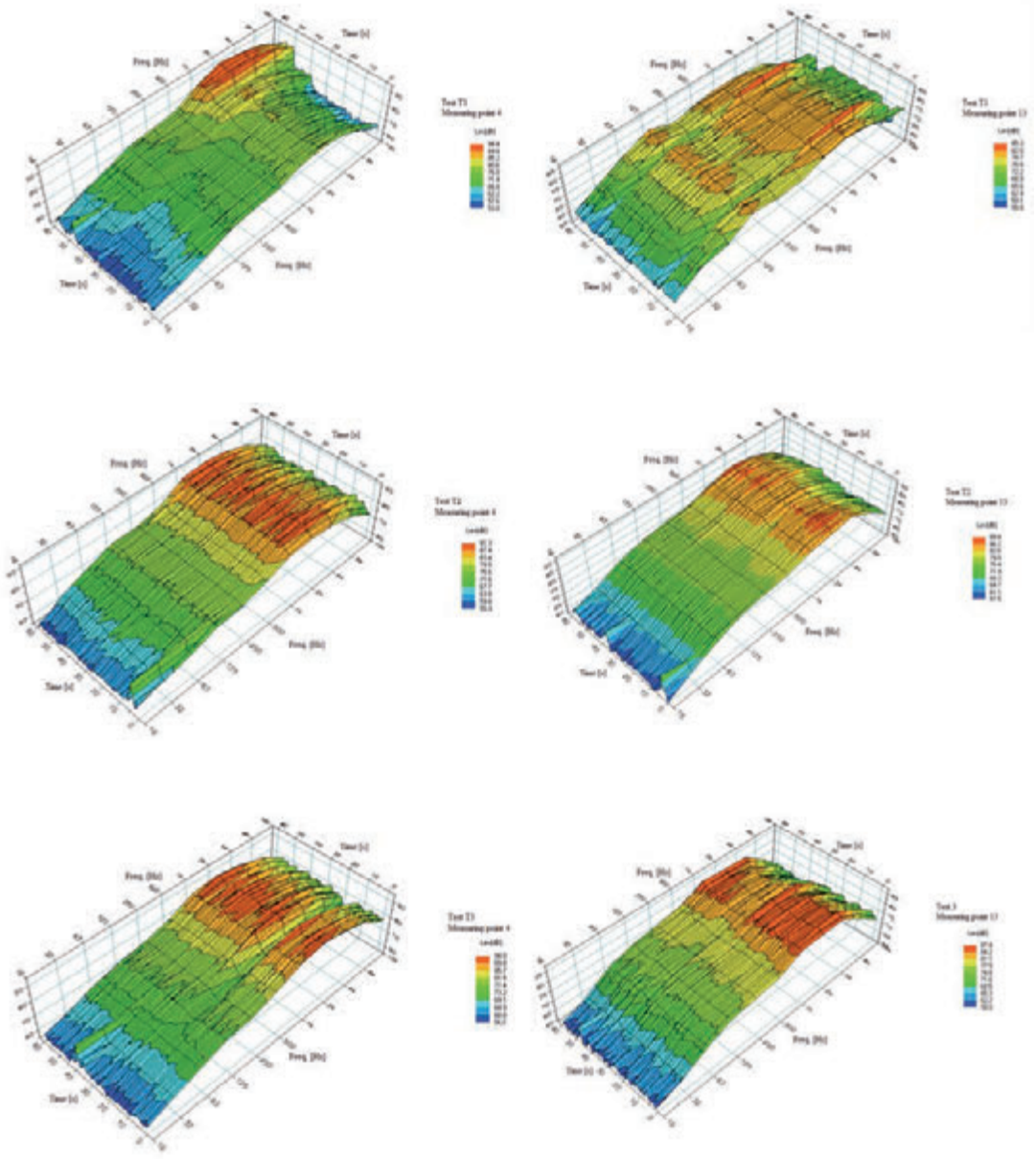

Figure 7. Spectral analysis regarding the measurement stations 4 and 13 for T1, T2 and T3.

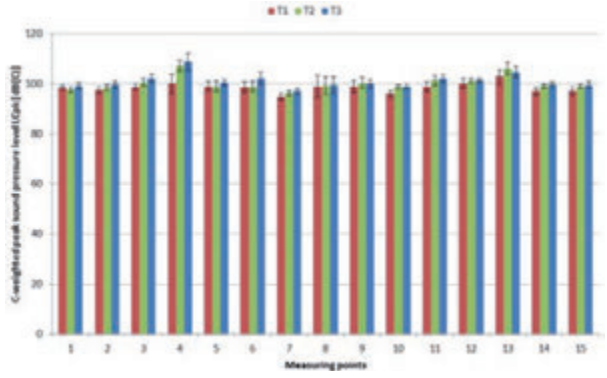

Figure 8. C-weighted peak sound pressure leves (L_{Cpk}).obtained in the tests T1, T2 and T3.

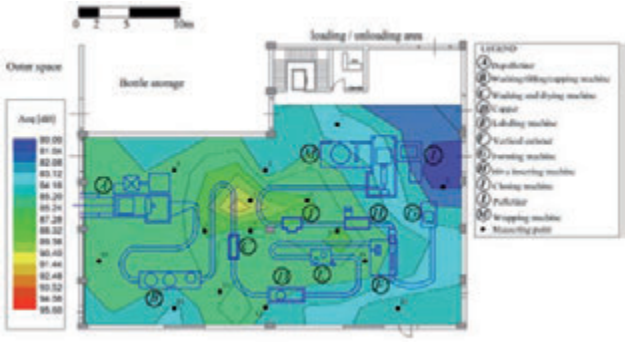

Figure 9. Map of equal loudness curves for test T1.

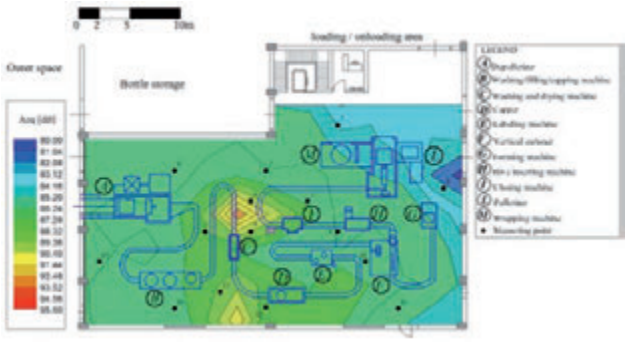

Figure 10. Map of equal loudness curves for test T2.

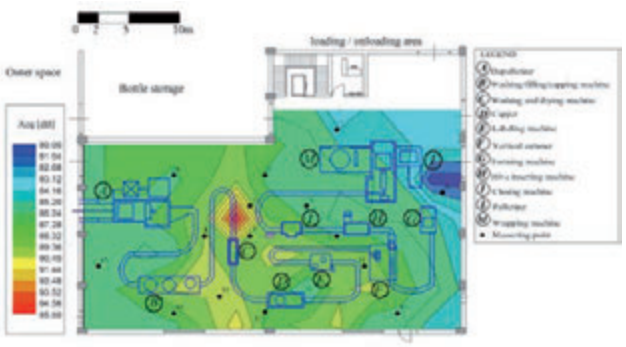

Figure 11. Map of equal loudness curves for test T3.

References

Deborah, I. N., Robert, Y. N., Marison, C. B., & Marilyn, F. The global burden of occupational noise induced hearing loss. American Journal of Industrial Medicine, 2005, 48(6), 446-458.

European Parliament and Council, Directive 2003/10/EC of the European Parliament and of the Council of 6 February 2003 on the minimum health and safety requirements regarding the exposure of workers to the risks arising from physical agents (noise).

International Labour Organization (ILO). Health, Safety and Environment: A Series of Trade Union Education Manuals for Agricultural Workers, 2004, ISBN:92-2-115 192-1.

Law Decree 81, 9 April 2008 of the Italian Republic.

Lowe C.M., Elkin W.I. Centenary review beer packaging in glass and recent developments. J. Inst. Brew., November-December, 1986, Vol. 92, 517-528.

Moselhi M., El-Sadik, Y. M. and El-Dakhakhny, A., A six year follow up study for evaluation of the 85 dBA safe criterion for noise exposure. Am. Ind. Hyg. Assoc. J., 1979, 40(5), 424-426.

Ologe F.E., Olajide T.G., Nwawolo C.C., Oyejola B.A. Deterioration of noise-induced hearing loss among bottling factory workers, Journal of Laryngology and Otology, 2008, 122(8), 786-794.

Oyedepo O.S., Saadu A.A., Assessment of noise level in sundry processing and manufacturing industries in Ilorin metropolis, Nigeria. Environ Monit Assess, 2010, 162, 453-464.

Sivak, R. F., Noise control design for packaging. Tech. Q. Master Brew. Assoc. Am., 1982, 19(3), 115-121.

Sorgatz, A., Voigt, T., Continuous control for buffering conveyors in beverage bottling plants. Packaging Technology and Science, 2012, DOI: 10.1002/pts.1997

A survey of safety issues in tree-climbing applications for forestry management

D. Longo, L. Caruso, A. Conti, D. Camillieri, G. Schillaci

DiGeSA, Mechanics and Mechanization Section, University of Catania, Catania, Italy

Abstract

Topping, trimming, consolidation, securing and felling are very common operations in arboriculture, in city park as well as in forests. In case of very large trees, these operations are often not possible from ground level using ladders or Mobile Elevating Work Platforms (MEWPs) because of excessive height or uneven/inaccessible terrain. In past years, different people start applying techniques, materials and procedures normally used in mountaineering and caving, to climb trees and these techniques start to be applied to forestry management operations; these techniques are now worldwide used. Work activities at height, as tree-climbing for forestry management purpose, are regulated in Italy by Legislative Decree 81/08 about safety in the workplace, as this activity expose operators to fall from height and many other risks. Moreover, as this activity involves the use of specific tools, operators must be trained (with periodic refreshment) and tools must been periodically checked by authorised operators. The objective of this work is to present and synthesise regulations and some technical aspects in order to allow operators to better understand different issues and general principles related to this activity.

Introduction

Forestry control measures are normally executed with long ladders or more often with Mobile Elevated Work Platforms (MEWP's) that can be used to efficiently and safely access areas whilst minimizing climbing requirements. Where ever these equipments (long ladders, MEWPs) are not suitable because of excessive tree height or for access issues, control measures can be done by using ropes and other tools with the tree climbing technique. This technique allows to execute the work from the inside of the canopy, without employing mechanical tools, preventing the weight of such tools damaging the branches, the roots and preventing soil compaction.

About 1980, in USA, different people start applying techniques, materials and procedures normally used in mountaineering and caving, to climb tree for recreational purpose (Tree climbing history, 2004). After few years these techniques start to be applied to tree forestry management operations and rapidly exported in other country.

In Italy, the health and safety at work are regulated by the Legislative Decree 81/2008. This Decree implements the European Directives, in particular the European Framework Directive on Safety and Health at Work (Directive 89/391 EEC), adopted in 1989, that guarantees a minimum safety level and health requirements throughout Europe. Tree-climbing for forestry management purpose, are regulated by Legislative Decree 81/08, about safety in the workplace. General guidelines of this decree for risk prevention and management can be summarised as:

- Pointing out risk factors and sources.
- Reduction of risk factors (risk probability and/or magnitude).
- Continuous check of used prevention devices/methodologies.
- Implementation of a global prevention methodology for the whole company.

Along this paper, different details of the Legislative Decree 81/08 about fall from height, risk prevention and managing approach, employer obligations, different risk sources for this activity and PPE management will be pointed out.

From technical point of view, different tools and techniques are available, most of them deriving from mountaineering and caving activities and some basic concept will be described in next sections.

Regulation aspects and risk source in tree-climbing operations

Work at height activities are regulated by Legislative Decree 81/08 (Title IV, Chapter 2, Article 105), about safety at workplace. Tree climbing activities for forestry management must be compliant to Legislative Decree 81/08 because Article 107 of Chapter 2 defines work at height all those works that exposes the operators to the risk of falling from a height greater than 2 m with respect to a safe surface. Generally, the employer must to comply with complete risks assessment for the health and safety of workers at workplace and must perform periodical and special inspections of used work equipment (Articles 17 and 71). The employer must maintains all used PPE (Personal Protective Equipment) with periodical check and ensure the necessary substitutions in accordance with any instructions provided by the PPE manufacturer (Article 77).

Tree-climbing activities for forestry management expose operators to fall from height risk. Moreover these workers are exposed to many other risks like physical factors as solar radiation, microclimate, wind

Correspondence: Domenico Longo, DiGeSA, Mechanics and Mechanization Section, University of Catania, via S. Sofia 100, 95123, Catania, Italy
e-mail: domenico.longo@unict.it

Keywords: legislative decree 81/08, tree-climbing, worker and workplace safety, fall from height, PPE directives, forestry management.

Contributions: the authors contributed equally.

Journal of Agricultural Engineering 2013; XLIV(s1):e141
doi:10.4081/jae.2013.(s1):e141

(Chapter VIII, Section I), like risk of electric shock due to lightning and operations near overhead power lines, biological risk as bites and stings of animals, insects etc. (Chapter X, Section I), like risk due to physical ergonomics and in particular biomechanical overload (Chapter VI, Section I and II), risk due to machinery and equipment as risk of cutting, dust, noise, vibration, burns (Chapter IV - Section I, Chapter VIII - Section II and III, Annex IV and VII). Another risk to be seriously considered, as it represents a deadly and rapidly evolving situation (ten – twenty minute), is Harness Hang Syndrome that can occur when a unconscious operator hang over her/his harness, even more if not in upright position (Progetto "Sospesi", 2010).

In particular, in work activities at height, the employer must choose the most suitable work equipment to ensure and maintain safe working conditions. The use of ladders is provided only in cases where the use of other safer work equipment is not considered justified because of the low level of risk and short duration of use or existing features on site that cannot change (Article 111 and 113). In many other cases, the employer can authorizes the use of access and positioning ropes, on which the worker is directly suspended, after having assessed any risk and verified that the work can be performed safely without residual risks and the use of other safer work equipment is not applicable.

The Legislative Decree prescribes fall arrest equipment and protection system against falls from a height after any collective protection measures have been implemented (Article 115).

In work activities at height, as tree-climbing for forestry management, the employer must follow some obligations regarding the access systems and positioning with ropes. The employer must also provide adequate training during the works with ropes, in particular the rescue. The employer must implement adequate supervision of the work to be able to immediately help the worker in case of need (emergency rescue). Article 37 obliges the employer to train workers while the Annex XXI - Legislative Decree 81/08, specify all the features the courses must fulfil. Optionally workers can obtain, from different certifying bodies, a specific certification recognised at European level (European Arboricultural Council).

The training for workers at height by using positioning ropes is structured in three modules. The basic module is mandatory to subsequent specific modules; the module A is specific for work at height using positioning ropes in natural or artificial environment; the module B is specific to access and work on trees. Every five years, the trained workers must follow a refresher course. There are other different training courses for personal in charge of supervision of the workers. Legislative Decree 81/08 specifies who can hold these courses. Lessons must be performed by personnel with at least two years of training experience, both in the field of prevention, health and safety in the workplace, and all the technical aspects that the use of ropes. Article 73 describes how the worksites must maintain appropriate levels of trained personnel to accommodate all foreseeable rescue scenarios. In order to limit physical risks (solar radiation, microclimate, wind and lightning), the employer shall carry out temporary work at a height only when the weather conditions do not endanger the safety and health of workers (Article 111) and make use of first category PPE.

With regard to electrical hazards, Article 83 states that works cannot be carried out in proximity of overhead power lines and at distances below limits, except with the adoption of appropriate measures to protect workers from these dangers.

In addition, during the risk assessment, it must be considered also the risks due to the poor or bad organization of work-site (transit or stationing of people, moving vehicles, the presence of buildings, removal of stumps) and lack of workers training (Chapter I, Section III, Article 36 and 37). If the workplaces contain danger areas and there is a risk of falls of workers or of dropping objects, these places must be marked and secured with barriers to prevent unauthorized workers from entering all those areas. Moreover, work-stations, traffic routes and other areas or outdoor installations which are used by the workers during their activities, must allow for a safe movement of pedestrians and vehicles (Annex IV).

Technical aspects in tree-climbing operations

Article 116 sets out the obligations of employers regarding the access and positioning systems with ropes. The systems should include at least two separately anchored ropes, one for access (for the descent and support), called work-rope and the other as back-up system, called safety-rope. The use of a single rope is allowed in exceptional circumstances where the use of the second rope would make the work more dangerous, and if, in any case, appropriate measures are taken to ensure the operator safety or eliminate the risks. Article 115 report devices to be used as protection against falls from a height. All that devices are derived, with suitable modifications, from similar devices used for mountaineering and caving and are classified as third category PPE (CAI, 2004). Most of manufacturers have normally two separate product lines, one for sport use and one for work at height activities; some of them have specific products for tree-climbing activities.

Aside specific techniques used in tree-climbing (that could be a bit different from techniques used in general purpose work at height activities), there are few basic common concepts that must be considered. The choice of correct devices and their use, rely on the two main concepts of "safety chain" and of "suitability/mutual compatibility". These two different concepts will have to be considered, among all other safety aspects, by the employer while selecting the correct PPE to be used by the worker.

The terms "safety chain" is referred to all those devices that support and sustain at height the operators and are represented by the anchor point(s), different connectors, ropes, harness, lanyard, shock absorbers and so on. The starting point of the safety chain is always the place where the main rope is attached (wall rock or tree branch for example) while the ending point is always the operator body. If any of the elements of the safety chain fails, the entire chain fails also, so a redundant retaining system (safety rope) must be used and connected to the operator by mean of specific dynamic retaining devices (Article 116). The whole safety chain must be carefully designed by trained person, especially as regard ropes anchors points. The main purpose of the safety chain is to sustain at height the operators, but in case of a fall, it not only should anyway sustain the operators but also should limit the impact force to a value that it is not dangerous or deadly. From different study (Crawford H., 2003; Leuthäusser U., 2012a; Leuthäusser U., 2012b), the impact force limit was set to 6 kN. This limit is mainly due to the maximum deceleration to that the operator body can be subjected to, without deadly consequences. It has been demonstrated that the maximum not deadly deceleration for a human body fall in upright position is about 15g. It is much less when the body falls in others positions. From these consideration, it comes that the safety chain must limit, without major damages or break, the impact force to the safe value of 6 kN, by converting the whole fall energy into heat (friction in hand-made knot, where they are allowed, friction between rope fibres or inside other dynamic retaining devices), by using it for generating some controlled break (shock absorber) or accumulate it in some elastic device (mainly ropes and rope lanyard). The residual impact force that is then applied to the operator body should be less than 6 kN. The severity of a fall is normally described in terms of Fall Factor (Figure 1). This number is the height of a potential fall divided by the initial length of the lanyard or rope that will support the operator at the end of the fall.

Standard semi-static rope allowed for work at height (EN1891A) can

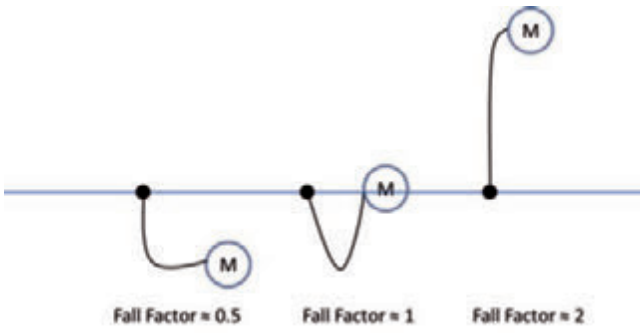

Figure 1. Fall factor definition.

normally survive to a fall with Fall Factor near one, but it must be remarked that, without using suitable devices (shock absorber), a fall with Fall Factor of just 0.3 can easily generate impact forces greater than 6 kN and these circumstances must be avoided. Close attention must be paid when hyper-static lanyard must be used. Normally these lanyard are made by Kevlar® or steel (for example anti-cut lanyard must be used when operator make use of a chainsaw). These lanyards have to be used only for operator positioning (Fall Factor very close to zero) and not as safety device in case of a fall as they can generate very high impact force. As general rule, scenarios with Fall Factor greater than two (possible in some outdoor sport activity) must be avoided. Another example of safety chain design could be some consideration about shock absorbers. These devices are used in all those situation where a potential fall will happen with high impact force. These devices are able to dissipate the fall energy by mean of a controlled break of specific areas of the device itself (they are normally made by folded and sewn webbing). Suitable clearance distance must be considered between operator working area and ground level, as the device can double or more its length during the fall. Lanyard length and additional safety clearance must be added. The operator must not impact the terrain neither hit some obstacle, so the whole fall trajectory must be carefully considered. Similar consideration will have to be done for all the other safety chain devices (ropes and ropes positioning, anchor points, connectors and so on). Workers must use full body harness whilst using this equipment to retain the fallen person in an upright position. Specific tools used by workers for specific operations, must be fixed to their belt. Second category PPE as helmets must always be worn.

Suitability/mutual compatibility concept of all the elements the safety chain is composed by, is referred to the specific directive that the device is compliant with. Only devices for work use are admitted along the entire safety chain. For example, different ropes are available on the market that are compliant to EN892 or EN1891A or EN1891B directives. Among these, only ropes compliant to EN1891A are admitted for work use while all the others can only be used for sport applications (suitability). On the other side, in a working contest, an EN1891A rope is not compatible with a harness compliant with EN12277C that is classified for sport use (mutual compatibility).

Conclusions

Tree climbing is a relatively new and worldwide used technique for forestry management. It has a lot of advantages in term of worker safety, tree damages and work speed. This activity rise different issues regarding operator safety, materials, tools and technical aspects. Safety issues can be eliminated or mitigated using guidelines reported in the Legislative Decree 81/08. It cover all aspect starting from basic safety best practice to procedures, material, operator training and responsibility sharing between employer and worker. From technical point of view, the mandatory training courses provide the basic knowledge about safety, work at height and tree climbing practice. Moreover different manual are available, so worker can easily have an in-deep sight of tree-climbing practice.

Information provided here are only for dissemination purpose and are neither complete nor sufficient to design any safety chain or any kind of work at height. Many others aspects must be considered as risk analysis, work organization, ropes techniques and so on. For a complete set of information, operators must attend to specific theoretical and practical courses hold by trained and authorised person. In any case work practice together to skilled operators is the best way to learn these techniques.

References

AA.VV., Arrampicata e lavoro su alberi. Tecniche di treeclimbing. Regione Piemonte, Torino 2010

Club Alpino Italiano (CAI), I manuali del CAI – 14 – Alpinismo su ghiaccio e misto, Milano, Club Alpino Italiano, 2004. ISBN 8879820117

Crawford H., Survivable Impact Forces on Human Body Constrained by Full Body Harness, UK Health and Safety Executive, 2003

European Arboricultural Council (EAC), http://www.eac-arboriculture.com/en/default.aspx

Health and Safety Executive, http://www.hse.gov.uk/

Legislative Decree 2008 n. 81, (Rev. 13°, May 2013), GU n. 101, 30 April 2008 web site http://www.lavoro.gov.it/Lavoro/SicurezzaLavoro/

Leuthäusser U., "Viscoelastic theory of climbing ropes", http://www.sigmadewe.com, 2012

Leuthäusser U., "Physics of climbing ropes: impact forces, fall factors and rope drag", http://www.sigmadewe.com, 2012

Progetto "Sospesi", http://www.camp.it/EN/template03.aspx?codicemenu=1414, 2010

Società Italiana Arboricoltura (SIA), http://www.isaitalia.org/

Tree climbing history, http://www.treeclimbingusa.com/history,owner.html, 2004

UIAA web site http://www.theuiaa.org/

Vibration risk evaluation in hand-held harvesters for olives

Giuseppe Manetto, Emanuele Cerruto

Department DiGeSA, Section of Mechanics and Mechanisation, University of Catania, Catania, Italy

Abstract

This research aims to evaluate the vibration transmitted to the hand-arm system by two electric portable harvesters, different for size and teeth features of the harvesting head. Moreover, being the bars of the two machines telescopic, they were operated at minimum and maximum length. The acceleration was measured, at different times, in two points, 1 m apart, next to the hand positions. Finally, measurements were carried out both at no load, in standard controlled conditions, and in field, under ordinary working conditions. To smooth the influence of external factors, the machines were operated by the same operator. The results showed that the greater and heavier harvesting head produced significantly higher acceleration at no load (10.7 m/s^2 vs. 5.5 m/s^2), and comparable acceleration at load (13.9 vs. 14.2 m/s^2). On average, the vibration was significantly higher at load (14.0 vs. 8.1 m/s^2). The difference between the two bar lengths was not statistically significant: 9.4 m/s^2 when using the minimum length and 9.8 m/s^2 when using the maximum one. Finally, the difference between the two measuring points was affected by the bar length: it was statistically significant when using the bar at its minimum length only. As far as the components are concerned, at no load the highest acceleration was measured along the bar axis for both harvesting heads (9.2 m/s^2 for the greater head and 4.2 m/s^2 for the smaller one). At load all the three components were comparable in the greater head (about 7.8 m/s^2) whereas the x component was predominant in the other one (11.4 vs. 4.8 (y) and 6.6 m/s^2 (z)).

Correspondence: Manetto Giuseppe, Dipartimento DiGeSA, Via S. Sofia 100, 95123 Catania, Italy.
Tel.:+39.095.7147515 - Fax: +39.095.7147600.
E-mail: gmanetto@unict.it

Key words: safety, vibration exposure, hand-arm system, facilitating machines

Contributions: the authors contributed equally.

Conflict of interests: the authors declare no potential conflict of interests.

Journal of Agricultural Engineering 2013; XLIV(s1):e142
doi:10.4081/jae.2013.(s1):e142

Introduction

Vibration is probably the most important risk connected with the use of portable machines for olive harvesting. Their large utilisation is aimed at reducing the production costs when farm fragmentation, tree structure, irregular tree layout, sloping lands, prevent the mechanical harvesting. In these cases, hand-held vibrating tools are approximately capable of triplicate the productivity of the workers with respect to the manual harvesting (Famiani *et al*., 2008).

Unfortunately, these tools have been characterised by lack of comfort and high levels of noise and vibration (Iannicelli and Ragni, 1994; Blandini *et al*., 1997; Deboli *et al*., 2008; Pascuzzi *et al*., 2008). Ergonomics and safety aspects are often underestimated by users, mainly interested in productivity. Workers, when operate with hand-held power tools, in most of the cases do not perceive acceleration levels as being too high, so increasing the exposure risk (Vergara *et al*., 2008) and the probability of appearance of the Raynaud syndrome (Chetter *et al*., 1998).

The factors influencing the biodynamic response of the hand-arm system are complex and numerous, such as frequency, direction and intensity of the vibration, features of the worker (mass, grip force), of the operating tool (handle, mechanical impedance), and of any anti-vibrating devices.

An increase in the operator's comfort was achieved when machines powered by electric motors were introduced, characterised by lightness, handiness and very effective in reducing the noise level with respect to those powered by two-stroke engines (Biocca *et al.*, 2008). The vibration level remains quite high and its reduction can be achieved after a proper design or an optimal selection of the operating parameters (Monarca *et al*., 2007; Pascuzzi *et al*., 2008; Mallick, 2010).

Based on the results of previous works (Cerruto *et al*., 2010; Cerruto *et al*., 2011; Cerruto *et al*., 2012), this research aims to evaluate the vibration transmitted to the hand-arm system by two electric portable harvesters at varying harvesting head size, bar length, and operating conditions (no load and under ordinary working conditions).

Materials and methods

The machines

Experimental tests were carried out by using two electric portable harvesters, assembled by a local manufacturer, different for size of the teeth (the small bars that beat branches and olives during the harvest) and size of the harvesting head. Moreover, being the bars of the two machines telescopic, they were operated at minimum (B1) and maximum length (B2).

Both harvesting head (H1 and H2) have a plastic-made box to which are connected two arms with opposed oscillations on a plane orthogonal to the motor shaft and inclined of about 20° with respect to the bar axis (Figure 1). Each arm carries 4 teeth; another tooth, of less length, is connected to the box, and then not oscillating. All the teeth are in

carbon fibres. The two harvesting heads differ in length of the two arms, in diameter and length of the teeth, and then in total mass. Their main features are reported in Table 1.

The telescopic bar is made from aluminium, with diameters of 28 (minimum) and 35 mm (maximum), 1 mm thick, and lengths of 1390 mm (minimum) and 2180 mm (maximum). Taking into account hand-grip, harvesting head, and a piece of bar (135 mm long) installed after the hand-grip, the total length of the harvesters ranges from 2060 up to 2850 mm. The total mass is 3.070 kg when using the head H1 and 2.960 kg when using H2.

The motor is powered by an external 12 V DC battery. The maximum power is about 900 W and the rotating speed about 6300 rpm, fixed by an electronic card. Its shaft is connected to a box that, with a gear ratio of 10:58, gets the arms with the teeth moving with oscillating frequency of 18 Hz.

The experimental activity

Experimental trials were carried out by operating the two machines at no load and on olive trees as under ordinary working conditions. To smooth the influence of external factors, they were operated by the same person. Moreover, to ensure the same power conditions, the battery was kept on charge during all the trials.

No load tests were carried out angling the bar according to three directions, so to cover all the possible orientations assumed during the working activity: vertical (90°), angled at about 45° and horizontal (0°). Moreover, vibration was measured, at different times, in two points (MP1 and MP2): the first near the hand-grip, the second on the bar, 1 m apart (Figure 2). Trials on olive trees were conducted in the same manner, but not considering the bar angle as a factor.

Overall, 24 measurement sessions (2 harvesting heads × 2 bar lengths × 2 measuring points × 3 angles) at no load and 8 (2 harvesting heads × 2 bar lengths × 2 measuring points) at load were carried out, each lasting about 6 minutes.

Figure 1. The two harvesting heads: H1 (left) and H2 (right).

Table 1. Main features of the portable harvesters.

	Harvesting head features		
	H1		H2
No. of teeth	8		8
Teeth diameter, mm	6		5
Teeth length, mm	330		360
Arm length, mm	155		110
Total width, mm	390		300
Mass, kg	1.400		1.290
Bar features			
Minimum length, mm	1390	Diameter, mm	35 / 28
Maximum length, mm	2180	Thickness, mm	1
Harvester features			
Total length (teeth excluded), mm		2060 / 2850	
Total mass, kg		3.070 (H1) / 2.960 (H2)	

Signal acquisition and analysis

Acceleration was measured by using three mono axial accelerometers arranged so to be equivalent to a triaxial accelerometer. The reference coordinate system was fixed in the measuring point MP1 (right hand) according to the UNI EN ISO 5349-1:2004 regulation (ISO, 2004): x-axis perpendicular to the palm surface area, y-axis parallel to the longitudinal axis of the grip, and z-axis directed along the third metacarpus bone of the hand. Considering that the operator, during the harvesting, rotates and changes continually the grip points, the accelerometers were only translated in the measuring point MP2, keeping parallel the reference axes. The accelerometer signals were recorded on the hard disk of a PC by means of a dB4 four-channel acquisition unit and the recording module of the dBFA Suite software (01dB-Metravib, Lyon, France).

Subsequently, they were analysed in laboratory according to the UNI EN ISO 5349-1:2004 regulation by using the post-processing module of the same dBFA Suite software, in the frequency range 5.6-1400 Hz (third of octave bands from 6.3 up to 1250 Hz). In addition, FFT spectra were computed so to detect the main harmonic for each operating condition. To evaluate the variability in time of the vibration level, 5 sub-samples of 1 min were extracted from each signal recorded and treated as replicates. On the other hand, being the maximum frequency of interest 1400 Hz, a signal length of about 10 s is enough for the digital analysis.

Frequency weighted root mean square (RMS) accelerations a_{hwx}, a_{hwy}, and a_{hwz} were computed via the third octave analysis for each axis, and then it was calculated the global weighted acceleration a_{hw} according to:

$$a_{hw} = \sqrt{a_{hwx}^2 + a_{hwy}^2 + a_{hwz}^2} \quad (1)$$

Global values were statistically analysed by means of analysis of variance to detect significant differences related to harvesting head, bar length, measuring point and working conditions (no load or harvesting). Raw data were transformed in order to achieve normal distribution of the residuals and constant variances. However, being the 1-minute sub-samples selected without an effective randomisation, mean separation was performed by the more robust non parametric Kruskal-Wallis test.

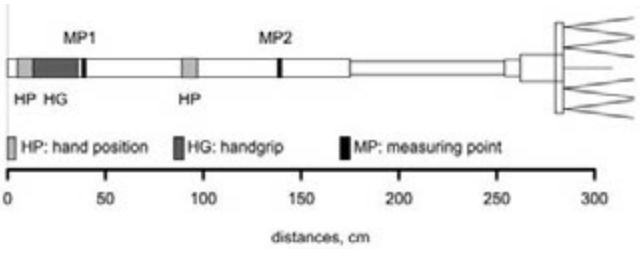

Figure 2. Schematic view of the portable harvesters.

Finally, the daily vibration exposure values, A(8), were computed according to:

$$A(8) = \sqrt{\frac{T}{8}} a_{hw} \quad (2)$$

being T the daily exposure time (h), and compared with the thresholds established by the Italian law 81/08: daily exposure action value of 2.5 m/s^2 and daily exposure limit value of 5.0 m/s^2.

All statistical analyses and graphical representations were carried out by using the open source software *R* (R Core Team, 2012).

Results and discussion

Global values

The comparisons among the levels of the main factors (harvesting head, bar length, operating condition, and measuring point) are summarised in Figure 3, whereas the first order interactions are reported in Table 2.

The box-plots in Figure 3 show a significant difference, confirmed by the analysis of variance (p-level < 0.001), between the two harvesting heads: on average H1 produces a vibration level much higher than H2 (11.5 vs. 7.7 m/s^2). Being the kinematic system of the two heads the same, the difference must be attributed to the different mass and geometry. Moreover, this difference is significantly affected by the working conditions (interaction significant for p-level < 0.001): the two harvesting heads produce different vibration only when used at no load (H1 = 10.7 m/s^2; H2 = 5.5 m/s^2), whereas produce the same vibration during the harvesting (H1 = 13.9 m/s^2; H2 = 14.2 m/s^2). Therefore, during the harvesting, due to the interaction with the tree canopy, the effect of mass and geometry of the harvesting head becomes negligible

Table 2. Global values of the accelerations (m/s^2) (mean separation by Kruskal-Wallis test for p-level = 0.05).

Head	Load	No load	Mean
H1	13.9^a	10.7^b	11.5^a
H2	14.2^a	5.5^c	7.7^b
Bar length	**Load**	**No load**	**Mean**
B1 (minimum)	14.1^a	7.9^b	9.4^a
B2 (maximum)	14.0^a	8.4^b	9.8^a
Measuring point	**Load**	**No load**	**Mean**
MP1	11.9^b	7.3^d	8.5^b
MP2	16.2^a	8.9^c	10.7^a
Mean	14.0^a	8.1^b	9.6
Measuring point	**^{B}1**	**^{B}2**	**Mean**
MP1	7.9^b	9.0^{ab}	8.5^b
MP2	10.9^a	10.5^a	10.7^a
Bar angle	0°	45°	90°
	7.7^a	8.3^a	8.4^a

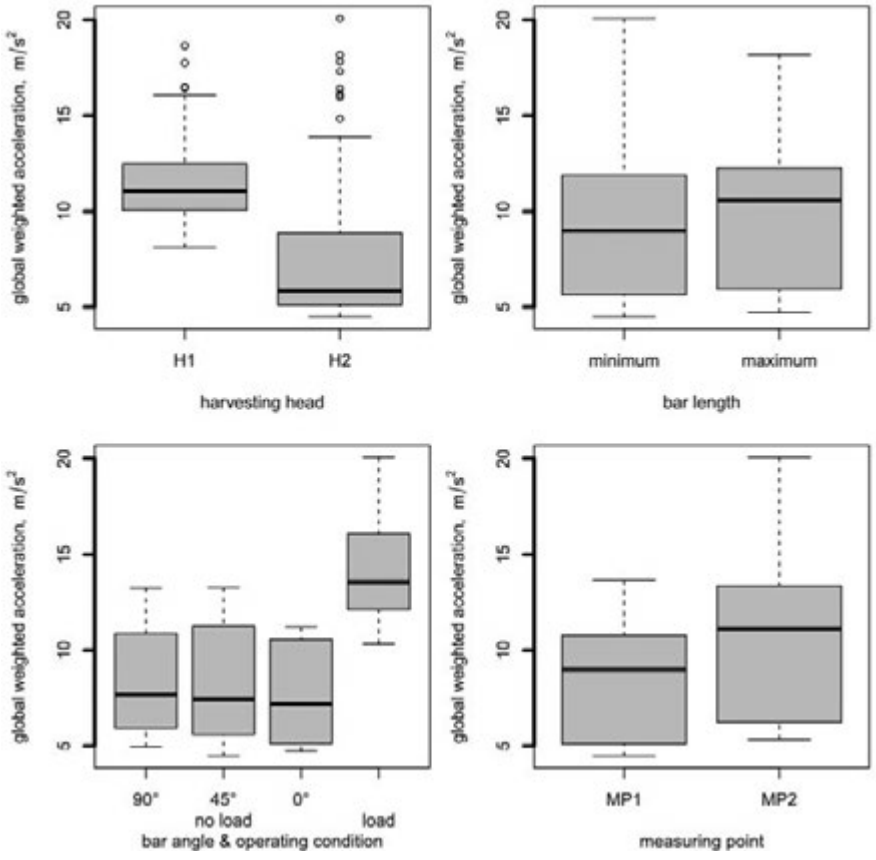

Figure 3. Comparisons among harvesting heads, bar lengths, operating conditions, and measuring points.

with respect to the mass and geometry of the canopy and the two heads vibrate in the same manner. On average, the vibration is significantly higher at load conditions: 14.0 vs. 8.1 m/s^2. This result confirms those reported in Cerruto *et al*. (2012): the vibration increases during the harvesting, due to both canopy effect and force exerted by the operator.

Moreover, the FFT analysis revealed that the working frequency was 18.0 Hz at no load for both harvesting heads and 15.1 Hz for H1 and 16.5 Hz for H2 at load. This decrease is due to the interference of the teeth with the canopy, greater in H1 due to the larger total width of the head (390 vs. 300 mm), that therefore is subjected to a resistant force higher than in H2. In addition, the force resistant is lower in H2 due to the greater flexibility of its teeth, characterised by greater length (360 vs. 330 mm) and smaller diameter (5 vs. 6 mm).

The difference between the two bar lengths (box-plots in Figure 3 and Table 2) is not statistically significant: the acceleration is on average equal to 9.4 m/s^2 when using the minimum length and 9.8 m/s^2 when using the maximum one. This difference is not affected by the working conditions: the interaction between bar length and working condition is not statistically significant, so the acceleration level is the same for the two bar lengths when the test condition (load or no load) is fixed.

The difference among the three bar angles, evaluated at no load, is not statistically significant (box-plots in Figure 3 and Table 2): each harvesting head produces the same vibration, independently of the bar angle.

Finally, the global acceleration in the measuring point MP2 is greater than that measured in MP1 (p-level < 0.001), but this result is affected by the bar length. In fact, the difference between the two measuring points is statistically significant when using the bar at its minimum length only.

The variability among the 1-minute sub-samples is very small: the coefficient of variation (CV), in fact, ranges from 0.8% up to 15.6%. As expected, the greatest variability is that measured at load: in these conditions the mean CV is 8.5%, whereas that measured at no load is 2.8%. This implies, on the one hand, that the operator is exposed to an almost constant level of vibration, and, on the other, that a measuring time of 1 2 min is enough for the measurement.

Table 3 reports the exposure times during harvesting activities corresponding to the A(8) daily exposure action value of 2.5 m/s^2 and the daily exposure limit value of 5.0 m/s^2, separately for each bar length and measuring point. The daily exposure limit value ranges from 0.7 up to 1.5 h, clearly incompatible with the standard work-day in agriculture, so the reduction of exposure times through rotating shifts of the operators should be recommended.

Vibration components

Figure 4 reports the acceleration components at varying harvesting head, working conditions, and measuring point. From it emerges that the main difference between the two harvesting heads at no load is due to the y component. In fact, whereas x and z components are on average comparable (3.4 and 2.8 m/s^2 the x component and 2.2 and 3.7 m/s^2 the z component for H1 and H2 respectively), the y component is 9.2 m/s^2 for H1 and 4.2 m/s^2 for H2.

When the working conditions change (from no load to load), the greatest increase in acceleration is observed in the x component (from 3.4 to 8.3 m/s^2 for H1 and from 2.8 to 11.4 m/s^2 for H2) and in the z component (from 3.7 to 7.2 m/s^2 for H1 and from 2.2 to 6.6 m/s^2 for H2), whereas the y component presents the smallest changes: from 9.2 to 8.0 m/s^2 for H1 and from 4.2 to 4.8 m/s^2 for H2. The variations of the x and z components from no load to load are explainable by observing that the teeth beat the branches along these two directions. Therefore the branches introduce another source of vibration that produces the increase in the global acceleration level.

Table 3. Exposure times (h) during harvesting corresponding to the A(8) daily exposure action value and daily exposure limit value.

Bar	Bar B1		Bar B2	
Measuring point	MP1	MP2	MP1	MP2
a_{hw}, m/s^2	11.4	16.8	12.4	15.7
A(8) = 2.5 m/s^2	0.4	0.2	0.3	0.2
A(8) = 5.0 m/s^2	1.5	0.7	1.3	0.8

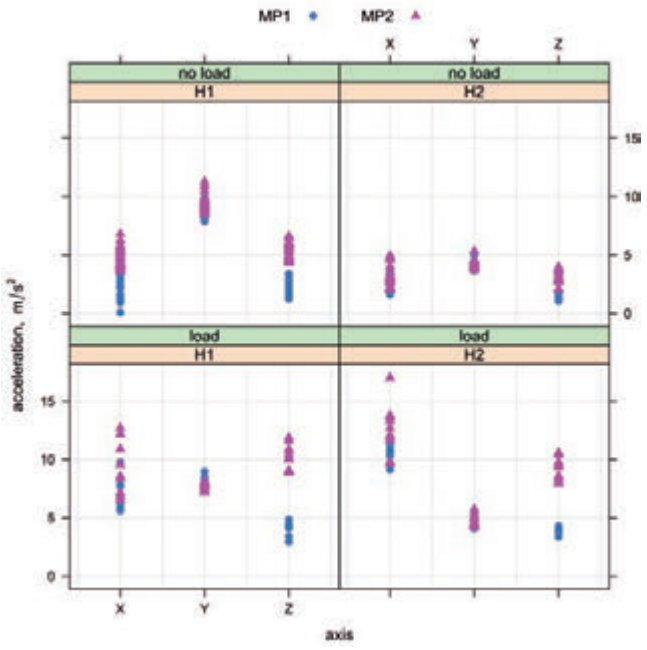

Figure 4. Acceleration components at varying harvesting head, working conditions, and measuring point.

Conclusions

The use of olive portable harvester if by one side has permitted to triplicate the productivity of the workers with respect to the manual harvesting, by another side has increased the risk for the safety of the operators due to the high acceleration level which are subjected. This is influenced by several aspects, but the main is the kinematic of the machine.

The research carried out has pointed out that:

- the branches produce a significant increase in the acceleration level with respect to the no load functioning; furthermore, the mass of the tree canopy nullifies the significant differences in the global acceleration levels between the two heads measured during the no load tests;
- the two harvesters studied, thank their kinematic, produce acceleration levels lower than those measured in other flap-type machines analysed in previous researches (Cerruto *et al*., 2012) (about 14 vs. 20 m/s^2); however, the stress for the workers remain so high that the daily exposure limit value ranges from 0.7 up to 1.5 h, incompatible with the standard work-day;

- the increase in the bar length with a telescopic system does not evidence significant difference in the global acceleration level between minimum and maximum length during both load and no load running; the variation in length, instead, has effect on the global acceleration measured in correspondence of the hand-grip: at the maximum bar length the global acceleration value increases and becomes statistically equal to that measured in the measuring point on the bar;
- the workers that operate with these machines are exposed to an almost constant level of vibration, as evidenced by the low coefficient of variations among the 1-minute sub-samples of the signal recorded during the tests (on average, 8.5%).

Finally, taking into account the results obtained, being the exposure time greater than the daily exposure limit, it is necessary to hypothesize rotating shifts among two or three operators during the work-day; on the other hand, to place the nets and to collect the olives from the ground require two operators. Therefore, operators must be informed about health risks and should take safety precautions to reduce continuous vibration exposures over long periods.

References

Biocca M., Fornaciari L., Vassalini G. 2008. Noise risk evaluation in electrical hand-held picking machines for olive harvesting. Proc. Int. Conf. Agr. Eng. "Agricultural and biosystems engineering for a sustainable world" June 23-25, Hersonissos, Crete, Greece, CD-ROM.

Blandini G., Cerruto E., Manetto G. 1997. Rumore e vibrazioni prodotti dai pettini pneumatici utilizzati per la raccolta delle olive. Proc. AIIA, September 11-12, Ancona, Italy, 4:229-38.

Cerruto E., Manetto G., Schillaci G. 2010. Vibrations produced by electric shakers for olive harvesting. Proc. Int. Conf. "Work Safety and Risk Prevention in Agro-Food and Forest Systems", September 16-18, Ragusa, Italy, CD-ROM.

Cerruto E., Manetto G., Schillaci G. 2011. Vibrations transmitted to the hand-arm system by electric shakers during olive harvesting. Proc. Int. Conf. XXXIV CIOSTA-CIGR V "Efficient and sale production processes in sustainable agriculture and forestry", June 29-July 1, Vienna, Austria, CD-ROM.

Cerruto E., Manetto G., Schillaci G. 2012. Vibration produced by hand-held olive electrical harvesters. Journal of Agricultural Engineering 2012, volume XLIII:e12, ISSN 1974-7071, doi:10.4081/jae.2012.e12, 79–85.

Chetter I.C., Kent P.J., Kester R.C. 1998. The hand arm vibration syndrome: a review. Cardiovasc. Surg. 6:1-9.

Deboli R., Calvo A., Preti C. 2008. The use of a capacitive sensor matrix to determine the grip forces applied to the olive hand held harvesters. Proc. Int. Conf. "Innovation Technology to Empower Safety, Health and Welfare in Agriculture and Agro-food Systems", September 15-17, Ragusa, Italy, CD-ROM.

Famiani F., Giurelli A., Proietti P., Nasini L., Farinelli D., Guelfi P. 2008. Sì alla raccolta agevolata in oliveti tradizionali ed intensivi. L'Informatore Agrario 4:103-7.

Iannicelli V., Ragni L. 1994. Agevolatrici vibranti per la raccolta delle olive. Riv. Ing. Agr. 25:248-56.

ISO, 2004. Mechanical vibration measurement and evaluation of human exposure to hand-transmitted vibration - part 1: general requirements. Norm ISO 5349-1:2004. International Organization for Standardization Publ., Geneva, Switzerland.

Italian Regulation. 2008. Attuazione dell'articolo 1 della legge 3 agosto 2007, n. 123, in materia di tutela della salute e della sicurezza nei luoghi di lavoro, LD 81/2008. In: Gazzetta Ufficiale no. 101, 30/04/2008, suppl. ordinario n. 108.

Mallick Z. 2010. Optimization of the operating parameters of a grass trimming machine. Appl. Ergonom. 41:260-5.

Monarca D., Cecchini M., Colantoni A. 2007. Study for the reduction of vibration levels on an "Olive electrical harvester". Proc. XXXII CIOSTA-CIGR Sect. V Conf., September 17-19, Nitra, Slovakia, Part II:503-9.

Pascuzzi S., Santoro F., Panaro V.N. 2008. Study of workers' exposures to vibrations produced by portable harvesters. Proc. Int. Conf. "Innovation Technology to Empower Safety, Health and Welfare in Agriculture and Agro-food Systems", September 15-17, Ragusa, Italy, CD-ROM.

R Core Team, 2012. R: A language and environment for statistical computing. R Foundation for Statistical Computing, Vienna, Austria. Available from: http://www.R-project.org/.

Vergara M., Sancho J.-L., Rodríguez P., Pérez-González A. 2008. Hand-transmitted vibration in power tools: Accomplishment of standards and users' perception. Int. J. Ind. Ergonom. 38:652-60.

Whole body vibrations during field operations in the vineyard

Pietro Catania,[1] Mariangela Vallone,[1] Maria Alleri,[1] Giuseppe Morello,[1] Giuseppe Spartà,[2] Pierluigi Febo[1]

[1]University of Palermo. Dipartimento di Scienze Agrarie e Forestali, Palermo, italy

[2]Assessorato Regionale Risorse Agricole e Alimentari, Palermo, Italy

Abstract

Human exposure to mechanical vibration can be a significant risk factor for exposed workers and this also occurs in the agricultural sector, in particular with reference to the driver of the tractor during field operations. The aim of this paper is the evaluation of Whole Body Vibrations for the operator driving tractors during the field operations in the vineyard. The experimental tests were performed using a wheeled and a track-laying tractor. They were coupled to four different machines: rototilling (RT), chisel plough (CP), flail mowers (FM) and vibro farmer (VF). Two homogeneous plots of vineyard, about 200 m long, were identified different only for slope: 0% and 30%. The tests were performed during the execution of the cultivation operations in flat conditions, uphill and downhill. For the evaluation of whole-body vibration we referred to ISO 2631-1:2008 standard. We used the portable vibration analyzer HD2070 by Delta Ohm, Italy. The mean square frequency-weighted acceleration [m s^{-2}] was evaluated along each of the three axial components of the acceleration vector (a_{wx}, a_{wy}, a_{wz})

$$a_w = \left[\frac{1}{T}\int_0^T a_w^2(t)dt\right]^{1/2}$$

The vibration total value to which the body is exposed (a_v) was determined by the following relationship:

$a_v = (kx^2\, awx^2 + ky^2\, awy^2 + kz^2\, awz^2)^{1/2}$

where kx = ky = 1.4 and kz = 1.

The study allowed to point out that during the use of the above mentioned operating machines coupled both with a track-laying tractor and a wheeled tractor, A(8) values were always higher than 0.5 m s^{-2} therefore, included in the "risk threshold" identified by the Italian Law Decree 81/2008. The machines coupled to the wheeled tractor always registered higher vibration values on the driving seat than the same machines coupled to the tracklying tractor. The operating machines showing higher vibration values are rototilling and vibro farmer in both tractors. Finally, the soil conditions in terms of slope caused no particular differences of vibration levels for all the machines used in the tests.

Correspondence: Pietro Catania, University of Palermo. Dipartimento di Scienze Agrarie e Forestali Viale delle Scienze Edificio 4, 90128 Palermo, Italy.
Tel. +39.91.23865608.
E-mail: pietro.catania@unipa.it

Key words: safety, tractor, whole body vibration.

Contributions: the authors contributed equally.

Conflict of interests: the authors declare no potential conflict of interests.

Conference presentation: part of this paper was presented at the 10th Italian Conference AIIA (Associazione Italiana di Ingegneria Agraria), 2013 September 8-12, Viterbo, Italy.

Journal of Agricultural Engineering 2013; XLIV(s1):e143
doi:10.4081/jae.2013.(s1):e143

Introduction

Human exposure to mechanical vibration may represent a significant risk factor for exposed workers in the agricultural sector, with particular reference to the operators driving tractors (Lines *et al.*, 1995; Matthews, 1966, Pessina *et al.*, 2012, Scarlett *et al.*, 2007).

The growing relevance of this risk in Europe and in the industrialized countries, both in terms health risk, and in terms of economic damage, led to the drafting of regulations and specific measures to reduce it. Directive 2002/44/EC of 25 June 2002 "on the minimum health and safety requirements regarding the exposure of workers to the risks arising from physical agents (vibration)" is the key step to ensure the implementation of specific protection measures for the prevention of risk exposure to vibration in the workplace.

This study would be a useful tool for users of machines and equipment that may result in exposure to vibrations within the agricultural sector in order to be in line with the provisions of the regulations on safety in the workplace.

The aim of the research was to assess the risk of exposure to whole-body vibration for the operator driving a wheeled and a tracklaying tractor during the execution of some agricultural operations carried out in the vineyard.

Materials and methods

Farm and experimental tests

The tests were carried out in a farm situated in the countryside of Santa Margherita Belice (province of Agrigento, Sicily).

The tests consisted in the evaluation of vibration values on the driving seat of a wheeled tractor (tractor A) and a tracklaying tractor (tractor B) during the execution of some agricultural operations with four different machines: rototilling (RT), chisel plough (CP), flail mowers (FM) and vibro farmer (VF).

Two homogeneous plots of vineyard, about 200 m long, were identified different only for slope: 0% and 30%. The tests were performed during the execution of the cultivation operations in the following conditions:

- flat, test named T1;
- uphill, test named T2;
- downhill, test named T3.

distinguishing between the tests performed with the wheeled tractor, known respectively as T1-A, T2-A and T3-A and those carried out with the tracklaying tractor, respectively called T1-B, T2-B and T3-B.

The average forward speed of the tractor was 2.5 km / h in test T2 and 3.0 km / h in tests T1 and T3.

Machines used in the tests

The tractors used during the tests are (Figure 1):

- the wheeled tractor Star 75 by Goldoni, named A, specialized for orchard and vineyard, 55 kW power, John Deere engine complete with soundproof cab and air conditioning (Table 1);
- the track-laying tractor Trekker 80F by Landini, named B, without cab, equipped with an anti-tip device, 58 kW power, Perkins engine 1104D-44 (Table 1).

Table 2 shows the characteristics of the machines used to carry out the tests (Figure 2).

Instruments used during the tests

For vibration measurements, a triaxial piezoelectric accelerometer, a signal conditioner, a digital archiving system, a frequency analyzer, connecting cables and a calibrator were used. The tests were performed according to ISO 2631–1, 2008. It defines standardized methods of measuring whole body vibration and provides some guidelines for the assessment of health effects.

The frequency spectrum and the direction and intensity of the acceleration were taken into account for the assessment of exposure to whole-body vibration.

ISO 2631–1: 2008 regulation defines the coordinate systems for accelerations measurement according to the entry point of the vibrations while keeping the axes x, y and z always in the same direction but with different origin according to the operator's position.

In whole-body vibration the z (vertical) axis is directed in the direction of the spinal column so this direction is the most dangerous for the drivers. Acceleration levels were measured as frequency-weighted root mean square values, in the frequency range 0.5 - 80 Hz. The measurements were made by inserting the triaxial accelerometer between the seat and the operator (Figure 3).

The accelerations (aw) detected on the x and y axes were further weighted by a factor of 1.4.

During the tests we used the portable vibration analyzer HD2070 by

Table 1. Main technical characteristics of the tractors used in the tests.

Tractor	Manifacturer	Mass [kg]	Wheel track [mm]	Wheelbase [mm]	Seat b1 b2 h [cm]	Year	Hours of work [n]
A	Goldoni	2700	1800	1900	42x39x41	2005	4480
B	Landini	3800	1650	-	40x41x39	2005	4390

Table 2. Main technical characteristics of the machines used in the tests.

Machine	Mass [kg]	Width [m]	Length [m]	Tillage depth [m]	Working tools [n]
Chisel plough	350	1.80	0.8	0.12	5
Vibro farmer	410	1.80	1.4	0.12	11
Rototilling	400	1.80	0.5	0.12	36
Flail mowers	495	1.80	0.85	0.00	14

Figure 1. Wheeled and tracklaying tractors used in the tests.

Delta Ohm, Italy (Fig.4). It is able to perform spectral analysis and statistics simultaneously on three channels.

The mean square frequency-weighted acceleration [m s^{-2}] was evaluated along each of the three axial components of the acceleration vector (awx, awy, awz):

$$a_w = \left[\frac{1}{T}\int_0^T a_w^2(t)dt\right]^{1/2} \quad (1)$$

The total vibration value to which the body is exposed (a_v) was determined by the following relationship:

$a_v = (kx^2\, a_{wx}^2 + ky^2\, a_{wy}^2 + kz^2\, a_{wz}^2)^{1/2}$ (2)

where kx = ky = 1.4 and kz = 1.

Acceleration data were correlated with the actual time of exposure in order to calculate the vibration risk assessment.

Results and discussion

Tests performed with the wheeled tractor

Wheeled tractor in flat (test T1-A)

Figure 5 shows that the highest aw value is obtained on the z axis for all the machines. In particular, RT provided the highest z-axis value (0.94 m/s^2), then FM (0.70 m/s^2), VF (0.63 m/s^2) and CP (0.63 m/s^2). Note that RT gave values higher than 30% respect to CP and VF. With regard to total a_v value, RT gave 1.42 m/s^2, then CP 1.04 m/s^2, FM 1.00 m/s^2 and VF 0.88 m/s^2.

It comes out that RT total a_v value is about 38% higher than VF that gave the lowest value. Regarding the A(8) daily values, calculated considering an effective duration of 7 hours, note that all the operating machines overcome the limit action value of 0.5 m/s^2. Even in this case RT has provided vibration values higher than about 34% compared to all the other operating machines. It follows that the maximum RT time of daily use is 0.99 h, against the maximum time of use of the other machines ranging between 1.86 and 2.56.

Wheeled tractor uphill (test T2-A)

In the tests performed uphill (T2-A), RT gave the highest vibration value on the z axes (0.99 m/s^2), then we have CP (0.57 m/s^2), VF (0.62 m/s^2) and FM (0.45 m/s^2). Note that FM shows a z-axis vibration value about 35% lower than the test performed in flat (T1-A). This difference could be attributed to the reduction of the forward speed from 3 to 2.5 km / h. Global weighted acceleration data and daily vibration exposure values are similar to those obtained in test T1-A.

Wheeled tractor downhill (test T3-A)

In the tests performed downhill (T3-A), RT gave the highest vibration value on the z axes (0.88 m/s^2), then we have CP (0.60 m/s^2), VF (0.58 m/s^2) and FM (0.58 m/s^2). Note that FM shows a z-axis vibration value about 17% lower than the test performed in flat (T1-A) and 24% higher than those in T2-A. Global weighted acceleration data and daily vibration exposure values are similar to those obtained in tests T1-A and T2-A.

Tests performed with the tracklying tractor

Tracklying tractor in flat (test T1-B)

Data show that FM, RT and VF provided very similar z-axis value (0.94 m/s^2) ranging between 0.52 and 0.58 m/s^2. CP, however, showed lower values of about 36% compared to the previous machines. Regarding total a_v value, FM and VF gave values about 22% higher than

Figure 2. Machines used in the tests.

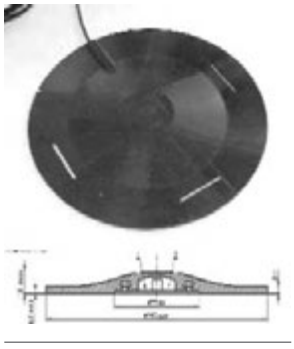

Figure 3. Triaxial accelerometer with adapter for the driving seat to measure whole-body vibrations.

Figure 4. HD2070 vibrometer by Delta Ohm, Italy.

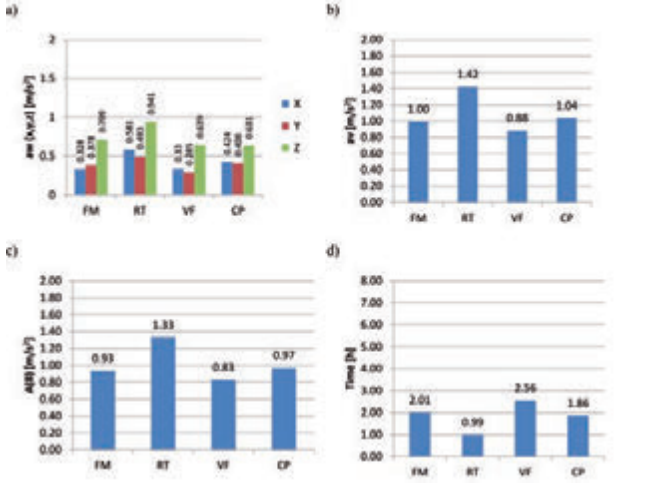

Figure 5. Frequency weighted vibration levels measured: a) on x, y and z axes; b) global weighted acceleration; c) daily vibration exposure value A(8); d) maximum exposure time measured on the driver's seat of the wheeled tractor during the tests with Flail-Mowers (FM), Rototilling (RT), Vibro farmer (VF) and Chisel Plough (CP) in test T1-A.

RT and CP. Concerning the A(8) daily values, note that all the operating machines overcome the limit action value of 0.5 m/s^2. FM and VF show the highest values (0.98 m/s^2) with a maximum time of daily use equal to 1.80 h respect to 2,56 h for RT and 2.99 h for CP.

Tracklying tractor uphill (test T2-B)

In the tests performed uphill (T2-B), the four operating machines gave very similar z axis vibration values going from a minimum of 0.51 m/s^2 for FM to a maximum of 0.66 for RT. This is attributed to the reduction of the forward speed from 3 to 2.5 km / h. With reference to global weighted acceleration data, VF show a value about 18% higher than FM and CP and about 10% higher than RT. The limit value of daily vibration exposure is exceeded by all the machines. VF and (1.05 m/s^2) and RT (0.95 m/s^2) gave the highest values with a maximum time of daily use respectively equal to 1.58 h and 1.95 h.

Tracklying tractor downhill (test T3-B)

In the tests performed downhill (T3-B), RT gave the highest vibration value on the z axis (0.74 m/s^2), then we have FM and CP (0.5 m/s^2), and VF (0.51 m/s^2). The maximum of global weighted acceleration data was obtained in RT equal to 1.32 m/s^2. The other machines show lower values respect to RT of about 18% (CP), 21% (FM) and 28% (VF). The limit value of daily vibration exposure is exceeded by all the machines. RT and (1.32 m/s^2) and CT (1.09 m/s^2) gave the highest values with a maximum time of daily use respectively equal to 1.14 h and 1.46 h.

Figure 11 shows one of several possible comparisons between the wheeled and the tracklying tractor time history both coupled with the rototilling.

Note that the highest peaks are in the z axis in the wheeled tractor (A), with a_v values of 1.2 - 1.3 m/s^2. In tractor B the peak values never exceed 1 m/s^2.

Conclusions

The study carried out in order to assess the levels of whole body vibration transmitted to the operator during the execution of the main tillage operations to the vineyard gave interesting results.

The use of four different operating machines as rototilling (RT), chisel plough (CP), flail mowers (FM) and vibro farmer (VF) coupled both with a wheeled and a tracklying tractor gave A(8) values always higher than 0.5 m/s^2 therefore, included in the "risk threshold" identified by the Italian Law Decree 81/2008. The employer, therefore, will have to apply the provisions aimed at avoiding or reducing vibration exposure of the worker as reported in Article 5 of Directive 2002/44/EC.

Finally, the results obtained allow to make the following considerations:

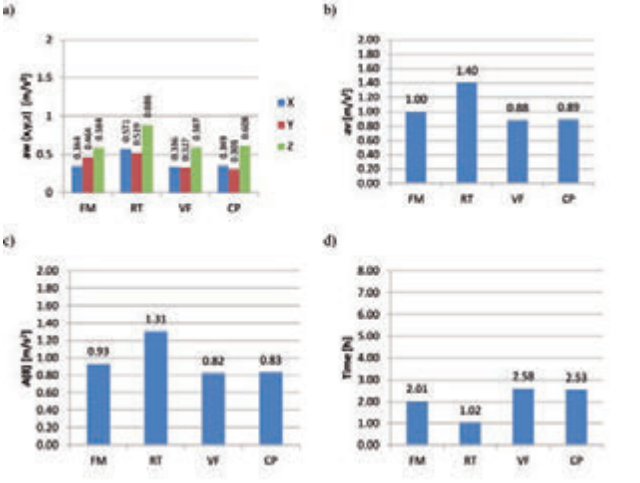

Figure 7. Frequency weighted vibration levels measured: a) on x, y and z axes; b) global weighted acceleration; c) daily vibration exposure value A(8); d) maximum exposure time measured on the driver's seat of the wheeled tractor during the tests with Flail-Mowers (FM), Rototilling (RT), Vibro farmer (VF) and Chisel Plough (CP) in test T3-A.

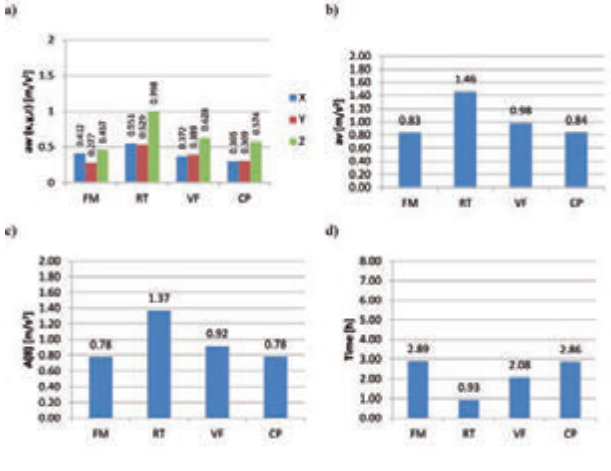

Figure 6. Frequency weighted vibration levels measured: a) on x, y and z axes; b) global weighted acceleration; c) daily vibration exposure value A(8); d) maximum exposure time measured on the driver's seat of the wheeled tractor during the tests with Flail-Mowers (FM), Rototilling (RT), Vibro farmer (VF) and Chisel Plough (CP) in test T2-A.

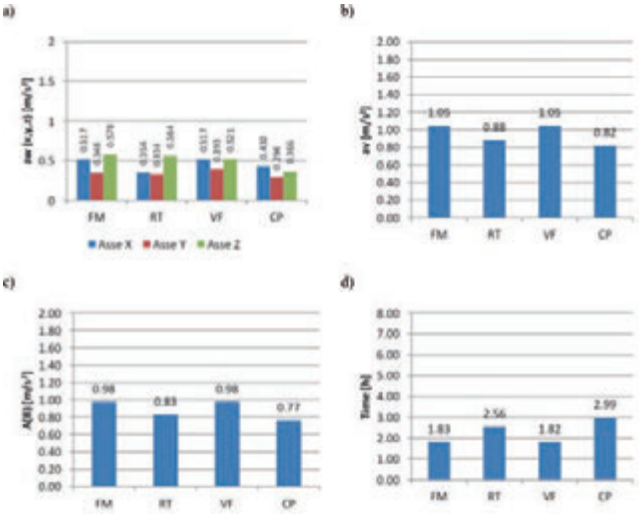

Figure 8. Frequency weighted vibration levels measured: a) on x, y and z axes; b) global weighted acceleration; c) daily vibration exposure value A(8); d) maximum exposure time measured on the driver's seat of the tracklying tractor during the tests with Flail-Mowers (FM), Rototilling (RT), Vibro farmer (VF) and Chisel Plough (CP) in test T1-B.

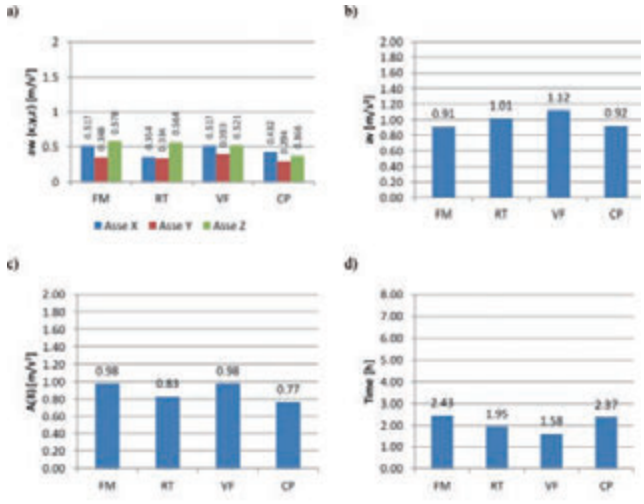

Figure 9. Frequency weighted vibration levels measured: a) on x, y and z axes; b) global weighted acceleration; c) daily vibration exposure value A(8); d) maximum exposure time measured on the driver's seat of the tracklying tractor during the tests with Flail-Mowers (FM), Rototilling (RT), Vibro farmer (VF) and Chisel Plough (CP) in test T2-B.

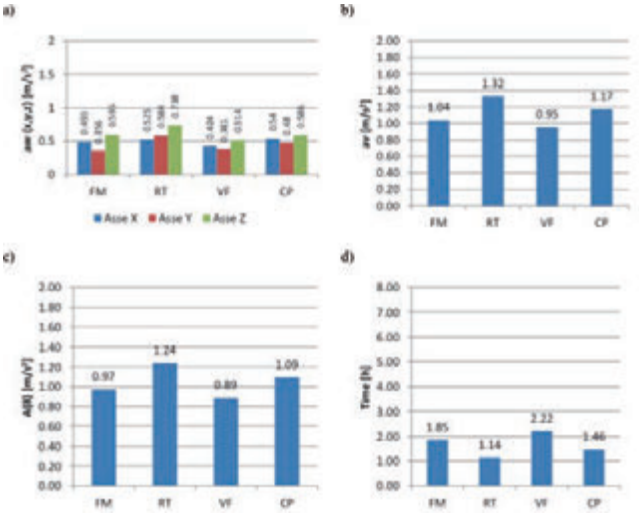

Figure 10. Frequency weighted vibration levels measured: a) on x, y and z axes; b) global weighted acceleration; c) daily vibration exposure value A(8); d) maximum exposure time measured on the driver's seat of the tracklying tractor during the tests with Flail-Mowers (FM), Rototilling (RT), Vibrofarmer (VF) and Chisel Plough (CP) in test T3-B.

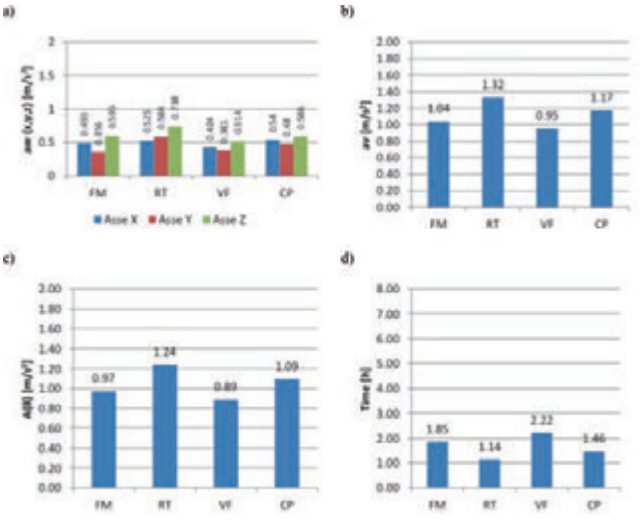

Figure 11. Time history of the vibration measurements on tractors A and B with rototilling in T1.

the machines coupled to the wheeled tractor always registered higher vibration values on the driving seat than the same machines coupled to the tracklying tractor. This may be attributed from the fact that the wheeled tractor has both a lower contact surface with the soil and a lower overall mass, about twice lower than the tracklying tractor;

the operating machines showing higher vibration values are rototilling and vibro farmer in both tractors;

the soil conditions in terms of slope caused no particular differences of vibration levels for all the machines used in the tests.

References

European Commission. 2002. European Directive of 25 June 2002 on the minimum health and safety requirements regarding the exposure of workers to the risks arising from physical agents (vibration) 2002/44/EC. In: Official Journal, L 177/13, 06/07/2002, 13-19.

ISO 2631–1, 2008. Mechanical Vibration and shock – Evaluation of Human Exposure to Whole-Body Vibration. Part – 1: General Requirements. International Standard Organization, Geneva.

Law Decree 81, 9 April 2008 of the Italian Republic.

Lines J.A., Stiles M., Whyte R.T. 1995. Whole body vibration during tractor driving. J Low Freq Noise Vib., 14(2), 87–104.

Matthews J. 1966. Ride comfort for tractor operators: II analysis of ride vibrations on pneumatic tyred tractors. J Agr Eng Res, 9(2), 147–58.

Pessina D., Facchinetti D., Bonalume V. 2012. Evaluation of vibration levels improves the efficiency of modern tracklaying tractors, XLIII, 43-47.

Scarlett A.J., Price J.S., Stayner R.M., 2007. Whole-body vibration: evaluation of emission and exposure levels arising from agricultural tractors. J. Terramechanics, 44, 65-73.

The heat stress for workers employed in a dairy farm

A. Marucci, D. Monarca, M. Cecchini, A. Colantoni, S. Di Giacinto, A. Cappuccini

Department of Agriculture, Forests, Nature and Energy (D.A.F.N.E.), Università degli Studi della Tuscia, Viterbo, Italy

Abstract

The italian dairy production is characterized by high heterogeneity. The typology quantitatively more important (80% of national production) is represented by cow's milk cheeses (Grana Padano cheese, string cheese, Parmesan cheese, etc.),while the cheese from buffalo's milk (especially string cheese such as mozzarella) and cheese from sheep and goats represents respectively 4% and 8% of the national dairy production, and are linked to specific regional contexts. Some phases of the cycle of milk processing occur at certain temperatures that not are comfortable for the operator also in relation to possible problems due to thermal shock. The aim of this study was to evaluate the risk of heat stress on workers operating in a dairy for processing of buffalo milk. The research was conducted at a dairy farm located in the province of Viterbo, Italy, during the spring-summer period. To carry out the research were detected major climatic parameters (air temperature, relative humidity, mean radiant temperature, air velocity) and the main parameters of the individual operators (thermal insulation provided by clothing and the energy expenditure required from the work done by employees in the work areas investigated). Subsequently were calculated main indices of heat stress assessment provided by the main technical standards. In particular have been calculated Predicted Mean Vote (PMV) and Predicted Percentage of Dissatisfied (PPD) in moderate environments, provided by the UNI EN ISO 7730 and the wet bulb globe temperature (WBGT) in severe hot environments required by UNI EN 27243. The results show some phases of risk from heat stress and possible solutions to improve the safety of the operators.

Introduction

Especially in Mediterranean areas the optimal temperatures are abundantly exceeded due to the high values of solar radiation, coming to 1000 W m^{-2}, and similarly for the high values of air temperature that during the summer can reach 40°C (Marucci *et al.*, *In Press*).

The issues related to the microclimate in the workplace are connected to the environmental factors that affect the thermal exchanges between man and the environment. In many agricultural and agro-industrial workplaces, the thermal comfort is difficult to achieve. In fact, the man is often found to operate outdoors or in the presence of animals, or in high temperature conditions (greenhouses) or very low (cold storage) or in situations where climatic parameters must be kept within specific microclimatic intervals, to ensure products conform to the standards of preparation, ripening and storage of products.

The main factors that influence these exchanges are: the weather conditions outside, the structural characteristics of the building, the characteristics of air conditioning (cold, hot), the number of occupants in environment to be examined and the type of activity.

Of particular importance is also, especially in the agro-food industries, the presence of thermal excursions such as to endanger the health of workers (Monarca *et al.*, 2012).

In dairy farms remain, even where the level of automation is high, numerous conditions of risk to workers' health (Di Giacinto *et al.*, 2012). Among these are included the sensation of thermal discomfort perceived by employees, caused to the microclimatic conditions (Marras *et al.*, 2005).

The milk processing within a dairy varies according to the type of product to be obtained with a consequent variation of the optimal microclimatic conditions which are often in contrast with those relating to the feeling of thermal comfort necessary for workers.

It is therefore necessary to analyze such working conditions, evaluate the impact on the worker's health and identify appropriate measures of technical, organizational and procedural be taken to improve the working conditions of staff (Marucci *et al.*, 2012).

The risk assessment of thermal stress is evaluated using microclimatic indices (Alfano *et al.*, 1998; Moran *et al.*, 2001; Pérez-Alonso *et al.*, 2011. Callejon-Ferre *et al.*, 2011) taken from the safety legislations that take into account climatic factors, the activities carried out by operators and clothing used (Budd, 2008).

The goal of this research is to assess the risk of heat stress for workers that operate within a dairy farm used as processing of buffalo's milk.

The research was conducted within a dairy farm located in a municipality of Alto Lazio, central Italy, during the spring-summer period and subsequent determination of the main indices of heat stress assessment provided by the main technical standards: UNI EN ISO 7730 for the determination of the Predicted Mean Vote (PMV) and Predicted Percentage of Dissatisfied (PPD) in moderate environments and UNI EN 27243 for the calculation of the wet bulb globe temperature (WBGT) in hot severe environments.

Materials and methods

The technical standards used for the risk assessment of thermal

Correspondence: A. Marucci, Department of Agriculture, Forests, Nature and Energy (D.A.F.N.E.), Università degli Studi della Tuscia, Viterbo, Italy.
Tel: +39(0)761.357365 - Fax: +39(0)761.357453.
E-mail: marucci@unitus.it

Key words: dairy farm, heat stress, microclimate.

Journal of Agricultural Engineering 2013; XLIV(s1):e144
doi:10.4081/jae.2013.(s1):e144

stress are those represented by the ISO standard, implemented in Italy as UNI. In particular, the following standards were applied:

- EN ISO 7730: 2006 Ergonomics of the thermal environment. Analytical determination and interpretation of thermal comfort using calculation of the PMV and PPD indices and local thermal comfort criteria;
- EN ISO 27243: 1996 Hot environments. Estimation of the heat stress on working man, based on the WBGT-index (wet bulb globe temperature);
- EN ISO 8996: 2005 Ergonomics of the thermal environment. Determination of metabolic rate;
- EN ISO 9920: 2009 Ergonomics of the thermal environment. Estimation of thermal insulation and water vapour resistance of a clothing ensemble;
- EN ISO 7726: 2002 Ergonomics of the thermal environment. Instruments for measuring physical quantities.

In order to determine the indices proposed by the reference standards were detected microclimatic parameters (temperature and relative humidity inside and outside) of a dairy farm (Figure 1) located in a municipality of Alto Lazio (Altitude: 464 m; Latitude: 42°32'17'' N; Longitude: 12°03'19''E) during the spring-summer period. The measurements were performed during the time of the mozzarella working (3 p.m.- 4 p.m.).

The measurement system used is the following (Figure 2):

1. multi-acquiring LSI BABUC M instrument with 6 inputs;
2. probes for measuring micro-climatic parameters (thermometer, psychrometer, anemometer and globe thermometer);
3. prop for probes;
4. tripod.

The probes were put into position on a tripod at a height of 1.50 m from the ground.

When measured microclimatic parameters were determined PMV and PPD.

The PMV (Predicted Mean Vote) is the average rating from a large sample of people present in the same environment14 and is a mathematical function (1) that depends on several factors:

$$PMV = f(M, W, I_{cl}, f_{cl}, t_a, t_r, v_{ar}, p_a, h_c, t_{cl}) \quad (1)$$

where:

M is the metabolic rate (Wm^{-2});
W is the effective mechanical power (Wm^{-2});
I_{cl} is the clothing insulation (m^2 K W^{-1});
f_{cl} is the clothing surface area factor;
t_a is the air temperature (°C);
t_r is the mean radiant temperature (°C);
v_{ar} is the relative air velocity (m s^{-1});
p_a is the water vapour partial pressure (Pa);
h_c is the convective heat transfer coefficient (W m^{-2} K^{-1});
t_{cl} is the clothing surface temperature (°C).

To determine climatic parameters have been used climate data collected on the farm, while the metabolism rate (M) and clothing insulation (I_{cl}) of workers have been determined on the basis of existing legislation. It was taken on a metabolic rate (M) equal to 116 W m^{-2} (2,0 met) as reported in legislation that corresponds to an medium activity and standing. The clothing used by workers is underpants, boiler suit, socks, shoes that corresponds to an I_{cl} equal to 0,75 clo (0,11 m^2 K W^{-1}).

ISO 7730 defines the scale of values of the PMV in range +3 (very hot) to -3 (very cold). There are intermediate situations where the 0 corresponds to thermal neutrality, the range between -0.5 and +0.5 corresponds to the thermal comfort. When -2 <PMV <-0.5 and +0.5 <PMV <+2 the thermal environment is moderate while the PMV values less than -2 and greater than +2 the thermal environment is severe.

The same standard defines PPD as the percentage of thermally dissatisfied people14 and is calculated according to the following function (2):

$$PPD = 100 - 95 \cdot e^{-\left[0.03353 PMV^4 + 0.2179 PMV^2\right]} \quad (2)$$

The PPD is equal to 10% in the case where the PMV is within the range of thermal comfort (-0.5 <PMV<+0.5), while for severe environments the PPD assumes values higher than 80%.

PMV has allowed us to classify the thermal environment into consideration as hot.

Consequently, it was necessary to calculate another index proposed

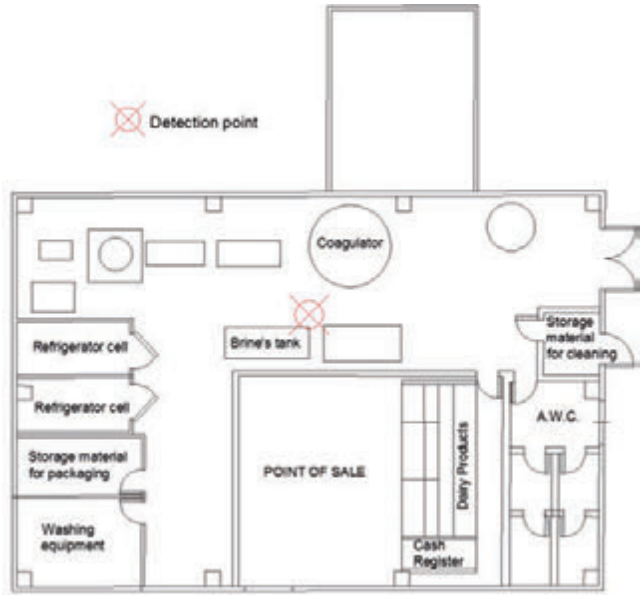

Figure 1. Plan of dairy farm object of study.

Figure 2. Measurement system used for the research.

legislation for harsh hot thermal environments: WBGT (Wet Bulbe Globe Temperature).

WBGT is used to determine the thermal stress for individuals acclimated. The current legislation proposes two equations for calculating the WBGT as a function of the presence or absence of sunshine. In this farm, the interior lighting is completely artificial and therefore without the entry of sunlight. Therefore, the equation that has been applied is that relating to environments not sunny (3):

$$WBGT = 0.7t_{nw} + 0.3t_g$$

for internal and external exposition without exposure to sun (3)

where:

t_{nw} is Natural wet-bulb temperature (°C);

t_g is globe thermometer temperature (°C).

The days when the measurements were performed are:

- April 10th, 2013;
- May 3rd, 2013;
- May 30th, 2013;
- June 11th, 2013;
- June 17th, 2013.

Results and discussion

The measured values of temperature and relative humidity of the air and the calculated values of PMV and PPD during the processing of milk in the test period have given the mean values reported in Table 1:

From the measurements performed in this period, the indoor air temperature is always higher than 20°C. In the last two measurement periods, which fall in June, the indoor air temperature was higher than 25°C.

The high values of the indoor air temperature in the dairy farm are due to the processing of milk and are positive for the production of mozzarella but they can cause serious health problems of the operators especially in the event of prolonged exposure.

The relative humidity measured inside the dairy farm is between 50% and 80%, has not been reached the saturation of the air and this has allowed to reduce the risks associated with the high air temperature.

Figure 3 shows the mean values of the PMV and PPD calculated with the measured values from 3 p.m. to 4 p.m. for each day of measurement inside the dairy and the limit (+2) beyond which the environment changes from moderate to severe hot.

On the first day of the experimental period (April 10), taking into account the thermal energy produced during metabolic activity by operators and thermal insulation of the clothing, the PMV is equal to +1.32 placing itself in the middle between "slightly warm "and" warm "in the seven-point thermal sensation scale reported by the legislation. The predicted percentage dissatisfied (PPD) associated with this PMV value was equal to 41.2%.

In the other days of measurements instead PMV index always exceeds the limit of +2 due to the high indoor values of air temperature and relative humidity measured, and other conditions being equal. Exceeding this limit allows to classify the processing environment as severe hot.

The day 17 June, the PMV was not calculated because the air temperature has exceeded the value of 30°C.

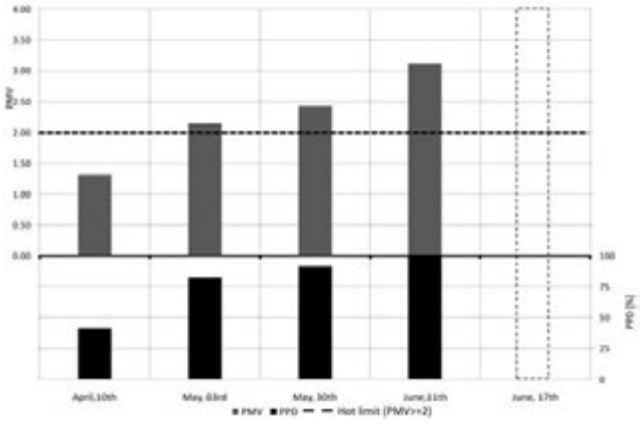

Figure 3. PMV, PPD and PMV limit established by the respective reference standards.

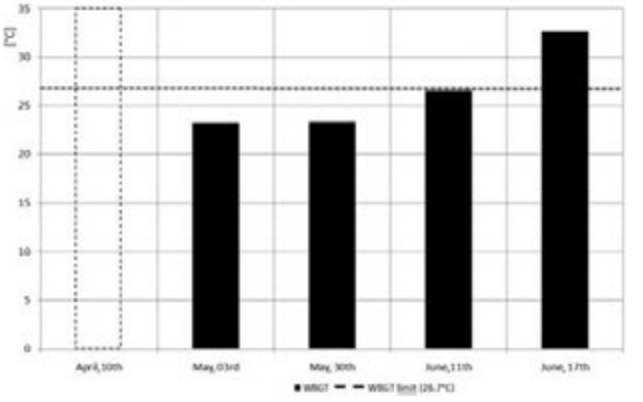

Figure 4. Mean values of WBGT index for the periods of experimentation.

Table 1. Mean values of indoor and outdoor air temperature and relative humidity, clothing insulation and metabolic rate.

	Indoor air temperature	Indoor relative humidity	Outdoor air temperature	Outdoor relative humidity	I_{cl}	M
	[°C]	[%]	[°C]	[%]	[clo]	[W m^{-2}]
April,10th	20.87	65.3	16.6	51.4	0.70	116
May, 03rd	22.90	64.8	21.1	59.2	0.70	116
May, 30th	22.75	78.4	17.1	56.6	0.70	116
June,11th	26.26	61.5	23.1	54.3	0.70	116
June, 17th	32.73	53.5	31.4	29.7	-	-

Where the PMV index exceeds the threshold of +2, and thus the work environment becomes "severe hot", and the indoor air temperature exceeds 30°C is necessary to calculate another index proposed by microclimate safety regulations: the WBGT, through which it is possible to verify if operators are subjected to heat stress.

Figure 4 shows the mean values of WBGT index for the periods of experimentation and the limit for acclimated subjects (26.7°C).

For the first day of observation (April, 10th) has not been calculated the WBGT index because the working environment was found to be moderate (+0.5<PMV<+2).

The WBGT values calculated for the later days of relief are higher than the limit established by law for acclimated subjects (26.7°C) only in the last day of the measurements. During these reliefs the WBGT was found to be equal to 32.7°C showing how the workers were subjected to a real thermal stress.

In general, the search results allow to affirm that, under the climatic conditions in which it is located the dairy farm , during the second part of the spring season (late April-mid June) the operators are in the presence of a situation of thermal discomfort but they are not subjected to thermal stress since the WBGT was found to be always lower than the limit established by law.

To reduce the thermal discomfort you might act on operator's clothing in order to reduce the I_{cl} index, a significant improvement of the conditions would be obtained to passing a clothing with I_{cl}=0.70 clo to another with I_{cl}=0.50 clo.

From mid June and for the entire duration of the hot season, the WBGT exceeds the limit set for acclimated workers and the employees find themselves operating under thermal stress conditions.

Since the WBGT index, unlike the PMV, is closely related to the air temperature you could intervene further reducing the value, whose control is generally entrusted only to the forced ventilation through fume hood.

Additional actions may be even the clothing of the operators described above and the programming of one or more breaks during the working shift to spend in areas of acclimatization.

Conclusions

The calculation of the indices, brought in accordance with the safety standards, has allowed us to assess the degree of risk of heat stress they are subjected to the operators involved in the preparation of buffalo's mozzarella in a dairy farm.

The survey data showed the presence of different situations of heat stress risk.

During the second part of the spring season (late April-mid June) the workers of buffalo's mozzarella, under the climatic conditions in which it is located the dairy farm, are in the presence of a situation of thermal discomfort because the calculated WBGT Index not exceeds the threshold established by the legislation.

In the last study period (mid-June) in the vicinity of the summer and in presence of significantly higher air temperatures, it is possible to affirm that operators are in presence of heat stress conditions.

In order to reduce this risk, the employer is required to:

- Provide appropriate clothing in order to reduce the I_{cl} index;
- Check the exposure times with programming breaks to spend in areas of acclimatization;
- Reduce the indoor air temperature of the workplace through an appropriate air conditioning system.

References

Alfano G., D'ambrosio R.F., Riccio G., 1998. Disagio e stress termico: Effetti, normative, valutazione e controllo. In Proc. dBA 1998: Dal rumore ai rischi fisici; valutazione, prevenzione bonifica degli ambienti di lavoro. 531-566 Modena, Italy.

Budd G. M., 2008. Wet-bulb globe temperature (WBGT): Its history and its limitation. J. Sci. Med. Sport, 11(1), 20-32.

Callejon-Ferre A.J., Manzano-Agugliaro F., Diaz-Perez M., Carreno-Sanchez J., 2011. Improving the climate safety of workers in Almeria-type greenhouse in Spain by predicting the periods when they are most likely to suffer thermal stress. Applied Ergonomics, 42, 391-396.

Di Giacinto S., Colantoni A., Cecchini M., Monarca D., Moscetti R., Massantini R., 2012. Dairy production in restricted environment and safety for the workers. Industrie Alimentari, 530, 5-12.

Marras T., Murgia L., Pazzona A, 2005. Valutazione del rischio biomeccanico in due caseifici industriali con differente grado di meccanizzazione. G. Ital. Med. Erg., 27 (1), 112-18.

Marucci A., Pagniello B., Monarca D., Cecchini M., Colantoni A., Biondi P., 2012. Heat stress suffered by workers employed in vegetable grafting in greenhouses. J. of Food, Agriculture & Environment, 10, 1117-1121.

Marucci A., Pagniello B., Monarca D., Cecchini M., Colantoni A., Biondi P., 2012. The heat stress for workers employed in laying hens houses. J. of Food, Agriculture & Environment, *In Press*.

Monarca D.,Bedini R., Cecchini M., Colantoni A., Di Giacinto S., Marucci A., Menghini G., Porceddu P.R., 2012. Il rischio da microclima nei caseifici e nelle sale di mungitura. Salute e sicurezza sul lavoro nel comparto zootecnico e caseario. Sassari, 26 ottobre 2011.

Moran D. S., Pandolf K.B., Shapiro Y., Heled Y., Shani Y., Mathew W. T., Gonzalez R.R., 2001. An environmental stress index (ESI) as a substitute for the wet bulbe temperature (WBGT). J. Of Thermal Biology, 26, 427-431.

Pérez-Alonso J., Callejón-Ferre Á.J., Carreño-Ortega Á., Sánchez-Hermosilla J., 2011. Approach to the evaluation of the thermal work environment in the greenhouse-construction industry of SE Spain. Building and Environment, 46(8), 1725-1734.

UNI EN ISO 7730:2006 Ergonomics of the thermal environment – Analytical determination and interpretation of thermal comfort using calculation of the PMV and PPD indices and local thermal comfort criteria.

UNI EN ISO 27243:1996 Hot environments. Estimation of the heat stress on working man, based on the WBGT index (wet bulb globe temperature).

UNI EN ISO 8996:2005 Ergonomics of the thermal environment Determination of metabolic rate.

UNI EN ISO 9920:2009 Ergonomics of the thermal environment. Estimation of thermal insulation and water vapour resistance of a clothing ensemble.

UNI EN ISO 7726:2002 Ergonomics of the thermal environment - Instruments for measuring physical quantities.

Spectral analysis of a standard test track profile during passage of an agricultural tractor

M. Cutini,[1] R. Deboli,[2] A. Calvo,[3] C. Preti,[2] M. Inserillo,[2] C. Bisaglia[1]

[1]Consiglio per la Ricerca e la Sperimentazione in Agricoltura, Unità di Ricerca per l'Ingegneria Agraria, Laboratorio di Treviglio, Treviglio (BG), Italy; [2]Italian National Research Council - Institute for Agricultural and Earthmoving Machines (IMAMOTER), Torino, Italy; [3]DISAFA, University of Turin, Grugliasco (TO), Italy

Abstract

National statistics on work safety are pointing out a decreasing trend about related injuries and fatalities but an increasing number of reports about professional diseases. In this frame are also considered the mechanical vibrations, in particular whole-body vibrations (WBV). This study aims to reproduce and analyse the vertical displacement of the wheel of an agricultural tractor during the passage on a standard surface (ISO 5008) for defining potential correlations between the surface contour and the effects on vehicle dynamic and driver comfort by analysis of the signals acting under the tractor tires. An agricultural tractor, in four setting conditions and four different forward speeds, was tested on an ISO 5008 standard test track. The accelerations at the hubs of the tractor were acquired and subsequently reproduced on a four hydraulic actuators test bench, at CRA-ING laboratories, Treviglio, Italy. The analysis of the spectrums generated have shown that a roughness surface induces a transformation of the part of energy developed by the forward speed of the vehicle in vertical acceleration that excites the elastic parts (*i.e.* tires, suspensions). These phenomena seem to indicate that vehicle's vibration entity is due to the combination of surface roughness and forward speed as amplitude and to the elastic properties of the vehicle as frequency.

Correspondence: Maurizio Cutini, Consiglio per la Ricerca e la Sperimentazione in Agricoltura, Unità di Ricerca per l'Ingegneria Agraria, Laboratorio di Treviglio, via Milano 43, 24047 Treviglio (BG), Italy.
Tel./Fax.: +39.0363.49603.
E-mail: maurizio.cutini@entecra.it

Keywords: ISO 5008, tractor vibration, WBV

Contributions: the authors contributed equally.

Conflict of interests: the authors declare no potential conflict of interests.

Acknowledgements: This study was funded by the PRIN project (2009): "Analysis of the rollover and the vibration in the agricultural tractors with respect to current safety legislation", Italian Ministry of Education, University and Research (MIUR) and the VIBRA.M.AG. project (2005): "Valutazione e controllo delle vibrazioni nei sistemi meccanici agrari con nuovi metodi d'indagine basati su banco vibrante", Italian Ministry of Agricultural, Alimentary and Forestry Policies, (MiPAAF).

Conference presentation: this paper was presented at the 10th AIIA Conference: "AIIA13 – Horizons in agricultural, forestry and biosystems engineering", Viterbo, University of Tuscia, Italy, on September 8-12, 2013.

Funding: this study was funded by the PRIN project (2009): "Analysis of the rollover and the vibration in the agricultural tractors with respect to current safety legislation", Italian Ministry of Education, University and Research (MIUR) and the VIBRA.M.AG. project (2005): "Valutazione e controllo delle vibrazioni nei sistemi meccanici agrari con nuovi metodi d'indagine basati su banco vibrante", Italian Ministry of Agricultural, Alimentary and Forestry Policies, (MiPAAF).

Journal of Agricultural Engineering 2013; XLIV(s1):e145

Introduction

National statistics on work safety are pointing out a decreasing trend about injuries and fatalities but an increasing number of reports about professional diseases. A mean value more has been observed of 36% in the last 5 years but data in agricultural environment are increased of 383% in the same period. It's difficult to associate these data specifically to some well identified causes but it is sure that the interest about the occupational diseases is increasing. In this frame are also considered the mechanical vibrations. In particular, whole-body vibrations (WBV) could affect an operator driving an agricultural tractor depending on intensity, duration and frequency.

European Parliament Directive 2002/44/EEC sets the minimum requirements for protection of workers from risks to their health and safety arising from exposure to mechanical vibrations; moreover, in 2008, Italy adopted a specific national regulation on safety (Decree Law n. 81/2008). Although most of the studies are directed to measure comfort (Deboli *et al.*, 2010), vibration dumping and developing models, one of the most important parameter as the surface profile, is not analyzed as expected, above all for the difficult its standardisation and measurement.

Vibrations with frequency lower than 2 Hz can cause smaller and temporary effects like motion sickness, which anyway interfere with the desired development of the work activity and produce a remarkable discomfort. A long-term exposure to vibrations with frequency ranging from 2 to 20 Hz can cause severe disease, like degenerative pathologies of the spine (Chiang *et al.*, 2006; Seidel and Heide, 1986).

The work has the goal to reproduce and analyse the vertical displacement of the wheel of an agricultural tractor during the passage on a standard surface (ISO 5008:2002) for defining potential correlations between the surface contour and the effects on vehicle dynamic and driver comfort.

State of the art

For agricultural tractors, considering normal conditions of use,

irregularity of working terrains and forward speed are the most important causes of vibrations transmitted to the driver (Scarlett *et al.*, 2007), on tool oscillations and impact on work quality (Bisaglia *et al.*, 2006; Cutini *et al.*, 2011).

For several years, tires have been the main element for attenuation of mechanical vibrations on agricultural tractors. Their effectiveness depends on factors such as eccentricity, load, resonance frequency, and elasticity characteristics (Nguyen and Hinaba, 2011; Sherwin *et al.* 2004; Park *et al.*, 2004; Taylor *et al.*, 2000). So, most of the studies have been directed to the tires' properties, dumping systems and/or their interaction.

However, as aforementioned, in agricultural machines an important factor characterizing the amplitude and frequency of vibrations is represented by the environment, in particular by the soil unevenness.

Soil unevenness has a stochastic character; its deformation has a nonlinear, visco-elastic-plastic behavior and its condition depends on a wide range of parameters (cultivation, cropping/tillage history, texture, organic residue, drainage conditions, etc.) so that it is almost impossible to standardize testing conditions in fields. For this reason, the experimental test has been carried out on the smoother ISO, 100 m track. To analyze the effect of surface outline on the vehicle body is necessary to obtain the displacement, or the accelerations, acting under the tires.

The most common existing approach (Anthonis, *et al.*, 2007; Bisaglia, *et al.*, 2006) consist in an iterative methodology. During the field test, the accelerations are measured at specific locations of the machine (usually at the hubs), then the machine is put on a test bench and the actuators (one for each tires) of the bench are driven in order to create, by a deconvolution method, input signals such that the sensor readings (one for each hubs) match with the measurements (accelerations) obtained in the field.

Theoretical considerations

An iterative deconvolution method is a computerized control technique that enables to duplicate, in the test laboratory, vehicle or component responses measured during field testing. The calculation of the control signals for the actuator of the test bench, called drive signals, is a multivariable tracking problem, currently solved with the so-called iterative deconvolution (ID) procedure (Soderling, *et al.*, 1999). ID is an off-line iterative feed forward procedure where the drive signals are updated by the measured frequency response function matrix (FRF) of the test arrangement and the tracking errors obtained in the previous iteration. Several commercial versions of the algorithm were developed. During the laboratory tests the Remote Parameter Control (RPC®) software from MTS Systems Corporation has been used. The drive signals obtained with this procedure can be considered an approximation of the real field surfaces subject to deformations.

Materials and methods

An agricultural tractor, in four setting conditions and four different forward speed, was tested on smoother ISO 5008 standard test track presents at CNR IMAMOTER testing facilities, located at Pratofiorito (Candiolo, TO). The tractor's hubs accelerations were acquired and subsequently reproduced on a four hydraulic actuators test bench, at CRA-ING laboratories of Treviglio (BG).

The vertical displacement of the hydraulic actuators were driven, by specific electronics, for reproducing the profiles defined as the vertical input of the surfaces.

The condition adopted and the relevant test code are reported.

Mass:
- With ballast (_Z)
- Without ballast (_N)

Tires inflation pressure
- 80 kPa (_08)
- 160 kPa (_16)

Forward speed
- 6 km/h (_6)
- 10 km/h (_10)
- 12 km/h (_12)
- 14km/h (_14)

Three repetitions were carried out for each tests. The sampling frequency was 1250 Hz.

The accelerations at the hubs of the tractor were acquired and subsequently reproduced, as above reported, on the four hydraulic actuators test bench by the deconvolution method.

Tested vehicle

The tested agricultural vehicle is a medium-range tractor, with a four-wheel drive (4WD) transmission, engine with 89 kW rated power, a closed rubber-mounted cabin and a mechanical suspended seat. The most relevant data for the tests are reported in Table 1.

The test track

The ISO 5008 track (Figure 1) consists of two parallel strips suitably spaced for the wheel track of the tractor. The surface of each strip is formed of wooden slats 80 mm wide, each slat separated from the next by a gap of 80 mm. Slats are sited firmly in a base framework. The surface of each track strip has been defined by the ordinates of elevation, with respect to a level base, listed in Tables of ISO 5008.

Operative conditions

During the tests, the tractor ran at four forward speeds (6, 10, 12 and 14 km/h), with tires at two inflation pressures (80 and 160 kPa). All tests were performed in unballast and ballast conditions. In the ballast tests, an 800 kg ballast was connected at the rear three-point hitch and a 320 kg ballast at the front.

One experienced operator (70 kg mass, 180 cm height) carried out all the tests.

Table 1. Tractor characteristics.

Item	Parameter	Unit/type	Value/type
Tractor	Power	kW	89
	Wheelbase	mm	2467
	Front width track	mm	1700
	Rear width track	mm	1800
	Front mass	kg	2230
	Rear mass	kg	2960
	Cab suspension	type	Rubber mounts
	Front axle suspension	type	None
	Seat suspension	type	Mechanical
Front tires	Overall size	ETRTO 2005	420/85R24
	Treads	n.	22x2
	Treads height	mm	41*
Rear tires	Overall size	ETRTO 2005	460/85R38
	Treads	n.	22x2
	Treads height	mm	42,5*

*Measured at 160 kPa at the midpoint of two consecutive noses, medium value of three measurements. The value was the same between right and left.

Acquisition times ranged between 59 s at 6 km/h forward speed and 25 s at 14 km/h.

Each test was replicated three times.

Four poster test bench

The CRA-ING four-post test bench is specifically designed to test large and heavy vehicles up to 15 t (Figure 2).

The test rig is composed of a seismic mass of 408 t weight, isolated from the ground by means of pneumatic springs, supporting four servo-hydraulic actuators, articulated for wheel-base/track adjustment. On the top of actuators are fixed four plates 1000 mm diameter upon which the tires of the vehicle are placed. Are also present a power hydraulic and a control unit, including a computer-based controller and a data acquisition unit.

Each actuator is controlled in position (up to a frequency of 100 Hz and a peak-to-peak amplitude of 250 mm) and excites one tire of the vehicle in vertical direction.

The displacements of the actuators are measured through linear variable differential transformer (LVDT) transducers, whose output signals are acquired and recorded.

Measure instrumentation

The vehicle was instrumented with a set of four piezo-electric monoaxial accelerometers (range ±50 g, sensitivity 100 mV/g) to measure the wheel hubs vertical acceleration. The output accelerometer signals were sent to a signal conditioner (Rogadaq 16) and then to a heavy-duty personal computer (Panasonic CF29).

Results

The acceleration registered on the standard track were reproduced at the four poster test bench.

A mean value of the root mean square error (RMSE) was 20.

Graphic example are reported in Figures 3 and 4.

Figure 3 shows the spectrum of both the desired (_des) and the reproduced signal (_res) in the test condition at 10 km/h, without ballast, tire pressure of 80 kPa, rear left hub (RL).

Figure 4 shows the spectrums of both the desired (_des) and the reproduced signal (_res) in the test condition at 10 km/h, without ballast, tire pressure of 160 kPa, front left hub (FL).

The analysis of the spectrums shows that, in each test, there is an energy peak proportional, as amplitude, to the forward tractor speed correlated to the elastic properties of the front tires. This peak must has been considered as an effect due to the specified tire models and not to the surface type.

In each test there are energy peaks corresponding to the vibration modes of the cabin. These peaks must be considered as a side effect correlated to the dynamics of the vehicle and to the test conditions and not to the surface type.

It can also be seen that, regardless of the surface type, moving towards and increasing forward speeds there is a correspondent increase of the spectrum magnitude in the whole range of frequency.

The surface types show similar frequency spectrum shapes, regardless of the forward speed: the power spectral density is most relevant at the lower frequencies (< 3 Hz); increasing frequency the spectrum magnitude rapidly decreases. Between 4 Hz and 10-12 Hz the spectral components are less relevant. Above 12 Hz the spectral components are negligible; over this frequency band the spectrum is flat and the signals can be considered "white".

Two auto spectral density spectrum (ASD) are reported as example in the N_16 setting: Figure 5 shows the mean value of the displacement of the two front plates and Figure 6 of the rear.

In the frame of the comfort analysis it must be considered that two filters have been applied to the spectrums of the plates' acceleration:

Figure 1. The standard test track.

Figure. 2. The four poster test bench.

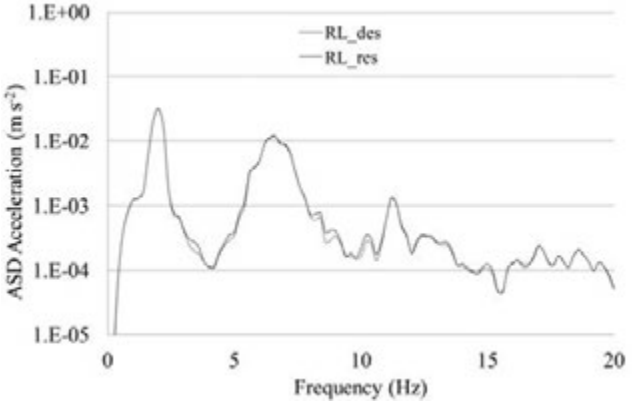

Figure 3. Example of reproducibility on the RL hub in R10_N08 condition.

the filter related to the vehicle (tire, cab, seat) and the filter related to the procedure (ISO 2631).

The outcome is that the frequency band of interest results 0.6-12 Hz with a major contribute between 1-4 Hz.

The interpretation of the results requires to consider the solicitation of the elastic part of the vehicle, as the change in rolling radius of the tires, when passing over a cleat. The forces induced depend from the surface forward curvature such as road unevenness. In the effort to evaluate the effect of rolling over an obstacle it is important to consider the increment in normal slope as height, curvature and length.

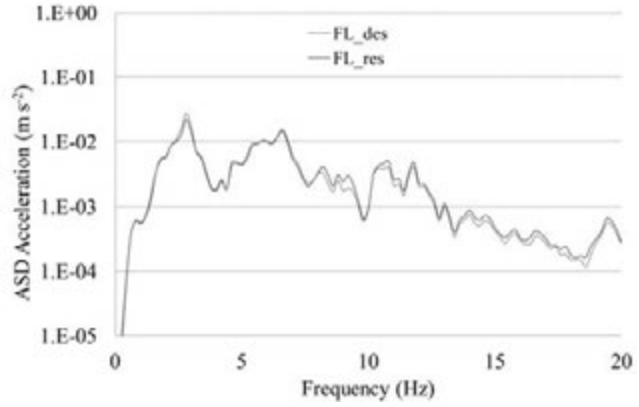

Figure 4. Example of reproducibility on the FL hub in R10_N16 condition.

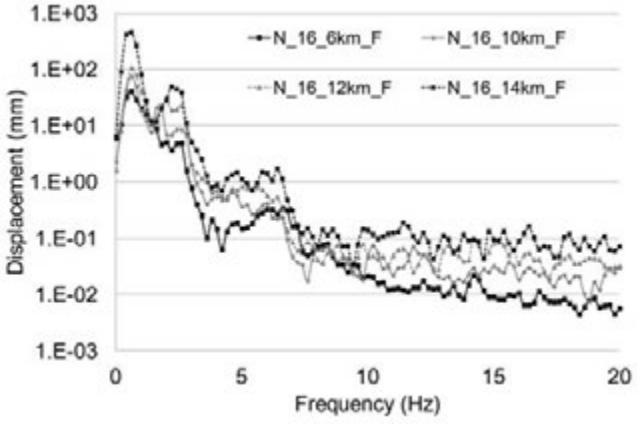

Figure. 5. ASD Spectrum of the settings N_16 on the front plates.

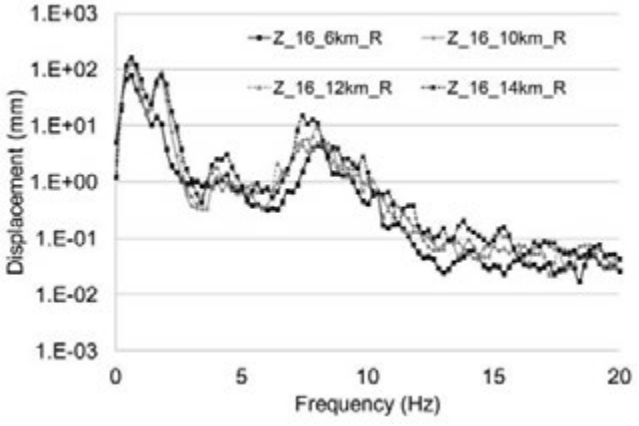

Figure. 6. ASD Spectrum of the setting N_16 on the rear plates.

Conclusions

This first essay permitted to verify the functionality of the four hydraulic actuators test bench to reproduce vertical solicitations at the wheel hubs of a tractor when crossing the ISO 5008 track at different forward speeds, with different settings and different tires pressure.

The analysis of the spectrums of the data obtained both in the smooth track and in the test bench have shown that a roughness surface induces a transformation of the forward speed of the vehicle in vertical acceleration that excites the elastic parts (*i.e.* tires, suspensions, …). These phenomena seem to indicate that vehicle's vibration entity is due to the combination of surface roughness and forward speed as amplitude and to the elastic properties of the elastic parts as frequency.

The comparison between the spectral power density of the accelerations of the wheel hubs achieved in the track with the same acquired in laboratory lead in new possibilities to redesign new artificial tracks to acquire vibration values over the tractor, which could convey to acceleration data at the operator seat.

References

Anthonis J., D. Vaes, K. Engelen, H. Ramon, J. Swevers 2007. Feedback Approach for Reproduction of Field Measurements on a Hydraulic Four Poster. Biosystems Engineering. 96(4): 435-445.

Bisaglia C., Cutini M., Gruppo G. 2006. Assessment of vibration reproducibility on agricultural tractors by a four poster test stand. Proc. XVI CIGR EurAgEng 2006. Bonn, Germany,1-6.

Chiang C. F., Liang C. C. 2006. A study on biodynamic models of seating human subjects exposed to vertical vibration. International Journal of Industrial Ergonomics. 36: 869-890.

Cutini M., Bisaglia C., Romano E. 2011. Measuring the radial eccentricity of agricultural tires for ride vibration assessment. Proc.39th Int. Symp. on Agr. Eng. Opatija, Croatia. 63-72.

Deboli R., Calvo A., Preti C. 2012. Transmissibility of agricultural tractors seats. Proc.Int. Conf. RagusaShwa. Ragusa, Italy. 368 – 374.

Italian Decree n. 81, Testo Unico in materia di tutela della salute e della sicurezza nei luoghi di lavoro, 9 April 2008

European Directives, 2002. Directive 2002/44/EC, Minimum health and safety requirements regarding the exposure of workers to the risks arising from physical agents (vibration), Official Journal, vols. L177, 06/07/2002, P. 0013-0020

International standards: ISO 5008: 2002. Agricultural wheeled tractors and field machinery — Measurement of whole-body vibration of the operator. International Organization for Standardization Publ., Geneva, Switzerland.

Nguyen V. N., Inaba S. 2011. Effects of tire inflation pressure and tractor velocity on dynamic wheel load and rear axle vibrations. J. of Terramechanics.48: 3–16.

Park S., Popov A.A., Cole D.J. 2004. Influence of soil deformation on off-road heavy vehicle suspension vibration. J. of Terramechanics. 41: 41-68.

Scarlett A. J., Price J. S., Stayner R. M. 2007. Whole body vibration:

Evaluation of emissions and exposure levels arising from agricultural tractors. J. of Terramechanics. 44: 65-73.

Seidel H., Heide R. 1986. Long-term effects of whole-body vibration: a critical survey of the literature. Int. Arch. of Occ. and Env. Health. 58(1): 1-26.

Sherwin L. M., Owende P. M. O., Kanali C. L., Lyons J., Ward S. M. 2004. Influence of tyre inflation pressure on whole-body vibrations transmitted to the operator in a cut-to-length timber. Applied Ergonomics. 35(3): 235-261.

Soderling, S., Sharp, M. Leser, C. 1999. Servo Controller Compensation Methods Selection of the Correct Technique for Test Applications. VII Int. MobilityTechnology Conf. Sao Paulo, Brazil: 30-35.

Taylor R.K., Bashford L.L., Schrock M.D. 2000. Methods for measuring vertical tire stiffness. Transactions of the ASAE. 43(6): 1415-1419.

Vibration transmitted to operator's back by machines with back-pack power unit: a case study on blower and spraying machines

Roberto Deboli,[1] Angela Calvo,[2] Venerando Rapisarda,[3] Christian Preti,[1] Marco Inserillo[1]

[1]Italian National Research Council, Institute for Agricultural and Earthmoving Machines (IMAMOTER), Torino, Italy ; [2]DISAFA, University of Turin, Grugliasco (TO), Italy; [3]Occupational Medicine Department, University of Catania, Catania, Italy

Abstract

To correctly evaluate the vibration transmitted to the operators, it is necessary to consider each body's point interested by the vibratory stimulus produced by machines. All the body's part in contact to the vibration, when a portable device with internal combustion engine is used, are: hands, back and shoulders. Some information for whole-body vibration are available in the ISO 2631-1997 standard, which otherwise refers to a seated operator. 'C' type standards for the vibration analysis exist for some portable machines with an internal combustion engine which is comprehensive in the machine (chainsaw, brush-cutter, blower). If the engine is not inside the machine, but it is on the operator's back, 'C' type standards on vibration measurements are quite incomplete. The IMAMOTER institute of CNR, the DISAFA Department (University of Turin) and the Occupational Medicine Department of the University of Catania started some tests to verify the vibration levels transmitted to an operator working with backed engine devices. Two machines have been examined: a blower and a spraying machine. Two operative conditions have been considered during all the tests: idling and full load. Three operators have been involved and each test has been repeated three times. The spraying machine has been tested both with the empty tank and with 10 litres of water, to simulate the load to be caused by the presence of liquid inside the tank. In this work the comfort condition of ISO 2631-1 standard was considered, using the frequency weighting Wc curve with the weighting factor 0.8 for X axis (back-ventral direction) and the Wd curve for Y and Z axis (shoulder - shoulder and buttocks - head) with weighting factors 0.5 and 0.4 (respectively for Y and Z axis). Data were examined using IBM SPSS Statistics 20 software package. The statistical analysis underlined that the running condition is the main factor to condition the vibration levels transmitted to the operator's back, while the ballast and the operators are influent when the running conditions are distinguished. Concerning medical investigation, lower back and shoulders are the main critical part of the body interested by vibration transmitted to each operator.

Correspondence: Roberto Deboli, Italian National Research Council, Institute for Agricultural and Earthmoving Machines (IMAMOTER), Strada delle Cacce 73, 10135 Torino, Italy.
Tel. +39.011.3977710 - Fax: +39.011.3489218.
E-mail: r.deboli@imamoter.cnr.it

Key words: back vibration, back-pack power machines, blower, spraying machine.

Journal of Agricultural Engineering 2013; XLIV(s1):e146
doi:10.4081/jae.2013.(s1):e146

Introduction

To correctly evaluate the exposure to the vibration transmitted to the workers, it is necessary to consider each body's point interested by the vibratory stimulus produced by machines. When an operator uses a portable machine equipped with an internal combustion engine (grass or leaves trimmer, blower, spraying machines or pole pruner) there are many points of the human body in contact with the vibrating tool: hands (sometimes only one), back (in function of the back pack shape more contact points may exist), shoulders (propped belts are surely contact points for vibration transmission, but also the back pack may be in contact with the shoulders).

A study carried out in 2010 on a sample of 103 green maintenance workers which used blowers (during all the four seasons, both to collect leaves and to sweep avenues and park paths) reported that the 83% of the interviewers manifested troubles using these machines, especially on shoulders and back (53%), less to hands (20%) and arms (15%) (Piana *et al.*, 2010).

Many studies report about whole body and hand-arm vibration (WBV and HAV) diseases for operators using these types of forestry and agricultural machines or others, for example: Haack, 1956; Bovenzi and Betta, 1994; Bovenzi, 1998; Sörenson *et al*., 1997, Lines *et al*., 1995; Luo *et al*., 2000, just to cite some works, but many others exist.

On the other hand it is difficult to find studies concerning vibration transmitted to the operators' back that had evaluated the clinical/biological effects during the occupational exposure. Many epidemiological and experimental studies on hand-arm transmitted vibration have shown an high incidence and prevalence of vascular and neurological disorders (Su *et al*., 2012; Heaver *et al*., 2011), but there are no studies that have measured the hemodynamic and neurologic changes of physiological functioning in workers exposed to back vibration. A work has been done to examine the myoelectric activity of back muscles submitted to random vibration to predict muscle forces (Bluthner *et al.*, 2001), but specific studies related to portable machines are not well known.

This fact can also be due to a lack of standards concerning this factor of risk. At the moment neither the ISO 5349-1:2001 standard gives information how to measure vibration at the operator's shoulders. For back measurements some information may be drawn from the ISO 2631-1:1997 standard, if the comfort condition of a sit person is considered.

If the internal combustion engine is a part of the machine, C stan-

dard type exist to obtain vibration levels, as the EN ISO 22867:2012, which considers chainsaws, brush cutters, blowers and pole pruner. Nevertheless, the models of these machines without an integrated engine, but as back pack power unit, have C standards on vibration measurements quite incomplete.

A short notice can be found in the ISO 11680-2:2011 where the EN ISO 22867 is cited to measure the vibration transmitted to the hands by the handle with the accelerator.

Nothing is written for the vibration transmitted to the shoulders, while for the back vibration measurements, the standard refers to the ISO 2631-1. This is the standard for the whole body vibration measurement, which only mentions the danger of the vibration transmitted to the operator's shoulders by the back pack power machines, but a standard for such types of measures is not actually available.

For these reasons, in a context of shortage of data, the CNR-Imamoter, DISAFA and the Occupational Medicine Departments started some tests to analyze the vibration level transmitted to the back of operators using back pack power machines. Aim of the work was also to highlight differences in vibration data obtained from different operators, different machine equipments and different racing cycles.

Material and methods

Tested machines

Two machines have been tested: a blower and a portable sprayer. Their technical characteristics are written in Tables 1 and 2.

Table 1. Technical characteristics of the blower.

Machine		Blower
Year of production		2006
Width	mm	469
Length	mm	328
Height	mm	483
Blow tube length	mm	1520
Output air speed	m/s	125
Output air volume	m3/min	20
Mass	kg	10.7
Max rpm	rpm	7070
Min rpm	rpm	2500
Power	kW	2.21

Table 2. Technical characteristics of the sprayer.

Machine		Sprayer
Year of production		2006
Width	mm	500
Length	mm	370
Height	mm	740
Mass	kg	11.4
Max rpm	rpm	6080
Min rpm	rpm	2290
Power	kW	3.5

Measurement chain

Test instruments were a vibration device Larson Davis (HVM100 model, specific for the whole body measures) coupled to a triaxial accelerometer (ICP®, Integrate Current Preamplifier, PCB manufacturer, 356B41 model, 10 g mass and with a sensitivity of 100 mV/g), for the contemporary acquisition of vibration along the three axes (x, y and z). The HVM100 output was connected to a computer to record the data. The frequency analysis was therefore made using the LabVIEW Signal Express software. Because the accelerometer could be tiresome for the operator's back, it was put inside a rubber shell, normally used for the whole body measures and true to the ISO 10326-1: 1992 requests (Figure 1 and 2).

To correctly evaluate the vibration transmitted to the back, the ISO 2631-1 concerning the seat back vibration was considered (4.2 paragraph). For these measures, the cited ISO uses weighing curves as well as weighting factors recommended for vibration evaluation with respect to health, comfort, perception and motion sickness: in this work the factors concerning the back vibration transmission have been treated (Table 3).

Only the X axis (back-ventral direction) with the frequency weighting W_c curve and the weighting factor 0.8 must be considered for the health condition evaluation (in this case, no concern for the Y and Z axis). For the comfort judgment, indeed, the W_d curve for Y and Z axis (shoulder - shoulder and buttocks - head) must be used: in this case the weighting factors are 0.8, 0.5 and 0.4 (respectively for X, Y and Z axis).

In this work the comfort condition was considered.

Operative conditions

The two typical working conditions for both the machines were test-

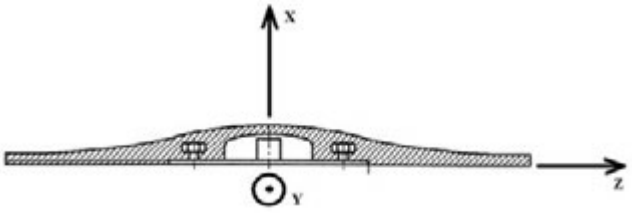

Figure 1. The semi rigid mounting disk with axes orientation

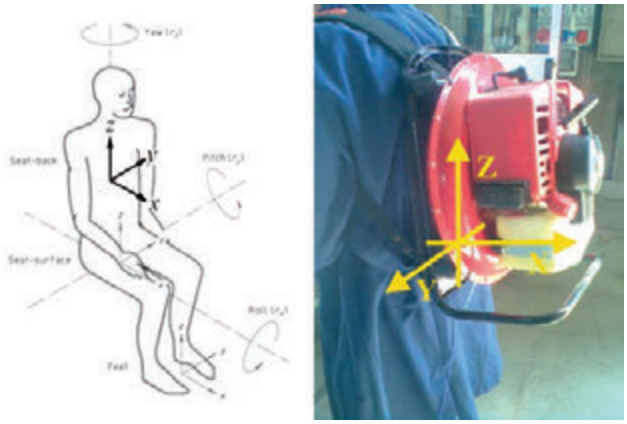

Figure 2. The whole body orientation axes for vibration measurements and application to the portable back pack blower

ed, idle and racing. Three operators used the machines and each test was repeated three times. Each operator adjusted the machine propped belts to correctly balance the weight and to adapt the padded backpack to his back. The blower was tested in the racing condition only with one operator. For the atomizer, more test were conducted: with the empty tank, with 5 or 10 litres of water, to simulate the load when the machine is used in the true operation. The software IBM Statistic SPSS 20 software package was used to perform statistical analysis of differences.

Medical investigations

The sensorineural evaluation was performed by the combination of aesthesiometric tests: two-point discrimination (TPD) ability and depth sense perception (DSP). The tests were carried out at on *quadratus lumborum* muscle in right area at the beginning of the test (basal conditions) and at the end of the test.

The evaluation of the aesthesiometric thresholds, TPD and DSP, are considered reliable screening test to discover a neurological damage in the initial stage (Bovenzi *et al*., 1997), even if the DSP had lower sensitivity (Coughlin *et al.,* 2001).

For the evaluation of TPD and DSP, it was used the Renfrew aesthesiometer (1969) modified by Carlson *et al*. (1979), already used in a previous study (Valentino *et al*., 2001) and here adapted for this specific anatomic area: the combination of aesthesiometric tests was used to evaluate the acute stimuli produced by the vibrations and for clinical-epidemiological evaluations in exposed workers.

In evaluating sensorineural, the survey also included the use of a questionnaire with questions designed to establish the possible occurrence in the back of subjective complaints such as: pain and paresthesias. The responses were graded according to the following scale: none, mild, moderate, persistent.

The hemodynamic analysis was conducted through an indirect assessment of the blood flow with measurement of the superficial skin temperature (SST) (Valentino *et al*., 2001-a). The measurement of the SST is derived from the assumption that this depends on the blood flow of cutaneous vessels.

Thermometric measurements were made on on *quadratus lumborum* muscle in right area, at the beginning of the test (baseline) and at the end of the test, until the return to baseline values.

For the SST measure was used a thermocouple thermometer (E 8105 Cole Parmer Instruments, USA) with a detection accuracy of 0.5 °C.

Results

For each machine, x, y, z and sum squares acceleration values are analysed and then differences among the different operative conditions are discussed. From the medical point of view, SST, TPD and DSP values obtained from each operator in the different operative conditions are reported.

Blower

Sum square values range between 0.451 to 1.082 m/s^2. Racing values are higher than idle ones, except for the operator B (Table 4).

Because of the few number of tests and the non normality of the distribution, the Kruskal-Wallis non parametric test (p=0.05) was used to evaluate vibration values uniformity among the operators along the three axis. Moreover, the analysis concerned a comparison among operators at the idle cycle and another for the operator A (idle and race cycles). In both comparisons, only the vertical Z axis is less affected by the operators or operative conditions.

Comparison among operators: idle cycle analysis

It does not exist uniformity in the acceleration values along the three axis among the three operators at the idling condition but, as it is confirmed by the Duncan test and it is also possible to see in Table 4, the difference is made by operator B: in fact, a consequent analysis without this operator demonstrated that there are not significant differences between the other two operators (A and C) along the X axis. Differences remain along Y and Z axis (with lower acceleration values than X axis, but with higher spread).

Comparison between idle and racing cycles

For this analysis only one operator was involved. Highly statistical differences exist comparing the two different operative conditions: in some cases along the X and Y axis the racing acceleration values double the idle ones (Table 4).

Atomizer

Table 5 shows that acceleration values for the atomizer are lower than the blower, independently from the examined axes and, as the blower, higher values are along the X axis, which is the most influencing the sum square.

Data (Table 6) are normally distributed but the Levene's test found the variables Y and Z heteroscedastic (with different variance): for this reason the Kruskal-Wallis non parametric test (p=0.05) was preferred to the ANOVA. In this first analysis along the X axis acceleration values were different in function of the operator and of the ballast presence (not for the rpm): the subsequent Dunnet test found that there were not differences between the 5 or 10 kg ballast.

Table 3. Frequency-weighting curves and weighting factors (source: ISO 2631-1).

Axis	Health		Comfort	
	Frequency weighting curve	Weighting factor (k)	Frequency weighting curve	Weighting factor (k)
X	W_c	0.8	W_c	0.8
Y	-	-	W_d	0.5

Table 4. Acceleration values obtained on the operators' back (X, Y, Z axis and sum square) when using the blower.

Operator	Engine status	X axis (m/s^2)	Y axis (m/s^2)	Z axis (m/s^2)	Sum square (m/s^2)
A	Racing	0,691	0,596	0,314	0,965
A	Racing	0,620	0,537	0,286	0,868
A	Racing	0,681	0,548	0,308	0,927
A	Idle	0,394	0,248	0,224	0,517
A	Idle	0,383	0,307	0,239	0,546
A	Idle	0,310	0,244	0,219	0,451
B	Idle	0,728	0,601	0,347	1,006
B	Idle	0,682	0,533	0,316	0,922
B	Idle	0,796	0,631	0,372	1,082
C	Idle	0,399	0,381	0,274	0,616
C	Idle	0,345	0,343	0,261	0,552
C	Idle	0,477	0,425	0,293	0,702

Idle average acceleration values are always higher than the corresponding race averages along all the axis and for the sum square (Figure 3), both in the unballast and ballast states.

The high number of tests with different operative conditions along the three axes (operator, rpm, unballast, ballast) condition the registered acceleration values: for this reason, different statistical analysis were performed, to enhance likeness or differences in function of the machine state (rpm), the operator presence and the ballast.

During the idle cycle, the operator is the factor conditioning the acceleration values along the X axis, apart from the ballast (Table 7).

Along the Y axis, values differences exist only when the ballast is present and the factor conditioning is the operator.

Z axis values are always different among the subsets.

Sum square values are always conditioned by the operators, as the X axis values (which are the most influencing the sum square).

During the racing cycle operators do not influence acceleration values along all the three axis (as well as the sum square): there are differences only along the Y axis in the unballast condition, Table 8. The ballast factor, instead, influences the acceleration values along the three axis (and, as a consequence, the sum square).

During the idling cycle, when the ballast is present, the operator always influences the acceleration values along the three axis; in the unballast conditions, instead, the operator presence influences the X axis, more affecting the back. In this case the values along this axis are undoubtedly higher than other values of Y and Z axis (Table 6): for this reason the sum square values are more influenced by the X axis. On the other hand the operator does not influence acceleration values in the racing cycle: in this case is the ballast which lets the results to vary (Table 8).

Medical investigations

The results collected in the medical tests are summarized in Table 9 and 10.

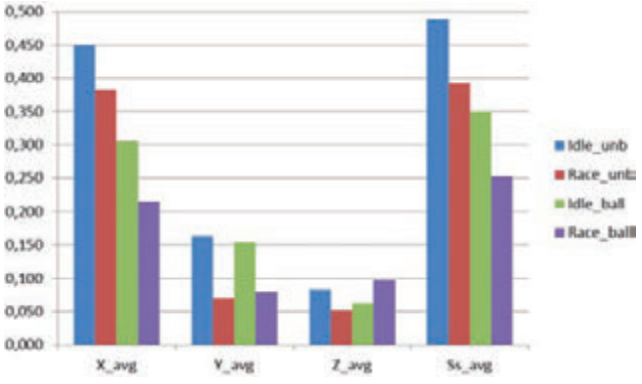

Figure 3. Averages of acceleration values along the X, Y and Z axis and sum square in idle and race states, unballast and ballast conditions.

Table 5. Descriptive statistic of atomizer acceleration values.

	X	Y	Z	Sum_square
Min	0.107	0.041	0.030	0.138
Max	0.547	0.178	0.542	0.572
Average	0.303	0.113	0.088	0.339
Dev.std	0.120	0.044	0.029	0.114

Analysis of results showed that values of SST, TPD and DSP were always altered after the tests compared to baseline values, both with blower and spraying machines. In particular, the SST was significantly reduced during the idle cycle. On the other hand, TPD and DSP values increased, more during the idling cycle than the racing. Data obtained

Table 6. Acceleration values obtained on the operators' back when using the atomizer.

Operator	Cycle	X	Y	Z	Sum square	Note
		RMS*k (m/s²)			(m/s²)	
A	idle	0,632	0,170	0,060	0,657	-
A	idle	0,618	0,165	0,061	0,643	-
A	idle	0,617	0,166	0,062	0,642	-
A	racing	0,457	0,083	0,062	0,468	-
A	racing	0,427	0,084	0,049	0,438	-
A	racing	0,358	0,080	0,047	0,370	-
C	idle	0,309	0,160	0,102	0,362	-
C	idle	0,326	0,171	0,097	0,381	-
C	idle	0,347	0,151	0,080	0,387	-
C	racing	0,363	0,067	0,051	0,373	-
C	racing	0,391	0,071	0,047	0,400	-
C	racing	0,381	0,073	0,045	0,390	-
B	idle	0,383	0,165	0,107	0,431	-
B	idle	0,362	0,166	0,100	0,411	-
B	idle	0,391	0,178	0,092	0,439	-
B	racing	0,374	0,057	0,059	0,382	-
B	racing	0,343	0,057	0,057	0,352	-
B	racing	0,347	0,055	0,052	0,355	-
B	idle	0,247	0,117	0,101	0,292	ballast 5 kg
B	idle	0,298	0,156	0,098	0,350	ballast 5 kg
B	idle	0,306	0,162	0,098	0,359	ballast 5 kg
B	racing	0,143	0,074	0,069	0,175	ballast 5 kg
B	racing	0,107	0,071	0,051	0,138	ballast 5 kg
B	racing	0,121	0,075	0,046	0,149	ballast 5 kg
B	idle	0,348	0,162	0,042	0,386	ballast 10 kg
B	idle	0,299	0,151	0,042	0,338	ballast 10 kg
B	idle	0,322	0,164	0,056	0,366	ballast 10 kg
B	racing	0,314	0,085	0,131	0,351	ballast 10 kg
B	racing	0,343	0,085	0,129	0,376	ballast 10 kg
B	racing	0,333	0,081	0,133	0,367	ballast 10 kg
A	idle	0,376	0,153	0,041	0,408	ballast 10 kg
A	idle	0,392	0,137	0,032	0,416	ballast 10 kg
A	idle	0,382	0,139	0,030	0,408	ballast 10 kg
A	racing	0,236	0,079	0,103	0,269	ballast 10 kg
A	racing	0,267	0,084	0,100	0,297	ballast 10 kg
A	racing	0,281	0,077	0,095	0,306	ballast 10 kg
C	idle	0,237	0,172	0,072	0,301	ballast 10 kg
C	idle	0,217	0,171	0,065	0,283	ballast 10 kg
C	idle	0,239	0,170	0,068	0,301	ballast 10 kg
C	racing	0,158	0,099	0,082	0,204	ballast 10 kg
C	racing	0,145	0,078	0,084	0,184	ballast 10 kg
C	racing	0,138	0,073	0,138	0,209	ballast 10 kg

in the 3 different ballast conditions (empty tank, 5 l and 10 l water) with the spraying machine didn't show significant differences.

Conclusions

Differences are highlighted about vibration values transmitted to the operators' back.

Table 7. Difference analysis obtained with operator and ballast variable conditioning along the three axis and the sum square in the idle cycle (p<0.05. No: there are significantly statistical differences. Yes: the sample may be considered homogeneous).

	Variable	X	Y	Z	Sum square
Variable conditioning: operator	With or without ballast	No	Yes	No	No
	With ballast	No	No	No	No
	Without ballast	No	Yes	No	No
Variable conditioning: ballast	With or without ballast	No	Yes	No	No
	With ballast	Yes	Yes	No	Yes

Table 8. Difference analysis obtained with operator and ballast variable conditioning along the three axis and the sum square in the racing cycle (p<0.05. No: there are significantly statistical differences. Yes: the samples may be considered homogeneous).

	Variable	X	Y	Z	Sum
Conditioning variable: operator	Operator with or without ballast	Yes	Yes	Yes	Yes
	Operator with ballast	Yes	Yes	Yes	Yes
	Operator without ballast	Yes	No	Yes	Yes
Conditioning variable: ballast	With or without ballast	No	No	No	No
	With ballast	No	No	No	No

In both the machines, X axis has always higher values: for the blower around 0.5 and 0.65 m/s^2 respectively in idling and racing cycle, for the atomizer around 0.37 and 0.28 m/s^2.

The blower has higher values along all the three axis than sprayer, both in the idling and racing cycles: moreover acceleration values in the race cycle are double than in the idle.

Concerning the sprayer, the operator influences nearly always the acceleration data, especially along the X axis, at lower rpm values. In the racing cycle, instead, accelerations are operator independent (with or without work experience), but they are influenced by the ballast.

Aesthesiometric thresholds increased after the tests in idle conditions, as well as the skin temperature was significantly reduced. These results could be explained by observing the amplitude of acceleration transmitted from tools to operators, which in fact were greater during the tests at low engine rpm.

Despite the small size of the sample studied, which does not allow generalized conclusions, we believe that the use of instruments backed induces changes in the sensitivity of the skin surface and of cutaneous temperature. Therefore, it is necessary to deepen study the biological effects produced by the use of these tools, increasing the sample and using screening instruments that can give information also on the musculoskeletal structures of the back of occupationally exposed workers.

References

Bluthner R., Seidel H., Hinz B. 2001. Examination of the myoelectric activity of back muscles during random vibration. Methodical approach and first results. Clinical Biomechanics. 16(1): S25-S30.

Bovenzi M., Betta A. 1994. Low-back disorders in agricultural tractor drivers exposed to whole-body vibration and postural stress. Appl. Ergon. 25(4): 231–241.

Bovenzi M., Apostoli P., Alessandro G., Vanoni O. 1997. Changes over a workshift in aesthesiometric and vibrotactile perception thresholds of workers exposed to intermittent hand transmitted vibration from impact wrenches. Occup. Environ. Med. 54: 577-587.

Table 9. Mean and standard deviation of SST, TPD and DSP values obtained from each operator when using the blower.

	Baseline	Idling cycle	Baseline	Racing cycle
SST (°C)	31.2 ±0.8	26.1 ±0.7	31.5 ±0.8	28.6 ±0.9
TPD mm	7,9 ±0,7	17,9 ±2,7	7,8 ±0,9	15,7 ±2,9
DSP mm	14,7 ±2,5	24,1 ±4,2	14,3 ±3,3	19,8 ±3,6

Table 10. Mean and standard deviation of SST, TPD and DSP values obtained from each operator using the spraying machine in 3 different ballast condition (empty tank, 5kg and 10 kg).

	Baseline	Idling cycle	Baseline	Racing cycle
SST (°C) -empty tank	31.4 ±0.8	26.5 ±0.6	31.7 ±0.7	28.5 ±0.9
TPD mm -empty tank	7,5 ±0,4	17,7 ±2,3	12,3 ± 2,3	15,3 ± 2,3
DSP mm -empty tank	14,5 ±2,1	24,3 ±4,7	14,4 ±3,7	20,1 ±3,3
SST (°C) 5 kg	32.7 ±0.9	26.9 ±1.1	32.9 ±0.9	30.6 ±1.1
TPD mm 5 kg	7,7 ±0,7	17,6 ±2,1	7,8 ±1,0	14,9 ±2,6
DSP mm 5 kg	15,1 ±2,9	25,4 ±4,9	14,6 ±3,1	21,0 ±3,5
SST (°C) 10 kg	32.3 ±0.5	28.7 ±0.5	32.8 ±0.8	31.3 ±0.6
TPD mm 10 kg	7,7 ±0,7	18,3 ±2,1	7,8 ±1,0	13,4 ±3,2
DSP mm 10 kg	14,7 ±2,4	26,2 ±4,5	15,1 ±3,8	22,4 ±4,1

Bovenzi M. 1998. Exposure-response relationship in the hand-arm vibration syndrome: an overview of current epidemiology research. Int. Arch. Occup. Environ. Health. 71: 509-519.

Carlson W.S., Samueloff S., Taylor W., Wasserman D.E. 1979. Instrumentation for measurement of sensory loss in fingertps. J Occup Med. 21: 260-264.

Coughlin P.A., Bonser R., Turton E.P., Kent P.J., Kester R.C. 2001. A comparison between two methods of aesthesiometric assessment in patients with hand-arm vibration syndrome. Occup. Med. 51: 272-277.

European Commission Enterprise And Industry. 2010. Guide to application of the Machinery Directive 2006/42/EC. Ian Fraser Editor.

International standards: ISO, 2001. Mechanical vibration - Measurement and evaluation of human exposure to hand-transmitted vibration. ISO 5349-1. International Organization for Standardization Publ., Geneva, Switzerland.

International standards: ISO 1997. Mechanical vibration and shock - Evaluation of human exposure to whole-body vibration. ISO 2631-1. International Organization for Standardization Publ., Geneva, Switzerland.

European standards: EN 1996. Mechanical vibration - Declaration and verification of vibration emission values. EN 12096. Brusseles, Belgium.

European standards: EN 2012. Forestry and gardening machinery - Vibration test code for portable hand held machines with internal combustion engine - Vibration at the handles. EN ISO 22867. Brusseles, Belgium.

International standards: ISO 2011. Machinery for forestry - Safety requirements and testing for pole-mounted powered pruners – ISO 11680-2. International Organization for Standardization Publ., Geneva, Switzerland.

International standards: ISO 1992. Mechanical vibration - Laboratory method for evaluating vehicle seat vibration. ISO 10326-1. International Organization for Standardization Publ., Geneva, Switzerland.

Haack M. 1956. Human tolerance to vibrations in farm machines. Agr. Eng. 37(4): 253-257.

Heaver C., Goonetilleke K.S., Ferguson H., Shiralkar S. 2011. Hand-arm vibration syndrome: a common occupational hazard in industrialized countries. J. Hand Surg. Eur. 36(5): 354-63.

Lines J.A., Stiles M., Whyte R.T. 1995. Whole Body Vibration During Tractor Driving. Journal of Low Frequency Noise and Vibration. 14(2): 87-104.

Luo J., Sakakibara H., Zhu SK. 2000. Effects of vibration magnitude and repetitive exposure on finger blood flow in healthy subjects. Int. Arch. Occup. Environ. Health. 73: 281-284.

Renfrew S. 1969. Fingertip sensation: a routine neurological test. Lancet. 1(7591): 396-7.

Sörensson A., Burström L. 1997. Transmission of vibration energy to different parts of the human hand-arm system. Int. Arch. Occup. Environ. Health. 70: 199-204.

Su A.T., Darus A., Bulgiba A., Maeda S., Miyashita K. 2012. The clinical features of hand-arm vibration syndrome in a warm environment-a review of the literature. J Occup Health. 54(5): 349-60.

Piana E.A., Marchesini A., Deboli R., Preti C. 2010. Rischio da esposizione a vibrazioni per l'uso di soffiatori a zaino: valutazione dell'esposizione a vibrazioni trasmesse al corpo intero e alla spalla. Atti del 37° Convegno Nazionale AIA. Siracusa, Italia.

Valentino M., Rapisarda V., Solina G., Cenerelli F. 2001. Esposizione a vibrazioni del sistema mano braccio: indagine di screening sulle modificazioni neurologiche. Atti del 64° Congresso Nazionale della Società Italiana di Medicina del Lavoro e Igiene Industriale, Roma, Italia. G. Ital. Med. Lav. 23: 266.

Valentino M., Rapisarda V., Paone N., Di Giulio G., Rossi G.L. 2001-a. Esposizione a vibrazioni del sistema mano-braccio. Atti del Congresso Nazionale della Società Italiana degli Igienisti Industriali, Napoli, Italia. 357-360.

Ergonomic analysis for the assessment of the risk of work-related musculoskeletal disorder in forestry operations

Raimondo Gallo, Fabrizio Mazzetto

Free University of Bozen-Bolzano, Faculty of Science and Technology, Bolzano (BZ) Italy

Abstract

The risk to run into a Work-Related Musculoskeletal Disorder (WMSD) is very high when operating in the primary sector. As a matter of fact the professional illnesses related to the WMSD in Italy are increasing. Nowadays the assessment of the WMSD in the primary sector is performed mainly in the agricultural sector, considering different agronomical activities; for the forestry sector, only few documents reported an ergonomic evaluation. The lack of available information on this topic in the forestry sector, as well as the similarity with the agricultural sector, drives the interest to the assessment of the conditions that expose workers to WMSD risks in forestry operations.

Four different assessment approaches were applied in this study. These tools permitted to classify which are the exposures and if there is the presence of WMSD risk for forest operators. The approaches are respectively the OCRA checklist and the RNLE equation, both recognized as ISO standards, as well as OWAS and REBA, recommended by ISO standards. The first approach focusses on the risk due to repetitive and stressed movements, while the second evaluates the risk of injures due to the manual movement of loads. Meanwhile OWAS and REBA detect the possibility of injures due to wrong postures during the work. These approaches were applied for the cutting operations with chainsaw. Since the evaluation requires high levels of attention and also because it was necessary to gain a good level of safety for the surveyor, a digital camera was used to film the operative activities. Then, the movies were analysed in office. Aim of the research is to analyse if it is possible to apply the approaches suggested by ISO standards in order to assess the most dangerous activities that, when not properly carried out, could be the cause of WMSD in forestry operations. The study showed that during the use of the chainsaw the index of risk of professional injures was overpassed several times, compromising the operator's safety.

Correspondence: Raimondo Gallo, Free University of Bozen-Bolzano, Faculty of Science and Technology, Piazza Universitá 5, 39100 Bolzano (BZ) Italy.
Email: raimondo.gallo@natec.unibz.it

Key words: physical ergonomics; biomechanical overload; exposure factors; postures assessment; risk of injures.

Journal of Agricultural Engineering 2013; XLIV(s1):e147
doi:10.4081/jae.2013.(s1):e147

Introduction

All typologies of manual work, even if with different levels, present the possibility to cause professional illnesses, constituting a risk for the operator's safety. In the specific literature these illnesses are called work-related musculoskeletal disorders – WMSD. The name WMSD refers to all disorders of joints as well as muscles due to traumas, micro-traumas repeated in the time and overload of muscles and joints (articulation) (Occhipinti, Colombini, 1996; Zanuttini, 2005). The national Institute for Occupational Safety and Health (Niosh, 1981) correlates the causes of WMSD to the heavy physical work, to the application of forces for lifting and moving loads, to the unbalanced lifting, to the bending and twisting of the articulation, to the velocity of movements and to the uncorrected postures. The assumption of a wrong posture causes the wrong coordination of the rachides' muscles, up to a failure. Other complementary factors that increment the risk of WMSD injuries are the use of equipment that transmits vibrations (Whole Body Vibration WBV and Hand Arm Vibration HAV) and the low temperature in the working place (Colombini *et al.* 2010, Calvo, 2009, Zanuttini, 2005). For this reason committees that treat health topics – international as well as national - edited standards, laws and guide lines about the procedure of monitoring and assessment of risk of injures due to manual handling of loads and postures. These methods evaluate the risk of WMSD for upper limbs (Colombini *et al.*, 2011; Colombini, Occhipinti, 2011; Colombini *et al.*, 2007) for rachides (Colombini *et al.*, 2010) and postures (Calvo, 2009; Zanuttini *et al.*, 2005; Hignett 2000).

Considering all factors of work-related injuries it is possible to assume that the primary productive sector is interested by having activities which could cause the arising of professional illness. Indeed, in a national report published in the 2012 by the INAIL – National Institute for the assessment of injures on work – is reported that WMSD in the primary sector increased about 620% since 2007. About 39% of those injures interest the intervertebral discs and about 26% the tendons. This is the reason for the importance to identify which are the levels of risk that determine WMSD in the operations of the primary productive sector.

Nowadays, consulting the specific literature, several documents treat the assessment of work-related musculoskeletal disorders in agriculture (Camilleri *et al.*, 2012; Colantoni *et al.*, 2012; Murgia *et al.*, 2012; Schillaci *et al.*, 2011; Cecchini *et al.*, 2010; Pressiani et al,. 2010; Colombini *et al.*, 2007), while only few of them refer to the forest sector (Calvo, 2009; Zanuttini 2005; Ashby, 2001). Aim of this work is to evaluate if the assessment methodologies already applied in the agricultural and in the industrial sector could be employed also in forestry. At this regard the assessment recommended by ISO 11228, EN 1005 – OCRA index, NIOSH index – and those recommended by standards – OWAS index, REBA index –, were applied for the WMSD assessment.

Materials and methods

As consequence of the importance of the operating time relief, the present study is done in parallel to ones that analyse the application of IT equipment for time monitoring during logging operations.

The study-case was set in a forest of spruce, where cultural operations of thinning were planned. The operations were organized in the municipality of Rodenek, in the Autonomous Province of Bozen (N-E of Italy) in a forest managed by the State-Owned Forest Company. Besides the silvicultural management task, the provincial company must execute all silvicultural exploitations. The harvesting operations consisted of thinning operations.

The filming was performed with a Nikon® S8000, a 14 megapixel digital camera that permitted to record the movies in high definition. For keeping the camera in the right position a tripod was used.

The forestry operations had interested a part of forest with 3rd and 4th class of slope, this means that it presents a slope from around 40% to 80%. (Hippoliti and Piegai, 2000). This morphological characteristic, associated to superficial humidity in the first hours of the day, characterized the working site to be very slippery and unstable.

The working operation of cutting and falling down, limbing (both branches and tops), cross-cutting, yarding, logging and transportation are reported in the specific literature (Hippoliti, Piegai, 2000, Cividini, 1991) as well as the sequence of forestry work. The present paper would focus its analysis on the ergonomic aspect of the cutting operations. Authors consider these operations as the most critical for the operator's safety due to the high number of movements with a load in hand – the chain saw –.The operation of cutting consists in the division of the aboveground biomass from the roots; causing a modification of the centre of gravity it is possible to change the tree's attitude from vertical to horizontal. Usually this operation is done through the use of a chain saw with cuts done with successive movements. At each movement, similar to the lever movement, every cutting tooth of the chains saw penetrates into the wood until the complete separation. Since this operation is done on the ground level, mainly on mountain steep sides, the operator is forced to assume, with a load in hand, wrong postures and also to do repetitive movements, those could be characterized by long periods of exposure (Figure 1).

Detection approaches

Checklist OCRA and RNLE by NIOSH as well as the OWAS and REBA methods were applied respectively in order to assess the index of exposure at WMSD and to identify the presence or not of risks of injuries.

The Checklist OCRA – Occupational Repetitive Actions – is a simplification of the OCRA index method. Through a rapid evaluation, the method permits to assess the presence of risks, their mapping and their first managing (Colombini *et al.*, 2011). Aim of this evaluation is to assess the risk of biomechanical overload of operators' upper limbs. The use of the checklist OCRA requires the recognition of the technical actions, considered as the elementary actions done by the operator in order to perform a task, also the evaluation of multiple risk factors like recovery period (RP), movements frequency (Fr), use of physical forces (F) and wrong posture evaluation as well as stereotypy (Ps). Besides these, also the evaluation of the net repetitive working time (NRWT) as well as the complementary factors (CF) (vibrations, low temperatures, equipment's kickbacks, etc.) was done (Colantoni *et al.*, 2012; Colombini *et al.*, 2011; Colombini, Occhipinti, 2011; Colombini *et al.*, 2007). In this case the equation that describes the Checklist OCRA index is:

Checklist OCRA = Fr x F x Ps x CF x mRP x mNRWT

(Colombini, Occhipinti, 2011)

In the equation, the RP and NRWT are reported as multiplicative factor.

Following the ISO 12295, the application of these methodologies must respect one of two criteria:

- The assessed operation must be composed by work cycles;
- The work must be characterized by the same repetitive technical actions for more than 50% of the working task.

The NIOSH (National Institution for Occupational Safety and Health) staff developed the RNLE – Revisited NIOSH Lifting Equation –. This equation permits the calculation of the risk of WMSD at rachides level. Thanks to this evaluation it is possible to obtain the lifting index (LI). The lifting index is "a term that provides a relative estimate of level of physical stress associated with a particular manual lifting task" (Waters *et al.*, 2007). In order to obtain the LI, a load constant (LC) – obtained according to gender and age of operator (Colombini *et al.*, 2010) – multiplied by factors of stress was calculated. The considered factors of stress are: the horizontal distance from load to operator (HM), the vertical height of the lift (VM), the vertical displacement during the lift (DM), the angle of asymmetry of the trunk (AM), the frequency and duration of lifting (FM), the quality of hand-object coupling (CM). With these data it is possible to calculate the recommended weight limit (WLR), as reported in the follow equation:

WRL = LC x HM x VM x DM x AM x FM x CM

(Waters, *et al.*, 1994)

The lifting index is based on the relationship between the weight of the load (L) listed during the task and the WRL, as reported in the equation below:

Figure 1. Example of possible wrong posture assumed by the operator during cutting operations.

$$LI = L/WRL$$

(Waters, *et al.*, 1994)

It is very important to underline that this method is usable if the load is more than 3 kg, or when the handling of the object happens more than once every 5 minutes (Colombini *et al.*, 2010) and for those repetitive operations that are cadenced by an industrial machine process (Zanuttini, 2005).

In order to analyse if the posture assumed by an operator is correct or could be in risk of WMSD, it is possible to employ two detecting tools: OWAS and REBA. The OWAS – Ovako Working-posture Analysis System – observes which are the positions of back, arms, legs and also the weight of the load lifted (Li, Buckle, 1999; Zanuttini, 2005). A codification for each of the above mentioned positions was done thanks to a comparison with references reported in literature (Lundqvist, Gustafsson, 1987). So each posture is described by a code – the OWAS code – with four scores, each of them evaluates the "weight" that each posture has on the global posture. Besides using the global postural codes in a multi-entry table it is possible to calculate the class of risk (1, 2, 3, 4) for each posture (Louhevaara, Suurnäkki, 1992). Considering the number of observation for each class of risk during the relief period it is possible to calculate the frequency of observation (a, b, c, d) of a posture for each task. The index of risk is calculated from the sum of the products between frequencies and respective class of risk, as reported in the following equation:

$$I = [(a \times 1) + (b \times 2) + (c \times 3) + (d \times 4)] \times 100$$

(Louhevaara, Suurnäkki, 1992)

Also REBA – Rapid Entire Body Assessment – is based on the association of scores, in relation to the posture assumed by the operators. REBA method assigns a code for each posture analysing the range between the angles of effective postures, taken during the working operation, and those of neutral positions. The analysed body parts are: the trunk, the neck, the legs (Group A), the upper arms, the lower arms and the wrists (Group B). The last groups are scored separately for different sides. Beside this, the method assigns a score – positive or negative – in relation to the frequency of the movements, to the presence of loads or to the application of forces and to the hand-object coupling (Hignett, McAtamney, 2000; McAtamney, Hignett, 2005). Using multi-entry tables, firstly specific for the two groups relieved then for a global evaluation, it is possible to calculate the total REBA score. The methodology is not based on a real equation but on a scoring sheet.

Anyhow, Authors suggest to refer to the specific literature for a more detailed description of the methodologies mentioned above (Colombini *et al.*, 2011; Colombini, Occhipinti, 2011; Colombini *et al.*, 2010; Colombini *et al.*, 2007; Li, Buckle, 1999; Zanuttini, 2005; Hignett, McAtamney, 2000; McAtamney, Hignett, 2005).

Procedure followed

The application of the cited assessment methodologies requires the direct analysis of the working operations in two different ways. Checklist OCRA and RNLE require an analysis of a period of work considered as sample. During this survey a dynamic assessment is made. So, the sample is representative of the whole working period. While OWAS and REBA, require the analysis of the singular posture assumed by the operator during his task. In this case the survey is made considering a static postural sample.

In order to obtain this observation, since the evaluation requires high levels of attention and also because it was necessary to gain a good level of safety for the surveyor, a digital camera was used to film the operative activities. Then, the movies were analysed in office in order to obtain the analysis for the different methodologies. At this regard KINOVEA, a free software for the video analyst, was used for all assessments. Indeed this software results useful both for the dynamic and for the static surveys, because it permits to make a photo sequence at fixed intervals: in our case every 5 seconds. Thanks to the KINOVEA software it was possible to measure also all joint angles for REBA assessment.

Finally, specific softwares developed by the epmresearch group of Milan (http://www.epmresearch.org) to calculate OCRA and NIOSH index and score sheets necessary to OWAS and REBA evaluation (Hignett, McAtamney, 2000, Louhevaara, Suurnäkki, 1992), were used in order to assess the level of risk or to identify it.

Results and discussions

The ergonomic assessment was done in parallel with a study of time monitoring for the application of systems for the automatic monitoring relief. Since the Authors wanted to evaluate the feasibility of the application of several methodologies for the ergonomic assessment, a sample period of half an hour of movie was taken. In this sample several operations of cutting were recorded. In office this movie was divided in movies, as many as the number of cutting operations. The Authors, in this context, consider that the cutting phase starts when the operator picks up the chain saw in order to use it and finishes when the cut is done and the operator turns it off.

Although the different methodologies require the analysis of different aspects, it was possible to use only one movie since it satisfied all ergonomic methodologies requirements. In the other movies, even if the positioning of the camera was done with care – considering felling direction, operator position – the trunk as well as the operator's body position did not permit a good and easy observation of the upper limbs movements and also the operator's postures. So the representative movie sample amounts to 87 second of recording on which OCRA and NIOSH index were analysed and 18 frames (5 second for each one) on which OWAS and REBA assessment were done.

As far as the assessment of the two indexes is concerned, a critical situation was found in both.

The application of the OCRA checklist approach is possible because the operations are characterized by repeated movements for more than half of the time of observation (Colombini *et al.*, 2010). Considering the OCRA index, from the analysis of the video, it was possible to recognize 44 and 19 technical actions respectively for the right and left upper limb (Table 1).

In this case the operator performed operative actions with a frequency of 30.3 actions/minute whit the right hand and 13.1 actions/minute with left hand. In Table 2 the summary of the assessment done through OCRA checklist approach is reported. According to Table 2, the operation of cutting presented two different values of OCRA checklist index.

Besides the numerical index, the classification by colours permits to easily identify the presence of criticism. Therefore the result of the assessment underlines the presence of a medium and high risk of WMSD for right and left limb respectively (values between 14.1 – 22.5, red colour; values ≥ 26.6, purple colour). This difference of the risk of injures is mainly due to the wrong postures that the woodman assumed during the cutting operations. Among all scores, the biggest role on the assessment is played by the long period in which the operator keeps the left arm rotated, in order to maintain a good grip on the handle of the chain saw, which affects the elbow. The use of this approach, indirectly, permits also the identification of the actions that are necessary to do in order to reduce, or eliminate, the reasons that could cause WMSD. Indeed, for example, only splitting the period of recovery (about 45 minutes) in four pauses, instead two, the value of the checklist OCRA decrease to 16.51 and 20.63 (red colour) respectively for right and left limbs.

The cutting operation is not characterized by having actions that are standardized like the industrial cycles. During the cutting operation no movement of loads is required, because the chain saw discharges its weight through the bar in the wood, and also because the penetration of the cutting tooth requires a very low force. However during the relief it was possible to identify an action where the operator moved loads whit repetitive movements: when he picked up the chain saw from the ground and moved it until the trunk and vice versa. Since the chain saw had a weight higher than 3 kg (chain saw Husqvarna 576 XP®, 6.8 kg), since it was moved more than once every 5 minutes and since the operator worked on a floor with poor characteristics of stability, Authors have considered the RNLE approach applicable for the risk assessment due to load movements. For this assessment it was estimated, cautiously due to the short sample period, that the chain saw was moved for 150 times per day of work. In fact the operator did not pick the equipment up from the ground before starting every cutting operation because he had it already in hand. On the other hand, several times the operator interrupted the cutting, put the chain saw on the ground, completed the felling operations through the use of a wedge, than picked the chain saw up again before leaving the place. Often the operator has done this movement while kneeling on the ground. So the geometry and respective factors of multiplication changed. Also this approach, as the checklist OCRA, gives as result a numerical value together with a colour classification. The assessment takes into account the operator's age and gender. Since in the present study-case the operator was a male older than 45 year, the assessed composite lifting index (CLI) is equal to 1.32. This value means a high intrinsic presence of work-correlated risk of injures. Considering the factors that had influenced the LI during the cutting operation, without any doubt, the most important was the horizontal distance. As a matter of fact, during the cutting, he often kept the equipment at a distance higher than 51 cm in order to ensure a good safety and at the same time to have a good visibility.

The results obtained from the OWAS and REBA assessment are reported in Table 3. In this Table all scores assigned with the two methods for each singular video frame are summarized. The two methodologies assessed different aspects of the posture that the operator assumed during the cutting operation. It is important to underline that the score scales are different for the two methods. In fact the OWAS scale classifies the risk of injures with values from 0 to 400 with intervals every 100 points, meanwhile the REBA with values from 1 to 15, divided in 5 different intervals. Considering these difference several video frames have substantial difference in the evaluation. For example the scores that the two methodologies assign to frame 5 and 6 are different. For the OWAS the posture in the frame number 5 and 6 is classified as a posture with negligible risk. Meanwhile, for the same posture, REBA assigns a score of high and very high risk of injures. Another difference between the two approaches is that REBA evaluates the posture of both sides of upper limbs. This factor is important to evaluate because the limbs do not always perform the same actions. Difference in the performed actions may cause different risks of

Table 1. Technical actions recognized during the video assessment.

Technical action	Right hand count	Left hand count
to take	5	-
to action	22	-
to place	3	3
to pull/push	9	12
to keep	1	2
to extract	2	2
to throw	2	-
TOT	44	19

Table 2. Scores attributed for each parameter evaluated.

Parameters of assessment	Limb Right	left
mRP	1.265	1.265
mNRWT	3.5	3.5
Fr	2.5	2.5
F	4	4
Ps	5.5	9.5
Ps (shoulder)	1	2
Ps (elbow)	1	8
Ps (wrist)	2	2
Ps (hand)	4	3
Ps (stereotypy)	1.5	1.5
CF	4	4
checklist OCRA	19.23	24.04

Table 3. Frames every 5 seconds of the video sample with respective OWAS and REBA scoring.

Operations	OWAS	REBA R	REBA L	Operations	OWAS	REBA R	REBA L
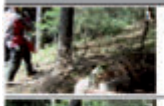	Evaluation felling direction	1	8	6		Back cut	4	11	11
	Cleaning	4	9	11		Back cut	4	12	12
	Control	4		8		Evaluation felling direction	4		9
	Undercut preparation	4	9	10		Back cut	4	10	10
	Evaluation felling direction	1	9	9		Felling	2		6
	Undercut preparation	1	10	11		Felling	2		6
	Undercut preparation	1	11	11		Docking	2	8	8
	Undercut preparation	4		11		Docking	2	8	8
	Moving	4	10	10		Control	2		6

injures.

Results for the OWAS assessment show that the operation of cutting involves a risk of injures equal to 278. This means that the operator performs a task with a medium risk of injuries.

Results of the REBA assessment show that in several evaluations a difference between the two upper limbs is present. The presence of more than one score for the REBA assessment (Table 3), even if equal, means a difference in the evaluation between the upper limbs postures.

Then, for each side, the percentage of presence was calculated. Since the approach does not foresee the calculation of a global index of risk the same procedure developed for the OWAS assessment was applied. So the global index of risk for cutting task equals to 406 and 411 for right and left upper limbs, recognising that the left upper limb could be more likely affected by risk of injures. Anyhow the result, compared to the REBA classification, highlights that the assessed operation presents a very high level of risk of injures and that it requires immediate action to reduce it.

It is important to underline that the specific literature regarding the methodology for the assessment of WMSD in forestry sector is very poor. In fact only two documents have been usable for a comparison, both only for the OWAS approach (Calvo, 2009; Zanuttini, 2005). From what reported in literature the index of risk results equal to 287 and 156 (Calvo 2009, Zanuttini 2005). Meanwhile the value obtained from this study is 278; in line with those reported in literature for the same operation and in analogues environment of work. So it is possible to draw the conclusion that the cutting phases presents a risk of WMSD ranged between slight and medium risk. The results are affected by the terrain morphology, which influence the working posture, and by the working habitudes.

Conclusions

The present work is an overview on the application of these different approaches for the assessment of the risk of injures in the primary forestry sector. The approaches applied were:

- OCRA checklist index, for the assessment of the level of risk of injures at upper limbs due to at repetitive movements;
- RNLE index, for the assessment of the level of risk of injures at rachides due to lifting movements;
- OWAS and REBA methods, for the assessment of the presence of risk of injures due to an incorrect posture assumed during the work.

Considering the four approaches applied, results showed that the cutting operation involves a substantial risk of injures, even if with different levels. All approaches presented a good feasibility in their application, thanks to the presence of specific software and also to the easy evaluations required. Considering the four different approaches, only the one related to RNLE is affected by uncertainties on its application due to the short period of sample. This happens because it is not clear if the movements of the chain saw respect the frequency of 1 every 5 minutes. Besides this it is necessary to validate the equation employed to assess the global index of risk for the REBA approach. Indeed the absence of a method to calculate the index for the entire task is a point of weakness of REBA approach. The comparison between the OWAS and REBA approaches showed that REBA has a higher detail level of assessment. Indeed this assessment is based on the measurement of the angles between the body structures. Beside this, it also analyses the body extremities as the wrist, the neck, the elbow and the shoulders for both sides; parameters that are not considered by OWAS approach. Besides these the REBA approach assesses also the type of handle coupling and the characteristics of the performed activities. Obviously due to these additional requirements the REBA approach takes more time for the assessment than the OWAS approach. The applications of these approaches have presented also the capability to obtain information on the posture, or on the action, that presents an intrinsic high risk of WMSD. So it is suitable for suggesting the intervention to be performed in order to decrease or delete the source of risk.

However, these approaches were not developed specifically for forestry operations, indeed several times they presented weakness points during the assessment. For example REBA approach does not assign any score when the operator has a kneeling posture. On the other hand, OWAS approach does not consider the posture of the body extremities. Therefore, in order to obtain a more accurate assessment, a review of the assessment parameters as well as the scores, mainly for posture assessment approaches, could be performed.

The position of the camera with respect to the operator, as well as its distance, is a fundamental factor to pay attention to during the filming. As a matter of fact, several videos were not usable because the recording angles, or the high distance from the operator, did not permit a good visibility of the assessment items. In the future, for the assessment of posture and RNLE, the camera will be placed in the front side – the same as the felling direction – and moved on lateral side out of the risk area. Meanwhile for the evaluation of OCRA checklist index the possibility to install a wide angle camera on the operator – on the helmet, or on a specific support clipped on the vest – directed to the hands will be evaluated. As consequence of the good results and in order to perform a global operative monitoring of the entire mechanised forest chain, this experience will be tested also for other forestry operations with the applications of sensors able to assess other ergonomic parameters like noise, vibration, etc.

In conclusion the use of OCRA checklist index, RNLE index, REBA index and OWAS index have presented a good applicability for the assessment of WMSD in the forestry sector, mainly to assess the cutting operations. Anyhow the research will assess also the other forest activities in order to evaluate if these approaches may be used for the analysis of all logging operations. The possibility to apply these assessment methods on the primary forestry sector, together with other ergonomic assessment methods, will permit the evaluation of the forestry firms in other to obtain quality certifications.

References

Ashby L., Bentley T., Parker R. 2001. Musculoskeletal disorder in silviculture and logging 1995-1999. Center Of Human Factors and Ergonomics (COHFE) Report. Volume 2(3).

Calvo A. 2009. Musculoskeletal Disorder (MSD) risk in forestry. A case Study to suggest an ergonomic analysis. Agricultural Engineering International: the CIGR Ejournal. Manuscript MES 1149, Vol. XI April.

Camilleri D., Caruso L., Schillaci G. 2012. Literature review: application of the OCRA method in agriculture and agro food activities. In: International Conference RAGUSA SHWA 2012 September 3-5. 2012 Ragusa – Italy "Safety Health and Welfare in Agro-food Agricultural and Forest Systems".

Cecchini, M., Massantini, R., Monarca, D. 2010. The ergonomics analysis tools for the assessment of the risk of musculoskeletal disorders due to the repetitive movements of the upper limbs of the workers employed in agriculture. In: "International Conference on Agricultural Engineering-AgEng 2010: towards environmental technologies, Clermont-Ferrand, France, 6-8 September 2010".

Cividini R. 1991. Elementi di tecnologia forestale. Materiale legno,

prodotti boschivi, mezzi e tecniche della raccolta, lavorazione dei prodotti boschivi. EdAgricole, Bologna. ISBN 88-206-2157-6.

Colantoni A., Marucci A., Monarca D., Pagniello B., Cecchini M., Bedini R. 2012. The risk of musculoskeletal disorders due to repetitive movements of upper limbs for workers employed to vegetable grafting. Journal of Food, Agriculture & Environment. Vol. 10 (3&4), July-October 2012.

Colombini D., Occhipinti E. 2011. La valutazione del rischio da sovraccarico biomeccanico degli arti superiori con strumenti semplificati: la minicheklist OCRA. Contenuti, campo applicativo e validazione. Med Lav 2011; 102, 1 000-000.

Colombini D., Occhipinti E., Cerbai M., Battevi N., Placci M. 2011. Aggiornamento di procedure e di criteri di applicazione della Checklist OCRA. Med Lav 2011; 102, 1 000-000.

Colombini D., Occhipinti E., Battevi N., Cerbai M., Fanti M., Menoni O., Placci M., 2010 – Movimentazione manuale dei carici. Manuale operativo dep l'applicazione del decreto legislativo 81/08. Dossier Ambiente n° 89. Ed., Associazione Ambiente e Lavoro. ISSN 1825-5396

Colombini D., Occhipinti E., Hernandez A., Alvarez, E. Montomoli L., Cerbai M., Fanti M., Ardissone S., Ruschioni A., Giambartolomei M., Sartorelli P. 2007. Repetitive movements of upper limbs in agriculture: set up of annual exposure level assessment models starting from OCRA checklist via simple and practical tools. In: International Conference on Agriculture Ergonomics in Developing Countries, AEDeC 2007.

Hignett, S., McAtamney, L. 2000. Rapid entire body assessment (REBA). Appl. Ergon. 31 (2). pp 201-05.

Hippoliti G., Piegai F. 2000. La raccolta del legno; tecniche e sistemi di lavoro. Compagnia delle Foreste-Arezzo. pp 157

Li G., Buckle P. 1999. Current techniques for assessing physical exposure to work-related musculoskeletal risks, with emphasis on posture-based methods, Ergonomics, 42:5. pp 674-95.

Louhevaara V, Suurnäkki T. 1992. OWAS: a method for the evaluation of postural load during work. Institute of Occupational Health Centre for Occupational Safety, Helsinky. pp 23.

Lundqvist P., Gustafsson B. 1987. Working postures in Dairy barns. IXth Joint International Ergonomics Symposium "Working postures in Agricolture and Forestry". Kuopio, Finland.

McAtamney L., Hignett S. 2005. Rapid Entire Body Assessment. In: Stanton N., Hedge A., Brookhuis K., Salas E., Hendrick H., "Handbook of Human Factors and Ergonomics Methods". CRC Press LLC. ISBN 0-415-28700-6.

Murgia l., Rosecrance J.C., Gallu T., Paulsen R. 2012. Risk evaluation of upper extremity musculoskeletal disorders among cheese processing workers: A comparison of exposure assessment techniques. In: International Conference RAGUSA SHWA 2012 September 3-5. 2012 Ragusa – Italy "Safety Health and Welfare in Agro-food Agricultural and Forest Systems".

Niosh, 1981. Work practices guide for manual lifting. Niosh Technical Report. Publication n° 81 – 122. US Department of Health and Human Service 1981.

Pressiani, S., & Colombini, D. 2010. Risk Assessment in plant nursery characterized by several working task with annual turnover. In International Conference Ragusa SHWA2010 "Work Safety and Risk Prevention in Agro-food and Forest Systems".

Schillaci G., Caruso L., Balloni S., Camilleri D 2011. I rischi da sovraccarico biomeccanico nelle attivitá del vivaio orticolo. In: Convegno di Medio Termine dell'Associazione Italiana di Ingegneria Agraria Belgirate, 22-24 settembre 2011.

Waters T.R., Lu M.L., Occhipinti E. 2007. New procedure for assessing sequential manual lifting jobs using the revised NIOSH lifting equation. Ergonomics. 50(11): 1761-1770.

Waters T.R., Putz-Anderson V., Garg A. 1994. Applications Manual for the Revised NIOSH Lifting Equation. DHHS(NIOSH) Publication No. 94–110. National Institute for Occupational Safety and Health, Centers for Disease Control and Prevention. Cincinnati, Ohio. 45226.

Zanuttini R., Cielo P., Poncino D. 2005. Il metodo OWAS. Prime applicazioni nella valutazione del rischio di patologie muscolo-scheletriche nel settore forestale in Italia. Forest@ 2(2). 242-55. [online] URL: http://www.sisef.it/

Fitting and testing roll-over protective structures on self-propelled agricultural machinery

Domenico Pessina, Davide Facchinetti

Dip. di Scienze Agrarie e Ambientali, Università degli Studi, Milan, Italy

Abstract

Roll-Over Protective Structure (ROPS) represents the state of art for the driver's protection in case of tractors roll-over. Despite their real risk of overturning, the ROPS approach for the Self-Propelled agricultural Machinery (SPM) is quite recent. Due to the several SPM categories available on the market, characterized by very different mass, dimension and working functions, the fitting of a ROPS and consequently the ascertainment of its protection level is quite complicated. SPM could be preliminarily divided into at least two categories:

- large SPM: combine, forage, potato, sugar-beet and grape harvesters; sprayer; etc.;
- small SPM: ride-on tractor, mower, comb side-delivery rake, etc.

The most followed approach at present is to check preliminarily the overturning behavior of the SPM considering its longitudinal and lateral stability; if a real risk of overturning is ascertained, in order to minimize the likelihood of driver's injury the manufacturer often installs a ROPS. The consequent need is to provide some test criteria of them. Sprayers between large SPM, and comb side-delivery rake between small SPM were the machine types on which ROPS were tested, adopting in both cases the procedure provided by Code 4 issued by the Organization for Economic and Cooperation Development (OECD), dedicated to ROPS fitted on conventional agricultural and forestry tractors. Notwithstanding the very different dimensions of these two SPM, this standard was selected considering the predictable roll-over behavior, also in relation with the front and rear track values. On the 4950 kg mass sprayer was fitted a closed cab, while on the 690 kg mass comb side-delivery rakes a 3-pillars frame was applied. In both cases the response of the tests was positive, so indicating a general suitability of OECD Code 4 to assure a ROPS good driver's protection level in case of overturning. On the other hand, to ascertain more in detail the roll-over behavior of the SPM, some further questions need to be deeply examined, such as the driver's place location, the height of the centre of gravity from the ground in different machine configurations (*i.e.* with crop tanks empty or full), the external silhouette, the axles mass distribution of the laden/unladen machine, etc.

Correspondence: Domenico Pessina, Dip. di Scienze Agrarie e Ambientali, Università degli Stud, Via Celoria, 2, 20133 Milan, italy.
E-mail: domenico.pessina@unimi.it

Key words: self-propelled machinery, stability, roll-over, tip-over, overturning, roll-over protective structure.

Journal of Agricultural Engineering 2013; XLIV(s1):e148
doi:10.4081/jae.2013.(s1):e148

Introduction

Beginning from the first experimental trials carried out in Scandinavian countries in early '50 of the last century, the Roll Over Protective Structures (ROPS) to be fitted on agricultural and forestry tractors for the driver's safety in case of roll-over have been considered worldwide the most effective mean against injury occurred in case of overturning (Springfeldt *et al*., 1998; Reynolds *et al*., 2000; Guzzomi *et al*., 2009; Harris *et al*., 2010; Biddle *et al*., 2012). Several national and international Standards dealing with ROPS tests were been in the meantime issued, considering progressively the strength test of the protective structures provided for almost all the various agricultural tractor categories: standard (or conventional), tracklaying, narrow track, etc. (Myers, 2000 ; Day *et al*., 2004 ; Alfaro *et al*., 2009; Murphy, 2010 ; Arana *et al*. 2011). Sometimes, further kind of tests were provided, such as those concerning the lateral stability and the non-continuous rolling of the narrow track tractors in case a two pillar front mounted folding roll-bar has to be fitted (Silleli *et al.*, 2009; Guan *et a*l., 2011).

More than 40 years ago, the OECD (Organization of Economic Cooperation Development) started to issue a number of Codes providing procedures to test the ROPS to be fitted on agricultural and forestry tractors, telehandlers used as tractors and other parts and accessories integrating the operator's safety on board in case of overturning, such as the safety belts attachment strength (OECD Codes 4, 6, 7, 8 and 9, 2013).

In recent years, mainly at a national level some rules and guidelines were issued trying to solve the problem of used tractors (Myers, 1995; Freeman, 1999; Franklin *et al*., 2006), in case they were used and/or introduced again on the market in absence of an international law providing the compulsory fitting of a homologated ROPS.

At present, ROPS on tractors have reached an excellent diffusion, and quite probably this is the most known and popular protection means in case of overturning. In spite of this fact, in Italy more than 130 fatal accidents due to tractor overturning are still occurring every year, mainly due to the use of very old and worn machines, but also because frequently operators working on narrow track tractors keep constantly the folding front roll-bar in the rest position, so nullifying any possible protection of that type of ROPS (Pessina *et al*., 2009).

In recent years, the accident statistics on agricultural machinery highlighted that not only the tractors can be subjected to a tip- or a roll-over, but also some other categories of large Self Propelled Machines (SPM), such as combine harvesters, grape harvesters, sprayers, etc. (Crandall *et al*., 1997; Day, 1999; Arana *et al.*, 2010) (Figure 1). In these cases, the problem consists of some technical characteristics and working conditions of these SPM, being them as follows: high overall mass, including the content of large tanks fitted on board; high centre of gravity, because the machine is working riding the crop (*i.e.* grape harvester and sprayer); development of high torque values; travelling on steep and rough slopes at high speed;

On the other hand, also small SPM, such as ride-on tractors, mowers, comb side-delivery rakes (Figure 2) are subjected to possible roll-over, due in this case not to a large mass or to a high centre of gravity, but rather to the roughness of the ground on which they travel at high speed, leading to skidding and bumps causing the lack of the vehicle control, especially when working on slope during forage management operation.

On the other hand, on small SPM the space reserved to the drive is often very narrow, and also for economical reason no closed cab is fitted, being the seat and the steering-wheel of the machine simply fitted on the main frame. No protection against high and low temperature, rain, wind, dust, noise, vibration, etc. is provided. In case of overturning, the operator on board cannot be protected in any way.

Because for both large and small SPM the overturning is a real hazard, their risk evaluation must consider the means to avoid or at least minimize this kind of hazard. Manufacturers have studied some systems to increase the stability of these machines, and also some international standards, such as EN 16231, provide a similar approach, taking into account the preliminary measurement of the static lateral and longitudinal stability of a given machine, thus comparing the limit angle values found with the limits established for the category in which the machine is included. If the stability does not satisfy the requirement, the manufacturer must consider the fitting of means able to reduce the driver's injury in case of overturning.

Thanks to the very long and deep expertise accumulated in more than 50 years for the similar question regarding the agricultural and forestry tractors, the manufacturers consider as a priority the fitting of a ROPS. On the large SPM, a suitable reinforcement of the cabs already fitted has to be provided. As an alternative, sometime a very stiff 2-pillars roll-bar or a 4-pillars frame is added to the original cab. Diversely, a simple 2, 3 or 4 pillars simple frame is applied to the small SPM.

Of course, these ROPS have to be tested, in order to ascertain if they are sufficiently strong to assure a suitable volume around the driver's place in case of overturning. At present, no dedicated Standards are available, and therefore those used normally for the ROPS to be fitted on agricultural and forestry tractors are considered.

The SPS (Self-Protective Structure)

On the other hand, the location of the driver's place on the tractors compared with that of SPM is often quite different: on the conventional tractors the seat and the steering wheel are normally located in a central-rear position, being them also central considering the lateral axis, lying on the longitudinal centre line. On the contrary, on the SPM the driver's place is often located in extreme front of rear positions and sometime is not central in the lateral axis.

Moreover, especially for large SPM the so called Self-Protective Structures (SPS) have to be considered for an extra protection in case of overturning. As defined in ISO 16231-1, the SPS are structural components of the machine with sufficient strength to provide a deflection limiting volume if the machine overturns.

The SPS can be represented by tanks, frames, shields, carters, etc. normally fitted on the machine, providing a certain energy absorption in case of overturning, avoiding partially (or sometime completely) the mechanical stress to which the cab structure should be subjected. Thus, the mechanical features of these structural elements have to be defined by adopting one (or more) testing method(s), allowing to identify and assess their strength in a reliable and repeatable way.

This is not a new principle, because in some standards dedicated to the testing of the ROPS to be fitted on earth-moving machinery (such as ISO 12117-2:2008/Cor 1:2010 "*Earth-moving machinery Laboratory tests and performance requirements for protective structures of excavators Part 2: Roll-over protective structures (ROPS) for excavators of over 6 t*") some simulated ground planes are defined. Each of them is ascertained by at least 3 stiff points located on the machine (deriving from

Figure 2. Some examples of small SPM. From left to right and from top to bottom: a self-propelled mower, a side-comb delivery rake, a multifunctional machine to clean the berth edge and a motor brush.

Figure 1. Some categories of large SPM, such as combine harvesters, grape harvesters and sprayers are subjected to tip- and roll-over due to their technical characteristics and working conditions (courtesy of INAIL – Rome, Italy).

SPS), which can provide protection for the operator in case of impact with the ground during a machine tip- or roll-over. In case the operator seat is off the machine longitudinal centre line, the worst condition has to be considered. Thus, a lateral, front, rear and upper boundary simulated ground planes (named respectively LBSGP, FBSGP, RBSGP and UBSGP, Figure 3) can be defined (INAIL, Rome-Italy, 2013).

The stiff points are lying on rigid structural members that remain fixed and unchanged on the machine in any configuration (including working on field and transport conditions), showing adequate strength to support the induced loads during a tip- or roll-over resulting in predictable deformation. Shall not be considered as stiff points interchangeable or detachable devices, *e.g.* for combine harvesters the header or the pick-up and stripping heads, and for grape harvesters detachable vine shoot tipping devices.

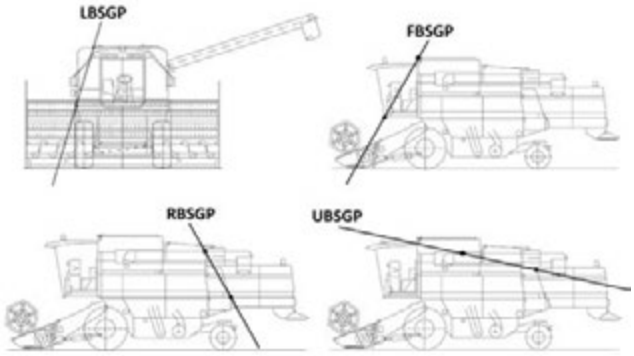

Figure 3. Example of lateral (LBSGP), front (FBSGP), rear (RBSGP)and upper (UBSGP) boundary simulated ground planes, referred to a combine harvester (courtesy of INAIL – Rome, Italy).

Figure 4. General drawings and view of the ROPS fitted on the large SPM, a self-propelled sprayer.

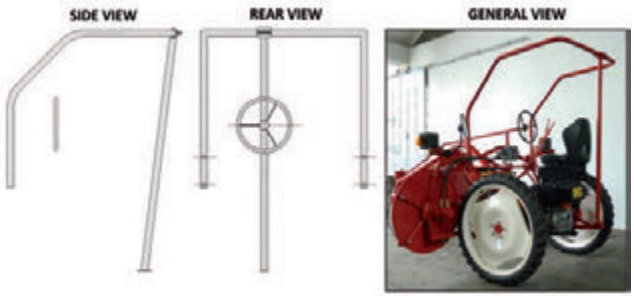

Figure 5. General drawings and view of the ROPS fitted on the small SPM, a comb side-delivery rake.

Some procedures have been proposed in order to test physically the strength of the stiff points. One of them provides to apply a static force equal to 2/3 of the machine weight in a perpendicular direction to the ground when the given point touches the terrain in case of overturning. In any case, with reference to the rigs at present available for the ROPS tests, considering the remarkable overall dimensions of the large SPM the execution of such tests could be very difficult and sometime really impossible. As an alternative, a virtual test (a computerized simulation) carried out by using the FEA method (Finite Element Analysis) could be profitably used (Karlinsky *et al.*, 2013). In fact, by now this kind of software has assured a high level of affordability and a reduced deviation of the output data in respect to the results of the real test.

Materials and methods

Waiting for the definite issue of Standards specifically dedicated to the large SPM (such as ISO 16231) and to the small ones, manufacturers asked with urgency for the testing of ROPS to be fitted on SPM, being it the most common (and quick) solution considered for the protection of the driver in case of tip- or roll-over. In the first instance, the lack of dedicated Standards leads to the application of those already used for similar machinery, mainly agricultural and forestry tractors, and sometime also earth-moving machines. On the subject, the OECD Code 4 appears at present the most known and applied standard. For this reason, two tests were carried out, respectively on the ROPS fitted on a self-propelled sprayer (large SPM), and on a comb side-delivery rake (small SPM). The most important technical characteristics of these two SPM (mainly their mass and front and rear track values) were into the range provided for the application of the OECD Code 4.

In detail, on the self-propelled sprayer a 4-pillars closed cab was fitted; on the contrary, due to technical and economical reasons, a simple 3-pillars frame was provided for the comb side-delivery rake (Figs. 4 and 5).

The OECD Code 4 provides a sequence of 4 tests, by absorbing defined energies (E, in J) or applying defined forces (F, in N) depending them on the machine mass (M, in kg), as shown in Table 1.

The machine mass appears a key feature on which are based the energies to be absorbed and the forces to be applied. Similarly, on SPM that are not harvesting of distributing material is easy to define a reference mass to calculate energy and force values, but for example the cases of combine and grape harvesters and also the self-propelled sprayers are more complicated, due to large mass variation occurring in the conditions of tank(s) empty or full. In such cases, the mass can double or more. Moreover, the tanks can be open or closed: in the first case, in the event of an overturning, all (or part) of the material could escape outside, thus decreasing the mass of the machine and the stress on its structure when touching the ground. On the other hand, no mass variation could occur in case of closed tank(s), but attention should be paid to the attachment of the tank(s), considering a possible complete

Table 1. Tests sequence and formulae used in OECD Code 4 for testing ROPS to be fitted on agricultural and forestry tractors.

Test sequence	Loading	Formula
1	Rear horizontal	E = 1.4 M
2	Rear vertical	F = 20 M
3	Side horizontal	E = 1.75 M
4	Front vertical	F = 20 M

E = energy, J; F = force, N; M = machine mass, kg.

detachment from the machine frame.

In Table 2 the main technical characteristics of the two SPM are shown, as far as the energies to be absorbed and the forces to be applied.

Results and discussion

Because cabs and frames are normally manufactured with vertical pillars, in the major part of the ROPS tests the horizontal loadings (to the rear and to the side in the case of OECD Code 4) result more severe rather than those applied vertically. The reason is that in the vertical direction the pillars are loaded in a buckling, while the horizontal tests load the structural components in their weakest section. Also in the two tests of ROPS fitted on SPM this condition has been verified, and as a consequence only the horizontal loadings have been investigated.

In Figs. 6 and 7 are shown the Force-Deflection (F-D) curves and the view at the end of the rear and side loadings of the ROPS fitted on the two SPM considered. On the F-D curves, also the values of permanent and elastic deflection were calculated, comparing them with the total deflection value.

In general, a ROPS is absorbing the energy provided by the formulae in the stress-strain field, so resulting a certain amount of both plastic (permanent) and elastic (temporary) deflection.

At the same time, the need to maintain protected the clearance zone (representing the presumable volume occupied by the driver properly attached to the seat when the machine overturns), as well as to limit at a reasonable size the ROPS, often constrains the designer to a compromise between the possibility to absorb energy in terms of both plastic and elastic deflection. In practice, a well designed ROPS shows a ratio plastic/elastic deflection ranging between 0.66 and 1.50. In other words, both the plastic and elastic deflection values range normally between 40% and 60% of the total.

As a consequence, a plastic deflection value higher than 60% of the total (and consequently an elastic deflection less than 40%) is typical of a very stiff ROPS, sometime fitted on narrow machines, where the deflection of the pillars has to be quite low, because the structure members must not enter into the safety zone. On the contrary, on large machines the possibility to fit "elastic" ROPS is higher, due to their largest overall dimensions.

The Plastic (PD) and Elastic (ED) Deflection values recorded for the tests of the ROPS fitted on the self-propelled sprayer confirmed this principle, being respectively 59%-41% (ratio PD/ED =1.44) for the rear loading, and 46%-54% (ratio PD/ED = 0.85) for the side loading. On the other hand, the ROPS type fitted was a closed cab made in the majority of its parts with shaped welded steel sheet and tubes. Different values were on the contrary recorded for the ROPS fitted on the comb side-delivery rake, being for the rear and side loadings respectively 39%-61% (ratio PD/ED = 0.64) and 36%-64% (ratio PD/ED = 0.56). In this case, for both loadings the ROPS revealed a poor plasticity, and consequently a very high elasticity. This was because the ROPS was a quite simple frame, manufactured with welded rounded tubes; at the same time, there was no criticism regarding the overall dimensions of the ROPS, having the machine a remarkable wheelbase and track values if compared with its low mass. Moreover, the frame was based on 3 pillars, a very unusual asymmetric design solution, considering that frames and roll-bars fitted normally on agricultural tractors have 2 or 4 pillars.

Table 2. Minimum values of energy to be absorbed and force to be applied to the ROPS fitted on the two SPM..

Loading	Formula	Self-propelled sprayer (Mref = 4950 kg; min track = 1800 mm wheelbase = 2820 mm)	Comb side-delivery rake (Mref = 690 kg min track = 1340 mm wheelbase = 2440 mm)
Rear horizontal	E = 1.4 M	E = 6.93 kJ	E = 0.97 kJ
Rear vertical	F = 20 M	F = 99.0 kN	F = 13.8 kN
Side horizontal	E = 1.75 M	E = 8.66 kJ	E = 1.21 kJ
Front vertical	F = 20 M	F = 99.0 kN	F = 13.8 kN

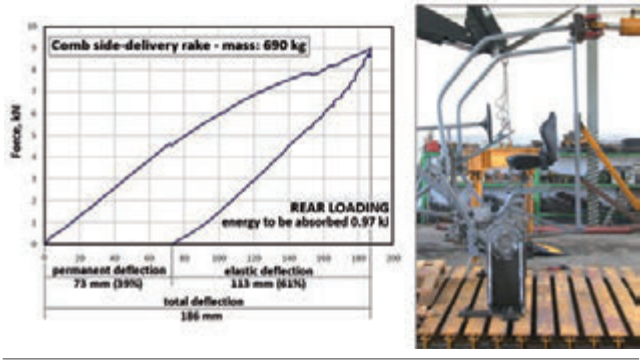

Figure 6. Force-deflection curves and condition at the end of the rear and side loadings of the ROPS fitted on the self-propelled sprayer.

Figure 7. Force-deflection curves and condition at the end of the rear and side loadings of the ROPS fitted on the comb side-delivery rake.

In Figs. 8 and 9 the final permanent deflections of the two ROPS are shown, resulting from the sequence of the 4 loadings. As expected, for both ROPS no high deflection occurred in the vertical plane, having recoded values ranging between 5 mm and 45 mm. This happens because this kind of structures show a remarkable stiffness being the force applied in the direction of their maximum resistance.

On the contrary, in the horizontal plane the behavior of the two ROPS was different. In the longitudinal direction (from back forwards), for the cab fitted on the self-propelled sprayer the permanent deflection was logically higher on the side where the loading was applied, while for the comb side-delivery rake the values of the left and right sides were similar, because the frame fitted had just one pillar at its back, more or less in the central position of the structure. Moreover, in this last case the deflection recorded was higher, due to the remarkable elasticity of this ROPS in comparison with the other.

Also the deflection values resulting in the lateral direction were noticeable, due to the high energy to be absorbed in the side loading, which is the most severe in the entire sequence of tests. The cab fitted on the self-propelled sprayer showed a higher deflection in its rear part, while the frame of the comb side-delivery rake highlighted the same deflection in the front and rear parts.

For both structures, the acceptance conditions of the tests carried out relative to the protection of the clearance zone were fulfilled. Thus, the two structures can be considered a roll-over protective structure in accordance with the OECD Code 4. On the other hand, the two SPM were not critical for their overall dimensions. The respect of the clearance zone could be difficult on other narrow SPM, such as self-propelled mower or some multifunctional machines used in the livestock breeding, such as for example that to clean the berth edge.

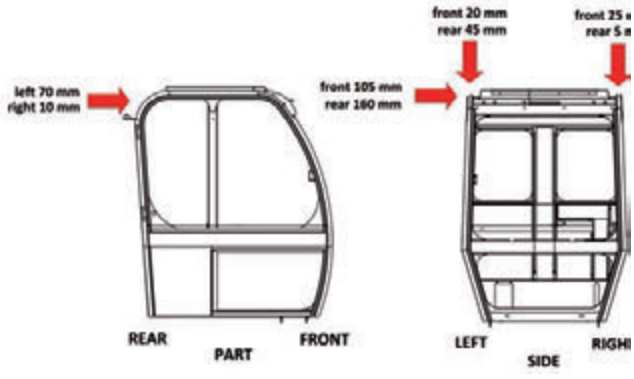

Figure 8. Permanent deflection values of the ROPS fitted on the self-propelled sprayer, resulting after the sequence of the 4 loadings provided by OECD Code 4.

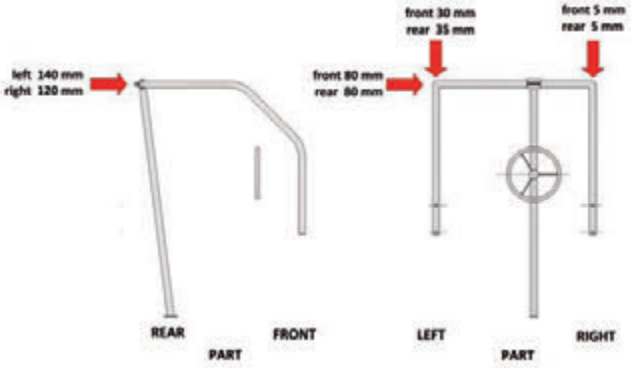

Figure 9. Permanent deflection values of the ROPS fitted on the comb side-delivery rake, resulting after the sequence of the 4 loadings provided by OECD Code 4.

Conclusions

On the SPM, the protection of the driver in case of overturning (and also that of a possible passenger on board) is still suffering for a lack of dedicated standards. The ISO 16231 is dealing with this question: the approach considered is quite interesting and well promising to solve the problem.

On the other hand, if the fitting of a ROPS is the solution selected by manufacturers to increase the driver's safety in case of overturning, the actual standards developed for agricultural and forestry tractors appear adequate for some categories of large SPM, such as some self-propelled sprayers, but not for several other categories (*e.g.* combine and grape harvesters), where the driver's place is located in the front part of the machine and sometime on one of the two sides.

The existing Self-Protective Structure (SPS) may modify remarkably the overturning dynamics of the SPM, depending on the stiffness of their points and the definition of the various boundary simulated ground planes. In some cases SPS could represent important means to reduce the mechanical stress of the cab, but in other situations could play a negative role just due to their stiffness, forcing the cab structure to absorb the great part of the energy developed in tip- or roll-over. This is for example the typical condition in case of front-side overturning when the driver's place is located in the front part of the machine.

The ISO 16231 primarily consider the stability of each SPM, and consequently the level of its risk of overturning. Only if the longitudinal and lateral stability values are lower than the limits established, the manufacturer is compelled to provide other means to reduce the risk. Very often the solution of fitting a ROPS is selected, due to the wide experience accumulated on agricultural and forestry tractors. Thus, the accurate and careful definition of the limit stability angles for each SPM category will have a great importance: several studies are in progress, devoted to evaluate the situation on the models currently on the market.

To come to a suitable solution of the general problem, the development of a series of specific standards for the testing of the ROPS designed to be fitted on SPM will be probably needed, considering that several both large and small SPM differ remarkably in design and function from the agricultural and forestry tractors.

References

Alfaro JR, Arana I, Arazuri S, Jaren C. Assessing the safety provided by SAE J2194 Standard and Code 4 Standard code for testing ROPS, using finite element analysis Biosystems Eng. 2010; 105(2):189-97.

Arana JI, Mangado J, Arnal P, et al. Evaluation of risk factors in fatal accidents in agriculture. Spanish Journal of Agricultural Research, 2010; 8(3):592-8.

Arana JI, Alfaro JR, Arazuri S, et al. A proposal to improve the sae standard and OECD code 4 standard code for testing ROPS. Transactions of the ASABE 2011, 54(4): 1189-97.

Biddle EA, Keane PR. Action Learning: A New Method to Increase

Tractor Roll-over Protective Structure (ROPS) Adoption. Journal of Agromedicine 2012; 17(4):398-409.
Crandall CS, Fullerton L, Olson L, et al. Farm-related injury mortality in New Mexico, 1980-91. Accid Anal Prev. 1997; 29(2):257-61.
Day LM Farm work related fatalities among adults in Victoria, Australia. The human cost of agriculture. Accident Analysis and Prevention 1999; 31:153–9.
Day LM, Rechnitzer G, Lough J. An Australian experience with tractor roll-over protective structure rebate programs: process, impact and outcome evaluation. Accid Anal Prev. 2004; 36(5):861-7.
Franklin RC, Stark K, Fragar L. Intervention strategies for the retro-fitment of Roll-over Protective Structures (ROPS) and fleet characteristic, farm tractors. Safety Science 2006; 44:771–83.
Freeman SA. Potential impact of a ROPS retrofit policy in central Iowa. J Agric Saf Health 1999; 5:11-20.
Guan J, Hsiao H, Zwiener JV, et al. Evaluating the protective capacity of two-post ROPS for a seat-belted occupant during a farm tractor overturn. Journal of Agricultural Safety and Health, 2011; 17(1):15-32.
Guzzomi AL, Rondelli V, Guarnieri A, et al. Available energy during the roll-over of narrow-track wheeled agricultural tractors. Biosystems Engineering 2009; 104:318-23.
Harris JR, McKenzie EA, Etherton JR, et al. ROPS performance during field upset and static testing. J. Agric. Safety and Health 2010; 16(1):5-18.
Karlinski J, Ptak M, Działak P. Simulation tests of roll-over protection structure. Archives of civil and mechanical engineering 2013 13:5 7-63.
Murphy D, Myers J, McKenzie Jr, et al. Tractors and roll-over protection in the United States. J Agromedicine 2010; 15:249-63.
Myers JR, Snyder KA. Roll-over protective structure use and the cost of retrofitting tractors in the United States, 1993. J Agric Saf Health 1995; 1:185-197.
Myers ML. Prevention effectiveness of roll-over protective structures, Part I: Strategy evolution. Journal of Agricultural Safety and Health 2000; 6(1):29-40.
Pessina D, Facchinetti D. Il ruolo del web nel monitoraggio degli incidenti mortali dovuti a ribaltamento nei trattori agricoli. Proc. of "Il nuovo Testo Unico e la sicurezza nel settore agroforestale", Viterbo (Italy), 2009, 1-18.
Reynolds SJ, Groves W. Effectiveness of roll-over protective structures in reducing farm tractor fatalities. American J. Prev. Med. 2000; 18(4S):63-9.
Silleli H, Ta ba H, Çay CI. A research on the evaluation of front hard point part of agricultural and forestry tractors. Tarim Bilimleri Dergisi 2009; 15(2):166-72.
Springfeldt B, Thorson J, Lee BC. Sweden's thirty-year experience with tractor roll-overs. J Agric Saf Health 1998; 4:173-80.
INAIL (Istituto Nazionale per l'Assicurazione contro gli Infortuni su Lavoro) "Self Protective Structure (SPS) and Roll Over Protective Structure (ROPS) for agricultural self-propelled machines", Rome (Italy), 2013.
ISO (International Organization for Standardization) "Earth-moving machinery Laboratory tests and performance requirements for protective structures of excavators Part 2: Roll-over protective structures (ROPS) for excavators of over 6 t. Norm ISO 12117-2:2008/Cor 1:2010, Geneva: International Organization for Standardization Publications; 2010.
ISO (International Organization for Standardization) "Self-propelled agricultural machinery. Assessment of stability. Norm ISO 16231 – Parts 1 and 2-2013, Geneva: International Organization for Standardization Publications; 2013.
OECD Codes 4, 6, 7, 8 and 9 (2013). OECD Standard Code for the Official Testing of Roll-over Protective Structures on Agricultural and Forestry Tractors. Organisation for the Economic Co-operation and Development, Paris, France.

Analysis of the building system of four mills and their suitability for heat treatment pest disinfestation

Loredana Strano, Giovanna Tomaselli

Department of Agri-food and Environmental Systems Management, Section: Building and Land Engineering, University of Catania, Catania, Italy

Abstract

The last century researchers at Kansas State University demonstrated the validity of the heat treatment as a method of pest control in more than 20 mills. However factors such as the high capital investment required to heat large buildings, inadequate control of high temperatures and the risk of damage to parts of the plants or the construction materials have prevented the large-scale adoption of this technique as a viable alternative to fumigants. Today the combination of the industrialization of the food industry, the technological and structural modernization of plants and developments in heat disinfection technologies have resulted in interesting results being obtained for the use of this system in primary and secondary production processing plants, both experimentally and in practice. However, the scientific literature highlights some of the factors that limit the efficiency of the treatment. This is related to aspects of the buildings and the plants and the environment of the buildings. The structure of the buildings appear to have an enormous impact on energy consumption, because this depends on the amount of heating time and the methods that have to be used when establishing a heat treatment regime. These factors are important if the fumigation temperatures are to be reached in the shortest possible time and can affect the choice of the technique used with current fumigants, especially when this is combined with the amount and cost of the energy consumed. The aim of this work is to analyse four Sicilians mills that intend to use the heat system for fumigation and pest control in order to identify those aspects of the buildings, plant and their environment which are "critical elements" and may discourage the use of this technology. Particular attention was paid to the type of construction materials and their thermal conductivity (roof, floors and walls), the number and volume of the buildings and the distance between them, the entrances and the links between different parts of the plant and the type of equipment used and its spatial organisation inside the buildings.

Correspondence: Giovanna Tomaselli, Department of Agri-food and Environmental Systems Management, Section: Building and Land Engineering, University of Catania, Via S. Sofia 100, 95123, Catania, Italy.
E-mail: gitomas@unict.it

Key words: buildings, heat, pest control, plant

Journal of Agricultural Engineering 2013; XLIV(s1):e149
doi:10.4081/jae.2013.(s1):e149

Introduction

The first example of the use of heat treatment pest disinfestation in the milling sector was in a document published by Duhamel du Monceau in France in 1762 (Beckett *et al.*, 2007).

In 1912 Professor G. A. Dean, an entomologist at Kansas State Agricultural College, demonstrated the efficicacy of heat treatment for controlling insect infestation in a study carried out at 20 mills in Ohio, Illinois, Indiana, Iowa, Nebraska and Southern Canada, and proposed that this method was a valid alternative to the use of fumigants (Dean, 1911, 1913; Field *et al.*, 1997; Dosland, 1996).

More recently pilot studies using heat treatment with biotesting have been carried out at mills in Canada and Europe by Kansas State University. These studies have demonstrated that the temperature at which the insects die was on average between 40 °C and 55 °C. The available data shows that most species of insects do not survive for more than: 24 hours at 40 °C, 12 hours at 45 °C, 5 minutes at 50 °C, and only 1 minute at 55 °C (Suss, 2007; Brijwani *et al.*, 2010, 2012).

In addition various experiments in agro-industrial plants in Italy and abroad have demonstrated that to reach 100% insect mortality one needs a treatment period of 36 to 48 hours at temperatures between 55°C and 60 °C.

An experiment carried out in a 11.500 m^3 brick-built mill in 2007 was able to evaluate the heat loss during treatment. 44% of the heat was absorbed by the floor and walls and 10% by the plant, while 46% was related to the heat loss of the building (Guerra, 2009).

The most recent reports in the literature have highlighted certain aspects of the buildings, plant and environment which may limit the efficacy of heat treatment.

It is known that the main critical points in mills are the "cold points", *i.e.* the spaces in which the temperatures do not reach the required levels. Certain studies have shown how, during treatment, various types of insect move to the areas where the temperatures do not reach lethal levels (Massara 2007; Suss, 2008; Guerra *et al.*, 2012). These critical points are linked to the characteristics of the materials used for the buildings and plant and the organisation of the buildings themselves. These factors influence the choices of how the treatment is applied (type of thermo-ventilator fans, season, time period and temperature of treatment), and thus the cost of the energy consumed, and the management of the operation (Braghieri *et al.*, 2007; Massara, 2007; Suss, 2008; Guerra, 2009).

At present it seems that innovations to the plant designed to ensure their efficiency when subjected to high temperatures are more advanced than the general level of innovation of the typical layout of the mills themselves, and also more advanced than the types of construction and the materials used to ensure a suitable environment for heat treatment.

Today, because of the good results of heat treatment pest disinfestation, more and more businesses are interested in and intend to use this system. However many of the buildings do not have the correct

characteristics and are not constructed of the right materials to guarantee good results.

Given that these problems exist, this paper studies four mills, in order to identify the critical points. The information obtained may be useful in helping to make existing structures suitable for heat treatment and also helpful when planning new mills.

Materials and methods

The paper studies four Sicilian mills whose owners intend to use heat treatment pest disinfestation. Thermo-ventilator fans will be used to heat the four mills, with each fan using about 20 kW/h of electricity. On average three ventilator fans will be used for a volume of 1000 m^3.

Mills 1 and 2 are in the Province of Syracusa and mill daily, respectively, 220 tons of durum wheat and 100 tons of common wheat. Mill 3 is in the Province of Enna and mills 0.3 tons of durum wheat per day, with the flour being to used in the bakery attached to the mill. Mill 4 is in the Province of Palermo and mills 220 tons of durum wheat per day for use in the bakery attached to the mill.

The mills are built according to the standard layout used by the major construction companies.

All the mills have a central building, with the height depending on the production capacity, divided into different floors, as can be seen in Figure 1. The standard layout is adequate for the production flow and, irrespective of the particular capacity, the silos are connected laterally to the central building. The plan in Figure 1 shows a mill with a capacity of 220 tons per day.

Analysis of the problems and direct observation of the mills has allowed us to acquire detailed information of the characteristics of the buildings and the relationships between them and the production processes.

The precise investigation of the critical points was only carried out in the places where heat treatment would be used. In order to do this aspect of the *buildings* and *plant* were used as indicators.

The *aspects of the buildings*, using meta-planning methods (Failla *et al.*, 2006; Strano *et al.*, 2012) as a point of reference, were extrapolated from the building systems used (UNI EN 10723:1998; UNI EN 10838:1999):

- the environment and type of building, in order to identify the critical points in heat distribution in the different areas and between the floors. In order to do this the volumes and the way that the different floors were connected were taken into consideration;
- the technological system, so as to identify the critical points in heat loss and the response of the materials used. In order to do this, the characteristics of the construction materials, the plant and the surface of the walls floors and roofs were taken into consideration.

For the *aspects of the plant,* the processing plant were analysed in order to identify possible equipment or parts of the plant which were "sensitive to heat treatment". The companies which construct many of the components supplied information on their heat resistance characteristics. In this way these values were acquired and systematised. For those components or plant where the information was not provided by the suppliers, laboratory tests were developed to check their resistance to high temperatures. To be more precise, samples of the sieves, the square sifters and the purifiers from the four mills, made up of wooden and aluminium sieve frames, assembled with cyanoacrylate adhesive or vinyl glue, were placed in a closed environment for 48 hours in a temperature of 63 °C.

Results and discussion

The results below take into consideration developments in the liter-

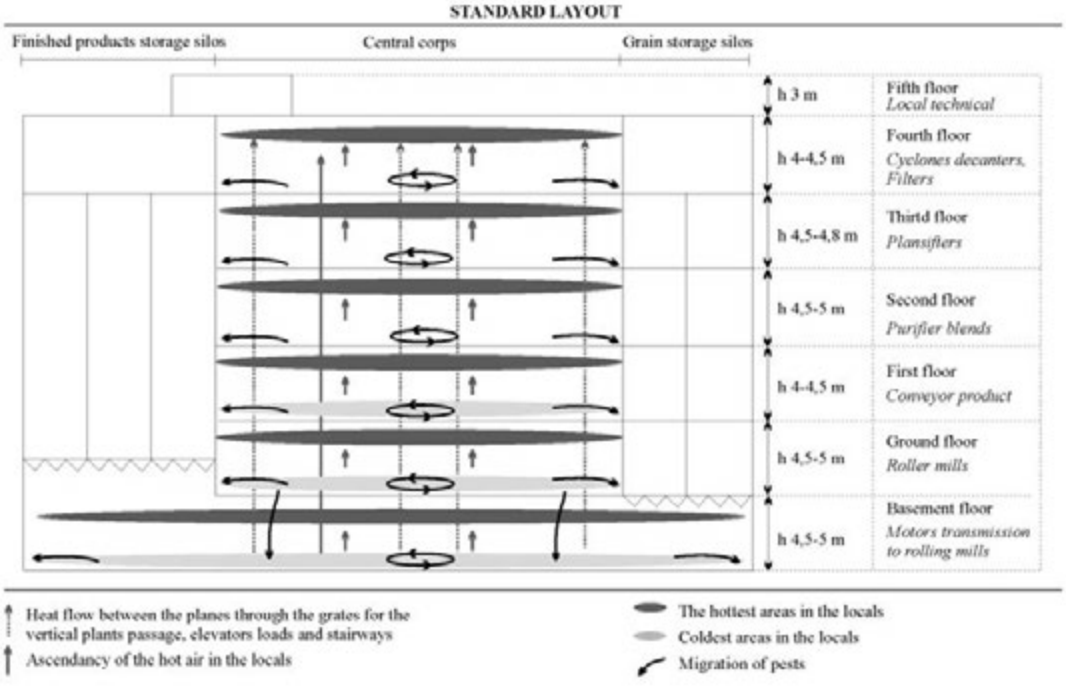

Figure 1. Heat distribution in the plans and possible migration of pests.

ature in recent years. Thus it is implicit that when highlighting the critical points in the mills we studied one must take into account the views expressed in the pricipal scientific literature for this sector (Beckett *et al.*, 2007; Massara, 2007; Süss, 2008; Guerra; 2009).

Aspects of the buildings and critical points

The characteristics of the building system used in the four mills are shown in Tables 1 and 2. The processing environment, in different places depending on the type of layout, although always compartmentalised, present points of continuity in correspondence with the many openings in the ceilings, which are necessary for connecting the different plant. As a result it is difficult to check the thermo-hygrometric parameters of each environment: to intervene in one would mean intervening in the whole volume of the building (Table 1).

Table 2 shows the construction system used for the four mills. They all of the traditional type and have insulating material only on the external walls.

The critical points identified in the analysed building systems

If one intends to use heat treatment in the mills, the critical points essentially refer to *heat movement* upwards from the lower floors to the upper ones. This causes temperature differences between the different floors and between the surfaces of the roofs, ceilings, walls and floors, as can be seen in Figure 1. Other critical points are linked to the *characteristics of the construction material used*.

Certain critical points were found in all four mills. To be precise, the areas used for the milling machines may be *critical points for heat transfer* due to the following aspects of the buildings:

- the longitudinal gratings of the vertical pneumatic conveyors of the products;
- openings in the horizontal partitions for housing the freight elevators;
- shutters.

Other specific points of heat loss in the different mills are:

Mill 1 (Figure 2A and 2B)

- transversal gratings between the walls and floors used for housing the Archimedian screws that transfer the grain. These are found between all the floors, from the basement to the fifth floor;
- open areas designed to house the iron silos for storing the flour awaiting packaging. These are found between the second and fourth floors of the mill;

Mill 2 (Figure 3)

- internal staircase without doors;
- openings in the ceiling between the basement and the ground floor in correspondence to the location of the flour storage silos;

Mill 3 (Figure 4)

- internal staircase without doors;

Mills 3 and 4 (Figure 4)

- trapdoors for the ramps for the sacks; central openings between the floors for the pneumatic machinery and for the conveyor belts.

The effects of the hot air rising and its stratification are particularly evident vertically, as the vertical areas are more difficult to heat uniformly than the horizontal ones.

In the mills under investigation the vertical spaces are found near the internal grain or flour storage silos or near the storage spaces for the unpackaged final products.

Other elements which may effect the uniform distribution of temperatures are the external walls, which are more exposed to heat exchange with the surrounding area.

At present the methods used for heat treatment use ventilator fans to circulate the air, This ensures that the ambient temperature is uniform and that the lower areas are also heated.

Analysis of studies on heat treatment in mills indicates that the zones where the pests migrate to often coincide with the following areas, which are those where it is most difficult to apply the heat treatment:

- the junctions between floors and walls, walls and walls, roofs and walls, as well as the spaces between the plant and the floors;
- crevices and cracks in the walls and floors;
- the spaces between the walls and the plant or the frames on which the machinery is mounted. (Dowdy, 1999; Dowdy and Field 2002; Mahroof *et al.*, 2003; Hulasare *et al.*, 2010; Guerra *et al.*, 2012)

Bearing in mind the observations of the migration of the pests, a report has been developed for the mills under consideration which indicates the colder points of the various work spaces (Figures 1, 2, 3 and 4).

The critical points inherent in the characteristics of the construction material are basically due to the way the material used for the buildings and plant aids heat loss.

From our observations and from information obtained during the experiment one can arrive at certain conclusions.

The mills generally have brick walls and concrete, granite or marble floors. These heat more slowly during the heating process. The plant and machinery are made of aluminium or iron and do not present any particular critical points during the heating process, although the seals may be damaged. The floors in mill 3 are connected by ramps covered in plastic, and this may be damaged by the high temperatures during heat treatment.

The heat retention of the buildings depends on the characteristics of the bricks used, which have different levels of conductivity, and the presence or absence of insulation (Table 2). The mills have insulated walls and roofs, with the exception of mill 3. Thus this is the one where there is likely to be more heat loss during treatment.

Other critical points may be the internal horizontal partitions which are not insulated, and so contribute to the upwards heat transfer in the buildings. The areas in the basements are always colder than the areas in the upper floors.

Mills 1 and 2 have external single glazed windows in aluminium frames, These prevent air escaping but are not efficacious for heat retention.

Mills 3 and 4 have windows with old iron frames which are often not airtight. During heat treatment even the smallest cracks may be significant critical points for heat loss.

Table 1. Volumes of local mills.

Production space	Volumes m³	Volumes bring thermal regime Total m³
Mill 1		
Grain storage	6576	23131
Milling	11589	
Durum wheat and waste storage	4966	
Mill 2		
Milling and storage	7295	7295
Finished products storage	5040	1175
Mill 3		
Milling and storage	-	5000
Mill 4		
Milling and storage	-	17514
Finished products storage		
Waste storage		

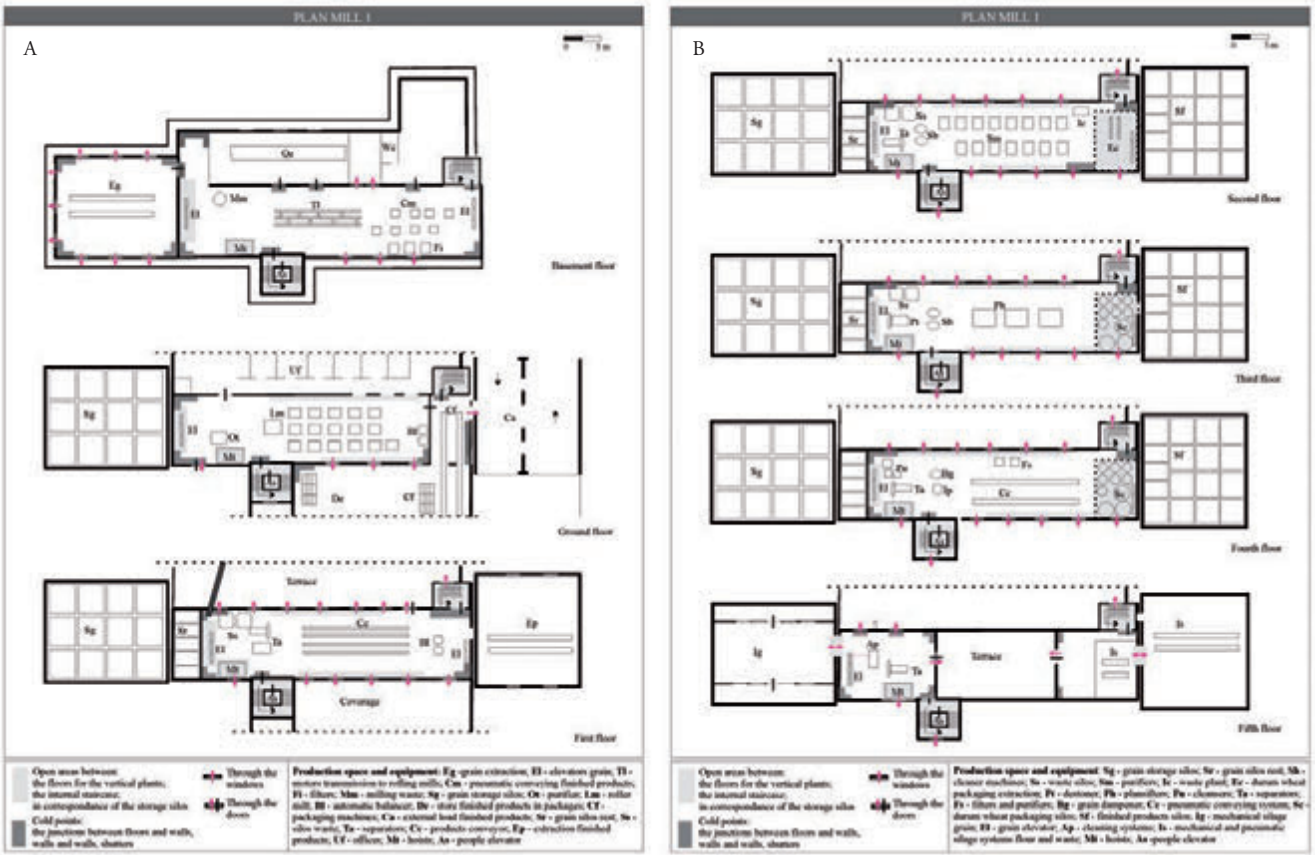

Figure 2. Critical points for transfer of heat.

Table 2. Construction characteristics of the mills and their critical points.

Production areas	Support structures	Lofts	Floors	External walls	Internal walls	Roofs	Ceilings	Doors		Windows
Mill 1								Internal	External	External
Grain store	Base with reinforced concrete grade beams and reinforced concrete foundations	A mixture of reinforced concrete with prefabricated reinforced concrete beams and brickwork	Industrial quartz flooring	Double brick walls with insulation in between them	Raw concrete/plaster	Reinforced concrete with insulation	Raw concrete/plaster	Idra REI 120	Aluminium and glass	Pre-painted aluminium and single glazing
Milling area					Raw concrete		Raw concrete	Fireproof doors		
Flour and waste store					Raw concrete/plaster		Raw concrete/plaster			
Mill 2										
Milling and storage areas	Reinforced concrete	Reinforced concrete	Industrial cement	Hollow brick with insulating material between them	Raw concrete/plastero	Reinforced concrete with insulation	Raw concrete	Absent	Aluminium and glass	Aluminium and single glazing
Final product store	Prefabricated in cement			Prefabricated in cement			Prefabricated in metal	-	Sectional doors	Metal and single glazing
Mill 3										
Milling and storage areas	Reinforced concrete	Reinforced concrete	Marble granite	Reinforced concrete blocks without insulation	Raw concrete/plaster	Reinforced concrete without insulation	Raw concrete	Absent	Iron and plexiglas	Iron and plexiglas
Mill 4										
Milling and storage areas	Reinforced concrete with beams and columns with closed mesh frames	Masonary cement screed and cement bricks	Marble granite	Calcarenite blocks in pomice blocks	Plaster	Reinforced concrete without insulation	Plaster	Iron and glass	Aluminium and glass	Iron and single glazing
Final products store										
Waste products store										
Critical points for heat loss										

Aspects of the plant and critical points

In mills transforming grain into flour involves the following processing stages: collection, pre-cleaning, storage, cleaning, drying, milling and processing, storage of the flour and packaging of the final product.

These processes involve the use of different machinery and plant (Table 3). These may be damaged by heat treatment.

Critical points identified in the plant

Analysis of the plant found that the storage silos in concrete or steel, zinc or iron sheet metal are not damaged by the temperatures used during heat treatment.

The cleaning, milling and sieving machinery in mills 1, 2 and 4 were made of stainless steel by Bühler S.p.A and there are no critical points at high temperature. There are also no problems for the aluminium or treated-wood sieves, the rubber components (seals, couplings, etc.), the PVC trapezoidal transmission belts, the flat leather transmission belts, the plexiglas bells, the fibreglass or wood rods or the special synthetic sleeving material.

The plant used in mill 3 for cleaning and milling are old machines from the 1980s made by Golfetto Italia. They are made of steel and/or wood with mahogany or American tulipwood equipment. The suppliers maintain that the materials used should be resistant to heat treatment.

However the information obtained during the research suggests that some equipment may be sensitive to heat treatment, especially the following:

- sieve frames used during sifting;
- parts and components of the packaging machinery;
- equipment and parts of machinery which have become worn out through use.

During sifting the critical points were identified as the sieve frames with nylon nets. The strength of the attachment depended on the type of glue used.

Tests on frames in wood and aluminium assembled using cyanoacrylate adhesive, found that the structures resisted high temperatures and the frames were not deformed.

The components of the packing and flour plant and machinery were found to be sensitive to the heat treatment (Table 3).

Conclusions

This study highlights the critical points for heat treatment in four representative mills. Most critical points were due to lack of insulation.

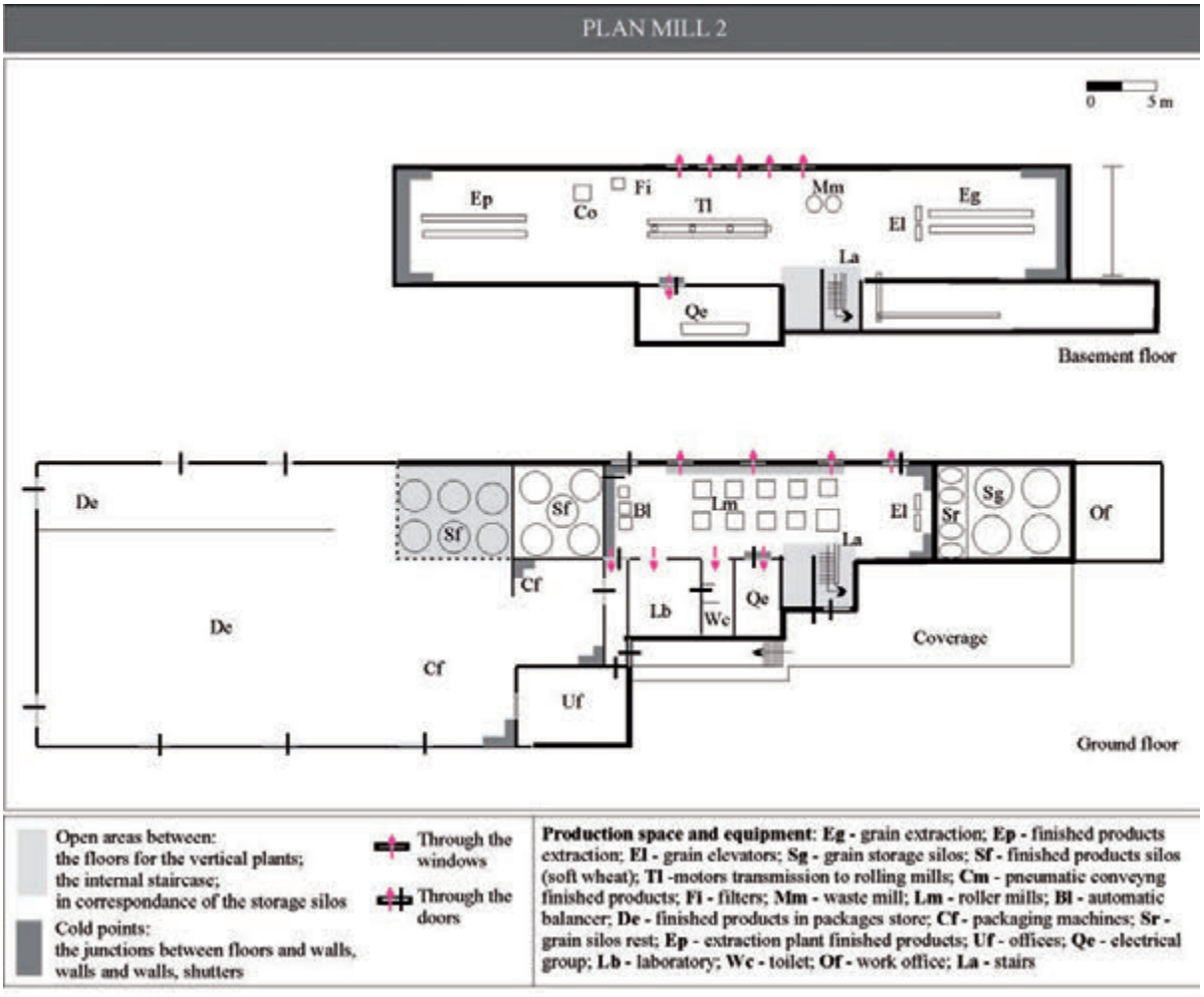

Figure 3. Critical points for transfer of heat.

This was only used for external walls in the various buildings.

Other aspects of planning, which are apparently of minor importance, such as for example isolating the different environments vertically, must be treated with particular care in buildings where heat treatment is intended to be used as a standard procedure for combating pest infestation.

Traditional mills may be built of different materials, usually metal structures, prefabricated panels or steel. These have the advantage of

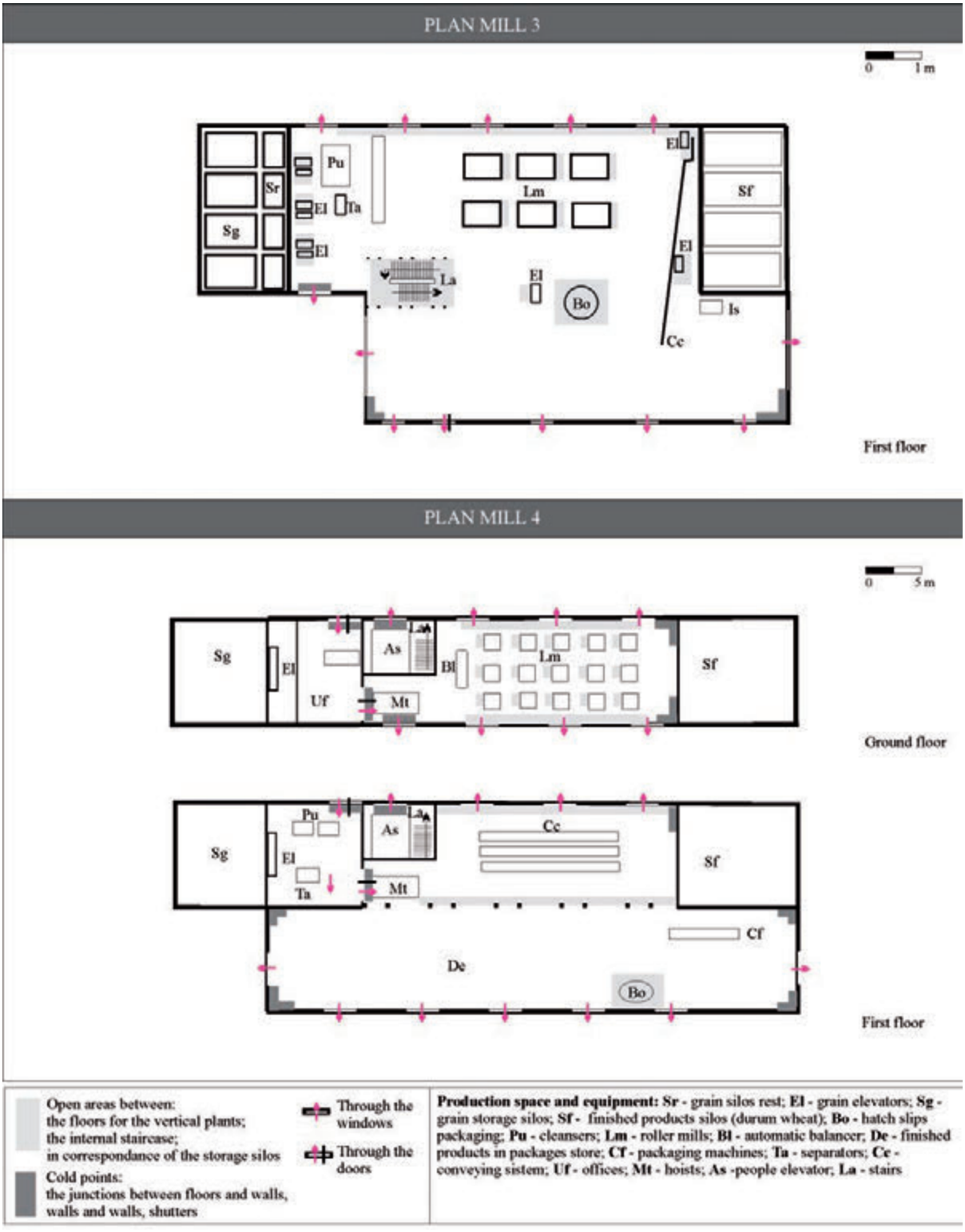

Figure 3. Critical points for transfer of heat.

Table 3. Identification of plant components susceptible to heat treatment.

Pneumatic and electrical components packaging machines	Operating temperature range ° C								
	0 ÷ +55	-20 ÷ +70	0 ÷ +50	-5 ÷ +70	-10 ÷ +60	<30 ÷ +110	-20 ÷ +80	-20 ÷ +70	-40 ÷ +60
Electrical equipment in general, internal panel, electronic control units, external electrical material, photocells / sensors	X	X (off)	-	-	-	-	-	-	-
Filter-reducing, electrovalves, lubricators 1700 series, electrodistributors	-	-	X	-	-	-	-	-	-
Non-rotating cylinder series 1348 ÷1350	-	-	-	X	-	-	-	-	-
PVC conveyor belts	-	-	-	-	X	-	-	-	-
Polyurethane conveyor belts	-	-	-	-	-	X	-	-	-
Pneumatic control valves series 224	-	-	-	X	-	-	-	-	-
PVC suction flexible hoses	-	-	-	-	-	-	X	-	-
Magnetic sensors	-	-	-	-	-	-	-	X	-
Pneumatic hoses, pneumatic plant	-	-	-	-	-	-	-	-	X

Components milling plants	Operating temperature range ° C		
	0 ÷ +100	0 ÷ +80	-20 ÷ +60
Flat Belts polyurethane elastomer-Z series	X	-	-
Flat belts in polyurethane leather-LT series	-	X	-
Flat belts in leather-LL series	-	X	-
Round belts and trapezoidal	-	-	X
Critical limit			

allowing the desired temperatures to be reached in a short time.

Very few critical points were found among the plant. The suppliers are ensuring that the components of the plant are suitable for the requirements of heat treatment.

The results of the analysis are of fundamental importance in establishing guide lines which can be used for existing buildings and when planning new mills, because heat treatment pest disinfestation is becoming ever more widely used n this sector.

References

Beckett S. J., Subramanyam B., Fields P. G. 2007. Disinfestation of Stored products and associated structures using heat. In: J. Tang, et al. (eds) Heat treatments for postharvest pest control. CABI, Wallingford, Oxfordshire, UK, pp 182-94.

Braghieri G., Nervi F & Zini N. 2007. Aspetti applicativi di nebbia secca e/o disinfestazioni con aria calda. pp 24-31 in Proc. Conf. L'eliminazione del bromuro di metile per la disinfestazione di industrie alimentari e strutture. Risultati di due anni di esperienze pratiche, 15 February, Bologna, Italy.

Brijwani M., Subramanyam B., Flinn P. W. 2012. Susceptibility of Tribolium castaneum Life Stages Exposed to Elevated Temperatures during Heat Treatments of a Pilot Flour Mill: Influence of Sanitation, Temperatures Attained Among Mills Floors, and Costs. Journal of Economic Entomology 2: 709-717.

Brijwani M., Subramanyam B., Flinn P.W., Langemeier M. R. 2010. Structural heat treatments against *Tribolium castaneum* (Herbst) (Coleoptera:Tenebrionidae): effect of flour depth, life stage and floor. Julius-Kühn-Archiv. 425:625-30.

Dean G. A. 1911. Heat for mill insects. Journal of Economic Entomology 4:142-58.

Dean G. A. 1913. Further data heat as a means of controlling mill insect. Journal of Economic Entomology 6:40-53.

Dosland O. 1996. Flour mills heating for insect control. Tecnica Molitoria 9: 867-75.

Dowdy A. K., Field P. G. 2002. Heat combined with diatomaceous earth to control the confused flour beetle (Coleoptera: Tenebrionidae) in a flour mill. Journal of Stored Products Research 38:11-22.

Dowdy A. K. 1999. Mortality of red flour beetle, Tribolium castaneum (Coleoptera: Tenebrionidae) exposed to high temperature and diatomaceous earth combinations. Journal of Stored Products Research. 35:175-82.

Failla A., Strano L., Tomaselli G.. 2006. Innovative Building Design Criteria for the Confectionary Industry. CIGR Ejournal 12, Vol. VIII.

Field P., Dowdy A., Marcotte M. 1997. Structural pest control: the use of an enahanced diatomaceus Earth product combined with heat treatment for the control of insect pests in food processing facilities. Agricolture and Agri-Food Canada and the United State Department of Agricolture: Environmental Bureau. Avaiable from: http//home.cc.umanitoba.ca/fieldspg/field/sheatde.htm. Accessed: May 2013.

Guerra P. 2009. Uso delle temperature elevate per il controllo degli insetti nei molini. Esperienze tecniche ed efficacia del metodo. Tecnica Molitoria 2:113-5.

Guerra P., Minetti S., De Cristofano J., Priolo F. 2012. High temperature treatment for pest control in pasta industries. Tecnica Molitoria 11:1110-21.

Mahroof R., Subramanyamb B., Eustace D. 2003. Temperature and relative humidity profiles during heat treatment of mills and its efficacy against Tribolium castaneum (Herbst) life stages. Journal of Stored Products Research 39:555-69.

Massara P. 2007. Disinfestare con aria calda. pp 34-40 in Proc. Conf. L'eliminazione del bromuro di metile per la disinfestazione di industrie alimentari e strutture. Risultati di due anni di esperienze pratiche, 15 February, Bologna, Italy.

Strano L., Russo P., Lanteri P., Tomaselli G. 2012. Defining the environmental and functional characteristics of the buildings used to produce prickly pear dried puree in terms of food hygiene and safety. Food Control 27:170-177.

Süss L. 2007. Quali possibilità per sostituire il bromuro di metile? pp 11-4 in Proc. Conf. L'eliminazione del bromuro di metile per la disinfestazione di industrie alimentari e strutture. Risultati di due anni di esperienze pratiche, 15 February, Bologna, Italy.

Süss L. 2008. L'impiego del calore nella disinfestazione di industrie alimentari. Igiene Alimenti - disinfestazione & igiene ambientale 3:27-8.

Hulasare R., Subramanyam B., Fields P. G., Abdelghany A.Y. 2010. Heat treatment: A viable methyl bromide alternative for managing stored-product insects in food-processing facilities. Julius-Kühn-Archiv. 425:664-70.

UNI EN, 1998. Processo edilizio - Classificazione e definizione delle fasi processuali degli interventi edilizi di nuova costruzione. Norma 10723:1998. Ente Nazionale Italiano Di Unificazione.

UNI EN, 1999. Terminologia riferita all'utenza, alle prestazioni, al processo edilizio e alla qualità edilizia. Norma 10838:1999. Ente Nazionale Italiano Di Unificazione.

Safety in the housing of horses

A. Checchi,[1] S. Casazza[2]

[1]University of Bologna, Dept. of Agri-Food Science and Technology, Bologna, Italy;
[2]Expert professional for safety in working environments, ASH srls, Brugherio (MB), Italy

Abstract

Safety within an equestrian facility is given also by the sizes of the places in which horses are lodged. The stalls are considered to be the basic modular element of breeding and hosting places, but in Italy there are no specific references about the most appropriate surface related both to different breeds and safety of the workers taking care of them. We sought to determine the size of individual spaces, based on the height at the withers of horses, and to formulate a specific forming and informing course for employees on the likely risks of contact which could generate traumatic events.

Introduction

The safety within an equestrian structure is also given by the size of spaces for stabling of horses. The stalls are considered the minimal units for housing and, for this reason, have been very often the subject of discussion. It's important to keep in mind that the welfare, safety and serenity of the horses are the starting point for the safety of the people working with and around them.

In the regulatory framework there is no reference document defining the most appropriate surface for proper housing of horses, and old bibliography does not respond to all the needs related to the size of animals of different breed and size.

Materials and methods

The Ministry of Health with "The Code for the Protection of the Horse" recently gave instructions about and showed some minimum parameters in the dimension of stalls:

Correspondence: A. Checchi, University of Bologna, Dept. of Agri-Food Science and Technology, Viale Fanin, 50, Bologna, Italy.
Tel. +39.051.2096101 - Fax +39.051.2096171.
E-mail: antonio.checchi@unibo.it

Key words: horses, farm risks, fire prevention

Journal of Agricultural Engineering 2013; XLIV(s1):e150
doi:10.4081/jae.2013.(s1):e150

Horses	3,00 m.	3,00 m.
Ponies	2,80 m.	2,80 m.
Mare&foal delivery boxes	3,00 m.	4,00 m.

On another side, the Scottish Animal Health and Welfare Act 2006 (the "'Act"), states that anyone who owns or operates an animal has a legal obligation to ensure his well-being and has the duty to treat him according to the "Five Freedoms" the first of which is given below:

"Freedom from discomfort ensuring an appropriate environment, including shelter and a comfortable resting area."

Starting from these two codes, we tried to introduce simple formulas that allow you to determine the size of individual spaces, estimated on the height at the withers of the subjects accommodated.

This does not mean that you should have different sizes of stalls for each horse depending on their size, but it does give directions, especially to farmers and horse riding schools. That is, for example, if you breed Haflinger horses or Frisian is should prepare boxes of different sizes, as well as if you are managing a pony school, needs will be different from a school that uses only horses.

To calculate stalls' dimensions, the area to be attributed to the relaying of each individual equine, with height at withers (hg) which can vary from 0.9 m. 2.0 m., refers to the following formula:

$$4\times(hg)\ 2$$

Similarly, in the case where the stalls are not square, the minimum width of the front of the stall can be defined, where the access door will be positioned:

$$1.8\times(hg)$$

The minimum ceiling height is important, on the one hand because of the risk of injury for equines bumping their head and, secondly, because it limits the amount of air circulating in the stable and thus influences its climatic conditions. Consequently, the recommended height of the lowest point is equal to twice the height at withers:

$$2\times(hg)$$

If it is planned to accommodate within the structure mares with foal, as they need more space to assure a correct movement of the foal, we must follow the formula:

$$5.2\times(hg)\ 2$$

The stall for stallions must be wider than the others, because they because they move more inside the stall, then you can consider the appropriate formula:

$$5.6\times(hg)\ 2$$

Interior features of stalls and accessories

Walls

All four walls of the stall must be closed from the bottom to a height equal to hg <hp <1.5 m where hp is the height of the wall. They must be strong enough to withstand kicks and sudden movements, must be anchored in stable way to the ground, so to support the weight of the animal in case he leans against them. This is important especially in the case of prefabricated structures that are usually positioned for

short periods, such as at trade shows, competitions and other temporary events. In addition to what is indicated, the walls must not have protrusions, either internally or externally, and if in the upper part have a grid, this should not allow the passage of the limbs.

Doors

The access door to the stall must have a minimum width of 1.5 m, because we must consider the transverse width of the body of man and horse, and a height not less than 2.5 m.

The door must open towards the outside of the stall or scroll on a top rail.

Generally the doors are made of two parts, a closed lower one, which must have a height proportional to the withers of the animal (the standard ones, considering an average size at the withers equal to 1.60 to 1.70 m, are about 1.30-1,40m.) and a top part that can be opened (this solution is mainly used in box with outer lane) or fixed, both filled or with grids. The opening of the top part in stables with an inside lane has some advantages but also some disadvantages related to the cleaning and maintenance of the lane. In fact, while the horse is eating he can dirty the outside of the stall, looking out during chewing and may interfere with the passage of the operators and users sticking out with the neck. However, there is the undeniable advantage that the possibility of extending his outside of the box allows the horse visual distraction and can so socialize with other horses. The best solution is that the upper grids can be opened, so you can close it during meal times and while the staff is working and leave it open in other moments so that the horse can "snoop" around.

Windows

The arrangement, number and size of windows are subject to the number of horses housed and the internal layout of the stable: their main function is to ensure adequate light and air circulation. Within each stable the air-entraining and illuminating ratio, i.e. the ratio between the windowed surface and that of the floor must be at least 1/10. Beware that not always illuminating windows can be opened, so when calculating the above-mentioned parameter you must take into account only the windows that you can open.

If positioned on the wall, opposite the door, it allows the horse to look outside the stall. In this case, the windows should have the possibility of being closed during the night or for other needs.

Their optimal position should be commensurate with the size of the horse at the withers; in this regard it is recommended to take as a reference the height of the lower shutter of the front door. This kind of window must have a height from the ground of 1.5-2.0 m. and a width of at least 1.0 m.

Other types of windows used in the stables are transom windows, placed at least 2.5 m. from the soil. They must be oriented so that the incoming air flows toward the ceiling and never directly on the horse. However they have the disadvantage that the horse cannot see outside. The important advantage of this type of opening is that they allow, with a good air circulation, in any season, to eliminate the high levels of ammonia that accumulate inside the stall. The most common sizes are equal to 1.2-1.4 m. wide and 0,70-0,90 m. in height.

If it is not possible to have the elements just described, it's advisable to provide for the presence of skylights on the roof of the structure, at least one for each stall, in order to assure a regular air change and the elimination of harmful gases. Keep in mind, however, that the skylights, in case of snow, cannot be opened and will not give light and therefore should not be the only air-entraining and illuminating source.

Accessories

All stalls must have within them some specific allocations: specifically, the drinking trough and feeder.

Feeders are trays with a round shape with a capacity of 20-25 liters and rounded and reinforced top edges, fastened to the wall.

The troughs are drinking systems connected to the water mains. The water level can be regulated automatically or by pressure on an inner tongue. It is recommended that each one has a separate shut-off valve, operable in case of malfunction. It 's very important that the water supply pipes are arranged perpendicular to the floor, so that it is more difficult for the horse to lean or damage them with their teeth or, if possible, recessed in the wall or protected.

Both elements must be positioned, respect to the ground, in proportion to the height at withers of the horse according to the following formula:

$$hg \times 0.70$$

The drinking trough and feeder inside the stall should be placed in opposite corners, on the diagonal of the stall, so to force the horse to walk a few steps and have a clear separation of drinking from the action of eating. It's also advisable to place the feeder on the same side of the door, for greater comfort of the operator who distributes the feed.

Conclusions

This article deals with some important issues towards which particular attention has been addressed over the last few years: animal welfare and safety at the workplace. We propose the design of a stable according to the parameters related to the welfare of the horses stabled, bearing in mind that this system allows you to resize the stalls as well as all the other spaces for the detention of horses of any breed, presenting the advantage of readjusting all the spaces within them.

Bibliography

Brandizzi G., Carbone E. (2004) Building for Sport, UTET

A. Checchi (1992), Stables: a guide for the design and construction, Edagricole

Chiumenti R. (2004), Rural Construction, Edagricole

Devenuto L. (2012) - Elements for the design of a riding club: Guidelines and functional diagrams - final work of the Master's Degree in "Architectural Design Sport facilities"

Ministry of Health (2011), The Ministry of Health for the horse - Standards, rules and protection projects

FVO - Federal Veterinary Office (2009), Minimum requirements for horse boxes

Wheeler E.F. (2006) - Horse stable and riding arena design - Blackwell

Levels of vibration transmitted to the operator of the tractor equipped with front axle suspension

Daniele Pochi, Roberto Fanigliulo, Laura Fornaciari, Gennaro Vassalini, Marco Fedrizzi, Gino Brannetti, Cesare Cervellini

Consiglio per la ricerca e la sperimentazione in agricoltura, CRA-ING Unità di ricerca per l'ingegneria agraria, Agricultural Engineering Research UnitMonterotondo (Rome), Italy

Abstract

In recent years the comfort and the preservation of the health of the operators became central issues in the evolution of agricultural machinery and led to the introduction of devices aimed at improving working conditions. Thereby, for instance, the presence of air conditioner, soundproof cab and driver seat suspension became normal on agricultural tractors. The vibrations are one of the most complex issues to deal with, being determined by the characteristics and interaction of elements such as tyres, axles, mainframe, cab and seat suspension. In this respect, manufacturers are trying to improve their products, even integrating these elements with new devices such as the suspension on the front axle of the tractor, aimed at reducing the level of vibrations during the transfers at high speed. One of these underwent tests at CRA-ING. Since its purpose is to reduce the level of vibration transmitted to the driver, their measurements in different points of the tractor and in different operating conditions, were compared in order to evaluate the effectiveness of the device, expressed as time of exposure. The suspension system of the front axle is designed to absorb the oscillations (especially pitching) determined by irregularities in the road surface, allowing an increased control of the vehicle at high speed, as demonstrated by the test results and confirmed by the driving impressions outlined by the operator. The action of the device under these conditions results in an increase of the exposure time, important fact because of the relevance of the road transfer operations of tractors with mounted implements or trailers to tow and of the tendency to increase the speed limit for the road tractors (in Germany were brought to 50 km h^{-1} for several years). The action just described is less evident with increasing irregularity of the road surface and with the decrease of the travel speed. Nevertheless, in such conditions, the device appears to positively work along the other directions, in particular in the Z-axis, improving the action of the suspension of the driver seat.

Correspondence: Daniele Pochi, Unità di ricerca per l'ingegneria agraria, Via della Pascolare, 16, 00015 Monterotondo (Rome), Italy.
Tel. +39.06.90675232 - Fax: +39.06.90625591.
E-mail: daniele.pochi@entecra.it

Keywords: vibrations, tractor suspensions, comfort, health protection.

Contributions: the authors contributed equally.

Conflict of interests: the authors declare no potential conflict of interests.

Journal of Agricultural Engineering 2013; XLIV(s1):e151
doi:10.4081/jae.2013.(s1):e151

Introduction

Since several years, the technological evolution of agricultural machinery focused the attention, beside the operative performances, on the aspects of comfort and health safe of the operator, introducing devices and measures aimed at improving the working conditions. Thereby, for example, the presence of the air conditioning and soundproofing systems in the cab of the tractor became normal, as well as driver's seats fitted with shock absorbers effective against the vibrations induced by the execution of the agricultural works (Ragni *et al*., 1999). Vibrations are one of the most important and complex problem to deal with, being determined by the characteristics and the interaction of different elements such as tires, axles, main frame, cab and driver seat (Fornaciari *et al*., 2008).

In relatively recent times, modern tractors, in addition to the suspension seat, are sometimes equipped with other devices aimed at improving the comfort of the driver, such as the front axle suspension and systems capable of changing the setting of the cockpit.

This paper reports the results of tests carried out on a tractor equipped with suspension of the front axle during transfer operations on different surfaces in order to observe its effect on the level of vibration at the driver seat.

Materials and methods

Tractor - The tests were conducted on a tractor of medium-high power (147 kW) suitable for the multiple farm needs and with a high level of comfort and ergonomics for the operator (Nuccitelli and Ragni, 1993). Considering the subject of the tests, beyond the driver seat with pneumatic suspension (in which a rubber cylinder containing pressurized air works as a spring), the front axle of the tractor was provided with an original suspension (Figure 1).

The front axle is hinged to the body of the tractor by means of arms, which allow the longitudinal or transverse oscillation and damping by means of the combined action of two hydraulic cylinders and of two nitrogen accumulators mounted in series. The oil leaking from the cylinders during the compression phases is received by the nitrogen accumulators which absorb the shocks.

The use of the suspended axle is recommended during road transfer, where it help to reduce the danger represented by bumps at high

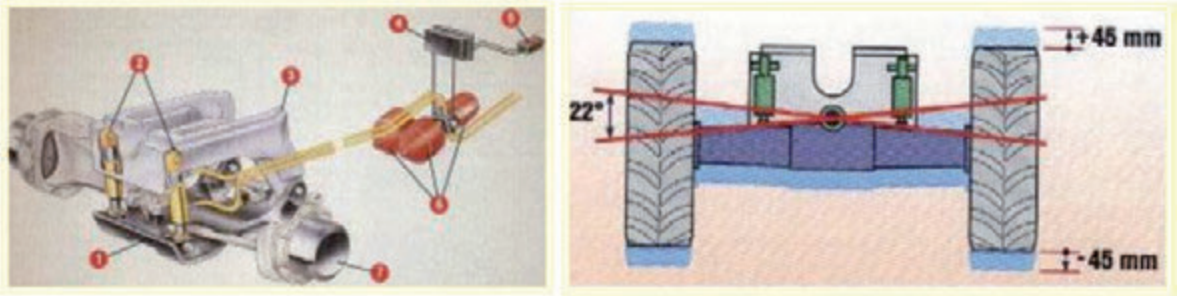

Figure 1. Left: scheme of the hydraulic-pneumatic suspension of the fron axle 1) mobile structure hinged to the main frame of the tractor; 2) double-acting hydraulic cylinders; 3) tractor main frame; 4) electronic controll unit; 5) on-off switch; 6) nitrogen accumulators; 7) Front axle. Right: Maximum amplitude of the oscillation allowed by the hydraulic cylinders.

travel speed. Under field conditions, its effectiveness is less evident and, at any rate, it is automatically disconnected whit the differential is locked.

Instruments - The instrumental chain use in the tests consisted of:

- two 6-channels signal conditioners Brüel & Kjær mod. 'Nexus';
- 8-channel digital recorder DAT-Herm;
- signal acquisition and processing system Brüel & Kjær, mod. Pulse;
- calibrator for accelerometers Brüel & Kjær, type 4294;
- tri-axial accelerometer adapted for driver seat Brüel & Kjær, type 4322;
- two tri-axial accelerometers Brüel & Kjær, type 4321, positioned on the cab floor and on the tractor mainframe

Methods - As previously said, the tests aimed at verifying the presence of effects of the introduction of the front axle suspension on the level of vibration. From this point of view, the basic parameter to measure, is the acceleration, a, expressed in ms^{-2}. As the effects of the vibrations depend on the frequency of the accelerations, these must be weighted by means of suitable filters, according to the standard ISO 2631-1:1997, and the Italian law (D.Lgs 81/2008) for the measurement of the levels of whole body vibrations transmitted to the operator by the driver seat (Scarlett *et al.*, 2007). The accelerometers were positioned with the purpose of measuring the vibration levels in correspondence of the main elements of the system that transmit the vibrations themselves. Therefore, an accelerometer was placed on the driver's seat, as the remaining two were placed, respectively, on the cab floor and on the main frame of the tractor, on the same vertical line of the first. The accelerometers were oriented accordingly to the requirements of the standard ISO 2631-1:1997, as described in the Figure 2.

The weighting filters are calculated as a function of the human body sensitiveness to the acceleration in the different sampling frequencies and provide an acceleration value called frequency weighted acceleration, a_w,

$$a_W = \left[\frac{1}{T}\int_0^T a_w^2(t)dt\right]^{\frac{1}{2}} \quad (1)$$

where:

$a_w(t)$ is the measured value of the acceleration; T is the acquisition time interval in seconds.

The three components of the acceleration along the X, Y and Z axes are simultaneously measured and the resultant vector of the acceleration a_v is provided by the relation:

$$a_v = (k_x^2 a_{wx}^2 + k_y^2 a_{wy}^2 + k_z^2 a_{wz}^2)^{\frac{1}{2}} \quad (2)$$

where:

a_{wx}, a_{wy}, a_{wz}: weighted RMS accelerations along the x, y and z axes;

k_x, k_y, k_z: indices the values of which were determined depending on the effects of the relative components of the acceleration on the health: for k_x e k_y a value of 1.4 is applied in the case of sitting positions, as they are equal to 1 for the upright position; k_z is equal to 1 in both positions.

The exposure to the vibrations can be quantified by normalizing the value of the acceleration a_v, measured during the daily exposure time (T_e), referring to a 8 hours time interval, according to the principle of "equal energy", providing the normalized acceleration, A(8) according to the formula:

$$A(8) = a_v \sqrt{\frac{T_e}{8}} \quad (3)$$

According to the standard ISO 2631-1, the calculation of A(8) aimed at the health risk assessment is made only considering the dominant axial a_w component. Considering the particular characteristic of agricultural work, in which all the axial accelerations are often relevant, this study, also provided the calculation of A(8) as function of the resultant acceleration, a_v and of the vertical weighted acceleration, a_{wz}, in order to observe how they affect the time of exposure. The determination of A(8) and the calculation of the maximum daily exposure times were made using the Excel data-sheet "Calculation of the exposure to vibrations" in the ENAMA website.

Tests - The tests consisted of transfer trials withour traction load (Figure 3) on asphalt track at 10.8 ms-1 (39 km h-1), on a macadam

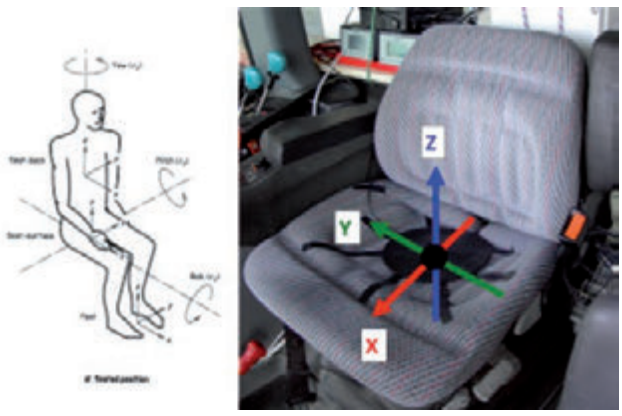

Figure 2. System of coordinates for the orientation of the accelerometer for seated operator and the driver seat with tri-axial accelerometer.

road at 7.7 ms-1 (27.7 km h-1) and on grassed headland at 4.5 ms-1 (16.3 km h-1).

The gear box rations were chosen in order to achieve, on each surface, the highest travel speed. As a consequence, considering the available test distance on each surface, the sampling intervals meanly resulted of 13.8 s on asphalt, 19.5 s on macadam and 33.3 s on the headland. Three replications were made in each condition, comparing the measurements with the front axle suspension disconnected (thesis A) and connected (thesis B).

Results and discussion

The Table 1 and the Figure 4 show the results of the transfer tests on the three surfaces. In all test conditions, the values of a_v increase passing from the frame of the tractor, to the cab floor, to the driver seat.

The amplification of the vibrations in the transition from one survey point another is related to the nature of the materials, to the constructive characteristics of the various elements, to the connections between them (geometries and characteristics of stiffness, etc..) and to the increasing distance from the points where the vibrations are generated and from which are transmitted (i.e. the contact area between tire and ground). This pattern was observed in all the theses and seemed more evident in the tests at higher speed (asphalt track and macadam).

From the observation of the axial components of the acceleration, a_w, (Table 1), it can be noticed that even in presence of a dominant component, the other two axial components often assumed relevant values.

In general, the peaks of the accelerations always occurred at low frequencies (between 1 and 3.15 Hz). Significant examples of such patterns are shown in the diagrams of Figure 5, reporting the results of the frequency analyses of the weighted accelerations with reference to the axes X and Z.

With reference to the three test surfaces, the following considerations can be made.

Asphalt track

The effect of the front suspension is more pronounced on the X-axis (pitch) where a clear reduction occurs of the weighted average accelerations, a_{wx} in the thesis B with respect to the thesis A (Table 1), on all three survey points (reduction from 39.83% to 48.57%). In absolute terms the reduction was higher at the driver's seat level (0,423 ms^{-2}).

This is confirmed by the analysis in frequency on X axis (Figure 5) which clearly shows that the linear reduction of the acceleration, a_x, is more evident in the range of frequencies between 1.6 and 4 Hz on all three observed points. Thereby, the suspension seems to also reduce

Figure 3. Tractor during the transfer tests on asphalt and on the headland.

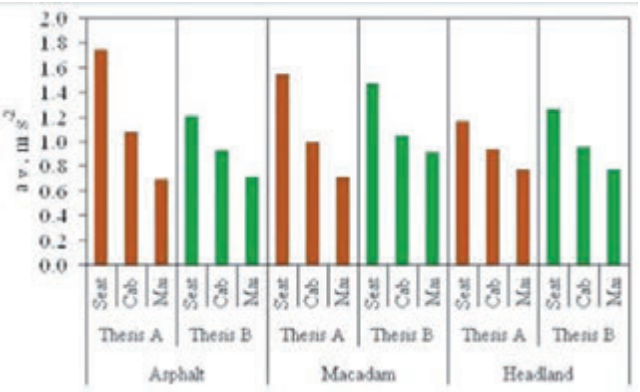

Figure 4. Average values of the vector acceleration, av, in the three point of application of the accelerometers.

Table 1. Values of the axial weighted accelerations aw , calculation of the resulting vector av, differences between the theses A and B in the different surfaces and values of the time of exposure. The time of exposure was calculated as function of the vertical acceleration awz (Te_{awz}), of the vector acceleration a_v (Te_{av}), and of the dominant wheighted axial acceleration a_{wDom} (Te_{awDom}). When the dominant axial acceleration is the a_{wz}, Te_{awz} and Te_{awDom} coincide.

Engine speed (min^{-1})	Active control	L_{Aeq} dB(A) Repetitions 1	2	3	Average	Stand. Dev.	Δ	L_{eq} dB Repetitions 1	2	3	Average	Stand. Dev.	Δ
600	OFF	76.3	75.4	75.6	75.8	0.46		89.5	89.3	89.8	89.6	0.26	
	ON	75.7	74.9	75.2	75.2	0.40	0.6	83.9	83.1	85.4	84.2	1.17	5.4
700	OFF	79.5	78.0	77.9	78.5	0.35		94.4	95.1	95.4	95.1	0.51	
	ON	77.8	77.0	77.0	77.3	0.45	0.9	87.5	87.7	88.1	87.8	0.42	7.7
800	OFF	78.7	78.4	78.2	78.4	0.25		93.3	93.6	93.4	93.5	0.22	
	ON	78.0	77.4	77.5	77.6	0.26	0.8	86.7	86.9	86.7	86.8	0.46	7.1
900	OFF	79.9	79.9	80.2	79.9	0.19		91.6	92.4	90.9	91.6	0.74	
	ON	73.4	73.5	80.0	73.6	0.33	6.3	87.9	88.4	88.7	88.3	0.39	3.3
1000	OFF	81.2	81.0	80.8	81.0	0.19		91.4	91.9	91.4	91.6	0.33	
	ON	80.6	80.6	80.7	80.7	0.11	0.3	86.2	86.2	86.7	86.5	0.57	5.0
1100	OFF	81.6	81.2	80.9	81.2	0.27		94.7	93.3	93.5	93.8	0.74	
	ON	81.1	80.9	80.8	81.0	0.14	0.3	88.9	88.7	90.0	89.2	0.71	4.6
1200	OFF	83.8	83.5	83.1	83.5	0.40		96.1	96.6	95.7	96.1	0.45	
	ON	83.1	82.4	82.7	82.7	0.35	0.7	90.9	90.7	91.7	91.1	0.49	5.0
1250	OFF	83.8	83.6	83.5	83.6	0.15		96.7	96.0	96.2	96.3	0.34	
	ON	83.5	83.4	83.4	83.4	0.06	0.2	91.9	92.2	91.8	91.9	0.21	4.4
1300	OFF	84.5	84.5	83.7	84.2	0.47		96.9	99.5	97.4	97.9	1.37	
	ON	84.0	84.0	83.4	83.8	0.33	0.4	92.2	92.3	92.3	92.3	0.06	5.6
1350	OFF	84.9	84.5	83.9	84.5	0.51		99.8	99.3	98.5	99.2	0.66	
	ON	83.7	83.7	83.6	83.6	0.10	0.9	92.6	92.8	91.9	92.5	0.55	6.7
1400	OFF	86.6	86.3	86.1	86.3	0.25		101.6	102.3	102.0	102.0	0.37	
	ON	83.7	83.5	83.5	83.6	0.10	2.7	93.5	93.6	93.1	93.5	0.36	8.5
1450	OFF	87.1	86.8	86.6	86.8	0.25		103.2	102.4	102.5	102.7	0.49	
	ON	84.7	84.9	84.8	84.8	0.10	2.0	94.6	95.1	94.7	94.8	0.40	7.9
1500	OFF	88.1	87.9	88.0	88.0	0.13		103.6	102.8	103.2	103.2	0.36	
	ON	85.5	85.4	85.8	85.6	0.19	2.4	95.0	94.4	95.5	95.0	0.56	8.2
1550	OFF	89.7	89.5	89.2	89.5	0.24		104.6	104.3	104.2	104.4	0.19	
	ON	87.2	87.3	86.8	87.1	0.51	2.5	97.3	97.5	95.2	96.7	1.27	7.7
1600	OFF	90.2	90.1	90.1	90.1	0.06		104.2	104.4	104.5	104.4	0.15	
	ON	88.2	88.1	87.3	87.9	0.48	2.2	96.3	96.8	96.3	96.8	1.30	6.6
1650	OFF	90.2	90.0	89.8	90.0	0.21		103.9	103.7	103.6	103.7	0.12	
	ON	88.5	88.1	88.3	88.3	0.19	1.7	98.5	98.4	98.2	98.4	0.15	5.4
1700	OFF	89.9	89.7	89.6	89.8	0.13		103.1	103.0	103.3	103.1	0.13	
	ON	88.2	88.4	88.9	88.5	0.34	1.3	97.6	98.5	99.4	98.6	0.79	4.5
1800	OFF	89.8	89.8	89.8	89.8	0.04		100.9	101.6	101.0	101.2	0.39	
	ON	89.1	91.2	90.3	90.2	1.06	0.4	97.5	101.9	100.2	99.8	2.23	1.4
1900	OFF	90.2	90.2	91.8	90.8	0.97		99.1	99.8	102.2	100.4	1.65	
	ON	90.2	90.8	92.3	91.1	1.08	0.3	98.0	99.0	102.0	99.7	2.04	0.7
2000	OFF	91.5	91.6	91.6	91.6	0.06		99.3	99.5	99.4	99.4	0.11	
	ON	91.3	91.5	91.8	91.4	0.16	0.1	98.6	98.9	98.7	98.7	0.11	0.7

the level of vibration at the tractor mainframe. The effect of amplification of the vibrations, passing from the frame to the seat, is evident as well.

On the Y-axis (roll), the front suspension causes a worsening in the level of vibrations at the mainframe and improvements in cabin and seat.

About the Z-axis, despite a_{wz} at the frame is higher for the thesis B (probably for effect of different surface irregularity in the two theses), a decrease of the vibration is detected specially at the driver seat, the shock absorber of which, combined with the front suspension, seems to increase its efficiency. Such a behaviour is visible in the diagram of the analysis in frequency (Figure 5) for frequencies between 3.2 and 20 Hz, where a_z, for the thesis B is always less than for the thesis A.

Macadam road

Despite the lower forward speed, the stresses caused by this surface were more severe than by the asphalt, as evidenced by the values of weighted accelerations averages a_{wx} and a_{wy} on the frame, and from those of a_v (Table 1).

Despite of the controversial behaviour of the axial weighted acceleration a_w (Table 1), the thesis A presents higher values of a_v at the frame and on the cab floor and lower at the driver seat, than the thesis B (Figure 4). The Z-axis resulted as the most stressed. The effect of the front suspension on the pitch (X-axis) can be observed in Figure 5. The linear acceleration, a_x, at the mainframe are similar for the two theses; passing at the driver-seat ax increases and is higher for the thesis B in the interval 1,25 - 2 Hz. The surface in macadam seems to produce shocks characterized by frequency values that tend to be lower than in asphalt and the evaluation of the effectiveness of the front suspension in such condition requires further tests.

The analysis in frequency on the Z-axis (Figure 5) shows that the linear acceleration is lower for the thesis B in the interval 1.6-16 Hz, with a relevant reduction on the peak point at 2.5 Hz.

Grassed headland

The resultant acceleration, a_v, is higher for the thesis B. As to the weighted accelerations, the dominant aw occur on the Z-axis for the Thesis A and on the Y-axis for the thesis B. This variable pattern indicates that, differently from the asphalt, in the headland there is not a prevailing pitch effect. The relatively low speed and the characteristics of the surface (limited and variable transversal slope, unevenness and compactness softened by the grass) probably had a damping effect that interfered with action of the suspension.

As to the action of the front suspension against the pitch, the analysis in frequency (Figure 5) shows that the linear acceleration a_x increases passing from the mainframe to the seat and that in the thesis B it has lower levels than in A. The higher values occurred in the interval of frequency between 1.6 and 3.15 Hz. The analysis in frequency on the Z-axis shows that the front suspension (thesis B) determines a reduction of the acceleration a_z in the interval 3.15 – 4 Hz, as it is increases in all remaining frequencies, with two relevant peaks a 2.5 and 8 Hz (Hz).

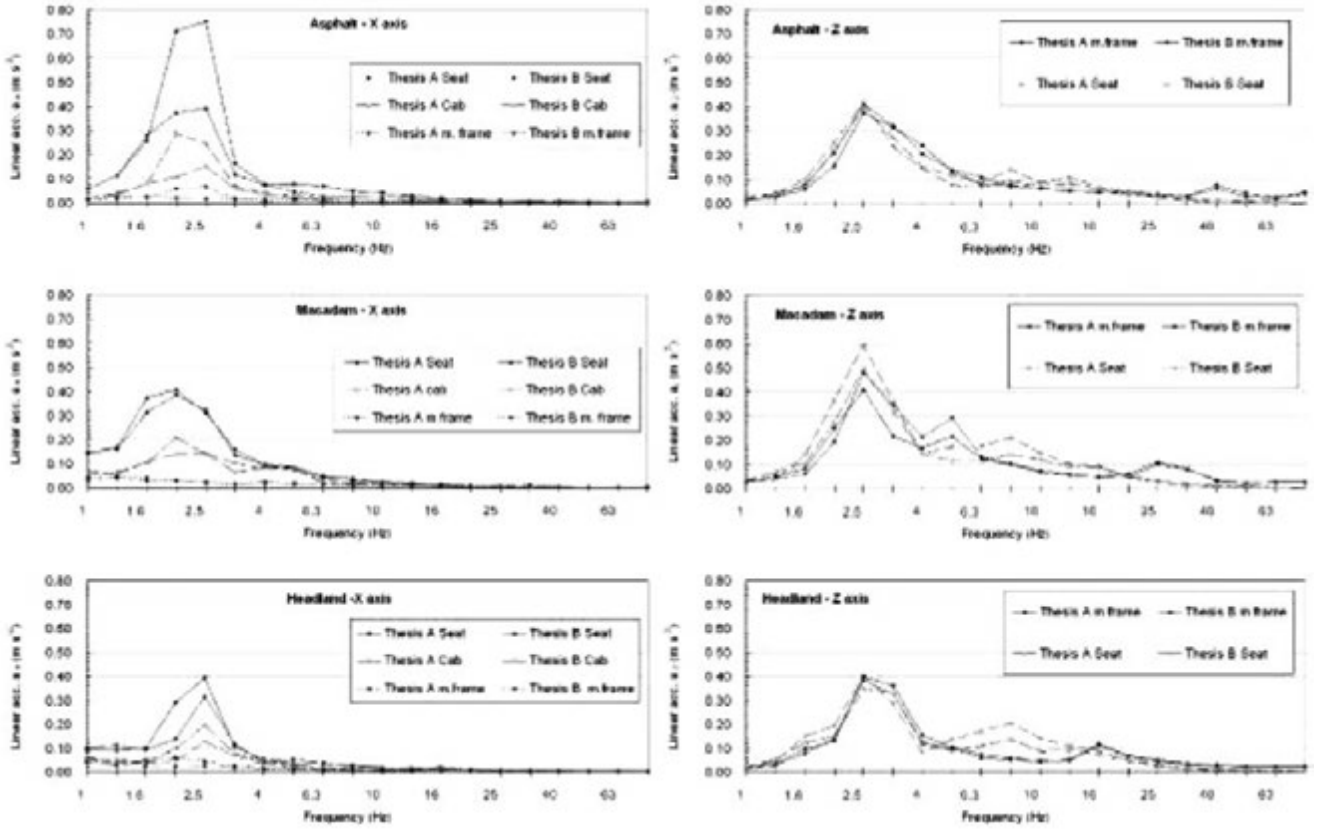

Figure 5. Frequency analysis of the accelerations during the transfer tests on the three surfaces with front axle suspension "off" (Th. A) nda and "on"(Th. B). Left: X-axis (aX) in the three points of observation. Right: Z-axis (aZ) only for the tractor mainframe and the driver seat, in order to achieve information about the shocks transmitted through the system by soil unevenness.

Finally, the Table 1 reports the exposure times calculated by means of the relation (3) as a function of the dominant axial acceleration Te_{awDom}, (according to the ISO 2631-1), of the resultant a_v ,Te_{av} and of the vertical component a_{wz}, Te_{awz}. The exposure times with the front suspension connected always resulted higher than suspension disconnected. Moreover, Te_{av} evidently resulted with lower values in all the tests, which demonstrates the relevant influence of all axial components, as expected. In this regard, for instance, observing the a_w values in Table 1, on asphalt/Thesis B, the weighted axial acceleration values are 0.64 ms^{-2}, 0.40 ms^{-2} and 0.59 ms^{-2} respectively for X, Y and Z, as a_v calculated with the relation (2) is 1,74 ms^{-2}. The calculation according the reference standard should be made using the dominant a_{wx} = 0.64 ms^{-2}, ignoring a_{wy} and a_{wz}, despite the values of the latter can be considered of the same order of magnitude of a_{wx} and heavily affect the determination of the resultant acceleration vector a_v. Unlike other work environments, the solicitations typical of agricultural work evidently involve all the spatial components and, as a consequence, the application of the common concept of "dominant axial component" may be improper and may contribute to an underestimation of the risks from exposure to the vibrations.

Conclusions

The front axle suspension represents a contribution to the improvement of the working conditions of the drivers of agricultural tractors from the point of view of the comfort and health protection.

The device resulted effective in the absorption of shocks and vibrations (mostly the pitch), due to the unevenness of the road surface. The best performances were observed in the tests at higher speeds and were confirmed by the impressions of the operators about an increased level control of driving. The increases of the time of exposure testifies the improvement of the quality of the working conditions. Such results are relevant with reference to the increasing importance of the road transfer operations, also considering the tendency to raise the speed limits for the tractors.

The effectiveness of the device is less evident at lower speeds and on more irregular surfaces, where, at any rate, its positive effects continue on the Z-axis, enhancing the action of the seat suspension.

References

Decreto Legislativo 9 aprile 2008, n. 81 Attuazione dell'articolo 1 della legge 3 agosto 2007, n. 123, per il riassetto e la riforma delle norme vigenti in materia di salute e sicurezza delle lavoratrici e dei lavoratori nei luoghi di lavoro, mediante il riordino e il coordinamento delle medesime in un unico testo normativo, G. U. n. 101 del 30 aprile 2008.

ISO. 1997. Mechanical vibration and shock – Evaluation of human exposure to whole-body vibration – Part 1: General requirements (ISO 2631-1:1997). International Organisation for Standardisation (ISO), Geneva, Switzerland.

Produzione documentale tecnica sulla problematica delle vibrazioni connessa all'uso delle macchine agricole ENAMA – Roma 2005. www.Enama.it

Pochi, D., Vassalini G., Fornaciari L., Gallucci. F. 2006. Valutazione delle vibrazioni trasmesse all'operatore da una trattrice a cingoli in varie condizioni di utilizzo. In Proc. dB(A) 2006 Rischi fisici negli ambienti di lavoro – Volume 1: Rumore e vibrazioni, Modena, Italy, 12-13 October.

Nuccitelli G., Ragni L. 1993. Influence of seat adjustment on the vibrations transmitted to the driver. Journal of Agricultural Engineering, 3: 143-150.

Fornaciari L., Pochi D., Vassalini G., Gallucci F. 2008. "Investigation of the vibrations transmitted by agricultural tractor to the driver under operative conditions" - International Conference: September 15-17, 2008 Ragusa – Italy.

Pochi D., Vassalini G., Fornaciari L., Gallucci F. 2007. "Hand-arm vibration levels measured under operating conditions in different types of agricultural tractors" – 11th International Conference on Hand-arm Vibration – 3-7 june 2007, Bologna.

Vassalini G., Fornaciari L. 2007. "Valutazione del rischio vibrazioni del parco macchine dell'azienda sperimentale del CRA-ISMA con il D. Lgs. 187/05" - Atti del 13° Convegno di Igiene Industriale – Le giornate di Corvara – 26-28 marzo 2007.

Pochi D., Vassalini G., Fornaciari L., Gallucci F. 2006 "Valutazione delle vibrazioni trasmesse all'operatore da una trattrice a cingoli in varie condizioni di utilizzo" – dB(A) 2006 Rischi fisici negli ambienti di lavoro – Volume 1: Rumore e vibrazioni.

Scarlett, A. J., J. S. Price, and R. M. Stayner. 2007. Whole-body vibration: evaluation of emission and exposure levels arising from agricultural tractors. Journal of Terramechanics, 44: 65-73.

First investigation on the applicability of an active noise control system on a tracked tractor without cab

Daniele Pochi,[1] Roberto Fanigliulo,[1] Lindoro Del Duca,[2] Pietro Nataletti,[3] Gennaro Vassalini,[1] Laura Fornaciari,[1] Luigi Cerini,[3] Filippo Sanjust,[3] Diego Annesi[3]

[1]Consiglio per la ricerca e la sperimentazione in agricoltura, CRA-ING Unità di ricerca per l'ingegneria agraria, Agricultural Engineering Research Unit, Monterotondo (Rome), Italy; [2]ACTIVE di Lindoro Del Duca, Rome, Italy; [3]INAIL Ricerca, Dipartimento di Igiene del Lavoro, Monte Porzio Catone (Rome), Italy

Abstract

In last years, several research teams pointed their attention on the application of active noise control systems (ANC) inside the cabs of agricultural tractor, with the purpose of reducing the driver exposition to noise, that is only partially controlled by the frame of the cab. This paper reports the results of a first experience that aimed at verifying the applicability of an ANC on a medium-high power, tracked tractor without cab. The tested tractor was a Fiat Allis 150 A, equipped with rear power take off, used in the execution of deep primary tillage in compact soils. It is a tracked tractor without cab, with maximum power of 108.8 kW at 1840 min^{-1} of the engine. The ANC consists of a control unit box based on a digital signal processor (DPS), two microphones, two speakers and a power amplifier. The instrumentation used in noise data collecting and processing consisted of a multichannel signal analyzer (Sinus - Soundbook), a ½" microphone capsule and an acoustic calibrator, both Bruel & Kjaer. The study aimed at evaluating the behaviour of the ANC by means of tests carried out under repeatable conditions, characterized by pre-defined engine speed values. Three replications have been made for each engine speed. The sampling time was 30 s. Two series of tests were performed in order to compare the results observed with the ANC on and off. The engine speed adopted in the study ranged from 600 min^{-1}, up to 2000 min^{-1} (maximum speed) with steps of 100 min^{-1}. The ANC proved to be effective in the interval of speed between 1400 and 1700 min^{-1}, where the samplings have been intensified, adopting steps of 50 min^{-1}. In such an interval, the attenuation observed with the ANC system on appeared evident both as weighed A sound pressure level (from 1.29 up to 2.46 dB(A)) and linear (from 4.54 up to 8.53 dB). The best performance has been observed at the engine speed of 1550 min^{-1}, with attenuations, respectively of 2.46 dB(A) and 7.67 dB. Outside of the engine speed interval 1400 - 1700 min^{-1}, the attenuations always resulted lower than 1 dB(A) for the weighed A sound pressure level and between 0.66 and 7.72 dB.

Correspondence: Daniele Pochi, Unità di ricerca per l'ingegneria agraria, Via della Pascolare, 16, 00015 Monterotondo (Rome), Italy.
Tel. +39.06.90675232 - Fax: +39.06.90625591.
E-mail: daniele.pochi@entecra.it

Keywords: sound pressure level, attenuation, tractor.

Contributions: the authors contributed equally.

Conflict of interests: the authors declare no potential conflict of interests.

Journal of Agricultural Engineering 2013; XLIV(s1):e152
doi:10.4081/jae.2013.(s1):e152

Introduction

At about twenty-five years since the beginning of systematic work on the active noise control, we can draw some important conclusions and suggest programs and reasonable results for the foreseeable future (Hasegawa *et al*., 1992; Kuo and Vijayan, 1994). The enthusiasm of the researchers, emerging from the reading of the considerable amount of works reported in the Proceedings of the Conference 'ACTIVE-95', the first conference dedicated exclusively to this area of research, gradually decreased over time. The few applications that were successful in industry were primarily the result of large investments in applied research of the products and were aimed at very large market segments (Elliot, 2000). For instance, it was the case of the active headphone and of the active-cancelling microphone. The problem of noise reduction in the cab of tractors, as well as other vehicles, it is very sensitive today both for the preservation of health and for a greater operator comfort. For several years, research groups turned their attention to the active noise control into cabs of tractors and industrial vehicles trying to reduce operator exposure to the noise, that is only partly controlled by the cab structure (Del Duca and Nataletti, 2009; Nataletti and Del Duca, 2010).

This work describes a first experience aimed at verifying and evaluating the application of a system for active noise control on an agricultural tracked tractor of medium-high power, without cab. This type of vehicles is largely diffused and has significant noise impact on the operators. The originality of this study lies precisely in the application of an active control system in absence of cab. The system used, ATH311, already successfully used in tractors with cab, consists of a control unit based on the digital signal processor DSP. A widespread feedback algorithm configuration was used in the experiment. It will be briefly described in the following. In experimental tests it was implemented in a configuration with two feedback channels (Figure 1).

Materials and methods

The active noise control, henceforth indicated with the term ANC (Active Noise Control), is a technique characterized by the fact that

the reduction of noise (primary noise) is obtained electronically generating a noise (secondary noise) that creates a destructive interference with the first, unlike the conventional techniques (passive) in which the reduction of noise is obtained with the use of sound absorbing and soundproofing materials and structures.

The tractor tested was a Fiat Allis 150 A, commonly employed in heavy works (plowing, subsoiling, etc.) in tenacious soil and fitted with a rear power take off. It is a tracked tractor, without cab, with maximum power of 108.8 kW at engine speed of 1840 min^{-1}. The diesel engine is turbocharged, with displacement of 8102 cm^3. Its total mass is approximately 12150 kg. It has steel tracks the tension of which is hydraulically adjustable. The gear box has three-speed gear ratios and a two gear range reducer (slow and fast). The maximum velocity is 2.41 m s^{-1} in III fast.

The system for the active control of the noise consisted of (Figure 2):

1. control unit based on the digital signal processor DSP;
2. stereo power amplifier Class D (600 W);
3. couple of electret microphones with cables and jacks,
4. woofer speaker pair of 13 ".

In the configuration, the standard algorithm was implemented with an original routine software aimed at increasing the efficiency, stability and reliability of the system.

The sound measurements were recorded with the following instrumental chain:

- Sound Book - eight channels datalogger / signal processor with special software "Samurai";
- microphone capsule ½" Brüel & Kjær, mod. 4189, with windscreen;
- microphone calibrator Brüel & Kjær, mod. 4231;

The tractor was fitted with a magnetic tachometer for measuring engine speed. The tests aimed at evaluating the system of active noise control.

For this purpose, the measurements were carried out in repeatable conditions at various rotation speeds of the engine, first with the active control system turned on, then off. For each speed, 3 replications were performed with a sampling time of 30 s. The measurements were made with engine speed increments of 100 min^{-1} in the range 600-2000 min^{-1}. In a second time, in the interval between 1400 and 1700 min^{-1}, in which the system resulted more efficient, the sampling occurred with increments of 50 min^{-1}.

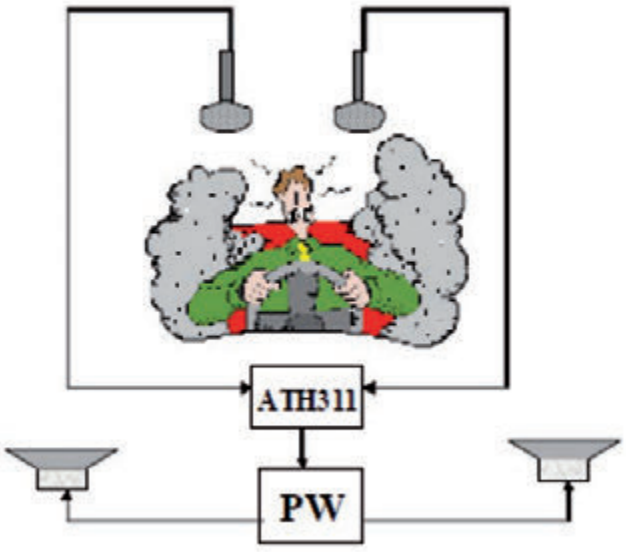

Figure 1. Configuration of the two channel feedback system.

Results

Figure 3 shows the frequency analysis in 1/3 of octave relating to the noise measured in the operator's station, with rotation speed of the engine of 600 min^{-1} (a), 1550 min^{-1} (b), and 2000 min^{-1} (c). The curves refer both to the ANC system "off " (brown and red lines) and "on" (blue and green).

In general, it can be noticed that the weighting filter A has the maximum effect on the frequencies ranging from 20 to 800-1000 Hz. Furthermore, it is evident that the frequency range in which the ANC system is more effective is between 40 and 200 Hz.

An attentive observation of the analysis in frequency shows that, in the cases in which the lower components of the spectrum (relative to the engine) prevail, the ANC system provides the best performance 40 Hz (Figure 3a and b).

Moreover, when the same low components of the spectrum are very pronounced in comparison to the other harmonic components, as in Figure 3 b, the best results are observed on the single frequencies which the system operates and on the total value in dB (A) as well.

Otherwise, from 1800 min^{-1} up to the max rotation speed (Figure 3 c), the lines of the spectrum are almost all at the same level, and the effect of attenuation results less effective.

The test results are reported in Table n. 1 and the above considerations indicate the opportunity to separate evaluation of the values obtained in linear and the A-weighted values. In the first case, the operation of the ANC system provides good attenuation, ranging from a

Figure 2. System for the active control of noise composed by a control unit based on the digital signal processor DSP and a power amplifier (A), two microphones (B), two speakers (C).

minimum of 3.0 dB to a maximum of 8.5 dB at engine speeds lower than 1700 min^{-1}.

As already mentioned above, for the rotation speeds higher than 1800 min^{-1}, the system is less effective, with attenuations ranging from 0.7 to 1.4 dB.

As to the A weighting filter, its action, inside the interval of the spectrum between 20 and 1000 Hz, almost completely cancels the ANC system action for engine speeds comprised between 600 and 1300 min^{-1}, where the maximum attenuation observed was 0.9 dB(A).

The attenuation level increased in the interval 1350-1800 min^{-1}, with values ranging from 0.9 up to 2.5 dB(A).

Even less significant differences were observed at higher engine speeds, with a light tendency to an increase of the global noise level at 1800 and at 1900 min^{-1}, while at 2000 min^{-1} the attenuation resulted of only 0.1 dB(A).

Considering the higher action value 85dB (A) and the limit value of 87 dB (A) defined in the Italian Legislative Decree no. 81/2008, for the first, the use of the system for the first ANC, at speeds of 1400 and 1450 min^{-1}, leads to a standardized level of exposure of the operator, for a working day of 8 h, which is within the range of lower risk.

As to the limit value, at the engine speeds of 1500 and 1550 min^{-1}, the ANC system seems capable to reduce the level below it (Table 1).

Conclusions

The study described in the present paper aimed at contributing to the improvement of the health safe and comfort levels through the reduction of the noise level to which the drivers of tractors without cab are exposed. The tests, carried out on a tracked tractor, using an active noise control system based with an original feedback configuration, provided good results. The most significant attenuations (up to 8.5 dB) occurred in the interval of engine speed between 1000 and 1400 min^{-1}, where the action of the ANC system appeared particularly effective towards the prevailing low frequencies. However, even at higher speeds, where the attenuation of the low frequencies is less significant in the prevention of the hearing damage, the ANC system could contribute to an increase of the level of comfort, through reduction of loss of attention and hearing fatigue. However, the link between the exposure to low frequency noise and the loss of attention and working efficiency should be suitably studied.

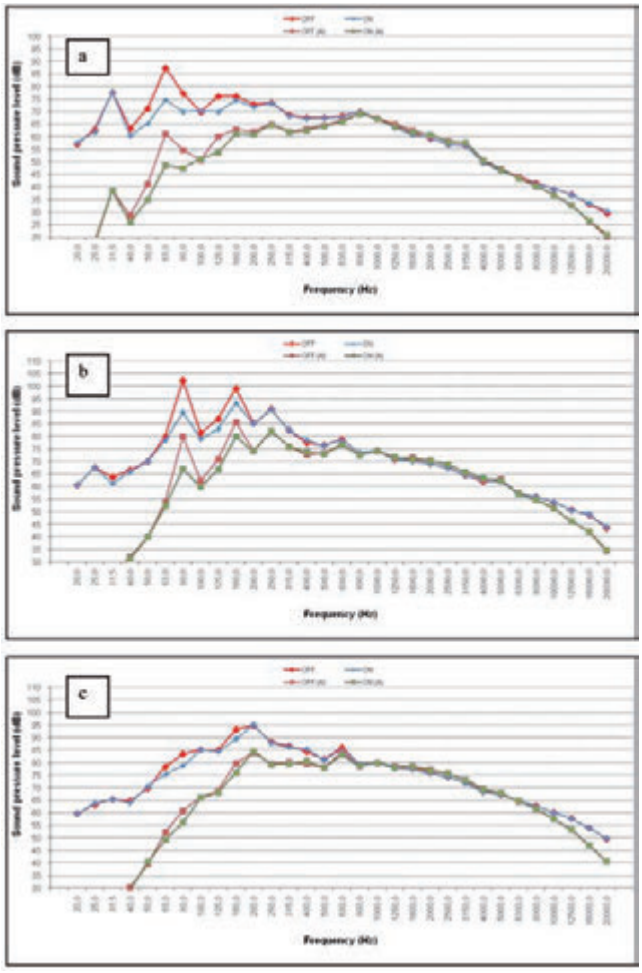

Figure 3. Spectrum in 1/3 of octave relating to the tests with the ANC system, "off" and "on" at the engine speeds of 600 min^{-1} (a), 1550 min^{-1} (b), 2000 min^{-1} (c).

Table 1. Results obtained in the noise measurements with the ANC system connected (on) and disconnected (off) at different engine speeds.

Engine speed (min^{-1})	Active control	L_{eq} dB(A) Repetitions 1	2	3	Average	Stand. Dev.	Δ	L_{eq} dB Repetitions 1	2	3	Average	Stand. Dev.	Δ
600	OFF	76.3	75.4	75.6	75.8	0.45		89.5	89.3	89.8	89.6	0.26	
	ON	75.7	74.8	75.2	75.2	0.46	0.6	83.9	83.1	85.4	84.2	1.17	5.4
700	OFF	79.5	78.0	77.9	78.5	0.85		94.4	95.5	95.4	95.1	0.61	
	ON	77.8	77.0	77.0	77.3	0.45	0.9	87.5	87.7	86.9	87.4	0.42	7.7
800	OFF	78.7	78.4	79.2	78.8	0.26		93.3	93.8	93.4	93.5	0.22	
	ON	76.0	77.4	77.5	77.4	0.36	0.8	86.7	86.9	86.7	86.8	0.40	7.1
900	OFF	79.8	79.8	80.2	79.9	0.19		91.8	92.4	90.9	91.6	0.76	
	ON	79.4	79.5	80.0	79.6	0.33	0.3	87.9	88.4	88.7	88.3	0.39	3.3
1000	OFF	81.2	81.0	80.8	81.0	0.19		91.4	91.9	91.4	91.6	0.33	
	ON	80.8	80.8	80.7	80.7	0.11	0.3	88.2	88.7	89.2	88.5	0.57	3.0
1100	OFF	81.5	81.2	80.9	81.2	0.27		94.7	93.1	93.5	93.8	0.74	
	ON	81.1	80.9	80.8	81.0	0.14	0.3	88.9	88.7	90.0	89.2	0.71	4.6
1200	OFF	83.9	83.5	83.1	83.5	0.40		96.1	96.6	96.7	96.5	0.35	
	ON	83.1	82.4	82.7	82.7	0.36	0.7	90.9	90.7	91.7	91.1	0.49	5.4
1250	OFF	83.8	83.6	83.5	83.6	0.15		96.7	96.0	96.2	96.3	0.34	
	ON	83.5	83.4	83.4	83.4	0.06	0.2	91.9	92.2	91.6	91.9	0.27	4.4
1300	OFF	84.5	84.5	83.7	84.2	0.47		96.9	99.3	97.4	97.9	1.27	
	ON	84.0	84.0	83.4	83.8	0.33	0.4	92.2	92.3	92.3	92.3	0.06	5.6
1350	OFF	84.9	84.5	83.9	84.5	0.51		99.9	99.3	98.5	99.2	0.66	
	ON	83.7	83.7	83.4	83.6	0.18	0.9	92.9	92.9	91.9	92.5	0.56	6.7
1400	OFF	86.6	86.3	86.1	86.3	0.26		101.6	102.3	102.0	102.0	0.37	
	ON	83.7	83.5	83.5	83.6	0.10	1.7	93.5	93.9	93.1	93.5	0.36	8.5
1450	OFF	87.1	86.8	86.6	86.8	0.25		103.2	102.4	102.5	102.7	0.40	
	ON	84.7	84.9	84.8	84.8	0.10	2.0	94.5	95.1	94.7	94.8	0.40	7.9
1500	OFF	88.1	87.9	88.0	88.0	0.13		103.6	102.9	103.2	103.2	0.35	
	ON	85.5	85.4	85.9	85.6	0.19	2.4	96.0	94.4	96.5	95.6	0.56	8.2
1550	OFF	89.7	89.5	89.7	89.5	0.24		104.6	104.7	104.7	104.6	0.19	
	ON	87.2	87.3	88.4	87.6	0.61	2.5	97.3	97.5	96.7	96.7	1.27	7.7
1600	OFF	90.2	90.1	90.1	90.1	0.08		104.2	104.4	104.5	104.4	0.15	
	ON	88.2	88.1	87.3	87.9	0.48	2.2	96.3	96.9	96.3	97.8	1.32	6.6
1650	OFF	90.2	90.0	89.8	90.0	0.21		103.9	103.7	103.6	103.7	0.12	
	ON	88.5	88.1	88.3	88.3	0.19	1.7	98.5	98.4	98.2	98.4	0.16	5.4
1700	OFF	89.9	89.7	89.8	89.8	0.13		103.1	103.8	103.3	103.5	0.13	
	ON	88.2	88.4	88.9	88.5	0.34	1.3	97.9	98.5	99.4	98.6	0.76	4.9
1800	OFF	89.8	89.8	89.8	89.8	0.04		100.9	101.6	101.0	101.2	0.36	
	ON	89.1	91.2	90.3	90.2	1.05	0.6	97.5	101.9	100.2	99.8	2.23	1.4
1900	OFF	90.3	90.3	91.8	90.8	0.87		99.1	99.9	102.2	100.4	1.65	
	ON	90.2	90.8	92.3	91.1	1.08	0.3	98.0	99.0	102.0	99.7	2.04	0.7
2000	OFF	91.6	91.6	91.6	91.6	0.06		99.3	99.5	99.4	99.4	0.11	
	ON	91.3	91.5	91.6	91.4	0.16	0.3	98.6	98.9	98.7	98.7	0.11	0.7

The results of these first experiences indicate that further tests are needed with the purpose of observing the behaviour of the ANC system during the execution of the classic operations the tractor is devoted to, such as ploughing or harrowing, and evaluating its capability of reaction to the variation of the conditions of working and, consequently, of noise.

Possible improvements of the system could be achieved through the use of audio components with more suitable characteristics, with reference to the working target represented by limited intervals of frequency (for instance between 40 and 200 Hz, as evidenced in the tests).

References

Del Duca L., Nataletti P. 2009. Il controllo attivo del rumore: stato dell'arte e prospettive future. Rivista Italiana di Acustica 33 (4): 9-23.

Nataletti P., Del Duca L. 2010. Active control of noise in the cabins of tractor and earth moving machinery. In Proc. 8th Int. Conf. IOHA, Rome, Italy.

Elliott S.J. 2000. Signal Processing for Active Control, Academic Press.

Hasegawa S., Tabata T., Kinoshita A., Hyoto H. 1992. The development of an active noise control system for automobiles. Soc. Of Automotive Engineers Technical Paper, N. 922086.

Kuo S.M., Vijayan D. 1994. Adaptive algorithms and experimental verification of feedback active noise control systems. Noise Control Eng. J., 42 (2): 37-46.

Safety settings in equestrian facilities

A. Checchi,[1] S. Casazza[2]

[1]University of Bologna, Dept. of Agri-Food Science and Technology, Bologna, Italy;
[2]Expert professional for safety in working environments, ASH srls, Brugherio (MB), Italy

Abstract

In recent years an increased attention has been paid to the risks that can emerge within the equestrian environment. In fact, the activities that are carried out every day, whether of working or sport nature, can cause serious traumatic events. The main problems are related to the following risks: biological and physical contact, followed by chemical, electrical, mechanical risks that are common to also a lot of other situations. All these specific risks, of which we talk about in this work, can be contained through proper training and information of workers. The likelihood of accidents can be reduced also applying appropriate behavioural requirements and certain quality and construction parameters used in structures. Inside the equestrian facilities all the main safety systems should be well indicated, also through appropriate signs.

Introduction

Analysis and definition of risks involves great difficulties due to the presence of horses both in permanent structures, that in an unknown environments such as a sport or show events. Safety rules should always be known to all the operators and put into effect in every phase of any activity that has an interaction between man and horse or horses' dedicated structures and should be respected, in every least detail, during the carrying out of any procedure. Beyond this, it is very important to check out the construction characteristics of the entire stable, laying on eye on dimensions of stalls, doors, passages and every place where a horse will transit along with a person on his side. All kinds of plants, installations and machineries, such as treadmills, drying lamps and so on, must strictly respond to the rules and be maintained in perfect conditions of use and each worker must know how to use them correctly.

Correspondence: A. Checchi, University of Bologna, Dept. of Agri-Food Science and Technology, Viale Fanin, 50, Bologna, Italy.
Tel. +39.051.2096101 - Fax: +39.051.2096171.
E-mail: antonio.checchi@unibo.it

Key words: horse, risks, prevention.

Journal of Agricultural Engineering 2013; XLIV(s1):e153
doi:10.4081/jae.2013.(s1):e153

Methods

The risk from physical contact with the horse

Among those who work around a horse, many, but not all, know that all his behaviours are intrinsically and instinctively aimed at the search for pleasure or to avoid pain and suffering, which can also be identified in the intolerance with respect to a person or a situation. However operators do not always consider the effect that the instinct has on the perception of these sensations: sometimes the stress caused by the frustration of instincts can be worse than the pain itself for a horse.

The stress state is of such importance in the horse that its presence is detected also by the increase in blood levels of cortisol and catecholamines. Consequently, an important equestrian safety parameter consists in understanding the instincts of the horse and acting so to create less emotional conflicts possible. Forcing the horse to do something against his will, is equivalent to significantly increase his level of emotional stress and to make him react in an unpredictable and dangerous manner.

This premise wants to indicate of the most frequent and harmful physical agent investigated: the aggressive action of the horse, which is manifested by kicking, biting and crushing with his limbs or body.

Evaluating the percentage of trauma occurring in equestrian activities, it has been shown that these activities are having one of the highest risk percentage of traumatic events among all sports, including motorcycling and motoring.

The most frequent causes of injuries are falls from the horse, the crushing from the horse, bites and kicks. The majority of serious and fatal injuries consists of head injuries that could have been less severe if the rider had worn properly a specific helmet. Even the use of shoes or boots with reinforced tips could prevent a good part of traumatic events or otherwise reduce their severity.

The obvious conclusion from what above is that the equestrian injuries are a serious health problem (still undervalued), which deserves a focused commitment to prevention, in each category of workers affected, by stressing the importance, for preventive purposes, of training the personnel in order to raise awareness of the correct perception of the risk, the use of personal protective equipment and the use of appropriate procedures.

The biological risk

There is talk of biological risk to human health in relation to exposure to organisms and pathogenic microorganisms or not, animals and human endoparasites, which may be present in the workplace.

The biological agent is any organism, even genetically modified, ecto-and endoparasites, of animal or human origin, being capable of causing infection, allergy or poisoning. According to the Legislative Decree 81/2008, biological agents are classified into specific classes according to the degree of danger.

This type of risk assumes a high importance in our context, thus diversifying this type of activity from those that, even if in the presence of animals, do not provide for such a close and ongoing relation-

ship with them and claiming, in this case, greater attention measures to be put in place.

The biological risk consists, on the one hand, in the danger that a disease of the horse can be transmitted to humans, generating in them a pathology similar for the etiological agent and often also for symptoms: in this case we speak about zoonoses.

Zoonoses can spread from animal to animal and from animals to humans and, usually, are not transmitted from man to man. Therefore a man gets sick only by contact with animal fluids or breath.

The assessment of this type of risk must be done in collaboration with the company physician, which must have a deep knowledge of diseases communicable to humans that can affect the horses with whom operators work and the related clinical manifestations in man himself. There must be a well-established and constant synergy between the Physician, the Responsible for the Service of Prevention and Protection and the Veterinarian who knows the health status of the stable in order to monitor the situation and immediately implement measures of organizational, technical and procedural to prevent transmission.

In this contest, a great relevance is given by the use of personal protective equipment, such as masks and goggles and work gloves.

Preventive and periodic visits must be carried out for the operators in the sector, which determines that do not exist conditions of particular sensitivity to infections, and to which a program of vaccine prophylaxis will follow along with the constant monitoring of the effectiveness of protection measures applied.

Another risk factor of great importance is the dust in stables, made up of particles that are derived from fodder, from litter trays, hair of horses and drying of manure. Workers subject to risk are those who have prolonged contact with animals and that manipulate bedding and feed. The danger of dust is due to the ability to carry pathogens, as well as animal and plant particles with allergenic effect, at the level of the respiratory system (eg, fungal spores). It is mainly the spores of fungi (mushrooms) and thermophilic actinomycetes, which originate from the hay and straw poorly preserved, the main cause of the onset of lung diseases such as eg. bronchial asthma, chronic bronchitis and a common disease known as farmer's lung.

In addition, the horse dander, dust mites, hair, saliva, droppings and debris from plant foods can cause allergic respiratory diseases, lung disease or pneumonia awareness, as well as chronic bronchitis. The same applies to environmental allergens such as pollens, richly present in the rural environment where this type of work is done.

To avoid as much as possible the exposure to various environmental pollutants, it is necessary to regularly use masks, in particular during the cleaning operations: it should be noted that the higher concentration of the different pollutants is revealed precisely in conjunction with these operations.

Outside housing

All animals must be kept in proper housing conditions which must follow the rules described below:

- minimal surfaces are defined by the height at the withers;
- the stall must be designed so that horses can lie down, rest and rise appropriately and beddings must be dry, abundant, free from dust and always kept clean;
- floors should not be slippery or dry;
- there must be provided in the paddock a rest area clean, dry, soft, which allows the horses to remain lying down for long times;
- in the stables where the horses are kept in groups, the lower-ranking animals must be able to avoid those of higher rank;
- horses kept permanently outdoors should have a place to find a protected shelter from strong winds, heavy rainfall and, taking advantage of the shadow, as a protection against flies,
- external soils must not be slippery and the mud must not exceed the crown of the foot,
- shelters must be easily accessible and spacious so that animals can lie down and get up normally, must be constructed in such a way that there is no risk of injury.

Working on walkers and treadmills

While bringing the horses to work within a walker or on a treadmill, the following procedures must be observed with attention.

The walker must always be completely stopped before opening the door to let the horse in. Once inside, you will reassure the horse and take off the halter. After closing the door, you can restart the walker, first at a moderate speed and then adjusted to the desired speed. At this point, it'a a good habit to follow the trend for some moment, keeping an eye on the attitude of the horse just introduced and on the other horses already present, and only after verifying that their attitude is quiet, it's possible to leave them alone, without ever leaving the situation totally uncontrolled.

More attention should be paid when placing horses on a treadmill, especially if the horse is not used to this type of equipment and movement. In fact, the walker is "down to earth" while the treadmill is on a structure slightly raised off the ground, which can also be adjusted with a variable inclination and the horse is moving alone, not in company of other horses that may calm him. It is therefore suggested to perform this operation with the presence of two operators, at least until the horse has acquired a familiarity with the equipment and the situation. With the treadmill turned off, you drive up the horse and then block the back side with the appropriate bar that is placed behind the horse's croup and the front side with a bar at chest level. Usually two lungs or chains with a safety release system for cases of emergency are used to tie the horse by the halter. Once set the treadmill in motion and settled the speed and time of training, the horse can be left to walk by himself, without being distracted or disturbed by external elements. The safety system of treadmills provides that if the horse bumps abruptly against the rear or front bar, the whole system stops and the front bar is unlocked. If the horse is not in difficulty he will remain stationary, tied on the platform, but in case of panic, the tie will break allowing him to get off the treadmill. Despite this safety system, the horse should never be left completely unattended during this workout and the treadmill should be located in a secluded and segregated place so that the horse cannot run away scared.

Grooming operations

The term "grooming" regards all the operations of cleaning and tidying of a horse performed in everyday life with which you shall keep clean the horse according to good standards of hygiene.

Wild horses are able to take care of themselves, of their skin and their mantle, but if domesticated and in captivity, they lose this instinct and man has to provide for them. It is important that at least once a day, in housed horses, all the cleaning operations are executed taking care of every single anatomic part, regardless of the use of the equine.

Thanks to the grooming operations is also possible to monitor the general conditions and preserve the horse from many diseases, both internal and external, because it turns out to be a thorough inspection of the body of the animal with the result of constant monitoring.

This kind of activity that places man in a very close contact with horses is definitely, of all the operations, the most risky, but cannot be avoided: nevertheless if approached with caution, attention, in proper operating conditions and supported by proper training, the residual risk can be reduced to an acceptable level.

The risks that operators may encounter during grooming are indeed many, from simple stepping on a foot, to small bites, up to the crushing of body and feet.

The intensity of the risk varies depending on the difficulty and the character of the horses with whom you have to deal: we must therefore pay close attention to every little gesture and the way in which it is accomplished. Keep in mind that a calm and reassuring voice predisposes the horse to a positive attitude towards the person who takes care of him: always takes advantage of this tool.

The grooming operations should always take place in "safe" areas, such as dedicated spaces inside the stables and never inside the stall.

It can happen that the horse identifies the stall as his home and may trigger in him an attitude of ownership and protection towards all those who access it. This aspect produces nervousness and does not allow man to be able to have confidence. Also, inside the stall, the necessary supports for tools are lacking and it is difficult to perform a correct and deep cleansing of the body (especially in the lower limbs) due to the presence of litter and dust, but especially this situation does not allow a convenient and ready escape.

The service areas should contain all the equipment needed to carry out these operations and the position of the working tools should be conceived to favour the ergonomics of the working phases and operator. These places must be kept clean and tidy and we recommend the reorganization after the passage of each horse. They should also be equipped with good lighting and escape routes.

You should pay particular attention to bring the tools near the body of the horse with kindness, in such a way that he will not be afraid, just as it would be good, before working in the lower parts of the body, that the horse perceives the presence of man and his intention.

The operator's concentration must remain always high and abrupt movements are not allowed.

Inside the service areas the horse should be tied "to the two winds", to avoid that he can turn abruptly and be kept as still as possible. It is also true, however, that certain horses, especially young ones, are very nervous when they feel immobilized and bounded, and so they start to pull on the lunge, with the risk of tipping, slipping, of injury in various ways and injuring the operator. With these subjects a balance must be seeken between the operator's safety and the horse's tranquillity, gradually getting them used to being tied, leaving them attached just to one side of the halter, in a confined place, with a loose lead rope and if necessary with the assistance of a second person. With patience and attention, even these difficult subjects can be made more tolerant to the situation.

After working, the horse must be taken back in his stall, he must proceed slowly and behind the man who, once inside, will have to move over to let the horse enter completely and then prepare to exit, releasing first the halter and closing the door behind him.

It is important that during this final operation man and horse never give each other the shoulders, and that, while the operator exits the stall, also the horse stands with his head turned towards the entrance.

Expected Results

Analyzing the procedures aims to encode and teach management habits for every worker, in order to protect their life and safety during the contact with horses and at the same time to assure to the stable good operating conditions and productivity that will make it competitive towards other stables in which the fundamental safety concepts are lacking. A working activity based on safety of structures, plants and procedures and on the application of rules of prevention surely brings to the appeasement of operators involved, which will be able to operate in greater serenity conditions.

Bibliography

Bozzi S., V. Bracaloni, Cialdella M.L. (2005), Handbook of safety in equine practice, University of Pisa

Checchi, S. Casazza - Guidelines towards an optimization of safety factors in equestrian shows - XXXIII CIOSTA conference

De Maria L. (1989) - The Big Book of the horse - De Agostini Geographic Institute

De Maria V. (2002), Horse and rider, Demeter

Di Pede, L. Vivaldi, M. Sabatini - Safety Manual in the horse industry - Azienda USL 5 Tuscany Pisa

DIPROVAL - Work safety in animal husbandry - Faculty of Agriculture, University of Bologna

Ministry of Health (2011), The Ministry of Health for the horse - Standards, rules and protection projects

Ministry of Health (2011), The sensory world of the horse

UFV-Federal Veterinary Office (2003), Horses: how to handle them

FVO - Federal Veterinary Office (2009), Requirements for the exit of horses

FVO - Federal Veterinary Office - (2011), Horses - I take care of my pet

Zorzan C. (2009), The Manual of the Horse - Breeds and choice. Psychology. Power. First Aid, Giunti Publishing.

Noise levels of a track-laying tractor during field operations in the vineyard

Pietro Catania, Mariangela Vallone

University of Palermo. Dipartimento di Scienze Agrarie e Forestali, Palermo, Italy

Abstract

Noise in agriculture is one of the risk factors to be taken into account in the assessment of the health and safety of workers; in particular, it is known that the tractor is a source of high noise. The Italian Low Decree 81/2008 defined the requirements for assessing and managing noise risk identifying a number of procedures to be adopted at different noise levels to limit workers exposure. This paper concerns the analysis of the noise risk arising from the use of a track-laying tractor during field operations carried out in the vineyard. The objective of this study was to evaluate the noise level that comes close to the ear of the operator driving the tractor measuring the values of equivalent sound level (Leq(A)) and peak sound pressure (LCpk). We considered four options related to the same tractor coupled with the following tools to perform some farming operations: rototilling, chisel plough, flail mowers and vibro farmer. We considered three test conditions: T1 in flat (slope 0%), T2 uphill and T3 downhill (both 30% slope). The instrument used for the measurements is a precision integrating portable sound level meter, class 1, model HD2110L by Delta OHM, Italy. Each survey lasted 2 minutes, with an interval of measurement equal to 0.5 s. The tests were performed in compliance with the standards ISO 9612 and ISO 9432. The results show that the measured sound levels exceed the limits allowed by the regulations in almost all the test conditions; values exceeding the threshold limit of 80 dB(A) were recorded coming up to a maximum value of 92.8 dB(A) for flail mowers in test T1. When limits imposed by the regulations are exceeded, the operator is obliged to wear the appropriate Personal Protective Equipment.

Correspondence: Mariangela Vallone, University of Palermo. Dipartimento di Scienze Agrarie e Forestali Viale Delle Scienze Edificio 4, 90128 Palermo, Italy.
Tel. +39.91.23865609.
E-mail: mariangela.vallone@unipa.it

Key words: noise risk, tractor, vineyard.

Contributions: the authors contributed equally.

Conflict of interests: the authors declare no potential conflict of interests.

Conference presentation: part of this paper was presented at the 10th Italian Conference AIIA (Associazione Italiana di Ingegneria Agraria), 2013 September 8-12, Viterbo, Italy.

Journal of Agricultural Engineering 2013; XLIV(s1):e154
doi:10.4081/jae.2013.(s1):e154

Introduction

Noise in agriculture is one of the risk factors to be taken into account for the evaluation of health and safety of workers. In particular, one of the major sources of discomfort for the workers operating a tractor is the noise to which they are subjected during work (Karamounsantas *et al.*, 2009).

In Italy, Law Decree 81/2008 has defined the obligations of noise assessment and risk management, identifying a series of procedures to be adopted at the different noise levels in order to limit the exposure of workers. Excessive noise, in fact, is a global occupational health hazard with considerable social and physiological impacts, including noise-induced hearing loss (NIHL) (Deborah *et al.*, 2005).

Directive 2003/10/EC of the European Parliament was enacted on the minimum health and safety requirements regarding the exposure of workers to the risks arising from physical agents (noise).

It stipulates an upper average limit of noise exposure of a worker during an eight hours shift of work at 85 dB(A). This level is supposed to inhibit hearing impairments of workers (Moselhi *et al.*, 1979). Even the ILO (International Labour Organization) indication agree with this.

Many authors carried out researches on noise risk in agriculture, in particular in the wood processing industry (Zimbalatti *et al.*, 2010), oil mill (Porceddu and Dionigi, 2010), pasta factory (Bianchi *et al.*, 2008), in mechanical harvest of hazelnuts (Cecchini *et al.*, 2010) and on tractors in field conditions with various implements (Dewangan *et al.*, 2005).

This paper concerns the analysis of the noise risk arising from the use of a track-laying tractor during field operations carried out in the vineyard; the aim is to evaluate noise at ear level of operators driving a track-laying tractor measuring the equivalent sound level (Leq(A)) and peak sound pressure (LCpk).

Materials and methods

Machines used in the tests

The tractor used during the tests is the track-laying tractor Trekker 80F by Landini (Figure 1), without cab, equipped with an anti-tip device, 58 kW power, Perkins engine 1104D-44 (Table 1).

Four test conditions were realized coupling the same tractor with the following tools to perform some farming operations in vineyard (Figure 2): rototilling, chisel plough, flail mowers and vibro farmer:

- rototilling (RT)
- chisel plough (CP)
- flail mowers (FM)
- vibro farmer (VF).

The tests were carried out in a vineyard situated in the countryside

of Santa Margherita Belice (province of Agrigento, Sicily). Two homogeneous plots of vineyard, about 200 m long, were identified different only for slope: 0% and 30%. The tests were performed during the execution of the cultivation operations in the following conditions:

- flat, test named T1;
- uphill, test named T2;
- downhill, test named T3.

The average forward speed of the tractor was 2.5 km / h in test T2 and 3.0 km / h in tests T1 and T3.

Instruments used during the tests

The instrument used in the tests is a precision integrating portable sound level meter by Delta OHM, Italy, model HD2110L.

Table 1. Main technical characteristics of the track-laying tractor used in the tests.

Mass [kg]	Wheel track [mm]	Wheelbase [mm]	Seat b1 b2 h [cm]	Year	Hours of work [n]
3800	1100	1650	40×41×39	2005	4390

Figure 1. Track-laying tractor Trekker 80F by Landini used in the tests.

Figure 2. Machines used during the tests.

The instrument complies with class 1 specifications of IEC 61672-1, IEC 60651 and IEC 60804 and is able to perform all the measurements required by Italian legislation on the protection of workers from the risk of noise exposure (Law Decree 81/2008 and UNI9432 standard). The constant percentage bandwidth filters are compliant with class 0 IEC 61260 specifications and the microphone with IEC 61094-4. The tests were carried out in compliance with ISO 9612 and ISO 9432 standards.

During the measurements the microphone was placed near the worker's ear at a distance of at least 0.1 m from the entrance of the external ear canal, approximately 0.04 m above the shoulder. Each measurement had a duration of 2 minutes (the case of stationary noise source) and the parameters were analyzed at intervals of 0.5 seconds.

We measured A-weighted time-averaged sound pressure level (LAeq) and C-weighted peak sound pressure level (LCpk). In addition, a C-weighted ex post measurement in the point of greatest noise was realized.

As required by article 189 of Law Decree 81/2008, the worker does not have to be exposed to $L_{Eex,8h}$ values (occupational noise) reported to 8 working hours higher than 80 dB(A) and to LCpk exceeding 135 dB(C).

$L_{Eex,8h}$ values is given by the following equation:

$$L_{EX,8h} = L_{Aeq,Te} + 10 \log (T_e / T_0)$$

where T_e is the effective duration, in hours, of the working day and T_0 is the reference duration equal to 8 hours. In this case T_e was assumed to be 4.5 hours.

Before each series of measurements the instrument calibration was performed applying a sound calibrator. The collected data were downloaded to the PC for further processing.

Tests were carried out in triplicates. Analysis of variance and Tukey's test were performed using Statgraphics Centurion by Statpoint inc., USA.

Results and discussion

A-weighted time-averaged sound pressure levels (LAeq) in test T1 are shown in Figure 3 for the 4 operating machines.

Noise pressure values obtained in T1 show a minimum of 86.5 dB(A) obtained by the chisel plough and a maximum of 92.8 dB(A) by the flail mowers. Figure 3 shows that the exposure limit value established by the article 189 of Law Decree 81/2008 (equal to 87 dB(A)) is exceeded

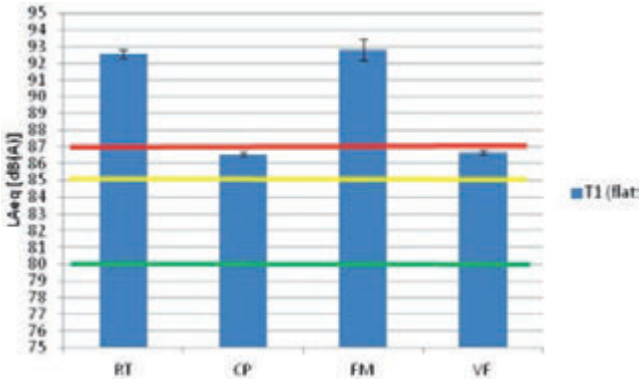

Figure 3. Noise pressure level in test T1 (flat) for rototilling (RT), chisel plough (CP), flail mowers (FM) and vibro farmer (VF) treatments (data are reported as means ± standard deviations of the three replicates).

only by rototilling and flail mowers. Both the upper action value of 85 dB(A) and the lower action value (equal to 80 dB(A)) are exceeded by all the machines. Statistical analysis ($p < 0.05$) shows significant differences between all the machines except chisel plough – vibro farmer and rototilling - flail mowers.

Figure 4 shows the A-weighted time-averaged sound pressure levels (LAeq) obtained by the four machines in test T2.

Noise pressure values obtained in T2 show a minimum of 86.6 dB(A) for chisel plough and a maximum of 92.2 dB(A) for flail mowers. The exposure limit value is exceeded by all the machines except chisel plough. Both the upper action value of 85 dB(A) and the lower action value (equal to 80 dB(A)) are exceeded by all the machines. Statistical analysis ($p < 0.05$) shows significant differences between all the machines.

Figure 5 shows the A-weighted time-averaged sound pressure levels (LAeq) in test T3.

Noise pressure values obtained in T3 show a minimum of 85.1 dB(A) for chisel plough and a maximum of 91.5 dB(A) for flail mowers. The exposure limit value is exceeded only by rototilling and vibro farmer. As obtained in T2, both the upper action value of 85 dB(A) and the lower action value (equal to 80 dB(A)) are exceeded by all the machines. Statistical analysis ($p < 0.05$) shows significant differences between all the machines.

C-weighted peak sound pressure leves (LCpk) obtained in the different tests are shown in Figure 6.

Neither the exposure limit value equal to 140 dB(C) according to the cited art. 189 of Law Decree 81/2008, or the upper and lower action values (equal to 137 dB(C) and 135 dB(C)) are reached or exceeded by any of the tested machines.

Finally, we determined the $L_{Ex,8h}$ values considering a daily duration of the operator personal exposure of 4.5 hours. The results are summarized in Table 2.

Conclusions

The results of the experiments carried out allow us to affirm that:

the highest noise pressure values were obtained by the flail mowers. This occurs in the three test conditions;

the other machine that gave high noise levels was rototilling in the three test conditions;

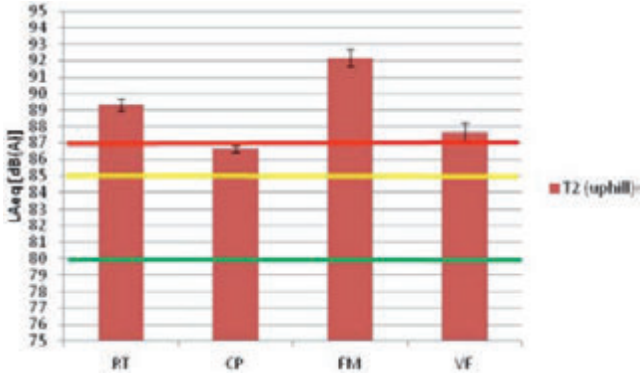

Figure 4. Noise pressure level in test T2 (uphill) for rototilling (RT), chisel plough (CP), flail mowers (FM) and vibro farmer (VF) treatments (data are reported as means ± standard deviations of the three replicates).

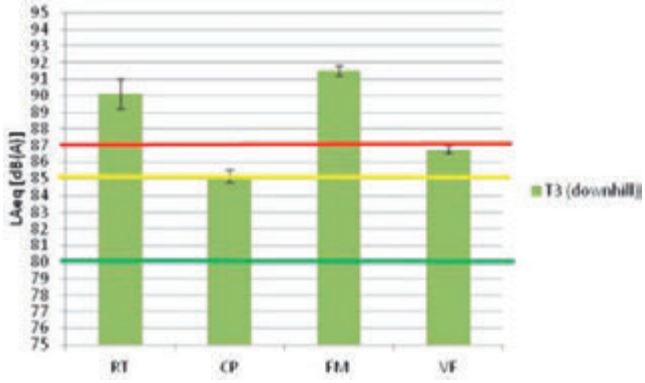

Figure 5. Noise pressure level in test T3 (downhill) for rototilling (RT), chisel plough (CP), flail mowers (FM) and vibro farmer (VF) treatments (data are reported as means ± standard deviations of the three replicates).

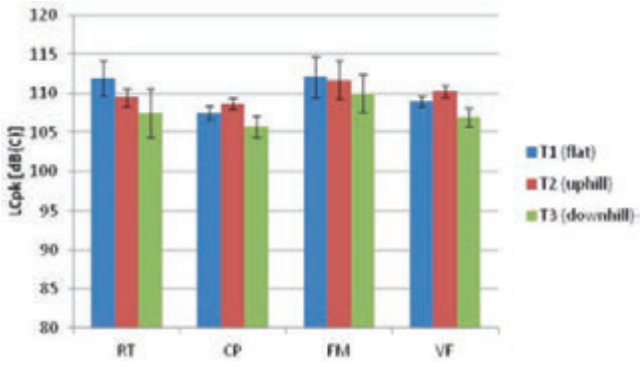

Figure 6. C-weighted peak sound pressure level LCpk in the three tests for rototilling (RT), chisel plough (CP), flail mowers (FM) and vibro farmer (VF) treatments (data are reported as means ± standard deviations of the three replicates).

Table 2. Daily noise exposure level $L_{Ex,8h}$.

		$L_{Ex,8h}$ [dB(C)]
T1	RT	90.07
	CP	84.04
	FM	90.30
	VF	84.20
T2	RT	86.80
	CP	84.12
	FM	89.66
	VF	85.19
T3	RT	87.65
	CP	82.64
	FM	89.01
	VF	84.25

noise pressure values measured during the three tests are always higher than the lower and the higher action values identified by law, respectively equal to 80 dB(A) and 85 dB(A);

the exposure limit value of 87 dB(A) is reached in T1 only by rototilling and flail mowers, in T2 by rototilling, flail mowers and vibro farmer and in T3 by rototilling and flail mowers again;

with reference to the peak values, neither the exposure limit value equal to 140 dB(C), or the upper and lower action values (equal to 137 dB(C) and 135 dB(C)) are reached or exceeded by any of the tested machines in the three tests;

daily noise exposure levels LEx,8h obtained by rototilling and flail mowers overcome the exposure limit value of 87 dB(A);

the use of appropriate PPE is required when limits imposed by the regulations are exceeded.

References

Bianchi B., Cassano F., Mongelli C. Experimental trials to evaluate risks from noise and particulate matter in a pasta factory. International Conference: "Innovation Technology to Empower Safety, Health and Welfare in Agriculture and Agro-food Systems", 2008, Ragusa, Italy, September 15-17.

Cecchini M., Monarca D., Guerrieri M., Lingero E., Bessone W., Bedini R., Menghini G. Noise Levels for Modern Hazelnut Harvesters. Proceedings of the International Conference "Work Safety and Risk Prevention in Agro-food and Forest Systems". September 16-18, 2010 Ragusa, Italy.

Deborah, I. N., Robert, Y. N., Marison, C. B., & Marilyn, F. The global burden of occupational noise induced hearing loss. American Journal of Industrial Medicine, 2005, 48(6), 446-458.

Dewangan K.N., Prasanna Kumar G.V., Tewari V.K. Noise characteristics of tractors and health effect on farmers, Applied Acoustics, 2005, 66, 1049–1062.

European Parliament and Council, Directive 2003/10/EC of the European Parliament and of the Council of 6 February 2003 on the minimum health and safety requirements regarding the exposure of workers to the risks arising from physical agents (noise).

International Labour Organization (ILO). Health, Safety and Environment: A Series of Trade Union Education Manuals for Agricultural Workers, 2004, ISBN:92-2-115 192-1.

Karamounsantas D., Varzakas T., Kanakis A., Dalamagas B.C., Noise levels produced by agricultural machinery and different farming processes. International Journal of Acoustics and Vibration, 2009, 14(4), 220-225.

Law Decree 81, 9 April 2008 of the Italian Republic.

Moselhi M., El-Sadik, Y. M. and El-Dakhakhny, A., A six year follow up study for evaluation of the 85 dBA safe criterion for noise exposure. Am. Ind. Hyg. Assoc. J., 1979, 40(5), 424-426.

Porceddu P.R., Dionigi M. Evaluation of Noise Levels in Olive Mills. Proceedings of the International Conference "Work Safety and Risk Prevention in Agro-food and Forest Systems". September 16-18, 2010 Ragusa, Italy.

Zimbalatti G., Proto A.R., Negri M. Acoustic Levels in the Wood Processing Industry in Northeast Italy. Proceedings of the International Conference "Work Safety and Risk Prevention in Agro-food and Forest Systems". September 16-18, 2010 Ragusa, Italy.

The assessment of the sawmill noise

P. D'Antonio, C. D'Antonio, C. Evangelista, V. Doddato

School of Agricultural Sciences, Forest and Environmental, University of Basilicata, Potenza, Italy

Abstract

Noise is a serious and widespread problem in many workplaces like in sawmill. The published data for the year 2010 about the total number of pathologies from work in Italia due to the noise, showed 5222 cases divided by sex, in fact for females there are instances in number of 221 while the male has a number of cases is equal to 4961. The aim of this work was to detect the sound level caused by the use of the machineries in a sawmill. The measurements were carried out through an instrument known as noise level meter, equipped with a microphone and connected to a computer for data processing and analysis of variance to a factor in excel, and able to assess noise levels at any particular point in the mill. The machines were subjected in relief and with several different types of wood materials. Obviously, in our case a fundamental role takes the moisture of wood. The drying operation is intended to obtain that degree of humidity of the wood, generally it must be between 7 and 16%, compatible with the type of glue used and, above all, appropriate to the target structures. The machines that have the highest sound pressure levels were trimmer and profiler, with values ranging between 85 dB(A) and 110 dB(A). Finally, it's possible conclude that the sound pressure level increases when the aspiration equipment is turned on, the noise of machinery decreases during the processing of wood and that, increasing the thickness, decreased the noise emitted by the machine.

Introduction

In Europe, around 50 million people are exposed to potentially hazardous levels of environmental noise, facing a risk of noise-induced hearing loss (NIHL). The loss in economic terms is substantial, at a minimum 0.2 % of national net income. This equals about 400 billion Euros annually at European Community level (Rantanen et al, 2001). This includes direct and indirect costs related to production. The indirect costs do not include factors related to reduced quality of life. The quality of life includes: social isolation, increased unemployment and difficulties in family life due to communication difficulties related to hearing handicap.Noise-induced hearing loss (NIHL) is considered to be one of the most common occupational health hazards of any country. When NIHL is moderate to severe, it leads to speech distortion, reduced word discrimination, noise intolerance and tinnitus. Reduced oral communication is a social handicap. NIHL also reduces the perception of warning signals, environmental sounds and music. Consequently, NIHL may lead to social isolation, decreased worker productivity and morale, and an increase of job-related accidents. There are no global or European Community figures available for the prevalence of NIHL. Such figures, if they did exist, would provide a database that would allow focused control methods to reduce the risk at national level and work place level; and even at an individual level.The most common counter measure is the use of Hearing Protective Devices (HPDs). In most cases, this should be sufficient, since the noise levels are generally below 95 dB in 90 % of the enterprises (Register on occupational exposures for physical and chemical agents, 1999). According to laboratory measurements (Comitee Europeen de Normalisation (CEN), parts 1 and 2, 1993), most earmuffs on the market can provide more than 20dB attenuation against typical industrial noise.In field conditions, the situation is more complicated as people lack motivation to use HPDs (Berger *et al.*, 1983; Foreshaw and Cruschley, 1981). Several researchers have shown that laboratory tests overestimate the attenuation of the protectors under investigation (Foreshaw and Cruzhley, 1981; Casali and Park, 1991; Merry *et al.*, 1992). Furthermore, if the protectors are in poor condition, the attenuation tends to further deteriorate.In studies, the usage rate of hearing protectors has varied a great deal. Between 1953 and 1992 in the paper mill, HPDs were used 55% of all work hours (Nieminen *et al.*, 2000). Recently, higher usage rates have been found at the shipyards at 70% (Pekkarinen, 1987), and in forest work at 90% (Pykko *et al.*, 1989). A recent Italian lex (D.Lgs. 81/2008) fixes the daily noise exposure levels and peak sound pressure for exposure limit values and exposure action values:

a) Exposure limit values: LEX,8h =87 dB(A) and P peak =200 Pa respectively.
b) Upper exposure action values: LEX,8h =85 dB(A) and P peak = 140 Pa respectively.
c) Lower action values: LEX,8h=80 dB(A) and P peak =112 Pa respectively.

When applying the exposure limit values, the determination of the worker's effective exposure shall take account of the attenuation provided by the individual HPDs worn by the worker. When the noise exposure level exceeds the lower exposure action values, the employer shall make HPDs available to workers, and HPDs shall be used where noise exposure levels match or exceed the upper action values. This study was intended to analyze the risk of noise in an Italian sawmill, relating to the use of the principal machineries for the timber transformation, taking in account the following factors: a) exposure to impulse noise, b) combined effects from the interactions between

Correspondence: P. D'Antonio, School of Agricultural Sciences, Forest and Environmental, University of Basilicata, Via dell'Ateneo, 85100 Potenza, Italy.
Tel. +39.0971205471 - Fax: +39.0971205429.
E-mail:dantonio@unibas.it

Key words: noise, sawmill, assessment, noise level meter, aspiration equipment.

Journal of Agricultural Engineering 2013; XLIV(s1):e155
doi:10.4081/jae.2013.(s1):e155

noise and the width of timber, c) analyzing the different type of the use of machineries and finally investigating about the use of HPDs in the sawmill.

Materials and methods

For each application you should check measurement technique and conditions in order to get valid and coherent results. The way of using the instrument has at least as much importance on result than device quality. During a normal working day, simultaneous measurements inside and outside the HPDs were conducted utilizing a miniature microphone and a portable 2-channel noise dose meter (Pekkarinen, 1987; Chang-Chun *et al.*, 1989). These measurements were done with 21 paper mill workers in 1985, 28 shipyard workers in 1986, and 20 forest workers in 1989. Each measurement consisted of a 10-minute sampling period. According to recent Italian legislation, employers must provide appropriate HPDs for the workers, and use is mandatory. However, when evaluating the worker's right for compensation due to hearing loss, the use of HPDs is not taken into account. Since the workers receive no monetary gain for overestimating their usage rate, the likelihood of overestimation is diminished. The Sound Level Meter has been designed to meet the measurementrequirements for industrial safety offices and sound quality control invarious environments,

- Ranges from 35 dB to 130 dB at frequencies between 31.5 Hz and 8 KHz;
- Display with 0.1 dB steps on a 4-digits LCD;
- With two weighting, A and C;
- Both AC and DC signals output is available from a singlestandard 3.5mm coaxial socket suitable for a frequency analyzer,level recorder, FFT analyzer, graphic recorder, etc.

The relief of the noise on the holding object of the measurements was made on the machinery being used during the production cycle:

- Planer on four sides;
- Profiling;
- Splicer;
- Trimmer - optimization.

It was not possible to carry out field surveys during a continuous production cycle, as it depended on the orders that came to the company, but data are collected when each piece of equipment was running, so it was possible to deduce the actual noise of the single machine without influences of other machinery on. On each machine were made more measures in such a way as to make a comparison between the different reliefs:

- An initial survey was carried out while the machine was switched on without aspiration and without the wood processing;
- A second measure with the suction on and without the wood being processed;
- A third and a fourth relief while they were working in wood of different thickness.

The wood species used in the trials was the silver Fir, aimed at different finished products such as beams and roof planks glued together with polystyrene which go to make up for insulated panels. All the machines in question were built according to CE standards and thus comply with the regulations in force and for each of them is available to the workers hearing protection.The data relating to the noisy machines were collected and analyzing thanks to the variance.

Results

The reliefs on the planer on four sides (Figure 2) have been set, as said earlier, comparing multiple variables in play. On this machine has not been possible to detect the sound pressure level while the machine was switched on without suction as it is an outbuilding that you can't turn off and then the analysis focused on data collected with different thicknesses.

The graph (Figure 3) will immediately notice that the that the sound pressure level for the planer falls below the 88 dB(A) and no higher than 95 dB(A), and this also shows that the most ups have occurred with the boards of fir thick white 160 x 360 mm, and less thick.

The values of sound pressure level registered onprofiling (Figure 4)

Figure1. Dosimeter.

Figure 2. The reliefs on the planer on four sides.

were higher than the values of the other machines. It is noted from the results of the graph (Figure 5) that the sound pressure level is around the threshold of 87 dB(A). The operator wears headphones because, as can be seen, some value goes beyond the threshold of exposure and therefore the law provides for the use of PPE.

The valuesthat are registered on this machine while working the wood are much higher than previous measurements, even compared to measurements found on the planer on four sides, even for us who did relief, and so we were in close contact with the machinery for a short period of time the noise was loud and annoying, so that an operator has to work with the machine for several hours the long term risk is considerable.

In Figure 3, unlike the previous machine, the results showed that the values of the sound pressure level ranging between 90 dB(A) and 110 dB(A) and are almost equal for both of the shims; while values increase compared to the observations made on the same machine without timber, with or without suction.The finished boards are glued with polystyrene and, as mentioned above are put in place to give rise to the panels to insulate roofs (Figure 6).

The optimizer, as showed in Table 1, it is not a very noisy machinery. The loudest noise is produced when the operator moves the plates from the plane of the trimmer to that of the splicing (Figure 7). Results show that the noise does not increase much, indeed, some values are decreased compared to the data detected while the machine is switched on without timber in processing.

In the graph (Figure 8), unlike the machinery above, the values of the sound pressure level ranging between 80 dB(A) and 100 dB(A) and are almost equal for both of the shims.

This machine is equipped with a laser inside that goes to note where the table has been marked by the operator with a marker (in order to eliminate the defects) and cuts the table where there is no defect. The splicer, however, has the task of "splice", that combine two tables with a joint system (Figure 9). It is equipped with soundproofing system, consisting of a soundproof room built around the machine as it is very noisy.

In the graph (Figure 10) the values of the sound pressure level ranging between 80 dB(A) and 100 dB(A) and, you will immediately notice that the values for the thickness 2 are higher than those of the thickness 1.

Ultimately, the values of the sound pressure level ranging between 75 dB(A) and 106 dB(A) and the values for the values for the thickness 2 are higher than those of the thickness 1. Furthermore, by comparing the averages of the values for the different machines, it notes that are scarcely different between a measurement and the other. The most noisy machinery is the profiling, even when the machine worked the timber with a different thickness. Below is the table (Table 1) that contains the data minimum, average and maximum values of different machinery analyzed with the use of the materials in different thickness.

The results showed that the profiling had sound pressure level higher than the other machines. As can be seen, the results do not fall below the 77 dB(A) but below the threshold of 100 dB(A). All this is not due to the timber used, or to its moisture, but just to the machinery itself

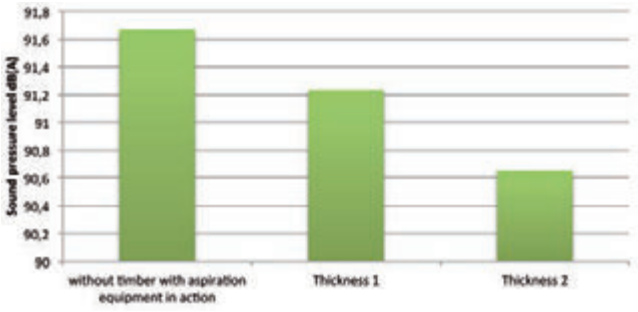

Figure 3. Graph of the sound pressure level of the planer.

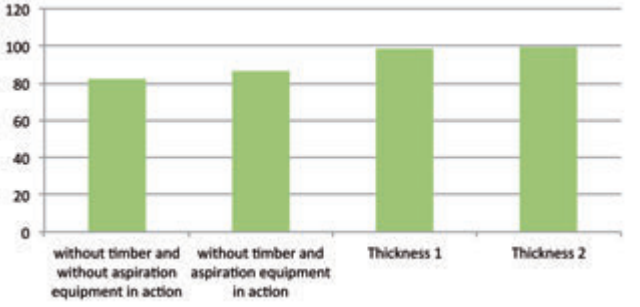

Figure 5. Graph of the sound pressure level of profiling/profiler.

Figure 4. Relief of noise on profiling.

Figure 6. Panels to insulate.

since, as can be seen from the findings, the noise is around values mentioned above even when it is switched on without that work. The other tested machineries with the highest sound pressure levels are the optimizer and the planer on 4 sides with values ranging between 85 dB(A) and 110 dB(A), depending on the thickness of the timber and the use of aspiration equipment.

Conclusions

The machines used are all cutting edge and all built according to CE standards, but the results of our measurements showed, often, as the sound pressure level exceeds the limits allowed by law and it is precisely at this time that IPR play a role in the hearing of the operator in contact with the machine at that time. The Silver Fir is heavy (dry density of 410 kg/m3), has good stability, retires on average and breaks, particularly well and dries well. Several factors can influence on increasing the sound pressure level emitted by the machine at the time of woodworking: moisture (whose increase causes a rise in), cover the timber with paints and lacquers that increase the logarithmic decrement. Obviously, in our case a fundamental role takes on the moisture content of wood processed. The drying operation is intended to obtain that degree of humidity of the wood compatible with the type of glue used, and especially suited to the destination of the structures. Generally it has to be between 7 and 16%. The results obtained are, as mentioned earlier, not much higher than the limits allowed by law, and considering the fact that the operator always wearing headphones at the time of the survey, we are in the norm. Perhaps the best way to reduce the noise of profiling is to construct, as in the case of the splicing, sound

Figure 7. Plan Optimization transition from the splicer.

Figure 9. Joint system.

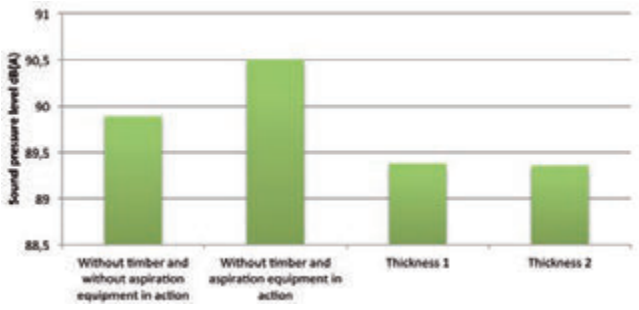

Figure 8. Graph of the sound pressure level trimmer.

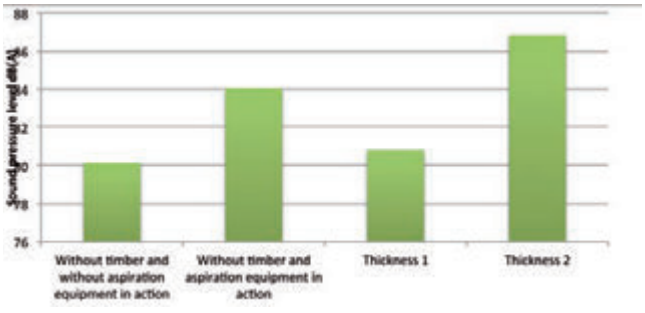

Figure 10. Graph of the sound pressure level of the splicing/splicer.

Table 1. Noise emission from machineries depending on wood thickness.

Values	Machinery							
	Trimmer		Planer on four sides		Splicer		Profiler	
	Thickness 1	Thickness 2	Thickness 1	Thickness 2	Thickness 1	Thickness 2	Thickness 1	Thickness 2
Min	79,9	80	88,3	88,2	77,6	85	85	84,4
Average	91,5	92,7	90,9	90,1	88,7	92,3	97,5	94,9
Max	96,1	97,2	93,4	92,7	96	100,2	104,3	105,9

proofing of machinery. Existing legislation envisages that workers exposed to values of LEP, 8h higher than 85 dB(A) must wear adequate individual protection devices (i.p.d.) (antinoise protection, such as ear plugs, headphones or similar devices). In work areas with levels of LEP, 8h in excess of 87 dB(A), the employer must mark the perimeter clearly and provide signposting limiting access solely to authorized personnel who must wear individual protection devices. These devices must ensure that the level of risk is maintained within values equal to or lower than 90 dB(A).The new directive (2003/10/EC) assumes that protectors are used always when noise level exceed 85 dB. This study shows that this assumption is not always valid and thus efforts must be made to promote the use of hearing protectors. In risk assessment the protection efficiency of HPDs is taken into account. The protection efficiency is predictable only if the HPDs are properly fitted and users are motivated. There are several other factors such as cold/heat, comfort of HPDs, and variation of noise levels that affect the usage rates. The effect of these factors must be studied case by case. The usage of HPDs was at an adequate level in the tested sawmill. It is likely that the usage rate will increase due to growing risk awareness and the fact that young people are used to wearing protectors from the beginning. Hearing conservation precautions are progressing well in the enterprise included in this study. However, this progress cannot be generalized between all workers.

References

2003/10/EC, 2003. Council directive on the minimum health and safety requirements regarding to the exposure of workers to the risks arising from physical factors (noise). European Commission, Brussels, 6p.

Berger E.H., Franks J.R., Lindgren F. 1983. International review of field studies of hearing protector attenuation, inScientific Basis of Noise-Induced Hearing loss,Axelsson A., Borchgrevink H., Hamenik R.P., Hellstrom P., Hendersson D., Salvi R.J. eds. Thieme Medical Publ. p361-367.

Casali J.G., Park M.J. (1991). Real-Ear Attenuation under Laboratory and Industrial Test Conditions as Provided by Selected Hearing Protectors, InProceedings of the Human Factors Society 35th Annual meeting,Vol. 2, San Francisco, California, September 2-6, 1991. Pp 1110-1114.

Chang-Chun L., Pekkarinen J., Starck J. 1989. Application of the probe microphone method to measure attenuation of hearing protectors against high impulse sound levels,Appl. Acoustics27:13-25.

ComiteEuropeen de Normalisation (CEN) (2003). Hearing protectors - Safety requirements and testing- part 2: Earplugs, (CEN Standard EN 352-2), Brussels: CEN pp15.

Foreshaw S., Cruchley J. 1981. Hearing protector problems in military operations. In:Personal hearing protection in industry,Alberti P., ed. New York: Raven Press: 387-402.

Nieminen O., Starck J., Toppila E., Pekkarinen, J., Pyykko I. (2000). Protection efficiency of hearing protectors among workers in a paper mill. Transactions of the XXV Congress of the Scandinavian Oto-Laryngological Society, Olofsson J. Ed., DavesTryckeri, Bergen, Norway,Scand. J. Audiol.P 51-53.

Pekkarinen, J. 1987. Industrial impulse noise, crest factor and the effect of earmuffs.Am. Ind. Hyg, Assoc. J.48:10:861-866.

Pykko I., Koskimies K., Starck J., Pekkarinen J., Inaba R. 1989. Risk factors in the genesis of sensory neural hearing loss in Finnish forestry workers.Br. J. Ind. Med.46: 439-446.

Rantanen J., Kauppinen T., Toikkanen J., Kurppa K., Lehtinen, S., Leino T. (2001). Work and health country profiles: country profiles and national surveillance indicators in occupational health and safety, People and work, Research report 44.

Rotella A., Campurra G. 2008. Il rischio rumore negli ambienti di lavoro. IPSOA INDICITALIA.

TESTO UNICO - Decreto legislativo 9 aprile 2008, n. 81 “Attuazione dell’articolo 1 della legge 3 agosto 2007, n. 123, in materia di tutela della salute e della sicurezza nei luoghi di lavoro” e successive modifiche. 2008.

Assessment of linear anionic polyacrylamide application to irrigation canals for seepage control

Hamil Uribe, Rodrigo Figueroa, Luis Llanos

National Institute for Agricultural Research, INIA, Chile

Abstract

South- central area of Chile area has a Mediterranean climate and high crop water requirements. Irrigation water is distributed through long channels which have low water conveyance efficiency (Ec), difficult to improve by conventional techniques. The objective of this study was to quantify Ec and to evaluate the use of Linear Anionic Polyacrylamide (LA-PAM) to reduce seepage losses. The study was carried out in south-central area of Chile, (UTM Coordinate N 5745000; E 725000 m, datum is WGS-84, zone 18S) in 250 km of channels whose flow varied between 0.12 and 24.6 m3 s^{-1}. Water users indicated channel reaches with potential low Ec, which were selected for LA-PAM application. In 11 reaches between 0.51 and 3 km in length, 1 to 3 LA-PAM applications were performed at rates of 10 kg ha^{-1}, considering the wet perimeter area as basis of calculation. Thirty-one LA-PAM applications were performed over a 30.5 km length. Most of the channels were large enough to allow motorboat moving against the current to carry-out LA-PAM application. Water flow was measured (StreamPro ADCP) at both ends of selected reaches before and after granular LA-PAM application. Weekly measurements were made to quantify treatment effect duration. Water turbidity and temperature were measured. Channels showed variable Ec from 87% to 94%. Two reaches showed 6% water gains. In more than 80% cases LA-PAM effect was positive, achieving loss reductions of 15 to 760 L s^{-1}. In other cases LA-PAM had a negative effect since it mainly affected water entry into the channel. It was determined that field conditions referred by users as indicators of Ec are not always correct and vary in time according to climatic conditions. Ec was estimated and it was possible to reduce seepage through LA-PAM applications. This allow increasing irrigation security in critical periods, especially under drought conditions.

Correspondence: Hamil Uribe, National Institute for Agricultural Research, INIA, Vicente Mendez 515 Chillan, Chile.
Tel. +56.42.206759 - Fax: +56.42.206799.
E-mail: huribe@inia.cl

Key words: canal seepage, irrigation, polyacrylamide.

Journal of Agricultural Engineering 2013; XLIV(s1):e156
doi:10.4081/jae.2013.(s1):e156

Introduction

Seepage from unlined water delivery canals occurs on a local and regional scale and that losses may be significant in particular areas. According to U.S. Geological Survey (USGS) the loss of water during transport through unlined water delivery and irrigation canals might be significant, with as much as 50 percent lost to seepage through the sides and bottoms of the canals (Carr, 1990). In Chile, as in many parts of the world, agriculture uses large volumes of irrigation water that must be driven through channels. Arumí *et al.* (2009) evaluated the water recharge in lower valley of the Cachapoal River, central Chile, concluding that 52 percent of them come from canals seepage. The Chilean National Irrigation Commission (CNR, 2012) estimates losses of water during transport through canals in more than 30 percent in average.

However, as water resources become further constrained, there is a need for cost-effective seepage reduction technologies that can be used in locations where traditional methods are cost-prohibitive. Traditional seepage-abatement technologies such as compacted earth, reinforced or unreinforced concrete, and buried geomembranes are typically used in situations where seepage rates are elevated and projected water savings offset their high construction and maintenance costs. Polyacrylamide (PAM) has been suggested as a means of sealing unlined water delivery canals to reduce seepage or infiltration losses (Zhu & Young, 2009). In contrast to traditional seepage-abatement technologies, LA-PAM is relatively inexpensive. Polyacrylamide or PAM is a generic term for polymers formed by the union of monomer acrylamide. Polyacrylamide (PAM) is a synthetic organic polymer used globally by a number of important industries. It also has a number of valuable applications in irrigated agriculture, including its use in furrow irrigation to control erosion and sediment loss in runoff, manage infiltration, and a growing use for reducing seepage losses in unlined irrigation canals and reservoirs (Lentz, 2009). Different formulations vary in molecular weight, charges (cationic, anionic or neutral) and if the molecules are linear or branched resulting in a large number of alternatives to be used (Sojka *et al.*, 2007). The granular form of linear anionic polyacrylamide (LA-PAM) has been identified as one such technology capable of cost-effectively reducing seepage rates from unlined water delivery canals (Susfalk *et al.*, 2008).

Granular LA-PAM is one type of a broader family of polyacrylamides that has a variety of uses, including as a flocculant in wastewater treatment, in food packaging, and paper manufacturing. Over the past decade, LA-PAM has been used to reduce erosion and sediment transport from crop fields under furrow irrigation and on construction sites. Water soluble PAM has been tested in reservoir reducing mean seepage rates an average 50% relative (Lentz, 2004).

Granular LA-PAM is easy to apply and can be targeted to specific canal reaches known to have high seepage rates. There is a conflictive empirical evidence of the longevity of a single LA-PAM application, but yearly or more frequent applications do not diminish its cost-effectiveness. This "short-term" seepage reduction of LA-PAM, relative to the

more permanent nature of traditional technologies, is a benefit, as it could be applied selectively during drought water years, and allowed to elapse if water savings are no longer needed.

Researches (Smith, 2008; Susfalk *et al.*, 2008) have found that this polymer would reduce water loss by seepage in channels at a cost that would justify their use from an economical point of view, allowing to increase the available flow and controlling the adverse effects of canal seepage. In addition, the polymer can be applied in the watering duration, achieving a reduction of losses of water in a short period of time, making it interesting to use in drought periods, in which an optimization of the transport of water in the channels would translate into a big economic impact for farmers. Research on the use of polymer are complex because there is not possible to compare channels situations which are exactly equal, since variables such as flow, the amount of sediment and the water temperature, that influence the behavior of polymer, are impossible to control.

The results of applications in channels have found that the use of the LA-PAM reduced leaks between 30% and 90% (Smith, 2008) and 28 and 87% in 8 of 11 field experiments. In other three experiments, the application did not reduce channel filtering, so it must study the conditions necessary so that the application of polymers reduce water loss by seepage (Susfalk *et al.*, 2008). The polymers used in agriculture are characterized by molecules anionic with a charge density of 18% and molecular weight between 12-15 Mg mol^{-1}(Sojka et al, 2007).

The Mediterranean climate of the area presents critical periods with peak demand of irrigation and minimum water availability, time in which could be appropriated for LA-PAM applications to have more water in the channels.

The objective of this study was to quantify water losses in channels and to evaluate the use of Linear Anionic Polyacrylamide (LA-PAM) to reduce seepage losses in south-central area of Chile under real water management conditions.

Materials and methods

The study area is shown in Figure 1. A big canal network belonging to South-Bio Bio, Chufquen and Allipen irrigation systems in the south-central area of Chile (UTM Coordinate N 5745000 ; E 725000 m, datum is WGS-84, zone 18S), was considered. The criteria used to select study sites, was the potential losses, according to water user's indication. The study was carried out in 11 reaches selected from 250 km of channels network whose flow varied between 0.12 and 24.6 m^3 s^{-1}. The length of the channels varies between 0.51 km and 3 km. In selected reaches LA-PAM applications and water flow monitoring was carried out.

Seepage rate estimates were focused on short-term and long term to study the effect of LA-PAM applications on water saving at 11 reaches. Water flow measurement and percentage of looses or profits were calculated to compare the pre and post treatment channel performance. The monitoring was just performed before and after LA-PAM application, in next day and weekly until the effect was lost.

From 2011 to 2013, seepage estimates were conducted before and after LA-PAM application. During field applications in 2011 and early 2012, application methods and monitoring protocols were being refined. The most of applications were in 2012 and early 2013.

Seepage was estimated by comparing surface water discharge above and below the reach of interest, avoiding presence of other inflows and outflows along the reach. In channels surface water discharge was measured with a Teledyne-RDI StreamPro (2007) (Poway, CA) acoustic Doppler current profiler (ADCP). Studies recently carried out in the United States has performed the measurements using Acoustic Doppler Profiler (ACDP) (Kinzli *et al.*, 2010) allowing to obtain repeatable results of profiles of speed and therefore acceptable errors in the determination of the flows.In small channels a Teledine Gurley N° 625 current meter was used when it was not possible to use the ADCP. The

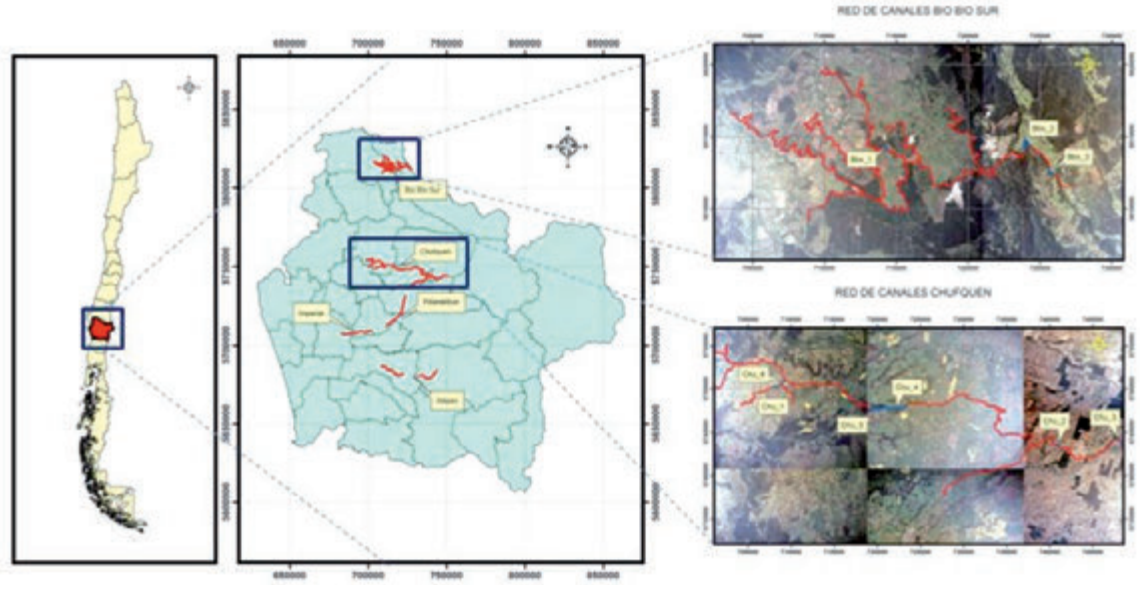

Figure 1. Aerial view of study area showing the location of the canals and reaches that were treated with PAM. UTM Coordinate in m, datum is WGS-84, zone 18S.

ADCP measure across the channel and delivers a flow value. The criteria used to ensure reliable values was four consecutive measurements with variation less than 5% over the average of them. Wrong data values were discarded.

Application rates of 10 kg of LA-PAM per wetted channel were targeted for each of the applications according to recommendation (Susfalk *et al.* 2008) taking into account the low sediment level. The LA-PAM used during these studies conformed specifications for use in irrigation channel. More specifically, the manufacturer certified that the LA-PAM a) complied with the NSF International/American National Standards Institute (ANSI) Health Effect Standard (NSF/ANSI-60); b) was an anionic charge density of 15 to 40 percent plus or minus 5 percent; c) had a molecular weight of at least 12 million g (Mg) mole^{-1}; and d) contained no more than 0.05 percent acrylamide monomer, by weight. The LA-PAM polymer used for field experiments was granulated Clarisol 4015, distributed by Aguasin Aguas Industriales ltda, Chile. This polymer was selected for not present toxicological effect in Daphnia magna after 24 and 48 hour, according to standard Chilean NCh 2083 of 1999 and testing of chronic toxicity at 21 days, according to US EPA, 1995.

In each reach, 1 to 3 LA-PAM applications were conducted by moving the point of LA-PAM application upstream while continuously dispersing granular LA-PAM onto the channel water surface by walking (small channels) or more commonly by boat (Zodiac motorboat 3.5 HP) (Table 1). In both cases a technician with hand sowing machine (Lhaura model 10502) distributed granulated LA-PAM on water surface. Water turbidity and temperature were measured (multi-parameter water quality checker Horiba U-50). In total, thirty-one LA-PAM applications were performed over a 30.5 km length in total.

The Table 1 resumes the principal reach characteristics of experiment. Some experimental reaches were partitioned into two or more subsets.

Analysis was based on comparison of the seepage rates of canal before and after the LA-PAM applications. Thanks to flow measurements at the beginning and end of the studied reaches, it was possible to calculate percentages of water losses with respect to the incoming flow. The average of the losses before LA-PAM applications was compared with the situation post application. Post application average considered a period between the application and the moment that effects of the polymer disappear. On these values average pre and post application was calculated the percentage of seepage-abatement respect to initial seepage rate. When water gains were found in some reaches studied the values of losses had negative sign and the focus was if the polymer produced an effect of increasing gains or reduction of them by sealing of the walls of the channel. The results were also expressed in terms of water saving in liters per second.

Results

Because some experimental reaches were partitioned into two or more subsets, in different measurement length or dates, the results are presented on 31 cases analysis. Water discharge monitoring with ADCP in the beginning and end of the reaches were carried out before and after LA-PAM applications. The Figure 2 shows typical graphics of water

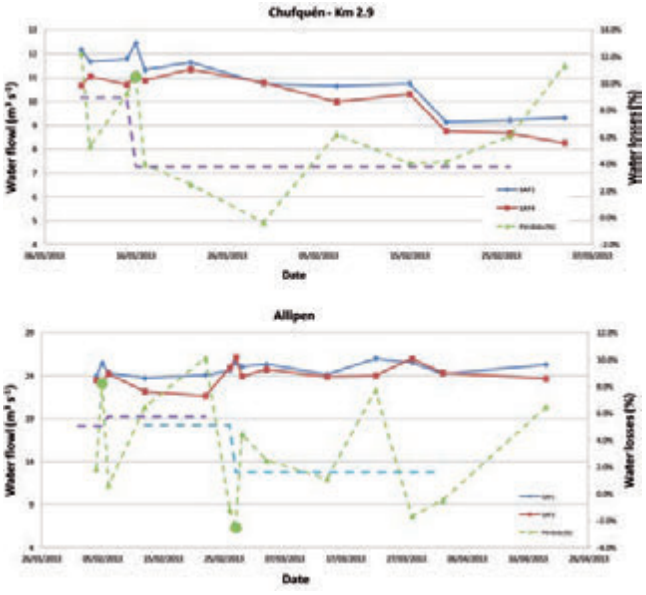

Figure 2. Graphics of water flow at the beginning (blue) and end (red) of reaches. The dots indicate LA-PAM applications. The green dashed lines indicate percentage of losses calculates from eater flow and the purple and ligh blue dashed lines indicate the average percentage of losses changing before and after LA-PAM application. Above: Chufquen canal in km 2.9. Under: Allipen canal.

Table 1. Summary of LA-PAM application locations and characteristics. Code refer to reaches.

Canal Code	Beginning N	Beginning E	End N	End E	Length (m)	Flow (m^3 s^{-1})	Irrigation system	Aplication type
All_1	5682451	742254	5680054	740613	3000	24,602	Allipen	Boat
Bbs_1	5814177	714411	5814046	714162	550	1,071	BioBio Sur	Walking
Bbs_2	5814368	724358	5813989	723933	1860	6,072	BioBio Sur	Boat
Chu_1	5750376	708545	5750234	707850	705	0,82	Chufquen	Walking
All_2	5814049	714161	5814177	714411	1367	0,12	Allipen	Walking
Chu_2	5743295	741049	5743488	740737	629	9,794	Chufquen	Boat
Chu_3	5744004	748164	5744140	747813	844	11,858	Chufquen	Boat
Chu_4	5748173	723390	5747908	721042	2686	6,393	Chufquen	Boat
Chu_5	5747920	721017	5748213	719155	2286	7,657	Chufquen	Boat
Bbs_3	5811533	726759	5812895	725661	513	7,1	BioBio Sur	Boat
Chu_6	5751008	709226	5750589	708909	651	1,721	Chufquen	Boat

UTM Coordinate in m, datum is WGS-84, zone 18S.

flow monitoring and water losses used in the analysis. Water flow monitoring on the time allowed to fallowing the losses of water before and after LA-PAM applications. The averages of losses of water before and after LA-PAM applications were calculated to study the LA-PAM application. The averages post application considered a period until effect of LA-PAM disappear. Negatives values result when water gains occurring instead of losses.

Table 2 resume the results focused to compare the reach condition before and after application in terms of loss by seepage or water gains.

In the analysis were compared to average water loss before and after each LA-PAM application. The average water loss in post application was considered for a period until the LA-PAM effects disappear. The percentage of water loss was calculated as the difference between the flow at the beginning and end of the section, divided by the flow at the beginning, expressed as a percentage.

Measurements pre application shown different cases: 7 reaches always showed losses, 1 reach always presented gains and 3 reaches showed losses or gains depending on the date of measurement. Must be noted that 2012-2013 irrigation season was atypically rainy until January 2013. In December 2012 fall 130 mm in Carillanca weather station, meaning two times monthly average rain.) Other important issue is the topography in the study area. In several cases the canal bordering a slope permitting water inflows through walls of canals, permitting a gain of water.

The results of Table 2 also indicate that in 5 cases, of a 31 in total, the LA-PAM application effects was different to the expected results , expressed as increased loss or reduction of gains post LA-PAM application. This could be explained by the presence of diffuse inputs of water by the walls of the channel, which could have been blocked by the polymer to a greater extent than the water seepage. The diffuse inputs were supported for more water than normal condition associated to abnormal summer rainy period 2012-2013.

The other 26 cases had an expected behavior , *i.e.* losses reduction or gains increased. In 8 cases LA-PAM was applied in reaches gaining water (negative losses), 5 of them were achieved more water gains and only 3 the gain was reduced.

Table 2. Resume of results.

Canal Code	Beginning UTM N*	Beginning UTM E*	End UTM N*	End UTM E*	Application date	**Pre loss	**Post loss	***Effect duration	**Loss variation	****Flow variation
All_1	5682451	742254	5680054	740613	05-02-2013	5,1	5,8	17	-0,70	-172
All_1	5682451	742254	5680054	740613	27-02-2013	4,5	1,6	34	2,90	728
Bbs_1	5814177	714411	5814046	714162	27-11-2012	-1,4	-3,9	37	2,50	27
Bbs_2	5814368	724358	5814321	723933	20-11-2012	-1,5	-5,1	13	3,60	219
Bbs_2	5814368	724358	5814321	723933	14-02-2013	2	-6,6	46	8,60	564
Bbs_2	5814368	724358	5813989	723933	20-11-2012	-6,5	-9,7	13	3,20	194
Bbs_2	5814368	724358	5813989	723933	14-02-2013	-0,7	-11,2	46	10,50	688
Bbs_2	5814321	723933	5813989	723933	20-11-2012	-4,9	-4,3	13	-0,60	-38
Bbs_2	5814321	723933	5813989	723933	14-02-2013	-3,3	-5,2	35	1,90	122
Chu_1	5750376	708545	5750234	707850	15-11-2012	12,9	10,6	7	2,30	19
Chu_1	5750376	708545	5750234	707850	31-01-2013	10,4	8	9	2,40	16
All_2	5814049	714161	5814177	714411	28-03-2012	37,5	22,6	14	14,90	18
Chu_2	5743295	741049	5743488	740737	14-03-2012	6,4	2,8	8	3,60	353
Chu_3	5744004	748164	5744140	747813	16-01-2013	9	3,8	41	5,20	617
Chu_3	5744004	748164	5744140	747813	14-11-2012	4,1	2,21	17	1,89	222
Chu_3	5744004	748164	5744025	747394	16-01-2013	4,2	1,1	41	3,10	368
Chu_3	5744004	748164	5744140	747813	11-04-2012	6,8	1,4	22	5,40	507
Chu_3	5744004	748164	5744140	747813	15-02-2012	5,5	1,8	43	3,70	391
Chu_4	5748173	723390	5747858	723018	29-10-2012	2,6	-0,3	15	2,90	213
Chu_4	5748173	723390	5747858	723018	15-01-2013	1,5	-4,5	15	6,00	454
Chu_4	5748173	723390	5747858	723018	20-02-2013	10,5	1,7	40	8,80	563
Chu_4	5748173	723390	5747908	721042	15-01-2013	3,6	1,3	15	2,30	174
Chu_4	5748173	723390	5747908	721042	20-02-2013	13,5	1,5	40	12,00	767
Chu_5	5747881	720770	5748041	719426	13-11-2012	4,7	0,8	15	3,90	299
Chu_5	5747920	721017	5748213	719155	10-01-2013	6,1	-1,4	25	7,50	541
Chu_5	5747920	721017	5748213	719155	20-02-2013	0,5	-1,2	40	1,70	96
Bbs_3	5811533	726759	5812895	725661	20-11-2012	-1,3	1,7	9	-3,00	-213
Bbs_3	5811533	726759	5812895	725661	14-02-2013	1,6	6,1	27	-4,50	-329
Bbs_3	5811533	726759	5812895	725661	13-04-2012	5	1,4	21	3,60	252
Chu_6	5751008	709226	5750589	708909	14-11-2012	11	9,4	44	1,60	28
Chu_6	5751008	709226	5750589	708909	31-01-2013	-4,2	-2,1	33	-2,10	-36

*, UTM Coordinate in m, datum is WGS-84, zone 18S; **, Losses pre and post LA-PAM Application (%); ***, Days; ****, Flow, liter per second.

The Figure 3 compare percentage water loss before and after 31 cases of LA-PAM applications separated for irrigation system: a) Bio Bio Sur; b) Chuquen and c) Allipen. It is possible to appreciate that most of the points are under red line indicating good result of LA-PAM application.

Discussion

The LA-PAM application is usually recommended for selected channels presenting water seepage, however in this case, on the basis of knowledge of irrigators, reaches where visually selected principally using wet areas as an indicator. In 25% of the cases water gains were presents before LA-PAM applications, indicating that in this area of Chile occurs an inputs and outputs of water thought the wall channels, dominated by the topography, rains and even irrigation recharge. In the main season (2012-2013), when the most of application were performed , atypical rains increased water gains. In normal or dry years would be expected to have water gains until November or December, , except in specific channels located on slopes hills that provide water. However the above, polymer was beneficial even in these conditions, permitting water saving.

The results corroborate that in 84% of cases was an effect of water saving (reduction of losses or profit increase) due to application of polymers. Others studies shown LA-PAM was effective (8 of 11 experiments), seepage rates measured within 24 hours were reduced between 28 and 87 percent. The average duration of effect was 25 days, with minimum of 7 and a maximum 46 days, while other research measured 30% to 100% seepage reduction in long term (more than 100 days) (Susfalk *et al.*, 2008). These results can be explained for low sediment level in water in the area.

Even in channels where there are water gains possible saving it is because the polymer could largely prevent outputs. Also keep in account that usually in channels in slopes losses occur in the walls of the channel slope down. Another important aspect to discuss is that there was no correlation of variables as level of sediment, size of channels , temperature, application dates of with the effect of the polymer, being very specific behaviors for each reach evaluated.

In absolute terms the application of polymer achievement recovers 2.623 m3 s^{-1}. 2.723 m3 s^{-1} were gains (increase gains or loss reduction), while 0.100 m3 s^{-1} were lost. These values are considered an average of saving water among all LA-PAM applications made in each reach. This occurred in 31 LA-PAM applications carried out in 15 kilometers of canal. In terms of irrigated area would mean more than 2500 has additional under drought conditions.

Conclusions

It was possible to quantify water loss in channels and to evaluate the use of Linear Anionic Polyacrylamide (LA-PAM) to reduce seepage losses.

Through water flow monitoring were estimated losses in irrigation channels, achieving a better understanding of the water behaviourn in a temporal and special basis. It was determined that some cases defined by water-users as water loss in channels were not such and also varied according to the rains and topography in the area. However, it was possible to find specifics reaches, not so extensive in length, pre-

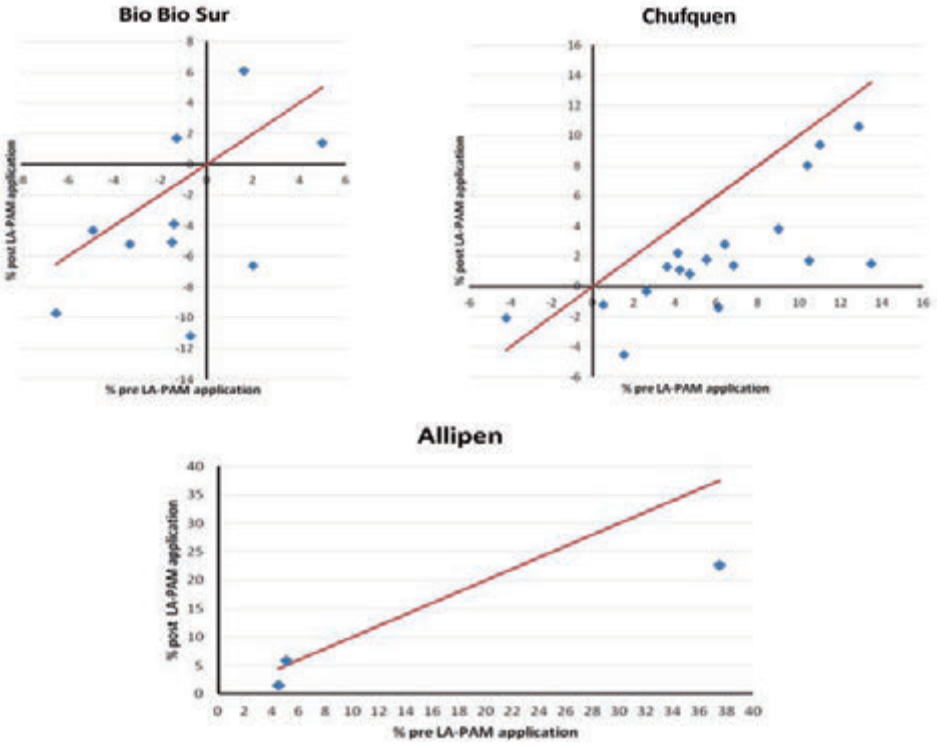

Figure 3. Comparison between percentage water loss (gains in negatives) pre and post LA-PAM applications in each irrigation systems: Bio Bio Sur; Chufquen and Allipen.

senting heavy losses that could be managed through LA- PAM applications. They were able to progress in the knowledge of LA-PAM applications according to local conditions. It was determined that the polymer application was positive since in the majority of cases (84%) it allowed water savings, through specific applications, maximum 3 per season, not affecting the environment and having low cost.

References

Arumí, J. L., D. Rivera, E. Holzapfel, P. Boochs, M. Billib, and A. Fernald. 2009. Effect of irrigation canal network on surface and groundwater connections in the lower valley of the Cachapoal River. Chile. Chilean Journal of Agricultural Research Vol. 69-(1) 12-20 (January-March 2009).

Carr, J.E. 1990. National water summary 1987: Hydrologic events and water supply and use. USGS Water Supply Pap. 2350. U.S. Gov. Print. Offi ce, Washington, DC.

Comisión Nacional de Riego (CNR). 2012. Revestimiento de canales, nuevas técnicas y sus beneficios. Revista CNR Riego, año 1/N° 1, septiembre de 2012, page 43-44..

Kinzli, K., M. Martinez, R. Oad, A. Prior and D. Gensler. 2010 Using an ADCP to determine canal seepage loss in an irrigation district Agricultural Water Management 97: 801-810.

Lentz, R.D. 2009. USDA-ARS perspective on PAM. Proceedings of the PAM and PAM Alternatives Workshop, February 26-27, 2008, Reno, Nevada. p. 3-5.

Lentz, R. D., and Kincaid, D. C. 2004. Polyacrylamide treatments for reducing infiltration and seepage in soil-lined ponds and channels: Field evaluations. Agron. Abstr. (CD-ROM). American Society of Agronomy, Madison, WI.

Smith, D. 2008. Field Application of PAM for Canal Seepage Reduction IN: Richard Susfalk (Ed.) POLYACRYLAMIDE (PAM) AND PAM ALTERNATIVES WORKSHOP February 26-27, 2008 Albany, California.

Sojka, R.E. , D.L. Bjorneberg, J.A. Entry, R.D. Lentz, W.J. Orts 2007 Polyacrylamide in Agriculture and Environmental Land Management Advances in Agronomy 92: 75-162

Susfalk, R. V., D. Sada, T Arrowood, Ch. Martin, B. Epstein, C. Rosamond, S. Labahn, M. Young, T. Gates, D. Moser ,T. Mihevc, M. Shanafield, B. Fitzgerald, J. Woodrow, G. Miller, D. Smith. Lessons from LA-PAM Application to Water Delivery Canals IN: Richard Susfalk (Ed.) POLYACRYLAMIDE (PAM) AND PAM ALTERNATIVES WORKSHOP February 26-27, 2008 Albany, California

Zhu, J., & Young, M. H. (2009). Sensitivity of Unlined Canal Seepage to Hydraulic Properties of Polyacrylamide-Treated Soil. Soil Science Society of America Journal, 73(3), 695-703.

Analysis of rainfed alfalfa evapotranspiration measured by an eddy covariance system

A. Vinci, L. Vergni, F. Todisco, F. Mannocchi

Department of Civil and Environmental Engineering, University of Perugia, Perugia, Italy

Abstract

The aim of this study was to quantify the evapotranspiration (ET_{ec}) of a rainfed alfalfa crop using the eddy covariance technique. The study was carried out during the alfalfa growing seasons (April-August 2009, April-August 2010) at the experimental farm of the University of Perugia. In central Italy alfalfa is grown for 3 to 4 years continuously, with at least 3 cutting cycles for year (usually between April and August) and a dormant period in winter. For the quantification of ET_{ec} an open-path eddy covariance system (EC) was used. The derivation of water and energy fluxes starting from raw wind, temperature and gas concentration data by means of the EC technique implies a remarkably long sequence of operations including calibration, corrections and statistical tests for assessing data quality. These operations were carried out by the EddyPro® software. After that, the output data were used for the flux-partitioning and all original data, flagged with a quality indicator with non-turbulent conditions, were dismissed. Then the gap-filling of the EC and meteorological data was performed to obtain reliable values. Furthermore the test of the energy balance closure gave satisfactory results. The ET_{ec} dynamics were consistent with the growth stages and the cuttings during both 2009 and 2010. Furthermore the comparison between the tabulated crop coefficients (K_c) and the ratio of ET_{ec} to reference evapotranspiration (ET_0) was performed. This analysis showed a good agreement during the 2nd cutting cycle (May-June) for both 2009 and 2010, whilst during the 3rd cutting cycle (July-August) the ratio ET_{ec}/ET_0 was considerably lower than K_c for both years. The reason of this behavior was found in the presence of water stress conditions during the last cutting cycle. This fact was confirmed by the application of a bucket soil water model, used as an exploratory, not confirmatory, tool to analyze the soil water availability dynamics during the growing season. Additional measurement campaigns will be carried out in order to deepen the knowledge about the K_c dynamics in rainfed crops and to assess the productivity of water under various meteorological and agricultural conditions.

Correspondence: A. Vinci, Department of Civil and Environmental Engineering, University of Perugia, Borgo XX Giugno 74, 06121, Perugia, Italy.
E-mail: avinci@unipg.it

Key words: crop coefficients, water stress, energy balance.

Journal of Agricultural Engineering 2013; XLIV(s1):e157
doi:10.4081/jae.2013.(s1):e157

Introduction

As the water demand is projected to increase (Giorgi and Lionello, 2008), a correct and detailed quantification of crop water use by evapotranspiration (ET) in different climatic and agronomical conditions is necessary to improve water use efficiency for both irrigated and rainfed crops (Smith, 2000; Parent and Anctil, 2012).

ET can be measured or modeled by several techniques. For practical purposes, ET is usually estimated by models having minimal requirement of meteorological data. The technique best known and most used is the one based on the FAO-56 approach (Allen *et al.*, 1998), according to which the potential evapotranspiration of a specific crop (ET_c) is estimated through the combination of reference evapotranspiration (ET_0) and crop coefficients (K_c). If some stress factor occurs (*e.g.* water stress) it is necessary to adjust the ET_c value, by introducing a stress coefficient K_s.

Direct methods to measure ET (such as lysimetry and micrometeorology) are more complex and demanding. The micrometeorological methods measure the components of the energy balance which allows to accurately estimate ET from large areas even at short time scales (Baldocchi, 2003). These are typically research methods, due both to the complex data processing and to the expensive instruments required, but they are very useful to improve the knowledge about evapotranspiration and K_c values.

A widely known micrometeorological method is eddy covariance. It is considered a direct and accurate method for measurements of both latent heat (ET) and sensible heat (H) fluxes (Stull, 1988; Rana and Katerji, 2000). The main idea of the eddy covariance method is to measure the turbulent transport of heat and water vapor in the vertical direction (Garratt, 1992; Campbell and Norman, 1998). The performance of the eddy covariance method is very good in hourly and daily time scales if sensors are placed in an appropriate geometrical configuration and special data corrections are made (Allen *et al.*, 2011a,b; Foken *et al.*, 2011a,b; Foken, 2008; Foken *et al.*, 2004; Twine *et al.*, 2000).

In this paper the eddy covariance method was applied in the monitoring of rainfed alfalfa evapotranspiration in Central Italy during two successive growing seasons (2009 and 2010).

Alfalfa (*Medicago sativa L.*) is one of the most grown forage crops in the Mediterranean where it plays an important economical and ecological role. In Central Italy it is a rainfed crop, grown for 3 to 4 years continuously, with 3-4 cutting cycles for year (usually between April and August) and a dormant period in winter.

The main objective of the paper was to derive actual crop coefficients (K_{c_act}) for rainfed alfalfa and to analyze their response to climatic factors and agricultural management. Indeed, alfalfa crop coefficients are largely documented in literature (Allen *et al.*, 1998;

Doorenbos and Pruitt, 1977), but they are mainly related to irrigated crops.

Materials and Methods

Experimental site, alfalfa data and instrumentation

The study was carried out at one site located in Central Italy (Deruta, Perugia) during the years 2009 and 2010. Measurements of energy balance terms were made with an open path eddy covariance (EC) system. The EC system was installed in the middle of a 20.63 ha (42° 57' 2.31" N , 12° 22' 53.73" E, 220 m a.s.l.) alfalfa farmland in both years. In this area, as already mentioned, alfalfa is grown for 3 to 4 years continuously after planting. The two years of experimentation corresponded to the 3rd and the 4th growing seasons respectively. The monitoring of evapotranspiration has been performed during the active growing season (from April to August). Each growing season was characterized by a series of three cutting cycles described by the sequence of four growth stages (Allen *et al.*, 1998): initial (IS), crop development (DS), mid-season (MS) and late (LS). The actual lengths of different stages and the cutting dates were dependent on the weather conditions and on the farm management. The beginning and the end of the growth stages were identified according to the guidelines provided by Allen *et al.* (1998) together with the monitoring of alfalfa phenological development. The MS and LS stages are considered as a whole in the paper, because the LS stage was frequently interrupted by the cuttings and alfalfa crop coefficients are not much variable in the two stages.

Results only refer to the second and third cutting cycles of each season, since the first cycle (after dormancy) is characterized by the considerable presence of other species.

In the EC system there are two types of platforms: a fast-response and a slow-response system. The first measures the variables needed to compute the sensible and latent heat flux and consists of a 3D sonic anemometer/thermometer (model CSAT3) and a Li-7500 CO_2-H_2O infrared gas analyzer. CSAT3 and Li-7500 measure three-dimensional fluctuations of wind, sonic temperature, and concentrations of H_2O and CO_2 at 20 Hz. These fast-response instruments were installed on a horizontal bar placed at the top of a tripod 1.7 m above the ground. The lateral separation between the two sensors was set at about 0.20 m. The slow-response system consists of a net radiometer, four heat flux plates (Hukseflux HFP01SC) and two soil temperature sensors for two level soil measurements (0.10 and 0.15 m depth). In the year 2010 a multi-depth soil water monitoring probe (EnviroSMART) was installed (0.30, 0.45, 0.60 m) and the Li-7500 was recalibrated. Checking and cleaning operations of the instruments were done weekly in correspondence of data download.

These instruments made it possible to measure independently the latent heat flux (ET), sensible heat flux (H), soil heat flux (G) and net radiation (Rn) in order to check energy balance closure. All the sensors were connected to a datalogger (model CR3000) and the 10-min statistics (average, variance and covariance) were computed.

Analysis of soil hydro-physical properties were carried out in the year 2010. In particular soil texture, water retention at field capacity and wilting point were determined at six depth up to 1.8 m. The available water content (AWC) between field capacity and wilting point is about 12% with a low variability among the different layers.

Eddy covariance measurements

H and ET were measured: during the year 2009 between May 9 and May 30 (corresponding to the first 22 days of the 2nd cutting cycle) and between July 9 and August 21 including the entire 3rd cutting cycle and the initial period of the successive regrowth,; during the year 2010 between May 24 and August 3, including completely the 2nd and 3rd cutting cycles.

H and ET are given in units of power per unit of area [Wm^{-2}], and they were calculated using the eddy covariance system (Baldocchi, 2003):

$$\lambda ET = \rho_a \lambda \overline{w'q'}$$
$$H = c_p \rho_a \overline{w'T'}$$

where $\overline{w'q'}$ is the covariance between fluctuations of vertical wind speed w' [m s^{-1}] and humidity q' [kg kg^{-1}], $\overline{w'T'}$ is the covariance between fluctuations of w' and sonic temperature T'[K], $_a$ is the air density [kg m^{-3}], c_p is the specific heat of dry air at constant pressure [J kg^{-1} K^{-1}], λ is the latent heat of water vaporization [MJ kg^{-1}] and *ET* is the crop evapotranspiration [kg m^{-2} s^{-1}]. The ratio of ET to λ enabled to obtain the measure of actual evapotranspiration ET_{ec}.

EC data processing and gap filling

The EC technique requires a considerable quality control process in order to obtain reliable measurements (Foken and Wichura, 1996).

For these reasons the EddyPro® software (open source) was used for processing raw eddy covariance data. EddyPro® allows calculating corrected fluxes starting from raw files through a long sequence of operations including filtering, calibration and other algorithms that user can configure to suit the research needs. In this study, the Advanced Mode was used for processing raw data and in particular: double axis rotation for tilt corrections of wind speed measurements, the block average detrend method for the corrections of the turbulent fluctuations and the covariance maximization for time lag compensation. Then, for the compensation of density fluctuations (WPL terms) an a posteriori correction (Webb *et al.*, 1980) was applied. It adjusts density fluctuations using measured sensible heat and evapotranspiration fluxes, corrected for spectral losses and water vapor effects. Furthermore the Fast Fourier Transform (FFT) was used for the frequency domain analysis (spectra and co-spectra) of the time series data. Finally a quality check (Mauder *et al.*, 2008) and a footprint estimation (Kljun *et al.*, 2004) were implemented. Flux crosswind-integrated footprints were provided as distances from the tower contributing 10%, 30%, 50%, 70% and 90% to measured fluxes. In particular the location of the peak contribution were 278.5 m and 75m (90%), 67 m and 31m (70%), 33 m and 19.43 m (50%) for 2009 and 2010 respectively.

Then the gap filling was applied to the EddyPro® output data. In particular, a tool that implements the standardized methods described in Reichstein *et al.* (2005) for processing half-hourly eddy covariance data (gap-filling and flux-partitioning) was used to replace the missing data. The missing value was replaced by the average value under similar meteorological conditions within a time-window of 7 days (because only the data of direct interest are missing, while all meteorological data are available). The similar meteorological conditions are present when the global radiation, the air temperature and the vapor pressure deficit do not deviate by more than 50Wm^{-2}, 2.5°C, and 5.0 hPa respectively. In the period June 1 – July 9 2009 the gap filling was not applied because in such long time-span there is a significant variation of crop characteristics that the method cannot consider. Furthermore the original data (not gap-filled) were used for the flux-partitioning..

Energy balance closure test

The plausibility of the datasets was valuated against the energy balance closure test (Farahani *et al.*, 2007). The slope of regression

between the energy measured by EC (H+ ET) and the available energy (Rn–G) indicates the degree of energy balance closure, which should be close to 1.

Reference ET (ET_0) and crop coefficients

Daily reference evapotranspiration was calculated by the FAO Penman-Monteith equation (Allen *et al.*, 1998). The daily agrometeorological data required by this equation and daily precipitation (for the soil water balance) were obtained from the closest meteorological station, about 600 m far from the considered alfalfa field.

Daily values of the actual crop coefficient K_{c_act} were calculated as the ratio of ET_{ec} to ET_0.

$$K_{c\_act} = \frac{ET_{ec}}{ET_0}$$

K_{c_act} is conceptually and numerically different from crop coefficients (K_c) usually available in literature. In fact K_c are used to quantify the crop evapotranspiration (ET_c) under the hypothesis of optimal environmental conditions with particular regard to water availability (*i.e.* under irrigation). The K_{c_act} coefficient refers instead to crops that could have suffered water shortage conditions and for which evapotranspiration could have been lower than ET_c for all or part of the growing season.

In this paper the tabulated Kc coefficients of Allen *et al.* (1998) have been considered as a term of comparison of K_{c_act}, taking into account the conceptual differences discussed above. The alfalfa K_c values given in Table 1 derive from Allen *et al.* (1998) after the adjustments proposed by the same authors for specific climatic and management conditions.

Soil water balance

A rough estimation of the alfalfa water availability was obtained by applying the following simplified water balance equation (Doorenbos and Kassam, 1986)

$$P - ET_{ec} - D = \Delta SW$$

where P is the measured precipitation, ET_{ec} is the actual evapotranspiration (measured by eddy covariance), D is the deep percolation and DSW the water storage variation in a 0-2 m soil depth. This soil layer was assumed as the effective root-zone depth (H) for alfalfa in the examined environmental conditions, considering the presence of a deep alluvial soil and the fact that at the 3rd and 4th year after seeding, alfalfa is well-established.

The drainage was quantified as the volume of water exceeding the maximum storage capacity of the soil, TAW=(AWC)·H.

In the water balance, surface runoff and capillary raise were both neglected due to the flat terrain conditions and to the deep groundwater table.

The soil water balance equation was applied in 2010 to estimate the soil water variation at a daily time scale (SW_t), assuming an initial condition (on May 24) equal to TAW (reliable hypothesis taking into consideration the abundant rainfall of April (66 mm) and May 2010 (108 mm), the relatively small evapotranspiration rate until the first cut and the information obtained from the water content probe.

At any rate, this simplified method can have several inaccuracies: uncertainty about the actual alfalfa rooting depth, the assumption of spatial uniformity of soil characteristics, soil rootzone assumed as a reservoir etc.

Table 1. Alfalfa crop coefficients (Allen *et al.*, 1998) for different growth stages under the specific climatic conditions of the case study.

Growth stage	Crop coefficient
Initial (IS)	$K_{c\text{-}ini}$=0.40
Development (DS)	Linear variation between Kc-ini and Kc-mid
Mid season (MS)	$K_{c\text{-}mid}$=1.15
Late season (LS)	Linear variation between Kc-mid and $K_{c\text{-}end}$=1.08

Results

Meteorological conditions

The growing season 2009 was characterized by lower than average rainfall amounts in April, May and July, and higher in June and August . Mean air temperature was usually higher than average with the exception of June (probably due to the high rainfall). The growing season 2010 was characterized by lower or near normal rainfall amounts in all months with the exception of May (much-above average rainfall). The mean air temperature was lower than average in most months.

These climatic conditions can be considered advantageous for a good growth and yield of rainfed alfalfa in both years, even if the rainfall occurrence led often to non-optimal choices with regards to cuts scheduling.

Energy balance closure test

Figure 1 shows mean daily values of Rn-G vs. H+ ET obtained from both years. The slope of the linear fit of Rn-G vs. H+ ET is 0.89. This little underestimation of the turbulent fluxes (by 11%) can be considered acceptable (Foken, 2008), and it may depends on non ideal conditions (a not completely flat field, the inhomogeneity of the crop).

Evapotranspiration by eddy covariance (ET_{ec}) and actual crop coefficients(K_{c_act})

The seasonal variation of daily ET_{ec} and of the 3-day means of K_{c_act} are shown in figures

2A and 2B, respectively. The same information for 2010 is given in figures 3A and 3B. Other variables and information, such as daily rainfall, ET_0, growth stages length, cutting dates, K_c (Allen *et al.*, 1998), are

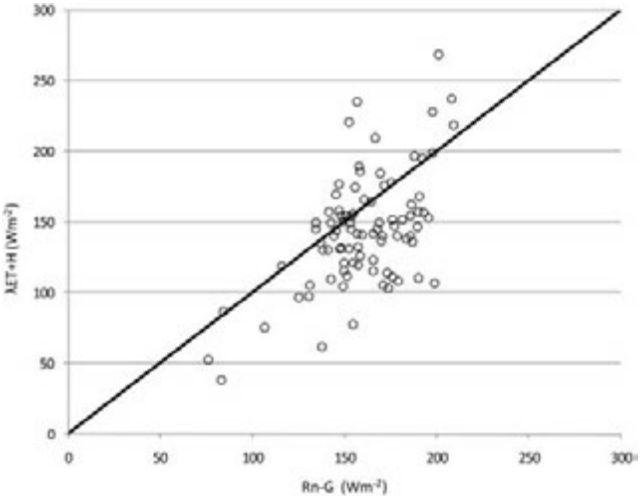

Figure 1. Daily energy balance of the turbulent flux λET+H and the available energy Rn-G, and 1:1 line. Data from 2009 and 2010 .

shown in the same figures. Summary statistics of daily values of ET_{ec}, ET_0 and K_{c_act} are shown in Table 2. Results are discussed separately for the year 2009 and 2010 in the next sections.

Growing season 2009

In 2009, ET_{ec} was first measured between May 8 and May 29, date on which data collection was suspended due to technical problems. During this cutting cycle (Figure 2A), the dynamics of ET_{ec} is consistent with that expected during the observed growth stages: in fact ET_{ec} shows a steady behavior after the cutting date (IS stage) and then a rapid increment during the following DS stage. The observation of this stage is not complete, but ET_{ec} during the last days is very close to ET_0, so that it can be assumed that during this cutting cycle almost optimal conditions occurred. This is confirmed by the dynamics of K_{c_act} (Figure 2B) that is aligned with that expected under optimal conditions (K_c). During the stage IS, the mean K_{c_act} is slightly lower than the K_c expected under optimal conditions (Table 2).

Data collection in 2009 restarted after the second cut (July 9), without interruptions until the last cut on August 18. For few days after cutting (Figure 2A), ETec is almost stationary, then it shows a rapid increment during the development stage (until July 25) with final values of about 6 mm/day (compared to ET0 of about 7 mm/day). During the next MS-LS stages ETec shows a decreasing trend until the beginning of August when it increases to values of about 6 mm/day. After, ETec shows again a decreasing trend until the final cutting. The observed dynamics of ETec can be likely attributable to the presence of non-optimal conditions (in particular water shortage). The dynamics of Kc_act compared to that of Kc (Figure 2B) clearly demonstrates this situation: a part from the slight difference during the stage IS (Figure 2B and Table 2), then Kc_act and Kc follow the same dynamics until about July 14. After this date, Kc_act continues to increase at a slower rate for some days, then it shows an evident decrease until the end of July. The abundant rainfalls of August 2 and 3 (Figures 2A and B) determine a temporary recovery of both ETec and Kc_act, but the consistent evapotranspirative demand of the period leads to a rapid decreasing of both variables until the end of the cutting cycle.

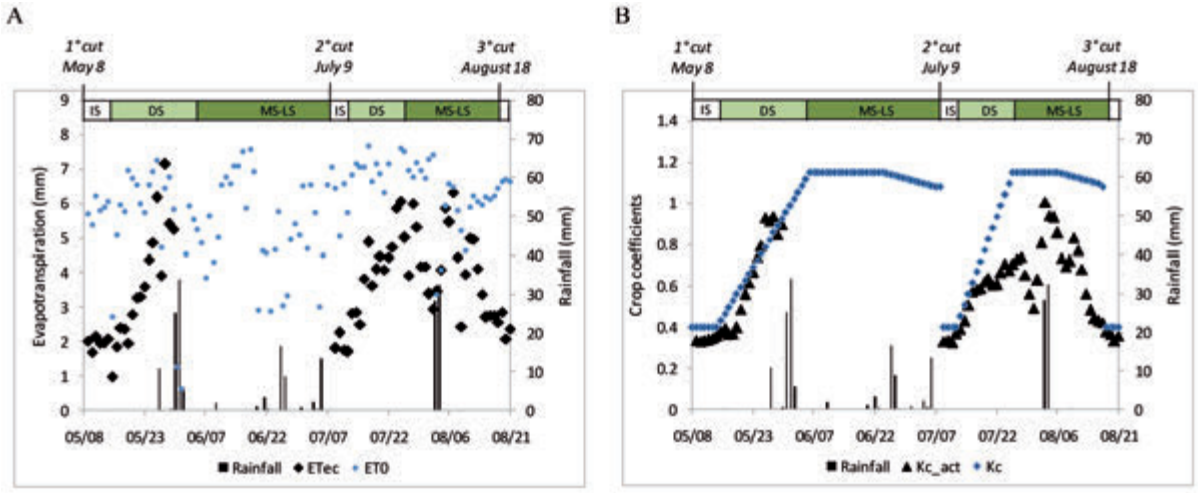

Figure 2. Daily values of rainfall, actual evapotranspiration measured by eddy covariance ET_{ec}, reference evapotranspiration ET_0 in 2009 (A). Daily values of rainfall, 3-day means of K_{c_act} (ET_{ec}/ET_0) and daily crop coefficients, K_c, by Allen *et al.* (1998) in 2009 (B). IS, initial stage; DS, development stage; MS-LS, mid and late season stages.

Table 2. Statistics of daily evapotranspiration measured by eddy covariance (ET_{ec}), reference evapotranspiration (ET_0), actual crop coefficients (K_{c_act}) in 2009 and 2010 during alfalfa growth stages.

Year	Growth stage	Period	ET_{ec} (mm/day)		ET_0 (mm/day)		K_{c_act}		
			Mean	Cumulated	Mean	Cumulated	Mean	Min	Max
2009	IS	8-14 May	1.98	11.90	5.85	35.10	0.34	0.31	0.35
	DS*	15 May-6 June	3.73	59.80	6.00	96.00	0.61	0.28	1.11
	MS-LS°	7 June-8 July	-	-	5.40	172.73	-	-	-
	IS	9-12 July	1.85	7.57	5.95	23.80	0.32	0.27	0.45
	DS	13-25 July	4.18	54.37	7.32	95.00	0.57	0.36	0.80
	MS-LS	26 July-17 August	4.20	96.78	6.16	141.65	0.70	0.40	1.03
2010	IS	24-28 May	2.20	10.90	4.88	24.41	0.45	0.42	0.53
	DS	29 May-12 June	3.38	50.76	5.06	75.92	0.66	0.39	0.90
	MS-LS	13-28 June	4.28	68.50	4.80	76.75	0.87	0.68	1.10
	IS	29 June-3 July	2.22	11.10	6.51	32.56	0.34	0.23	0.47
	DS	4 July-18 July	2.93	44.05	6.42	96.24	0.45	0.28	0.60
	MS-LS	19 July-1 August	2.68	37.51	5.81	81.38	0.48	0.24	1.06

IS, Initial stage; DS, development stage; MS-LS, mid and late season stages; * This stage has been observed until May 30; ° This stage was not observed due to technical problems.

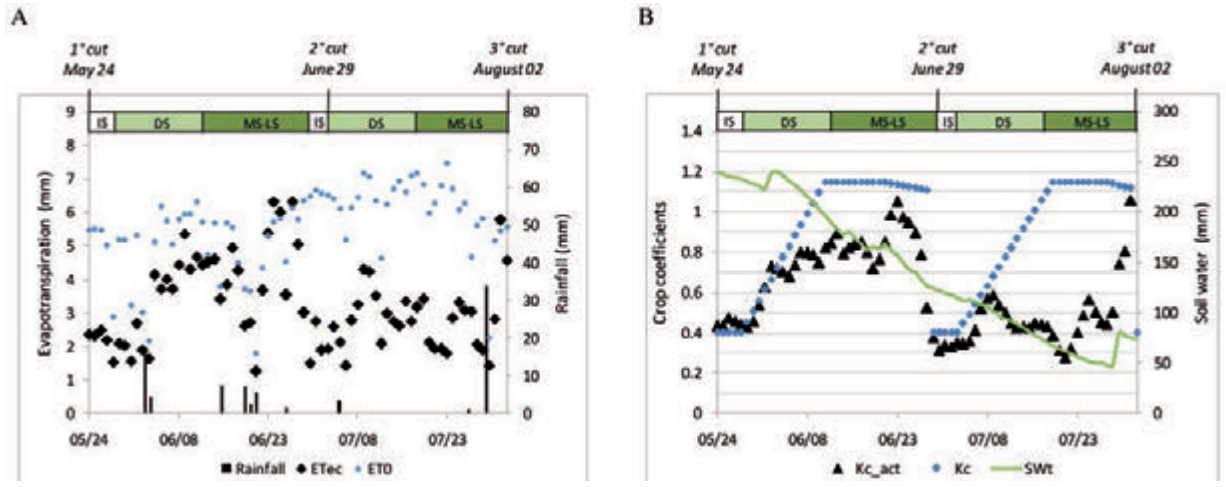

Figure 3. Daily values of rainfall, actual evapotranspiration measured by eddy covariance ET_{ec}, reference evapotranspiration ET_0 in 2010 (A). 3-day means of K_{c_act} (ET_{ec}/ET_0), daily crop coefficients, K_c (Allen *et al.*,1998) and simulated soil water dynamics (SWt) in 2010 (B). IS, initial stage; DS, development stage; MS-LS, mid and late season stages.

Growing season 2010

In 2010 ET_{ec} was monitored between May 24 and August 2 (Figure 3A), including two complete cutting cycles. A preliminary comparison between 2009 and 2010 (Figure 2A and 3A respectively) shows that in 2010 ET_{ec} has a weaker relationship with growth stages. During the first monitored cutting cycle (May 24- June 29) ET_{ec} shows a increasing tendency until June 20, followed by few days with very low values, after which ET_{ec} rises to about 6 mm/day in the proximity of the cutting (Figure 3A). The ET_{ec} drop after June 20 can be partially explained by the corresponding reduction of ET_0 (Figure 3A) in correspondence of some cold and rainy days. The analysis of the K_{c_act} dynamics, compared to K_c (Figure 3B) depicts a probable condition of water stress after the first week of June, partially reduced by some rainfall events and by the ET_0 reduction around June 20.

During the second monitored cutting cycle of 2010 (June 29 – August 2) low values for both ET_{ec} and K_{c_act} (Figure 3A and B, Table 2) were recorded. In particular, the K_{c_act} dynamics can be considered aligned (although lower) with that of K_c only during the IS stage and during the first week of the DS stage. During the rest of the cycle, until the rainfall event of July 30 (34 mm), K_{c_act} is always lower than 0.6 reaching a minimum of 0.24 on July 23. Both ET_{ec} and K_{c_act} increase after the considerable rainfall event of July 30, confirming that the low evapotranspiration during this cycle has been mainly dependent on water shortage.

Figure 3B shows also the dynamics of the simulated soil water availability SWt in 2010. This information confirms the presence of a relevant water shortage during the last cutting cycle. On the other hand, the SWt computed from the single-layer soil water balance can just provide general information and it is not well correlated with short-term variations of K_{c_act} and actual ET (*e.g.* the brief K_{c_act} recovery on June 20 and July 30, due to rainfall events).

Conclusions and discussion

The paper shows an analysis of rainfed alfalfa evapotranspiration, measured by eddy covariance technique. The main objective was to obtain a precise evaluation of actual crop coefficients of rainfed alfalfa and their response to climatic factors and agricultural management. The tabulated crop coefficients for optimal conditions were used as term of comparison. The main results can be summarized as follows:

- in most cases, the K_{c_act} during the days following the cutting was slightly lower than the tabulated K_c value (Allen *et al.*, 1998) for the same stage (K_{c_ini}). Since ET in this phase is mainly ruled by the evaporation process, the detected differences were unlikely dependent on crop water shortage. Local conditions (cutting height, crop density, wetting/drying cycles) are the most probable influencing factors of actual ET in this stage that can be adequately described only by a direct measurement (like EC).
- during the DS stage, K_{c_act} was often aligned with that expected under optimal conditions. In contrast, during the MS stage, K_{c_act} was almost always lower than $K_{c\text{-}mid}$ =1.15 apart after heavy rainfalls. This shows how in non-irrigated conditions, the considerable demand of water of alfalfa at full cover can be unlikely supplied by the soil water storage and precipitation;
- after persistent periods of water scarcity (*e.g.* last cutting cycles of 2009 and 2010), evapotranspiration moves back to high values if significant rainfalls occur, but this increase could be mainly due to evaporation.

The detected intra and inter-annual variability of K_{c_act} makes it opportune to plan other measurement campaigns in order to obtain more information about evapotranspiration dynamics in rainfed crops.

References

Allen R.G., Pereira L.S., Raes D., Smith M. 1998. Crop evapotranspiration - Guidelines for computing crop water requirements , Irrigation and Drainage Paper56 , UN-FAO, Rome, Italy.

Allen R.G., Pereira L.S., Howell T.A., Jensen M.E. 2011a. Evapotranspiration information reporting: I. Factors governing measurement accuracy. Agric. Water Manage. 98: 899-920.

Allen R.G., Pereira L.S., Howell T.A., Jensen M.E. 2011b. Evapotranspiration information reporting: II. Recommended documentation. Agric. Water Manage. 98: 921-29.

Baldocchi D.D. 2003. Assessing the eddy covariance technique for evaluating carbon dioxide exchange rates of ecosystems: past, present and future. Glob. Change Biol. 9:479-492.

Campbell G.S., Norman J.M. 1998. An introduction to environmental biophysics, 2nd ed. Springer, New York.

Doorenbos J., Pruitt W.O. 1977. Guidelines for predicting crop water requirements, Irrigation and Drainage Paper 24 , UN-FAO, Rome, Italy.

Doorenbos J., Kassam A.H. 1986. Yield response to water. Irrigation and drainage Paper 33. UN-FAO, Rome, Italy.

Farahani S.H.J., Howell T.A., Shuttleworth W.J., Bausch W.C. 2007. Evapotranspiration: progress in measurement and modeling in agriculture. Transactions of the ASABE 50: 1627–38.

Foken T., Wichura B. 1996. Tools for quality assessment of surface-based flux measurements. Agric. For. Meteorol. 78: 83-105.

Foken T., Göckede M., Mauder M., Mahrt L., Amiro B.D., Mauger J.M. 2004. Post-field data quality control. In: Lee X. et al., eds. Handbook of Micrometeorology: a guide for surface flux measurement and analysis. Kluwer, Dodrecht, 181-208.

Foken T. 2008. The energy balance closure problem – An overview. Ecolog. Appl. 18:1351-67.

Foken T., Aubinet, M., Leuning, R., 2011a. The eddy covariance method. In: Aubinet M., et al. eds. Eddy covariance: a practical guide to measurement and data analysis. Springer, Berlin, Heidelberg.

Foken T., Leuning R., Oncley S.P., Mauder M., Aubinet M. 2011b. Corrections and data quality. In: Aubinet M., et al. eds., Eddy covariance: a practical guide to measurement and data analysis. Springer, Berlin, Heidelberg.

Garratt J.R., 1992. The Atmospheric Boundary Layer. Cambridge University Press, New York.

Giorgi F., Lionello P. 2008. Climate change projections for the Mediterranean region. Global Planet. Change. 63:90-104.

Kljun N., Calanca P., Rotach M.W., et al. 2004. A Simple Parameterisation for Flux footprint Predictions, Boundary-Layer Meteorol. 112: 503-23.

Mauder M., Foken T., Clement R., Elbers J., Eugster W., Grünwald T., Heusinkveld B., Kolle O. 2008. Quality control of CarboEurope flux data - Part 2: Inter-comparison of eddy-covariance software. Biogeosci. 5:451-62.

Parent A.C., Anctil F. 2012. Quantifying evapotranspiration of a rainfed potato crop in South-eastern Canada using eddy covariance techniques. Agric. Water Manage. 113: 45-56.

Rana G., Katerji N. 2000. Measurement and estimation of actual evapotranspiration in the field under Mediterranean climate: a review. Eur. J. Agron. 13: 125-53.

Reichstein M., et al. 2005. On the separation of net ecosystem exchange into assimilation and ecosystem respiration: review and improved algorithm. Global Change Biol. 11: 1424-39.

Smith M. 2000. The application of climatic data for planning and management of sustainable rainfed and irrigated production. Agric. For. Meteorol.103: 99-108.

Stull R.B. 1988. An introduction to boundary layer meteorology. Atmospheric Science Library, Kluwer Academic Publishers, Dordrecht, Netherlands.

Twine T.E., Kustas W.P., Norman J.M., Cook D.R., Houser P.R., Meyers T.P., Prueger J.H., Starks P.J., Wesely M.L. 2000. Correcting eddy-covariance flux understimates over a grassland. Agric. For. Meteorol. 103: 279-300.

Webb E.K., Pearman G.L., Leuning R. 1980. Correction of flux measurements for density effects due to heat and water vapour transfer. Q.J.R. Meteorol. Soc. 106: 85-100.

A neuro-fuzzy model to predict the inflow to the guardialfiera multipurpose dam (Southern Italy) at medium-long time scales

L.F. Termite, F. Todisco, L. Vergni, F. Mannocchi

Department of Civil and Environmental Engineering, University of Perugia, Perugia, Italy

Abstract

Intelligent computing tools based on fuzzy logic and artificial neural networks have been successfully applied in various problems with superior performances. A new approach of combining these two powerful tools, known as neuro-fuzzy systems, has increasingly attracted scientists in different fields. Few studies have been undertaken to evaluate their performances in hydrologic modeling. Specifically are available rainfall-runoff modeling typically at very short time scales (hourly, daily or event for the real-time forecasting of floods) with in input precipitation and past runoff (*i.e.* inflow rate) and in few cases models for the prediction of the monthly inflows to a dam using the past inflows as input. This study presents an application of an Adaptive Network-based Fuzzy Inference System (ANFIS), as a neuro-fuzzy-computational technique, in the forecasting of the inflow to the Guardialfiera multipurpose dam (CB, Italy) at the weekly and monthly time scale. The latter has been performed both directly at monthly scale (monthly input data) and iterating the weekly model. Twenty-nine years of rainfall, temperature, water level in the reservoir and releases to the different uses were available. In all simulations meteorological input data were used and in some cases also the past inflows. The performance of the defined ANFIS models were established by different efficiency and correlation indices. The results at the weekly time scale can be considered good, with a Nash-Sutcliffe efficiency index $E = 0.724$ in the testing phase. At the monthly time scale, satisfactory results were obtained with the iteration of the weekly model for the prediction of the incoming volume up to 3 weeks ahead ($E = 0.574$), while the direct simulation of monthly inflows gave barely satisfactory results ($E = 0.502$). The greatest difficulties encountered in the analysis were related to the reliability of the available data. The results of this study demonstrate the promising potential of ANFIS in the forecasting of the short term inflows to a reservoir and in the simulation of different scenarios for the water resources management in the longer term.

Correspondence: Lorenzo Francesco Termite, Department of Civil and Environmental Engineering, University of Perugia, Borgo XX Giugno 74, 06121 Perugia, Italy
E-mail: lorisfrancesco.termite@studenti.unipg.it

Key words: ANFIS, streamflow forecasting, weekly time scale, model iteration.

Journal of Agricultural Engineering 2013; XLIV(s1):e158
doi:10.4081/jae.2013.(s1):e158

Introduction

River flow forecasting is a very important issue; in particular, when the river flows are stored in artificial reservoirs, the inflows forecasting allows to plan and adequately support the decision making for multipurpose reservoir releases both in the real time and at the inter and intra seasonal time scale. The traditional hydrological modeling techniques have been joined in recent years by alternative methods based on artificial intelligence systems, including systems based on artificial neural networks (ANNs), that bypass the problem of the parameterization of typical rainfall-runoff models and allow a significant reduction in the number of input data, while requiring long time series as input. From the combination of ANNs with fuzzy logic (Zadeh, 1965) derived neuro-fuzzy networks, which combine the main advantages of the two methodologies.

The first applications of ANNs to the problem of flow forecasting date back to the early '90s (Halff *et al.*, 1993; Hjelmfet and Wang, 1993; Karunanithi *et al.*, 1994). In the following years ANNs or neuro-fuzzy based models have found more applications to hydrologic problems. In particular, though it is possible to find in literature applications at weekly (Zealand *et al*., 1999) or monthly scale (Jeong and Kim, 2005; Cannas *et al*., 2006; Jain and Kumar, 2007), most of the applications of such models refers to the prediction of the flow at short time scales as hourly, daily or single event time scale (Minns and Hall, 1996; Dawson and Wilby, 1998; Campolo *et al*., 1999; Nayak *et al*., 2004, 2005; Vernieuwe *et al*., 2005; Chen *et al*., 2006; Aquil *et al*., 2007; Firat and Gungor, 2007, 2008; Talei *et al*., 2010; Sarkar and Kumar, 2012). These models are useful to take timely decisions in case of extreme events, but they are not useful to plan the water resource management. On the other hand, longer time scale models have the limitation of using many input, sometimes not readily available, as for example the measured evaporation in Jeong and Kim (2005); moreover, within the same application, are sometimes used different networks for different time scales, or networks trained separately for the forecasting of low, medium and high values of the flow regime.

This study presents an application of neuro-fuzzy networks to forecast the inflows to the Guardialfiera artificial reservoir (Southern Italy). The objective is to build a single model that may be efficient in the short-medium term (weekly scale) and that may, at the same time, enlarge the forecasting time scale trough iterations, giving indications about the inflows in the next periods in relation to possible meteorological scenarios. The implemented models use a limited number of input data, easy to find or to predict: observed values of inflows at the previous time steps and elaborations of precipitation and temperature data.

Materials and methods

The Guardialfiera Lake is a multipurpose artificial reservoir on the Biferno river (Molise Region, Southern Italy). The lake has a maxi-

mum surface area of 7.45 km^2, a gross storage capacity of 173 Mm^3 and a live storage capacity of 137 Mm^3. The catchment area is 1043 km^2. The water is used for domestic, irrigation, industrial and hydropower uses.

Daily values of rainfall, minimum and maximum temperature at 12 stations upstream and 4 downstream, in the period 1974÷2006, are available. Rainfall time series have a percentage of missing data lower than 6.19% in 13 stations; for 3 stations the percentage increases up to a maximum of 27.93%. The percentage of missing data is more consistent for the temperature: from 48.01% to 85.63% for 9 stations, while for only 6 stations the percentage is lower than 11.41%. Nevertheless, for every year data from a number of stations at least equal to 4 are available: thus, it was possible to reconstruct the missing data, using the inverse distance method (Wei and McGuinnes, 1973) for precipitation and the formulation proposed by Vergni and Todisco (2011), based on the correlation coefficient, for temperature. After the reconstruction of missing data, an estimate of the average daily temperature was obtained as the mean of the minimum and maximum daily values. Then, the time series of daily areal rainfall R^A (Thiessen, 1911) and mean daily areal temperature T^A, relative to the upstream catchment area, were obtained after calculating the area A_i associated to each station i (Figure 1) with Thiessen's polygons method (Thiessen, 1911; Boots, 1986).

With regards to the reservoir, daily values of water level and corresponding volume for the period 1978÷2011 are available. For the same period, daily values of the releases for the different uses are also available. Unfortunately, as inflows data are not available, an indirect estimate was obtained by inverting the reservoir water balance equation. However, due to error sources such as occasional incorrect readings of water level or periods of non-operation of the releases measuring instruments, there are some uncertainties in the storage and releases data, and consequently also in the estimation of the inflows. In particular, there are some more or less evident anomalies in the estimate of daily inflows, consisting mostly in very low or even negative values. Some of these outliers (8.41% of the total data) have been corrected with a simple averaging procedure. Analyzing the time series of the flow at a gauge station located 30 km upstream from the reservoir, a minimum threshold for the inflow of 0.5 m^3/s (corresponding to a daily inflow volume of 43200 m^3) was identified; all values below this threshold were replaced with greater or equal values, performing media operation.

Table 1 shows a summary of climatologic data of the Biferno basin and storage volumes, inflows and outflows.

The potential of the Adaptive Network-based Fuzzy Inference (ANFIS) model (Jang, 1993) in weekly scale forecasting have been investigated and then the forecasting time horizon has been enlarged both implementing monthly scale models and iterating the best weekly model. ANFIS is the best known neuro-fuzzy model, based on ANNs and fuzzy logic.

ANNs are adaptive mathematical models constituted by a group of interconnections of informations and can be used to represent complex relationships between input and output data, that other analytical functions fail to represent. Structurally they are composed of a series of interconnected processing elements called "artificial neurons", arranged in layers. In the input layer, each neuron receives input data, in the output layer neurons provide the final result of data processing. Between these two layers there are one or more intermediate layers called "hidden layers", which have the task to process the data to arrive at the final result. In the training phase pairs of known input and corresponding output data are provided. During the training, the network modifies the parameters of the functions defined in its nodes through learning algorithms (Satyabrata and Uttam, 2013) that are iterated for a number of times said "training epochs". In this way the network acquires generalization capability, *i.e.* the ability to produce a plausible output starting from input data not included in the training data set.

The fuzzy logic (Zadeh, 1965) is based on the concept of fuzzy sets, defined as sets with no crisp boundaries; unlike the two-valued Boolean logic, fuzzy logic uses any real value between 0 (completely false) and 1 (completely true), which is known as membership value; the function representing such values is called membership function. On this basis, inferential systems such as the Takagi-Sugeno one (Takagi and Sugeno, 1985) are built.

The ANFIS model acquires knowledge from data using typical ANNs' algorithms, but represent it using fuzzy rules.

Figure 1. Basin of the Biferno river within Molise region and division in Thiessen polygons .

Table 1. Principal characteristics of Biferno basin climate regime and Guardialfiera Lake storage, inflow and outflow volumes .

	Minimum	Maximum	Mean
Annual R^A (mm)	635.3	1242.0	942.2
Mean T^A_{min} (°C)	7.4	10.3	8.9
Mean T^A_{max} (°C)	16.2	19.7	18.0
Mean T^A_{mean} (°C)	11.8	14.8	13.4
V_{min} (Mm^3)	22.89	110.11	78.74
V_{max} (Mm^3)	50.50	154.94	129.21
Mean I (Mm^3)	0.35	1.71	0.84
Mean O_1 (Mm^3)	0.09	1.52	0.55
Mean O_2 (Mm^3)	0.02	0.04	0.02
Mean O_3 (Mm^3)	0.01	0.56	0.22
Mean O_4 (Mm^3)	0.00	0.08	0.03

Annual R^A: annual areal rainfall (1974-2006); Mean T^A_{min}: mean of the minimum daily areal temperature (1974-2006); Mean T^A_{max}: mean of the maximum daily areal temperature (1974-2006); Mean T^A_{mean}: mean of the mean daily areal temperature (1974-2006); V_{min}: annual minimum storage volume (1978-2011); V_{max}: annual maximum storage volume (1978-2011); mean I: mean daily inflow volume (1978-2011); mean O_1: mean daily bed release volume (1978-2011); mean O_2: mean daily release volume for civil use (1985-2011); mean O_3: mean daily release volume for industrial and agricultural use (1978-2011); mean O_4: mean daily release volume for hydroelectric use (1999-2011).

In order to select the input data among the various elaborations of available data, analyses of correlation between inflows and meteorological data were carried out. Different ANFIS models for inflows simulation were then implemented, varying the input/output combinations (Table 2) and the network's structure. Given the different periods covered by the meteorological data (1974 ÷ 2006) and those relating to the management of the reservoir (1978 ÷ 2011), it was possible to use only the common period data (1978÷2006), with a total of 10592 values of daily inflows and a number of input/output vectors varying from 10542 to 10592 depending on timely data aggregation. In all simulations, data from 1978 to 1996 and from 2002 to 2006 (number of vectors varying from 8716 to 8766) were used as training data, while those from 1997 to 2001 (1826 vectors) were selected as testing data. This choice is justified by the fact that the period 1997÷2001 is characterized by a fairly standardized inflows trend, while up to 1992 and from 2003 onwards there are inflow peaks that is worthwhile to insert in the training data.

The implemented models were evaluated with: a) standard regression indices, as the slope and the intercept of the observed vs. simulated data linear regression line; Pearson's correlation coefficient *r* and the coefficient of determination R^2; b) adimensional efficiency indices, as the efficiency index *E* (Nash and Sutcliffe, 1970); the modified efficiency index E_1 (Legates and McCabe, 1999); the index of agreement *d* (Willmott, 1981) and the modified index of agreement d_1 (Wilmott *et al*. 1985); c) error indices, as the Root Mean Square Error *RMSE*; the Mean Absolute Error *MAE*; the Mean Absolute Percentage Error *MAPE*; the percent-bias index *PBIAS* (Gupta *et al*., 1999) and the RMSE-observation Standard deviation Ratio *RSR* (Singh *et al*., 2004).

Particular attention is given to *E*, *PBIAS* and *RSR* values, that have been compared with the ranges identified by Moriasi *et al.* (2007) in their guidelines for the evaluation of hydrological simulation models.

Results and discussion

The weekly time scale model that gave the best results, called *Liscione_67*, has the input/output combination n. 6 in Table 2. The model was built with 4 triangular membership functions for each input and constant function for the output; it was trained for 200 epochs with the hybrid learning algorithm.

The use of input as meteorological data relative to the same period of the forecasted inflows obviously introduces new variables when these models are actually applied. However, today's weather prediction models allow to have a fairly good estimate of rainfall within the next 6 days (Chou *et al*., 2000; Collischonn *et al*., 2007). Graphical results on the testing data are presented in Figures 2 and 3. Table 3 shows the results in term of statistical indices for both training and testing data. The results on the training data can be defined "very good" for all *E, PBIAS* and *RSR* indices according to the classification proposed by Moriasi *et al.* (2007). In particular, the *PBIAS* index shows the optimal value 0.000. With regards to the testing data, the value of *E* equal to 0.724 and *RSR* equal to 0.525 allow to classify the model as "good"; the *PBIAS* value -20.151 instead fall within the range of "satisfactory" values and reveals the general tendency of the model to overestimate the inflows.

Anyway, the guidelines proposed by Moriasi *et al.* (2007) refer to simulations at monthly scale, while the *Liscione_67* model uses a weekly scale. According to the authors, less restrictive evaluation criteria can be adopted in case of time scales shorter than monthly, and also in the case of considerable uncertainties on the data used for the simulation and when the objective of the study is to investigate the technology potential and to perform a base research: all these conditions fall in this study, so the results can be considered very satisfactory.

Table 2. Input and output data of the implemented models.

Combination number	Input	Target/output	Number of input/output vectors
1	$R^A(t\div t+6)$, $T^A_{mean}(t\div t+6)$	I(t÷t+6)	10591
2	$R^A(t-1\div t+5)$, $T^A_{mean}(t-1\div t+5)$	I(t÷t+6)	10587
3	RA(t-1÷t+5), I(t-7÷t-1)	I(t÷t+6)	10580
4	$R^A(t-1\div t+5)$, $T^A_{mean}(t-1\div t+5)$, I(t-7÷t-1)	I(t÷t+6)	10580
5	$R^A(t-7\div t-1)$, $T^A_{mean}(t-7\div t-1)$, I(t-7÷t-1)	I(t÷t+6)	10585
6	$R^A(t\div t+6)$, $T^A_{mean}(t\div t+6)$, I(t-7÷t-1)	I(t÷t+6)	10579
7	I(t-7÷t-1), $I_{stat}(t\div t+6)$	I(t÷t+6)	10585
8	$R^A(t-7\div t-1)$, $R^A_{stat}(t\div t+6)$, $T^A_{mean}(t-7\div t-1)$, $T^A_{mean,stat}(t\div t+6)$, I(t-7÷t-1)	I(t÷t+6)	10585
9	I(t-7÷t-1), I_{stat} (t-7÷t-1), $I_{stat}(t\div t+6)$	I(t÷t+6)	10585
10	$R^A_{stat}(t\div t+6)$, $T^A_{mean,stat}(t\div t+6)$, I(t-7÷t-1)	I(t÷t+6)	10585
11	$R^A(t\div t+6)$, $R^A_{stat}(t\div t+6)$, $T^A_{mean}(t\div t+6)$, $T^A_{mean,stat}(t\div t+6)$, $I_{stat}(t\div t+6)$	I(t÷t+6)	10586
12	$R^A(t-90\div t-1)$, $T^A_{mean}(t-15\div t-1)$	I(t÷t+29)	10592
13	$R^A(t-90\div t-1)$, $T^A_{mean}(t-15\div t-1)$, I(t-30÷t-1)	I(t÷t+29)	10562
14	$R^A(t-9\div t+20)$, $T^A_{mean}(t-9\div t+20)$, I(t-30÷t-1)	I(t÷t+29)	10542
15	$R^A(t-9\div t+20)$, $T^A_{mean}(t-9\div t+20)$	I(t÷t+29)	10572
16	$R^A(t-9\div t+20)$, I(t-30÷t-1)	I(t÷t+29)	10542

R^A: areal rainfall (cumulated values from t+i to t+j, with i,jϵ $\mathbb{Z}$); R^A_{stat}: mean of areal rainfall (cumulated values from t+i to t+j, with i,jϵ $\mathbb{Z}$) in the period 1974÷2006;
TA_{mean}: daily areal temperature (mean value from t+i to t+j, with i,jϵ $\mathbb{Z}$); $T^A_{mean,\ stat}$: mean value of daily areal temperature (mean value from t+i to t+j, with i,jϵ $\mathbb{Z}$) in the period 1974÷2006; I: inflow (cumulated values from t+i to t+j, with i,jϵ $\mathbb{Z}$); I_{stat}: mean value of inflow (cumulated values from t+i to t+j, with i,jϵ $\mathbb{Z}$) in the period 1974÷2006.

Nevertheless, analyses were carried to understand the principal causes of error.

The analysis of the absolute frequencies of observed and simulated values showed a tendency to overestimate lower values, as shown also in Figure 3. Moreover, the analysis of the absolute frequencies of the differences between observed and simulated values confirms a general model's tendency to overestimate, already indicated by the negative value of the *PBIAS* index. It was also verified that, with respect to the testing data, in 6% of cases the absolute difference between the observed and simulated value is greater than 5 Mm^3; these cases (white dots in Figure 3) greatly influence the efficiency index *E* and are mainly due to overestimation of the lower values and underestimation of the higher ones. It was also analyzed the cumulative frequency of the data used as input, both for all testing data and only for those cases in which the absolute difference between observed and simulated data exceeds 5 Mm^3. It was thus possible to observe that the largest errors occur when precipitation values are higher than the average ones, when temperature values are lower than the average ones and in correspondence of high differences between the inflows of consecutive weeks (percentage difference higher than 100%). This analysis suggests that in order to reduce the prediction error it is reasoning to focus the attention on some particular periods of the year, especially autumn and winter. Beyond these considerations, an interesting result was obtained by analyzing the dates with absolute differences greater than 5 Mm^3. The analysis showed that they are grouped into 14 periods of few consecutive days; most of these periods are characterized by initial uncertainties on the values of the inflows and in many cases the inflow values have been reconstructed as described previously. It is therefore reasonable to think that these uncertainties had a decisive weight in the model performance. In order to verify the weight of the initial uncertainties, it was constructed, trained and tested a new model, called *Liscione_67_b*, obtained removing from both the training and the testing set all the input/output vectors that contain reconstructed values of the inflows. Because of the weekly aggregation of the inflows in both the input and output data, this led to a reduction of the input/output vectors of 31.4% in the training set and of 55.3% in the testing set. The simulation results on the training and testing data, reported in Table 3, show an improvement over *Liscione_67* in terms of the statistical indices. With regard to the testing data, the efficiency index *E* increases from 0.724 to 0.761 and *RSR* decreases from 0.525 to 0.489. The model performance rating on both these indices, according to Moriasi *et al.* (2007), changes from "good" to "very good." The value of *PBIAS* improves too, decreasing from -20.151 to -17.891, however the performance rating on this index remains "satisfactory".

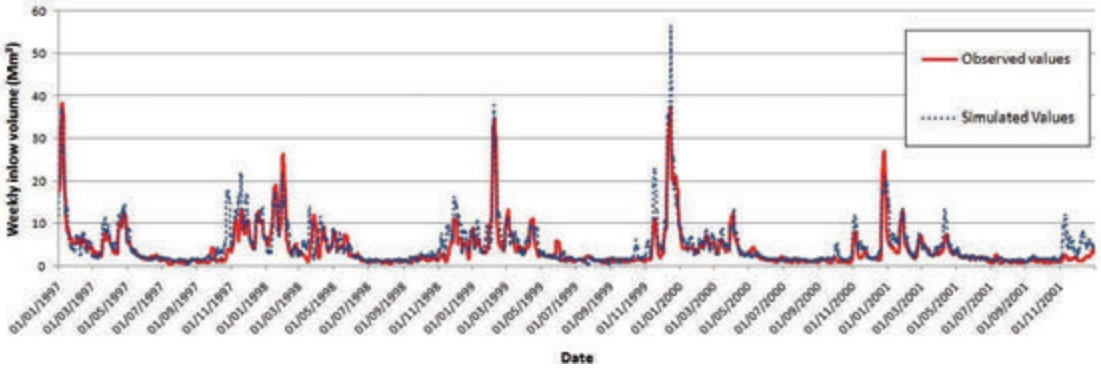

Figure 2. Observed and simulated weekly inflow volumes in the testing period (1997-2001) for Liscione_67 Model.

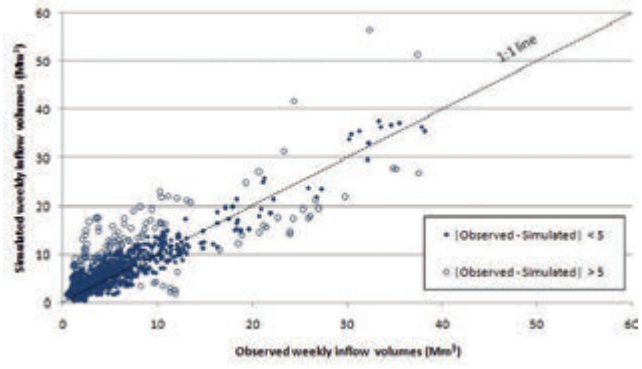

Figure 3. Observed vs simulated weekly inflow volumes in the testing period (1997-2001) for Liscione_67 Model.

Table 3. Results of the weekly time scale models Liscione_67 and Liscione_67_b.

	Liscione_67 Model		Liscione_67_b Model	
	Training data	Testing data	Training data	Testing data
Slope	0.797	0.946	0.812	0.951
Intercept	1.28E+06	1.02E+06	1.44E+06	1.36E+06
r	0.893	0.886	0.901	0.904
R2	0.797	0.785	0.812	0.817
E	0.797	0.724	0.812	0.761
E1	0.633	0.486	0.643	0.478
d	0.940	0.933	0.946	0.942
d1	0.809	0.751	0.815	0.740
RMSE	3.87E+06	2.57E+06	4.07E+06	2.86E+06
MAE	1.97E+06	1.53E+06	2.15E+06	1.90E+06
MAPE	39.92	54.07	31.75	43.66
PBIAS	0.000	-20.151	0.000	-17.891

The monthly scale model that gave the best results has the input/output combination n. 16 in Table 2, with total precipitation from day *t-9* to day *t+20* and observed inflows from *t-30* to *t-1* as inputs. Typically, when ANNs are used for the simulation of flows at monthly scale, the input data used are the flow values at previous time steps (Atiya *et al*., 1999; Cannas *et al*., 2006; Jain and Kumar, 2007). In fact, it is difficult to relate the upcoming month flow value with past meteorological data, especially in small basins in which the rainfall-runoff process is exhausted in a short time. Indeed, the results obtained using these kind of input have not proved satisfactory. On the other hand, the use of future values of rainfall as input data involves uncertainties related to the their prediction beyond a certain time horizon, although in literature there are examples of meteorological modeling that produce accurate predictions even at a monthly or seasonal time scale (Chou *et al*. 2000; Chou *et al*. 2005). The model was built with 4 triangular membership functions for each input and constant function for the output, and trained for 200 epochs with the hybrid learning algorithm. Good results on the training data contrast with poorer results on the testing data, with a barely satisfactory efficiency index $E = 0.502$.

Another possible way to enlarge the forecasting time scale is the iteration of the same model (Atiya *et al*., 1999), when among the input data there is the same variable produced as output (for example, when the upcoming flow value is simulated using the flow values at previous time steps as input). The *Liscione_67* model was thus iterated, using the output inflow value as input for the next step. The output values from all the simulation steps were then added together and compared with the total inflow values in the corresponding days. The performance get worse at every iteration, due to the casual propagation of errors; in particular, satisfactory results were obtained up to the second iteration, with an efficiency index $E = 0.574$ relative to the forecast of the inflow volumes up to 20 days ahead.

Conclusions

ANFIS models for the forecasting of the inflow volumes to the Guardialfiera dam at the weekly and monthly time scale were implemented in this study. These models allow to use a smaller number of input data compared to the traditional hydrologic modeling and make it possible to simulate the flow regimes even from just a few and readily available data such as meteorological ones; in particular, in this study daily data of rainfall, temperature and storage volume in the period 1978÷2006 were used.

The results at the weekly scale have proved good, with an efficiency index $E = 0.724$ on the testing data. The model tends to overestimate the inflows, especially the lower values. At the monthly scale the results are poorer, because it's more difficult to relate monthly values of the inflows with rainfall and temperature data. The best result of the direct simulation of the monthly inflows gave an efficiency index $E = 0.502$. Moreover, iterations of the best performing weekly model were performed, thus obtaining forecasts of the cumulated values of inflows in the upcoming weeks. In this case there is a casual error propagation at every iteration and the model performance get worse compared to the first step. In particular, satisfactory results were obtained up to the second iteration, with an efficiency index $E = 0.574$, thus obtaining satisfactory forecasts of the inflow volumes up to 20 days ahead.

The principal causes of error were investigated and it was found that these type of models are very sensitive to input data that differ much from their mean values. Moreover, especially when the number of input data is small, it is necessary that the input time series are accurate and without uncertainties, since the latter strongly influence the performance of the models, as demonstrated in this work. Data preprocessing, aimed to reduce the weight of the outliers, is thus useful. In addition, it is appropriate to ensemble a training set including all possible cases or, however, the extreme cases, in terms of both minimum and maximum, among the available data. In this study, the division into training and testing set was made a priori, including all the extreme values of the inflows in the training set and choosing a testing set characterized by rather standardized values of the inflow volumes. However, it could be interesting to check the model performance varying the training and testing sets with a cross-validation technique.

The best performing models use future values of rainfall and temperature as inputs, that obviously would not be known a priori in case of their actual application. However, today it is possible to obtain very accurate estimations of rainfall and temperature values in the upcoming week and even at longer term.

In conclusion, with the implemented ANFIS model it is possible to forecast fairly accurately the inflow volumes in the short term, while for longer periods it is possible to simulate different scenarios, varying predictions on meteorological data, and formulate hypotheses of water resource management.

References

Aqil M., Kita I., Yano A., Nishiyama S. 2007. A comparative study of artificial neural networks and neuro-fuzzy in continuous modeling of the daily and hourly behaviour of runoff. J. Hydrol. 337:22-34.

Atiya A. F., El-Shoura S. M., Shaheen S. I., El-Sherif M. S. 1999. A comparison between neural-network forecasting techniques - Case study: river flow forecasting. IEEE T. Neural Networ. 10:402-9.

Boots B. N. 1986. Voronoi (Thiessen) Polygons. Concepts and Techniques in Modern Geography 45, Geo Book, Norwich.

Campolo M., Andreussi P., Soldati A. 1999. River flow forecasting with a neural network model. Water Resour. Res. 35:1191-97.

Cannas B., Fanni A., See L., Sias G. 2006. Data preprocessing for river flow forecasting using neural networks: Wavelet transforms and data partitioning. Phys. Chem. Earth 31:1164-71.

Chen S.-H., Lin Y.-H., Chang L.-C., Chang,F.-J. 2006. The strategy of building a flood forecast model by neuro-fuzzy network. Hydrol.Process. 20:1525-40.

Chou S. C., Nunes A. M. B., Cavalcanti I. F. A. 2000. Extended range forecasts over South America using the regional Eta model. J. Geophys. Res. 105:10147-60.

Chou S. C., Bustamante J. F., Gomes J, L. 2005. Evaluation of Eta model seasonal precipitation forecasts over South America. Nonlinear Proc. Geoph. 12:537-55.

Collischonn W., Morelli Tucci C. E., Clarke R. T., Chou S. C., Guilhon L. G., Cataldi M., Allasia D. 2007. Medium-range reservoir inflow predictions based on quantitative precipitation forecasts. J. Hydrol. 344:112-22.

Dawson C. W., Wilby R. 1998. An artificial neural network approach to rainfall-runoff modelling. Hydrolog. Sci. J. 43:47-66.

Firat M., Gungor M. 2007. River flow estimation using adaptive neuro fuzzy inference system. Math. Comput. Simulat. 75:87-96.

Firat, M., Gungor M. 2008. Hydrological time-series modeling using an adaptive neuro-fuzzy inference system. Hydrolo. Process. 22:2122-32.

Gupta H. V., Sorooshian S., Yapo P. O. 1999. Status of automatic calibration for hydrologic models: comparison with multilevel expert calibration. J. Hydrol. Eng. 4:135-43.

Halff A. H., Halff H. M., Azmoodeh M. 1993. Predicting runoff from rainfall using neural networks. Proc. Engng. Hydrol., ASCE, New York, 760-5.

Hjelmfelt A. T., Wang M. 1993. Artificial neural networks as unit hydrograph applications. Proc. Engng. Hydrol., ASCE, New York, 1993, 754-9.

Jain A., Kumar A. M. 2007. Hybrid neural network models for hydrologic time series forecasting. Appl. Soft Comput. 7:585-92.

Jang J.-S. R. 1993. ANFIS: Adaptive-Network-Based Fuzzy Inference System. IEEE T. Syst. Man Cyb. 23:665-85.

Jeong D.-I., Kim, Y.-O. 2005. Rainfall-runoff models using artificial neural networks for ensemble streamflow prediction. Hydrol. Process. 19:3819-35.

Karunanithi N., Grenney W. J., Whitley D., Bovee K. 1994. Neural networks for river flow prediction. J.Comput. Civil Eng. 2:203-19.

Legates D. R., McCabe G. J. 1999. Evaluating the use of "goodness-of-fit" measures in hydrologic and hydroclimatic model validation. Water Resour. Res. 35:233-41.

Minns A. W., Hall M. J. 1996. Artificial neural networks as rainfall-runoff models. Hydrolog. Sci. J. 41:399-418.

Moriasi D. N., Arnold J. G., Van Liew M. W., Bingner R. L., Harmel R. D., Veith T. L. 2007. Model evaluation guidelines for systematic quantification of accuracy in watershed simulations. T. ASABE 50:885-900.

Nash J. E., Sutcliffe J. V. 1970. River flow forecasting through conceptual models: Part 1. A discussion of principles. J. Hydrol. 10:282-90.

Nayak P. C., Sudheer K. P., Rangan D. M., Ramasastri K. S. 2004. A neuro-fuzzy computing technique for modeling hydrological time series. J. Hydrol. 291:52-66.

Nayak P. C., Sudheer K. P., Rangan D. M., Ramasastri K. S. 2005. Short-term flood forecasting with a neurofuzzy model. Water Resour. Res. 41, article W04004.

Sarkar A., Kumar R. 2012. Artificial neural networks for event based rainfall-runoff modeling. J. Water Resour. Prot. 4:891-897.

Satyabrata P., Uttam R. 2013. ANFIS based weld metal deposition prediction system in mag welding using hybrid learning algorithm. Int. J. Fuzzy Log. Syst. 3:33-46.

Singh J., Knapp H. V., Demissie M. 2004. Hydrologic modeling of the Iroquois river watershed using HSPF and SWAT. ISWS CR 2004-08. Champaign, Ill.: Illinois State Water Survey.

Takagi T., Sugeno M. 1985. Fuzzy identification of systems and its applications to modeling and control. IEEE T. Syst. Man Cyb. 15:116-32.

Talei A., Chua L. H. C., Quek C. 2010. A novel application of a neuro-fuzzy computational technique in event-based rainfall-runoff modeling. Expert Syst. Appl. 37:7456-68.

Thiessen A. H. 1911. Precipitation averages for large areas. Mon. Weather Rev. 39:1082-4.

Vergni L., Todisco F. 2011. Spatio-temporal variability of precipitation, temperature and agricultural drought indices in Central Italy. Agr. Forest Meteorol. 151:301-13.

Vernieuwe H., Georgieva O., De Baets B., Pauwels V. R. N., Verhoest N. E. C., De Troch F. P. 2005. Comparison of data-driven Takagi-Sugeno models of rainfall-discharge dynamics. J. Hydrol. 302:173-86.

Wei T. C., McGuinnes J. L. 1973. Reciprocal distance squared method, a computer technique for estimating area precipitation. Technical Report ARS-Nc-8. US Agricultural Research Service, North Central Region, Ohio.

Willmott C. J. 1981. On the validation of models. Phys. Geogr. 2:184-94.

Willmott C. J., Ackleson S. G., Davis R. E., Feddema,J. J., Klink K. M., Legates D. R., O'Donnell J., Rowe C. M. 1985. Statistics for the evaluation and comparison of models. J. Geophys. Res.90:8995-9005.

Zadeh L. A. 1965. Fuzzy sets. Inform. Control 8:338-53.

Zealand C. M., Burn D. H., Simonovic,S. P. 1999. Short term streamflow forecasting using artificial neural networks. J. Hydrol. 214:32-48.

Water balance of rice plots under three different cultivation methods: first season results

Enrico Antonio Chiaradia,[1] Arianna Facchi,[1] Olfa Gharsallah,[1] Marco Romani,[2] Gian Battista Bischetti,[1] Claudio Gandolfi[1]

[1]DiSAA, Università degli Studi di Milano, Milano, Italy; [2]CRR, Ente Nazionale Risi, Castello d'Agogna (PV), Italy

Abstract

In the last years rice cultivation methods have been the object of an intense research activity aiming to implement new irrigation methods in addition to traditional flooding, in order to reduce water use. This change has concerned also the traditional paddy-rice territories of the north-west of Italy, where rice has been traditionally cultivated as flooded and where paddy fields are a strong landscape landmark and represent a central feature in the Italian and European network for nature protection. The new techniques introduced in these territories consist in a dry seeding followed by field flooding after about one month (third-fourth leaf), and in a full aerobic cultivation with intermittent irrigations, similarly to standard irrigated crops. This paper presents the results obtained after the first year of a monitoring activity carried out at the Ente Nazionale Risi Experimental Station of Castello d'Agogna-Mortara (PV, Italy), where the main terms of water balance have been measured or estimated during the whole crop season. Because there is a substantial lack of data concerning the water balance related to the new water management techniques, the data are of wide interest despite this study covered only one season. The results here presented show that dry seeding-delayed flooding method required a rather similar amount of water respect to the traditional flooding method (2200 mm and 2491 mm, respectively), whereas the aerobic technique required one order of magnitude less water (298 mm), also due to the very shallow depth of the surface aquifer. Since evapotranspiration was nearly the same for the three methods (578 mm, 555 mm, and 464 mm, respectively for traditional flooded, dry seeding-delayed flooding and aerobic methods), percolation was very high in the case of the two flooded methods and very limited in the case of the aerobic cultivation with intermittent irrigations. These results suggest that, if the aerobic cultivation of rice represents a highly effective water-saving technique at the field scale, at the same time if applied on a large scale in traditional paddy areas, as the north-west of Italy, it could be a potential threat for groundwater dynamics, due to the dramatic decrease of groundwater recharge, and in general for traditional landscape conservation and nature protection.

Correspondence: Gian Battista Bischetti, DiSAA via Celoria 2 , 20133 Milano, Italy.
Tel. +39.02.50316904 - Fax: +39.02.50316911.
E-mail: bischetti@unimi.it

Key words: water balance, rice, soil hydrology.

Contributions: the authors contributed equally.

Conflict of interests: the authors declare no potential conflict of interests

Funding: the work was supported by Regione Lombardia under the grants "Fondo per la promozione di accordi istituzionali, "Project "BIOGESTECA" – Piattaforma di biotecnologie verdi e di tecniche gestionali per un sistema agricolo ad elevata sostenibilità ambientale Project, n. 4779, 14/05/2009.

Acknowledgments: the authors wish to thank Daniele Ferrari, Ezio Naldi, Gianluca Beltarre and its staff for the field assistance.

Journal of Agricultural Engineering 2013; XLIV(s1):e159
doi:10.4081/jae.2013.(s1):e159

Introduction

Rice is one of the most extended cultivations around the world and represents the main food for millions of people. As it requires a larger amount of water compared with other crops (e.g. Feng *et al.* 2007), it is at risk of water scarcity (Tuong and Bouman 2003) and represents an important target for reductions in water use worldwide. In South and Southeast Asia, for example, Tuong and Bouman (2003) estimate that by 2025 approximately 15 million hectares may experience "physical water scarcity" and 22 million hectares "economic water scarcity".

This has stimulated the application of new water-saving methods for rice cultivation, consisting of wetting and drying fields (Bouman and Tuong, 2001; Belder *et al.*, 2004), continuous soil saturation (Borell *et al.*, 1997), dry seeding (Tabbal *et al.*, 2002) and aerobic cultivation as in standard irrigated crops (Bouman *et al.,* 2005). The amounts of water saved by implementing the different water-saving systems vary greatly with climate, soil type and hydrological conditions (Cabangon*et al.*, 2004; Li, 2001; Mao, 1993; Bouman *et al.,* 2005; Yang *et al.*, 2005) and general guidelines cannot yet be drawn.

Although in Italy rice cultivation is only 0.2% of the world's surface (FAOSTAT data for 2011), in some areas it represents a relevant crop both in terms of cultivated land and economic value, as well as from an environmental and landscape perspective.

In Piedmont and western Lombardy, in particular, rice cultivation extends for more than 227,000 hectares (over 92% of the rice cultivated surface in Italy and about a half in Europe; Ente Nazionale Risi and FAOSTAT data for 2011), representing nearly 10% of the total value of the agriculture sector. In these territories, moreover, paddy rice fields have been one of the main landscape markers from centuries, and one of the main wetland in the north-western part of Italy where it represents a keystone in the European protection policy for wild bird migratory species. The paddy fields of Piedmont and Lombardy, in fact, are a

portion of the European ecological network NATURA 2000 and on the official list of the European Special Protection Areas (Habitat Directive, 92/43/EEC), which together with the Birds Directive (79/409/EEC) forms the cornerstone of Europe's nature conservation policy.

In such territories water has never been scarce, but due to increasing competition from new water uses (industry, hydropower, dilution of chemicals in natural water bodies, etc.) and the European Water Framework Directive, which requires more efficient water use in agriculture, the traditional flooded rice cultivation is being questioned and some water-saving methods are appearing. In particular dry seedling followed by delayed flooding (after approximately one month, at third-fourth leaf emission) now represents approximately one third of the whole cultivated area in Piedmont and Lombardy, whereas full aerobic cultivation is gaining increasing popularity.

Studies aiming to quantify the reduction of water inputs as a consequence of the application of water-saving techniques are increasing (Bouman *et al.*, 2005; Feng *et al.*, 2007; Luo *et al.,* 2009; Alberto *et al.*, 2011), but they are mainly carried out in Asian regions where pedo-climatic conditions and cultivation methods are very different from Europe and Italy. Moreover, most of these studies lack on analysis of the hydrological processes on which the water requirement reduction is due (transpiration, evaporation, percolation, etc.) and the dynamics of water fluxes related to irrigation methods is still poorly investigated and understood (Bouman *et al.*, 2007). As a consequence, the scaling-up of the results obtained so far, from field to larger spatial scales, cannot be used to analyse the potential effects of extensive adoption of the new techniques on water requirements at the regional scale and on environment and landscape characteristics, as well as on irrigation service organization.

This paper, contributing to fill such a gap, presents results obtained after the first year of a monitoring activity carried out on three experimental plots, cultivated following one of the three mentioned irrigation techniques adopted (or being adopted) in Piedmont and Lombardy's traditional rice cultivation areas.

Materials and methods

Field experiments were conducted at the Ente Nazionale Risi Rice Research Centre's experimental station located in Castello d'Agogna-Mortara (PV, Italy), within a traditional rice cultivated area. Three on a total of six experimental plots have been instrumented for water fluxes and water storage monitoring (Figure 1).

In order to characterise the soil, five profiles were dug outside of the experimental plots and 112 observations (at three depths each) were carried out inside the plots, according to a regular grid, by a bucket auger. Results led to a detailed pedological map (Figure 2) that guided the positioning of tensiometers and water content probes. Fundamentally three soil type were identified (A, B, C), plus a transitional type between A and C (AC).

In type A, classified as "Aeric Epiaquept" or "Aeric Epiaqualf" (Soil Taxonomy, USDA, 2010), three horizons were identified: Apg (0-35 cm, 1.4-1.5 g cm^{-3}, silt loam), B acting as plough pan or hard pan (35-75 cm, 1.5-1.6 g cm^{-3}, silt loam) and subsoil (>75 cm, 1.4-1.5 g cm^{-3}, sand). Type B is similar to type A (silt loam) but the first horizon appeared darker and thicker. In type C, classified as "Aquic Ustipsamment", four horizons can be identified: Apg1 (0-35 cm, 1.5-1.6 g cm^{-3}, loam), Apg2 representing the hard pan (35-50 cm, 1.6-1.7 g cm^{-3}, loam), B and C (>50 cm, 1.4-1.5 g cm^{-3}, sand).

Each plot (approximately 20 m x 80 m) has been cultivated under one of the three cited irrigation methods (two replicates each): i) traditional flooding, ii) dry seeding and delayed flooding, and iii) aerobic cultivation (noted in the course of the paper- see Figure 1 and 2- as T2, T1 and T3, respectively). The land was prepared in all plots by ploughing and harrowing under dry conditions for all the treatments.

Flooded cultivation consisted of flooding the fields just after tilling, without any puddling, and seeding in water. Few drying periods were done to allow weed control operations and fertilization until the final drying (06/09) before harvesting (21/09).

Dry seeding and delayed flooding consisted of making all tillage operations and seeding before any field flooding, that was done approximately after one month when the third or the fourth leaf appears. After the first flooding, fields were dried only once (11/07-14/7) to allow rice blast control operations and fertilization, and then flooded again until the final drying (06/09) required for harvesting (21/09).

Aerobic method consisted of rice cultivation like standard irrigated crops, maize for example, providing irrigation when necessary.

The seeded rice cultivar was Gladio type for all the plots, and sowing dates were 15/05 for aerobic (T3) and dry seeding-delayed flooding (T1) methods, and 28/05 for the traditional flooded irrigation (T2).

No transplantation have been adopted in any treatment as such practice was abandoned in Europe from several decades. All plots were kept free from weeds, pests, and diseases, by application of chemicals.

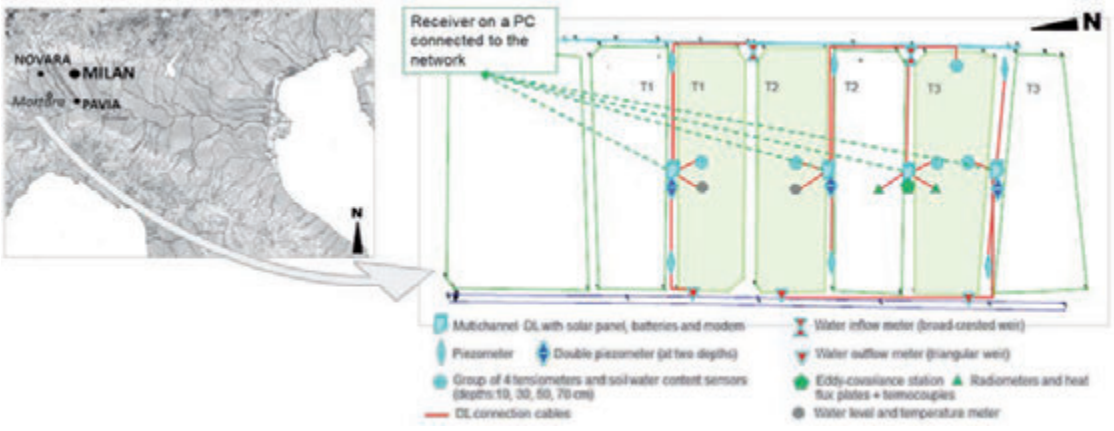

Figure 1. Location of the experimental site and plots with the installed instruments positions.

Aerobic treatment was irrigated nine times during the season (approximately every 7-10 days), with the last irrigation approximately one month before harvesting (24/08) that was done on 21/09.

Continuous measures and records were made for several variables. For all the treatments: inflow and outflow discharge, ground water level by 1.5 m screen piezometers placed along the levees at the two extremity of plots with their bottom at 2.3 m; a couple of a 0.1 m screen piezometer at the middle of levees, with bottom at 1.0 m and 2.4 m, were also placed. In T1 and T2 ponded water depth was also monitored, whereas in T3 plot (aerobic method), three tensiometer groups were installed considering the three soil types. Each tensiometer group was coupled with a multiple depth sensor probe for water content measurements (EnviroSCAN Sentek) placed aside each group. A probe for water content monitoring and four tensiometers were also installed in T1 plot, and removed just before plot flooding.

Standard meteorological variables (rainfall, radiation, temperature, humidity, wind speed, wind direction) were measured on an hourly time step over a grass coverage by a station of the regional meteorological network (ARPA), located in the ENR centre at a distance of about 100 m from the experimental fields.

In addition, an eddy covariance station was installed on the edge between the traditional flooding and the aerobic rice treatments, but its data were not used for this work (for more details about the eddy covariance system and results see Facchi *et al.*, 2013). Details on the experimental design and the installed instrumentation is presented in a companion paper (Chiaradia *et al.*, 2013).

In addition to the continuous automatic monitoring, some periodic measurement campaigns (11 dates) were carried out to monitor the crop growth (leaf area index, crop height, depth of roots).

Irrigation (I), outflow (O) and rainfall (R) were directly measured, and summed for the periods covering the crop growth from seeding (or flooding in the case of the traditional flooding method) to harvesting. Evaporation from soil (E_s), from the water surface during the flooding periods (E_a) and transpiration (T) from the canopy, were estimated by direct application of Penman-Monteith type equations at hourly time steps for all the three irrigation treatments. As some of the requested meteorological data were not available, the adjustments suggested by Rana and Katerji (2009) relating meteorological data monitored over a standard grass cover to those expected over a rice canopy, were adopted. For more detail on ET estimation see Facchi *et al.* (2013).

Soil water content at the beginning and at the end of the cropping season were obtained from each treatment from the available soil water potential and soil water content measurements.

Finally, fluxes at the bottom of the hard pan (percolation P plus capillary rise CR) have been obtained as the closure term of water budget in agreement with other authors (e.g. Bouman *et al.*, 2005).

Water application efficiency (AE) can be calculated as (Bouman *et al.*, 2005):

$$AE = \frac{ET}{I + R}$$

In Piedmont and Lombardy systems, however, outflow cannot be considered a loss as it is used to feed downstream fields and AE can be calculated as:

$$AE' = \frac{ET}{I + R - O}$$

Results and discussion

The water balance for the three plots is reported in Table 1. The irrigation provided to T1 is greater than the one provided to T2, but the same can be observed for the outflow discharge. In this way the water actually provided by irrigation in T1 is 88% of T2 amount. This can be essentially due to percolation and water evaporation in the first month when T2 was flooded and T1 was not. In the case of T3, the water provided by irrigation is 12% of T2 and 14% of T1.

The actual water consumption due to evapotranspiration of the crop under the three different treatments, on the contrary, is approximately the same for T1 and T2 and slightly less in T3 (96% and 80% of T2 for T1 and T3 respectively). Looking at the single components of ET, it can be noted that transpiration is nearly the same (104% and 91% of T2 for T1 and T3 respectively), whereas the major difference between T3 and the other two treatments depends, as obvious, on evaporation amounts. In T3 water evaporation is null and in T1 it is two thirds of T2 as a consequence of the delay in flooding. The smaller value of transpiration in

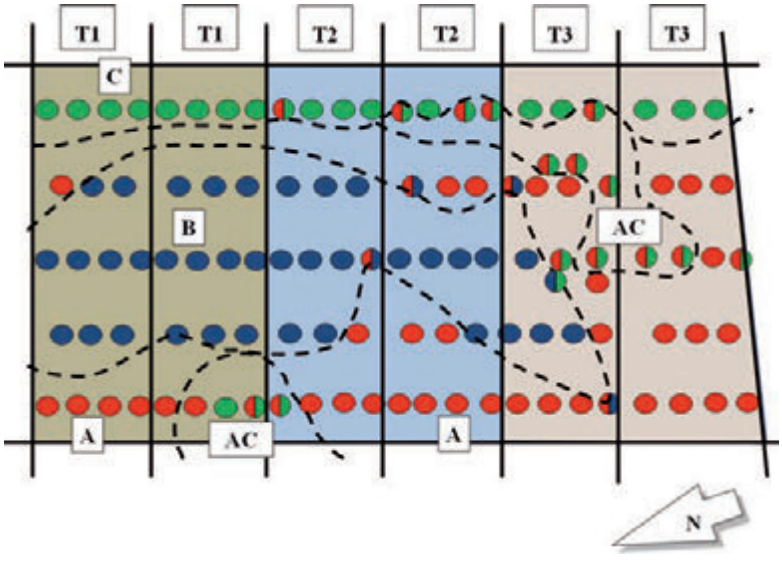

Figure 2. Soil type distribution in the experimental plots.

T3 can be ascribed to lower values of LAI during the season as showed in Figure 3a.

In terms of daily trend during the season, in the first period ET for T1 treatment was equal to aerobic (T3), whereas after flooding it became similar to the T2 treatment (Figure 3b).

The fact that the closure term represents vertical fluxes (percolation and capillary rise), and that seepage between plots with different irrigation treatments can be excluded.

It can be noted that, as expected, high percolation values concerns the traditional flooded treatment and secondarily the delayed flood one. For the aerobic cultivation the net flux is almost null, indicating that in this treatment the percolation flux basically equates the capillary rise, making groundwater recharge negligible. A better exploration of this issue will be addressed by applying mathematical simulation models to the experimental datasets.

The EA' values, as a consequence, are a little greater than 20% in flooded and delayed flooded cultivation and close to 100% for aerobic rice.

Table 1. Seasonal water budget for the three treatments (different rainfall volumes are due to small difference in plot size).

Term of water balance	Flooded cultivation (T2)	Dry seeding (T1)	Aerobic cultivation (T3)
Season duration (days)	120	122.0	122.0
Rainfall (mm)	133	133	133
Irrigation (mm)	4728	5322	884
Plot outflow (mm)	-2237	-3123	-585
Evapotranspiratipon (mm)	-691	-678	-568
Soil evaporation (mm)	-40	-37	-67
Water evaporation (mm)	-100	-67	-
Transpiration (mm)	-551	-574	-501
Soil (40 cm) storage variation (mm)	-10	-10	-28
Percolation and capillary rise (mm)	-2056	-1788	18
AE' (%)	22	24	1.08

Conclusions

The results of this study, although preliminary, indicate that rice cultivated in aerobic conditions has a great potentiality as a water-saving technique. The amount of water required during the season, in fact, is of one order of magnitude less than traditional flooded and dry seeding-delayed flooding methods, which required approximately the same quantity of water. The delay in flooding resulted in saving less than 300 mm (approx. 10%) compared to traditional flooding.

The rate of water saving is considerably higher than those obtained in Asian experiments (Bouman *et al.*, 2005; Feng *et al.*, 2007), and in our interpretation this is mainly due to a greater attention given in our experiments to aerobic rice irrigation and/or to difference in cultivation, as for example doing or not puddling, and groundwater levels, which can significantly affect the percolation rate.

The amount of evapotranspiration, on the contrary, is comparable to the values reported in other studies (Singh *et al.*, 2006; Alberto *et al.*, 2011). The differences can be ascribed, besides climate and irrigation management, to the length of the agricultural season, that in the case study was quite short (about 120 days). ET was found to be approximately the same for flooded and dry seeding irrigation methods (691 and 678 mm respectively) and 12-14% less for aerobic rice (568 mm).

In conclusion, the results obtained in the first year of experimentation suggest that water saving related to aerobic cultivation of rice fundamentally strongly reduces the vertical flux towards the water table, affecting the groundwater recharge. If this undoubtedly is considerable in terms of irrigation efficiency at the field scale, however, a massive conversion of the traditional irrigation methods on a regional scale must be properly evaluated, as it could dramatically impact on groundwater resources and on landscape conservation and nature protection .

References

Alberto MCR,, Wassmann R., Hirano T. , Miyata A. , Hatano R., Kumar A., Padre A., Amante M. 2011. Comparisons of energy balance and evapotranspiration between flooded and aerobic rice fields in the Philippines. Agric. Water Manag. 98: 1417– 1430

Belder P., Bouman B.A.M., Cabangon R., Lu G., Quilang E.J.P., Li Y.,

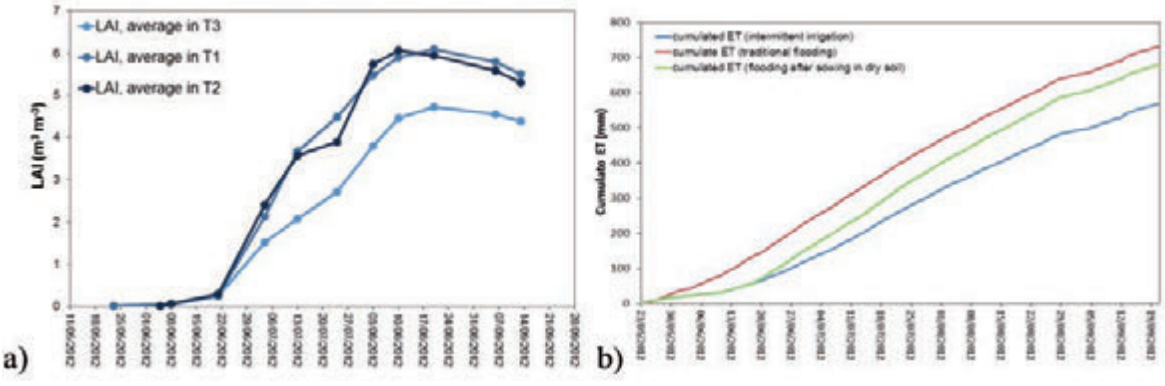

Fig. 3. a) the leaf area index values during the season (measured by a LP-80 AccuPAR Ceptometer) shows that aerobic rice produced a smaller amount of aboveground biomass with respect to the other two treatments, affecting the transpiration term; b) cumulated ET values during the season simulated by Penman-Monteith type models show that delayed flooding treatment behave exactly like the aerobic rice in the first stage of the season and as traditional flooded rice in the second.

Spiertz J.H.J., Tuong T.P. 2004. Effect of water-saving irrigation on rice yield and water use in typical lowland conditions in Asia. Agric. Water Manage. 65: 193–210.

Borell A., Garside A., Fukai S. 1997. Improving efficiency of water for irrigated rice in a semi-arid tropical environment. Field Crops Res. 52: 231–248.

Bouman B.A.M., Tuong T.P. 2001. Field water management to save water and increase its productivity in irrigated rice. Agric. Water Manage. 49: 11–30.

Bouman B.A.M., Feng L., Tuong T.P., Lu G., Wang H., Feng Y. 2007. Exploring options to grow rice using less water in northern China using a modelling approach: II. Quantifying yield, water balance components, and water productivity. Agric. Water Manag. 88: 23-33

Cabangon R.J., Tuong T.P., Castillo E.G., Bao L.X., Lu G., Wang G.H., Cui L., Bouman B.A.M., Li Y., Chen C., Wang J. 2004. Effect of irrigation method and N-fertilizer management on rice yield, water productivity and nutrient-use efficiencies in typical lowland rice conditions in China. Paddy Water Environ. 2: 195–206.

Chiaradia E.A., Ferrari D., Bischetti G.B., Facchi A., Gharsallah O., Gandolfi C. 2013. Monitoring water fluxes in rice plots under three different cultivation methods, 10th AIIA Conference: "AIIA13 – Horizons in agricultural, forestry and biosystems engineering", Viterbo (Italy), September 8-12, 2013.

Ente Nazionale Risi 2013, Data base delle superfici coltivate (Data base of cultivated extension), http://www.enterisi.it (Accessed: May 2013)

Facchi A., Gharsallah O., Chiaradia E.A., Bischetti G.B., Gandolfi C. 2013. Monitoring and modelling evapotranspiration in flooded and aerobic rice fields, *Four Decades of Progress in Monitoring and Modeling of Processes in the Soil-Plant-Atmosphere System: Applications and Challenges*, *Procedia Environmental Sciences.*

FAOSTAT 2013. Food and Agriculture Organization. FAOSTAT on-line electronic database. http://faostat.fao.org/site/291/default.aspx (accessed: May 2013)

Feng L., Bouman B.A.M., Tuong T.P., Cabangon R.J., Li Y., Lu G., Feng Y. 2007. Exploring options to grow rice using less water in northern China using a modelling approach: I. Field experiments and model evaluation Agricultural Water Management, 88: 1-13

Li Y. 2001. Research and practice of water saving irrigation for rice in China. In: Barker, R., Loeve, R., Li, Y., Tuong, T.P. (Eds.), Proceedings of the International Workshop on Water-saving Irrigation for Rice, March 23–25, Wuhan, China. International Water Management Institute, Colombo, Sri Lanka, pp. 135–144.

Luo Y. Khan S., Cui Y., Peng S. 2009, Application of system dynamics approach for time varying water balance in aerobic paddy fields. Paddy Water Environ. 7:1–9

Mao Z. 1993. Study on evaluation of irrigation performance in China. In: Proceedings of the Asian Regional Symposium on Maintenance and Operation of Irrigation/Drainage Scheme and Improved Performance, Beijing, China, pp. 6–35.

Rana G., Katerji N. 2009. Operational model for direct determination of evapotranspiration for well watered crops in Mediterranean region. *Theor. Appl. Climatol.*, 97: 243-253.

Singh R., van Dam J.C., Feddes R.A. 2006. Water productivity analysis of irrigated crops in Sirsa district, India. Agricultural Water Management, 82: 253–278

Tabbal D.F., Bouman B.A.M., Bhuiyan S.I., Sibayan E.B., Sattar M.A. 2002. On-farm strategies for reducing water input in irrigated rice; case studies in the Philippines. Agric. Water Manage. 56:93–112.

Tuong T.P., Bouman B.A.M. 2003. Rice production in water-scarce environments. In: Kijne, J.W., Barker, R., Molden, D. (Eds.), Water Productivity in Agriculture: Limits and Opportunities for Improvement. CABI Publishing, UK, pp. 53–67

Yang X., Bouman B.A.M., Wang H., Wang Z., Zhao J., Chen B., 2005. Performance of temperate aerobic rice under different water regimes in North China. Agric. Water Manage. 74, 107–122.

Effect of different plant species in pilot constructed wetlands for wastewater reuse in agriculture

Salvatore Barbagallo, Giuseppe L. Cirelli, Alessia Marzo, Mirco Milani, Attilio Toscano

Department of Agri-food and Environmental Systems Management, University of Catania, Catania, Italy

Abstract

In this paper the first results of an experiment carried out in Southern Italy (Sicily) on the evapotranspiration (ET) and removal in constructed wetlands with five plant species are presented. The pilot plant used for this study is made of twelve horizontal sub-surface flow constructed wetlands (each with a surface area of 4.5 m^2) functioning in parallel, and it is used for tertiary treatment of part of the effluents from a conventional municipal wastewater treatment plant (trickling filter). Two beds are unplanted (control) while ten beds are planted with five different macrophyte species: *Cyperus papyrus*, *Vetiveria zizanoides*, *Miscanthus x giganteus*, *Arundo donax* and *Phragmites australis* (*i.e.*, every specie is planted in two beds to have a replication). The influent flow rate is measured in continuous by an electronic flow meter. The effluent is evaluated by an automatic system that measure the discharged volume for each bed. Physical, chemical and microbiological analyses were carried out on wastewater samples collected at the inlet of CW plant and at the outlet of the twelve beds. An automatic weather station is installed close to the experimental plant, measuring air temperature, wind speed and direction, rainfall, global radiation, relative humidity. This allows to calculate the reference Evapotranspiration (ET_0) with the Penman-Monteith formula, while the ET of different plant species is measured through the water balance of the beds. The first results show no great differences in the mean removal performances of the different plant species for TSS, COD and *E.coli*, ranged from, respectively, 82% to 88%, 60% to 64% and 2.7 to 3.1 Ulog. The average removal efficiency of nutrient (64% for TN; 61 for NH_4-N, 31% for PO_4-P) in the *P.australis* beds was higher than that other beds. From April to November 2012 ET measured for plant species were completely different from ET_0 and $ET_{control}$, underlining the strong effect of vegetation. The cumulative evapotranspiration highest value was measured in the CWs vegetated with *P.australis* (4,318 mm), followed by *A.donax* (2,706 mm), *V.zizanoides* (1,904), *M.giganteus* (1,804 mm), *C.papyrus* (1,421 mm).

Correspondence: Alessia Marzo, Department of Agri-food and Environmental Systems Management, University of Catania, Via Santa Sofia 100, Catania 95123, Italy.
Tel. +39.095.7147.593 - Fax: +39.095.7147.600.
E-mail: alessia.marzo@unict.it

Key words: *constructed wetlands, cyperus papyrus, vetiveria zizanoides, miscanthus x giganteus, arundo donax, phragmites australis*.

Journal of Agricultural Engineering 2013; XLIV(s1):e160
doi:10.4081/jae.2013.(s1):e160

Introduction

Agriculture sector is the main user of water in the Mediterranean region. The increasing competition for good-quality water among different water-use sectors in the Mediterranean region has decreased freshwater allocation to agriculture. The general decreasing trend for water supply and the need for sustainable use of the available water resources make essential to find alternative water sources like urban treated wastewater (TWW) through reuse practice (Barbagallo *et al.*, 2012). The use of treated wastewater for irrigation in agriculture combines two advantages. First, using the fertilizing properties of the water eliminates part of the demand for synthetic fertilizers and contributes to decrease the level of nutrients in rivers. Second, the practice increases the available agricultural water resources.

Although the reuse of wastewater is potentially beneficial, it raises concerns such as soil and crop contamination by pathogens and thus public health issues. As a consequence, the wastewater methods used to treat wastewater for agricultural irrigation, have to be able to produce a final effluent that ensures the safely use of wastewater without risk to human health, and that complies with national quality standards for reclaimed wastewater (Toscano *et al.*, 2013).

The Department of Agri-food and Environmental Systems Management, of Catania University, conducts, since 1990, studies on the possibility to reuse wastewater for irrigation purposes with tertiary treatment performed by constructed wetlands (CWs). The adoption of CWs, widely applied for the treatment of different varieties of wastewater (Vymazal, 2009), combined with conventional treatment plants, seem to be an attractive solution for wastewater purification, able to improve water quality through efficient pollutant removal, with low cost and no environmental impact (Katsenovich *et al.*, 2009).

An important issue to consider when constructed wetlands is used for wastewater treatment, is the hydrological regime. In subsurface flow wetlands, the key components of the hydrologic cycle, are rainfall and evapotranspiration (ET), the process by which water moves from wetlands into the atmosphere through plants and medium. In CWs these variables may influence pollutant removal efficiency since precipitation dilutes the pollutant concentration and increases throughflow (IWA, 2000), shortening the contact time between waterborne substances and the wetland ecosystem. By contrast, ET decreases wastewater volume reducing outflow and concentrating the pollutants, but it does increase retention time which allows longer interaction with the wetland ecosystem (Kadlec and Wallace, 2009).

In mild temperate climates annual rainfall slightly exceeds annual

ET and there is little effect of atmospheric gains and losses over the course of a year. But most climatic regions have a dry season and a wet season, which vary depending upon geographical setting. As a consequence ET losses may have a seasonally variable impact (Kadlec and Wallace, 2009). Unfortunately, the specific effects of ET on constructed wetland performance have not been thoroughly investigated because good ET estimates are hard to obtain (USEPA, 2000), even if better evaluation of ET can improve CW design and produce better predictions of simulation models.

The main objectives of this study, were to compare the individual performances of five emergent plant species, planted in a pilot-scale horizontal subsurface flow (H-SSF) CW, in term of capability to comply with Italian limits (Italian regulation, 2003) and with WHO guidelines (2006) for wastewater reuse in agriculture. The evapotranspiration (ET) rates and crop coefficients of the tested plant species were also assessed. Materials and methods

Site characteristics

The research activity was carried out in San Michele di Ganzaria, a small community (5,000 inhabitants) of Eastern Sicily, 90 km South-West of Catania (Sicily). The site is at an altitude of 490 m above sea level and is of coordinates 37°17 0 N and 14°26 0 E. The climate is Mediterranean. This means that it is mild with temperatures generally not much lower than 0ºC in winter and not much higher than 36ºC in summer, despite sometime over 40ºC were measured in July/August. Rain is not well distributed throughout the year with spring/summer being the driest period (occasional rainfall) and autumn/winter being the wettest. Every year the area receives an average rainfall of 500 mm.

Constructed wetland pilot plant

The CW pilot plant is located close to the municipal wastewater treatment plant (WWTP) and is made of 2 parallel lines, each one consisting of 6 horizontal sub surface flow (H-SSF) constructed wetland functioning in parallel (Figure 1). In each line, five beds are planted with different macrophyte species, while one bed is unvegetated. In particular *Cyperus papirus* was planted in H-SSF1 and H-SSF7, *Vetiveria zizanoides* in H-SSF2 and H-SSF8, *Miscanthus x giganteus* in H-SSF3 and H-SSF9, *Arundo donax* in H-SSF4 and H-SSF10, *Phragmites australis* in H-SSF5 and H-SSF11, while H-SSF6 and H-SSF12 are unplanted. *Phragmites*, *Arundo*, *Vetivera* and *Typha* are typically used in constructed wetland applications. *Miscanthus x giganteus*, perennial herbaceous plant suitable for renewable energy source since its high bio-

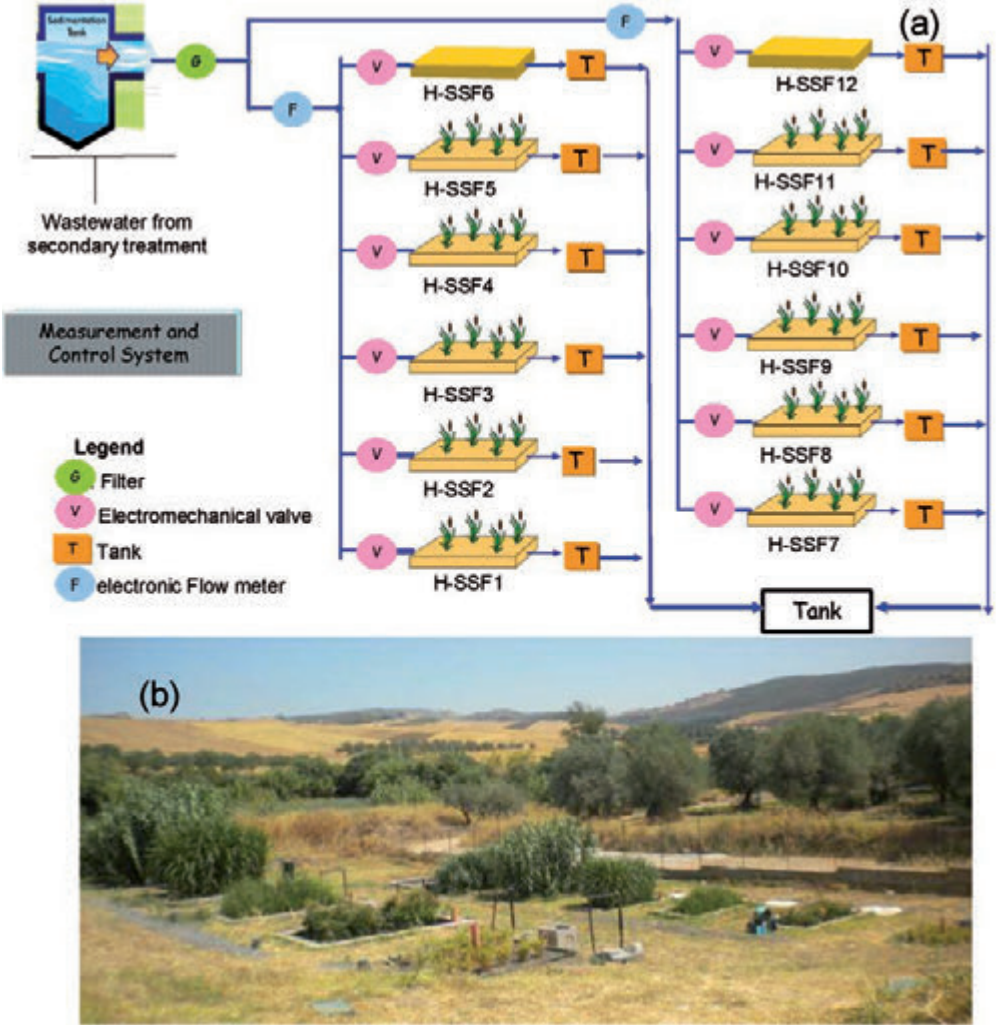

Figure 1. Constructed wetland pilot-scale: schema (a); picture (b).

mass production (Chou, 2009), is not used in constructed wetland systems. This species was used to compare its removal efficiencies with common wetland-type plants, such as *Phragmites*, *Arundo*, *Vetivera* and *Typha.* All these emergent herbaceous plants were planted in CWs in November 2011, except *Cyperus papyrus* that was planted later (January 2012).

Each CW bed is rectangular with a surface area of 4.5 m^2 (1.5 m × 3.0 m), built of concrete and waterproofed with an impermeable liner. Volcanic gravel (10 – 15 mm) was used to fill the bed to an average depth of 0.6 m.

The pilot-scale wetlands were fed in sequence with domestic wastewater treated by WWTP, with a pre-treatment step followed by an Imhoff tank, a trickling filter and secondary settlement. Wastewater from the effluent of the secondary clarifier, first passes through a filter (G), to prevent clogging of wastewater distribution pipes, and then is diverted to the two lines. The influent is distributed at the bed-head through a perforated 5 mm PEBD pipe transversal to flow direction to allow homogeny wastewater distribution into the bed. Wastewater in the terminal section is intercepted downstream by a transversal perforated pipe connected to an adjustable outlet (spiral plastic pipe) to allow water level control in the filtering bed. Wastewater effluent from each bed, first is collected a in plastic tank (T) (one per bed), where a submersible pump with a water level sensor is located for intermittent emptying of the tank, and then is used for the irrigation of a green area close to the pilot plant. The flow rate treated in the CW plant (about 65 L/h) was measured by 2 electronic flow meters (F), installed at the inlet pipe of each line and connected to a control panel to record the influent wastewater flow rate. For each bed, a control panel records the influent flow rate, the effluent discharged volume and regulates the open/closing time of the electromechanical valves (V), the latter installed in the inlet pipe of each bed.

A CR510 automatic weather station (Campbell Scientific, Logan, UT) was installed close to the experimental plant to measure air temperature, wind speed and direction, rainfall, global radiation and relative humidity.

Physicochemical and microbiological parameters

The monitoring campaign was from January 2012 until December 2012, during which water quality was assessed once per month. Thirteen samples were analyzed per monitoring event, one at the inlet and twelve at the outlet in each reed bed, totalling 126 samples. These samples were analysed according to standard methods (APHA, AWWA, AEF, 2005) for physicochemical parameters such as: total suspended solids (TSS) at 105 C, COD, orthophosphates (PO_4), Ammonia (NH_4) and total nitrogen (TN). COD of CW effluent were evaluated on samples filtered by GF/C Whatmann fiber glass.

A total of 64 samples (about 5 from each sampling point) were collected form April 2012 to November 2012. These samples were analysed for microbiological indicators, such as *Escherichia coli* and *Salmonella*. The *E. coli* were analysed by standard methods (APHA, AWWA, WEF, 2005) while *Salmonella* was examined according to the methodology described by Giammanco *et al.* (2002).

For the physicochemical parameters, the evaluation of treatment performance was based on the removal efficiency percentage, calculated as mean removal percentage of the two beds planted with the same specie. For microbiological parameters, log reductions of cell numbers were calculated.

Water balance and evapotranspiration

The reference ET (ET_0) was calculated with a spreadsheet program, PMday.xls (Snyder and Eching, 2009). The program calculates ET_0 (mm d^{-1}) using the standardized Penman-Monteith equation (ASCE-EWRI, 2004):

$$ET_0 = R_0 + A_0 \quad (1)$$

where R_0 and A_0 are the radiation and aerodynamic terms of the Penman-Monteith equation for short canopy reference ET with wind speed at 2 m height (U_2, m s^{-1}). The influent wastewater flow rate and the effluent wastewater discharged volume, combined with precipitation data measured by a meteorological station located close to plant, were used to estimate the evapotranspiration (ET) rates of the plant species during the vegetative period (from Spring to late Autumn), using a water balance method, as:

$$ET = \frac{Q_i}{A} + P - \frac{D_v}{A} \quad (2)$$

where:

ET (mm day^{-1}) is the evapotranspiration of the macrophytes, Q_i is the influent flow rate (m^3 day^{-1}), A is surface area of H-SSF CW bed (m^2), P is net precipitation (mm day^{-1}) and D_v is the discharged volume (m^3 day^{-1}).

ET values were cumulated and averaged over 10-day periods and were used to calculate 10-day plant coefficient (K_c), according to FAO-56 crop coefficient approach (Allen *et al.*, 1998):

$$K_c = \frac{ET}{ET_0} \quad (3)$$

Results and discussion

Environmental conditions

The air temperature trend increased from the beginning of April to the beginning of July, followed by an almost constant phase till the end of August and a tendency to decrease up to the end of November. The daily minimum air temperatures ranged from 1.5 to 22.2°C and the maximums from 15.0 to 43.4°C with an average seasonal value of 20.1 °C (Table 1).

Total rainfall from April to November was 102.8 mm. During the observation period, the seasonal average wind speed and seasonal total solar radiation were about 0.9 ms^{-1} and 5253.28 MJ $m^{-2}d^{-1}$ (Table 1).

Water balance and evapotranspiration

10-day average ET_0 and 10-day average ET_{con} (ET measured in unplanted CWs) trends were very similar (Figure 2).

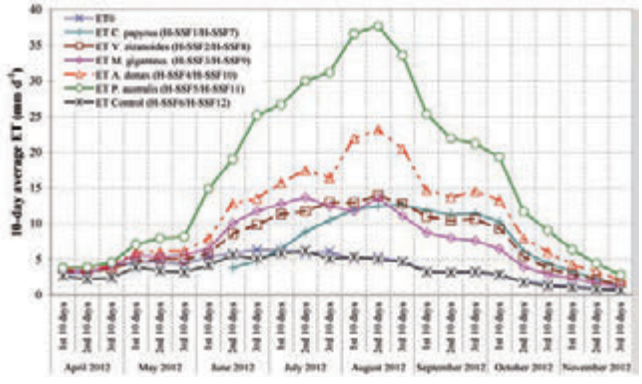

Figure 2. 10-day average ET (from April to December 2012).

10-day average ET_{con} increased from the first 10 days of April (2.2 mm d^{-1}) to the second 10 days of June (5.8 mm d^{-1}), followed by an almost constant phase till the end of August (average value of 5.3 mm d^{-1}) and a tendency to decrease up to the end of the monitored period (minimum value of 0.6 mm d^{-1} in the third decade of October November). From April to November 2012, cumulative ET_{con} was 856 mm (average daily value of 3.5 mm) and cumulative ET_0 was 961 mm (average daily value of 3.9 mm).

ET measured for plant species were completely different from ET_0 and ET_{con} underlining the strong effect of vegetation. The 10-day average ET maximum value was detected in the second 10 days of August, with the exception of *Cyperus papyrus*. Thereafter, 10-day ET declined steadily until the last decade of November. The 10-day average ET trend of *C.papyrus*, transplanted in the middle of June 2012, was different than those other herbaceous species, transplanted in November 2011. In particular, 10-day average ET of *C.papyrus* increased from the second 10 days of June (3.8 mm d^{-1}) to the third 10 days of August (12.6 mm d^{-1}), followed by an almost constant phase till the end of September then decreased to 1.2 at the end of November.

The cumulative evapotranspiration (Figure 3) highest value was measured in the CWs vegetated with *Phragmites australis* (4,318 mm) followed by *Arundo donax* (2,706 mm), *Vetiveria zizanoides* (1,904 mm), *Myscanthus x giganteus* (1,804 mm) and *Cyperus papyrus* (1,421). Note that the *C.papyrus* results was obtained with a 173 day cycle growth whereas the other plant species results were in 244 days.

The average water loss through evapotranspiration process ranged from about 2 (*M.giganteus*, *V.zizanoide*s, *C.papyrus*) to 5% (*P.australis*) of the influent flow rate, with the highest percentage in August (from 4 to 12%).

The plant coefficient time patterns of all plant species tested, were similar to the classic trapezium shape of K_c for agricultural crops (Figure 4). For *P.australis* and *A.donax*, 10-day K_c increased continuously from 1.3 and 1.2 at the start of April to 7.3 and 4.4 at the beginning of August. Thereafter, the values remained almost constant until the first 10 days of October, then decreased to 3.3 (*P.australis*) and 2.3 (*A.donax*) at the end of November. The other plant species showed a 10-day K_c constant phase shorter than a month: from first 10-day of September to first 10-day of October (*V.zizanoides* and *C.papyrus*) and from the middle of August to the mid-September (*M.giganteus*).

Physicochemical and microbiological parameters

The obtained results show a typical performance of H-SSF constructed wetlands with very high removal of organics and suspended solids comparable with results reported in other studies (Vymazal, 2002; Kadlec and Wallace, 2009). Total Suspended Solids (TSS) removal remained stable in all CW beds despite high variations in influent concentrations, including a spike in concentration recorded in November, greater than 200 mgL^{-1}. Except for some samples (about one or two samples per bed), all vegetated beds produced a final TSS effluent concentration of less than 14 mgL^{-1} with a mean removal efficiency up to 88% (±15) achieved in *Phragmites australis* CW (Table 2). An older CW with emergent plants and an extensive root system can enhance TSS removal efficiency by providing a larger surface area, reducing the water velocity and reinforcing settling and filtration in the root network

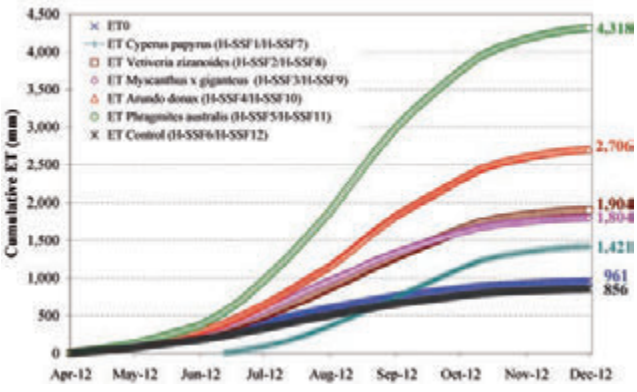

Figure 3. Cumulative ET (from April to December 2012).

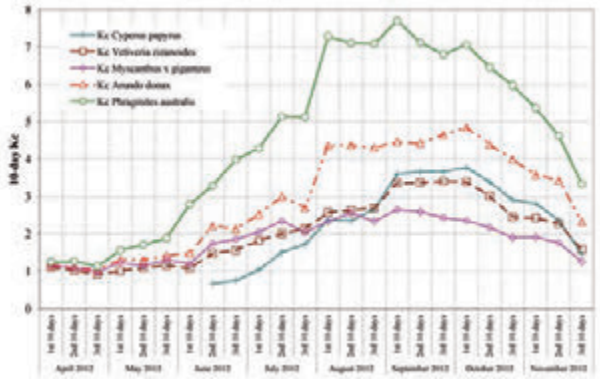

Figure 4. 10-day Kc (from April to December 2012).

Table 1. Monthly meteorological data for the calculation of ET_0.

Variables	Units	Apr	May	Jun	Jul	Aug	Sep	Oct	Nov	Average Season
Cumulative rain	mm	66.0	5.6	0.0	4.4	0.0	8.0	18.2	0.6	102.8*
Absolute Minimum Air Temp.	°C	1.5	3.9	8.2	13.4	13.9	11.7	3.3	3.4	12.5
Absolute Maximum Air Temp.	°C	27.1	29.5	37.5	43.4	42.2	35.6	34.5	25.6	28.1
Average Air Temperature	°C	13.3	16.8	23.1	26.3	26.1	22.0	19.0	14.4	20.1
Average wind speed	ms–1	1.8	1.0	0.9	0.8	0.8	0.7	0.6	0.7	0.9
Average Relative Humidity	%	73.9	61.9	48.1	47.5	49.2	66.0	75.3	83.5	63.1
Average Solar Radiation	$MJm^{-2}d^{-1}$	22.2	26.7	29.9	27.6	24.2	19.6	13.5	8.4	5253.2*

*cumulative value

(Brix 1997, Tanner 2001). Since the wetlands in San Michele di Ganzaria have only been working for 1 year, the observed TSS removal efficiencies could mostly be related to the processes of sedimentation and filtration to the wetland media (Toscano *et al.*, 2013; Stowell *et al.*, 1981).

There was no great difference in the removal performances of organic matter between the vegetated beds, since the mean COD removal was about 60-64%. It has to note that, during the monitor campaign, the *Phragmites australis* planted bed provided better results than the other planted beds. The average COD effluent concentration was 26 (±18) mgL^{-1} in the *Cyperus parirus* CW, 27 mgL^{-1} (±13) in *Vetiveria zizanoides,* 27 (±12) in *Myscanthus x giganteus,* 28 (±14) in *Arundo donax,* and the lowest value of 25 mgL^{-1} (±13) was detected in *Phragmites australis* CW effluent (Table 2). The COD concentration detected in the effluent of the unvegetated beds (about 36 mgL^{-1}) was higher than COD concentration recorded in the effluents of planted beds.

Total nitrogen is the sum of all inorganic (ammonium NH_4, nitrite NO_2 and nitrate NO_3) and organic forms of nitrogen. Despite plant uptake of nitrogen generally being non-significant for removal of this element in most wetlands receiving treated municipal wastewater (US EPA, 2000), a positive effect of the plants was observed. The average removal efficiencies of TN and NH_4 in the vegetated beds were always higher than that in the unplanted beds. *Phragmites australis* CW provided the lowest concentration and the highest removal rate with a mean TN value 9 mgL^{-1} in the effluent and an average reduction efficiency of 64 % (±12).

A slight removal for PO_4 (from 24% to 31%) was observed with little differences between the beds (planted or not). This was probably due the very low influent PO_4 values (3-5 mgL^{-1}), already close to the "background concentration", and due to the type of substrate used. The major phosphorus removal processes in wetlands are adsorption and precipitation within to soil particles contented Fe, Ca, Al minerals (US EPA, 2000; Faulkner and Richardson, 1989). Gravel material (volcanic material) used in CW pilot plant located in Sam Michele di Ganzaria do not provide a large amounts of phosphorus adsorption due its not low concentrations of Al, Fe or Ca, and therefore, the removal effect is low.

CW systems were highly efficient in reduction of *E. coli* concentrations, in spite of monthly fluctuations observed in the influent (incoming range 5.2-6.0 Ulog). Similar *E. coli* treatment trends for all planted wetlands were observed with a mean reduction more than 2.5 log units, similar with the results reported in other studies (Kadlec and Wallace, 2009). In particular, *E. coli* were reduced to a mean value of 2.8 Ulog in the effluent of *Cyperus parirus* CW and of *Arundo donax*, a mean value of 2.9 Ulog (±0.5) in *Vetiveria zizanoides* and in *Myscanthus x giganteus*. Maximum *E.coli* removal (up to 4.3 Ulog) was achieved in *Phragmites australis* CW with a mean concentration value of 2.5 Ulog (±0.6) in the effluent (Table 2). The performance was excellent for *Salmonella* removal, which was never detected in the effluent of CWs, despite sometime was revealed in the influent.

The slight differences between the performance of the different plant species could be explained by two reasons: probably the plant root system is not yet fully developed since the macrophytes species were planted in November 2011 and the monitoring campaign started in January 2012, and second the nominal residence time (the theoretical time that wastewater should spend in the wetland and during which wastewater can interact with the reactive surfaces) was quite short, about 10-13 hours. The highest evapotranspiration rate highlighted in the *P.australis* CWs determined longest HRTs, increasing treatment performance.

It could be reductive to evaluate constructed wetland performance just according to removal efficiency. Constructed wetlands, and in general all wastewater treatment plants, are designed to meet at least discharge limits. For this reason, samples expressed as percentages below the wastewater Italian limits for discharge into surface waters (Italian regulation, 2006) and for agriculture reuse (Italian regulation, 2003) have been calculated. In all effluents, COD and TSS concentrations were always below the Italian discharge concentration (35 and 125 mgL^{-1}, respectively). Furthermore, the wetland beds always reduced COD and TN to acceptable concentrations for irrigation (100 and 35 mgL^{-1} respectively). Despite constructed wetlands have shown a good removal of microbial indicators (up to 4.3 log units in the bed planted with *Phragmites australis*), they did not produce effluent with *E. coli* levels matching the Italian wastewater reuse standard (50 UFC/100 ml [Maximum value to be detected in 80% samples for natural treatment systems.]). This result highlights the need for further treatment to achieve the Italian limits required for irrigation reuse.

The tolerable infection risk, associated with the use of wastewaters in "unrestricted irrigation" that includes irrigation of vegetable and salad crops that might be eaten uncooked, was also assessed by applying the microbial risk analyses proposed in the WHO guidelines (2006). Following the WHO reuse guidelines (2006), in 100% of samples *E. coli* contamination was less than 10^4 CFU $100mL^{-1}$ (Figure 5), correspon-

Table 2. Mean influent (±SD) and effluent (±SD) wastewater concentrations and mean (±SD) pollutant removal efficiencies (R) throughout the monitoring period.

	(mg/L)	SST		COD		NH_4		N_{tot}		PO_4		*E. Coli**	
Influent		102	(71)	82	(36)	10	(4)	25	(8)	4	(1)	5.6	(0.4)
Cyperus papirus	out (mg/L)	9	(4)	26	(18)	4	(2)	9	(3)	3	(1)	2.8	(0.2)
	R (%)	82	(24)	60	(30)	48	(38)	53	(21)	24	(20)	2.8	(0.4)
Vetiveria zizanoides	out (mg/L)	13	(19)	27	(13)	4	(2)	10	(4)	3	(1)	2.9	(0.5)
	R (%)	85	(16)	63	(19)	53	(18)	58	(13)	25	(19)	2.7	(0.5)
Myscanthus × giganteus	out (mg/L)	13	(18)	27	(12)	4	(2)	10	(4)	3	(1)	2.9	(0.6)
	R (%)	84	(14)	62	(19)	52	(23)	57	(15)	24	(28)	2.8	(0.6)
Arundo donax	out (mg/L)	13	(20)	28	(14)	4	(1)	10	(5)	3	(1)	2.8	(0.4)
	R (%)	87	(13)	61	(23)	58	(22)	61	(15)	29	(24)	2.8	(0.4)
Phragmites australis	out (mg/L)	9	(14)	25	(13)	4	(2)	9	(5)	3	(1)	2.5	(0.6)
	R (%)	88	(15)	64	(21)	61	(21)	64	(12)	31	(25)	3.1	(0.6)
Unplanted	out (mg/L)	16	(21)	36	(17)	6	(3)	14	(5)	3	(1)	3.4	(0.8)
	R (%)	78	(18)	49	(27)	40	(10)	46	(9)	22	(18)	2.2	(0.7)

*Concentration and removal values in Ulog.

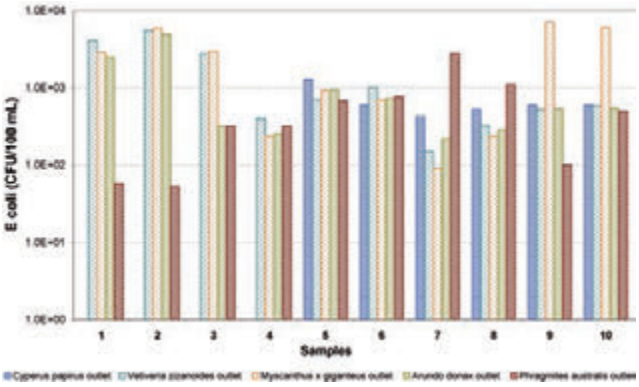

Figure 5. ***E. Coli*** **concentration trend.**

ding to a median risk rotavirus infection of 10^{-3} pppy, in unrestricted irrigation. So wastewater reclaimed by the constructed wetland system could be used for unrestricted crop irrigation if combined with some post-treatment health protection control measures, such as withholding periods between the last application of a wastewater and harvesting of fruits, in order to obtain the supplementary 2-3 log reduction needed to achieve the health based target of 10^{-6} DALY.

Conclusions

The H-SSF constructed wetland pilot plant, located in San Michele di Ganzaria (Sicily), was highly efficient in the reduction of main chemical, physical and microbiological pollutant concentrations in municipal wastewater. The vegetated beds have showed a better performance in the removal process for all the investigated parameters than unvegetated beds, underlining the active role of macrophytes in the wastewater treatment. The best removal performances obtained in the beds planted with *Phragmites australis*, confirm that this is the plant specie most suitable to be used in constructed wetlands for wastewater treatment. About the capability to treat wastewater for reuse purposes, *E. coli* concentration in the CW effluents was not always under the maximum limit for wastewater reuse fixed by Italian legislation. This limited impact on *Escherichia coli* removal means that further treatments are necessary to reuse treated wastewater in agriculture. For example, after CW treatment, stabilization reservoirs could be used to further reduce the microbiological load. On the other hand, the number of *E. coli* in the CW effluents (always less than 10^4 CFU $100mL^{-1}$) ensures that health-based targets proposed by the WHO guidelines (2006) are easily achievable by combining constructed wetland systems with some post-treatment health protection control measures (such as natural pathogen die-off after the last irrigation).

Finally, during the monitoring period, *Phragmites australis* showed the highest evapotranspiration rates. For this specie the very high ET rates and Kp values were detected only over a relatively short period (about 30 days, between early and late August), in which the amount of water lost was higher than what is usually considered negligible (about 10%) by the most common hydraulic and hydrological models. However, the highest evapotranspiration rate highlighted in the *P.australis* CWs determined longest HRTs, increasing treatment performance. The small experimental plant may have led to over-estimating macrophytes evapotranspiration, due to the clothesline and oasis effects. However, the results are useful for estimating ET in small subsurface flow (SSF) CWs which serve individual homes. Furthermore, it should be noted that even real scale SSF CWs, which have an area ranging from a few dozen up to several hundred square meters, are affected by advective energy exchanges. So even if the experimental results can not be indiscriminately extrapolated to full-scale systems, they represent a reliable guide for estimating the ET of *Phragmites australis*, *Vetiveria zizanoides*, M*yscanthus x giganteus*, *Arundo donax* and *Cyperus papyrus* (Milani and Toscano, 2013; Borin *et al.*, 2011).

References

Allen R.G., Pereira L.S., Raes D., Smith M. 1998. Crop evapotranspiration: Guidelines for computing crop requirements, FAO Irrigation and Drainage Paper 56. FAO- FAO - Food and Agriculture Organization of the United Nations Press, Rome, Italy.

APHA, AWWA, AEF 2005. Standard methods for the examination of water & wastewater. 21st edn. Baltimore: American Public Health Association (APHA), AmericanWaterWorks Association (AWWA), and American Environment Federation (AEF). Washington, DC, USA.

ASCE-EWRI. 2004. The ASCE Standardized Reference Evapotranspiration Equation. Technical Committee Report to the Environmental and Water Resources Institute of the American Society of Civil Engineers from the Task Committee on Standardization of Reference Evapotranspiration.

Barbagallo S., Cirelli G.L., Consoli S., Licciardello F., Marzo A., Toscano A. 2012. Analysis of treated wastewater reuse potential for irrigation in Sicily. Water Sci. Technol. 65: 2024–2033.

Borin M., Milani M., Salvato M., Toscano A. 2011. Evaluation of Phragmites australis (Cav.) Trin. evapotranspiration in Northern and Southern Italy. Ecol. Eng. 37: 721–728.

Brix H. 1997. Do macrophytes play a role in constructed wetlands? Water Sci. Technol. 35:11–17.

Chou C.-H. 2009. Miscanthus plants used as an alternative biofuel material: The basic studies on ecology and molecular evolution. Renew. Energ. 34: 1908–1912.

Faulkner S.P., Richardson C.J. 1989. Physical and chemical characteristics of freshwater wetland soils. In: Hammer, D.A. (Ed.), Constructed Wetlands for Wastewater Treatment. Municipal, Industrial and Agricultural. Lewis Publishers, Chelsea, MI, pp. 41-72.

Giammanco G., Pignato S., Alliot M., Polgatti M. 2002. Rapid method for Salmonella enumeration in wastewater. Proc. Iternational Symposium on Salmonella and Salmonellosis. St. Brieuc, France.

Italian regulation, 2003. Italian Technical Guidelines for Wastewater Reuse. D.M. 185/2003. In: Official Journal No. 169, 23/07/2003.

Italian regulation, 2006. Italian Technical Guidelines for Wastewater Dischage in water bodies. D. Lgs 152/2006. In: Official Journal No.88, 03/04/2006.

IWA, 2000. Constructed Wetlands for Pollution Control, Scientific and Technical Report No. 8, IWA Publishing. London, England.

Kadlec R. H., Wallace S. 2009. Treatment Wetlands, 2nd Edition, CRC press, New York, USA.

Katsenovich Y., Hummel-Batista A., Ravinet A. J., Miller J. F. 2009. Performance evaluation of constructed wetlands in a tropical region. Ecol Eng. 35: 1529–1537.

Milani M., Toscano A. 2013. Evapotranspiration from pilot-scale constructed wetlands planted with Phragmites australis in a Mediterranean environment. J. Environ. Sci. Health. A Tox Hazard. Subst. Environ. Eng. 48:568-80.

Snyder R.L., Eching S. 2009. Daily reference evapotranspiration calcu-

lator user's guide for PMday.xls. University of California, Davis, California.
Stowell R., Tchoba G,. Ludwig R., Colt J. 1981. Concepts in aquatic treatment design. J. Env. Eng. Div. 107: 919–940.
Tanner C. 2001. Plant as ecosystem engineers in subsurface flow treatment wetlands. Water Sci. Technol. 44: 9–17.
Toscano A., Hellio C., Marzo A., Milani M., Lebret K., Cirelli G.L., Langergraber G. 2013. Removal efficiency of a constructed wetland combined with ultrasound and UV devices for wastewater reuse in agriculture. Environ. Technol., (doi 10.1080/09593330.2013.767284).
US Environmental Protection Agency (EPA), 2000. Constructed Wetlands Treatment of Municipal Wastewaters. Office of Research and Development, Cincinnati, Ohio, USA.
Vymazal J. 2002. The use of sub-surface constructed wetlands for wastewater treatment in the Czech Republic: 10 years experience. Ecol. Eng. 18: 633–646.
Vymazal J. 2009. The use constructed wetlands with horizontal sub-surface flow for various types of wastewater. Ecol. Eng. 35: 1–17.
World Health Organization 2006. Guidelines for the safe use of wastewater, excreta and greywater, Volume 2: Wastewater Use in Agriculture. World Health Organization Press, Geneva, Sweezerland.

Monitoring water fluxes in rice plots under three different cultivation methods

Enrico Antonio Chiaradia,[1] Daniele Ferrari,[1] Gian Battista Bischetti,[1] Arianna Facchi,[1] Olfa Gharsallah,[1] Marco Romani,[2] Claudio Gandolfi[1]

[1]DiSAA, Università degli Studi di Milano, Milano, Italy; [2]CRR, Ente Nazionale Risi, Castello d'Agogna (PV), Italy

Abstract

Italy is the leading producer of rice in Europe with over half of total production, almost totally concentrated in a large traditional paddy rice area between the Lombardy and Piedmont regions, in the north-western part of the country. In this area irrigation of rice has been traditionally carried out by flooding. The introduction of new combined irrigation and agronomic management practices (dry seeding followed by field flooding and in a full aerobic cultivation with intermittent irrigations), aiming to reduce the water consumption, can determine considerable effect on the landscape and the water cycle. With the aim to study in depth the water fluxes during the whole crop season, three experimental plots at the Ente Nazionale Risi-Rice Research Centre's Experimental Station of Castello d'Agogna (PV) were instrumented. In each plot the following instruments have been installed: 1) a long throated flume and a double shaped (V-notch and rectangular) thin plate for superficial inputs and outputs, 3) a set of piezometers for groundwater levels, 4) one stage level gauge in each submerged field, 5) four tensiometers and moisture sensors clusters, 6) one eddy covariance station for vapour fluxes estimation. Most of the instruments were equipped with electrical sensors connected by cables to a wireless data logger that, in turn, send the data to a PC placed within ENR offices and web-connected by a LAN. In this way, besides the automatic download of data, it was possible to remotely control the devices, to quickly fix troubles, and to better plan the field trips. The management of the whole framework was done by a specifically developed software. In this paper the whole system, which presents some degree of innovation, is described in detail.

Correspondence: Gian Battista Bischetti, DiSAA via Celoria 2 , 20133 Milano, Italy.
Tel. +39.02.50316904 - Fax: +39.02.50316911.
E-mail: bischetti@unimi.it

Key words: water balance, rice, monitoring.

Contributions: the authors contributed equally.

Conflict of interests: the authors declare no potential conflict of interests

Funding: the work was supported by Regione Lombardia under the grants "Fondo per la promozione di accordi istituzionali, "Project "BIOGESTECA" – Piattaforma di biotecnologie verdi e di tecniche gestionali per un sistema agricolo ad elevata sostenibilità ambientale.

Acknowledgments: the authors thanks Daniele Masseroni, Ezio Naldi, Gianluca Beltarre and its staff for the field assistance

Journal of Agricultural Engineering 2013; XLIV(s1):e161
doi:10.4081/jae.2013.(s1):e161

Introduction

Rice cultivation has a great importance in many economies, at the world level and in Italy as well. In Piedmont and Lombardy, in particular, rice represents a significant crop for the whole agricultural sector both in terms of extension and economic value. Although these territories are traditionally rich in water, and agriculture has always been the principal user, in the last years its management is the object of an increasing number of conflicts due to both a growing demand by other stakeholders and new goals related to water quality (Chiaradia *et al.*, 2013).

As the traditional method for rice cultivation requires great volumes of water to keep paddy field flooded, irrigation methods requiring less water have been proposed and increasingly applied (Chiaradia *et al.*, 2013).

In order to study the effect of different rice irrigation systems, the Department of Agricultural and Environmental Sciences - hydraulic group, developed a non-standard and innovative prototypal system for water fluxes monitoring. The system, specifically thought for rice cultivation, has been implemented at the experimental station of the ENR-Rice Research Center located in Castello d'Agogna-Mortara (Pavia, Italy) , This paper describes in detail the prototypal monitoring system.

The monitoring system

The experimental setup involves three pairs of rice plots. 20 x 80 m^2 in size, each characterized by a different water management strategy (see Figure 1). The monitoring system has been installed in three of the plots, one for each type of irrigation management. These included: i) traditional flooding, ii) dry seeding and delayed flooding, and iii) aerobic cultivation, noted in the course of the paper as T2, T1 and T3, respectively (see Figure 1).

A total of 5 dataloggers, 12 stilling wells for groundwater measurements, 6 device for discharge measurements, 20 tensiometers, 16 of which automatically recorded and connected to the datalogger, 4 soil moisture measurements multilevel probes, automatically read and, finally, an eddy-covariance station were installed.

Devices and sensors

Superficial water fluxes

Inflow discharge for each plot was measured by a RBC long throated flume equipped with a level gauge (Figure 1a). Advantages in using this kind of device are: 1) their hydraulic performance can be theoretically predicted, 2) low level of theoretical error (less than 2%), 3) little problem with sedimentation (Clemmens *et al.*, 2001); in addition, long RBC flumes work well also with small upstream head values that was one of the constrains of this installation. The RBC flumes were built by a 1.26 m long metal sheet trapezoidally shaped in section. Channel base is 0.09 m large and walls are inclined of 63.4°. Throat was obtained by a trapezoidal element at the bottom of the flume. A stilling well was connected by a PVC tube to the upstream section and two metal walls increased the handcraft stiffness. Discharge scale was calculated using the WinFlume software version num. 1.06.0004 (www.usbr.gov/pmts/hydraulics_lab/winflume) and verified by volumetric sampling. Attention was given in placing correctly the base of flumes with respect to the seed bed to avoid backwater when fields were flooded.

Triangular V-notch weirs were instead used to measure outflow discharge (Figure 1b). Weirs were installed on a metal box 1.2 m long, 1.0 m width and 0.4 m height. At the internal side of the box a woody gate was used to regulate water depth inside paddy fields. A stilling well was placed in the middle of a lateral wall of the box. The outflow from the box passed through a mobile V shaped plate able to measure low discharges (less than 5 l/s), whereas during high flow (up to 30 l/s) the plate was removed and the weir became rectangular. Both the sections have been associated to a specific stage-discharge relationship, calibrated by some volumetric tests.

Both flumes and V-notch weirs, have been equipped with pressure transmitters for industrial applications (serie 41X by Keller, www.keller-druck.com) to measure the water level within the stilling wells . The sensors have a full scale, FS, of 30 mbar (relative pressure), *i.e.* 30.6 cm of water, and an error 0.1-0.2 % FS (*i.e.* <1 mm). Measures were recorded every 10 minutes.

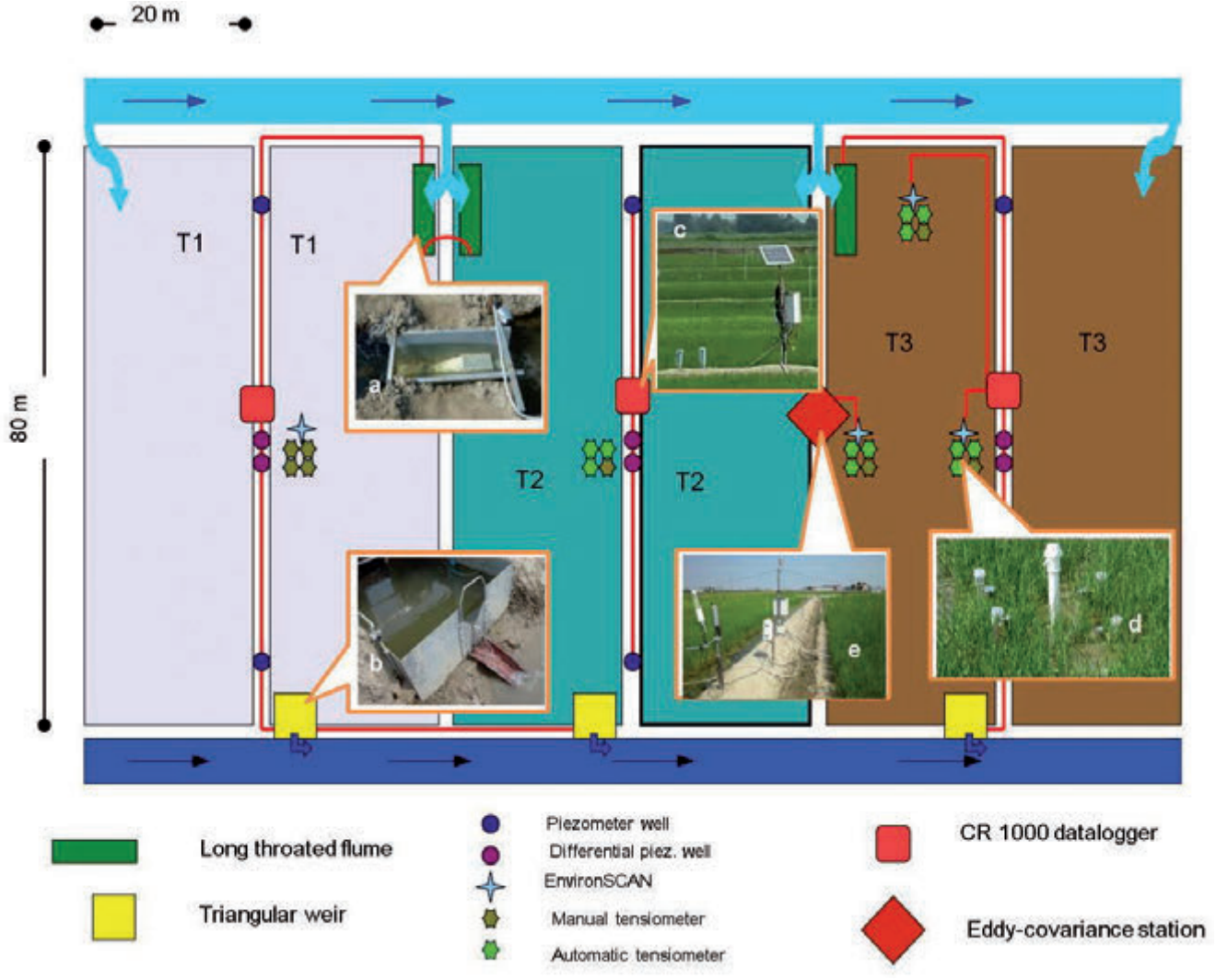

Figure 1. Diagram of the experimental plant: T1, T2 and T3 are the three different treatments, duplicated in two field of 40×80 m. a) long throated flume, b) V-shaped weir, c) the heads of the piezometer tubes and the datalogger system, d) a cluster of tensiometer and one moisture sensors column, e) eddy covariance station.

Ground water levels

Ground water levels were monitored in 12 1"1/5-piezometric wells (Figure 1c). The wells were positioned along the levees dividing two paired plots with the same treatment (Figure 1). Along each levee, the two wells positioned at upstream and downstream sides of the plot have a 1.5 m long windowed tube, whereas the central couple of wells had a smaller windowed segment of 0.10 m positioned at 3 and 1.5 m in depth. The central wells are used as differential piezometer. Each piezometer was endowed by a pressure transmitter PR-46X by Keller with 100 mbar FS (1.02 m) and error less than 0.1% FS (1.02 mm). Measures were recorded hourly.

Soil water content and potential

Soil water content was measured by 4 EnviroSCAN (Sentek Pty. Ltd., South Australia) sensors. EnviroSCANs are multiple sensor capacitance probes capable of continuous measurement of soil moisture; in the present case four depths, 10, 30, 50, 70 cm, were set (Figure 1d).Volumetric water content is obtained by a scaled frequency reading using a site specific calibration equation. Calibration tests were made by volumetric measures on undisturbed soil volumes sampled at the end of the season.

The soil moisture tension was measured by tensiometer devices (Figure 1d). A total of 5 groups of tensiometers for a total number of 20 were installed in clusters, 12 of which able to automatically record the data. In each cluster, tensiometers were placed at a different depth: 10, 30, 50 and 70 cm respectively, the same depths monitored by EnvironSCAN sensors. The data were recorded every 10 minutes.

Aerial water fluxes

A 3D sonic anemometer, model num. 81000 (Young Co., 2010) and an infrared gas analyser, model LI-7500 (LI-COR, 2009) for the measurement of energy and gas (H_2O, CO^2) exchanges were installed on the levee separating the two irrigation treatment T3 and T2, as shown in Figure 1e. This in order to monitor two rice treatments with only one eddy covariance station; this was possible because the limited size of the experimental fields. Instruments were held at one meter over the average canopy height, changing the vertical position of the sensors, during all the monitoring period (18 July – 21 September 2012). Net radiometers CNR-1 (Kipp & Zonen, 2002) and devices for the measurements of the heat flux in the soil were installed in both fields. In particular, one heat flux plate HFP01 (Hukseflux, 2010) for each irrigation treatment was installed at 8 cm below the soil surface. Two soil thermocouples (Campbell, 2012a), installed at 2 and 6 cm, allowed the calculation of the ground heat flux (G, in W m^{-2}) at the soil surface for the intermittent irrigation treatment (T3). As G calculation required an accurate set-up on the flooded rice field, the challenge was to measure the storage term (G) in the water. To do that, in addition to the two soil thermocouples, also the water temperature and the water level in the field T2 were measured over time by means of a pressure transmitter (serie 41X by Keller, www.keller-druck.com). A thermohygrometer (Vaisala, 2006) completed the installation. The data were recorded every 30 minutes.

Acquisition and storing system

The number of dataloggers were defined according to: 1) total number of sensors, 2) maximum cable length to limit noise and voltage loss, 3) permitting machines passage for cultivation works, 4) best distribution of recording work between each instrument, 5) costs of the instruments.

Three CR1000 and one CR5000 Campbell Scientifics dataloggers (Campbell, 2012b) were installed on each of the three instrumented

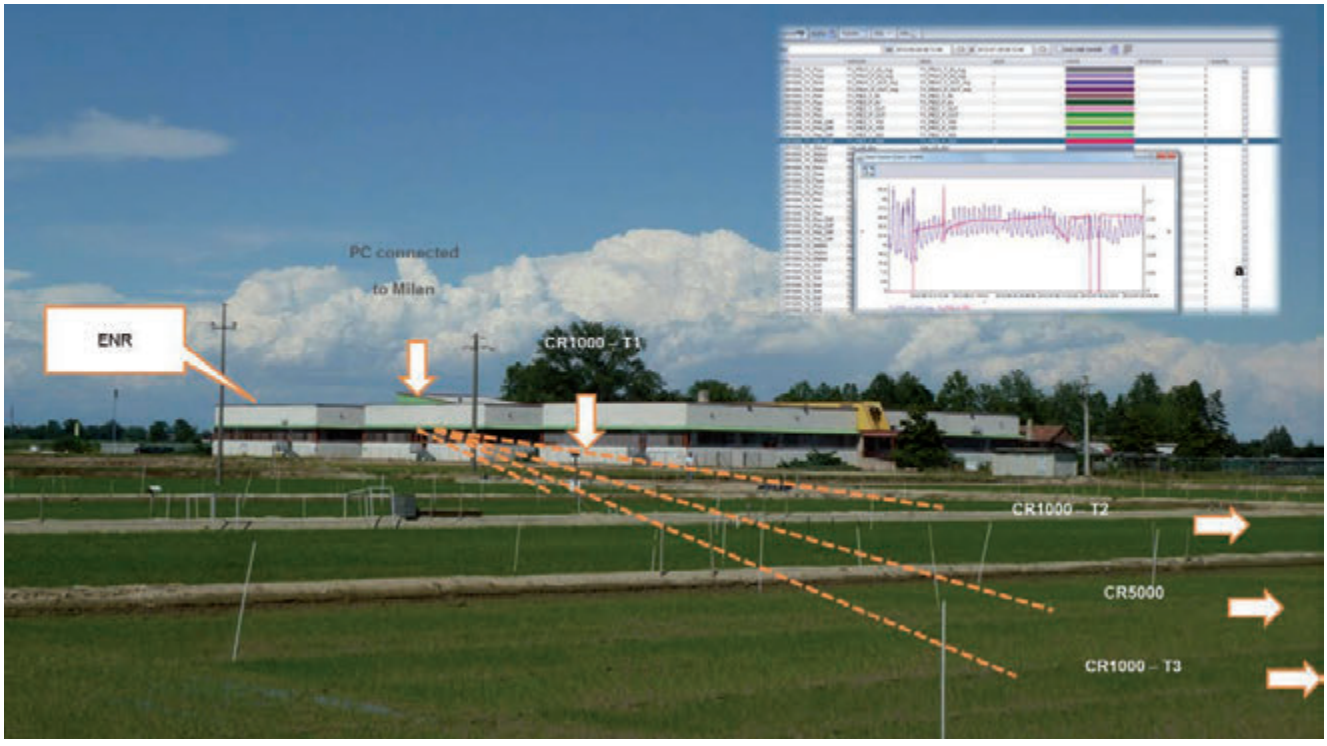

Figure 2. A view to the ENR building in Castello d'Agogna (PV); dashed lines describe theradio connections between dataloggers and the PC positioned in the office; a) an example of the custom made Java software.

levee and for the Eddy Station (Figure 1c). Each CR1000 DL can manage up to 16 single-ended analog input channels, 2 pulse input and 8 digital ports, whereas CR5000 DL 40 single-ended analog input channels, 2 pulse input and 8 digital ports.

Each datalogger was powered by a 12 V/ 12 Ah rechargeable sealed lead-acid battery automatically recharged by a standard solar panel (CanadianSolar Mo. Type CS5F-14M) with a nominal maximum power of 14W through a 12 V charge controller (Steca Solsum 8.8F). All groups were protected by an industrial control panel enclosure (Stahlin).

Finally, a set of tensiometer was controlled by a standalone datalogger Watchdog 2000 series (Spectrum, 2009).

Remote control, backup and data analysis

All dataloggers were wireless connected, through a RF416 radio (Campbell, 2011), to a RF432 radio (Campbell, 2011) installed on a PC placed in one of the offices in the ENR building. All the radio were coupled with a 0 dBd, ¼ wave whip antenna (model num. 15730, Campbell, 2011).

The storing procedure was programmed by the software LoggerNet 4.3.1 (Campbell, 2012c). Connection was operating every day from 8.00 a.m. for data download and storage (Figure 2). An automatic procedure produced, every day after the download, a compressed backup file of the stored data that were sent via FTP to a remote storage device in Milan by standard web network.

The PC at ENR was remotely controlled and, besides downloading data, permitted to check the system operation at any time, limiting the number of direct visits and the data loss.

To manage the huge quantity of data, a custom graphical software written in Java language and supported by SQLite database, have been developed to provide a complete framework for rapidly data visualization, queries, post-acquisition correction and exportation to text file (Figure 2a).

Table 1. Cost of instrument and sensors installed during the research activity.

material	individual cost (€)	Number	Total cost (€)
Keller pressure sensor 41X	€ 310,00	8	€ 2.480,00
Material for RBC flumes and V-noch weirs		€ 1.138,51	
Surface flow			€ 3.618,51
Keller pressure sensor PR-46X	€ 300,00	12	€ 3.600,00
Piezometer wells		€ 531,19	
USB-driver for Interface converter K-104	€ 80,00	1	€ 80,00
Additional cables		€ 228,00	
Groundwater			€ 4.439,19
EnviroSCAN	€ 2.400,00	4	€ 9.600,00
Tensiometers Irrometer con manometro,	€ 150,00	20	€ 3.000,00
Pressure transducers for tensiometers	€ 350,00	2	€ 700,00
Pressure transducers for tensiometers	€ 392,00	4	€ 1.568,00
Soil water			€ 14.868,00
3D sonic anemometer	€ 7.500,00	1	€ 7.500,00
Infrared gas analyser	€ 18.120,00	1	€ 18.120,00
CGR 3 pyrgeometer	€ 1.300,00	1	€ 1.300,00
CMP 3 pyranometer	€ 760,00	1	€ 760,00
Heat flux plate HFP01	€ 512,00	1	€ 512,00
Thermocouples	€ 53,00	2	€ 106,00
Eddy station			€ 28.298,00
CR1000	€ 1.438,00	3	€ 4.314,00
CR5000	1	€ 3.500,00	
Case	€ 270,00	3	€ 810,00
Mast Mount bracket	€ 79,00	3	€ 237,00
Interfaccia SDI-12 per sonde EnviroSmart	€ 438,00	3	€ 1.314,00
Modulo I/O a 1 canale seriale, protocollo RS232, 485 e 422 (NO CR5000)	€ 210,00	3	€ 630,00
Data logger			€ 10.805,00
12 V/ 12 Ah rechargeable sealed lead-acid battery	€ 65,00	3	€ 195,00
14 W solar panel	€ 27,30	6	€ 163,80
SOLSUM8.8 Regolatore di carica 8.8A Solsum	€ 31,20	3	€ 93,60
Power supply			€ 452,40
RF416 radio	€ 466,00	3	€ 1.398,00
RF432 radio	€ 486,00	1	€ 486,00
Whip antenna	€ 35,00	4	€ 140,00
Remote transmission			€ 2.024,00
Cables,		€ 708,29	
Connectors and other material		€ 597,00	
Cables, etc.			€ 1.305,29

Shadowed cells indicate that instruments and sensor were already available for the research.

Costs and work

To establish the described system, instruments and sensor already available to group and new bought ones were used. In Table 1 are reported costs of the instruments, sensors and other material required for installing the system. It can noted that the whole value of instrumentation is approximately 65,000 euros, 64% of which already available to the research activity. Among the different components of the system nearly half is imputable to gas fluxes measurement, approximately 20% to soil tension and soil water content measurement and approximately 15% to data loggers; surface flow and groundwater measurement, and data transmission, power supply and consumables required only few per cent of the total investment.

In terms of human effort, it is not easy carrying out an accurate estimate, also due to the number of people involved in the different activities (7 people). It was impossible tracing the time spent in choosing the right combination of instruments and in programming the sensor and data loggers in laboratory. A rough (underestimated) evaluation of in-field only activity gives a value of 67 man-days; 29 for the system installation, 24 days for management during the crop season, 14 day for removing the system to allow field operations to the new season.

As such data refer to the first experience in installing the system, it is expected that some time could be save for a new installation (approximately a half). On the contrary, no time can be expected to be saved during the season and in removing the system.

Conclusions

An experimental setup for the integrated monitoring of the water fluxes in three rice plots, using a variety of sensors and probes, has been presented in the paper. If on one hand the use of single sensors and probes does not represent a novelty, on the other their use in a such massive and synergic way was a challenge in practice. In such a perspective, the possibility to verify if all the instruments were working correctly from remote, without the necessity to visit daily the experimental plots represented a crucial point in limiting the loss of data and in reducing the research costs. Much effort was spent in choosing the right combination of instruments in order to guarantee the proper connection and communication between sensors and dataloggers over a local net and using different protocols. Most of the sensors, in fact, are from different manufacturers, each with its own communication protocol an then requiring a hard work to make them connected without conflicts. Problems related to energy supplies, noises in the acquisition, remote connectivity and limits due to the environmental characteristics (high temperature and high humidity) required a great attention as well.

After a first season of monitoring activity, a nearly complete set of data were obtained from field measurements: maximum data losses amounted to 9.4% in all the monitored period.

The first years' experience suggested some adjustments, which were considered for the current season (2013). All the system, in fact, have to be removed before the new season to allow ploughing and all the operations for the cultivation,

For example, triangular weirs have been substituted by RBC flumes similar to those installed for inflow monitoring as the latter are easier to be placed and to calibrate. The pressure sensors for water level measure inside the flumes, have proven to better work when horizontally installed instead of vertically (as suggested by their datasheets) in order to prevent any possible presences of air balls inside the threaded pin during very high temperature values. During the first year we had, in fact, some problems due to such phenomenon and a specific post processing algorithm had to be developed to remove the errors.

A new monitoring season is currently undergoing and already resulted in strongly reduction of installation time.

References

Campbell, 2011. RF401-Series & RF430-Series Spread Spectrum Radio Modems. www.campbellsci.com

Campbell, 2012a. Model 108 Temperature Probe Instruction Manual. www.campbellsci.com

Campbell, 2012b. CR1000 Measurement and Control System Operator's Manual. www.campbellsci.com

Campbell, 2012c. LoggerNet Version 4.1 Instruction Manual. www.campbellsci.com

Clemmens A.J., Wahl T.L., Bos M.G., Replogle J.A., 2001. Water measurement with flumes and weir. International Institute for Land Reclamation and Improvement / ILRI, Wageningen, The Netherlands.

Chiaradia E.A., Facchi A., Gharsallah O., Romani M., Bischetti G.B., Gandolfi, C. 2013. Water balance of rice plots under three different cultivation methods: first season results, Proceedings of AIIA 2013, Viterbo (Italy), September 8-12 2013.Kipp & Zonen, 2002. CNR- 1 Net radiometer Instruction Manual. www.kippzonen.com

Hukseflux, 2010. HFP01 Heat flux plate/ heat flux sensor (Brochure). www.hukseflux.com

Vaisala, 2006. Vaisala HUMICAP® Indicator HMI41 and Probes HMP41/45/46 Vaisala User's guide. http://www.vaisala.com.

LI-COR, inc., 2009. LI-7500A Open Path CO2/H2O Analyzer Instruction Manual.

Young Co., 2010. Ultrasonic anemometer Model 81000 Instructions. www.youngusa.com

Spectrum, 2009.Watchdog 2000 Series Weather Stations product manual. www.specmeters.com

Effects of water distribution uniformity on waxy (*Zea mays* L.) yield: first results

L. Bortolini, M. Martello

Dip. TESAF - University of Padova, Padova, Italy

Introduction

In 2050 an increase in water consumption up to 11% and a duplication in food production needs have been predicted (UNESCO-WWAP, 2003). For this reason the correct choice of irrigation method along with a rational irrigation water management will be essential to increase the water use efficiency. Therefore a reduction in water losses and a utilization of low irrigation volume are needed, integrating the irrigation practice into a sustainable cultivation with a rational water use (Castaldi, 2009; Bortolini, 2008).

The irrigation system performance is evaluated in the study area on the basis of adaptability, efficiency and distribution uniformity. The distribution uniformity is a parameter to indicate the irrigation system capability to apply the same application rate to a surface unit for the surface and sprinkler methods, or to discharge the same water volume from each emitters for the microirrigation methods. Without an appropriate uniformity distribution it is impossible to irrigate in a appropriate and efficient manner and with a good water use efficiency. In fact, with a scarce distribution uniformity some zones will be over-watered and other ones will be under-watered (Burt, 1997; Camp, 1997; Lameck, 2011).

The irrigation uniformity can affect the crop yield and influence more or less heavily the environmental impact of the irrigation (Salmeron, 2012).

Corn is a very important crop in the North of Italy, especially in the Po Valley Plain where it is cultivated with high water and fertilizer use and often with high energy consumption.

The limitation of high crop yield is especially due to an incorrect use both of water and fertilizer elements. For these reasons, it is advisable to use fertigation technique that allows for an optimum use of water and the fertilizers are easily and uniformly distributed near the roots in the correct time and quantities.

The proper use of production inputs is an indispensable condition not only for the farm finances but even for the collectivity, and especially for irrigation water, evermore subjected to use limitation and withdrawal restriction, and its efficient use have to involve both engineering aspects of the distribution system and the management strategies of the irrigation operations (Ghinassi, 2010).

The scope of this work is to quantify the impact of water distribution uniformity of a drip irrigation system on the waxy corn yield and on water use efficiency, by comparing this system with the more traditional sprinkler irrigation system, even on the profitability basis, in order to evaluate its real possible use in the Venetian Plain.

Correspondence: Lucia Bortolini, Dip. Territorio e Sistemi Agro-Forestali Università degli Studi di Padova, Viale dell'Università 16, 35020 Legnaro (PD), Italy. E-mail: lucia.bortolini@unipd.it

Journal of Agricultural Engineering 2013; XLIV(s1):e162
doi:10.4081/jae.2013.(s1):e162

Materials and methods

The trials were carried out during summer 2012 on the farm of Società Cooperativa Agricola Zootecnica "La Torre" located in Isola della Scala (Verona, Italy), in a drip irrigated plot of 12 ha, subdivided into 3 irrigation zones of 4 ha, and in a gun sprinkler irrigated plot of 1 ha.

The soil is a sandy loam (USDA classification), with a good organic matter content. A 30 cm plough was done during autumn burying 42 t ha^{-1} of cattle slurry, corresponding to about 170 unit of nitrogen. A FAO 600 cultivar was seeded, with a plant spacing of 0.16 m and row spacing of 0.75 m.

Fertigation in three different applications was done in the drip irrigated area using N 30 liquid fertilizer, while urea was distributed during hoeing operation in the sprinkler irrigated area, for a total of about 100 unit of nitrogen per ha in each.

The waxy corn harvesting was done on the 9th of August.

The drip system was made up of a centrifugal pump with a 37 kW diesel engine, a hydrocyclon and self-cleaning screen filter of 120 mesh, and a Venturi fertigation pump. The drip lines were Aqua-Traxx® PC drip tape of 22 mm of diameter with 1.14 L h^{-1} of flow rate at 0.8 bar and 20 cm emitter spacing, installed 5 cm underground, located in the furrow and in every other row, supplied by a layflat 5" manifold.

The solid-set sprinkler system was made up of a multistage centrifugal pump containing three impellers with a flow rate of 67 m^3 h^{-1}, a head of 70 m and an engine of 130 kW. The sprinklers were turbine gun sprinklers with a nozzle of 28 mm operating at 5 bar pressure (measured with a Pitot tube) with a flow rate of 1096 L min^{-1}, positioned with 40 x 40 m spacing and supplied by aluminum pipes of 100 mm of diameter.

To define the distribution uniformity of the drip irrigation system the discharge was measured at 24 points within each irrigation zone according to ISO 9261; as the sprinkler system, 100 catch cans were positioned with a grid of 5 m apart, covering an area of 160 m^2 equal to the distance between gun sprinklers and the application rate was measured at each survey point (Figures 1 and 2).

The waxy corn yield was carried out weighing the whole epigeous part of the crops harvested in each survey point for drip system and in 16 points for sprinkler system (all plants of two rows x 1.2 m of length),

excluding the borders, and then transformed in kg ha^{-1}.

In order to observe the soil water content variations, even to calculate the water use efficiency indexes, fiber glass tubes where positioned at various points and located between rows and on rows in order to use the soil moisture profile probe (a device with 4 FDR sensors at 10 – 20 – 30 – 40 cm depth).

The irrigation was scheduled from the 14th of June to 7th of August distributing 15 mm every three days (corresponding to about 5 mm of daily crop ET) for drip irrigation. Regarding sprinkler system, only supplemental irrigations were chosen according to the procedure typically used in Venetian Plain.

To calculate the non-irrigated waxy corn yield six rows were not irrigated.

Distribution uniformity and efficiency parameters

To evaluate the distribution uniformity two indexes suitable for drip irrigation were used. The first one is the Low Quarter Distribution uniformity DU_{lq} which emphasizes the areas which receive the least irrigation by focusing on the low quarter

$$DU_{lq} = \frac{q_{avglq}}{q_{avg}} \quad (1)$$

where:

q_{avglq} = average discharge rate of the lowest one-fourth of the field data readings (L h^{-1})

q_{avg} = average discharge rate of all field data checked (L h^{-1})

The second index calculated is the *CU* uniformity coefficient developed by Christiansen (Christiansen, 1942) that treats overirrigation and underirrigation equally compared to the mean:

$$CU = 100 \cdot \left[1 - \frac{\sum_{i=1}^{n} |x|}{M \cdot n}\right] \quad (2)$$

where:

x is the total absolute value of deviations from average of the application rate of each survey point regarding the average application rate M measured in n control points. To determine this, catch cans were distributed according to a grid within the irrigated area.

For drip system *CU* coefficient modified by Merriam and Keller (Merriam, 1978) was used

$$CU = 100 \left(1 - \frac{\sum |z - m|}{\sum z}\right) \quad (3)$$

where:

z = discharge rate of each emitter (L h^{-1})

m = average discharge rate of total emitters (L h^{-1}).

The values of the parameters depend on constructive and hydraulic features, and the age of the emitters and are influenced by the obstruc-

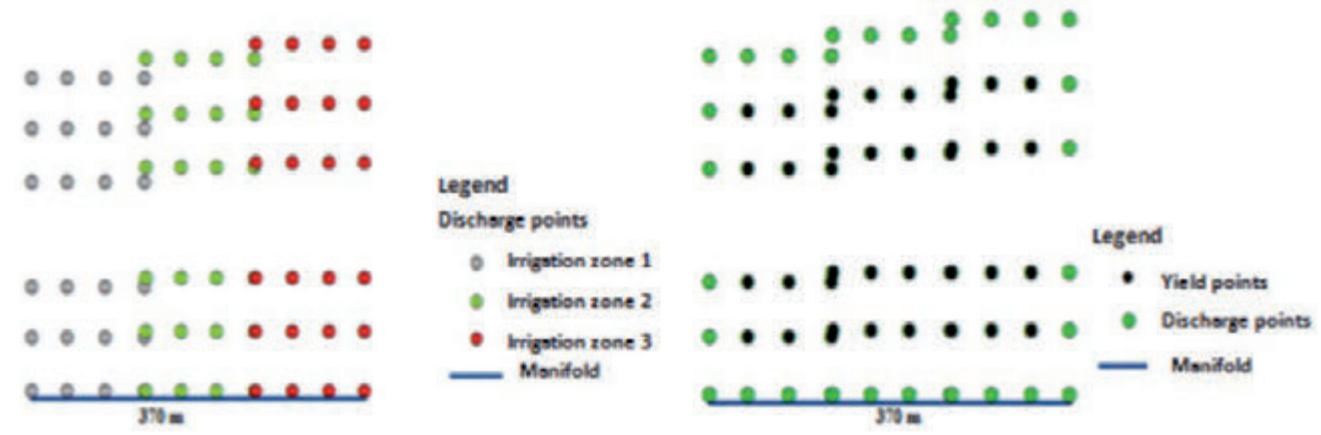

Figure 1. Map of the survey points in each zone of the plot with drip irrigation system.

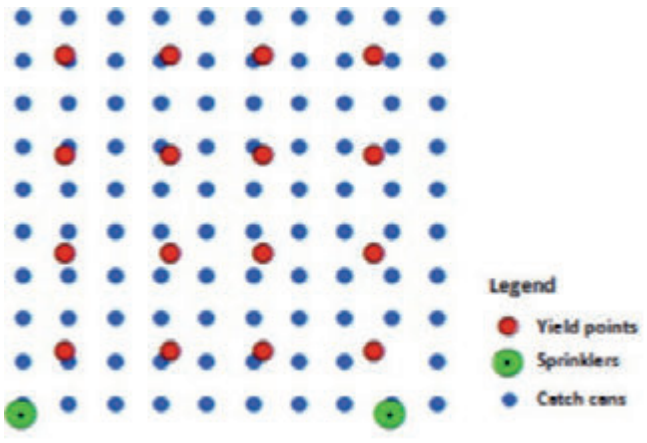

Figure 2. Map of the survey points of the area with sprinkler irrigation system.

tion level of the emitters. By means of these indexes it is possible to evaluate the efficiency of water filtration system and the system maintenance. For this reason these indexes should be used with both new and old systems.

To determinate the water use efficiency, the WUE_b index, which considers the total amount of water distributed, and the IWU_e index, used to characterize the yield increase in relation to the water applied during irrigation, were calculated (Lameck, 2011).

The two indexes are illustrated with the following formulas

$$WUE_b = \frac{Y}{(P_e + IR + \Delta SW)} \quad (4)$$

where:
WUE_b = water use efficiency at biomass-basis (kg m^{-3})
Y = crop yield (kg ha^{-1})
Pe = rainfall (m^3 ha^{-1})
IR = irrigation volume (m^3 ha^{-1})
ΔSW = soil water stock (m^3 ha^{-1})

$$IWU_e = \frac{(Y_i - Y_d)}{IR} \quad (5)$$

where:
IWU_e = irrigation water use efficiency (kg m^{-3})
Yi = irrigated crop yield (kg ha^{-1})
Yd = non-irrigated crop yield (kg ha^{-1})
IR = irrigation volume (m^3 ha^{-1})

To visualize and better analyze the distribution uniformity, the crop yield and the efficiency parameters, ArcGIS 10 (ESRI®) with IDW (Inverse Distance Weighting) geostatistical interpolation technique (the most suitable given the quantity and distance of the survey points) were used to create the maps.

Profitability

The profitability of the two irrigation systems was calculated and compared.

As regards sprinkler irrigation, in order to simplify analysis and at the same time make the results more useful, a travelling gun system was considered. The parameters used for the choice of the most appropriate model to the acquired data were: gun sprinkler with a nozzle of 28 mm, pressure 5 bar at the sprinkler, PE pipe with diameter of 100 mm and length of 300 m.

The cost of the system is € 20 000 of which € 12 000 for the travelling gun system and € 8 000 for the pump. From these data an annual amortization in 12 years of € 58 per ha with a 6 h ha^{-1} management time for labour of seven irrigation operations was obtained (Ghinassi, 2012).

For the drip system, the real costs sustained were for the purchase of the drip system components. With the same procedure used for the sprinkler system, fixed costs of the system head were calculated considering a 6 years amortization for the manifolds. It is important to note that, for this type of microirrigation system, it is necessary to consider variable costs regarding the purchase of lateral drip tapes.

For the Value of Production (VP) a price of € 40 per ton of silo maize was considered. Regarding diesel consumption, real costs of € 1 L^{-1} were used.

Finally, the profitability of both irrigation systems was calculated taking into consideration the VP and total costs.

Results

Uniformity distribution and efficiency

The analysis of the distribution uniformity for the drip system shows that both the indexes present good but not optimum results, indicating a discrete variability of the discharge rates probably due to elevated length of the area, and therefore the consequent lost of pressure along the water distribution lines. In fact, considering the three irrigation zones individually (Table 1), it can be noted that the second zone, with an inferior length of the manifold, achieves the best distribution uniformity. The third zone has suffered a loss of load due to the greater length of both the manifold and the lateral lines, given the worst performance.

As regarding the crop yield, the non-irrigated plot was unproductive, because the plants were completed wilted after flowering, while it was observed in the irrigated part that the third zone has given the best average yield (respectively, +10% compared to the first zone and +3% compared to the second one).

It is interesting to note the difference between the three zones, principally caused by the actual discharge rate of the drippers. The third zone, with an inferior total irrigation volume distributed, gives a better efficiency: in fact, the WUE_b is more than 15% compared to the first zone and 12% regarding the second zone, while the IWU_e was more than 19% regarding the other two zones.

By observing both application rate and crop yield maps (Figure 3) it can be noted that, in the zone in which the irrigation volumes distributed were higher, the yields obtained were lower. In hypothesis, these results are due to prolonged and repeated moments of water saturated soil in which the plants were in anoxia caused by excessive irrigation volumes distributed.

It must be noted that, in spite of these differences, the average yield was 89,7 t ha^{-1}, therefore very high.

Even observing the water use efficiency maps it is evident that, both for the IWU_e and for the WUE_b indexes, in the area where the distributed volume were lower both indexes are better.

As regards the sprinkler system, both distribution uniformity parameters are very low, above all the DU_{lq} (Table 2). In fact, in Figure 4 it can be noted that there is a wide zone opposite to the sprinklers, where the application rate was up to 50% lower regarding the average value.

In the same maps it can be noted that the zone with higher application rate has obtained lower yield regarding the central part where the application rate was near the average value. It possible to hypothesize that in the over-irrigated part, even in this case, the lower yield was caused by the soil water saturation conditions, therefore the plants suf-

Table 1. Average crop yields, seasonal irrigation volumes, total water supplies, distribution uniformity and efficiency parameters of the three drip irrigation zones.

Drip zone	Average yield (t ha^{-1})	Irrigation volume (mm)	Rainfall (mm)	Water supply (mm)	DU_{lq}	CU %	WUE_b (kg m^{-3})	IWU_e (kg m^{-3})
1	84.4	334	196	530	0.75	86.70	15.9	25.3
2	90.9	355	196	551	0.80	88.84	16.5	25.6
3	93.4	300	196	496	0.70	82.06	18.8	31.1

fered anoxia. However, the waxy corn yields were more than 80 t ha^{-1}, underlining the superior production of irrigated corn in the studied area (Table 2).

In the water use efficiency maps (Figure 4) it can be noted that the area immediate to the gun sprinklers has lower values due to high application rate and inferior average yields, while in the central zone it was found to be higher. In the opposite zone higher IWU_b values were obtained, due to low application rate, even if the crop yield was near average.

Profitability

Table 3 shows that the Value of Production (VL) is higher for the drip irrigation system of € 316 per ha, equal to 9% more than travelling gun system. On the contrary, the travelling gun system has an amortization lower than 35% and almost half of the variable costs. The higher cost of the drip system is caused by the cost of the drip tapes (€ 450 per ha), as for travelling system, costs are more connected to diesel consumption that were 44% higher than drip system. Instead, as regards labour, due to time needed for installation and dis-installation of the drip lines, the costs are higher by 56% for the drip system.

The income is slightly higher for the travelling gun system (+ 0,5%), despite the cost of diesel, demonstrating the importance of the cost of the drip tapes on the total costs.

Discussion

Comparing the two irrigation methods (Table 2) it can be noted that the average yield of the drip irrigation system was higher by only 8.6% in regard to sprinkler system, even if the seasonal irrigation volume distributed was more than 50%.

This difference is shown in WUE_b value where a superior value of 25% of the sprinkler system can be seen. Comparing the two irrigation

Table 3. Profitability of the drip and sprinkler (travelling gun) irrigation systems.

	Drip	Sprinkler
Value of Production (€ ha^{-1})	3588	3272
Amortization (€ ha^{-1})	89	58
Variable costs (€ ha^{-1})	828	456
Diesel (€ ha^{-1})	214	384
Labour (€ ha^{-1})	164	72
Income (€ ha^{-1})	2292	2303

Table 2. Comparison between drip and sprinkler irrigation of average crop yields, seasonal irrigation volumes, total water supplies, distribution uniformity and efficiency parameters.

	Average yield (t ha^{-1})	Irrigation volume (mm)	Rainfall (mm)	Water supply (mm)	DU_{lq}	CU %	WUE_b (kg m^{-3})	IWU_e (kg m^{-3})
Drip	89.7	330	196	526	0.73	84.74	17.1	27.2
Sprinkler	81.9	165	196	361	0.33	59	22.7	49.6

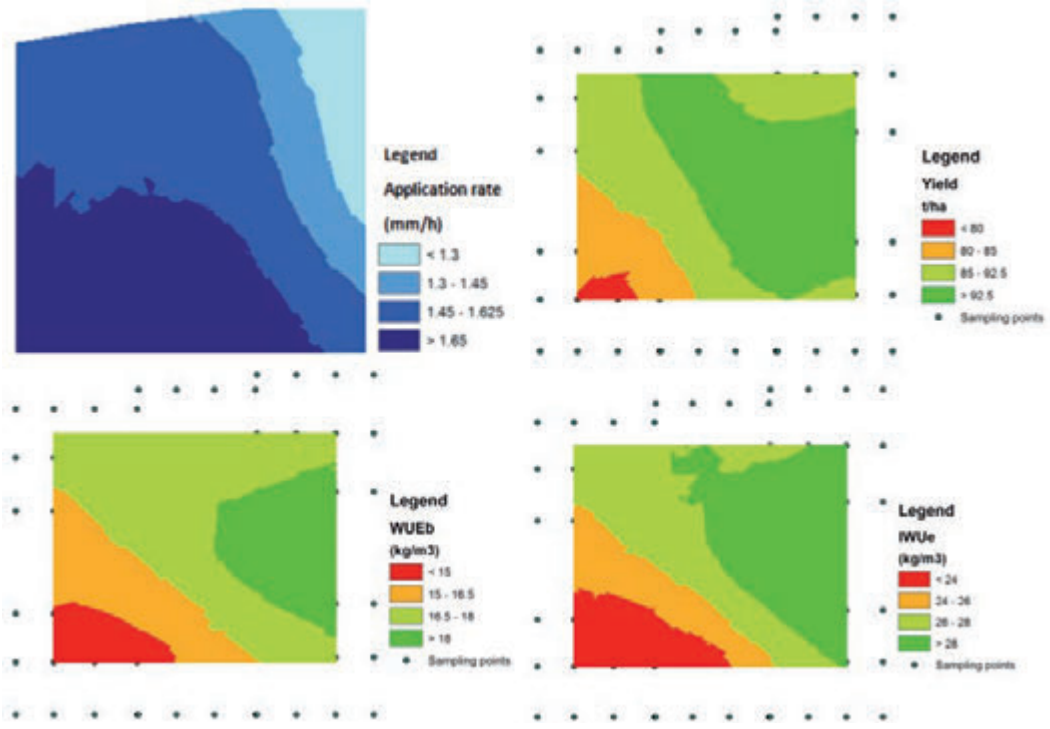

Figure 3. Maps with surface interpolation of Application rate, Yield, WUE_b, and IWU_e of the drip irrigation system.

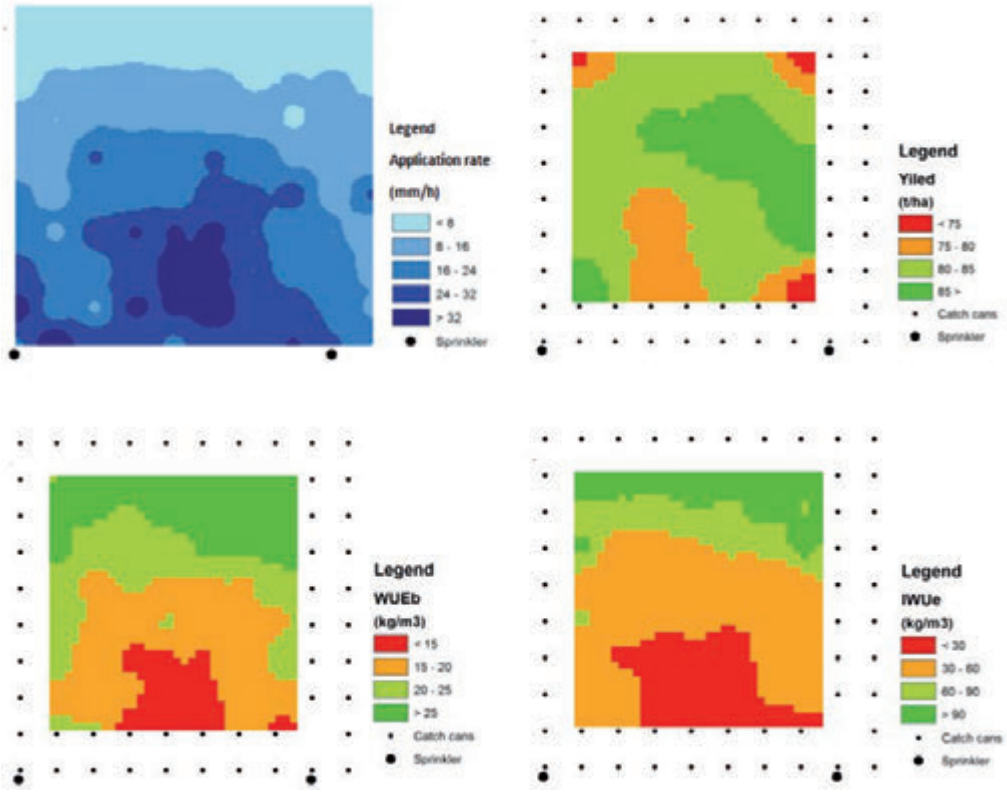

Figure 4. Maps with surface interpolation of Application rate, Yield, WUE_b, and IWU_e of the sprinkler irrigation system.

methods in IWU_e terms, it turns out that water use efficiency is 45% higher than for the drip system, showing that the rational management of the irrigation volumes has a greater influence than the uniformity distribution.

Observing results, for the both systems it can be hypothesized that in the over-irrigated part the inferior crop yield was caused by periods in which the soil was saturated, with a subsequent state of anoxia, while better production were obtained in the areas with average application rate.

The profitability of the two systems shows that the income is better by 0.5% for the travelling gun system in respect of drip irrigation system. From the calculation, it turns out that the annual cost of the drip lines are elevated, while for the travelling system elevated costs are due to diesel consumption. In latter case, lower cost could be found by simply using a pump with a lower kW engine, more useful for the flow rate and pressure needs of the system.

Conclusions

The trials carried out during summer 2012 have shown how the drip irrigation system easily allows for a good distribution uniformity, but careful designing is necessary in order to reduce the head loss into the drip lines.

The drip irrigation management with pre-scheduled irrigation plan based on hypothetical average crop daily ET does not optimized the use of water, lowering the water use efficiency.

Despite of a particularly dry summer, in general irrigation has allowed for very high yields on average, even if relatively lower in the over-irrigated zones.

The income of the drip irrigation system is slightly lower than the sprinkler irrigation system, mostly due to the use of "throw away" drip lines (*i.e.* used only for one crop season) that can have future consequence only if supported by justifiable financing because of a rational use of water, energy, fertilizers, including the possibility to distribute the liquid fraction of slurry.

It is very important to evaluate the correct irrigation volumes and operation times in order to reduce to a minimum the number and the duration of irrigation, and consequently the energy consumption. For this reason new trials will take place on summer 2013.

References

Bortolini L, 2008. Irrigazione razionale: da sfruttamento a uso strategico. Informatore Agrario. 19: 31-33.

Burt CM, Clemmens AJ, Strelkoff TS, Solomon KH, Bliesner RD, Hardy LA, Howell TA, Eisenhauer DE, Irrigation performance measures: efficiency and uniformity. J. Irrig. Drain. Division ASCE, 1997, 123(6), 423-442.

Burt CM, Clemmens AJ, Strelkoff TS, Solomon KH, Bliesner RD, Hardy LA, Howell TA, Eisenhauer DE, Irrigation performance measures: efficiency and uniformity. J. Irrig. Drain. Division ASCE, 1997, 123(6), 423-442.

Camp C, Sadler E, Busscher W, 1997. A comparison of uniformity measures for drip irrigation systems. Trans. ASAE, 40:1013-1020.

Castaldi R, 2009. Bassi volumi irrigui per un uso razionale dell'acqua. Informatore Agrario. 45:36-40.

Christiansen JE, 1942. Irrigation by sprinkling, University of California Agricultural Experiment Station Bulletin n. 670, p 124.

Ghinassi G, 2012. Comparazione dell'efficacia agronomica ed economica dell'irrigazione effettuata con macchine irrigatrici semoventi e linee gocciolanti. DEISTAF, Università degli studi di Firenze.

Ghinassi G, Zammarchi L, 2010. Irrigazione a goccia o a pioggia? Confronto costi e PLV su mais. Informatore Agrario. 23:40-43.

ISO9261, 2004. Agricultural irrigation equipment Emitters and emitting pipe Specification and test methods, Wien: Austrian Standards Institute 2010.

Lameck O, William L, Dean E, 2011. Irrigation Efficiency and Uniformity, and Crop Water Use Efficiency, University of Nebraska Lincoln Extension.

Merriam J L, Keller J, 1978. Farm irrigation system evaluation: A guide to management. Logan, Utah, Utah State Univ.

Salmerón M, Urrego Y, Isla R, Cavero J, 2012. Effect of non-uniform sprinkler irrigation and plant density on simulated maize yield. Agricultural Water Management, Volume 113, pp. 1-9.

UNESCO-WWAP, 2003. Water for people water for life, Unesco.

An analytic-geospatial approach for sustainable water resource management: a case study in the province of Perugia

Stefano Casadei,[1] Michele Bellezza,[2] Luca Casagrande,[2] Arnaldo Pierleoni[2]

[1]Department of Civil and Environmental Engineering, University of Perugia, Italy;
[2]T4E S.r.l. one Technology four Elements, Spin-Off UNIPG, Perugia, Italy

Abstract

Water is a strategic, but also highly vulnerable, natural resource. This because the increasing demand from multiple uses, in many cases competing amongst them, seems to influence the concepts of sustainability of the exploitation. From the operational point of view, the studied system is an integrated decision support system. It is not only a platform to exchange information and assessments, but also a tool for conflict resolution, in the management of water resources, to obtain the consensus among all participants in the decisional processes. So the canonical "top-down" approach has been replaced with a "bottom-up" approach where all stakeholders become decision makers themselves. The application of the aforementioned approach was studied for the Tiber River basin and has been applied to the Province of Perugia area. The study focused to the building of a spatial database of hydrological data and multipurpose water withdrawals, together with the setting of the evaluation model for the surface water resources. This model bases its algorithms on regionalization procedures of flow parameters. For the definition of the river condition, hydrological indices calculated from the hydrological database have been used, while for the existing withdrawals, an analysis procedure has been developed, that from the point of interest directly selected on the map, finds out the upstream basin and, by means of overlay procedures, identifies the upstream water uses and the total flow that could be extracted. The potential of the system and the technologies used are contained in a WEB platform that allows the analysis of the database of water uses/withdrawals on the cartography, and the comparison with the hydrogeological characteristics of the sub-basin examined.

Correspondence: Stefano Casadei, Department of Civil and Environmental Engineering, University of Perugia, Borgo XX Giugno 74, 06121 Perugia, Italy.
Tel. +39.075.5856043 - Fax: +39.075.5856049.
E-mail: casadei@unipg.it

Key words: water resource, decision support system, WebGIS

Acknowledgments: this research is part of the project defined and funded by the Province of Perugia - Division of Defence and Management Hydraulics

Journal of Agricultural Engineering 2013; XLIV(s1):e163
doi:10.4081/jae.2013.(s1):e163

The purpose of this study is to provide software tools that can be used as a support in water resource evaluation and management policies at the basin scale.

Introduction

The new approach in water resources management is based on the building of a spatial database of hydrological data and multipurpose water withdrawals, together with the setting of the evaluation model for the surface water resources.

This model bases its algorithms on regionalization procedures of flow parameters derived from the geomorphologic features of the basin, Area and Base Flow Index (BFI) (Casadei, 1995). The output is a set of Flow Duration Curves (FDCs) for each arc of the simplified network (Vogel and Fennessy, 1995). For the definition of the river condition, hydrological indices such as BFI, $Q_{7,10}$, Q_{355}, Q_{347}, entire FDC are used (Singh and Stall, 1974; Smakhtin, 2001). They are calculated from the hydrological database, while for the existing withdrawals an analysis procedure has been developed, that from the point of interest directly selected on the map, finds out the upstream basin and, by means of overlay procedures, identifies the upstream water uses and the total flow that could be extracted.

In this work hydrological topics are linked with the Information and Communication Technologies (ICT) for environmental sustainability. The use of the Web Processing Service (WPS) protocol makes possible to perform the typical operation of Desktop GIS application, through a Web interface and via an HTTP protocol. The main procedures require as search parameters both numerical inputs (such as the kind of water use, the maximum allowed withdrawal, etc) and geographical (such as withdrawals upstream of a certain section of the network). For this specific kind of search it is necessary to use the potentialities of a GIS software since it implies the spatial analysis of the river network, together with a database containing the information of the basin. Therefore the system is composed of a relational database with geospatial extension for vectorial data; the GIS engine that performs all the geospatial operations and finally the PyWPS that is a Python implementation of the WPS protocol. The WEB interface offers various thematisms in order to provide a better support to the decisional process. The thematisms are shown by means of a the Web Map Service protocol taking advantage of the javascript framework OpenLayers. The project is entirely based on Open Source Technology (Neteler and Mitasova, 2008).

Materials and methods

Data analysis and modeling processes

The first step has been the creation of a shared database at the

basin scale (Tiber River) of all data and information together with user friendly procedures for its periodical update.

This final goal has been achieved by a software platform that could allow a free sharing of information, which is provided by a WEB-BASED architecture.

The creation of the database leads to the developing of a series of procedures concerning the analysis of the data. These procedures can be both numerical and graphical, according to the typology of the data and the kind of analysis concerned.

The computational side of the data analysis also foresees the possibility of performing statistical evaluations, and in this field there is a wide range of possibilities (Katz *et al.*, 2002) that perform nicely in a WEB-GIS environment.

At present, the procedures implemented are aimed towards the definition of various hydrological indexes for defining the base flow value in low-flow conditions in order to be able to correctly assess the water resources and/or the available amount in a section of a network, either in order to issue or renew a withdrawal license or to study the state of the watercourse.

BFI calculation

The analysis of hydrographs of daily flow is a useful technique in a wide variety of studies in the field of water resources. In particular, the breakdown of flow rates in the two components of base flow and surface runoff is often used to identify contributions from springs and groundwater (Sloto *et al.*, 1991). In this context, it is now definitely clear that there is a close relation between the geology of the basin and the base flow.

The hydrogeological features of a basin (intensity limit infiltration, effective porosity, permeability of rock formations, etc.), directly affect low flow regimes of a stream. It is therefore of great interest to establish a quantitative relationship between base flow and these features. Unfortunately it is difficult to summarize in a single parameter the complex hydrological features mentioned above, unless we assume as a measure of these characteristics the effects that they produce, *i.e.* the base flow itself.

From an operative point of view, the BFI calculation (Figure1) is made according to Lvovich method (Lvovich, 1972). The index is the ratio between the volume of base flow, area under yellow line, and the total volume, area under the total hydrograph (blue line). The yellow line is obtained by means of a procedure of data analysis conducted on the minimum flow of 5oups, then processed in groups of three values in a moving average and finally filtered according to the following conditions: 0.9 Qmin(I) ≤ Qmin(I+1) and 0.9 Qmin(I) ≤ Qmin(I-1), for I=2, N-1.

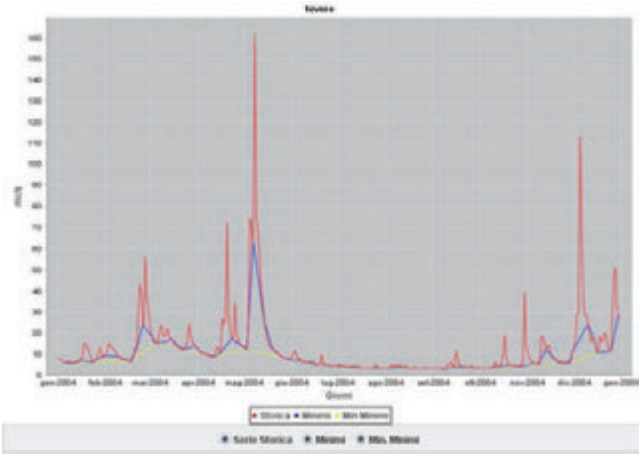

Figure 1. Example of applet view of BFI calculation by measured data at S. Lucia station, Tiber River.

The BFI of the basin is the average of the time series of annual BFI, but it is also possible elaborate the consecutive time series of flow data.

As mentioned, the index of the base flow is closely related to the nature of the hydrogeological formations in the basin. Indeed with increasing occurrence of permeable formations there is a direct variation of the BFI calculated on the basis of observed data, while an increase in the occurrence of impermeable formations inverts the relation (Manciola and Casadei, 1991) .

The BFI of the ungauged basin is thus obtained using a weighted average method, compared to areas, with BFI typical of single formations, assuming that every formation has a specific value of BFI which is evaluated in the gauged basins:

$$BFI_{est,j} = \sum_{i=1}^{n} \frac{A_{j,i}}{A_{j,tot}} \cdot BFI_{frm,i} \quad (1)$$

Where:

$A_{j,i}$ = superficial extension of the i^{th} hydrogeological formation in the j^{th} basin

$A_{j,tot}$= total area j^{th} basin

$BFI_{est,j}$ = extimated BFI in the j^{th} basin

$BFI_{frm,i}$ = BFI associated to the i^{th} hydrogeological formation

This last term has been evaluated in the studied area, where every hydrogeological formation has been linked to a value of BFI by means of a technique which minimizes the estimation error in the gauged station (Manciola and Casadei, 1991).

$Q_{n,m}$ calculation

The value of $Q_{n,m}$ describes the low flow characteristics of the river, represented by the series of annual minimum flow averaged over an interval of *n* consecutive days with a return time of *m* years. This index is implemented by various US Agencies for environmental protection, that generally adopt the $Q_{7,10}$ value.

For the calculation of $Q_{n,m,}$ a series of steps that begin with the calculation of minimum average daily flow over n-days are required. This calculation is performed for each year of the series. From these values the average and variance are calculated in order to evaluate the parameters of the Weibull-Gumbel distribution:

$$P(x) = 1 - \exp\left[-\left(\frac{x-\varepsilon}{\theta-\varepsilon}\right)^{1/\lambda}\right] \quad (2)$$

Where:

ε = lower limit of the distribution

λ = shape parameter

θ = scale parameter

So, in order to produce estimates of the parameters of the distribution, more procedures have been implemented, especially for the estimation of the parameter λ, from which also derives the parameter ε, and this one is essential to locate the minimum value of the distribution itself (Manciola *et al.*, 2004).

The regionalization process of the minimum flow of 7 days with return time of 10 years ($Q_{7,10}$) is based on the study of regressions between calculated data and hydrogeological parameters of the gauged basin. From a methodological point of view an estimate of the $Q_{7,10}$ that can fit the entire basin is still to be made, instead estimates for different portions of it, identifying one or more relations like the following:

$$\frac{Q_{7,10}}{A_{tot}} = \sum_{k=1}^{3} a_k \cdot BFI^k + a_0 \quad (3)$$

where the constants are taken from the interpolation procedure conducted starting from the values of calculated $Q_{7,10}$, possibly on natural and naturalized flow values (*i.e.* not influenced by human factors). The methodological approach does not vary with the change of the characteristics of the index in terms of *n* and *m*, it should be noted that the polynomial estimate does not exceed in any case the third order (Ubertini et al, 1996) .

Flow duration curves

The FDCs are meant as a synthesis of the hydrological status, before and after the human modifications, of each section of the river network.

The use of FDC as a tool for assessing available water resources is possible by means of regionalization procedures, using characteristic parameters of the basin, automatically calculated by querying the GIS engine that performs the analysis of the geomorphology of the basin (BFI and Area, see Bellezza *et al.*, 2007).

In this case, the main river network is divided into sections for which it is possible to know all relevant information that influence the availability of water. These data, through the theoretical regionalization procedure, allow the determination of the hypothetical natural flow for each section (Figure 2).

This information can be evaluated in terms of low flow indexes, *i.e.* Q 355-days and 347-days duration, or overlapped to the minimum instream flow for this section (DMV), if defined.

However, this information cannot be considered enough for the management of the resource at the scale of the basin concerned, in fact it is necessary to overlay the hydrological and hydrogeological information that quantifies the natural resources available, with the information about all the licences of water withdrawal.

Water withdrawals management

This step, of course, implies an expansion of the database with the information about water withdrawals. These data are from different administrations and authorities and are highly non- homogeneous and incomplete to the point that the recent legislation has many times imposed a reorganization of the public water resources dataset (Ministry of the Environment, 2004). Achieving this result can surely be made easier through the creation of a unified database of withdrawals at the basin scale. This database should also be made accessible to the several administrations concerned via a WEB portal where they can operate or modify, update present data and insert new ones. Indeed, we think that sharing a single database is the only effective way to reorganize this strategic sector of the water resources management.

For this reason, the main technologies used within the system are contained in the section of the portal that allows the analysis of the database of water uses/withdrawals on the cartography. This is probably the most significant section, in terms of low flow management, because the search can easily point out the situation, even at the sub-basin scale, and make a comparison with the hydrogeological features of the sub-basin examined, that are particularly influential especially during droughts, also making easily understandable the spatial distribution of licences and their information.

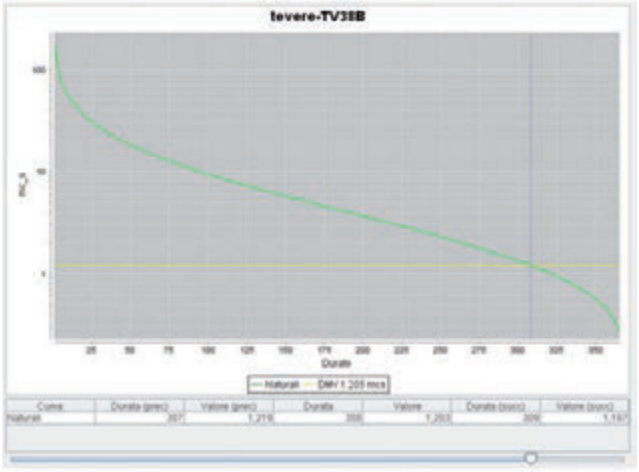

Figure 2. Example of applet view of flow duration curve.

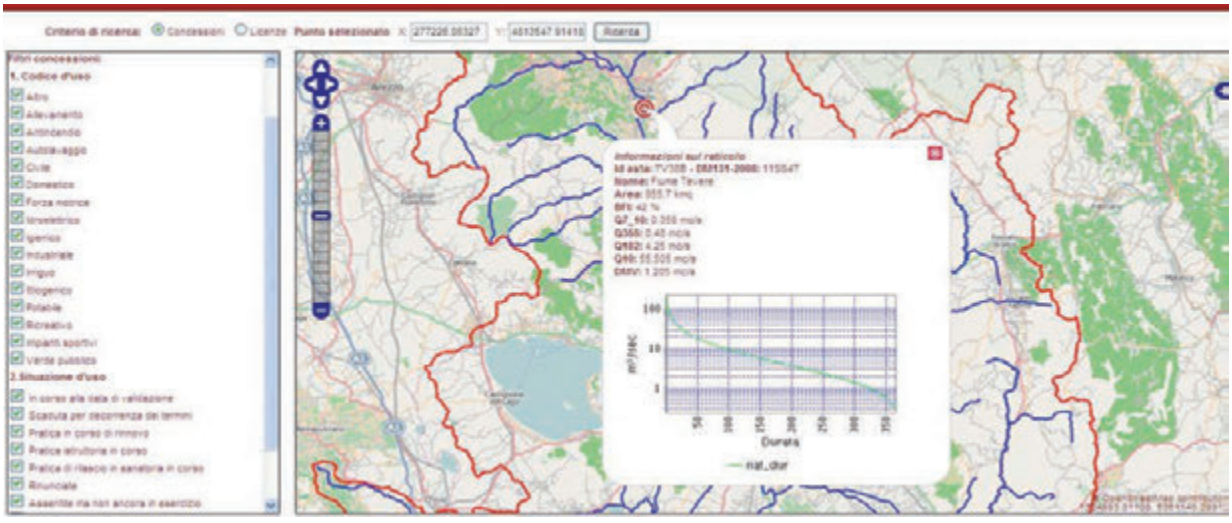

Figure 3. Search example of the hydrological status in a sub-basin.

In order to evaluate the river conditions the previous hydrological indices were used (Figure 3), while for the existing water withdrawals an analysis procedure has been developed, that from the point of interest selected directly on the map, finds out the upstream basin and, by means of overlay procedures, identifies the upstream water uses which are geo-referenced on the map. To search the water body in more details, a filtered search has been developed so that the uses can be retrieved on the base of their type, the allowed amount of water, and their administrative status (Figure 4).

Results and discussion

The development of this study shows the greatest difficulty in the fragmentation of responsibilities among administrations located in succession along the river network, this is why administrations downstream do not know the upstream situation (water availability), while those upstream are not able to evaluate the amount of water withdrawn downstream. At the moment this situation generates a stalemate, for this reason a web tool operating on a single database of licences, that should be constantly kept updated by all the administrations involved, can be very useful.

This is the reason why the initial case study has been the total Tiber River Basin, which has 17462 Km^2 of area distributed over 6 Regions and 8 main Province. The second step has been an in depth analysis the area managed by the Province of Perugia.

In order to make the technical-administrative side of the management of the superficial water resource in a much easier and immediate way, a web site (Province of Perugia, 2012) has been created. In this portal all the methodologies described above are becoming operative and accessible.

The data collection and validation phase brought to the compilation of a hydrological database, already accessible online, that has different levels of access according to the typology of user and the kind of information required. It is made of about 11800 years of hydro-meteorological data and about 10000 information regarding the uses and the water withdrawal licenses. The data can be viewed both in a numeric format and a graphic visualization and if needed, easily exportable in various file formats.

The main result obtained in this study is in demonstrating that it is technically possible to conduct a spatial analysis, at the level of the basin or sub-basin, between the use of surface water resources and the availability of water in low flow condition. The final data show some no-balanced conditions, and many limit conditions, demonstrating the bad water management politics in the last decades.

Therefore, this situation has directed the study toward finding solutions, which using the same tool for spatial analysis, could propose the use of non-conventional water resources.

These analysis also highlighted the presence of a large number of small reservoirs, especially in the Apennines area, whose data were available in the Province of Perugia. So, the same application was extended in order to include data regarding small reservoirs, with the aim of evaluating the possibility of exploitation of this resource that is usually almost completely neglected, even during dry periods.

The results were very encouraging, in fact the possible use of small reservoirs for irrigation can contribute in many cases to restore the equilibrium in the water balance (Figure 5).

In addition, this result indicates that the application can also be extended to the possible use of well water or other available water resources in the area, but only when data are properly recorded and cataloged.

Conclusions

The purpose of this study is to provide software tools that can serve as a support in water resource evaluation and management policies at the basin scale, with particular attention given to the creation of a database of uniform data that can be easily updated, and to the development of mathematical models that are easy to use, both as regards the interpretation of output data and the choosing of management hypotheses.

The database of water withdrawals, with its related tools, is one of the most significant parts of the work, and if adopted, it will allow to define a more accurate scenario of water use at the basin level. This result may highlight imbalances and failures, and then point out the need for other water resources. The latter may be identified, for example, in small reservoirs, wells, wastewater reuse, and in any case will be handled by the system as geospatial data in the water balance of the basin.

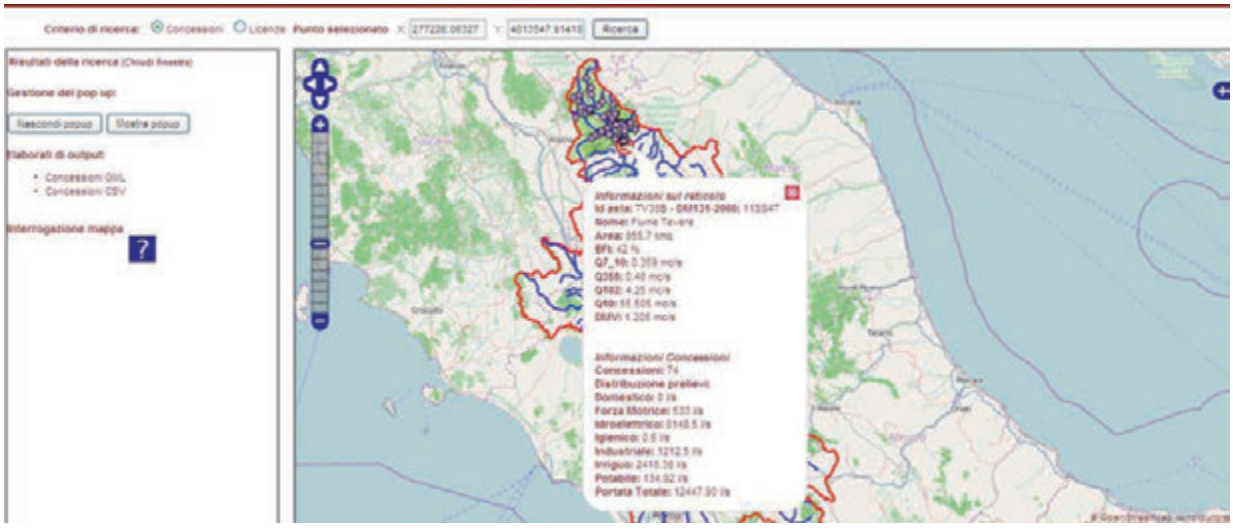

Figure 4. Search example of water withdrawals in a sub-basin versus low flow indeces.

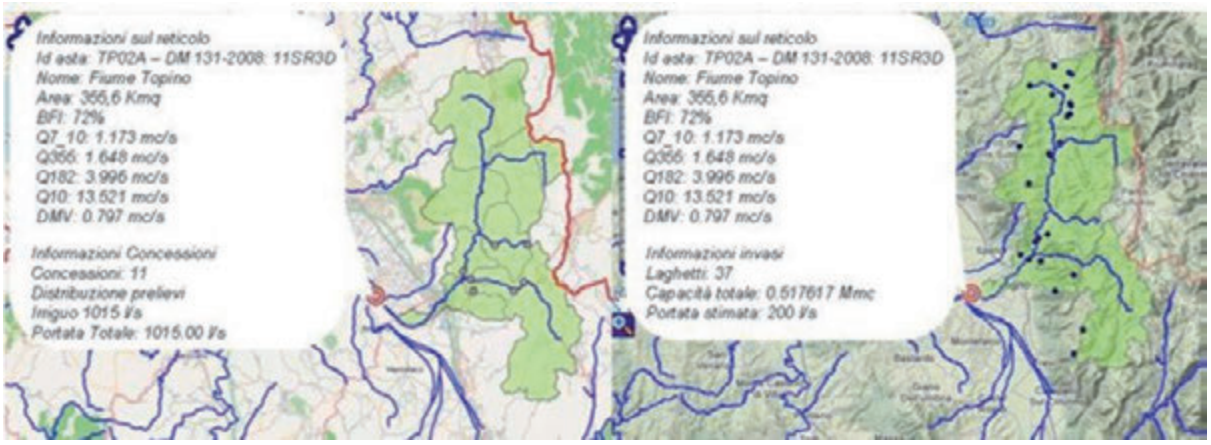

Figure 5. Example of limit condition in water resources management (A) and available water integration from small reservoir (B).

Because of this, the ICT approach and the WebGIS platform represent the added value of the project. The use of algorithmic geospatial analysis within the common GIS software, needs a certain know-how ranging from the use of different data formats to the concept of reference systems, but the overall system is high-performance.

The case study carried on in the Province of Perugia confirms the good performance of the results of the research in the practical field, in particular all the problems underlying the concept of water withdrawal must be assessed carefully, taking into account the existing withdrawals and hydrological situation of the basin concerned.

Future developments cannot only concern techno-scientific investigations, but they will need more information about water resource data management. This problem will involve Institutions and all the stakeholders taking part in the decisional process. This means that only a real and complete sharing of the tool amongst all the participants in the managing process will allow further development in the study and research presented in this paper.

References

Bellezza M., Casadei S., Manciola, P., Pierleoni, A. 2007. Mathematical model for multipurpose water resource management. In: Proc. 22nd European Regional Conference ICID-CIID ERWG Water Resources Management and Irrigation and Drainage Systems Development in the European Environment, Pavia, Italy.

Casadei S. 1995. Analisi dell'indice del deflusso di base (BFI) di alcuni bacini dell'Italia Centrale. Idrotecnica 3: 177-191.

Katz R. W., Parlange M. B., Naveau P. 2002. Statistics of extremes in hydrology. Adv. Water Resour. 25: 1287-1304.

Lvovich M.I. 1972. Hydrologic budget of continents and estimate of the balance of global fresh water resources. Sov. Hydrol. 4: 360-439.

Manciola P., Casadei S. 1991. Low flow index and hydrogeological characteristics. Proc. of the National Conference on Hydraulic Engineering, ASCE, Nashville, July 29-August 2: 930-936.

Manciola P., Pierleoni A., Bellezza M., Casadei S. 2004. Weibull distribution parameters computation in low flow phenomena. Proc. of the IASTED International Conference on Environmental Modelling and Simulation, St. Thomas, US Virgin Island: 192-196.

Ministry of the Environment, 2004. Guidelines for the preparation of the basin water balance and criteria for the water withdrawals evaluation and for the definition of minimum instream flow, art. 22, paragraph 4, of Legislative Decree No. 152 of 11 May 1999. In: Official Journal No. 268, 15/11/2004.

Neteler M., Mitasova H. 2008. Open source GIS: a GRASS GIS approach. 2nd ed., Springer.

Province of Perugia, 2012. Available from: http://demo.t4e.it/pivrid/

Singh K.P., Stall I.B. 1974. Hydrology of 7-day 10-yr low flow. J. Hydraul. ENG-ASCE, 100, 1753-1771.

Sloto R.A., 1991. A computer method for estimating ground-water contribution to streamflow using hydrograph-separation techniques. In: U.S. Geological Survey Water-Resources Investigations. Report 90-4162: 101-110.

Smakhtin V. U. 2001. Low flow hydrology: a review. J. Hydrol. 240, 147-186.

Ubertini L., Manciola L., Casadei S. 1996. Evaluation of the minimum instream flow of the Tiber river basin. Environmental Monitoring and Assessment, vol. 41, n.2, 125-136.

Vogel R. M. and Fennessy N. M. 1995. Flow duration curve II: a review of application in water resources planning. Water Resour. Bull. 31,6, 1029–1039.

Farms as a resilience factors to land degradation in peri-urban areas

Paolo Zappavigna, Andrea Brugnoli

Department of Agricultural and Food Sciences (DISTAL), University of Bologna, Italy

Abstract

The purpose of this study was the analysis of the effects induced by urban pressures on the socio-economic and territorial characteristics of the rural peri-urban areas in order to identify planning and intervention strategies aimed at enhancing the quality of agriculture and landscape. A survey was conducted in the surroundings of Parma on farms located in the vicinity of urban areas. The structural, productive and social characteristics of the family-farm units were analyzed. The survey updated an identical survey, carried out in 1986, in which it was examined a sample of 208 farms. The units surveyed were evaluated in two aspects: the "vitality", which takes into account the structural characteristics (size, production, labour force, etc.), and the "stability", in which a crucial role is played by the age of the conductor and the presence of a successor. It was found that only 28% of the original farm sample is still alive, one third has disappeared, 30% was absorbed by existing farms, 8% has been abandoned. The factors most favourable to the survival resulted those referred to the vitality, especially the physical and economic size of the farm, the presence of cattle, the percentage of land in property, the presence of young labour. Among the factors that predispose to the abandonment, the urbanization processes were found to be determinants, in terms of expansion of both the built-up area and of that planned as urbanisable. The research has highlighted the importance of the vitality of the farms together with a context that has maintained its original rural features. These combined aspects can better define what we call the resiliency of the land-farms system *i.e.* the capability of positively reacting to the variable modifications of the internal and external conditions.

Introduction

The future of the landscape and environment characters of rural land is closely linked to the future of the productive primary structure that determined its identity over time. This is why the preservation of the agricultural space in its typical traits cannot be separated from the maintenance of a substrate of solid and viable farms, especially in areas with high urban pressure where the expectations of ground rent may overcome the much more modest profitability of enterprise.

Who looks with attention to the phenomena of transformation taking place in these areas, must recognize as the dynamic expansion of urban systems has given rise to a type of landscape with very heterogeneous and not uniquely defined characters, in which the signs of agricultural production mingle with the signs of urban activities causing an environmental scenario disarticulated and lacking its own identity. A landscape where intensive farming can coexist with industrial complexes, greenhouses sprout between the nuclei built, the wasteland mingle with emerging neighborhoods, fields tend to lose their attendance warping stripping trees, livestock contracts in few farms survivors.

This state of affairs suggests that a simple passive protection of land use, exclusively entrusted to restrictions of planning tools, is not sufficient to ensure over time the maintenance of landscape-environmental characteristics typical of the places and how the matter should be to leverage the inherent capacity of the agricultural production system to perform its own decisive function for an active protection of the territory. Which means to assign to agricultural enterprises a leading role, often unrecognized, of territorial processes.

Correspondence: Paolo Zappavigna, Department of Agricultural and Food Sciences (DISTAL), University of Bologna, Viale G. Fanin 50, 40127 Bologna, Italy.
E-mail: paolo.zappavigna@unibo.it

Key words: rural areas, periurban, farms, planning.

Journal of Agricultural Engineering 2013; XLIV(s1):e164
doi:10.4081/jae.2013.(s1):e164

Materials and methods

This view, which takes on the farms as co-protagonists of the destinies of the suburban areas, has inspired a research that we conducted in 2011 in Parma hinterland (municipalities of Parma, Collecchio and Sorbolo), as an update of a similar survey carried out in 1986 in the same context, in order to evaluate the effects of the dynamics of urbanization on primary production structure and the surrounding area.

In the first survey 208 farms had been examined by means of questionnaires administered to the conductor, located in different position with respect to the urban perimeter. Twenty-five years later, the survey has been repeated taking as object the same production units in order to ascertain the processes of adaptation/survival put in place by farms to be able to resist the urbanization pressure or, conversely, the degradation processes and the factors, structural or planning, which led to them.

In both surveys, the units surveyed were evaluated in two respects: "vitality" and "stability."

The vitality takes into account the structural characteristics and management activities and is parameterized according to certain thresholds of Standard Gross Margin (RLS), both overall and in relation to the total work units (ULT); stability concerns, on the one hand, the composition of family (with particular attention to the age of the farm manager and the presence of young people) and, on the other hand, the workforce, especially the family labour entity.

With regard to the vitality the following classes of farms have been

defined: a) vital, when both RLS and RLS/ULT thresholds are exceeded; b) potentially vital but unprofitable when the only RLS absolute threshold is exceeded; c) profitable but not autonomous, when only the RLS/ULT threshold is exceeded; d) not vital, when none of the two thresholds is exceeded.

With regard to stability the following types of farms have been defined: stable, tended to be stable, potentially stable, tended to be unstable, unstable.

Combining the two indicators, vitality and stability, three classes of "value" have been identified, in order to obtain a ranking of "merit" for possible protection and support actions on the part of government policies in the area. So the farms have been grouped according to the scheme shown in the following Table 1 and defined as follows: deserving (A), intermediate (B), not deserving (C).

Results

In previous research a dynamic transformation in the territory had been found aiming at the progressive loss of traditional agricultural connotations and the contraction/extensification of production, the more intense the closer to urban areas. However, it was also revealed the existence of a significant number of farms vital and quite stable able to respond to pressure from settlements with a strengthening of their production capacity. On the other hand an important role in order to stay on the farm of rural families was carried out by the strong bond with the land and the high value assigned to live in the country.

The general situation in which the farms are operating has changed however: both in terms of the of settlements growth, further increased and spread, and the conditions under which the production activity takes place (market trends, Common Agricultural Policy). But even more relevant has been, in this period, the continuation of the processes of productive extensification and aging of the workers, which were already established in the previous research The result was, as we shall see further, a significant impairment of the primary production tissue and, consequently, of the territorial scenario pertaining to it.

Without going into a detailed analysis of the results, which will be done in other places, we here briefly indicate the most significant.

The deterioration of the productive structure is evidenced by the following data: the disappearance due to urban expansion of a substantial proportion (about one third) of the units then surveyed, some of which had been regarded as vital; the downgrading of another 30 % consisting of units absorbed by outer companies (mainly due to the advanced age of the owners); the decay of a further 8% of farms that are now managed without labour or simply abandoned.

Only 28% of the old sample is still present and active. A portion undoubtedly modest, but still potentially capable of maintaining even the connotation of rurality at least in some, more preserved, areas of peri-urban belt.

Table 1. Reference scheme for the attribution of the three value classes: A = deserving; B = intermediate; C = not deserving.

	Stable	Tend. st.	Pot. st.	Tend.un.	Unst.
Vital	A	A	B	B	B
Pot. vital	A	B	B	C	C
Prof.not aut.	B	B	C	C	C
Not vital	B	C	C	C	C

In fact, this sample, which appeared then mainly composed of vital and stable units, over time has become differentiating in two opposites addresses: a portion of farms where the aging process has led to a situation of high instability (manager and family very elderly); a portion, while smaller, of farms which have chosen the path of expanding the production capacity and income (also as a result of a fairly frequent replacement of families) reaching today an even higher level of vitality and stability. Such farms able to strengthen the policies for protecting the quality of landscape and environment are mainly located in the outer bands of the survey area, but there are some really interesting in the vicinity of the settled areas.

Among the factors that most influenced the evolution of the productive structure, urban sprawl is by far the one that led to the disappearance of most farms; on the other hand, the factor that has acted more favourably on permanence of survived farms was the, objective, structural consistency (size and profitability) of the farms, rather than the, subjective, composition of the family unit and its active involvement in agriculture (they are also companies which had in the past a low age of workers).

Among the new elements that have come to light, there was a phenomenon of the incorporation of many companies which were in the past autonomous in other companies, valid and vital, located in outer areas; an absorption process that we might consider of "farm relocation", which places these units in a limbo from which it will be difficult to come back to a new production autonomy. It is, however, a phenomenon that has not only negative aspects as it has enabled a significant enhancement of the "absorbent" farms. An ad hoc survey actually showed how these farms are equipped structurally and sociologically to a great vitality with a strong presence of youth. In these cases the divestiture has not resulted in the productive abandonment, but has indeed kept alive the agricultural activity and offered a possibility of strengthening and survival to other companies potentially better equipped and able to offer a more stable future to the adjacent territorial context.

There are however various signals that indicate how much of the surviving companies are in a situation which is still in transition, starting with the persistence of the aging processes and productive extensification (*e.g.* loss of cattle).

Of these signals, we can include also the novelty of some farms whose owners perform functions related to agriculture, but paying almost exclusively their work outside and then using the farm only as a home base for their activities (contractors, traders).

Turning our attention to the territory, the reading of the transformations of primary production, plus the analysis of the processes of urban sprawl and planning decisions taken in the period made it possible to highlight some important features in significant parts of the peri-urban space. In fact, some spatial sectors which remained not affected by the development of the city are clearly put into evidence, where the farm tissue and landscape are still quite intact.

These areas, mainly composed of four country wedges that penetrate so landlocked in the urban area, have proved to be strategic areas for a conversion of planning tools to take on the agricultural production as a factor structuring the decisions regarding the management of territory.

Discussion

Compared to the previous investigation, the research has brought to light some limitations of the classification adopted at the time, which was based on the capacity of the individual farming units to withstand external stresses, measured through an equal combination of vitality and stability indicators, as determined on the basis of the situation

existing on the date of the survey.

Indeed, if we assume a vision of perspective, which looks at trends of medium to long term by trying to define (promote) desirable future scenarios, it must be recognized that the concept of "resistance" which briefly is the expression of the two indicators mentioned above presents limitations arising from the fact that the judgment on the merits, operated according to this principle, is based on an examination of the status quo referred to a given period. It has been seen that the evolutionary dynamics that have affected our farms in the past quarter-century have led to strong changes the original structure, in particular the family organization and farm management, often mainly for their intrinsic reasons, primarily the natural tendency to aging of household members; regardless of the external pressures.

On the other hand, the state of affairs in a given period is inevitably destined to change in time for the changing external conditions: market trends, agricultural and planning policies, technological and production innovation, social expectations etc..

A search that intends to foreshadow more sustainable future organization should therefore refer not so much to a current survival capacity corresponding to the conditions detected at a given time, as an ability "potential" to develop suitable alternative arrangements able to react positively to the possible amendments to the socio-economic and environmental scenario. Modifications which, in addition to family structure (including the possible exit of the managing family), may relate with the different public policies (planning, grants, etc..), the integrations with productive chains, the new opportunities offered by the multi-functionality, with particular reference to the urban proximity etc..

This observation has led us to reduce the importance given in the past to the criterion of farm stability (based, as we have said, on the family conditions and labour supply) because highly variable over time, and give greater weight, decisive for our purposes, to the criterion of viability, based mainly on longer-lasting structural characteristics.

This indicator, indeed, proved to be able to justify by itself the permanence of most farms survivors. It is demonstrated on the one hand by the fact that many of the surveyed farms are still fully functional even if run by families very old (in this, probably also thanks to the contribution of families co-inhabitants, a situation greatly increased in the period). On the other hand it is confirmed by a new phenomenon observed, *i.e.* taking charge of some divested farms by other more viable farms; phenomenon which, in addition to having propitiated an increasing efficiency of incorporating farms, has allowed to maintain unchanged the physical-environmental context of the absorbed ones. Even a phenomenon that can affect much on profitability, which is the significant reduction of the cattle husbandry (more than halved in the meantime), it was not enough, for the farms involved, to determine the abandonment of production.

Based on these considerations, we considered it more appropriate to replace the concept of resistance with the concept of "resilience" of the system farms-territory, meaning by this term the susceptibility of a given socio-economic and environmental organization to react positively to changes in external conditions, to grasp opportunities for development and innovation, to be able to create a new, more adaptable and durable structure: in both farming and territorial level.

On this basis, and on the basis of the findings of our research, we could distinguish, as useful for our purposes, two different levels of resilience: a farm level, which measures the ability to provide a positive response to the expected/possible changes according to objective and subjective (to a lesser extent) conditions existing in individual enterprises; a territorial level, in which the positive response to changes (*i.e.* consistent with a given project on the area) depends on the integrity and the favourable disposition of the spatial and environmental context.

The synergistic presence of both conditions, *i.e.* strength of the family-farm unit and integrity of the territory of belonging, can significantly increase the potential capacity of resilience of the system land-farms.

A situation of this type has been highlighted by our research which has put into evidence important portions of the territory where the absence of expansionary actions of the city, the preserved integrity of land organization and the presence of a farm tissue alive and vital have positively contributed to the maintenance of the original connotation of rurality and of its landscape-environmental values. These areas may, in our opinion, be considered as primary for the protection and support on the part of government policies.

Conclusions

The considerations made suggest an original method to select the areas of intervention of territorial policies and offer guidance to develop the most appropriate strategies.

Beside the structural and social endowment of individual farms become also important, on a larger scale, some factors (structural and locational) that can make farms, situated in areas subject to external pressure, vital and profitable. For example, greater importance is assumed by: a) the size of the farm rather than the presence of animal husbandry; b) the localization in the context of particular attractiveness and/or accessibility for the urban population; c) the ability to offer products to the consumer citizens (zero km); d) the ability to perform multiple integrative activities, even non-agricultural; e) the possibility of offering services to the city functions as recreation and ecological regeneration; f) the sensitivity to the distribution of public funds.

With these assumptions innovative policies can be put in place for the protection and development of the territory, where in particular the rural areas better preserved should be taken into account rather than those compromised and the areas with a widespread presence of farms with high level of vitality rather than those with a prevalence of farms without autonomous capacity. Thus realizing integrated and efficient systems which ensure, with their own resources, permanence and development in the near and long term future. So configuring an active integrated protection of which the defensive actions of territorial planning will only become a prerequisite.

In this view, resilience is configured as a criterion of judgment and operating especially useful in areas where there are competitive factors and criticality. The rural development measures will act more effective if aimed at increasing resilience in a territorial sense.

Bibliography

Ambrosio-Albalá M., Bastiaensen J. 2010. The new territorial paradigm of rural development: Theoretical foundations from systems and institutional theory, *Discussion Paper/2010.02*. pp. 1-68. http://www.ua.ac.be/objs/00251118.pdf.

Arzeni A., Sotte F. 2013. Imprese e non imprese nell'agricoltura italiana. Una analisi sui dati del Censimento dell'Agricoltura 2010*, Working paper Gruppo 2013*, n.20, marzo 2013. www.gruppo2013.it

Brugnoli A. 1990. Valutazione dell'impatto urbano sulla struttura produttiva agricola, *Genio Rurale*. 4: 52-64.

Brugnoli A., Zappavigna P. 1991. Strutture agricole e sistemi urbani: indagine su aree periurbane del parmense, in Maggioli U. (a cura di), *Trasformazioni d'uso del suolo agricolo*, Milano, Franco Angeli. pp.173-226.

Ministero delle politiche Agricole Alimentari e Forestali (Mipaaf). 2010. *PSN 2007-13 Piano strategico nazionale per lo sviluppo rurale,* testo approvato dalla Conferenza Stato-Regioni del 2 ottobre 2010

http://www.regione.toscana.it.
Pascucci S. 2008. Agricoltura periurbana e strategie di sviluppo rurale: una riflessione, in *QA Rivista dell'Associazione Rossi-Doria.* 2.
Quaranta G., Salvia R., (2012) Resilienza e politiche di sviluppo nei sistemi socio-ecologici rurali, *Territori*, anno III, giugno 2012: 2-8.
Torquati B., Giacchè G., Musotti F., Taglioni C. 2009. Agricoltura periurbana tra adattamento aziendale, funzioni riconosciute e funzioni percepite, *Rivista di Economia Agraria,* a. LXIV, 3-4: 401- 441.
B. Walker, C. S. Holling, S. R. Carpenter, A. Kinzig. 2004. Resilience, Adaptability and Transformability in Social-ecological Systems, *Ecology and Society* 9 (2). 5:1-9. http://www.ecologyandsociety.org/vol.9/iss2/art5/

Alternative method for vegetables cultivation in Benin

Lucia Recchia,[1] Paolo Boncinelli,[2] Enrico Cini[1]

[1]Dipartimento di Gestione dei Sistemi Agrari, Alimentari e Forestali (GESAAF), Università degli Studi di Firenze; [2]Consorzio per la Ricerca e la Dimostrazione sulle Energie Rinnovabili Re-CORD, San Casciano Val di Pesa (FI), Italy

Abstract

In the developing countries populations, which are already vulnerable and food insecure, are likely to be the most seriously affected by the effects of climate change, *e.g.* yield decreases and price increases for the most important agricultural crops. The IPCC's Fourth Assessment Report for Africa describes a trend of warming at a rate faster than the global average and increasing aridity: in many parts of Africa, it seems that warmer climates and changes in precipitation will destabilise agricultural production and aggravates food security. The present work concerns the vegetables cultivation in the Parakou region in Benin, where agriculture employs approximately 70% of the active population and contributes to 36% of the Gross Domestic Product and 88% of export earnings. However, the agricultural sector has been regarded as unproductive with low adaptation capacities because of structural factors (*e.g.* high level of poverty among rural populations, weak mechanization and intensification of production modes), but also because of natural constraints (*e.g.* poor management of water and soils, leading to soil degradation). Considering the aridity, the low carbon content and the reduced level of nutrients available in the soil, the use of an hydroponic module has been hypothesised. In this way sufficient yields of the crops may be assured and no agricultural machines will be needed for the tillage operations. In addition, the nutrients can be added to the growing solution using residual materials as poultry manure, ashes and green wastes. In order to verify if some construction or maintenance problems can occur and if a growing solution can be easily obtained using agricultural wastes, some tests have been carried out. Moreover laboratory analyses have been done for different solutions that may be adopted with different shares of water, poultry manure, ashes and green wastes. The tests have indicated that the hydroponic module could be used in Benin without incurring in technical problems and that a growing solution containing poultry manure, ashes and green wastes can supply to the crops a significant amount of nutrients.

Correspondence: Lucia Recchia, Dipartimento di Gestione dei Sistemi Agrari, Alimentari e Forestali (GESAAF), Università degli Studi di Firenze, P.le delle Cascine 15, 50144 Firenze, Italy.
Tel. +39.055.3288315 - Fax: +39.055.331794.
Email: lucia.recchia@unifi.it

Key words: vegetables, hydroponic cultivation, African food security.

Acknowledgements: authors wish to acknowledge Mr. Riccardo Pempori and Mr. Federico Lotti which developed their Master Thesis of Agriculture in Benin, such as Eng. Badii which funded the research project on the implementation of simplified hydroponic systems in Parakou, Benin.

Journal of Agricultural Engineering 2013; XLIV(s1):e165
doi:10.4081/jae.2013.(s1):e165

Introduction

In the developing countries populations, which are already vulnerable and food insecure, are likely to be the most seriously affected by the climate change (Nelson *et al.*, 2009), *e.g.* yield decreases and price increases for the most important agricultural crops. The IPCC's Fourth Assessment Report for Africa (Ziervogel et al, 2008) describes a trend of warming at a rate faster than the global average and increasing aridity: in many parts of Africa, it seems that warmer climates and changes in precipitation will destabilise agricultural production and aggravates food security. Moreover, the impacts of climate change are evident and mostly felt by the rural poor who depend on rainfed agriculture for their livelihood. Although farmers are aware of climate change and adapt differently, many are still very vulnerable in their production systems: it seems that more than 30% percent of farmers do not employ any adaptation method on their farms (Onyeneke and Madukwe, 2010). Despite the urgency of adapting to climate change, a number of factors impedes effective actions in developing countries, *i.e.* the low level of awareness of climate change and its risks, the lack of knowledge, the poor sharing.

Considering all these assumptions, the present work concerns a simple proposal for improving the vegetables cultivation in the Parakou region by means of introducing a simple system based on the hydroponic method. Particularly, a simplified hydroponic system has been proposed and tested: in fact, advanced hydroponic systems can be intensive and expensive, but the simplified ones are much simpler and cheaper with low operational and maintenance costs. Even if yields from such systems are lower in comparison to the advanced hydroponics, the yield still outweighs the regular farming yields.

The main aim of the simplified hydroponics is for a family to be able to feed itself and to produce a small income; it is appropriate for low-resource populations; it uses very low cost, simple technology; it requires almost no investment; it allows the growth of a wide variety of vegetables (*e.g.* lettuce, tomatoes, carrots, garlic, aubergine, beans, radish, leek, strawberries, melons, etc.). In brief, the hydroponic vegetable production presents the following advantages:

- the produced vegetables can be of high quality and need little washing. The produced fruits and vegetables have a high biological and nutritional value, since they are harvested immediately before their use;
- no good soil to grow vegetables is needed;

- soil preparation and weeding is almost eliminated;
- the production presents very high yields because of the optimisation of the environmental conditions;
- the water is used efficiently;
- it is a low-cost and easy-to-learn technique.

The scope of the present work depends on the statement that in Benin, agriculture employs approximately 70% of the active population and contributes to 36% of the Gross Domestic Product and 88% of export earnings. However, the agricultural sector has been regarded as unproductive with low adaptation capacities because of structural factors (*e.g.* high level of poverty among rural populations, weak mechanization and intensification of production modes), but also because of natural constraints (*e.g.* poor management of water and soils, leading to soil degradation). Moreover, the soil of the small farms is often poor of nutrients and organic substance. Based on the aridity, the low carbon content and the reduced level of nutrients available in the soil, the use of an hydroponic module has been hypothesised, taking into account the necessity of reducing costs for the plant production and the system management.

Materials and methods

Description of the farm

The farm selected for this study was previously analysed and characterised by the University of Florence (Pempori, 2009). It is located in the S.Francisco Domaine, about 500 meters from the road that connects Parakou with Beterou (RNIE6) in Benin. The area is characterized by an increasing human presence living in small clusters of mud houses; the agriculture is mainly characterised by small plots of corn, peanut, soybean, sesame (*Sesamum indicum*) and yam. The vegetation is dense, usually dominated by tall grass (*Imperata cylindrica, Striga spp.*) and shrubs of various species (see Figure 1). Concerning the farm, arranged at random along its whole extension, there are various trees of cashew (*Anacardium spp.*), mango (*Magnifera indica*), shea (*Vitellaria paradoxa*), papaya (*Carica papaya*) and neem (*Azadirachta spp.*).

The climate is characterized by a few rainy days, with a reduced average monthly rainfall, as illustrated in Table 1. Taking into account these aspects and the presence in the farm of poultry manure and agroforestry residues, it was assumed to perform a simple hydroponic module to save water and agricultural land, allowing the reuse of wastewater directly into the field.

Description of the tests

The work is based on the results of two Master Thesis developed in 2009 (Pempori, 2009; Lotti, 2009) with a close collaboration with the local NGO Envole Afrique, that have permitted a detailed collection of climatic, agricultural and socio-economic information about the Parakou province. The work has been privately founded and developed by the GESAAF Department of the University of Florence with the support of the Re-Cord consortium for the laboratory analyses.

Firstly, a market research has been carried out identifying the adeguate hydroponic system according to the operative conditions of the typical farms in Parakou. In general two different hydroponic systems are used to produce vegetables: the open bag, or drain to waste system, and the gravel flow, or re-circulating system. In the drain to waste system, the plants grow in containers and the nutrient solution is supplied to plants by means of a dripper, for up to 12 times per day. In the gravel flow system, the nutrient solution is re-circulated and the roots of the plants stand in a thin film of nutrient solution all the time. Gravel or sand is used most often as growth medium.

Figure 1. Example of vegetation of the farm in S. Francisco Domaine, Parakou, Benin.

Figure 2. Well of the farm in S.Francisco Domaine, Parakou, Benin.

Table 1. Climatic data in Parakou, Benin, as monthly average of historical data from 1961 to 1990 (Source: http://gb.weather.gov.hk).

	Jan	Feb	Mar	Apr	May	Jun	Jul	Aug	Set	Oct	Nov	Dec
Maximum temperature (°C)	34.1	36.0	36.2	34.9	32.8	30.7	29.2	28.6	29.5	31.5	33.6	33.6
Average temperature (°C)	26.5	28.7	29.6	29.0	27.5	26.1	25.1	24.7	25.0	26.1	26.6	26.1
Minimum temperature (°C)	18.9	21.3	22.9	23.1	22.2	21.4	21.0	20.8	20.5	20.8	19.7	18.5
Precipitation (mm of rain)	3.8	9.2	39.4	85.5	130.8	172.0	189.9	208.8	205.6	91.1	6.3	6.6
Days of rain (n°)	0	1	3	5	9	11	12	13	15	7	1	1

Considering that the technological level of the farms is very low as also the farmers knowledge, a gravel flow system has been preferred, bought and installed in a plot in Florence, Italy. The experimented system is provided by an automatic irrigation: a water tank is filled and then, thanks to gravity, the water is distributed to the plants. This layout is completely replicable in the S.Francisco Domaine where the water may be pumped from the existing well to the collection tank (see Figure 2).

Moreover, different growing solution have been applied, all obtained reusing residuals and wastes available in a typical farm of Parakou, adequately shredded and mixed with water:

- only poultry manure (100%);
- green residuals (88%), poultry manure (6%), ash (6%);
- green residuals (94%), poultry manure (3%), ash (3%).

Particularly, the green residuals consist of wood pruning and herbaceous crops residues. In order to measure the pH, the nutrients and the micro-elements, the different growing solutions have been analysed.

Table 2. Results of the chemical analyses of a sample for 1.5 liters of the growing solution with poultry manure (100%). The analyses have been carried out by the Re-Cord laboratory on Febrary, 20th 2012.

Parameters	Value	Analysis method
pH (sample as received)	10.70	-
pH (filtered sample)	9.93	-
Nitrogen (N)	4.1 g/L	UNI EN ISO 10304-1
Phosphorus (P)	110.4 g/L	UNI EN ISO 10304-1
Potassium (K)	19.9 mg/L	AAS method
Calcium (Ca)	6.8 mg/L	AAS method
Magnesium (Mg)	0.2 mg/L	AAS method
Sodium (Na)	4.3 mg/L	AAS method

Table 3. Results of the chemical analyses of a sample for 1.5 liters of the growing solution with green wastes (88%), poultry manure (6%) and ash (6%). The analyses have been carried out by the Re-Cord laboratory on August, 27th 2012.

Parameters	Value	Analysis method
pH (sample as received)	7.68	-
pH (filtered sample)	8.02	-
Nitrogen (N)	2.7 ppm	UNI EN ISO 10304-1
Phosphorus (P)	12.0 ppm	UNI EN ISO 10304-1
Potassium (K)	47.7 ppm	UNI EN 15290 (adapted)
Calcium (Ca)	8.5 ppm	UNI EN 15290 (adapted)
Magnesium (Mg)	7.7 ppm	UNI EN 15290 (adapted)
Sodium (Na)	5.7 ppm	UNI EN 15290 (adapted)

Table 4. Results of the chemical analyses of a sample for 1.5 liters of the growing solution with green wastes (94%), poultry manure (3%) and ash (3%). The analyses have been carried out by the Re-Cord laboratory on August, 27th 2012.

Parameters	Value	Analysis method
pH (sample as received)	7,98	-
pH (filtered sample)	8,14	-
Nitrogen (N)	3,0 ppm	UNI EN ISO 10304-1
Phosphorus (P)	21,7 ppm	UNI EN ISO 10304-1
Potassium (K)	103,7 ppm	UNI EN 15290 (adapted)
Calcium (Ca)	15,3 ppm	UNI EN 15290 (adapted)
Magnesium (Mg)	6,4 ppm	UNI EN 15290 (adapted)
Sodium (Na)	12,1 ppm	UNI EN 15290 (adapted)

Results and discussion

Considering that the performances of the gravel flow hydroponic system depends on the hydraulic behaviour, the system has be monitored for about 6 months and no obstructions have been noticed.

Tables 2, 3 and 4 report the results of the chemical analyses of the different growing solutions.

As results shown, the mixture of water and only poultry manure indicates that in order to correct the pH, the addition of some vegetable component for acidifying is needed. In fact a proper pH value allows the plants to absorb the right nutrients for healthy growth. Moreover, the precise value of pH that determines the precipitation of macro-nutrients is due to the combined concentrations of calcium and sulfate: for instance, if the pH of the solution is too high, greater than 6.5-7.0, a precipitation of salts not absorbed by plants could stop the irrigation system.

Conclusions

The hydroponic system constitutes a good response to the agricultural difficulties in the Parakou region: sufficient yields of the crops may be assured and no agricultural machines will be needed for the tillage operations. Moreover, the proposed solution does not provide the use of chemical fertiliser, promoting the use of residual materials, as poultry manure, ashes and green wastes, that may be added to the growing solution.

Therefore, in order to verify if some construction or maintenance problems can occur and if a growing solution can be easily obtained using agro-forestry wastes, some tests have been carried out. Moreover laboratory analyses have been done for different water solutions that may be adopted mixing with different shares of water, poultry manure, ashes and green wastes.

The tests have indicated that the hydroponic module could be used without incurring in technical problems and that a growing solution containing poultry manure, ashes and green wastes can supply to the crops a significant amount of nutrients. In substance, the present study, developed at the request of the NGO Envole Afrique and privately funded, highlighted that a business improvementis feasible, also at limited or no cost. Only few years ago, this type of project was not considered viable for the implementation; currently, mainly because of the increased difference between rich and poor areas, *i.e.* between rich farmers and farmers who derive from agriculture the only chance of survival, the outlook seems completely opposite.

For this reason, based on the positive results obtained, a future development and implementation of the work carried out is expected: Table 5 reports a synthesis of the structure and the objectives for the future project.

Table 5. Main structure and objectives of the future project, developing and implementing the present work.

	Operational logics	Indicators verifiable	Validation sources	External conditions
General objective	Contribution at the improvement of the food security and the living conditions in rural areas of Parakou			
Specific objective	Increasing and diversification of the agricultural production within the Domaine San Francisco through the cultivation of new areas	- At the end of the project 500 m^2 of land are allocated to vegetable crops - The local NGO Envole Afrique choose a technician specifically trained for the maintenance of the cultivated area	- Technical reports, administrative and project monitoring - Statistical data - Photographic documentation	- Climatic conditions in accordance with the historical data - Choice of the staff
Results	Result 1: Construction of a small irrigation system Result 2: Preparation of an area of 500 m^2 for vegetables production	- After the installation and the start-up of the hydroponic kit, the irrigation system is functioning and the whole area has been cultivated put under cultivation the area identified	- Daily technical report of the construction and the maintenance of the hydraulic system - Daily technical report on the management of the agronomic practices - Photographic documentation	- Climatic conditions in accordance with the historical data - Availability of the water - Retrieval of all the tools and materials needed
Topics	Topic 1: - Identification of the site and construction of the irrigation system - Training of personnel on the operation and maintenance of the tank and the plant Topic 2: - Tillage in an area of 500 m^2 and sowing of various horticultural crops			

References

Lotti, 2009. Lotti F. Insediamento agroproduttivo in Benin: primo approccio di analisi per filiera, Master Thesis of Agriculture, University of Florence, 2009.

Nelson *et al.*, 2009. Nelson GC, Rosegrant MW, Koo J, Robertson R, Sulser T, Zhu T, Ringler C, Msangi S, Palazzo A, Batka M, Magalhaes M, Valmonte-Santos R, Ewing M, Lee D. Climate change: impact on agriculture and costs of adaptation. International Food Policy Research Institute, Washington D.C., October 2009.

Onyeneke and Madukwe, 2010. Onyeneke RU, Madukwe DK. Adaptation measures by crop farmers in the southeast rainforest zone of Nigeria to climate change. Science World Journal, 2010, 5(1):32-34.

Pempori, 2009. Pempori R. Insediamento agroproduttivo in Benin: proposte progettuali di strutture per l'allevamento zootecnico, Master Thesis of Agriculture, University of Florence, 2009.

Ziervogel *et al.*, 2008. Ziervogel G, Taylor A, Hachigonta S, Hoffmaister J. Climate adaptation in southern Africa: addressing the needs of vulnerable communities, Stockholm Environment Institute, Commissioned by Oxfam GB, July 15th, 2008.

Aerated lagooning of agro-industrial wastewater: depuration performance and energy requirements

Serafina Andiloro, Giuseppe Bombino, Vincenzo Tamburino, Demetrio Antonio Zema, Santo Marcello Zimbone

Department "AGRARIA", "Mediterranea" University of Reggio Calabria, loc. Feo di Vito, Reggio Calabria, Italy

Abstract

Intensive depuration plants have often shown low reliability and economic sustainability, when utilised for agro-industrial wastewater treatment, due to the particular wastewater properties: high organic load and essential oil concentrations, acidity, nutrient scarcity and qualitative-quantitative variability of effluents. Aerated lagooning systems represent a suitable alternative, because they are able to assure good reliability and low energy requirements, avoiding the drawbacks shown by the intensive depuration plants. In order to optimize performance of the lagooning systems, particularly in terms of energy requirements, depuration processes of aerobic-anaerobic aerated lagoons were investigated, both at full- and laboratory-scale. Citrus processing wastewater were subject to bubble aeration with low flow rates and limited time; the removal rate of organic load was evaluated and energy requirements of different depuration schemes were compared. The experimental investigations in full-scale aerated lagoons showed a low energy supply (0.21-0.59 kWh per kg of COD (Chemical Oxygen Demand) removed with an average value of 0.45 kWh kg_{COD}^{-1}), an adequate equalisation capability and constantly good depurative performance also with high concentrations of essential oil (500-1000 ppm). The experimental investigations in lab-scale aerated tanks under controlled conditions indicated the possibility of decreasing energy requirements (down to 0.16 kWh kg_{COD}^{-1}) by reducing aeration power (down to 0.6 W m^{-3}) and limiting aeration time to night 12 hours only, when energy price is lower. In spite of the low aeration, the COD removal rates were on the average six-fold higher compared to the anaerobic tank. Other outcomes indicated an ability of the spontaneous microflora to adapt to high concentrations of essential oils, which however did not provide an increase of the removal rate of the organic load in the experimented scheme.

Correspondence: Demetrio Antonio Zema, Department "Agraroa", "Mediterranea" University of Reggio Calabria, loc. Feo di Vito, I-89124 Reggio Calabria, Italy.
E-mail: dzema@unirc.it

Key words: aerated lagoon, agro-industrial wastewater, depuration, energy requirement, essential oil, Chemical Oxygen Demand.

Acknowledgements: this work was supported by the research project "PRIN 2008 - Depuration and Reuse of Citrus Processing Wastewater" (Scientific responsibility: Vincenzo Tamburino).

Contributions: the contributions of the authors to this work can be considered equivalent.

Journal of Agricultural Engineering 2013; XLIV(s1):e166
doi:10.4081/jae.2013.(s1):e166

Introduction

Depuration of citrus processing wastewater (water from washing fruits machinery, and floors as well as from the extraction of juice and essential oils, peel drying and cooling, Kimball, 1999) poses heavy environmental and economic difficulties, because of high essential oil (EO) content, high oxygen demand and energy requirement, high acidity, lack of nutrients and qualitative and quantitative variability.

Citrus processing wastewater, like other agro-industrial effluents, have been often depurated in intensive biological plants, mainly by activated sludge, often designed by the same criteria used for urban wastewater depuration, which neglect peculiar citrus wastewater characteristics. These intensive depuration processes have often shown low reliability and high energy costs. In order to overcome the drawbacks of the intensive plants and lower the energy requirements, aerated lagooning systems have been proposed for such kind of wastewater with positive results (Tamburino *et al.*, 2007; Van Dyke *et al.*, 2003).

In aerated lagoons, wastewater is usually stored in large and deep basins with long retention time (Jail *et al.*, 2010). The most common lagoons are aerobic-anaerobic with low-intensity aeration (less than 2.5 W m^{-3}) determining low concentrations of dissolved oxygen (DO) and suspended solids; the sludge settles at the bottom where it is subject to anaerobic digestion. Biological processes in aerated lagoons do not require the constant settleability of sludge large flocs, as required by activated sludge plants; in these plants sludge settlement is a crucial phase which is negatively affected by EO concentrations over 50 ppm, high COD/N/P ratios and low DO concentrations (Tamburino *et al.*, 2007; Bombino *et al.*, 2009)

In order to enhance reduction of energy requirements, the management operations of aerated lagooning systems should be further investigated. To this aim, in this paper depuration processes of citrus processing wastewater were investigated at full scale (in an aerobic-anaerobic aerated lagoon) and at laboratory scale (in aerated tanks simulating the aerobic surface layer of an aerated lagoon under controlled environmental conditions), in order to evaluate the performances and energy efficiency of lagooning systems with different aeration rates and times as well as EO oil concentrations.

Materials and methods

Full-scale investigation

The investigations were carried out in an aerobic-anaerobic aerated pond of a lagooning system treating effluents of a medium-size citrus processing company. The aerated lagoon depurated the citrus processing wastewater with the highest organic load (up to 20-30 g L^{-1} of COD) and EO concentration (over 600 ppm).

The lagoon (Figure 1) consisted of an earth pond with plastic waterproofing; the storage volume was 10.000 m^3 and the lagoon maximum depth was 7 m. Aeration was ensured by 1-3 floating aerators, each one with an electric power equal to 15 kW, operating only during the night hours and the week-end. The aeration intensity was in the range 1.4-4.1 W m^{-3}, depending on the number of floating aerators contemporarily operating. The electrical energy supply was setup to maintain a low concentration of dissolved oxygen in the wastewater surface layer (0.3-1.5 mg L^{-1}), which maximizes the oxygen transfer efficiency to the aerobic surface layer, but avoids bad smell exhalation from the deep anaerobic layer.

Since 2006 to 2010 the values of pH, DO and temperature of the stored wastewater were automatically surveyed each 6 hours from April to December, while the COD and EO concentrations were monthly measured; the amount of electric energy supplied and the aeration time were also evaluated.

Laboratory-scale investigations

Citrus processing wastewater was treated from July 2010 to February 2011 (first cycle, 240 days) and from December 2011 to June 2012 (second cycle, 210 days) in an experimental depuration plant, consisting of cylindrical 1-m^3 tanks simulating the aerobic layer of an aerobic-anaerobic lagoon (Figure 2).

In the following discussion each tank will be indicated by the symbol "$T_{xx, xx, xx}$", where: the first two numbers of the subscript refer to either the position of the air diffuser ("0" for positioning above the tank bottom and "1/2" for placing at mid-depth) or other information about the experimental conditions ("IN" for tank with "*inoculum*" wastewater and "NA" for the tank not aerated); the intermediate numbers refer to the air flow rate ("7" or "14" L m^{-3} h^{-1}); and the final two numbers refer to the aeration time ("12" or "24" hours). For example "$T_{1/2, 7, 12}$" indicates the tank with the diffuser placed at mid-depth and subject to an air flow rate of 7 L m^{-3} h^{-1} supplied for 12 hours per day. Finally, in the case of equal experimental conditions (for example for the tanks "$T_{0, 7, 12}$" a superscript has been added ("I" or "II") indicating the first ("I", 2010-2011) or second ("II", 2011-2012) depuration cycle.

All tanks, except one ($T_{NA, 0, 0}$) were subject to fine bubble aeration through an air diffuser fed by a blower (Table 1). The air flow rates and the power per volume unit (0.6-1.2 W m^{-3}) felt among the lowest values adopted in aerated aerobic-anaerobic lagoons at full scale.

During the first depuration cycle the energy requirements under different aeration times (permanent, *i.e.* 24 hours per day, in the tank $T_{0, 7, 24}$, or limited to the 12 night hours, in the other aerated tanks) was evaluated. After six months, the EO concentration of wastewater in the tank $T_{0, 7, 12}$ was gradually increased up to 1400 ppm by weekly additions of 100 ppm.

During the second cycle the intermittent aeration, which provided the highest OM removal rates in the previous cycle, was setup. Air flow was provided by a fine bubble diffuser fed by a blower; the diffuser was placed 5-cm above the bottom (0.85-m deep below the wastewater surface, Figure 2a) in all tanks, except for tank $T_{1/2, 7, 12}$. In this latter the diffuser was placed at mid-depth with the lower anaerobic layer partially separated by the upper aerobic one by a wood disk, thus limiting wastewater mixing due to air bubble lift (Figure 2b).

Fifty per cent of the wastewater in one tank ($T_{IN, 7, 12}$) was an *inoculum* consisting of citrus wastewater from the previous depuration cycle and containing a spontaneous microflora already adapted to EO concentration in the range 600-1000 ppm. One tank ($T_{NA, 0, 0}$) was not aerated.

A preliminary characterisation of the wastewater showed an initial COD concentration close to 5-6 g L^{-1}. The ratio COD:N:P was close to 600:5:1. During the experiment, in order to restore COD consumed by microorganisms, COD was kept in the range 3-12 g L^{-1}, adding periodically organic matter as saccharose, in order to assure food for microorganisms. Initial EO concentrations, close to 500 ppm, were always kept in the range 300-600 ppm by adding periodically EO.

The mean values of wastewater temperature ranged from 11.3 °C (January) to 29.4 °C (August) in the first cycle and from 7.4 (February) to 29.5 (June) in the second cycle.

During the depuration cycles the COD and the EO concentrations of wastewater were evaluated every month on 0.5-L samples of supernatant (in duplicate) using standard methods (APHA 1998; Scott and Veldhuis 1966). Dissolved Oxygen, temperature and pH of wastewater were measured weekly (or daily, after EO addition), 0.3 m under the wastewater surface, using a digital multimeter (HACH Lange HQ40).

In order to estimate the oxygen transfer to wastewater, the oxygen deficit was calculated as the difference between the saturation concentration at the measured temperature and the actual DO concentration. The ratio between the energy supplied and the measured COD removal rates was calculated to estimate energy requirement in the aerated tanks.

Figure 1. The full-scale aerobic-anaerobic aerated lagoon under investigation.

Results and discussion

Full-scale investigation

The initial acidity of wastewater (pH = 3.3-4, Table 2), which disturbs activated sludge processes (Tamburino *et al.*, 2007; Bombino *et al.*, 2009), was due to organic acid components of citrus fruits and the lactic fermentation of sugars and other carbohydrates, producing organic acids under oxygen shortage. The depuration processes acting in the aerated lagoon progressively increased the pH up to the final values of 4.8-8.3, Table 2), due to degradation of organic acids, and reduced the EO concentrations (on the average by 88%, Table 2). EO

concentration generally higher than 600 ppm (with peaks of 1000 ppm) never slowed down depuration processes; conversely, in activated sludge plants biological instability has been described when EO concentrations are higher than 50 ppm, due to their antimicrobial activity (Lane, 1983; Ratcliff, 1990; Kimball, 1999). No bad smell exhalations (typical of anaerobic processes) were detected in proximity of the lagoon thanks to the aeration of the surface layer.

The investigation showed a good depuration capacity of the organic load with a COD removal efficiency from 59% (in 2010) to 97% (in 2006); the COD removal rates varied from 0.59 (in 2010) to 2.50 (in 2007) g L^{-1} $month^{-1}$, with a high variability due to:

- the effects (contrasting each others) of COD settling and releasing from sludge in the lagoon bottom;
- the incidence of anaerobic processes in the lagoon bottom with respect to aerobic degradation in the surface layer;
- the variation in aeration times and intensity, this latter depending from the number of floating aerators contemporarily activated.

An adequate capacity of equalization in stored wastewater, which limited the variability of physico-chemical characteristics (thanks to the high retention time and volume of the lagoon), was detected.

Depuration performance did not suffer from the high EO concentrations, the high ratio COD:N:P and the very low values of wastewater pH (Table 2).

An analysis of the depuration input factors showed a significant reduction of:

Table 1. Experimental characteristics of the tanks utilised for depurating citrus processing wastewater at laboratory scale.

Tank	Air flow rate (L m^{-3} h^{-1})	Aeration time (h)	Specific power (W m^{-3})	Air diffuser position	Other experimental conditions
I cycle (July 2010 - February 2011)					
$T_{0, 14, 12}$	14	12	1.2	Bottom	
$T_{0, 7, 24}$	7	24	0.6		
$T^{I}_{0, 7, 12}$	7	12	0.6		
II cycle (December 2011 - June 2012)					
$T^{II}_{0, 7, 12}$	7	12	0.6	Bottom	
$T_{IN, 7, 12}$	7	12	0.6		*Inoculum* with citrus wastewater from a previous treatment cycle
$T_{1/2, 7, 12}$	7	12	0.6	Mid-depth	Separation of upper (aerobic) and lower (anaerobic) layer
$T_{NA, 0, 0}$	-	-	-	-	Not aerated

Table 2. Initial (April) and final (December) values of the main qualitative characteristics of citrus processing wastewater treated in the full-scale aerated lagoon.

Parameter	Year									
	2006		2007		2008		2009		2010	
	Apr	Dec	Apr	Dec	Apr	Dec	Apr	Dec	Apr	Dec
COD concentration (g L^{-1})	18.2	0.3	27.2	7.2	17.4	9.7	12.2	6.7	14.8	10.1
pH	4.0	8.3	3.5	6.8	3.6	4.8	3.4	5.4	3.3	6.6
EO concentration (ppm)	620	70	1030	40	810	50	380	17	440	120

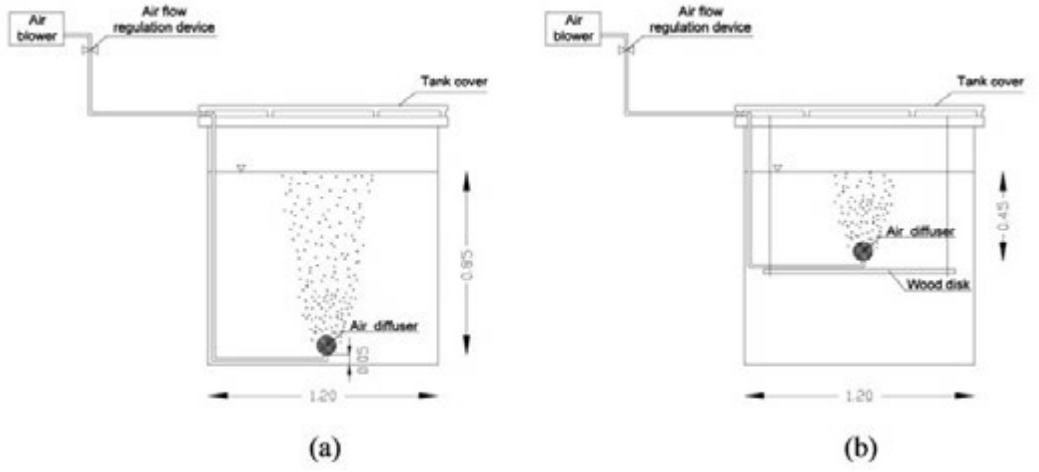

Figure 2. Scheme of the 1-m^3 in tanks simulating aerated lagoons (measures in metres).

- personnel requirement (lower by 75% compared to a common activated sludge plant);
- frequency of water quality analysis (about a control per month against the daily sampling of activated sludge plants) thanks to the low wastewater qualitative variability.

Furthermore, the depuration process do not need lime (due to the natural stabilisation of pH in stored wastewater) and nutrient addition (thanks to the release of nitrogen and phosphorous from activated sludge on the lagoon deep bottom).

The most relevant results were related to the energy aspects. The monthly electrical energy supply per unit of removed COD was in the range 0.21 (in 2008) to 0.59 (in 2006) kWh kg^{-1}_{COD} (Table 3) with an average value of 0.45 kWh kg^{-1}_{COD}. The cost savings are mostly appreciable, because aerators worked only in the night and during the weekend (in which the energy price is lower).

The reduction of the energy requirements in the aerated lagoon under investigation can be related to:

- the significant incidence of anaerobic processes in the high-depth wastewater layer, in which the organic matter is degraded without energy requirements (Zema *et al.*, 2012);
- the higher efficiency of oxygen transfer, due to the high DO oxygen deficit (98-99% of saturation) thanks to the low DO concentrations in wastewater (generally in the range 0.5-1.5 mg L^{-1} with few exceptions) induced by the low aeration intensity (Zema *et al.*, 2012). Conversely, in the activated sludge plants DO concentrations over 2-3 mg L^{-1}, Masotti, 2002; Tchobanoglous *et al.*, 2006) are usual in order to assure oxygen penetration in sludge large flocs with consequent higher energy requirements.

Laboratory-scale investigations

During the investigation in the aerated tanks the pH increased from 4.2-5.5 up to values close to 6.3-8.0, due to degradation of organic acids in oxidation processes. The evolution of pH was similar among the investigated tanks (with mean differences under 5%) and seemed to be independent on air supply. When the organic matter was added, a pH reduction was always detected, presumably due to the lactic fermentation of sugars. The lowest pH increase was recorded in the tank $T_{NA, 0, 0}$ (from 5.5 to 5.7), due to less intense oxidation processes in the absence of aeration.

In the aerated tanks the low DO concentrations, due to the limited air flow rates, determined a high oxygen deficit (close to 95-99% of the saturation concentration). This DO deficit induced a very high efficiency of oxygen transfer to the stored wastewater, which can be estimated as over 20% more compared to a standard activated sludge plant, in which values of oxygen deficit around 80% are usual. Furthermore, the low DO concentration highlighted that in the aerated tanks the oxygen supplied was fully and quickly utilised by microorganisms, even at low temperature and high EO concentration.

The COD monthly removal rate in the aerated tanks was on the average six-fold higher compared to the anaerobic tank ($T_{NA, 0, 0}$, 0.36 g L^{-1} $month^{-1}$). The comparison of energy requirements under different aeration times (12 or 24 hours per day) showed that aeration in the 12 night hours determined an increase of 12% of the monthly removal rate of COD (0.76 g L^{-1} $month^{-1}$, $T_{0, 14, 12}$) compared to the permanently aerated tank (0.68 g L^{-1} $month^{-1}$, $T^{I}_{0, 7, 24}$), although having the same total air supply (Figure 3). As a consequence the energy supply per unit of COD removed were about 10% lower (0.57 kWh kg_{COD}^{-1}, tank $T_{0, 14, 12}$, ver-

Table 3. COD removal and electrical energy supply in the full-scale aerated lagoon.

Parameter	Year					Mean
	2006	2007	2008	2009	2010	
COD total reduction (10^3 kg)	182	236	145	125	111	160
Total supply of electrical energy (MWh)	107	79	30	45	47	62
Mean supply of electrical energy (MWh month-1)	12.8	10.0	3.8	5.0	5.3	7.4
COD removal rate (g L^{-1} $month^{-1}$)	2.24	2.50	0.64	0.68	0.59	1.33
Mean energy supply for unit of removed COD (kWh kg^{-1}_{COD})	0.59	0.34	0.21	0.55	0.54	0.45

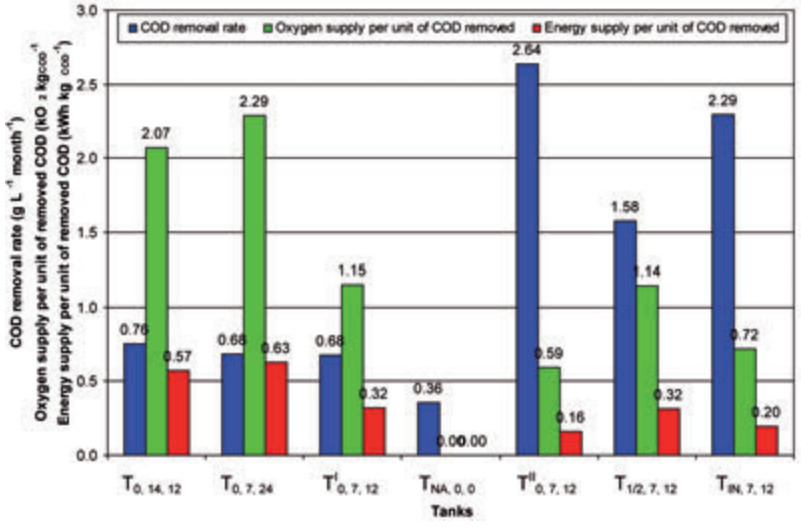

Figure 3. COD monthly removal rate as well as of oxygen and energy supply per unit of COD removed (mean and standard deviation) in the aerated tanks for depurating citrus processing wastewater at laboratory scale.

sus 0.63 kWh kg_{COD}^{-1}, tank $T_{0,7,24}$, Figure 3), which could be presumably due to the higher incidence of anaerobic processes. This result shows that limiting aeration to the 12 night hours allows a total cost saving of nearly 30%, given the present price of off-peak energy in Italy, about lower by 20% than the mean daily price.

Halving the night air flow rates in the tank $T^{I}_{0,7,12}$ from 14 to 7 L m^{-3} h^{-1} reduced by 10% the removal rate of COD (0.68 g L^{-1} $month^{-1}$) compared to tank $T_{0,14,12}$. Given the reduction of 50% in oxygen supply, the energy requirement per unit of COD removed (0.32 kWh kg_{COD}^{-1}) was consequently reduced by more than 40% (Figure 3).

These results confirm the possibility of reducing energy requirement by maximising the incidence of anaerobic processes, thanks to the reduced aeration intensity (down to 0.6 W m^{-3}) and to the limitation of air supply during the 12 night hours.

The highest COD monthly removal rate (2.64 g L^{-1} $month^{-1}$) was measured in the tank $T^{II}_{0,7,12}$ (Figure 3). No positive effect of *inoculum* (tank $T_{IN,7,12}$) was detected, being COD removal rate (2.29 g L^{-1} $month^{-1}$) 13% lower than in the tank $T^{II}_{0,7,12}$ (Figure 3).

The COD monthly removal rate detected in the tank $T_{1/2,7,12}$ (1.58 g L^{-1} $month^{-1}$) was 40% lower than in the tank $T^{II}_{0,7,12}$ (Figure 3). This may be due to the fact that part of oxygen supplied in the upper layer was not presumably transferred to the wastewater, due to the shorter contact time among air bubbles and wastewater because of the halved water depth: this confirms the influence of diffuser submergence on oxygen transfer efficiency, as reported in other studies (Casey, 2009; Popel and Wagner, 1994).

The lowest energy requirement per unit of COD removed was detected in the tank $T^{II}_{0,7,12}$ (0.16 kWh kg_{COD}^{-1}). Tanks $T_{IN,7,12}$ (0.2 kWh kg_{COD}^{-1}) and $T_{1/2,7,12}$ (0.32 kWh kg_{COD}^{-1}) recorded values respectively by 25% and 100% higher (Figure 3), while the energy requirements in the first depuration cycle were 2 to 4-fold, presumably because of the different composition of the citrus processing wastewater.

The comparison of the average COD removal rate recorded in the lab-scale investigations (0.37 kWh kg_{COD}^{-1}) evidences an energy requirement of the same order of magnitude as the full-scale aerated lagoon (0.45 kWh kg_{COD}^{-1}, Table 2).

The low energy requirements detected in aerated lagoons during this investigation are not achievable in activated sludge plants treating agro-industrial wastewater (usually 2.0 kWh kg_{COD}^{-1} in the smallest plants, Cheng *et al.*, 2011). In high loading rate activated sludge processes lower energy requirements (down to 0.5 kWh kg_{COD}^{-1}) are observed only for large and well regulated plants treating urban wastewater, Masotti, 2002; Tchobanoglous *et al.*, 2006).

The depuration processes were not influenced by the low DO and nutrient concentrations, which instead negatively affect biomass settleability and recirculation level in the activated sludge plants, where filamentous bacteria can take advantage of large flocs of sludge, because of their higher surface/volume ratio (Martins *et al.*, 2004; Liu and Liu, 2006). Given that sludge settleability plays a secondary role in aerated ponds, filamentous bacteria did not induce any negative impact on the overall treatment performance.

The gradual addition of EO up to 1400 ppm (tank $T^{I}_{0,7,12}$) did not slow down the removal rate of the organic load. The increase of the EO tolerance recorded in the experimental tank may be presumably attributed to microbial adaptation to terpenes contained in EO and/or non uniform EO concentration in the tank, due to the incomplete mixing of wastewater. The tolerance to high EO concentrations in aerated ponds is more than one order of magnitude higher than the maximum concentration of 50 ppm tolerated by activated sludge processes (Ratcliff, 1990; Kimball, 1999).

Conclusions

This study has investigated depuration processes of citrus wastewater with high concentration of EO in aerobic-anaerobic aerated lagoons at full and laboratory scales. The outcomes of these investigations basically confirm that aerated lagoons are able to reduce the high organic load of agro-industrial wastewater with high EO concentrations at low energy costs.

The monitoring of five citrus wastewater depuration campaigns in the full-scale lagoon highlighted that biological processes, also at high EO concentrations (600-1000 ppm) go regularly, because they do not depend on sludge settleability, contrarily to the activated sludge plants affected by biological instability when EO concentrations are higher than 50 ppm.

Lab-scale investigations indicated that:

- it is possible to increase energy efficiency by limiting aeration to the 12 night hours (with a total cost saving of about 30%) or by halving the night air flow rate to 7 L h^{-1} m^{-3} (with a reduction of 40% in energy requirement);
- a gradual increase of EO concentration up to 1400 ppm seems to induce a microbial adaptation which allows regular biological processes, but an *inoculum* of 50% of wastewater with microflora already adapted to high EO concentration does not induce any positive effect on the removal rate of the organic load;
- positioning the air diffuser 0.45-m above the tank bottom (instead of 0.05-m) determines a decrease of COD removal rate, presumably due to a reduced oxygen absorption by the wastewater due to the reduced water depth.

On the whole, the results of the investigations confirm that depuration of agro-industrial wastewater in aerated lagoons is a valid alternative to the intensive biological plants (as the most common activated sludge processes), thanks to their higher reliability and lower energy requirements.

References

APHA. 1998. Standard methods for the examination of water and wastewater, XX Ed., Washington, APHA, USA.

Bombino G., Tamburino V., Zema D.A., Zimbone S.M. 2009. Depuration of citrus processing wastewater in aerated biological ponds. Proceedings of the Congress of the Italian Association of Agricultural Engineers. Ischia (Italy), 12-16 September.

Casey T.J. 2009. Diffused air aeration systems for the activated sludge process. Design performance testing. Aquavarra Research Publications – Water Engineering Papers. Available from http://www.aquavarra.ie/AerationP4.pdf. Accessed: February 2013.

Jail A., Boukhoubza F., Nejmeddine A., Duarte J.C., Sayadi S., Hassani L. 2010. Traitement des effluents d'huileries par un procédé combinant un traitement intensif (Jet_Loop Reactor) suivi d'un traitement extensif (bassins de stabilisation), Environ. Technol., 31: 533-543 (in French).

Kimball D.A. 1999. Citrus processing, 2nd Edition. Aspen Publishers, Inc. Gaithersburg, MD, USA.

Lane A.G. 1983. Removal of peel oil from citrus peel press liquors before anaerobic digestion, Environ. Technol. Lett. 4: 65–72.

Liu Y., Liu Q.-S. 2006. Causes and control of filamentous growth in aerobic granular sludge sequencing batch reactors. Biotechnology Advances 24: 115-127.

Martins A.M.P., Pagilla K., Heijne J.J., van Loosdrecht M.C.M. 2004.

Filamentous bulking sludge - a critical review. Water Research 38: 793-817.

Masotti L. 2002. Depurazione delle acque reflue. Il Sole 24 Ore Edagricole (Ed.), Bologna (Italy), (in Italian).

Popel H.J., Wagner M. 1994. Modelling of oxygen transfer in deep diffused-aeration tanks and comparison with full-scale data. Water Science Techn. 30(4): 71-80.

Ratcliff M.W. 1990. Citrus processing waste prevention, handling and treatment, Citrus world, Lake Wales, Florida, USA.

Scott W.C., Veldhuis M.K. 1966. Rapid estimation of recoverable oil in citrus juices by bromate titration. J. AOAC Int., 49: 628–633.

Tamburino V., Zema D.A., Zimbone S.M. 2007. Depuration processes of citrus wastewater, Proceedings of the 3rd International Symposium of CIGR Section VI "Food and agricultural products: processing and innovations". Naples (Italy), 24-26 September.

Tchobanoglous G., Burton F.L., Burton F., Stensel H.D. 2002. Wastewater engineering. Treatment and reuse, Inc Metcalf & Eddy, McGraw-Hill Company, New York, USA.

Van Dyke S., Jones S., Ong S.K. 2003. Cold weather nitrogen removal deficiencies of aerated lagoons, Environ. Technol. 24: 767–777.

Zema D.A., Andiloro S., Bombino G., Tamburino V., Sidari R., Caridi A. 2012. Performance of aerated ponds in depurating citrus processing wastewater with high concentrations of essential oils. Environmental Technology 33 (11): 1255-1260.

Time domain reflectometry-measuring dielectric permittivity to detect soil non-acqeous phase liquids contamination-decontamination processes

A. Comegna,[1] A. Coppola,[2] G. Dragonetti,[3] N. Chaali,[1] A. Sommella[4]

[1]School of Agricultural Forestry Food and Environmental Sciences (SAFE), University of Basilicata, Potenza, Italy; [2]Department of European and Mediterranean Cultures-Architecture, Environment, Cultural Heritage (DiCEM), Hydraulics and Hydrology Division, University of Basilicata, Matera, Italy; [3]Mediterranean Agronomic Institute, Land and Water Division, IAMB, Bari, Italy; [4]Division of Water Resources Management, University of Naples "Federico II", Italy

Abstract

Contamination of soils with non-aqueous phase liquids (NAPL) constitutes a serious geo-environmental problem, given the toxicity level and high mobility of these organic compounds. To develop effective decontamination methods, characterisation and identification of contaminated soils are needed. The objective of this work is to explore the potential of dielectric permittivity measurements to detect the presence of NAPLs in soils. The dielectric permittivity was measured by Time Domain Reflectometry method (TDR) in soil samples with either different volumetric content of water (θ_w) and NAPL (θ_{NAPL}) or at different stages during immiscible displacement test carried out with two different flushing solutions. A mixing model proposed by Francisca and Montoro, was calibrated to estimate the volume fraction of contaminant present in soil. Obtained results, showed that soil contamination with NAPL and the monitoring of immiscible fluid displacement, during soil remediation processes, can be clearly identified from dielectric measurements.

Introduction

Subsurface contamination of soil and groundwater with organic compounds from waste disposal sites, industrial spills, gasoline stations, mine tailings and industrial processes constitutes a serious geo-environmental problem. The detrimental effects are limited not only to deterioration of chemical, physical and mechanical properties of soils, but also constitute a real risk to human health and the well-being of other living species.

Non-aqueous phase liquids (NAPLs), are organic compounds immiscible with water. They have low solubility that may still be several orders of magnitude higher than that of acceptable drinking water standards. NAPLs can be further subdivided into those that are denser than water (DNAPLs) and those that are lighter than water (LNAPLs). Chlorinated solvents such as trichloroethylene (TCE) and tetrachloroethylene (PCE) and polychlorinated biphenyl oils (PCBs) are common examples of DNAPLs. Hydrocarbon fuels such as gasoline, kerosene and jet fuels are common LNAPL contaminants which pollute the environment extensively (Illangasekare, 1998; Jury and Horton, 2004).

Following a near-surface release, NAPLs penetrate the subsurface as an immiscible oil phase that migrates in response to gravity and capillary forces. This results in substantial sensitivity to the local distribution of soil and aquifer properties (*e.g.* permeability and porosity) beneath the source (Gerhard *et al.*, 2007). As a result, the NAPL body (*e.g.* the source zone) is often expected to exhibit a complex heterogeneous distribution of both mobile pools (*i.e.* connected-phase accumulations) and immobile residuals (*i.e.* disconnected blobs and ganglia (Mercer and Cohen, 1990).

The remediation of contaminated soil sites requires knowledge of the contaminant distribution in the soil profile and groundwater. Methods commonly used to characterize contaminated sites are coring, soil sampling and the installation of monitoring wells for the collection of groundwater samples (Mercer and Cohen, 1990).

Given the high cost of the above methods, other non-invasive methods have been sought to extensively characterize sites and provide volume-averaged properties that support localized measurements provided by sampling and coring. Indirect detection with geophysical methods (*e.g.* radar, resistivity and conductivity) offers an attractive alternative (Redman *et al.*, 1991). In particular, the time domain reflectometry (TDR) technique has been proposed as potentially exhibiting sufficient sensitivity and lateral and vertical resolution for characterization of saturation of NAPLs (θ_{NAPL}). This is because commonly encountered NAPLs have a dielectric permittivity of 2-10 versus 81 for water, 1 for air, and 4-5 for soil mineral grains (Ajo-Franklin *et al.*, 2006).

Most studies have demonstrated estimation of θ_{NAPL} essentially in saturated coarse-grained media (Redman and DeRyck, 1994; Chenaf and Amara, 2001; Persson and Berndtsson, 2002; Haridy *et al.*, 2004; Mohamed and Said, 2005; Ajo-Franklin *et al.*, 2006; Moroizumi and Sasaki, 2006; Francisca and Montoro, 2012). Little is known about the dielectric behaviour of contaminated fine-grained soils. The complexity of these soils, arises due to polarization of the diffuse-double layer, whereas coarse-grained soils do not possess polarization at which most of the cited studies have been conducted. Moreover, in these studies

Correspondence: A. Comegna, School of Agricultural Forestry Food and Environmental Sciences (SAFE), University of Basilicata, Potenza, Italy.
E-mail: alessandro.comegna@unibas.it

Key words: soil-NAPL-water mixtures; dielectric permittivity; mixing models, remediation processes.

Journal of Agricultural Engineering 2013; XLIV(s1):e167
doi:10.4081/jae.2013.(s1):e167

estimation of θ_{NAPL} using TDR measurements of dielectric properties relies greatly on various mixing models (van Dam *et al.*, 2005) relating the measured dielectric permittivity to the volume fractions of the pore fluids and various soil phases such as solid, water, air and NAPLs.

New laboratory-controlled experiments are still needed to extend the above research on TDR identification of organic contaminated soils by dielectric permittivity measurements. The experimentation strategy of the present research emphasized, in a preliminary approach, the study of the potential use of TDR to monitor or map θ_f (= θ_w+θ_{NAPL}) in soil. The specific aims include: i) evaluation of correlations between θ_f in variable saturated volcanic Vesuvian soil, and dielectric permittivity, ii) examination and validation of the mixing model provided by Francisca and Montoro (Francisca and Montoro, 2012) for predicting the dielectric permittivity of contaminated soil; iii) exploration of the potential application of electromagnetic waves to evaluate the effect of contaminant removal in soil in context.

TDR and complex dielectric permittivity of soil

The time domain reflectometry technique is a widely accepted geophysical method to estimate the complex dielectric permittivity (ε^*) of the soil. The complex dielectric permittivity consists of two parts, a real and an imaginary part, and can be expressed by the relation of Ledieu (Ledieu *et al.,* 1986):

$$\varepsilon^* = \varepsilon' + i\left[\varepsilon'' + \frac{\sigma}{\omega\varepsilon_0}\right] \quad (1)$$

where ε^* is the complex dielectric permittivity of the medium, ε' is the real part (which represents the polarizability of the material), i is the imaginary unit (= $\sqrt{-1}$), ε'' is the imaginary part (which captures the losses due to conduction and polarization), s (Siemens/m) is the zero frequency conductivity, w (radians/s) is the angle frequency and ε_0 (=8.85*10^{-12} Farads/m) is the permittivity in free space.

At the highest effective frequency of the TDR Tester (200 MHz to 1.5 GHz) the complex dielectric permittivity ε^* is considered to represent the real part only (ε', Heimovaara *et al.*, 1994). Besides, in the frequency range transmitted from the TDR instrument the ε' of most soil is almost independent of frequency.

Without introducing serious errors, under these assumptions, the propagation velocity (v) of electromagnetic waves through an homogeneous medium can be expressed as:

$$v = \frac{c}{\sqrt{\varepsilon'}} \quad (2)$$

where c(=3•10^8 m/s) is the velocity of an electromagnetic wave in free space (Topp *et al.*, 1980).

Materials and methods

Soil properties

The soil used for this study was sampled from an Ap horizon of a soil pedologically classified as Andosol, localized in Campania region (Italy). In Table 1 we have also exploited the main physico-chemical soil properties.

The soil texture was determined using hydrometer and sieving analysis (Day, 1965); organic content (*OC*) was determined by Walkley-Black method (Allison, 1965), The specific surface area (S_e) was determined with ethylene glycol monoethyl ether (Carter *et al.*, 1986).

Dielectric permittivity measurement of soil-NAPL mixtures

A first group of experiments refers to dielectric permittivity measurement conducted on mixtures with known different volumetric content of water (θ_w) and NAPL (θ_{NAPL}).

Experimental setup

The experimental setup consists of an excitation unit constituted by a TDR signal generator (Tektronix 1502C) and a three-wire TDR probe, with wave guides 15 cm long, connected to the signal generator by a coaxial cable 2 m long. The reflected signals are collected by a PC-based data acquisition and processing system. The reflected signal carries the signature of the sample under study. Estimation of ε' was calculated from the signal using Win-TDR software (developed by the Soil Physics Group at Utah State University). Figure 1 gives a picture of the dielectric measurement system used in these experiment.

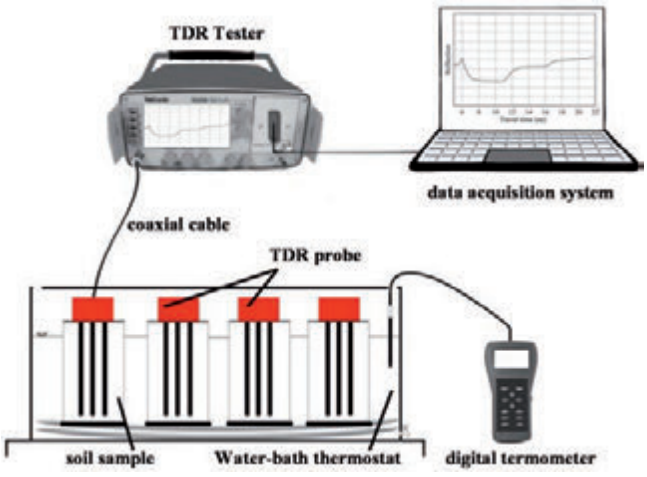

Figure 1. Experimental setup used in the experiment.

Table 1. Main physico-chemical properties of the soil.

Horizon	Depth (cm)	Soil texture (IUSS) Coarse sand %	Fine sand %	Silt %	Clay %	Al_o+1/2Fe_o %	*OC* %	*Se* m^2g^{-1}
Ap	0-20	30.0	50.0	12.0	8.0	1.05	1.90	125.4

Sample preparation and testing procedures

Soil samples were oven dried at 105°C and passed through a 2 mm sieve. Corn oil, a non-volatile and non-toxic LNAPL, was used as soil contaminant. The dielectric permittivity and density of the oil were 3.2 (at 25°C) and 0.905 g/cm^3 respectively. Known amounts of soil, water and oil were mixed together, shaken and then kept for 24 hours in sealed plastic bags to avoid any evaporation and to ensure a uniform distribution of oil and water within the sample, and good oil and water adsorption by the soil matrix. The soil is then placed in PVC soil containers of cylindrical geometry (16 cm high and 9.5 cm in diameter). In all, there were 40 oil-contaminated soil samples, used for a full factorial analysis presented in Table 2.

For all tests the soil was placed in the PVC containers in several steps during which it was compacted until a 1.09 g/cm^3 bulk density was attained. At each step the compacted surface was scraped to avoid the appearance of plane boundaries which give the sample a stratified behaviour responsible for parasitic reflections on the TDR signal. Soil samples were kept at a fairly constant temperature (25°C) through the TDR measurements using a water-bath thermostat.

Dielectric permittivity measurements of soil-NAPL mixtures flushed with washing solution

A second group of experiments refers to dielectric permittivity measurements conducted in soil samples initially contaminated with NAPL and then flushed with two different washing solutions.

Experimental setup

The experimental setup consist of: i) a Techtronix cable tester; ii) a three-wire TDR probe with wave guides 15 cm long inserted vertically into the soil samples; iii) a testing cell of 8 cm in diameter and 16 cm high; iv) a peristaltic pump for upward injection of washing solution. Figure 2 gives a picture of experimental system used in these experiments.

Sampling preparation and testing procedures

Soil columns tests were carried out employing the following procedure: i) two soil columns were contaminated with corn-oil (by following the same procedure described in section 3.2.2) to obtain a saturation degree (θ_{NAPL}) close to 0.3, ii) upward injection of several flushing volumes N_f (defined as the volume of displacing fluid V_d with respect to volume of soil sample V) of two washing solutions: a) distilled water; b) distilled water (90%) with commercial detergent (1%) and methanol (9%) were supplied at a rate q=1.5 cm^3/min, which corresponds to a darcian velocity v=6.0 cm/h; iii) the out coming fluid, from the soil columns was collected, water and oil was separated and the amount of oil that is remediated from the soil is recorded.

Mixing models

In the present study, from among the many physical models of dielectric permittivity that describe soil as a mixture of particles, water and air, the a model was used (Roth *et al.*, 1990).

$$\varepsilon' = \left[\sum_{i=1}^{n} V_i \varepsilon_i^{\alpha}\right]^{\frac{1}{\alpha}} \quad (3)$$

where ε' is the permittivity of the mixture, ε_i and V_i are the permittivity and volume of the *"i"* phase respectively, the exponent a is an empirical constant related to the geometry of the grains and their spatial distri-

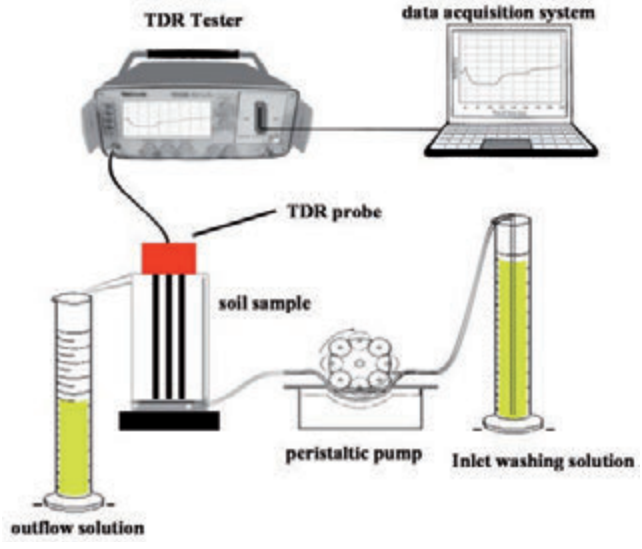

Figure 2. Experimental setup used in the NAPL removal experiment.

Table 2. Combinations of moisture volume (V_w) and NAPL volume (V_{NAPL}) at fixed values of volume fraction of NAPL (β).

volumetric fluid content θ_f	volume of fluids (cm^3)	relative volume of NAPL in water: β					volumetric fluid content θ_f	volume of fluids (cm^3)	relative volume of NAPL in water: β				
		1	0.75	0.5	0.25	0			1	0.75	0.5	0.25	0
0.05	V_w	0	13	27	40	53	0.025	V_w	0	67	133	200	267
	V_{NAPL}	53	40	27	13	0		V_{NAPL}	267	200	133	67	0
0.10	V_w	0	27	53	80	107	0.30	V_w	0	80	160	240	320
	V_{NAPL}	107	80	53	27	0		V_{NAPL}	320	240	160	80	0
0.15	V_w	0	40	80	120	160	0.35	V_w	0	93	187	280	373
	V_{NAPL}	160	120	80	40	0		V_{NAPL}	373	280	187	93	0
0.20	V_w	0	53	107	160	213	0.40	V_w	0	107	213	320	427
	V_{NAPL}	213	160	107	53	0		V_{NAPL}	427	320	213	107	0

bution (Hilrost, 1998; Coppola *et al.*, 2013). For an homogeneous and isotropic medium, a can be assumed equal to 0.5 (Alharti *et al.*, 1986) and the mixing model is then referred to as the complex refractive index model (CRIM, *e.g.* Hiusman *et al.*, 2003). The CRIM model does not account for the microgeometry of the components. However, despite this limitation, and the apparent simplicity of using the CRIM model, remarkably good agreement was found in modeling the dielectric properties of geological materials (Knight, 2001) and soil-water-NAPL mixture (Francisca and Montoro, 2012).

For mixtures of soil and water, the CRIM formula yields:

$$\varepsilon'_{sw} = \left[(1-\phi)\varepsilon'^{\alpha}_{s} + \phi\varepsilon'^{\alpha}_{w} + \phi(1-S)\varepsilon'^{\alpha}_{a}\right]^{1/\alpha} \quad (4)$$

where ε'_{sw} is the permittivity of soil-water mixture, ε'_s, ε'_w, ε'_a are the permittivities of soil particles, water and air respectively, S is the degree of saturation and ϕ is the porosity of the sample.

Similarly for soil-organic mixtures, the CRIM formula becomes:

$$\varepsilon'_{sNAPL} = \left[(1-\phi)\varepsilon'^{\alpha}_{s} + \phi S\varepsilon'^{\alpha}_{NAPL} + \phi(1-S)\varepsilon'^{\alpha}_{a}\right]^{1/\alpha} \quad (5)$$

where ε'_{sNAPL} is the permittivity of the soil-NAPL mixture and ε_{NAPL} is the permittivity of NAPL. Mixtures of soil particles, water, NAPL and air can be considered as mixtures of soil-air and water (equation 4) with soil-air and NAPL (equation 5):

$$\varepsilon'_{sw-sNAPL} = \left[\beta\varepsilon'^{\alpha}_{sNAPL} + (1-\beta)\varepsilon'^{\alpha}_{sw}\right]^{1/\alpha} \quad (6)$$

where $\varepsilon'_{sw-NAPL}$ is the permittivity of the soil-water-NAPL mixture and b is the relative volume of NAPL (θ_{NAPL}) in water (θ_w):

$$\beta = \theta_{NAPL}/(\theta_{NAPL} + \theta_w) \quad (7)$$

Results and discussion

Figure 3 shows a comparison between the measured dielectric permittivity and CRIM models (equations 4-5), fitted to the experimental data, corresponding to fully uncontaminated soil and fully contaminated soil respectively, as a function of the volumetric fluid content in the samples ($\theta_f = \theta_w$ or θ_{NAPL}).

In the CRIM model, to achieve accurate modeling, we adopt for the dielectric permittivity of the solid phase (ε'_s) a value of 4.18, measured with the immersion method (Robinson et al., 2003; Kameyama and Miyamoto, 2008), which is, until recently the most common method for measuring ε'_s of soils. Figure 3 shows that: i) dielectric permittivity increases with volumetric content of fluids θ_f ($=\theta_w$ or θ_{NAP}), while the presence of NAPL reduces the dielectric permittivity of the soil. The observed higher and lower dielectric permittivity values of the soil-water and soil-NAPL mixtures can be attributed here respectively to the presence of a larger amount of polar molecules in soil-water mixtures and to the non-polar nature of NAPL molecules in the soil-NAPL mixture, ii) the agreement of the CRIM model (equation 4) to the experimental data is fairly acceptable, iii) the CRIM model (equation 5) tends to underestimate the dielectric permittivity in the case of contaminated soil with NAPL (in particular in the range $0<\theta_f<0.2$); obtained differences, even small, may arise from experimental errors and from adopted values of a=0.5.

The model as given by Francisca and Montoro (equation 6), was then evaluated for different volume fractions of NAPL (b=0.75, 0.5, 0.25) and the resulting curves were plotted together with experimental data in Figure 4 as a function of volumetric fluid content θ_f ($=\theta_{NAPL}+\theta_w$) in the soil samples. The model is adequate to forecast the dielectric permittivity only for values of volumetric fluid content (θ_f) greater than 0.20; notice that the slope of the curves becomes steeper as the NAPL content (b) in the pore fluids decreases.

The volumetric content of NAPL (θ_{NAPL}), at a fixed, and thus known volumetric fluid content θ_f, can be computed from equations 6 and 7, deriving ε'_{sNAPL}, ε'_{sw} from Figure 3, and the dielectric permittivity measured in the contaminated soil $\varepsilon'_{sw-sNAPL}$. Parameters can be early obtained either in laboratory or in the field. Additionally Figure 4 can be very useful during an in situ remediation process to monitor the removal process.

Figure 5 presents a 1:1 plot for estimated and measured dielectric permittivity values to verify the accuracy of the dielectric mixing model (equation 6). The model adopted, showed that the estimated dielectric permittivity values were reasonable close to the measured, meaning that with TDR methodology it is possible to achieve sufficient accuracy in predicting the presence of a contaminant, mixed with water, in the soil, that is, the root mean square error (RMSE), is 0.719, 0.584, 0.438, 0.413, 0.267 for b=1, 0.75, 0.5, 0.25, 0 respectively. Figure 6 reveals the effects of flushing volumes N_f on measured dielectric permittivity (ε') for the two samples initially contaminated with oil. As the flushing flow began to displace oil, the ε' increased because of the larger dielectric permittivity of the washing solution. As the solution continued to flow, the rate of increase of ε' lessened and asymptotically approaches a constant value. This constant value was reached after displacing approximately 15 times the total flushing volume N_f in the column.

This steady-value was less than that obtained when the soil samples

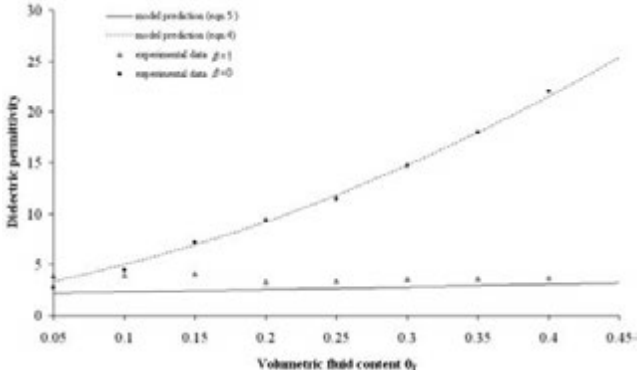

Figure 3 Effect of volumetric fluid content (θ_f) on dielectric permittivity of soil-water (ε'_{sw}) and soil-water-NAPL (ε'_{sNAPL}) mixtures.

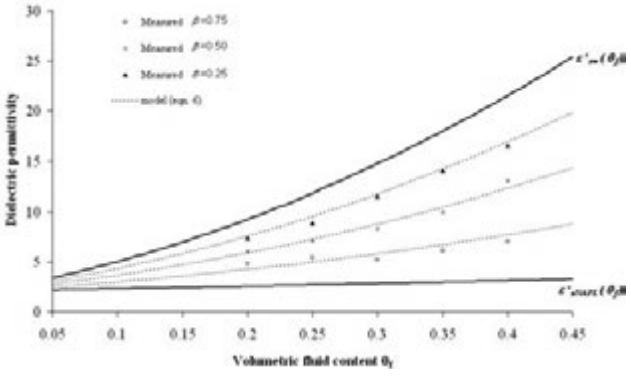

Figure 4. Dielectric permittivity of soil-water-NAPL mixtures ($\varepsilon'_{sw-NAPL}$) for different volumetric fluid contents (θ_f) and volume fractions of NAPL (β).

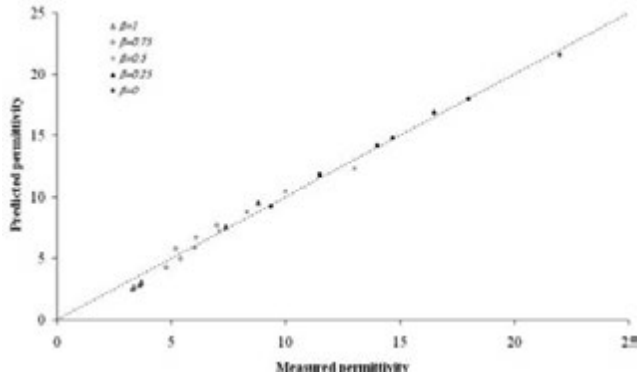

Figure 5. Relationship between calculated and measured dielectric permittivity ($\varepsilon'_{sw-NAPL}$) at different β values.

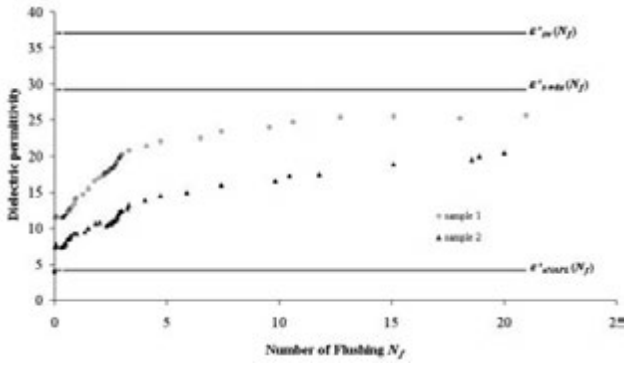

Figure 6. Dielectric permittivity of oil-contaminated soil samples, subjected to flushing with water-detergent-alcohol (sample 1) and distilled water (sample 2) washing solutions.

Table 3: Volumes of NAPL recovered at different Nf values, for each washing solution.

Number of Flushing N_f	Volume (%) of NAPL Removed by: Water-Detergent-Alcohol	Water	Number of Flushing N_f
0.00	0.00	0.00	0.00
0.02	9.07	18.5	0.05
0.40	36.21	18.5	0.38
0.51	37.11	19.2	0.51
0.72	39.98	22.33	0.86
0.90	42.49	23.97	1.47
1.49	47.60	27.16	2.10
2.19	56.78	28.35	2.80
2.44	58.90	31.63	2.92
2.63	60.50	32.85	3.30
2.79	63.02	36.18	4.72
3.31	67.30	39.23	7.43
6.49	73.70	43.39	10.45
10.61	80.20	50.89	15.15
15.08	86.00	53.66	18.90
21.30	86.72	55.88	20.10

were completely saturated only by flushing solutions. This differences in values is due to oil trapped in soil pores. Contaminated sample (sample 1), flushed with a solution of water, detergent and methanol (wda), yields higher values of measured dielectric permittivity, as compared to the sample (sample 2) flushed with only distilled water. This effect was attributed to the potential of detergent and alcohol reducing the soil interfacial tension and contact angle. Finally a comparison of oil removed in soil samples, from direct volume measurements of the immiscible fluid in the discharge, is given, in Table 3, for the applications.

Table 3 clearly reveals that the inclusion of detergent and alcohol in the displacing fluid improves the removal efficiency considerable.

Conclusions

From the results of our experiment it can be concluded as follows: i) the dielectric properties of contaminated soil were analyzed using mixing models extended from two to three and four components. The models that better represent the dielectric properties of contaminated soil are the models proposed by Francisca and Montoro; ii) the curves of dielectric permittivity obtained from contaminated soil and different volume of water (θ_w) and NAPL (θ_{NAPL}), were considered as upper and lower bounds respectively. The amount of contaminant in the soil can be inferred from the plots of Figure 3 and 4 or with the aid of mixing models. In any case

the volumetric fluid content θ_f must be known in advance; and iii) removal of oil during flushing, produced an increment in soil dielectric permittivity which allows evaluating the evolution of NAPL saturation degree during remediation processes and computing the organic contaminant content at different stages during remediation.

References

Ajo-Franklin J.B., Geller J.T., Harris J.M. 2006. A survey of the geophysical properties of chlorinated DNAPLs. J. Appl Geophys. 59, 177-189.

Alharti A., Lange J., Whitaker E. 1986 Immiscible fluid flow in porous media: Dielectric properties. J. Contam. Hydrol. 1, 107-118.

Allison L.E., 1965. Organic carbon. In A. Klute (ed.). Methods of Soil Analysis, Part 1, Madison, Agron. Monograph, vol 9, ASA and SSSA, pp. 1367-1378.

Carter D.L., Mortland M.M., Kemper W.D.M. 1986. Specific Surface. Methods of Soil Analysis, Part I. Physical and Mineralogical Methods-Agron, Monograph vol. 9 (2nd Edition), ASA and SSSA, Madison, 1986, p 413-423.

Chenaf D., Amara N. 2001. Time domain reflectometry for the characterization of diesel contaminated soils. Proc. Second Int. Symp. and Workshop on Time Domain Reflectometry for Innovative Geotechnical Applications (5-7 September 2001), Infrastructure Technology Institute, Northwestern University, Evanston, Illinois, USA.

Coppola A., Dragonetti G.,. Comegna A., Lamaddalena N.,. Caushi B., Haikal M.A., Basile A. 2013. Measuring and modeling water content in stony soils. Soil Till. Res. 128, 9-22.

Day P.R. 1965. Particle fractionation and particle-size analysis. In Black CA, editor, Methods of Soil Analysis, Part 1, Madison, American Society of Agronomy, pp 545-567.

Francisca M., Montoro M.A. 2012 Measuring the dielectric properties of soil-organic mixtures using coaxial impedance dielectric reflectometry. Journal of Applied Geophysics. 80, 101-109.

Gerhard J.I., Pang T., Kueper B.H. 2007. Time scales of DNAPL migration in sandy aquifers. Ground Water. 45, 147-157.

Haridy S.A., Persson M., Berndtsson R. 2004 Estimation of LNAPL saturation in fine sand using time-domain reflectometry. Hydrological Sciences. 49, 987-1000.

Heimovaara T.J., Bouten W., Verstraten J.M. 1994. Frequency domain analysis of time domain reflectometry waveforms, 2, A four-component complex dielectric mixing model for soils. Water Resour. Res. 30, 201-210.

Hilhorst M.A. 1998. Dielectric characterisation of soil. PhD dissertation, Wageningen Agricultural University.

Huisman J.A., Hubbard S.S., Redman J.D., Annan A.P. 2003. Measuring soil water content with ground penetrating radar: A review. Vadose Zone J. 2, 476-491.

Illangasekare H.T. 1998. Flow and entrapment of Non-Aqueous-Phase Fluids in heterogeneous soil formation. In. M.H. Selim, Ma L, (ed.). Physical nonequilibrium in soils. Michigan, Ann Arbor Press, pp 417-435.

Kameyama K., Miyamoto T. 2008. Measurement of solid phase permittivity for soils by time domain reflectometry. European Journal of Soil Science. 59, 1253–1259.

Knight R. 2001. Ground penetrating radar for environmental applications. Annu. Rev. Earth Planet Sci. 29, 229-255.

Ledieu J., De Bidder P., De Clerck P., Dautrebande S. 1986. A method of measuring soil moisture by time-domain reflectometry. J. Hydrol. 88, 319-328.

Jury W.A., Horton R. 2004. Soil Physics. New Jersey, John Wiley & Sons.

Mercer J.W., Cohen R.M. 1990. A review of immiscible fluids in the subsurface: properties, models, characterization, and remediation. J. Contam. Hydrol. 6, 107-163.

Mohamed A.M.O., Said R.A. 2005. Detection of organic pollutants in sandy soils via TDR and eigendecomposition. J. Contain. Hydrol. 76, 235-249.

Moroizumi T., Sasaki Y. 2006. Estimating the nonaqueous-phase liquid content in saturated sandy soil using amplitude domain reflectometry. Soil Sci. Soc. Am. J. 72, 1520-1526.

Persson M., Berndtsson R. 2002. Measuring nonaqueous phase liquid saturation in soil using time domain reflectometry, Water Resour. Res. 38, doi: 10.1029/2001WR000523.

Redman J.D., Kueper B.H., Annan A.P. 1991. Dielectric stratigraphy of a DNAPL spill and implications for detection with ground penetrating radar. Ground Water Monitoring and Geophysical Methods, 5th National Outdoor Action Conference, Natl. Ground Water Assoc., Las Vegas, Nev.

Redman J.D., DeRyck S.M. 1994. Monitoring non-aqueous phase liquids in the subsurface with multilevel time domain reflectometry probes. Proc Symp. on Time Domain Reflectometry in Environmental, Infrastructure, and Mining Applications, Evanston, IL. Spec. Publ. SP19-94. U.S. Bur. of Mines, Washington, DC.

Roth K., Schulin R., Fluhler H., Attinger W. 1990. Calibration of time domain reflectometry for water content measurements using a composite dielectric approach. Water Resour. Res. 26, 2267-2273.

Topp C.G., Davis J.L., Annan A.P. 1980 Electromagnetic determination of soil water content: measurements in coaxial transmission lines. Water Resour. Res. 16, 574-582.

van Dam R.L., Borchers B., Hendrickx J.M.H. 2005. Methods for prediction of soil dielectric properties: a review. available on http://www.ees.nmt.edu/hydro/landmine.

Robinson D.A., Jones S.B., Wraith J.M., Or D. 2003 A review of advances in dielectric and electric conductivity measurements using time domain reflectometry, Vadose Zone J. 2, 444-475.

A simplified method to determine the first primary drying and wetting curves of water diffusivity of unsaturated soil

A. Sommella,[1] A. Comegna,[2] M. Palladino,[1] A. Coppola[3]

[1]Division of Water Resources Management, University of Naples "Federico II", Italy; [2]School of Agricultural Forestry Food and Environmental Sciences (SAFE), University of Basilicata, Potenza, Italy; [3]Department of European and Mediterranean Cultures-Architecture, Environment, Cultural Heritage (DiCEM), Hydraulics and Hydrology Division, University of Basilicata, Matera, Italy

Abstract

Within the framework of a research project examining the spatial variability of hydraulic characteristics of soil intended for irrigation, some of the more frequently used analytical expressions describing the laws linking diffusivity D to the water content of the soil θ were verified. By studying the flow field of soil samples tested in the laboratory, under one-dimensional wetting and drying cycles, it has been found that the laws of hydraulic diffusivity of the exponential types can be ascribed to them. Finally, a simplified laboratory method was proposed which, with the aid of nomographs, allows the definition of the law D(θ) to be easily arrived at.

Introduction

Soil hydraulic properties such as the soil water retention curve h(θ), unsaturated hydraulic conductivity K(θ) and diffusivity D(θ), are very important in all computational models for predicting water flow. Of the three hydraulic properties, only two are necessary since any of the three can be obtained from the other two which are independent. Direct measurements of these properties is quite expensive and time-consuming.

Methods to measure soil water diffusivity in the laboratory have been extensively explored. Initially Gardner (1956) presented a method for experimentally calculating diffusivity from volumetric measurements of water outflow with time from a soil sample subjected to an abrupt change in soil water pressure. The impedance to flow offered by the membrane was neglected in his mathematical description. Miller and Elrick (1958) improved this pressure outflow method by including membrane impedance in the solution. Rijtema (1959) presented a procedure for obtaining the membrane and soil contact impedance from the experimental data. The simplified method of Kunze and Kirkham (1962) not only reduced the number of steps required to calculate the diffusivity but eliminated the necessity of measuring membrane impedance. Experimental and theoretical determination of the diffusivity by the above methods requires three basic assumptions: i) soil water content be a linear function of the soil water pressure within the applied pressure increment, ii) that diffusivity be constant throughout the imposed water content range; and iii) that Darcy's law be applicable to unsaturated soil water movement.

Gardner (1962) presented the pressure outflow equation in a slightly different form by assuming that water content does not vary appreciably with sample depth during outflow and calculated the diffusivity and average water content directly from the instantaneous outflow rate. This procedure has been used by Doering (1965), Gupta *et al.* (1974), Passioura (1976), Valiantzas (1990), and Londra and Valiantzas (2011), and is referred to as the one-step outflow method which can be ascribed to so-called direct laboratory methods. On the other hand, within the indirect approach, parameter estimation methods have been applied together with laboratory outflow experiments to determine hydraulic properties (Kool *et al.*, 1987; Parker *et al.*, 1985; Eching *et al.*, 1994; Ciollaro and Romano, 1995). Parameter estimation techniques enable simultaneous determination of the functions h(θ), K(θ) and D(θ) just from outflow experiments. An assumption of particular mathematical forms of the hydraulic properties is however required. The indirect method is certainly more flexible than the direct one, but nonetheless there are some drawbacks concerning the way the problem is posed, instability and lack of solution uniqueness.

The above procedures assume that volumetric water content θ is uniquely related to the water potential h during the drying and wetting process. However, in unsaturated zones of the flow domain, the potential h is not a unique function of θ and thus hydraulic characterisation of the medium extended to hysteresis phenomena envisages, at the very least, definition of the two primary functions of D(θ) and K(θ), respectively of wetting and drying.

Given the onerous task of conducting laboratory tests required for complete soil hydraulic characterisation, in this work we examined the possibility of characterising soil samples through exponential laws obtained with more straightforward, rapid testing techniques. Thus we examined the wetting and drying processes in the laboratory, using a vertical experiment, and the results of tests were compared with the theoretical solutions of flow domains supplied by Scott and Hanks (1962) and obtained by approximating the law D(θ) through an exponential expression suggested by Klute *et al.* (1965).

Contrary to the conventional one-step outflow method the present method requires only the measurement of the average volumetric soil

Correspondence: A. Comegna, School of Agricultural Forestry Food and Environmental Sciences (SAFE), University of Basilicata, Potenza, Italy.
E-mail: alessandro.comegna@unibas.it

Key words: soil hydraulic characterization, soil water diffusivity, laboratory method.

Journal of Agricultural Engineering 2013; XLIV(s1):e168
doi:10.4081/jae.2013.(s1):e168

water content. The advantage of the proposed method over existing methods is that it provides a rapid, easy method to determine D(θ) without requiring the laborious recording and analysis of all outflow volumes over time.

Theory

For one-dimensional vertical flow the continuity equation takes the form:

$$\frac{\partial \theta}{\partial t} = \frac{\partial q}{\partial z} \quad (1)$$

where θ is volumetric soil water content, q is the soil water flux density, z is taken positive downwards and t is time. Combined with the generalized Darcy law:

$$q = -K(\theta)\frac{\partial H}{\partial z} \quad (2)$$

the soil water transfer equation can be written as:

$$\frac{\partial \theta}{\partial t} = \frac{\partial}{\partial z}\left[K(\theta)\left(\frac{\partial h}{\partial z} - 1\right)\right] \quad (3)$$

where h is soil water pressure head relative to atmospheric pressure ($h \leq 0$), K is hydraulic conductivity as a function of θ, and H is hydraulic head defined as:

$$H = h(\theta) - z \quad (4)$$

For non-swelling soil (Childs and Collins-George, 1950; Coppola *et al.*, 2012), equation 3 can be expressed as a θ dependent equation by introducing the concept of soil water diffusivity:

$$\frac{\partial \theta}{\partial t} = \frac{\partial}{\partial z}\left[D(\theta)\frac{\partial \theta}{\partial z} - K(\theta)\right] \quad (5)$$

where D(θ) is diffusivity defined by:

$$D(\theta) = K(\theta)\frac{\partial h}{\partial \theta} \quad (6)$$

Equation 5, generally known as the Fokker-Planck equation (Jury 2004), is a diffusivity equation with diffusivity dependent on θ. Because of this dependence, a diffusivity versus soil water content relation must be secured prior to solving equation 5.

To define the function D(θ) various expressions have been proposed. Exponential expressions proposed in 1958 by Gardner and Mayhugh (1958) have long been used, where:

$$D(\theta) = -\alpha\exp(\beta\theta) \quad (7)$$

with α and β constant for an assigned soil.

An exponential expression was also adopted in the theoretical studies of Scott and Hanks (1962) and Klute *et al.* (1965) on wetting and drying phenomena occurring in a horizontal experiment. Scott and Hanks (1962) examine a semi-infinite flow domain, with transient flow determined initially under constant water content when there occurs an unexpected variation in θ in correspondence with the initial section, at x=0.

The following conditions are thus set for drying:

$$0 < x < \infty \quad t > 0$$

$$\theta(x,t) = \theta_0 \quad t > 0$$

$$\theta(x,0) = \theta_2$$

The following conditions are thus set for wetting:

$$0 < x < \infty \quad t > 0$$

$$\theta(x,t) = \theta \quad t > 0$$

$$\theta(x,0) = \theta_1$$

leading to

$$0 < \theta_2 < \theta_0 < \theta_1$$

The solution is obtained numerically with the aid of a mathematical model. For both transients, we supply graphs of the distributions of water content in the medium, using parametric curve for ratios D_1/D_0 or D_0/D_2 at each of the two transients in question.

For the initial section, x=0, the infiltration velocity i is expressed by the relation:

$$i = -\frac{\omega}{\beta}\sqrt{\frac{\alpha}{2t}} = -\frac{\omega^*}{\beta}\sqrt{\frac{\alpha\exp(\beta\theta_0)}{2t}} \quad (8)$$

The outflow volumes W at time t are supplied by the expression:

$$W(t) = -\frac{\omega^* A}{\beta}\sqrt{2\alpha\exp(\beta\theta_0)\cdot t} \quad (9)$$

A being the area of the transversal section of the column, α and β characteristic parameters of the medium, and ω^* a parameter defined in drying by the ratio D_0/D_2 and in wetting by the ratio D_1/D_0.

Klute ed al. (1965) consider the same transients in a column of finite length L, consisting of a medium of hydraulic diffusivity

$$D(\theta) = D_r\exp(\beta)\frac{(\theta - \theta_r)}{(\theta_s - \theta_r)} \quad (10)$$

D_r being the diffusivity corresponding to hygroscopic water content θ_r and β a characteristic parameter of the porous medium.

Klute *et al.* (1965) also make reference to adimensional variables:

$$\xi = \frac{x}{L}$$

$$\tau = \frac{D_r}{L^2}$$

They then express the water volume present at time τ in the sample still susceptible of exchange with the environment by means of the relation:

$$\sigma = \int_0^1 (\theta - \theta_r)/(\theta_s - \theta_r)\,d\xi \quad (11)$$

and set at the terminal sample section, x=L, the further condition of zero flow:

$$\left[\frac{\partial \theta(\xi,t)}{\partial \xi}\right]_{\xi=1} = 0 \quad t \geq 0$$

The solution to the problem is likewise obtained numerically with the aid of the mathematical model.

For assigned values of parameter β the distributions of water content in the medium are supplied for assigned values of τ. Once again, for media with the assigned value of β, we supply the functions σ(τ) using the curves reported for drying and for wetting respectively in Figures 1 and 2.

Further, in the nomograph below we provide the values in time of the infiltration velocity in the initial section by means of the dimensional expression:

$$J(\tau) = \frac{L_1(t)}{D_r(\theta_s - \theta_r)} \quad (12)$$

Of particular interest is the nomograph reported in Figure 3, and that in Figure 2. It is evident that, for all the values of parameter β considered, there may even be a 60% reduction in average water content in

the porous medium without $J(\tau)$ being affected by the actual length L of the column.

In the range $1 \le \sigma \le 0.6$ it would thus appear appropriate to express water volumes acquired by the porous medium through more straightforward solutions relative to the semi-infinite flow domain.

Materials and methods

This study concerns the hydraulic characterisation of undisturbed *terra rossa* samples from Nardò in the region of Puglia (south-eastern Italy), taken from horizons Ap and B of a modal soil profile whose properties are reported in the Appendix. The samples (diameter: 80 mm; height: 150 mm) were brought to hygroscopic water content θ_r and subjected to the wetting process from the bottom. At the end of the wetting transient, with the stabilising of condition $\theta=\theta_1$, the samples were brought to maximum water content θ_s, after which we proceeded to determine, under constant hydraulic head, the maximum value of hydraulic conductivity K_s.

Having thus impeded the flow of water at the lower base, the samples underwent the drying process. Sample drying was obtained by letting the water evaporate from the upper surface using a ventilator with a turbine of the same diameter as the sample and positioned at a height of about 12 cm. When the ventilator is started, the drying process develops through an initial phase of constant water flow θ, of little variability in relation to the properties of the sample in question (Ciollaro and Comegna, 1981). The duration t_c of this first phase is conditioned by the possibility that, at any point of the domain, as the local value of the water content diminishes, the corresponding decrease in hydraulic conductivity K is compensated by the accentuation of hydraulic head gradients.

When the water content at the surface of the porous medium reaches the value corresponding to hygroscopic water content θ_r, the condition of constant flow can no longer be guaranteed. In the subsequent drying phase the transient is characterised by the parallel reduction of local gradients in the potential and in conductivity K.

In various tests conducted on the same sample, the reduction in the initial constant water flow θ leads to a corresponding increase in duration t_c, the value qt_c of the evaporated volume remaining substantially constant.

For $t>t_c$ the completion of drying occurs according to the law which varies little for the various values of water flow q. Yet in the same system it depends essentially on the volume of liquid still present in the same system. With the rapid exhaustion of the influence of initial conditions, there remains a curve which represents the completion of the transient with regard essentially to the characteristics of the porous medium.

In conducting our research, we examined the second phase of the transient, which is completed for $t>t_c$ insofar as Klute's analysis refers only to the second part of the evaporative process and may be extended to the case of vertically arranged samples, given the modest height of the dried samples. In particular, a comparison was established between wetting-drying phenomena found for the soil samples tested, according to the techniques recalled above, and those defined by using the scheme proposed by Klute. In the course of both transients, the corresponding wetting and drying functions were measured by continuously recording sample weight.

Results and discussion

In Figure 4 the two functions determined during the characterisation tests of an undisturbed red soil sample are illustrated as an example in plane $\theta(t)$. The test measurements were elaborated under the hypothesis that, for water contents close to θ_r, hydraulic diffusivity assumes the same value in both phases, namely wetting and drying.

Interpretation of the observations draws on the results of the theoretical investigations mentioned above, through calculations facilitated by the use of appropriately designed nomographs (Figures 5 and 6).

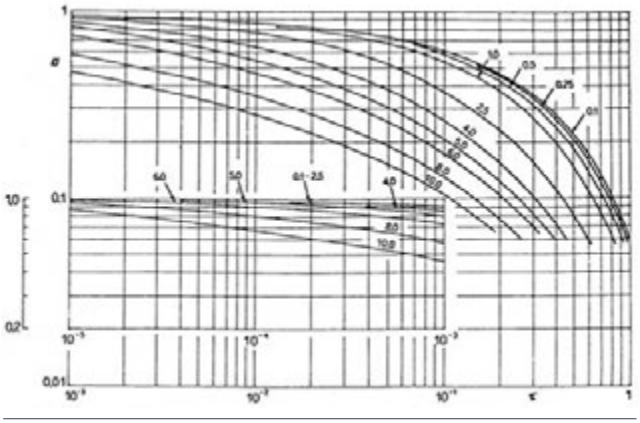

Figure 1. Values of $\sigma(\tau)$ for β=constant, for the drying process.

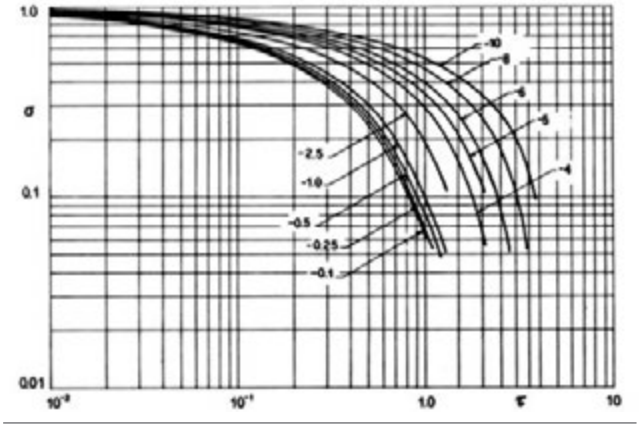

Figure 2. Values of $\sigma(\tau)$ for β=constant, for the wetting process.

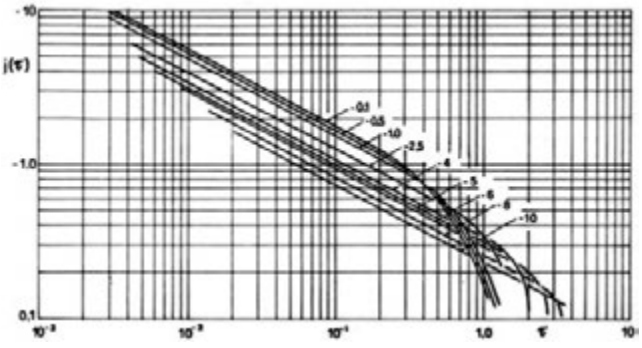

Figure 3. Values of $J(\tau)$ for β=constant, for the wetting process.

Use of the first (Figure 5) envisages, for longer durations t_c of constant water flux evaporation, the acquisition of two values, σ_1 and $\sigma_2=\sigma_1+0.2$ and times t_1, t_2 and t_3 corresponding to the values σ_1, σ_2 and $\sigma_3=0.5(\sigma_1+\sigma_2)$.

On the basis of the measured value of σ_1 and the $(t_2-t_1)/(t_3-t_1)$ ratio using the abacus in Figure 1, by interpolation we obtain the value of parameter β. For the values of β, σ_1 and σ_2, once again by interpolation, we obtain the corresponding values of τ_1 and τ_2.

Finally, for the relation

$$\tau = \frac{D_t t}{L^2}$$

we arrive at determining diffusivity D_b for $\theta=\theta_s$ using the expression

$$D_t = (\tau_2 - \tau_1)L^2/(t_2 - t_1)_m .$$

As regards the wetting phase, the extreme values θ_r and θ_1 are supplied by experience. Hence for a pair of values σ and τ, found experimentally, for σ no less than 0.4, the characteristic parameters of the medium may be determined, satisfying the equation

$$W = \frac{\omega^* A}{\beta}\sqrt{t}$$

in respect of ω^* values which are obtained by using the nomograph in Figure 6, representative of the theoretical results of Scott and Hanks.

As an example, in the ratios $(\theta_s-\theta)/(\theta_s-\theta_r)$ *vs* D Figure 7 shows the representative curves of equation (7) obtained in characterising soil samples n° 71, 42 and 2.

For each sample in Table 1 we report for the applications the values assumed on the basis of soil hydraulic characterisation.

It is easy to detect that hysteresis phenomena condition the behaviour of the samples in question to a much greater extent than local variabilities which characterise natural media.

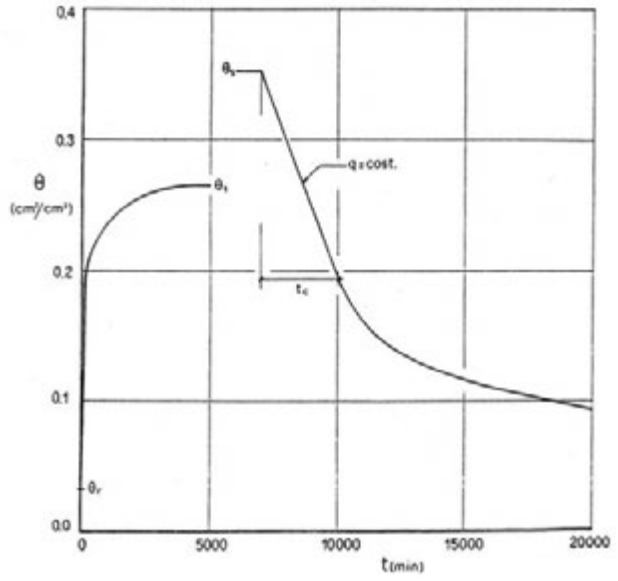

Figure 4. Laws *θ(t)* in wetting and subsequent drying phases.

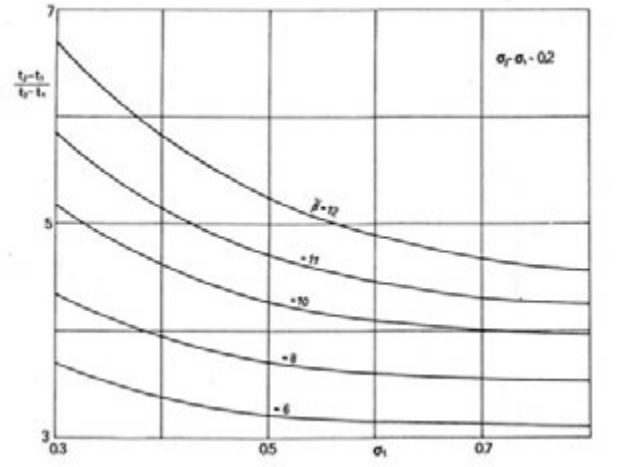

Figure 5. Values of $\frac{t_2-t_1}{t_3-t_1}$ *vs* (σ) for β=constant.

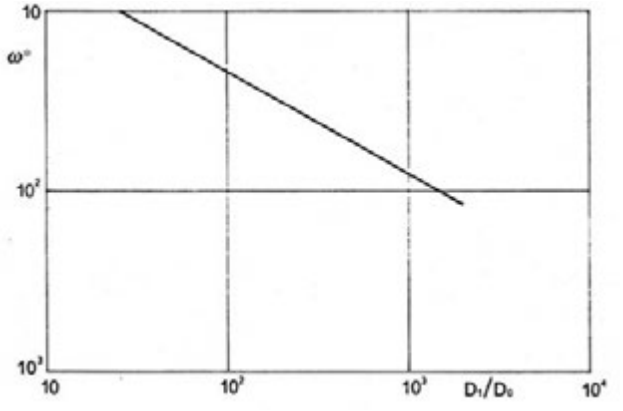

Figure 6. Values of ω^* *vs* (D_1/D_0) in the wetting process.

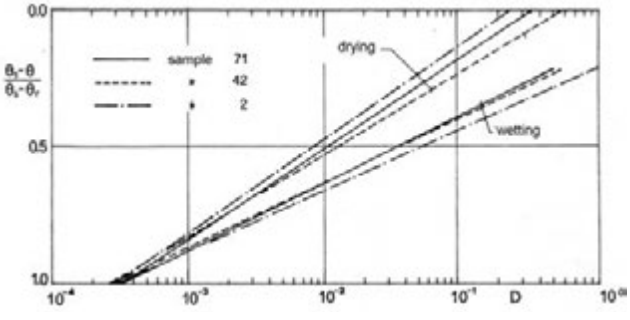

Figure 7. Values of $(\theta_s-\theta)/(\theta_s-\theta_r)$ *vs* *D*.

Table 1. Basic soil hydraulic properties.

Sample No.	θ_r cm^3/cm^3	θ_1 cm^3/cm^3	θ_s cm^3/cm^3	D_r cm^2/min	D_1 cm^2/min	D_s cm^2/min	K_s cm/min
71	0.031	0.264	0.351	0.00030	0.45	0.33	0.0253
42	0.036	0.280	0.329	0.00025	0.50	0.57	0.0852
2	0.037	0.25	0.345	0.00027	1.00	0.23	0.0469

Conclusions

The test method proposed requires that only the sample's mean water content be recorded by weighing. Experimental findings highlighted the validity of wetting and subsequent drying test in hydraulic characterization of soil samples.

Interpretation of the results, developed in light of theoretical data, allows straightforward definition of both primary wetting and drying curves of hydraulic diffusivity of the medium. It is easy to detect that hysteresis conditions the behaviour of the samples in question to a much greater extent than local variabilities which characterise natural media. Our results show that it may be useful to extend observations to other soil types. The proposed method may be considered an effective investigation tool when hydraulic characterisation of different pedological units is carried out on a statistical basis.

Appendix

Sample n°71) Undisturbed, sampled at Nardò (LE) from horizon Ap, between the depths of 10 and 25 cm; classified as sandy (SISS): 81% sand; 6% silt; 13% clay; height L=11 cm; bulk density r=1.59g/cm^3.

Sample n°42) Undisturbed, sampled at Nardò from horizon B, between the depths of 25 and 40 cm; classified as sandy-clayey (SISS): 76% sand; 6% silt; 18% clay; height L=13 cm; bulk density r=1.57/cm^3.

Sample n°2) Undisturbed, sampled at Nardò from horizon B, between the depths of 50 and 65 cm; classified as sandy-clayey (SISS): 76% sand; 6% silt; 18% clay; height L=12.5 cm; bulk density r=1.52cm^3.

References

Childs E.C., Collis-George C. 1950. The permeability of porous materials. Proc. R. Soc. London Ser.(A). 201: 392-405.

Ciollaro G., Comegna V. 1981. La caratterizzazione idraulica del suolo nell'intervento irriguo. Pubblicazione dell'Istituto di Idraulica Agraria di Napoli. Università di Napoli.

Ciollaro G., Romano N. 1995. Spatial variability of the hydraulic properties of a volcanic soil. Geoderma. 65: 263-282.

Coppola A., Gerke H.H., Comegna A., Basile A., Comegna V. 2012. Dual-permeability model for flow in shrinking soil with dominant horizontal deformation. Water Resour. Res. 48: W08527, doi:10.1029/2011WR011376.

Doering E.J. 1965. Soil-water diffusivity by the one-step method. Soil Sci. 99:322-326.

Eching S.O., Hopmans J.W., Wendroth O. 1994. Unsaturated hydraulic conductivity from transient multistep outflow and soil water pressure data. Soil Sci. Soc. Am. J. 58: 687-695.

Gardner W.R., 1956. Calculation of capillary conductivity from pressure outflow data. Soil Sci. Soc. Am. Proc. 20: 317-320.

Gardner W.R., Mayhugh M.S. 1958. Solutions and tests of the diffusion equation for the movement of water in soil: Soil Sci. Soc. Am. Proc. 22: 197-201.

Gardner W.R. 1962. Note on the separation and solution of diffusion type equations. Soil Sci. Soc. Am. Proc. 26: 404.

Gupta S.C., Farrel D.A., Larson W.E. 1974. Determining effective soil water diffusivities from one-step outflow experiments. Soil Sci. Soc. Am. J. 38: 710-716.

Jury W.A., Horton R. 2004. Soil Physics, John Wiley and Sons, Inc.

Klute A., Whisler F.D., Scott E.J. 1965. Numerical solution of the nonlinear diffusion equation for water flow in a horizontal soil column of finite length. Soil Sci. Soc. Am. Proc. 4: 353-358.

Kool J.B., Parker J.C., van Genuchten M.Th. 1987. Parameter estimation for unsaturated flow and transport models-A review. J. Hydrol. 91: 255-293.

Kunze R.J., Kirkham D. 1962. Simplified accounting for membrane impedance in capillary conductivity determinations. Soil Sci. Soc. Am. Proc. 26: 421-426.

Londra P.A., Valiantzas, J.D. 2011. Soil water diffusivity determination using a new two-point outflow method. Soil Sci. Soc. Am. J., 75: 1343–1346.

Scott E.J., Hanks R.J. 1962 Solution of the one dimensional diffusion equation for exponential and linear diffusivity functions by power series applied to moisture flow in soils. Soil Sci. 94: 314-322.

Parker J.C., Kool J.B., van Genuchten M.Th. 1985. Determining soil hydraulic properties from one-step outflow experiments by parameter estimation: II. Experimental studies. Soil Sci. Soc. Am. J. 49: 1354-1359.

Passioura J.B. 1976. Determining soil water diffusivities from one step outflow experiments. Aust. J. Soil Res. 15:1-8. doi:10.1071/SR9770001.

Rijtema P.E. 1959. Calculation of capillary conductivity from pressure plate outflow data with non-negligible membrane impedance. Netherlands J. Agr, Sci. 7:209-215.

Valiantzas J.D. 1990. Analysis of outflow experiments subject to significant plate impedance. Water Resour. Res. 26:2921-2929. doi:10.1029/ WR026i012p02921.

Evapotranspiration models for a maize agro-ecosystem in irrigated and rainfed conditions

Arianna Facchi, Olfa Gharsallah, Claudio Gandolfi

DiSAA, Università degli Studi di Milano, Milano, Italy

Abstract

A high level of accuracy in the estimation of crop evapotranspiration (ET) may lead to significant savings of economic and water resources in irrigated agriculture. Although ET is a fundamental process in many applications, it cannot be directly measured but it has to be estimated by monitoring the exchange of energy/water above the vegetated surface (micrometeorological methods), or as a residual term of the hydrological balance (lysimeters, soil water budget). The techniques to be adopted are often complex, costly and require specific equipment. Thus, since the '50s, many researchers have devoted their activity to the development of models for its estimation. The available approaches can be classified in "direct" methods, based on the original Penman-Monteith (PM) equation, in which the canopy resistance r_c is modelled, and "indirect" methods, based on the preliminary calculation of ET for a well-watered reference grass (ET_0) with a constant r_c, which is then multiplied by a crop coefficient K_c and, in case, by a stress coefficient K_s to obtain ET. Even if the latter approaches are more widely adopted for their practical simplicity, many authors show that the former often provide better ET estimates in absence of calibration of crop parameters. In this study the performances of different direct and indirect methods were evaluated in the case of a surface irrigated and of a rainfed maize grown in the Padana Plain (Northern Italy). The following models were considered: the "one-layer" original PM equation with three different models for r_c (Monteith, Jarvis, Katerji-Perrier), the "two-layers" PM model proposed by Shuttleworth and Wallace, the "single" and "double" crop coefficient models illustrated in the Paper FAO-56. Latent heat fluxes measured in 2006 and 2011 in an experimental maize field by eddy-covariance were used to evaluate the models accuracy. Crop, soil and meteo data monitored contextually were used for the implementation of the different models. Results confirm that direct methods are more performing for both irrigated (2006) and rainfed (2011) conditions, with the SW model providing the best results and the FAO-56 models with generalized crop coefficients overestimating ET, especially during the middle growth stage.

Correspondence: Arianna Facchi, DiSAA via Celoria 2 , 20133 Milano, Italy.
Tel. +39.02.50316909 - Fax: +39.02.50316911.
E-mail arianna.facchi@unimi.it

Key words: evapotranspiration, Penman Monteith equation, canopy resistance, Paper FAO-56, crop coefficient, eddy covariance.

Contributions: the authors contributed equally.

Conflict of interests: the authors declare no potential conflict of interests

Funding: This research was financed by Regione Lombardia – D.G. Agricoltura.

Acknowledgments: this research was financed by Regione Lombardia – D.G. Agricoltura which is gratefully acknowledged. The authors wish to thank the PoliMi- DIIAR group coordinated by Prof. Marco Mancini with whom the monitoring activity was conducted.

Journal of Agricultural Engineering 2013; XLIV(s1):e169
doi:10.4081/jae.2013.(s1):e169

Introduction

As the water resources available for agriculture become limited due to population growth, competition among different water uses, droughts, and water quality degradation, the importance of quantifying evapotranspiration (ET), which is the major component of water use in agriculture, grows (Farahani *et al.*, 2007). ET cannot be directly measured but it has to be estimated by monitoring the exchange of energy/water above the vegetated surface (micrometeorological methods), or as a residual term of the hydrological balance (lysimeters, soil water budget). The techniques that can be adopted are often complex, costly and require specific equipment, thus they are generally applied only in scientific research.

In most practical situations where crop ET rates are required, the available economic and human resources are not sufficient to allow use of the ET measurement techniques mentioned above, and models are used instead. Since the '50s, many researchers have devoted their activity to the development of models that seek to estimate crop ET from near surface climate data. Early ET models were based on the perception that surface atmosphere exchange was a simple physical phenomenon little influenced by any overlying vegetation cover. This led to empirical relationships between climatic data and the potential rate of evaporation (or evapotranspiration) (*e.g.*, Thornthwaite, 1948; Blaney and Criddle, 1950). In this context, the equation of Penman (1948, 1963) was a benchmark. Penman's contribution was to derive a "combination equation" by combining two terms, one of which accounted for the energy required to maintain evaporation ("available energy" term), and the second for the atmosphere's ability to remove water vapour ("aerodynamic" or "sink"term) (Farahani *et al.*, 2007). After that, the modification of Monteith (1965) to the previous equation of Penman moved the axis of the research from a representation of the phenomenon by purely physical laws to one where physiological controls play a fundamental role (Ziemer, 1979). Subsequently, further progress was made in building compartment models based on two or more combination equations, allowing the description of sparse canopies and the partitioning of ET (*e.g.*, Shuttleworth and Wallace, 1985).

Difficulties in applying combination formulas (particularly related to a lack of consolidated information on the required aerodynamic and surface resistances for different crops and to the need of meteorological data measured above the canopy) led researchers towards an alternative "indirect" approach to estimate the crop evapotranspiration (ET_c). This approach is based on a "two-step" procedure: in the first step, the rate of ET was estimated for a reference crop (ET_0) in well-watered conditions. This rate was then multiplied by a crop specific coefficient with the objective of estimating ET_c for different crops. The ratio of ET_c to the ET_0 for a reference crop (short grass or alfalfa), called crop coefficient, K_c (Jensen, 1968), was then experimentally determined for different growth stages for many crops as the basis for this now long established two step approach for estimating crop water use. The use of ET_0 (estimated using local climate data) and associated crop coefficients, K_c, became an accepted way to estimate ET_c for well watered crops, and the K_c methodology was adopted by the UN's Food and Agriculture Organization (FAO) in the 1970s (Doorenbos and Pruitt, 1977). Its subsequent worldwide promotion was a significant step forward in irrigation engineering and water management (Farahani *et al.*, 2007). Later, in the 1980s and 1990s, there was further rapid progress in data acquisition, remote data access, automation, and in eddy correlation and other measurement techniques. Transfer of technology made available daily values of ET_0, facilitating early computer applications for irrigation scheduling (Martin *et al.*, 1990). The superior realism and value of combination equations was recognized, and the PM equation was adopted to estimate ET_0 in the K_c approach (Allen *et al.*, 1994; Allen *et al.*, 1998).

Despite the practical simplicity of using the "indirect" approach is indisputable, many authors in the last fifteen years demonstrated that the adoption of generalized crop coefficient curves can lead to relevant errors in the estimation of ET, since the differences between the K_c values reported in the FAO-56 Paper (Allen *et al.*, 1998) and the values obtained from locally observed data are up to ± 40%, especially during the middle growth cycle (Katerji and Rana 2006). This is mainly due to the complexity of the crop coefficient, which actually integrates several physical and biological factors. On the contrary, many researchers assessed the validity of "direct" approaches (Kato *et al.*, 2004; Farahani and Bausch, 1995; Lafleur and Rouse, 1990), concluding that their ability to simulate the processes is good, provided that the resistances involved are calculated appropriately (Brisson *et al.*, 1998). In order to adopt these models for operational uses, however, the main problems limiting their practical application must be solved.

Both the "direct" and "indirect" methods have their merits and demerits, but certainly very few experiments were conducted applying the different models jointly to the same dataset.

The objective of this study was the investigation of the performance of the most popular "direct" and "indirect" ET methods for a maize agro-ecosystem under well-irrigated and under water-stressed conditions in Northern Italy. In particular, the exercise was conducted using the datasets collected in two agricultural seasons: the first in which the field was irrigated, and the second in which no irrigation event was applied. This allowed to compare the models' performance under different soil water conditions and, at the same time, in conditions ranging from bare to full covered soils. Latent heat fluxes measured by an eddy-covariance tower placed in the field were used to test the models performance at the daily time step.

Materials and methods

The Landriano experimental site

Data used in this work were collected during the cropping seasons 2006 and 2011 in a 10 ha maize field located in Northern Italy (Landriano), in an experimental farm of the State University of Milan (45°19' N, 9°15' E, 88 m a.s.l.). Long-season Zea Mays varieties (FAO class 600–700) were seeded both years. The crop in 2006 was for silage, seeded after ryegrass and harvested green (emergence: DoY=157, harvesting: DoY=283). In 2011 maize was for forage as well, but it was harvested at the dough stage (maize silage with cobs; emergence DoY=110, harvesting: DoY=244). Maize was chosen for the study since it is the main crop in Northern Italy, covering more than 30% of the arable land.

Instruments for detailed monitoring of water and energy fluxes were installed in 2005. A micrometeorological eddy covariance (EC) station was located in the centre of the field. Instruments for the monitoring of soil water content and potential were positioned at different depth in a soil profile. Due to the presence of a shallow water table (90-120 cm below the topographic surface), a shallow piezometer with a pressure transducer device was also installed. Data were averaged and registered on half an hour basis. Several campaigns were carried out to monitor crop biometric parameters (leaf area index, crop height, rooting depth) and soil properties in both agricultural seasons. Standard meteorological variables were measured on hourly time step by an agro-meteorological station installed in a grass parcel located at 200 m distance from the experimental field.

The site has a humid subtropical climate according to the Koppen classification system.

During the cropping season 2006 the field was irrigated twice: at DoY=159 with the sprinkler method to promote crop emergence, and at DoY=195 with the border method. The water amount applied was estimated to be respectively 25 mm and 140 mm in the two events (Baroni *et al.* 2010). No irrigation was applied in 2011.

Eddy covariance data were post-processed using the TK2 software (Mauder and Foken, 2004). The energy balance closure for daytime (R_n>0) 30-min data was equal to 83% for 2006 and 92% for 2011. The gap-filling of missing/eliminated daytime data was conducted determining a regression between half-hourly values of ET and both available energy (R_n-G) and vapour pressure deficit (VPD), only for the days in which at least the 80% of daytime data were available. Daily ET values were finally calculate summing up the 30-min data. More information about the experimental site and the processing of eddy covariance data are illustrated in Facchi *et al.* (2013).

Direct methods

One-layer Penman-Monteith (PM) model

The Penman Monteith (1965) "one-layer" model (PM) schematizes the vegetation cover as a single "big leaf" placed at a certain height within the vegetation. The vegetation is taken into account through the canopy and the aerodynamic resistances. The aerodynamic resistance (r_a) is a function of wind and vegetation height. The canopy resistance (r_c) is a "bulk" resistance describing the resistance of vapour flow through stomata openings, through the canopy total leaf area and within the soil to the soil surface.

A problem with the PM "one-layer" approach is that areas with partial or sparse vegetation cover don't satisfy completely the hypothesis of "big leaf". The difficulty of providing accurate ET estimates using the PM model in partial canopy conditions (LAI<1.5-2) has been underlined by several authors (Farahani and Bausch, 1995; Lafleur and

Rouse, 1990).

In this study, the following three approaches for estimating r_c have been selected: a) Monteith, b) Jarvis and c) Katerji and Perrier.

Canopy resistance following Monteith

For a thick crop canopy it can be assumed that all the leaves behave as resistances in parallel and r_c is computed from the ratio between the minimal stomatal resistance (r_s) and the leaf area directly involved in the energy exchange (LAI_{eff}):

$$r_c = \frac{r_s}{LAI_{eff}} \quad (1)$$

Several earlier studies fixed the value of the minimal stomatal resistance r_s at 100 s m^{-1} for grass type fields (Monteith, 1965; Szeicz and Long, 1969). Subsequently, many authors demonstrated that this variable ranges between 100 and 300 s m^{-1} as a function of the crop type. In this study a value of 252 s $m^{-1}$was adopted, as suggested by Howell *et al.* (1997) for maize.

In a fully developed canopy only a fraction of the leaf area index effectively contributes to transpiration, since the photosynthetically active radiation varies through the canopy. A functional relationship between LAI and LAI_{eff} suitable for all crops has not yet been found. For a maize crop, Gardiol *et al.* (2003) reported LAI_{eff}=LAI for LAI≤2, LAI_{eff}=0.5 LAI for LAI≥4 and LAI_{eff}=2 for intermediate LAI values (2<LAI<4). In this paper an update of this formula is proposed. The PM model with r_c by Monteith applies only to well watered soil conditions, since this resistance does not take into account of soil or crop water status.

Canopy resistance following Jarvis

For more than thirty years, the most widespread approaches to parameterize the effect of environmental factors on stomatal behaviour have been the Jarvis-type models, in which the canopy resistance is expressed as a function of the minimal stomatal resistance r_s and a series of independent stress functions F_i combined in a multiplicative way (each function representing the influence of one factor and providing values ranging from 0 to 1). In particular, the Jarvis-type model proposed by Noilhan and Planton (1989) is set as follows:

$$r_c = \frac{r_s}{LAI\, F_1 F_2 F_3 F_4} \quad (2)$$

In this study, for consistency with the r_c modelled following the Monteith approach, LAI=LAI_{eff} and r_s=252 s m^{-1} (Howell *et al.*, 1997) were adopted. F_1, F_2, F_3 and F_4 represent respectively the influence on r_c of photosynthetically active radiation, vapour pressure deficit, air temperature and effective soil water content, and they were modelled as reported in Gharsallah *et al.* (2013). In particular, the F_4 factor was modified with respect to the original version of Noilhan and Planton (1989), becoming:

$$F_4 = \begin{cases} 1, if\ \theta > \theta_t \\ \dfrac{\theta - \theta_{wilt}}{\theta_t - \theta_{wilt}}, if\ \theta_{wilt} \le \theta \le \theta_t \\ 0, if\ \theta < \theta_{wilt} \end{cases} \quad (3)$$

where θ is the effective soil water content ($m^3\ m^{-3}$), θ_{wilt} is the soil water content at the wilting point ($m^3\ m^{-3}$) while θ_t is set at the critical soil water content under which the evaporative stress begins following what proposed by Allen *et al.* (1998). Due to the F_4 function, the PM equation with r_c following Jarvis is expected to provide good results both under well-watered and water-stressed conditions.

Canopy resistance following the Katerji and Perrier approach

According to Katerji and Perrier (1983), the latent heat flux is governed by three resistances: the aerodynamic resistance r_a, the climatic resistance r*, depending only on weather variables, and the canopy resistance r_c. Through dimensional analysis the authors demonstrated that the resistances r_c and r* are linked as follows:

$$\frac{r_c}{r_a} = a\frac{r^*}{r_a} + b \quad (4)$$

where a and b are calibration parameters which vary with the crop type, its phenological stage and its water status, but, according to the authors, they are not site-specific (Rana *et al.*, 1997a). Parameters values for a few crops in different growth stages (active development and senescence) and water conditions (different intervals of leaf water potential) were provided by Rana *et al.* (1997a, 1997b, 2001). Unfortunately, maize is not among those crops, thus in this study the two parameters were derived from the available data. This is the only calibration operation in the study, performed using some days of the dataset collected at Landriano in 2011. In particular, the dataset was divided into three periods: active development in the absence of crop water stress conditions, active development under crop water stress conditions and senescence. Three representative days for each period were selected, the daytime (R_n>0) 30-min canopy resistance r_c was determined from the corresponding eddy covariance data by the inversion of the PM equation, a linear regression between the ratio r_c/r_a and r^*/r_a was then fitted and the parameters a and b were identified. Obviously, r_c from the eddy covariance data, r* and r_a were calculated starting from the half-hourly data acquired in the selected days. The a and b values found for the first period of 2011 agricultural season (*i.e.* active development with absence of water stress) were used for the whole 2006 season, since maize was well-watered and harvested very early that year. Instead, for the agricultural season 2011, a e b values found for the three periods where respectively used. Data used for the a and b calibration were eliminated from the 2011 eddy covariance dataset used for the models' validation. Since the a e b parameter values were identified even under water-stressed conditions, the model is expected to work properly for all soil water status.

Two-layers Shuttleworth (SW) model

The SW model (Shuttleworth and Wallace, 1985; Shuttleworth and Gurney, 1990) combines two PM type equations for crop transpiration and soil evaporation. Canopy and surface resistances regulate the heat and mass transfer at the plant and soil surfaces and aerodynamic resistances regulate those between the two surfaces and the atmospheric boundary layer. The two terms are computed by the following equations:

$$\lambda ET = \lambda T + \lambda E = C_c \lambda T0 + C_s \lambda E0 \quad (5)$$

where λET is the sum of the latent heat flux from the crop (λT) and the soil (λE) (W m^{-2}). λT0 and λE0 are the terms similar to the PM model and C_c and C_s are respectively the canopy resistance and soil surface resistance coefficients.

Different resistances play they role in the model. The soil surface resistance r_{ss} is interpreted as the resistance for the water vapour to diffuse through the top layer of the soil. Shuttleworth and Wallace (1985) proposed values respectively of 0, 500 and 2000 s m^{-1} for r_{ss} in various soil water conditions. The canopy resistance r_{sc} was calculated following Eq. 1, while the aerodynamic resistances r_{aa} and r_{as} as well as the soil surface resistance coefficients C_c and C_s were computed as reported by Shuttleworth and Gurney (1990) and Kato *et al.* (2004). The SW model is expected to provide affordable results for bare to full covered soils under water stressed and well-watered conditions.

Indirect methods

The FAO-56 "single crop coefficient" model

In the FAO-56 "single crop coefficient" approach (Allen *et al.*, 1998), crop evapotranspiration ET_c in optimal water conditions is estimated multiplying the reference evapotranspiration ET_0 (calculated applying the PM equation to a "reference grass" having fixed crop parameters) and the crop coefficient K_c, specific for the crop type and its stage of development. Crop development stages (L_{ini}, L_{dev}, L_{mid}, L_{late}) and the corresponding K_c values ($K_{c\,ini}$, $K_{c\,mid}$, $K_{c\,end}$) are tabulated in the Paper FAO-56 for different crops grown in various regions.

For the case study, K_c curves for years 2006 and 2011 were built considering the length of the crop growth stages observed in the field and adjusting the tabulated crop coefficients with the local data following the procedures indicated by Allen et al (1998). Since maize in 2006 was harvested green and FAO-56 does not provide $K_{c\,end}$ value for silage maize, K_c was kept constant and equal to $K_{c\,mid}$ till harvesting. Crop stages length and adjusted K_c values for 2006 and 2011 are reported in Table 1. More details can be found in Facchi *et al.* (2013).

To estimate the evapotranspiration in water-stressed condition $ET_{c\,adj}$, ET_c must be multiplied by a stress coefficient K_s, which depends on the average soil water content in the root zone as calculated by a daily water balance (Allen *et al.*, 1998).

Since the simple balance model proposed by FAO-56 does not take into account adequately the capillary rise, the "single crop coefficient" approach was applied in this study only for 2006 (for which $ET_{c\,adj}$=ET_c). As a matter of fact, the capillary rise is very important in soil water-stressed conditions when the water table depth is very shallow, as for the experimental site.

The FAO-56 "double crop coefficient" model

In the FAO-56 "double crop coefficient" approach (Allen *et al.*, 1998) the separation between the soil evaporation and the crop transpiration fluxes is achieved by splitting the K_c in two different coefficients: the basal crop (K_{cb}) and the soil evaporation (K_e) coefficients, the latter being calculated as a function of the basal crop coefficient and other variables. As for the "single crop coefficient", crop development stages and the corresponding K_{cb} ($K_{cb\,ini}$, $K_{cb\,mid}$, $K_{cb\,end}$) values are tabulated in FAO-56. In the case of soil water stress, $ET_{c\,adj}$ is calculated from ET_c considering the two stress coefficients K_s and K_r respectively computed from the average water content in the transpirative and in the evaporative zone by daily water balances (Allen *et al.*, 1998).

In this study, K_{cb} curves for 2006 and 2011 were built by considering the growing periods length observed in the field and the tabulated K_{cb} values after the adjustments suggested by Allen *et al.* (1998). The resulting values are reported in Table 1.

The calculation of daily K_r and K_s values was carried out with the support of the ALHyMUS model (Gandolfi *et al.*, 2006; Baroni *et al.*, 2010), computing ET_c on the basis of the "double crop coefficient" proposed by FAO-56. In this model, capillary rise is simulated following Liu *et al.* (2006).

Time step and performance indicators

Eddy covariance ET measurements were used to test the models performance for the two datasets at the daily time step. The PM and SW models were applied at the hourly time step, to determine the daily ET amount the sum of hourly daytime outputs (R_n>0) was then carried out. Since the FAO-56 "single" and "double crop coefficient" models were implemented using daily ET_0 estimates, they provided directly the daily ET values.

The statistical evaluation of the models' performance was carried out evaluating the linear correlation between observed and measured data (slope of the regression, M, and regression coefficient, R^2, were considered) and calculating the root mean square error (RMSE), the mean relative error (MRE) and the Nash-Sutcliffe Efficiency (NSE) indices.

$$RMSE = \left[\frac{1}{N}\sum_{i=1}^{N}(C_i - M_i)^2\right]^{\frac{1}{2}} \quad (6)$$

$$MRE = \frac{1}{N}\sum_{i=1}^{N}\frac{(C_i - M_i)}{M_i}100 \quad (7)$$

$$NSE = 1 - \frac{\sum_{i=1}^{N}(C_i - M_i)^2}{\sum_{i=1}^{N}(M_i - M_{avg})^2} \quad (8)$$

Results and discussion

Development of a new LAIeff function for maize crop

With the aim of identifying a new and more general equation for LAI_{eff} for maize crop, five ET data series measured by the eddy covariance technique were considered. Alongside the data series measured at Landriano in 2006 and 2011, also the one (incomplete) acquired in 2010 at the same site and the two measured in 2010 and 2011 at the Livraga experimental site (45°11' N, 9° 34' E, 60 m a.s.l.) were used. For more information about the datasets refer to Facchi *et al.* (2013). The need to identify a new function emerged because the Gardiol *et al.* (2003) model, which showed to work well for the 2006 dataset (Gharsallah *et al.*, 2013), led to an unacceptable LAI_{eff} pattern for 2011, characterized by a fast increase in the LAI_{eff} value for LAI≥4. As a matter of fact, the maximum LAI value measured in 2006 was around 4 $m^2\,m^{-2}$, while in 2011 this parameter reached a value of about 6 $m^2\,m^{-2}$.

Once daily ET data were obtained for the five eddy covariance datasets, ET values for days characterized by soil water stress conditions were eliminated. Soils were considered in water conditions preventing the occurrence of evapotranspirative stress when the average water content in the rooting depth is higher than 0.15 m^3m^{-3} and 0.22 m^3m^{-3} respectively for the Landriano and Livraga sites (Facchi *et al.*, 2013).

Crop resistance r_c was obtained for each day by inverting the PM equation following the Monteith approach for r_c. The obtained r_c, as well as the measured LAI values, were then plotted in function of the cumulative ground degrees days (GDD) starting from the seeding date

Table 1. Crop stages length observed in the field and K_c and K_{cb} adjusted considering local data.

Parameter	2006	2011
L_{ini}	25	29
L_{dev}	26	40
L_{mid}	56	51
L_{late}	27	26
$K_{c\,ini}$	0.29	0.28
$K_{c\,mid}$	1.16	1.14
$K_{c\,end}$	1.16*	0.57
$K_{cb\,ini}$	0.15	0.15
$K_{cb\,mid}$	1.11	1.09
$K_{cb\,end}$	1.11*	0.52

* crop was harvested green

(Facchi *et al.*, 2013). The use of GDD instead of the number of days reduces the data dispersion due to the different climatic conditions, and allows to consider data of a second crop maize (Landriano 2006) together with those of a first crop maize. The obtained data are shown in Figure 1.

Two approaches for the estimation of LAI_{eff} are proposed. The first one can be applied when measured LAI values are available. In that case, the Gardiol *et al.* (2003) model is modified as follows: LAI_{eff}=LAI for LAI≤2, LAI_{eff}=2 until the end of the middle season stage, LAI_{eff} linearly decreasing from 2 to 0.3 in the case of a complete senescence, to 0.35 for a dough stage harvesting, to 0.5 for silage maize.

The second approach can be adopted when measured LAI data are not available: LAI_{eff}=0.2 for initial stage (L_{ini}), LAI_{eff} between 0.2 and 2 for the crop development stage (L_{dev}), LAI_{eff}=2 for the middle season stage (L_{mid}), and LAI_{eff} as in the first approach for the late season stage (L_{late}).

Comparsion of ET models under well-watered conditions (2006)

Results of the models application and performance indices are reported in Figure 2 and Table 2.

All the "direct" approaches for ET estimation provide a very good agreement with the observations during the entire agricultural season. In particular, as expected given the lack of soil water stress conditions, the result provided by the model of PM with r_c by Jarvis is very close to that obtained with r_c by Monteith. Slightly lower performances are provided by the PM model with r_c by KP, even if the result is very satisfactory considering that the parameters a and b were calibrated using an independent data set (*i.e.* 2011). The SW model shows the best performance, behaving well also for days with sparse canopy and peak evaporation rate following irrigation and rainfall events. ET values estimated with the "single" and "double crop coefficient" approaches are higher than the observed, probably because of the excessively high values of K_c and K_{cb} obtained following the methodology FAO-56 when compared with those obtained from experimental observations in Northern Italy (Facchi *et al.*, 2013).

Comparsion of ET models under water-stressed conditions (2011)

Figure 3 and Table 3 show the performances of ET models under water-stress conditions, which basically confirm the results obtained

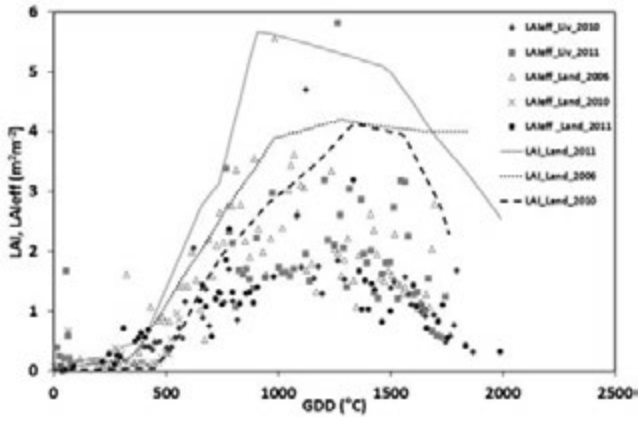

Figure 1. LAIeff derived from field measurements, measured LAI and average LAI_{eff}.

Table 2. Performance indices calculated for the ET models at Landriano in 2006.

ET models	M	R2	RMSE	MRE	NSE
PM (rc Monteith)	0.98	0.86	0.52	-1.25	0.87
PM (rc Jarvis)	0.96	0.86	0.53	-3.20	0.86
PM (rc KP)	1	0.73	0.69	9.56	0.76
SW	1.05	0.93	0.42	7.43	0.91
FAO-56 "single crop"	1.12	0.82	0.79	16.8	0.68
FAO-56 "double crop"	1.24	0.82	1.17	23.53	0.31

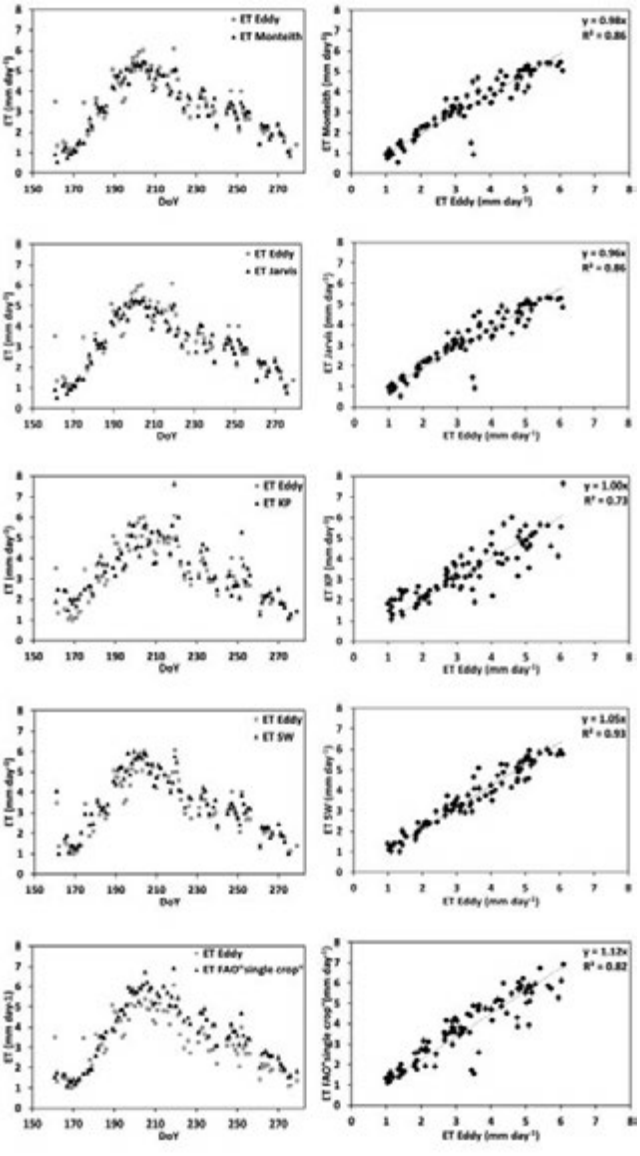

Figure 2. On the left: daily ET estimated by the different ET models and measured by the eddy covariance technique at Landriano in 2006. On the right: correlation between the measured and estimated data series.

Table 3. Performance indices calculated for the ET models at Landriano in 2011.

ET models	M	R^2	RMSE	MRE	NSE
PM (r_c Jarvis)	0.97	0.56	0.65	2.75	0.72
PM (r_c KP)	1.01	0.74	0.51	7.89	0.78
SW (r_c Jarvis)	0.99	0.67	0.56	6.78	0.73
FAO-56_adj"double crop"	1.16	0.68	1.05	267.43	0.04

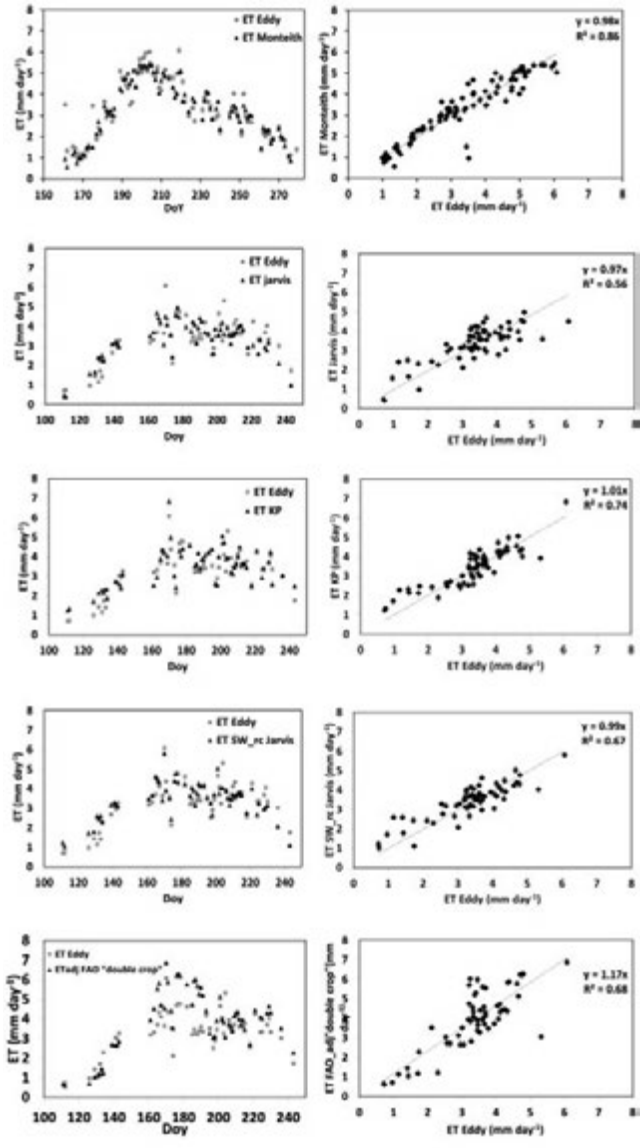

Figure 3. On the left: daily ET estimated by the different ET models and measured by the eddy covariance technique at Landriano in 2011. On the right: correlation between the measured and estimated data series.

under well-watered conditions, with the "direct" approaches giving the best results. It can be noted that the PM equation with r_c modelled following KP gives the best results, outperforming the PM with r_c by Jarvis, probably because the parameters a and b were calibrate using data of the 2011 dataset. Anyway, the performances for the three "direct" methods are comparable. As in the well-watered case, the performance of the FAO-56 model is the poorest.

A comparison between indices in Table 2 and Table 1 shows that in water-stressed conditions, even if the index values indicate good performances for all the "direct" models, these are slightly lower than those found for the well-watered case. In particular, the dispersion around the regression line increases, especially - but not only - at lower ET values (with a decreasing of R^2), and the NSE values are higher. This can be explained by the fact that in water-stressed condition ET deviates from its potential value, becoming more difficult to estimate, since it starts to depend from a higher number of factors.

Conclusions

The main findings of this study are: i) in absence of calibration of the crop parameters, direct methods provide better performances than the indirect methods, confirming the findings of several authors in the literature; ii) the use of a new and simple function for estimating LAI_{eff} for a maize crop in the different growth stages, proposed in this study, improves the performances of direct models at high values of LAI, compared to the most widely used functions reported in the literature; iii) the SW model is a robust model providing very good performance for the entire agricultural season under different soil water status conditions, but it requires complex procedures to estimate the various resistances involved; iv) the one-layer PM equation also provides good results in well-watered and water-stressed conditions with r_c by Jarvis and KP; v) the "single" and "double crop coefficient" FAO-56 models overestimate ET for the entire agriculture season; this is due to the fact that the crop coefficients, even if adjusted with local data, are overestimated, pointing to the necessity of determining site-specific crop coefficients ; vi) the main obstacle to the routine use of direct approaches, such as both PM and SW models, is the need of micrometeorological measurements taken above the crop (*e.g.*, R_n, VPD, wind speed) and the lack of consolidated information on surface resistances for the different crops, which call for further research to make these methods more applicable operatively.

References

Allen R. G., M. Smith., Perrier L., Pereira L. S. 1994. An update for the definition of reference evapotranspiration. ICID Bull. 43 A. (2): 1-34.

Allen R.G., Pereira L.S., Raes D., Smith M. 1998. Crop evapotranspiration (guidelines for computing crop water requirements). Irrigation and Drainage Paper 56. FAO. Food and Agriculture Organization of the United Nations. Rome, Italy.

Baroni G., Facchi A., Gandolfi C., Ortuani B., Horeschi D., Van Dam J.C. 2010. Uncertainty in the determination of soil hydraulic parameters and its influence on the performance of two hydrological models of different complexity. Hydrol. Earth. Syst. Sci (HESS). 6: 4065-4105.

Blaney H. F., Criddle W. D. 1950. Determining water requirements in irrigated areas from climatological and irrigation data. TP-96. Washington, D.C.: USDA Soil Conservation service.

Brisson N., Itier B., L'Hotel J.C., Lorendeau J.Y. 1998. Parameterisation of the Shuttleworth-Wallace model to estimate daily maximum transpiration for use in crop models. Ecol. Model. 107 (2–3): 159–169.

Doorenbos J., Pruitt W.O. 1977. Crop water requirements. Irrigation and Drainage Paper FAO 24. Food and Agriculture Organization of the United Nations. Rome, Italy, Rome, Italy

Facchi A., Gharsallah O., Gandolfi C., Corbari C., Mancini M. 2013. Eddy covariance for the determination of crop coefficients and crop water requirements for maize in Northern Italy. Accepted by Agric. Water Manage.

Farahani H.J., Bausch W.C. 1995. Performance of evapotranspiration models for maize: Bare soil to closed canopy. Trans. ASAE. 38: 1049–1059.

Farahani H. J., Howell T. A., Shuttleworth W. J., Bausch W. C. 2007. Evapotranspiration: progress in measurement and modelling in agriculture. Transactions of the ASABE. 50(5):1627-1638.

Gandolfi C., Facchi A., Maggi D. 2006. Comparison of 1D Models of Water Flow in Unsaturated Soils. Environ. Model. Soft. 21: 1759-1764.

Gharsallah O., Facchi A., Gandolfi C., 2013. Comparison of six evapotranspiration models for a surface irrigated maize agro-ecosystem in Northern Italy. Accepted by Agric. Water Manage.

Gardiol J.M., Serio L.A., Maggiora A.I.D. 2003. Modelling evapotranspiration of corn (Zea mays) under different plant densities. J. Hydrol .217, 188–196.

Howell T.A., Steiner J.L., Schneider A.D., Evett S.R., Tolk J.A. 1997. Seasonal and maximum daily evapotranspiration of irrigated winter wheat, sorghum, and corn-Southern High Plains. Trans. ASAE. 40(3): 623–634.

Jarvis, P.G., 1976. The interpretation of the variation in leaf water potential and stomatal conductance found in canopies in the field. Philos. Trans. Roy. Soc. London, Ser B. 273: 593-610.

Jensen M. E. 1968. Water consumption by agricultural plants. In Water Deficits and Plant Growth, 1-22. T. T. Kozlowski, ed. New York, N.Y.: Academic Press.

Kato T., Kimura R., Kamichika M. 2004. Estimation of evapotranspiration, transpiration ratio and water-use efficiency from a sparse canopy using a compartment model. Agric. Water Manage. 65 :173–191.

Katerji N., Perrier A. 1983. Modélisation de l'évapotranspiration réelle d'une parcelle de luzerne : rôle d'un coefficient cultural. Agron. J. 3(6): 513-521.

Katerji N., Rana G., 2006. Modelling evapotranspiration of six irrigated crops under Mediterranean climate conditions. Agric For Meteorol. 138: 142–155.

Lafleur P.M., Rouse W.R. 1990. Application of an energy combination model for evaporation from sparse canopies. Agric For Meteorol. 49(2) : 135-153.

Liu Y., Pereira L. S., Fernando R.M. 2006. Fluxes through the bottom boundary of the root zone in silty soils: parametric approaches to estimate groundwater contribution and percolation. Agric. Water Manag. 84: 27–40.

Mauder M., Foken T. 2004. Documentation and Instruction Manual of the Eddy Covariance Software Package TK2. University Bayreuth, Abt. Micrometeorologies, Germany.

Martin D. L., Heermann D. F., Fereres E. 1990. Irrigation scheduling principles. In Management of Farm Irrigation Systems: 155-203.

Monteith J.L. 1965. Evaporation and environment. In: Fogg, B.D. (Ed.) The State and Movement of Water in Living Organism. Symp. Soc. Exp. Biol. 19: 205–234.

Noilhan J., Planton S. 1989. A Simple Parameterisation of Land and Surface Process for Meteorological Models. American. Meteorol. Soc. 117: 536-549.

Penman H.L. 1948. Natural evaporation from open water, bare soil and grass. Proc. Roy. Soc. Ser A. 193: 120-146.

Penman H. L. 1963. Vegetation and hydrology. Tech. Comm. No. 53. Harpenden, U.K.: Commonwealth Bureau of Soils. Expression et paramètres donnant l'évapotranspiration réelle d'une surface mince. Ann. Agron .26 : 105-123.

Rana G., Katerji N., Mastrorilli M., El Moujabber M. 1997a. A model for predicting actual evapotranspiration under water stress conditions in a Mediterranean region. Theor. Appl. Climatol. 56: 45-55.

Rana G., Katerji N., Mastrorilli M., El Moujabber M. 1997b. Canopy resistance modelling for crops in contrasting water conditions. Phys. Chem. Earth. 23(4): 433-438.

Rana G., Katerji N., Perniola M. 2001. Evapotranspiration of sweet sorghum: a general model and multilocal validity in semiarid environmental conditions. Water. Resour. Res. 37(12): 3237-3246.

Shuttleworth W.J., Wallace J.S. 1985. Evaporation from sparse crops-an energy combination theory. Q. J. R. Meteorol. Soc. 111: 839–855.

Shuttleworth W.J., Gurney R.J., 1990. The theoretical relationship between foliage temperature and canopy resistance in sparse crops. Q. J. R. Meteorol. Soc. 116: 497–519.

Szeicz G., Long I.F. 1969. Surface resistance of crop canopies. Water. Resour. Res. 5: 622-633.

Thornthwaite C. W. 1948. An approach toward a rational classification of climate. Geography Rev. 38(1): 55-94.

Ziemer R.R. 1979. Evaporation and transpiration. Reviews of geophysics and space physics. 17(6): 1175-1186.

Manually operated pile driver for use in the south Iraqi Marshlands

Massimo Monti, Giuseppe Rossi, Stefano Simonini, Francesco Sorbetti Guerri, Matteo Barbari

Dipartimento di Gestione dei Sistemi Agrari, Alimentari e Forestali (GESAAF), Sezione Ingegneria Agraria, Forestale e dei Biosistemi, Università di Firenze, Firenze, Italy

Abstract

Anthropizations are necessary to implement the maintenance, recovery and utilization of wetlands. These interventions should be sustainable in every sense, in particular they should be marked by a low environmental impact. In general this aim can be achieved by using natural materials and carrying out procedures minimally invasive. In Developing Countries the latter point is often supported by the lack of equipment and energy availability, normally obtainable in Industrialized Countries. In practice, to build micro-infrastructures with the above said characteristics, it is normally necessary to drive poles, in our case in wood, in marshland's soil. In order to accomplish this task a manually operated pile driver was designed and built. To operate in the water, a floating pier consisting of removable modular elements was also designed.

Introduction

Aim of the work

The aim of this work is to design, build and make actually executive tools and methods of use that would allow the construction, in appropriate ways, of micro-infrastructures necessary to wise-use of wetlands. These tools and ways to operate should be sustainable. Such characteristic is essential particularly in developing Countries, both from the environmental point of view and from the economic-social one.

Correspondence: Matteo Barbari, Dipartimento di Gestione dei Sistemi Agrari, Alimentari e Forestali (GESAAF), Sezione Ingegneria Agraria, Forestale e dei Biosistemi, Università di Firenze, Italy.
E-mail: matteo.barbari@unifi.it

Key words: wood pile driver, floating pier, wetland ecosystems, Marshlands, Iraq.

Acknowledgments: study carried out within the project funded by Italian Ministry of Foreign Affairs – DGCS Task Force Iraq, titled "Rational management of water resources for agricultural development of rural areas in South Iraq".

Journal of Agricultural Engineering 2013; XLIV(s1):e170
doi:10.4081/jae.2013.(s1):e170

Wetland ecosystems

Worldwide wetlands are areas with a very high conservation value, significantly contributing to human well-being. In these areas water is the primary factor to control environment and associated plant and animal life . Wetland ecosystems are essentials for the conservation of the biodiversity . Article 1.1 of the Ramsar Convention officially defines "Wetlands" .

More than three billion people (around half the world's population) obtain their basic water needs from inland freshwater wetlands. A similar number of people rely on rice as their staple food, a crop largely growing in natural and artificial wetlands. In some parts of the world, such as the Kilombero Wetland in Tanzania, almost the entire local population relies on wetland cultivation for their livelihoods .

Throughout history, in many places, a lot of attempts to "reclamation" have been carried out, that is, in this case, to wetlands draining, conversion and destruction, originated by reasons of particularistic, social, political and health nature. More than 50% of wetlands in North America, Europe, Australia and New Zealand were destroyed during the twentieth century, and many others in many parts of the world degraded (MA, Millennium Ecosystem Assessment, 2005).

To counter these trends, organizations with the mission to protect wetlands are born and developed, giving rise to international and national legislation and regulations (Shine and de Klemm, 1999).

Iraqi Marshlands

Until a few decades ago the Iraqi Marshlands, having an area of over 20,000 km^2, were the largest wetland ecosystem in Western Eurasia (UNEP and Partow, 2001). However, over the past 30 years, they were subject to a gradual drying, which reduced their surface area by about 70%. This drying is due in part to the construction, by neighboring countries, of dams on the rivers, especially the Euphrates, which descend from the mountains of Northern Iraq. But above all the will of Saddam Hussein's Government was decisive to eradicate, and even physically eliminate, Shiite populations gravitating on Marshlands, on which he could not take full control (USAID, 2004; Alwash *et al*., 2008).

The Marshlands were, and still partly are, inhabited by populations with cultural peculiarities and way of life fully integrated in the marsh environment (Kubba, 2011).

For some years some international projects are in progress to reflood Iraqi Marshlands and revitalize activities linked to them, in order to favor their sustainable development (Eden Again, 2003; AMAR International Charitable Foundation, 2001).

Wise use of wetlands and wustainable anthropizations

Protected wetlands are often considered as "nature sanctuaries", rather than valuable ecosystems that can also be used sustainably by communities. Nevertheless, in the course of time, in some of these ecosystems a human presence was established, which, in many cases

and for very long periods, utilized resources from animal and plant environment employing means and methods compatible with the sustainability.

Man, sometimes unconscious of wetlands fragility, in attempt to increase their productivity, has greatly disturbed the natural system, not only severely damaging it, but also causing a productivity decline.

In order to be properly maintained and protected, economically sustainable activities have to be performed in wetlands. They can also provide jobs and livelihood for people living in and around them (Russi *et al*., 2013). All this goals can be reached by practicing the "wise use".

The wise use of wetlands is defined as "the maintenance of their ecological character, achieved through the implementation of ecosystem approaches, within the context of sustainable development". "Wise use" therefore has at its heart the conservation and sustainable use of wetlands and their resources, for the benefit of humankind (Ramsar Convention on Wetlands, 2010). "Sustainable development" is intended as defined in "Our Common Future" Report (United Nations, 1987).

Wetlands provide a different range of valuable services. In general, merely by their existence, they perform functions such as reduction of the damaging impact of floods, control of pollution and regulation of the climate. Among the many functions that wetlands can perform, those related to direct or indirect productivity are particularly interesting in our study. The following products can be mentioned: fish and timber, wildlife (directly harvested or used indirectly for ecotourism or scientific research purposes), housing materials such as reeds, medicinal plants, agricultural, livestock and pastoral products, water supply for domestic and irrigation (CBD, 2004; UNEP, 2007; Russi *et al*., 2013; Ramsar Convention on Wetlands; UNWTO, 2012). These products and activities have direct and immediate benefits for local communities and peoples living in or close to wetlands.

All these activities, in order to be carried out, require changes of the nature, even in the slightest degree: namely, small anthropizations are realized. The most important feature of anthropizations, to be consistent with the implementation of a sustainable development, is not so much the small size, as their reversibility. They should be in maximum degree deconstructible (Barbari *et al*., 2012a). The degree of deconstructibility, which in some cases may reach 100%, essentially depends on the used materials and construction methods. Suitable materials can be considered those of natural origin (wood, reeds, straw, and other fibrous materials mainly made of cellulose, raw earth, stone) and steel, which to some extent is almost always indispensable and, in any case, is a 100% recyclable material (Barbari *et al*., 2012 b; Berge, 2001).

Natural materials are often regarded as low-tech or outdated. On the contrary, we want strongly to affirm here that "there are no low-tech or outdated materials, but only low-tech or outdated ways of using them".

Infrastructures, or rather micro-infrastructures, which are necessary for the sustainable use and exploitation of wetlands are, for example: riparian adjustments, small channels dams, landings and moorings, boardwalks, small earth roads, pathways, shelters for boats, shacks, small buildings for the management of activities (fishing, breeding, cultivations, fish farming, pastoralism, bird-watching, etc.) and other anthropizations, which are part of a fully-fledged system of sustainable management of wetlands.

Materials and methods

Piles

In wetlands for the construction of all the above-mentioned infrastructures, the placement of piles is always required, specifically wooden piles or, secondly, steel piles, driven into the soil. The piles serve as foundation, support and anchorage for constructions. These functions can also be provided by other types of structures, for example concrete arrangements, but these are not compatible with sustainability objectives above outlined.

The major criticisms regarding the use of wood can be the difficulty of supplying, because sometimes the wood is not naturally present in the vicinity of the place of use, and the poor durability.

As regards the first aspect, it can be underlined that steel and concrete are never naturally present in the vicinity of the place of use. Given the density/mechanical strength ratio of the materials, it is presumable that the specific transportation environmental impact related to the wood is lower than for the other materials. As regards the second aspect, the durability of the wood depends on the species used and can actually be lower than that of the concrete, which anyway is not unlimited. However, the advantages of the use of wood in relation to sustainability (Barbari *et al.*, 2012b) are such as to justify its use. Moreover timber is widely applied worldwide in wetlands.

The diameter of the wooden piles used for the type of construction considered in this study can vary roughly from 10 cm to 16-18 cm.

Piles driving

To drive small diameter piles, such as those here required, in industrialized countries hydraulically or pneumatically operated machineries are generally employed, in which the energy is supplied by a thermal engine. Very popular are the vibratory pile drivers applied to the arm of excavators, pile drivers connected to the power takeoff of farm tractors, pneumatic pile drivers connected to compressors. When the piles have to be driven in submerged soil, the pile drivers should be placed on floating docks.

When operating in ecosystems having high natural value, transportation, placement and operation of pile drivers and of related actuator machinery could lead to serious problems of environmental impact.

In developing countries, and particularly in wetlands, machines of the above type are not usually available. Even if they were, they would have costs that fall outside of the actual economic availability of local populations. In addition, the fragility of ecosystems requires the utmost caution relating to materials and methods used.

For all the above aspects, the use of a manually operated pile driver, hammering body type, can be considered the optimal solution.

This type of pile drivers has a history of millennia and, given that since ancient times a highly efficient technology has been adopted, in the course of time it had no major developments. The model of pile drivers present in the Department GESAAF of University of Firenze (Figure 1) probably is not very different from the machinery used by Julius Caesar to build the bridges on the Rhein river, 55 BC and 53 BC.

Today manually operated pile drivers are not produced, with the exception of very small types, which, however, can effectively perform the limited functions to which they are intended.

On the basis of specific needs shown in this paper, the researchers of Department have designed and constructed a manually operated pile driver, and designed a floating pier to build on site.

Design

Border conditions

The pile driver and the floating pier have been designed taking into account the below boundary conditions:

- The pile driver and the floating pier should be used, and replicated, in areas in which there is, in contrast to industrialized countries, large supply of cheap manpower. In such areas local populations have generally kept the "the art of getting by", ability that, con-

versely, technological progress has greatly reduced in the "Northern hemisphere".
- The pile driver should be manually operated.
- The materials used in construction should be readily available on site at low cost. If some materials are not available, they have to be replaced with others having the above characteristics, with a reasonably moderate drop in overall efficiency.
- The pile driver and the floating pier should be made by very simple mechanical parts, in order to be built in a basic blacksmith workshop and replicated on site. For example, for the vertical raising of the truss the solution in hinged portions operated by the winch has been rejected, because it would involve excessive complications and machining precision.
- The pile driver and the floating pier should consist of easily transportable elements and they should be easily assembled on the site of use, therefore hand movable and not longer than 3 m.

Pile driver

General design

The pile driver has been structurally designed, also according to the relevant Eurocodes (EN, 2007) (Figure 2).

Given the type of soil on which to operate, the piles to be used for the construction of micro-infrastructures generally are of the "suspended" type. Moreover their resistance to horizontal actions are important at least as the resistance to vertical actions. However it must be considered that the values of these last actions are far less than those generally encountered in pilings for ordinary buildings and civil works for which, moreover, the eligible permanent deformations are far lower than those tolerated in the designed micro-infrastructures.

The formulas for the calculation of the vertical lift of the piles (Davidian, 1973) are based or on the knowledge of refusal (so-called dynamic), or on knowledge of the characteristics of the soil (so-called static). The latter is also necessary for the calculation of the resistance to horizontal actions (ASABE, 2000; Giacomin *et al*., 2005).

Of course the refusal is unknown; the values of density, internal friction and cohesion of the soil are only vaguely conceivable. The maximum mass of the pile is about 60 kg (pile Ø 16 cm, l = 6 m). Given these uncertainties, the pile driver is designed so that both the mass of the hammer and the stroke are largely alterable in a simple manner. For the mass of the hammer actually realized a value is adopted to allow the movement by hand.

When the pile driver has to be actually used, being very unlikely to have reliable data on soil characteristics, it could be necessary to drive some attempt piles, in order to develop the optimal values of the mass of the hammer and the stroke.

Relevant design specifications

The structure consists of 4 main pieces which can be assembled together on-site: the chassis CH1 (approximately: length=3.00 m, mass=100 kg), the lower truss TR1 (approximately: length=2.50 m, mass=70 kg), the middle truss TR2 (approximately: length=2.50 m, mass=60 kg), which can be replicated in order to increase the stroke of the hammer, and the upper truss TR3 (approximately: length=2.70 m, mass=70 kg). Other removable components are the hammer (rough mass 70 kg) and the Pile Ties (rough mass 10 kg). The mass of the hammer can be increased by applying steel sheets, if necessary.

The chassis consists of a tube frame and rests on 4 adjustable bases of the type used for scaffolds. Four supports are welded to the frame by 4 castor wheels. Four coach screws are used for the connection of the base plate of the element TR1. The coach screws are fitted with double nut and lock nut in order to make adjustable the slant of the truss with respect to the chassis. The hoist winch is bolted to the chassis; to the chassis the pulley for the transmission of the hoist rope is also connected. The pulley is equipped with a tube-frame in order to prevent the derailment of the rope. This transmission can be avoided joining directly the hoist rope to the pulley at the head of the truss, thereby reducing the friction of the system. The bending moment is minimized acting on the truss. In the realized configuration the winch has a reduction ratio of about 1/6.

The 3 elements TR1, TR2, TR3, which constitute the truss, were constructed using prefabricated elements, to which the rail of the hammer stroke and the pulleys on the head have been applied. It was decided to use these prefabricated elements in order to reduce the process-

Figure 1. Pile driver model, owned by the GESAAF, and a present-day hand operated pile driver in Venice.

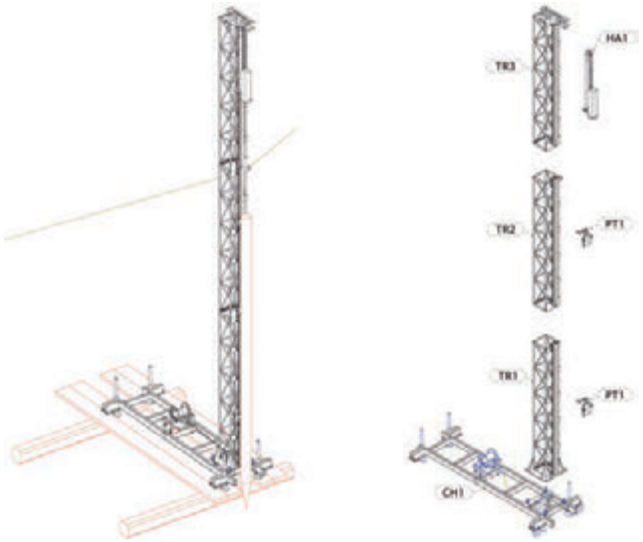

Figure 2. The pile driver on ground, and its major components.

ing times. However, the implementation of these elements in the workshop presents no difficulties. In order to obtain a perfectly rectilinear rail, consisting in a IPE80 section bar, this was applied on the truss fully assembled and horizontally disposed. To guarantee the easiness and the precision of the mutual coupling of the elements in the on-site assembly phase, appropriate slide elements have been affixed. The pulleys on the head are equipped with a tube-frame in order to prevent the derailment of the rope. For the pulleys normal wheels for sliding gates were used.

The hammer and the pile-ties run on the flange of the IPE section bar, lubricated with grease, by means of steel sliding blocks sufficiently long and loose as to avoid any jamming.

For the uplifting chains and steel ropes anchored to stakes driven into the ground with a mallet are used. Such stakes are expressly designed equipped with variable height fastening. Lifting is implemented by means of a griphoist. The horizontal actions on the pile driver (mainly wind) are countered by two stays in synthetic fiber fitted with hoist and cam-cleats. The lifting rope is of the type with great flexibility and small elongation under stress (sheet rope).

Construction

In order to demonstrate that the pile driver, as well as designed, can be built by unskilled personnel in small blacksmith workshops, it was completely built in the workshop held by GESAAF, by staff belonging to the Department, then by non-professionals of mechanical constructions. The workshop is equipped with the following major equipment: drill press for holes up to Ø16 mm, miter saw for elements having transverse dimension not exceeding 100 mm, wire welding and electrode welding, lathe. All equipment is of usual level (Figure 3).

Piles preparing for driving

The head of the pile must be circled with a frettage to avoid splitting under the blows of the hammer. A simple method, specifically designed, consists in fixing chain, strongly tightened with a bolt, located few centimeters away from the upper surface (Figure 4).

The tip of the pile must be formed so that it is as much as possible aligned with the axis of the pile. If the pile is constituted by green wood the tip can be hardened by subjecting it to a strong heating in order to evaporate moisture, however without coming to burn.

Floating pier

Design

The floating pier has been structurally designed, also according to the relevant Eurocodes (EN, 2007).

The floating pier was conceived as a 3D truss which can be assembled on-site, backed into the water from empty oil barrels, having the capacity of 216.5 l (ISO, 2002) (Figure 5).

The elementary components of the floating pier have dimensions 1210x910x460 mm and a mass ranging from 35 kg to 42 kg; therefore they are movable by hand.

To avoid that the entire floating pier has to be launched, assembly must take place in water. For this purpose a system of connection joints has been designed, so that the bolting must be performed only in the part of the structure that emerges above the surface of the water. Above the floating reticular structure a deck of wood boards has to be placed.

The floating pier could not be built in Firenze because the shipping costs would have far exceeded the cost of construction. However, the extreme simplicity of the structure allows that it is made in-situ with ease and economy.

Figure 3. Pile driver under construction; uplifting; stays hooking system, and pile driver in working position.

Figure 4. Pile head frettage.

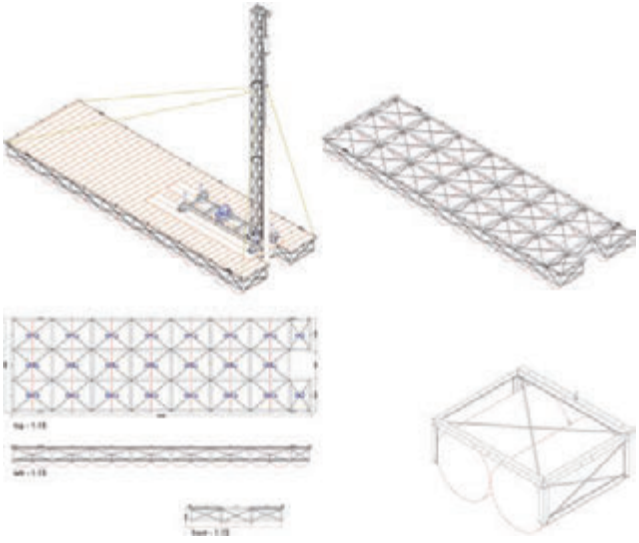

Figure 5. The pile driver on the floating pier; the complete 3D Truss; pile driver views; a modular component of the floating pier.

Results

In order to test the proper functioning and effectiveness of the pile driver, it has been assembled and positioned within the competence area of the GESAAF. The soil on which the test was carried out has physical and mechanical characteristics different from those on which the pile driver should carry out his work. However, the trial was intended to establish the correctness of the overall functioning of the mechanism, and a generic indication of its effectiveness.

Conclusions

All the activities were carried out with satisfactory results. The effectiveness of the machine was verified, and in particular it was demonstrated that the pile driver can be placed and removed with the use of only 3 people. In essence the tests give reasonable assurance that the tools can be effectively used in the expected places and conditions of employment.

References

[1] Alwash, A., Alwash, S., and Cattarossi, A. (2008). Iraq's Marshlands - Demise and the Impending Rebirth of an Ecosystem. Baghdad: Iraq Foundation.

[2] AMAR International Charitable Foundation (2001). The Iraqi Marshlands. AMAR International Charitable Foundation.

[3] ASABE - American Society of Agricultural and Biological Engineers (2000, October). ANSI/ASAE 486.1 - Shallow Post Foundation Design. USA: ASABE -American Society of Agricultural and Biological Engineers.

[4] Barbari, M., Conti, L., Monti, M., Pellegrini, P., Rossi, G., Simonini, S., and Sorbetti Guerri, F. (2012). Antropizzazioni decostruibili per il non-consumo del territorio rurale - Parte I: dallo sviluppo sostenibile alle antropizzazioni decostruibili. L'Edilizia Rurale tra Sviluppo Tecnologico e Tutela del Territorio. Firenze: AIIA - Associazione Italiana di Ingegneria Agraria.

[5] Barbari, M., Conti, L., Monti, M., Pellegrini, P., Rossi, G., Simonini, S., and Sorbetti Guerri, F. (2012). Antropizzazioni decostruibili per il non-consumo del territorio rurale - Parte II: progettazione per la decostruibilità. L'Edilizia Rurale tra Sviluppo Tecnologico e Tutela del Territorio. FIRENZE: AIIA - Associazione Italiana di Ingegneria Agraria.

[6] Berge, B. (2001). Ecology of Building Materials. Oxford, UK: Architectural Press.

[7] CBD, Convention on Biological Diversity. (2004). The CBD Guidelines on biodiversity and tourism development. Montreal, Canada: Secretariat of the Convention on Biological Diversity.

[8] CBD, Convention on Biological Diversity; UNEP, United Nations Environment Programme. (2007, Feb). Users' Manual on the CBD Guidelines on Biodiversity and Tourism Development. Montreal, Canada: Secretariat of the Convention on Biological Diversity.

[9] Davidian, Z. (1973). Pali e fondazioni su pali. Bologna: C.E.L.I.

[10] Eden Again (2003). Building a Scientific Basis for Restoration of the Mesopotamian Marshlands. Baghdad: The Iraq Foundation.

[11] EN (2007). EN 1993-1-1 - Eurocode 3 - Design of steel structures.

[12] Giacomin, A., Monti, M., Pellegrini, P., and Sorbetti Guerri, F. (2005). Resistenza alle azioni orizzontali di pali in legno infissi nel terreno. Verifiche sperimentali. L'ingegneria agraria per lo sviluppo sostenibile dell'area mediterranea. Catania: AIIA.

[13] ISO - International Organization for Standardization (2002). ISO 15750-2:2002. Packaging — Steel drums — Part 2: Non-removable head (tight head) drums with a minimum total capacity of 212 l, 216,5 l and 230 l.

[14] IWMI - International Water Management Institute (2010). Using wetlands sustainably. Colombo: International Water Management Institute. doi:10.5337/2010.231

[15] Kubba, S. (2011). The Iraqi Marshlands and the Marsh Arabs. Reading, UK: Ithaca Press.

[16] MA, Millennium Ecosystem Assessment. (2005). Ecosystems and human well-being: wetlands and water synthesis. Washington, DC, USA: World Resources Institute.

[17] Niemann, G. (1967). Elementi di macchine. Springer.

[18] Ramsar Convention on Wetlands (1971, Feb 2). The Convention on Wetlands text, as originally adopted in 1971. Retrieved from http://www.ramsar.org/cda/en/ramsar-documents-texts-convention-on-20708/main/ramsar/1-31-38%5E20708_4000_0__

[19] Ramsar Convention on Wetlands (2008, Oct-Nov). The Changwon Declaration on human well-being and wetlands. "Healthy wetlands, healthy people". Changwon, Republic of Korea.

[20] Ramsar Convention on Wetlands (2010). The Ramsar Handbooks for the wise use of wetlands (IV ed.). Gland, Switzerland: Ramsar Convention Secretariat.

[21] Ramsar Convention on Wetlands; UNWTO, World Tourism Organization (2012). Destination wetlands: supporting sustainable tourism. Secretariat of the Ramsar Convention on Wetlands, Gland, Switzerland, & World Tourism Organization (UNWTO), Madrid, Spain.

[22] Russi, D., ten Brink, P., Farmer, A., Badura, T., Coates, D., Forster, J., and Davidson, N. (2013). The economics of ecosystems and biodiversity for water and wetlands. London, UK: IEEP, Institute for European Environmental Policy, GB; Ramsar Convention Bureau; Wetlands International; CBD, Convention on Biological Diversity; IUCN, International Union for Conservation of Nature; UFZ, Helmholtz Zentrum für Umweltforschung, DE.

[23] Shine, C., and de Klemm, C. (1999). Wetlands, Water and the Law. Using law to advance wetland conservation and wise use. Gland, Switzerland, Cambridge, UK and Bonn, Germany: IUCN, International Union for Conservation of Nature.

[24] UNEP, and Partow, H. (2001). The Mesopotamian Marshlands: Demise of an Ecosystem. Nairobi, Kenya: United Nations Environment Programme - Division of Early Warning and Assessment.

[25] United Nations - World Commission on Environment and Development (1987). Our Common Future.

[26] United Nations (1992, May 22). Convention on Biological Diversity. Nairobi, KENYA.

[27] USAID - United States Agency for International Development (2004). The Iraq Marshlands Restoration Program. USAID. Retrieved from www.usaid.gov/iraq.

Experiences of improving water access in rural areas in Guatemala

Elena Bresci, Antonio Giacomini, Federico Preti

Dipartimento di Gestione dei Sistemi Agrari, Alimentari e Forestali (GESAAF), Sezione di Ingegneria Agraria, Forestale e dei Biosistemi, Università di Firenze, Firenze, Italy

Abstract

The GESAAF Department of the UNIFI has been involved in the project *"Gestione ambientale e del rischio nel dipartimento di Sololà"* in the period 2011-'12 aiming at guaranteeing water access to people leaving in rural areas in the Sololà Department in Guatemala, in collaboration with the two NGOs *Movimento Africa '70* and *Oxfam Italia*. Appropriate technologies, such as EMAS pump and well drilled with the Baptista-Boliviana technique, have been proposed and utilized for improving water access in areas where lack of water represented a limiting factor for the human development. They can be both considered compatible with local, cultural and economic conditions: in fact locally available materials are used and the tools can be maintained and operationally controlled by the local users. At the end of the project, 52 EMAS pumps have been installed and 19 wells drilled, 33 pumps have been installed in already existing wells tank. Formation activities of local people played an important role: diffusion actions of the methodology started from schools, 20 workers participated to an in class course and more than 100 participated in the field work. Monitoring activities on the 52 installed pumps have been carried out in order to check the performances of the pumps and the knowledge level acquired by the users. After some months of operation, more than 80% of the pumps were correctly functioning and the required maintenance activities have been carried out in collaboration with the local users. In order to analyze the project results, a SWOT analysis (Strengths, Weaknesses, Opportunities, and Threats) has been carried out for developing a strategy able to tackle the weaknesses and threats of the procedure. The application of the SWOT analysis showed to be an useful tool to analyse the current situation coming from the ended project. It has been helpful to gauge how the project performed. The analysis results may be also utilized for exploring strengths and weaknesses of a possible transferring of the methodology to other sites.

Correspondence: Prof. Elena Bresci, Università degli Studi di Firenze
Dipartimento GESAAF, Via San Bonaventura 13, 50145 Firenze, Italy
E.mail: elena.bresci@unifi.it

Key words: Bolivian Baptist well drilling technique, EMAS pump, SWOT analysis, improved water access.

Journal of Agricultural Engineering 2013; XLIV(s1):e171
doi:10.4081/jae.2013.(s1):e171

Introduction

One of the World Health Organization (WHO) Millennium Development Goals has been established in cutting in half the proportion of people without access to safe drinking water and basic sanitation by 2015 (Sachs, 2005). WHO has declared 2005–2015 the decade of water, with the goal of establishing the framework to eventually provide full access to water supply and sanitation for all people. In order to achieve that goal, the increase of the percentage of residences in rural areas with household connections for drinking water has been set by WHO. In Guatemala, the percentage went from 34% of all households in 1990 to 53% in 2002. Even the increase of that percentage, nearly half of Guatemala's inhabitants of undeveloped areas is obtaining drinking water of doubtful quality from nearby lakes or streams, cisterns, shallow wells, or spring-fed gravity-flow systems. Numerous health problems are still associated with contaminated water consumption, including amoebic dysentery, hepatitis and cholera (Martin and Elmore, 2007). In rural areas of Guatemala, although municipal governments are compelled by law to disinfect water, water treatment to guarantee safe drinking water is not routinely performed. Even though local users consider their water to be clean, it is generally thought by the scientific community as unsafe water in rural areas. Water sources in these areas consist of reservoirs fed by springs or wells and available water is frequently contaminated by both human and animal faeces (Lopez *et al.*, 2003). Disinfecting water by boiling at home, before drinking, is the most common and utilized household water treatment. But without a safe storage, boiled water can be immediately vulnerable to recontamination (Rosa *et al.*, 2010). The WHO (2000) individuated the availability of clean water for drinking as an important concern in developing countries, particularly in Latin America (Elmore and Fahrenholtz, 2007). The access to safe water became more difficult after the 2010 tropical storm, Agatha, made landfall on the Pacific coast of Guatemala on May 29. It resulted in more than 426 mm of rain in a short period of time. Flooding caused extensive damage across a large part of the country. Simultaneously, an eruption of Pacaya Volcano limited search and rescue operations as well as the provision of humanitarian relief. Communities lost homes or had their homes damaged. The loss of crops and livelihoods risks increasing food insecurity. People then lack food and clean drinking water. In 2011, the Department of Agricultural, Food and Forestry Systems (GESAAF) of the University of Florence (UNIFI) has been involved in the project *"Gestione ambientale e del rischio nel dipartimento di Sololà"* aiming at guaranteeing water access to people leaving in rural areas in the Sololà Department in Guatemala, in collaboration with the two NGOs, *Movimento Africa '70* and *Oxfam Italia*. The use of appropriate technologies has been tested on the field, EMAS (*Escuela Móvil del Agua y Saneamiento, http://paulcloesen.50webs.com/DocEMAS/SistemasEMAS.pps#256,1,Sistemas de Agua EMAS*) pump and drilling well with the Baptista-Boliviana technique, have been proposed and utilized for improving water access in areas where lack of water is representing a limiting factor for the human development (Petrone *et al.*, 2009). The term improved water access is used accord-

ing to the definition proposed by Montgomery *et al.*, (2007), representing households that obtain water from sources that are superior to traditional, unprotected ones. Strengths, weakness, opportunities and threats (SWOT) analysis has been applied in order to analyze the project results, and developing a strategy able to tackle the weaknesses and threats of the procedure. Based on that, modifications will be applied before transferring the methodology to some other rural areas both in Guatemala and in some other countries, characterized by similarity in the difficulty of water access.

Materials and methods

Study area

The study is conducted over a period of two years (2011-2012) in the Municipality of Sololà, Department of Sololà, in Guatemala (Figure 1). The Department covers an area of 1061 km^2, representing the 9% of the VI Region, made up of other five departments: Totonicapán, Quetzalenango, San Marcos, Suchitepéquez and Retalhuleu. In 2008, the population of the Department was of about 398000 people (49% male and 51% female). More than 96% of the population belongs to the Mayan ethnicities: Tzutujiles, Quichés and Kakchiqueles. Its main subsistence is agriculture with a minority relying in industry and commercial activities. Literacy is 50% and, in some areas, reaches only the 10%. An estimated 77% of the population in the Department is classified as poor and 18% as extreme poor. In these rural communities, it has been estimated that more than 40% of the families does not have permanent access to water, and the situation became worst after the hurricane Agatha. In fact, the most common water resource, spring water, has not been any more available after the hurricane for both quantity and quality reasons.

The project *Gestione ambientale e del rischio nel dipartimento di Sololà*

The Department of Agricultural, Food and Forestry Systems (GESAAF) of the University of Florence (UNIFI) has been involved in the project *"Gestione ambientale e del rischio nel dipartimento di Sololà"* in the period 2011-'12 aiming at improving life conditions of people, leaving in rural areas in the Sololà Department in Guatemala, in collaboration with the two Italian NGOs, *Movimento Africa '70* and *Oxfam Italia* (funded also by Tuscany Region and Italian Ministry of Education and Research, Cooperation funds). In particular, the GESAAF focused the attention on improving water access to families living in rural areas, providing a safe and reliable source of water, applying the participatory approach and using appropriate technologies.

Figure 1. The study area.

Participatory approach, in the bottom up form, involved beneficiaries starting from scratch, through the analysis of the information given from the interactive participation (Pimbert and Pretty, 1994). Surveys carried out on the field, through questionnaires and interviews to people in rural areas in the Sololà Department, showed water access as a priority to favouring the human development in that area. Appropriate technologies, such as the EMAS (*Escuela Móvil del Agua y Saneamiento*) pump and the Bolivian Baptista well drilling technique (http://www.waterforallinternational.org/Documents/WFA%20Bolivian%20Baptist%20Drilling%20System.pps), have been proposed and utilized for improving water access in areas where lack of water represented a limiting factor for the human expansion. They can be both considered compatible with local, cultural and economic conditions: in fact, locally available materials are used and the tools can be maintained and operationally controlled by the local users, once trained. Many local associations have been involved in the project to ensure the local participation: *Asociacíon Amigos del Lago* (AALA), *Asociacíon para el Mejoramiento Habitacional de Guatemala* (MEJORHA), *Oficina Municipal de Agua de Sololà*, *Oficina Municipal Indígena de Sololà, Oficina Municipal de Agua (OMA)*.

The individuation of sites for well drilling has been carried out through the interactive participation of local people in joint analysis, to strengthen the role of local institutions. In fact, interdisciplinary methodologies, seeking multiple objectives (social, medical, sanitary, etc.) have been tested. In such a way, local groups may have control on the decisions and in the long term, will have a stake in maintaining operational the structures (well and pump). Some criteria considered for well drilling localization were represented by: water table depth according to local people information, soil type, family priorities (number of children, income, number of women), number of family utilizing the same well, collaboration offered by the families in well drilling, collaboration offered by people of the community in the case of collective well drilling (school, public sites, etc.). Formation activities of local people played an important role: diffusion actions of the methodology started from schools, 20 workers participated to an in class course and more than 100 participated in the field work.

The well drilling and EMAS pump construction (Figure 2a) have been carried out by trained on the field workers, some of them were the owner of the well and some other were simple workers that have learned or where learning the technique. In fact, it happened that people working for a well became the responsible for the training in a nearby well. The OMA engaged itself to provide water quality analysis for each location of pump installed. Accuracy has been paid on well protection by contamination from the surface, but obviously, nothing could be made on the original quality of the water. Monitoring activities on the 52 installed pumps have been carried out in order to check the performances of the pumps (Figure 2b) and the acquired knowledge level by the users. More than 70% of the pumps were correctly functioning and the required maintenance activities have been carried out in collaboration with the local users.

The SWOT analysis

Strengths, Weakness, Opportunities and Threats (SWOT) approach involves thinking and diagnosis of factors related to a new product, technology, management or planning (Weihrich, 1982). It is considered a common and useful tool in strategic planning, where all factors influ-

a) b)

Figure 2. a) The EMAS pump in a drilled well. 2b) Performing analysis on the EMAS pump in an existing well tank.

encing the operational environment are diagnosed with greater details (Kotler, 1994; Smith, 1999; Hill and Westbrook, 1997). In particular, it allows analysts to classify factors into internal (strengths, weaknesses) and external (opportunities, threats) as they relate to a decision and thus enables them to compare opportunities and threats with strengths and weaknesses. One of the main limitation of the approach is that the importance and the value of each factor cannot be measured quantitatively. It appears clear, then, that it is difficult to assess which is the factor influencing the strategic decision most (Pesonen *et al.*, 2000).

The actions to be undertaken deduced from the matrix analysis are represented by: build on strengths; eliminate weaknesses; exploit opportunities; mitigate the effect of threats.

Results

At the end of the project, 52 EMAS pumps have been installed and 19 wells drilled, 33 pumps have been installed in already existing wells tank. The main characteristics of the two situations are presented, respectively, in Table 1 and 2.

As regards, the well drilling, the Baptista Bolivian technique seemed to be adequate to the local situation, only in two cases out of 19, it has been necessary the abandonment of the original site of drilling, due to the presence of a rock stratum. In all the other cases, there were mainly sandy strata. This is the reason why the numbers go from 1 to 21. The mean value of the well depth is 4.8 m (with a standard deviation of 2.09 m) below the water level. The mean values of the number of days needed for the drilling is around 13 (with a standard deviation of 5), and obviously it depends on the strataum type found in the aquifer. When rock is present it takes much longer.

33 EMAS pumps have been located in existing wells of the tank type. The number of days, variable from 1 to 3, have been necessary for the pump construction, generally one day, and for realizing the cement structure for closing the well, once the pump have been installed. In fact, attention have to be put on avoiding contamination on the well water. As we can see from Table 2, the water level in the existing wells is much closer to the topographic surface (mean value of 2.7 m with a standard deviation of 2.1 m) than in the case of drilled wells. The mean value of work days is 2.6 (with a standard deviation of 0.68). All the existing wells were belonging to families; that's why the new drilled wells have been located in area where the use could be collective. Water was previously withdrawn with a pail and the well was opened, subjected to contamination from the above. The utilization of the hand pump and the possibility of closing the well to avoiding contamination made users very pleased with proposed tools.

The monitoring phase has been carried out in the month of June 2012, after 2-3 months of pump operation. All the 52 pumps have been tested to verify their performances. The 85% of the pumps (44 out of 52) were functioning. The water volume extracted in the unit time (1 minute) has been compared with the ideal value, taken as 15 l/min

Table 1. Drilled wells with the Baptista Bolivian technique and EMAS pump positioning.

N.	Well location	Access type*		Depth [m]		Work days
		D	C	Water	Well	
1	Escuela Central Chuiquel		×	10.5	16	24
2	Aldea San Juan Argueta		×	3	11	11
3	Escuela Central Xajaxac		×	2.5	4.3	23
4	Escuela Central Los Encuentros		×	17	23	11
5	Central Los Encuentros	×		15	22	6
6	Cantón Chiuel	×		20	24.5	25
7	Escuela Nueva Amanecer		×	20.5	26	15
8	Cantón Xajaxac	×		8.5	12	13
9	Sector Nueva Amanecer	×		25	29	8
10	Escuela San Francisco		×	15.5	20.30	12
12	Escuela El Ascenso		×	16.5	21.8	17
13	Central Los Encuentros	×		12	23.85	8
14	Central Los Encuentros	×		24	28.3	10
16	Caserío San Francisco	×		16	21	9
17	Escuela Pacoxom		×	3.5	7.85	14
18	Escuela El Encanto		×	16	20.2	9
19	Caserío Chujulimul		×	17.5	23	10
20	Caserío El Rosario		×	25.5	29.3	9
21	Caserío El Paraíso	×		22	25.8	17

* D: Domestic; C: Collective.

Table 2. EMAS pumps in existing well tanks.

N.	Well and pump location	Access type*		Depth [m]		Work days
		D	C	Water	Well	
1	Cantón Xajaxac	×		2.80	4.35	3
2	Cantón Xajaxac	×		1.50	2.65	5
3	Cantón Xajaxac	×		13.40	15.80	4
4	Sector Nueva Amanecer	×		1.70	8.20	2
5	Sector Nueva Amanecer	×		3.60	12.90	2
6	Cantón Chiuel	×		3.25	10.10	2
7	Sector Nueva Amanecer	×		2.10	10.30	2
8	Sector Nueva Amanecer	×		1.90	9.80	2
9	Aldea Los Encuentros	×		2.90	10.20	2
10	Sector Nueva Amanecer	×		1.90	7.80	2
11	Aldea Los Encuentros	×		3.90	15.30	2
12	Aldea Los Encuentros	×		2.20	9.90	2
13	Aldea Los Encuentros	×		2.10	6.20	2
14	Aldea Los Encuentros	×		1.90	6.10	2
15	Caserío San Francisco	×		1.90	8.40	2
16	Caserío San Francisco	×		2.60	7.80	3
17	Caserío El Rosario	×		2.10	9.50	3
18	Caserío El Rosario	×		2.00	7.10	2
19	Caserío El Rosario	×		1.90	8.40	2
20	Caserío Vista Hermosa	×		0.90	23.20	2
21	Caserío Vista Hermosa	×		1.68	12.50	2
22	Caserío Paxocon	×		2.60	17.50	3
23	Caserío Chujulimul	×		1.60	14.50	2
24	Caserío Chujulimul	×		2.60	8.00	2
25	Caserío Paxocon	×		2.10	4.65	3
26	Caserío Valle del Norte	×		1.50	16.10	2
27	Caserío Valle del Norte	×		2.40	8.90	2
28	Caserío Valle del Norte	×		5.50	12.00	2
29	Caserío Valle del Norte	×		2.10	10.60	2
30	Caserío La Fé	×		2.40	16.80	2
31	Caserío La Fé	×		1.90	9.40	2
32	Caserío Central	×		2.00	4.10	2
33	Caserío Chuiquel	×		2.30	11.20	2

* D: Domestic; C: Collective.

Table 3. The SWOT matrix.

Internal	External
Strengths • Availability of pump material construction on the local market • Easily repaired • Hand operated (men, women, children) • Low cost of the EMAS pump • Pumping up to 40 m depth • Water can be pumped directly into an elevated storage tank	Opportunities • Improved water access • Access to water of a better quality • Partnership with other communities for system implementation and pump construction
Weaknesses • Lack of interest in recognizing low pump performance from the users • Testing of acquired competence • Differences in time needed for pump installation	Threats • Lack of hydrogeological map • Difficulties in well drilling in presence of rocks • Groundwater quality concerns

(pump mobile part excursion equal to 45 cm and 50 pumping per minute). 26% of the pumps (5 out of 19) had a performance mean value of 90% (with a standard deviation of 7%), for the 73% of the pumps there were problems in the wells for producing water both in terms of quantity (42%) and quality (32%) due to the presence of too much sediments. Then, activities related to improving well water production, has been carried out and, afterwards, the analysis of the produced water volume. The performance of the pumps, located in the existing wells, showed a mean value of 93% (with a standard deviation of 7%). It appears clear that problems of water production were mainly depending on the well drilling.

In order to analyze the project results, a SWOT analysis (Strengths, Weaknesses, Opportunities, and Threats) has been carried out for developing a strategy able to tackle the weaknesses and threats of the proposed model. The internal system is represented by the use of the EMAS pump and the Baptista Bolivian technique for well drilling, the external system is the environment.

In Table 3 the SWOT matrix is presented.

Conclusions

In the framework of the project *"Gestione ambientale e del rischio nel dipartimento di Sololà"* (2011-'12) the GESAAF Department of the University of Florence (UNIFI) tested the utilization of appropriate technologies, the EMAS pump and the well drilling Baptista-Boliviana technique, for improving water access to people leaving in rural areas in the Sololà Department in Guatemala, in collaboration with the two NGOs, *Movimento Africa '70* and *Oxfam Italia*. A total of 52 pumps have been installed, respectively, 19 in drilled wells and 32 in existing wells tank. More than 100 workers contributed to field activities and more than 250 people have been provided with groundwater. The application of the SWOT analysis showed to be an useful tool to analyse the current situation in terms of internal strength. The matrix analysis may be also explored for eliminating internal weaknesses and work on the exploitation of the external opportunities and mitigating the effect of external threats. Based on that analysis, the possible transferring of the methodology to other sites would be characterized by less uncertainty.

References

Ballestero M., Reyes V., Astorga Y. 2007. Groundwater in central America: its importance, development and use, with particular reference to its role in irrigated agriculture. In Giordano M., Villholth K.G., 2007. The Agricultural Groundwater Revolution: Opportunities and Threats to development. CAB International, IWMI.

Danca A. 2000. An explanation of the SWOT analysis process. http://www.stfrancis.edu/ba/ghkickul/stuwebs/btopics/works/swot.htm

Elmore A.C., Fahrenholtz W.G., 2007. Using Science, Engineering and Education to Address Water Supply Challenges in the Highlands of Guatemala. World Environmental and water Resources Congress 2007: Restoring our Natural habitat.

González-Gómez F., Guardiola J., Lendechy Grajales A. 2011. The challenges of water access in Yucatán, México. Proceedings of the ICE - Municipal Engineer,Volume 164, Issue 1, 01 March 2011,45-53.

Hill T., Westbrook, R. 1997. SWOT analysis: it's time for a product recall. Long Range Planning 30(1):46-52.

http://www.waterforallinternational.org/Documents/WFA%20Bolivian%20Baptist%20Drilling%20System.pps.

http://paulcloesen.50webs.com/DocEMAS/SistemasEMAS.pps#256,1,Sistemas de Agua EMAS.

Karppi I., Kokkonen M., Lähteenmäki-Smith K., 2001. SWOT analysis as a basis for regional strategies. Nordregio Working Paper 2001:4, ISSN 1403-2511.

Kotler P., 1994. Marketing Management: Analysis, Planning, Implementation and Control, 8th Edition Printice-Hall, Englewood Cliffs, NJ.

Lopez B., Alvarez M., Mendoza C., Gerba C., Naranjo J., Luby S., Klein R. 2003. Quality of Source Water in A Rural Area of Guatemala. Epidemiology, Vol. 14, Issue 5.

Martin J.H., Elmore A.C. 2007. Water drinking attitudes and behaviours in Guatemala: an assessment and intervention. Journal of Rural and Tropical Health. 6:54-60.

Montgomery M.A., Elimelech M., 2007. Water and sanitation in developing countries: including health in the equation. Environmental Science and Technology, 17-24.

Pesonen M., Kurttila M., Kangas J., Kajanus M., Heinonen P. 2000. Assessing the priorities using A'WOT among resource management strategies at the Finish Forest and Park Service. Forest Science 47(4), 534-541.

Petrone A., Giacomin A., Preti, F. 2009. Sistemi appropriati e sostenibili per l'uso di risorse idriche da parte di comunità rurali: monitoraggio e sperimentazioni. IX Convegno Nazionale dell'Associazione Italiana di Ingegneria Agraria, Ischia Porto, 12-16 settembre 2009, memoria n. 977.

Pimbert M. Pretty J. 1994. Parks, People and Professionals: Putting "Participation" into Protected Area Management. Discussion Paper No. 57. Geneva: UNRISD.

Rosa G., Miller L., Clasen T. 2010. Microbiological effectiveness of disinfecting water by boiling in rural Guatemala. Am. J. Trop. Med. Hyg., 82(3):473-477.

Sachs J.D. 2005. Investing in Development: A Practical Plan To Achieve the Millennium Development Goals; UN Development Programme: New York.

Smith J.A. 1999. The behaviour and performance of young micro firms: evidence from businesses in Scotland. Small Business economics 13:185-200.

Weihrich H. 1982. The TOWS matrix – a tool for situation analysis. Long Range Planning 15(2), 54-66.

Wickramasinghe V., Takano S. 2009. Application of a Combined SWOT and Analysis Hierarchy Process (AHP) for Tourism Revival Strategic Marketing Planning: a case of Sri Lanka Tourism. Journal of the Eastern Asia Society for Transportation Studies, Vol. 8.

World Health Organization (WHO) 2000. Global water supply and sanitation report 2000. UNICEF, New York.